THE UNIVERSITY OF CHICAGO

SITE-SELECTIVE DIFUNCTIONALIZATION OF ARENES AND HETEROARENES ENABLED BY PALLADIUM/NORBORNENE COOPERATIVE CATALYSIS

A DISSERTATION SUBMITTED TO

THE FACULTY OF THE DIVISION OF THE PHYSICAL SCIENCES

IN CANDIDACY FOR THE DEGREE OF

DOCTOR OF PHILOSOPHY

DEPARTMENT OF CHEMISTRY

BY

RENHE LI

CHICAGO, ILLINOIS

AUGUST 2021

To my family

TABLE OF CONTENTS

LIST OF ABBREVIATIONS xii

LIST OF SCHEMES xv

LIST OF TABLES xxi

LIST OF FIGURES xxiv

ACKNOWLEDGEMENT lxi

ABSTRACT lxiii

PREFACE lxvi

Chapter 1: Structurally Modified Norbornenes: A Key Factor to Modulate Reaction Selectivity in the Palladium/Norbornene Cooperative Catalysis 1

1.1. Introduction 1

1.2 C1-Substituted smNBEs 4

1.3 C2-Substituted smNBEs 7

1.3.1 Pd(II)-Catalyzed Meta C−H Functionalization Involving C2-Substituted smNBEs 8

1.3.2 Pd(II)-Initiated Vicinal Difunctionalization Involving C2-Substituted smNBEs 17

1.3.3 Pd(0)-Initiated Difunctionalization of Aryl Halides Involving C2-Substituted smNBEs 20

1.3.4 Pd(0)-Initiated Difunctionalization of Alkenyl Halides Involving C2-Substituted smNBEs 27

1.4 C5-Substituted or C5, C6-Disubstituted smNBEs 30

1.4.1 Pd(0)-Initiated Difunctionalization of Aryl Halides Involving C5-Substituted or C5, C6-Disubstituted smNBEs 30

1.4.2 Pd(II)-Initiated Difunctionalization of Aryl Halides Involving C5-Substituted or C5, C6-Disubstituted smNBEs 40

1.4.3 Pd(II)-Catalyzed Distal C−H Functionalization with C5, C6-Disubstituted smNBEs 41

1.5 Conclusion and Outlook 44

1.6 References 46

Chapter 2: Direct Annulation between Aryl Iodides and Epoxides via Palladium/Norbornene Cooperative Catalysis 55

2.1 Introduction 55

2.2 Results and Discussion 58

2.2.1 Reaction Discovery and Optimization 58

2.2.2 Substrates Scope 60

2.2.3 Synthetic Utility 62

2.3 Conclusion 65

2.4. Experimental Procedures and Characterization Data 66

2.4.1 General Information 66

2.4.2 Preparation of Aryl Iodide 1k 67

2.4.3 Preparation of Substituted NBEs (N2–N8) 68

2.4.4 General Procedure of Palladium and Norbornene Catalyzed Direct Annulation Reaction 71

2.4.5 Large Scale Reaction 86
2.4.6 Direct Annulation with Chiral Epoxide (S)-2h 87
2.4.7 Synthetic Application 90
2.5 NMR Spectra 93
2.6 Crystallographic Data 128
2.7 References 129
Chapter 3: Palladium-Catalyzed Asymmetric Annulation between Aryl Iodides and Racemic Epoxides Using a Chiral Norbornene Cocatalyst 134
3.1 Introduction 134
3.2 Results and Discussion 136
3.2.1 Reaction Discovery and Optimization 136
3.2.2 Substrates Scope 142
3.2.3 Preliminary Mechanistic Study 143
3.3 Conclusion 145
3.4 Experimental Procedures and Characterization Data 146
3.4.1 General Information 146
3.4.2 Chiral Resolution of Ester Substituted NBE 147
3.4.3 General Procedure for Synthesis of Chiral NBEs 149
3.4.4 Enantioselective Transformation Using Chiral NBE-CO_2*i*Pr (N1*) 158
3.4.5 Match and Mismatch for the Stereochemistry of NBE and Epoxide 165
3.5 NMR Spectra 167
3.6 Crystallographic Data 185
3.7 References 187

Chapter 4: Redox-Neutral Ortho Functionalization of Aryl Boroxines via Palladium/Norbornene Cooperative Catalysis 190

4.1 Introduction 190

4.2 Results and Discussion 194

4.2.1 Reaction Discovery and Optimization 194

4.2.2 Substrates Scope 195

4.2.3 Unsuccessful or Less Successful Examples 199

4.2.4 Deuterium Labelling Studies 200

4.2.5 Synthetic Utility 201

4.2.6 Ortho Amination 203

4.3 Conclusion 205

4.4 Experimental Procedures and Characterization Data 206

4.4.1 General Information 206

4.4.2 Condition screening 207

4.4.3 Preparation of Aryl Boroxines 1a-m 211

4.4.4 Preparation of Substituted Benzoic Anhydrides 212

4.4.5 General Procedure of Palladium and Norbornene Catalyzed Ortho Acylation Reaction 213

4.4.6 Analysis of The Side Products in The Reaction of Aryl Boroxine 1i 231

4.4.7 Mechanistic study 232

4.4.8 General Procedure of Palladium and Norbornene Catalyzed Ortho Amination Reaction 235

4.4.9 Synthetic Utility 238

4.5 NMR Spectra 252

4.6 Reference 334

Chapter 5: Sulfenamide-Enabled Ortho Thiolation of Aryl Iodides via Palladium/Norbornene Cooperative Catalysis 342

5.1 Introduction 342

5.2 Results and Discussion 344

5.2.1 Reaction Discovery and Optimization 344

5.2.2 Substrates Scope 347

5.2.3 Synthetic Utility 350

5.3 Conclusion 352

5.4 Experimental Procedures and Characterization Data 353

5.4.1 General Information 353

5.4.2 Control Experiments 354

5.4.3 Preparation of Aryl Iodides and Thiolating Reagents 355

5.4.4 General Procedure of Palladium/Norbornene-Catalyzed Ortho Thiolation Reaction 368

5.4.5 Synthetic Applications 385

5.5 NMR Spectra 392

5.6 Crystallographic Data 460

5.7 References 467

Chapter 6: Direct Vicinal Difunctionalization of Thiophenes Enabled by the Palladium/Norbornene Cooperative Catalysis 474

6.1 Introduction 474

6.2 Results and Discussion 478

6.2.1 Reaction Discovery and Optimization 478
6.2.2 Substrates Scope 486
6.2.3 Synthetic Utility 490
6.2.4 Kinetic Study 491
6.3 Conclusion 493
6.4 Experimental Procedures and Characterization Data 494
6.4.1 General Information 494
6.4.2 Substrates Preparation 495
6.4.3 General Procedure of Direct Difunctionalization of Thiophenes 501
6.4.4 Synthetic Applications 521
6.4.5 Kinetic Study 526
6.5 NMR Spectra 528
6.6 References 575
Chapter 7: Site-Selective Vicinal Difunctionalization of Five-Membered Heteroarenes: Mechanism and Applications 582
7.1 Introduction 582
7.2 Results and Discussion 586
7.2.1 Reaction Discovery and Optimization 586
7.2.2 Substrates Scope 591
7.2.3 Ortho Alkynylation and Ortho Methylation of Heteroarenes 597
7.2.4 Synthetic Utility 599
7.2.5 Mechanistic Study 601
7.3 Conclusion 606

7.4 Experimental Procedures and Characterization Data 607
7.4.1 General Information 607
7.4.2 Preparation of Heteroarene Substrates 608
7.4.3 General Procedure of Vicinal Difunctionalization of Indoles 610
7.4.4 General Procedure of Vicinal Difunctionalization of Pyrroles 626
7.4.5 General Procedure of Vicinal Difunctionalization of Furans 647
7.4.6 General Procedure of Ortho Methylation and Alkynylation 658
7.4.7 Synthetic Utility 664
7.4.8 Kinetic Study 669
7.5 NMR Spectra 684
7.6 Crystallographic Data 787
7.7 References 791
Chapter 8: Site-Selective Vicinal Double C−H Functionalization of Five-Membered Heteroarenes with Dual Electrophiles 794
8.1 Introduction 794
8.2 Results and Discussion 799
8.2.1 Reaction Discovery and Optimization 799
8.2.2 Substrates Scope 802
8.2.3 Exploration of the Reaction Pathway 804
8.2.4 Synthetic Utility 807
8.3 Conclusion 811
8.4. Experimental Procedures and Characterization Data 812
8.4.1 General Information 812

8.4.2 Preparation of Alkynyl Bromide Substrates 813
8.4.3 Preparation of Structurally Modified Norbornenes (smNBEs) 814
8.4.4 General Procedure of Direct Difunctionalization of Pyrroles..... 816
8.4.5 General Procedure of Direct Difunctionalization of Thiophenes 825
8.4.6 General Procedure of Direct Difunctionalization of Furans 835
8.4.7 General Procedure of Ortho Methylation of Pyrrole 1a..... 838
8.4.8 Mechanistic Study..... 840
8.4.9 Synthetic Utility..... 844
8.5 NMR Spectra 864
8.6 Crystallographic Data 937
8.7 References..... 938

LIST OF ABBREVIATIONS

smNBE	structurally modified norbornene
NBE	norbornene
E	electrophile
Nu	nucleophile
FG	functional group
S_NAr	nucleophilic aromatic substitution
ANP	aryl-norbornyl-palladacycle
L	ligand
Cy	cyclohexyl
EAS	electrophilic aromatic substitution
RuPhos	2-dicyclohexylphosphino-2',6'-diisopropoxybiphenyl
SPhos	2-dicyclohexylphosphino-2',6'-dimethoxybiphenyl
XPhos	2-dicyclohexylphosphino-2',4',6'-triisopropylbiphenyl

DFT	density functional theory
CMD	concerted metalation deprotonation
R.E.	reductive elimination
EWG	electron withdrawing group
DG	directing group
DCE	1,2-dichloroethane
DCM	dichloromethane
BNDHP	1,1'-binaphthyl-2,2'-diyl hydrogenphosphate
TBME	*tert*-butyl methyl ether
HFIP	1,1,1,3,3,3-hexafluoro-2-propanol
Ac-Gly-OH	*N*-acetylglycine
DMAP	4-dimethylaminopyridine
BQ	1,4-benzoquinone
DHBF	2,3-dihydrobenzofuran
DMF	dimethylformamide

PhDavePhos	2'-(diphenylphosphino)-*N*,*N*'-dimethyl-(1,1'-biphenyl)-2-amine
TFP	tri(2-furyl)phosphine
DTBPF	1,1'-bis(di-*tert*-butylphosphino)ferrocene
THF	tetrahydrofuran
NMP	1-methyl-2-pyrrolidinone
dba	dibenzylideneacetone
DMA	*N*,*N*-dimethylacetamide
DME	1,2-dimethoxyethane
TIPS	triisopropylsilyl
MOM	methoxymethyl
Ph	phenyl
NBS	N-bromosuccinimide
PCC	pyridinium chlorochromate

LIST OF SCHEMES

Scheme 1.1. Pd/NBE Cooperative Catalysis 3

Scheme 1.2. Overcoming the Ortho Constraint with C1-smNBEs..... 5

Scheme 1.3. Scope and Late-Stage Functionalization of Bioactive Compounds 6

Scheme 1.4. C2-Substituted smNBEs..... 8

Scheme 1.5. Meta Alkylation and Arylation of Substituted Phenylacetamides Using C2-Substituted smNBEs 9

Scheme 1.6. Meta Amination, Alkynylation and Chlorination of Aniline and Phenol Derivatives 11

Scheme 1.7. Enantioselective Meta C–H Arylation and Alkylation Enabled by a Chiral smNBE 13

Scheme 1.8. Direct Meta Arylation of Electron-Rich Arenes, Electron-Deficient Heteroarenes and Fluorobenzenes. 15

Scheme 1.9. Remote C–H Arylation of Benzoazines, Tetrahydroisoquinolines and Phenylpropanoic Acids 17

Scheme 1.10. Vicinal Difunctionalization of Thiophenes 19

Scheme 1.11. Direct Annulation between Aryl Iodides and Epoxides..... 21

Scheme 1.12. Asymmetric Annulation between Aryl Iodides and Epoxides 23

Scheme 1.13. Asymmetric ortho arylation of Aryl Iodides 24

Scheme 1.14. NBE Effect for the Meta-Substituted Aryl Iodides..... 26

Scheme 1.15. Ortho/Ipso Difunctionalization of Vinyl Triflates/Halides *via* Pd/NBE Catalysis 28

Scheme 1.16. Reported C5-Substituted and C5, C6-Disubstituted NBEs..... 30

Scheme 1.17. Ortho Acylation of Haloarenes Enabled by C5 Methylamide-Substituted NBE ... 32

Scheme 1.18. Pd/NBE-Catalyzed Ortho Alkylation Reaction with Epoxides 33
Scheme 1.19. Ortho Alkylation/Ipso Redox-Relay Heck Cascade 34
Scheme 1.20. Aziridines as Electrophiles in Catellani-type Reactions 35
Scheme 1.21. Ortho Thiolation of Aryl Iodide with Thiosulfonates 36
Scheme 1.22. Ortho Methylation of Aryl Halides 37
Scheme 1.23. Ortho Glycosylation of Aryl Iodides 39
Scheme 1.24. Pd(II)-Initiated Ortho Alkylation and Arylation of Arylboronates 41
Scheme 1.25. Pd(II)-Catalyzed Meta Alkylation of Nosyl-Protected Phenylalanines 42
Scheme 1.26. Pd(II)-Catalyzed Distal Alkenyl C−H Functionalization 43
Scheme 2.1. Synthesis of DHBFs 57
Scheme 2.2. Synthesis of Insecticide Fufenozide 64
Scheme 2.3. Preparation of Aryl Iodide 1k 67
Scheme 2.4. Preparation of N8 68
Scheme 2.5. Preparation of C2 Ester-Substituted NBEs 69
Scheme 2.6. Direct Annulation Reaction via Pd/NBE Catalysis 71
Scheme 2.7. Gram-Scale Preparation of 3aa and 3ja 86
Scheme 2.8. Direct Annulation with Chiral Epoxide (S)-2h 87
Scheme 2.9. Concise Synthesis of Fufenozide 90
Scheme 3.1. Annulation Between Aryl Iodides and Racemic Epoxides 135
Scheme 3.2. Preparation of Enantiomerically Enriched N1* 137
Scheme 3.3. Examination of N10*, N11* and N13* Cocatalysts with the XPhos Ligand 142
Scheme 3.4. Substrate Scope with Enantiomerically Enriched N1* 143
Scheme 3.5. Chiral Resolution of C2-Substituted NBE 147

Scheme 3.6. Chiral NBE Preparation 149

Scheme 3.7. Preparation of C2 Amide-Substituted NBEs..... 153

Scheme 3.8. Asymmetric Annulation Enabled by Pd/Chiral NBE..... 158

Scheme 3.9. Asymmetric Annulation with Enantioenriched 2b and N1 165

Scheme 4.1. Palladium/Norbornene Cooperative Catalysis 191

Scheme 4.2. Proposed Catalytic Cycle 193

Scheme 4.3. Deuterium Labelling Studies..... 201

Scheme 4.4. Tolerance of Aryl Iodide Moieties 202

Scheme 4.5. Controlling the Reaction Sequence Enabled by Orthogonal Chemoselectivity..... 203

Scheme 4.6. General Procedure of the Preparation of Aryl Boroxines 211

Scheme 4.7. Preparation of Anhydride 2o 212

Scheme 4.8. Redox-Neutral Ortho Acylation of Aryl Boroxines 213

Scheme 4.9. Preparation of 1-Naphthylboroxine-d7 232

Scheme 4.10. Deuterium Labelling Study with 1-Naphthylboroxine-d_7 233

Scheme 4.11. Deuterium labelling study with D_2O 234

Scheme 4.12. Redox-Neutral Ortho Amination of Aryl Boroxines..... 235

Scheme 4.13. Preparation of Tethered Substrate 6 238

Scheme 4.14. Sequential Functionalization of 6..... 241

Scheme 4.15. Sequential Functionalization of 5..... 243

Scheme 4.16. Preparation of 1t 245

Scheme 4.17. Preparation of 1u 247

Scheme 4.18. Sequential Functionalization of 1t..... 248

Scheme 4.19. Sequential Functionalization of 1u..... 250

Scheme 5.1. Synthetic Applications 351
Scheme 5.2. Preparation of Aryl Iodides 1n 355
Scheme 5.3. Preparation of Aryl Iodides 1r 356
Scheme 5.4. Preparation of Thiolating Regent 3a 361
Scheme 5.5. Pd/NBE-Catalyzed Ortho Thiolation Reaction 368
Scheme 5.6. Selective Oxidation of the Ortho Thiolation Product 385
Scheme 5.7. Ipso Functionalization with Arylboronates 388
Scheme 5.8. Ipso Sonogashira Coupling 389
Scheme 5.9. Gram-Scale Preparation 390
Scheme 6.1. Direct C−H Functionalization of Heterocycles 476
Scheme 6.2. Potential Challenges for the Proposed Approach 477
Scheme 6.3. Side Product Analysis 480
Scheme 6.4. Preparation of 1r 495
Scheme 6.5. Preparation of 1o 496
Scheme 6.6. Preparation of 1m 498
Scheme 6.7. Preparation of 1s 500
Scheme 6.8. Vicinal Difunctionalization of Thiophenes 501
Scheme 6.9. Gram-Scale Preparation 521
Scheme 6.10. Direct Difunctionalization of Furans 523
Scheme 6.11. Direct C4 Arylation of Thiophenes 524
Scheme 6.12. Kinetic Profile and Competition Reaction 526
Scheme 7.1. Direct C−H Functionalization of Heterocycles 583
Scheme 7.2. Difunctionalization of Indole with C1- and C2-Substituted NBEs 586

Scheme 7.3. Gram-scale Preparation 599
Scheme 7.4. Total Synthesis of (±)-Rhazinilam 600
Scheme 7.5. Kinetic Isotope Effect of C−H Activation 602
Scheme 7.6. Preparation of Proposed Resting State 605
Scheme 7.7. Preparation of 5l 608
Scheme 7.8. Preparation of 7h 609
Scheme 7.9. Vicinal Difunctionalization of Indoles 611
Scheme 7.10. Vicinal Difunctionalization of Pyrroles 626
Scheme 7.11. Vicinal Difunctionalization of Furans 647
Scheme 7.12. Ortho Methylation of Pyrrole 5a 659
Scheme 7.13. Ortho Methylation of Thiophene 9a 660
Scheme 7.14. Ortho Alkynylation of Pyrroles and Thiophenes 661
Scheme 7.15. Gram-scale Preparation 664
Scheme 7.16. Total Synthesis of (±)-Rhazinilam 665
Scheme 7.17. Parallel KIE of Indole 669
Scheme 8.1. The General Reaction Modes of the Pd/NBE Cooperative Catalysis 797
Scheme 8.2. Potential Challenges Associated with the Proposed Reaction 798
Scheme 8.3. Control Experiments 805
Scheme 8.4. Product Derivatizations 808
Scheme 8.5. Synthetic Applications 809
Scheme 8.6. Preparation of 3d 813
Scheme 8.7. Preparation of N1 814
Scheme 8.8. Preparation of N6 815

Scheme 8.9. Pyrrole Difunctionalization with Ortho-Substituted Aryl Iodide 816

Scheme 8.10. Pyrrole Difunctionalization with Ortho-Unsubstituted Aryl Iodide 823

Scheme 8.11. Thiophene Difunctionalization with Ortho-Substituted Aryl Iodide 825

Scheme 8.12. Furan Difunctionalization with Ortho-Substituted Aryl Iodide 835

Scheme 8.13. Ortho Methylation of Pyrrole 1a 839

Scheme 8.14. Control Experiments 840

Scheme 8.15. Gram-Scale Preparation 844

Scheme 8.16. Using 1 mol% $Pd(OAc)_2$ 845

Scheme 8.17. Product Derivatizations 845

Scheme 8.18. Stepwise Tetrafunctionalization of Thiophene 12 850

Scheme 8.19. Direct Tetrafunctionalization of Pyrrole 17 852

Scheme 8.20. Synthesis of ETAr Spacer 22 853

Scheme 8.21. Preparation of Alkynyl Bromide 27 857

Scheme 8.22. Preparation of Thiophenyl Bromide 26 858

Scheme 8.23. Synthesis of P38α MAPK Inhibitor Analogue 30 860

LIST OF TABLES

Table 2.1. Control Experiments for Annulation with Epoxides 59

Table 2.2. Substrates Scope with Aryl iodides[a] 61

Table 2.3. Substrates Scope with Epoxides[a] 62

Table 2.4. Crystallographic Data of 3ah 128

Table 3.1. Optimization Study Based on N1*[a] 139

Table 3.2. Testing Different Substituted Chiral NBEs[a] 140

Table 3.3. Reactions with N12* Using Different Buchwald Ligands 141

Table 3.4. Match and Mismatch between Chiral NBE and Epoxide 165

Table 3.5. Crystallographic Data of A 185

Table 3.6. Crystallographic Data of B 186

Table 4.1. Control Experiments for Ortho Acylation with 2-Tolylboroxine[a] 194

Table 4.2. Substrates Scope with Respect to Anhydrides[a] 197

Table 4.3. Substrates Scope with Respect to Aryl Boroxines [a] 198

Table 4.4. Unsuccessful or Less Successful Examples 200

Table 4.5. Substrates Scope of the Ortho Amination Reaction[a] 204

Table 4.6. Early Pd Pre-Catalyst Screening 207

Table 4.7. Early Base Effect Study 207

Table 4.8. Early Solvent Effect Study 208

Table 4.9. Water Effect 208

Table 4.10. Pd Pre-Catalyst Screening 209

Table 4.11. Ligand effect I 210

Table 4.12. Ligand effect II 211

Table 5.1. Electrophiles for the Pd/NBE-Catalyzed Ortho Thiolation of Aryl Iodides[a] 345

Table 5.2. The Aryl Iodide Scope of the Ortho Thiolation[a] 348

Table 5.3. The Sulfenamide and Olefin Scope of the Ortho Thiolation[a] 349

Table 5.4. Less Successful Substrates 350

Table 5.5 Control Experiments 354

Table 5.6. X-Ray Structure and Crystallographic Data of 4e 460

Table 5.7. X-Ray Structure and Crystallographic Data of S11 461

Table 5.8. X-Ray Structure and Crystallographic Data of S12 462

Table 5.9. X-Ray Structure and Crystallographic Data of S13 463

Table 5.10. X-Ray Structure and Crystallographic Data of S19 464

Table 5.11. X-Ray Structure and Crystallographic Data of 3c 465

Table 5.12. X-Ray Structure and Crystallographic Data of S14 466

Table 6.1. Preliminary Condition Screening 479

Table 6.2. Preliminary NBEs Screening 481

Table 6.3. Solvents Screening 483

Table 6.4. Key Parameters 483

Table 6.5. Temperature Effect 484

Table 6.6. Control Experiments 485

Table 6.7. Thiophene Derivatives Scope[a] 487

Table 6.8. Aryl Iodides and Olefin Scope[a] 488

Table 6.9. Less Successful or Unsuccessful Substrates 489

Table 6.10. Functionalization of Complex Bioactive Compounds[a] 490

Table 7.1. NBE Effect[a] 588

Table 7.2. Control Experiments 590

Table 7.3. Substrates Scope of Indoles[a] 592

Table 7.4. Substrates Scope of Pyrroles[a] 595

Table 7.5. Substrates Scope of Furans[a] 596

Table 7.6. Substrates Scope of Ortho Alkynylation[a] 598

Table 7.7. Crystallographic Data of 4f 787

Table 7.8. Crystallographic Data of 6b 788

Table 7.9. Crystallographic Data of 8g 789

Table 7.10. Crystallographic Data of 11d 790

Table 8.1. Control Experiments 801

Table 8.2. Substrates Scope[a] 803

Table 8.3. Crystal Data of 5q 937

LIST OF FIGURES

Figure 2.1 Bioactive Compounds Containing DHBFs 56

Figure 2.2. Proposed Catalytic Circle 57

Figure 2.3. HPLC of Racemic 3ah 88

Figure 2.4. HPLC of Enantiomeric 3ah* 89

Figure 2.5 ^{1}H NMR Spectrum of 1k 93

Figure 2.6 ^{13}C NMR Spectrum of 1k 93

Figure 2.7 ^{1}H NMR Spectrum of N3 94

Figure 2.8 ^{13}C NMR Spectrum of N3 94

Figure 2.9 ^{1}H NMR Spectrum of N4 95

Figure 2.10 ^{13}C NMR Spectrum of N4 95

Figure 2.11 ^{1}H NMR Spectrum of N5 96

Figure 2.12 ^{13}C NMR Spectrum of N5 96

Figure 2.13 ^{1}H NMR Spectrum of 3aa 97

Figure 2.14 ^{13}C NMR Spectrum of 3aa 97

Figure 2.15 ^{1}H NMR Spectrum of 3ba 98

Figure 2.16 ^{13}C NMR Spectrum of 3ba 98

Figure 2.17 ^{1}H NMR Spectrum of 3ca 99

Figure 2.18 ^{13}C NMR Spectrum of 3ca 99

Figure 2.19 ^{1}H NMR Spectrum of 3da 100

Figure 2.20 ^{13}C NMR Spectrum of 3da 100

Figure 2.21 ^{1}H NMR Spectrum of 3ea 101

Figure 2.22 ^{13}C NMR Spectrum of 3ea 101

Figure 2.23 ^{1}H NMR Spectrum of 3fa 102
Figure 2.24 ^{13}C NMR Spectrum of 3fa 102
Figure 2.25 ^{1}H NMR Spectrum of 3ga 103
Figure 2.26 ^{13}C NMR Spectrum of 3ga 103
Figure 2.27 ^{19}F NMR Spectrum of 3ga 104
Figure 2.28 ^{1}H NMR Spectrum of 3ha 105
Figure 2.29 ^{13}C NMR Spectrum of 3ha 105
Figure 2.30 ^{19}F NMR Spectrum of 3ha 106
Figure 2.31 ^{1}H NMR Spectrum of 3ia 107
Figure 2.32 ^{13}C NMR Spectrum of 3ia 107
Figure 2.33 ^{1}H NMR Spectrum of 3ja 108
Figure 2.34 ^{13}C NMR Spectrum of 3ja 108
Figure 2.35 ^{1}H NMR Spectrum of 3ka 109
Figure 2.36 ^{13}C NMR Spectrum of 3ka 109
Figure 2.37 ^{1}H NMR Spectrum of 3la 110
Figure 2.38 ^{13}C NMR Spectrum of 3la 110
Figure 2.39 ^{1}H NMR Spectrum of 3ma 111
Figure 2.40 ^{13}C NMR Spectrum of 3ma 111
Figure 2.41 ^{1}H NMR Spectrum of 3na 112
Figure 2.42 ^{13}C NMR Spectrum of 3na 112
Figure 2.43 ^{1}H NMR Spectrum of 3oa 113
Figure 2.44 ^{13}C NMR Spectrum of 3oa 113
Figure 2.45 ^{1}H NMR Spectrum of 3pa 114

Figure 2.46 ^{13}C NMR Spectrum of 3pa 114
Figure 2.47 ^{1}H NMR Spectrum of 3ab 115
Figure 2.48 ^{13}C NMR Spectrum of 3ab 115
Figure 2.49 ^{1}H NMR Spectrum of 3ac 116
Figure 2.50 ^{13}C NMR Spectrum of 3ac 116
Figure 2.51 ^{1}H NMR Spectrum of 3ad 117
Figure 2.52 ^{13}C NMR Spectrum of 3ad 117
Figure 2.53 ^{1}H NMR Spectrum of 3ae 118
Figure 2.54 ^{13}C NMR Spectrum of 3ae 118
Figure 2.55 ^{1}H NMR Spectrum of 3af 119
Figure 2.56 ^{13}C NMR Spectrum of 3af 119
Figure 2.57 ^{1}H NMR Spectrum of 3ag 120
Figure 2.58 ^{13}C NMR Spectrum of 3ag 120
Figure 2.59 ^{1}H NMR Spectrum of 3ah 121
Figure 2.60 ^{13}C NMR Spectrum of 3ah 121
Figure 2.61 ^{1}H NMR Spectrum of 3ai 122
Figure 2.62 ^{13}C NMR Spectrum of 3ai 122
Figure 2.63 ^{1}H NMR Spectrum of 3aj 123
Figure 2.64 ^{13}C NMR Spectrum of 3aj 123
Figure 2.65 ^{1}H NMR Spectrum of 3ak 124
Figure 2.66 ^{13}C NMR Spectrum of 3ak 124
Figure 2.67 ^{1}H NMR Spectrum of 3al 125
Figure 2.68 ^{13}C NMR Spectrum of 3al 125

Figure 2.69 ^{1}H NMR Spectrum of 3qc 126

Figure 2.70 ^{13}C NMR Spectrum of 3qc 126

Figure 2.71 ^{1}H NMR Spectrum of Fufenozide 127

Figure 2.72 ^{13}C NMR Spectrum of Fufenozide 127

Figure 3.1. Bioactive Compounds Containing Chiral 2,3-Dihydrobenzofurans 135

Figure 3.2. Proposed Catalytic Cycle 137

Figure 3.3. X-Ray Crystal Structures of Chiral NBEs A and B 138

Figure 3.4. Match and Mismatch between Chiral NBE and Epoxide 144

Figure 3.5. HPLC of Racemic N1 151

Figure 3.6. HPLC of Enantiomeric N1* 151

Figure 3.7. HPLC of Racemic 3aa 159

Figure 3.8. HPLC of Enantiomeric 3aa* 160

Figure 3.9. HPLC of Racemic 3ba 161

Figure 3.10. HPLC of Enantiomeric 3ba* 161

Figure 3.11. HPLC of Racemic 3ab 162

Figure 3.12. HPLC of Enantiomeric 3ab* 163

Figure 3.13. HPLC of Racemic 3ac 164

Figure 3.14. HPLC of Enantiomeric 3ac* 164

Figure 3.15. ^{1}H NMR of A 167

Figure 3.16. ^{13}C NMR of A 167

Figure 3.17. ^{1}H NMR of B 168

Figure 3.18. ^{1}H NMR of B 168

Figure 3.19. ^{1}H NMR of N1* 169

Figure 3.20. ^{13}C NMR of N1* 169
Figure 3.21. ^{1}H NMR of N2*..... 170
Figure 3.22. ^{13}C NMR of N2* 170
Figure 3.23. ^{1}H NMR of N3*..... 171
Figure 3.24. ^{13}C NMR of N3* 171
Figure 3.25. ^{1}H NMR of N4*..... 172
Figure 3.26. ^{13}C NMR of N4* 172
Figure 3.27. ^{1}H NMR of N5*..... 173
Figure 3.28. ^{13}C NMR of N5* 173
Figure 3.29. ^{1}H NMR of N7*..... 174
Figure 3.30. ^{13}C NMR of N7* 174
Figure 3.31. ^{1}H NMR of N8*..... 175
Figure 3.32. ^{13}C NMR of N8* 175
Figure 3.33. ^{1}H NMR of N9*..... 176
Figure 3.34. ^{13}C NMR of N9* 176
Figure 3.35. ^{1}H NMR of N10*..... 177
Figure 3.36. ^{13}C NMR of N10* 177
Figure 3.37. ^{1}H NMR of N11*..... 178
Figure 3.38. ^{13}C NMR of N11* 178
Figure 3.39. ^{1}H NMR of N12*..... 179
Figure 3.40. ^{13}C NMR of N12* 179
Figure 3.41. ^{1}H NMR of N13*..... 180
Figure 3.42. ^{13}C NMR of N13* 180

Figure 3.43. ^{1}H NMR of 3aa* 181
Figure 3.44. ^{13}C NMR of 3aa* 181
Figure 3.45. ^{1}H NMR of 3ba* 182
Figure 3.46. ^{13}C NMR of 3ba* 182
Figure 3.47. ^{1}H NMR of 3ab* 183
Figure 3.48. ^{13}C NMR of 3ab* 183
Figure 3.49. ^{1}H NMR of 3ac* 184
Figure 3.50. ^{13}C NMR of 3ac* 184
Figure 4.1. ^{1}H NMR Spectrum of 2-Mentylphenylboronic Acid from Combi-Blocks 252
Figure 4.2. ^{1}H NMR Spectrum of 2-Mentylphenylboronic Acid from Sigma-Aldrich 252
Figure 4.3. ^{1}H NMR Spectrum of 2-Mentylphenylboronic Acid from Oakwood 253
Figure 4.4. ^{1}H NMR Spectrum of 2o 254
Figure 4.5. ^{13}C NMR Spectrum of 2o 254
Figure 4.6. ^{1}H NMR Spectrum of 3aa 255
Figure 4.7. ^{13}C NMR Spectrum of 3aa 255
Figure 4.8. ^{1}H NMR Spectrum of 3ab 256
Figure 4.9. ^{13}C NMR Spectrum of 3ab 256
Figure 4.10. ^{1}H NMR Spectrum of 3ac 257
Figure 4.11. ^{13}C NMR Spectrum of 3ac 257
Figure 4.12. ^{1}H NMR Spectrum of 3ad 258
Figure 4.13. ^{13}C NMR Spectrum of 3ad 258
Figure 4.14. ^{19}F NMR Spectrum of 3ad 259
Figure 4.15. ^{1}H NMR Spectrum of 3ae 259

Figure 4.16. ^{13}C NMR Spectrum of 3ae 260
Figure 4.17. ^{1}H NMR Spectrum of 3af 260
Figure 4.18. ^{13}C NMR Spectrum of 3af 261
Figure 4.19. ^{1}H NMR Spectrum of 3ag 261
Figure 4.20. ^{13}C NMR Spectrum of 3ag 262
Figure 4.21. ^{1}H NMR Spectrum of 3ah 262
Figure 4.22. ^{13}C NMR Spectrum of 3ah 263
Figure 4.23. ^{1}H NMR Spectrum of 3ai 263
Figure 4.24. ^{13}C NMR Spectrum of 3ai 264
Figure 4.25. ^{19}F NMR Spectrum of 3ai 264
Figure 4.26. ^{1}H NMR Spectrum of 3aj 265
Figure 4.27. ^{13}C NMR Spectrum of 3aj 265
Figure 4.28. ^{1}H NMR Spectrum of 3ak 266
Figure 4.29. ^{13}C NMR Spectrum of 3ak 266
Figure 4.30. ^{1}H NMR Spectrum of 3al 267
Figure 4.31. ^{13}C NMR Spectrum of 3al 267
Figure 4.32. ^{1}H NMR Spectrum of 3am 268
Figure 4.33. ^{13}C NMR Spectrum of 3am 268
Figure 4.34. ^{1}H NMR Spectrum of 3an 269
Figure 4.35. ^{13}C NMR Spectrum of 3an 269
Figure 4.36. ^{1}H NMR Spectrum of 3ao 270
Figure 4.37. ^{13}C NMR Spectrum of 3ao 270
Figure 4.38. ^{1}H NMR Spectrum of 3ap 271

Figure 4.39. ^{13}C NMR Spectrum of 3ap 271
Figure 4.40. ^{1}H NMR Spectrum of 3aq 272
Figure 4.41. ^{13}C NMR Spectrum of 3aq 272
Figure 4.42. ^{1}H NMR Spectrum of 3ar 273
Figure 4.43. ^{13}C NMR Spectrum of 3ar 273
Figure 4.44. ^{1}H NMR Spectrum of 3as 274
Figure 4.45. ^{13}C NMR Spectrum of 3as 274
Figure 4.46. ^{1}H NMR Spectrum of 3at 275
Figure 4.47. ^{13}C NMR Spectrum of 3at 275
Figure 4.48. ^{1}H NMR Spectrum of 3bb 276
Figure 4.49. ^{13}C NMR Spectrum of 3bb 276
Figure 4.50. ^{19}F NMR Spectrum of 3bb 277
Figure 4.51. ^{1}H NMR Spectrum of 3cb 278
Figure 4.52. ^{13}C NMR Spectrum of 3cb 278
Figure 4.53. ^{19}F NMR Spectrum of 3cb 279
Figure 4.54. ^{1}H NMR Spectrum of 3db 280
Figure 4.55. ^{13}C NMR Spectrum of 3db 280
Figure 4.56. ^{19}F NMR Spectrum of 3db 281
Figure 4.57. ^{1}H NMR Spectrum of 3eb 282
Figure 4.58. ^{13}C NMR Spectrum of 3eb 282
Figure 4.59. ^{19}F NMR Spectrum of 3eb 283
Figure 4.60. ^{1}H NMR Spectrum of 3fb 284
Figure 4.61. ^{13}C NMR Spectrum of 3fb 284

Figure 4.62. ^{19}F NMR Spectrum of 3fb 285
Figure 4.63. ^{1}H NMR Spectrum of 3gb 286
Figure 4.64. ^{13}C NMR Spectrum of 3gb 286
Figure 4.65. ^{19}F NMR Spectrum of 3gb 287
Figure 4.66. ^{1}H NMR Spectrum of 3hb 288
Figure 4.67. ^{13}C NMR Spectrum of 3hb 288
Figure 4.68. ^{19}F NMR Spectrum of 3hb 289
Figure 4.69. ^{1}H NMR Spectrum of 3ib 290
Figure 4.70. ^{13}C NMR Spectrum of 3ib 290
Figure 4.71. ^{19}F NMR Spectrum of 3ib 291
Figure 4.72. ^{1}H NMR Spectrum of 3jb 292
Figure 4.73. ^{13}C NMR Spectrum of 3jb 292
Figure 4.74. ^{19}F NMR Spectrum of 3jb 293
Figure 4.75. ^{1}H NMR Spectrum of 3kb 294
Figure 4.76. ^{13}C NMR Spectrum of 3kb 294
Figure 4.77. ^{19}F NMR Spectrum of 3kb 295
Figure 4.78. ^{1}H NMR Spectrum of 3lb 296
Figure 4.79. ^{13}C NMR Spectrum of 3lb 296
Figure 4.80. ^{19}F NMR Spectrum of 3lb 297
Figure 4.81. ^{1}H NMR Spectrum of 3mb 298
Figure 4.82. ^{13}C NMR Spectrum of 3mb 298
Figure 4.83. ^{19}F NMR Spectrum of 3mb 299
Figure 4.84. ^{1}H NMR Spectrum of 3nb 300

Figure 4.85. ^{13}C NMR Spectrum of 3nb 300
Figure 4.86. ^{19}F NMR Spectrum of 3nb 301
Figure 4.87. ^{1}H NMR Spectrum of 3ob 302
Figure 4.88. ^{13}C NMR Spectrum of 3ob 302
Figure 4.89. ^{19}F NMR Spectrum of 3ob 303
Figure 4.90. ^{1}H NMR Spectrum of 3pb 304
Figure 4.91. ^{13}C NMR Spectrum of 3pb 304
Figure 4.92. ^{19}F NMR Spectrum of 3pb 305
Figure 4.93. ^{1}H NMR Spectrum of 3qb 306
Figure 4.94. ^{13}C NMR Spectrum of 3qb 306
Figure 4.95. ^{19}F NMR Spectrum of 3qb 307
Figure 4.96. ^{1}H NMR Spectrum of 3rb 308
Figure 4.97. ^{13}C NMR Spectrum of 3rb 308
Figure 4.98. ^{19}F NMR Spectrum of 3rb 309
Figure 4.99. ^{1}H NMR Spectrum of 3sb 310
Figure 4.100. ^{13}C NMR Spectrum of 3sb 310
Figure 4.101. ^{19}F NMR Spectrum of 3sb 311
Figure 4.102. ^{1}H NMR Spectrum of 3sb-*d* 312
Figure 4.103. ^{1}H NMR Spectrum of 3ab-*d* 312
Figure 4.104. ^{1}H NMR Spectrum of 4aa 313
Figure 4.105. ^{13}C NMR Spectrum of 4aa 313
Figure 4.106. ^{1}H NMR Spectrum of 4ga 314
Figure 4.107. ^{13}C NMR Spectrum of 4ga 314

Figure 4.108. ^{1}H NMR Spectrum of 4la 315
Figure 4.109. ^{13}C NMR Spectrum of 4la 315
Figure 4.110. ^{1}H NMR Spectrum of 4na 316
Figure 4.111. ^{13}C NMR Spectrum of 4na 316
Figure 4.112. ^{1}H NMR Spectrum of 4sa 317
Figure 4.113. ^{13}C NMR Spectrum of 4sa 317
Figure 4.114. ^{1}H NMR Spectrum of 4ab 318
Figure 4.115. ^{13}C NMR Spectrum of 4ab 318
Figure 4.116. ^{1}H NMR Spectrum of 5 319
Figure 4.117. ^{13}C NMR Spectrum of 5 319
Figure 4.118. ^{1}H NMR Spectrum of 12 320
Figure 4.119. ^{13}C NMR Spectrum of 12 320
Figure 4.120. ^{1}H NMR Spectrum of 7 321
Figure 4.121. ^{13}C NMR Spectrum of 7 321
Figure 4.122. ^{19}F NMR Spectrum of 7 322
Figure 4.123. ^{1}H NMR Spectrum of 8 323
Figure 4.124. ^{13}C NMR Spectrum of 8 323
Figure 4.125. ^{19}F NMR Spectrum of 8 324
Figure 4.126. ^{1}H NMR Spectrum of 9 325
Figure 4.127. ^{13}C NMR Spectrum of 9 325
Figure 4.128. ^{1}H NMR Spectrum of 15 326
Figure 4.129. ^{13}C NMR Spectrum of 15 326
Figure 4.130. ^{1}H NMR Spectrum of 18 327

Figure 4.131. ^{13}C NMR Spectrum of 18 327
Figure 4.132. ^{1}H NMR Spectrum of 3tb 328
Figure 4.133. ^{13}C NMR Spectrum of 3tb 328
Figure 4.134. ^{19}F NMR Spectrum of 3tb 329
Figure 4.135. ^{1}H NMR Spectrum of 3ub 330
Figure 4.136. ^{13}C NMR Spectrum of 3ub 330
Figure 4.137. ^{19}F NMR Spectrum of 3ub 331
Figure 4.138. ^{1}H NMR Spectrum of 4uba 332
Figure 4.139. ^{13}C NMR Spectrum of 4uba 332
Figure 4.140. ^{19}F NMR Spectrum of 4uba 333
Figure 5.1. Project Background and Design for Ortho C-H Thiolation via Pd/NBE Cooperative Catalysis 343
Figure 5.2. X-Ray Structures of Selected Lactam-Derived Sulfenamides[a] 346
Figure 5.3. ^{1}H NMR Spectrum of S4 392
Figure 5.4. ^{13}C NMR Spectrum of S4 392
Figure 5.5. ^{1}H NMR Spectrum of S6 393
Figure 5.6. ^{13}C NMR Spectrum of S6 393
Figure 5.7. ^{1}H NMR Spectrum of S5 394
Figure 5.8. ^{13}C NMR Spectrum of S5 394
Figure 5.9. ^{1}H NMR Spectrum of S7 395
Figure 5.10. ^{13}C NMR Spectrum of S7 395
Figure 5.11. ^{1}H NMR Spectrum of S10 396
Figure 5.12. ^{13}C NMR Spectrum of S10 396

Figure 5.13. ^{1}H NMR Spectrum of S14 397
Figure 5.14. ^{13}C NMR Spectrum of S14 397
Figure 5.15. ^{1}H NMR Spectrum of S15 398
Figure 5.16. ^{13}C NMR Spectrum of S15 398
Figure 5.17. ^{1}H NMR Spectrum of S17 399
Figure 5.18. ^{13}C NMR Spectrum of S17 399
Figure 5.19. ^{1}H NMR Spectrum of S18 400
Figure 5.20. ^{13}C NMR Spectrum of S18 400
Figure 5.21. ^{1}H NMR Spectrum of 17 401
Figure 5.22. ^{13}C NMR Spectrum of 17 401
Figure 5.23. ^{1}H NMR Spectrum of S19 402
Figure 5.24. ^{13}C NMR Spectrum of S19 402
Figure 5.25. ^{1}H NMR Spectrum of S21 403
Figure 5.26. ^{13}C NMR Spectrum of S21 403
Figure 5.27. ^{1}H NMR Spectrum of 3a 404
Figure 5.28. ^{13}C NMR Spectrum of 3a 404
Figure 5.29. ^{1}H NMR Spectrum of 3b 405
Figure 5.30. ^{13}C NMR Spectrum of 3b 405
Figure 5.31. ^{1}H NMR Spectrum of 3c 406
Figure 5.32. ^{13}C NMR Spectrum of 3c 406
Figure 5.33. ^{1}H NMR Spectrum of 3d 407
Figure 5.34. ^{13}C NMR Spectrum of 3d 407
Figure 5.35. ^{1}H NMR Spectrum of 3e 408

Figure 5.36. ^{13}C NMR Spectrum of 3e 408
Figure 5.37. ^{1}H NMR Spectrum of 3f 409
Figure 5.38. ^{13}C NMR Spectrum of 3f 409
Figure 5.39. ^{1}H NMR Spectrum of 3g 410
Figure 5.40. ^{13}C NMR Spectrum of 3g 410
Figure 5.41. ^{1}H NMR Spectrum of 3h 411
Figure 5.42. ^{13}C NMR Spectrum of 3h 411
Figure 5.43. ^{1}H NMR Spectrum of 3i 412
Figure 5.44. ^{13}C NMR Spectrum of 3i 412
Figure 5.45. ^{1}H NMR Spectrum of 3j 413
Figure 5.46. ^{13}C NMR Spectrum of 3j 413
Figure 5.47. ^{1}H NMR Spectrum of 3k 414
Figure 5.48. ^{13}C NMR Spectrum of 3k 414
Figure 5.49. ^{1}H NMR Spectrum of 1n 415
Figure 5.50. ^{13}C NMR Spectrum of 1n 415
Figure 5.51. ^{1}H NMR Spectrum of 1r 416
Figure 5.52. ^{13}C NMR Spectrum of 1r 416
Figure 5.53. ^{1}H NMR Spectrum of 4a 417
Figure 5.54. ^{13}C NMR Spectrum of 4a 417
Figure 5.55. ^{1}H NMR Spectrum of 4b 418
Figure 5.56. ^{13}C NMR Spectrum of 4b 418
Figure 5.57. ^{1}H NMR Spectrum of 4c 419
Figure 5.58. ^{13}C NMR Spectrum of 4c 419

Figure 5.59. ^{1}H NMR Spectrum of 4d 420
Figure 5.60. ^{13}C NMR Spectrum of 4d 420
Figure 5.61. ^{1}H NMR Spectrum of 4e 421
Figure 5.62. ^{13}C NMR Spectrum of 4e 421
Figure 5.63. ^{1}H NMR Spectrum of 4f 422
Figure 5.64. ^{13}C NMR Spectrum of 4f 422
Figure 5.65. ^{1}H NMR Spectrum of 4g 423
Figure 5.66. ^{13}C NMR Spectrum of 4g 423
Figure 5.67. ^{1}H NMR Spectrum of 4h 424
Figure 5.68. ^{13}C NMR Spectrum of 4h 424
Figure 5.69. ^{1}H NMR Spectrum of 4i 425
Figure 5.70. ^{13}C NMR Spectrum of 4i 425
Figure 5.71. ^{1}H NMR Spectrum of 4j 426
Figure 5.72. ^{13}C NMR Spectrum of 4j 426
Figure 5.73. ^{1}H NMR Spectrum of 4k 427
Figure 5.74. ^{13}C NMR Spectrum of 4k 427
Figure 5.75. ^{1}H NMR Spectrum of 4l 428
Figure 5.76. ^{13}C NMR Spectrum of 4l 428
Figure 5.77. ^{1}H NMR Spectrum of 4m 429
Figure 5.78. ^{13}C NMR Spectrum of 4m 429
Figure 5.79. ^{1}H NMR Spectrum of 4n 430
Figure 5.80. ^{13}C NMR Spectrum of 4n 430
Figure 5.81. ^{1}H NMR Spectrum of 4o 431

Figure 5.82. ^{13}C NMR Spectrum of 4o 431
Figure 5.83. ^{1}H NMR Spectrum of 4p 432
Figure 5.84. ^{13}C NMR Spectrum of 4p 432
Figure 5.85. ^{1}H NMR Spectrum of 4q 433
Figure 5.86. ^{13}C NMR Spectrum of 4q 433
Figure 5.87. ^{1}H NMR Spectrum of 4r 434
Figure 5.88. ^{13}C NMR Spectrum of 4r 434
Figure 5.89. ^{1}H NMR Spectrum of 4s 435
Figure 5.90. ^{13}C NMR Spectrum of 4s 435
Figure 5.91. ^{1}H NMR Spectrum of 4t 436
Figure 5.92. ^{13}C NMR Spectrum of 4t 436
Figure 5.93. ^{1}H NMR Spectrum of 4u 437
Figure 5.94. ^{13}C NMR Spectrum of 4u 437
Figure 5.95. ^{1}H NMR Spectrum of 5a 438
Figure 5.96. ^{13}C NMR Spectrum of 5a 438
Figure 5.97. ^{1}H NMR Spectrum of 5b 439
Figure 5.98. ^{13}C NMR Spectrum of 5b 439
Figure 5.99. ^{1}H NMR Spectrum of 5c 440
Figure 5.100. ^{13}C NMR Spectrum of 5c 440
Figure 5.101. ^{1}H NMR Spectrum of 5d 441
Figure 5.102. ^{13}C NMR Spectrum of 5d 441
Figure 5.103. ^{19}F NMR Spectrum of 5d 442
Figure 5.104. ^{1}H NMR Spectrum of 5e 443

Figure 5.105. ^{13}C NMR Spectrum of 5e 443
Figure 5.106. ^{1}H NMR Spectrum of 5f 444
Figure 5.107. ^{13}C NMR Spectrum of 5f 444
Figure 5.108. ^{1}H NMR Spectrum of 5g 445
Figure 5.109. ^{13}C NMR Spectrum of 5g 445
Figure 5.110. ^{19}F NMR Spectrum of 5g 446
Figure 5.111. ^{1}H NMR Spectrum of 5h 447
Figure 5.112. ^{13}C NMR Spectrum of 5h 447
Figure 5.113. ^{1}H NMR Spectrum of 5i 448
Figure 5.114. ^{13}C NMR Spectrum of 5i 448
Figure 5.115. ^{19}F NMR Spectrum of 5i 449
Figure 5.116. ^{1}H NMR Spectrum of 5j 450
Figure 5.117. ^{13}C NMR Spectrum of 5j 450
Figure 5.118. ^{1}H NMR Spectrum of 5k 451
Figure 5.119. ^{13}C NMR Spectrum of 5k 451
Figure 5.120. ^{1}H NMR Spectrum of 5l 452
Figure 5.121. ^{13}C NMR Spectrum of 5l 452
Figure 5.122. ^{1}H NMR Spectrum of 5m 453
Figure 5.123. ^{13}C NMR Spectrum of 5m 453
Figure 5.124. ^{1}H NMR Spectrum of 5n 454
Figure 5.125. ^{13}C NMR Spectrum of 5n 454
Figure 5.126. ^{1}H NMR Spectrum of 5o 455
Figure 5.127. ^{13}C NMR Spectrum of 5o 455

Figure 5.128. ^{1}H NMR Spectrum of 6a 456
Figure 5.129. ^{13}C NMR Spectrum of 6a 456
Figure 5.130. ^{1}H NMR Spectrum of 6b 457
Figure 5.131. ^{13}C NMR Spectrum of 6b 457
Figure 5.132. ^{1}H NMR Spectrum of 9 458
Figure 5.133. ^{13}C NMR Spectrum of 9 458
Figure 5.134. ^{1}H NMR Spectrum of 11 459
Figure 5.135. ^{13}C NMR Spectrum of 11 459
Figure 6.1. Examples of Polysubstituted Thiophenes and Furans 475
Figure 6.2. Reaction Discovery and Product Characterization 478
Figure 6.3. Kinetic Profile of the Model Reaction 492
Figure 6.4. ^{1}H NMR Spectrum of 4a 528
Figure 6.5. ^{13}C NMR Spectrum of 4a 528
Figure 6.6. ^{1}H NMR Spectrum of 4b 529
Figure 6.7. ^{13}C NMR Spectrum of 4b 529
Figure 6.8. ^{1}H NMR Spectrum of 4c 530
Figure 6.9. ^{13}C NMR Spectrum of 4c 530
Figure 6.10. ^{1}H NMR Spectrum of 4d 531
Figure 6.11. ^{13}C NMR Spectrum of 4d 531
Figure 6.12. ^{1}H NMR Spectrum of 4e 532
Figure 6.13. ^{13}C NMR Spectrum of 4e 532
Figure 6.14. ^{1}H NMR Spectrum of 4f 533
Figure 6.15. ^{13}C NMR Spectrum of 4f 533

Figure 6.16. ^{1}H NMR Spectrum of 4g 534

Figure 6.17. ^{13}C NMR Spectrum of 4g 534

Figure 6.18. ^{1}H NMR Spectrum of 4h 535

Figure 6.19. ^{13}C NMR Spectrum of 4h 535

Figure 6.20. ^{1}H NMR Spectrum of 4i 536

Figure 6.21. ^{13}C NMR Spectrum of 4i 536

Figure 6.22. ^{1}H NMR Spectrum of 4j 537

Figure 6.23. ^{13}C NMR Spectrum of 4j 537

Figure 6.24. ^{1}H NMR Spectrum of 4k 538

Figure 6.25. ^{13}C NMR Spectrum of 4k 538

Figure 6.26. ^{1}H NMR Spectrum of 4l 539

Figure 6.27. ^{13}C NMR Spectrum of 4l 539

Figure 6.28. ^{1}H NMR Spectrum of 4m 540

Figure 6.29. ^{13}C NMR Spectrum of 4m 540

Figure 6.30. ^{1}H NMR Spectrum of 4n 541

Figure 6.31. ^{13}C NMR Spectrum of 4n 541

Figure 6.32. ^{1}H NMR Spectrum of 4o 542

Figure 6.33. ^{13}C NMR Spectrum of 4o 542

Figure 6.34. ^{1}H NMR Spectrum of 5a 543

Figure 6.35. ^{13}C NMR Spectrum of 5a 543

Figure 6.36. ^{1}H NMR Spectrum of 5b 544

Figure 6.37. ^{13}C NMR Spectrum of 5b 544

Figure 6.38. ^{19}F NMR Spectrum of 5b 545

Figure 6.39. ^{1}H NMR Spectrum of 5c 546
Figure 6.40. ^{13}C NMR Spectrum of 5c 546
Figure 6.41. ^{1}H NMR Spectrum of 5d 547
Figure 6.42. ^{13}C NMR Spectrum of 5d 547
Figure 6.43. ^{1}H NMR Spectrum of 5e 548
Figure 6.44. ^{13}C NMR Spectrum of 5e 548
Figure 6.45. ^{1}H NMR Spectrum of 5f 549
Figure 6.46. ^{13}C NMR Spectrum of 5f 549
Figure 6.47. ^{1}H NMR Spectrum of 5g 550
Figure 6.48. ^{13}C NMR Spectrum of 5g 550
Figure 6.49. ^{1}H NMR Spectrum of 5h 551
Figure 6.50. ^{13}C NMR Spectrum of 5h 551
Figure 6.51. ^{1}H NMR Spectrum of 5i 552
Figure 6.52. ^{13}C NMR Spectrum of 5i 552
Figure 6.53. ^{1}H NMR Spectrum of 5j 553
Figure 6.54. ^{13}C NMR Spectrum of 5j 553
Figure 6.55. ^{19}F NMR Spectrum of 5j 554
Figure 6.56. ^{1}H NMR Spectrum of 6a 555
Figure 6.57. ^{13}C NMR Spectrum of 6a 555
Figure 6.58. ^{1}H NMR Spectrum of 6b 556
Figure 6.59. ^{13}C NMR Spectrum of 6b 556
Figure 6.60. ^{1}H NMR Spectrum of 6c 557
Figure 6.61. ^{13}C NMR Spectrum of 6c 557

Figure 6.62. ^{1}H NMR Spectrum of 6d 558
Figure 6.63. ^{13}C NMR Spectrum of 6d 558
Figure 6.64. ^{1}H NMR Spectrum of 6e 559
Figure 6.65. ^{13}C NMR Spectrum of 6e 559
Figure 6.66. ^{1}H NMR Spectrum of 6f 560
Figure 6.67. ^{13}C NMR Spectrum of 6f 560
Figure 6.68. ^{1}H NMR Spectrum of 6g 561
Figure 6.69. ^{13}C NMR Spectrum of 6g 561
Figure 6.70. ^{1}H NMR Spectrum of 7a 562
Figure 6.71. ^{13}C NMR Spectrum of 7a 562
Figure 6.72. ^{1}H NMR Spectrum of 7b 563
Figure 6.73. ^{13}C NMR Spectrum of 7b 563
Figure 6.74. ^{1}H NMR Spectrum of 7b' 564
Figure 6.75. ^{13}C NMR Spectrum of 7b' 564
Figure 6.76. ^{1}H NMR Spectrum of 7c 565
Figure 6.77. ^{13}C NMR Spectrum of 7c 565
Figure 6.78. ^{1}H NMR Spectrum of 7d 566
Figure 6.79. ^{13}C NMR Spectrum of 7d 566
Figure 6.80. ^{1}H NMR Spectrum of 7e 567
Figure 6.81. ^{13}C NMR Spectrum of 7e 567
Figure 6.82. ^{1}H NMR Spectrum of 9a 568
Figure 6.83. ^{13}C NMR Spectrum of 9a 568
Figure 6.84. ^{1}H NMR Spectrum of 1r 569

Figure 6.85. ^{13}C NMR Spectrum of 1r 569
Figure 6.86. ^{1}H NMR Spectrum of 1o 570
Figure 6.87. ^{13}C NMR Spectrum of 1o 570
Figure 6.88. ^{1}H NMR Spectrum of 1m 571
Figure 6.89. ^{13}C NMR Spectrum of 1m 571
Figure 6.90. ^{1}H NMR Spectrum of 1n 572
Figure 6.91. ^{13}C NMR Spectrum of 1n 572
Figure 6.92. ^{1}H NMR Spectrum of 1s 573
Figure 6.93. ^{13}C NMR Spectrum of 1s 573
Figure 6.94. ^{1}H NMR Spectrum of 8 574
Figure 6.95. ^{13}C NMR Spectrum of 8 574
Figure 7.1. Examples of Polysubstituted Five-membered Heteroarenes 583
Figure 7.2. Proposed Reaction Mechanism 584
Figure 7.3. Indole C−H Palladation Transition States. 601
Figure 7.4. Initial-Rate Dependence on N2 671
Figure 7.5. Initial-Rate Dependence on N2 (Formation of Direct Alkenylation Side Product) . 673
Figure 7.6. Initial-Rate Dependence on 1a 676
Figure 7.7. Initial-Rate Dependence on 2a 678
Figure 7.8. Initial-Rate Dependence on 3a 680
Figure 7.9. Initial-Rate Dependence on [Pd] 682
Figure 7.10. ^{1}H NMR Spectrum of 1l 684
Figure 7.11. ^{13}C NMR Spectrum of 1l 684
Figure 7.12. ^{1}H NMR Spectrum of 7h 685

Figure 7.13. ^{1}H NMR Spectrum of 7h 685
Figure 7.14. ^{1}H NMR Spectrum of 6m 686
Figure 7.15. ^{1}H NMR Spectrum of 6m 686
Figure 7.16. ^{1}H NMR Spectrum of 6n 687
Figure 7.17. ^{1}H NMR Spectrum of 6n 687
Figure 7.18. ^{1}H NMR Spectrum of 6a 688
Figure 7.19. ^{1}H NMR Spectrum of 6a 688
Figure 7.20. ^{1}H NMR Spectrum of 6b 689
Figure 7.21. ^{13}C NMR Spectrum of 6b 689
Figure 7.22. ^{1}H NMR Spectrum of 6c 690
Figure 7.23. ^{13}C NMR Spectrum of 6c 690
Figure 7.24. ^{1}H NMR Spectrum of 6d 691
Figure 7.25. ^{13}C NMR Spectrum of 6d 691
Figure 7.26. ^{1}H NMR Spectrum of 6e 692
Figure 7.27. ^{13}C NMR Spectrum of 6e 692
Figure 7.28. ^{1}H NMR Spectrum of 6f 693
Figure 7.29. ^{13}C NMR Spectrum of 6f 693
Figure 7.30. ^{1}H NMR Spectrum of 6g 694
Figure 7.31. ^{13}C NMR Spectrum of 6g 694
Figure 7.32. ^{1}H NMR Spectrum of 6h 695
Figure 7.33. ^{13}C NMR Spectrum of 6h 695
Figure 7.34. ^{19}F NMR Spectrum of 6h 696
Figure 7.35. ^{1}H NMR Spectrum of 6i 697

Figure 7.36. ^{13}C NMR Spectrum of 6i 697
Figure 7.37. ^{1}H NMR Spectrum of 6j 698
Figure 7.38. ^{13}C NMR Spectrum of 6j 698
Figure 7.39. ^{1}H NMR Spectrum of 6k 699
Figure 7.40. ^{13}C NMR Spectrum of 6k 699
Figure 7.41. ^{1}H NMR Spectrum of 6l 700
Figure 7.42. ^{13}C NMR Spectrum of 6l 700
Figure 7.43. ^{1}H NMR Spectrum of 6o 701
Figure 7.44 ^{13}C NMR Spectrum of 6o 701
Figure 7.45. ^{1}H NMR Spectrum of 6p 702
Figure 7.46. ^{13}C NMR Spectrum of 6p 702
Figure 7.47. ^{19}F NMR Spectrum of 6p 703
Figure 7.48. ^{1}H NMR Spectrum of 6q 704
Figure 7.49. ^{13}C NMR Spectrum of 6q 704
Figure 7.50. ^{1}H NMR Spectrum of 6r 705
Figure 7.51. ^{13}C NMR Spectrum of 6r 705
Figure 7.52. ^{1}H NMR Spectrum of 6s 706
Figure 7.53. ^{13}C NMR Spectrum of 6s 706
Figure 7.54. ^{1}H NMR Spectrum of 6t 707
Figure 7.55. ^{13}C NMR Spectrum of 6t 707
Figure 7.56. ^{1}H NMR Spectrum of 6u 708
Figure 7.57. ^{13}C NMR Spectrum of 6u 708
Figure 7.58. ^{1}H NMR Spectrum of 6v 709

Figure 7.59. ^{1}H NMR Spectrum of 6v 709
Figure 7.60. ^{1}H NMR Spectrum of 6w 710
Figure 7.61. ^{13}C NMR Spectrum of 6w 710
Figure 7.62. ^{1}H NMR Spectrum of 6x 711
Figure 7.63. ^{13}C NMR Spectrum of 6x 711
Figure 7.64. ^{1}H NMR Spectrum of 6y 712
Figure 7.65. ^{13}C NMR Spectrum of 6y 712
Figure 7.66. ^{1}H NMR Spectrum of 6ah 713
Figure 7.67. ^{1}H NMR Spectrum of 6ah 713
Figure 7.68. ^{19}F NMR Spectrum of 6ah 714
Figure 7.69. ^{1}H NMR Spectrum of 6af 715
Figure 7.70. ^{13}C NMR Spectrum of 6af 715
Figure 7.71. ^{19}F NMR Spectrum of 6af 716
Figure 7.72. ^{1}H NMR Spectrum of 6aa 717
Figure 7.73. ^{13}C NMR Spectrum of 6aa 717
Figure 7.74. ^{1}H NMR Spectrum of 6z 718
Figure 7.75. ^{13}C NMR Spectrum of 6z 718
Figure 7.76. ^{19}F NMR Spectrum of 6z 719
Figure 7.77. ^{1}H NMR Spectrum of 6ag 720
Figure 7.78. ^{13}C NMR Spectrum of 6ag 720
Figure 7.79. ^{1}H NMR Spectrum of 6ac 721
Figure 7.80. ^{13}C NMR Spectrum of 6ac 721
Figure 7.81. ^{19}F NMR Spectrum of 6ac 722

Figure 7.82. ^{1}H NMR Spectrum of 6ae 723
Figure 7.83. ^{13}C NMR Spectrum of 6ae 723
Figure 7.84. ^{1}H NMR Spectrum of 6ak 724
Figure 7.85. ^{13}C NMR Spectrum of 6ak 724
Figure 7.86. ^{1}H NMR Spectrum of 6al 725
Figure 7.87. ^{13}C NMR Spectrum of 6al 725
Figure 7.88. ^{1}H NMR Spectrum of 6am 726
Figure 7.89. ^{13}C NMR Spectrum of 6am 726
Figure 7.90. ^{1}H NMR Spectrum of 6ao 727
Figure 7.91. ^{13}C NMR Spectrum of 6ao 727
Figure 7.92. ^{1}H NMR Spectrum of 6ap 728
Figure 7.93. ^{13}C NMR Spectrum of 6ap 728
Figure 7.94. ^{1}H NMR Spectrum of 6aq 729
Figure 7.95. ^{13}C NMR Spectrum of 6aq 729
Figure 7.96. ^{1}H NMR Spectrum of 6ar 730
Figure 7.97. ^{13}C NMR Spectrum of 6ar 730
Figure 7.98. ^{1}H NMR Spectrum of 6as 731
Figure 7.99. ^{13}C NMR Spectrum of 6as 731
Figure 7.100. ^{19}F NMR Spectrum of 6as 732
Figure 7.101. ^{1}H NMR Spectrum of 4a 733
Figure 7.102. ^{13}C NMR Spectrum of 4a 733
Figure 7.103. ^{1}H NMR Spectrum of 4b 734
Figure 7.104. ^{13}C NMR Spectrum of 4b 734

Figure 7.105. ^{1}H NMR Spectrum of 4c 735
Figure 7.106. ^{13}C NMR Spectrum of 4c 735
Figure 7.107. ^{1}H NMR Spectrum of 4d 736
Figure 7.108. ^{13}C NMR Spectrum of 4d 736
Figure 7.109. ^{19}F NMR Spectrum of 4d 737
Figure 7.110. ^{1}H NMR Spectrum of 4f 738
Figure 7.111. ^{13}C NMR Spectrum of 4f 738
Figure 7.112. ^{1}H NMR Spectrum of 4e 739
Figure 7.113. ^{13}C NMR Spectrum of 4e 739
Figure 7.114. ^{1}H NMR Spectrum of 4g 740
Figure 7.115. ^{13}C NMR Spectrum of 4g 740
Figure 7.116. ^{1}H NMR Spectrum of 4h 741
Figure 7.117. ^{13}C NMR Spectrum of 4h 741
Figure 7.118. ^{1}H NMR Spectrum of 4i 742
Figure 7.119. ^{13}C NMR Spectrum of 4i 742
Figure 7.120. ^{1}H NMR Spectrum of 4j 743
Figure 7.121. ^{13}C NMR Spectrum of 4j 743
Figure 7.122. ^{1}H NMR Spectrum of 4k 744
Figure 7.123. ^{13}C NMR Spectrum of 4k 744
Figure 7.124. ^{1}H NMR Spectrum of 4l 745
Figure 7.125. ^{13}C NMR Spectrum of 4l 745
Figure 7.126. ^{1}H NMR Spectrum of 4n 746
Figure 7.127. ^{13}C NMR Spectrum of 4n 746

Figure 7.128. ^{1}H NMR Spectrum of 4m 747
Figure 7.129. ^{13}C NMR Spectrum of 4m 747
Figure 7.130. ^{1}H NMR Spectrum of 4o 748
Figure 7.131. ^{13}C NMR Spectrum of 4o 748
Figure 7.132. ^{1}H NMR Spectrum of 4p 749
Figure 7.133. ^{13}C NMR Spectrum of 4p 749
Figure 7.134. ^{19}F NMR Spectrum of 4p 750
Figure 7.135. ^{1}H NMR Spectrum of 4q 751
Figure 7.136. ^{13}C NMR Spectrum of 4q 751
Figure 7.137. ^{1}H NMR Spectrum of 4r 752
Figure 7.138. ^{13}C NMR Spectrum of 4r 752
Figure 7.139. ^{1}H NMR Spectrum of 4s 753
Figure 7.140. ^{13}C NMR Spectrum of 4s 753
Figure 7.141. ^{1}H NMR Spectrum of 4t 754
Figure 7.142. ^{13}C NMR Spectrum of 4t 754
Figure 7.143. ^{1}H NMR Spectrum of 4t’ 755
Figure 7.144. ^{13}C NMR Spectrum of 4t’ 755
Figure 7.145. ^{1}H NMR Spectrum of 4u 756
Figure 7.146. ^{13}C NMR Spectrum of 4u 756
Figure 7.147. ^{1}H NMR Spectrum of 4v 757
Figure 7.148. ^{13}C NMR Spectrum of 4v 757
Figure 7.149. ^{1}H NMR Spectrum of 4w 758
Figure 7.150. ^{13}C NMR Spectrum of 4w 758

Figure 7.151. ^{1}H NMR Spectrum of 4x 759
Figure 7.152. ^{13}C NMR Spectrum of 4x 759
Figure 7.153. ^{1}H NMR Spectrum of 4y 760
Figure 7.154. ^{13}C NMR Spectrum of 4y 760
Figure 7.155. ^{1}H NMR Spectrum of 4z 761
Figure 7.156. ^{13}C NMR Spectrum of 4z 761
Figure 7.157. ^{1}H NMR Spectrum of 8a 762
Figure 7.158. ^{13}C NMR Spectrum of 8a 762
Figure 7.159. ^{1}H NMR Spectrum of 8b 763
Figure 7.160. ^{13}C NMR Spectrum of 8b 763
Figure 7.161. ^{1}H NMR Spectrum of 8c 764
Figure 7.162. ^{13}C NMR Spectrum of 8c 764
Figure 7.163. ^{1}H NMR Spectrum of 8d 765
Figure 7.164. ^{13}C NMR Spectrum of 8d 765
Figure 7.165. ^{1}H NMR Spectrum of 8e 766
Figure 7.166. ^{13}C NMR Spectrum of 8e 766
Figure 7.167. ^{1}H NMR Spectrum of 8f 767
Figure 7.168. ^{13}C NMR Spectrum of 8f 767
Figure 7.169. ^{1}H NMR Spectrum of 8g 768
Figure 7.170. ^{13}C NMR Spectrum of 8g 768
Figure 7.171. ^{1}H NMR Spectrum of 8h 769
Figure 7.172. ^{13}C NMR Spectrum of 8h 769
Figure 7.173. ^{1}H NMR Spectrum of 8i 770

Figure 7.174. ^{13}C NMR Spectrum of 8i 770
Figure 7.175. ^{1}H NMR Spectrum of 8j 771
Figure 7.176. ^{13}C NMR Spectrum of 8j 771
Figure 7.177. ^{19}F NMR Spectrum of 8j 772
Figure 7.178. ^{1}H NMR Spectrum of 8k 773
Figure 7.179. ^{13}C NMR Spectrum of 8k 773
Figure 7.180. ^{1}H NMR Spectrum of 8l 774
Figure 7.181. ^{13}C NMR Spectrum of 8l 774
Figure 7.182. ^{1}H NMR Spectrum of 8m 775
Figure 7.183. ^{13}C NMR Spectrum of 8m 775
Figure 7.184. ^{1}H NMR Spectrum of 8n 776
Figure 7.185. ^{13}C NMR Spectrum of 8n 776
Figure 7.186. ^{1}H NMR Spectrum of 8o 777
Figure 7.187. ^{13}C NMR Spectrum of 8o 777
Figure 7.188. ^{1}H NMR Spectrum of 8q 778
Figure 7.189. ^{13}C NMR Spectrum of 8q 778
Figure 7.190. ^{1}H NMR Spectrum of 8p 779
Figure 7.191. ^{13}C NMR Spectrum of 8p 779
Figure 7.192. ^{1}H NMR Spectrum of 8r 780
Figure 7.193. ^{13}C NMR Spectrum of 8r 780
Figure 7.194. ^{1}H NMR Spectrum of 13 781
Figure 7.195. ^{13}C NMR Spectrum of 13 781
Figure 7.196. ^{1}H NMR Spectrum of 14 782

Figure 7.197. ^{1}H NMR Spectrum of 14 782

Figure 7.198. ^{1}H NMR Spectrum of 21 783

Figure 7.199. ^{13}C NMR Spectrum of 21 783

Figure 7.200. ^{1}H NMR Spectrum of 23 784

Figure 7.201. ^{13}C NMR Spectrum of 23 784

Figure 7.202. ^{1}H NMR Spectrum of 24 785

Figure 7.203. ^{13}C NMR Spectrum of 24 785

Figure 7.204. ^{1}H NMR Spectrum of 15 786

Figure 7.205. ^{13}C NMR Spectrum of 15 786

Figure 8.1. Examples of Polysubstituted Heterocycles 795

Figure 8.2. Kinetic Profile of the Model Reaction 806

Figure 8.3. Structurally Modified Norbornenes 814

Figure 8.4. Kinetic Profile 843

Figure 8.5. ^{1}H NMR of 3d 864

Figure 8.6. ^{13}C NMR of 3d 864

Figure 8.7. ^{1}H NMR of N1 865

Figure 8.8. ^{13}C NMR of N1 865

Figure 8.9. ^{19}F NMR of N1 866

Figure 8.10. ^{1}H NMR of N6 867

Figure 8.11. ^{13}C NMR of N6 867

Figure 8.12. ^{19}F NMR of N6 868

Figure 8.13. ^{1}H NMR of 4a 869

Figure 8.14. ^{13}C NMR of 4a 869

Figure 8.15. ^{1}H NMR of 4b 870
Figure 8.16. ^{13}C NMR of 4b 870
Figure 8.17. ^{1}H NMR of 4c 871
Figure 8.18. ^{13}C NMR of 4c 871
Figure 8.19. ^{19}F NMR of 4c 872
Figure 8.20. ^{1}H NMR of 4d 873
Figure 8.21. ^{13}C NMR of 4d 873
Figure 8.22. ^{1}H NMR of 4e 874
Figure 8.23. ^{13}C NMR of 4e 874
Figure 8.24. ^{1}H NMR of 4f 875
Figure 8.25. ^{13}C NMR of 4f 875
Figure 8.26. ^{13}C NMR of 4g 876
Figure 8.27. ^{1}H NMR of 4g 876
Figure 8.28. ^{19}F NMR of 4g 877
Figure 8.29. ^{1}H NMR of 4h 878
Figure 8.30. ^{13}C NMR of 4h 878
Figure 8.31. ^{1}H NMR of 4i 879
Figure 8.32. ^{13}C NMR of 4i 879
Figure 8.33. ^{1}H NMR of 4j 880
Figure 8.34. ^{13}C NMR of 4j 880
Figure 8.35. ^{1}H NMR of 4k 881
Figure 8.36. ^{13}C NMR of 4k 881
Figure 8.37. ^{1}H NMR of 4l 882

Figure 8.38. ^{13}C NMR of 4l 882
Figure 8.39. ^{1}H NMR of 4m 883
Figure 8.40. ^{13}C NMR of 4m 883
Figure 8.41. ^{1}H NMR of 5a 884
Figure 8.42. ^{13}C NMR of 5a 884
Figure 8.43. ^{1}H NMR of 5b 885
Figure 8.44. ^{13}C NMR of 5b 885
Figure 8.45. ^{1}H NMR of 5c 886
Figure 8.46. ^{13}C NMR of 5c 886
Figure 8.47. ^{1}H NMR of 5d 887
Figure 8.48. ^{13}C NMR of 5d 887
Figure 8.49. ^{1}H NMR of 5e 888
Figure 8.50. ^{13}C NMR of 5e 888
Figure 8.51. ^{1}H NMR of 5f 889
Figure 8.52. ^{13}C NMR of 5f 889
Figure 8.53. ^{1}H NMR of 5g 890
Figure 8.54. ^{13}C NMR of 5g 890
Figure 8.55. ^{1}H NMR of 5h 891
Figure 8.56. ^{13}C NMR of 5h 891
Figure 8.57. ^{1}H NMR of 5i 892
Figure 8.58. ^{13}C NMR of 5i 892
Figure 8.59. ^{1}H NMR of 5j 893
Figure 8.60. ^{13}C NMR of 5j 893

Figure 8.61. ^{1}H NMR of 5k 894
Figure 8.62. ^{13}C NMR of 5k 894
Figure 8.63. ^{1}H NMR of 5l 895
Figure 8.64. ^{13}C NMR of 5l 895
Figure 8.65. ^{1}H NMR of 5m 896
Figure 8.66. ^{13}C NMR of 5m 896
Figure 8.67. ^{1}H NMR of 5n 897
Figure 8.68. ^{13}C NMR of 5n 897
Figure 8.69. ^{1}H NMR of 5o 898
Figure 8.70. ^{13}C NMR of 5o 898
Figure 8.71. ^{1}H NMR of 5p 899
Figure 8.72. ^{13}C NMR of 5p 899
Figure 8.73. ^{1}H NMR of 5p 900
Figure 8.74. ^{1}H NMR of 5u 901
Figure 8.75. ^{13}C NMR of 5u 901
Figure 8.76. ^{1}H NMR of 5q 902
Figure 8.77. ^{13}C NMR of 5q 902
Figure 8.78. ^{1}H NMR of 5r 903
Figure 8.79. ^{13}C NMR of 5r 903
Figure 8.80. ^{1}H NMR of 5s 904
Figure 8.81. ^{13}C NMR of 5s 904
Figure 8.82. ^{1}H NMR of 5t 905
Figure 8.83. ^{13}C NMR of 5t 905

Figure 8.84. ^{1}H NMR of 5v 906
Figure 8.85. ^{13}C NMR of 5v 906
Figure 8.86. ^{1}H NMR of 5w 907
Figure 8.87. ^{13}C NMR of 5w 907
Figure 8.88. ^{1}H NMR of 6a 908
Figure 8.89. ^{13}C NMR of 6a 908
Figure 8.90. ^{1}H NMR of 6b 909
Figure 8.91. ^{13}C NMR of 6b 909
Figure 8.92. ^{1}H NMR of 6c 910
Figure 8.93. ^{13}C NMR of 6c 910
Figure 8.94. ^{1}H NMR of 6d 911
Figure 8.95. ^{13}C NMR of 6d 911
Figure 8.96. ^{1}H NMR of 11a 912
Figure 8.97. ^{13}C NMR of 11a 912
Figure 8.98. ^{1}H NMR of 11b 913
Figure 8.99. ^{13}C NMR of 11b 913
Figure 8.100. ^{1}H NMR of 11c 914
Figure 8.101. ^{13}C NMR of 11c 914
Figure 8.102. ^{1}H NMR of 11d 915
Figure 8.103. ^{13}C NMR of 11d 915
Figure 8.104. ^{1}H NMR of 11e 916
Figure 8.105. ^{13}C NMR of 11e 916
Figure 8.106. ^{1}H NMR of 13 917

Figure 8.107. ^{13}C NMR of 13 917
Figure 8.108. ^{1}H NMR of 14 918
Figure 8.109. ^{13}C NMR of 14 918
Figure 8.110. ^{1}H NMR of 18 919
Figure 8.111. ^{13}C NMR of 18 919
Figure 8.112. ^{1}H NMR of S6 920
Figure 8.113. ^{13}C NMR of S6 920
Figure 8.114. ^{1}H NMR of 20 921
Figure 8.115. ^{13}C NMR of 20 921
Figure 8.116. ^{1}H NMR of 21 922
Figure 8.117. ^{13}C NMR of 21 922
Figure 8.118. ^{1}H NMR of 22 923
Figure 8.119. ^{13}C NMR of 22 923
Figure 8.120. ^{1}H NMR of 26 924
Figure 8.121. ^{13}C NMR of 26 924
Figure 8.122. ^{19}F NMR of 26 925
Figure 8.123. ^{1}H NMR of 27 926
Figure 8.124. ^{13}C NMR of 27 926
Figure 8.125. ^{1}H NMR of 28 927
Figure 8.126. ^{13}C NMR of 28 927
Figure 8.127. ^{19}F NMR of 28 928
Figure 8.128. ^{1}H NMR of S10 929
Figure 8.129. ^{13}C NMR of S10 929

Figure 8.130. ^{19}F NMR of S10 930
Figure 8.131. ^{1}H NMR of 30 931
Figure 8.132. ^{13}C NMR of 30 931
Figure 8.133. ^{19}F NMR of 30 932
Figure 8.134. ^{1}H NMR of 9 933
Figure 8.135. ^{13}C NMR of 9 933
Figure 8.136. ^{1}H NMR of 10 934
Figure 8.137. ^{13}C NMR of 10 934
Figure 8.138. ^{1}H NMR of 4a’ 935
Figure 8.139. ^{13}C NMR of 4a’ 935
Figure 8.140. ^{1}H NMR of 8 936
Figure 8.141. ^{13}C NMR of 8 936

ACKNOWLEDGEMENT

First and foremost, I would like to thank my advisor, Prof. Guangbin Dong, for offering me the opportunity to join in the group and explore the interesting palladium/norbornene chemistry. I would not have finished those projects without his leadership and mentorship over the past five years. I still remembered the first discussion with Guangbin when I was a visiting prospective student in the University of Chicago, I was quite impressed by both the chemistry he has done and his personality and enthusiasm toward chemistry. After I joined in the group and started doing my own project, he always offered tons of useful ideas and suggestions and many of them eventually worked out. I always admire his curiosity, creativity and imagination as well as enthusiasm and patience, which indeed taught me a lot and will further guide me to become a good researcher in the future. I am very grateful for what he did. Second, I would like to thank my undergraduate advisor, Prof. Baiquan Wang, who was also my first organic chemistry professor in the college. He gave me the opportunity to join his lab during my first summer and soon I was able to work on my own project and published my first paper. The research experience in his lab focusing on ruthenium-catalyzed C–H functionalization eventually led me to choose the field of palladium/norbornene catalysis to dig in. I would also like to thank Prof. Peng Liu for his helpful suggestions on DFT calculation in my last project.

Then, I would like to thank my committee members, Prof. Scott Snyder and Prof. Viresh Rawal, for agreeing to serve on my dissertation committee, generously offering their time to read this thesis and offering valuable feedback and being supportive of my future career goals. Prof. Snyder, Prof. Rawal and Prof. Bryan Dickinson also served on my Ph.D. candidacy committee, and I am very grateful for their feedback and advice.

Next, I would like to thank those who I have closely worked with over the past few years. Special thanks to my co-workers: Yun Zhou, Feipeng Liu, Jianchun Wang, Zhe Dong, Xiaolong Xu, Ki-Young Yoon and Xiaotian Qi. I would not have finished those projects without their help. I would also like to thank Jianchun Wang, Zhongxing Huang, Zhe Dong, Yan Xu, Chengpeng Wang, Jiaxin Xie, Lin Deng, Alex Rago, Yibin Xue, Sihua Hou, Zhao Wu, Xin Liu, Jun Zhu, Ming Chen and Ziqiang Rong for helpful discussion. In addition, I would like to thank Ki-Young Yoon, Shusuke Ochi and Xin Liu for solving the crystal structures.

Finally, I would like to thank my family for their support during my graduate study. I deeply thank my mom, dad, aunt, uncle, and my grandmother, who unfortunately didn't have the opportunity to read this thesis. Most importantly, I would like to thank my fiancée, Xiaotong, for her trust, love and support over the past seven years. She will also obtain her chemistry Ph.D. soon and I cannot imagine the life without her. I dedicate this thesis to all of them.

Renhe Li

University of Chicago

July 2021

ABSTRACT

Poly-substituted aromatics are frequently found in pharmaceuticals and agrochemicals. During the past decades, cross-coupling reactions and nucleophilic aromatic substitutions (S_NAr) have become indispensable tools for preparing functionalized arenes from readily available aryl halides. Recently, ortho-metalation approaches, mediated by either stoichiometric organometallics or catalytic transition metals, enabled broadly useful ortho C−H functionalization. We were motivated by the merits of merging cross-coupling and ortho-metalation, two powerful organic reactions, into a single palladium/norbornene (Pd/NBE)-catalyzed transformation. Pd/NBE catalysis, namely Catellani reaction, has recently emerged as a powerful approach for vicinal difunctionalization of arenes. Using simple aryl iodides as substrates, a number of nucleophiles and electrophiles have been installed at the ipso and ortho positions respectively through selective reactions with the aryl-norbornyl-palladacycle (ANP) intermediate.

Considering this relatively long and complicated catalytic cycle involving both Pd(II) and Pd(IV) intermediates, some intrinsic challenges still exist in developing new Catellani-type transformation. First, the initially generated Pd(0) precatalyst must react with aryl iodide instead of the electrophile; thus, a fast/facile oxidative addition process is necessary. Regarding most of literature reported Catellani-type reactions aryl iodide was proved to be the only suitable substrate (*Aryl Iodide Constraint*). Second, the electrophile must selectively oxidize ANP instead of initially generated Pd(II) intermediate, which leads to a very limited electrophiles scope (*Electrophile Constraint*). Third, the NBE extrusion will only take place when two ortho positions of aryl iodide are blocked, otherwise undesired difunctionalization product or NBE-containing side products will be formed (*Ortho Constraint*).

To address the aforementioned “Electrophile Constraint”, we developed a direct annulation strategy between aryl iodides and epoxides, affording the desired 2,3-dihydrobenzofuran derivatives in decent yields and regioselectivity. The readily available epoxide served as a new class of electrophile and alkylating reagent; asymmetric synthesis was also realized using enantiopure epoxide. Application of this method into a concise synthesis of insecticide fufenozide was also demonstrated. In addition, inspired by our previously reported ortho amination of aryl iodide, we developed an ortho thiolation strategy enabled by a new class of sulfenamide electrophile, derived from a seven-membered lactam. The arene ipso functionalization is simultaneously achieved through Heck, Suzuki or Sonogashira termination. The broad substrate scope and high chemoselectivity could make this method attractive for synthesis of complex sulfur-containing aromatic compounds.

To overcome the “Aryl Iodide Constraint”, a redox-neutral ortho functionalization of aryl boroxines was developed. The reaction was initiated by a transmetalation of aryl boroxine to Pd(II) and terminated by a protodepalladation process, thereby avoiding stoichiometric amount of oxidant and reductant as well as tolerating a broader functional group including aryl iodide. In addition, a direct vicinal difunctionalization of thiophene was developed; this transformation was initiated by direct C−H palladation at C2 position of thiophene without aids of directing group, allowing for simultaneously installing two different functional groups at vicinal positions in a site- and regioselective manner. The synthetic utility of this method was demonstrated by late-stage functionalization of a range of bioactive compounds. Then this difunctionalization method was successfully extended to other heteroarenes, including furans, pyrroles and indoles. Besides ortho arylation, ortho alkylation and ortho alkynylation were all realized with decent yields and regioselective. Meanwhile, a concise synthesis of Rhazinilam was realized to demonstrate the

synthetic utility. Finally, a vicinal double C−H functionalization of five-membered heteroarenes with two different electrophiles in a site-selective and redox-neutral manner was realized by using aryl iodide as the first electrophile and alkynyl bromide as the second electrophile, enabling regioselective difunctionalization of a variety of five-membered heteroarenes at their C4 and C5 positions. Moreover, the mechanistic exploration discloses the origin of the high selectivity of this difunctionalization reaction.

PREFACE

Each chapter of this dissertation is numbered independently. A given compound may have a different number in different chapters. All experimental details, references and notes for individual chapters are included at the end of each chapter.

CHAPTER 1

Structurally Modified Norbornenes: A Key Factor to Modulate Reaction Selectivity in the Palladium/Norbornene Cooperative Catalysis

1.1. Introduction

Since the seminal discovery by Catellani in 1997, the palladium/norbornene (Pd/NBE) co-catalyzed arene functionalization reactions have received increasing amounts of attention and led to many synthetic applications in the past two decades.[1] Compared to the widely adopted cross-coupling and nucleophilic aromatic substitution (S_NAr) reactions where the number and position of newly installed functional groups (FGs) are dictated by those of the leaving groups in the substrates, the Catellani-type reactions can introduce multiple different FGs simultaneously in a site-selective manner (Scheme 1.1a). Considering that polysubstituted aromatics are ubiquitously found in pharmaceuticals and agrochemicals, the Pd/NBE catalysis could become an incredible useful tool for functionalization and streamlined syntheses of complex arenes and heteroarenes.

Despite the great promise, some intrinsic constraints due to the use of the NBE co-factor had nevertheless become roadblocks to practical applications of these reactions.

As illustrated in Scheme 1.1b, a general mechanism of the Catellani reaction involves first forming an aryl-Pd(II) species from either oxidative addition of Pd(0) with aryl halides or transmetallation or direct C−H palladation from a Pd(II) catalyst. The subsequent NBE migratory insertion and palladation at the ortho position give a unique aryl-norbornyl-palladacycle (ANP) intermediate that can react with an electrophile to introduce an ortho FG (relative to the original reaction site).[2] After β-carbon elimination to exclude NBE, the resulting aryl-Pd(II) species can either react with a nucleophile (including olefins) to install an ipso FG and regenerate the Pd(0) catalyst, or be quenched by a proton to regenerate the Pd(II) catalyst. Due to the high complexity of the mechanism, many competing side reactions can take place. For example, the ANP can undergo direct C−C reductive elimination to form benzocyclobutenes (step **G**);[3] the reaction with electrophiles can oxidize the $C(sp^3)$−Pd bond in ANP instead of the desired $C(sp^2)$−Pd bond (step **H**);[4-5] the β-carbon elimination of NBE could be problematic in the absence of an existing sizable ortho substituent and a second C−H palladation may take place (known as "ortho constraint", step **I**),[6] etc. Clearly, the structure of NBE plays critical roles in almost every single step of the catalytic cycle, and most side-products contain the NBE moieties. Thus, in the past five years researchers in this field have been motivated to use structurally modified NBEs (smNBE) to solve these selectivity problems in the Catellani-type reactions.

Scheme 1.1. Pd/NBE Cooperative Catalysis

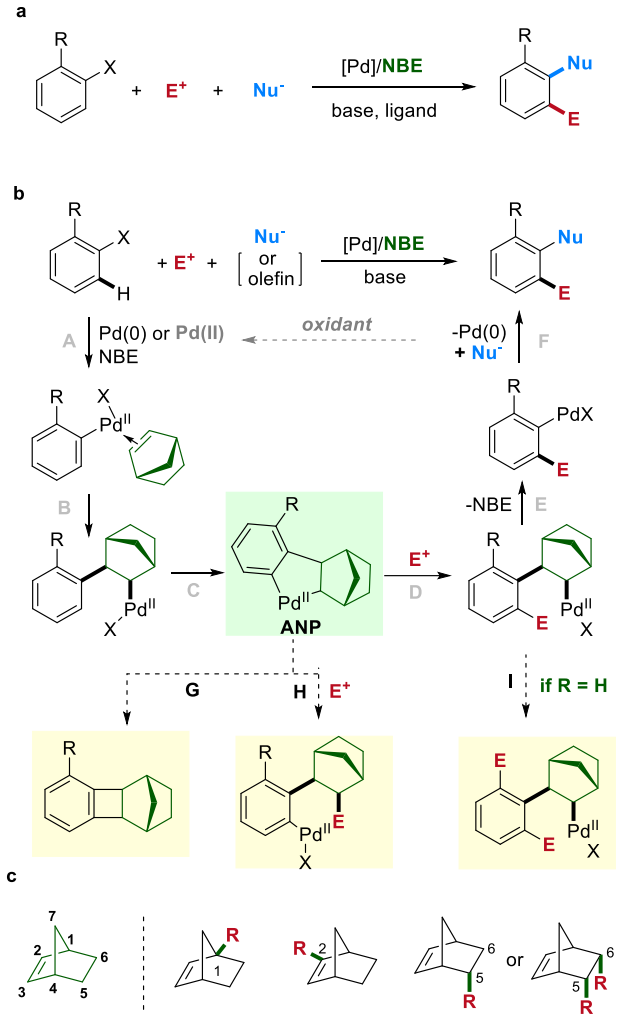

The strained and rigid [2.2.1] bicyclic scaffold of NBE offers unique features for the success of the Catellani-type reactions: it enables rapid migratory insertion to outcompete direct ipso functionalization, avoids β-hydrogen elimination to promote the desired ortho C−H palladation, and allows β-carbon elimination to regenerate NBE. Hence, the current successful modifications on NBE usually maintain the original [2.2.1] skeleton, and to date effective variations are located at the C1, C2, C5 and C6 positions (Scheme 1.1c). In general, the size and position of the substituents are critical. For instance, increasing the steric hindrance of NBE would promote β-carbon elimination, but reduce its binding affinity to Pd, thereby causing formation of more

undesired direct ipso functionalization side-products. The C1-substituted NBEs can inhibit the undesired second C−H metalation and promote β-carbon elimination; thus, they were developed for addressing the "ortho constraint" issue. The reactivity of the C5- and C6-substituted NBEs are close to (*yet sometimes more reactive than*) simple unsubstituted NBE. The C2-substituted NBEs play a more complex role: they can inhibit direct reductive elimination of ANP to form norbornyl benzocyclobutenes, prompt NBE insertion and C−H palladation (when the C2-substituent can form hydrogen bonding). More detailed discussions are provided in the following sections.

This perspective article was inspired by several excellent review articles published recently[7-17] and will primarily focus on three types of smNBE cocatalysts: C1-substituted, C2-substituted and C5-substituted or C5, C6-disubstituted smNBEs.[18]

1.2 C1-Substituted smNBEs

Typically, the aryl-halide substrates used in the Pd/NBE catalysis contain an ortho-substituent. When ortho unsubstituted haloarenes were used, di-ortho-functionalization (with para-substituted substrates) or formation of a mixture of NBE-containing side-products (with meta-substituted substrates) would dominate, whereas the desired mono-ortho-functionalization generally cannot be achieved (Scheme 1.2a). This has been referred as "ortho constraint".[6] The origin of the problem is due to slow β-carbon elimination of NBE in the absence of the ortho substituent, which promotes a second ortho C−H palladation or pre-mature termination.

Scheme 1.2. Overcoming the Ortho **Constraint with C1-smNBEs**

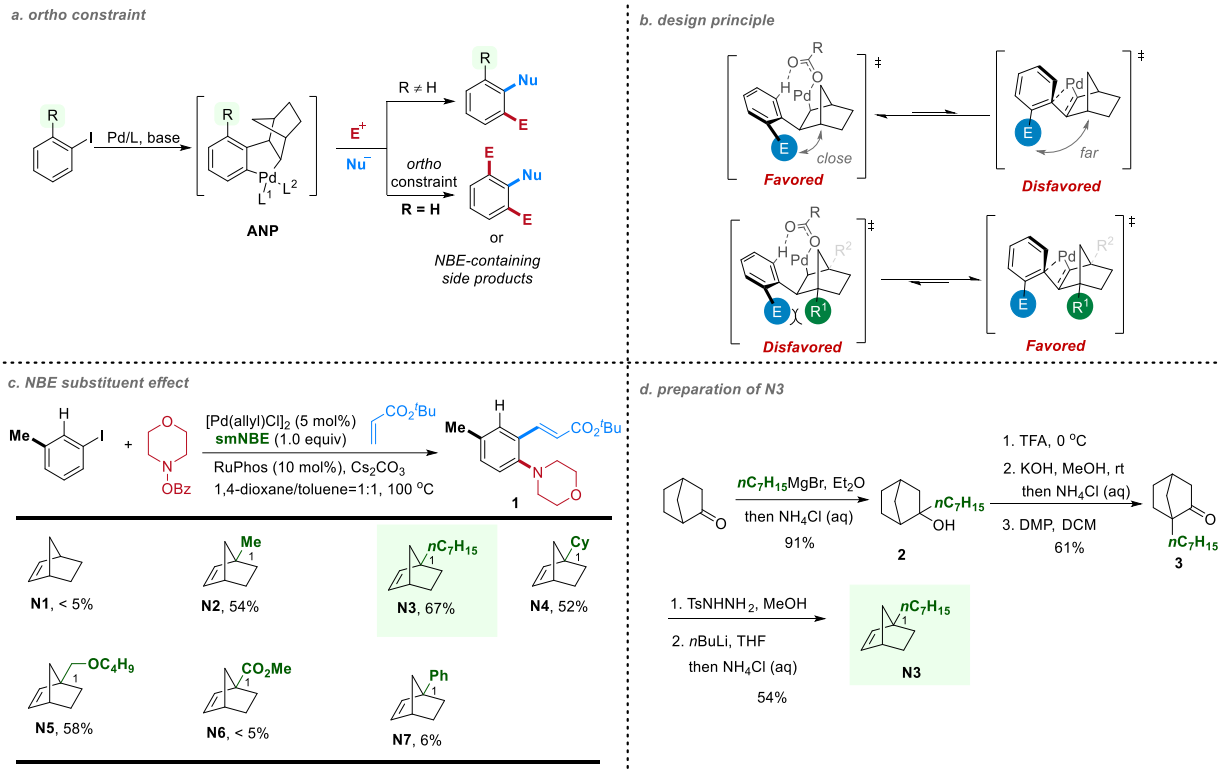

To address this challenge, the Dong group developed a class of C1-substituted smNBEs in 2018, which effectively allowed the use of ortho-unsubstituted aryl halides as substrates for mono-ortho-functionalization.[6] Compared to regular NBE, the bridgehead substitution was anticipated to inhibit the undesired second C−H palladation by destabilizing its transition state (TS) through repulsive interaction with the newly installed ortho FG; meanwhile, it can also reduce the barrier for β-carbon elimination to extrude NBE through controlling the orientation of the arene (Scheme 1.2b). The C1 alkyl-substituted NBEs, e.g. **N2-N5**, were found particularly effective when the ortho amination was used as the model reaction (Scheme 1.2c).[19] Stoichiometric smNBEs were used here to minimize undesired ipso functionalization. The typical procedure for synthesis of C1-substituted smNBEs is shown in Scheme 1.2d with **N3** as an example.

While the *n*-heptyl-substituted **N3** smNBE was optimal for most meta-substituted substrates, the cyclohexyl-substituted **N4** was more effective when the meta-substituents are small, such as F, OMe and CO_2Me (Scheme 1.3). Higher yield was observed when aryliodides with a bulkier meta substituent were used (**4-6**). Heck reaction (**4-6**), hydrogenation (**7**), Suzuki (**8**) and Sonogashira (**9**) reactions could all take place at the ipso position; besides ortho amination, ortho acylation (**10**) and arylation (**11**) also worked under slightly modified reaction conditions. Without such ortho constraint, vicinal difunctionalization or site-selective derivatization of complex bioactive molecules (**12-15**) could now be conveniently realized via a two-step sequence—arene iodination and this method. When ipso hydrogenation was employed, complementary site-selectivity to electrophilic aromatic substitution (EAS) was achieved for arene C−H functionalization because FGs can be installed at the positions that are not favorable for EAS reactions.

Scheme 1.3. Scope and Late-Stage Functionalization of Bioactive Compounds

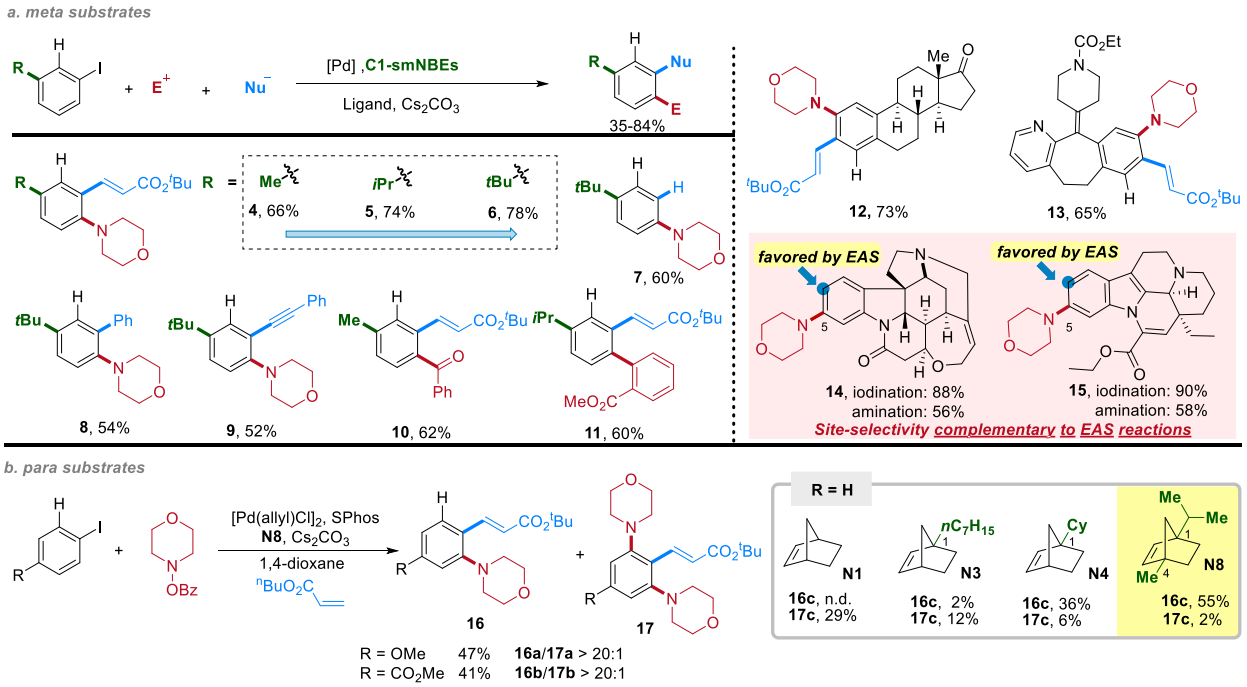

Finally, selective mono ortho functionalization of the more challenging para-substituted aryl iodides could be realized with a doubly bridgehead-substituted NBE (**N8**). The density functional theory (DFT) calculation suggested that steric repulsion caused by the bridgehead substituents in **N8** significantly increased the barrier of the second C–H metalation step (thus preventing di-ortho-functionalization), whereas the β-carbon elimination and migratory insertion steps exhibit reduced activation energy, which makes forming the mono-ortho-product kinetically favored.

The C1-substituted smNBEs provide a viable approach to address the longstanding ortho constraint in the Catellani-type transformations. Future work may focus on improving the efficiency of C1-smNBEs and enabling new synthetic applications.

1.3 C2-Substituted smNBEs

Compared to C1-substituted smNBEs, the C2-substituted ones exhibit different functions. First, the C2 substituents directly introduce steric hindrance on the carbon that binds to Pd, which greatly suppresses direct C−C reductive elimination of ANP (Scheme 1.4a).[20] Second, the electron-withdrawing C2 substituent can promote migratory insertion of NBE from the electronic prospect to compromise the weakened olefin binding and steric disadvantage (Scheme 1.4b). Third, when a secondary amide moiety is introduced at the C2 position, the resulting hydrogen bonding with the concerted metalation deprotonation (CMD) ligand on Pd can reduce the overall activation barrier (*vide infra*, Scheme 1.13).[21] While a number of C2-substituted smNBEs have been prepared, to date the most effective two types are: the ester-substituted one pioneered by Yu[20] and the amide-substituted ones developed by Dong (Scheme 1.4c).[22-23] The preparation of **N9** was shown as an example (Scheme 1.4d).[24]

Scheme 1.4. C2-Substituted smNBEs

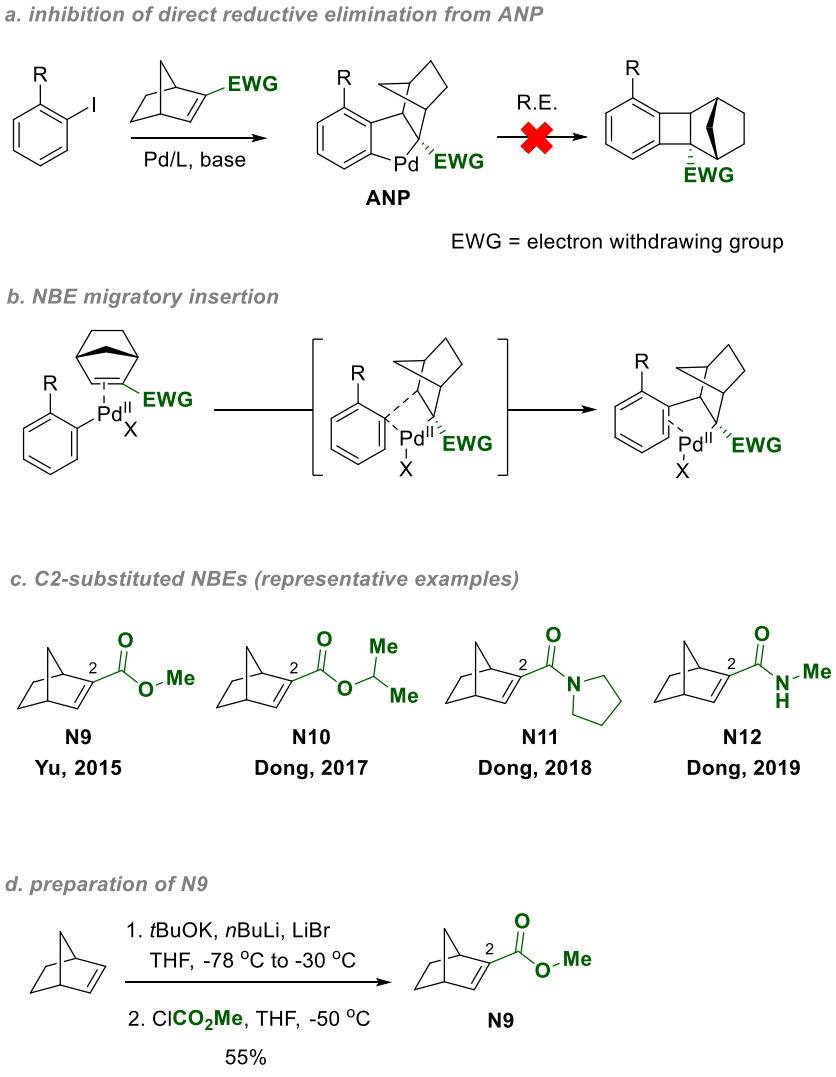

1.3.1 Pd(II)-Catalyzed Meta C−H Functionalization Involving C2-Substituted smNBEs

While the directing group (DG)-promoted meta C−H arylation and alkylation of arenes *via* the Pd/NBE cooperative catalysis was firstly realized using simple NBE,[25,26] these reactions suffered from relatively limited substrate scopes. For example, aryl iodides without an ortho DG typically gave less than 5% yield, and formation of norbornyl benzocyclobutene side-products outcompeted the desired meta-alkylation pathway, especially when using alkyl iodides bearing β-hydrogens. To address these drawbacks, Yu and co-workers utilized a C2 methyl carboxylate-substituted NBE

(**N9**) to greatly expand the scope of aryl and alkyl electrophiles for meta C−H functionalization (Scheme 1.5).[20] The new condition allowed the use of simple alkyl iodides with β-hydrogens and aryl iodides without an ortho DG; it also minimized benzocyclobutene side-products. The ester moiety was more effective than a more electron-withdrawing ketone or nitrile group as the corresponding **N13** and **N14** NBEs showed much lower reactivity.

Scheme 1.5. Meta Alkylation and Arylation of Substituted Phenylacetamides Using C2-Substituted smNBEs

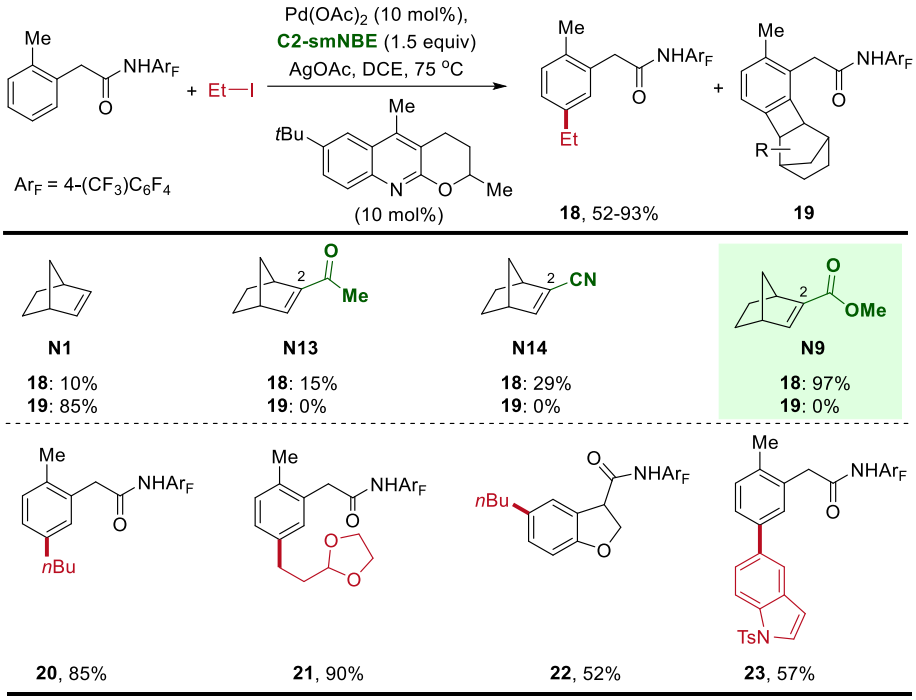

Besides aryl and alkyl iodides, other electrophiles such as *o*-benzoyl hydroxylamines and alkynyl bromides were successfully utilized in the C−H activation-initiated meta-functionalization reactions. Owing to the use of C2 methyl carboxylate-substituted smNBE (**N9**) as well as the 2-pyridone-type ligands, the Yu group realized the first meta amination and alkynylation (Scheme 1.6a) of aniline- and phenol-derivatives in 2016.[27] For example, the yield of meta amination product was improved significantly by switching simple NBE **N1** to **N9**. Heterocycles including

indole, indoline and indazole were compatible in the meta amination and alkynylation reactions. In terms of the alkyne electrophiles, only bulky silyl-protected alkynyl bromides afforded the desired products in good yields at the current stage, while simple alkyl and aryl alkynyl bromides only led to trace amounts of meta products. In addition, smNBE **N9** also enabled the first Pd(II)-initiated meta C−H chlorination of aniline and phenol derivatives also by Yu in 2017 (Scheme 1.6b).[28] An aryl chlorosulfate reagent[29] was used as a mild chlorinating reagent to exclusively oxidize Pd(II) to Pd(IV)[30] without direct ortho C−H chlorination. The two new hydroxypyridine ligands **L1** and **L2** were also important for enhanced yields and scope. As an important application, the chloride group in the products could be conveniently converted to other FGs through various cross-coupling reactions.

Scheme 1.6. Meta Amination, Alkynylation and Chlorination of Aniline and Phenol Derivatives

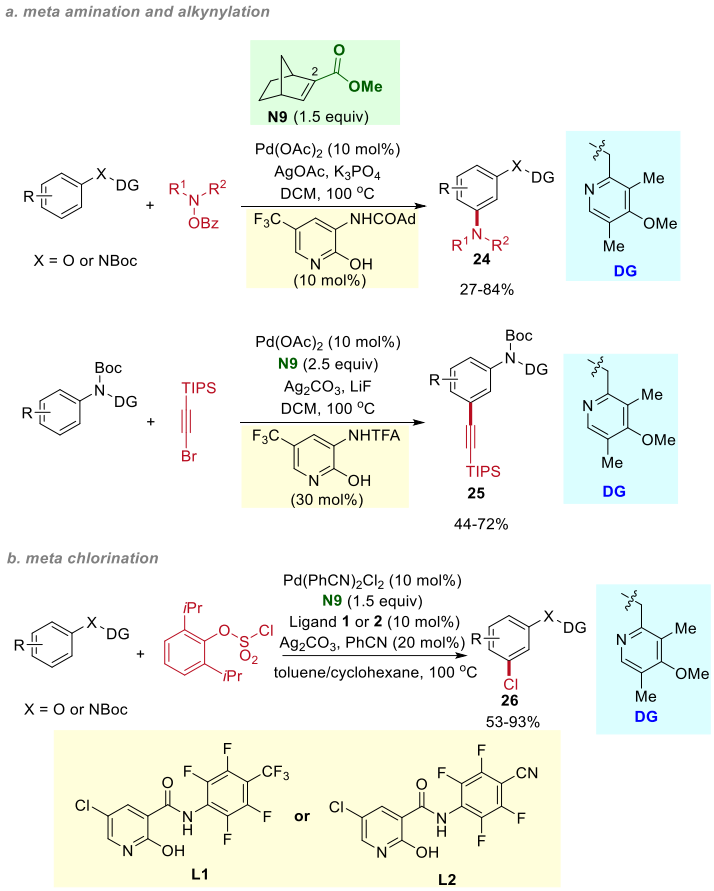

The unsymmetrical structure of C2-substituted smNBEs also offers opportunities for developing enantioselective transformations. In 2018, the Yu group reported the first example of enantioselective meta C−H arylation and alkylation using enantiopure **N9*** (Scheme 1.7).[31] It was proposed that the chiral NBE structure could differentiate the enantiomeric ortho C−H palladation intermediates during the NBE migratory insertion step. Compared with other smNBEs, the C2 substitution was more important for the enantio-determining step. Addition of a catalytic amount of chiral or achiral phosphoric acids as the additive was beneficial for both yield and

enantioselectivity, while control experiments indicated that the enantioenriched smNBE was mostly responsible for the chiral induction.

Besides diarylbenzylamines, homobenzylamines can also be used as the substrates, despite forming a more distal stereocenter (Scheme 1.7b). The use of nosyl-protected amines as DGs proved to be efficient. Besides desymmetrization, kinetic resolution of unsymmetrical aryl substrates was also achieved. Note that a contemporary discovery of an enantioenriched C2-smNBE-promoted Pd(0)-catalyzed asymmetric annulation with aryl iodides was reported by Dong (*vide infra*, Scheme 1.12).[22]

Scheme 1.7. Enantioselective Meta C–H Arylation and Alkylation Enabled by a Chiral smNBE

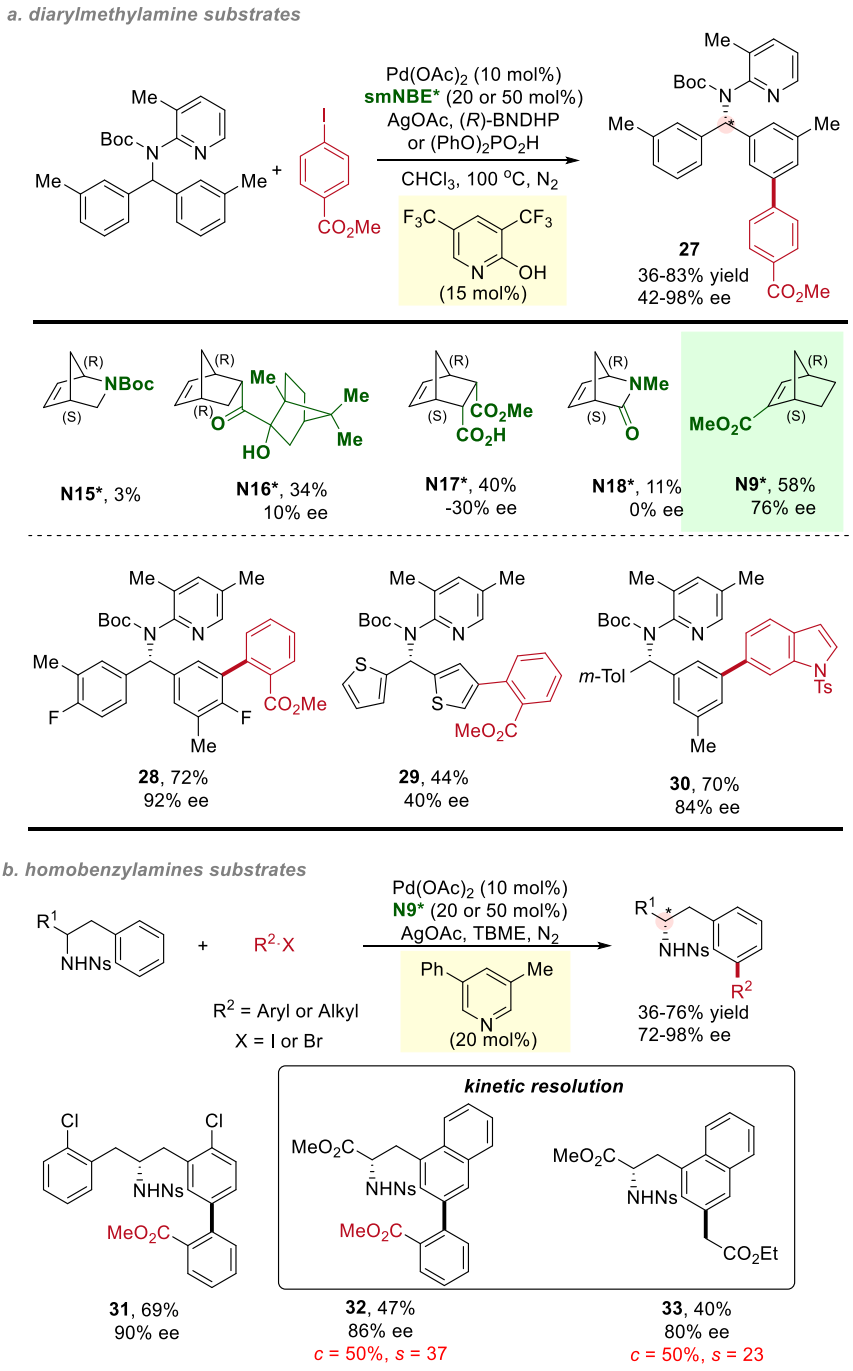

The meta C−H functionalization could also be realized for substrates without covalently bound auxiliary DGs, in which the C2-substiutted smNBEs were again found to be important. In 2019,

the Yu group reported the meta C−H arylation of aryl ethers, which offered complementary site-selectivity to EAS reactions (Scheme 1.8a).[32] Interestingly, a dual-ligand system was applied: an electron-deficient quinoxaline-6-carbonitrile **L3** along with a 3-pyridinesulfonic acid **L4** were used to generate more electrophilic cationic Pd(II) species, thus facilitating the first C−H palladation. A series of aryl ethers can be used as substrates; besides anisoles, 2,3-dihydrobenzofuran and chromane moieties (**36** and **37**) were also suitable, affording exclusively meta selectivity. Heterocycles, such as pyridine (**34**), were tolerated. Various complex moieties such as estrone (**35**) and tasimelteon (**36**) were also comparable. Based on the DFT calculation, the first C−H palladation was proved to be the rate-determining step.[33] Very recently, this method has been extended to electron-deficient heterocycles[34] and fluorobenzenes[35] by the Yu group (Scheme 1.8b).

Scheme 1.8. Direct Meta Arylation of Electron-Rich Arenes, Electron-Deficient Heteroarenes and Fluorobenzenes.

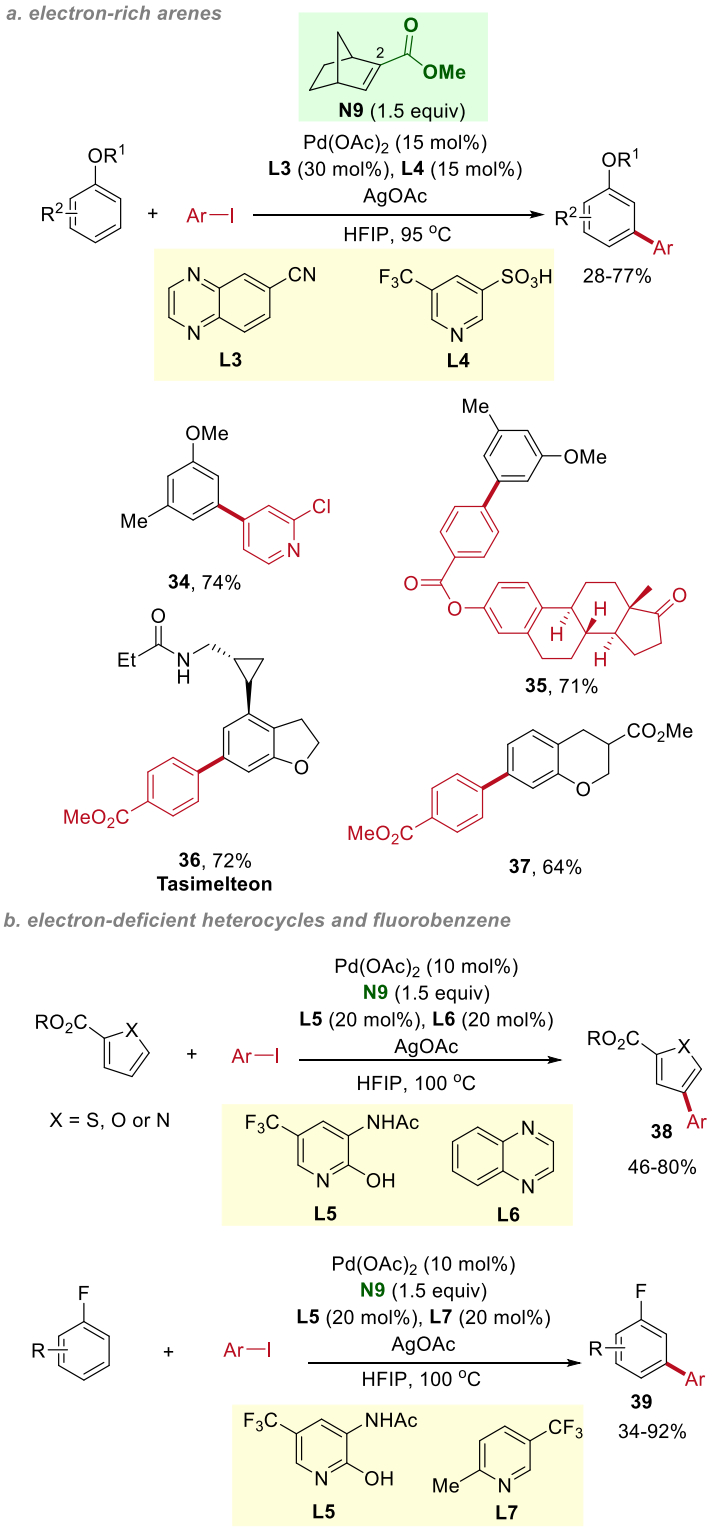

Very recently, a remote site-selective C−H arylation of quinolines and other heterocycles was achieved by Yu and Houk using the **N9** smNBE (Scheme 1.9a).[36] This work merged their previously developed template-directed approach[37] and the Pd/NBE catalysis to realize complementary remote site-selectivity. The DFT calculation indicated that the nitrile group on the side arm of the Pd template directed the initial C−H palladation with the second Pd center to reach the C5 position of the quinoline substrate, and an *N*-acetylglycine ligand promoted the CMD step. This approach was applicable to a variety of heterocycles, including quinolines (**40**), benzoxazoles (**41**) and benzothiazoles (**42**). A late-stage modification of an antileukemic and antitumor alkaloid, camptothecin (**43**), was demonstrated. Besides the nitrile template, this strategy also worked with their previously reported U-shape templates (Scheme 1.9b). Tetrahydroisoquinolines (**44**) was able to undergo C−H arylation at the C7 position, which is one bond further away from the "normal" C8 selectivity offered by the U-shape DG alone. Finally, para arylation of phenylpropanoic acid derivatives (**45**) was realized in a similar manner, while the two ortho positions adjacent to the DG had to be blocked likely due to the ortho *constraint* of the Catellani-type reactions (*vide supra*, Scheme 1.2).

Scheme 1.9. Remote C–H Arylation of Benzoazines, Tetrahydroisoquinolines and Phenylpropanoic Acids

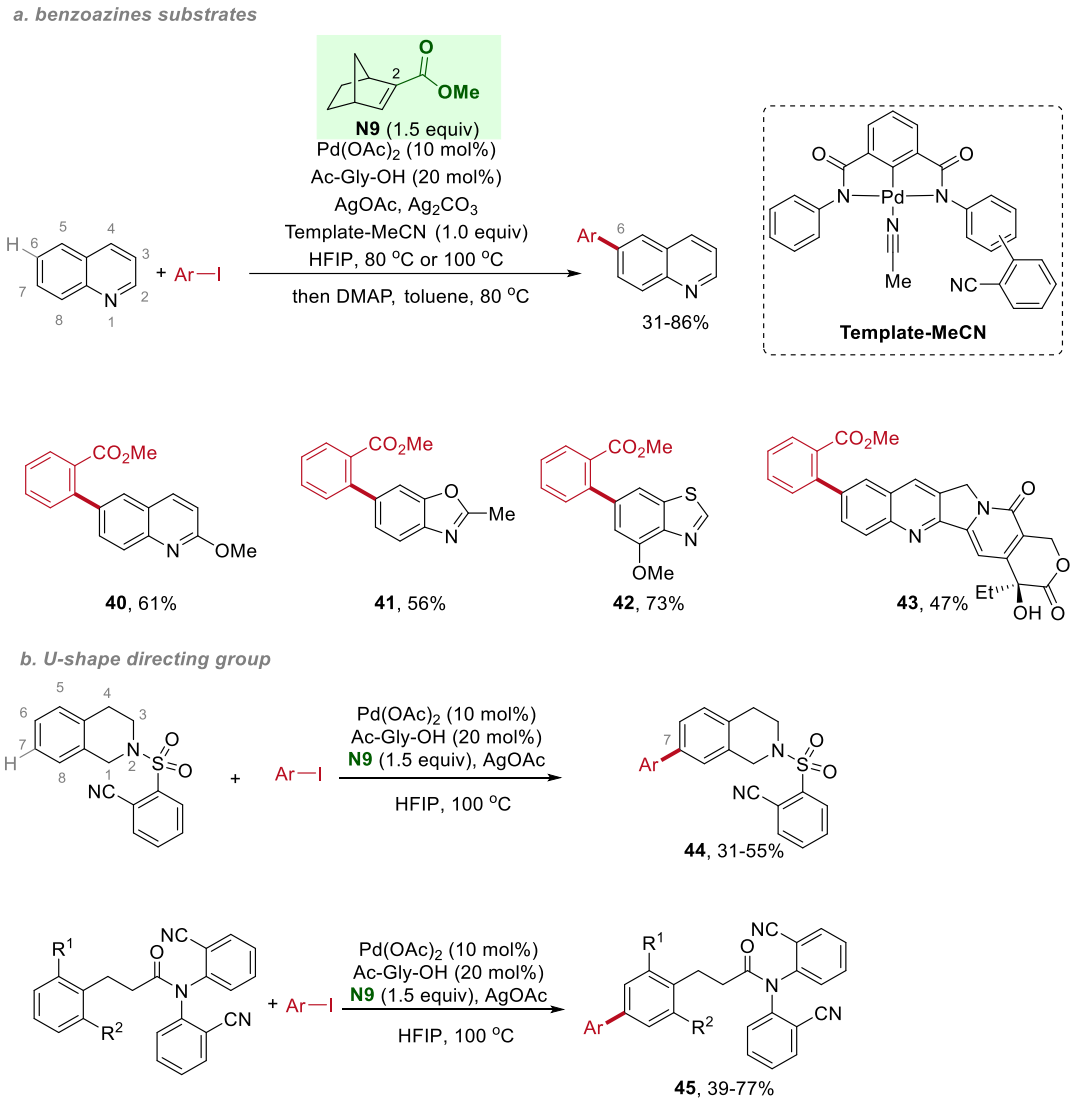

1.3.2 Pd(II)-Initiated Vicinal Difunctionalization Involving C2-Substituted smNBEs

While the meta C−H functionalization *via* the Pd/NBE cooperative catalysis has been extensively developed, the corresponding vicinal difunctionalization through sequential double C−H activation was not reported until 2019. From the synthetic efficiency viewpoint, it could be attractive to simultaneously convert two adjacent C−H bonds into different FGs in a site-selective

manner. In 2019, the Dong group reported a direct vicinal difunctionalization of thiophenes and furans without aid of DGs, where a C2 amide-substituted smNBE (**N12**) was found superior to other NBEs (Scheme 1.10a).[38] **N12** has been known to prompt both the migratory insertion and CMD processes (*vide infra*, Scheme 1.14). The reaction was initiated through a reversible C−H palladation at thiophene C2 (or C5) positions. The use of a weakly coordinative π-acidic arsine ligand was important to prevent chelation of the sulfur moiety on the palladium without compromising the ANP formation.[26] The scope of the ortho arylation/ipso Heck reaction was relatively broad (Scheme 1.10b). A series of mono- and disubstituted thiophenes were difunctionalized site- and regio-selectively at the C4 and C5 positions in good yields. Various FGs including bromide (**51**) and internal alkynes (**50**) were tolerated. Preliminary success was obtained with a furan substrate (**49**). In addition, this method was applied to vicinal difunctionalization of complex bioactive compounds (**52-55**). Besides, an open-flask gram-scale preparation was demonstrated using commercial ethyl acetate without further purification (Scheme 1.10c). Finally, a kinetic study implied a simultaneous difunctionalization pathway instead of a stepwise functionalization pathway. The high reactivity and selectivity shown by the C2-amide-substituted smNBE (**N12**) could inspire vicinal di-C−H-functionalization of other arenes and heteroarenes.

Scheme 1.10. Vicinal Difunctionalization of Thiophenes

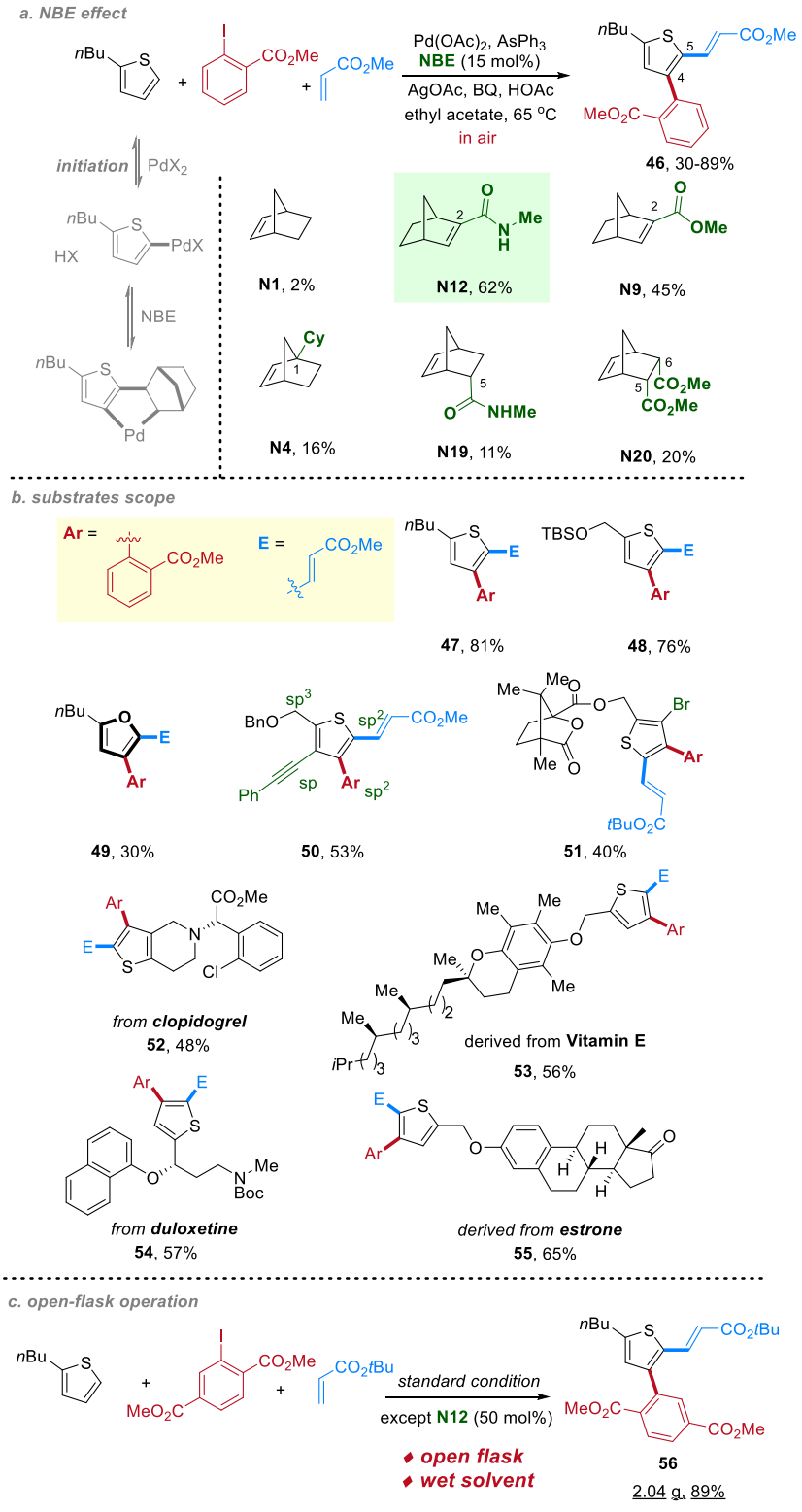

1.3.3 Pd(0)-Initiated Difunctionalization of Aryl Halides Involving C2-Substituted smNBEs

In most of Pd(0)-initiated Catellani-type reactions, simple NBE is sufficient to achieve good yields and selectivity. However, in some special cases, particularly those with less reactive electrophiles or substrates, side reactions, e.g. multi-NBE insertion or direct reductive elimination from ANP,[3, 39] can dominate; the C2-substiutted smNBEs have been found to be effective to enhance selectivity of such reactions. For example, when epoxides were employed as the electrophile in an annulation with aryl iodides for synthesis of 2,3-dihydrobenzofurans (DHBFs), the use of simple NBE (**N1**) generated a significant amount of multi-NBE insertion products (Scheme 1.11).[40] This was likely due to the relatively low electrophilicity of epoxides, which makes them less reactive to couple with ANP compared with **N1**. The Dong group in 2017 disclosed that the multi-NBE insertion pathway can be effectively suppressed using C2-substituted smNBEs as the steric hindrance introduced in the ANP intermediate can prevent insertion of another bulky smNBE. While the C2 isopropyl ester-substituted NBE (**N10**) proved to be optimal, further increasing the steric hindrance, e.g. use of *tert*-butyl ester-substituted **N23**, significantly diminished the yield. Note that, while most prior Pd/NBE-catalyzed reactions require a high loading of or excess NBE due to the formation of undesired NBE-attached side-product (*vide supra*, Scheme 1.1), only 20 mol% **N10** was found to be sufficient in this reaction. In addition, a bulky phosphine-derived Buchwald's precatalyst, Ruphos-Pd-G4,[41] was employed to inhibit β−H elimination of the Pd alkoxide intermediate and promote the final C−O reductive elimination step.[42-43]

Scheme 1.11. Direct Annulation between Aryl Iodides and Epoxides

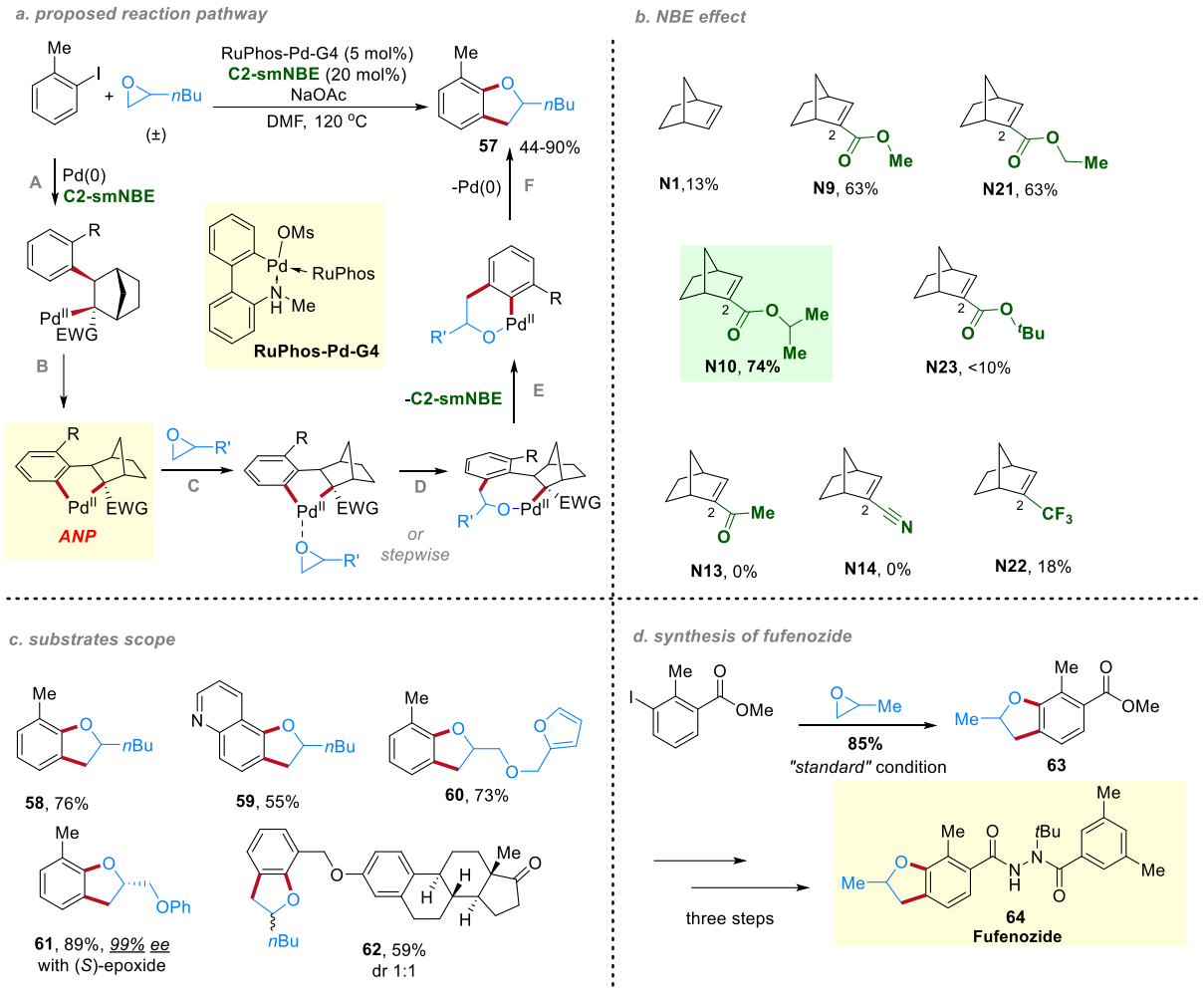

This reaction tolerates various primary epoxides and aryl iodides with diverse FGs and heterocycles. When an enantiopure epoxide was used as the coupling partner, the annulation reaction proceeded with complete stereo-retention (**61**). Finally, this method was used to realize a concise synthesis of fufenozide. Note that almost concurrently, Zhou reported an elegant transformation using epoxides as electrophiles in an ortho alkylation/ipso Heck reaction, whereas a C5-substituted NBE was found more important (*vide infra*, Scheme 1.18).[44-45]

While enantioenriched epoxides can be obtained from kinetic resolution or asymmetric synthesis, it would still be attractive to utilize more available racemic epoxides to realize an asymmetric

synthesis of DHBFs. In 2018, the Dong group reported their initial study on a Pd-catalyzed asymmetric annulation between aryl iodides and epoxides enabled by an enantioenriched C2-substituted smNBE cocatalyst.[22] This work represents the first chiral NBE scaffold-promoted asymmetric reaction *via* Pd(0)-initiated Catellani-type reactions. The chirality of the enantiopure NBE was anticipated to create a chiral pocket around the metal center in ANP, consequently promoting one enantiomer of the epoxide to react faster than the other (Scheme 1.12a). A reliable route was first developed to prepare these enantiopure smNBEs using 2,10-camphorsultam as a chiral auxiliary (Scheme 1.12b). The pyrrolidine amide-substituted (+)-**N11** gave the highest enantioselectivity (45% ee) but diminished reactivity; the enantiopure isopropyl ester-substituted NBE (−)-**N10** gave slightly lower enantioselectivity but significantly better yield (Scheme 1.12c). The kinetic monitoring of the reaction suggested that the stereochemistry of (−)-**N10** matches the (*S*)-epoxide, which nevertheless reacted significantly slower if using another enantiomer of NBE (+)-**N10** (Scheme 1.12d).

Scheme 1.12. Asymmetric Annulation between Aryl Iodides and Epoxides

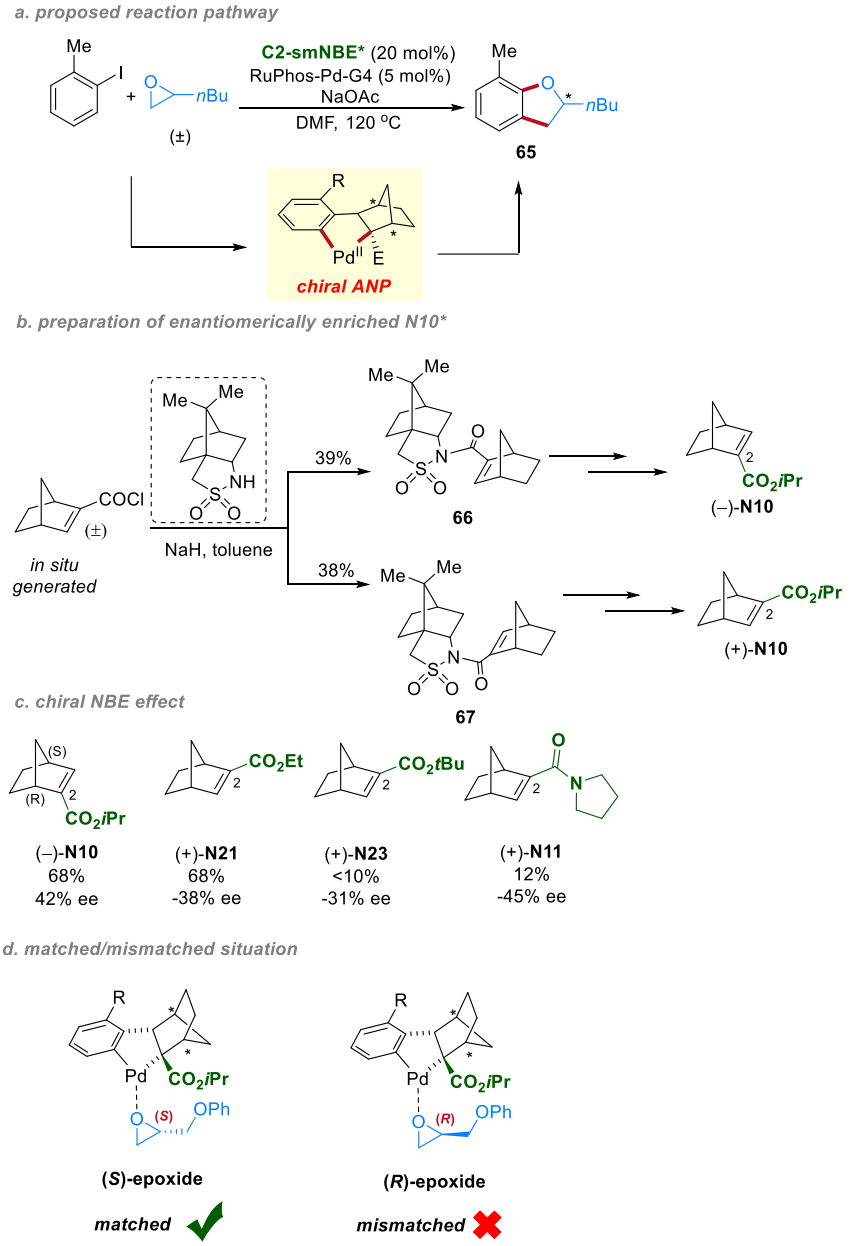

The Pd(0)-initiated asymmetric Catellani-type reactions enabled by chiral smNBEs was further expanded to asymmetric ortho arylation reaction by Zhou group very recently (Scheme 1.13).[46] The C2 ethyl ester-substituted **N21*** gave the highest enantioselectivity (96% ee), while the methylamide-substituted **N12*** afforded 86% ee and diminished reactivity. In contrast, the C5 ester-substituted **N33*** and C5 acid-substituted **N34*** gave significantly lower reactivity and

enantioselectivity. A series of axially chiral biaryl compounds were obtained in decent yield and enantioselectivity and good FG tolerance was demonstrated as well. Note that besides Heck reaction, other ipso quenching, e.g. Sonogashira coupling (**70**), was also realized. When an ortho acetyl aryl bromide was used, a fluorenol product (**71**) was obtained in decent yield and enantioselectivity, which is consistent with Lautens' prior observation.[47] In terms of the stereo-induction model, it was proposed that the aryl moiety is located at the planar position of the Pd(IV) complex to minimize the steric repulsion; the coordination of the ester group would help fixing the orientation of the aryl moiety through a stable dihedral angle (Scheme 1.13b).

Scheme 1.13. Asymmetric ortho arylation of Aryl Iodides

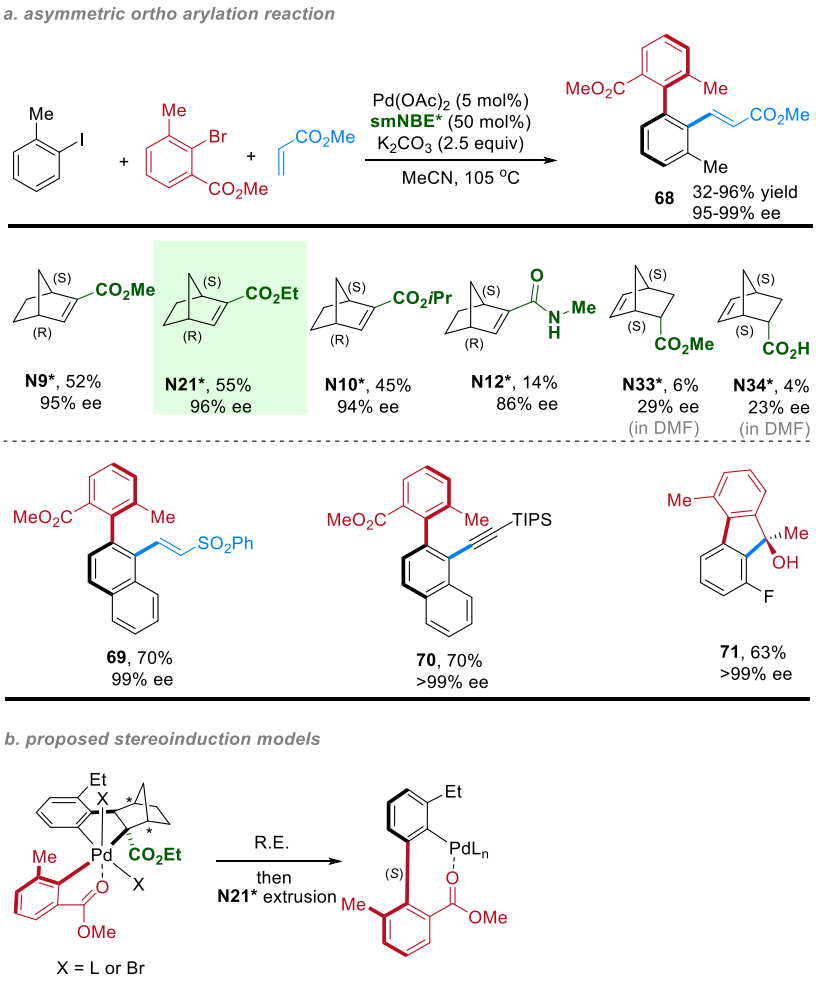

One long-standing limitation of the Catellani-type reactions is that sizeable substituents (e.g. methyl or isopropyl group) at the meta position of aryl halides inhibit ortho functionalization, which has been referred as "*meta constraint*".[48] The steric hindrance at the meta position makes the ANP formation and the following steps more difficult. Electron-withdrawing meta substituents were also detrimental to the reaction. These substrates often lead to NBE-attached side-products or direct ipso substitution. In 2020, the Dong group reported the use of C2 amide-derived smNBEs to realize Catellani-type reactions with aryl iodides bearing diverse meta substituents, which provided rapid access to 1,2,3,4-tetrasubstituted arenes (Scheme 1.14).[21] Compared with other NBEs, the C2 smNBE that contains a secondary amide moiety (**N12**) proved to be most efficient. Based on the DFT calculations, **N12** with a mild electron-withdrawing substituent exhibited the lowest barrier for the NBE-insertion step through balancing the opposite electronic requirements in the NBE binding and the migratory insertion steps. In addition, the existence of a hydrogen bonding interaction between the N−H bond of the amide moiety in **N12** and the oxygen of the CMD promoter stabilizes the transition state of the ortho C−H palladation step (**TS2**), which is the turnover-limiting step. Moreover, the C2 substituent should also inhibit the direct reductive elimination of ANP to form norbornyl benzocyclobutene side-products. It is noteworthy that, while mechanistically only a catalytic amount of NBE is sufficient to promote this transformation, a higher NBE concentration can suppress the undesired direct ipso-Heck pathway.

Scheme 1.14. NBE Effect for the Meta-Substituted Aryl Iodides

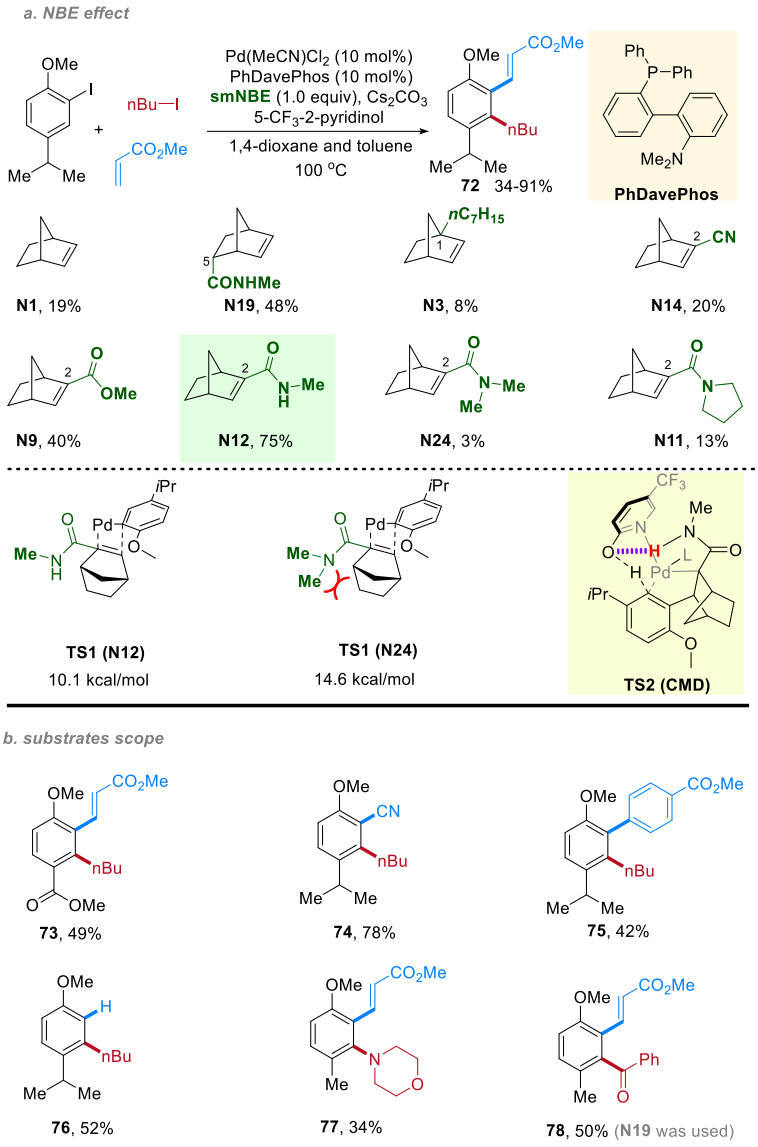

Through addressing such meta constraint, the substrate scope of the Catellani-type reaction was substantially expanded (Scheme 1.14b). Meta substituents with different sizes and electronic properties (**72**-**76**) were tolerated, and diverse ipso/ortho functionalizations were realized (**77**-**78**). Consequently, streamlined syntheses of several bioactive compounds were demonstrated with this method.

1.3.4 Pd(0)-Initiated Difunctionalization of Alkenyl Halides Involving C2-Substituted smNBEs

Beyond arene substrates, alkene-based substrates were seldom used in the Pd/NBE cooperative catalysis. One major difficulty was caused by the more reactive olefin π bond toward the undesired cyclopropanation reactions (Scheme 1.15a). In addition, the lack of an ortho substituent in general alkenyl substrates also makes the NBE extrusion more challenging. In 2019, the Dong group found the same C2-methylamide smNBE (**N12**) was highly efficient for the vicinal difunctionalization of alkenyl halides and triflates, which offers a rapid approach to build all-carbon tetrasubstituted olefins (Scheme 1.15b).[23] The undesired 3-*exo*-trig process (cyclopropane formation, **80**) was significantly inhibited by the rigid amide moiety; meanwhile the β-carbon elimination was promoted due to the bulkiness of **N12**.[6, 38] For comparison, regular NBE **N1**, the C2-ester smNBE **N9** and those with substituents at other positions were not reactive and/or selective.

Scheme 1.15. Ortho/Ipso Difunctionalization of Vinyl Triflates/Halides *via* Pd/NBE Catalysis

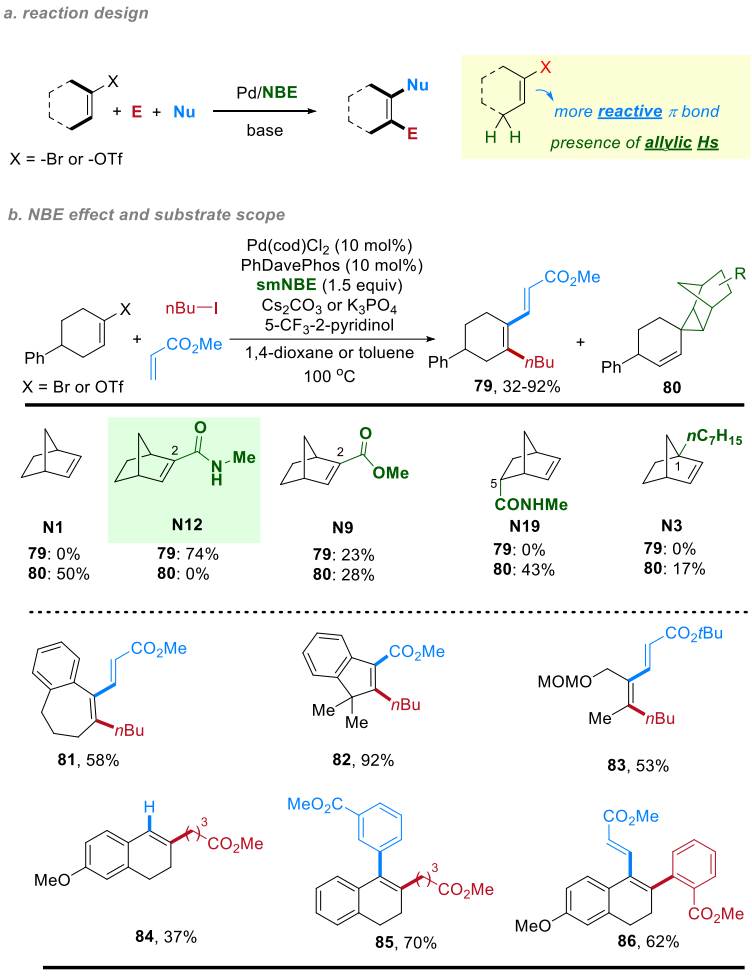

Both cyclic and linear vinyl triflates or bromides were competent substrates. Besides ipso Heck reaction, other ipso terminating reactions, such as hydrogenation (**84**) and Suzuki (**85**) coupling, could also take place. Both ortho alkylation and arylation were realized. As an interesting feature, the PhDavePhos ligand underwent in situ C−H/P−C bond activation to generate the corresponding phosphafluorene as the actual active ligand.

Overall, compared to the simple unsubstituted NBE **N1** and other smNBEs, the C2-substituted smNBEs own some unique features due to the direct substitution on the reactive C=C double bond. Adjusting the steric and electronic properties of the C2 substituents can greatly influence the NBE-

insertion and the downstream reactions with ANP, thereby capable of expanding the reaction capacity. They also provide promising directions for developing enantioselective transformations.

1.4 C5-Substituted or C5, C6-Disubstituted smNBEs

In general, C5-substituted and C5, C6-disubstituted smNBEs exhibit similar reactivity as simple unsubstituted NBE, while in some specific cases they have been found to be more efficient. To date, at least eleven types of C5-substituted or C5, C6-disubstituted NBEs have been developed and employed in Pd/NBE cooperative catalysis (Scheme 1.16). All of them contain EWGs, as the skeletons are typically prepared *via* the Diels−Alder reaction between cyclopentandiene and electron-deficiency alkenes.[49] Unlike C1- or C2-substituted smNBEs, the steric and electronic environment of the NBE alkene in these smNBEs is almost identical to simple NBE, though the remote steric effect or coordinative properties of the C5/C6 substituents could play an important role in modulating reaction selectivity.

Scheme 1.16. Reported C5-Substituted and C5, C6-Disubstituted NBEs

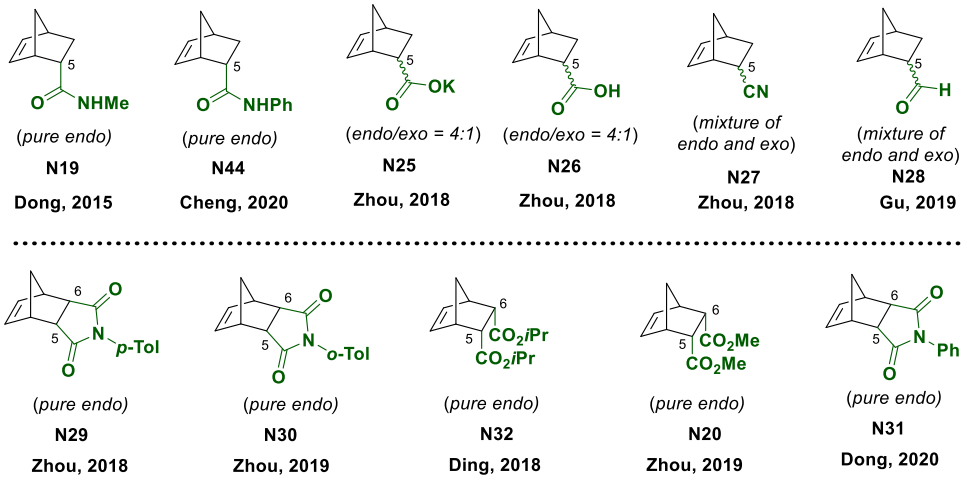

1.4.1 Pd(0)-Initiated Difunctionalization of Aryl Halides Involving C5-Substituted or C5, C6-Disubstituted smNBEs

The first use of a C5-substituted smNBE was reported by the Dong group in the ortho C−H acylation of haloarenes in 2015 (Scheme 1.17a),[50] which also represents *the first use of smNBEs* in the catalytic Catellani reactions. In the ortho acylation/ipso hydrogenation reaction, a

bifunctional isopropyl-carbonate anhydride was employed as both an acyl electrophile and a "masked" hydride source, i.e. isopropoxide, which prevented undesired esterification if homo-anhydrides and isopropanol were used. The C5 methylamide-substituted NBE (**N19**) not only provided consistently higher yields than unsubstituted NBE, but also eased isolation of pure products from NBE-containing side-products due to the polar amide moiety. This transformation tolerated a broad range of FGs, including various heterocycles. Besides ipso hydrogenation, Heck (**92**) and Suzuki (**93**) couplings could also be used for the ipso quench under similar conditions. Note that the ortho acylation of haloarenes was also concurrently reported by the Liang[51] and Gu[52] groups. This ortho acylation approach was further extended to a rapid construction of substituted indenones *via* direct annulation between aryl iodides and unsaturated carboxylic acid anhydrides by the same group in 2019.[53] Significant yield improvement was found using the C5-amide NBE (**N19**) compared to simple NBE (**N1**) (Scheme 1.17b). Diverse aryl iodides and conjugated anhydrides were suitable substrates. Mechanistic studies indicated the ipso functionalization was likely realized through a Heck-type coupling. Utility of this method was demonstrated in concise syntheses of indenone-based nature products, pauciflorol F and acredinone A. Notably, the total synthesis of acredinone A features a strategy involving two Pd/**N19**-catalyzed ortho acylations to construct both penta-substituted arene cores, including the use of a new ortho acylation/ipso borylation method.[54]

Scheme 1.17. Ortho Acylation of Haloarenes Enabled by C5 Methylamide-Substituted NBE

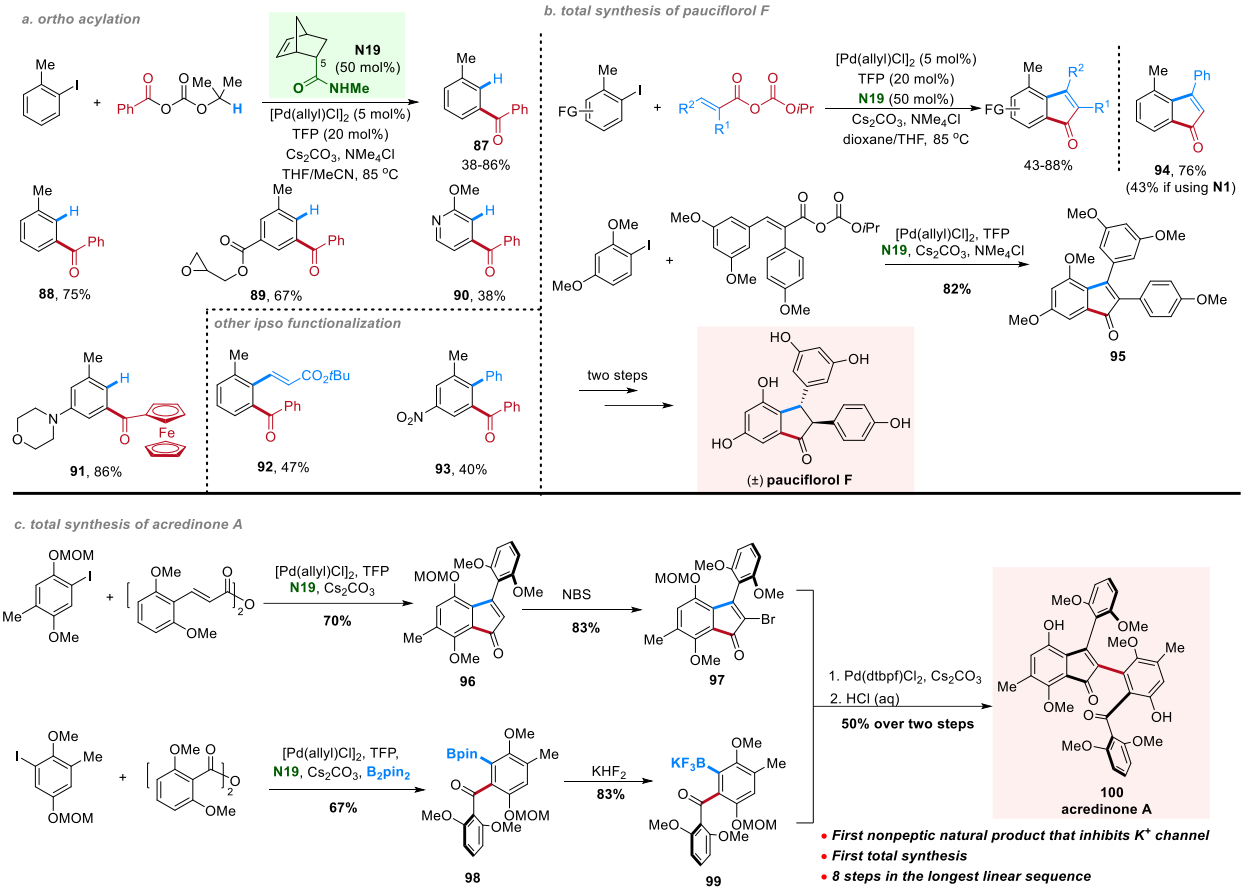

In 2018, the Zhou group reported the successful use of a unique potassium salt of 5-norbornene-2-carboxylic acid (**N25**) in the Pd/NBE-catalyzed ortho alkylation with epoxides as the electrophile (Scheme 1.18).[44] The carboxylate moiety in **N25** was proposed to serve as a CMD promoter to promote the ortho C−H activation, while comparable yield was obtained using the combination of simple NBE **N1** and CsOAc. Unlike the direct annulation approach (*vide supra*, Scheme 1.11), olefins were utilized here as the termination reagent. With additional base, a one-pot *oxa*-Michael addition could be realized, providing a rapidly access to isochroman scaffolds (Scheme 1.18b). The substrate scope was broad for both aryl iodides and terminal epoxides. Stereo-retention was observed (**101**) using an enantiopure epoxide; pyridine (**102**) and styrene (**103**)

were all tolerated. Note that an intramolecular ortho alkylation/ipso Heck coupling was achieved using an alkene-tethered epoxide, which afforded 14- and 13-membered macrocycles (**104** and **105**). Finally, a gram-scale preparation was demonstrated using only 1 mol% $Pd(OAc)_2$.

Scheme 1.18. Pd/NBE-Catalyzed Ortho Alkylation Reaction with Epoxides

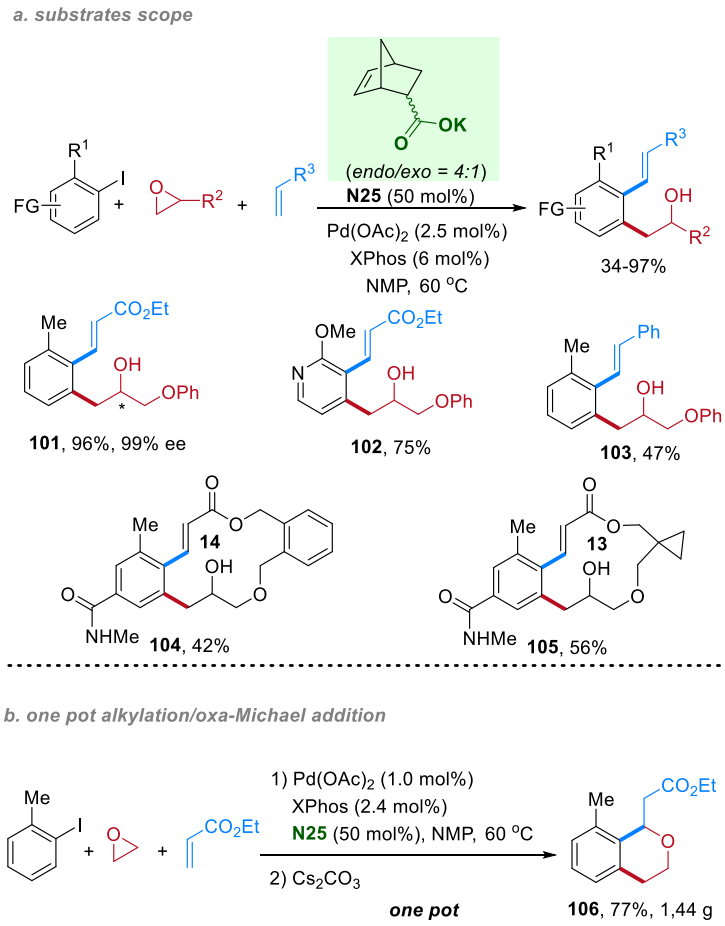

In 2018, the same group extended the use of *in situ* generated 5-norbornene-2-carboxylate in an ortho alkylation/redox-Heck relay reaction, which allowed for a rapid construction of tetrahydronaphthalene and indane scaffolds that contain quaternary centers (Scheme 1.19).[55,56] Interestingly, the C5/C6-dicarboxylic acid-derived NBE was also examined but only giving a trace amount of product. Regarding the reaction scope, both allyl and homo-allyl alcohols could be employed as the reagent to yield the corresponding aldehydes and ketones as the products, and

various aryl iodides (e.g. **107** and **108**) were suitable substrates. An indane-type product (**108**) was obtained in moderate yield when using a shorter-linked reagent. Besides carbon linkers, substrates bearing an oxygen linker (**109**) were also suitable, affording a seven-membered product albeit in lower yield. The synthetic utility was nicely demonstrated through a concise synthesis of (±)-eptazocine (Scheme 1.19b). The asymmetric ortho alkylation/ipso redox-relay Heck cascade has also been investigated using a chiral phosphine ligand (**L8**) and an achiral C5, C6-disubstituted smNBE (**N29**). Promising enantioselectivity (78% ee) was obtained albeit in 27% yield (Scheme 1.19c).

Scheme 1.19. Ortho Alkylation/Ipso Redox-Relay Heck Cascade

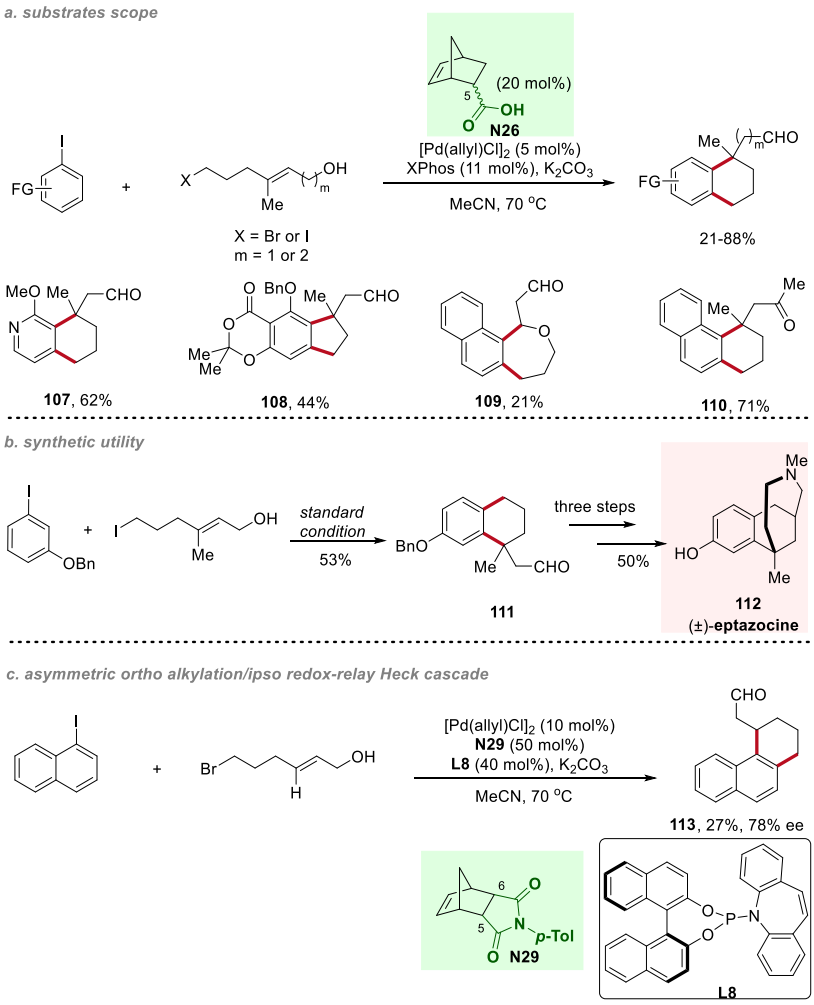

Analogous to epoxides, aziridines have also been used as electrophiles in ortho alkylation of aryl iodides. In 2018, Liang and coworkers reported a direct annulation between aryl iodides and Ts-aziridines to form indoline-type products using unsubstituted simple NBE (**N1**).[57] Shortly after, the Zhou group discovered that the C5, C6-disubstituted imide-type NBE (**N29**) was more effective than other smNBEs or simple NBE for the aziridine alkylation when using olefins as the ipso terminating reagent (Scheme 1.20).[58] By large, C5-substiutted and C5,C6-disubstiuted smNBEs were more efficient than the C2-substituted one in this reaction. Owing to a broad substrate scope and good FG tolerance, this method provides a streamlined assembly of substituted tetrahydroisoquinolines in a stereoselective manner from readily available starting materials.

Scheme 1.20. Aziridines as Electrophiles in Catellani-type Reactions

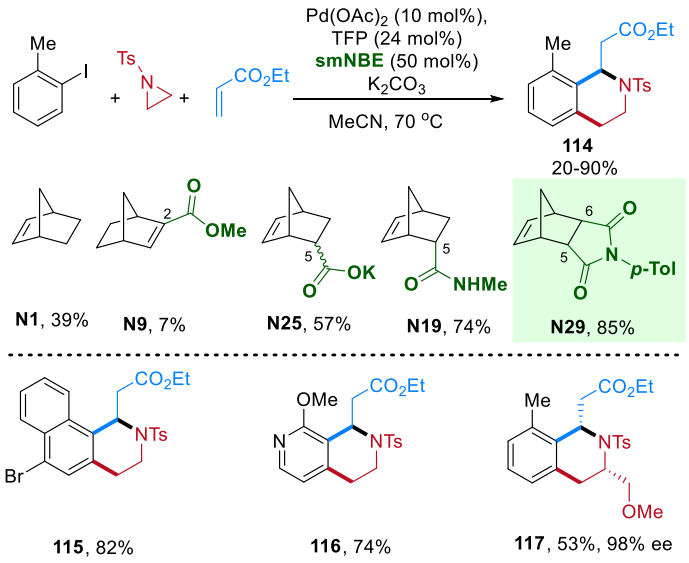

Considering that sulfur-substituted aromatic compounds are widely found in pharmaceuticals, agrochemicals, and organic materials, the ortho-thiolation of aryl halides *via* the Pd/NBE catalysis has attracted significant attentions. In 2019, the Gu[59] and Dong[60] groups independently reported ortho thiolation reactions of aryl iodides with different thiolating reagents (Scheme 1.21).

Thiosulfonates and sulfenamides were used as the electrophiles by the two groups, respectively. This also represents the first time when a heteroatom besides nitrogen was installed at the ortho position of aryl halides via the Pd/NBE catalysis. Gu's work features the use of a C5 aldehyde-substituted NBE (**N28**), which gave a better result than simple NBE (**N1**). Both aryl and alkyl thiolate moieties can be installed using this method.

Scheme 1.21. Ortho Thiolation of Aryl Iodide with Thiosulfonates

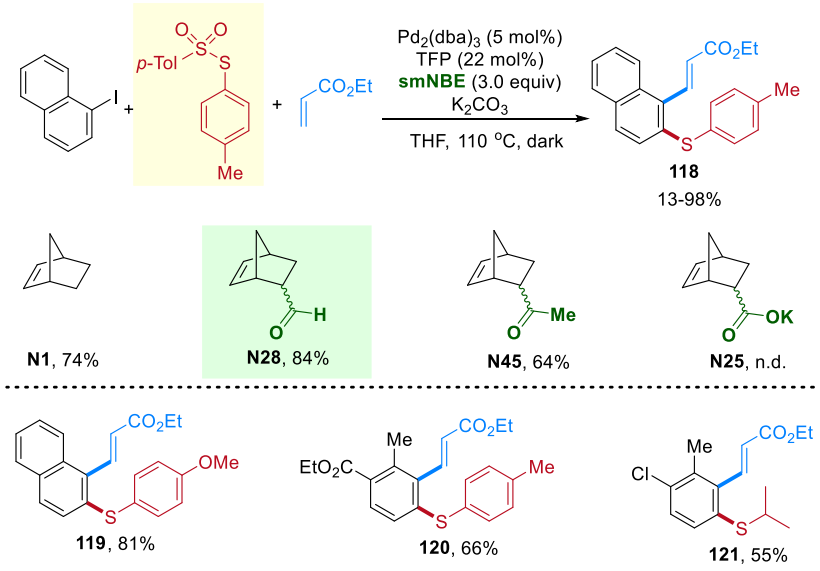

Methyl groups have played a profound role in medicinal chemistry, as the introduction of a methyl group could potentially modulate physical properties and even conformation of drug candidates.[61] The coupling of a methyl group at the arene ortho positions via the Catellani reaction was first reported in 2007 by Lautens using methyl iodide as the electrophile with simple NBE.[62] The use of MeONs and tetramethylammonium salts as electrophiles in the Pd/NBE catalysis were later reported in 2018 and 2019, respectively.[21,63] In 2019, the Zhou group systematically studied the ortho methylation and trideuteriomethylation of haloarenes, and they nicely enhanced the efficiency and expanded the scope of the reaction (Scheme 1.22).[64] Besides simple NBE, the C5

nitrile-substituted NBE (**N27**) was found to be an efficient and general co-catalyst. Two types of methyl electrophiles, MeOTs and trimethylphosphate, were utilized as electrophiles. The ipso position of substrates could be terminated by a range of olefins and nucleophiles, e.g. *t*-butyl acrylate (**122** and **123**), arylboronic acids (**124**), terminal alkynes (**125**), zinc cyanide (**126**), $B_2(pin)_2$ (**127**) and sodium formate as a hydride source (**128**), suggesting broad utilities in modification of bioactive compounds. For the ipso hydrogenation, a C5, C6-disubstituted NBE (**N30**) was found to be more effective. Finally, use of the corresponding CD_3OTs or $^{13}CH_3OTs$ as the electrophiles instead led to isotope-labelled methylation (**123** and **128**).

Scheme 1.22. Ortho Methylation of Aryl Halides

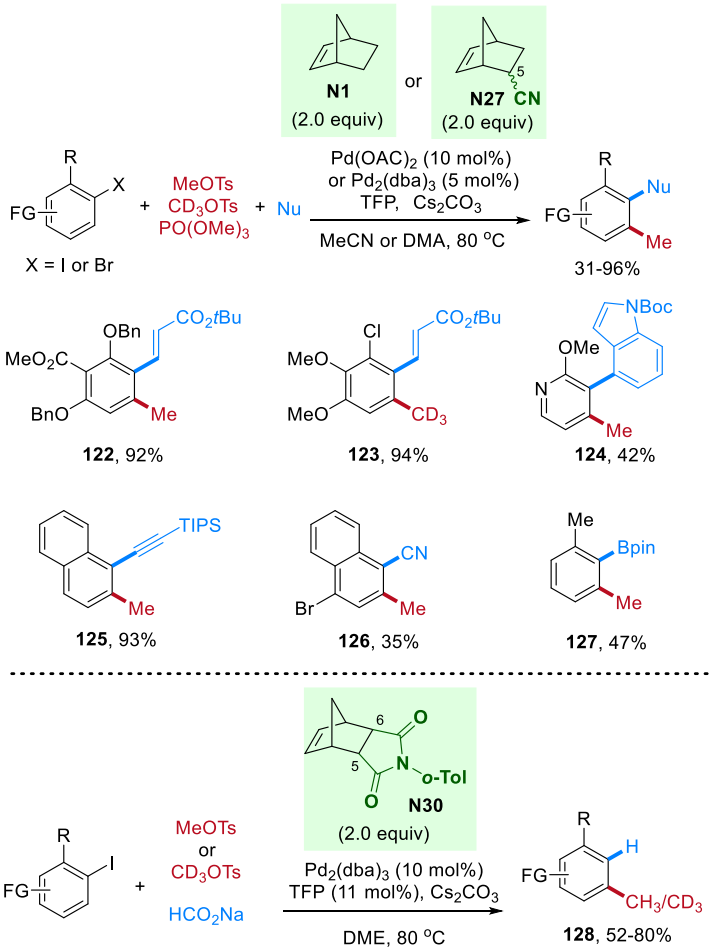

Given that C-linked glycosides have been widely used as carbohydrate mimetics owing to their relatively high chemical and metabolic stability compared to O-linked glycoside, developing a transition metal-catalyzed C−H glycosylation reaction has attracted significant attentions.[65] In 2020, the Liang[66] and Cheng[67] groups independently realized the Pd/NBE-catalyzed ortho glycosylation reaction of aryl iodides using glycosyl chlorides as the electrophile (Scheme 1.23). Liang's work features the use of a 5-norbornene-2-carbonitrile (**N27**), which gave a better result than other NBEs. The major side reaction was observed to be the direct ipso Heck termination, which was significantly inhibited using C5-substituted (**N27**, **N36** and **N38**) and C5, C6-disubstituted (**N31**) NBEs. In Cheng's work a C5 anilide-substituted NBE (**N44**) proved to be the optimal co-catalyst. Note that both reactions proceed in a stereoselective manner: α isomers of the resulting C−aryl glycoside products were obtained predominantly in most examples.

Scheme 1.23. Ortho Glycosylation of Aryl Iodides

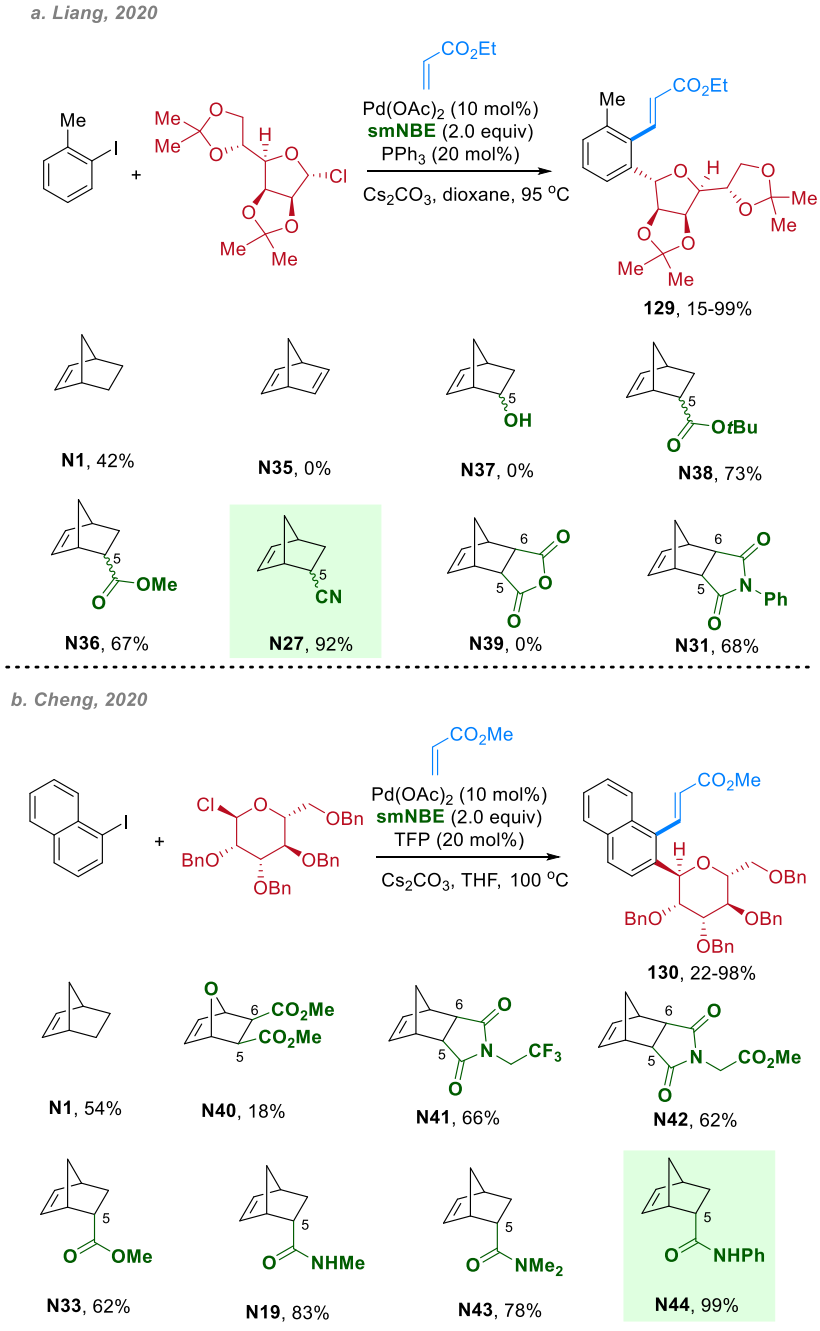

1.4.2 Pd(II)-Initiated Difunctionalization of Aryl Halides Involving C5-Substituted or C5, C6-Disubstituted smNBEs

Besides through oxidative addition of Pd(0) with aryl halides, as illustrated in Scheme 1b, the initial aryl-Pd(II) species can also be formed through transmetallation of arylboronic acids to Pd(II). After the Catellani process, the Pd(II) catalyst can be regenerated *via* oxidation of the Pd(0) after ipso termination. In 2018, the Zhang[68] and Zhou[69] groups independently reported a Pd(II)-initiated Catellani-type reaction with arylboron substrates. While simple NBE was efficient for vicinal difunctionalization of arylboronic acids in Zhang's method, Zhou found 5-norbornene-2-carbonitrile (**N27**) was more efficient than other NBEs when using arylboronic acid pinacol esters as substrates (Scheme 1.24a). Besides ortho alkylation, ortho arylation of arylboronic acid pinacol esters was also realized by the Zhou group in 2019 using aryl bromides as the electrophiles, in which a C5, C6 diester-substituted NBE (**N20**) proved to be optimal (Scheme 1.24b).[70] Air was employed as the terminal oxidant in Zhou's reactions, which is beneficial compared to the use of stoichiometric metallic oxidants. In this context, a related redox-neutral arylboron-based Pd(II)-initiated ortho functionalization was reported by Dong[71] and later Zhou[72], in which the Pd(II) was regenerated through a protonation process, therefore avoiding stoichiometric oxidants and bases. A key merit of the Pd(II)-initiated processes is the tolerance of aryl iodides and bromides that are otherwise reactive under the Pd(0) conditions. Such orthogonal reactivity could be beneficial for strategic planning.

Scheme 1.24. Pd(II)-Initiated Ortho Alkylation and Arylation of Arylboronates

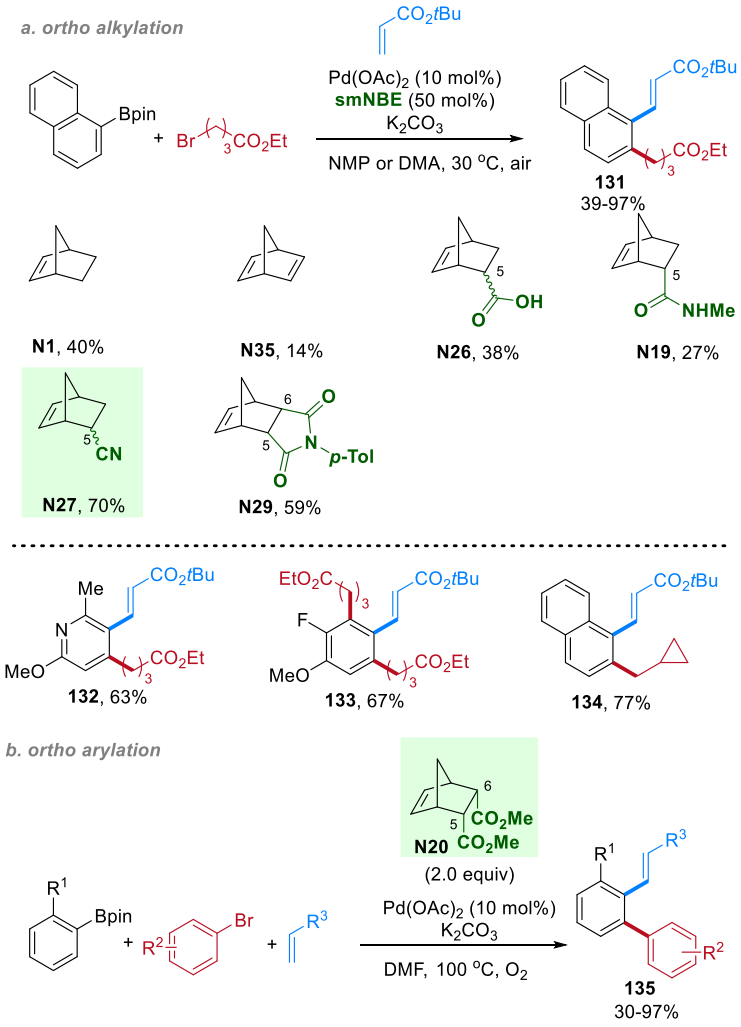

1.4.3 Pd(II)-Catalyzed Distal C−H Functionalization with C5, C6-Disubstituted smNBEs

In 2018, the Ding group reported a meta alkylation reaction of nosyl-protected phenethylamines, which was enabled by a C5, C6-disubstituted NBE (**N32**) and a simple pyridine ligand (Scheme 1.25).[73] Compared to Yu's C2 ester smNBE (**N9**) or simple NBE, the 5,6-di-isopropyl ester-substituted NBE (**N32**) afforded much enhanced yields. While high efficiency was generally observed for using alkyl electrophiles without β-hydrogens, moderate yield was nevertheless obtained for the ortho ethylation reaction.

Scheme 1.25. Pd(II)-Catalyzed Meta Alkylation of Nosyl-Protected Phenylalanines

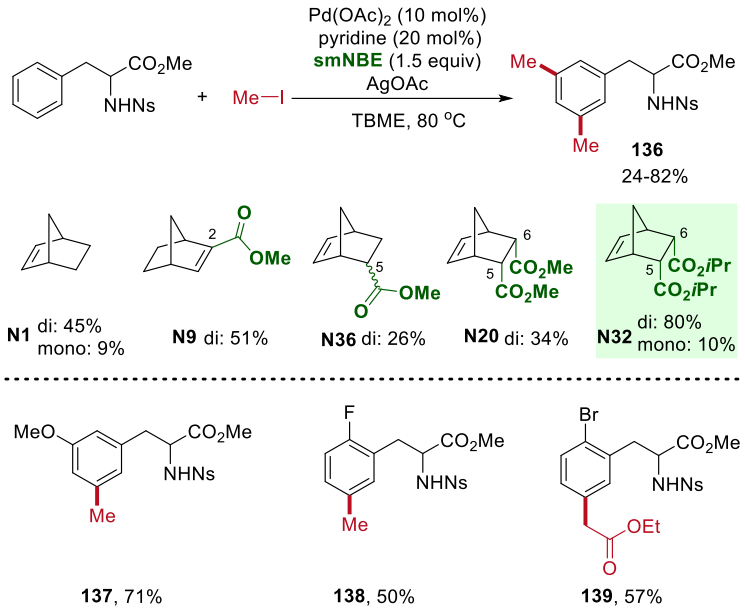

The concept of the distal C−H functionalization *via* the Pd/NBE catalysis was recently extended to alkene substrates by the Dong group, which provides a regio- and stereo-selective preparation of trisubstituted alkenes from 1,2-disubstituted ones (Scheme 1.26).[74] Given that the π bond in olefin substrates is more reactive than arene substrates and easily undergoes various π-breaking side-reactions,[23] the key of this reaction was to use an appropriate combination of a DG and a NBE cocatalyst to realize a fast and reversible proximal C−H palladation. The *N*-Ph-imide-based NBE (**N31**) was found to be most efficient; an oxime ether-based DG proved to be superb as it can be easily installed and removed. Both alcohol and amine-based substrates could be used. Besides distal C−H arylation, alkylation with α-halogenated esters was realized in good yield under slightly modified conditions (**143**).

Scheme 1.26. Pd(II)-Catalyzed Distal Alkenyl C−H Functionalization

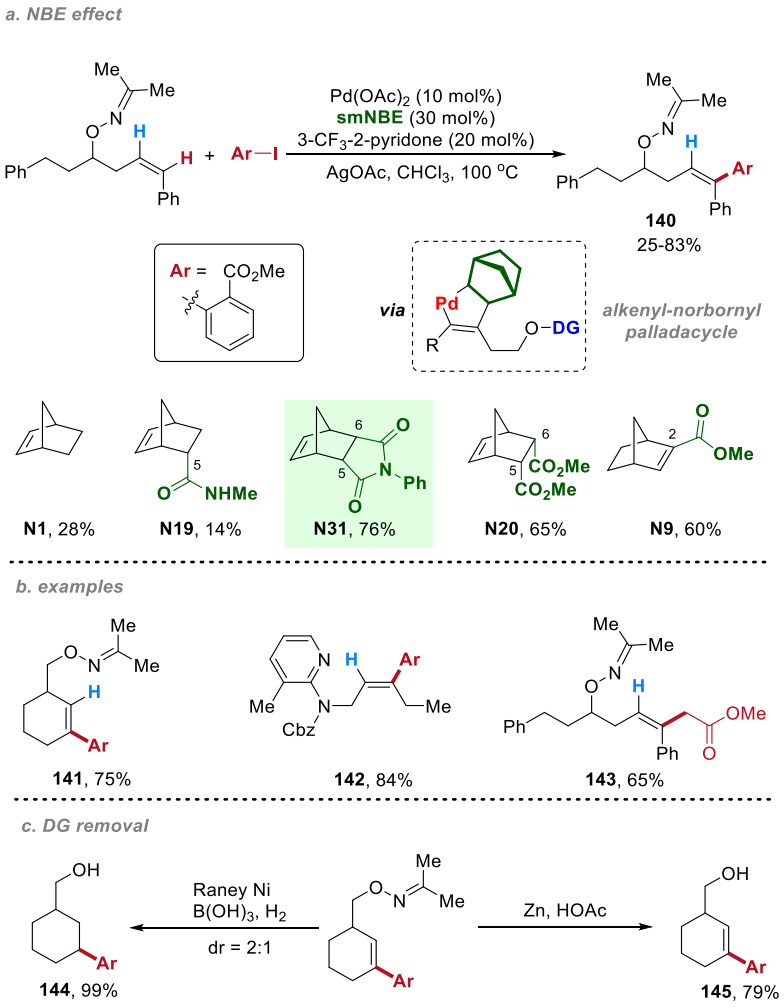

While C5-substituted and C5, C6-disubstituted smNBEs generally exhibit similar reactivity/selectivity to simple unsubstituted NBE, remarkably improved efficiency can nevertheless be observed in many cases shown above. Compared to C1- and C2-substituted smNBEs, the effect of the C5/C6 substituents that are distal to the reactive site remains to be well understood, which could be an important topic to be explored in the future.

1.5 Conclusion and Outlook

In summary, the Pd/NBE cooperative catalysis has emerged as a powerful tool for regio- and site-selective functionalization of arenes, heteroarenes and alkenes, and smNBEs have significantly contributed to the growth of this field. Many breakthroughs, including broader scope, better reactivity, higher selectivity, and new applications, have been realized, and some intrinsic limitations have been overcome owing to these structural modifications on the NBE scaffold. For example, the ortho constraint in the Catellani-type reactions was addressed using the C1-substituted smNBE; the meta constraint and the problem of forming norbornyl benzocyclobutene side-products were solved by the C2-substituted smNBEs; enhanced reaction efficiency can be achieved through modifying the NBE C5 and C6 positions. In addition, the Pd/NBE-catalyzed alkene C−H functionalization and enantioselectivity transformations have also been enabled by smNBEs.

Despite the enormous achievements made to date, future advancement in the field of Pd/NBE catalysis would benefit from developing more versatile smNBEs. First, the catalyst efficiency in most reactions still requires further improvement. Due to the complex nature of the Catellani-type reactions, the amounts of NBE or smNBEs used are typically 50% or higher, and the loading of Pd pre-catalysts is often 10 mol%. It is anticipated that deep and systematic mechanistic understanding of these reactions could guide development of more efficient catalyst systems. In addition, it would be attractive to realize more synthetically useful enantioselective transformations. Given that most of the smNBEs contain a chiral skeleton, there is sufficient room for developing new asymmetric Pd/NBE catalysis methods. Moreover, the applicability of the Pd/NBE catalysis would be aided by a broadened reaction scope. For example, discovery of new and compatible electrophiles for ortho functionalization has been an ongoing challenge. These

"tailor-made" smNBEs with fine-tuned steric and electronic properties are expected to become a key factor for accommodating unusual electrophiles that are currently unknown for the Catellani-type reactions. It is our expectation that, through addressing these challenges, the Pd/NBE catalysis could ultimately become one of the "go-to" methods for preparing polysubstituted arenes and alkenes in the future.

1.6 References

(1) Catellani, M.; Frignani, F.; Rangoni, A., A Complex Catalytic Cycle Leading to a Regioselective Synthesis of o,o′-Disubstituted Vinylarenes. *Angew. Chem. Int. Ed.* **1997**, *36*, 119-122.

(2) An, Z.-w.; Catellani, M.; Chiusoli, G. P., Palladium-catalyzed synthesis of coumarin. *J. Organomet. Chem.* **1989**, *371*, C51-C52.

(3) Bocelli, G.; Catellani, M.; Chiusoli, G. P., Palladium-catalyzed C–C bond formation involving aromatic C–H activation: III. Aspects of aromatic substitution and structure of 1-bromo-3-[3-(2-methylenecyclohex-5-en-1-yl)bicyclo[2.2.1]hept-2-yl]-4-bicyclo[2.2.1]hept-2-ylbenzene. *J. Organomet. Chem.* **1985**, *279*, 225-232.

(4) Catellani, M.; Chiusoli, G. P., Palladium-catalyzed synthesis of 1,2,3,4,4a,12b-hexahydro-1,4-methanotriphenylenes. *J. Organomet. Chem.* **1985**, *286*, c13-c16.

(5) Maestri, G.; Motti, E.; Della Ca', N.; Malacria, M.; Derat, E.; Catellani, M., Of the Ortho Effect in Palladium/Norbornene-Catalyzed Reactions: A Theoretical Investigation. *J. Am. Chem. Soc.* **2011**, *133*, 8574-8585.

(6) Wang, J.; Li, R.; Dong, Z.; Liu, P.; Dong, G., Complementary site-selectivity in arene functionalization enabled by overcoming the ortho constraint in palladium/norbornene catalysis. *Nat. Chem.* **2018**, *10*, 866-872.

(7) Catellani, M., Catalytic Multistep Reactions via Palladacycles. *Synlett* **2003**, *2003*, 0298-0313.

(8) Catellani, M., Novel Methods of Aromatic Functionalization Using Palladium and Norbornene as a Unique Catalytic System. *Top. Organomet. Chem.* **2005**, *14*, 21-53.

(9) Catellani, M.; Motti, E.; Della Ca', N., Catalytic Sequential Reactions Involving Palladacycle-Directed Aryl Coupling Steps. *Acc. Chem. Res.* **2008**, *41*, 1512-1522.

(10) Martins, A.; Mariampillai, B.; Lautens, M., Synthesis in the Key of Catellani: Norbornene-Mediated ortho C–H Functionalization. *Top. Curr. Chem.* **2009**, *292*, 1-33.

(11) Ye, J.; Lautens, M., Palladium-catalysed norbornene-mediated C–H functionalization of arenes. *Nat. Chem.* **2015**, *7*, 863.

(12) Della Ca', N.; Fontana, M.; Motti, E.; Catellani, M., Pd/Norbornene: A Winning Combination for Selective Aromatic Functionalization via C–H Bond Activation. *Acc. Chem. Res.* **2016**, *49*, 1389-1400.

(13) Wegmann, M.; Henkel, M.; Bach, T., C–H alkylation reactions of indoles mediated by Pd(ii) and norbornene: applications and recent developments. *Org. Biomol. Chem.* **2018**, *16*, 5376-5385.

(14) Liu, Z.-S.; Gao, Q.; Cheng, H.-G.; Zhou, Q., Alkylating Reagents Employed in Catellani-Type Reactions. *Chem. Eur. J.* **2018**, *24*, 15461-15476.

(15) Zhao, K.; Ding, L.; Gu, Z., Development of New Electrophiles in Palladium/Norbornene-Catalyzed ortho-Functionalization of Aryl Halides. *Synlett* **2019**, *30*, 129-140.

(16) Cheng, H.-G.; Chen, S.; Chen, R.; Zhou, Q., Palladium(II)-Initiated Catellani-Type Reactions. *Angew. Chem. Int. Ed.* **2019**, *58*, 5832-5844.

(17) Wang, J.; Dong, G., Palladium/Norbornene Cooperative Catalysis. *Chem. Rev.* **2019**, *119*, 7478-7528.

(18) The use of norbornadiene and 7-oxa-[2.2.1]bicyclic alkenes as stoichiometric reagents will not be covered.

(19) Dong, Z.; Dong, G., *Ortho* vs *Ipso*: Site-Selective Pd and Norbornene-Catalyzed Arene C–H Amination Using Aryl Halides. *J. Am. Chem. Soc.* **2013**, *135*, 18350-18353.

(20) Shen, P.-X.; Wang, X.-C.; Wang, P.; Zhu, R.-Y.; Yu, J.-Q., Ligand-Enabled Meta-C–H Alkylation and Arylation Using a Modified Norbornene. *J. Am. Chem. Soc.* **2015**, *137*, 11574-11577.

(21) Wang, J.; Zhou, Y.; Xu, X.; Liu, P.; Dong, G., Entry to 1,2,3,4-Tetrasubstituted Arenes through Addressing the "Meta Constraint" in the Palladium/Norbornene Catalysis. *J. Am. Chem. Soc.* **2020**, *142*, 3050-3059.

(22) Li, R.; Liu, F.; Dong, G., Palladium-catalyzed asymmetric annulation between aryl iodides and racemic epoxides using a chiral norbornene cocatalyst. *Org. Chem. Front.* **2018**, *5*, 3108-3112.

(23) Wang, J.; Dong, Z.; Yang, C.; Dong, G., Modular and regioselective synthesis of all-carbon tetrasubstituted olefins enabled by an alkenyl Catellani reaction. *Nat. Chem.* **2019**, *11*, 1106-1112.

(24) Verkruijsse, H. D.; Brandsma, L., Preparative metallation of norbornene and norbornadiene. *Recl. Trav. Chim. Pays-Bas* **1986**, *105*, 66-68.

(25) Wang, X.-C.; Gong, W.; Fang, L.-Z.; Zhu, R.-Y.; Li, S.; Engle, K. M.; Yu, J.-Q., Ligand-enabled meta-C–H activation using a transient mediator. *Nature* **2015**, *519*, 334.

(26) Dong, Z.; Wang, J.; Dong, G., Simple Amine-Directed Meta-Selective C–H Arylation via Pd/Norbornene Catalysis. *J. Am. Chem. Soc.* **2015**, *137*, 5887-5890.

(27) Wang, P.; Li, G.-C.; Jain, P.; Farmer, M. E.; He, J.; Shen, P.-X.; Yu, J.-Q., Ligand-Promoted meta-C–H Amination and Alkynylation. *J. Am. Chem. Soc.* **2016**, *138*, 14092-14099.

(28) Shi, H.; Wang, P.; Suzuki, S.; Farmer, M. E.; Yu, J.-Q., Ligand Promoted *meta*-C–H Chlorination of Anilines and Phenols. *J. Am. Chem. Soc.* **2016**, *138*, 14876-14879.

(29) DeBergh, J. R.; Niljianskul, N.; Buchwald, S. L., Synthesis of Aryl Sulfonamides via Palladium-Catalyzed Chlorosulfonylation of Arylboronic Acids. *J. Am. Chem. Soc.* **2013**, *135*, 10638-10641.

(30) Zhao, X.; Dimitrijević, E.; Dong, V. M., Palladium-Catalyzed C−H Bond Functionalization with Arylsulfonyl Chlorides. *J. Am. Chem. Soc.* **2009**, *131*, 3466-3467.

(31) Shi, H.; Herron, A. N.; Shao, Y.; Shao, Q.; Yu, J.-Q., Enantioselective remote meta-C–H arylation and alkylation via a chiral transient mediator. *Nature* **2018**, *558*, 581-585.

(32) Liu, L.-Y.; Qiao, J. X.; Yeung, K.-S.; Ewing, W. R.; Yu, J.-Q., meta C–H Arylation of Electron-Rich Arenes: Reversing the Conventional Site Selectivity. *J. Am. Chem. Soc.* **2019**, *141*, 14870-14877.

(33) Ma, X.; Zhao, X.; Zhu, R.; Zhang, D., Computational Study on Why and How of Nonconventional meta-C–H Arylation of Electron-Rich Arenes via Pd/Quinoxaline-Based Ligand/Norbornene Cooperative Catalysis. *J. Org. Chem.* **2020**, *85*, 5995-6007.

(34) Liu, L.-Y.; Qiao, J. X.; Ewing, W. R.; Yeung, K.-S.; Yu, J.-Q., β-Selective C−H Arylation of Electron-Deficient Thiophenes, Pyrroles, and Furans. *Isr. J. Chem.* **2020**, *60*, 416-418.

(35) Liu, L.-Y.; Qiao, J. X.; Yeung, K.-S.; Ewing, W. R.; Yu, J.-Q., meta-Selective C−H Arylation of Fluoroarenes and Simple Arenes. *Angew. Chem. Int. Ed.* **2020**, *59*, 13831-13835.

(36) Shi, H.; Lu, Y.; Weng, J.; Bay, K. L.; Chen, X.; Tanaka, K.; Verma, P.; Houk, K. N.; Yu, J.-Q., Differentiation and functionalization of remote C–H bonds in adjacent positions. *Nat. Chem.* **2020**, *12*, 399-404.

(37) Zhang, Z.; Tanaka, K.; Yu, J.-Q., Remote site-selective C–H activation directed by a catalytic bifunctional template. *Nature* **2017**, *543*, 538-542.

(38) Li, R.; Zhou, Y.; Xu, X.; Dong, G., Direct Vicinal Difunctionalization of Thiophenes Enabled by the Palladium/Norbornene Cooperative Catalysis. *J. Am. Chem. Soc.* **2019**, *141*, 18958-18963.

(39) Catellani, M.; Cugini, F., A Catalytic Process Based on Sequential Ortho-alkylation and Vinylation of Ortho-alkylaryl Iodides via Palladacycles. *Tetrahedron* **1999**, *55*, 6595-6602.

(40) Li, R.; Dong, G., Direct Annulation between Aryl Iodides and Epoxides through Palladium/Norbornene Cooperative Catalysis. *Angew. Chem. Int. Ed.* **2018**, *57*, 1697-1701.

(41) Bruno, N. C.; Niljianskul, N.; Buchwald, S. L., N-Substituted 2-Aminobiphenylpalladium Methanesulfonate Precatalysts and Their Use in C–C and C–N Cross-Couplings. *J. Org. Chem.* **2014**, *79*, 4161-4166.

(42) Torraca, K. E.; Huang, X.; Parrish, C. A.; Buchwald, S. L., An Efficient Intermolecular Palladium-Catalyzed Synthesis of Aryl Ethers. *J. Am. Chem. Soc.* **2001**, *123*, 10770-10771.

(43) Kuwabe, S.-i.; Torraca, K. E.; Buchwald, S. L., Palladium-Catalyzed Intramolecular C−O Bond Formation. *J. Am. Chem. Soc.* **2001**, *123*, 12202-12206.

(44) Cheng, H.-G.; Wu, C.; Chen, H.; Chen, R.; Qian, G.; Geng, Z.; Wei, Q.; Xia, Y.; Zhang, J.; Zhang, Y.; Zhou, Q., Epoxides as Alkylating Reagents for the Catellani Reaction. *Angew. Chem. Int. Ed.* **2018**, *57*, 3444-3448.

(45) Wu, C.; Cheng, H.-G.; Chen, R.; Chen, H.; Liu, Z.-S.; Zhang, J.; Zhang, Y.; Zhu, Y.; Geng, Z.; Zhou, Q., Convergent syntheses of 2,3-dihydrobenzofurans via a Catellani strategy. *Org. Chem. Front.* **2018**, *5*, 2533-2536.

(46) Liu, Z.-S.; Hua, Y.; Gao, Q.; Ma, Y.; Tang, H.; Shang, Y.; Cheng, H.-G.; Zhou, Q., Construction of axial chirality via palladium/chiral norbornene cooperative catalysis. *Nat. Catal.* **2020**, *3*, 727-733.

(47) Zhao, Y.-B.; Mariampillai, B.; Candito, D. A.; Laleu, B.; Li, M.; Lautens, M., Exploiting the Divergent Reactivity of Aryl–Palladium Intermediates for the Rapid Assembly of Fluorene and Phenanthrene Derivatives. *Angew. Chem. Int. Ed.* **2009**, *48*, 1849-1852.

(48) Lautens, M.; Paquin, J.-F.; Piguel, S.; Dahlmann, M., Palladium-Catalyzed Sequential Alkylation−Alkenylation Reactions and Their Application to the Synthesis of Fused Aromatic Rings. *J. Org. Chem.* **2001**, *66*, 8127-8134.

(49) Davies, D. I.; Gomez, P. M.; Hallett, P., Synthesis of 2,5- and 2,6-norbornane derivatives with prostaglandin-like side chains. *J. Chem. Soc., Perkin Trans. 1* **1984**, 843-848.

(50) Dong, Z.; Wang, J.; Ren, Z.; Dong, G., *Ortho* C–H Acylation of Aryl Iodides by Palladium/Norbornene Catalysis. *Angew. Chem. Int. Ed.* **2015**, *54*, 12664-12668.

(51) Zhou, P.-X.; Ye, Y.-Y.; Liu, C.; Zhao, L.-B.; Hou, J.-Y.; Chen, D.-Q.; Tang, Q.; Wang, A.-Q.; Zhang, J.-Y.; Huang, Q.-X.; Xu, P.-F.; Liang, Y.-M., Palladium-Catalyzed Acylation/Alkenylation of Aryl Iodide: A Domino Approach Based on the Catellani–Lautens Reaction. *ACS Catal.* **2015**, *5*, 4927-4931.

(52) Huang, Y.; Zhu, R.; Zhao, K.; Gu, Z., Palladium-Catalyzed Catellani ortho-Acylation Reaction: An Efficient and Regiospecific Synthesis of Diaryl Ketones. *Angew. Chem. Int. Ed.* **2015**, *54*, 12669-12672.

(53) Liu, F.; Dong, Z.; Wang, J.; Dong, G., Palladium/Norbornene-Catalyzed Indenone Synthesis from Simple Aryl Iodides: Concise Syntheses of Pauciflorol F and Acredinone A. *Angew. Chem. Int. Ed.* **2019**, *58*, 2144-2148.

(54) Shi, H.; Babinski, D. J.; Ritter, T., Modular C–H Functionalization Cascade of Aryl Iodides. *J. Am. Chem. Soc.* **2015**, *137*, 3775-3778.

(55) Liu, Z.-S.; Qian, G.; Gao, Q.; Wang, P.; Cheng, H.-G.; Wei, Q.; Liu, Q.; Zhou, Q., Palladium/Norbornene Cooperative Catalysis To Access Tetrahydronaphthalenes and Indanes with a Quaternary Center. *ACS Catal.* **2018**, *8*, 4783-4788.

(56) Liu, Z.-S.; Qian, G.; Gao, Q.; Wang, P.; Cheng, H.-G.; Hua, Y.; Zhou, Q., 5-Norbornene-2-carboxylic acid: Another catalytic mediator for Catellani-type reactions. *Tetrahedron* **2019**, *75*, 1774-1780.

(57) Liu, C.; Liang, Y.; Zheng, N.; Zhang, B.-S.; Feng, Y.; Bi, S.; Liang, Y.-M., Synthesis of indolines via a palladium/norbornene-catalyzed reaction of aziridines with aryl iodides. *Chem. Commun.* **2018**, *54*, 3407-3410.

(58) Qian, G.; Bai, M.; Gao, S.; Chen, H.; Zhou, S.; Cheng, H.-G.; Yan, W.; Zhou, Q., Modular One-Step Three-Component Synthesis of Tetrahydroisoquinolines Using a Catellani Strategy. *Angew. Chem. Int. Ed.* **2018**, *57*, 10980-10984.

(59) Cai, W.; Gu, Z., Selective Ortho Thiolation Enabled by Tuning the Ancillary Ligand in Palladium/Norbornene Catalysis. *Org. Lett.* **2019**, *21*, 3204-3209.

(60) Li, R.; Zhou, Y.; Yoon, K.-Y.; Dong, Z.; Dong, G., Sulfenamide-enabled ortho thiolation of aryl iodides via palladium/norbornene cooperative catalysis. *Nat. Commun.* **2019**, *10*, 3555.

(61) Schönherr, H.; Cernak, T., Profound Methyl Effects in Drug Discovery and a Call for New C□H Methylation Reactions. *Angew. Chem. Int. Ed.* **2013**, *52*, 12256-12267.

(62) Mariampillai, B.; Alliot, J.; Li, M.; Lautens, M., A Convergent Synthesis of Polysubstituted Aromatic Nitriles via Palladium-Catalyzed C−H Functionalization. *J. Am. Chem. Soc.* **2007**, *129*, 15372-15379.

(63) Dong, Z.; Lu, G.; Wang, J.; Liu, P.; Dong, G., Modular ipso/ortho Difunctionalization of Aryl Bromides via Palladium/Norbornene Cooperative Catalysis. *J. Am. Chem. Soc.* **2018**, *140*, 8551-8562.

(64) Gao, Q.; Shang, Y.; Song, F.; Ye, J.; Liu, Z.-S.; Li, L.; Cheng, H.-G.; Zhou, Q., Modular Dual-Tasked C–H Methylation via the Catellani Strategy. *J. Am. Chem. Soc.* **2019**, *141*, 15986-15993.

(65) Wang, Q.; An, S.; Deng, Z.; Zhu, W.; Huang, Z.; He, G.; Chen, G., Palladium-catalysed C−H glycosylation for synthesis of C-aryl glycosides. *Nat. Catal.* **2019**, *2*, 793-800.

(66) Ding, Y.-N.; Shi, W.-Y.; Liu, C.; Zheng, N.; Li, M.; An, Y.; Zhang, Z.; Wang, C.-T.; Zhang, B.-S.; Liang, Y.-M., Palladium-Catalyzed ortho-C–H Glycosylation/ipso-Alkenylation of Aryl Iodides. *J. Org. Chem.* **2020**, *85*, 11280-11296.

(67) Lv, W.; Chen, Y.; Wen, S.; Ba, D.; Cheng, G., Modular and Stereoselective Synthesis of C-Aryl Glycosides via Catellani Reaction. *J. Am. Chem. Soc.* **2020**, *142*, 14864-14870.

(68) Shi, G.; Shao, C.; Ma, X.; Gu, Y.; Zhang, Y., Pd(II)-Catalyzed Catellani-Type Domino Reaction Utilizing Arylboronic Acids as Substrates. *ACS Catal.* **2018**, *8*, 3775-3779.

(69) Chen, S.; Liu, Z.-S.; Yang, T.; Hua, Y.; Zhou, Z.; Cheng, H.-G.; Zhou, Q., The Discovery of a Palladium(II)-Initiated Borono-Catellani Reaction. *Angew. Chem. Int. Ed.* **2018**, *57*, 7161-7165.

(70) Wang, P.; Chen, S.; Zhou, Z.; Cheng, H.-G.; Zhou, Q., Chemoselective Borono-Catellani Arylation for Unsymmetrical Biaryls Synthesis. *Org. Lett.* **2019**, *21*, 3323-3327.

(71) Li, R.; Liu, F.; Dong, G., Redox-Neutral ortho Functionalization of Aryl Boroxines via Palladium/Norbornene Cooperative Catalysis. *Chem* **2019**, *5*, 929-939.

(72) Chen, S.; Wang, P.; Cheng, H.-G.; Yang, C.; Zhou, Q., Redox-neutral ortho-C–H amination of pinacol arylborates via palladium(ii)/norbornene catalysis for aniline synthesis. *Chem. Sci.* **2019**, *10*, 8384-8389.

(73) Liu, J.; Ding, Q.; Fang, W.; Wu, W.; Zhang, Y.; Peng, Y., Pd(II)/Norbornene-Catalyzed Meta-C–H Alkylation of Nosyl-Protected Phenylalanines. *J. Org. Chem.* **2018**, *83*, 13211-13216.

(74) Wu, Z.; Fatuzzo, N.; Dong, G., Distal Alkenyl C–H Functionalization via the Palladium/Norbornene Cooperative Catalysis. *J. Am. Chem. Soc.* **2020**, *142*, 2715-2720.

(Some contents of this chapter were published in *J. Am. Chem. Soc.* **2020**, *142*, 17859-17875.)

CHAPTER 2

Direct Annulation between Aryl Iodides and Epoxides via Palladium/Norbornene Cooperative Catalysis

2.1 Introduction

Dihydrobenzofuran (DHBF) moiety is frequently found in pharmaceuticals and agrochemicals (Fig. 2.1).[1] While a number of methods are available for its synthesis, only a few can directly give DHBFs from simple starting materials.[2] For example, DHBFs can be synthesized via a sequence of ortho-allylation of phenols and then hydroalkoxylation,[3] in which strong bases and/or acids are used (Scheme 2.1a). A (3+2) coupling between benzynes and epoxides appears to be a more attractive approach; however, the poor regioselectivity with unsymmetrical benzynes and the need for more reactive aryl epoxides limited its application.[4] Hence, a general approach that can synthesize DHBFs directly from readily available feedstock chemicals remained to be realized. In this communication, we describe the development of a simple and direct DHBF synthesis method

through annulation between aryl iodides and terminal epoxides via palladium/norbornene (NBE) cooperative catalysis (Scheme 2.1b).

Figure 2.1 Bioactive Compounds Containing DHBFs

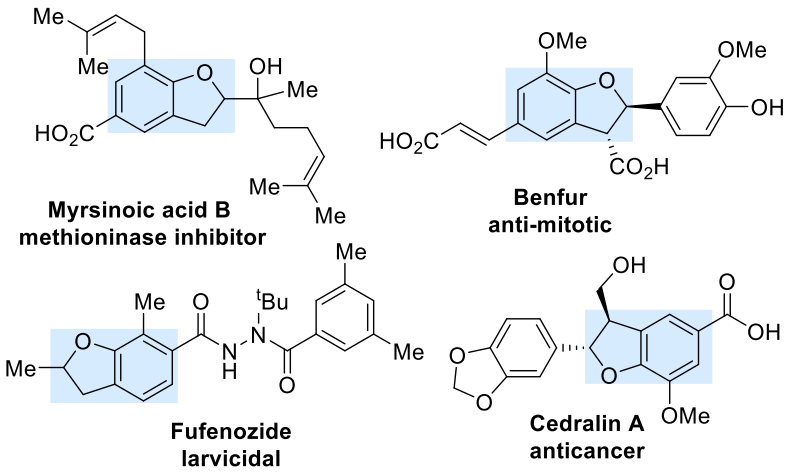

Pd/NBE catalysis, namely Catellani reaction, has recently emerged as a powerful approach for vicinal bis-functionalization of arenes.[5] Using simple aryl iodides as substrates, a number of nucleophiles and electrophiles have been coupled at the ipso and ortho positions respectively through selective reactions with the aryl-NBE-palladacycle (ANP) intermediate (Fig. 2.2).[6-10] In particular, Lautens and coworkers have developed a suite of elegant annulation methods through tethering an electrophile with a nucleophile for synthesis of various benzo-fused rings.[11]

Scheme 2.1. Synthesis of DHBFs

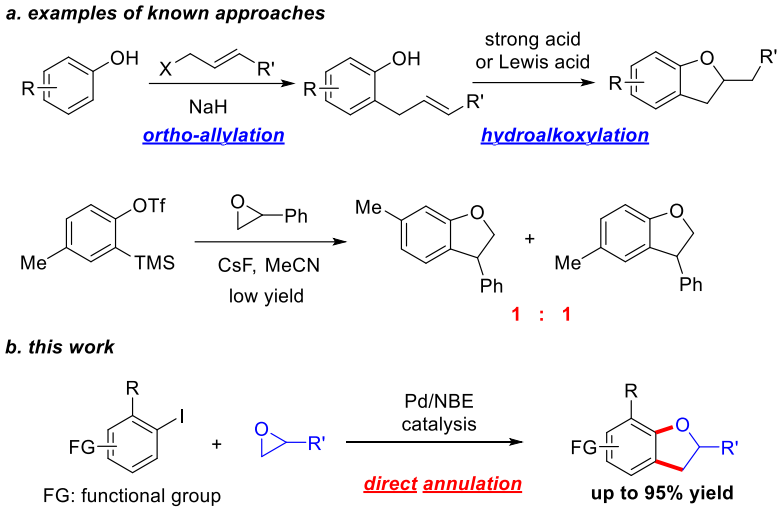

Figure 2.2. Proposed Catalytic Circle

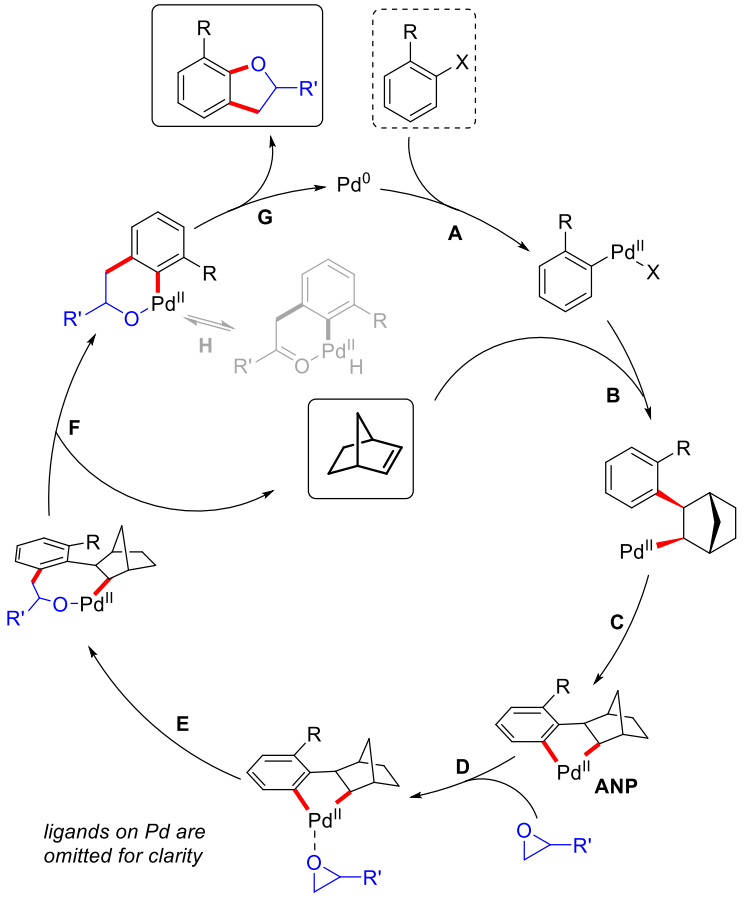

2.2 Results and Discussion

2.2.1 Reaction Discovery and Optimization

Despite the successful cyclization with highly strained *2H*-azirines (44-48 kcal/mol),[11g] the use of simple epoxides as the coupling partner in Pd/NBE catalysis has not been reported. The challenge is three-fold. First, activation of epoxides typically requires acids or Lewis acids,[12] while the Pd/NBE catalysis operates under slightly basic conditions. Second, the alkoxide generated from epoxide ring opening (step E, Fig. 2.2) is an excellent hydride donor and can lead to ipso reduction via β-hydrogen elimination.[7f,8a,9b] Third, coupling with oxygen nucleophiles with β-hydrogen has not been reported previously for Pd/NBE catalysis, likely due to the difficulty of the C−O bond reductive elimination versus β-hydrogen elimination (steps G and H, Fig. 2.2).

To address the aforementioned challenges, we propose that 1) use of polar aprotic solvents would promote S_N2-type ring opening of epoxides; and 2) use of a sterically hindered phosphine ligand, such as Buchwald's ligands, would inhibit β-hydrogen elimination and promote the C−O reductive elimination.[13] Indeed, after a careful survey of the reaction parameters, the desired DHBF product **3aa** was observed with RuPhos/DMF as the ligand/solvent combination (Table 2.1). Use of less polar solvents (entries 2 and 3) or other mono-dentate phosphines (entries 6 and 7) gave no annulation product. An improved yield (74%) was obtained using 5 mol% Buchwald's Ruphos-Pd-G4 precatalyst.[14] While regular NBE (**N1**) provided the desired annulation product (entry 9), multi-NBE insertion became the major side reaction, as the **ANP** intermediate is known to react further with additional NBE when the electrophile is not reactive enough.[15] Thus, we hypothesized that use of a *less reactive NBE*, such as those with a substitution at the C2 position, would hinder the multi-NBE insertion pathway. To our delight, the isopropyl ester-derived NBE (**N4**) was found to be most efficient for this transformation.[16] NBEs with less sterically hindered ester groups (**N2**

and **N3**) gave lower yields, while bulky *t*-butyl-ester substituted one (**N5**) significantly diminished the reactivity. Interestingly, the CF_3-substiutted NBE (**N8**) still afforded the desired product albeit in a low yield. It is noteworthy that, while most prior Pd/NBE catalyzed reactions require a high loading or excess NBE, only 20 mol% **N4** was found sufficient in this reaction. NaOAc proved to be an optimal base (entries 10 and 11). While 4 equiv of epoxide **2a** was used due to its volatility, reducing the loading to 2 equiv still provided DHBF **3aa** in 57% yield (entry 12).

Table 2.1. Control Experiments for Annulation with Epoxides

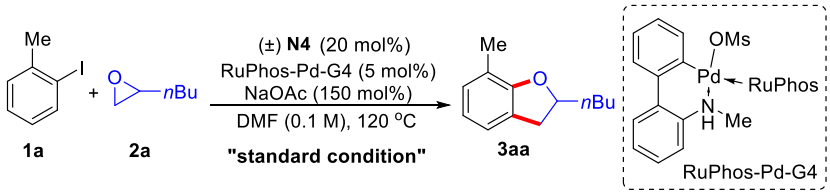

1a **2a** **3aa**

Entry	Change from the "standard condition"	Yield [%][a]
1	none	74
2	toluene instead of DMF	0
3	dioxane instead of DMF	0
4	no RuPhos-Pd-G4	0
5	$Pd(OAc)_2$ + RuPhos	41
6	$Pd(OAc)_2$ + PPh_3	0
7	$Pd(OAc)_2$ + $P(furyl)_3$	0
8	no **N4**	0
9	other NBEs	see below
10	no NaOAc	0
11	KOAc instead of NaOAc	0
12	2.0 equiv of **2a**	57

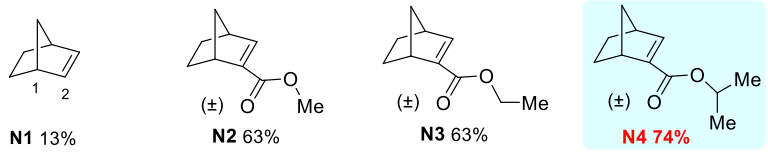

N1 13% **N2** 63% **N3** 63% **N4** 74%

N5 <10% **N6** 0% **N7** 0% **N8** 18%

[a]The reaction was run with 0.1 mmol **1a** and 0.4 mmol **2a** in 1 mL DMF for 24h. [b]Yields are determined by ^{1}H NMR Spectrum analysis using 1,3,5-trimethoxybenzene as the internal standard.

2.2.2 Substrates Scope

With the optimal reaction conditions in hand, the scope of the aryl iodides was examined first (Table 2.2). To our delight, substrates with electron-donating and -withdrawing groups all worked well giving the direct annulation products in moderate to excellent yields. One important feature of this transformation is that a variety of functional groups, including alkyl, TBS-silyl protected benzyl alcohol, methyl ester, methoxy, fluoride, chloride, amide, Weinreb amide and free tertiary alcohol, were all tolerated (**3ba**-**3ma**). It is worthy to mention that aryl chloride (**3ia**), which is reactive under the Pd/RuPhos conditions, survived in this reaction.[14] Notably, polyaryl iodide (**3na**) and heteroaryl iodide (**3oa**) were also suitable substrates. Furthermore, more complex estrone-derived substrate (**3pa**) is competent in this transformation, giving the desired DHBF in 59% yield. Altogether, this method exhibits excellent chemoselectivity.

Next, the scope of epoxides was explored (Table 2.3).[17] Direct annulation with simple ethylene oxide, propyl oxide and other 2-alkyloxiranes occurred smoothly (**3ab**-**3ae)**. Epoxides containing phenyl, ether or ester moieties all delivered the products in good to excellent yields (**3ag**-**3al**). Note that benzyl ether (**3ag)** and furan (**3aj**) are compatible under the reaction conditions.

Table 2.2. Substrates Scope with Aryl iodides[a]

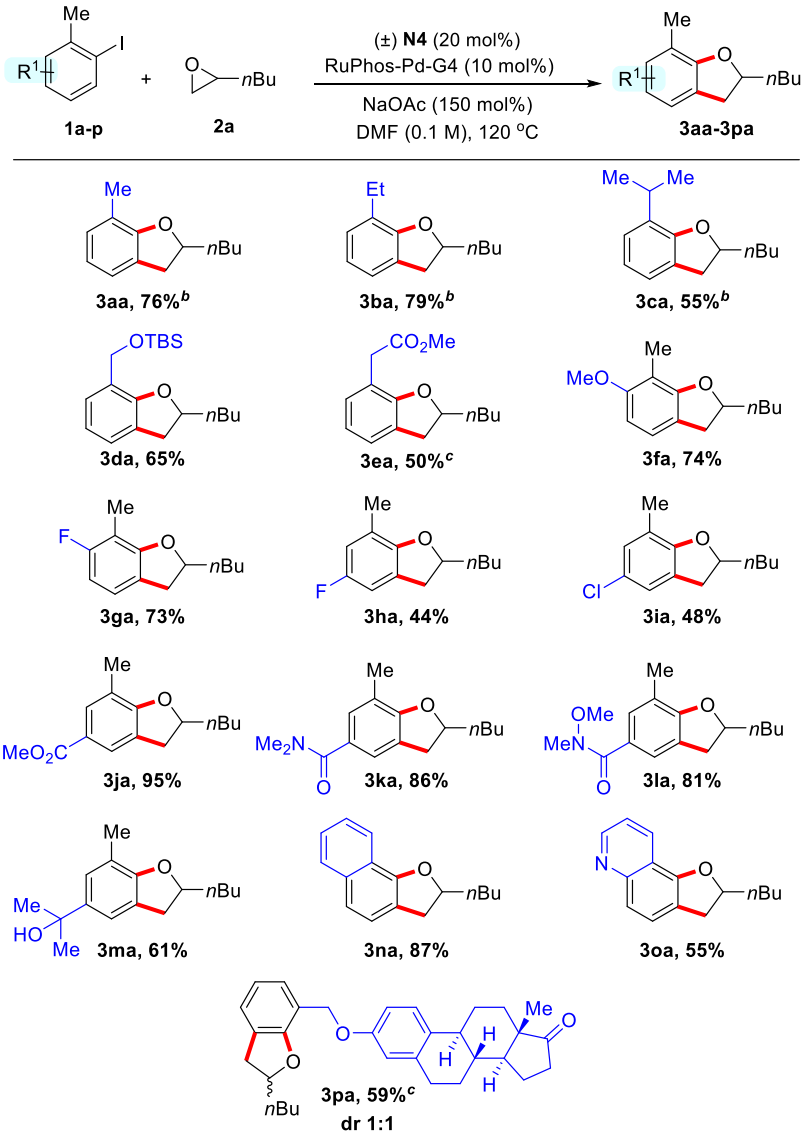

[a]All reactions were run with 0.3 mmol **1a-p** and 1.2 mmol **2a** in 3 mL DMF for 24h. Isolated yields are reported. [b]5.0 mol% of RuPhos-Pd-G4 was used. [c]20 mol% of RuPhos-Pd-G4 was used.

Table 2.3. Substrates Scope with Epoxides[a]

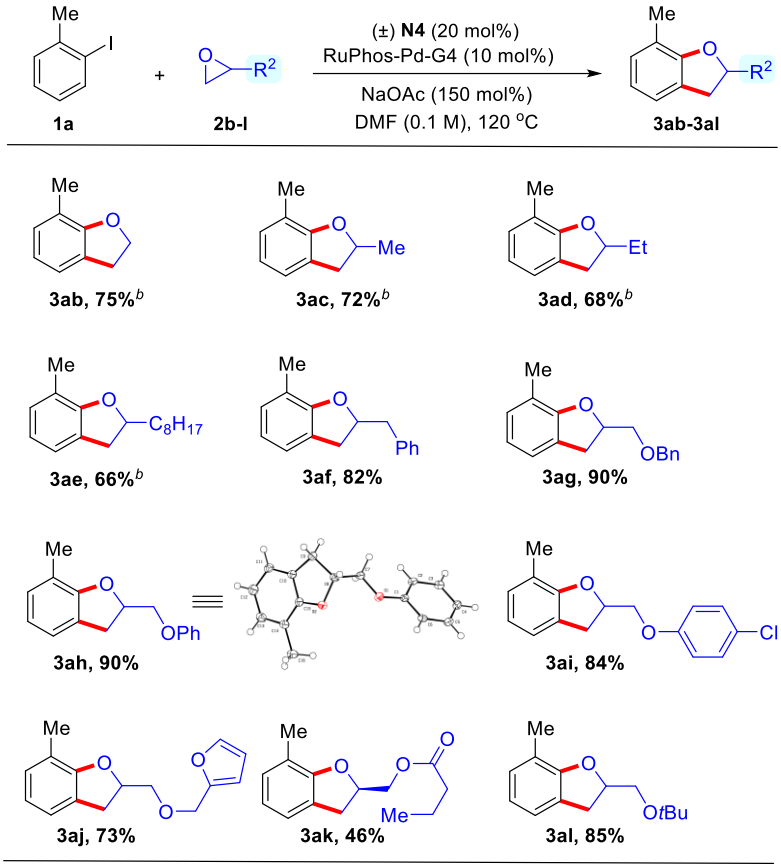

[a]All reactions were run with 0.3 mmol **1a** and 1.2 mmol epoxide in 3 mL DMF for 24h. Isolated yields are reported. [b]5.0 mol% of RuPhos-Pd-G4 was used.

2.2.3 Synthetic Utility

The synthetic utility of this method was first demonstrated by gram-scale preparations. The reaction is scalable (Eq 1 and 2). Using 1.75 g of aryl iodide **1a** (8.0 mmol), DHBF **3aa** was isolated in 80% yield with only 4.0 mol% [Pd]. Also, another DHBF **3ja** was obtained in 99% yield when using 1.38g of **1j** (5.0 mmol) and epoxide **2a**. In addition, when an enantiopure epoxide (*S*)-**2h** was used, the annulation reaction proceeded with stereo-retention and afforded chiral DHBF **3ah*** in 99% ee with 89% yield (Eq 3). Given the wide availability of enantiopure epoxides,

this transformation is anticipated to be useful for building chiral complex target molecules with DHBF moieties.

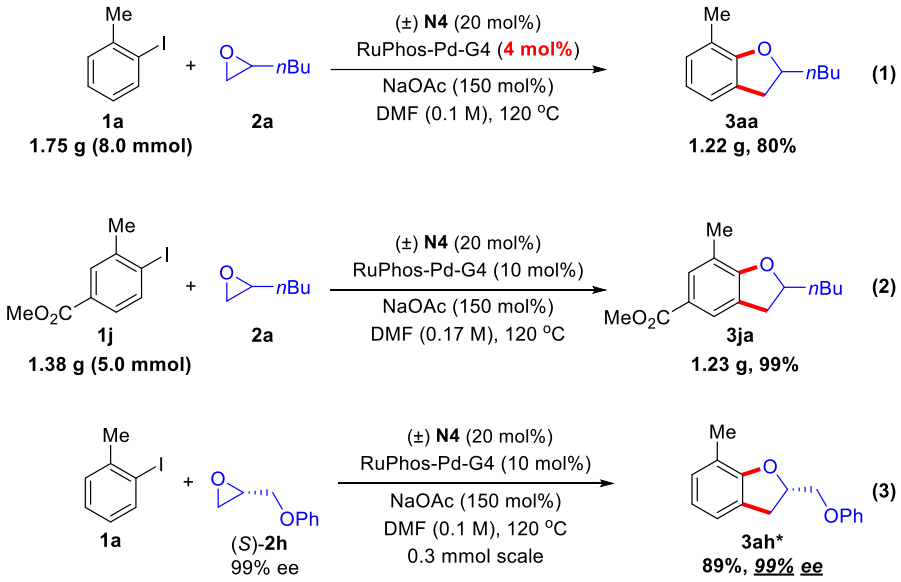

Finally, the synthetic utility of this method is demonstrated in a concise synthesis of fufenozide (Scheme 2.2),[18] which is a novel insect growth regulator showing high insecticidal activities towards *plutella*, *xylostella* and *mythimna*.[19] Starting from the commercially available aryl iodide **1q** and propyl oxide **2c**, their direct annulation provided the key DHBF intermediate (**3qc)** in 85% yield. Subsequent hydrolysis and peptide coupling with hydrazine **5** accomplished the synthesis of fufenozide in an excellent yield.

Scheme 2.2. Synthesis of Insecticide Fufenozide

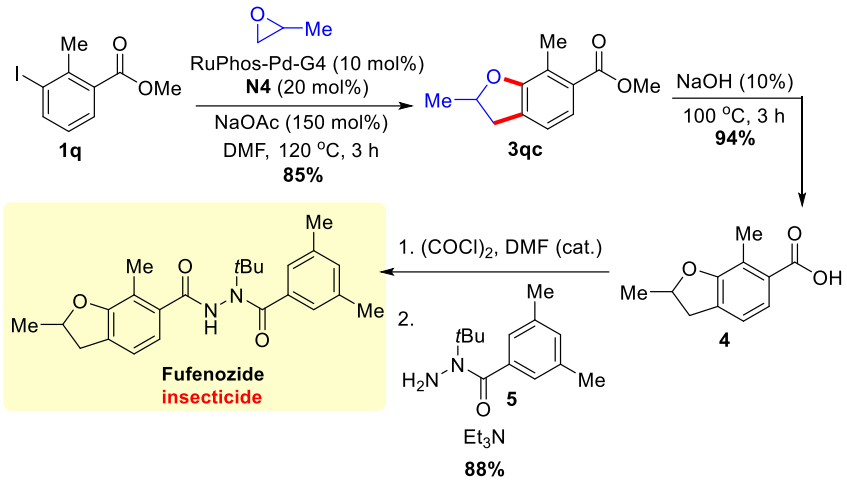

2.3 Conclusion

In summary, a direct annulation between aryl iodides and epoxides is developed via Pd/NBE cooperative catalysis. A variety of 2,3-dihydrobenzofuran derivatives was obtained in moderate to excellent yield. The use of easily available reactants, high chemo-selectivity and scalability should make this method attractive for practical applications. The discovery of an asymmetric reaction with an enantiopure NBE should have broad implications beyond this work.

2.4. Experimental Procedures and Characterization Data

2.4.1 General Information

Unless noted otherwise, all solvents were dried by filtration through a Pure-Solv MD-5 Solvent Purification System (Innovative Technology). Dimethylformamide was then vacuum-distilled freshly over calcium hydride and carefully freeze-pump-thawed. Reaction temperatures were reported as the temperatures of the bather surrounding the flasks or vials. Sensitive reagents and solvents were transferred under nitrogen into a nitrogen-filled glovebox with standard techniques. Sodium acetate was purchased from STREM, stored and used directly in the glovebox. Analytical thin-layer chromatography (TLC) was carried out using 0.2 mm commercial silica gel plates (silica gel 60, F254, EMD chemical). Vials (15 x 45 mm 1 dram (4 mL) with PTFE lined cap attached) were purchased from Qorpak and flame-dried and cooled in a desiccator prior to usage. High resolution mass spectra (HR-MS) were recorded on an Agilent 6530 LC Q-TOF mass spectrometer using electrospray ionization with fragmentation voltage set at 115 V and processed with an Agilent MassHunter Operating System. Infrared spectra were recorded on a Nicolet 380 FTIR using neat thin film technique. Nuclear magnetic resonance spectra (^{1}H NMR and ^{13}C NMR) were recorded with a Bruker DMX 400 (400 MHz, ^{1}H at 400 MHz, ^{13}C at 101 MHz) or Bruker Model DMX 500 (500 MHz, ^{1}H at 500 MHz, ^{13}C at 126 MHz). Chemical shifts were reported in parts per million (ppm, δ), downfield from tetramethylsilane (TMS, δ=0.00ppm) and were referenced to residual solvent ($CDCl_3$, δ=7.26 ppm (^{1}H) and 77.00 ppm (^{13}C)). All the ^{19}F chemical shifts were not referenced. Coupling constants were reported in Hertz (Hz). Data for ^{1}H NMR spectra were reported as follows: chemical shift (ppm, referenced to protium, s = singlet, d = doublet, t = triplet, q = quartet, quin = quintet, dd = doublet of doublets, td = triplet of doublets, ddd = doublet of

doublet of doublets, m = multiplet, coupling constant (Hz), and integration). All other materials were obtained from Sigma-Aldrich Corporation or Combi-Blocks Inc and were used as received.

2.4.2 Preparation of Aryl Iodide 1k

Scheme 2.3. Preparation of Aryl Iodide 1k

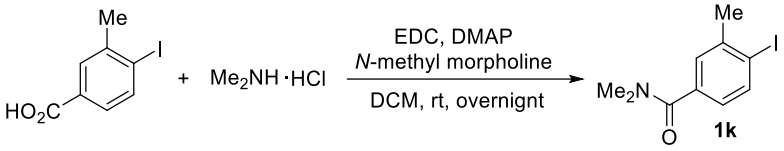

4-Iodo-3-methylbenzoic acid (2.6 g, 10.0 mmol, 1.0 equiv), dimethylamine hydrochloride (0.90 g, 11.0 mmol, 1.1 equiv), 1-ethyl-3-(3-dimethylaminopropyl)carbodiimide hydrochloride (2.30 g, 12.0 mmol, 1.2 equiv), 4-dimethylaminopyridine (122 mg, 1.0 mmol, 10 mol%) and *N*-methyl morpholine (1.01 g, 10.0 mmol, 1.0 equiv) were dissolved in dichloromethane (30 mL). Then the reaction mixture was stirred at room temperature. After 12 h it was diluted with diethyl ether, washed with water and brine, dried over $MgSO_4$, and then purified on silica gel (hexanes/ethyl acetate = 2:1) to afford **1k** as a colorless oil (2.6 g, 90%).

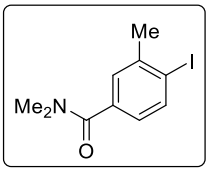

1k: Colorless oil (90%). R_f = 0.1 (hexane/ethyl acetate = 5:1). **^{1}H NMR** (500 MHz, $CDCl_3$) δ 7.78 (d, *J* = 8.1 Hz, 1H), 7.25 (s, 1H), 6.86 (dd, *J* = 8.1, 2.2 Hz, 1H), 3.04 (s, 3H), 2.92 (s, 3H), 2.40 (s, 3H). **^{13}C NMR** (126 MHz, $CDCl_3$) δ 170.67, 141.78, 138.84, 136.39, 128.21, 125.80, 102.43,

39.54, 35.33, 28.09. **IR** (KBr): υ 3486, 3016, 2925, 1633, 1444, 1396, 1261, 1180, 1090, 1014, 825, 754 cm^{-1}. **HRMS** (ESI): Calculated for $C_{10}H_{13}ONI$ ($M+H^+$): 290.0036, found: 290.0044.

2.4.3 Preparation of Substituted NBEs (N2–N8)

N2[20], **N6**[21], **N7**[22] was prepared following the literature reported procedures.

Scheme 2.4. Preparation of N8

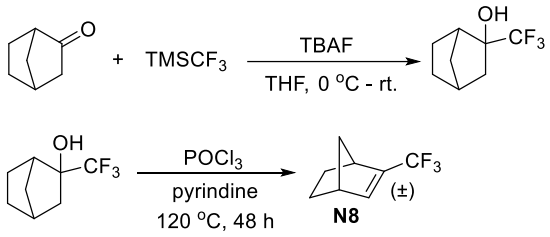

A mixture of norcamphor (3.3 g, 30 mmol, 1.0 equiv) and $TMSCF_3$ (5.1 g, 36 mmol, 1.2 equiv) in 30 mL of THF cooled to 0 °C was treated with TBAF (60 mg, 0.23 mmol, 0.77 mol%).[23] The reaction mixture was brought to ambient temperature and stirred for 12 h. Then 3 mL 4 M hydrochloric acid was added to the reaction mixture to hydrolyze the resulting siloxy compound. After the reaction, the mixture was extracted with ether (75 mL), and the ether extracts were washed with water (50 mL) and brine (50 mL), dried over $MgSO_4$, concentrated under vaccum and then purified on silica gel (pentane/Et_2O = 20:1) to afford the 2-hydroxy-2-trifluoromethylnorbornane in 89% yield.

2-Hydroxy-2-trifluoromethylnorbornane (18.0 g, 100 mmol) and phosphoryl chloride (46.0 g, 300 mmol) were dissolved in 200 mL pyridine. The reaction was stirred at 120 °C for 48 h. Then the mixture was diluted with diethyl ether, and the diluted solution was slowly poured into 200 mL mixture of 4M hydrochloric acid and ice at 0° C with vigorous stirring. Subsequently, the aqueous

layer was extracted three times with diethyl ether and the combined organic layers was dried over $MgSO_4$ and concentrated under reduced pressure. Then the crude mixture was purified through vacuum distillation to afford the desired product **N8** in 16% yield. Both the ^{1}H NMR and ^{13}C NMR match the literature reported data.[24]

Scheme 2.5. Preparation of C2 Ester-Substituted NBEs

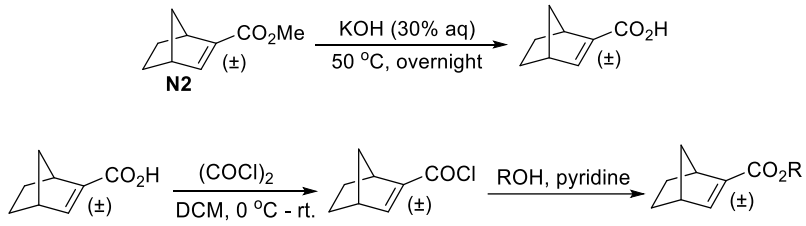

Methyl ester substituted NBE **N2** (152 mg, 0.1 mmol) was added to a 4 mL vial charged with a stir bar. Then 2.0 mL of 30% aqueous KOH solution was added and the reaction mixture was stirred at 50 °C for 12 h until the disappearance of **N2** was confirmed by TLC. After the reaction was done the mixture was diluted to 10 mL with water and then washed with diethyl ether for two times. The aqueous layer was acidified using 4 M hydrochloric acid and then extracted with dichloromethane for three times. The combined organic layers were dried over $MgSO_4$ and the solvent was removed under reduced pressure to afford the desired NBE-CO_2H, which was used directly in the next step without further purification.

To a solution of NBE-CO_2H (276 mg, 2.0 mmol, 1.0 equiv) and 1 drop of DMF in dichloromethane (1.0 mL) was added oxalyl chloride (267 mg, 2.1 mmol, 1.05 equiv) dropwise at 0 °C. The reaction mixture was stirred at room temperature for another 1 h until the bubbling stopped. A mixture of the corresponding alcohol (3.0 mmol, 1.5 equiv) and pyridine (475 mg, 6.0 mmol, 3.0 equiv) was

then added and the reaction was stirred for another 3 h until it was completed. The organic layer was washed with 1 M hydrochloric acid and then concentrated under vacuum. The corresponding ester substituted NBE was isolated by column (hexane/Et_2O = 20:1).

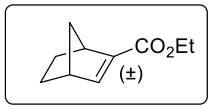

CAS: 15023-43-5

N3: Colorless oil (47%). R_f = 0.5 (hexane/ethyl acetate = 20:1). **^{1}H NMR** (500 MHz, $CDCl_3$) δ 7.26 (d, *J* = 3.1 Hz, 1H), 4.53 (q, *J* = 7.0 Hz, 2H), 3.61 (s, 1H), 3.36 (s, 1H), 2.09 (dtt, *J* = 15.1, 11.6, 7.6 Hz, 2H), 1.83 (d, *J* = 8.5 Hz, 1H), 1.64 (t, *J* = 7.1 Hz, 3H), 1.54 (d, *J* = 8.6 Hz, 1H), 1.44 (tdt, *J* = 7.6, 5.1, 2.3 Hz, 2H). **^{13}C NMR** (101 MHz, $CDCl_3$) δ 165.10, 146.78, 141.21, 60.15, 48.33, 43.61, 42.03, 24.78, 24.65, 14.48. **IR** (KBr): υ 2977, 2874, 1712, 1596, 1370, 1341, 1278, 1258, 1160, 1079, 753 cm^{-1}. **HRMS** (ESI): Calculated for $C_{10}H_{15}O_2$ ($M+H^+$): 167.1067, found: 167.1061. Both the ^{1}H NMR and ^{13}C NMR match the literature reported data.[25]

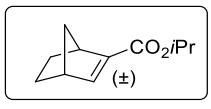

N4: Colorless oil (78%). R_f = 0.6 (hexane/ethyl acetate = 20:1). **^{1}H NMR** (500 MHz, $CDCl_3$) δ 6.88 (d, *J* = 3.2 Hz, 1H), 5.05 (hept, *J* = 6.1 Hz, 1H), 3.24 (s, 1H), 3.00 (s, 1H), 1.74 (th, *J* = 13.0, 3.3 Hz, 2H), 1.52 – 1.43 (m, 1H), 1.26 (dd, *J* = 6.3, 4.1 Hz, 6H), 1.18 (d, *J* = 8.7 Hz, 1H), 1.07 (dt, *J* = 7.4, 2.3 Hz, 2H). **^{13}C NMR** (101 MHz, $CDCl_3$) δ 164.68, 146.41, 141.62, 67.33, 48.29, 43.58, 42.02, 24.82, 24.67, 22.10. **IR** (KBr): υ 2978, 2874, 1707, 1279, 1259, 1163, 1110, 1076, 753 cm^{-1}. **HRMS** (ESI): Calculated for $C_{11}H_{17}O_2$ ($M+H^+$): 181.1223, found: 181.1219.

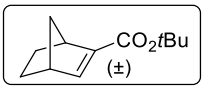

N5: White solid (50%). R_f = 0.6 (hexane/ethyl acetate = 20:1). Mp = 51.6 – 52.8 °C. **^{1}H NMR** (500 MHz, $CDCl_3$) δ 6.79 (d, *J* = 3.1 Hz, 1H), 3.19 (s, 1H), 2.98 (s, 1H), 1.78 – 1.68 (m, 2H), 1.48 (s, 10H), 1.16 (d, *J* = 8.5 Hz, 1H), 1.07 (qd, *J* = 8.5, 2.2 Hz, 2H). ^{13}C NMR (101 MHz, $CDCl_3$) δ 164.56, 145.64, 142.78, 80.01, 48.30, 43.53, 42.05, 28.37, 24.88, 24.66. **IR** (KBr): υ 2976, 2873, 1702, 1596, 1284, 1260, 1154, 1077, 756 cm^{-1}. **HRMS** (ESI): Calculated for $C_{12}H_{18}O_2Na$ ($M+Na^+$): 217.1199, found: 217.1184.

2.4.4 General Procedure of Palladium and Norbornene Catalyzed Direct Annulation Reaction

Scheme 2.6. Direct Annulation Reaction via Pd/NBE Catalysis

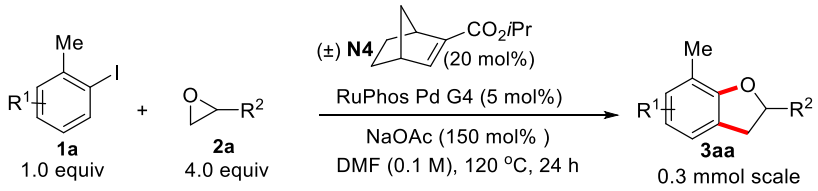

A flame-dried 4.0 mL vial was charged with RuPhos Pd G4 (12.8 mg, 0.015 mmol, 5 mol%), aryl iodide (0.3 mmol, 1.0 equiv) and NaOAc (36.9 mg, 0.45 mmol, 1.5 equiv). Then the vial was directly transferred into a nitrogen-filled glovebox without caps. After that **N4** (10.8 mg, 0.06 mmol, 20 mol%) and epoxides (1.2 mmol, 4.0 equiv) was added, 3 mL of degassed DMF was added to the vial. Then the vial was tightly sealed, transferred out of glovebox and stirred on a pie-block preheated to 120 °C for 24 hours. After completion of the reaction, the mixture was filtered through a thin pad of celite. The filter cake was washed with dichloromethane and diethyl ether,

and the combined filtrate was concentrated. The residue was loaded to a small amount of silica gel and then purified by flash column chromatography on silica gel to give the desired product.

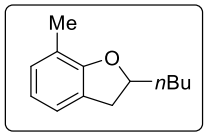

3aa: Pale yellow oil (76%). R_f = 0.4 (hexane/ethyl acetate = 40:1). **^{1}H NMR** (400 MHz, $CDCl_3$) δ 7.00 (d, *J* = 6.9 Hz, 1H), 6.93 (ddq, *J* = 7.5, 1.5, 0.8 Hz, 1H), 6.74 (t, *J* = 7.4 Hz, 1H), 4.76 (dddd, *J* = 8.9, 7.8, 6.9, 6.2 Hz, 1H), 3.28 (dd, *J* = 15.4, 8.9 Hz, 1H), 2.86 (dd, *J* = 15.4, 7.8 Hz, 1H), 2.22 (s, 3H), 1.93 – 1.79 (m, 1H), 1.73 – 1.62 (m, 1H), 1.55 – 1.34 (m, 4H), 0.95 (t, *J* = 7.1 Hz, 3H). **^{13}C NMR** (126 MHz, $CDCl_3$) δ 158.17, 129.19, 126.31, 122.36, 119.99, 119.55, 83.09, 36.02, 35.93, 27.74, 22.80, 15.41, 14.20. **IR** (KBr): υ 3025, 2956, 2931, 2859, 1599, 1467, 1260, 1186, 759 cm^{-1}. **HRMS** (ESI): Calculated for $C_{13}H_{19}O$ ($M+H^+$): 191.1430, found: 191.1428.

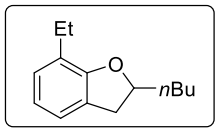

3ba: Pale yellow oil (79%). R_f = 0.4 (hexane/ethyl acetate = 40:1). **^{1}H NMR** (400 MHz, $CDCl_3$) δ 7.02 (dt, *J* = 7.3, 1.3 Hz, 1H), 6.97 (dp, *J* = 7.5, 0.8 Hz, 1H), 6.78 (t, *J* = 7.4 Hz, 1H), 4.82 – 4.72 (m, 1H), 3.35 – 3.22 (m, 1H), 2.93 – 2.81 (m, 1H), 2.62 (qd, *J* = 7.5, 1.6 Hz, 2H), 1.93 – 1.79 (m, 1H), 1.68 (ddt, *J* = 13.2, 11.1, 5.4 Hz, 1H), 1.58 – 1.34 (m, 4H), 1.24 (tt, *J* = 7.4, 0.9 Hz, 3H), 0.96 (ddd, *J* = 7.4, 6.2, 1.0 Hz, 3H). **^{13}C NMR** (126 MHz, $CDCl_3$) δ 157.73, 127.43, 126.48, 125.91,

122.43, 120.10, 83.01, 36.02, 35.86, 27.71, 23.16, 22.80, 14.19, 14.11. **IR** (KBr): υ 3049, 2959, 2930, 2872, 2859, 1596, 1455, 1265, 1190, 740 cm^{-1}. **HRMS** (ESI): Calculated for $C_{14}H_{21}O$ ($M+H^+$): 205.1587, found: 205.1592.

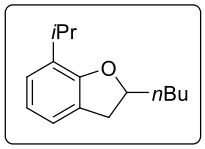

3ca: Pale yellow oil (55%). R_f = 0.5 (hexane/ethyl acetate = 40:1). **^{1}H NMR** (400 MHz, $CDCl_3$) δ 7.03 – 6.98 (m, 2H), 6.83 – 6.77 (m, 1H), 4.77 (dtd, J = 9.0, 7.2, 6.0 Hz, 1H), 3.28 (ddt, J = 15.4, 9.0, 0.9 Hz, 1H), 3.10 (hept, J = 6.9 Hz, 1H), 2.86 (ddt, J = 15.4, 7.5, 1.0 Hz, 1H), 1.85 (dddd, J = 13.4, 9.9, 7.0, 5.2 Hz, 1H), 1.73 – 1.61 (m, 1H), 1.55 – 1.35 (m, 4H), 1.26 (dd, J = 6.9, 2.6 Hz, 6H), 0.95 (t, J = 7.1 Hz, 3H). **^{13}C NMR** (101 MHz, $CDCl_3$) δ 157.19, 130.46, 126.60, 124.82, 122.34, 120.13, 82.91, 36.01, 35.79, 28.48, 27.73, 22.79, 22.49, 22.34, 14.22. **IR** (KBr): υ 3049, 2958, 2871, 1595, 1451, 1301, 1188, 994, 868, 740 cm^{-1}. **HRMS** (ESI): Calculated for $C_{15}H_{23}O$ ($M+H^+$): 219.1743, found: 219.1745.

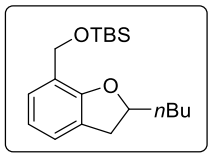

3da: Pale yellow oil (65%). R_f = 0.4 (hexane/ethyl acetate = 40:1). **^{1}H NMR** (400 MHz, $CDCl_3$) δ 7.23 (d, *J* = 7.6 Hz, 1H), 7.05 (d, *J* = 6.6 Hz, 1H), 6.83 (t, *J* = 7.5 Hz, 1H), 4.82 – 4.70 (m, 3H), 3.26 (dd, *J* = 15.4, 8.9 Hz, 1H), 2.84 (dd, *J* = 15.4, 7.7 Hz, 1H), 1.90 – 1.77 (m, 1H), 1.66 (ddt, *J* = 13.4, 10.1, 5.5 Hz, 1H), 1.55 – 1.32 (m, 4H), 0.98 – 0.90 (m, 12H), 0.11 (s, 6H). **^{13}C NMR** (101

MHz, $CDCl_3$) δ 156.31, 126.42, 125.98, 123.41, 123.24, 120.10, 83.63, 60.08, 36.00, 35.58, 27.68, 26.14, 22.79, 18.61, 14.19, -5.13. **IR** (KBr): υ 2956, 2930, 2857, 1456, 1258, 1190, 1108, 837, 776 cm^{-1}. **HRMS** (ESI): Calculated for $C_{19}H_{32}O_2SiNa$ ($M+Na^+$): 343.2064, found: 343.2055.

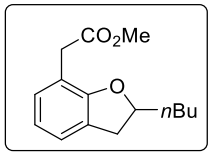

3ea: Yellow oil (50%). R_f = 0.2 (hexane/ethyl acetate = 40:1). **^{1}H NMR** (400 MHz, $CDCl_3$) δ 7.06 (d, *J* = 7.3 Hz, 1H), 7.00 (dd, *J* = 7.6, 0.7 Hz, 1H), 6.77 (d, *J* = 7.4 Hz, 1H), 4.77 (dtd, *J* = 9.0, 7.2, 5.9 Hz, 1H), 3.70 (s, 3H), 3.60 (s, 2H), 3.29 (dd, *J* = 15.4, 9.0 Hz, 1H), 2.86 (dd, *J* = 15.5, 7.4 Hz, 1H), 1.81 (dddd, *J* = 13.5, 12.3, 6.3, 3.1 Hz, 1H), 1.64 (ddt, *J* = 13.5, 11.7, 4.8 Hz, 1H), 1.52 – 1.32 (m, 4H), 0.98 – 0.87 (m, 3H). **^{13}C NMR** (101 MHz, $CDCl_3$) δ 172.05, 158.13, 129.00, 126.94, 124.02, 120.19, 115.78, 83.47, 52.06, 35.93, 35.79, 35.19, 27.59, 22.74, 14.18. **IR** (KBr): υ 2954, 2922, 2960, 1742, 1460, 1435, 1248, 1188, 1155, 755, 668 cm^{-1}. **HRMS** (ESI): Calculated for $C_{15}H_{21}O_3$ ($M+H^+$): 249.1485, found: 249.1477.

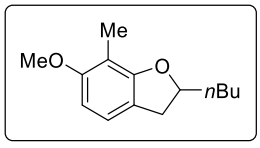

3fa: Pale yellow oil (74%). R_f = 0.4 (hexane/ethyl acetate = 40:1). **^{1}H NMR** (500 MHz, $CDCl_3$) δ 6.90 (d, *J* = 8.0 Hz, 1H), 6.34 (d, *J* = 8.1 Hz, 1H), 4.76 (dt, *J* = 14.9, 7.1 Hz, 1H), 3.80 (s, 3H), 3.22 (dd, *J* = 14.9, 8.8 Hz, 1H), 2.80 (dd, *J* = 14.9, 7.7 Hz, 1H), 2.08 (s, 3H), 1.92 – 1.78 (m, 1H), 1.75 – 1.61 (m, 1H), 1.55 – 1.31 (m, 4H), 0.94 (t, *J* = 7.0 Hz, 3H). **^{13}C NMR** (101 MHz, $CDCl_3$)

δ 159.21, 158.14, 121.30, 118.97, 108.43, 102.14, 84.03, 56.03, 36.03, 35.50, 27.76, 22.80, 14.20, 8.70. **IR** (KBr): υ 2933, 2859, 1625, 1604, 1489, 1268, 1152, 1113, 967, 783 cm^{-1}. **HRMS** (ESI): Calculated for $C_{14}H_{21}O_2$ ($M+H^+$): 221.1536, found: 221.1538.

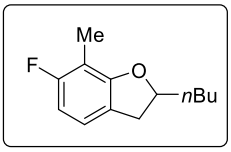

3ga: Pale yellow oil (73%). R_f = 0.6 (hexane/ethyl acetate = 40:1). **^{1}H NMR** (500 MHz, $CDCl_3$) δ 6.88 (d, *J* = 7.9 Hz, 1H), 6.49 (dd, *J* = 9.9, 8.1 Hz, 1H), 4.80 (dt, *J* = 14.9, 7.5 Hz, 1H), 3.22 (dd, *J* = 15.0, 9.0 Hz, 1H), 2.81 (dd, *J* = 15.1, 7.8 Hz, 1H), 2.11 (d, *J* = 1.6 Hz, 3H), 1.90 – 1.78 (m, 1H), 1.71 – 1.60 (m, 1H), 1.54 – 1.33 (m, 4H), 0.94 (t, *J* = 7.0 Hz, 3H). **^{13}C NMR** (126 MHz, $CDCl_3$) δ 161.54 (d, *J* = 240.6 Hz), 159.41 (d, *J* = 10.2 Hz), 121.66 (d, *J* = 10.5 Hz), 121.49 (d, *J* = 2.6 Hz), 107.66 (d, *J* = 22.2 Hz), 106.31 (d, *J* = 23.9 Hz), 84.66, 35.98, 35.48, 27.68, 22.76, 14.16, 7.94 (d, *J* = 4.2 Hz). **^{19}F NMR** (470 MHz, $CDCl_3$) δ -121.15. **IR** (KBr): υ 2957, 2931, 2860, 1628, 1607, 1487, 1455, 1079, 968, 793 cm^{-1}. **HRMS** (ESI): Calculated for $C_{13}H_{18}OF$ ($M+H^+$): 209.1336, found: 209.1336.

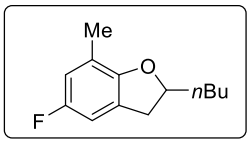

3ha: Pale yellow oil (44%). R_f = 0.5 (hexane/ethyl acetate = 40:1). **^{1}H NMR** (500 MHz, $CDCl_3$) δ 6.65 (dd, *J* = 26.5, 8.9 Hz, 2H), 4.75 (p, *J* = 7.1 Hz, 1H), 3.23 (dd, *J* = 15.6, 8.8 Hz, 1H), 2.83 (dd, *J* = 15.6, 7.9 Hz, 1H), 2.17 (s, 3H), 1.89 – 1.76 (m, 1H), 1.71 – 1.60 (m, 1H), 1.53 – 1.31 (m, 4H),

0.93 (t, *J* = 6.9 Hz, 3H). **^{13}C NMR** (101 MHz, $CDCl_3$) δ 157.01 (d, *J* = 235.8 Hz), 153.93 (d, *J* = 1.4 Hz), 127.11 (d, *J* = 9.2 Hz), 119.96 (d, *J* = 8.2 Hz), 115.03 (d, *J* = 23.5 Hz), 109.03 (d, *J* = 24.4 Hz), 83.44, 36.02 (d, *J* = 1.9 Hz), 35.77, 27.55, 22.64, 15.37 (d, *J* = 1.3 Hz), 14.05. **^{19}F NMR** (470 MHz, $CDCl_3$) δ -125.69. **IR** (KBr): υ 2957, 2931, 2860, 1478, 1202, 1116, 964, 856, 805, 716 cm^{-1}. **HRMS** (ESI): Calculated for $C_{13}H_{17}OFNa$ ($M+Na^+$): 231.1156, found: 231.1167.

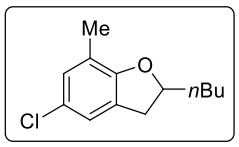

3ia: Pale yellow oil (48%). R_f = 0.6 (hexane/ethyl acetate = 40:1). **^{1}H NMR** (400 MHz, $CDCl_3$) δ 6.95 – 6.86 (m, 2H), 4.76 (dddd, *J* = 9.0, 7.8, 6.9, 6.1 Hz, 1H), 3.24 (dd, *J* = 15.6, 8.9 Hz, 1H), 2.82 (dd, *J* = 15.6, 7.7 Hz, 1H), 2.16 (s, 3H), 1.82 (dddd, *J* = 13.2, 9.9, 6.9, 4.9 Hz, 1H), 1.71 – 1.60 (m, 1H), 1.52 – 1.32 (m, 4H), 0.93 (t, *J* = 7.1 Hz, 3H). **^{13}C NMR** (101 MHz, $CDCl_3$) δ 156.86, 128.86, 127.99, 124.31, 122.35, 120.81, 83.70, 35.90, 35.82, 27.63, 22.75, 15.33, 14.18. **IR** (KBr): υ 2957, 2931, 2860, 1467, 1200, 956, 860, 778, 720 cm^{-1}. **HRMS** (ESI): Calculated for $C_{13}H_{18}OCl$ ($M+H^+$): 225.1041, found: 225.1048.

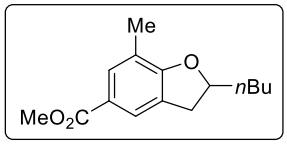

3ja: Pale yellow oil (95%). R_f = 0.2 (hexane/ethyl acetate = 40:1). **^{1}H NMR** (400 MHz, $CDCl_3$) δ 7.70 – 7.65 (m, 2H), 4.89 – 4.78 (m, 1H), 3.85 (s, 3H), 3.28 (dd, *J* = 15.5, 9.0 Hz, 1H), 2.85 (dd, *J* = 15.5, 7.7 Hz, 1H), 2.21 (s, 3H), 1.90 – 1.78 (m, 1H), 1.74 – 1.62 (m, 1H), 1.54 – 1.32 (m, 4H),

0.93 (t, *J* = 7.1 Hz, 3H). **^{13}C NMR** (126 MHz, $CDCl_3$) δ 167.38, 162.40, 131.93, 126.61, 124.38, 122.15, 119.27, 84.41, 51.83, 35.97, 35.26, 27.55, 22.71, 15.26, 14.13. **IR** (KBr): υ 2954, 2860, 1715, 1607, 1434, 1306, 1161, 954, 771 cm^{-1}. **HRMS** (ESI): Calculated for $C_{15}H_{21}O_3$ ($M+H^+$): 249.1485, found: 249.1492.

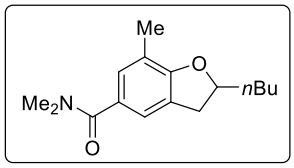

3ka: Yellow oil (86%). R_f = 0.1 (hexane/ethyl acetate = 5:1). **^{1}H NMR** (500 MHz, $CDCl_3$) δ 7.09 (s, 1H), 7.03 (s, 1H), 4.79 (p, *J* = 7.3 Hz, 1H), 3.27 (dd, *J* = 15.5, 9.0 Hz, 1H), 3.05 (s, 6H), 2.85 (dd, *J* = 15.5, 7.7 Hz, 1H), 2.20 (s, 3H), 1.89 – 1.77 (m, 1H), 1.72 – 1.60 (m, 1H), 1.48 (ddt, *J* = 12.2, 9.2, 6.2 Hz, 1H), 1.40 (dtt, *J* = 10.6, 6.8, 4.1 Hz, 3H), 0.94 (t, *J* = 7.0 Hz, 3H). **^{13}C NMR** (126 MHz, $CDCl_3$) δ 172.19, 159.34, 128.98, 128.04, 126.30, 121.98, 119.02, 83.71, 35.90, 35.55, 27.55, 22.67, 15.27, 14.09. **IR** (KBr): υ 2950, 2930, 2859, 1633, 1608, 1475, 1389, 1288, 1158, 762 cm^{-1}. **HRMS** (ESI): Calculated for $C_{16}H_{24}NO_2$ ($M+H^+$): 262.1802, found: 262.1801.

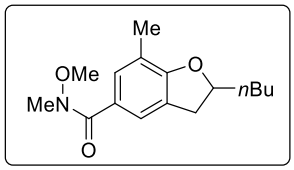

3la: Yellow oil (81%). R_f = 0.2 (hexane/ethyl acetate = 5:1). **^{1}H NMR** (500 MHz, CD_2Cl_2) δ 7.34 (d, *J* = 18.6 Hz, 2H), 4.81 (dt, *J* = 14.9, 7.4 Hz, 1H), 3.57 (s, 3H), 3.34 – 3.25 (m, 4H), 2.87 (dd, *J*

= 15.5, 7.8 Hz, 1H), 2.19 (s, 3H), 1.89 – 1.78 (m, 1H), 1.67 (ddd, *J* = 13.2, 10.6, 5.6 Hz, 1H), 1.55 – 1.34 (m, 4H), 0.94 (t, *J* = 7.0 Hz, 3H). **^{13}C NMR** (126 MHz, CD_2Cl_2) δ 170.38, 160.69, 130.62, 126.49, 126.31, 123.46, 118.95, 84.39, 61.01, 36.25, 35.74, 34.40, 27.92, 23.04, 15.35, 14.22. **IR** (KBr): υ 2956, 2932, 2860, 1640, 1607, 1466, 1409, 1370, 1153, 955, 751 cm^{-1}. **HRMS** (ESI): Calculated for $C_{16}H_{24}NO_3$ ($M+H^+$): 278.1751, found: 278.1754.

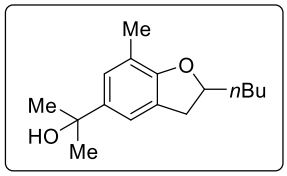

3ma: Yellow oil (61%). R_f = 0.3 (hexane/ethyl acetate = 5:1). **^{1}H NMR** (500 MHz, $CDCl_3$) δ 7.09 (d, *J* = 38.5 Hz, 2H), 4.85 – 4.70 (m, 1H), 3.26 (dd, *J* = 15.3, 8.9 Hz, 1H), 2.85 (dd, *J* = 15.4, 7.8 Hz, 1H), 2.21 (s, 3H), 1.85 (ddt, *J* = 13.2, 9.8, 6.0 Hz, 1H), 1.77 (s, 1H), 1.70 – 1.63 (m, 1H), 1.56 (s, 6H), 1.51 – 1.35 (m, 4H), 0.94 (t, *J* = 6.9 Hz, 3H). **^{13}C NMR** (126 MHz, $CDCl_3$) δ 157.00, 141.12, 126.21, 125.51, 118.73, 118.68, 83.40, 72.47, 36.02, 36.01, 32.08, 32.07, 27.73, 22.77, 15.60, 14.17. **IR** (KBr): υ 3393, 2959, 2930, 2860, 1482, 1361, 1184, 963, 872, 732 cm^{-1}. **HRMS** (ESI): Calculated for $C_{16}H_{23}O$ ($M+H^+$-H_2O): 231.1743, found: 231.1743.

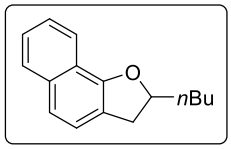

3na: Orange oil (87%). R_f = 0.5 (hexane/ethyl acetate = 40:1). **^{1}H NMR** (500 MHz, $CDCl_3$) δ 7.99 (dd, *J* = 8.0, 1.6 Hz, 1H), 7.82 (dd, *J* = 8.0, 1.6 Hz, 1H), 7.48 – 7.40 (m, 2H), 7.37 (d, *J* = 8.2 Hz, 1H), 7.33 (d, *J* = 8.2 Hz, 1H), 5.00 (dd, *J* = 15.1, 7.5 Hz, 1H), 3.47 (dd, *J* = 15.1, 9.3 Hz, 1H), 3.05 (dd, *J* = 15.1, 7.6 Hz, 1H), 1.96 (dddd, *J* = 13.6, 10.2, 7.1, 5.2 Hz, 1H), 1.83 – 1.73 (m, 1H), 1.65 – 1.54 (m, 1H), 1.54 – 1.39 (m, 3H), 0.98 (t, *J* = 7.2 Hz, 3H). **^{13}C NMR** (126 MHz, $CDCl_3$) δ 155.09, 134.07, 127.94, 125.60, 125.19, 123.12, 121.65, 120.69, 119.79, 84.30, 36.43, 36.21, 27.71, 22.83, 22.81, 14.21. **IR** (KBr): υ 3055, 2955, 2931, 2858, 1575, 1402, 1375, 1279, 1068, 1003, 801, 773, 565 cm^{-1}. **HRMS** (ESI): Calculated for $C_{16}H_{19}O$ ($M+H^+$): 227.1430, found: 227.1438.

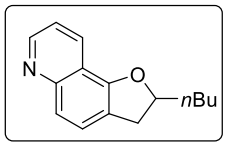

3oa: Yellow oil (55%). R_f = 0.2 (hexane/ethyl acetate = 5:1). **^{1}H NMR** (400 MHz, $CDCl_3$) δ 8.82 (dd, *J* = 4.2, 1.8 Hz, 1H), 8.27 (ddd, *J* = 8.4, 1.8, 0.8 Hz, 1H), 7.60 (d, *J* = 8.4 Hz, 1H), 7.51 (d, *J* = 8.3 Hz, 1H), 7.30 (dd, *J* = 8.4, 4.2 Hz, 1H), 5.07 – 4.95 (m, 1H), 3.45 (dd, *J* = 15.3, 9.2 Hz, 1H), 3.03 (dd, *J* = 15.3, 7.8 Hz, 1H), 1.92 (dddd, *J* = 13.6, 10.0, 7.1, 5.2 Hz, 1H), 1.75 (ddt, *J* = 13.7, 10.2, 5.5 Hz, 1H), 1.61 – 1.51 (m, 1H), 1.49 – 1.36 (m, 3H), 0.94 (t, *J* = 7.1 Hz, 3H). **^{13}C NMR** (101 MHz, $CDCl_3$) δ 154.78, 150.16, 148.59, 130.27, 126.29, 121.09, 120.65, 120.12, 115.78, 85.16, 36.16, 36.11, 27.62, 22.74, 14.18. **IR** (KBr): υ 3068, 3037, 2955, 2931, 2859, 1590, 1569, 1466, 1403, 1371, 1277, 1064, 826, 804, 566 cm^{-1}. **HRMS** (ESI): Calculated for $C_{15}H_{17}NO$ ($M+H^+$): 228.1383, found: 228.1389.

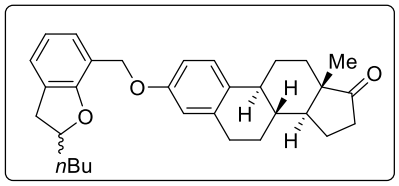

3pa: White solid (59%). R_f = 0.5 (hexane/ethyl acetate = 5:1). Mp = 120.0 – 130.0 °C. **^{1}H NMR** (400 MHz, $CDCl_3$) δ 7.22 (dd, *J* = 17.8, 8.2 Hz, 2H), 7.11 (dd, *J* = 7.3, 1.3 Hz, 1H), 6.86 – 6.79 (m, 2H), 6.77 (d, *J* = 2.8 Hz, 1H), 5.03 (s, 2H), 4.82 (dt, *J* = 14.8, 7.3 Hz, 1H), 3.30 (dd, *J* = 15.5, 8.9 Hz, 1H), 2.95 – 2.81 (m, 3H), 2.51 (dd, *J* = 18.9, 8.4 Hz, 1H), 2.45 – 2.32 (m, 1H), 2.26 (t, *J* = 10.7 Hz, 1H), 2.20 – 1.91 (m, 4H), 1.86 (dddd, *J* = 13.3, 9.9, 6.9, 5.1 Hz, 1H), 1.74 – 1.64 (m, 1H), 1.64 – 1.33 (m, 10H), 0.98 – 0.88 (m, 6H). **^{13}C NMR** (101 MHz, $CDCl_3$) δ 221.10, 157.38, 157.04, 137.76, 132.15, 127.58, 127.11, 126.36, 124.59, 120.33, 118.80, 114.96, 114.95, 112.58, 112.56, 83.83, 64.66, 50.54, 48.15, 44.13, 38.50, 36.01, 35.97, 35.61, 31.72, 29.79, 27.66, 26.70, 26.04, 22.77, 21.72, 14.19, 13.99. **IR** (KBr): υ 2953, 2929, 2859, 1739, 1607, 1499, 1457, 1255, 1054, 1006, 862, 760, 668 cm^{-1}. **HRMS** (ESI): Calculated for $C_{31}H_{39}O$ ($M+H^+$): 459.2894, found: 459.2885. Elemental analysis [%] found (calculated for $C_{31}H_{38}O_3$): C 80.64 (81.18), H 8.39 (8.35).

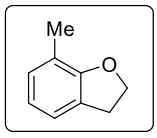

CAS: 17359-45-4

3ab: colorless oil (75%). R_f = 0.4 (hexane/ethyl acetate = 40:1). **^{1}H NMR** (400 MHz, $CDCl_3$) δ 7.05 (d, *J* = 7.1 Hz, 1H), 6.95 (ddt, *J* = 7.5, 1.5, 0.7 Hz, 1H), 6.77 (t, *J* = 7.4 Hz, 1H), 4.61 – 4.53 (m, 2H), 3.22 (t, *J* = 8.7 Hz, 2H), 2.23 (s, 3H). **^{13}C NMR** (101 MHz, $CDCl_3$) δ 158.48, 129.25, 126.20, 122.37, 120.34, 119.69, 70.84, 30.20, 15.37. **IR** (KBr): υ 2924, 2854, 1598, 1480, 1464,

1260, 1187, 983, 760 cm^{-1}. **HRMS** (ESI): Calculated for $C_9H_{11}O$ ($M+H^+$): 135.0804, found: 135.0802.

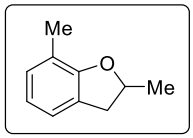

CAS: 3199-41-5

3ac: colorless oil (72%). R_f = 0.4 (hexane/ethyl acetate = 40:1). **^{1}H NMR** (400 MHz, $CDCl_3$) δ 7.00 (d, *J* = 7.3 Hz, 1H), 6.94 (d, *J* = 7.5 Hz, 1H), 6.75 (t, *J* = 7.4 Hz, 1H), 4.98 – 4.86 (m, 1H), 3.32 (dd, *J* = 15.3, 8.8 Hz, 1H), 2.83 (dd, *J* = 15.1, 8.0 Hz, 1H), 2.22 (s, 3H), 1.49 (d, *J* = 6.2 Hz, 3H). **^{13}C NMR** (101 MHz, $CDCl_3$) δ 158.10, 129.25, 126.37, 122.39, 120.11, 119.58, 79.23, 37.60, 22.01, 15.43. **IR** (KBr): υ 2917, 2851, 1598, 1467, 1380, 1196, 908, 854, 759 cm^{-1}. **HRMS** (ESI): Calculated for $C_{10}H_{13}O$ ($M+H^+$): 149.0961, found: 149.0964. Both the ^{1}H NMR and ^{13}C NMR match the literature reported data.[26]

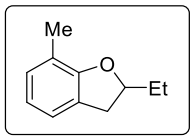

3ad: colorless oil (68%). R_f = 0.5 (hexane/ethyl acetate = 40:1). **^{1}H NMR** (500 MHz, $CDCl_3$) δ 6.99 (d, *J* = 7.3 Hz, 1H), 6.93 (d, *J* = 7.5 Hz, 1H), 6.73 (d, *J* = 7.4 Hz, 1H), 4.76 – 4.66 (m, 1H), 3.27 (dd, *J* = 15.4, 8.9 Hz, 1H), 2.86 (dd, *J* = 15.4, 7.7 Hz, 1H), 2.21 (s, 3H), 1.86 (dp, *J* = 14.3, 7.3 Hz, 1H), 1.71 (ddd, *J* = 13.9, 7.6, 6.5 Hz, 1H), 1.03 (t, *J* = 7.4 Hz, 3H). **^{13}C NMR** (126 MHz, $CDCl_3$) δ 158.23, 129.20, 126.29, 122.36, 120.00, 119.54, 84.19, 35.47, 29.17, 15.40, 9.72. **IR**

(KBr): υ 2960, 2924, 2853, 1464, 1378, 1195, 924, 757 cm^{-1}. **HRMS** (ESI): Calculated for $C_{11}H_{15}O$ ($M+H^+$): 163.1117, found: 163.1126.

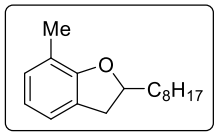

3ae: colorless oil (66%). R_f = 0.6 (hexane/ethyl acetate = 40:1). **^{1}H NMR** (500 MHz, $CDCl_3$) δ 6.99 (d, *J* = 7.3 Hz, 1H), 6.92 (d, *J* = 7.5 Hz, 1H), 6.73 (t, *J* = 7.4 Hz, 1H), 4.75 (tt, *J* = 8.7, 6.8 Hz, 1H), 3.27 (dd, *J* = 15.4, 8.9 Hz, 1H), 2.85 (dd, *J* = 15.4, 7.8 Hz, 1H), 2.21 (s, 3H), 1.84 (dddd, *J* = 13.5, 10.2, 6.9, 5.3 Hz, 1H), 1.65 (tdd, *J* = 11.6, 8.2, 5.5 Hz, 1H), 1.53 – 1.47 (m, 1H), 1.45 – 1.39 (m, 1H), 1.37 – 1.25 (m, 10H), 0.89 (t, *J* = 6.9 Hz, 3H). **^{13}C NMR** (126 MHz, $CDCl_3$) δ 158.20, 129.20, 126.33, 122.36, 119.99, 119.57, 83.12, 36.32, 35.96, 32.03, 29.73, 29.68, 29.41, 25.58, 22.83, 15.40, 14.25. **IR** (KBr): υ 3025, 2926, 2855, 1599, 1486, 1260, 1196, 758 cm^{-1}. **HRMS** (ESI): Calculated for $C_{17}H_{27}O$ ($M+H^+$): 247.2056, found: 247.2062.

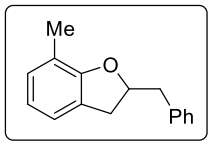

3af: pale yellow oil (82%). R_f = 0.4 (hexane/ethyl acetate = 40:1). **^{1}H NMR** (500 MHz, $CDCl_3$) δ 7.43 – 7.30 (m, 5H), 7.04 (dd, *J* = 16.6, 7.4 Hz, 2H), 6.83 (t, *J* = 7.4 Hz, 1H), 5.06 (dq, *J* = 9.2, 6.9 Hz, 1H), 3.33 – 3.16 (m, 2H), 3.00 (ddd, *J* = 24.1, 14.4, 6.9 Hz, 2H), 2.31 (s, 3H). **^{13}C NMR** (126 MHz, $CDCl_3$) δ 157.91, 137.72, 129.59, 129.30, 128.59, 126.66, 125.93, 122.44, 120.27, 119.74,

83.22, 42.25, 35.36, 15.42. **IR** (KBr): υ 3027, 2917, 2854, 1598, 1467, 1454, 1260, 1194, 1072, 980, 756, 699 cm^{-1}. **HRMS** (ESI): Calculated for $C_{16}H_{17}O$ ($M+H^+$): 225.1274, found: 225.1280.

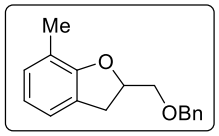

3ag: Colorless oil (90%). R_f = 0.2 (hexane/ethyl acetate = 40:1). **^{1}H NMR** (500 MHz, $CDCl_3$) δ 7.36 (d, *J* = 4.3 Hz, 4H), 7.33 – 7.27 (m, 1H), 7.00 (d, *J* = 7.3 Hz, 1H), 6.94 (d, *J* = 7.0 Hz, 1H), 6.76 (t, *J* = 7.5 Hz, 1H), 5.02 – 4.93 (m, 1H), 4.64 (q, *J* = 12.2 Hz, 2H), 3.72 (dd, *J* = 10.4, 6.3 Hz, 1H), 3.63 (dd, *J* = 10.3, 4.7 Hz, 1H), 3.28 (dd, *J* = 15.6, 9.4 Hz, 1H), 3.02 (dd, *J* = 15.5, 7.4 Hz, 1H), 2.24 (s, 3H). **^{13}C NMR** (126 MHz, $CDCl_3$) δ 158.07, 138.25, 129.34, 128.56, 128.54, 127.87, 127.83, 125.66, 122.41, 120.41, 120.41, 119.81, 81.31, 73.62, 72.34, 32.80, 15.45. **IR** (KBr): υ 3027, 2918, 2857, 1598, 1467, 1453, 1260, 1194, 1118, 759, 698 cm^{-1}. **HRMS** (ESI): Calculated for $C_{17}H_{19}O_2$ ($M+H^+$): 255.1380, found: 255.1371.

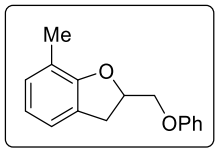

3ah: White solide (90%). R_f = 0.3 (hexane/ethyl acetate = 40:1). Mp = 77.8 – 78.6 °C. ^{1}H NMR (400 MHz, $CDCl_3$) δ 7.35 – 7.25 (m, 2H), 7.04 (ddd, *J* = 7.3, 1.4, 0.7 Hz, 1H), 7.03 – 6.91 (m, 4H), 6.79 (t, *J* = 7.4 Hz, 1H), 5.15 (dddd, *J* = 9.4, 7.0, 5.9, 5.3 Hz, 1H), 4.24 (dd, *J* = 9.9, 5.9 Hz, 1H), 4.10 (dd, *J* = 9.9, 5.3 Hz, 1H), 3.40 (dd, *J* = 15.7, 9.4 Hz, 1H), 3.17 (dd, *J* = 15.7, 7.1 Hz, 1H), 2.23

(s, 3H). **^{13}C NMR** (101 MHz, $CDCl_3$) δ 158.84, 157.92, 129.60, 129.47, 125.39, 122.47, 121.24, 120.63, 119.96, 114.84, 80.22, 69.90, 32.92, 15.44. **IR** (KBr): υ 3040, 2920, 2857, 1599, 1497, 1468, 1243, 1193, 1050, 754, 691 cm^{-1}. **HRMS** (ESI): Calculated for $C_{16}H_{17}O_2$ ($M+H^+$): 241.1223, found: 241.1221.

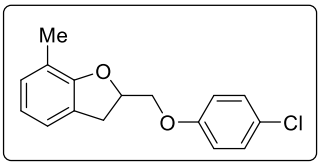

3ai: White solide (84%). R_f = 0.3 (hexane/ethyl acetate = 40:1). Mp = 78.2 – 79.6 ^oC **^{1}H NMR** (400 MHz, $CDCl_3$) δ 7.27 – 7.25 (m, 1H), 7.24 (d, *J* = 2.3 Hz, 1H), 7.05 (d, *J* = 7.3 Hz, 1H), 6.97 (ddd, *J* = 7.5, 1.5, 0.7 Hz, 1H), 6.89 (d, *J* = 2.3 Hz, 1H), 6.87 (d, *J* = 2.2 Hz, 1H), 6.80 (t, *J* = 7.4 Hz, 1H), 5.13 (dddd, *J* = 9.4, 7.0, 5.9, 5.0 Hz, 1H), 4.19 (dd, *J* = 9.9, 5.9 Hz, 1H), 4.08 (dd, *J* = 10.0, 5.0 Hz, 1H), 3.39 (dd, *J* = 15.7, 9.5 Hz, 1H), 3.15 (dd, *J* = 15.7, 7.0 Hz, 1H), 2.23 (s, 3H). **^{13}C NMR** (101 MHz, $CDCl_3$) δ 157.83, 157.48, 129.52, 129.44, 126.12, 125.25, 122.45, 120.71, 119.95, 116.16, 80.08, 70.31, 32.79, 15.41. **IR** (KBr): υ 3044, 2920, 2858, 1597, 1492, 1469, 1243, 1193, 824. 762 cm^{-1}. **HRMS** (ESI): Calculated for $C_{16}H_{16}O_2Cl$ ($M+H^+$): 275.0833, found: 275.0825.

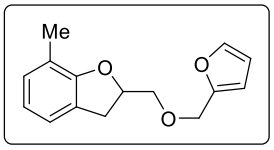

3aj: Yellow oil (73%). R_f = 0.2 (hexane/ethyl acetate = 40:1). **^{1}H NMR** (400 MHz, $CDCl_3$) δ 7.43 (dd, *J* = 1.8, 0.9 Hz, 1H), 7.00 (d, *J* = 7.0 Hz, 1H), 6.94 (ddq, *J* = 7.5, 1.5, 0.8 Hz, 1H), 6.76 (t, *J* = 7.4 Hz, 1H), 6.38 – 6.32 (m, 2H), 4.94 (dddd, *J* = 9.4, 7.5, 6.3, 4.8 Hz, 1H), 4.65 – 4.52 (m, 2H), 3.73 (dd, *J* = 10.4, 6.3 Hz, 1H), 3.64 (dd, *J* = 10.4, 4.8 Hz, 1H), 3.26 (dd, *J* = 15.6, 9.4 Hz, 1H), 3.00 (dd, *J* = 15.6, 7.5 Hz, 1H), 2.23 (d, *J* = 0.6 Hz, 3H). **^{13}C NMR** (101 MHz, $CDCl_3$) δ 157.98, 151.69, 142.97, 129.32, 125.59, 122.41, 120.41, 119.81, 110.40, 109.65, 81.22, 72.07, 65.40, 32.75, 15.45. **IR** (KBr): υ 3119, 3049, 2919, 2857, 1599, 1468, 1261, 1194, 1151, 1073. 920, 758, 600 cm^{-1}. **HRMS** (ESI): Calculated for $C_{15}H_{17}O_3$ ($M+H^+$): 245.1172, found: 245.1174.

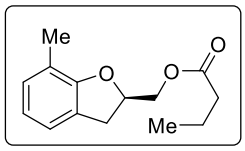

3ak: Yellow oil (46%). R_f = 0.2 (hexane/ethyl acetate = 40:1). **^{1}H NMR** (400 MHz, $CDCl_3$) δ 7.00 (d, *J* = 7.3 Hz, 1H), 6.94 (d, *J* = 7.0 Hz, 1H), 6.76 (t, *J* = 7.4 Hz, 1H), 5.02 – 4.92 (m, 1H), 4.34 – 4.21 (m, 2H), 3.31 (dd, *J* = 15.6, 9.5 Hz, 1H), 2.99 (dd, *J* = 15.6, 7.2 Hz, 1H), 2.32 (t, *J* = 7.4 Hz, 2H), 2.21 (s, 3H), 1.64 (q, *J* = 7.4 Hz, 2H), 0.94 (t, *J* = 7.4 Hz, 3H). **^{13}C NMR** (101 MHz, $CDCl_3$) δ 173.68, 157.82, 129.50, 125.19, 122.33, 120.62, 119.92, 79.67, 65.81, 36.17, 32.58, 18.53, 15.35, 13.75. **IR** (KBr): υ 3024, 2955, 2876, 1738, 1599, 1468, 1260, 1175, 761 cm^{-1}. **HRMS** (ESI): Calculated for $C_{14}H_{19}O_3$ ($M+H^+$): 235.1329, found: 235.1327.

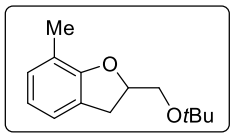

3al: Pale yellow oil (85%). R_f = 0.2 (hexane/ethyl acetate = 40:1). **^{1}H NMR** (400 MHz, $CDCl_3$) δ 7.01 (d, *J* = 7.3 Hz, 1H), 6.94 (ddd, *J* = 7.5, 1.4, 0.7 Hz, 1H), 6.76 (t, *J* = 7.4 Hz, 1H), 4.87 (ddt, *J* = 9.3, 6.8, 6.1 Hz, 1H), 3.66 (dd, *J* = 9.4, 6.1 Hz, 1H), 3.44 (dd, *J* = 9.4, 6.2 Hz, 1H), 3.29 (dd, *J* = 15.7, 9.3 Hz, 1H), 3.01 (dd, *J* = 15.8, 6.8 Hz, 1H), 2.22 (s, 3H), 1.23 (s, 9H). **^{13}C NMR** (101 MHz, $CDCl_3$) δ 158.09, 129.22, 125.82, 122.47, 120.25, 119.72, 81.46, 73.42, 64.54, 33.19, 27.65, 15.44. **IR** (KBr): υ 3025, 2974, 2921, 2868, 1599, 1466, 1363, 1192, 1093, 986, 759 cm^{-1}. **HRMS** (ESI): Calculated for $C_{14}H_{21}O_2$ ($M+H^+$): 221.1536, found: 221.1539.

2.4.5 Large Scale Reaction

Scheme 2.7. Gram-Scale Preparation of 3aa and 3ja

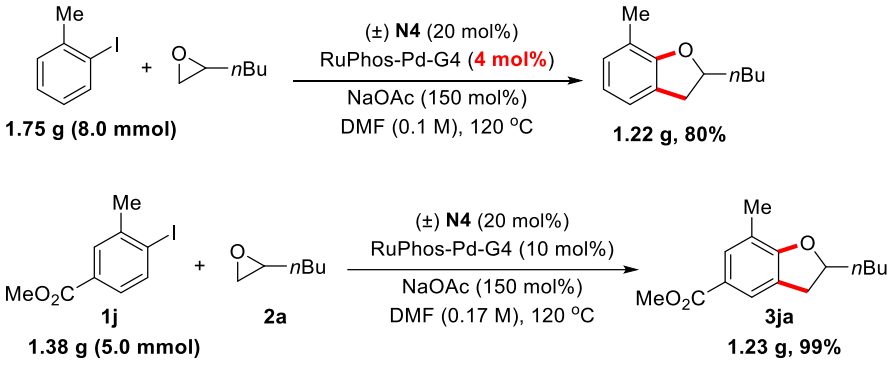

A flame-dried 150 mL flask was charged with RuPhos-Pd-G4 (273 mg, 0.32 mmol, 4 mol%), aryl iodide **1a** (1.74 g, 8.0 mmol, 1.0 equiv) and NaOAc (984 mg, 12.0 mmol, 1.5 equiv). Then the flask was directly transferred into a nitrogen-filled glovebox without caps. After NBE **N4** (288 mg, 1.6 mmol, 20 mol%) and 64 mL of degassed DMF was added to the flask, 1,2-epoxyhexane (3.2 g, 32.0 mmol, 4.0 equiv) was added. Then the flask was tightly sealed, transferred out of glovebox and stirred in the oil bath preheated to 120 °C for 24 hours. After completion of the reaction, the

mixture was filtered through a thin pad of celite. The filter cake was washed with dichloromethane and diethyl ether, and the combined filtrate was concentrated. The residue was loaded to a small amount of silica gel and then purified by flash column chromatography on silica gel to give the desired product **3aa** (1.22g, 80%).

A flame-dried 150 mL flask was charged with RuPhos-Pd-G4 (427 mg, 0.5 mmol, 10 mol%), aryl iodide **1j** (1.38 g, 5.0 mmol, 1.0 equiv) and NaOAc (615 mg, 7.5 mmol, 1.5 equiv). Then the flask was directly transferred into a nitrogen-filled glovebox without caps. After NBE **N4** (180 mg, 1.0 mmol, 20 mol%) and 30 mL of degassed DMF was added to the flask, 1,2-epoxyhexane **2a** (2.0 g, 20.0 mmol, 4.0 equiv) was added. Then the flask was tightly sealed, transferred out of glovebox and stirred in the oil bath preheated to 120 ^{o}C for 24 hours. After completion of the reaction, the mixture was filtered through a thin pad of celite. The filter cake was washed with dichloromethane and diethyl ether, and the combined filtrate was concentrated. The residue was loaded to a small amount of silica gel and then purified by flash column chromatography on silica gel to give the desired product **3ja** (1.23g, 99%).

2.4.6 Direct Annulation with Chiral Epoxide (S)-2h

Scheme 2.8. Direct Annulation with Chiral Epoxide (S)-2h

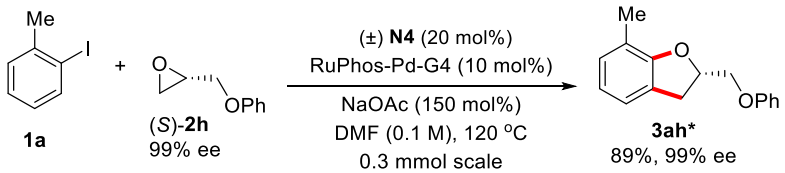

A flame-dried 4 mL vial was charged with RuPhos-Pd-G4 (25.6 mg, 0.03 mmol, 10 mol%), aryl iodide **1a** (65.4 mg, 0.3 mmol, 1.0 equiv), epoxide (*S*)-**2h** (180 mg, 1.2 mmol, 4.0 equiv) and NaOAc (36.9 mg, 0.45 mmol, 1.5 equiv). Then the vial was directly transferred into a nitrogen-filled glovebox without caps. After NBE **N4** (10.8 mg, 0.06 mmol, 20 mol%) and 3 mL degassed DMF was added, the flask was tightly sealed, transferred out of glovebox and stirred on a pie-block preheated to 120 ^{o}C for 24 hours. After completion of the reaction, the mixture was filtered through a thin pad of celite. The filter cake was washed with dichloromethane and diethyl ether, and the combined filtrate was concentrated. The residue was loaded to a small amount of silica gel and then purified by flash column chromatography on silica gel to give the desired product **3ah*** in 89% yield with 99% ee.

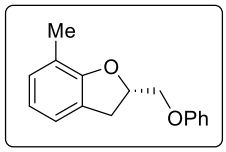

Chiral HPLC (Chiralpak OD-H, hexane/isopropanol = 95:5, 0.5 mL/min, 260 nm): t_{minor} = 18.037, t_{major} = 25.037. $[\alpha]_D$ = 36.2 (c=1.52, dichloromethane, 22.5 ^{o}C) at 99% ee.

Figure 2.3. HPLC of Racemic 3ah

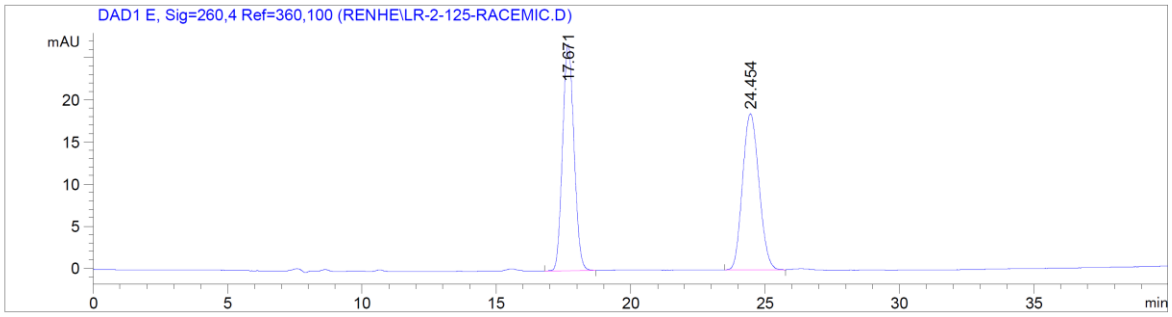

Figure 2.3. HPLC of Racemic 3ah (continued)

Signal 5: DAD1 E, Sig=260,4 Ref=360,100

Peak #	RetTime [min]	Type	Width [min]	Area [mAU*s]	Height [mAU]	Area %
1	17.671	BB	0.4647	793.81140	26.86917	50.1011
2	24.454	BB	0.6778	790.60815	18.52917	49.8989
Totals :				1584.41956	45.39834	

Figure 2.4. HPLC of Enantiomeric 3ah*

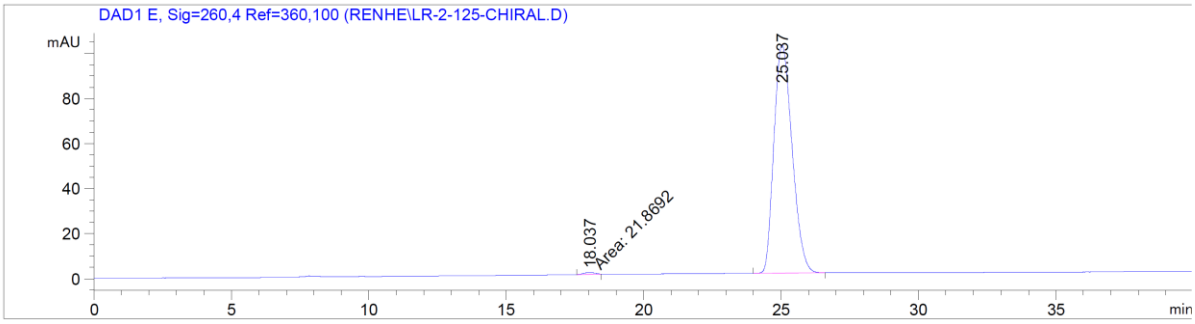

Signal 5: DAD1 E, Sig=260,4 Ref=360,100

Peak #	RetTime [min]	Type	Width [min]	Area [mAU*s]	Height [mAU]	Area %
1	18.037	MM	0.4594	21.86923	7.93394e-1	0.4659
2	25.037	BB	0.7329	4671.96484	101.52334	99.5341
Totals :				4693.83408	102.31673	

2.4.7 Synthetic Application

Scheme 2.9. Concise Synthesis of Fufenozide

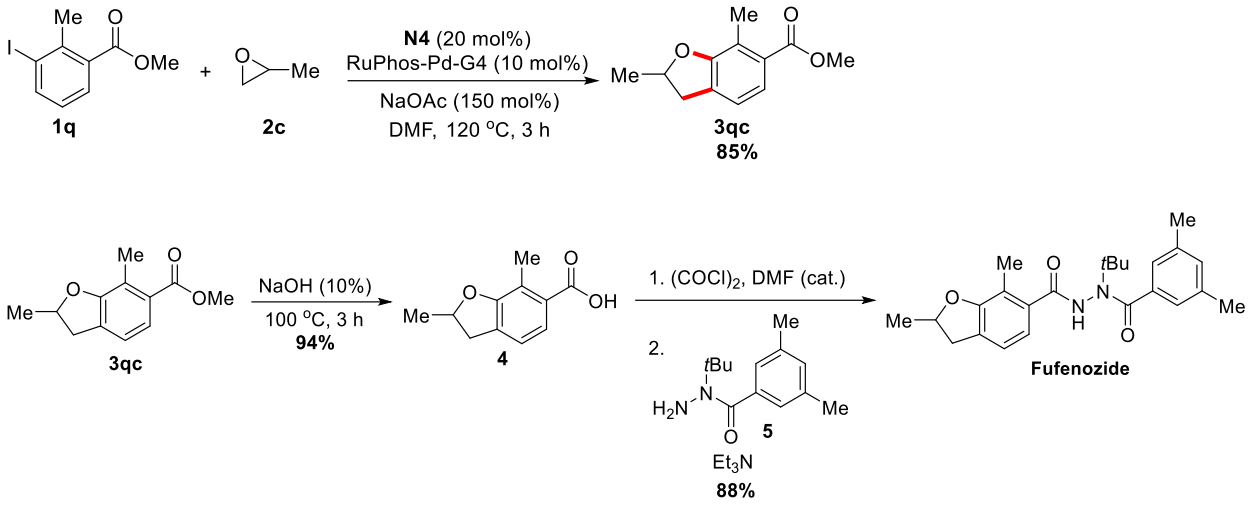

A flame-dried 40 mL vial was charged with RuPhos-Pd-G4 (256 mg, 0.3 mmol, 10 mol%), aryl iodide **1q** (828 mg, 3.0 mmol, 1.0 equiv) and NaOAc (369 mg, 4.5 mmol, 1.5 equiv). Then the vial was directly transferred into a nitrogen-filled glovebox without caps. After NBE **N4** (108 mg, 0.6 mmol, 20 mol%) and 20 mL degassed DMF was added to the flask, epoxide **2c** (696 mg, 12.0 mmol, 4.0 equiv) was added. Then the flask was tightly sealed, transferred out of glovebox and stirred on a pie-block preheated to 120 °C for 3 hours. After completion of the reaction, the mixture was filtered through a thin pad of celite. The filter cake was washed with dichloromethane and diethyl ether, and the combined filtrate was concentrated. The residue was loaded to a small amount of silica gel and then purified by flash column chromatography on silica gel to give the desired product **3qc** in 85% yield.

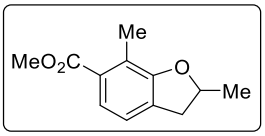

3qc: Pale yellow solid (85%). R_f = 0.5 (hexane/ethyl acetate = 20:1). Mp = 57.8 – 58.5 °C. **^{1}H NMR** (400 MHz, $CDCl_3$) δ 7.41 (d, *J* = 7.8 Hz, 1H), 7.00 (d, *J* = 7.7 Hz, 1H), 4.98 – 4.87 (m, 1H), 3.86 (s, 3H), 3.33 (dd, *J* = 16.0, 8.9 Hz, 1H), 2.84 (dd, *J* = 16.0, 8.0 Hz, 1H), 2.42 (s, 3H), 1.47 (d, *J* = 6.2 Hz, 3H). **^{13}C NMR** (101 MHz, $CDCl_3$) δ 168.30, 158.98, 130.67, 129.68, 123.12, 121.70, 121.64, 79.42, 51.86, 37.79, 21.96, 13.26. **IR** (KBr): υ 2977, 2950, 2926, 1716, 1449, 1257, 1055, 804, 768 cm^{-1}. **HRMS** (ESI): Calculated for $C_{12}H_{15}O_3$ ($M+H^+$): 207.1016, found: 207.1016. Elemental analysis [%] found (calculated for $C_{12}H_{14}O_3$): C 69.58 (69.89), H 6.93 (6.84).

Compound **3qc** (61.8 mg, 0.3 mmol) was added to a 4 mL vial charged with a stir bar. Then 1.0 mL of 10% aqueous NaOH solution was added and the reaction mixture was stirred at 100 °C for 3 h until the disappearance of **3qc** was confirmed by TLC. After the reaction was done the mixture was diluted to 10 mL with water and then washed with diethyl ether for two times. Then the aqueous layer was acidified using 1 M hydrochloric acid and extracted with dichloromethane for three times. The combined organic layers were dried over $MgSO_4$ and the solvent was removed under reduced pressure to afford the desired acid **4** (54.3 mg, 94%), which was used directly in the next step without further purification.

To a flame-dried round bottom flask #1 was added the solution of acid **4** (96.1 mg, 0.5 mmol, 1.0 equiv) and 1 drop of DMF as catalyst in dichloromethane (1.0 mL). Then oxalyl chloride (69.8 mg, 0.55 mmol, 1.1 equiv) was added dropwise at 0 °C. The reaction mixture was stirred at room temperature for another 1 h until the bubbling stopped. The excess oxalyl chloride was removed under reduced pressure. To another flame-dried round bottom flask #2 was added the known *N*-*t*-butyl-*N*-benzoylhydrazine (165 mg, 0.75 mmol, 1.5 equiv)[5], triethylamine (83.5 mg, 0.825 mmol,

1.65 equiv) and 1 mL dichloromethane. The generated acyl chloride in flask #1 was dissolved in dichloromethane and then was added dropwise to flask #2 under 0 °C. After stirring at room temperature overnight, the reaction mixture was washed successively with water and brine and then dried over $MgSO_4$. The solvent was removed under reduced pressure and the desired compound Fufenozide was isolated by silica gel chromatography.

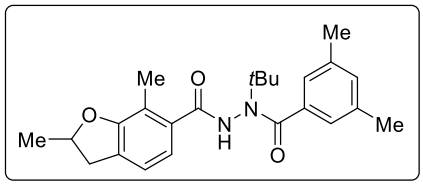

CAS: 467427-81-1

Fufenozide: White solid (88%). R_f = 0.2 (hexane/ethyl acetate = 5:1). Mp = 169.2 – 170.8 °C. **^{1}H NMR** (400 MHz, $CDCl_3$) δ 7.63 (d, *J* = 2.0 Hz, 1H), 7.03 (s, 2H), 6.96 (dd, *J* = 1.6, 0.8 Hz, 1H), 6.80 (d, *J* = 7.5 Hz, 1H), 6.13 (t, *J* = 7.7 Hz, 1H), 4.86 (ddq, *J* = 8.8, 7.6, 6.2 Hz, 1H), 3.24 (dd, *J* = 15.8, 8.9 Hz, 1H), 2.74 (dddd, *J* = 15.8, 7.8, 3.5, 1.1 Hz, 1H), 2.24 (dd, *J* = 1.7, 0.7 Hz, 6H), 1.90 (d, *J* = 5.2 Hz, 3H), 1.57 (s, 9H), 1.41 (dd, *J* = 6.2, 1.4 Hz, 3H). **^{13}C NMR** (101 MHz, $CDCl_3$) δ 173.90, 168.15, 158.76 (d, *J* = 3.6 Hz), 137.99 (d, *J* = 1.1 Hz), 137.72, 133.45 (d, *J* = 1.5 Hz), 131.08, 129.11 (d, *J* = 4.7 Hz), 124.13, 121.86 (d, *J* = 1.2 Hz), 118.75 (d, *J* = 1.3 Hz), 118.51, 79.57 (d, *J* = 3.9 Hz), 61.35, 37.46 (d, *J* = 2.3 Hz), 27.98, 21.92 (d, *J* = 2.2 Hz), 21.27, 11.74 (d, *J* = 2.4 Hz). **IR** (KBr): υ 3241, 2977, 2916, 2850, 1634, 1601, 1363, 1274, 855, 736 cm^{-1}. **HRMS** (ESI): Calculated for $C_{24}H_{31}N_2O_3$ ($M+H^+$): 395.2329, found: 395.2331. Elemental analysis [%] found (calculated for $C_{24}H_{30}N_2O_3$): C 72.58 (73.07), H 7.58 (7.67), N 6.95 (7.10). ^{1}H NMR matches the literature reported data.[27]

2.5 NMR Spectra

Figure 2.5 ^{1}H NMR Spectrum of 1k

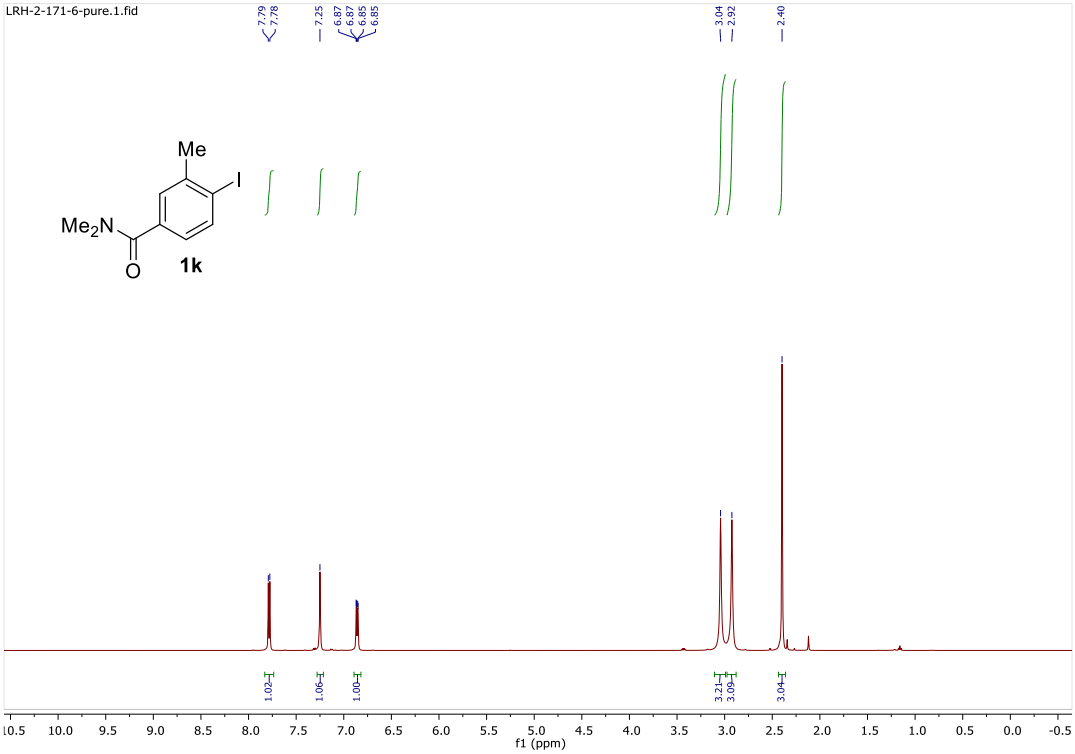

Figure 2.6 ^{13}C NMR Spectrum of 1k

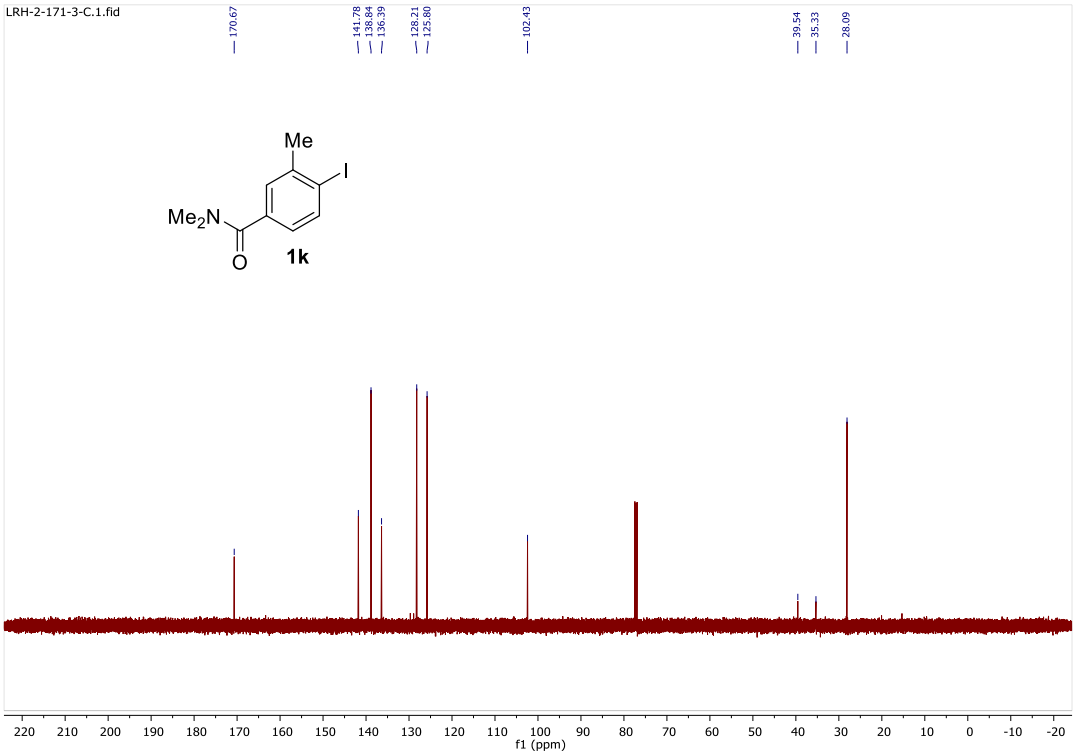

Figure 2.7 ^{1}H NMR Spectrum of N3

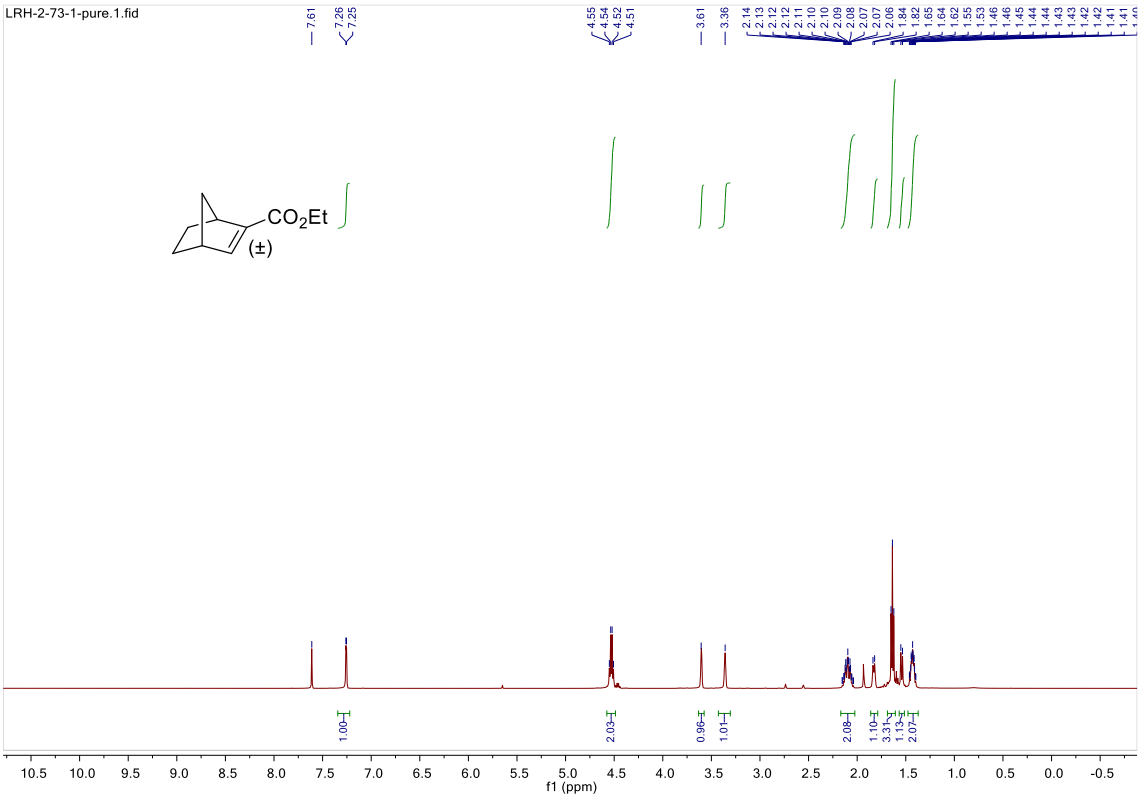

Figure 2.8 ^{13}C NMR Spectrum of N3

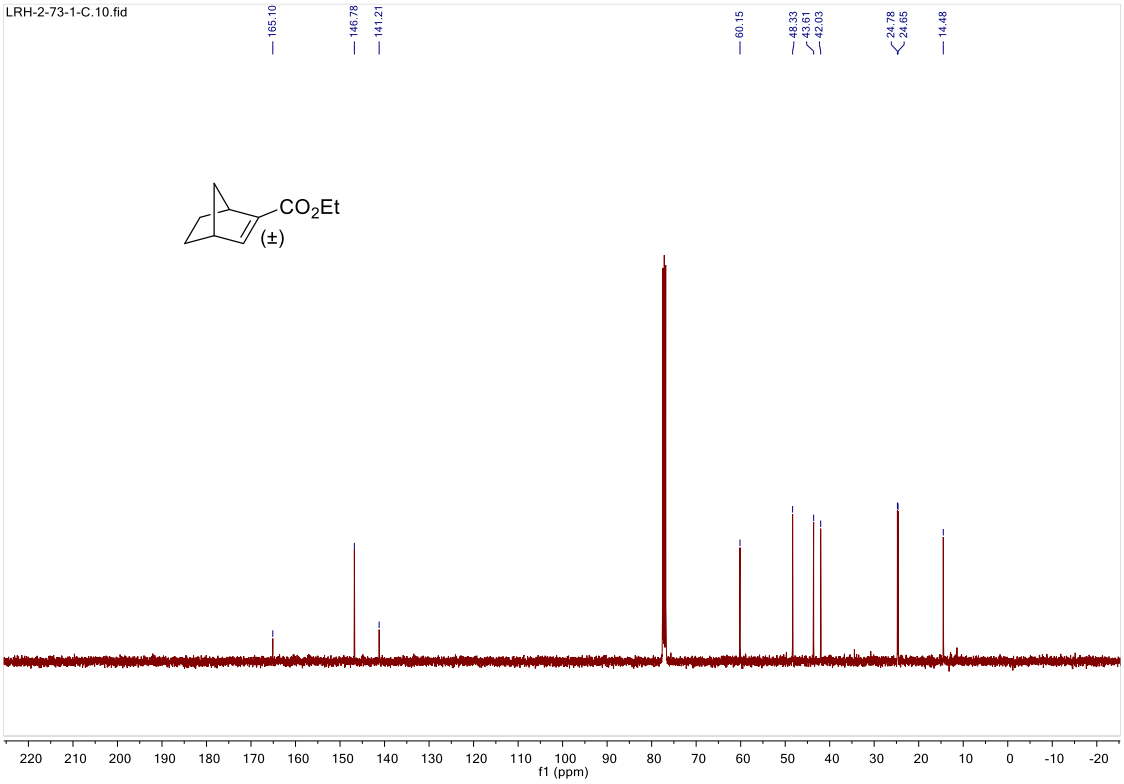

Figure 2.9 ^{1}H NMR Spectrum of N4

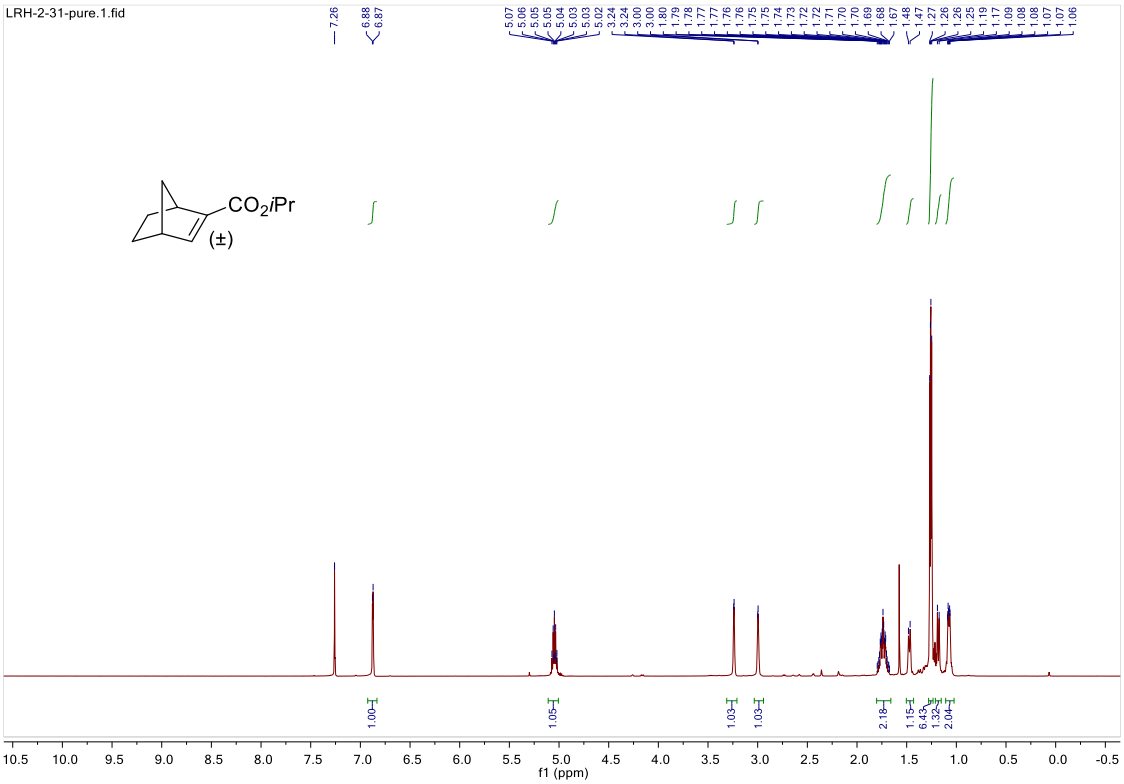

Figure 2.10 ^{13}C NMR Spectrum of N4

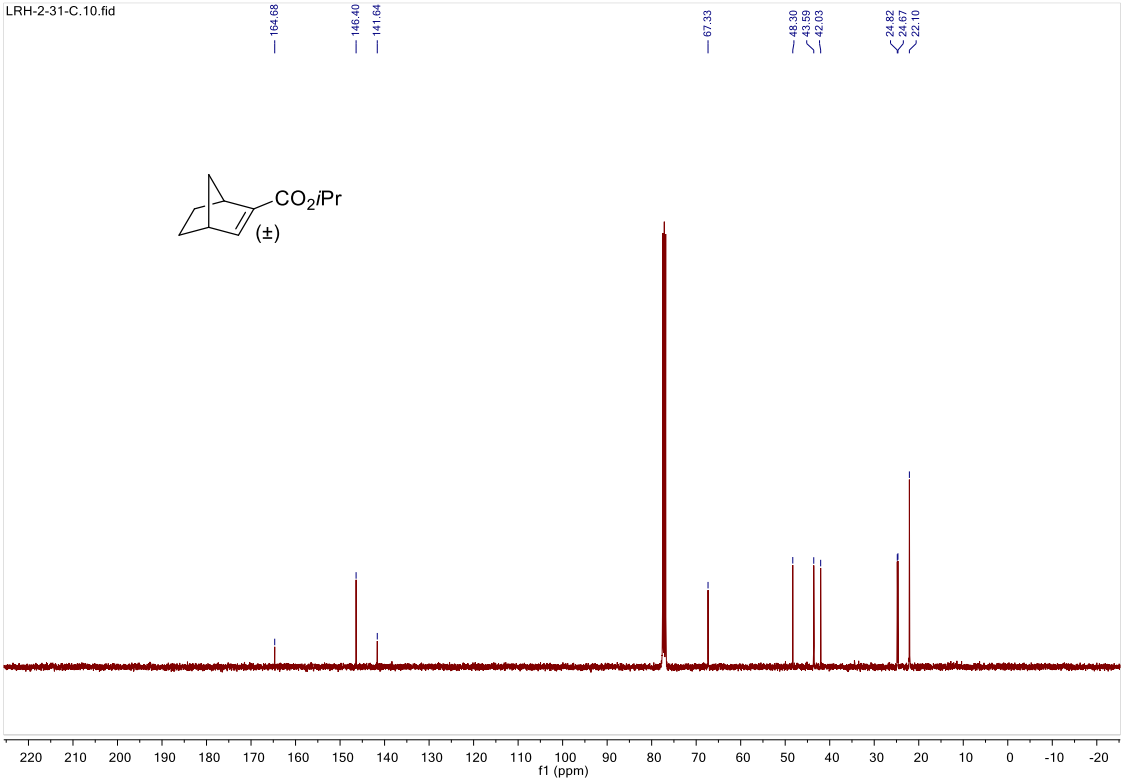

Figure 2.11 ^{1}H NMR Spectrum of N5

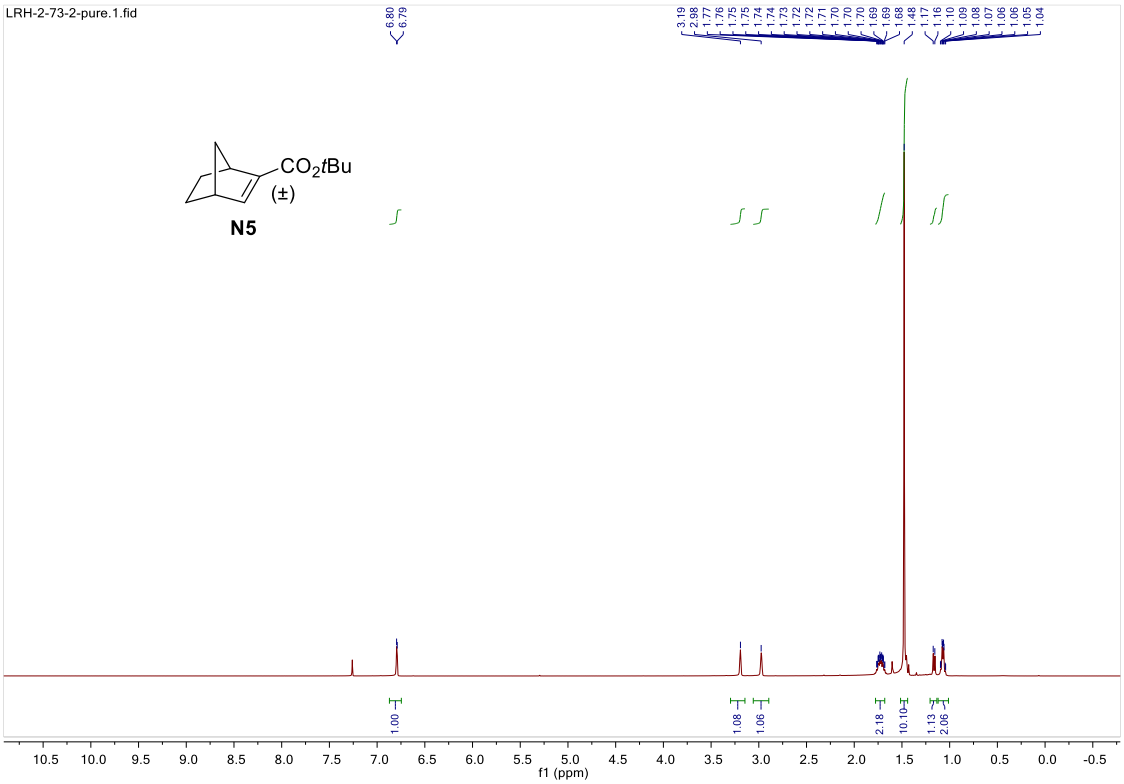

Figure 2.12 ^{13}C NMR Spectrum of N5

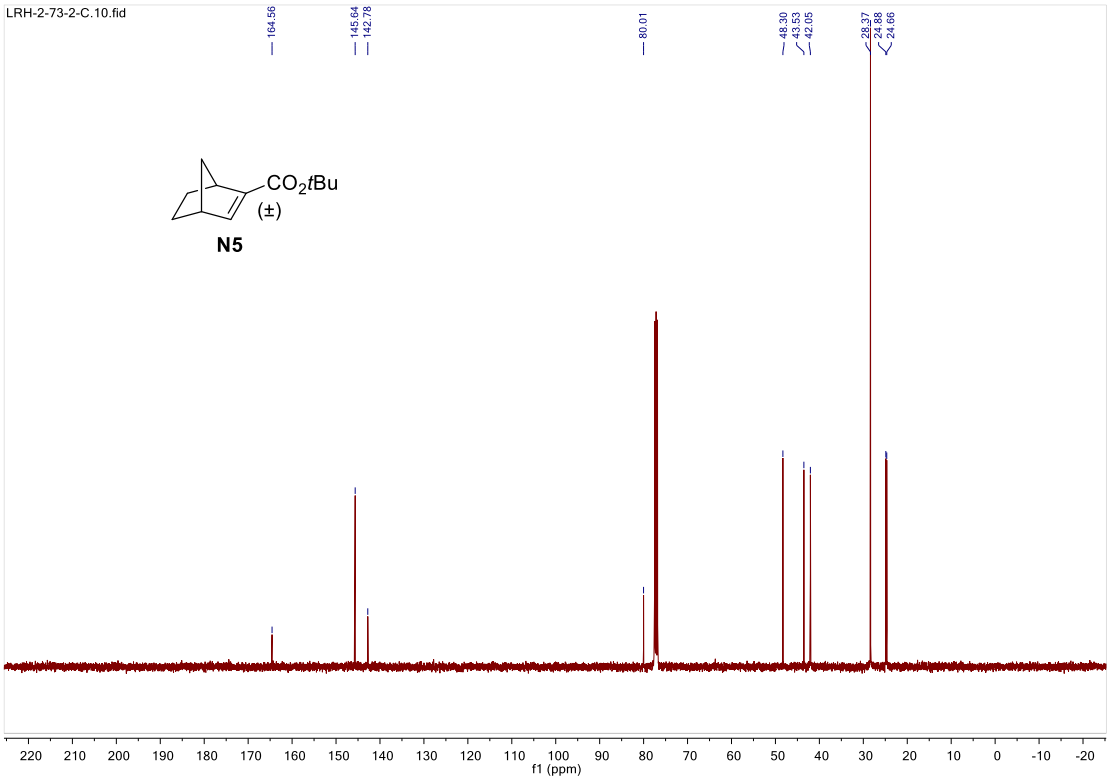

Figure 2.13 ^{1}H NMR Spectrum of 3aa

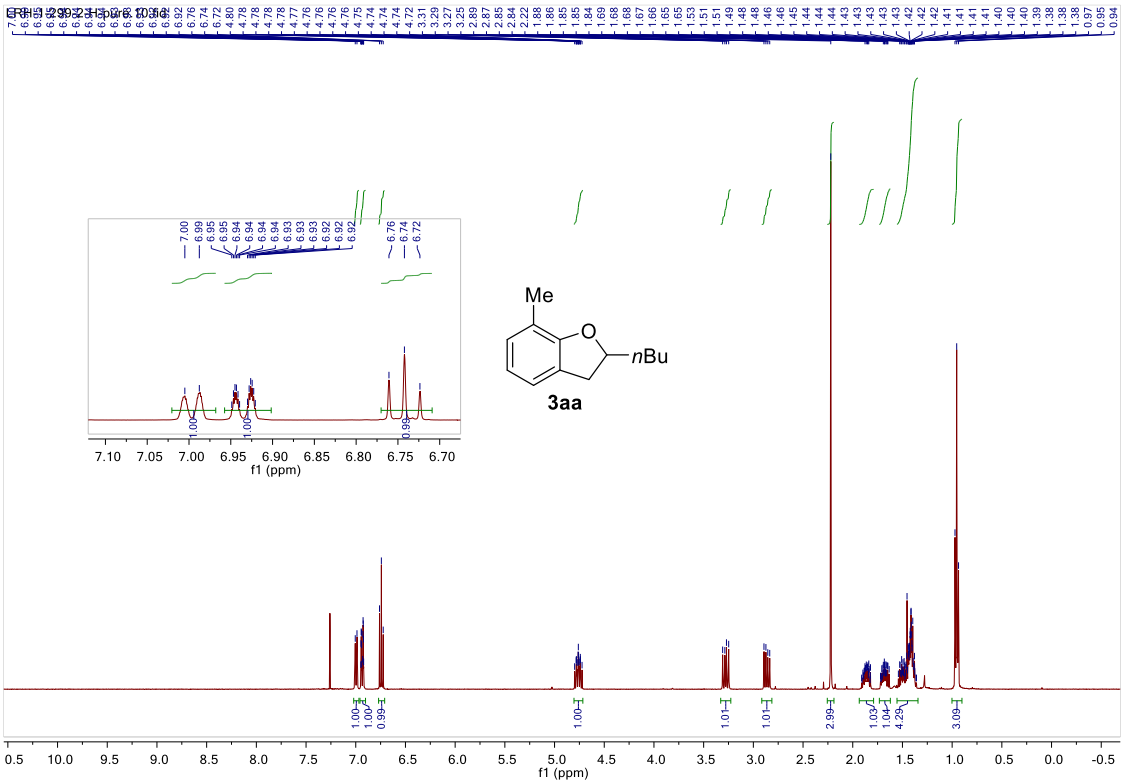

Figure 2.14 ^{13}C NMR Spectrum of 3aa

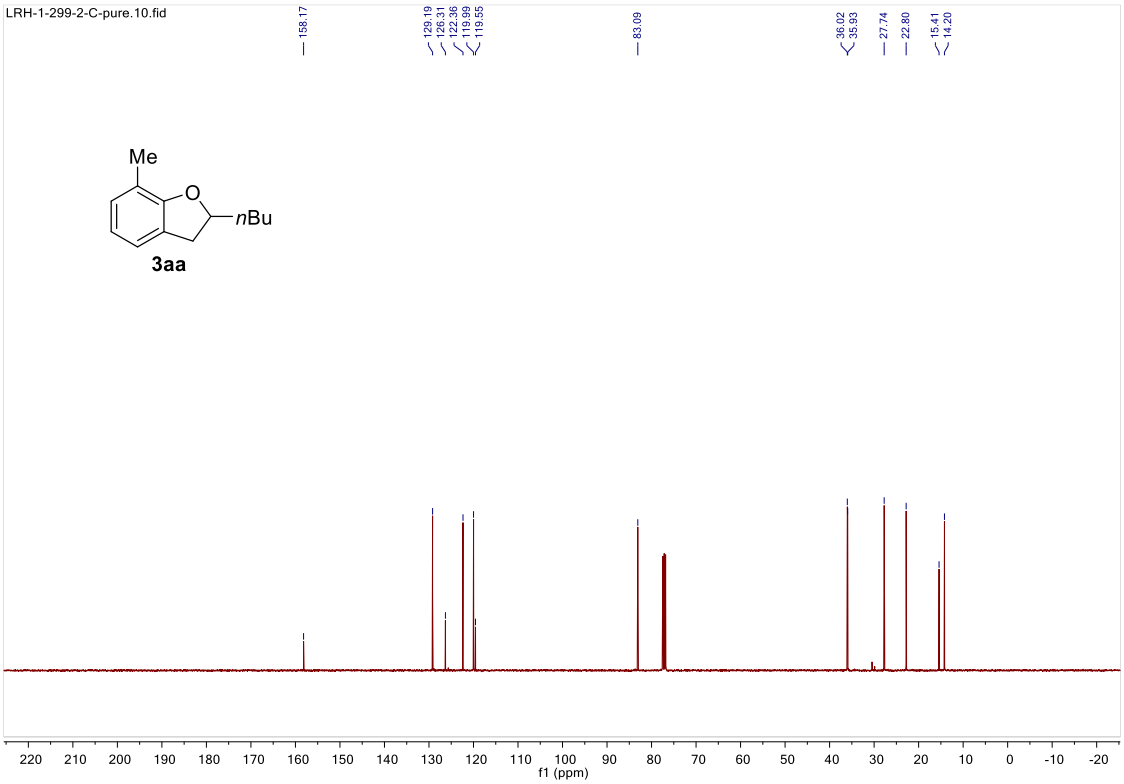

Figure 2.15 ^{1}H NMR Spectrum of 3ba

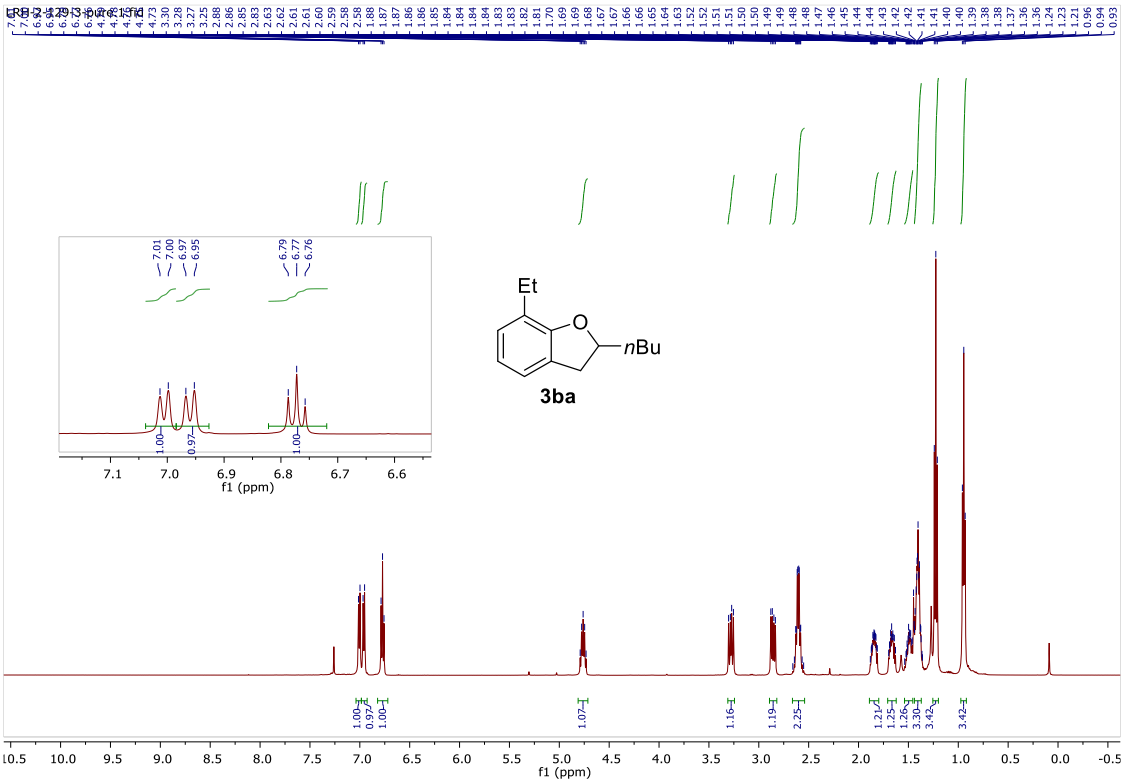

Figure 2.16 ^{13}C NMR Spectrum of 3ba

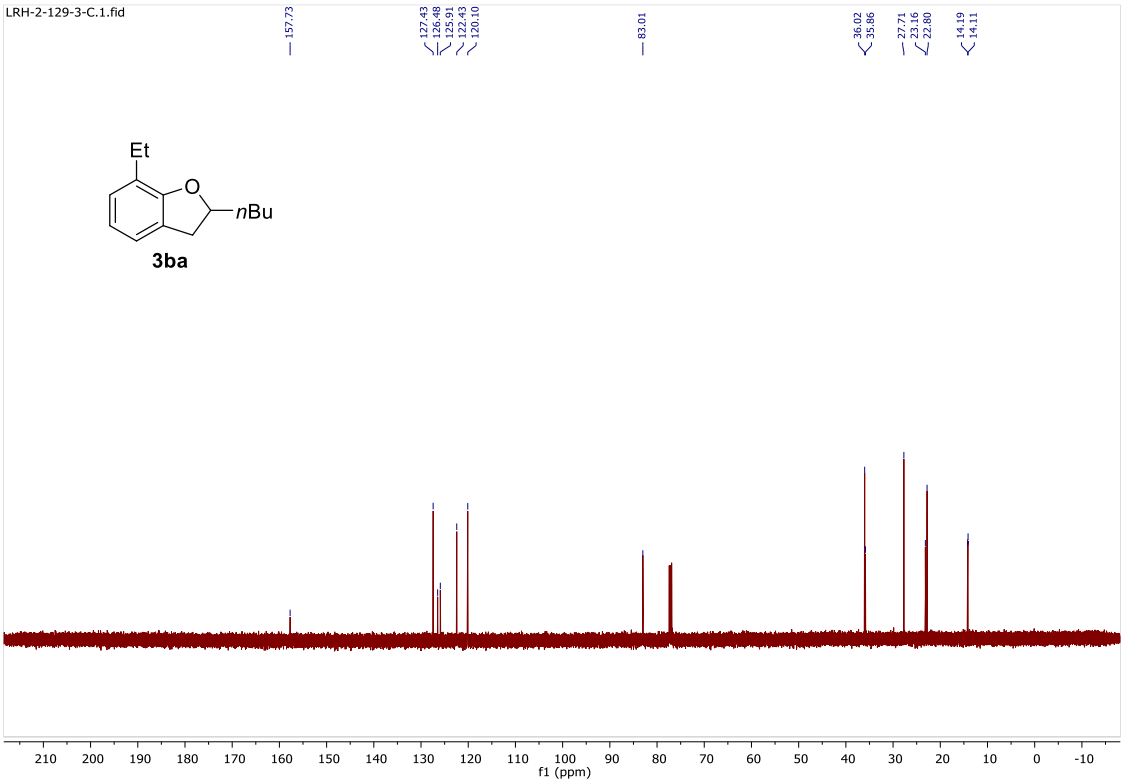

Figure 2.17 ^{1}H NMR Spectrum of 3ca

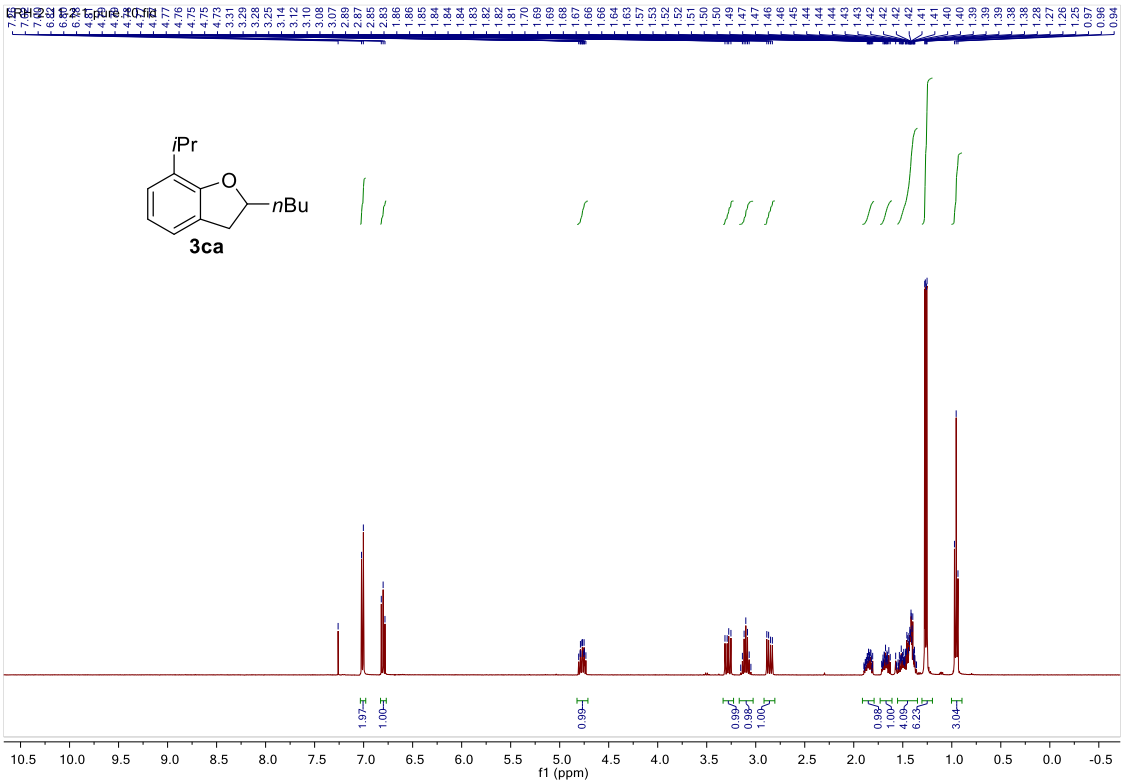

Figure 2.18 ^{13}C NMR Spectrum of 3ca

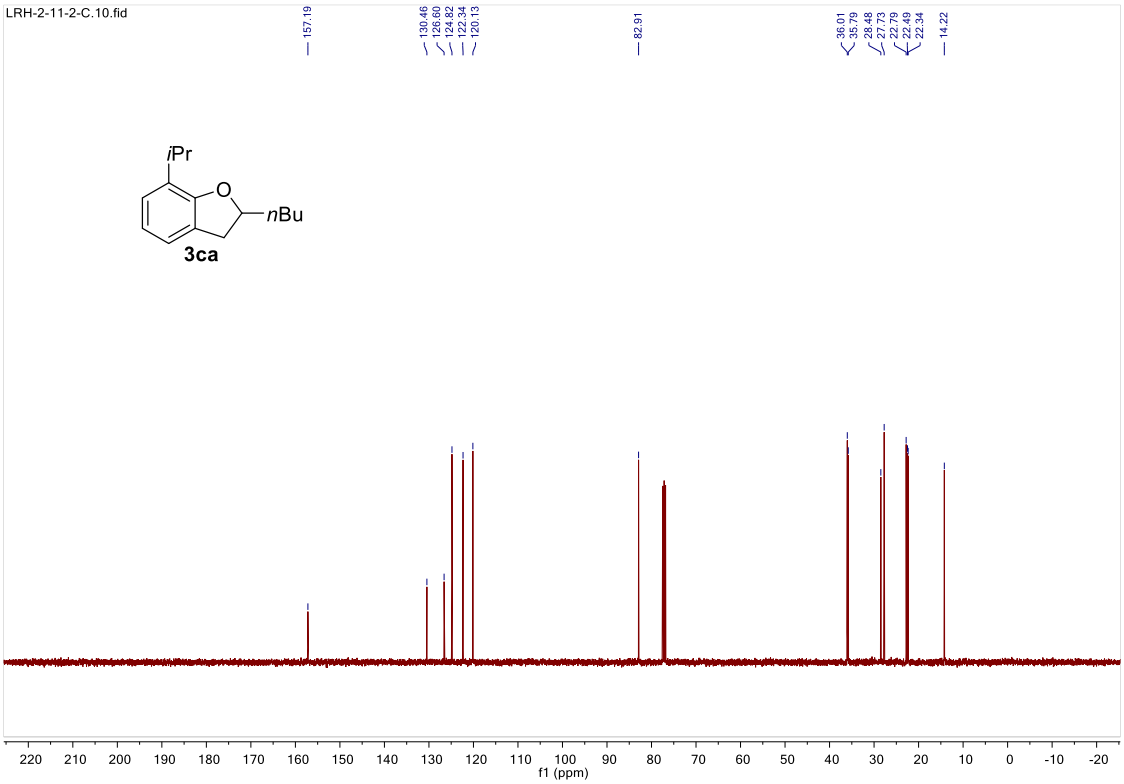

Figure 2.19 ^{1}H NMR Spectrum of 3da

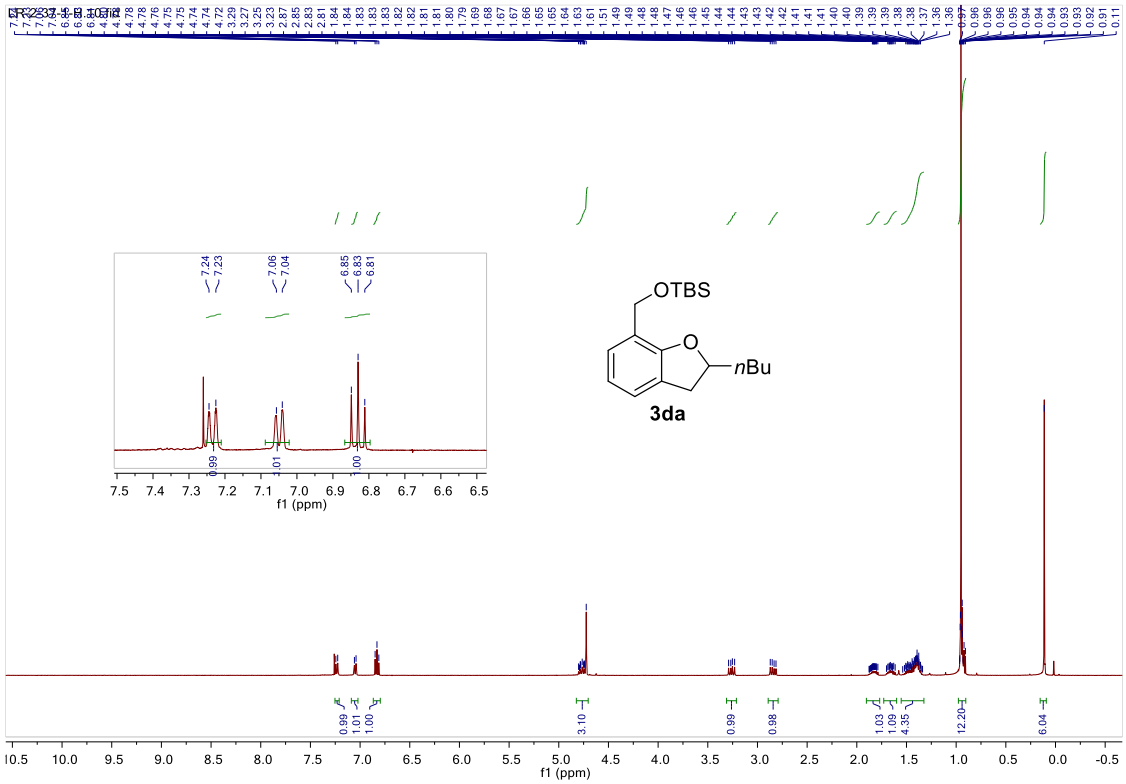

Figure 2.20 ^{13}C NMR Spectrum of 3da

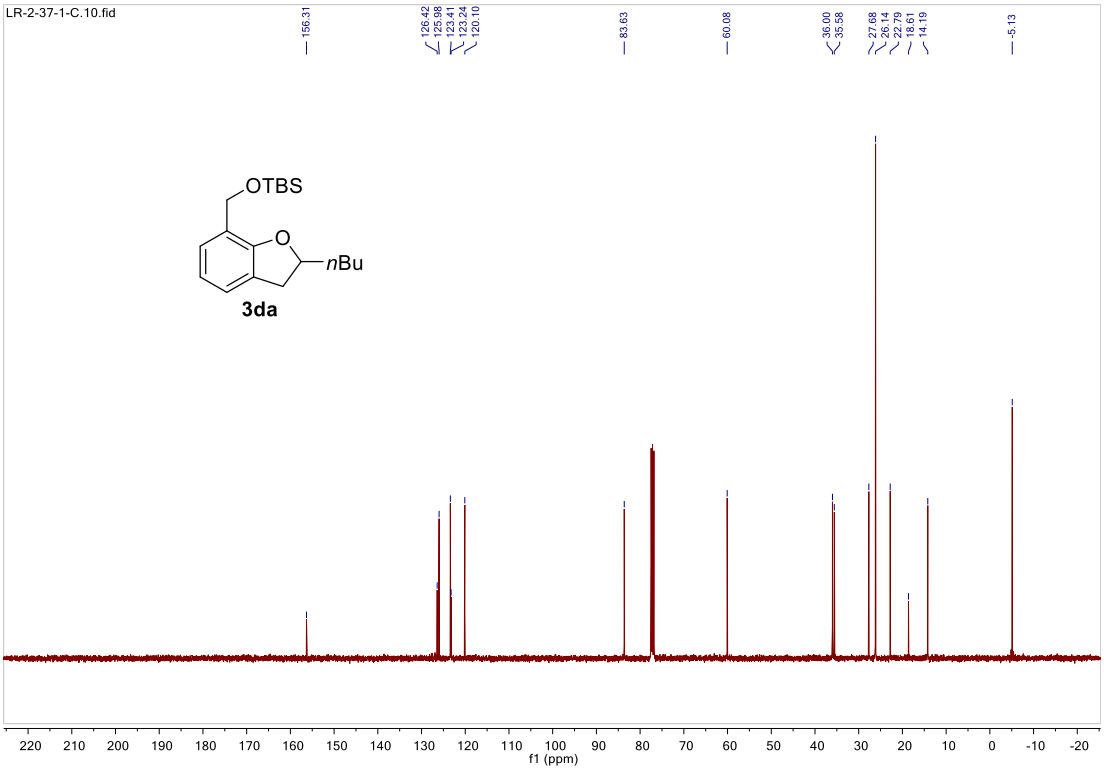

Figure 2.21 ^{1}H NMR Spectrum of 3ea

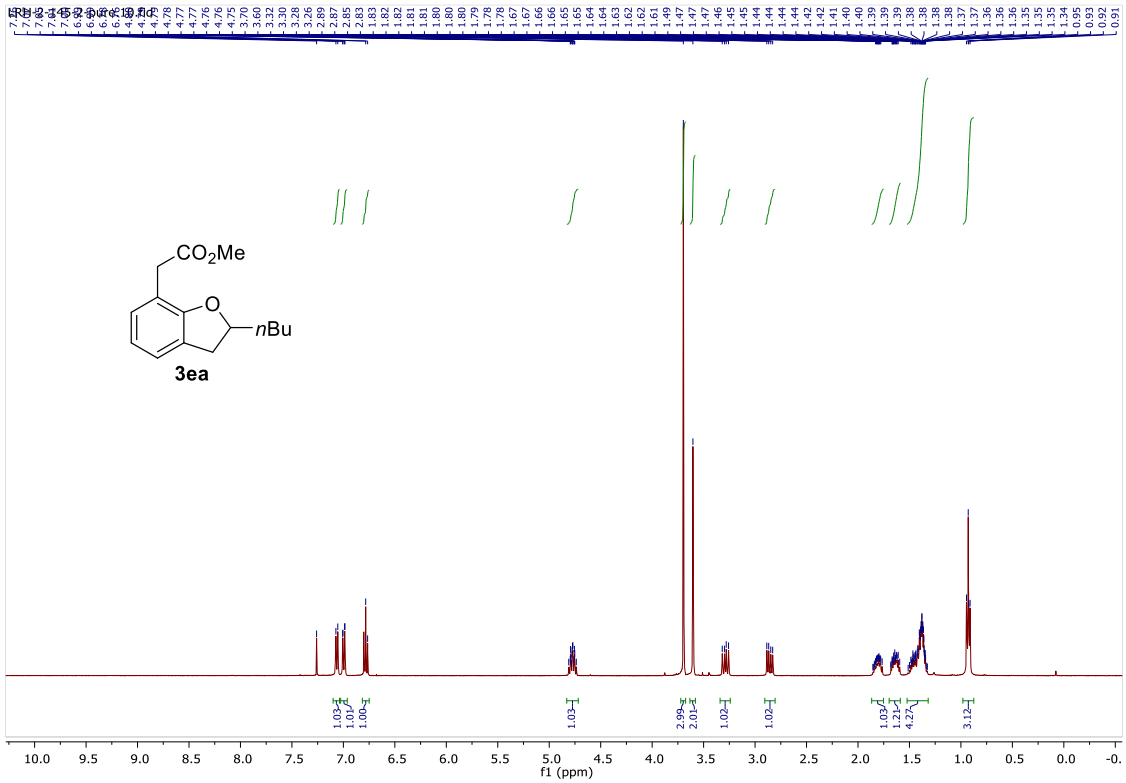

Figure 2.22 ^{13}C NMR Spectrum of 3ea

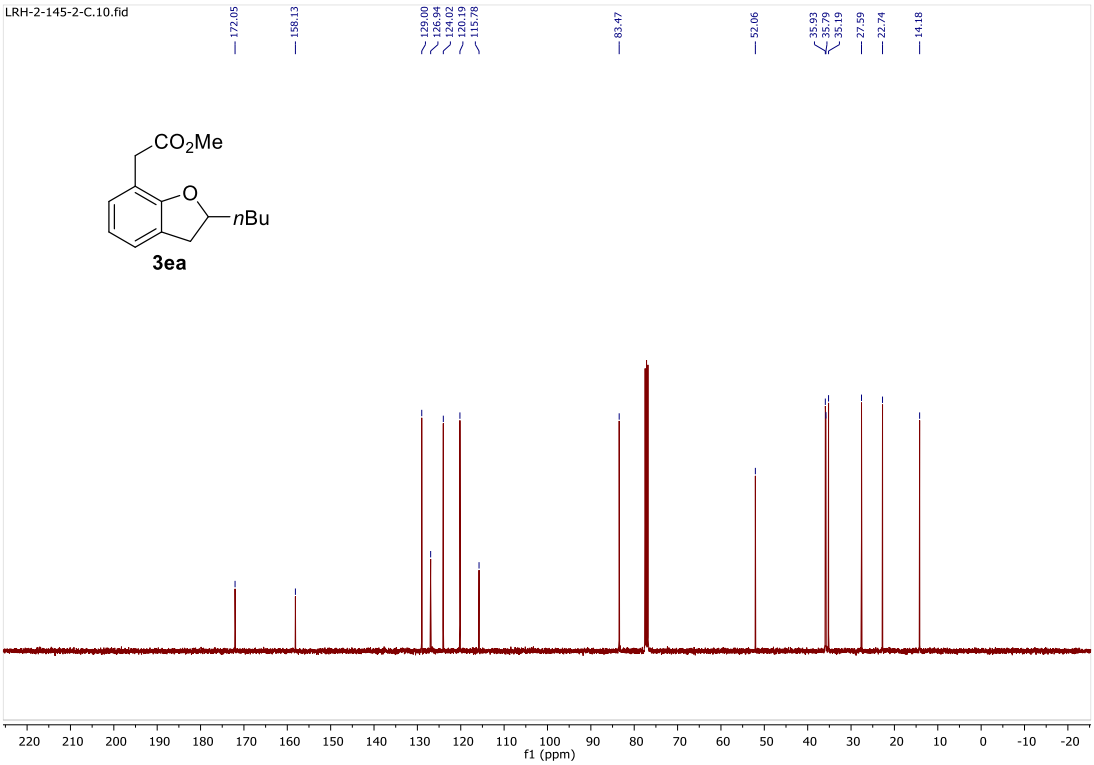

Figure 2.23 ^{1}H NMR Spectrum of 3fa

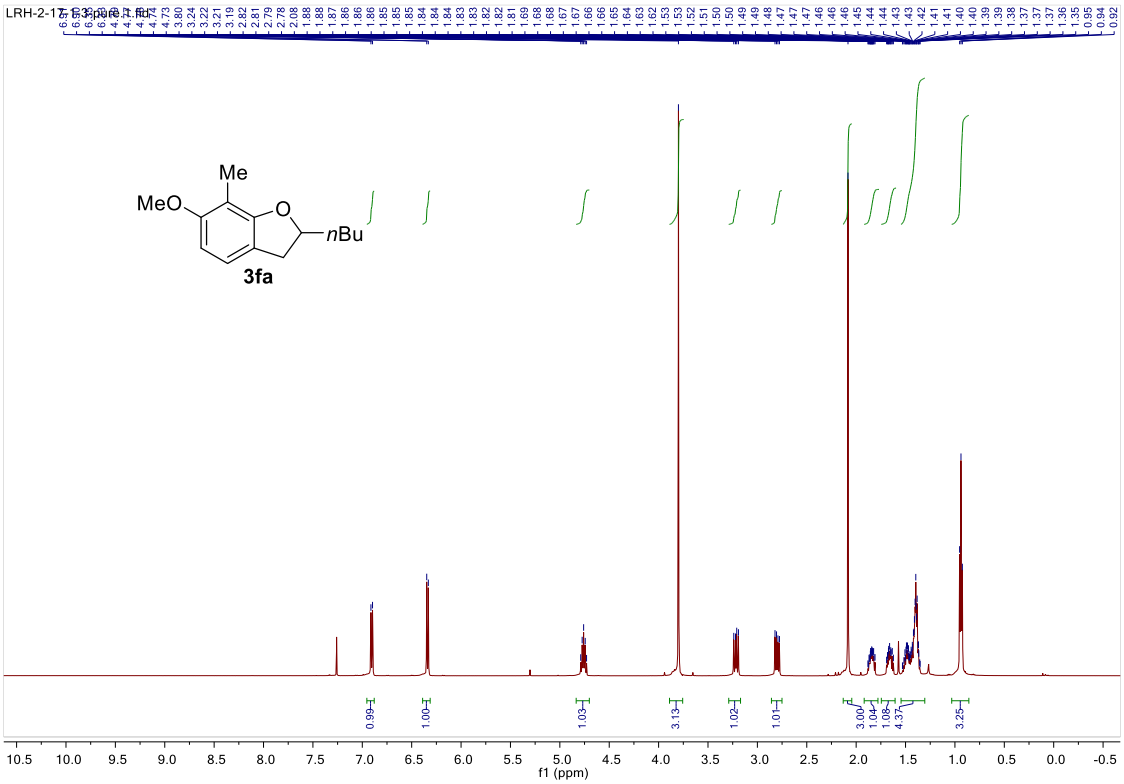

Figure 2.24 ^{13}C NMR Spectrum of 3fa

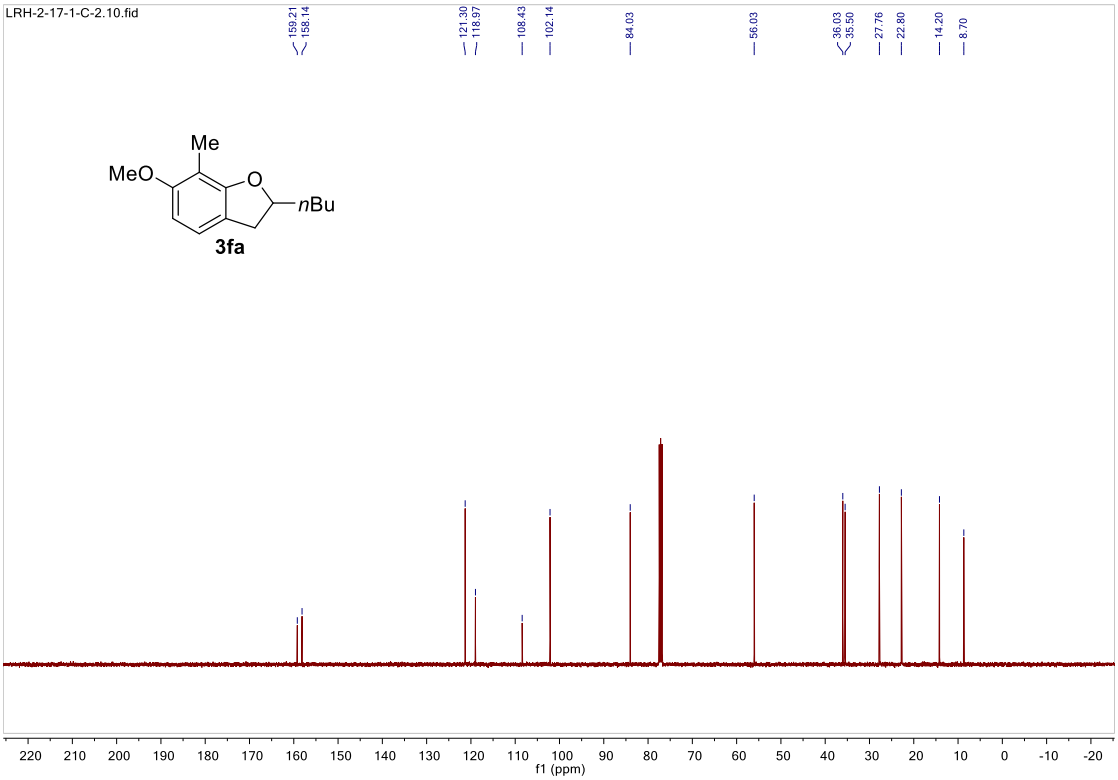

Figure 2.25 ^{1}H NMR Spectrum of 3ga

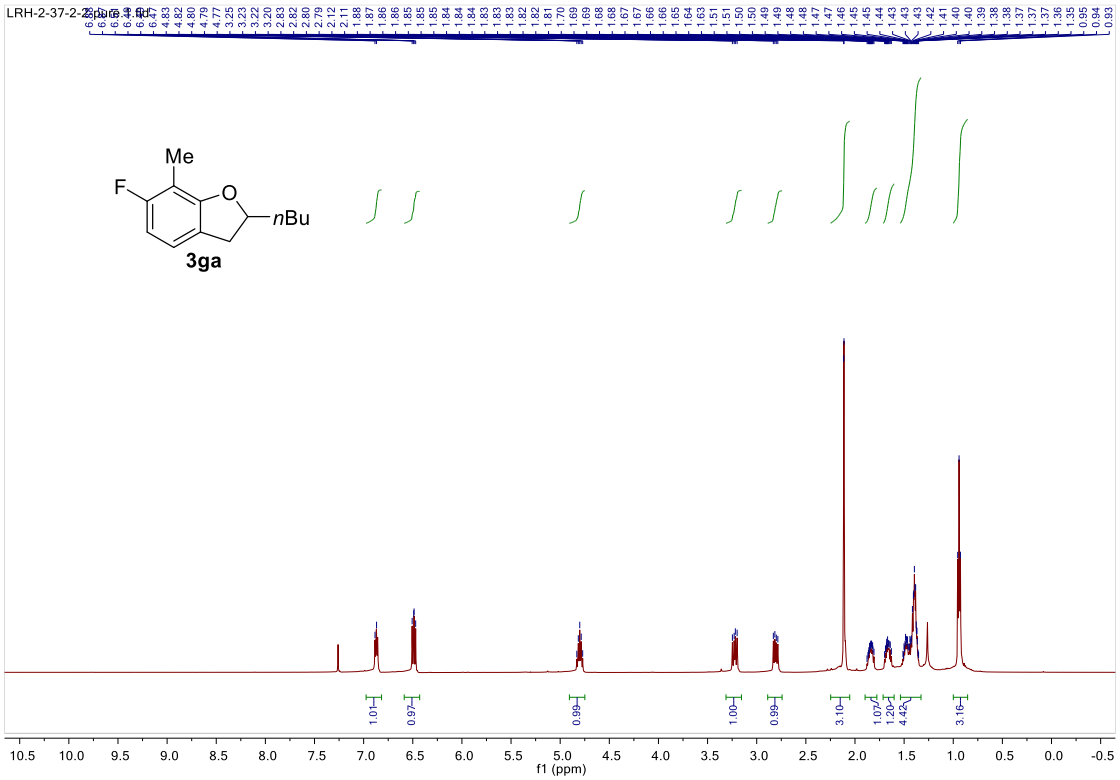

Figure 2.26 ^{13}C NMR Spectrum of 3ga

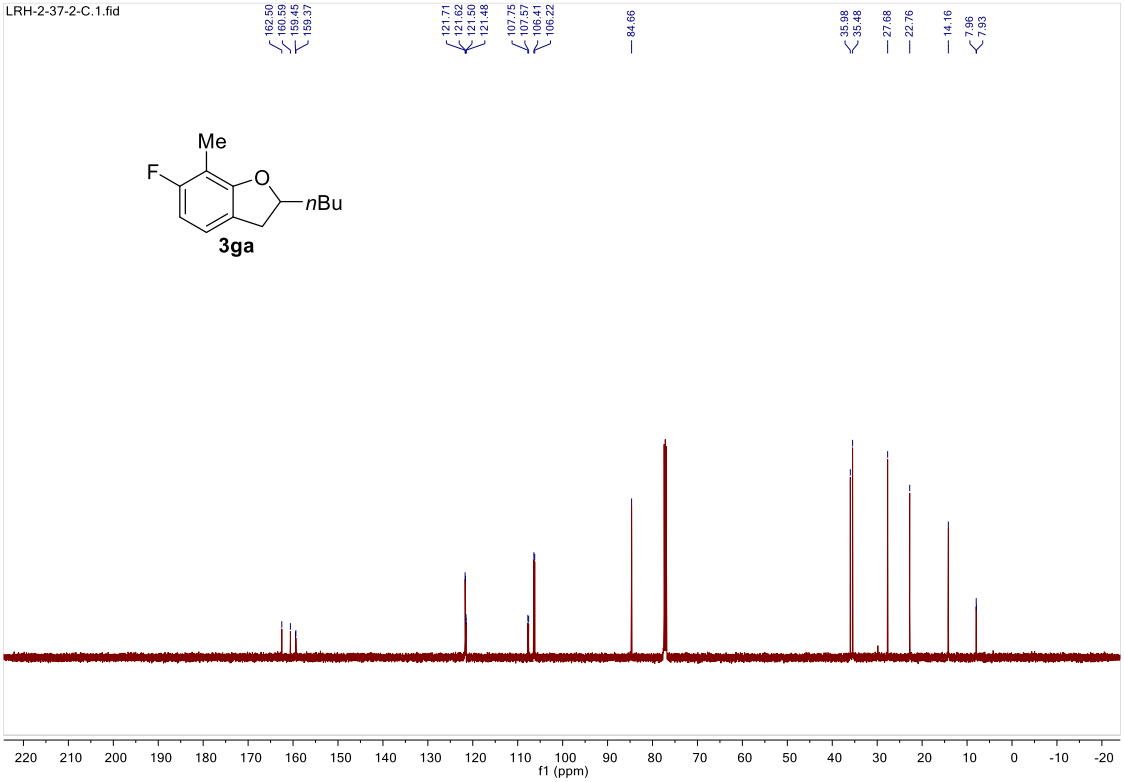

Figure 2.27 ^{19}F NMR Spectrum of 3ga

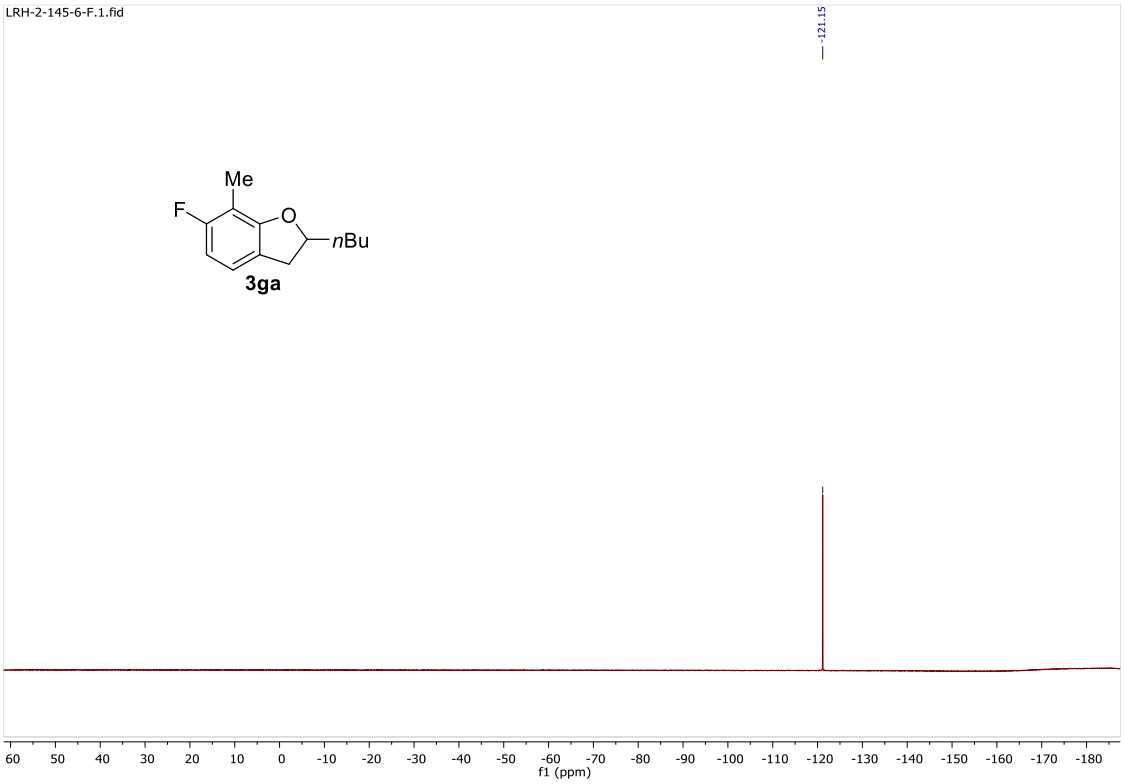

Figure 2.28 ^{1}H NMR Spectrum of 3ha

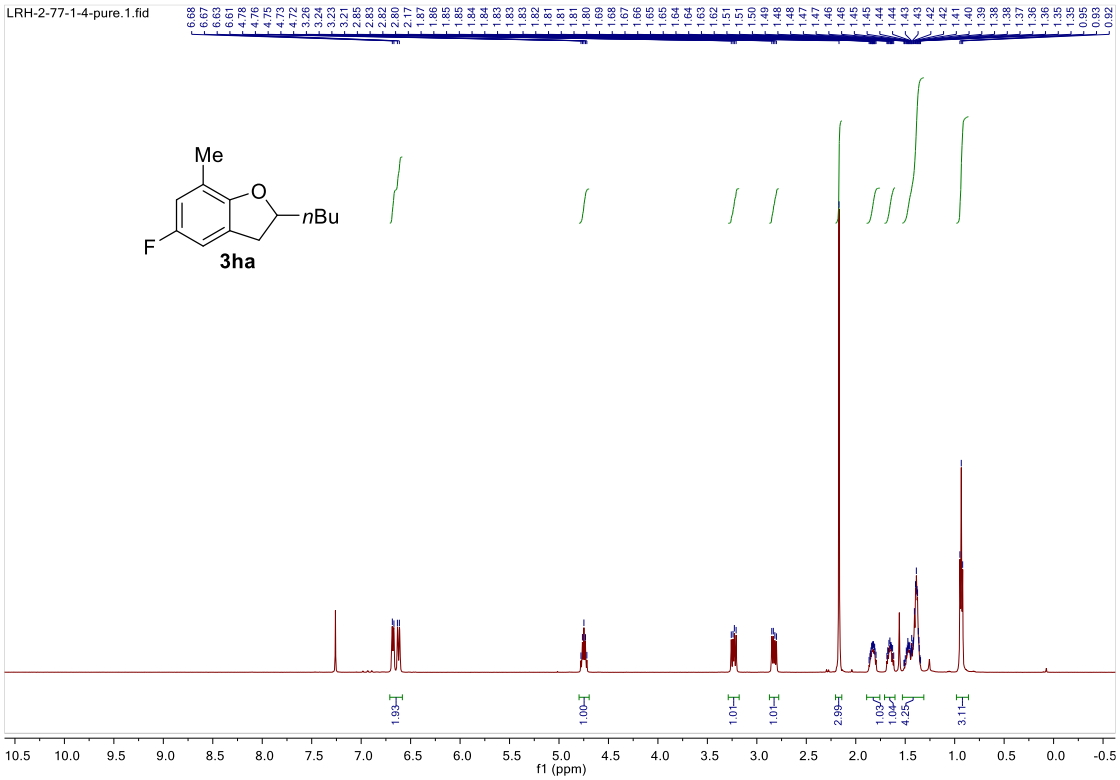

Figure 2.29 ^{13}C NMR Spectrum of 3ha

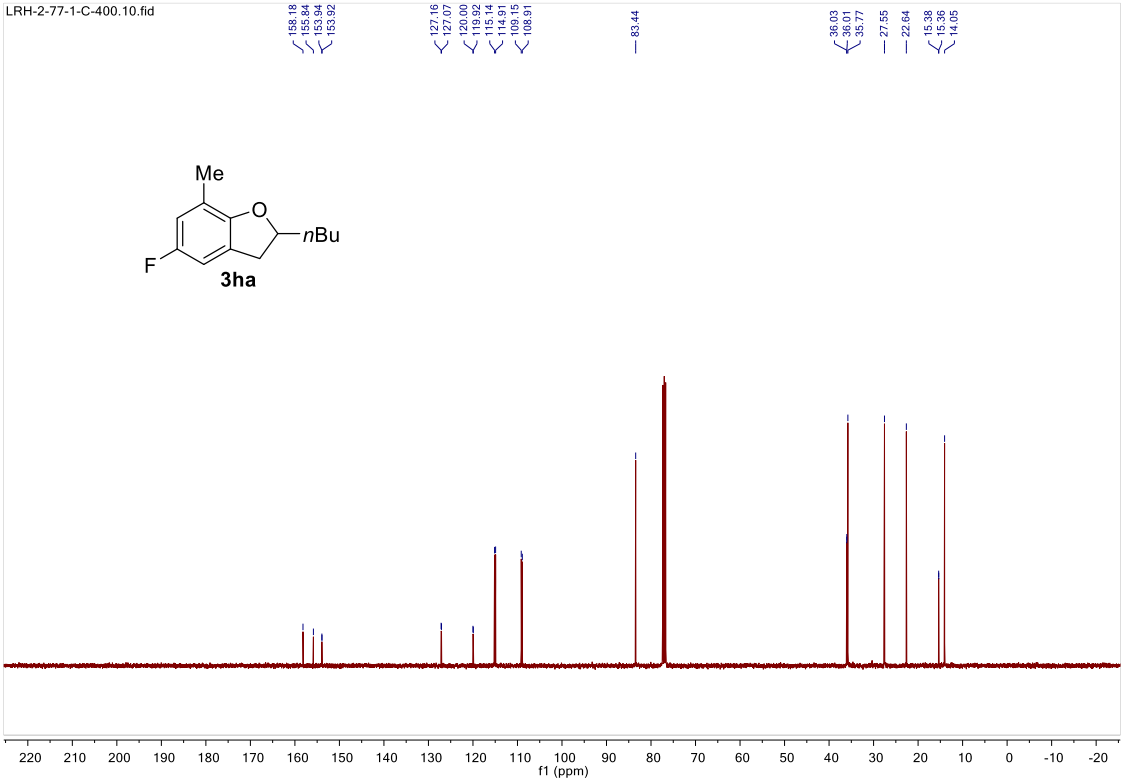

Figure 2.30 ^{19}F NMR Spectrum of 3ha

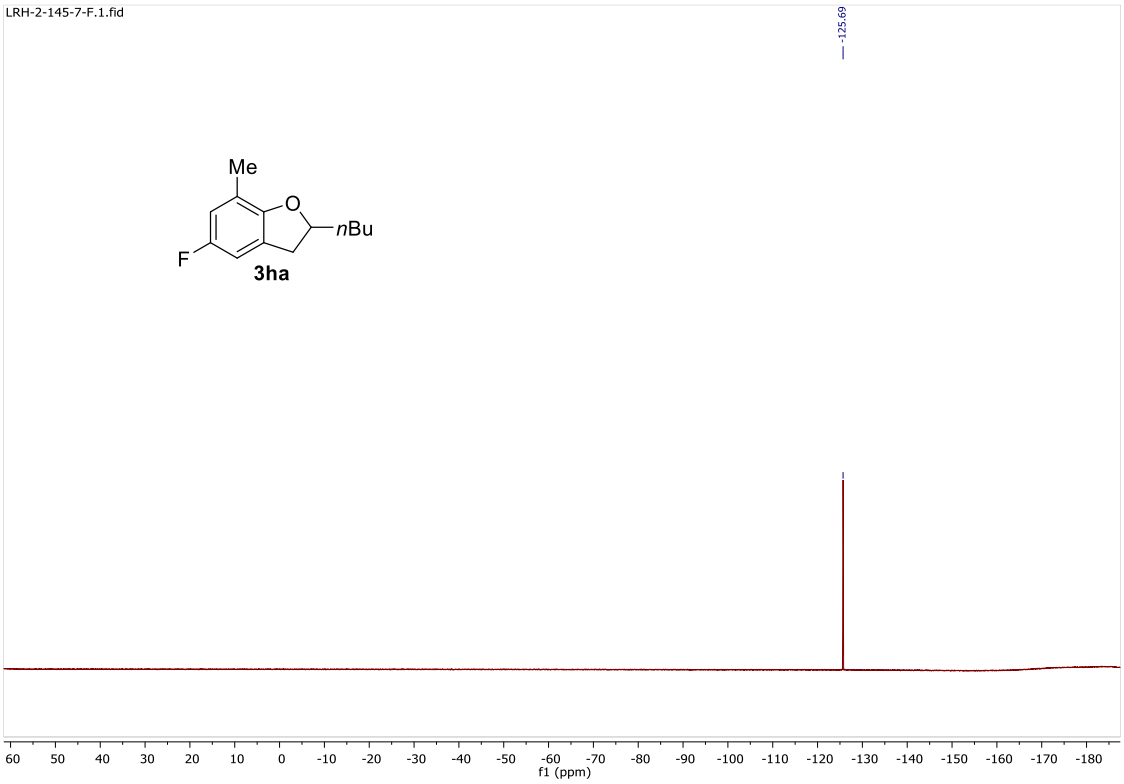

Figure 2.31 ^{1}H NMR Spectrum of 3ia

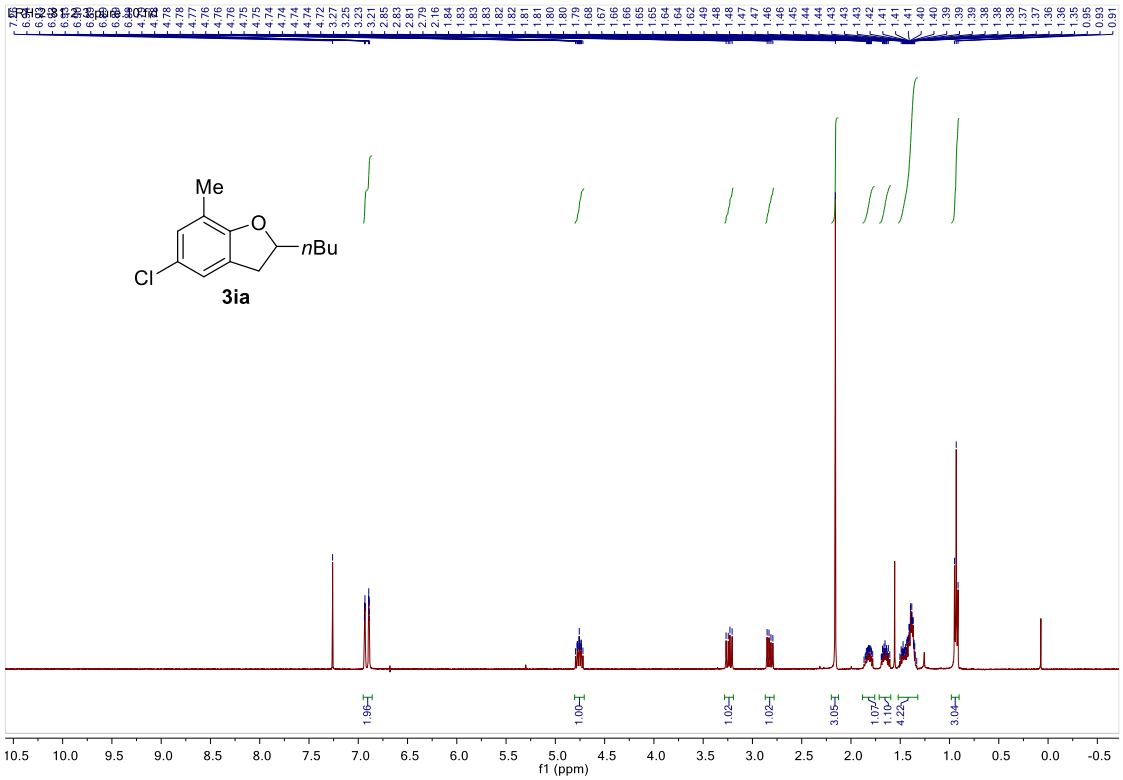

Figure 2.32 ^{13}C NMR Spectrum of 3ia

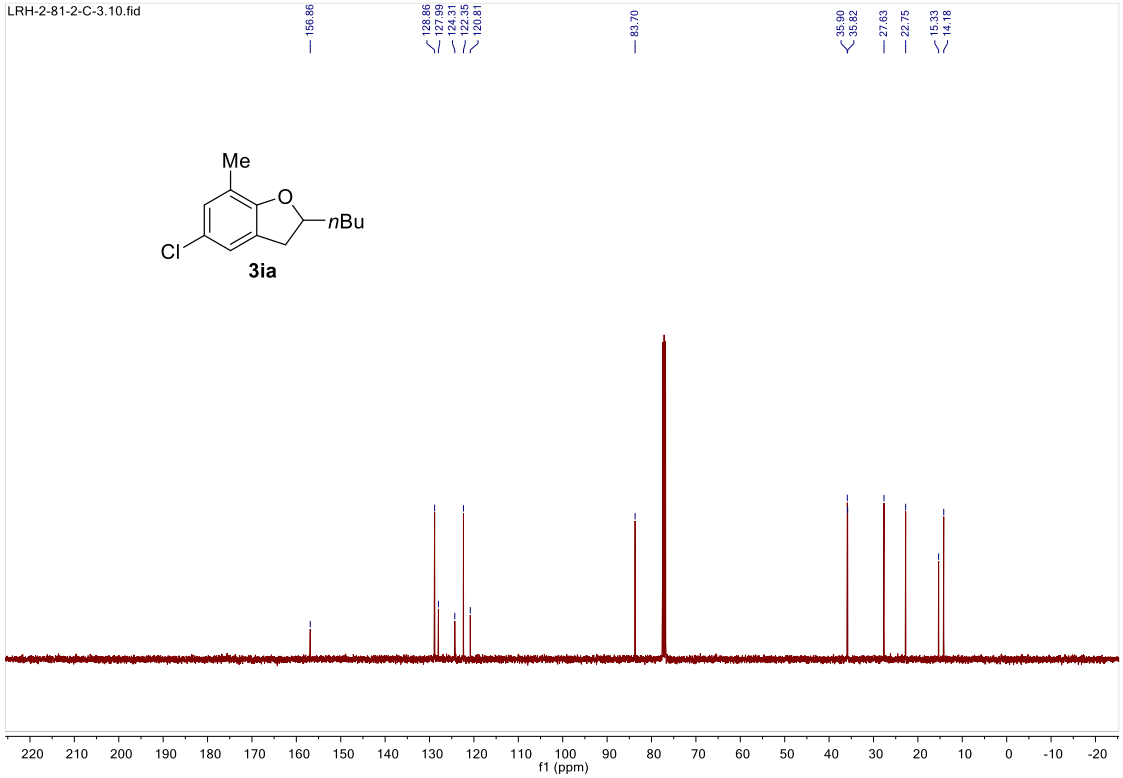

Figure 2.33 ^{1}H NMR Spectrum of 3ja

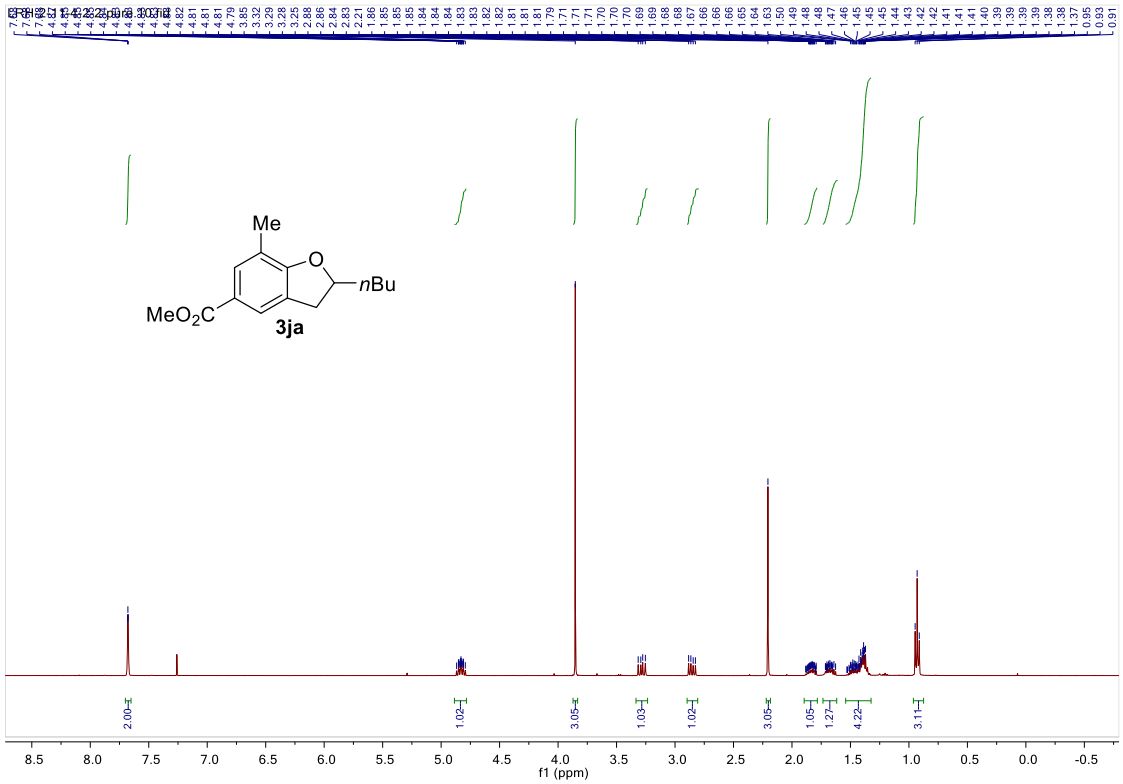

Figure 2.34 ^{13}C NMR Spectrum of 3ja

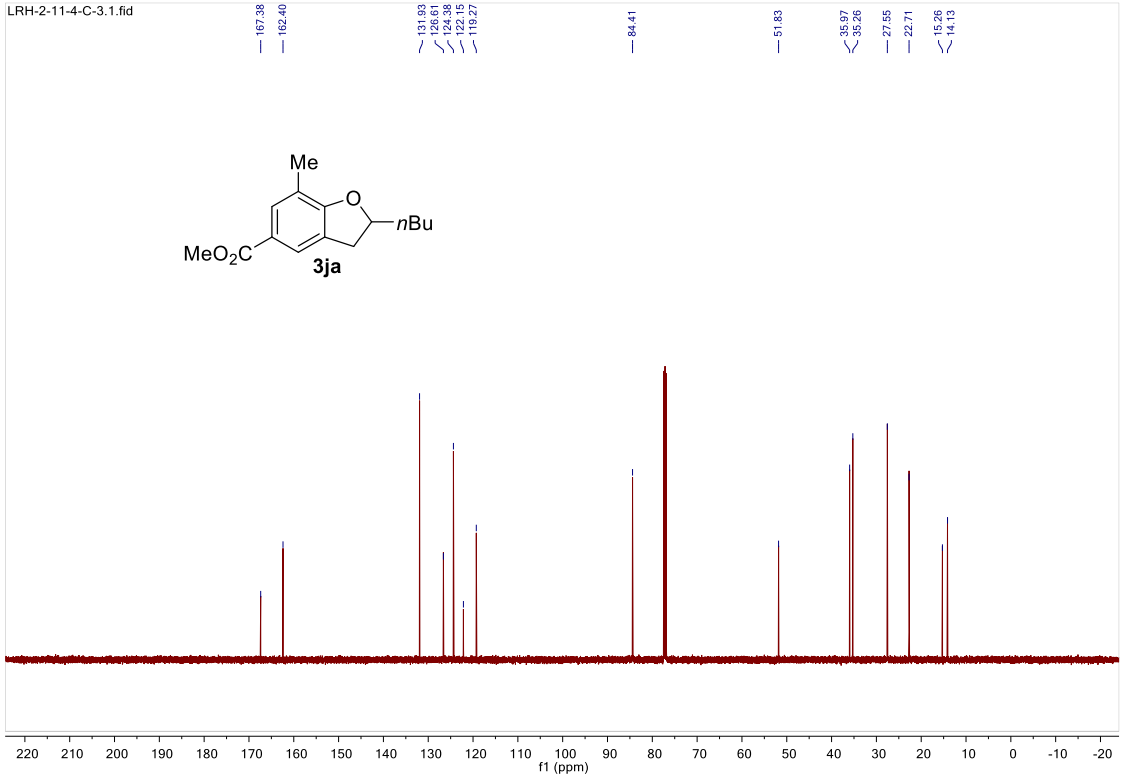

Figure 2.35 ^{1}H NMR Spectrum of 3ka

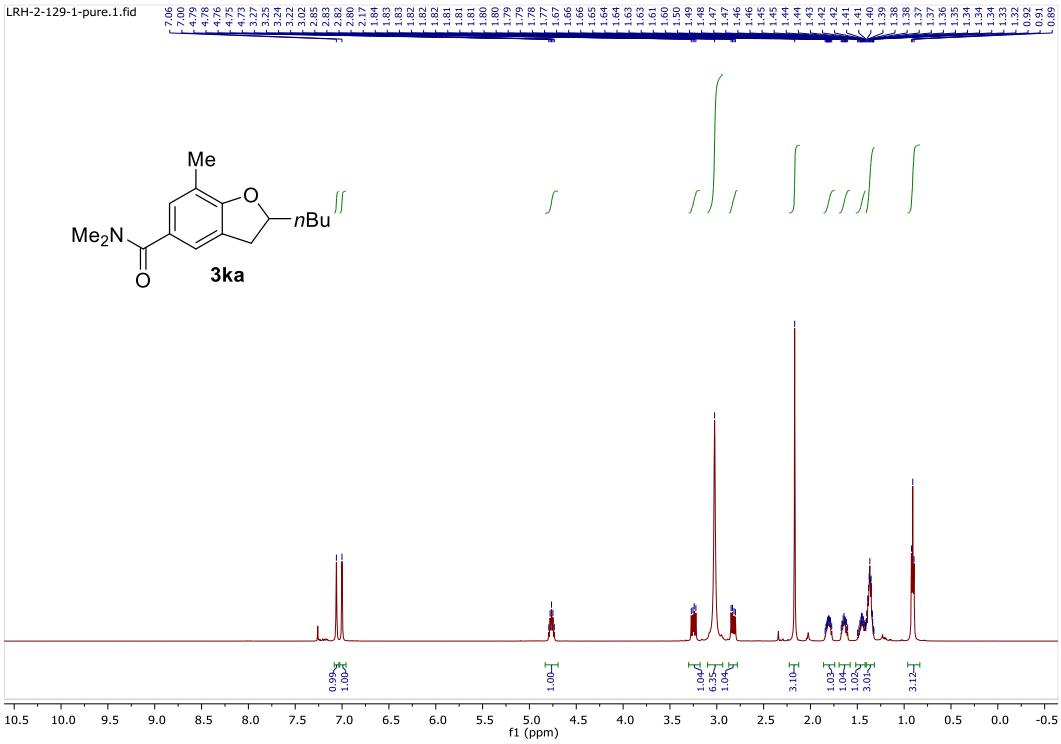

Figure 2.36 ^{13}C NMR Spectrum of 3ka

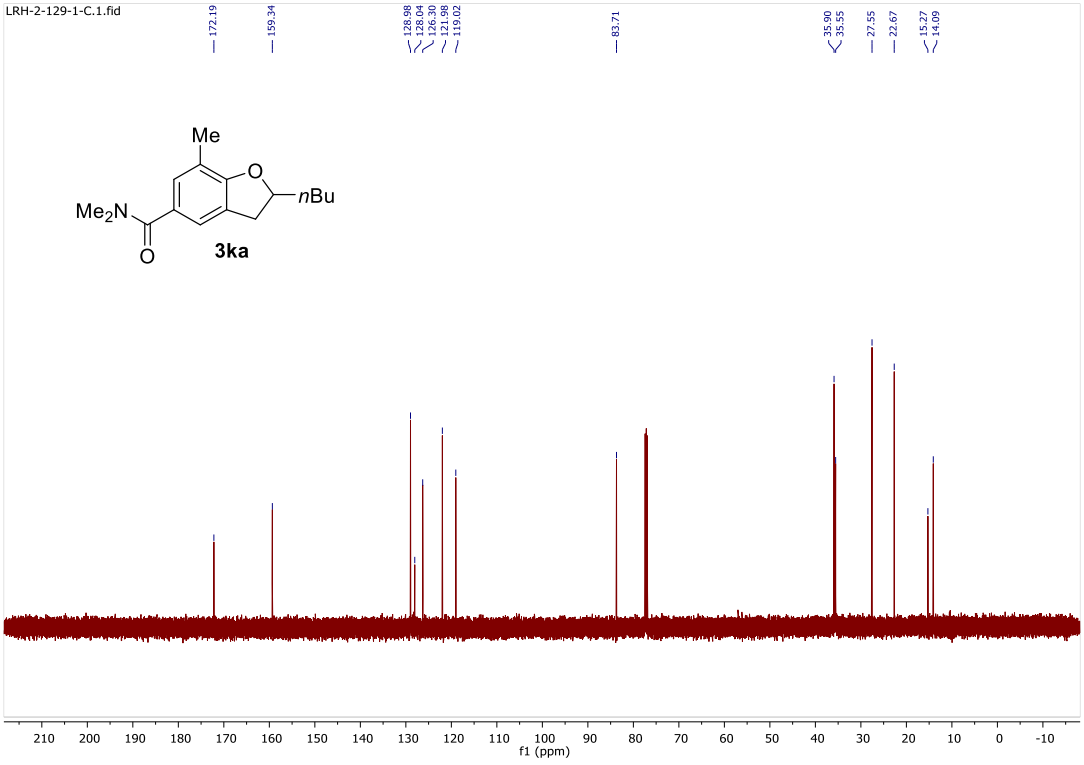

Figure 2.37 ^{1}H NMR Spectrum of 3la

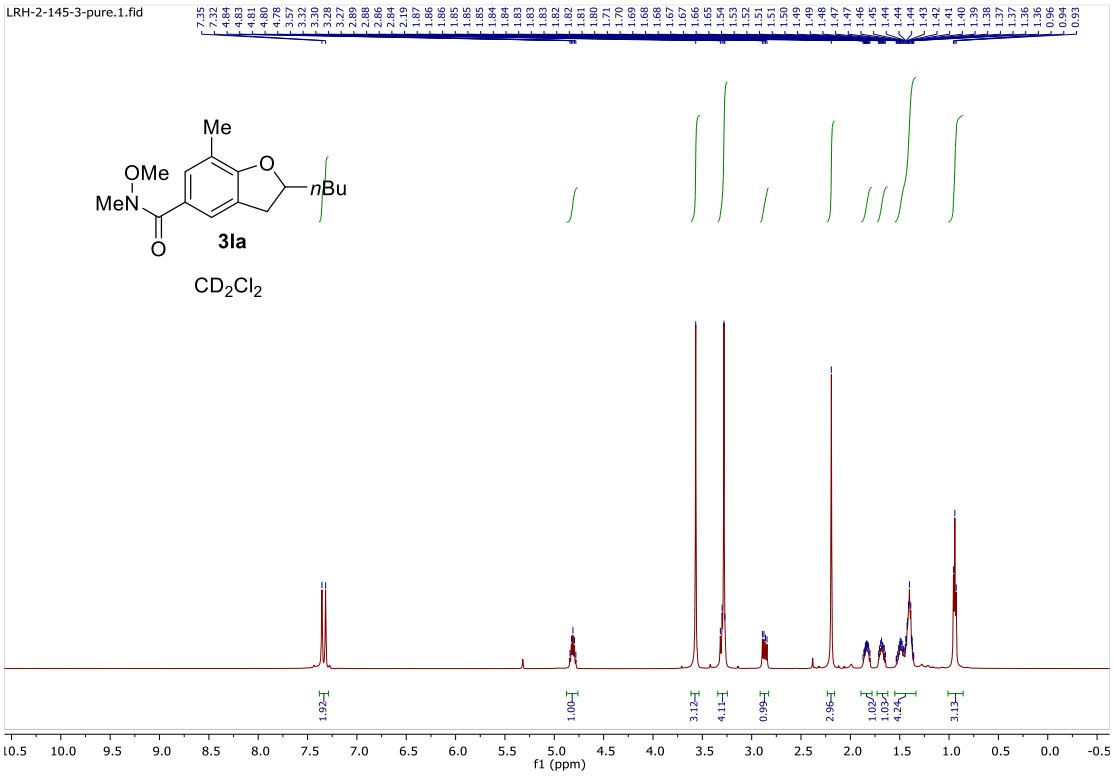

Figure 2.38 ^{13}C NMR Spectrum of 3la

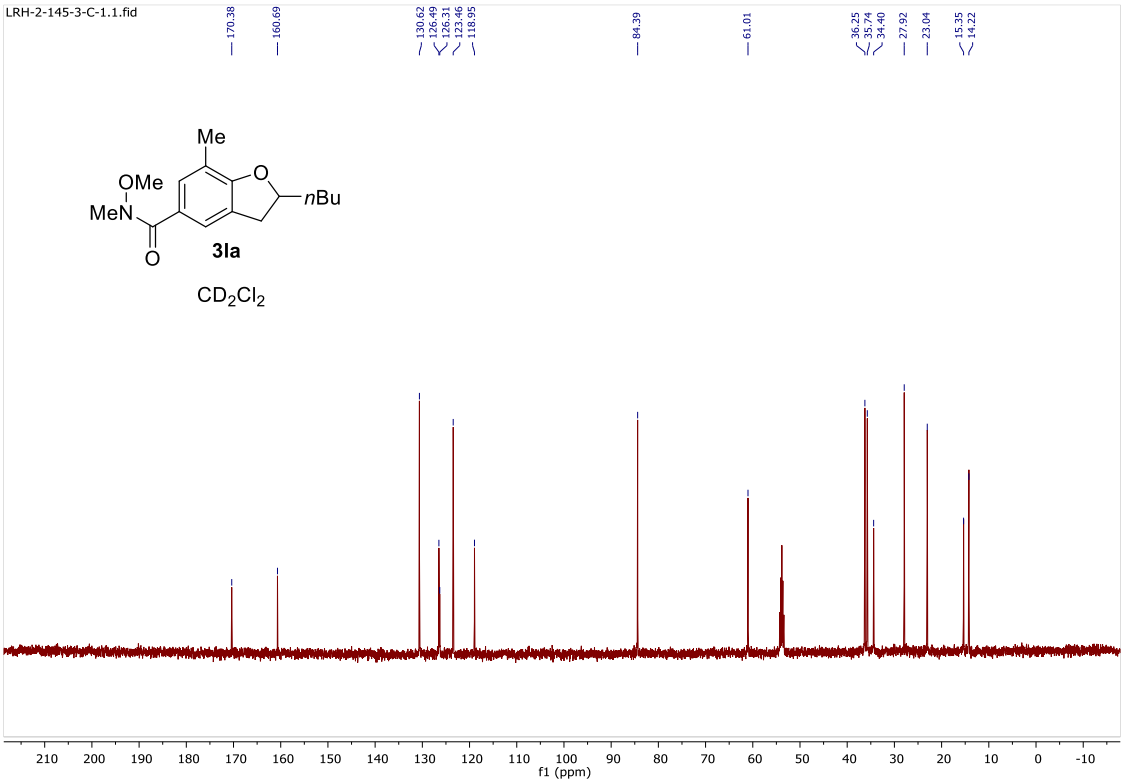

Figure 2.39 ^{1}H NMR Spectrum of 3ma

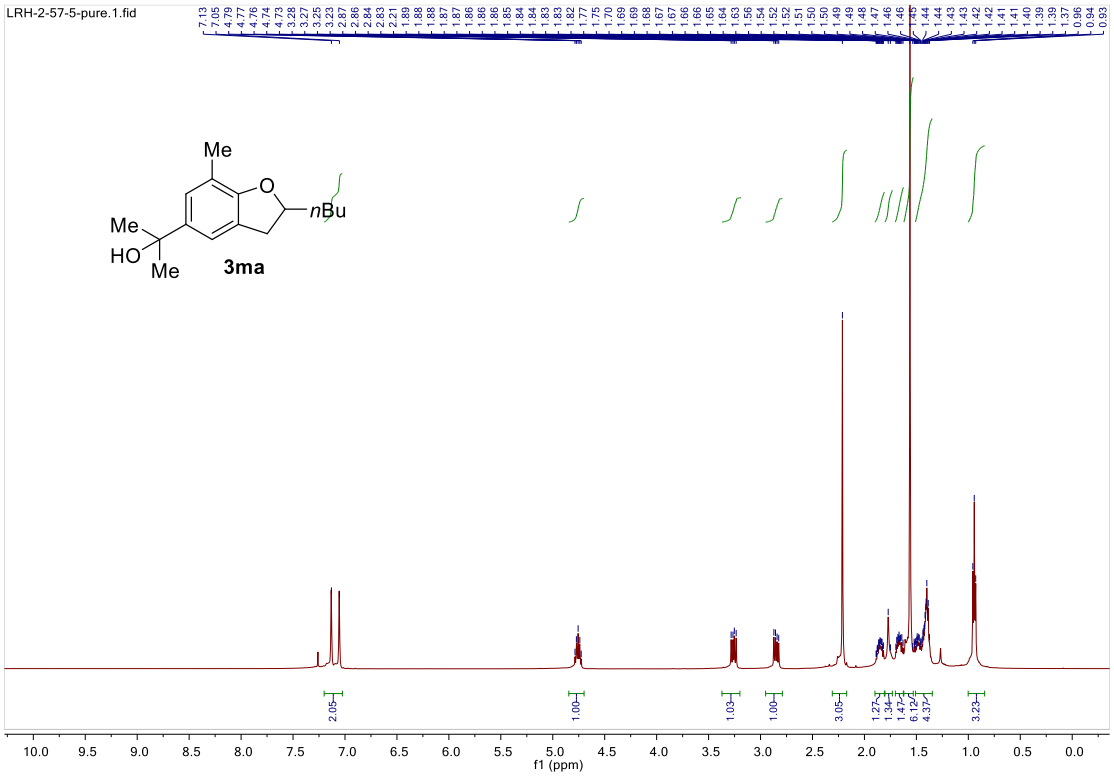

Figure 2.40 ^{13}C NMR Spectrum of 3ma

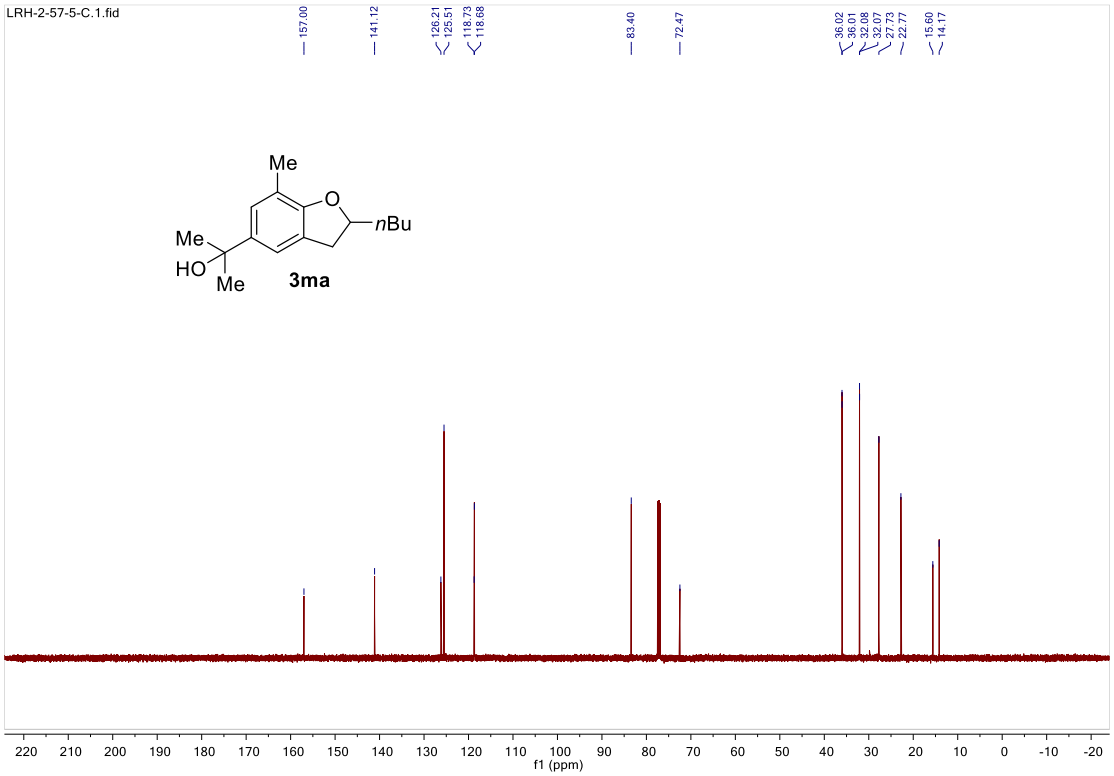

Figure 2.41 ^{1}H NMR Spectrum of 3na

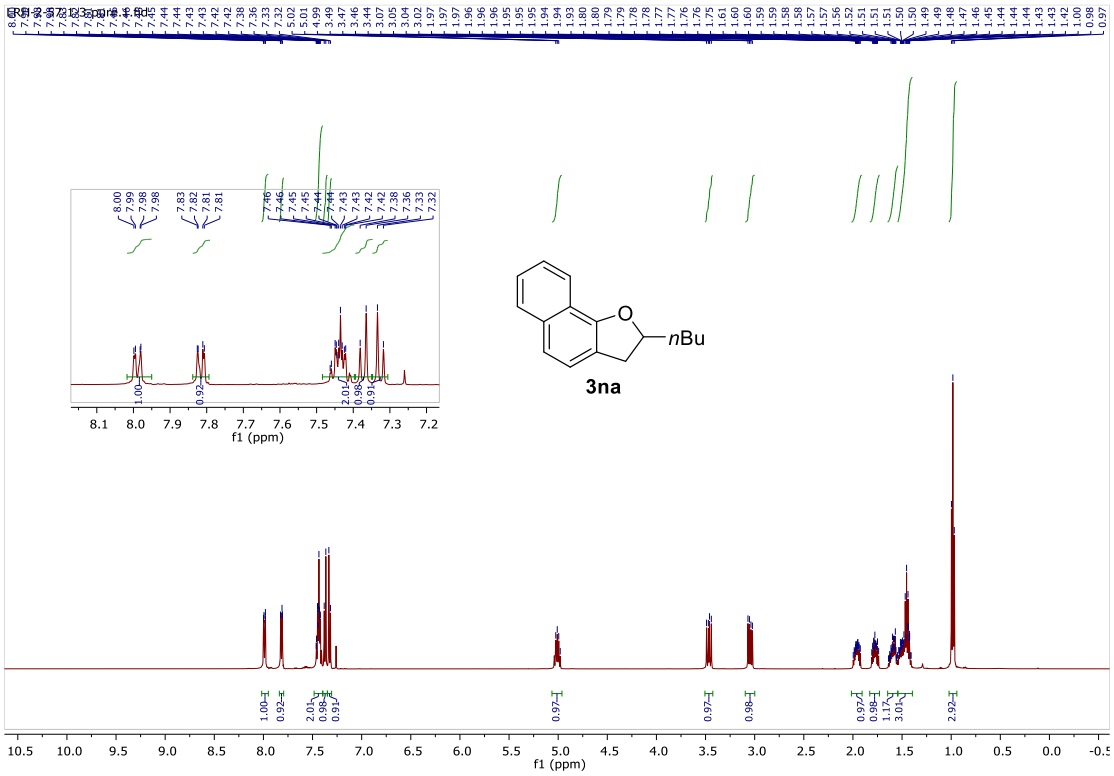

Figure 2.42 ^{13}C NMR Spectrum of 3na

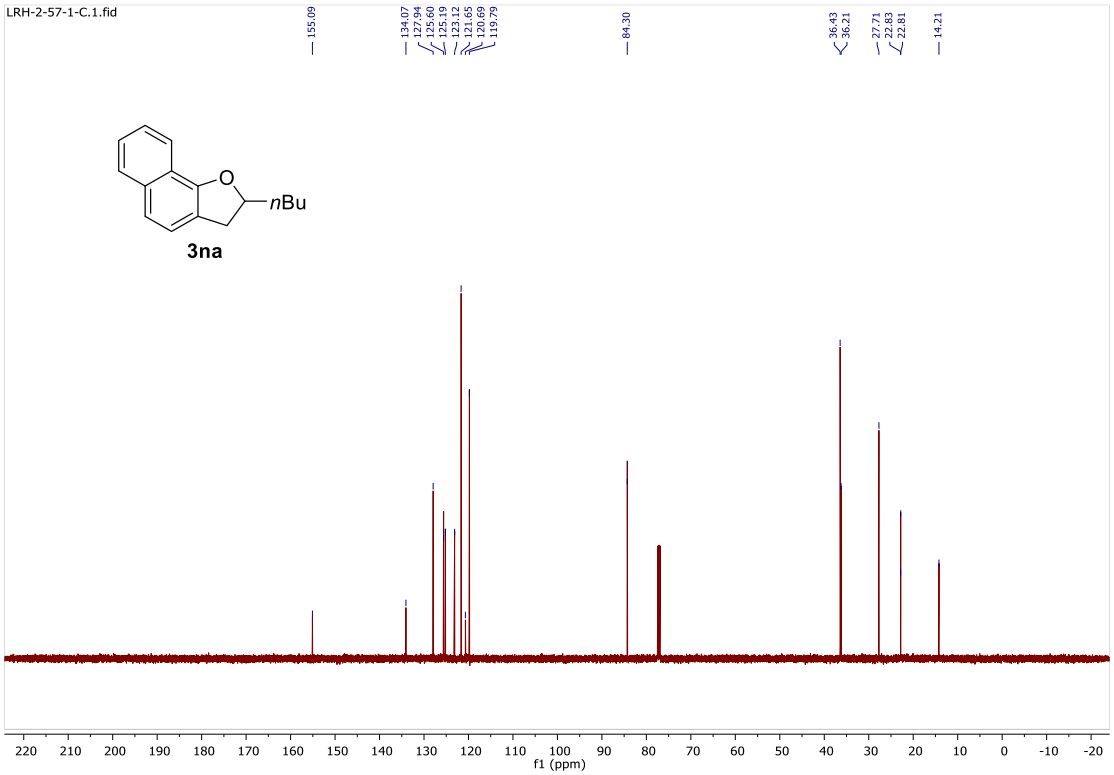

Figure 2.43 ^{1}H NMR Spectrum of 3oa

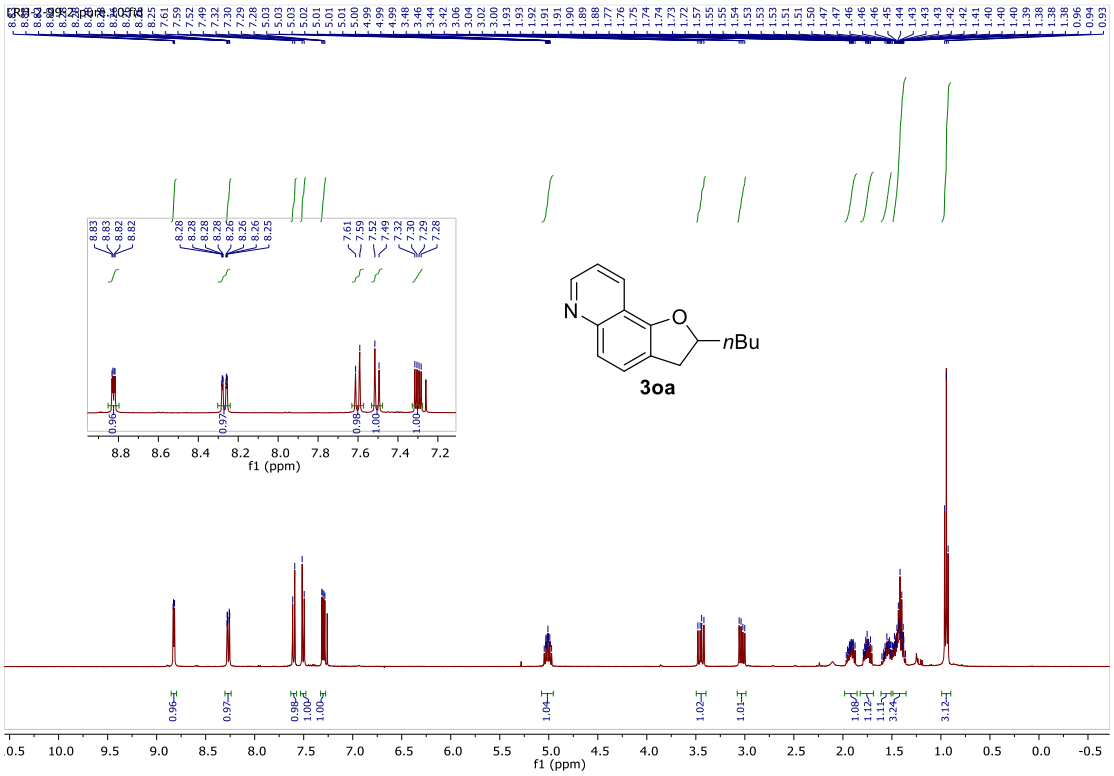

Figure 2.44 ^{13}C NMR Spectrum of 3oa

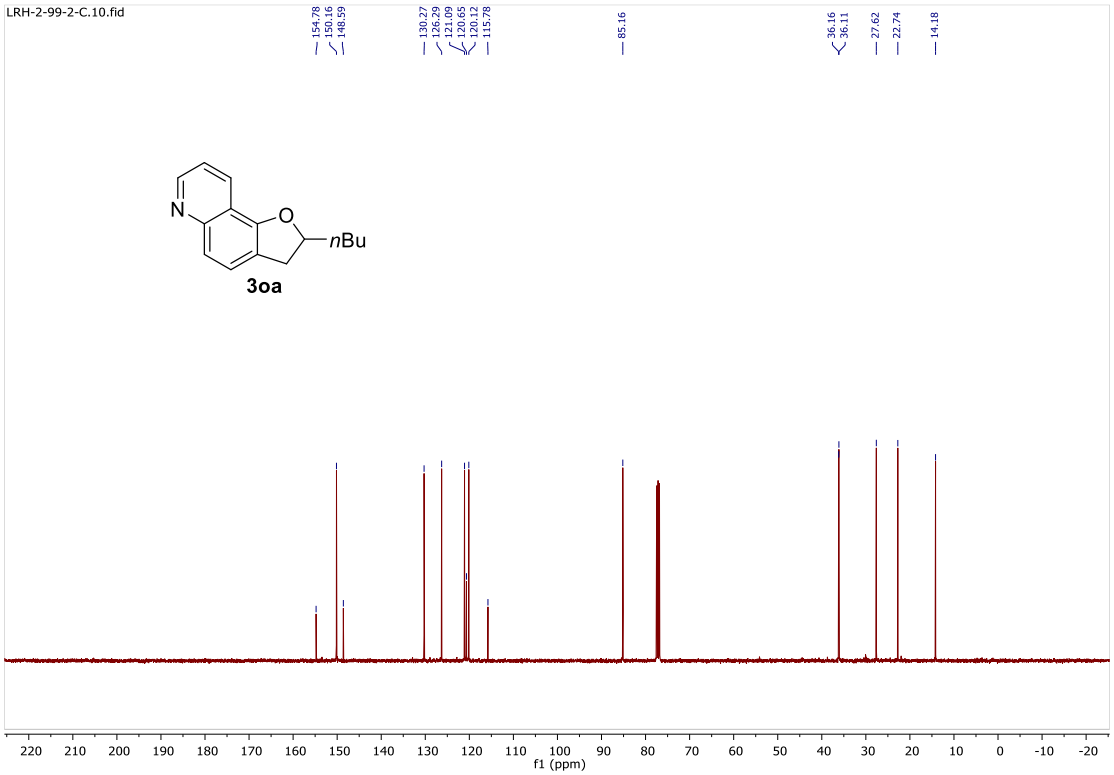

Figure 2.45 ^{1}H NMR Spectrum of 3pa

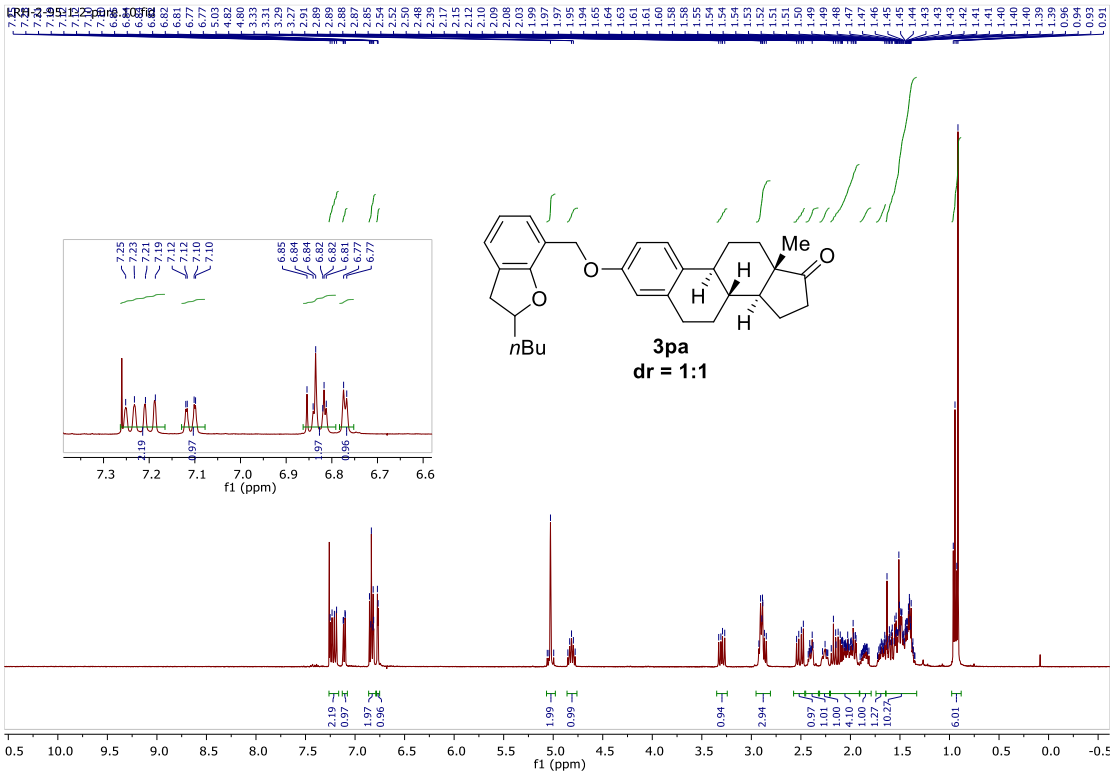

Figure 2.46 ^{13}C NMR Spectrum of 3pa

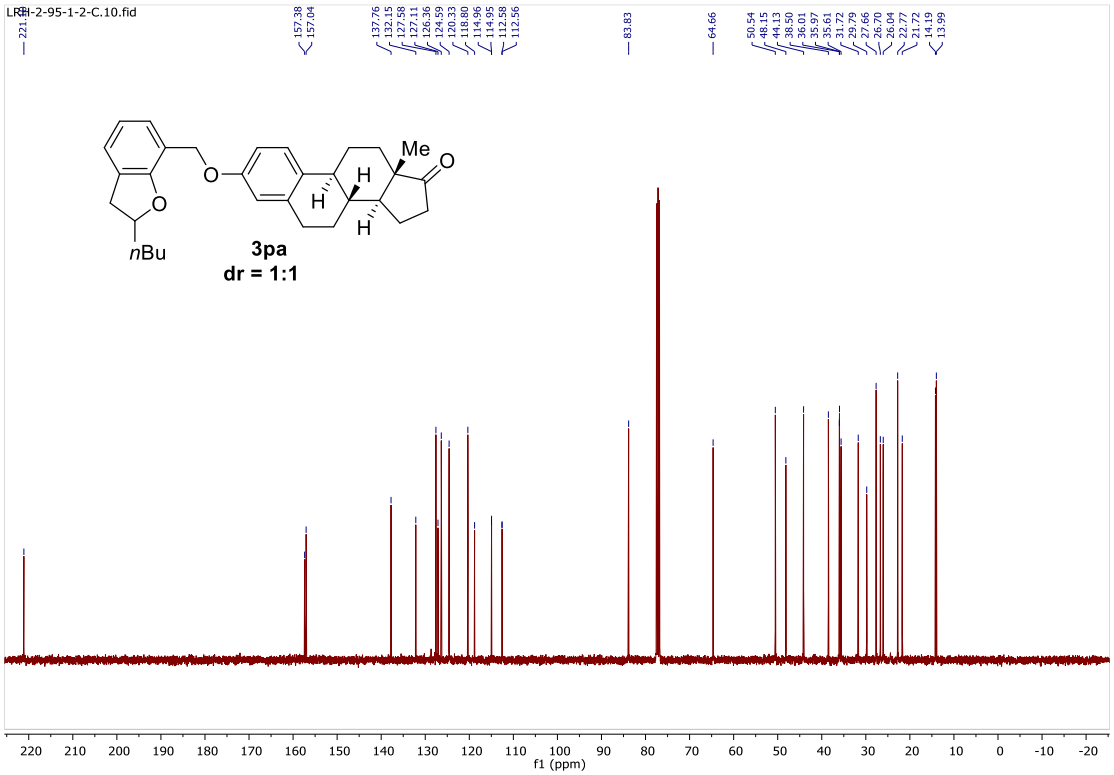

Figure 2.47 ^{1}H NMR Spectrum of 3ab

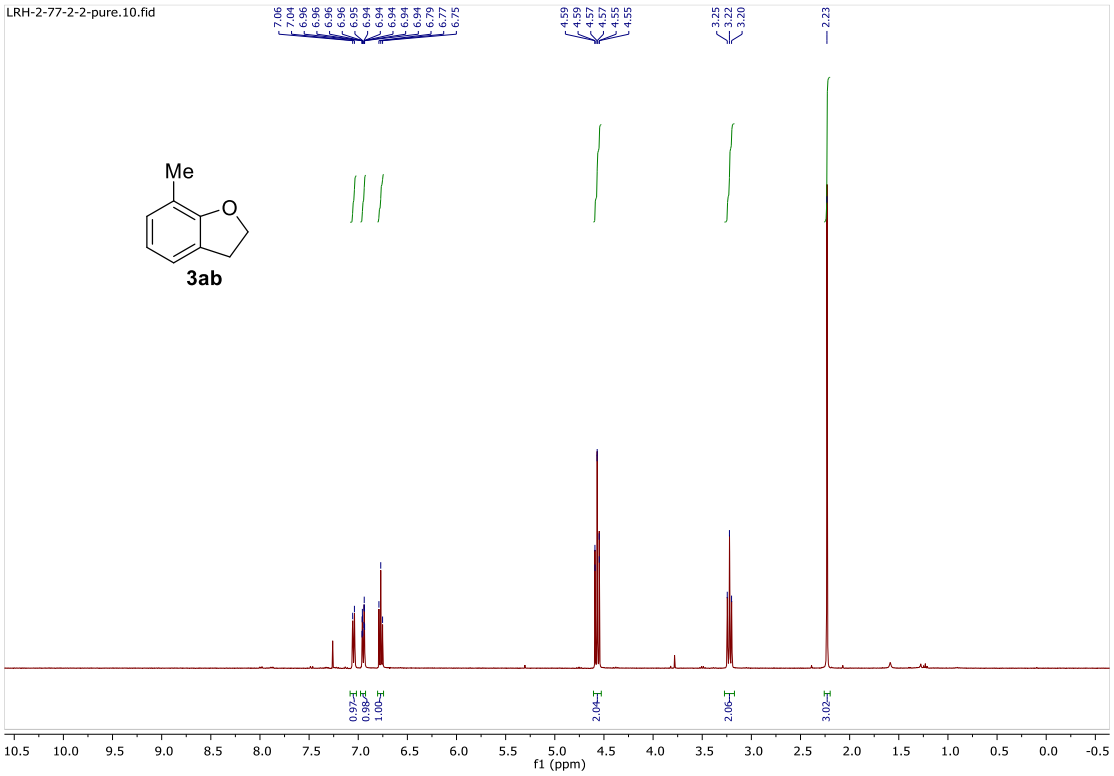

Figure 2.48 ^{13}C NMR Spectrum of 3ab

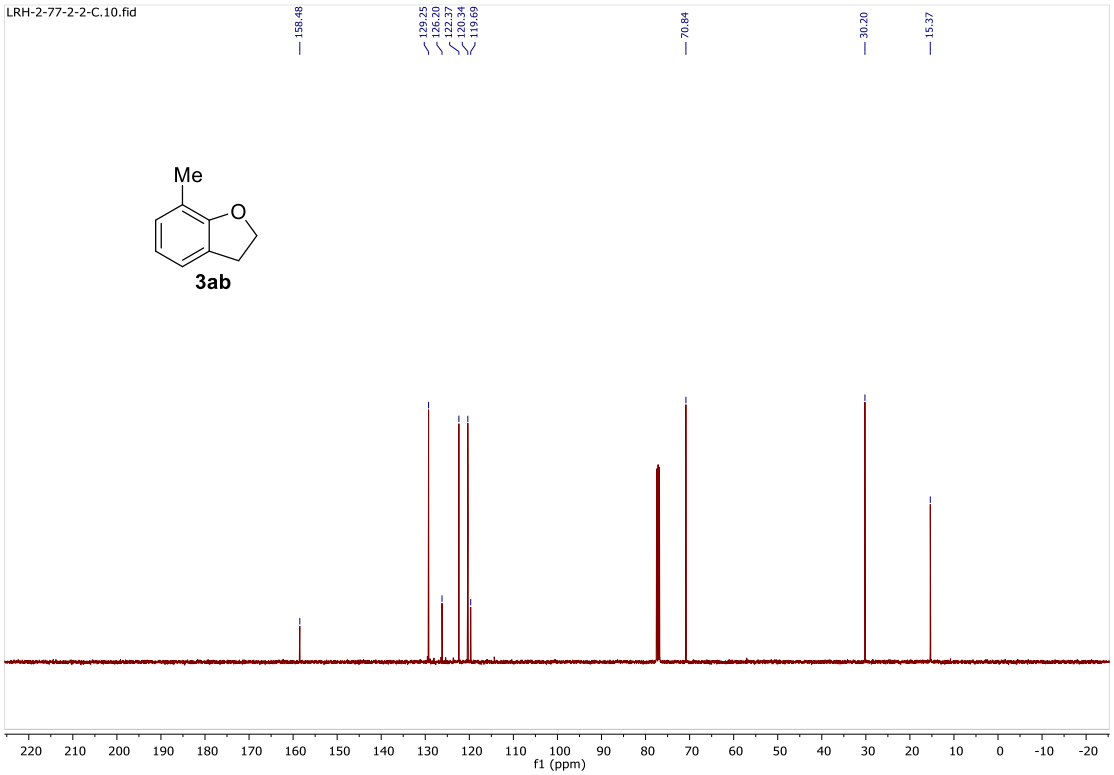

Figure 2.49 ^{1}H NMR Spectrum of 3ac

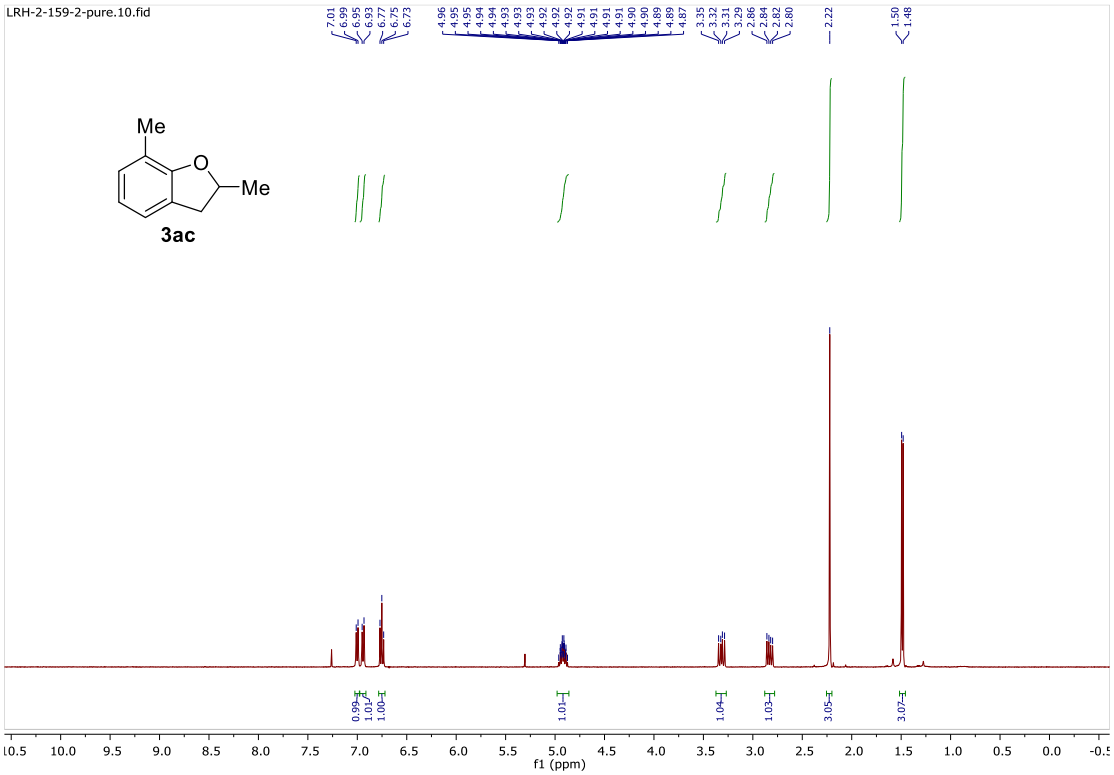

Figure 2.50 ^{13}C NMR Spectrum of 3ac

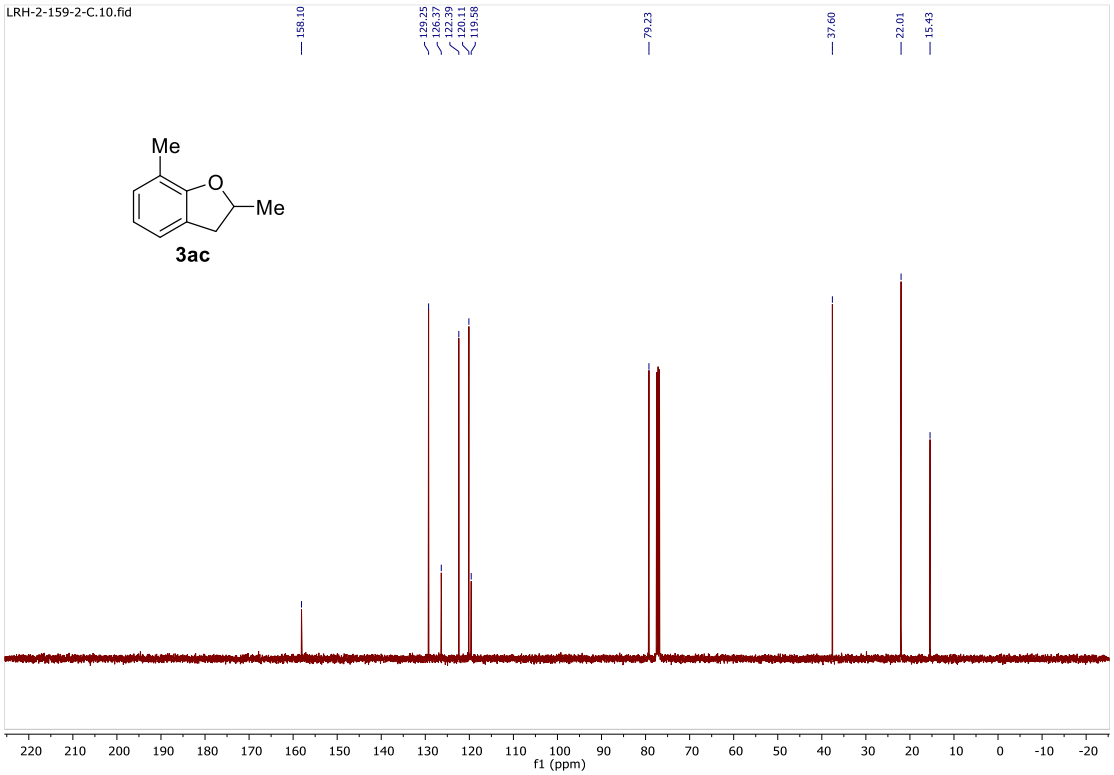

Figure 2.51 ^{1}H NMR Spectrum of 3ad

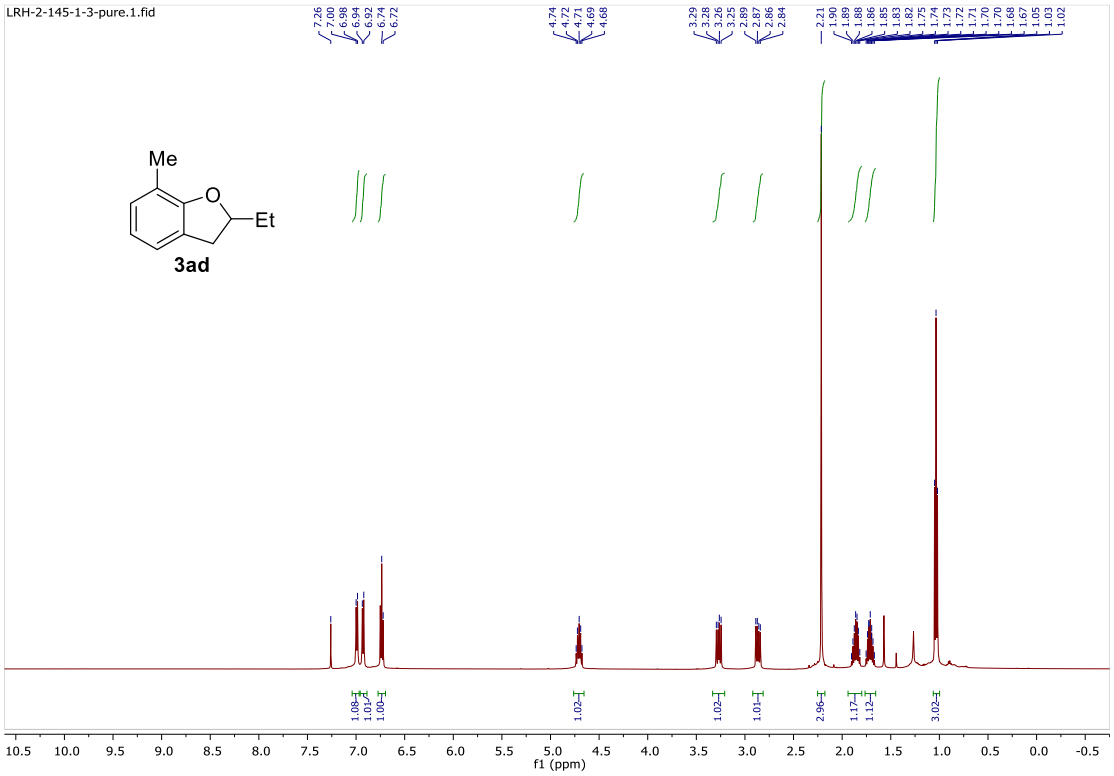

Figure 2.52 ^{13}C NMR Spectrum of 3ad

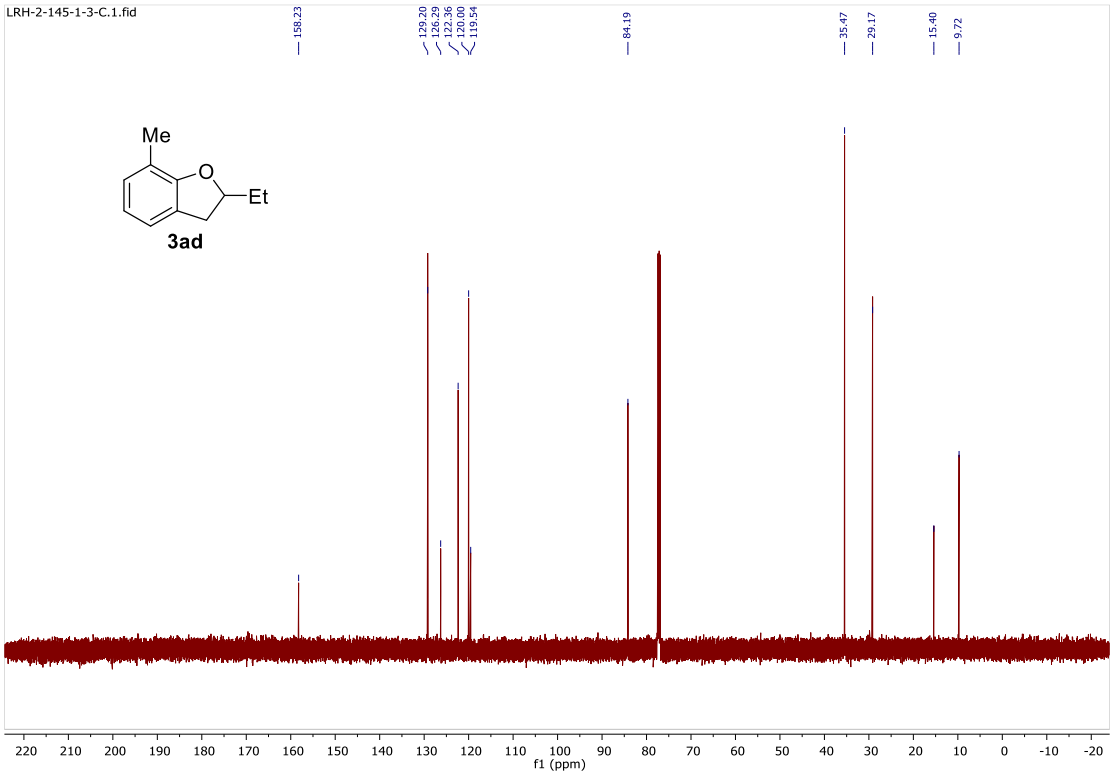

Figure 2.53 ^{1}H NMR Spectrum of 3ae

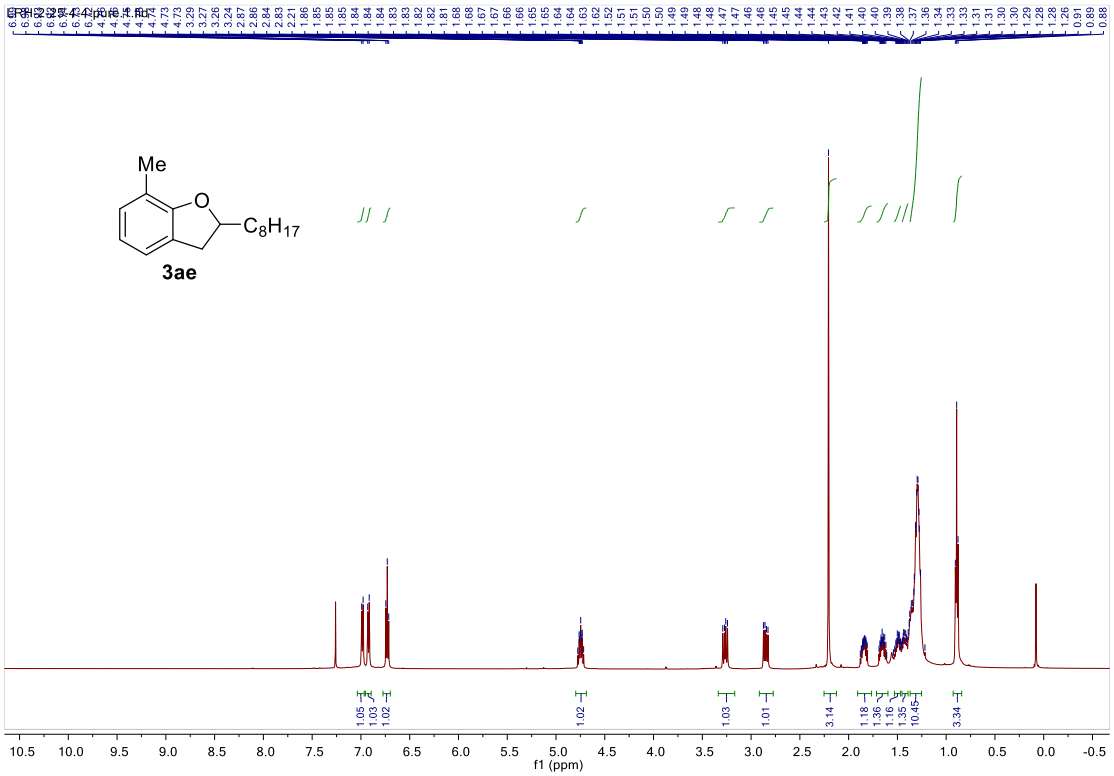

Figure 2.54 ^{13}C NMR Spectrum of 3ae

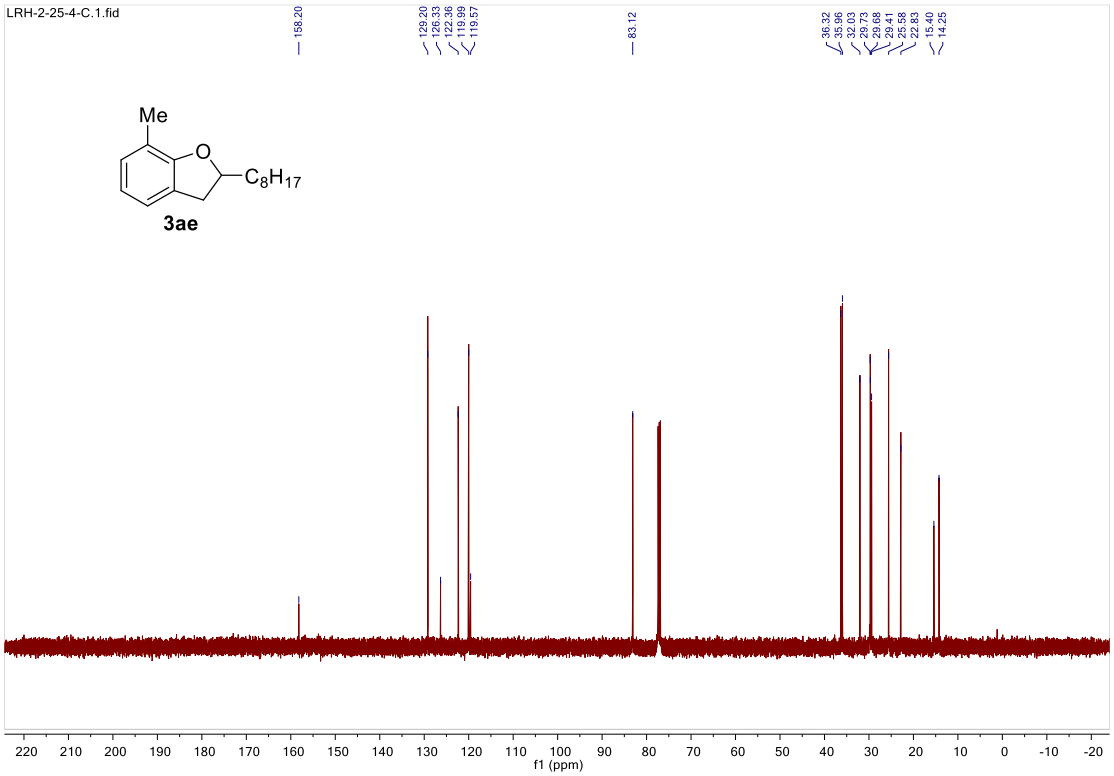

Figure 2.55 ^{1}H NMR Spectrum of 3af

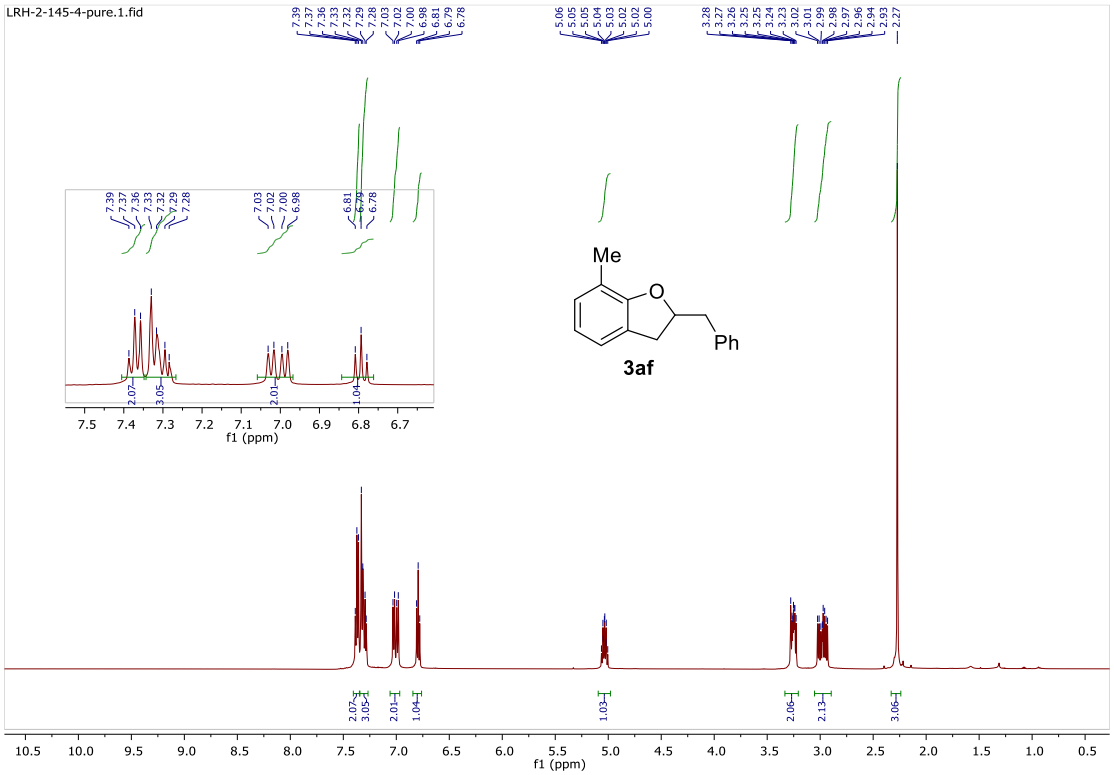

Figure 2.56 ^{13}C NMR Spectrum of 3af

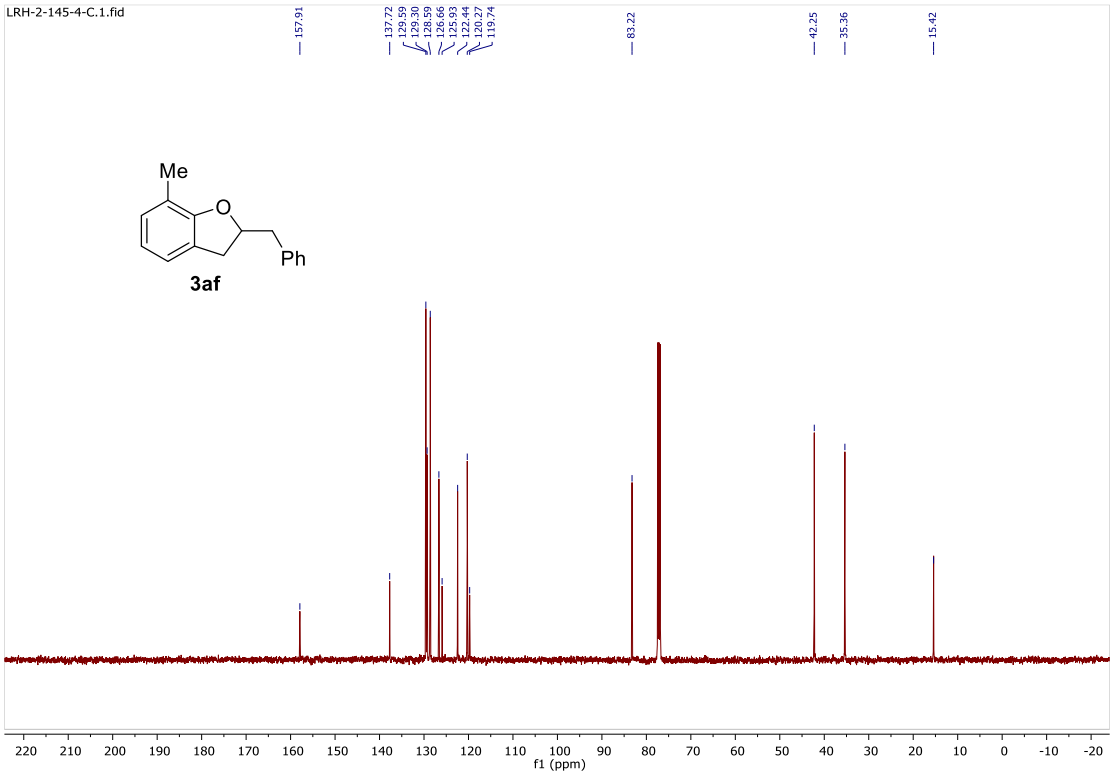

Figure 2.57 ^{1}H NMR Spectrum of 3ag

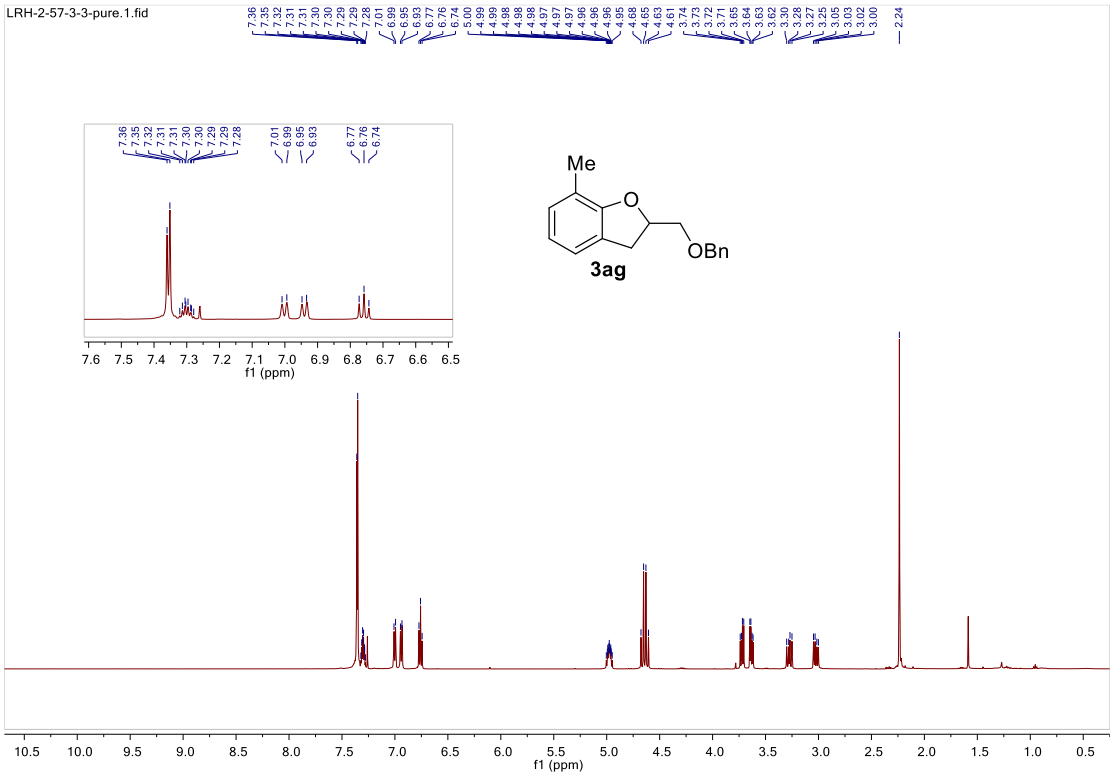

Figure 2.58 ^{13}C NMR Spectrum of 3ag

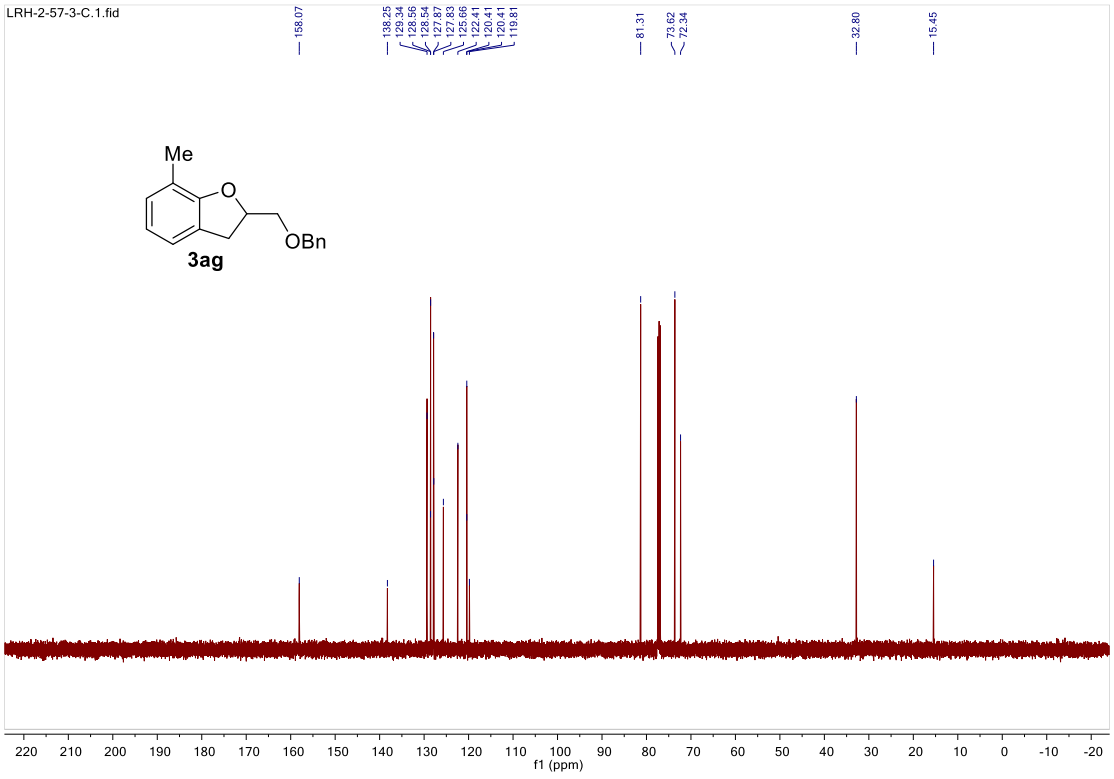

Figure 2.59 ^{1}H NMR Spectrum of 3ah

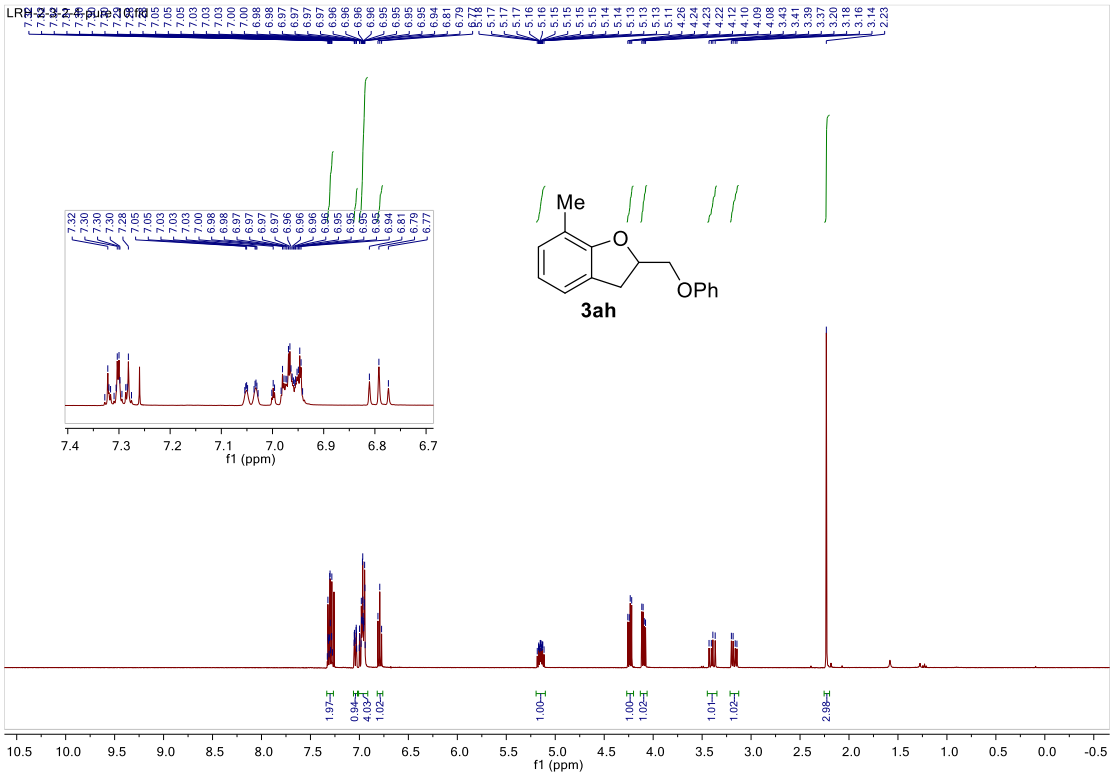

Figure 2.60 ^{13}C NMR Spectrum of 3ah

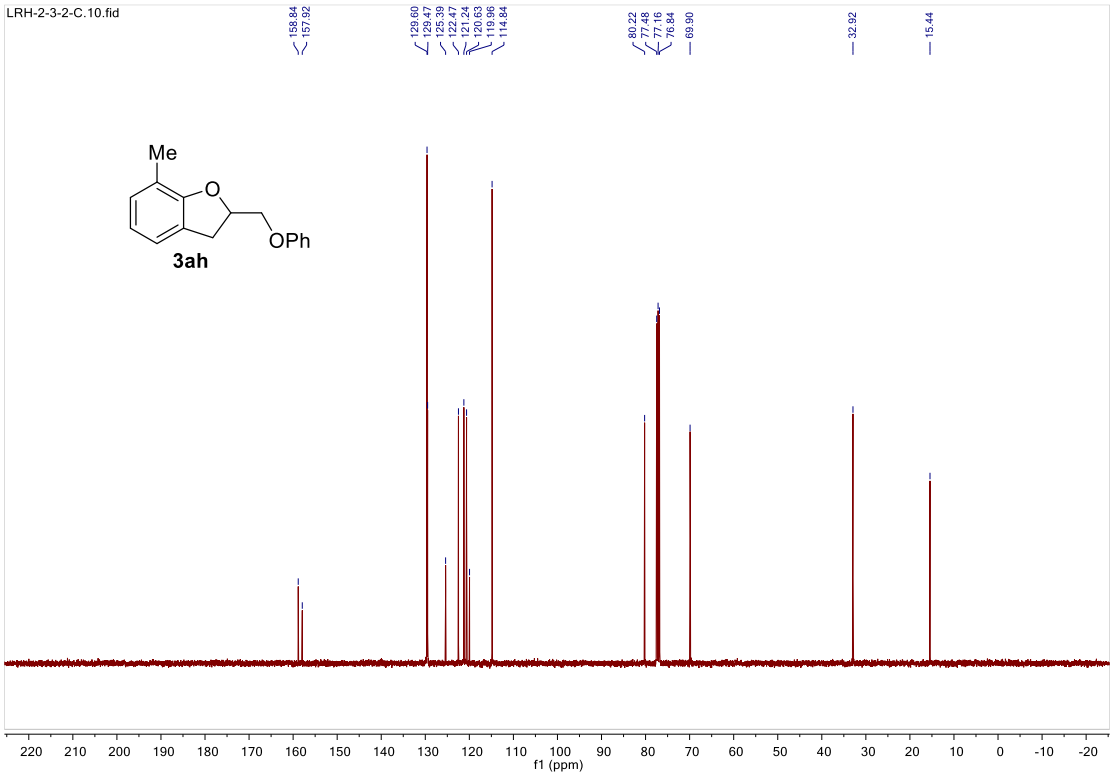

Figure 2.61 ^{1}H NMR Spectrum of 3ai

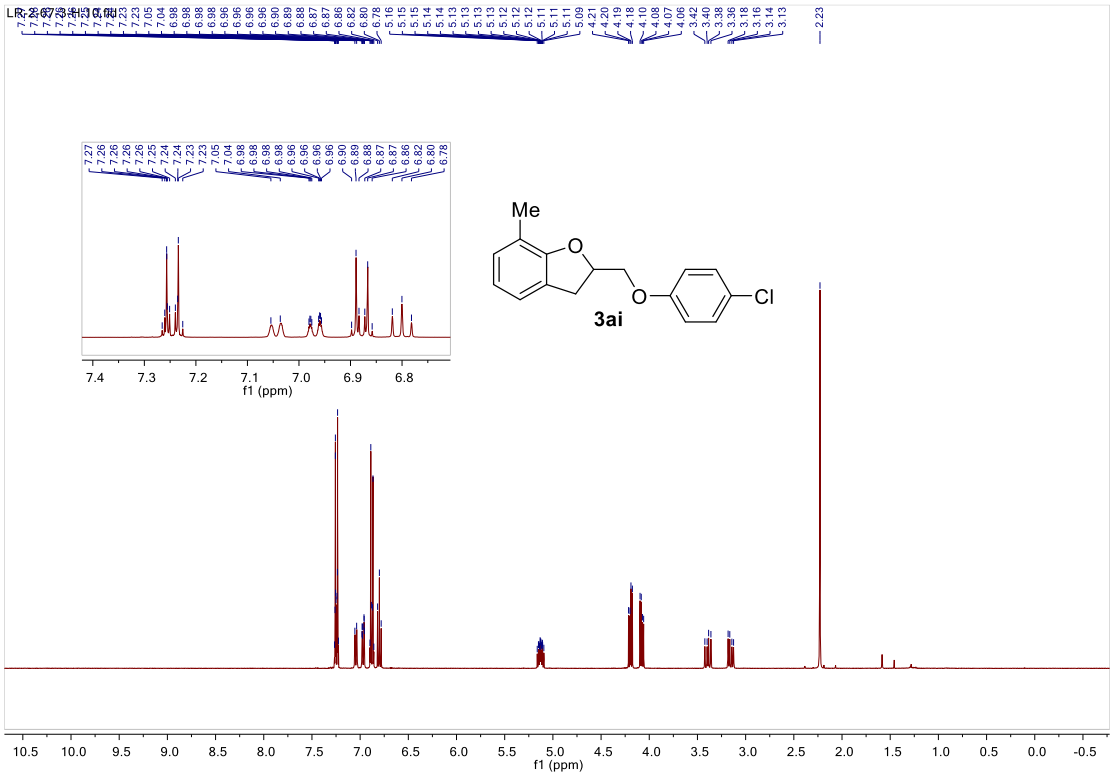

Figure 2.62 ^{13}C NMR Spectrum of 3ai

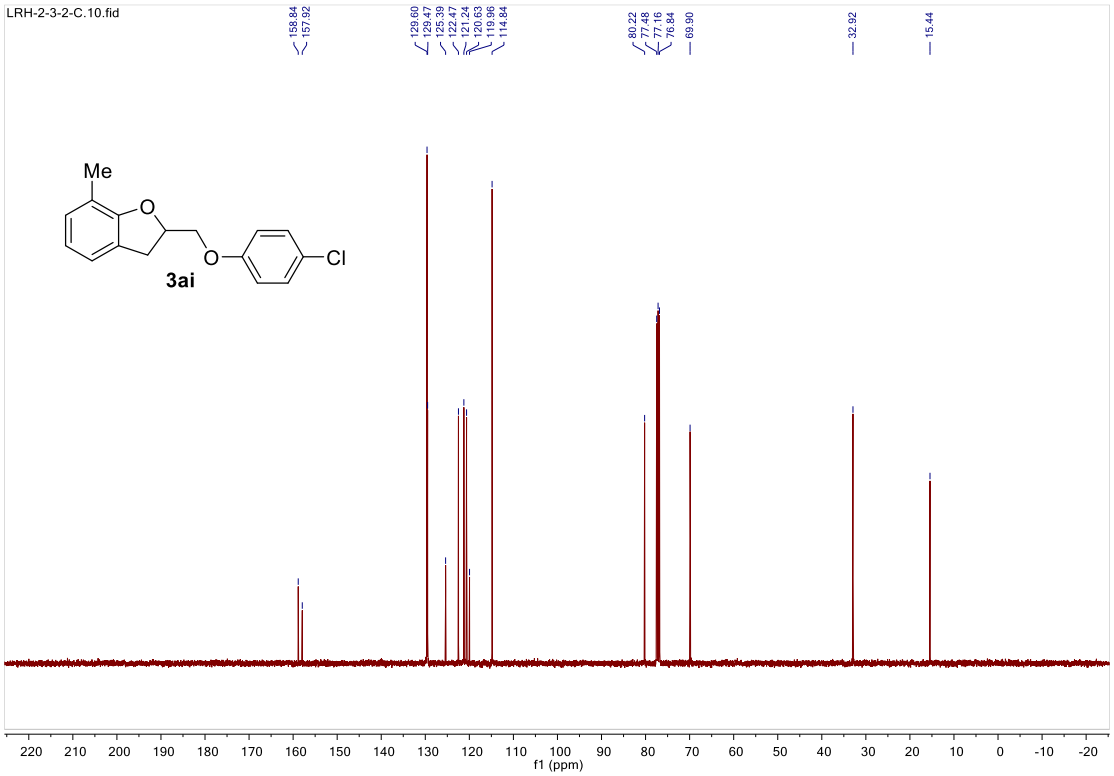

Figure 2.63 ^{1}H NMR Spectrum of 3aj

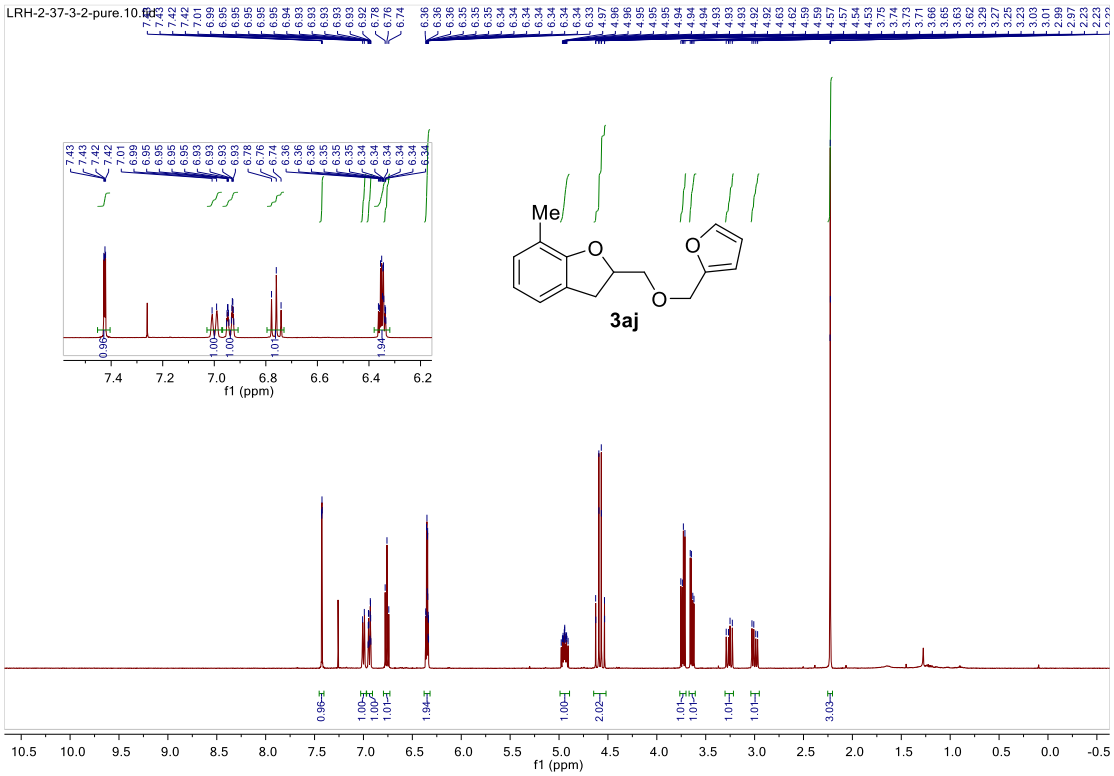

Figure 2.64 ^{13}C NMR Spectrum of 3aj

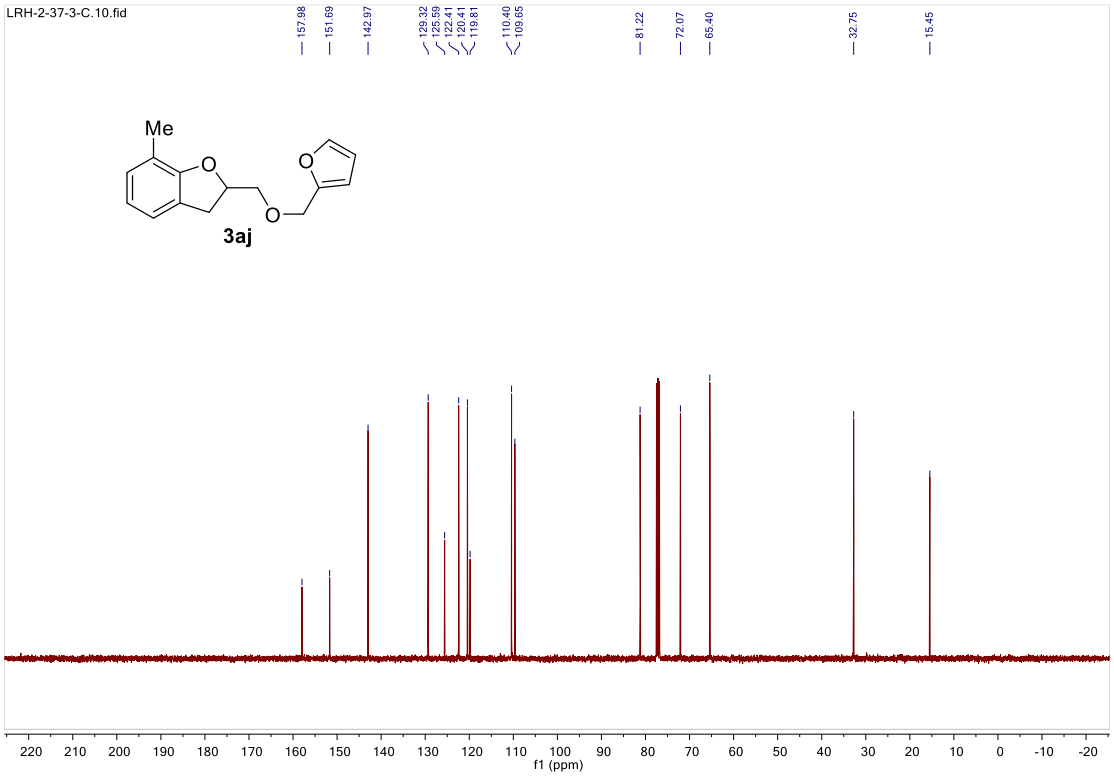

Figure 2.65 ^{1}H NMR Spectrum of 3ak

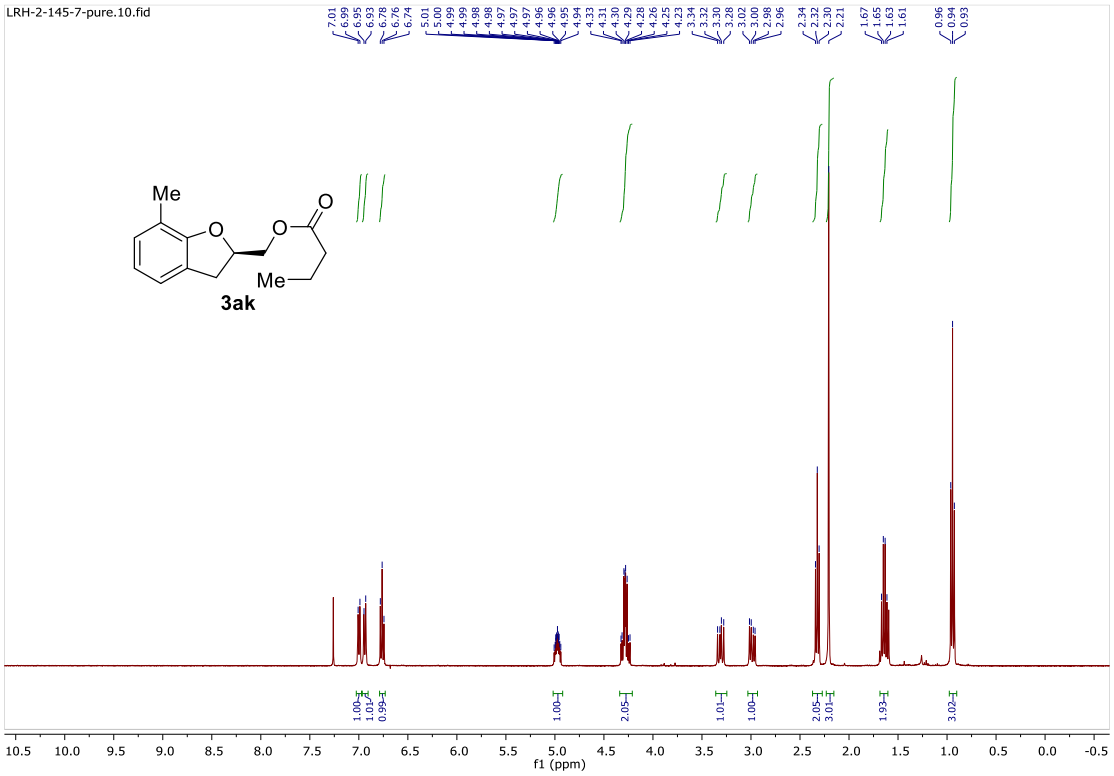

Figure 2.66 ^{13}C NMR Spectrum of 3ak

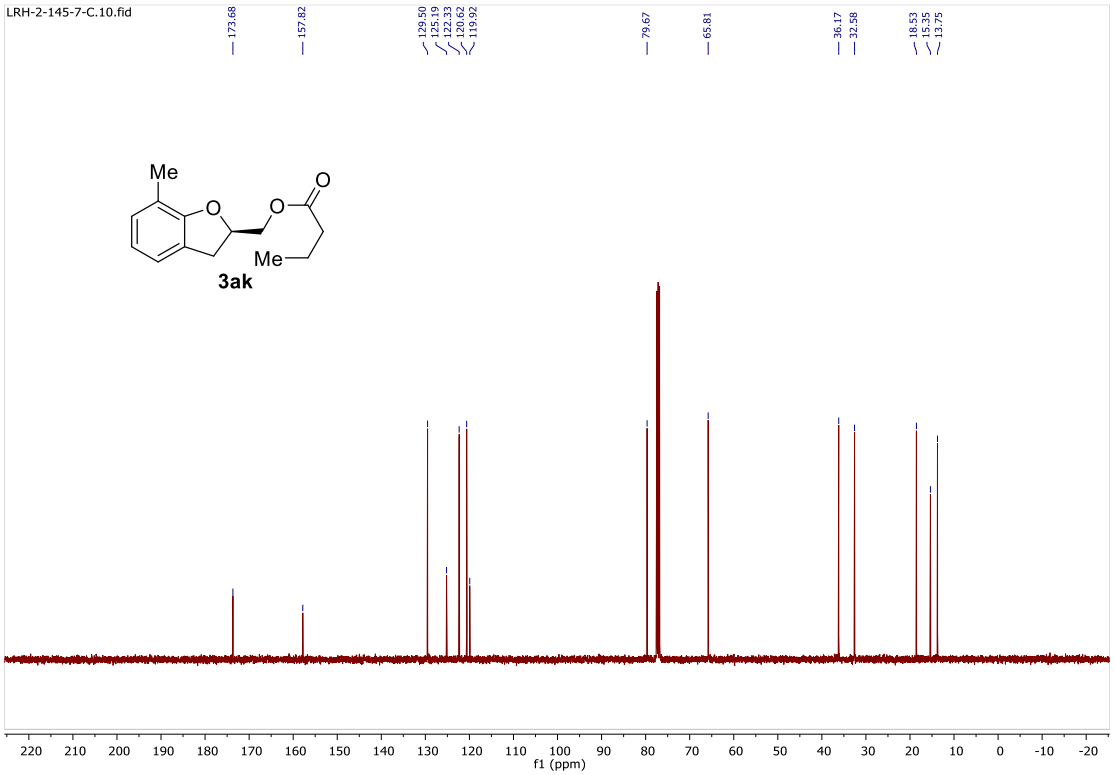

Figure 2.67 ^{1}H NMR Spectrum of 3al

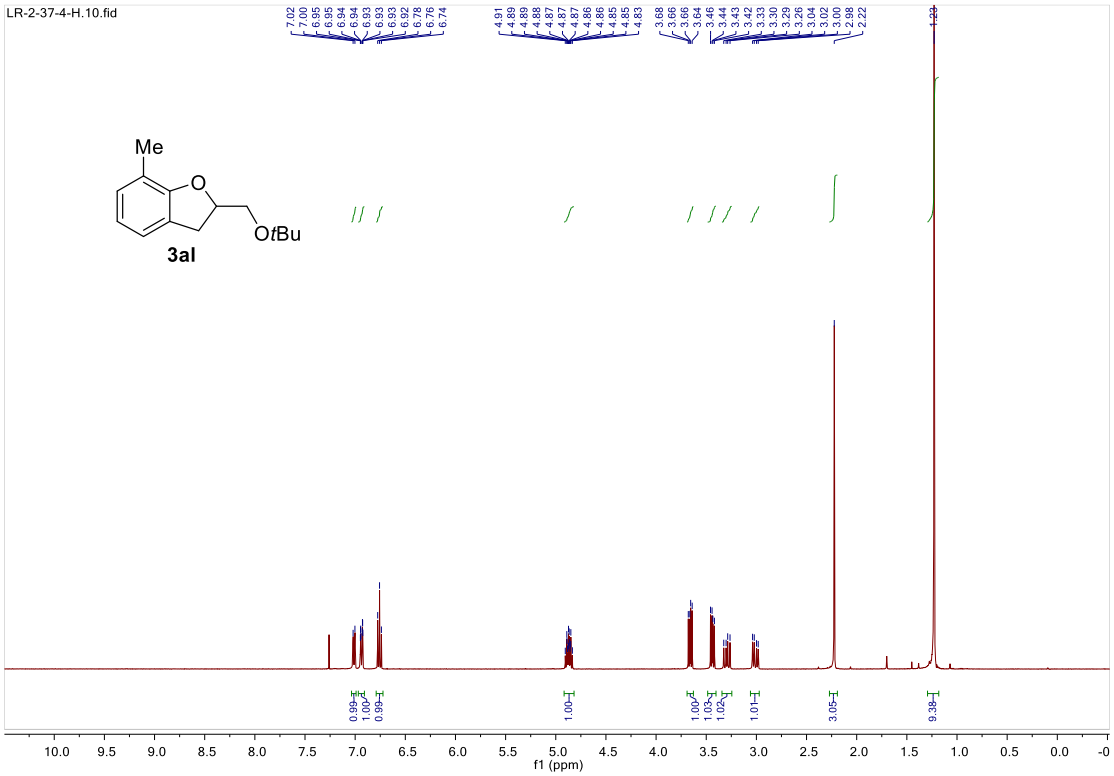

Figure 2.68 ^{13}C NMR Spectrum of 3al

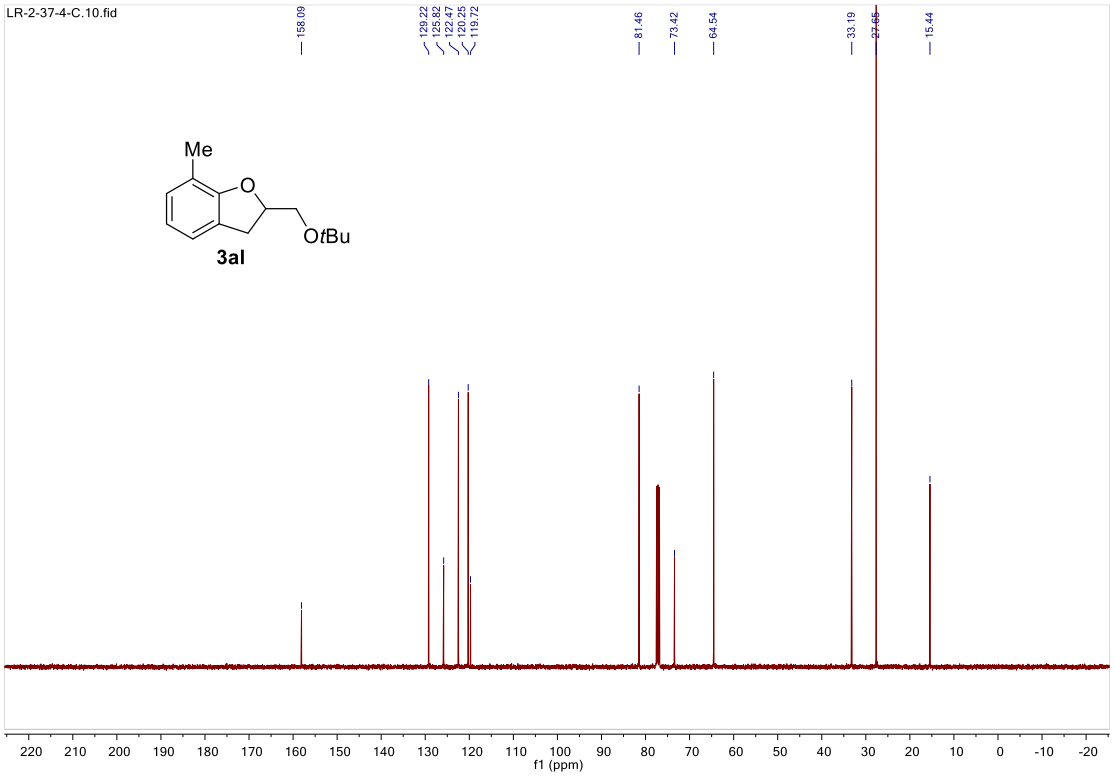

Figure 2.69 ^{1}H NMR Spectrum of 3qc

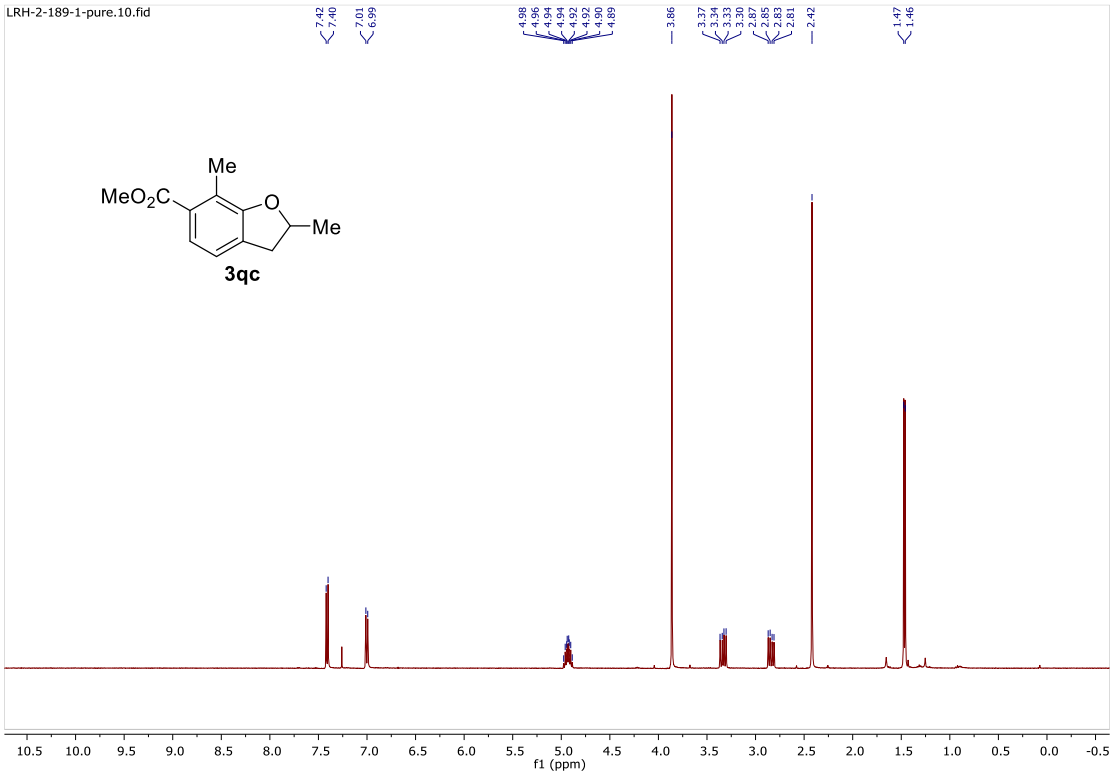

Figure 2.70 ^{13}C NMR Spectrum of 3qc

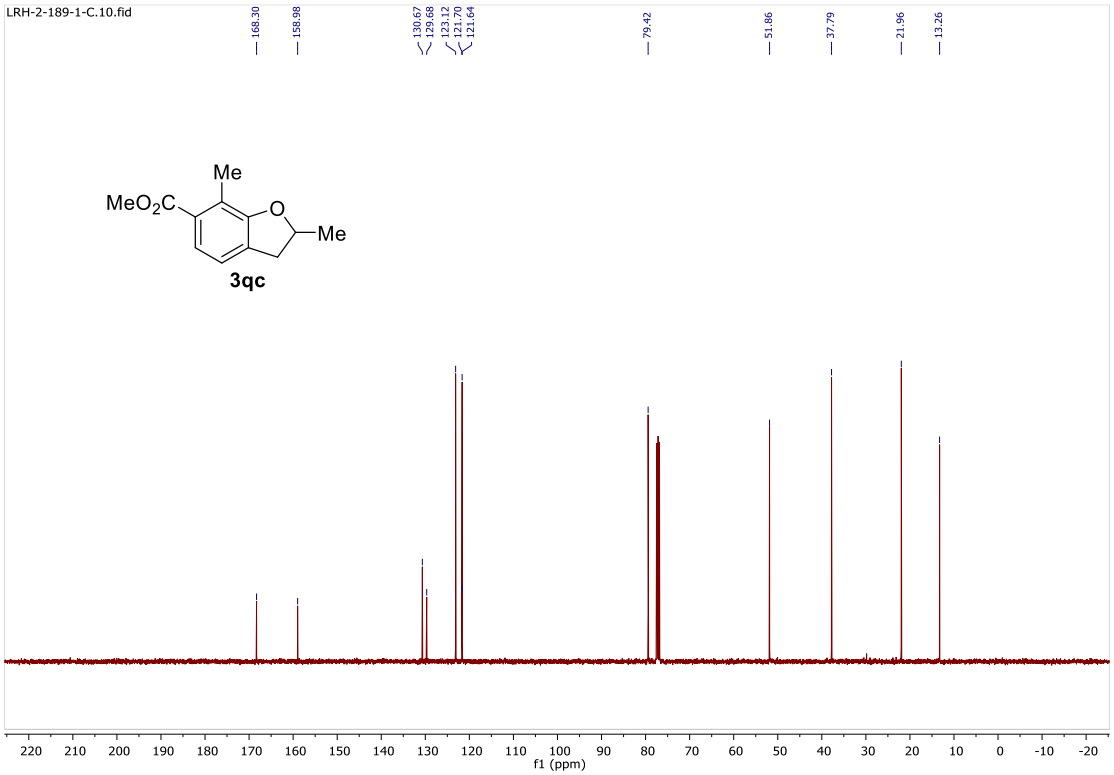

Figure 2.71 ^{1}H NMR Spectrum of Fufenozide

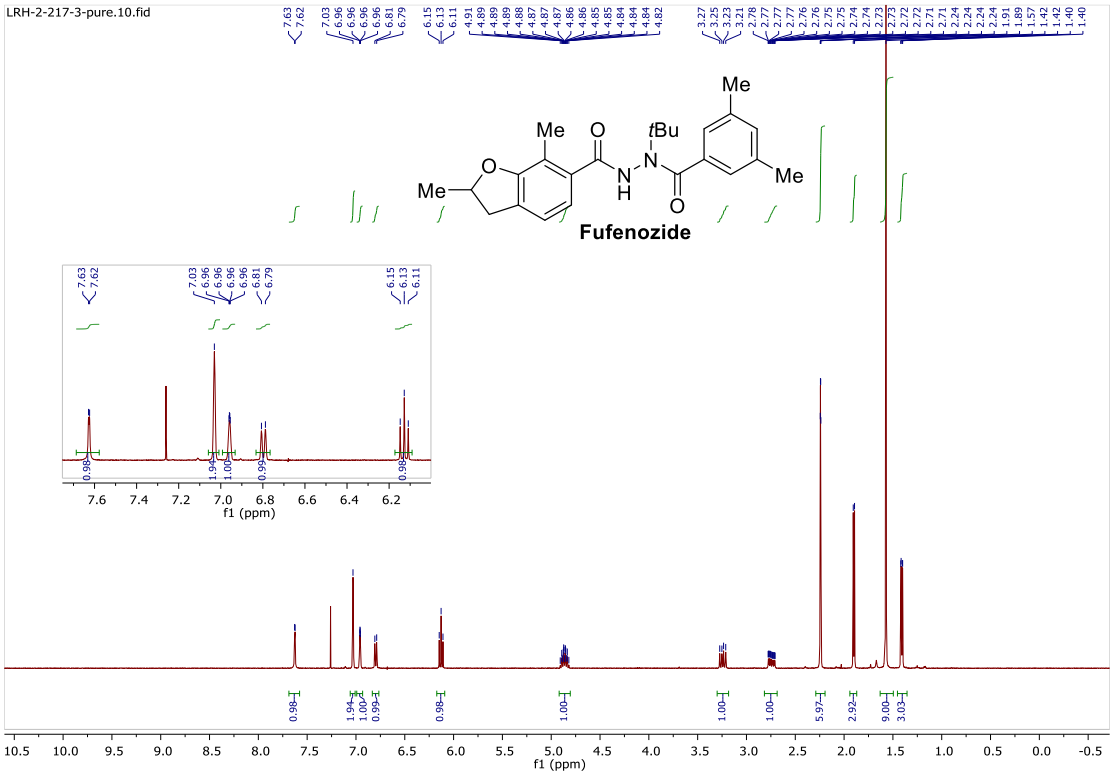

Figure 2.72 ^{13}C NMR Spectrum of Fufenozide

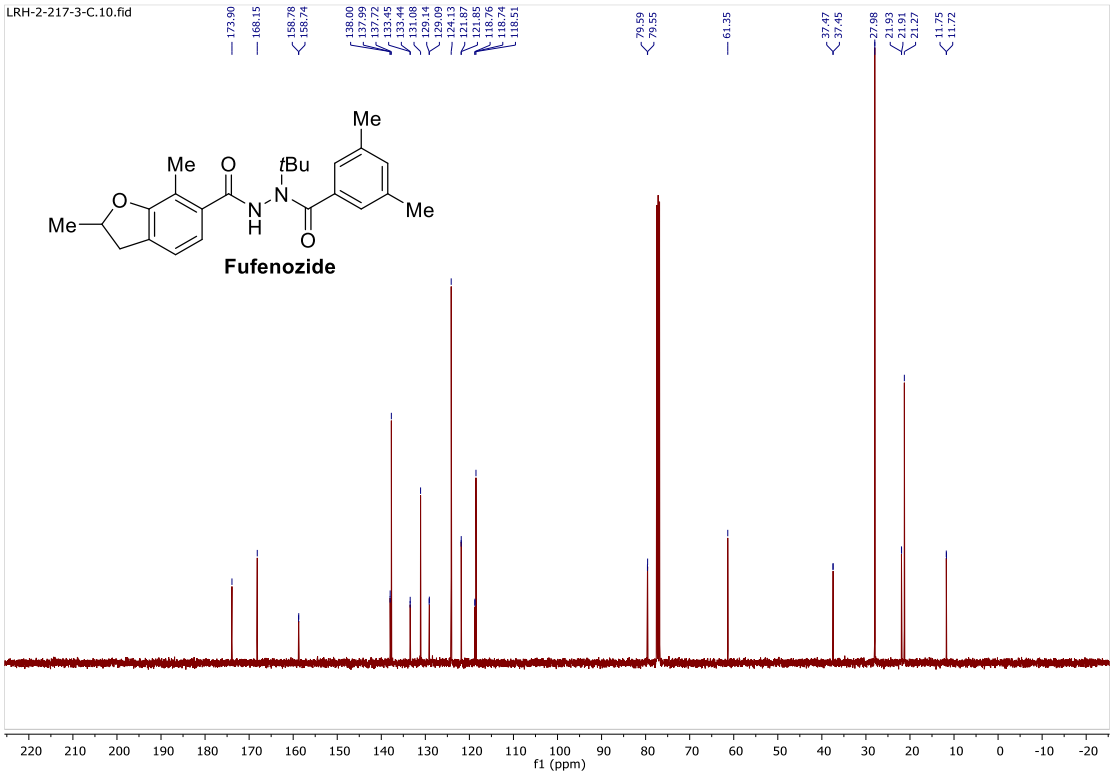

2.6 Crystallographic Data

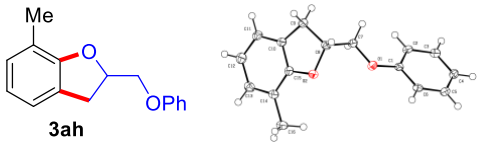

3ah

Table 2.4. Crystallographic Data of 3ah

Identification code	LRH-2-165-1
Empirical formula	$C_{16}H_{16}O_2$
Formula weight	240.29
Temperature/K	100.0
Crystal system	monoclinic
Space group	$P2_1/c$
a/Å	22.201(3)
b/Å	5.2045(6)
c/Å	10.8034(12)
α/°	90
β/°	97.896(3)
γ/°	90
Volume/Å^3	1236.4(2)
Z	4
ρ_{calc}g/cm^3	1.291
μ/mm^{-1}	0.084
F(000)	512.0
Crystal size/mm^3	0.05 × 0.05 × 0.035
Radiation	MoKα (λ = 0.71073)
2Θ range for data collection/°	1.852 to 55.142
Index ranges	$-28 \leq h \leq 28$, $-6 \leq k \leq 6$, $-14 \leq l \leq 14$
Reflections collected	19036
Independent reflections	2855 [R_{int} = 0.0557, R_{sigma} = 0.0385]
Data/restraints/parameters	2855/0/164
Goodness-of-fit on F^2	1.071
Final R indexes [I>=2σ (I)]	R_1 = 0.0524, wR_2 = 0.1160
Final R indexes [all data]	R_1 = 0.0763, wR_2 = 0.1314
Largest diff. peak/hole / e Å^{-3}	0.33/-0.23

2.7 References

(1) (a) D. E. Nichols, A. J. Hoffman, R. A. Oberlender, R. M. Riggs, *J. Med. Chem.* **1986**, *29*, 302-304; (b) M. Saito, M. Ueo, S. Kametaka, O. Saigo, S. Uchida, H. Hosaka, K. Sakamoto, T. Nakahara, A. Mori, K. Ishii, *Biol. Pharm. Bull.* **2008**, *31*, 1959-1963; (c) Z. Huang, Q. Cui, L. Xiong, Z. Wang, K. Wang, Q. Zhao, F. Bi, Q. Wang, *J. Agric. Food. Chem.* **2009**, *57*, 2447-2456; (d) I.-S. Lee, H.-J. Kim, U.-J. Youn, Q.-C. Chen, J.-P. Kim, D. T. Ha, T. M. Ngoc, B.-S. Min, S.-M. Lee, H.-J. Jung, M.-K. Na, K.-H. Bae, *Helv. Chim. Acta* **2010**, *93*, 272-276; (e) A. Radadiya, A. Shah, *Eur. J. Med. Chem.* **2015**, *97*, 356-376.

(2) For a recent review of the synthesis of 2,3-dihydrobenzofurans, see: (a) F. Bertolini, M. Pineschi, *Org. Prep. Proced. Int.* **2009**, *41*, 385-418; (b) T. D. Sheppard, *J. Chem. Res.* **2011**, *35*, 377−385.

(3) For selected examples on synthesizing DHBFs through hydroalkoxylation reactions, see: (a) Ohkawa, S.; Fukatsu, K.; Miki, S.; Hashimoto, T.; Sakamoto, J.; Doi, T.; Nagai, Y.; Aono, T. *J. Med. Chem.* **1997**, *40*, 559; (b) S. Kantevari, D. Addla, B. Sridhar, *Synthesis* **2010**, *2010*, 3745-3754; (c) J. Schlüter, M. Blazejak, L. Hintermann, *ChemCatChem* **2013**, *5*, 3309-3315.

(4) S. Beltrán-Rodil, D. Peña, E. Guitián, *Synlett* **2007**, *8*, 1308-1310.

(5) For reviews on Catellani reaction, see: (a) M. Catellani, *Top. Organomet. Chem.* **2005**, *14*, 21-53; (b) M. Catellani, E. Motti, N. Della Ca', *Acc. Chem. Res.* **2008**, *41*, 1512-1522; (c) A. Martins, B. Mariampillai, M. Lautens, *Top. Curr. Chem.* **2010**, *292*, 1-33; (d) R. Ferraccioli, *Synthesis* **2013**, *45*, 581-591; (e) J. Ye, M. Lautens, *Nat. Chem.* **2015**, *7*, 863-870; (f) N. Della Ca', M. Fontana, E. Motti, M. Catellani, *Acc. Chem. Res.* **2016**, *49*, 1389-1400.

(6) For representative examples involving *ortho* alkylation, see: (a) M. Catellani, F. Frignani, A. Rangoni, *Angew. Chem. Int. Ed.* **1997**, *36*, 119-122; *Angew. Chem.* **1997**, *109*, 142-145; (b) M. Catellani, E. Motti, M. Minari, *Chem. Commun.* **2000**, 157-158; (c) A. Martins, M. Lautens, *Org. Lett.* **2008**, *10*, 5095-5097; (d) L. Jiao, T. Bach, *J. Am. Chem. Soc.* **2011**, *133*, 12990-12993; (e) H. Weinstabl, M. Suhartono, Z. Qureshi, M. Lautens, *Angew. Chem. Int. Ed.* **2013**, *52*, 5305-5308; *Angew. Chem.* **2013**, *125*, 5413-5416; (f) H. Zhang, P. Chen, G. Liu, *Angew. Chem. Int. Ed.* **2014**, *53*, 10174-10178; *Angew. Chem.* **2014**, *126*, 10338-10342; (g) Z. Qureshi, W. Schlundt, M. Lautens, *Synthesis* **2015**, *47*, 2446-2456. (h) C. Lei, X. Jin, J. Zhou, *Angew. Chem. Int. Ed.* **2015**, *54*, 13397-13400; *Angew. Chem.* **2015**, *127*, 13595-13598; (i) C. Lei, X. Jin, J. Zhou, *ACS Catal.* **2016**, *6*, 1635-1639; (j) C. Lei, J. Cao, J. Zhou, *Org. Lett.* **2016**, *18*, 6120-6123; (k) X. Sui, L. Ding, Z. Gu, *Chem. Commun.* **2016**, *52*, 13999-14002; (l) F. Sun, M. Li, Z. Gu, *Org. Chem. Front.* **2016**, *3*, 309.

(7) For representative examples involving *ortho* arylation, see: (a) M. Catellani, E. Motti, S. Baratta, *Org. Lett.* **2001**, *3*, 3611-3614; (b) F. Faccini, E. Motti, M. Catellani, *J. Am. Chem. Soc.* **2004**, *126*, 78-79; (c) B. Mariampillai, J. Alliot, M. Li, M. Lautens, *J. Am. Chem. Soc.* **2007**, *129*, 15372-15379; (d) Y.-B. Zhao, B. Mariampillai, D. A. Candito, B. Laleu, M. Li, M. Lautens, *Angew. Chem. Int. Ed.* **2009**, *48*, 1849-1852; *Angew. Chem.* **2009**, *121*, 1881-1884; (e) A. Martins, D. A. Candito, M. Lautens, *Org. Lett.* **2010**, *12*, 5186-5188; (f) E. Motti, N. Della Ca', D. Xu, A. Piersimoni, E. Bedogni, Z.-M. Zhou, M. Catellani, *Org. Lett.* **2012**, *14*, 5792-5795; (g) D. Xu, L. Dai, M. Catellani, E. Motti, N. Della Ca, Z. Zhou, *Org. Biomol. Chem.* **2015**, *13*, 2260-2263; (h) X.-C. Wang, W. Gong, L.-Z. Fang, R.-Y. Zhu, S. Li, K. M. Engle, J.-Q. Yu, *Nature* **2015**, *519*, 334-338; (i) Z. Dong, J. Wang, G. Dong, *J. Am. Chem. Soc.* **2015**, *137*, 5887-5890; (j) K. Zhao, S. Xu, C. Pan, X. Sui, Z. Gu, *Org. Lett.* **2016**, *18*, 3782-3785; (k) D. Rasina, A. Kahler-Quesada, S.

Ziarelli, S. Warratz, H. Cao, S. Santoro, L. Ackermann, L. Vaccaro, *Green Chem.* **2016**, *18*, 5025-5030.

(8) For *ortho* amination, see: (a) Z. Dong, G. Dong, *J. Am. Chem. Soc.* **2013**, *135*, 18350-18353; (b) Z.-Y. Chen, C.-Q. Ye, H. Zhu, X.-P. Zeng, J.-J. Yuan, *Chem. Eur. J.* **2014**, *20*, 4237-4241; (c) C. Ye, H. Zhu, Z. Chen, *J. Org. Chem.* **2014**, *79*, 8900-8905; (d) H. Shi, D. J. Babinski, T. Ritter, *J. Am. Chem. Soc.* **2015**, *137*, 3775-3778; (e) F. Sun, Z. Gu, *Org. Lett.* **2015**, *17*, 2222-2225; (f) S. Pan, X. Ma, D. Zhong, W. Chen, M. Liu, H. Wu, *Adv. Synth. Catal.* **2015**, *357*, 3052-3056; (g) B. Luo, J.-M. Gao, M. Lautens, *Org. Lett.* **2016**, *18*, 4166-4169; (h) B. Majhi, B. C. Ranu, *Org. Lett.* **2016**, *18*, 4162-4165; (i) P. Wang, G.-C. Li, P. Jain, M. E. Farmer, J. He, P.-X. Shen, J.-Q. Yu, *J. Am. Chem. Soc.* **2016**, *138*, 14092-14099; j) J. Wang, Z. Gu, *Adv. Synth. Catal.* **2016**, *358*, 2990-2995; k) W. C. Fu, B. Zheng, Q. Zhao, W. T. K. Chan, F. Y. Kwong, *Org. Lett.* **2017**, *19*, 4335-4338.

(9) For *ortho* acylation, see: (a) P.-X. Zhou, Y.-Y. Ye, C. Liu, L.-B. Zhao, J.-Y. Hou, D.-Q. Chen, Q. Tang, A.-Q. Wang, J.-Y. Zhang, Q.-X. Huang, P.-F. Xu, Y.-M. Liang, *ACS Catal.* **2015**, *5*, 4927-4931; (b) Z. Dong, J. Wang, Z. Ren, G. Dong, *Angew. Chem. Int. Ed.* **2015**, *54*, 12664-12668; *Angew.Chem.* **2015**, *127*,12855–12859; (c) Y. Huang, R. Zhu, K. Zhao, Z. Gu, *Angew. Chem. Int. Ed.* **2015**, *54*, 12669-12672; *Angew. Chem.* **2015**, *127*, 12860-12863; (d) X. Li, J. Pan, S. Song, N. Jiao, *Chem. Sci.* **2016**, *7*, 5384-5389; (e) F. Sun, M. Li, C. He, B. Wang, B. Li, X. Sui, Z. Gu, *J. Am. Chem. Soc.* **2016**, *138*, 7456-7459.

(10) For ortho carboxylation, see: J. Wang, L. Zhang, Z. Dong, G. Dong, *Chem*, *1*, 581-591.

(11) For seminal works, see: (a) M. Lautens, S. Piguel, *Angew. Chem. Int. Ed.* **2000**, *39*, 1045-1046; *Angew. Chem.* **2000**, *112*, 1087-1088; (b) C. Bressy, D. Alberico, M. Lautens, *J. Am. Chem. Soc.* **2005**, *127*, 13148-13149; (c) A. Rudolph, N. Rackelmann, M. Lautens, *Angew. Chem. Int. Ed.*

2007, *46*, 1485-1488; *Angew. Chem.* **2007**, *119*, 1507-1510; (d) P. Thansandote, M. Raemy, A. Rudolph, M. Lautens, *Org. Lett.* **2007**, *9*, 5255-5258; (e) K. M. Gericke, D. I. Chai, N. Bieler, M. Lautens, *Angew. Chem. Int. Ed.* **2009**, *48*, 1447-1451; *Angew. Chem.* **2009**, *121*, 1475-1479; (f) D. A. Candito, M. Lautens, *Angew. Chem. Int. Ed.* **2009**, *48*, 6713-6716; *Angew. Chem.* **2009**, *121*, 6841-6844; (g) D. A. Candito, M. Lautens, *Org. Lett.* **2010**, *12*, 3312-3315; (h) H. Liu, M. El-Salfiti, M. Lautens, *Angew. Chem. Int. Ed.* **2012**, *51*, 9846-9850; *Angew. Chem.* **2012**, *124*, 9984-9988.

(12) C.-Y. Huang, A. G. Doyle, *Chem. Rev.* **2014**, *114*, 8153-8198.

(13) (a) K. E. Torraca, X. Huang, C. A. Parrish, S. L. Buchwald, *J. Am. Chem. Soc.* **2001**, *123*, 10770-10771; (b) S.-i. Kuwabe, K. E. Torraca, S. L. Buchwald, *J. Am. Chem. Soc.* **2001**, *123*, 12202-12206; (c) A. V. Vorogushin, X. Huang, S. L. Buchwald, *J. Am. Chem. Soc.* **2005**, *127*, 8146-8149.

(14) N. C. Bruno, N. Niljianskul, S. L. Buchwald, *J. Org. Chem.* **2014**, *79*, 4161-4166.

(15) M. Catellani, G. P. Chiusoli, S. Ricotti, F. Sabini, *Gazz. Chim. Ital.* **1985**, *115*, 685-689.

(16) (a) For the first preparation of an ester-substituted NBE, see: R. A. Finnegan, R. S. McNees, *J. Org. Chem.* **1964**, *29*, 3234-3241; (b) For the first use of an ester-substituted NBE in a *meta*-functionalization of arene, see: P.-X. Shen, X.-C. Wang, P. Wang, R.-Y. Zhu, J.-Q. Yu, *J. Am. Chem. Soc.* **2015**, *137*, 11574-11577.

(17) Di- and tri-substituted epoxides are not reactive under the current conditions.

(18) (a) X. Zhang, Y. Li, L. Zhu, L. Liu, X. Sha, H. Xu, H. Ma, F. Wang, Y. Ni, L. Guo, CN 1313276, **2001**. (b) N. Xu, Y. Zhang, X. Zhang, J. Ni, J. Xiong, M. Shen, CN 1918986, **2007**.

(19) Z. Huang, Y. Liu, Y. Li, L. Xiong, Z. Cui, H. Song, H. Liu, Q. Zhao, Q. Wang, *J. Agric. Food. Chem.* **2011**, *59*, 635-644.

(20) H. D. Verkruijsse, L. Brandsma, *Recl. Trav. Chim. Pays-Bas* **1986**, *105*, 66-68.

(21) L. A. M. Cornelius, R. G. A. Bone, R. H. Hastings, M. A. Deardorff, R. A. Scharlach, B. E. Hauptmann, C. S. Stankovic, H. W. Pinnick, *J. Org. Chem.* **1993**, *58*, 3188-3190.

(22) K. Nozaki, US Patent 5399647 A, **1995**.

(23) R. Krishnamurti, D. R. Bellew, G. K. S. Prakash, *J. Org. Chem.* **1991**, *56*, 984-989.

(24) Wang, Q. M.; Huang, R. Q. *Phosphorus Sulfur* **2000**, *161*, 173-179.

(25) P. Mayo, W. Tam, *Tetrahedron* **2002**, *58*, 9527-9540.

(26) X. Zhu, G. Li, F. Xu, Y. Zhang, M. Xue, Q. Shen, *Tetrahedron* **2017**, *73*, 1451-1458.

(27) (a) X. Zhang, Y. Li, L. Zhu, L. Liu, X. Sha, H. Xu, H. Ma, F. Wang, Y. Ni, L. Guo, CN 1313276, **2001**; (b) N. Xu, Y. Zhang, X. Zhang, J. Ni, J. Xiong, M. Shen, CN 1918986, **2007**.

(Some contents of this chapter were published in *Angew. Chem. Int. Ed.* **2018**, *57*, 1697-1701.)

CHAPTER 3

Palladium-catalyzed Asymmetric Annulation between Aryl Iodides and Racemic Epoxides Using a Chiral Norbornene Cocatalyst

3.1 Introduction

Dihydrobenzofuran (DHBF) moiety is frequently found in pharmaceuticals and agrochemicals The 2,3-dihydrobenzofuran (DHBF) moiety is frequently found in pharmaceuticals and agrochemicals that are commonly prepared in their enantiopure form (Fig. 3.1).[1] While a number of approaches have been developed for DHBFs, asymmetric synthesis of this structural motif is rare.[2,3] Recently, we reported a direct annulation between simple aryl iodides and terminal epoxides for synthesis of DHBFs via palladium/norbornene (Pd/NBE) cooperative catalysis, also known as Catellani-type reactions (Scheme 3.1a).[4-6] The reaction shows a reasonably broad substrate scope with high yields and excellent functional group tolerance; however, the DHBF products generated in this reaction are racemic. While using an enantiopure epoxide as a coupling partner can lead to enantiomerically

enriched products,[4] prior chiral resolution or asymmetric synthesis of epoxides would be needed.[7] Given the wide availability of racemic epoxides from both commercial and preparative prospects, it would be attractive if one enantiomer of racemic epoxides could selectively react *during* their annulative coupling with aryl iodides.[8] Herein, we describe our preliminary results on a palladium-catalyzed asymmetric DHBF synthesis between aryl iodides and racemic epoxides using an enantiopure NBE cocatalyst (Scheme 3.1b). To the best of our knowledge, this should represent the first chiral NBE scaffold-promoted asymmetric reactions in aryl halide-mediated Pd/NBE catalysis.[9,10,11]

Figure 3.1. Bioactive Compounds Containing Chiral 2,3-Dihydrobenzofurans

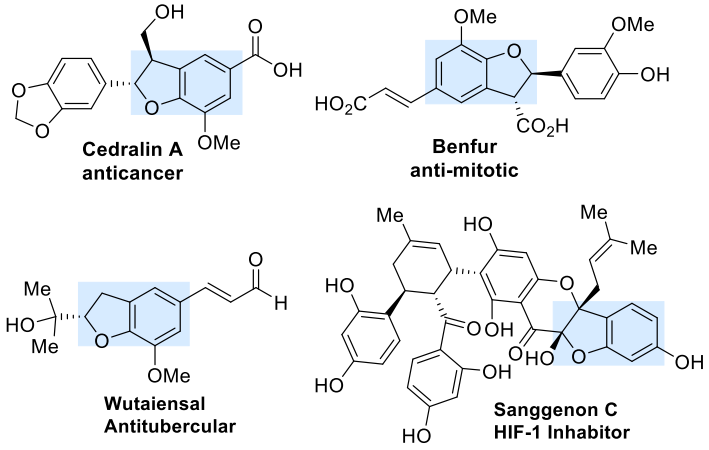

Scheme 3.1. Annulation Between Aryl Iodides and Racemic Epoxides

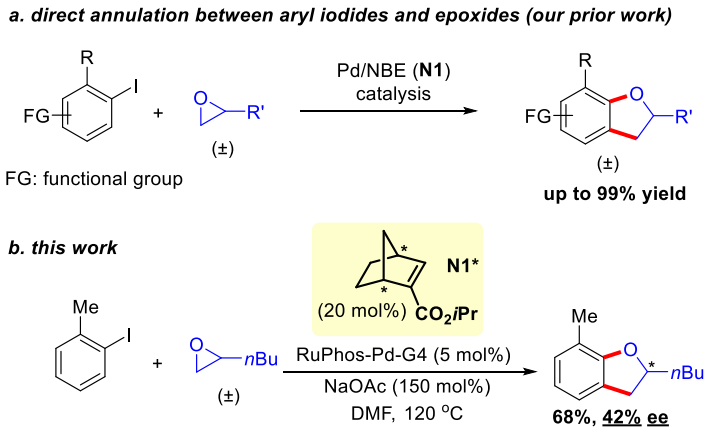

3.2 Results and Discussion

3.2.1 Reaction Discovery and Optimization

The optimal NBE cocatalyst found in this annulation reaction was the isopropyl ester-derived NBE (**N1**).[12] Given that the scaffold of **N1** is chiral, we were motivated to examine the feasibility of realizing a kinetic resolution in the coupling with racemic epoxides using enantiopure **N1**. We hypothesized that, during the reaction of the key **ANP** intermediate, the chirality of NBE **N1** would create a chiral pocket around the palladium, which could consequently promote one enantiomer of the epoxide to react faster than the other one (Step D, Fig. 3.2).

To test the hypothesis, a reliable route was first developed to prepare enantiopure **N1*** (Scheme 3.2). Using 2,10-camphorsultam as a chiral auxiliary, the diastereomeric amide-derived NBEs (**A** and **B**) were separated through silica gel chromatography, and each could be isolated in good yields. The structures of NBEs **A** and **B** have also been characterized through X-ray crystallography (Fig. 3.3). Subsequent hydrolysis and esterification afforded the desired enantiomerically enriched **N1*** in 42% yield (98% ee).

Figure 3.2. Proposed Catalytic Cycle

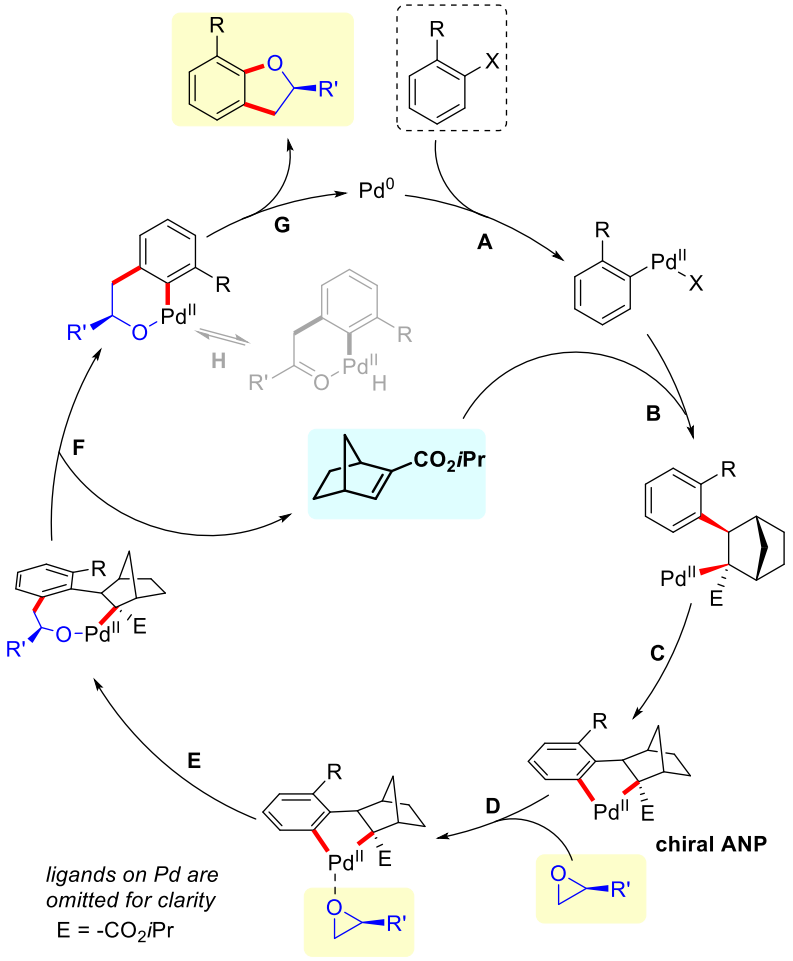

Scheme 3.2. Preparation of Enantiomerically Enriched N1*

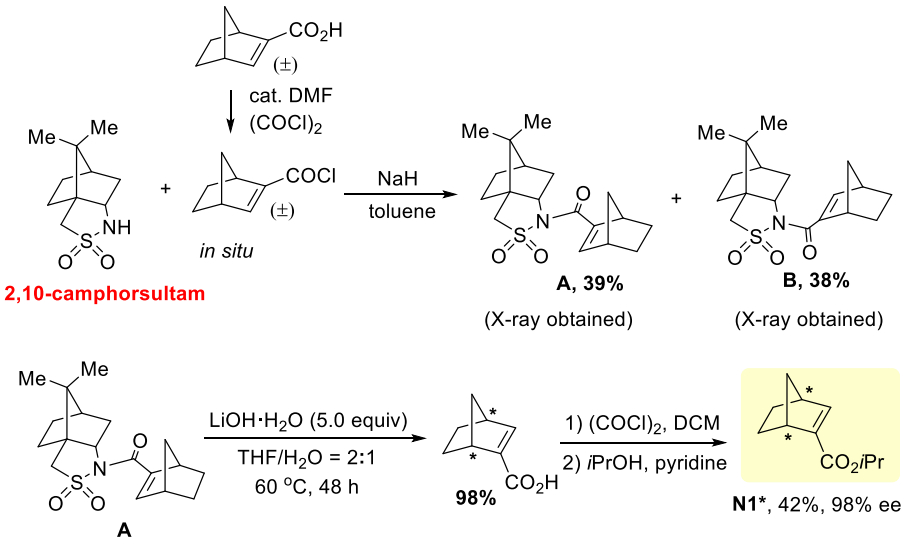

Figure 3.3. X-Ray Crystal Structures of Chiral NBEs A and B

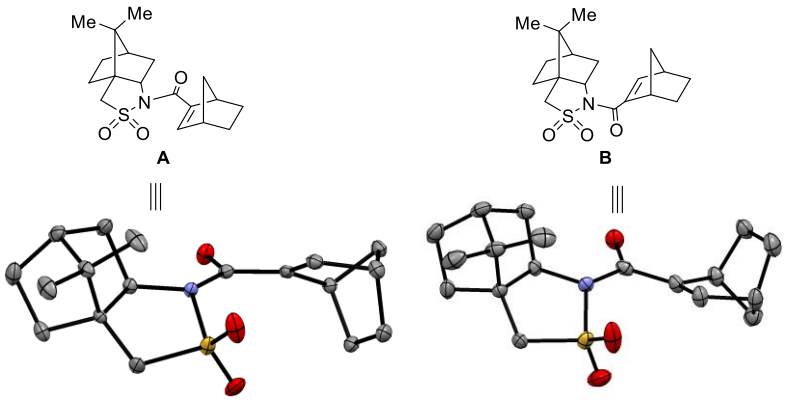

To our delight, the preliminary result shows that, when 20 mol% **N1*** was employed as the ligand, promising enantioselectivity (42% ee) could be obtained (Table 3.1, entry 1). It is worthy to mention that direct use of sulfonamide NBE **A** could also give the desired product with moderate enantioselectivity (Table 3.1, entry 2). To further optimize the enantioselectivity, different reaction conditions were applied (Table 3.1). First, using different reaction temperatures (entries 3-5), adding more **N1*** (entry 6), running the reaction with a mixed solvent (entry 7) or changing the reaction time (entries 8-9) nearly had no influence on the enantioselectivity. In addition, employing a metal-Salen complex as a chiral Lewis acid cocatalyst (entries 10-12) completely shut down the reaction. Decreasing the amount of epoxide **2a** from 4.0 equiv to 0.5 equiv (entries 13-15) gave lower yield and lower enantioselectivity, though the exact reason is unclear.

Table 3.1. Optimization Study Based on N1*[a]

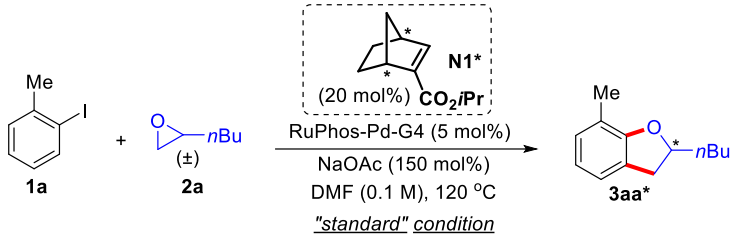

Entry	Change from the standard condition	Yield [%][c]	ee [%][d]
1	**none**	68	**42**
2[b]	**A** instead of **N1***	45	33
3	100 °C	67	41
4	80 °C	31	43
5	60 °C	19	44
6	40 mol% **N1***	31	41
7	DMF/dioxane = 4:1	80	40
8	5 h	37	41
9	10 h	60	41
10	adding 5 mol% Co(Salen)	trace	-
11	adding 5 mol% Cr(Salen)	trace	-
12	adding 5 mol% Mn(Salen)	trace	-
13	2.0 equiv **2a**	66	31
14	1.0 equiv **2a**	53	28
15	0.5 equiv **2a**	32	33

[a]The reaction was run with 0.2 mmol **1a** and 0.8 mmol **2a** in 2 mL DMF for 24h. [b]150 mol% of **A** was used. [c]Yields are determined by ^{1}H NMR analysis using 1,3,5-trimethoxybenzene as the internal standard. [d]The ee was determined using chiral HPLC.

On the other hand, a series of chiral NBEs (**N1*-N13***) with ester or amide substituents have been prepared in their enantiopure forms via a similar fashion as **N1***. Their reactivity and enantioselectivity have been examined in the annulation reaction (Table 3.2). Some interesting trends have been observed. For various ester-substituted NBEs (**N1*-N6***), the isopropyl ester-derived **N1*** still gave the highest ee. Increasing or decreasing steric hindrance around the ester led to lower enantioselectivity. It is worth noting that **N3*** with a *t*-butyl ester moiety showed low

reactivity. Amide and imide-substituted NBEs were also investigated. Encouragingly, the pyrrolidine amide-derived **N7*** gave the highest enantioselectivity (45% ee or 72.5:27.5 e.r.) albeit in a low yield. Evans auxiliary-type NBEs based on chiral oxazolidinone (**N9*-N13***) have also been synthesized.[13] While the simple oxazolidinone-derived **N9*** gave a good yield and promising ee, the bulkier **N10*-N13*** cocatalysts with additional stereocenters on auxiliaries unfortunately showed no reactivity under the current conditions.

Table 3.2. Testing Different Substituted Chiral NBEs[a]

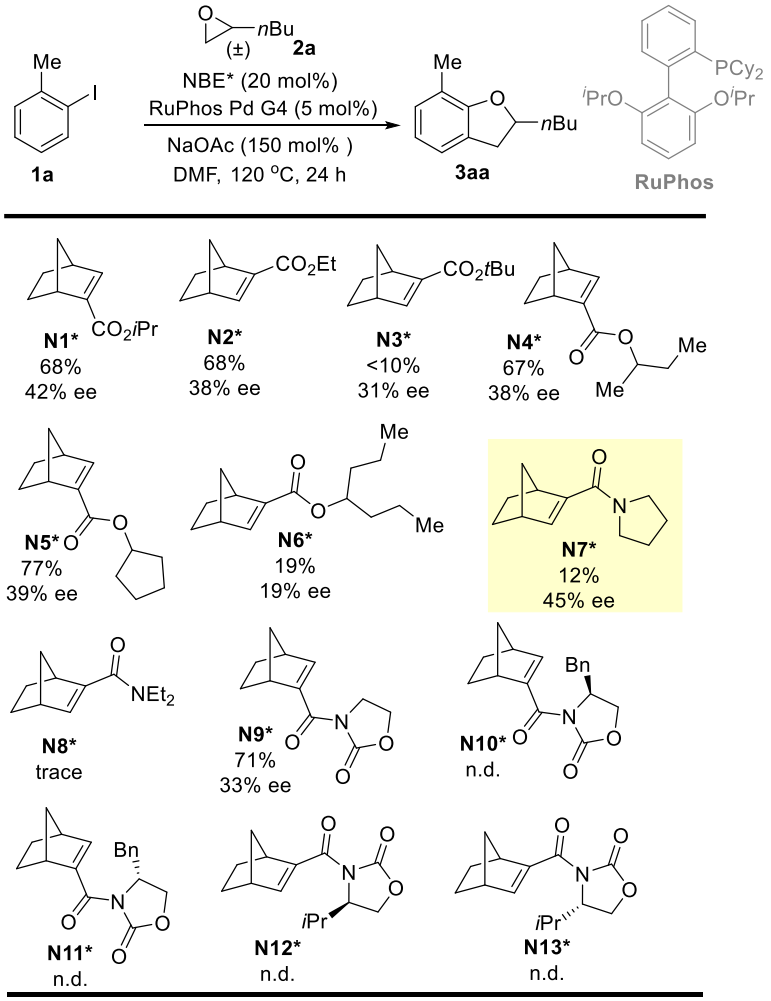

[a]The reaction was run with 0.2 mmol **1a** and 0.8 mmol **2a** in 2 mL DMF for 24h. [b]Yields are determined by ^{1}H NMR analysis using 1,3,5-trimethoxybenzene as the internal standard. [c]The ee was determined using chiral HPLC based on isolated pure products.

Considering the sharp reactivity difference between **N9*** and **N10-13***, we postulated that the steric interaction between the bulky RuPhos ligand and the additional substituent on oxazolidinone might be the reason for the low reactivity. Hence, other Buchwald phosphine ligands[14] were explored using **N12*** as the cocatalyst (Table 3.3). Interestingly, when XPhos and CPhos were employed as the ligands, the reaction with **N12*** could then provide the desired product **3aa*** in 25% ee and 31% ee, respectively (entries 1 and 2). Other Buchwald ligands still showed no reactivity similar to the case with Ruphos (entries 3-5).

Table 3.3. Reactions with N12* Using Different Buchwald Ligands

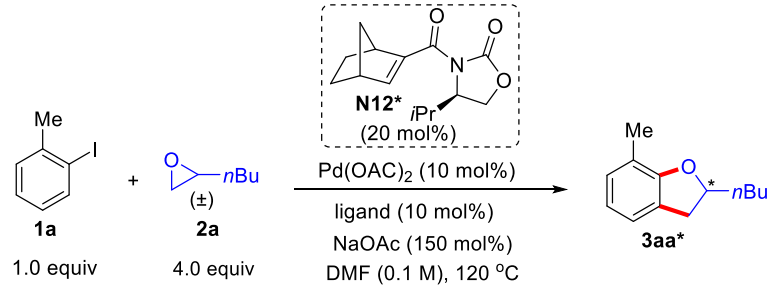

Entry	ligand	Yield [%]	ee [%]
1	XPhos	57	25
2	CPhos	24	31
3	BrettPhos	trace	-
4	DavePhos	trace	-
5	SPhos	trace	-

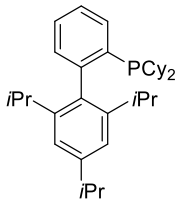

XPhos

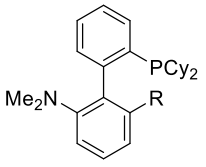

R= NMe_2 **CPhos**
R= H **Davephos**

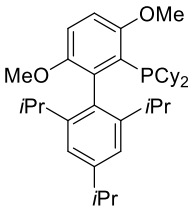

BrettPhos

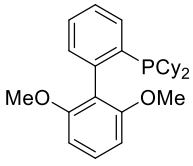

SPhos

[a]The reaction was run with 0.2 mmol **1a** and 0.8 mmol **2a** in 2 mL DMF for 24h. [b]Yields were determined by ^{1}H NMR analysis using 1,3,5-trimethoxybenzene as the internal standard. [c]The ee was determined using chiral HPLC based on isolated pure products.

Considering that XPhos ligand was the most effective ligand when using the bulky **N12*** cocatalyst, other oxazolidinone-derived **N10***, **N11*** and **N13*** were also examined under the XPhos conditions (Scheme 3.2). While **N10*** and **N11*** indeed showed good reactivity, the enantioselectivity remained moderate. Surprisingly, **N13***, a diastereomer of **N12***, only gave a trace amount of product, suggesting that the reaction is very sensitive to the steric environment around the palladium catalyst.

Scheme 3.3. Examination of N10*, N11* and N13* Cocatalysts with the XPhos Ligand

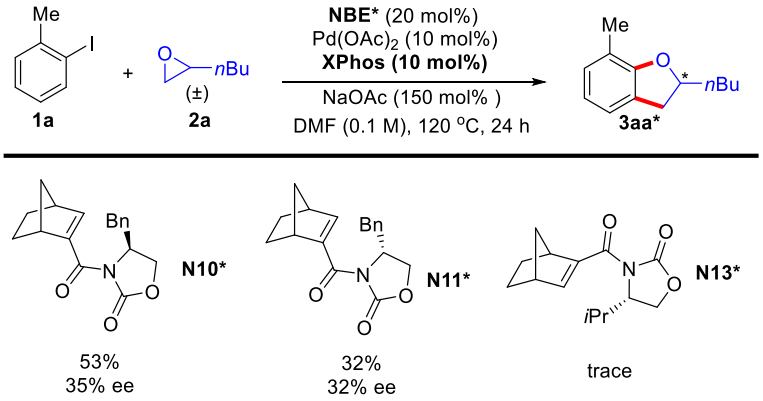

3.2.2 Substrates Scope

Then the substrate scope was briefly examined using **N1*** as the cocatalyst (Scheme 3.3). Substituted aryl iodides and more functionalized racemic epoxides were all competent substrates. The highest ee (42%) was still obtained from simple 2-iodotoluene with 1,2-epoxyhexane. Ester substitution at the para position of the aryl iodide decreased both the yield and the ee (**3ba***). In addition, glycidyl ether-type epoxides gave high yield but moderate enantioselectivity (**3ac*** and **3ab***).

Scheme 3.4. Substrate Scope with Enantiomerically Enriched N1*

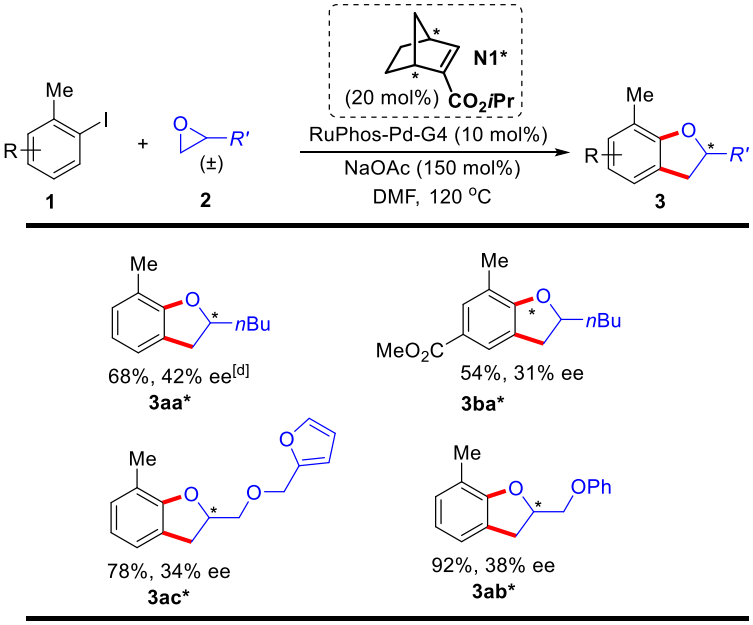

[a]The reaction was run with 0.2 mmol **1** and 0.8 mmol **2** in 2 mL DMF for 24h. [b]Yields are determined by ^{1}H NMR analysis using 1,3,5-trimethoxybenzene as the internal standard. [c]The ee was determined using chiral HPLC based on isolated pure products. [d]5 mol% of Ruphos-Pd-G4 was used.

3.2.3 Preliminary Mechanistic Study

Finally, in order to figure out the match and mismatch for the stereochemistry of NBE and epoxide, chiral epoxide (*S*)-**2b** was treated with aryl iodide **1a** in the presence of two enantiomers **(+) N1*** and **(-)N1*** as cocatalyst (Fig. 3.4). It is easily to tell from the following graph that the stereochemistry of **(-)N1*** matches epoxide (*S*)-**2b**, which gave 88% of desired product within an hour. Instead, the stereochemistry of another enantiomer **(+)N1*** doesn't match epoxide (*S*)-**2b**, which only gave 19% of desired product during the same reaction time.

Figure 3.4. Match and Mismatch between Chiral NBE and Epoxide

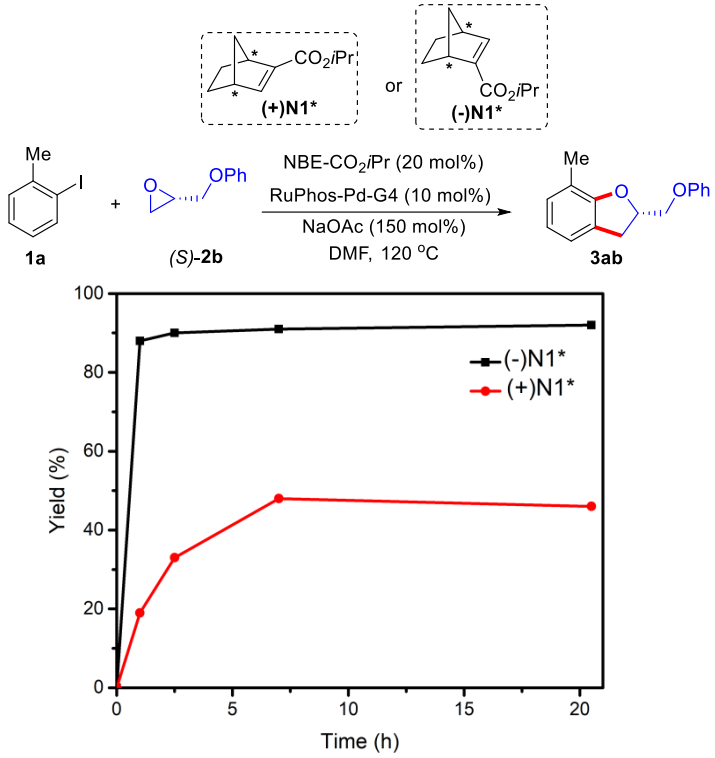

3.3 Conclusion

In summary, we describe our initial efforts on developing an asymmetric annulation reaction between aryl iodides and racemic epoxides *via* Pd/NBE cooperative catalysis. A series of enantiopure NBEs have been prepared with a reliable synthetic route. In particular, the isopropyl ester-substituted NBE (**N1***) could afford the DHBF product in good yield and promising enantioselectivity. While the ee at this stage is still moderate, the availability of such a family of chiral/enantiopure NBE cocatalysts should now open the door for developing various asymmetric Catellani-type reactions. Efforts on better understanding of the chiral induction step through DFT calculation and further improving the enantioselectivity via a better catalyst design are underway in our laboratory.

3.4 Experimental Procedures and Characterization Data

3.4.1 General Information

Unless noted otherwise, all solvents were dried by filtration through a Pure-Solv MD-5 Solvent Purification System (Innovative Technology). Dimethylformamide was then vacuum-distilled freshly over calcium hydride and carefully freeze-pump-thawed. Reaction temperatures were reported as the temperatures of the bather surrounding the flasks or vials. Sensitive reagents and solvents were transferred under nitrogen into a nitrogen-filled glovebox with standard techniques. Sodium acetate was purchased from STREM, stored and used directly in the glovebox. Analytical thin-layer chromatography (TLC) was carried out using 0.2 mm commercial silica gel plates (silica gel 60, F254, EMD chemical). Vials (15 x 45 mm 1 dram (4 mL) with PTFE lined cap attached) were purchased from Qorpak and flame-dried and cooled in a desiccator prior to usage. Mass spectra were recorded on an Agilent 6530 LC Q-TOF mass spectrometer using electrospray ionization with fragmentation voltage set at 115 V and processed with an Agilent MassHunter Operating System. X-ray diffraction data were collected at 100(2) K on a Bruker-Nonius Kappa CCD or Agilent SuperNova AtlasS2 CCD. Infrared spectra were recorded on a Nicolet 380 FTIR using neat thin film technique. Nuclear magnetic resonance spectra (^{1}H NMR and ^{13}C NMR) were recorded with a Bruker (400 MHz, ^{1}H at 400 MHz, ^{13}C at 101 MHz) or Bruker Model DMX 500 (500 MHz, ^{1}H at 500 MHz, ^{13}C at 126 MHz). Chemical shifts were reported in parts per million (ppm, δ), downfield from tetramethylsilane (TMS, δ=0.00ppm) and were referenced to residual solvent ($CDCl_3$, δ=7.26 ppm (^{1}H) and 77.00 ppm (^{13}C)). All the ^{19}F chemical shifts were not referenced. Coupling constants were reported in Hertz (Hz). Data for ^{1}H NMR spectra were reported as follows: chemical shift (ppm, referenced to protium, s = singlet, d = doublet, t = triplet, q = quartet, quin = quintet, dd = doublet of doublets, td = triplet of doublets, ddd = doublet of

doublet of doublets, m = multiplet, coupling constant (Hz), and integration). All other materials were obtained from Aldrich Chemical Company or Combi-blocks and were used as received.

3.4.2 Chiral Resolution of Ester Substituted NBE

Scheme 3.5. Chiral Resolution of C2-Substituted NBE

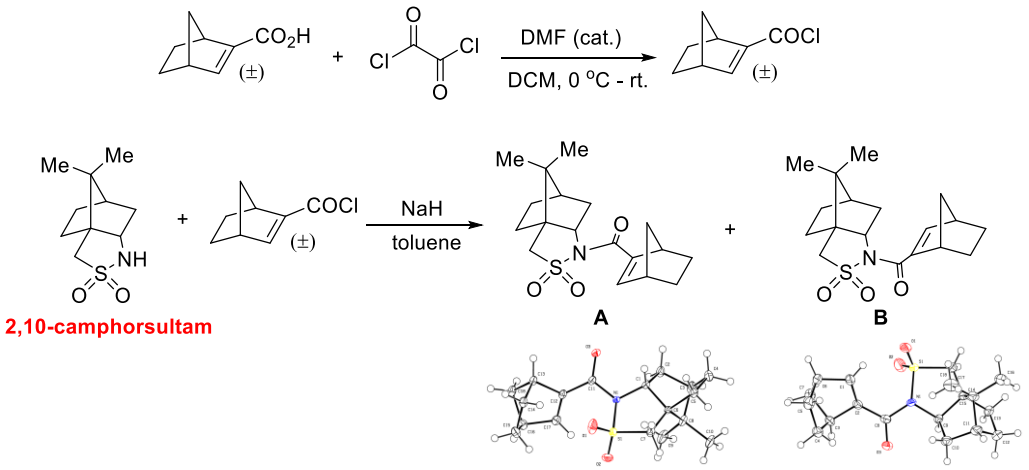

To a solution of NBE-CO_2H (700 mg, 5.1 mmol, 1.0 equiv) and 1 drop of DMF in DCM (5 mL) was added oxalyl chloride (648 mg, 5.1 mmol, 1.0 equiv) dropwise at 0 °C.[16] The reaction mixture was stirred at room temperature for another 1 h until the bubbling stopped. To another flame-dried round bottom flask was added sulfonamide (1.65g, 7.65 mmol, 1.5 equiv) and dry toluene (50 mL). Then NaH (3.06g, 76.5 mmol, 15 equiv) was added slowly to the flask and the reaction mixture was stirred at room temperature for another 30 min. After that, the generated acid chloride from the first flask was transferred into the second flask dropwise and the reaction mixture was stirred at room temperature until the reaction was completed. Then the reaction was quenched by 1M HCl and the aqueous lays was extracted by DCM for three times. The combined organic layers were

dried over $MgSO_4$. Sulfonamide **A** and **B** were isolated via silica gel chromatography as a pair of diastereomers.

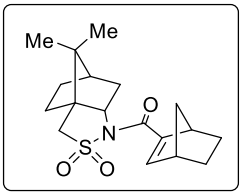

A: White solid (666 mg, 39%). R_f = 0.4 (hexane/ethyl acetate = 5:1). Mp = 125.7 – 127.1 °C. **^{1}H NMR** (500 MHz, $CDCl_3$) δ 7.11 (d, *J* = 3.4 Hz, 1H), 4.06 (dd, *J* = 7.7, 4.7 Hz, 1H), 3.47 (d, *J* = 13.6 Hz, 1H), 3.37 (d, *J* = 13.7 Hz, 2H), 3.03 (s, 1H), 2.03 (dd, *J* = 13.7, 7.7 Hz, 1H), 1.99 – 1.84 (m, 4H), 1.79 – 1.65 (m, 2H), 1.61 (dt, *J* = 8.6, 2.2 Hz, 1H), 1.45 – 1.24 (m, 5H), 1.21 (s, 3H), 0.98 (s, 3H). **^{13}C NMR** (101 MHz, $CDCl_3$) δ 165.30, 148.53, 141.13, 65.84, 53.81, 49.80, 47.96, 47.82, 45.28, 43.72, 43.08, 38.49, 33.34, 26.65, 24.21, 24.03, 21.36, 20.06. **IR** (KBr): υ 2960, 2874, 1671, 1590, 1332, 1286, 1172, 1140, 754, 536 cm^{-1}. **HRMS** (ESI): Calculated for $C_{18}H_{26}NO_3S$ ($M+H^+$): 336.1628, found: 336.1631.

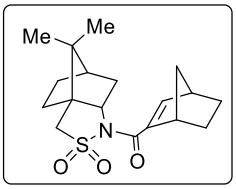

B: White solid (652 mg, 38%) R_f = 0.3 (hexane/ethyl acetate = 5:1). Mp = 169.2 – 170.0 °C. **^{1}H NMR** (500 MHz, $CDCl_3$) δ 6.91 (d, *J* = 3.2 Hz, 1H), 4.04 (dd, *J* = 7.7, 4.7 Hz, 1H), 3.49 (d, *J* = 13.6 Hz, 1H), 3.39 (d, *J* = 13.6 Hz, 1H), 3.23 (s, 1H), 3.08 (s, 1H), 2.05 – 1.91 (m, 3H), 1.90 – 1.83 (m, 2H), 1.76 (ttd, *J* = 12.8, 9.4, 3.6 Hz, 2H), 1.56 (dt, *J* = 8.8, 2.2 Hz, 1H), 1.41 (ddd, *J* = 10.9, 9.1, 2.3 Hz, 1H), 1.37 (s, 1H), 1.21 (s, 4H), 1.19 – 1.12 (m, 1H), 1.11 – 1.05 (m, 1H), 0.98 (s, 3H). **^{13}C NMR** (101 MHz, $CDCl_3$) δ 167.12, 148.31, 142.38, 65.78, 53.74, 48.07, 47.81, 46.72,

45.36, 44.34, 43.99, 38.65, 33.34, 26.64, 25.24, 25.20, 21.44, 20.05. **IR** (KBr): υ 2962, 2876, 1668, 1586, 1334, 1288, 1139, 1054, 748, 536 cm^{-1}. **HRMS** (ESI): Calculated for $C_{18}H_{26}NO_3S$ ($M+H^+$): 336.1628, found: 336.1632.

3.4.3 General Procedure for Synthesis of Chiral NBEs

Scheme 3.6. Chiral NBE Preparation

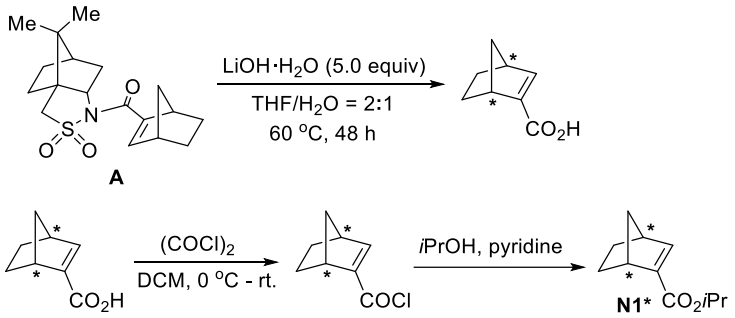

To a solution (18 mL, H_2O/THF = 1:2) of sulfonamide (565 mg, 1.69 mmol, 1.0 equiv) was added LiOH • H_2O (354 mg, 8.42 mmol, 5.0 equiv). The reaction was stirred at 60 °C for 48 h until the reaction mixture became clear. Then the aqueous layer was washed by diethyl ether for two times and then acidified by 1 M hydrochloric acid until pH < 7. Then the reaction mixture was extracted by dichloromethane for three times and the combined organic layers were dried over $MgSO_4$. The solvent was removed under vacuum to afford the chiral NBE-CO_2H as a colorless oil, which was used directly in the next step without further purification.

To a solution of NBE-CO_2H (276 mg, 2.0 mmol, 1.0 equiv) in DCM (2 mL) with 1 drop of DMF was added oxalyl chloride (254 mg, 2.0 mmol, 1.0 equiv) dropwise at 0 °C. The reaction mixture was stirred at room temperature for another 1 h until the bubbling stopped. Then a mixture of the corresponding alcohol (6.0 mmol, 3.0 equiv) and pyridine (949.2 mg, 12.0 mmol, 6.0 equiv) was added dropwise and the reaction mixture was stirred at room temperature for another 3 h until the

reaction was completed. The organic layer was washed with 1 M hydrochloric acid and then concentrated under vacuum. The corresponding ester substituted NBE was isolated by silica gel chromatography (hexane/Et_2O = 20:1) as a colorless oil.

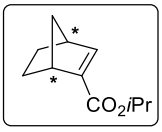

N1*: Colorless oil (151 mg, 42%). R_f = 0.6 (hexane/ethyl acetate = 20:1). **^{1}H NMR** (500 MHz, $CDCl_3$) δ 6.88 (d, *J* = 3.2 Hz, 1H), 5.05 (hept, *J* = 6.1 Hz, 1H), 3.24 (s, 1H), 3.00 (s, 1H), 1.74 (th, *J* = 13.0, 3.3 Hz, 2H), 1.52 – 1.43 (m, 1H), 1.26 (dd, *J* = 6.3, 4.1 Hz, 6H), 1.18 (d, *J* = 8.7 Hz, 1H), 1.07 (dt, *J* = 7.4, 2.3 Hz, 2H). **^{13}C NMR** (101 MHz, $CDCl_3$) δ 164.7, 146.4, 141.6, 67.3, 48.3, 43.6, 42.0, 24.8, 24.7, 22.1. **IR** (KBr): υ 2978, 2874, 1707, 1279, 1259, 1163, 1110, 1076, 753 cm^{-1}. **HRMS** (ESI): Calculated for $C_{11}H_{17}O_2$ ($M+H^+$): 181.1223, found: 181.1219. **Chiral HPLC** (Chiralpak IC, hexane/isopropanol = 98:2, 0.5 mL/min, 230 nm): t_{minor} = 12.308 min, t_{major} = 12.778. $[\alpha]_D$ = -139.6 (c = 0.53, dichloromethane, 21.0 ^oC) at 98% ee.

Figure 3.5. HPLC of Racemic N1

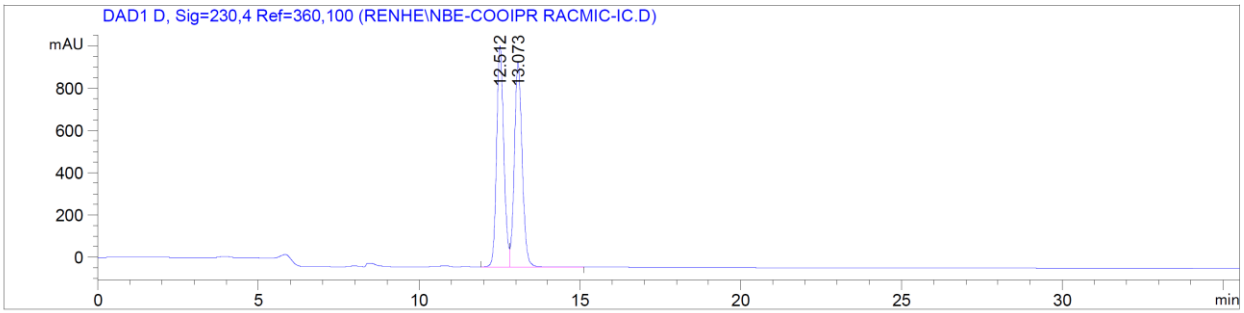

Signal 4: DAD1 D, Sig=230,4 Ref=360,100

Peak #	RetTime [min]	Type	Width [min]	Area [mAU*s]	Height [mAU]	Area %
1	12.512	BV	0.2362	1.61599e4	1045.99609	49.6824
2	13.073	VB	0.2588	1.63666e4	970.13281	50.3176
Totals :				3.25265e4	2016.12891	

Figure 3.6. HPLC of Enantiomeric N1*

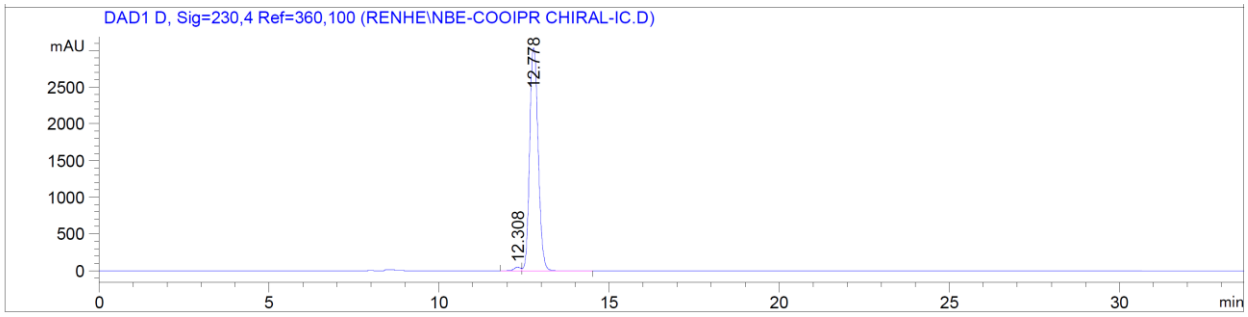

Signal 4: DAD1 D, Sig=230,4 Ref=360,100

Peak #	RetTime [min]	Type	Width [min]	Area [mAU*s]	Height [mAU]	Area %
1	12.308	BV	0.2035	637.26788	47.82213	1.1954
2	12.778	VB	0.2705	5.26707e4	3034.12402	98.8046
Totals :				5.33080e4	3081.94615	

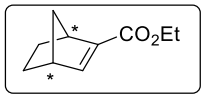

N2*: Colorless oil (47%). R_f = 0.5 (hexane/ethyl acetate = 20:1). **^{1}H NMR** (500 MHz, $CDCl_3$) δ 7.26 (d, *J* = 3.1 Hz, 1H), 4.53 (q, *J* = 7.0 Hz, 2H), 3.61 (s, 1H), 3.36 (s, 1H), 2.09 (dtt, *J* = 15.1, 11.6, 7.6 Hz, 2H), 1.83 (d, *J* = 8.5 Hz, 1H), 1.64 (t, *J* = 7.1 Hz, 3H), 1.54 (d, *J* = 8.6 Hz, 1H), 1.44 (tdt, *J* = 7.6, 5.1, 2.3 Hz, 2H). **^{13}C NMR** (101 MHz, $CDCl_3$) δ 165.1, 146.8, 141.2, 60.2, 48.3, 43.6, 42.0, 24.8, 24.6, 14.5. **IR** (KBr): υ 2977, 2874, 1712, 1596, 1370, 1341, 1278, 1258, 1160, 1079, 753 cm^{-1}. **HRMS** (ESI): Calculated for $C_{10}H_{15}O_2$ ($M+H^+$): 167.1067, found: 167.1061. $[\alpha]_D$ = 155.6 (c = 0.32, dichloromethane, 22.0 ºC).

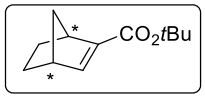

N3*: White solid (48%). R_f = 0.6 (hexane/ethyl acetate = 20:1). Mp = 52.0 – 54.0 ºC. **^{1}H NMR** (500 MHz, $CDCl_3$) δ 6.79 (d, *J* = 3.1 Hz, 1H), 3.19 (s, 1H), 2.98 (s, 1H), 1.78 – 1.68 (m, 2H), 1.48 (s, 10H), 1.16 (d, *J* = 8.5 Hz, 1H), 1.07 (qd, *J* = 8.5, 2.2 Hz, 2H). ^{13}C NMR (101 MHz, $CDCl_3$) δ 164.6, 145.6, 142.8, 80.0, 48.3, 43.5, 42.0, 28.4, 24.9, 24.7. **IR** (KBr): υ 2976, 2873, 1702, 1596, 1284, 1260, 1154, 1077, 756 cm^{-1}. **HRMS** (ESI): Calculated for $C_{12}H_{18}O_2Na$ ($M+Na^+$): 217.1199, found: 217.1184. $[\alpha]_D$ = 148.9 (c = 0.91, dichloromethane, 22.0 ºC).

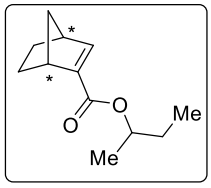

N4*: Colorless oil (50%, dr = 1:1). R_f = 0.5 (hexane/ethyl acetate = 20:1). **^{1}H NMR** (500 MHz, $CDCl_3$) δ 6.89 (dd, *J* = 6.6, 3.2 Hz, 1H), 4.88 (h, *J* = 6.1, 5.7 Hz, 1H), 3.24 (s, 1H), 3.00 (s, 1H), 1.74 (tt, *J* = 9.6, 1.9 Hz, 2H), 1.68 – 1.60 (m, 1H), 1.48 (d, *J* = 8.5 Hz, 1H), 1.23 (dd, *J* = 6.3, 5.2 Hz, 4H), 1.20 – 1.16 (m, 1H), 1.11 – 1.04 (m, 2H), 0.90 (td, *J* = 7.5, 5.6 Hz, 3H). **^{13}C NMR** (101 MHz, $CDCl_3$) δ 164.86, 164.83, 146.45, 146.31, 141.64, 141.59, 71.85, 71.82, 48.28, 48.23, 43.57,

43.55, 42.04, 42.01, 29.08, 29.05, 24.83, 24.80, 24.67, 19.73, 19.67, 9.86, 9.85. **IR** (KBr): υ 2974, 1708, 1596, 1449, 1364, 1337, 1278, 1257, 1162, 933, 752 cm^{-1}. **HRMS** (ESI): Calculated for $C_{12}H_{19}O_2$ ($M+H^+$): 195.1380, found: 195.1370. $[\alpha]_D$ = -133.3 (c = 0.95, dichloromethane, 21.8 °C).

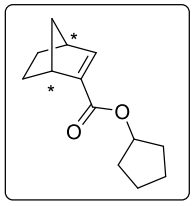

N5*: White solid (45%). R_f = 0.5 (hexane/ethyl acetate = 20:1). Mp = 60.2 – 60.8 °C. **^{1}H NMR** (500 MHz, $CDCl_3$) δ 6.79 (d, *J* = 3.2 Hz, 1H), 5.14 (dq, *J* = 6.0, 3.1 Hz, 1H), 3.16 (s, 1H), 2.92 (s, 1H), 1.80 (dtd, *J* = 12.5, 6.6, 6.0, 3.0 Hz, 2H), 1.71 – 1.60 (m, 6H), 1.58 – 1.47 (m, 2H), 1.40 (dt, *J* = 8.6, 2.1 Hz, 1H), 1.11 (d, *J* = 8.5 Hz, 1H), 1.04 – 0.96 (m, 2H). **^{13}C NMR** (101 MHz, $CDCl_3$) δ 164.9, 146.3, 141.6, 76.6, 48.2, 43.5, 42.0, 32.9, 32.8, 24.8, 24.6, 23.91, 23.90. **IR** (KBr): υ 2871, 1703, 1593, 1449, 1369, 1341, 1277, 1217, 1116, 1078, 879, 753 cm^{-1}. **HRMS** (ESI): Calculated for $C_{13}H_{19}O_2$ ($M+H^+$): 207.1380, found: 207.1374. $[\alpha]_D$ = -130.1 (c = 0.99, dichloromethane, 22.0 °C).

Scheme 3.7. Preparation of C2 Amide-Substituted NBEs

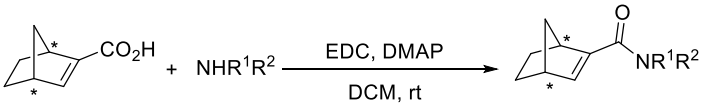

NBE-CO_2H (138 mg, 1.0 mmol, 1.0 equiv), amine (1.1 mmol, 1.1 equiv), 1-ethyl-3-(3-dimethylaminopropyl)carbodiimide hydrochloride (230 mg, 1.2 mmol, 1.2 equiv) and 4-dimethylaminopyridine (12.2 mg, 0.1 mmol, 10 mol%) were dissolved in dichloromethane (5 mL). The reaction mixture was stirred at room temperature overnight. Then it was diluted with diethyl

ether, washed with water and brine, dried over $MgSO_4$, and purified on silica gel chromatography (hexanes/ethyl acetate = 2:1) to afford the corresponding amide-derived norbornene **N7*** and **N8***.

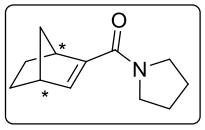

N7*: Colorless oil (49%). R_f = 0.3 (hexane/ethyl acetate = 2:1). **^{1}H NMR** (400 MHz, $CDCl_3$) δ 6.30 (d, *J* = 3.1 Hz, 1H), 3.65 – 3.33 (m, 4H), 3.26 (s, 1H), 2.99 (s, 1H), 1.99 – 1.76 (m, 4H), 1.71 (d, *J* = 6.0 Hz, 2H), 1.37 (d, *J* = 8.3 Hz, 1H), 1.29 – 1.20 (m, 1H), 1.15 – 1.00 (m, 2H). **^{13}C NMR** (101 MHz, $CDCl_3$) δ 165.9, 144.4, 139.4, 48.4, 47.1, 46.3, 44.3, 43.8, 26.6, 25.3, 25.2, 24.2. **IR** (KBr): υ 2968, 2871, 1722, 1612, 1577, 1426, 1341, 1311, 1166, 875, 748 cm^{-1}. **HRMS** (ESI): Calculated for $C_{12}H_{18}NO$ ($M+H^+$): 192.1383, found: 192.1374. $[\alpha]_D$ = 76.9 (c = 1.27, dichloromethane, 21.6 ^oC).

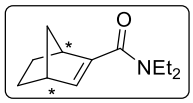

N8*: Colorless oil (50%). R_f = 0.3 (hexane/ethyl acetate = 2:1). **^{1}H NMR** (400 MHz, $CDCl_3$) δ 6.10 (d, *J* = 3.1 Hz, 1H), 3.54 – 3.39 (m, 2H), 3.31 (dq, *J* = 14.1, 7.1 Hz, 2H), 3.12 (s, 1H), 2.97 (s, 1H), 1.76 – 1.66 (m, 2H), 1.44 – 1.33 (m, 2H), 1.13 (t, *J* = 7.1 Hz, 8H). **^{13}C NMR** (101 MHz, $CDCl_3$) δ 168.6, 143.2, 135.8, 47.4, 45.5, 43.5, 42.7, 39.4, 25.5, 25.4, 14.8, 13.0. **IR** (KBr): υ 2971, 2872, 1620, 1585, 1427, 1379, 1285, 1150, 1064, 812, 743 cm^{-1}. **HRMS** (ESI): Calculated for $C_{12}H_{20}NO$ ($M+H^+$): 194.1539, found: 194.1535. $[\alpha]_D$ = 125.7 (c = 0.97, dichloromethane, 22.0 ^oC).

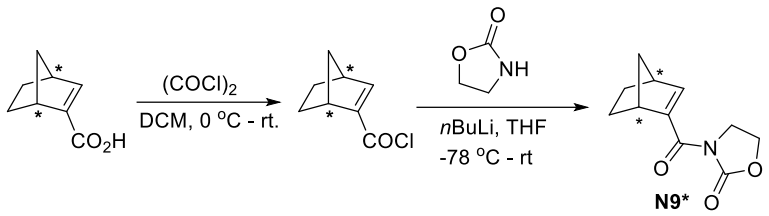

To a solution of NBE-CO_2H (138 mg, 1.0 mmol, 1.0 equiv) in DCM (1 mL) with1 drop of DMF was added oxalyl chloride (152 mg, 1.2 mmol, 1.2 equiv) dropwise at 0 °C. The reaction mixture was stirred at room temperature for another 1 h until the bubbling stopped. To another flame-dried round bottom flask was added 2-oxazolidinone (95.8 mg, 1.1 mmol, 1.1 equiv) and dry THF (10 mL). Then, *n*BuLi (0.81 mL, 1.6 M in hexane, 1.3 mmol, 1.3 equiv) was added dropwise to the flask at -78 °C and the reaction mixture was stirred at -78 °C for another 30 min. After that, the generated acyl chloride from the first flask was transferred into the second flask dropwise using dry THF. Then the reaction mixture was warmed to room temperature slowly and stirred for another 2 h. The reaction was quenched by 5 mL H_2O and the aqueous lays was extracted by ethyl acetate for three times. The combined organic layers were dried over $MgSO_4$ and then purified by silica gel chromatography to afford **N9***.

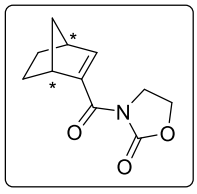

N9*: White solid (48%). R_f = 0.2 (hexane/ethyl acetate = 2:1). Mp = 85.4 – 87.9 °C. **^{1}H NMR** (400 MHz, $CDCl_3$) δ 6.83 (d, *J* = 3.3 Hz, 1H), 4.41 – 4.27 (m, 2H), 4.02 (ddd, *J* = 10.9, 9.0, 7.9 Hz, 1H), 3.91 (ddd, *J* = 10.8, 8.6, 5.9 Hz, 1H), 3.21 (s, 1H), 3.03 (s, 1H), 1.76 – 1.64 (m, 2H), 1.55 (dt, *J* = 8.6, 2.1 Hz, 1H), 1.20 – 1.00 (m, 3H). **^{13}C NMR** (101 MHz, $CDCl_3$) δ 165.7, 153.3, 148.3, 140.1, 62.2, 47.3, 44.2, 44.0, 43.6, 25.10, 25.06. **IR** (KBr): υ 2971, 2872, 1783, 1664, 1587, 1478,

1383, 1301, 1199, 1115, 1080, 1039, 987, 746, 698 cm^{-1}. **HRMS** (ESI): Calculated for $C_{11}H_{14}NO_3$ ($M+H^+$): 208.0968, found: 208.0966. $[\alpha]_D$ = -65.9 (c = 0.97, dichloromethane, 22.0 ^oC).

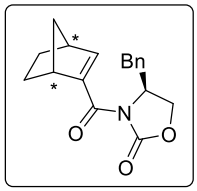

N10*: White solid (63%). R_f = 0.2 (hexane/ethyl acetate = 2:1). Mp = 105.9 – 107.2 ^oC. **^{1}H NMR** (400 MHz, $CDCl_3$) δ 7.33 – 7.27 (m, 3H), 7.19 – 7.13 (m, 2H), 6.89 (d, *J* = 3.0 Hz, 1H), 4.80 (tdd, *J* = 8.7, 5.1, 3.6 Hz, 1H), 4.25 (t, *J* = 8.6 Hz, 1H), 4.13 (dd, *J* = 8.9, 5.2 Hz, 1H), 3.32 – 3.21 (m, 2H), 3.11 (s, 1H), 2.83 (dd, *J* = 13.5, 8.9 Hz, 1H), 1.86 – 1.73 (m, 2H), 1.61 (dq, *J* = 6.4, 2.1 Hz, 1H), 1.28 – 1.18 (m, 2H), 1.17 – 1.10 (m, 1H). **^{13}C NMR** (101 MHz, $CDCl_3$) δ 166.0, 153.4, 148.9, 140.7, 135.4, 129.6, 129.0, 127.4, 66.3, 55.5, 47.1, 44.3, 44.0, 38.0, 25.3, 25.3. **IR** (KBr): υ 2972, 2872, 1785, 1660, 1497, 1453, 1348, 1290, 1212, 1114, 746, 702 cm^{-1}. **HRMS** (ESI): Calculated for $C_{18}H_{20}NO_3$ ($M+H^+$): 298.1438, found: 298.1439. $[\alpha]_D$ = -7.5 (c = 0.99, dichloromethane, 22.0 ^oC).

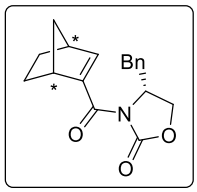

N11*: White solid (47%). R_f = 0.2 (hexane/ethyl acetate = 2:1). Mp = 92.4 – 93.1 ^oC. **^{1}H NMR** (400 MHz, $CDCl_3$) δ 7.36 – 7.30 (m, 2H), 7.30 – 7.25 (m, 1H), 7.24 – 7.20 (m, 2H), 6.86 (d, *J* = 3.2 Hz, 1H), 4.64 (ddt, *J* = 9.6, 7.3, 3.6 Hz, 1H), 4.24 – 4.11 (m, 2H), 3.40 (dd, *J* = 13.4, 3.3 Hz, 1H), 3.32 (s, 1H), 3.09 (s, 1H), 2.80 (dd, *J* = 13.4, 9.6 Hz, 1H), 1.85 – 1.73 (m, 2H), 1.68 (dt, *J* =

8.6, 2.1 Hz, 1H), 1.28 – 1.10 (m, 3H). **^{13}C NMR** (101 MHz, $CDCl_3$) δ 165.7, 153.3, 147.6, 140.6, 135.6, 129.6, 129.0, 127.4, 66.3, 56.4, 47.7, 44.2, 44.1, 37.6, 25.1, 25.0. **IR** (KBr): υ 2973, 1785, 1659, 1453, 1350, 1293, 1211, 1114, 1084, 745, 702 cm^{-1}. **HRMS** (ESI): Calculated for $C_{18}H_{20}NO_3$ ($M+H^+$): 298.1438, found: 298.1441. $[\alpha]_D$ = -128.7 (c = 0.97, dichloromethane, 22.0 ^oC).

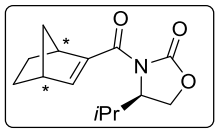

N12*: White solid (61%). R_f = 0.3 (hexane/ethyl acetate = 2:1). Mp = 84.1 – 86.2 ^oC. **^{1}H NMR** (400 MHz, $CDCl_3$) δ 6.88 (dt, *J* = 3.4, 1.0 Hz, 1H), 4.56 (dt, *J* = 9.0, 4.7 Hz, 1H), 4.30 (t, *J* = 8.9 Hz, 1H), 4.15 (dd, *J* = 9.0, 4.9 Hz, 1H), 3.24 (s, 1H), 3.09 (s, 1H), 2.27 (pd, *J* = 7.0, 4.4 Hz, 1H), 1.83 – 1.70 (m, 2H), 1.60 (dt, *J* = 8.6, 2.1 Hz, 1H), 1.22 – 1.15 (m, 2H), 1.12 – 1.05 (m, 1H), 0.87 (dd, *J* = 9.7, 7.0 Hz, 6H). **^{13}C NMR** (101 MHz, $CDCl_3$) δ 166.1, 153.9, 148.6, 140.9, 63.5, 58.4, 46.9, 44.4, 44.0, 28.8, 25.4, 25.3, 17.9, 15.2. **IR** (KBr): υ 2965, 2873, 1783, 1665, 1587, 1485, 1388, 1363, 1289, 1203, 886, 764, 745 cm^{-1}. **HRMS** (ESI): Calculated for $C_{14}H_{20}NO_3$ ($M+H^+$): 250.1438, found: 250.1433. $[\alpha]_D$ = 37.2 (c = 1.13, dichloromethane, 22.0 ^oC).

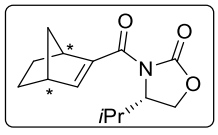

N13*: White solid (54%). R_f = 0.3 (hexane/ethyl acetate = 2:1). Mp = 85.5 – 89.4 ^oC. **^{1}H NMR** (400 MHz, $CDCl_3$) δ 6.81 (d, *J* = 3.3 Hz, 1H), 4.45 (dt, *J* = 8.6, 4.3 Hz, 1H), 4.28 (t, *J* = 8.7 Hz, 1H), 4.17 (dd, *J* = 8.9, 4.5 Hz, 1H), 3.28 (s, 1H), 3.05 (s, 1H), 2.42 (pd, *J* = 7.0, 4.1 Hz, 1H), 1.82 – 1.66 (m, 3H), 1.24 (dd, *J* = 8.6, 1.1 Hz, 1H), 1.19 – 1.11 (m, 2H), 0.90 (dd, *J* = 8.2, 7.0 Hz, 6H).

^{13}C NMR (101 MHz, $CDCl_3$) δ 165.6, 154.0, 146.8, 141.1, 63.5, 59.0, 48.3, 44.2, 43.8, 28.4, 24.9, 24.8, 18.0, 15.0. **IR** (KBr): υ 2965, 2672, 1783, 1672, 1589, 1465, 1387, 1341, 1293, 1201, 1079, 888, 766, 744 cm^{-1}. **HRMS** (ESI): Calculated for $C_{14}H_{20}NO_3$ ($M+H^+$): 250.1438, found: 250.1429. $[\alpha]_D$ = 132.5 (c = 1.02, dichloromethane, 22.0 °C).

3.4.4 Enantioselective Transformation Using Chiral NBE-CO_2*i*Pr (N1*)

Scheme 3.8. Asymmetric Annulation Enabled by Pd/Chiral NBE

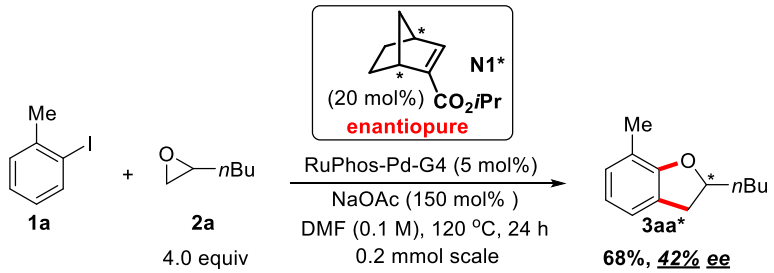

A flame-dried 4.0 mL vial was charged with aryl iodide **1a** (43.6 mg, 0.2 mmol, 1.0 equiv), NaOAc (24.6 mg, 0.3 mmol, 1.5 equiv) and RuPhos-Pd-G4 (8.5 mg, 0.01 mmol, 5 mol%). Then the vial was directly transferred into a nitrogen-filled glovebox without caps. After enantiomeric NBE-CO_2*i*Pr **N1*** (7.2 mg, 0.04 mmol, 20 mol%) and 1,2-epoxyhexane (80 mg, 0.8 mmol, 4.0 equiv) was added to the vial, 2 mL of degassed DMF was added. Then the vial was tightly sealed, transferred out of glovebox and stirred on a pie-block preheated to 120 °C for 24 hours. After completion of the reaction, the mixture was filtered through a thin pad of celite. The filter cake was washed with dichloromethane and diethyl ether, and the combined filtrate was concentrated. The residue was absorbed onto a small amount of silica gel and then purified by flash column chromatography on silica gel to give the desired product.

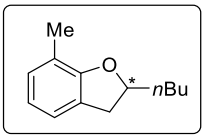

3aa*: Pale yellow oil (68%). R_f = 0.4 (hexane/ethyl acetate = 40:1). **^{1}H NMR** (400 MHz, $CDCl_3$) δ 7.00 (d, *J* = 6.9 Hz, 1H), 6.93 (ddq, *J* = 7.5, 1.5, 0.8 Hz, 1H), 6.74 (t, *J* = 7.4 Hz, 1H), 4.76 (dddd, *J* = 8.9, 7.8, 6.9, 6.2 Hz, 1H), 3.28 (dd, *J* = 15.4, 8.9 Hz, 1H), 2.86 (dd, *J* = 15.4, 7.8 Hz, 1H), 2.22 (s, 3H), 1.93 – 1.79 (m, 1H), 1.73 – 1.62 (m, 1H), 1.55 – 1.34 (m, 4H), 0.95 (t, *J* = 7.1 Hz, 3H). **^{13}C NMR** (126 MHz, $CDCl_3$) δ 158.2, 129.2, 126.3, 122.4, 120.0, 119.6, 83.1, 36.0, 35.9, 27.7, 22.8, 15.4, 14.2. **IR** (KBr): υ 3025, 2956, 2931, 2859, 1599, 1467, 1260, 1186, 759 cm-1. **HRMS** (ESI): Calculated for $C_{13}H_{19}O$ ($M+H^+$): 191.1430, found: 191.1428. **Chiral HPLC** (Chiralpak OD-H, hexane/isopropanol = 99:1, 0.5 mL/min, 230 nm): t_{minor} = 11.161, t_{major} = 10.094. 42% ee.

Figure 3.7. HPLC of Racemic 3aa

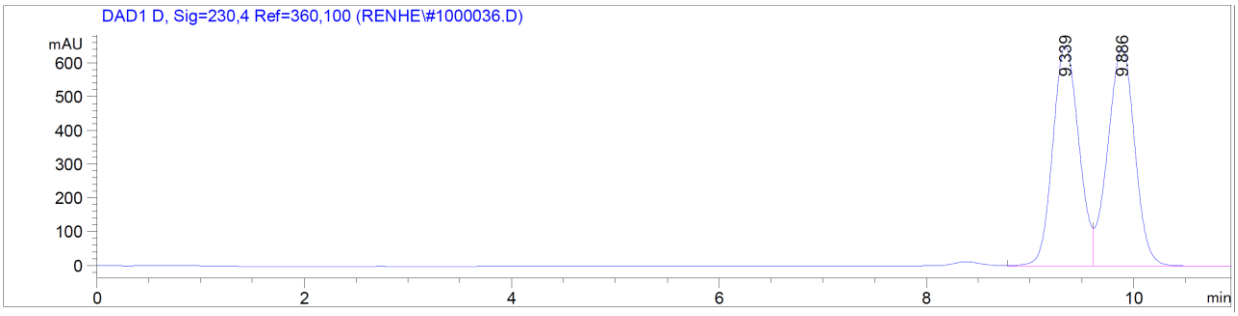

Signal 4: DAD1 D, Sig=230,4 Ref=360,100

Peak #	RetTime [min]	Type	Width [min]	Area [mAU*s]	Height [mAU]	Area %
1	9.339	VV	0.2748	1.14719e4	653.63702	49.4863
2	9.886	VBA	0.2817	1.17100e4	645.41187	50.5137
Totals :				2.31819e4	1299.04889	

Figure 3.8. HPLC of Enantiomeric 3aa*

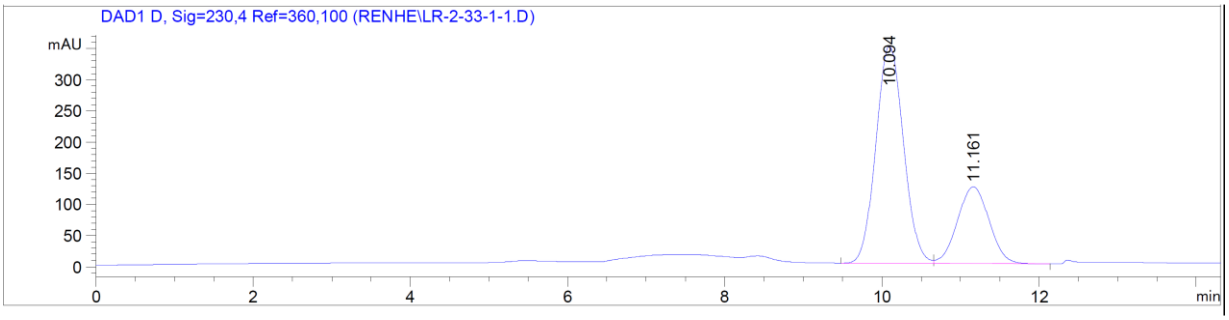

Signal 4: DAD1 D, Sig=230,4 Ref=360,100

Peak #	RetTime [min]	Type	Width [min]	Area [mAU*s]	Height [mAU]	Area %
1	10.094	BV	0.3827	8513.32520	348.88733	71.0521
2	11.161	VB	0.4418	3468.47949	123.45961	28.9479
Totals :				1.19818e4	472.34694	

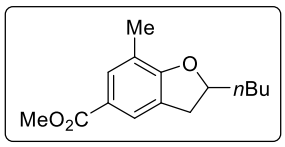

3ba*: Pale yellow oil (54%). R_f = 0.2 (hexane/ethyl acetate = 40:1). **^{1}H NMR** (400 MHz, $CDCl_3$) δ 7.70 – 7.65 (m, 2H), 4.89 – 4.78 (m, 1H), 3.85 (s, 3H), 3.28 (dd, *J* = 15.5, 9.0 Hz, 1H), 2.85 (dd, *J* = 15.5, 7.7 Hz, 1H), 2.21 (s, 3H), 1.90 – 1.78 (m, 1H), 1.74 – 1.62 (m, 1H), 1.54 – 1.32 (m, 4H), 0.93 (t, *J* = 7.1 Hz, 3H). **^{13}C NMR** (126 MHz, $CDCl_3$) δ 167.4, 162.4, 131.9, 126.6, 124.4, 122.2, 119.3, 84.4, 51.8, 36.0, 35.3, 27.6, 22.7, 15.3, 14.1. **IR** (KBr): υ 2954, 2860, 1715, 1607, 1434, 1306, 1161, 954, 771 cm^{-1}. **HRMS** (ESI): Calculated for $C_{15}H_{21}O_3$ ($M+H^+$): 249.1485, found: 249.1492. **Chiral HPLC** (Chiralpak OD-H, hexane/isopropanol = 99:1, 0.5 mL/min, 260 nm): t_{minor} = 21.892, t_{major} = 14.268. 31% ee.

Figure 3.9. HPLC of Racemic 3ba

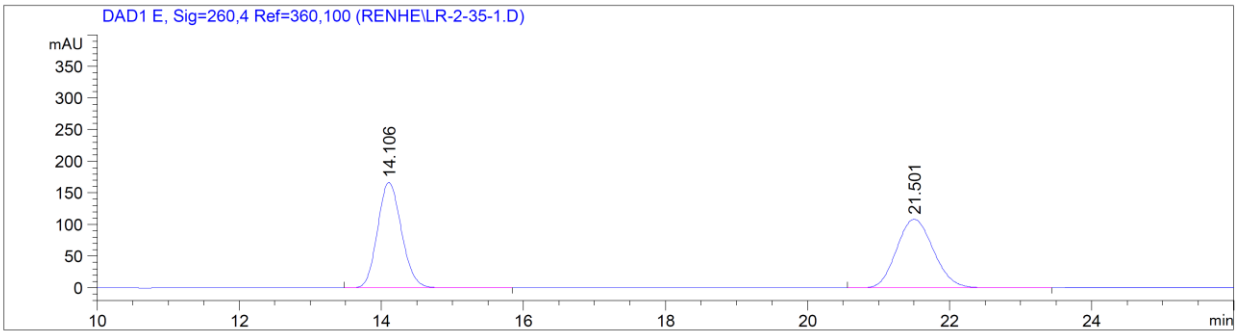

Signal 5: DAD1 E, Sig=260,4 Ref=360,100

Peak #	RetTime [min]	Type	Width [min]	Area [mAU*s]	Height [mAU]	Area %
1	14.106	BB	0.3649	3900.03076	166.73305	49.9833
2	21.501	BB	0.5676	3902.63062	108.50792	50.0167
Totals :				7802.66138	275.24097	

Figure 3.10. HPLC of Enantiomeric 3ba*

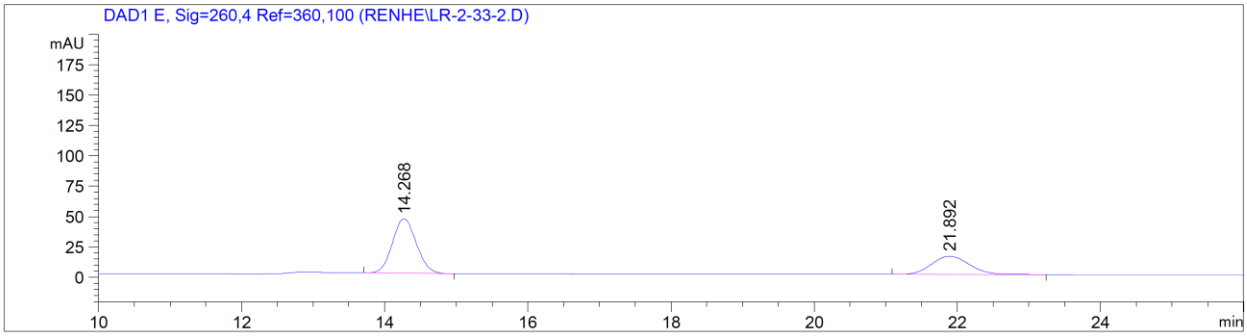

Signal 5: DAD1 E, Sig=260,4 Ref=360,100

Peak #	RetTime [min]	Type	Width [min]	Area [mAU*s]	Height [mAU]	Area %
1	14.268	BB	0.3624	1039.04126	44.82608	65.5087
2	21.892	BB	0.5756	547.07068	14.99671	34.4913
Totals :				1586.11194	59.82279	

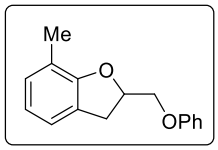

3ab*: White solid (92%). R_f = 0.3 (hexane/ethyl acetate = 40:1). Mp = 77.8 – 78.6 °C. **^{1}H NMR** (400 MHz, $CDCl_3$) δ 7.35 – 7.25 (m, 2H), 7.04 (ddd, *J* = 7.3, 1.4, 0.7 Hz, 1H), 7.03 – 6.91 (m, 4H), 6.79 (t, *J* = 7.4 Hz, 1H), 5.15 (dddd, *J* = 9.4, 7.0, 5.9, 5.3 Hz, 1H), 4.24 (dd, *J* = 9.9, 5.9 Hz, 1H), 4.10 (dd, *J* = 9.9, 5.3 Hz, 1H), 3.40 (dd, *J* = 15.7, 9.4 Hz, 1H), 3.17 (dd, *J* = 15.7, 7.1 Hz, 1H), 2.23 (s, 3H). **^{13}C NMR** (101 MHz, $CDCl_3$) δ 158.8, 157.9, 129.6, 129.5, 125.4, 122.5, 121.2, 120.6, 120.0, 114.8, 80.2, 69.9, 32.9, 15.4. **IR** (KBr): υ 3040, 2920, 2857, 1599, 1497, 1468, 1243, 1193, 1050, 754, 691 cm^{-1}. **HRMS** (ESI): Calculated for $C_{16}H_{17}O_2$ ($M+H^+$): 241.1223, found: 241.1221. **Chiral HPLC** (Chiralpak OD-H, hexane/isopropanol = 98:2, 0.5 mL/min, 230 nm): t_{minor} = 23.912, t_{major} = 34.968. 38% ee.

Figure 3.11. HPLC of Racemic 3ab

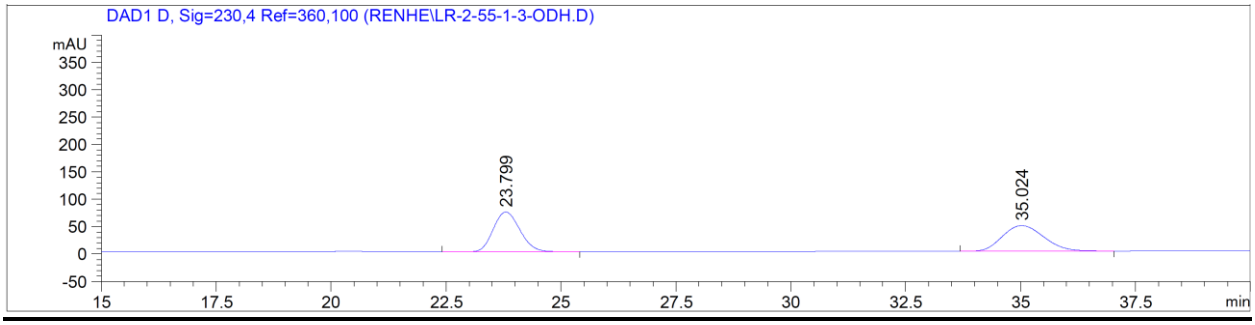

Signal 4: DAD1 D, Sig=230,4 Ref=360,100

Peak #	RetTime [min]	Type	Width [min]	Area [mAU*s]	Height [mAU]	Area %
1	23.799	BB	0.6346	2908.75586	72.41602	49.9844
2	35.024	BB	0.9928	2910.56860	46.59019	50.0156
Totals :				5819.32446	119.00621	

Figure 3.12. HPLC of Enantiomeric 3ab*

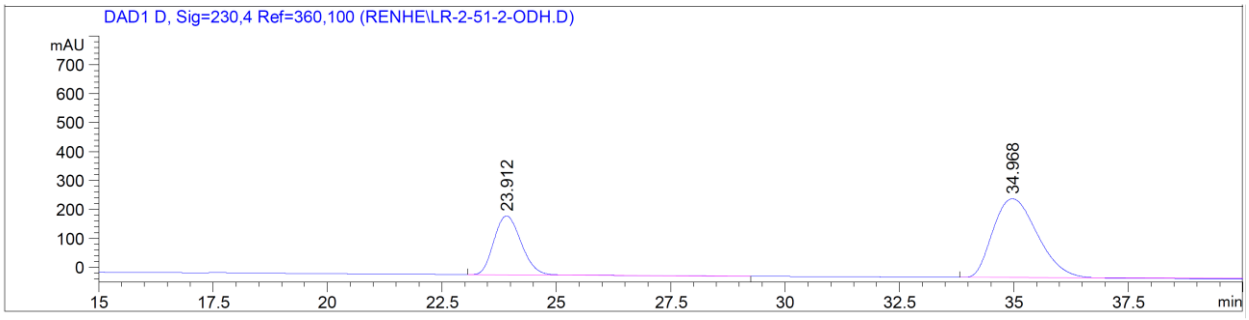

Signal 4: DAD1 D, Sig=230,4 Ref=360,100

Peak #	RetTime [min]	Type	Width [min]	Area [mAU*s]	Height [mAU]	Area %
1	23.912	BB	0.6562	8405.07129	203.36694	31.2355
2	34.968	BBA	1.0753	1.85036e4	272.80038	68.7645
Totals :				2.69087e4	476.16733	

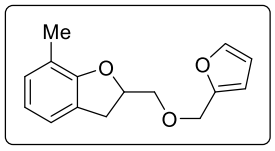

3ac*: Yellow oil (78%). R_f = 0.2 (hexane/ethyl acetate = 40:1). **^{1}H NMR** (400 MHz, $CDCl_3$) δ 7.43 (dd, *J* = 1.8, 0.9 Hz, 1H), 7.00 (d, *J* = 7.0 Hz, 1H), 6.94 (ddq, *J* = 7.5, 1.5, 0.8 Hz, 1H), 6.76 (t, *J* = 7.4 Hz, 1H), 6.38 – 6.32 (m, 2H), 4.94 (dddd, *J* = 9.4, 7.5, 6.3, 4.8 Hz, 1H), 4.65 – 4.52 (m, 2H), 3.73 (dd, *J* = 10.4, 6.3 Hz, 1H), 3.64 (dd, *J* = 10.4, 4.8 Hz, 1H), 3.26 (dd, *J* = 15.6, 9.4 Hz, 1H), 3.00 (dd, *J* = 15.6, 7.5 Hz, 1H), 2.23 (d, *J* = 0.6 Hz, 3H). **^{13}C NMR** (101 MHz, $CDCl_3$) δ 158.0, 151.7, 143.0, 129.3, 125.6, 122.4, 120.4, 119.8, 110.4, 109.6, 81.2, 72.1, 65.4, 32.8, 15.4. **IR** (KBr): υ 3119, 3049, 2919, 2857, 1599, 1468, 1261, 1194, 1151, 1073. 920, 758, 600 cm^{-1}. **HRMS** (ESI): Calculated for $C_{15}H_{17}O_3$ ($M+H^+$): 245.1172, found: 245.1174. **Chiral HPLC** (Chiralpak OD-H, hexane/isopropanol = 95:5, 0.5 mL/min, 230 nm): t_{minor} = 27.530, t_{major} = 44.530. 34% ee.

Figure 3.13. HPLC of Racemic 3ac

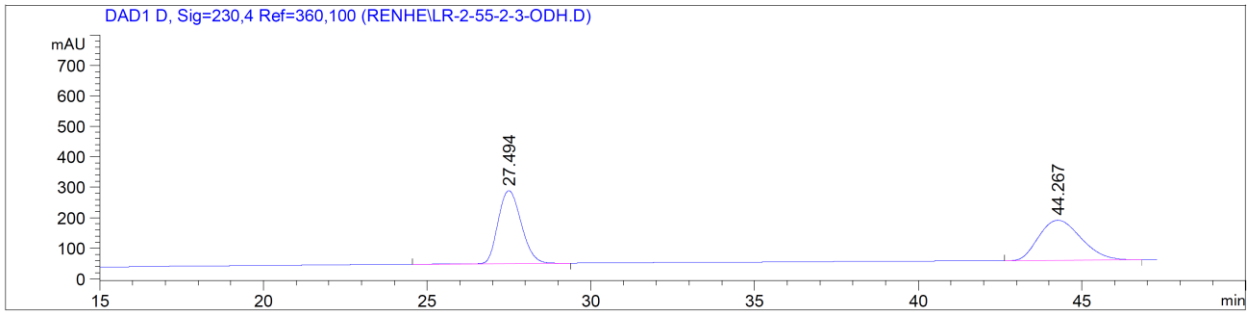

Signal 4: DAD1 D, Sig=230,4 Ref=360,100

Peak #	RetTime [min]	Type	Width [min]	Area [mAU*s]	Height [mAU]	Area %
1	27.494	BB	0.7824	1.17421e4	239.31871	49.8019
2	44.267	BB	1.4292	1.18355e4	131.60634	50.1981
Totals :				2.35776e4	370.92505	

Figure 3.14. HPLC of Enantiomeric 3ac*

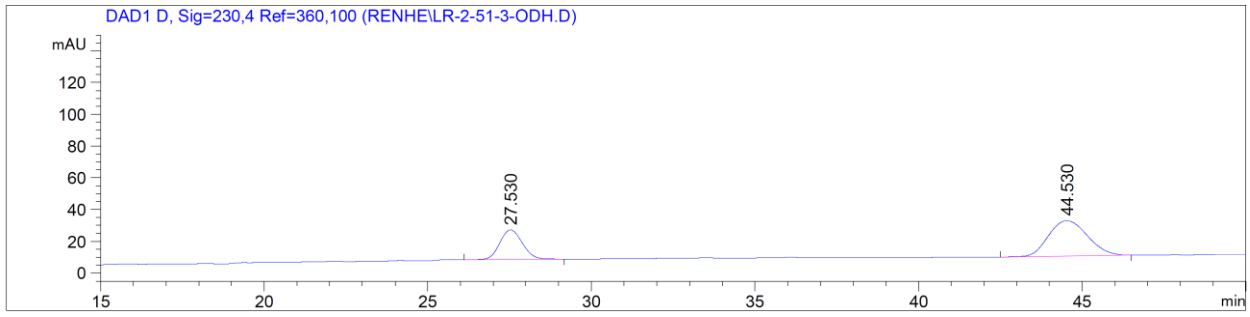

Signal 4: DAD1 D, Sig=230,4 Ref=360,100

Peak #	RetTime [min]	Type	Width [min]	Area [mAU*s]	Height [mAU]	Area %
1	27.530	BB	0.7585	912.32776	18.72223	33.0027
2	44.530	BB	1.2981	1852.07678	22.31998	66.9973
Totals :				2764.40454	41.04220	

3.4.5 Match and Mismatch for the Stereochemistry of NBE and Epoxide

Scheme 3.9. Asymmetric Annulation with Enantioenriched 2b and N1

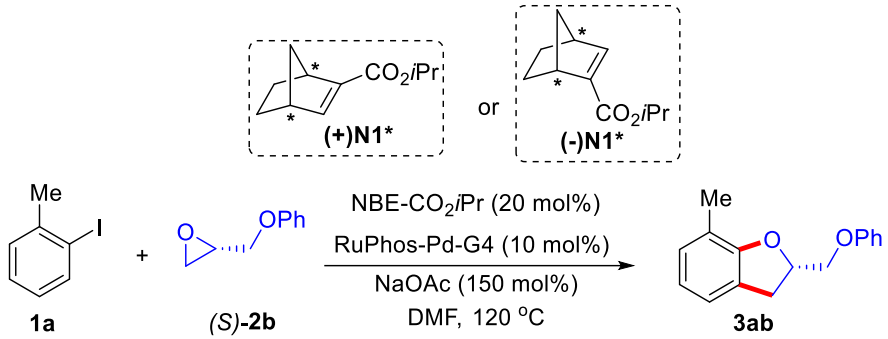

A flame-dried 4.0 mL vial was charged with aryl iodide **1a** (21.8 mg, 0.1 mmol, 1.0 equiv), NaOAc (12.3 mg, 0.15 mmol, 1.5 equiv) and RuPhos-Pd-G4 (8.5 mg, 0.01 mmol, 10 mol%). Then the vial was directly transferred into a nitrogen-filled glovebox without caps. After enantiomeric NBE-CO_2*i*Pr **N1*** (3.6 mg, 0.02 mmol, 20 mol%) and chiral epoxide (*S*)-**2b** (60 mg, 0.4 mmol, 4.0 equiv) was added to the vial, 1 mL of degassed DMF was added. Then the vial was tightly sealed, transferred out of glovebox and stirred on a pie-block preheated to 120 °C. After completion of the reaction, the mixture was filtered through a thin pad of celite. The filter cake was washed with dichloromethane and diethyl ether, and the combined filtrate was concentrated. The residue was absorbed onto a small amount of silica gel and then purified by flash column chromatography on silica gel to give the desired product.

Table 3.4. Match and Mismatch between Chiral NBE and Epoxide

	1 h	2.5 h	7.0 h	20.5 h
Yield% **(-)N1***	88%	90%	91%	92%
Yield% **(+)N1***	19%	33%	48%	46%

Table 3.4. Match and Mismatch between Chiral NBE and Epoxide (continued)

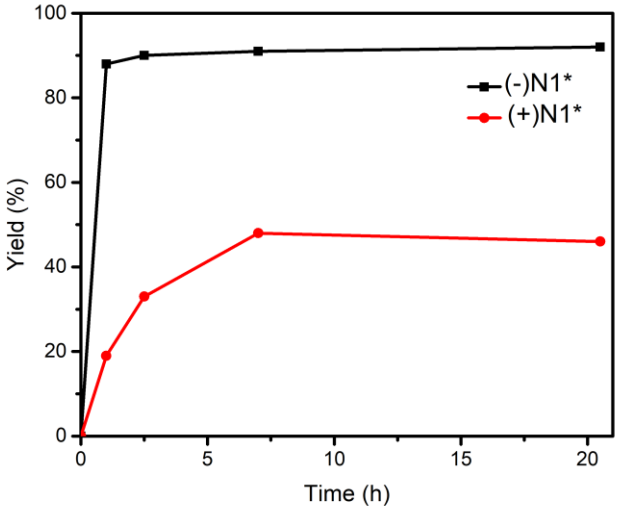

3.5 NMR Spectra

Figure 3.15. ^{1}H NMR of A

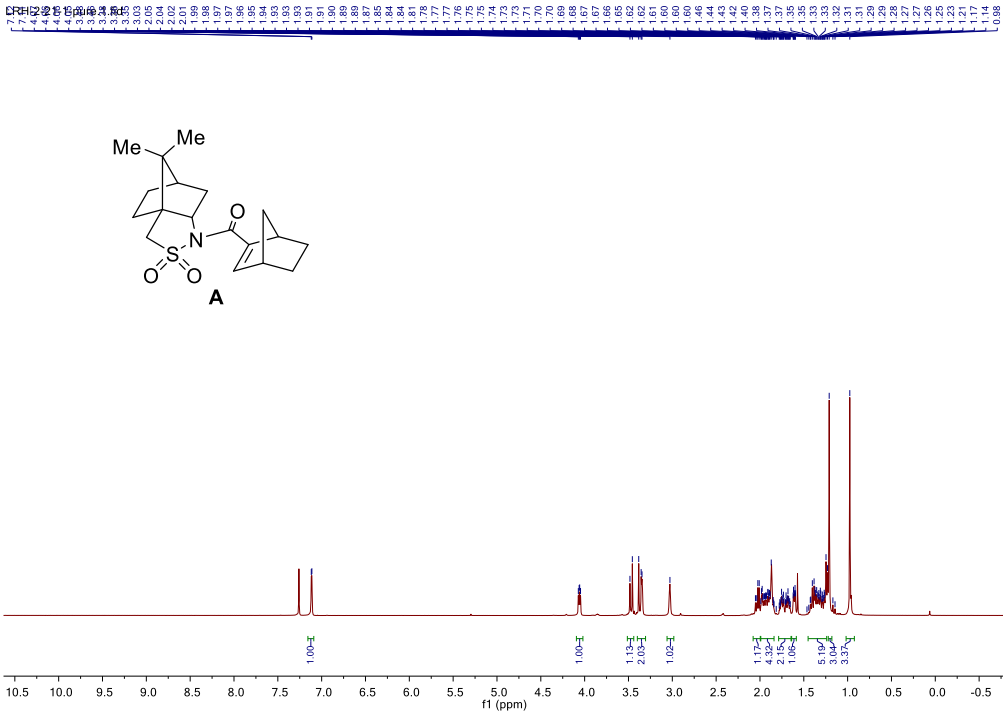

Figure 3.16. ^{13}C NMR of A

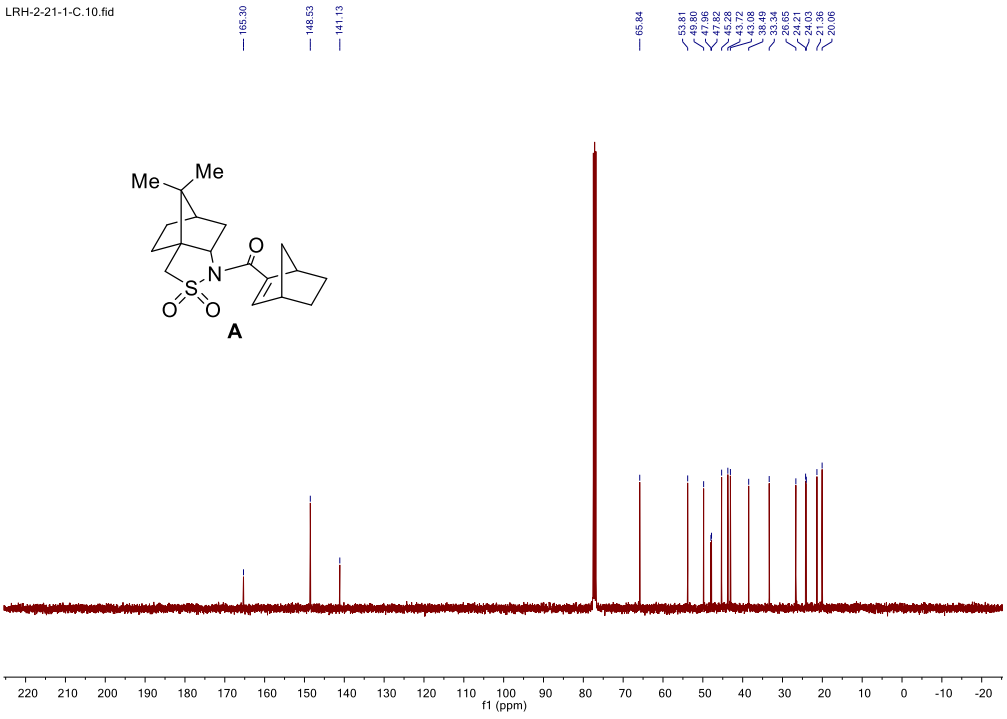

Figure 3.17. ^{1}H NMR of B

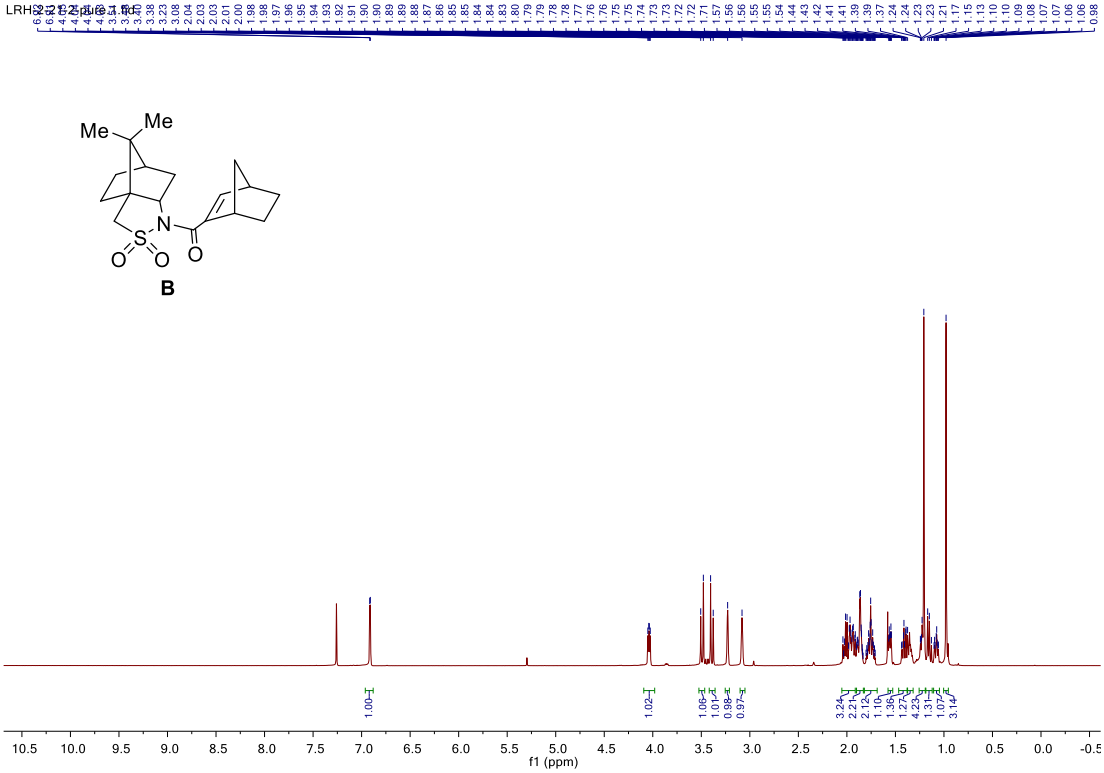

Figure 3.18. ^{1}H NMR of B

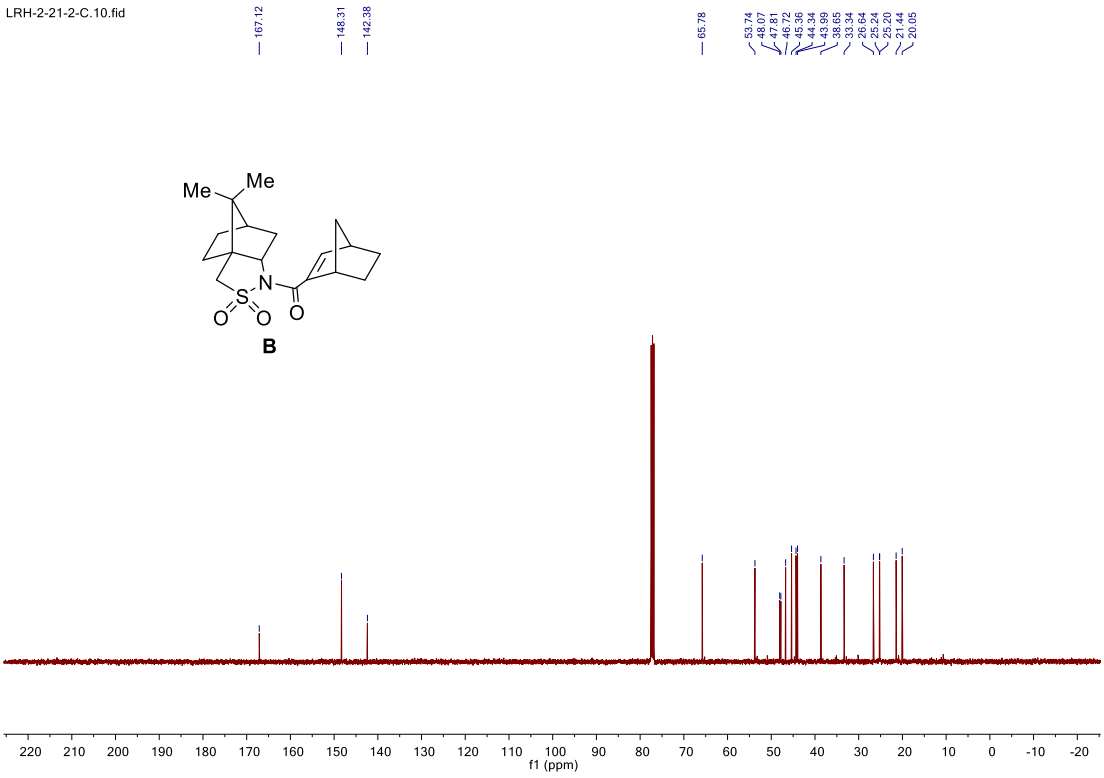

Figure 3.19. ^{1}H NMR of N1*

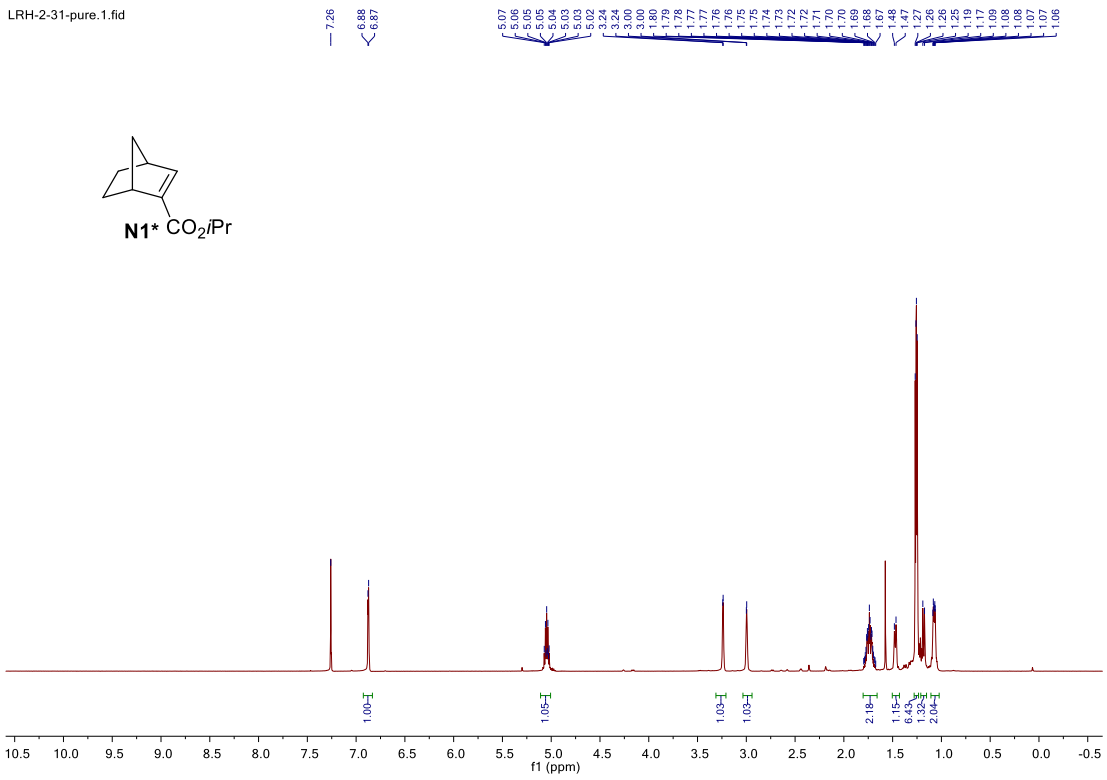

Figure 3.20. ^{13}C NMR of N1*

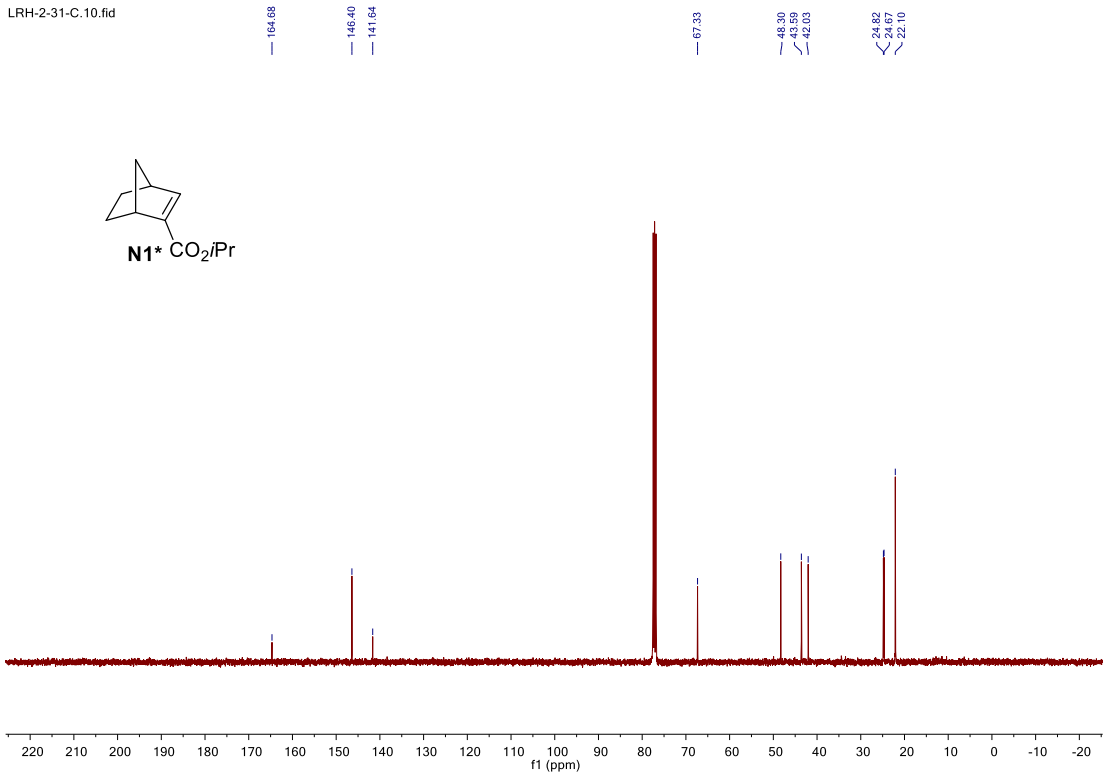

Figure 3.21. ^{1}H NMR of N2*

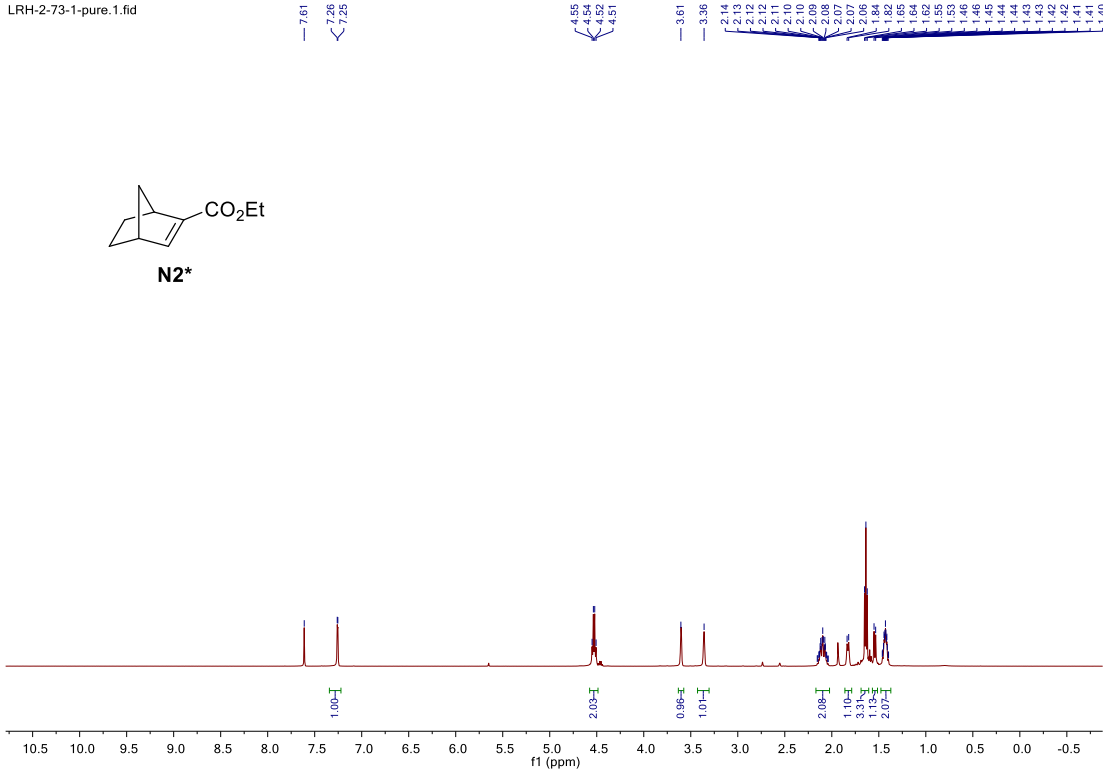

Figure 3.22. ^{13}C NMR of N2*

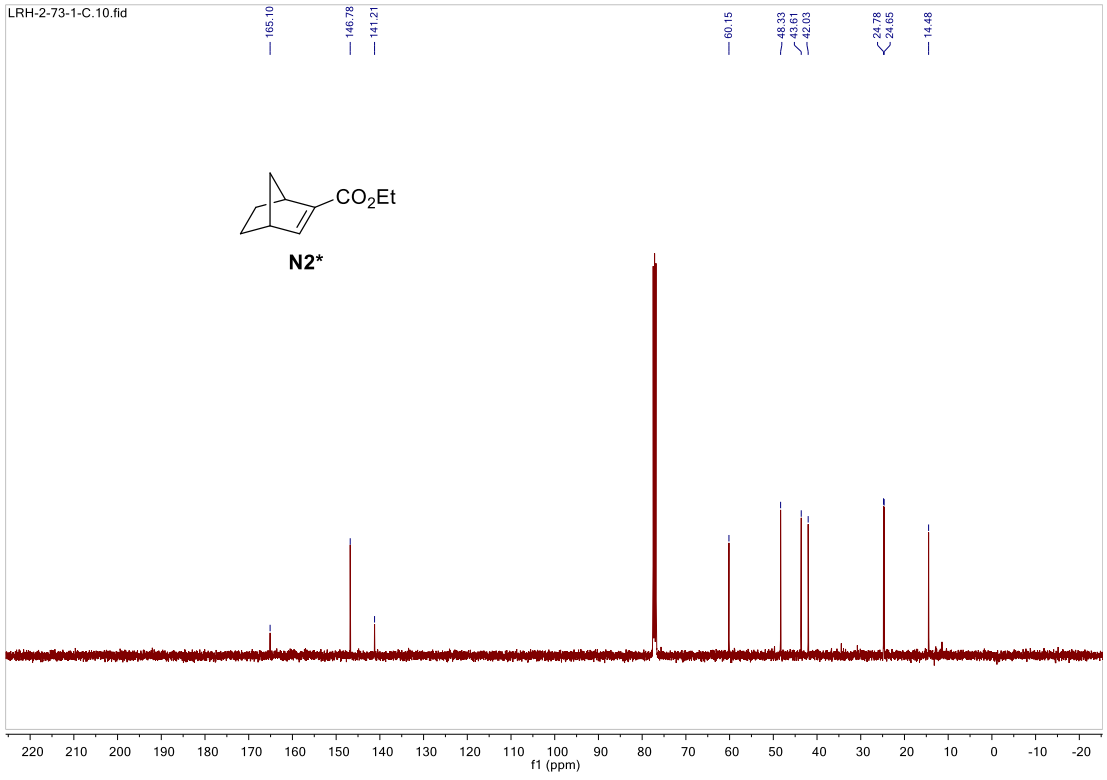

Figure 3.23. ^{1}H NMR of N3*

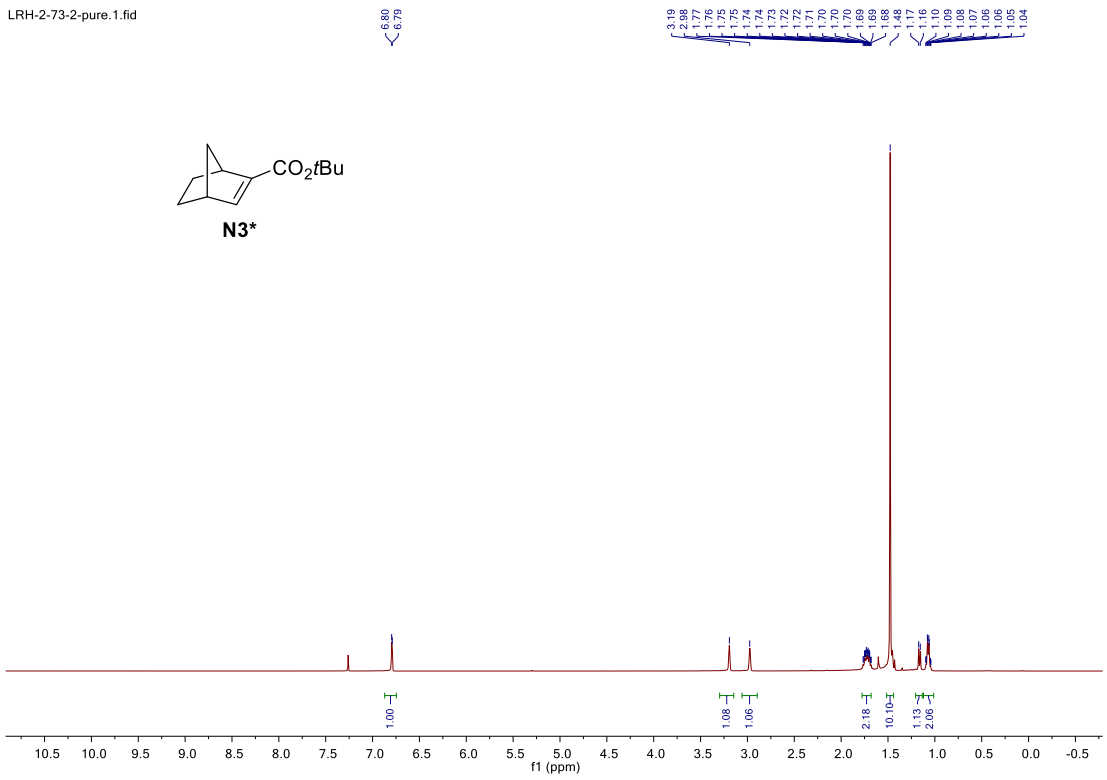

Figure 3.24. ^{13}C NMR of N3*

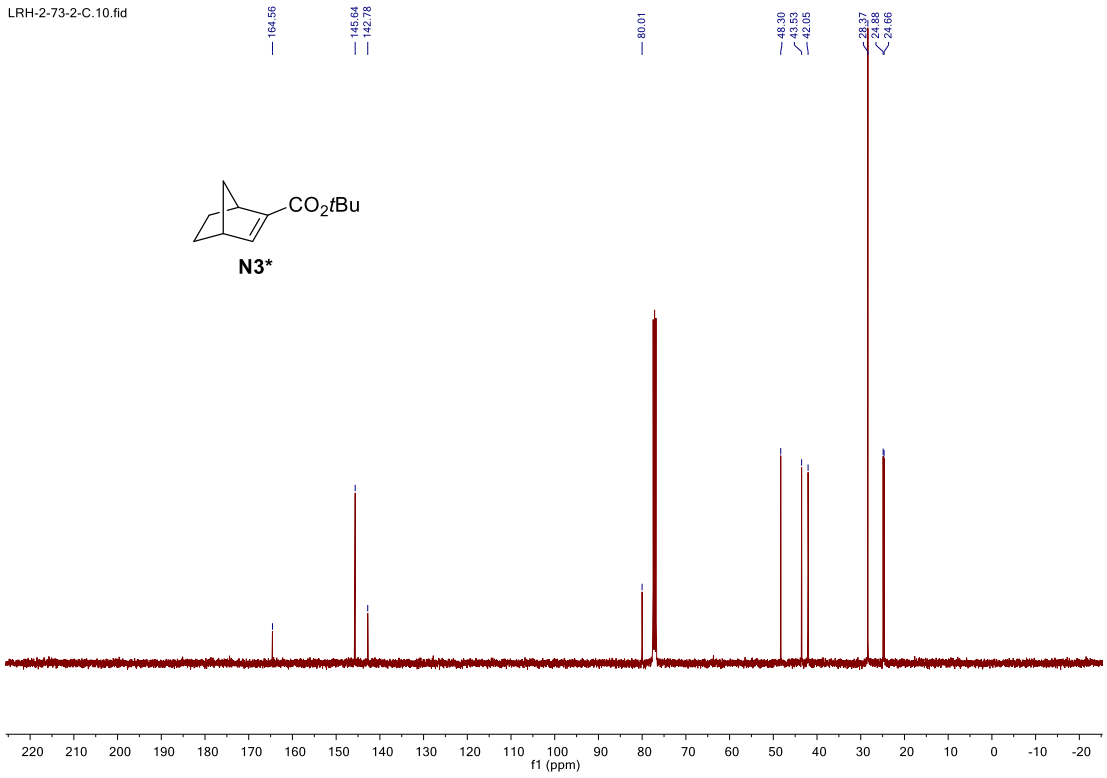

Figure 3.25. ^{1}H NMR of N4*

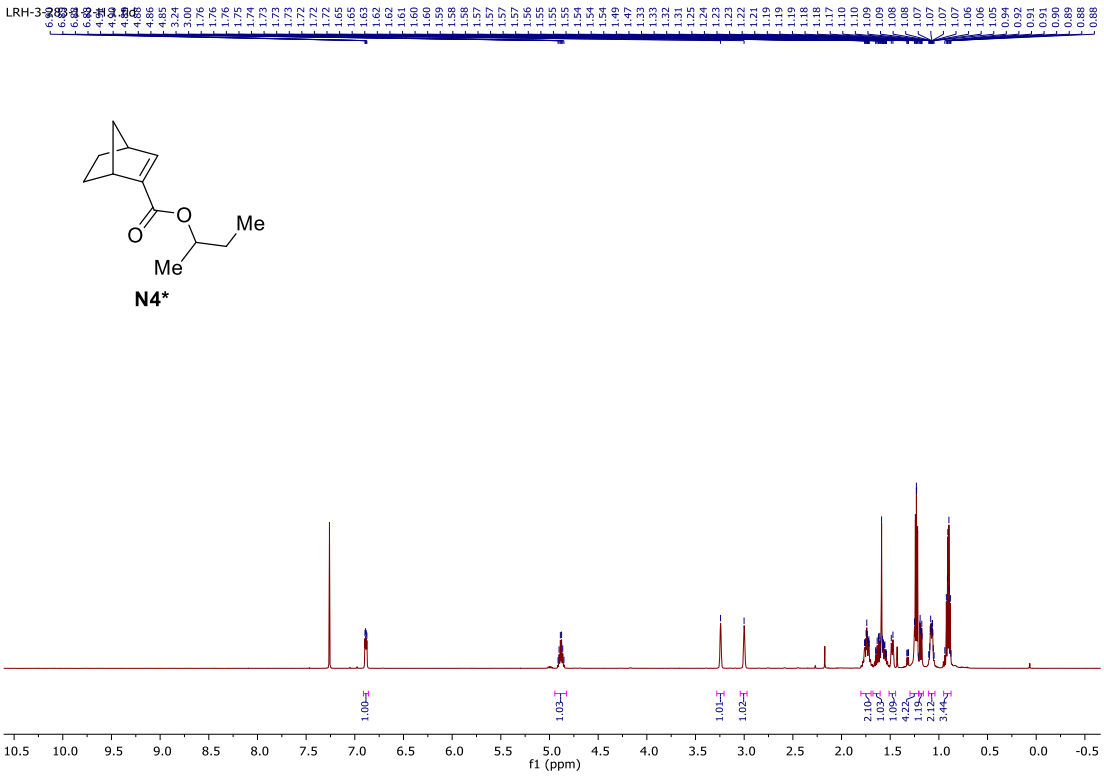

Figure 3.26. ^{13}C NMR of N4*

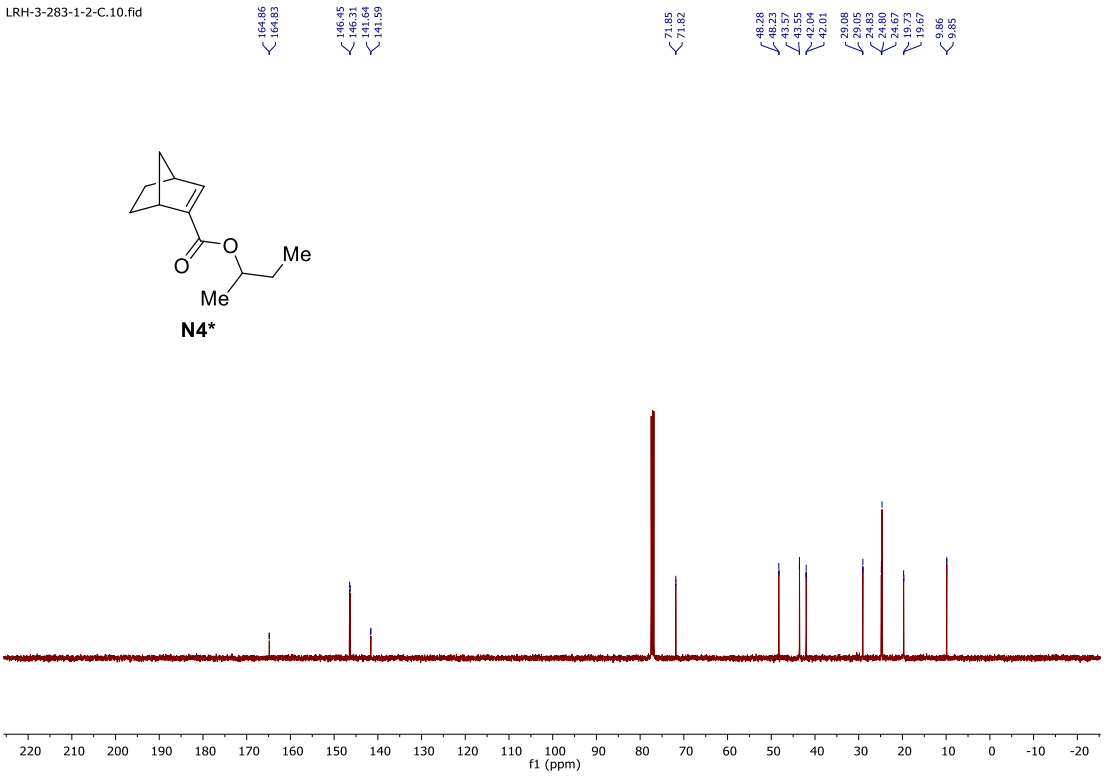

Figure 3.27. ^{1}H NMR of N5*

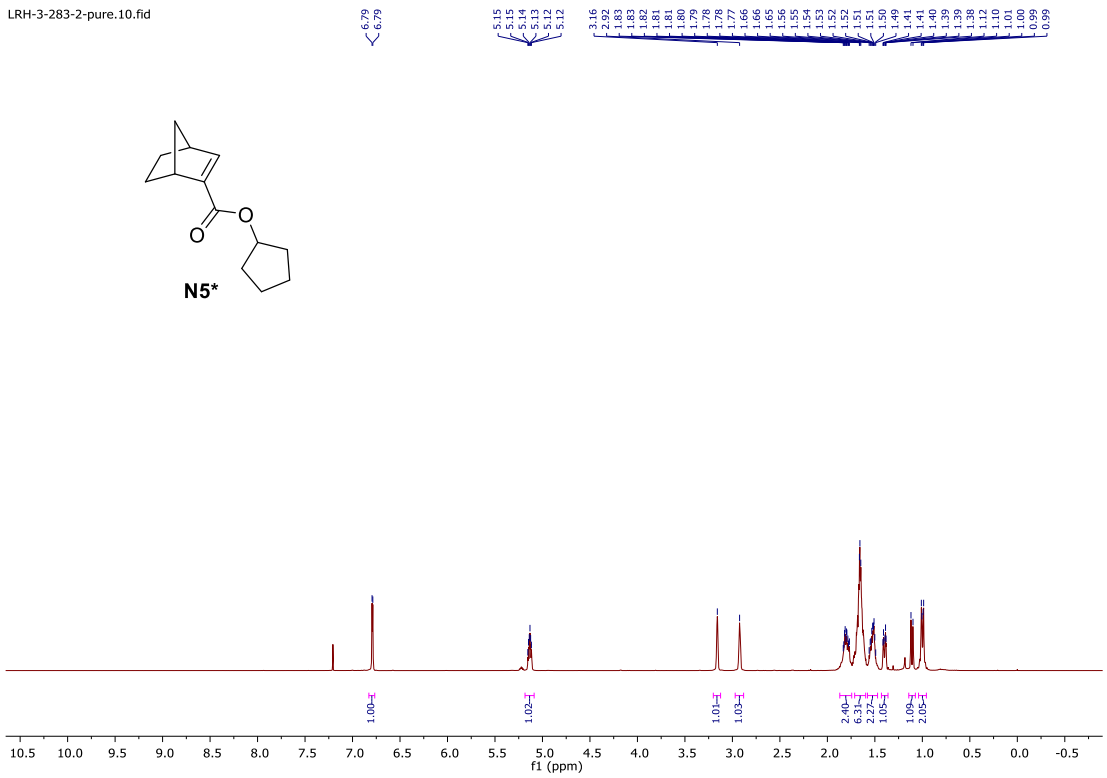

Figure 3.28. ^{13}C NMR of N5*

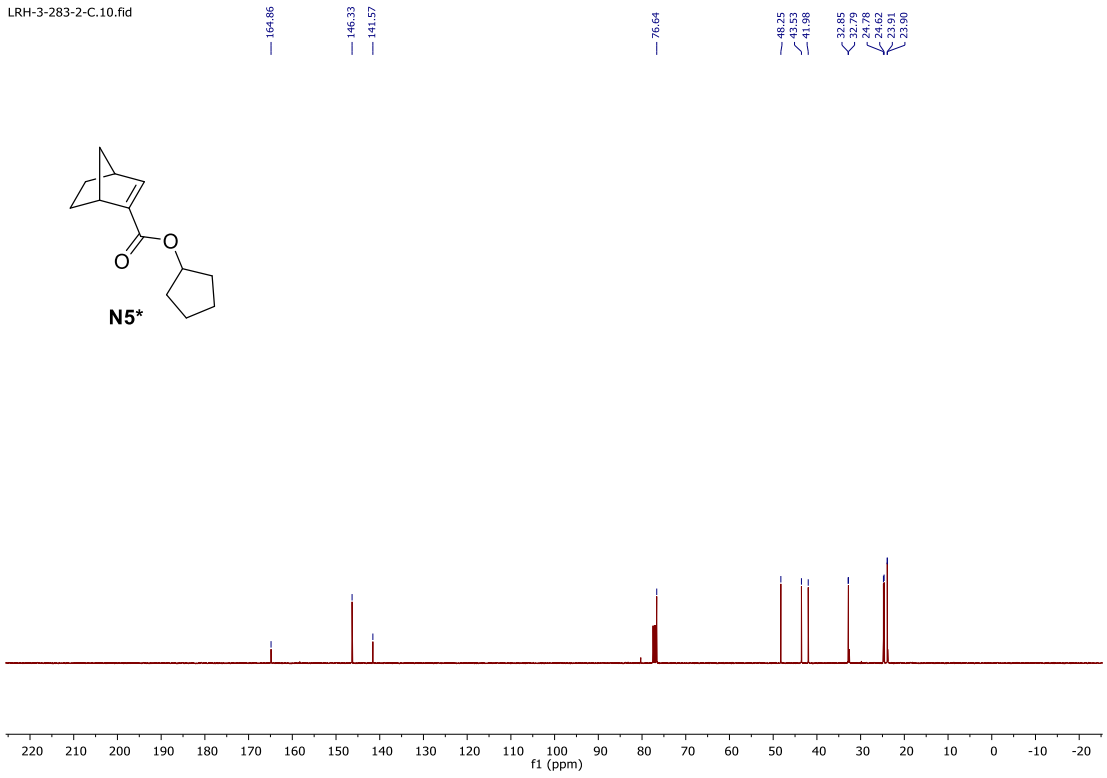

Figure 3.29. ^{1}H NMR of N7*

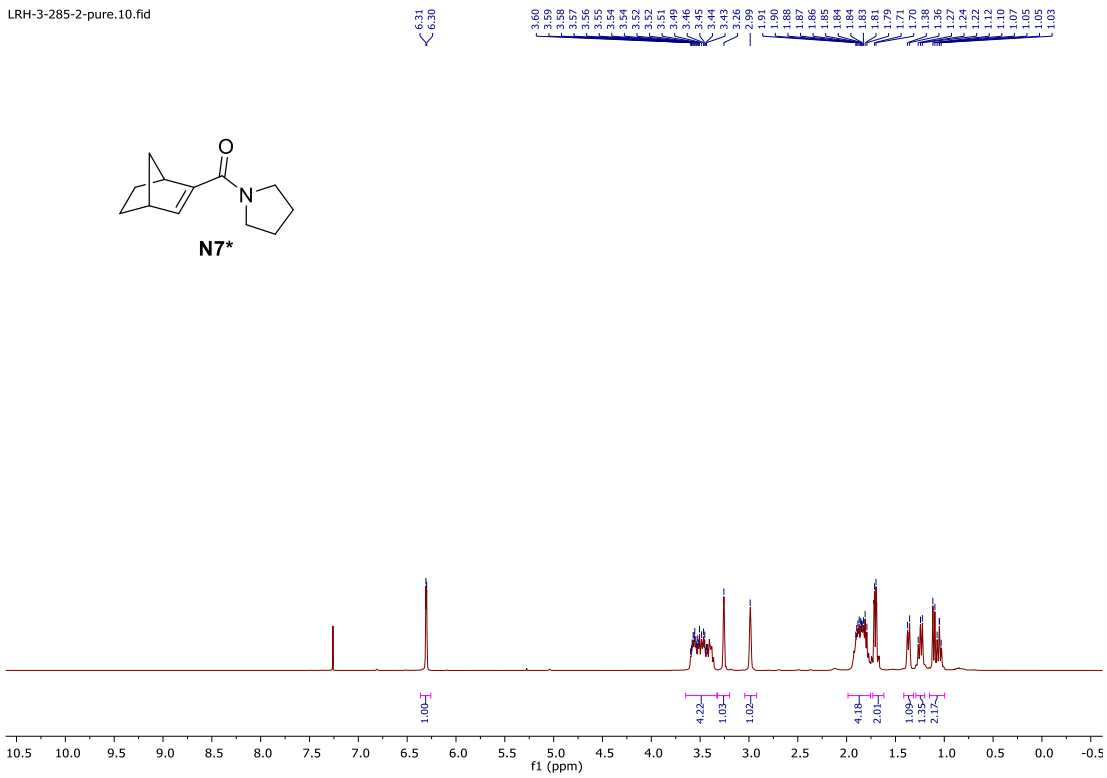

Figure 3.30. ^{13}C NMR of N7*

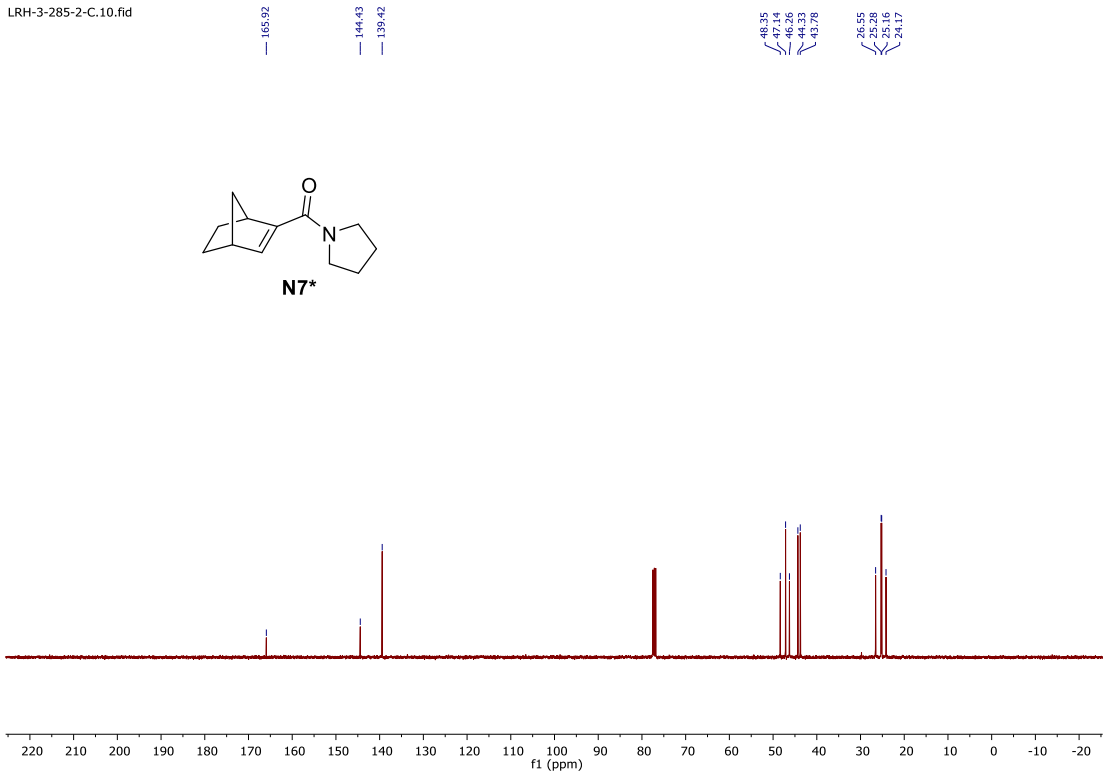

Figure 3.31. ^{1}H NMR of N8*

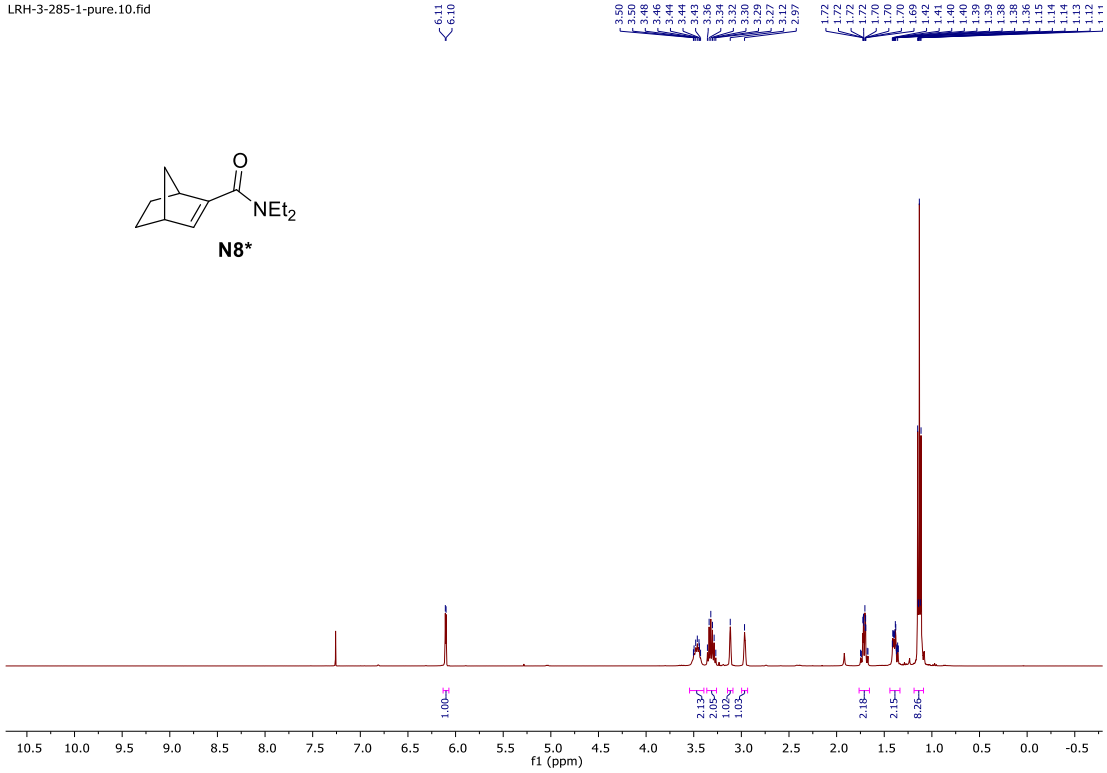

Figure 3.32. ^{13}C NMR of N8*

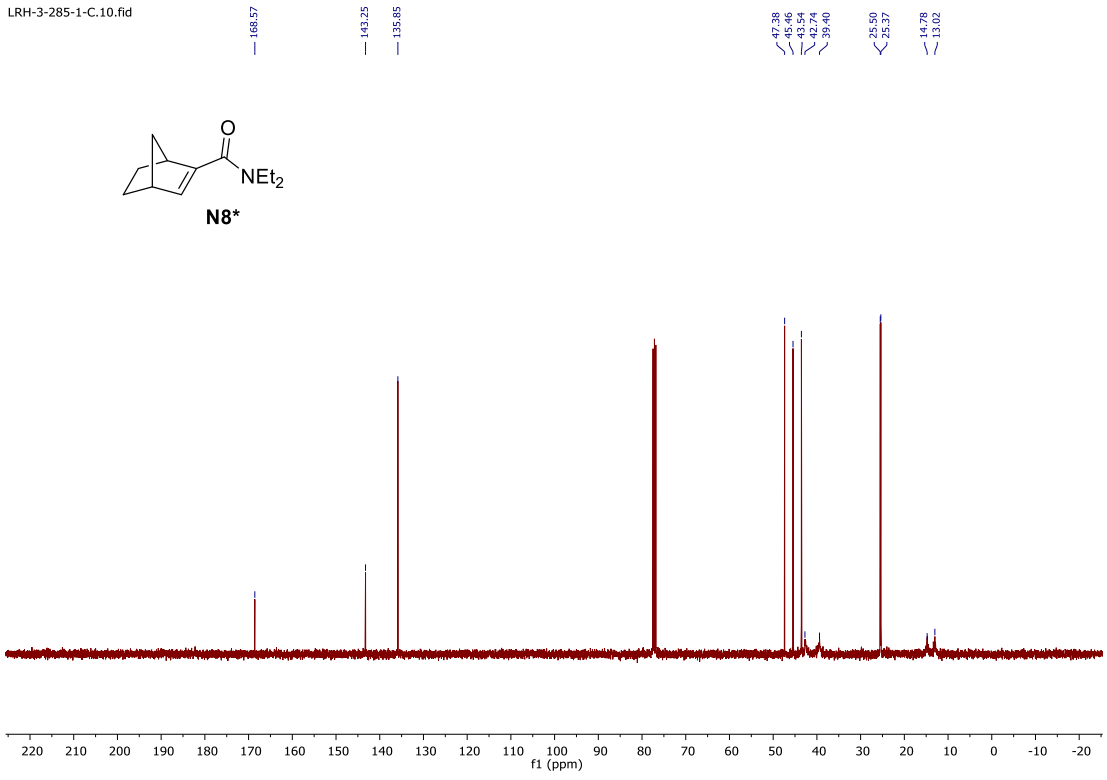

Figure 3.33. ^{1}H NMR of N9*

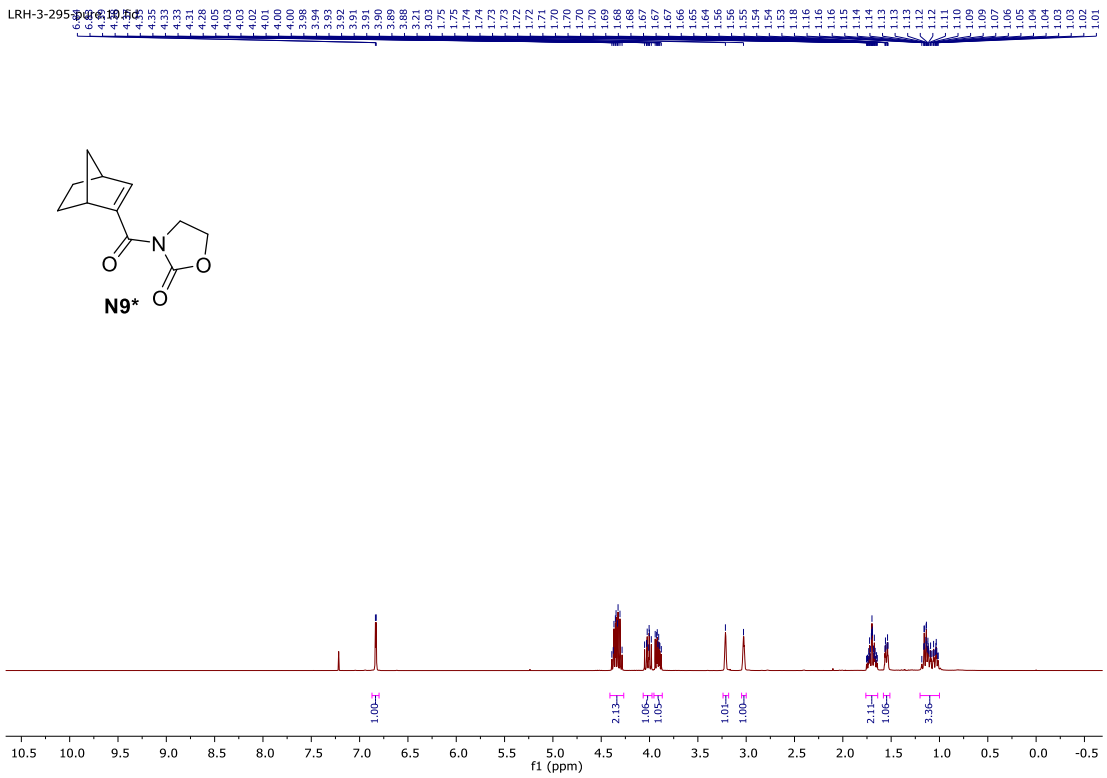

Figure 3.34. ^{13}C NMR of N9*

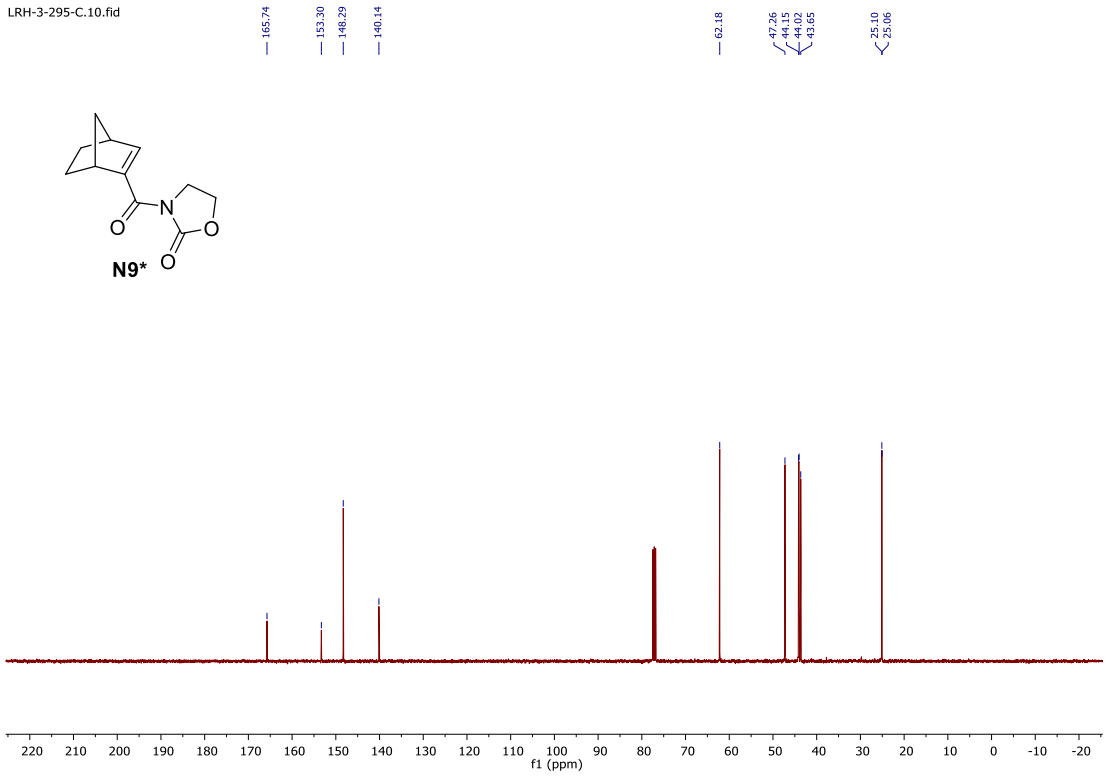

Figure 3.35. ^{1}H NMR of N10*

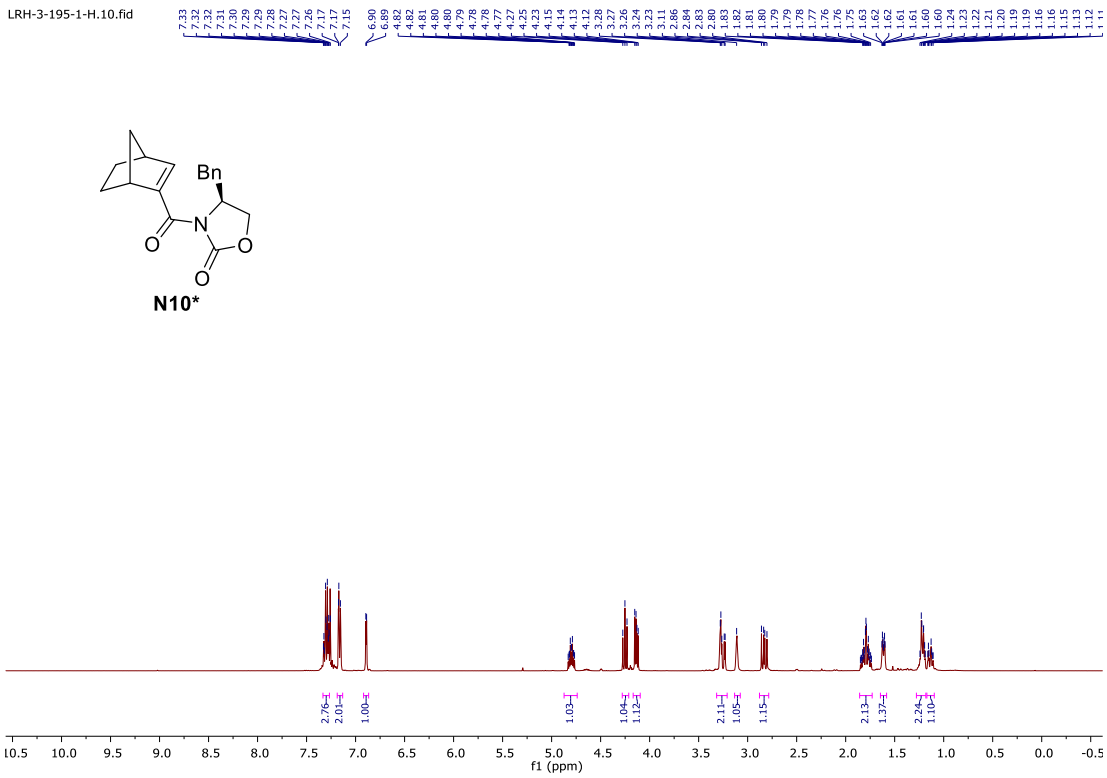

Figure 3.36. ^{13}C NMR of N10*

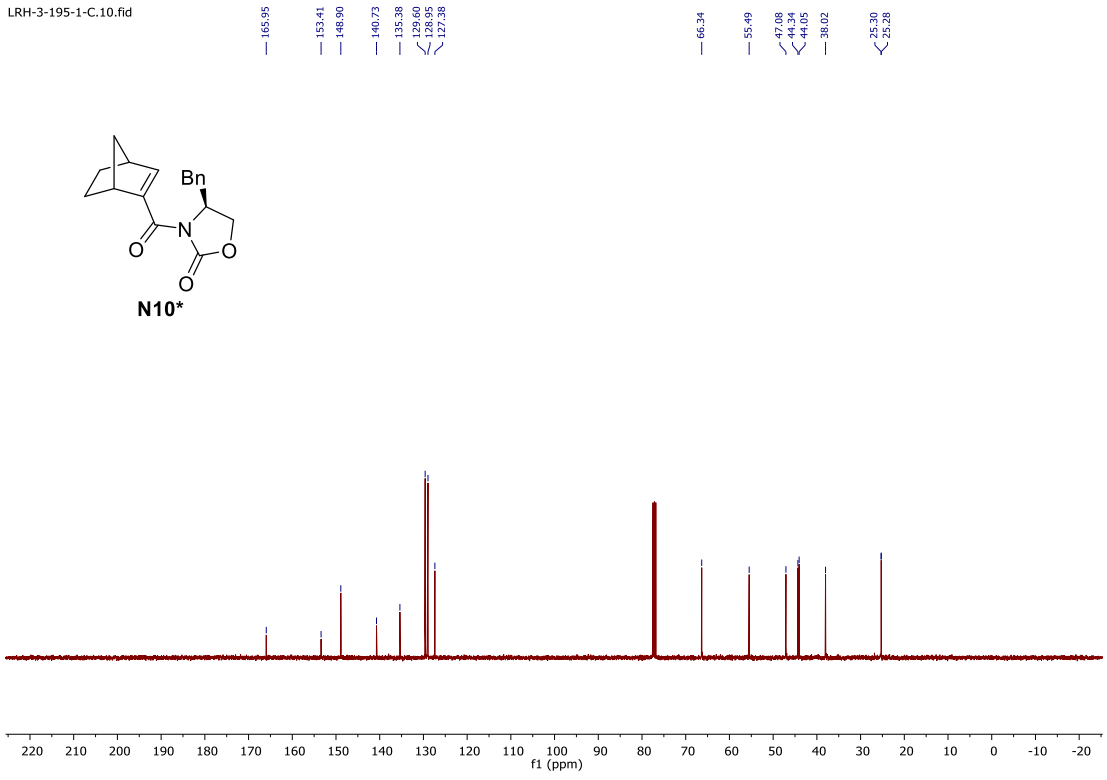

Figure 3.37. ^{1}H NMR of N11*

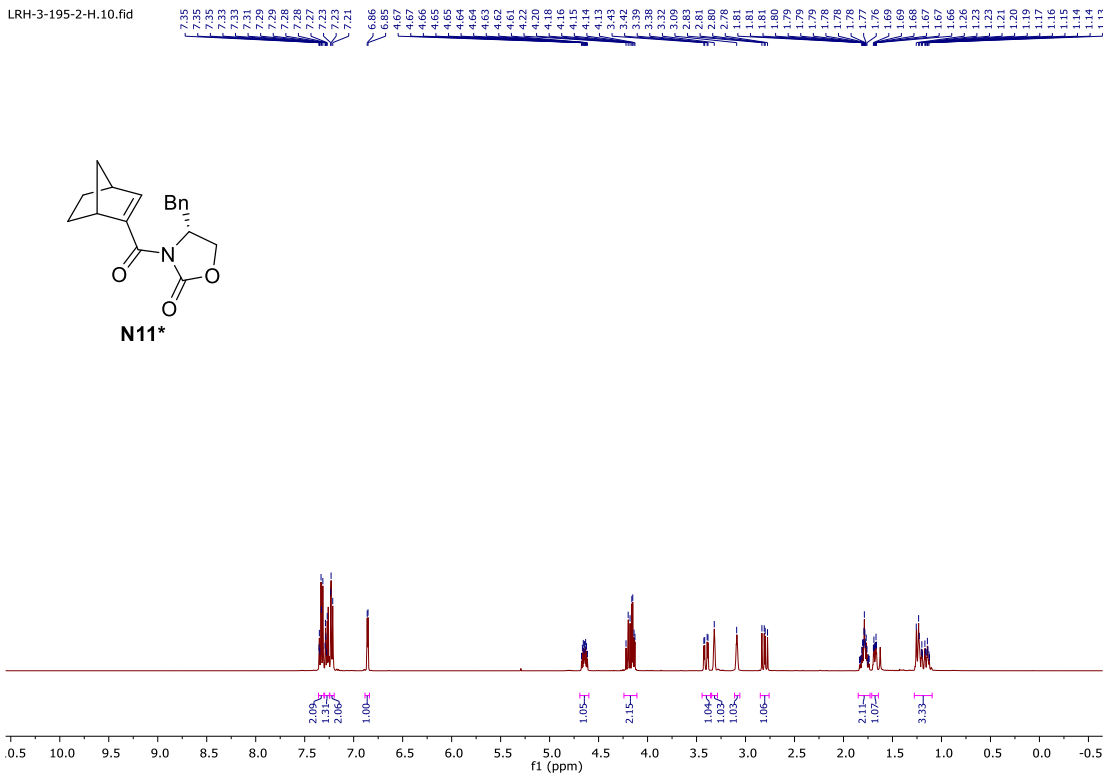

Figure 3.38. ^{13}C NMR of N11*

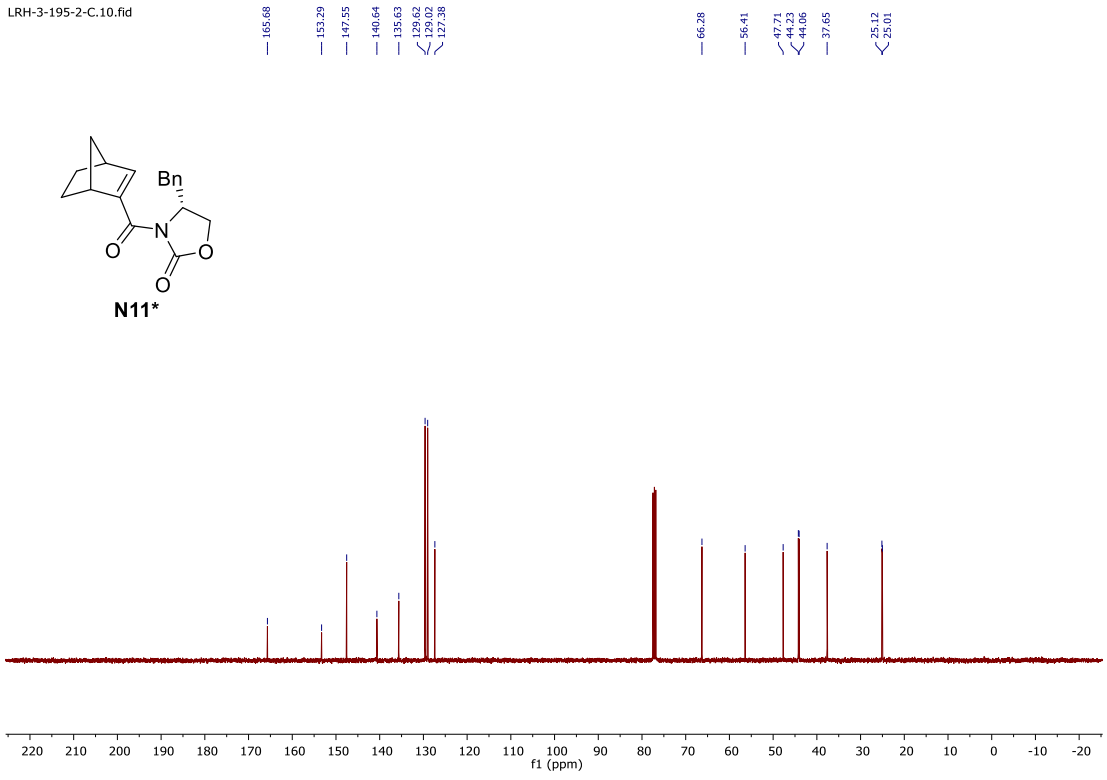

Figure 3.39. ^{1}H NMR of N12*

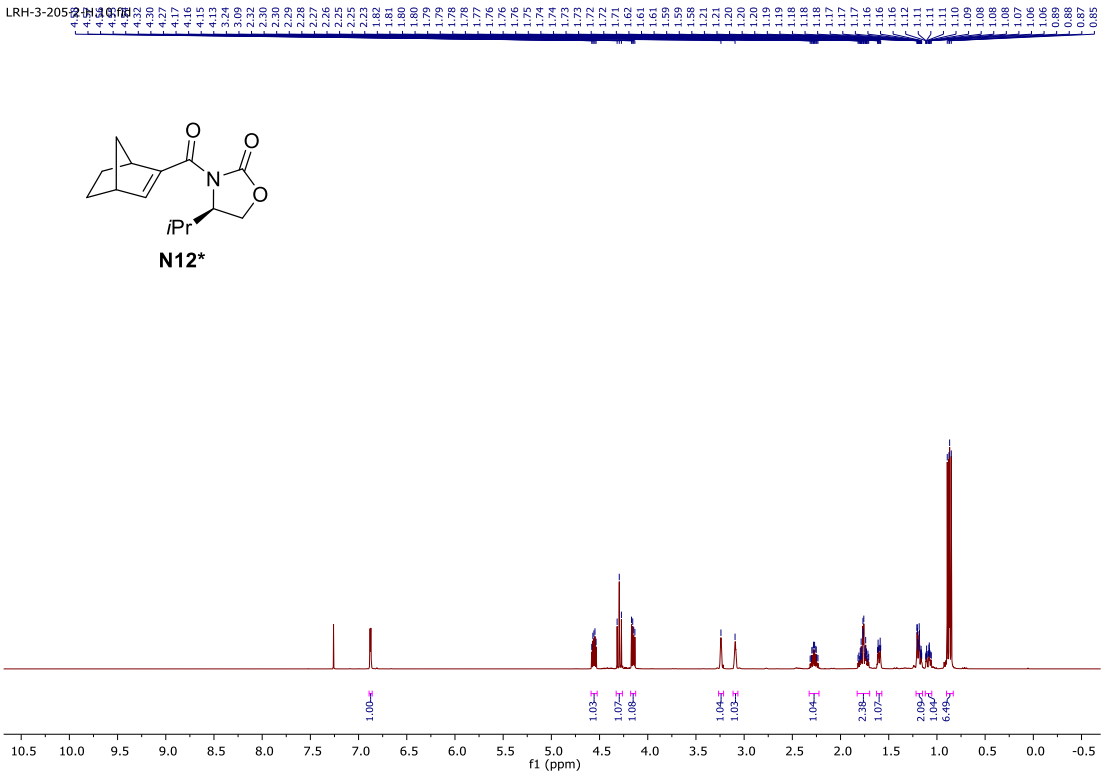

Figure 3.40. ^{13}C NMR of N12*

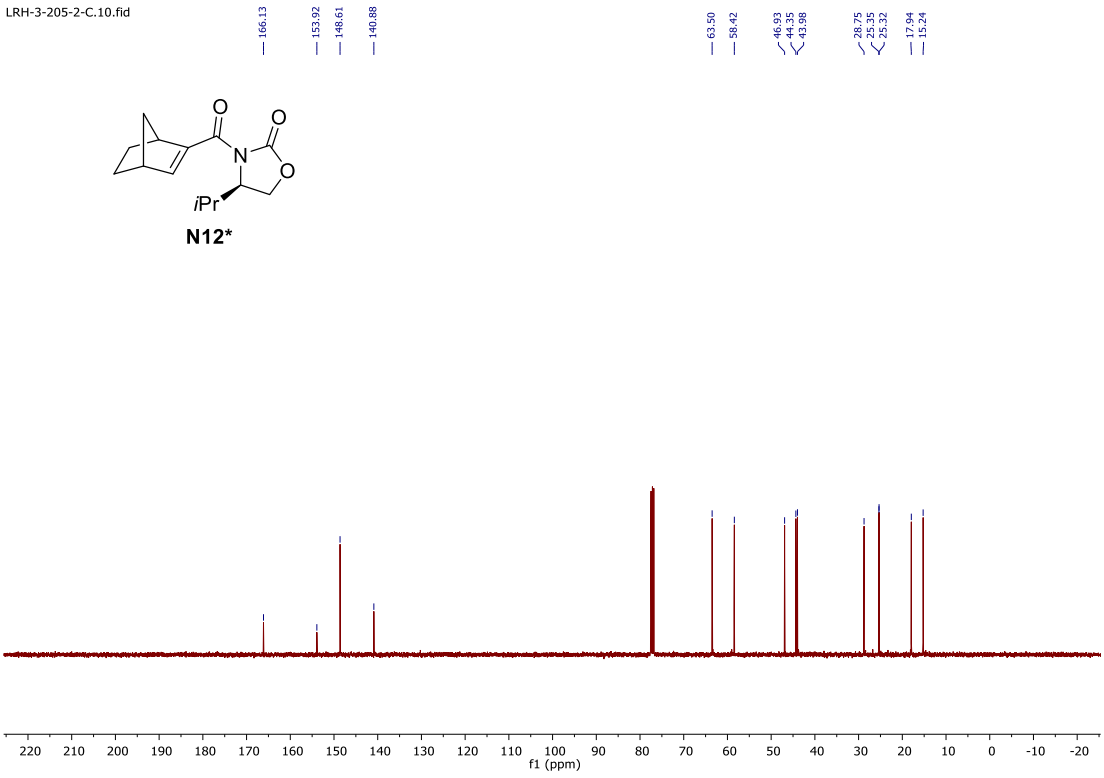

Figure 3.41. ^{1}H NMR of N13*

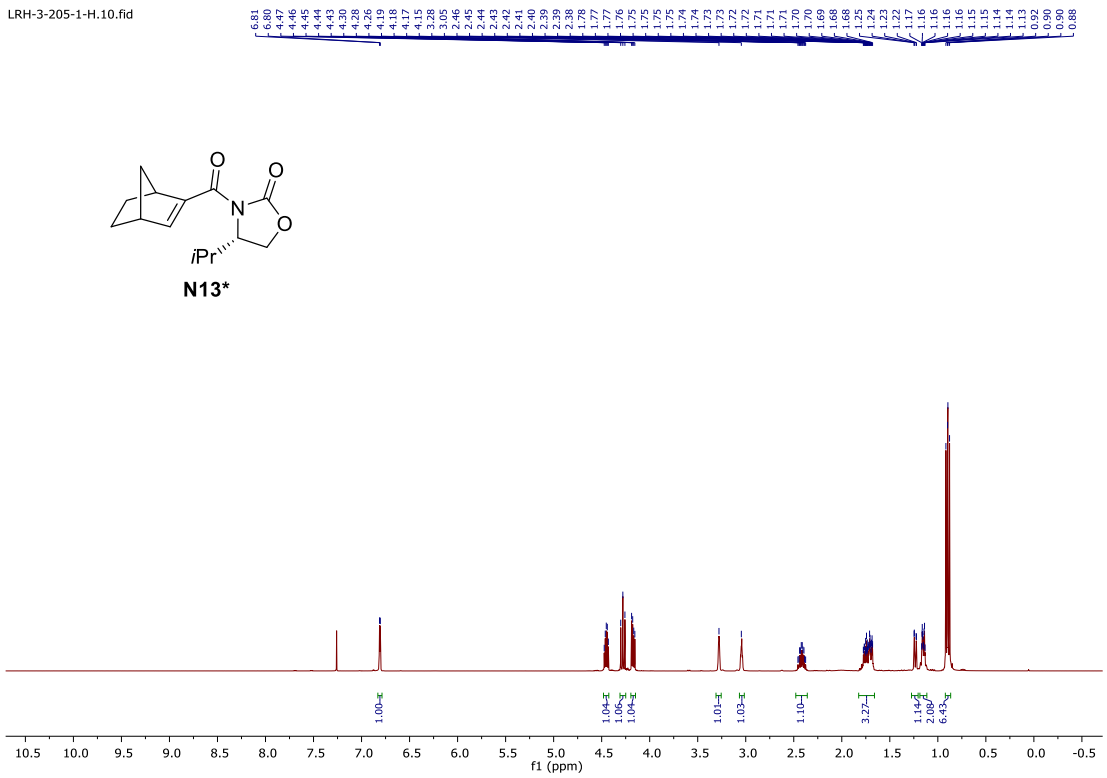

Figure 3.42. ^{13}C NMR of N13*

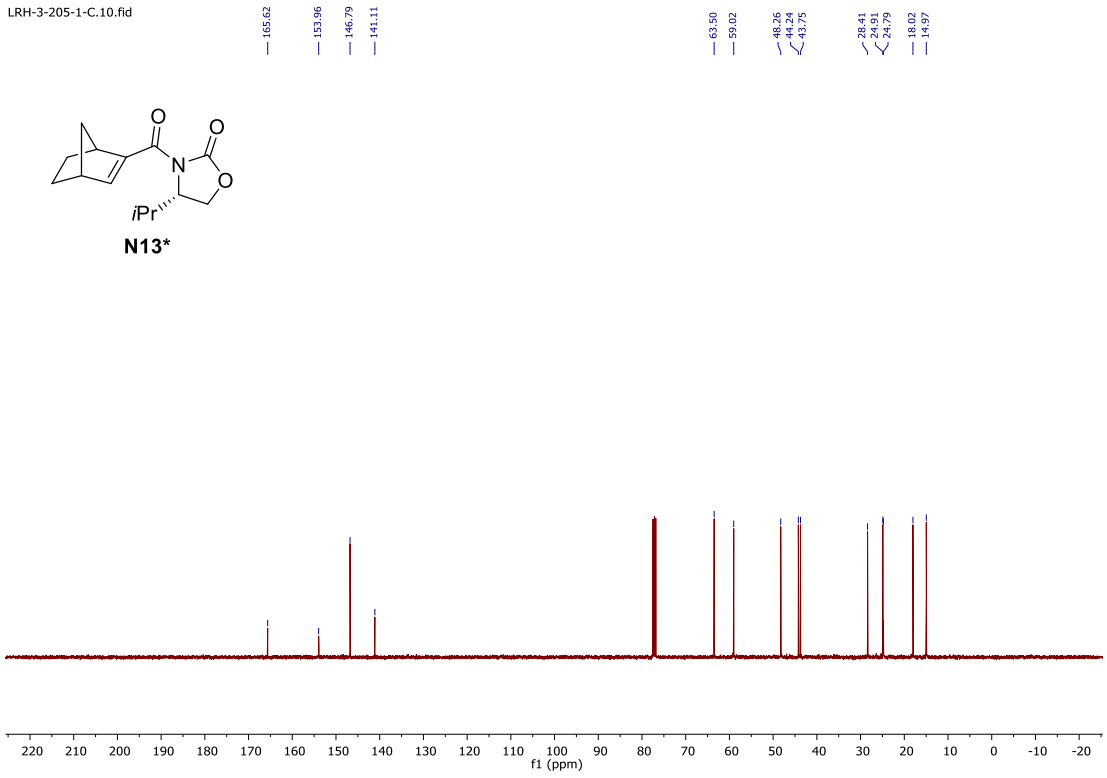

Figure 3.43. ^{1}H NMR of 3aa*

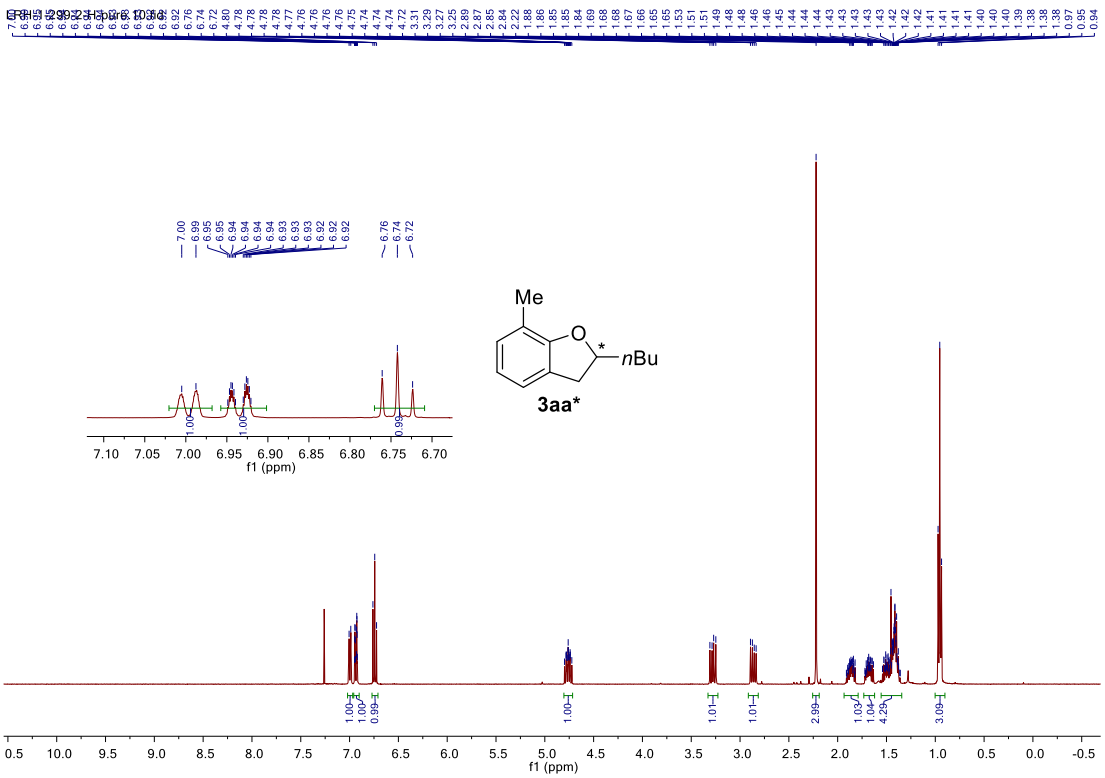

Figure 3.44. ^{13}C NMR of 3aa*

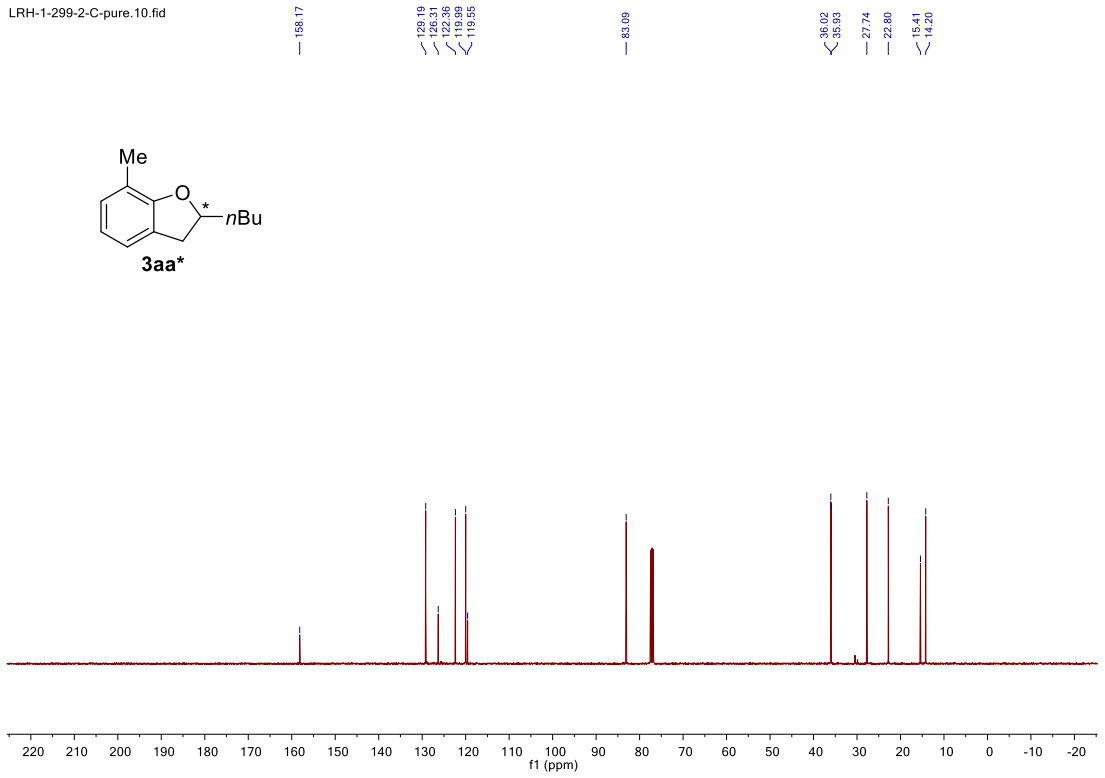

Figure 3.45. ^{1}H NMR of 3ba*

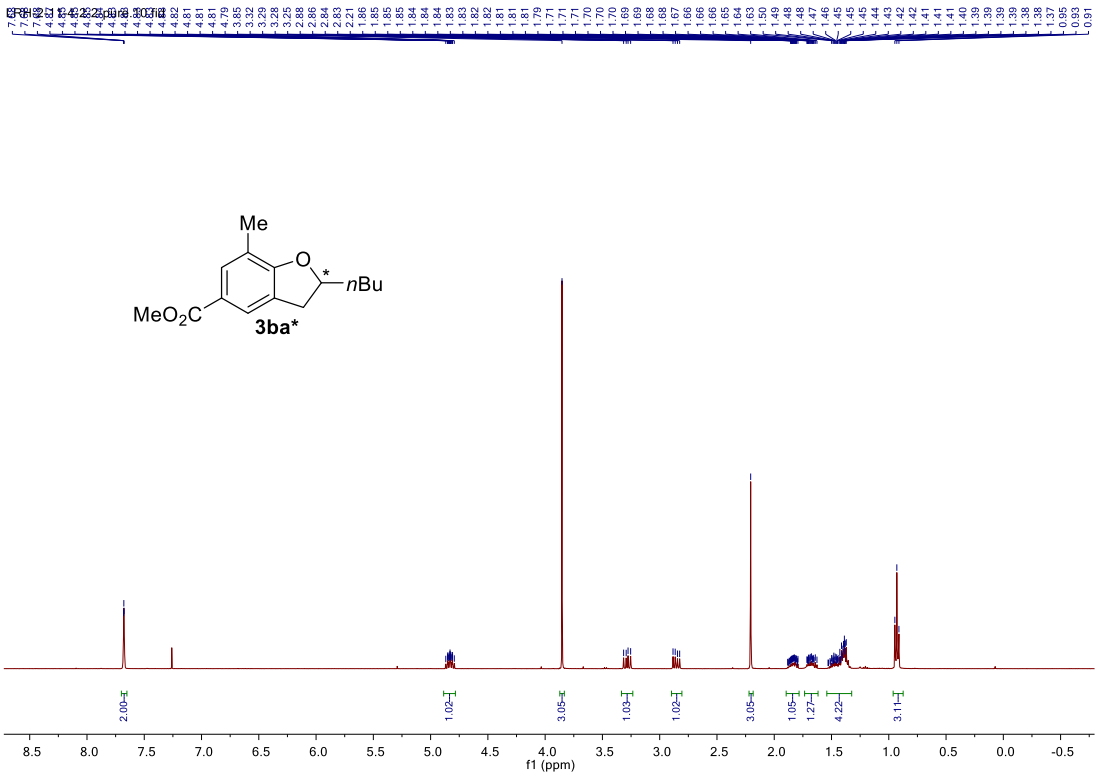

Figure 3.46. ^{13}C NMR of 3ba*

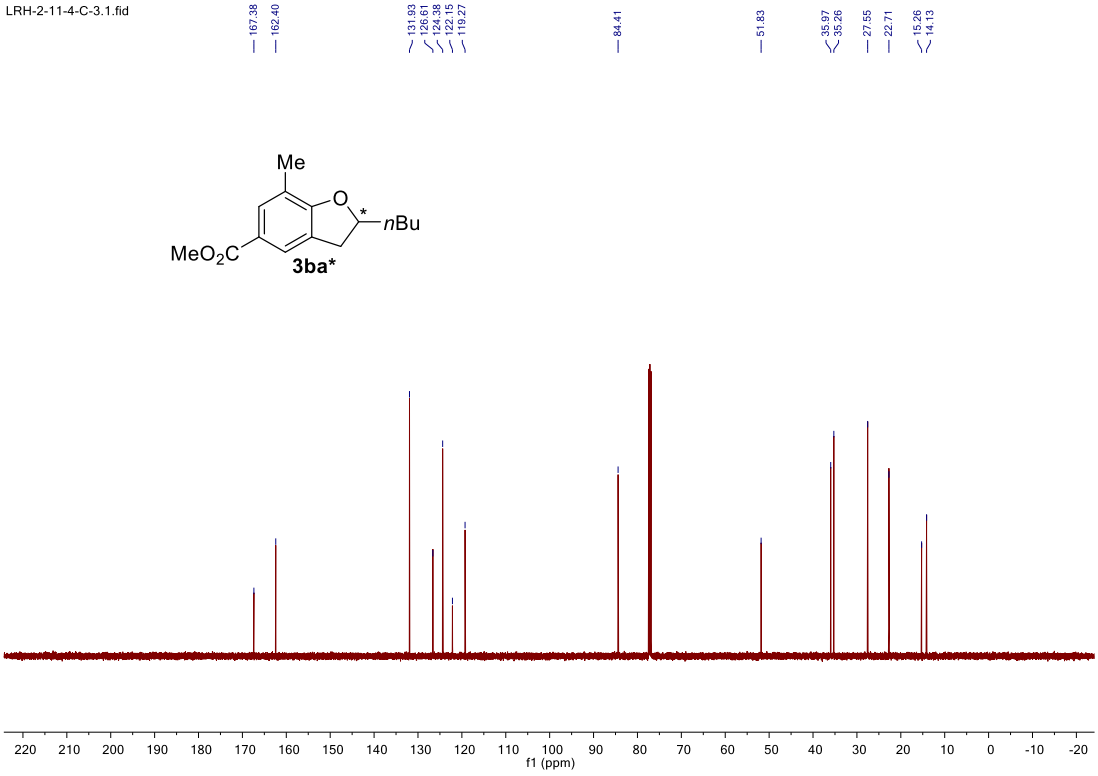

Figure 3.47. ^{1}H NMR of 3ab*

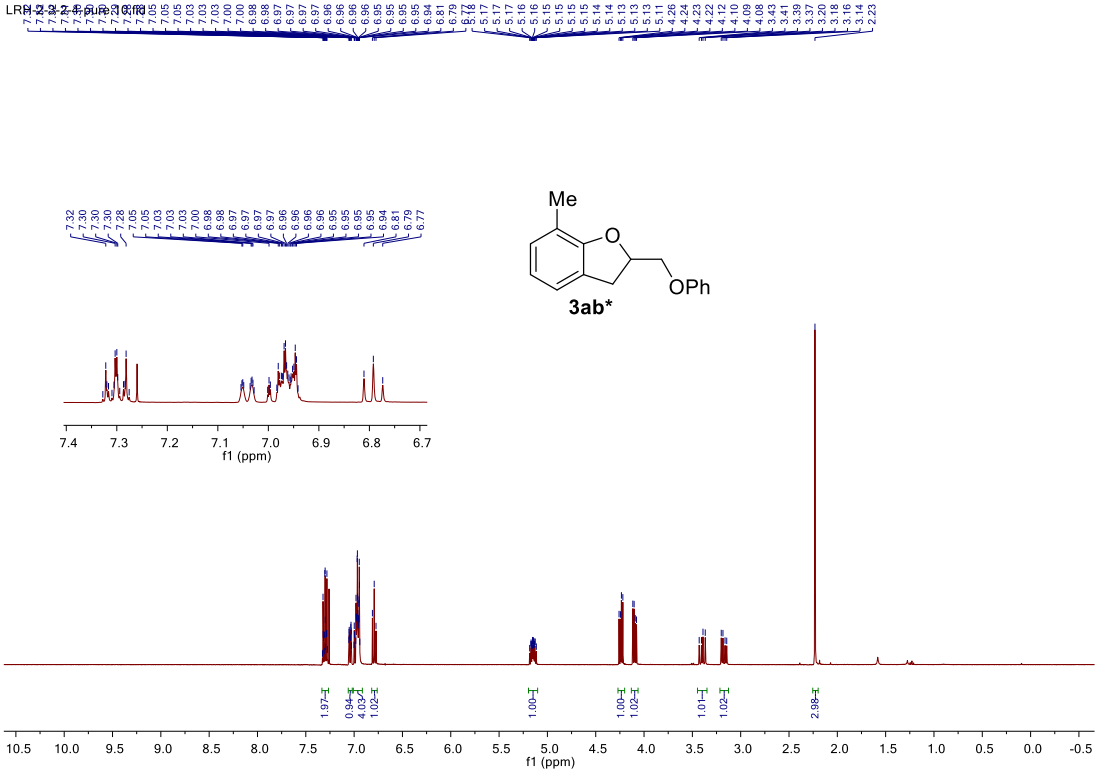

Figure 3.48. ^{13}C NMR of 3ab*

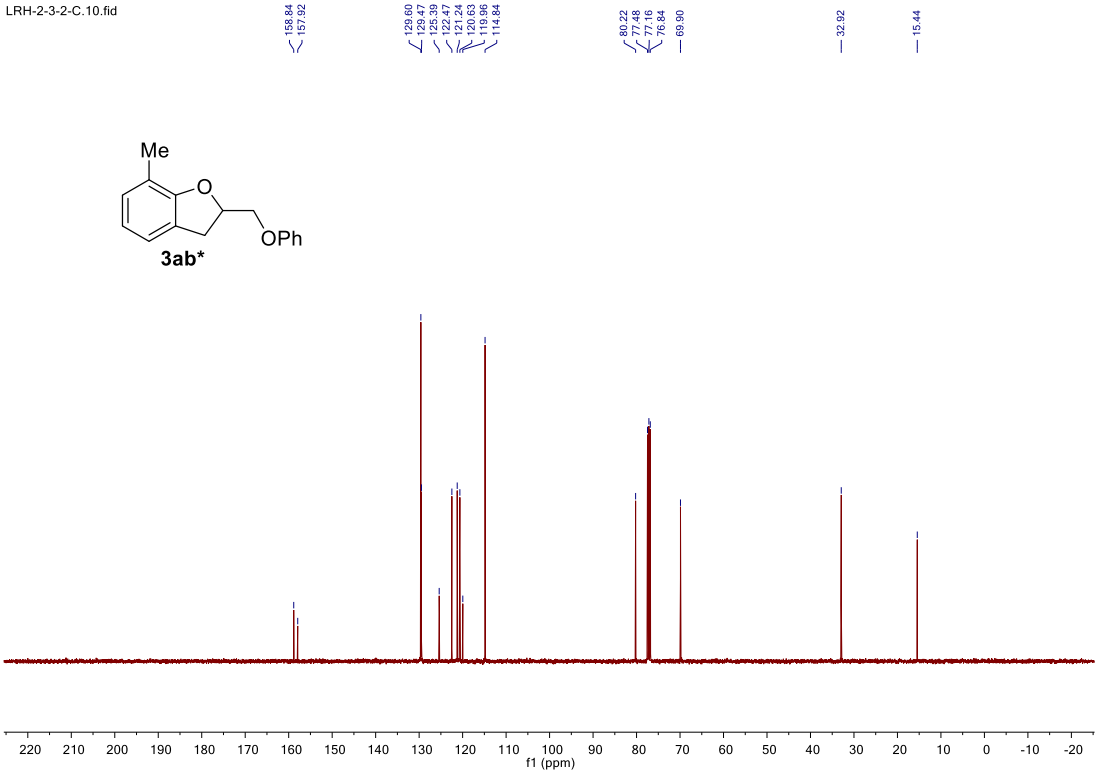

Figure 3.49. ^{1}H NMR of 3ac*

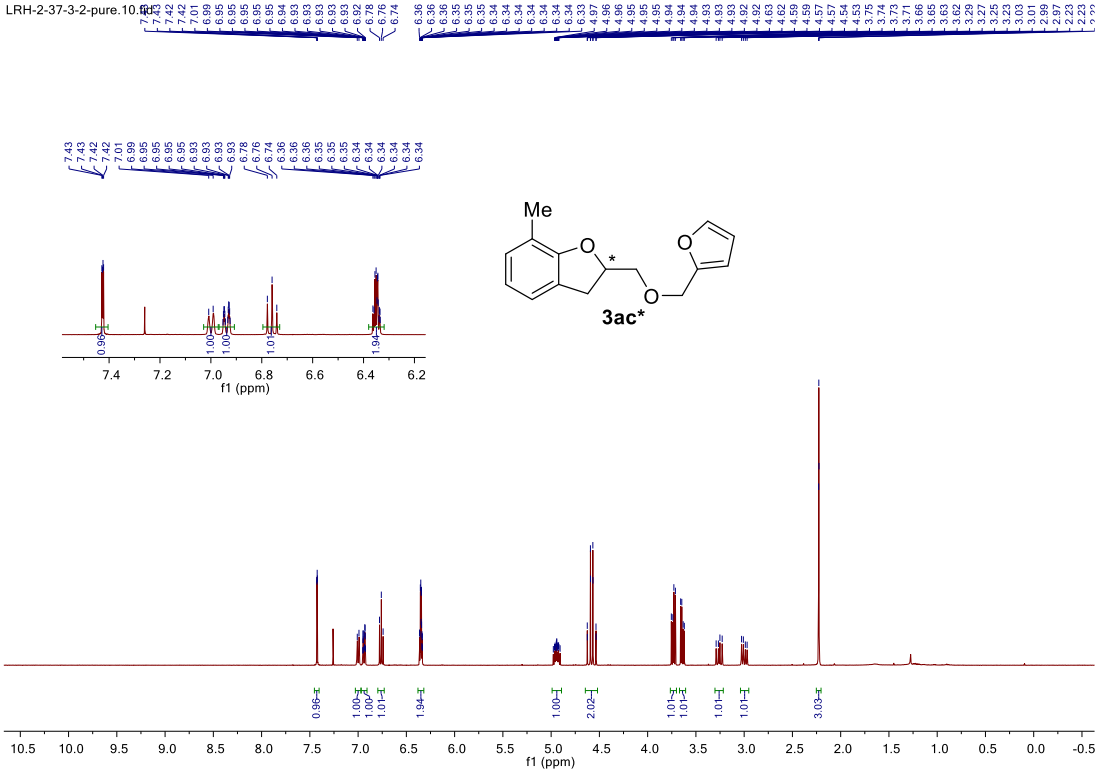

Figure 3.50. ^{13}C NMR of 3ac*

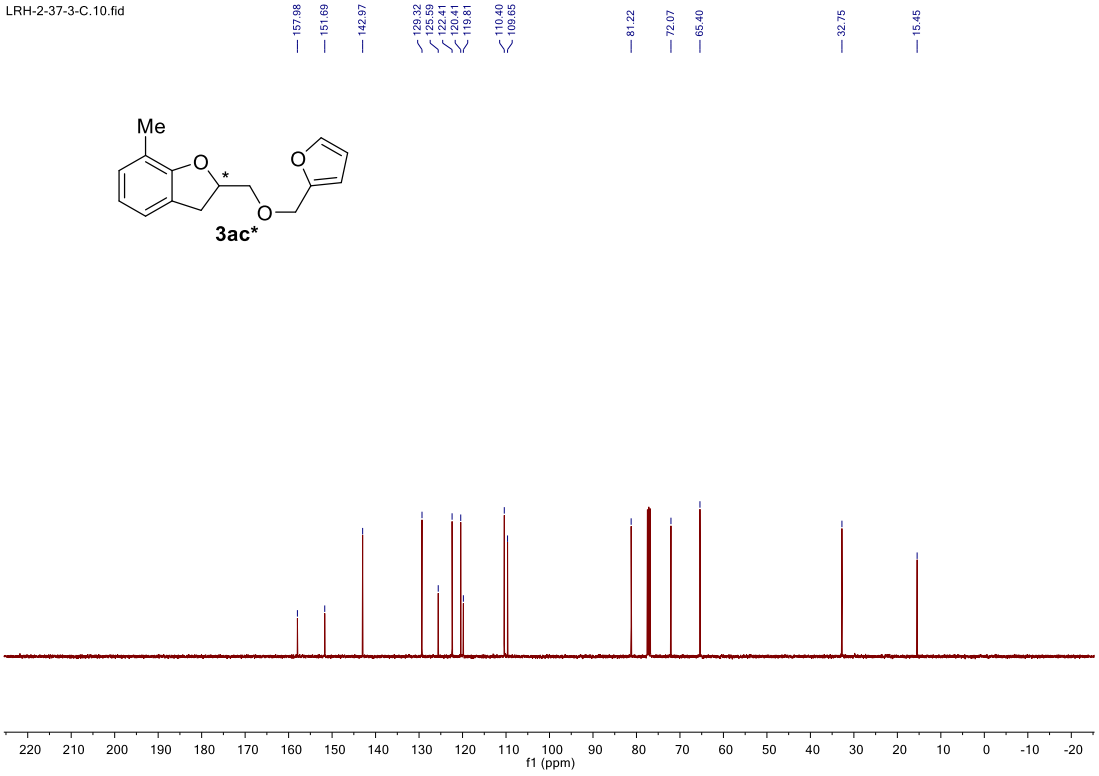

3.6 Crystallographic Data

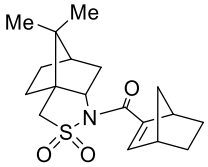

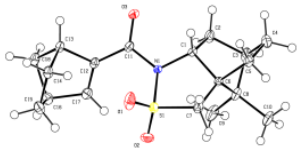

Table 3.5. Crystallographic Data of A

Empirical formula	$C_{18}H_{25}NO_3S$
Formula weight	335.45
Temperature	100(2) K
Wavelength	0.71073 Å
Crystal system	orthorhombic
Space group	P 21 21 21
Unit cell dimensions	a = 7.8259(6) Å □= 90°.
	b = 9.5135(8) Å □= 90°.
	c = 22.6470(18) Å □ = 90°.
Volume	1686.1(2) $Å^3$
Z	4
Density (calculated)	1.321 Mg/m^3
Absorption coefficient	0.207 mm^{-1}
F(000)	720
Crystal size	0.510 x 0.380 x 0.320 mm^3
Theta range for data collection	2.754 to 30.819°.
Index ranges	-11<=h<=11, -13<=k<=13, -32<=l<=32
Reflections collected	60626
Independent reflections	5259 [R(int) = 0.0409]
Completeness to theta = 25.242°	99.9 %
Absorption correction	Semi-empirical from equivalents
Max. and min. transmission	1.00 and 0.912
Refinement method	Full-matrix least-squares on F^2
Data / restraints / parameters	5259 / 0 / 214
Goodness-of-fit on F^2	1.044
Final R indices [I>2sigma(I)]	R1 = 0.0304, wR2 = 0.0758
R indices (all data)	R1 = 0.0350, wR2 = 0.0771
Absolute structure parameter	0.039(12)
Extinction coefficient	n/a
Largest diff. peak and hole	0.295 and -0.406 $e.Å^{-3}$

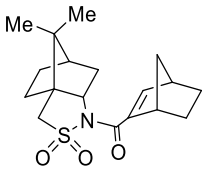

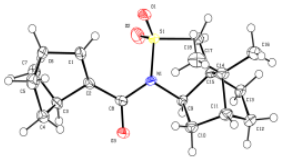

Table 3.6. Crystallographic Data of B

Identification code	LRH 2-21-2
Empirical formula	$C_{18}H_{25}NO_3S$
Formula weight	335.45
Temperature/K	100.0
Crystal system	monoclinic
Space group	$P2_1$
a/Å	7.9608(8)
b/Å	9.0050(9)
c/Å	11.9856(12)
α/°	90
β/°	105.827(2)
γ/°	90
Volume/Å^3	826.64(14)
Z	2
ρ_{calc}g/cm^3	1.348
μ/mm^{-1}	0.211
F(000)	360.0
Crystal size/mm^3	0.1 × 0.06 × 0.05
Radiation	MoKα (λ = 0.71073)
2Θ range for data collection/°	5.318 to 54.998
Index ranges	$-10 \leq h \leq 10$, $-11 \leq k \leq 11$, $-15 \leq l \leq 14$
Reflections collected	12941
Independent reflections	3792 [R_{int} = 0.0422, R_{sigma} = 0.0432]
Data/restraints/parameters	3792/1/210
Goodness-of-fit on F^2	1.053
Final R indexes [I>=2σ (I)]	R_1 = 0.0393, wR_2 = 0.0827
Final R indexes [all data]	R_1 = 0.0478, wR_2 = 0.0864
Largest diff. peak/hole / e Å^{-3}	0.30/-0.27
Flack parameter	0.02(3)

3.7 References

(1) (a) D. E. Nichols, A. J. Hoffman, R. A. Oberlender, R. M. Riggs, *J. Med. Chem.* **1986**, *29*, 302; (b) M. Saito, M. Ueo, S. Kametaka, O. Saigo, S. Uchida, H. Hosaka, K. Sakamoto, T. Nakahara, A. Mori, K. Ishii, *Biol. Pharm. Bull.* **2008**, *31*, 1959; (c) H.-Y. Huang, T. Ishikawa, C.-F. Peng, I.-L. Tsai, I.-S. Chen, *J. Nat. Prod.* **2008**, *71*, 1146; (d) Z. Huang, Q. Cui, L. Xiong, Z. Wang, K. Wang, Q. Zhao, F. Bi, Q. Wang, *J. Agric. Food. Chem.* **2009**, *57*, 2447; (e) I.-S. Lee, H.-J. Kim, U.-J. Youn, Q.-C. Chen, J.-P. Kim, D. T. Ha, T. M. Ngoc, B.-S. Min, S.-M. Lee, H.-J. Jung, M.-K. Na, K.-H. Bae, *Helv. Chim. Acta* **2010**, *93*, 272; (f) A. Radadiya, A. Shah, *Eur. J. Med. Chem.* **2015**, *97*, 356-376.

(2) For a recent review of the synthesis of 2,3-dihydrobenzofurans, see: (a) F. Bertolini, M. Pineschi, *Org. Prep. Proced. Int.* **2009**, *41*, 385; (b) T. D. Sheppard, *J. Chem. Res.* **2011**, *35*, 377.

(3) For examples of asymmetric synthesis of 2,3-dihydrobenzofurans, see: (a) R. M. Trend, Y. K. Ramtohul, B. M. Stoltz, *J. Am. Chem. Soc.* **2005**, *127*, 17778; (b) Y. Natori, H. Tsutsui, N. Sato, S. Nakamura, H. Nambu, M. Shiro, S. Hashimoto, *J. Org. Chem.* **2009**, *74*, 4418; c) D. Belmessieri, L. C. Morrill, C. Simal, A. M. Z. Slawin, A. D. Smith, *J. Am. Chem. Soc.* **2011**, *133*, 2714.

(4) R. Li, G. Dong, *Angew. Chem. Int. Ed.* **2018**, *57*, 1697.

(5) For reviews on Catellani-type reactions, see: (a) M. Catellani, *Top. Organomet. Chem.* **2005**, *14*, 21; (b) M. Catellani, E. Motti, N. Della Ca', *Acc. Chem. Res.* **2008**, *41*, 1512; (c) A. Martins, B. Mariampillai, M. Lautens, *Top. Curr. Chem.* **2010**, *292*, 1; (d) R. Ferraccioli, *Synthesis* **2013**, *45*, 581; (e) J. Ye, M. Lautens, *Nat. Chem.* **2015**, *7*, 863; (f) N. Della Ca', M. Fontana, E. Motti, M. Catellani, *Acc. Chem. Res.* **2016**, *49*, 1389.

(6) For other Pd/NBE-catalyzed reactions using epoxides and related aziridines as electrophiles, see: (a) H.-G. Cheng, C. Wu, H. Chen, R. Chen, G. Qian, Z. Geng, Q. Wei, Y. Xia, J. Zhang, Y. Zhang, Q. Zhou, *Angew. Chem. Int. Ed.* **2018**, *57*, 3444; (b) C. Liu, Y. Liang, N. Zheng, B.-S. Zhang, Y. Feng, S. Bi, Y.-M. Liang, *Chem. Commun.* **2018**, *54*, 3407-3410; (c) C. Wu, H.-G. Cheng, R. Chen, H. Chen, Z.-S. Liu, J. Zhang, Y. Zhang, Y. Zhu, Z. Geng, Q. Zhou, *Org. Chem. Front.* **2018**, DOI: 10.1039/c8qo00348c; (d) G. Qian, M. Bai, S. Gao, H. Chen, S. Zhou, H.-G. Cheng, W. Yan, Q. Zhou, *Angew. Chem. Int. Ed.* **2018**, doi: 10.1002/anie.201806780.

(7) For selected reviews on asymmetric epoxidation reactions, see: (a) D. Yang, *Acc. Chem. Res.* **2004**, *37*, 497; (b) Q. H. Xia, H. Q. Ge, C. P. Ye, Z. M. Liu, K. X. Su, *Chem. Rev.* **2005**, *105*, 1603; (c) E. Rose, B. Andrioletti, S. Zrig, M. Quelquejeu-Ethève, *Chem. Soc. Rev.* **2005**, *34*, 573; (d) O. A. Wong, Y. Shi, *Chem. Rev.* **2008**, *108*, 3958; (e) G. De Faveri, G. Ilyashenko, M. Watkinson, *Chem. Soc. Rev.* **2011**, *40*, 1722-1760; f) Y. Zhu, Q. Wang, R. G. Cornwall, Y. Shi, *Chem. Rev.* **2014**, *114*, 8199;

(8) C.-Y. Huang, A. G. Doyle, *Chem. Rev.* **2014**, *114*, 8153-8198.

(9) The key results of this manuscript were first submitted as a part of a communication to *JACS* on 11/10/2017 as ja-2017-11930x. After the paper was rejected, the racemic portion of the manuscript was reported as ref 4.

(10) For seminal works on asymmetric ipso functionalization via Pd/NBE catalysis using chiral phosphine ligands, see: a) K. Zhao, S. Xu, C. Pan, X. Sui, Z. Gu, *Org. Lett.* **2016**, *18*, 3782; b) L. Ding, X. Sui, Z. Gu, *ACS Catal.* **2018**, *8*, 5630.

(11) During the preparation of this manuscript, an elegant work on enantioselective *meta* C−H arylation using a similar chiral NBE was reported by Yu and coworkers, see: H. Shi, A. N. Herron, Y. Shao, Q. Shao, J.-Q. Yu, *Nature* **2018**, *558*, 581.

(12) The class of ester-substituted NBEs was first used by Yu and coworkers in the arene *meta* C−H functionalization, see: P.-X. Shen, X.-C. Wang, P. Wang, R.-Y. Zhu, J.-Q. Yu, *J. Am. Chem. Soc.* **2015**, *137*, 11574.

(13) D. A. Evans, J. Bartroli and T. L. Shih, *J. Am. Chem. Soc.* **1981**, *103*, 2127.

(14) (a) R. Martin, S. L. Buchwald, *Acc. Chem. Res.* **2008**, *41*, 1461; (b) P. Ruiz-Castillo, S. L. Buchwald, *Chem. Rev.* **2016**, *116*, 12564; (c) D. S. Surry, S. L. Buchwald, *Angew. Chem. Int. Ed.* **2008**, *47*, 6338.

(15) CCDC 1859743 (**NBE A**) and 1859744 (**NBE B**) contain the supplementary crystallographic data for this paper. These data can be obtained free of charge from The Cambridge Crystallographic Data Centre.

(16) M. Inai, T. Nishii, A. Tanaka, H. Kaku, M. Horikawa, T. Tsunoda, *Eur. J. Org. Chem.* **2011**, *2011*, 2719-2729.

(Some contents of this chapter were published in *Org. Chem. Front.* **2018**, *5*, 3108-3112.)

CHAPTER 4

Redox-Neutral Ortho Functionalization of Aryl Boroxines via Palladium/Norbornene Cooperative Catalysis

4.1 Introduction

Site-selectivity control still represents an ongoing quest in organic synthesis.[1-2] Especially, site-selective functionalization of arenes has been playing a key role in preparing aromatic moieties ubiquitously found in drugs and agrichemicals. Recently, the palladium/norbornene (Pd/NBE) cooperative catalysis, pioneered by Catellani[3] and Lautens[4], has emerged as a useful set of tools to access poly-substituted arenes. In a typical Catellani reaction, a nucleophile and an electrophile are coupled at the ipso and ortho positions, respectively, through selective reactions with the aryl-NBE palladacycle (ANP) intermediate (Scheme 4.1A).[3-33] In particular, when the nucleophile is a hydride equivalent, a reductive ortho functionalization is realized. While efficient, the Catellani reaction contains a non-productive process, which is the removal of the generated HX with

stoichiometric bases. In addition, the reaction needs to be terminated by a nucleophile or reductant in order to reform the Pd(0) catalyst. Moreover, the compatibility between the nucleophile and the electrophile is an inevitable concern, and typically, only masked or weak nucleophiles are suitable. Very recently, Zhang[34] and Zhou[35] concurrently reported a novel arylboronic acid-based Catellani reaction also through coupling an electrophile/nucleophile pair, but stoichiometric bases and oxidants were still required (Scheme 4.1B).

Scheme 4.1. Palladium/Norbornene Cooperative Catalysis

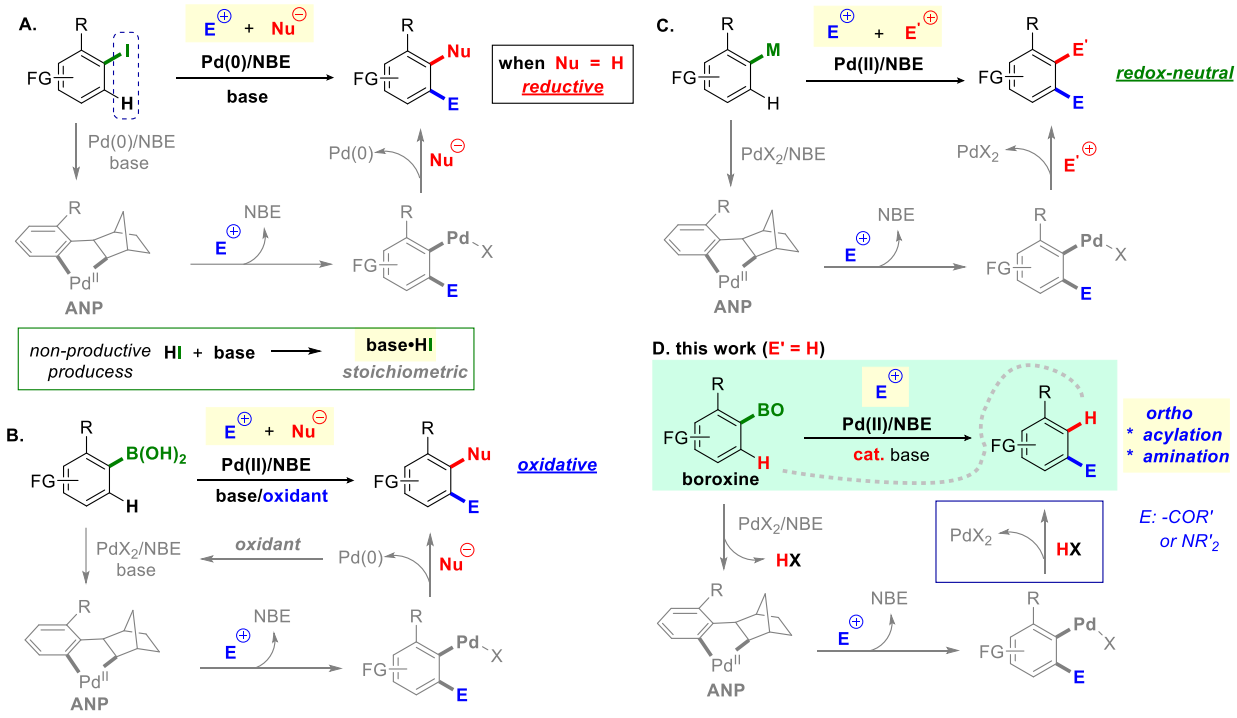

Stimulated by these intrinsic constraints in the Catellani reaction, we felt it could be attractive to develop a redox-neutral arene ortho functionalization, in which an aryl nucleophile (e.g. aryl boron compounds) could be coupled with *two electrophiles* without the need for stoichiometric bases or oxidants (Scheme 4.1C). Mechanistically, after the ortho functionalization with ANP followed by NBE extrusion, the resulting aryl-Pd(II) species could then react with another electrophile (instead

of a nucleophile or reductant) to regenerate the Pd(II) catalyst. Seminal work by Lautens has shown that such a aryl-Pd(II) species could attack an adjacent carbonyl group, but this has been limited to an intramolecular transformation.[15] Clearly, many challenges can be envisioned with this redox-neutral strategy, including the difficulty of controlling site-selectivity and the choice of suitable electrophiles. Thus, at this preliminary stage, we have been focused on a simplified system with one electrophile being a proton source (Scheme 4.1D).[31-33] In this reaction, the acid generated during the ANP formation could be re-coupled at the ipso position, which leads to a net proton swap.

The proposed catalytic cycle is depicted in Scheme 4.2. The reaction starts with transmetalation to generate an aryl-Pd(II) species (Step A), which then undergoes analogous transformations as the regular Catellani-type reactions, such as NBE migratory insertion (Step B) and ortho palladation (Step C) to give the key aryl-norbornyl-palladacycle (**ANP**) intermediate. The reaction between **ANP** and the anhydride should furnish the ortho acylation (Step D). The resulting Pd(II) intermediate could undergo β-carbon elimination to generate a new aryl-Pd(II) species (Step E), which could then be protonated by the acid (HX) produced in the ortho metalation step (Step C) to afford the ortho acylation product and re-generate the Pd(II) catalyst (Step F). Hence, the proposed catalytic cycle does not involve a Pd(0) intermediate, and use of additional stoichiometric oxidants and bases appear unnecessary.

Herein, we describe our initial development of Pd/NBE-catalyzed redox-neutral acylation and amination using aryl boroxines as substrates, which directly introduces a functional group at the arene ortho position without extra stoichiometric oxidants or reductants.

Scheme 4.2. Proposed Catalytic Cycle

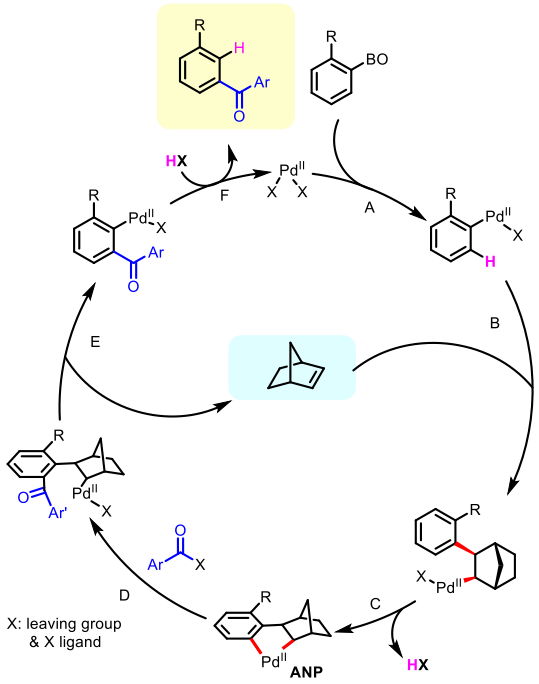

The challenges for developing such a redox-neutral transformation are two-fold. First, given that the aryl-Pd(II) intermediate formed after the NBE extrusion is typically less nucleophilic, protonation of such a species could be difficult.[36] Second, transmetalation of aryl boronates is generally promoted by basic conditions, while the final protonation step requires the presence of an acid. Hence, the compatibility of these two steps could be another concern. We hypothesized that the key for the success of this reaction would be to discover a catalyst system that can promote both transmetalation and protonation. The use of arsine-type ligands caught our attention because first, $AsPh_3$ is known to promote fast transmetalation in Stille reactions;[37] and second, $AsPh_3$ was also found to be the most efficient ligand in our previous meta C−H arylation reaction[32], which requires facile de-protonation and re-protonation at the arene ortho position.

4.2 Results and Discussion

4.2.1 Reaction Discovery and Optimization

Table 4.1. Control Experiments for Ortho Acylation with 2-Tolylboroxine[a]

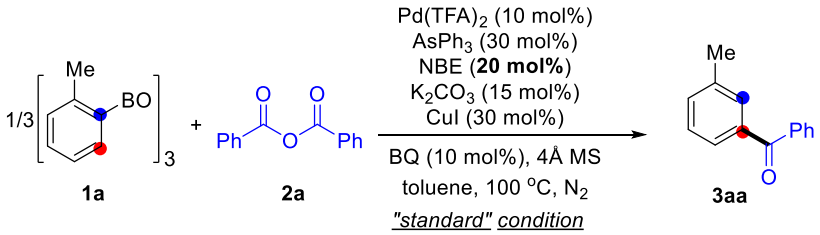

Entry	Change from the "standard" condition	Yield[b]
1	none	65%
2	w/o $Pd(TFA)_2$	0%
3	w/o NBE	0%
4	w/o $AsPh_3$	0%
5	$Pd(OAc)_2$ instead of $Pd(TFA)_2$	43%
6	PPh_3 instead of $AsPh_3$	12%
7	$(2\text{-furyl})_3P$ instead of $AsPh_3$	6%
8	w/o BQ	32%
9	w/o CuI	53%
10	w/o K_2CO_3	51%
11	w/o 4Å MS	43%[c]
12	H_2O (1.0 equiv) instead of 4Å MS	0%
13	commerical "$ArB(OH)_2$" instead of $(ArBO)_3$	52%[d]
14	ArBpin instead of $(ArBO)_3$	0%

[a]The reaction was run with 0.2 mmol **1a** (monomer of the boroxine) and 0.4 mmol **2a** in 4 mL toluene for 14h. [b]Determined by ^{1}H NMR analysis using 1,1,2,2-tetrachloroethane as the internal standard. [c]Toluene after freeze-pump-thaw treatment was used. [d]Purchased from Combi-Blocks, containing 28% free 2-toylboronic acid determined by ^{1}H NMR analysis.

To test this hypothesis, ortho acylation was studied as the model reaction; 2-tolylboroxine (**1a**) and benzoic anhydride (**2a**) were employed as the initial model substrates. After careful evaluation of various reaction parameters, the $Pd(TFA)_2/AsPh_3$ combination indeed provided the desired ortho acylation product **3aa** in 65% yield (Table 4.1, entry 1). No direct ipso substitution between the

aryl boroxine and benzoic anhydride was observed in this case. A number of control experiments were subsequently carried out. First, the Pd salt, NBE and $AsPh_3$ were all essential to this reaction (entries 2-4). Other Pd(II) precatalysts or phosphine-based ligands were less efficient (entries 5-7). It is noteworthy that, while the majority of the prior Pd/NBE-catalyzed reactions use a high loading or excess NBE,[5-10] only 20 mol% NBE was sufficient in this reaction. A catalytic amount of benzoquinone could improve the reaction yield (entry 8), which likely serves as a Pd(0) scavenger or a π-ligand[38-40] to prevent catalyst decomposition. A catalytic amount of CuI and K_2CO_3 also enhanced the yield, though their roles were not critical (entries 9 and 10).[41] One hypothesis is that a catalytic amount of carbonate base may facilitate the transmetalation of boroxines or promote the concerted metalation deprotonation step to form the ANP. The reaction was sensitive to water, and adding molecular sieves significantly increased the yield (entries 11 and 12). Use of aryl boroxines instead of boronic acids was beneficial, though the commercial "boronic acid" that contains ~28% $ArB(OH)_2$ and ~72% boroxine still afforded the desired product in 52% yield (entry 13). In contrast, the corresponding pinacol-derived substrate was not reactive, likely due to its difficulty in the transmetalation step (entry 14).[42]

4.2.2 Substrates Scope

The scope of the reaction with respect to the acyl part was examined first (Table 4.2). Anhydrides with electron-donating and -withdrawing groups all afforded the desired ortho acylation products in moderate to good yields. Generally, the more electron-deficient aromatic anhydrides (e.g. **3ab** and **3ae**) gave slightly higher yields than the electron-richer ones, probably owing to their enhanced reactivity towards the ANP intermediate. One important feature is that a number of

functional groups, including aryl fluoride (**3ab**-**3ad**), chloride (**3ae** and **3af**), bromide (**3ag**), iodide (**3ah**, *vide infra*, Schemes 3 and 4), trifluoromethyl (**3ai**), ester (**3aj**) and anisole moieties (**3am**-**3ao**), were tolerated. Ortho-substituted aromatic anhydrides (**3ak** and **3ao**) are competent substrates. It is noteworthy that pinacol boronates were compatible (**3ap**), which could serve as a handle for further functionalization. In addition, ferrocene- (**3aq**) and thiophene-derived ketone products (**3ar**) could be isolated in moderate yields. Encouragingly, aliphatic carboxylic acid anhydrides also proved to be suitable coupling partners (**3as** and **3at**).

Table 4.2. Substrates Scope with Respect to Anhydrides[a]

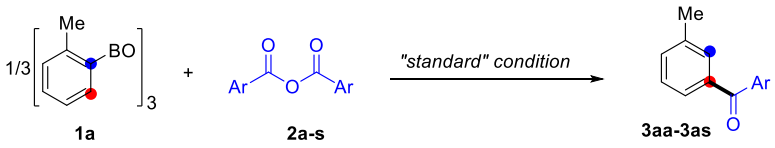

1a **2a-s** **3aa-3as**

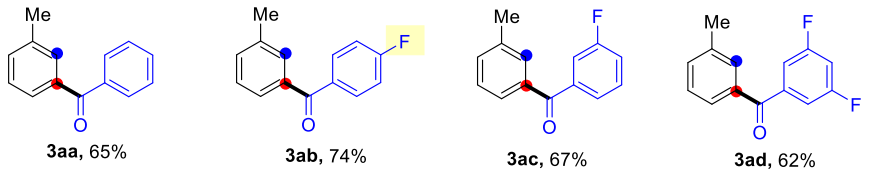

3aa, 65%

3ab, 74%

3ac, 67%

3ad, 62%

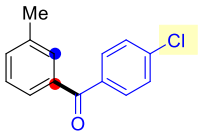

3ae, 66%

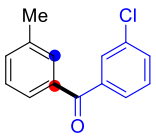

3af, 66%

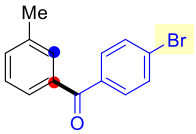

3ag, 61%

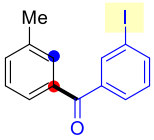

3ah, 31%

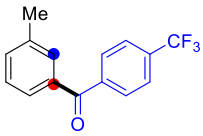

3ai, 63%

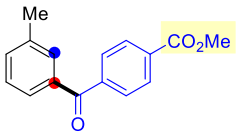

3aj, 53%

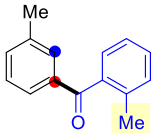

3ak, 48%

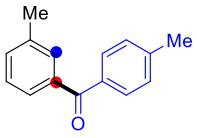

3al, 52%

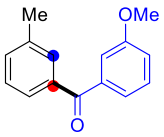

3am, 58%

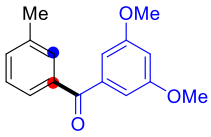

3an, 51%

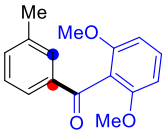

3ao, 37%

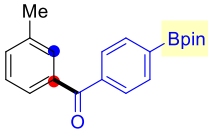

3ap, 41%

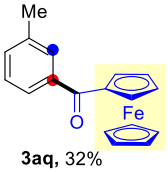

3aq, 32%

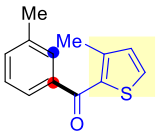

3ar, 33%

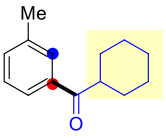

3as, 50%

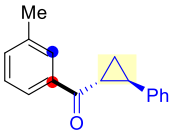

3at, 60%

[a]The reaction was run with 0.3 mmol **1a** and 0.6 mmol **2a** in 4 mL toluene for 14h.

Table 4.3. Substrates Scope with Respect to Aryl Boroxines [a]

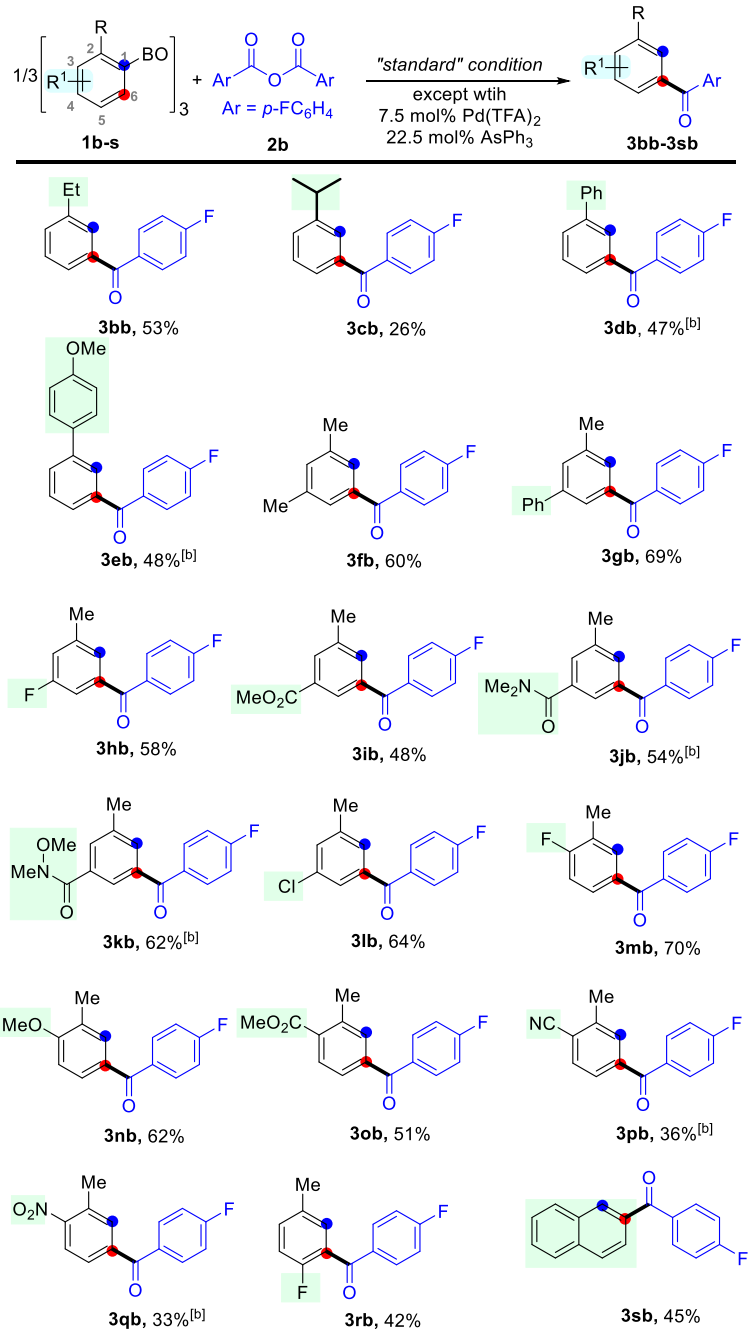

[a]The reaction was run with 0.3 mmol **1b-s** and 0.6 mmol **2b** in 4 mL toluene for 14h. [b]10 mol% of $Pd(TFA)_2$ and 30 mol% of $AsPh_3$ was used.

Next, the scope of the aryl boroxines was explored. Notably, a *lower* palladium loading (7.5 mol%) was applied in these reactions (Table 4.3). Substitutions at C2, C3, C4 and C5 positions of aryl boroxines could all be tolerated. For the para-substituted aryl boroxines, aryl fluoride (**3hb**), chloride (**3lb**), ester (**3ib**), amide (**3jb**), Weinreb amide (**3kb**), phenyl (**3gb**) and alkyl groups (**3fb**) were compatible. In addition, aryl boroxines that contain an electron-donating or -withdrawing substituent smoothly provided the ortho acylation products in moderate to good yields. While the trend of the electronic effect with the aryl boroxine substrates was not obvious, those bearing a strong electron-withdrawing group at the C3 position (**3pb** and **3qb**) typically gave lower yields. Moreover, a naphthalene-derived substrate (**3sb**) also provided the desired ketone product.

4.2.3 Unsuccessful or Less Successful Examples

However, there are still some limitations for this transformation (Table 4.4). First, only alkyl type group was tolerated at the ortho position of arylboroxine. Trifluoromethyl and ester group at ortho position gave no more than 30% yield of desired product. Some electron rich boroxine also failed to desired product. It is noteworthy that TBS protected phenol and benzyl alcohol type boroxine gave the ipso acylation product instead of desired ortho acylation product, likely owing to the difficulty in migratory insertion of NBE. In addition, electron rich benzoyl anhydride and heterocycle-derived anhydride were not tolerated. 4-cyano benzoyl anhydride reacted with boroxine to give desired product in only 15% yield.

Table 4.4. Unsuccessful or Less Successful Examples

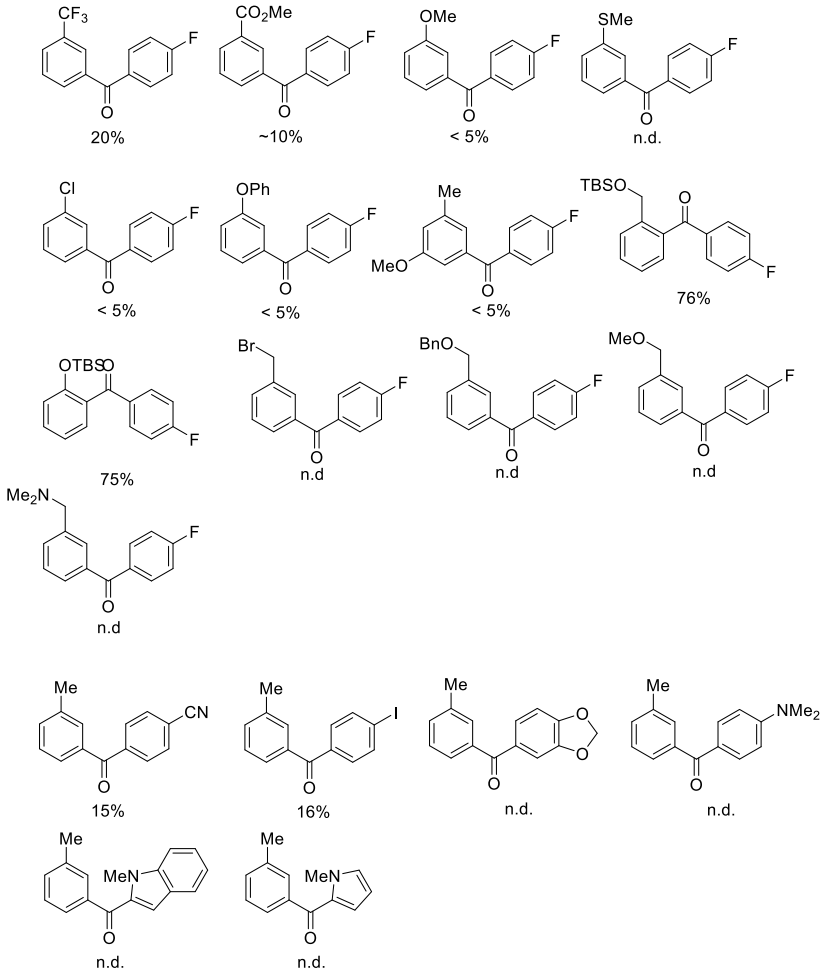

4.2.4 Deuterium Labelling Studies

To gain some mechanistic insight into this reaction, deuterium labelling studies were performed (Scheme 4.3). When the fully deuterated substrate **1s-*d*** reacted with anhydride **2b**, the desired product (**3sb-*d***) was isolated with 60% deuterium incorporated at the ipso position (Scheme 4.3, Eq. 1). The erosion of deuterium incorporation was possibly due to the H-D exchange with adventitious water in the reaction system. To examine the possibility of the H-D exchange, a

reverse control experiment was conducted. Using regular 2-toylboroxine **1a** as the substrate, the standard reaction was run in the presence of 2.0 equiv of D_2O (Scheme 4.3, Eq. 2). Although the reaction still contained a significant amount of molecular sieves, 38% deuterium was nevertheless observed as the ipso position of the product. These results are consistent with an ipso-protonation pathway proposed in Scheme 4.1D.

Scheme 4.3. Deuterium Labelling Studies

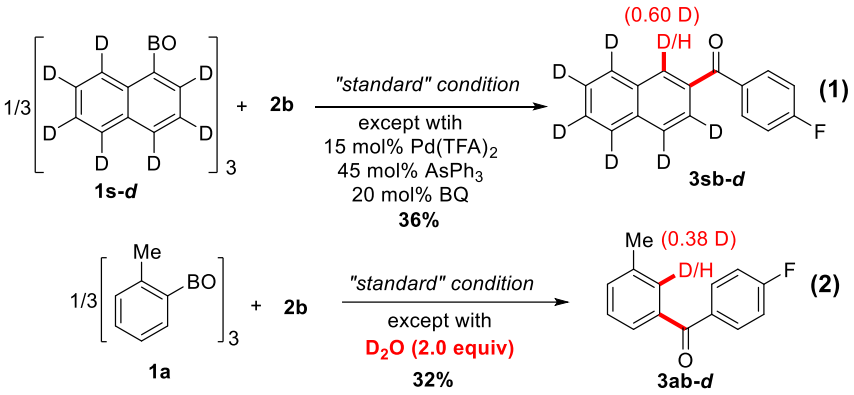

4.2.5 Synthetic Utility

One potential merit of aryl boroxine-mediated reactions is the compatibility of aryl iodide moieties,[35] which are otherwise highly reactive under the typical Pd/NBE catalysis conditions (Scheme 4.4A).[5-10] First, in the presence of aryl iodide **4a**, ortho acylation of 2-tolylboroxine **1a** still proceeded selectively with a full recovery of unreacted aryl iodide **4a**. Encouragingly, a more complex aryl iodide (**4b**) derived from strychnine remained intact under the reaction conditions, while the ortho acylation with boroxine **1a** provided the desired product (**3ab**) in 55% yield.[43] In addition, substrates bearing halogens and boroxines on the same aromatic ring were tested (Scheme 4.4B). Gratifyingly, both the aryl bromide (**1t**) and iodide (**1u**) groups survived under the

standard ortho acylation conditions; such compatibility allows for convenient sequential functionalization of the arene substrates.

Scheme 4.4. Tolerance of Aryl Iodide Moieties

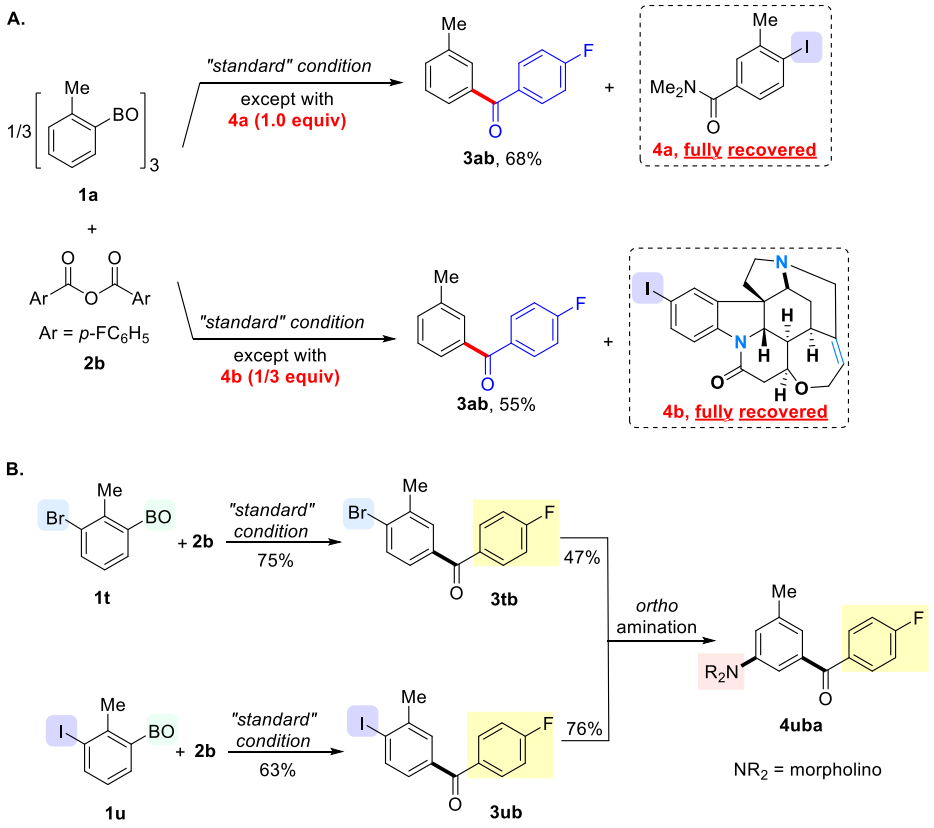

Encouraged by the unique chemoselectivity in the aryl boroxine-mediated reactions, *orthogonal* reactivity between aryl iodide (I) and boroxine (B) moieties was next explored, which, if successful, would provide a convenient way to control the reaction sequence without significant alteration of the substrates (Scheme 4.5). Diaryl compound **5** containing both "I" and "B" groups was employed as the model substrate. First, as expected, the "*B first, then I*" sequence worked smoothly, which first gave an ortho acylation on the boroxine site and then an ortho amination on the iodide site. On the other hand, the "*I first, then B*" sequence was also successful: the Pd(0)-catalyzed reductive ortho amination of the aryl iodide tolerated the pinacol boronate moiety; the

resulting intermediate after hydrolysis then participated in the Pd(II)-catalyzed ortho acylation uneventfully. Thus, without the need to prepare different substrates, the order of the reaction sequence between the boroxine and iodide sites could be controlled by different catalytic systems.

Scheme 4.5. Controlling the Reaction Sequence Enabled by Orthogonal Chemoselectivity

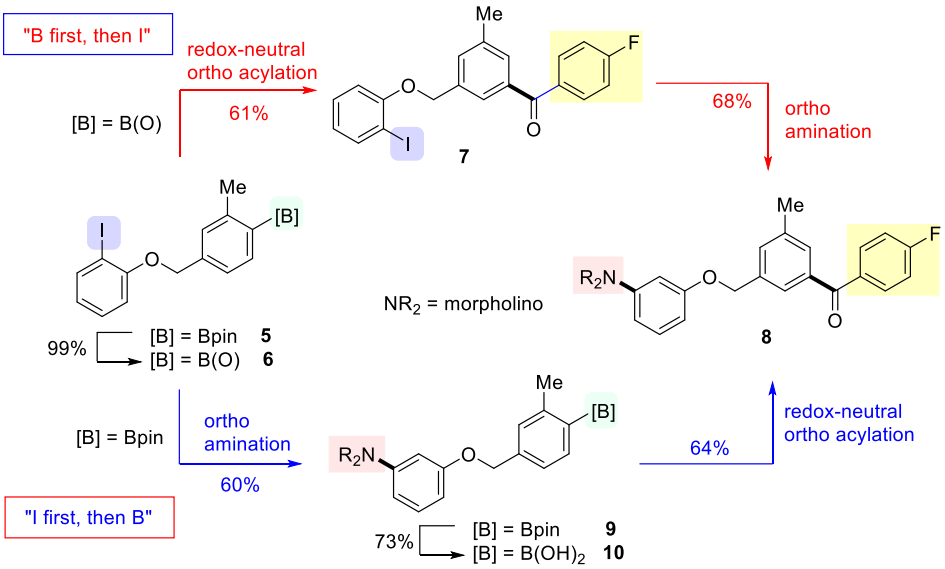

4.2.6 Ortho Amination

Besides the ortho acylation, preliminary success has also been obtained for achieving the ortho amination under the redox-neutral conditions (Table 4.5). *O*-benzoyl hydroxylamines were found to be suitable electrophiles. Under modified reaction conditions, the desired ortho amination products could be obtained in moderate to good yields without the need of reductants.[17] Phosphite ligands, e.g. $P(OPh)_3$, proved to work better than arsine ligands, while other types of ligands were less efficient. To the best of our knowledge, phosphite ligands have not been used in the Pd/NBE catalysis previously. A piperazine-derived electrophile also afforded the desired amination product

(**4ab**) in 58% yield. Efforts on further enhancing the efficiency and scope of this ortho amination reaction through detailed mechanistic studies are ongoing.

Table 4.5. Substrates Scope of the Ortho Amination Reaction[a]

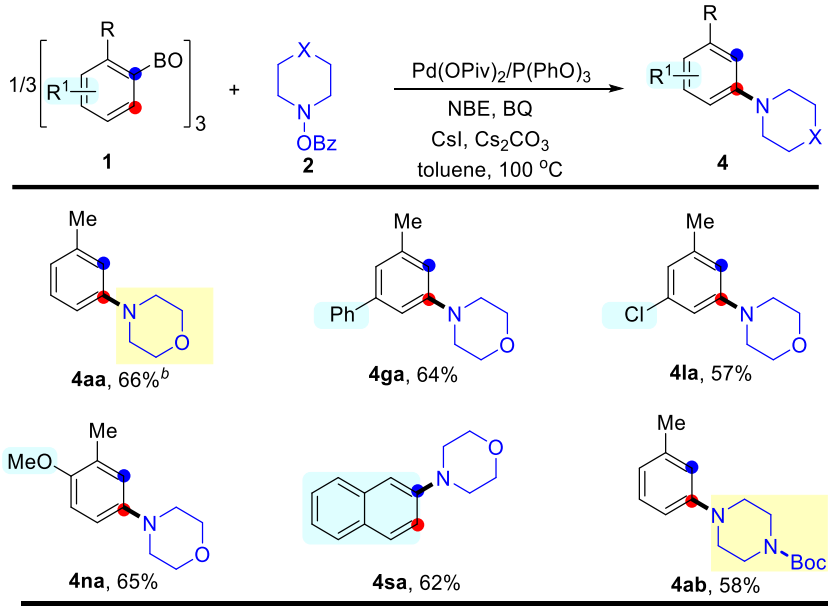

[a]Reaction conditions: **1** (0.5 mmol), **2** (0.2 mmol), $Pd(OPiv)_2$ (20 mol%), $P(OPh)_3$ (40 mol%), NBE (50 mol%), BQ (15 mol%), Cs_2CO_3 (50 mol%), CsI (50 mol%), toluene (4 mL), 100 °C, 12 h. [b]When 10 mol% Pd was used instead, 55% isolated yield was observed.

4.3 Conclusion

In summary, a redox-neutral Catellani-type transformation is developed using aryl boroxines as substrates. The reaction is enabled by a arsine or phosphite ligand and a palladium(II) catalyst, showing broad functional group compatibility. Compared to the classical reductive Catellani-type reactions, this approach does not require stoichiometric bases or reductants; in addition, it can tolerate various aryl halide moieties. While the efficiency of these methods remains to be further improved, the unique mechanistic pathway discovered here could have important implications on developing a new class of Pd/NBE-catalyzed reactions.

4.4 Experimental Procedures and Characterization Data

4.4.1 General Information

Unless noted otherwise, all solvents were dried by filtration through a Pure-Solv MD-5 Solvent Purification System (Innovative Technology). Dimethylformamide was then vacuum-distilled freshly over calcium hydride and carefully freeze-pump-thawed. Reaction temperatures were reported as the temperatures of the bath surrounding the flasks or vials. Sensitive reagents and solvents were transferred under nitrogen into a nitrogen-filled glovebox with standard techniques. Sodium acetate was purchased from STREM, stored and used directly in the glovebox. Analytical thin-layer chromatography (TLC) was carried out using 0.2 mm commercial silica gel plates (silica gel 60, F254, EMD chemical). Vials (15 x 45 mm 1 dram (4 mL) with PTFE lined cap attached) were purchased from Qorpak and flame-dried and cooled in a desiccator prior to usage. High resolution mass spectra (HR-MS) were recorded on an Agilent 6530 LC Q-TOF mass spectrometer using electrospray ionization with fragmentation voltage set at 115 V and processed with an Agilent MassHunter Operating System. Infrared spectra were recorded on a Nicolet 380 FTIR using neat thin film technique. Nuclear magnetic resonance spectra (^{1}H NMR and ^{13}C NMR) were recorded with a Bruker DMX 400 (400 MHz, ^{1}H at 400 MHz, ^{13}C at 101 MHz) or Bruker Model DMX 500 (500 MHz, ^{1}H at 500 MHz, ^{13}C at 126 MHz). Chemical shifts were reported in parts per million (ppm, δ), downfield from tetramethylsilane (TMS, δ=0.00ppm) and were referenced to residual solvent ($CDCl_3$, δ=7.26 ppm (^{1}H) and 77.00 ppm (^{13}C)). All the ^{19}F chemical shifts were not referenced. Coupling constants were reported in Hertz (Hz). Data for ^{1}H NMR spectra were reported as follows: chemical shift (ppm, referenced to protium, s = singlet, d = doublet, t = triplet, q = quartet, quin = quintet, dd = doublet of doublets, td = triplet of doublets, ddd = doublet of

doublet of doublets, m = multiplet, coupling constant (Hz), and integration). All other materials were obtained from Sigma-Aldrich Corporation or Combi-Blocks Inc and were used as received.

4.4.2 Condition screening

Table 4.6. Early Pd Pre-Catalyst Screening

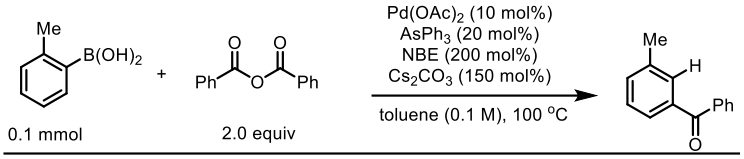

0.1 mmol 2.0 equiv

Entry	Change from the *above* condition	Yield[a]
1	none	25%
2	**$Pd(TFA)_2$**	**31%**
3	$PdCl_2$	12%
4	$Pd(OPiv)_2$	22%
5	$Pd(MeCN)_2Cl_2$	20%
6	$Pd(PhCN)_2Cl_2$	10%

[a]Yields were determined by ^{1}H NMR analysis using 1,1,2,2-tetrachloroethane as the internal standard.

Table 4.7. Early Base Effect Study

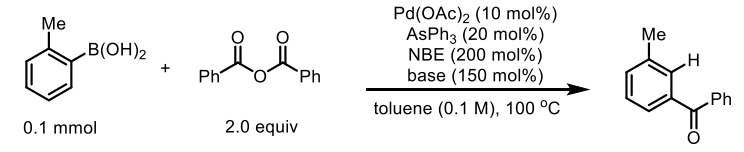

0.1 mmol 2.0 equiv

Entry	Base	Yield[a]
1	Cs_2CO_3	25%
2	**K_2CO_3**	**26%**
3	Na_2CO_3	17%
4	NaOAc	22%
5	KOAc	26%
6	K_3PO_4	<5%
7	$K_3PO_4 \cdot H_2O$	<5%
8	K_2HPO_4	<5%
9	NaTFA	-
10	$CsHCO_3$	18%

[a]Yields were determined by ^{1}H NMR analysis using 1,1,2,2-tetrachloroethane as the internal standard.

Table 4.8. Early Solvent Effect Study

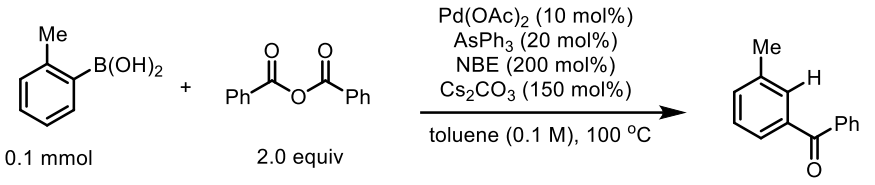

0.1 mmol 2.0 equiv

Entry	Change from the *"standard"* condition	Yield[a]
1	**none**	**26%**
2	1,4-dioxane	<10%
3	DMF	<5%
4	MeCN	15%
5	THF	<5%
6	DCE	<5%
7	DCM	<5%

[a]Yields were determined by ^{1}H NMR analysis using 1,1,2,2-tetrachloroethane as the internal standard.

Table 4.9. Water Effect

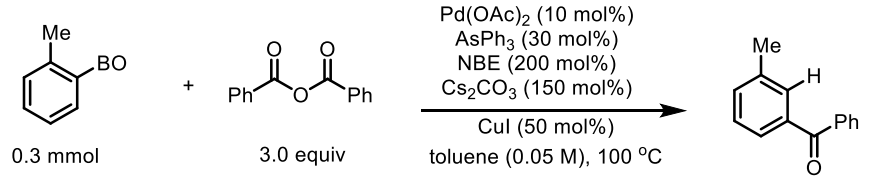

0.3 mmol 3.0 equiv

Entry	Change from the *"standard"* condition	Yield[a]
1	**none**	**43%**
2	H_2O 10 mol%	41%
3	H_2O 20 mol%	35%
4	H_2O 30 mol%	26%
5	H_2O 40 mol%	21%
6	H_2O 50 mol%	18%

[a]Yields were determined by ^{1}H NMR analysis using 1,1,2,2-tetrachloroethane as the internal standard.

Table 4.10. Pd Pre-Catalyst Screening

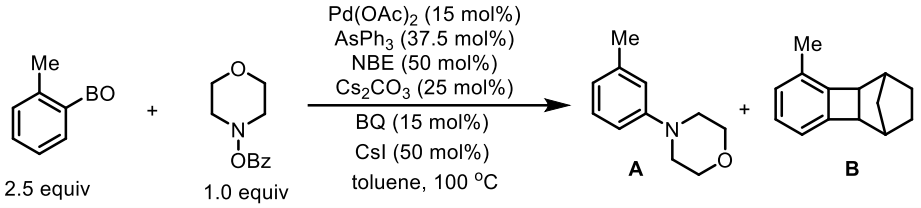

Entry	Change from the "*standard*" condition	**A** Yield[a]	**B** Yield[a]
1	none	38%	31%
2	$Pd(TFA)_2$	17%	36%
3	$PdCl_2$	12%	24%
4	PdI_2	21%	29%
5	$Pd(MeCN)Cl_2$	26%	41%
6	$Pd(COD)Cl_2$	24%	36%
7	$Pd(COD)Br_2$	19%	44%
8	**$Pd(OPiv)_2$**	**42%**	**34%**
9	$[Pd(allyl)Cl]_2$	18%	30%
10	$Pd(TFP)_2Cl_2$	9%	14%
11	$Pd(dba)_2$	29%	19%

[a]Yields were determined by ^1H NMR analysis using 1,1,2,2-tetrachloroethane as the internal standard.

Table 4.11. Ligand effect I

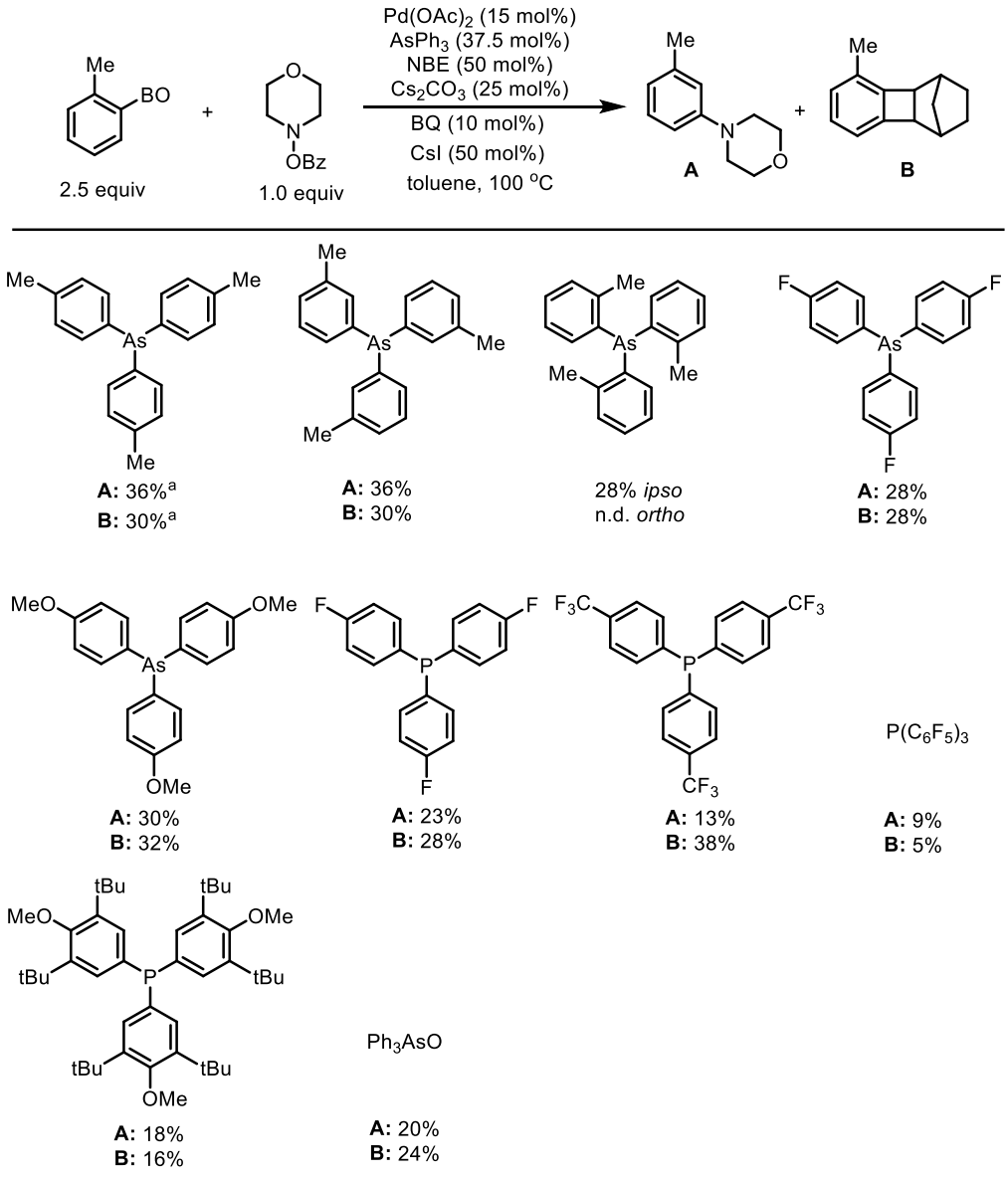

[a]Yields were determined by ^{1}H NMR analysis using 1,1,2,2-tetrachloroethane as the internal standard.

Table 4.12. Ligand effect II

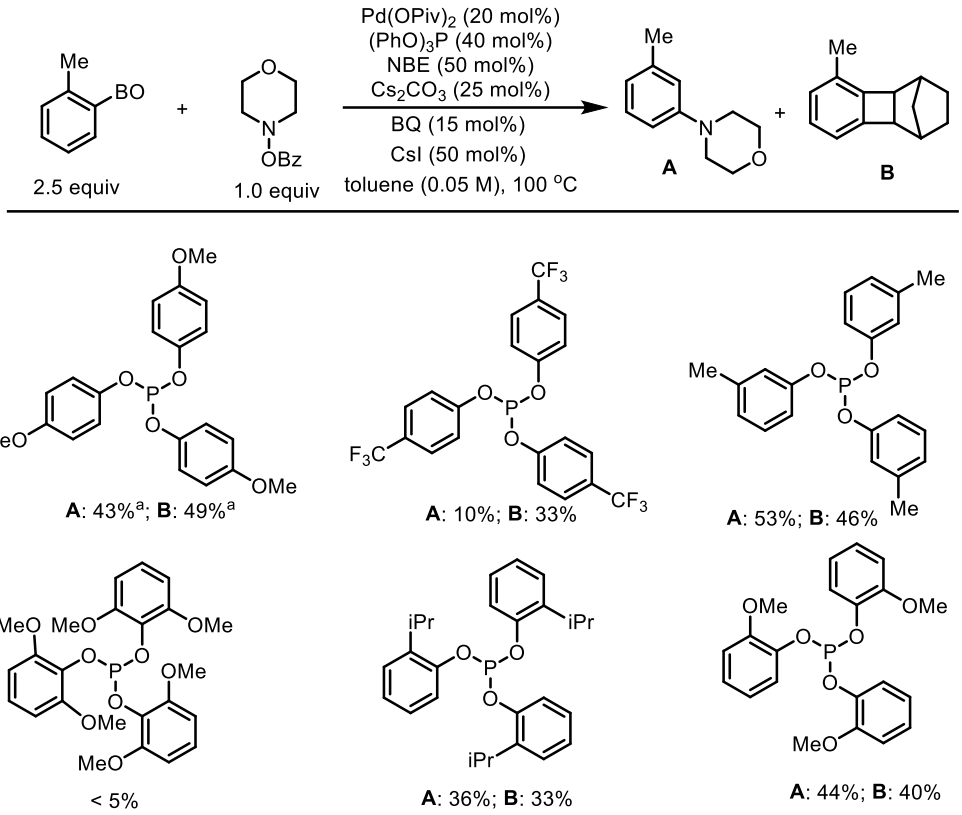

[a]Yields were determined by ^{1}H NMR analysis using 1,1,2,2-tetrachloroethane as the internal standard.

4.4.3 Preparation of Aryl Boroxines 1a-m

Scheme 4.6. General Procedure of the Preparation of Aryl Boroxines

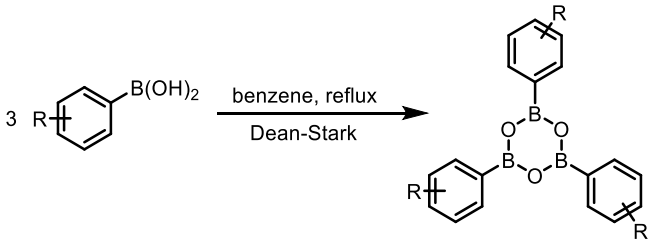

In a 100 mL round bottom flask was added arylboronic acid (15.0 mmol) and a stir bar. Then benzene (50 mL) was added and the solution was refluxed for 12 h using Dean-Stark trap to remove water. The solution was allowed to cool to room temperature and the solvent was removed under

vacuum to give the desired arylboroxine as a white solid. After washed with hexane for three time and dried under vacuum, the arylboroxine product was directly used in the acylation reaction without further purification.

4.4.4 Preparation of Substituted Benzoic Anhydrides

2b-o, **2q-r** and **2t** were prepared by following the literature reported procedures.[44-45]

Scheme 4.7. Preparation of Anhydride 2o

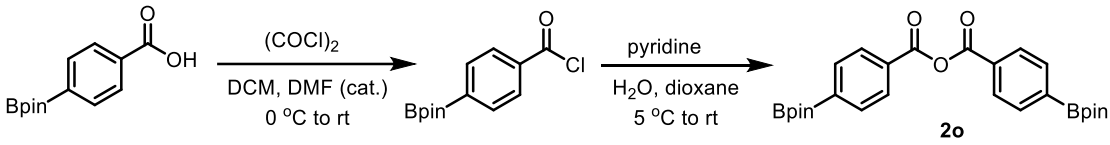

To a solution of substituted benzoic acid (4.96 g, 20.0 mmol, 1.0 equiv) and 10 drops of DMF in dichloromethane (100 mL) was added oxalyl chloride (5.1 g, 40.0 mmol, 2.0 equiv) dropwise at 0 °C. The reaction mixture was stirred at room temperature for another 1 h until the bubbling stopped. Then the solvent was removed under vacuum and the generated acyl chloride was used in the next step without further purification.

Acyl chloride was added to 40 mL dry dioxane and cooled to 5 °C. Dry pyridine (1.9 g, 24.0 mmol, 1.2 equiv) was added and the mixture was stirred for 30 minutes below 10 °C. Then, 0.4 mL water (0.4g, 22.0 mmol, 1.1 equiv) was added dropwise and the mixture was agitated vigorously for 10 minutes at 0 °C. After a mixture of 15 mL concentrated HCl, 15 g cracked ice and 140 mL H_2O was added to the solution, a white precipitate was formed and filtered. The solid was washed with 5% cold $NaHCO_3$ (20 mL) and cold water. 3.2 g (67% yield) of a white solid was obtained after being dried under vacuum.

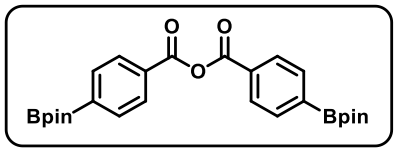

2p: White solid (67%). m.p. = 173–175 °C. **^{1}H NMR** (400 MHz, $CDCl_3$) δ 8.18 – 8.09 (m, 4H), 7.98 – 7.91 (m, 4H), 1.37 (s, 24H). **^{13}C NMR** (101 MHz, $CDCl_3$) δ 162.4, 135.0, 130.8, 129.5, 84.4, 24.9. **IR** (KBr): υ 2979, 1790, 1728, 1509, 1400, 1271, 1213, 1144, 1088, 1040 cm^{-1}. **HRMS** (ESI): Calculated for $C_{26}H_{32}B_2O_7Na$ ($M+Na^+$): 501.2226, found: 501.2228.

4.4.5 General Procedure of Palladium and Norbornene Catalyzed Ortho Acylation Reaction

Scheme 4.8. Redox-Neutral Ortho Acylation of Aryl Boroxines

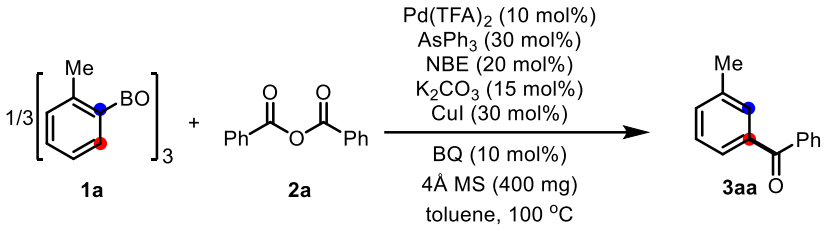

A flame-dried 4.0 mL vial was charged with $Pd(TFA)_2$ (9.9 mg, 0.03 mmol, 10 mol%), benzoquinone (3.3 mg, 0.03 mmol, 10 mol%), CuI (17.1 mg, 0.09 mmol, 30 mol%), $AsPh_3$ (27.6 mg, 0.09 mmol, 30 mol%), arylboroxine (0.3 mmol, 1.0 equiv, based on monomer) and substituted benzoic anhydride (0.6 mmol, 2.0 equiv). The vial was directly transferred into a nitrogen-filled glovebox without caps. Then, K_2CO_3 (6.2 mg, 0.045 mmol, 15 mol%) and 4Å molecular sieves (400 mg) were added. In another 4.0 mL vial, NBE (16.9 mg, 0.18 mmol) was dissolved in 1.5 mL dry toluene. 0.5 mL of this NBE solution (5.64 mg, 0.06 mmol, 20 mol%) was transferred into the reaction mixture, before another 3.5 mL dry toluene was added. The vial was tightly sealed, transferred out of glovebox and stirred on a pie-block preheated to 100 °C for 14 hours. After completion of the reaction, the mixture was filtered through a thin pad of silica gel. The filter cake

was washed with ethyl acetate and the combined filtrate was concentrated. The residue was loaded to a small amount of silica gel and then purified by flash column chromatography on silica gel to give the desired ortho acylation product.

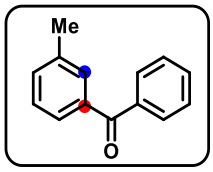

CAS: 643-65-2

3aa: Pale yellow oil (65%). R_f = 0.3 (hexane/ethyl acetate = 20:1). **^{1}H NMR** (400 MHz, $CDCl_3$) δ 7.83 – 7.78 (m, 2H), 7.64 (s, 1H), 7.57 (ddt, J = 8.0, 6.7, 1.3 Hz, 2H), 7.47 (td, J = 7.5, 1.4 Hz, 2H), 7.42 – 7.32 (m, 2H), 2.41 (s, 3H). **^{13}C NMR** (101 MHz, $CDCl_3$) δ 196.9, 138.1, 137.7, 137.6, 133.2, 132.6, 130.4, 130.0, 128.2, 128.1, 127.4, 21.4. Both the ^{1}H NMR and ^{13}C NMR match the literature reported data.[46]

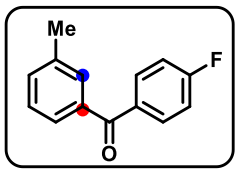

CAS: 1996-79-8

3ab: Pale yellow solid (74%). R_f = 0.2 (hexane/ethyl acetate = 20:1). **^{1}H NMR** (400 MHz, $CDCl_3$) δ 7.88 – 7.81 (m, 2H), 7.59 (s, 1H), 7.54 (d, J = 7.4 Hz, 1H), 7.43 – 7.34 (m, 2H), 7.20 – 7.12 (m, 2H), 2.43 (s, 3H). **^{13}C NMR** (101 MHz, $CDCl_3$) δ 195.6, 165.5 (d, J = 254.0 Hz), 138.4, 137.7, 134.1 (d, J = 3.1 Hz), 133.4, 132.8 (d, J = 9.1 Hz), 130.4, 128.3, 127.3, 115.6 (d, J = 21.8 Hz), 21.5. Both the ^{1}H NMR and ^{13}C NMR match the literature reported data.[47]

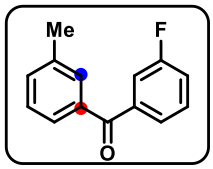

CAS: 864087-22-9

3ac: Pale yellow oil (67%). R_f = 0.2 (hexane/ethyl acetate = 20:1). **^{1}H NMR** (400 MHz, $CDCl_3$) δ 7.62 (t, J = 0.9 Hz, 1H), 7.59 – 7.53 (m, 2H), 7.53 – 7.32 (m, 4H), 7.32 – 7.25 (m, 1H), 2.43 (s, 3H). **^{13}C NMR** (101 MHz, $CDCl_3$) δ 195.6 (d, J = 2.1 Hz), 162.6 (d, J = 248.0 Hz), 140.0 (d, J = 6.4 Hz), 138.5, 137.2, 133.7, 130.5, 130.1 (d, J = 7.7 Hz), 128.4, 127.5, 125.9 (d, J = 3.1 Hz), 119.5 (d, J = 21.4 Hz), 116.9 (d, J = 22.4 Hz), 21.5. Both the ^{1}H NMR and ^{13}C NMR match the literature reported data.[47]

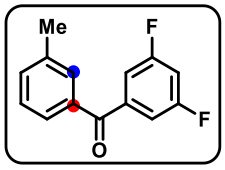

CAS: 844885-06-9

3ad: Pale yellow solid (62%). R_f = 0.3 (hexane/ethyl acetate = 20:1). **^{1}H NMR** (400 MHz, $CDCl_3$) δ 7.61 (s, 1H), 7.56 (d, *J* = 7.3 Hz, 1H), 7.44 (d, *J* = 7.2 Hz, 1H), 7.39 (t, *J* = 7.5 Hz, 1H), 7.34 – 7.27 (m, 2H), 7.04 (tt, *J* = 8.5, 2.4 Hz, 1H), 2.43 (s, 3H). **^{13}C NMR** (101 MHz, $CDCl_3$) δ 194.3, 164.1, 164.0, 161.6, 161.5, 140.9, 140.9, 140.8, 138.7, 136.5, 134.1, 130.5, 128.5, 127.4, 113.2, 113.1, 113.0, 112.9, 108.0, 107.7, 107.5, 21.5. **^{19}F NMR** (470 MHz, CDCl3) δ -108.2. **IR** (KBr): υ 3085, 2924, 1665, 1594, 1438, 1326, 1259, 1185, 1123, 987 cm^{-1}. **HRMS** (ESI): Calculated for $C_{14}H_{11}F_2O$ ($M+H^+$): 233.0772, found: 233.0772.

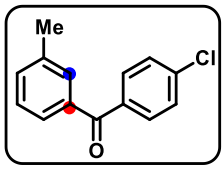

CAS: 35256-82-7

3ae: White solid (66%). R_f = 0.2 (hexane/ethyl acetate = 20:1). **^{1}H NMR** (400 MHz, $CDCl_3$) δ 7.78 – 7.72 (m, 2H), 7.59 (s, 1H), 7.54 (d, *J* = 7.1 Hz, 1H), 7.48 – 7.43 (m, 2H), 7.41 (d, *J* = 8.3 Hz, 1H), 7.36 (t, *J* = 7.5 Hz, 1H), 2.42 (s, 3H). **^{13}C NMR** (101 MHz, $CDCl_3$) δ 195.8, 138.9, 138.4, 137.4, 136.1, 133.5, 131.5, 130.5, 128.7, 128.3, 127.3, 21.5. Both the ^{1}H NMR and ^{13}C NMR match the literature reported data.[48]

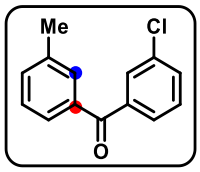

CAS: 71372-41-3

3af: Pale yellow solid (66%). R_f = 0.2 (hexane/ethyl acetate = 20:1). **^{1}H NMR** (400 MHz, $CDCl_3$) δ 7.78 (t, *J* = 1.9 Hz, 1H), 7.66 (dt, *J* = 7.7, 1.3 Hz, 1H), 7.62 (s, 1H), 7.56 (ddd, *J* = 8.1, 2.3, 1.1 Hz, 2H), 7.46 – 7.35 (m, 3H), 2.43 (s, 3H). **^{13}C NMR** (101 MHz, $CDCl_3$) δ 195.6, 139.6, 138.5, 137.1, 134.7, 133.8, 132.4, 130.5, 130.0, 129.7, 128.4, 128.2, 127.4, 21.5. Both the ^{1}H NMR and ^{13}C NMR match the literature reported data.[49]

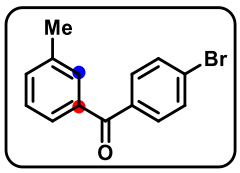

CAS: 27428-61-1

3ag: White solid (61%). R_f = 0.2 (hexane/ethyl acetate = 20:1). **^{1}H NMR** (400 MHz, $CDCl_3$) δ 7.70 – 7.60 (m, 4H), 7.59 (d, *J* = 1.6 Hz, 1H), 7.54 (dt, *J* = 7.4, 1.7 Hz, 1H), 7.43 – 7.39 (m, 1H), 7.36 (t, *J* = 7.5 Hz, 1H), 2.42 (s, 3H). **^{13}C NMR** (101 MHz, $CDCl_3$) δ 196.0, 138.5, 137.3, 136.6,

133.6, 131.7, 131.7, 130.5, 128.3, 127.5, 127.3, 21.5. Both the ^{1}H NMR and ^{13}C NMR match the literature reported data.[50]

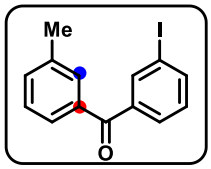

CAS: 951887-36-8

3ah: White solid (31%). R_f = 0.2 (hexane/ethyl acetate = 20:1). **^{1}H NMR** (400 MHz, $CDCl_3$) δ 8.13 (t, *J* = 1.7 Hz, 1H), 7.95 – 7.88 (m, 1H), 7.73 (dt, *J* = 7.7, 1.3 Hz, 1H), 7.61 (td, *J* = 1.7, 0.8 Hz, 1H), 7.54 (dt, *J* = 7.3, 1.6 Hz, 1H), 7.45 – 7.40 (m, 1H), 7.37 (t, *J* = 7.5 Hz, 1H), 7.22 (t, *J* = 7.8 Hz, 1H), 2.43 (s, 3H). **^{13}C NMR** (101 MHz, $CDCl_3$) δ 195.3, 141.0, 139.6, 138.5, 138.4, 136.9, 133.6, 130.4, 129.9, 129.1, 128.2, 127.3, 94.0, 21.4. **IR** (KBr): υ 3057, 2920, 1659, 1558, 1413, 1278, 1206, 1134, 997, 738 cm^{-1}. **HRMS** (ESI): Calculated for $C_{14}H_{12}IO$ ($M+H^+$): 322.9927, found: 322.9931.

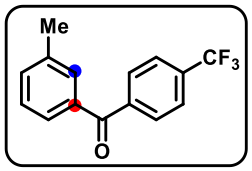

CAS: 1273961-09-3

3ai: White solid (63%). R_f = 0.2 (hexane/ethyl acetate = 20:1). **^{1}H NMR** (400 MHz, $CDCl_3$) δ 7.89 (d, *J* = 7.8 Hz, 2H), 7.75 (d, *J* = 8.1 Hz, 2H), 7.63 (s, 1H), 7.57 (d, *J* = 7.5 Hz, 1H), 7.44 (d, *J* = 7.1 Hz, 1H), 7.38 (t, *J* = 7.6 Hz, 1H), 2.43 (s, 3H). **^{13}C NMR** (101 MHz, $CDCl_3$) δ 195.9, 141.0 (d, *J* = 1.4 Hz), 138.6, 136.9, 134.1, 133.8 (q, *J* = 32.6 Hz), 130.6, 130.3, 128.5, 127.6, 125.5 (q, *J* = 3.8 Hz), 123.8 (q, *J* = 272.7 Hz), 21.5. **^{19}F NMR** (470 MHz, CDCl3) δ -63.0. **IR** (KBr): υ 2924,

1654, 1599, 1408, 1328, 1168, 1133, 1067, 858, 717 cm^{-1}. **HRMS** (ESI): Calculated for $C_{15}H_{12}F_3O$ ($M+H^+$):265.0835, found: 255.0831.

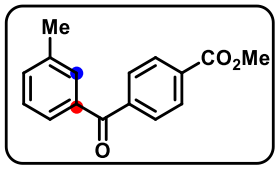

CAS: 288846-46-8

3aj: Yellow solid (53%). R_f = 0.1 (hexane/ethyl acetate = 20:1). **^{1}H NMR** (400 MHz, $CDCl_3$) δ 8.18 – 8.10 (m, 2H), 7.87 – 7.79 (m, 2H), 7.62 (s, 1H), 7.56 (d, *J* = 7.4 Hz, 1H), 7.42 (d, *J* = 7.6 Hz, 1H), 7.37 (t, *J* = 7.5 Hz, 1H), 3.96 (s, 3H), 2.41 (s, 3H). **^{13}C NMR** (101 MHz, $CDCl_3$) δ 196.3, 166.4, 141.6, 138.5, 137.1, 133.8, 133.2, 130.6, 129.9, 129.6, 128.4, 127.5, 52.6, 21.5. Both the ^{1}H NMR and ^{13}C NMR match the literature reported data.[51]

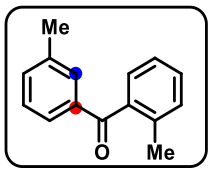

CAS: 22682-29-7

3ak: Pale yellow oil (48%). R_f = 0.3 (hexane/ethyl acetate = 20:1). **^{1}H NMR** (400 MHz, $CDCl_3$) δ 7.65 (s, 1H), 7.56 (d, *J* = 7.6 Hz, 1H), 7.39 (t, *J* = 7.0 Hz, 2H), 7.34 (d, *J* = 7.6 Hz, 1H), 7.32 – 7.22 (m, 3H), 2.40 (s, 3H), 2.33 (s, 3H). **^{13}C NMR** (101 MHz, $CDCl_3$) δ 199.0, 139.0, 138.5, 137.9, 136.8, 134.1, 131.1, 130.5, 130.3, 128.6, 128.5, 127.7, 125.3, 21.5, 20.1. Both the ^{1}H NMR and ^{13}C NMR match the literature reported data.[52]

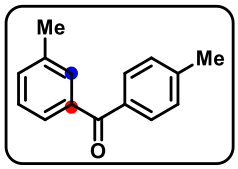

CAS: 13152-94-8

3al: White solid (52%). R_f = 0.3 (hexane/ethyl acetate = 20:1). **^{1}H NMR** (400 MHz, $CDCl_3$) δ 7.75 – 7.70 (m, 2H), 7.61 (s, 1H), 7.56 (d, *J* = 7.3 Hz, 1H), 7.42 – 7.33 (m, 2H), 7.28 (d, *J* = 7.9 Hz, 2H), 2.44 (s, 3H), 2.42 (s, 3H). **^{13}C NMR** (101 MHz, $CDCl_3$) δ 196.9, 143.3, 138.2, 138.1, 135.2, 133.1, 130.5, 130.4, 129.1, 128.1, 127.3, 21.8, 21.5. Both the ^{1}H NMR and ^{13}C NMR match the literature reported data.[53]

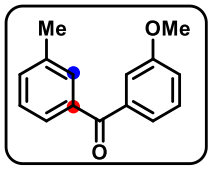

CAS: 71372-40-2

3am: Pale yellow oil (58%). R_f = 0.1 (hexane/ethyl acetate = 20:1). **^{1}H NMR** (400 MHz, $CDCl_3$) δ 7.63 (s, 1H), 7.58 (d, *J* = 7.4 Hz, 1H), 7.42 – 7.31 (m, 5H), 7.13 (ddd, *J* = 7.8, 2.7, 1.4 Hz, 1H), 3.86 (s, 3H), 2.42 (s, 3H). **^{13}C NMR** (101 MHz, $CDCl_3$) δ 196.9, 159.7, 139.2, 138.3, 137.8, 133.3, 130.6, 129.3, 128.2, 127.5, 123.0, 118.9, 114.4, 55.6, 21.5. Both the ^{1}H NMR and ^{13}C NMR match the literature reported data.[54]

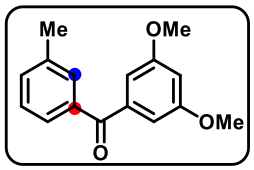

CAS: 1046145-53-2

3an: Colorless oil (51%). R_f = 0.1 (hexane/ethyl acetate = 10:1). **^{1}H NMR** (400 MHz, $CDCl_3$) δ 7.63 (s, 1H), 7.58 (d, *J* = 7.4 Hz, 1H), 7.37 (dt, *J* = 15.0, 7.6 Hz, 2H), 6.92 (d, *J* = 2.3 Hz, 2H), 6.67 (t, *J* = 2.3 Hz, 1H), 3.82 (s, 6H), 2.42 (s, 3H). **^{13}C NMR** (101 MHz, $CDCl_3$) 196.7, 160.6,

139.8, 138.3, 137.7, 133.4, 130.5, 128.2, 127.5, 108.0, 104.8, 55.7, 21.5. Both the ^{1}H NMR and ^{13}C NMR match the literature reported data.[55]

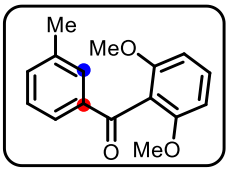

CAS: 855287-60-4

3ao: Colorless oil (37%). R_f = 0.2 (hexane/ethyl acetate = 5:1). **^{1}H NMR** (400 MHz, $CDCl_3$) δ 7.64 (s, 1H), 7.52 (d, *J* = 7.6 Hz, 1H), 7.30 – 7.18 (m, 3H), 6.55 (d, *J* = 8.4 Hz, 2H), 3.63 (s, 6H), 2.31 (s, 3H). **^{13}C NMR** (101 MHz, $CDCl_3$) δ 195.5, 157.5, 138.1, 137.6, 134.0, 130.6, 129.5, 128.3, 127.0, 118.1, 104.0, 55.9, 21.3. **IR** (KBr): υ 2937, 2839, 1735, 1595, 1473, 1433, 1294, 1253, 1111, 1074 cm^{-1}. **HRMS** (ESI): Calculated for $C_{16}H_{17}O_3$ ($M+H^+$): 257.1172, found: 257.1177.

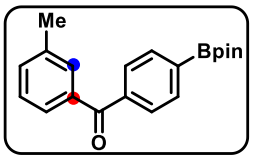

3ap: Yellow oil (41%). R_f = 0.2 (hexane/ethyl acetate = 10:1). **^{1}H NMR** (400 MHz, $CDCl_3$) δ 7.94 – 7.88 (m, 2H), 7.80 – 7.74 (m, 2H), 7.62 (td, *J* = 1.8, 0.9 Hz, 1H), 7.57 (dt, *J* = 7.1, 1.6 Hz, 1H), 7.43 – 7.33 (m, 2H), 2.41 (s, 3H), 1.37 (s, 12H). **^{13}C NMR** (101 MHz, $CDCl_3$) δ 197.3, 140.1, 138.3, 137.6, 134.6, 133.4, 130.69, 129.1, 128.3, 127.5, 84.3, 25.0, 21.5. **IR** (KBr): υ 2978, 1659, 1508, 1397, 1360, 1309, 1270, 1144, 1088, 1040 cm^{-1}. **HRMS** (ESI): Calculated for $C_{20}H_{24}BO_3$ ($M+H^+$): 323.1813, found: 323.1819.

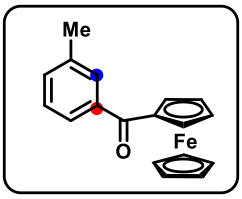

CAS: 33153-78-5

3aq: Red solid (32%). R_f = 0.1 (hexane/ethyl acetate = 10:1). **^{1}H NMR** (400 MHz, $CDCl_3$) δ 7.75 – 7.66 (m, 2H), 7.42 – 7.33 (m, 2H), 4.94 – 4.87 (m, 2H), 4.62 – 4.54 (m, 2H), 4.21 (s, 5H), 2.45 (s, 3H). **^{13}C NMR** (101 MHz, $CDCl_3$) δ 199.3, 139.8, 138.0, 132.2, 128.6, 128.0, 125.3, 78.3, 72.5, 71.5, 70.2, 21.4. Both the ^{1}H NMR and ^{13}C NMR match the literature reported data.[56]

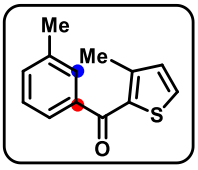

CAS: 56824-86-3

3ar: Colorless oil (33%). R_f = 0.2 (hexane/ethyl acetate = 10:1). **^{1}H NMR** (400 MHz, $CDCl_3$) δ 7.65 – 7.59 (m, 2H), 7.48 (d, *J* = 4.9 Hz, 1H), 7.40 – 7.31 (m, 2H), 7.00 (d, *J* = 5.0 Hz, 1H), 2.48 (s, 3H), 2.42 (s, 3H). **^{13}C NMR** (101 MHz, $CDCl_3$) δ 190.0, 145.8, 140.1, 138.2, 135.2, 133.0, 132.2, 130.9, 129.7, 128.2, 126.4, 21.5, 16.9. **IR** (KBr): υ 2922, 1637, 1601, 1519, 1399, 1370, 1277, 1204, 933, 749 cm^{-1}. **HRMS** (ESI): Calculated for $C_{13}H_{13}OS$ ($M+H^+$): 217.0682, found: 217.0685.

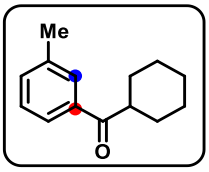

CAS: 3277-78-9

3as: Colorless oil (50%). R_f = 0.3 (hexane/ethyl acetate = 20:1). **^{1}H NMR** (400 MHz, $CDCl_3$) δ 7.73 (d, *J* = 7.9 Hz, 2H), 7.38 – 7.31 (m, 2H), 3.25 (tt, *J* = 11.5, 3.2 Hz, 1H), 2.41 (s, 3H), 1.86

(tdd, *J* = 15.0, 5.8, 2.6 Hz, 4H), 1.74 (ddd, *J* = 12.3, 2.9, 1.5 Hz, 1H), 1.55 – 1.37 (m, 4H), 1.36 – 1.26 (m, 1H). **^{13}C NMR** (101 MHz, $CDCl_3$) δ 204.3, 138.5, 136.6, 133.6, 128.9, 128.6, 125.6, 45.8, 29.6, 26.1, 26.0, 21.5. Both the ^{1}H NMR and ^{13}C NMR match the literature reported data.[57]

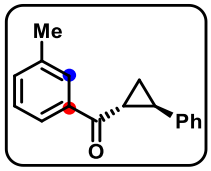

CAS: 1801328-76-6

3at: Colorless oil (60%). R_f = 0.3 (hexane/ethyl acetate = 20:1). **^{1}H NMR** (400 MHz, $CDCl_3$) δ 7.83 (d, *J* = 6.7 Hz, 2H), 7.44 – 7.31 (m, 4H), 7.29 – 7.20 (m, 3H), 2.94 (ddd, *J* = 8.1, 5.3, 4.0 Hz, 1H), 2.74 (ddd, *J* = 9.0, 6.6, 4.0 Hz, 1H), 2.44 (s, 3H), 1.95 (ddd, *J* = 9.2, 5.3, 4.1 Hz, 1H), 1.59 (ddd, *J* = 8.1, 6.5, 4.1 Hz, 1H). **^{13}C NMR** (101 MHz, $CDCl_3$) δ 198.7, 140.5, 138.3, 137.7, 133.6, 128.6, 128.5, 128.4, 126.5, 126.2, 125.3, 29.9, 29.3, 21.3, 19.3. Both the ^{1}H NMR and ^{13}C NMR match the literature reported data.[58]

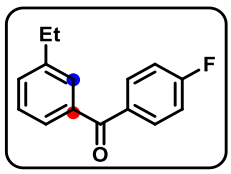

CAS: 1506583-26-1

3bb: Colorless oil (53%). R_f = 0.25 (hexane/ethyl acetate = 20:1). **^{1}H NMR** (400 MHz, $CDCl_3$) δ 7.94 – 7.80 (m, 2H), 7.62 (s, 1H), 7.56 (dq, *J* = 7.3, 1.5 Hz, 1H), 7.48 – 7.35 (m, 2H), 7.19-7.14 (m, 2H), 2.72 (q, *J* = 7.6 Hz, 2H), 1.27 (t, *J* = 7.6 Hz, 3H). **^{13}C NMR** (101 MHz, $CDCl_3$) δ 195.5, 165.3 (d, *J* = 253.9 Hz), 144.6, 137.5, 134.0 (d, *J* = 3.0 Hz), 132.6 (d, *J* = 9.1 Hz), 132.1, 129.2, 128.2, 127.4, 115.4 (d, *J* = 21.8 Hz), 28.7, 15.5. **^{19}F NMR** (470 MHz, $CDCl_3$) δ -106.2. **IR** (KBr):

υ 2967, 2933, 1660, 1598, 1504, 1301, 1279, 1229, 1156, 851 cm^{-1}. **HRMS** (ESI): Calculated for $C_{15}H_{14}FO$ ($M+H^+$): 229.1023, found: 229.1026.

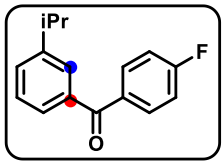

3cb: Colorless oil (26%). R_f = 0.30 (hexane/ethyl acetate = 20:1). **^{1}H NMR** (400 MHz, $CDCl_3$) δ 7.92 – 7.78 (m, 2H), 7.66 (t, *J* = 1.8 Hz, 1H), 7.55 (dt, *J* = 7.5, 1.5 Hz, 1H), 7.47 (dt, *J* = 7.7, 1.6 Hz, 1H), 7.40 (t, *J* = 7.6 Hz, 1H), 7.23 – 7.12 (m, 2H), 2.99 (dq, *J* = 13.8, 6.9 Hz, 1H), 1.28 (d, *J* = 6.9 Hz, 6H). **^{13}C NMR** (101 MHz, $CDCl_3$) δ 195.6, 165.3 (d, *J* = 254.0 Hz), 149.2, 137.5, 134.0 (d, *J* = 3.1 Hz), 132.6 (d, *J* = 9.1 Hz), 130.7, 128.2, 127.8, 127.6, 115.4 (d, *J* = 21.8 Hz), 34.0, 23.9. **^{19}F NMR** (470 MHz, $CDCl_3$) δ -106.2. **IR** (KBr): υ 2962, 2870, 1660, 1598, 1505, 1408, 1302, 1268, 1230, 1155 cm^{-1}. **HRMS** (ESI): Calculated for $C_{16}H_{16}FO$ ($M+H^+$): 243.1180, found: 243.1178.

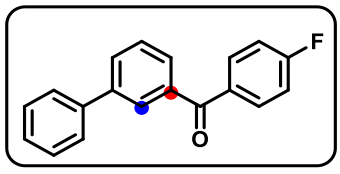

3db: Colorless oil (47%). R_f = 0.20 (hexane/ethyl acetate = 20:1). **^{1}H NMR** (500 MHz, $CDCl_3$) δ 7.99 (s, 1H), 7.90 (dd, *J* = 8.7, 5.5 Hz, 2H), 7.83 (d, *J* = 7.8 Hz, 1H), 7.74 (d, *J* = 7.8 Hz, 1H), 7.61 (d, *J* = 7.3 Hz, 2H), 7.57 (t, *J* = 7.7 Hz, 1H), 7.47 (t, *J* = 7.7 Hz, 2H), 7.39 (t, *J* = 7.4 Hz, 1H), 7.18 (t, *J* = 8.6 Hz, 2H). **^{13}C NMR** (126 MHz, $CDCl_3$) δ 195.2, 165.5 (d, *J* = 254.4 Hz), 141.5, 140.1, 138.1, 133.8 (d, *J* = 3.0 Hz), 132.7 (d, *J* = 9.2 Hz), 131.1, 128.9, 128.8, 128.7, 128.4, 127.8, 127.2,

115.5 (d, *J* = 21.9 Hz). **^{19}F NMR** (470 MHz, $CDCl_3$) δ -105.73. **IR** (KBr): υ 3062, 2925, 1660, 1597, 1504, 1477, 1408, 1312, 1269, 1240, 1096 cm^{-1}. **HRMS** (ESI): Calculated for: $C_{19}H_{14}FO$ ($M+H^+$): 277.1023, found: 277.1033.

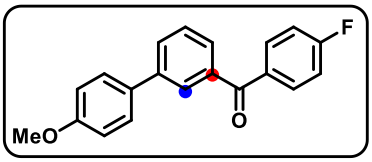

3eb: White solid (48%). m. p. = 89–91 ° C. R_f = 0.20 (hexane/ethyl acetate = 20:1). **^{1}H NMR** (400 MHz, $CDCl_3$) δ 7.95 (td, *J* = 1.8, 0.5 Hz, 1H), 7.92 – 7.87 (m, 2H), 7.78 (ddd, *J* = 7.7, 1.9, 1.1 Hz, 1H), 7.68 (ddd, *J* = 7.7, 1.7, 1.2 Hz, 1H), 7.61 – 7.47 (m, 3H), 7.21 – 7.14 (m, 2H), 7.03 – 6.96 (m, 2H), 3.86 (s, 3H). **^{13}C NMR** (101 MHz, $CDCl_3$) δ 195.3, 165.4 (d, *J* = 254.3 Hz), 159.6, 139.6 (d, *J* = 307.3 Hz), 133.8 (d, *J* = 3.1 Hz), 132.7 (d, *J* = 9.1 Hz), 132.5, 130.6, 128.7, 128.2, 128.0 (d, *J* = 15.5 Hz), 122.6, 115.6, 115.4, 114.4, 55.4. **IR** (KBr): υ 3041, 2985, 1662, 1597, 1518, 1431, 1280, 1263, 1181, 1150, 1023 cm^{-1}. **HRMS** (ESI): Calculated for: $C_{20}H_{16}FO_2$ ($M+H^+$): 307.1129, found: 307.1131.

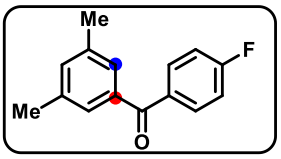

CAS: 1152684-96-2

3db: Colorless oil (60%). R_f = 0.3 (hexane/ethyl acetate = 20:1). **^{1}H NMR** (400 MHz, $CDCl_3$) δ 7.87 – 7.78 (m, 2H), 7.40-7.34 (m, 2H), 7.22 (s, 1H), 7.19 – 7.11 (m, 2H), 2.37 (s, 3H), 2.37 (s, 3H). **^{13}C NMR** (101 MHz, $CDCl_3$ δ 195.6, 165.2 (d, *J* = 253.8 Hz), 138.0, 137.6, 134.1, 134.0 (d, *J* = 3.1 Hz), 132.6 (d, *J* = 9.1 Hz), 127.6, 115.3 (d, *J* = 21.8 Hz), 21.2. **^{19}F NMR** (470 MHz, $CDCl_3$)

δ -106.3. **IR** (KBr): υ 2918, 1659, 1598, 1504, 1315, 1234, 1155, 968, 847, 764 cm^{-1}. **HRMS** (ESI): Calculated for $C_{15}H_{14}FO$ ($M+H^+$): 229.1023, found: 229.1026.

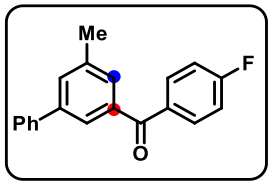

3gb: White solid (61%). m. p. = 53–55 ° C. R_f = 0.3 (hexane/ethyl acetate = 20:1). **^{1}H NMR** (400 MHz, $CDCl_3$) δ 7.92 – 7.86 (m, 2H), 7.76 (d, *J* = 1.8 Hz, 1H), 7.65-7.63 (m, 1H), 7.62 – 7.55 (m, 3H), 7.49 – 7.42 (m, 2H), 7.40 – 7.35 (m, 1H), 7.21 – 7.14 (m, 2H), 2.49 (d, *J* = 0.7 Hz, 3H).**^{13}C NMR** (101 MHz, $CDCl_3$) δ 195.4, 165.4 (d, *J* = 254.2 Hz), 141.4, 140.2, 138.7, 138.1, 133.9(d, *J* = 3.1 Hz), 132.7 (d, *J* = 9.2 Hz), 131.9, 129.2, 128.9, 127.7, 127.2, 125.8, 115.5(d, *J* = 21.9 Hz), 21.5. **^{19}F NMR** (470 MHz, $CDCl_3$) δ -105.1. **IR** (KBr): υ 3061, 2920, 1661, 1597, 1505, 1330, 1253, 1240, 1155, 850, 757 cm^{-1}. **HRMS** (ESI): Calculated for $C_{20}H_{16}FO$ ($M+H^+$): 291.1180, found: 291.1184.

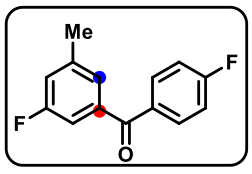

CAS: 1332348-95-4

3hb: Colorless oil (58%). R_f = 0.25 (hexane/ethyl acetate = 20:1). **^{1}H NMR** (400 MHz, $CDCl_3$) δ 7.80 – 7.74 (m, 2H), 7.31 – 7.26 (m, 1H), 7.19 – 7.15 (m, 1H), 7.13 – 7.07 (m, 2H), 7.07-7.02 (m, 1H), 2.35 (s, 3H).**^{13}C NMR** δ 194.1 (d, *J* = 2.3 Hz), 165.5 (d, *J* = 254.7 Hz), 162.3 (d, *J* = 247.6 Hz), 140.8 (d, *J* = 7.6 Hz), 139.2(d, *J* = 6.9 Hz), 133.4 (d, *J* = 3.1 Hz), 132.6 (d, *J* = 9.2 Hz), 126.1 (d, *J* = 2.7 Hz), 120.0 (d, *J* = 21.2 Hz), 115.6 (d, *J* = 21.9 Hz), 113.8 (d, *J* = 22.7 Hz), 21.3 (d, *J* =

1.8 Hz). **^{19}F NMR** (470 MHz, $CDCl_3$) δ -105.4, -113.0. **IR** (KBr): υ 3076, 2924, 1662, 1596, 1505, 1452, 1317, 1255, 1234, 1156, 846 cm^{-1}. **HRMS** (ESI): Calculated for $C_{14}H_{11}F_2O$ ($M+H^+$): 233.0772, found: 233.0776.

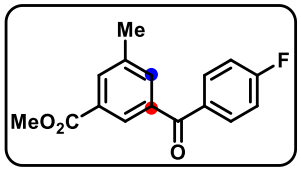

3ib: White solid (48%). m. p. = 80–82 °C. R_f = 0.30 (hexane/ethyl acetate = 10:1). **^{1}H NMR** (400 MHz, $CDCl_3$) δ 8.20 – 8.15 (m, 1H), 8.10-8.07 (m, 1H), 7.86 – 7.81 (m, 2H), 7.79-7.77 (m, 1H), 7.22 – 7.14 (m, 2H), 3.92 (s, 3H), 2.48 (s, 3H). **^{13}C NMR** δ 194.5, 166.4, 165.5 (d, *J* = 254.8 Hz), 138.9, 137.8, 134.4, 133.9, 133.4 (d, *J* = 3.0 Hz), 132.7 (d, *J* = 9.2 Hz), 130.2, 128.1, 115.7(d, *J* = 21.9 Hz), 52.4 , 21.2 .**^{19}F NMR** (470 MHz, $CDCl_3$) δ -106.2. **IR** (KBr): υ 2952, 1726, 1661, 1597, 1505, 1441, 1328, 1248, 1208, 1156, 849 cm^{-1}. **HRMS** (ESI): Calculated for $C_{16}H_{14}FO_3$ ($M+H^+$): 273.0921, found: 273.0926.

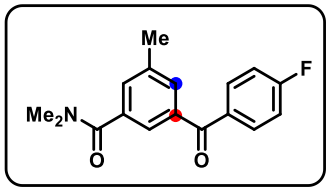

3jb: Yellow oil (54%). R_f = 0.20 (hexane/ethyl acetate = 5:1). **^{1}H NMR** (500 MHz, $CDCl_3$) δ 7.85 (dd, *J* = 8.6, 5.6 Hz, 2H), 7.64 (s, 1H), 7.56 (s, 1H), 7.49 (s, 1H), 7.18 (t, *J* = 8.6 Hz, 2H), 3.12 (s, 3H), 2.99 (s, 3H), 2.46 (s, 3H). **^{13}C NMR** (126 MHz, $CDCl_3$) δ 194.7, 170.7, 165.5 (d, *J* = 254.7 Hz), 138.9, 137.7, 136.6, 133.5 (d, *J* = 3.0 Hz), 132.6 (d, *J* = 9.2 Hz), 131.6, 131.2, 125.4, 115.6

(d, J = 21.8 Hz), 37.5 (d, J = 528.4 Hz), 21.3. **IR** (KBr): υ 3058, 2928, 1710, 1670, 1633, 1504, 1399, 1269, 1231, 1156, 1060 cm^{-1}. **HRMS** (ESI): Calculated for: $C_{17}H_{17}FNO_2$ ($M+H^+$): 286.1238, found: 286.1242.

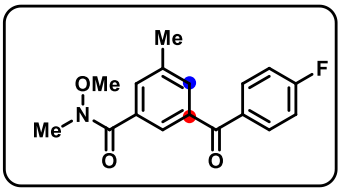

3kb: Colorless oil (62%). R_f = 0.20 (hexane/ethyl acetate = 5:1). **^{1}H NMR** (400 MHz, $CDCl_3$) δ 7.81 – 7.72 (m, 3H), 7.64 (s, 1H), 7.62 (s, 1H), 7.13 – 7.06 (m, 2H), 3.48 (s, 3H), 3.29 (s, 3H), 2.39 (s, 3H). **^{13}C NMR** (101 MHz, $CDCl_3$) δ 194.8, 167.9 (d, J = 230.6 Hz), 164.2, 138.6, 137.3, 134.2, 133.5 (d, J = 3.0 Hz), 132.8, 132.7, 132.4 (d, J = 41.7 Hz), 126.8, 115.6 (d, J = 21.9 Hz), 61.2, 33.5, 21.3. **^{19}F NMR** (470 MHz, $CDCl_3$) δ 35.28, -105.47. **IR** (KBr): υ 3068, 2934, 1712, 1660, 1597, 1504, 1383, 1307, 1276, 1257,1156 cm^{-1}. **HRMS** (ESI): Calculated for: $C_{17}H_{17}FNO_3$ ($M+H^+$): 302.1187, found: 302.1197.

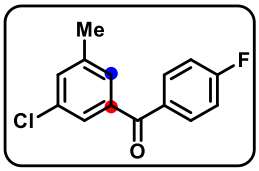

CAS: 1503093-93-3

3lb: Pale yellow oil (64%). R_f = 0.25 (hexane/ethyl acetate = 20:1). **^{1}H NMR** (400 MHz, $CDCl_3$) δ 7.86 – 7.80 (m, 2H), 7.54 – 7.48 (m, 1H), 7.46-7.44 (m, 1H), 7.40-7.37 (m, 1H), 7.20 – 7.14 (m, 2H), 2.40 (d, J = 0.7 Hz, 3H). **^{13}C NMR** (101 MHz, $CDCl_3$) δ 194.0, 165.5 (d, J = 254.9 Hz), 140.2, 139.0, 134.2, 133.3 (d, J = 3.1 Hz), 132.9, 132.6 (d, J = 9.2 Hz), 128.5, 126.9, 115.6 (d, J = 21.9

Hz), 21.1 .**^{19}F NMR** (470 MHz, $CDCl_3$) δ -105.2. **IR** (KBr): υ 3073, 2924, 1663, 1599, 1505, 1303, 1285, 1156, 982, 849 cm^{-1}. **HRMS** (ESI): Calculated for $C_{14}H_{11}ClFO$ ($M+H^+$): 249.0477, found: 249.0480.

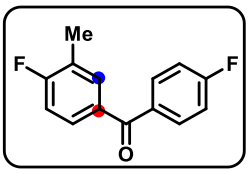

CAS: 59396-50-8

3mb: White solid (70%). R_f = 0.25 (hexane/ethyl acetate `= 20:1). **^{1}H NMR** (400 MHz, $CDCl_3$) δ 7.85 – 7.76 (m, 2H), 7.67 (ddd, *J* = 7.5, 2.3, 0.9 Hz, 1H), 7.59 (dddd, *J* = 8.1, 5.1, 2.4, 0.7 Hz, 1H), 7.20 – 7.12 (m, 2H), 7.09 (t, *J* = 8.9 Hz, 1H), 2.34 (s, 3H). **^{13}C NMR** (101 MHz, $CDCl_3$) δ 194.2, 166.1 (d, *J* = 132.5 Hz), 163.5 (d, *J* = 131.4 Hz), 134.0 (d, *J* = 3.1 Hz), 133.7 (d, *J* = 6.4 Hz), 133.6 (d, *J* = 3.4 Hz), 132.6 (d, *J* = 9.1 Hz), 130.0 (d, *J* = 9.2 Hz), 125.5 (d, *J* = 17.9 Hz), 115.6 (d, *J* = 21.9 Hz), 115.1 (d, *J* = 23.0 Hz), 14.7 (d, *J* = 3.5 Hz). **^{19}F NMR** (470 MHz, $CDCl_3$) δ -106.0, -110.0. **IR** (KBr): υ 2918, 1651, 1593, 1502, 1269, 1232, 1156, 1114, 911, 850 cm^{-1}. **HRMS** (ESI): Calculated for $C_{14}H_{11}F_2O$ ($M+H^+$): 233.0772, found: 233.0755.

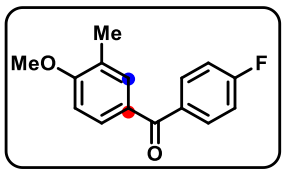

CAS: 1017160-10-9

3nb: Pink oil (62%). R_f = 0.25 (hexane/ethyl acetate = 20:1). **^{1}H NMR** (400 MHz, $CDCl_3$) δ 7.83 – 7.76 (m, 2H), 7.68 – 7.61 (m, 2H), 7.18 – 7.11 (m, 2H), 6.89 – 6.85 (m, 1H), 3.91 (s, 3H), 2.26 (s, 3H). **^{13}C NMR** (101 MHz, $CDCl_3$) δ 194.5, 165.1 (d, *J* = 252.9 Hz), 161.7, 134.7 (d, *J* = 3.1

Hz), 132.7, 132.4 (d, *J* = 9.0 Hz), 130.5, 129.62, 127.0, 115.4 (d, *J* = 21.8 Hz), 109.1, 55.7, 16.4. **^{19}F NMR** (470 MHz, $CDCl_3$) δ -107.2. **IR** (KBr): υ 2947, 2839, 1651, 1601, 1504, 1305, 1269, 1226, 1156, 1123, 1029 cm^{-1}. **HRMS** (ESI): Calculated for $C_{15}H_{14}FO_2$ ($M+H^+$): 245.0972, found: 245.0988.

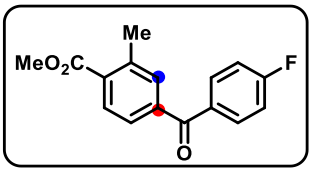

3ob: White solid (51%). m. p. = 101–103 °C. R_f = 0.2 (hexane/ethyl acetate = 20:1). **^{1}H NMR** (400 MHz, $CDCl_3$) δ 7.98 (d, *J* = 8.0 Hz, 1H), 7.88 – 7.81 (m, 2H), 7.61 (s, 1H), 7.57 (dd, *J* = 7.8, 1.4 Hz, 1H), 7.21 – 7.12 (m, 2H), 3.93 (s, 3H), 2.64 (s, 3H). **^{13}C NMR** (101 MHz, $CDCl_3$) δ 194.8, 167.5, 165.7 (d, *J* = 255.0 Hz), 140.4, 140.3, 133.4 (d, *J* = 3.0 Hz), 133.1, 132.9 (d, *J* = 9.3 Hz), 132.7, 130.6, 127.0, 115.8 (d, *J* = 21.9 Hz), 52.3, 21.8. **^{19}F NMR** (470 MHz, $CDCl_3$) δ -105.1. **IR** (KBr): υ 2954, 1734, 1597, 1436, 1405, 1296, 1269, 1250, 1160, 1080, 852 cm^{-1}. **HRMS** (ESI): Calculated for $C_{16}H_{14}FO_3$ ($M+H^+$): 273.0921, found: 273. 0913.

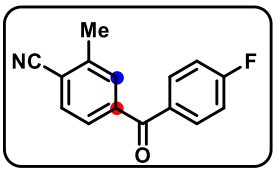

3pb: White solid (36%). m. p. = 103–105 °C. R_f = 0.2 (hexane/ethyl acetate = 20:1). **^{1}H NMR** (400 MHz, $CDCl_3$) δ 7.86 – 7.78 (m, 2H), 7.73 (d, *J* = 8.0 Hz, 1H), 7.69 (d, *J* = 0.8 Hz, 1H), 7.61 (d, *J* = 8.0 Hz, 1H), 7.22 – 7.14 (m, 2H), 2.63 (s, 3H). **^{13}C NMR** (101 MHz, $CDCl_3$) δ 194.0, 166.0 (d, *J* = 255.9 Hz), 141.9 (d, *J* = 140.5 Hz), 132.88, 132.9 (d, *J* = 9.3 Hz), 132.7, 131.1, 127.3, 117.4,

116.3, 116.1, 115.9, 20.7. **^{19}F NMR** (470 MHz, $CDCl_3$) δ -104.18. **IR** (KBr): υ 3074, 2922, 2228, 1663, 1597, 1505, 1410, 1267, 1157, 854, 766, 687 cm^{-1}. **HRMS** (ESI): Calculated for $C_{15}H_{10}FNO$ ($M+H^+$): 240.0819, found: 240.0835.

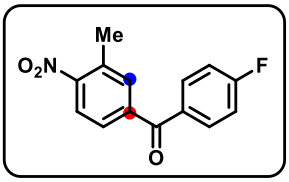

3qb: Colorless oil (33%). R_f = 0.2 (hexane/ethyl acetate = 20:1). **^{1}H NMR** (400 MHz, $CDCl_3$) δ 7.86 – 7.78 (m, 2H), 7.73 (d, *J* = 8.0 Hz, 1H), 7.69 (d, *J* = 0.8 Hz, 1H), 7.61 (d, *J* = 8.0 Hz, 1H), 7.22 – 7.14 (m, 2H), 2.63 (s, 3H). **^{13}C NMR** (101 MHz, $CDCl_3$) δ 193.4, 165.9 (d, *J* = 256.1 Hz), 151.2, 141.2, 133.8, 132.8, 132.7, 128.0, 124.6, 116.0, 115.8, 20.2. **^{19}F NMR** (470 MHz, $CDCl_3$) δ -104.02. **IR** (KBr): υ 3077, 2925, 1791, 1726, 1667, 1598, 1525, 1350, 1310, 1232, 1159 cm^{-1}. **HRMS** (ESI): Calculated for: $C_{14}H_{10}FNNaO_3$ ($M+Na^+$):282.0537, found: 282.0529.

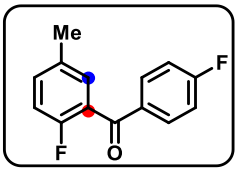

CAS: 59396-49-5

3rb: White solid (42%). R_f = 0.3 (hexane/ethyl acetate = 20:1). **^{1}H NMR** (400 MHz, $CDCl_3$) δ 7.89-7.85(m, 2H), 7.37 – 7.27 (m, 2H), 7.18 – 7.11 (m, 2H), 7.08 – 7.01 (m, 1H), 2.37 (s, 3H). **^{13}C NMR** (101 MHz, $CDCl_3$) δ 192.3, 166.1 (d, *J* = 255.3 Hz), 158.2 (d, *J* = 249.3 Hz), 134.3 (d, *J* = 3.6 Hz), 134.0 (d, *J* = 2.7 Hz), 133.9 (d, *J* = 8.0 Hz), 132.6 (dd, *J* = 9.5, 1.4 Hz), 130.9 (d, *J* = 2.7 Hz), 126.5 (d, *J* = 15.1 Hz), 116.1 (d, *J* = 21.9 Hz), 115.8 (d, *J* = 22.0 Hz), 20.7. **^{19}F NMR** (470

MHz, $CDCl_3$) δ -104.6, -116.1. **IR** (KBr): υ 2927, 1666, 1597, 1505, 1412, 1308, 1285, 1229, 1155, 965 cm^{-1}. **HRMS** (ESI): Calculated for $C_{14}H_{11}F_2O$ ($M+H^+$): 233.0772, found: 233.0769.

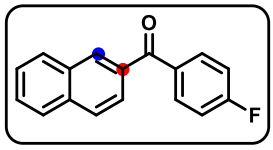

CAS: 1543-56-2

3sb: White solid (45%). R_f = 0.2 (hexane/ethyl acetate = 20:1). **^{1}H NMR** (400 MHz, $CDCl_3$) δ 8.24 (s, 1H), 7.99 – 7.88 (m, 6H), 7.60 (dddd, *J* = 22.6, 8.1, 6.9, 1.4 Hz, 2H), 7.25 – 7.17 (m, 2H). **^{13}C NMR** (101 MHz, $CDCl_3$) δ 195.4, 165.5 (d, *J* = 254.1 Hz), 135.4, 134.9, 134.2 (d, *J* = 3.1 Hz), 132.8 (d, *J* = 9.1 Hz), 132.4, 131.7, 129.5, 128.5, 128.0, 127.0, 125.8, 115.7 (d, *J* = 21.9 Hz). **^{19}F NMR** (470 MHz, $CDCl_3$) δ -106.0. Both the ^{1}H NMR and ^{13}C NMR match the literature reported data.[59]

4.4.6 Analysis of The Side Products in The Reaction of Aryl Boroxine 1i

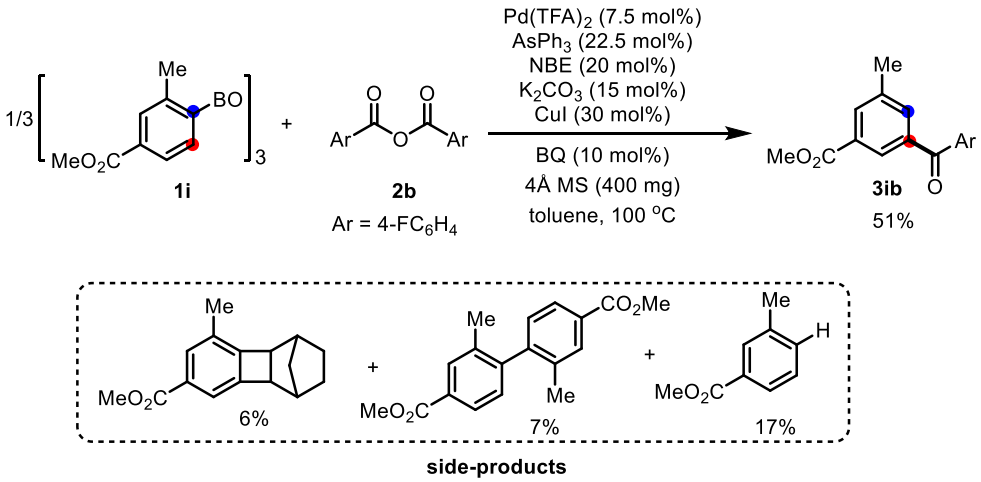

Yields were determined by ^{1}H NMR analysis using 1,1,2,2-tetrachloroethane as the internal standard.

Aryl boroxine **1i** was chosen as a substrate to study the side products generated in the ortho acylation. Protodeboronation was found to be the major side reaction.

4.4.7 Mechanistic study

1-Bromonaphthalene-*d*$_7$ was prepared according to the literature reported procedure.[60] NBS (2.14 g, 12.0 mmol) and $AuCl_3$ (4 mg, 0.012 mmol, 0.1 mol%) were added in a 40 mL vial. Then naphthalene-*d*$_8$ (1.64 g, 12.0 mmol) and DCE (24 mL) were added in succession. The resulting reaction mixture was allowed to stir for about 15 h at 80 °C. Then the solvent was removed under vacuum and the residue was purified by flash column chromatography to give 1-bromonaphthalene-*d*$_7$ (2.0 g, 78%). Both the ^{1}H NMR and ^{13}C NMR match the literature reported data.[61]

Scheme 4.9. Preparation of 1-Naphthylboroxine-d7

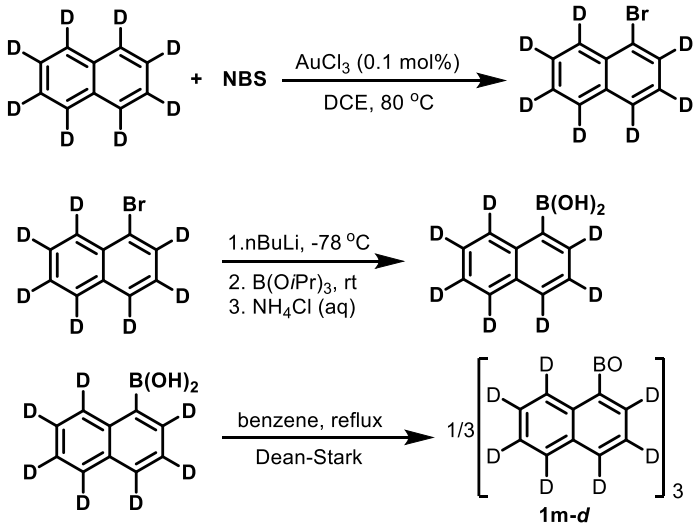

1-Bromonaphthalene-*d*$_7$ (1.90 g, 8.7 mmol) was dissolved in 50 mL dry THF and cooled down to -78 °C. Then nBuLi (7.1 mL, 10.6 mmol, 1.5 M in hexane) was added dropwise to the reaction

mixture. The temperature was maintained at -78 °C for 2 h and afterwards B(O*i*Pr)$_3$ (3.32 g, 17.7 mmol) was added. The resulting reaction mixture was allowed to warm to rt and stirred overnight. The reaction was quenched by aq NH_4Cl and extracted with ethyl acetate for three times. The desired boronic acid was isolated through flash column chromatography as a white solid (599.2 mg, 38%). Both the ^{1}H NMR and ^{13}C NMR match the literature reported data.[61]

In a 50 mL round bottom flask was added 1-bromonaphthalene-*d*$_7$ (600 mg) and a stir bar. Then 30 mL benzene was added and the solution was refluxed for 12 h using Dean-Stark trap to remove water. The solution was allowed to cool down to room temperature and the solvent was removed under vacuum to give the desired 1-naphthylboroxine-d$_7$ as a white solid. After washed with hexane for three time and dried under vacuum, the arylboroxine product was directly used in the acylation reaction without further purification.

Scheme 4.10. Deuterium Labelling Study with 1-Naphthylboroxine-d$_7$

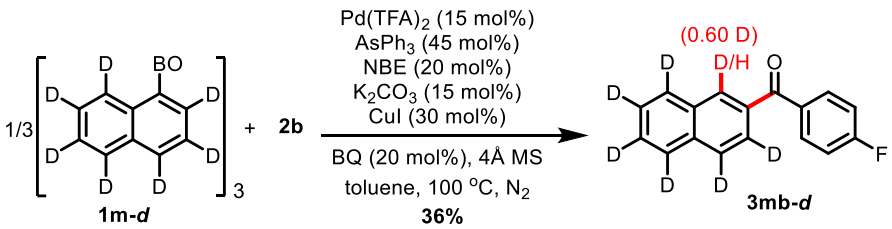

A flame-dried 4.0 mL vial was charged with Pd(TFA)$_2$ (9.9 mg, 0.03 mmol, 15 mol%), benzoquinone (4.4 mg, 0.04 mmol, 20 mol%), CuI (11.4 mg, 0.06 mmol, 30 mol%), AsPh$_3$ (27.6 mg, 0.09 mmol, 45 mol%), **1m-*d*** (32.2 mg, 0.2 mmol, 1.0 equiv, based on monomer) and 4-fluorobenzoic anhydride (104.9 mg, 0.4 mmol, 2.0 equiv). Then the vial was directly transferred into a nitrogen-filled glovebox without caps. Then K_2CO_3 (4.1 mg, 0.03 mmol, 15 mol%) and 4Å molecular sieves (400 mg) were added. In another 4.0 mL vial, NBE (11.3 mg, 0.12 mmol) was

dissolved in 1.5 mL dry toluene. 0.5 mL of this NBE solution (3.8 mg, 0.04 mmol, 20 mol%) was transferred into the reaction mixture, before another 3.5 mL dry toluene was added. The vial was tightly sealed, transferred out of glovebox and stirred on a pie-block preheated to 100 °C for 14 hours. After completion of the reaction, the mixture was filtered through a thin pad of silica gel. The filter cake was washed with ethyl acetate and the combined filtrate was concentrated. The residue was loaded to a small amount of silica gel and then purified by flash column chromatography on silica gel to give the desired ortho acylation product **3mb-*d*** as a white solid.

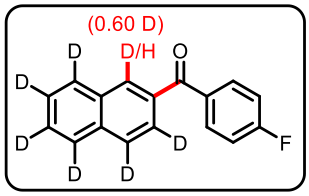

3mb-*d*: White solid (36%). R_f = 0.2 (hexane/ethyl acetate = 20:1). **^{1}H NMR** (400 MHz, $CDCl_3$) δ 8.24 (s, 0.4H + 0.6D), δ 7.96 – 7.86 (m, 2H), 7.24 – 7.16 (m, 2H).

Scheme 4.11. Deuterium labelling study with D_2O

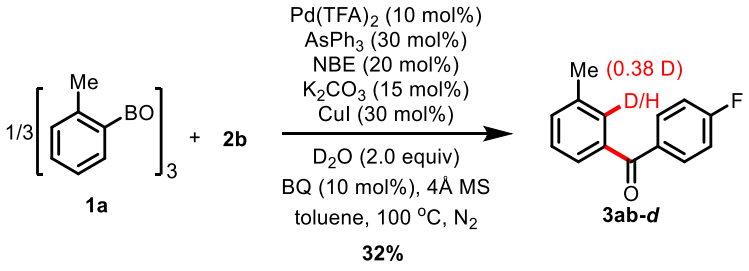

A flame-dried 4.0 mL vial was charged with $Pd(TFA)_2$ (9.9 mg, 0.03 mmol, 10 mol%), benzoquinone (3.3 mg, 0.03 mmol, 10 mol%), CuI (17.1 mg, 0.09 mmol, 30 mol%), $AsPh_3$ (27.6 mg, 0.09 mmol, 30 mol%), 2-toylboroxine (35.4 mg, 0.3 mmol, 1.0 equiv, based on monomer) 4-flrorobenzoic anhydride (157.4 mg, 0.6 mmol, 2.0 equiv) and D_2O (12 mg, 0.6 mmol, 2.0 equiv). The vial was directly transferred into a nitrogen-filled glovebox without caps. Then K_2CO_3 (6.2

mg, 0.045 mmol, 15 mol%) and 4Å molecular sieves (200 mg) were added. In another 4.0 mL vial, NBE (16.9 mg, 0.18 mmol) was dissolved in 1.5 mL dry toluene. 0.5 mL of this NBE solution (5.64 mg, 0.06 mmol, 20 mol%) was transferred into the reaction mixture, before another 3.5 mL dry toluene was added. The vial was tightly sealed, transferred out of glovebox and stirred on a pie-block preheated to 100 °C for 14 hours. After completion of the reaction, the mixture was filtered through a thin pad of silica gel. The filter cake was washed with ethyl acetate and the combined filtrate was concentrated. The residue was loaded to a small amount of silica gel and then purified by flash column chromatography on silica gel to give the desired ortho acylation product **3ab-*d*.**

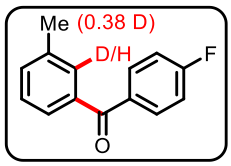

3mb-*d*: Colorless oil (32%). R_f = 0.3 (hexane/ethyl acetate = 20:1). **^{1}H NMR** (400 MHz, Chloroform-d) δ 7.89 – 7.80 (m, 2H), 7.59 (s, 0.62H + 0.38D), 7.54 (d, *J* = 7.4 Hz, 1H), 7.45 – 7.34 (m, 2H), 7.20 – 7.13 (m, 2H), 2.42 (s, 3H).

4.4.8 General Procedure of Palladium and Norbornene Catalyzed Ortho Amination Reaction

Scheme 4.12. Redox-Neutral Ortho Amination of Aryl Boroxines

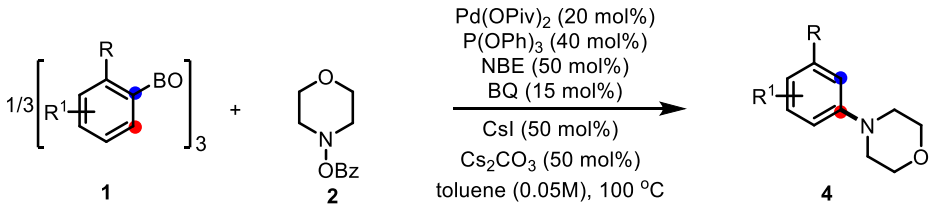

1 2 4

A flame-dried 4.0 mL vial was charged with $Pd(OPiv)_2$ (12.4 mg, 0.04 mmol, 20 mol%), benzoquinone (3.3 mg, 0.03 mmol, 15 mol%), $P(OPh)_3$ (24.8 mg, 0.08 mmol, 40 mol%), 2-toylboroxine (59 mg, 0.5 mmol, 2.5 equiv, based on the monomer) and *O*-benzoyl hydroxylamines (41.4 mg, 0.2 mmol, 1.0 equiv). The vial was directly transferred into a nitrogen-filled glovebox without caps. Then Cs_2CO_3 (32.6 mg, 0.1 mmol, 50 mol%) and CsI (26.0 mg, 0.1 mmol, 50 mol%) were added. In another 4.0 mL vial, NBE (37.6 mg, 0.40 mmol) was dissolved in 2.0 mL dry toluene. 0.5 mL of this NBE solution (9.4 mg, 0.1 mmol, 50 mol%) was transferred into the reaction mixture, before another 3.5 mL of dry toluene was added. The vial was tightly sealed, transferred out of glovebox and stirred on a pie-block preheated to 100 °C for 12 hours. After completion of the reaction, the mixture was filtered through a thin pad of silica gel. The filter cake was washed with ethyl acetate and the combined filtrate was concentrated. The residue was loaded to a small amount of silica gel and then purified by flash column chromatography on silica gel to give the desired ortho amination products **4aa-4sa**.

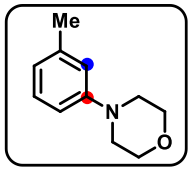

CAS: 7025-91-4

4aa: Colorless oil (66%). R_f = 0.2 (hexane/ethyl acetate = 10:1). **^{1}H NMR** (400 MHz, $CDCl_3$) δ 7.18 (t, *J* = 7.9 Hz, 1H), 6.78 – 6.68 (m, 3H), 3.92 – 3.84 (m, 4H), 3.21 – 3.12 (m, 4H), 2.33 (s, 3H). **^{13}C NMR** (101 MHz, $CDCl_3$) δ 151.3, 138.9, 129.0, 120.9, 116.5, 112.8, 67.0, 49.4, 21.8. Both the ^{1}H NMR and ^{13}C NMR match the literature reported data.[62]

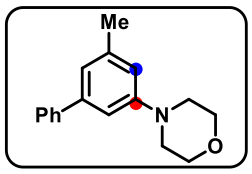

CAS: 152275-19-9

4ga: White solid (64%). m. p. = 54–56 °C. R_f = 0.2 (hexane/ethyl acetate = 10:1). **^{1}H NMR** (400 MHz, $CDCl_3$) δ 7.61 – 7.55 (m, 2H), 7.48 – 7.40 (m, 2H), 7.38 – 7.31 (m, 1H), 6.98 – 6.92 (m, 2H), 6.76 (s, 1H), 3.93 – 3.85 (m, 4H), 3.27 – 3.18 (m, 4H), 2.40 (s, 3H). **^{13}C NMR** (101 MHz, $CDCl_3$) δ 151.7, 142.3, 141.8, 139.2, 128.6, 127.2, 127.2, 120.2, 115.5, 112.0, 67.0, 49.5, 21.8. **IR** (KBr): υ 2959, 2852, 2822, 1594, 1449, 1221, 1122, 1007, 890, 762, 699 cm^{-1}. **HRMS** (ESI): Calculated for: $C_{17}H_{20}NO$ ($M+H^+$): 254.1539, found: 254.1533.

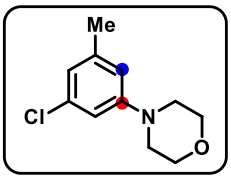

4la: Colorless oil (57%). R_f = 0.2 (hexane/ethyl acetate = 10:1). **^{1}H NMR** (400 MHz, $CDCl_3$) δ 6.69 (d, *J* = 1.8 Hz, 2H), 6.59 (s, 1H), 3.87 – 3.81 (m, 4H), 3.17 – 3.10 (m, 4H), 2.29 (s, 3H). **^{13}C NMR** (101 MHz, $CDCl_3$) δ 152.2, 140.2, 134.7, 120.6, 114.5, 112.7, 66.7, 49.0, 21.6. **IR** (KBr): υ 2961, 2854, 1601, 1573, 1449, 1249, 1122, 992, 891, 827, 684, 658 cm^{-1}. **HRMS** (ESI): Calculated for: $C_{11}H_{15}ClNO$ ($M+H^+$): 212.0837, found: 212.0844.

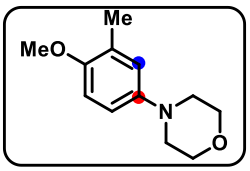

4na: pink solid (65%). m. p. = 74–76 °C. R_f = 0.1 (hexane/ethyl acetate = 10:1). **^{1}H NMR** (400 MHz, $CDCl_3$) δ 6.83 – 6.65 (m, 3H), 3.92 – 3.82 (m, 4H), 3.78 (s, 3H), 3.14 – 2.90 (m, 4H), 2.21 (s, 3H). **^{13}C NMR** (101 MHz, $CDCl_3$) δ 152.3, 145.2, 127.3, 120.0, 114.3, 110.7, 67.0, 55.7, 50.8, 16.5. **IR** (KBr): υ 2821, 2955, 1505, 1454, 1237, 1120, 1029, 1003, 879, 804, 704 cm^{-1}. **HRMS** (ESI): Calculated for: $C_{12}H_{18}NO_2$ ($M+H^+$): 208.1332, found: 208.1336.

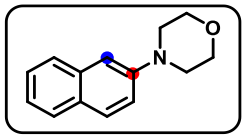

CAS: 7508-21-6

4sa: Yellow solid (62%). R_f = 0.2 (hexane/ethyl acetate = 10:1). **^{1}H NMR** (400 MHz, $CDCl_3$) δ 7.73 – 7.57 (m, 3H), 7.32 (ddd, *J* = 8.2, 6.8, 1.4 Hz, 1H), 7.22 (ddd, *J* = 8.0, 6.8, 1.3 Hz, 1H), 7.15 (dd, *J* = 9.1, 2.4 Hz, 1H), 7.02 (d, *J* = 2.4 Hz, 1H), 3.87 – 3.76 (m, 4H), 3.24 – 3.10 (m, 4H). **^{13}C NMR** (101 MHz, $CDCl_3$) δ 149.0, 134.4, 128.8, 128.6, 127.4, 126.7, 126.3, 123.5, 118.8, 110.0, 66.9, 49.7. Both the ^{1}H NMR and ^{13}C NMR match the literature reported data.[62]

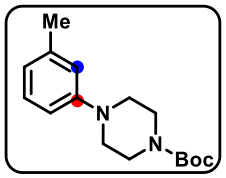

CAS: 1121596-67-5

4ab: Yellow solid (58%). **^{1}H NMR** (400 MHz, $CDCl_3$) δ 7.19 – 7.13 (m, 1H), 6.78 – 6.69 (m, 3H), 3.62 – 3.49 (m, 4H), 3.17 – 3.06 (m, 4H), 2.32 (s, 3H), 1.48 (s, 9H). **^{13}C NMR** (126 MHz, $CDCl_3$) δ 154.9, 151.5, 139.0, 129.2, 121.3, 117.6, 113.9, 80.0, 49.7, 28.6, 21.9, 21.9. Both the ^{1}H NMR and ^{13}C NMR match the literature reported data.[63]

4.4.9 Synthetic Utility

Scheme 4.13. Preparation of Tethered Substrate 6

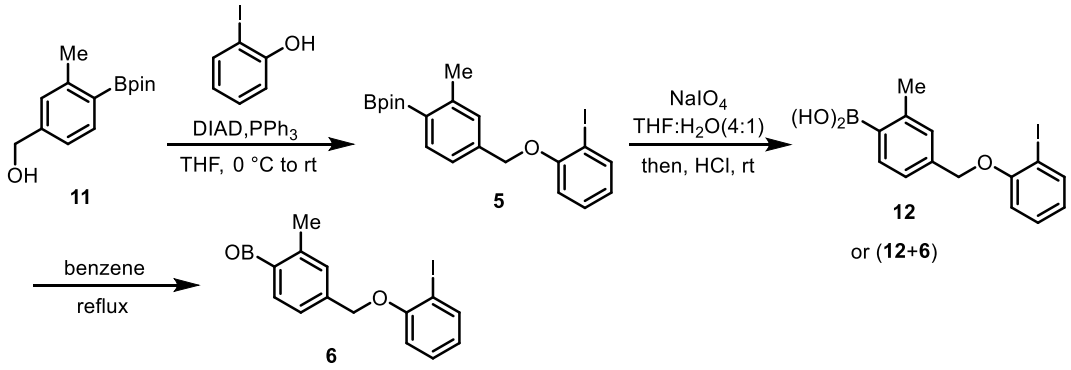

To a 100 mL flask equipped with a stir bar was charged with benzyl alcohol **11** (1.95g, 8 mmol, 1.0 equiv), 2-iodophenol (1.94g, 8.8 mmol, 1.1 equiv), triphenylphosphine (2.52g, 9.6 mmol, 1.2

equiv) and THF (40 ml). The pure diisopropyl azodicarboxylate (1.78 g, 8.8 mmol, 1.1 equiv) was added dropwise at zero degree. When the addition was finished, the solution was warmed to room temperature and stirred overnight. The reaction was monitored by TLC until full conversion was observed. The solution was concentrated under vacuum and the residue was purified by column chromatography on silica gel (hexane/ethyl acetate = 20:1 to 10:1) to give the tethered product **5** as a yellow oil (2.01g) in 56% yield. [64]

To a solution of pinacol boronate ester **5** (450 mg, 1.0 mmol, 1.0 equiv) in THF/H_2O (4:1, 15 mL), sodium periodate (643 mg, 3.0 mmol, 3.0 equiv) was added at room temperature. The reaction mixture was stirred for 30 min and then 1 N HCl (1.0 mL, 1.0 mmol, 1.0 equiv) was added. After 4 h, the reaction mixture was extracted with ethyl acetate (3 × 30 mL), and the combined organic extracts were washed with water and brine, dried over Na_2SO_4 and concentrated in vacuo. The residue was purified by column chromatography on silica gel (MeOH/DCM = 20:1) to give boronic acid **12** (or a mixture of boronic acid **12** and boroxine **6**) as a white solid (364 mg) in 99% yield.

In a 100 mL round bottom flask was added arylboronic acid **12** (15.0 mmol) and a stir bar. Then, benzene (50 mL) was added and the solution was refluxed for 12 h using Dean-Stark trap to remove water. The solution was allowed to cool to room temperature and the solvent was removed under vacuum to give the desired arylboroxine as a white solid. After washed with hexane for three time and dried under vacuum, the arylboroxine product **6** was directly used in the acylation reaction without further purification.

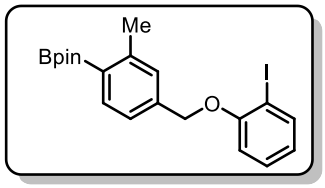

5: Yellow oil (56%). R_f = 0.4 (hexane/ethyl acetate = 10:1). **^{1}H NMR** (400 MHz, $CDCl_3$) δ 7.83 – 7.77 (m, 2H), 7.32 – 7.28 (m, 2H), 7.28-7.22 (m, 1H), 6.82 (dd, *J* = 8.3, 1.4 Hz, 1H), 6.74-6.70 (m, 1H), 5.13 (s, 2H), 2.57 (s, 3H), 1.35 (s, 12H). **^{13}C NMR** (101 MHz, $CDCl_3$) δ 157.1, 145.2, 139.5, 139.1, 136.2, 129.4, 128.1, 123.2, 122.7, 112.7, 86.7, 83.4, 70.7, 24.9, 22.3. **IR** (KBr): υ 3062, 2921, 1660, 1598, 1505, 1476, 1438, 1317, 1233, 1155, 1053 cm^{-1}. **HRMS** (ESI): Calculated $C_{20}H_{28}BINO_3$ ($M+NH_4^+$): 468.1201, found: 468.1205.

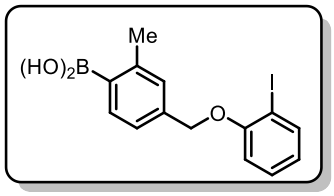

12: White solid (99%). m. p. = 103–105 °C. R_f = 0.2 (DCM/ethyl acetate = 5:1). **^{1}H NMR** (400 MHz, Acetone-*d*) δ 7.83 (dd, *J* = 7.8, 1.6 Hz, 1H), 7.61 (d, *J* = 7.5 Hz, 1H), 7.39 – 7.27 (m, 3H), 7.15 (s, 2H), 7.09 (dd, *J* = 8.3, 1.4 Hz, 1H), 6.78 (td, *J* = 7.6, 1.3 Hz, 1H), 5.20 (s, 2H), 2.53 (s, 3H). **^{13}C NMR** (101 MHz, Acetone-*d*) δ 157.4, 142.4, 139.4, 137.8, 133.9, 133.9, 129.6, 128.3, 123.4, 122.7, 113.0, 86.0, 70.4, 21.8. **IR** (KBr): υ 3052, 2924, 1611, 1582, 1474, 1438, 1417, 1348, 1270, 1245, 1054cm^{-1}. **HRMS** (ESI): Calculated $C_{14}H_{12}BINaO_2$ ($M+Na-H_2O^+$): 372.9867, found: 372.9854.

Scheme 4.14. Sequential Functionalization of 6

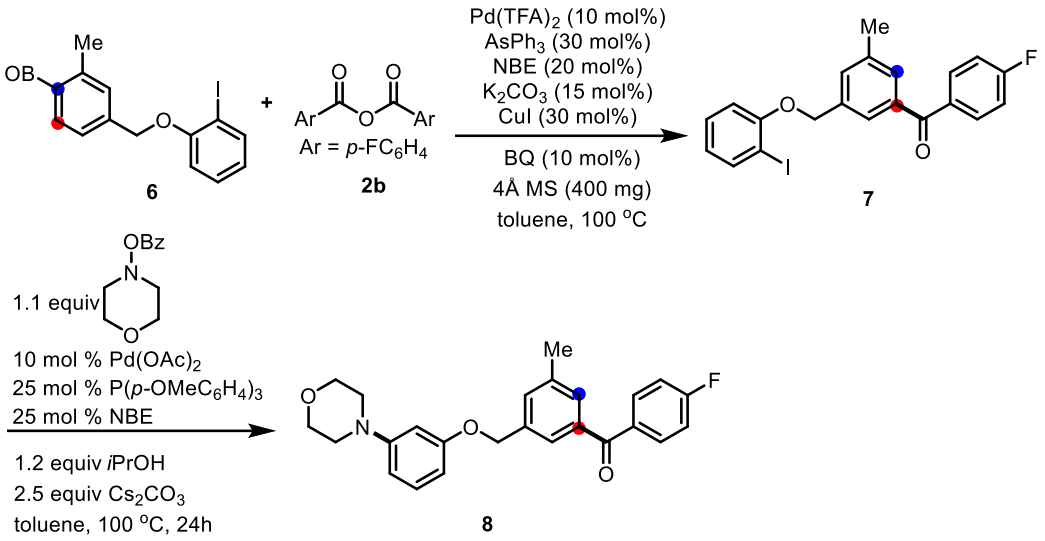

A flame-dried 4.0 mL vial was charged with $Pd(TFA)_2$ (9.9 mg, 0.03 mmol, 10 mol%), benzoquinone (3.3 mg, 0.03 mmol, 10 mol%), CuI (17.1 mg, 0.09 mmol, 30 mol%), $AsPh_3$ (27.6 mg, 0.09 mmol, 30 mol%), **6** (105.0 mg, 0.3 mmol, 1.0 equiv, based on monomer) and substituted 4-fluorobenzoic anhydride (157.4 mg, 0.6 mmol, 2.0 equiv). The vial was directly transferred into a nitrogen-filled glovebox without caps. Then, K_2CO_3 (6.2 mg, 0.045 mmol, 15 mol%) and 4Å molecular sieves (400 mg) were added. In another 4.0 mL vial, NBE (16.9 mg, 0.18 mmol) was dissolved in 1.5 mL dry toluene. 0.5 mL of this NBE solution (5.6 mg, 0.06 mmol, 20 mol%) was transferred into the reaction mixture, before more dry toluene (3.5 mL) was added. The vial was tightly sealed, transferred out of glovebox and stirred on a pie-block preheated to 100 °C for 14 hours. After completion of the reaction, the mixture was filtered through a thin pad of silica gel. The filter cake was washed with ethyl acetate and the combined filtrate was concentrated. The residue was loaded to a small amount of silica gel and then purified by flash column chromatography (hexane : ethyl acetate = 40 : 1) on silica gel to give **7** (81.7mg) as a white solid in 61% yield.

An flame-dried 4 mL vial was charged with aryl iodide **7** (44.6 mg, 0.1 mmol 1.0 equiv), *O*-Benzoyl hydroxylamines (22.8 mg, 0.11 mmol, 1.1 equiv), Cs_2CO_3 (82 mg, 0.25 mmol, 2.5 equiv), isopropanol (7.1 mg, 0.12 mmol, 1.2 equiv), norbornene (2.3 mg, 0.025 mmol, 0.25 equiv), $Pd(OAc)_2$ (2.2 mg, 0.01 mmol, 0.10 equiv) and tris(4-methoxyphenyl)phosphine (8.8 mg, 0.025 mmol, 0.25 equiv), which was sealed outside and transferred in a nitrogen-filled glovebox. Toluene (2 ml) was added into the vial, then the vial was sealed with PTFE lined cap in the glovebox again and stirred at RT for 10 minutes until the $Pd(OAc)_2$ was fully dissolved. The vial was subsequently transferred out of glovebox and stirred on a pie-block preheated to 100℃ for 24 hours. The mixture was then filtered through a thin pad of celite. The filter cake was washed with diethyl ether, and the combined filtrate was concentrated. The residue was directly purified by flash column chromatography (hexane : ethyl acetate =20 : 1) on silica gel to give the desired product **8** (27.6 mg) in 68% yield as a yellow oil.[62]

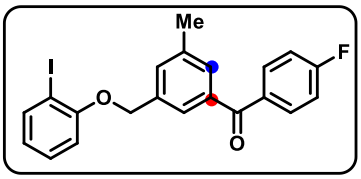

7: White solid (61%). m. p. = 77–79 ° C. **^{1}H NMR** (400 MHz, Chloroform-*d*) δ 7.87 – 7.82 (m, 2H), 7.80 (dd, *J* = 7.8, 1.6 Hz, 1H), 7.69 (s, 1H), 7.57-7.56 (m, 2H), 7.35 – 7.27 (m, 1H), 7.19 – 7.10 (m, 2H), 6.86 (dd, *J* = 8.2, 1.3 Hz, 1H), 6.77-6.73 (m, 1H), 5.16 (s, 2H), 2.46 (s, 3H). **^{13}C NMR** (101 MHz, Chloroform-*d*) δ 195.2, 165.4 (d, *J* = 254.2 Hz), 156.8, 139.6, 138.8, 137.8, 136.7, 133.7 (d, *J* = 3.1 Hz), 132.7 (d, *J* = 9.2 Hz), 131.8, 129.9, 129.5, 125.9, 123.0, 115.5 (d, *J* = 21.8 Hz), 112.7, 86.8, 70.3, 21.4. **IR** (KBr): υ 3062, 2921, 1660, 1598, 1505, 1476, 1438, 1317, 1233, 1155, 1053 cm^{-1}. **HRMS** (ESI): Calculated for $C_{21}H_{17}FIO_2$ ($M+H^+$): 447.0252, found: 447.0251.

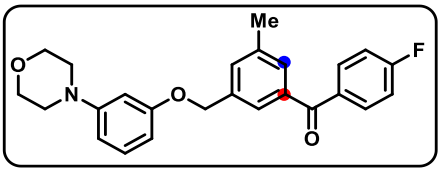

8: Yellow oil (68%). **^{1}H NMR** (400 MHz, $CDCl_3$) δ 7.81 (ddd, *J* = 9.8, 5.1, 2.3 Hz, 2H), 7.60 (s, 1H), 7.53 (s, 1H), 7.49 (s, 1H), 7.24 – 7.09 (m, 3H), 6.62 – 6.51 (m, 2H), 6.48 (dd, *J* = 8.1, 2.4 Hz, 1H), 5.07 (s, 2H), 3.95 – 3.80 (m, 4H), 3.25 – 3.08 (m, 4H), 2.44 (s, 3H). **^{13}C NMR** (101 MHz, $CDCl_3$) δ 195.32, 165.49 (d, *J* = 254.1 Hz), 159.67, 152.84, 138.83, 137.93, 137.54, 133.89 (d, *J* = 3.0 Hz), 132.79 (d, *J* = 9.2 Hz), 132.29, 130.08, 130.04, 126.25, 115.58 (d, *J* = 21.8 Hz), 109.03, 105.51, 103.27, 69.50, 66.97, 49.31, 21.49. **^{19}F NMR** (470 MHz, $CDCl_3$) δ -105.87. **IR** (KBr): υ 3054, 2960, 1732, 1660, 1598, 1495, 1449, 1315, 1232, 1191, 1115 cm^{-1}. **HRMS** (CI): Calculated for $C_{25}H_{25}FNO_3$ ($M+H^+$): 406.1813, found: 406.1815.

Scheme 4.15. Sequential Functionalization of 5

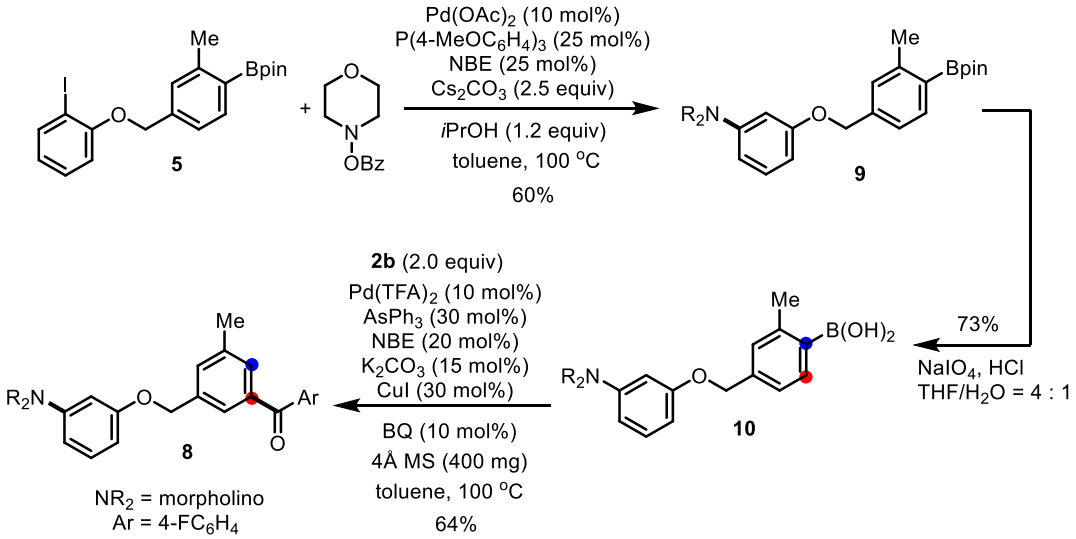

An flame-dried 7.0 mL vial was charged with aryl iodide **5** (135.0 mg, 0.3 mmol 1.0 equiv), *O*-Benzoyl hydroxylamines (124.3 mg, 0.6 mmol, 2.0 equiv), $Pd(OAc)_2$ (6.7 mg, 0.03 mmol, 0.10 equiv) and tris(4-methoxyphenyl)phosphine (26.4 mg, 0.075 mmol, 0.25 equiv), which was transferred into a nitrogen-filled glovebox without caps. Then Cs_2CO_3 (244.4 mg, 0.75 mmol,2.5

equiv), isopropanol (21.6 mg, 0.36 mmol, 1.2 equiv) and norbornene (7.1 mg, 0.075 mmol, 0.25 equiv) were added. Toluene (6 ml) was added into the vial, then the vial was sealed with PTFE lined cap in the glovebox and stirred at RT for 10 minutes until the $Pd(OAc)_2$ was fully dissolved (the solution takes on a light yellow color). The vial was subsequently transferred out of glovebox and stirred on a pie-block preheated to 100℃ for 24 hours. The mixture was then filtered through a thin pad of celite. The filter cake was washed with diethyl ether, and the combined filtrate was concentrated. The residue was directly purified by flash column chromatography (hexane : ethyl acetate =10 : 1) on silica gel to give the desired product **9** (73.7 mg) in 60% yield as a colorless oil.[62]

To a solution of pinacol boronate ester **9** (0.95 g, 2.32 mmol, 1.0 equiv) in THF/H_2O (4:1, 40 mL), sodium periodate (1.5 g, 7.0 mmol, 3.0 equiv) was added at room temperature. The reaction mixture was stirred for 30 min and then 1 N HCl (1.7 mL, 1.7 mmol, 0.7 equiv) was added. The reaction was monitored by TLC until full conversion, then 50 mL H_2O was added and the mixture was extracted with ethyl acetate. The combined organic extracts were washed with water and brine, dried over Na_2SO_4 and concentrated in vacuo. The residue was purified by column chromatography on silica gel (DCM/MeOH = 50:1 to 20:1) to give the boronic acid **10** as a yellow oil in 73% yield.

A flame-dried 4.0 mL vial was charged with $Pd(TFA)_2$ (6.6 mg, 0.02 mmol, 10 mol%), benzoquinone (2.2 mg, 0.02 mmol, 10 mol%), CuI (11.4 mg, 0.06 mmol, 30 mol%), $AsPh_3$ (18.4 mg, 0.06 mmol, 30 mol%), **11** (65.4 mg, 0.2 mmol, 1.0 equiv, based on monomer) and substituted 4-fluorobenzoic anhydride (104.9 mg, 0.4 mmol, 2.0 equiv). The vial was directly transferred into a nitrogen-filled glovebox without caps. Then, K_2CO_3 (4.1 mg, 0.03 mmol, 15 mol%) and 4Å molecular sieves (400 mg) were added. In another 4.0 mL vial, NBE (15.0 mg, 0.16 mmol) was

dissolved in 2.0 mL dry toluene. 0.5 mL of this NBE solution (3.76 mg, 0.04 mmol, 20 mol%) was transferred into the reaction mixture, before more dry toluene (3.5 mL) was added. The vial was tightly sealed, transferred out of glovebox and stirred on a pie-block preheated to 100 ^{o}C for 14 hours. After completion of the reaction, the mixture was filtered through a thin pad of silica gel. The filter cake was washed with ethyl acetate and the combined filtrate was concentrated. The residue was loaded to a small amount of silica gel and then purified by flash column chromatography (hexane : ethyl acetate = 20 : 1) on silica gel to give **8** (51.9 mg) as a yellow oil in 64% yield.

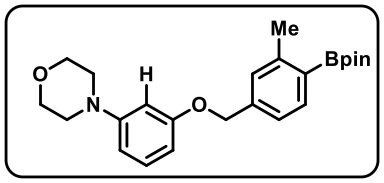

9: Colorless oil (60%). R_f = 0.2 (hexane/ethyl acetate = 10:1). **^{1}H NMR** (500 MHz, $CDCl_3$) δ 7.78 (d, *J* = 7.5 Hz, 1H), 7.25 – 7.20 (m, 2H), 7.18 (t, *J* = 8.5 Hz, 1H), 6.58 – 6.52 (m, 2H), 6.52 – 6.47 (m, 1H), 5.03 (s, 2H), 3.89 – 3.82 (m, 4H), 3.18 – 3.12 (m, 4H), 2.56 (s, 3H), 1.35 (s, 12H). **^{13}C NMR** (101 MHz, $CDCl_3$) δ 160.0, 152.8, 145.4, 139.9, 136.4, 130.0, 128.7, 123.7, 108.8, 105.7, 103.3, 83.6, 70.0, 67.0, 49.4, 25.0, 22.4. **IR** (KBr): υ 2976, 2856, 1610, 1579, 1495, 1450, 1340, 1191, 1065, 859, 829, 687, 665 cm^{-1}. **HRMS** (ESI): Calculated for $C_{24}H_{33}BNO_4$ ($M+H^+$): 410.2497, found: 410.2508.

Scheme 4.16. Preparation of 1t

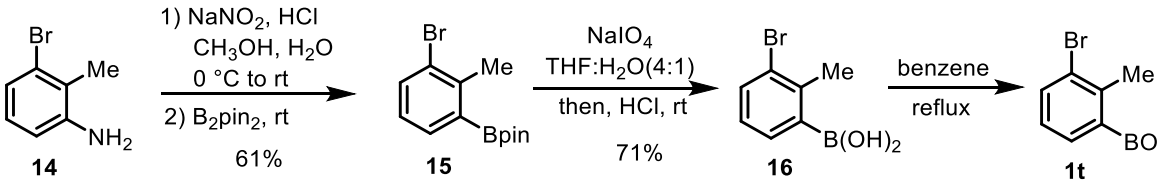

To a solution of aryl amine **14** (3.72 g, 20.0 mmol, 1.0 equiv) in MeOH (40 mL) was added HCl (20 mL, 60 mmol, 3.0 equiv) followed by H_2O (20 ml). This mixture was stirred for 2 min, and $NaNO_2$ (1.52g, 22 mmol, 1.1 equiv) in 10 mL H_2O was added dropwise. This mixture was stirred at 0–5 °C for 30 min followed by adding B_2pin_2 (15.2 g, 60 mmol, 3.0 equiv) in MeOH (40 mL) solution. This reaction mixture was stirred for another 1h. Then H_2O (30 mL) was added and the mixture was extracted with DCM (100 mL× 3). The combined organic layers were washed with sat. $NaHCO_3$, dried over Na_2SO_4 and concentrated in vacuo. The crude residue was purified by column chromatography on silica gel (hexane/ethyl acetate = 40:1) to give the corresponding pinacolboronate ester **15** as a yellow oil (3.56 g) in 61%.[65]

To a solution of pinacol boronate ester **15** (1.04 g, 3.5 mmol, 1.0 equiv) in THF/H_2O (4:1, 40 mL), sodium periodate (1.89 g, 8.8 mmol, 2.5 equiv) was added at room temperature. The reaction mixture was stirred for 30 min and then 2 N HCl (0.9 mL, 1.8 mmol, 0.5 equiv) was added. After 4 h, the reaction mixture was extracted with ethyl acetate (3 × 30 mL), and the combined organic extracts were washed with water and brine, dried over Na_2SO_4 and concentrated in vacuo. The residue was purified by column chromatography on silica gel (DCM/ethyl acetate = 10:1 to 5:1) to give the boronic acid **16** (752 mg) as a yellow oil in 71% yield.

In a 100 mL round bottom flask was added arylboronic acid **16** (15.0 mmol) and a stir bar. Then benzene (50 mL) was added and the solution was refluxed for 12 h using Dean-Stark trap to remove water. The solution was allowed to cool to room temperature and the solvent was removed under vacuum to give the desired arylboroxine as a white solid. After washed with hexane for three time and dried under vacuum, the arylboroxine product **1t** was directly used in the acylation reaction without further purification.

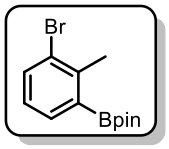

CAS: 2057523-47-2

15: Yellow oil (61%). R_f = 0.2 (hexane/ethyl acetate = 40:1). **^{1}H NMR** (400 MHz, $CDCl_3$) δ 7.69 (dd, *J* = 7.4, 1.4 Hz, 1H), 7.61 (dd, *J* = 7.9, 1.4 Hz, 1H), 7.05-7.01 (m,1H), 2.63 (s, 3H), 1.35 (s, 12H). **^{13}C NMR** (101 MHz, $CDCl_3$) δ 134.9, 134.8, 126.4, 83.8, 24.8, 22.1.

Scheme 4.17. Preparation of 1u

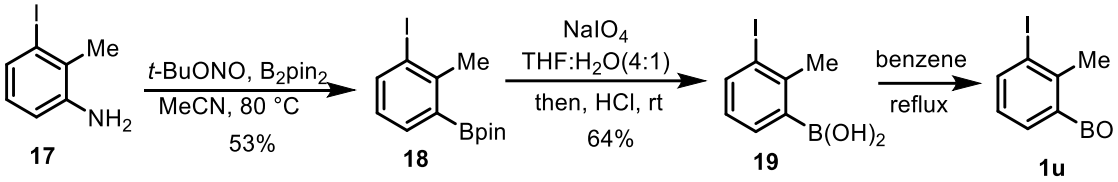

B_2pin_2 (140 mg, 0.55mmol, 1.1 equiv) and aniline **17** (117 mg, 0.5 mmol, 1.0 equiv) were weighed in a 25 mL round-bottom flask. MeCN (2mL) and *t*-BuONO (86 mg, 0.75 mmol, 1.5 equiv) were then added in succession. The resulting reaction solution was stirred for 3 h at 80 °C (N_2 evolution completed within 5 to 15 min). The solution was then concentrated under reduced pressure, and the crude residue was purified by flash chromatography (silica gel, hexane/EtOAc = 40:1) to give pinacol boronate ester **18** (91.2 mg) in 53% yield. The following deprotection and dean-stark procedure was same as preparing **1t**.[66]

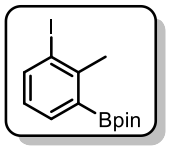

18: Yellow oil (53%). R_f = 0.2 (hexane/ethyl acetate = 40:1). **^{1}H NMR** (400 MHz, $CDCl_3$) δ 7.91 (dd, *J* = 7.8, 1.4 Hz, 1H), 7.75 (dd, *J* = 7.4, 1.4 Hz, 1H), 6.86 (t, *J* = 7.6 Hz, 1H), 2.69 (s, 3H), 1.36 (s, 12H).**^{13}C NMR** (101 MHz, $CDCl_3$) δ 146.8, 141.6, 138.2, 135.7, 126.5, 103.6, 83.8, 27.8, 24.8.

IR (KBr): υ 3056, 2977, 1583, 1422, 1344, 1270, 1251, 1212, 1141, 1111, 1068 cm^{-1}. **HRMS** (ESI): Calculated for $C_{13}H_{19}BIO_2$ ($M+H^+$): 345.0517, found: 345.0510.

Scheme 4.18. Sequential Functionalization of 1t

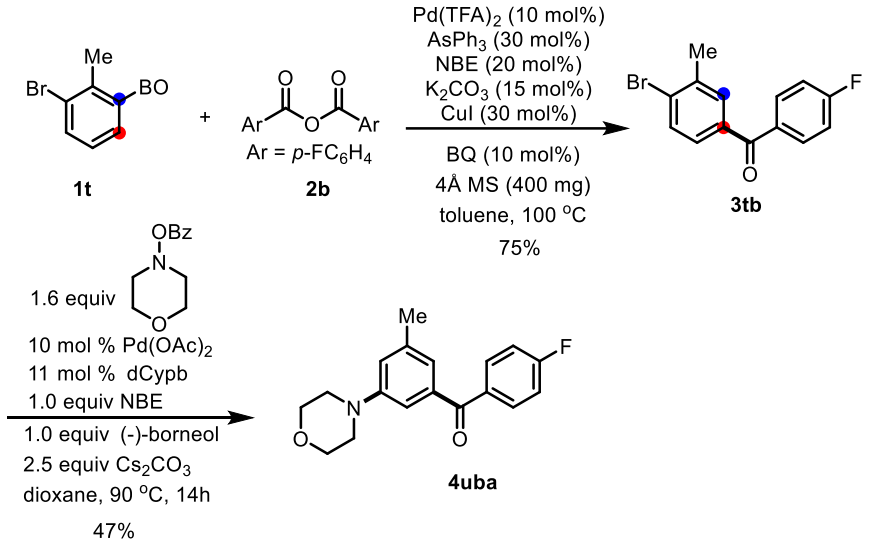

A flame-dried 4.0 mL vial was charged with $Pd(TFA)_2$ (9.9 mg, 0.03 mmol, 10 mol%), benzoquinone (3.3 mg, 0.03 mmol, 10 mol%), CuI (17.1 mg, 0.09 mmol, 30 mol%), $AsPh_3$ (27.6 mg, 0.09 mmol, 30 mol%), **1t** (59.1mg, 0.3 mmol, 1.0 equiv, based on monomer) and substituted 4-fluorobenzoic anhydride (157.4mg, 0.6 mmol, 2.0 equiv). The vial was directly transferred into a nitrogen-filled glovebox without caps. Then, K_2CO_3 (6.2 mg, 0.045 mmol, 15 mol%) and 4Å molecular sieves (400 mg) were added. In another 4.0 mL vial, NBE (16.9 mg, 0.18 mmol) was dissolved in 1.5 mL dry toluene. 0.5 mL of this NBE solution (5.64 mg, 0.06 mmol, 20 mol%) was transferred into the reaction mixture, before another 3.5 mL dry toluene was added. The vial was tightly sealed, transferred out of glovebox and stirred on a pie-block preheated to 100 °C for 14 hours. After completion of the reaction, the mixture was filtered through a thin pad of silica gel. The filter cake was washed with ethyl acetate and the combined filtrate was concentrated. The

residue was loaded to a small amount of silica gel and then purified by flash column chromatography (hexane : ethyl acetate = 40 : 1) on silica gel to give **3tb** (65.8mg) as a white solid in 75% yield .

A flame-dried 4 mL vial was charged with **3tb** (43.9 mg, 0.15 mmol, 1.0 equiv), O-benzoyl hydroxylamine (49.7 mg, 0.24 mmol, 1.6 equiv), (-)-borneol (23.1 mg, 0.15mmol, 1.0 equiv), norbornene (14.1 mg, 0.15 mmol, 1.0 equiv) and $Pd(OAc)_2$ (3.4 mg, 0.015 mmol, 0.1 equiv). The vial was sealed in the air and transferred into a nitrogen-filled glovebox. dCypb (7.5 mg, 0.017 mmol, 0.11 equiv) and Cs_2CO_3 (123 mg, 0.38 mmol, 2.5 equiv) were added to the vial in the glove box. 1,4-dioxane (1.5 ml) was added, and the vial was then sealed with PTFE lined cap in the glovebox. The resulting mixture was stirred at room temperature for 10 minutes until the all the $Pd(OAc)_2$ was fully dissolved. The vial was subsequently transferred out of glovebox and stirred on a pie-block preheated to 90 ^oC for 14 hours. After completion of the reaction, the mixture was filtered through a thin pad of celite. The filter cake was washed with ethyl acetate, and the combined filtrate was concentrated. The residue was directly purified by flash column chromatography (hexane : ethyl acetate = 10 : 1) on silica gel to yield the desired **4uba** (21.2 mg) as a yellow oil in 47% yield.[67]

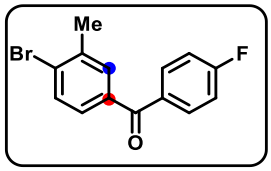

3tb: White solid (75%). m. p. = 81–83 ^{o}C. R_f = 0.2 (hexane/ethyl acetate = 20:1). **^{1}H NMR** (400 MHz, $CDCl_3$) δ 7.85 – 7.78 (m, 2H), 7.65 (d, *J* = 4.8 Hz, 1H), 7.64 (s, 1H), 7.41 (ddd, *J* = 8.3, 2.1, 0.7 Hz, 1H), 7.20 – 7.13 (m, 2H), 2.46 (s, 3H). **^{13}C NMR** (101 MHz, $CDCl_3$) δ 194.4, 165.4 (d, *J* = 254.6 Hz), 138.4, 136.5, 133.5 (d, *J* = 3.1 Hz), 132.5 (d, *J* = 9.2 Hz), 132.4, 131.8, 129.9, 128.6,

115.5 (d, *J* = 21.9 Hz), 23.0. **^{19}F NMR** (470 MHz, $CDCl_3$) δ -105.52. **IR** (KBr): υ 3043, 2924, 1651, 1590, 1431, 1342, 1269, 1207,1109, 1063 cm^{-1}. **HRMS** (CI): Calculated for $C_{14}H_{11}BrFO$ ($M+H^+$): 292.9972, found: 292.9966.

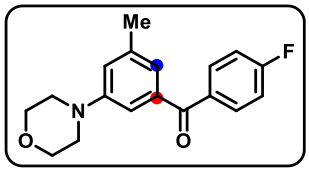

4uba: Yellow oil (47%). R_f = 0.1 (hexane/ethyl acetate = 10:1). **^{1}H NMR** (400 MHz, $CDCl_3$) δ 7.91 – 7.79 (m, 2H), 7.20 – 7.12 (m, 2H), 7.11 (s, 1H), 7.02 (s, 1H), 6.95 (s, 1H), 3.90 – 3.82 (m, 4H), 3.25 – 3.14 (m, 4H), 2.37 (s, 3H). **^{13}C NMR** (101 MHz, $CDCl_3$) δ 195.8, 165.3 (d, *J* = 253.9 Hz), 151.3, 138.9, 138.4, 134.1 (d, *J* = 3.1 Hz), 132.6 (d, *J* = 9.1 Hz), 122.4, 120.3, 115.4 (d, *J* = 21.8 Hz), 113.8, 66.8, 49.1, 21.8. **^{19}F NMR** (470 MHz, $CDCl_3$) δ -106.20. **IR** (KBr): υ 3066, 2960, 1659, 1596, 1505, 1449, 1408, 1353, 1287, 1236, 1155, 1070 cm^{-1}. **HRMS** (ESI): Calculated for $C_{18}H_{19}FNO_2$($M+H^+$): 300.1394, found: 300.1402.

Scheme 4.19. Sequential Functionalization of 1u

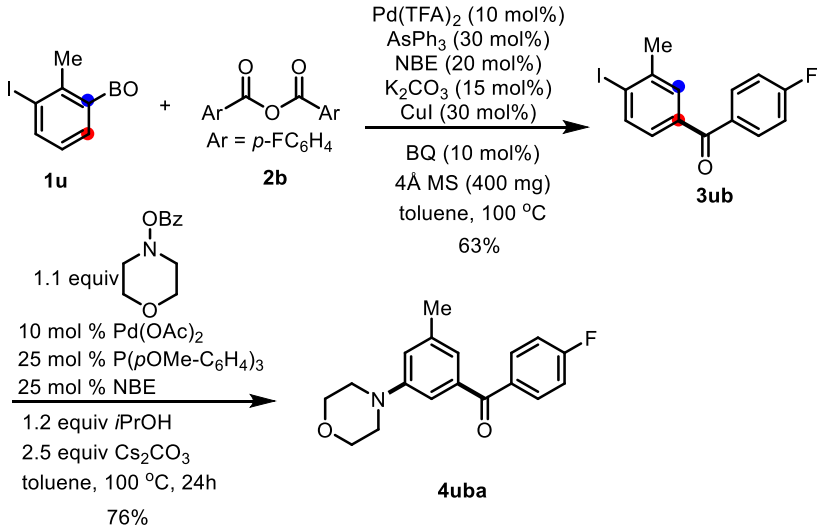

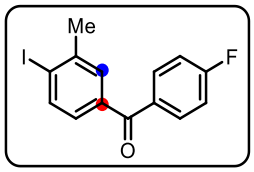

3ub: White solid (63%). m. p. = 93–95 ^{o}C. R_f = 0.2 (hexane/ethyl acetate = 20:1). **^{1}H NMR** (500 MHz, $CDCl_3$) δ 7.93 (d, *J* = 8.1 Hz, 1H), 7.85 – 7.78 (m, 2H), 7.61 (d, *J* = 2.1 Hz, 1H), 7.22 (dd, *J* = 8.1, 2.2 Hz, 1H), 7.16 (t, *J* = 8.6 Hz, 2H), 2.50 (s, 3H). **^{13}C NMR** (126 MHz, $CDCl_3$) δ 194.52, 165.44 (d, *J* = 254.6 Hz), 141.98, 139.03, 137.46, 133.51 (d, *J* = 3.1 Hz), 132.53 (d, *J* = 9.2 Hz), 130.41, 128.38, 115.62, 106.82, 28.11. **^{19}F NMR** (470 MHz, $CDCl_3$) δ -105.46. **IR** (KBr): υ 3053, 2988, 1652, 1597, 1503, 1466, 1437, 1289, 1262, 1228, 1156 cm^{-1}. **HRMS** (ESI): Calculated for $C_{14}H_{11}FIO$ ($M+H^+$): 340.9833, found: 340.9830.

4.5 NMR Spectra

Figure 4.1. ^{1}H NMR Spectrum of 2-Mentylphenylboronic Acid from Combi-Blocks

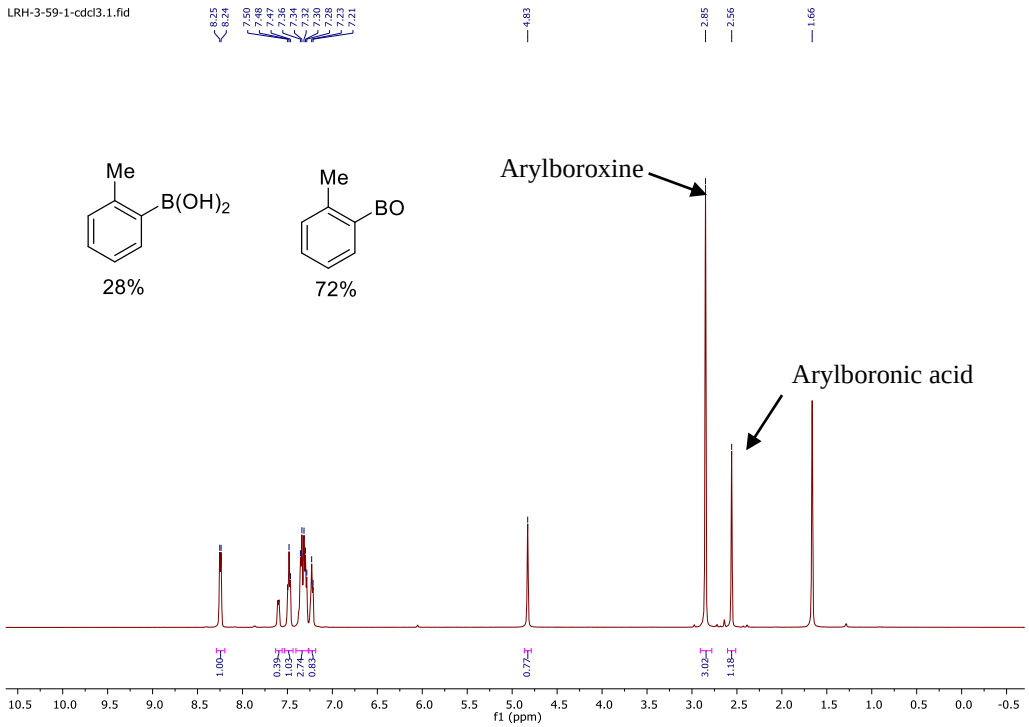

Figure 4.2. ^{1}H NMR Spectrum of 2-Mentylphenylboronic Acid from Sigma-Aldrich

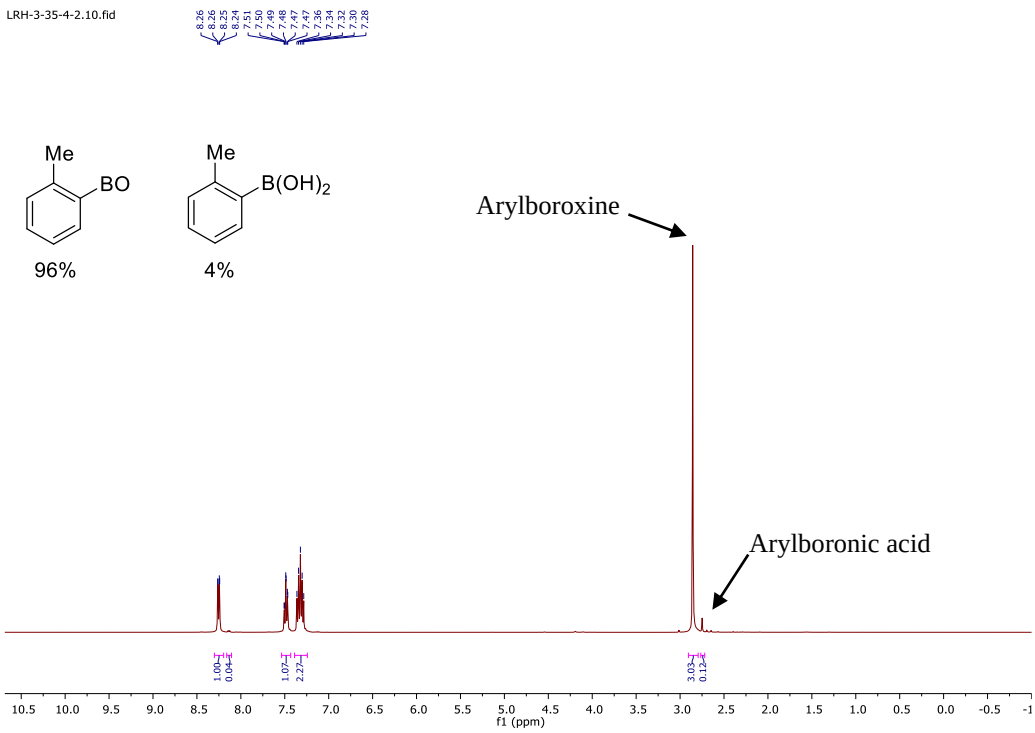

Figure 4.3. ^{1}H NMR Spectrum of 2-Mentylphenylboronic Acid from <u>Oakwood</u>

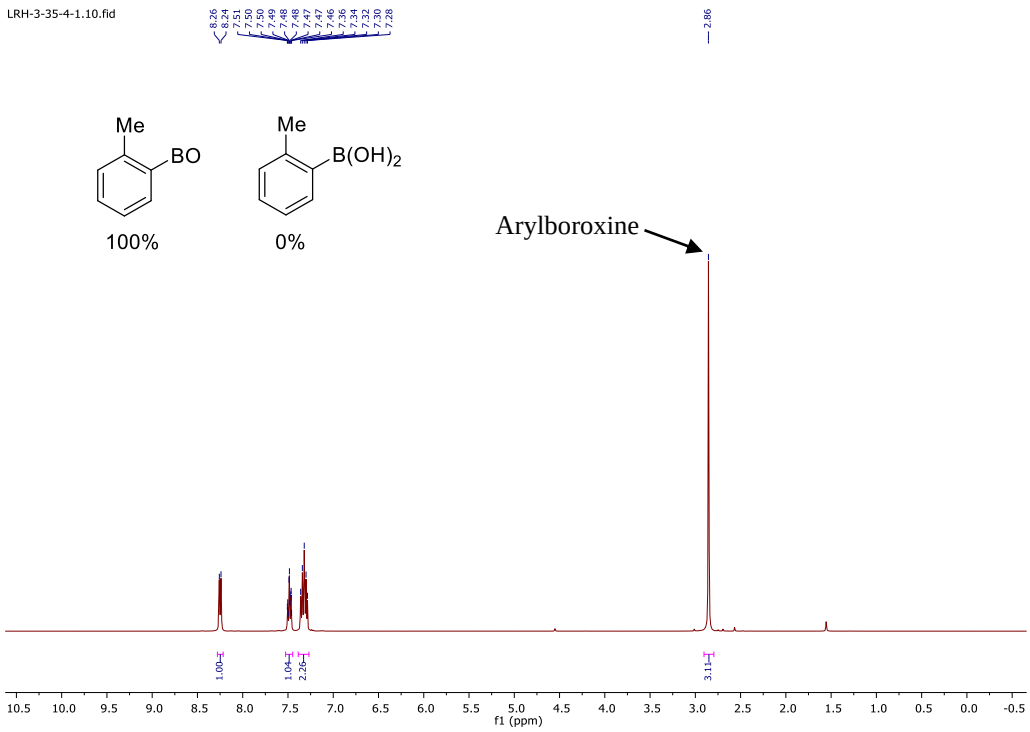

Figure 4.4. ^{1}H NMR Spectrum of 2o

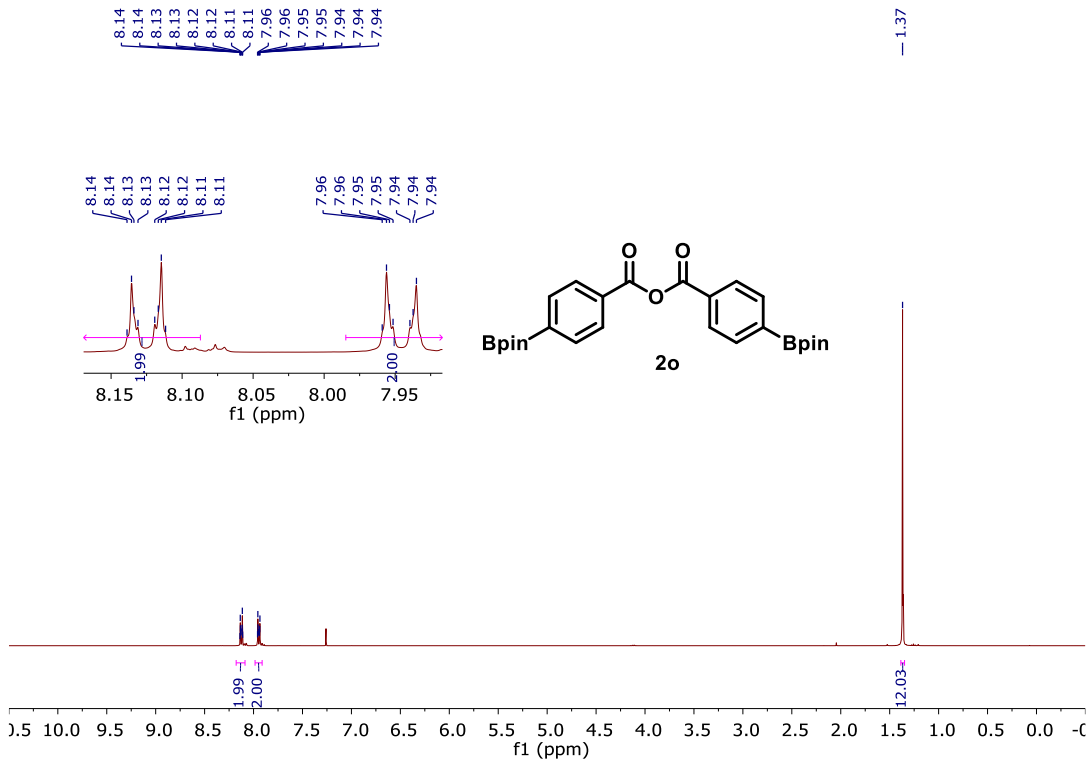

Figure 4.5. ^{13}C NMR Spectrum of 2o

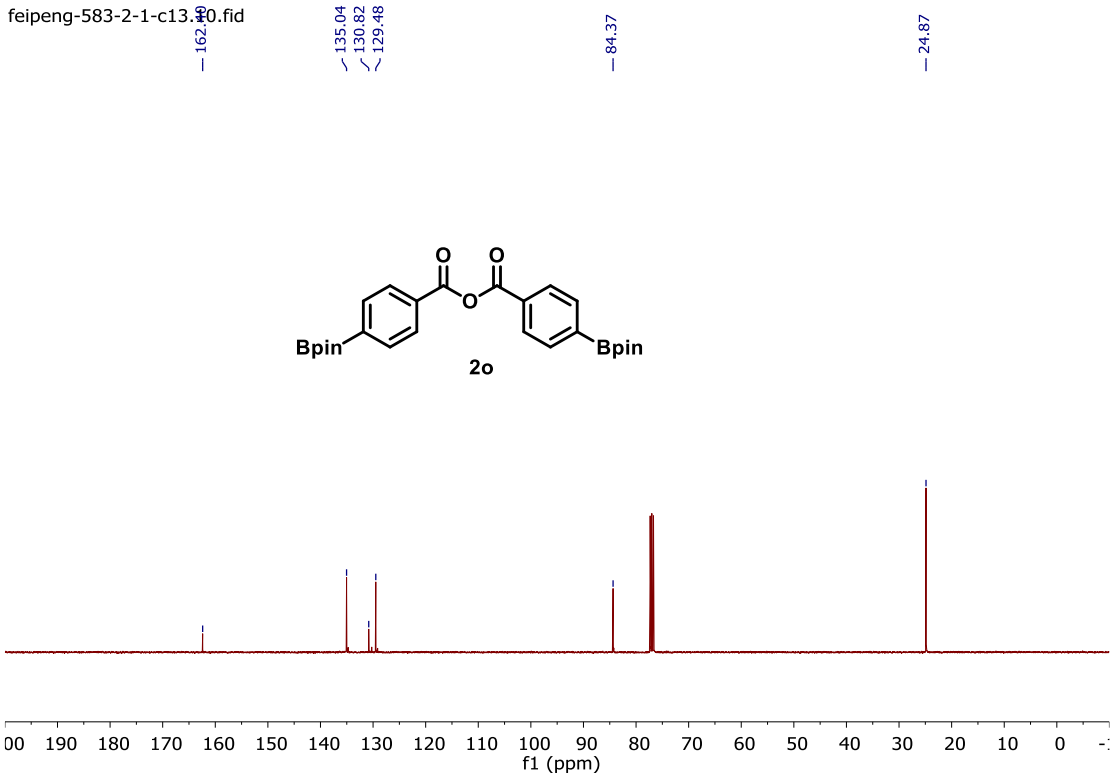

Figure 4.6. ^{1}H NMR Spectrum of 3aa

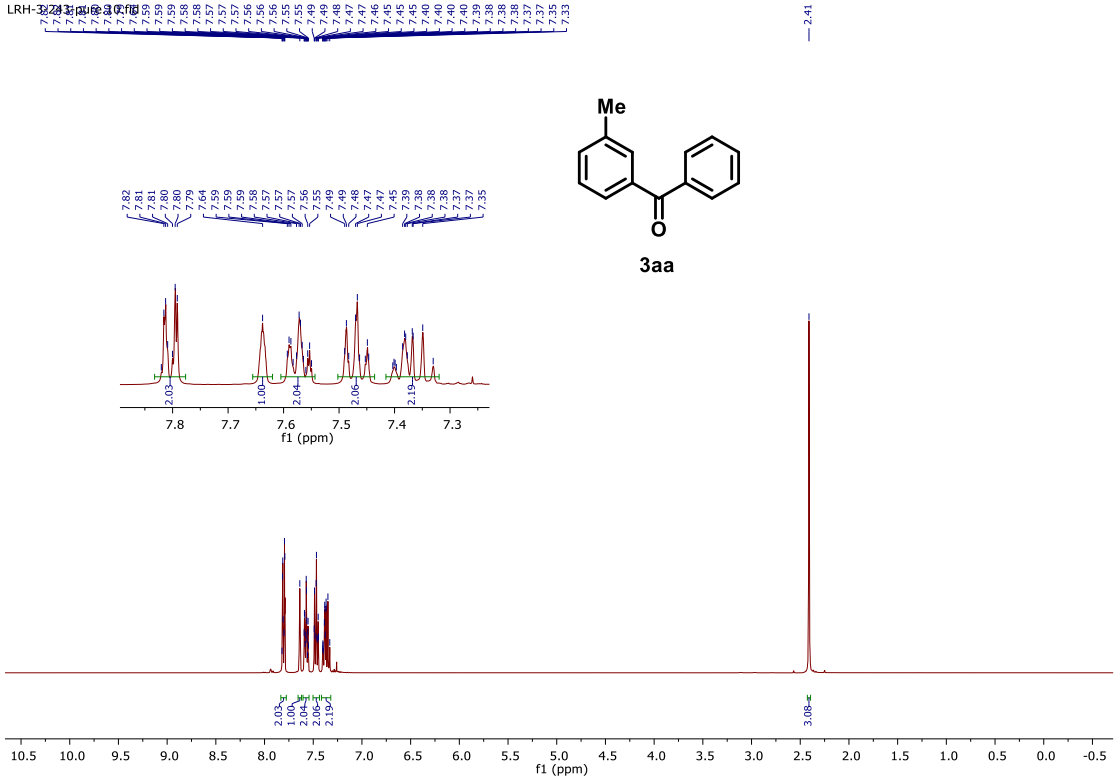

Figure 4.7. ^{13}C NMR Spectrum of 3aa

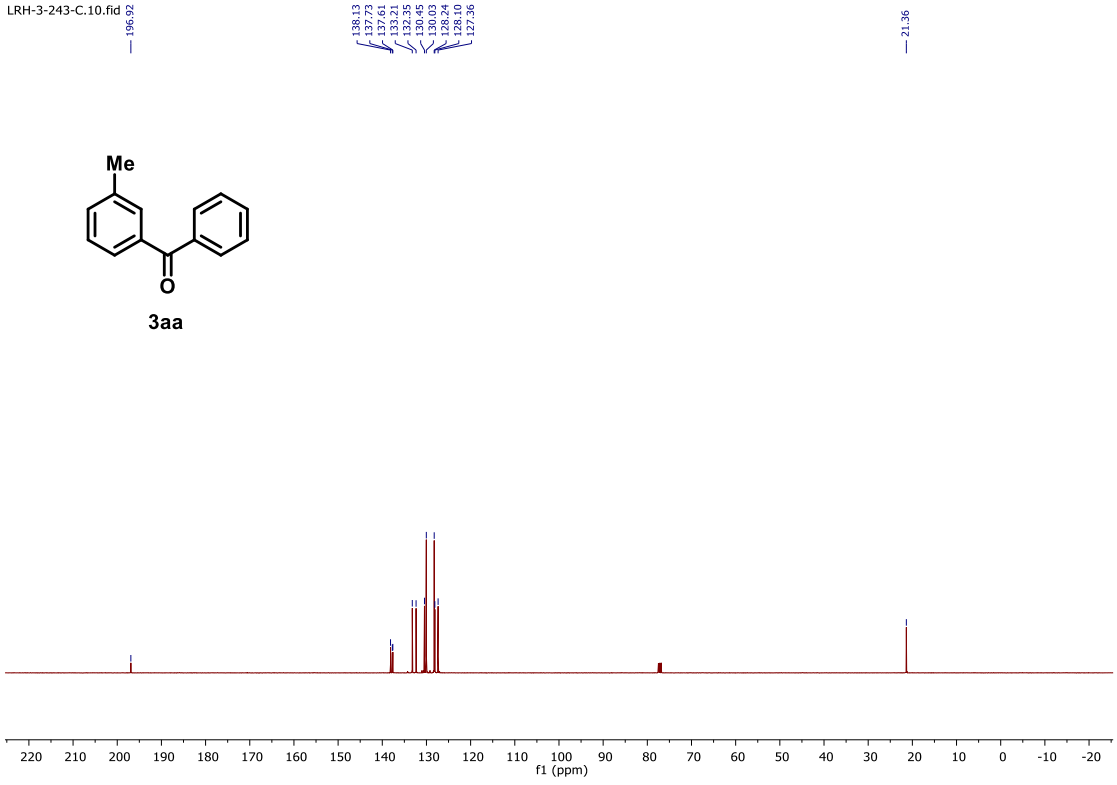

Figure 4.8. ^{1}H NMR Spectrum of 3ab

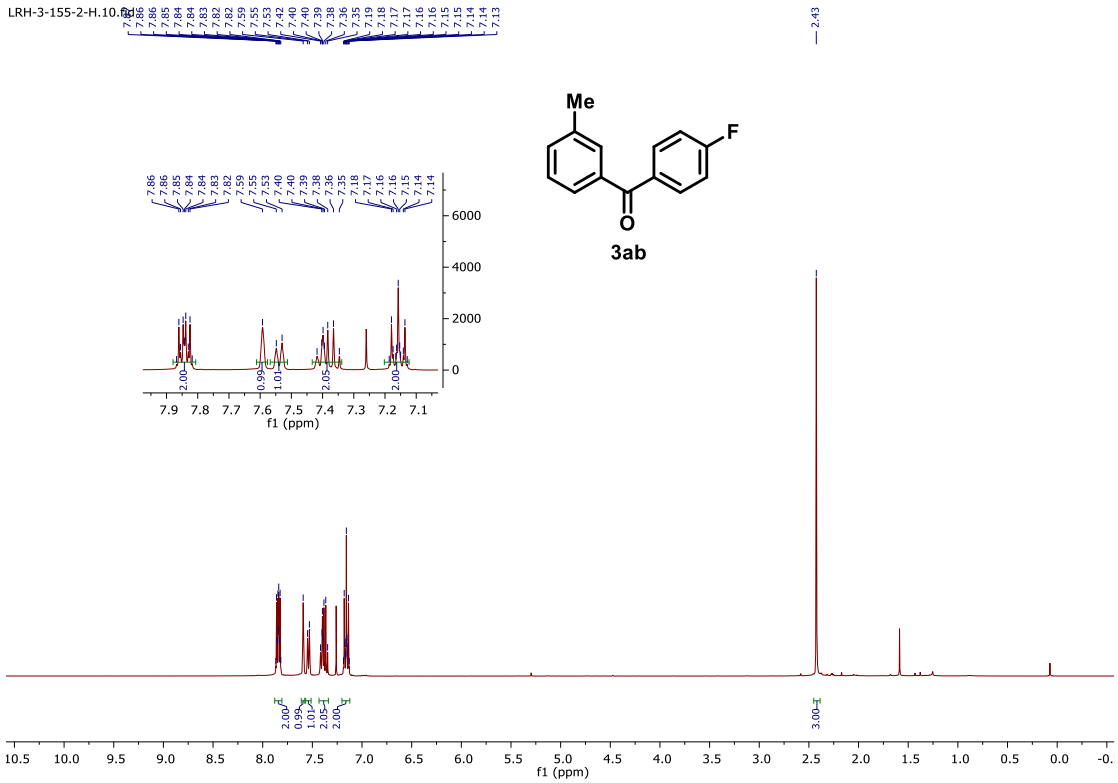

Figure 4.9. ^{13}C NMR Spectrum of 3ab

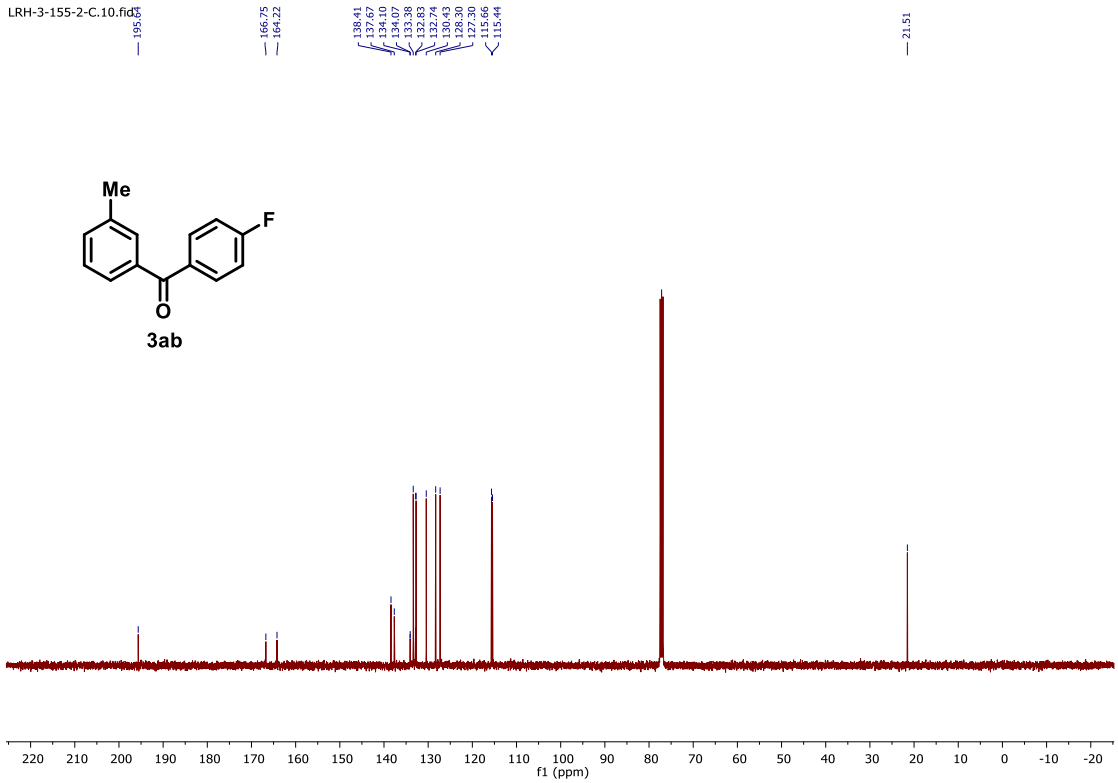

Figure 4.10. ^{1}H NMR Spectrum of 3ac

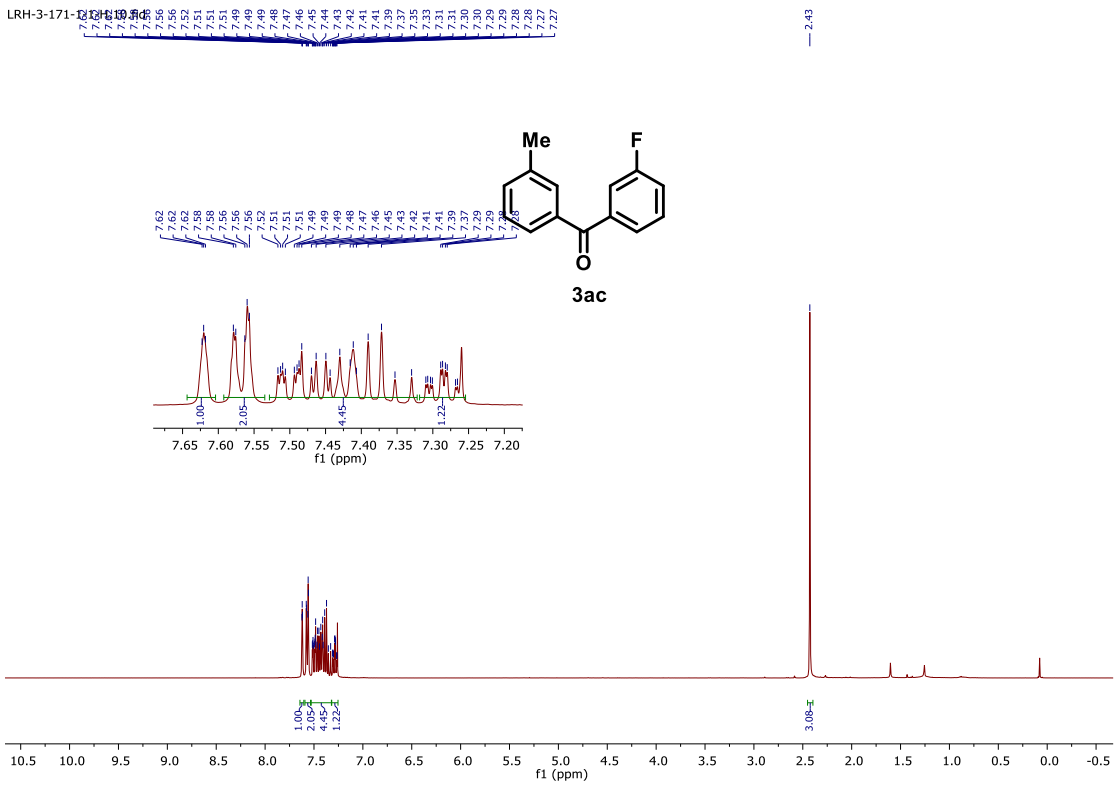

Figure 4.11. ^{13}C NMR Spectrum of 3ac

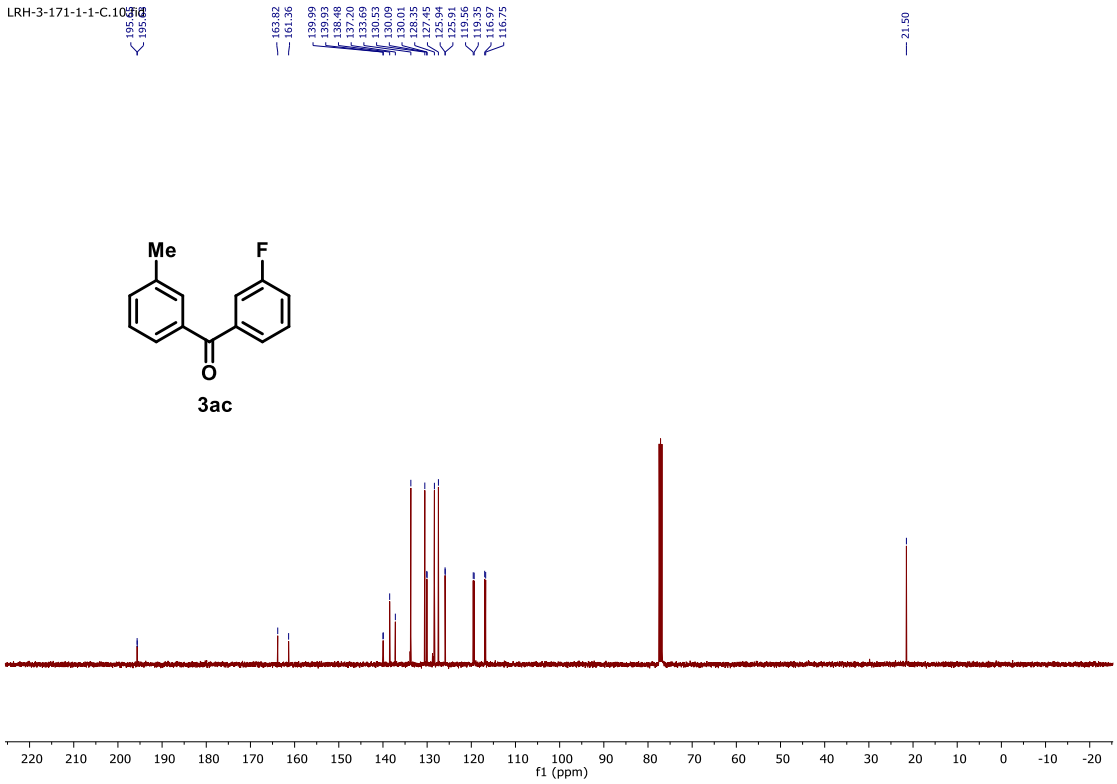

Figure 4.12. ^{1}H NMR Spectrum of 3ad

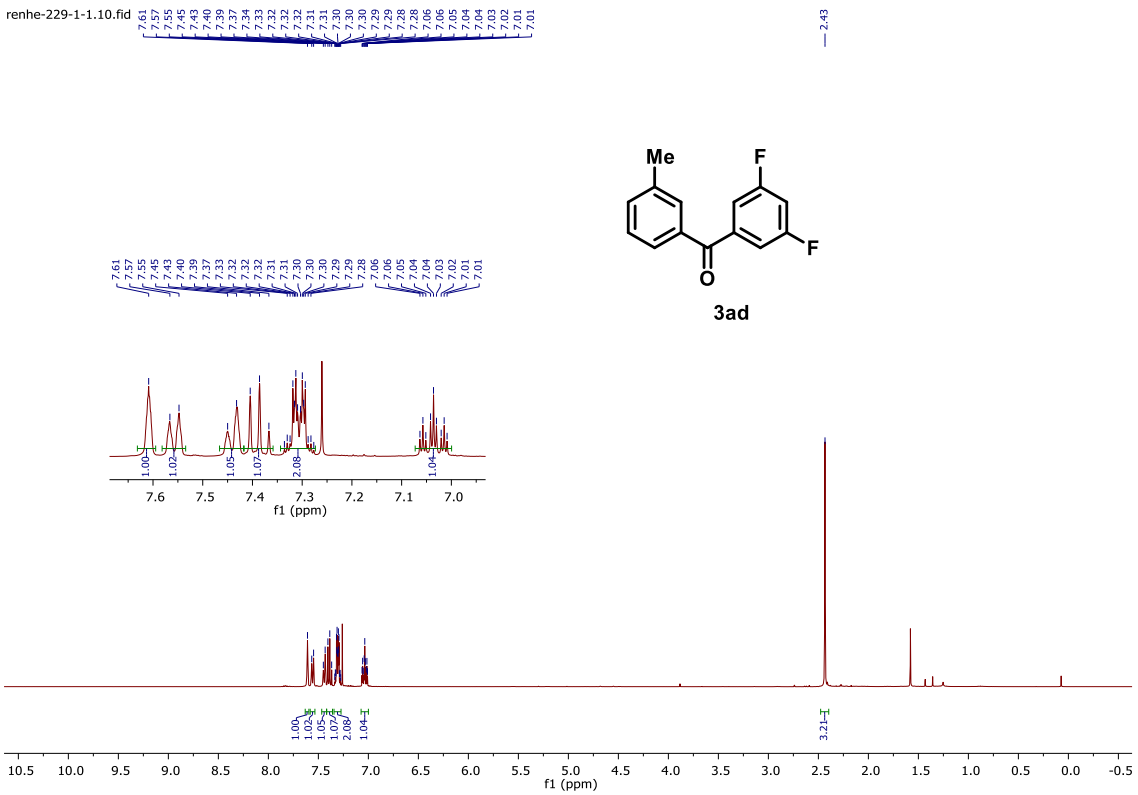

Figure 4.13. ^{13}C NMR Spectrum of 3ad

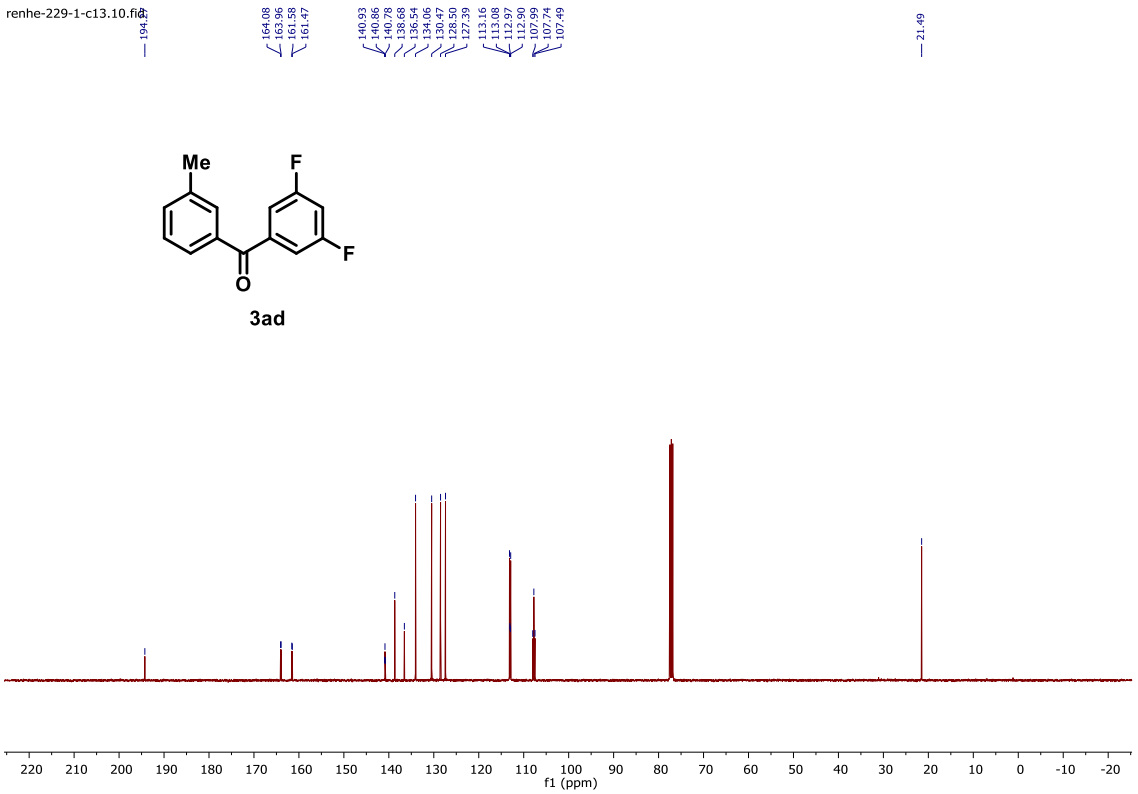

Figure 4.14. ^{19}F NMR Spectrum of 3ad

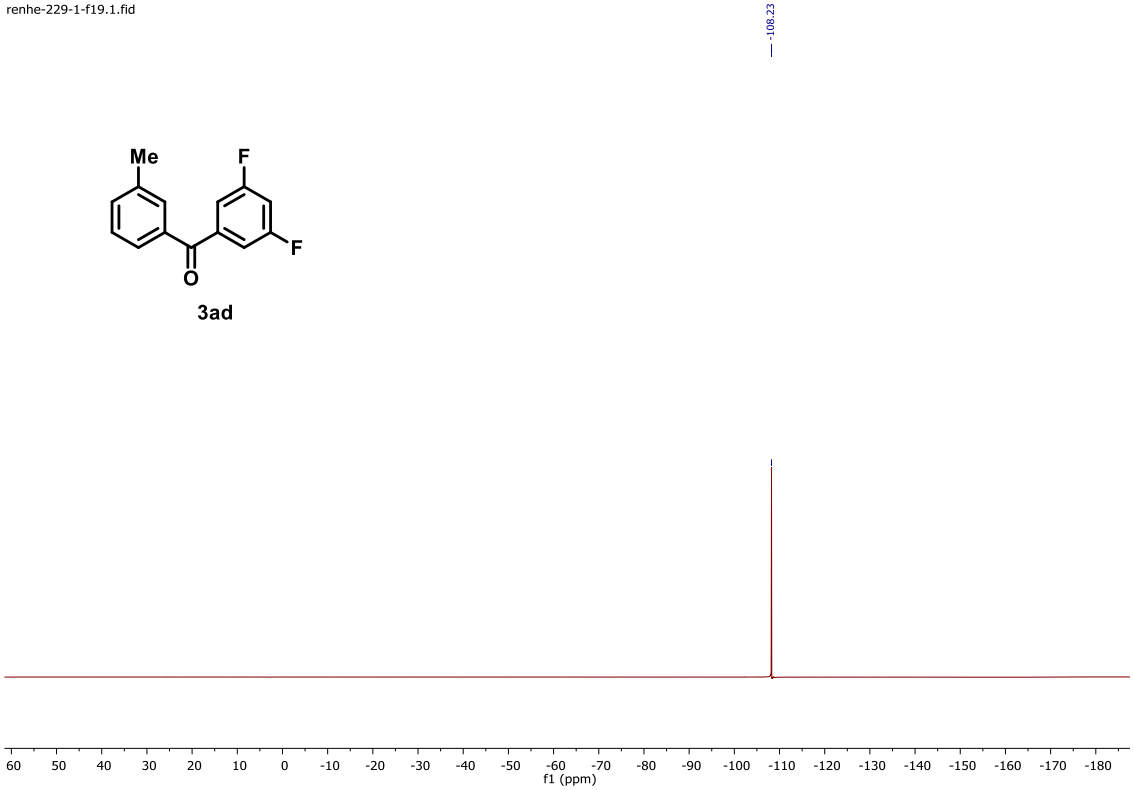

Figure 4.15. ^{1}H NMR Spectrum of 3ae

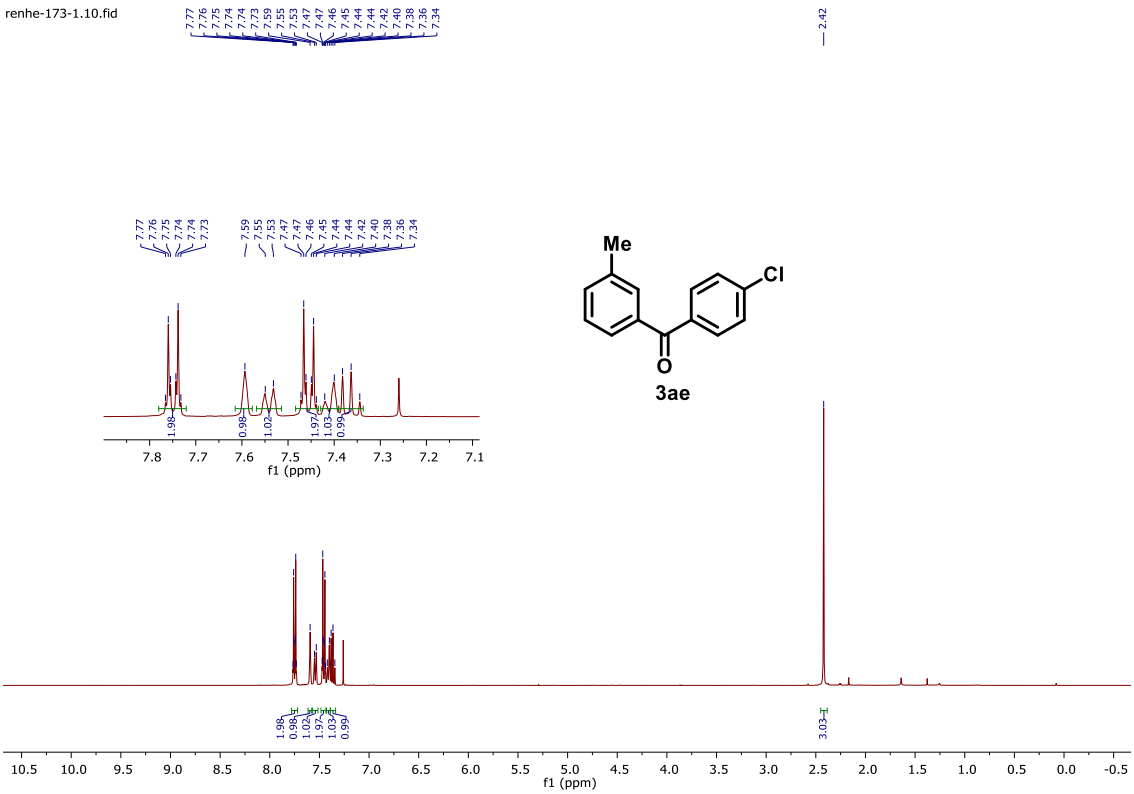

Figure 4.16. ^{13}C NMR Spectrum of 3ae

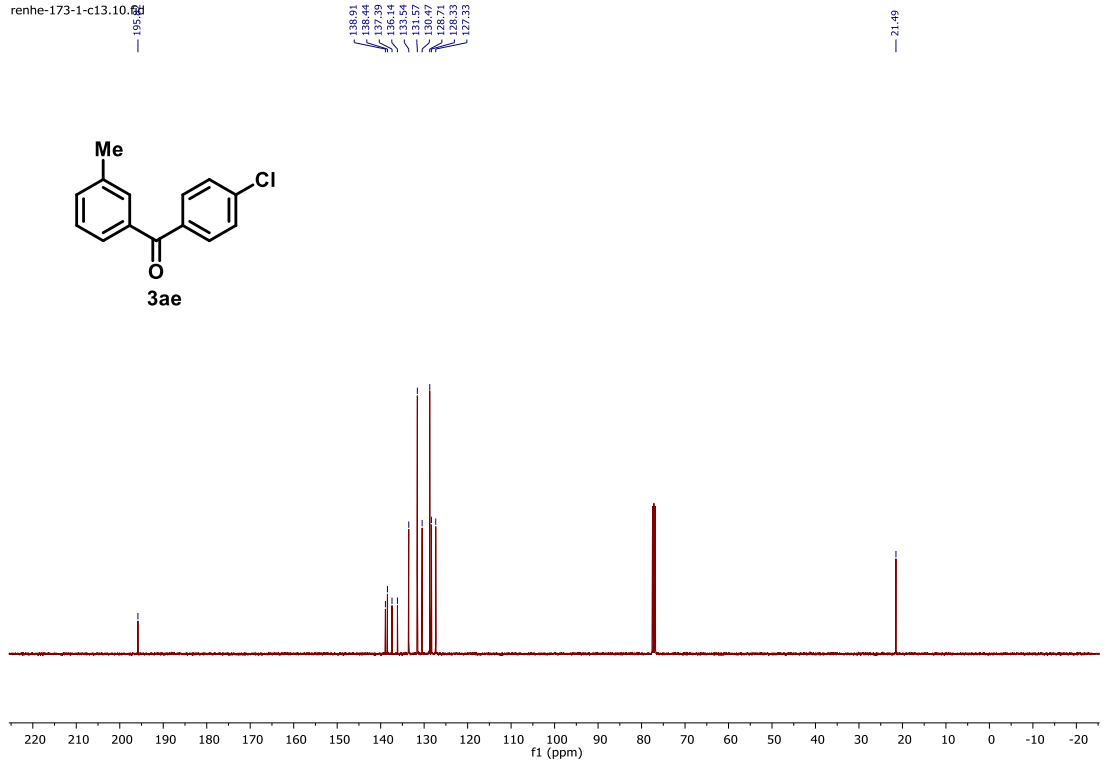

Figure 4.17. ^{1}H NMR Spectrum of 3af

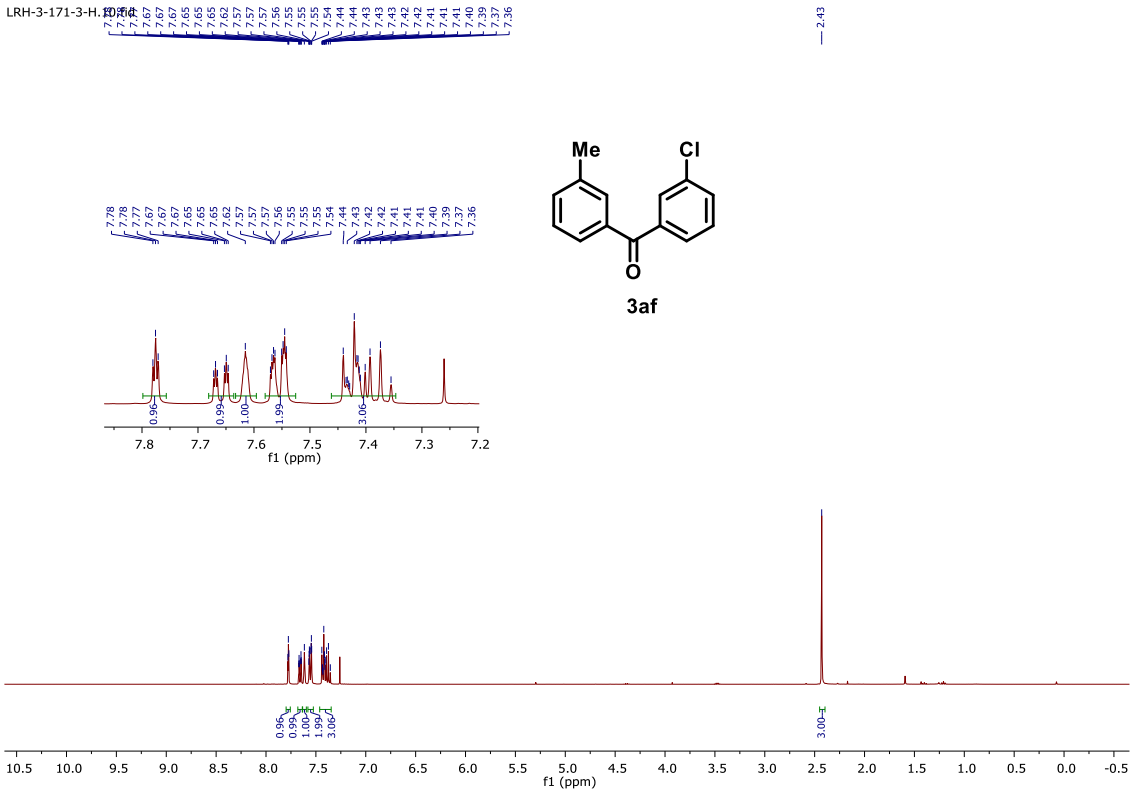

Figure 4.18. ^{13}C NMR Spectrum of 3af

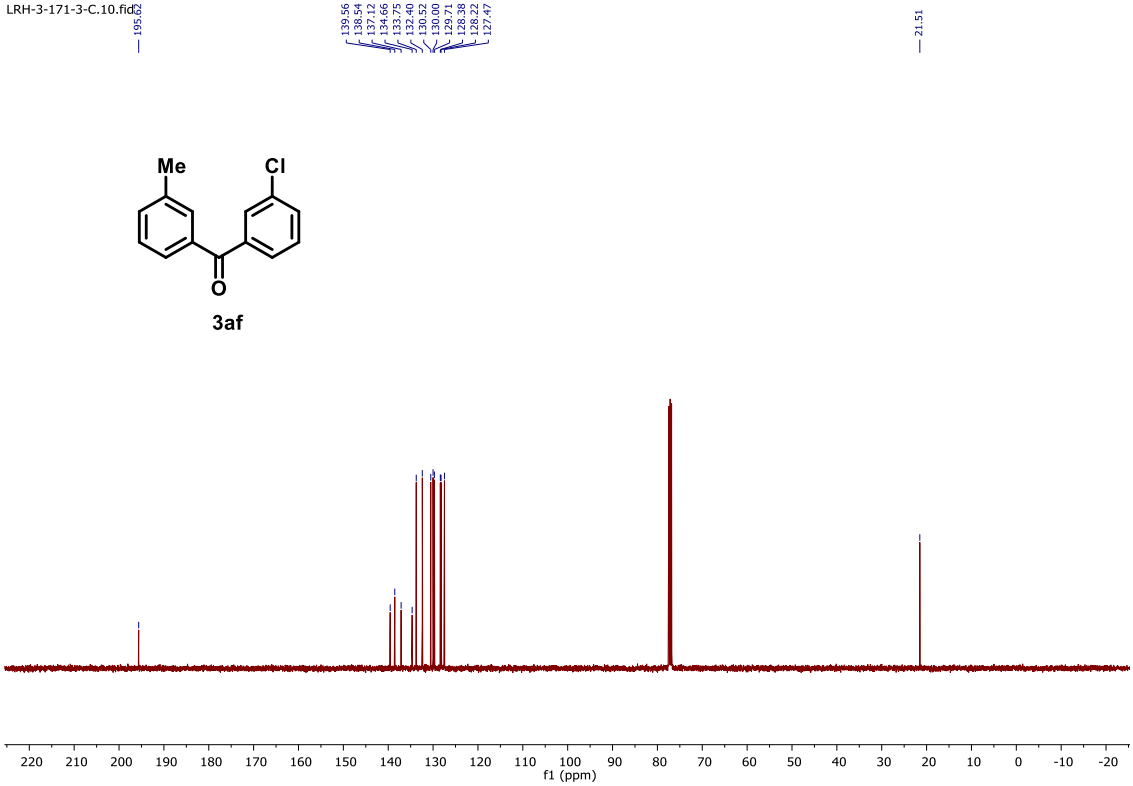

Figure 4.19. ^{1}H NMR Spectrum of 3ag

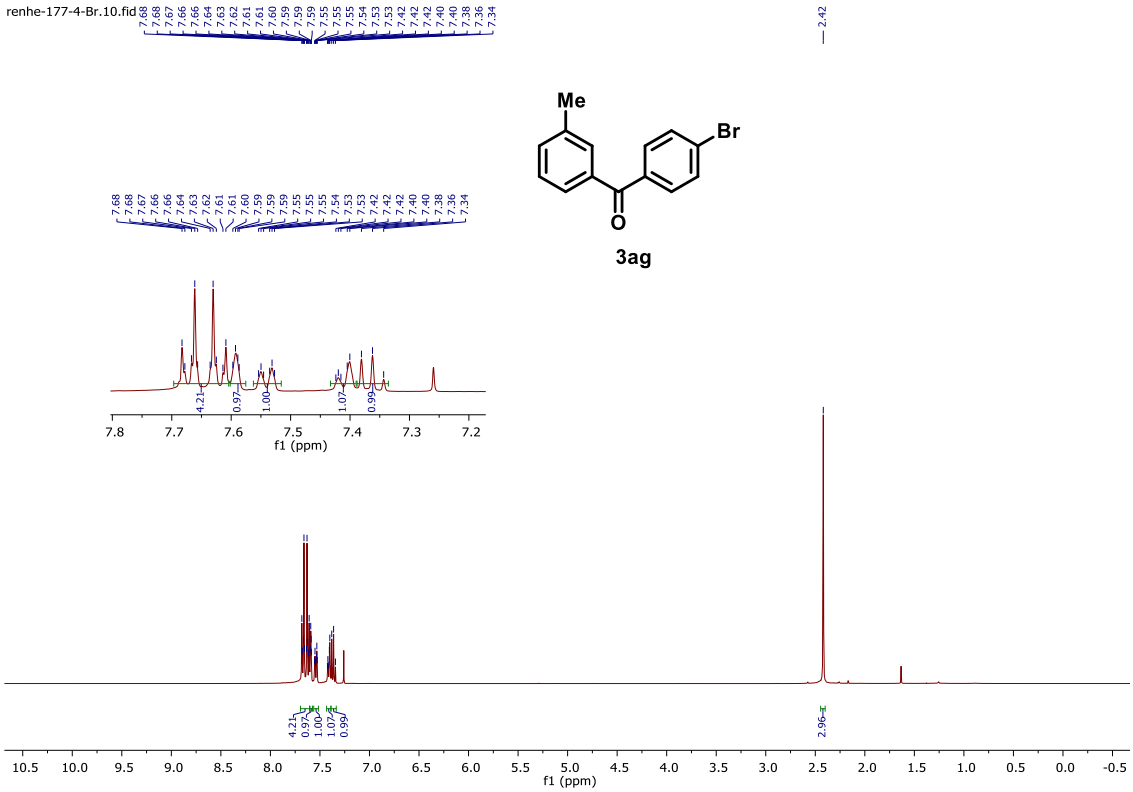

Figure 4.20. ^{13}C NMR Spectrum of 3ag

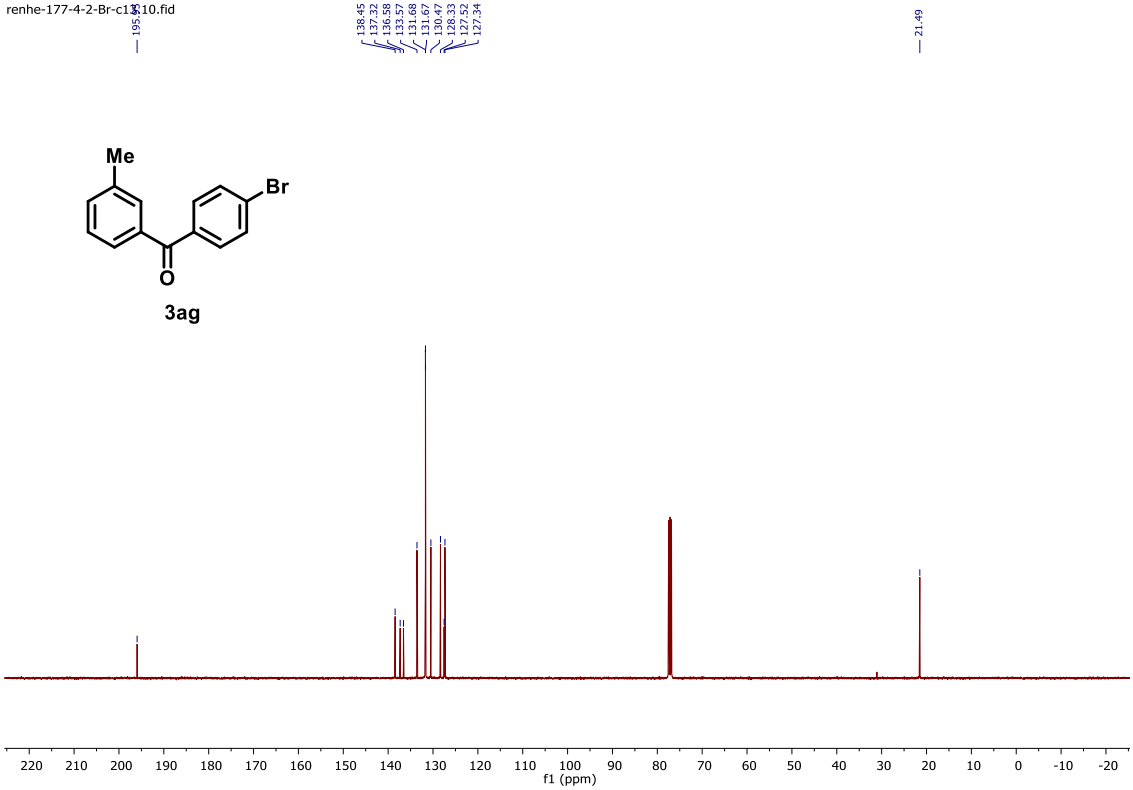

Figure 4.21. ^{1}H NMR Spectrum of 3ah

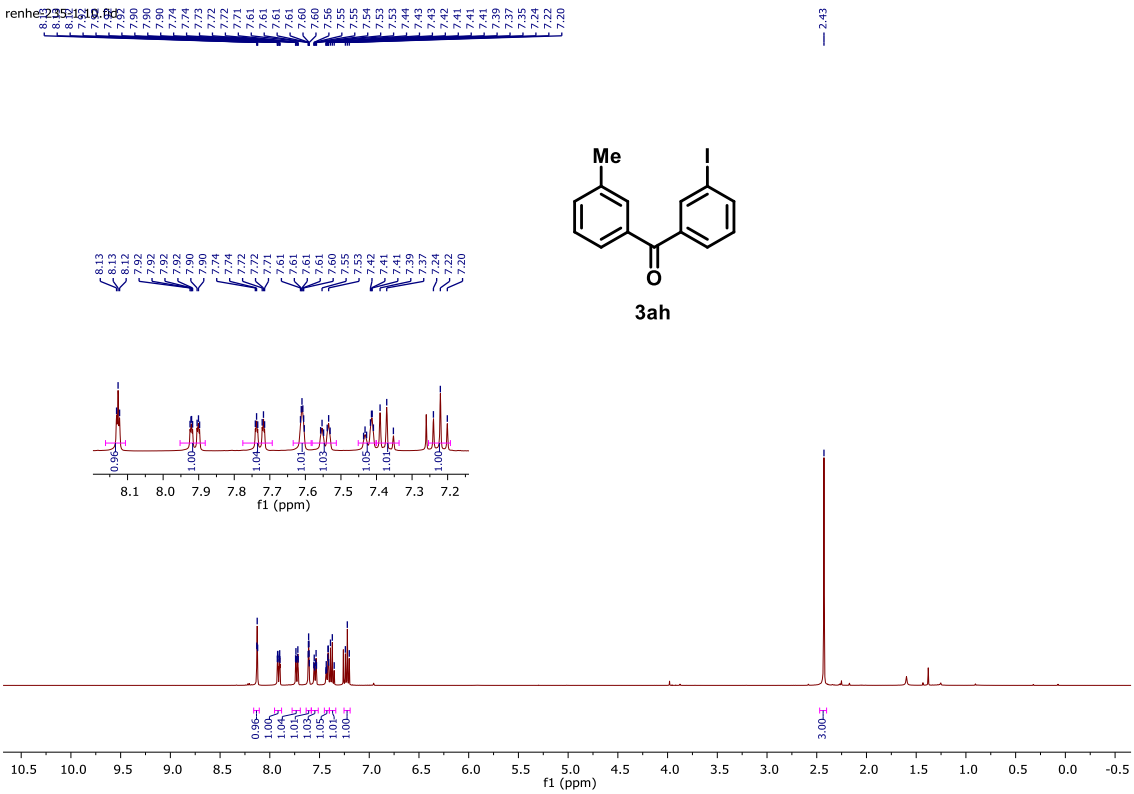

Figure 4.22. ^{13}C NMR Spectrum of 3ah

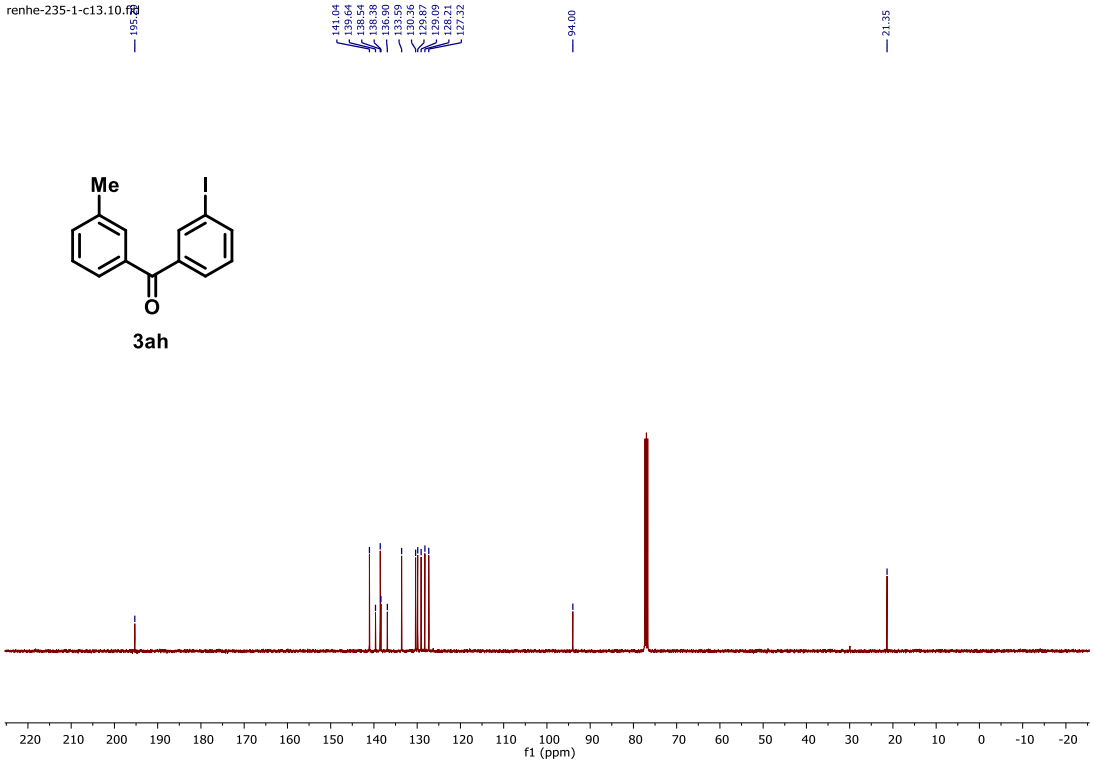

Figure 4.23. ^{1}H NMR Spectrum of 3ai

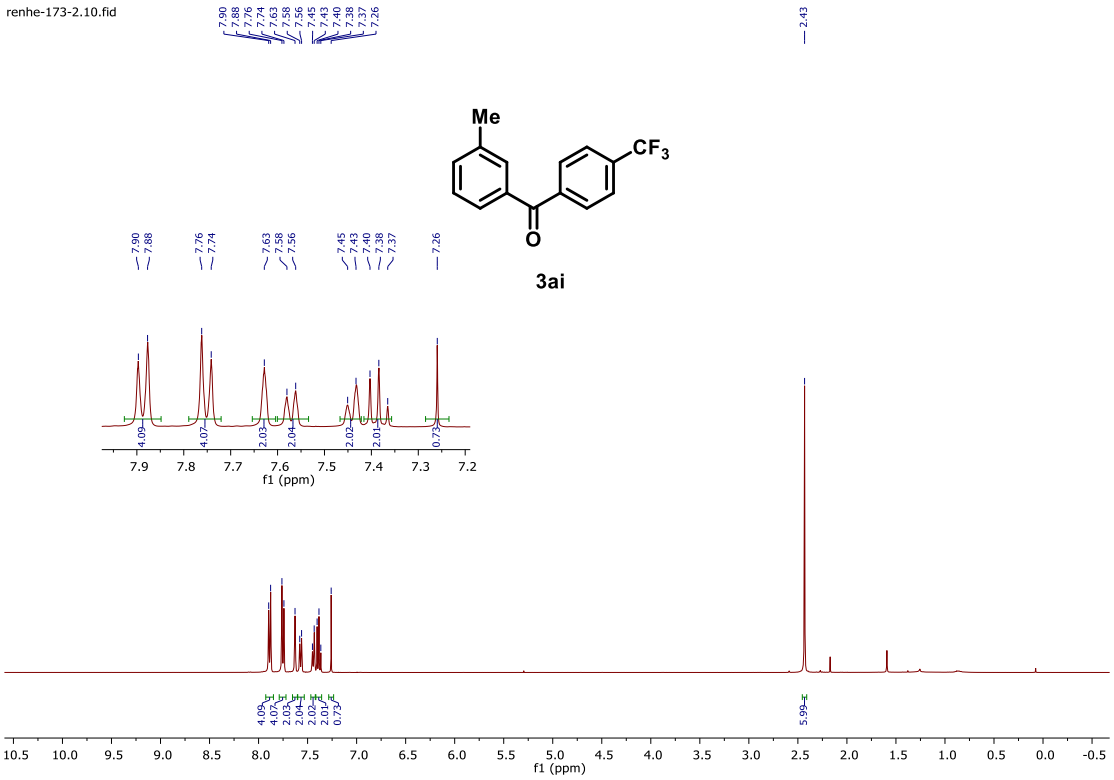

Figure 4.24. ^{13}C NMR Spectrum of 3ai

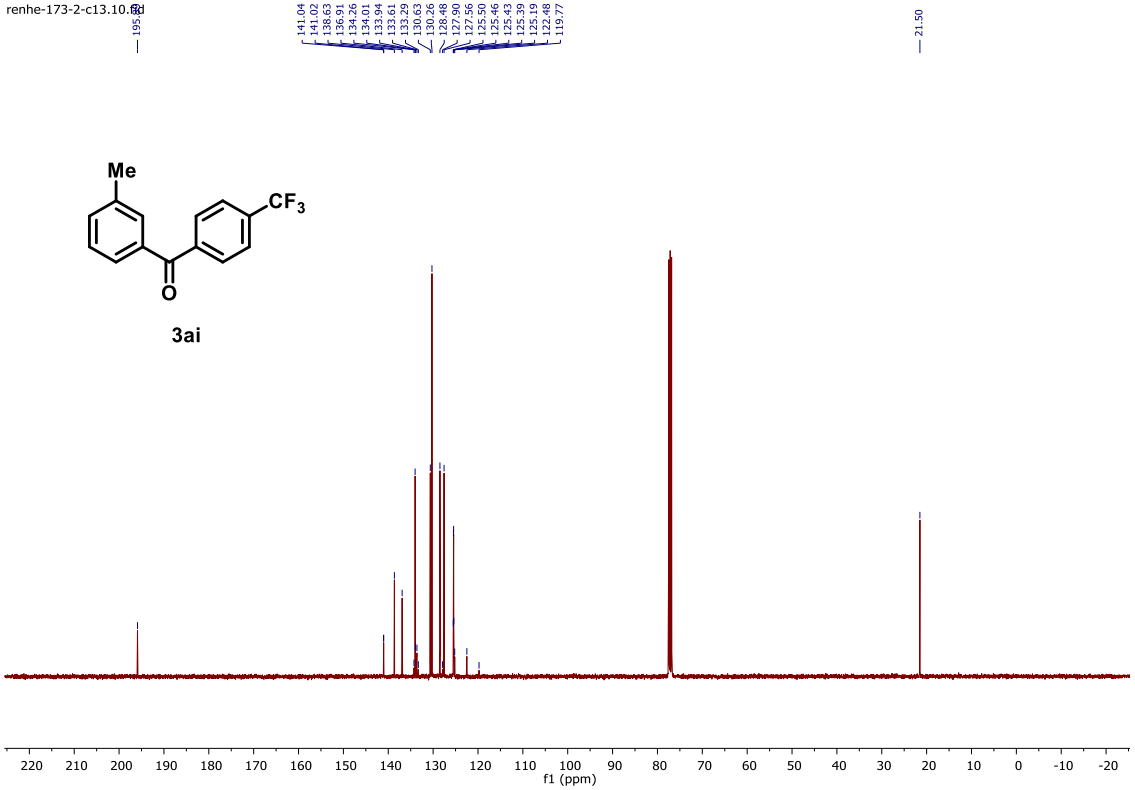

Figure 4.25. ^{19}F NMR Spectrum of 3ai

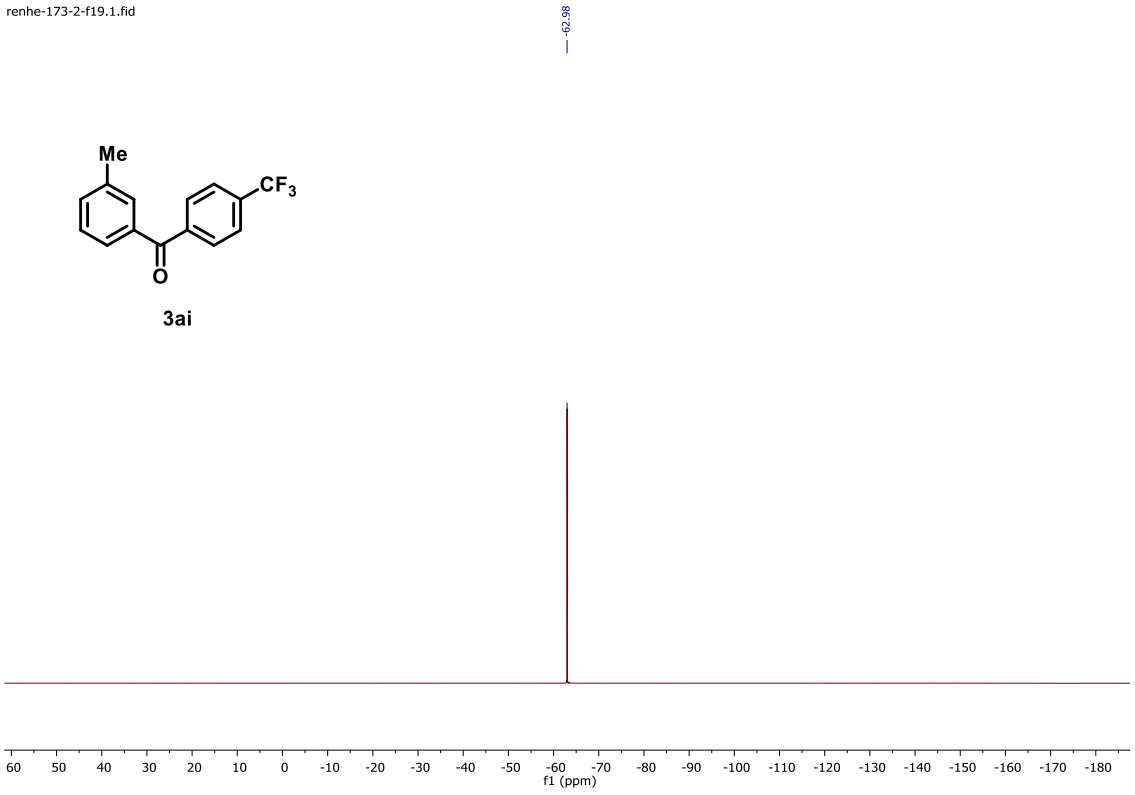

Figure 4.26. ^{1}H NMR Spectrum of 3aj

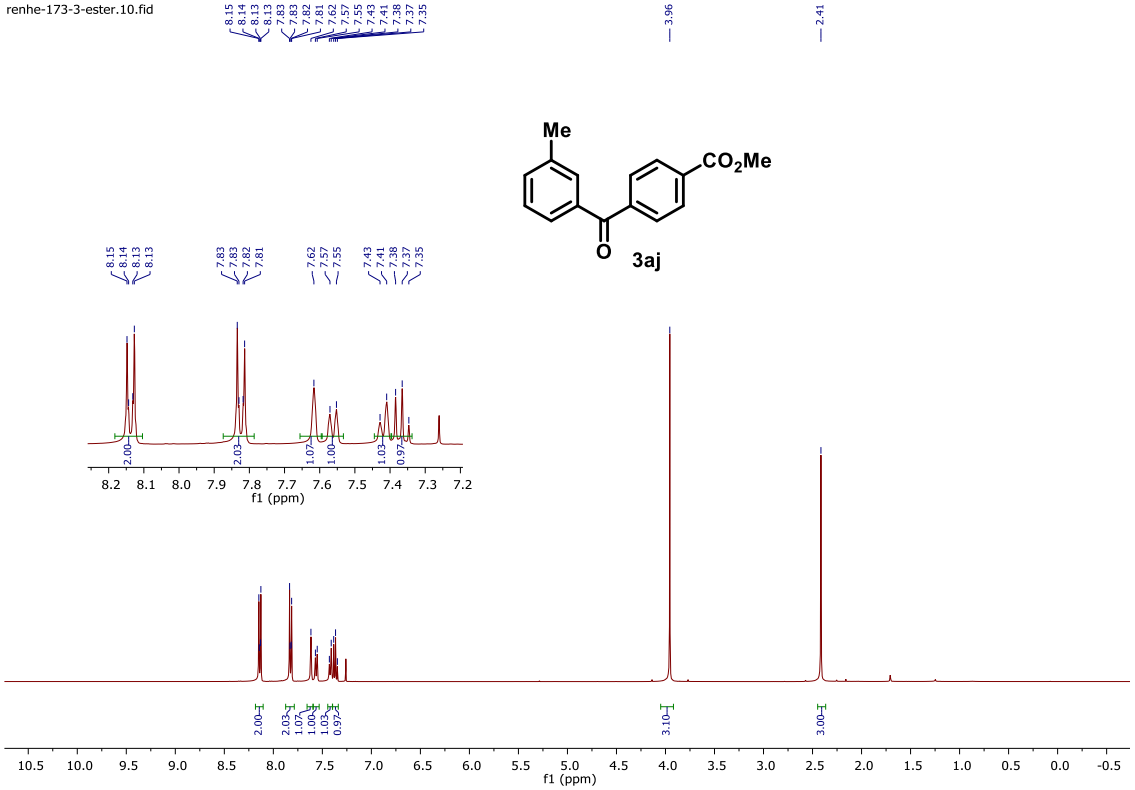

Figure 4.27. ^{13}C NMR Spectrum of 3aj

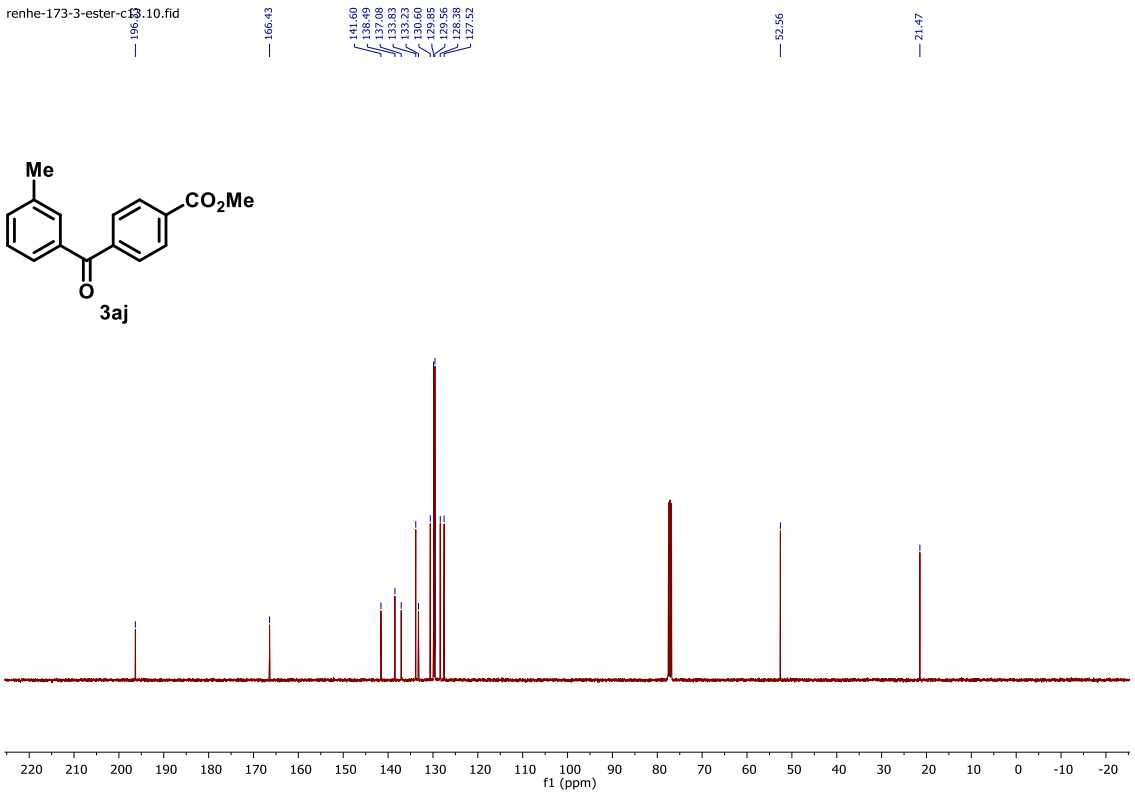

Figure 4.28. ^{1}H NMR Spectrum of 3ak

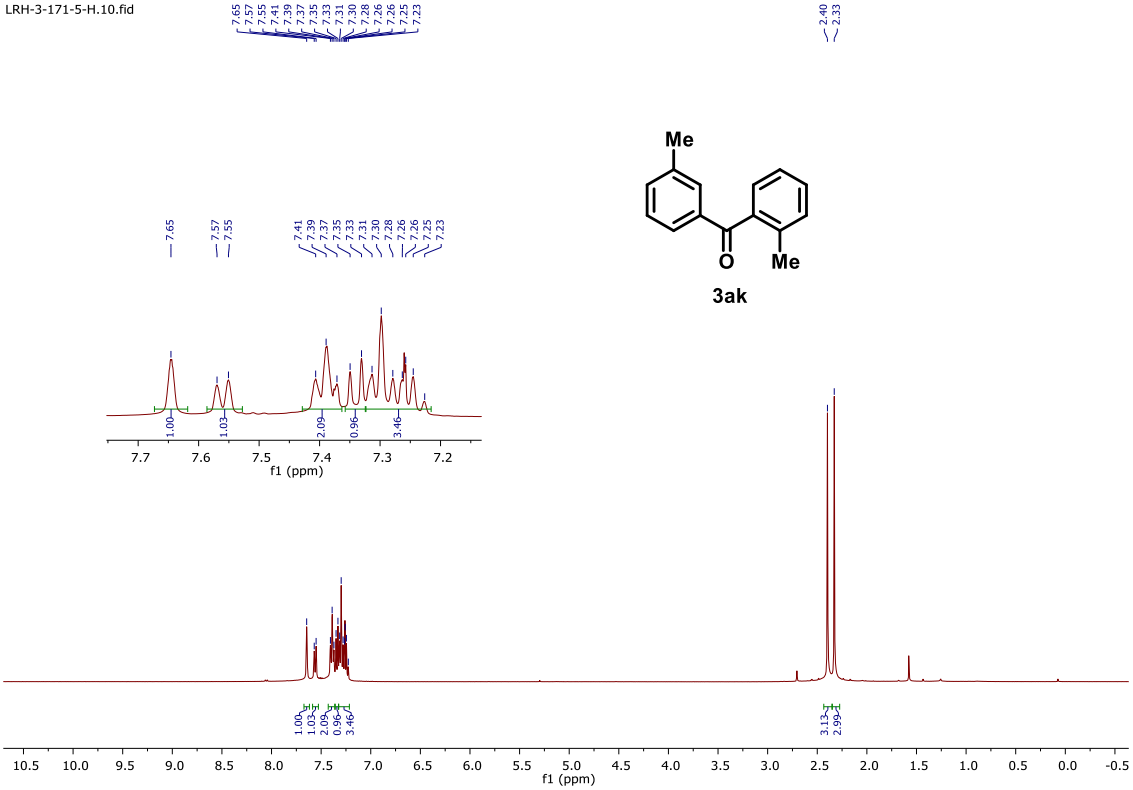

Figure 4.29. ^{13}C NMR Spectrum of 3ak

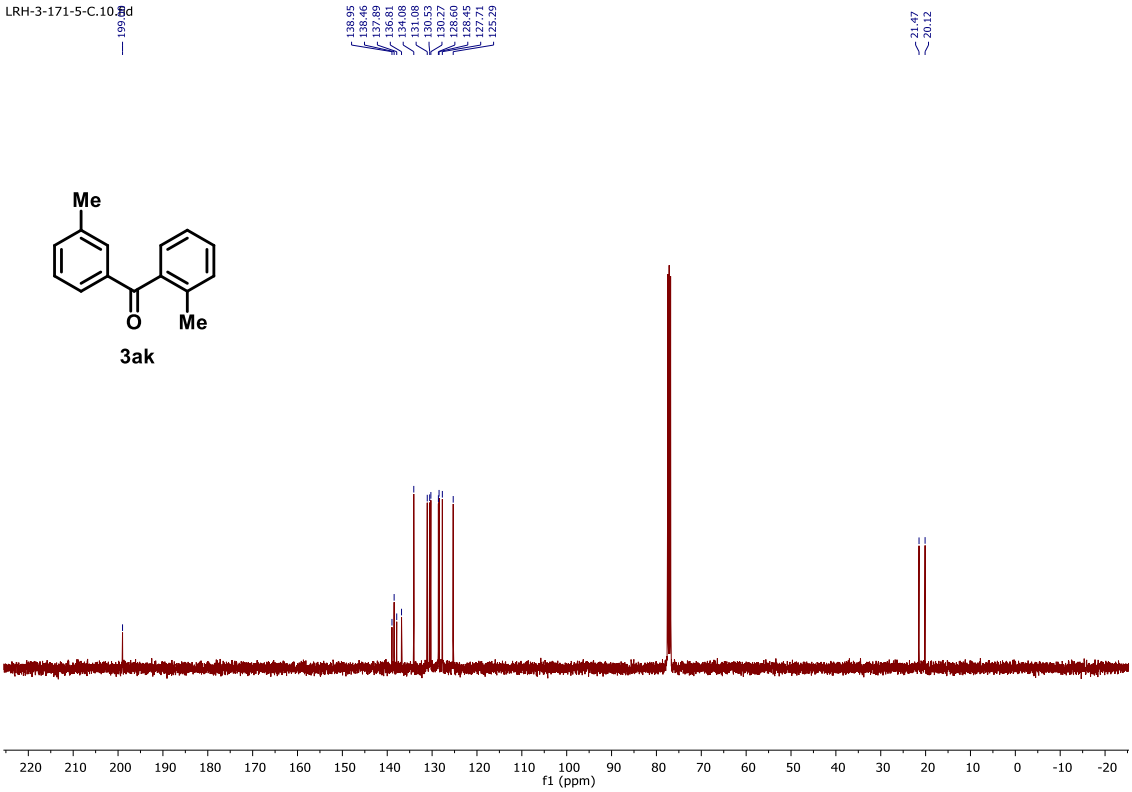

Figure 4.30. ^{1}H NMR Spectrum of 3al

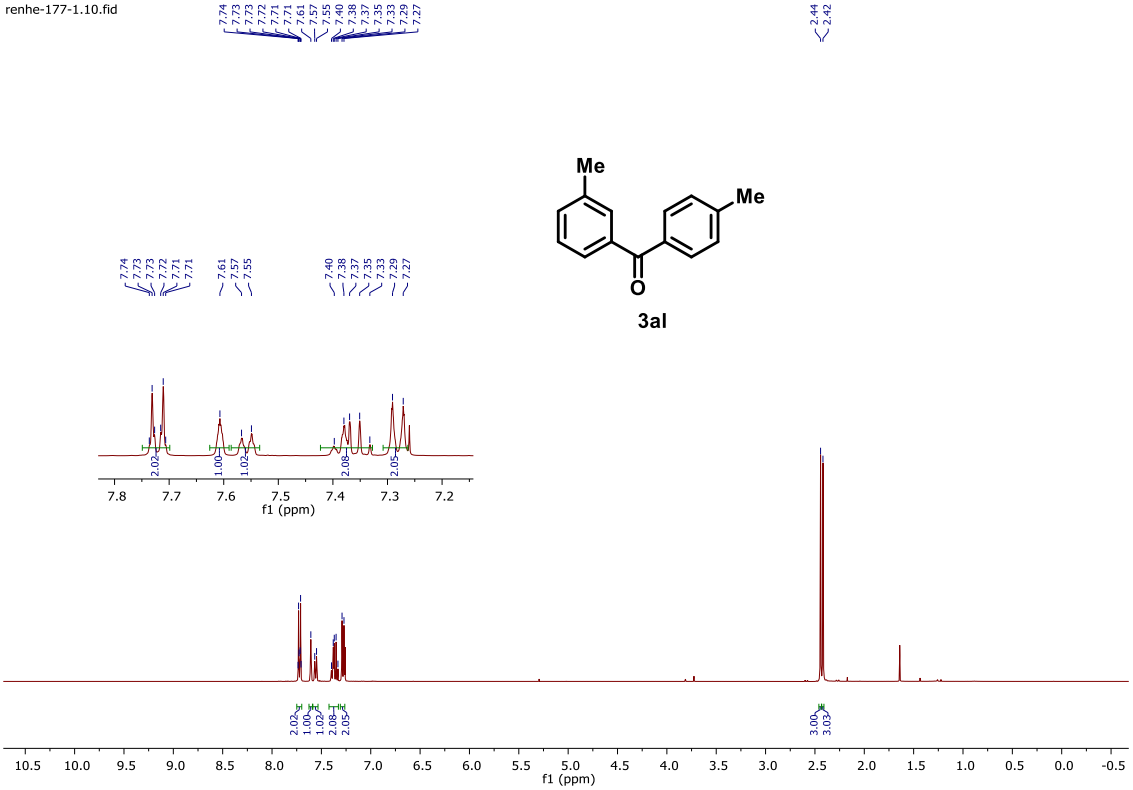

Figure 4.31. ^{13}C NMR Spectrum of 3al

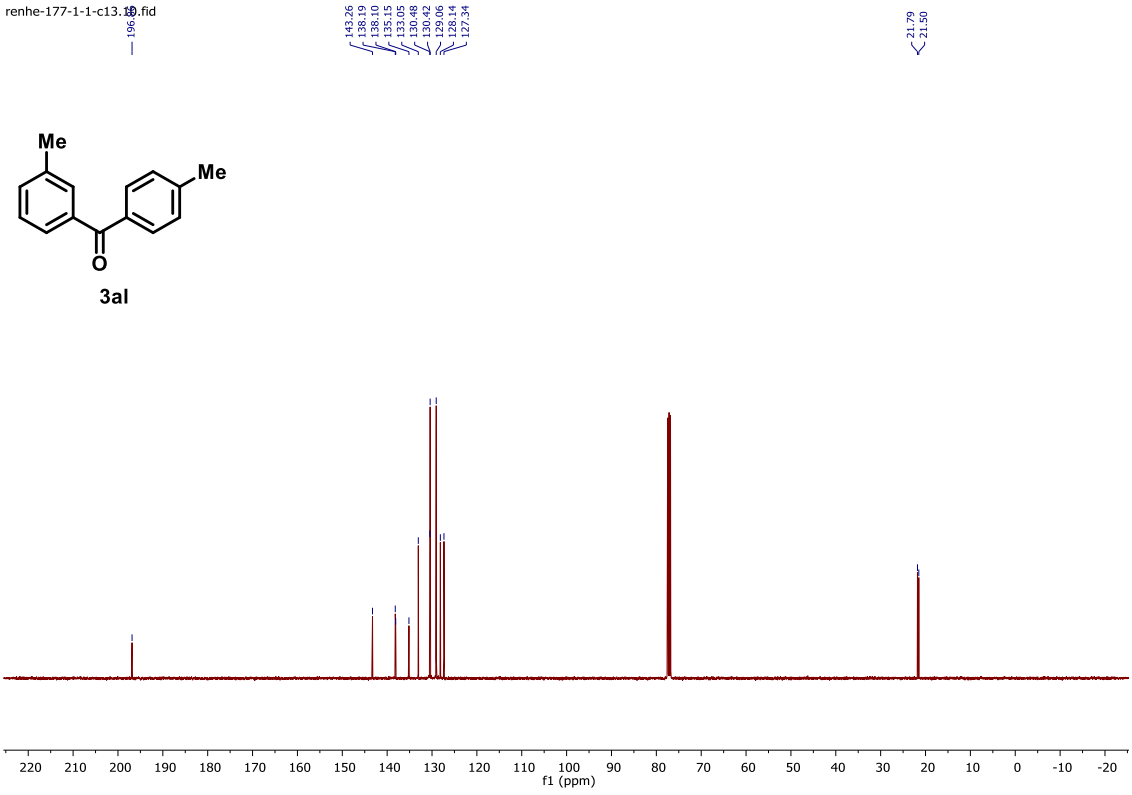

Figure 4.32. ^{1}H NMR Spectrum of 3am

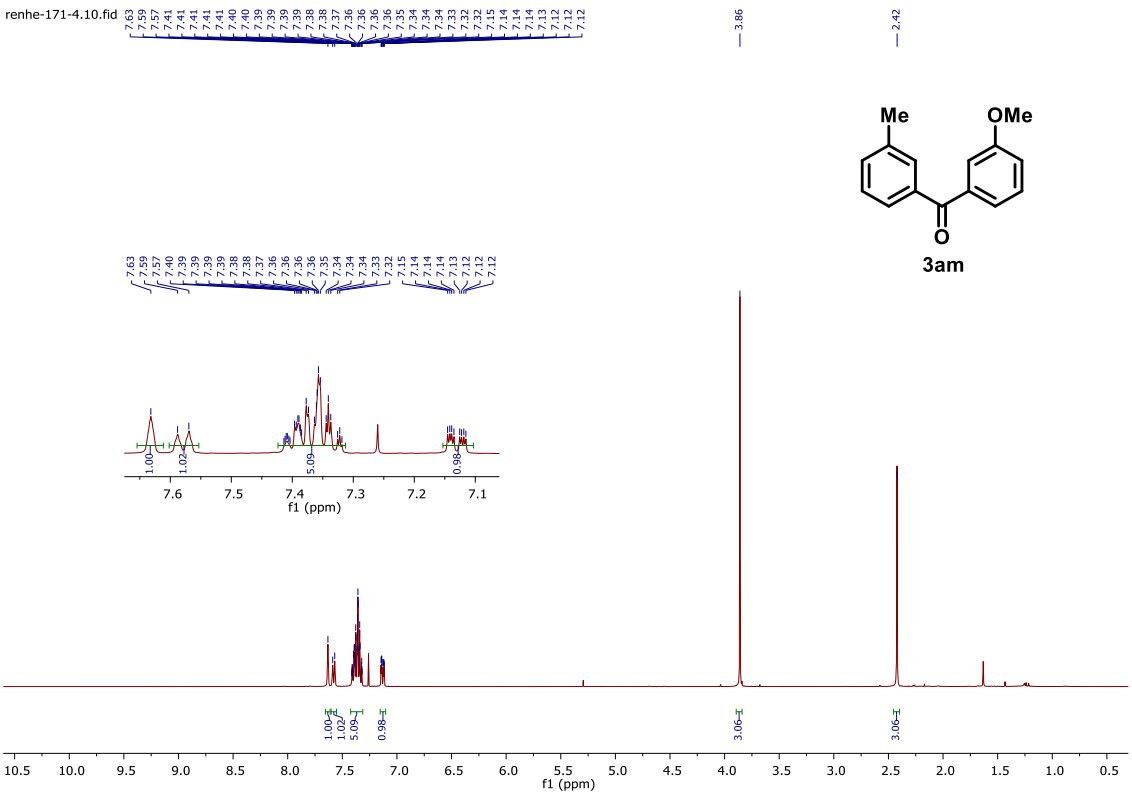

Figure 4.33. ^{13}C NMR Spectrum of 3am

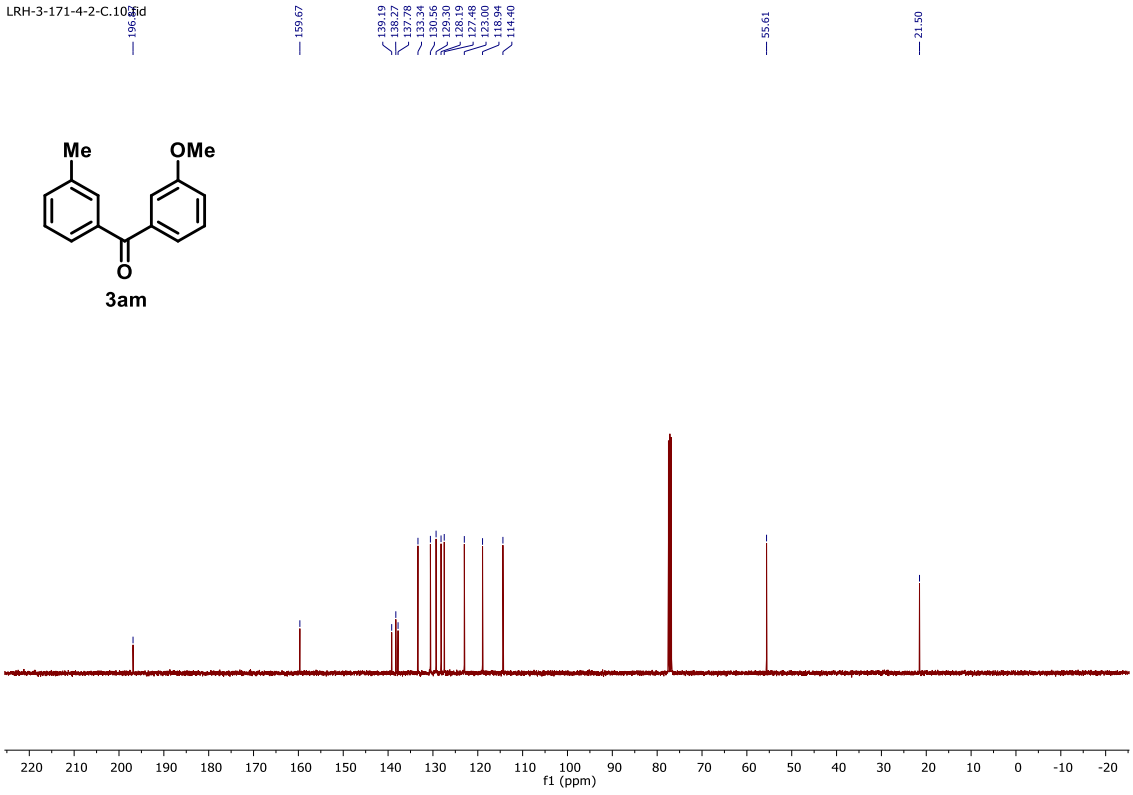

Figure 4.34. ^{1}H NMR Spectrum of 3an

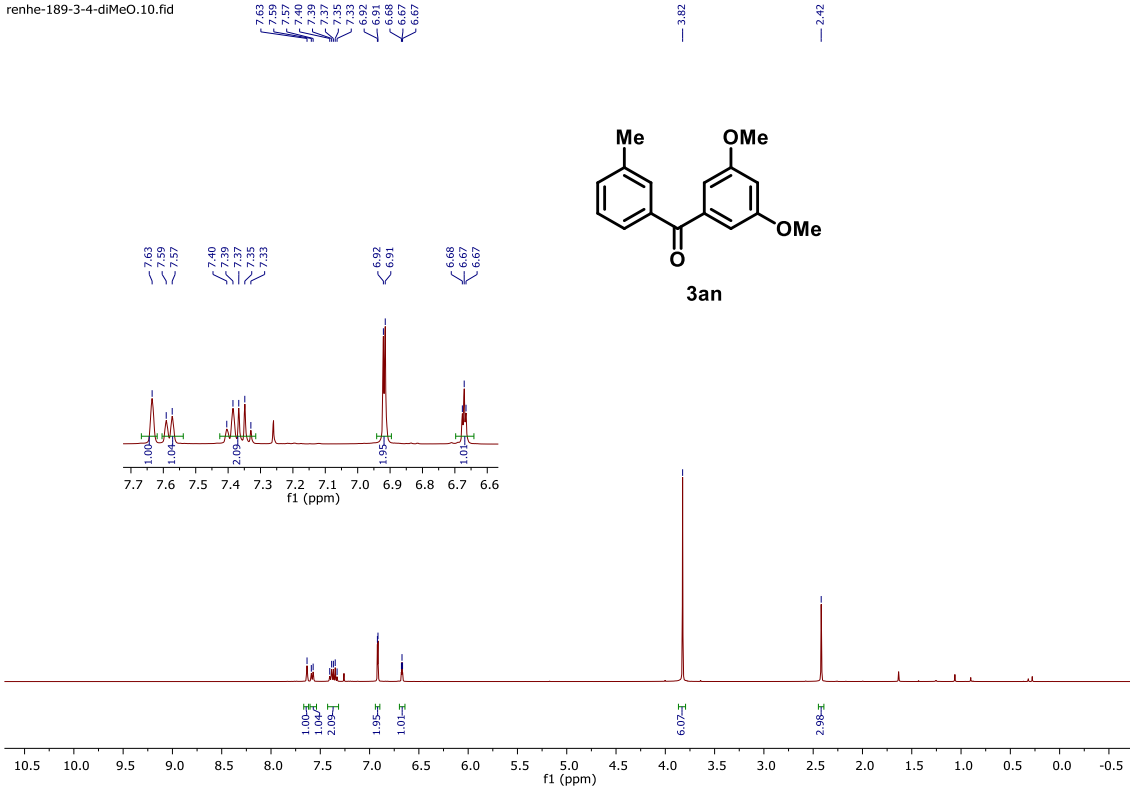

Figure 4.35. ^{13}C NMR Spectrum of 3an

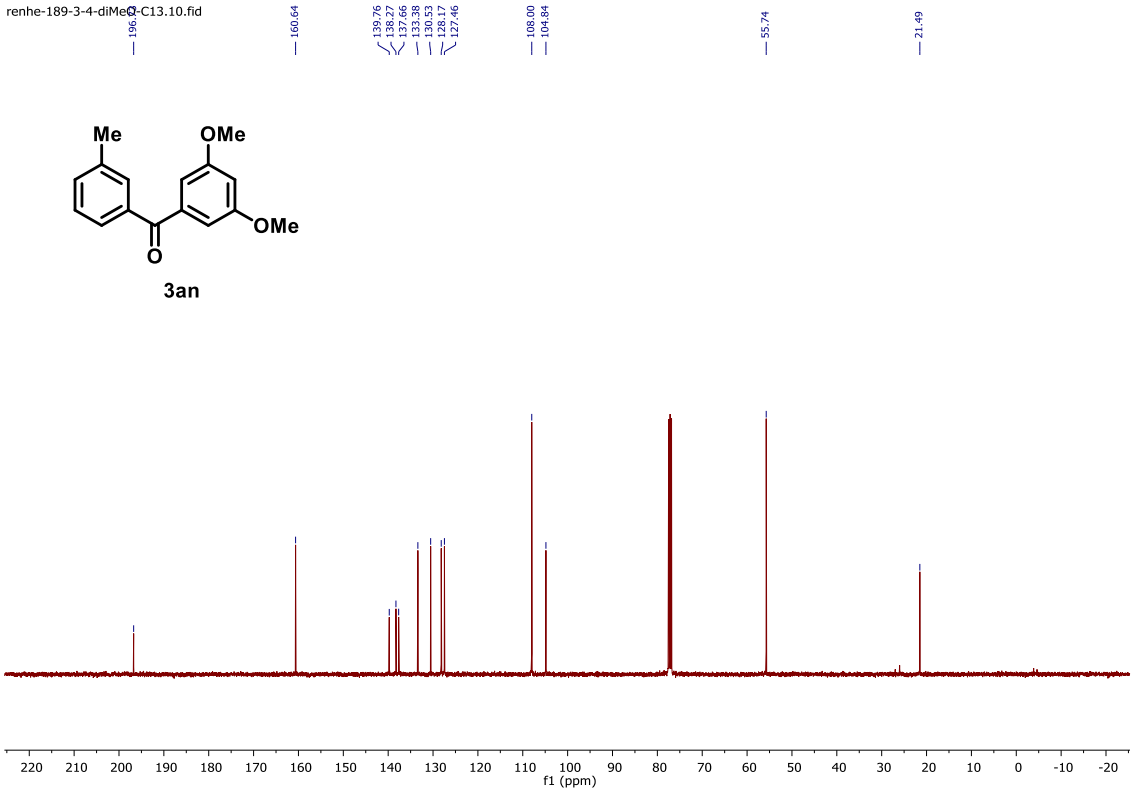

Figure 4.36. ^{1}H NMR Spectrum of 3ao

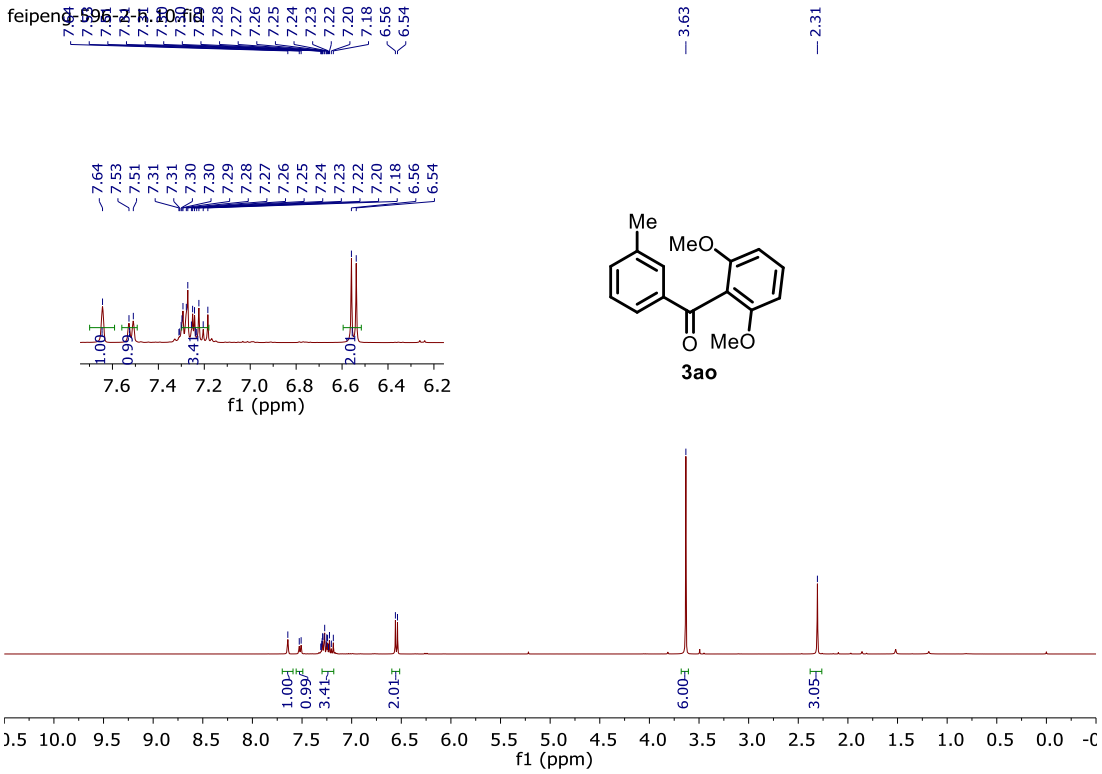

Figure 4.37. ^{13}C NMR Spectrum of 3ao

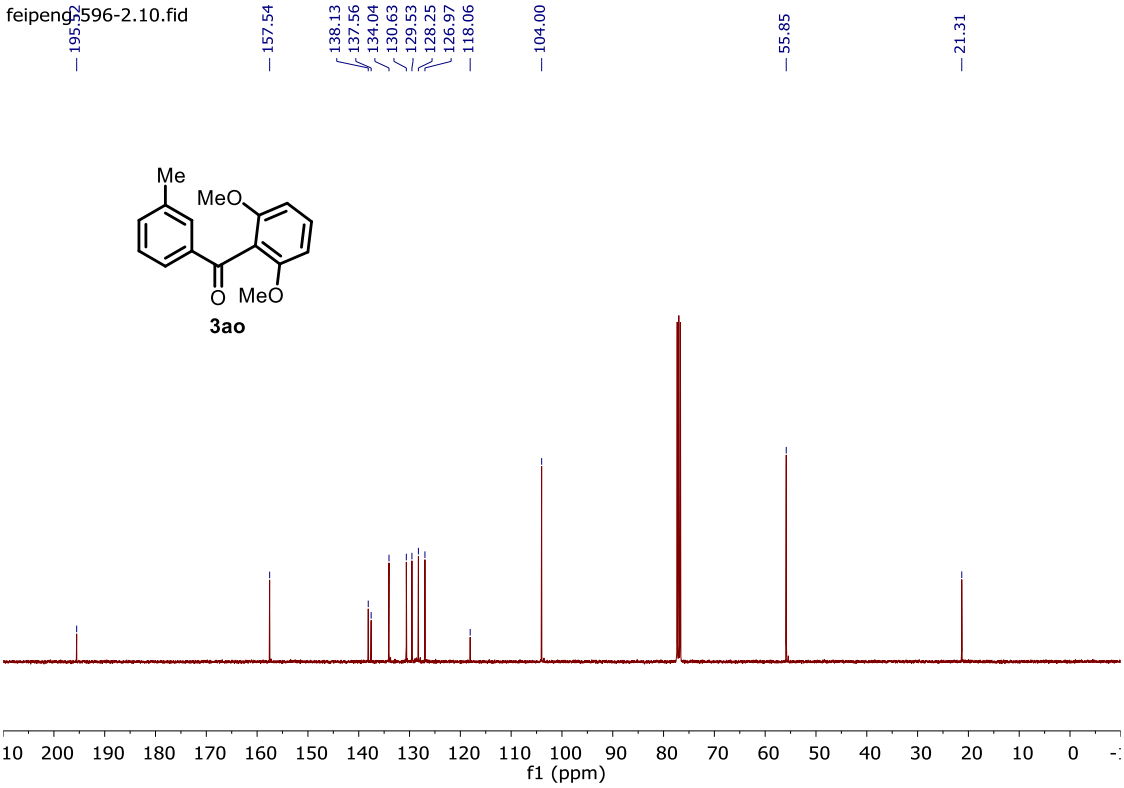

Figure 4.38. ^{1}H NMR Spectrum of 3ap

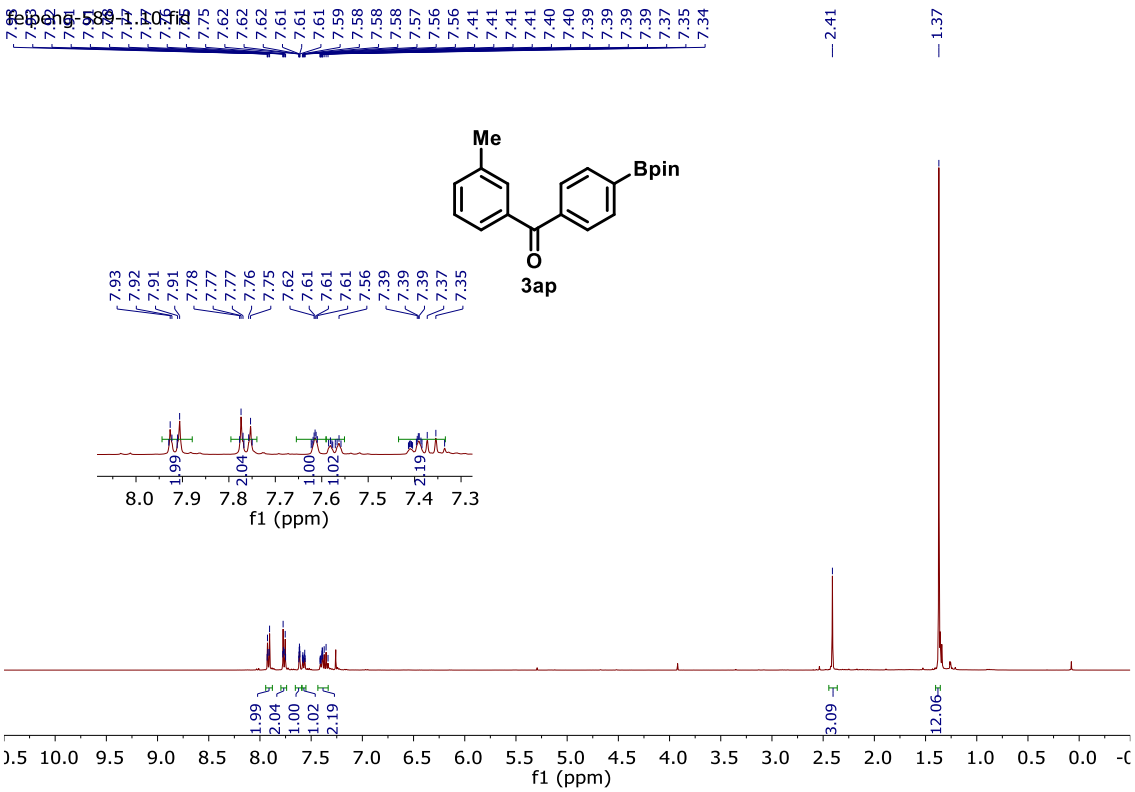

Figure 4.39. ^{13}C NMR Spectrum of 3ap

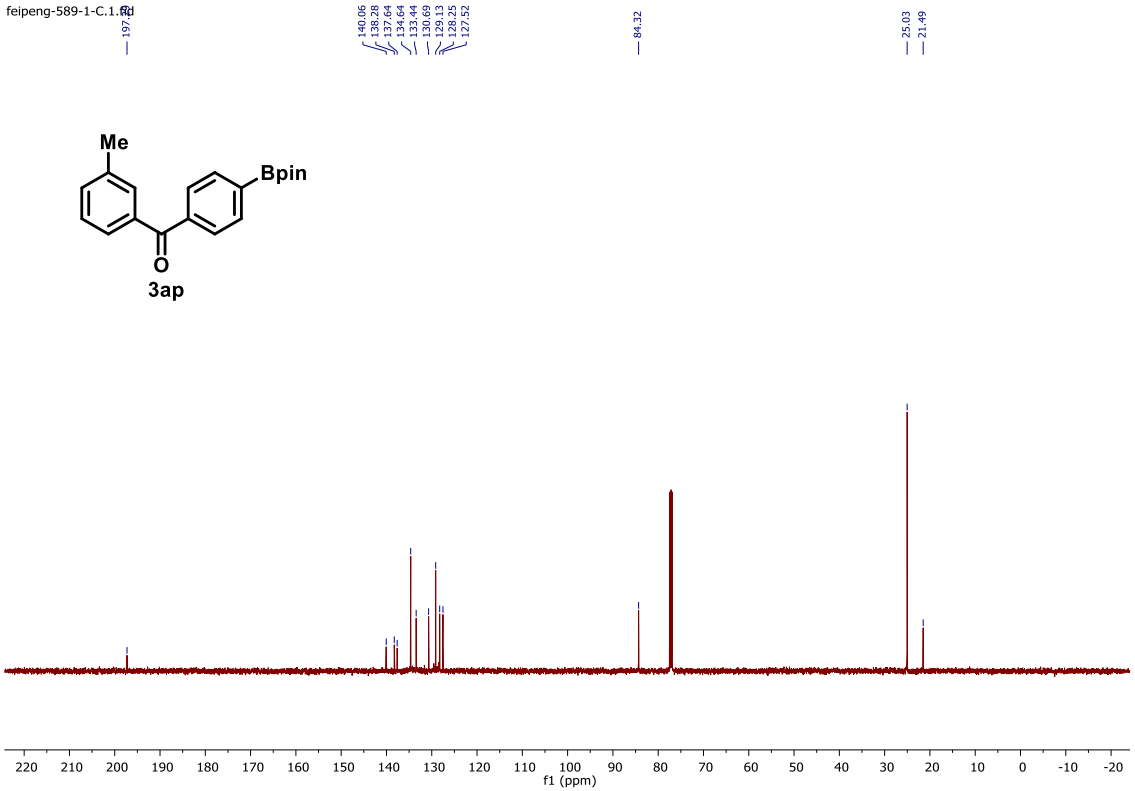

Figure 4.40. ^{1}H NMR Spectrum of 3aq

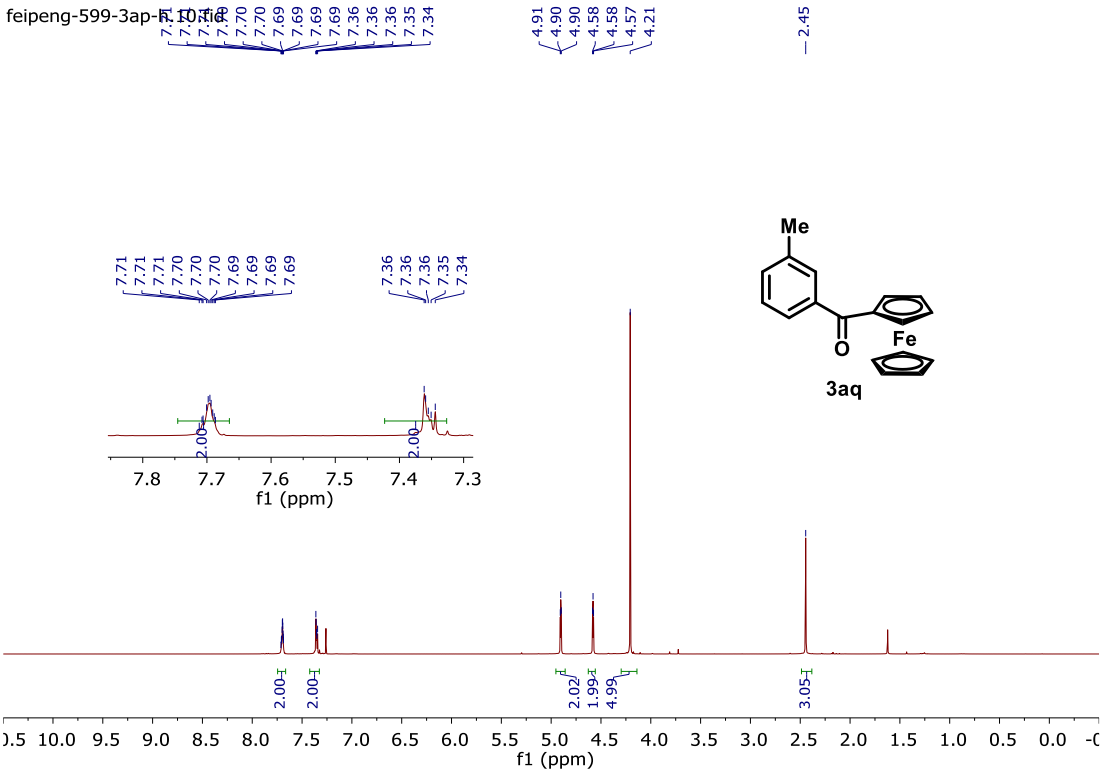

Figure 4.41. ^{13}C NMR Spectrum of 3aq

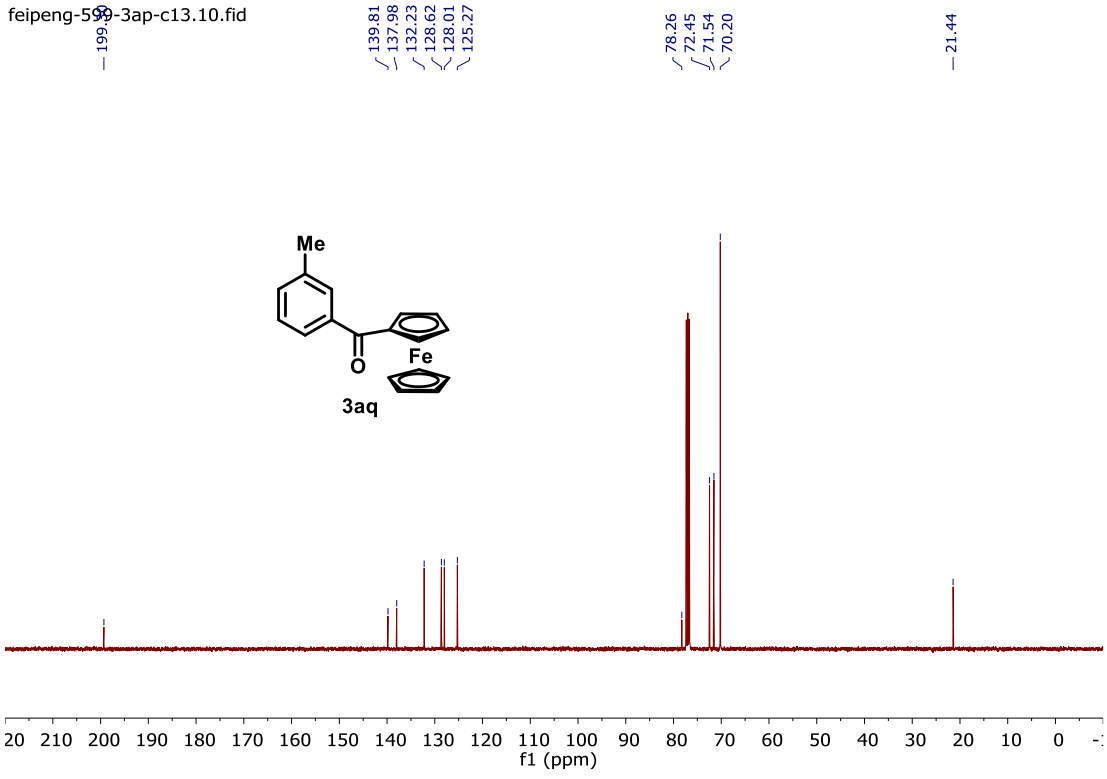

Figure 4.42. ^{1}H NMR Spectrum of 3ar

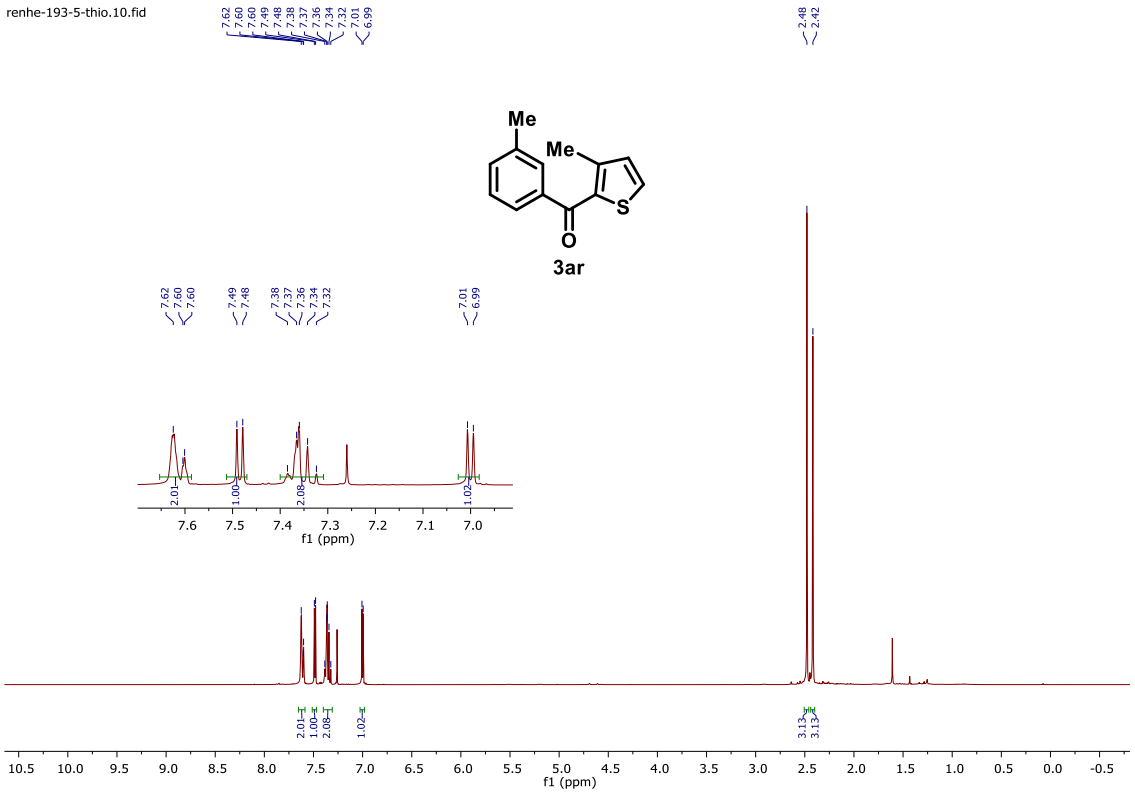

Figure 4.43. ^{13}C NMR Spectrum of 3ar

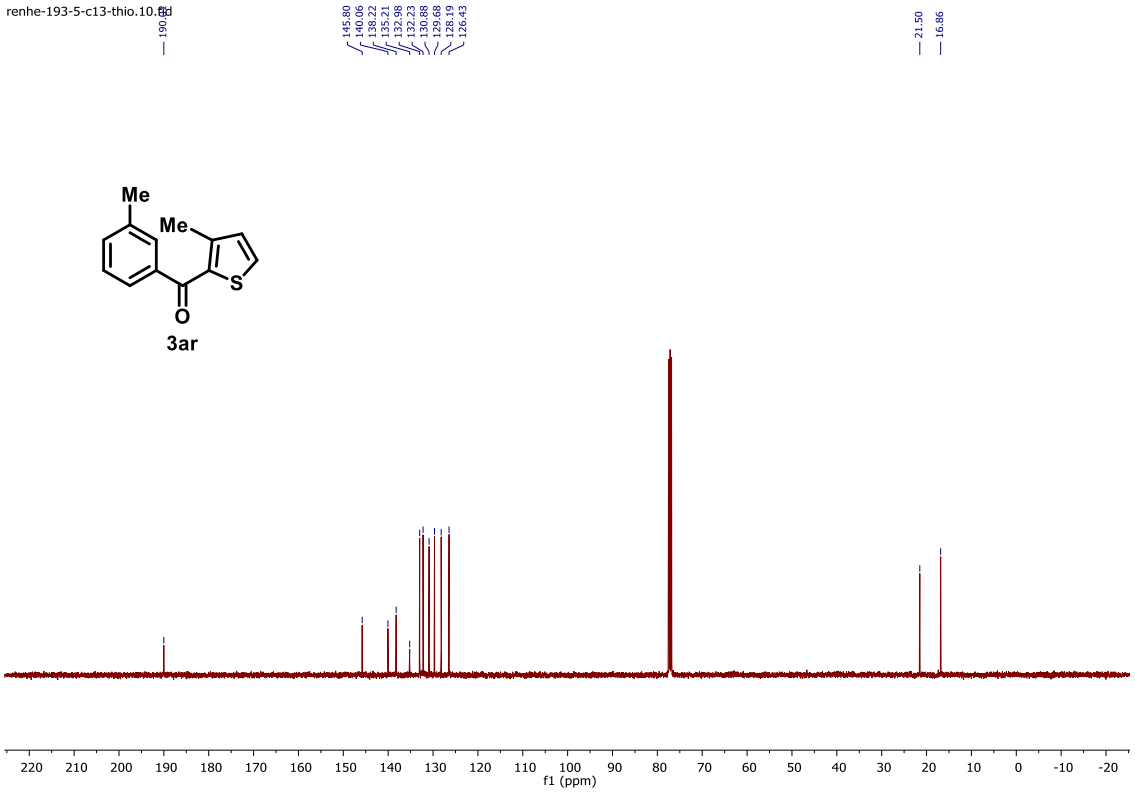

Figure 4.44. ^{1}H NMR Spectrum of 3as

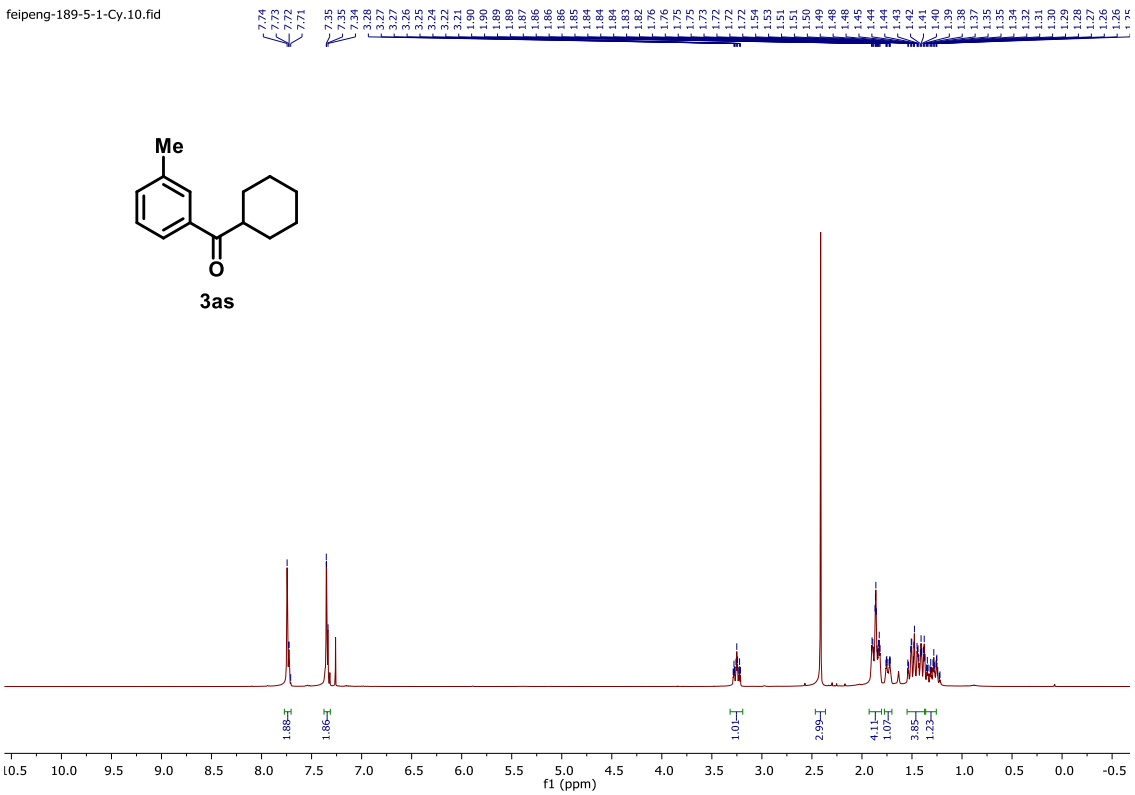

Figure 4.45. ^{13}C NMR Spectrum of 3as

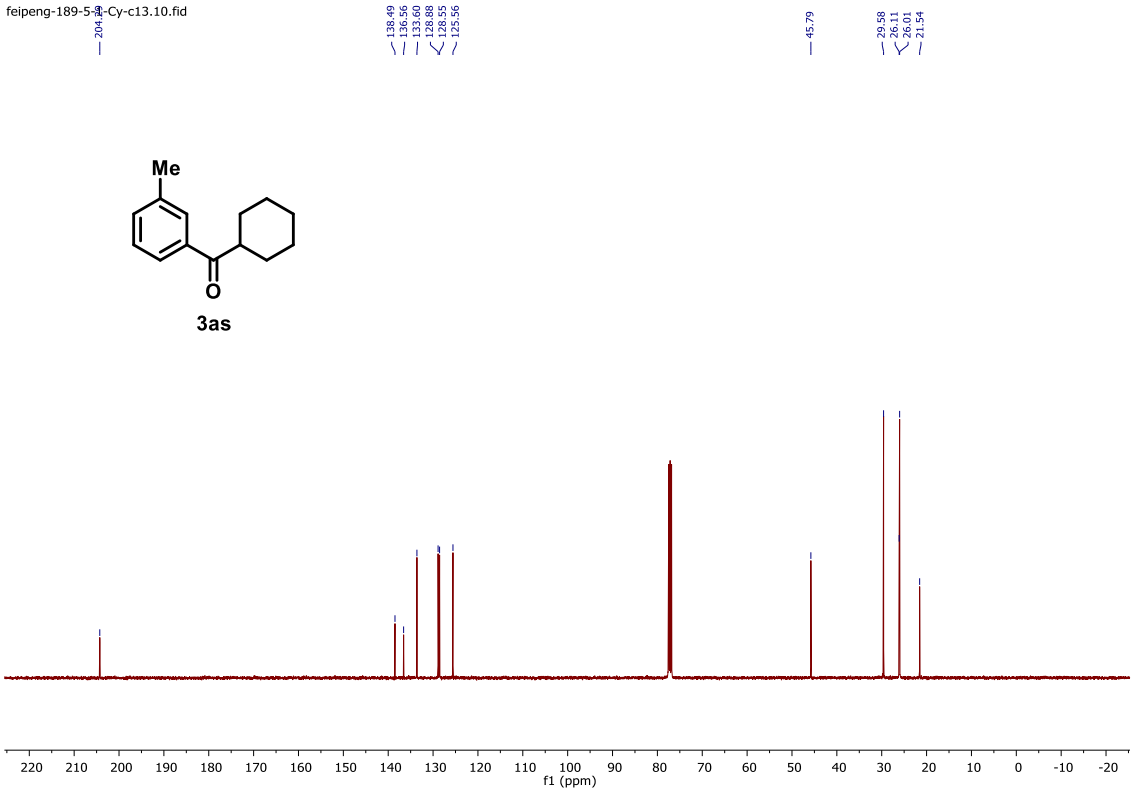

Figure 4.46. ^{1}H NMR Spectrum of 3at

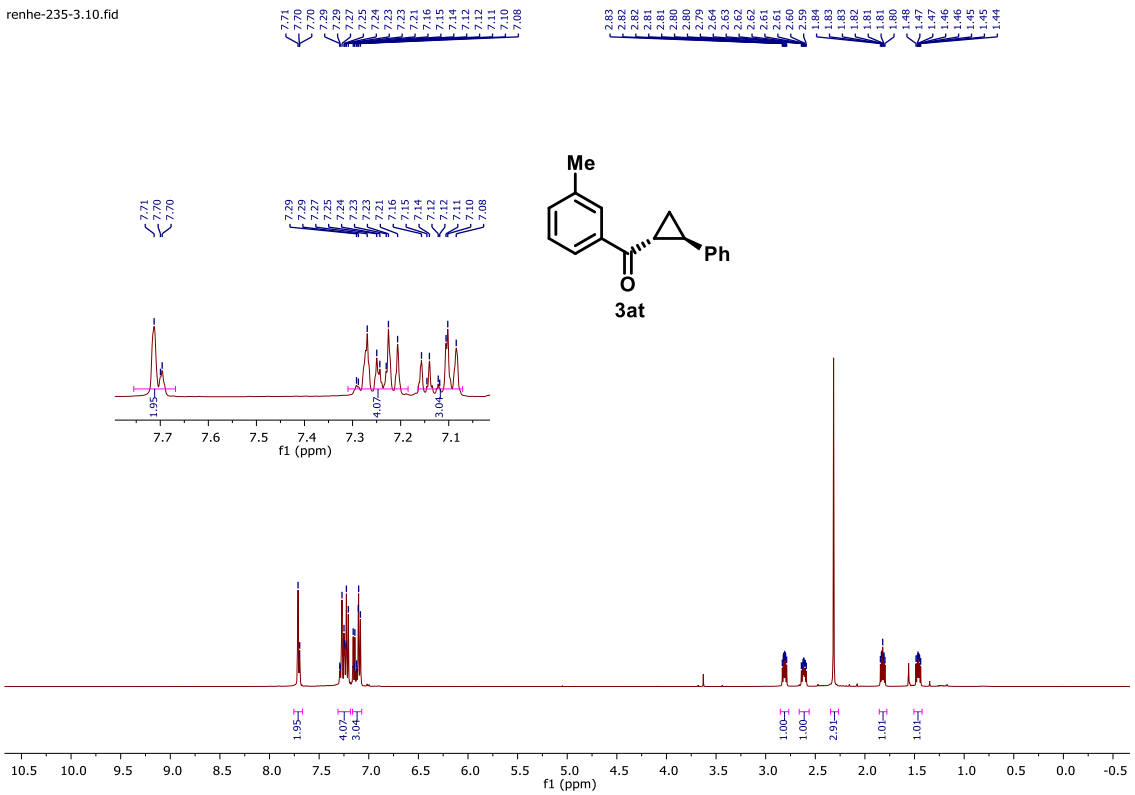

Figure 4.47. ^{13}C NMR Spectrum of 3at

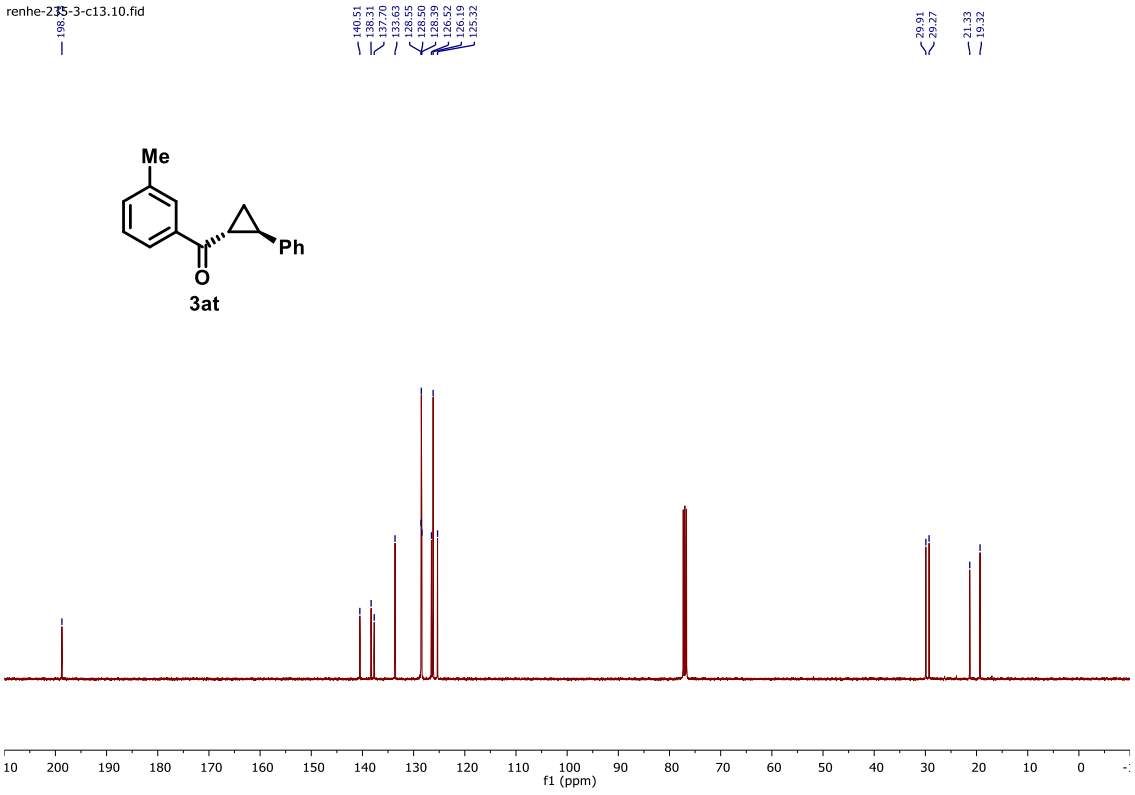

Figure 4.48. ^{1}H NMR Spectrum of 3bb

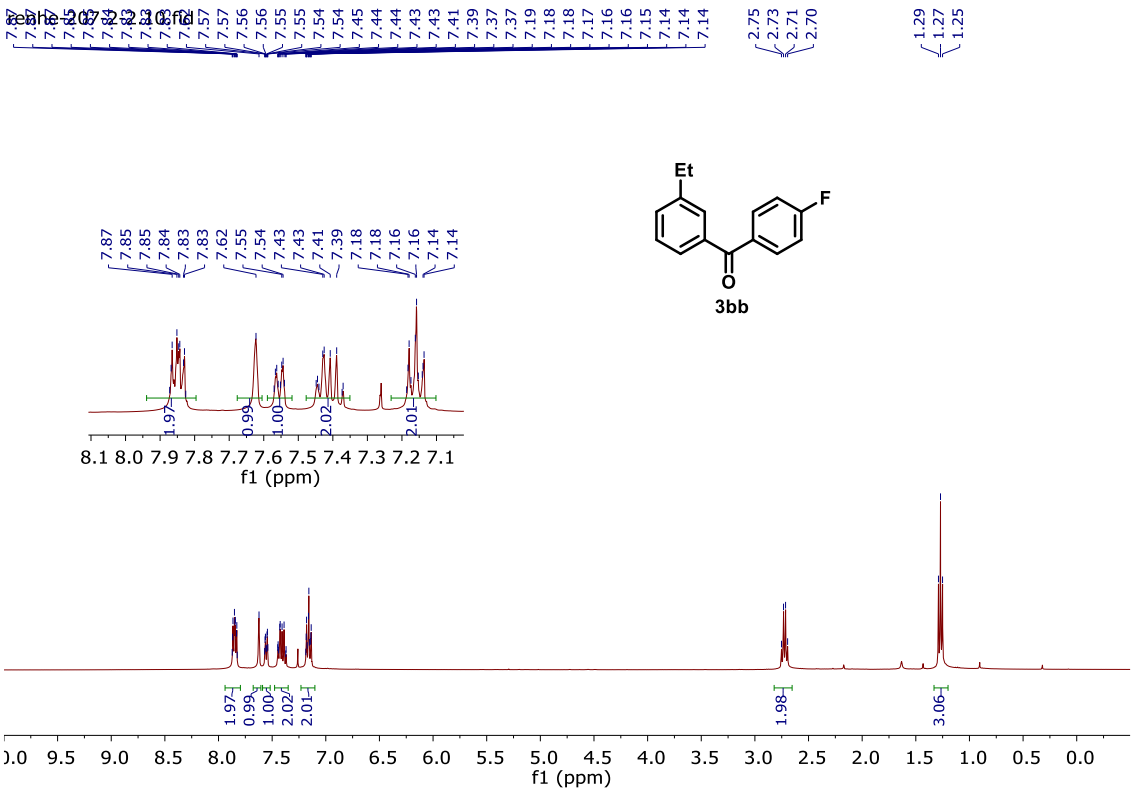

Figure 4.49. ^{13}C NMR Spectrum of 3bb

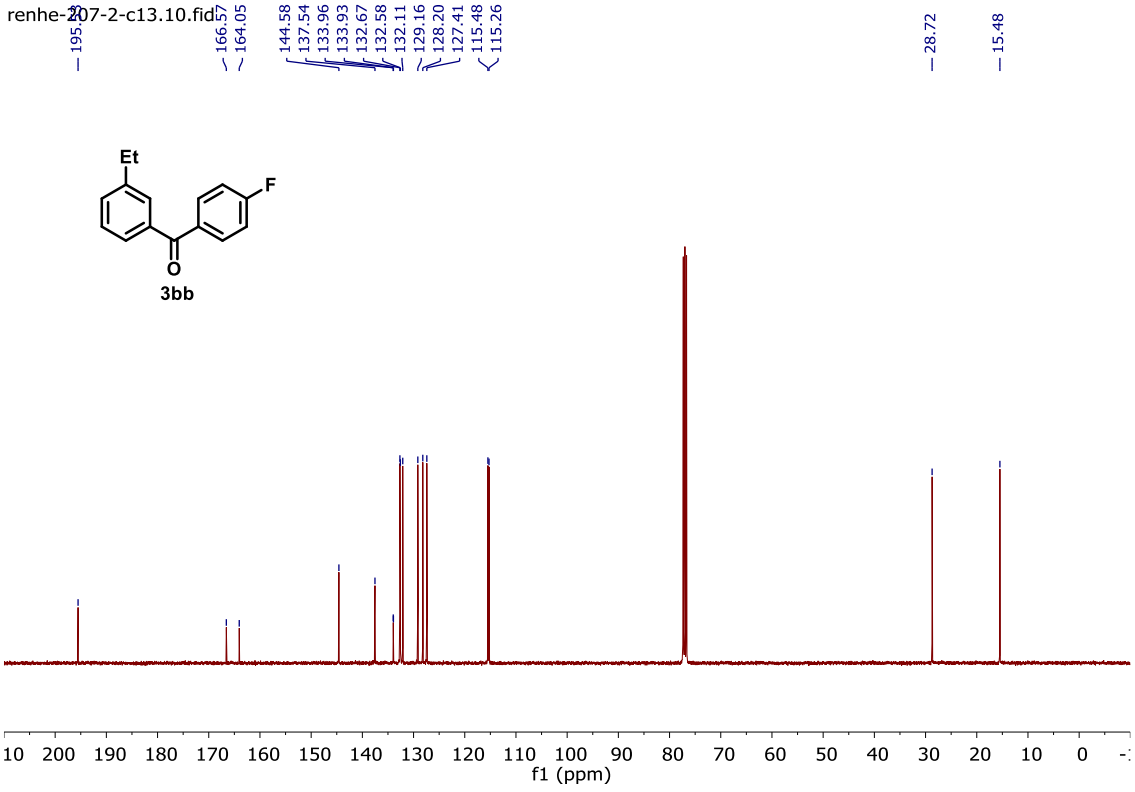

Figure 4.50. ^{19}F NMR Spectrum of 3bb

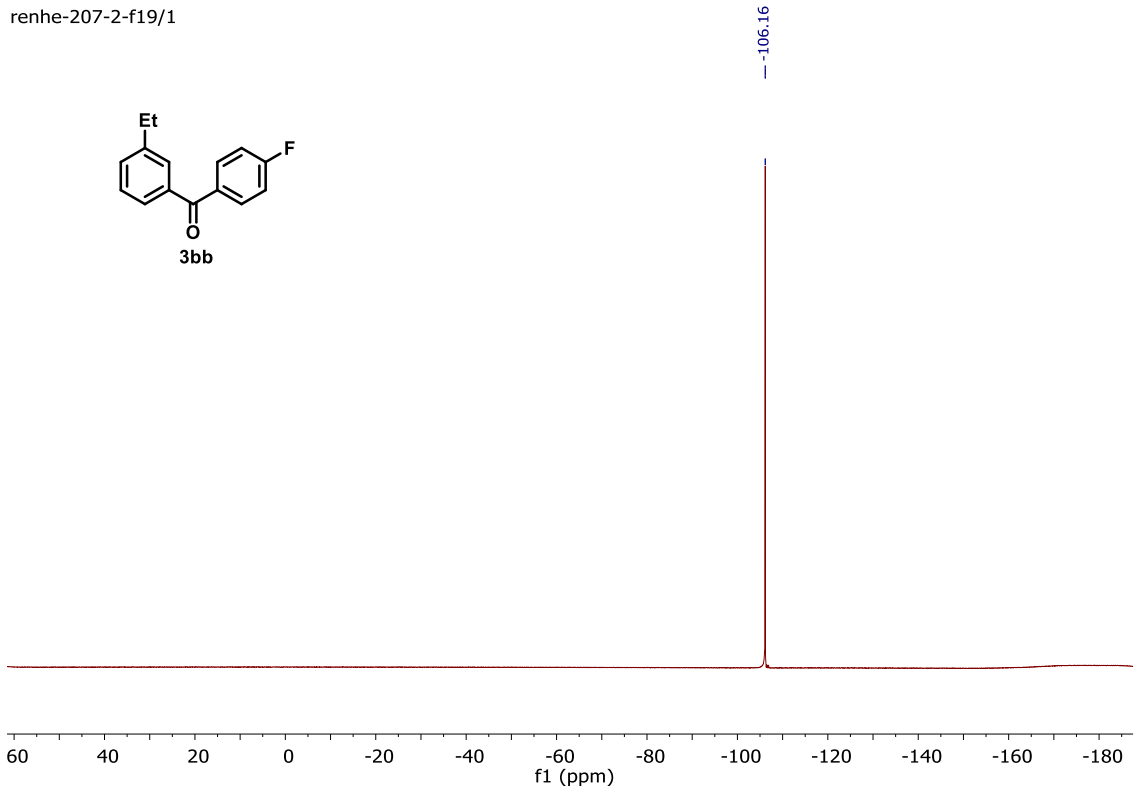

Figure 4.51. ^{1}H NMR Spectrum of 3cb

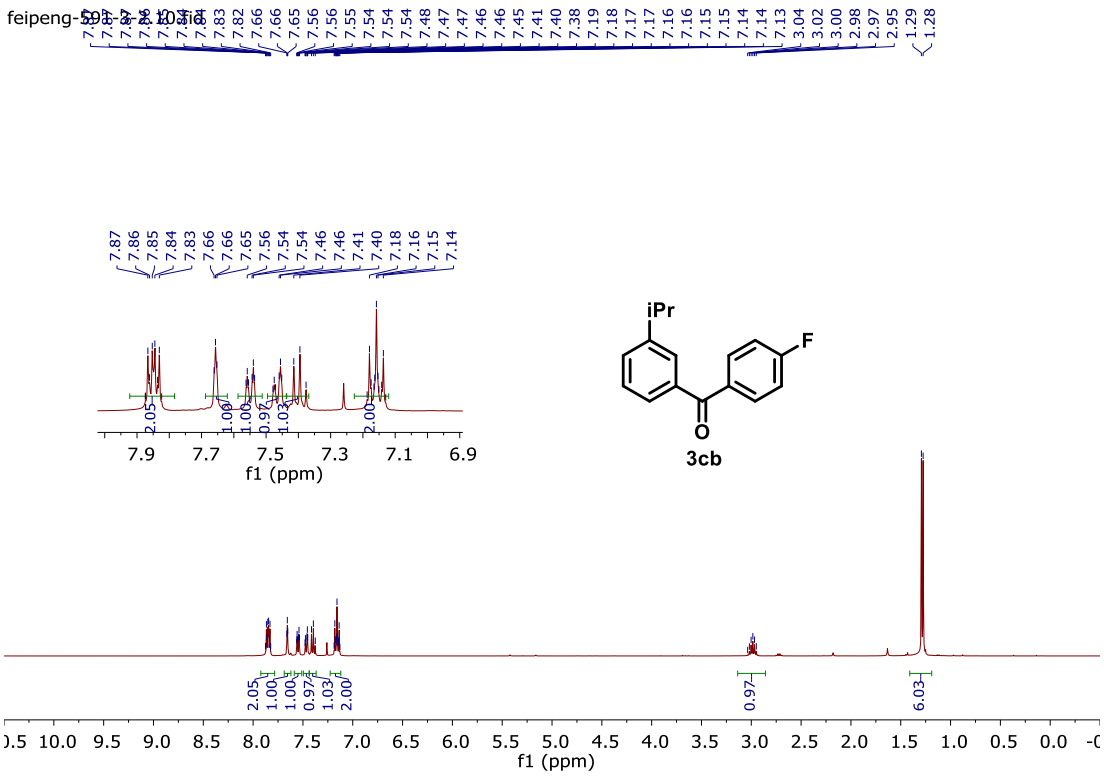

Figure 4.52. ^{13}C NMR Spectrum of 3cb

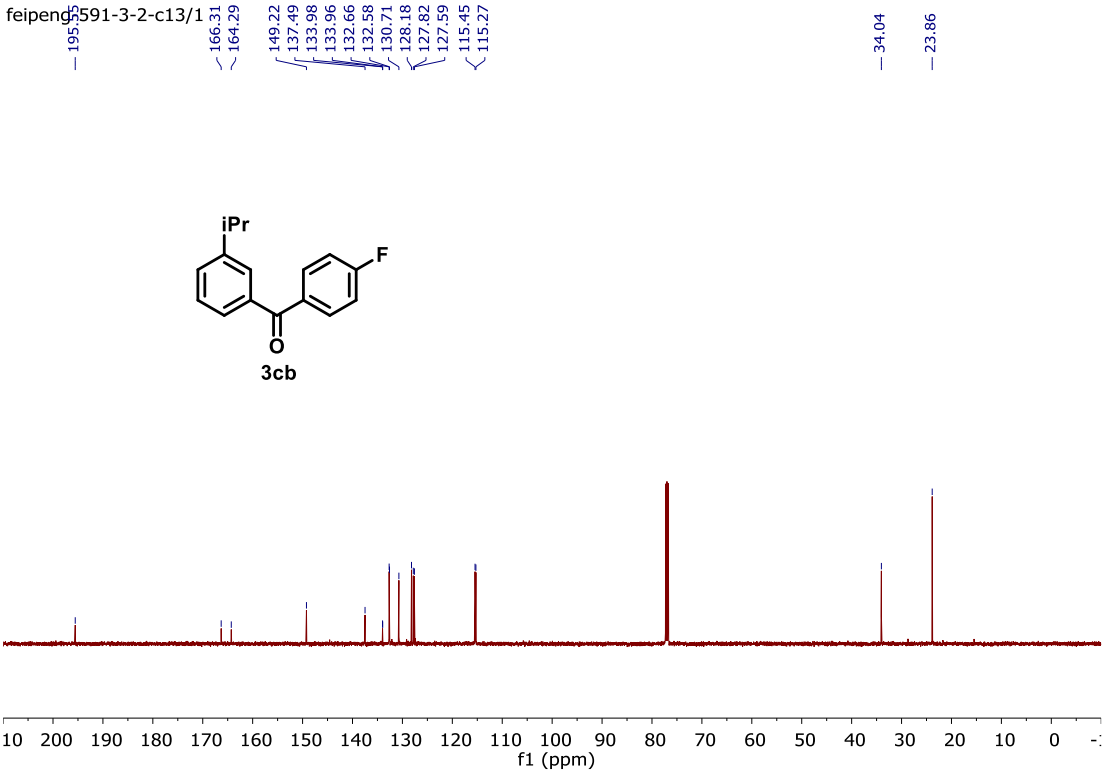

Figure 4.53. ^{19}F NMR Spectrum of 3cb

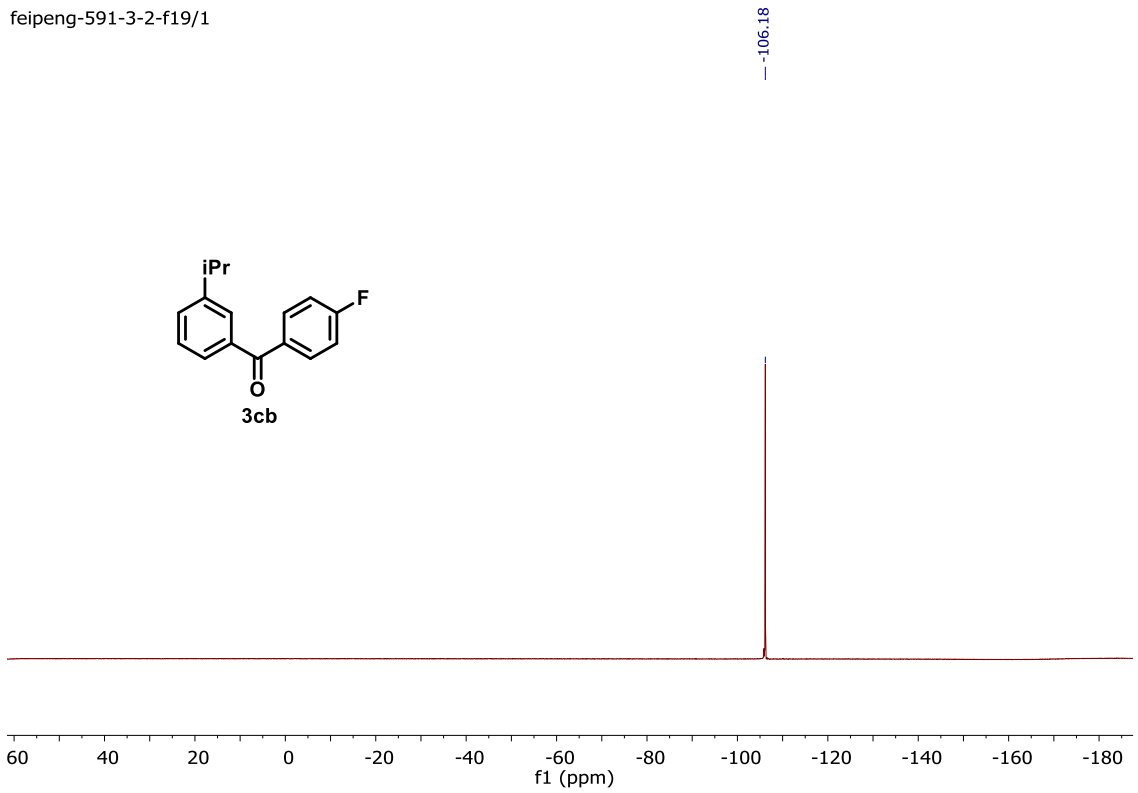

Figure 4.54. ^{1}H NMR Spectrum of 3db

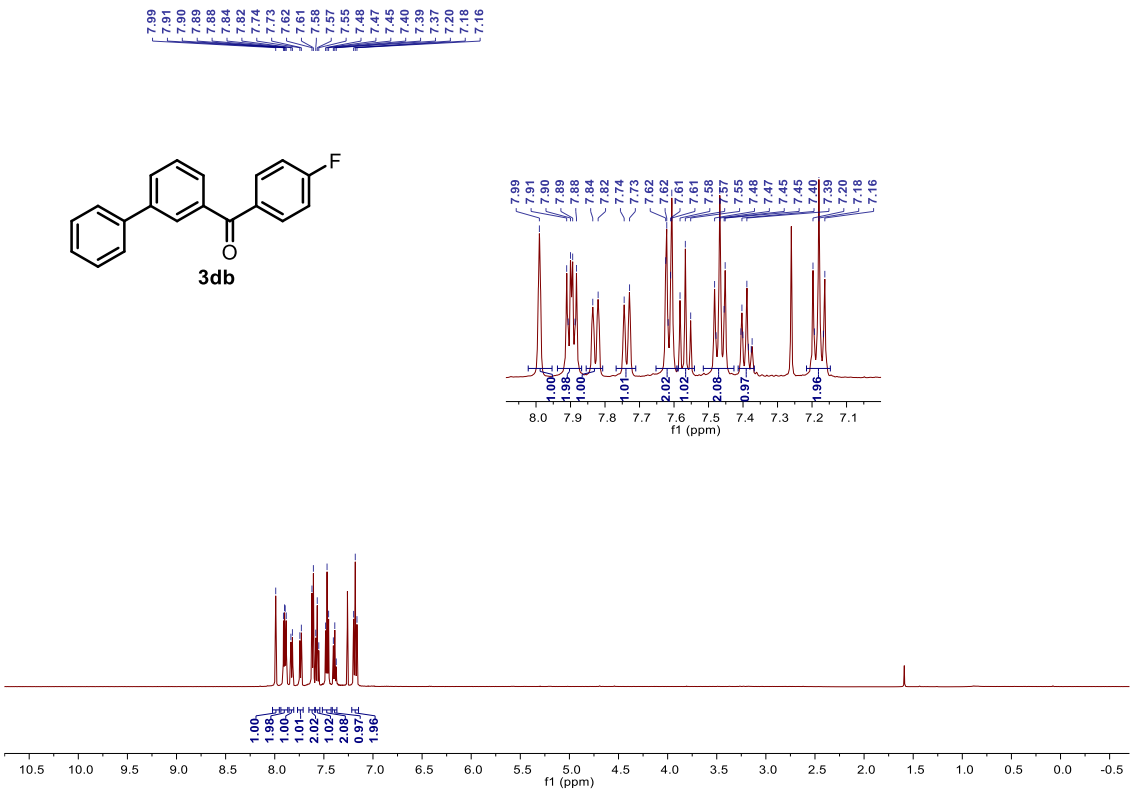

Figure 4.55. ^{13}C NMR Spectrum of 3db

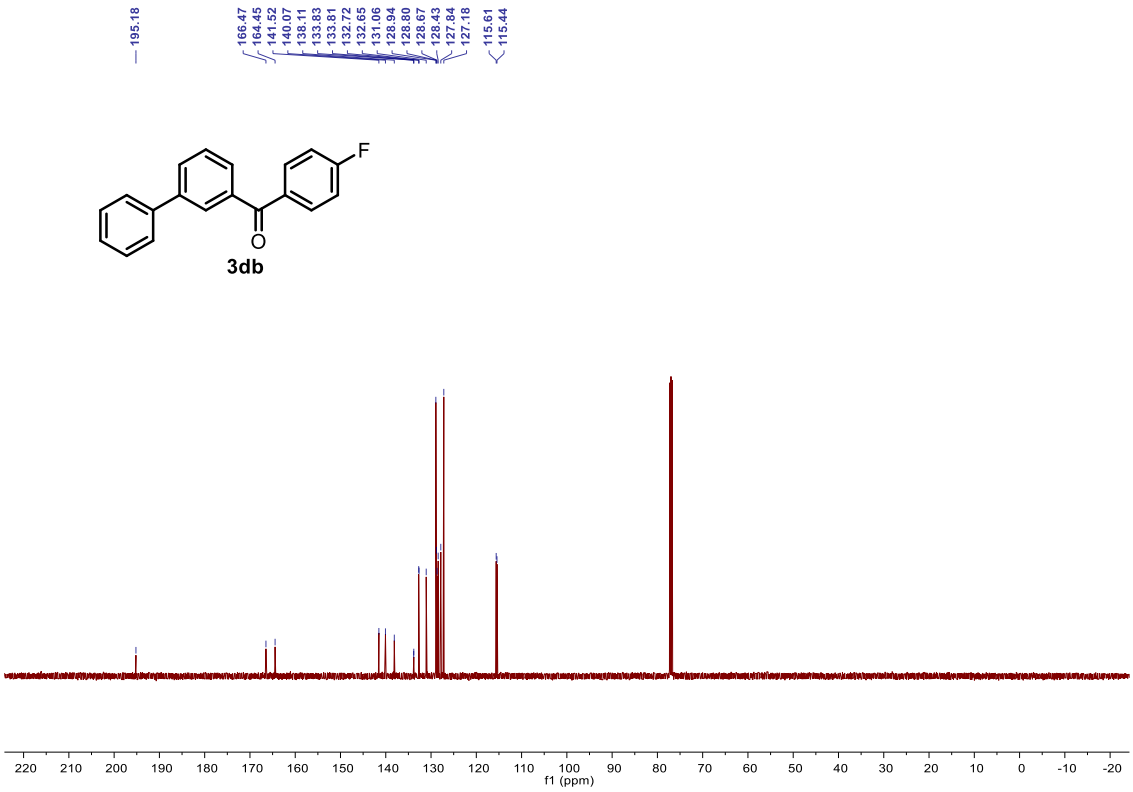

Figure 4.56. ^{19}F NMR Spectrum of 3db

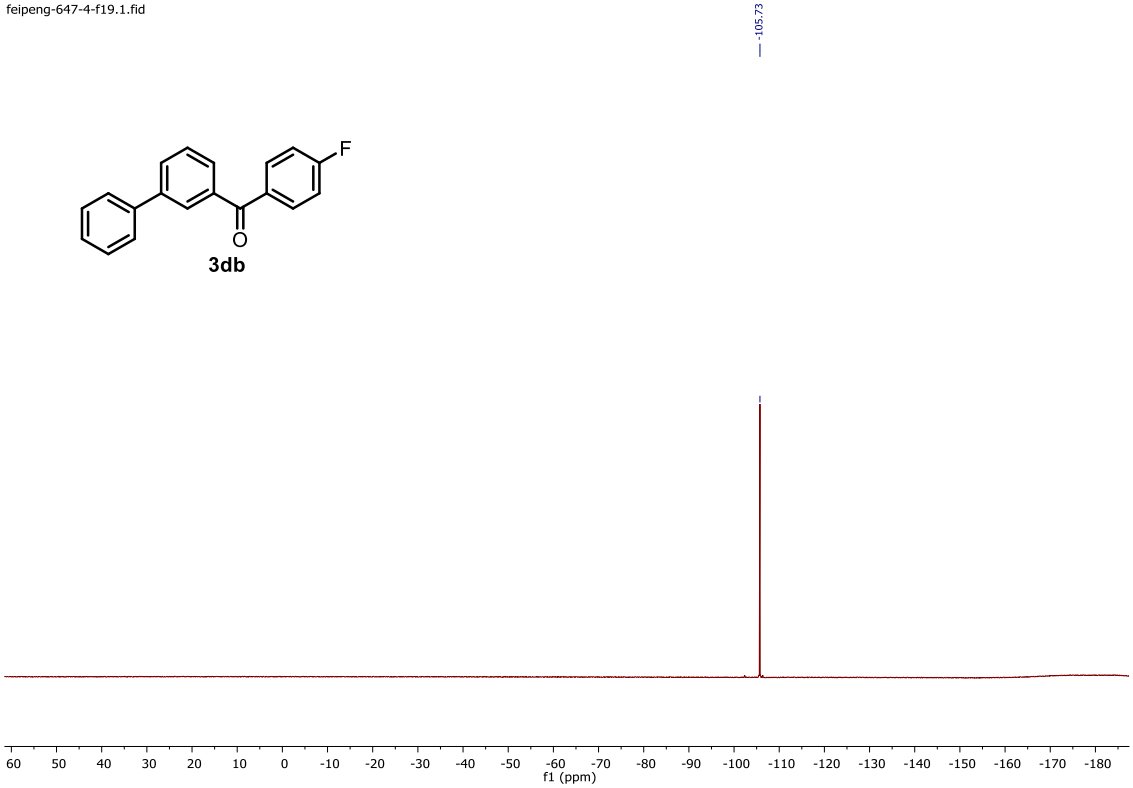

Figure 4.57. ^{1}H NMR Spectrum of 3eb

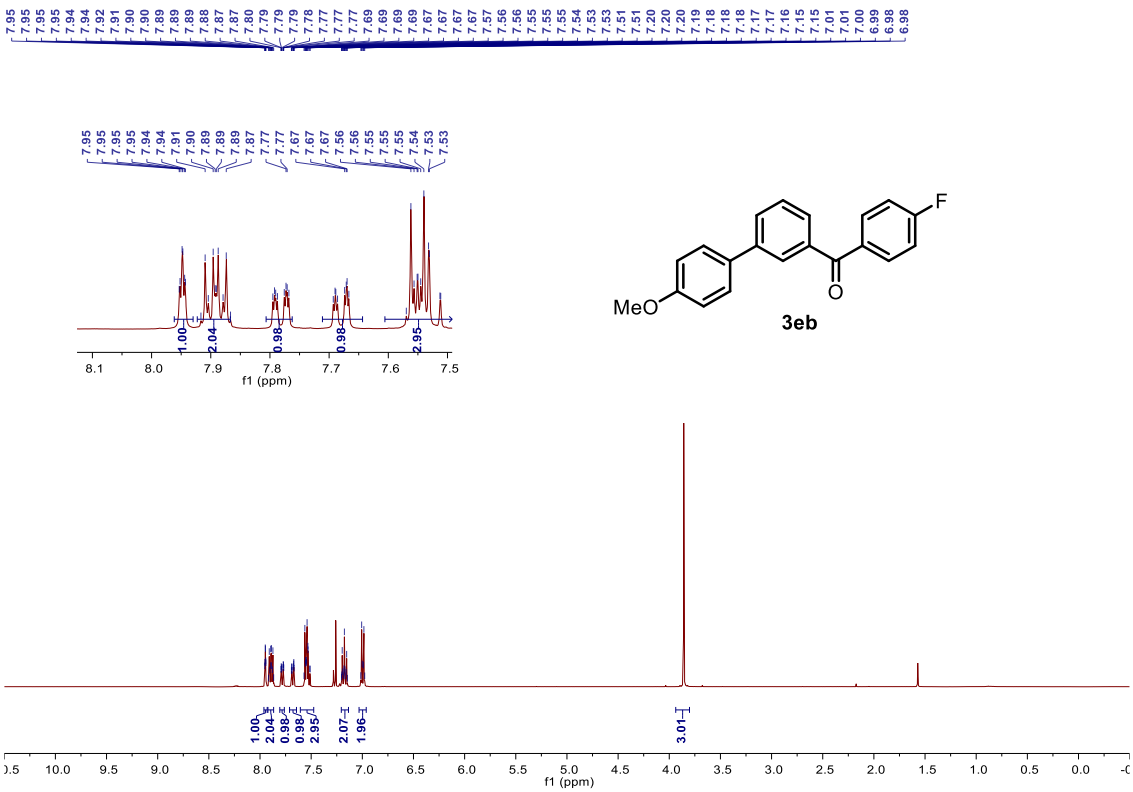

Figure 4.58. ^{13}C NMR Spectrum of 3eb

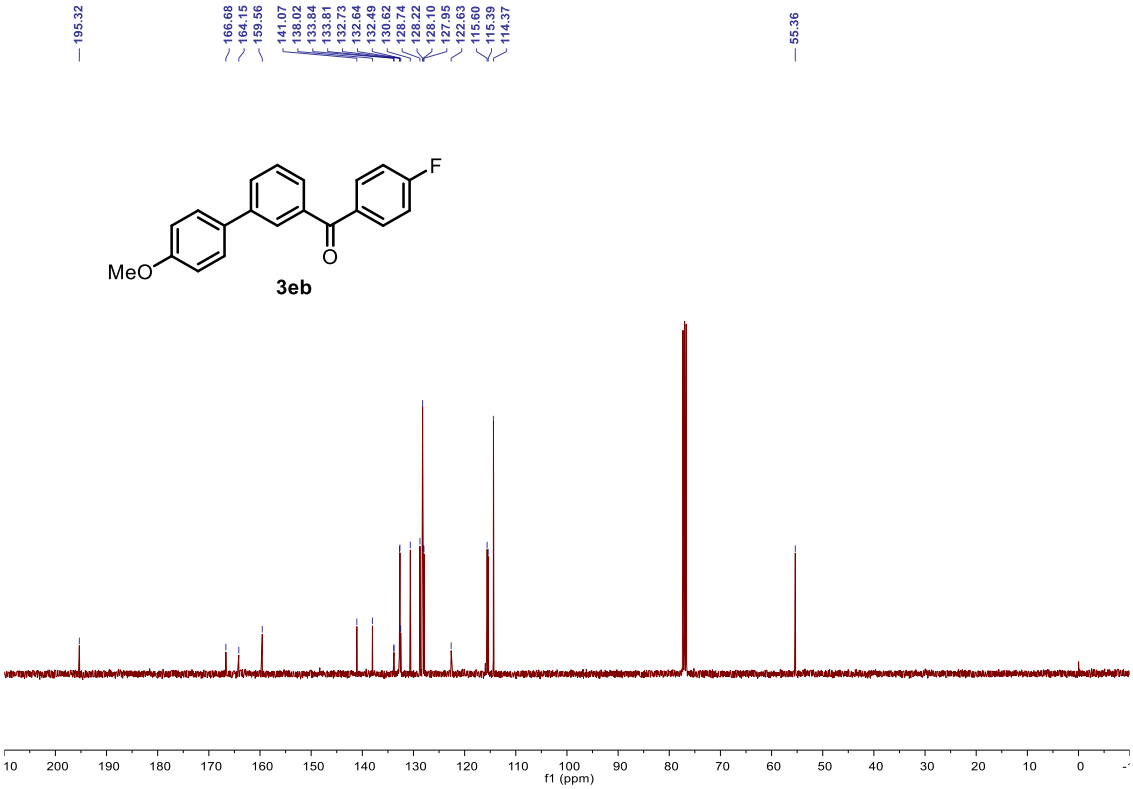

Figure 4.59. ^{19}F NMR Spectrum of 3eb

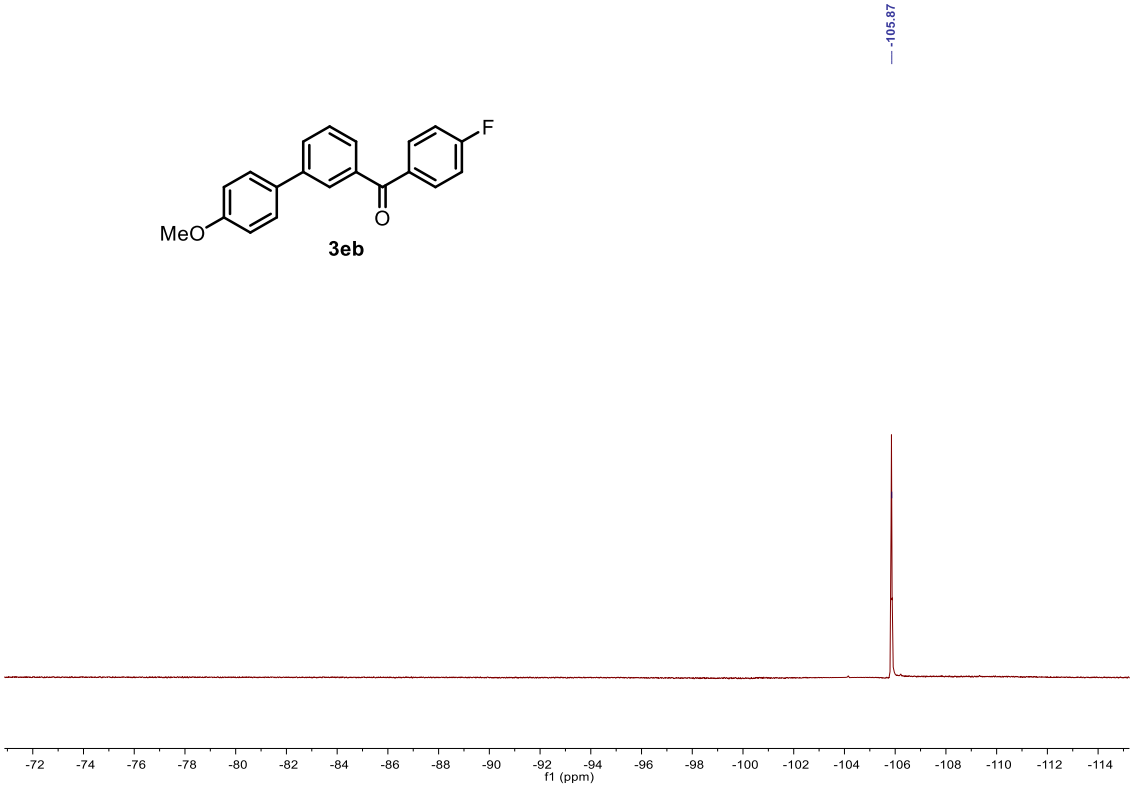

Figure 4.60. ^{1}H NMR Spectrum of 3fb

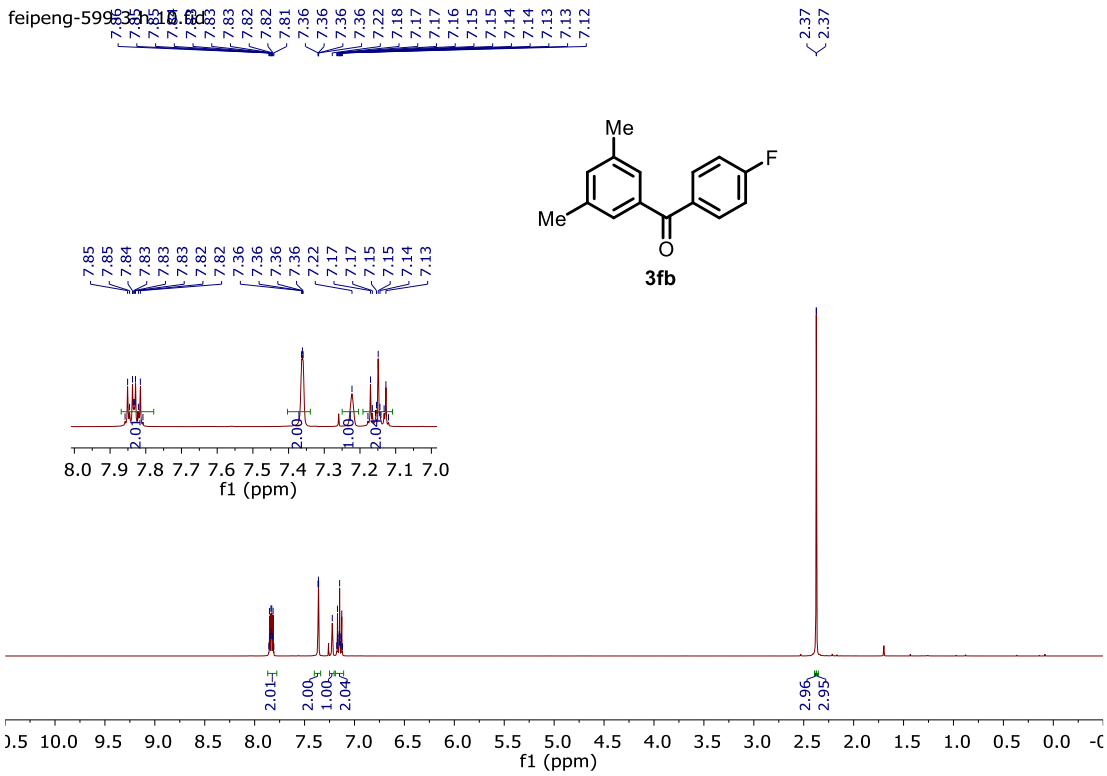

Figure 4.61. ^{13}C NMR Spectrum of 3fb

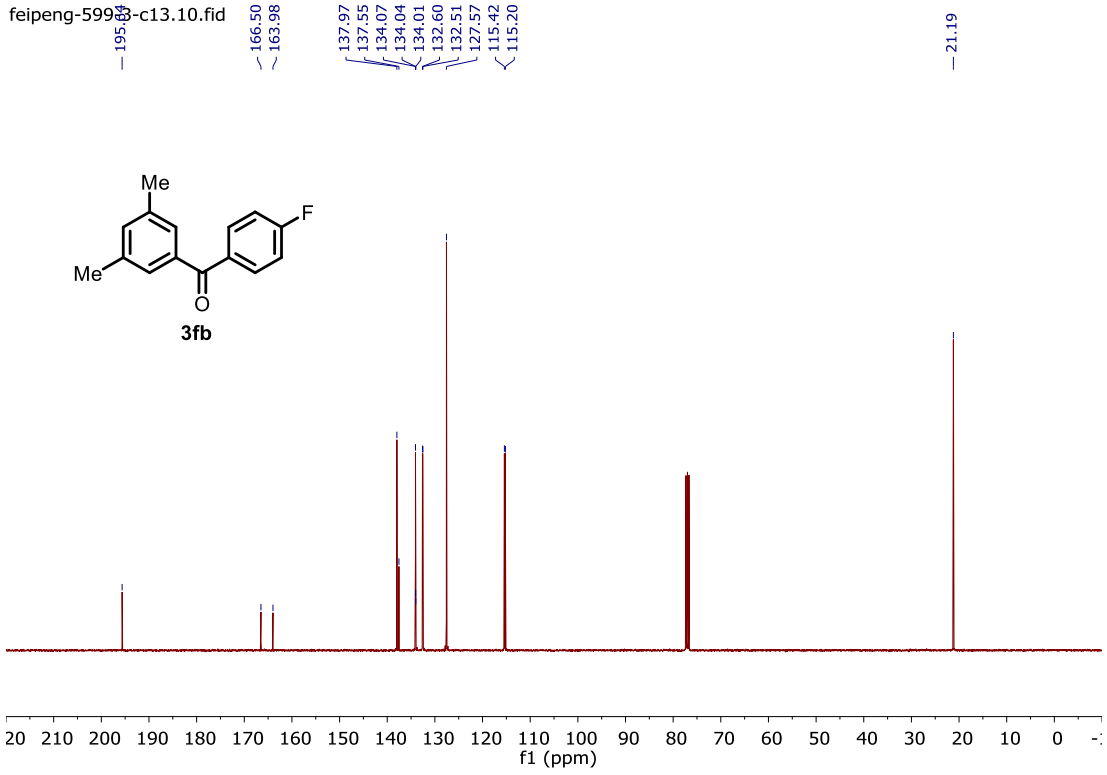

Figure 4.62. ^{19}F NMR Spectrum of 3fb

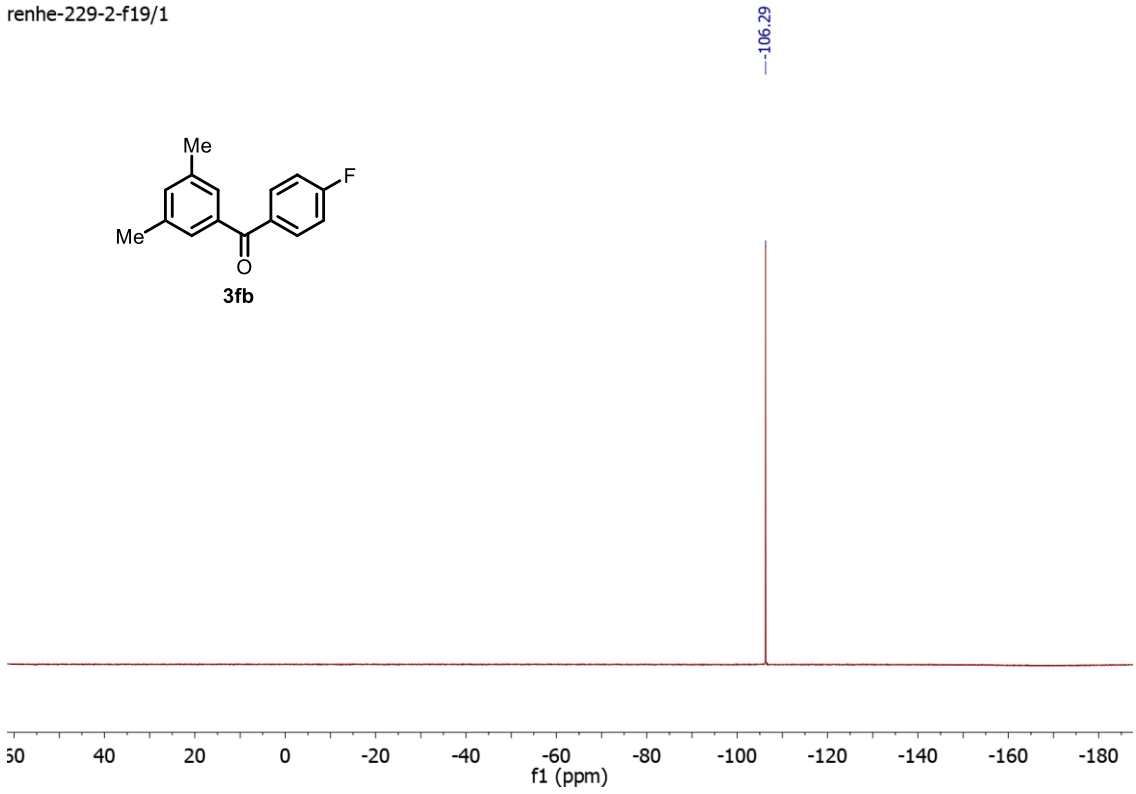

Figure 4.63. ^{1}H NMR Spectrum of 3gb

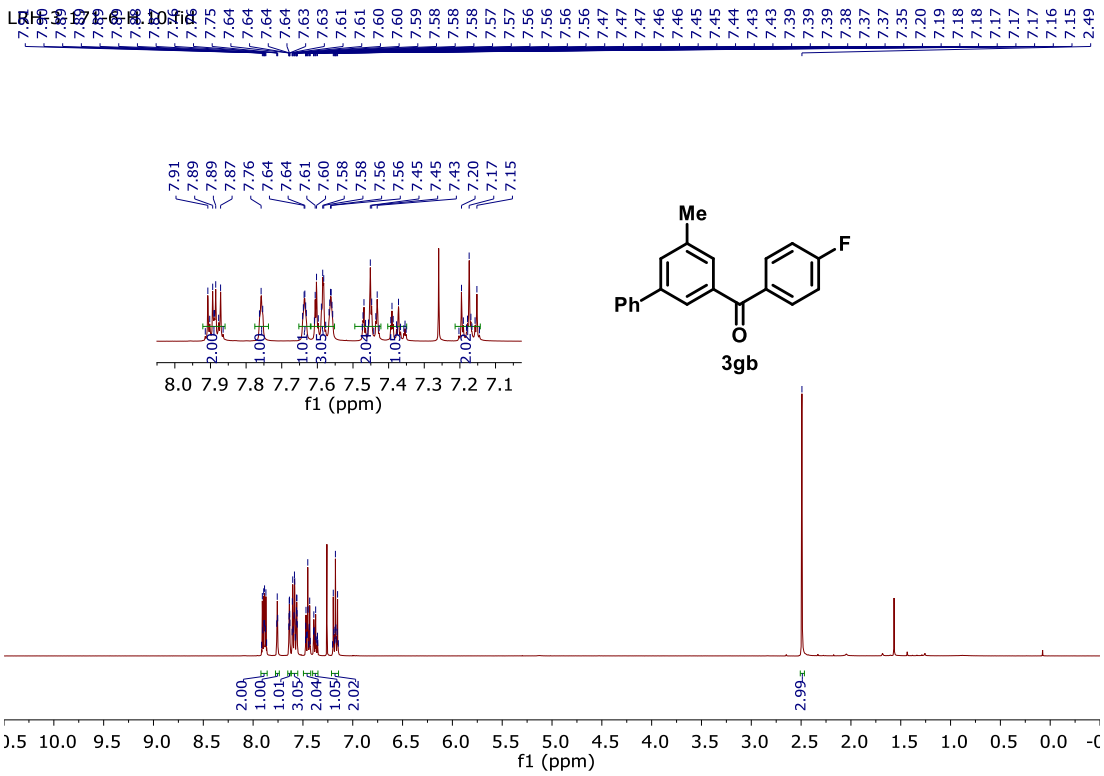

Figure 4.64. ^{13}C NMR Spectrum of 3gb

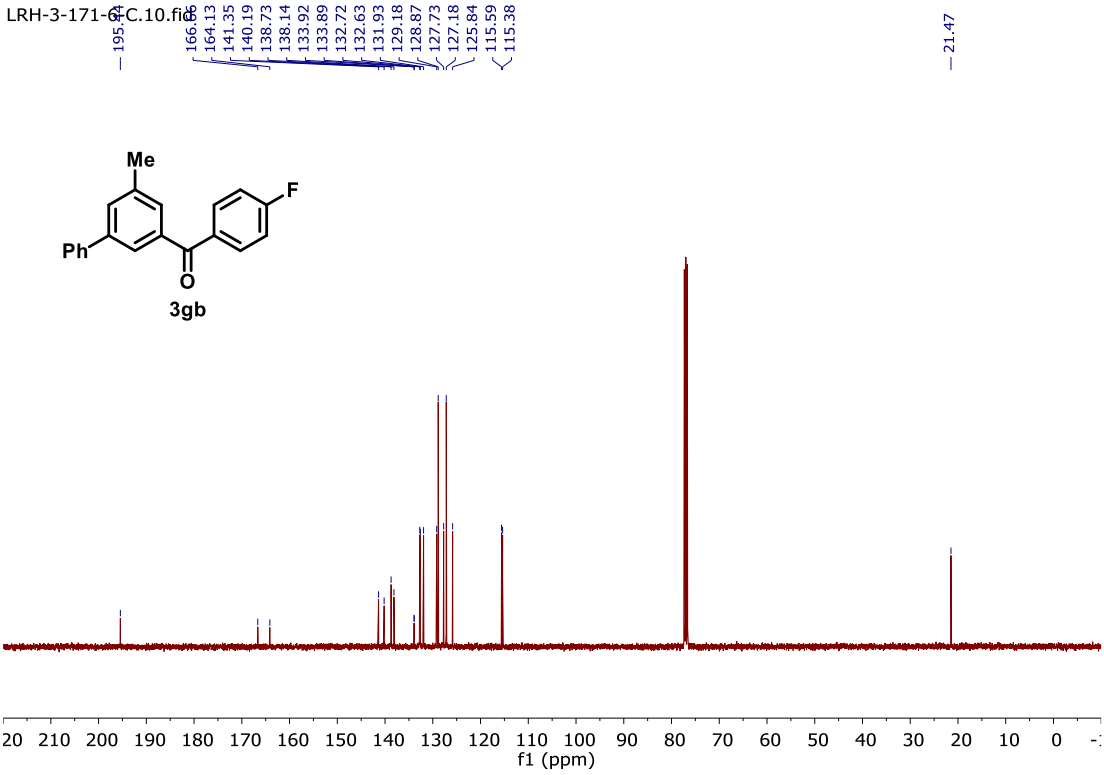

Figure 4.65. ^{19}F NMR Spectrum of 3gb

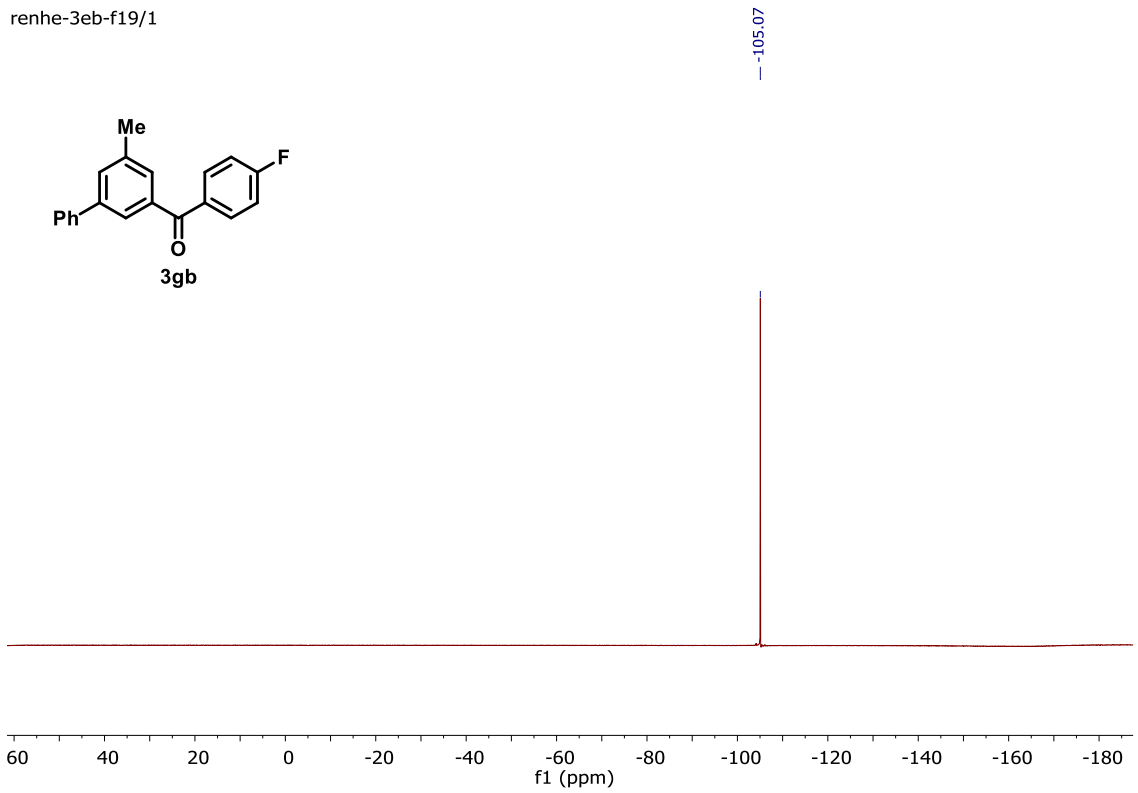

Figure 4.66. ^{1}H NMR Spectrum of 3hb

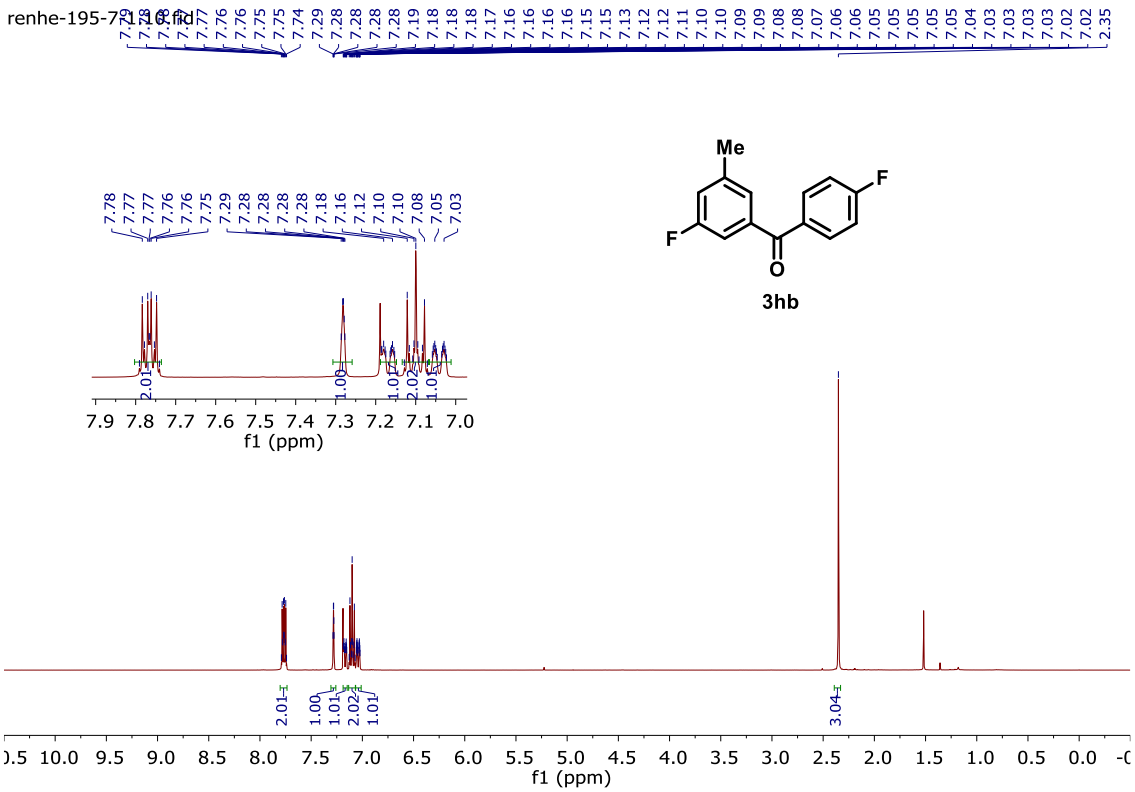

Figure 4.67. ^{13}C NMR Spectrum of 3hb

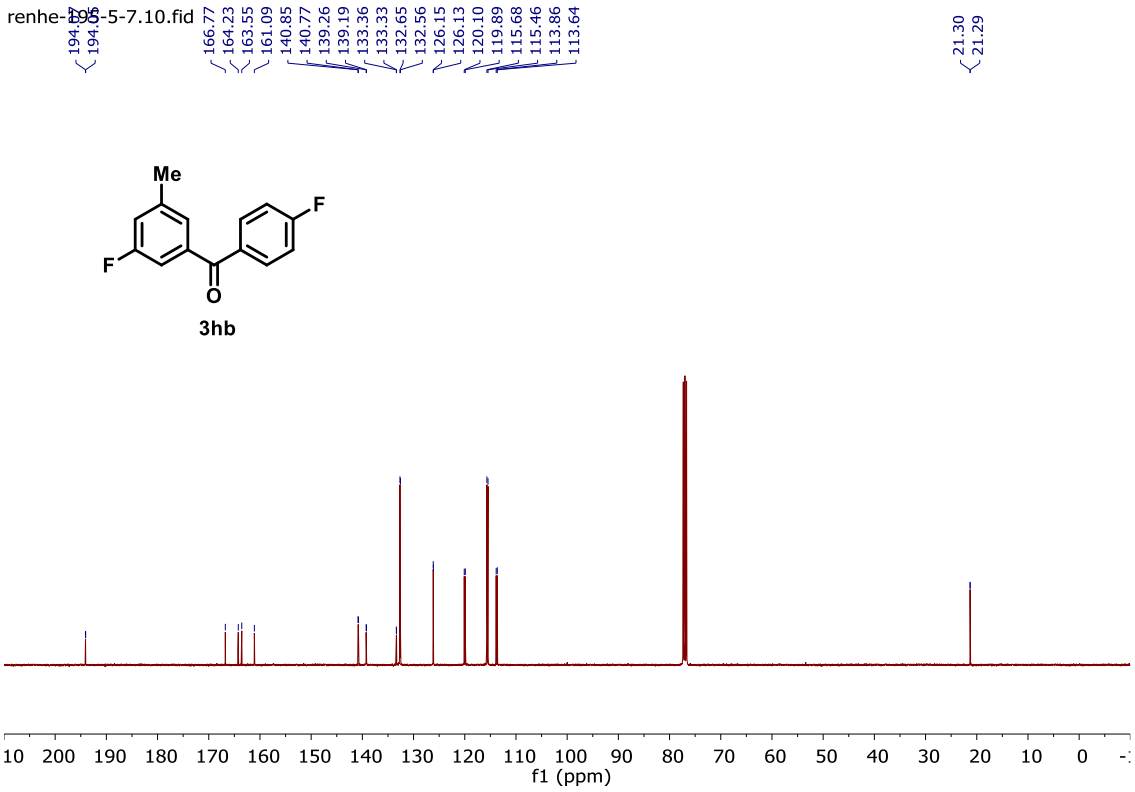

Figure 4.68. ^{19}F NMR Spectrum of 3hb

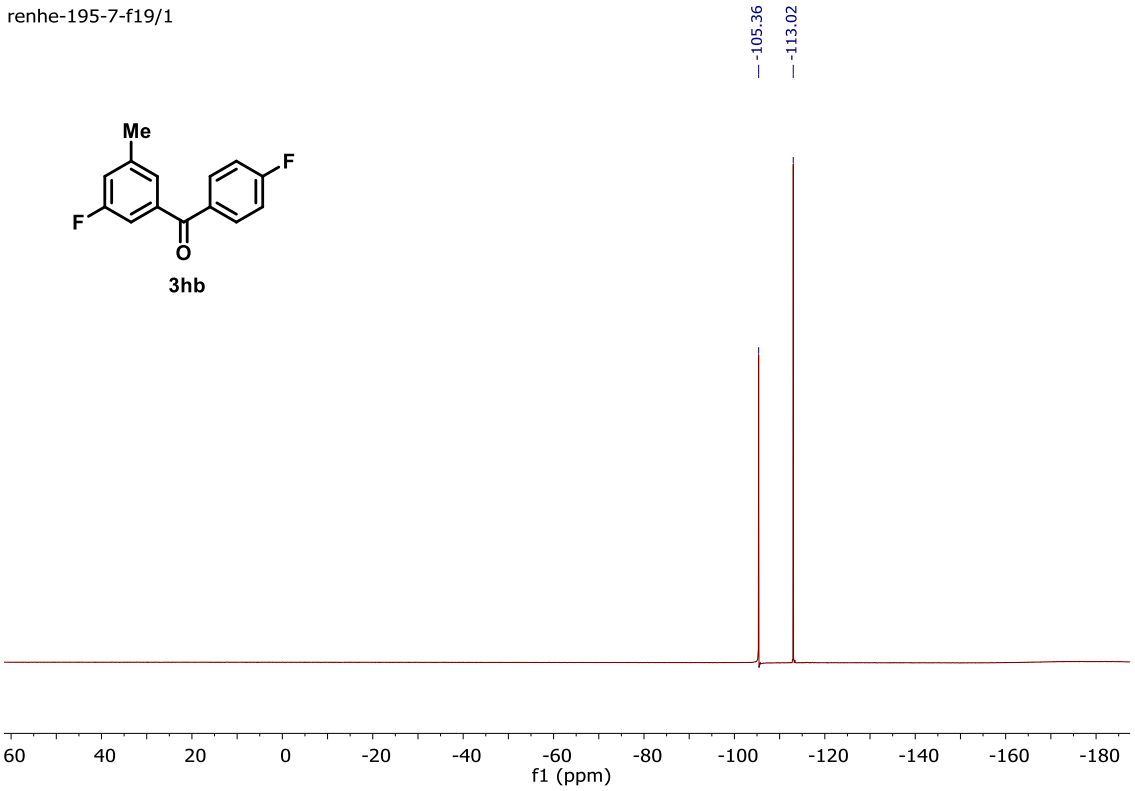

Figure 4.69. ^{1}H NMR Spectrum of 3ib

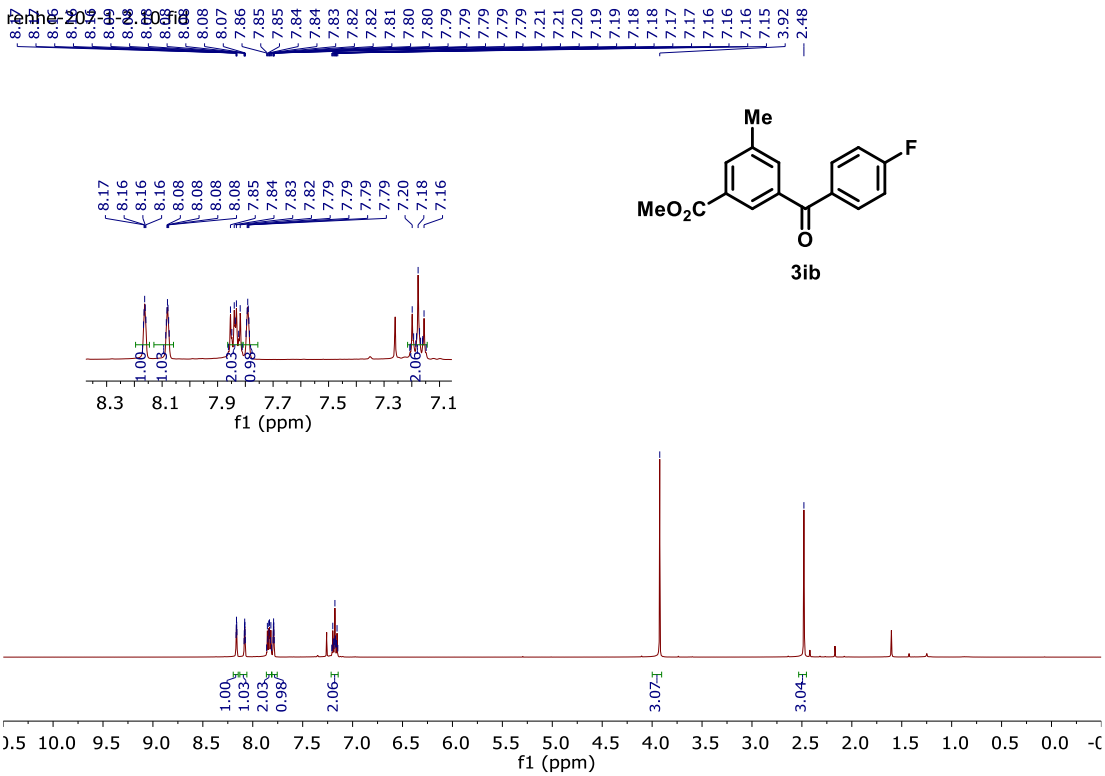

Figure 4.70. ^{13}C NMR Spectrum of 3ib

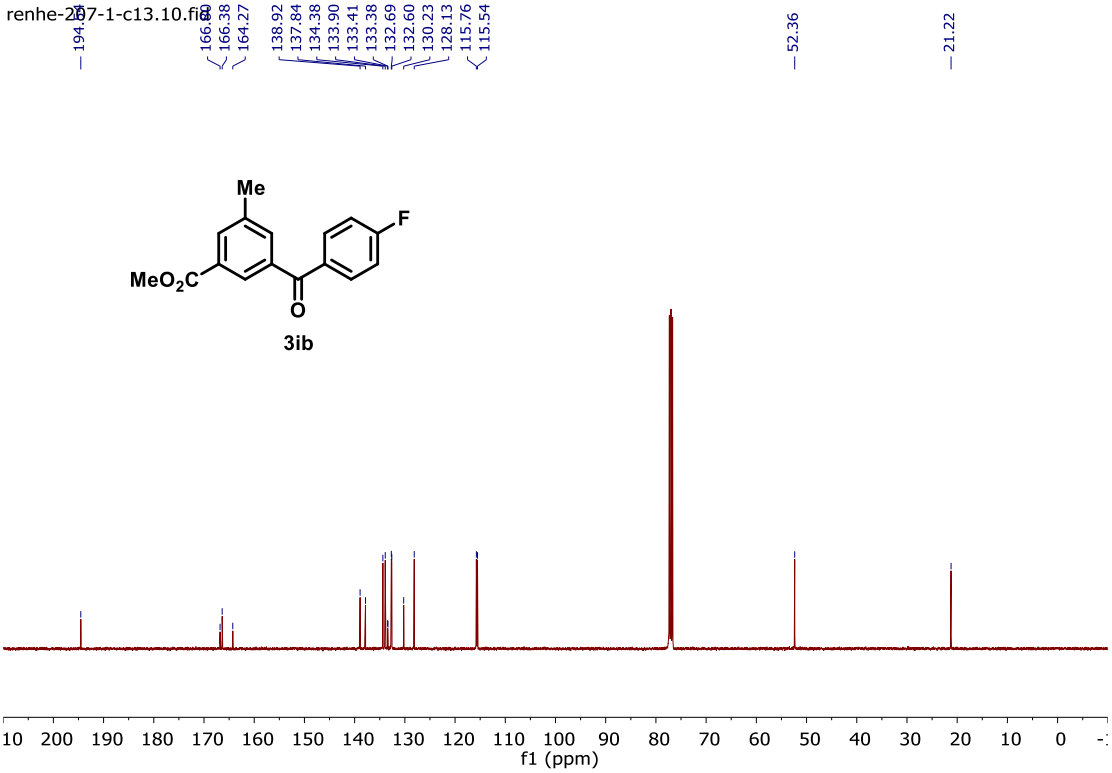

Figure 4.71. ^{19}F NMR Spectrum of 3ib

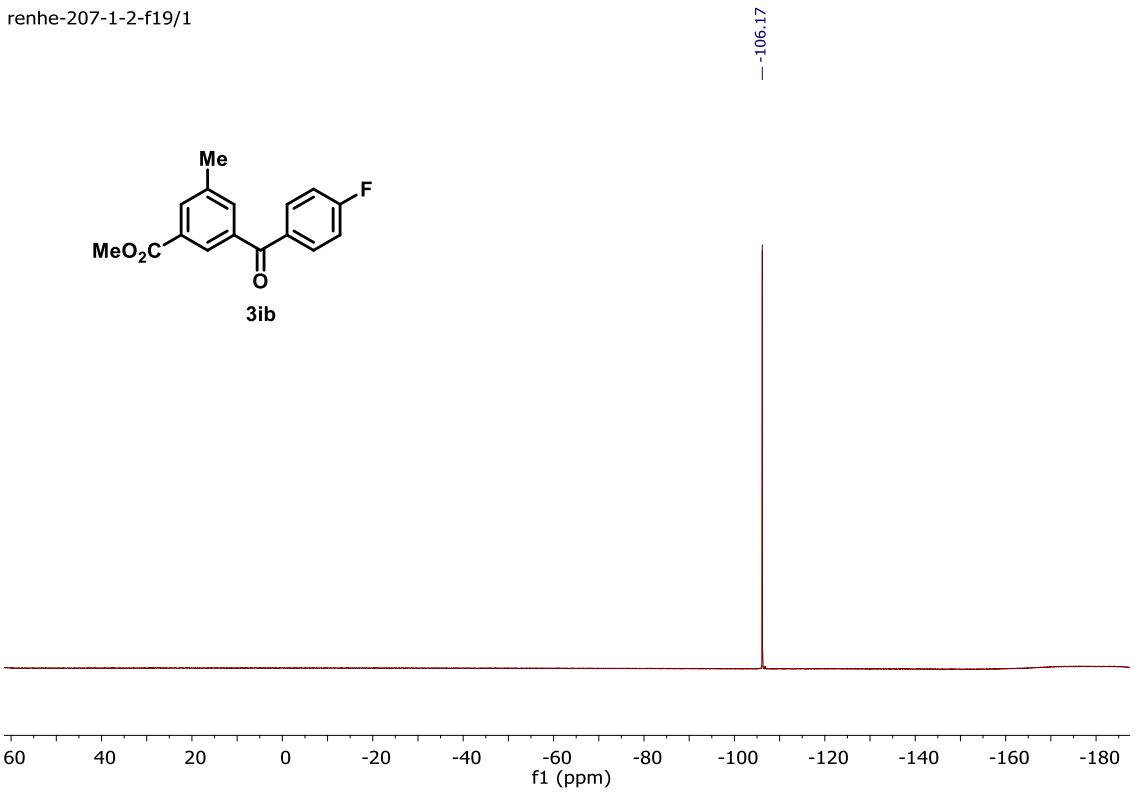

Figure 4.72. ^{1}H NMR Spectrum of 3jb

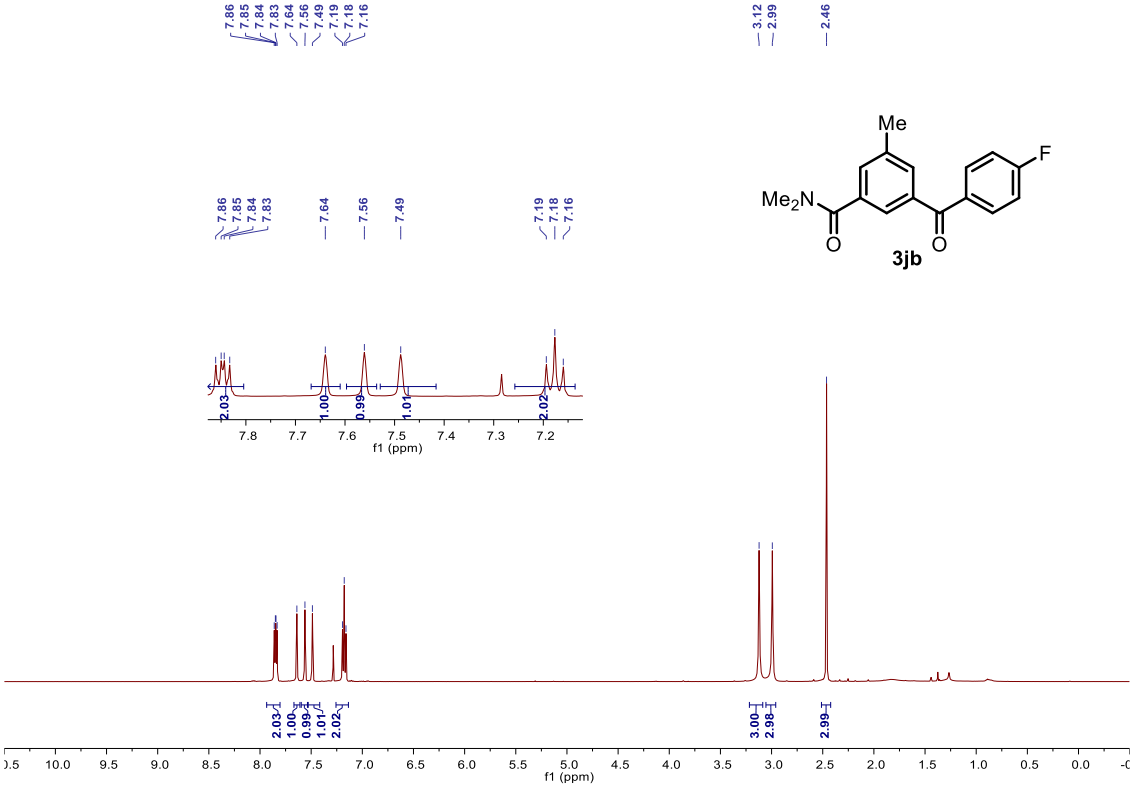

Figure 4.73. ^{13}C NMR Spectrum of 3jb

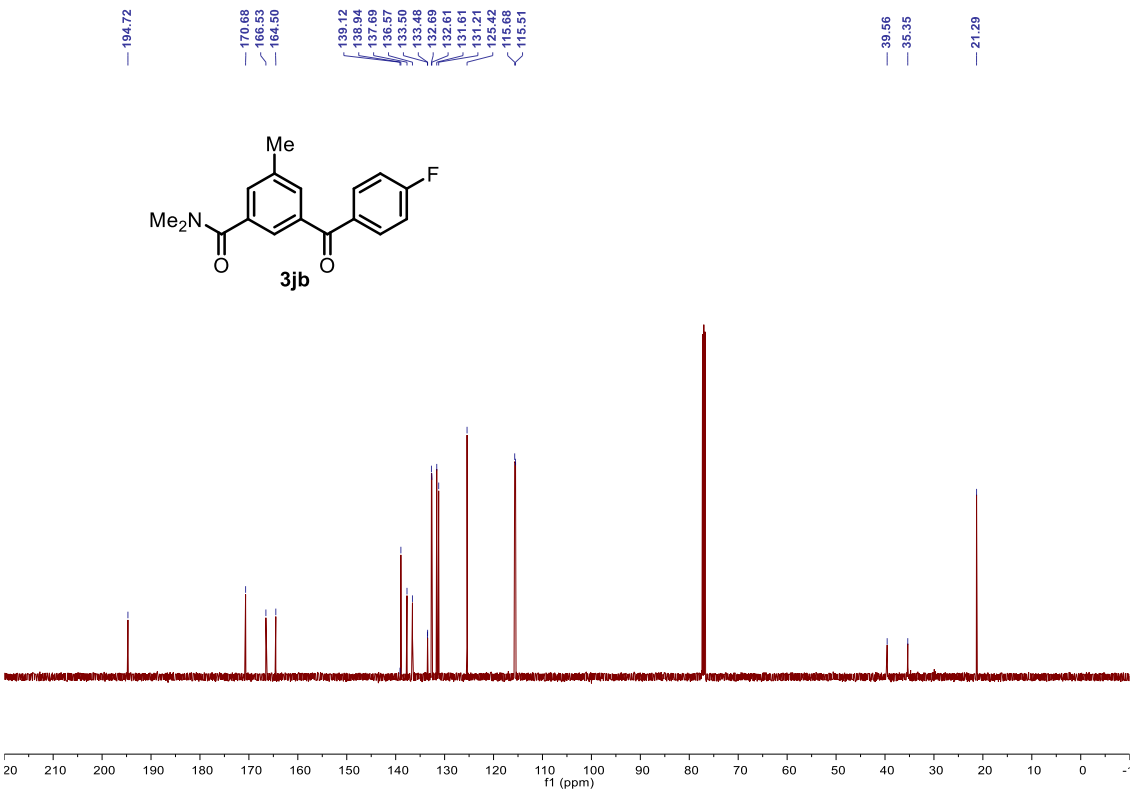

Figure 4.74. ^{19}F NMR Spectrum of 3jb

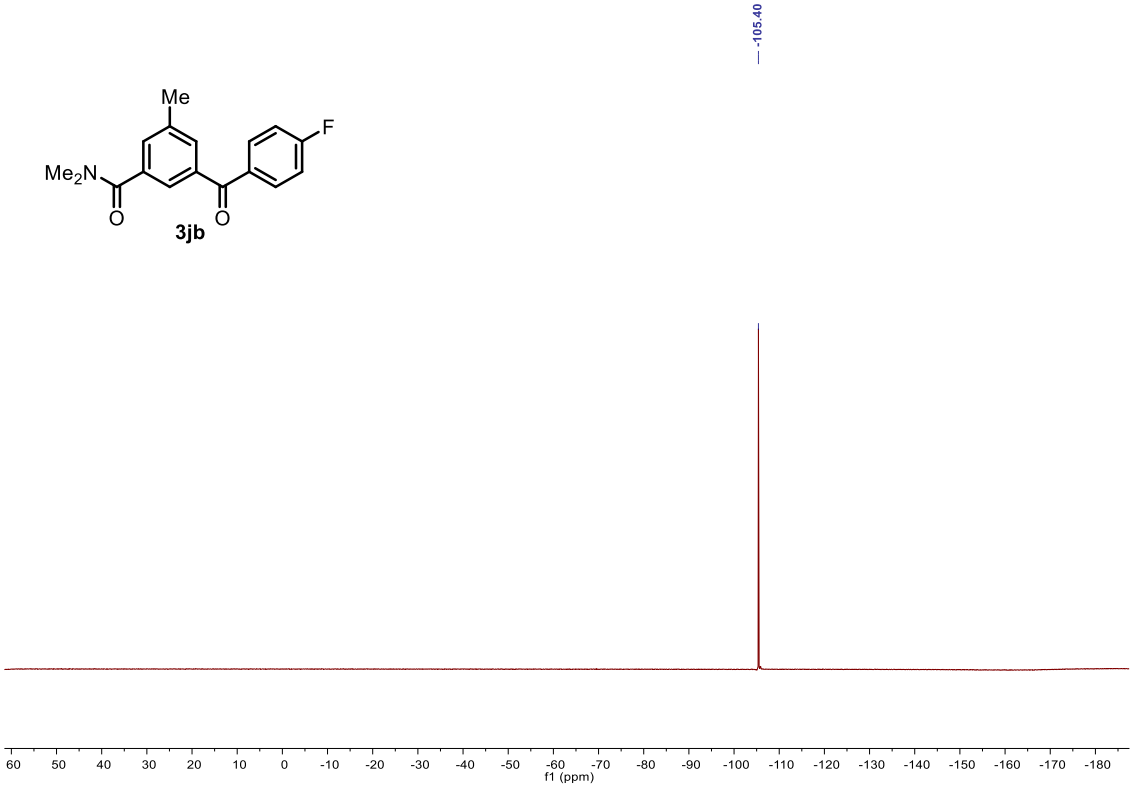

Figure 4.75. ^{1}H NMR Spectrum of 3kb

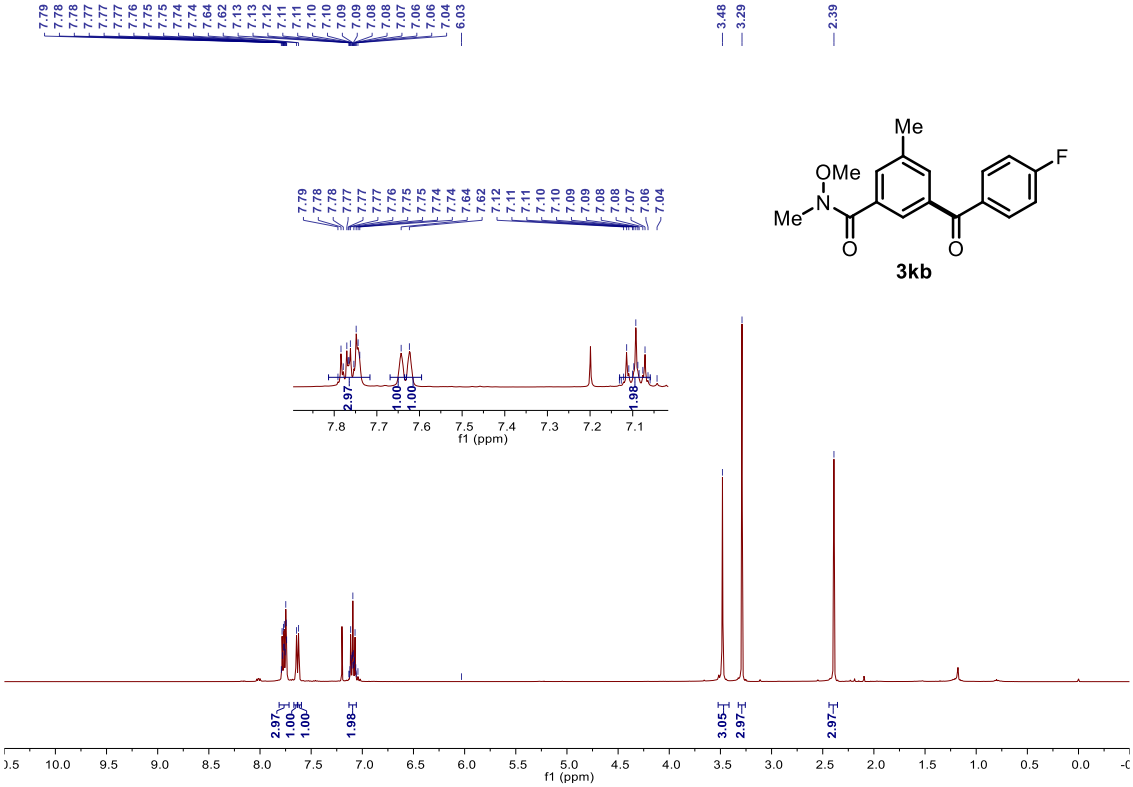

Figure 4.76. ^{13}C NMR Spectrum of 3kb

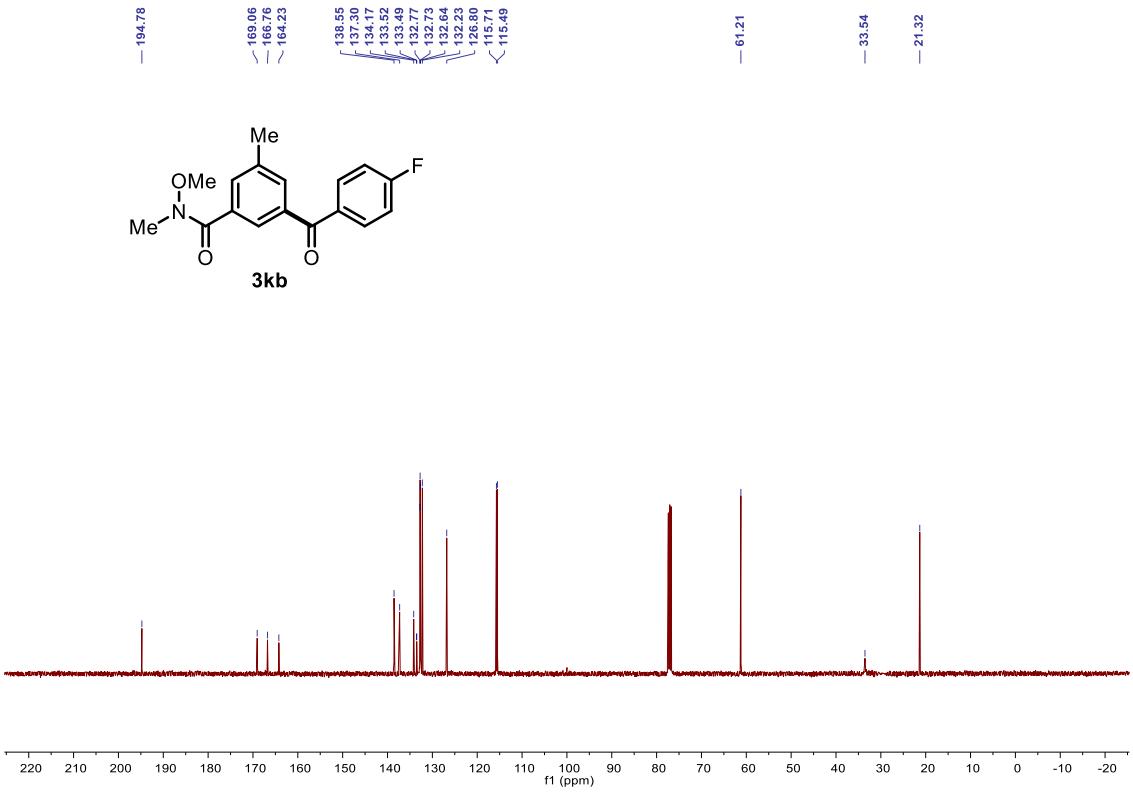

Figure 4.77. ^{19}F NMR Spectrum of 3kb

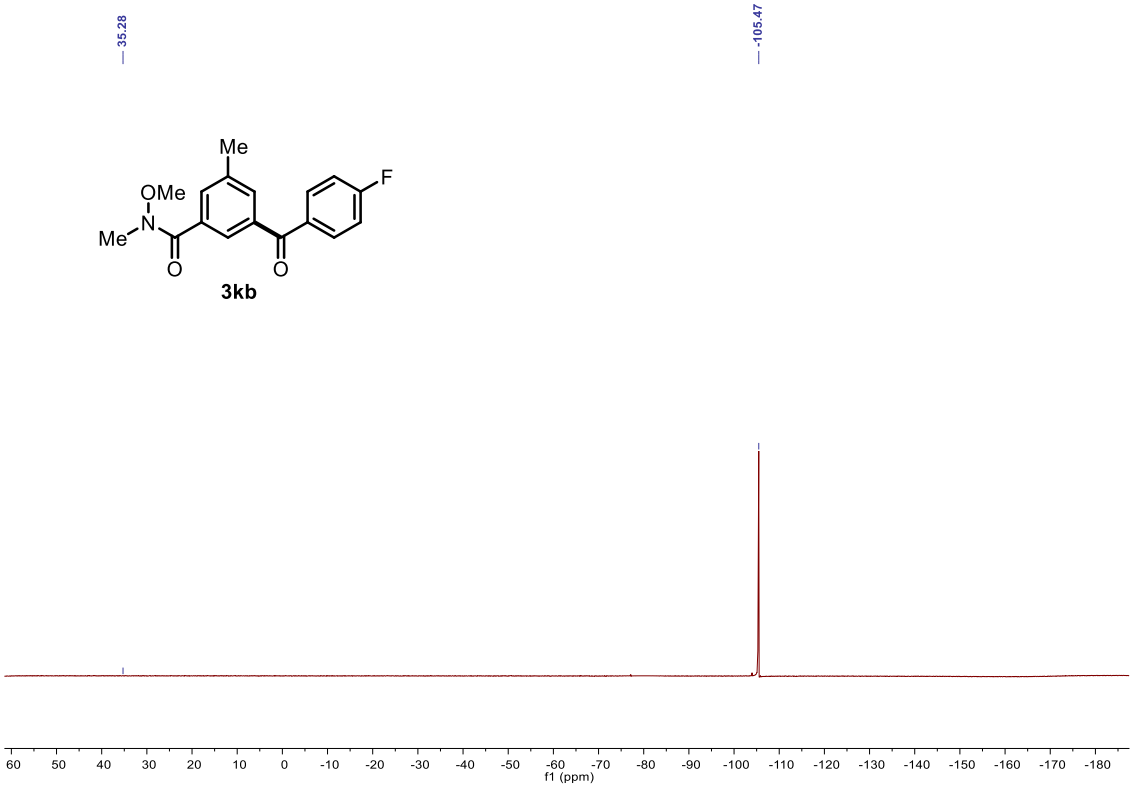

Figure 4.78. ^{1}H NMR Spectrum of 3lb

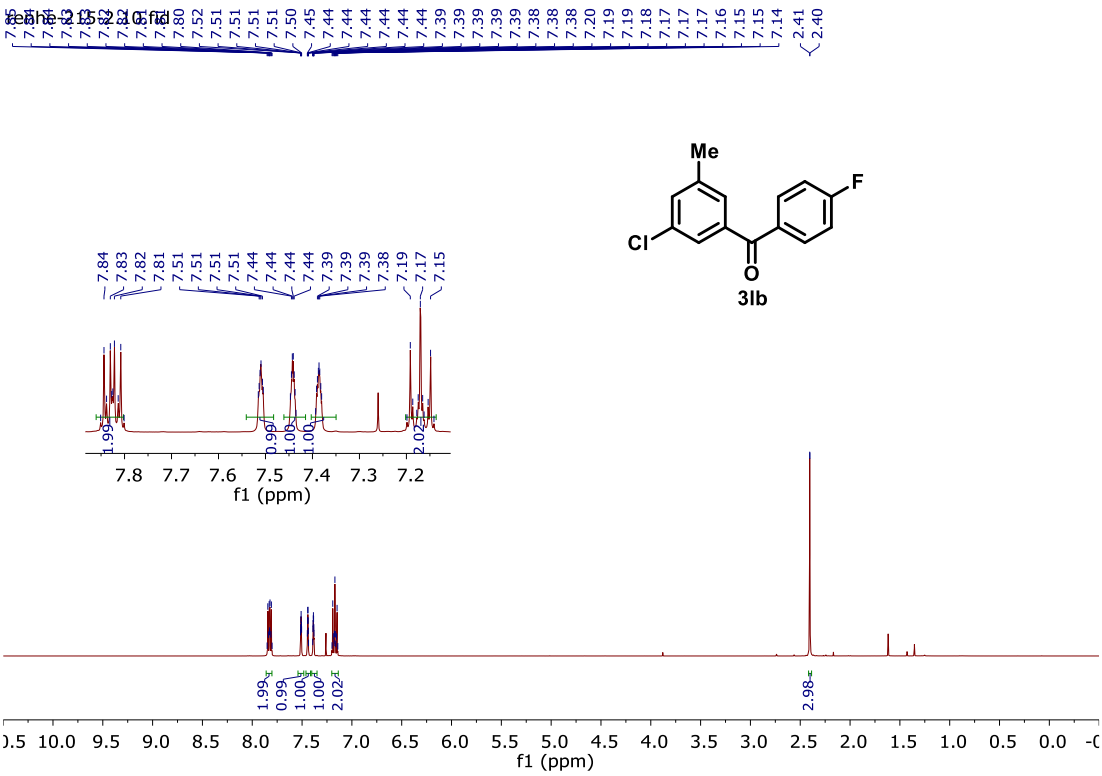

Figure 4.79. ^{13}C NMR Spectrum of 3lb

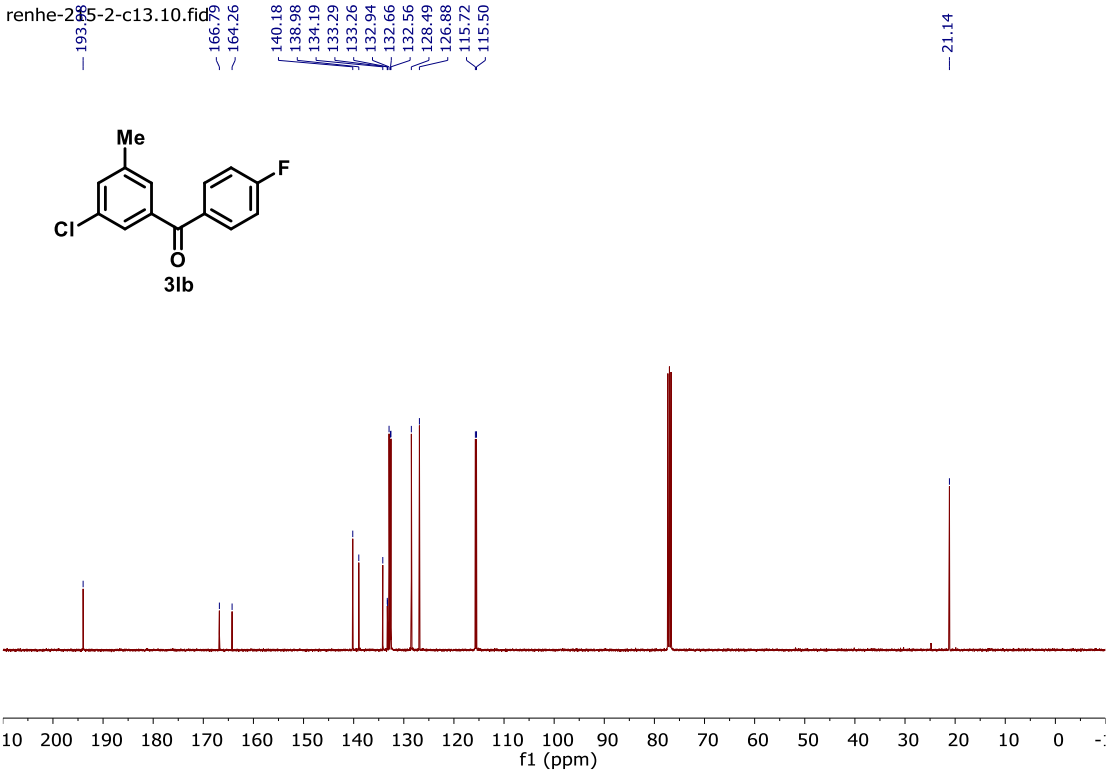

Figure 4.80. ^{19}F NMR Spectrum of 3lb

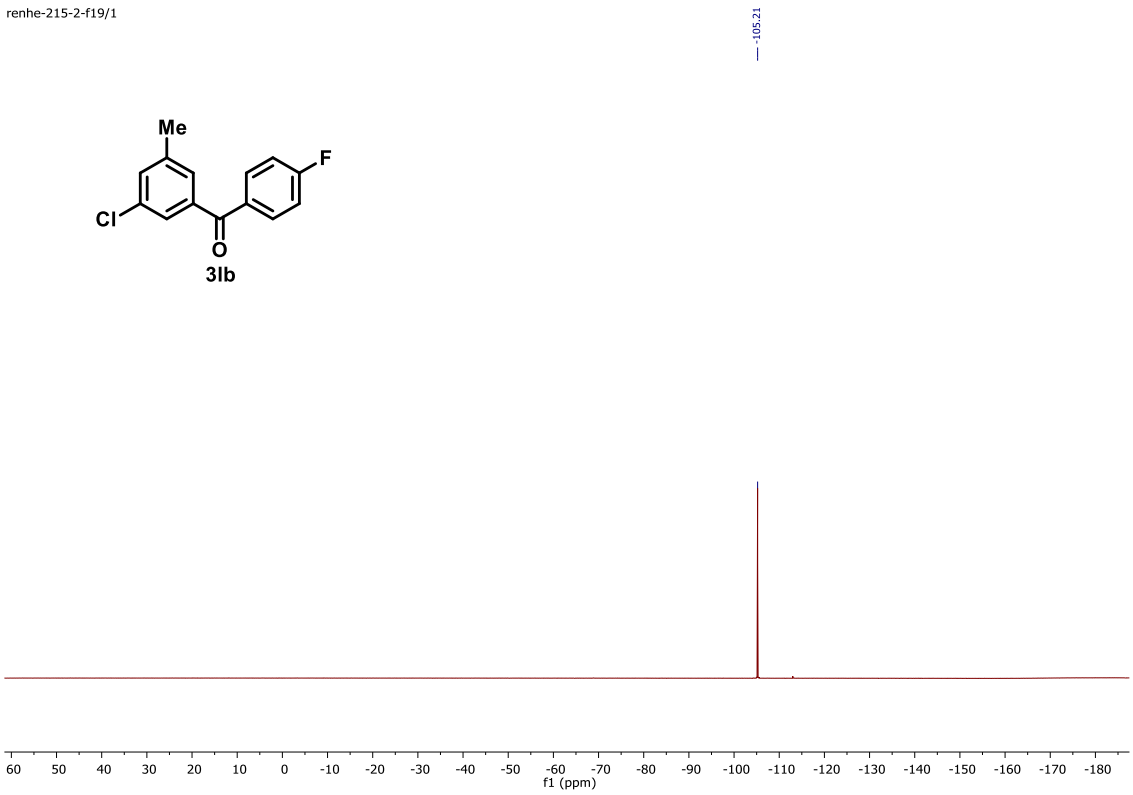

Figure 4.81. ^{1}H NMR Spectrum of 3mb

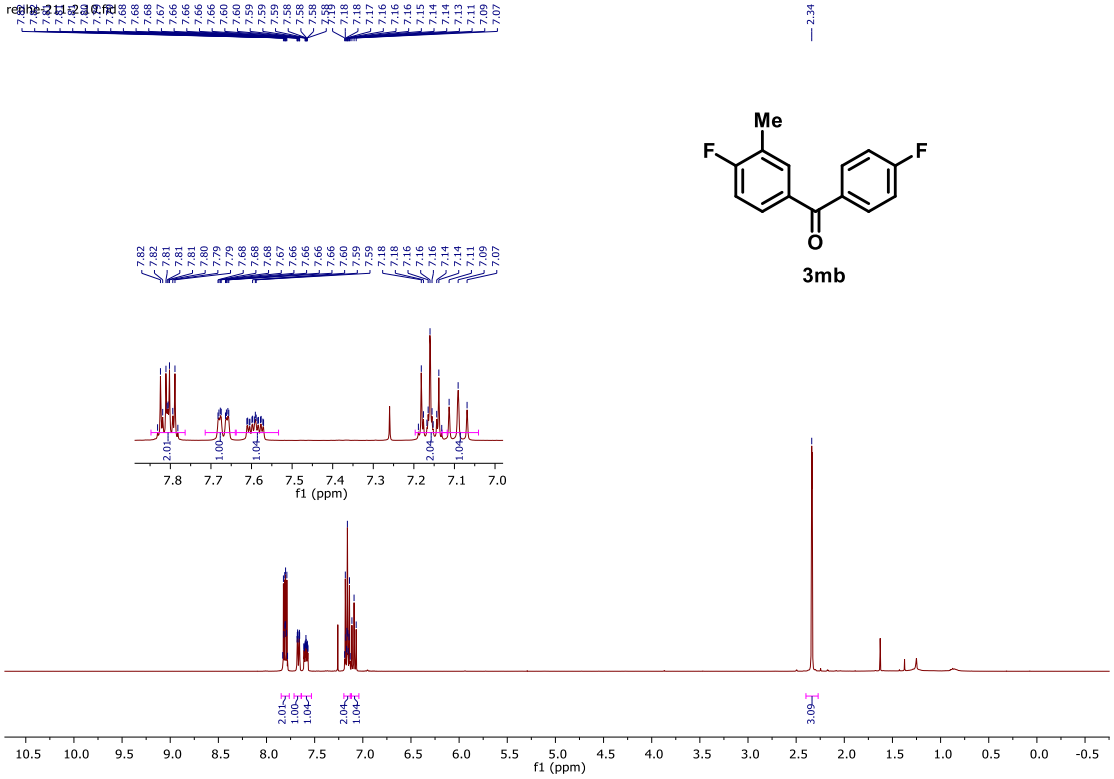

Figure 4.82. ^{13}C NMR Spectrum of 3mb

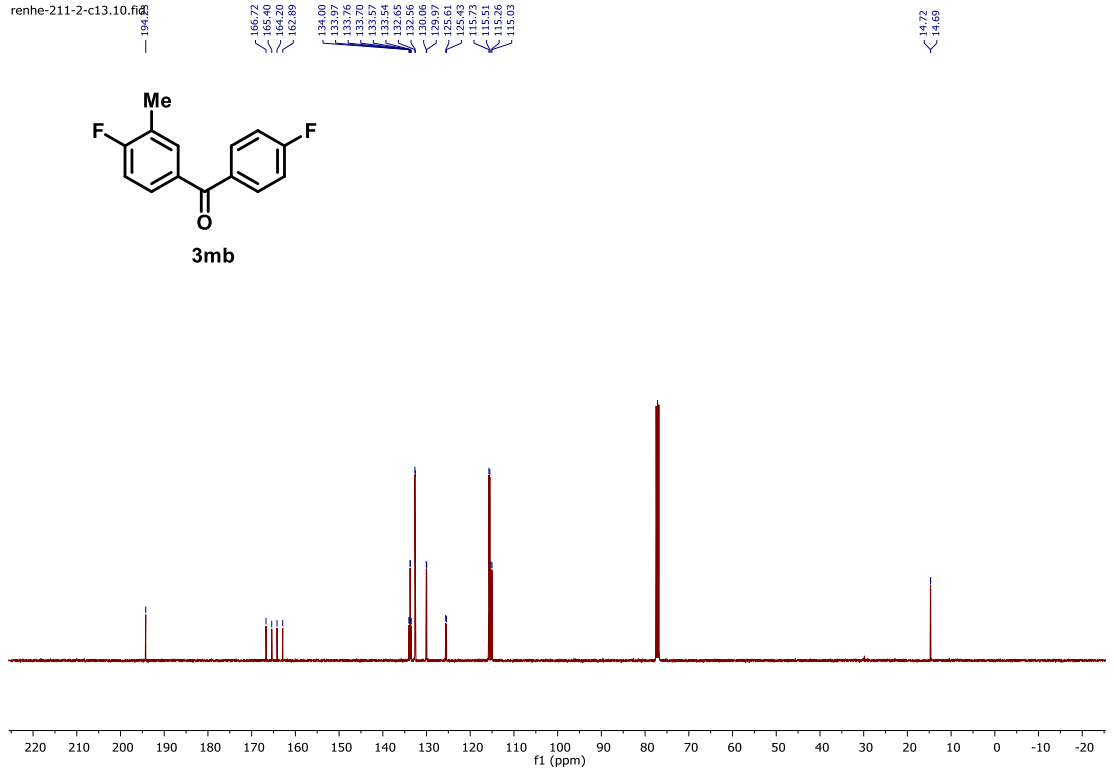

Figure 4.83. ^{19}F NMR Spectrum of 3mb

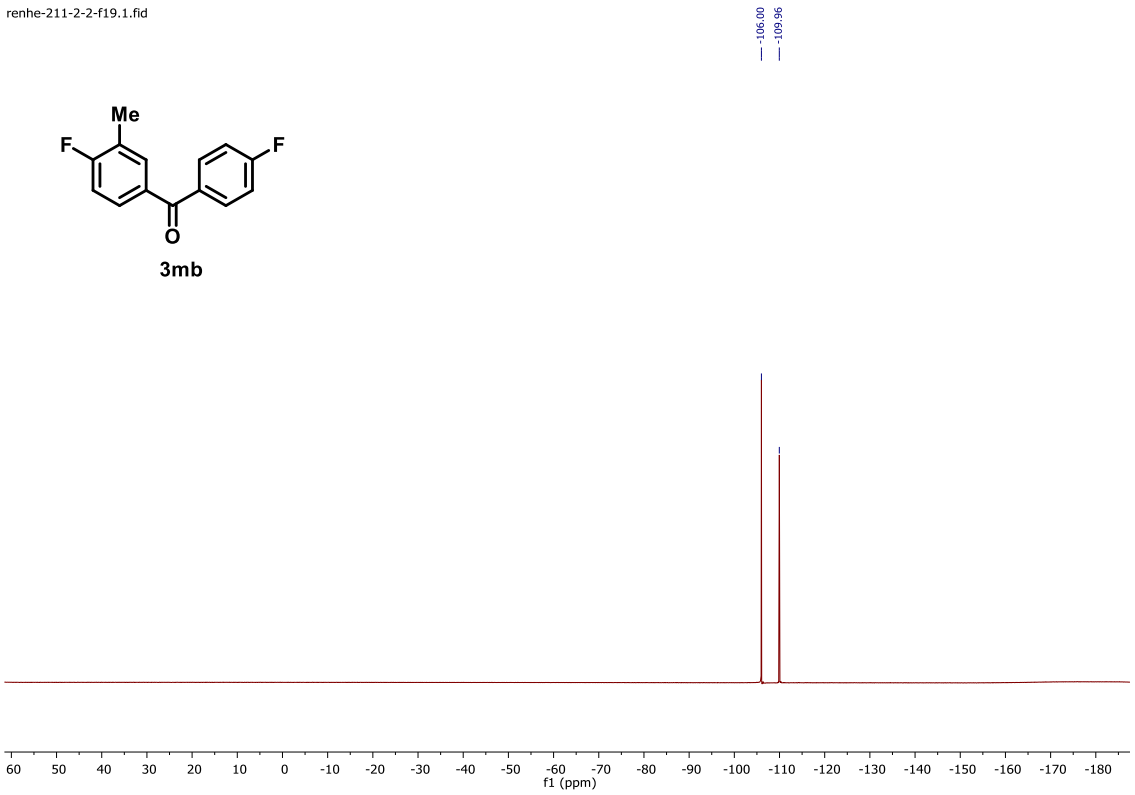

Figure 4.84. ^{1}H NMR Spectrum of 3nb

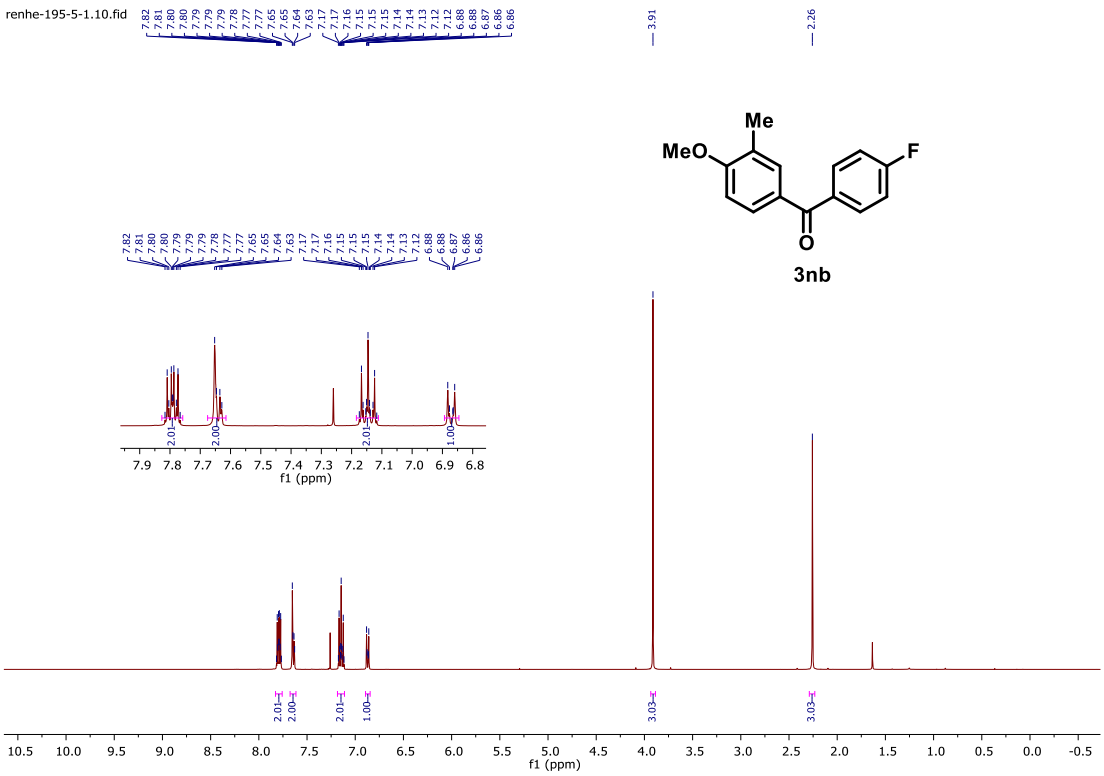

Figure 4.85. ^{13}C NMR Spectrum of 3nb

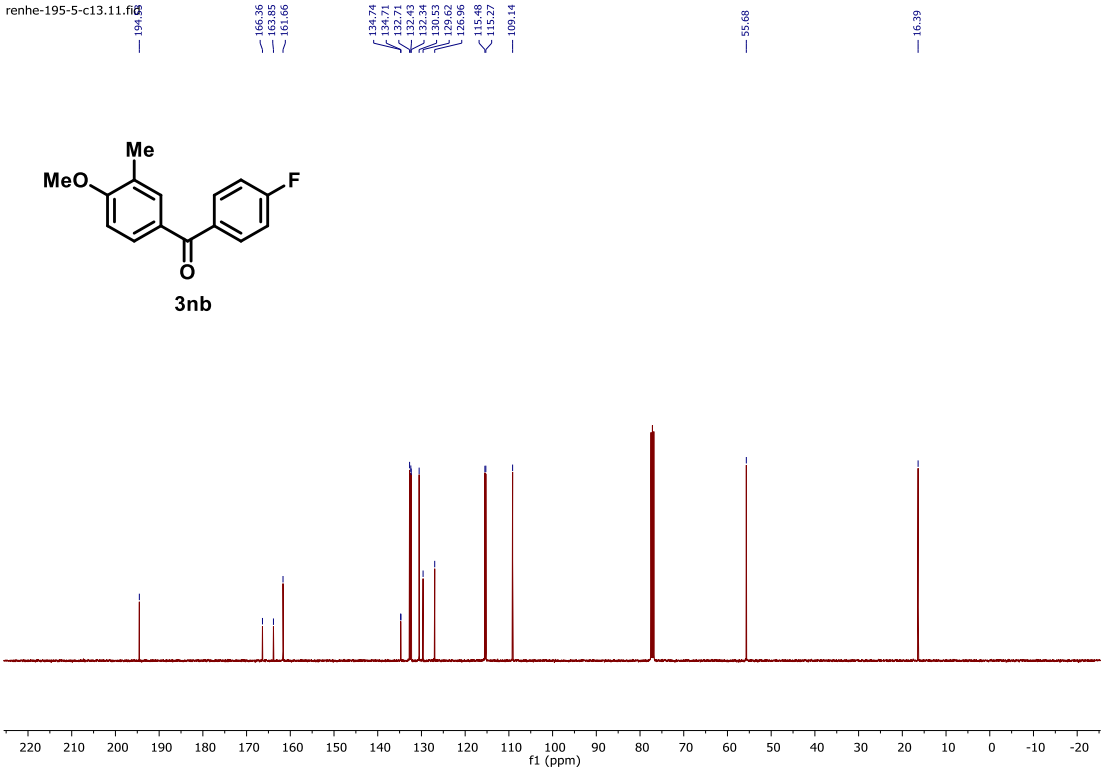

Figure 4.86. ^{19}F NMR Spectrum of 3nb

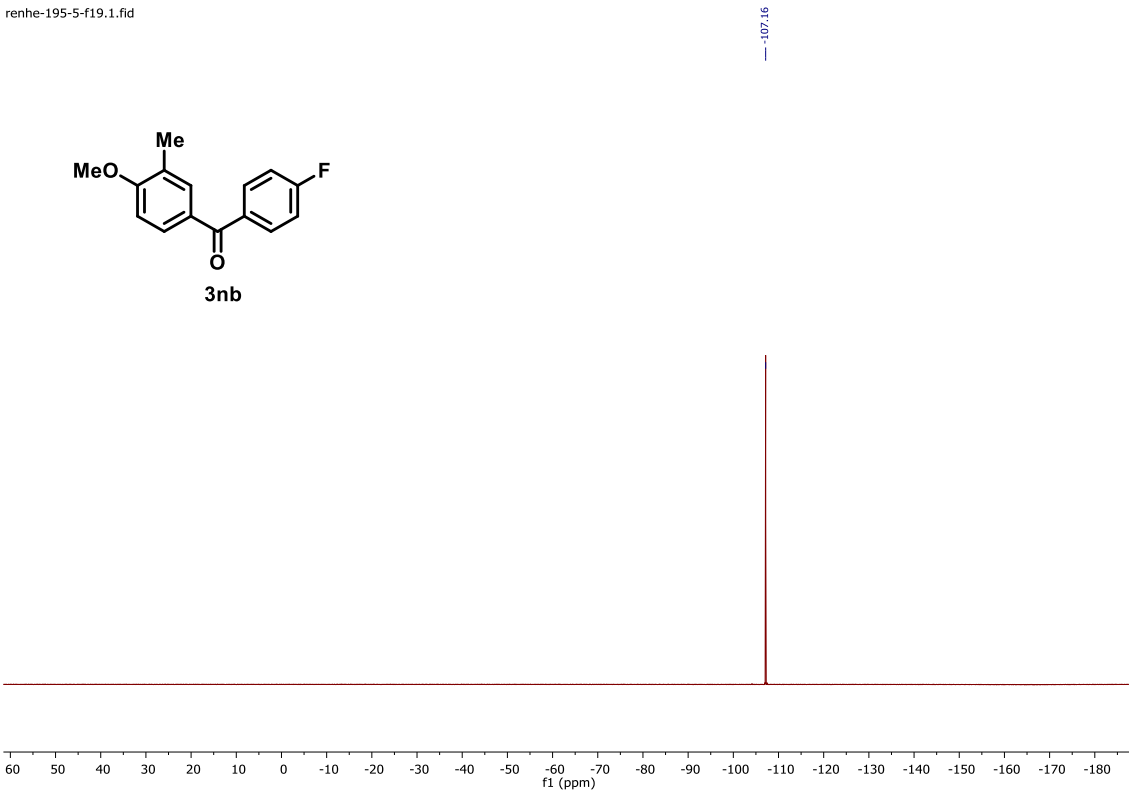

Figure 4.87. ^{1}H NMR Spectrum of 3ob

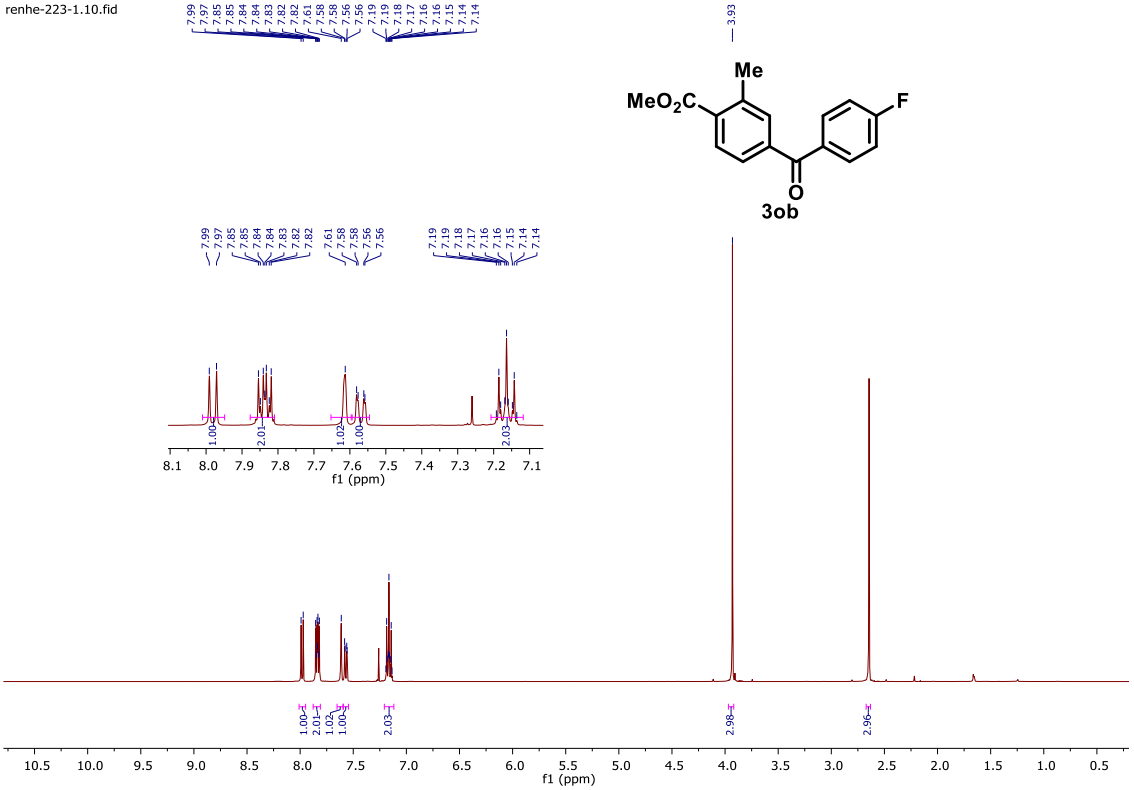

Figure 4.88. ^{13}C NMR Spectrum of 3ob

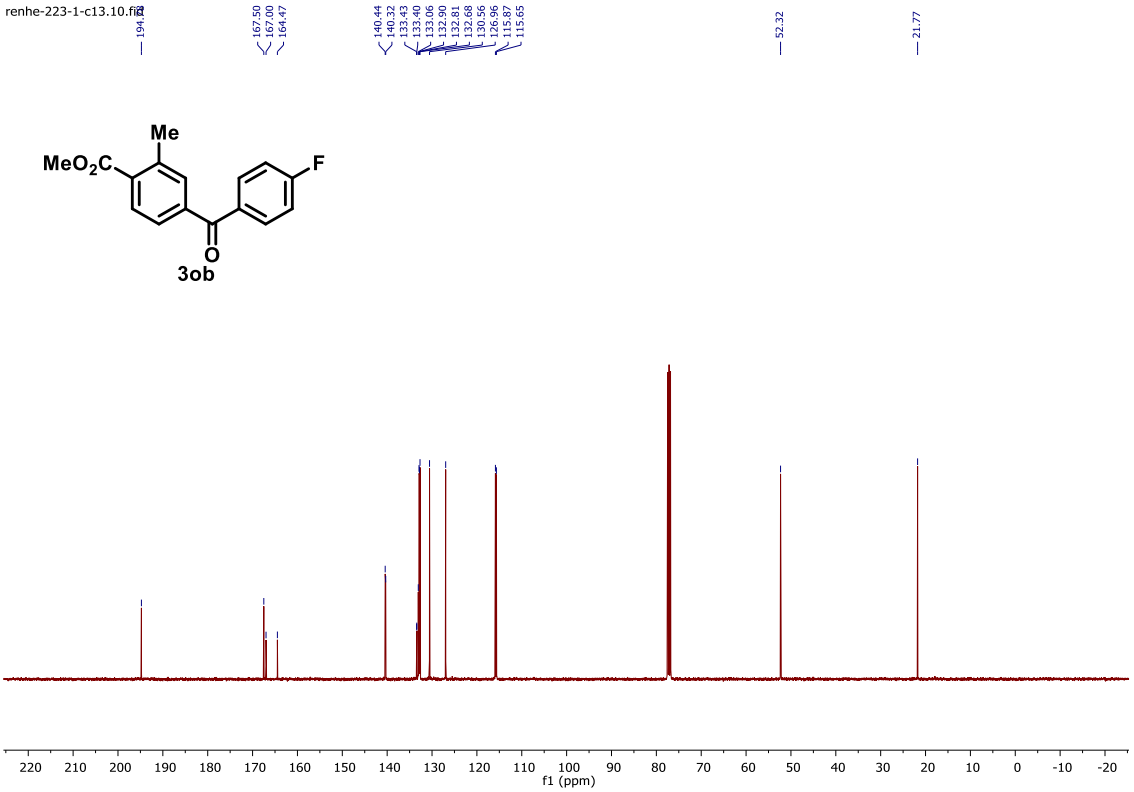

Figure 4.89. ^{19}F NMR Spectrum of 3ob

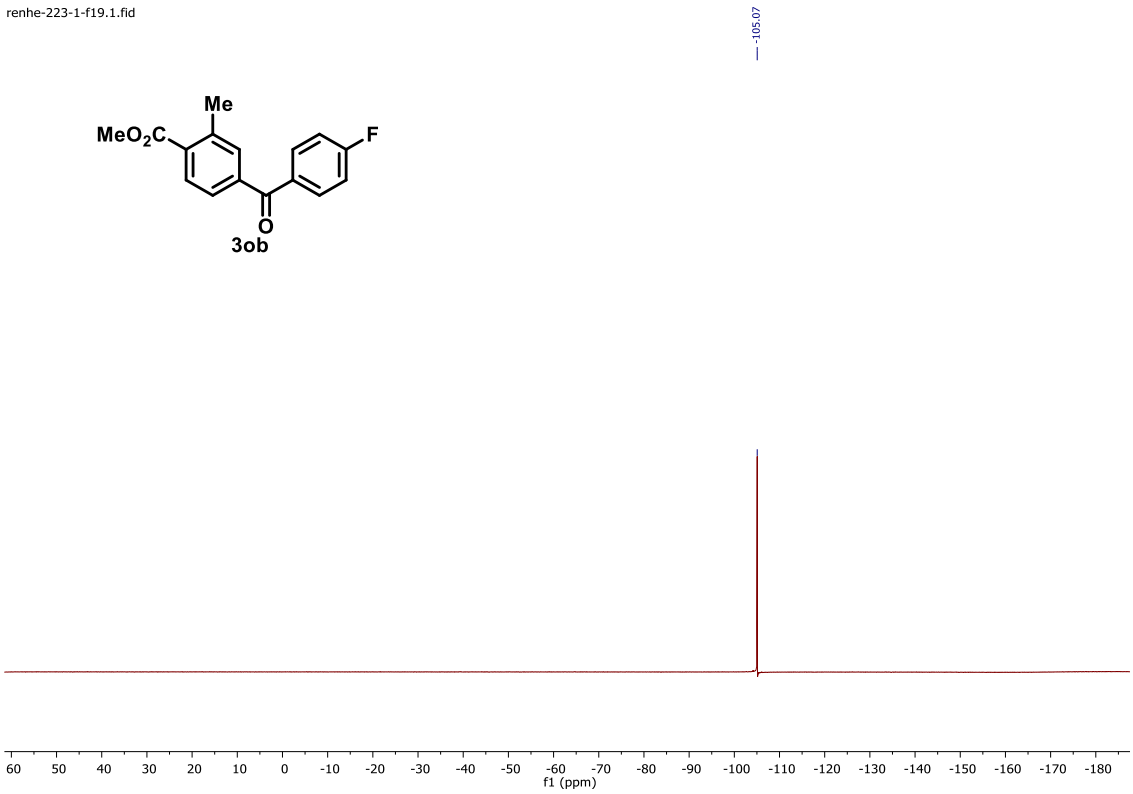

Figure 4.90. ^{1}H NMR Spectrum of 3pb

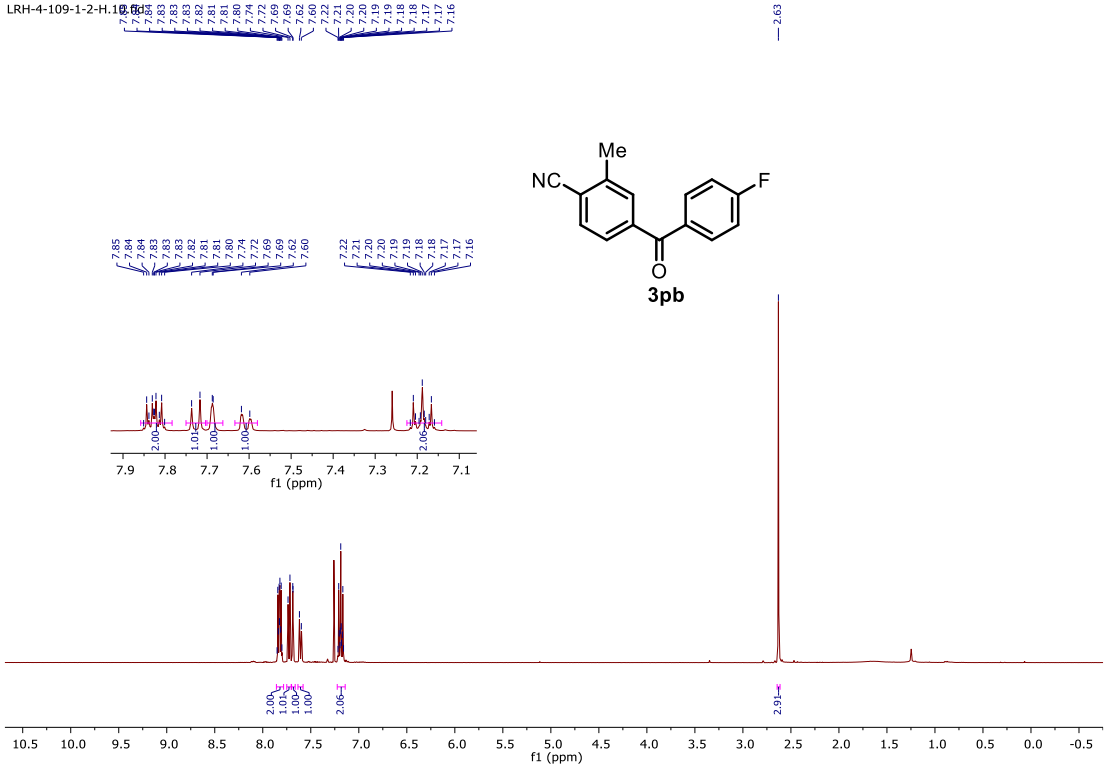

Figure 4.91. ^{13}C NMR Spectrum of 3pb

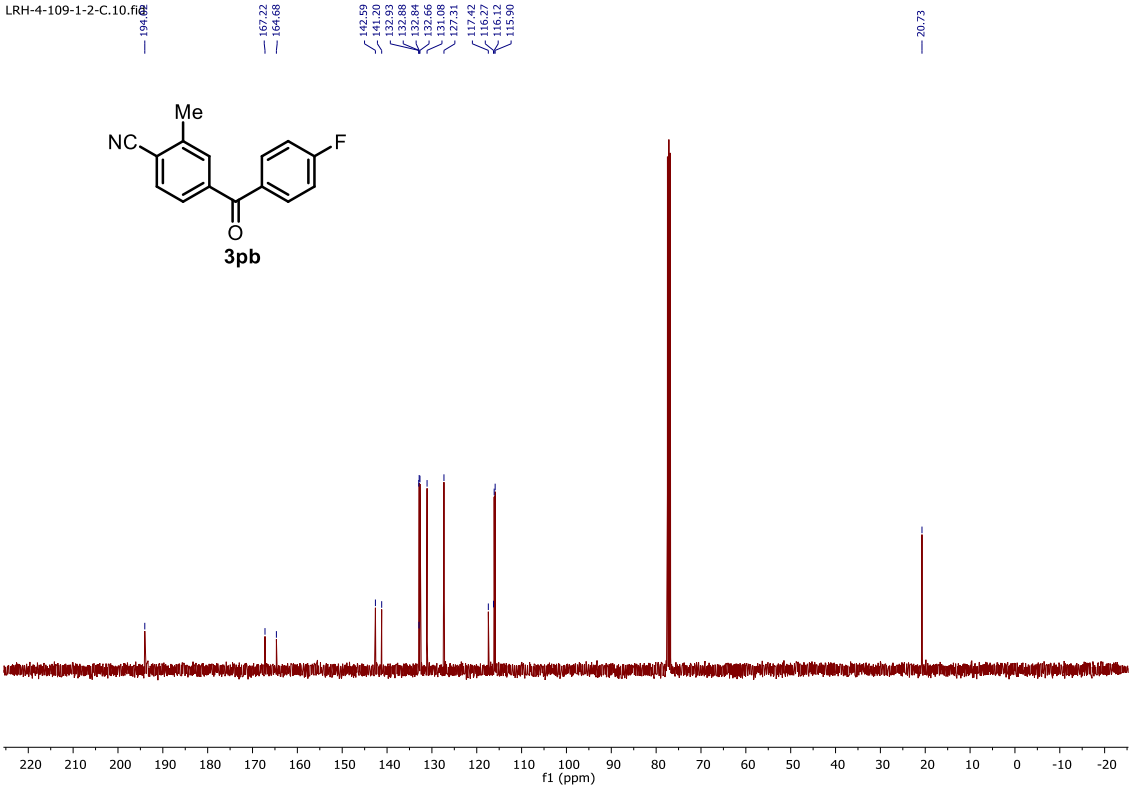

Figure 4.92. ^{19}F NMR Spectrum of 3pb

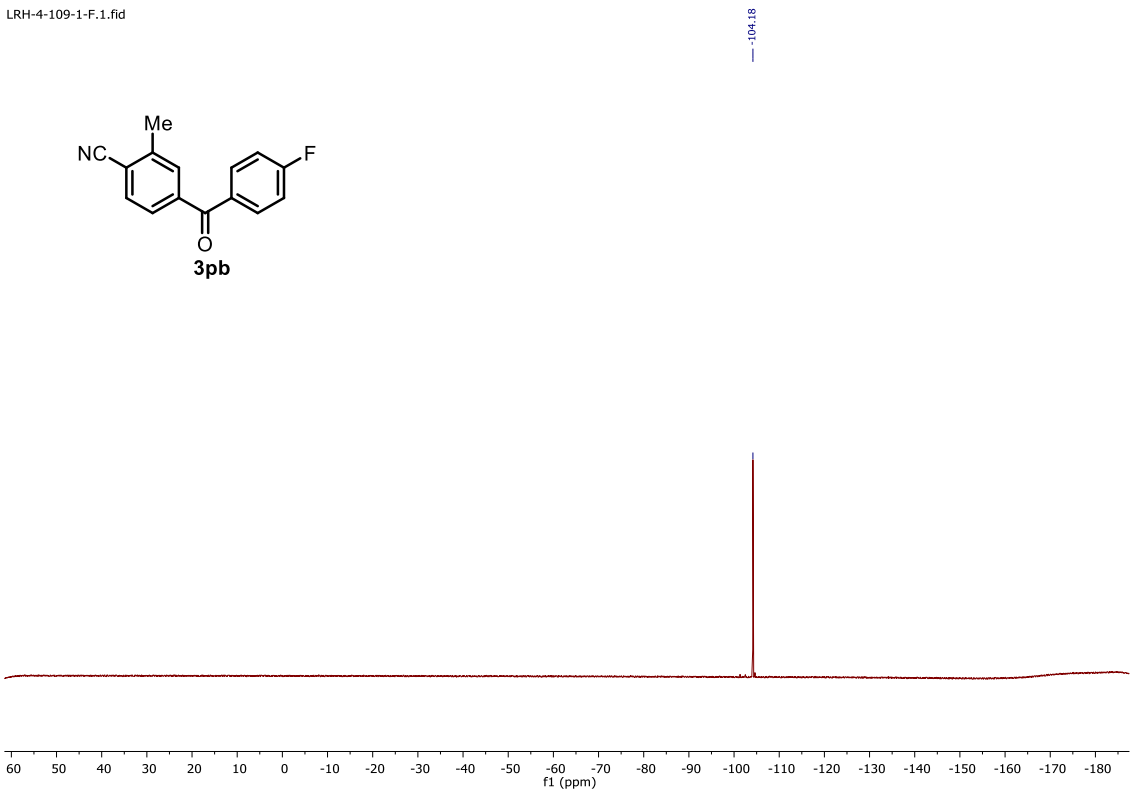

Figure 4.93. ^{1}H NMR Spectrum of 3qb

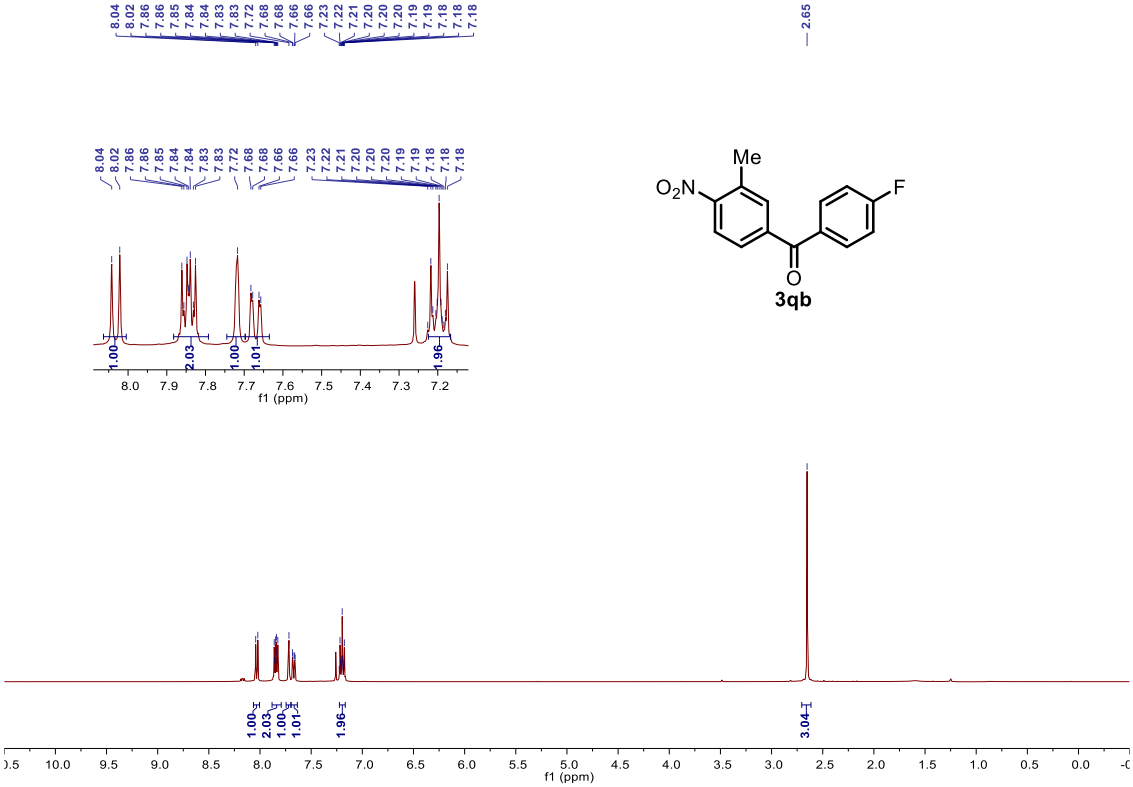

Figure 4.94. ^{13}C NMR Spectrum of 3qb

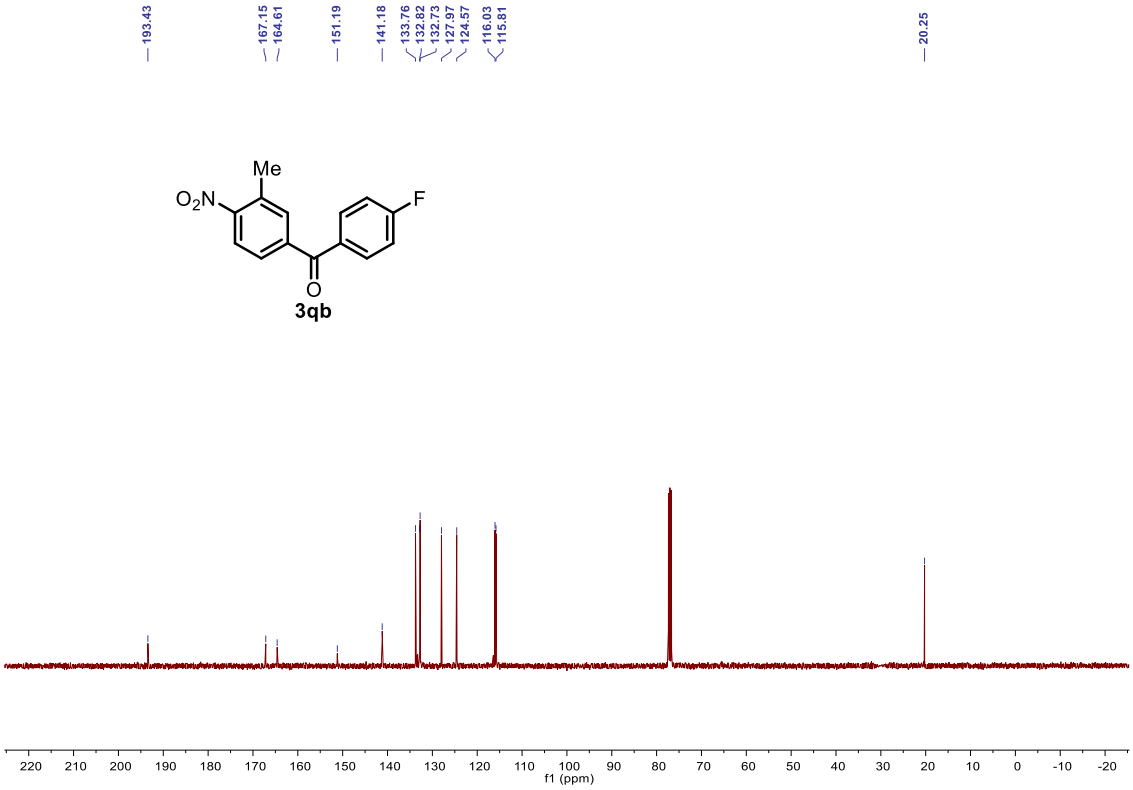

Figure 4.95. ^{19}F NMR Spectrum of 3qb

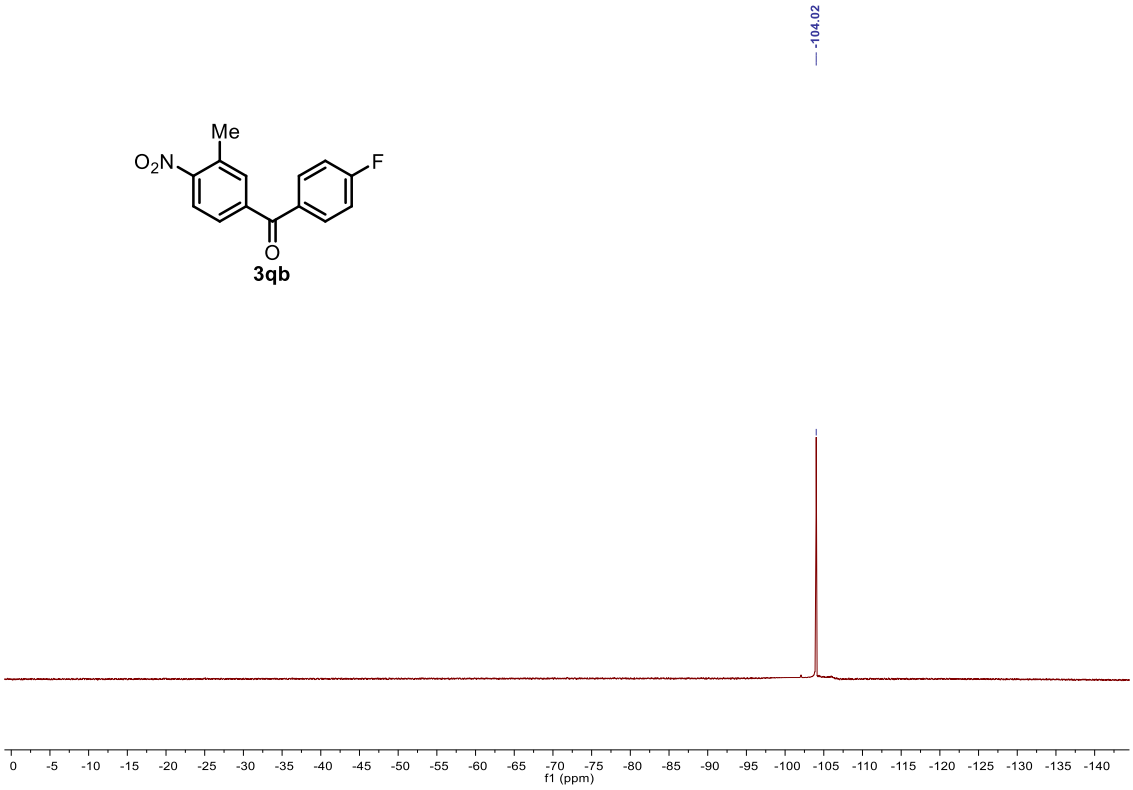

Figure 4.96. ^{1}H NMR Spectrum of 3rb

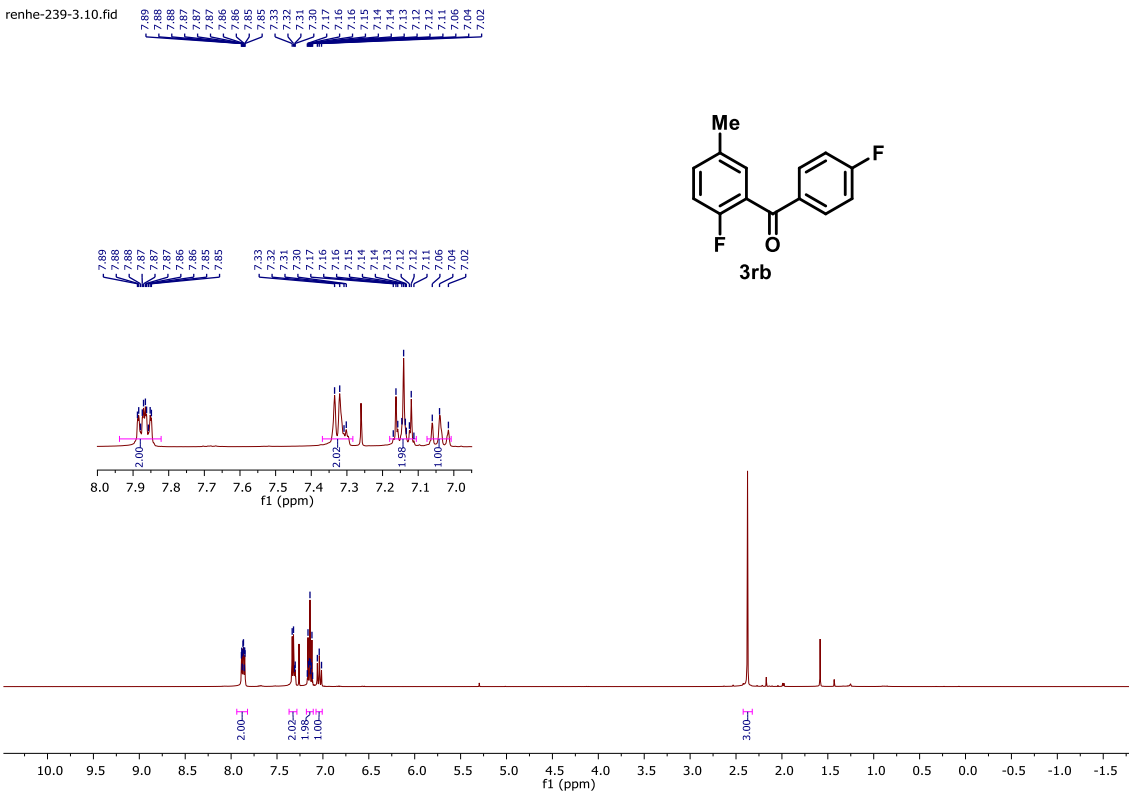

Figure 4.97. ^{13}C NMR Spectrum of 3rb

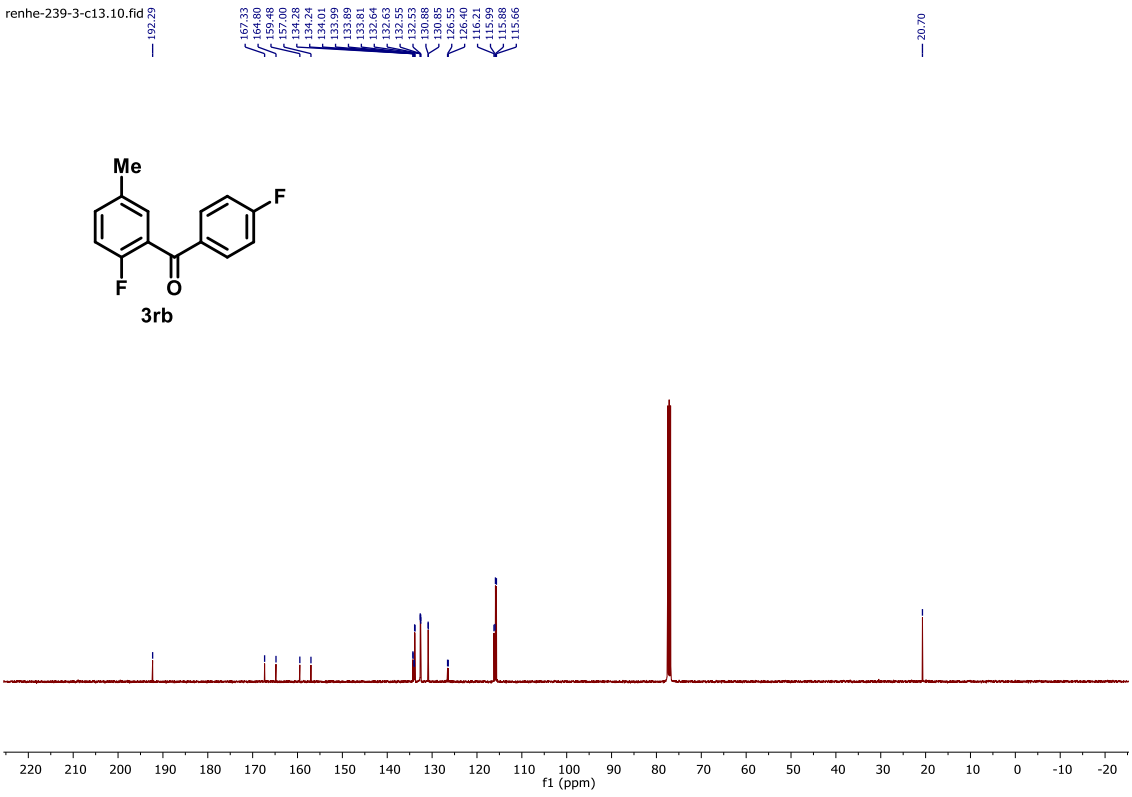

Figure 4.98. ^{19}F NMR Spectrum of 3rb

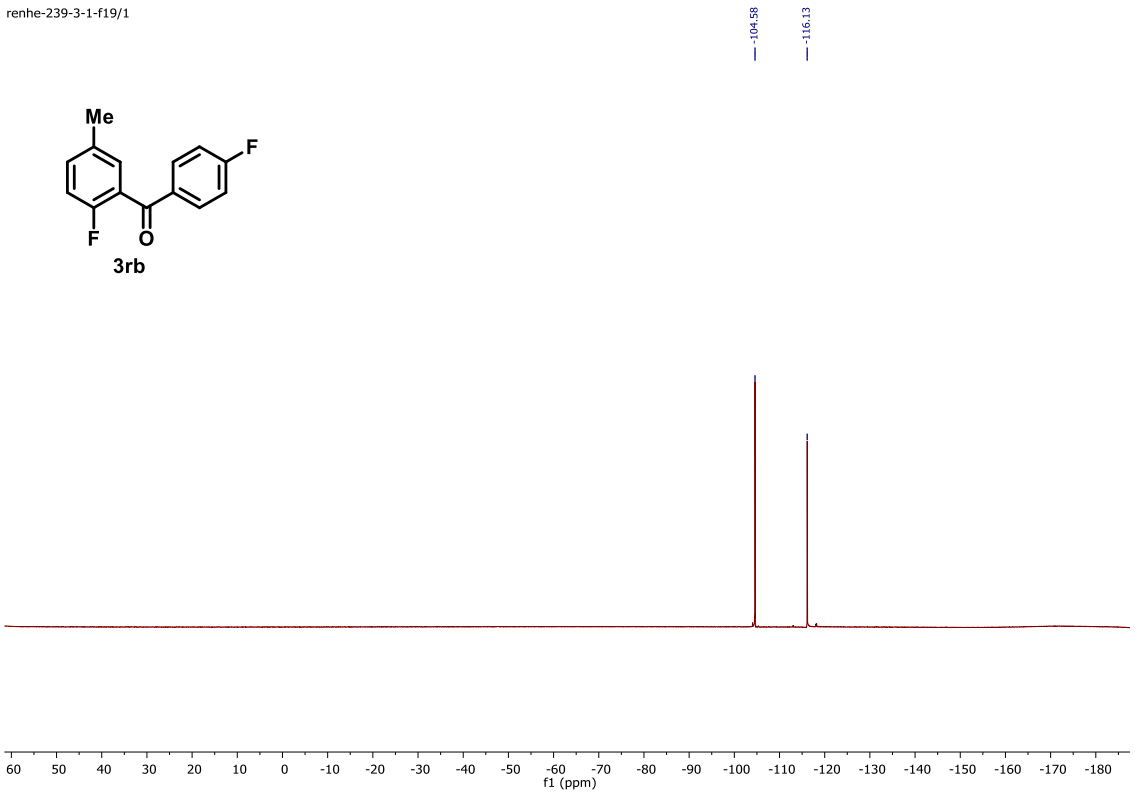

Figure 4.99. ^{1}H NMR Spectrum of 3sb

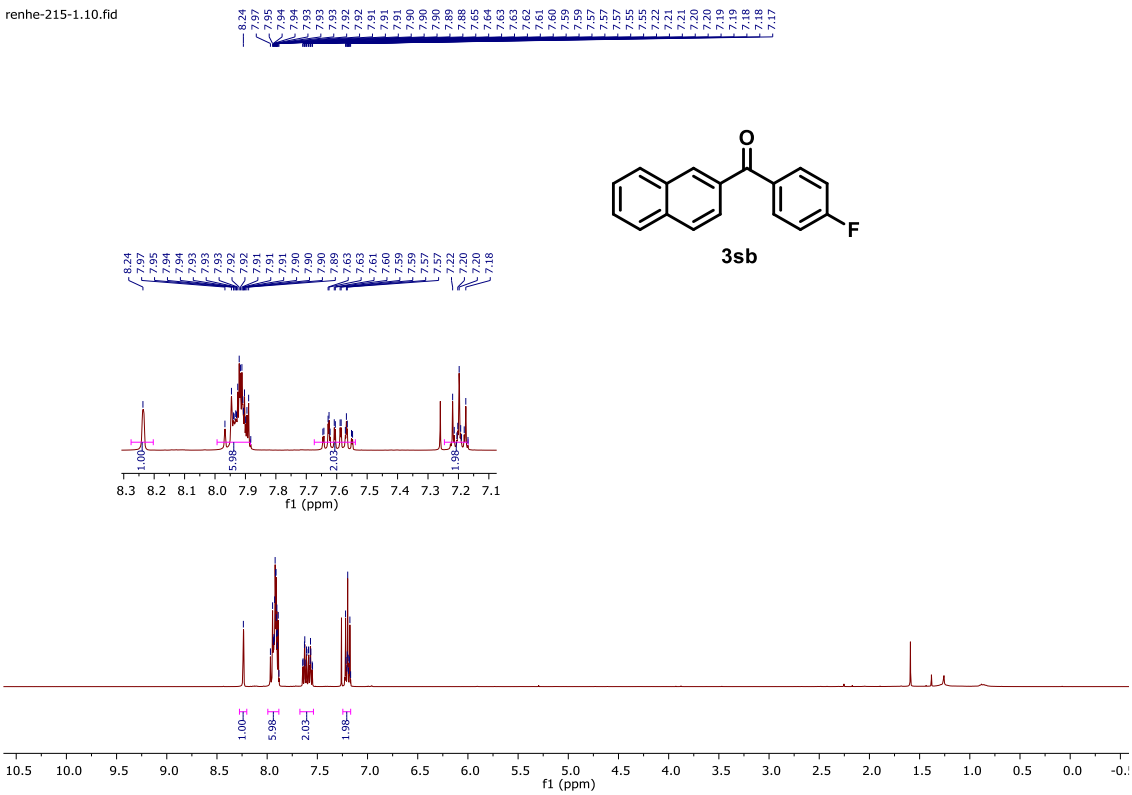

Figure 4.100. ^{13}C NMR Spectrum of 3sb

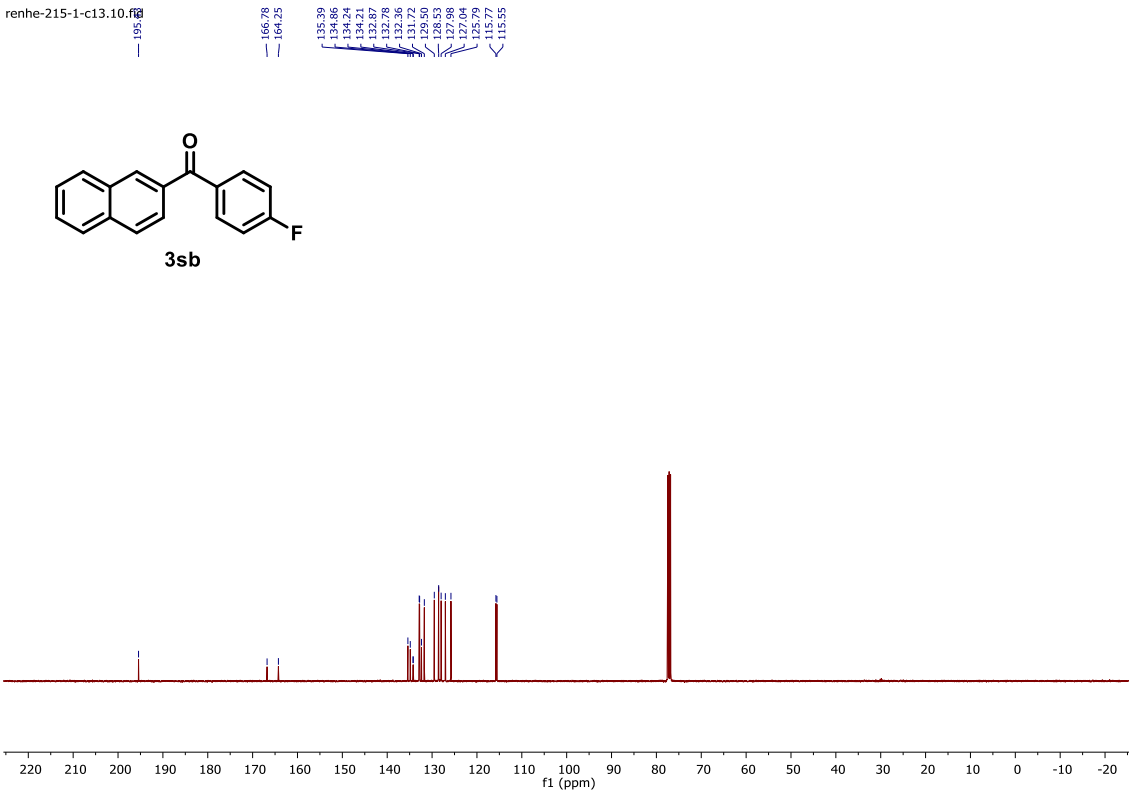

Figure 4.101. ^{19}F NMR Spectrum of 3sb

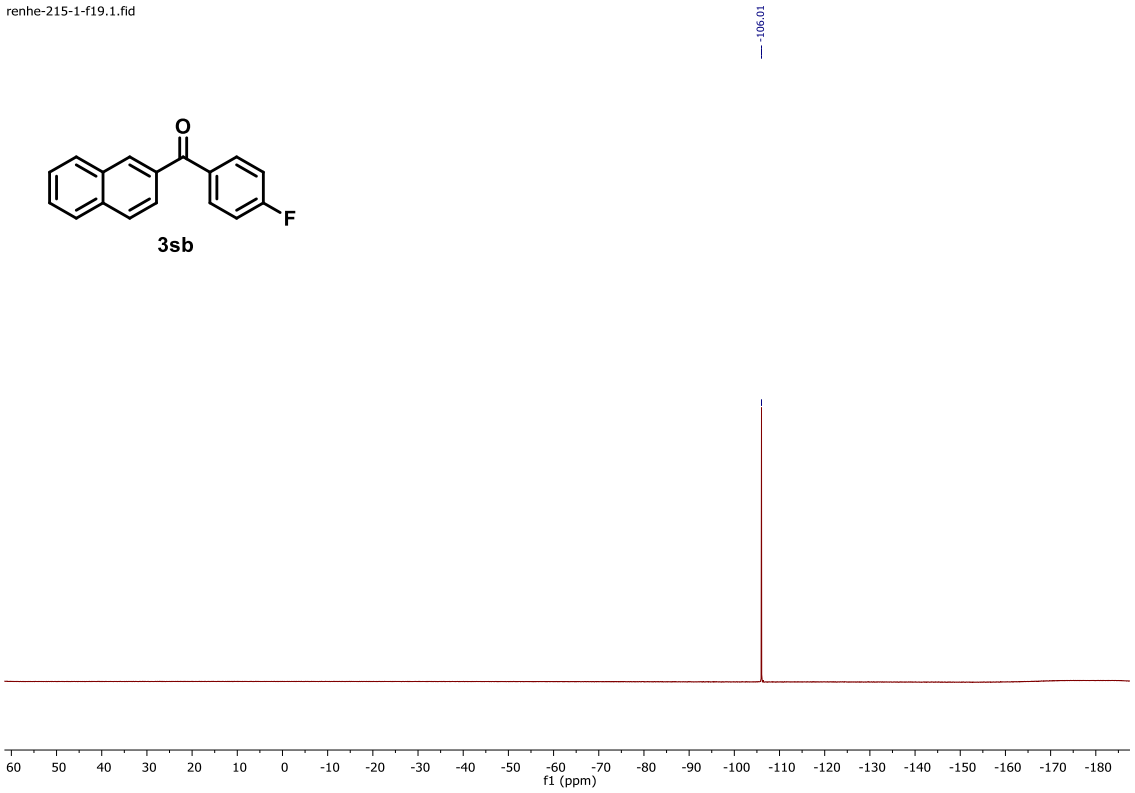

Figure 4.102. ^{1}H NMR Spectrum of 3sb-*d*

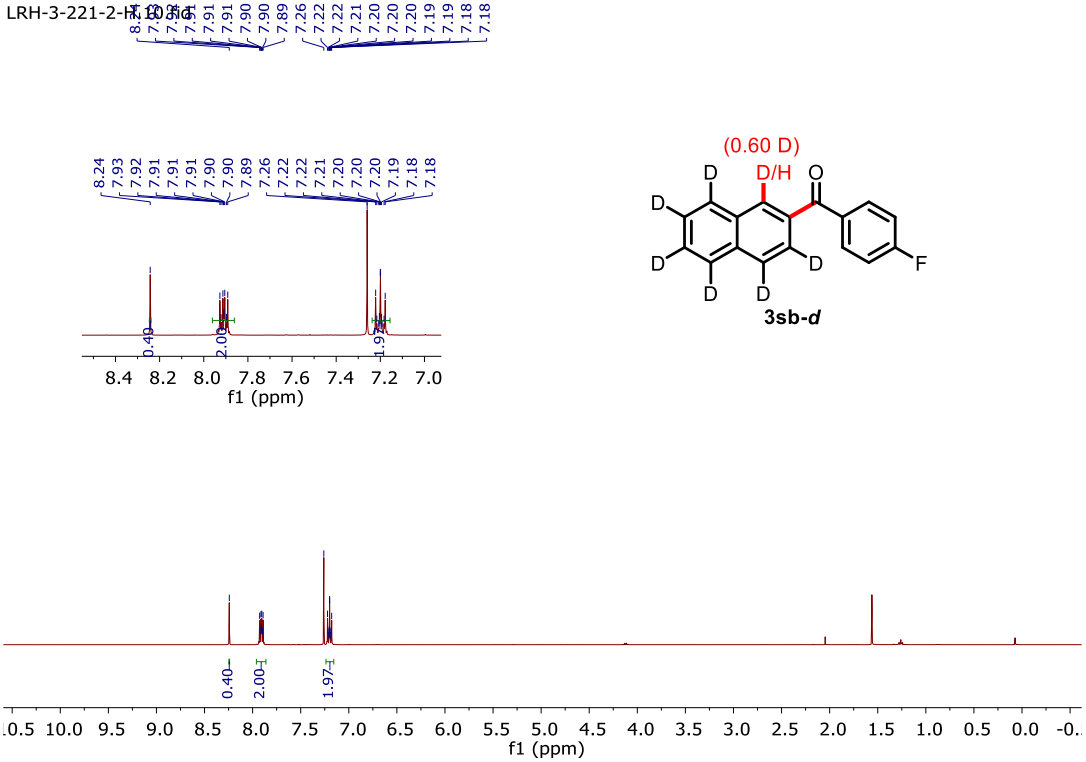

Figure 4.103. ^{1}H NMR Spectrum of 3ab-*d*

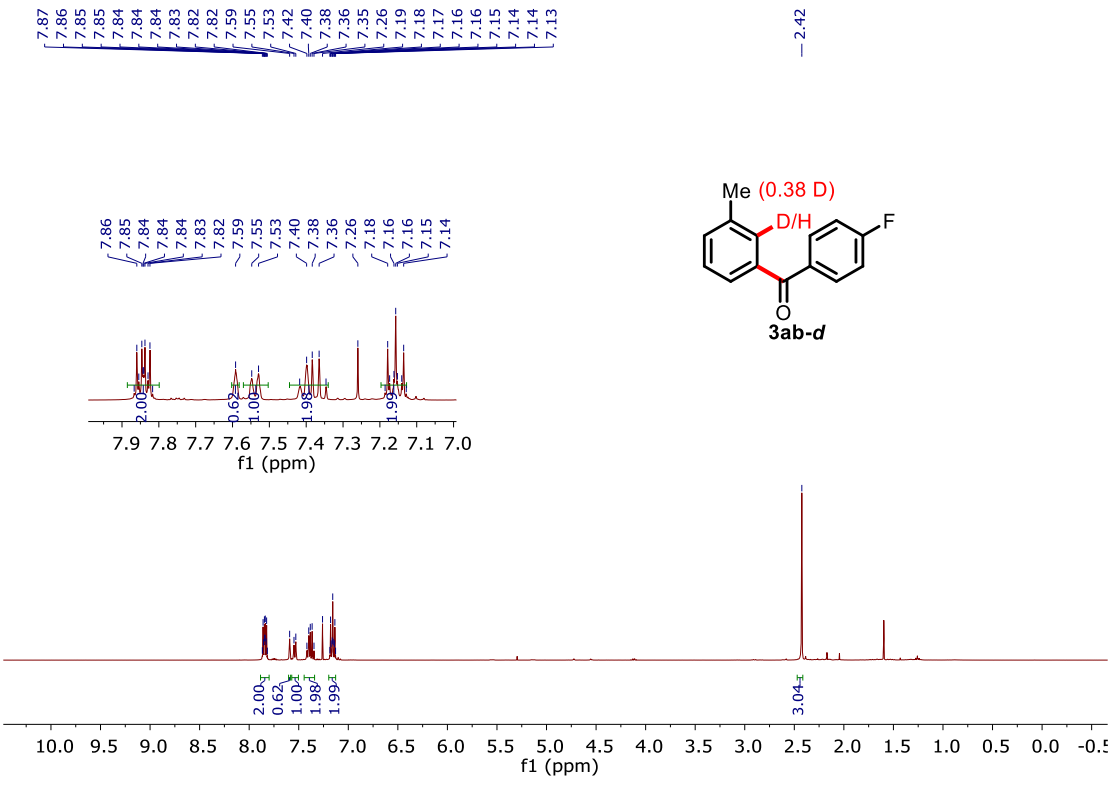

Figure 4.104. ^{1}H NMR Spectrum of 4aa

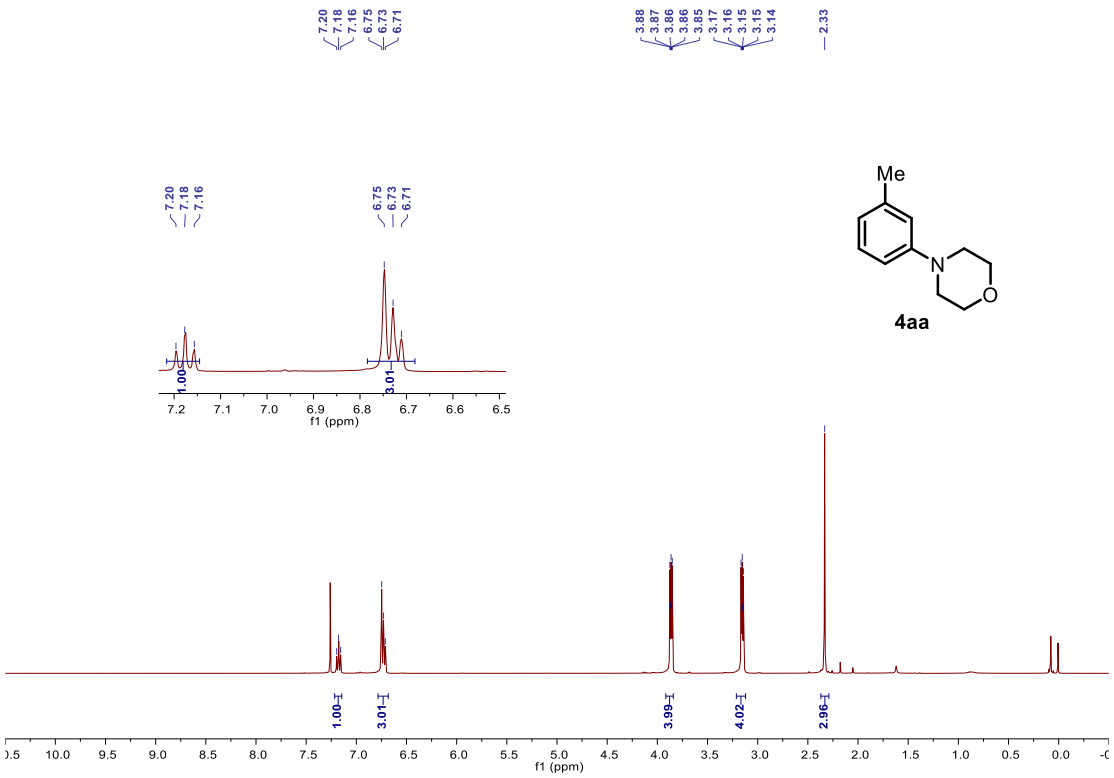

Figure 4.105. ^{13}C NMR Spectrum of 4aa

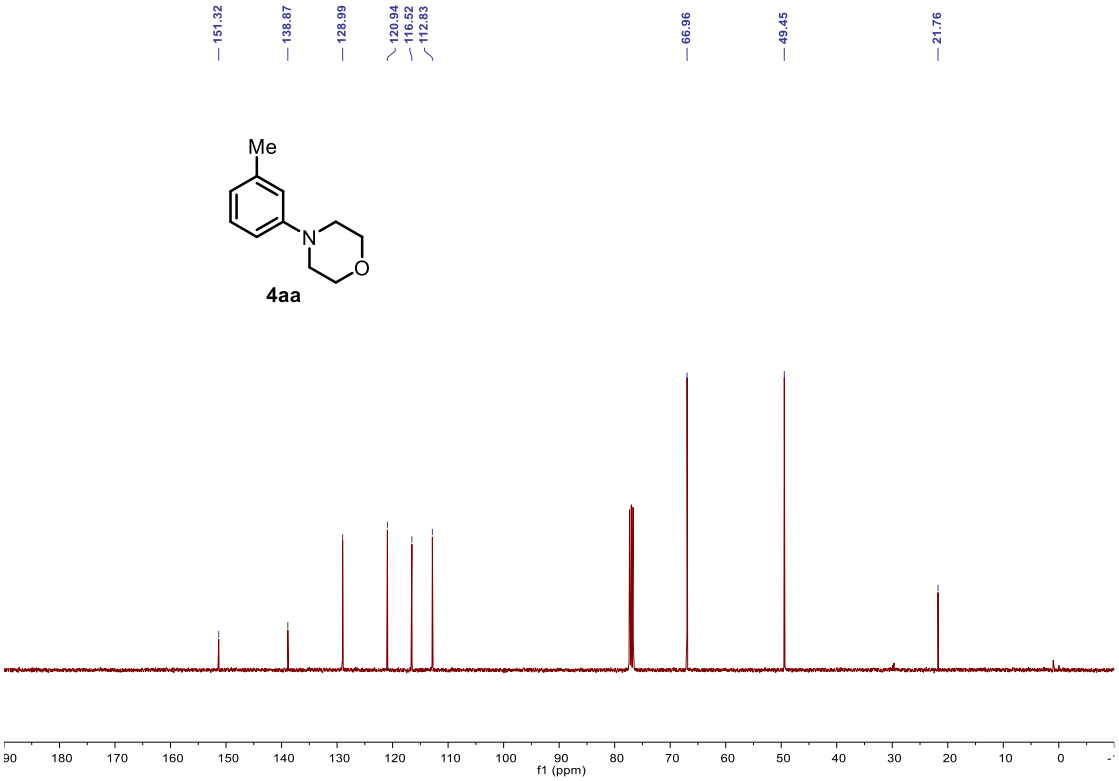

Figure 4.106. ^{1}H NMR Spectrum of 4ga

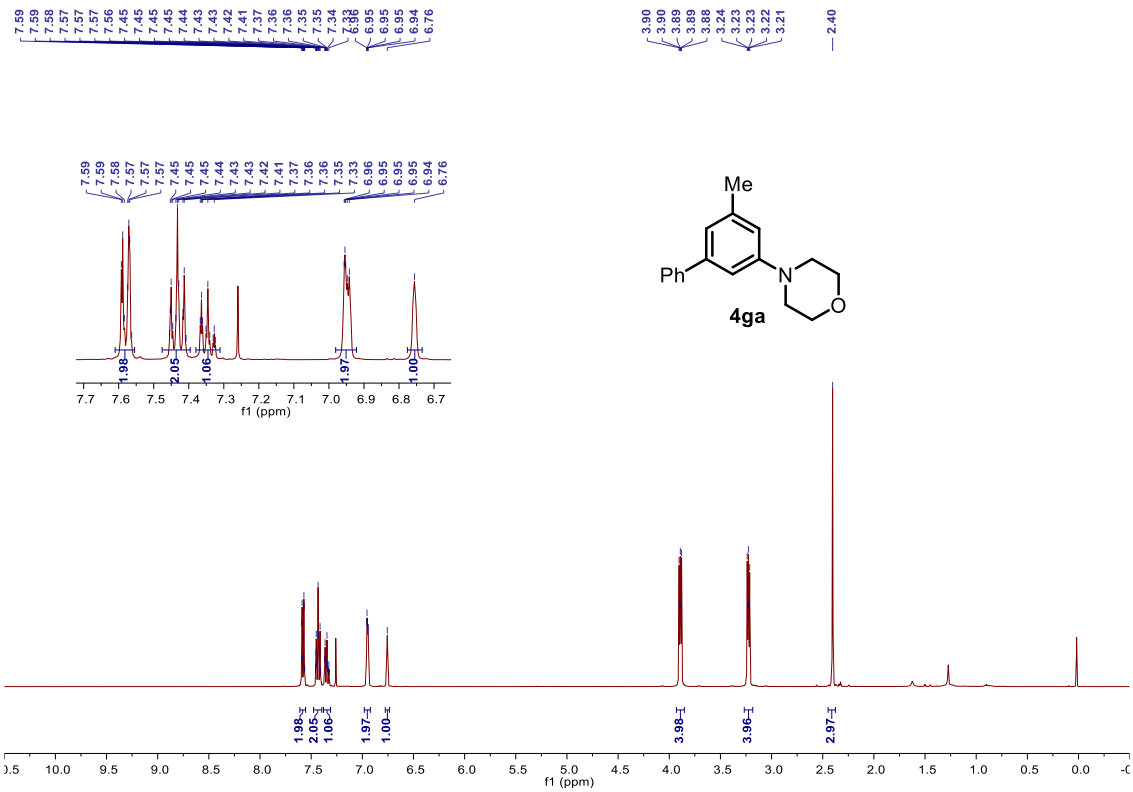

Figure 4.107. ^{13}C NMR Spectrum of 4ga

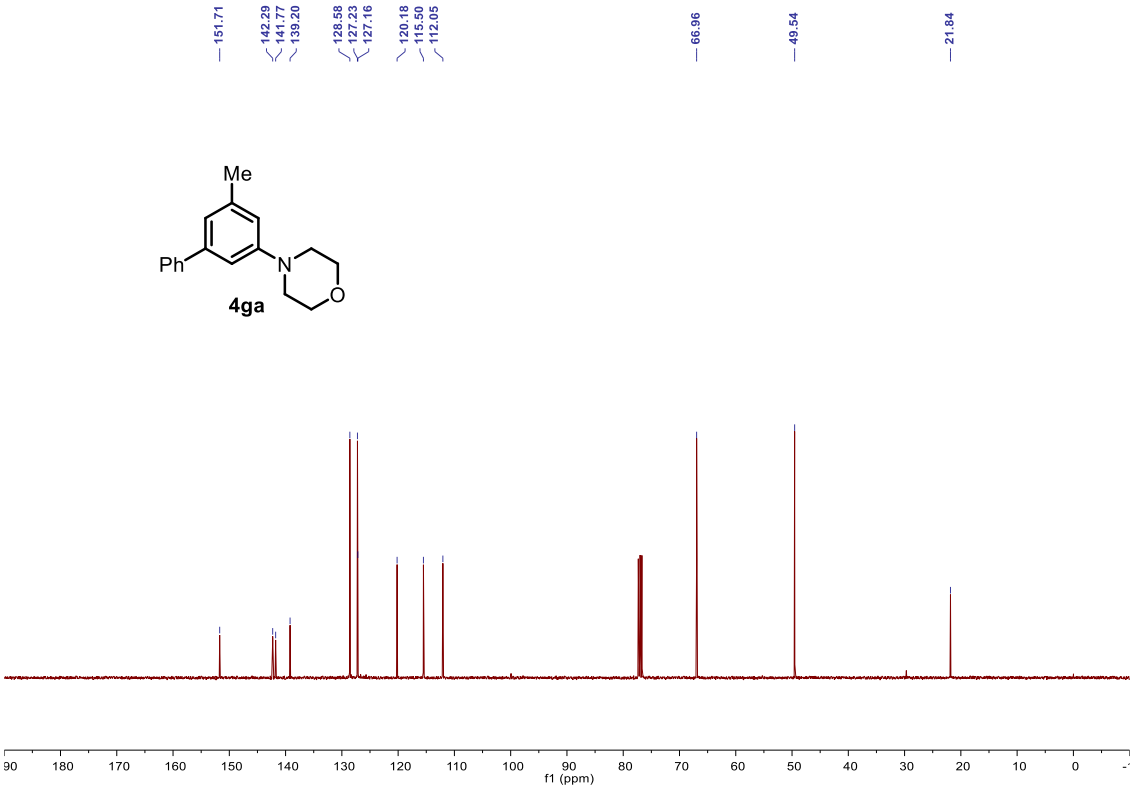

Figure 4.108. ^{1}H NMR Spectrum of 4la

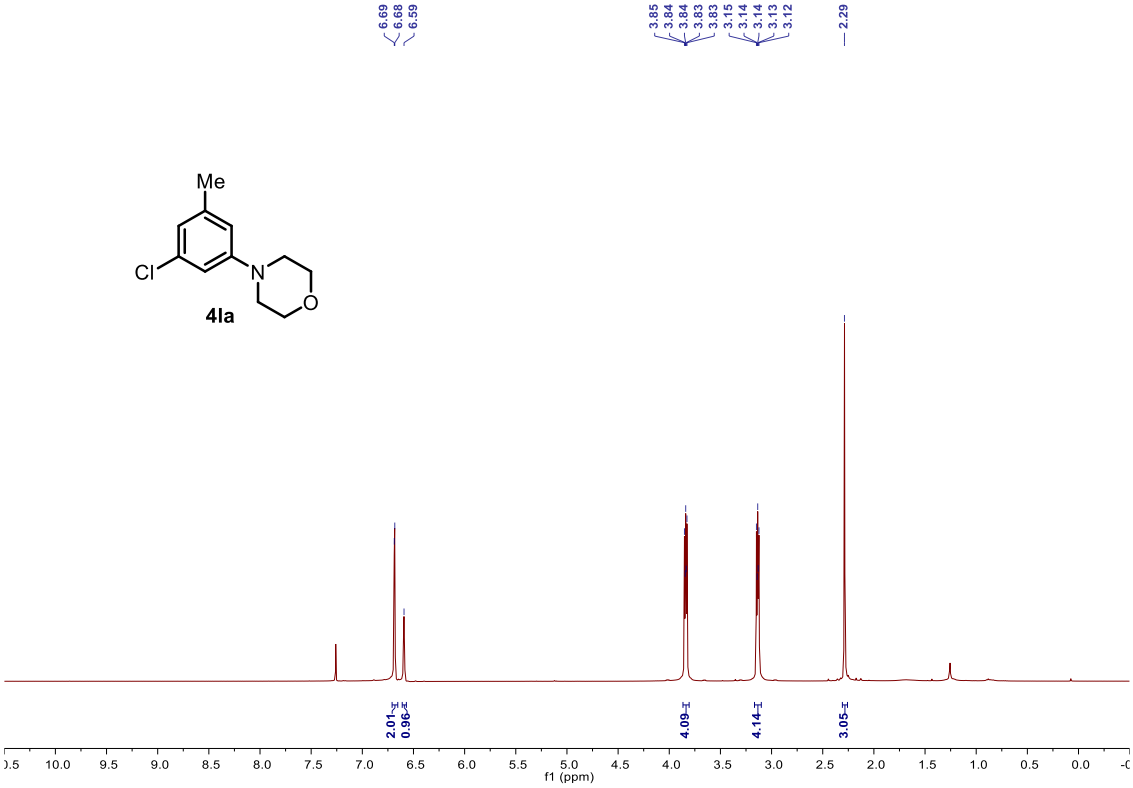

Figure 4.109. ^{13}C NMR Spectrum of 4la

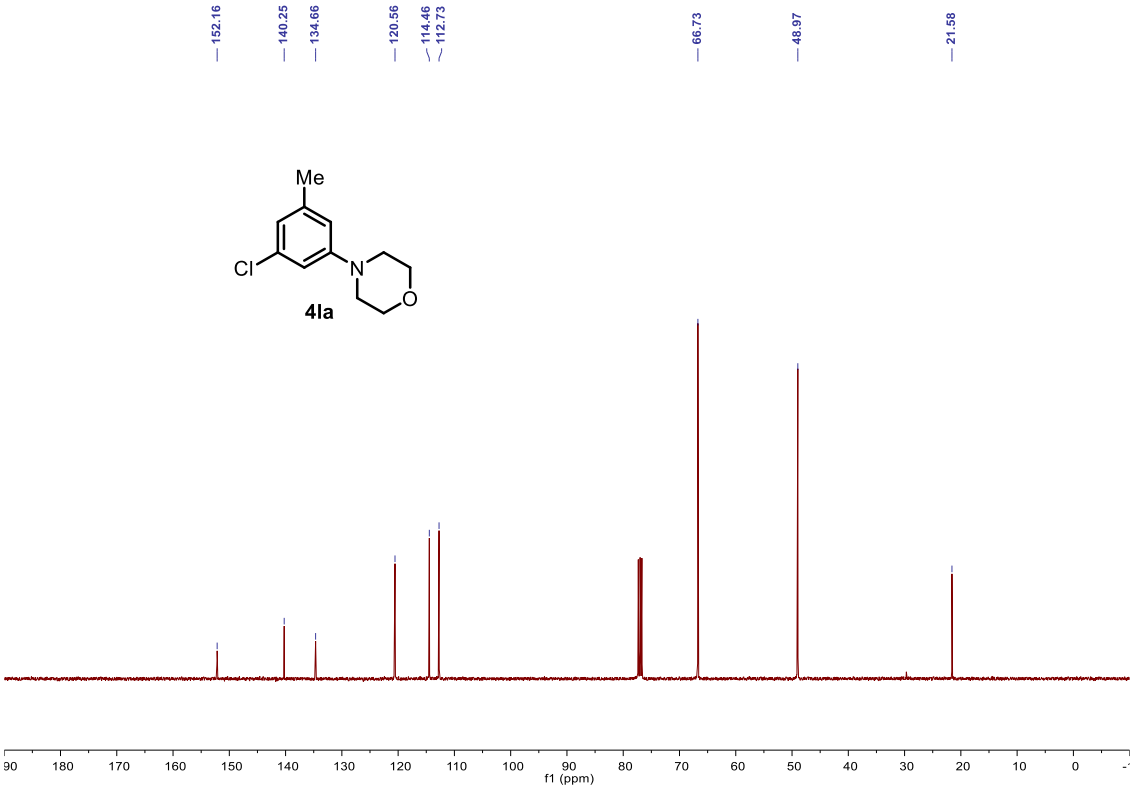

Figure 4.110. ^{1}H NMR Spectrum of 4na

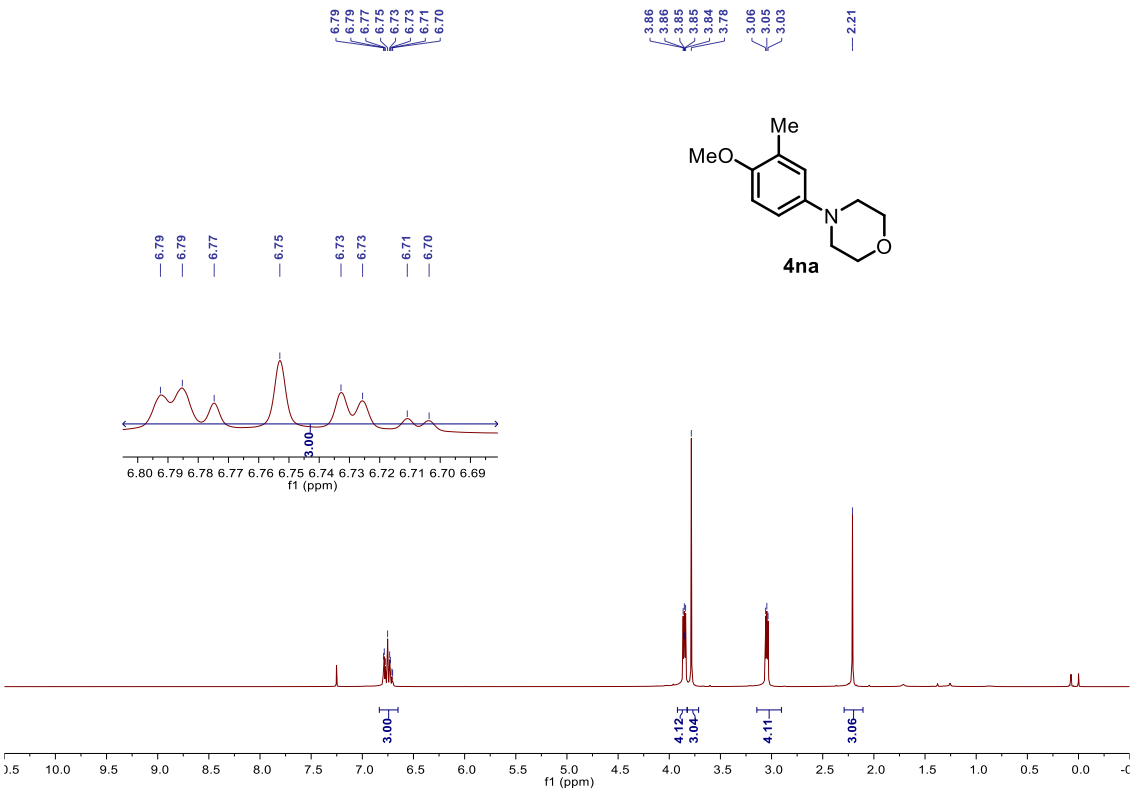

Figure 4.111. ^{13}C NMR Spectrum of 4na

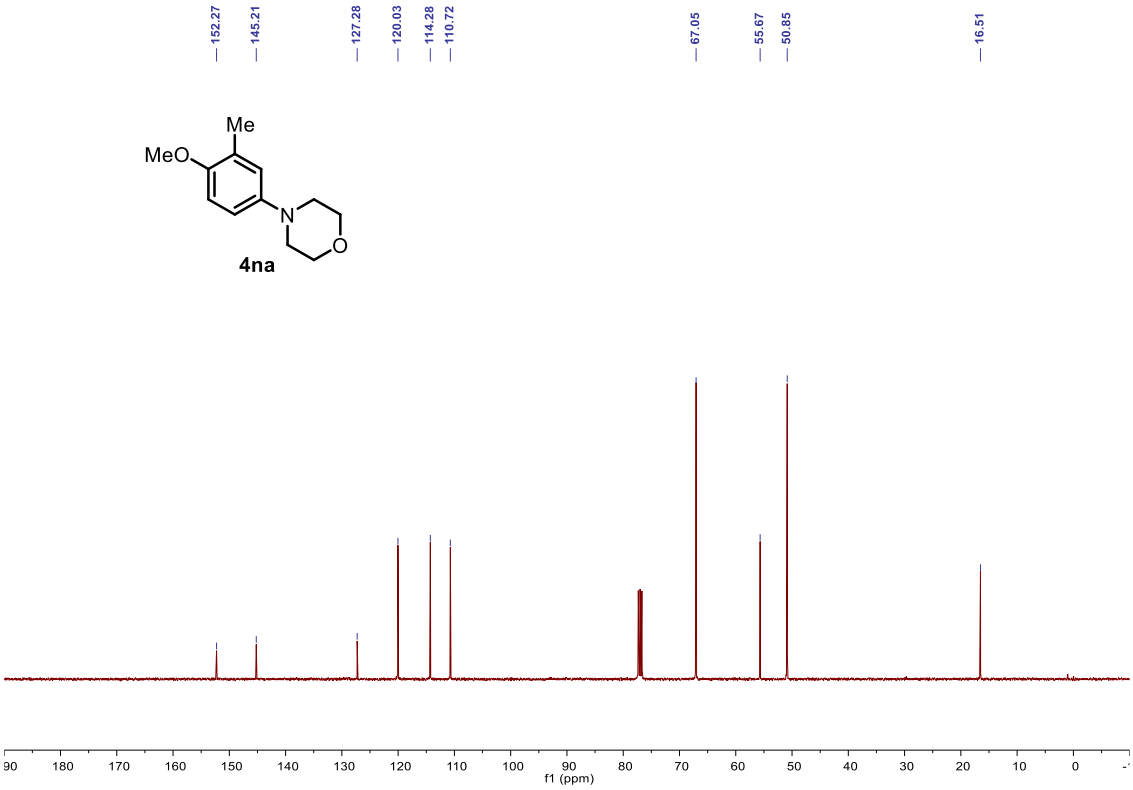

Figure 4.112. ^{1}H NMR Spectrum of 4sa

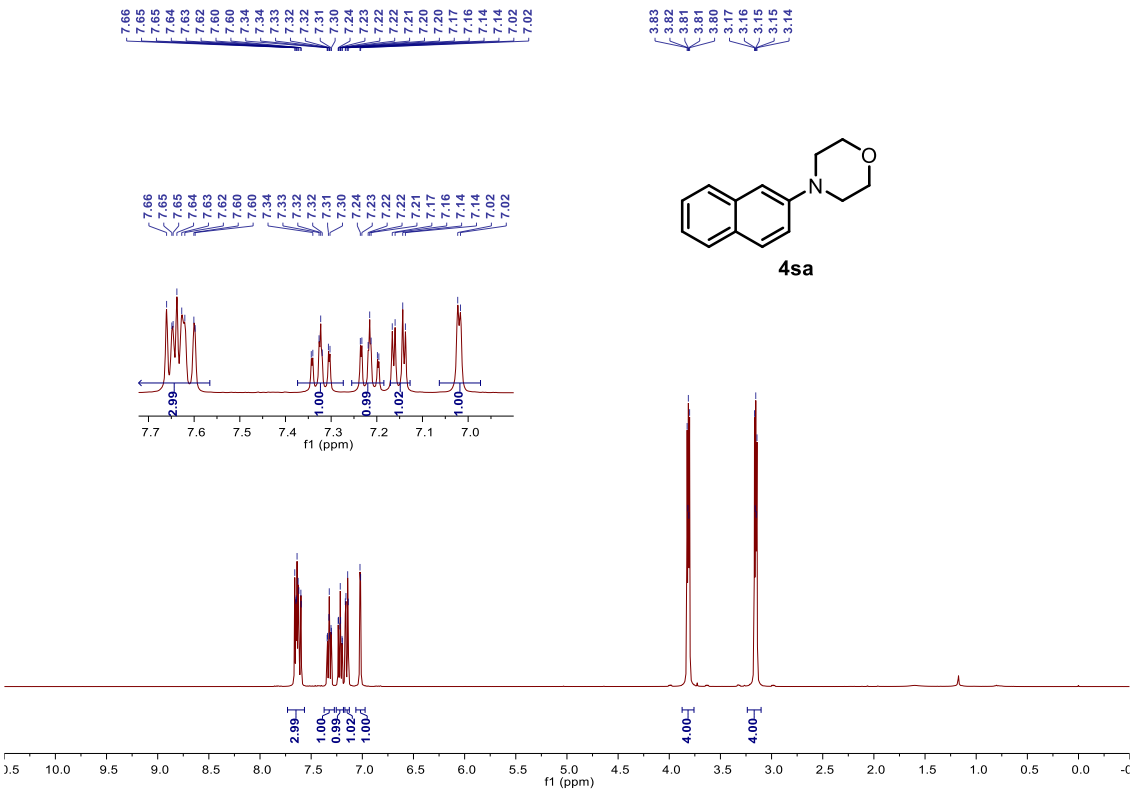

Figure 4.113. ^{13}C NMR Spectrum of 4sa

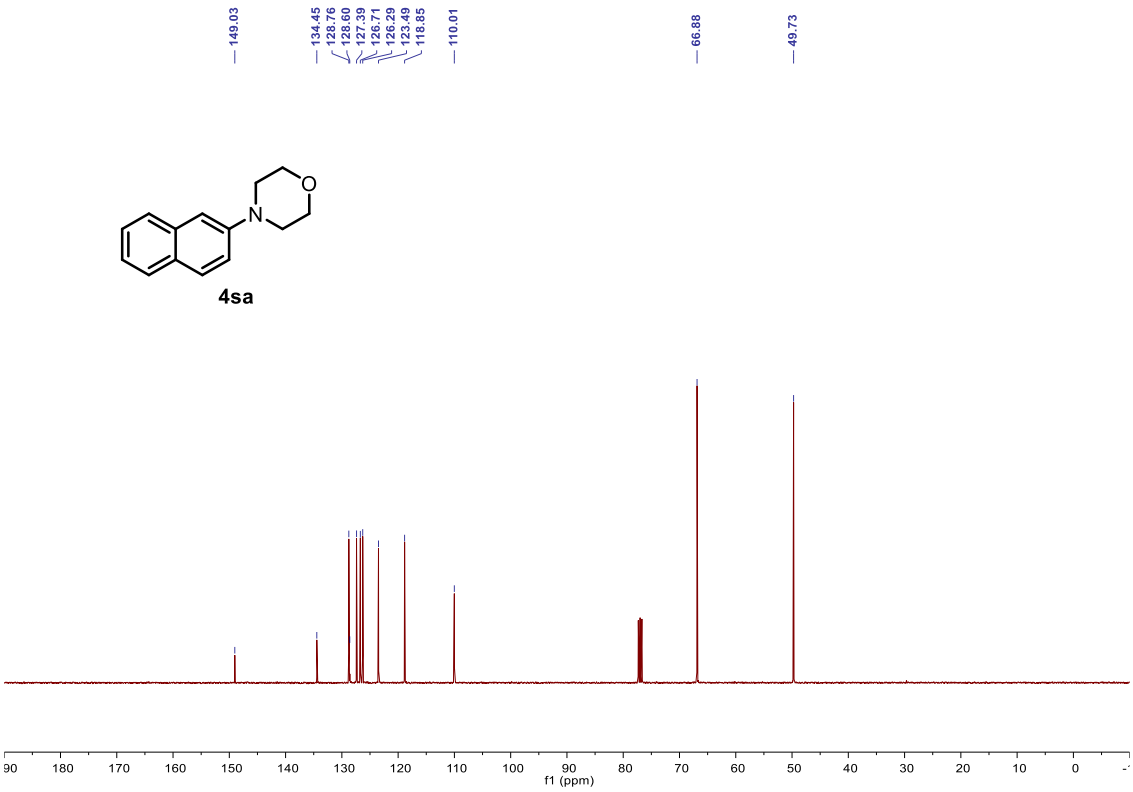

Figure 4.114. ^{1}H NMR Spectrum of 4ab

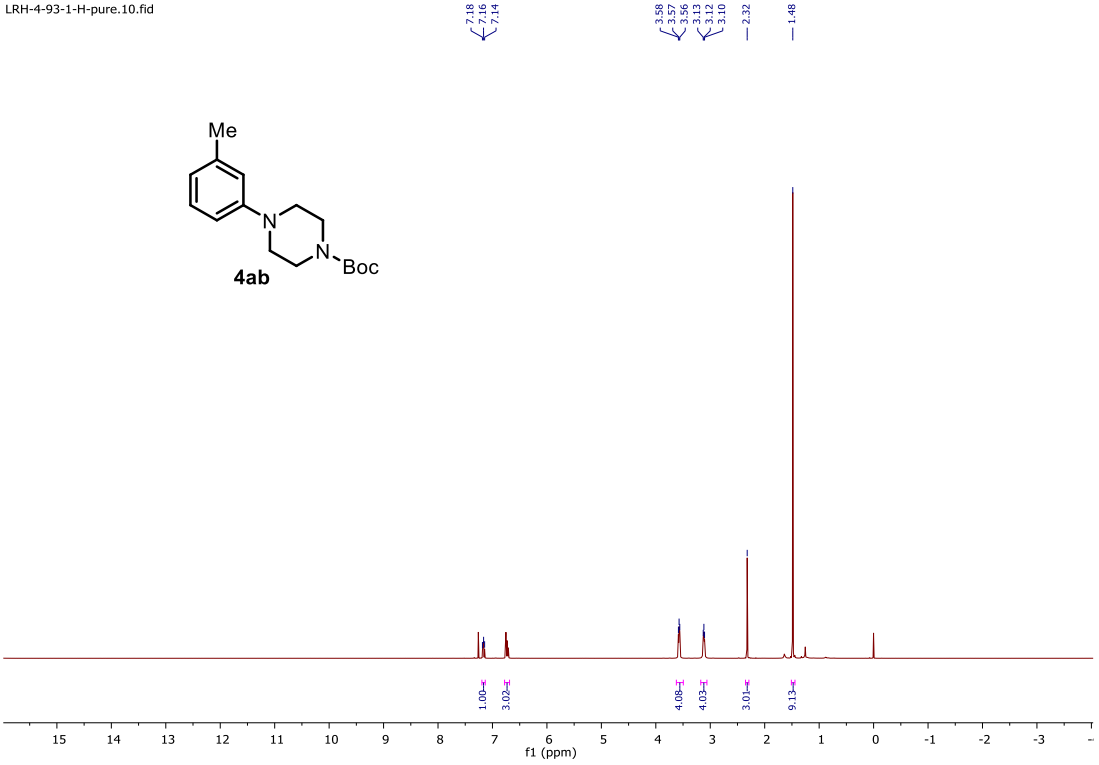

Figure 4.115. ^{13}C NMR Spectrum of 4ab

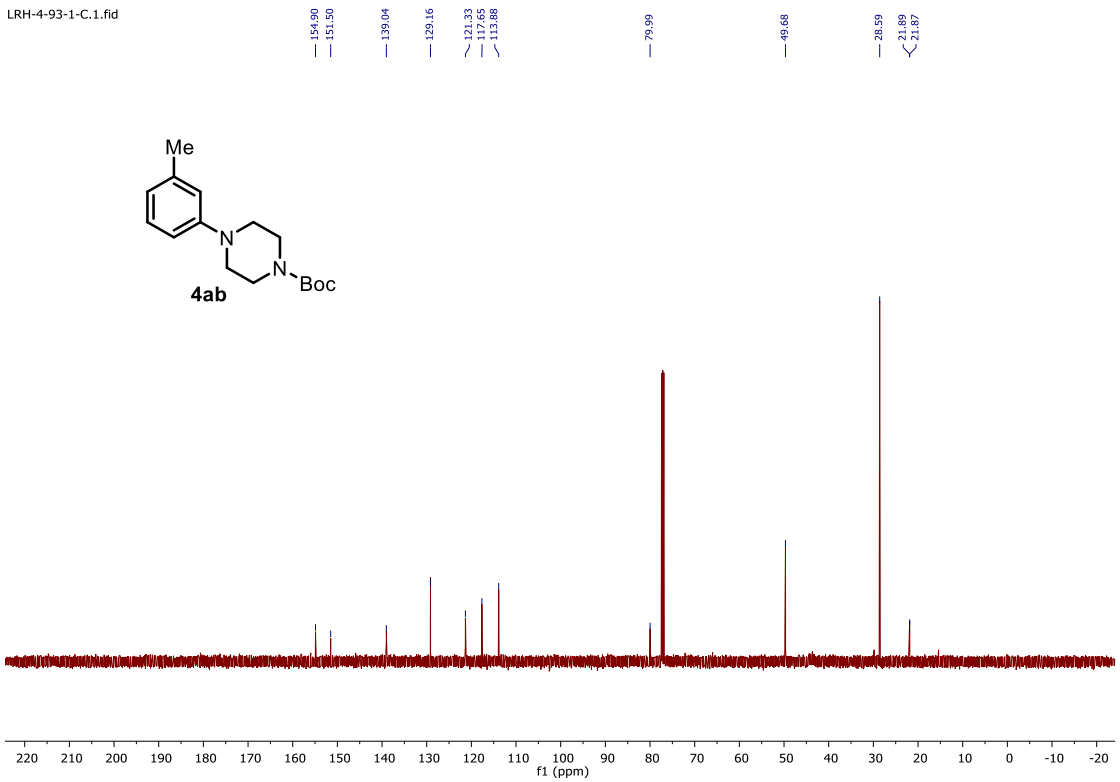

Figure 4.116. ^{1}H NMR Spectrum of 5

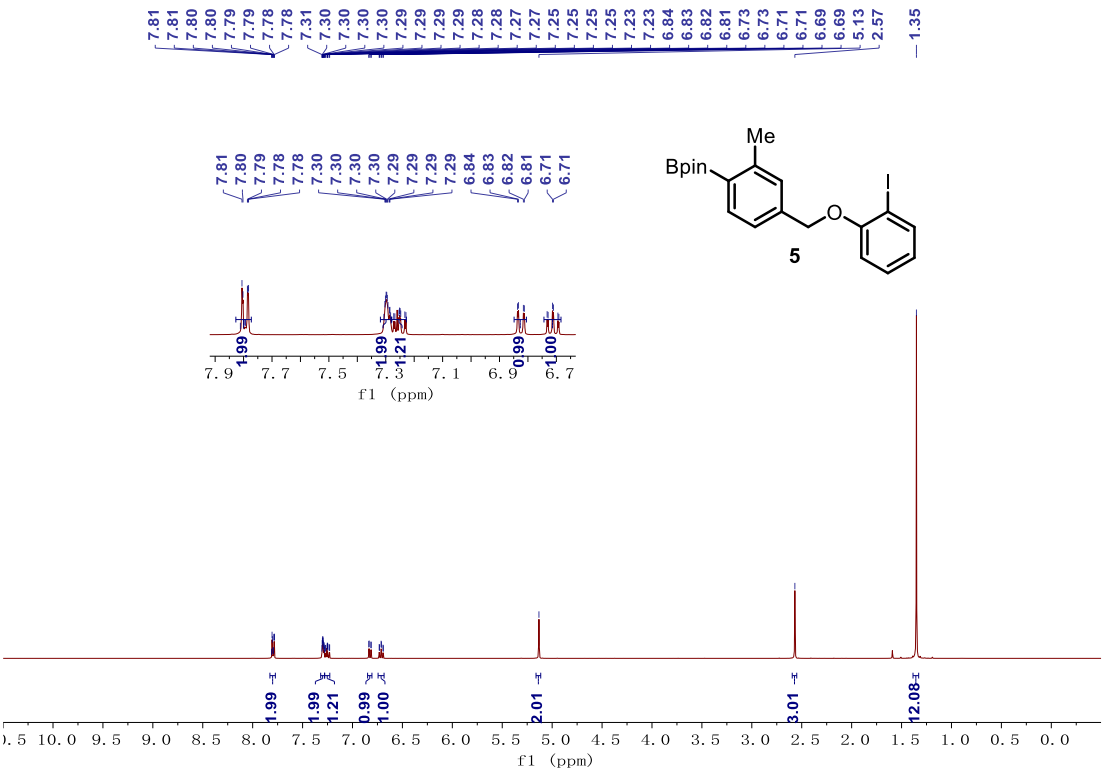

Figure 4.117. ^{13}C NMR Spectrum of 5

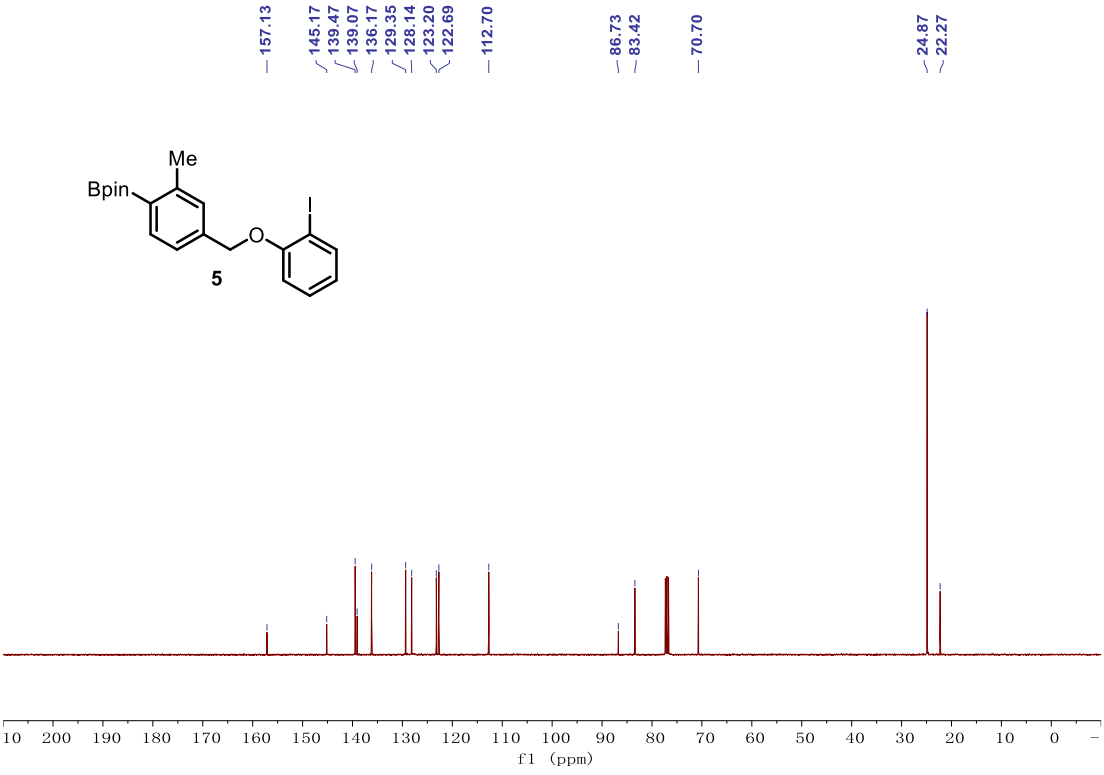

Figure 4.118. ^{1}H NMR Spectrum of 12

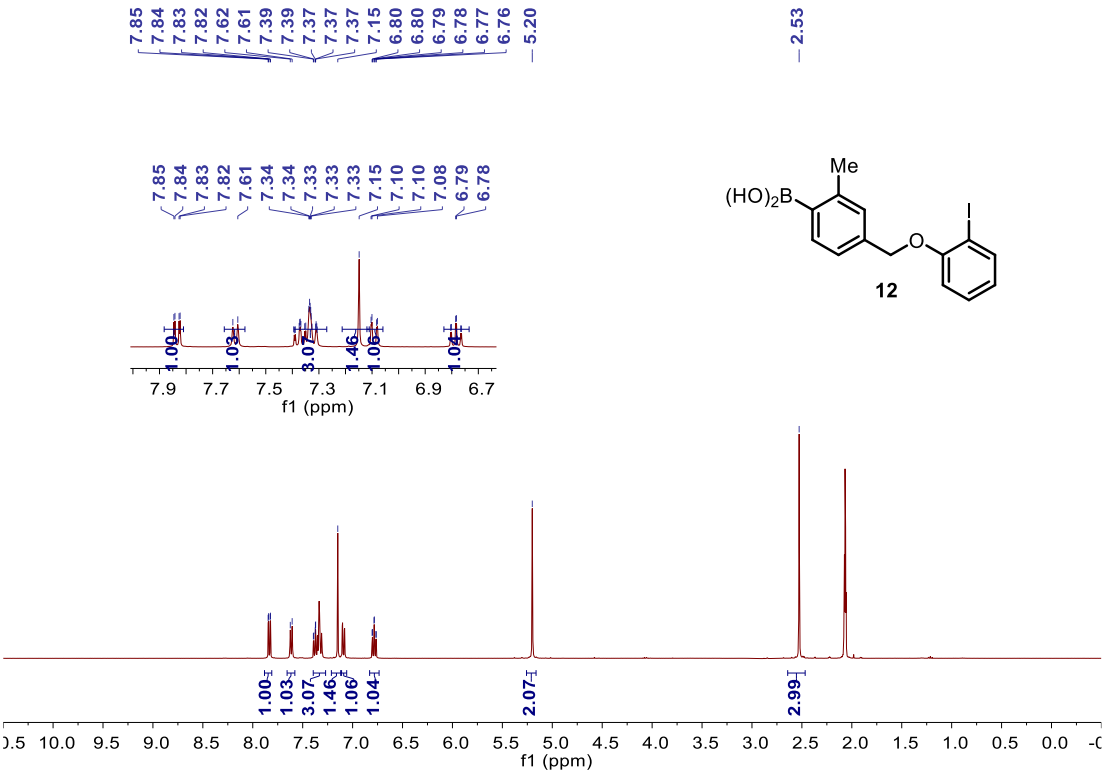

Figure 4.119. ^{13}C NMR Spectrum of 12

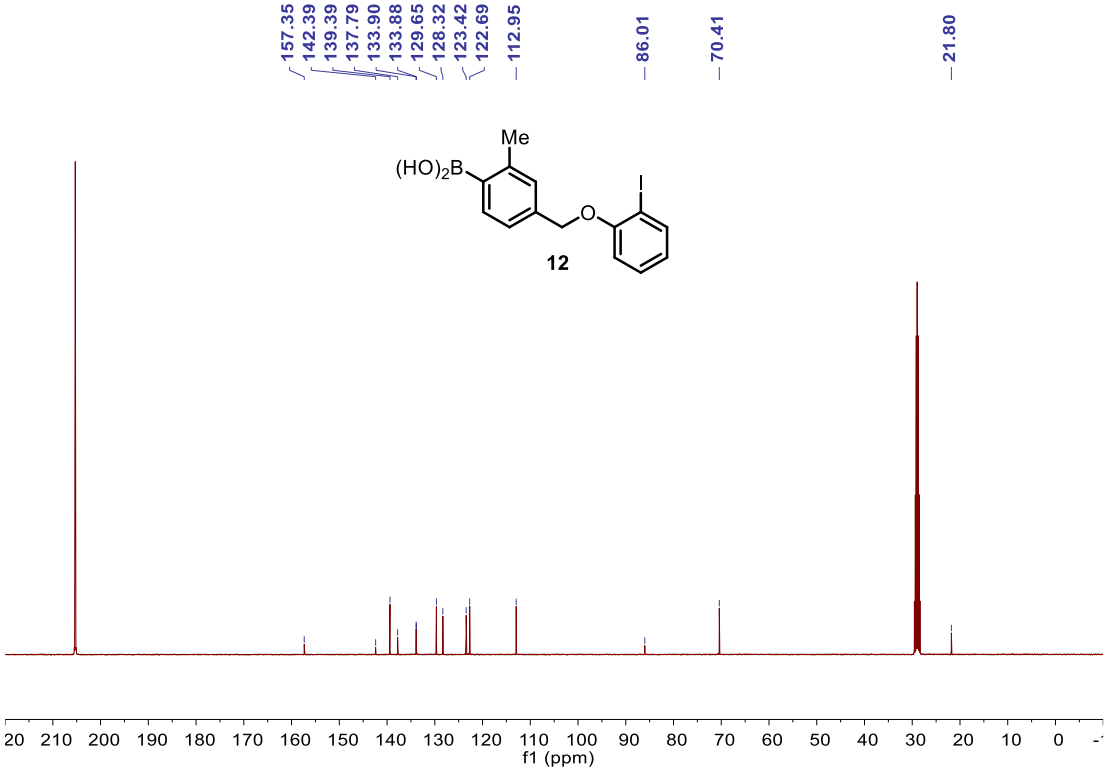

Figure 4.120. ^{1}H NMR Spectrum of 7

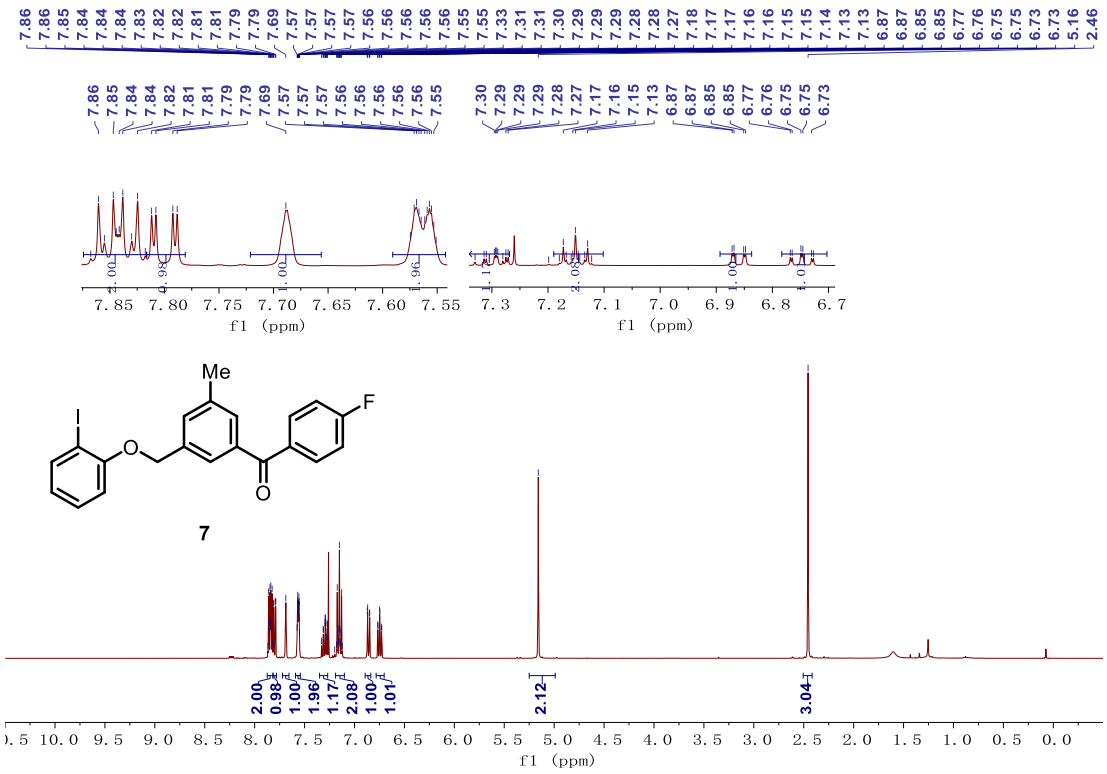

Figure 4.121. ^{13}C NMR Spectrum of 7

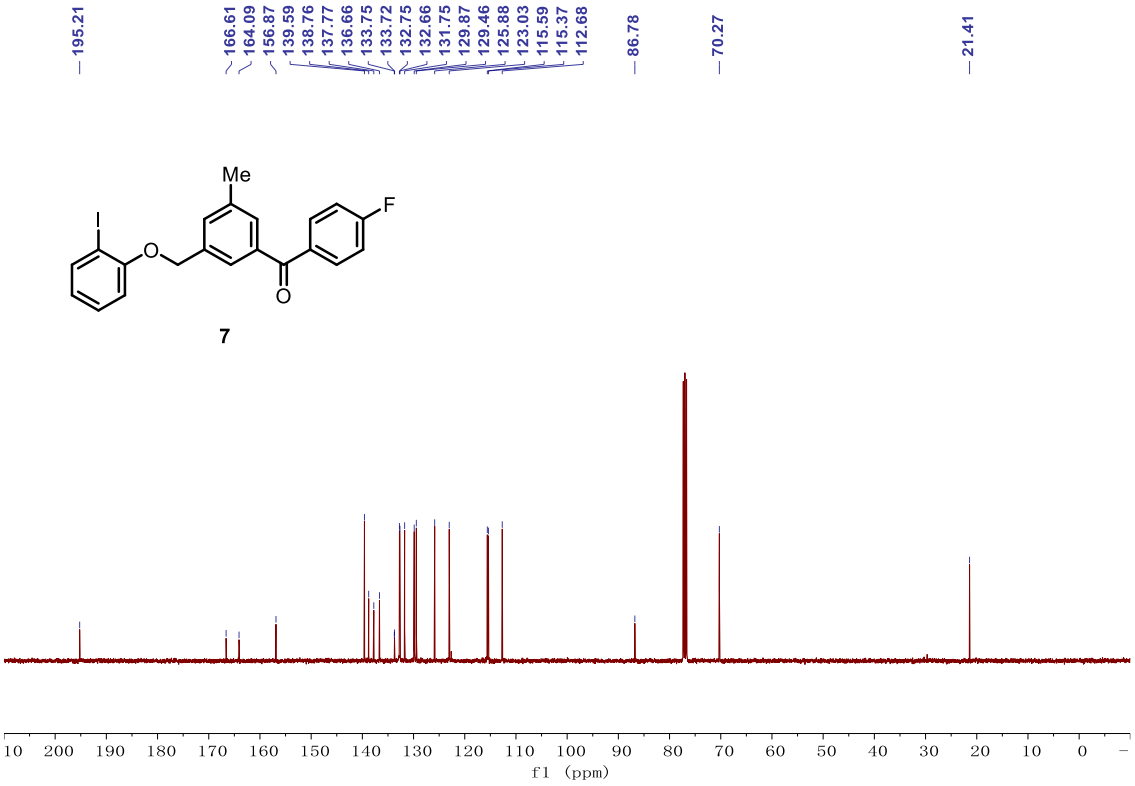

Figure 4.122. ^{19}F NMR Spectrum of 7

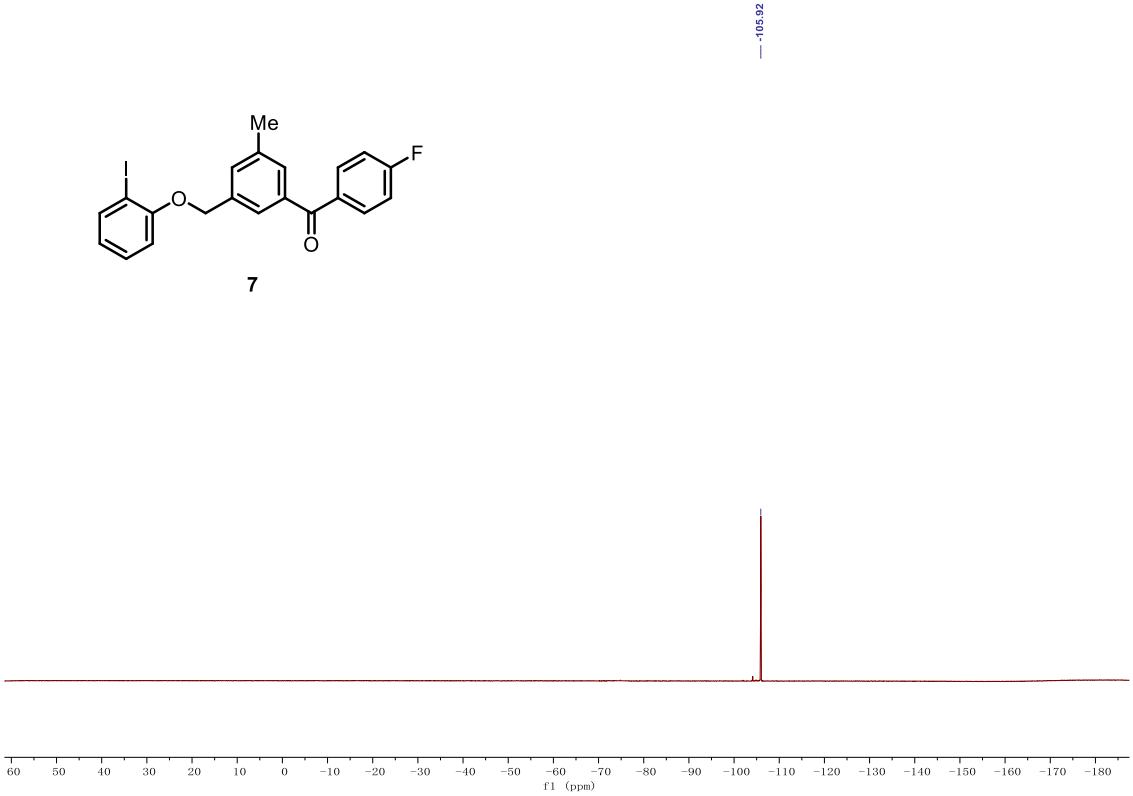

Figure 4.123. ^{1}H NMR Spectrum of 8

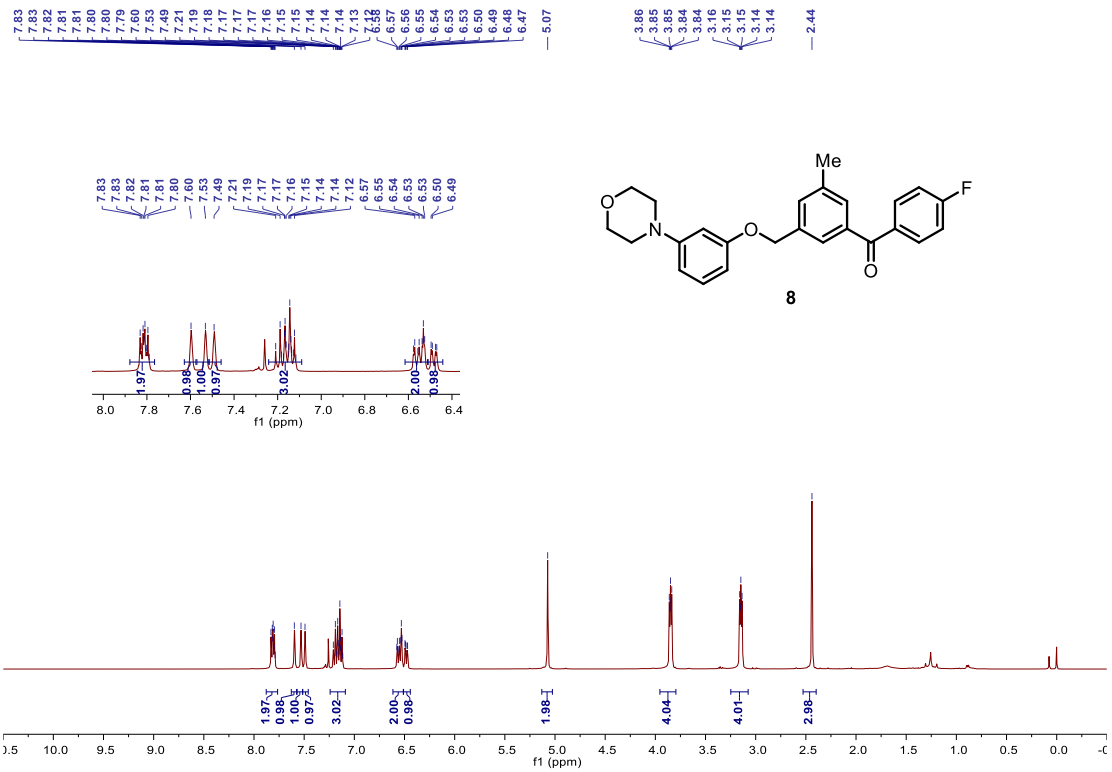

Figure 4.124. ^{13}C NMR Spectrum of 8

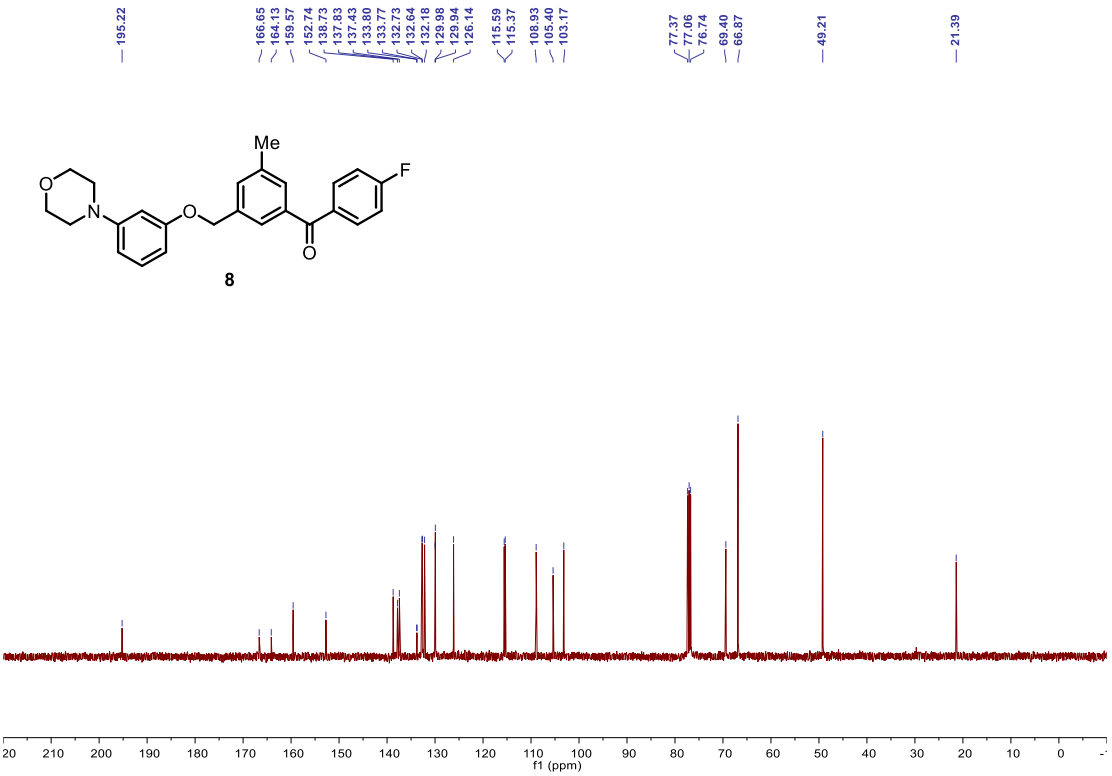

Figure 4.125. ^{19}F NMR Spectrum of 8

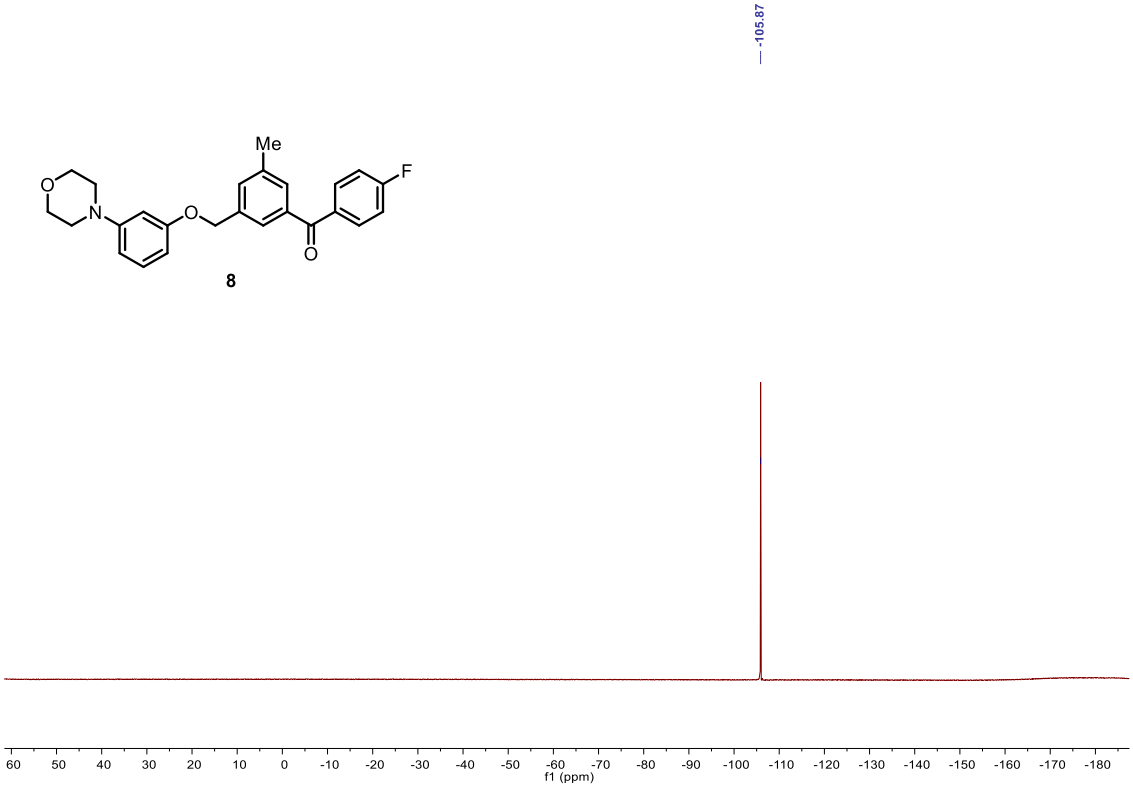

Figure 4.126. ^{1}H NMR Spectrum of 9

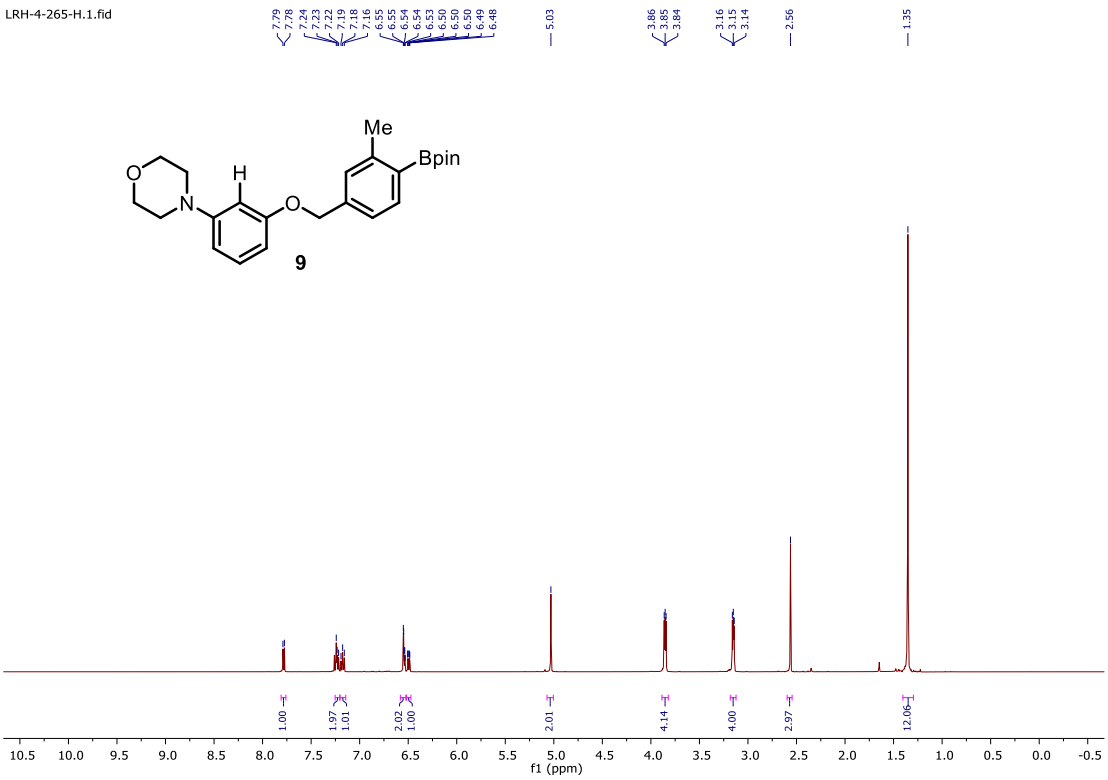

Figure 4.127. ^{13}C NMR Spectrum of 9

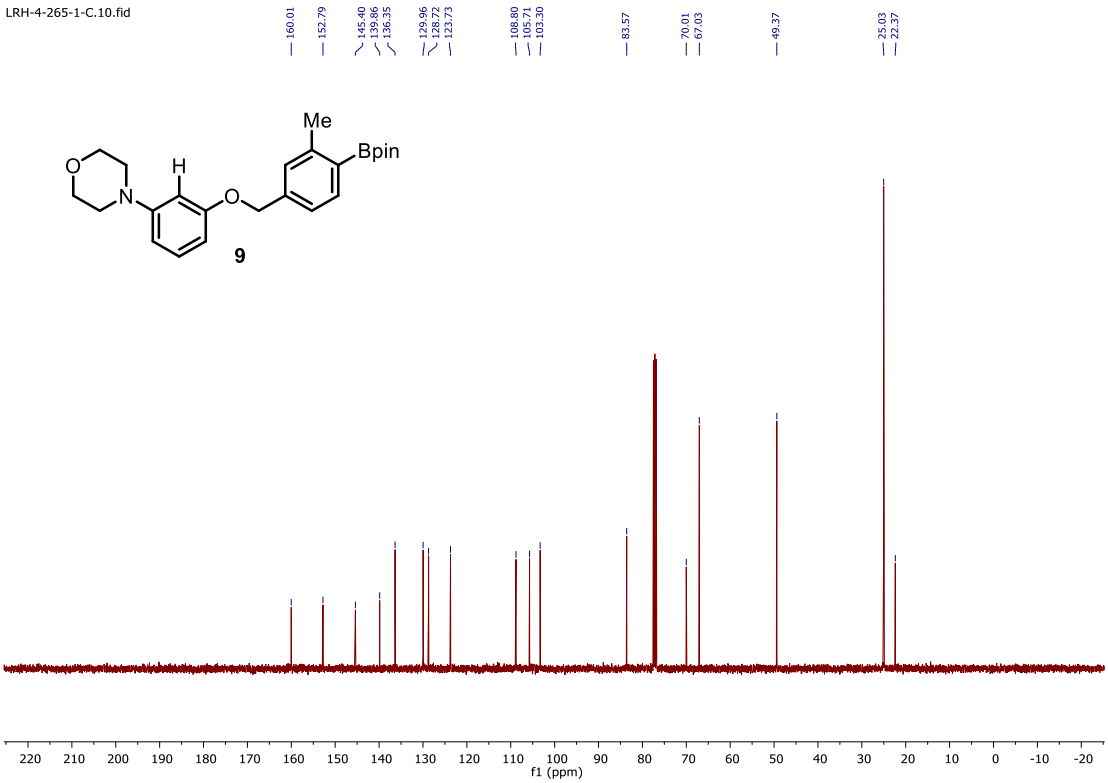

Figure 4.128. ^{1}H NMR Spectrum of 15

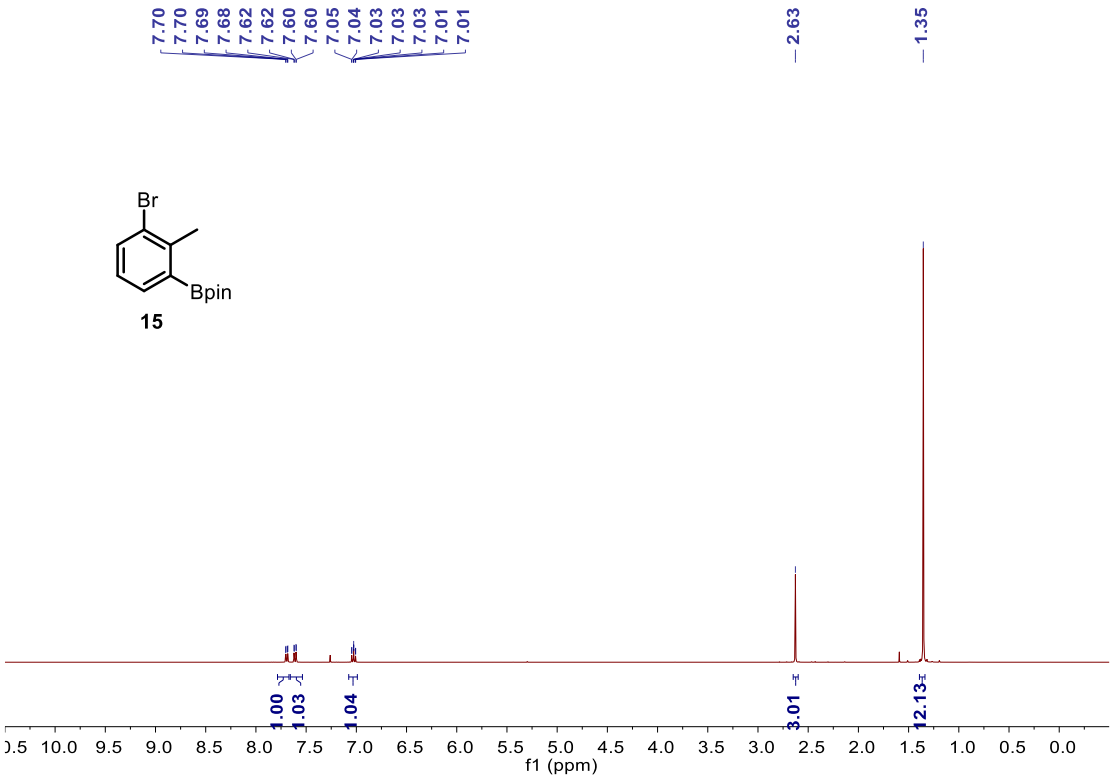

Figure 4.129. ^{13}C NMR Spectrum of 15

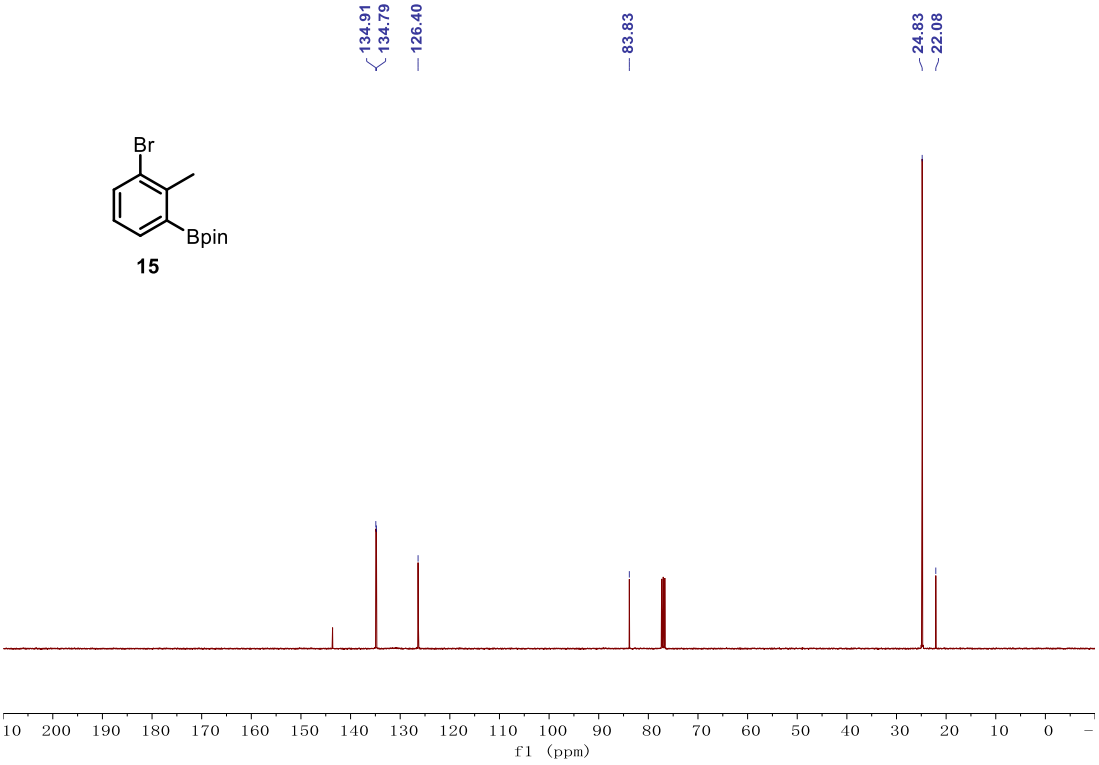

Figure 4.130. ^{1}H NMR Spectrum of 18

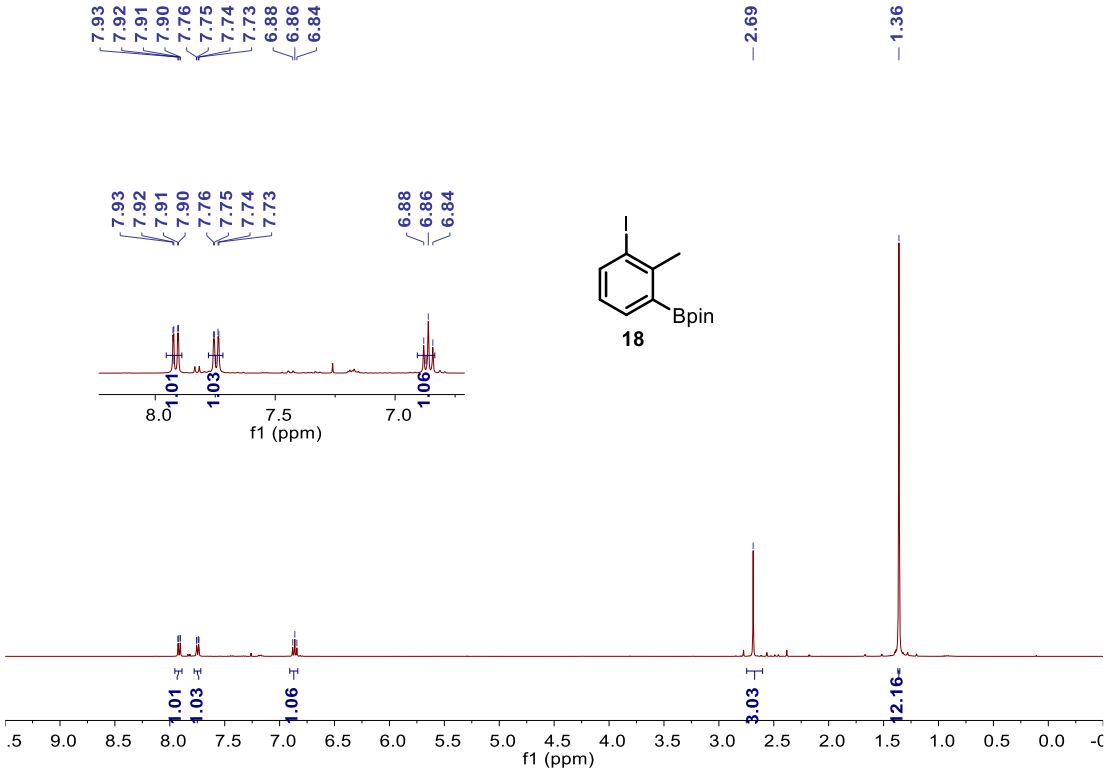

Figure 4.131. ^{13}C NMR Spectrum of 18

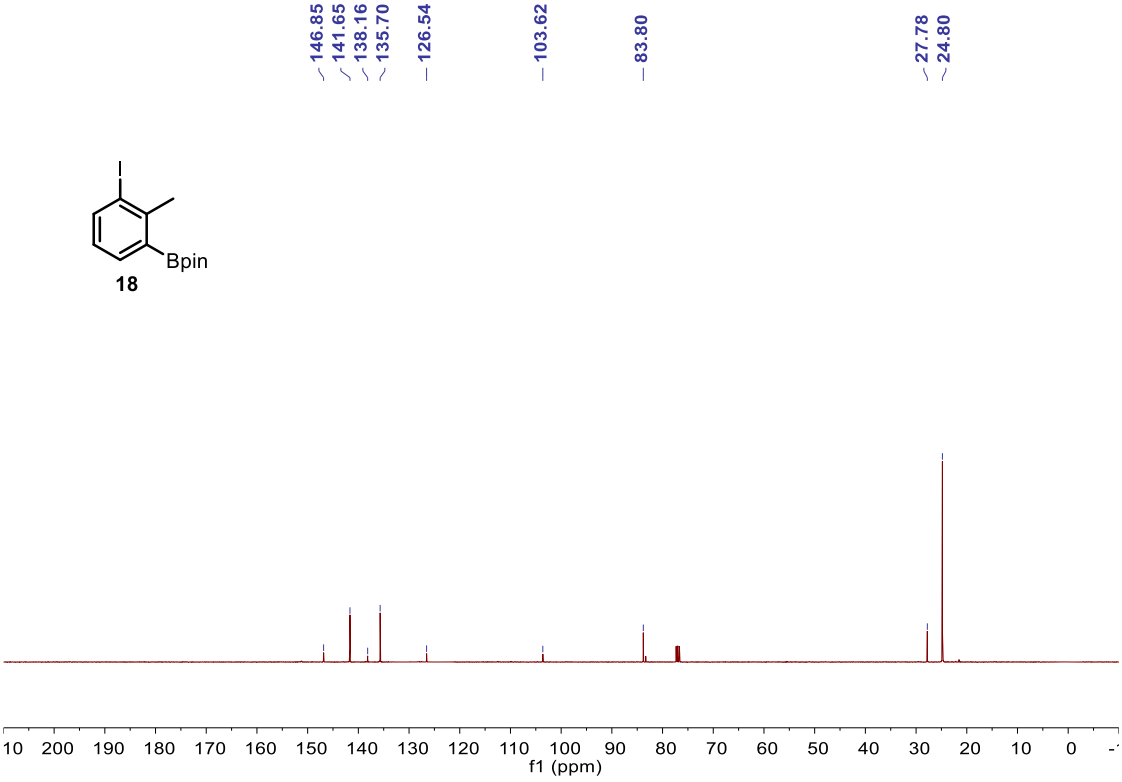

Figure 4.132. ^{1}H NMR Spectrum of 3tb

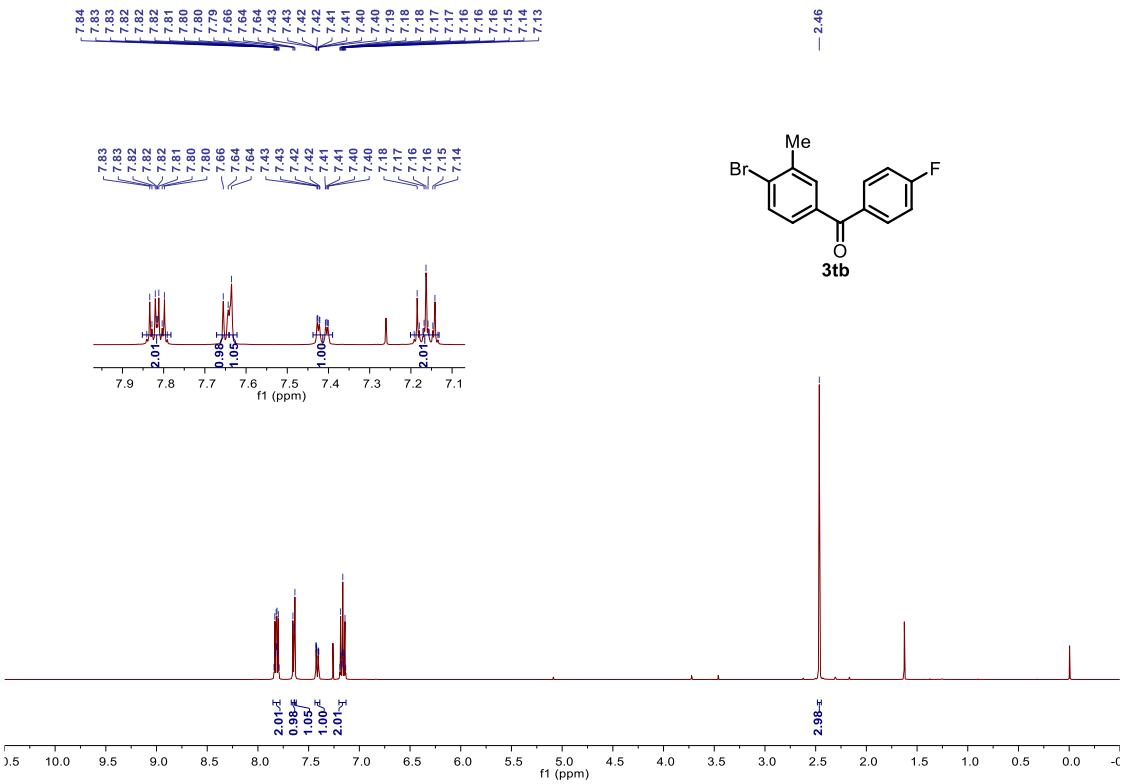

Figure 4.133. ^{13}C NMR Spectrum of 3tb

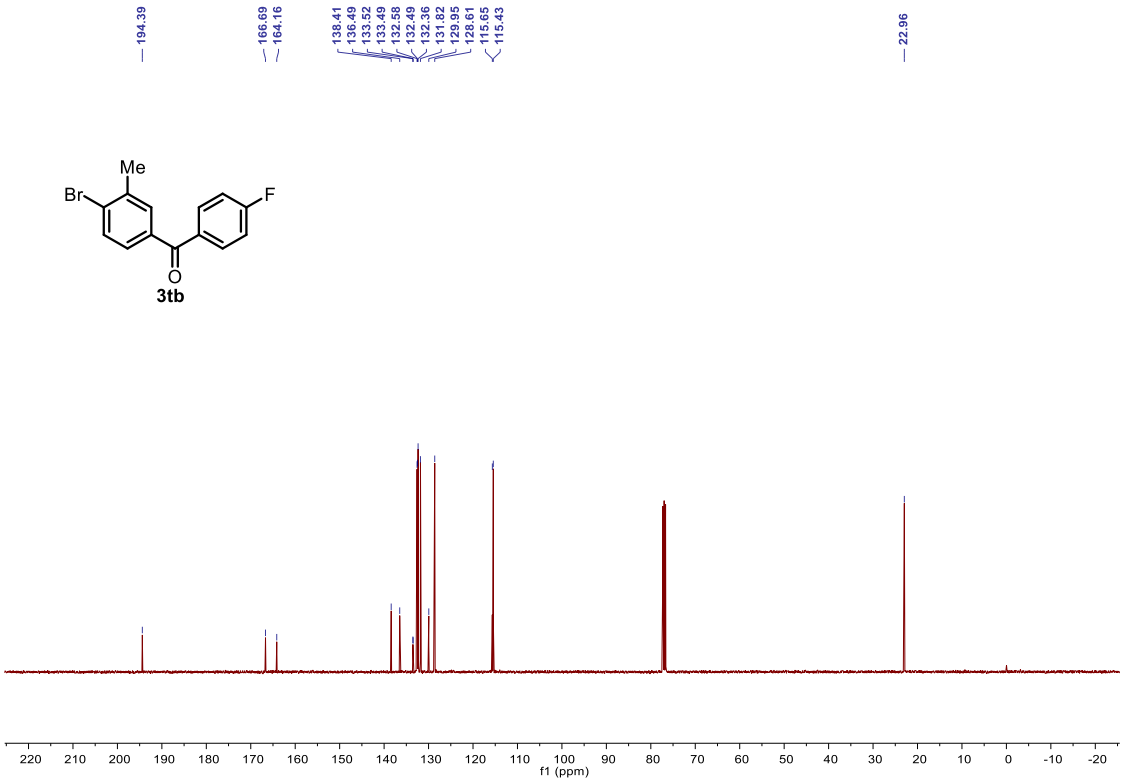

Figure 4.134. ^{19}F NMR Spectrum of 3tb

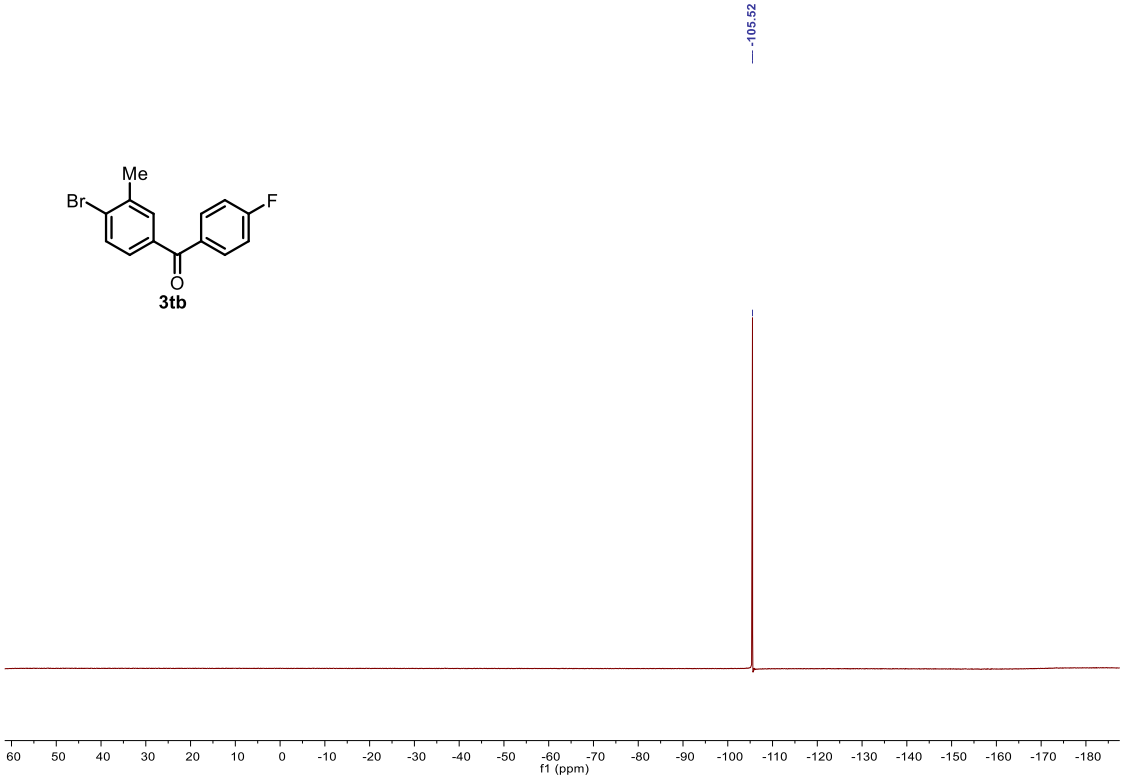

Figure 4.135. ^{1}H NMR Spectrum of 3ub

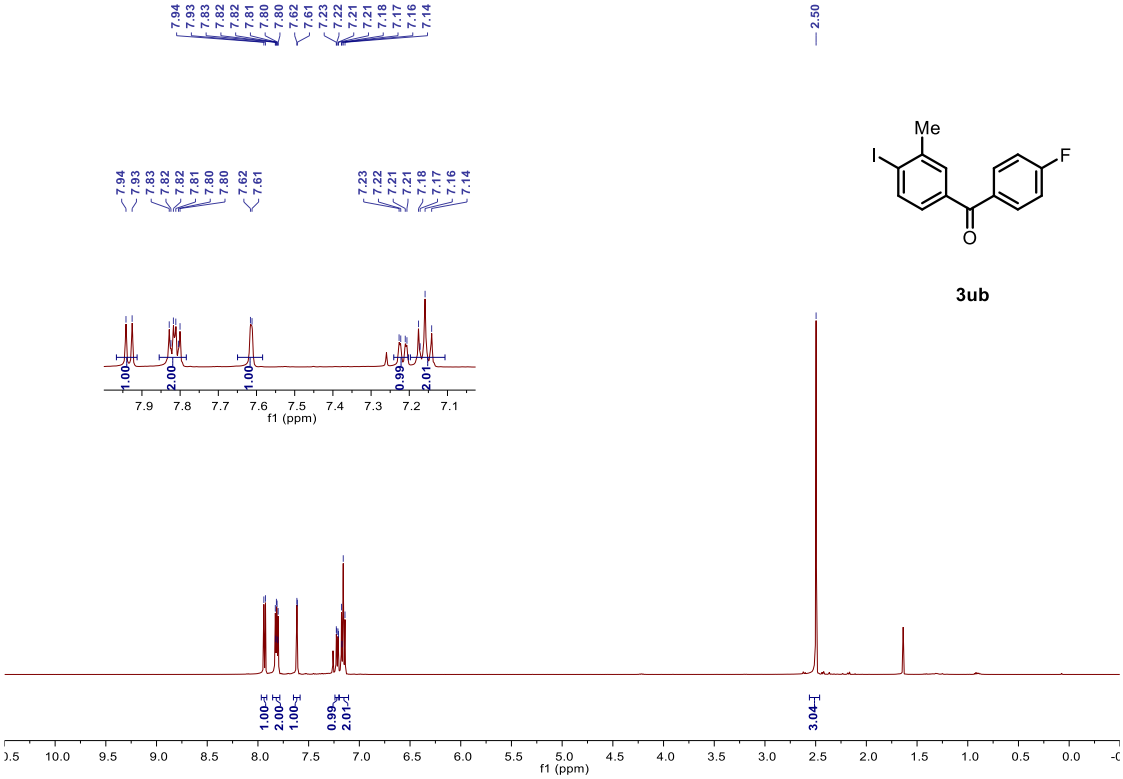

Figure 4.136. ^{13}C NMR Spectrum of 3ub

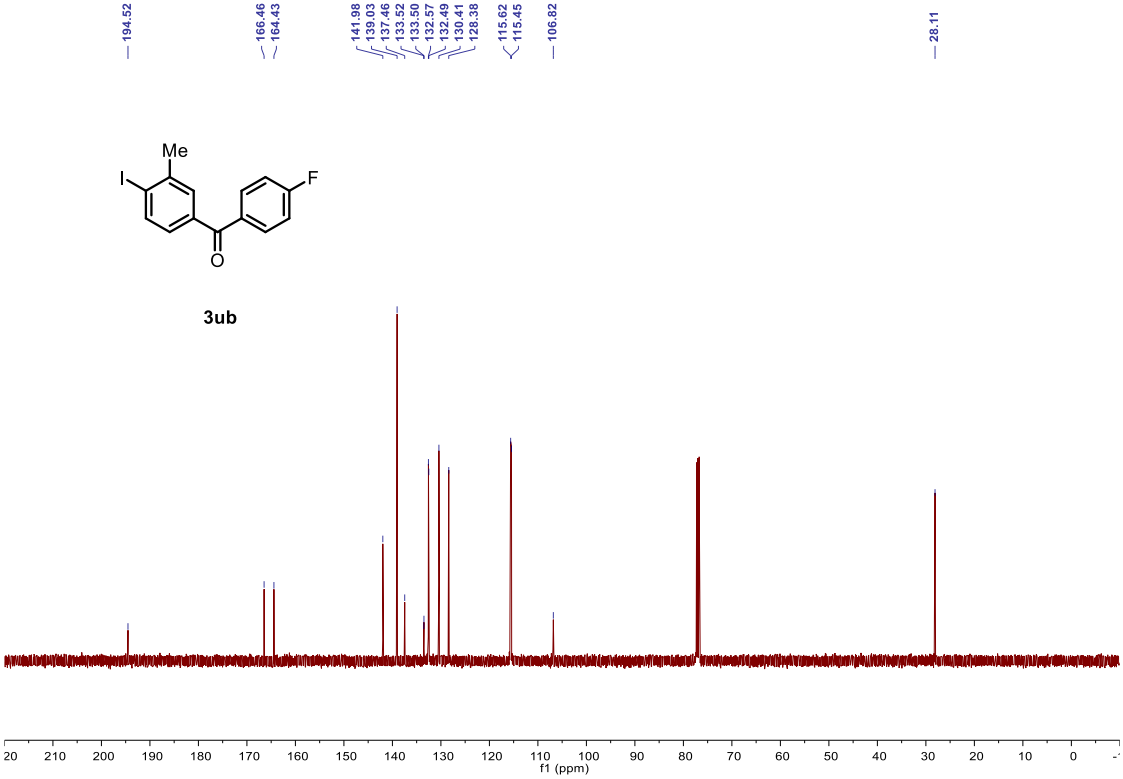

Figure 4.137. ^{19}F NMR Spectrum of 3ub

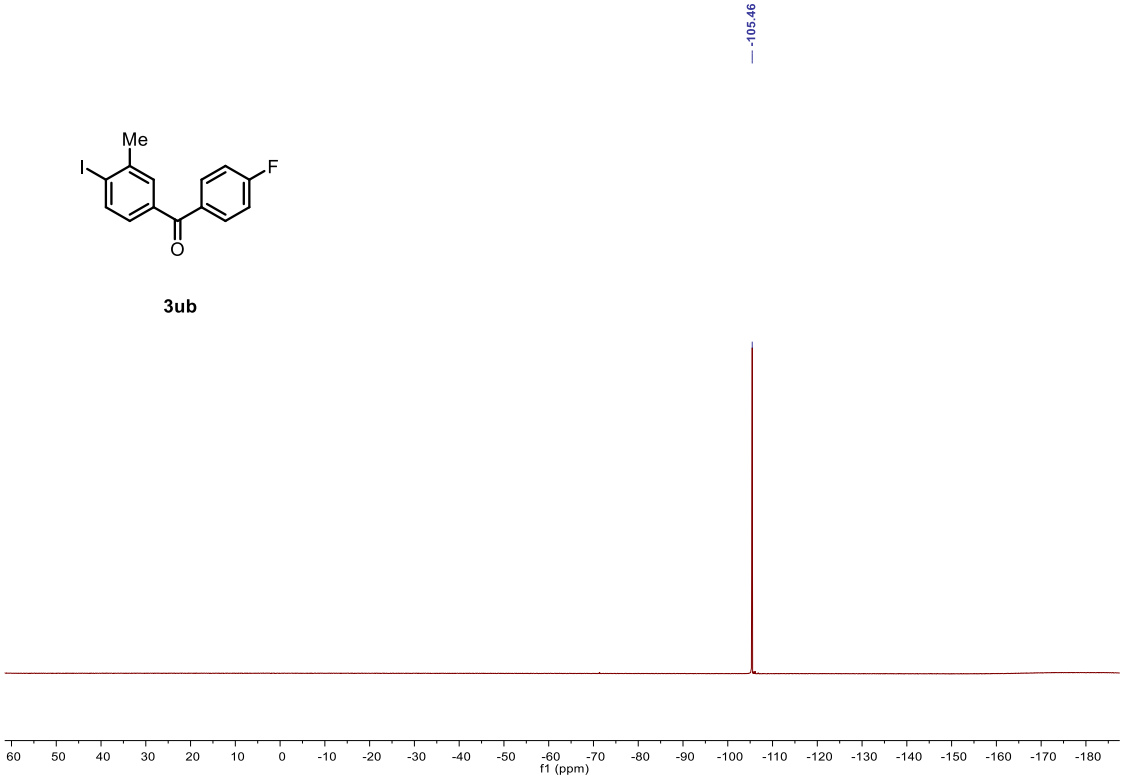

Figure 4.138. ^{1}H NMR Spectrum of 4uba

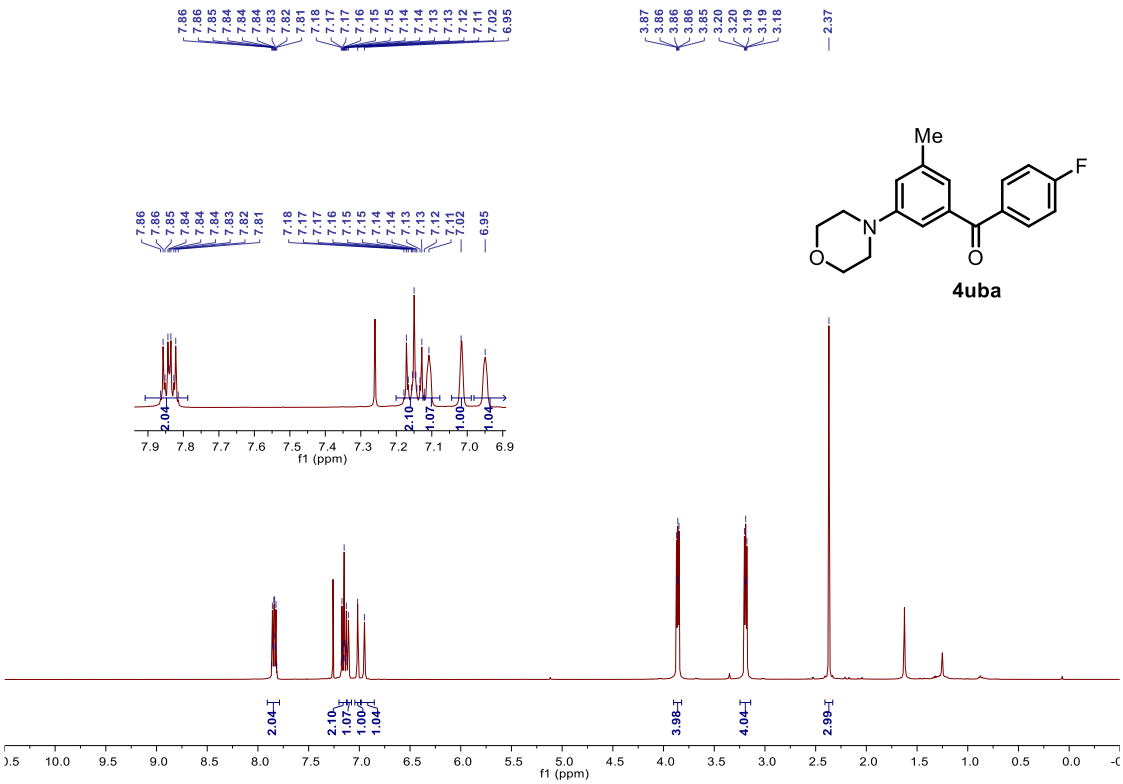

Figure 4.139. ^{13}C NMR Spectrum of 4uba

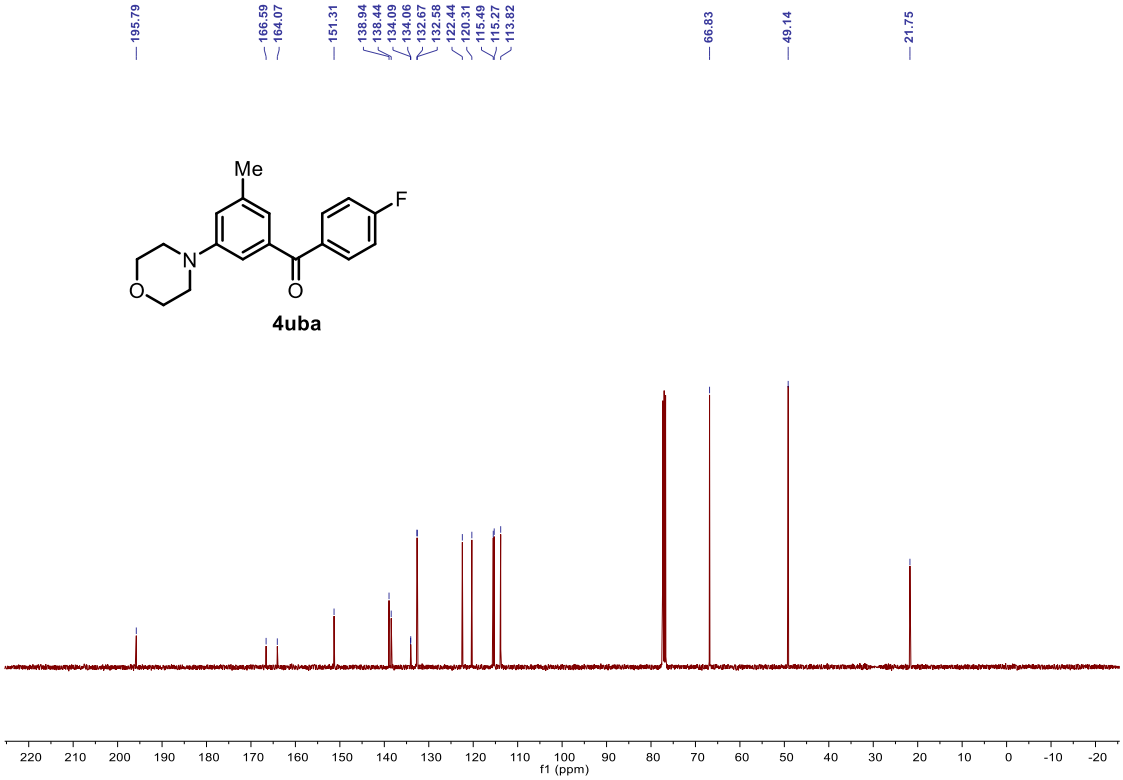

Figure 4.140. ^{19}F NMR Spectrum of 4uba

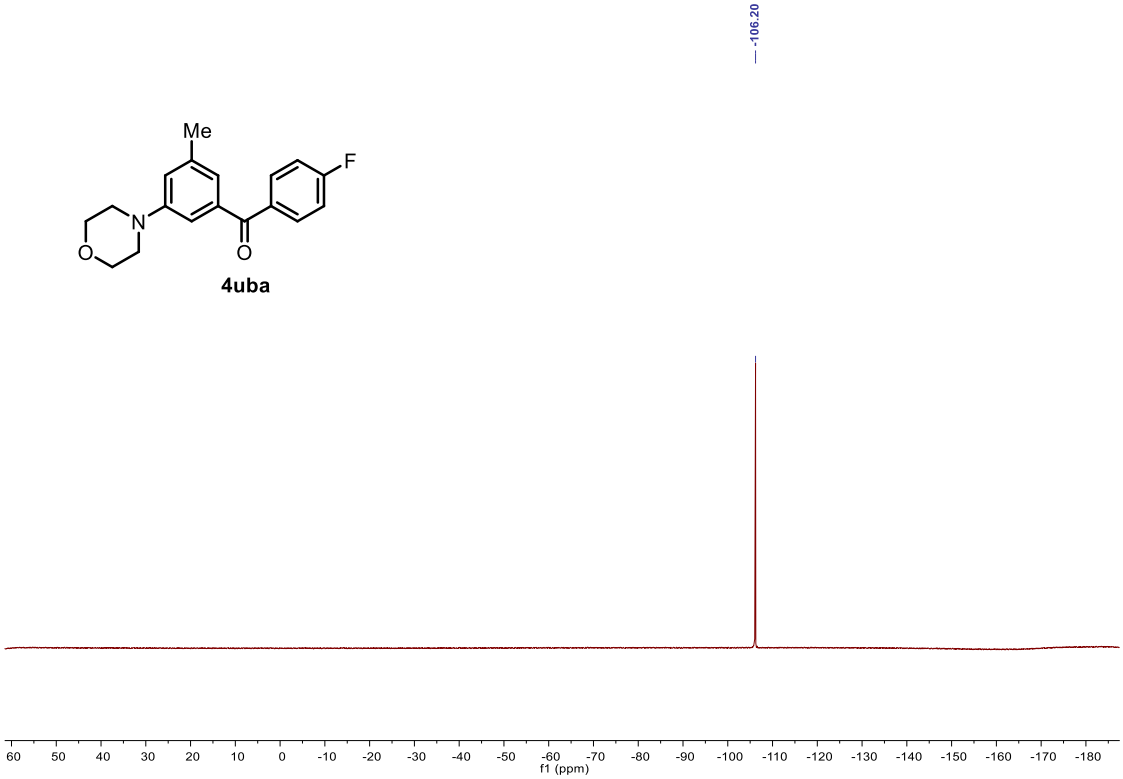

4.6 Reference

(1) Huang, Z., and Dong, G. Site-Selectivity Control in Organic Reactions: A Quest to Differentiate Reactivity among the Same Kind of Functional Groups. *Acc. Chem. Res.* **2017**. *50*, 465-471.

(2) Toste, F.D., Sigman, M.S., and Miller, S.J. Pursuit of Noncovalent Interactions for Strategic Site-Selective Catalysis. *Acc. Chem. Res.* **2017**, *50*, 609-615.

(3) Catellani, M., Frignani, F., and Rangoni, A. A Complex Catalytic Cycle Leading to a Regioselective Synthesis of o,o′-Disubstituted Vinylarenes. *Angew. Chem. Int. Ed.* **1997**, *36*, 119-122.

(4) Lautens, M., and Piguel, S. A New Route to Fused Aromatic Compounds by Using a Palladium-Catalyzed Alkylation–Alkenylation Sequence. *Angew. Chem. Int. Ed.* **2000**, *39*, 1045-1046.

(5) Catellani, M. Novel Methods of Aromatic Functionalization Using Palladium and Norbornene as a Unique Catalytic System. *Top. Organomet. Chem.* **2005**, *14*, 21-53.

(6) Catellani, M., Motti, E., and Della Ca', N. Catalytic Sequential Reactions Involving Palladacycle-Directed Aryl Coupling Steps. *Acc. Chem. Res.* **2008**, *41*, 1512-1522.

(7) Martins, A.; Mariampillai, B.; Lautens, M. Synthesis in the Key of Catellani: Norbornene-Mediated ortho C–H Functionalization. *Top. Curr. Chem.* **2010**, *292*, 1-33.

(8) Ferraccioli, R. Palladium-Catalyzed Synthesis of Carbo- and Heterocycles through Norbornene-Mediated ortho C–H Functionalization. *Synthesis* **2013**, *45*, 581-591.

(9) Ye, J., and Lautens, M. Palladium-catalysed norbornene-mediated C–H functionalization of arenes. *Nat. Chem.* **2015**, *7*, 863.

(10) Della Ca', N., Fontana, M., Motti, E., and Catellani, M. Pd/Norbornene: A Winning Combination for Selective Aromatic Functionalization via C–H Bond Activation. *Acc. Chem. Res.* *49*, **2016**, 1389-1400.

(11) Catellani, M.; Motti, E.; Baratta, S. A Novel Palladium-Catalyzed Synthesis of Phenanthrenes from ortho-Substituted Aryl Iodides and Diphenyl- or Alkylphenylacetylenes. *Org. Lett.* **2001**, *3*, 3611-3614.

(12) Faccini, F.; Motti, E.; Catellani, M. A New Reaction Sequence Involving Palladium-Catalyzed Unsymmetrical Aryl Coupling. *J. Am. Chem. Soc*. **2004**, *126*, 78-79.

(13) Mariampillai, B., Alliot, J., Li, M., and Lautens, M. A Convergent Synthesis of Polysubstituted Aromatic Nitriles via Palladium-Catalyzed C−H Functionalization. *J. Am. Chem. Soc*. **2007**, *129*, 15372-15379.

(14) Martins, A.; Lautens, M. Aromatic ortho-Benzylation Reveals an Unexpected Reductant. *Org. Lett.* **2008**, *10*, 5095-5097.

(15) Zhao, Y.-B.; Mariampillai, B.; Candito, D. A.; Laleu, B.; Li, M.; Lautens, M. Exploiting the Divergent Reactivity of Aryl‑Palladium Intermediates for the Rapid Assembly of Fluorene and Phenanthrene Derivatives. *Angew. Chem. Int. Ed.* **2009**, *48*, 1849-1852.

(16) Weinstabl, H., Suhartono, M., Qureshi, Z., and Lautens, M. Total Synthesis of (+)-Linoxepin by Utilizing the Catellani Reaction. *Angew. Chem. Int. Ed.* **2013**, *52*, 5305-5308.

(17) Dong, Z.; Dong, G. Ortho vs Ipso: Site-Selective Pd and Norbornene-Catalyzed Arene C–H Amination Using Aryl Halides. *J. Am. Chem. Soc.* **2013**, *135*, 18350-18353.

(18) Zhou, P.-X.; Ye, Y.-Y.; Liu, C.; Zhao, L.-B.; Hou, J.-Y.; Chen, D.-Q.; Tang, Q.; Wang, A.-Q.; Zhang, J.-Y.; Huang, Q.-X.; Xu, P.-F.; Liang, Y.-M. Palladium-Catalyzed

Acylation/Alkenylation of Aryl Iodide: A Domino Approach Based on the Catellani–Lautens Reaction. *ACS Catal.* **2015**, *5*, 4927-4931.

(19) Dong, Z.; Wang, J.; Ren, Z.; Dong, G. Ortho C-H Acylation of Aryl Iodides by Palladium/Norbornene Catalysis. *Angew. Chem. Int. Ed.* **2015**, *54*, 12664-12668.

(20) Shi, H.; Babinski, D. J.; Ritter, T. Modular C–H Functionalization Cascade of Aryl Iodides. *J. Am. Chem. Soc.* **2015**, *137*, 3775-3778.

(21) Wang, J., Zhang, L., Dong, Z., and Dong, G. Reagent-Enabled *ortho*-Alkoxycarbonylation of Aryl Iodides via Palladium/Norbornene Catalysis. *Chem* **2016**, *1*, 581-591.

(22) Sun, F., Li, M., He, C., Wang, B., Li, B., Sui, X., and Gu, Z. Cleavage of the C(O)–S Bond of Thioesters by Palladium/Norbornene/Copper Cooperative Catalysis: An Efficient Synthesis of 2-(Arylthio)aryl Ketones. *J. Am. Chem. Soc.* **2016**, *138*, 7456-7459.

(23) For a recent related intramolecular lactam formation, see: Li, X.; Pan, J.; Song, S.; Jiao, N. Pd-catalyzed Dehydrogenative Annulation Approach for the Efficient Synthesis of Phenanthridinones. *Chem. Sci.* **2016**, *7*, 5384-5389.

(24) Li, Renhe., and Dong, Guangbin., Direct Annulation between Aryl Iodides and Epoxides through Palladium/Norbornene Cooperative Catalysis. *Angew. Chem. Int. Ed.* **2018**, 57, 1697-1701.

(25) Cheng, H.-G., Chenggui, W., Han, C., Ruiming, C., Guangyin, Q., Zhi, G., Qiang, W., Yuanyuan, X., Jingyang, Z., Yuming, Z. Epoxides as Alkylating Reagents for the Catellani Reaction. *Angew. Chem. Int. Ed.* **2018**, *57*, 3444-3448.

(26) Dong, Z., Lu, G., Wang, J., Liu, P., and Dong, G. Modular ipso/ortho Difunctionalization of Aryl Bromides via Palladium/Norbornene Cooperative Catalysis. *J. Am. Chem. Soc.* **2018**, *140*, 8551-8562.

(27) Liu, C., Liang, Y., Zheng, N., Zhang, B.-S., Feng, Y., Bi, S., and Liang, Y.-M. Synthesis of indolines via a palladium/norbornene-catalyzed reaction of aziridines with aryl iodides. *Chem. Commun.* **2018**, *54*, 3407-3410.

(28) Qian, G., Bai, M., Gao, S., Chen, H., Zhou, S., Cheng, H.-G., Yan, W., and Zhou, Q. Modular One-Step Three-Component Synthesis of Tetrahydroisoquinolines Using a Catellani Strategy. *Angew. Chem. Int. Ed.* **2018**, *57*, 10980-10984.

(29) Wang, J., Li, R., Dong, Z., Liu, P., and Dong, G. Complementary site-selectivity in arene functionalization enabled by overcoming the ortho constraint in palladium/norbornene catalysis. *Nat. Chem.* **2018**, *10*, 866-872.

(30) Jiao, L., and Bach, T. Palladium-Catalyzed Direct 2-Alkylation of Indoles by Norbornene-Mediated Regioselective Cascade C–H Activation. *J. Am. Chem. Soc.* **2011**, *133*, 12990-12993.

(31) Wang, X.-C.; Gong, W.; Fang, L.-Z.; Zhu, R.-Y.; Li, S.; Engle, K. M.; Yu, J.-Q. Ligand-enabled Meta-C-H Activation Using a Transient Mediator. *Nature* **2015**, *519*, 334-338.

(32) Dong, Z.; Wang, J.; Dong, G. Simple Amine-Directed Meta-Selective C‑H Arylation via Pd/Norbornene Catalysis. *J. Am. Chem. Soc.* **2015**, *137*, 5887-5890.

(33) Shi, H., Herron, A. N., Shao, Y., Shao, Q., and Yu, J.-Q. Enantioselective remote meta-C–H arylation and alkylation via a chiral transient mediator. *Nature* **2018**, *558*, 581-585.

(34) Shi, G., Shao, C., Ma, X., Gu, Y., and Zhang, Y. Pd(II)-Catalyzed Catellani-Type Domino Reaction Utilizing Arylboronic Acids as Substrates. *ACS Catal.* **2018**, *8*, 3775-3779.

(35) Chen, S., Liu, Z.-S., Yang, T., Hua, Y., Zhou, Z., Cheng, H.-G., and Zhou, Q. The Discovery of a Palladium(II)-Initiated Borono-Catellani Reaction. *Angew. Chem. Int. Ed.* **2018**, *57*, 7161-7165.

(36) O'Duill, M.L., and Engle, K.M. Protodepalladation as a Strategic Elementary Step in Catalysis. *Synthesis* **2018**, *50*, 4699-4714.

(37) Farina, V., and Krishnan, B. Large rate accelerations in the stille reaction with tri-2-furylphosphine and triphenylarsine as palladium ligands: mechanistic and synthetic implications. *J. Am. Chem. Soc.* **1991**, *113*, 9585-9595.

(38) Chen, M.S., Prabagaran, N., Labenz, N.A., and White, M.C. Serial Ligand Catalysis: A Highly Selective Allylic C−H Oxidation. *J. Am. Chem. Soc.* **2005**, *127*, 6970-6971.

(39) Lin, S., Song, C.-X., Cai, G.-X., Wang, W.-H., and Shi, Z.-J. Intra/Intermolecular Direct Allylic Alkylation via Pd(II)-Catalyzed Allylic C−H Activation. *J. Am. Chem. Soc.* **2008**, *130*, 12901-12903.

(40) Braun, M.-G., and Doyle, A.G. Palladium-Catalyzed Allylic C–H Fluorination. *J. Am. Chem. Soc.* **2013**, *135*, 12990-12993.

(41) Cu(I) salts are known to promote transmetalation in Stille reactions as a ligand scavenger; see: Farina, V., Kapadia, S., Krishnan, B., Wang, C., and Liebeskind, L.S. On the Nature of the "Copper Effect" in the Stille Cross-Coupling. *J. Org. Chem.* **1994**, *59*, 5905-5911.

(42) Lennox, A.J.J., and Lloyd-Jones, G.C. Selection of boron reagents for Suzuki-Miyaura coupling. *Chem. Soc. Rev.* **2014**, *43*, 412-443.

(43) The slight decrease in yield was likely due to the presence of the basic amine moiety in the alkaloid.

(44) H. Adkins, Q. E. Thompson, Diacylation of Water and of Hydrogen Sulfide with Acyl Chloride--Pyridine Compounds. *J. Am. Chem. Soc.* **1949**, *71*, 2242-2244.

(45) R. Kocz, J. Roestamadji, S. Mobashery, A Convenient Triphosgene-Mediated Synthesis of Symmetric Carboxylic Acid Anhydrides. *J. Org. Chem.* **1994**, *59*, 2913-2914.

(46) Q. Zhou, S. Wei, W. Han, In Situ Generation of Palladium Nanoparticles: Ligand-Free Palladium Catalyzed Pivalic Acid Assisted Carbonylative Suzuki Reactions at Ambient Conditions. *J. Org. Chem.* **2014**, *79*, 1454-1460.

(47) F. Jin, W. Han, Transition-metal-free, ambient-pressure carbonylative cross-coupling reactions of aryl halides with potassium aryltrifluoroborates. *Chem. Commun.* **2015**, *51*, 9133-9136.

(48) H. Yi, C. Bian, X. Hu, L. Niu, A. Lei, Visible light mediated efficient oxidative benzylic sp3 C-H to ketone derivatives obtained under mild conditions using O_2. *Chem. Commun.* **2015**, *51*, 14046-14049.

(49) K. Kikukawa, T. Idemoto, A. Katayama, K. Kono, F. Wada, T. Matsuda, Reaction of diazonium salts with transition metals. Part 13. Palladium-catalyzed carbonylative coupling of arenediazonium salts with organotin reagents to give aromatic ketones. *J. Chem. Soc., Perkin Trans. 1*. **1987**, 1511-1514.

(50) B. A. T., G. Frank, Intermolecular N-Heterocyclic Carbene Catalyzed Hydroacylation of Arynes. *Angew. Chem. Int. Ed.* **2010**, *49*, 9761-9764.

(51) SANOFI-AVENTIS - US2011/112097, 2011, A1

(52) J. Chen, C. Chen, C. Ji, Z. Lu, Cobalt-Catalyzed Asymmetric Hydrogenation of 1,1-Diarylethenes. *Org. Lett.* **2016**, *18*, 1594-1597.

(53) G. Prasanjit, G. Bhaskar, D. Sajal, Pd-NHC catalysed Carbonylative Suzuki coupling reaction and its application towards the synthesis of biologically active 3-aroylquinolin-4 (1H)-one and acridone scaffolds. *Appl. Organomet. Chem.* **2018**, *32*, e4173.

(54) K. M. Bjerglund, T. Skrydstrup, Carbonylative Suzuki Couplings of Aryl Bromides with Boronic Acid Derivatives under Base-Free Conditions. G. A. Molander, *Org. Lett.* **2014**, *16*, 1888-1891.

(55) M. Krishnamurthy, S. Gurley, B. M. Moore, Exploring the substituent effects on a novel series of C1'-dimethyl-aryl Delta8-tetrahydrocannabinol analogs. *Biorg. Med. Chem.* **2008**, *16*, 6489-6500.

(56) C. Lorenzo, C. Antonella, F. Barbara, Arylferrocenylmethanols: a new family of ferrocenes to be used as mediators in biosensors. *Appl. Organomet. Chem.* **2003**, *17*, 589-599.

(57) S. Roslin, L. R. Odell, Palladium and visible-light mediated carbonylative Suzuki-Miyaura coupling of unactivated alkyl halides and aryl boronic acids. *Chem. Commun.* **2017**, *53*, 6895-6898.

(58) C. Pietro, M. Antonio, C. Francesco, M. Antonella, N. Angelo, Palladium-Catalyzed Cross-Coupling of Styrenes with Aryl Methyl Ketones in Ionic Liquids: Direct Access to Cyclopropanes. *Angew. Chem. Int. Ed.* **2014**, *53*, 13563-13567.

(59) S. Ushijima, S. Dohi, K. Moriyama, H. Togo, Facile preparation of aromatic ketones from aromatic bromides and arenes with aldehydes. *Tetrahedron* **2012**, *68*, 1436-1442.

(60) M. Fanyang, Y. J. Mingtao, Q. Di, L. Fei, Z. Yan, W. Jianbo, Gold-Catalyzed Halogenation of Aromatics by N-Halosuccinimides. *Angew. Chem. Int. Ed.* **2010**, *49*, 2028-2032.

(61) P. A. Bonvallet, C. J. Breitkreuz, Y. S. Kim, E. M. Todd, K. Traynor, C. G. Fry, M. D. Ediger, R. J. McMahon, Organic Glass-Forming Materials: 1,3,5-Tris(naphthyl)benzene Derivatives. *J. Org. Chem.* **2007**, *72*, 10051-10057.

(62) Z. Dong, G. Dong, *Ortho* vs *Ipso*: Site-Selective Pd and Norbornene-Catalyzed Arene C–H Amination Using Aryl Halides. *J. Am. Chem. Soc.* **2013**, *135*, 18350-18353.

(63) F.-F. Yong, Y.-C. Teo, K.-N. Tan, Efficient copper-catalyzed cross-coupling of 1-Boc-piperazine with aryl iodides and its application in the synthesis of trazodone. *Tetrahedron Lett.* **2013**, *54*, 5332-5334.

(64) J. R. Falck, M. Bondlela, S. K. Venkataraman, D. Srinivas, Bromo-Boronolactonization of Olefins1. *J. Org. Chem.* **2001**, *66*, 7148-7150.

(65) C.-J. Zhao, D. Xue, Z.-H. Jia, C. Wang, J. Xiao, Methanol-Promoted Borylation of Arylamines: A Simple and Green Synthetic Method to Arylboronic Acids and Arylboronates. *Synlett* **2014**, *25*, 1577-1584.

(66) D. Qiu, L. Jin, Z. Zheng, H. Meng, F. Mo, X. Wang, Y. Zhang, J. Wang, Synthesis of Pinacol Arylboronates from Aromatic Amines: A Metal-Free Transformation. *J. Org. Chem.* **2013**, *78*, 1923-1933.

(67) Z. Dong, G. Lu, J. Wang, P. Liu, G. Dong, Modular ipso/ortho Difunctionalization of Aryl Bromides via Palladium/Norbornene Cooperative Catalysis. *J. Am. Chem. Soc.* **2018**, *140*, 8551-8562.

(Some contents of this chapter were published in *Chem* **2019**, *5*, 929-939.)

CHAPTER 5

Sulfenamide-Enabled Ortho Thiolation of Aryl Iodides via Palladium/Norbornene Cooperative Catalysis

5.1 Introduction

Aromatic sulfur compounds are commonly found in drugs,[1] agrochemicals,[2] organic electronics[3] and polymers[4] (Figure 5.1a). In addition, aryl sulfides often serve as versatile intermediates to access the corresponding sulfoxides,[5] sulfones[6] and benzothiophenes.[7] Common ways to prepare aryl sulfides heavily rely on nucleophilic aromatic substitution[8] and cross-coupling reactions[9] between aryl halides and thiols. Both methods form carbon−sulfur (C−S) bonds at the ipso position of aryl halides; thus, the position of the installed sulfur moiety is restricted by the position of the halide. On the other hand, C−H thiolation offers an attractive approach to introduce sulfur to an non-pre-functionalized position;[10] however, control of site-selectivity generally requires use of directing groups[11] or electron-rich arenes.[12] Hence, a general method that site-selectively

introduces sulfur functional groups to unbiased and unactivated arene positions would be highly attractive for preparing multi-substituted aromatic sulfur compounds. This has motivated us to explore the approach using palladium/norbornene (Pd/NBE) cooperative catalysis.

Figure 5.1. Project Background and Design for Ortho C-H Thiolation via Pd/NBE Cooperative Catalysis

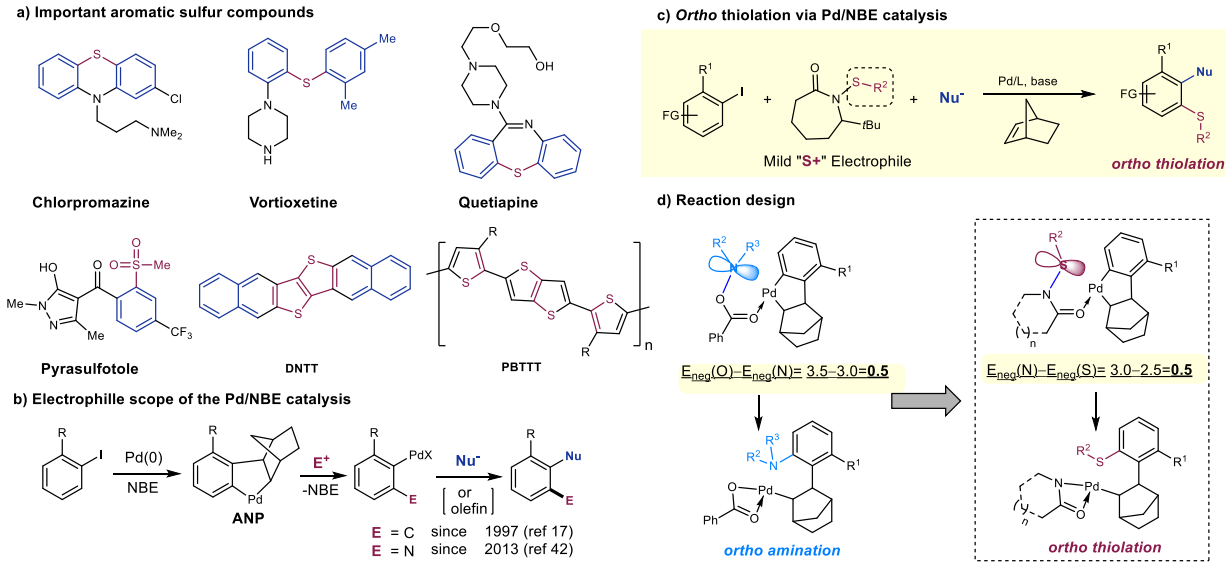

Pd/NBE cooperative catalysis,[13] originally discovered by Catellani,[14] has emerged as a useful tool for preparing multi-substituted arenes.[15] Compared to the conventional arene functionalization, this approach enables simultaneous functionalization of arene vicinal positions regioselectively using simple aryl halides as substrates (Figure 5.1b). Specifically, through forming an aryl-NBE-palladacycle (ANP) intermediate, a nucleophile and an electrophile are coupled at the arene ipso and ortho positions, respectively. While the scope of nucleophiles in this reaction is broad,[13a, 16] finding suitable electrophiles that can participate in the Catellani reaction nevertheless remains a formidable challenge,[17] because the electrophile must react with ANP selectively in the presence of Pd(0) species and has to be compatible with the nucleophile and NBE. Currently, the scope of

electrophiles is mainly limited to carbon[14, 18] and nitrogen[19]-based reagents. In 2017, Yu used aryl chlorosulfates for a directed Pd(II)-catalyzed meta chlorination of arenes;[20] however, compatibility of this reagent with Pd(0) catalysts could be a concern.[21] More recently, Zhang[22] and Cheng[23] independently reported an interesting ortho silyation with disilanes; unfortunately, NBE cannot be extruded in this reaction. Clearly, it would be attractive if other elements, besides C and N, could be introduced at the arene ortho position in the Pd(0)-catalyzed Catellani reaction. Herein, we report a Pd/NBE-catalyzed ortho thiolation of aryl iodides, which is enabled by sulfenamide-type electrophiles (FIgure 5.1c). This approach provides a general platform to introduce various sulfur moieties to the arene ortho positon and simultaneously install other functional groups at the arene ipso position. The generality, scability and high chemoselectivity could make this method attractive for preparing complex sulfur-containing aromatic compounds.

5.2 Results and Discussion

5.2.1 Reaction Discovery and Optimization

Hypothesis. Compared to other ortho functionalizations, ortho thiolation exhibits its unique challenges. First, many electrophilic sulfur-based compounds, such as PhSSPh or PhSCl, readily react with Pd(0),[24] therefore preventing arene functionalization. Second, thiolates (RS^-) are known as strong ligands for soft Pd species; thus, decomposition of the thiolation agent would likely generate RS^- that could lead to direct ipso thiolation.[25] Hence, developing a stable but also reactive electrophilic thiolation agent would be a key for realizing the ortho thiolation reaction. Based on our prior efforts on developing the ortho amination reaction,[19] sulfenamides[26] were anticipated to be a suitable electrophile for the Pd/NBE catalysis for two reasons (FIgure 5.1d): 1) the

electronegativity (E_{neg}, Pauling scale) difference between N and S matches well with that between O and N;[27] 2) analogous to the ortho amination, the amide carbonyl could serve as a directing moiety to facilitate selective reactions with ANP. Thus, we hypothesized that sulfenamides might show similar stability and reactivity as *O*-benzoyl hydroxylamines. It is noteworthy that, during the review process of this work, an interesting ortho thiolation using thiosulfonate reagents was reported by Gu.[28]

Table 5.1. Electrophiles for the Pd/NBE-Catalyzed Ortho Thiolation of Aryl Iodides[a]

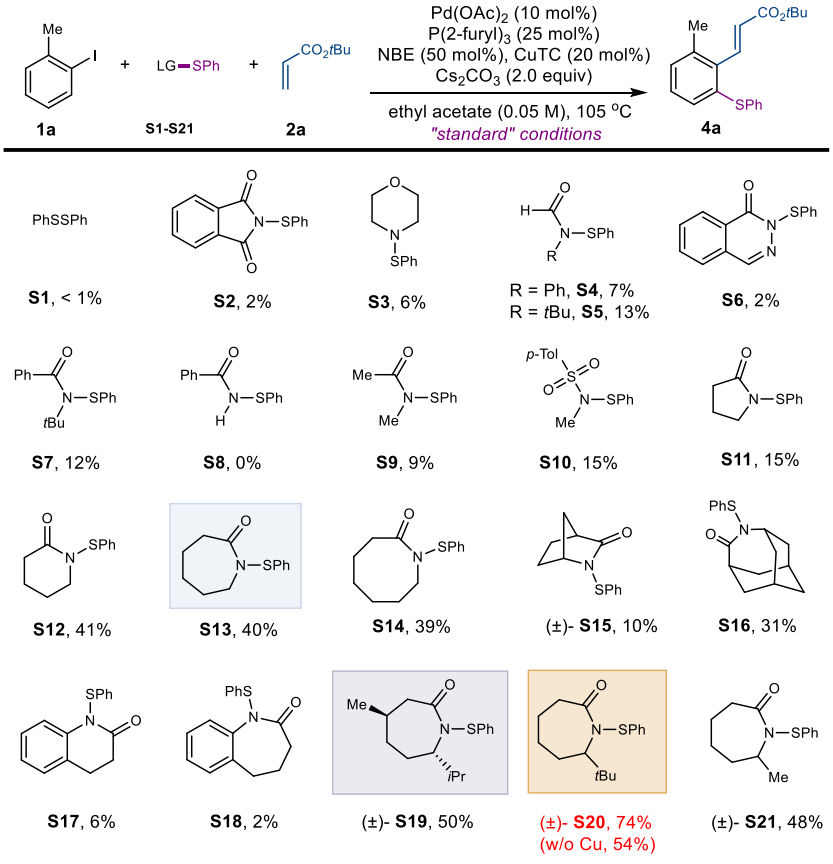

[a]The reaction was run with **1** (0.15 mmol), **2** (0.30 mmol), sulfur electrophile (0.30 mmol), $Pd(OAc)_2$ (0.015 mmol), $P(2\text{-furyl})_3$ (0.0375 mmol), NBE (0.075 mmol), Cs_2CO_3 (0.30 mmol) and CuTC (0.03 mmol) in ethyl acetate (3.0 mL) at 105 °C for 12 h. The yield was determined by ^{1}H-NMR using 1,3,5-trimethoxylbenzene as the internal standard. LG: leaving group. CuTC: copper(I) thiophene-2-carboxylate.

To test this hypothesis, a range of sulfenamide-based thiolation agents were examined with 2-iodotoluene (**1a**) as the standard substrate, and the ipso position was functionalized via Heck termination with acrylate **2a** (Table 5.1). As a control experiment, PhSSPh **S1**, previously used in the Pd-catalyzed C−H thiolation,[11] gave almost no desired product with a low conversion of **1a**. In contrast, various sulfenamides indeed afforded the desired ortho thiolation product (**4a**). First, neither imide- or amine-derived sulfenamides (**S2** and **S3**) were as effective as amide-based ones. In particular, the lactam-derived sulfenamides (**S11-S21**) were found most reactive. Interestingly, the six, seven and eight-membered sulfenamides (**S12-S14**) gave significantly improved yields compared to the five-membered one (**S11**). Use of more strained or benzofused lactams (**S15-S18**) gave inferior results. Surprisingly, increasing the bulkiness around the lactam nitrogen with an adjacent isopropyl group significantly enhanced the yield (**S19**). Ultimately, the optimal result was obtained using the *t*-butyl-substituted sulfenamide **S20**.

Figure 5.2. X-Ray Structures of Selected Lactam-Derived Sulfenamides[a]

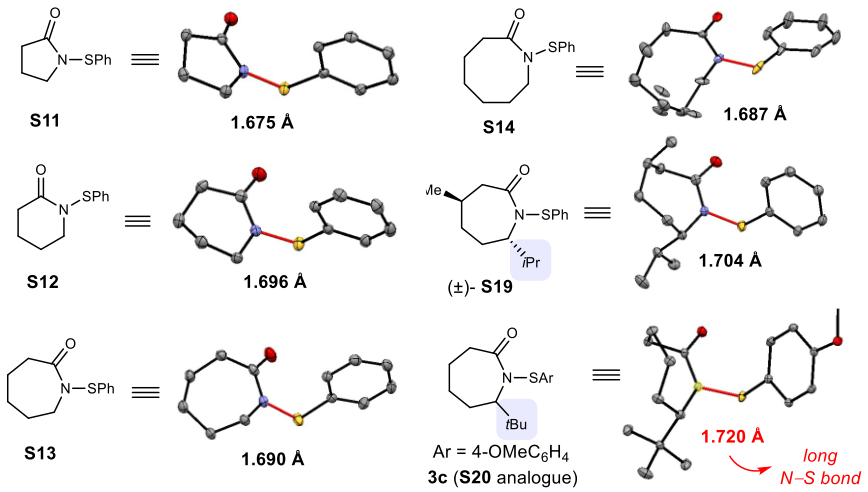

[a]The nitrogen−sulfur bond lengths are labelled in ångström (Å).

To understand these counterintuitive results in terms of the role of the bulk substituent, X-ray crystal structures of **S11-S14**, **S19** and **S20** analogue (**3c**) were obtained (Figure 5.2). A clear trend is that increasingly the steric hindrance around the amide moiety elongated the N−S bond, which correlates to the performance of these reagents. Hence, the *t*-butyl group in **S20** weakened the N−S bond, thereby making it more reactive. Note that adding copper(I) thiophene-2-carboxylate (20 mol%) enhanced the yield, which may serve as a thiolate scavenger (for full control experiments, see Supplementary Table 1).

5.2.2 Substrates Scope

With the optimized conditions in hands, the aryl iodide scope was examined first (Table 5.2). Different substituents at the ortho position of aryl iodides were tolerated, including methyl (**4a**), methoxy (**4b**), MOM ether (**4c**), 4-bromobenzyl ether (**4d**), acetate and silyl-protected benzyl alcohols (**4e** and **4f**) and an estrone derivative (**4g**). In addition, a broad range of functional groups, such as aryl chloride (**4h**), aryl bromide (**4i**), Weinreb amide (**4j**), dialkyl aniline (**4k**), carbamate (**4l**), fluoride (**4m**) and Vitamin E moiety (**4n**). Importantly, the reaction is suitable for a variety of heteroarenes and polycyclic arenes, including quinoline derivative (**4o** and **4p**), indole (**4q**), thiophene (**4r**), naphthalene (**4s**), phenanthrene (**4t**) and pyrene (**4u**).

Next, the scope of the thiolation agents and the olefin coupling partners was explored (Table 5.3). Besides PhS-, other aryl sulfur groups that contain electron-donating or withdrawing groups could be introduced at the ortho position in good to excellent yields. Notably, the ortho-substituted aryl sulfide (**5h**) still afforded a high yield of product. While it was challenging to prepare the corresponding alkyl thiolation agents based on the *t*Bu-substituted lactam, use of simple ε-lactam-

derived sulfenamide **6** nevertheless delivered the desired methylthiolated product (**5k**) in moderate efficiency. In addition to *t*Bu acrylate, other acrylates and acrylamides (**5l-5o**) were also competent coupling partners for ipso functionalization.

Table 5.2. The Aryl Iodide Scope of the Ortho Thiolation[a]

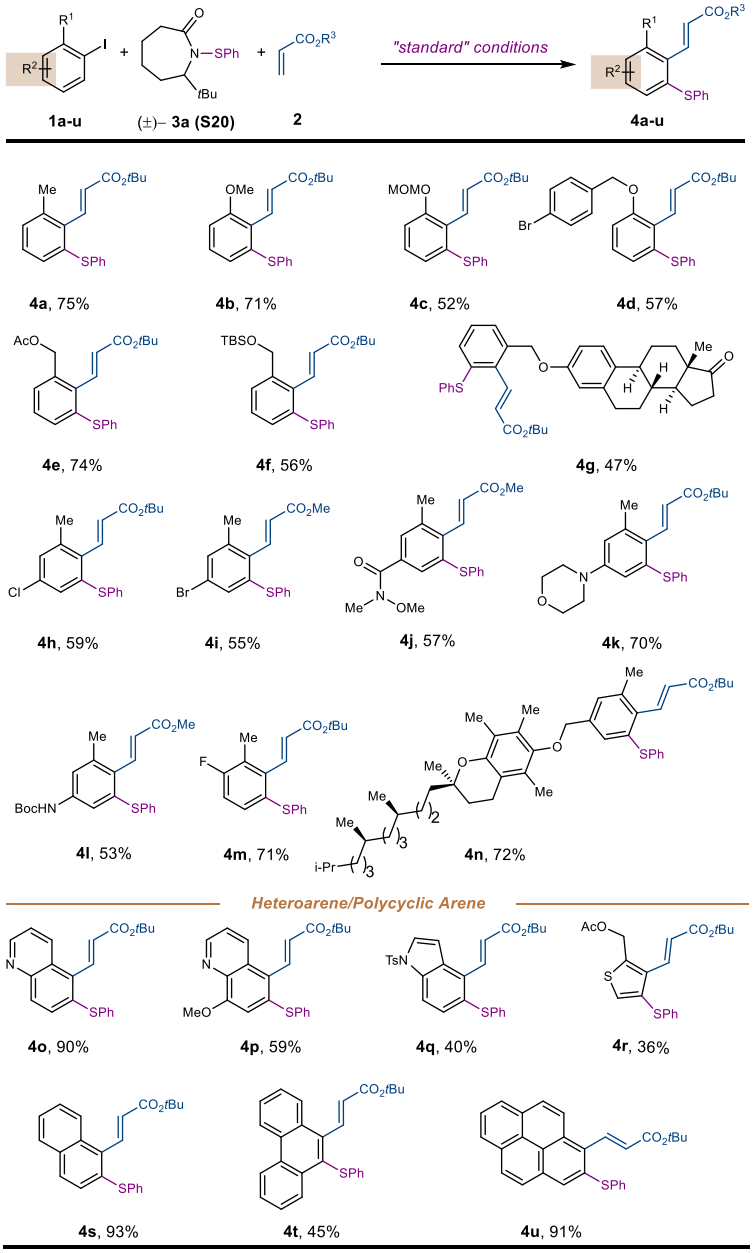

[a]All reactions were run with 0.2 mmol **1**, 0.4 mmol **3a** (**S20**) and 0.4 mmol **2** in ethyl acetate (0.5 M) at 105 °C for 12h. Isolated yields are reported.

Table 5.3. The Sulfenamide and Olefin Scope of the Ortho Thiolation[a]

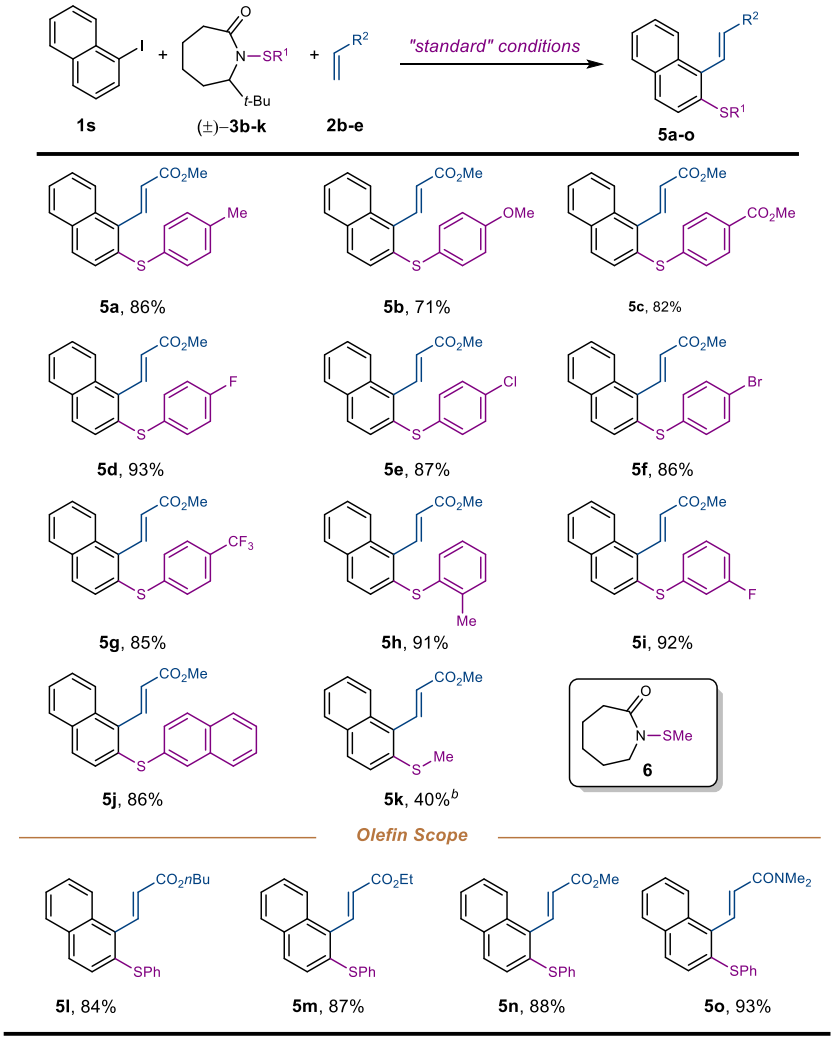

[a]All reactions were run with 0.2 mmol 1s, 0.4 mmol 3 and 0.4 mmol 2 in ethyl acetate (0.5 M) at 105 °C for 12h. Isolated yields are reported. [b]Sulfenamide **6** was used instead of **2**.

It is worth to point out that there are a few unsuccessful examples (Table 5.4). For the scope of aryl iodides, unsatisfying results were obtained when the ortho substituent is small or electron-withdrawing or too bulky. Some heteroaryl iodide also failed to afford the desired, e.g., pyridine and quinoline, probably owning to strong chelation effect from the heteroatoms.

Table 5.4. Less Successful Substrates

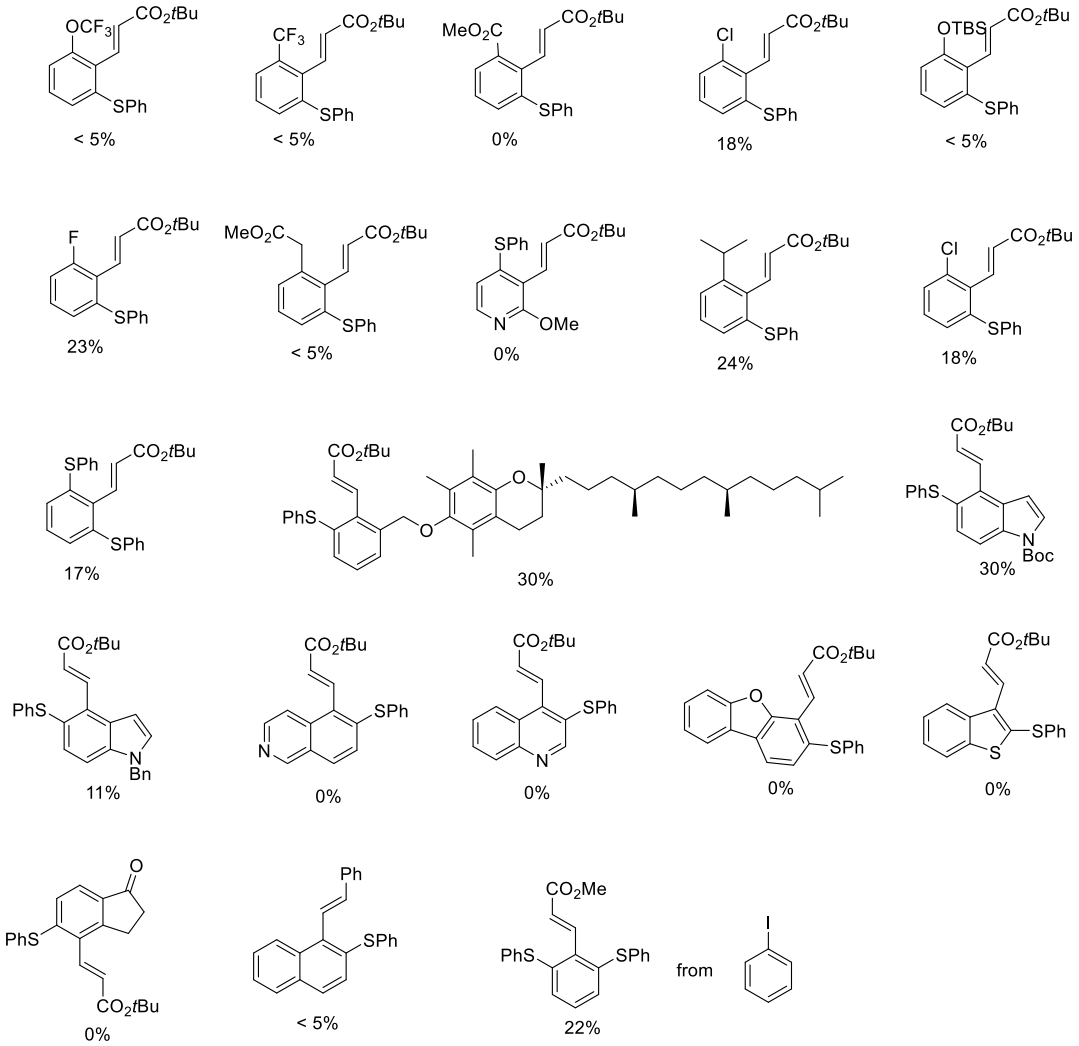

5.2.3 Synthetic Utility

From a practical viewpoint, the lactam byproduct **3a'** was recovered in 86% yield after the reaction, which could be used to regenerate the sulfenamide reagent (Scheme 5.1a). The reaction is scalable: a high yield was still obtained on a gram scale (Scheme 5.1b). Besides aryl sulfides, the corresponding sulfoxides and sulfones could be conveniently accessed through selective oxidation of the ortho thiolation product (Scheme 5.1c). In addition to Heck coupling, preliminary success

has been obtained with Suzuki quench (Scheme 5.1d) and Sonogashira quench (Scheme 5.1e) to install an aryl group or alkyne group at the ipso position, respectively.[13b]

Scheme 5.1. Synthetic Applications

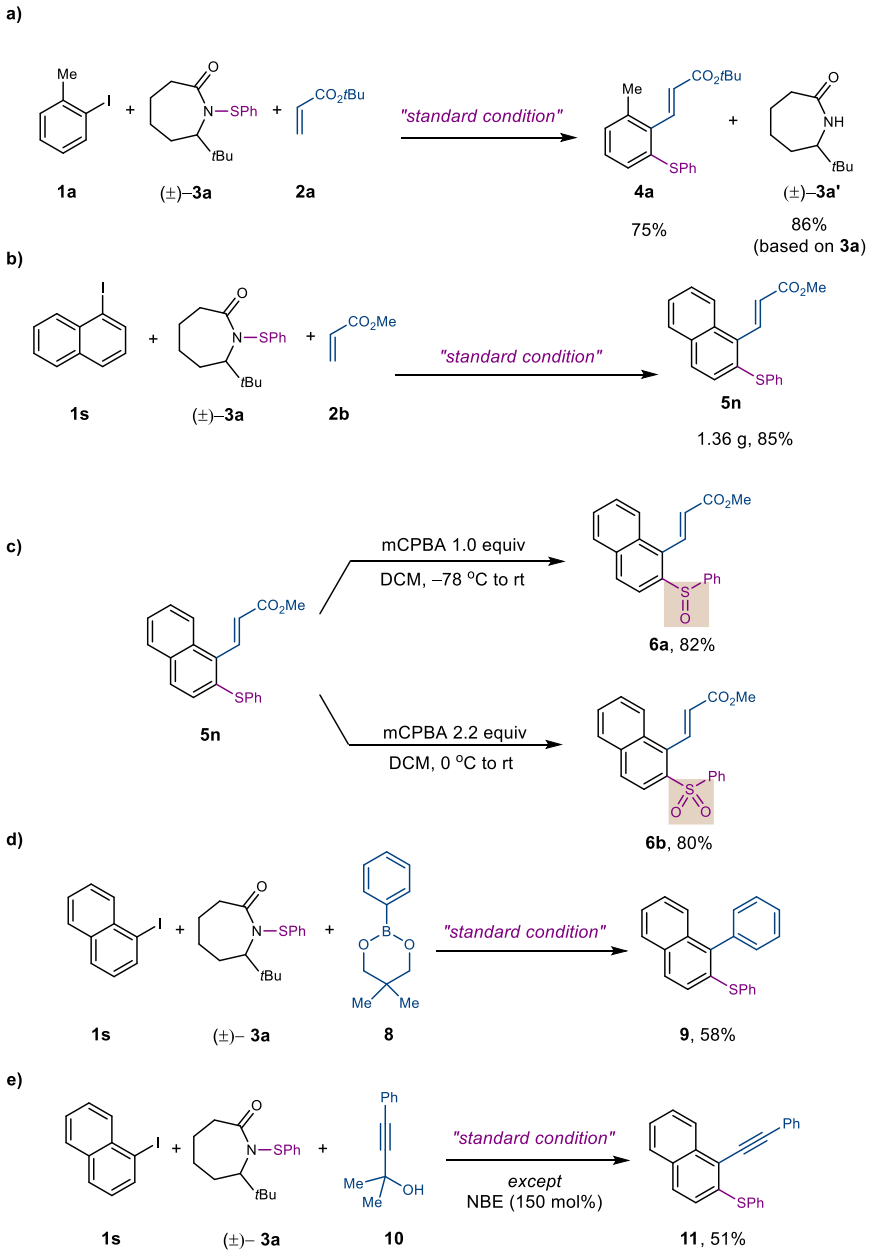

5.3 Conclusion

In summary, a unique class of electrophilic thiolation reagents, sulfenamides, is developed for the Pd/NBE catalysis, which enables ortho thiolation of a wide range of aryl and heteroaryl iodides. The broad substrate scope, scalability and high chemoselectivity could make this method attractive for complex molecule synthesis. The substituent effect observed in tuning the sulfenamide reactivity could have implications beyond this work. Efforts on expanding the reaction scope and understanding the detailed mechanism of the C–S bond formation are underway.

5.4 Experimental Procedures and Characterization Data

5.4.1 General Information

Unless noted otherwise, all solvents were dried by filtration through a Pure-Solv MD-5 Solvent Purification System (Innovative Technology). Ethyl acetate was distilled freshly over calcium hydride and carefully freeze-pump-thawed. Reaction temperatures were reported as the temperatures of the bather surrounding the flasks or vials. Sensitive reagents and solvents were transferred under nitrogen into a nitrogen-filled glovebox with standard techniques. Cesium carbonate was purchased from STREM, stored and used directly in the glovebox. Analytical thin-layer chromatography (TLC) was carried out using 0.2 mm commercial silica gel plates (silica gel 60, F254, EMD chemical). Vials (15 x 45 mm 1 dram (4 mL) with PTFE lined cap attached) were purchased from Qorpak and flame-dried and cooled in a desiccator prior to usage. High resolution mass spectra (HR-MS) were recorded on an Agilent 6530 LC Q-TOF mass spectrometer using electrospray ionization with fragmentation voltage set at 115 V and processed with an Agilent MassHunter Operating System. Infrared spectra were recorded on a Nicolet 380 FTIR using neat thin film technique. Nuclear magnetic resonance spectra (^{1}H NMR and ^{13}C NMR) were recorded with a Bruker DMX 400 (400 MHz, ^{1}H at 400 MHz, ^{13}C at 101 MHz) or Bruker Model DMX 500 (500 MHz, ^{1}H at 500 MHz, ^{13}C at 126 MHz). Chemical shifts were reported in parts per million (ppm, δ), downfield from tetramethylsilane (TMS, δ=0.00ppm) and were referenced to residual solvent ($CDCl_3$, δ=7.26 ppm (^{1}H) and 77.00 ppm (^{13}C)). All the ^{19}F chemical shifts were not referenced. Coupling constants were reported in Hertz (Hz). Data for ^{1}H NMR spectra were reported as follows: chemical shift (ppm, referenced to protium, s = singlet, d = doublet, t = triplet, q = quartet, quin = quintet, dd = doublet of doublets, td = triplet of doublets, ddd = doublet of

doublet of doublets, m = multiplet, coupling constant (Hz), and integration). All other materials were obtained from Sigma-Aldrich Corporation or Combi-Blocks Inc and were used as received.

5.4.2 Control Experiments

Table 5.5 Control Experiments

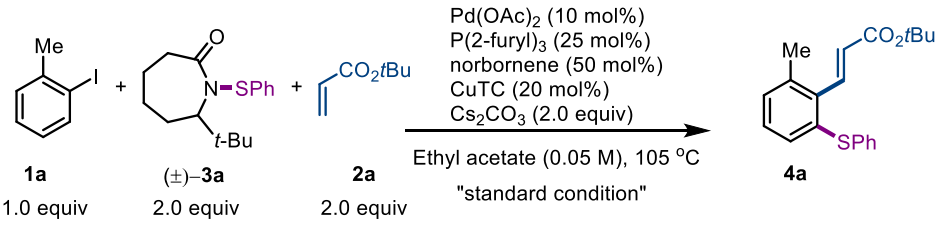

1a 1.0 equiv | (±)–**3a** 2.0 equiv | **2a** 2.0 equiv | **4a**

Entry	Change from the "standard condition"	Yield [%][a]
1	none	74
2	no $Pd(OAc)_2$	0
3	no norbornene	0
4	no Cs_2CO_3	6
5	no CuTC	54
6	5 mol% $Pd(OAc)_2$	15
7	$P(tBu)_3$• HBF_4 instead of $P(2\text{-furyl})_3$	trace
8	PCy_3 instead of $P(2\text{-furyl})_3$	0
9	XPhos instead of $P(2\text{-furyl})_3$	7
10	PPh_3 instead of $P(2\text{-furyl})_3$	3
11	$P(4\text{-}OMeC_6H_4)_3$ instead of $P(2\text{-furyl})_3$	2
12	dioxane instead of EtOAc	66
13	toluene instead of EtOAc	32
14	85 °C	23

[a]Unless otherwise noted, the reaction was run with **1** (0.15 mmol), **2** (0.30 mmol), sulfur electrophile (0.30 mmol), $Pd(OAc)_2$ (0.015 mmol), $P(2\text{-furyl})_3$ (0.0375 mmol), NBE (0.075 mmol), Cs_2CO_3 (0.30 mmol) and CuTC (0.03 mmol) in ethyl acetate (3.0 mL) at 105 °C for 12 h. The yield was determined by ^{1}H-NMR using 1,3,5-trimethoxylbenzene as the internal standard.

5.4.3 Preparation of Aryl Iodides and Thiolating Reagents

Preparation of aryl iodides

Scheme 5.2. Preparation of Aryl Iodides 1n

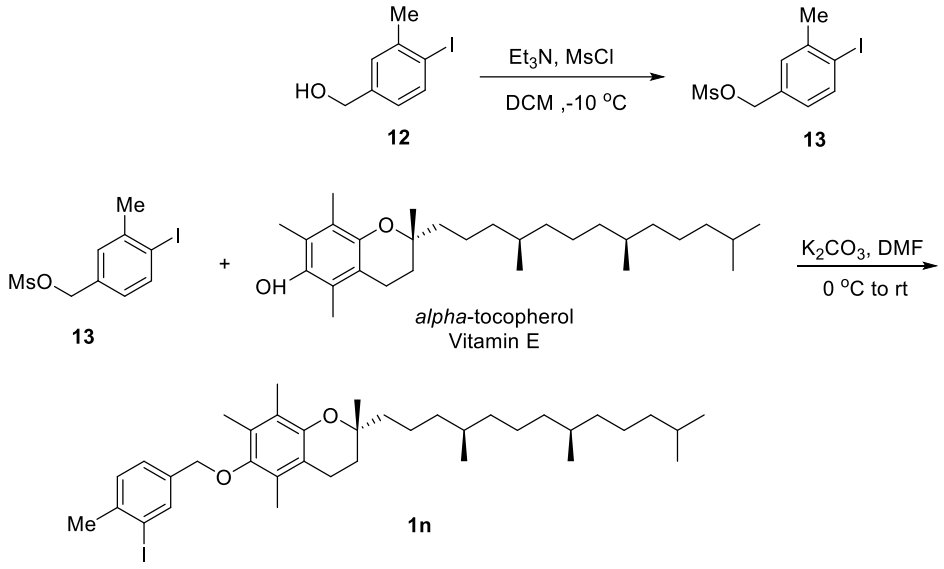

A solution of **12** (2.13 g, 8.6 mmol, 1.0 equiv) and Et_3N (1.8 mL, 12.9 mmol, 1.5 equiv) in DCM (100 mL) was cooled to -10 °C using NaCl/ice cooled water bath. MsCl(1.18 g, 10.3 mmol, 1.2 equiv) was added dropwise over 5 min. The reaction mixture was stirred for 25min, maintaining a temperature between 0 and -10 °C, before pouring it into ice water (100 mL). The layers were separated and the organic layer was washed subsequently with additional ice water (100 mL), NH_4Cl solution (sat., 2x100 mL), $NaHCO_3$ solution (sat., 2x100 mL) and brine (100 mL). The resulting solution was then dried over $MgSO_4$, filtrated and concentrated under reduced pressure to give crude **13** (2.7 g, 96%).[29]

To a 40 mL vial charged with a stirred bar was added **13** (1.17 g, 3.6 mmol, 1.2 equiv) and vitamin E (1.29 g, 3.0 mmol, 1.0 equiv). 16 mL anhydrous DMF was added to the vial and the reaction was cooled at 0 °C followed by adding K_2CO_3 (829 mg, 6.0 mmol, 2.0 equiv). The reaction was then warmed to room temperature and stirred overnight. Upon completion, as judged by TLC

analysis, the mixture was filtered through Celite and poured into water. The aqueous phase was extracted with Et_2O for three times and then washed with water, brine and dried over Na_2SO_4. The solvent was removed under reduced pressure and the residue was purified by silica gel chromatography to afford compound **1n** (1.3 g, 66 %) as a yellow oil.

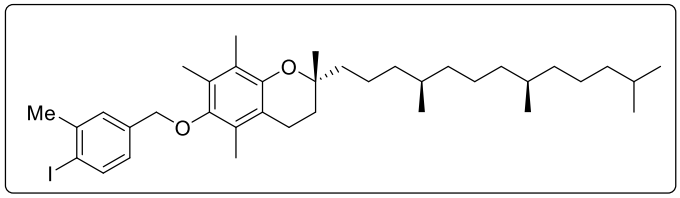

1n: Yellow oil (66%). **^{1}H NMR** (400 MHz, Chloroform-*d*) δ 7.83 (d, *J* = 8.1 Hz, 1H), 7.39 (d, *J* = 2.0 Hz, 1H), 7.02 (dd, *J* = 8.1, 2.1 Hz, 1H), 4.62 (s, 2H), 2.62 (s, 2H), 2.48 (s, 3H), 2.21 (s, 3H), 2.16 (s, 3H), 2.12 (s, 3H), 1.88 – 1.72 (m, 2H), 1.63 – 1.49 (m, 3H), 1.49 – 1.36 (m, 4H), 1.33 – 1.22 (m, 10H), 1.21 – 1.03 (m, 7H), 0.93 – 0.82 (m, 12H). **^{13}C NMR** (101 MHz, $CDCl_3$) δ 148.1, 148.1, 141.6, 139.1, 138.5, 129.0, 128.0, 126.7, 126.0, 123.1, 117.8, 100.1, 75.0, 74.0, 40.2, 39.5, 37.5, 32.9, 32.8, 31.4, 28.3, 28.1, 25.0, 25.0, 24.6, 24.0, 22.9, 22.8, 21.2, 20.8, 19.9, 19.8, 19.8, 13.0, 12.2, 12.0. **IR** (KBr): υ 2925, 2866, 1725, 1512, 1460, 1415, 1377, 1257, 1166, 1088 cm^{-1}. **HRMS** (ESI): Calculated for $C_{37}H_{58}IO_2$ ($M+H^+$):661.3476, found:661.3475.

Scheme 5.3. Preparation of Aryl Iodides 1r

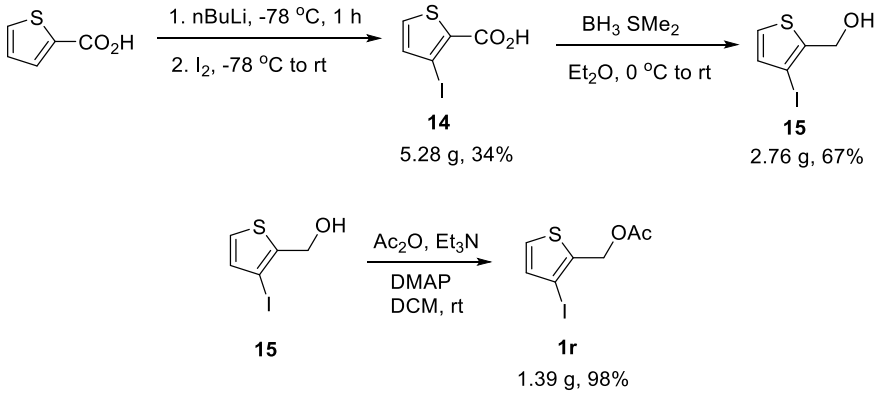

14 and **15** were prepared according to the literature reported procedure.[30] To a solution of Ac_2O (766 mg, 7.5 mmol, 1.5 equiv)), Et_3N (759 mg, 7.5 mmol, 1.5 equiv) and DMAP (48.9 mg, 0.4 mmol, 0.08 equiv) in DCM (10 mL) was added **15** (1.2 g, 5 mmol, 1.0 equiv). The reaction mixture was then stirred at room temperature for 19 h. Upon completion, HCl (2M, 60 mL) was added into the reaction flask. The mixture was extracted with Et_2O and organic layers were washed with sat. $NaHCO_3$, brine and dried over $MgSO_4$. The solvent was removed under reduced pressure and the residue was purified by silica gel chromatography to afford compound **1r** (1.39 g, 98 %) as a colorless oil.

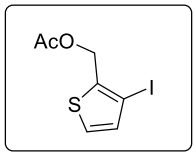

1r: Colorless oil (98%). **^{1}H NMR** (400 MHz, Chloroform-*d*) δ 7.31 (d, *J* = 5.3 Hz, 1H), 7.05 (d, *J* = 5.2 Hz, 1H), 5.22 (s, 2H), 2.11 (s, 3H). **^{13}C NMR** (101 MHz, $CDCl_3$) δ 170.7, 136.7, 135.2, 128.2, 82.5, 62.3, 21.0. **IR** (KBr): υ 3105, 2950, 1743, 1438, 1375, 1223, 1023, 857, 776, 710 cm^{-1}.

Preparation of thiolation reagent

S3-S18 were prepared according to literature reported procedure[31].

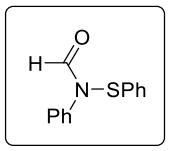

S4: Yellow oil (60%). **^{1}H NMR** (400 MHz, $CDCl_3$) δ = 8.75 (d, *J*=33.0, 1H), 7.47 – 7.25 (m, 10H). **^{13}C NMR** (101 MHz, $CDCl_3$) δ = 167.4, 163.9, 129.5, 129.1, 128.3, 127.4, 126.6, 125.6, 125.0.

IR (KBr): υ 3060, 1696, 1593, 1489, 1440, 1253, 1126, 1024, 739, 689 cm^{-1}. **HRMS** (ESI): Calculated for $C_{13}H_{12}NOS$ ($M+H^+$): 230.0634, found: 230.0632.

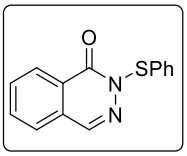

S6: White solid (52%). **^{1}H NMR** (400 MHz, $CDCl_3$) δ = 8.40 – 8.32 (m, 1H), 8.12 (s, 1H), 7.73 (dtd, *J*=16.6, 7.4, 1.4, 2H), 7.64 – 7.58 (m, 1H), 7.58 – 7.48 (m, 2H), 7.29 – 7.19 (m, 3H). **^{13}C NMR** (101 MHz, $CDCl_3$) δ = 161.1, 141.0, 135.9, 134.1, 132.3, 130.0, 129.6, 129.4, 129.1, 128.0, 127.9, 126.4. **IR** (KBr): υ 3058, 1674, 1594, 1475, 1440, 1321, 1287, 1232, 1136, 1051 cm^{-1}. **HRMS** (ESI): Calculated for $C_{14}H_{10}N_2OS$ (M^+): 254.0508, found: 254.0517.

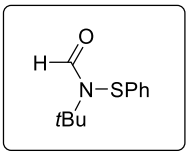

S5: Colorless oil (56%). **^{1}H NMR** (400 MHz, $CDCl_3$) δ = 8.58 (s, 1H), 7.33 – 7.09 (m, 5H), 1.40 (s, 9H). **^{13}C NMR** (101 MHz, $CDCl_3$) δ = 170.0, 164.0, 129.2, 127.0, 124.5, 61.5, 28.8. **IR** (KBr): υ 2976, 1689, 1582, 1478, 1440, 1366, 1258, 1207, 1146, 740 cm^{-1}. **HRMS** (ESI): Calculated for $C_{11}H_{15}NOSNa$ ($M+Na^+$): 232.0764, found: 232.0774.

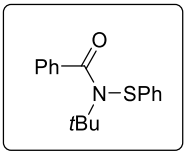

S7: Colorless oil (50%). **^{1}H NMR** (400 MHz, $CDCl_3$) δ = 7.43 – 7.37 (m, 2H), 7.26 – 7.17 (m, 5H), 7.11 – 7.04 (m, 3H), 1.51 (s, 9H). **^{13}C NMR** (101 MHz, $CDCl_3$) δ = 178.0, 141.0, 138.6,

129.8, 129.0, 127.8, 127.0, 126.3, 123.9, 63.4, 29.3. **IR** (KBr): υ 3059, 2975, 1663, 1581, 1478, 1393, 1363, 1287, 1187, 1117 cm^{-1}. **HRMS** (ESI): Calculated for $C_{17}H_{19}NOSNa$ ($M+Na^+$): 308.1080, found: 308.1090.

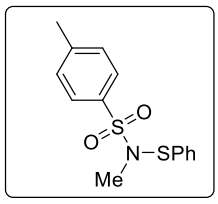

S10: White solid (43%). **^{1}H NMR** (400 MHz, $CDCl_3$) δ = 7.85 – 7.80 (m, 2H), 7.46 – 7.41 (m, 2H), 7.39 – 7.33 (m, 4H), 7.30 – 7.24 (m, 1H), 3.29 (s, 3H), 2.46 (s, 3H). **^{13}C NMR** (101 MHz, $CDCl_3$) δ = 144.2, 136.8, 135.3, 129.8, 129.2, 127.8, 127.7, 126.4, 42.5, 21.7. **IR** (KBr): υ 1580, 1437, 1350, 1302, 1164, 1088, 849, 819, 739, 707, 678 cm^{-1}. **HRMS** (ESI): Calculated for $C_{14}H_{15}NO_2S_2$ (M^+): 293.0539, found: 293.0544.

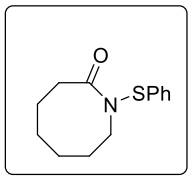

S14: Yellow solid (36%). **^{1}H NMR** (400 MHz, $CDCl_3$) δ = 7.37 – 7.29 (m, 4H), 7.26 – 7.20 (m, 1H), 3.91 – 3.74 (m, 2H), 2.79 – 2.67 (m, 2H), 1.87 (m, *J* =10.0, 8.8, 6.1, 2H), 1.75 (dt, *J* =11.8, 6.0, 2H), 1.58 (dt, *J* =12.1, 6.0, 2H), 1.49 (dt, *J* =10.2, 6.1, 2H). **^{13}C NMR** (101 MHz, $CDCl_3$) δ = 177.5, 137.4, 129.1, 127.2, 126.8, 53.5, 34.5, 29.6, 29.0, 26.1, 24.2. **IR** (KBr): υ 2926, 1664, 1477, 1439, 1374, 1245, 1120, 1084, 738, 690 cm^{-1}. **HRMS** (ESI): Calculated for $C_{13}H_{17}NOS$ (M^+): 235.1025, found: 235.1017.

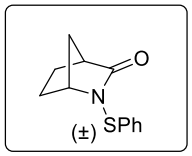

S15: Yellow solid (83%). **^{1}H NMR** (400 MHz, $CDCl_3$) δ = 7.36 – 7.27 (m, 4H), 7.26 – 7.19 (m, 1H), 3.99 (s, 1H), 2.96 (dd, *J*=2.7, 1.2, 1H), 2.13 – 2.01 (m, 1H), 1.98 – 1.88 (m, 1H), 1.81 (ddd, *J*=9.9, 5.8, 1.4, 1H), 1.76 – 1.62 (m, 2H), 1.49 (d, *J*=9.7, 1H). **^{13}C NMR** (101 MHz, $CDCl_3$) δ = 180.3, 137.9, 129.2, 127.3, 126.4, 66.4, 45.2, 40.1, 28.5, 24.3. **IR** (KBr): υ 2951, 2875, 1722, 1581, 1476, 1439, 1331, 1209, 1141, 1101 cm^{-1}. **HRMS** (ESI): Calculated for $C_{12}H_{13}NOS$ (M^+): 219.0712, found: 219.0720.

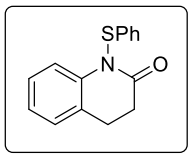

S17: Yellow solid (21%). **^{1}H NMR** (400 MHz, $CDCl_3$) δ = 7.57 (dd, *J*=8.2, 0.7, 1H), 7.24 – 7.09 (m, 7H), 6.97 (td, *J*=7.4, 1.0, 1H), 2.92 (dd, *J*=8.6, 5.6, 2H), 2.85 – 2.76 (m, 2H). **^{13}C NMR** (101 MHz, $CDCl_3$) δ = 172.0, 142.1, 137.1, 129.3, 127.8, 127.8, 127.4, 127.0, 124.9, 124.1, 118.5, 33.2, 25.6. **IR** (KBr): υ 2759, 1701, 1603, 1582, 1485, 1457, 1438, 1347, 1292, 1251 cm^{-1}. **HRMS** (ESI): Calculated for $C_{15}H_{13}NOSNa$ ($M+Na^+$): 278.0610, found: 278.0618.

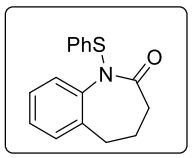

S18: Yellow solid (80%). **^{1}H NMR** (400 MHz, $CDCl_3$) δ = 7.47 (dd, *J*=8.0, 0.9, 1H), 7.44 – 7.38 (m, 2H), 7.36 – 7.24 (m, 4H), 7.15 (dtd, *J*=9.0, 7.5, 1.4, 2H), 2.60 (t, *J*=6.9, 2H), 2.49 (t, *J*=6.9, 2H), 2.18 (s, 2H). **^{13}C NMR** (101 MHz, $CDCl_3$) δ = 174.9, 145.2, 137.5, 134.6, 129.2, 128.9, 128.1,

128.0, 127.8, 127.0, 124.3, 33.50, 29.90, 28.4. **IR** (KBr): υ 2946, 1694, 1580, 1484, 1455, 1338, 1304, 1265, 1222, 1140 cm^{-1}. **HRMS** (ESI): Calculated for $C_{16}H_{15}NOS$ (M^+): 269.0874, found: 269.0872.

Scheme 5.4. Preparation of Thiolating Regent 3a

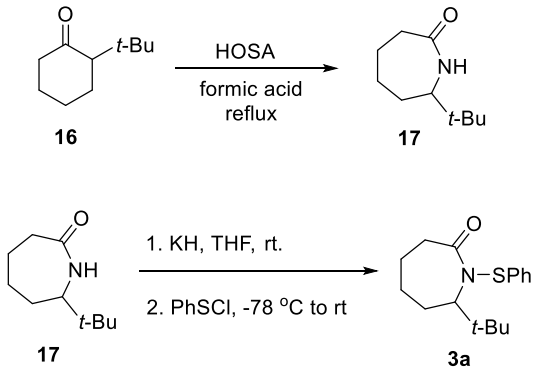

The seven-membered lactam was prepared according to the literature reported procedure.[32] In a 100 ml Schlenk flask, dry potassium hydride solid (0.48 g, 12 mmol, 1.2 equiv) was suspended in 15 ml dry THF solution. A 10 ml THF solution of the corresponding amide (10 mmol) was added dropwise at room temperature. The resulting solution was stirred at room temperature for two hours until no more hydrogen gas was released. The solution was cooled to -78°C before a 10 ml THF solution of the corresponding sulfenyl chloride (freshly distilled) was added dropwise.[33] The resulting solution was allowed to warm up to room temperature slowly and stirred overnight. The reaction was quenched by 10% citric acid (50 ml), and the aqueous layer was extracted three times with ethyl acetate (75 ml X 3). The combined organic phases were washed with sodium bicarbonate solution (100 ml), water (100 ml) and brine. The mixture was dried over $MgSO_4$ and the solvent was removed under reduced pressure. The residue was purified by silica gel chromatography to afford the corresponding sulfenamide compound.

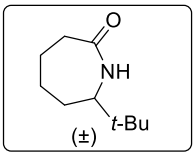

S17: White solid (59%). **^{1}H NMR** (400 MHz, Chloroform-*d*) δ 5.57 (s, 1H), 3.00 (ddd, *J* = 9.8, 5.9, 1.0 Hz, 1H), 2.55 – 2.45 (m, 1H), 2.44 – 2.36 (m, 1H), 1.99 (dddq, *J* = 10.2, 4.3, 2.9, 1.5 Hz, 1H), 1.91 (ddd, *J* = 13.7, 4.5, 3.0 Hz, 1H), 1.87 – 1.80 (m, 1H), 1.59 – 1.40 (m, 2H), 1.19 (dddd, *J* = 13.8, 12.5, 9.6, 3.1 Hz, 1H), 0.93 (s, 9H). **^{13}C NMR** (101 MHz, $CDCl_3$) δ 177.5, 63.0, 36.4, 33.6, 30.4, 29.9, 26.4, 23.4. **IR** (KBr): υ 3216, 3067, 2941, 2863, 1652, 1443, 1415, 1372, 1344, 1190 cm^{-1}. HRMS (ESI): Calculated for $C_{10}H_{19}NONa(M+Na^{+})$:192.1359, found:192.1367. Both ^{1}H NMR and ^{13}C NMR match the literature reported data.[34]

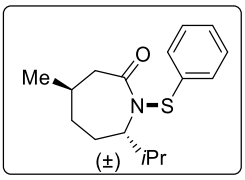

S19: White solid (74%). Mp = 96.1 – 96.6 °C. **^{1}H NMR** (400 MHz, Chloroform-*d*) δ 7.47 (d, *J* = 7.3 Hz, 2H), 7.29 (td, *J* = 7.3, 1.1 Hz, 2H), 7.25 – 7.19 (m, 1H), 3.57 (ddd, *J* = 10.3, 8.1, 2.7 Hz, 1H), 2.73 (dd, *J* = 13.6, 3.7 Hz, 1H), 2.63 (dd, *J* = 13.7, 6.8 Hz, 1H), 2.31 (dp, *J* = 9.2, 6.6 Hz, 1H), 2.06 – 1.93 (m, 1H), 1.91 – 1.73 (m, 2H), 1.54 (dt, *J* = 15.9, 8.5 Hz, 1H), 1.35 – 1.21 (m, 1H), 0.95 (dd, *J* = 12.4, 6.8 Hz, 9H). **^{13}C NMR** (101 MHz, $CDCl_3$) δ 176.5, 129.2, 128.9, 127.9, 72.8, 43.2, 31.5, 30.2, 28.1, 26.7, 20.8, 19.7. **IR** (KBr): υ 3751, 3650, 2961, 2870, 1793, 1701, 1654, 1533, 1457, 1388 cm^{-1}. **HRMS** (ESI): Calculated for $C_{16}H_{23}NOSNa(M+Na^{+})$: 300.1393, found: 300.1387.

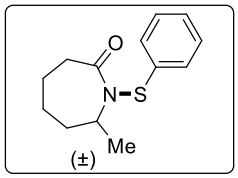

S21: Orange solid (76%). Mp = 96.1 – 96.6 ºC. **^{1}H NMR** (400 MHz, Chloroform-*d*) δ 7.27 (d, *J* = 1.4 Hz, 4H), 7.17 (ddt, *J* = 7.1, 5.6, 2.2 Hz, 1H), 4.24 – 4.11 (m, 1H), 2.88 (ddd, *J* = 14.5, 8.9, 3.2 Hz, 1H), 2.75 (ddd, *J* = 14.1, 8.4, 3.0 Hz, 1H), 1.86 – 1.52 (m, 6H), 1.37 (d, *J* = 6.9 Hz, 3H). **^{13}C NMR** (101 MHz, $CDCl_3$) δ 178.4, 139.5, 129.1, 126.7, 125.8, 60.2, 37.3, 35.8, 26.5, 23.1, 20.7. **IR** (KBr): υ 2973, 2931, 2858, 1673, 1477, 1439, 1293, 1185, 739, 690 cm^{-1}. **HRMS** (ESI): Calculated for $C_{13}H_{17}NOSNa(M+Na^{+})$: 258.0923, found: 258.0930.

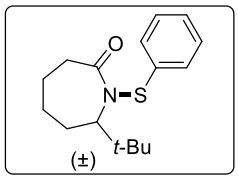

3a: Yellow oil (82%). **^{1}H NMR** (400 MHz, Chloroform-*d*) δ 7.51 – 7.45 (m, 2H), 7.33 – 7.23 (m, 3H), 3.73 (dd, *J* = 9.8, 6.8 Hz, 1H), 2.84 – 2.70 (m, 1H), 2.63 (d, *J* = 13.7 Hz, 1H), 1.82 – 1.69 (m, 2H), 1.68 – 1.56 (m, 2H), 1.50 (dt, *J* = 23.5, 8.8 Hz, 1H), 1.27 – 1.12 (m, 1H), 1.06 (s, 9H). **^{13}C NMR** (101 MHz, $CDCl_3$) δ 177.8, 138.0, 130.3, 128.9, 128.3, 74.8, 37.4, 34.6, 28.0, 26.4, 22.6. **IR** (KBr): υ 2950, 2868, 1670, 1478, 1439, 1401, 1275, 1164, 1080, 1024 cm^{-1}. **HRMS** (ESI): Calculated for $C_{16}H_{23}NOS(M^{+})$: 300.1495, found: 300.1487.

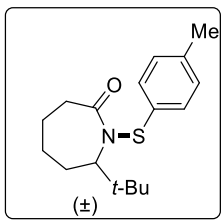

3b: Orange oil (82%). **^{1}H NMR** (400 MHz, $CDCl_3$) δ 7.42 (d, *J* = 8.1 Hz, 2H), 7.08 (d, *J* = 7.9 Hz, 2H), 3.80 – 3.64 (m, 1H), 2.74 – 2.48 (m, 2H), 2.29 (s, 3H), 1.59 (m, 5H), 1.03 (s, 10H). **^{13}C NMR** (101 MHz, $CDCl_3$) δ 177.5, 138.9, 134.2, 131.6, 129.6, 74.7, 37.3, 34.3, 27.8, 26.1, 22.5, 21.3. **IR** (KBr): υ 2950, 2868, 1669, 1491, 1479, 1401, 1366, 1275, 1164, 1141 cm^{-1}. **HRMS** (ESI): Calculated for $C_{17}H_{25}NOS$ (M^+):291.1651, found: 291.1659.

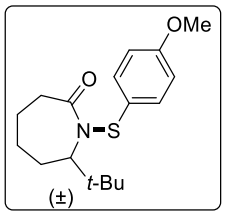

3c: Yellow solid (67%). **^{1}H NMR** (400 MHz, $CDCl_3$) δ 7.66 – 7.58 (m, 2H), 6.88 – 6.78 (m, 2H), 3.84 – 3.78 (m, 3H), 3.75 (dd, *J* = 12.6, 6.3 Hz, 1H), 2.66 (ddd, *J* = 10.3, 9.6, 4.5 Hz, 1H), 2.52 (s, 1H), 1.84 – 1.31 (m, 6H), 1.07 (s, 9H). **^{13}C NMR** (101 MHz, $CDCl_3$) δ 177.4, 160.8, 135.5, 128.5, 114.4, 114.4, 74.2, 55.3, 37.2, 34.2, 27.7, 25.8, 22.5. **IR** (KBr): υ 2950, 2868, 1664, 1590, 1493, 1428, 1172, 1140, 1028, 831 cm^{-1}. **HRMS** (ESI): Calculated for $C_{17}H_{25}NO_2S$ (M^+): 307.1601, found: 307.1603.

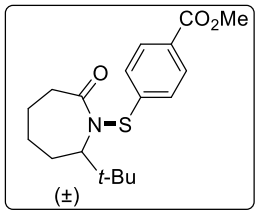

3d: Orange oil (30%). **^{1}H NMR** (400 MHz, $CDCl_3$) δ 8.00 – 7.88 (m, 2H), 7.31 (d, *J* = 8.4 Hz, 2H), 3.88 (s, 3H), 3.71 (dd, *J* = 9.6, 5.9 Hz, 1H), 2.78 (dt, *J* = 12.4, 7.4 Hz, 2H), 1.90 – 1.68 (m, 4H), 1.55 (dd, *J* = 22.4, 10.6 Hz, 1H), 1.42 (m, 1H), 1.04 (s, 9H). **^{13}C NMR** (101 MHz, $CDCl_3$) δ 178.1, 166.7, 144.7, 130.0, 128.4, 126.3, 74.7, 52.2, 37.1, 34.8, 28.1, 27.2, 23.4, 22.7. **IR** (KBr):

υ 2951, 2869, 1720, 1674, 1593, 1479, 1436, 1399, 1276, 1177 cm^{-1}. **HRMS** (ESI): Calculated for $C_{18}H_{25}NO_3SNa(M+Na^+)$: 358.1447, found: 358.1449.

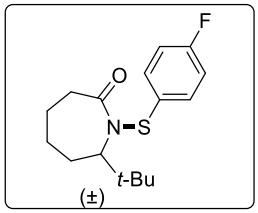

3e: Orange oil (85%). **^{1}H NMR** (400 MHz, $CDCl_3$) δ 8.28 – 8.06 (m, 2H), 7.37 – 7.23 (m, 2H), 3.83 – 3.67 (m, 1H), 2.85 (s, 2H), 1.75 (m, 6H), 1.08 (s, 9H). **^{13}C NMR** (101 MHz, Chloroform-*d*) δ 177.43, 163.12 (d, *J* = 249.5 Hz), 134.22 (d, *J* = 6.5 Hz), 132.97 (d, *J* = 2.8 Hz), 74.89, 37.25, 34.22, 27.81, 26.07, 22.43. **IR** (KBr): υ 2951, 2869, 1668, 1587, 1489, 1394, 1275, 1223, 1164, 1141 cm^{-1}. **HRMS** (ESI): Calculated for $C_{16}H_{22}FNOSNa$ ($M+Na^+$): 318.1298, found: 318.1295.

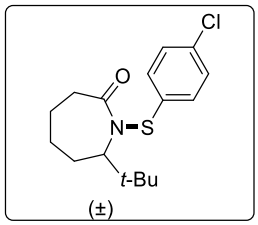

3f: Orange oil (74%). **^{1}H NMR** (400 MHz, $CDCl_3$) δ 7.44 (d, *J* = 8.5 Hz, 2H), 7.31 – 7.25 (m, 2H), 3.72 (dd, *J* = 9.8, 6.8 Hz, 1H), 2.80 – 2.55 (m, 2H), 1.85 – 1.42 (m, 5H), 1.20 (m, 1H), 1.05 (s, 9H). **^{13}C NMR** (101 MHz, $CDCl_3$) δ 177.8, 136.4, 134.4, 131.7, 129.1, 74.8, 37.2, 34.4, 27.9, 26.4, 22.5. **IR** (KBr): υ 2950, 2868, 1670, 1570, 1474, 1401, 1275, 1260, 1163, 1114 cm^{-1}. **HRMS** (ESI): Calculated for $C_{16}H_{22}ClNOS(M^+)$: 311.1105, found: 311.1104.

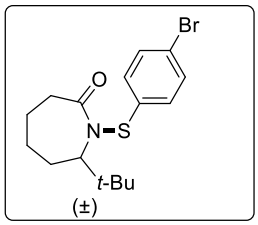

3g: Orange oil (70%). **^{1}H NMR** (400 MHz, $CDCl_3$) δ 7.43 – 7.38 (m, 2H), 7.33 (d, *J* = 8.5 Hz, 2H), 3.69 (dd, *J* = 9.8, 6.7 Hz, 1H), 2.77 – 2.5zxcVds5 (m, 2H), 1.83 – 1.40 (m, 5H), 1.22 (m, 1H), 1.03 (s, 9H). **^{13}C NMR** (101 MHz, $CDCl_3$) δ 177.9, 137.2, 132.1, 131.8, 122.5, 75.0, 37.3, 34.6, 28.1, 26.6, 22.7. **IR** (KBr): υ 2950, 2868, 1670, 1472, 1401, 1275, 1260, 1230, 1163, 1008 cm^{-1}. **HRMS** (ESI): Calculated for $C_{16}H_{22}BrNOSNa(M+Na^{+})$: 378.0498, found: 378.0506.

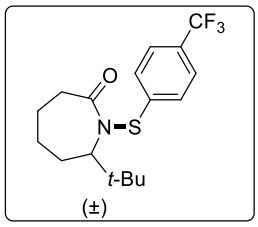

3h: Orange oil (87%). **^{1}H NMR** (400 MHz, 126.9, 125.7 (q, *J* = 3.8 Hz), δ 124.1 (q, *J* = 272.0 Hz). 74.7, 37.1, 34.8, 28.0, 27.2, 23.6, 22.6. **IR** (KBr): υ $CDCl_3$) δ 7.52 (d, *J* = 8.4 Hz, 2H), 7.37 (d, *J* = 8.2 Hz, 2H), 3.71 (dd, *J* = 9.6, 6.0 Hz, 1H), 2.87 – 2.66 (m, 2H), 1.90 – 1.62 (m, 4H), 1.55 gi(dd, *J* = 22.9, 10.9 Hz, 1H), 1.45 – 1.32 (m, 1H), 1.04 (s, 9H). **^{13}C NMR** (101 MHz, Chloroform-*d*) δ 178.0, 143.3, 128.9 (q, *J* = 32.7 Hz), 2953, 2870, 1675, 1605, 1479, 1400, 1326, 1164, 1123, 1088 cm^{-1}. **HRMS** (ESI): Calculated for $C_{17}H_{22}F_3NOS(M^{+})$: 345.1369, found: 345.1361.

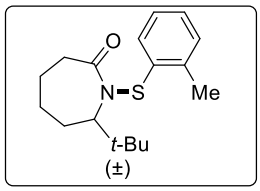

3i: Yellow solid (87%). Mp = 95.5 – 96.3 °C. **^{1}H NMR** (400 MHz, $CDCl_3$) δ 7.28 – 7.03 (m, 4H), 3.72 (dd, *J* = 9.6, 6.7 Hz, 1H), 2.82 – 2.62 (m, 2H), 2.36 (s, 3H), 1.88 – 1.56 (m, 5H), 1.46 – 1.31 (m, 1H), 1.06 (s, 9H). **^{13}C NMR** (101 MHz, $CDCl_3$) δ 177.9, 136.9, 135.1, 130.2, 128.2, 126.8,

126.4, 74.8, 37.4, 34.7, 28.2, 26.9, 19.8. **IR** (KBr): υ 2951, 2868, 1670, 1589, 1466, 1401, 1275, 1230, 1164, 1141 cm^{-1}. **HRMS** (ESI): Calculated for $C_{17}H_{25}NOS(M^+)$:291.1651, found:291.1645.

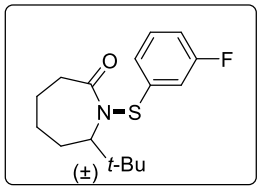

3j: Orange oil (81%). **^{1}H NMR** (400 MHz, $CDCl_3$) δ 7.34 – 7.08 (m, 3H), 6.92 (tdd, *J* = 8.4, 2.5, 1.0 Hz, 1H), 3.72 (dd, *J* = 9.7, 6.4 Hz, 1H), 2.87 – 2.60 (m, 2H), 1.88 – 1.62 (m, 4H), 1.55 (d, *J* = 10.8 Hz, 1H), 1.37 – 1.19 (m, 1H), 1.05 (s, 9H). **^{13}C NMR** (101 MHz, Chloroform-*d*) δ 177.9, 162.6 (d, *J* = 249.0 Hz), 140.4 (d, *J* = 7.2 Hz), 124.2, 115.7 (d, *J* = 23.4 Hz), 114.7 (d, *J* = 21.3 Hz), 74.8, 37.1, 34.6, 28.0, 26.7, 23.0, 22.6. **IR** (KBr): υ 2952, 2869, 1671, 1598, 1579, 1472, 1402, 1367, 1262, 1215 cm^{-1}. **HRMS** (ESI): Calculated for $C_{16}H_{22}FNOSNa(M+Na^+)$: 318.1298, found: 318.1303.

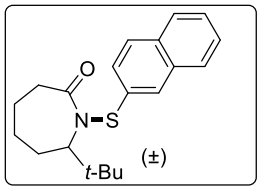

3k: Orange oil (81%). **^{1}H NMR** (400 MHz, $CDCl_3$) δ 7.93 (s, 1H), 7.79 (ddd, *J* = 8.8, 5.7, 3.3 Hz, 3H), 7.59 (dd, *J* = 8.6, 1.8 Hz, 1H), 7.52 – 7.43 (m, 2H), 3.77 (dd, *J* = 9.6, 7.0 Hz, 1H), 2.91 – 2.59 (m, 2H), 1.81 – 1.45 (m, 5H), 1.22 – 1.02 (m, 10H). **^{13}C NMR** (101 MHz, $CDCl_3$) δ 178.0, 135.4, 133.4, 133.0, 129.1, 128.7, 128.0, 127.8, 126.7, 126.6, 74.7, 37.4, 34.6, 28.0, 26.5, 22.7. **IR** (KBr): υ 2950, 2868, 1667, 1624, 1500, 1478, 1402, 1366, 1275, 1164 cm^{-1}. **HRMS** (ESI): Calculated for $C_{20}H_{25}NOS(M^+)$: 327.1651, found: 327.1647.

5.4.4 General Procedure of Palladium/Norbornene-Catalyzed Ortho Thiolation Reaction

Scheme 5.5. Pd/NBE-Catalyzed Ortho Thiolation Reaction

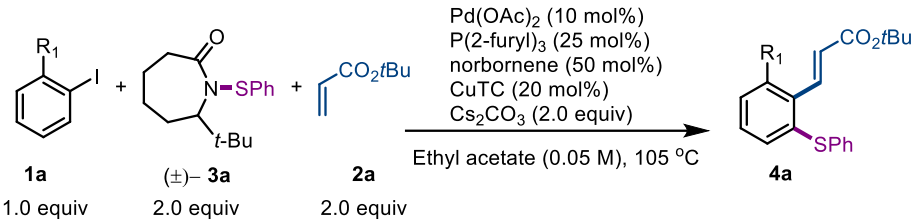

A flame-dried 7.0 mL vial A was charged with $Pd(OAc)_2$ (4.6 mg, 0.02 mmol, 10 mol%), CuTC (7.6 mg, 0.04 mmol, 20 mol%), TFP (11.6 mg, 0.05 mmol, 25 mol%) and ArI (0.2 mmol, 1.0 equiv). To another 4.0 mL vial B was weighed the thiolation reagent (0.6 mmol). The two vials were directly transferred into a nitrogen-filled glovebox without caps. Then, Cs_2CO_3 (130.4 mg, 0.4 mmol, 2.0 equiv) was added to vial A. In the third empty 4.0 mL vial C, NBE (18.8 mg, 0.2 mmol) was dissolved in 1.0 mL dry ethyl acetate. Half of this NBE solution (0.5 mL, 0.1 mmol, 50 mol%) was transferred into vial A. To the 4.0 mL vial B containing thiolation reagent was added 0.75 mL dry ethyl acetate. Two thirds of this thiolation reagent solution (0.5 mL, 0.4 mmol, 2.0 equiv) was transferred into vial A, before another 3.0 mL dry ethyl acetate was added. After acrylate **2** (0.4 mmol, 2.0 equiv) was added, vial A was tightly sealed, transferred out of glovebox and stirred on a pie-block preheated to 105 °C for 12 hours. After completion of the reaction, the mixture was filtered through a thin pad of silica gel. The filter cake was washed with ethyl acetate and the combined filtrate was concentrated. The residue was loaded to a small amount of silica gel and subjected to flash column chromatography to give the desired ortho thiolation product.

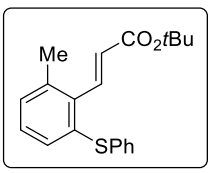

4a: Colorless oil (75%). R_f = 0.3 (hexane/ethyl acetate = 20:1). **^{1}H NMR** (400 MHz, $CDCl_3$) δ 7.83 (d, *J* = 16.3 Hz, 1H), 7.31 – 7.22 (m, 5H), 7.11 (d, *J* = 1.6 Hz, 3H), 6.01 (d, *J* = 16.4 Hz, 1H), 2.38 (s, 3H), 1.52 (s, 9H). **^{13}C NMR** (101 MHz, $CDCl_3$) δ 165.9, 141.0, 137.6, 136.2, 135.9, 135.6, 131.7, 129.7, 129.3, 128.6, 127.3, 126.8, 80.6, 28.3, 21.5. **IR** (KBr): υ 3057, 2977, 2930, 1711, 1639, 1583, 1478, 1367, 1314, 1152 cm^{-1}. **HRMS** (ESI): Calculated for $C_{20}H_{23}O_2S$ ($M+H^+$): 327.1413, found: 327.1403.

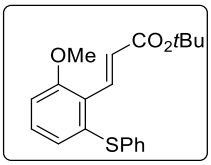

4b: Colorless oil (71%). R_f = 0.2 (hexane/ethyl acetate = 20:1). **^{1}H NMR** (400 MHz, $CDCl_3$) δ 8.08 (d, *J* = 16.1 Hz, 1H), 7.32 – 7.21 (m, 5H), 7.17 (t, *J* = 8.1 Hz, 1H), 6.89 (dd, *J* = 7.9, 1.1 Hz, 1H), 6.83 (d, *J* = 8.3 Hz, 1H), 6.67 (d, *J* = 16.1 Hz, 1H), 3.89 (s, 3H), 1.51 (s, 9H). **^{13}C NMR** (101 MHz, $CDCl_3$) δ 167.2, 159.5, 139.0, 137.3, 135.5, 131.6, 130.0, 129.3, 127.4, 125.6, 124.8, 124.3, 110.0, 80.2, 55.8, 28.4. **IR** (KBr): υ 2976, 2935, 1704, 1624, 1462, 1433, 1312, 1266, 1150, 1041 cm^{-1}. **HRMS** (ESI): Calculated for $C_{20}H_{22}O_3S$ Na($M+Na^+$): 365.1182, found: 365.1185.

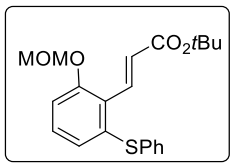

4c: White solid (52%). R_f = 0.2 (hexane/ethyl acetate = 20:1). Mp = 96.4 – 97.2 °C. **^{1}H NMR** (400 MHz, Chloroform-*d*) δ 8.04 (d, *J* = 16.1 Hz, 1H), 7.34 – 7.27 (m, 4H), 7.26 – 7.22 (m, 1H), 7.14 (dd, *J* = 8.3, 7.7 Hz, 1H), 7.07 (ddd, *J* = 8.3, 1.3, 0.5 Hz, 1H), 6.92 (dd, *J* = 7.7, 1.3 Hz, 1H), 6.62 (d, *J* = 16.1 Hz, 1H), 5.25 (s, 2H), 3.49 (s, 3H), 1.51 (s, 9H). **^{13}C NMR** (101 MHz, $CDCl_3$) δ 167.0,

157.0, 138.8, 137.3, 135.3, 131.7, 130.0, 129.4, 127.4, 125.9, 125.8, 125.0, 113.6, 94.7, 80.4, 28.3. **IR** (KBr): υ 2977, 2932, 1705, 1626, 1565, 1455, 1367, 1312, 1254, 1150 cm^{-1}. **HRMS** (ESI): Calculated for $C_{21}H_{24}O_4S$ Na($M+Na^+$): 395.1288, found: 395.1294.

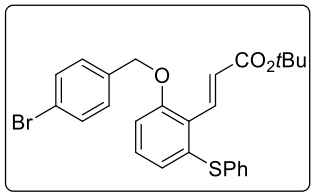

4d: White solid (57%). R_f = 0.2 (hexane/ethyl acetate = 20:1). Mp = 129.5 – 130.1 °C. **^{1}H NMR** (400 MHz, Chloroform-*d*) δ 8.06 (d, *J* = 16.1 Hz, 1H), 7.54 – 7.47 (m, 2H), 7.35 – 7.26 (m, 7H), 7.12 (t, *J* = 8.1 Hz, 1H), 6.87 (dd, *J* = 7.9, 1.0 Hz, 1H), 6.80 (dt, *J* = 8.3, 0.8 Hz, 1H), 6.67 (d, *J* = 16.2 Hz, 1H), 5.12 (s, 2H), 1.50 (s, 9H). **^{13}C NMR** (101 MHz, $CDCl_3$) δ 166.8, 157.9, 139.2, 136.8, 135.4, 135.0, 131.8, 131.8, 129.8, 129.3, 128.8, 127.4, 126.0, 124.9, 124.5, 122.0, 111.3, 80.2, 70.0, 28.2. **IR** (KBr): υ 2976, 1704, 1627, 1581, 1449, 1367, 1312, 1267, 1150, 1071 cm^{-1}. **HRMS** (ESI): Calculated for $C_{26}H_{25}BrO_3S$ Na($M+Na^+$):519.0600, found:519.0595.

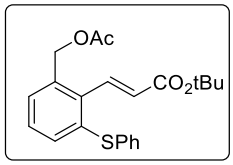

4e: White solid (74%). R_f = 0.2 (hexane/ethyl acetate = 10:1). Mp = 89.1 – 90.3 °C. **^{1}H NMR** (400 MHz, Chloroform-*d*) δ 7.81 (d, *J* = 16.2 Hz, 1H), 7.36 – 7.26 (m, 6H), 7.25 – 7.18 (m, 2H), 5.99 (d, *J* = 16.2 Hz, 1H), 5.12 (s, 2H), 2.11 (s, 3H), 1.52 (s, 9H). **^{13}C NMR** (101 MHz, $CDCl_3$) δ 170.73, 165.27, 139.49, 137.15, 136.37, 134.85, 134.74, 132.18, 131.38, 129.46, 128.88, 128.59, 127.82, 127.74, 80.91, 64.39, 28.29, 21.13. **IR** (KBr): υ 3059, 2978, 1743, 1710, 1640, 1367, 1316, 1233, 1151, 1025 cm^{-1}. **HRMS** (ESI): Calculated for $C_{22}H_{24}O_4S$ (M^+): 384.1390, found: 384.1390.

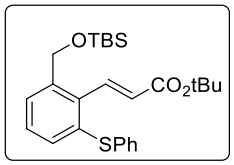

4f: Colorless oil (56%). R_f = 0.2 (hexane/ethyl acetate = 10:1). **^{1}H NMR** (500 MHz, Chloroform-*d*) δ 7.81 (d, *J* = 16.2 Hz, 1H), 7.42 (dd, *J* = 7.3, 1.5 Hz, 1H), 7.28 (dd, *J* = 4.0, 0.9 Hz, 4H), 7.24 – 7.17 (m, 3H), 6.10 (d, *J* = 16.2 Hz, 1H), 4.67 (s, 2H), 1.51 (s, 9H), 0.94 (s, 9H), 0.11 (s, 6H). **^{13}C NMR** (126 MHz, $CDCl_3$) δ 165.7, 140.4, 139.8, 136.1, 135.6, 135.4, 131.6, 131.0, 129.3, 127.4, 127.3, 127.3, 80.6, 63.5, 28.3, 26.1, 18.5, -5.1. **IR** (KBr): υ 3059, 2955, 2929, 2884, 2857, 1712, 1639, 1583, 1473, 1440, 1151 cm^{-1}. **HRMS** (ESI): Calculated for $C_{26}H_{36}O_3SSiNa$ ($M+Na^+$): 479.2047, found: 479.2044.

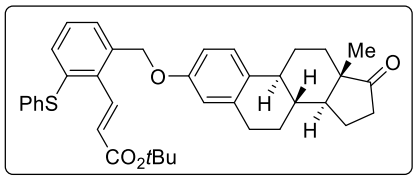

4g: Colorless oil (47%). R_f = 0.2 (hexane/ethyl acetate = 20:1). **^{1}H NMR** (400 MHz, Chloroform-*d*) δ 7.85 (d, *J* = 16.2 Hz, 1H), 7.49 – 7.44 (m, 1H), 7.34 – 7.29 (m, 4H), 7.29 – 7.26 (m, 1H), 7.25 – 7.22 (m, 2H), 7.22 – 7.18 (m, 1H), 6.75 (dd, *J* = 8.6, 2.8 Hz, 1H), 6.69 (d, *J* = 2.8 Hz, 1H), 6.02 (d, *J* = 16.3 Hz, 1H), 5.02 (s, 2H), 2.95 – 2.86 (m, 2H), 2.51 (dd, *J* = 18.7, 8.6 Hz, 1H), 2.43 – 2.36 (m, 1H), 2.27 (d, *J* = 10.0 Hz, 1H), 2.20 – 1.92 (m, 4H), 1.68 – 1.49 (m, 6H), 1.47 (s, 9H), 0.91 (s, 3H). **^{13}C NMR** (126 MHz, $CDCl_3$) δ 165.4, 156.6, 139.6, 138.0, 136.7, 136.4, 135.9, 135.1, 132.8, 131.9, 131.4, 129.4, 129.0, 128.1, 127.7, 127.6, 126.5, 115.3, 112.8, 80.8, 68.3, 50.6, 48.2, 44.2, 38.5, 36.0, 31.7, 28.3, 26.7, 26.1, 21.7, 14.0. **IR** (KBr): υ 2929, 1738, 1709, 1608, 1498, 1477, 1440, 1368, 1315, 1152 cm^{-1}. **HRMS** (ESI): Calculated for $C_{38}H_{42}O_4S$ Na($M+Na^+$):617.2696, found: 617.2705.

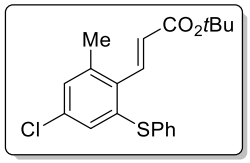

4h: Colorless oil (59%). R_f = 0.3 (hexane/ethyl acetate = 20:1). **^{1}H NMR** (400 MHz, Chloroform-*d*) δ 7.74 (d, *J* = 16.3 Hz, 1H), 7.37 – 7.29 (m, 5H), 7.07 (dt, *J* = 1.3, 0.6 Hz, 1H), 6.95 (d, *J* = 2.1 Hz, 1H), 6.03 (d, *J* = 16.3 Hz, 1H), 2.37 – 2.32 (m, 3H), 1.52 (s, 9H). **^{13}C NMR** (101 MHz, $CDCl_3$) δ 165.5, 139.9, 139.6, 139.0, 134.0, 133.7, 133.3, 132.7, 129.5, 128.9, 128.1, 127.7, 127.2, 80.8, 28.2, 21.2. **IR** (KBr): υ 2977, 1711, 1639, 1572, 1549, 1478, 1392, 1367, 1314, 1150 cm^{-1}. **HRMS** (ESI): Calculated for $C_{20}H_{20}ClOS$ Na[(M+Na^+)+(-H_2O)]:365.0737, found: 365.0734.

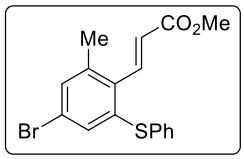

4i: Colorless oil (55%). R_f = 0.3 (hexane/ethyl acetate = 20:1). **^{1}H NMR** (400 MHz, Chloroform-*d*) δ 7.82 (d, *J* = 16.3 Hz, 1H), 7.39 – 7.29 (m, 5H), 7.25 – 7.22 (m, 1H), 7.10 (d, *J* = 2.0 Hz, 1H), 6.13 (d, *J* = 16.4 Hz, 1H), 3.80 (s, 3H), 2.34 (d, *J* = 0.6 Hz, 3H). **^{13}C NMR** (101 MHz, $CDCl_3$) δ 166.8, 141.2, 139.3, 139.3, 133.8, 133.7, 132.7, 132.0, 130.7, 129.7, 128.3, 125.3, 122.7, 52.0, 21.1. **IR** (KBr): υ 3059, 2949, 2925, 2360, 1722, 1639, 1565, 1438, 1306, 1272, 1195, 1172, 748, 690 cm^{-1}. **HRMS** (ESI): Calculated for $C_{17}H_{16}BrO_2S$ (M+H^+): 363.0049, found: 363.0058.

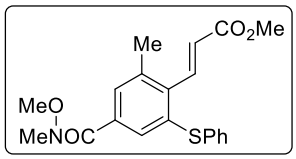

4j: Colorless oil (57%). R_f = 0.2 (hexane/ethyl acetate = 2:1). **^{1}H NMR** (400 MHz, Chloroform-*d*) δ 7.91 (d, *J* = 16.4 Hz, 1H), 7.41 (s, 1H), 7.37 – 7.26 (m, 6H), 6.15 (d, *J* = 16.3 Hz, 1H), 3.81 (s, 3H), 3.44 (s, 3H), 3.27 (s, 3H), 2.40 (s, 3H). **^{13}C NMR** (101 MHz, $CDCl_3$) δ 168.9, 166.7, 141.6, 137.5, 137.4, 136.7, 134.7, 134.4, 132.2, 129.5, 129.1, 128.5, 127.9, 125.5, 61.2, 52.0, 33.7, 21.3. **IR** (KBr): υ 2950, 1722, 1644, 1439, 1309, 1274, 1197, 1172, 748, 692 cm^{-1}. **HRMS** (ESI): Calculated for $C_{20}H_{21}NO_4SNa$ ($M+Na^+$): 394.1083, found: 394.1087.

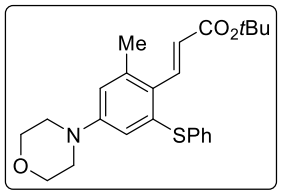

4k: White solid (64%). R_f = 0.2 (hexane/ethyl acetate = 10:1). Mp = 93.4 – 94.3 °C. **^{1}H NMR** (400 MHz, Chloroform-*d*) δ 7.81 (d, *J* = 16.3 Hz, 1H), 7.19 (dd, *J* = 4.1, 0.8 Hz, 4H), 7.16 – 7.10 (m, 1H), 6.64 (d, *J* = 2.6 Hz, 1H), 6.59 (d, *J* = 2.6 Hz, 1H), 5.93 (d, *J* = 16.3 Hz, 1H), 3.75 – 3.67 (m, 4H), 3.06 – 2.97 (m, 4H), 2.32 (s, 3H), 1.42 (s, 9H). **^{13}C NMR** (101 MHz, $CDCl_3$) δ 166.5, 150.8, 140.8, 139.3, 137.5, 136.0, 131.0, 129.2, 127.0, 124.3, 117.0, 116.9, 80.3, 66.7, 48.3, 28.3, 22.5. **IR** (KBr): υ 2974, 2855, 1704, 1627, 1588, 1538, 1478, 1449, 1367, 1310 cm^{-1}. **HRMS** (ESI): Calculated for $C_{23}H_{29}NO_3S$ Na($M+Na^+$): 434.1760, found: 434.1760.

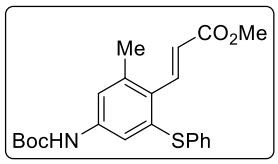

4l: Colorless oil (55%). R_f = 0.3 (hexane/ethyl acetate = 5:1). **^{1}H NMR** (500 MHz, Chloroform-*d*) δ 7.93 (d, *J* = 16.3 Hz, 1H), 7.46 (s, 1H), 7.29 (d, *J* = 3.9 Hz, 4H), 7.24 (td, *J* = 3.3, 2.1 Hz, 1H), 6.84 (d, *J* = 2.3 Hz, 1H), 6.37 (s, 1H), 6.11 (d, *J* = 16.3 Hz, 1H), 3.78 (s, 3H), 2.38 (s, 3H), 1.47 (s,

9H). **^{13}C NMR** (101 MHz, $CDCl_3$) δ 167.3, 152.4, 141.9, 139.2, 138.9, 137.5, 135.2, 131.8, 129.4, 127.5, 123.6, 119.6, 119.2, 81.1, 51.8, 28.4, 21.9. **IR** (KBr): υ 3332, 2978, 1703, 1577, 1516, 1272, 1228, 1158, 1069, 739, 690 cm^{-1}. **HRMS** (ESI): Calculated for $C_{22}H_{25}NO_4S$ Na($M+Na^+$): 422.1397, found: 422.1400.

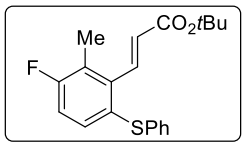

4m: Colorless oil (71%). R_f = 0.3 (hexane/ethyl acetate = 20:1). **^{1}H NMR** (400 MHz, Chloroform-*d*) δ 7.75 (d, *J* = 16.4 Hz, 1H), 7.28 – 7.15 (m, 7H), 6.95 (t, *J* = 8.9 Hz, 1H), 5.91 (d, *J* = 16.3 Hz, 1H), 2.28 (d, *J* = 2.6 Hz, 3H), 1.50 (s, 9H). **^{13}C NMR** (101 MHz, Chloroform-*d*) δ 165.5, 161.2 (d, *J* = 245.9 Hz), 140.2 (d, *J* = 2.7 Hz), 139.3 (d, *J* = 4.8 Hz), 136.3, 132.3 (d, *J* = 8.8 Hz), 130.4, 130.1 (d, *J* = 3.5 Hz), 129.2, 127.7, 126.9, 124.8 (d, *J* = 17.4 Hz), 115.7 (d, *J* = 23.9 Hz), 80.8, 28.3, 12.8 (d, *J* = 5.4 Hz). **IR** (KBr): υ 2978, 2932, 1712, 1641, 1582, 1479, 1456, 1392, 1367, 1152 cm^{-1}. **HRMS** (ESI): Calculated for $C_{21}H_{22}FO_2S$ ($M+H^+$): 345.1319, found: 345.1325.

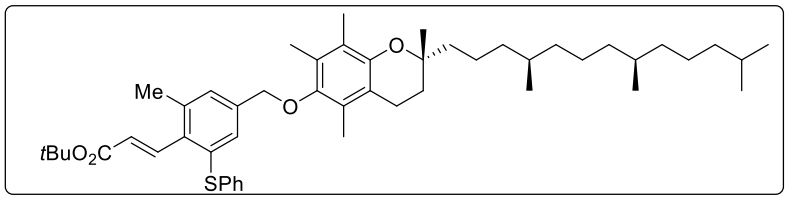

4n: Colorless oil (72%). R_f = 0.2 (hexane/ethyl acetate = 20:1). **^{1}H NMR** (400 MHz, Chloroform-*d*) δ 7.84 (d, *J* = 16.3 Hz, 1H), 7.34 – 7.29 (m, 3H), 7.28 – 7.19 (m, 4H), 6.03 (d, *J* = 16.3 Hz, 1H), 4.55 (s, 2H), 2.57 (t, *J* = 6.9 Hz, 2H), 2.43 (s, 3H), 2.15 – 2.05 (m, 9H), 1.87 – 1.72 (m, 2H), 1.52 (s, 10H), 1.46 – 1.33 (m, 5H), 1.33 – 1.23 (m, 11H), 1.17 – 1.03 (m, 7H), 0.86 (dd, *J* = 9.3, 6.5 Hz, 12H). **^{13}C NMR** (101 MHz, $CDCl_3$) δ 165.9, 148.1, 148.0, 140.8, 138.5, 137.9, 136.6, 135.4, 135.2,

131.7, 129.3, 129.0, 128.8, 127.9, 127.4, 126.8, 126.0, 123.1, 117.7, 80.7, 75.0, 74.0, 40.2, 39.5, 37.5, 32.9, 32.8, 31.4, 28.3, 28.1, 25.0, 25.0, 24.6, 24.0, 22.9, 22.8, 21.6, 21.2, 20.8, 19.9, 19.84, 19.78, 13.0, 12.1, 12.0. **IR** (KBr): υ 2927, 2867, 1712, 1638, 1553, 1460, 1366, 1313, 1256, 1150 cm^{-1}. **HRMS** (ESI): Calculated for $C_{50}H_{72}O_4SNa$ ($M+Na^+$):769.5224, found:769.52.

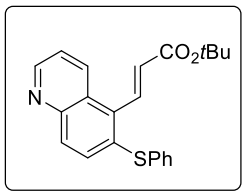

4o: Pale yellow oil (90%). R_f = 0.1 (hexane/ethyl acetate = 5:1). **^{1}H NMR** (400 MHz, $CDCl_3$) δ 8.80 (dd, *J* = 4.1, 1.5 Hz, 1H), 8.39 (ddd, *J* = 8.6, 1.5, 0.8 Hz, 1H), 8.04 (d, *J* = 16.2 Hz, 1H), 7.85 (d, *J* = 9.0 Hz, 1H), 7.41 – 7.21 (m, 7H), 6.11 (d, *J* = 16.2 Hz, 1H), 1.49 (s, 9H). **^{13}C NMR** (126 MHz, $CDCl_3$) δ 165.4, 150.3, 147.5, 138.7, 135.5, 134.3, 133.3, 132.8, 132.6, 131.4, 130.5, 129.6, 129.0, 128.1, 126.8, 122.0, 81.2, 28.4. **IR** (KBr): υ 2977, 1710, 1633, 1579, 1488, 1367, 1312, 1286, 1151, 1024 cm^{-1}. **HRMS** (ESI): Calculated for $C_{22}H_{21}NO_2SNa$ ($M+Na^+$): 386.1185, found: 386.1192.

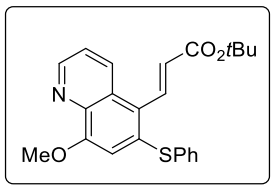

4p: Yellow solid (59%). R_f = 0.1 (hexane/ethyl acetate = 5:1). Mp = 139.7 – 140.2 ^oC. **^{1}H NMR** (400 MHz, $CDCl_3$) δ 8.91 (dd, *J* = 4.2, 1.6 Hz, 1H), 8.49 (dd, *J* = 8.7, 1.7 Hz, 1H), 8.10 (d, *J* = 16.2 Hz, 1H), 7.48 (dd, *J* = 8.6, 4.2 Hz, 1H), 7.43 – 7.38 (m, 2H), 7.37 – 7.28 (m, 3H), 6.84 (s, 1H), 6.15 (d, *J* = 16.2 Hz, 1H), 3.86 (s, 3H), 1.56 (s, 9H). **^{13}C NMR** (101 MHz, $CDCl_3$) δ 165.6, 155.3, 149.0, 138.5, 136.1, 134.4, 133.5, 132.3, 129.4, 128.0, 127.7, 127.5, 125.0, 122.5, 110.0,

80.9, 56.0, 28.2. **IR** (KBr): υ 2976, 1707, 1572, 1497, 1456, 1366, 1290, 1246, 1148, 1124 cm^{-1}. **HRMS** (ESI): Calculated for $C_{23}H_{23}NO_3SNa$ ($M+Na^+$): 416.1291, found: 416.1292.

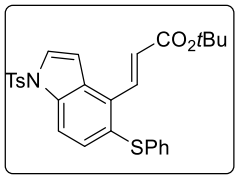

4q: Colorless oil (40%). R_f = 0.2 (hexane/ethyl acetate = 10:1). **^{1}H NMR** (400 MHz, $CDCl_3$) δ 8.13 (d, *J* = 16.2 Hz, 1H), 7.91 (dd, *J* = 8.7, 0.8 Hz, 1H), 7.77 (d, *J* = 8.4 Hz, 2H), 7.65 (d, *J* = 3.7 Hz, 1H), 7.38 (d, *J* = 8.7 Hz, 1H), 7.27 (d, *J* = 0.9 Hz, 1H), 7.25 (dd, *J* = 1.7, 0.9 Hz, 1H), 7.22 (dd, *J* = 2.3, 1.2 Hz, 1H), 7.21 (d, *J* = 0.9 Hz, 1H), 7.20 – 7.14 (m, 3H), 6.91 (dd, *J* = 3.7, 0.8 Hz, 1H), 6.27 (d, *J* = 16.2 Hz, 1H), 2.37 (s, 3H), 1.50 (s, 9H). **^{13}C NMR** (101 MHz, $CDCl_3$) δ 165.9, 145.5, 140.2, 136.9, 135.1, 134.8, 131.0, 130.5, 130.2, 130.1, 130.0, 129.9, 129.2, 127.8, 127.0, 126.7, 125.7, 114.8, 108.2, 80.8, 28.3, 21.8. **IR** (KBr): υ 2977, 2359, 2341, 1706, 1633, 1596, 1582, 1478, 1375, 1170 cm^{-1}. **HRMS** (ESI): Calculated for $C_{28}H_{27}NO_4S_2$ (M^+):505.1376, found:505.1381.

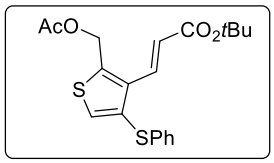

4r: Pale yellow solid (36%). R_f = 0.2 (hexane/ethyl acetate = 10:1). Mp = 84.5 – 85.2 ºC. **^{1}H NMR** (400 MHz, $CDCl_3$) δ 7.60 (d, *J* = 16.2 Hz, 1H), 7.37 (s, 1H), 7.25 (m, 2H), 7.22 – 7.15 (m, 3H), 6.22 (d, *J* = 16.2 Hz, 1H), 5.29 (s, 2H), 2.13 (s, 3H), 1.48 (s, 9H). **^{13}C NMR** (101 MHz, $CDCl_3$) δ 170.6, 165.9, 138.7, 136.3, 136.0, 134.8, 130.8, 129.7, 129.3, 129.1, 126.8, 124.6, 80.8, 59.5, 28.3, 21.0. **IR** (KBr): υ 2977, 1745, 1707, 1632, 1582, 1478, 1367, 1312, 1284, 1150 cm^{-1}. **HRMS** (ESI): Calculated for $C_{20}H_{22}O_4S_2$ Na($M+Na^+$): 413.0852, found: 413.0861.

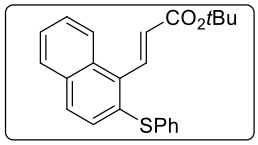

4s: Colorless oil (93%). R_f = 0.3 (hexane/ethyl acetate = 20:1). **^{1}H NMR** (400 MHz, $CDCl_3$) δ 8.13 – 8.02 (m, 2H), 7.79 – 7.66 (m, 1H), 7.60 (d, *J* = 8.7 Hz, 1H), 7.43 (dddd, *J* = 17.5, 8.1, 6.9, 1.4 Hz, 2H), 7.27 – 7.15 (m, 6H), 6.14 (d, *J* = 16.3 Hz, 1H), 1.49 (s, 9H). **^{13}C NMR** (101 MHz, $CDCl_3$) δ 165.8, 140.0, 135.6, 133.8, 133.7, 132.6, 131.8, 131.7, 129.4, 129.2, 128.7, 128.5, 128.4, 127.5, 127.3, 126.3, 125.2, 80.9, 28.4. **IR** (KBr): υ 3056, 2977, 2930, 1709, 1635, 1582, 1477, 1367, 1312, 1284 cm^{-1}. **HRMS** (ESI): Calculated for $C_{23}H_{22}O_2SNa(M+Na^+)$: 385.1233, found: 385.1236.

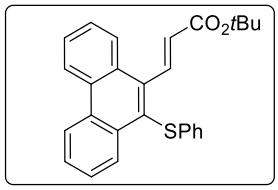

4t: White solid (45%). R_f = 0.4 (hexane/ethyl acetate = 20:1). Mp = 174.8 – 175.4 °C. **^{1}H NMR** (500 MHz, $CDCl_3$) δ 8.77 (d, *J* = 8.3 Hz, 1H), 8.73 (d, *J* = 8.2 Hz, 1H), 8.67 (dd, *J* = 8.3, 0.9 Hz, 1H), 8.29 – 8.20 (m, 2H), 7.74 (ddd, *J* = 8.3, 7.0, 1.2 Hz, 1H), 7.69 (ddd, *J* = 8.3, 7.0, 1.2 Hz, 1H), 7.64 (ddd, *J* = 8.2, 7.1, 1.1 Hz, 1H), 7.60 (ddd, *J* = 8.1, 7.0, 1.1 Hz, 1H), 7.12 (t, *J* = 7.5 Hz, 2H), 7.09 – 6.99 (m, 3H), 6.02 (d, *J* = 16.4 Hz, 1H), 1.55 (s, 9H). **^{13}C NMR** (101 MHz, $CDCl_3$) δ 165.5, 141.7, 140.0, 137.7, 132.0, 131.3, 130.8, 130.1, 128.9, 127.9, 127.9, 127.8, 127.6, 127.6, 127.5, 127.2, 127.1, 127.1, 125.3, 123.0, 122.8, 80.7, 28.2. **IR** (KBr): υ 3854, 3712, 3629, 2360, 2343, 1735, 1712, 1654, 1560, 1154 cm^{-1}. **HRMS** (ESI): Calculated for $C_{27}H_{25}O_2S$ $(M+H^+)$: 413.1570, found: 413.1578.

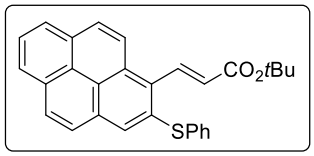

4u: Yellow solid (91%). R_f = 0.4 (hexane/ethyl acetate = 10:1). Mp = 116.4 – 117.9 °C. **^{1}H NMR** (400 MHz, Chloroform-*d*) δ 8.43 – 8.33 (m, 2H), 8.18 (t, *J* = 7.3 Hz, 2H), 8.14 – 7.98 (m, 4H), 7.87 (dd, *J* = 8.9, 1.1 Hz, 1H), 7.39 – 7.26 (m, 5H), 6.28 (d, *J* = 16.2 Hz, 1H), 1.60 (s, 9H). **^{13}C NMR** (101 MHz, $CDCl_3$) δ 165.7, 140.7, 135.9, 133.5, 131.8, 131.7, 131.5, 131.3, 130.8, 129.8, 129.5, 128.8, 128.7, 128.7, 128.2, 127.4, 126.9, 126.5, 125.9, 125.7, 124.6, 124.6, 124.2, 80.9, 28.4. **IR** (KBr): υ 3048, 2977, 2930, 1708, 1635, 1581, 1530, 1478, 1367, 1150 cm^{-1}. . **HRMS** (ESI): Calculated for $C_{29}H_{24}O_2SNa$ ($M+Na^+$): 459.1389, found: 459.1387.

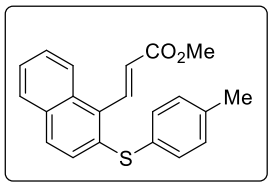

5a: Colorless oil (86%). R_f = 0.3 (hexane/ethyl acetate = 20:1). **^{1}H NMR** (400 MHz, Chloroform-*d*) δ 8.30 (d, *J* = 16.2 Hz, 1H), 8.15 – 8.09 (m, 1H), 7.81 – 7.76 (m, 1H), 7.69 – 7.62 (m, 1H), 7.55 – 7.43 (m, 2H), 7.30 (d, *J* = 8.2 Hz, 2H), 7.22 (d, *J* = 8.7 Hz, 1H), 7.18 – 7.13 (m, 2H), 6.36 (d, *J* = 16.3 Hz, 1H), 3.88 (s, 3H), 2.36 (s, 3H). **^{13}C NMR** (101 MHz, $CDCl_3$) δ 166.9, 141.3, 138.1, 135.2, 132.8, 132.3, 132.2, 131.6, 131.1, 129.4, 128.6, 127.6, 127.4, 126.1, 126.1, 124.9, 52.0, 21.3. **IR** (KBr): υ 2948, 1721, 1636, 1584, 1492, 1434, 1308, 1280, 1171, 1127 cm^{-1}. **HRMS** (ESI): Calculated for $C_{21}H_{19}O_2S$ ($M+H^+$): 335.1100, found: 335.1096.

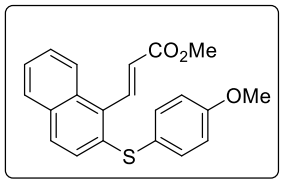

5b: Yellow oil (71%). R_f = 0.2 (hexane/ethyl acetate = 20:1). **^{1}H NMR** (400 MHz, Chloroform-*d*) δ 8.29 (d, *J* = 16.3 Hz, 1H), 8.10 (dd, *J* = 8.6, 1.2 Hz, 1H), 7.77 (dd, *J* = 8.0, 1.5 Hz, 1H), 7.63 (d, *J* = 8.8 Hz, 1H), 7.55 – 7.37 (m, 4H), 7.11 (d, *J* = 8.8 Hz, 1H), 6.90 (d, *J* = 8.8 Hz, 2H), 6.38 (d, *J* = 16.3 Hz, 1H), 3.88 (s, 3H), 3.83 (s, 3H). **^{13}C NMR** (101 MHz, $CDCl_3$) δ 167.0, 160.1, 141.2, 136.5, 135.7, 132.0, 131.5, 130.8, 129.3, 128.6, 127.4, 126.5, 126.1, 125.9, 124.7, 124.4, 115.2, 55.5, 52.0. **IR** (KBr): υ 2948, 1721, 1636, 1584, 1492, 1434, 1308, 1280, 1171, 1127 cm^{-1}. **HRMS** (ESI): Calculated for $C_{21}H_{19}O_3S$ ($M+H^+$): 351.1049, found: 351.1039.

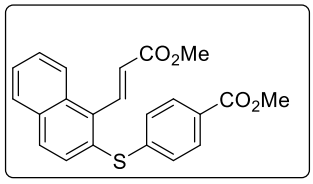

5c: Yellow solid (82%). R_f = 0.3 (hexane/ethyl acetate = 5:1). Mp = 94.5 – 95.1 °C. **^{1}H NMR** (400 MHz, $CDCl_3$) δ 8.20 – 8.02 (m, 2H), 7.87 – 7.67 (m, 4H), 7.49 (ddd, *J* = 5.6, 4.2, 2.1 Hz, 2H), 7.38 (d, *J* = 8.6 Hz, 1H), 7.17 – 7.07 (m, 2H), 6.20 (d, *J* = 16.3 Hz, 1H), 3.81 (s, 3H), 3.76 (s, 3H). **^{13}C NMR** (101 MHz, $CDCl_3$) δ 166.7, 166.7, 143.3, 141.3, 136.3, 133.4, 131.8, 130.5, 130.4, 130.3, 129.9, 128.7, 128.5, 128.0, 127.6, 127.1, 126.5, 125.5, 52.3, 52.0. **IR** (KBr): υ 2950, 2360, 1720, 1636, 1594, 1559, 1506, 1435, 1399, 1308 cm^{-1}. **HRMS** (ESI): Calculated for $C_{22}H_{19}O_4S$ ($M+H^+$): 379.0999, found: 379.1002.

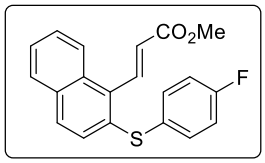

5d: Colorless oil (82%). R_f = 0.3 (hexane/ethyl acetate = 20:1). **^{1}H NMR** (400 MHz, Chloroform-*d*) δ 8.28 (d, *J* = 16.3 Hz, 1H), 8.15 – 8.09 (m, 1H), 7.80 (dd, *J* = 8.2, 1.5 Hz, 1H), 7.68 (d, *J* = 8.7 Hz, 1H), 7.57 – 7.45 (m, 2H), 7.36 (dd, *J* = 8.8, 5.2 Hz, 2H), 7.21 (d, *J* = 8.7 Hz, 1H), 7.03 (t, *J* = 8.7 Hz, 2H), 6.34 (d, *J* = 16.3 Hz, 1H), 3.87 (s, 3H). **^{13}C NMR** (101 MHz, Chloroform-*d*) δ 166.83, 162.63 (d, *J* = 248.5 Hz), 141.18, 134.52 (d, *J* = 8.2 Hz), 134.37, 132.70, 132.43, 131.56, 130.09 (d, *J* = 3.4 Hz), 129.54, 128.59, 127.72, 127.48, 126.35, 126.32, 124.94, 116.67 (d, *J* = 22.0 Hz), 52.01. **^{19}F NMR** (470 MHz, $CDCl_3$) δ -113.3. **IR** (KBr): υ 2949, 1719, 1636, 1588, 1505, 1489, 1435, 1280, 1172, 1127 cm^{-1}. **HRMS** (ESI): Calculated for $C_{20}H_{16}FO_2S$ ($M+H^+$): 339.0850, found: 339.0856.

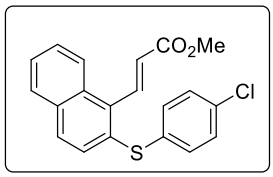

5e: Colorless oil (82%). R_f = 0.3 (hexane/ethyl acetate = 20:1). **^{1}H NMR** (400 MHz, $CDCl_3$) δ 8.18 (d, *J* = 16.3 Hz, 1H), 8.08 – 8.02 (m, 1H), 7.74 (dd, *J* = 7.1, 2.3 Hz, 1H), 7.64 (d, *J* = 8.7 Hz, 1H), 7.45 (dqd, *J* = 8.4, 6.9, 1.6 Hz, 2H), 7.25 – 7.12 (m, 5H), 6.23 (d, *J* = 16.3 Hz, 1H), 3.78 (s, 3H). **^{13}C NMR** (101 MHz, $CDCl_3$) δ 166.8, 141.2, 134.2, 134.0, 133.6, 133.0, 132.8, 132.6, 131.6, 129.7, 129.6, 128.7, 128.6, 127.5, 126.6, 126.4, 125.1, 52.0. **IR** (KBr): υ 3055, 2948, 1721, 1637, 1475, 1434, 1309, 1280, 1193, 1172 cm^{-1}. **HRMS** (ESI): Calculated for $C_{20}H_{16}ClO_2S$ ($M+H^+$): 335.0554, found: 335.0552.

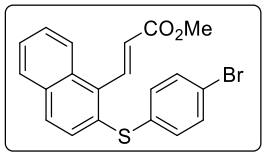

5f: Colorless oil (86%). R_f = 0.3 (hexane/ethyl acetate = 20:1). **^{1}H NMR** (400 MHz, $CDCl_3$) δ 8.19 (d, *J* = 16.3 Hz, 1H), 8.06 (dd, *J* = 8.5, 1.0 Hz, 1H), 7.76 (dd, *J* = 7.0, 2.4 Hz, 1H), 7.66 (d, *J* = 8.7 Hz, 1H), 7.51 – 7.41 (m, 2H), 7.38 – 7.31 (m, 2H), 7.25 (d, *J* = 8.7 Hz, 1H), 7.16 – 7.05 (m, 2H), 6.25 (d, *J* = 16.3 Hz, 1H), 3.80 (s, 3H). **^{13}C NMR** (101 MHz, $CDCl_3$) δ 166.8, 141.2, 135.0, 134.2, 132.8, 132.7, 132.7, 132.5, 131.6, 129.7, 128.8, 128.6, 127.5, 126.7, 126.4, 125.2, 121.4, 52.0. **IR** (KBr): υ 3853, 3745, 3649, 3055, 2948, 2360, 1719, 1636, 1471, 1172 cm^{-1}. **HRMS** (ESI): Calculated for $C_{25}H_{16}BrO_2S$ ($M+H^+$): 399.0049, found: 399.0044.

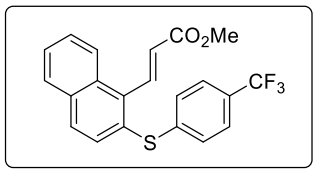

5g: White solid oil (85%). R_f = 0.2 (hexane/ethyl acetate = 20:1). Mp = 76.0 – 77.0 °C. **^{1}H NMR** (400 MHz, Chloroform-*d*) δ 8.24 (d, *J* = 16.3 Hz, 1H), 8.18 – 8.11 (m, 1H), 7.90 – 7.83 (m, 1H), 7.81 – 7.77 (m, 1H), 7.60 – 7.54 (m, 2H), 7.53 – 7.42 (m, 3H), 7.28 (d, *J* = 0.8 Hz, 2H), 6.28 (d, *J* = 16.3 Hz, 1H), 3.84 (s, 3H). **^{13}C NMR** (101 MHz, Chloroform-*d*) δ 166.7, 141.9, 141.3, 136.2, 133.4, 131.8, 130.4, 130.3, 130.0, 129.2, 128.7, 127.6, 127.5 – 119.4 (m), 127.1, 126.6, 126.0 (q, *J* = 3.8 Hz), 125.5, 52.0. **^{19}F NMR** (470 MHz, $CDCl_3$) δ -62.5. **IR** (KBr): υ 3853, 3057, 2951, 1723, 1639, 1605, 1436, 1327, 1280, 1170 cm^{-1}. **HRMS** (ESI): Calculated for $C_{21}H_{16}F_3O_2S$ ($M+H^+$): 389.0818, found: 389.0818.

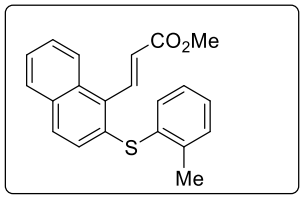

5h: Colorless oil (91%). R_f = 0.2 (hexane/ethyl acetate = 20:1). **^{1}H NMR** (400 MHz, $CDCl_3$) δ 8.20 (d, *J* = 16.3 Hz, 1H), 8.09 – 7.99 (m, 1H), 7.77 – 7.64 (m, 1H), 7.55 (d, *J* = 8.8 Hz, 1H), 7.40 (dddd, *J* = 20.5, 8.0, 6.9, 1.3 Hz, 2H), 7.23 (d, *J* = 7.5 Hz, 1H), 7.20 – 7.12 (m, 2H), 7.06 (ddd, *J* = 8.4, 5.5, 2.4 Hz, 1H), 6.98 (d, *J* = 8.7 Hz, 1H), 6.29 (d, *J* = 16.3 Hz, 1H), 3.78 (s, 3H), 2.26 (s, 3H). **^{13}C NMR** (101 MHz, $CDCl_3$) δ 167.0, 141.2, 140.6, 134.6, 134.0, 133.5, 132.3, 132.1, 131.6, 130.9, 129.4, 128.6, 128.5, 127.4, 127.0, 127.0, 126.1, 126.1, 124.8, 52.0, 20.9. **IR** (KBr): υ 3058, 2948, 1721, 1637, 1584, 1434, 1280, 1172, 1059, 1036 cm^{-1}. **HRMS** (ESI): Calculated for $C_{21}H_{19}O_2S$ ($M+H^+$): 335.1100, found: 335.1098.

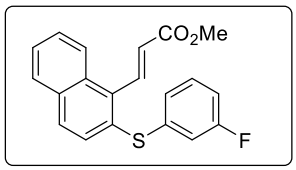

5i: White solid (92%). R_f = 0.2 (hexane/ethyl acetate = 20:1). Mp = 80.4 – 81.2 °C. **^{1}H NMR** (400 MHz, $CDCl_3$) δ 8.18 (d, *J* = 16.3 Hz, 1H), 8.11 – 8.00 (m, 1H), 7.82 – 7.73 (m, 1H), 7.68 (d, *J* = 8.7 Hz, 1H), 7.55 – 7.41 (m, 2H), 7.32 (d, *J* = 8.7 Hz, 1H), 7.19 – 7.13 (m, 1H), 6.97 (ddd, *J* = 7.8, 1.6, 1.0 Hz, 1H), 6.91 – 6.81 (m, 2H), 6.22 (d, *J* = 16.3 Hz, 1H), 3.78 (s, 3H). **^{13}C NMR** (101 MHz, Chloroform-*d*) δ 166.75, 163.10 (d, *J* = 248.9 Hz), 141.32, 138.49 (d, *J* = 7.8 Hz), 135.10, 133.09, 131.74 (d, *J* = 9.5 Hz), 130.56 (d, *J* = 8.5 Hz), 129.71 (d, *J* = 14.5 Hz), 128.64, 127.52, 126.85, 126.42, 126.03 (d, *J* = 3.0 Hz), 125.32, 117.23 (d, *J* = 23.2 Hz), 114.10 (d, *J* = 21.2 Hz), 52.03. **^{19}F NMR** (470 MHz, Chloroform-*d*) δ -111.75 (q, *J* = 8.7 Hz). **IR** (KBr): υ 3060, 2949, 1721,

1639, 1597, 1580, 1473, 1433, 1309, 1281 cm^{-1}. **HRMS** (ESI): Calculated for $C_{20}H_{16}FO_2S$ ($M+H^+$): 339.0850, found: 339.0847.

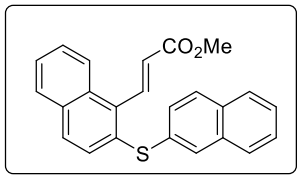

5j: White solid (86%). R_f = 0.2 (hexane/ethyl acetate = 20:1). Mp = 122.0 – 123.0 °C. **^{1}H NMR** (400 MHz, $CDCl_3$) δ 8.27 (d, *J* = 16.3 Hz, 1H), 8.09 (d, *J* = 8.3 Hz, 1H), 7.82 (s, 1H), 7.77 – 7.66 (m, 4H), 7.61 (d, *J* = 8.7 Hz, 1H), 7.51 – 7.38 (m, 4H), 7.31 – 7.19 (m, 2H), 6.30 (d, *J* = 16.3 Hz, 1H), 3.78 (s, 3H). **^{13}C NMR** (101 MHz, $CDCl_3$) δ 166.9, 141.3, 134.0, 133.9, 133.4, 132.6, 132.60, 132.5, 131.6, 130.9, 129.5, 129.2, 129.2, 128.6, 128.6, 127.9, 127.6, 127.4, 126.9, 126.6, 126.4, 126.3, 125.1, 52.0. **IR** (KBr): υ 3053, 2947, 1720, 1636, 1584, 1557, 1500, 1434, 1309, 1281 cm^{-1}. **HRMS** (ESI): Calculated for $C_{24}H_{19}O_2S$ ($M+H^+$): 371.1100, found: 371.1096.

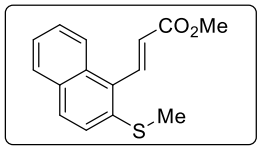

5k: Colorless oil (40%). R_f = 0.2 (hexane/ethyl acetate = 20:1). **^{1}H NMR** (400 MHz, $CDCl_3$) δ 8.21 (d, *J* = 16.3 Hz, 1H), 8.07 (dd, *J* = 8.6, 1.1 Hz, 1H), 7.90 (dd, *J* = 10.6, 8.0 Hz, 1H), 7.85 – 7.77 (m, 2H), 7.54 – 7.41 (m, 3H), 6.36 (d, *J* = 16.3 Hz, 1H), 5.97 (d, *J* = 16.3 Hz, 1H), 3.87 (s, 3H), 2.56 (s, 3H). **^{13}C NMR** (101 MHz, $CDCl_3$) δ 167.0, 141.2, 136.1, 131.6, 131.4, 130.8, 129.4, 128.6, 127.4, 126.0, 125.7, 124.5, 124.2, 52.0, 16.9. **IR** (KBr): υ 3685, 2947, 1720, 1633, 1583, 1504, 1434, 1281, 1191, 1172 cm^{-1}. **HRMS** (ESI): Calculated for $C_{15}H_{15}O_2S$ ($M+H^+$):259.0787, found:259.0793.

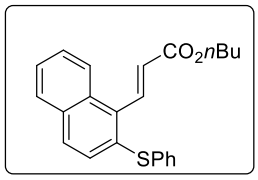

5l: Colorless oil (84%). R_f = 0.3 (hexane/ethyl acetate = 20:1). **^{1}H NMR** (400 MHz, Chloroform-*d*) δ 8.28 (d, *J* = 16.2 Hz, 1H), 8.14 (d, *J* = 8.2 Hz, 1H), 7.81 (dd, *J* = 8.1, 1.4 Hz, 1H), 7.69 (d, *J* = 9.1 Hz, 1H), 7.57 – 7.46 (m, 2H), 7.37 – 7.24 (m, 6H), 6.32 (d, *J* = 16.3 Hz, 1H), 4.27 (t, *J* = 6.7 Hz, 2H), 1.73 (ddt, *J* = 8.8, 7.9, 6.6 Hz, 2H), 1.53 – 1.39 (m, 2H), 0.99 (t, *J* = 7.4 Hz, 3H). **^{13}C NMR** (101 MHz, $CDCl_3$) δ 166.5, 141.0, 135.4, 133.8, 133.6, 132.6, 131.7, 131.6, 129.4, 128.6, 128.6, 127.5, 127.4, 126.7, 126.4, 125.1, 64.8, 30.9, 19.4, 13.9. **IR** (KBr): υ 2958, 2872, 1714, 1639, 1582, 1477, 1306, 1280, 1257, 1174 cm^{-1}. **HRMS** (ESI): Calculated for $C_{23}H_{23}O_2S$ ($M+H^+$): 363.1413, found: 363.1418.

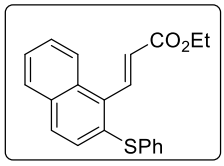

5m: Colorless oil (87%). R_f = 0.3 (hexane/ethyl acetate = 20:1). **^{1}H NMR** (400 MHz, Chloroform-*d*) δ 8.28 (d, *J* = 16.3 Hz, 1H), 8.17 – 8.11 (m, 1H), 7.81 (dd, *J* = 8.1, 1.4 Hz, 1H), 7.69 (d, *J* = 8.9 Hz, 1H), 7.57 – 7.47 (m, 2H), 7.40 – 7.26 (m, 6H), 6.32 (d, *J* = 16.2 Hz, 1H), 4.33 (q, *J* = 7.1 Hz, 2H), 1.38 (t, *J* = 7.1 Hz, 3H). **^{13}C NMR** (101 MHz, $CDCl_3$) δ 166.5, 141.1, 135.4, 133.9, 133.5, 132.6, 131.8, 131.6, 129.4, 128.6, 128.6, 127.5, 127.4, 126.6, 126.4, 125.1, 60.8, 14.5. **IR** (KBr): υ 3056, 2980, 1715, 1638, 1582, 1477, 1440, 1368, 1305, 1281 cm^{-1}. **HRMS** (ESI): Calculated for $C_{21}H_{19}O_2S$ ($M+H^+$): 335.1100, found: 335.1107.

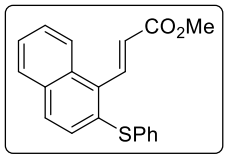

5n: Pale yellow oil (88%). R_f = 0.2 (hexane/ethyl acetate = 20:1). **^{1}H NMR** (400 MHz, Chloroform-*d*) δ 8.30 (d, *J* = 16.3 Hz, 1H), 8.17 – 8.10 (m, 1H), 7.84 – 7.78 (m, 1H), 7.70 (d, *J* = 8.9 Hz, 1H), 7.58 – 7.46 (m, 2H), 7.37 – 7.25 (m, 6H), 6.34 (d, *J* = 16.3 Hz, 1H), 3.87 (s, 3H). **^{13}C NMR** (101 MHz, $CDCl_3$) δ 166.9, 141.4, 135.4, 133.9, 133.4, 132.6, 131.7, 131.6, 129.5, 129.4, 128.6, 128.6, 127.6, 127.4, 126.4, 126.2, 125.1, 52.0. **IR** (KBr): υ 3056, 2948, 2360, 2342, 1721, 1638, 1582, 1434, 1280, 1172 cm^{-1}. **HRMS** (ESI): Calculated for $C_{20}H_{17}O_2S$ ($M+H^+$): 321.0944, found: 321.0950.

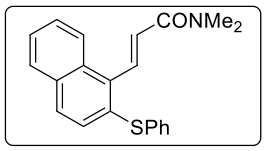

5o: White solid (93%). R_f = 0.2 (hexane/ethyl acetate = 5:1). Mp = 120.7 – 121.4 °C. **^{1}H NMR** (400 MHz, Chloroform-*d*) δ 8.19 – 8.11 (m, 2H), 7.80 (dd, *J* = 7.7, 1.8 Hz, 1H), 7.68 (d, *J* = 8.7 Hz, 1H), 7.54 – 7.45 (m, 2H), 7.35 – 7.21 (m, 6H), 6.73 (d, *J* = 15.8 Hz, 1H), 3.07 (d, *J* = 13.5 Hz, 6H). **^{13}C NMR** (101 MHz, $CDCl_3$) δ 166.3, 138.2, 136.0, 135.1, 132.7, 132.6, 132.0, 131.4, 129.3, 129.0, 128.9, 128.4, 127.3, 127.1, 126.6, 126.3, 125.4, 37.5, 36.0. **IR** (KBr): υ 3054, 2928, 1653, 1617, 1582, 1477, 1395, 1140, 1056, 1023 cm^{-1}. **HRMS** (ESI): Calculated for $C_{21}H_{20}NOS$ ($M+H^+$): 334.1260, found: 334.1269.

5.4.5 Synthetic Applications

Scheme 5.6. Selective Oxidation of the Ortho Thiolation Product

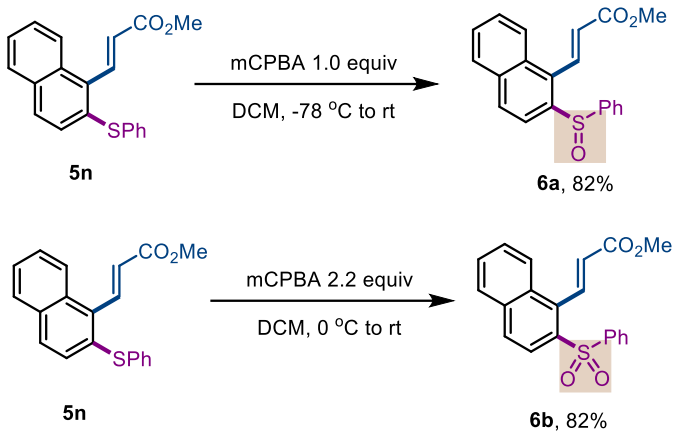

A Schlenk tube was charged with a solution of **5n** (96.1 mg, 0.3 mmol) in DCM (5 mL). A solution of mCPBA (67.2 mg, 77%, 0.3 mmol, 1.0 equiv) in DCM (5 mL) was then added dropwise at -78 °C. The resulting mixture was allowed to warm to room temperature overnight. Subsequently, the reaction mixture was washed by saturated aq. Na_2CO_3 (10 mL) solution three time. The organic layers were washed with water and brine before they were dried over $MgSO_4$ and concentrated. The residual was then purified by silica gel chromatography (acetone/hexane = 1/5) to afford **6a** (82.3 mg, 82%) as a white solid.

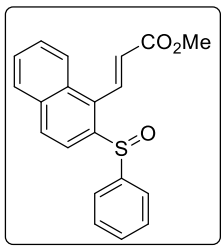

6a: White solid (82%). R_f = 0.2 (hexane/acetone = 5:1). Mp = 151.7 – 152.1 °C. **^{1}H NMR** (400 MHz, Chloroform-*d*) δ 8.26 (d, *J* = 16.3 Hz, 1H), 8.11 – 8.06 (m, 1H), 8.05 – 7.96 (m, 2H), 7.91 – 7.84 (m, 1H), 7.64 – 7.53 (m, 4H), 7.45 – 7.36 (m, 3H), 6.32 (d, *J* = 16.3 Hz, 1H), 3.90 (s, 3H). **^{13}C NMR** (101 MHz, $CDCl_3$) δ 166.0, 144.9, 141.7, 139.1, 134.6, 132.5, 131.2, 130.8, 130.7, 129.4, 128.9, 128.2, 128.2, 127.9, 125.5, 125.3, 120.1, 52.3. **IR** (KBr): υ 3745, 3057, 2950, 1844,

1718, 1675, 1670, 1570, 1419, 1280 cm^{-1}. **HRMS** (ESI): Calculated for $C_{20}H_{16}O_3SNa(M+Na^+)$: 359.0712, found: 359.0703.

A Schlenk tube was charged with a solution of **5n** (96.1 mg, 0.3 mmol) in DCM (5 mL). A solution of mCPBA (147.9 mg, 77%, 0.66 mmol, 2.2 equiv) in DCM (5 mL) was then added dropwise at 0 ^oC. The resulting mixture was allowed to warm to room temperature overnight. Subsequently, the reaction mixture was washed by saturated aq. Na_2CO_3 (10 mL) solution three time. The organic layers were washed with water and brine before they were dried over $MgSO_4$ and concentrated. The residual was then purified by silica gel chromatography (acetone/hexane = 1/5) to afford **6b** (85.5 mg, 80%) as a white solid.

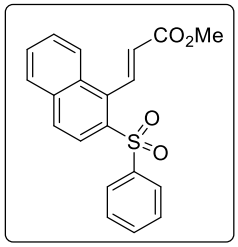

6b: White solid (80%). R_f = 0.25 (hexane/acetone = 5:1). Mp = 130.7 – 131.3 ^oC. **^{1}H NMR** (400 MHz, $CDCl_3$) δ 8.29 (dd, *J* = 23.9, 12.6 Hz, 2H), 8.04 (dd, *J* = 28.6, 8.7 Hz, 2H), 7.95 – 7.82 (m, 3H), 7.71 – 7.48 (m, 3H), 7.44 (dd, *J* = 10.5, 4.8 Hz, 2H), 5.81 (d, *J* = 16.4 Hz, 1H), 3.88 (s, 3H). **^{13}C NMR** (101 MHz, $CDCl_3$) δ 165.9, 141.5, 140.0, 136.4, 135.6, 135.2, 133.4, 131.1, 129.4, 129.1, 128.9, 128.6, 128.2, 128.0, 127.7, 126.7, 123.8, 52.2. **IR** (KBr): υ 2950, 2360, 2341, 1722, 1582, 1446, 1309, 1280, 1170, 1151 cm^{-1}. **HRMS** (ESI): Calculated for $C_{20}H_{17}O_4S(M+H^+)$: 353.0842, found: 353.0853.

Scheme 5.7. Ipso Functionalization with Arylboronates

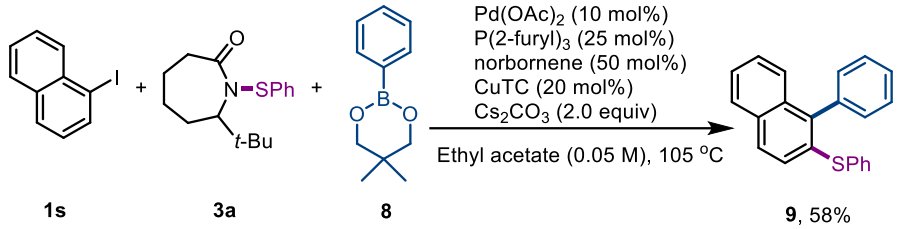

A flame-dried 7.0 mL vial A was charged with $Pd(OAc)_2$ (4.6 mg, 0.02 mmol, 10 mol%), CuTC (7.6 mg, 0.04 mmol, 20 mol%), TFP (11.6 mg, 0.05 mmol, 25 mol%), phenylboronate **8** (76 mg, 0.4 mmol, 2.0 equiv) and ArI (0.2 mmol, 1.0 equiv). To another 4.0 mL vial B was weighed **3a** (0.6 mmol). Two vials were directly transferred into a nitrogen-filled glovebox without caps. Then, Cs_2CO_3 (130.4 mg, 0.4 mmol, 2.0 equiv) was added to the vial A. In the third empty 4.0 mL vial C, NBE (18.8 mg, 0.2 mmol) was dissolved in 1.0 mL dry ethyl acetate. Half of this NBE solution (0.5 mL, 0.1 mmol, 50 mol%) was transferred into the vial A. To the 4.0 mL vial B containing **3a** was added 0.75 mL dry ethyl acetate. Two thirds of this **3a** solution (0.5 ml, 0.4 mmol, 2.0 equiv) was transferred into the vial A, before another 3.0 mL dry ethyl acetate was added. Vial A was tightly sealed, transferred out of glovebox and stirred on a pie-block preheated to 105 °C for 12 hours. After completion of the reaction, the mixture was filtered through a thin pad of silica gel. The filter cake was washed with ethyl acetate and the combined filtrate was concentrated. The residue was loaded to a small amount of silica gel and then purified by flash column chromatography to give the desired ortho thiolation product.

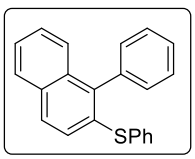

9: Colorless oil (58%). R_f = 0.4 (hexane/ethyl acetate = 20:1). **^{1}H NMR** (400 MHz, $CDCl_3$) δ 7.78 – 7.72 (m, 1H), 7.66 (d, *J* = 8.7 Hz, 1H), 7.44 – 7.35 (m, 4H), 7.31 – 7.14 (m, 10H). **^{13}C NMR**

(101 MHz, $CDCl_3$) δ 140.3, 138.8, 136.2, 133.3, 133.0, 132.4, 131.8, 130.4, 129.2, 128.4, 128.4, 128.2, 128.0, 127.8, 127.2, 126.7, 126.5, 125.9. **IR** (KBr): υ 3054, 2953, 1581, 1560, 1505, 1491, 1476, 1439, 1379, 1070 cm^{-1}. **HRMS** (ESI): Calculated for $C_{22}H_{17}S$ ($M+H^+$): 313.1045, found: 313.1055.

Scheme 5.8. Ipso Sonogashira Coupling

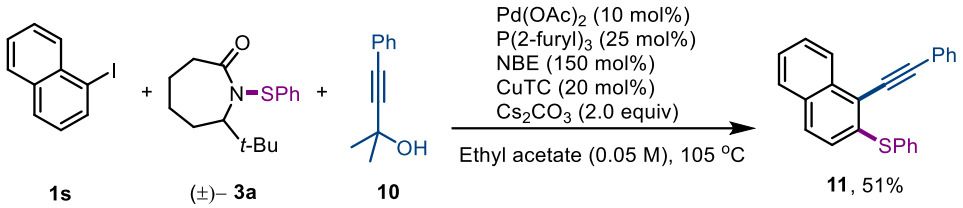

A flame-dried 7.0 mL vial A was charged with $Pd(OAc)_2$ (4.6 mg, 0.02 mmol, 10 mol%), CuTC (7.6 mg, 0.04 mmol, 20 mol%), TFP (11.6 mg, 0.05 mmol, 25 mol%), **10** (64.1 mg, 0.4 mmol, 2.0 equiv) and ArI (0.2 mmol, 1.0 equiv). To another 4.0 mL vial B was weighed thiolation reagent (0.6 mmol). Two vials were directly transferred into a nitrogen-filled glovebox without caps. Then, NBE (28.2 mg, 0.3 mmol, 150 mol%) and Cs_2CO_3 (130.4 mg, 0.4 mmol, 2.0 equiv) was added to the vial A. To the 4.0 mL vial B containing thiolation reagent was added 0.75 mL dry ethyl acetate. 0.5 mL of this thiolation reagent solution (0.4 mmol, 2.0 equiv) was transferred into the vial A, before another 3.5 mL dry ethyl acetate was added. Vial A was tightly sealed, transferred out of glovebox and stirred on a pie-block preheated to 105 °C for 12 hours. After completion of the reaction, the mixture was filtered through a thin pad of silica gel. The filter cake was washed with ethyl acetate and the combined filtrate was concentrated. The residue was loaded to a small amount of silica gel and then purified by flash column chromatography on silica gel to give the desired ortho thiolation product.

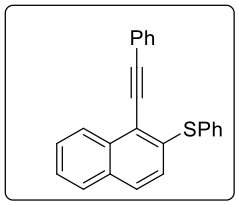

11: Yellow oil (51%). R_f = 0.4 (hexane/ethyl acetate = 20:1). **^{1}H NMR** (400 MHz, Chloroform-*d*) δ 8.42 (dd, *J* = 8.4, 1.1 Hz, 1H), 7.80 – 7.75 (m, 1H), 7.69 – 7.63 (m, 3H), 7.60 (ddd, *J* = 8.3, 6.9, 1.3 Hz, 1H), 7.55 – 7.51 (m, 2H), 7.48 (ddd, *J* = 8.1, 6.9, 1.3 Hz, 1H), 7.43 – 7.33 (m, 6H), 7.13 (d, *J* = 8.7 Hz, 1H). **^{13}C NMR** (101 MHz, $CDCl_3$) δ 139.1, 133.7, 133.3, 131.7, 131.4, 129.5, 128.7, 128.6, 128.4, 128.2, 128.1, 127.5, 126.1, 126.1, 125.9, 123.3, 119.2, 101.2, 85.5. **IR** (KBr): υ 3055, 2921, 1616, 1581, 1555, 1489, 1129, 1085, 1068, 1024 cm^{-1}. **HRMS** (ESI): Calculated for $C_{24}H_{17}S$ ($M+H^+$): 337.1045, found: 337.1055.

Scheme 5.9. Gram-Scale Preparation

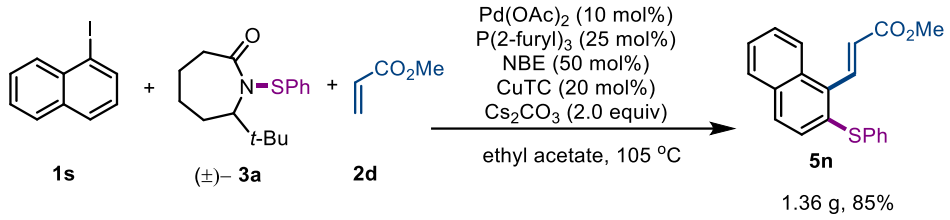

A flame-dried 100 mL vessel was charged with $Pd(OAc)_2$ (115 mg, 0.5 mmol, 10 mol%), CuTC (190 mg, 1.0 mmol, 20 mol%), TFP (290 mg, 1.25 mmol, 25 mol%), sulfenamide **3a** (2.77 g, 10.0 mmol, 2.0 equiv) and ArI **1s** (1.27 g, 5.0 mmol, 1.0 equiv). The vessel was directly transferred into a nitrogen-filled glovebox without caps. Then, NBE (235 mg, 2.5 mmol, 50 mol%) and Cs_2CO_3 (3.26 g, 10 mmol, 2.0 equiv) was added. 100 mL dry ethyl acetate was added before acrylate **2d** (860 mg, 10 mmol, 2.0 equiv) was added. Then the vessel was tightly sealed, transferred out of glovebox and stirred in an oil bath preheated to 105 °C for 12 hours. After completion of the reaction, the mixture was filtered through a thin pad of silica gel. The filter cake was washed with

ethyl acetate and the combined filtrate was concentrated. The residue was loaded to a small amount of silica gel and subjected to flash column chromatography to give the desired ortho thiolation product **5n** (1.36 g, 85%).

5.5 NMR Spectra

Figure 5.3. ^{1}H NMR Spectrum of S4

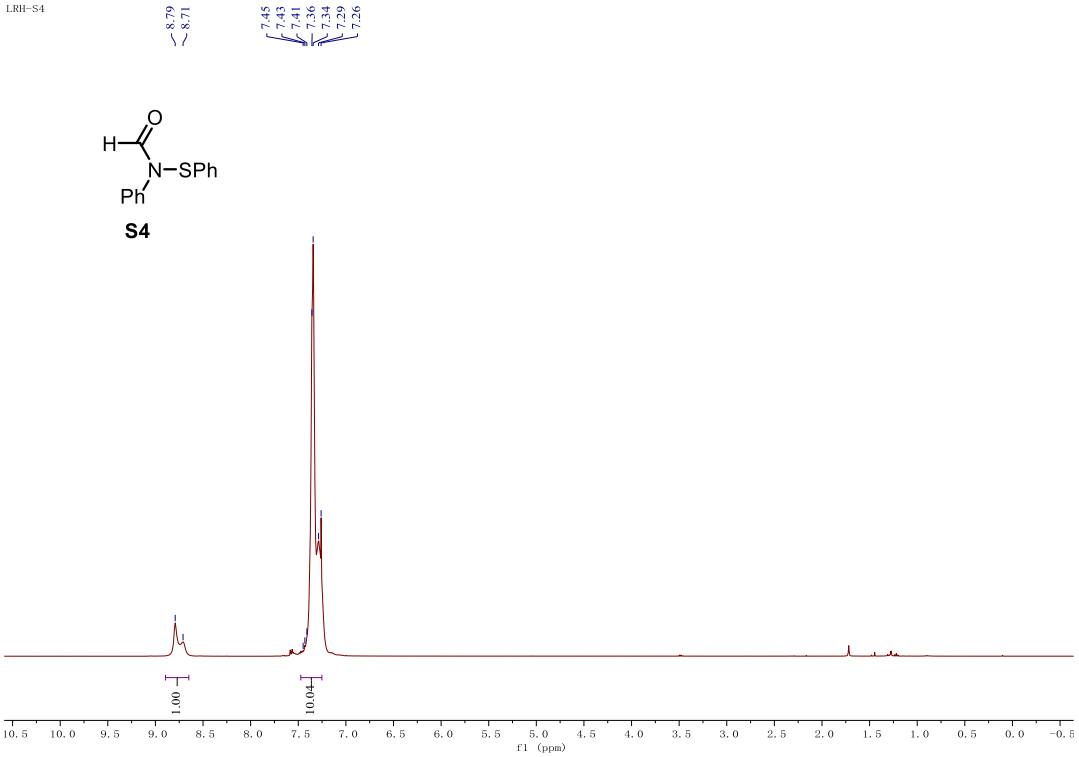

Figure 5.4. ^{13}C NMR Spectrum of S4

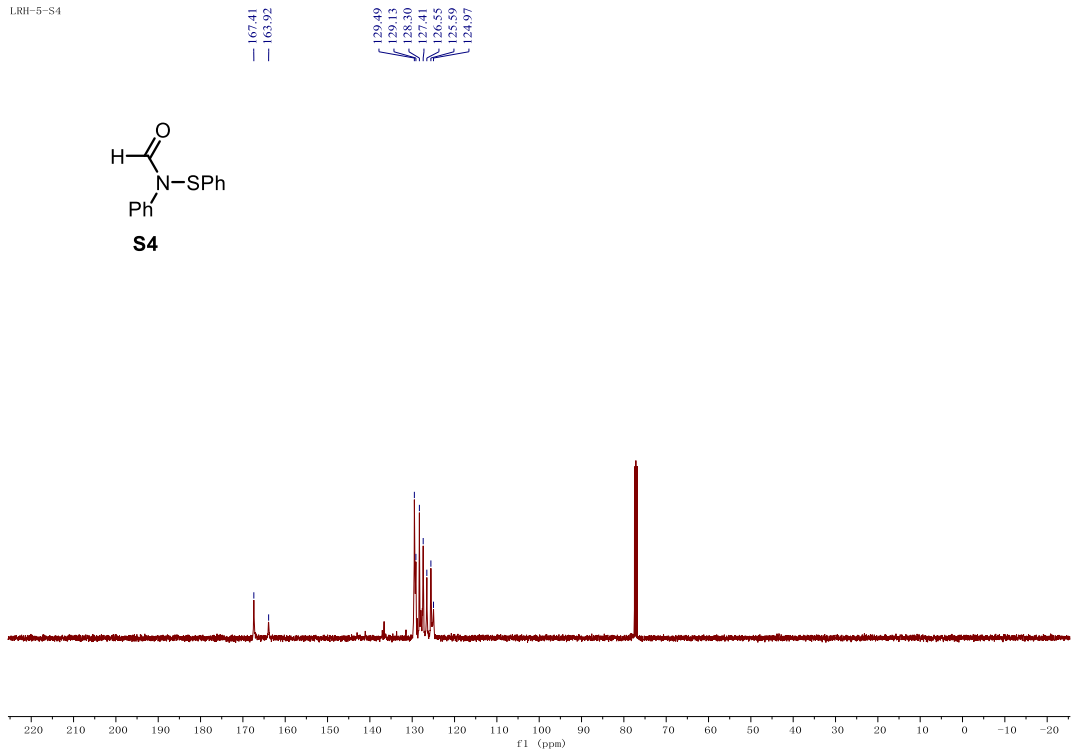

Figure 5.5. ^{1}H NMR Spectrum of S6

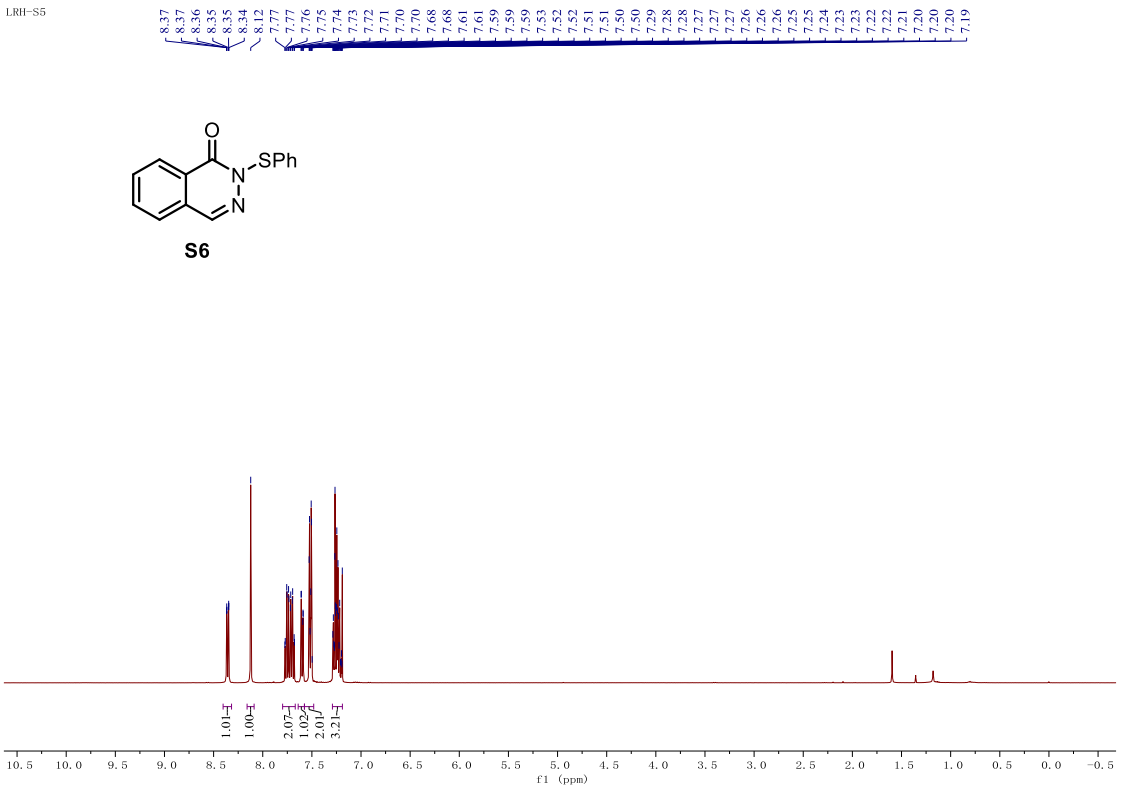

Figure 5.6. ^{13}C NMR Spectrum of S6

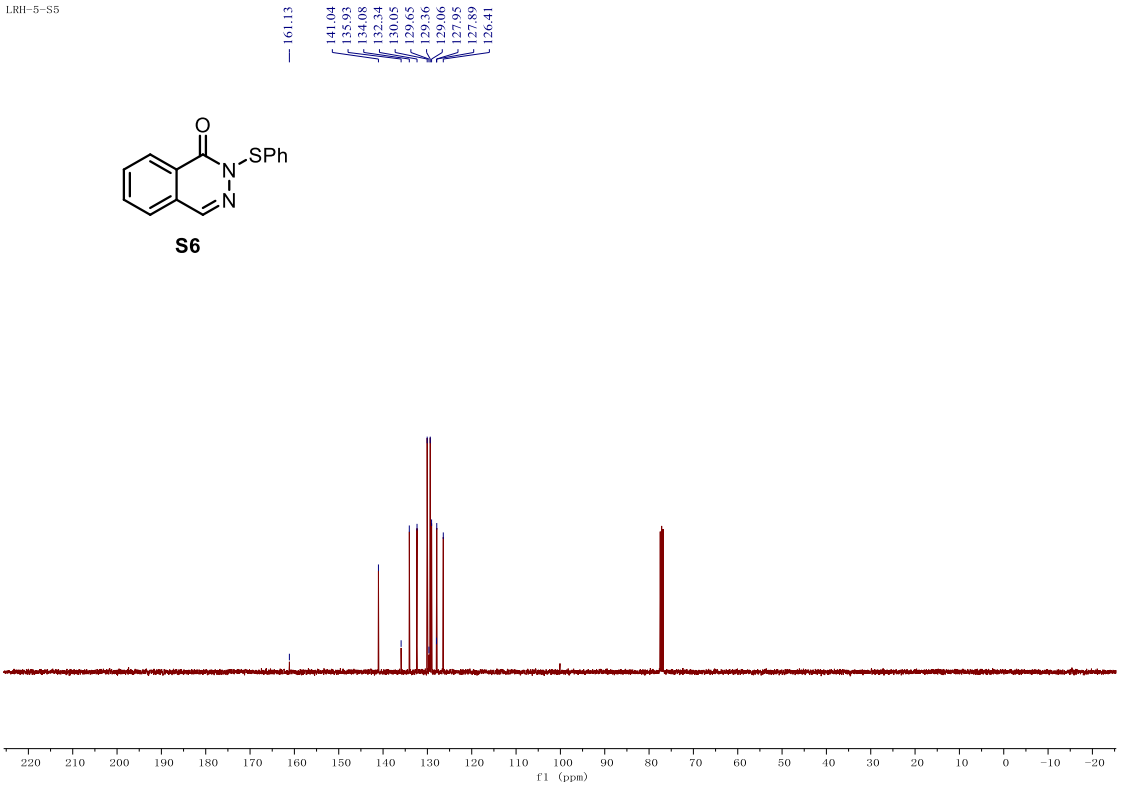

Figure 5.7. ^{1}H NMR Spectrum of S5

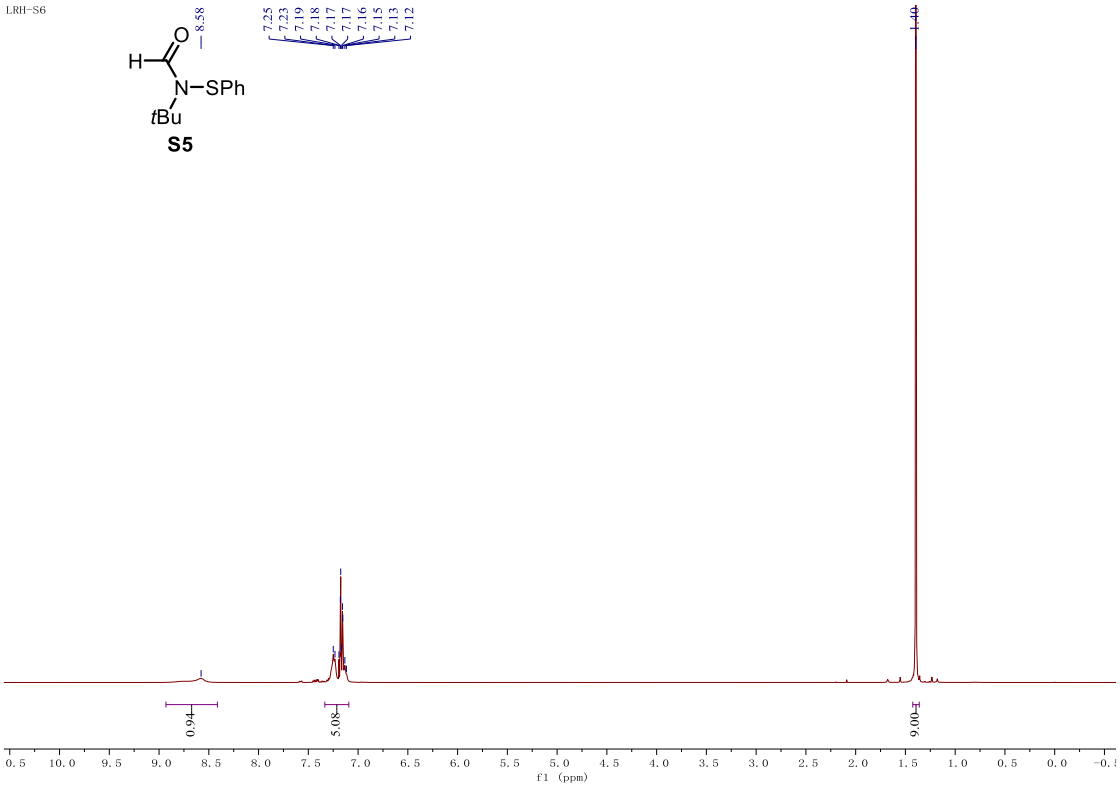

Figure 5.8. ^{13}C NMR Spectrum of S5

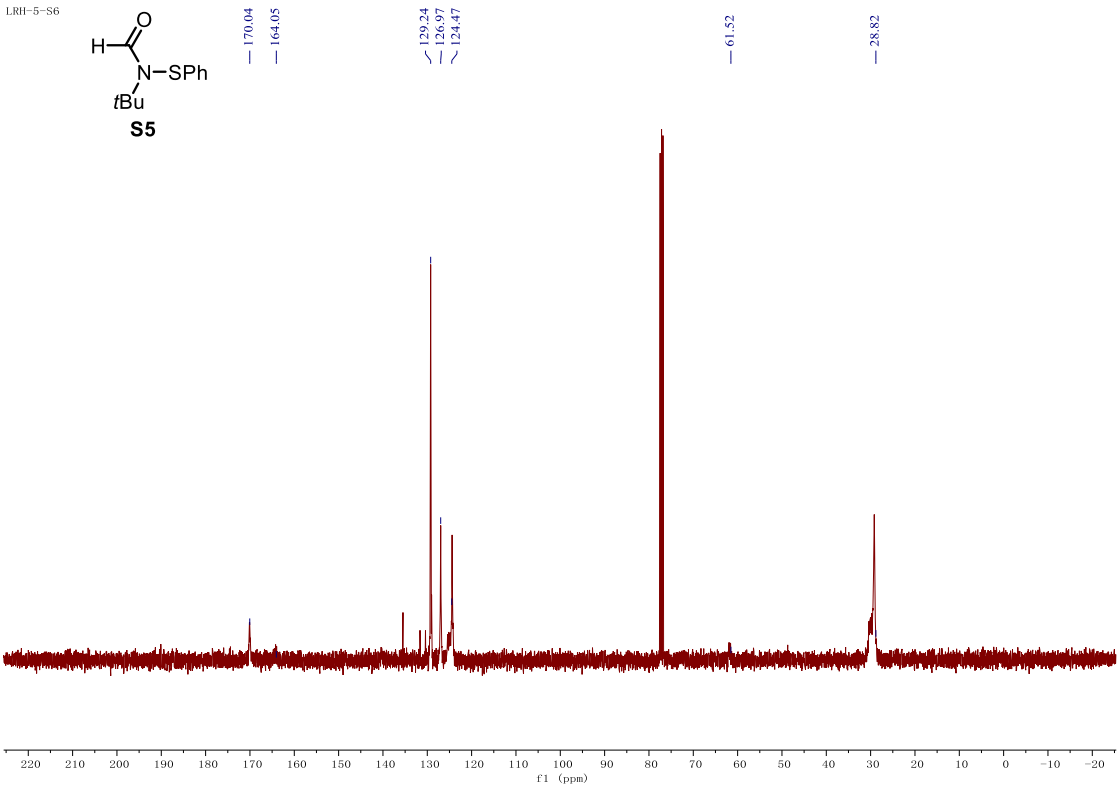

Figure 5.9. ^{1}H NMR Spectrum of S7

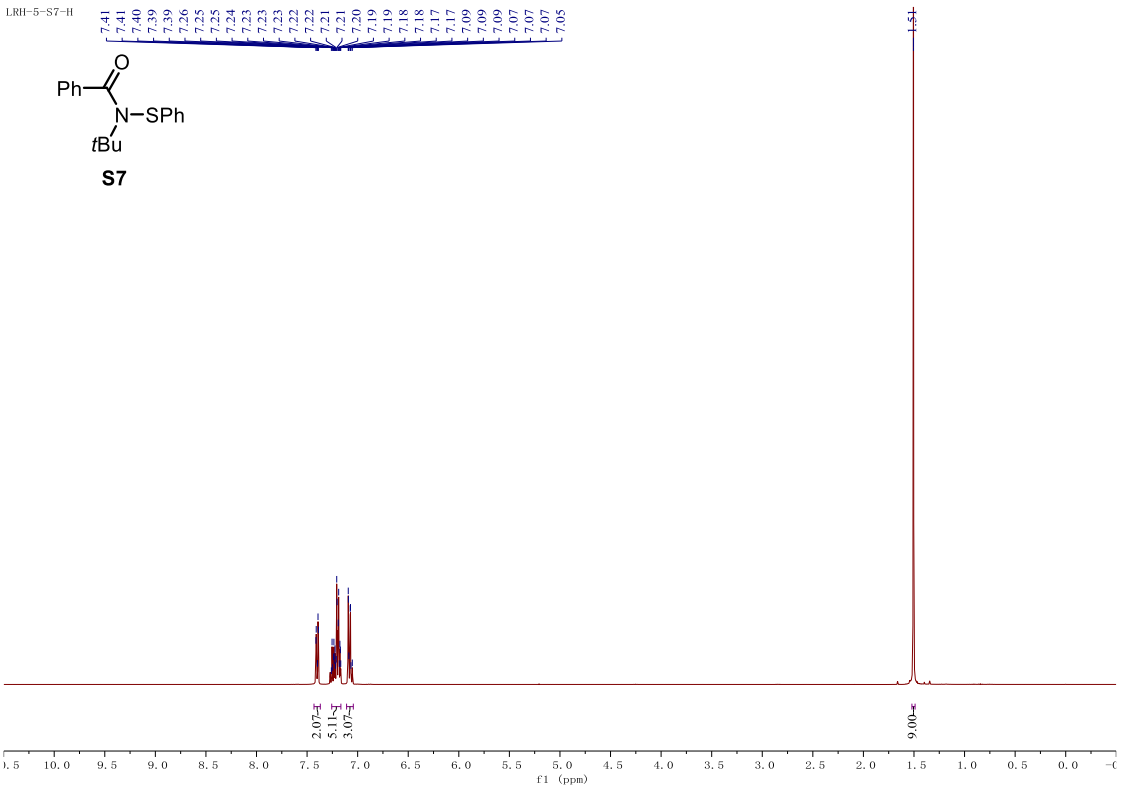

Figure 5.10. ^{13}C NMR Spectrum of S7

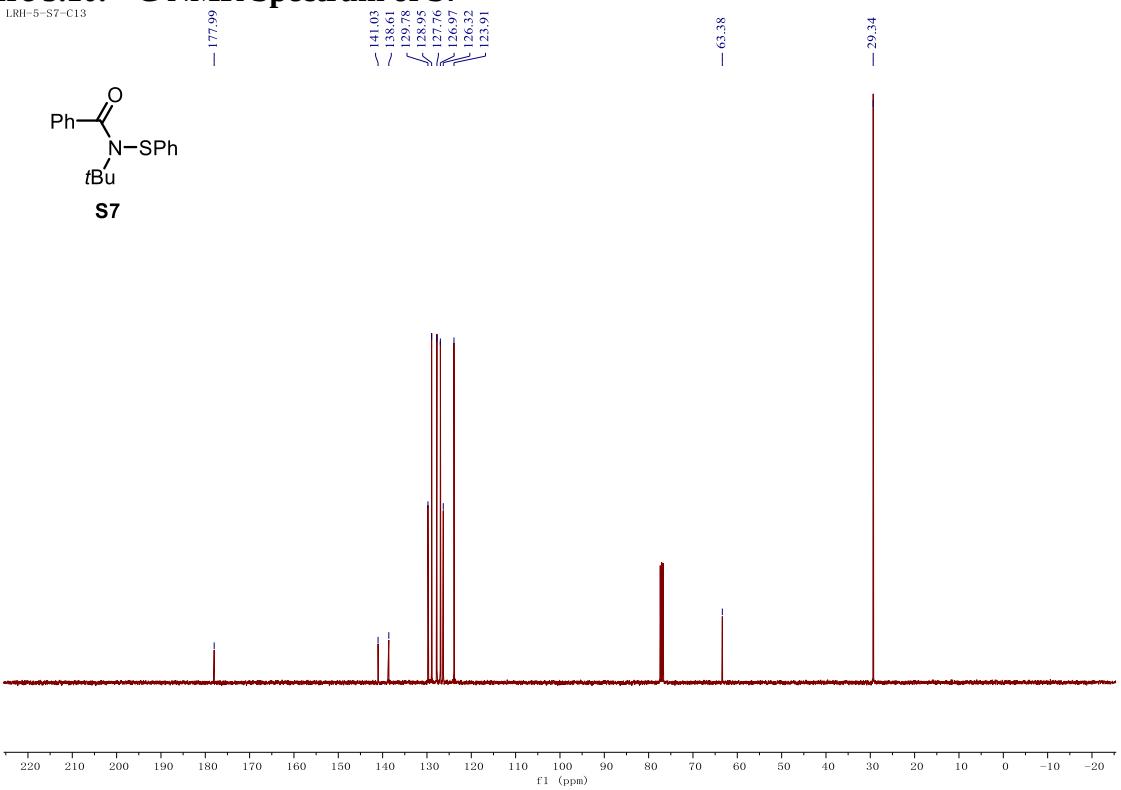

Figure 5.11. ^{1}H NMR Spectrum of S10

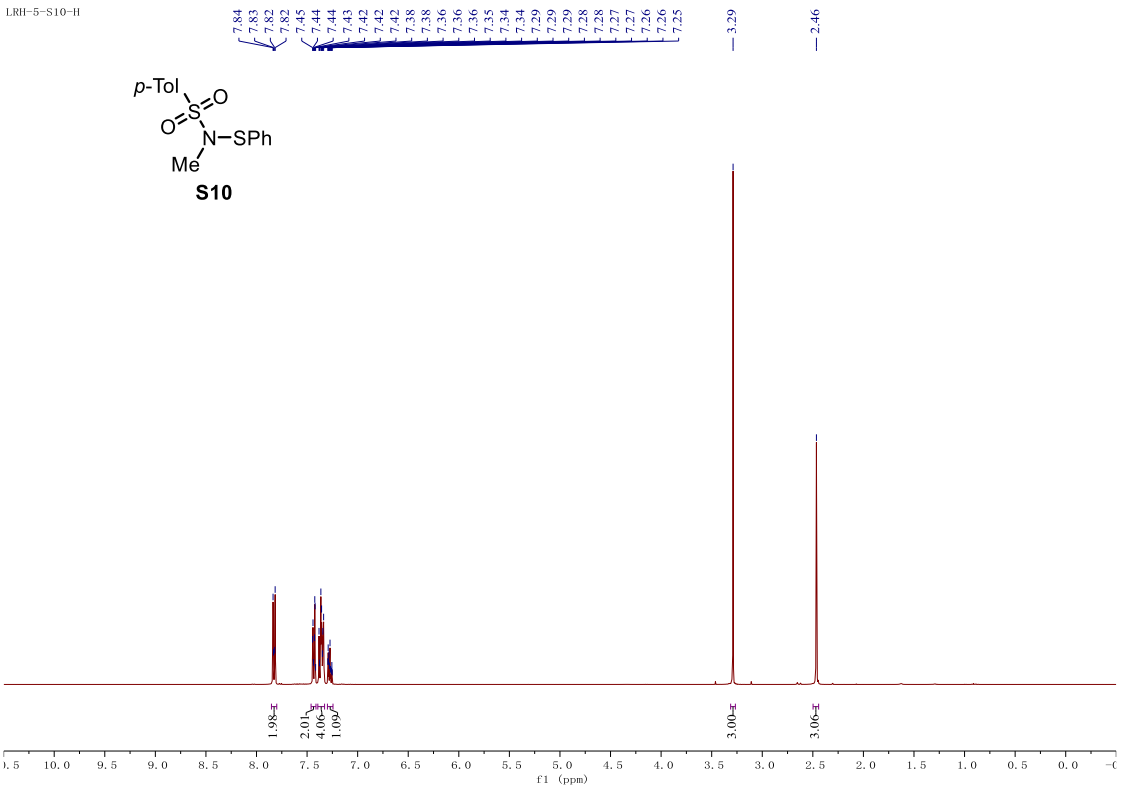

Figure 5.12. ^{13}C NMR Spectrum of S10

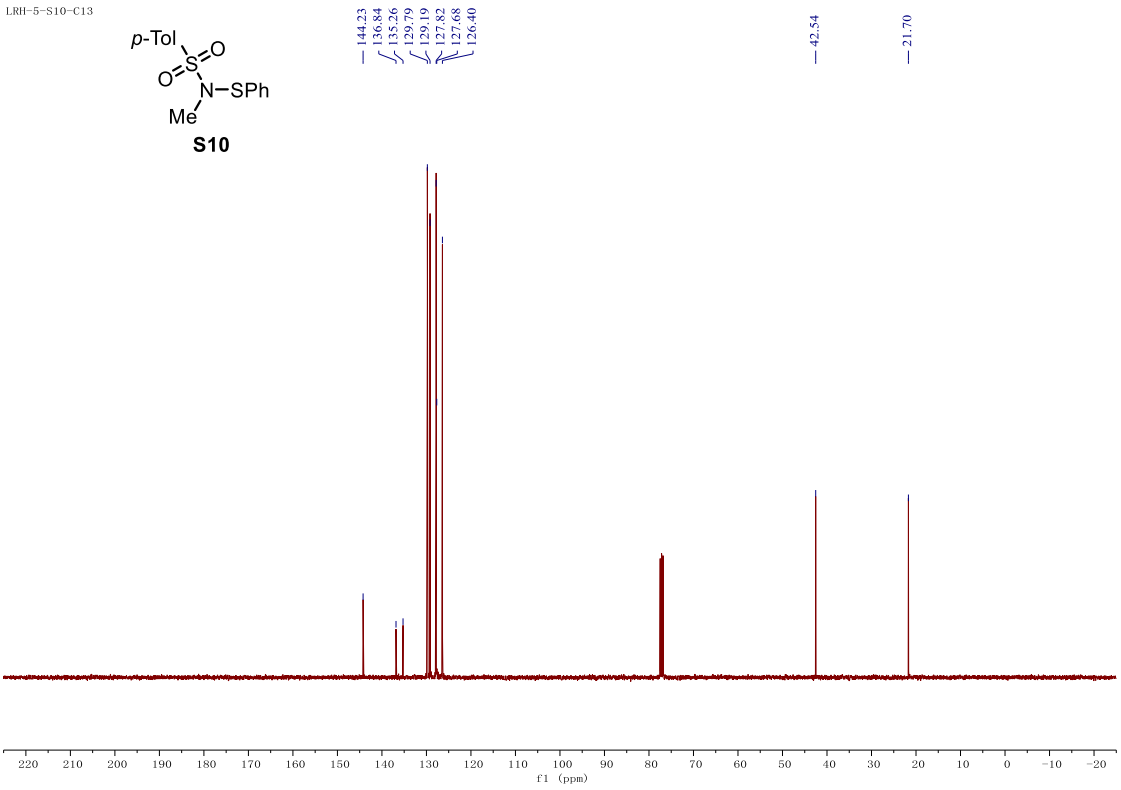

Figure 5.13. ^{1}H NMR Spectrum of S14

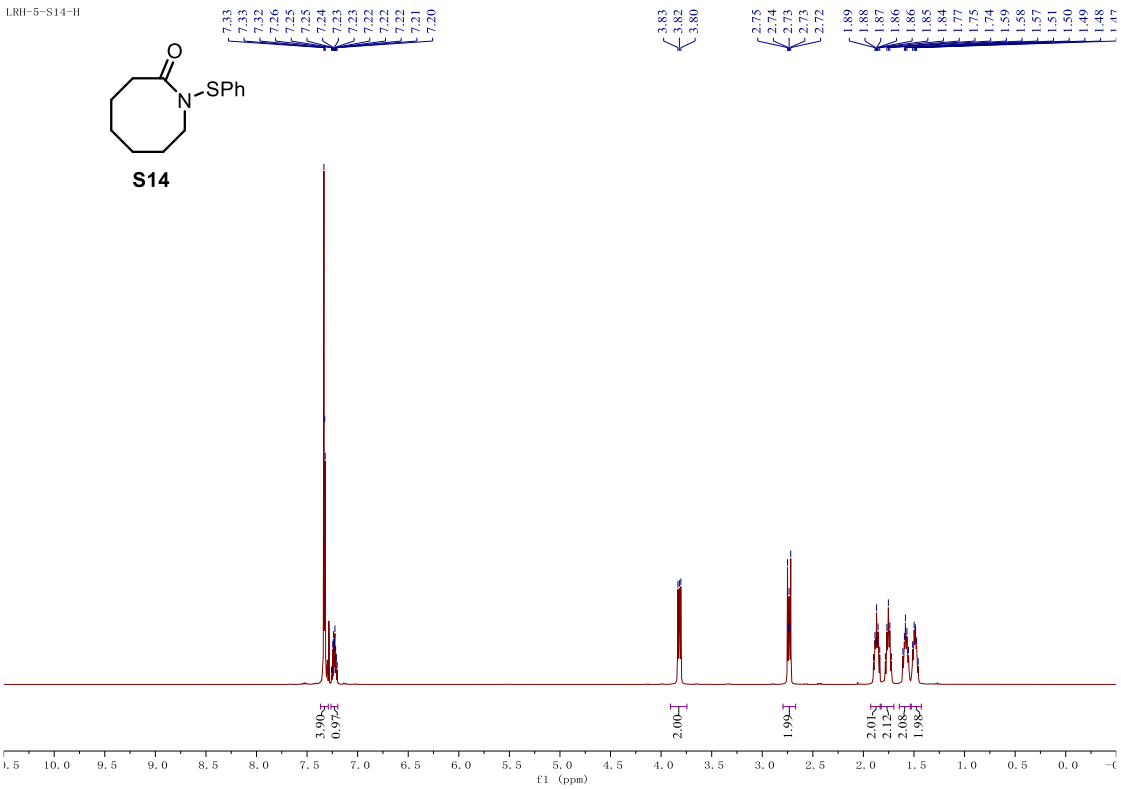

Figure 5.14. ^{13}C NMR Spectrum of S14

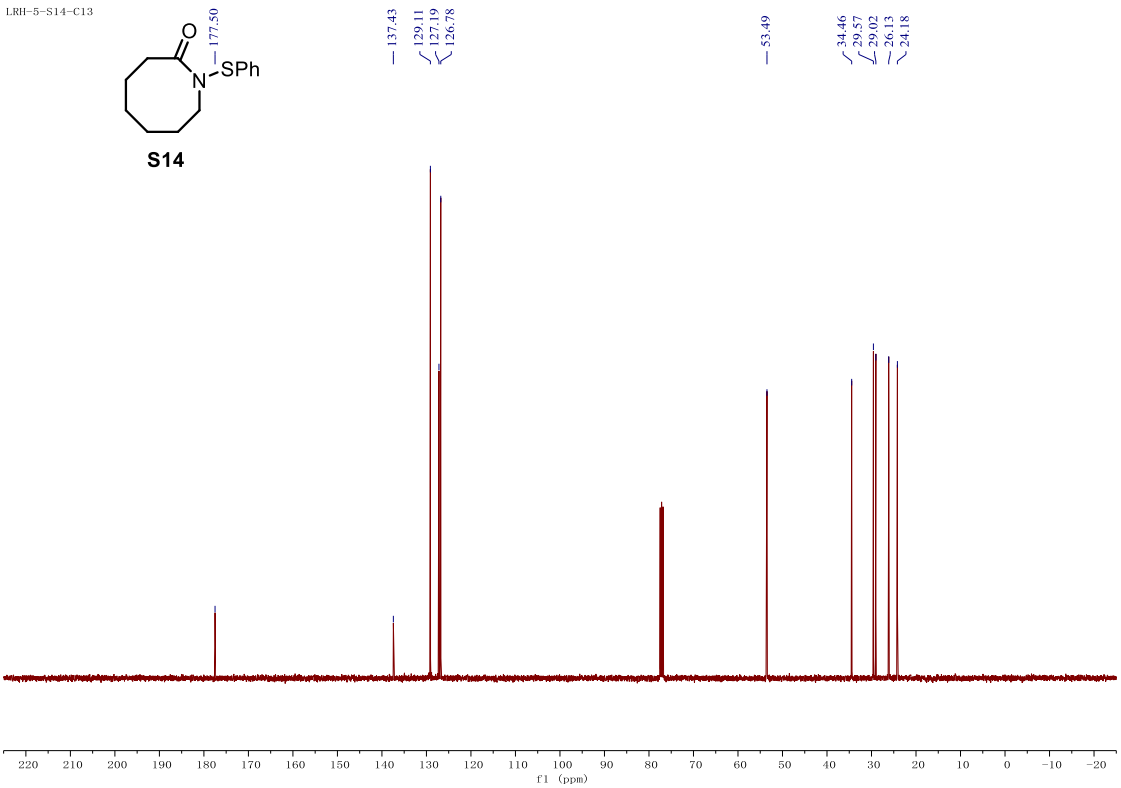

Figure 5.15. ^{1}H NMR Spectrum of S15

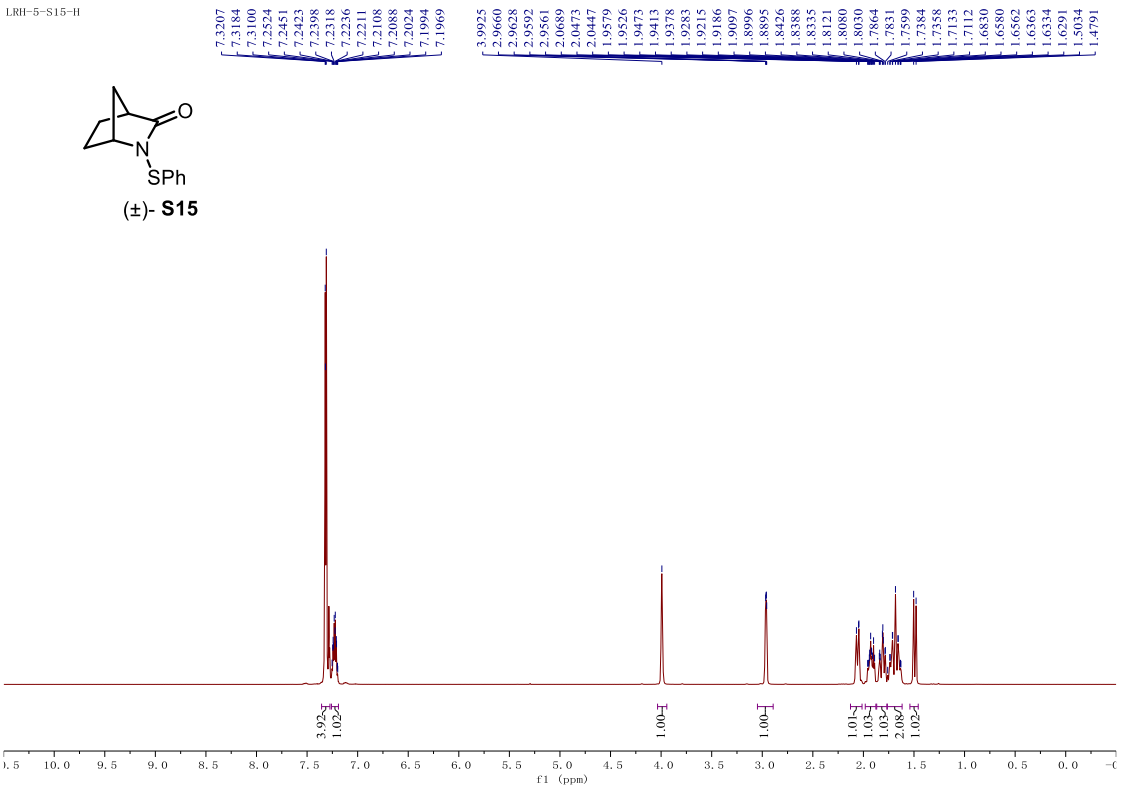

Figure 5.16. ^{13}C NMR Spectrum of S15

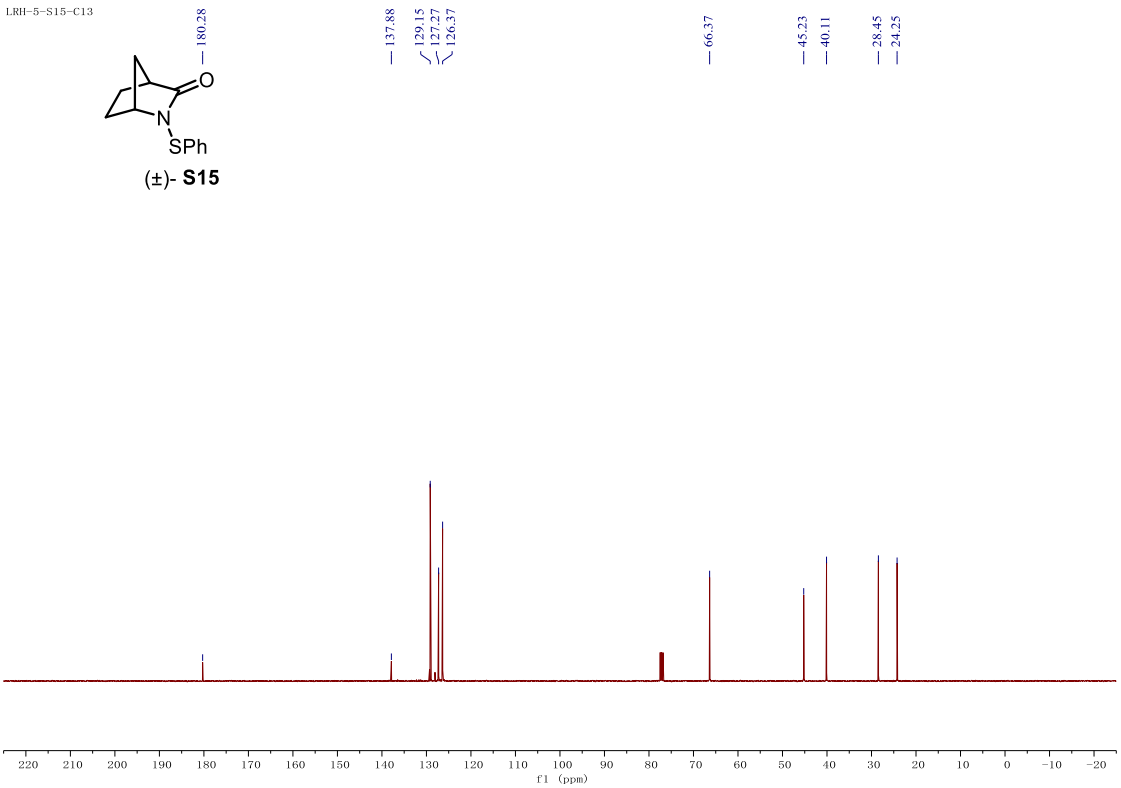

Figure 5.17. ^{1}H NMR Spectrum of S17

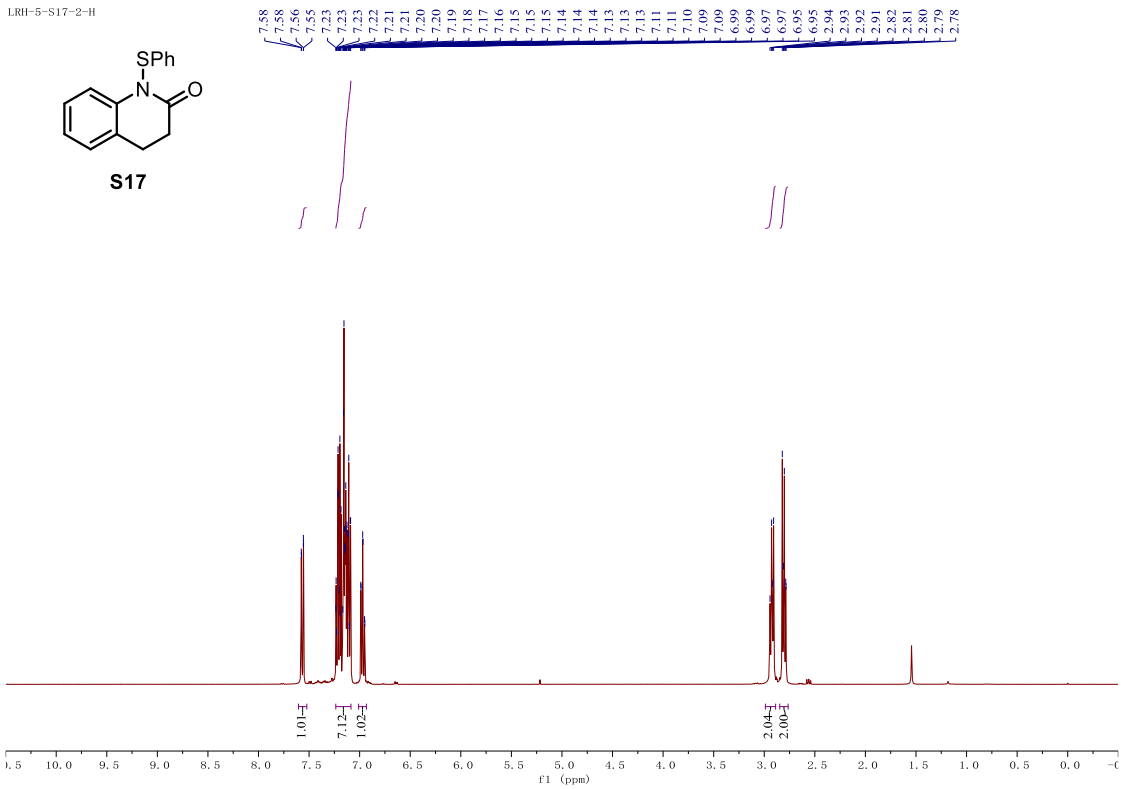

Figure 5.18. ^{13}C NMR Spectrum of S17

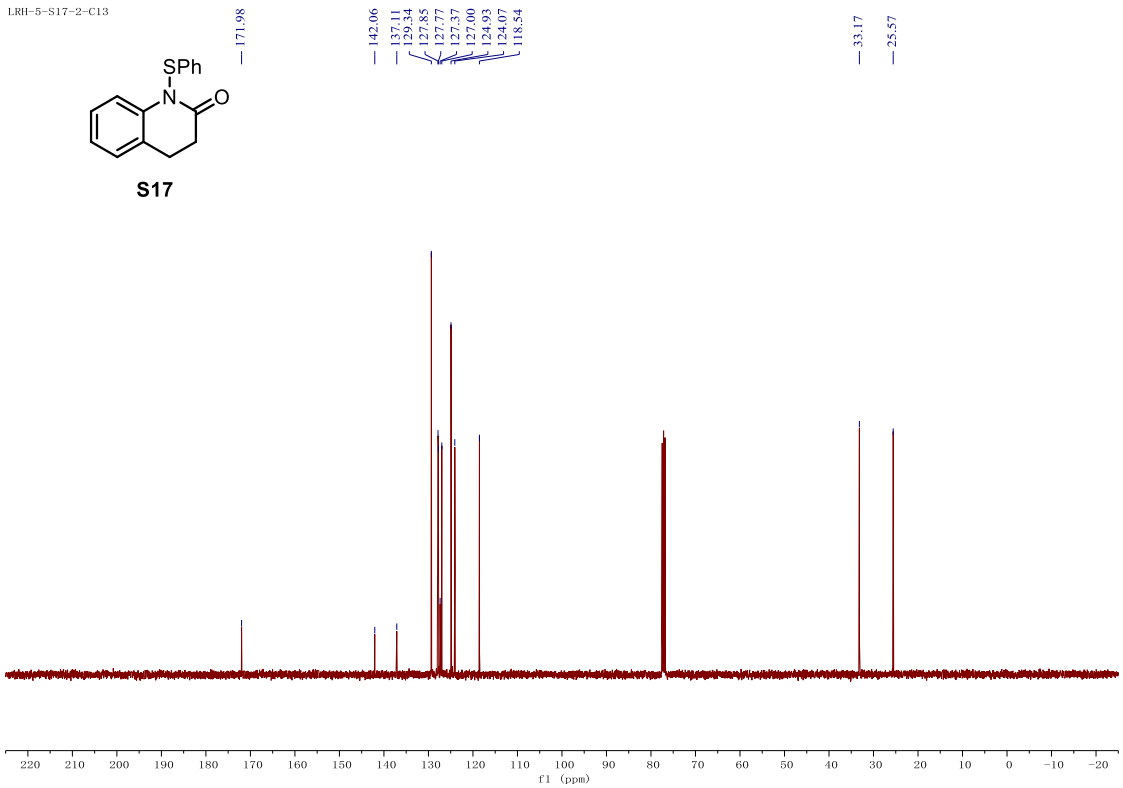

Figure 5.19. ^{1}H NMR Spectrum of S18

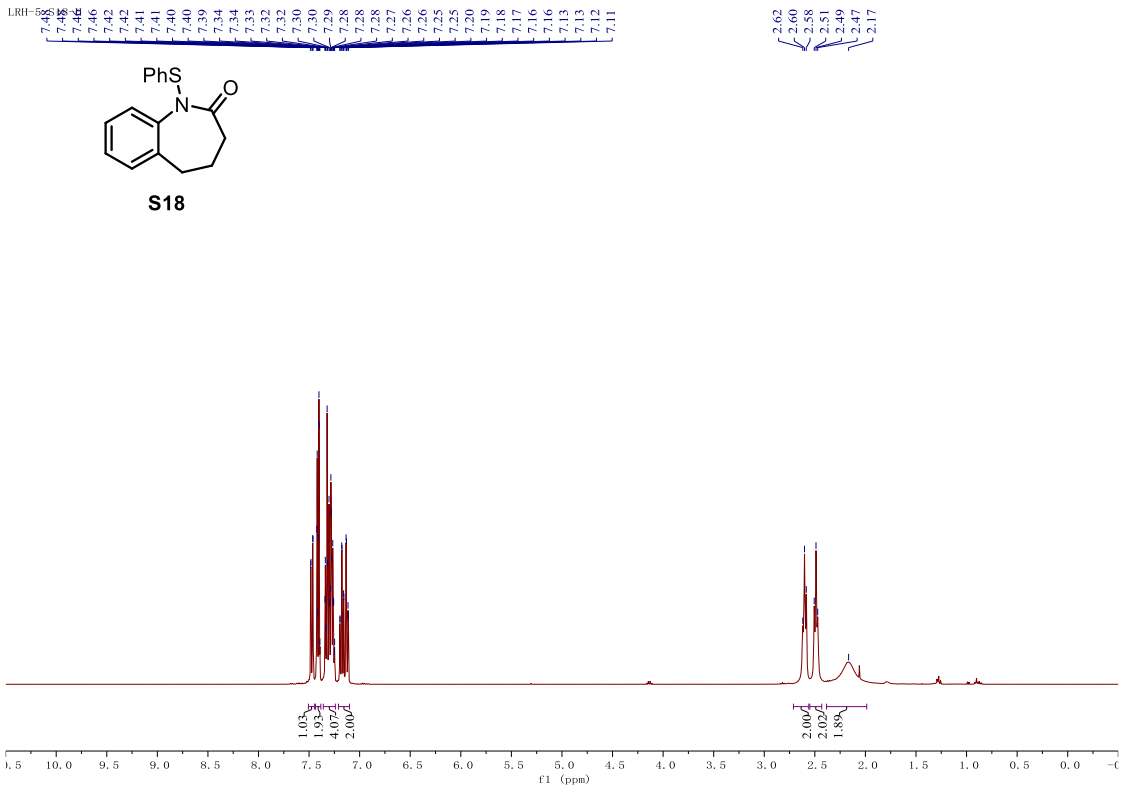

Figure 5.20. ^{13}C NMR Spectrum of S18

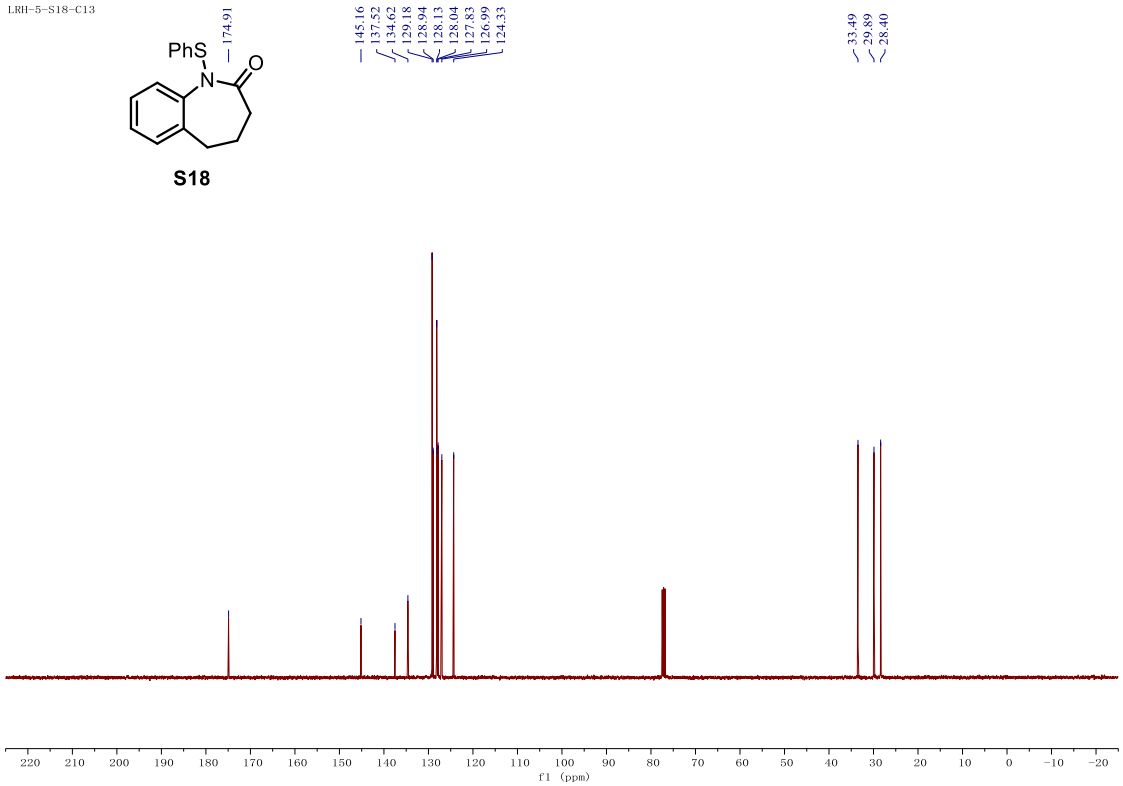

Figure 5.21. ^{1}H NMR Spectrum of 17

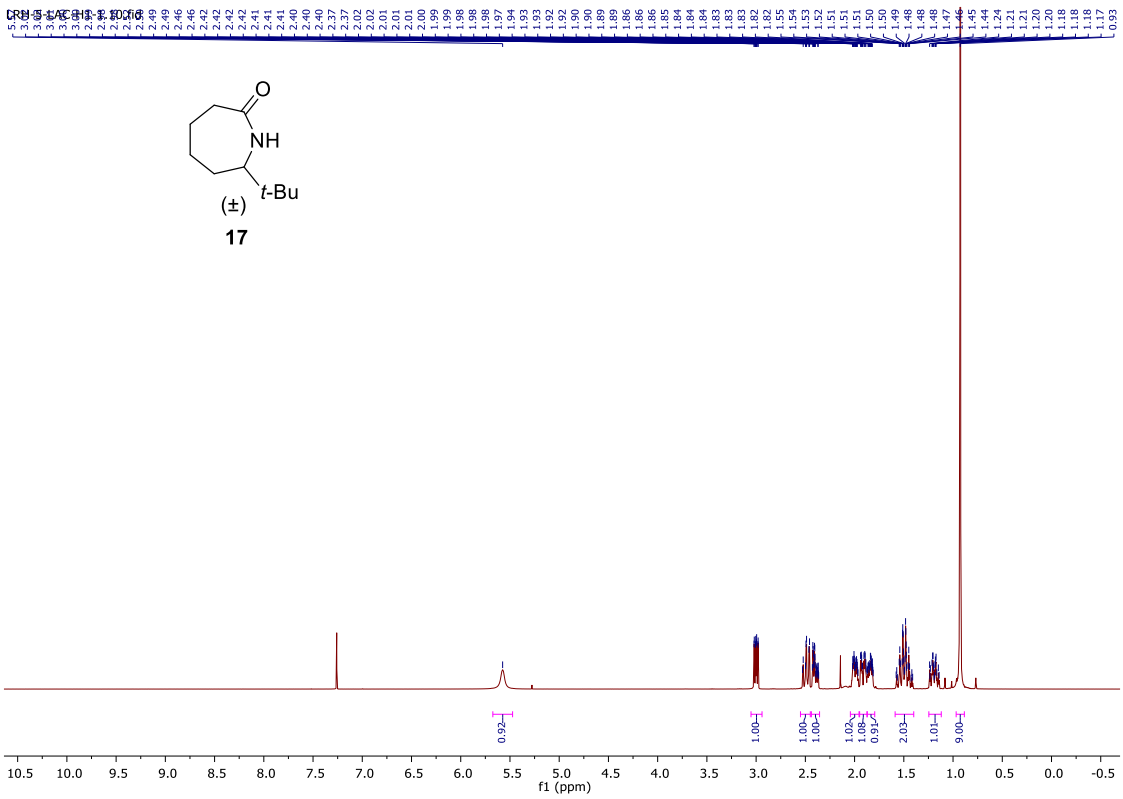

Figure 5.22. ^{13}C NMR Spectrum of 17

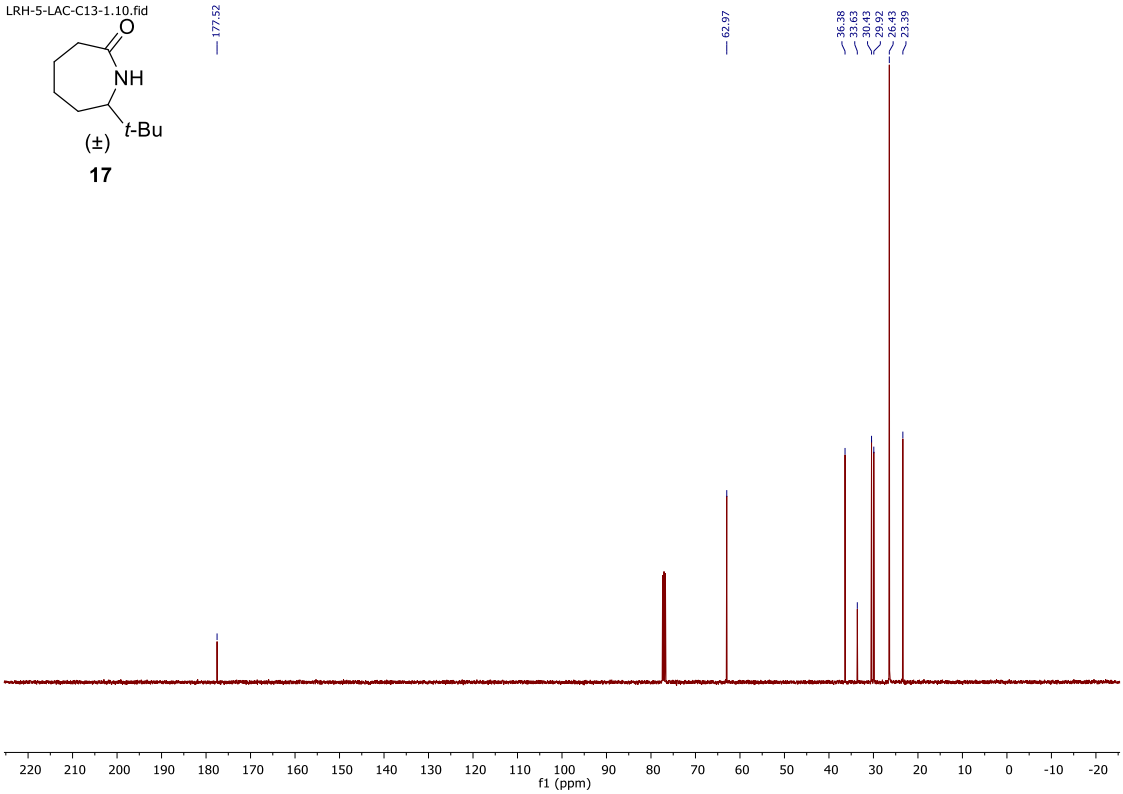

Figure 5.23. ^{1}H NMR Spectrum of S19

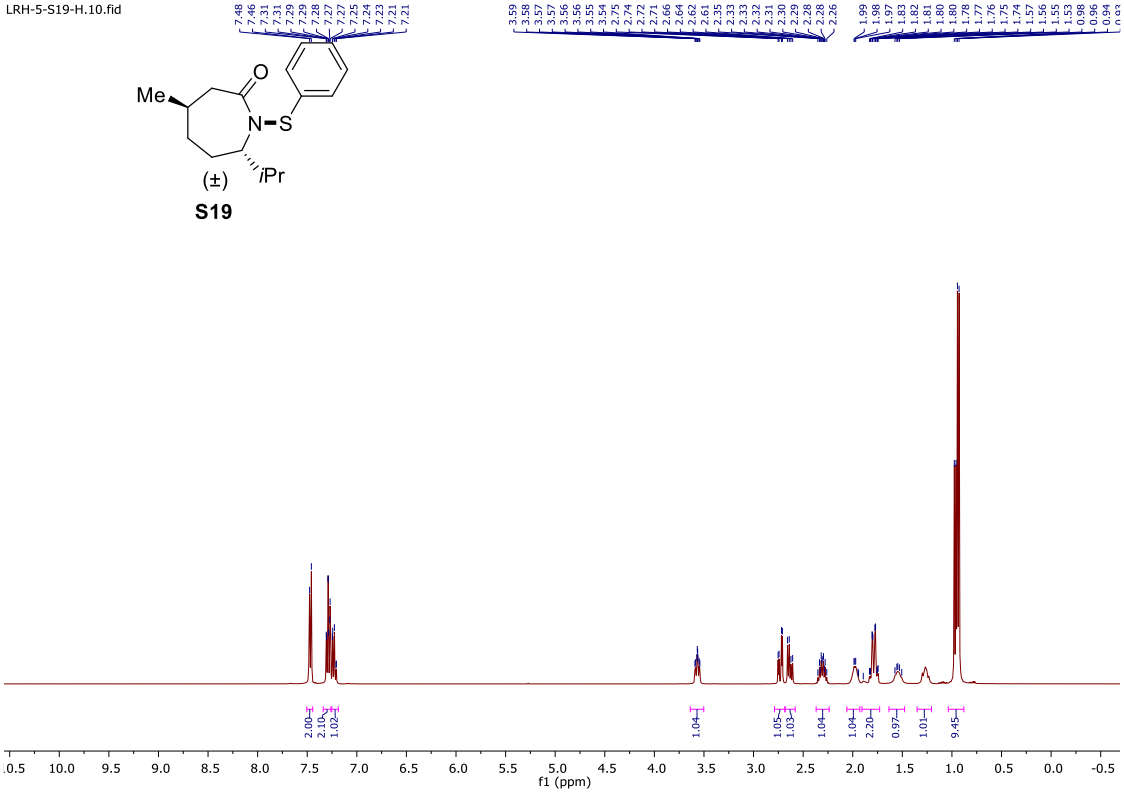

Figure 5.24. ^{13}C NMR Spectrum of S19

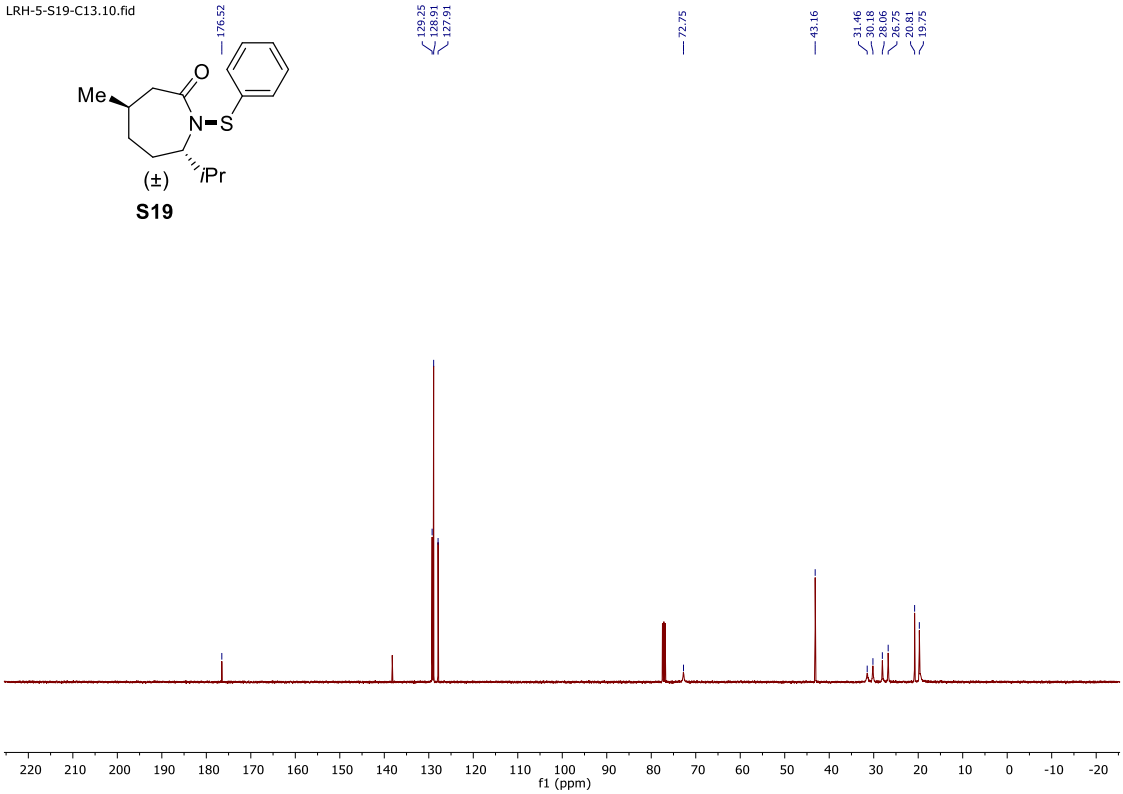

Figure 5.25. ^{1}H NMR Spectrum of S21

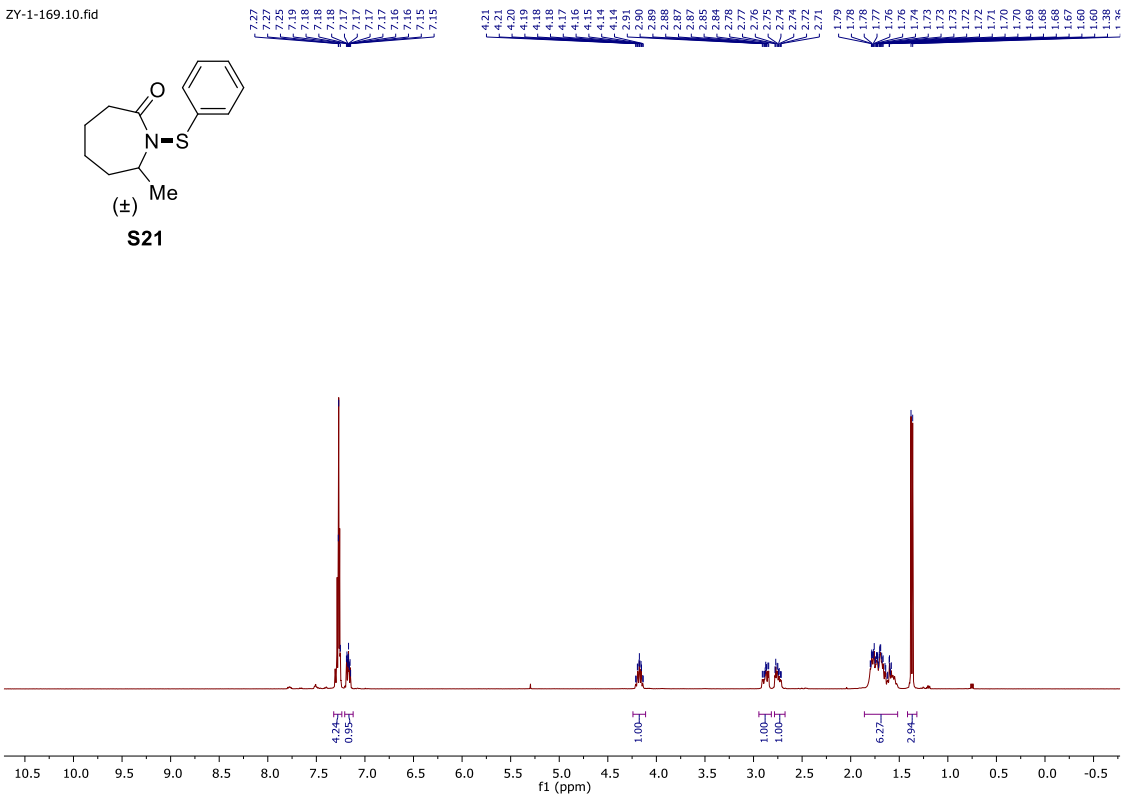

Figure 5.26. ^{13}C NMR Spectrum of S21

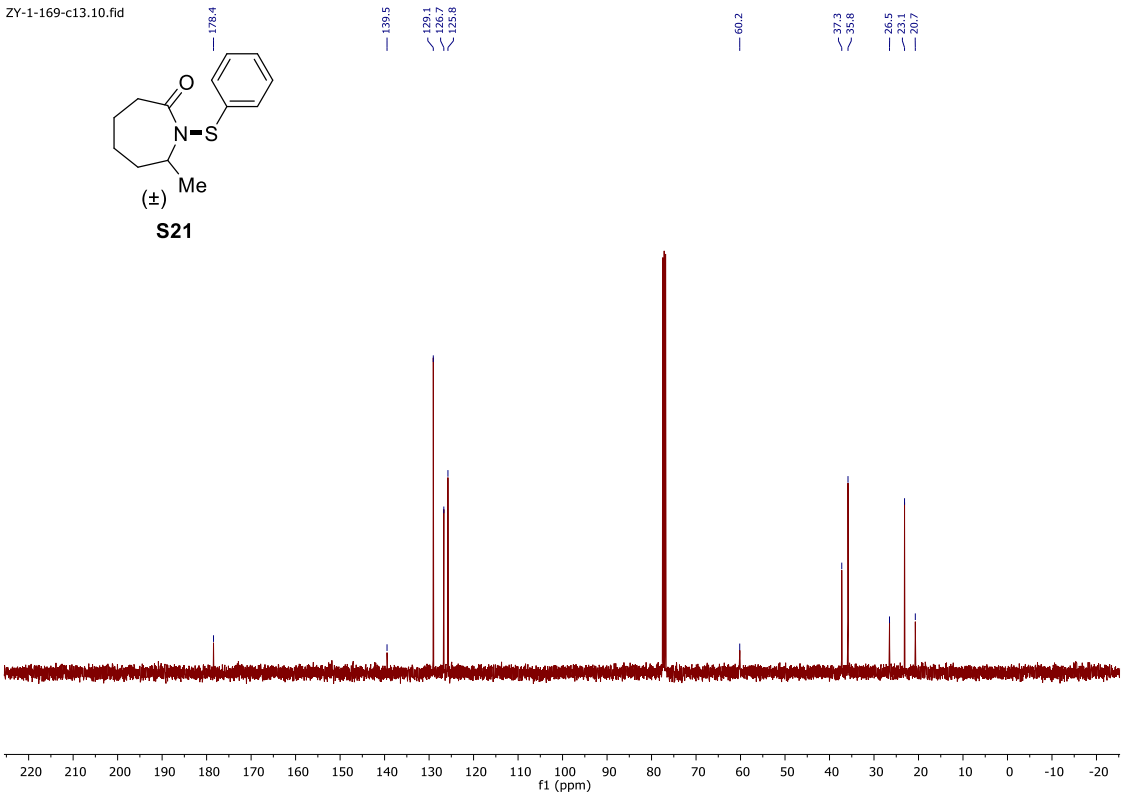

Figure 5.27. ^{1}H NMR Spectrum of 3a

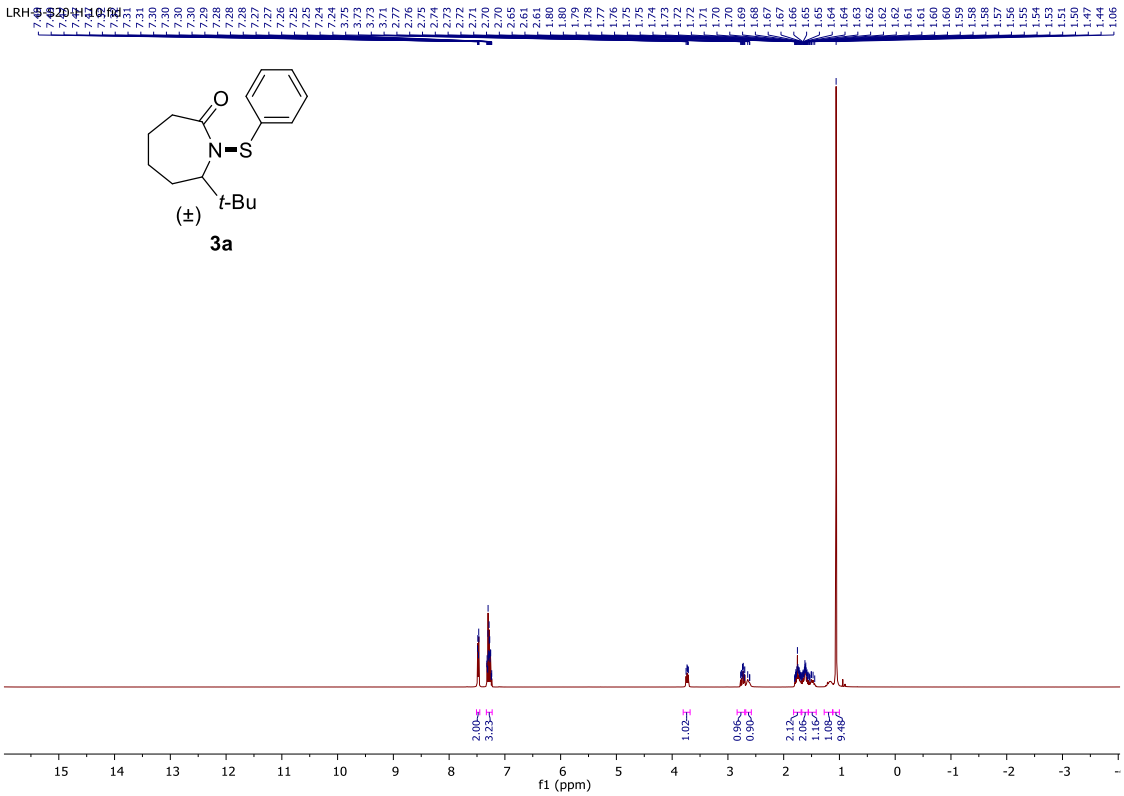

Figure 5.28. ^{13}C NMR Spectrum of 3a

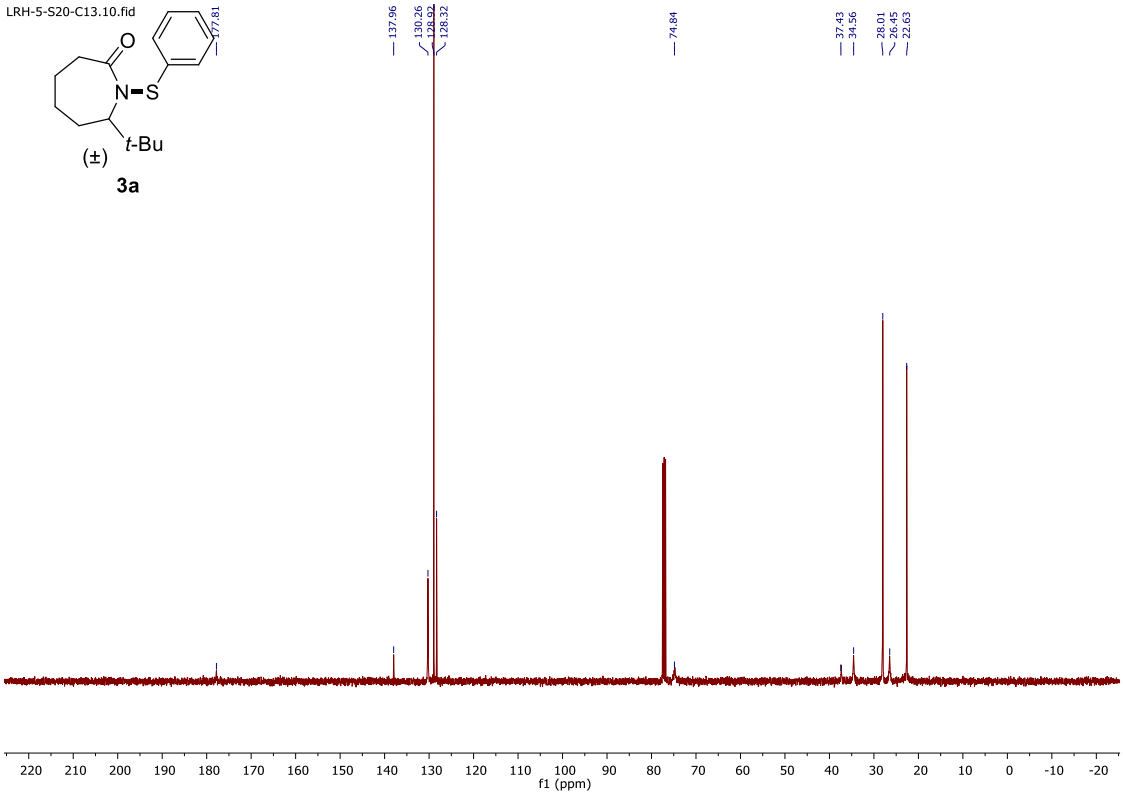

Figure 5.29. ^{1}H NMR Spectrum of 3b

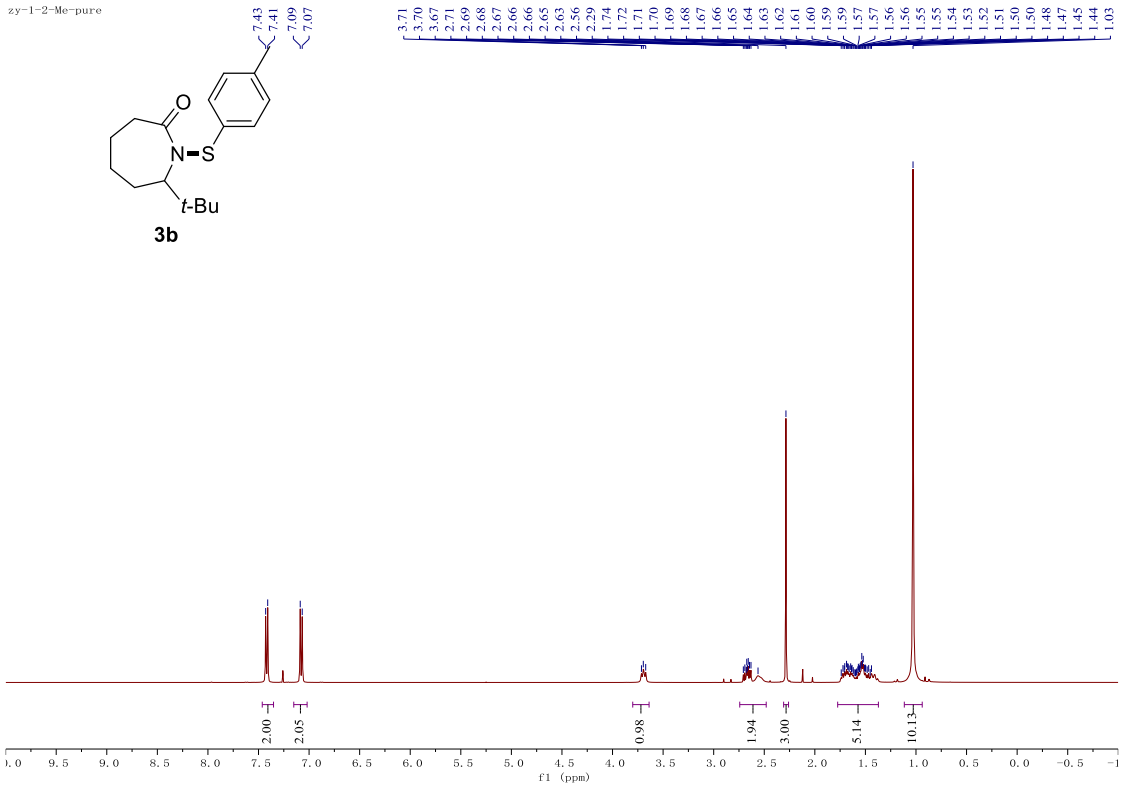

Figure 5.30. ^{13}C NMR Spectrum of 3b

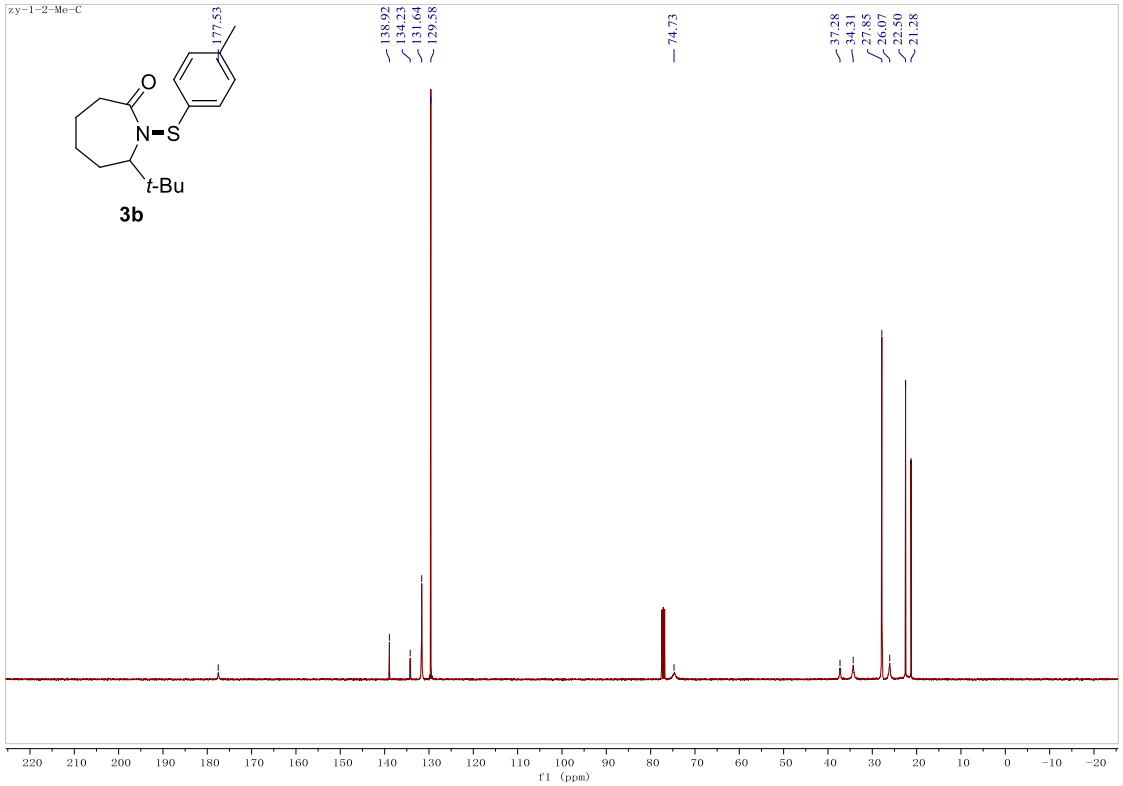

Figure 5.31. ^{1}H NMR Spectrum of 3c

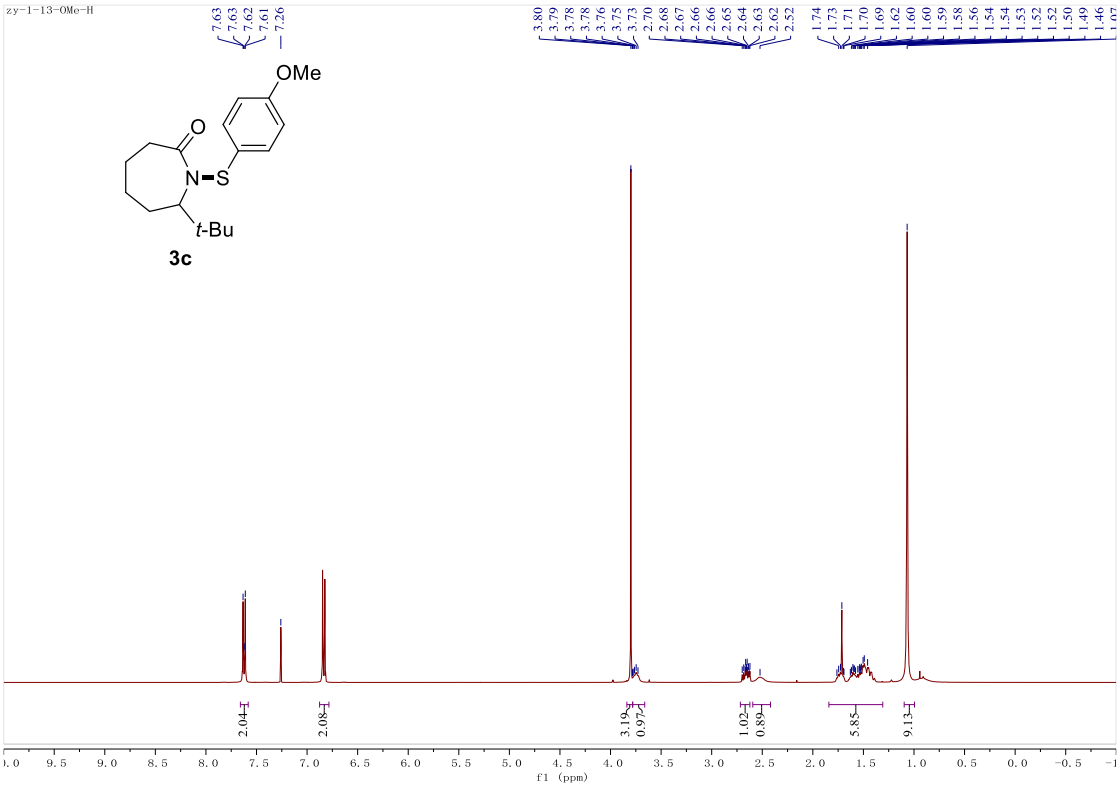

Figure 5.32. ^{13}C NMR Spectrum of 3c

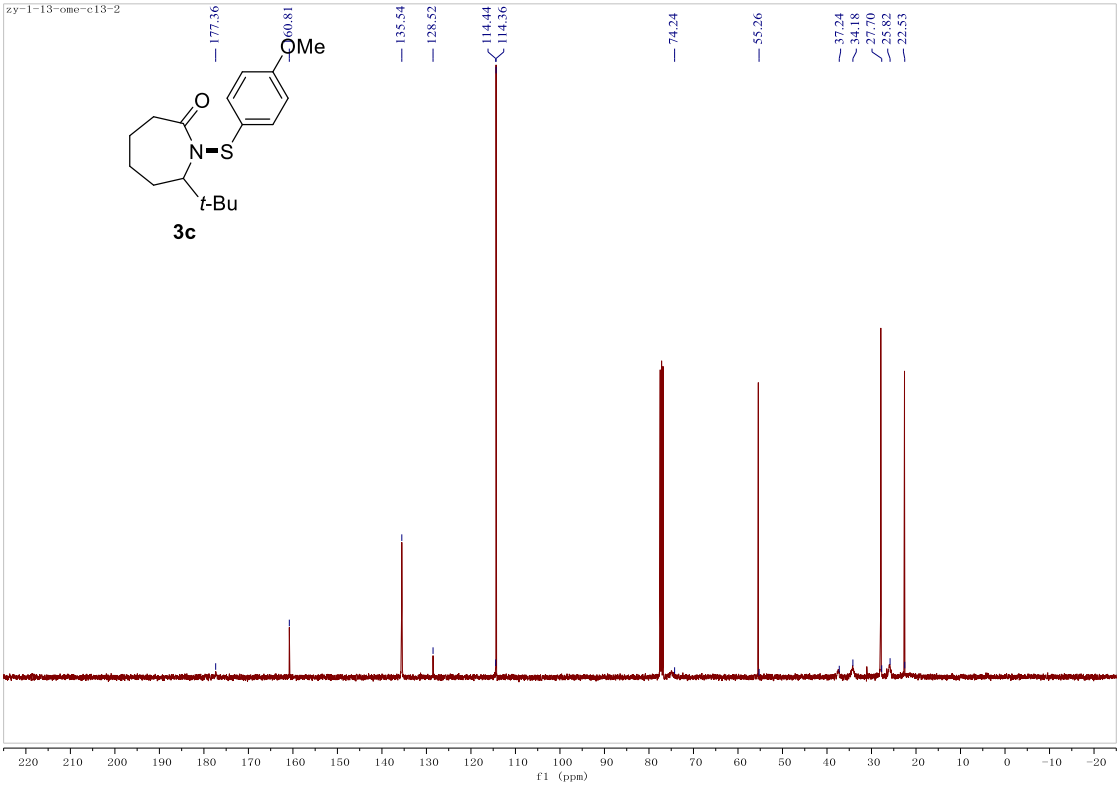

Figure 5.33. ^{1}H NMR Spectrum of 3d

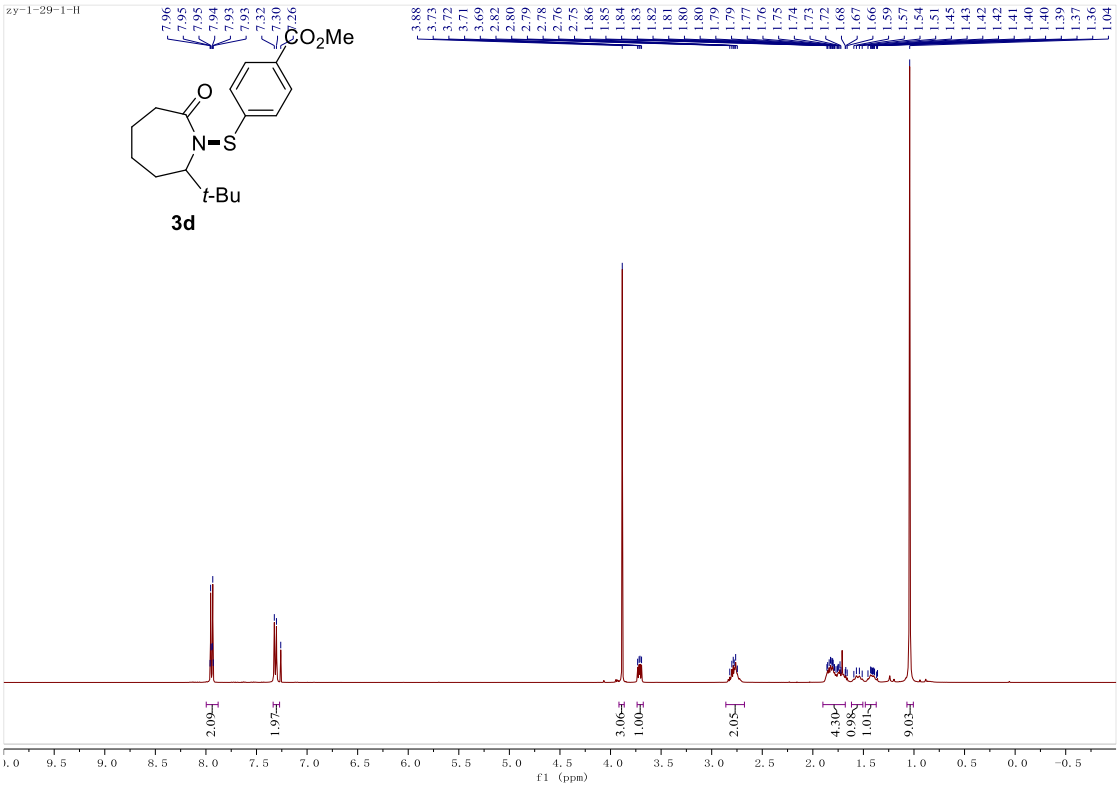

Figure 5.34. ^{13}C NMR Spectrum of 3d

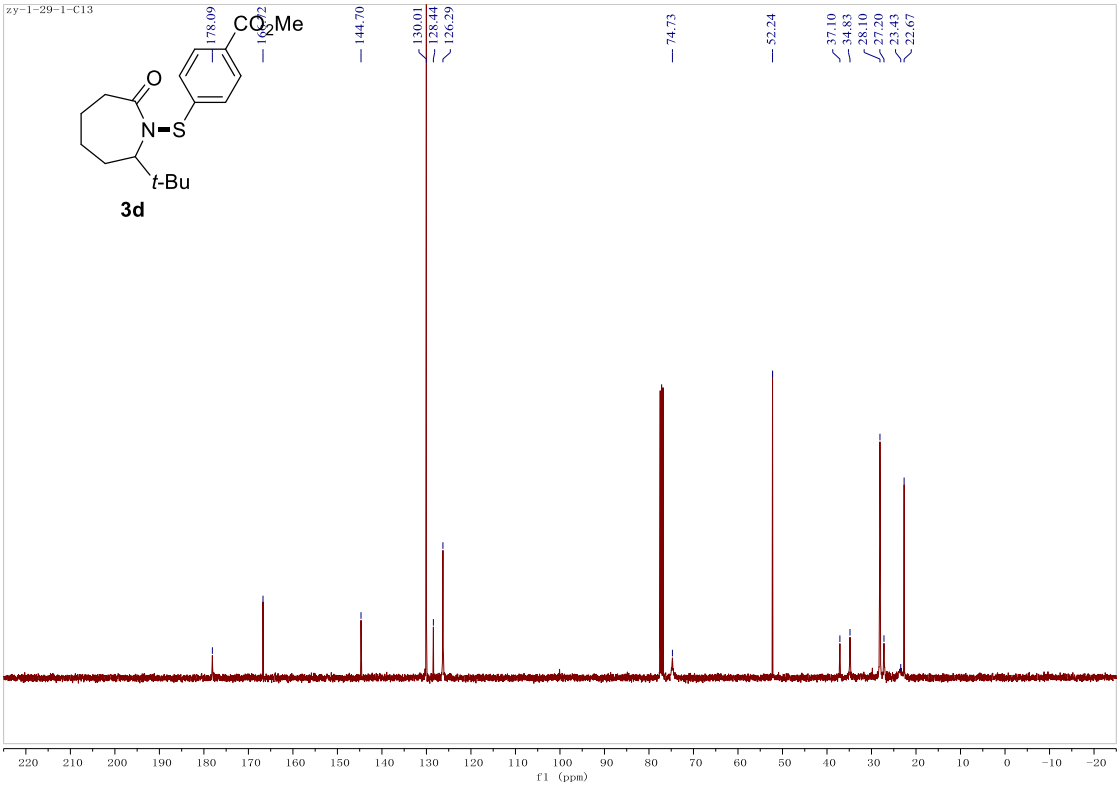

Figure 5.35. ^{1}H NMR Spectrum of 3e

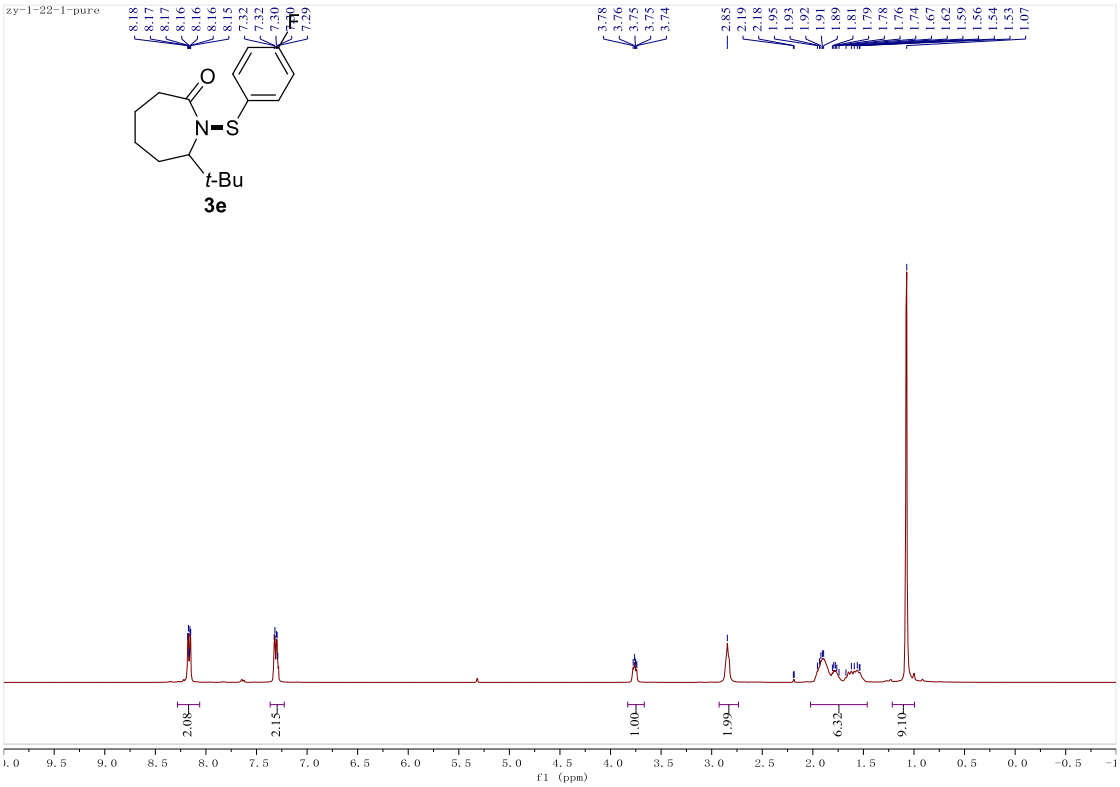

Figure 5.36. ^{13}C NMR Spectrum of 3e

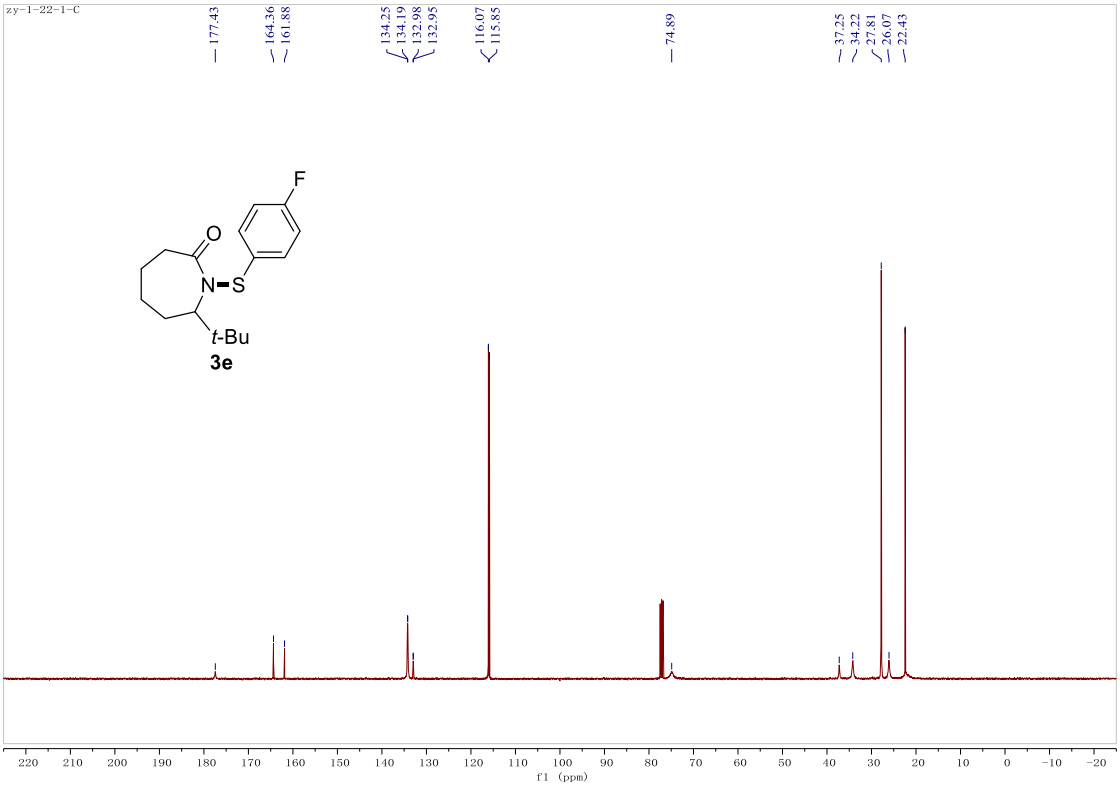

Figure 5.37. ^{1}H NMR Spectrum of 3f

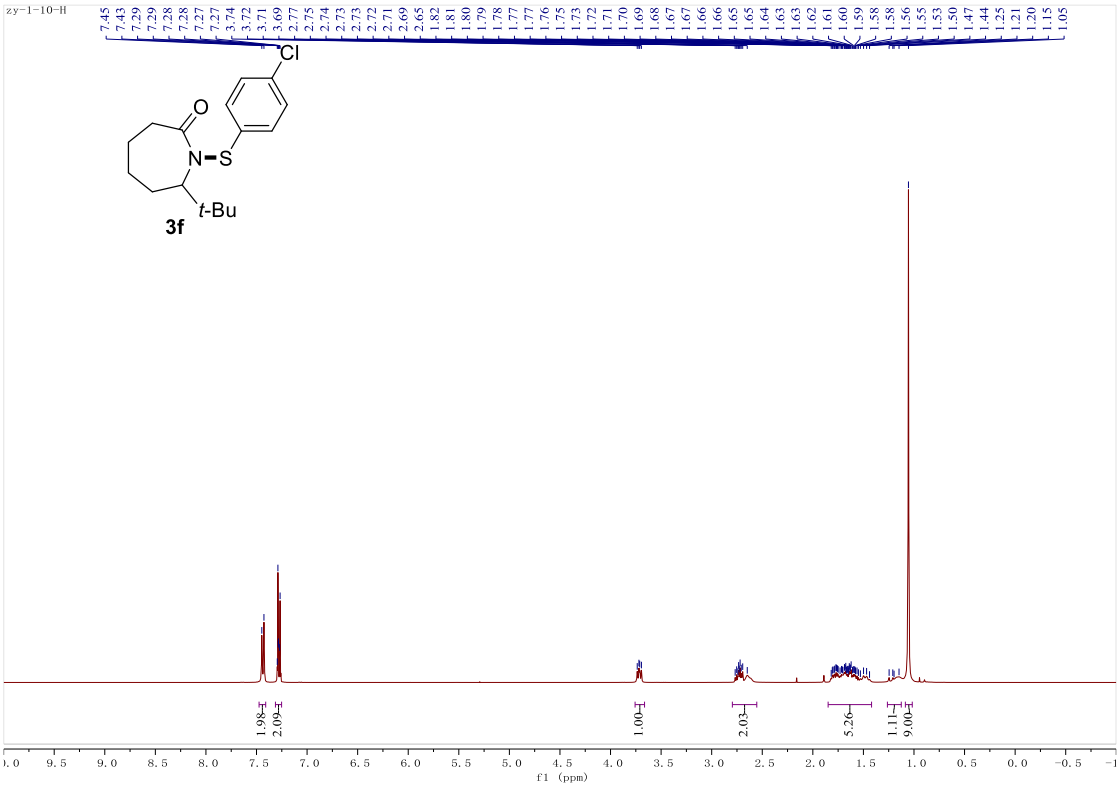

Figure 5.38. ^{13}C NMR Spectrum of 3f

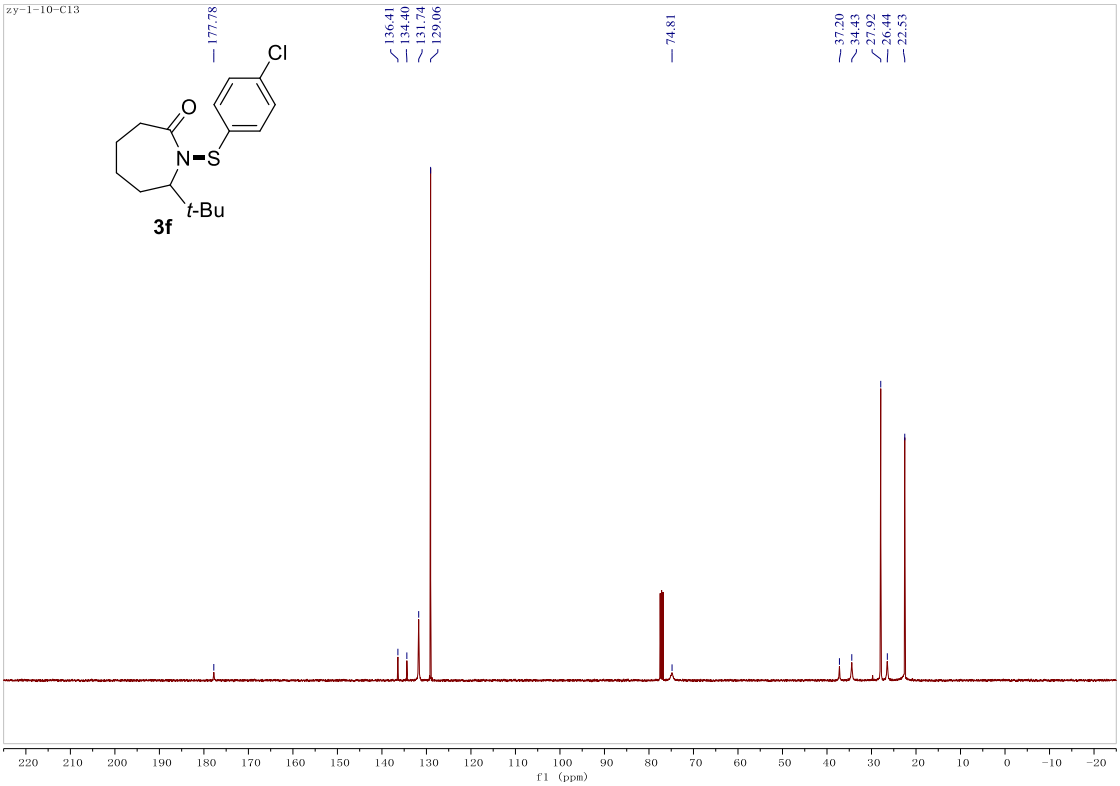

Figure 5.39. ^{1}H NMR Spectrum of 3g

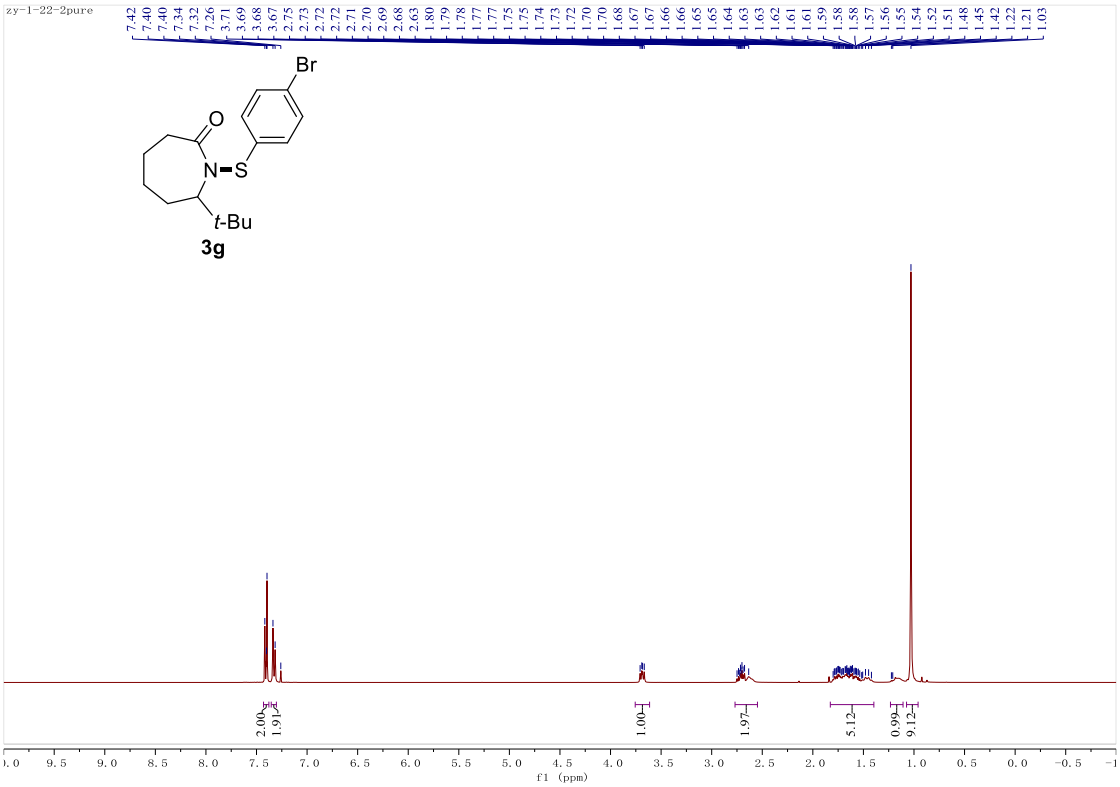

Figure 5.40. ^{13}C NMR Spectrum of 3g

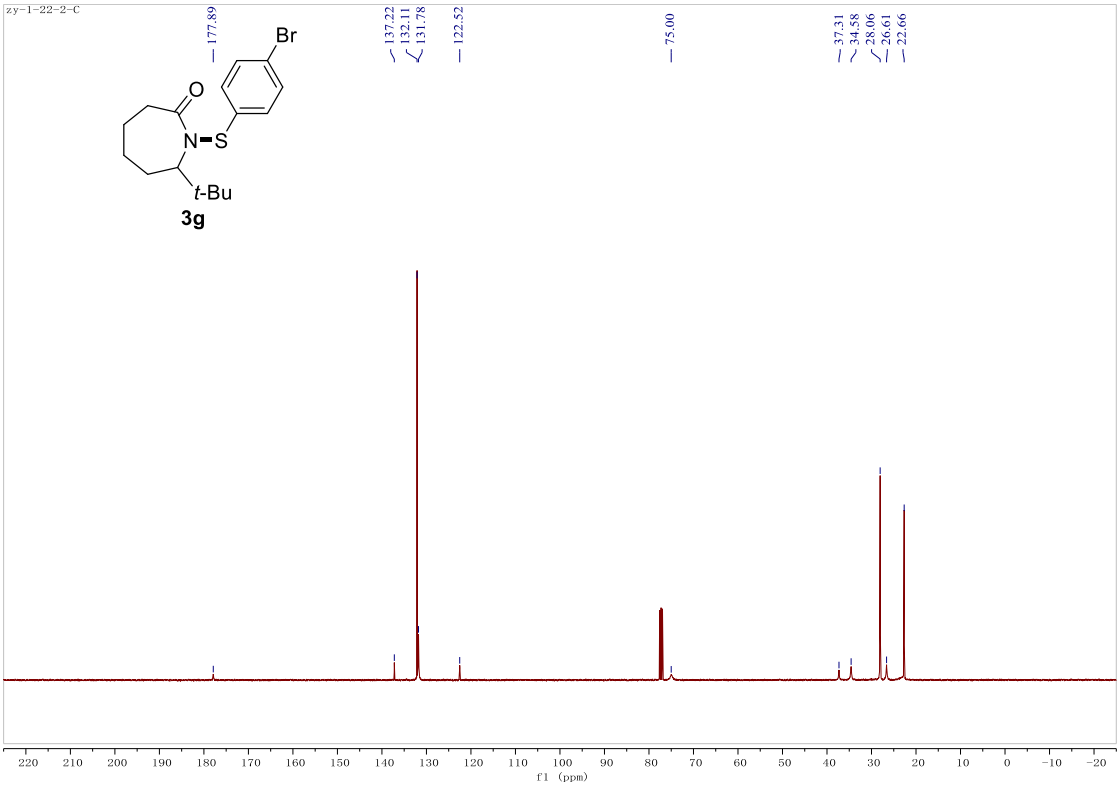

Figure 5.41. ^{1}H NMR Spectrum of 3h

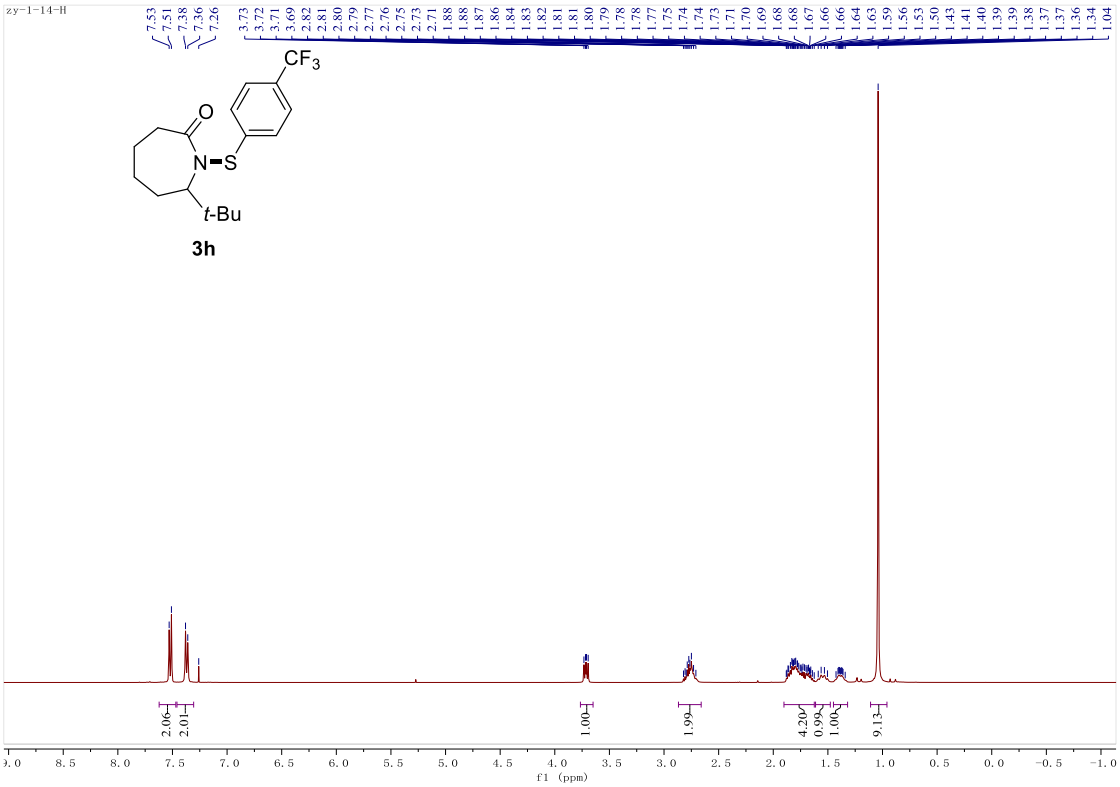

Figure 5.42. ^{13}C NMR Spectrum of 3h

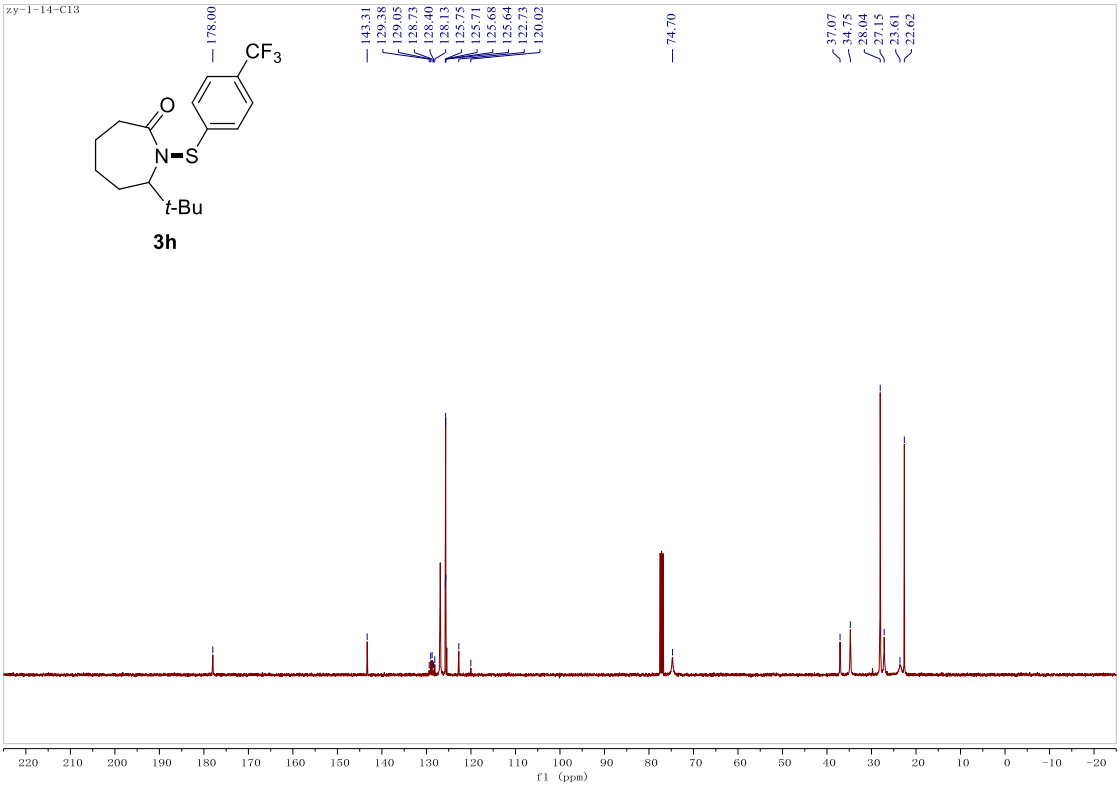

Figure 5.43. ^{1}H NMR Spectrum of 3i

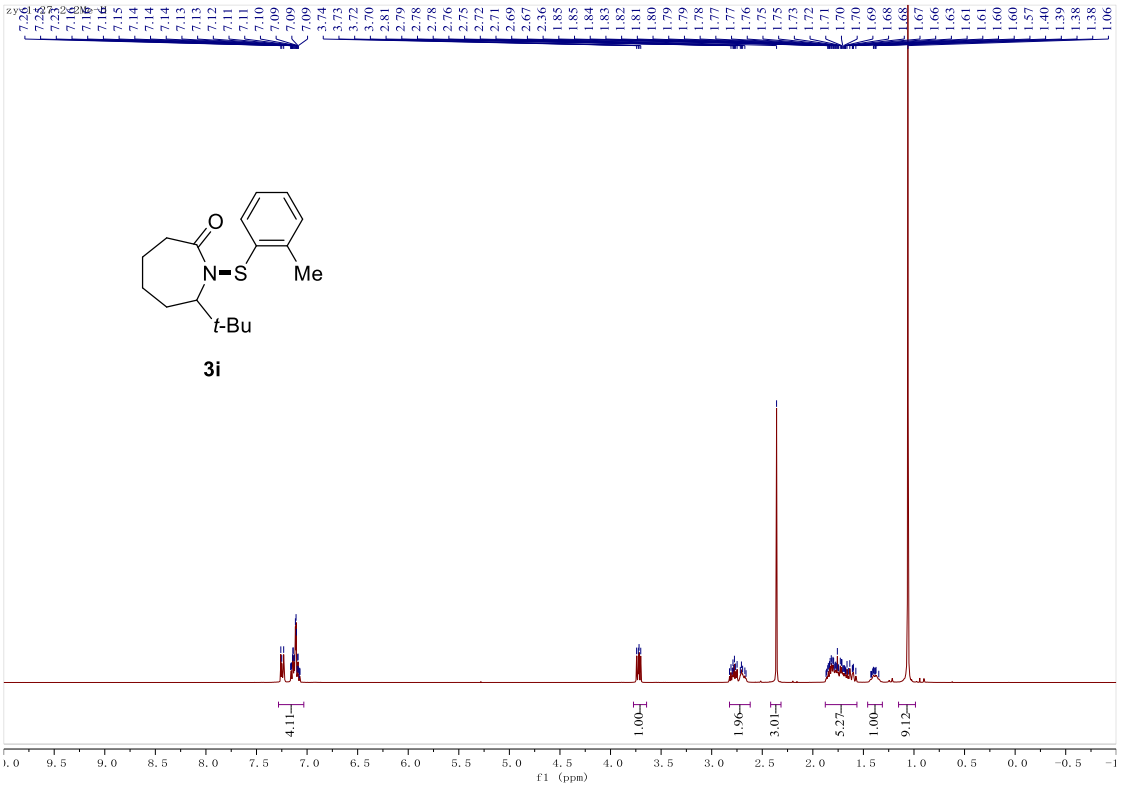

Figure 5.44. ^{13}C NMR Spectrum of 3i

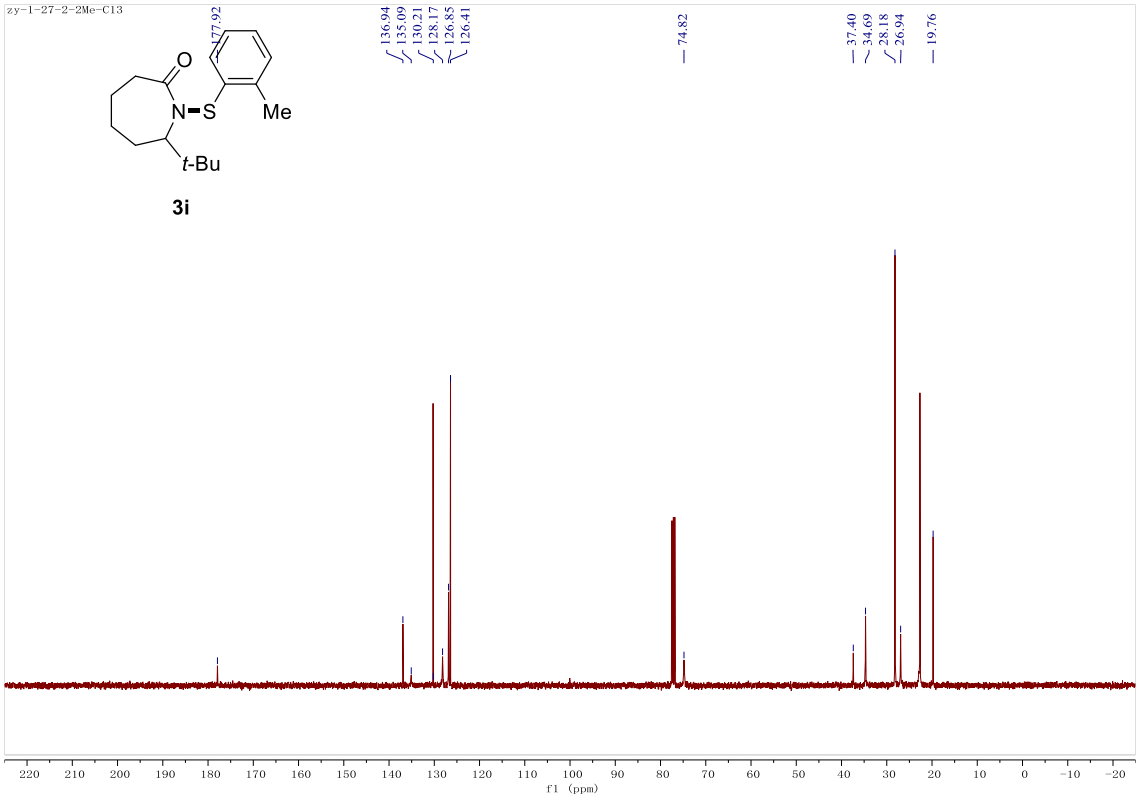

Figure 5.45. ^{1}H NMR Spectrum of 3j

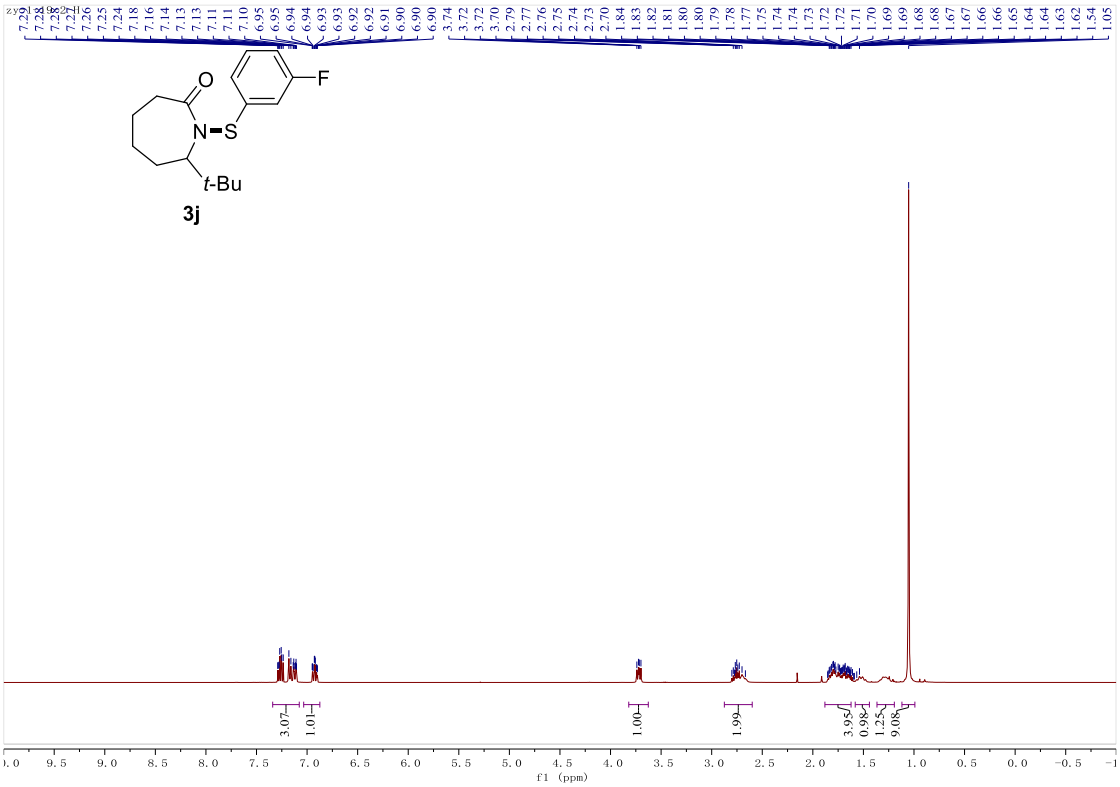

Figure 5.46. ^{13}C NMR Spectrum of 3j

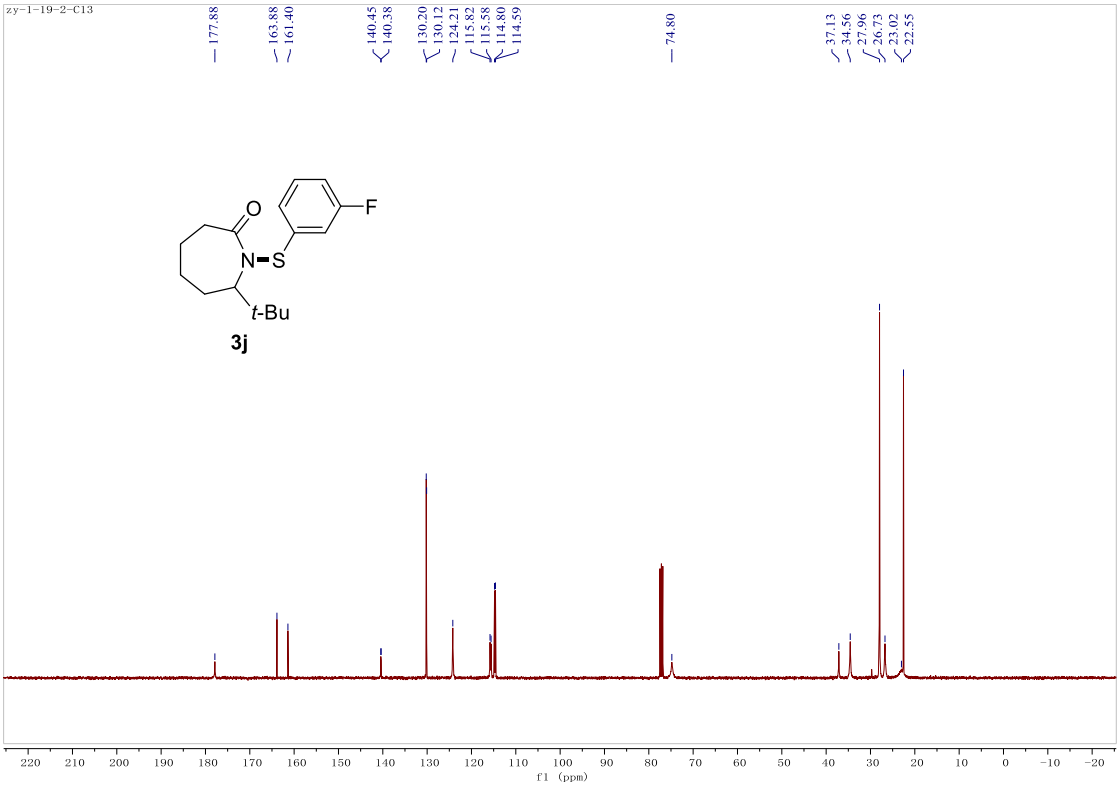

Figure 5.47. ^{1}H NMR Spectrum of 3k

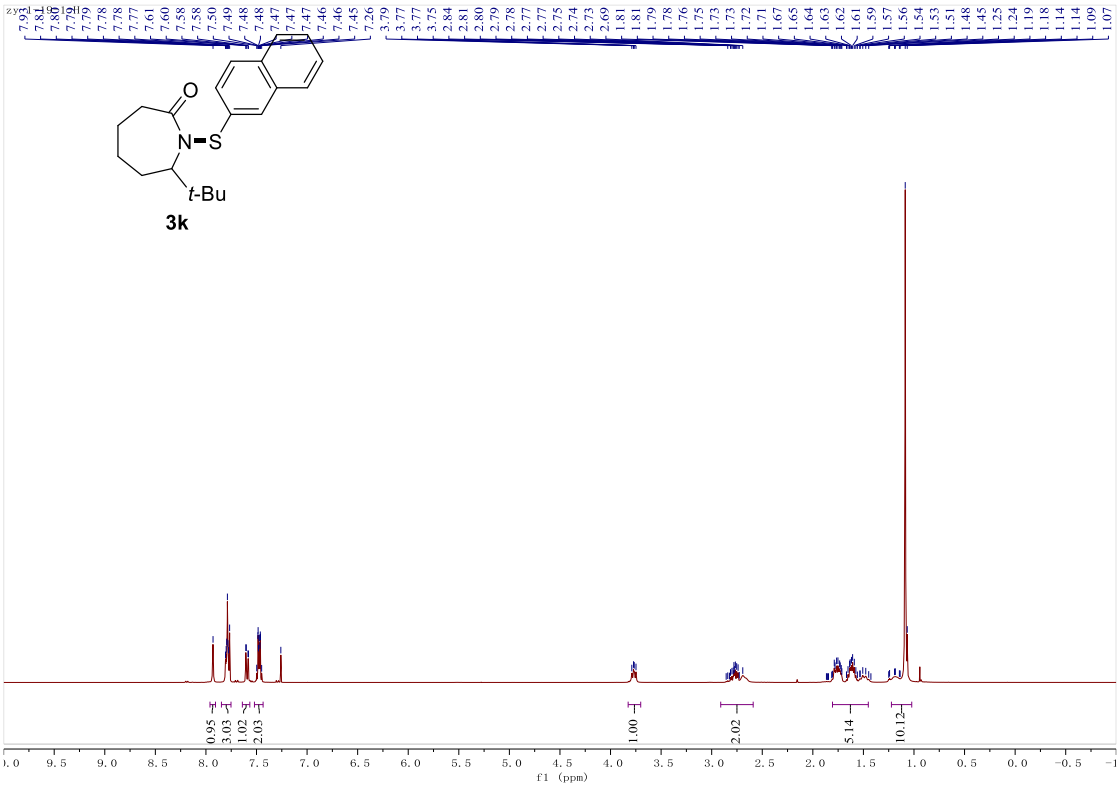

Figure 5.48. ^{13}C NMR Spectrum of 3k

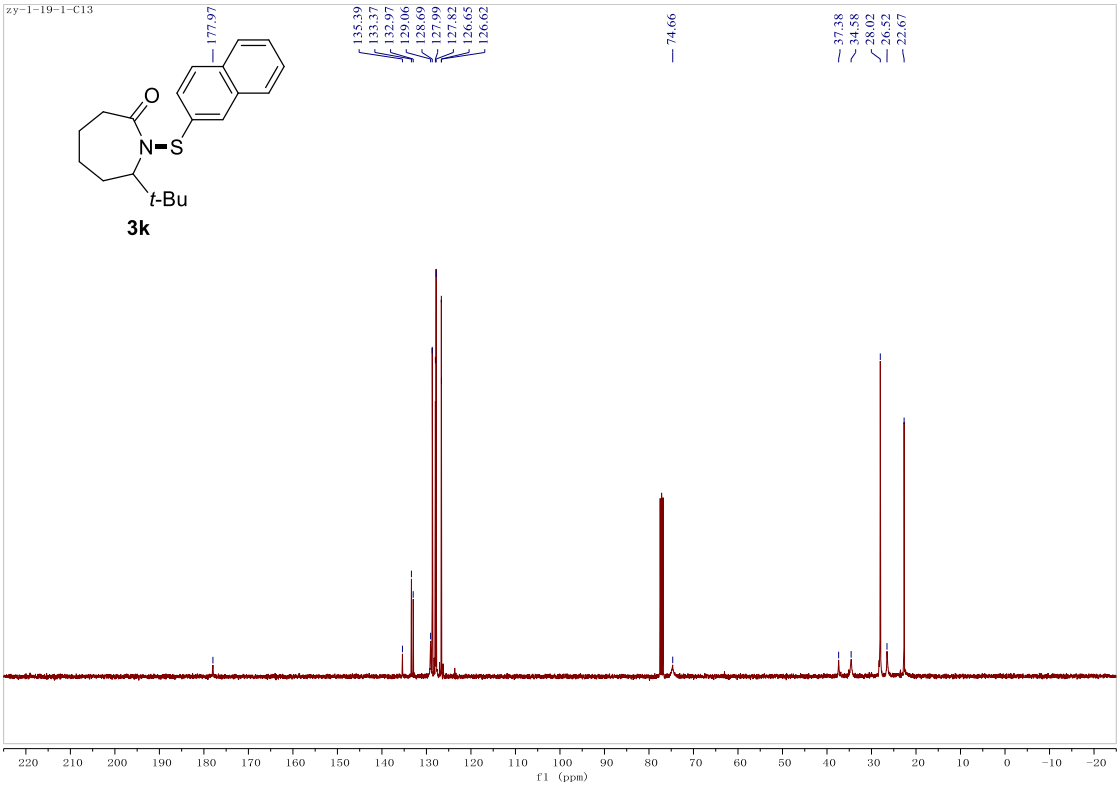

Figure 5.49. ^{1}H NMR Spectrum of 1n

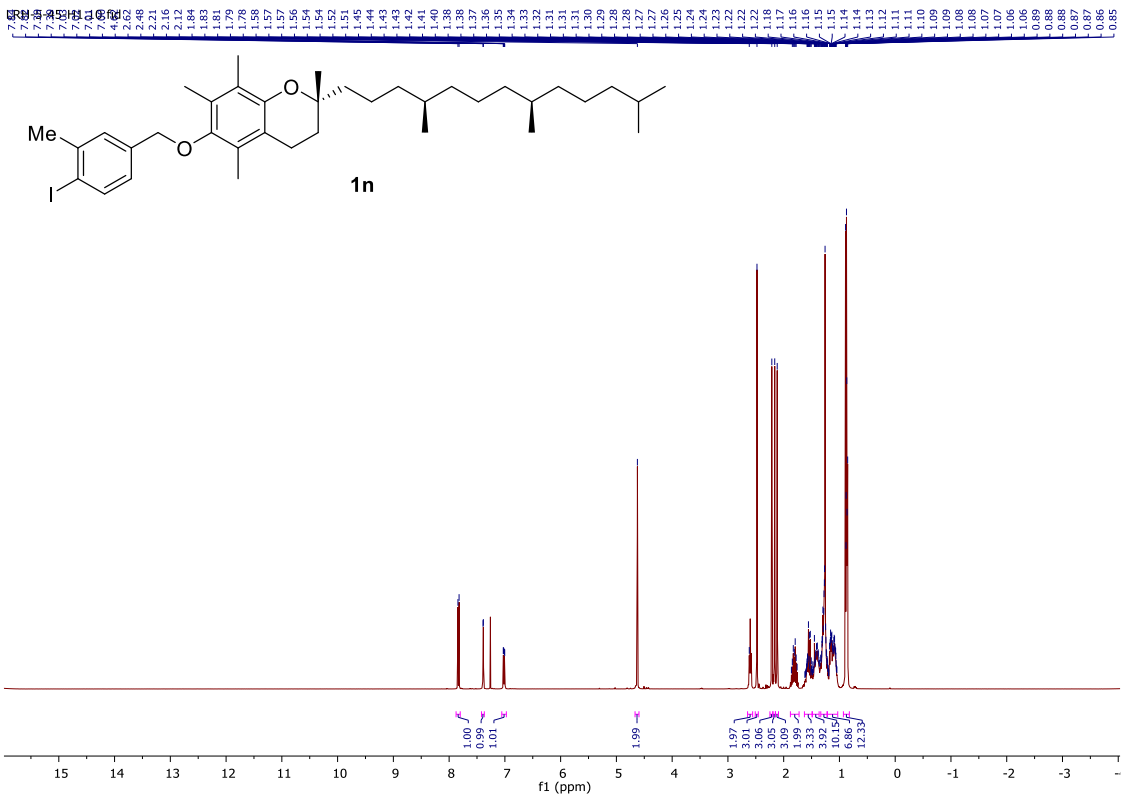

Figure 5.50. ^{13}C NMR Spectrum of 1n

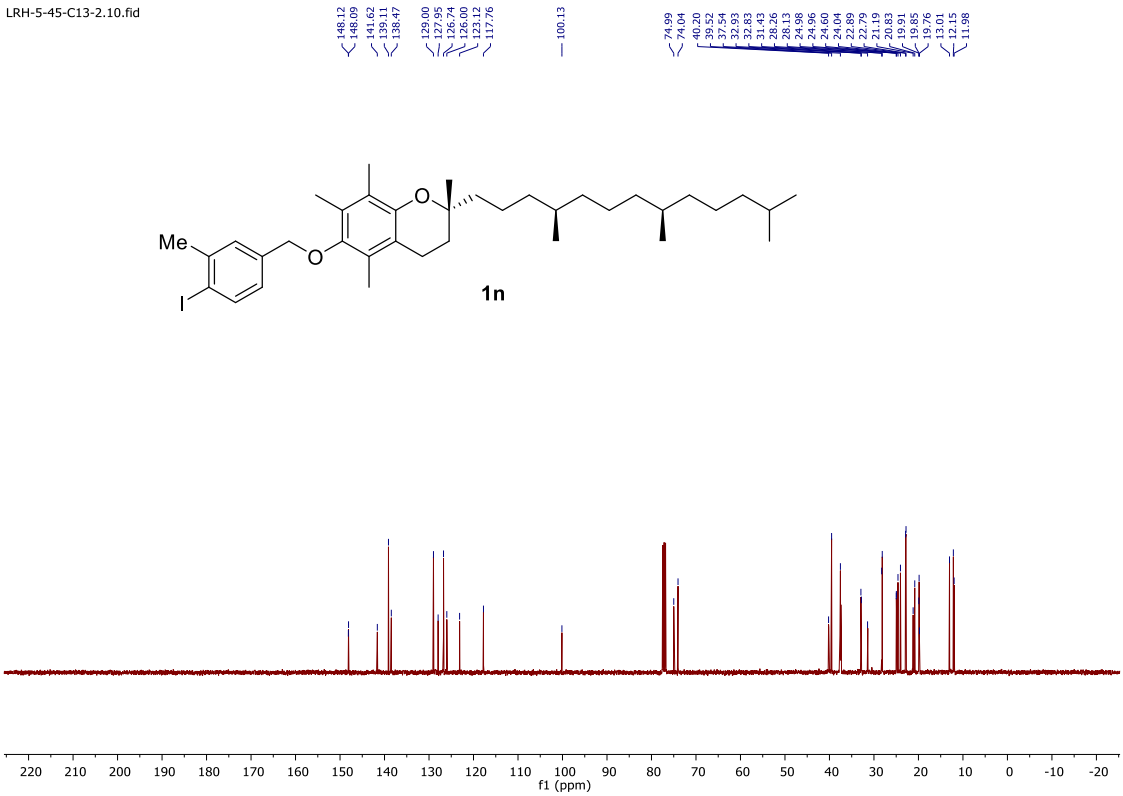

Figure 5.51. ^{1}H NMR Spectrum of 1r

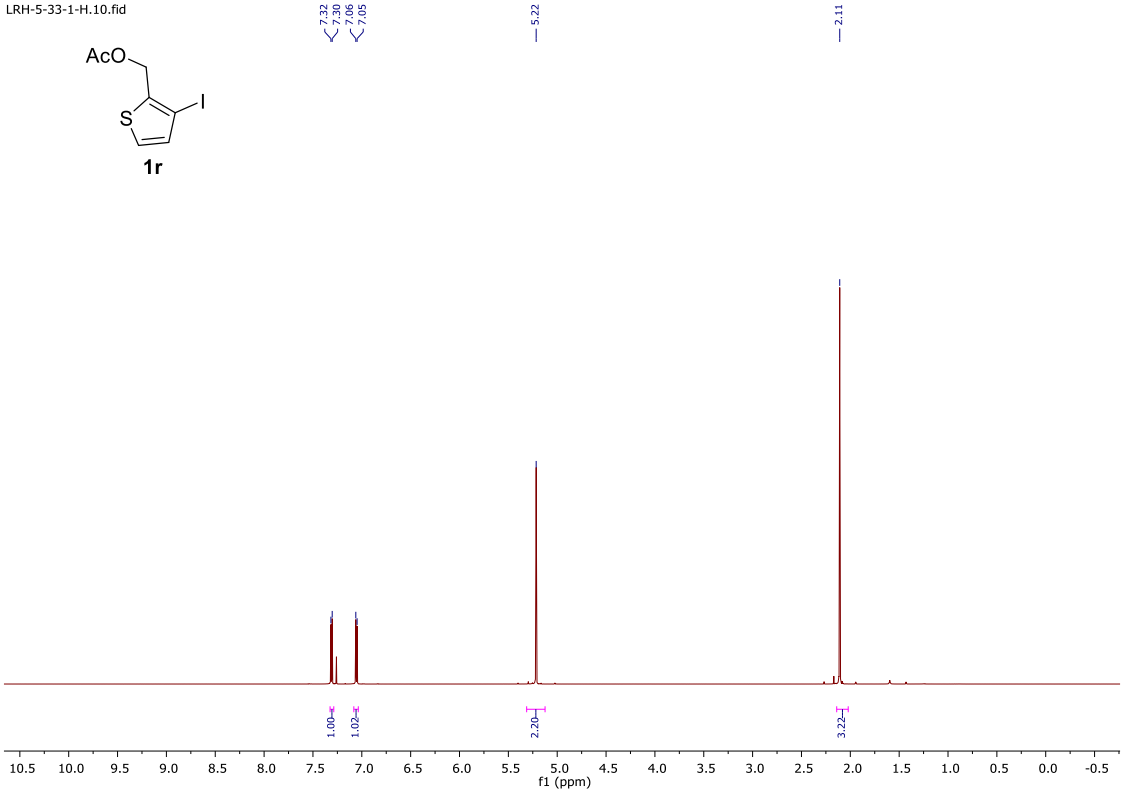

Figure 5.52. ^{13}C NMR Spectrum of 1r

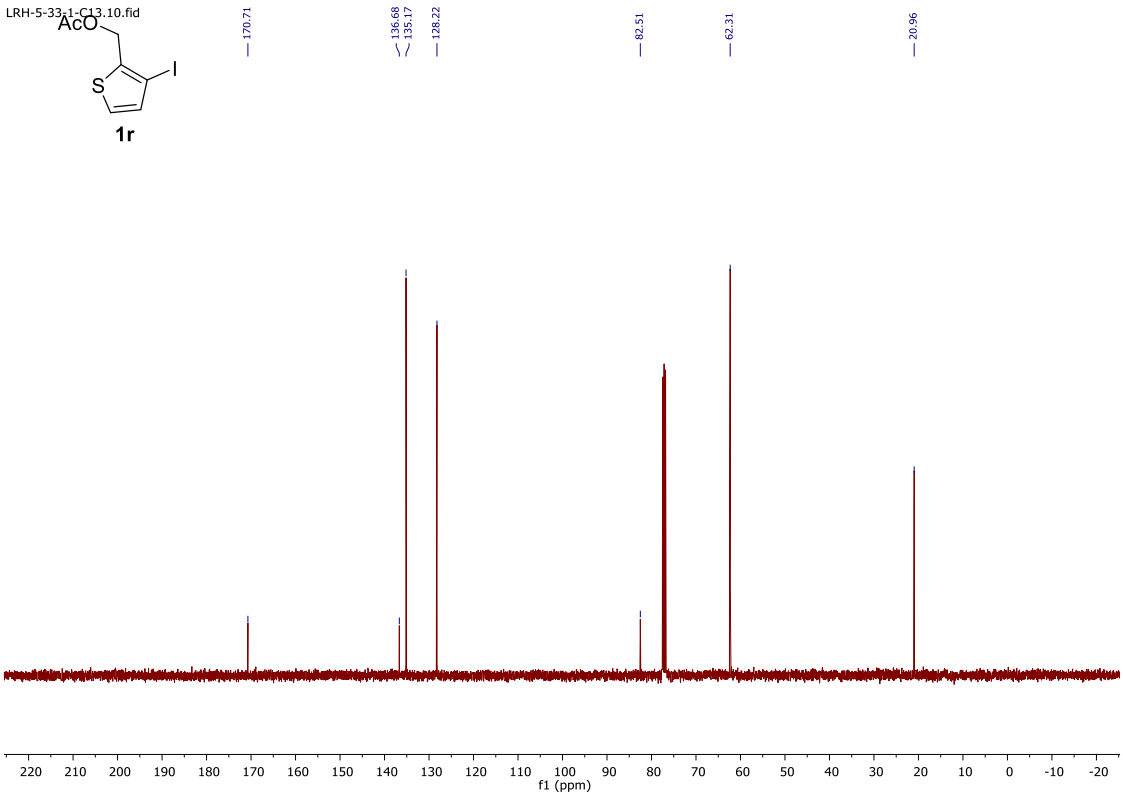

Figure 5.53. ^{1}H NMR Spectrum of 4a

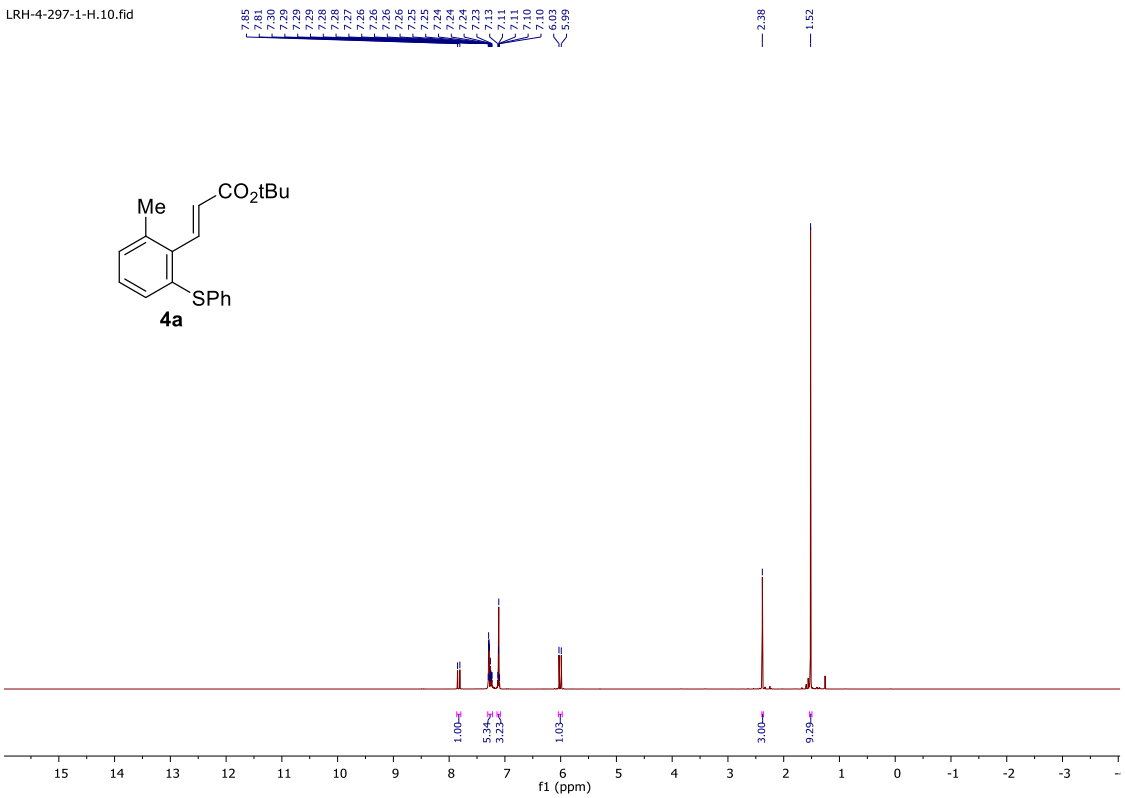

Figure 5.54. ^{13}C NMR Spectrum of 4a

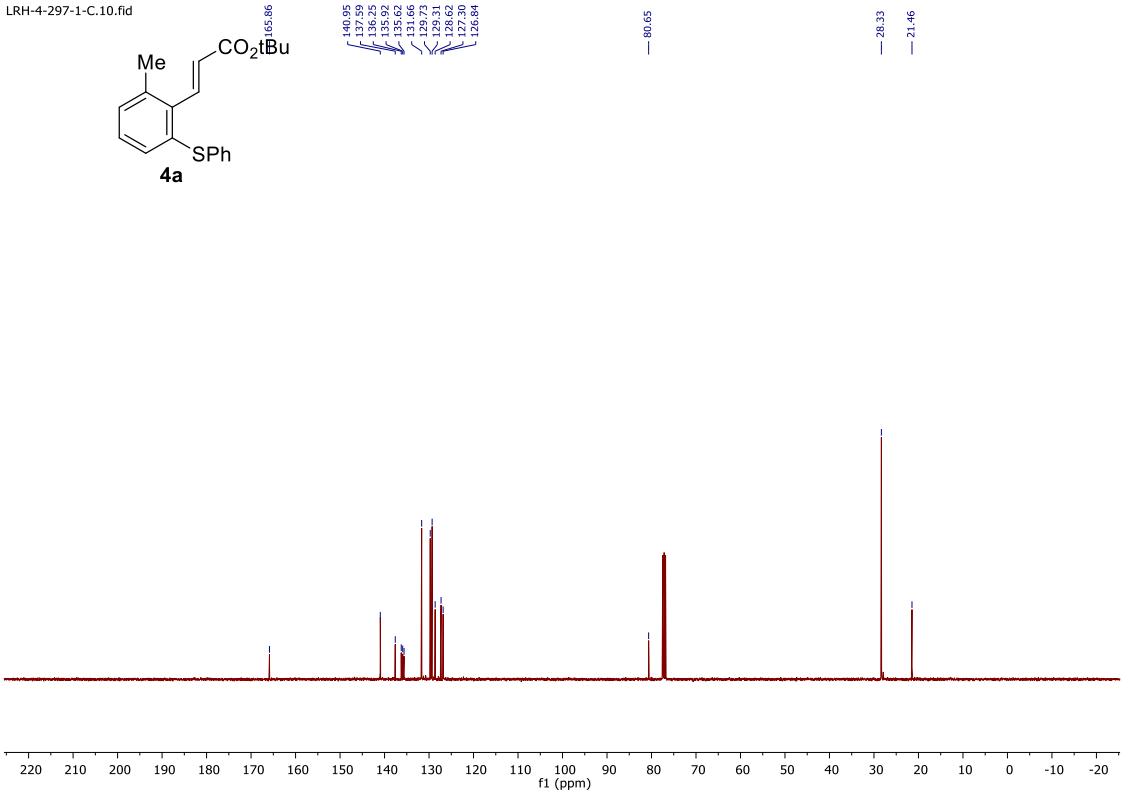

Figure 5.55. ^{1}H NMR Spectrum of 4b

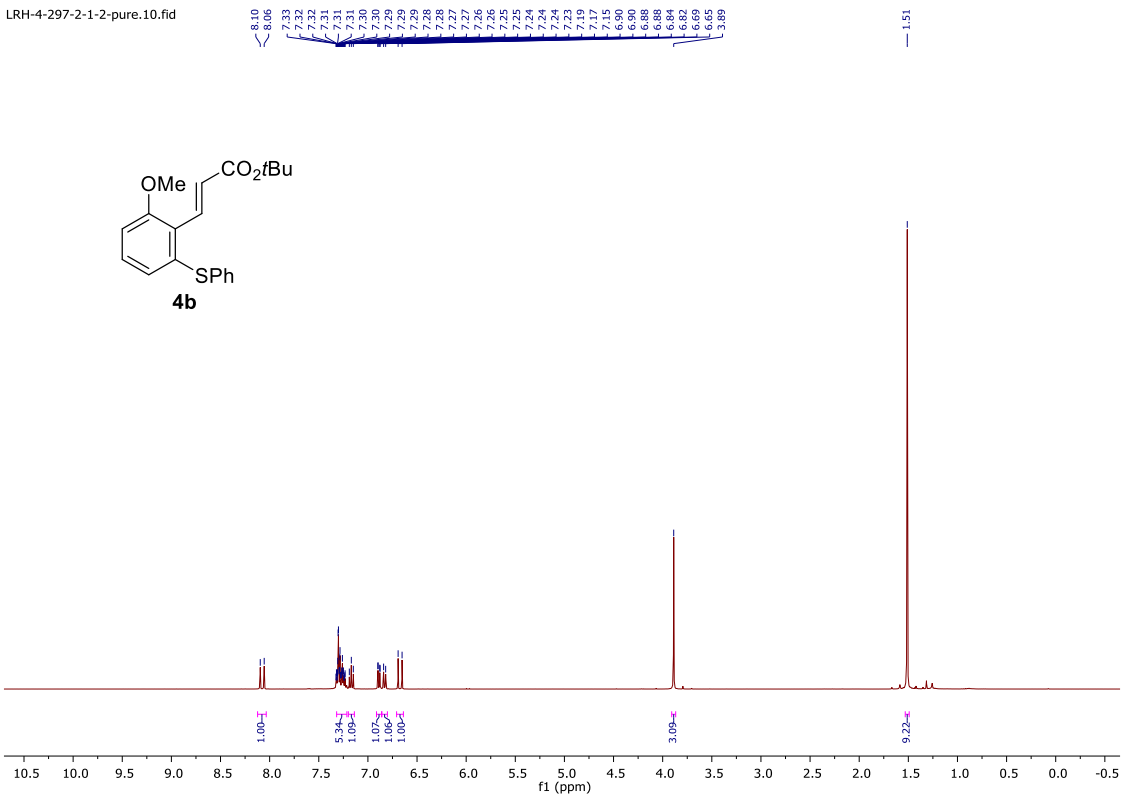

Figure 5.56. ^{13}C NMR Spectrum of 4b

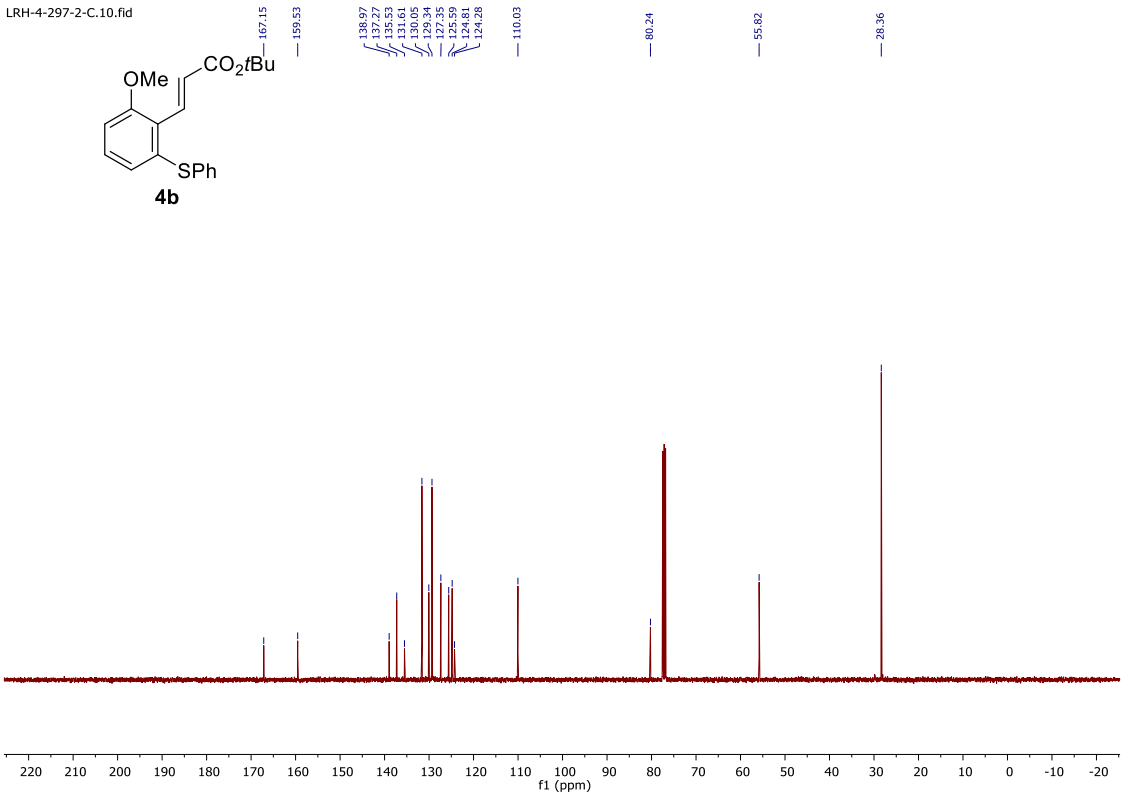

Figure 5.57. ^{1}H NMR Spectrum of 4c

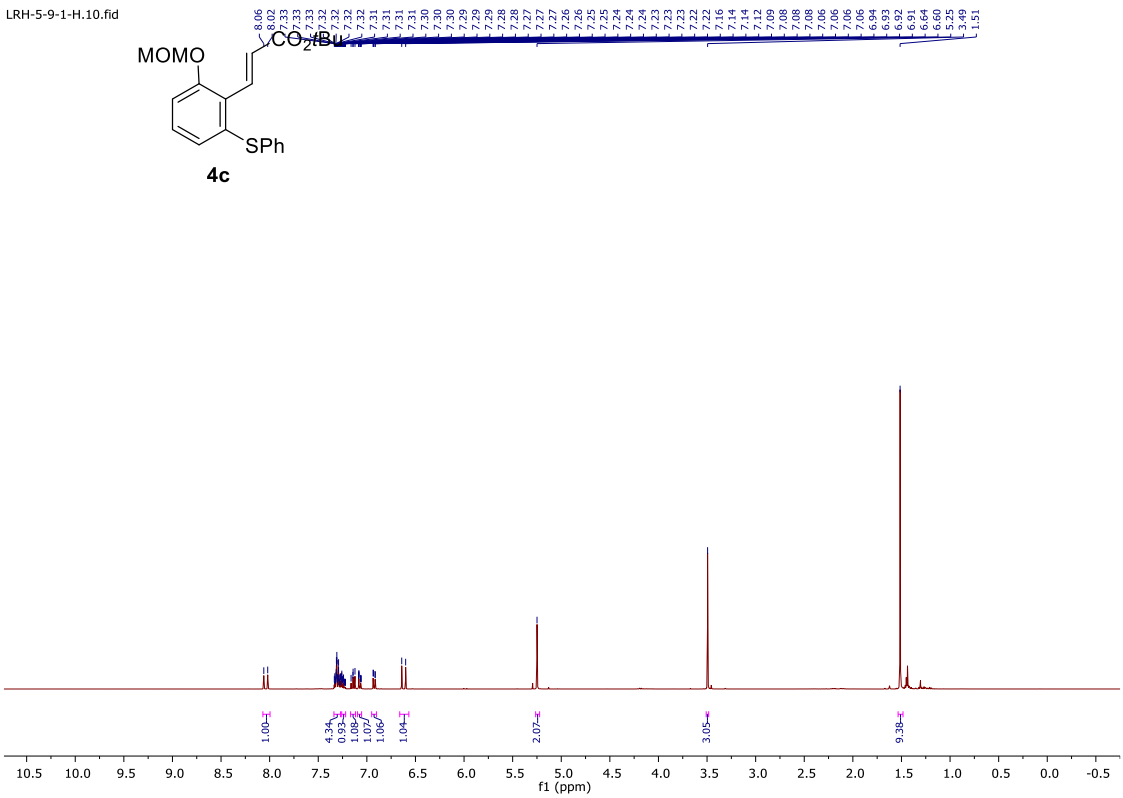

Figure 5.58. ^{13}C NMR Spectrum of 4c

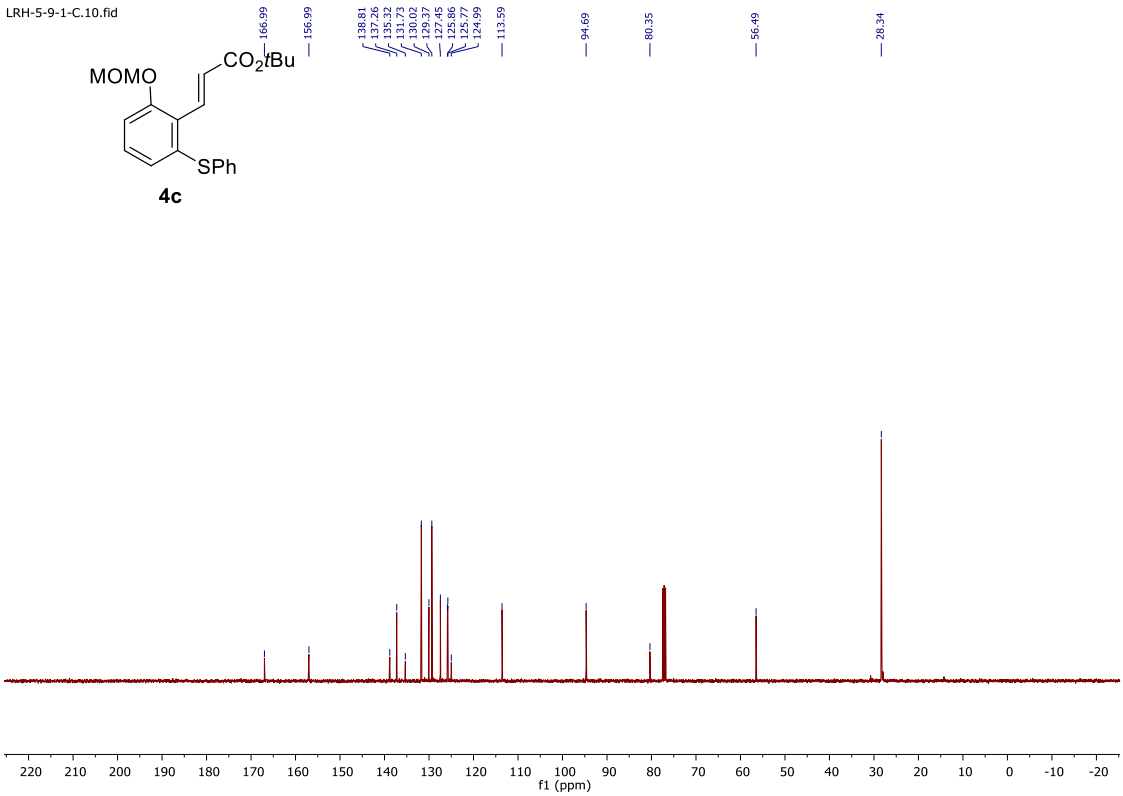

Figure 5.59. ^{1}H NMR Spectrum of 4d

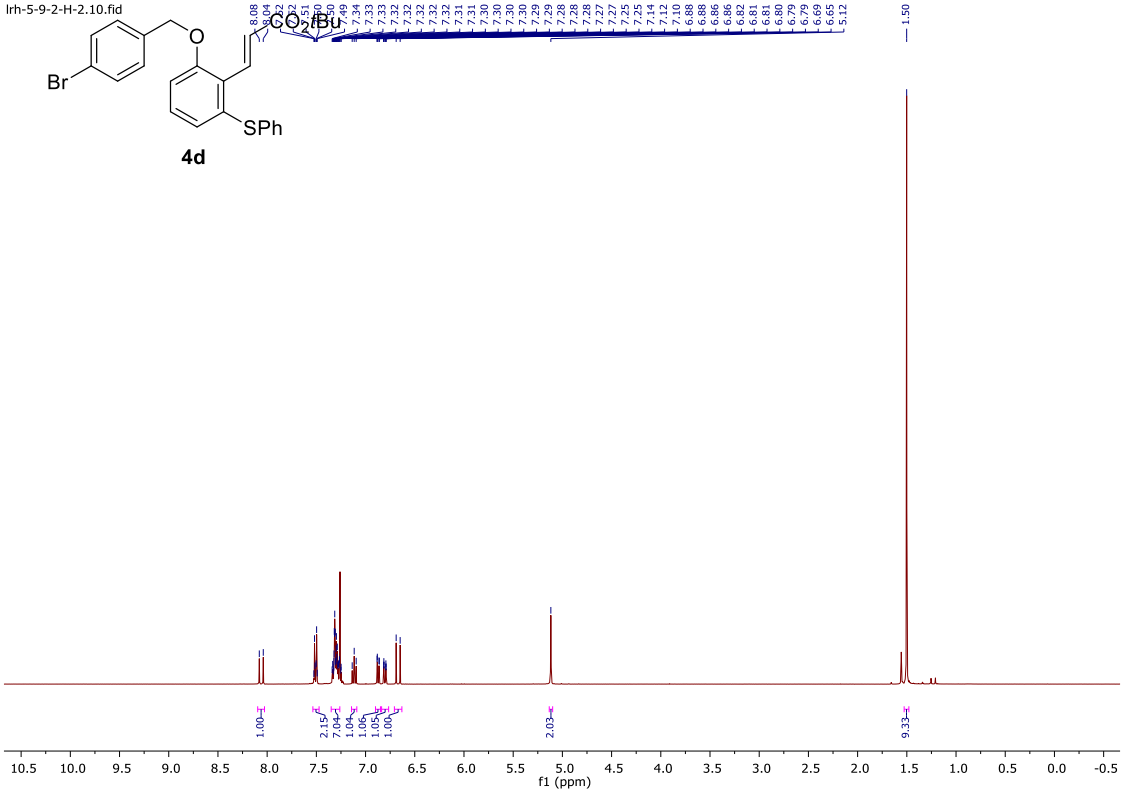

Figure 5.60. ^{13}C NMR Spectrum of 4d

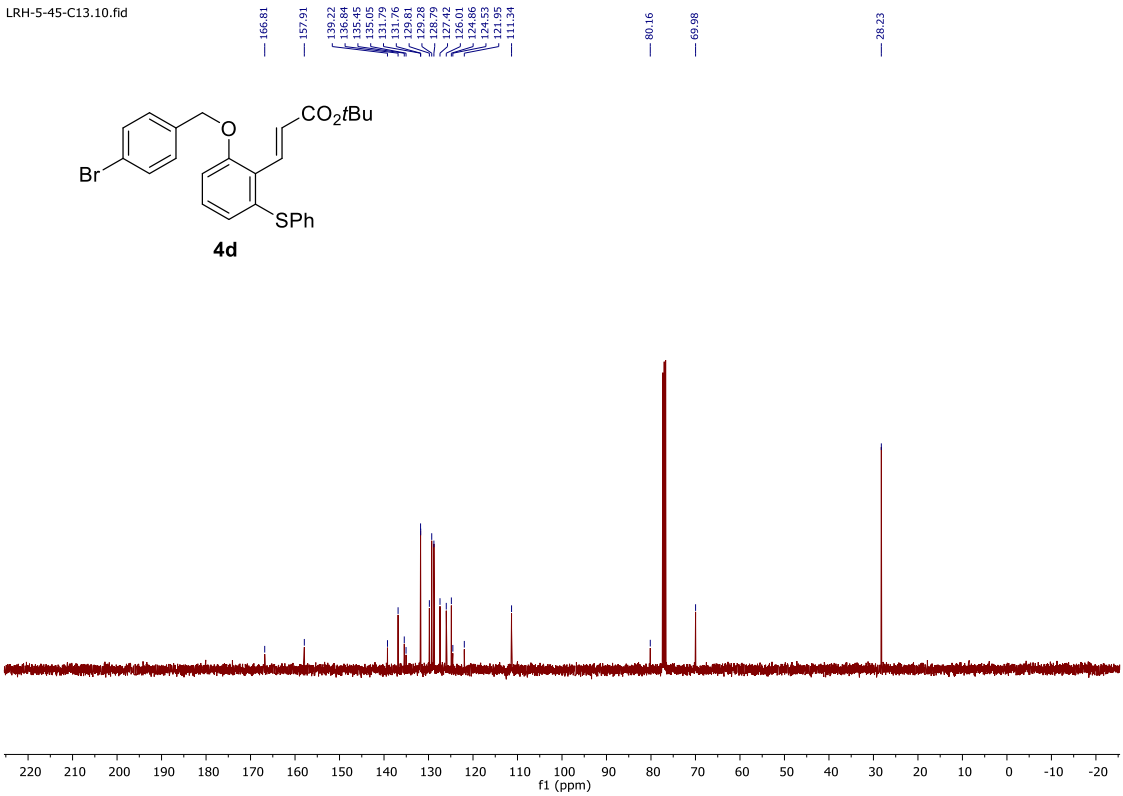

Figure 5.61. ^{1}H NMR Spectrum of 4e

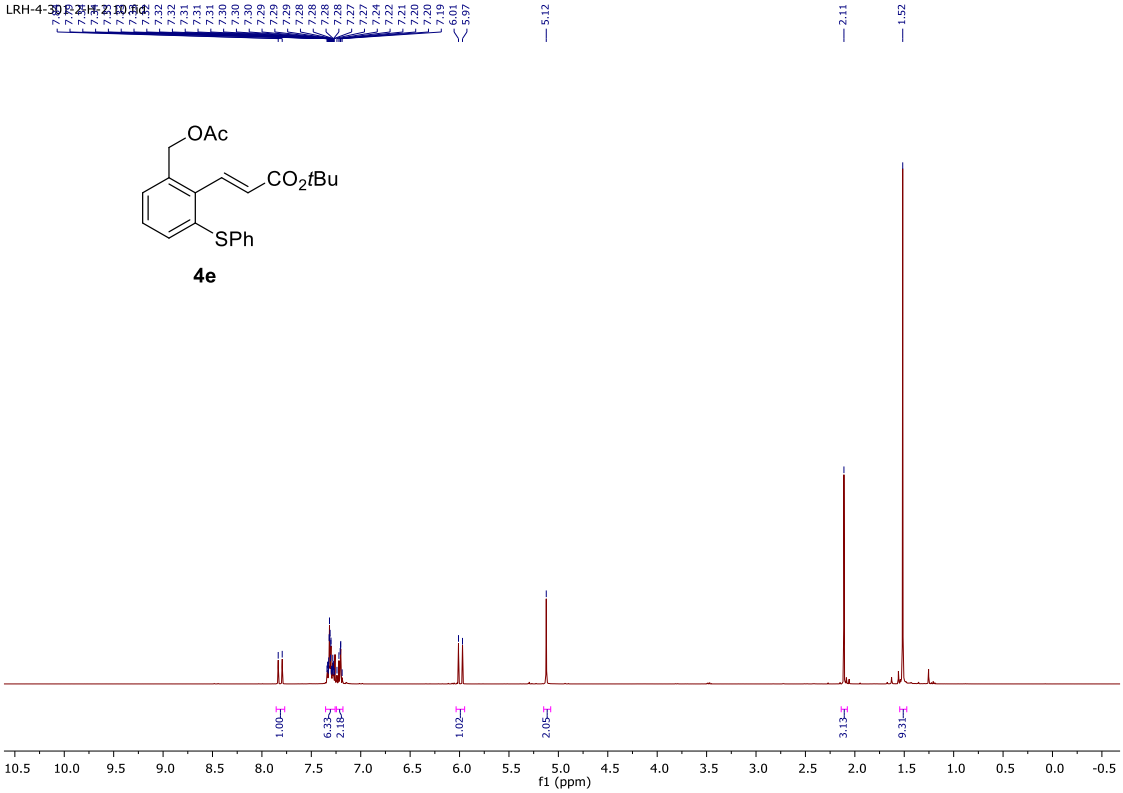

Figure 5.62. ^{13}C NMR Spectrum of 4e

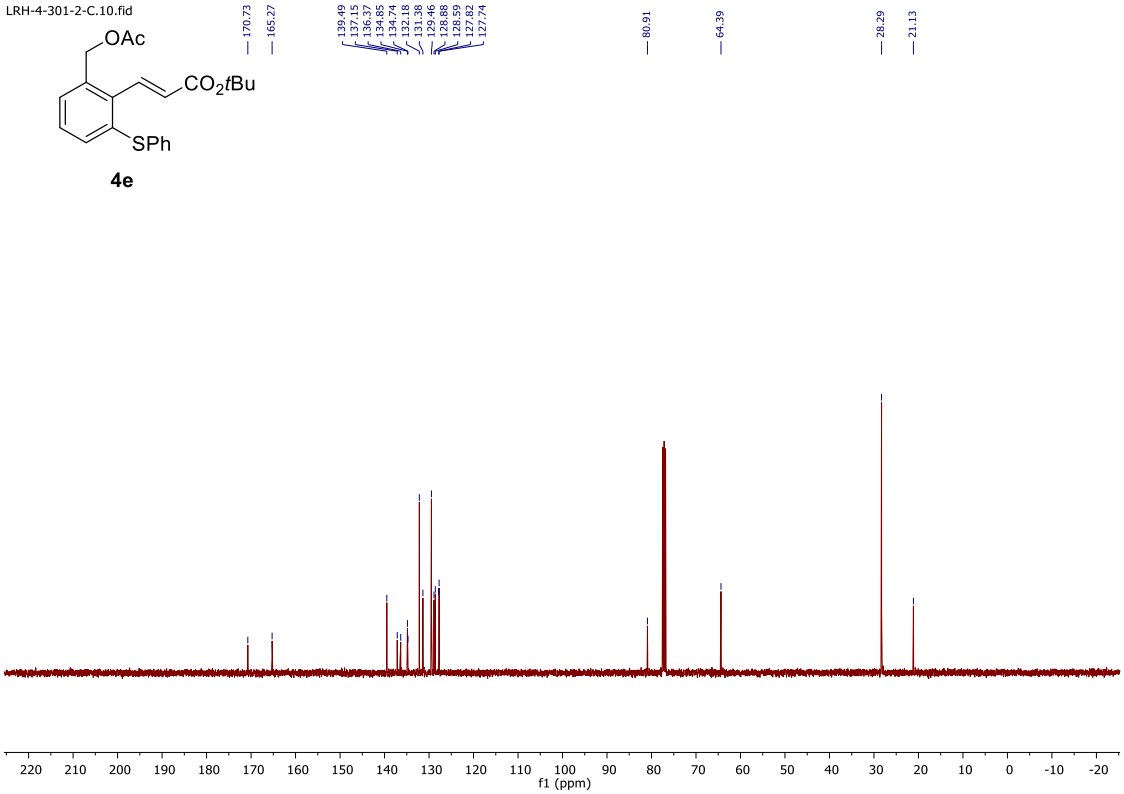

Figure 5.63. ^{1}H NMR Spectrum of 4f

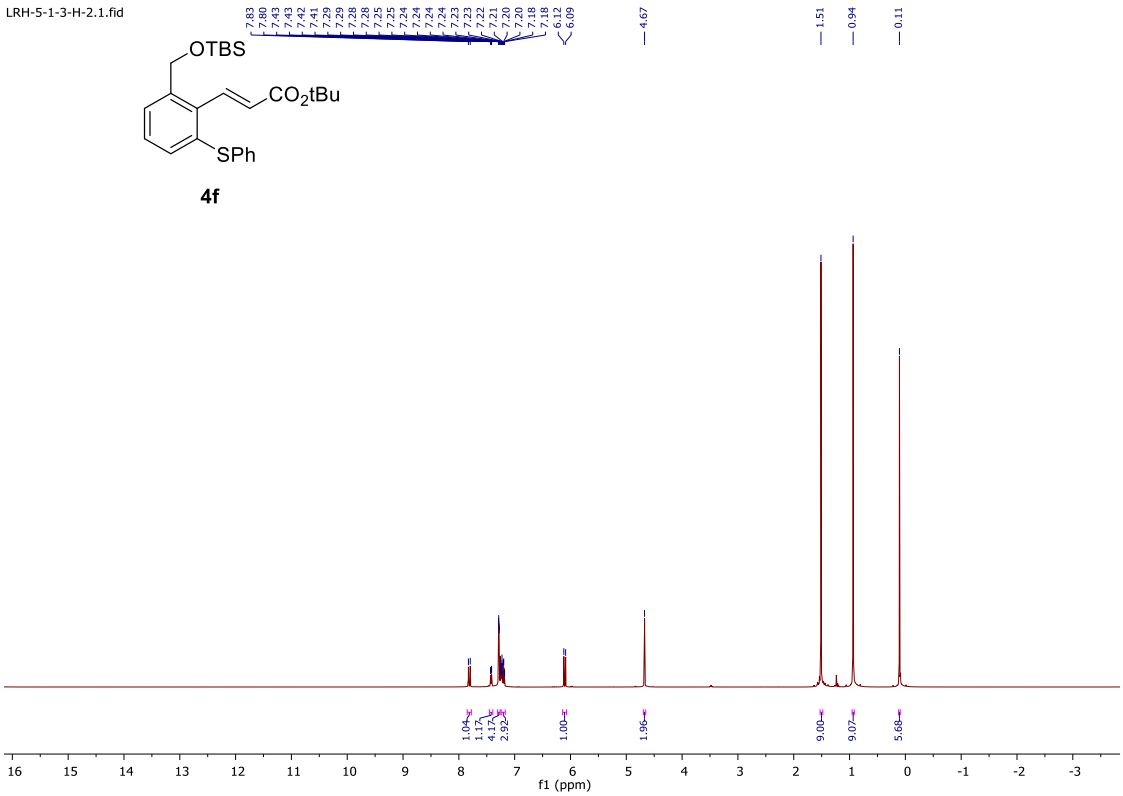

Figure 5.64. ^{13}C NMR Spectrum of 4f

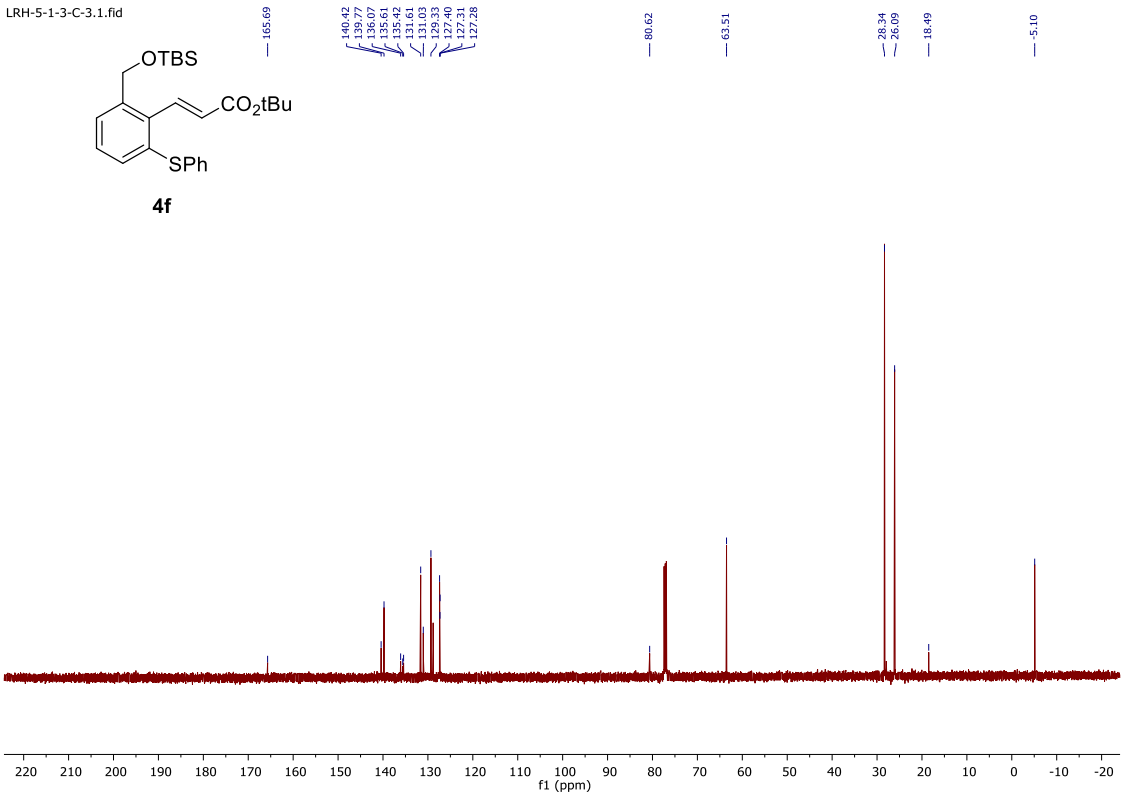

Figure 5.65. ^{1}H NMR Spectrum of 4g

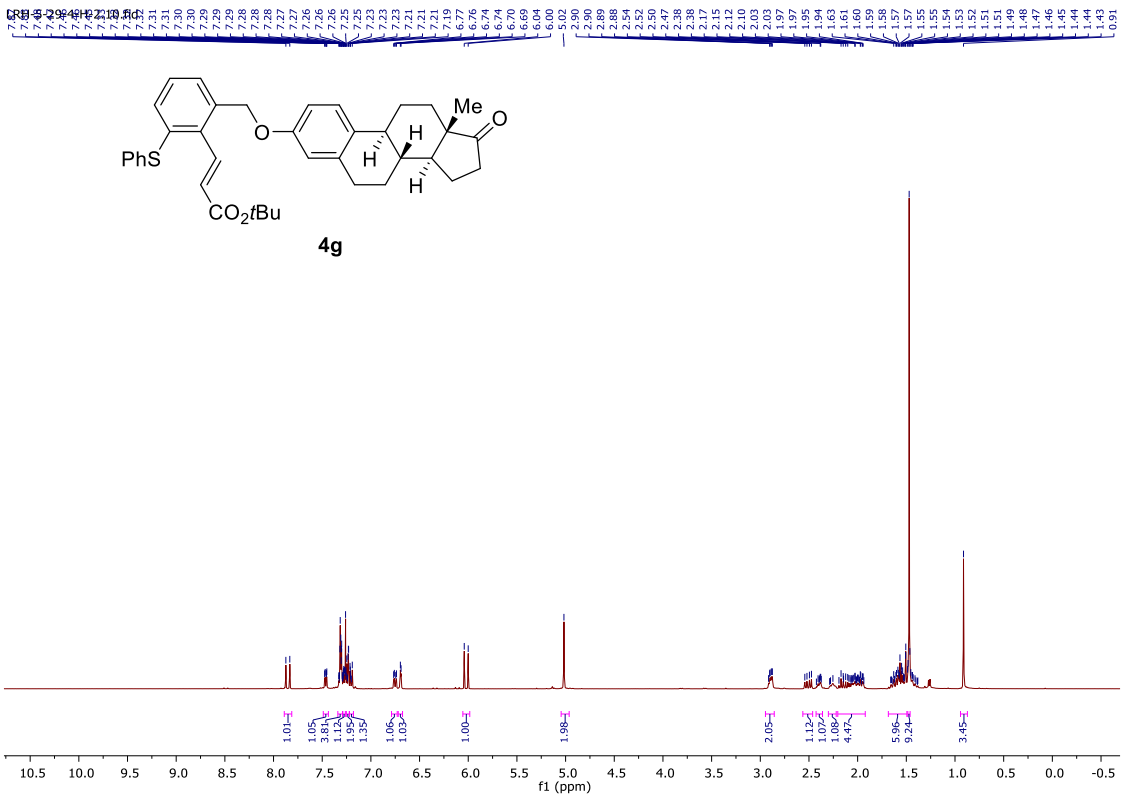

Figure 5.66. ^{13}C NMR Spectrum of 4g

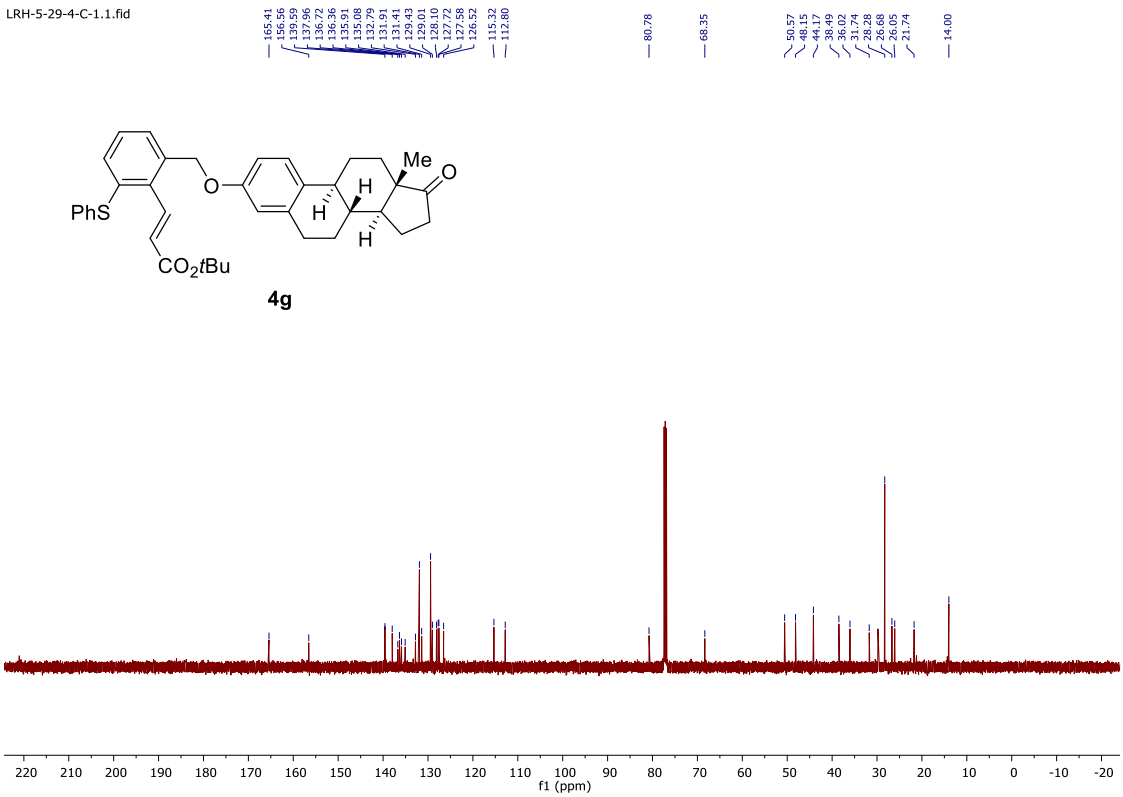

Figure 5.67. ^{1}H NMR Spectrum of 4h

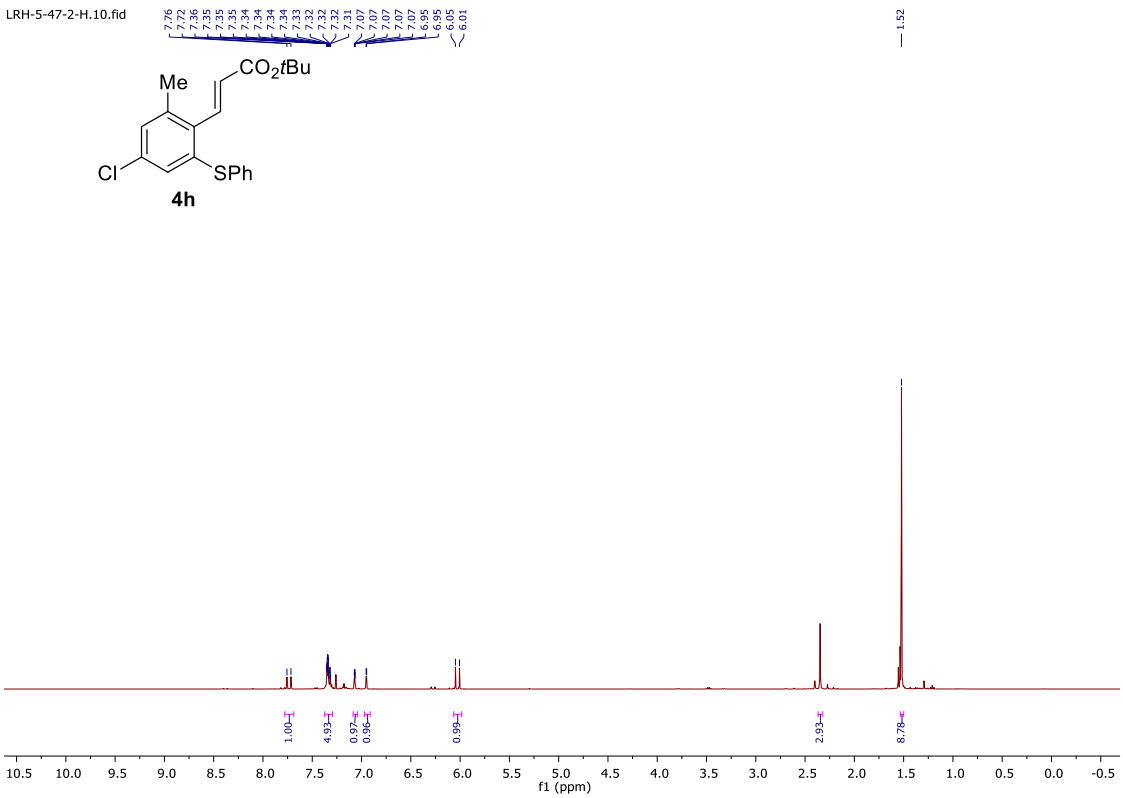

Figure 5.68. ^{13}C NMR Spectrum of 4h

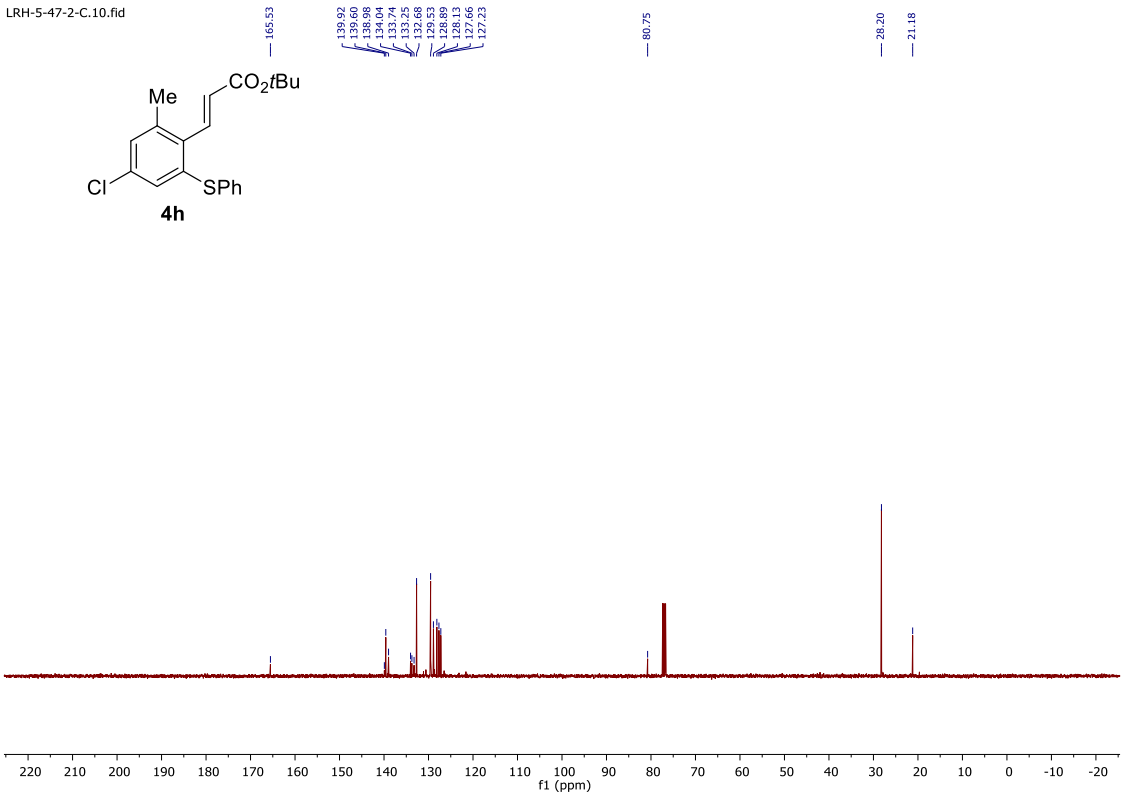

Figure 5.69. ^{1}H NMR Spectrum of 4i

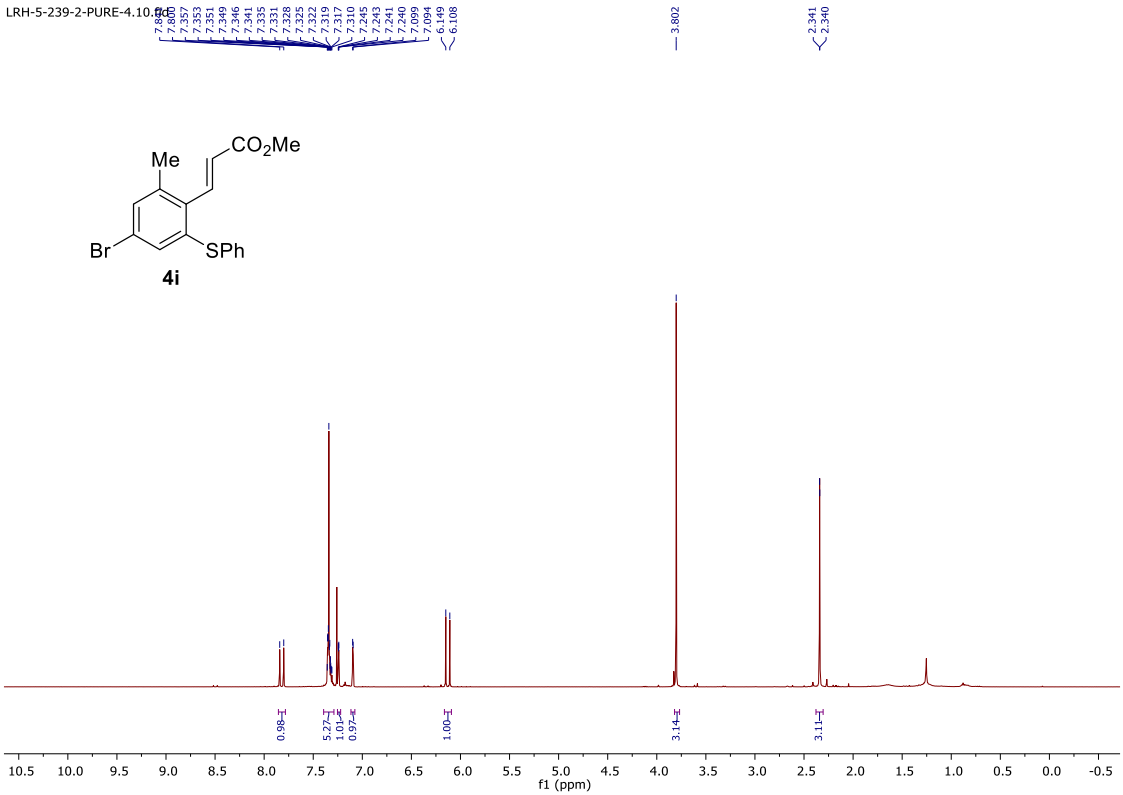

Figure 5.70. ^{13}C NMR Spectrum of 4i

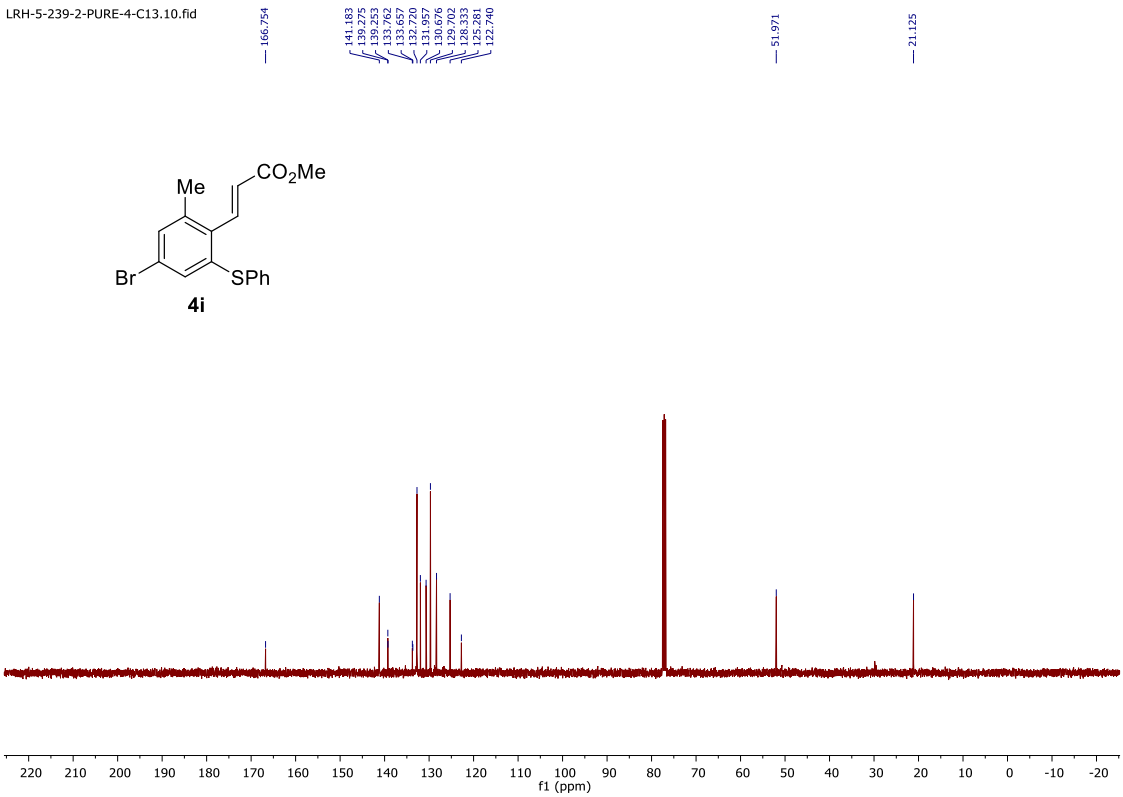

Figure 5.71. ^{1}H NMR Spectrum of 4j

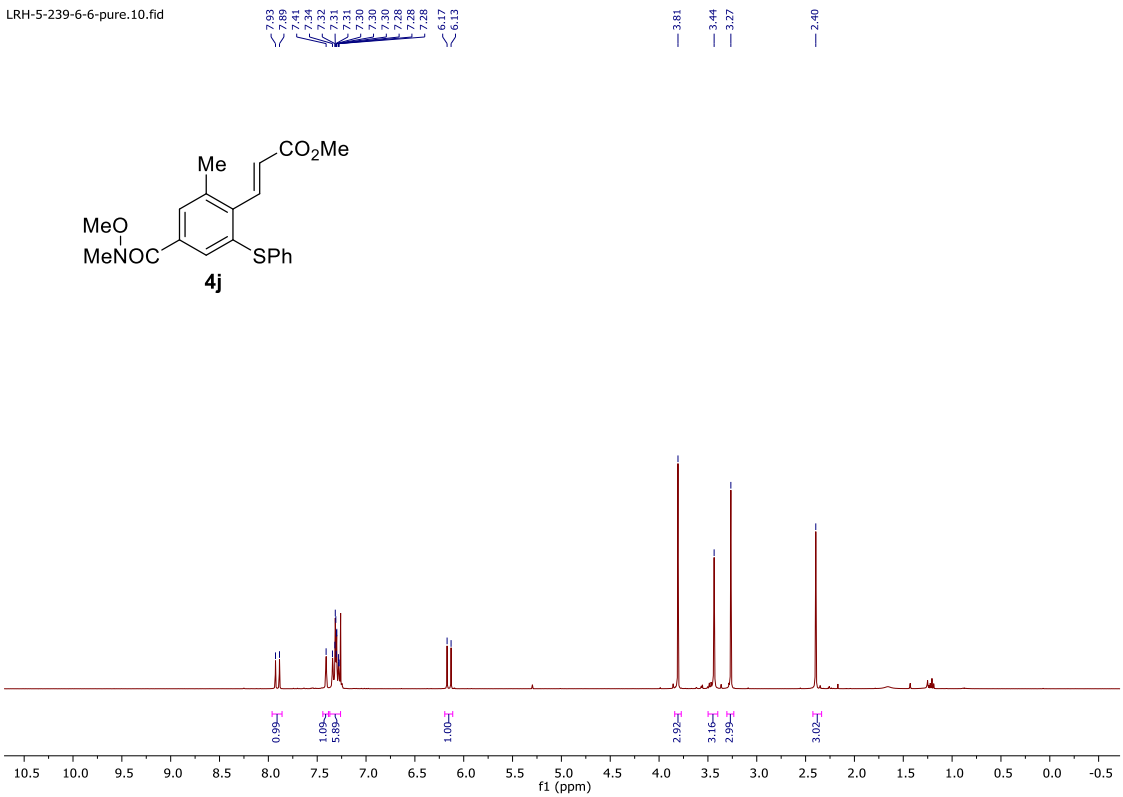

Figure 5.72. ^{13}C NMR Spectrum of 4j

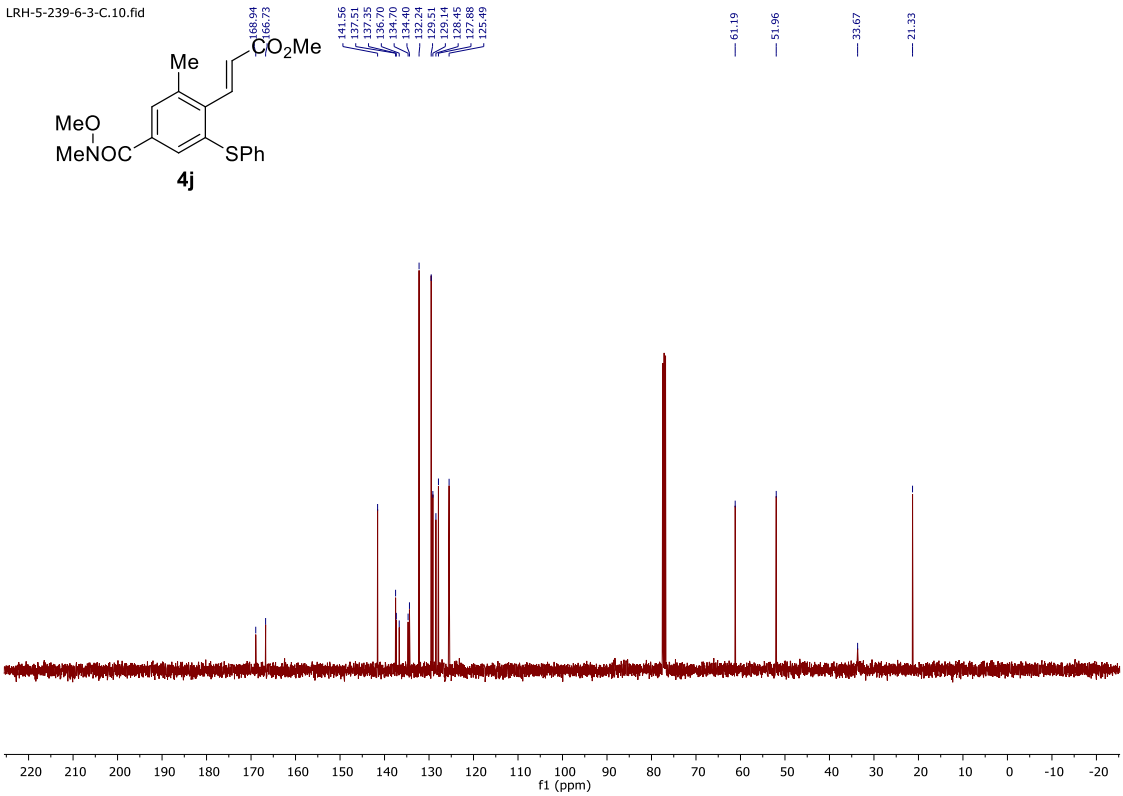

Figure 5.73. ^{1}H NMR Spectrum of 4k

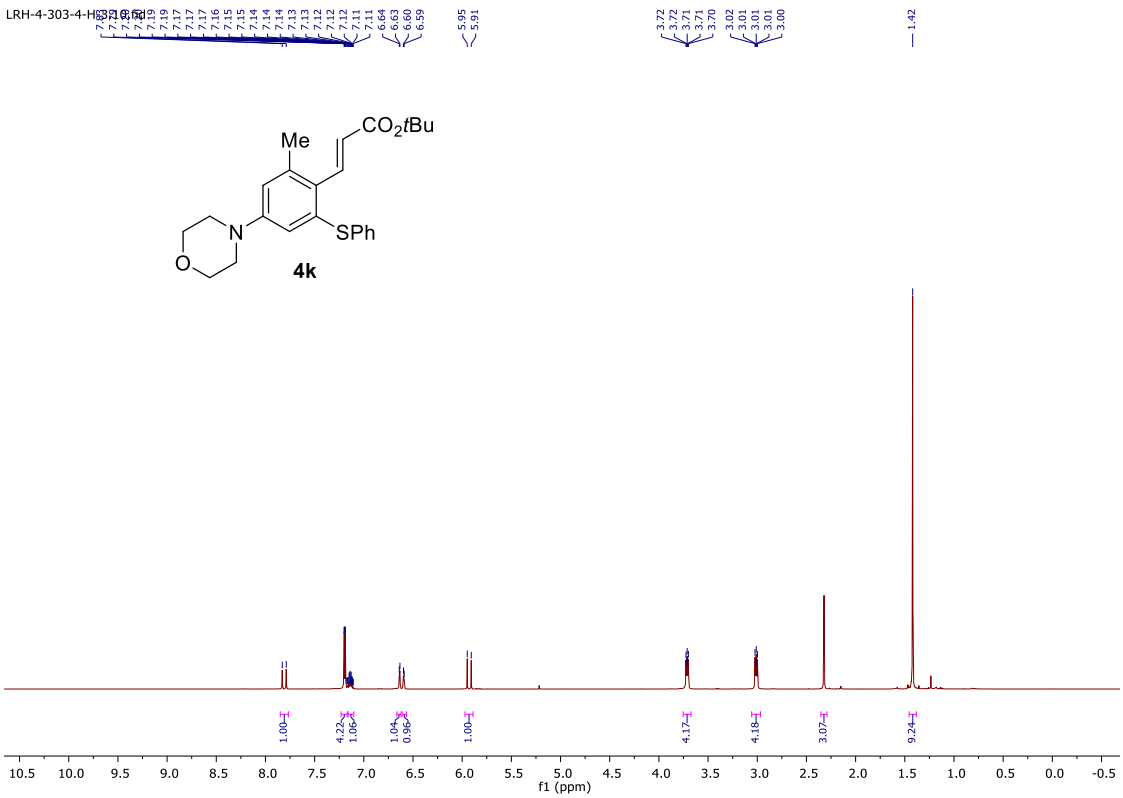

Figure 5.74. ^{13}C NMR Spectrum of 4k

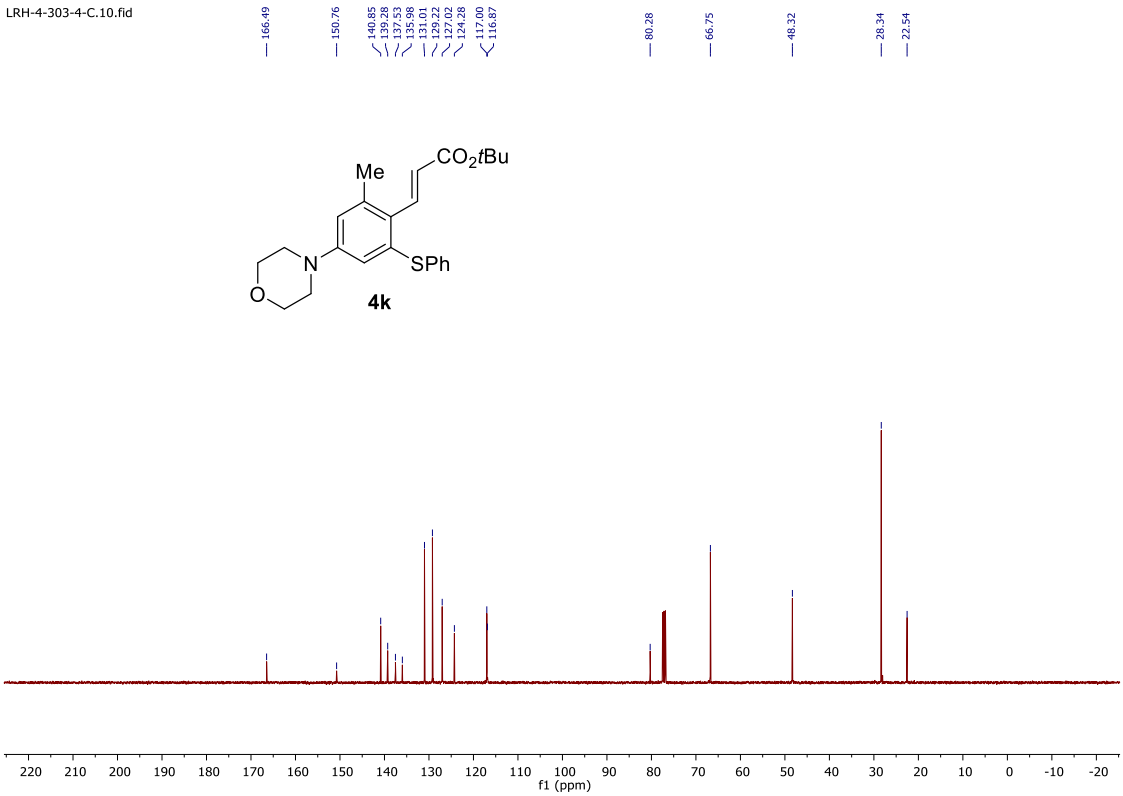

Figure 5.75. ^{1}H NMR Spectrum of 4l

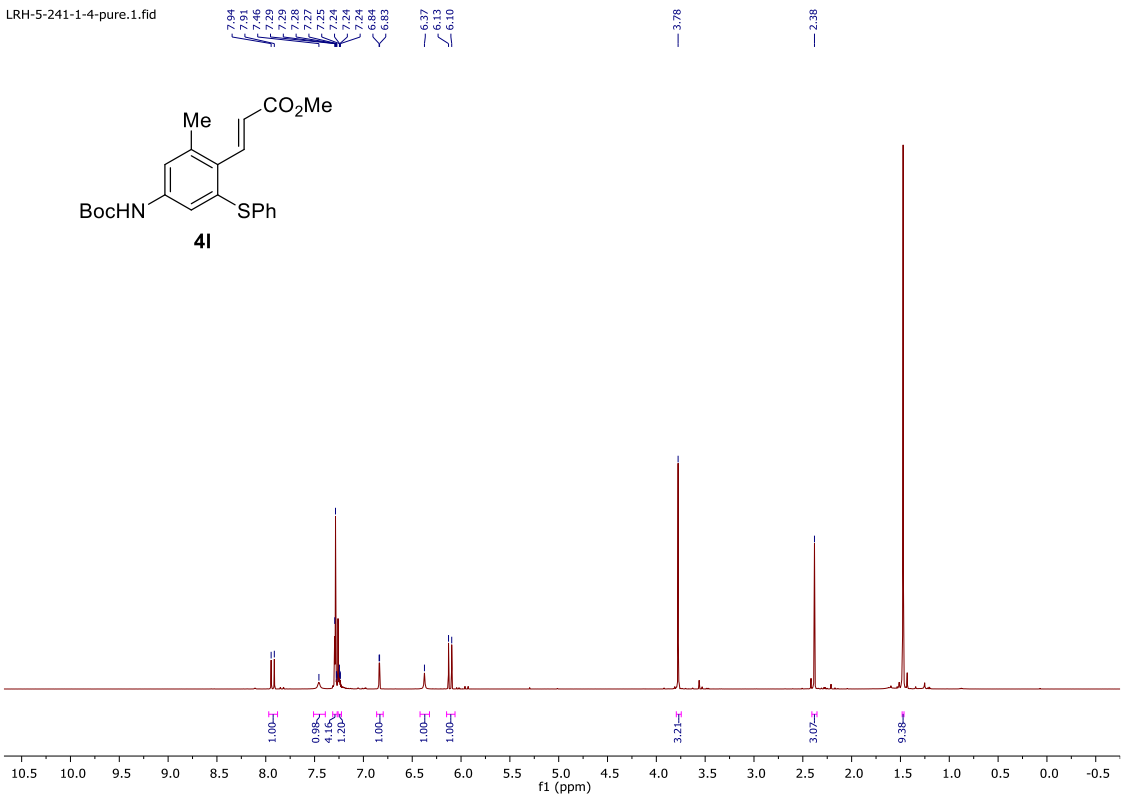

Figure 5.76. ^{13}C NMR Spectrum of 4l

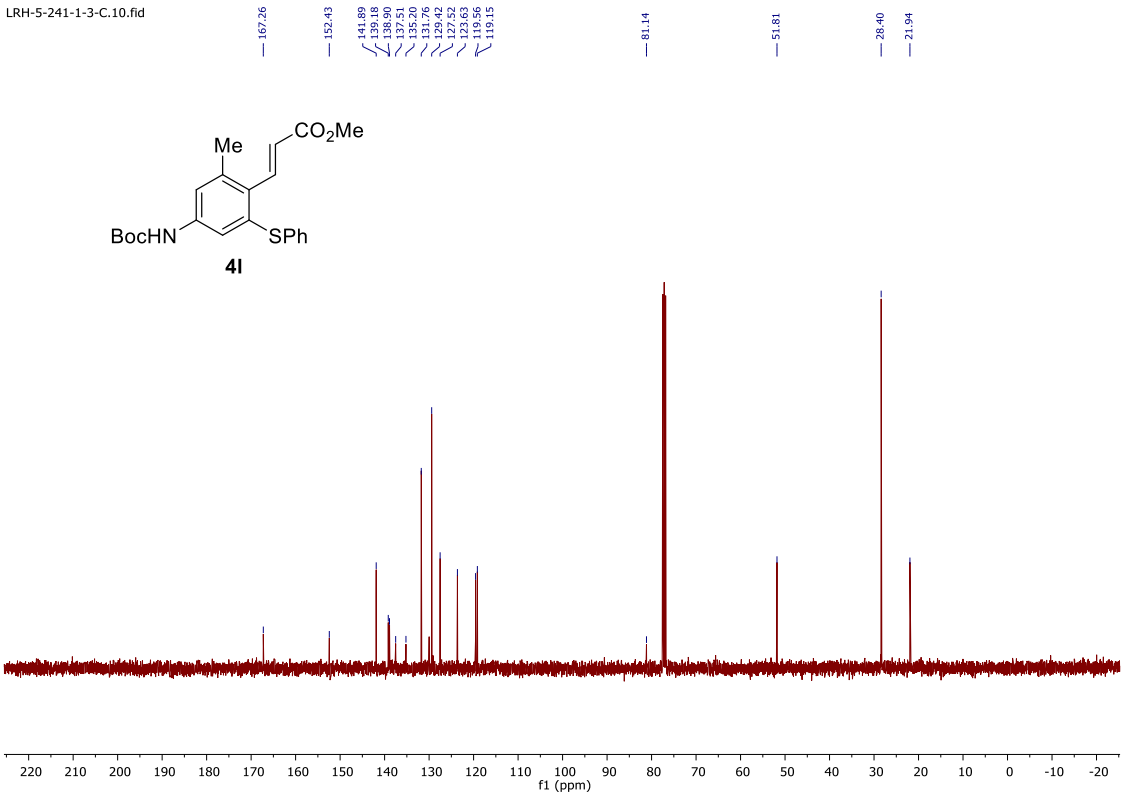

Figure 5.77. ^{1}H NMR Spectrum of 4m

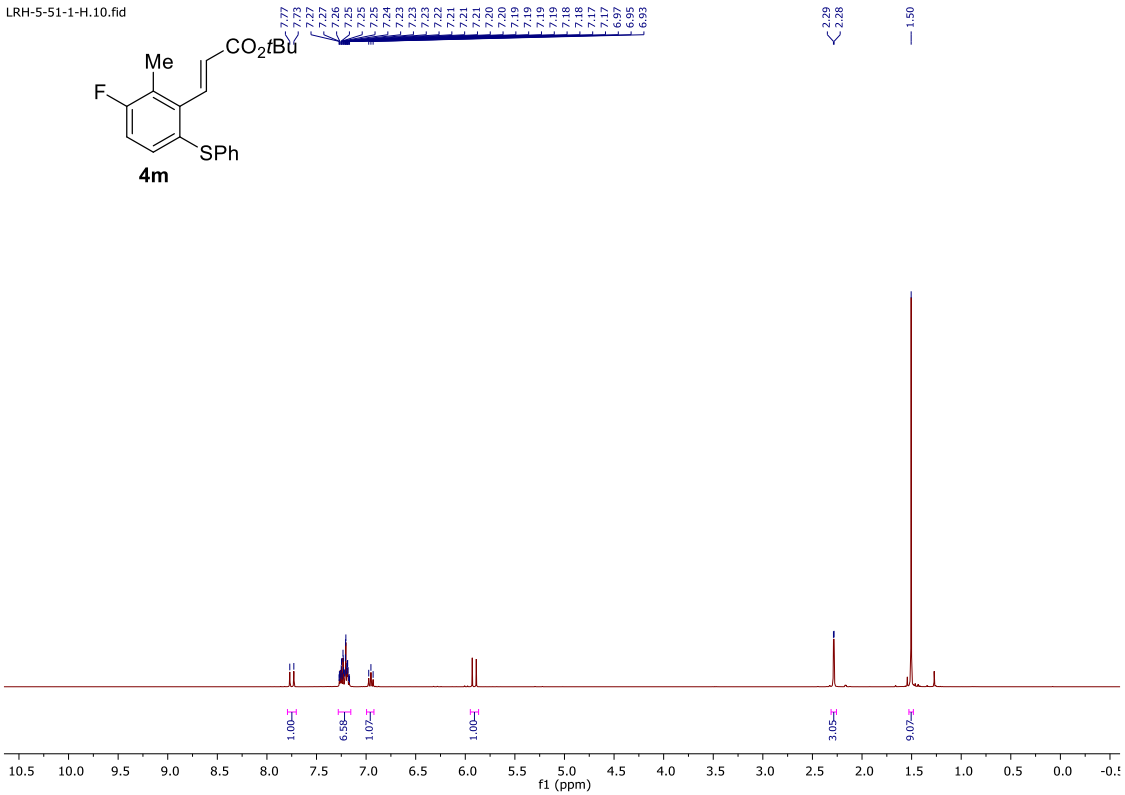

Figure 5.78. ^{13}C NMR Spectrum of 4m

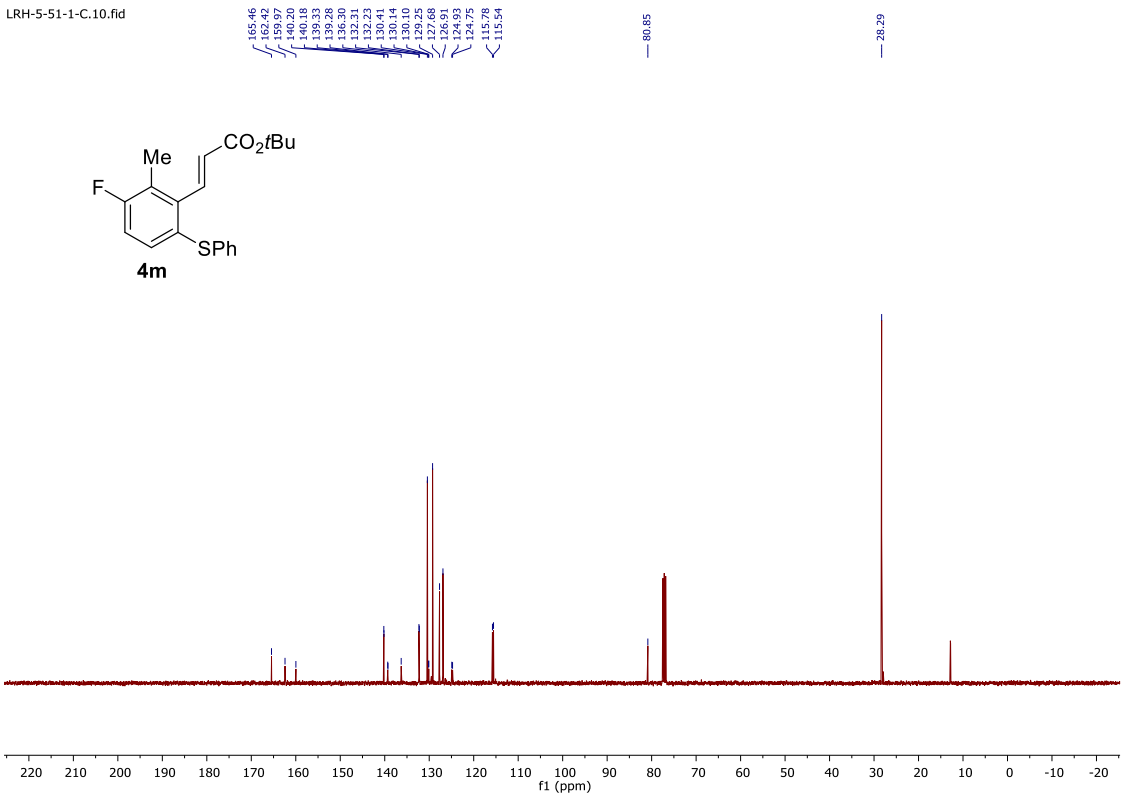

Figure 5.79. ^{1}H NMR Spectrum of 4n

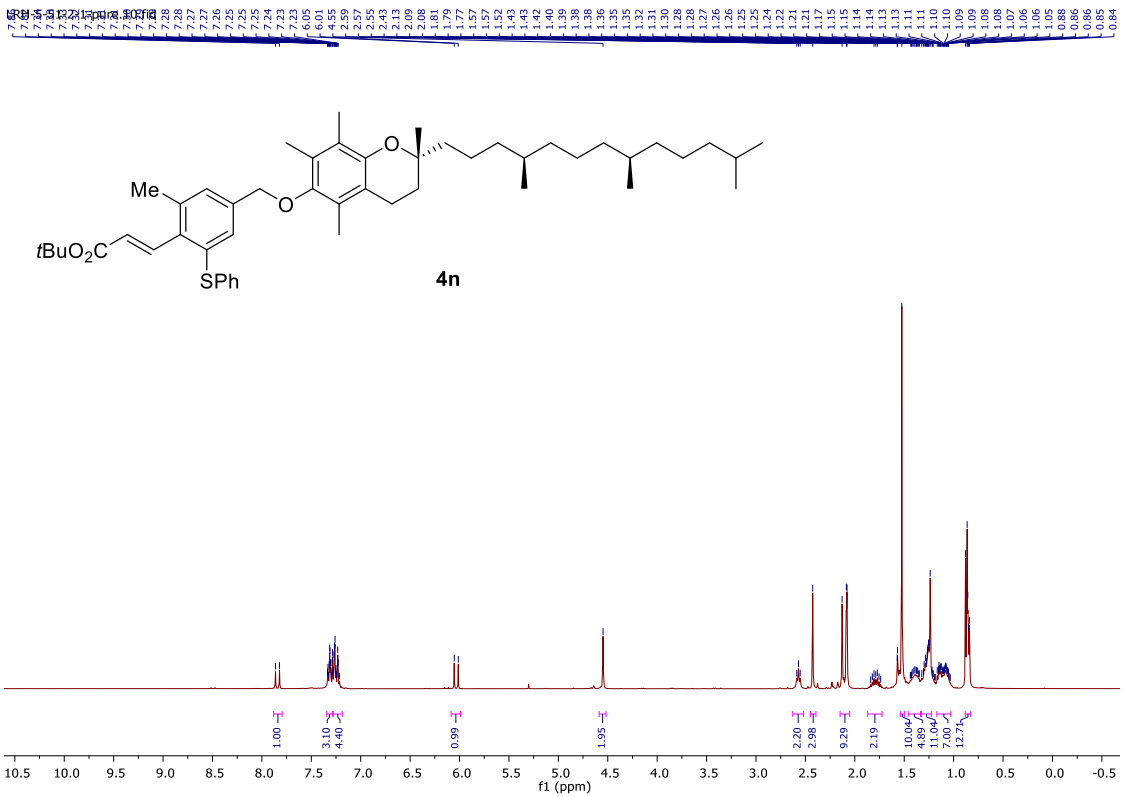

Figure 5.80. ^{13}C NMR Spectrum of 4n

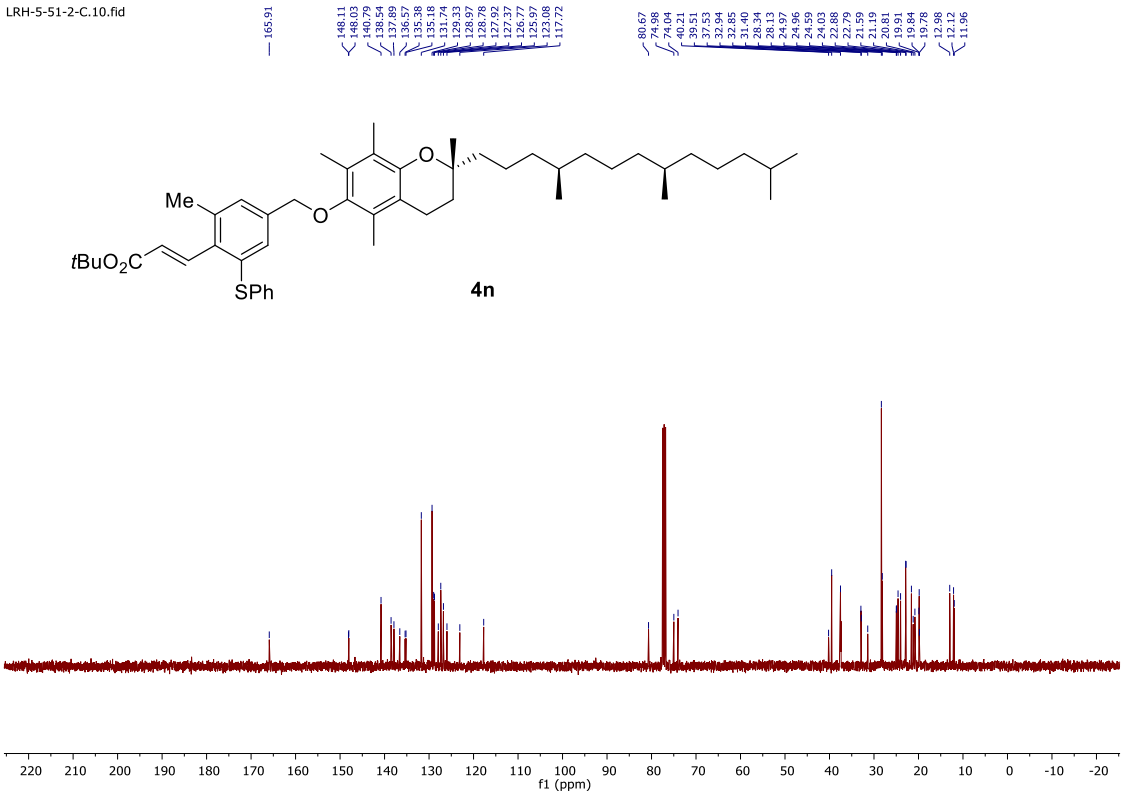

Figure 5.81. ^{1}H NMR Spectrum of 4o

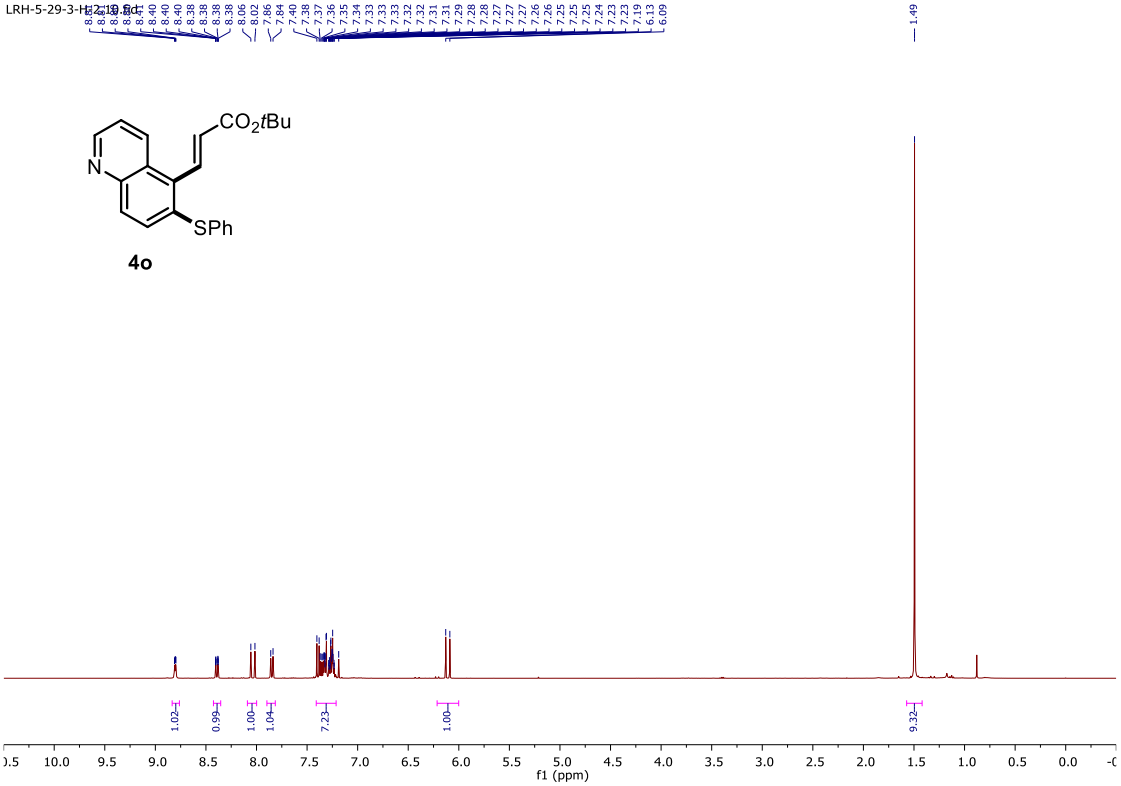

Figure 5.82. ^{13}C NMR Spectrum of 4o

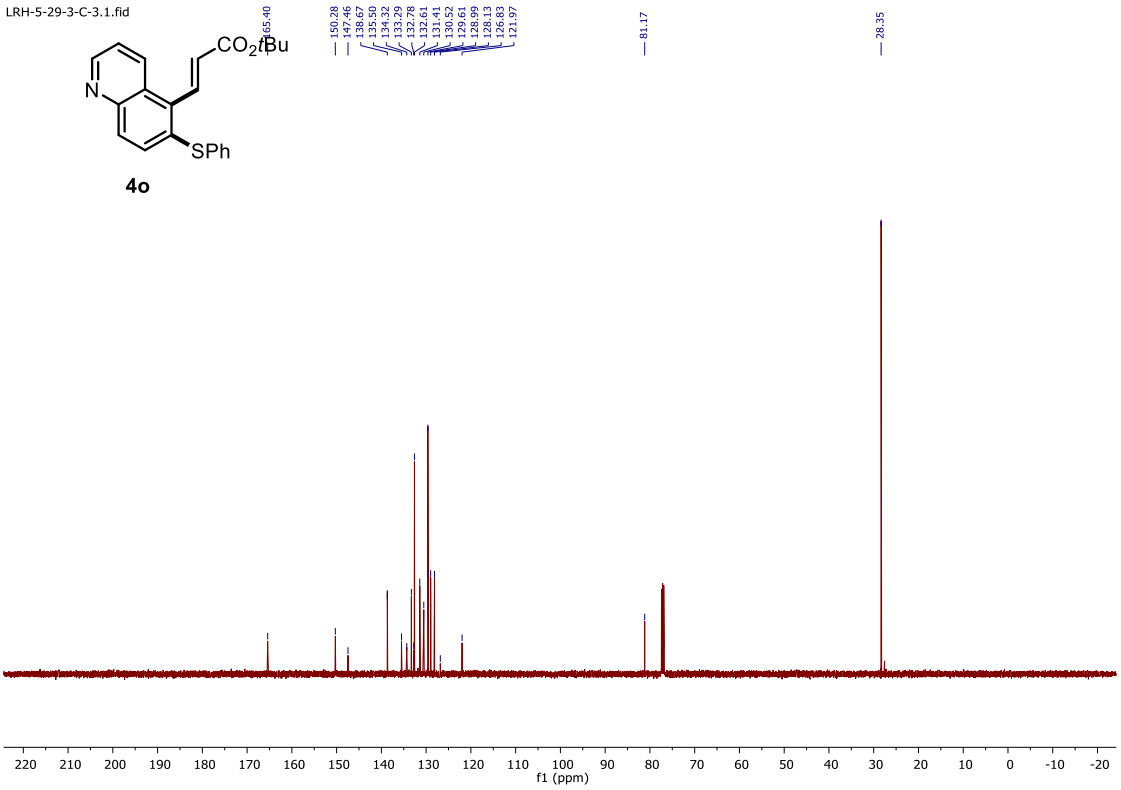

Figure 5.83. ^{1}H NMR Spectrum of 4p

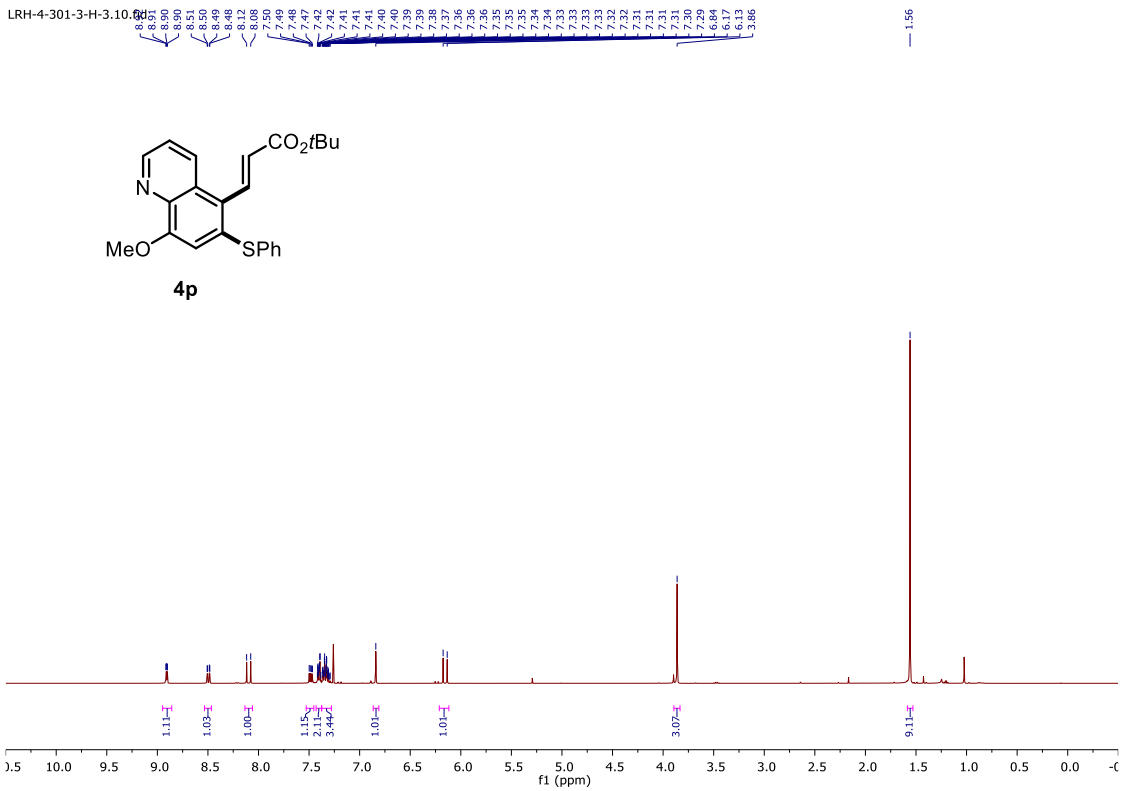

Figure 5.84. ^{13}C NMR Spectrum of 4p

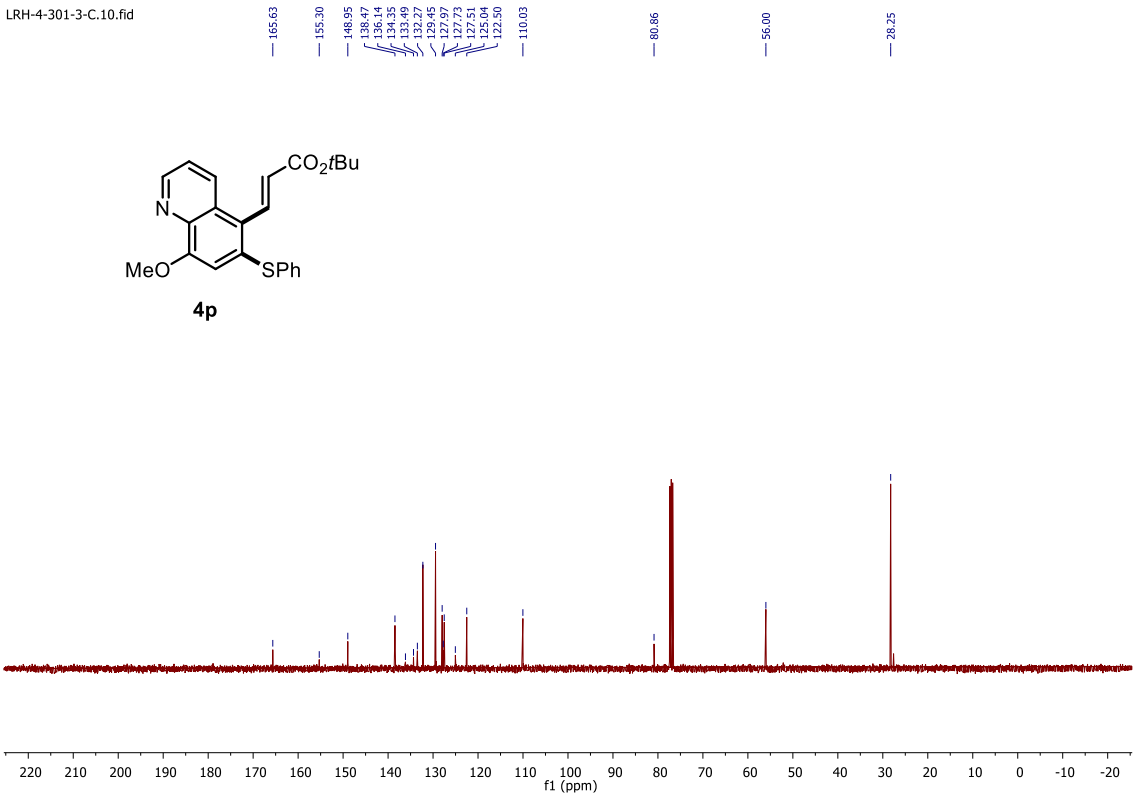

Figure 5.85. ^{1}H NMR Spectrum of 4q

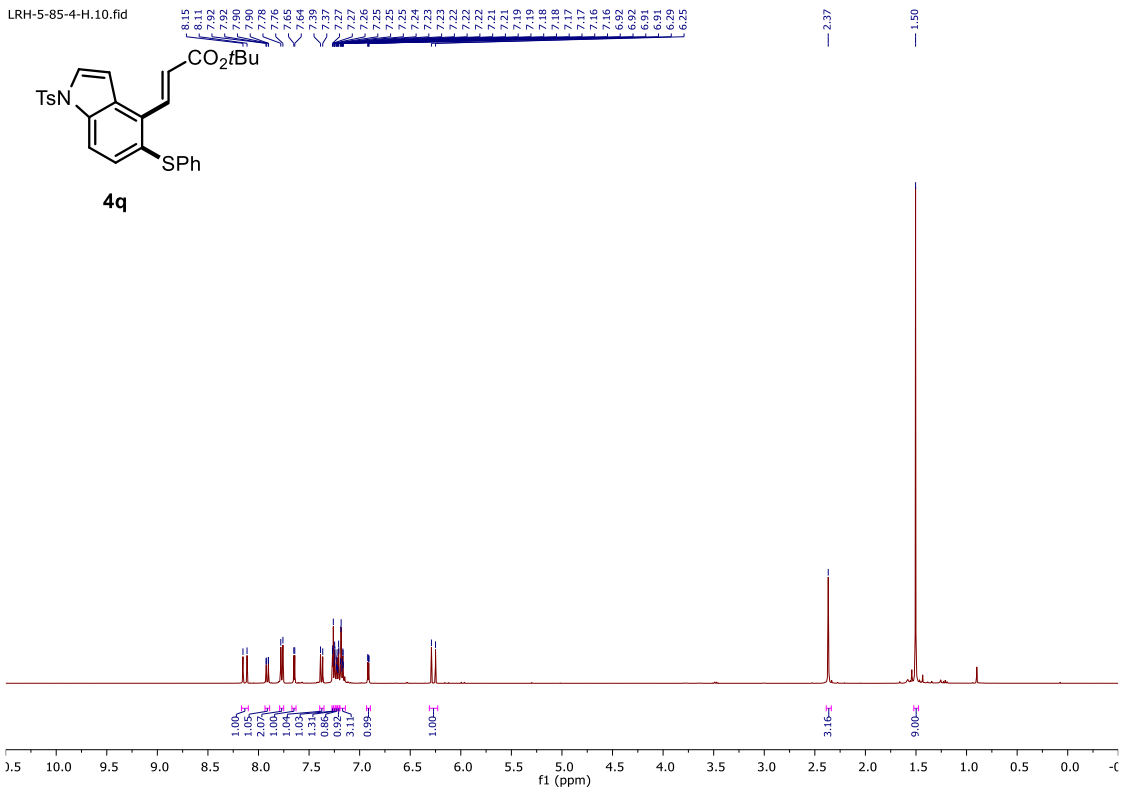

Figure 5.86. ^{13}C NMR Spectrum of 4q

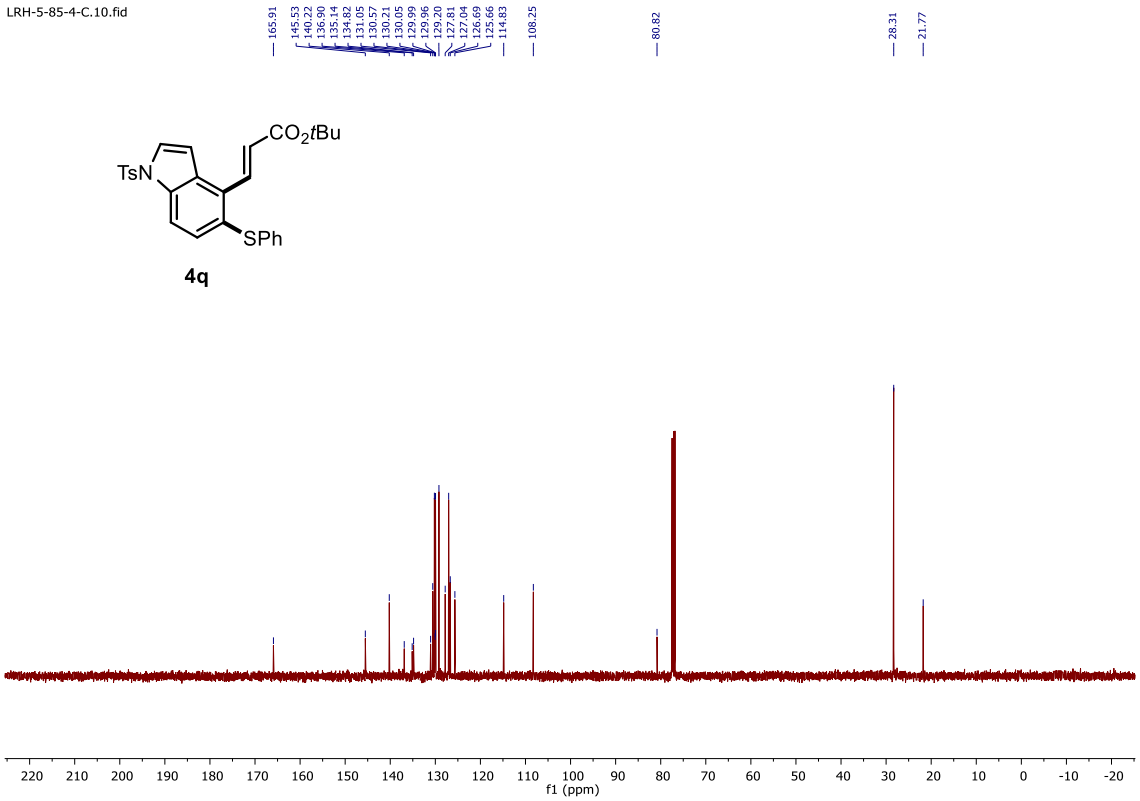

Figure 5.87. ^{1}H NMR Spectrum of 4r

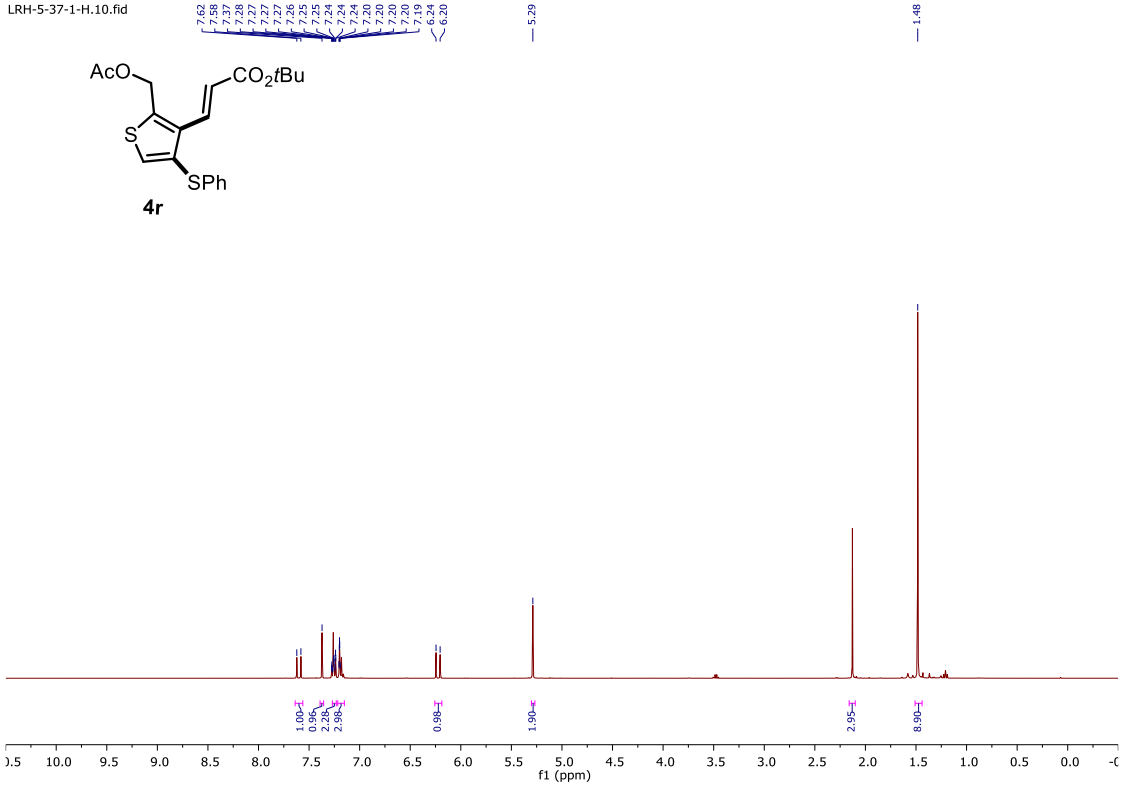

Figure 5.88. ^{13}C NMR Spectrum of 4r

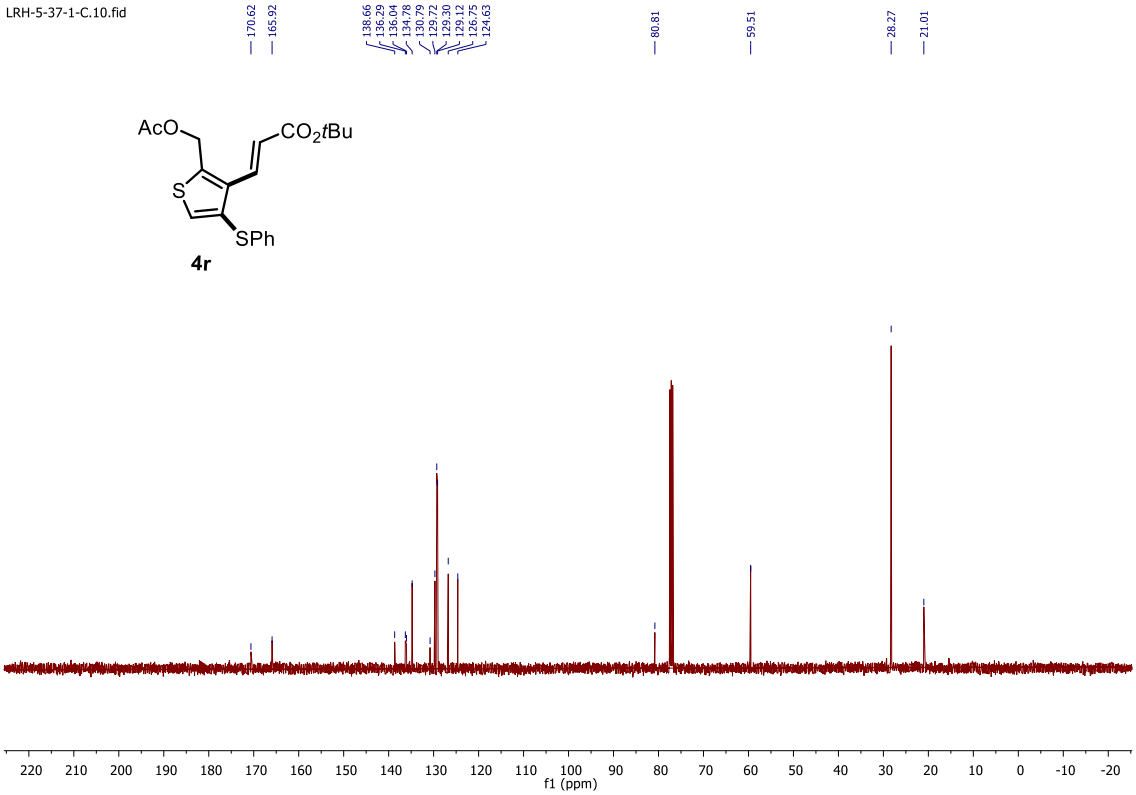

Figure 5.89. ^{1}H NMR Spectrum of 4s

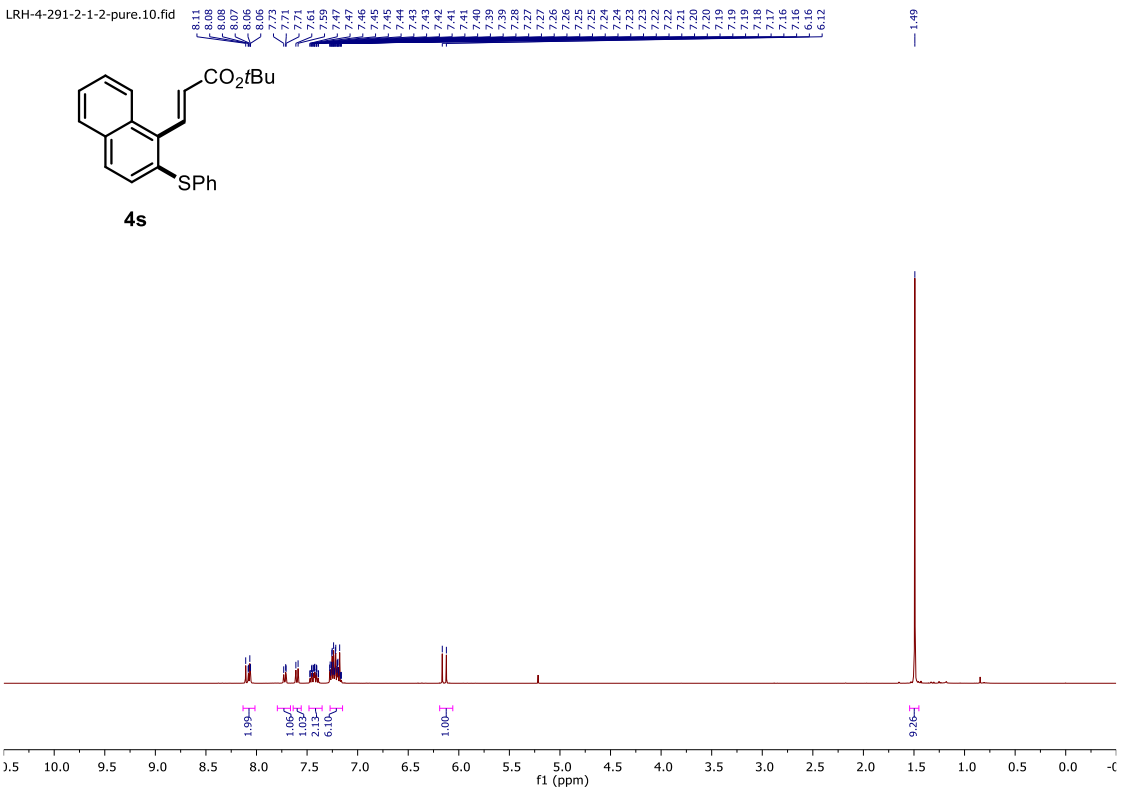

Figure 5.90. ^{13}C NMR Spectrum of 4s

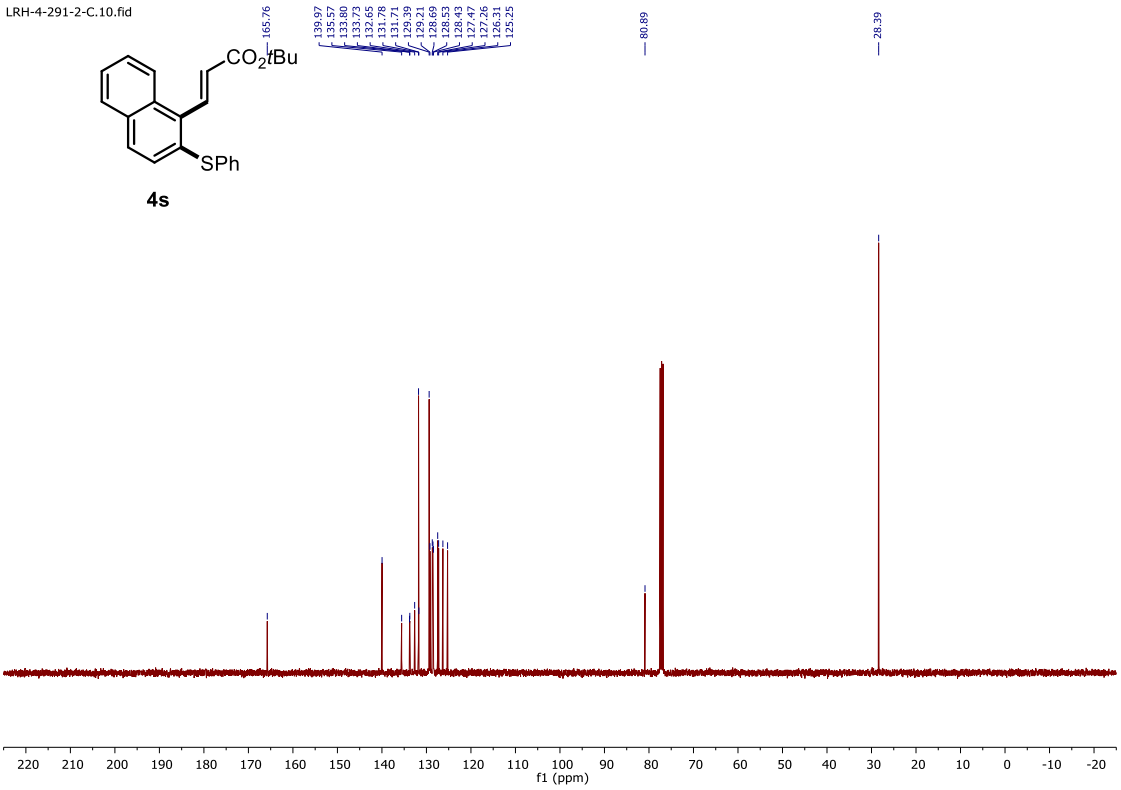

Figure 5.91. ^{1}H NMR Spectrum of 4t

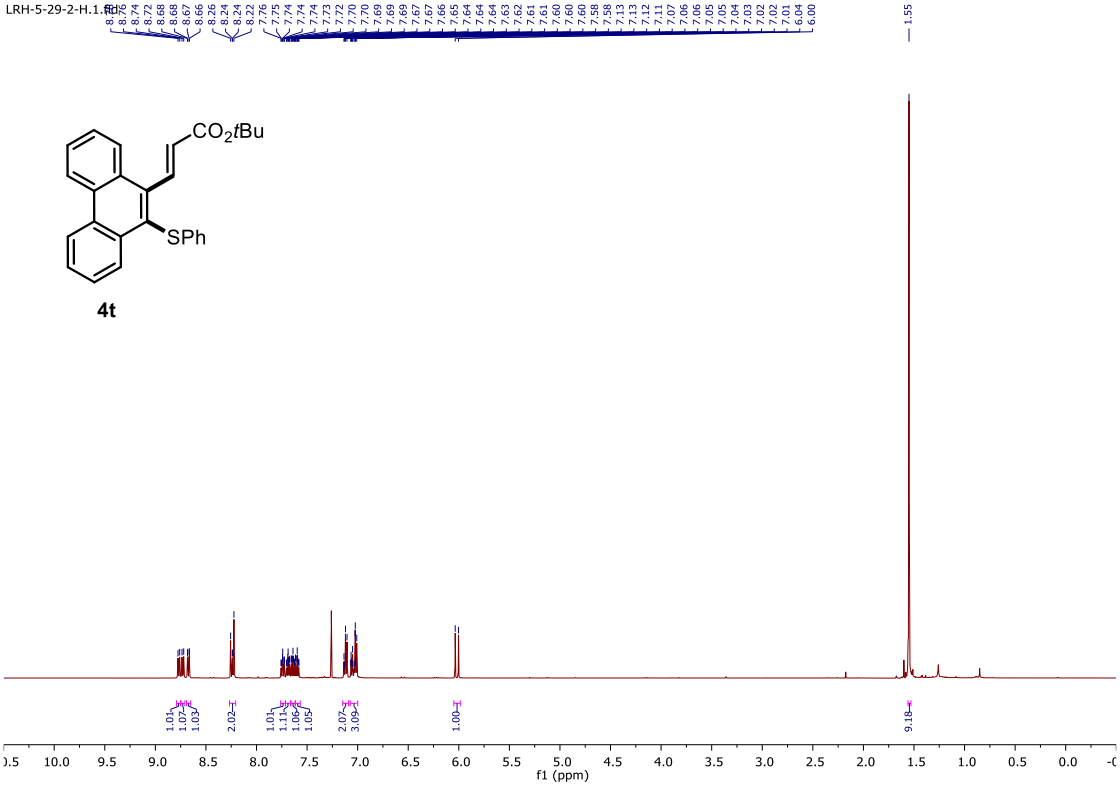

Figure 5.92. ^{13}C NMR Spectrum of 4t

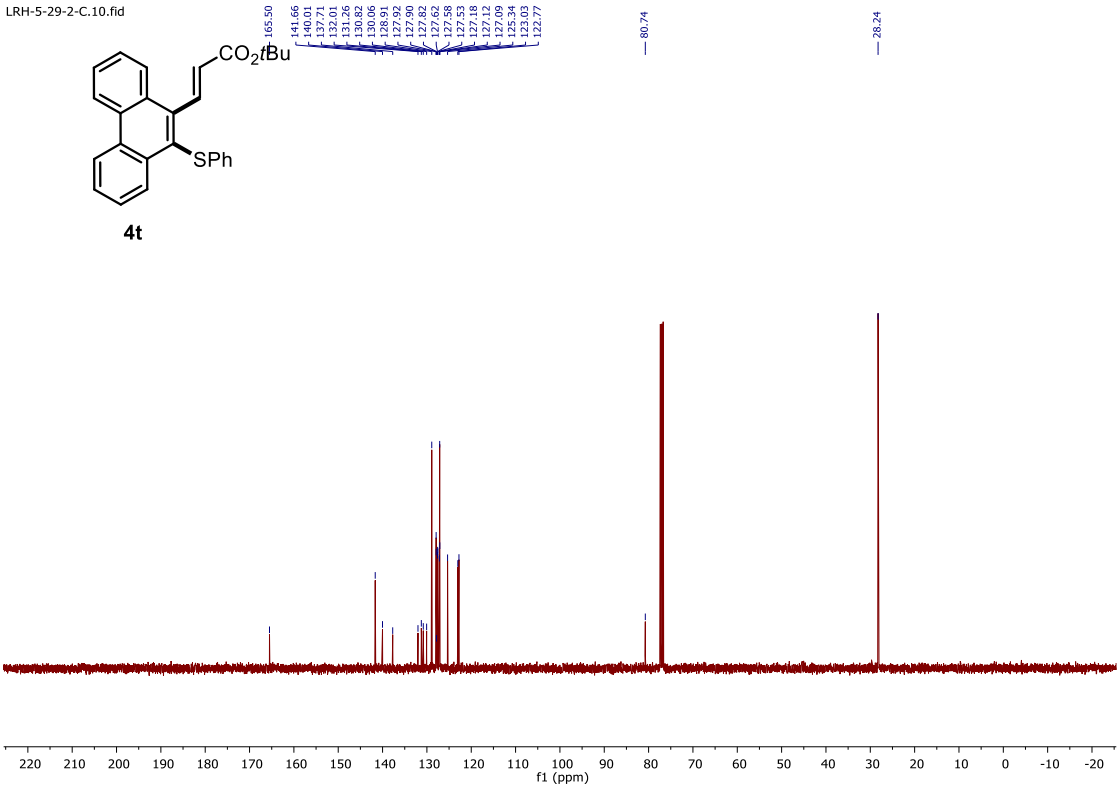

Figure 5.93. ^{1}H NMR Spectrum of 4u

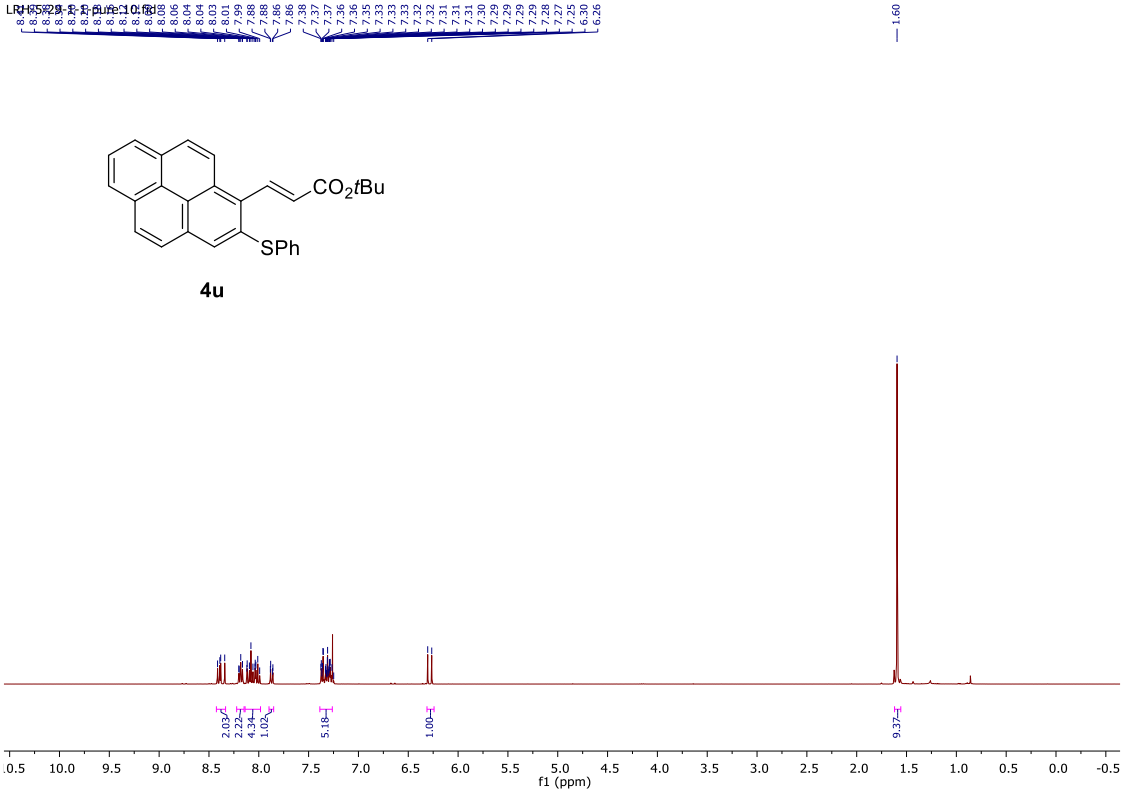

Figure 5.94. ^{13}C NMR Spectrum of 4u

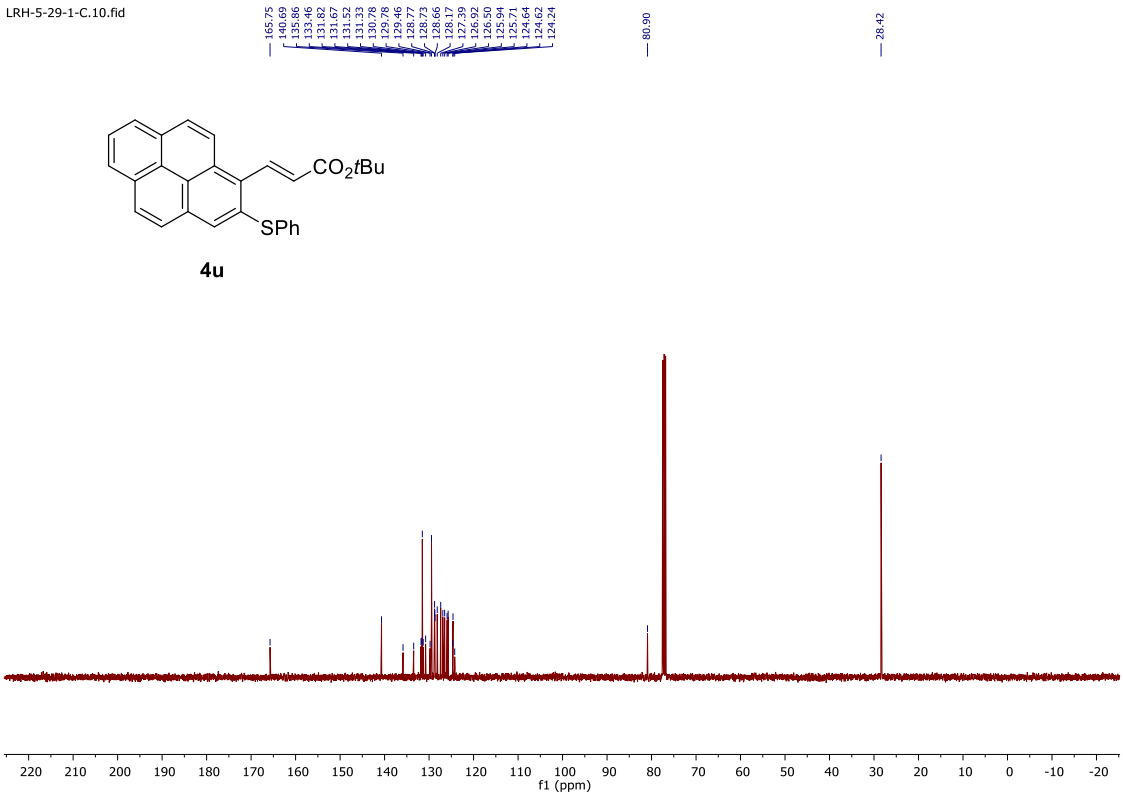

Figure 5.95. ^{1}H NMR Spectrum of 5a

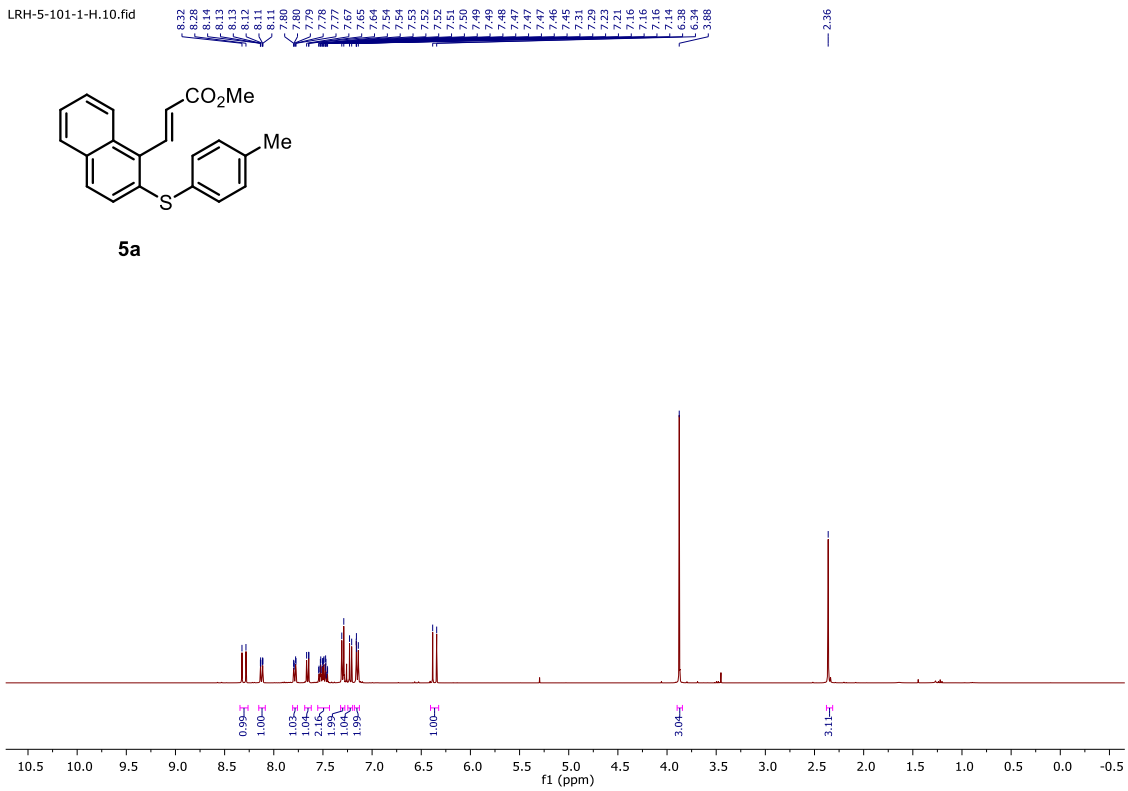

Figure 5.96. ^{13}C NMR Spectrum of 5a

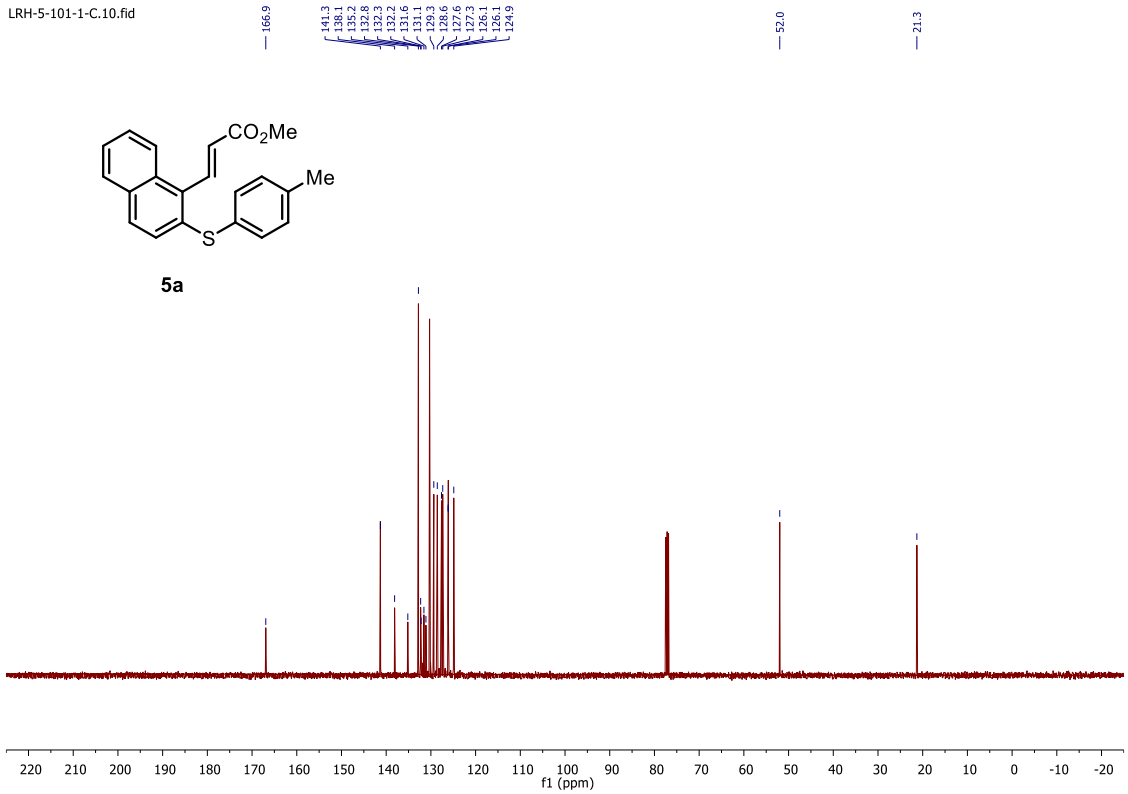

Figure 5.97. ^{1}H NMR Spectrum of 5b

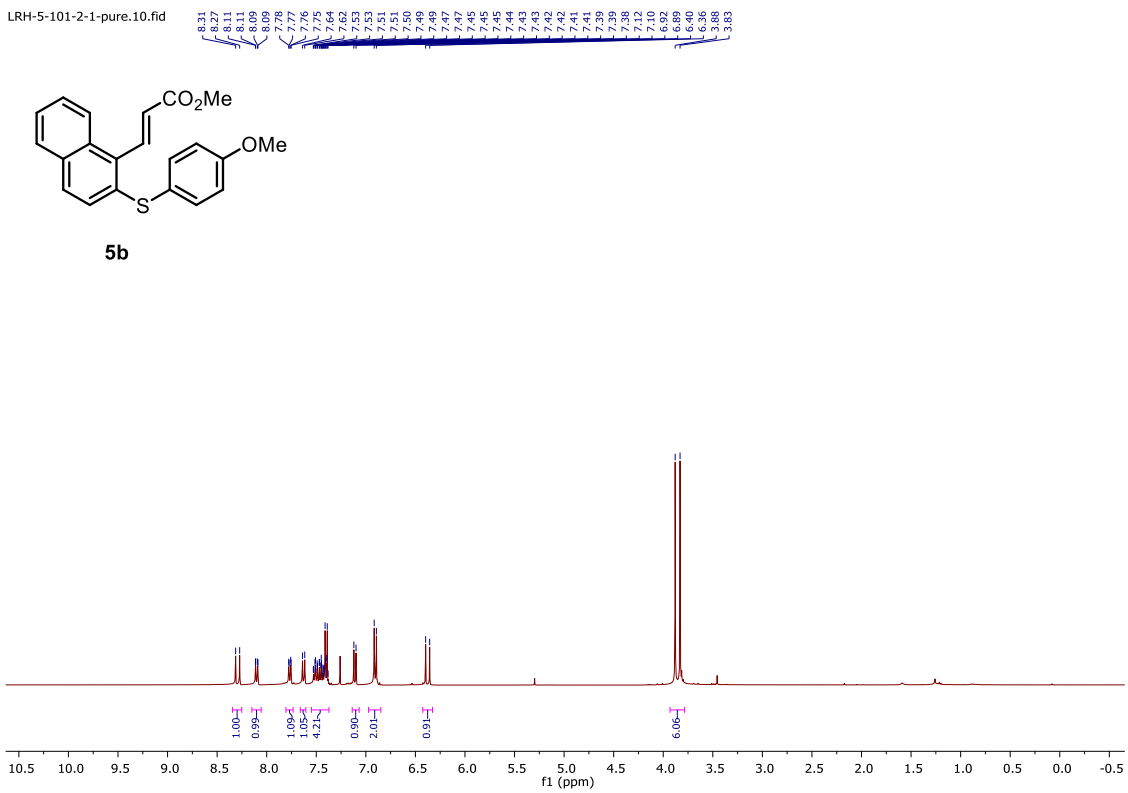

Figure 5.98. ^{13}C NMR Spectrum of 5b

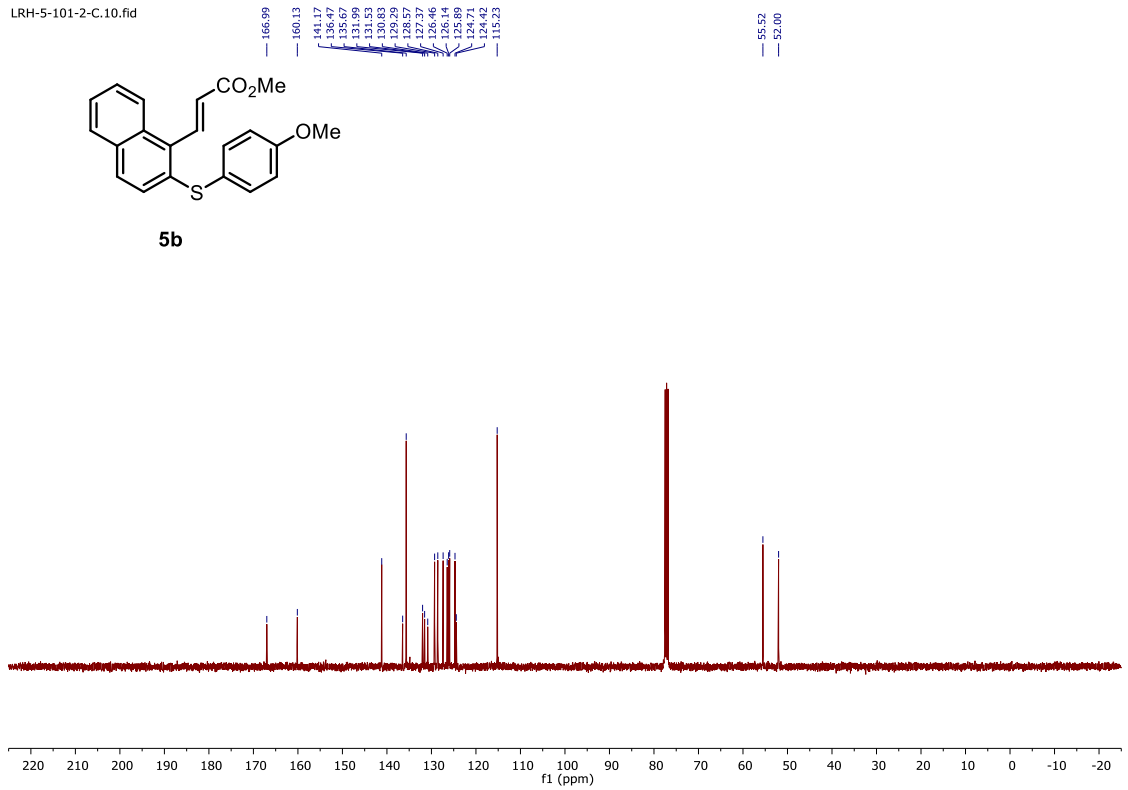

Figure 5.99. ^{1}H NMR Spectrum of 5c

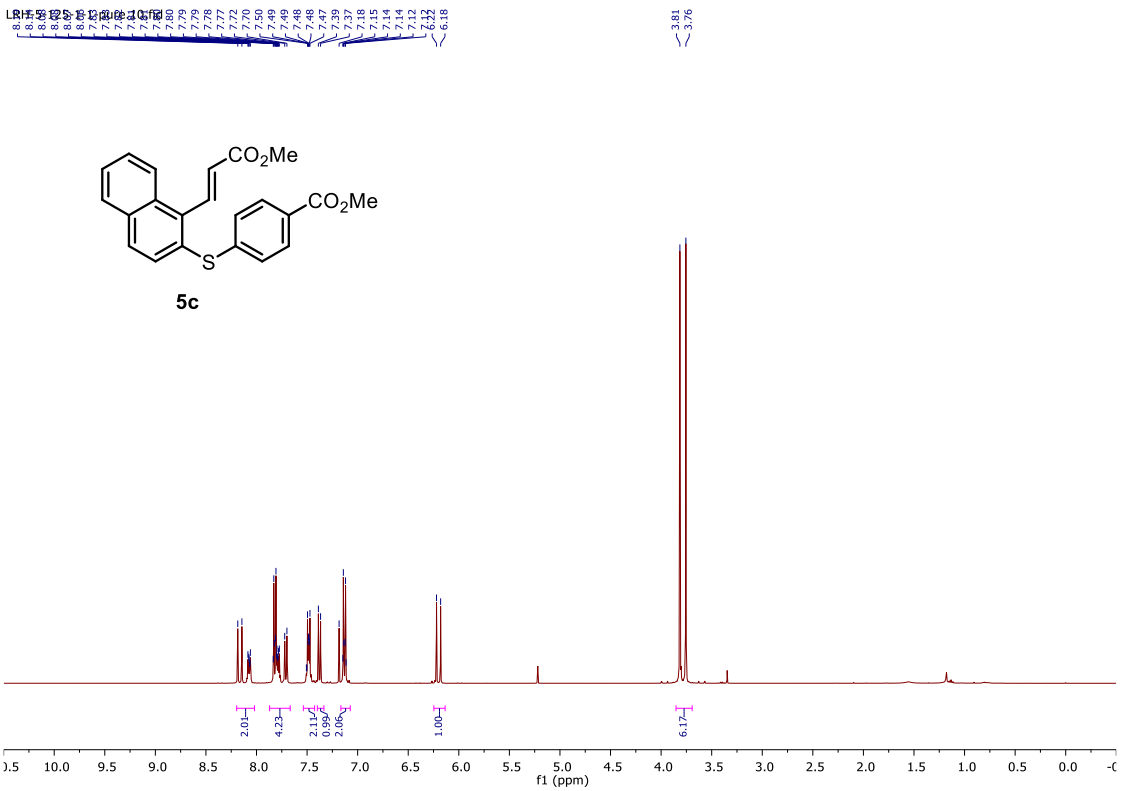

Figure 5.100. ^{13}C NMR Spectrum of 5c

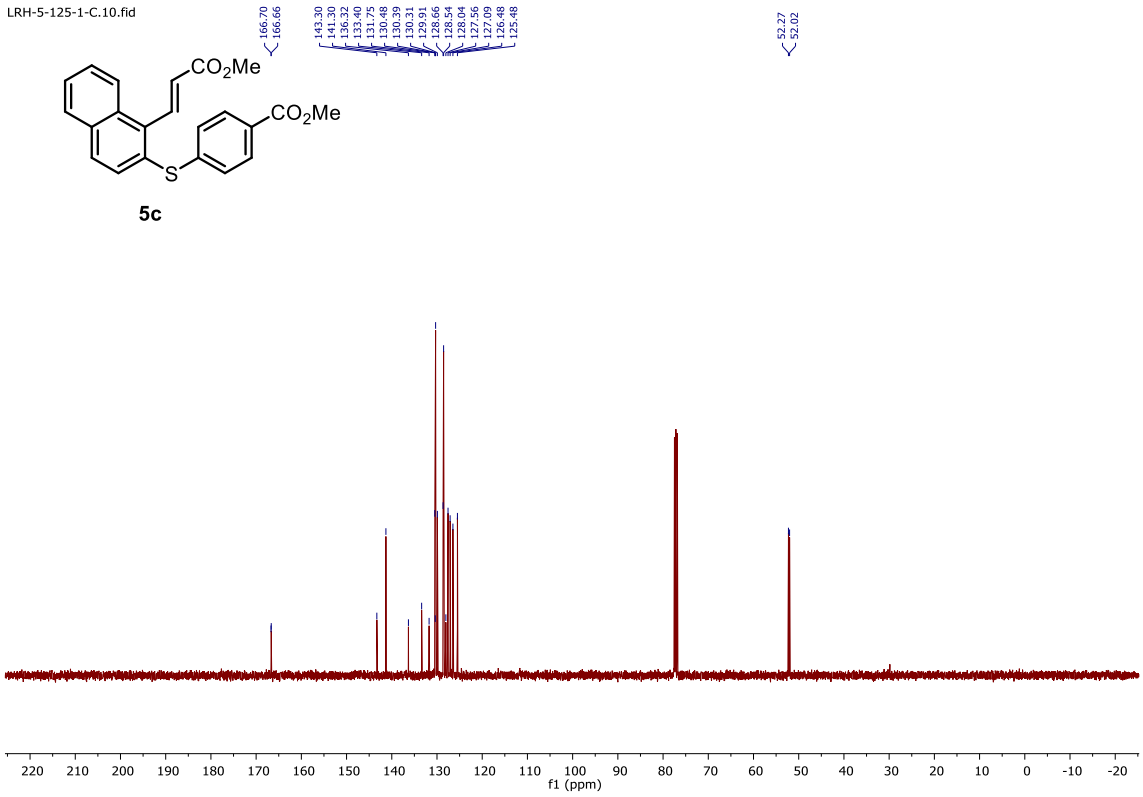

Figure 5.101. ^{1}H NMR Spectrum of 5d

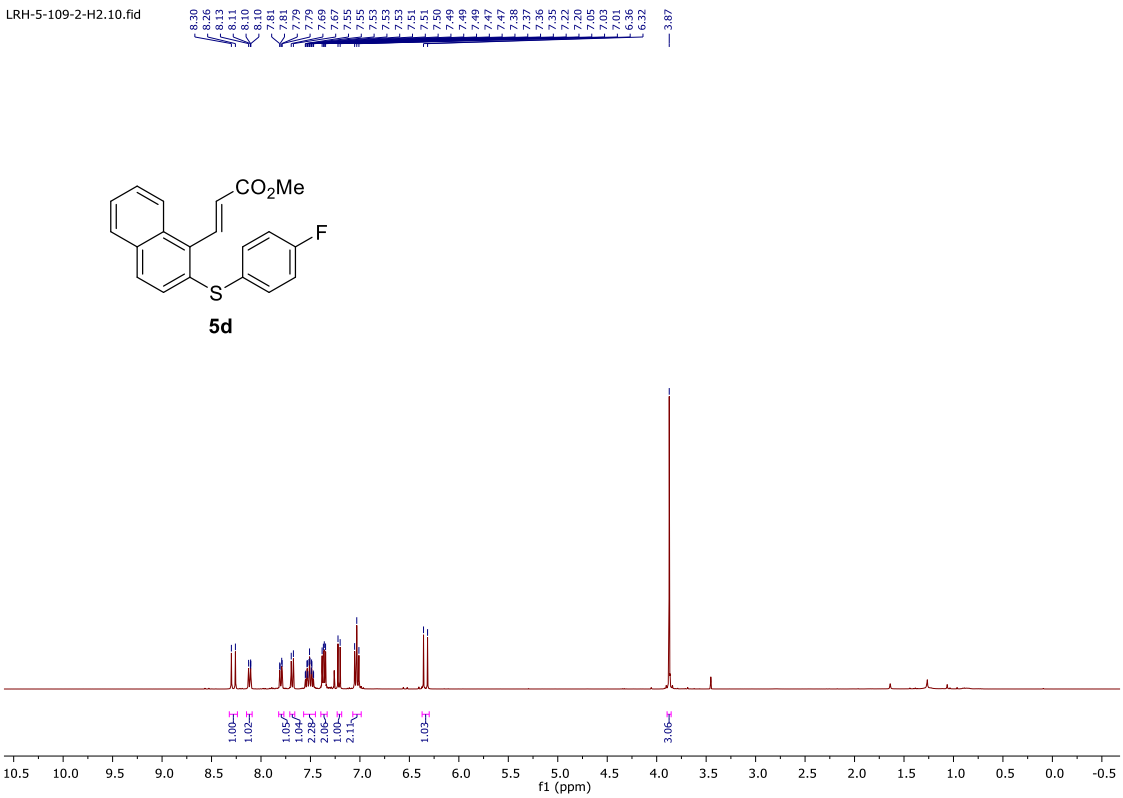

Figure 5.102. ^{13}C NMR Spectrum of 5d

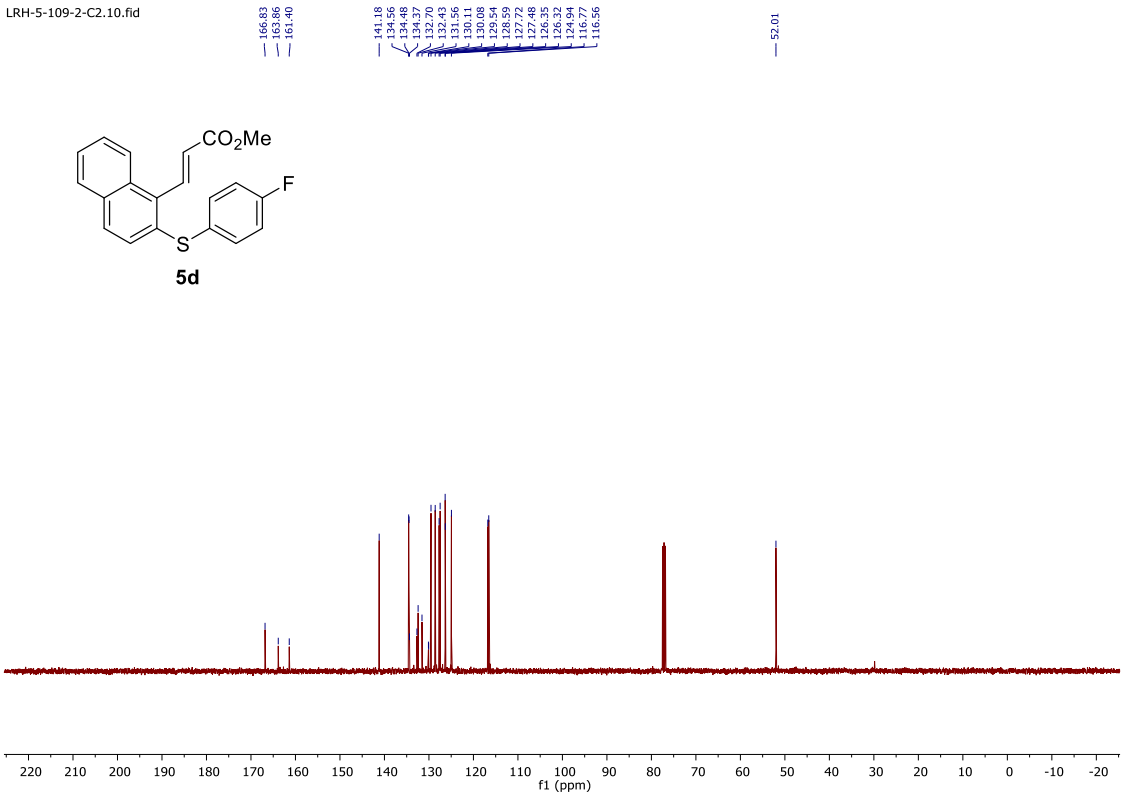

Figure 5.103. ^{19}F NMR Spectrum of 5d

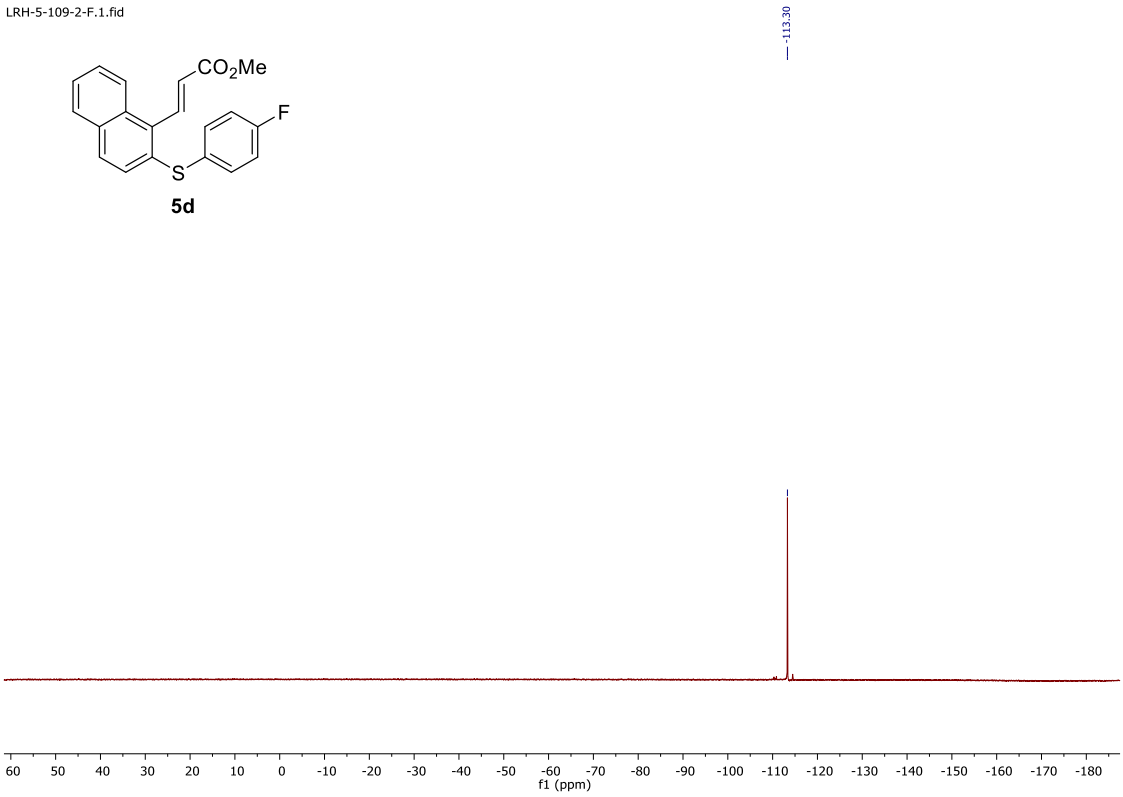

Figure 5.104. ^{1}H NMR Spectrum of 5e

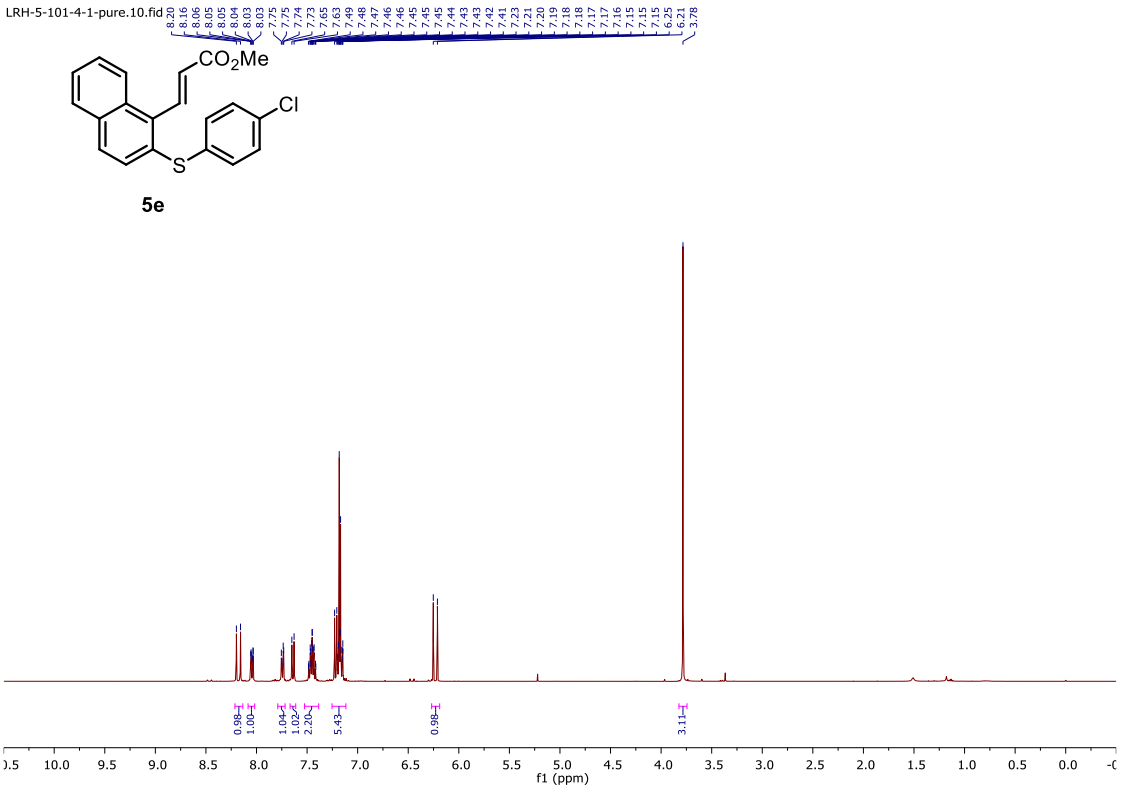

Figure 5.105. ^{13}C NMR Spectrum of 5e

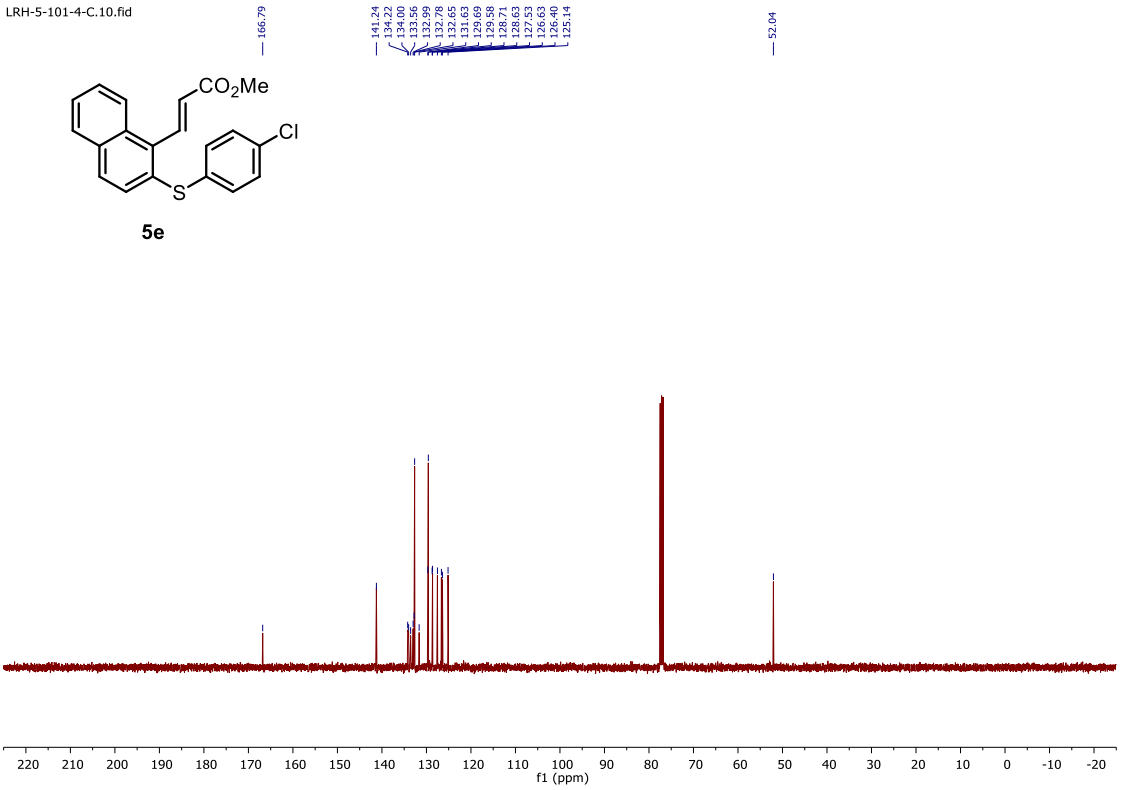

Figure 5.106. ^{1}H NMR Spectrum of 5f

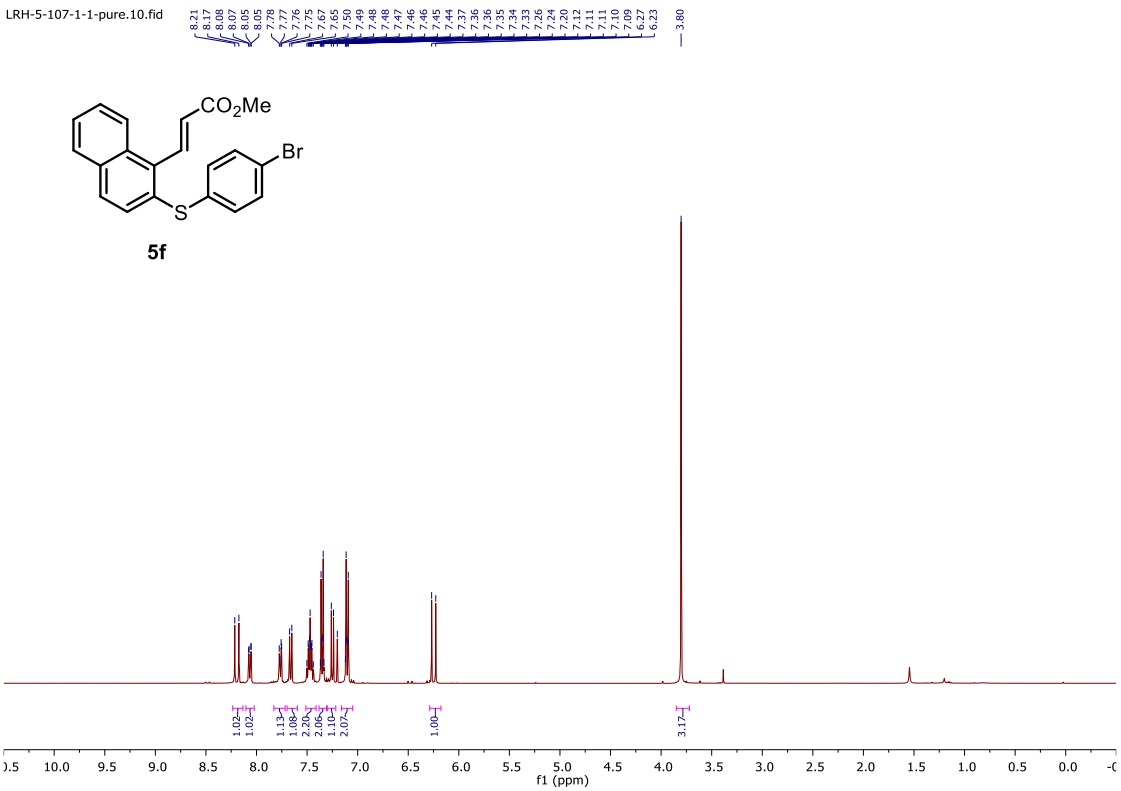

Figure 5.107. ^{13}C NMR Spectrum of 5f

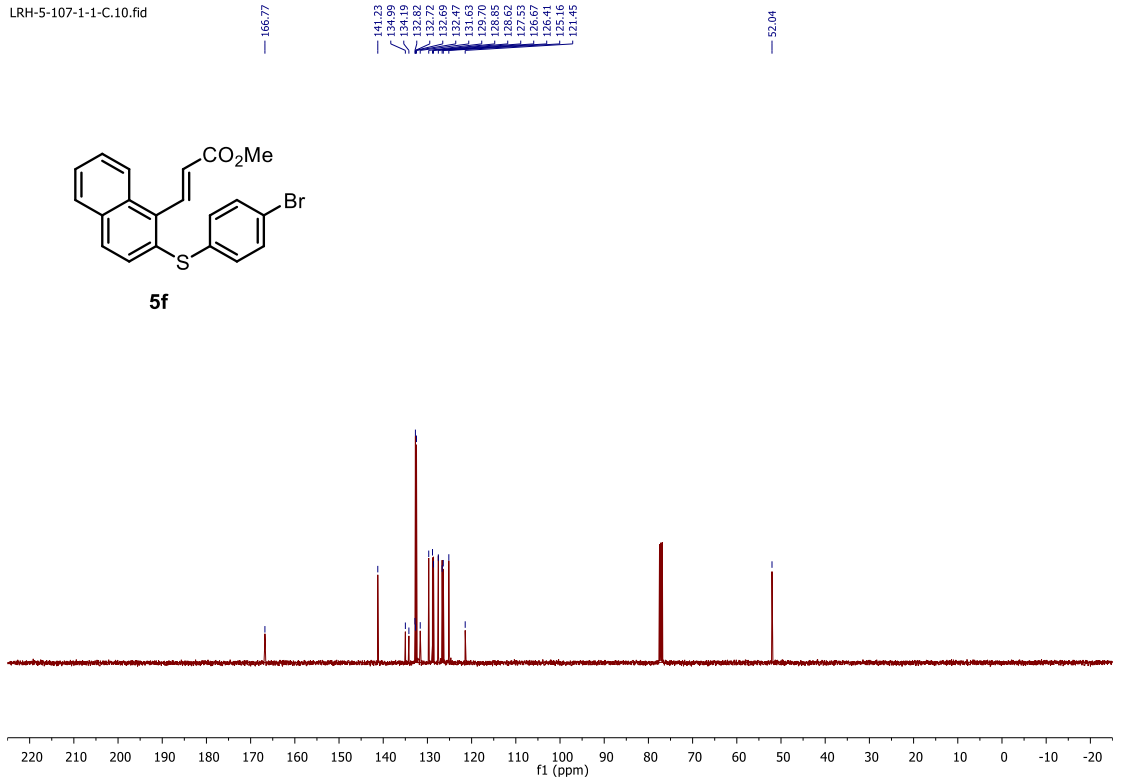

Figure 5.108. ^{1}H NMR Spectrum of 5g

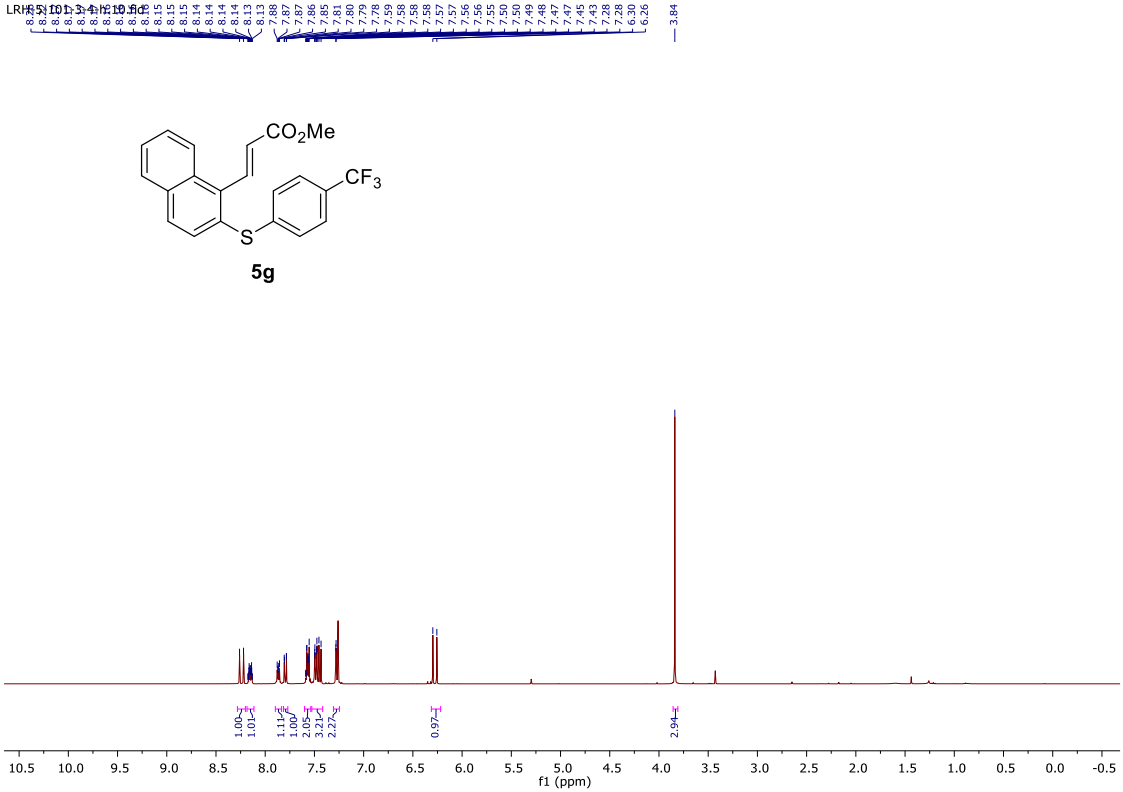

Figure 5.109. ^{13}C NMR Spectrum of 5g

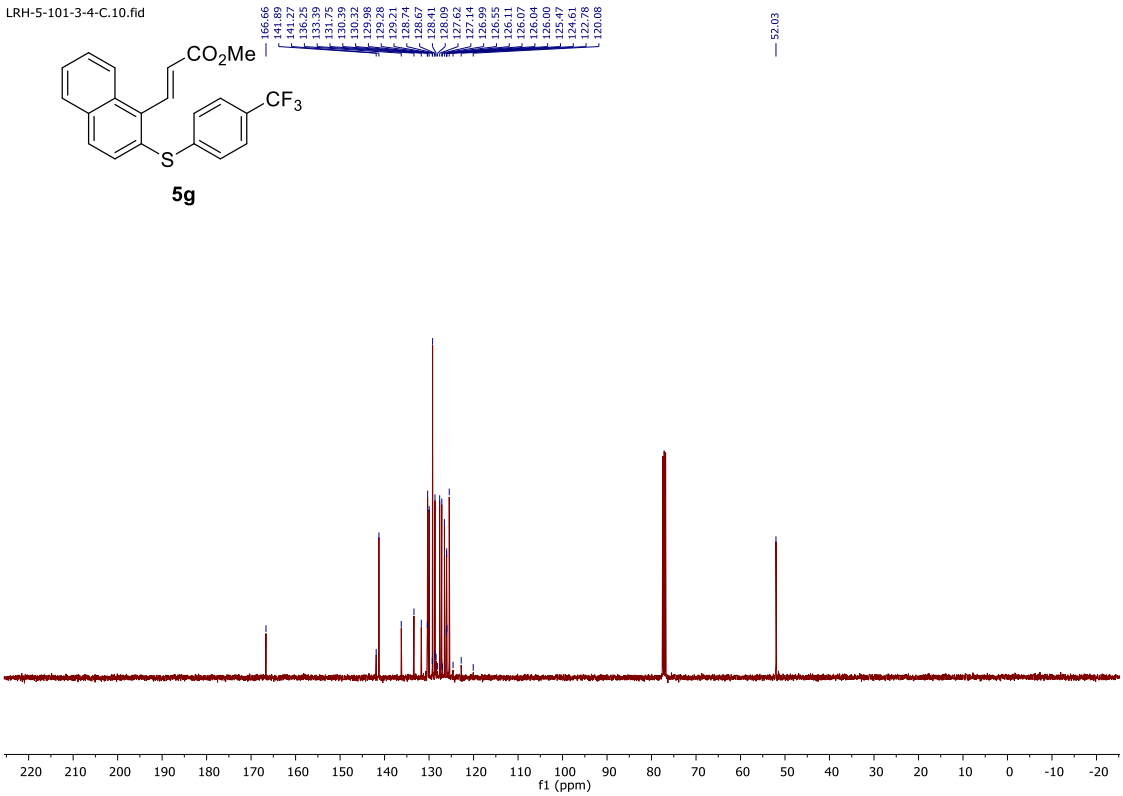

Figure 5.110. ^{19}F NMR Spectrum of 5g

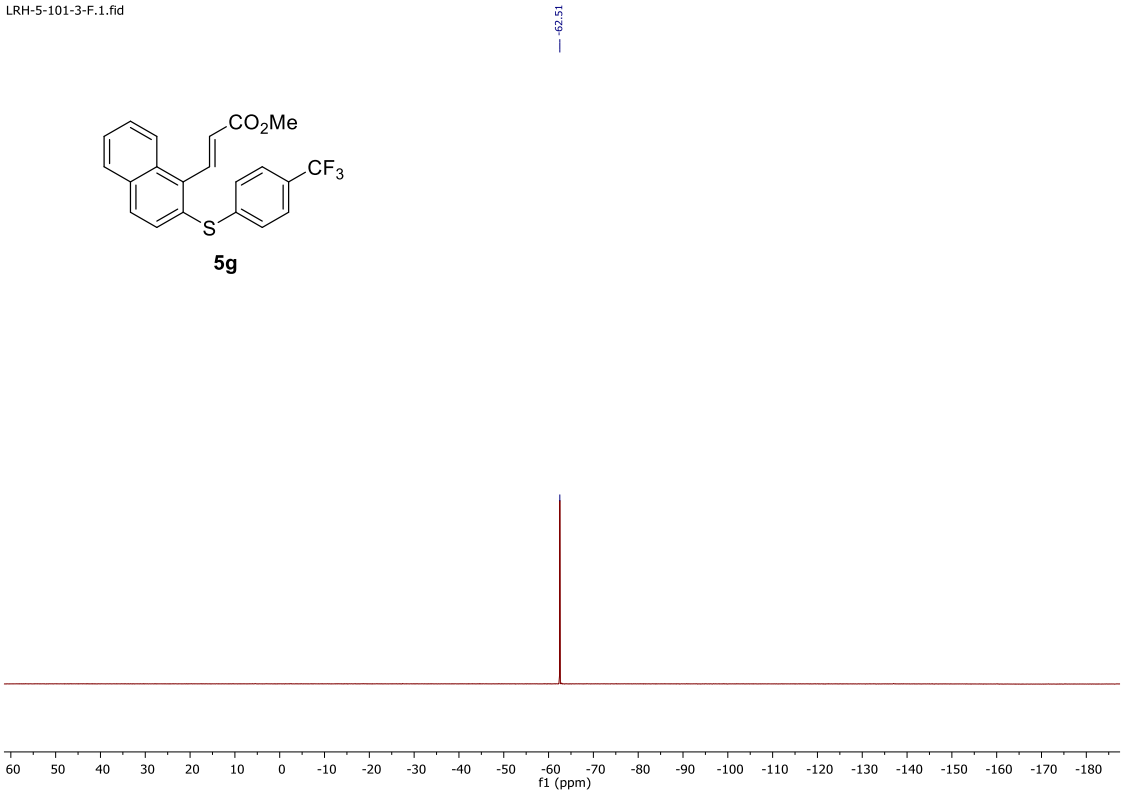

Figure 5.111. ^{1}H NMR Spectrum of 5h

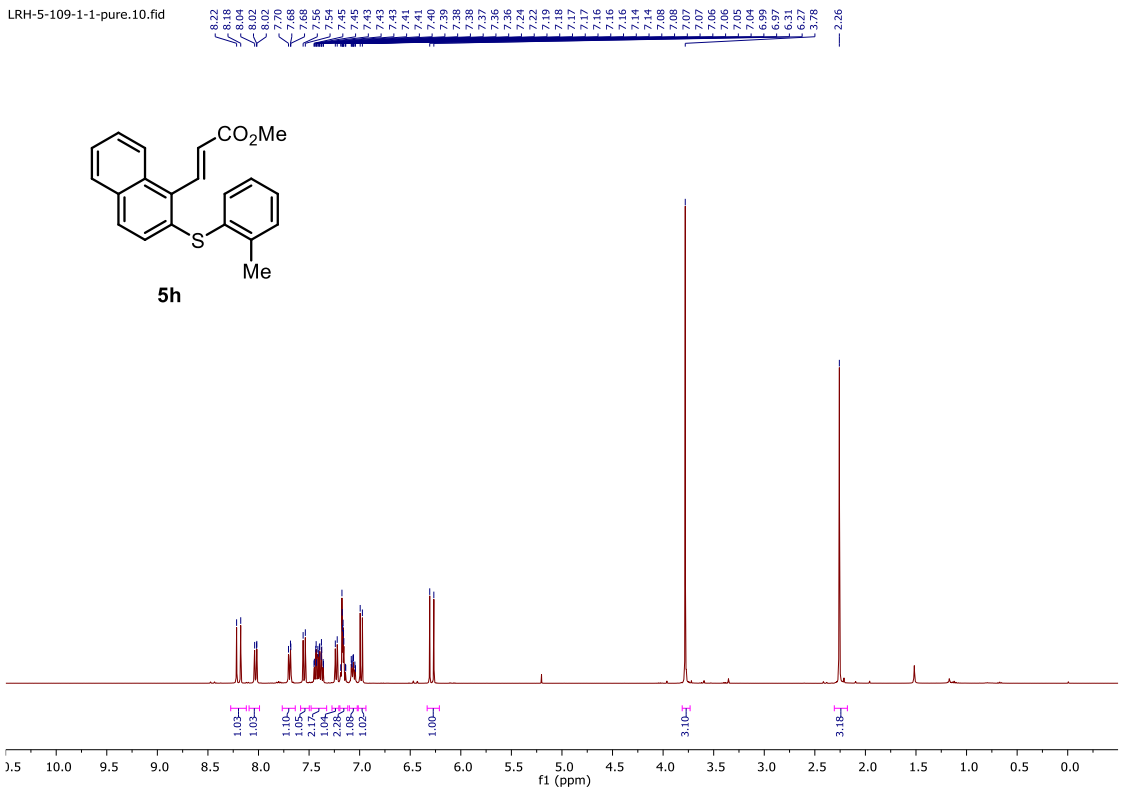

Figure 5.112. ^{13}C NMR Spectrum of 5h

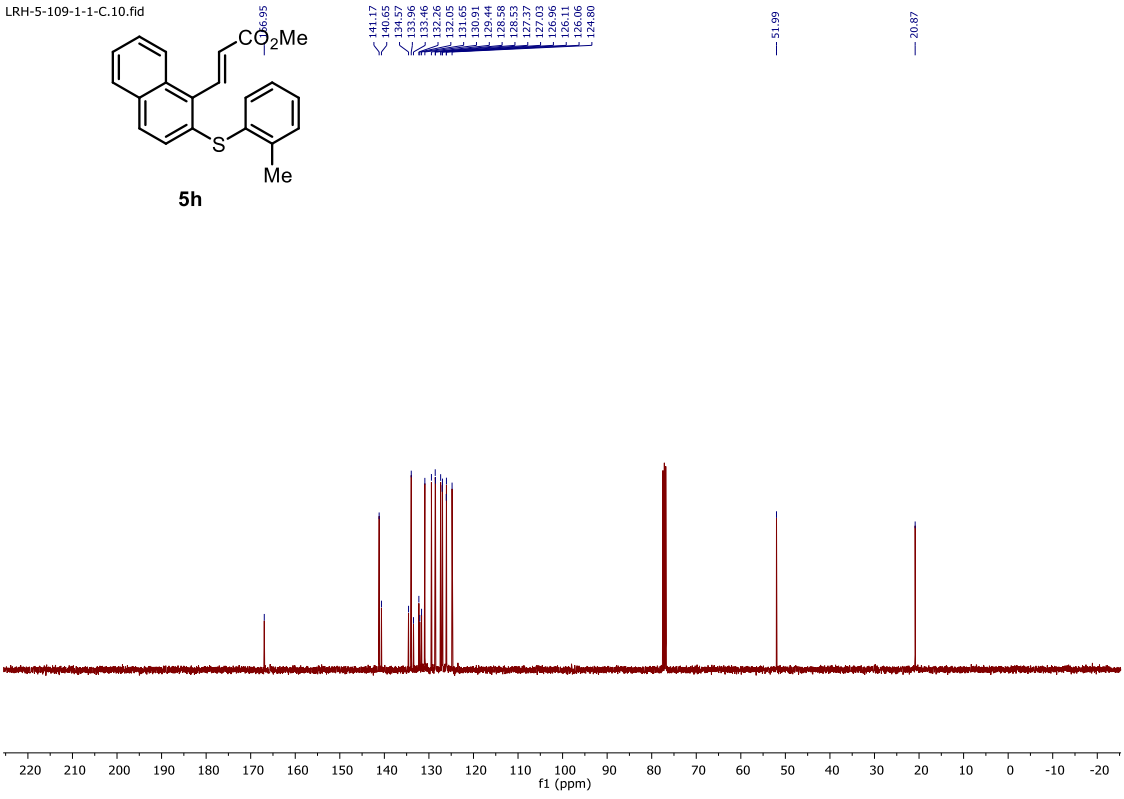

Figure 5.113. ^{1}H NMR Spectrum of 5i

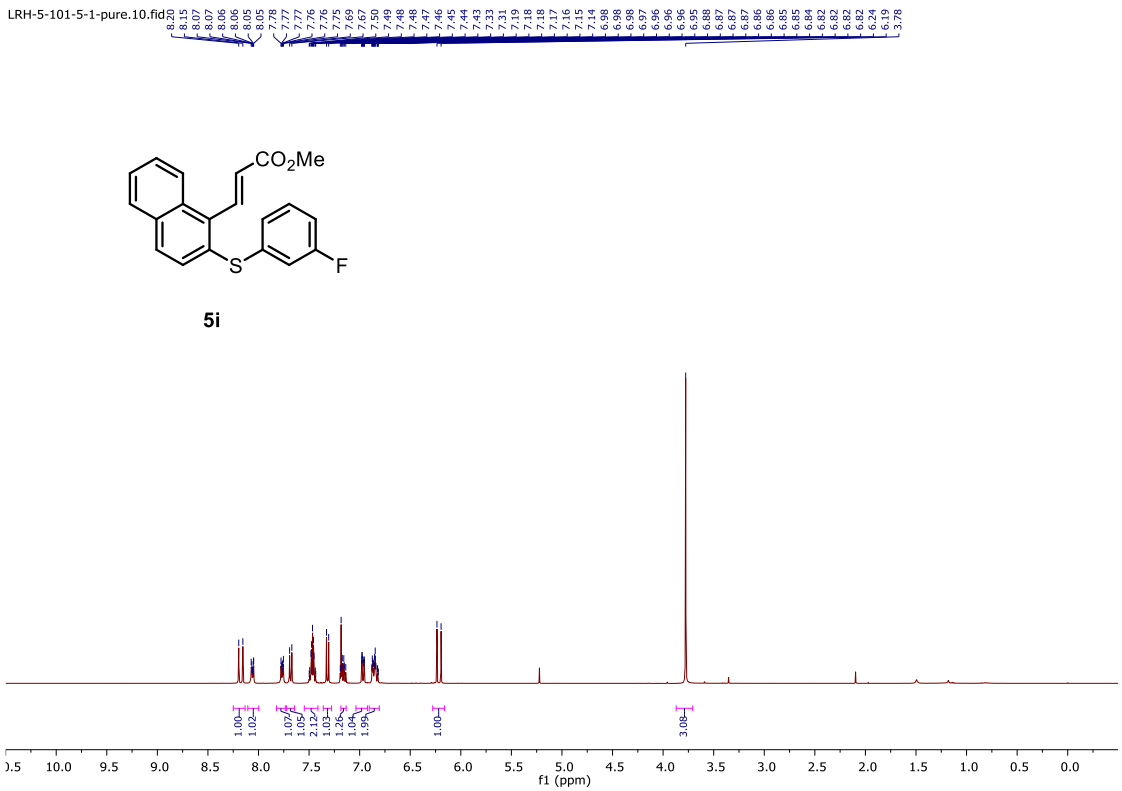

Figure 5.114. ^{13}C NMR Spectrum of 5i

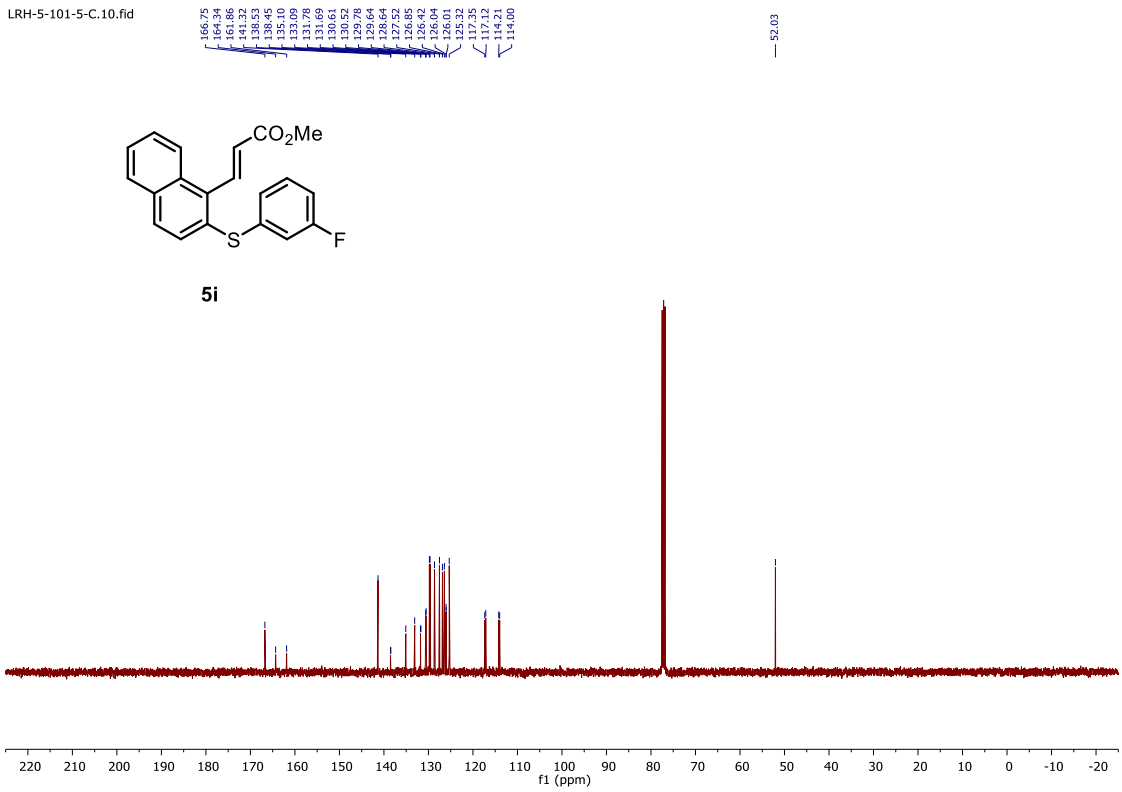

Figure 5.115. ^{19}F NMR Spectrum of 5i

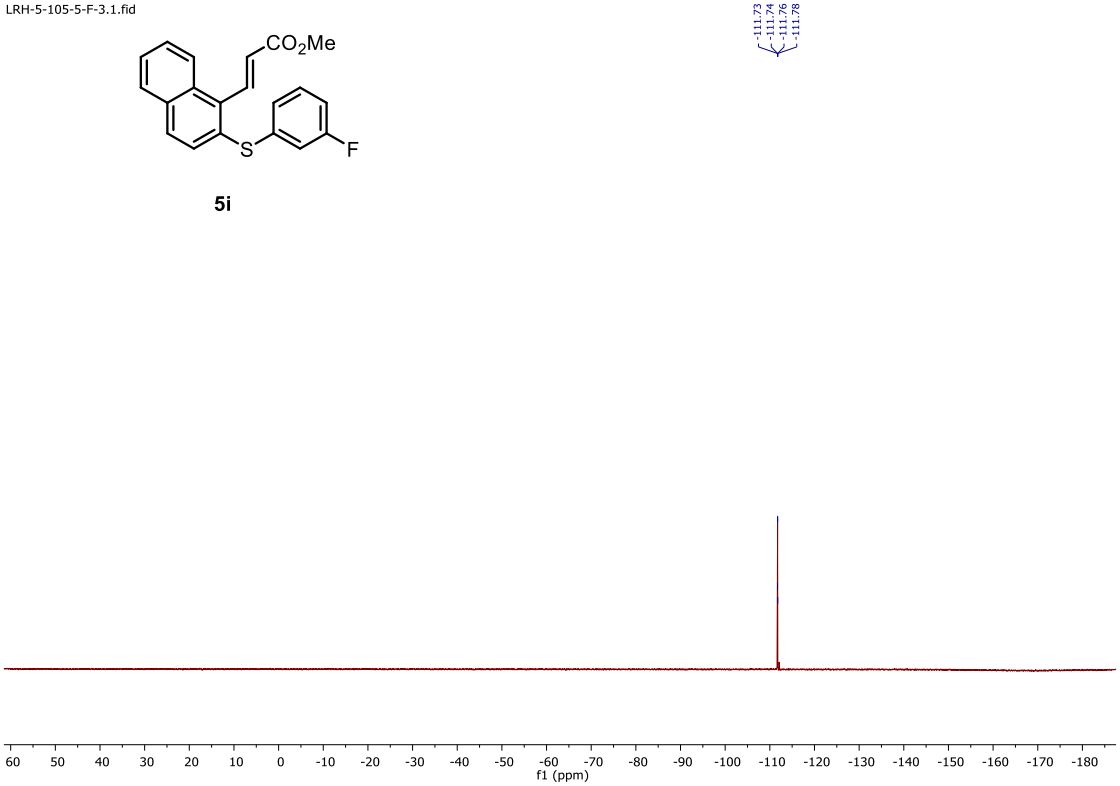

5i

Figure 5.116. ^{1}H NMR Spectrum of 5j

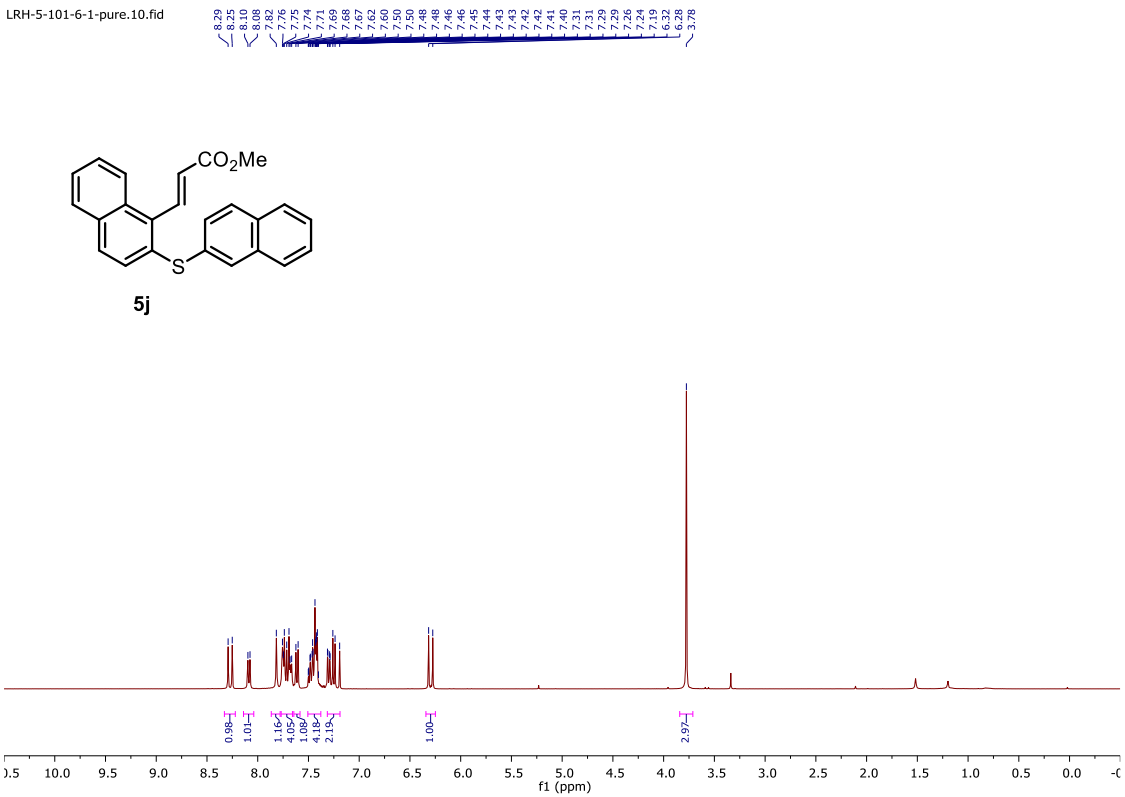

Figure 5.117. ^{13}C NMR Spectrum of 5j

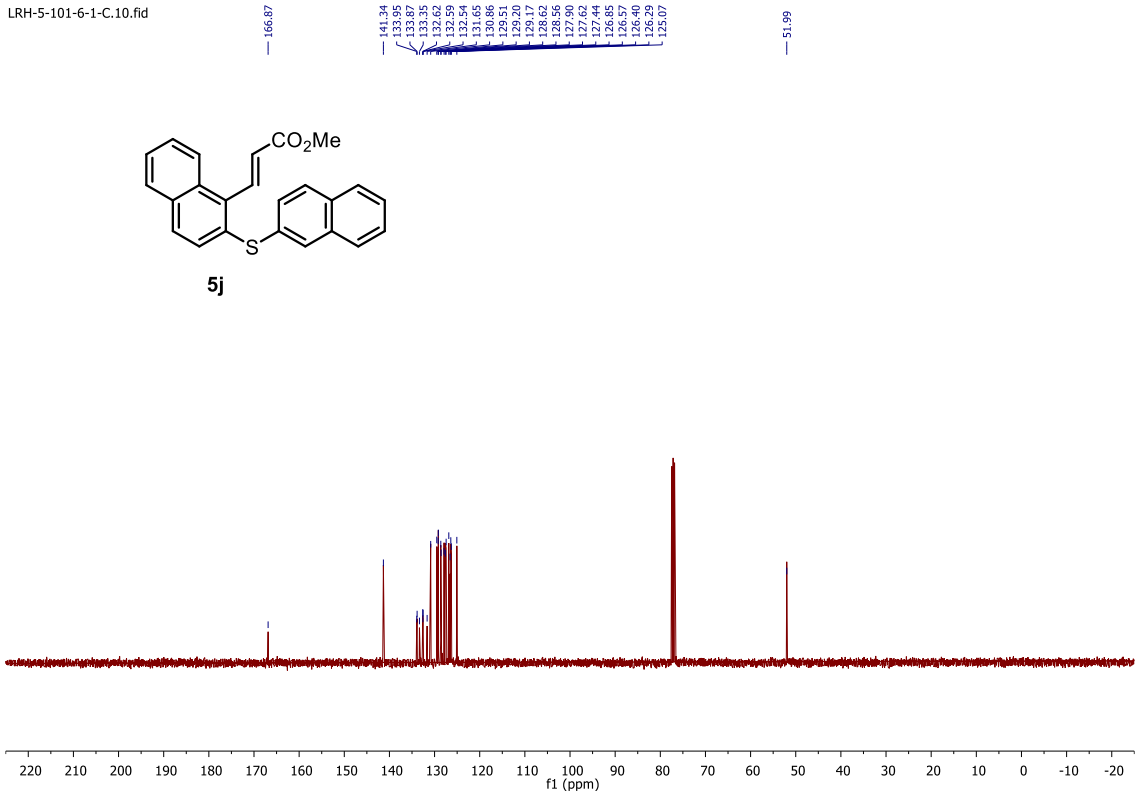

Figure 5.118. ^{1}H NMR Spectrum of 5k

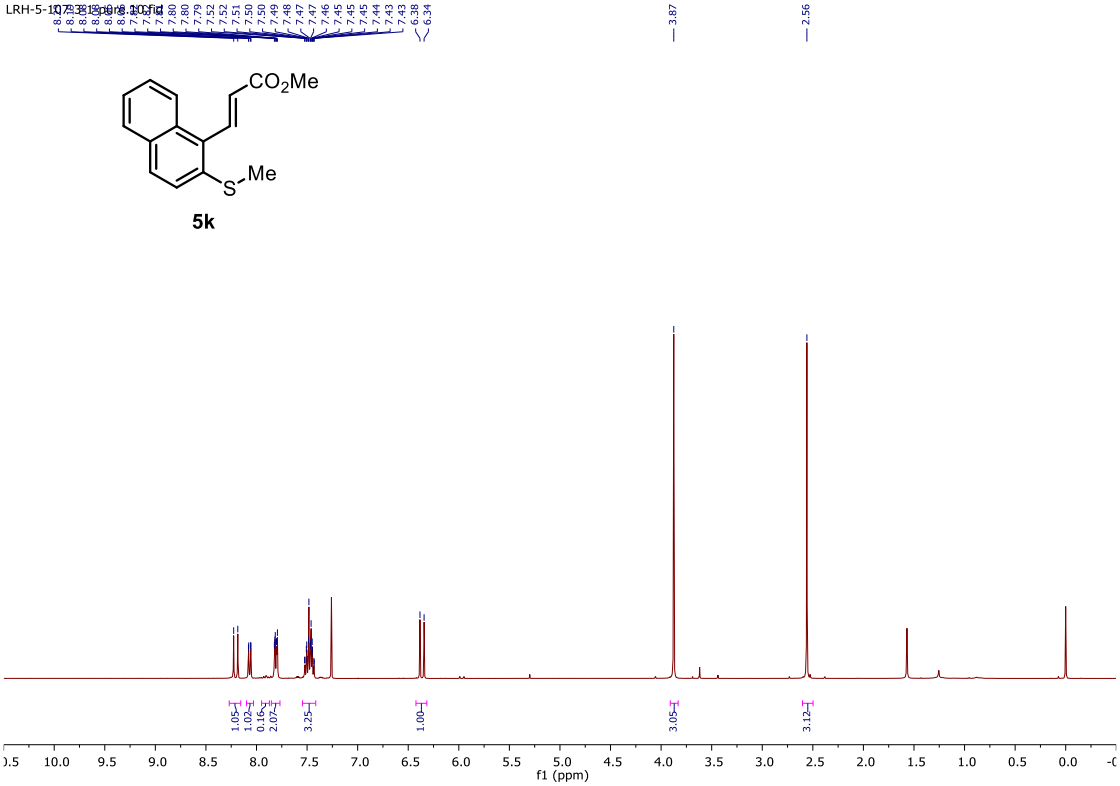

Figure 5.119. ^{13}C NMR Spectrum of 5k

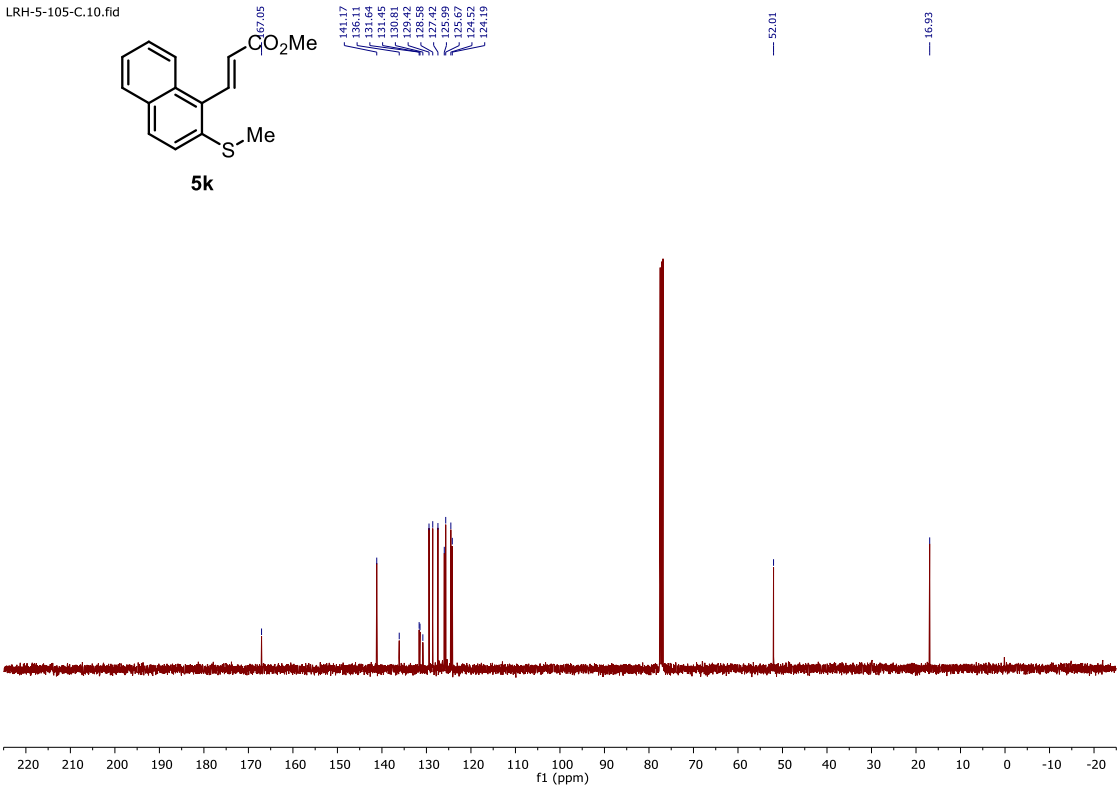

Figure 5.120. ^{1}H NMR Spectrum of 5l

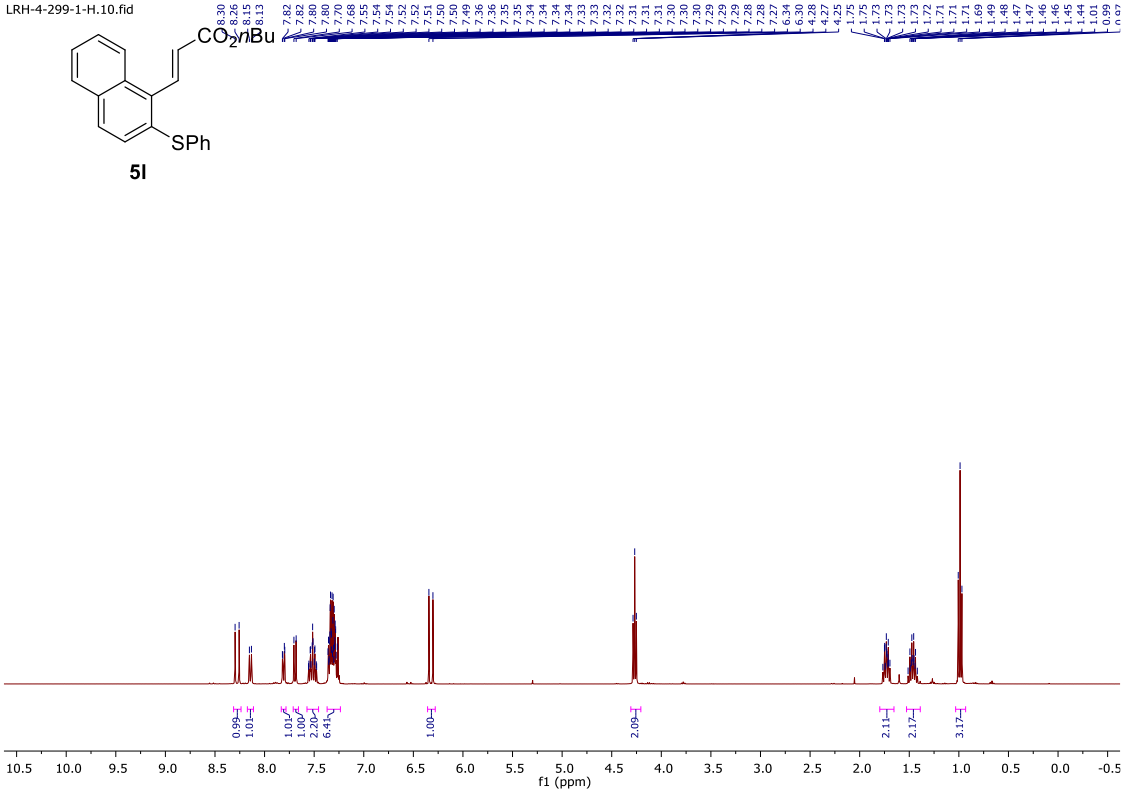

Figure 5.121. ^{13}C NMR Spectrum of 5l

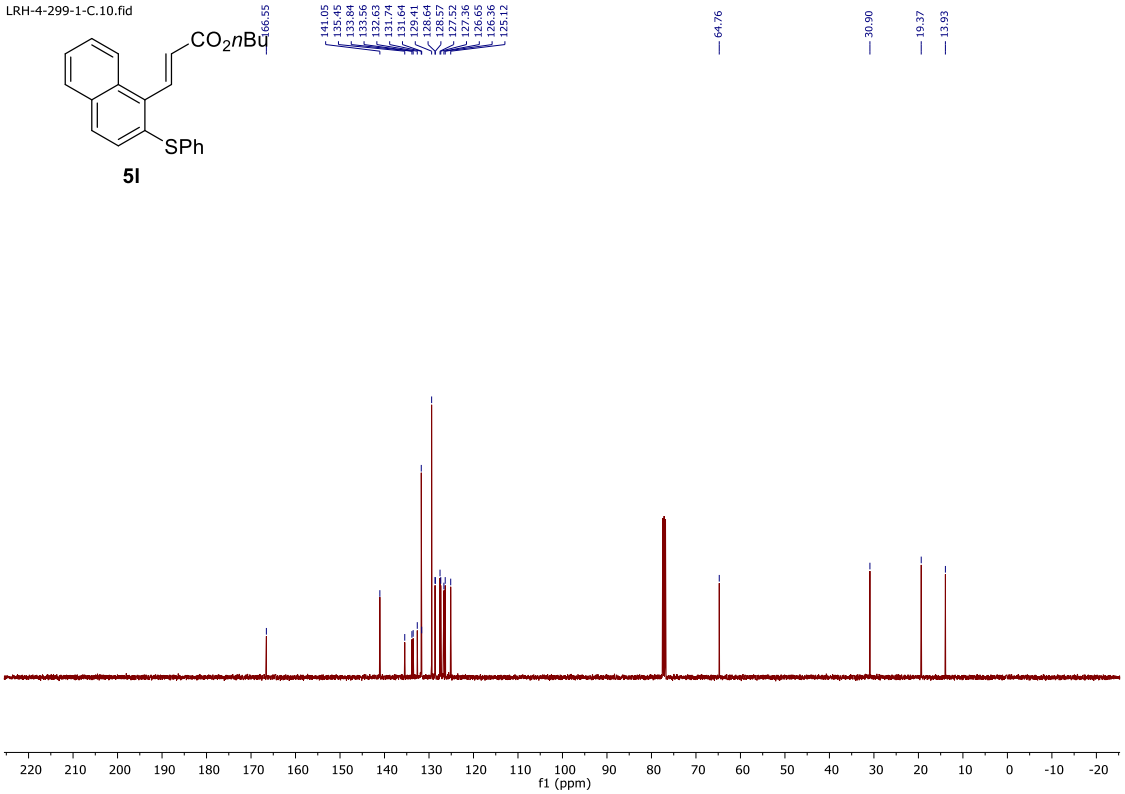

Figure 5.122. ^{1}H NMR Spectrum of 5m

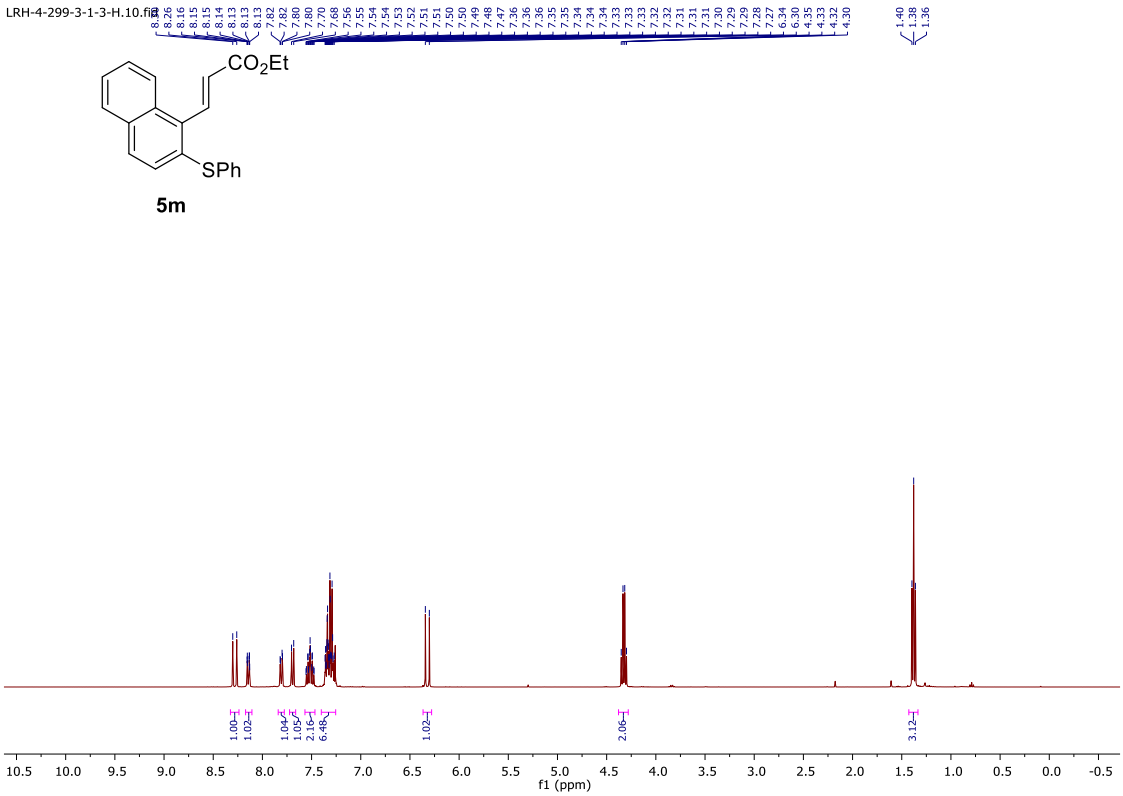

Figure 5.123. ^{13}C NMR Spectrum of 5m

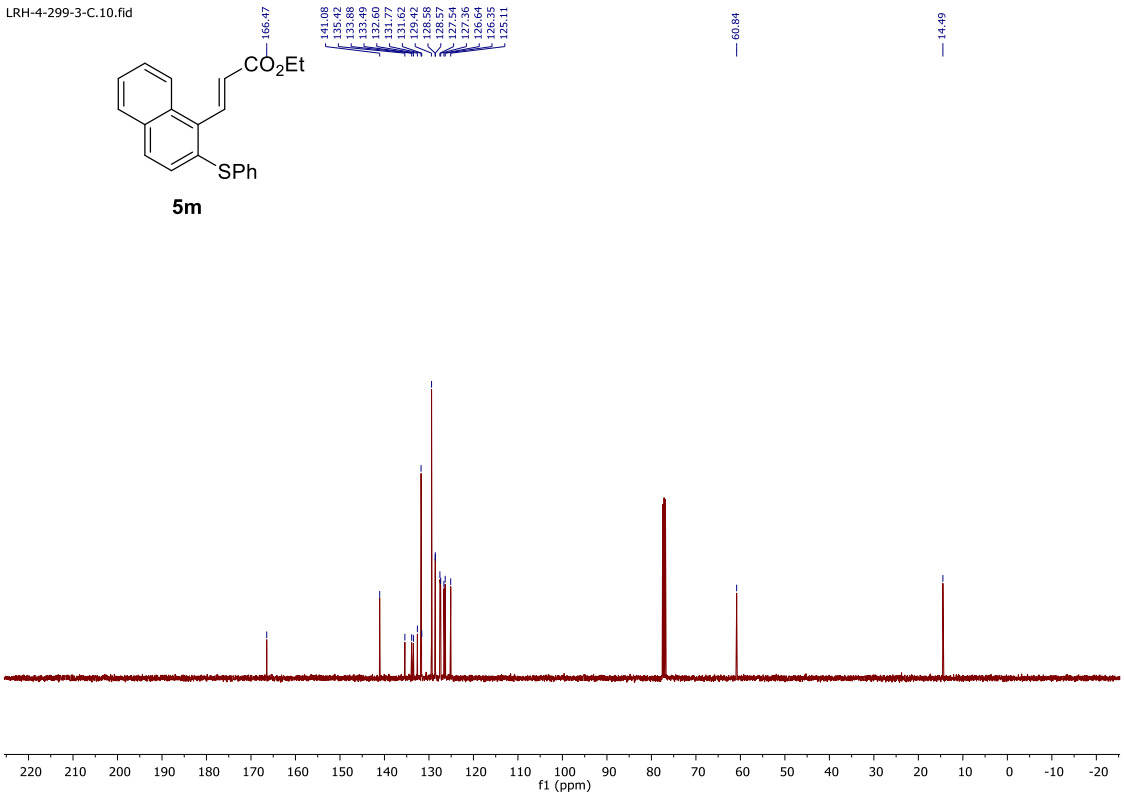

Figure 5.124. ^{1}H NMR Spectrum of 5n

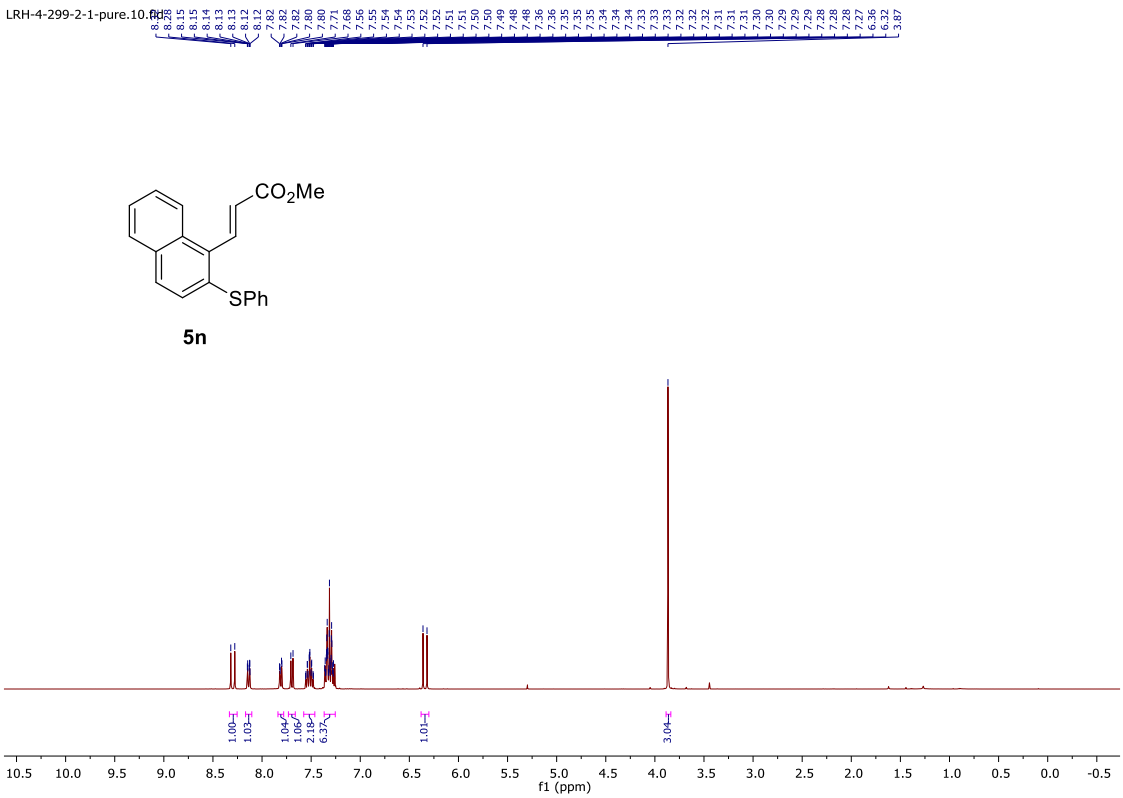

Figure 5.125. ^{13}C NMR Spectrum of 5n

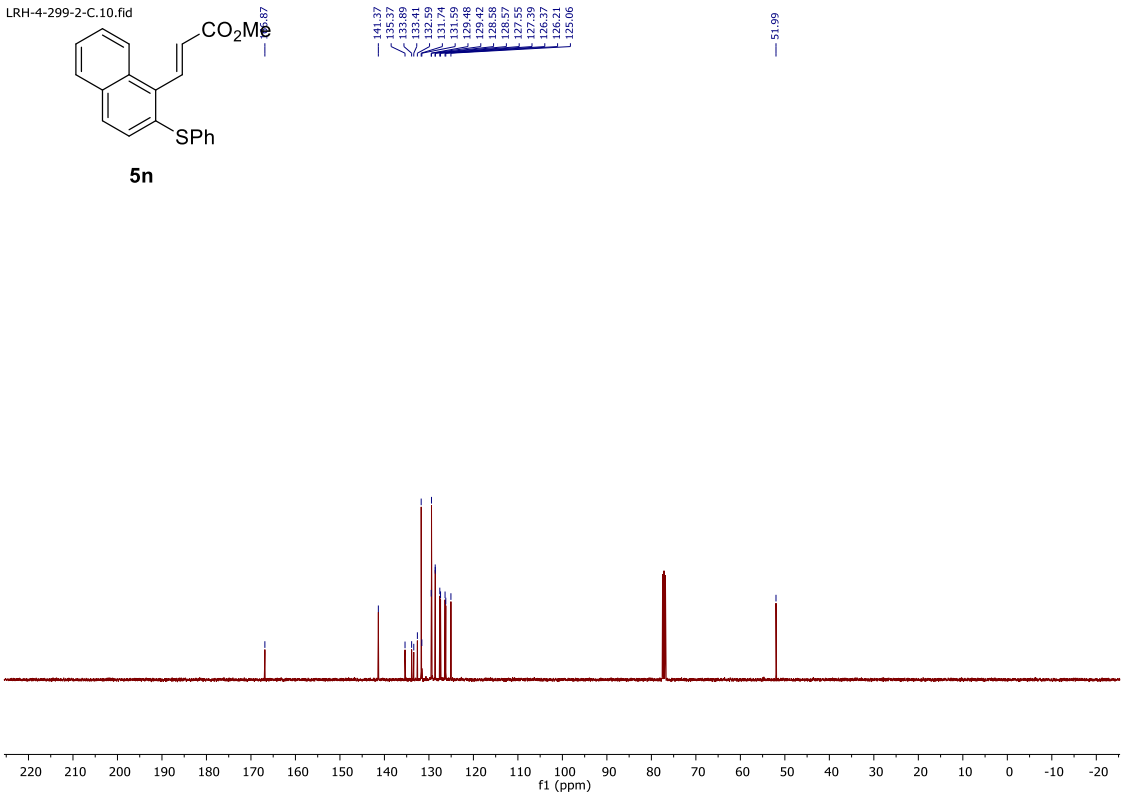

Figure 5.126. ^{1}H NMR Spectrum of 5o

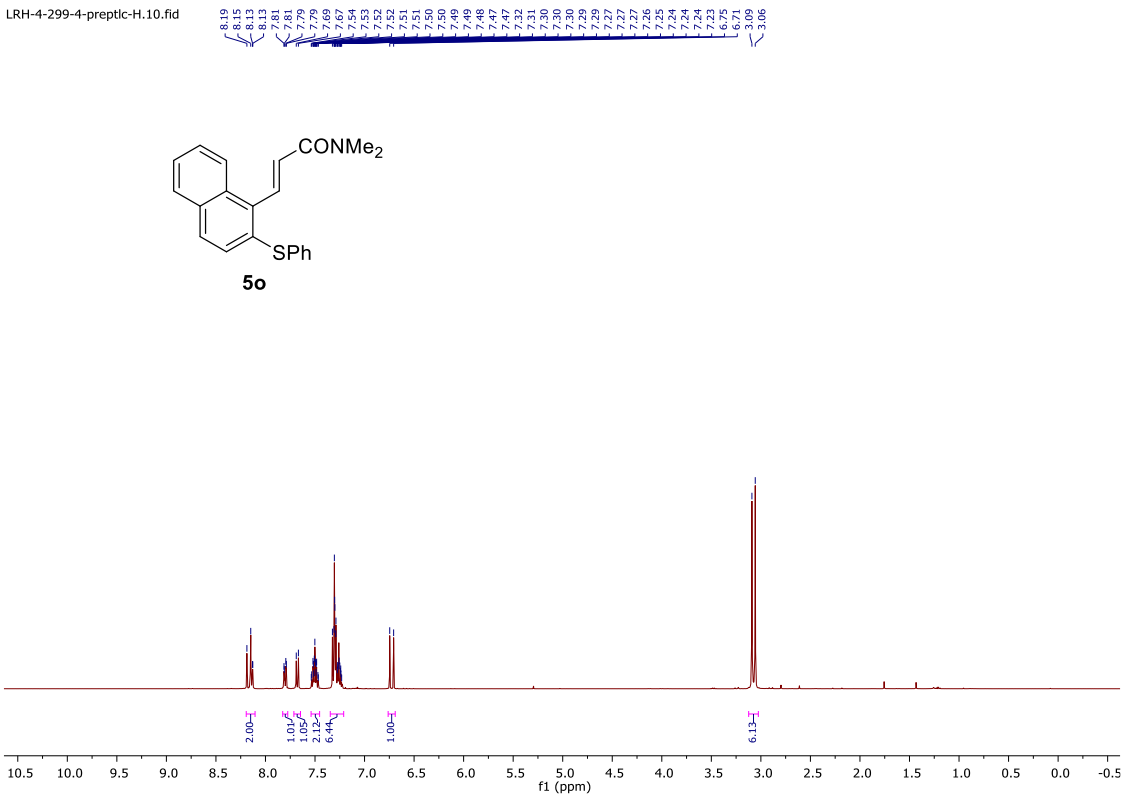

Figure 5.127. ^{13}C NMR Spectrum of 5o

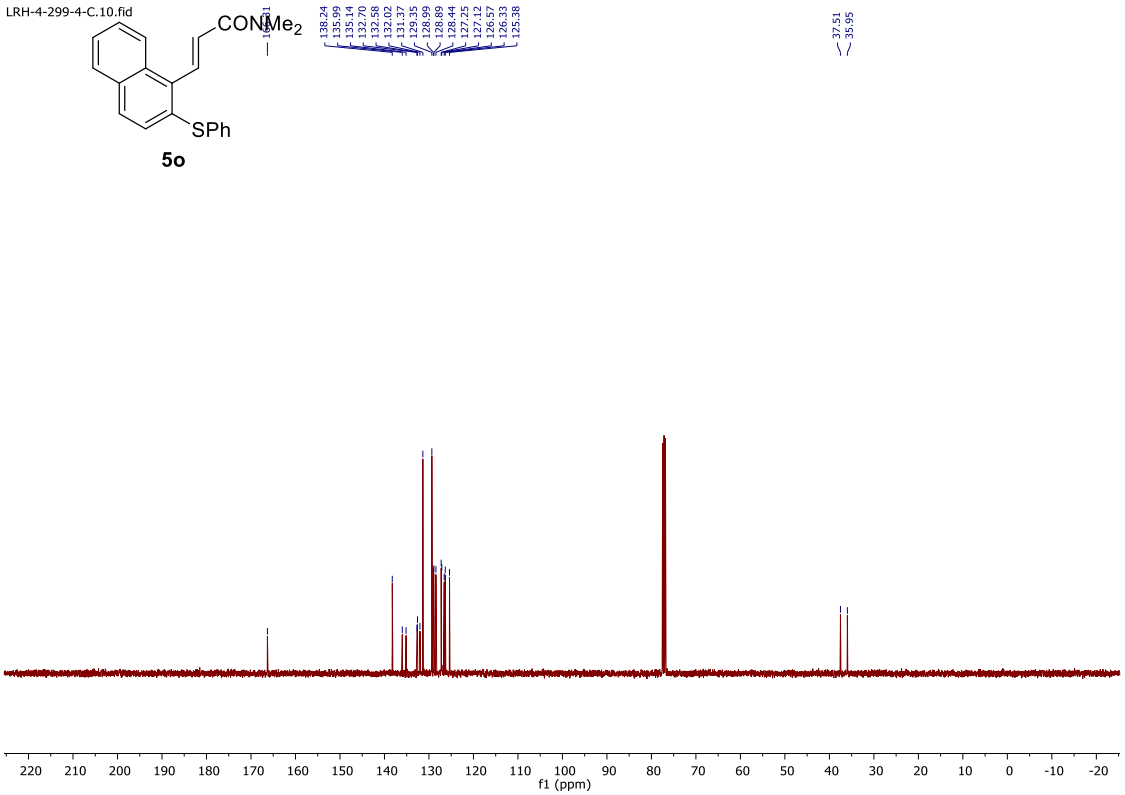

Figure 5.128. ^{1}H NMR Spectrum of 6a

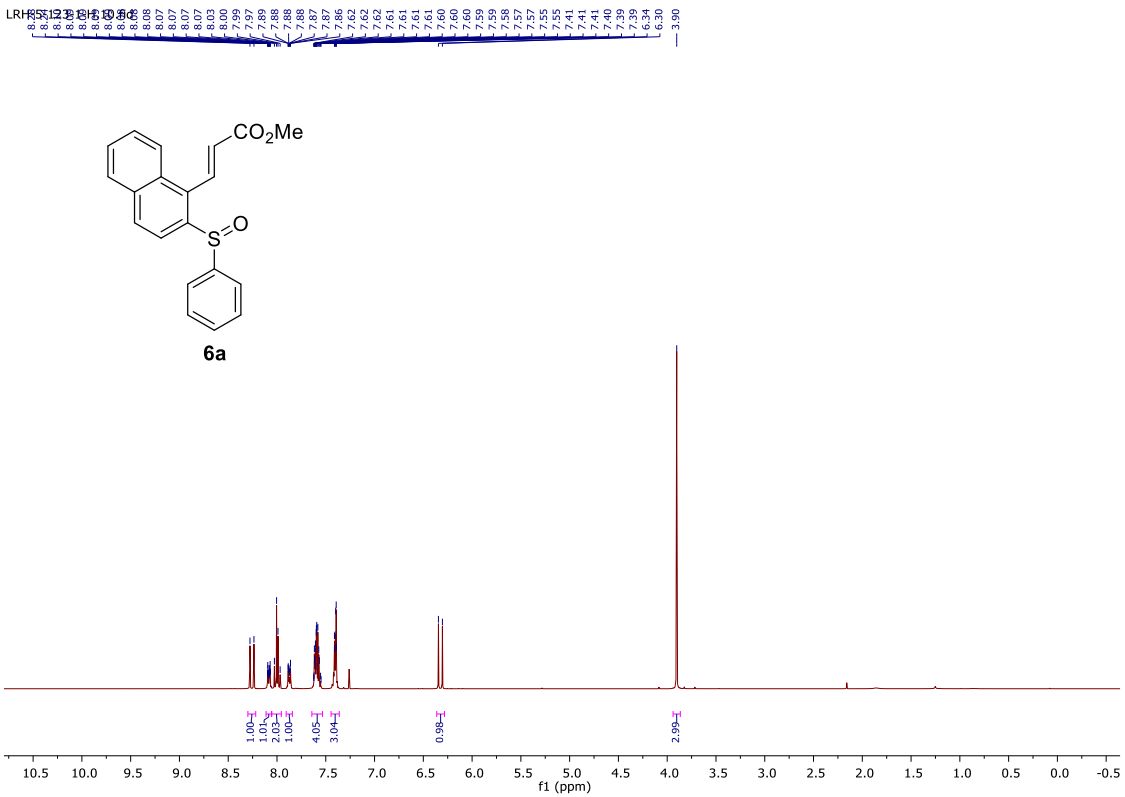

Figure 5.129. ^{13}C NMR Spectrum of 6a

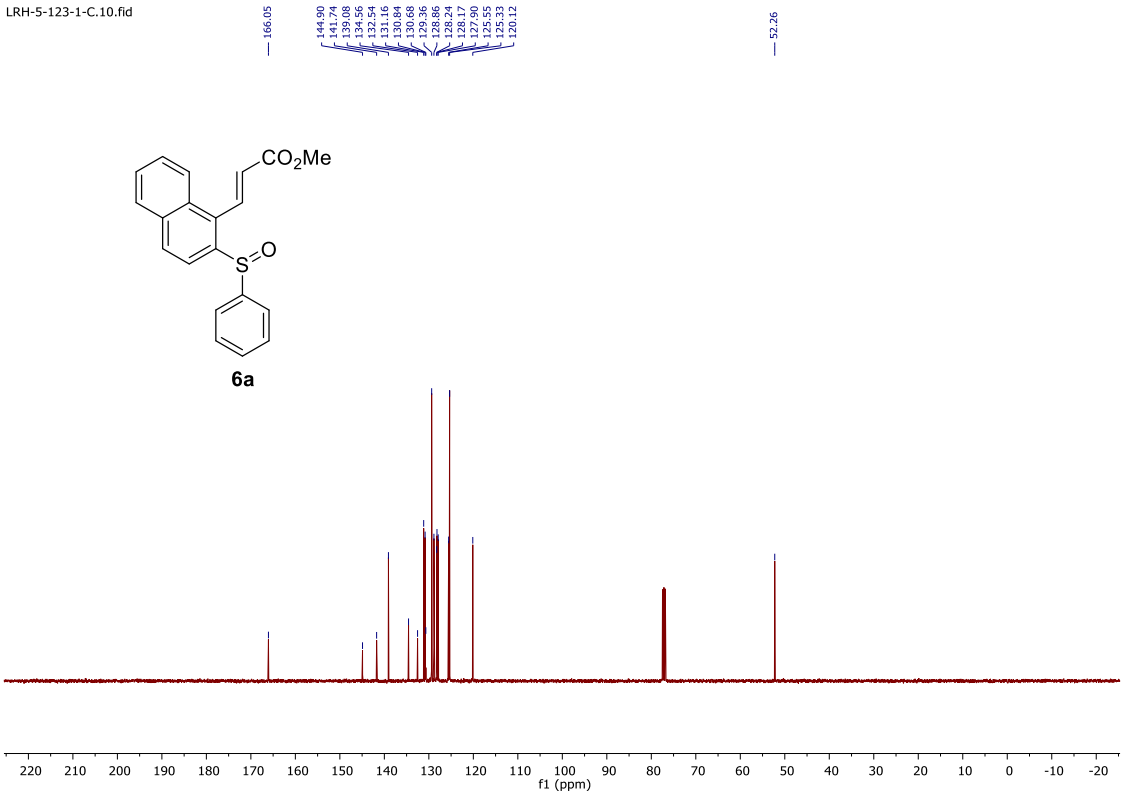

Figure 5.130. ^{1}H NMR Spectrum of 6b

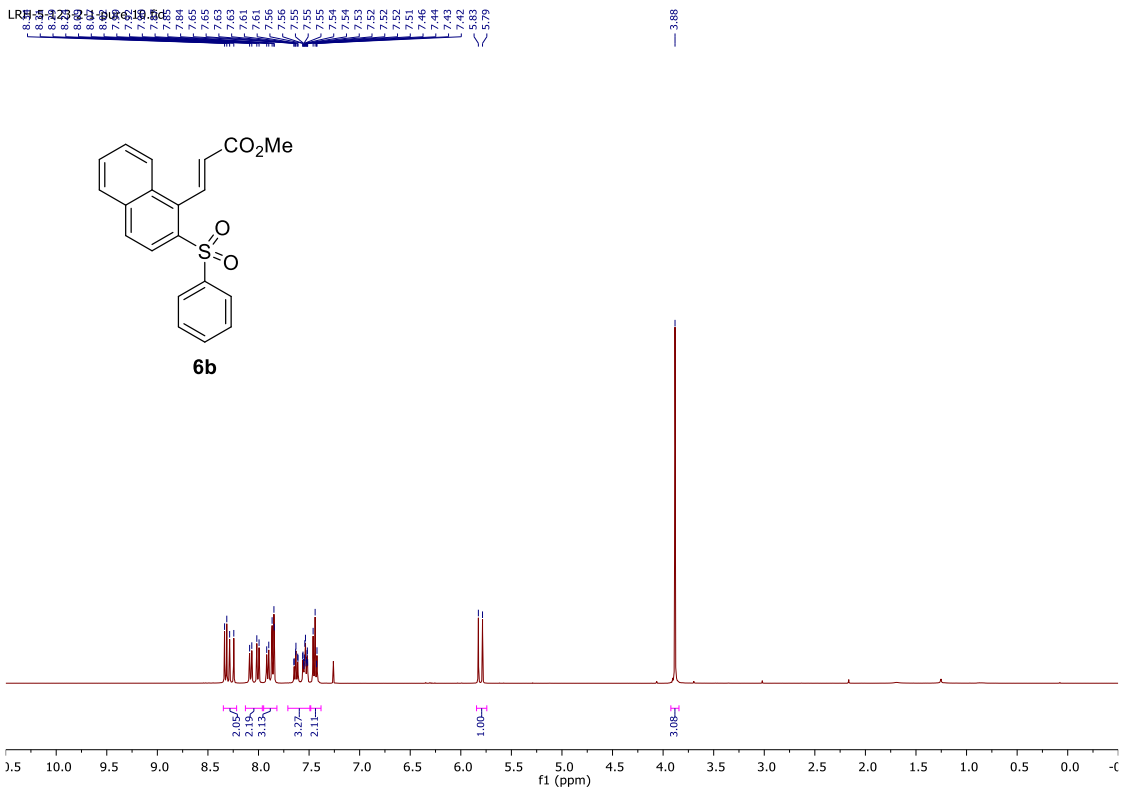

Figure 5.131. ^{13}C NMR Spectrum of 6b

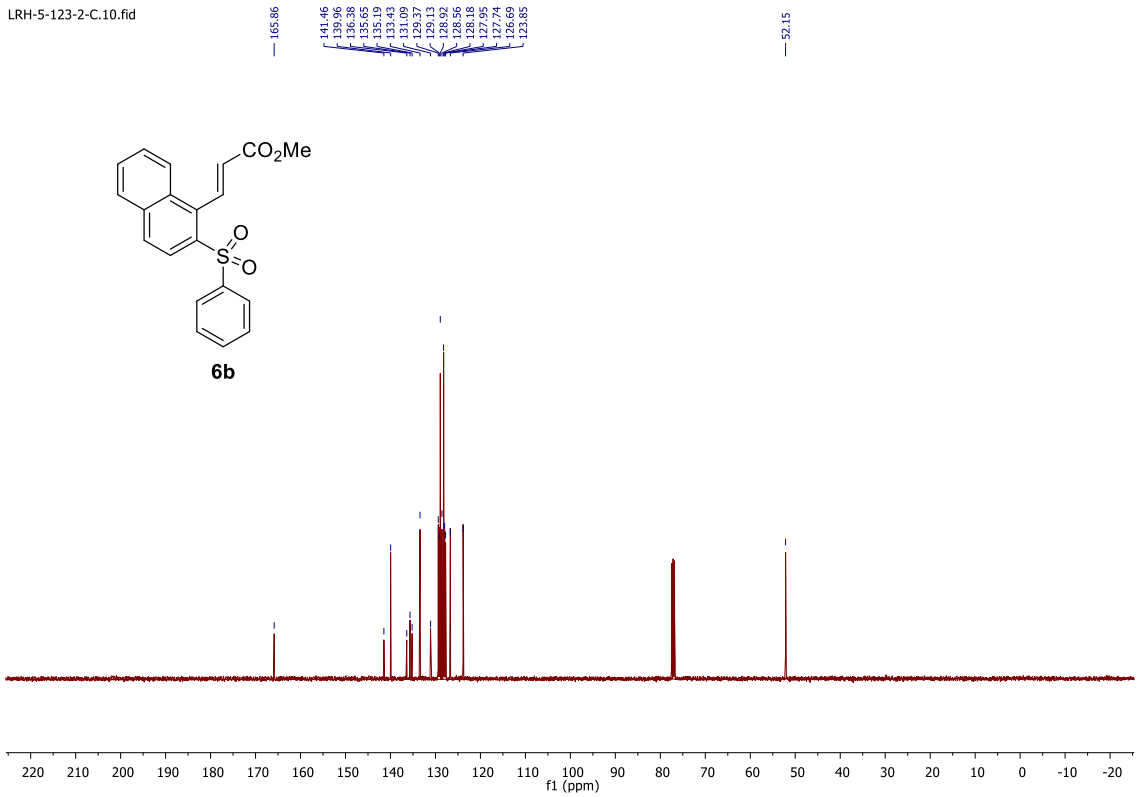

Figure 5.132. ^{1}H NMR Spectrum of 9

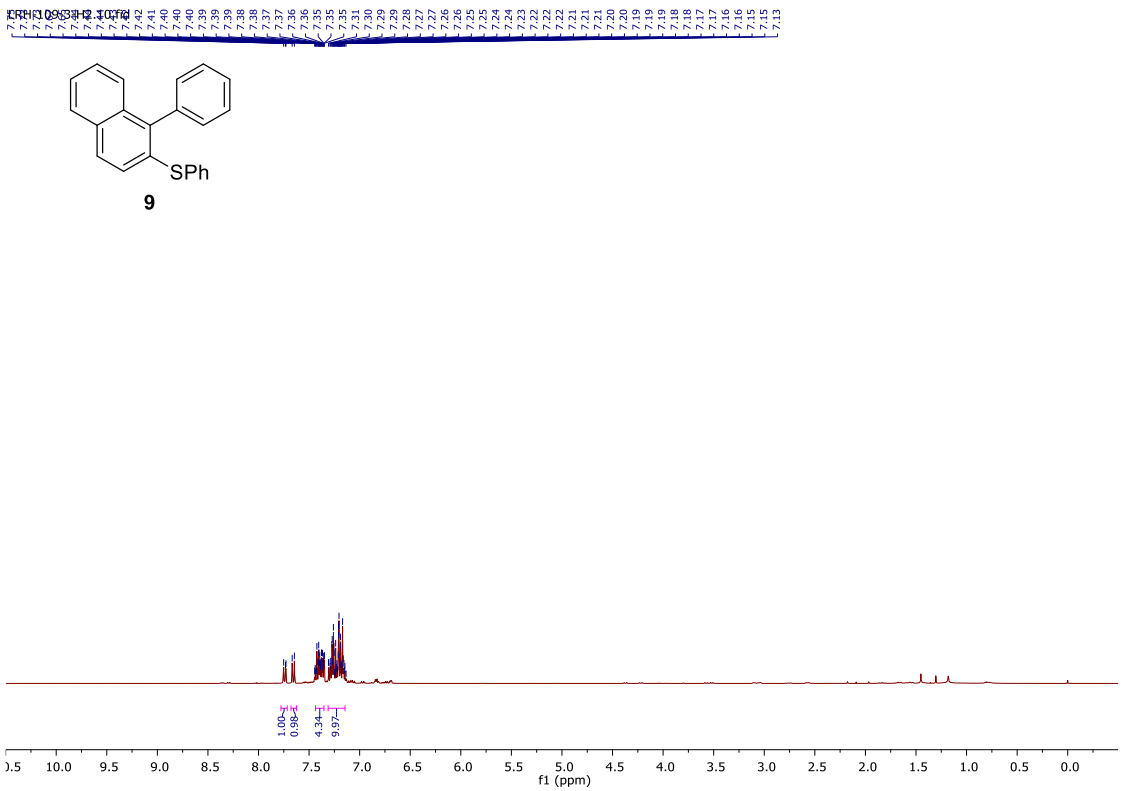

Figure 5.133. ^{13}C NMR Spectrum of 9

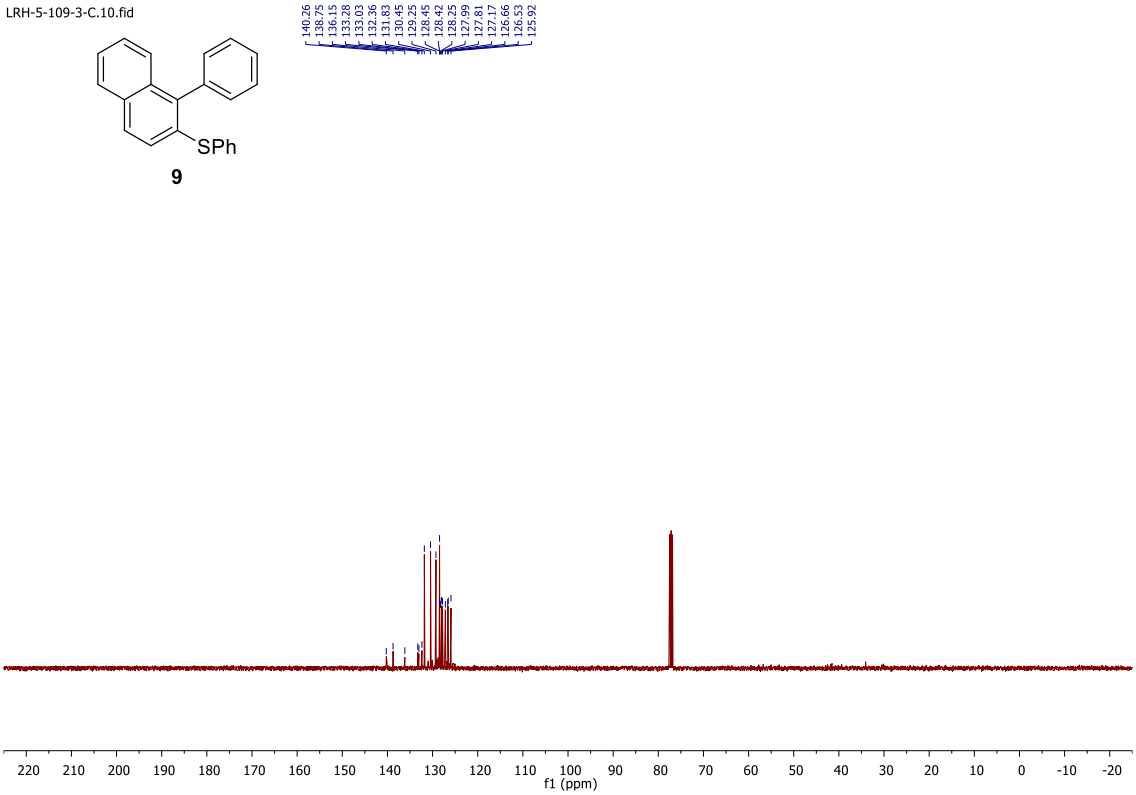

Figure 5.134. ^{1}H NMR Spectrum of 11

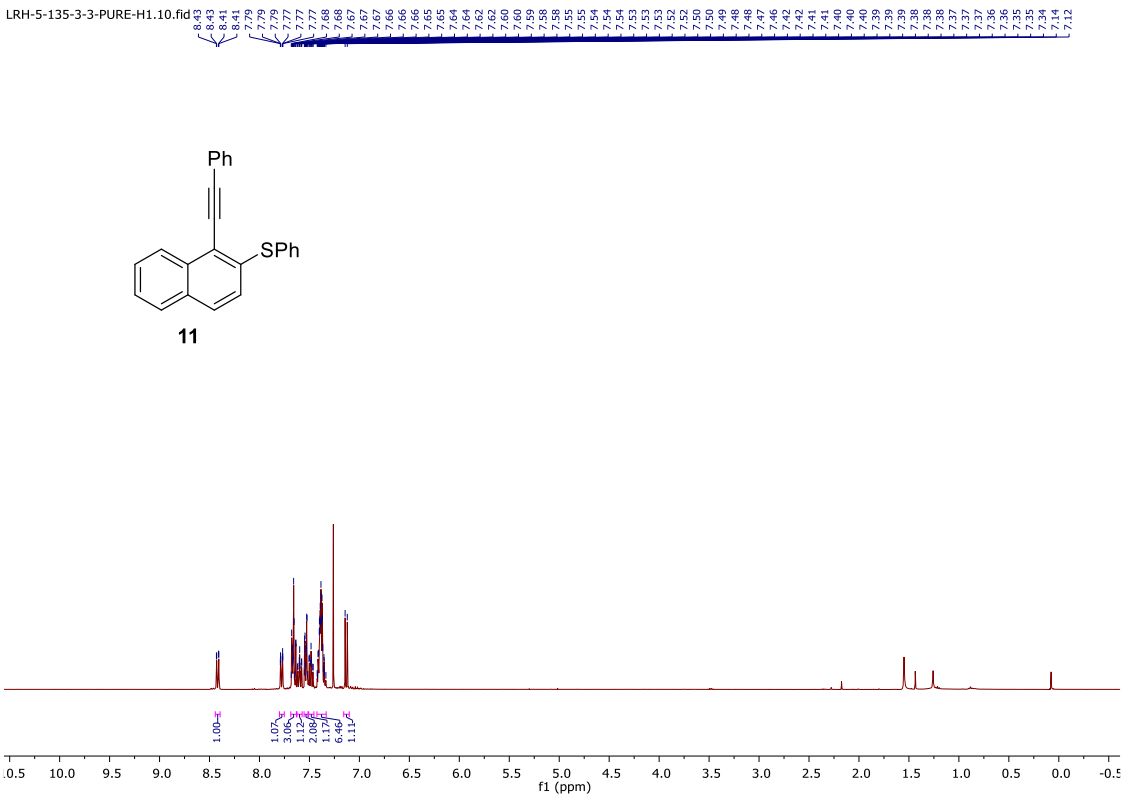

Figure 5.135. ^{13}C NMR Spectrum of 11

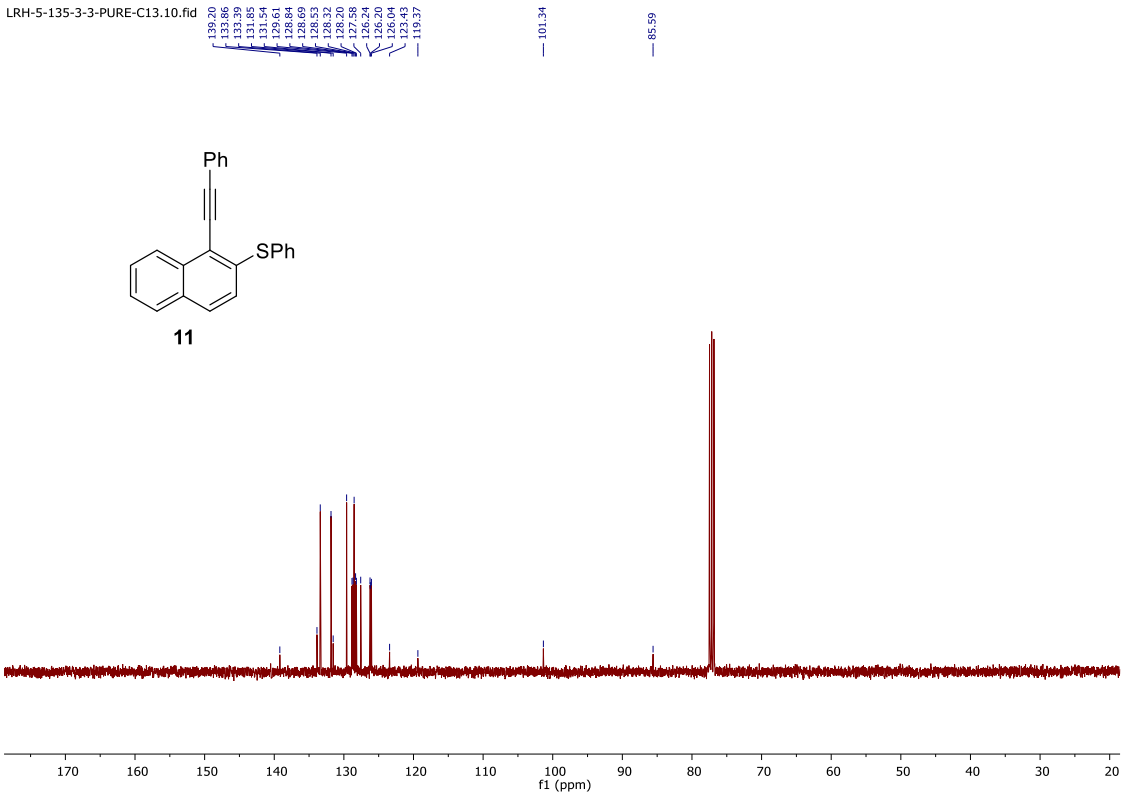

5.6 Crystallographic Data

Table 5.6. X-Ray Structure and Crystallographic Data of 4e

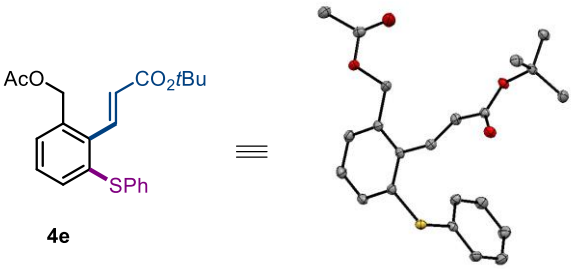

4e

CCDC: 1906772

Identification code	RHL-key
Empirical formula	$C_{22}H_{24}O_4S$
Formula weight	384.47
Temperature/K	100(2)
Crystal system	triclinic
Space group	P-1
a/Å	5.5071(5)
b/Å	11.5833(10)
c/Å	15.6570(14)
α/°	97.152(2)
β/°	93.856(2)
γ/°	102.375(2)
Volume/Å^3	963.41(15)
Z	2
ρ_{calc}g/cm^3	1.325
μ/mm^{-1}	0.193
F(000)	408.0
Crystal size/mm^3	0.1 × 0.1 × 0.03
Radiation	MoKα (λ = 0.71073)
2Θ range for data collection/°	4.786 to 55.092
Index ranges	-7 ≤ h ≤ 7, -15 ≤ k ≤ 15, -20 ≤ l ≤ 20
Reflections collected	27080
Independent reflections	4421 [R_{int} = 0.0392, R_{sigma} = 0.0311]
Data/restraints/parameters	4421/0/248
Goodness-of-fit on F^2	1.031
Final R indexes [I>=2σ (I)]	R_1 = 0.0377, wR_2 = 0.0811
Final R indexes [all data]	R_1 = 0.0538, wR_2 = 0.0877
Largest diff. peak/hole / e Å^{-3}	0.38/-0.24

Table 5.7. X-Ray Structure and Crystallographic Data of S11

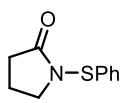

S11

≡

CCDC: 1906766

Identification code	RHL-5ring
Empirical formula	$C_{10}H_{11}NOS$
Formula weight	193.26
Temperature/K	100(2)
Crystal system	orthorhombic
Space group	$P2_12_12_1$
a/Å	9.3377(19)
b/Å	9.727(2)
c/Å	9.976(2)
α/°	90
β/°	90
γ/°	90
Volume/Å^3	906.1(3)
Z	4
ρ_{calc}g/cm^3	1.417
μ/mm^{-1}	0.312
F(000)	408.0
Crystal size/mm^3	0.07 × 0.05 × 0.03
Radiation	MoKα (λ = 0.71073)
2Θ range for data collection/°	5.85 to 60.79
Index ranges	$-13 \le h \le 12$, $-13 \le k \le 8$, $-12 \le l \le 14$
Reflections collected	7220
Independent reflections	2454 [R_{int} = 0.0249, R_{sigma} = 0.0318]
Data/restraints/parameters	2454/0/118
Goodness-of-fit on F^2	1.100
Final R indexes [I>=2σ (I)]	R_1 = 0.0318, wR_2 = 0.0775
Final R indexes [all data]	R_1 = 0.0386, wR_2 = 0.0831
Largest diff. peak/hole / e Å^{-3}	0.41/-0.31
Flack parameter	0.01(3)

Table 5.8. X-Ray Structure and Crystallographic Data of S12

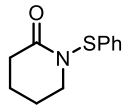

S12

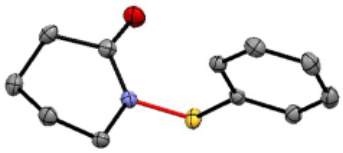

CCDC: 1906767

Identification code	RHL-6ring
Empirical formula	$C_{11}H_{13}NOS$
Formula weight	207.28
Temperature/K	100(2)
Crystal system	tetragonal
Space group	$P4_2/n$
a/Å	16.5787(10)
b/Å	16.5787(10)
c/Å	7.4975(5)
α/°	90
β/°	90
γ/°	90
Volume/Å^3	2060.7(3)
Z	8
ρ_{calc}g/cm^3	1.336
μ/mm^{-1}	0.279
F(000)	880.0
Crystal size/mm^3	0.12 × 0.1 × 0.08
Radiation	MoKα (λ = 0.71073)
2Θ range for data collection/°	4.914 to 61.264
Index ranges	$-21 \le h \le 20$, $-22 \le k \le 19$, $-10 \le l \le 10$
Reflections collected	16147
Independent reflections	2895 [R_{int} = 0.0293, R_{sigma} = 0.0291]
Data/restraints/parameters	2895/0/127
Goodness-of-fit on F^2	1.038
Final R indexes [I>=2σ (I)]	R_1 = 0.0374, wR_2 = 0.0798
Final R indexes [all data]	R_1 = 0.0557, wR_2 = 0.0862
Largest diff. peak/hole / e Å^{-3}	0.31/-0.17

Table 5.9. X-Ray Structure and Crystallographic Data of S13

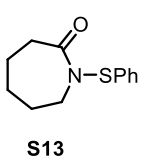

S13

≡

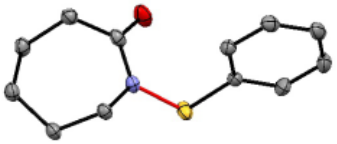

CCDC: 1906768

Identification code	RHL-7membered
Empirical formula	$C_{12}H_{15}NOS$
Formula weight	221.31
Temperature/K	100(2)
Crystal system	monoclinic
Space group	$P2_1/c$
a/Å	9.1705(6)
b/Å	8.8692(6)
c/Å	14.0231(9)
α/°	90
β/°	92.720(2)
γ/°	90
Volume/Å^3	1139.28(13)
Z	4
ρ_{calc}g/cm^3	1.290
μ/mm^{-1}	0.257
F(000)	472.0
Crystal size/mm^3	0.2 × 0.15 × 0.1
Radiation	MoKα (λ = 0.71073)
2Θ range for data collection/°	5.436 to 60.54
Index ranges	$-12 \le h \le 12$, $-12 \le k \le 11$, $-19 \le l \le 19$
Reflections collected	16162
Independent reflections	3136 [R_{int} = 0.0263, R_{sigma} = 0.0208]
Data/restraints/parameters	3136/27/136
Goodness-of-fit on F^2	1.049
Final R indexes [I>=2σ (I)]	R_1 = 0.0331, wR_2 = 0.0780
Final R indexes [all data]	R_1 = 0.0418, wR_2 = 0.0823
Largest diff. peak/hole / e Å^{-3}	0.35/-0.20

Table 5.10. X-Ray Structure and Crystallographic Data of S19

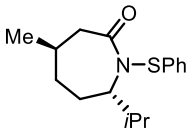

(±)- **S19**

≡

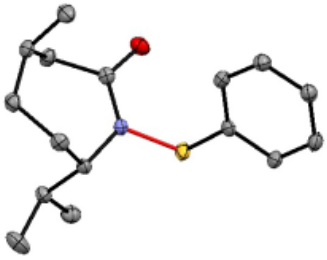

CCDC: 1906771

Identification code	zhe1
Empirical formula	$C_{16}H_{23}NOS$
Formula weight	277.41
Temperature/K	293(2)
Crystal system	orthorhombic
Space group	$P2_12_12_1$
a/Å	9.4262(12)
b/Å	11.2142(14)
c/Å	14.1135(17)
α/°	90
β/°	90
γ/°	90
Volume/Å^3	1491.9(3)
Z	4
ρ_{calc}g/cm^3	1.235
μ/mm^{-1}	0.210
F(000)	600.0
Crystal size/mm^3	? × ? × ?
Radiation	MoKα (λ = 0.71075)
2Θ range for data collection/°	6.342 to 61.016
Index ranges	-13 ≤ h ≤ 13, -16 ≤ k ≤ 15, -19 ≤ l ≤ 19
Reflections collected	23427
Independent reflections	4390 [R_{int} = 0.0213, R_{sigma} = 0.0156]
Data/restraints/parameters	4390/0/176
Goodness-of-fit on F^2	1.056
Final R indexes [I>=2σ (I)]	R_1 = 0.0257, wR_2 = 0.0671
Final R indexes [all data]	R_1 = 0.0269, wR_2 = 0.0678
Largest diff. peak/hole / e Å^{-3}	0.30/-0.20
Flack parameter	0.01(6)

Table 5.11. X-Ray Structure and Crystallographic Data of 3c

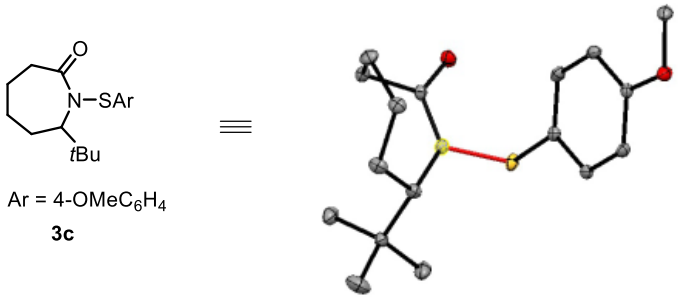

CCDC: 1906769

Identification code	RHL-7ring
Empirical formula	$C_{17}H_{25}NO_2S$
Formula weight	307.44
Temperature/K	100(2)
Crystal system	orthorhombic
Space group	Pbca
a/Å	10.0223(5)
b/Å	16.1566(8)
c/Å	20.2915(10)
α/°	90
β/°	90
γ/°	90
Volume/Å^3	3285.7(3)
Z	8
ρ_{calc}g/cm^3	1.243
μ/mm^{-1}	0.202
F(000)	1328.0
Crystal size/mm^3	0.1 × 0.1 × 0.1
Radiation	MoKα (λ = 0.71073)
2Θ range for data collection/°	5.042 to 61.126
Index ranges	-11 ≤ h ≤ 14, -22 ≤ k ≤ 22, -24 ≤ l ≤ 28
Reflections collected	28148
Independent reflections	4691 [R_{int} = 0.0299, R_{sigma} = 0.0274]
Data/restraints/parameters	4691/0/194
Goodness-of-fit on F^2	1.032
Final R indexes [I>=2σ (I)]	R_1 = 0.0405, wR_2 = 0.0968
Final R indexes [all data]	R_1 = 0.0591, wR_2 = 0.1059
Largest diff. peak/hole / e Å^{-3}	0.44/-0.22

Table 5.12. X-Ray Structure and Crystallographic Data of S14

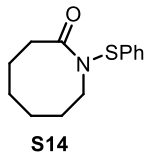

S14

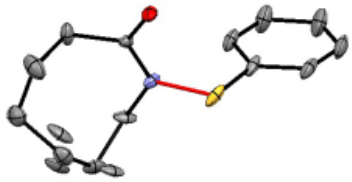

CCDC: 1906770

Identification code	RHL-8membered
Empirical formula	$C_{13}H_{17}NOS$
Formula weight	235.33
Temperature/K	100(2)
Crystal system	monoclinic
Space group	$P2_1/n$
a/Å	11.001(2)
b/Å	5.9033(12)
c/Å	18.619(4)
α/°	90
β/°	90.427(7)
γ/°	90
Volume/Å^3	1209.2(4)
Z	4
ρ_{calc}g/cm^3	1.293
μ/mm^{-1}	0.246
F(000)	504.0
Crystal size/mm^3	0.1 × 0.1 × 0.1
Radiation	MoKα (λ = 0.71073)
2Θ range for data collection/°	4.314 to 49.032
Index ranges	$-12 \le h \le 12$, $-6 \le k \le 6$, $-21 \le l \le 21$
Reflections collected	9404
Independent reflections	1999 [R_{int} = 0.0658, R_{sigma} = 0.0577]
Data/restraints/parameters	1999/93/172
Goodness-of-fit on F^2	1.052
Final R indexes [I>=2σ (I)]	R_1 = 0.0797, wR_2 = 0.2105
Final R indexes [all data]	R_1 = 0.1016, wR_2 = 0.2246
Largest diff. peak/hole / e Å^{-3}	0.45/-0.43

5.7 References

1. Feng, M.; Tang, B.; H. Liang, S.; Jiang, X., Sulfur Containing Scaffolds in Drugs: Synthesis and Application in Medicinal Chemistry. *Curr. Top. Med. Chem.* **2016**, *16*, 1200-1216.

2. Devendar, P.; Yang, G.-F., Sulfur-Containing Agrochemicals. *Top. Curr. Chem.* **2017**, *375*, 82.

3. Lee, E. K.; Lee, M. Y.; Park, C. H.; Lee, H. R.; Oh, J. H., Toward Environmentally Robust Organic Electronics: Approaches and Applications. *Adv. Mater.* **2017**, *29*, 1703638.

4. Roncali, J., Conjugated poly(thiophenes): synthesis, functionalization, and applications. *Chem. Rev.* **1992**, *92*, 711-738.

5. Varma, R. S.; Naicker, K. P., The Urea−Hydrogen Peroxide Complex: Solid-State Oxidative Protocols for Hydroxylated Aldehydes and Ketones (Dakin Reaction), Nitriles, Sulfides, and Nitrogen Heterocycles. *Org. Lett.* **1999**, *1*, 189-192.

6. Voutyritsa, E.; Triandafillidi, I.; Kokotos, C. G., Green Organocatalytic Oxidation of Sulfides to Sulfoxides and Sulfones. *Synthesis* **2017**, *49*, 917-924.

7. Tobisu, M.; Masuya, Y.; Baba, K.; Chatani, N., Palladium(ii)-catalyzed synthesis of dibenzothiophene derivatives via the cleavage of carbon–sulfur and carbon–hydrogen bonds. *Chem. Sci.* **2016**, *7*, 2587-2591.

8. Terrier, F., Synthetic Aspects of Intermolecular SNAr Reactions. In *Modern Nucleophilic Aromatic Substitution*, John Wiley & Sons, Inc.: 2013; pp 205-278.

9. Beletskaya, I. P.; Ananikov, V. P., Transition-Metal-Catalyzed C−S, C−Se, and C−Te Bond Formation via Cross-Coupling and Atom-Economic Addition Reactions. *Chem. Rev.* **2011**, *111*, 1596-1636.

10. Vásquez-Céspedes, S.; Ferry, A.; Candish, L.; Glorius, F., Heterogeneously Catalyzed Direct C–H Thiolation of Heteroarenes. *Angew. Chem. Int. Ed.* **2015**, *54*, 5772-5776.

11. (a) Iwasaki, M.; Iyanaga, M.; Tsuchiya, Y.; Nishimura, Y.; Li, W.; Li, Z.; Nishihara, Y., Palladium-Catalyzed Direct Thiolation of Aryl C□H Bonds with Disulfides. *Chem. Eur. J.* **2014**, *20*, 2459-2462; (b) Lin, C.; Li, D.; Wang, B.; Yao, J.; Zhang, Y., Direct ortho-Thiolation of Arenes and Alkenes by Nickel Catalysis. *Org. Lett.* **2015**, *17*, 1328-1331.

12. Saravanan, P.; Anbarasan, P., Palladium Catalyzed Aryl(alkyl)thiolation of Unactivated Arenes. *Org. Lett.* **2014**, *16*, 848-851.

13. (a) Della Ca', N.; Fontana, M.; Motti, E.; Catellani, M., Pd/Norbornene: A Winning Combination for Selective Aromatic Functionalization via C–H Bond Activation. *Acc. Chem. Res.* **2016**, *49*, 1389-1400; (b) Wang, J.; Dong, G., Palladium/Norbornene Cooperative Catalysis. *Chem. Rev.* **2019**, *119*, 7478-7528; (c) Ye, J.; Lautens, M., Palladium-catalysed norbornene-mediated C–H functionalization of arenes. *Nat. Chem.* **2015**, *7*, 863.

14. Catellani, M.; Frignani, F.; Rangoni, A., A Complex Catalytic Cycle Leading to a Regioselective Synthesis of o,o′ -Disubstituted Vinylarenes. *Angew. Chem. Int. Ed.* **1997**, *36*, 119-122.

15. (a) Lautens, M.; Piguel, S., A New Route to Fused Aromatic Compounds by Using a Palladium-Catalyzed Alkylation-Alkenylation Sequence. *Angew. Chem. Int. Ed.* **2000**, *39*, 1045-1046; (b) Bressy, C.; Alberico, D.; Lautens, M., A Route to Annulated Indoles via a Palladium-Catalyzed Tandem Alkylation/Direct Arylation Reaction. *J. Am. Chem. Soc.* **2005**, *127*, 13148-13149; (c) Jiao, L.; Bach, T., Palladium-Catalyzed Direct 2-Alkylation of Indoles by Norbornene-Mediated Regioselective Cascade C–H Activation. *J. Am. Chem. Soc.* **2011**, *133*, 12990-12993;

(d) Sui, X.; Zhu, R.; Li, G.; Ma, X.; Gu, Z., Pd-Catalyzed Chemoselective Catellani Ortho-Arylation of Iodopyrroles: Rapid Total Synthesis of Rhazinal. *J. Am. Chem. Soc.* **2013**, *135*, 9318-9321; (e) Zhang, H.; Chen, P.; Liu, G., Palladium-Catalyzed Cascade C□H Trifluoroethylation of Aryl Iodides and Heck Reaction: Efficient Synthesis of ortho-Trifluoroethylstyrenes. *Angew. Chem. Int. Ed.* **2014**, *53*, 10174-10178; (f) Wang, X.-C.; Gong, W.; Fang, L.-Z.; Zhu, R.-Y.; Li, S.; Engle, K. M.; Yu, J.-Q., Ligand-enabled Meta-C-H Activation Using a Transient Mediator. *Nature* **2015**, *519*, 334-338; (g) Dong, Z.; Wang, J.; Dong, G., Simple Amine-Directed Meta-Selective C–H Arylation via Pd/Norbornene Catalysis. *J. Am. Chem. Soc.* **2015**, *137*, 5887-5890; (h) Lei, C.; Jin, X.; Zhou, J., Palladium-Catalyzed Heteroarylation and Concomitant ortho-Alkylation of Aryl Iodides. *Angew. Chem. Int. Ed.* **2015**, *54*, 13397-13400; (i) Shi, H.; Babinski, D. J.; Ritter, T., Modular C–H Functionalization Cascade of Aryl Iodides. *J. Am. Chem. Soc.* **2015**, *137*, 3775-3778; (j) Sun, F.; Li, M.; He, C.; Wang, B.; Li, B.; Sui, X.; Gu, Z., Cleavage of the C(O)–S Bond of Thioesters by Palladium/Norbornene/Copper Cooperative Catalysis: An Efficient Synthesis of 2-(Arylthio)aryl Ketones. *J. Am. Chem. Soc.* **2016**, *138*, 7456-7459; (k) Wang, J.; Li, R.; Dong, Z.; Liu, P.; Dong, G., Complementary site-selectivity in arene functionalization enabled by overcoming the *ortho* constraint in palladium/norbornene catalysis. *Nat. Chem.* **2018**, *10*, 866-872; (l) Dong, Z.; Lu, G.; Wang, J.; Liu, P.; Dong, G., Modular ipso/ortho Difunctionalization of Aryl Bromides via Palladium/Norbornene Cooperative Catalysis. *J. Am. Chem. Soc.* **2018**, *140*, 8551-8562; (m) Zhang, B.-S.; Li, Y.; An, Y.; Zhang, Z.; Liu, C.; Wang, X.-G.; Liang, Y.-M., Carboxylate Ligand-Exchanged Amination/C(sp3)–H Arylation Reaction via Pd/Norbornene Cooperative Catalysis. *ACS Catal.* **2018**, *8*, 11827-11833; (n) Wang, Z.; Li, T.; Zhao, J.; Shi, X.; Jiao, D.; Zheng, H.; Chen, C.; Zhu, B., Expeditious Synthesis of 6-Fluoroalkyl-Phenanthridines via Palladium-Catalyzed Norbornene-Mediated Dehydrogenative Annulation. *Org. Lett.* **2018**, *20*,

6640-6645; (o) Li, R.; Liu, F.; Dong, G., Redox-Neutral *ortho* Functionalization of Aryl Boroxines via Palladium/Norbornene Cooperative Catalysis. *Chem* **2019**, *5*, 929-939; (p) Liu, F.; Dong, Z.; Wang, J.; Dong, G., Palladium/Norbornene-Catalyzed Indenone Synthesis from Simple Aryl Iodides: Concise Syntheses of Pauciflorol F and Acredinone A. *Angew. Chem. Int. Ed.* **2019**, *58*, 2144-2148.

16. (a) Ye, J.; Lautens, M., Palladium-catalysed norbornene-mediated C-H functionalization of arenes. *Nat. Chem.* **2015**, *7*, 863-870; (b) Wang, J.; Dong, G., Palladium/Norbornene Cooperative Catalysis. *Chem. Rev.* **2019**.

17. (a) Liu, Z.-S.; Gao, Q.; Cheng, H.-G.; Zhou, Q., Alkylating Reagents Employed in Catellani-Type Reactions. *Chem. Eur. J.* **2018**, *24*, 15461-15476; (b) Zhao, K.; Ding, L.; Gu, Z., Development of New Electrophiles in Palladium/Norbornene-Catalyzed *ortho*-Functionalization of Aryl Halides. *Synlett* **2019**, *30*, 129-140.

18. (a) Faccini, F.; Motti, E.; Catellani, M., A New Reaction Sequence Involving Palladium-Catalyzed Unsymmetrical Aryl Coupling. *J. Am. Chem. Soc.* **2004**, *126*, 78-79; (b) Zhou, P.-X.; Ye, Y.-Y.; Liu, C.; Zhao, L.-B.; Hou, J.-Y.; Chen, D.-Q.; Tang, Q.; Wang, A.-Q.; Zhang, J.-Y.; Huang, Q.-X.; Xu, P.-F.; Liang, Y.-M., Palladium-Catalyzed Acylation/Alkenylation of Aryl Iodide: A Domino Approach Based on the Catellani–Lautens Reaction. *ACS Catal.* **2015**, 4927-4931; (c) Dong, Z.; Wang, J.; Ren, Z.; Dong, G., Ortho C−H Acylation of Aryl Iodides by Palladium/Norbornene Catalysis. *Angew. Chem. Int. Ed.* **2015**, *54*, 12664-12668; (d) Huang, Y.; Zhu, R.; Zhao, K.; Gu, Z., Palladium-Catalyzed Catellani ortho-Acylation Reaction: An Efficient and Regiospecific Synthesis of Diaryl Ketones. *Angew. Chem. Int. Ed.* **2015**, *54*, 12669-12672; (e) Wang, J.; Zhang, L.; Dong, Z.; Dong, G., Reagent-Enabled *ortho*-Alkoxycarbonylation of Aryl Iodides via Palladium/Norbornene Catalysis. *Chem* **2016**, *1*, 581-591; (f) Li, R.; Dong, G., Direct

Annulation between Aryl Iodides and Epoxides through Palladium/Norbornene Cooperative Catalysis. *Angew. Chem. Int. Ed.* **2018**, *57*, 1697-1701.

19. Dong, Z.; Dong, G., *Ortho* vs *Ipso*: Site-Selective Pd and Norbornene-Catalyzed Arene C–H Amination Using Aryl Halides. *J. Am. Chem. Soc.* **2013**, *135*, 18350-18353.

20. Shi, H.; Wang, P.; Suzuki, S.; Farmer, M. E.; Yu, J.-Q., Ligand Promoted *meta*-C–H Chlorination of Anilines and Phenols. *J. Am. Chem. Soc.* **2016**, *138*, 14876-14879.

21. DeBergh, J. R.; Niljianskul, N.; Buchwald, S. L., Synthesis of Aryl Sulfonamides via Palladium-Catalyzed Chlorosulfonylation of Arylboronic Acids. *J. Am. Chem. Soc.* **2013**, *135*, 10638-10641.

22. Ma, X.; Lu, A.; Ji, X.; Shi, G.; Zhang, Y., Disilylation of Palladacycles that were Generated through the C−H Activation of Aryl Halides. *Asian J. Org. Chem.* **2018**, *7*, 1403-1410.

23. Lv, W.; Wen, S.; Yu, J.; Cheng, G., Palladium-Catalyzed Ortho-Silylation of Aryl Iodides with Concomitant Arylsilylation of Oxanorbornadiene: Accessing Functionalized (Z)-β-Substituted Vinylsilanes and Their Analogues. *Org. Lett.* **2018**, *20*, 4984-4987.

24. Kuniyasu, H.; Sugoh, K.; Su, M. S.; Kurosawa, H., The First Evidence of Insertion of Isocyanide into a Metal−Sulfur Bond: Catalytic and Stoichiometric Behavior of Isocyanide and Thiolate Ligands on Palladium and Platinum. *J. Am. Chem. Soc.* **1997**, *119*, 4669-4677.

25. Baranano, D.; Hartwig, J. F., Carbon-Heteroatom Bond-Forming Reductive Elimination. Mechanism, Importance of Trapping Reagents, and Unusual Electronic Effects during Formation of Aryl Sulfides. *J. Am. Chem. Soc.* **1995**, *117*, 2937-2938.

26. (a) Zhang, X.-S.; Li, G.; Zhang, X.-G.; Zhang, X.-H., Pd(II)-catalyzed selective sulfenylation of arene C–H bonds using N-arylthiobenzamides as thiolation reagent and oxidant. *Tetrahedron*

2015, *71*, 5458-5464; (b) Craine, L.; Raban, M., The chemistry of sulfenamides. *Chem. Rev.* **1989**, *89*, 689-712.

27. Pauling, L., The Nature of the Chemical Bond. IV. The Engergy of Single Bonds and the Relative Electronegativity of Atoms. *J. Am. Chem. Soc.* **1932**, *54*, 3570-3582.

28. Cai, W.; Gu, Z., Selective Ortho Thiolation Enabled by Tuning the Ancillary Ligand in Palladium/Norbornene Catalysis. *Org. Lett.* **2019**, *21*, 3204-3209.

29. Burkhardt, I.; Dickschat, J. S., Synthesis and Absolute Configuration of Natural 2-Pyrones. *Eur. J. Org. Chem.* **2018**, *2018*, 3144-3157.

30. Duffault, J.-M.; Tellier, F., A New Route to the Synthesis of Bicyclo [3.3.2] Nonene by Radical Cyclisation. *Synth. Commun.* **1998**, *28*, 2467-2481.

31. (a) Bao, M.; Shimizu, M.; Shimada, S.; Tanaka, M., Efficient synthesis of N-acylarenesulfenamides by acylation of arenesulfenamides. *Tetrahedron* **2003**, *59*, 303-309; (b) Biallas, P.; Mensak, T. M.; Kunz, K.-A.; Kirsch, S. F., The Deazidoalkoxylation: Sequential Nucleophilic Substitutions with Diazidated Diethyl Malonate. *J. Org. Chem.* **2019**, *84*, 1654-1663; (c) Esker, J. L.; Newcomb, M., Amidyl radicals from N-(phenylthio)amides. *Tetrahedron Lett.* **1993**, *34*, 6877-6880; (d) Gaykar, R. N.; Bhattacharjee, S.; Biju, A. T., Transition-Metal-Free Thioamination of Arynes Using Sulfenamides. *Org. Lett.* **2019**, *21*, 737-740; (e) Lee, C.; Lim, Y. N.; Jang, H.-Y., Copper-Catalyzed Synthesis of N-Formyl/Acylsulfenamides and -thiosulfonamides. *Eur. J. Org. Chem.* **2015**, *2015*, 5934-5938; (f) Winter, D. K.; Drouin, A.; Lessard, J.; Spino, C., Photochemical Rearrangement of N-Chlorolactams: A Route to N-Heterocycles through Concerted Ring Contraction. *J. Org. Chem.* **2010**, *75*, 2610-2618.

32. Winnacker, M.; Tischner, A.; Neumeier, M.; Rieger, B., New insights into synthesis and oligomerization of ε-lactams derived from the terpenoid ketone (−)-menthone. *RSC Adv.* **2015**, *5*, 77699-77705.

33. Li, Z.-S.; Wang, W.-M.; Lu, W.; Niu, C.-W.; Li, Y.-H.; Li, Z.-M.; Wang, J.-G., Synthesis and biological evaluation of nonsymmetrical aromatic disulfides as novel inhibitors of acetohydroxyacid synthase. *Biorg. Med. Chem. Lett.* **2013**, *23*, 3723-3727.

34. Ramalingan, C.; Park, Y.-T., Mercury-Catalyzed Rearrangement of Ketoximes into Amides and Lactams in Acetonitrile. *J. Org. Chem.* **2007**, *72*, 4536-4538.

(Some contents of this chapter were published in *Nat. Commun.* **2019**, *10*, 3555.)

CHAPTER 6

Direct Vicinal Difunctionalization of Thiophenes Enabled by the Palladium/Norbornene Cooperative Catalysis

6.1 Introduction

Polysubstituted aromatic heterocycles are commonly found in pharmaceuticals, agrochemicals and organic materials (Figure 1).[1] Site-selective conversion of unactivated C−H bonds directly to new functional groups (FGs) represents an important and straightforward approach for efficient functionalization of heteroarenes.[2] To date, great success has been achieved for site-selectively introducing one FG to heteroarenes without aids of directing groups (DGs);[3] it remains challenging to simultaneously install two *different* FGs,[4] particularly at vicinal positions in a regioselective manner. However, such a transformation would constitute significant interests because it could rapidly increase molecular complexity, thereby facilitating streamlined synthesis of polysubstituted heteroarenes.

Figure 6.1. Examples of Polysubstituted Thiophenes and Furans

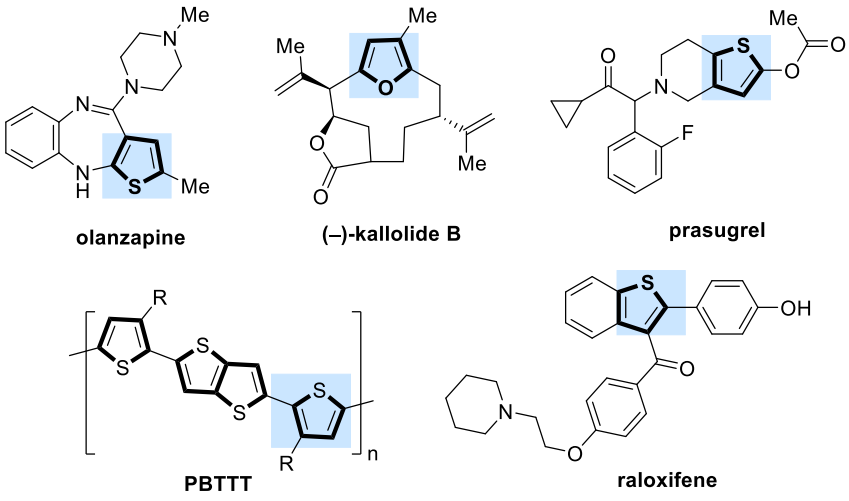

The palladium/norbornene (Pd/NBE) cooperative catalysis, also known as Catellani-type reactions, has emerged as a versatile approach for vicinal difunctionalization of arenes.[5] Seminal efforts led by Catellani[6] and Lautens[7] show that, using aryl halides as substrates, an electrophile and a nucleophile could be coupled simultaneously at arene ipso and ortho positions, respectively (Scheme 1a). Beyond using aryl halides as substrates,[8] in 2015 the Yu[9a] and our[9b] groups independently disclosed the direct meta functionalizations of arenes initiated by a directed ortho C−H palladation (Scheme 1b). Very recently, a meta arylation of electron-rich alkoxyarenes was developed by Yu through a related approach.[10] However, to the best of our knowledge, vicinal difunctionalization of arenes through the C−H-initiated Pd/NBE catalysis (either directed or non-directed) has not been reported yet. The primary challenge is associated with the fact that, for the proposed difunctionalization, acidic conditions are often beneficial for the C−H palladation step,[11] which could result in an ipso protonation process instead of further couplings.[9] Additional difficulties could be envisaged for using heteroarene substrates in the Pd/NBE catalysis, as many aromatic heterocycles can behave as good ligands for Pd and they are often less stable than arenes under the oxidative conditions. Herein, stimulated by these challenges and given the therapeutic

importance of thiophene derivatives,[12] we describe the initial development of a double C−H functionalization of thiophenes at the C4 and C5 positons via the Pd/NBE catalysis using a unique catalytic system (Scheme 1c).

Scheme 6.1. Direct C−H Functionalization of Heterocycles

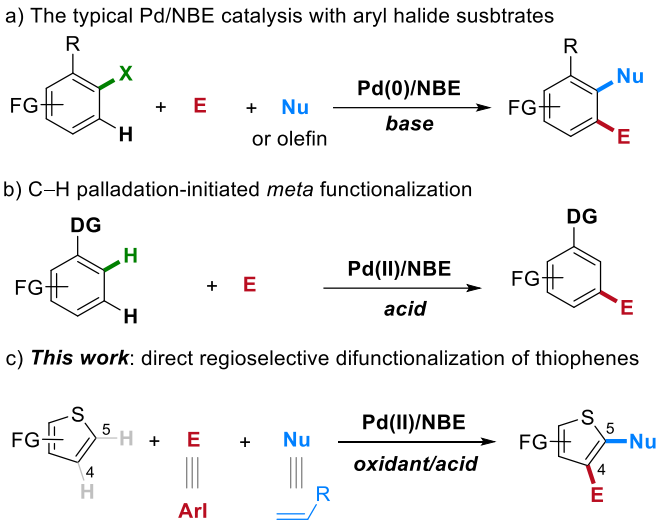

The C5 (or C2) position of thiophene is generally considered to be most electron-rich, and a number of direct C−H metalation methods have been successfully developed.[13] However, directly merging the C5-palladation with the Pd/NBE catalysis would still be nontrivial because of (1) the lack of an ortho substituent to promote the NBE extrusion (namely the "*ortho constraint*")[14] and (2) the coordinative ability of the sulfur that could retard the C4 palladation and NBE extrusion (Scheme 2). For example, the use of α-halothiophenes as substrates for the Catellani-type reactions has been elusive.[15] We hypothesized that one key to address the sulfur coordination problem is to use *a weak and π-acidic ligand* that could facilitate dechelation from the sulfur on thiophene but not inhibit the C−H palladium and the Catellani process. In addition, the use of a *bulkier NBE* was also anticipated to be beneficial over simple NBE for assisting the NBE extrusion step via β-carbon elimination.[5c]

Scheme 6.2. Potential Challenges for the Proposed Approach

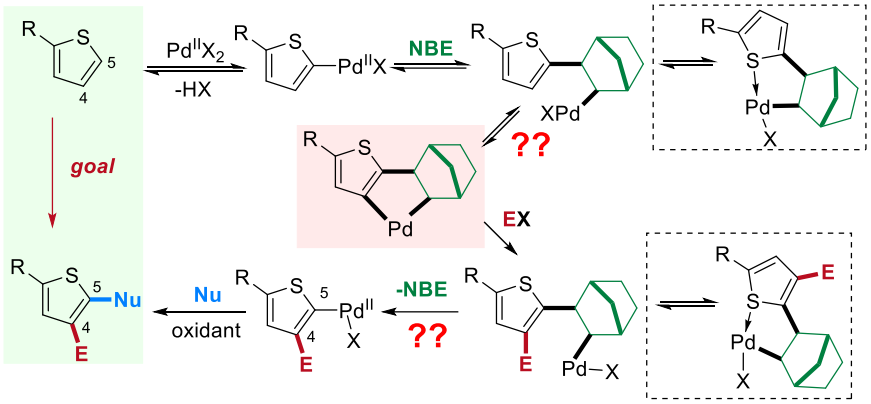

6.2 Results and Discussion

6.2.1 Reaction Discovery and Optimization

To test the hypothesis, 2-butylthiophene (**1a**) was used as the model substrate, and ortho arylation/ipso Heck reaction was examined at this initial stage (Figure 6.2). To our delight, 2% desired difunctionalization product was isolated through careful prep TLC separation and fully characterized, while the formation of other side products was observed as well. To further confirm the structure and regioselectivity of the difunctionalization product, a complimentary experiment using 2-iodo-5-*n*butylthiophene was performed. We are delighted to find that same product was generated.

Figure 6.2. Reaction Discovery and Product Characterization

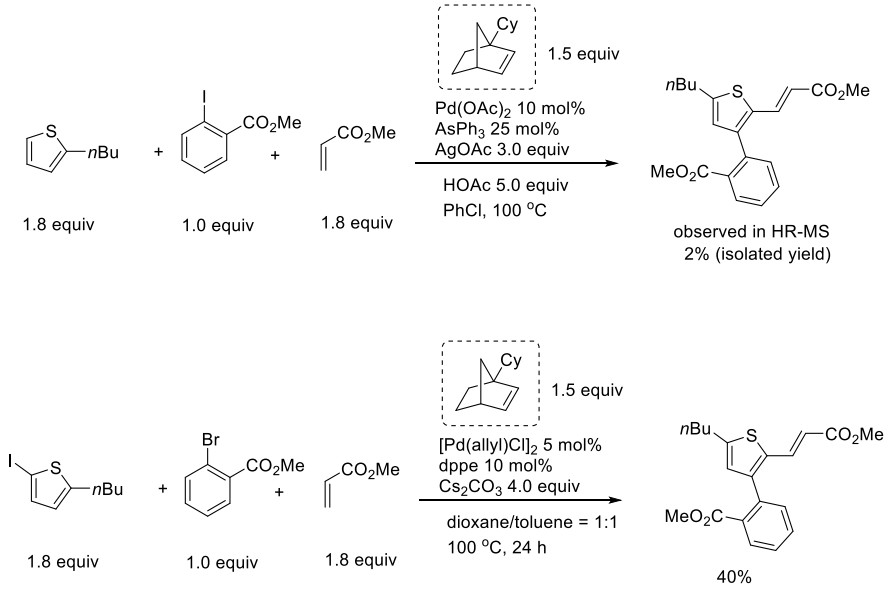

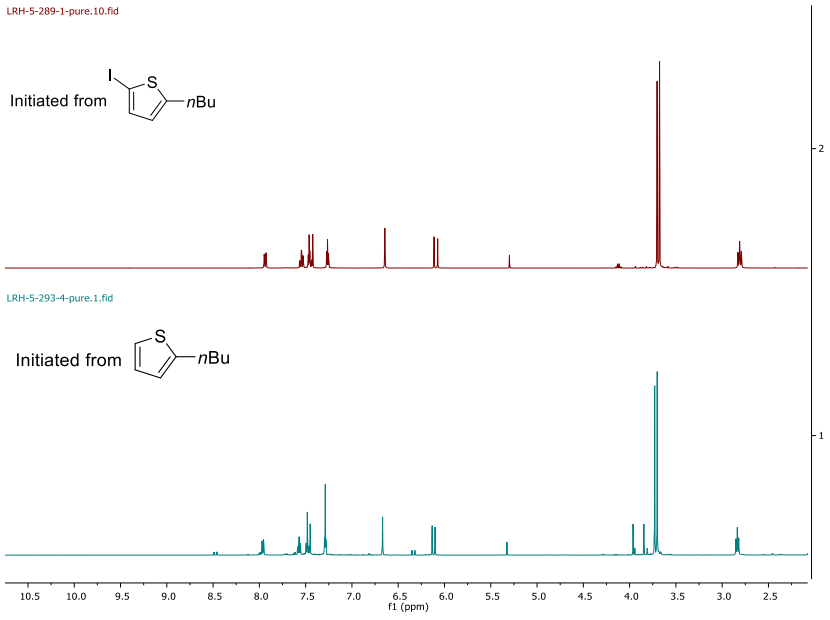

Then, preliminary condition screening was performed (Table 6.1). The yield was significantly increased to 26% when adding BQ as a co-oxidant, which probably because BQ is likely to be a better oxidant towards Pd(0), or BQ is known to be a ligand. The bulky bridgehead-substituted NBE was chosen to promote the β-carbon elimination step. Other ligands, for example 2-pyridone ligand, didn't give the desired difunctionalization product.

Table 6.1. Preliminary Condition Screening

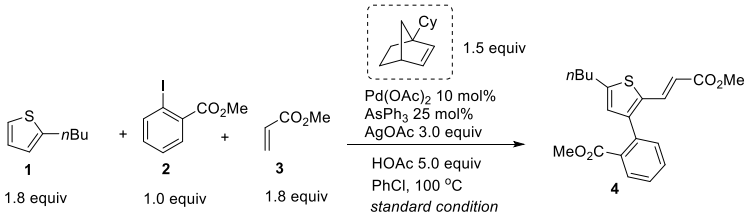

Entry	Change from the *"standard condition"*	**4** Yield
1	none	5%
2	**1** as 1.0 equiv	5%
3	under air	3%
4	w/ BQ 1.0 equiv	26%
5	w/o HOAc	5%
6	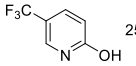 25 mol%	0%

Scheme 6.3. Side Product Analysis

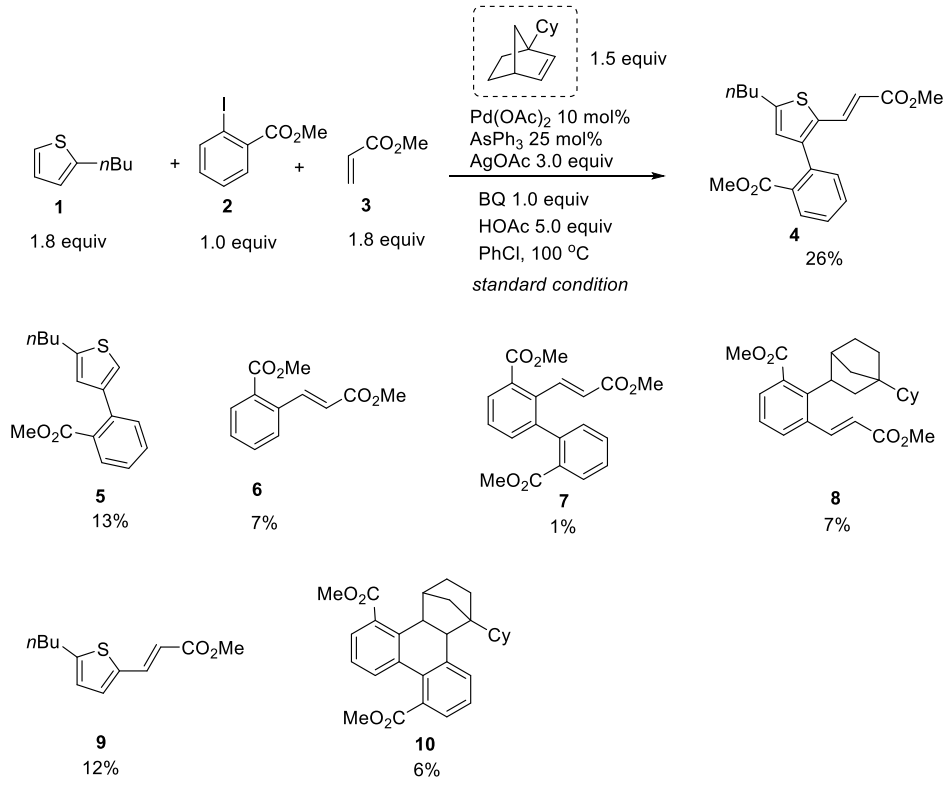

Based on the current best reaction condition, we carefully separated all the promising side products by prep TLC (Scheme 6.3). The major side product was the direct 4-arylation product **5** as well as the ArI dimerization product **10**. We also observed the ortho Heck product **8**. We were thinking the desired C−H activation-initiated Catellani process is relatively slow when comparing with Pd(0)-initiated Catellani process, especially at high temperature.

Table 6.2. Preliminary NBEs Screening

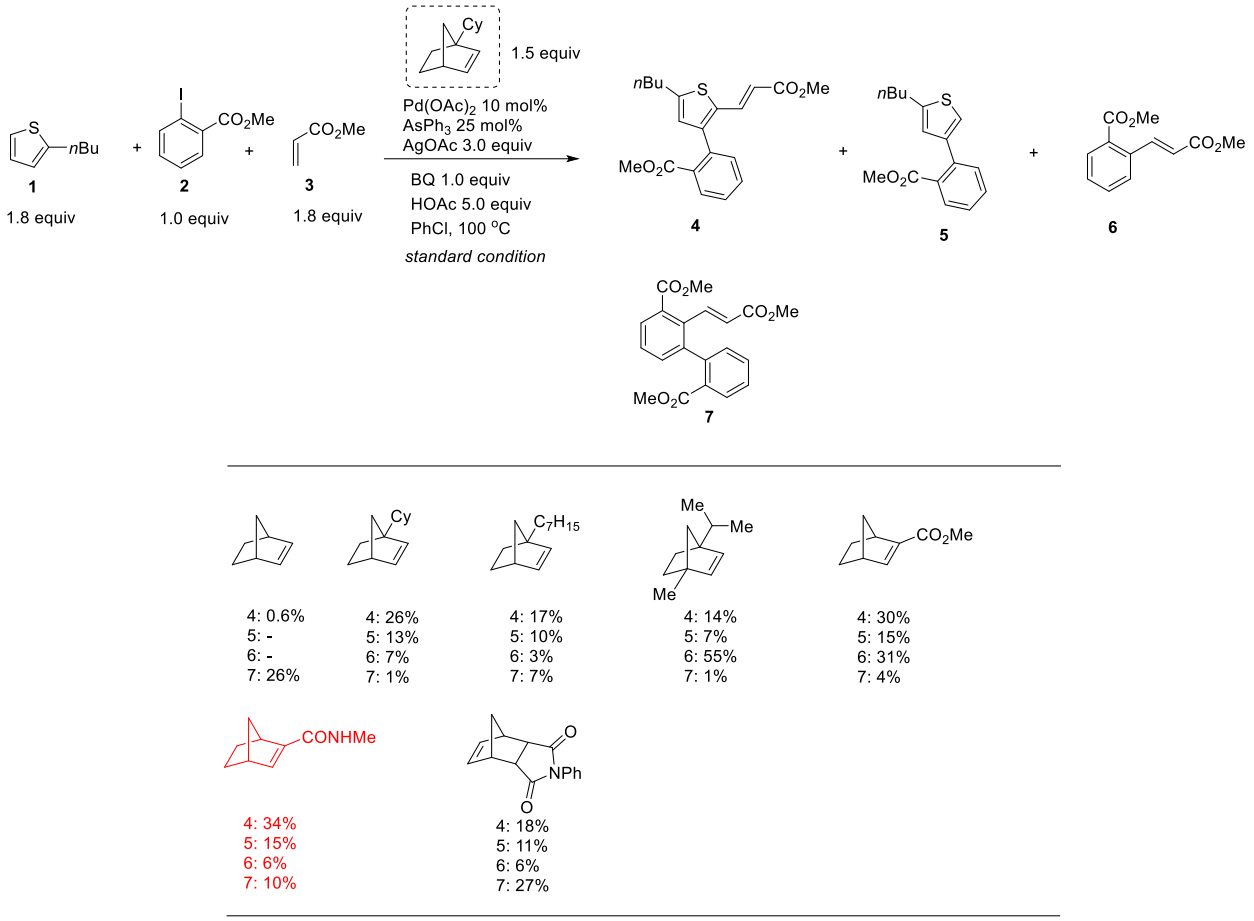

Other bulky NBEs were also tested to exam reaction efficiency (Table 6.2). We were delighted to see that C2 methyl amide-substituted NBE gave the higher yield than cyclohexyl bridgehead-substituted NBE, which probably owing to the formation of hydrogen bonding to stabilize the transition state. Double bridgehead-substituted NBE showed significantly lower reactivity, and the direct heck became to the major side product. It is noteworthy that C2 methyl ester-substituted NBE gave comparable yield as amide-substituted NBE at this stage.

Then the solvents screening turned out that higher mass balance as well as higher yield was obtained when using ethyl acetate as the solvent (Table 6.3). More acidic solvent such as chloroform (dry) also gave the desired product in 22%, while higher yield (27%) was observed

when using wet chloroform (entries 7-8). In addition, adding more HOAc is likely to facilitate both C−H activation and direct protonation steps, thereby giving better conversion as well as more direct protonation side product (entries 10-11). The Reaction was not sensitive to air (Table 6.4); the yield was significantly increased to 55% when a lower temperature (85 ^{o}C) was applied. We proposed that the Pd(0)-initiated Catellani reaction (dimerization of ArI, **7**) was largely inhibited at lower temperature, while the desired difunctionalization pathway was not affected at all. Finally, direct use of commercially available ethyl acetate gave a comparable yield as treated dry ethyl acetate.

Table 6.3. Solvents Screening

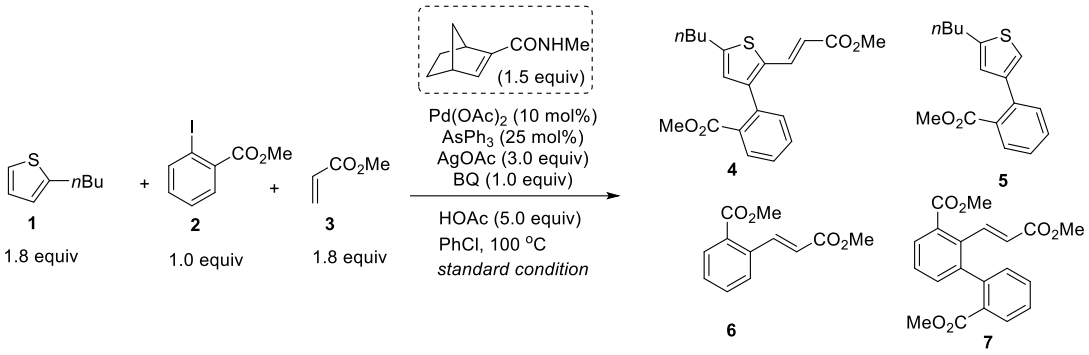

Entry	Change from the *"standard condition"*	S.M.	**4** Yield	**5** Yield	**6** Yield	**7** Yield
1	none	-	34%	16%	6%	5%
2	freshly distilled PhCl	-	29%	13%	7%	5%
3	**EA**	**8%**	**39%**	**8%**	**7%**	**5%**
4	toluene	-	33%	12%	5%	9%
5	dioxane	5%	21%	3%	12%	8%
6	DCE	-	37%	18%	7%	6%
7	chloroform (dry)	-	22%	18%	8%	10%
8	chloroform (wet)	-	27%	16%	7%	14%
9	HFIP	-	trace	-	19%	43%
10	w/o HOAc	5%	17%	3%	11%	7%
11	HOAc (2.5 equiv)	-	31%	10%	8%	6%

Table 6.4. Key Parameters

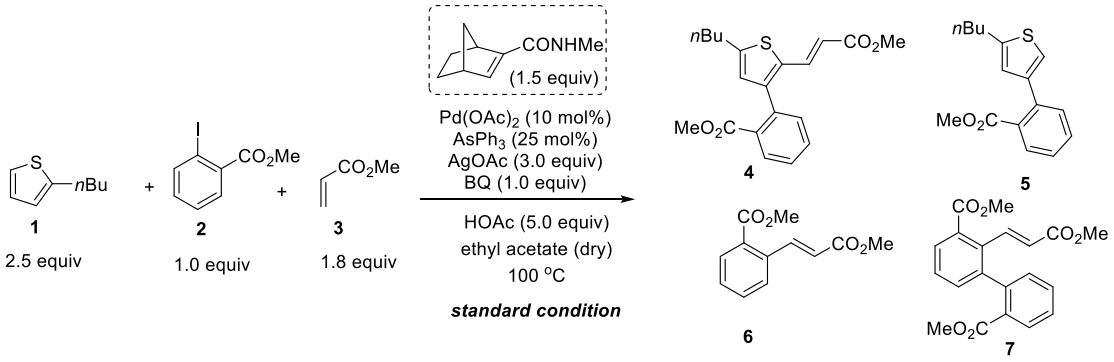

Entry	Change from the *"standard condition"*	S.M.	**4** Yield	**5** Yield	**6** Yield	**7** Yield
1	none	8%	39%	8%	7%	5%
2	HOAc (7.5 equiv)	-	50%	13%	5%	2%
3	under air	6%	36%	8%	6%	7%
4	85 °C instead of 100 °C (36 h)	-	55%	8%	6%	0.6%
5	ethyl acetate (drum)	-	63%	12%	8%	2%

The reaction was not sensitive to temperature (Table 6.5), while highest yield (77%, entry 4) was obtained at 65 °C and less than 8% of C4 arylation side product was formed.

Table 6.5. Temperature Effect

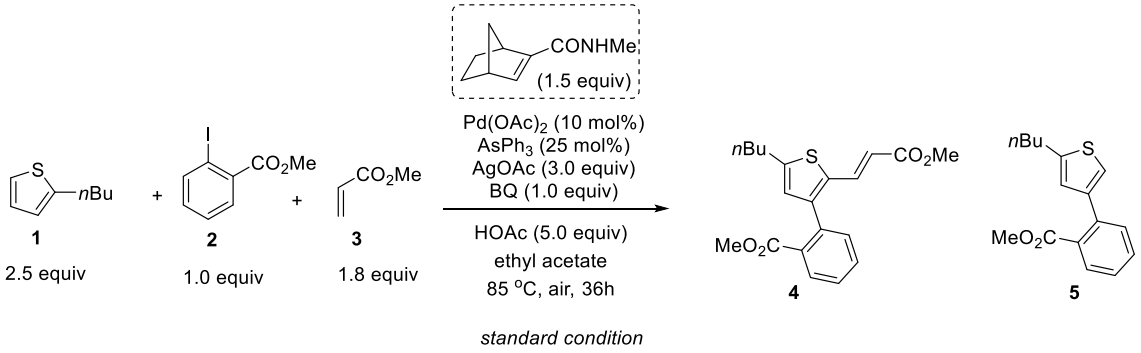

Entry	Change from the *"standard condition"*	S.M.	**4** Yield	**5** Yield
1	95 °C	-	75%	~8%
2	85 °C	-	65%	
3	75 °C	-	72%	
4	65 °C	-	77%	

To examine the optimal reaction condition, a series of control experiments were carried out (Table 6.6). Indeed, $AsPh_3$, previously employed for dechelating the amine directing group in our meta arylation reaction,[9b] was found to be superior over phosphine and phosphite ligands (entries 1-4) and delivered the desired C4,5-difunctionalized thiophene product (**4a**) in 82% yield after systematic optimization. Unsurprisingly, no desired product was observed in the absence of Pd or NBE (entries 5 and 6). The C2 methyl amide-substituted NBE (**N1**) proved to be most efficient,[16] and 72% yield was still obtained with 25 mol% **N1** (entry 7). Other substituted NBEs were less optimal. For example, tertiary amide-derived NBEs (**N2** and **N3**)[17] showed significantly reduced reactivity likely due to excessive steric hindrance. In addition, the C2 ester-substituted one (**N4**) is slightly less effective.[18] While simple NBE (**N7**) gave almost no desired product, the bulkier

bridgehead-substituted NBEs (**N5** and **N6**)[14] or the remotely substituted NBEs (**N8-10**)[18,19] could indeed afford the desired product in higher yields.

Table 6.6. Control Experiments

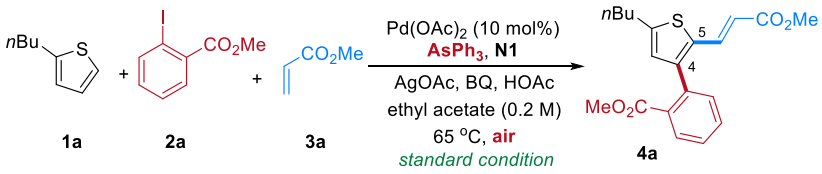

1a 2a 3a 4a

Entry	Change from the *"standard condition"*	yield of **4a** (%)[a]
1	none	82(81)
2	w/o $AsPh_3$	2
3	PPh_3 instead of $AsPh_3$	1
4	$(PhO)_3P$ instead of $AsPh_3$	0
5	w/o $Pd(OAc)_2$	0
6	w/o **N1**	0
7	25 mol% **N1**	72
	NBE Effect (15 mol% NBE used instead)[b]	
	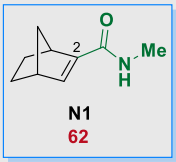 **N1** 62	
	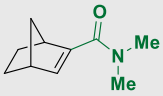 **N2** 5	
	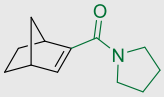 **N3** 15	
	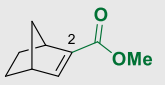 **N4** 45	
	 **N5** 16	
	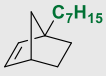 **N6** 18	
	 **N7** 2	
	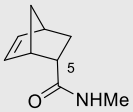 **N8** 11	
	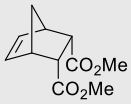 **N9** 20	
	 **N10** 10	
8	w/o BQ	11
9	w/o AgOAc	13
10	w/o HOAc	51
11	0.1 M	72[b]
12	**1a/2a** = 1 : 1 (1 equiv)	71[c]

[a]The reaction was run with 0.15 mmol **1a**, 0.1 mmol **2a**, 0.18 mmol **3a**, $Pd(OAc)_2$ (0.01 mmol), **N1** (0.15 mmol), $AsPh_3$ (0.025 mmol), AgOAc (0.3 mmol), BQ (0.1 mmol) and HOAc (0.5 mmol) in 0.5 mL ethyl acetate for 48 h. Yields were determined by ^1H NMR analysis using dibromomethane as the internal standard. [b]1 mL ethyl acetate was used. [c] 0.1 mmol **1a** was used.

The difunctionalization reaction requires stoichiometric oxidants to regenerate the Pd(II) catalyst. Both BQ and AgOAc were found necessary (entries 8 and 9); it is likely that BQ could promote fast oxidation of Pd(0) to Pd(II) by acting as a redox active ligand,[20] while AgOAc could assist activation of the C−I bond through forming AgI. Adding HOAc was beneficial, though 51% yield could still be achieved without HOAc (entry 10). The reaction was less efficient at a lower concentration (entry 11). Finally, when substrates **1a** and **2a** were used in an equal molar ratio, the desired product **4a** was afforded in a good yield (entry 12). It is noteworthy that the reaction can run directly in air at a relatively low reaction temperature (65 ^{o}C).

6.2.2 Substrates Scope

With the optimized reaction condition in hand, the scope with respect to thiophenes was examined first (Table 6.7). A range of thiophenes with various substituents at the C2 position were found to be suitable substrates for vicinal difunctionalization. Besides alkyl substitution (**4a-4e**), aryl-derived thiophenes (**4f-4h**) still delivered the desired products in good to excellent yields; both electron-rich (**4g**) and deficient (**4h**) aryl groups were tolerated. Interestingly, for **4g**, the C−H functionalization took place site-selectively at the thiophene site instead of the electron-rich alkoxyarenes. Many FGs were found compatible, including methoxy group (**4c**), benzyl and silyl-protected primary alcohols (**4d** and **4e**) and esters (**4h**). Note that 2-chloro and bromo thiophenes (**4i** and **4j**) were also reactive; the halogen FGs could potentially be used as a handle for further functionalization. The C2 and C3 disubstituted thiophenes also proved to be competent substrates, giving fully substituted products that are nontrivial to be prepared via conventional approaches. In

particular, the reaction can tolerate internal alkyne (**4m**) and generate a tetrasubstituted thiophene bearing all carbon groups with three different hybridizations.

Table 6.7. Thiophene Derivatives Scope[a]

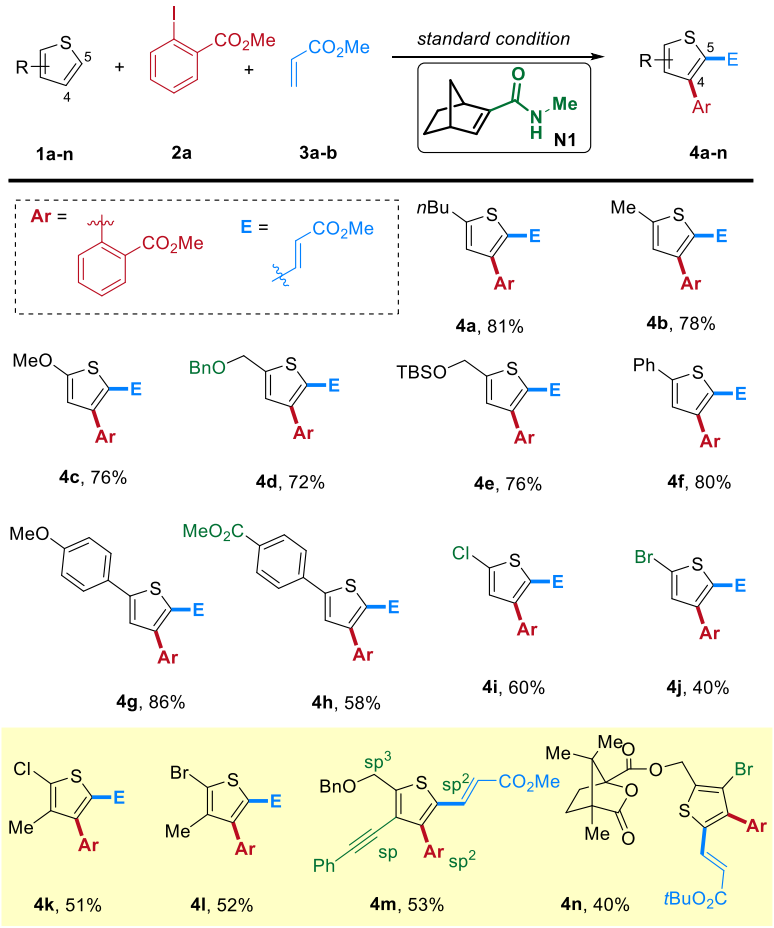

[a]The reaction was run with 0.3 mmol **1**, 0.2 mmol **2** and 0.36 mmol **3** in 1.0 mL ethyl acetate for 48 h.

The scope with respect to aryl iodides and olefins was next explored (Table 6.8). Aryl iodides with an ortho electron-withdrawing group (EWG) were found to be most efficient, which is consistent with the preference in the standard Catellani ortho arylation[5] and our prior observation[9b]. Ester, amide, ketone and nitro-substituted aryl iodides served as effective electrophiles. Notably, a

second iodide moiety (**5d**) not ortho to the EWG was compatible. Use of other aryl iodides, particularly the less reactive electron-rich ones, was challenging under the current conditions, though 3,5-bistrifluoromethylphenyl iodide gave the desired difunctionalization product in 37% yield. In addition to methyl acrylate, other Michael acceptors, such as conjugated esters (**6a-c**), amides (**6d**, **6e**) and ketones (**6f**), are also excellent coupling partners for the C5 functionalization. Encouragingly, the more electron-neutral styrene could also be efficiently coupled in 81% yield (**6g**).

Table 6.8. Aryl Iodides and Olefin Scope[a]

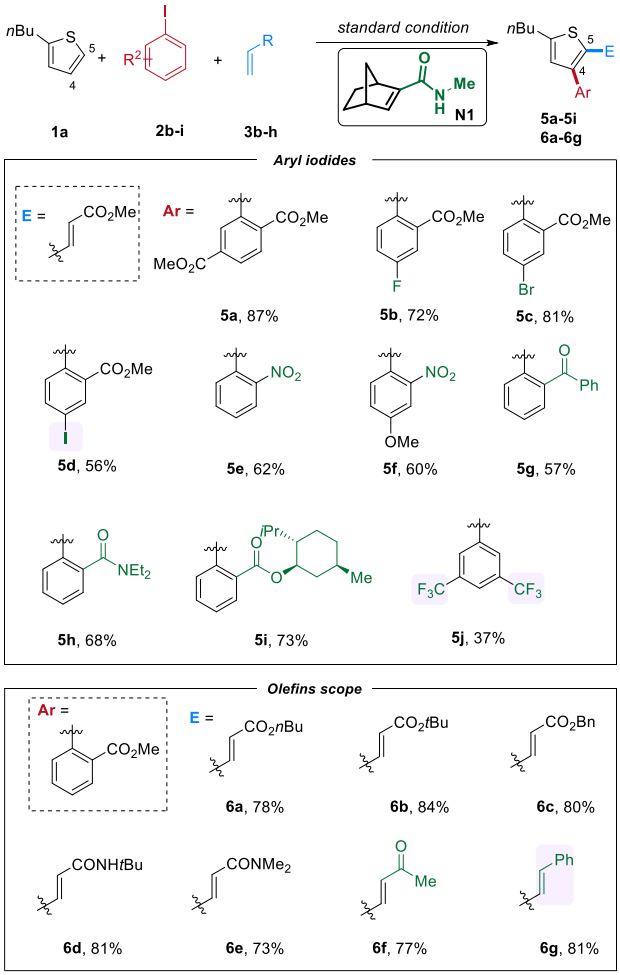

[a]The reaction was run with 0.3 mmol **1a**, 0.2 mmol **2** and 0.36 mmol **3** in 1.0 mL ethyl acetate for 48 h.

It is worth to point out that there are a few unsuccessful examples (Table 6.9). In terms of the heterocycles, less successful results were obtained when electron deficient heterocycles, e.g., pyridine and thiophene bearing EWG, were used. In addition, benzofuran and benzothiophene all afforded poor conversion, while the exact reaction is unclear. C3-substituted thiophene also provided less than 20% yield, which might be due to the competitive undesired C2 palladation pathway. For the scope of aryl iodides, unsatisfying results were obtained when using electron rich or bulky substrates. Ortho DGs were also proved to be essential. Regarding the olefins, some pyridine-containing olefins and aliphatic terminal olefin were not compatible in this method.

Table 6.9. Less Successful or Unsuccessful Substrates

Heterocycles:

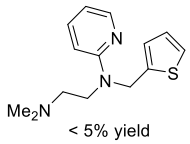

< 5% yield
53% recovery

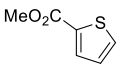

< 5% yield
63% recovery

19% yield

< 5% yield
> 95% recovery

< 5% yield
80% recovery

n.r.

Aryl iodides:

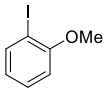

< 5% yield

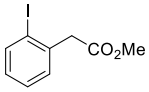

< 5% yield

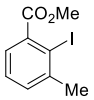

10%

Olefins:

n.r.

n.r.

complex mixture

6.2.3 Synthetic Utility

The synthetic utility of this method was first tested in the derivatization of complex bioactive compounds that contain thiophenes (Table 6.10). Reactions with derivatives from vitamin E (**7a**), estrone (**7d**) and hexahydro-1,4-diazepine-L-proline adduct (**7e**), clopidogrel (**7b**) and Boc-protected duloxetine (**7c**) all worked smoothly to afford the desired difunctionalized products in moderate to good yields. Additional chemoselectivity could be observed from the tolerance of electron-rich arenes (**7a**, **7c**, **7d**), ketones, tertiary amines (**7b**, **7e**) and epimerizable stereocenters (**7b**, **7e**). In addition, this reaction is robust and scalable: a high yield was obtained on a gram scale in an open-flask operation (Eq. 1). The commercial ethyl acetate can be directly used as solvent without further purification.

Table 6.10. Functionalization of Complex Bioactive Compounds[a]

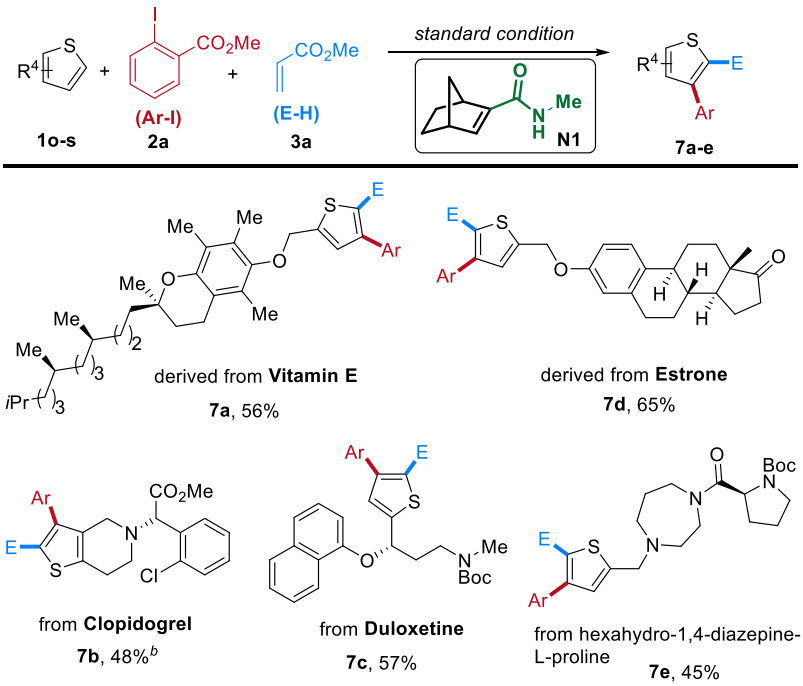

[a]The reaction was run with 0.3 mmol **1**, 0.2 mmol **2a** and 0.36 mmol **3a** in 1.0 mL ethyl acetate for 48 h. [b]A pair of rotational isomers was isolated in a 1:1 ratio.

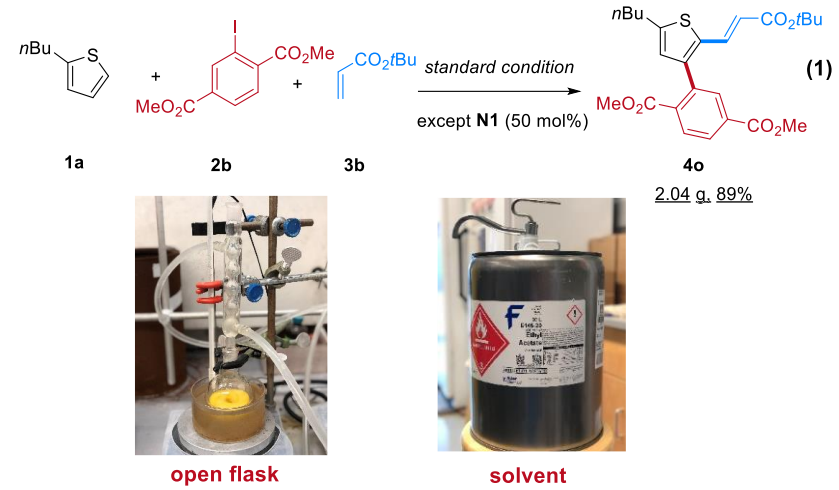

Beyond thiophenes, preliminary success was achieved using a simple furan substrate. When 2-butylfuran **1t** was subjected to the standard conditions with 1.0 equiv of **N1**, the desired trisubstituted product (**8**) was obtained in 30% yield (Eq. 2). In addition, the direct C4 arylation with protonation at the C5 position was realized with excess HOAc in the absence of acrylate **3a** (Eq. 3).[21]

6.2.4 Kinetic Study

Regarding the mechanistic pathway, an intriguing question is whether the reaction goes through a "coupled" difunctionalization as a regular Catellani pathway (**path a**) or a sequential stepwise

C4/C5 functionalization (**path b**), i.e. C4 arylation followed by an independent C5 C−H/Heck reaction. To address this question, the kinetic profile of the model reaction was obtained (Fig. 6.3), which indicates that the difunctionalization product (**4a**) was formed immediately at the beginning of the reaction and there was no accumulation of the C4-arylation intermediate (**9a**) during the course of the reaction. A competition experiment further indicated that direct difunctionalization is more favorable than the C5 alkenylation (C−H/Heck) of **9a** (Eq. 4). Taken together, these results suggest that the Heck quench at the C5 position is preferred compared to the protonation, thus supporting the "coupled" difunctionalization pathway (path **a**).

Figure 6.3. Kinetic Profile of the Model Reaction

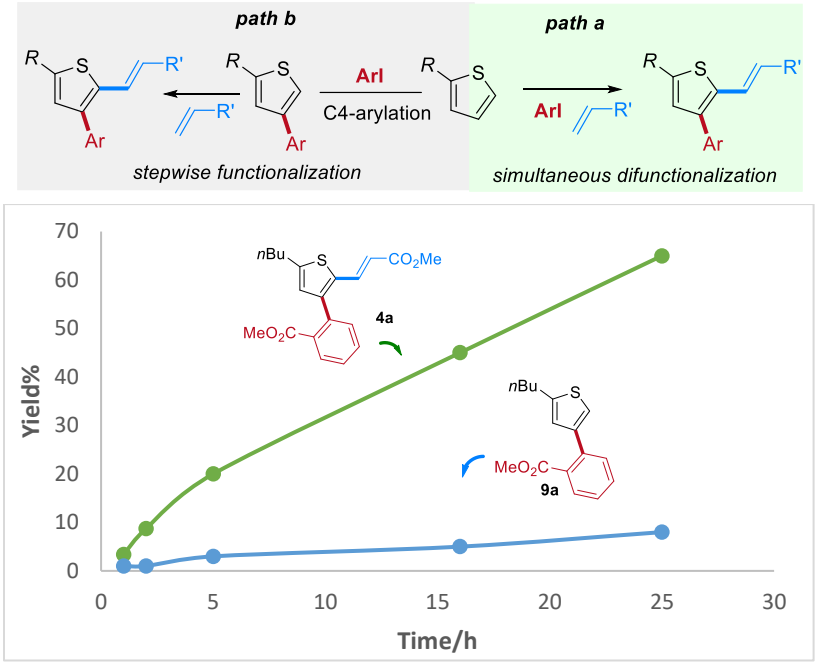

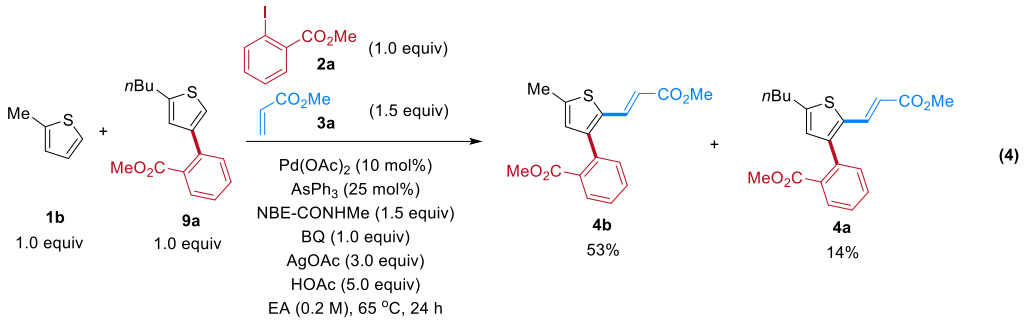

6.3 Conclusion

In summary, a direct method for vicinal difunctionalizations of thiophenes has been developed through the Pd/NBE cooperative catalysis. The reaction exhibits excellent FG tolerance and complete site- and regio-selectivity. The mild and robust reaction condition should make it attractive for preparing complex poly-substituted thiophenes and late-stage functionalization of bioactive compounds. Efforts on disclosing the detailed mechanism, including the exact role of the amide-derived NBE cofactor, and expanding the reaction scope to other types of difunctionalizations and other electron-rich heterocycles (beside thiophenes and furans) are ongoing.

6.4 Experimental Procedures and Characterization Data

6.4.1 General Information

Unless noted otherwise, all solvents were dried by filtration through a Pure-Solv MD-5 Solvent Purification System (Innovative Technology). Ethyl acetate was purchased from Fisher and used directly without further purification. Reaction temperatures were reported as the temperatures of the bather surrounding the flasks or vials. Sensitive reagents and solvents were transferred under nitrogen into a nitrogen-filled glovebox with standard techniques. Analytical thin-layer chromatography (TLC) was carried out using 0.2 mm commercial silica gel plates (silica gel 60, F254, EMD chemical). Vials (15 x 45 mm 1 dram (4 mL) with PTFE lined cap attached) were purchased from Qorpak and flame-dried and cooled in a desiccator prior to usage. High resolution mass spectra (HR-MS) were recorded on an Agilent 6530 LC Q-TOF mass spectrometer using electrospray ionization with fragmentation voltage set at 115 V and processed with an Agilent MassHunter Operating System. Infrared spectra were recorded on a Nicolet 380 FTIR using neat thin film technique. Nuclear magnetic resonance spectra (^{1}H NMR and ^{13}C NMR) were recorded with a Bruker DMX 400 (400 MHz, ^{1}H at 400 MHz, ^{13}C at 101 MHz) or Bruker Model DMX 500 (500 MHz, ^{1}H at 500 MHz, ^{13}C at 126 MHz). Chemical shifts were reported in parts per million (ppm, δ), downfield from tetramethylsilane (TMS, δ=0.00ppm) and were referenced to residual solvent ($CDCl_3$, δ=7.26 ppm (^{1}H) and 77.160 ppm (^{13}C)). All the ^{19}F chemical shifts were not referenced. Coupling constants were reported in Hertz (Hz). Data for ^{1}H NMR spectra were reported as follows: chemical shift (ppm, referenced to protium, s = singlet, d = doublet, t = triplet, q = quartet, quin = quintet, dd = doublet of doublets, td = triplet of doublets, ddd = doublet of doublet of doublets, m = multiplet, coupling constant (Hz), and integration). All other materials were obtained from Sigma-Aldrich Corporation or Combi-Blocks Inc and were used as received.

6.4.2 Substrates Preparation

Scheme 6.4. Preparation of 1r

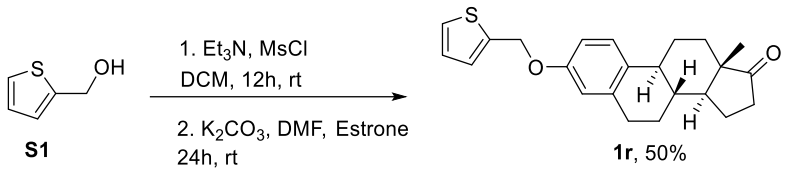

Under a N_2 atmosphere, triethylamine (84 ml, 60.0 mmol, 3.0 equiv.) and methanesulfonyl chloride (3.1 mL, 40.0 mmol, 2.0 equiv.) were added slowly to a dichloromethane solution of 2-thiophenemethanol **S1** (2.28 g, 20.0 mmol, 1.0 equiv.). The reaction mixture was stirred for 12 hours at room temperature. The the reaction mixture was then quenched with water, extracted with dichloromethane, dried over Na_2SO_4, and concentrated. The crude product was directly used in the following step without further purification.

Following a known procedure[22]: At 0 ^oC, estrone (5.4 g, 20.0 mmol, 1.0 equiv.) and K_2CO_3 (5.5 g, 40.0 mmol, 2.0 equiv.) were stirred in dimethylformamide (50 mL) for 5 min. **11** was added to the reaction mixture, and then the reaction was stirred for 24 hours at room temperature. The reaction was quenched with water, extracted with ethyl acetate, dried over Na_2SO_4, and purified on silica gel chromatography (hexane/ethyl acetate = 1:1) to afford the desired product **1r**.

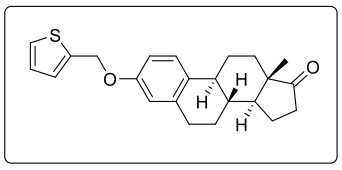

1r: White solid (50%). m. p. = 172–173 ^{o}C **^{1}H NMR** (400 MHz, Methylene Chloride-d_2) δ 7.34 (dd, J = 5.1, 1.2 Hz, 1H), 7.20 (d, J = 8.5 Hz, 1H), 7.12 – 7.09 (m, 1H), 7.01 (dd, J = 5.1, 3.5 Hz, 1H), 6.75 (dd, J = 8.6, 2.8 Hz, 1H), 6.70 (d, J = 2.7 Hz, 1H), 5.18 (s, 2H), 2.91 – 2.85 (m, 2H),

2.49 – 2.35 (m, 2H), 2.28 – 2.21 (m, 1H), 2.12 – 1.99 (m, 3H), 1.94 – 1.86 (m, 1H), 1.67 – 1.57 (m, 2H), 1.52 – 1.39 (m, 4H), 0.89 (s, 3H). **^{13}C NMR** (101 MHz, Methylene Chloride-d_2) δ 220.9, 156.7, 140.4, 138.6, 133.4, 127.3, 126.8, 126.6, 115.4, 112.8, 65.3, 50.9, 48.4, 44.5, 38.9, 36.3, 32.2, 30.2, 27.0, 26.5, 22.0, 14.2. **IR** (KBr): υ 3471, 2928, 2859, 1736, 1611, 1498, 1454, 1375, 1280, 1247 cm^{-1}. **HRMS** (ESI): Calculated for $C_{23}H_{27}O_2S(M+H^+)$: 367.1726, found: 367.1729.

Scheme 6.5. Preparation of 1o

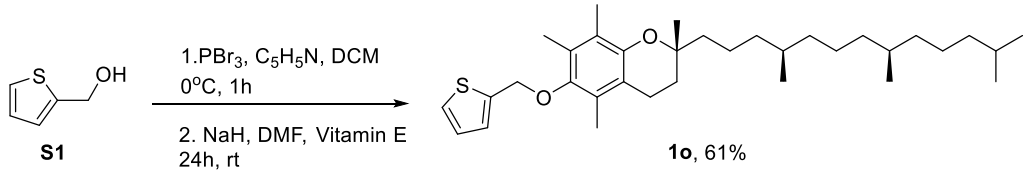

Following a known procedure[23]: under a N_2 atmosphere, a solution of 2-thiophenemethanol **S1** (0.69 g, 6 mmol, 1.0 equiv), phosphorus tribromide (9.0 mL, 1 M in DCM, 9.0 mmol, 1.5 equiv), and three drops of dry pyridine in dry dichloromethane (40 mL) at 0 °C, was stirred for 1 h. During this period, the reaction mixture was allowed to reach room temperature. Water was then added, and the organic phase was separated. The aqueous layer was extracted with dichloromethane (2×30 mL). All the combined organic extracts were washed with saturated sodium bicarbonate, dried over Na_2SO_4, filtered, and concentrated under reduced pressure to afford the crude product as a light-yellow oil.

Following a known procedure[24]: under a N_2 atmosphere, to a solution of Vitamin E (2.2 g, 5 mmol, 1.0 equiv) in anhydrous DMF (15 mL) at 0 °C was added sodium hydride (0.4 g, 10 mmol, 60 % in mineral oil, 2.0 equiv) in several portions. The suspension was stirred for 20 min at 0 °C, before crude 2-(bromomethyl)thiophene was slowly added. The mixture was stirred at room temperature until completion. An aqueous solution of ammonium chloride was added to the reaction mixture,

and then the aqueous layer was extracted with ether (3 × 30 mL). The combined organic layers were washed with water and brine, dried over Na_2SO_4, and concentrated under reduced pressure. The crude residue was purified by flash chromatography (hexane/EtOAc = 3:1) to afford the desired product **1o**.

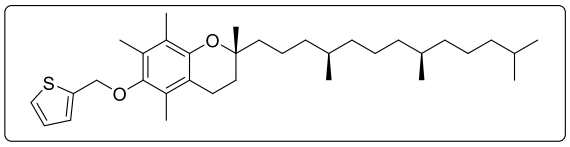

1o: Yellow oil (61%). **^{1}H NMR** (400 MHz, Chloroform-*d*) δ 7.34 (dd, *J* = 5.1, 1.2 Hz, 1H), 7.09 (d, *J* = 2.5 Hz, 1H), 7.02 (dd, *J* = 5.1, 3.5 Hz, 1H), 4.84 (s, 2H), 2.59 (t, *J* = 6.8 Hz, 2H), 2.22 (s, 3H), 2.17 (s, 3H), 2.10 (s, 3H), 1.87 – 1.74 (m, 2H), 1.56 – 1.47 (m, 3H), 1.43 – 1.36 (m, 3H), 1.31 – 1.19 (m, 12H), 1.15 – 1.04 (m, 6H), 0.86 (dd, *J* = 9.2, 6.5 Hz, 12H). **^{13}C NMR** (101 MHz, Chloroform-*d*) δ 148.17, 147.97, 140.45, 128.13, 126.85, 126.65, 126.19, 126.08, 123.06, 117.73, 75.00, 69.38, 37.70, 37.60, 37.54 (d, *J* = 2.5 Hz), 37.46 (d, *J* = 5.3 Hz), 32.93 (d, *J* = 2.0 Hz), 32.83 (d, *J* = 1.9 Hz), 31.40 (d, *J* = 4.8 Hz), 24.96 (d, *J* = 1.4 Hz), 24.59, 24.03, 22.88, 22.78, 21.19, 20.82, 19.87 (d, *J* = 6.6 Hz), 19.90 – 19.66 (m), 13.08, 12.22, 11.98. **IR** (KBr): υ 2926, 2867, 1461, 1414, 1376, 1254, 1159, 1086, 996, 698 cm^{-1}. **HRMS** (ESI): Calculated for $C_{34}H_{55}O_2S$ ($M+H^+$): 527.3917, found: 527.3919.

Scheme 6.6. Preparation of 1m

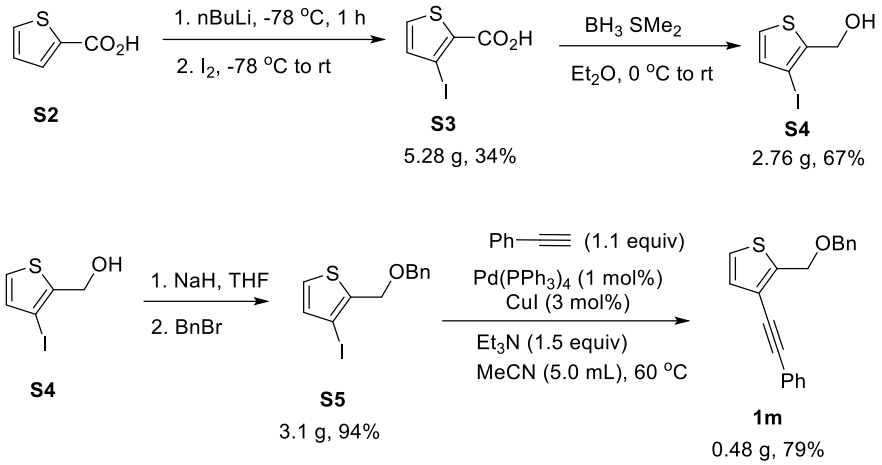

S3 and **S4** were prepared according to the literature reported procedures.[25] Following a known procedure[26], in a 50 mL Schlenk flask, **S4** (2.4 g, 10.0 mmol, 1.0 equiv) was dissolved in dry THF (10 mL). At 0 °C, sodium hydride (60% dispersion) (0.6 g, 15.0 mmol, 1.5 equiv) was added portionwise. The yellow suspension was allowed to warm up to rt under stirring for 20 min. Subsequently, benzyl bromide (1.8 mL, 15.0 mmol, 1.5 equiv) was added dropwise at 0 °C followed by stirring at rt for 3 h. When TLC indicated a full conversion, an aqueous solution of ammonium chloride was added. The aqueous layer was extracted with diethyl ether and the combined organic phase was washed with aqueous $NaHCO_3$, brine and dried over Na_2SO_4. The solvent was removed under reduced pressure and the residue was purified by flash chromatography to yield the title compound **S5** as a yellow liquid (3.1 g, 94%). The synthesis of **1m** was followed the general Sonogashira procedure,[27] except that it was performed at 60 °C, with **1r** (660 mg, 2.0 mmol, 1.0 equiv), phenylacetylene (224 mg, 2.2 mmol, 1.1 equiv), $Pd(PPh_3)_4$ (23 mg, 0.02 mmol, 1 mol %), CuI (11.4 mg, 0.06 mmol, 3 mol%) and Et_3N (303 mg, 3.0 mmol, 1.5 equiv) in MeCN (5.0 mL) to afford the title compound as an orange oil (480 mg, 79%).

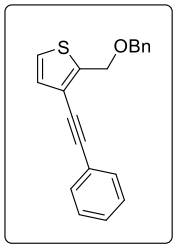

1m: orange oil (79%). **^{1}H NMR** (400 MHz, Chloroform-*d*) δ 7.51 – 7.47 (m, 2H), 7.46 – 7.41 (m, 2H), 7.40 – 7.34 (m, 5H), 7.33 – 7.27 (m, 2H), 7.14 (dd, *J* = 5.2, 1.6 Hz, 1H), 4.92 (s, 2H), 4.67 (s, 2H). **^{13}C NMR** (101 MHz, Chloroform-*d*) δ 144.3, 138.0, 131.6, 129.6, 128.6, 128.5, 128.4, 128.0, 127.8, 125.1, 123.2, 121.2, 92.4, 83.4, 77.5, 77.2, 76.8, 72.1, 65.5. **IR** (KBr): 2856, 1597, 1488, 1453, 1442, 1348, 1155, 1070, 1027, 755 cm^{-1}. **HRMS** (ESI): Calculated for $C_{20}H_{16}OSNa$ ($M+Na^{+}$): 327.0814, found: 327.0815.

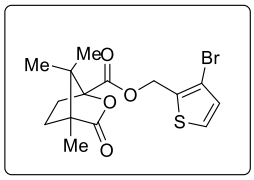

1n: White solid. m. p. = 104–105 ºC **^{1}H NMR** (400 MHz, Chloroform-*d*) δ 7.36 (d, *J* = 5.3 Hz, 1H), 7.00 (d, *J* = 5.3 Hz, 1H), 5.40 (d, *J* = 1.3 Hz, 2H), 2.50 – 2.42 (m, 1H), 2.09 – 2.02 (m, 1H), 1.97 – 1.90 (m, 1H), 1.73 – 1.67 (m, 1H), 1.11 (s, 3H), 1.04 (s, 3H), 0.93 (s, 3H).**^{13}C NMR** (101 MHz, Chloroform-*d*) δ 178.04, 167.28, 131.60, 130.30, 127.37, 112.75, 91.02, 60.34, 54.88, 54.48, 30.69, 29.02, 16.87, 16.78, 9.78. **IR** (KBr): υ 3450, 2968, 1789, 1753, 1634, 1446, 1311, 1263, 1168, 1102 cm^{-1}. **HRMS** (ESI): Calculated for $C_{15}H_{17}BrO_4SNa$ ($M+Na^{+}$): 394.9923, found: 394.9922.

Scheme 6.7. Preparation of 1s

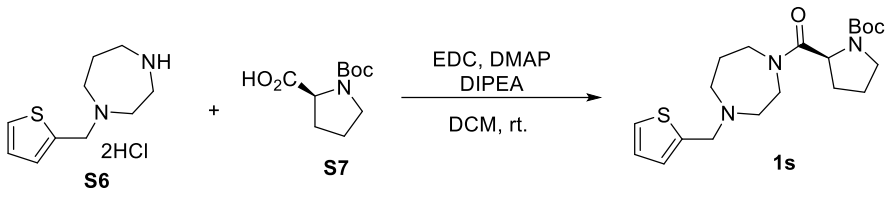

To a 100 mL round bottom flask were added Boc-Pro-OH (710.2 mg, 3.3 mmol, 1.0 equiv), 1-(2-Thienylmethyl)-1,4-diazepane dihydrochloride (1.35 g, 5.0 mmol, 1.5 equiv), EDC (1.27 g, 6.6 mmol, 2.0 equiv), DMAP (80.5 mg, 0.66 mmol, 20 mol%) and DCM (20 mL). DIPEA (2.13 g, 16.5 mmol, 5.0 equiv) was then added and the reaction was stirred at room temperature overnight. When the TLC indicated a full conversion, aqueous ammonium chloride was added to quench the reaction. The aqueous layer was extracted with ethyl acetate three times, and the combined organic phase was washed with aqueous $NaHCO_3$ and brine, dried over Na_2SO_4 and concentrated under reduced pressure. The desired product **1s** was purified through flash column chromatography on silica gel (hexane/acetone = 1:1) in 77% yield.

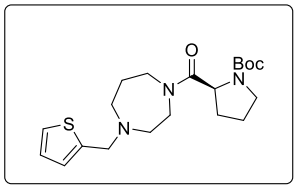

1s: Light yellow oil (77%). **^{1}H NMR** (400 MHz, Chloroform-*d*) δ 7.24 – 7.18 (m, 1H), 6.96 – 6.86 (m, 2H), 4.56 (dddd, *J* = 50.8, 15.3, 7.9, 3.4 Hz, 1H), 3.92 – 3.78 (m, 2H), 3.75 – 3.37 (m, 6H), 2.85 – 2.55 (m, 4H), 2.18 – 1.98 (m, 2H), 1.95 – 1.77 (m, 4H), 1.42 (d, *J* = 16.9 Hz, 10H). **^{13}C NMR** (101 MHz, Chloroform-*d*) δ 173.24 – 171.94 (m), 154.22 (d, *J* = 57.3 Hz), 142.64 (d, *J* = 5.3 Hz), 126.46 (d, *J* = 3.3 Hz), 125.62 (d, *J* = 3.0 Hz), 125.28 – 124.75 (m), 79.40 (dd, *J* = 14.2, 1.5 Hz), 57.58 – 56.13 (m), 55.67 (d, *J* = 4.1 Hz), 55.57 – 53.10 (m), 47.62 (d, *J* = 28.5 Hz), 46.99

– 46.15 (m), 45.86 – 44.17 (m), 30.43 (dd, *J* = 85.5, 5.4 Hz), 28.77 – 28.27 (m), 27.54 (d, *J* = 26.6 Hz), 24.22 (d, *J* = 1.9 Hz), 23.42. **IR** (KBr): υ 3477, 2974, 2876, 1694, 1651, 1478, 1402, 1365, 1165, 1134 cm^{-1}. **HRMS** (ESI): Calculated for $C_{20}H_{31}N_3O_3SNa$ ($M+Na^+$): 416.1978, found: 416.1969.

6.4.3 General Procedure of Direct Difunctionalization of Thiophenes

Scheme 6.8. Vicinal Difunctionalization of Thiophenes

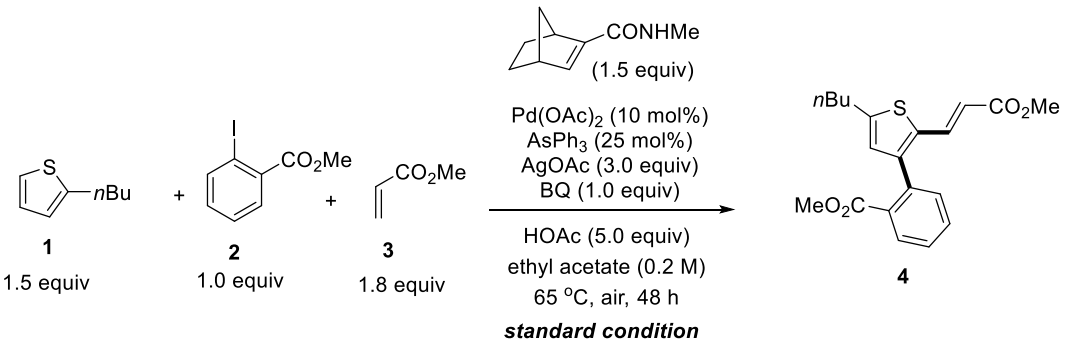

A flame-dried 4.0 mL vial was charged with $Pd(OAc)_2$ (4.6 mg, 0.02 mmol, 10 mol%), $AsPh_3$ (15.2 mg, 0.05 mmol, 25 mol%), BQ (21.6 mg, 0.2 mmol, 1.0 equiv), NBE-CONHMe (45.4 mg, 0.3 mmol, 1.5 equiv), AgOAc (100 mg, 0.6 mmol, 3.0 equiv), thiophene **1** (0.3 mmol, 1.5 equiv) and aryl iodide **2** (0.2 mmol, 1.0 equiv) in air. Ethyl acetate (1.0 mL) was then added. After HOAc (60 mg, 1.0 mmol, 5.0 equiv) and acrylate **3** (0.36 mmol, 1.8 equiv) was added, the vial was tightly sealed and stirred on a pie-block preheated to 65 °C for 48 hours. After completion of the reaction, the mixture was filtered through a thin pad of silica gel. The filter cake was washed with ethyl acetate and the combined filtrate was concentrated under reduced pressure. The residue was loaded to a small amount of silica gel and subjected to flash column chromatography to give the desired product **4**.

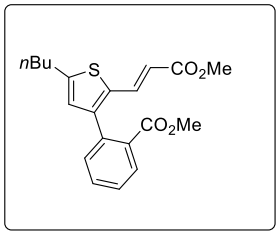

4a: Light yellow oil (81%). R_f = 0.3 (hexane/ethyl acetate = 10:1). **^{1}H NMR** (400 MHz, Chloroform-*d*) δ 7.93 (dd, *J* = 7.8, 1.4 Hz, 1H), 7.54 (td, *J* = 7.5, 1.5 Hz, 1H), 7.49 – 7.40 (m, 2H), 7.26 (dd, *J* = 7.6, 1.3 Hz, 1H), 6.64 (s, 1H), 6.09 (d, *J* = 15.6 Hz, 1H), 3.70 (s, 3H), 3.67 (s, 3H), 2.86 – 2.76 (m, 2H), 1.75 – 1.63 (m, 2H), 1.47 – 1.35 (m, 2H), 0.94 (t, *J* = 7.3 Hz, 3H). **^{13}C NMR** (101 MHz, Chloroform-*d*) δ 167.9, 167.6, 147.7, 145.1, 136.6, 136.1, 132.5, 131.7, 131.7, 131.2, 130.5, 128.2, 127.9, 115.4, 52.3, 51.6, 33.5, 30.2, 22.3, 13.9. **IR** (KBr): υ 2953, 2927, 2854, 1721, 1619, 1491, 1433, 1379, 1258, 1168 cm^{-1}. **HRMS** (ESI): Calculated for $C_{20}H_{23}O_4S$ ($M+H^+$): 359.1312, found: 359.1303.

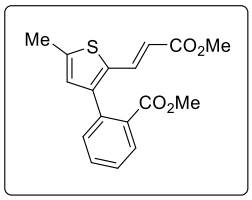

4b: Light yellow oil (78%). R_f = 0.3 (hexane/ethyl acetate = 10:1). **^{1}H NMR** (400 MHz, Chloroform-*d*) δ 7.95 (dd, *J* = 7.8, 1.2 Hz, 1H), 7.54 (td, *J* = 7.5, 1.4 Hz, 1H), 7.48 – 7.44 (m, 1H), 7.41 (d, *J* = 15.6 Hz, 1H), 7.26 – 7.23 (m, 1H), 6.64 (d, *J* = 1.0 Hz, 1H), 6.08 (d, *J* = 15.6 Hz, 1H), 3.70 (s, 6H), 2.50 (d, *J* = 0.8 Hz, 3H). **^{13}C NMR** (101 MHz, Chloroform-*d*) δ 167.7, 167.6, 145.3, 141.7, 136.5, 136.2, 132.9, 131.8, 131.7, 131.1, 130.5, 129.1, 128.2, 115.5, 52.3, 51.7, 15.9. **IR** (KBr): υ 2950, 1717, 1618, 1492, 1432, 1376, 1310, 1191, 1168, 1076 cm^{-1}. **HRMS** (ESI): Calculated for $C_{17}H_{16}O_4SNa$ ($M+Na^+$): 339.0662, found: 339.0660.

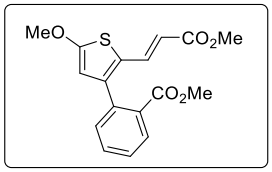

4c: White solid (76%). m. p. = 112–113 °C R_f = 0.2 (hexane/ethyl acetate = 10:1). **^{1}H NMR** (400 MHz, Methylene Chloride-d_2) δ 7.93 (dd, *J* = 7.8, 1.4 Hz, 1H), 7.58 (td, *J* = 7.6, 1.5 Hz, 1H), 7.49 (td, *J* = 7.6, 1.4 Hz, 1H), 7.36 – 7.27 (m, 2H), 6.13 (s, 1H), 5.90 (d, *J* = 15.5 Hz, 1H), 3.93 (s, 3H), 3.70 (s, 3H), 3.65 (s, 3H). **^{13}C NMR** (101 MHz, Methylene Chloride-d_2) δ 167.92, 167.67, 167.39, 144.92, 136.86, 136.31, 132.08, 131.89, 131.87, 130.68, 128.83, 122.01, 113.52, 108.11, 60.76, 52.66, 51.79. **IR** (KBr): υ 2950, 1715, 1615, 1540, 1498, 1422, 1311, 1292, 1168, 1076 cm^{-1}. **HRMS** (ESI): Calculated for $C_{17}H_{16}O_5SNa$ ($M+Na^+$): 355.0611, found: 355.0612.

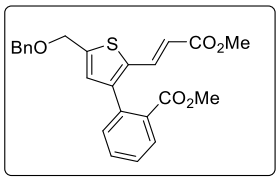

4d: Light yellow oil (72%). R_f = 0.1 (hexane/ethyl acetate = 10:1). **^{1}H NMR** (400 MHz, Chloroform-*d*) δ 7.97 (dd, *J* = 7.8, 1.2 Hz, 1H), 7.56 (td, *J* = 7.5, 1.4 Hz, 1H), 7.50 – 7.42 (m, 2H), 7.39 – 7.34 (m, 4H), 7.32 (dt, *J* = 6.8, 2.8 Hz, 1H), 7.27 – 7.25 (m, 1H), 6.85 (s, 1H), 6.18 (d, *J* = 15.6 Hz, 1H), 4.70 – 4.67 (m, 2H), 4.61 (s, 2H), 3.71 (s, 3H), 3.68 (s, 3H). **^{13}C NMR** (101 MHz, Chloroform-*d*) δ 167.6, 167.4, 144.6, 142.4, 137.7, 136.3, 135.9, 135.0, 131.9, 131.8, 131.0, 130.7, 129.5, 128.7, 128.4, 128.1, 128.0, 116.7, 72.2, 66.7, 52.3, 51.8. **IR** (KBr): υ 2949, 2851, 1717, 1620, 1495, 1453, 1432, 1310, 1270, 1191 cm^{-1}. **HRMS** (ESI): Calculated for $C_{24}H_{22}O_5SNa$ ($M+Na^+$): 445.1080, found: 445.1082.

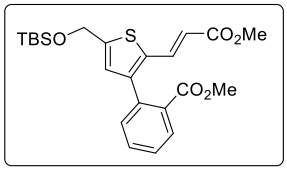

4e: Colorless oil (76%). R_f = 0.3 (hexane/ethyl acetate = 10:1). **^{1}H NMR** (400 MHz, Chloroform-*d*) δ 7.79 (dd, *J* = 7.8, 1.3 Hz, 1H), 7.39 (td, *J* = 7.5, 1.4 Hz, 1H), 7.32 – 7.28 (m, 1H), 7.09 (d, *J* = 7.5 Hz, 2H), 6.60 (s, 1H), 5.99 (d, *J* = 15.6 Hz, 1H), 4.72 – 4.68 (m, 2H), 3.55 (s, 3H), 3.52 (s, 3H), 0.78 (s, 9H), -0.03 (s, 6H). **^{13}C NMR** (101 MHz, Chloroform-*d*) δ 167.7, 167.5, 147.1, 144.7, 136.6, 136.1, 133.8, 131.8, 131.8, 131.1, 130.6, 128.3, 126.6, 116.2, 61.1, 52.3, 51.7, 26.0, 18.5, -5.1. **IR** (KBr): υ 2952, 2930, 2857, 1716, 1621, 1472, 1433, 1463, 1310, 1256 cm^{-1}. **HRMS** (ESI): Calculated for $C_{23}H_{30}O_5SSiNa$ ($M+Na^+$): 469.1475, found: 469.1474.

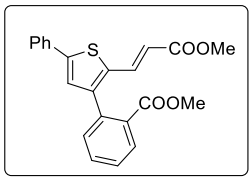

4f: Colorless oil (80%). R_f = 0.3 (hexane/ethyl acetate = 10:1). **^{1}H NMR** (400 MHz, Methylene Chloride-d_2) δ 7.99 (dd, *J* = 7.8, 1.4 Hz, 1H), 7.69 – 7.64 (m, 2H), 7.61 (dd, *J* = 7.5, 1.5 Hz, 1H), 7.53 (td, *J* = 7.6, 1.4 Hz, 1H), 7.45 – 7.38 (m, 3H), 7.38 – 7.31 (m, 2H), 7.23 (s, 1H), 6.21 (d, *J* = 15.6 Hz, 1H), 3.69 (s, 3H), 3.68 (s, 3H). **^{13}C NMR** (101 MHz, Methylene Chloride-d_2) δ 167.9, 167.4, 146.5, 145.1, 136.2, 136.2, 134.5, 133.8, 132.3, 132.1, 131.8, 130.9, 129.6, 129.1, 128.9, 126.9, 126.4, 117.0, 52.7, 52.0. **IR** (KBr): υ 2949, 1716, 1616, 1481, 1455, 1431, 1374, 1312, 1271, 1076 cm^{-1}. **HRMS** (ESI): Calculated for $C_{22}H_{18}O_4SNa$ ($M+Na^+$): 401.0818, found: 401.0817.

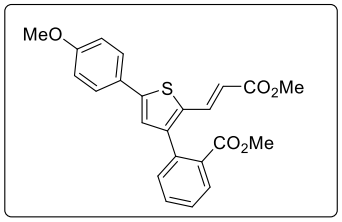

4g: Yellow oil (86%). R_f = 0.2 (hexane/ethyl acetate = 10:1). **^{1}H NMR** (400 MHz, Chloroform-*d*) δ 7.99 (dd, *J* = 7.8, 1.4 Hz, 1H), 7.69 – 7.64 (m, 2H), 7.61 (dd, *J* = 7.5, 1.5 Hz, 1H), 7.53 (td, *J* = 7.6, 1.4 Hz, 1H), 7.45 – 7.38 (m, 3H), 7.38 – 7.31 (m, 2H), 7.23 (s, 1H), 6.21 (d, *J* = 15.6 Hz, 1H), 3.69 (s, 3H), 3.68 (s, 3H). **^{13}C NMR** (101 MHz, Chloroform-*d*) δ 167.7, 167.4, 160.0, 146.1, 145.0, 136.3, 135.9, 133.1, 131.8, 131.6, 131.1, 130.6, 128.4, 127.4, 126.2, 125.3, 115.8, 114.5, 55.5, 52.3, 51.7. **IR** (KBr): υ 2999, 2950, 2838, 1715, 1615, 1573, 1512, 1484, 1454, 1431 cm^{-1}. **HRMS** (ESI): Calculated for $C_{23}H_{20}O_5SNa$ ($M+Na^+$): 431.0924, found: 431.0929.

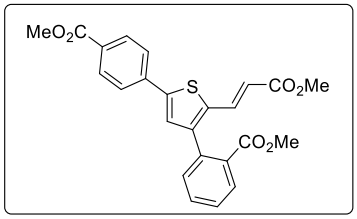

4h: Light yellow oil (58%). R_f = 0.1 (hexane/ethyl acetate = 10:1). **^{1}H NMR** (400 MHz, Chloroform-*d*) δ 8.08 – 8.03 (m, 2H), 8.02 (dd, *J* = 7.8, 1.2 Hz, 1H), 7.70 – 7.66 (m, 2H), 7.59 (td, *J* = 7.5, 1.4 Hz, 1H), 7.50 (td, *J* = 7.6, 1.3 Hz, 1H), 7.45 (d, *J* = 15.6 Hz, 1H), 7.31 (dd, *J* = 7.6, 1.1 Hz, 1H), 7.29 (s, 1H), 6.24 (d, *J* = 15.6 Hz, 1H), 3.93 (s, 3H), 3.72 (s, 3H), 3.70 (s, 3H). **^{13}C NMR** (101 MHz, $CDCl_3$) δ 167.4, 167.2, 166.6, 146.1, 143.1, 137.6, 135.9, 135.7, 135.4, 132.0, 131.7, 130.9, 130.8, 130.4, 129.7, 128.6, 127.7, 125.7, 117.3, 52.4, 52.3, 51.8. **IR** (KBr): υ 2951, 1722, 1619, 1606, 1484, 1435, 1411, 1312, 1279, 1191 cm^{-1}. **HRMS** (ESI): Calculated for $C_{24}H_{20}O_6SNa$ ($M+Na^+$): 459.0873, found: 459.0873.

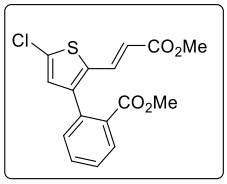

4i: Light yellow oil (60%). R_f = 0.4 (hexane/ethyl acetate = 10:1). **^{1}H NMR** (400 MHz, Chloroform-*d*) δ 8.00 (dd, *J* = 7.8, 1.3 Hz, 1H), 7.57 (td, *J* = 7.5, 1.5 Hz, 1H), 7.49 (td, *J* = 7.6, 1.4 Hz, 1H), 7.34 (d, *J* = 15.7 Hz, 1H), 7.24 (dd, *J* = 7.6, 1.2 Hz, 1H), 6.80 (s, 1H), 6.07 (d, *J* = 15.7 Hz, 1H), 3.73 (s, 3H), 3.71 (s, 3H). **^{13}C NMR** (101 MHz, $CDCl_3$) δ 167.2, 167.1, 144.5, 135.5, 135.1, 133.5, 132.1, 131.7, 130.9, 130.8, 129.7, 128.8, 125.4, 116.9, 52.4, 51.8. **IR** (KBr): υ 2950, 1724, 1621, 1484, 1425, 1310, 1273, 1192, 1169, 1076 cm^{-1}. **HRMS** (ESI): Calculated for $C_{16}H_{13}Cl\ O_4SNa$ ($M+Na^+$): 359.0115, found: 359.0116.

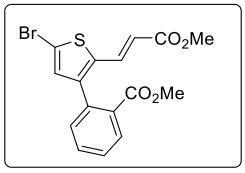

4j: Light yellow oil (40%). R_f = 0.4 (hexane/ethyl acetate = 10:1). **^{1}H NMR** (400 MHz, Chloroform-*d*) δ 8.00 (dd, *J* = 7.8, 1.3 Hz, 1H), 7.57 (td, *J* = 7.5, 1.5 Hz, 1H), 7.49 (td, *J* = 7.6, 1.4 Hz, 1H), 7.34 (d, *J* = 15.7 Hz, 1H), 7.24 (dd, *J* = 7.6, 1.1 Hz, 1H), 6.93 (s, 1H), 6.09 (d, *J* = 15.7 Hz, 1H), 3.72 (s, 3H), 3.71 (s, 3H). **^{13}C NMR** (101 MHz, Chloroform-*d*) δ 167.2, 167.1, 145.2, 136.3, 135.3, 134.9, 133.4, 132.1, 131.7, 130.9, 130.8, 128.8, 117.2, 114.4, 52.4, 51.8. **IR** (KBr): υ 2950, 1723, 1621, 1434, 1420, 1309, 1273, 1192, 1170, 1076 cm^{-1}. **HRMS** (ESI): Calculated for $C_{16}H_{13}BrO_4SNa$ ($M+Na^+$): 402.9610, found: 402.9606.

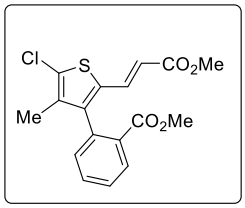

4k: white solid (51%). m. p. = 116-117 ºC R_f = 0.3 (hexane/ethyl acetate = 10:1). **^{1}H NMR** (400 MHz, Chloroform-*d*) δ 8.08 (dd, *J* = 7.8, 1.2 Hz, 1H), 7.60 (td, *J* = 7.5, 1.4 Hz, 1H), 7.52 (td, *J* = 7.7, 1.4 Hz, 1H), 7.22 (d, *J* = 15.6 Hz, 1H), 7.17 (dd, *J* = 7.5, 1.1 Hz, 1H), 6.03 (d, *J* = 15.6 Hz, 1H), 3.72 (s, 3H), 3.68 (s, 3H), 1.83 (s, 3H). **^{13}C NMR** (101 MHz, $CDCl_3$) δ 167.2, 166.7, 145.5, 136.0, 135.9, 135.8, 132.5, 131.8, 131.6, 131.1, 130.7, 128.9, 127.2, 116.2, 52.4, 51.7, 12.9. **IR** (KBr): υ 2950, 1726, 1682, 1643, 1621, 1548, 1462, 1433, 1308, 1259 cm^{-1}. **HRMS** (ESI): Calculated for $C_{17}H_{15}ClO_4SNa$ ($M+Na^+$): 373.0272, found: 373.0273.

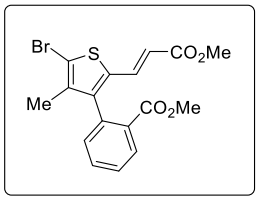

4l: Light yellow oil (52%). R_f = 0.3 (hexane/ethyl acetate = 10:1). **^{1}H NMR** (400 MHz, Chloroform-*d*) δ 8.09 (dd, *J* = 7.8, 1.2 Hz, 1H), 7.60 (td, *J* = 7.5, 1.4 Hz, 1H), 7.52 (td, *J* = 7.7, 1.3 Hz, 1H), 7.21 (d, *J* = 15.7 Hz, 1H), 7.16 (dd, *J* = 7.5, 1.1 Hz, 1H), 6.05 (d, *J* = 15.7 Hz, 1H), 3.71 (s, 3H), 3.68 (s, 3H), 1.83 (s, 3H). **^{13}C NMR** (101 MHz, $CDCl_3$) δ 167.2, 166.7, 145.6, 138.6, 136.0, 135.8, 134.5, 132.5, 131.8, 131.1, 130.7, 128.9, 116.5, 112.3, 52.4, 51.8, 14.6. **IR** (KBr): υ 2950, 1724, 1622, 1573, 1493, 1432, 1366, 1274, 1196, 1158 cm^{-1}. **HRMS** (ESI): Calculated for $C_{17}H_{15}BrO_4SNa$ ($M+Na^+$): 416.9767, found: 416.9771.

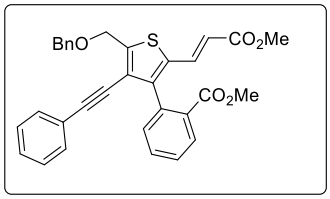

4m: Yellow oil (53%). R_f = 0.2 (hexane/ethyl acetate = 10:1). **^{1}H NMR** (400 MHz, Methylene Chloride-d_2) δ 8.10 (dd, *J* = 7.8, 1.4 Hz, 1H), 7.65 (td, *J* = 7.5, 1.5 Hz, 1H), 7.56 (td, *J* = 7.7, 1.4 Hz, 1H), 7.48 (d, *J* = 15.7 Hz, 1H), 7.44 – 7.39 (m, 2H), 7.39 – 7.24 (m, 7H), 7.24 – 7.18 (m, 2H), 6.26 (d, *J* = 15.7 Hz, 1H), 4.90 (s, 2H), 4.66 (s, 2H), 3.70 (s, 3H), 3.66 (s, 3H). **^{13}C NMR** (101 MHz, CD_2Cl_2) δ 167.6, 167.2, 146.6, 145.8, 138.4, 136.2, 135.2, 134.1, 132.9, 132.4, 131.8, 131.1, 129.2, 129.0, 128.9, 128.8, 128.4, 128.3, 123.2, 123.0, 118.1, 94.9, 82.5, 72.9, 66.5, 52.6, 52.1. **IR** (KBr): υ 2949, 1722, 1622, 1598, 1496, 1433, 1349, 1315, 1270, 1195 cm^{-1}. **HRMS** (ESI): Calculated for $C_{32}H_{26}O_5SNa$ ($M+Na^+$): 545.1393, found: 545.1394.

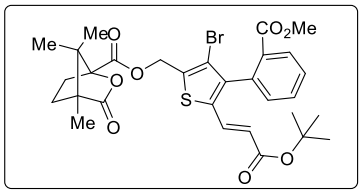

4n: Light yellow oil (40%). R_f = 0.1 (hexane/ethyl acetate = 5:1). **^{1}H NMR** (400 MHz, Chloroform-*d*) δ 8.11 (dd, *J* = 7.8, 1.2 Hz, 1H), 7.25 (d, *J* = 15.7 Hz, 1H), 7.20 (d, *J* = 7.5 Hz, 1H), 6.14 (d, *J* = 15.7 Hz, 1H), 5.42 (s, 2H), 3.71 (d, *J* = 0.7 Hz, 3H), 2.54 – 2.42 (m, 1H), 2.13 – 2.05 (m, 1H), 1.99 – 1.90 (m, 1H), 1.74 – 1.66 (m, 1H), 1.44 (s, 9H), 1.12 (s, 3H), 1.08 (d, *J* = 2.2 Hz, 3H), 0.97 (s, 3H). **^{13}C NMR** (101 MHz, Chloroform-*d*) δ 178.0 (d, *J* = 1.5 Hz), 167.3 (d, *J* = 1.5 Hz), 166.4, 165.7, 144.5, 135.7, 134.9, 134.4, 132.5, 132.2, 131.7 (d, *J* = 4.5 Hz), 131.1, 130.8, 129.2, 120.6, 115.6 (d, *J* = 4.8 Hz), 91.0 (d, *J* = 2.3 Hz), 81.0, 61.2, 55.0, 54.6, 52.4, 30.8, 29.1,

28.2, 17.0, 16.9, 9.8. **IR** (KBr): υ 2974, 1792, 1728, 1705, 1625, 1449, 1368, 1314, 1262, 1154 cm^{-1}. **HRMS** (ESI): Calculated for $C_{30}H_{33}BrO_8SNa$ ($M+Na^+$): 655.0972, found: 655.0981.

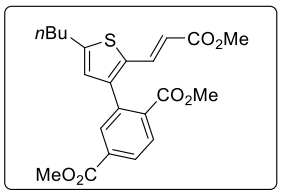

5a: Light yellow oil (87%). R_f = 0.1 (hexane/ethyl acetate = 10:1). **^{1}H NMR** (400 MHz, Chloroform-*d*) δ 7.97 (dd, *J* = 7.8, 1.4 Hz, 1H), 7.55 (td, *J* = 7.5, 1.5 Hz, 1H), 7.47 (td, *J* = 7.6, 1.4 Hz, 1H), 7.42 (d, *J* = 15.7 Hz, 1H), 7.24 (dd, *J* = 7.5, 1.3 Hz, 1H), 6.92 (s, 1H), 6.17 (d, *J* = 15.6 Hz, 1H), 5.22 (s, 2H), 3.70 (s, 3H), 3.69 (s, 3H), 2.11 (s, 3H). **^{13}C NMR** (101 MHz, Chloroform-*d*) δ 167.4, 167.2, 166.0, 148.1, 143.7, 136.3, 136.0, 135.2, 133.0, 132.8, 132.5, 130.4, 129.1, 127.7, 115.9, 52.7, 52.6, 51.7, 33.5, 30.2, 22.2, 13.9. **IR** (KBr): υ 2954, 1727, 1620, 1435, 1365, 1279, 1249, 1193, 1168, 1114 cm^{-1}. **HRMS** (ESI): Calculated for $C_{22}H_{24}O_6SNa$ ($M+Na^+$): 439.1186, found: 439.1177.

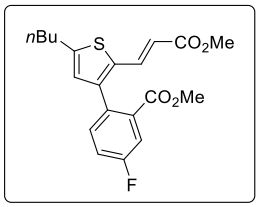

5b: Light yellow oil (72%). R_f = 0.3 (hexane/ethyl acetate = 10:1). **^{1}H NMR** (400 MHz, Chloroform-*d*) δ 7.58 (ddd, *J* = 9.1, 2.0, 1.0 Hz, 1H), 7.32 (d, *J* = 15.6 Hz, 1H), 7.20 – 7.16 (m, 2H), 6.55 (s, 1H), 6.02 (d, *J* = 15.6 Hz, 1H), 3.64 (s, 3H), 3.62 (s, 3H), 2.74 (t, *J* = 7.6 Hz, 2H), 1.66 – 1.58 (m, 2H), 1.35 (dt, *J* = 14.8, 7.4 Hz, 2H), 0.88 (t, *J* = 7.4 Hz, 3H). **^{13}C NMR** (101 MHz, Chloroform-*d*) δ 167.47, 166.53 (d, *J* = 2.5 Hz), 162.05 (d, *J* = 249.0 Hz), 145.82 (d, *J* = 404.5

Hz), 136.23, 133.81, 133.44 (d, *J* = 7.7 Hz), 132.86 (d, *J* = 7.5 Hz), 132.76, 132.19 (d, *J* = 3.6 Hz), 131.28 (d, *J* = 509.3 Hz), 127.86, 118.84 (d, *J* = 21.2 Hz), 117.47 (d, *J* = 23.6 Hz), 115.65, 52.52, 51.67, 33.47, 30.18, 22.24, 13.90. **^{19}F NMR** (376 MHz, Chloroform-*d*) δ -112.8. **IR** (KBr): υ 2954, 1717, 1619, 1499, 1435, 1378, 1308, 1273, 1193, 1167 cm^{-1}. **HRMS** (ESI): Calculated for $C_{20}H_{21}FO_4SNa$ ($M+Na^+$): 399.1037, found: 399.1043.

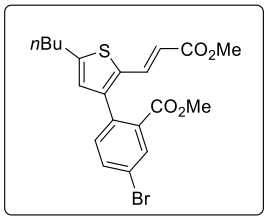

5c: Light yellow oil (81%). R_f = 0.3 (hexane/ethyl acetate = 10:1). **^{1}H NMR** (400 MHz, Chloroform-*d*) δ 8.07 (d, *J* = 2.1 Hz, 1H), 7.67 (dd, *J* = 8.2, 2.1 Hz, 1H), 7.38 (d, *J* = 15.6 Hz, 1H), 7.14 (d, *J* = 8.2 Hz, 1H), 6.61 (s, 1H), 6.09 (d, *J* = 15.6 Hz, 1H), 3.71 (s, 3H), 3.68 (s, 3H), 2.80 (t, *J* = 7.6 Hz, 2H), 1.71 – 1.64 (m, 2H), 1.47 – 1.36 (m, 2H), 0.94 (t, *J* = 7.3 Hz, 3H). **^{13}C NMR** (101 MHz, Chloroform-*d*) δ 167.4, 166.4, 148.0, 143.6, 136.1, 135.0, 134.7, 133.4, 133.2, 132.8, 132.8, 127.6, 122.2, 115.9, 52.6, 51.7, 33.5, 30.2, 22.3, 13.9. **IR** (KBr): υ 2953, 2931, 1717, 1620, 1487, 1433, 1309, 1283, 1192, 1168 cm^{-1}. **HRMS** (ESI): Calculated for $C_{20}H_{21}BrO_4SNa$ ($M+Na^+$): 459.0236, found: 459.0238.

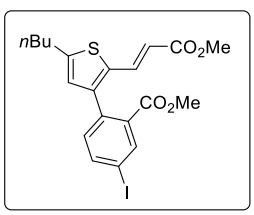

5d: Light yellow oil (56%). R_f = 0.3 (hexane/ethyl acetate = 10:1). **^{1}H NMR** (400 MHz, Chloroform-*d*) δ 8.26 (d, *J* = 1.9 Hz, 1H), 7.86 (dd, *J* = 8.1, 1.9 Hz, 1H), 7.38 (d, *J* = 15.6 Hz, 1H),

6.99 (d, *J* = 8.1 Hz, 1H), 6.61 (s, 1H), 6.09 (d, *J* = 15.6 Hz, 1H), 3.71 (s, 3H), 3.68 (s, 3H), 2.80 (t, *J* = 7.6 Hz, 2H), 1.71 – 1.63 (m, 2H), 1.46 – 1.36 (m, 2H), 0.94 (t, *J* = 7.3 Hz, 3H). **^{13}C NMR** (101 MHz, Chloroform-*d*) δ 167.4, 166.3, 148.0, 143.7, 140.6, 139.2, 136.1, 135.6, 133.2, 132.8, 132.8, 127.6, 115.9, 93.4, 52.5, 51.7, 33.5, 30.2, 22.2, 13.9. **IR** (KBr): υ 2952, 1717, 1619, 1485, 1433, 1309, 1281, 1192, 1168, 1084 cm^{-1}. **HRMS** (ESI): Calculated for $C_{20}H_{21}IO_4SNa$ ($M+Na^+$): 507.0097, found: 507.0100.

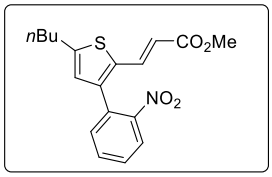

5e: Yellow solid (62%). m. p. = 93–94 ºC R_f = 0.1 (hexane/ethyl acetate = 10:1). **^{1}H NMR** (400 MHz, Chloroform-*d*) δ 7.99 (dd, *J* = 8.1, 1.2 Hz, 1H), 7.65 (td, *J* = 7.5, 1.3 Hz, 1H), 7.55 (td, *J* = 7.9, 1.5 Hz, 1H), 7.42 (d, *J* = 15.6 Hz, 1H), 7.35 (dd, *J* = 7.6, 1.4 Hz, 1H), 6.63 (s, 1H), 6.13 (d, *J* = 15.6 Hz, 1H), 3.71 (s, 3H), 2.80 (t, *J* = 7.6 Hz, 2H), 1.73 – 1.62 (m, 2H), 1.48 – 1.35 (m, 2H), 0.94 (t, *J* = 7.3 Hz, 3H). **^{13}C NMR** (101 MHz, Chloroform-*d*) δ 167.4, 149.4, 148.8, 140.3, 135.6, 133.6, 132.9, 132.8, 130.3, 129.2, 126.7, 124.7, 116.5, 51.8, 33.4, 30.2, 22.3, 13.9. **IR** (KBr): υ 2955, 2931, 1717, 1621, 1528, 1432, 1350, 1310, 1281, 1170 cm^{-1}. **HRMS** (ESI): Calculated for $C_{18}H_{19}NO_4SNa$ ($M+Na^+$): 368.0927, found: 368.0930.

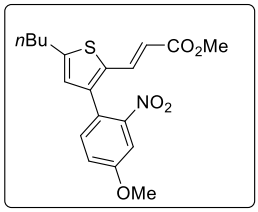

5f: Light red oil (60%). R_f = 0.3 (hexane/ethyl acetate = 1:1). **^{1}H NMR** (400 MHz, Chloroform-*d*) δ 7.50 (d, *J* = 2.6 Hz, 1H), 7.41 (d, *J* = 15.6 Hz, 1H), 7.24 (d, *J* = 8.5 Hz, 1H), 7.17 (dd, *J* = 8.5, 2.6 Hz, 1H), 6.60 (s, 1H), 6.11 (d, *J* = 15.6 Hz, 1H), 3.92 (s, 3H), 3.71 (s, 3H), 2.79 (t, *J* = 7.6 Hz, 2H), 1.70 – 1.61 (m, 2H), 1.45 – 1.36 (m, 2H), 0.94 (t, *J* = 7.3 Hz, 3H). **^{13}C NMR** (101 MHz, Chloroform-*d*) δ 167.5, 159.9, 149.8, 148.6, 140.4, 135.9, 133.8, 133.5, 127.0, 122.3, 119.1, 116.2, 109.7, 56.1, 51.7, 33.4, 30.2, 22.3, 13.9. **IR** (KBr): υ 2956, 1715, 1621, 1566, 1532, 1402, 1433, 1351, 1169, 1066 cm^{-1}. **HRMS** (ESI): Calculated for $C_{19}H_{21}NO_5SNa$ ($M+Na^+$): 398.1033, found: 398.1037.

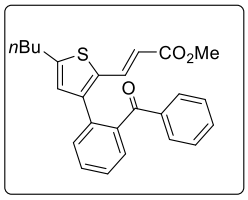

5g: Light yellow oil (57%). R_f = 0.2 (hexane/ethyl acetate = 10:1). **^{1}H NMR** (400 MHz, Chloroform-*d*) δ 7.61 – 7.58 (m, 2H), 7.58 – 7.53 (m, 3H), 7.53 – 7.49 (m, 1H), 7.40 (tt, *J* = 7.1, 1.3 Hz, 1H), 7.34 (dd, *J* = 7.8, 1.1 Hz, 1H), 7.27 – 7.24 (m, 2H), 6.50 (s, 1H), 6.00 (d, *J* = 15.6 Hz, 1H), 3.73 (s, 3H), 2.60 (t, *J* = 7.5 Hz, 2H), 1.53 – 1.44 (m, 2H), 1.27 – 1.19 (m, 2H), 0.89 (d, *J* = 7.3 Hz, 3H). **^{13}C NMR** (101 MHz, Chloroform-*d*) δ 198.2, 167.5, 148.3, 144.0, 139.8, 137.4, 136.4, 134.4, 133.2, 132.9, 131.0, 130.7, 129.7, 129.2, 128.6, 128.2, 128.0, 115.9, 51.7, 33.3, 29.9, 22.0, 13.9. **IR** (KBr): υ 2955, 2930, 1716, 1666, 1619, 1597, 1486, 1449, 1431, 1312 cm^{-1}. **HRMS** (ESI): Calculated for $C_{25}H_{24}O_3SNa$ ($M+Na^+$): 427.1388, found: 427.1342.

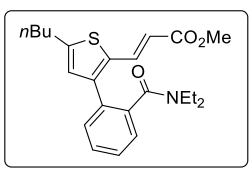

5h: Light yellow oil (68%). R_f = 0.2 (hexane/ethyl acetate = 1:1). **^{1}H NMR** (400 MHz, Chloroform-*d*) δ 7.61 (d, *J* = 15.5 Hz, 1H), 7.46 – 7.41 (m, 2H), 7.40 – 7.36 (m, 1H), 7.26 – 7.23 (m, 1H), 6.89 (s, 1H), 6.15 (d, *J* = 15.5 Hz, 1H), 3.80 – 3.68 (m, 4H), 2.96 (s, 2H), 2.76 (t, *J* = 7.6 Hz, 3H), 1.70 – 1.59 (m, 2H), 1.44 – 1.33 (m, 2H), 0.92 (t, *J* = 7.3 Hz, 6H), 0.82 (t, *J* = 7.1 Hz, 3H). **^{13}C NMR** (101 MHz, Chloroform-*d*) δ 170.0, 167.6, 148.0, 143.7, 137.4, 136.5, 133.2, 131.8, 131.1, 128.9, 128.9, 128.5, 126.9, 115.9, 51.7, 42.6, 38.4, 33.4, 30.2, 22.3, 13.9, 13.7, 12.3. **IR** (KBr): υ 2957, 2932, 1717, 1621, 1492, 1460, 1429, 1380, 1309, 1168 cm^{-1}. **HRMS** (ESI): Calculated for $C_{23}H_{29}NO_3SNa$ (M+Na$^+$): 422.1760, found: 422.1758.

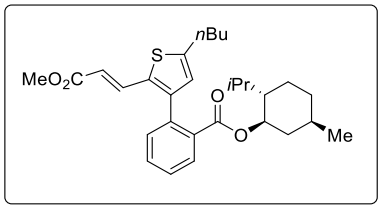

5i: Light yellow oil (73%). R_f = 0.4 (hexane/ethyl acetate = 10:1). **^{1}H NMR** (400 MHz, Chloroform-*d*)) δ 7.96 – 7.91 (m, 1H), 7.52 (td, *J* = 7.5, 1.5 Hz, 1H), 7.45 (td, *J* = 7.6, 1.4 Hz, 1H), 7.40 (d, *J* = 15.6 Hz, 1H), 7.23 (dd, *J* = 7.5, 1.1 Hz, 1H), 6.63 (s, 1H), 6.06 (d, *J* = 15.6 Hz, 1H), 4.71 (td, *J* = 10.8, 4.4 Hz, 1H), 3.69 (s, 3H), 2.86 – 2.76 (m, 2H), 1.93 – 1.85 (m, 1H), 1.75 – 1.57 (m, 6H), 1.43 (dq, *J* = 14.6, 7.3 Hz, 3H), 1.18 (t, *J* = 11.7 Hz, 1H), 1.04 (d, *J* = 4.1 Hz, 1H), 0.95 (t, *J* = 7.3 Hz, 3H), 0.86 (d, *J* = 6.5 Hz, 3H), 0.81 – 0.74 (m, 4H), 0.67 (d, *J* = 6.9 Hz, 3H). **^{13}C NMR** (101 MHz, Chloroform-*d*) δ 167.5, 167.1, 147.6, 145.6, 137.9, 136.7, 136.0, 132.6, 132.2, 131.5, 131.4, 130.4, 128.2, 115.3, 75.0, 51.6, 47.0, 40.4, 34.3, 33.5, 31.4, 30.3, 26.1, 23.2, 22.5, 22.2, 21.0 16.1, 14.0. **IR** (KBr): υ 2955, 2870, 1717, 1620, 1490, 1456, 1370, 1290, 1166, 1111cm^{-1}. **HRMS** (ESI): Calculated for $C_{29}H_{39}O_4S$ (M+H$^+$): 483.2564, found: 483.2570.

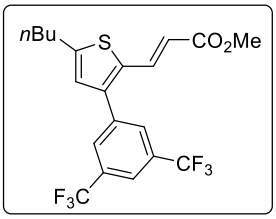

5j: Light red oil (37%). R_f = 0.5 (hexane/ethyl acetate = 10:1). **^{1}H NMR** (400 MHz, Chloroform-*d*) δ 7.92 – 7.87 (m, 1H), 7.79 (s, 2H), 7.60 (d, *J* = 15.6 Hz, 1H), 6.84 (s, 1H), 6.22 (d, *J* = 15.5 Hz, 1H), 3.75 (s, 3H), 2.90 – 2.79 (m, 2H), 1.78 – 1.66 (m, 2H), 1.44 (dt, *J* = 14.9, 7.4 Hz, 2H), 0.96 (t, *J* = 7.3 Hz, 3H). **^{13}C NMR** (101 MHz, Chloroform-*d*) δ 167.1, 149.6, 142.0, 137.7, 135.2, 133.7, 132.2 (q, *J* = 33.3 Hz), 129.3 (d, *J* = 3.8 Hz), 123.3 (q, *J* = 272.8 Hz). 127.1, 121.6 (p, *J* = 3.9 Hz), 117.8, 51.9, 33.5, 30.2, 22.3, 13.9. **^{19}F NMR** (376 MHz, $CDCl_3$) δ -62.9. **IR** (KBr): υ 2959, 1722, 1622, 1541, 1434, 1348, 1280, 1170, 1137, 1040 cm^{-1}. **HRMS** (ESI): Calculated for $C_{20}H_{19}F_6O_2S$ ($M+H^+$): 437.1004, found: 437. 1000.

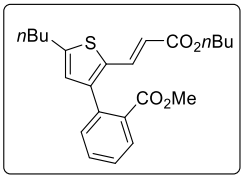

6a: Light yellow oil (78%). R_f = 0.4 (hexane/ethyl acetate = 10:1). **^{1}H NMR** (400 MHz, Chloroform-*d*) δ 7.93 (dd, *J* = 7.8, 1.3 Hz, 1H), 7.53 (td, *J* = 7.5, 1.4 Hz, 1H), 7.47 – 7.42 (m, 2H), 7.26 (dd, *J* = 7.6, 1.1 Hz, 1H), 6.64 (s, 1H), 6.09 (d, *J* = 15.6 Hz, 1H), 4.10 (t, *J* = 6.6 Hz, 2H), 3.67 (s, 3H), 2.81 (t, *J* = 7.6 Hz, 2H), 1.71 – 1.65 (m, 2H), 1.64 – 1.58 (m, 2H), 1.45 – 1.33 (m, 4H), 0.93 (dt, *J* = 11.8, 7.4 Hz, 6H). **^{13}C NMR** (101 MHz, Chloroform-*d*) δ 167.9, 167.3, 147.6, 145.0, 136.4, 136.1, 132.6, 131.7, 131.7, 131.2, 130.4, 128.1, 127.9, 115.9, 64.3, 52.3, 33.5, 30.8, 30.2, 22.2, 19.3, 13.91, 13.85. **IR** (KBr): υ 2957, 2932, 1716, 1618, 1491, 1456, 1433, 1379, 1257, 1167cm^{-1}. **HRMS** (ESI): Calculated for $C_{23}H_{28}O_4SNa$ ($M+Na^+$): 423.1601, found: 423.1607.

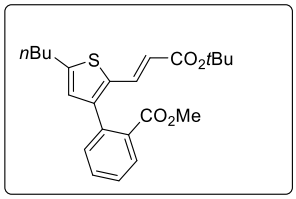

6b: Light yellow oil (84%). R_f = 0.4 (hexane/ethyl acetate = 10:1). **^{1}H NMR** (400 MHz, Chloroform-*d*) δ 7.91 (dd, *J* = 7.8, 1.3 Hz, 1H), 7.52 (td, *J* = 7.5, 1.4 Hz, 1H), 7.43 (dd, *J* = 7.7, 1.3 Hz, 1H), 7.41 – 7.36 (m, 1H), 7.28 – 7.25 (m, 1H), 6.63 (s, 1H), 6.04 (d, *J* = 15.5 Hz, 1H), 3.67 (s, 3H), 2.80 (t, *J* = 7.5 Hz, 2H), 1.70 – 1.64 (m, 2H), 1.45 (s, 9H), 1.43 – 1.37 (m, 2H), 0.94 (t, *J* = 7.3 Hz, 3H). **^{13}C NMR** (101 MHz, Chloroform-*d*) δ 167.9, 166.6, 147.1, 144.6, 136.2, 135.5, 132.7, 131.7, 131.7, 131.2, 130.4, 128.0, 127.8, 117.7, 80.3, 52.2, 33.5, 30.2, 28.3, 22.2, 13.9. **IR** (KBr): υ 2957, 2932, 1732, 1704, 1619, 1491, 1456, 1433, 1391, 1367 cm^{-1}. **HRMS** (ESI): Calculated for $C_{23}H_{28}O_4S$ Na (M+Na$^+$): 423.1601, found: 423.1605.

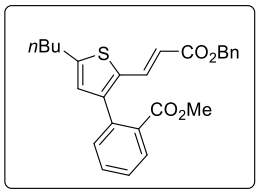

6c: Light yellow oil (80%). R_f = 0.2 (hexane/ethyl acetate = 10:1). **^{1}H NMR** (400 MHz, Chloroform-*d*) δ 7.85 (dd, *J* = 7.8, 1.3 Hz, 1H), 7.48 – 7.40 (m, 2H), 7.39 – 7.34 (m, 1H), 7.28 – 7.21 (m, 5H), 7.20 – 7.16 (m, 1H), 6.57 (s, 1H), 6.07 (d, *J* = 15.5 Hz, 1H), 5.08 (s, 2H), 3.58 (s, 3H), 2.73 (t, *J* = 7.6 Hz, 2H), 1.65 – 1.56 (m, 2H), 1.39 – 1.28 (m, 2H), 0.86 (t, *J* = 7.3 Hz, 3H). **^{13}C NMR** (101 MHz, Chloroform-*d*) δ 167.8, 166.9, 147.9, 145.3, 137.0, 136.3, 136.1, 132.5, 131.7, 131.7, 131.2, 130.4, 128.6, 128.2, 128.1, 127.9, 115.3, 66.1, 52.2, 33.4, 30.2, 22.2, 13.9. **IR** (KBr): υ 2955, 2931, 1716, 1617, 1491, 1455, 1433, 1375, 1293, 1159 cm^{-1}. **HRMS** (ESI): Calculated for $C_{26}H_{26}O_4SNa$ (M+Na$^+$): 457.1444, found: 457.1444.

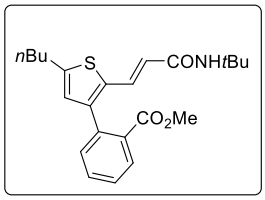

6d: White solid (81%). m. p. = 142–143 ^{o}C R_f = 0.3 (hexane/ethyl acetate = 1:1). **^{1}H NMR** (400 MHz, Chloroform-*d*) δ 7.89 (dd, *J* = 7.8, 1.1 Hz, 1H), 7.50 (td, *J* = 7.5, 1.4 Hz, 1H), 7.41 (dd, *J* = 7.7, 1.2 Hz, 1H), 7.36 (d, *J* = 15.1 Hz, 1H), 7.29 – 7.24 (m, 1H), 6.60 (s, 1H), 6.01 (d, *J* = 15.1 Hz, 1H), 5.49 (s, 1H), 3.66 (s, 3H), 2.78 (t, *J* = 7.6 Hz, 2H), 1.71 – 1.62 (m, 2H), 1.41 (dt, *J* = 13.3, 6.6 Hz, 2H), 1.35 (s, 9H), 0.93 (t, *J* = 7.3 Hz, 3H). **^{13}C NMR** (101 MHz, Chloroform-*d*) δ 168.0, 165.4, 145.8, 143.9, 136.3, 132.9, 132.2, 131.7, 131.1, 130.3, 127.9, 127.7, 119.9, 52.1, 51.5, 33.5, 30.1, 28.9, 22.2, 13.9. **IR** (KBr): υ 2960, 2930, 1731, 1651, 1612, 1552, 1491, 1433, 1454, 11363 cm^{-1}. **HRMS** (ESI): Calculated for $C_{23}H_{29}NO_3SNa$ ($M+Na^+$): 422.1760, found: 422.1762.

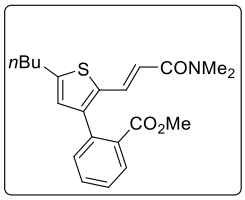

6e: Red oil (73%). R_f = 0.3 (hexane/ethyl acetate = 1:1). **^{1}H NMR** (400 MHz, Chloroform-*d*) δ 7.91 (dd, *J* = 7.8, 1.2 Hz, 1H), 7.51 (td, *J* = 7.5, 1.4 Hz, 1H), 7.46 (d, *J* = 15.0 Hz, 1H), 7.41 (td, *J* = 7.6, 1.3 Hz, 1H), 7.26 (dd, *J* = 7.6, 1.1 Hz, 1H), 6.61 (s, 1H), 6.52 (d, *J* = 15.0 Hz, 1H), 3.67 (s, 3H), 3.08 (s, 3H), 2.98 (s, 3H), 2.80 (t, *J* = 7.5 Hz, 2H), 1.70 – 1.63 (m, 2H), 1.42 (dt, *J* = 14.8, 7.4 Hz, 2H), 0.94 (t, *J* = 7.3 Hz, 3H). **^{13}C NMR** (101 MHz, Chloroform-*d*) δ 167.9, 166.7, 146.1, 144.0, 136.5, 134.4, 133.3, 131.8, 131.8, 131.0, 130.4, 128.0, 127.9, 115.3, 52.2, 37.4, 36.0, 33.5,

30.1, 22.2, 13.9. **IR** (KBr): υ 2954, 2931, 1730, 1644, 1599, 1543, 1492, 1392, 1292, 1257 cm^{-1}. **HRMS** (ESI): Calculated for $C_{21}H_{25}NO_3SNa$ ($M+Na^+$): 394.1447, found: 394.1449.

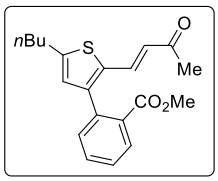

6f: Light yellow oil (77%). R_f = 0.3 (hexane/ethyl acetate = 10:1). **^{1}H NMR** (400 MHz, Chloroform-*d*) δ 7.92 (dd, *J* = 7.8, 1.2 Hz, 1H), 7.55 (td, *J* = 7.5, 1.4 Hz, 1H), 7.46 (td, *J* = 7.6, 1.3 Hz, 1H), 7.30 – 7.26 (m, 2H), 6.68 (s, 1H), 6.38 (d, *J* = 15.8 Hz, 1H), 3.67 (s, 3H), 2.82 (t, *J* = 7.5 Hz, 2H), 2.19 (s, 3H), 1.73 – 1.65 (m, 2H), 1.42 (dt, *J* = 14.8, 7.4 Hz, 2H), 0.94 (t, *J* = 7.4 Hz, 3H). **^{13}C NMR** (101 MHz, Chloroform-*d*) δ 197.9, 168.0, 148.5, 145.7, 135.9, 135.2, 132.7, 131.7, 131.5, 131.4, 130.4, 128.2, 128.1, 125.2, 52.3, 33.4, 30.2, 27.5, 22.2, 13.9. **IR** (KBr): υ 2955, 2931, 1731, 1684, 1661, 1588, 1433, 1360, 1293, 1254 cm^{-1}. **HRMS** (ESI): Calculated for $C_{20}H_{22}O_3SNa$ ($M+Na^+$): 365.1182, found: 365.1192.

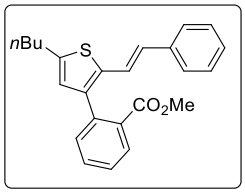

6g: Yellow oil (81%). R_f = 0.5 (hexane/ethyl acetate = 20:1). **^{1}H NMR** (400 MHz, Methylene Chloride-d_2) δ 7.87 (dd, *J* = 7.8, 1.3 Hz, 1H), 7.60 – 7.54 (m, 1H), 7.45 (td, *J* = 7.6, 1.3 Hz, 1H), 7.37 – 7.26 (m, 5H), 7.22 – 7.17 (m, 1H), 6.92 (d, *J* = 16.0 Hz, 1H), 6.81 (d, *J* = 16.0 Hz, 1H), 6.65 (s, 1H), 3.64 (s, 3H), 2.82 (d, *J* = 7.5 Hz, 2H), 1.74 – 1.67 (m, 2H), 1.48 – 1.41 (m, 2H), 0.97 (t, *J* = 7.4 Hz, 3H). **^{13}C NMR** (101 MHz, Methylene Chloride-d_2) δ 168.3, 143.6, 139.4, 137.2,

136.4, 135.4, 131.9, 131.5, 131.3, 129.8, 128.6, 127.5, 127.4, 127.3, 127.2, 126.1, 120.8, 52.0, 33.6, 29.9, 22.2, 13.6. **IR** (KBr): υ 2954, 2929, 1733, 1598, 1491, 1448, 1292, 1252, 1126, 1076 cm^{-1}. **HRMS** (ESI): Calculated for $C_{24}H_{24}O_2SNa$ ($M+Na^+$): 399.1389, found: 399.1385.

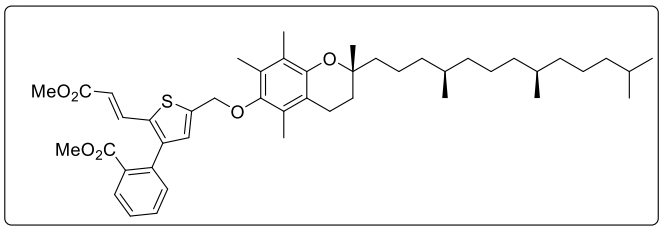

7a: Light yellow oil (56%). R_f = 0.2 (hexane/ethyl acetate = 10:1). **^{1}H NMR** (400 MHz, Chloroform-*d*) δ 7.98 (dd, *J* = 7.8, 1.2 Hz, 1H), 7.57 (td, *J* = 7.5, 1.4 Hz, 1H), 7.51 – 7.45 (m, 2H), 7.29 (dd, *J* = 7.6, 1.0 Hz, 1H), 6.94 (s, 1H), 6.22 (d, *J* = 15.6 Hz, 1H), 4.83 (s, 2H), 3.72 (s, 3H), 3.71 (s, 3H), 2.60 (t, *J* = 6.7 Hz, 2H), 2.23 (s, 3H), 2.19 (s, 3H), 2.11 (s, 3H), 1.81 (dp, *J* = 19.9, 6.9 Hz, 2H), 1.60 – 1.49 (m, 3H), 1.39 (dd, *J* = 11.5, 4.7 Hz, 3H), 1.32 – 1.20 (m, 12H), 1.17 – 1.06 (m, 6H), 0.88 – 0.84 (m, 12H). **^{13}C NMR** (101 MHz, Chloroform-*d*) δ 167.5, 167.2, 148.2, 147.7, 144.5, 141.4, 136.3, 135.8, 134.9, 131.8, 131.7, 131.0, 130.5, 129.3, 128.3, 127.9, 126.0, 123.1, 117.7, 116.7, 74.9, 69.4, 52.2, 51.6, 40.1 (d, *J* = 4.3 Hz), 39.4, 37.6 (d, *J* = 1.6 Hz), 37.5, 37.4 (d, *J* = 2.2 Hz), 37.3 (d, *J* = 4.8 Hz), 32.8 (d, *J* = 1.9 Hz), 32.7 (d, *J* = 2.1 Hz), 31.3 (d, *J* = 4.9 Hz), 28.0, 24.8 (d, *J* = 1.3 Hz), 24.5, 23.9, 22.8, 22.7, 21.1, 20.7, 19.8 (d, *J* = 6.6 Hz), 19.7 – 19.6 (m), 13.0, 12.1, 11.9. **IR** (KBr): υ 2928, 2867, 1722, 1622, 1457, 1434, 1378, 1309, 1191, 1168 cm^{-1}. **HRMS** (ESI): Calculated for $C_{46}H_{64}O_6SNa$ ($M+Na^+$): 767.4316, found: 767.4313.

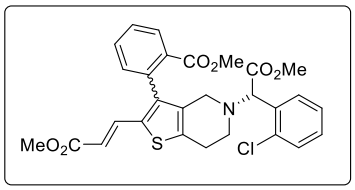

(1:1 separable rotational isomers)

7b: Light yellow oil (24%). R_f = 0.3 (hexane/ethyl acetate = 2:1). **^{1}H NMR** (400 MHz, Chloroform-*d*) δ 7.97 (dd, *J* = 7.8, 1.2 Hz, 1H), 7.52 – 7.46 (m, 2H), 7.41 (td, *J* = 7.6, 1.3 Hz, 1H), 7.32 – 7.28 (m, 1H), 7.22 (d, *J* = 3.6 Hz, 1H), 7.21 – 7.16 (m, 2H), 7.09 (dd, *J* = 7.5, 1.1 Hz, 1H), 6.02 (d, *J* = 15.6 Hz, 1H), 4.76 (s, 1H), 3.64 (s, 3H), 3.63 (s, 3H), 3.59 (s, 3H), 3.34 (d, *J* = 14.5 Hz, 1H), 3.16 (d, *J* = 14.5 Hz, 1H), 2.95 – 2.81 (m, 4H). ^{13}C NMR (101 MHz, Chloroform-*d*) δ 171.2, 167.6, 166.8, 143.3, 136.6, 136.0, 135.2, 134.8, 134.7, 133.8, 132.6, 132.2, 131.8, 131.0, 130.7, 129.9, 129.8, 129.5, 128.6, 127.1, 115.3, 67.5, 52.4, 52.1, 51.6, 49.9, 47.2, 26.2. **IR** (KBr): υ 2950, 1728, 1619, 1433, 1308, 1260, 1196, 1160, 1130, 1079 cm^{-1}. **HRMS** (ESI): Calculated for $C_{28}H_{26}ClNO_6SNa$ ($M+Na^+$): 562.1062, found: 562.1063.

7b': Red oil (24%). R_f = 0.25 (hexane/ethyl acetate = 2:1). **^{1}H NMR** (400 MHz, Chloroform-*d*) δ 7.99 (dd, *J* = 7.8, 1.2 Hz, 1H), 7.55 – 7.49 (m, 2H), 7.46 – 7.42 (m, 1H), 7.36 – 7.32 (m, 1H), 7.22 (dd, *J* = 8.9, 4.9 Hz, 3H), 7.15 – 7.12 (m, 1H), 6.03 (d, *J* = 15.6 Hz, 1H), 4.80 (s, 1H), 3.66 (s, 3H), 3.65 (s, 3H), 3.58 (s, 3H), 3.34 (d, *J* = 14.5 Hz, 1H), 3.19 (d, *J* = 14.5 Hz, 1H), 2.86 (dddd, *J* = 38.9, 23.6, 11.3, 5.0 Hz, 4H).**^{13}C NMR** (101 MHz, Chloroform-*d*) δ 171.3, 167.5, 166.9, 143.4, 136.5, 136.0, 135.2, 134.9, 134.8, 133.8, 132.7, 132.3, 131.8, 130.9, 130.7, 129.9, 129.9, 129.6, 128.6, 127.2, 115.3, 67.2, 52.4, 52.2, 51.6, 50.2, 47.0, 25.9. **IR** (KBr): υ 2950, 1728, 1619, 1499, 1433, 1308, 1260, 1196, 1160, 1079 cm^{-1}. **HRMS** (ESI): Calculated for $C_{28}H_{26}ClNO_6S$ Na ($M+Na^+$): 562.1062, found: 562.1065.

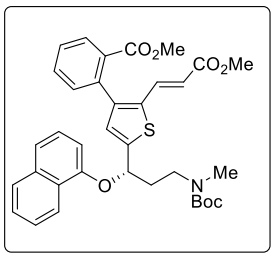

7c: Colorless oil (57%). R_f = 0.2 (hexane/ethyl acetate = 2:1). **^{1}H NMR** (400 MHz, Chloroform-*d*) δ 8.34 (dd, *J* = 6.8, 2.8 Hz, 1H), 7.96 – 7.91 (m, 1H), 7.79 (dt, *J* = 6.8, 2.9 Hz, 1H), 7.56 – 7.49 (m, 3H), 7.47 – 7.42 (m, 2H), 7.40 (d, *J* = 9.6 Hz, 1H), 7.29 (t, *J* = 8.0 Hz, 1H), 7.24 – 7.20 (m, 1H), 6.91 (s, 1H), 6.85 (d, *J* = 7.6 Hz, 1H), 6.10 (d, *J* = 15.6 Hz, 1H), 5.61 (s, 1H), 3.68 (s, 3H), 3.48 (s, 5H), 2.87 (s, 3H), 2.53 – 2.28 (m, 2H), 1.35 (s, 9H). **^{13}C NMR** (101 MHz, Chloroform-*d*) δ 167.1, 159.6, 156.9, 155.8, 152.9, 144.6, 136.0, 135.4, 134.6, 134.0, 131.7, 131.6, 131.0, 130.6, 128.3, 127.9, 127.6, 126.5, 125.9, 125.6, 125.5, 121.9, 121.0, 116.8, 106.6, 79.5, 73.5, 52.0, 51.6, 45.7, 37.2, 29.7, 28.3. **IR** (KBr): υ 2976, 2950, 1718, 1695, 1621, 1597, 1578, 1433, 1397, 1310 cm^{-1}. **HRMS** (ESI): Calculated for $C_{35}H_{37}NO_7SNa$ ($M+Na^+$): 638.2183, found: 638.2188.

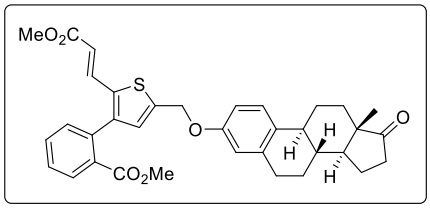

7d: Colorless oil (65%). R_f = 0.2 (hexane/ethyl acetate = 2:1). **^{1}H NMR** (400 MHz, Chloroform-*d*) δ 7.97 (dd, *J* = 7.8, 1.3 Hz, 1H), 7.56 (td, *J* = 7.5, 1.4 Hz, 1H), 7.50 – 7.41 (m, 2H), 7.27 – 7.24 (m, 1H), 7.21 (d, *J* = 8.6 Hz, 1H), 6.93 (s, 1H), 6.79 (dd, *J* = 8.6, 2.7 Hz, 1H), 6.73 (d, *J* = 2.7 Hz, 1H), 6.17 (d, *J* = 15.6 Hz, 1H), 5.17 (s, 2H), 3.70 (s, 3H), 3.66 (s, 3H), 2.90 (dd, *J* = 9.6, 4.8 Hz, 2H), 2.50 (dd, *J* = 18.8, 8.5 Hz, 1H), 2.44 – 2.22 (m, 2H), 2.17 – 1.95 (m, 4H), 1.59 – 1.43 (m, 6H), 0.91 (s, 3H). **^{13}C NMR** (101 MHz, Chloroform-*d*) δ 221.1, 167.5, 167.3, 156.2, 144.6, 140.8, 138.1, 136.2, 135.8, 135.1, 133.1, 131.9, 131.8, 131.0, 130.7, 129.5, 128.4, 126.6, 116.9, 115.2, 112.5, 65.3, 52.3, 51.8, 50.5, 48.1, 44.1, 38.4, 36.0, 31.7, 29.8, 26.6, 26.0, 21.7, 14.0. **IR** (KBr): υ 3447, 2947, 2360, 1717, 1622, 1497, 1433, 1375, 1255, 1167 cm^{-1}. **HRMS** (ESI): Calculated for $C_{35}H_{36}O_6SNa$ ($M+Na^+$): 607.2125, found: 607.2125.

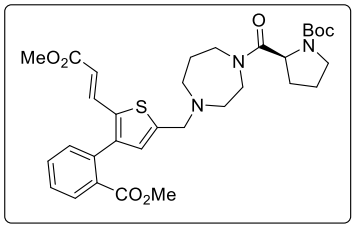

7e: Light red oil (45%). R_f = 0.2 (hexane/acetone = 1:1). **^{1}H NMR** (400 MHz, Chloroform-*d*) δ 7.99 – 7.94 (m, 1H), 7.55 (dt, *J* = 7.5, 3.8 Hz, 1H), 7.49 – 7.41 (m, 2H), 7.25 (s, 1H), 6.76 (d, *J* = 4.5 Hz, 1H), 6.13 (d, *J* = 15.6 Hz, 1H), 4.66 – 4.50 (m, 1H), 3.84 – 3.78 (m, 2H), 3.71 – 3.48 (m, 12H), 2.84 – 2.66 (m, 4H), 2.24 – 2.06 (m, 2H), 1.95 – 1.81 (m, 4H), 1.45 – 1.41 (m, 9H). **^{13}C NMR** (101 MHz, Chloroform-*d*) δ 172.4, 167.4, 154.7, 154.0, 151.8, 144.7, 136.4, 136.0, 134.2, 131.9, 131.8, 131.1, 130.6, 128.8, 128.3, 116.3, 79.7, 57.7, 56.9, 56.2, 54.5, 52.3, 51.7, 47.0, 44.7, 31.0, 30.1, 28.7, 24.4, 23.6. **IR** (KBr): υ 3440, 2950, 1699, 1652, 1620, 1433, 1402, 1366, 1272, 1167 cm^{-1}. **HRMS** (ESI): Calculated for $C_{32}H_{41}N_3O_7SNa$ ($M+Na^+$): 634.2557, found: 634.2565.

6.4.4 Synthetic Applications

Scheme 6.9. Gram-Scale Preparation

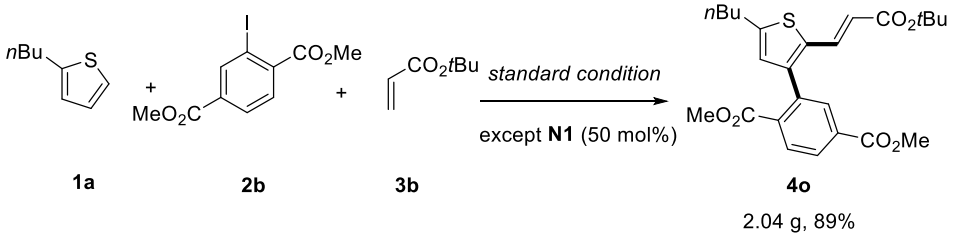

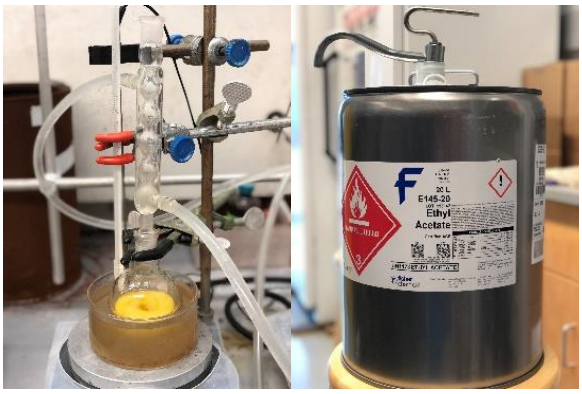

Reaction set-up **Solvent**

A flame-dried 100 mL round bottom flask was charged with $Pd(OAc)_2$ (112.2 mg, 0.5 mmol, 10 mol%), $AsPh_3$ (382.8 mg, 1.25 mmol, 25 mol%), BQ (540.4 mg, 5.0 mmol, 1.0 equiv), NBE-CONHMe (378 mg, 2.5 mmol, 50 mol%), AgOAc (2.50 g, 15 mmol, 3.0 equiv), thiophene **1a** (1.051 g, 7.5 mmol, 1.5 equiv) and aryl iodide **2b** (1.6 g, 5.0 mmol, 1.0 equiv) in air. Ethyl acetate (25 mL) was then added. After HOAc (1.501 g, 25 mmol, 5.0 equiv) and *t*butyl acrylate **3b** (1.154 g, 9.0 mmol, 1.8 equiv) was added, the flask was equipped with a reflux condenser and stirred on a oil bath preheated to 65 ^oC for 48 hours. After completion of the reaction, the mixture was filtered through a thin pad of silica gel. The filter cake was washed with ethyl acetate and the combined filtrate was concentrated under reduced pressure. The residue was loaded to silica gel and subjected to flash column chromatography to give the desired product **4o** in 89% yield.

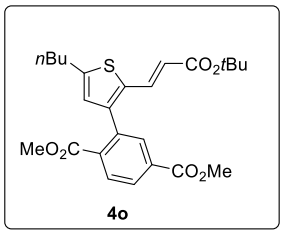

4o: Orange oil (89%). R_f = 0.2 (hexane/ethyl acetate = 10:1). **^{1}H NMR** (400 MHz, Chloroform-*d*) δ 8.08 (dd, *J* = 8.1, 1.7 Hz, 1H), 7.98 – 7.92 (m, 2H), 7.29 (d, *J* = 15.5 Hz, 1H), 6.65 (s, 1H), 6.04 (d, *J* = 15.5 Hz, 1H), 3.93 (s, 3H), 3.69 (s, 3H), 2.81 (t, *J* = 7.6 Hz, 2H), 1.72 – 1.63 (m, 2H), 1.44

(s, 9H), 1.43 – 1.37 (m, 2H), 0.94 (t, J = 7.3 Hz, 3H). **^{13}C NMR** (101 MHz, Chloroform-*d*) δ 167.3, 166.4, 166.0, 147.6, 143.2, 136.4, 135.3, 135.0, 133.2, 132.8, 132.5, 130.3, 129.0, 127.5, 118.3, 80.4, 52.6, 52.5, 33.5, 30.2, 28.3, 22.2, 13.9. **IR** (KBr): υ 2955, 2932, 1729, 1704, 1619, 1457, 1435, 1392, 1367, 1313 cm^{-1}. **HRMS** (ESI): Calculated for $C_{25}H_{30}O_6SNa$ ($M+Na^+$): 481.1655, found: 481.1662.

Scheme 6.10. Direct Difunctionalization of Furans

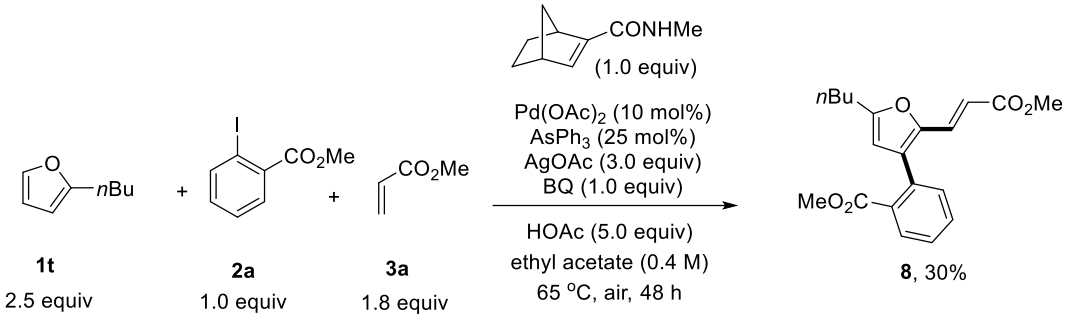

A flame-dried 4.0 mL vial was charged with $Pd(OAc)_2$ (4.6 mg, 0.02 mmol, 10 mol%), $AsPh_3$ (15.2 mg, 0.05 mmol, 25 mol%), BQ (21.6 mg, 0.2 mmol, 1.0 equiv), NBE-CONHMe (30.2 mg, 0.2 mmol, 1.0 equiv), AgOAc (100 mg, 0.6 mmol, 3.0 equiv), 2-butylfuran **1t** (62.0 mg, 0.5 mmol, 2.5 equiv) and methyl 2-iodobenzote **2a** (52.4 mg, 0.2 mmol, 1.0 equiv) in air. Ethyl acetate (0.5 mL) was then added. After HOAc (60 mg, 1.0 mmol, 5.0 equiv) and methyl acrylate **3a** (0.36 mmol, 1.8 equiv) was added, the vial was tightly sealed and stirred on a pie-block preheated to 65 ^oC for 48 hours. After completion of the reaction, the mixture was filtered through a thin pad of silica gel. The filter cake was washed with ethyl acetate and the combined filtrate was concentrated under reduced pressure. The residue was loaded to a small amount of silica gel and subjected to flash column chromatography to give the desired product **8**.

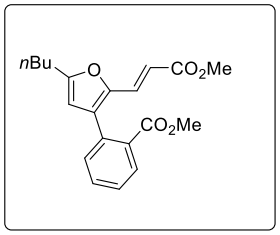

8: Yellow oil (30%). R_f = 0.3 (hexane/ethyl acetate = 10:1). **^{1}H NMR** (400 MHz, Chloroform-*d*) δ 7.89 (dd, *J* = 7.8, 1.5 Hz, 1H), 7.53 (td, *J* = 7.6, 1.5 Hz, 1H), 7.43 (td, *J* = 7.6, 1.4 Hz, 1H), 7.29 (dd, *J* = 7.6, 1.3 Hz, 1H), 7.23 (d, *J* = 15.6 Hz, 1H), 6.27 (d, *J* = 15.5 Hz, 1H), 6.12 (d, *J* = 1.0 Hz, 1H), 3.73 (d, *J* = 2.6 Hz, 6H), 2.69 (t, *J* = 7.4 Hz, 2H), 1.71 – 1.64 (m, 2H), 1.41 (dt, *J* = 13.6, 6.9 Hz, 2H), 0.95 (t, *J* = 7.4 Hz, 3H). **^{13}C NMR** (101 MHz, $CDCl_3$) δ 168.1, 168.0, 158.7, 145.5, 133.0, 131.8, 131.7, 131.4, 131.3, 130.4, 130.0, 128.1, 114.1, 110.4, 52.3, 51.7, 30.0, 28.0, 22.4, 13.9. **IR** (KBr): υ 2953, 1777, 1722, 1658, 1631, 1573, 1461, 1433, 1293, 1257 cm^{-1}. **HRMS** (ESI): Calculated for $C_{20}H_{22}O_5Na$ ($M+Na^+$): 365.1359, found: 365.1358.

Scheme 6.11. Direct C4 Arylation of Thiophenes

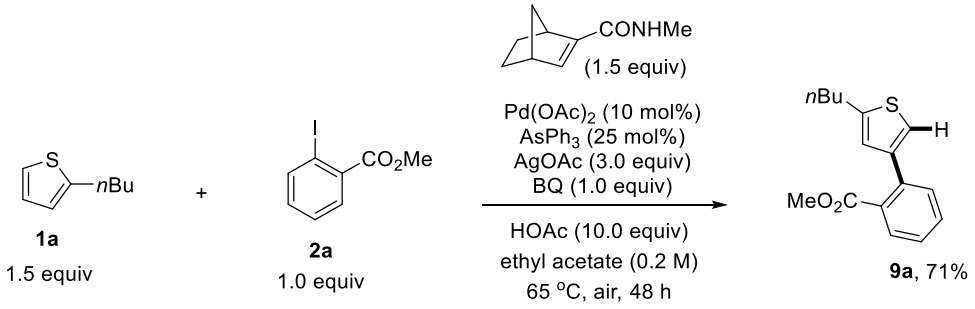

A flame-dried 4.0 mL vial was charged with $Pd(OAc)_2$ (4.6 mg, 0.02 mmol, 10 mol%), $AsPh_3$ (15.2 mg, 0.05 mmol, 25 mol%), BQ (21.6 mg, 0.2 mmol, 1.0 equiv), NBE-CONHMe (45.4 mg, 0.3 mmol, 1.5 equiv), AgOAc (100 mg, 0.6 mmol, 3.0 equiv), 2-butylthiophene **1a** (42 mg, 0.3 mmol, 1.5 equiv) and methyl 2-iodobenzote **2a** (52.4 mg, 0.2 mmol, 1.0 equiv) in air. Ethyl acetate (1.0 mL) was then added. After HOAc (120 mg, 2.0 mmol, 10.0 equiv) was added, the vial was

tightly sealed and stirred on a pie-block preheated to 65 °C for 48 hours. After completion of the reaction, the mixture was filtered through a thin pad of silica gel. The filter cake was washed with ethyl acetate and the combined filtrate was concentrated under reduced pressure. The residue was loaded to a small amount of silica gel and subjected to flash column chromatography to give the desired product **9a**.

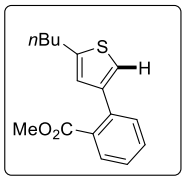

9a: Light yellow oil (71%). R_f = 0.5 (hexane/ethyl acetate = 10:1). **^{1}H NMR** (400 MHz, Chloroform-*d*) δ 7.71 (ddd, *J* = 7.7, 1.4, 0.5 Hz, 1H), 7.48 (td, *J* = 7.5, 1.5 Hz, 1H), 7.42 (ddd, *J* = 7.7, 1.5, 0.5 Hz, 1H), 7.35 (td, *J* = 7.5, 1.5 Hz, 1H), 7.01 (d, *J* = 1.5 Hz, 1H), 6.76 (q, *J* = 1.0 Hz, 1H), 3.72 (s, 3H), 2.86 – 2.79 (m, 2H), 1.75 – 1.63 (m, 2H), 1.42 (dq, *J* = 14.5, 7.3 Hz, 2H), 0.95 (t, *J* = 7.4 Hz, 3H). **^{13}C NMR** (101 MHz, $CDCl_3$) δ 169.6, 145.5, 140.9, 136.9, 131.1, 131.0, 130.3, 129.3, 127.0, 125.4, 119.7, 52.1, 33.8, 29.7, 22.2, 13.8. **IR** (KBr): υ 2955, 2930, 2871, 2858, 1732, 1600, 1493, 1455, 1433, 1293 cm^{-1}. **HRMS** (ESI): Calculated for $C_{16}H_{18}O_2SNa$ ($M+Na^+$): 297.0920, found: 297.0920.

6.4.5 Kinetic Study

Scheme 6.12. Kinetic Profile and Competition Reaction

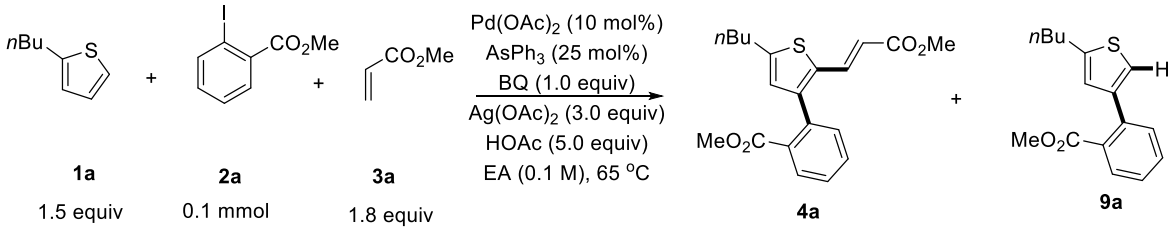

1a 1.5 equiv | **2a** 0.1 mmol | **3a** 1.8 equiv | **4a** | **9a**

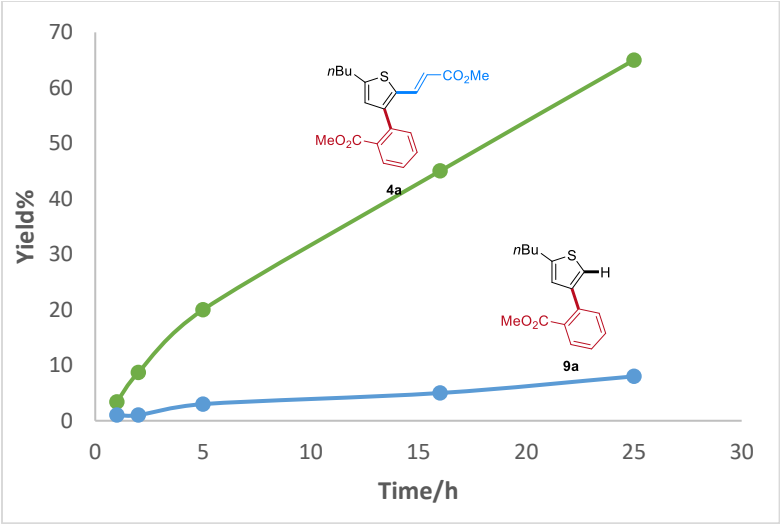

Time	1 h	2 h	5 h	16 h	25 h
4a	3%	9%	20%	45%	65%
9a	1%	1%	3%	5%	8%

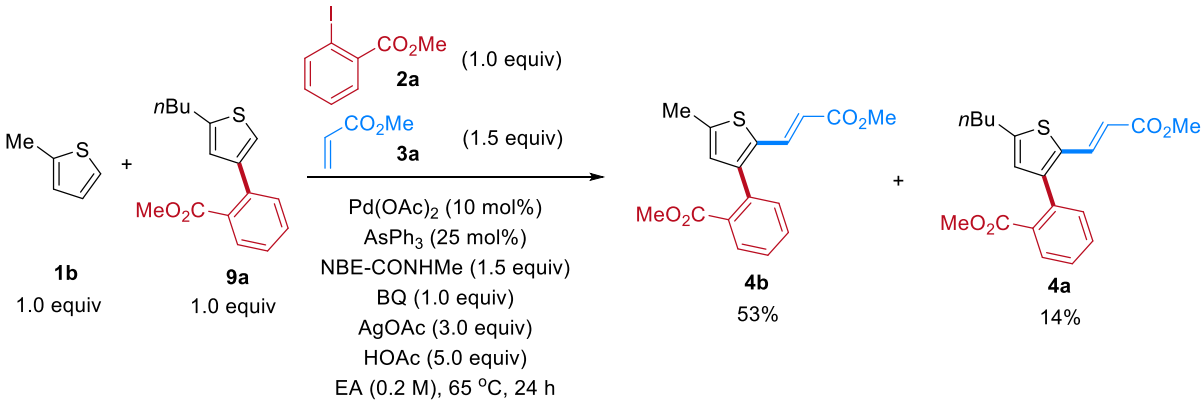

1b 1.0 equiv | **9a** 1.0 equiv | **4b** 53% | **4a** 14%

A flame-dried 4.0 mL vial was charged with $Pd(OAc)_2$ (2.3 mg, 0.01 mmol, 10 mol%), $AsPh_3$ (7.6 mg, 0.025 mmol, 25 mol%), BQ (10.8 mg, 0.1 mmol, 1.0 equiv), NBE-CONHMe (22.7 mg, 0.15 mmol, 1.5 equiv), AgOAc (50 mg, 0.3 mmol, 3.0 equiv), 2-methylthiophene **1b** (9.8 mg, 0.1 mmol, 1.0 equiv), **9a** (27.4 mg, 0.1 mmol, 1.0 equiv) and methyl 2-iodobenzote **2a** (26.2 mg, 0.1 mmol, 1.0 equiv) in air. Ethyl acetate (0.5 mL) was then added. After HOAc (30 mg, 0.5 mmol, 5.0 equiv) and **3a** (12.9 mg, 0.15 mmol, 1.5 equiv) were added, the vial was tightly sealed and stirred on a pie-block preheated to 65 ^{o}C for 24 hours. After completion of the reaction, the mixture was filtered through a thin pad of silica gel. The filter cake was washed with ethyl acetate and the combined filtrate was concentrated under reduced pressure. The yields of **4b** (53%) and **4a** (14%) were determined by crude ^{1}H NMR using dibromomethane as the internal standard. The competition experiment between the C4-arylated substrate (**9a**) and regular substrate (**1b**) indicates that difunctionalization is more favorable than the C5 C−H alkenylation reaction.

6.5 NMR Spectra

Figure 6.4. ^{1}H NMR Spectrum of 4a

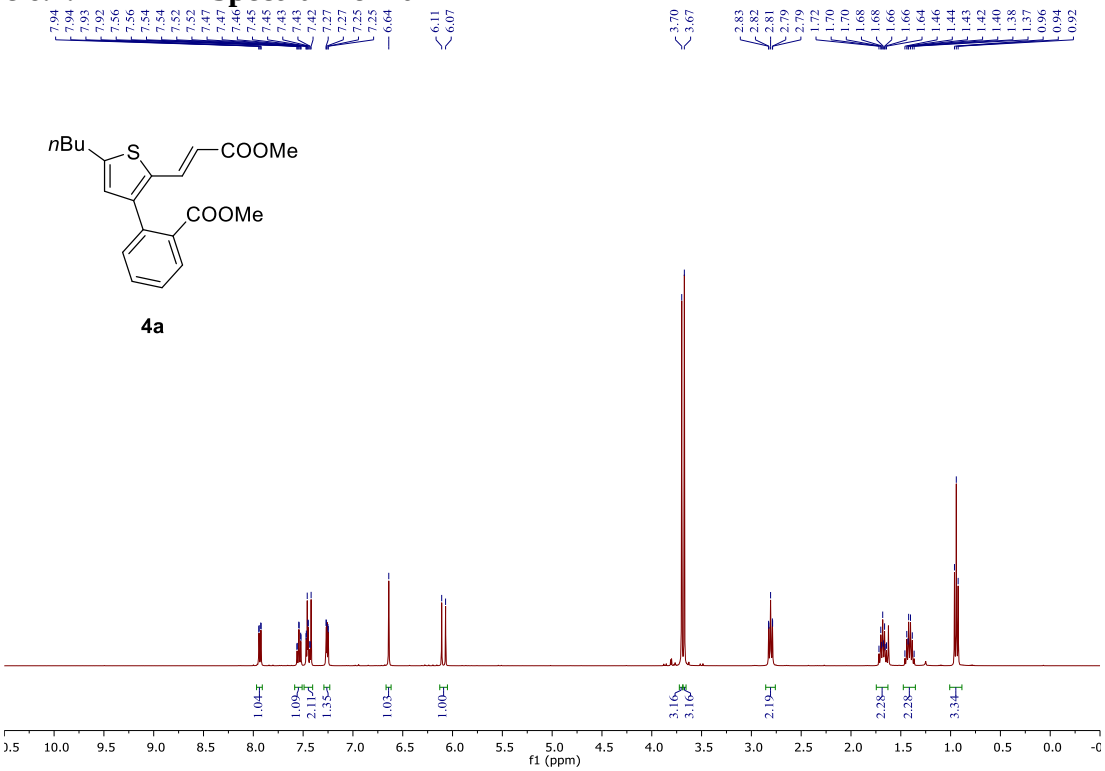

Figure 6.5. ^{13}C NMR Spectrum of 4a

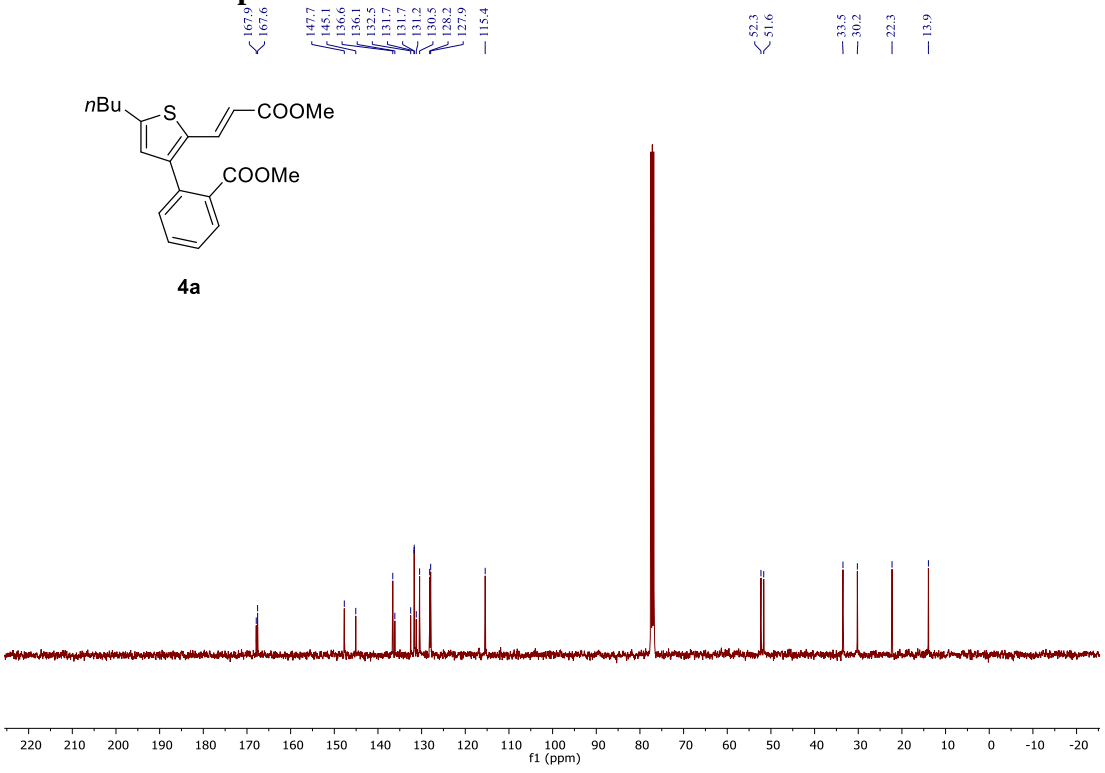

Figure 6.6. ^{1}H NMR Spectrum of 4b

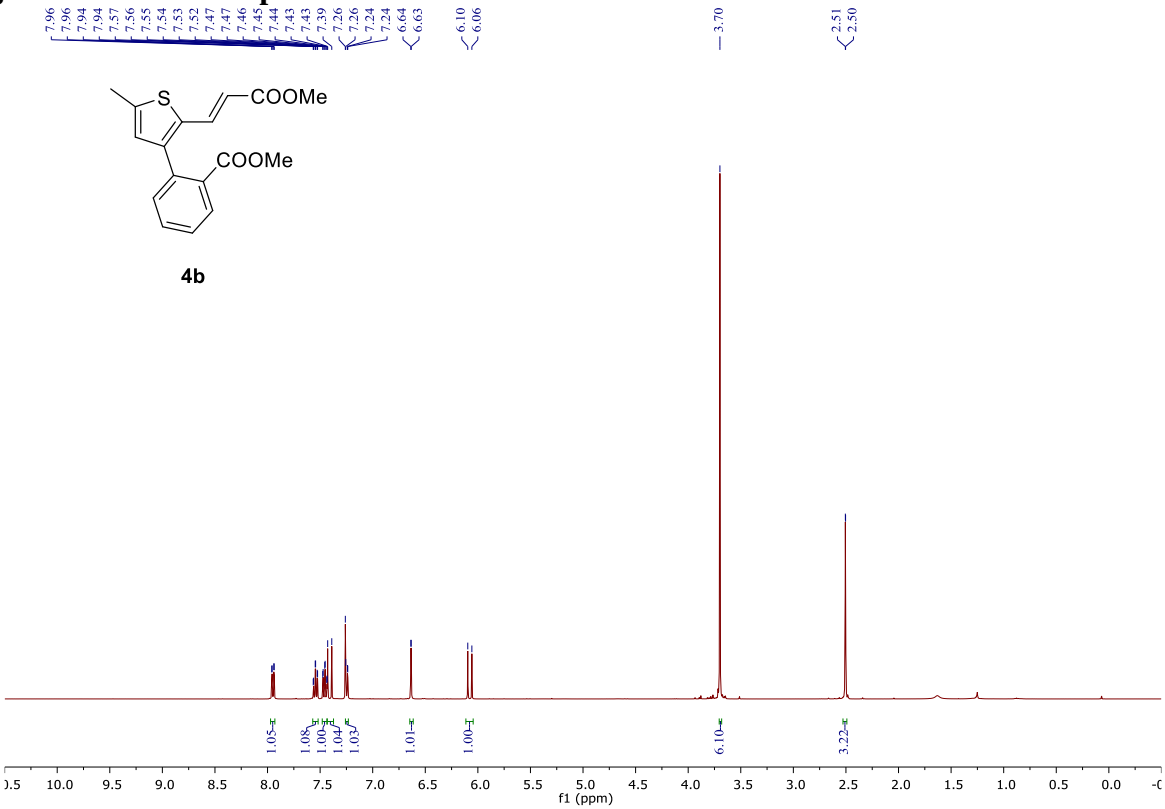

Figure 6.7. ^{13}C NMR Spectrum of 4b

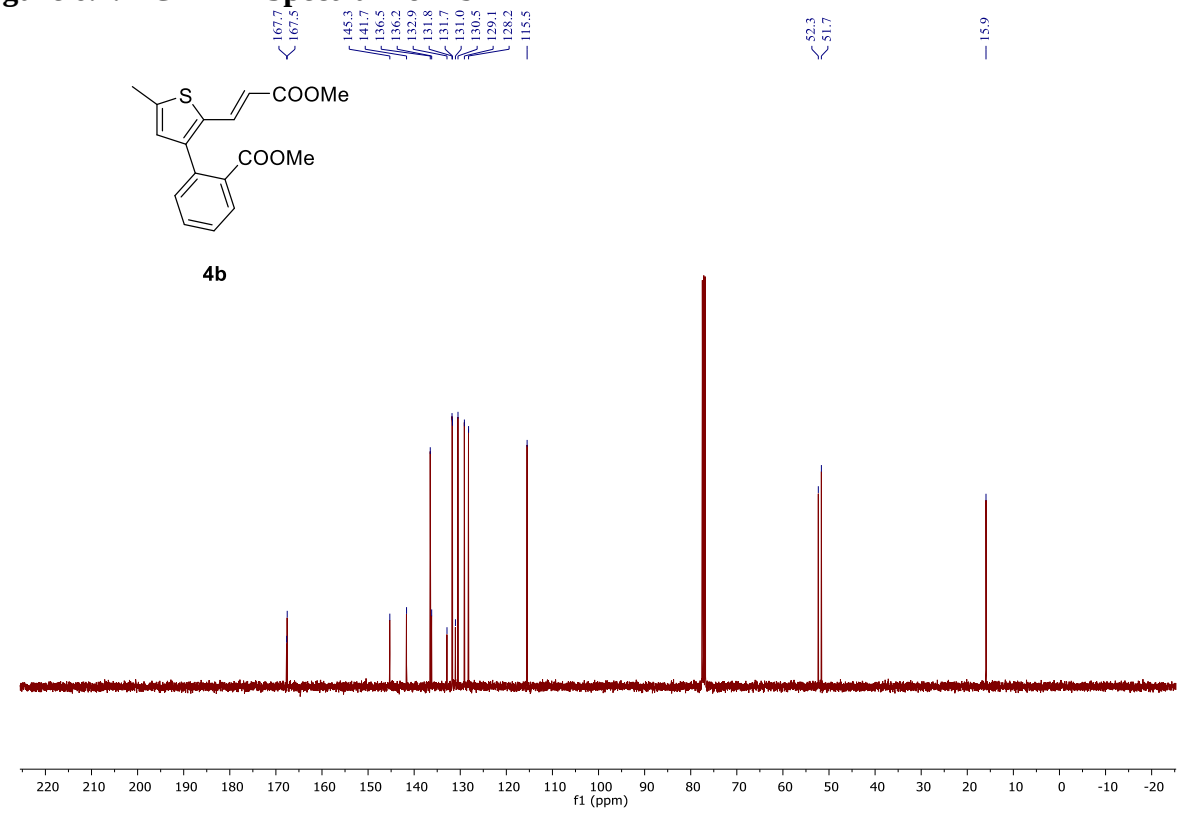

Figure 6.8. ^{1}H NMR Spectrum of 4c

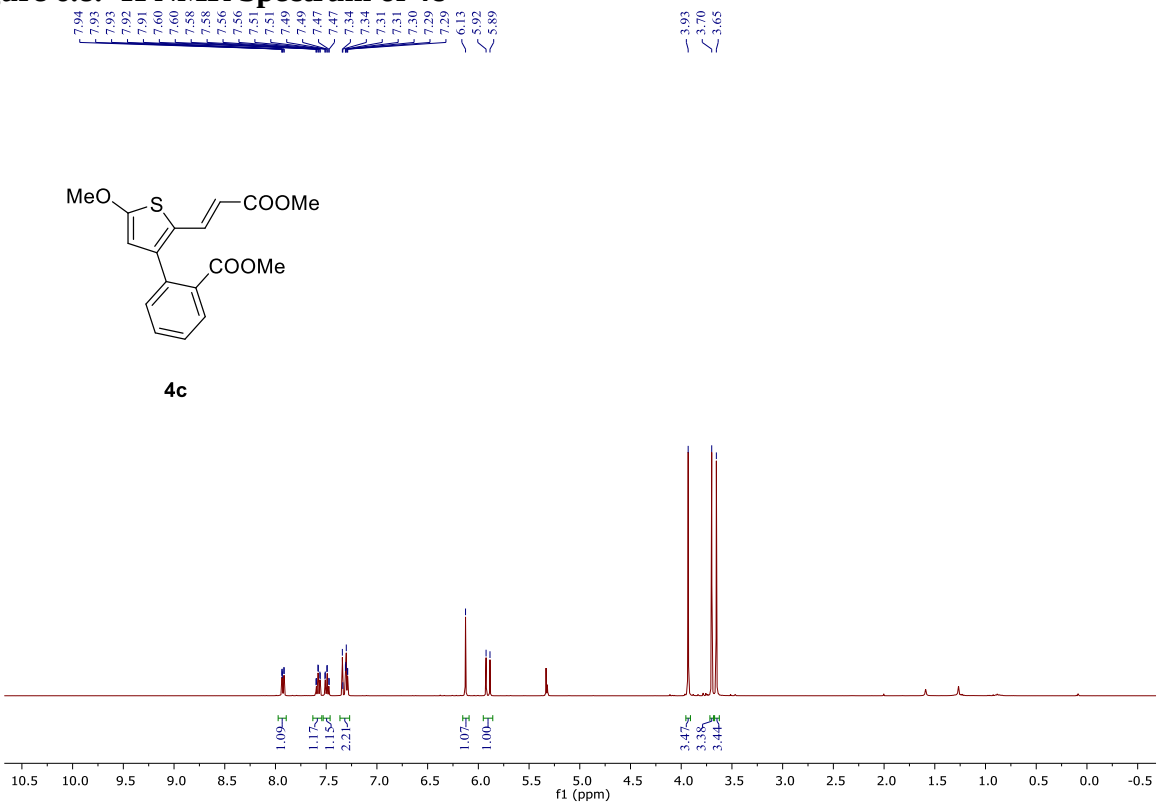

4c

Figure 6.9. ^{13}C NMR Spectrum of 4c

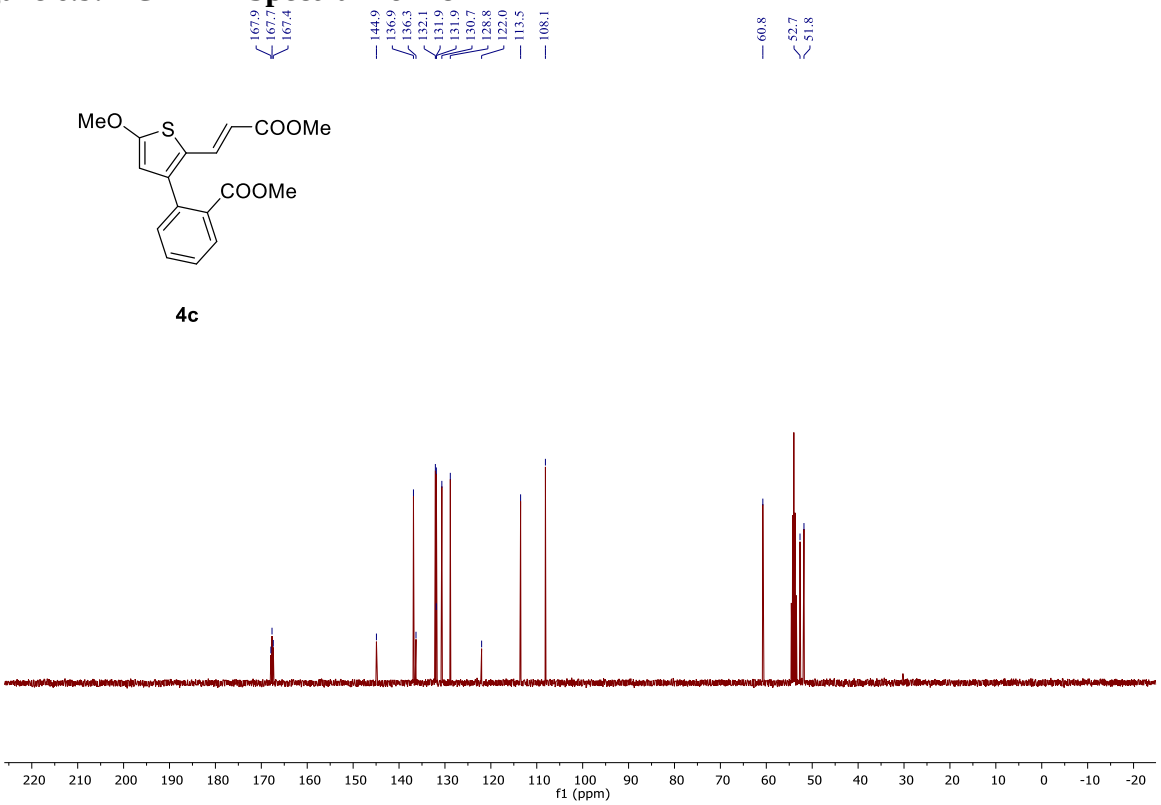

4c

Figure 6.10. ^{1}H NMR Spectrum of 4d

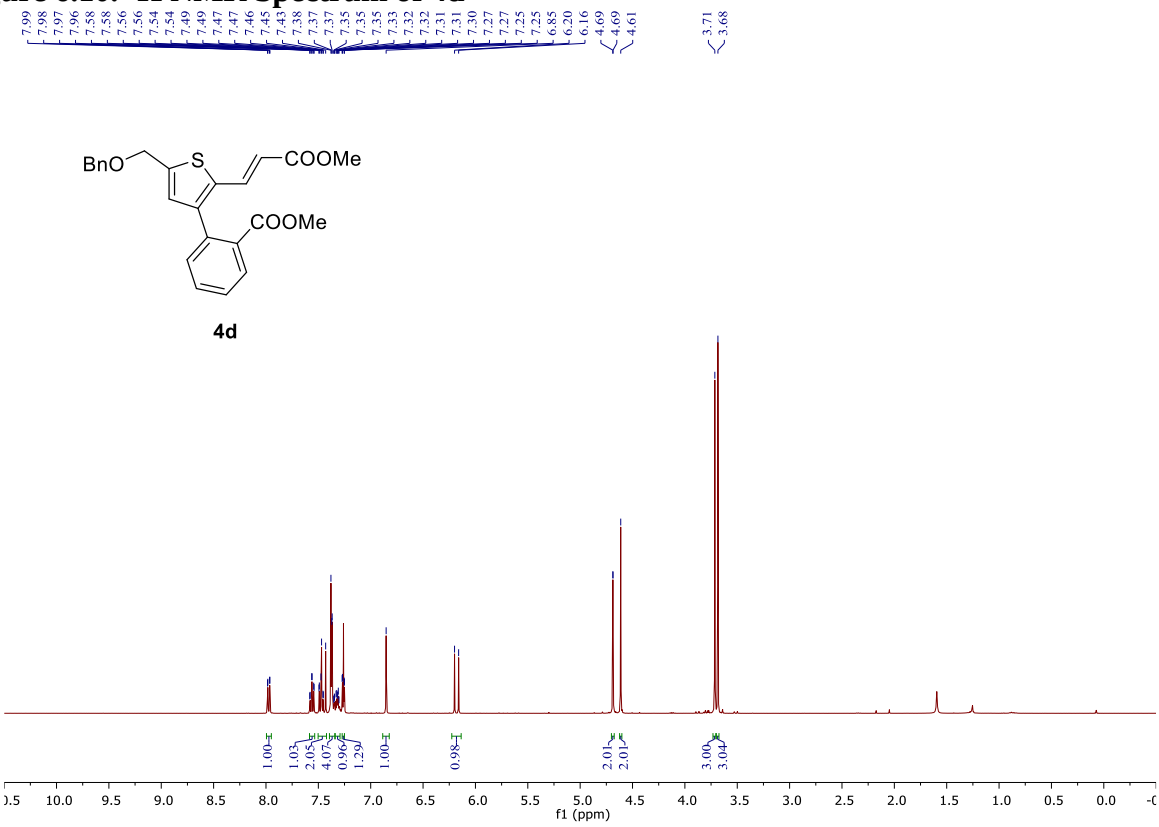

Figure 6.11. ^{13}C NMR Spectrum of 4d

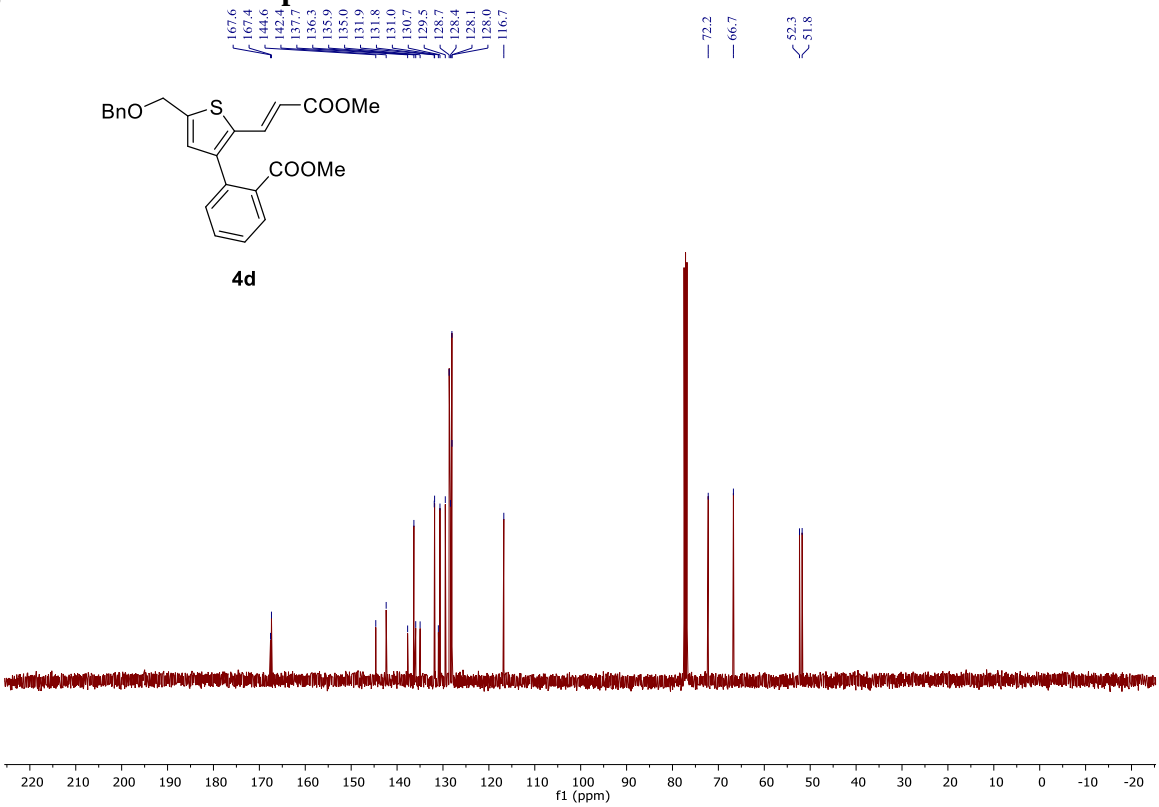

Figure 6.12. ^{1}H NMR Spectrum of 4e

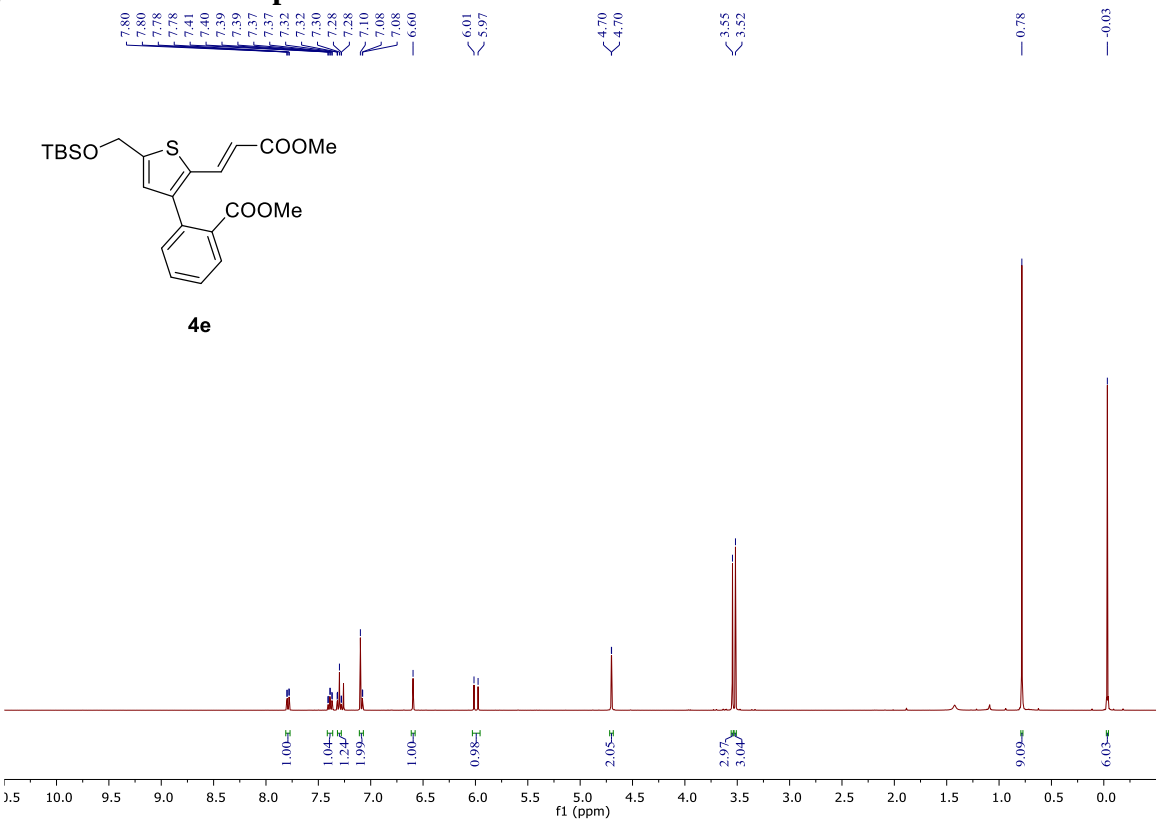

Figure 6.13. ^{13}C NMR Spectrum of 4e

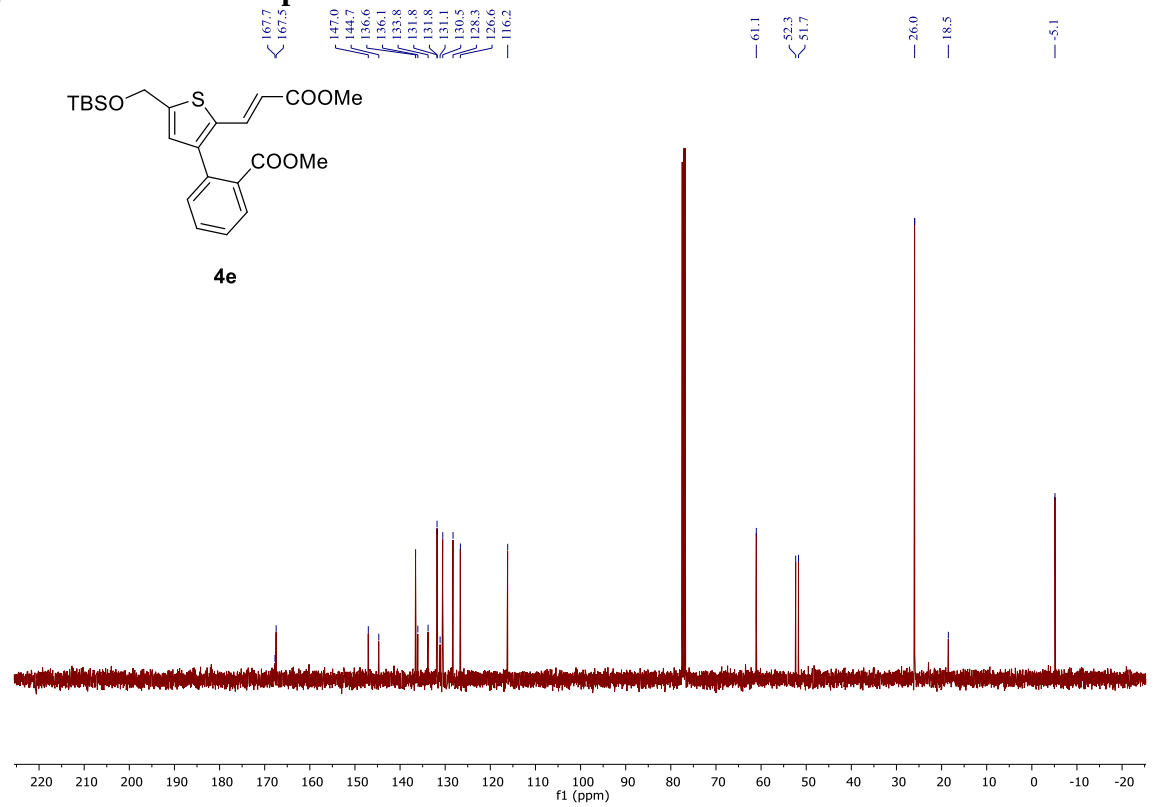

Figure 6.14. ^{1}H NMR Spectrum of 4f

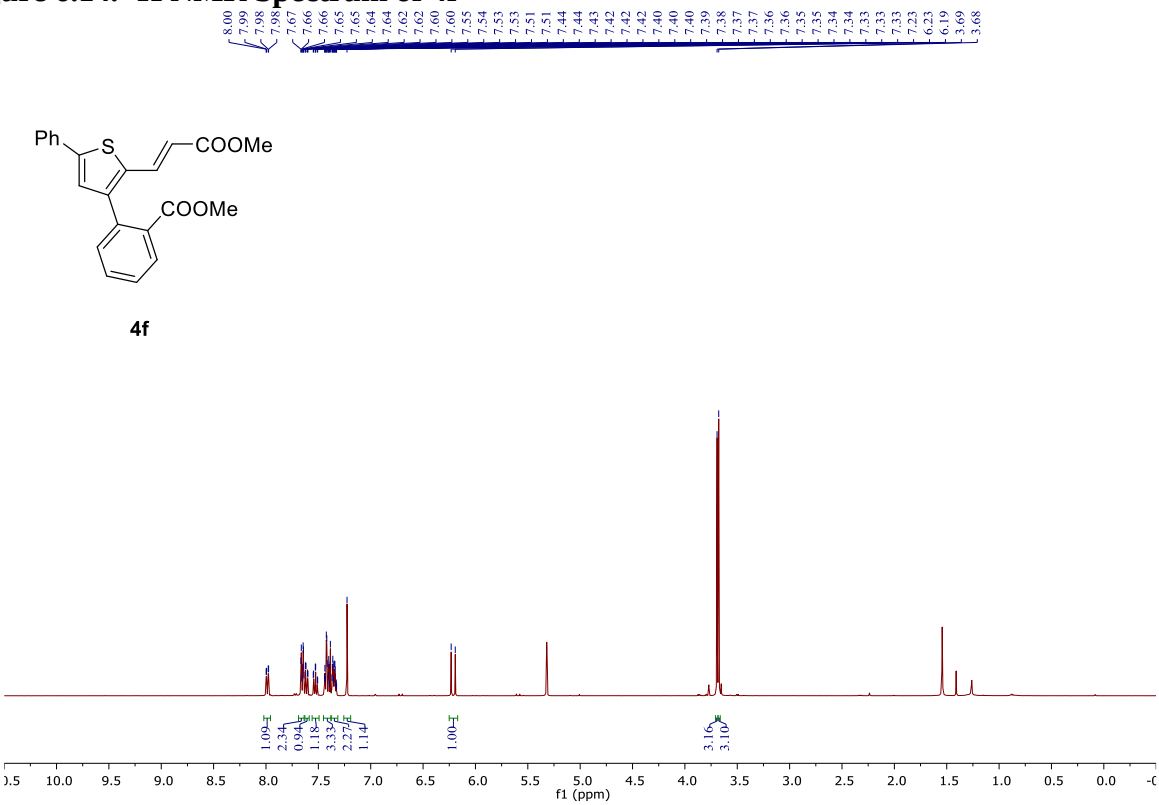

Figure 6.15. ^{13}C NMR Spectrum of 4f

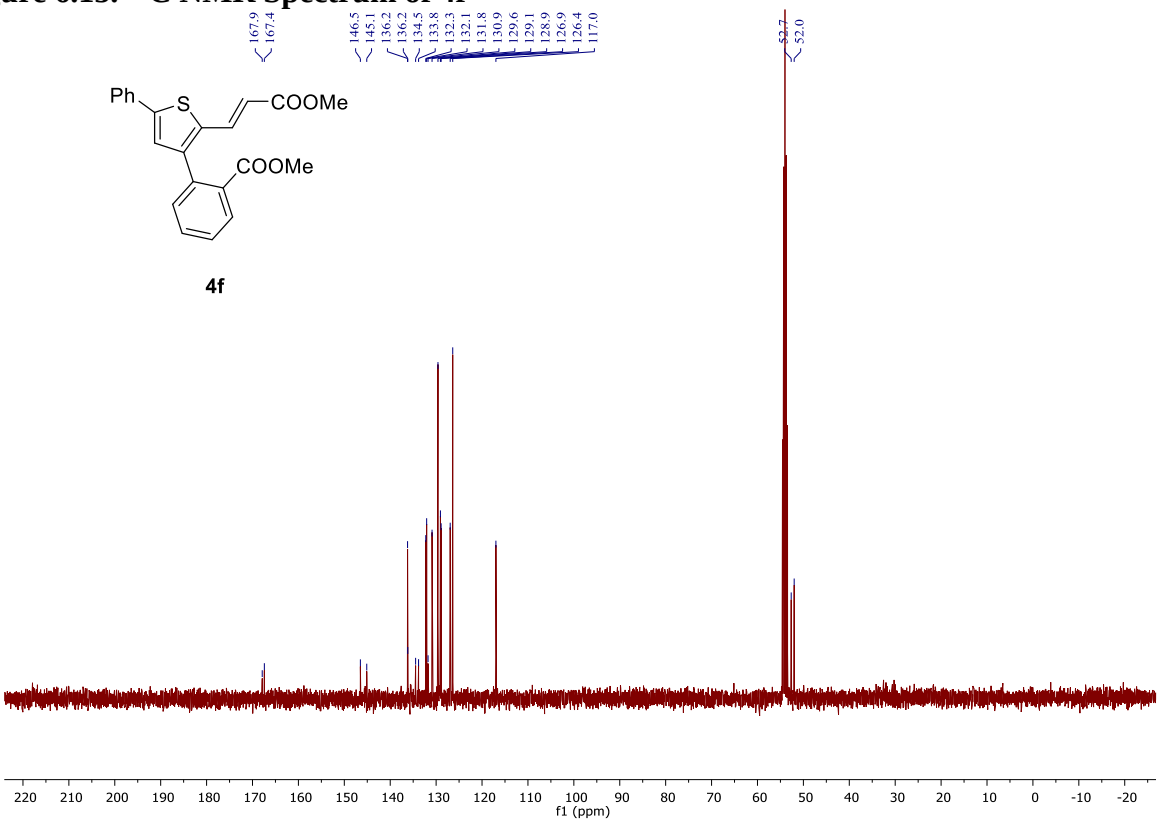

Figure 6.16. ^{1}H NMR Spectrum of 4g

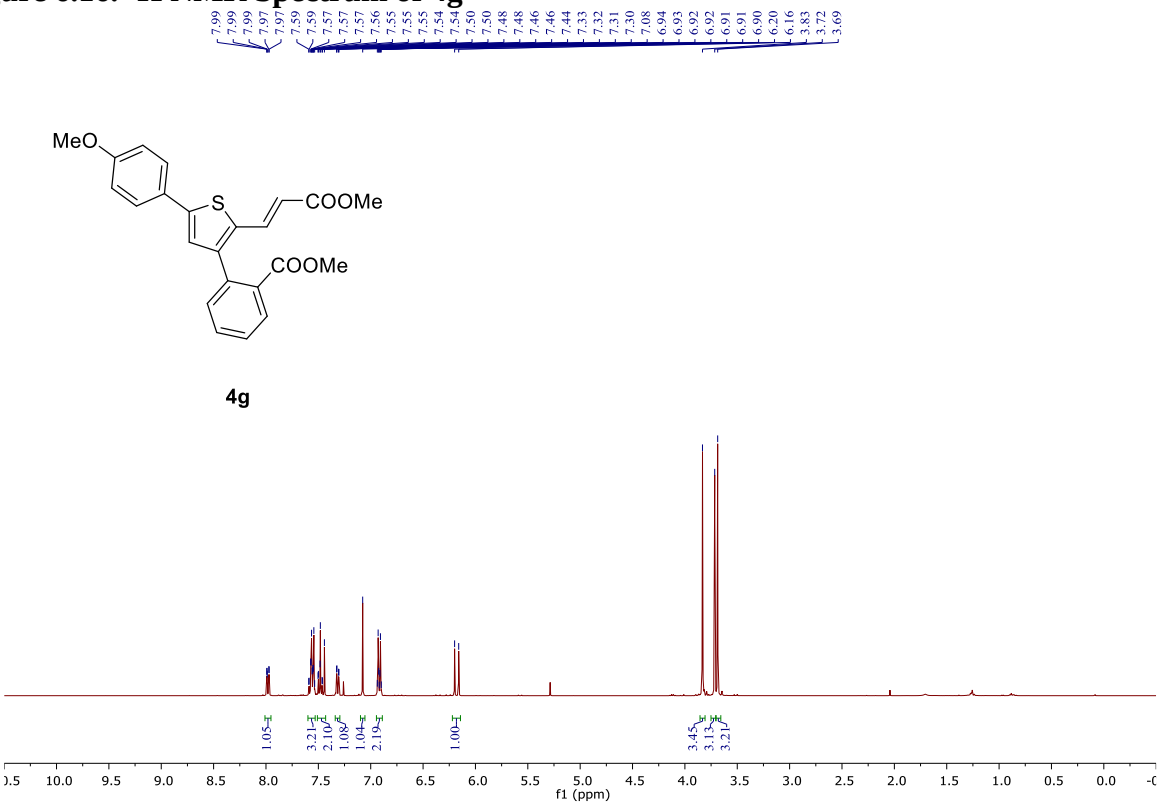

Figure 6.17. ^{13}C NMR Spectrum of 4g

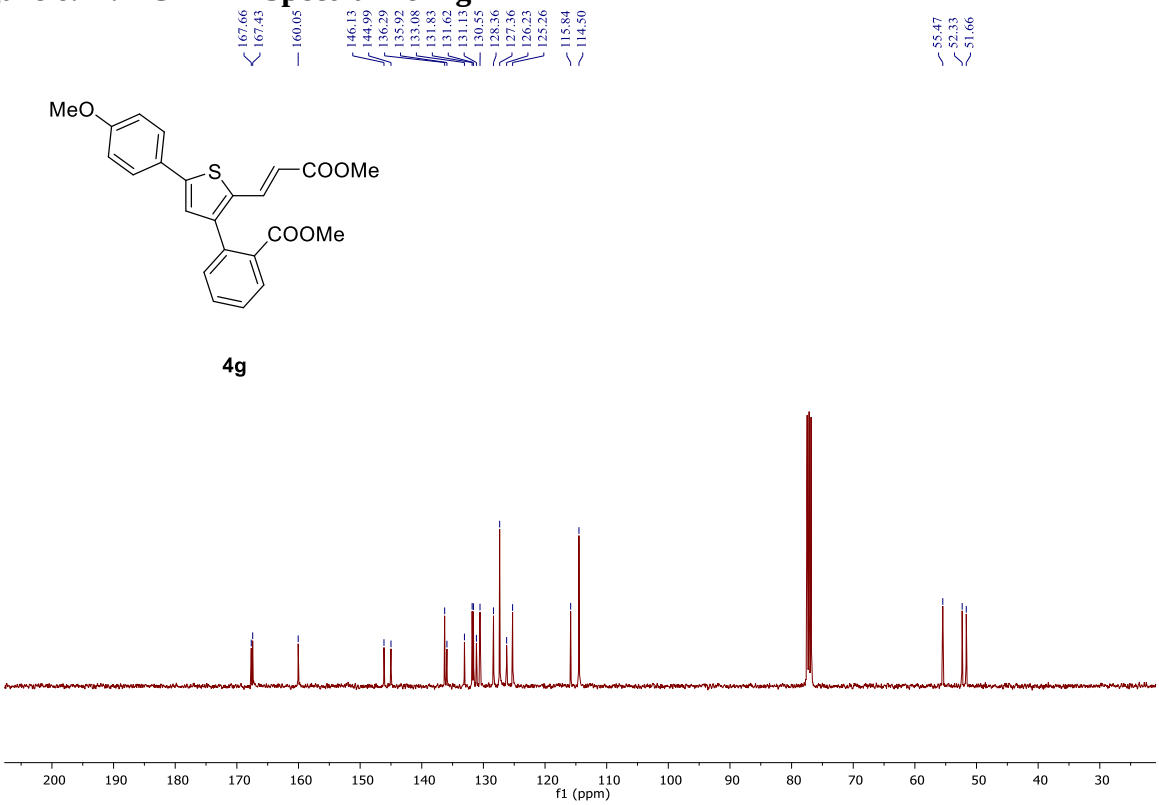

Figure 6.18. ^{1}H NMR Spectrum of 4h

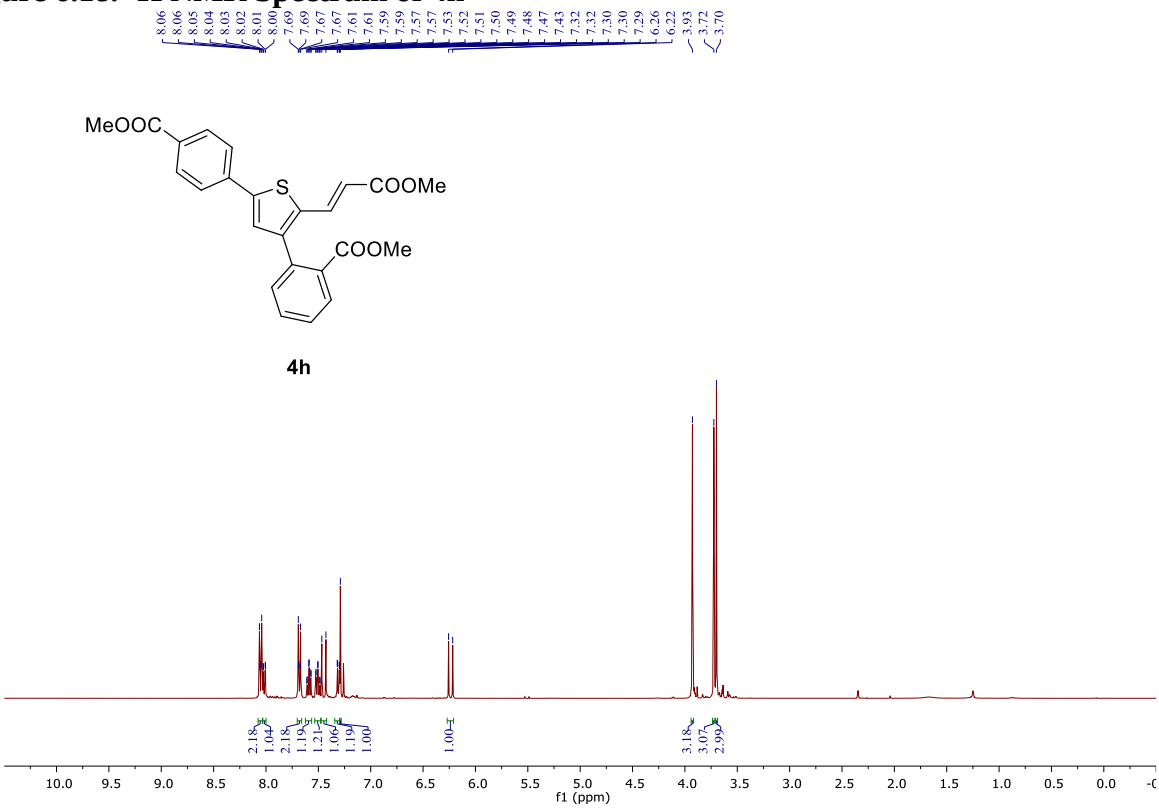

Figure 6.19. ^{13}C NMR Spectrum of 4h

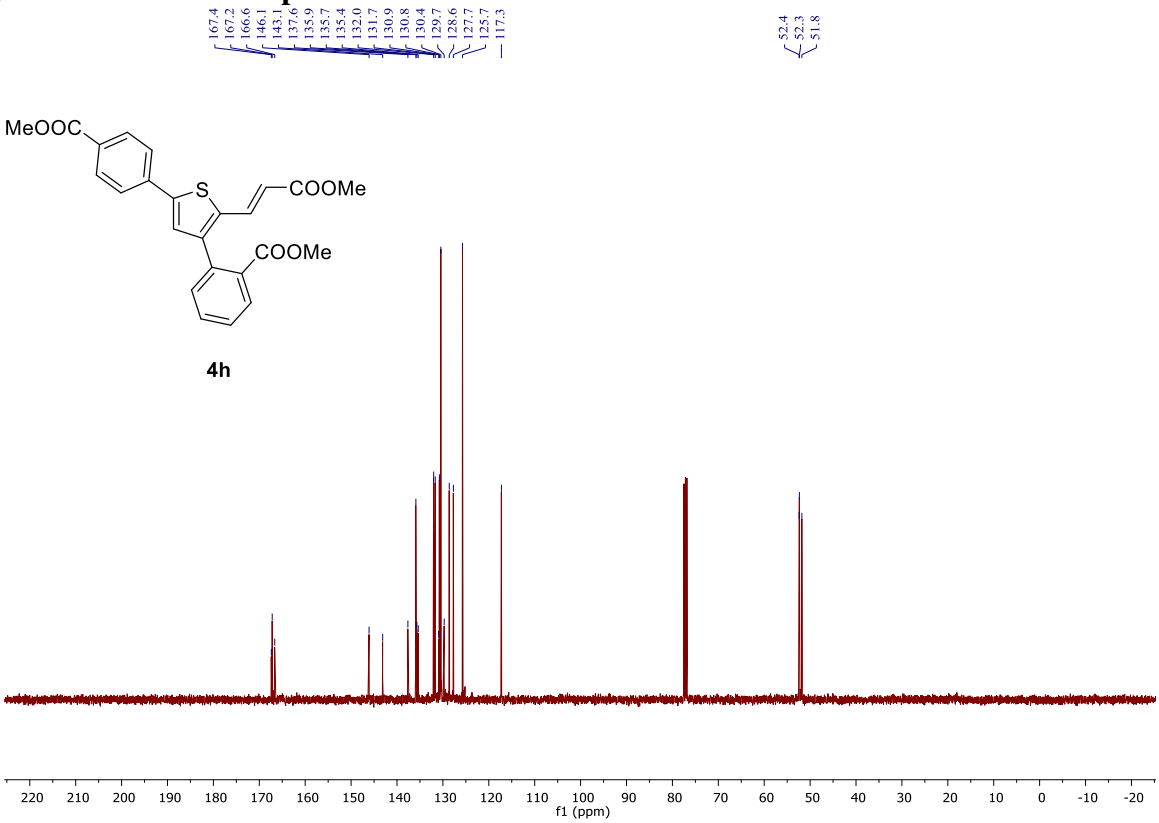

Figure 6.20. ^{1}H NMR Spectrum of 4i

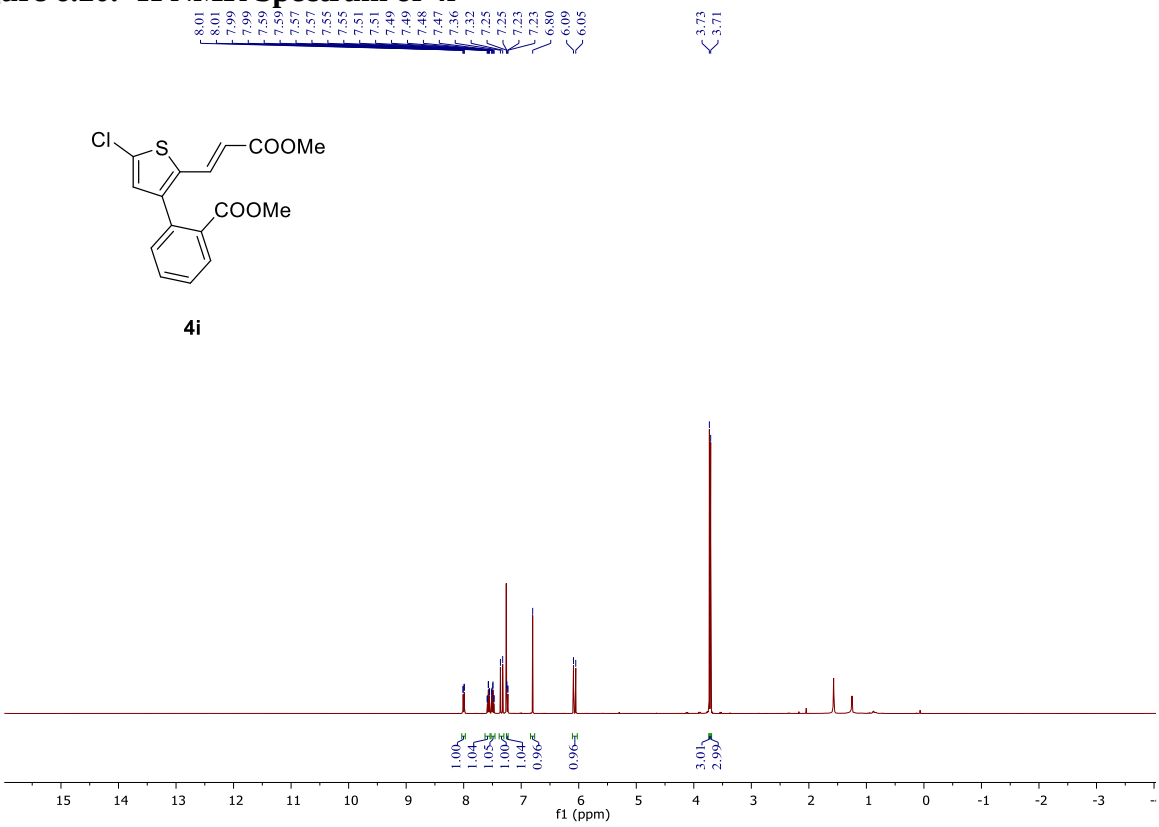

Figure 6.21. ^{13}C NMR Spectrum of 4i

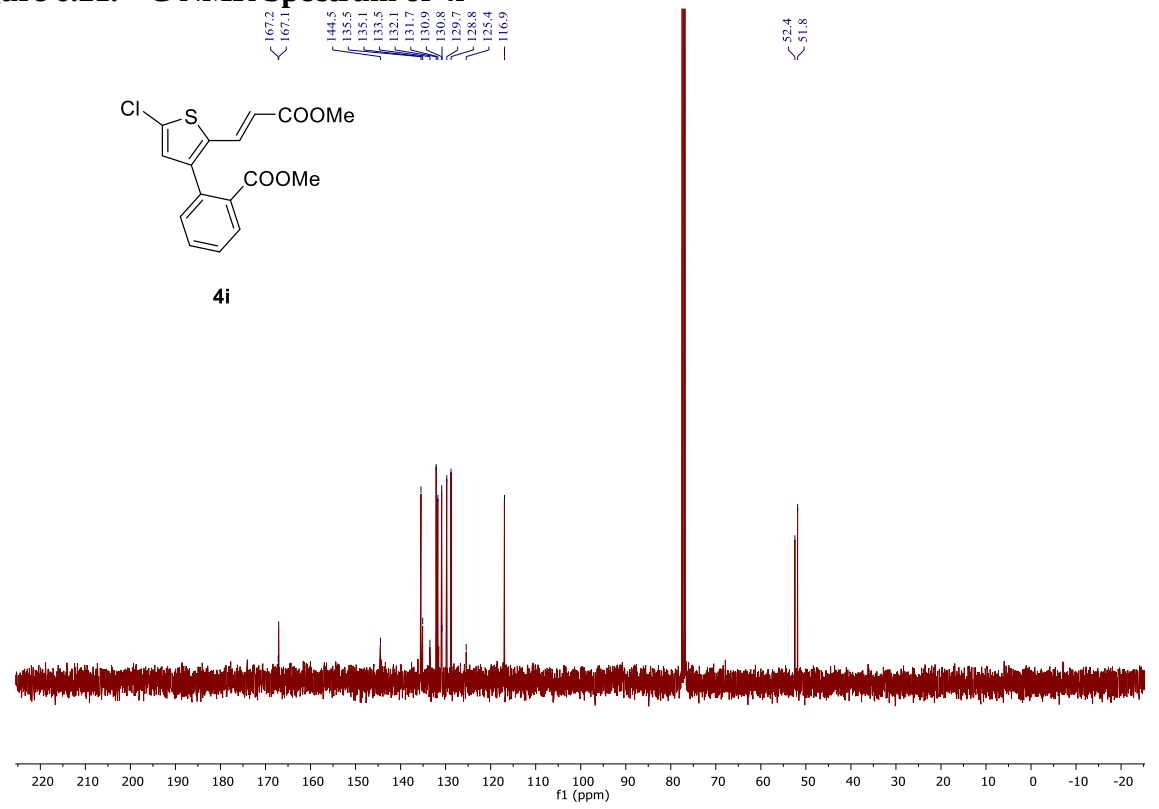

Figure 6.22. ^{1}H NMR Spectrum of 4j

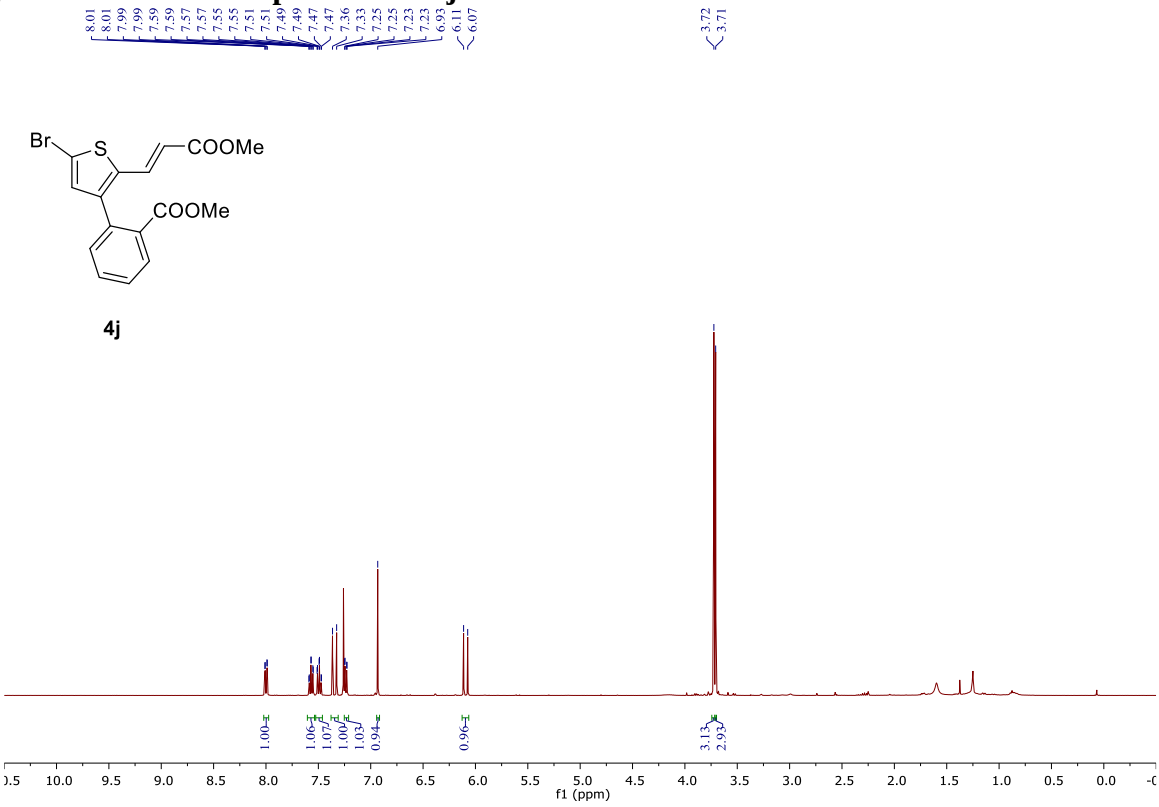

Figure 6.23. ^{13}C NMR Spectrum of 4j

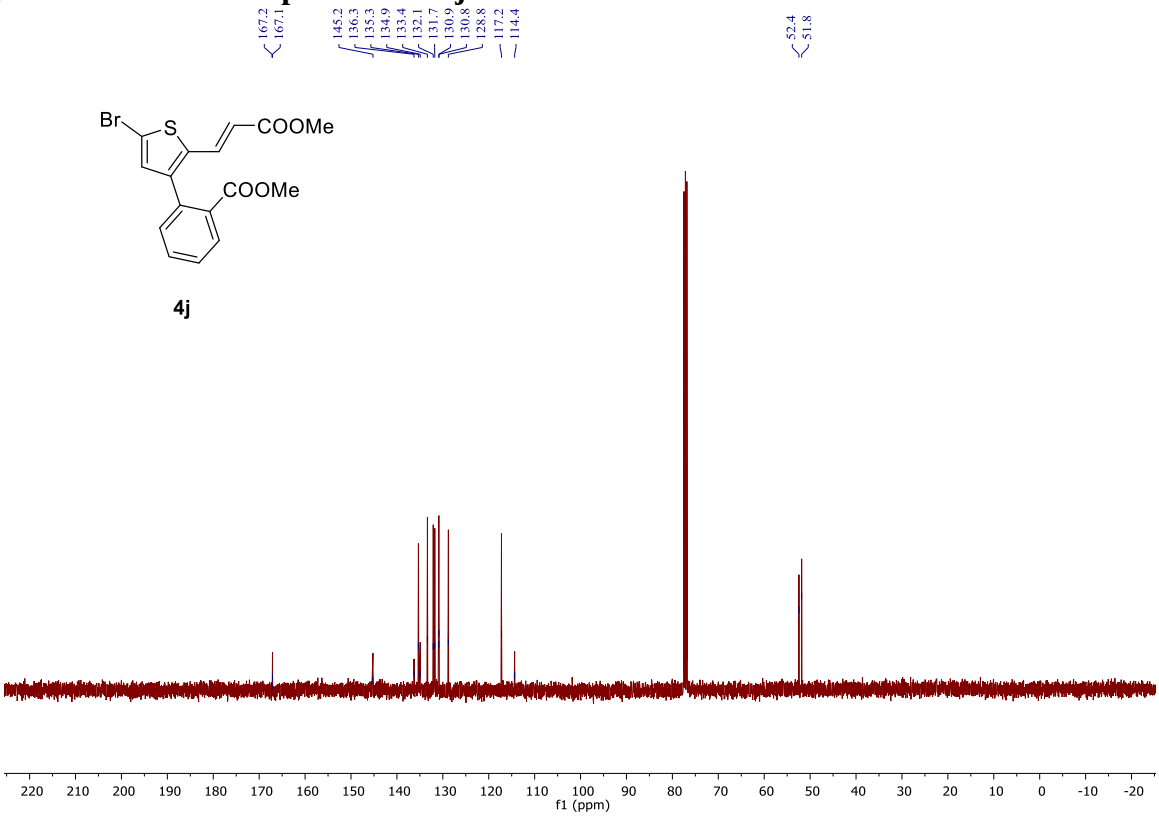

Figure 6.24. ^{1}H NMR Spectrum of 4k

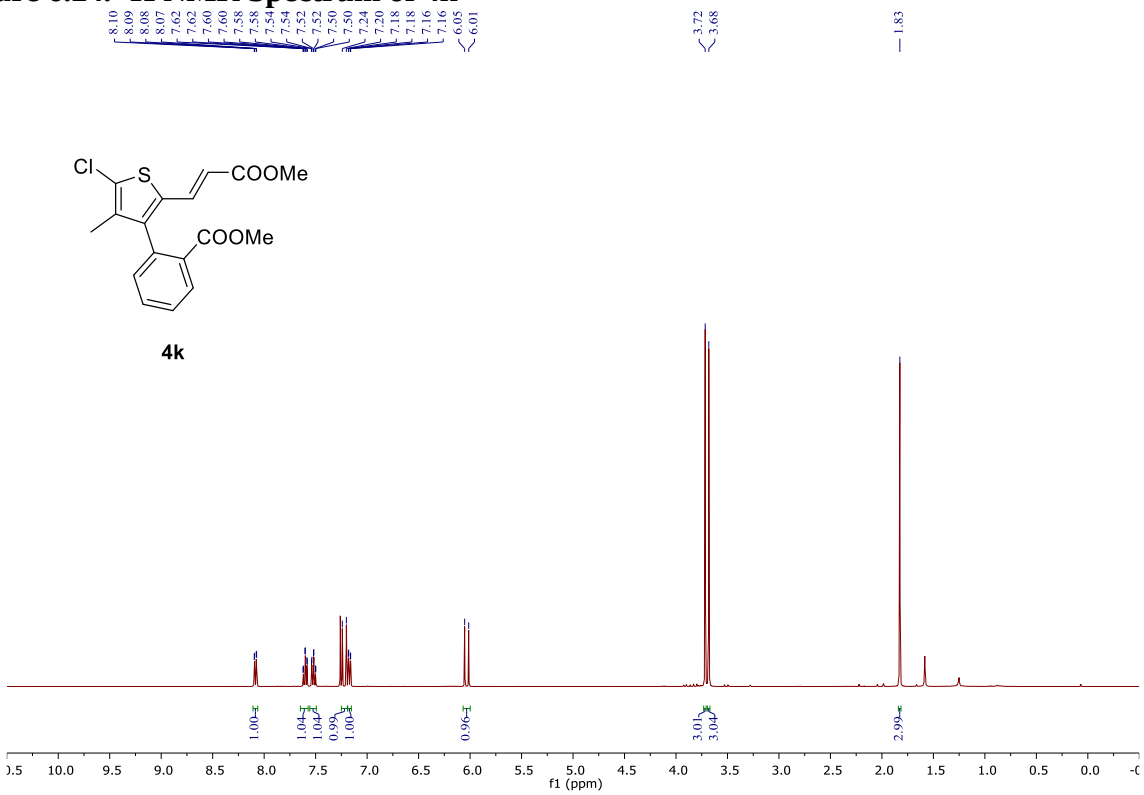

Figure 6.25. ^{13}C NMR Spectrum of 4k

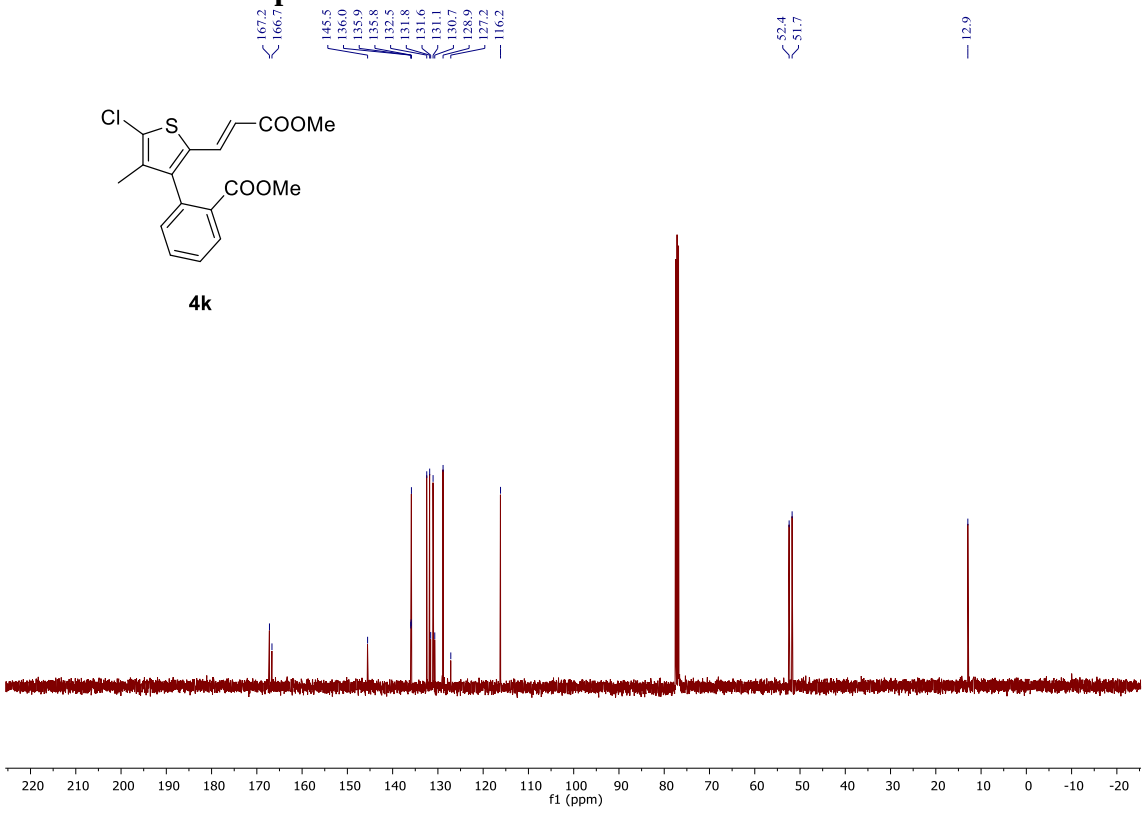

Figure 6.26. ^{1}H NMR Spectrum of 4l

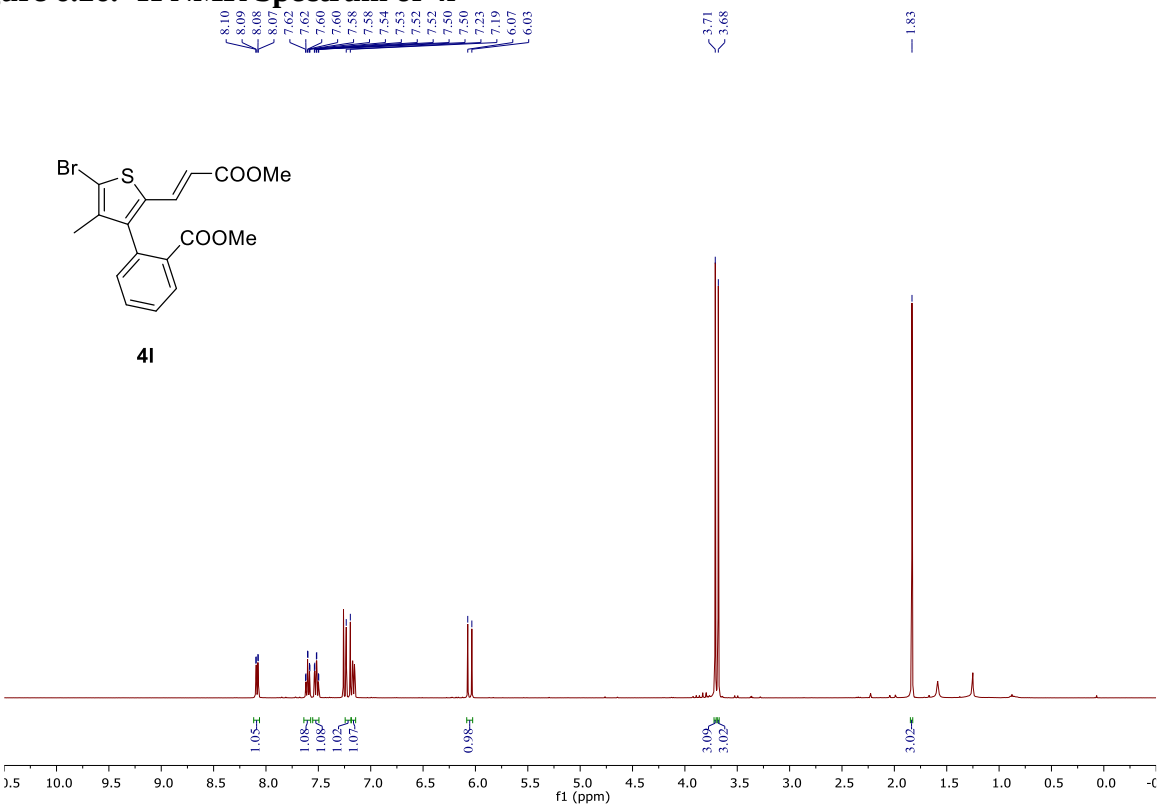

Figure 6.27. ^{13}C NMR Spectrum of 4l

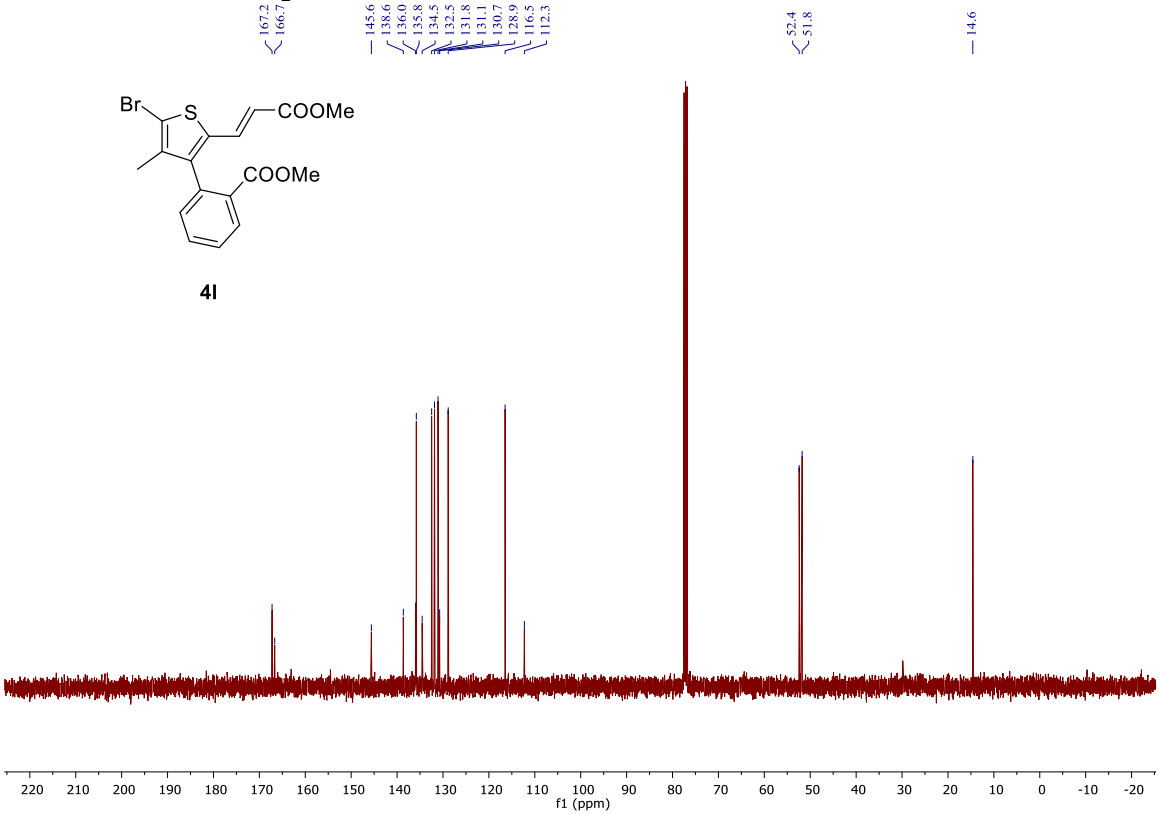

Figure 6.28. ^{1}H NMR Spectrum of 4m

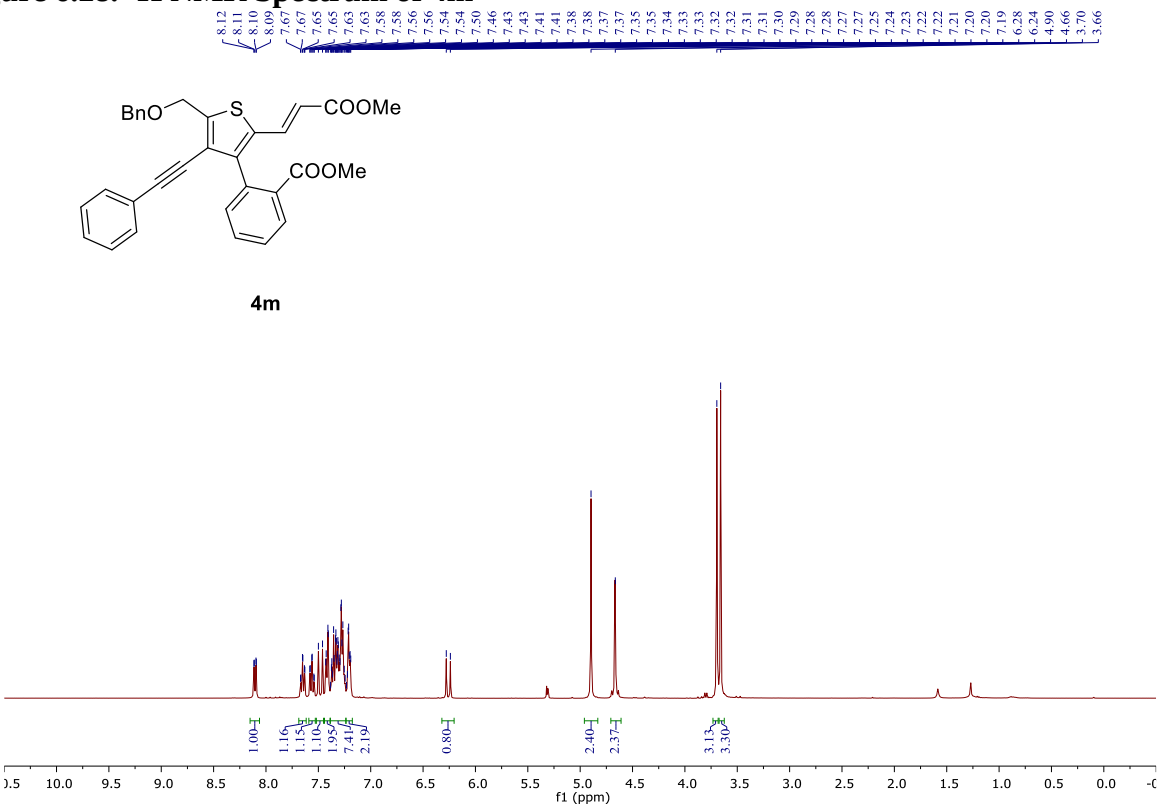

Figure 6.29. ^{13}C NMR Spectrum of 4m

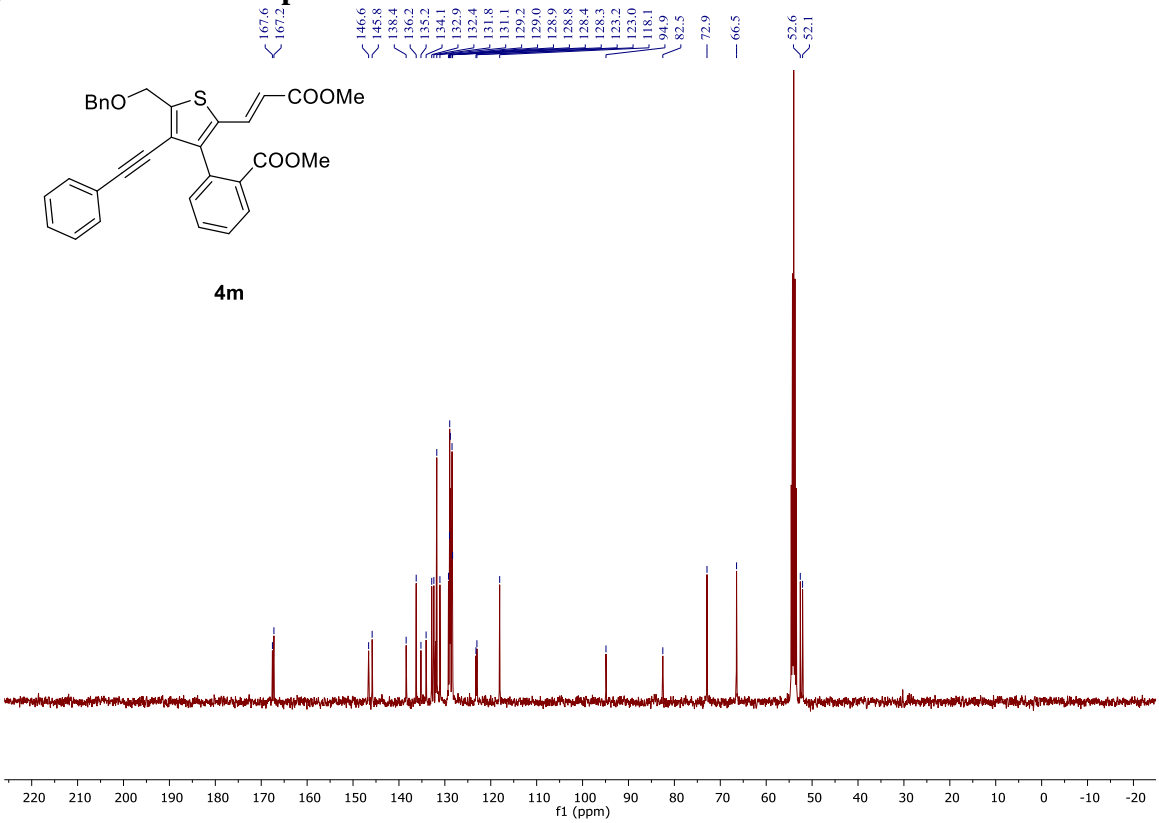

Figure 6.30. ^{1}H NMR Spectrum of 4n

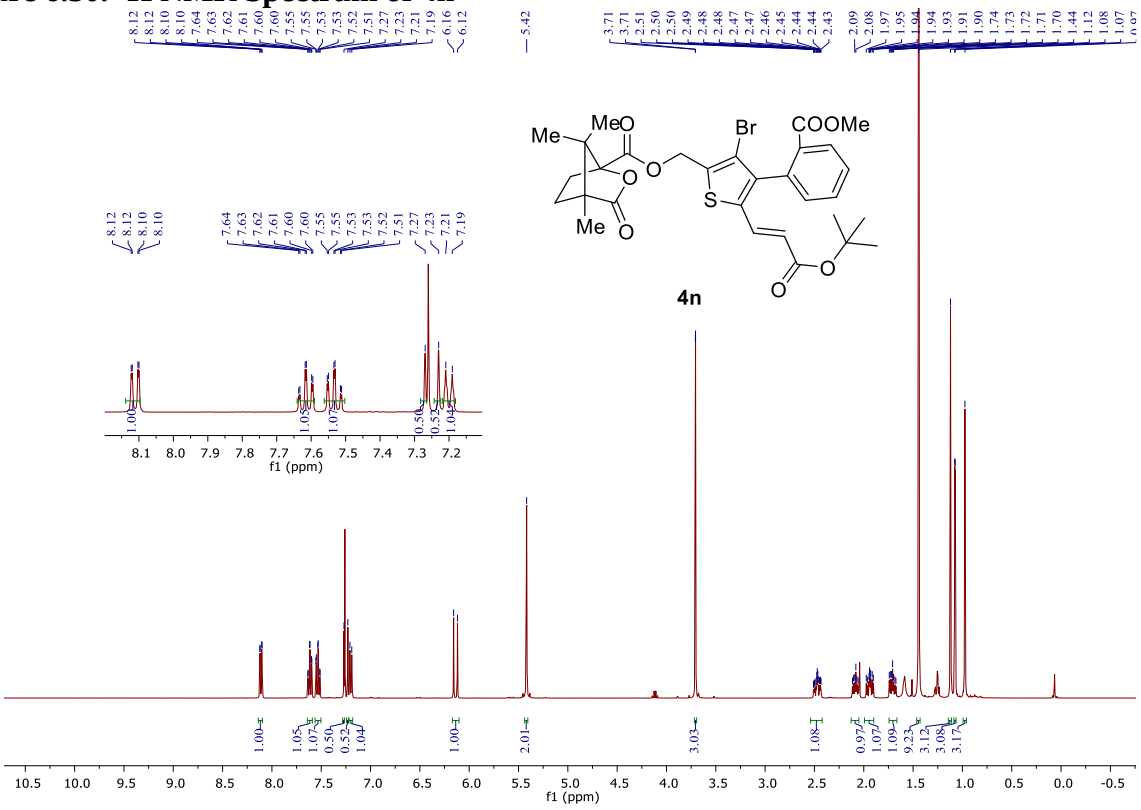

Figure 6.31. ^{13}C NMR Spectrum of 4n

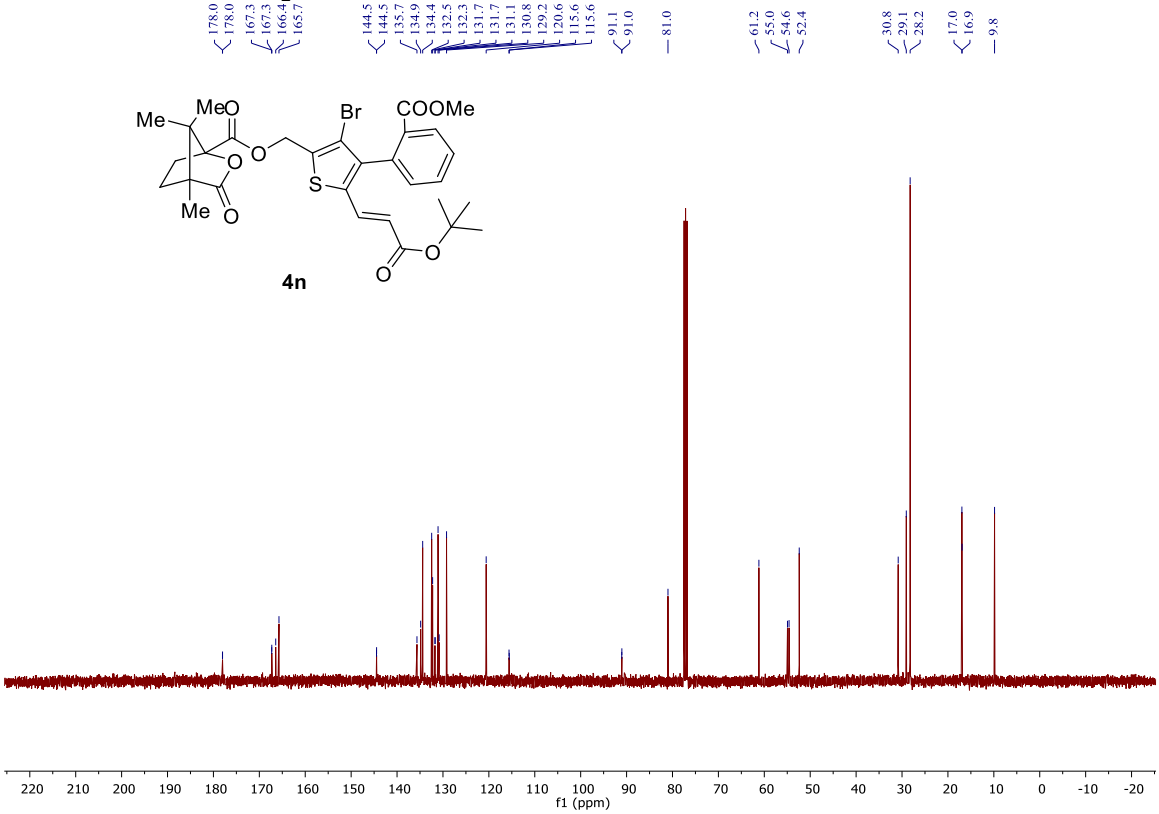

Figure 6.32. ^{1}H NMR Spectrum of 4o

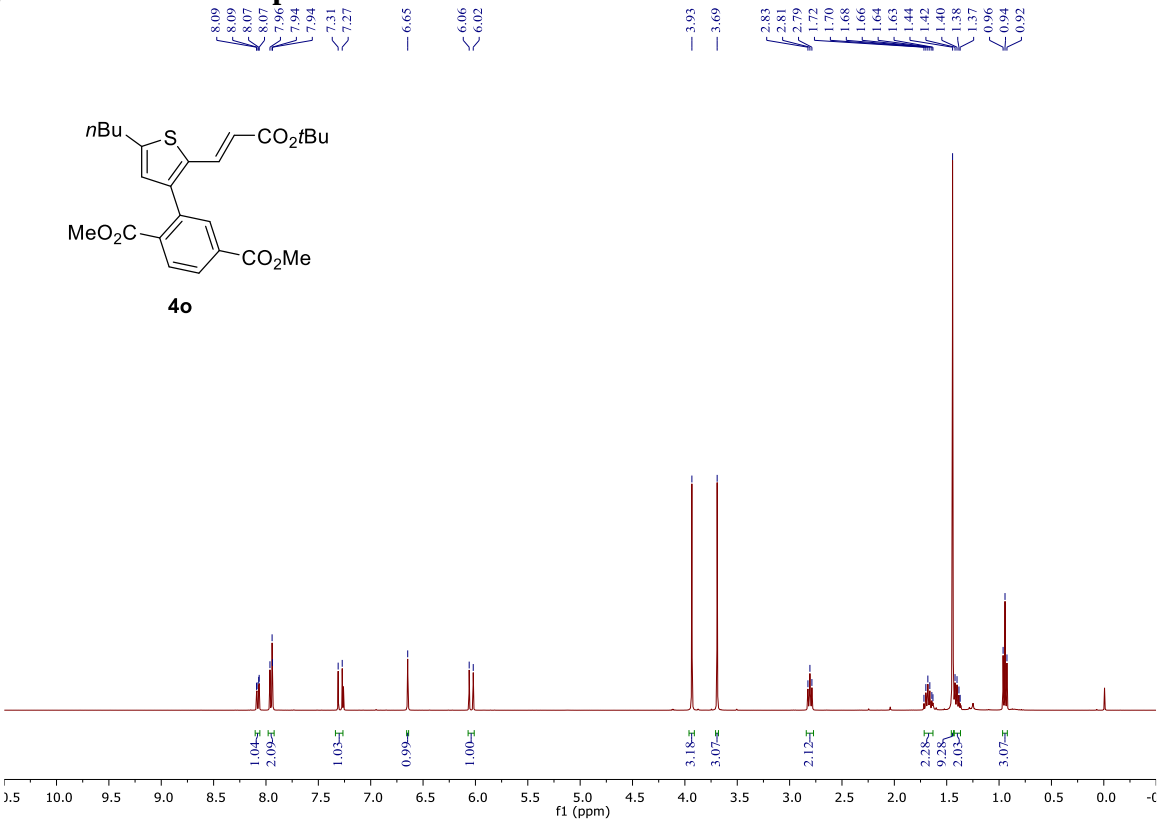

Figure 6.33. ^{13}C NMR Spectrum of 4o

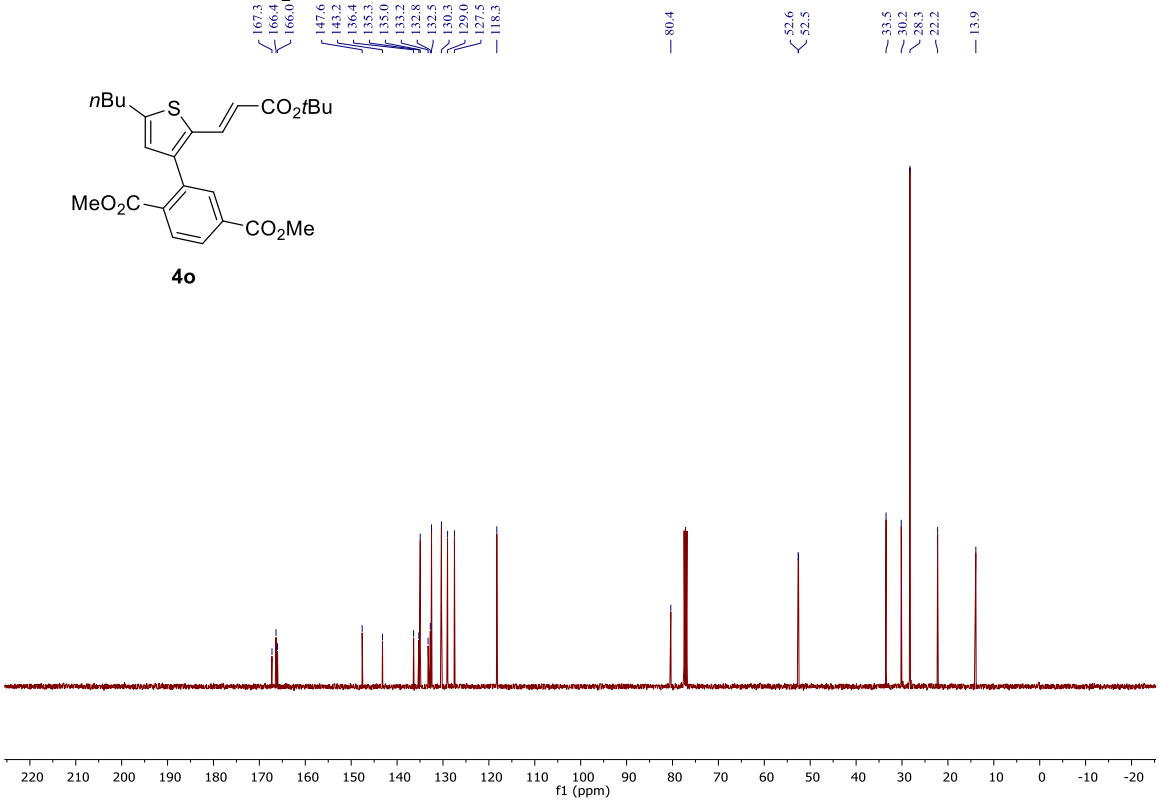

Figure 6.34. ^{1}H NMR Spectrum of 5a

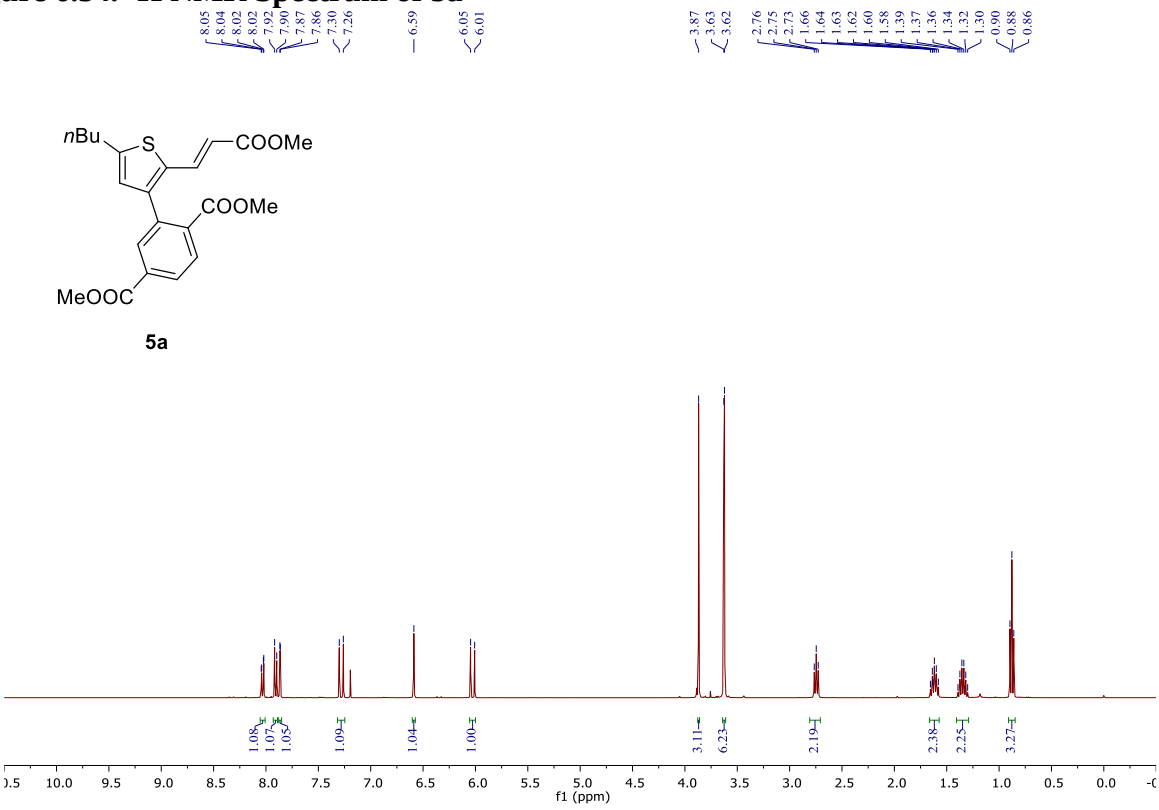

Figure 6.35. ^{13}C NMR Spectrum of 5a

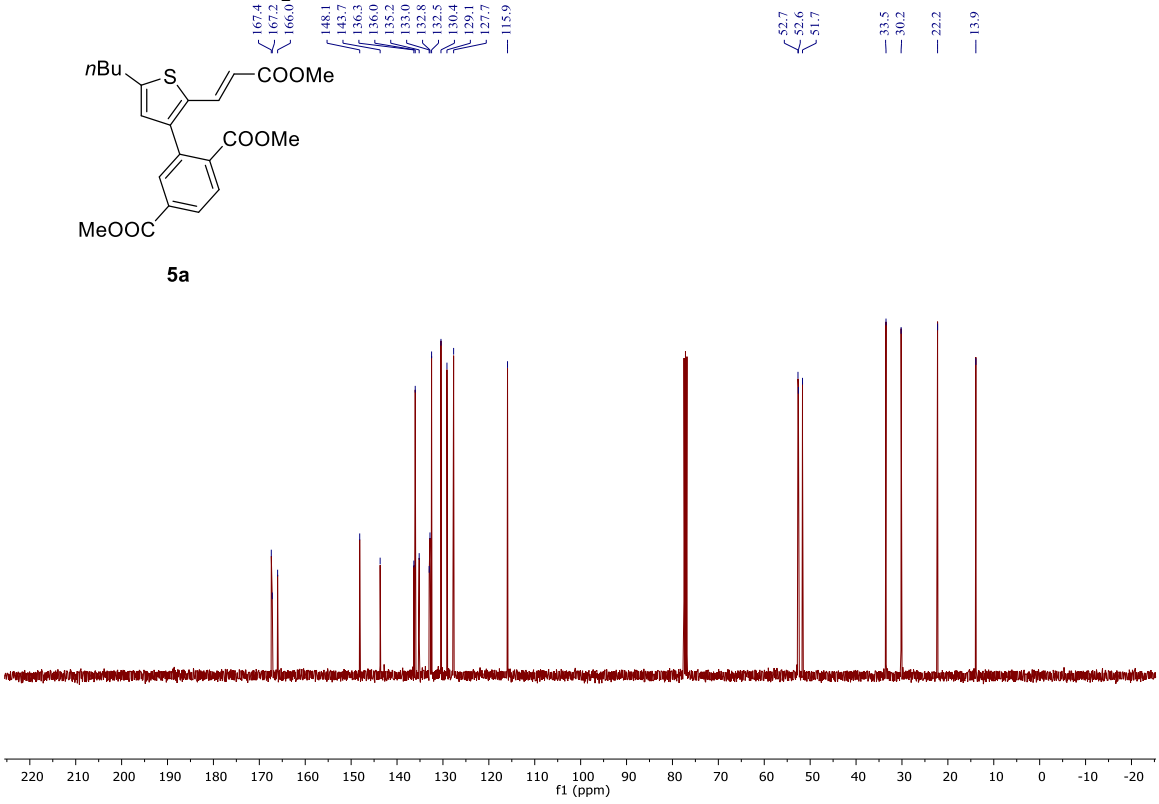

Figure 6.36. ^{1}H NMR Spectrum of 5b

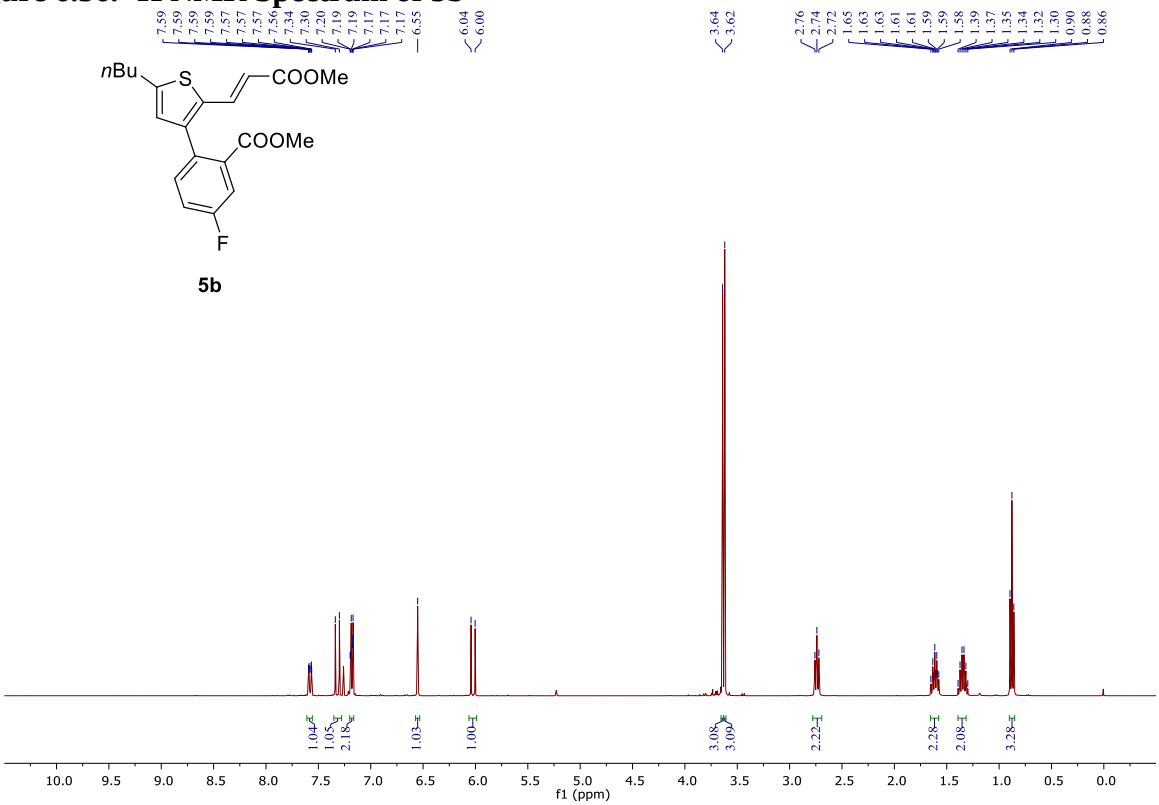

Figure 6.37. ^{13}C NMR Spectrum of 5b

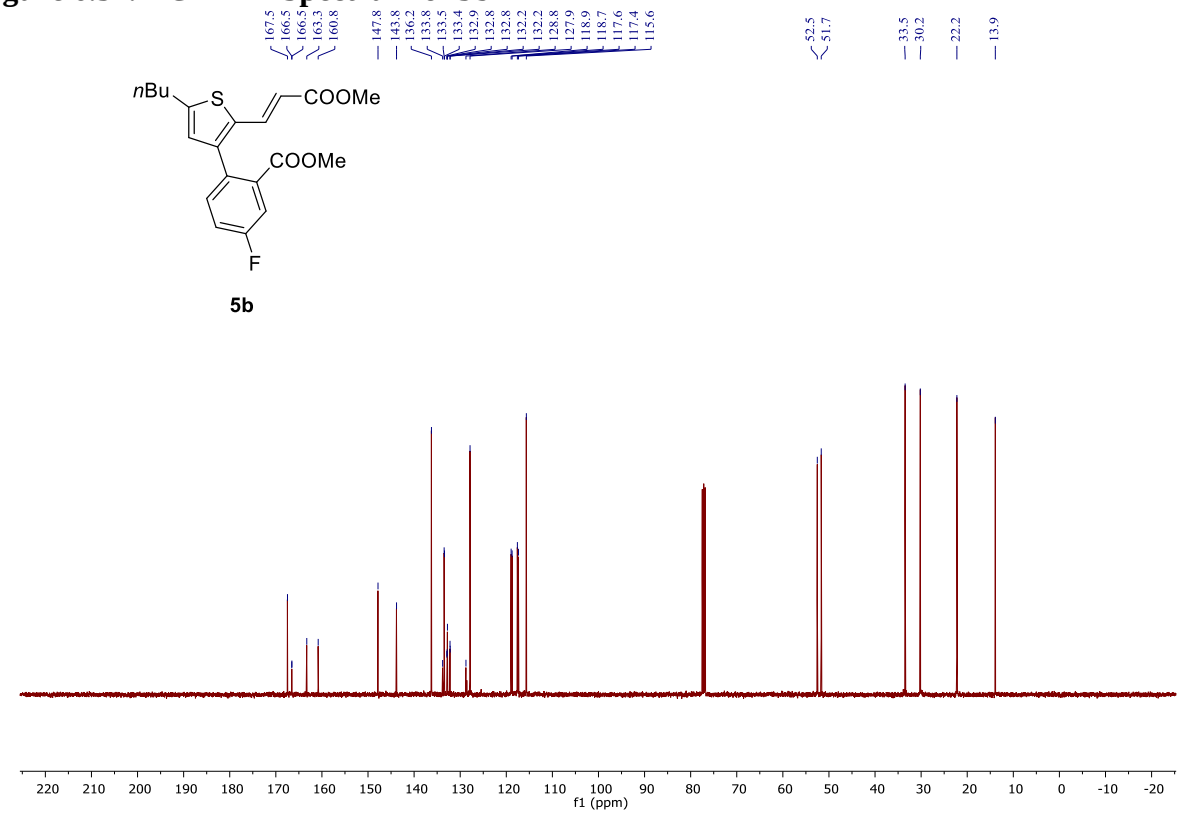

Figure 6.38. ^{19}F NMR Spectrum of 5b

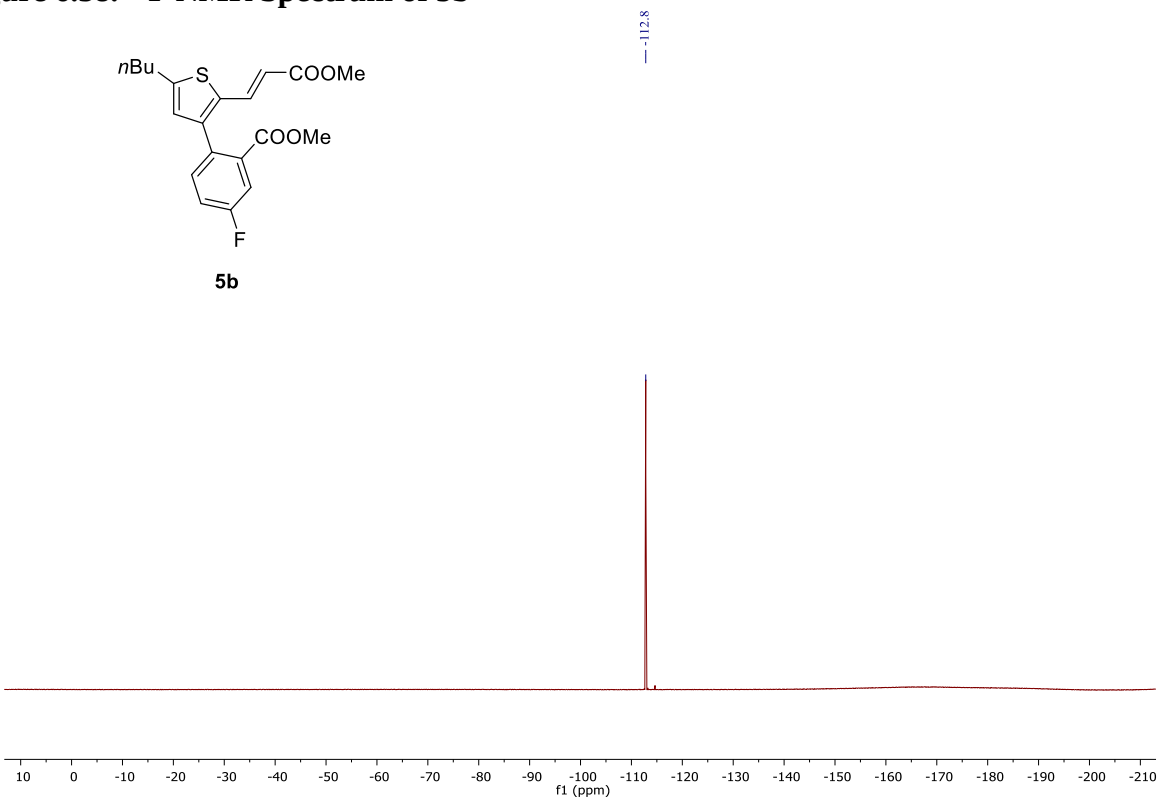

5b

Figure 6.39. ^{1}H NMR Spectrum of 5c

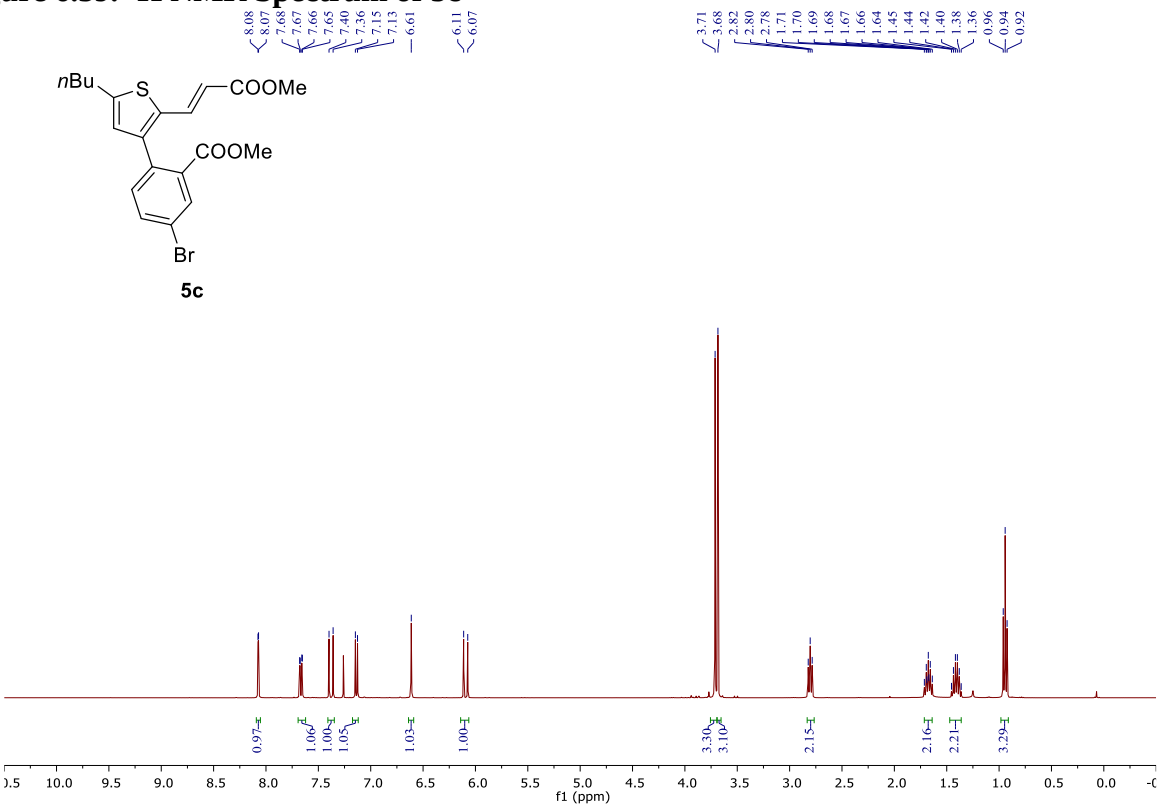

Figure 6.40. ^{13}C NMR Spectrum of 5c

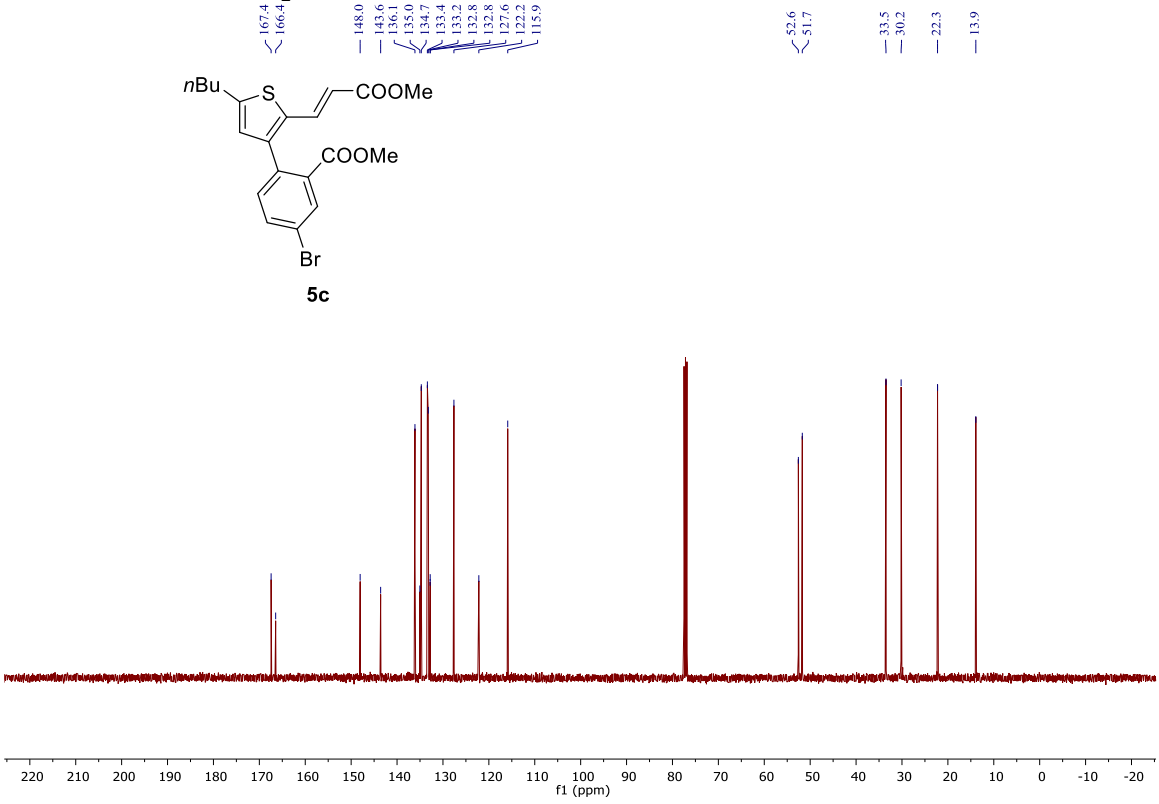

Figure 6.41. ^{1}H NMR Spectrum of 5d

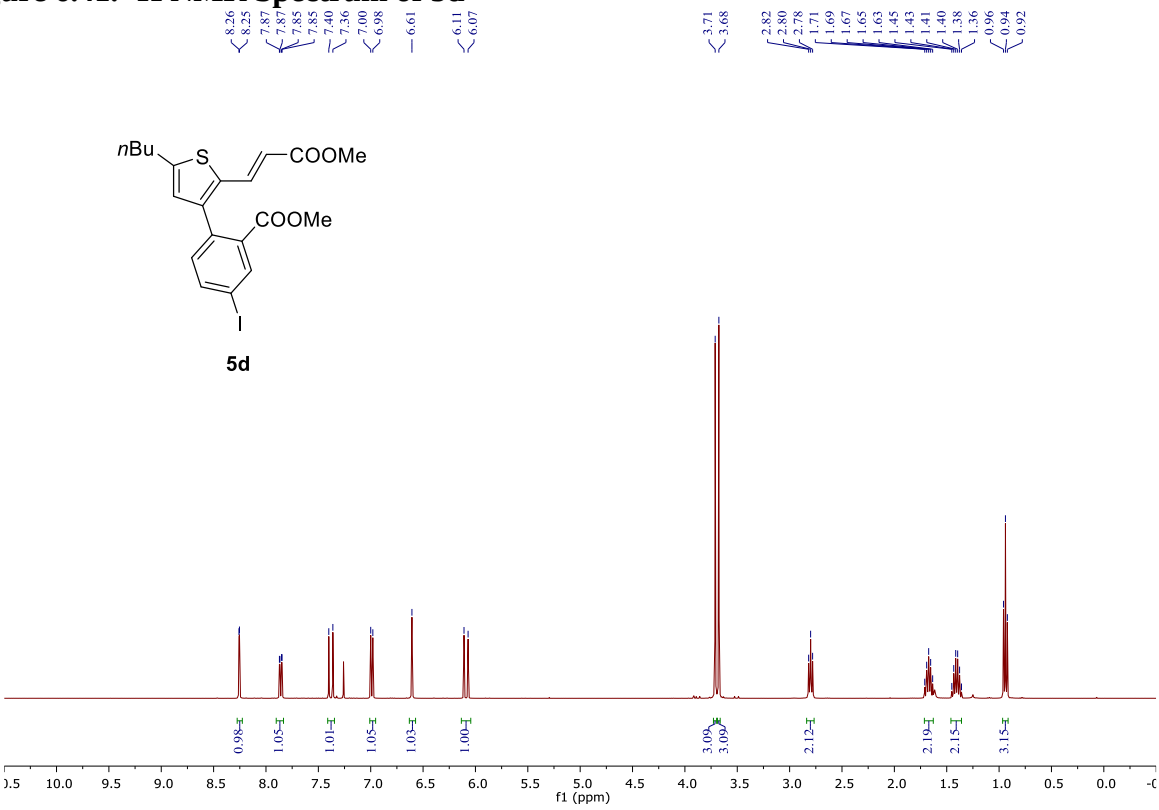

Figure 6.42. ^{13}C NMR Spectrum of 5d

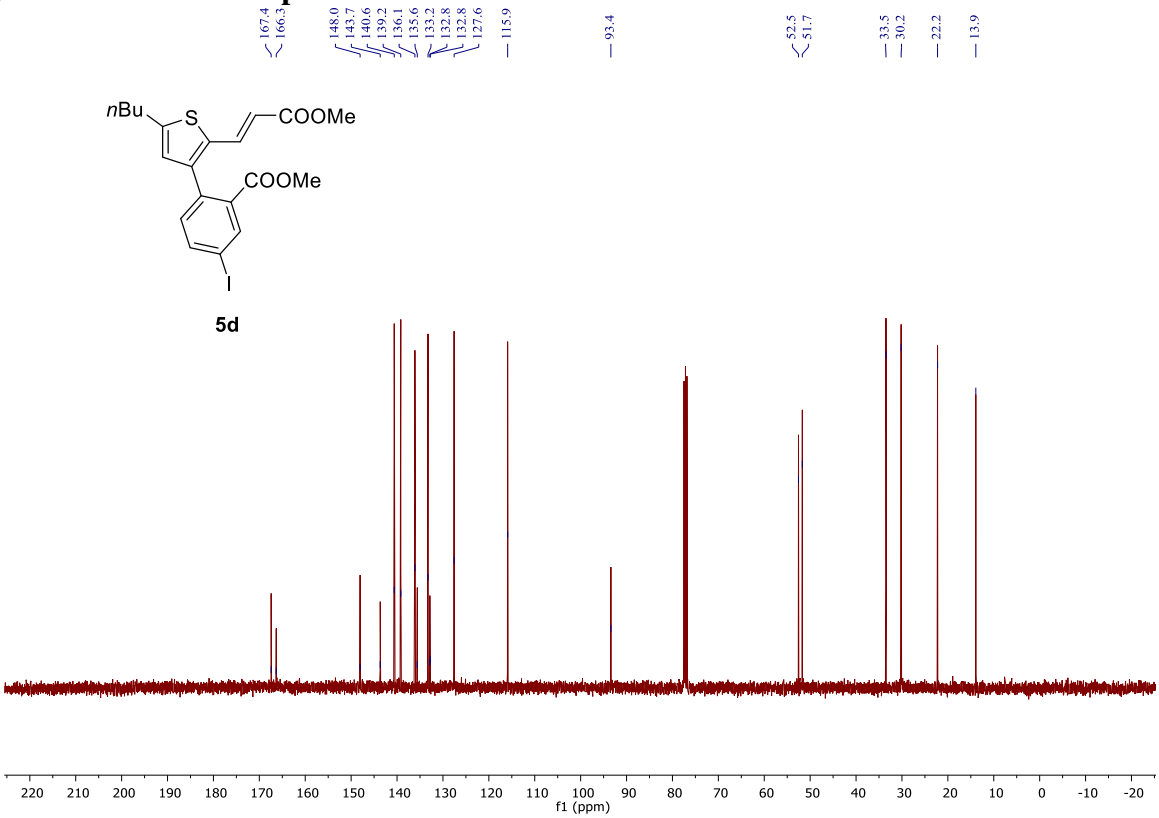

Figure 6.43. ^{1}H NMR Spectrum of 5e

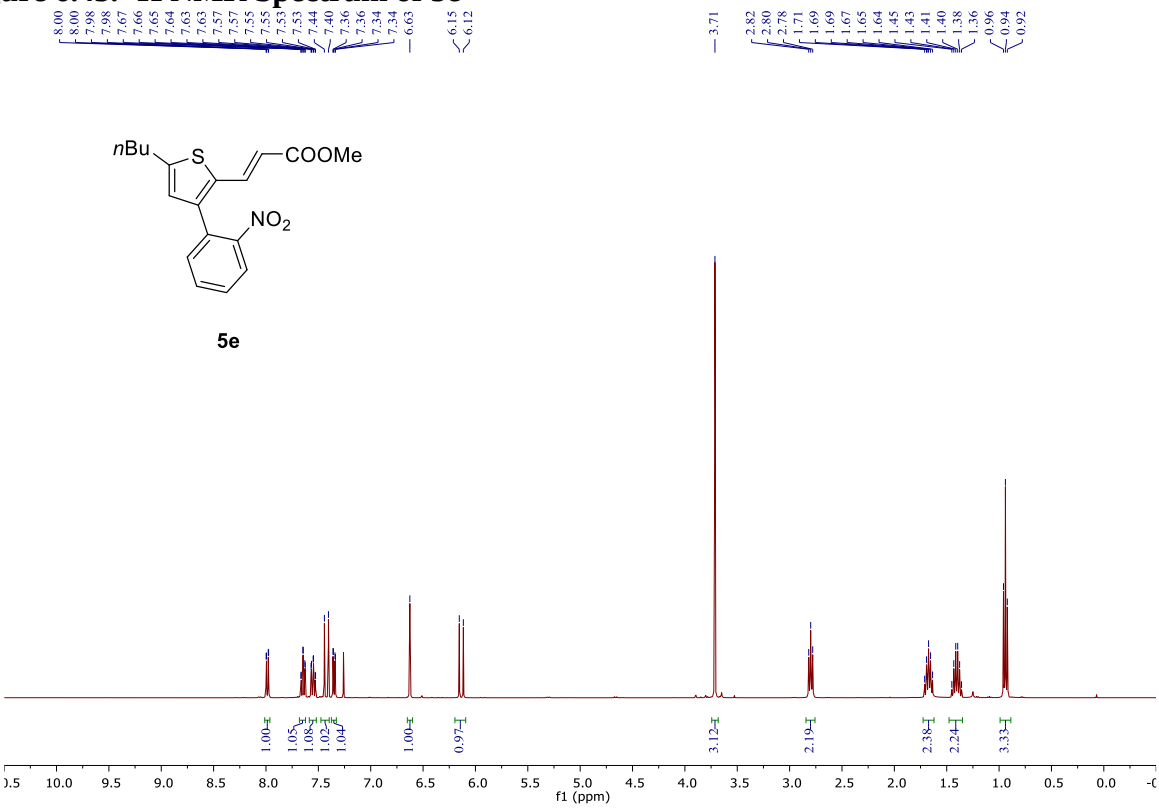

Figure 6.44. ^{13}C NMR Spectrum of 5e

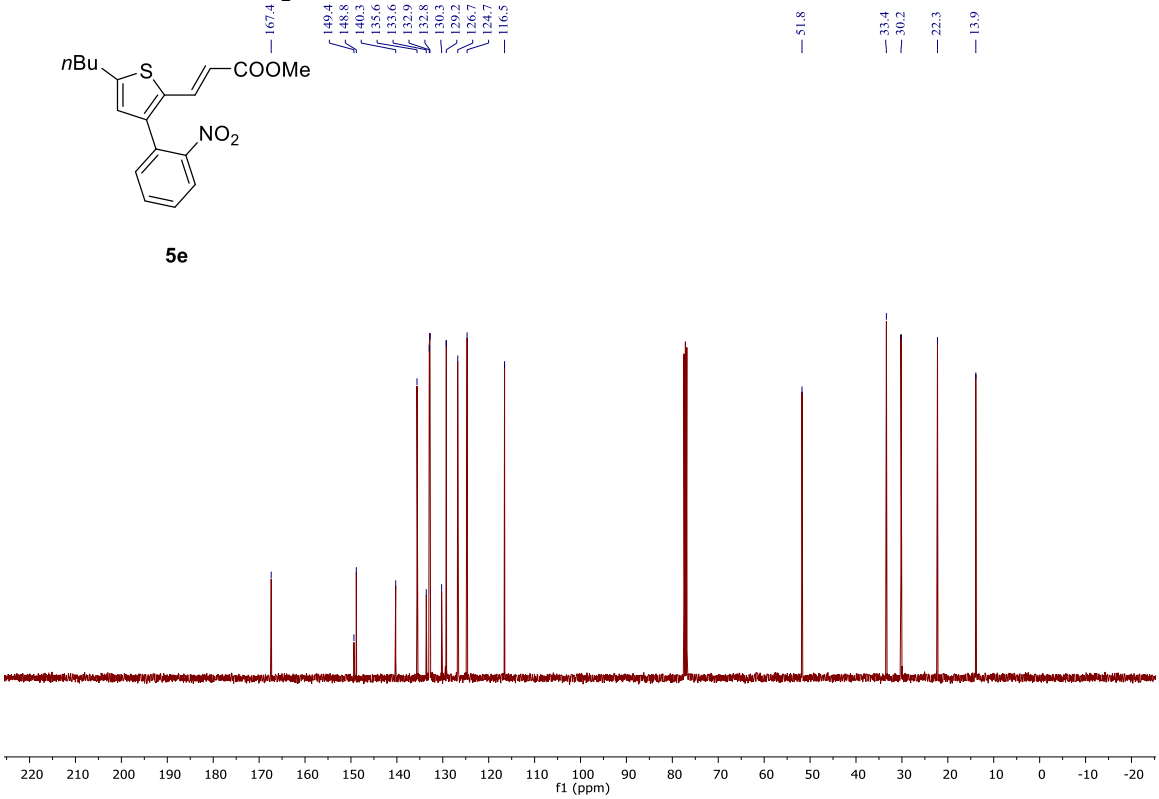

Figure 6.45. ^{1}H NMR Spectrum of 5f

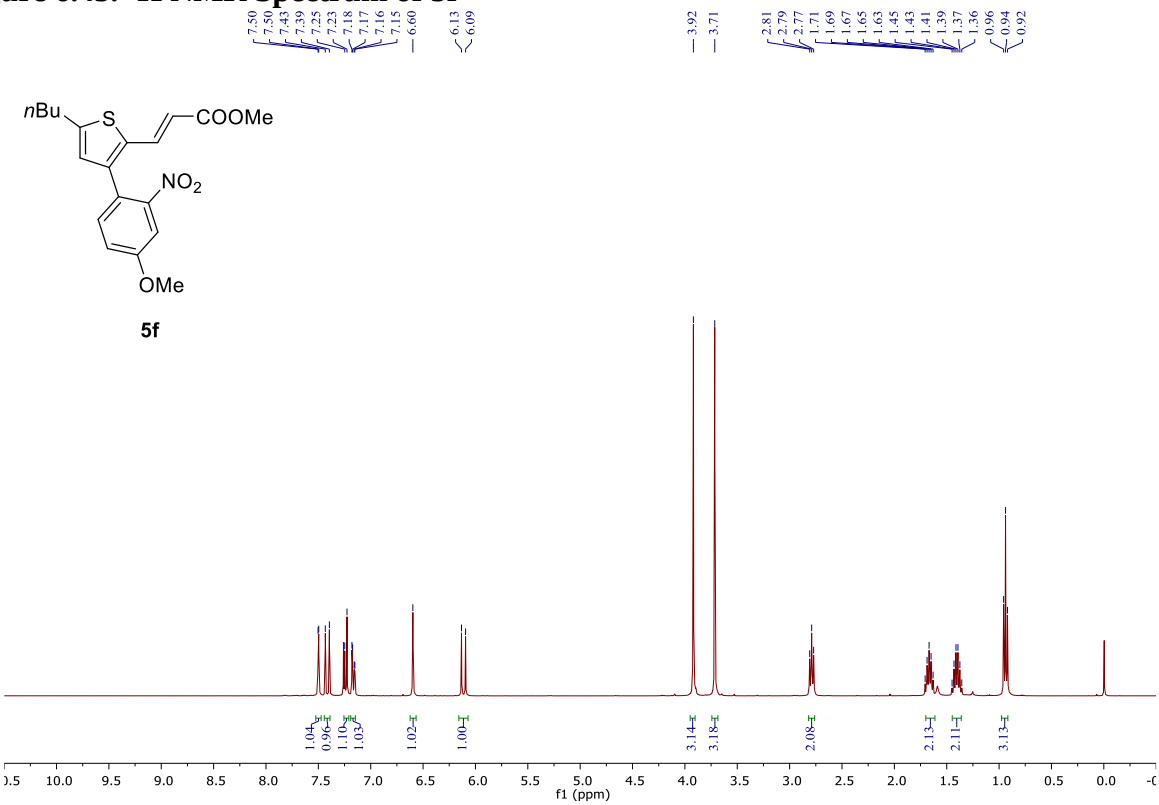

Figure 6.46. ^{13}C NMR Spectrum of 5f

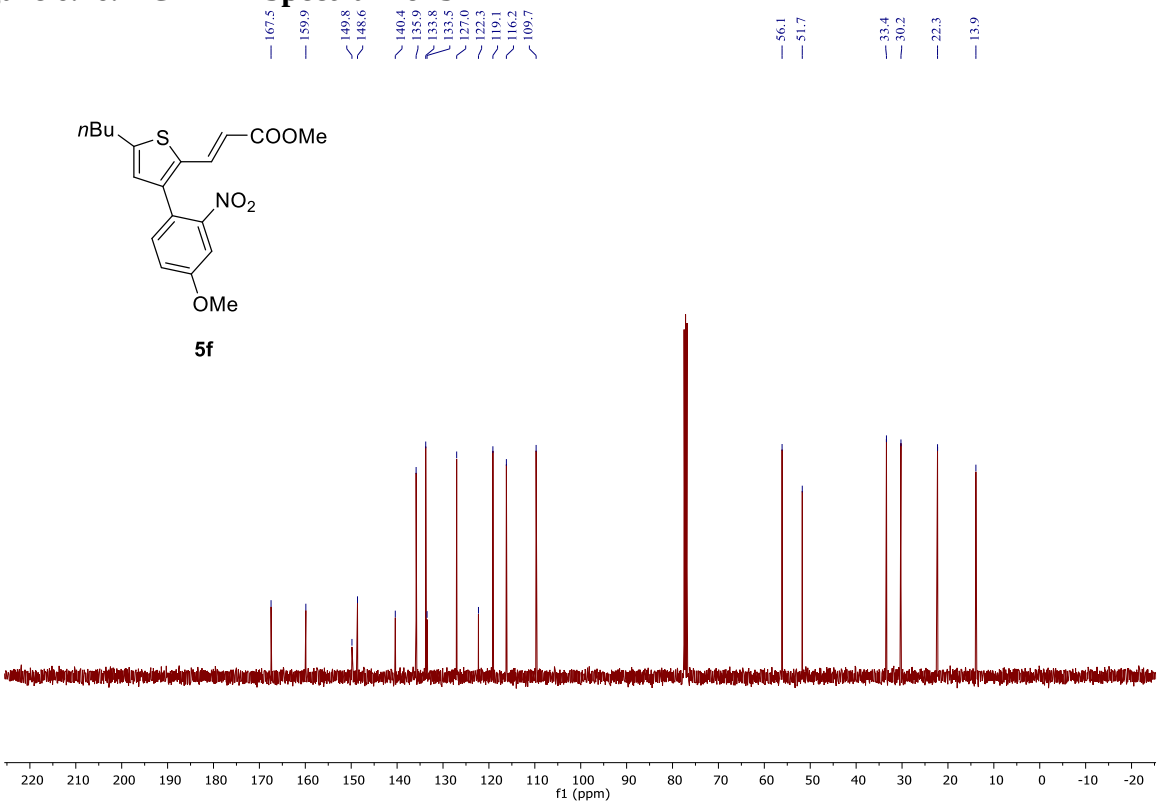

Figure 6.47. ^{1}H NMR Spectrum of 5g

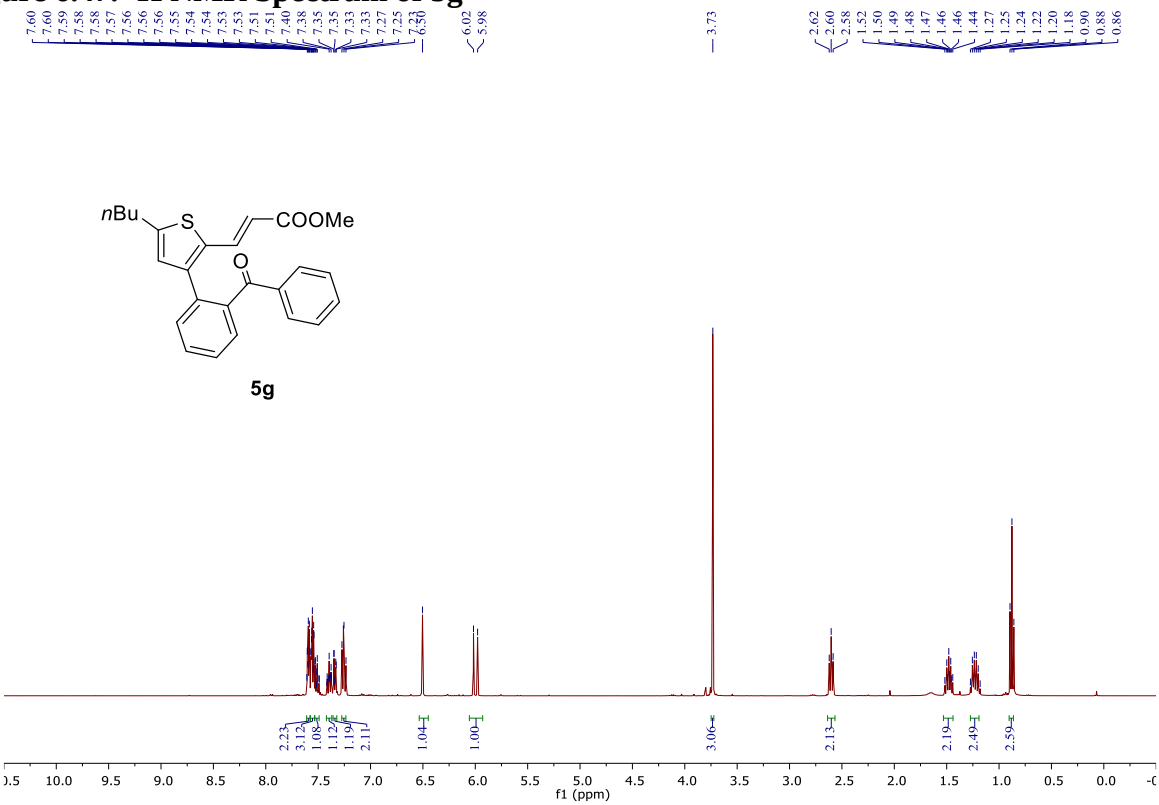

Figure 6.48. ^{13}C NMR Spectrum of 5g

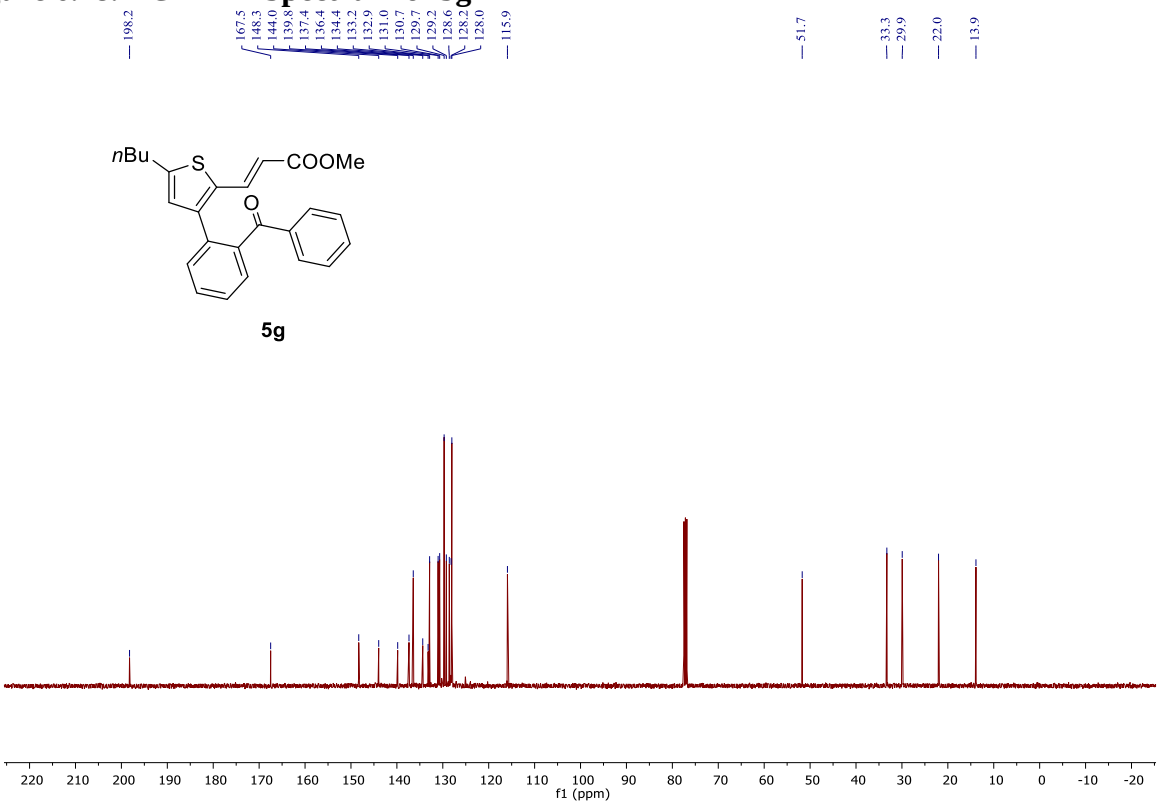

Figure 6.49. ^{1}H NMR Spectrum of 5h

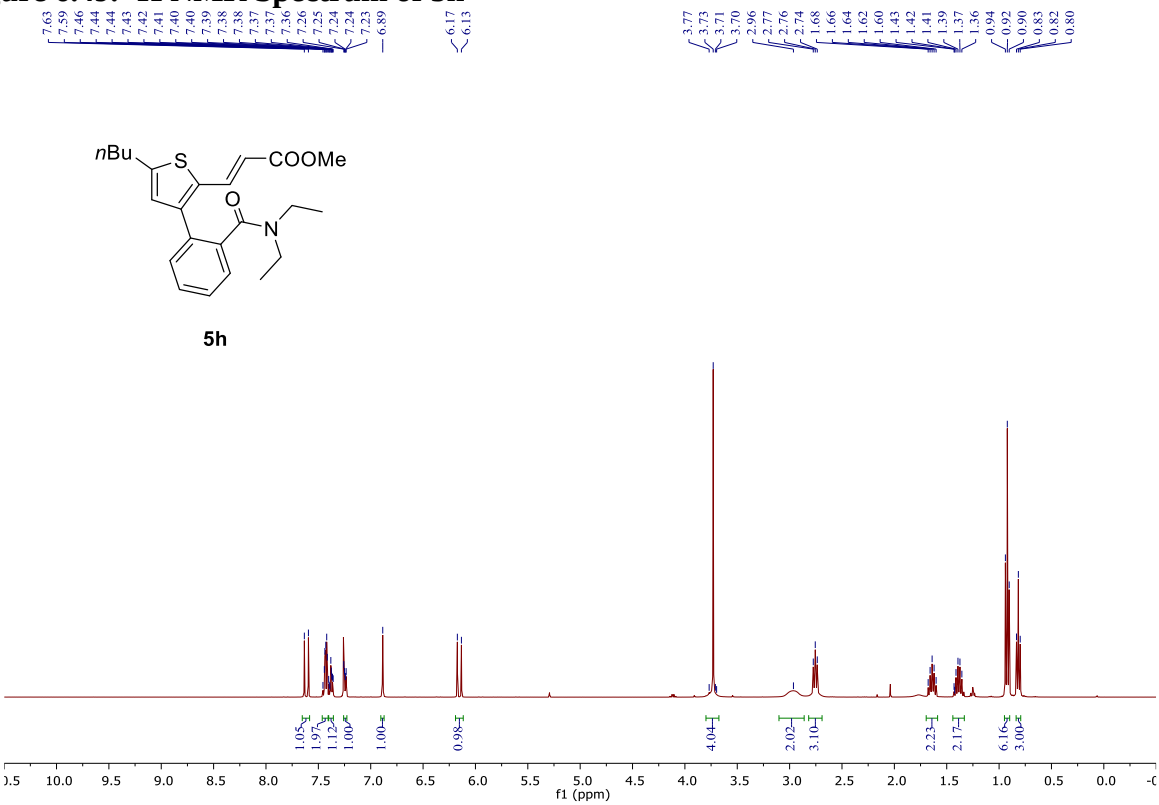

Figure 6.50. ^{13}C NMR Spectrum of 5h

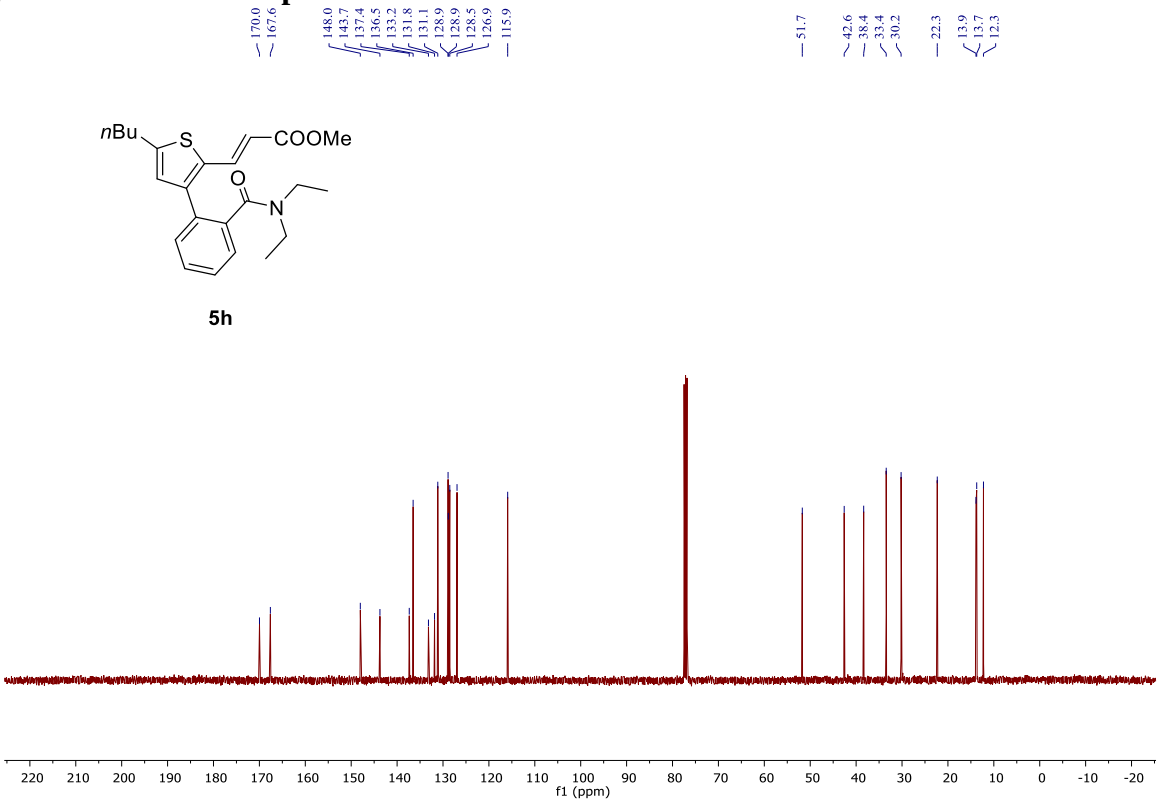

Figure 6.51. ^{1}H NMR Spectrum of 5i

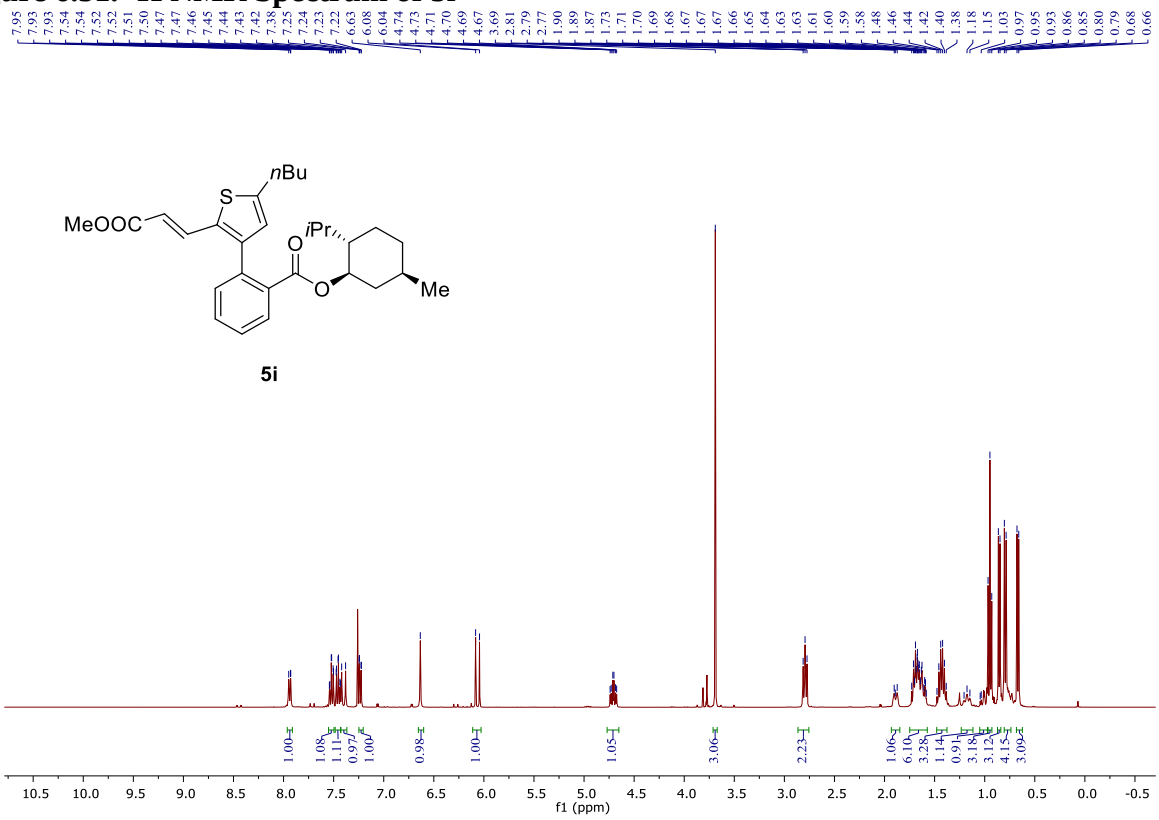

Figure 6.52. ^{13}C NMR Spectrum of 5i

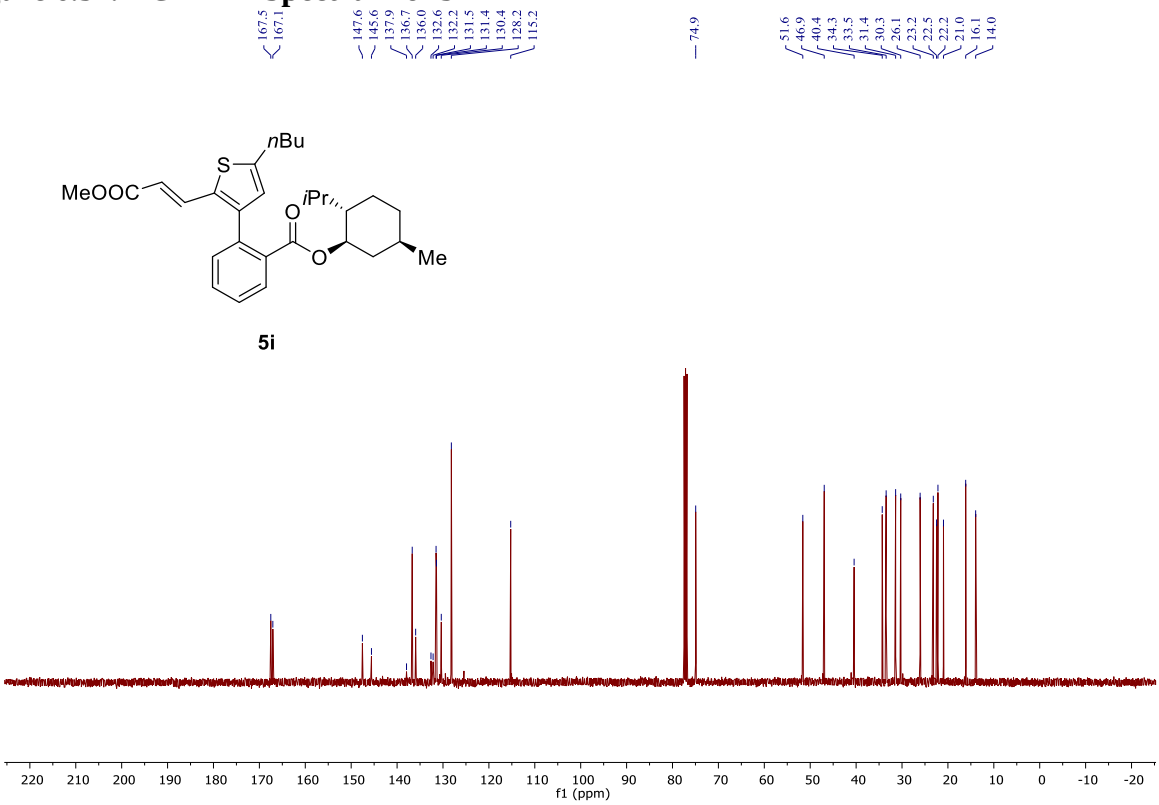

Figure 6.53. ^{1}H NMR Spectrum of 5j

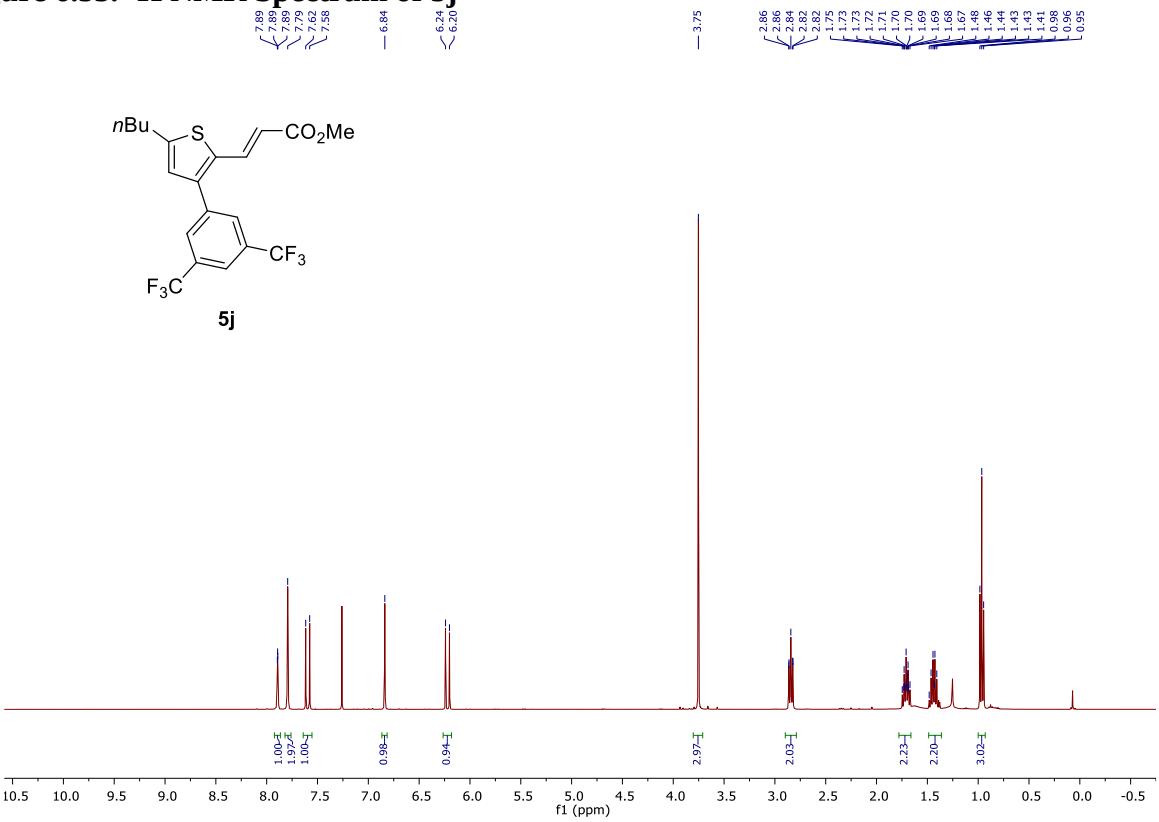

Figure 6.54. ^{13}C NMR Spectrum of 5j

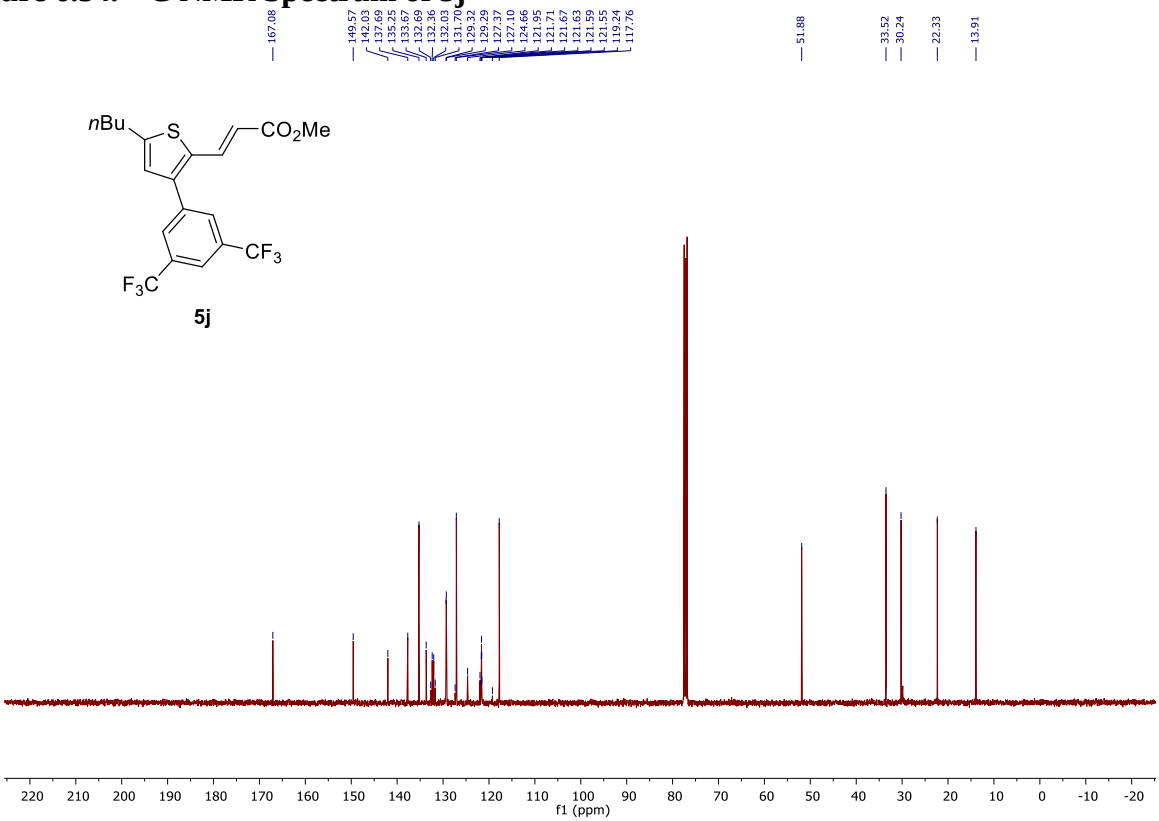

Figure 6.55. ^{19}F NMR Spectrum of 5j

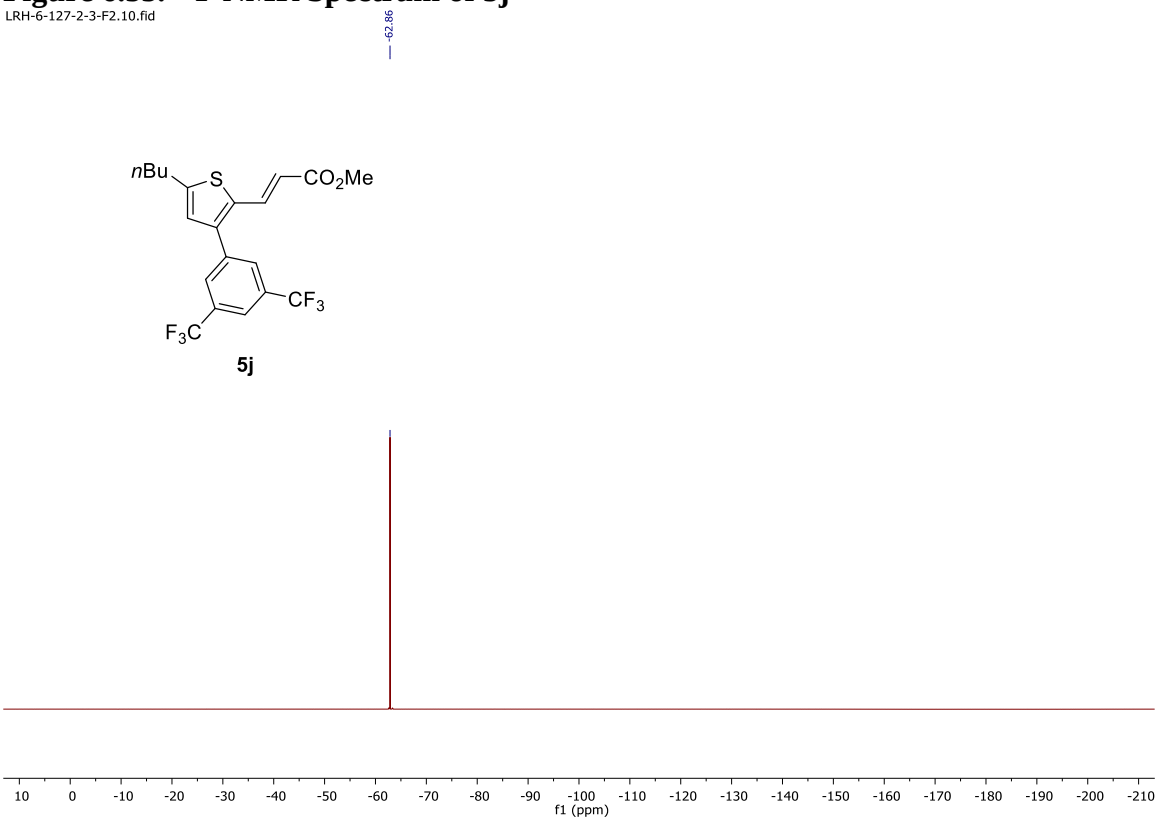

Figure 6.56. ^{1}H NMR Spectrum of 6a

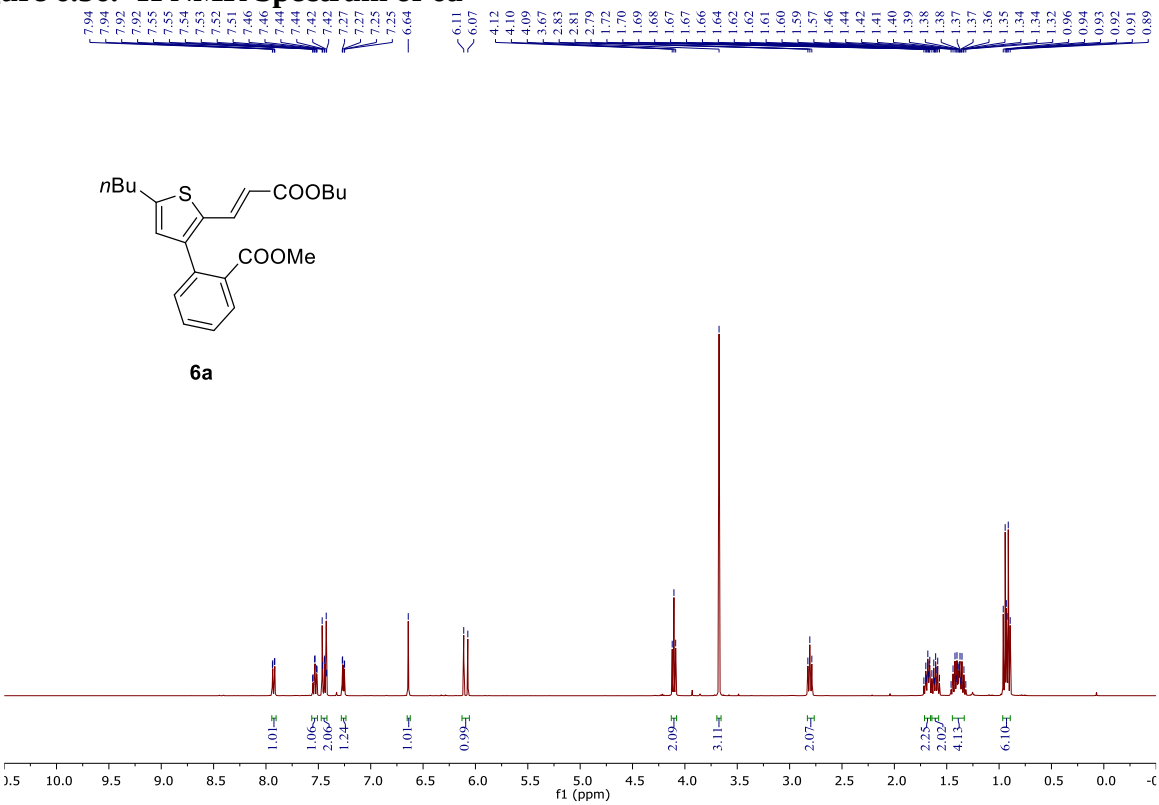

Figure 6.57. ^{13}C NMR Spectrum of 6a

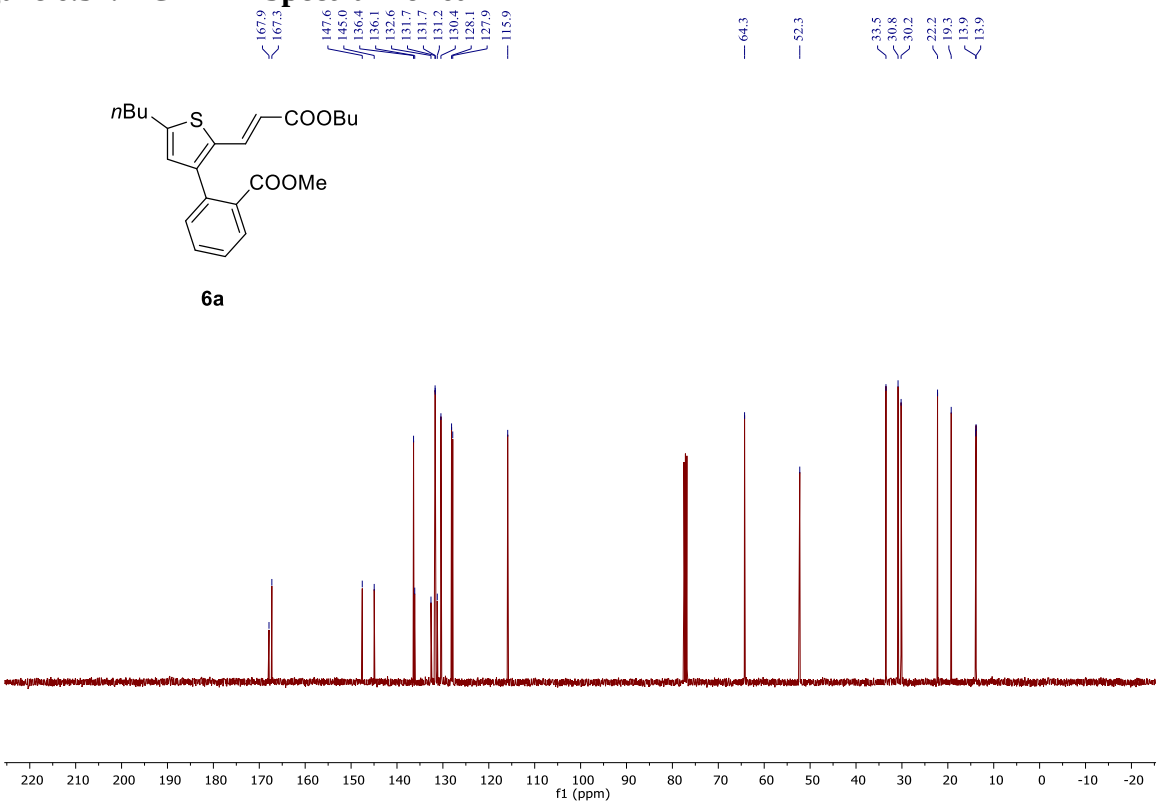

Figure 6.58. ^{1}H NMR Spectrum of 6b

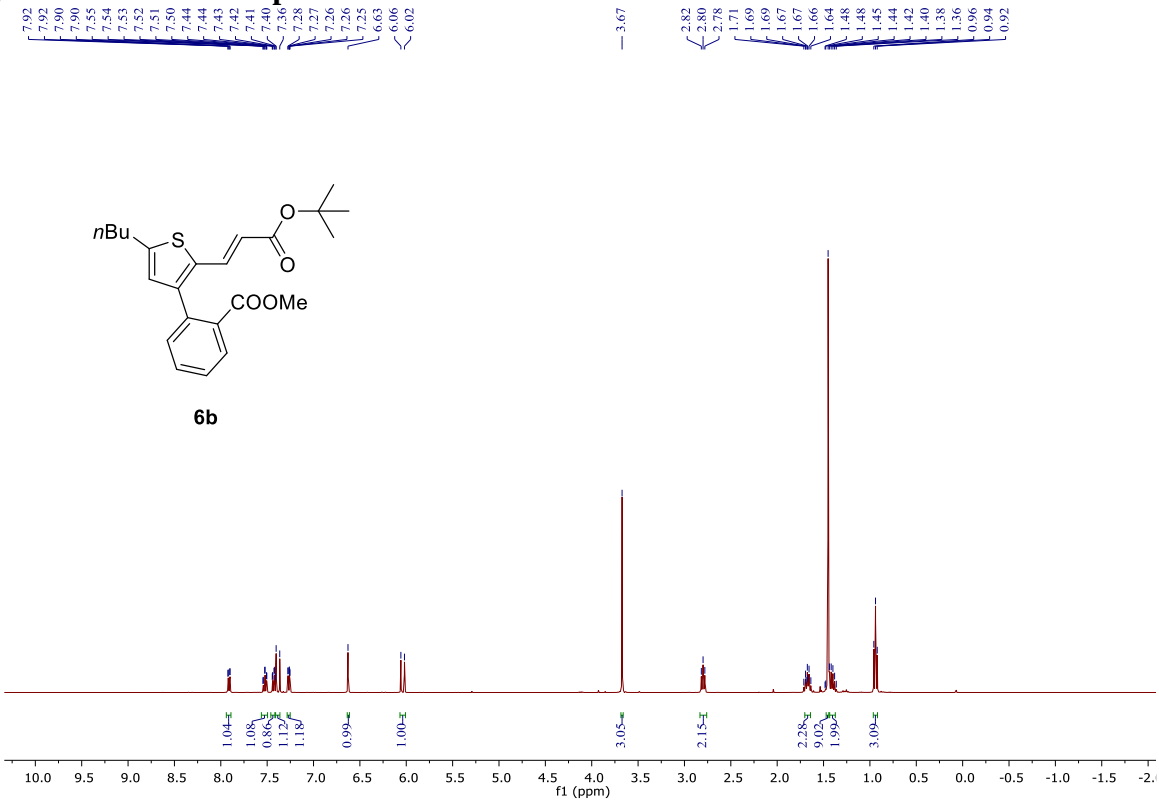

Figure 6.59. ^{13}C NMR Spectrum of 6b

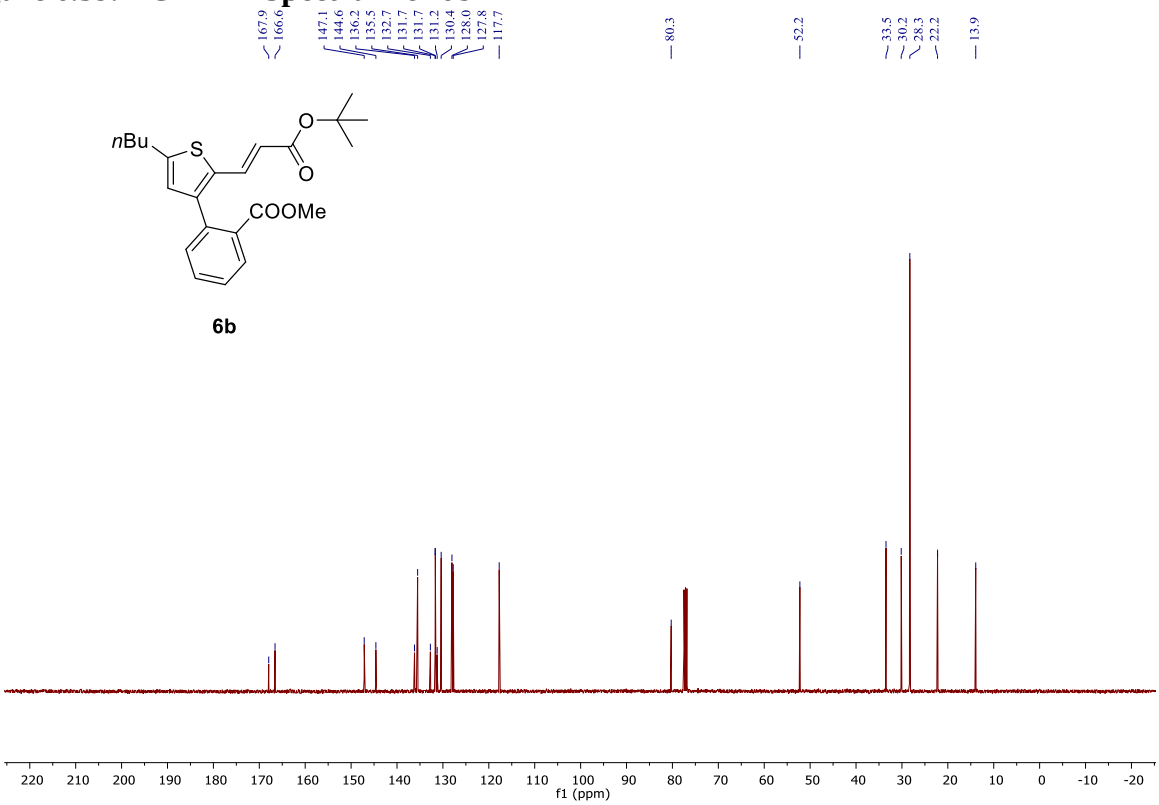

Figure 6.60. ^{1}H NMR Spectrum of 6c

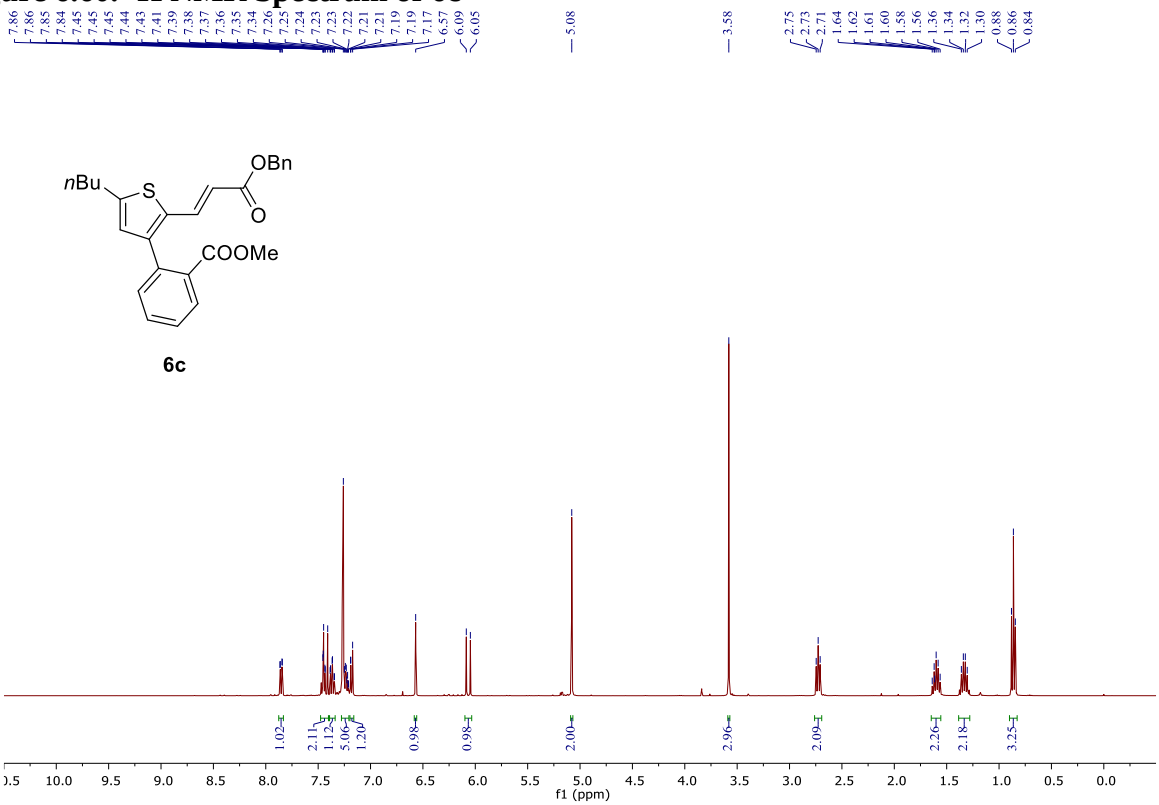

Figure 6.61. ^{13}C NMR Spectrum of 6c

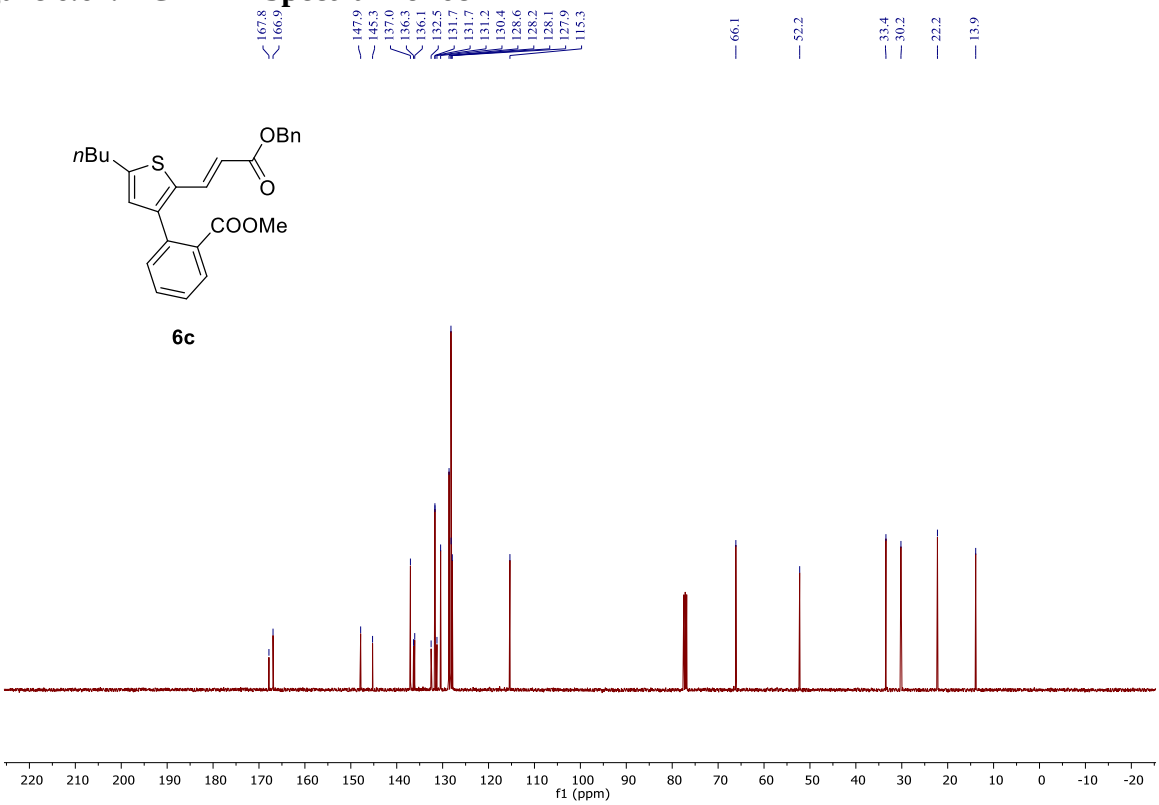

Figure 6.62. ^{1}H NMR Spectrum of 6d

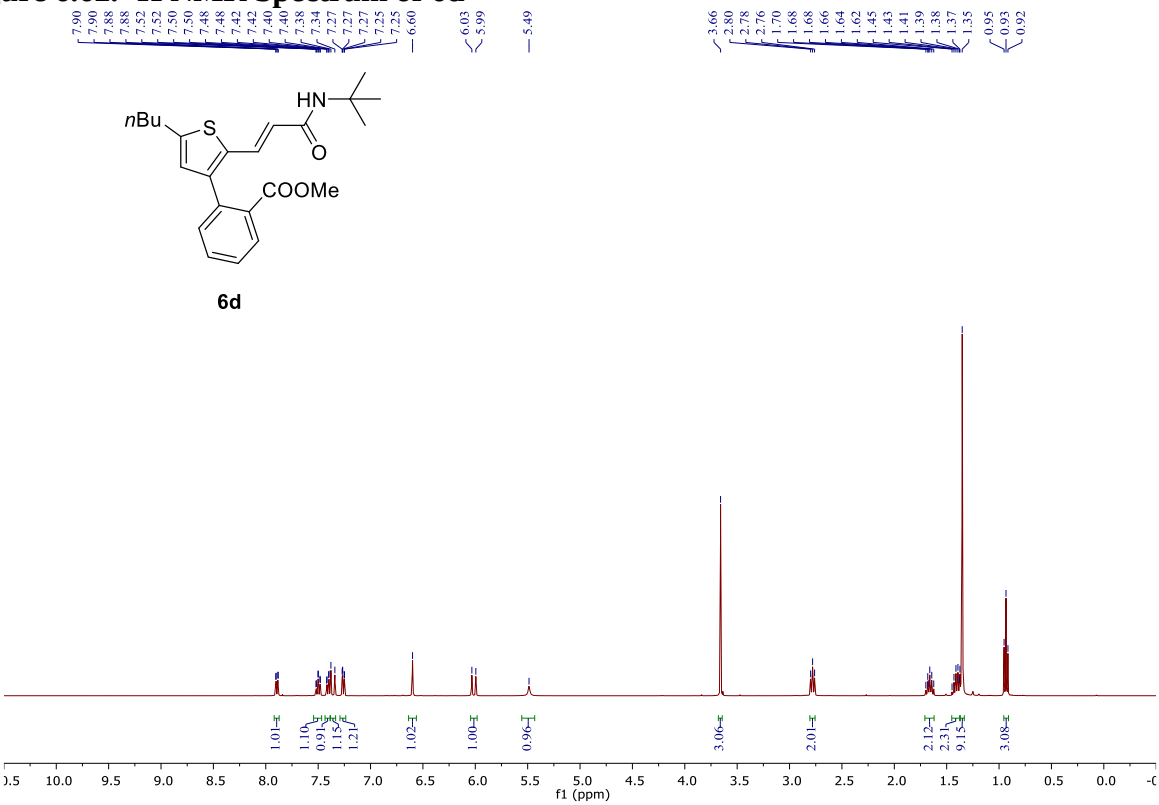

Figure 6.63. ^{13}C NMR Spectrum of 6d

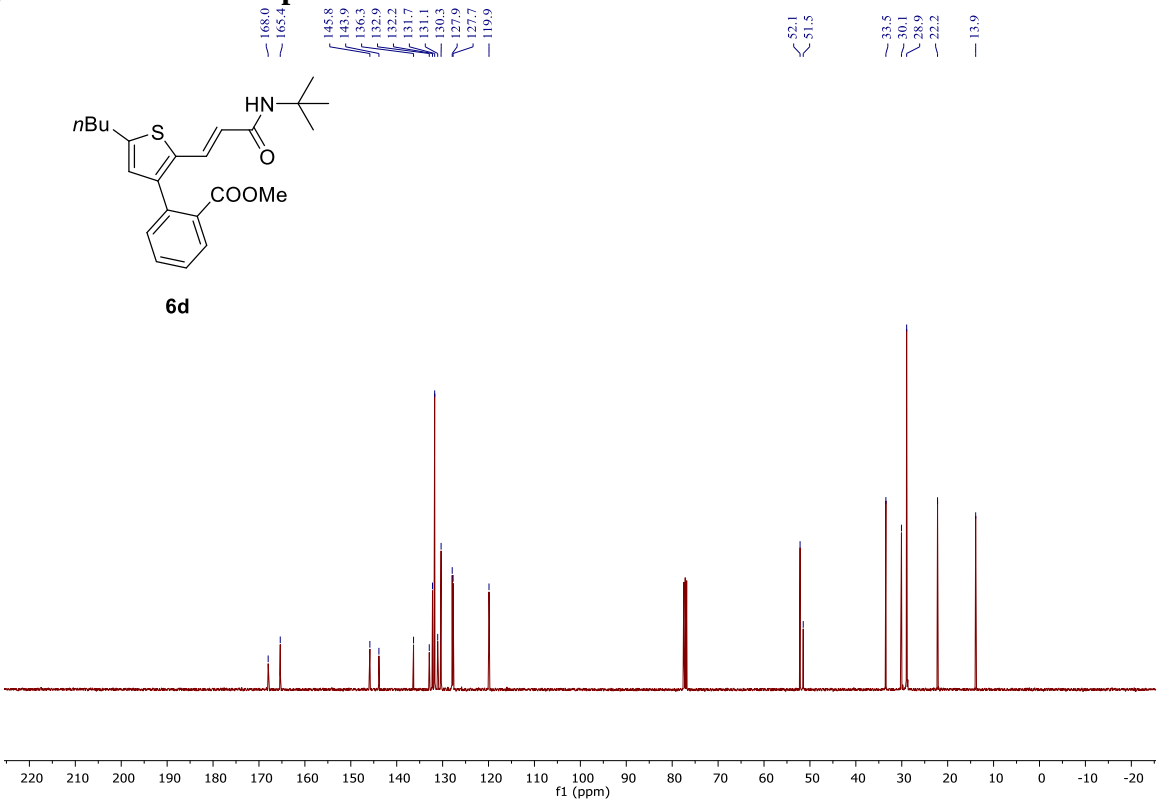

Figure 6.64. ^{1}H NMR Spectrum of 6e

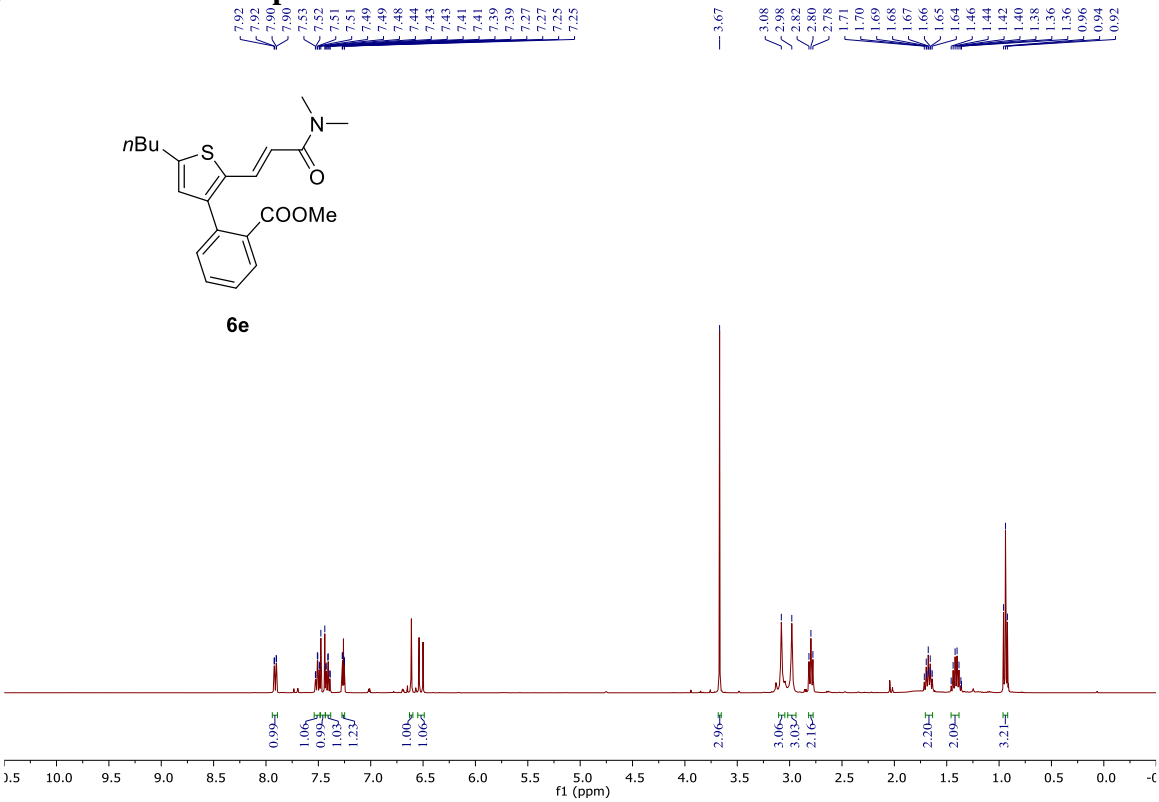

Figure 6.65. ^{13}C NMR Spectrum of 6e

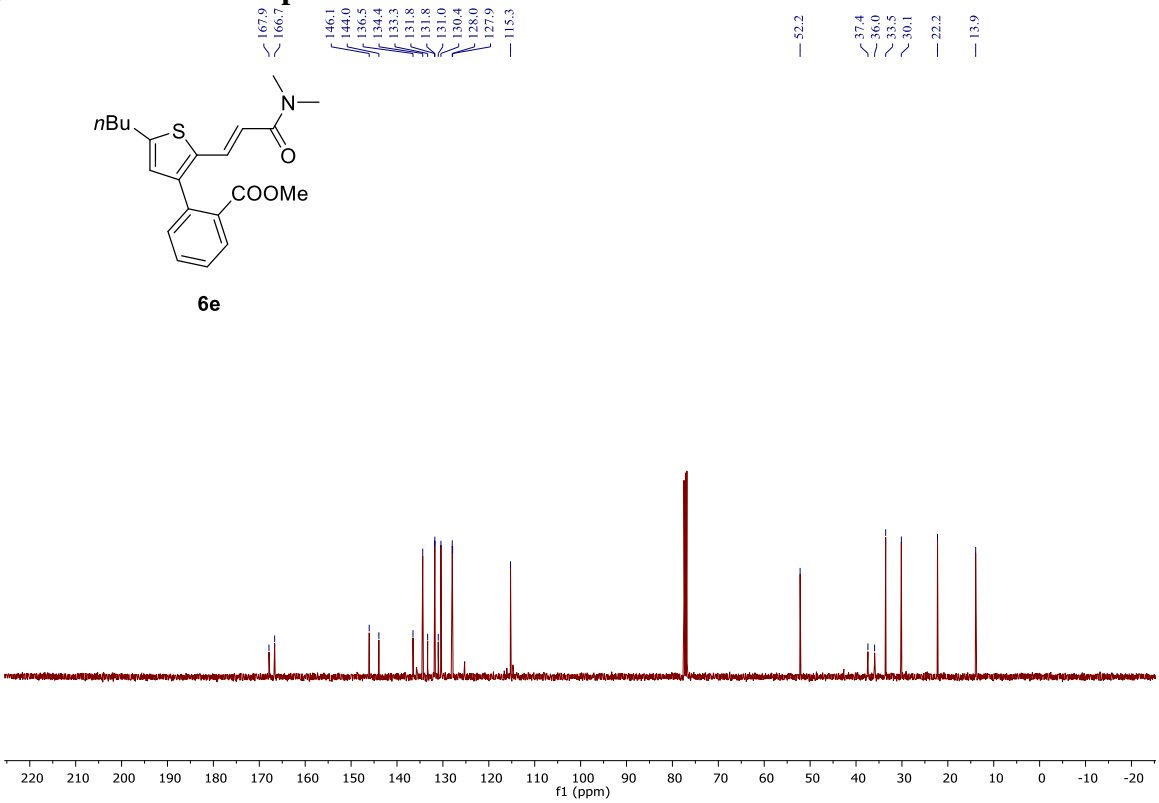

Figure 6.66. ^{1}H NMR Spectrum of 6f

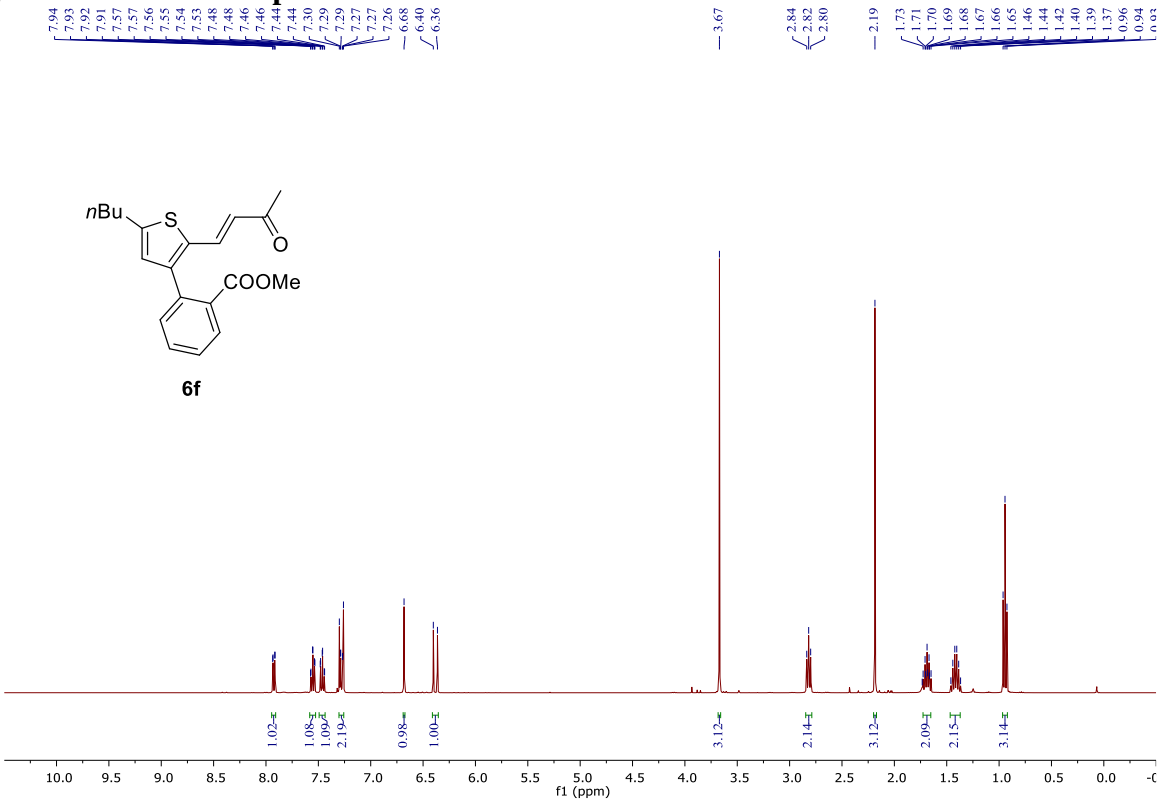

Figure 6.67. ^{13}C NMR Spectrum of 6f

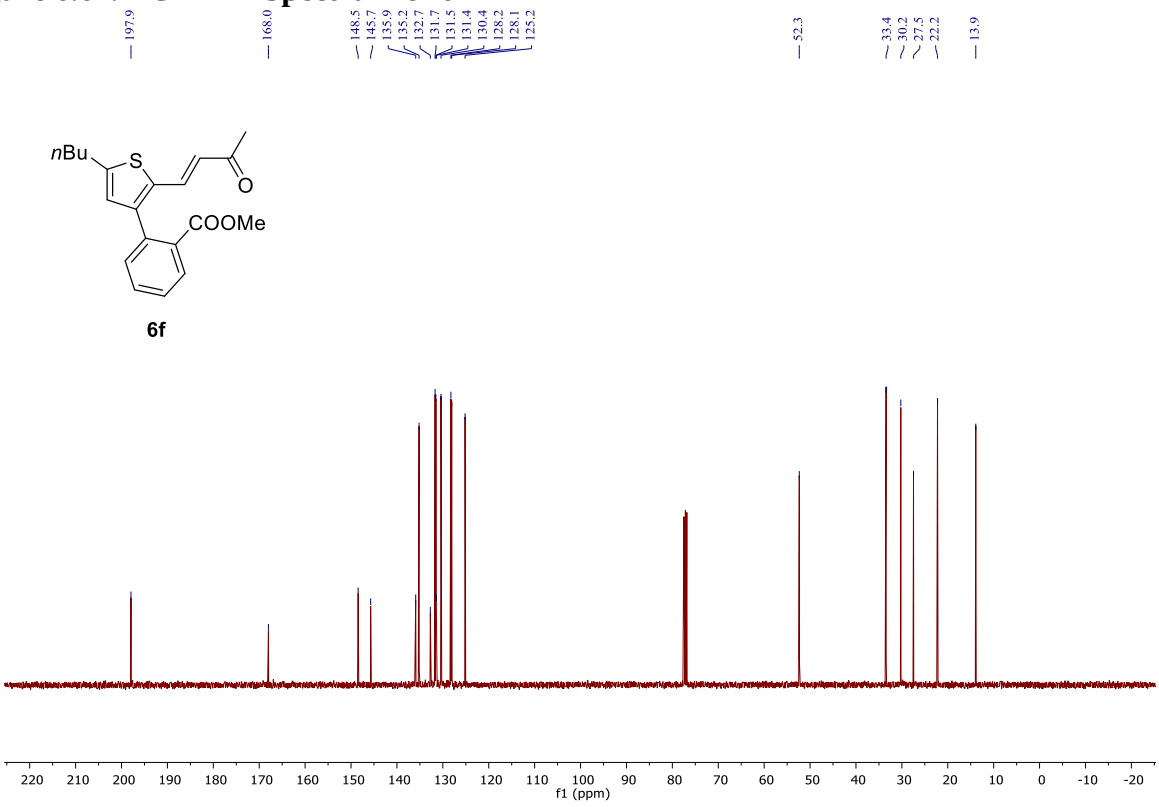

Figure 6.68. ^{1}H NMR Spectrum of 6g

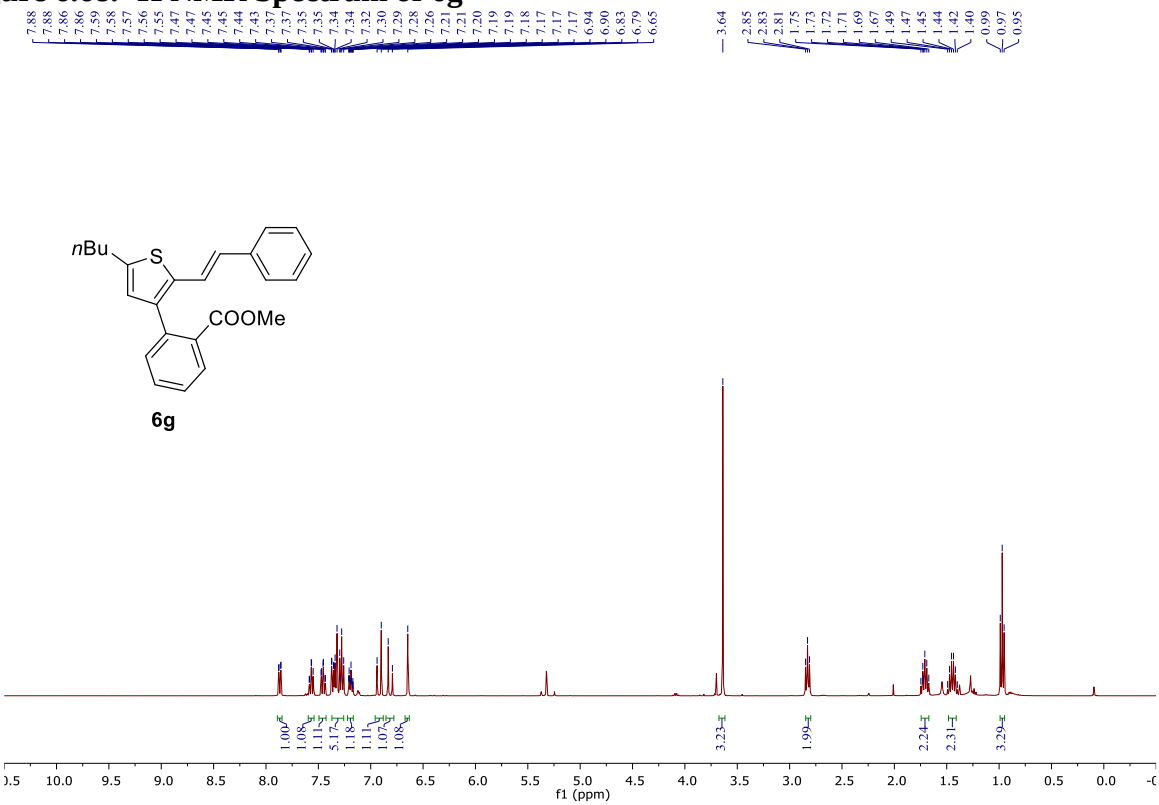

Figure 6.69. ^{13}C NMR Spectrum of 6g

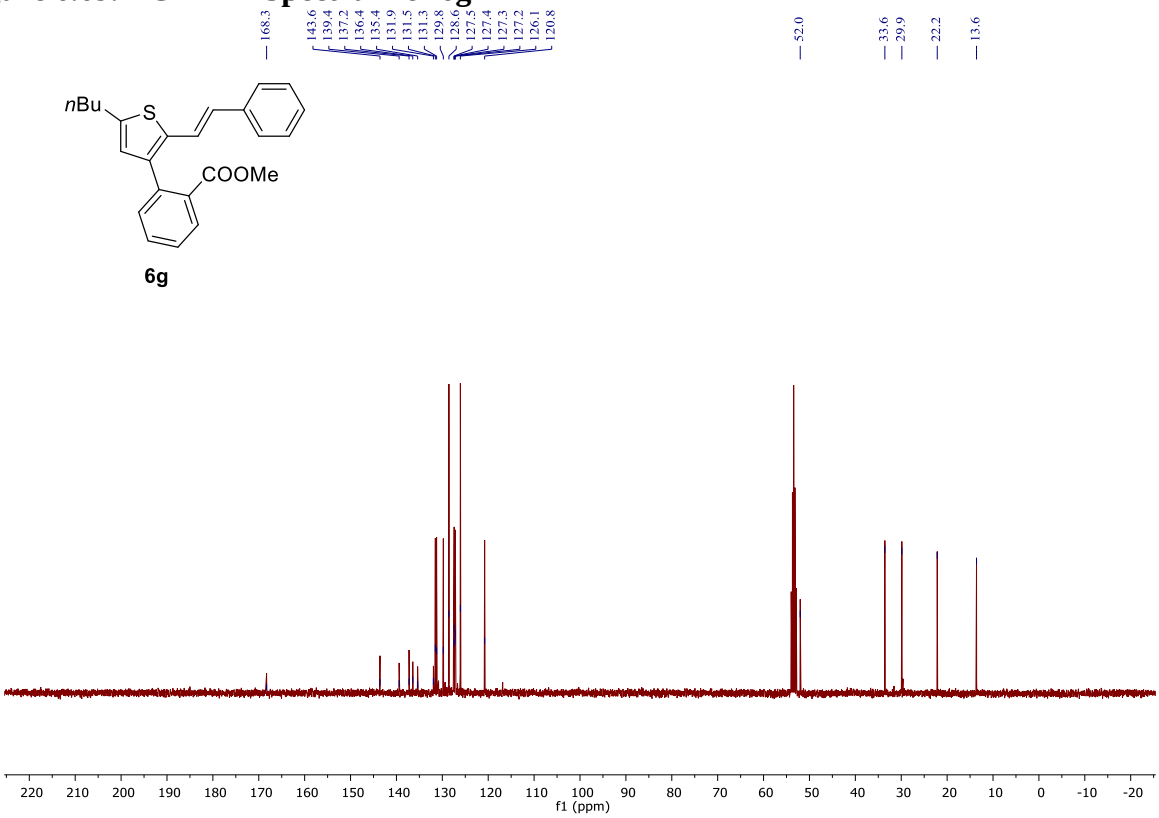

Figure 6.70. ^{1}H NMR Spectrum of 7a

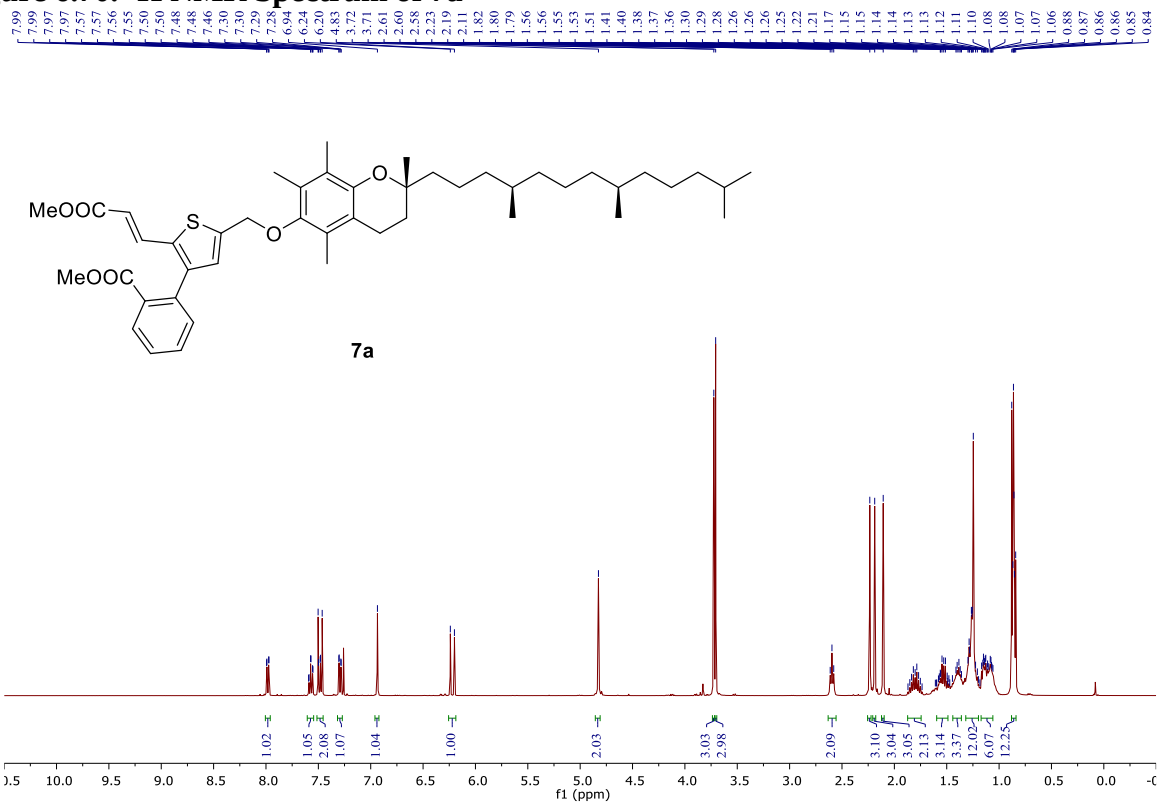

Figure 6.71. ^{13}C NMR Spectrum of 7a

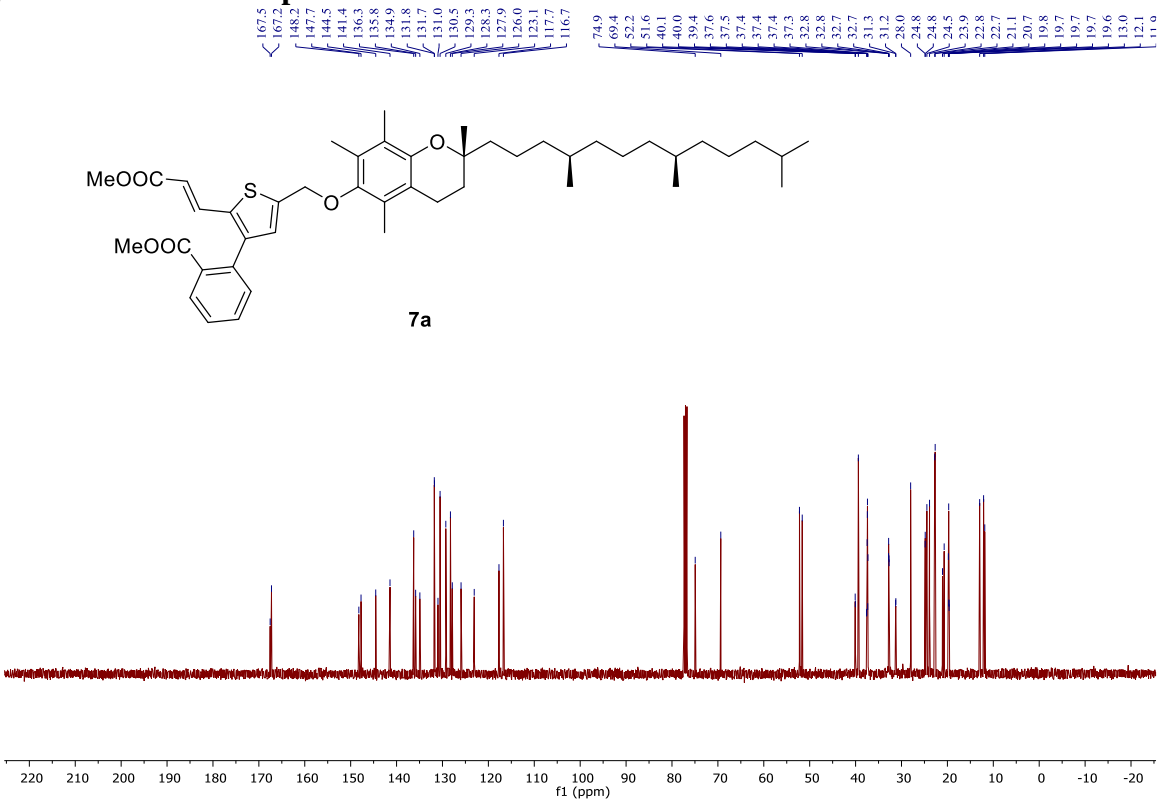

Figure 6.72. ^{1}H NMR Spectrum of 7b

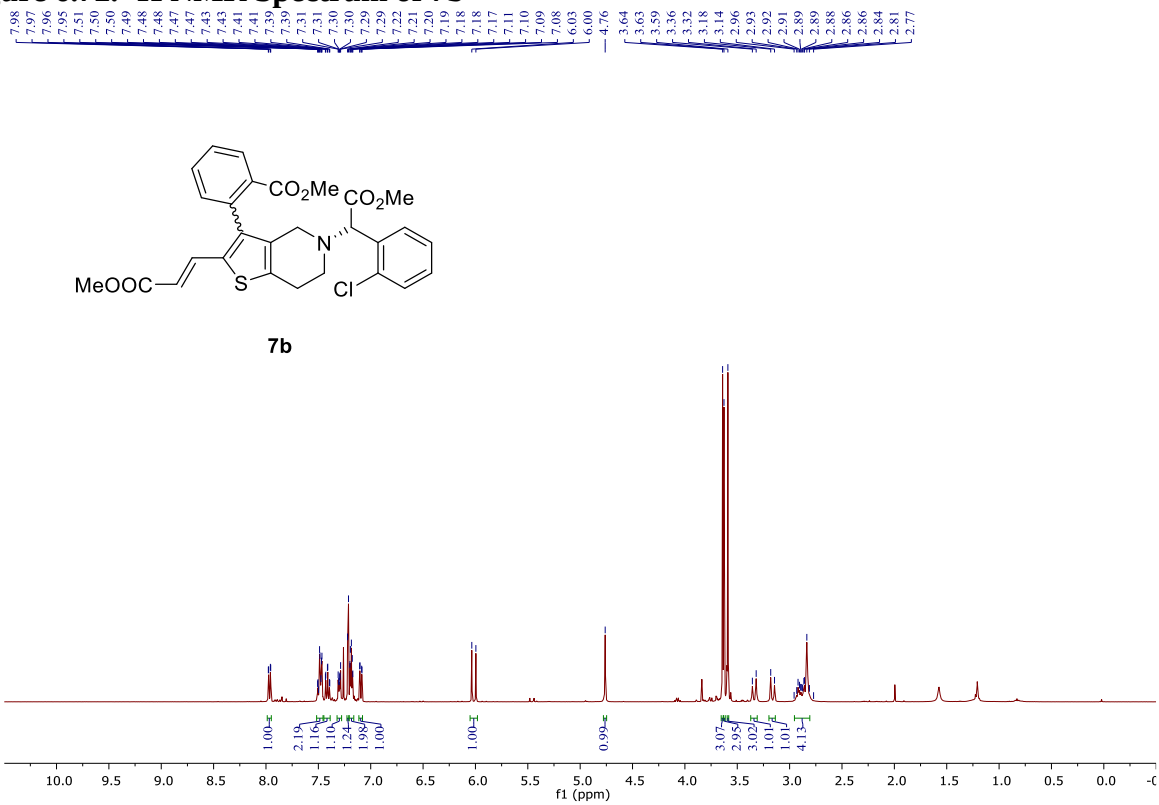

Figure 6.73. ^{13}C NMR Spectrum of 7b

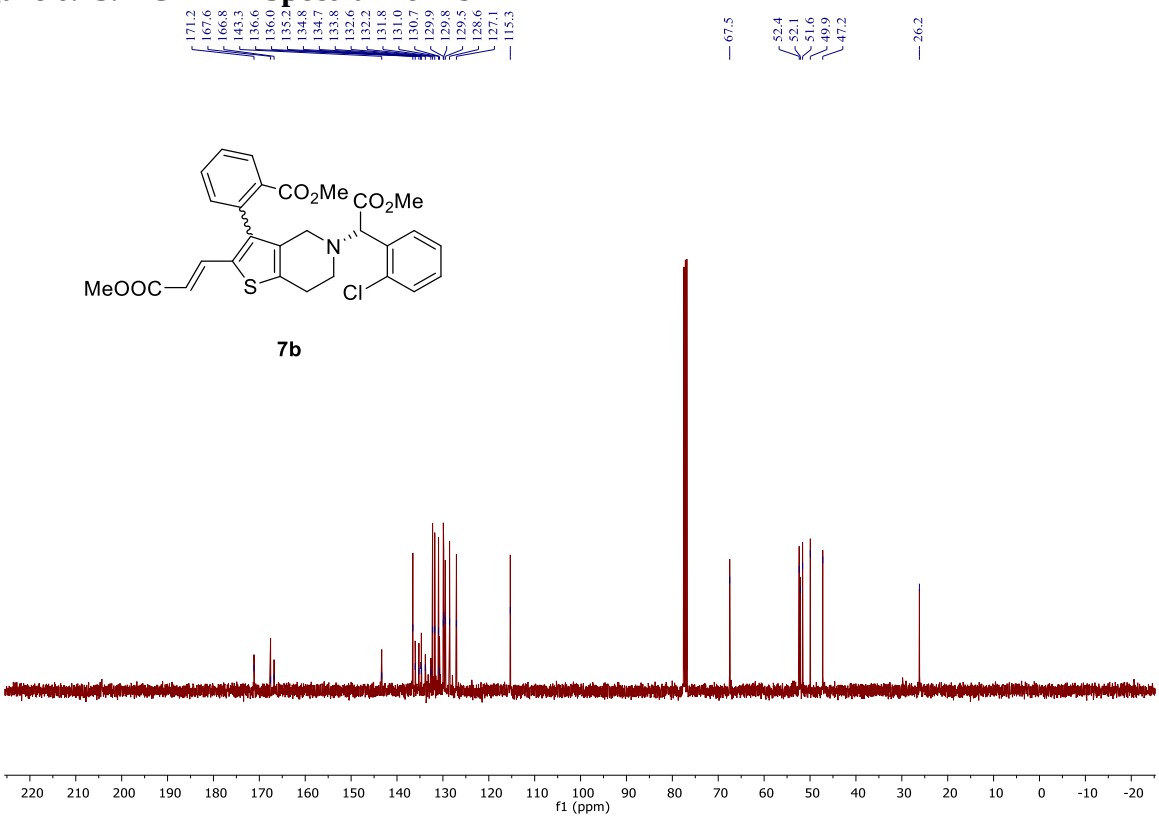

Figure 6.74. ^{1}H NMR Spectrum of 7b'

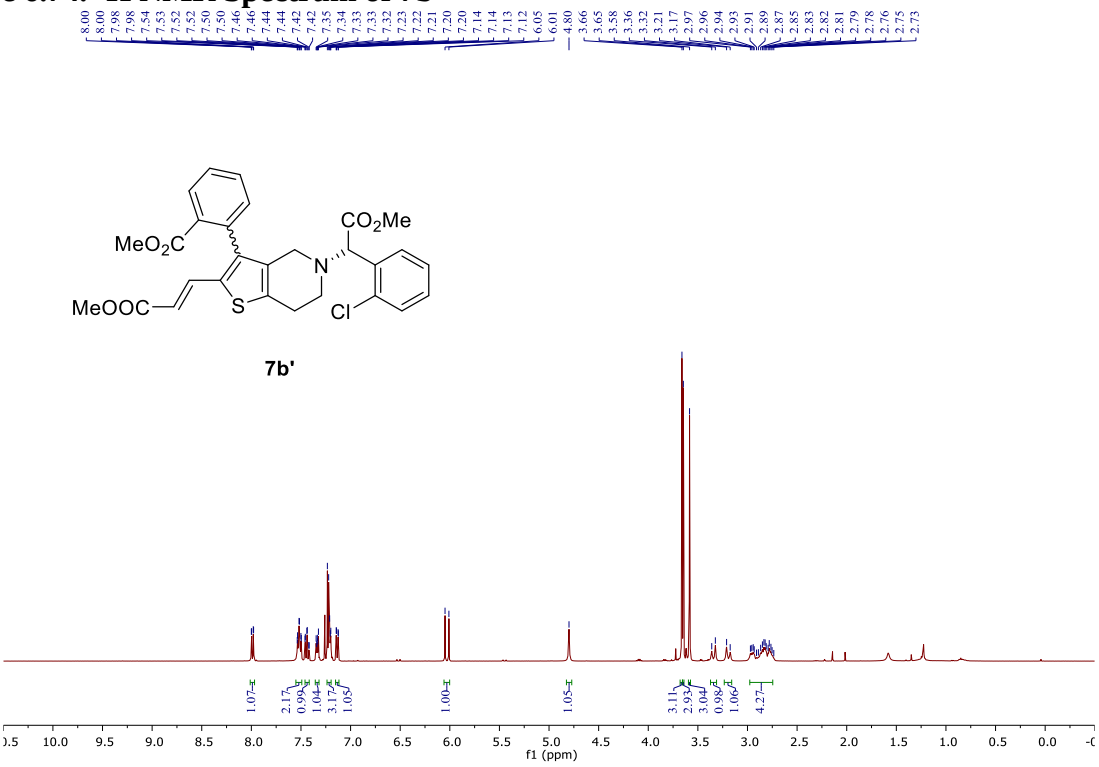

Figure 6.75. ^{13}C NMR Spectrum of 7b'

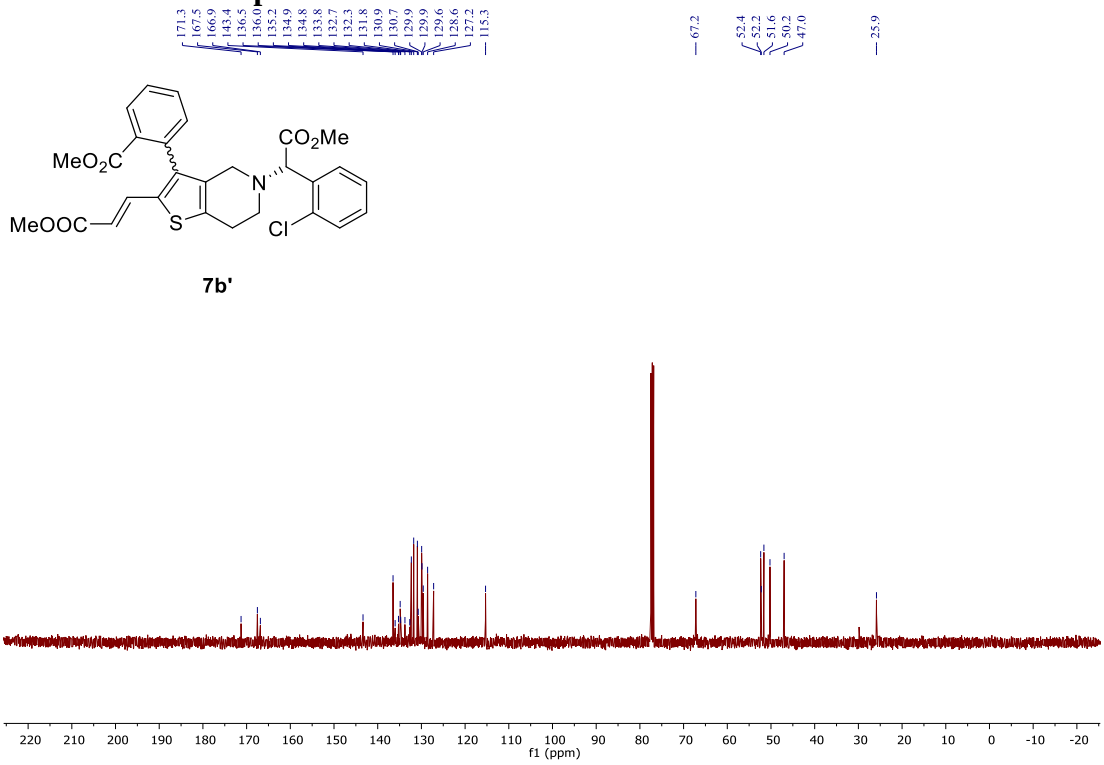

Figure 6.76. ^{1}H NMR Spectrum of 7c

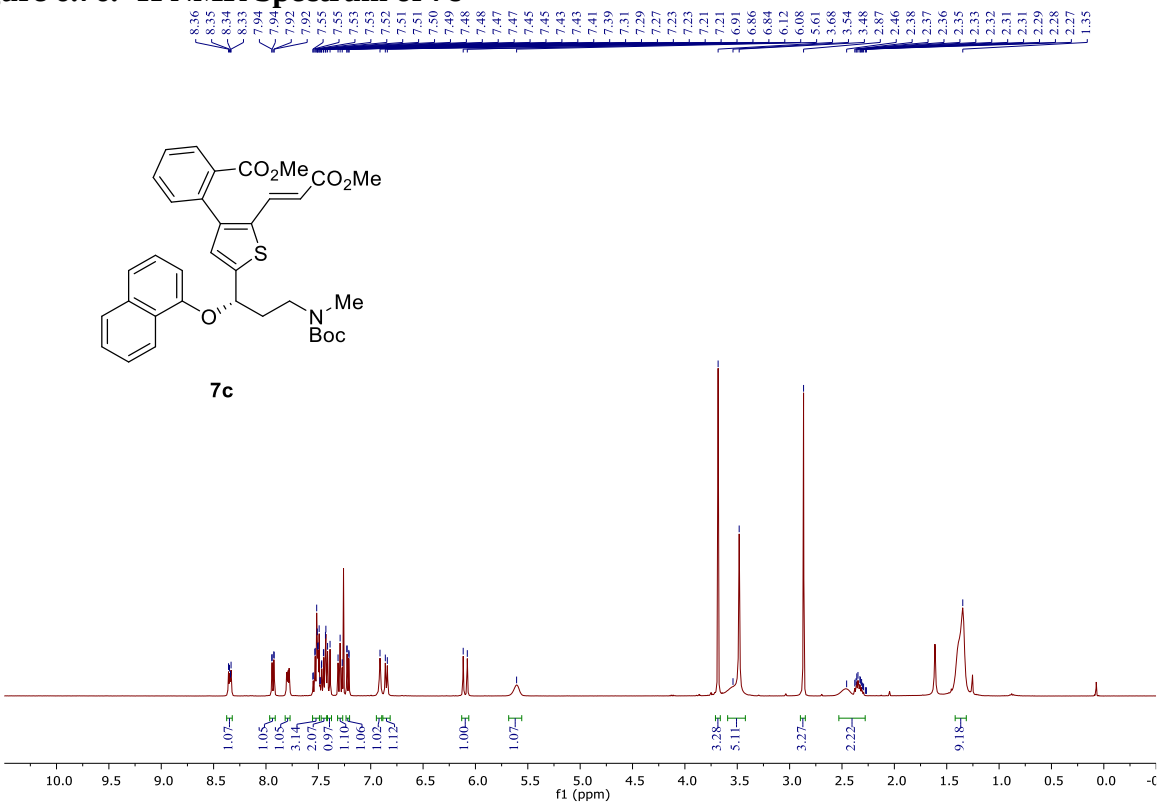

Figure 6.77. ^{13}C NMR Spectrum of 7c

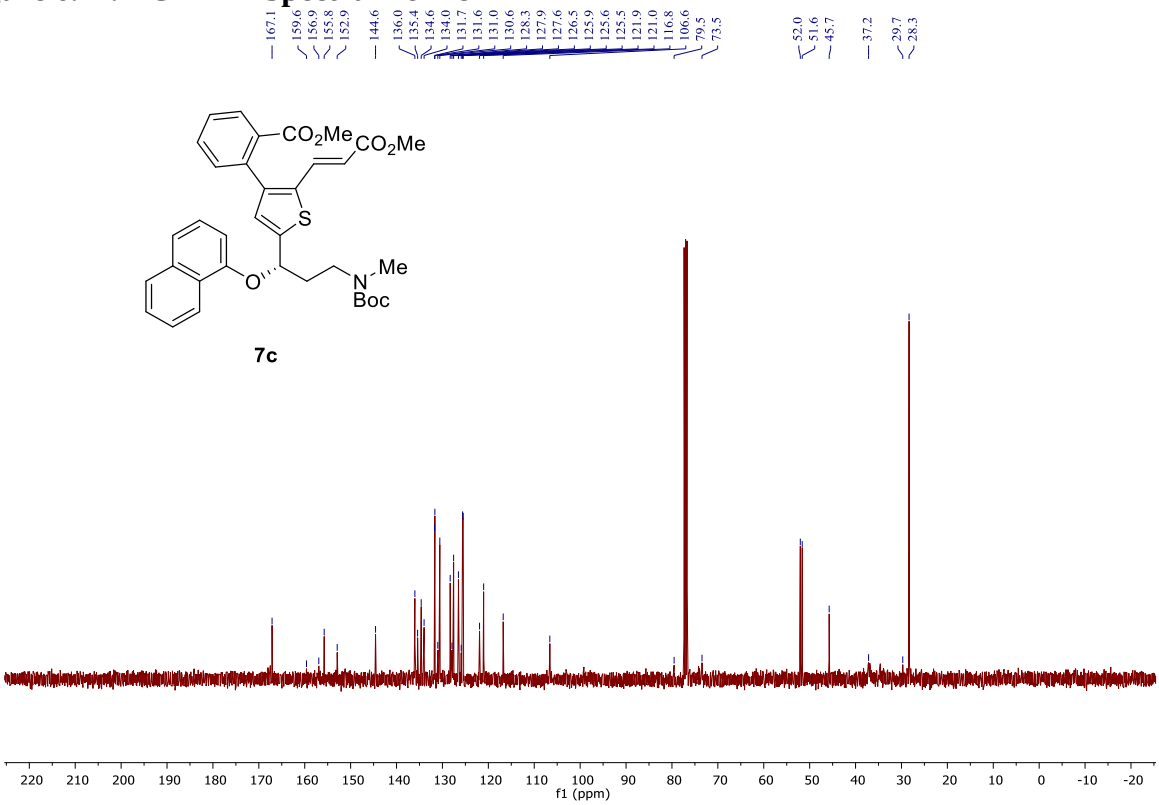

Figure 6.78. ^{1}H NMR Spectrum of 7d

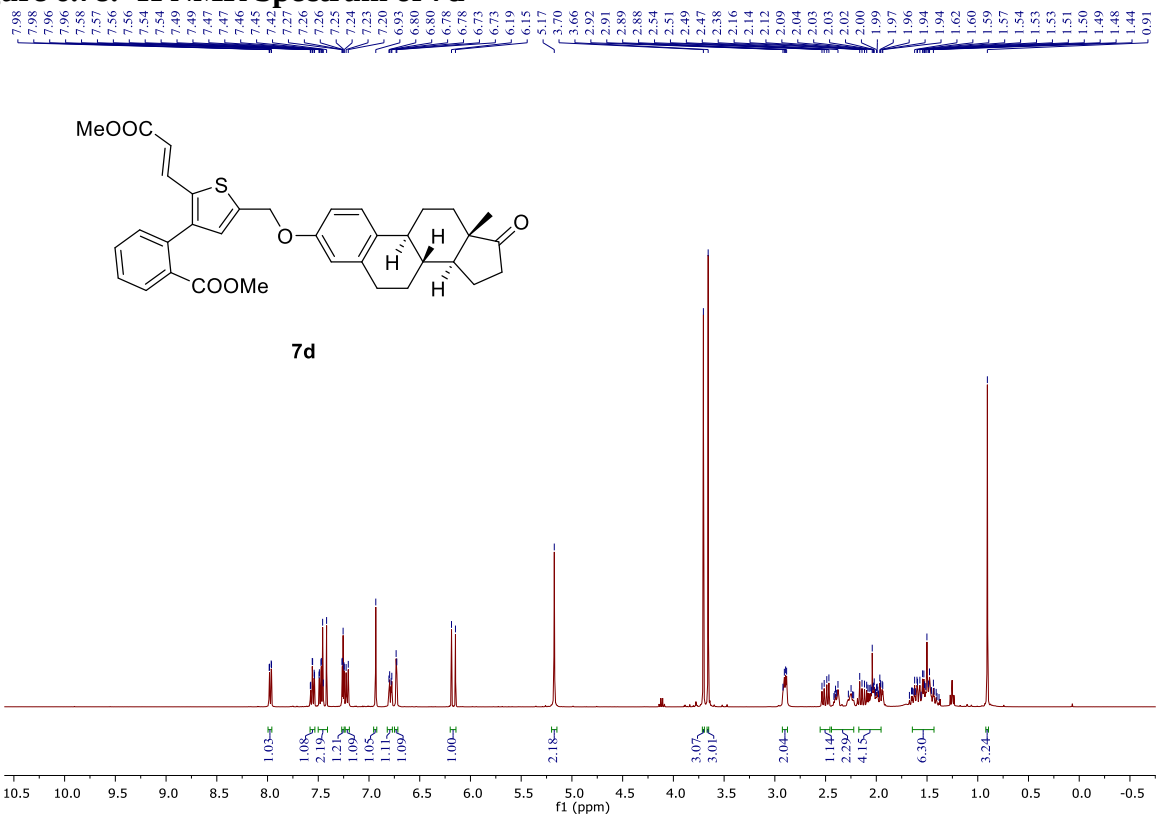

Figure 6.79. ^{13}C NMR Spectrum of 7d

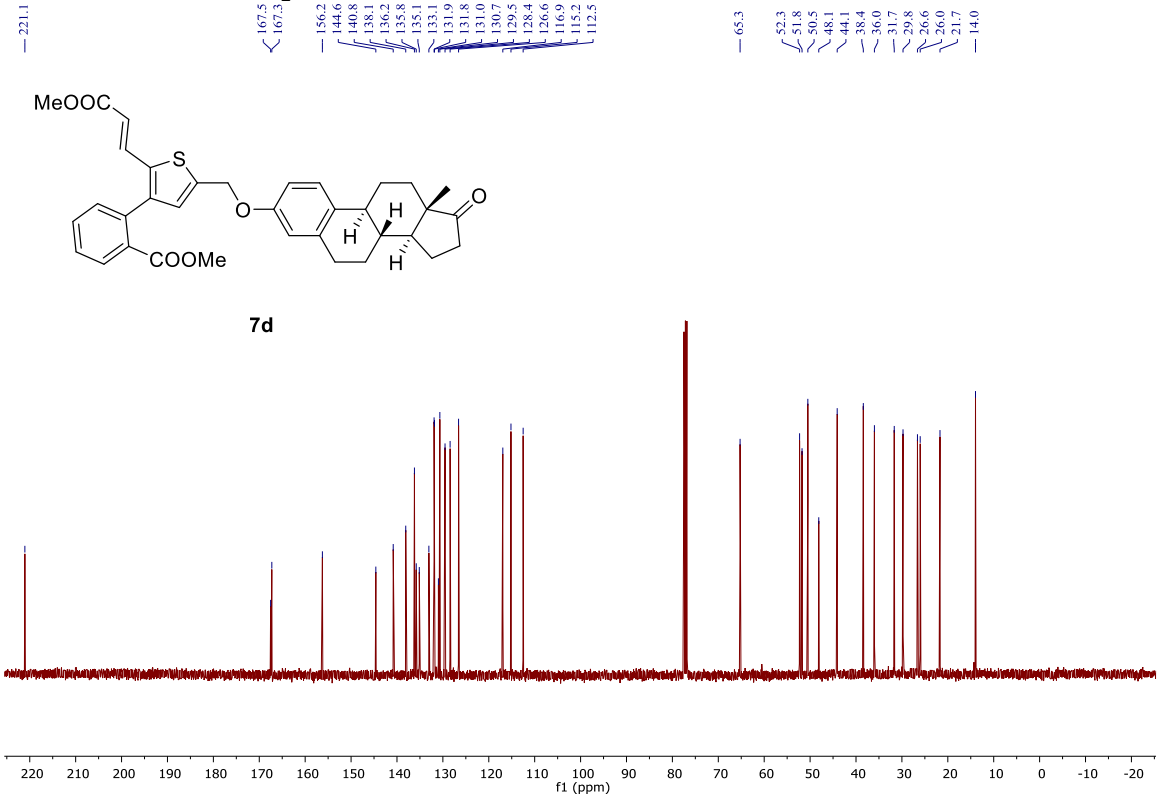

Figure 6.80. ^{1}H NMR Spectrum of 7e

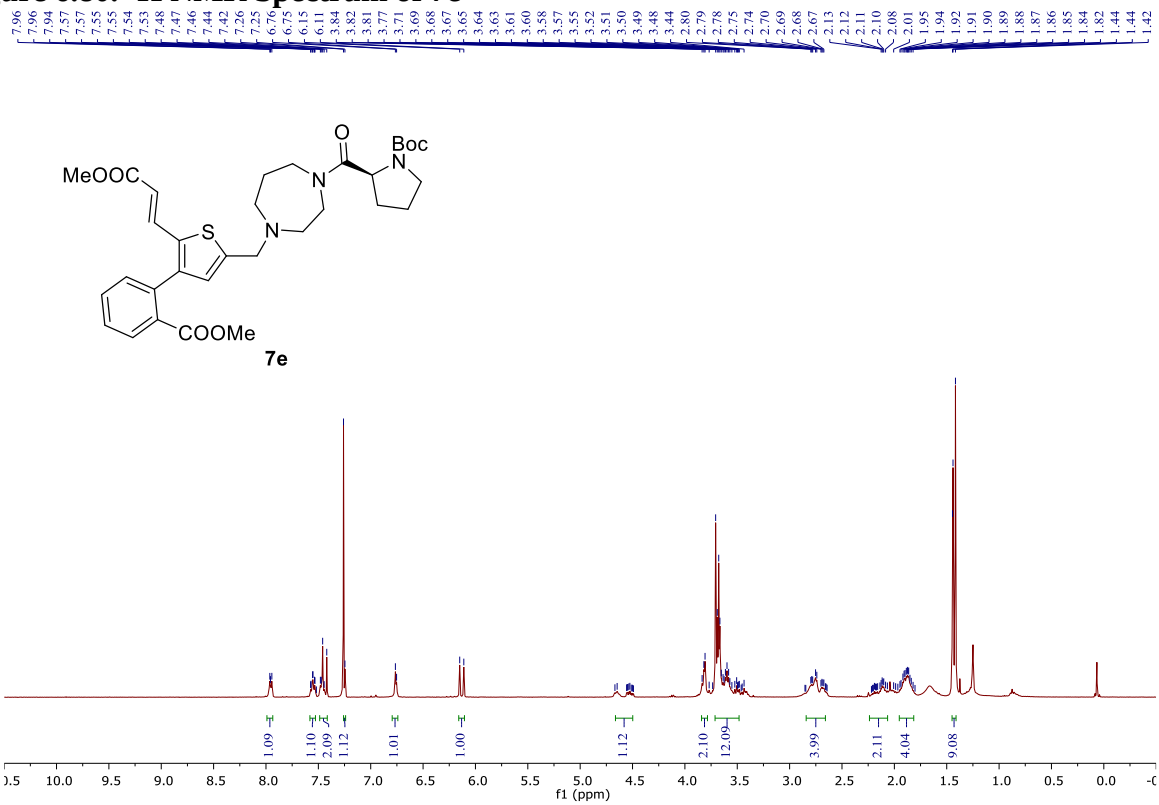

Figure 6.81. ^{13}C NMR Spectrum of 7e

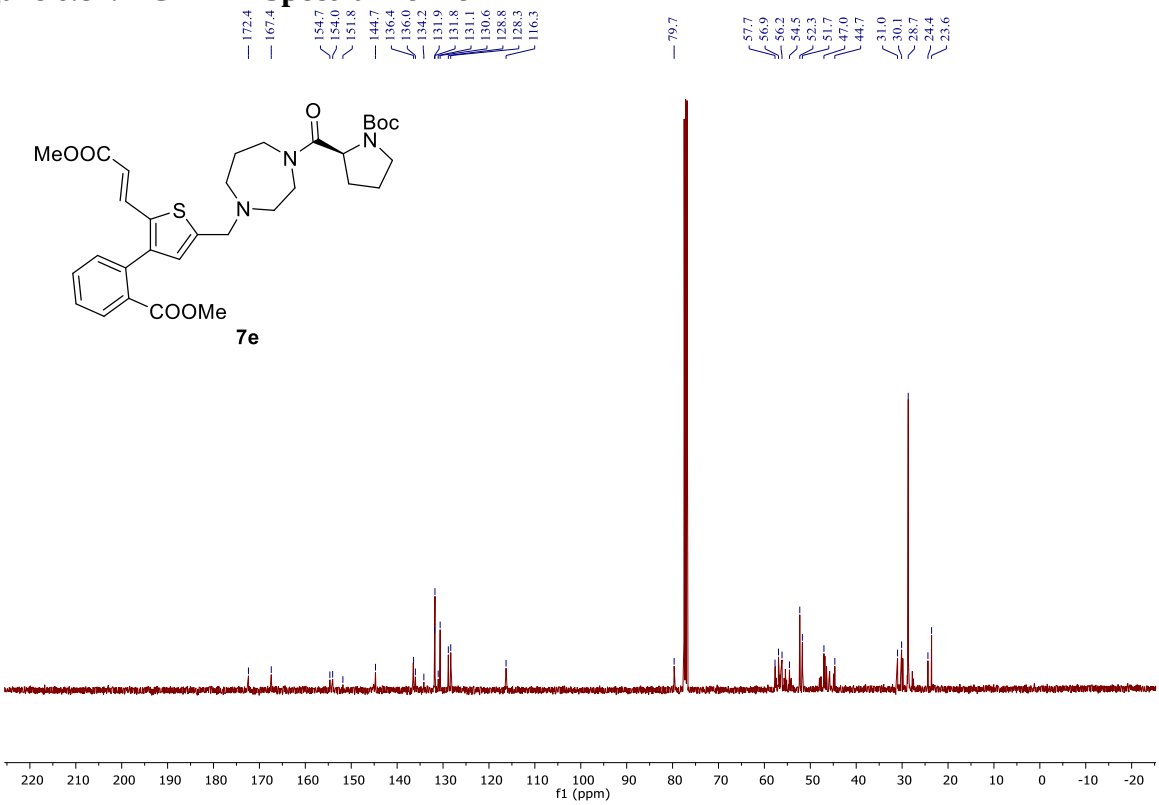

Figure 6.82. ^{1}H NMR Spectrum of 9a

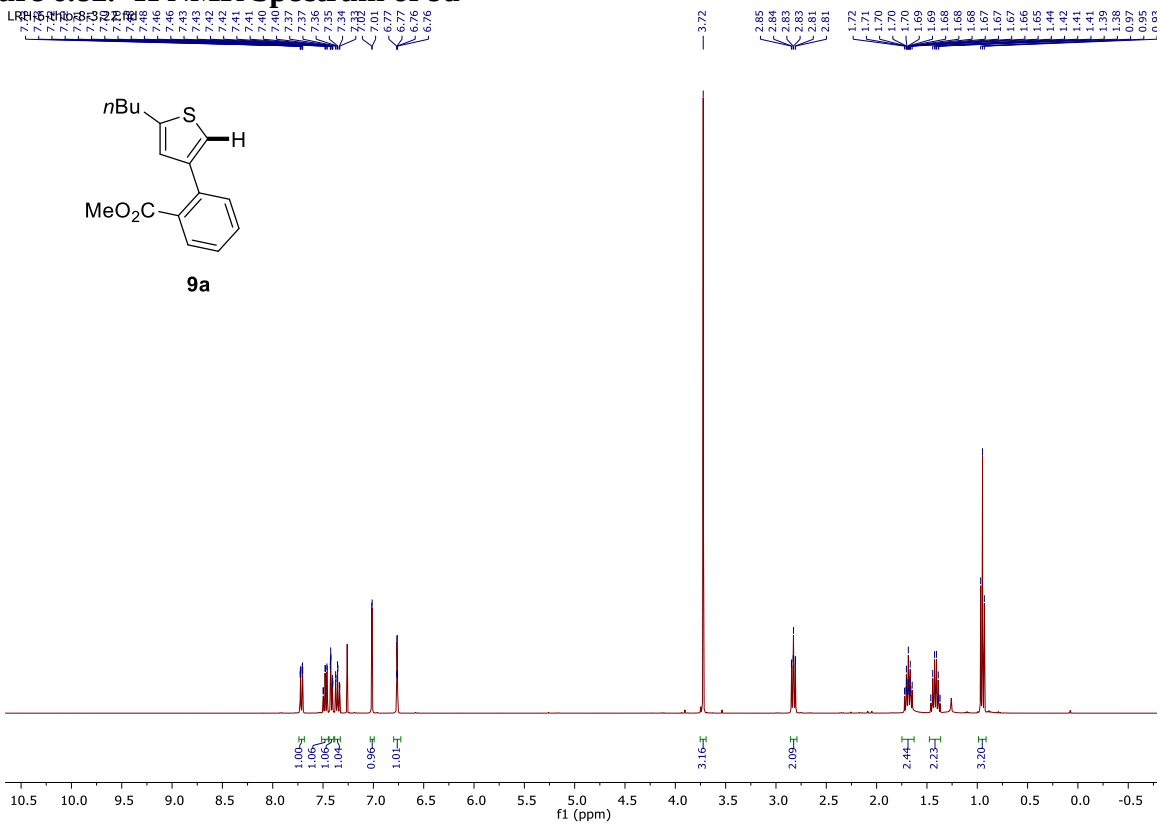

Figure 6.83. ^{13}C NMR Spectrum of 9a

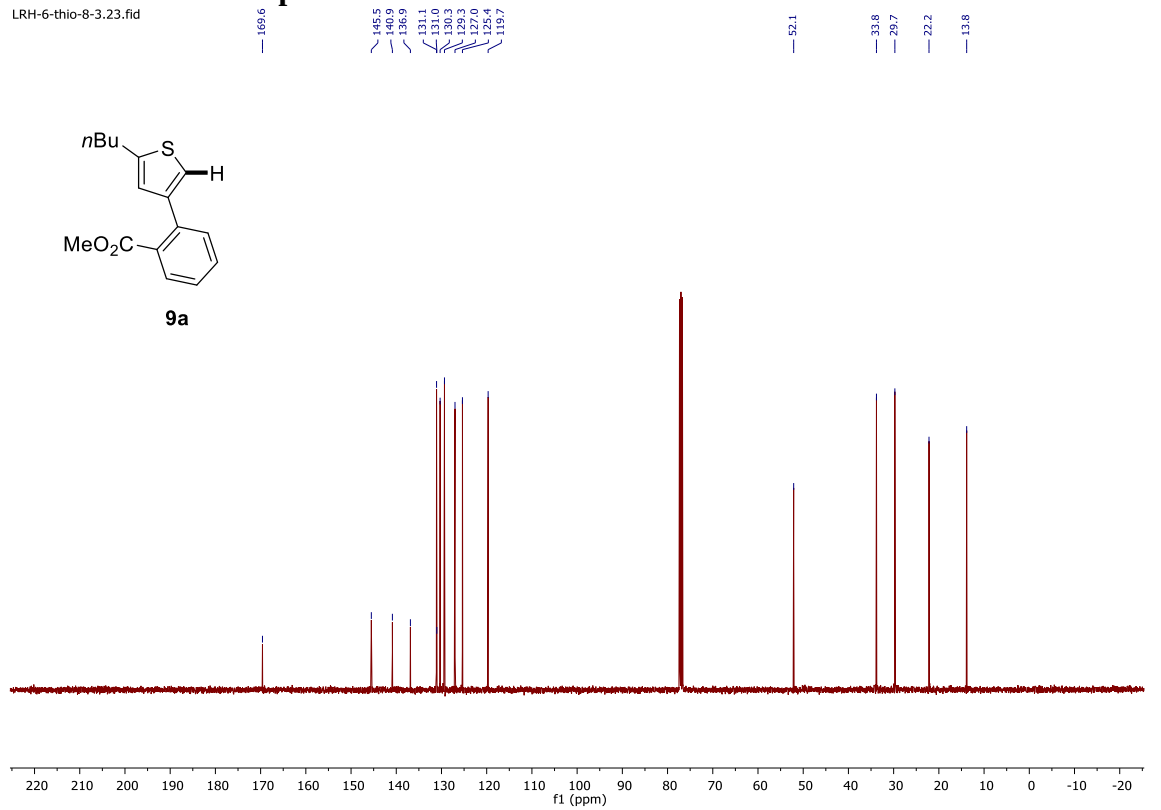

Figure 6.84. ^{1}H NMR Spectrum of 1r

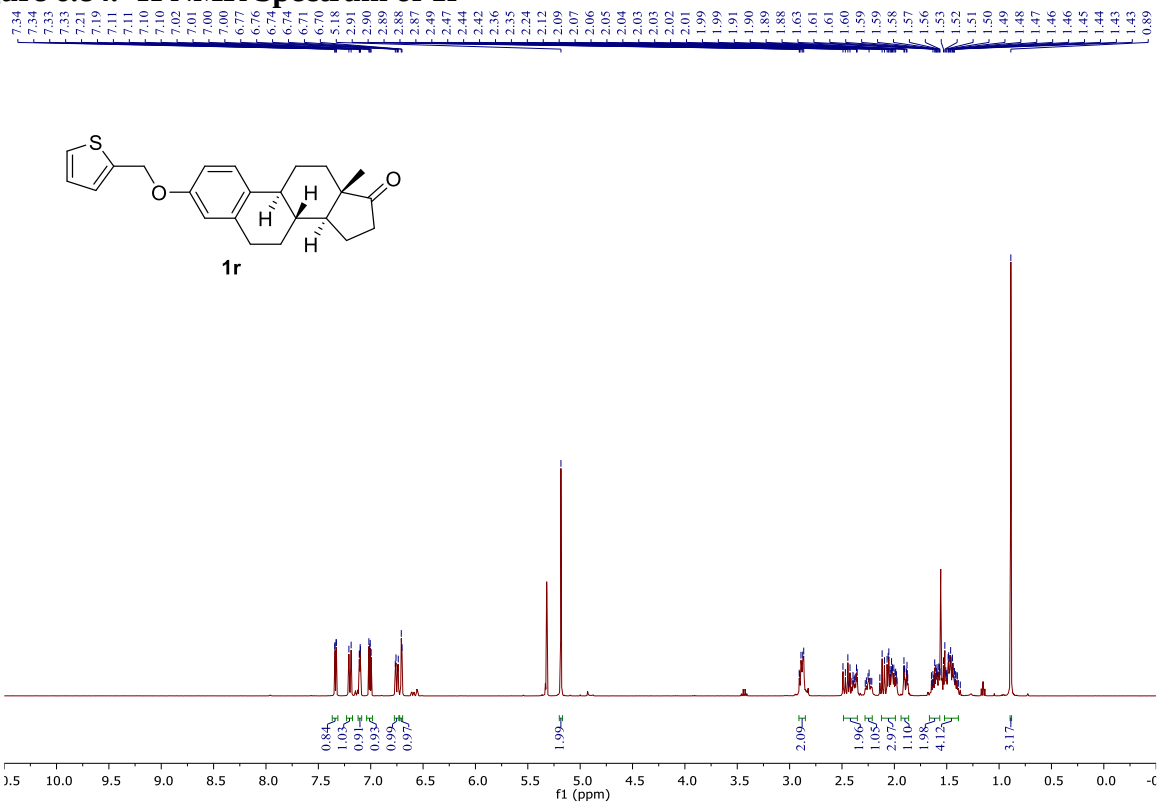

Figure 6.85. ^{13}C NMR Spectrum of 1r

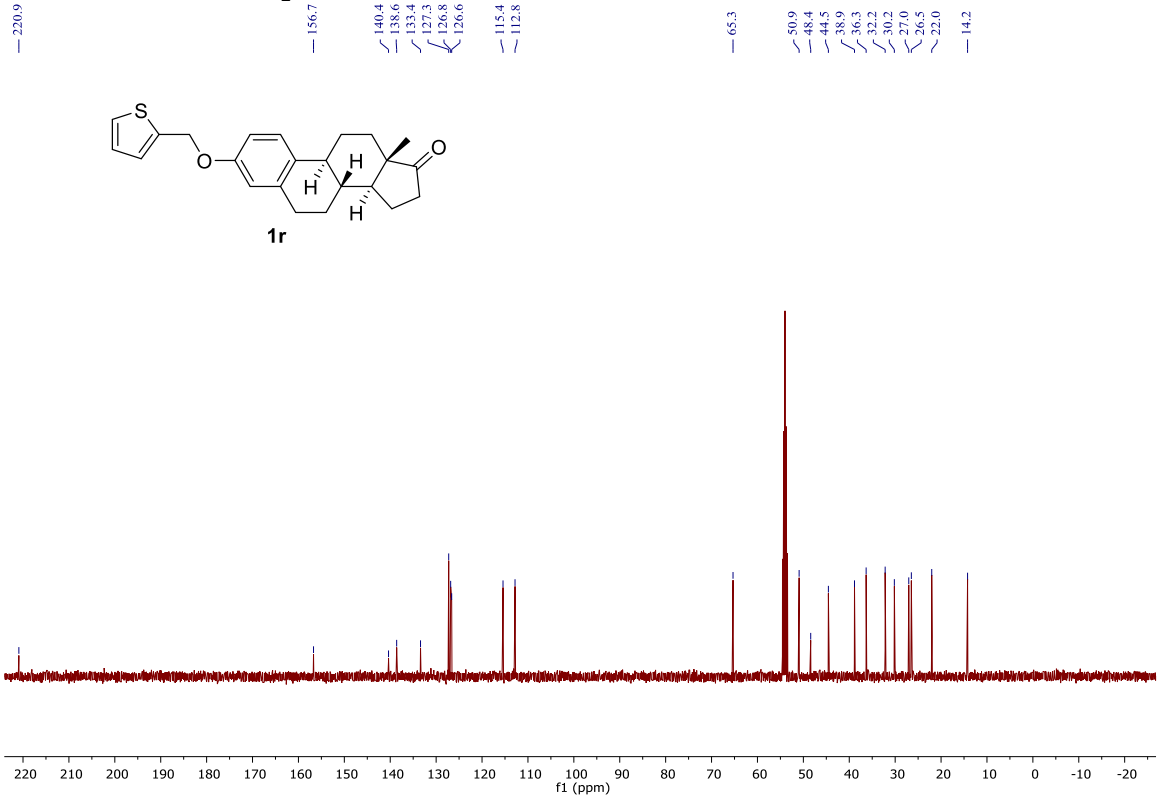

Figure 6.86. ^{1}H NMR Spectrum of 1o

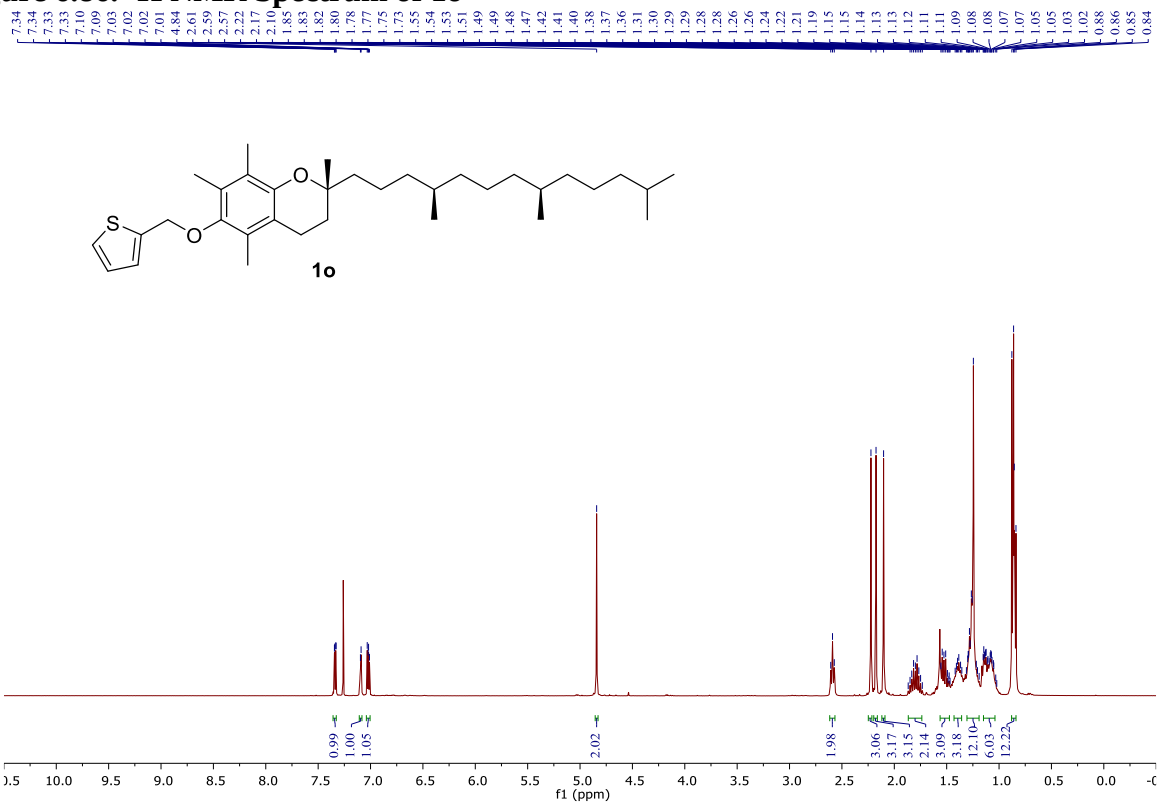

Figure 6.87. ^{13}C NMR Spectrum of 1o

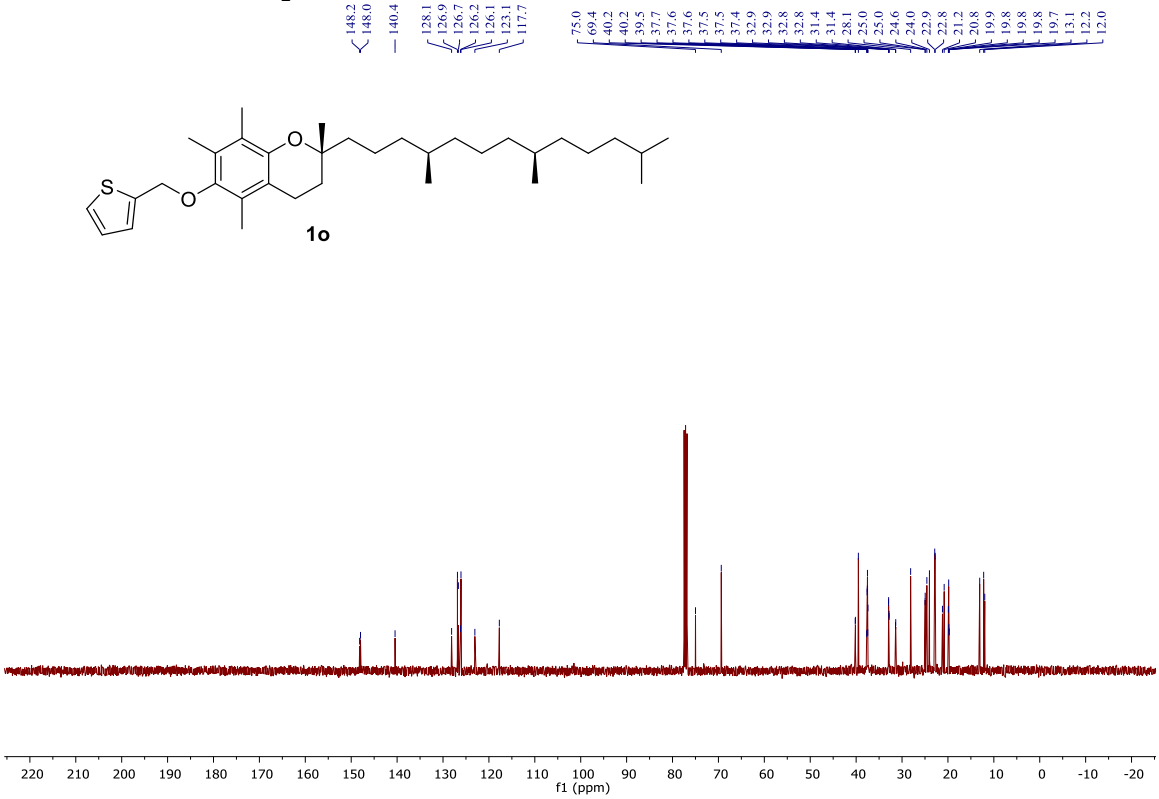

Figure 6.88. ^{1}H NMR Spectrum of 1m

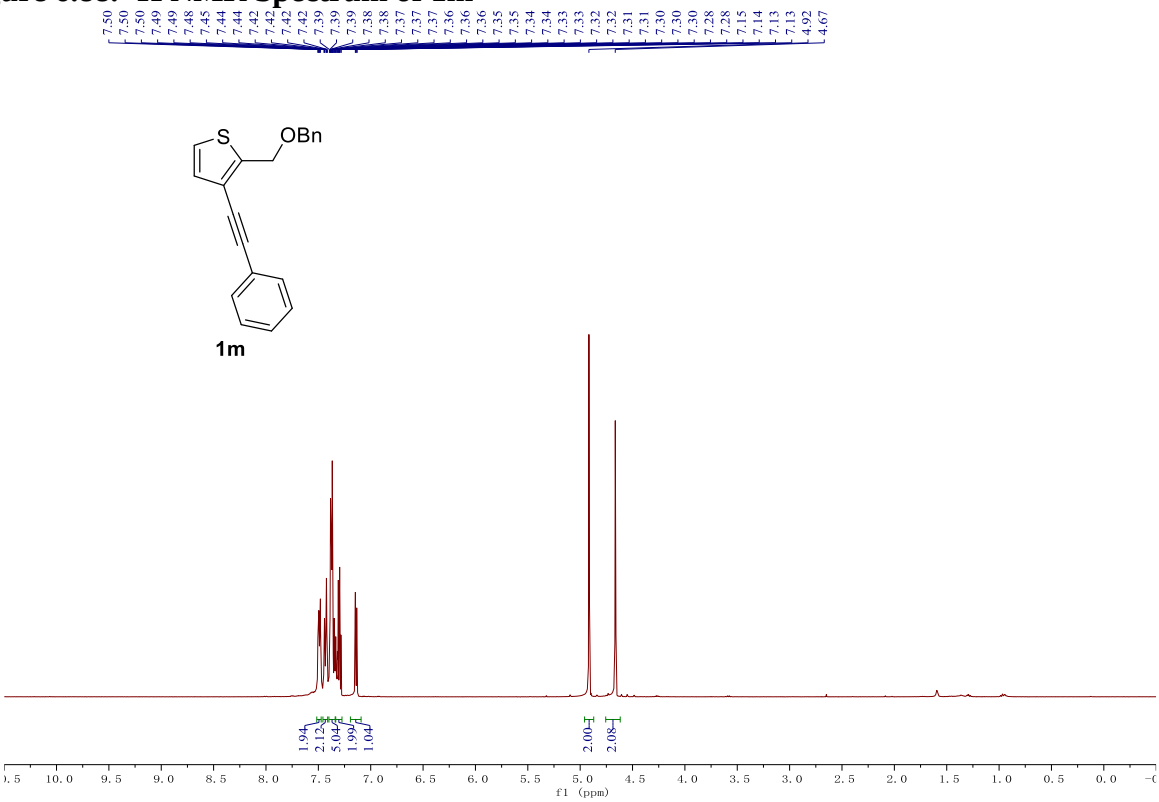

Figure 6.89. ^{13}C NMR Spectrum of 1m

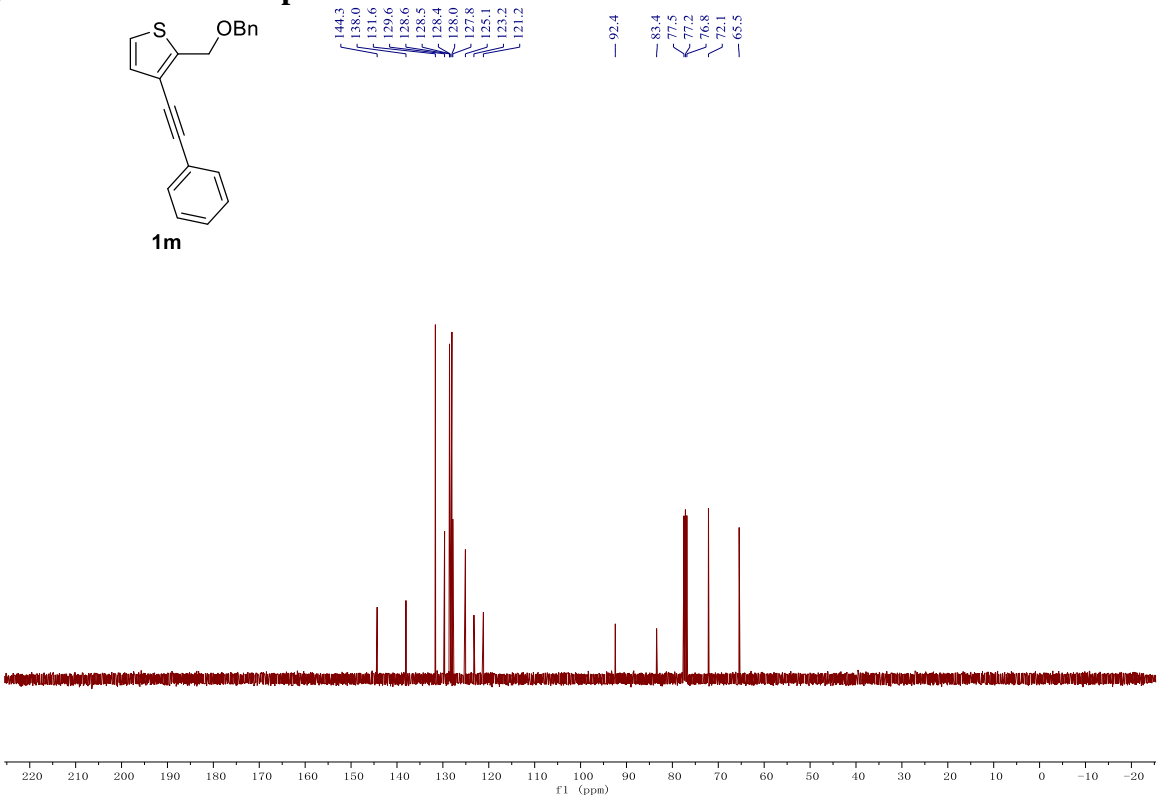

Figure 6.90. ^{1}H NMR Spectrum of 1n

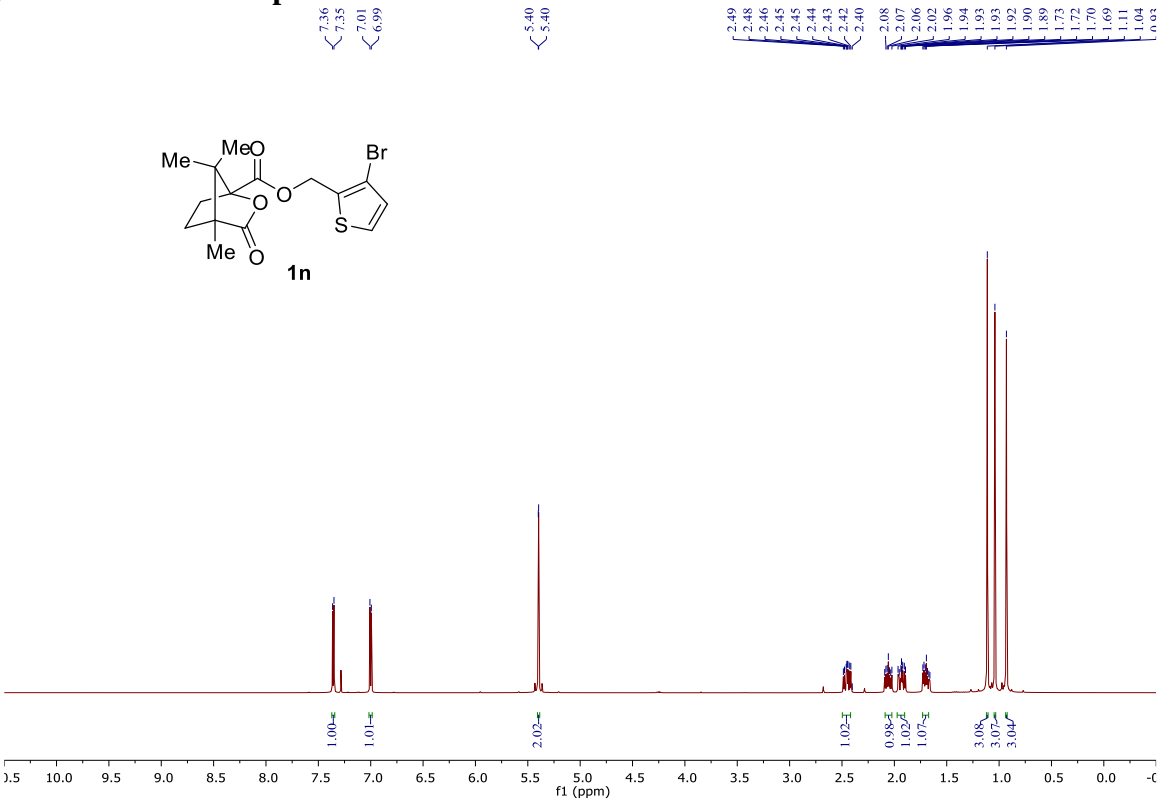

Figure 6.91. ^{13}C NMR Spectrum of 1n

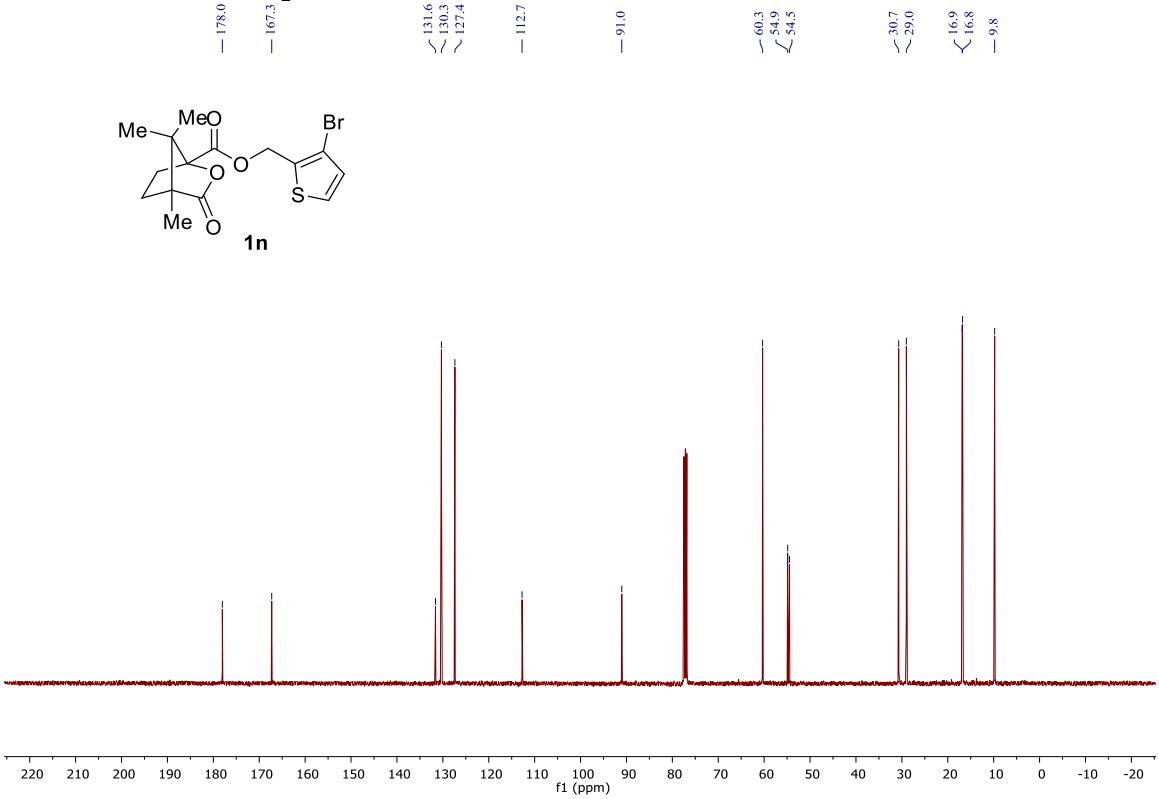

Figure 6.92. ^{1}H NMR Spectrum of 1s

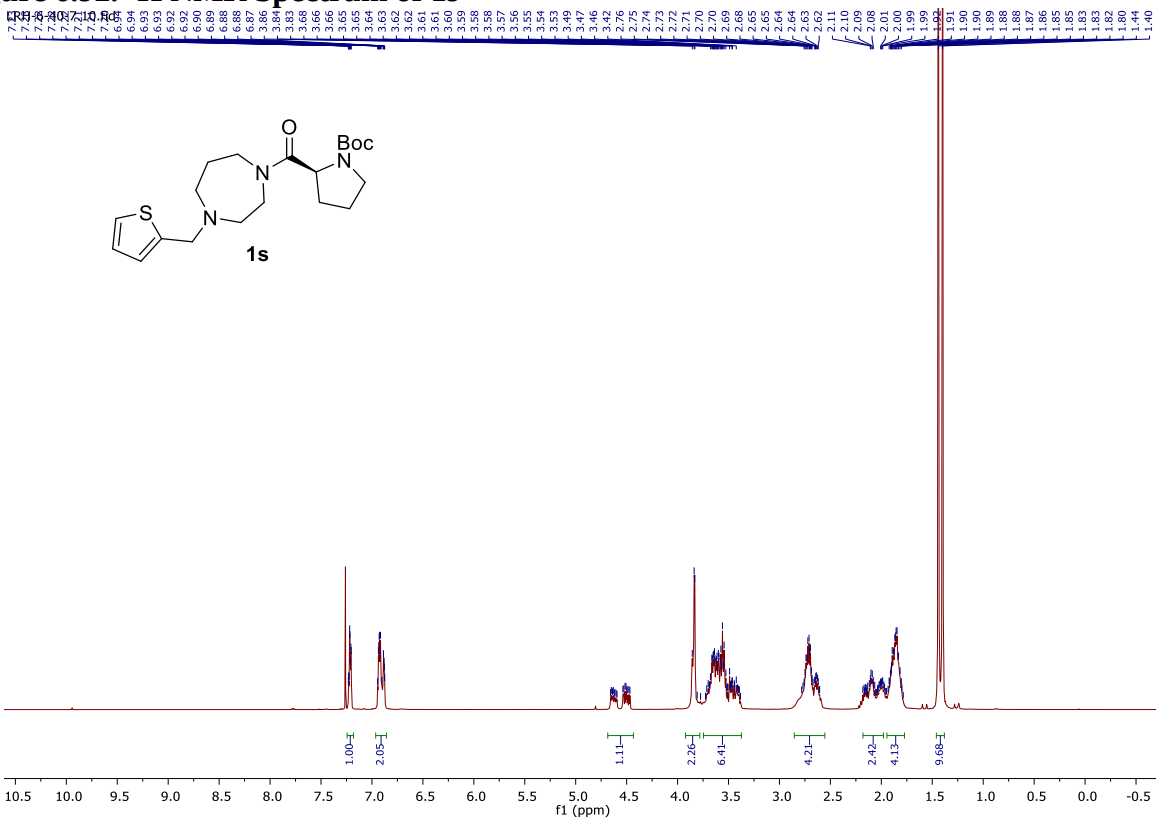

Figure 6.93. ^{13}C NMR Spectrum of 1s

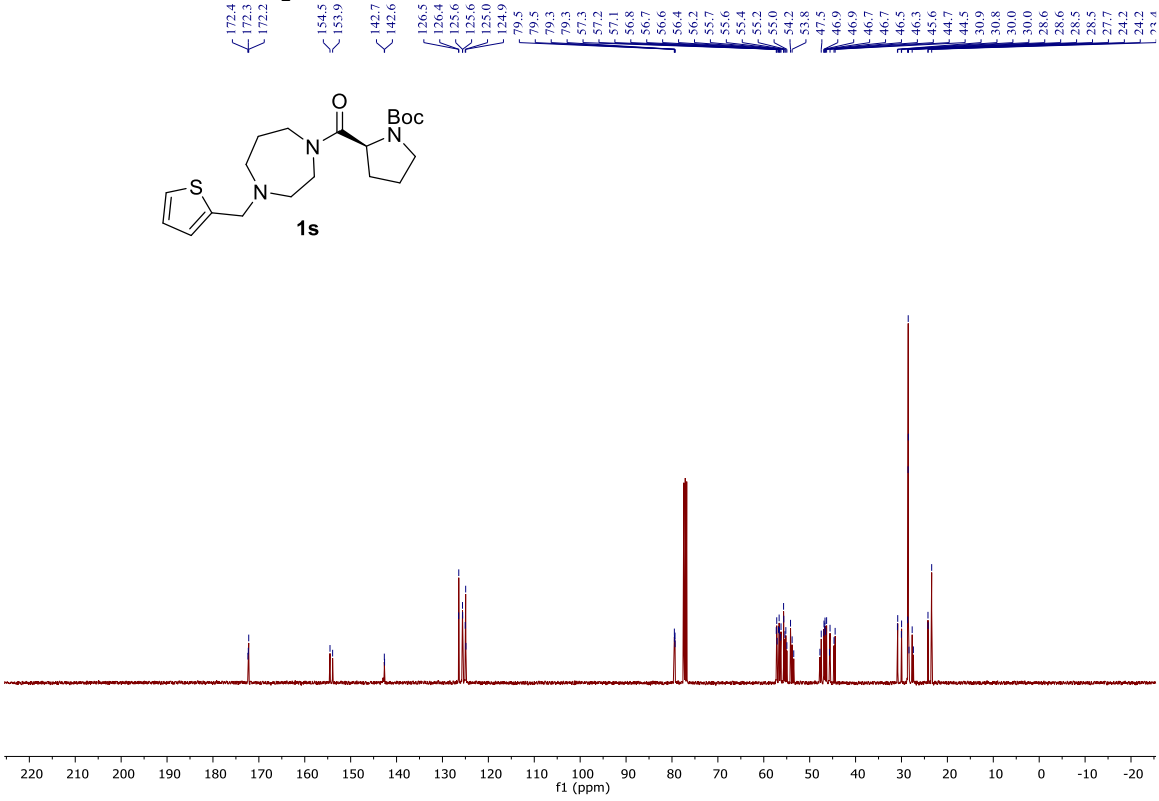

Figure 6.94. ^{1}H NMR Spectrum of 8

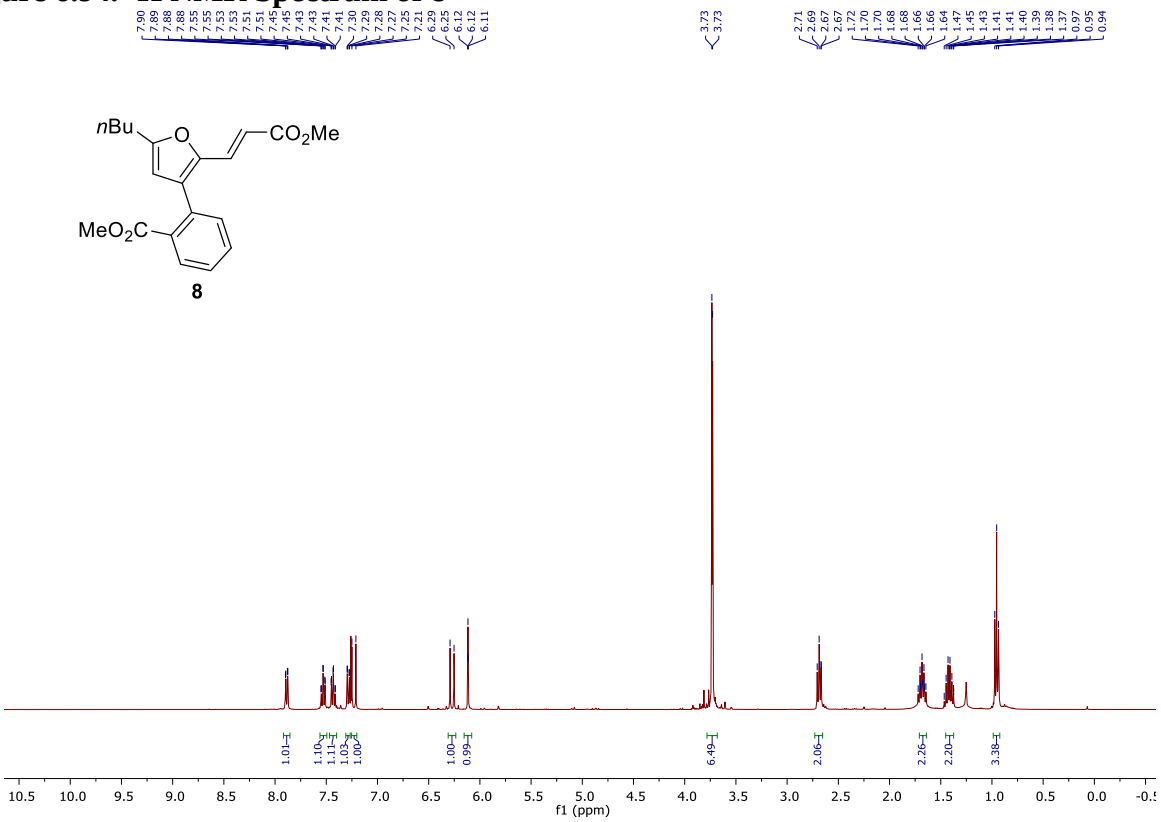

Figure 6.95. ^{13}C NMR Spectrum of 8

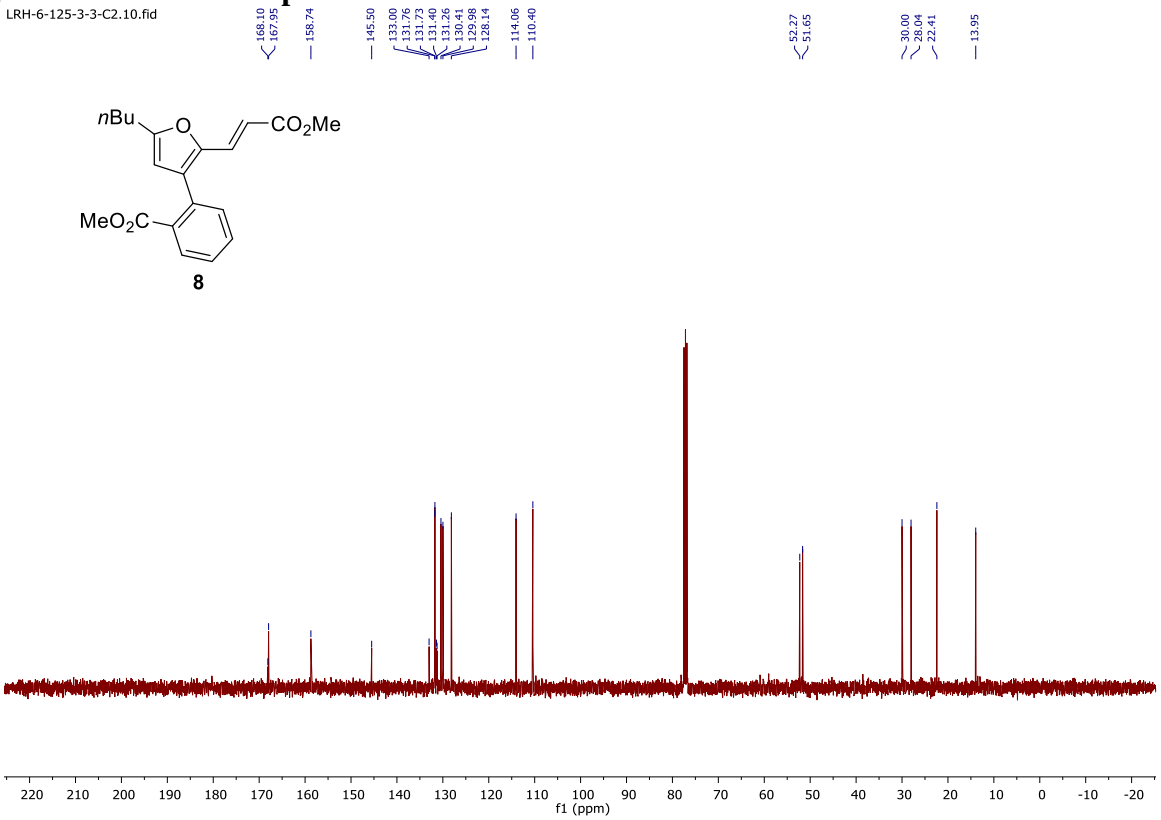

6.6 References

(1) Joule, J. A.; Mills, K., *Heterocyclic Chemistry*; Wiley: Weinheim, **2013**.

(2) For recent reviews, see: (a) Mkhalid, I. A. I.; Barnard, J. H.; Marder, T. B.; Murphy, J. M.; Hartwig, J. F., C−H Activation for the Construction of C−B Bonds. *Chem. Rev.* **2010**, *110*, 890-931. (b) Yeung, C. S.; Dong, V. M., Catalytic Dehydrogenative Cross-Coupling: Forming Carbon−Carbon Bonds by Oxidizing Two Carbon−Hydrogen Bonds. *Chem. Rev.* **2011**, *111*, 1215-1292. (c) Lyons, T. W.; Sanford, M. S., Palladium-Catalyzed Ligand-Directed C−H Functionalization Reactions. *Chemical Reviews* **2010**, *110*, 1147-1169. (d) Hartwig, J. F., Catalyst-Controlled Site-Selective Bond Activation. *Accounts of Chemical Research* **2017**, *50*, 549-555. (e) Toste, F. D.; Sigman, M. S.; Miller, S. J., Pursuit of Noncovalent Interactions for Strategic Site-Selective Catalysis. *Acc. Chem. Res.* **2017**, *50*, 609-615. (f) Rouquet, G.; Chatani, N., Catalytic Functionalization of C(sp2)−H and C(sp3)−H Bonds by Using Bidentate Directing Groups. *Angew. Chem. Int. Ed.* **2013**, *52*, 11726-11743. (g) Huang, Z.; Dong, G., Site-Selectivity Control in Organic Reactions: A Quest To Differentiate Reactivity among the Same Kind of Functional Groups. *Accounts of Chemical Research* **2017**, *50*, 465-471.

(3) For selected examples, see: (a) Joo, J. M.; Touré, B. B.; Sames, D., C−H Bonds as Ubiquitous Functionality: A General Approach to Complex Arylated Imidazoles via Regioselective Sequential Arylation of All Three C−H Bonds and Regioselective N-Alkylation Enabled by SEM-Group Transposition. *J. Org. Chem.* **2010**, *75*, 4911-4920. (b) Guo, P.; Joo, J. M.; Rakshit, S.; Sames, D., C–H Arylation of Pyridines: High Regioselectivity as a Consequence of the Electronic Character of C–H Bonds and Heteroarene Ring. *J. Am. Chem. Soc.* **2011**, *133*, 16338-16341. (c) Bae, S.; Jang, H.-L.; Jung, H.; Joo, J. M., Catalytic C–H Allylation and Benzylation of Pyrazoles. *J. Org. Chem.* **2015**, *80*, 690-697. (d) Kim, O. S.; Jang, J. H.; Kim, H. T.; Han, S. J.; Tsui, G. C.; Joo, J.

M., Synthesis of Fluorescent Indazoles by Palladium-Catalyzed Benzannulation of Pyrazoles with Alkynes. *Org. Lett.* **2017**, *19*, 1450-1453. (e) Yamamoto, K.; Li, J.; Garber, J. A. O.; Rolfes, J. D.; Boursalian, G. B.; Borghs, J. C.; Genicot, C.; Jacq, J.; van Gastel, M.; Neese, F.; Ritter, T., Palladium-catalysed electrophilic aromatic C–H fluorination. *Nature* **2018**, *554*, 511. (b) Berger, F.; Plutschack, M. B.; Riegger, J.; Yu, W.; Speicher, S.; Ho, M.; Frank, N.; Ritter, T., Site-selective and versatile aromatic C−H functionalization by thianthrenation. *Nature* **2019**, *567*, 223-228. (c) Cheng, C.; Hartwig, J. F., Rhodium-Catalyzed Intermolecular C–H Silylation of Arenes with High Steric Regiocontrol. *Science* **2014**, *343*, 853.

(4) (a) Ghosh, I.; Khamrai, J.; Savateev, A.; Shlapakov, N.; Antonietti, M.; König, B., Organic semiconductor photocatalyst can bifunctionalize arenes and heteroarenes. *Science* **2019**, *365*, 360. (b) Kim, H. T.; Ha, H.; Kang, G.; Kim, O. S.; Ryu, H.; Biswas, A. K.; Lim, S. M.; Baik, M.-H.; Joo, J. M., Ligand-controlled Regiodivergent C−H Alkenylation of Pyrazoles and its Application to the Synthesis of Indazoles. *Angew. Chem. Int. Ed.* **2017**, *56* , 16262-16266. (c) Goikhman, R.; Jacques, T. L.; Sames, D., C−H Bonds as Ubiquitous Functionality: A General Approach to Complex Arylated Pyrazoles via Sequential Regioselective C-Arylation and N-Alkylation Enabled by SEM-Group Transposition. *J. Am. Chem. Soc.* **2009**, *131*, 3042-3048. (d) Okazawa, T.; Satoh, T.; Miura, M.; Nomura, M., Palladium-Catalyzed Multiple Arylation of Thiophenes. *J. Am. Chem. Soc.* **2002**, *124*, 5286-5287.

(5) (a) Ye, J.; Lautens, M., Palladium-catalysed norbornene-mediated C–H functionalization of arenes. *Nat. Chem.* **2015**, *7*, 863. (b) Della Ca', N.; Fontana, M.; Motti, E.; Catellani, M., Pd/Norbornene: A Winning Combination for Selective Aromatic Functionalization via C–H Bond Activation. *Acc. Chem. Res.* **2016**, *49*, 1389-1400. (c) Wang, J.; Dong, G., Palladium/Norbornene Cooperative Catalysis. *Chem. Rev.* **2019**, *119*, 7478-7528. (d) Cheng, H.-G.; Chen, S.; Chen, R.;

Zhou, Q., Palladium(II)-Initiated Catellani-Type Reactions. *Angew. Chem. Int. Ed.* **2019**, *58*, 5832-5844.

(6) (a) Catellani, M.; Frignani, F.; Rangoni, A., A Complex Catalytic Cycle Leading to a Regioselective Synthesis of o,o′-Disubstituted Vinylarenes. *Angew. Chem. Int. Ed.* **1997**, *36*, 119-122. (b) Motti, E.; Ippomei, G.; Deledda, S.; Catellani, M., Synthesis of Selectively Substituted ortho-Vinylbiphenyls by Palladium-Catalysed Reaction of ortho-Substituted Aryl Iodides with Olefins. *Synthesis* **2003**, *2003*, 2671-2678.

(7) Lautens, M.; Piguel, S., A New Route to Fused Aromatic Compounds by Using a Palladium-Catalyzed Alkylation – Alkenylation Sequence. *Angew. Chem. Int. Ed.* **2000**, *39*, 1045-1046.

(8) For the first Pd(II)-initated Pd/NBE catalysis, see: (a) Jiao, L.; Bach, T., Palladium-Catalyzed Direct 2-Alkylation of Indoles by Norbornene-Mediated Regioselective Cascade C–H Activation. *J. Am. Chem. Soc.* **2011**, *133*, 12990-12993. For representative works on transmetallation-initiated Pd/NBE catalysis, see: (b) Shi, G.; Shao, C.; Ma, X.; Gu, Y.; Zhang, Y., Pd(II)-Catalyzed Catellani-Type Domino Reaction Utilizing Arylboronic Acids as Substrates. *ACS Catal.* **2018**, *8*, 3775-3779. (c) Chen, S.; Liu, Z.-S.; Yang, T.; Hua, Y.; Zhou, Z.; Cheng, H.-G.; Zhou, Q., The Discovery of a Palladium(II)-Initiated Borono-Catellani Reaction. *Angew. Chem. Int. Ed.* **2018**, *57*, 7161-7165. (d) Li, R.; Liu, F.; Dong, G., Redox-Neutral ortho Functionalization of Aryl Boroxines via Palladium/Norbornene Cooperative Catalysis. *Chem* **2019**, *5*, 929-939.

(9) (a) Wang, X.-C.; Gong, W.; Fang, L.-Z.; Zhu, R.-Y.; Li, S.; Engle, K. M.; Yu, J.-Q., Ligand-enabled meta-C–H activation using a transient mediator. *Nature* **2015**, *519*, 334. (b) Dong, Z.; Wang, J.; Dong, G., Simple Amine-Directed Meta-Selective C–H Arylation via Pd/Norbornene Catalysis. *J. Am. Chem. Soc.* **2015**, *137*, 5887-5890.

(10) Liu, L.-Y.; Qiao, J. X.; Yeung, K.-S.; Ewing, W. R.; Yu, J.-Q., meta C–H Arylation of Electron-Rich Arenes: Reversing the Conventional Site Selectivity. *J. Am. Chem. Soc.* **2019**, *141*, 14870-14877.

(11) Gómez, M.; Granell, J.; Martinez, M., Mechanisms of Cyclopalladation Reactions in Acetic Acid: Not So Simple One-Pot Processes. *Eur. J. Inorg. Chem.* **2000**, *2000*, 217-224.

(12) (a) Gramec, D.; Peterlin Mašič, L.; Sollner Dolenc, M., Bioactivation Potential of Thiophene-Containing Drugs. *Chem. Res. Toxicol* **2014**, *27*, 1344-1358. (b) Dalvie, D. K.; Kalgutkar, A. S.; Khojasteh-Bakht, S. C.; Obach, R. S.; O'Donnell, J. P., Biotransformation Reactions of Five-Membered Aromatic Heterocyclic Rings. *Chem. Res. Toxicol* **2002**, *15*, 269-299. (c) Valadon, P.; Dansette, P. M.; Girault, J.-P.; Amar, C.; Mansuy, D., Thiophene Sulfoxides as Reactive Metabolites: Formation upon Microsomal Oxidation of a 3-Aroylthiophene and Fate in the Presence of Nucleophiles in Vitro and in Vivo. *Chem. Res. Toxicol* **1996**, *9*, 1403-1413.

(13) For reviews, see: (a) Tetsuya, S.; Masahiro, M., Catalytic Direct Arylation of Heteroaromatic Compounds. *Chem. Lett.* **2007**, *36*, 200-205. (b) Bellina, F.; Rossi, R., Recent advances in the synthesis of (hetero)aryl-substituted heteroarenes via transition metal-catalysed direct (hetero)arylation of heteroarene C–H bonds with aryl halides or pseudohalides, diaryliodonium salts, and potassium aryltrifluoroborates. *Tetrahedron* **2009**, *65*, 10269-10310. For selected works, see: (c) Liégault, B.; Lapointe, D.; Caron, L.; Vlassova, A.; Fagnou, K., Establishment of Broadly Applicable Reaction Conditions for the Palladium-Catalyzed Direct Arylation of Heteroatom-Containing Aromatic Compounds. *J. Org. Chem.* **2009**, *74*, 1826-1834. (d) Gorsline, B. J.; Wang, L.; Ren, P.; Carrow, B. P., C–H Alkenylation of Heteroarenes: Mechanism, Rate, and Selectivity Changes Enabled by Thioether Ligands. *J. Am. Chem. Soc.* **2017**, *139*, 9605-9614. (e) Colletto, C.; Panigrahi, A.; Fernández-Casado, J.; Larrosa, I., Ag(I)–C–H Activation Enables

Near-Room-Temperature Direct α-Arylation of Benzo[b]thiophenes. *J. Am. Chem. Soc.* **2018**, *140*, 9638-9643.(f) Doba, T.; Matsubara, T.; Ilies, L.; Shang, R.; Nakamura, E., Homocoupling-free Iron-catalysed Twofold C–H Activation/Cross-couplings of Aromatics via Transient Connection of Reactants, *Nat. Catal.* **2019**, *2*, 400-406.

(14) Wang, J.; Li, R.; Dong, Z.; Liu, P.; Dong, G., Complementary site-selectivity in arene functionalization enabled by overcoming the ortho constraint in palladium/norbornene catalysis. *Nat. Chem.* **2018**, *10*, 866-872.

(15) Mitsudo, K.; Thansandote, P.; Wilhelm, T.; Mariampillai, B.; Lautens, M., Selectively Substituted Thiophenes and Indoles by a Tandem Palladium-Catalyzed Multicomponent Reaction. *Org. Lett.* **2006**, *8*, 3939-3942.

(16) The exact reason for the high efficiency of **N1** remains unclear, which is a topic for the ongoing investigation.

(17) Li, R.; Liu, F.; Dong, G., Palladium-Catalyzed Asymmetric Annulation Between Aryl Iodides and Racemic Epoxides Using a Chiral Norbornene Cocatalyst. *Org. Chem. Front.* **2018**, *5*, 3108-3112.

(18) NBE **N4** was first used by Yu in the Pd/NBE catalysis: Shen, P.-X.; Wang, X.-C.; Wang, P.; Zhu, R.-Y.; Yu, J.-Q., Ligand-Enabled Meta-C–H Alkylation and Arylation Using a Modified Norbornene. *J. Am. Chem. Soc.* **2015**, *137*, 11574-11577.

(19) (a) For the first used of **N8**, see: Dong, Z.; Wang, J.; Ren, Z.; Dong, G., Ortho C−H Acylation of Aryl Iodides by Palladium/Norbornene Catalysis. *Angew. Chem. Int. Ed.* **2015**, *54*, 12664-12668. (b) For the first used of **N10**, see: Chen, S.; Liu, Z.-S.; Yang, T.; Hua, Y.; Zhou, Z.; Cheng,

H.-G.; Zhou, Q., The Discovery of a Palladium(II)-Initiated Borono-Catellani Reaction. *Angew. Chem. Int. Ed.* **2018**, *57*, 7161-7165.

(20) Chen, M. S.; Prabagaran, N.; Labenz, N. A.; White, M. C., Serial Ligand Catalysis: A Highly Selective Allylic C−H Oxidation. *J. Am. Chem. Soc.* **2005**, *127*, 6970-6971.

(21) (a) Ueda, K.; Yanagisawa, S.; Yamaguchi, J.; Itami, K., A General Catalyst for the β-Selective C–H Bond Arylation of Thiophenes with Iodoarenes. *Angew. Chem. Int. Ed.* **2010**, *49*, 8946-8949. (b) Kirchberg, S.; Tani, S.; Ueda, K.; Yamaguchi, J.; Studer, A.; Itami, K., Oxidative Biaryl Coupling of Thiophenes and Thiazoles with Arylboronic Acids through Palladium Catalysis: Otherwise Difficult C4-Selective C□H Arylation Enabled by Boronic Acids. *Angew. Chem. Int. Ed.* **2011**, *50*, 2387-2391. (c) Tang, D.-T. D.; Collins, K. D.; Glorius, F., Completely Regioselective Direct C–H Functionalization of Benzo[b]thiophenes Using a Simple Heterogeneous Catalyst. *J. Am. Chem. Soc.* **2013**, *135*, 7450-7453. (d) Tang, D.-T. D.; Collins, K. D.; Ernst, J. B.; Glorius, F., Pd/C as a Catalyst for Completely Regioselective C□H Functionalization of Thiophenes under Mild Conditions. *Angew. Chem. Int. Ed.* **2014**, *53*, 1809-1813. (e) Funaki, K.; Sato, T.; Oi, S., Pd-Catalyzed β-Selective Direct C–H Bond Arylation of Thiophenes with Aryltrimethylsilanes. *Org. Lett.* **2012**, *14*, 6186-6189. (f) Yuan, K.; Doucet, H., Benzenesulfonyl chlorides: new reagents for access to alternative regioisomers in palladium-catalysed direct arylations of thiophenes. *Chem. Sci.* **2014**, *5*, 392-396. (g) Colletto, C.; Islam, S.; Juliá-Hernández, F.; Larrosa, I., Room-Temperature Direct β-Arylation of Thiophenes and Benzo[b]thiophenes and Kinetic Evidence for a Heck-type Pathway. *J. Am. Chem. Soc.* **2016**, *138*, 1677-1683.

(22) Li, R.; Zhou, Y.; Yoon, K.-Y.; Dong, Z.; Dong, G., Sulfenamide-enabled ortho thiolation of aryl iodides via palladium/norbornene cooperative catalysis. *Nat. Commun.* **2019,** *10* (1), 3555.

(23) Prazeres, V. F. V.; Tizón, L.; Otero, J. M.; Guardado-Calvo, P.; Llamas-Saiz, A. L.; van Raaij, M. J.; Castedo, L.; Lamb, H.; Hawkins, A. R.; González-Bello, C., Synthesis and Biological Evaluation of New Nanomolar Competitive Inhibitors of Helicobacter pylori Type II Dehydroquinase. Structural Details of the Role of the Aromatic Moieties with Essential Residues. *J. Med. Chem.* **2010,** *53* (1), 191-200.

(24) Kern, N.; Dombray, T.; Blanc, A.; Weibel, J.-M.; Pale, P., Silver(I)-Catalyzed Deprotection of p-Methoxybenzyl Ethers: A Mild and Chemoselective Method. *J. Org. Chem.* **2012,** *77* (20), 9227-9235.

(25) Duffault, J.-M.; Tellier, F., A New Route to the Synthesis of Bicyclo [3.3.2] Nonene by Radical Cyclisation. *Synth. Commun.* **1998,** *28* (13), 2467-2481.

(26) Rentner, J.; Breinbauer, R., An efficient labeling strategy of drug like molecules with functionalized alkyl linkers using CH-activation. *Chem. Commun.* **2012,** *48* (83), 10343-10345.

(27) Moulton, B. E.; Whitwood, A. C.; Duhme-Klair, A. K.; Lynam, J. M.; Fairlamb, I. J. S., Regiochemistry in Cobalt-Mediated Intermolecular Pauson–Khand Reactions of Unsymmetrical Internal Heteroaromatic Alkynes with Norbornene. *J. Org. Chem.* **2011,** *76* (13), 5320-5334.

(Some contents of this chapter were published in *J. Am. Chem. Soc.* **2019**, *141*, 18958-18963.)

CHAPTER 7

Site-Selective Vicinal Difunctionalization of Five-Membered Heteroarenes: Mechanism and Applications

7.1 Introduction

Polysubstituted aromatic heterocycles are commonly found in pharmaceuticals, agrochemicals and organic materials (Figure 7.1).[1] Therefore, site-selective functionalization of arenes and heteroarenes has been playing a key role in preparing aromatic moieties ubiquitously found in natural products, drugs and bioactive compounds. While numerous methods are available for site-selectively introducing one functional group (FG) to heteroarenes without aids of directing groups (DGs), only a few can directly install two different FGs, particularly at vicinal positions in a regioselective manner. Therefore, the development of a direct multi-functionalization method for heterocycles, which can rapidly increase molecular complexity, is still highly demanded.

Figure 7.1. Examples of Polysubstituted Five-membered Heteroarenes

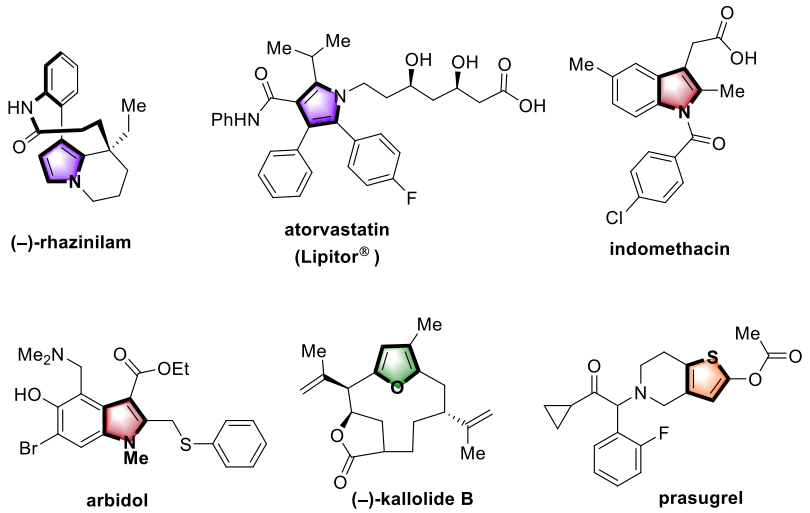

Scheme 7.1. Direct C−H Functionalization of Heterocycles

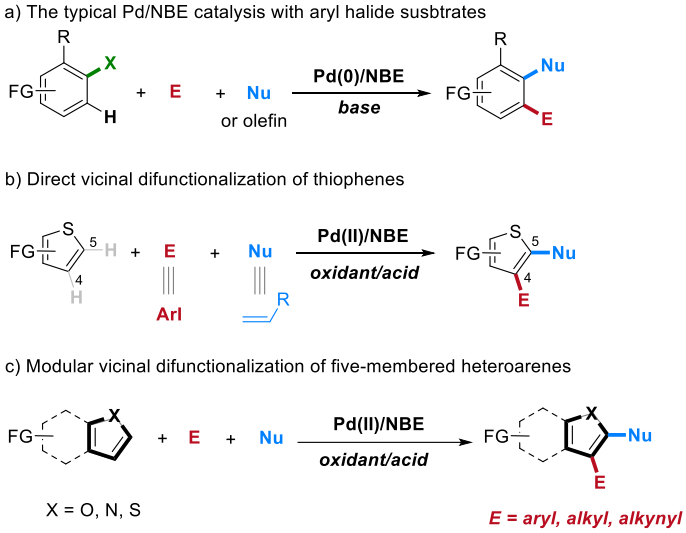

The palladium/norbornene (Pd/NBE) cooperative catalysis, pioneered by Catellani[2] and Lautens[3], has emerged as a versatile approach for vicinal difunctionalization of arenes. By using aryl halides as substrates, an electrophile and a nucleophile can be installed at arene ortho and ipso positions, respectively (Scheme 7.1a).[4] By means of this unique and efficient transformation, we have recently developed a direct vicinal difunctionalization of thiophenes, which was enabled by an arsine ligand and a unique amide-based NBE (Scheme 7.1b).[5] A series of mono- and disubstitued

thiophenes can be difunctionalized site- and regio-selectively at the C4 and C5 positions in moderate to excellent yield. Great functional group tolerance was exhibited, and the synthetic utility has been shown in derivatizations of complex bioactive compounds and an open-flask gram-scale preparation. The mild and robust reaction condition should make it attractive for preparing complex polysubstituted thiophenes and late-stage functionalization of bioactive compounds.

Figure 7.2. Proposed Reaction Mechanism

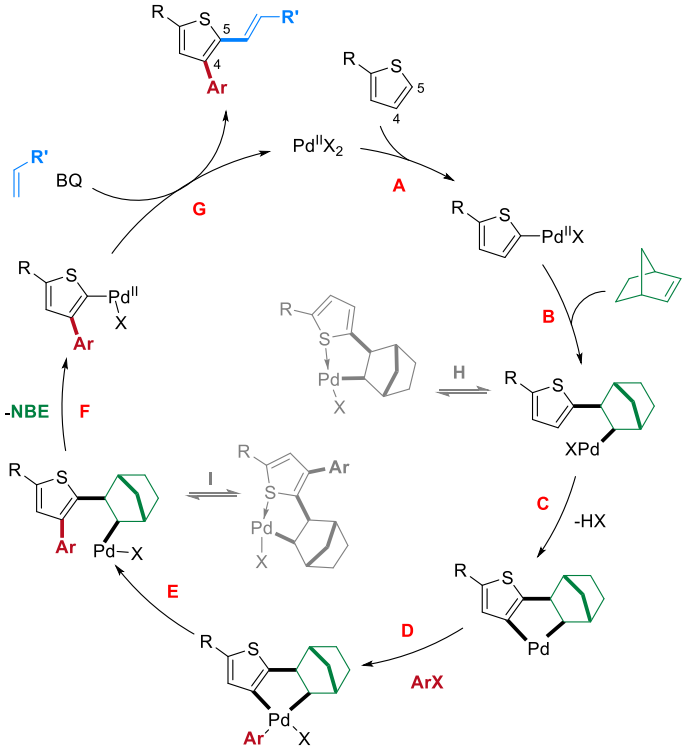

The key to realize the direct vicinal difunctionalization of thiophenes can be attributed to the use of a bulky C2 amide-substituted NBE as a cocatalyst and triphenylarsine as a ligand, which will be better understood from the reaction mechanism (Figure 7.2). It was speculated that the reaction is initiated by the well-established C5-palladation of thiophene (Step A),[6] followed by NBE migratory insertion (Step B) and C–H activation to form the aryl-norbornyl-palladacycle (ANP) intermediate (Step C), which can reactive with aryl iodide to introduce a aryl group at the C4

position. The following NBE de-insertion takes place via β-carbon elimination (Step F) and the resulting thiophenyl-Pd(II) species reacts with an acrylate to deliver the difunctionalized product, meanwhile the Pd(II) is regenerated in the presence of BQ (Step G). Considering the strong chelating ability of thiophene, the use of a weakly coordinative π-acidic arsine ligand was important to prevent chelation of the sulfur moiety on the palladium without compromising the ANP formation (Step H).[7] In addition, the use of a bulky C2 amide-substituted NBE would promote the desired β-carbon elimination pathway, avoiding the undesired chelation on the palladium (Step I).[5]

As an extension of current work, we would like to further study the reactivity of other heterocycles, including furans, pyrroles and indoles. Besides ortho arylation, ortho alkynylation and ortho methylation were also realized with different structurally-modified NBE and modified reaction condition. A unique NBE effect was observed when we studied the reactivity of indole, where only C1-substitued NBEs can effectively afford the desired difunctionalized product, while other substituted NBEs all gave significantly diminished yield or even no desired product. Detailed kinetic study and DFT calculation were performed to disclose this NBE effect and the rate-determining step was also assigned. In addition to the mechanistic investigation, we have also exploited the synthetic utility of this difunctionalization method to the total synthesis of *rhazinilam*.

7.2 Results and Discussion

7.2.1 Reaction Discovery and Optimization

Scheme 7.2. Difunctionalization of Indole with C1- and C2-Substituted NBEs

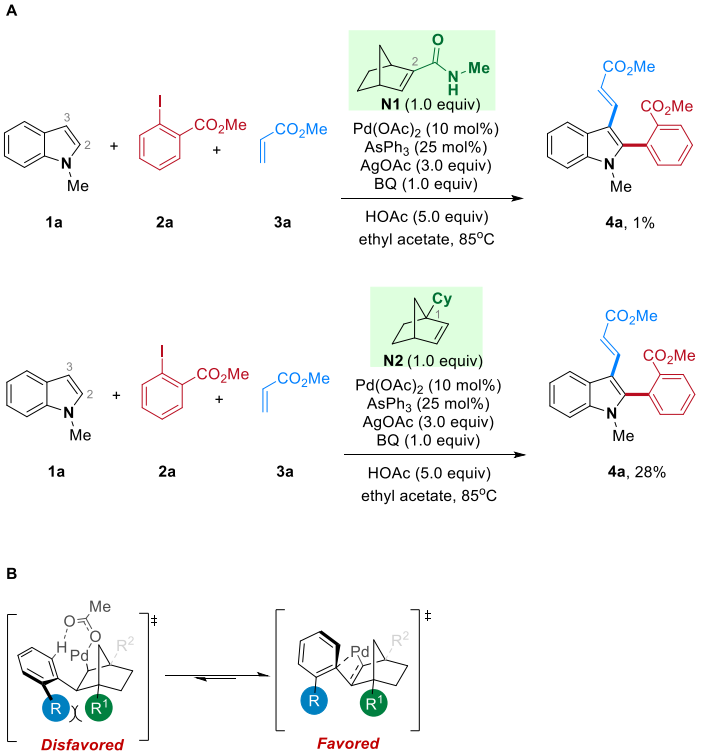

NBE Effect. To further explore the compatibility of the direct vicinal difunctionalization method toward other heteroarenes, the reaction of *N*-methylindole (**1a**), methyl 2-iodobenzoate (**2a**) and methyl acrylate (**3a**) were tested under previously reported standard condition except at higher reaction temperature (Scheme 7.2A). Fortunately, the ortho arylation/ipso olefination product **4a** was isolated in 1% yield with desired regioselectivity when using C2 methyl amide-substituted NBE **N1**, which served as the optimal NBE co-catalyst in our previous work. The structure of the product indicates that the initial C−H palladation takes place at C3 position instead of C2 position. In stark contrast, the reaction exhibited unexpected reactivity when C1-substituted NBE **N2** was used instead of **N1**, affording the same product in moderate yield. The C1-substituted NBEs are

known to inhibit the undesired second C−H metalation and promote β-carbon elimination;[8] thus, they were developed for addressing the "ortho constraint" issue (Scheme 7.2B). Compared with simple NBE and electron deficient C2-subsittuted NBEs, C1-substituted NBEs typically have weaker binding affinity and slower migratory insertion rate due to the increased steric hindrance, which usually lead to a faster β-carbon elimination, particularly when the ortho position of arene is occupied.[9] However, the successful difunctionalization using **N2** contradicted the mechanistic interpretation.

Motivated by this unique reactivity difference caused by using different substituted NBEs, the NBE effect was then carefully examined (Table 7.1). After careful evaluation of various reaction parameters, the desired ortho arylation/ipso olefination product **4a** was ultimately obtained in 71% yield using **N2** as the optimal co-catalyst, along with two side products **4a'** and **4a''**, which were formed through a direct Heck reaction and an aryl iodide-initiated Catellani pathway, respectively. Three types of structurally modified NBEs were investigated. Interestingly, only C1-substitued NBEs (**N2**, **N13**-**N15**) gave a notably improvement, while C2-substituted NBEs and C5-substituted NBEs afford significantly diminished yield or even no desired product. In general, more direct Heck product **4a'** was formed when using C2-substituted NBE, and more **4a''** was formed when using C5-substituted NBE. The side product **4a'** potentially comes from the competitive migratory insertion of methyl acrylate **3a**. Thus, both electronic effect and steric effects of NBE should play a role. Strongly electron-withdrawing substituents like CF_3 and C_8F_{17} greatly disfavor the NBE binding. As a result, they majorly afforded the direct Heck product **4a'**. As a comparison, less electron deficient C2 amide-substituted NBEs (**N1**, **N3**-**N6**)[10] and C2 ester-substituted NBEs (**N8**-**N10**)[11] formed less direct Heck product.

Table 7.1. NBE Effect[a]

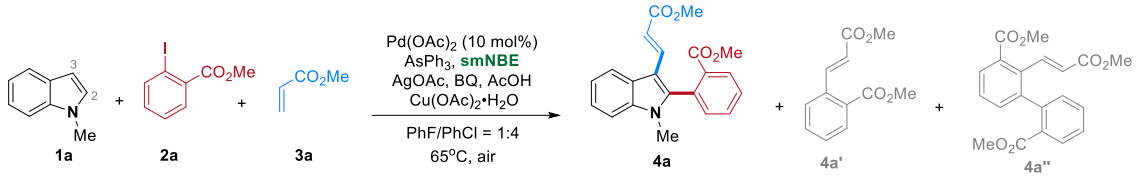

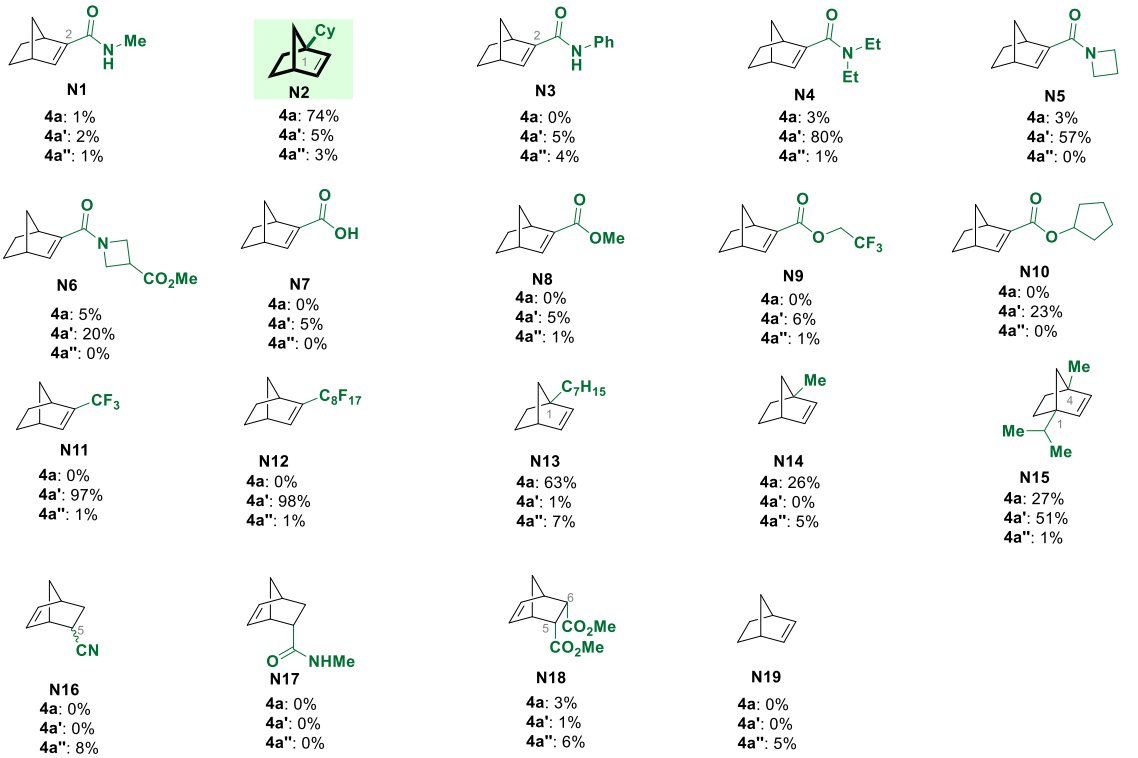

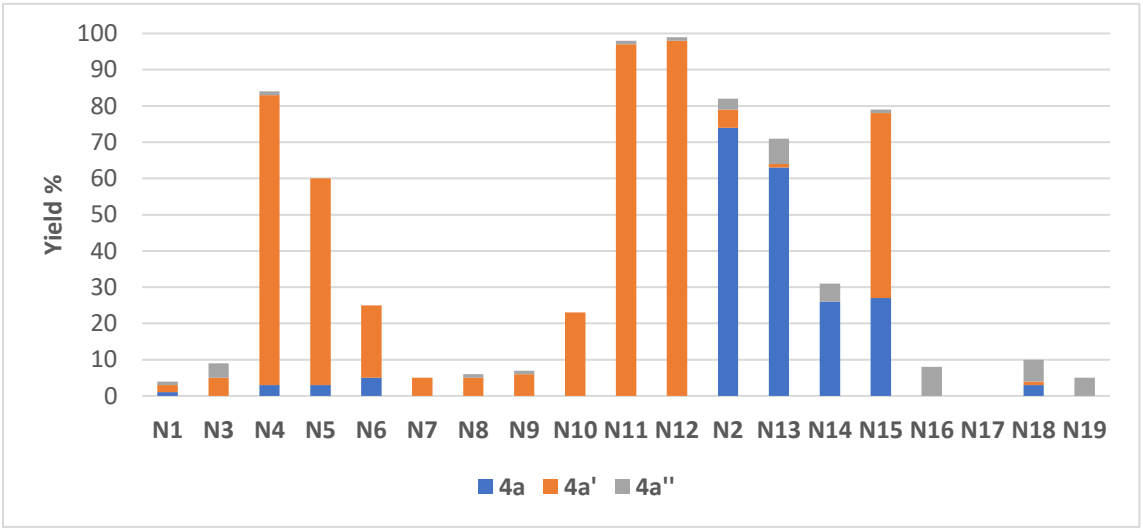

Table 7.1. NBE Effect[a] (continued)

[a]The reaction was run with 0.15 mmol **1a**, 0.1 mmol **2a**, 0.3 mmol **3a**, $Pd(OAc)_2$ (0.01 mmol, 10 mol%), smNBE (0.15 mmol, 1.5 equiv), $AsPh_3$ (0.025 mmol, 25 mol%), BQ (0.06 mmol, 60 mol%), $Cu(OAc)_2 \cdot H_2O$ (0.05 mmol, 50 mol%), AgOAc (0.3 mmol, 3.0 equiv), and HOAc (0.5 mmol, 5.0 equiv) in 0.5 mL solvent (PhF/PhCl = 4:1) for 72 h. Yields were determined by ^1H NMR analysis using dibromomethane as the internal standard.

In terms of steric effect, similar trends were observed in both amide- and ester-substituted NBEs: bulkier substitutes, e.g. tertiary amides (**N4**-**N6**) and secondary ester (**N10**) afforded more **4a'** than secondary amides (**N4**-**N6**) and primary esters (**N8** and **N9**), likely due to the higher energy barrier during migratory insertion transition state. The side product **4a''** comes from a Pd(0)-initiated Catellani-type side pathway, as aryl iodide **2a** is known to easily undergo dimerization in the presence of Pd/NBE. Our hypothesis is, when C5-substituted or C5,C6-disubstituted NBEs were used, the direct heck pathway was largely inhibited owing to faster migratory insertion comparted to the use of C2-substituted NBEs. However, the indole C3-H activation-initiated Catellani reaction, the major pathway, was slow, which would result in the accumulation of the dimerization side product **4a''**. The simple NBE **N19** behaved as similar as C5-substituted NBEs, affording **4a''** as the major side product. Surprisingly, none of the three products were observed when **N17** was used and the reason is not clear.[12] A combined experimental and computational investigation were conducted later to demonstrate the unique NBE effect when using C1-substituted NBEs.

Control Experiments. A series of control experiments were also performed (Table 7.2). The $Pd(OAc)_2/AsPh_3$ combination, which previously was successfully applied in Pd(II)-initiated Catellani reactions,[13] indeed provided the desired ortho arylation/ipso alkynylation product **4a** in 74% yield (entry 1). Not surprisingly, no desired product was observed in the absence of Pd, ligand or NBE (entries 2-3, 6). The direct Heck would become the predominant pathway in the absence

of NBE (entry 6). Other phosphine-based ligands were less effective, probably owing to the stability under this oxidative condition (entries 4-5). It is worthy noting that the reaction proceeded well in the presence of catalytic amount of **N2** with only slightly decreased yield (entry 7). The silver salt was beneficial, likely serving as the halide scavenger to promote the oxidative addition of aryl iodide **2a** (entry 8). Benzoquinone was also critical, which served as the oxidant to regenerate the Pd(II) from Pd(0) (entry 9). Adding catalytic amount of copper acetate was also helpful possibly through acting as a co-oxidant (entry 10).[14] The addition of 5 equivalents of HOAc improved the yield probably by promoting the initial C−H palladation on the indole (entry 11).[6b] The yield was slightly improved by use of a mixed solvent system (entry 12) while the exact reason is not clear. In addition, reduction of the Pd loading to 5 mol% only slightly diminished the yield (entry 13). Finally, similar yield was obtained when indole **1a** was used as the limiting reagent (entry 14).

Table 7.2. Control Experiments

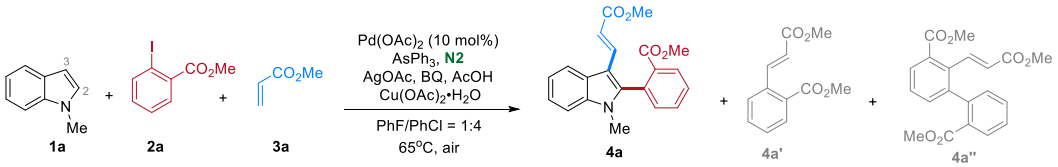

1a **2a** **3a** **4a** **4a'** **4a''**

Entry	Change from the *"standard condition"*	**4a** (%)[a]	**4a'** (%)[a]	**4a''** (%)[a]
1	none	74	5	3
2	w/o $Pd(OAc)_2$	0	0	0
3	w/o $AsPh_3$	0	25	4
4	TFP instead of $AsPh_3$	0	20	4
5	PPh_3 instead of $AsPh_3$	7	27	8
6	w/o NBE	0	76	0
7	NBE (50 mol%)	60	18	2
8	w/o AgOAc	26	10	1
9	w/o BQ	13	19	8
10	w/o $Cu(OAc)_2•H_2O$	62	17	3
11	w/o HOAc	33	21	10
12	PhCl instead of PhF/PhCl	70	7	3
13	[Pd] (5 mol%)	68[b]	5[b]	4[b]
14	**1a** as 1.0 equiv	71[c]	17[c]	9[c]

Table 7.2. Control Experiments (continued)

[a]The reaction was run with 0.15 mmol **1a**, 0.1 mmol **2a**, 0.3 mmol **3a**, $Pd(OAc)_2$ (0.01 mmol, 10 mol%), **N2** (0.15 mmol, 1.5 equiv), $AsPh_3$ (0.025 mmol, 25 mol%), BQ (0.06 mmol, 60 mol%), $Cu(OAc)_2 \cdot H_2O$ (0.05 mmol, 50 mol%), AgOAc (0.3 mmol, 3.0 equiv), and HOAc (0.5 mmol, 5.0 equiv) in 0.5 mL solvent (PhF/PhCl = 4:1) for 72 h. Yields were determined by ^1H NMR analysis using dibromomethane as the internal standard. [b]$Pd(OAc)_2$ (0.005 mmol, 5 mol%) and $AsPh_3$ (0.0125 mmol, 12.5 mol%) were used. [c]**1a** (0.1 mmol, 1.0 equiv) and **2a** (0.15 mmol, 1.5 equiv) were used.

7.2.2 Substrates Scope

Substrates Scope of Indoles. With the optimized reaction condition in hand, the scope with respect to indole was examined first (Table 7.3). A range of indoles with various substituents at the C5, C6 and C7 positions, including alkyl (**4b** and **4m**), methoxy (**4c** and **4j**), halogen atoms (**4d**-**4f** and **4k**-**4l**), cyano (**4g**), aldehyde (**4h**) and ester (**4i**) groups were all compatible substrates in this transformation. Note that aryl iodide moiety, which is reactive in Pd(0)-catalyzed cross-coupling reaction, can be tolerated in current reaction condition and serve as a handle for further derivatization. The X-ray structure of **4f** was obtained to confirm the regioselectivity of this difunctionalization method. Besides methyl, benzyl protected indole (**4n**) can undergo difunctionalization reaction smoothly with slightly diminished yield. In terms of the aryl iodides and olefin scopes, aryl iodides with an ortho EWGs were found to be most efficient, which is consistent with our previous observation. A series of functional group, including easter (**4o**-**4q** and **4t**), halogen atoms (**4p**-**4q**), ketone (**4r**) and amide (**4s**) groups were all well tolerated in this method. Notably, a menthol derived aryl iodide can also be couple at C2 position of indole in good yield, while a pair of rotational isomers were observed in 1:1 ratio. In addition to methyl acrylate,

other Michael acceptors, such as conjugated esters (**4u**-**4w**), amides (**4x**-**4y**), and ketones (**4z**), are also excellent coupling partners for the C3 functionalization.

Table 7.3. Substrates Scope of Indoles[a]

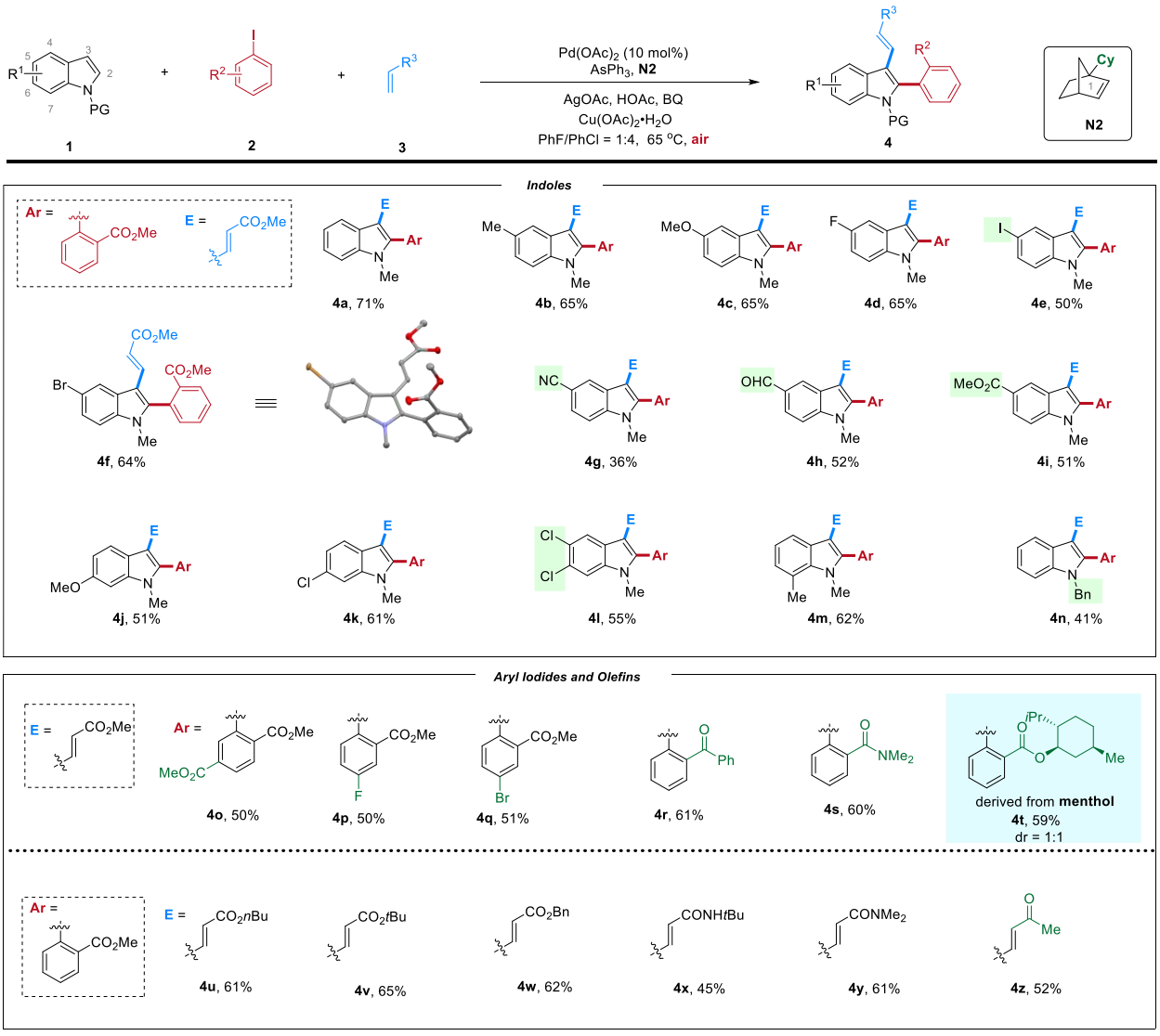

[a]The reaction was run with 0.3 mmol **1**, 0.2 mmol **2**, 0.6 mmol **3**, $Pd(OAc)_2$ (0.02 mmol, 10 mol%), **N2** (0.3 mmol, 1.5 equiv), $AsPh_3$ (0.05 mmol, 25 mol%), BQ (0.12 mmol, 60 mol%), $Cu(OAc)_2 \cdot H_2O$ (0.1 mmol, 50 mol%), AgOAc (0.6 mmol, 3.0 equiv), and HOAc (1.0 mmol, 5.0 equiv) in 1.0 mL solvent (PhF/PhCl = 4:1) for 72 h.

Substrates Scope of Pyrroles. Besides indoles, pyrroles are also excellent substrates. A series of mono- and di-substituted pyrroles underwent difunctionalization reaction smoothly in modified reaction condition using **N5** as the optimal co-catalyst (Table 7.4). The regioselectivity of pyrrole difunctionalization, which was confirmed by X-ray (**6b**), is different from indole since the initial C−H palladation takes place at pyrrole C2 (C5 if C2-substituted pyrrole) position. In particular, both electron-rich (**6c** and **6g**) and electron-deficient (**6d** and **6h**) could afforded the corresponding desired difunctionalized product in moderate to good yield. Notably, a C2 thiophenyl-substituted pyrrole (**6j**) was also suitable substrate, where the pyrrole instead of thiophene was difunctionalized in a chemo- and regioselective manner. Note that C3-substituted pyrrole (**6k**) was compatible in this method; C2 and C3 disubstituted pyrrole (**6l**) also proved to be a suitable substrate, giving fully substituted products that are nontrivial to be prepared via conventional approaches. In addition, simple *N*-methylpyrrole **6m** and *N*-benzylpyrrole **6n** were compatible, affording disubstituted pyrroles in one step with moderate yields. Regarding the aryl iodides scope, aryl iodides bearing ortho EWGs, including ester (**6o**-**6r**, **6x**), amide (**6w**), nitro (**6s**-**6u**) and ketone (**6v**) groups could all be coupled at pyrrole ortho position in moderate to good yield. A second heteroarene could also be coupled by using thiophenyl iodide as the coupling partner (**6y**). It is worth mentioning that ortho EWG is *not* necessary for this difunctionalization method: aryl iodides bearing para (**6z**-**6ac**) and meta (**6ad**-**6ai**) substituents could all undergo difunctionalization method smoothly, affording desired product in moderate to good yields. Notably, electron-rich 3-iodoanisole (**6ad**) and neutral phenyl iodide were also compatible substrates. Given the diversity of aryl moieties that can be coupling with pyrrole substrates, this method would serve as an efficient way to prepare polysubstituted biaryl moiety-containing heteroarenes. In addition to electron-deficient Michael acceptors (**6ak**-**6aq**), electron-neutral (**6ar**) and moderate electron-

deficient (**6as**) styrenes were good coupling partners. Encouragingly, cyclic olefin (**6at**) was also an excellent coupling partner for pyrrole C5 functionalization.

Table 7.4. Substrates Scope of Pyrroles[a]

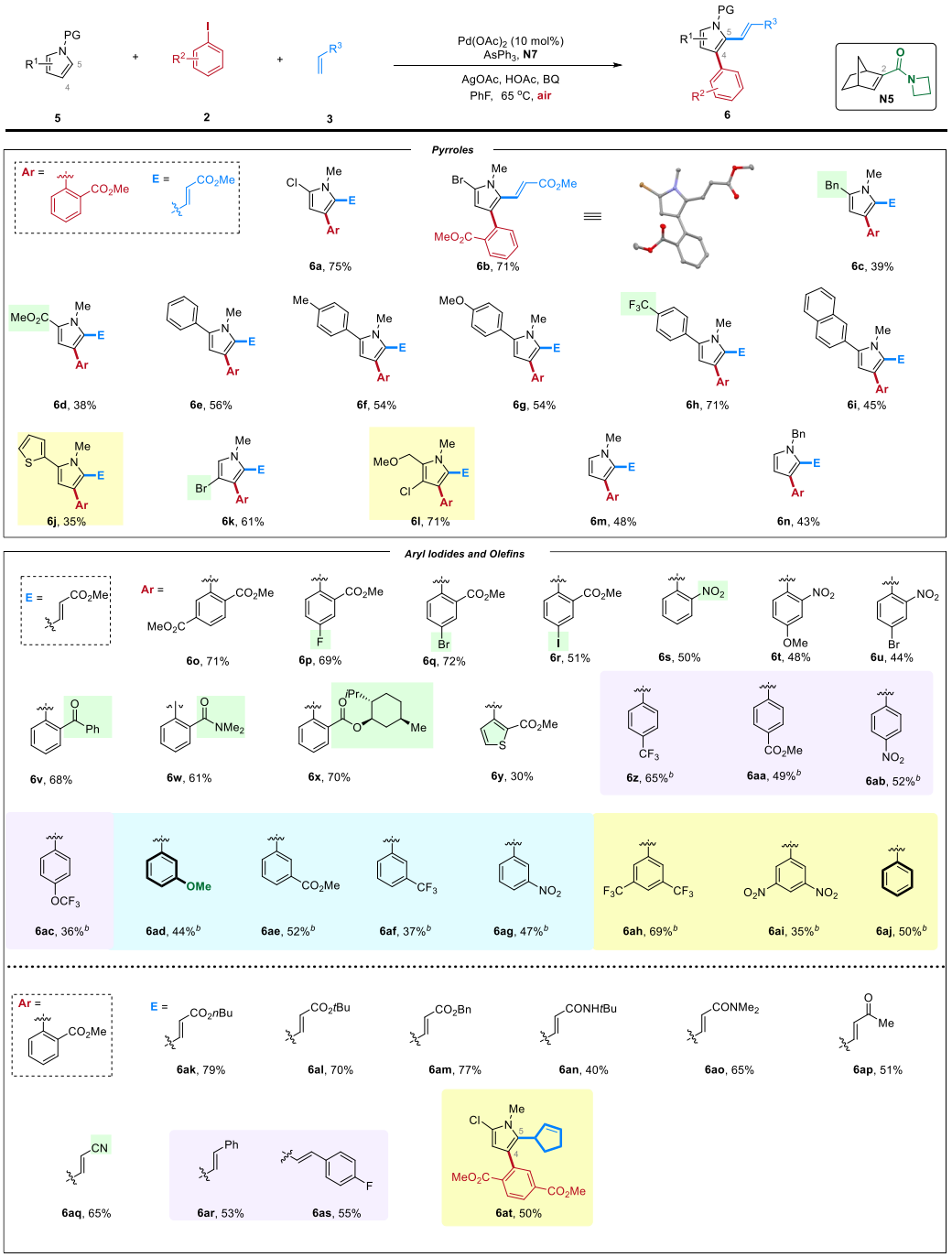

[a]The reaction was run with 0.2 mmol **5**, 0.4 mmol **2**, 0.6 mmol **3a**, $Pd(OAc)_2$ (0.02 mmol, 10 mol%), **N5** (0.3 mmol, 1.5 equiv), $AsPh_3$ (0.05 mmol, 25 mol%), BQ (0.2 mmol, 1.0 equiv), AgOAc (0.6 mmol, 3.0 equiv), and HOAc (1.0 mmol, 5.0 equiv) in 1.0 mL fluorobenzene for 72 h. [b]**N16** (0.4 mmol, 2.0 equiv), AgOAc (0.8 mmol, 4.0 equiv) and TBME (*tert*-butyl methyl ether) were used.

Table 7.5. Substrates Scope of Furans[a]

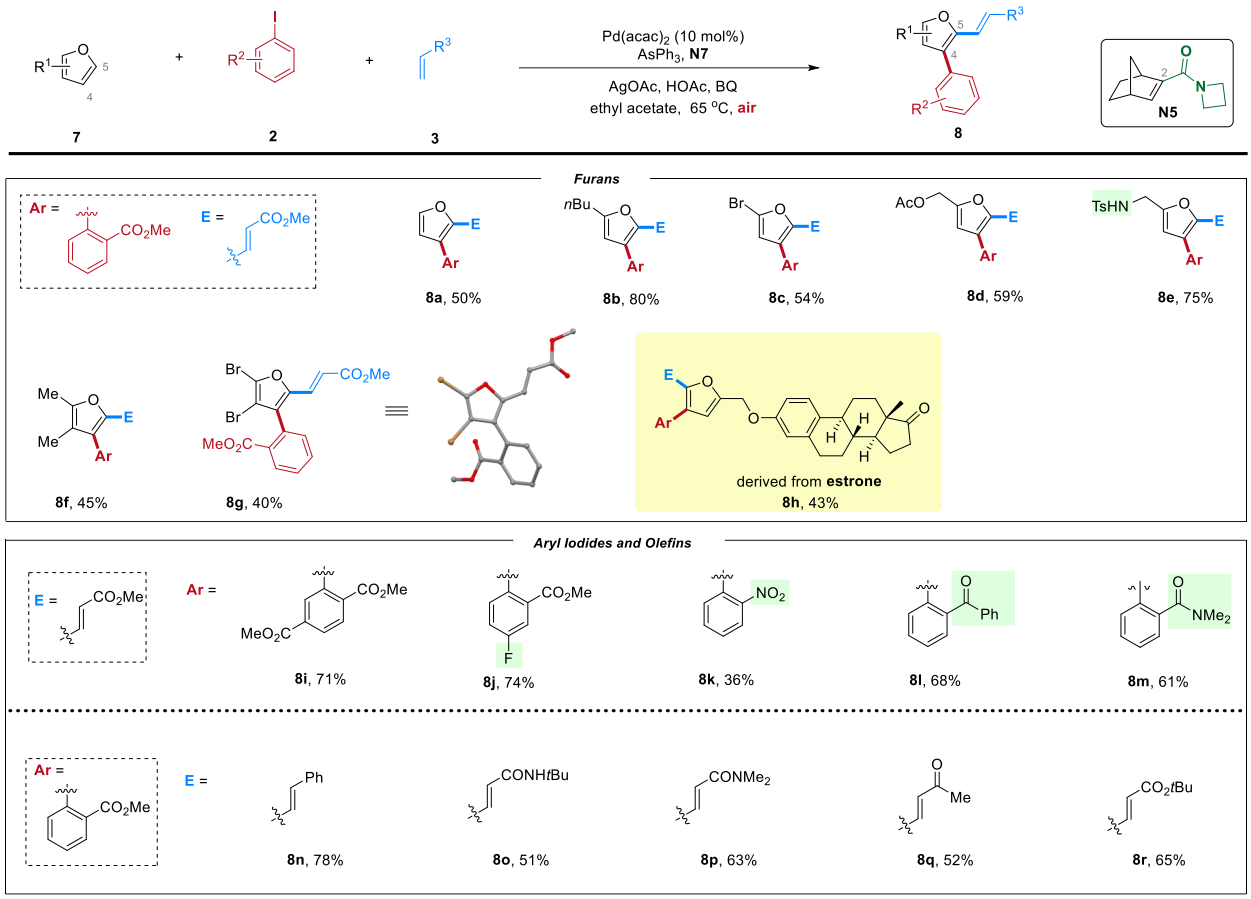

[a]The reaction was run with 0.5 mmol **7**, 0.2 mmol **2**, 0.36 mmol **3a**, $Pd(acac)_2$ (0.02 mmol, 10 mol%), **N5** (0.3 mmol, 1.5 equiv), $AsPh_3$ (0.05 mmol, 25 mol%), BQ (0.2 mmol, 1.0 equiv), AgOAc (0.7 mmol, 3.5 equiv), and HOAc (1.0 mmol, 5.0 equiv) in 0.67 mL ethyl acetate for 72 h.

Substrates Scope of Furans. The third type of heteroarene furan also proved to be excellent substrates. Using a different Pd precatalyst $Pd(acac)_2$, a range of mono- and di-substituted furan can be difunctionalized in moderate to good yields (Table 7.5). The regioselectivity of furan difunctionalization, which was confirmed by X-ray structure (**8g**), is same as pyrroles and thiophenes. In addition, more functionalization groups including protected primary alcohol (**8d**)

and amine (**8e**) at C2 position were all compatible in this method. Notably, a more complex substituted furan derived from bioactive estrone (**8h**) could be difunctionalized smoothly in moderate yield. Besides, aryl iodides bearing different substituents (**8i**-**8m**) as well as a series of electron-deficient olefins (**8n**-**8r**) were all suitable substrates.

7.2.3 Ortho Alkynylation and Ortho Methylation of Heteroarenes

Ortho Alkynylation and Ortho Methylation. To demonstrate the modularity and generality of this heteroarenes difunctionalization method, different ortho functionalization was then investigated. Apart from ortho arylation, ortho alkynylation could also be realized by using alkynylation bromide as the electrophile (Table 7.6). While the meta C−H alkynylation was realized by Yu in 2016, a complex DG was necessary and only proton was coupled at ortho position, which largely limited the application of this method.[15] To the best of our knowledge, the ortho alkynylation via Catellani-type difunctionalization has not been realized yet. In a slightly modified reaction condition with **N2** as the co-catalyst, four substituted thiophenes and pyrroles were able to undergo ortho alkynylation/ipso Heck coupling, affording the desired difunctionalized heteroarenes, albeit in moderate yields (**11a**-**11d**). The regioselectivity of this method was confirmed by X-ray structure (**11d**). Besides using aryl iodides and alkynyl bromide as the electrophile, preliminary success on employing methyl iodide as the electrophile has been achieved. When 2-chloro-1-methylpyrrole (**5a**) was subjected to the standard reaction condition with **N1** as the co-catalyst, the desired C4 methylated/C5-alkenylated pyrrole (**13**) was isolated in 43% yield (Eq. 1). Likewise, when 1-butylthiophene was subjected to the slightly modified reaction condition, the desired methylated thiophene (**14**) was isolated in 20% yield (Eq. 2). Further optimization of the reaction is underway in our laboratory. Considering the importance of methyl group in drug design, the method is expected to be useful in medicinal chemistry research.

Table 7.6. Substrates Scope of Ortho Alkynylation[a]

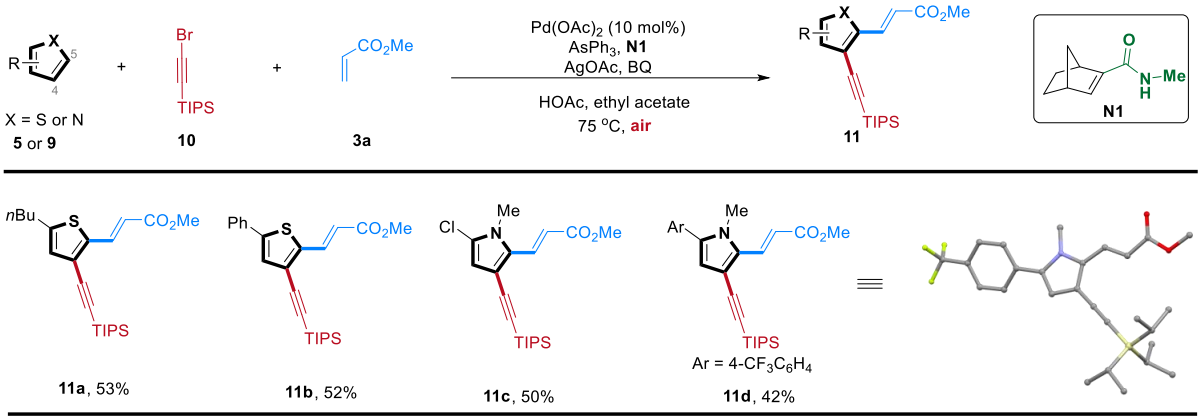

[a]The reaction was run with 0.2 mmol **5** or **9**, 0.4 mmol **10**, 0.48 mmol **3a**, $Pd(OAc)_2$ (0.02 mmol, 10 mol%), N1 (0.4 mmol, 2.0 equiv), $AsPh_3$ (0.05 mmol, 25 mol%), BQ (0.2 mmol, 1.0 equiv), AgOAc (0.6 mmol, 3.0 equiv), and HOAc (1.0 mmol, 5.0 equiv) in 1.0 mL ethyl acetate for 72 h.

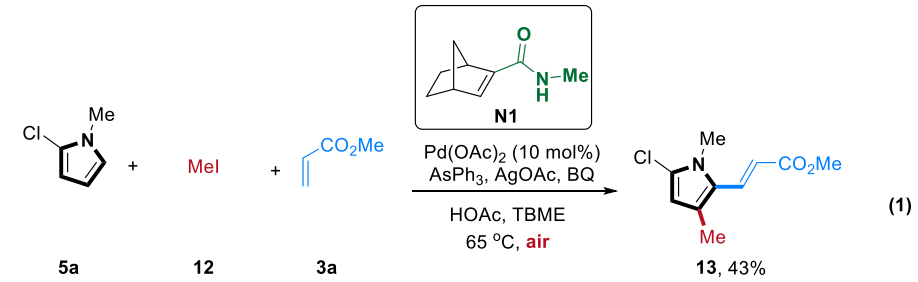

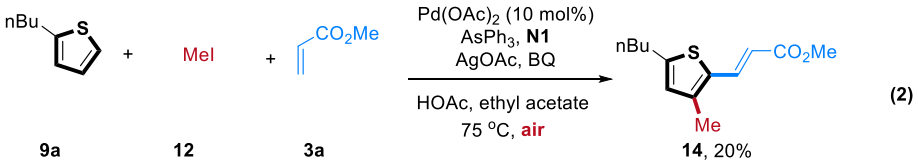

7.2.4 Synthetic Utility

The synthetic utilities of this method were then explored. From the scalability prospect, it is encouraging that the reaction appears to be robust. On a gram scale, excellent yield can be obtained with an open-flask setup and untreated solvent (Scheme 7.3).

Scheme 7.3. Gram-scale Preparation

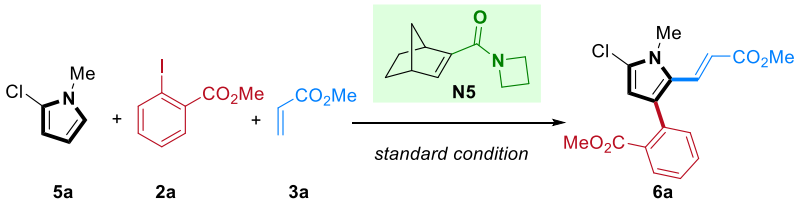

open flask

solvent

The other synthetic utility of this method was demonstrated in a concise synthesis of (±)-rhazinilam, which displays cytotoxic activity toward various cancer cell lines in the low micromolar range in vitro, where it shows the inhibition of microtubule assembly and disassembly as well as the formation of abnormal tubulin spirals. In 2013, a decent work by Gu demonstrated a rapid synthesis of rhazinal using a Pd(0)-initiated Catellani-type ortho arylation/annulation cascade, where an electron-withdrawing aldehyde substituent is necessary in order to enhance the reactivity of the 2-iodopyrrole intermediate.[16] Also, the iodide moiety is also necessary to initiate the Catellani reaction. We believe this modular difunctionalization strategy would have a great opportunity to construct the polysubstituted pyrrole intermediate **16** directly from commercially

available 2-nitroiodobenzene and an alkyl protected pyrrole **17**, which was prepared according to a literature reported procedure. Hence, the preparation of highly unstable 2-iodopyrrole intermediate and the necessity of electron-withdrawing substituent can be avoided. (Scheme 7.4A).

Scheme 7.4. Total Synthesis of (±)-Rhazinilam

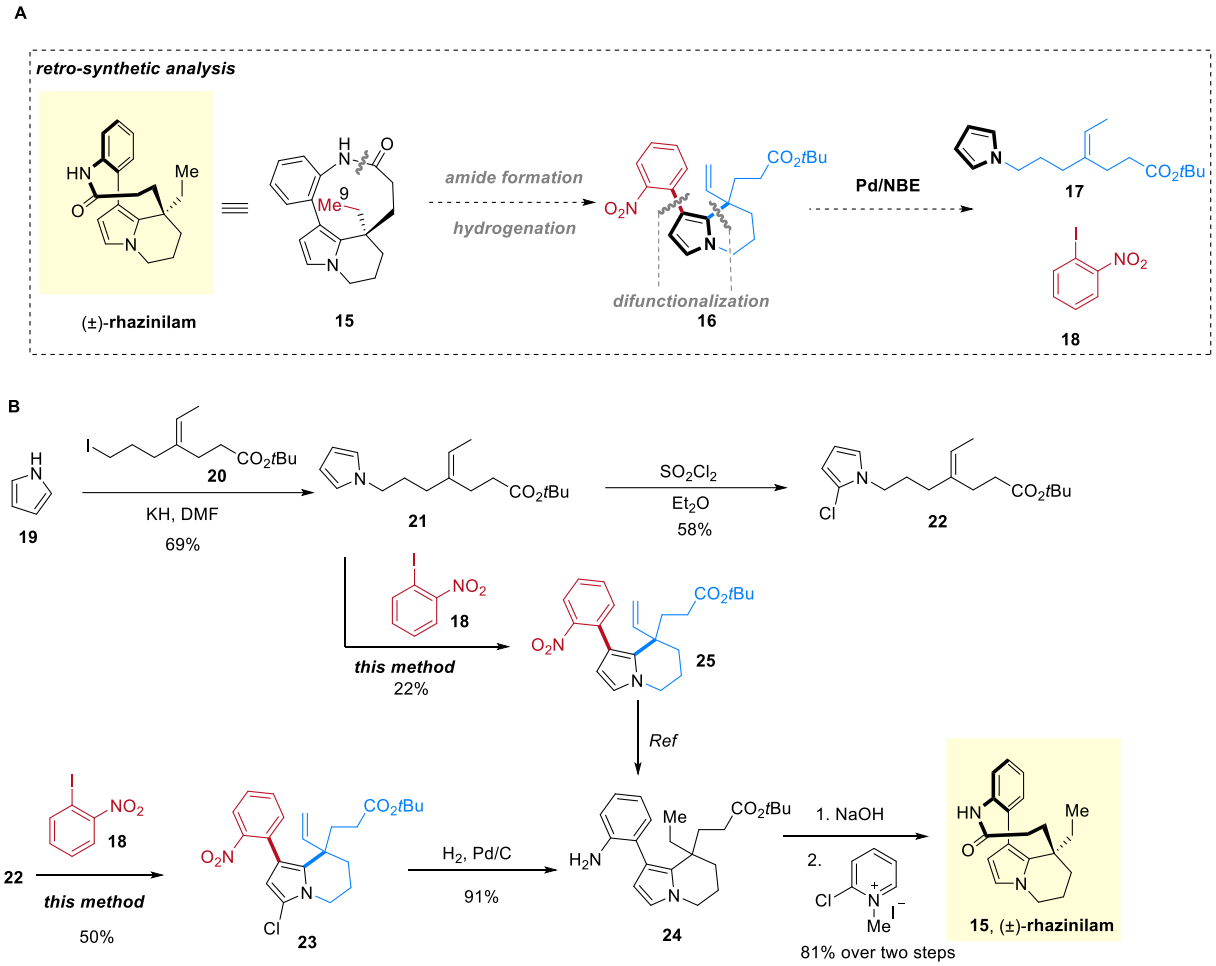

Starting from alkylation of simple pyrrole **19** with alkyl iodide **20**, the affording alkyl pyrrole **21** then underwent chlorination to deliver 2-chloropyrrole **22**. It is worth noting that while intermediate **21** could be directly difunctionalized to afford **25** in a diminished yield, the newly introduced chloride moiety can serve as a promoter to largely enhance the conversion of following difunctionalization reaction. Then the terminal double bonds generated from ipso heck coupling

was reduced under Pd/C, followed by hydrolysis and Mukaiyama condensation to deliver the (±)-rhazinilam in decent yield (Scheme 7.4B).

7.2.5 Mechanistic Study

NBE Effect. Considering the critical roles that NBE plays in the catalytic cycle, especially the unique reactivity and selectivity of indoles difunctionalization enabled by C1-substituted NBE, investigation of this NBE effect would become an important approach to address limitations and modulate reaction selectivity in Pd/NBE catalysis, which meanwhile would serve as the guidance for further design of structurally modified NBEs. Hence, a combined experimental and computational investigation was undertaken to understand the beneficial role of the C1-substituted NBE (**N2**) in the context of enabling indoles difunctionalization reaction. In a regular Pd(0)-initiated Catellani reaction of aryl halide, the position of first oxidative addition is dictated by the position of halide moiety, while in the current method the reaction is initiated by C−H palladation. First, DFT calculation was carried out to study the regioselectivity of the first indole C−H palladation. In line with our proposed mechanism, the computed energy barrier of **TS-2**, which is the transition state of indole C3−H palladation, is 1.6 kcal/mol lower than that of TS-2b, which is the transition state of C2−H palladation (Figure 7.3).

Figure 7.3. Indole C−H Palladation Transition States.

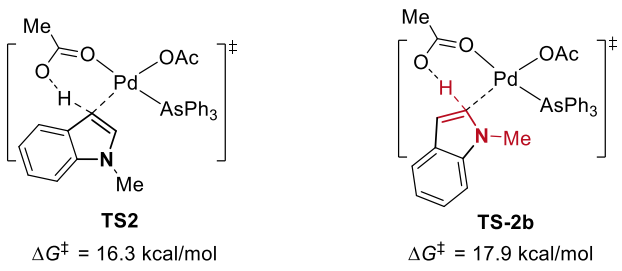

Kinetic isotope effect. To gain some insight into C−H activation steps, the parallel kinetic isotope effect (KIE) of the first C−H palladation (Scheme 7.5A) and the second C−H palladation (Scheme 7.5B) were measured by employing 3-deuteroincole and 2-deuteroincole, respectively. The k_H/k_D values were obtained by ^{1}H NMR analysis of four parallel reactions. The KIE of C3−H palladation was found to be 1.3 and the KIE of C2−H palladation was found to be 1.4, indicating both C−H activation steps may not be the rate-determining step.

Scheme 7.5. Kinetic Isotope Effect of C−H Activation

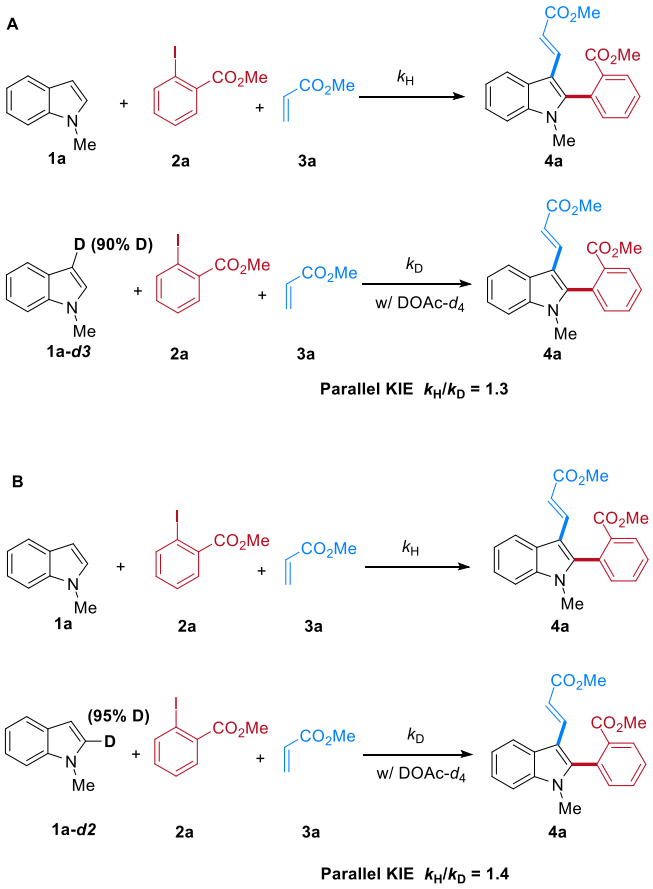

Kinetic study. In order to find the rate-determining step of this reaction, first, the kinetic profile of this transformation was measured to determine the reaction order of each reaction component. The order of each component was determined by the initial-rate method. The dependence of the

initial rate on [**N2**] was explored first: a saturation dependence was observed. Interestingly, an indole C3 direct Heck side pathway was predominant when the concentration of **N2** is low, indicating a direct competition between NBE migratory insertion and acrylate **3a** migratory insertion, with the former promoted by higher **N2** concentration. Under the condition of saturating [**N2**], the catalytic rate law exhibits a first-order dependence on [Pd]/[AsPh3] and [**2a**], saturation dependences on [**1a**], and a zero-order dependence on [**3a**]. The experimental data presented above indicates that the Pd catalyst and aryl iodide should be involved in the rate-determining step and indole both C−H activations are ruled out as the rate-determining step. Thus, the oxidative addition of ANP with aryl iodide **2a** is more likely to be the rate-determining step when saturating **1a** and **N3** are present in the reaction and the indole-norbornene-palladium complex might be the catalyst resting state. The dependences of the rate on **1a** and **N2** are presumably due to the change of resting state when [**1a**] and [**N2**] are low, for example the indole direct Heck side pathway will become predominant in the presence of lower [**1a**]. The experimental data presented above and DFT calculation indicate that the indole-norbornene-palladium complex might be the catalyst resting state and the oxidative addition of ANP with **2a** might be the turnover-limiting step when saturating **1a** and **N3** are present in the reaction. The dependences of the rate on **1a** and **N3** are presumably due to the change of resting state when the concentrations of **1a** and **N3** are low.

Stoichiometric study. We wonder whether the resting state can be trapped in the real reaction system. In the model study when NBE **2** was used, the desired indole-NBE-Pd complex **4** could be synthesized by a modified procedure in 10% yield as the single isomer (Scheme 7.6). However, two regioisomers **7** and **8** were formed in a ratio of 2:1 when C1-substituted **5** was used, where the major isomer is consistent with the one proposed in DFT calculation. The same scenario was observed when **9** was used, while the ratio between two formed regioisomers **11** and **12** was 3:2

and the major isomer has the desired selectivity, which was further confirmed by NOESY. Direct reduction of this inseparable mixture by NaBH4 formed two NBE-attached products **13** and **14**, which has the same ratio and the structures were confirmed by ^{1}H NMR. Interestingly, a ratio of over 20:1 between **16** and **15** was observed when the real ligand $AsPh_3$ was used in replace of PPh_3, where the undesired **16** was the major regioisomer. The structure and ratio were further confirmed by reduction of the complex mixture with $NaBH_4$. Based on DFT calculation the rational is that NBE migratory insertion step might be reversable and only the formation of desired regioisomer (Cy pointing in) will trigger the following irreversible C–H palladation. The steric repulsion between Cy and $AsPh_3$ will destabilized the reaction resting state, thereby promoting the following oxidative addition with ANP and NBE extrusion.

Scheme 7.6. Preparation of Proposed Resting State

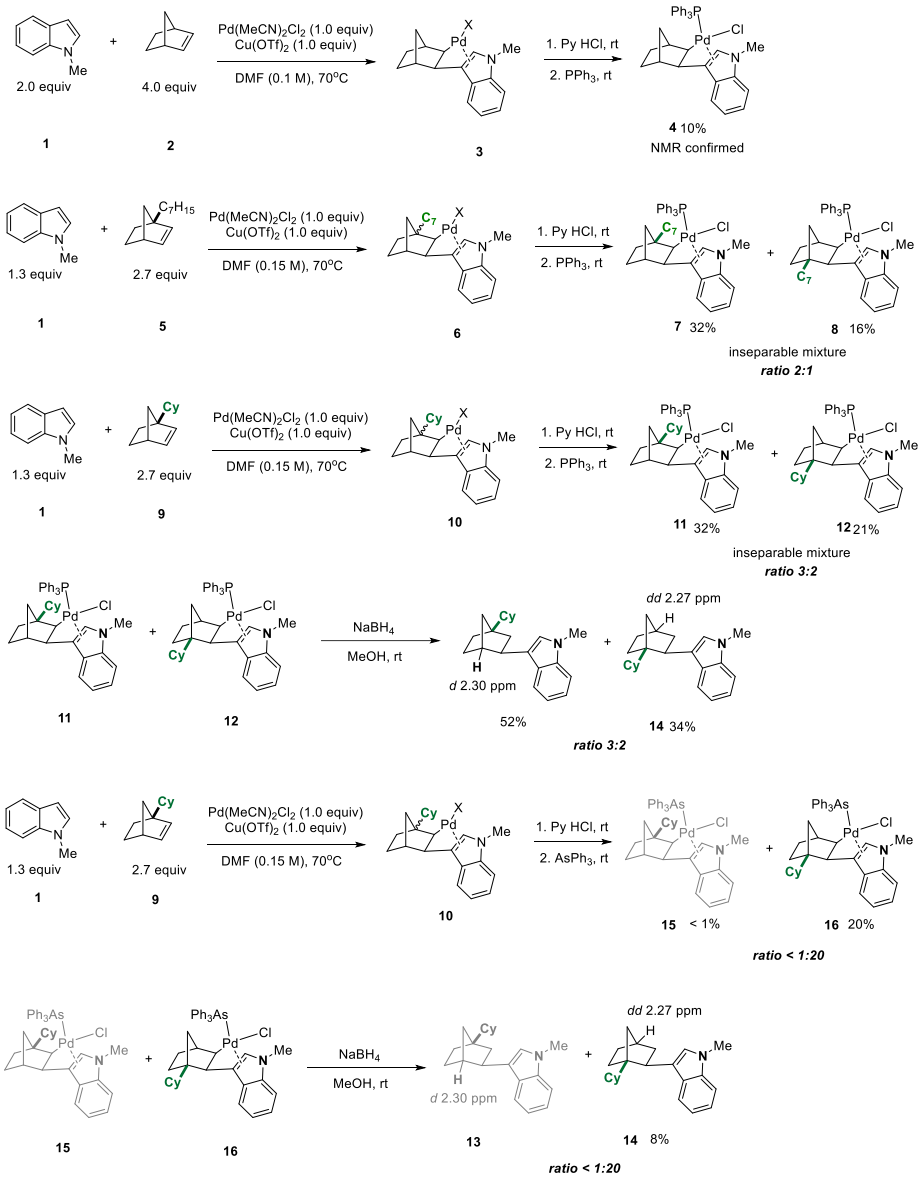

Computational study. In process.

7.3 Conclusion

In Summary, the development of a direct multi-functionalization method for heteroarenes, which can rapidly increase molecular complexity, is still highly demanded. In this full paper, we report a site-selective vicinal difunctionalization of five-membered heteroarenes enabled by the palladium/norbornene (Pd/NBE) cooperative catalysis. A wide range of heteroarenes, including indoles, pyrroles, furans and thiophenes were able to be difunctionalized in a site- and regio-selective manner. Besides ortho arylation, ortho alkynylation was also realized by using alkynyl bromide as the electrophile, which previously has not been achieved in the Catellani-type difunctionalization reaction. In addition, preliminary success has been achieved using methyl iodide as the electrophile to give the C4-alkylation/C5-alkenylation of pyrrole and thiophene. Moreover, considering the versatility of the heteroarene moieties in natural products and bioactive compounds, a concise synthesis of (±)-rhazinilam was realized by using this direct difunctionalization strategy. Finally, given that the C1-substituted NBEs have been found most effective in the indoles difunctionalization reaction, a combined experimental and computational study was performed to disclose the unique role of this type of NBE.

7.4 Experimental Procedures and Characterization Data

7.4.1 General Information

Unless noted otherwise, all solvents were dried by filtration through a Pure-Solv MD-5 Solvent Purification System (Innovative Technology). Ethyl acetate and *t*-butyl methyl ether were used directly without further purification. Reaction temperatures were reported as the temperatures of the bather surrounding the flasks or vials. Sensitive reagents and solvents were transferred under nitrogen into a nitrogen-filled glovebox with standard techniques. Sodium acetate was purchased from STREM, stored and used directly in the glovebox. Analytical thin-layer chromatography (TLC) was carried out using 0.2 mm commercial silica gel plates (silica gel 60, F254, EMD chemical). Vials (15 x 45 mm 1 dram (4 mL) with PTFE lined cap attached) were purchased from Qorpak and flame-dried and cooled in a desiccator prior to usage. High resolution mass spectra (HR-MS) were recorded on an Agilent 6530 LC Q-TOF mass spectrometer using electrospray ionization with fragmentation voltage set at 115 V and processed with an Agilent MassHunter Operating System. Infrared spectra were recorded on a Nicolet 380 FTIR using neat thin film technique. Nuclear magnetic resonance spectra (^{1}H NMR and ^{13}C NMR) were recorded with a Bruker DMX 400 (400 MHz, ^{1}H at 400 MHz, ^{13}C at 101 MHz) or Bruker Model DMX 500 (500 MHz, ^{1}H at 500 MHz, ^{13}C at 126 MHz). Chemical shifts were reported in parts per million (ppm, δ), downfield from tetramethylsilane (TMS, δ=0.00ppm) and were referenced to residual solvent ($CDCl_3$, δ=7.26 ppm (^{1}H) and 77.00 ppm (^{13}C)). All the ^{19}F chemical shifts were not referenced. Coupling constants were reported in Hertz (Hz). Data for ^{1}H NMR spectra were reported as follows: chemical shift (ppm, referenced to protium, s = singlet, d = doublet, t = triplet, q = quartet, quin = quintet, dd = doublet of doublets, td = triplet of doublets, ddd = doublet of doublet of doublets, m

= multiplet, coupling constant (Hz), and integration). All other materials were obtained from Sigma-Aldrich Corporation or Combi-Blocks Inc and were used as received.

7.4.2 Preparation of Heteroarene Substrates

Scheme 7.7. Preparation of 5l

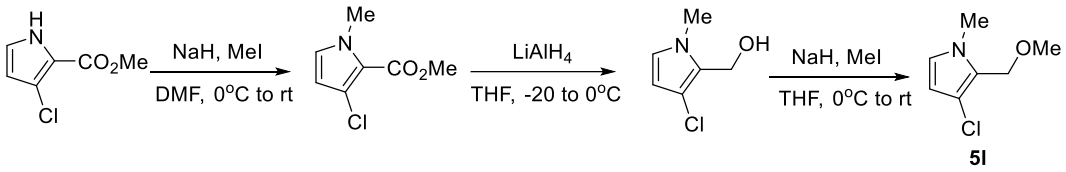

Following a similar reported procedure,[17] under N_2 atmosphere, methyl 3-chloro-1H-pyrrole-2-carboxylate (0.64 g, 4.0 mmol, 1.0 equiv.) was added to a solution of NaH (0.26 g, 6.4 mmol, 1.6 equiv.) in 15 ml DMF slowly at 0 °C. The mixture was stirred for 0.5h at rt, then adding MeI (0.32 ml, 5,2 mmol, 1.3 equiv.) at 0 °C. The resulting mixture was stirred for 8 h. Then the reaction mixture was quenched with water, extracted with Et_2OAc, dried over Na_2SO_4, and concentrated. The crude product was directly used in the following step without further purification.

Under N_2 atmosphere, the corresponding crude product was added to a solution of $LiAlH_4$ (0.35 g, 9.2 mmol, 2.3 equiv.) in 15 ml THF at -20 °C. The resulting mixture allowed to warm to 0 °C and stirring for 2 h. Water (20 mL) and 2 M aqueous NaOH (20 mL) were added to the reaction mixture, and the solid formed was filtered and washed with EtOAc. The filtrate was extracted with EtOAc and the combined organic extract was washed with saturated NaCl solution and then concentrated under vacuum to obtain the crude alcohol product. The crude alcohol product was directly used in the following step without further purification.

Under N_2 atmosphere, the crude alcohol product was added to a solution of NaH (0.26 g, 6.4 mmol, 1.6 equiv.) in 15 ml THF slowly at 0 ^oC. The mixture was stirred for 0.5 h at rt, then adding MeI (0.32 ml, 5,2 mmol, 1.3 equiv) at 0 ^oC. The resulting mixture was stirred for 8 h. Then the reaction mixture was quenched with water, extracted with Et_2O, dried over Na_2SO_4, and purified on silica gel chromatography (hexane/ethyl acetate = 20:1) to afford the desired product in 60% yield.

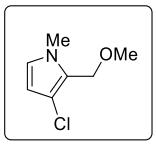

5l: Light yellow oil (60%). R_f = 0.3 (hexane/ethyl acetate = 20:1) **^{1}H NMR** (400 MHz, Chloroform-d) δ 6.54 (d, J = 2.9 Hz, 1H), 6.04 (d, J = 2.9 Hz, 1H), 4.43 (s, 2H), 3.62 (s, 3H), 3.29 (s, 3H). **^{13}C NMR** (101 MHz, $CDCl_3$) δ 124.7, 122.1, 112.9, 107.1, 62.5, 57.2, 34.8. **IR** (KBr): 2926, 1500, 1429, 1318, 1183, 1083, 1028, 946, 926, 898 cm^{-1}. **HRMS** (ESI): Calculated for $C_7H_{11}ClNO$ ($M+H^+$): 160.0524, found: 160.0520.

Scheme 7.8. Preparation of 7h

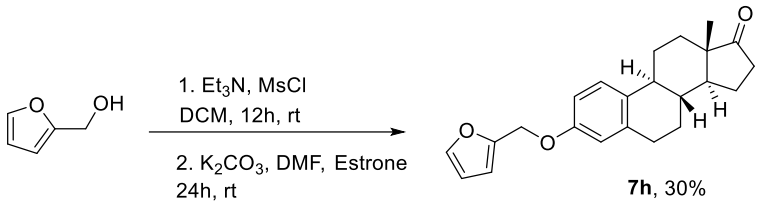

Following a known procedure,[18] triethylamine (4.2 ml, 30.0 mmol, 3.0 equiv) and methanesulfonyl chloride (1.6 mL, 20.0 mmol, 2.0 equiv) were added slowly to a dichloromethane solution of furan-2-ylmethanol (1.0 g, 10.0 mmol, 1.0 equiv) under N_2 atmosphere. The reaction mixture was stirred for 12 hours at room temperature. Then the reaction mixture was quenched with water, extracted

with dichloromethane, dried over Na_2SO_4, and concentrated. The crude product was directly used in the following step without further purification.

At 0 ^oC, estrone (2.7 g, 10.0 mmol, 1.0 equiv) and K_2CO_3 (2.8 g, 20.0 mmol, 2.0 equiv) was stirred in dimethylformamide (20 mL) for 5 min. The crude product was added to the reaction mixture, and then stirred at room temperature for 24 hours. The reaction mixture was quenched with water, extracted with ethyl acetate, dried over Na_2SO_4, and purified on silica gel chromatography (hexane/ethyl acetate = 3:1) to afford the desired product.

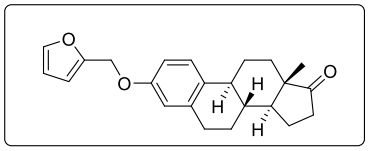

7h: White solid (40%). R_f = 0.2 (hexane / ethyl acetate =3:1). Mp = 181.6– 182.0 ^oC. **^{1}H NMR** (400 MHz, Chloroform-*d*) δ 7.44 (dd, *J* = 1.8, 0.8 Hz, 1H), 7.21 (d, *J* = 8.6 Hz, 1H), 6.80 (dd, *J* = 8.6, 2.8 Hz, 1H), 6.73 (d, *J* = 2.7 Hz, 1H), 6.42 (d, *J* = 3.2 Hz, 1H), 6.38 (dd, *J* = 3.2, 1.9 Hz, 1H), 4.97 (s, 2H), 2.90 (dd, *J* = 10.8, 4.4 Hz, 2H), 2.54 – 2.47 (m, 1H), 2.42 – 2.37 (m, 1H), 2.28 – 2.21 (m, 1H), 2.19 – 1.91 (m, 5H), 1.65 – 1.60 (m, 1H), 1.55 – 1.44 (m, 4H), 0.91 (s, 3H). **^{13}C NMR** (101 MHz, $CDCl_3$) δ 221.1, 156.5, 150.6, 143.2, 138.0, 132.8, 126.5, 115.2, 112.5, 110.6, 109.9, 62.6, 50.6, 48.2, 44.1, 38.5, 36.0, 31.7, 29.8, 26.7, 26.0, 21.7, 14.0. **IR** (KBr):2926, 1737, 1608, 1498, 1454, 1373, 1281, 1247, 1155, 1055 cm^{-1}. **HRMS** (ESI): Calculated for $C_{23}H_{27}O_3$ ($M+H^+$): 351.1955, found: 351.1952.

7.4.3 General Procedure of Vicinal Difunctionalization of Indoles

Scheme 7.9. Vicinal Difunctionalization of Indoles

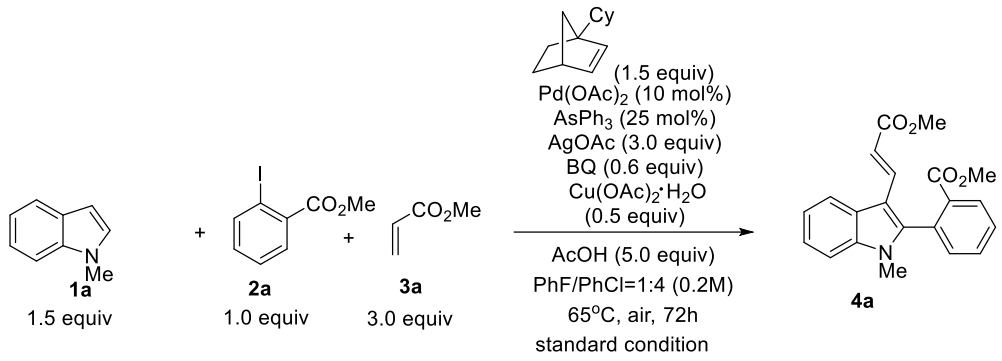

A flame-dried 4.0 mL vial was charged with $Pd(OAc)_2$ (4.6 mg, 0.02 mmol, 10 mol%), $AsPh_3$ (15.2 mg, 0.05 mmol, 25 mol%), BQ (13.0 mg, 0.12 mmol, 0.6 equiv), $Cu(OAc)_2.H_2O$ (20.0 mg, 0.1 mmol, 0.5 equiv.), NBE-Cy (53.0 mg, 0.3 mmol, 1.5 equiv), AgOAc (100 mg, 0.6 mmol, 3.0 equiv), Indole **1a** (39.4 mg, 0.2 mmol, 1.5 equiv) and aryl iodide **2a** (52.4 mg, 0.2 mmol, 1.0 equiv). Then, 1.0 mL chlorobenzene /fluorobenzene = 4:1 was added. After acrylate **3a** (51.6 mg/60 µL, 0.6 mmol, 3.0 equiv) and AcOH (60 mg/56 µL, 1.0 mmol, 5.0 equiv) and was added, the vial was tightly sealed and stirred on a pie-block preheated to 65 °C for 72 hours. After completion of the reaction, the mixture was filtered through a thin pad of silica gel. The filter cake was washed with ethyl acetate and the combined filtrate was concentrated. The residue was loaded to a small amount of silica gel and subjected to flash column chromatography to give the desired difunctionalization product **6a**.

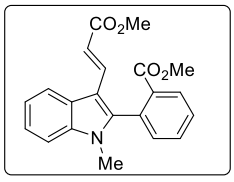

4a: Light yellow solid (71%). R_f = 0.3 (hexane/ ethyl acetate = 3:1). Mp = 123.1– 123.6 °C. **^{1}H NMR** (400 MHz, Chloroform-*d*) δ 8.17 (dd, *J* = 7.7, 1.4 Hz, 1H), 7.97 (d, *J* = 7.4 Hz, 1H), 7.71 –

7.60 (m, 2H), 7.48 (d, *J* = 15.9 Hz, 1H), 7.41 – 7.27 (m, 4H), 6.33 (d, *J* = 15.9 Hz, 1H), 3.70 (s, 3H), 3.64 (s, 3H), 3.47 (s, 3H). **^{13}C NMR** (101 MHz, $CDCl_3$) δ 169.0, 166.4, 144.7, 138.6, 137.8, 133.0, 132.5, 131.7, 131.4, 131.1, 129.9, 125.8, 123.0, 121.7, 120.8, 111.9, 110.3, 110.0, 52.5, 51.3, 30.9. **IR** (KBr): 2949, 1727, 1620, 1470, 1429, 1434, 1408, 1373, 1286, 1172 cm^{-1}. **HRMS** (ESI): Calculated for $C_{21}H_{19}NO_4Na$ ($M+Na^+$): 372.1206, found: 372.1206.

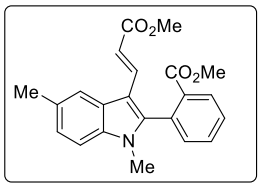

4b: Light yellow oil (65%). R_f = 0.3 (hexane/ ethyl acetate = 3:1). **^{1}H NMR** (400 MHz, Acetone-d_6) δ 8.16 (dd, *J* = 7.8, 1.3 Hz, 1H), 7.85 – 7.74 (m, 3H), 7.52 (dd, *J* = 7.5, 1.2 Hz, 1H), 7.46 – 7.34 (m, 2H), 7.20 – 7.15 (m, 1H), 6.27 (d, *J* = 15.9 Hz, 1H), 3.62 (s, 3H), 3.61 (s, 3H), 3.51 (s, 3H), 2.52 (s, 3H). **^{13}C NMR** (101 MHz, Acetone) δ 168.6, 166.9, 145.8, 139.0, 137.3, 133.7, 133.2, 133.1, 132.0, 131.6, 131.3, 130.8, 126.8, 125.0, 120.9, 111.7, 110.8, 110.2, 52.6, 51.1, 31.1, 21.7. **IR** (KBr): 2948, 1727, 1615, 1478, 1434, 1407, 1372, 1286, 1260, 1159 cm^{-1}. **HRMS** (ESI): Calculated for $C_{22}H_{21}NO_4Na$ ($M+Na^+$): 386.1363, found: 386.1367.

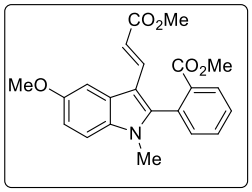

4c: Light yellow solid (52%). R_f = 0.3 (hexane/ ethyl acetate = 2:1). Mp = 153.1– 153.5 °C. **^{1}H NMR** (400 MHz, Chloroform-*d*) δ 8.16 (dd, *J* = 7.7, 1.3 Hz, 1H), 7.70 – 7.60 (m, 2H), 7.48 (d, *J*

= 15.9 Hz, 1H), 7.41 – 7.35 (m, 2H), 7.28 (d, *J* = 8.9 Hz, 1H), 6.98 (dd, *J* = 8.8, 2.4 Hz, 1H), 6.20 (d, *J* = 15.9 Hz, 1H), 3.92 (s, 3H), 3.70 (s, 3H), 3.65 (s, 3H), 3.44 (s, 3H). **^{13}C NMR** (101 MHz, $CDCl_3$) δ 169.0, 166.4, 155.8, 145.0, 138.7, 133.0, 132.9, 132.5, 131.7, 131.5, 131.0, 129.9, 126.3, 112.6, 111.2, 110.7, 109.9, 103.2, 56.2, 52.5, 51.3, 31.0. **IR** (KBr): 2948, 1726, 1614, 1484, 1432, 1409, 1292, 1261, 1160, 1046 cm^{-1}. **HRMS** (ESI): Calculated for $C_{22}H_{21}NO_5Na$ ($M+Na^+$): 402.1312, found: 402.1312.

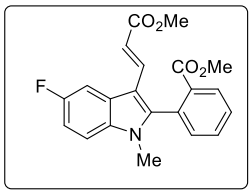

4d: Light yellow solid (65%). R_f = 0.3 (hexane/ ethyl acetate = 3:1). Mp = 155.4– 155.8 °C. **^{1}H NMR** (400 MHz, Chloroform-*d*) δ 8.18 (dd, *J* = 7.7, 1.4 Hz, 1H), 7.72 – 7.59 (m, 3H), 7.43 (d, *J* = 16.0 Hz, 1H), 7.37 (dd, *J* = 7.4, 1.3 Hz, 1H), 7.30 (dd, *J* = 8.9, 4.4 Hz, 1H), 7.07 (td, *J* = 9.0, 2.4 Hz, 1H), 6.21 (d, *J* = 16.0 Hz, 1H), 3.70 (s, 3H), 3.66 (s, 3H), 3.46 (s, 3H). **^{13}C NMR** (101 MHz, Chloroform-*d*) δ 168.8, 166.2, 160.4, 158.0, 145.9, 138.1, 134.3, 132.9, 132.6, 131.6, 131.1, 130.1, 126.1 (d, *J* = 10.0 Hz), 112.0, 111.1 (d, *J* = 26.0 Hz), 110.7 (d, *J* = 9.7 Hz), 110.1 (d, *J* = 4.4 Hz), 106.2 (d, *J* = 24.6 Hz), 52.6, 51.4, 31.1. **^{19}F NMR** (376 MHz, $CDCl_3$) δ -122.1. **IR** (KBr): 2950, 1726, 1618, 1481, 1434, 1409, 1373, 1289, 1194, 1161 cm^{-1}. **HRMS** (ESI): Calculated for $C_{21}H_{18}FNO_4Na$ ($M+Na^+$): 390.1112, found: 390.1113.

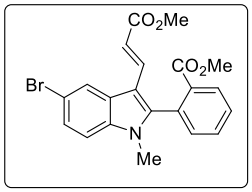

4f: White solid (64%). R_f = 0.3 (hexane/ ethyl acetate = 3:1). Mp = 161.7– 162.1°C. **^{1}H NMR** (400 MHz, Chloroform-*d*) δ 8.18 (dd, *J* = 7.7, 1.4 Hz, 1H), 8.08 (d, *J* = 1.7 Hz, 1H), 7.73 – 7.61 (m, 2H), 7.44 – 7.35 (m, 3H), 7.25 (d, *J* = 8.4 Hz, 1H), 6.25 (d, *J* = 16.0 Hz, 1H), 3.71 (s, 3H), 3.65 (s, 3H), 3.44 (s, 3H). **^{13}C NMR** (101 MHz, $CDCl_3$) δ 168.7, 166.2, 145.5, 137.8, 136.4, 132.8, 132.6, 131.5, 131.2, 130.9, 130.2, 127.3, 125.8, 123.3, 115.0, 112.6, 111.4, 109.7, 52.6, 51.4, 31.0. **IR** (KBr): 2949, 1726, 1622, 1467, 1433, 1405, 1366, 1285, 1168, 1092 cm^{-1}. **HRMS** (ESI): Calculated for $C_{21}H_{18}BrNO_4Na$ ($M+Na^+$): 450.0311, found: 450.0310.

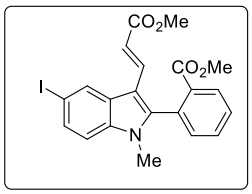

4e: Light yellow oil (50%). R_f = 0.3 (hexane/ ethyl acetate = 3:1). **^{1}H NMR** (400 MHz, Chloroform-*d*) δ 8.27 (d, *J* = 1.4 Hz, 1H), 8.18 (dd, *J* = 7.7, 1.4 Hz, 1H), 7.72 – 7.62 (m, 2H), 7.58 (dd, *J* = 8.6, 1.6 Hz, 1H), 7.40 (d, *J* = 16.0 Hz, 1H), 7.36 (dd, *J* = 7.4, 1.3 Hz, 1H), 7.16 (d, *J* = 8.6 Hz, 1H), 6.24 (d, *J* = 16.0 Hz, 1H), 3.71 (s, 3H), 3.65 (s, 3H), 3.44 (s, 3H). **^{13}C NMR** (101 MHz, $CDCl_3$) δ 168.7, 166.2, 145.1, 137.8, 136.9, 132.8, 132.6, 131.6, 131.3, 131.2, 130.9, 130.2, 129.4, 128.0, 112.6, 111.9, 109.4, 85.4, 52.6, 51.4, 30.9. **IR** (KBr): 2948, 1726, 1621, 1467, 1433, 1367, 1284, 1262, 1167, 1092 cm^{-1}. **HRMS** (ESI): Calculated for $C_{21}H_{18}BrNO_4Na$ ($M+Na^+$): 498.0173, found: 498.0173.

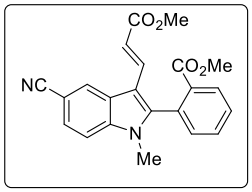

4g: White solid (36%). R_f = 0.3 (hexane/ ethyl acetate = 2:1). Mp = 181.6 – 182.0 ^{o}C. **^{1}H NMR** (400 MHz, Acetone-d_6) δ 8.49 – 8.44 (m, 1H), 8.25 – 8.20 (m, 1H), 7.88 (td, *J* = 7.5, 1.5 Hz, 1H), 7.81 (td, *J* = 7.7, 1.5 Hz, 1H), 7.76 (d, *J* = 8.5 Hz, 1H), 7.65 (dd, *J* = 8.5, 1.5 Hz, 1H), 7.58 (dd, *J* = 7.5, 1.1 Hz, 1H), 7.40 (d, *J* = 16.1 Hz, 1H), 6.35 (d, *J* = 16.1 Hz, 1H), 3.64 (s, 3H), 3.63 (s, 3H), 3.61 (s, 3H). **^{13}C NMR** (101 MHz, Acetone) δ 168.2, 166.6, 147.7, 140.2, 137.2, 133.6, 133.6, 132.6, 131.7, 131.4, 131.2, 126.4, 126.2, 126.0, 120.7, 114.3, 112.4, 110.9, 105.2, 52.7, 51.3, 31.5. **IR** (KBr): 2950, 2221, 1724, 1626, 1478, 1434, 1406, 1376, 1287, 1264 cm^{-1}. **HRMS** (ESI): Calculated for $C_{22}H_{18}N_2O_4Na$ ($M+Na^+$): 397.1159, found: 397.1162.

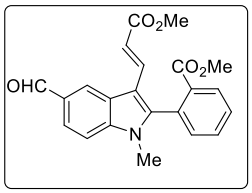

4h: Light yellow oil (52%). R_f = 0.2 (hexane/ ethyl acetate = 2:1). **^{1}H NMR** (400 MHz, Chloroform-*d*) δ 10.11 (s, 1H), 8.47 – 8.44 (m, 1H), 8.21 (dd, *J* = 7.7, 1.4 Hz, 1H), 7.90 (dd, *J* = 8.5, 1.4 Hz, 1H), 7.74 – 7.65 (m, 2H), 7.50 – 7.43 (m, 2H), 7.39 (dd, *J* = 7.4, 1.3 Hz, 1H), 6.40 (d, *J* = 16.1 Hz, 1H), 3.73 (s, 3H), 3.68 (s, 3H), 3.51 (s, 3H). **^{13}C NMR** (101 MHz, $CDCl_3$) δ 192.4, 168.5, 166.1, 146.2, 141.0, 137.3, 132.9, 132.8, 131.4, 131.3, 130.9, 130.8, 130.4, 125.7, 125.4, 123.5, 113.9, 111.5, 110.6, 52.6, 51.5, 31.2. **IR** (KBr): 2949, 2359, 1724, 1685, 1623, 1574, 1457,

1435, 1405, 1288 cm^{-1}. **HRMS** (ESI): Calculated for $C_{22}H_{19}NO_5Na$ ($M+Na^+$): 400.1155, found: 400.1158.

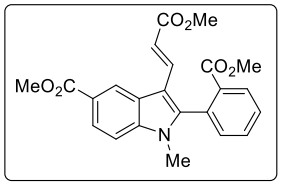

4i: Light yellow solid (51%). R_f = 0.2 (hexane/ ethyl acetate = 2:1). Mp = 163.2 – 163.6 °C. **^{1}H NMR** (400 MHz, Chloroform-*d*) δ 8.20 (dd, *J* = 7.7, 1.4 Hz, 1H), 8.15 (s, 1H), 7.97 (s, 2H), 7.73 – 7.63 (m, 2H), 7.46 (d, *J* = 16.0 Hz, 1H), 7.38 (dd, *J* = 7.4, 1.3 Hz, 1H), 6.31 (d, *J* = 16.0 Hz, 1H), 3.97 (s, 3H), 3.71 (s, 3H), 3.65 (s, 3H), 3.53 (s, 3H). **^{13}C NMR** (101 MHz, $CDCl_3$) δ 168.7, 167.9, 166.1, 147.3, 137.8, 137.2, 132.7, 132.7, 131.4, 131.3, 130.9, 130.3, 129.3, 124.4, 122.6, 120.2, 113.0, 112.3, 110.4, 52.6, 52.2, 51.4, 31.1. **IR** (KBr): 2950, 1715, 1623, 1464, 1433, 1379, 1289, 1264, 1242, 1171 cm^{-1}. **HRMS** (ESI): Calculated for $C_{23}H_{21}NO_6Na$ ($M+Na^+$): 430.1261, found: 4301263.

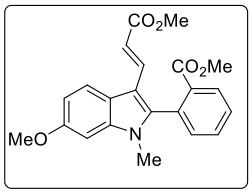

4j: Light yellow oil (51%). R_f = 0.3 (hexane/ ethyl acetate = 2:1). **^{1}H NMR** (400 MHz, Chloroform-*d*) δ 8.15 (dd, *J* = 7.7, 1.3 Hz, 1H), 7.84 (d, *J* = 8.7 Hz, 1H), 7.64 (dtd, *J* = 21.8, 7.5, 1.4 Hz, 2H), 7.43 (d, *J* = 15.9 Hz, 1H), 7.37 (dd, *J* = 7.4, 1.3 Hz, 1H), 6.93 (dd, *J* = 8.7, 2.3 Hz, 1H), 6.84 (d, *J* = 2.2 Hz, 1H), 6.31 (d, *J* = 15.9 Hz, 1H), 3.91 (s, 3H), 3.70 (s, 3H), 3.65 (s, 3H),

3.42 (s, 3H). **^{13}C NMR** (101 MHz, $CDCl_3$) δ 169.0, 166.4, 157.0, 143.9, 138.8, 138.6, 133.1, 132.4, 131.8, 131.4, 131.0, 129.8, 121.5, 119.9, 111.6, 110.7, 110.3, 94.0, 55.9, 52.5, 51.3, 30.9. **IR** (KBr): 2949, 1727, 1617, 1575, 1472, 1433, 1381, 1350, 1290, 1169 cm^{-1}. **HRMS** (ESI): Calculated for $C_{22}H_{21}NO_5Na$ ($M+Na^+$): 402.1312, found: 402.1310.

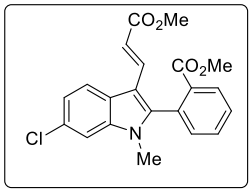

4k: Light yellow oil (61%). R_f = 0.3 (hexane/ ethyl acetate = 3:1). **^{1}H NMR** (400 MHz, Acetone-d_6) δ 8.20 (dd, *J* = 7.8, 1.3 Hz, 1H), 7.98 (d, *J* = 8.5 Hz, 1H), 7.87 – 7.77 (m, 2H), 7.63 (d, *J* = 1.9 Hz, 1H), 7.55 (dd, *J* = 7.5, 1.2 Hz, 1H), 7.38 (d, *J* = 16.0 Hz, 1H), 7.29 (dd, *J* = 8.5, 1.9 Hz, 1H), 6.25 (d, *J* = 16.0 Hz, 1H), 3.63 (s, 3H), 3.62 (s, 3H), 3.55 (s, 3H). **^{13}C NMR** (101 MHz, Acetone) δ 168.4, 166.7, 146.6, 139.3, 138.1, 136.2, 133.6, 133.4, 132.8, 131.5, 131.1, 129.0, 125.1, 122.5, 122.2, 112.9, 111.3, 110.5, 52.7, 51.2, 31.3. **IR** (KBr): 2949, 1726, 1621, 1473, 1433, 1407, 1287, 1289, 1170, 1091 cm^{-1}. **HRMS** (ESI): Calculated for $C_{21}H_{18}ClNO_4Na$ ($M+Na^+$): 406.0817, found: 406.0817.

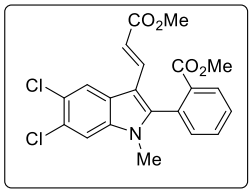

4l: Light yellow solid (55%). R_f = 0.3 (hexane/ ethyl acetate = 3:1). Mp = 182.9 – 183.2 °C. **^{1}H NMR** (400 MHz, Chloroform-*d*) δ 8.19 (dd, *J* = 7.7, 1.4 Hz, 1H), 8.01 (s, 1H), 7.73 – 7.63 (m,

2H), 7.48 (s, 1H), 7.40 – 7.34 (m, 2H), 6.22 (d, *J* = 16.0 Hz, 1H), 3.71 (s, 3H), 3.67 (s, 3H), 3.42 (s, 3H). **^{13}C NMR** (101 MHz, $CDCl_3$) δ 168.5, 166.0, 146.2, 137.4, 136.6, 132.8, 132.7, 131.4, 131.3, 130.6, 130.4, 126.8, 125.7, 125.2, 121.7, 113.1, 111.6, 109.7, 52.6, 51.5, 31.1. **IR** (KBr): 2949, 1726, 1623, 1469, 1435, 1406, 1324, 1291, 1169, 1092 cm^{-1}. **HRMS** (ESI): Calculated for $C_{21}H_{18}Cl_2NO_4$ ($M+H^+$): 418.0607, found: 418.0611.

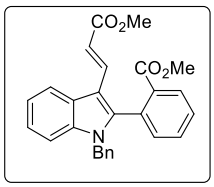

4n: Light yellow oil (41%). R_f = 0.3 (hexane/ ethyl acetate = 3:1). **^{1}H NMR** (400 MHz, Chloroform-*d*) δ 8.15 – 8.09 (m, 1H), 8.02 – 7.97 (m, 1H), 7.60 – 7.52 (m, 2H), 7.48 (d, *J* = 16.0 Hz, 1H), 7.26 (td, *J* = 4.3, 3.5, 2.0 Hz, 4H), 7.21 – 7.17 (m, 3H), 6.92 (dd, *J* = 6.6, 2.9 Hz, 2H), 6.36 (d, *J* = 16.0 Hz, 1H), 5.24 – 4.95 (m, 2H), 3.71 (s, 3H), 3.61 (s, 3H). **^{13}C NMR** (101 MHz, $CDCl_3$) δ 168.9, 166.3, 144.5, 138.4, 137.5, 136.9, 133.1, 132.3, 131.8, 131.1, 131.0, 129.9, 128.7, 127.6, 126.6, 126.1, 123.2, 121.8, 120.8, 112.5, 111.0, 110.9, 52.5, 51.4, 48.2. **IR** (KBr): 2949, 1727, 1621, 1574, 1462, 1419, 1365, 1292, 1263, 1172 cm^{-1}. **HRMS** (ESI): Calculated for $C_{27}H_{23}NO_4Na$ ($M+Na^+$): 448.1519, found: 448.1522.

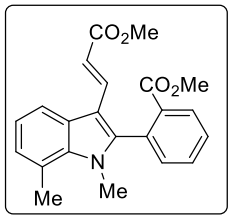

4m: Light yellow solid (62 %). R_f = 0.2 (hexane / ethyl acetate = 5:1). Mp = 167.5 – 168.0 ºC. **^{1}H NMR** (400 MHz, Benzene-d_6) δ 8.01 (d, *J* = 16.0 Hz, 1H), 7.91 – 7.83 (m, 2H), 7.08 (d, *J* = 7.7 Hz, 1H), 7.03 – 6.96 (m, 3H), 6.92 (d, *J* = 7.2 Hz, 1H), 6.65 (d, *J* = 16.0 Hz, 1H), 3.43 (s, 3H), 3.22 (s, 3H), 3.12 (s, 3H), 2.34 (s, 3H). **^{13}C NMR** (101 MHz, CDCl3) δ 168.34, 166.26, 145.05, 138.26, 137.07, 132.85, 132.63, 132.08, 131.95, 130.76, 129.54, 127.57, 126.28, 122.04, 121.64, 119.11, 113.03, 110.72, 51.81, 50.78, 33.99, 20.22. **IR** (KBr): 2950, 2923, 1728, 1618, 1540, 1475, 1456, 1434, 1286, 1172 cm^{-1}. **HRMS** (ESI): Calculated for $C_{22}H_{22}NO_4$ ($M+H^+$): 364.1543, found: 364.1544.

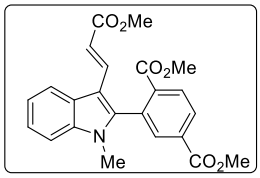

4o: Light yellow oil (50%). R_f = 0.2 (hexane/ ethyl acetate = 2:1). **^{1}H NMR** (400 MHz, Chloroform-*d*) δ 8.28 (dd, *J* = 8.2, 1.7 Hz, 1H), 8.21 (d, *J* = 8.2 Hz, 1H), 8.04 (d, *J* = 1.4 Hz, 1H), 7.97 (d, *J* = 7.6 Hz, 1H), 7.44 – 7.38 (m, 2H), 7.37 – 7.32 (m, 1H), 7.30 (td, *J* = 7.5, 7.0, 1.4 Hz, 1H), 6.34 (d, *J* = 15.9 Hz, 1H), 3.95 (s, 3H), 3.70 (s, 3H), 3.66 (s, 3H), 3.48 (s, 3H). **^{13}C NMR** (101 MHz, $CDCl_3$) δ 168.9, 165.8, 165.7, 143.1, 138.0, 137.9, 135.7, 133.7, 133.5, 131.7, 131.0, 130.9, 125.7, 123.2, 121.8, 120.8, 112.5, 110.7, 110.1, 52.9, 52.8, 51.4, 31.0. **IR** (KBr): 2949, 1727, 1621, 1574, 1462, 1419, 1365, 1292, 1263, 1172 cm^{-1}. **HRMS** (ESI): Calculated for $C_{23}H_{21}NO_6Na$ ($M+Na^+$): 430.1261, found: 430.1265.

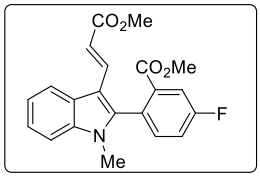

4p: Light yellow oil (50%). R_f = 0.3 (hexane/ ethyl acetate = 3:1). **^{1}H NMR** (400 MHz, Chloroform-*d*) δ 7.97 (d, *J* = 7.6 Hz, 1H), 7.87 (dd, *J* = 9.0, 2.1 Hz, 1H), 7.44 (d, *J* = 16.0 Hz, 1H), 7.41 – 7.26 (m, 5H), 6.34 (d, *J* = 15.9 Hz, 1H), 3.71 (s, 3H), 3.66 (s, 3H), 3.47 (s, 3H). **^{13}C NMR** (101 MHz, Chloroform-*d*) δ 168.9, 165.2 (d, *J* = 2.5 Hz), 163.1 (d, *J* = 251.7 Hz), 143.3, 138.2, 137.8, 134.9 (d, *J* = 8.0 Hz), 133.8 (d, *J* = 7.7 Hz), 127.4 (d, *J* = 3.7 Hz), 125.7, 123.1, 121.7, 120.8, 119.7 (d, *J* = 21.3 Hz), 118.3 (d, *J* = 23.7 Hz), 112.3, 110.6, 110.0, 52.8, 51.4, 30.9. **^{19}F NMR** (376 MHz, $CDCl_3$) δ -109.7. **IR** (KBr): 2950, 1732, 1710, 1621, 1575, 1470, 1435, 1411, 1287, 1195 cm^{-1}. **HRMS** (ESI): Calculated for $C_{21}H_{18}FNO_4Na$ ($M+Na^+$): 390.1112, found: 390.1117.

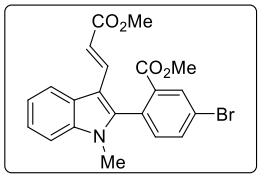

4q: Light yellow oil (51%). R_f = 0.3 (hexane/ ethyl acetate = 3:1). **^{1}H NMR** (400 MHz, Chloroform-*d*) δ 8.31 (d, *J* = 2.1 Hz, 1H), 7.96 (d, *J* = 7.7 Hz, 1H), 7.81 (dd, *J* = 8.1, 2.1 Hz, 1H), 7.43 (d, *J* = 15.9 Hz, 1H), 7.40 – 7.24 (m, 4H), 6.36 (d, *J* = 15.9 Hz, 1H), 3.72 (s, 3H), 3.66 (s, 3H), 3.47 (s, 3H). **^{13}C NMR** (101 MHz, $CDCl_3$) δ 168.9, 165.0, 143.1, 138.1, 137.9, 135.5, 134.4, 134.1, 133.3, 130.2, 125.6, 124.3, 123.2, 121.8, 120.8, 112.5, 110.5, 110.0, 52.8, 51.4, 30.9. **IR** (KBr): 2949, 1732, 1708, 1621, 1470, 1434, 1411, 1287, 1253, 1172 cm^{-1}. **HRMS** (ESI): Calculated for $C_{21}H_{18}BrNO_4Na$ ($M+Na^+$): 450.0311, found: 450.0312.

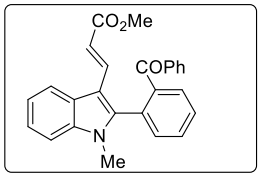

4r: Light yellow oil (61%). R_f = 0.3 (hexane/ ethyl acetate = 2:1). **^{1}H NMR** (400 MHz, Chloroform-*d*) δ 7.77 (d, *J* = 7.9 Hz, 1H), 7.72 – 7.62 (m, 3H), 7.61 – 7.57 (m, 2H), 7.52 (d, *J* = 15.9 Hz, 1H), 7.47 (d, *J* = 7.4 Hz, 1H), 7.39 – 7.34 (m, 1H), 7.29 (d, *J* = 3.5 Hz, 1H), 7.26 – 7.17 (m, 4H), 6.22 (d, *J* = 15.9 Hz, 1H), 3.72 (s, 3H), 3.55 (s, 3H). **^{13}C NMR** (101 MHz, $CDCl_3$) δ 197.0, 168.7, 143.4, 141.4, 138.4, 137.9, 136.6, 133.1, 132.3, 130.9, 129.8, 129.8, 129.4, 129.4, 128.1, 125.5, 123.1, 121.7, 120.5, 112.4, 111.2, 110.1, 51.3, 31.4. **IR** (KBr): 3056, 2947, 1706, 1663, 1621, 1597, 1469, 1433, 1288, 1172 cm^{-1}. **HRMS** (ESI): Calculated for $C_{26}H_{21}NO_3Na$ ($M+Na^+$): 418.1414, found: 418.1414.

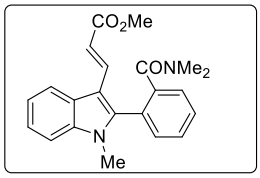

4s: Light yellow oil (60%). R_f = 0.3 (toluene/ ethyl acetate = 5:1). **^{1}H NMR** (400 MHz, Chloroform-*d*) δ 7.95 (d, *J* = 7.6 Hz, 1H), 7.62 – 7.50 (m, 3H), 7.49 – 7.43 (m, 1H), 7.41 – 7.26 (m, 4H), 6.42 (d, *J* = 15.9 Hz, 1H), 3.72 (s, 3H), 3.57 (s, 3H), 2.79 (d, *J* = 1.4 Hz, 6H). **^{13}C NMR** (101 MHz, $CDCl_3$) δ 169.6, 168.9, 143.9, 138.7, 138.6, 138.2, 132.2, 129.9, 129.2, 128.2, 127.1, 125.5, 123.2, 121.7, 120.7, 111.8, 110.7, 110.6, 51.3, 39.3, 34.8, 31.7. **IR** (KBr): 3056, 2947, 1706, 1663, 1621, 1597, 1469, 1433, 1288, 1172 cm^{-1}. **HRMS** (ESI): Calculated for $C_{22}H_{22}N_2O_3Na$ ($M+Na^+$): 385.1523, found: 385.1526.

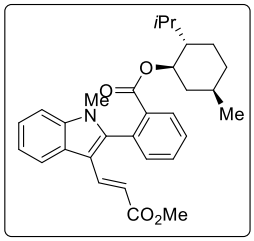

4t: Light yellow oil (60%, dr =1:1). R_f = 0.3 (hexane / ethyl acetate = 3:1). **^{1}H NMR** (400 MHz, Chloroform-*d*) δ 8.21 (dd, *J* = 7.3, 1.6 Hz, 1H), 7.97 (d, *J* = 7.7 Hz, 1H), 7.66 (tt, *J* = 6.6, 3.6 Hz, 2H), 7.51 (d, *J* = 15.9 Hz, 1H), 7.39 – 7.28 (m, 4H), 6.33 (d, *J* = 15.9 Hz, 1H), 4.63 (td, *J* = 10.9, 4.3 Hz, 1H), 3.70 (s, 3H), 3.43 (s, 3H), 1.78 – 1.71 (m, 1H), 1.52 – 1.24 (m, 6H), 0.83 (dd, *J* = 13.0, 3.2 Hz, 1H), 0.73 (d, *J* = 6.5 Hz, 3H), 0.58 – 0.52 (m, 6H), 0.41 – 0.33 (m, 1H). **^{13}C NMR** (101 MHz, $CDCl_3$) δ 168.92, 165.84, 145.16, 138.58, 137.69, 132.69, 132.66, 132.30, 131.44, 130.84, 129.97, 125.77, 122.98, 121.70, 120.79, 111.88, 110.43, 109.82, 75.03, 51.32, 46.66, 40.47, 34.08, 31.24, 30.83, 25.66, 22.76, 22.04, 20.80, 15.83. **IR** (KBr): 2953, 1711, 1621, 1470, 1433, 1409, 1288, 1254, 1171, 1090 cm^{-1}. **HRMS** (ESI): Calculated for $C_{30}H_{35}NO_4Na$ ($M+Na^+$): 496.2458, found: 496.2466.

4t': **^{1}H NMR** (400 MHz, Chloroform-*d*) δ 8.13 – 8.05 (m, 1H), 7.94 (d, *J* = 7.5 Hz, 1H), 7.70 – 7.60 (m, 2H), 7.46 – 7.28 (m, 5H), 6.27 (d, *J* = 16.0 Hz, 1H), 4.61 (td, *J* = 10.7, 4.4 Hz, 1H), 3.69 (s, 3H), 3.48 (s, 3H), 1.68 – 1.64 (m, 1H), 1.56 – 1.46 (m, 3H), 1.27 (dd, *J* = 9.7, 2.5 Hz, 2H), 0.90 – 0.85 (m, 2H), 0.68 (dd, *J* = 13.7, 6.8 Hz, 6H), 0.55 (d, *J* = 6.9 Hz, 3H), 0.35 (q, *J* = 12.1 Hz, 1H). **^{13}C NMR** (101 MHz, $CDCl_3$) δ 168.71, 166.11, 138.23, 137.56, 133.48, 132.11, 131.77, 130.62, 129.82, 129.01, 126.02, 125.80, 122.86, 121.57, 120.50, 111.84, 110.62, 109.83, 75.05, 51.18, 46.71, 40.14, 33.98, 31.09, 30.77, 25.81, 22.82, 21.87, 20.73, 15.75. **IR** (KBr): 2952, 1714, 1620, 1470, 1433, 1373, 1287, 1255, 1170, 1132 cm^{-1}. **HRMS** (ESI): Calculated for $C_{30}H_{35}NO_4Na$ ($M+Na^+$): 496.2458, found: 496.2465.

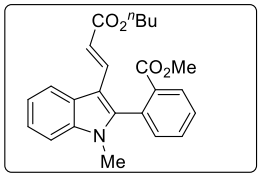

4u: Light yellow oil (61%). R_f = 0.3 (hexane / ethyl acetate = 3:1). **^{1}H NMR** (400 MHz, Chloroform-*d*) δ 8.17 (dd, *J* = 7.7, 1.3 Hz, 1H), 7.99 (d, *J* = 7.3 Hz, 1H), 7.69 – 7.60 (m, 2H), 7.46 (d, *J* = 15.9 Hz, 1H), 7.40 – 7.27 (m, 4H), 6.35 (d, *J* = 15.9 Hz, 1H), 4.11 (t, *J* = 6.6 Hz, 2H), 3.65 (s, 3H), 3.48 (s, 3H), 1.65 – 1.60 (m, 2H), 1.43 – 1.33 (m, 2H), 0.92 (t, *J* = 7.4 Hz, 3H). **^{13}C NMR** (101 MHz, $CDCl_3$) δ 168.7, 166.4, 144.7, 138.4, 137.8, 133.1, 132.4, 131.8, 131.4, 131.0, 129.9, 125.7, 122.9, 121.6, 120.8, 112.4, 110.3, 110.0, 63.9, 52.5, 31.0, 30.9, 19.4, 13.9. **IR** (KBr): 2956, 1728, 1704, 1619, 1574, 1470, 1433, 1373, 1284, 1172 cm^{-1}. **HRMS** (ESI): Calculated for $C_{24}H_{25}NO_4Na$ ($M+Na^+$): 414.1676, found: 414.1677.

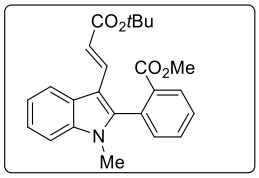

4v: Light yellow oil (65%). R_f = 0.3 (hexane / ethyl acetate = 3:1). **^{1}H NMR** (400 MHz, Chloroform-*d*) δ 8.15 (dd, *J* = 7.8, 1.3 Hz, 1H), 7.99 (d, *J* = 7.4 Hz, 1H), 7.63 (dtd, *J* = 24.0, 7.5, 1.4 Hz, 2H), 7.42 – 7.27 (m, 5H), 6.32 (d, *J* = 15.9 Hz, 1H), 3.64 (s, 3H), 3.47 (s, 3H), 1.47 (s, 9H). **^{13}C NMR** (101 MHz, $CDCl_3$) δ 168.2, 166.4, 144.5, 137.8, 137.4, 133.1, 132.4, 131.8, 131.5, 131.0, 129.8, 125.8, 122.8, 121.5, 120.9, 114.2, 110.3, 109.9, 79.6, 52.5, 30.9, 28.5. **IR** (KBr): 2919, 1728, 1699, 1617, 1471, 1470, 1434, 1368, 1288, 1149 cm^{-1}. **HRMS** (ESI): Calculated for $C_{24}H_{25}NO_4Na$ ($M+Na^+$): 414.1676, found: 414.1680.

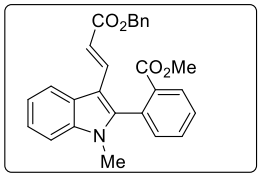

4w: Light yellow oil (62%). R_f = 0.3 (hexane / ethyl acetate = 3:1). **^{1}H NMR** (400 MHz, Chloroform-*d*) δ 8.17 (dd, *J* = 7.7, 1.4 Hz, 1H), 7.97 (d, *J* = 7.6 Hz, 1H), 7.70 – 7.61 (m, 2H), 7.52 (d, *J* = 15.9 Hz, 1H), 7.41 – 7.27 (m, 9H), 6.40 (d, *J* = 15.9 Hz, 1H), 5.17 (s, 2H), 3.64 (s, 3H), 3.48 (s, 3H). **^{13}C NMR** (101 MHz, $CDCl_3$) δ 168.4, 166.4, 145.0, 139.1, 137.8, 136.8, 133.0, 132.4, 131.8, 131.3, 131.1, 129.9, 128.6, 128.2, 128.1, 125.7, 123.0, 121.7, 120.9, 111.7, 110.4, 110.0, 65.8, 52.5, 30.9. **IR** (KBr): 2950, 1727, 1618, 1574, 1470, 1434, 1409, 1377, 1284, 1168 cm^{-1}. **HRMS** (ESI): Calculated for $C_{27}H_{23}NO_4Na$ ($M+Na^+$): 448.1519, found: 448.1522.

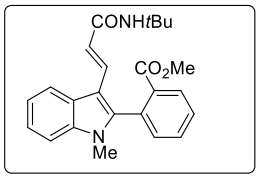

4x: Light yellow oil (45%). R_f = 0.3 (toluene / ethyl acetate = 5:1). **^{1}H NMR** (400 MHz, Chloroform-*d*) δ 8.07 (dd, *J* = 7.8, 1.2 Hz, 1H), 7.88 (d, *J* = 7.8 Hz, 1H), 7.60 – 7.49 (m, 2H), 7.36 – 7.29 (m, 3H), 7.26 – 7.22 (m, 1H), 7.17 (d, *J* = 7.0 Hz, 1H), 6.21 (d, *J* = 15.5 Hz, 1H), 5.22 (s, 1H), 3.56 (s, 3H), 3.38 (s, 3H), 1.31 (s, 9H). **^{13}C NMR** (101 MHz, $CDCl_3$) δ 166.8, 166.3, 143.8, 137.6, 133.9, 133.1, 132.4, 131.6, 131.5, 130.9, 129.6, 125.7, 122.5, 121.0, 120.5, 116.3, 110.0, 109.8, 52.3, 51.2, 30.7, 29.1. **IR** (KBr): 3290, 2964, 1727, 1651, 1607, 1552, 1470, 1453, 1290, 1261 cm^{-1}. **HRMS** (ESI): Calculated for $C_{24}H_{26}N_2O_3Na$ ($M+Na^+$): 413.1836, found: 413.1838.

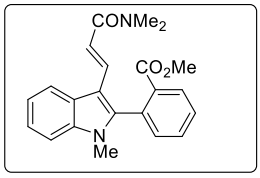

4y: Light yellow oil (61%). R_f = 0.3 (hexane / ethyl acetate = 3:1). **^{1}H NMR** (400 MHz, Chloroform-*d*) δ 8.17 – 8.12 (m, 1H), 7.93 (d, *J* = 7.8 Hz, 1H), 7.66 (td, *J* = 7.4, 1.3 Hz, 1H), 7.59 (td, *J* = 7.6, 1.3 Hz, 1H), 7.53 (d, *J* = 15.4 Hz, 1H), 7.39 (d, *J* = 7.6 Hz, 2H), 7.35 – 7.27 (m, 2H), 6.69 (d, *J* = 15.4 Hz, 1H), 3.64 (s, 3H), 3.48 (s, 3H), 3.04 (s, 6H). **^{13}C NMR** (101 MHz, $CDCl_3$) δ 168.1, 166.4, 143.5, 137.7, 136.0, 133.1, 132.6, 132.0, 131.7, 131.0, 129.7, 126.0, 122.6, 121.2, 120.4, 111.9, 110.6, 110.0, 52.5, 30.8, 29.8. **IR** (KBr): 2924, 1727, 1643, 1593, 1470, 1434, 1386, 1275, 1129, 1091 cm^{-1}. **HRMS** (ESI): Calculated for $C_{22}H_{22}N_2O_3Na$ ($M+Na^+$): 385.1523, found: 385.1527.

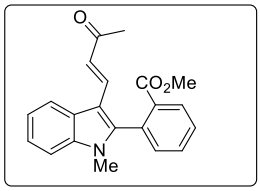

4z: Light yellow oil (52%). R_f = 0.2 (hexane/ethyl acetate = 3:1). **^{1}H NMR** (400 MHz, Chloroform-*d*) δ 8.17 (dd, *J* = 7.7, 1.2 Hz, 1H), 8.00 (d, *J* = 7.6 Hz, 1H), 7.73 – 7.63 (m, 2H), 7.41 – 7.29 (m, 5H), 6.70 (d, *J* = 16.1 Hz, 1H), 3.65 (s, 3H), 3.50 (s, 3H), 2.19 (s, 3H). **^{13}C NMR** (101 MHz, $CDCl_3$) δ 198.6, 166.4, 145.4, 138.0, 137.5, 132.9, 132.4, 131.9, 131.2, 131.0, 130.0, 125.7, 123.2, 122.5, 121.9, 120.9, 110.4, 110.1, 52.6, 31.0, 27.4. **IR** (KBr): 2924, 1727, 1676, 1585, 1572, 1470, 1408, 1374, 1357, 1284 cm^{-1}. **HRMS** (ESI): Calculated for $C_{21}H_{19}NO_3Na$($M+Na^+$): 356.1257, found: 356.1260.

7.4.4 General Procedure of Vicinal Difunctionalization of Pyrroles

Scheme 7.10. Vicinal Difunctionalization of Pyrroles

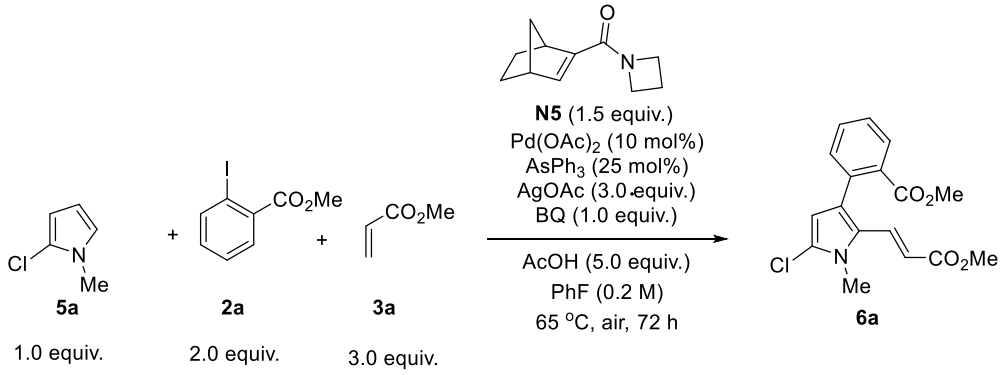

Unless otherwise noted, a flame-dried 4.0 mL vial was charged with $Pd(OAc)_2$ (4.6 mg, 0.02 mmol, 10 mol%), $AsPh_3$ (15.2 mg, 0.05 mmol, 25 mol%), BQ (21.6 mg, 0.2 mmol, 1.0 equiv), **N5** (53.2 mg, 0.3 mmol, 1.5 equiv), AgOAc (100 mg, 0.6 mmol, 3.0 equiv), Pyrrole **5a** (23.2 mg, 0.2 mmol, 1.0 equiv) and aryl iodide **2a** (104.8 mg, 0.4 mmol, 2.0 equiv). Then, 1.0 mL fluorobenzene was added. After acrylate **3a** (51.6 mg/60 µL, 0.6 mmol, 3.0 equiv) and AcOH (60 mg/56 µL, 1.0 mmol, 5.0 equiv) and was added, the vial was tightly sealed and stirred on a pie-block preheated to 65 ^oC for 72 hours. After completion of the reaction, the mixture was filtered through a thin pad of silica gel. The filter cake was washed with ethyl acetate and the combined filtrate was concentrated. The residue was loaded to a small amount of silica gel and subjected to flash column chromatography to give the desired difunctionalization product **6a**.

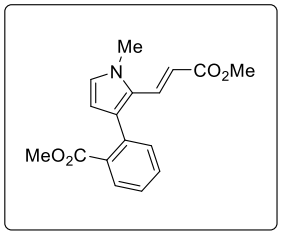

6m: Light yellow oil (48%). R_f = 0.3 (hexane/ethyl acetate = 3:1). **^{1}HNMR** (400 MHz, Chloroform-d) δ 7.86 (dd, J = 7.8, 1.2 Hz, 1H), 7.57 – 7.47 (m, 2H), 7.39 (td, J = 7.6, 1.3 Hz, 1H), 7.30 (dd, J = 7.6, 1.0 Hz, 1H), 6.78 (d, J = 2.6 Hz, 1H), 6.12 (d, J = 2.6 Hz, 1H), 5.68 (d, J = 16.1

Hz, 1H), 3.79 (s, 3H), 3.70 (s, 3H), 3.68 (s, 3H). **^{13}C NMR** (101 MHz, $CDCl_3$) δ 168.4, 168.3, 136.9, 132.6, 132.0, 131.6, 131.4, 130.1, 130.1, 127.4, 126.9, 125.4, 112.4, 110.8, 52.1, 51.5, 36.0. **IR** (KBr): 3057, 2951, 1728, 1621, 1495, 1434, 1417, 1354, 1291, 1173 cm^{-1}. **HRMS** (ESI): Calculated for $C_{17}H_{17}NO_4$ (M^+): 299.1152, found: 299.1157.

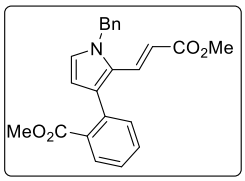

6n: Light yellow oil (43%). R_f = 0.3 (hexane/ethyl acetate = 3:1). **^{1}H NMR** (400 MHz, Chloroform-*d*) δ 7.88 (dd, *J* = 7.8, 1.1 Hz, 1H), 7.53 – 7.46 (m, 2H), 7.42 – 7.29 (m, 5H), 7.10 (d, *J* = 7.2 Hz, 2H), 6.87 (d, *J* = 2.7 Hz, 1H), 6.21 (d, *J* = 2.6 Hz, 1H), 5.51 (d, *J* = 16.0 Hz, 1H), 5.28 (s, 2H), 3.66 (s, 3H), 3.60 (s, 3H). **^{13}C NMR** (101 MHz, $CDCl_3$) δ 168.5, 168.2, 137.5, 136.9, 132.1, 131.9, 131.7, 131.6, 130.2, 130.0, 129.1, 127.9, 127.5, 126.4, 126.3, 125.1, 113.3, 111.6, 52.1, 51.6, 51.5. **IR** (KBr): 2949, 1712, 1621, 1497, 1433, 1454, 1350, 1293, 1253, 1171 cm^{-1}. **HRMS** (ESI): Calculated for $C_{23}H_{21}NO_4Na$ ($M+Na^+$): 398.1363, found: 398.1368.

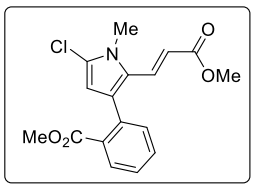

6a: Light yellow oil (75%). R_f = 0.3 (hexane/ ethyl acetate = 3:1). **^{1}H NMR** (400 MHz, Chloroform-*d*) δ 7.82 (dd, *J* = 7.8, 1.2 Hz, 1H), 7.44 (td, *J* = 7.5, 1.4 Hz, 1H), 7.39 (d, *J* = 16.1 Hz, 1H), 7.34 (td, *J* = 7.6, 1.3 Hz, 1H), 7.21 – 7.19 (m, 1H), 6.04 (s, 1H), 5.56 (d, *J* = 16.1 Hz, 1H),

3.66 (s, 3H), 3.65 (s, 3H), 3.60 (s, 3H). **^{13}C NMR** (101 MHz, $CDCl_3$) δ 168.18, 167.92, 135.94, 132.08, 131.93, 131.86, 131.26, 130.31, 129.13, 127.80, 125.23, 122.11, 113.02, 109.84, 52.19, 51.59, 32.22. **IR** (KBr): 2950, 1731, 1622, 1572, 1485, 1459, 1424, 1352, 1282, 1252 cm^{-1}. **HRMS** (ESI): Calculated for $C_{17}H_{16}ClNO_4Na(M+Na^+)$: 356.0660, found: 356.0661.

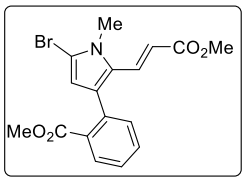

6b: White solid (71%). R_f = 0.3 (hexane/ethyl acetate = 3:1). Mp = 138.4 – 138.8 °C. **^{1}H NMR** (400 MHz, Chloroform-*d*) δ 7.89 (dd, *J* = 7.8, 1.2 Hz, 1H), 7.54 – 7.44 (m, 2H), 7.41 (td, *J* = 7.6, 1.3 Hz, 1H), 7.27 (dd, *J* = 7.5, 1.1 Hz, 1H), 6.21 (s, 1H), 5.62 (d, *J* = 16.0 Hz, 1H), 3.75 (s, 3H), 3.71 (s, 3H), 3.67 (s, 3H). **^{13}C NMR** (101 MHz, $CDCl_3$) δ 168.1, 167.9, 135.9, 132.1, 131.9, 131.9, 131.2, 130.3, 129.8, 127.8, 126.7, 113.7, 113.3, 109.1, 52.2, 51.6, 34.0. **IR** (KBr): 2949, 1714, 1621, 1455, 1417, 1350, 1280, 1251, 1192, 1173 cm^{-1}. **HRMS** (ESI): Calculated for $C_{17}H_{16}BrNO_4Na$ ($M+Na^+$): 400.0155, found: 400.0159.

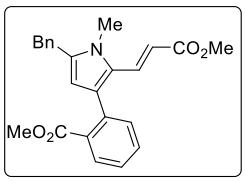

6c: Yellow oil (39%). R_f = 0.4 (hexane/ethyl acetate = 3:1). **^{1}H NMR** (400 MHz, Chloroform-*d*) δ 7.83 (dd, *J* = 7.8, 1.2 Hz, 1H), 7.54 (d, *J* = 16.0 Hz, 1H), 7.49 (td, *J* = 7.6, 1.4 Hz, 1H), 7.38 (td, *J* = 7.6, 1.3 Hz, 1H), 7.34 – 7.29 (m, 3H), 7.23 (dd, *J* = 8.4, 6.2 Hz, 1H), 7.17 (d, *J* = 7.0 Hz, 2H),

5.94 (s, 1H), 5.64 (d, *J* = 16.0 Hz, 1H), 4.01 (s, 2H), 3.69 (s, 3H), 3.67 (s, 3H), 3.56 (s, 3H). **^{13}C NMR** (101 MHz, $CDCl_3$) δ 168.6, 168.6, 138.3, 136.8, 136.6, 132.7, 131.9, 131.6, 131.5, 130.0, 129.2, 128.8, 128.5, 127.3, 126.7, 125.6, 112.0, 111.6, 52.1, 51.5, 33.4, 32.1. **IR** (KBr): 2949, 1713, 1616, 1496, 1456, 1433, 1397, 1357, 1282, 1251 cm^{-1}. **HRMS** (ESI): Calculated for $C_{24}H_{23}NO_4Na$ ($M+Na^+$): 412.1519, found: 412.1516.

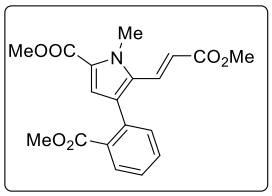

6d: Yellow oil (38%). R_f = 0.3 (Hexane/ethyl acetate = 1:1). Pyrrole **1f** (2.5 equiv) , ArI **2a** (1.0 equiv) and acrylate **3a** (3.0 equiv) were used. **^{1}H NMR** (400 MHz, Chloroform-*d*) δ 7.92 (dd, *J* = 7.8, 1.1 Hz, 1H), 7.58 – 7.50 (m, 2H), 7.42 (td, *J* = 7.6, 1.3 Hz, 1H), 7.27 – 7.25 (m, 1H), 6.87 (s, 1H), 5.68 (d, *J* = 16.1 Hz, 1H), 4.08 (s, 3H), 3.82 (s, 3H), 3.70 (s, 3H), 3.68 (s, 3H).**^{13}C NMR** (101 MHz, $CDCl_3$) δ 167.7, 167.4, 161.7, 136.3, 132.1, 131.9, 131.5, 131.5, 131.0, 130.5, 127.9, 127.4, 124.8, 119.0, 118.7, 52.2, 51.8, 51.5, 33.4. **IR** (KBr): 2951, 1711, 1627, 1455, 1400, 1292, 1246, 1166, 1094, 1078 cm^{-1}. **HRMS** (ESI): Calculated for $C_{19}H_{19}NO_6Na$ ($M+Na^+$): 380.1105, found: 380.1109.

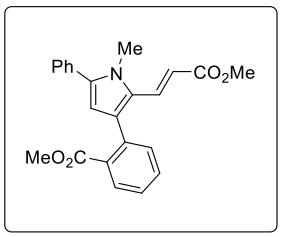

6e: Brown oil (56%). R_f = 0.3 (hexane/ethyl acetate = 3:1). **^{1}H NMR** (400 MHz, Chloroform-d) δ 7.87 (dd, J = 7.8, 1.1 Hz, 1H), 7.61 (d, J = 16.1 Hz, 1H), 7.53 (td, J = 7.5, 1.4 Hz, 1H), 7.46 – 7.35 (m, 7H), 6.25 (s, 1H), 5.76 (d, J = 16.1 Hz, 1H), 3.75 (s, 3H), 3.72 (s, 3H), 3.70 (s, 3H). **^{13}C NMR** (101 MHz, $CDCl_3$) δ 168.5, 168.4, 139.6, 136.5, 132.9, 132.2, 132.0, 131.6, 131.6, 130.1, 130.0, 129.2, 128.7, 127.9, 127.4, 127.2, 112.6, 112.1, 52.1, 51.5, 34.0. **IR** (KBr): 2949, 1712, 1615, 1481, 1462, 1433, 1357, 1286, 1251, 1170 cm^{-1}. **HRMS** (ESI): Calculated for $C_{23}H_{21}NO_4Na$ ($M+Na^+$): 398.1372, found: 398.1377.

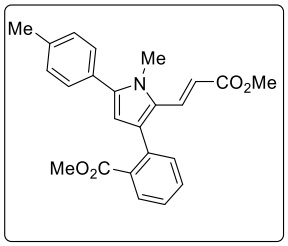

6f: Brown oil (54%). R_f = 0.3 (hexane/ethyl acetate = 3:1). **^{1}H NMR** (400 MHz, Chloroform-d) δ 7.86 (dd, J = 7.8, 1.2 Hz, 1H), 7.59 (d, J = 16.0 Hz, 1H), 7.52 (td, J = 7.5, 1.4 Hz, 1H), 7.42 – 7.32 (m, 4H), 7.24 (s, 2H), 6.21 (s, 1H), 5.75 (d, J = 16.0 Hz, 1H), 3.74 (s, 3H), 3.72 (s, 3H), 3.69 (s, 3H), 2.40 (s, 3H). **^{13}C NMR** (101 MHz, CDCl3) δ 168.6, 168.5, 139.8, 137.9, 136.6, 133.0, 132.0, 131.6, 130.1, 130.0, 129.4, 129.3, 129.2, 127.4, 127.0, 112.2, 111.9, 52.2, 51.5, 34.0, 21.4. IR (KBr): 2949, 1731, 1712, 1615, 1487, 1460, 1433, 1357, 1283, 1251 cm-1. HRMS (ESI): Calculated for $C_{24}H_{23}NO_4Na$ ($M+Na^+$): 412.1519, found: 412.1523.

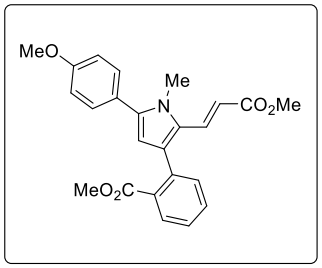

6g: Yellow oil (56%). R_f = 0.2 (toluene/ethyl acetate = 5:1). **^{1}H NMR** (400 MHz, Chloroform-*d*) δ 7.86 (dd, *J* = 7.8, 1.2 Hz, 1H), 7.59 (d, *J* = 16.0 Hz, 1H), 7.52 (td, *J* = 7.5, 1.4 Hz, 1H), 7.42 – 7.34 (m, 4H), 7.00 – 6.95 (m, 2H), 6.19 (s, 1H), 5.75 (d, *J* = 16.0 Hz, 1H), 3.85 (s, 3H), 3.72 (d, *J* = 1.4 Hz, 6H), 3.69 (s, 3H). **^{13}C NMR** (101 MHz, $CDCl_3$) δ 168.6, 168.5, 159.5, 139.6, 136.6, 133.0, 132.0, 131.6, 130.6, 130.05, 130.07, 127.3, 126.8, 124.7, 114.2, 112.0, 111.7, 55.5, 52.2, 51.5, 34.0. **IR** (KBr): 2949, 1731, 1712, 1615, 1488, 1460, 1433, 1290, 1250, 1170 cm^{-1}. **HRMS** (ESI): Calculated for $C_{24}H_{23}NO_5Na$ ($M+Na^+$): 428.1468, found: 428.1470.

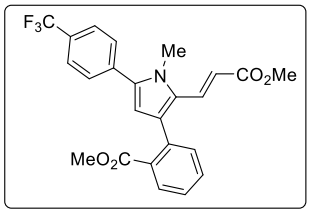

6h: White solid (71%). R_f = 0.3 (hexane/ethyl acetate = 3:1). Mp = 180.6– 181.0 °C. **^{1}H NMR** (400 MHz, Chloroform-*d*) δ 7.92 – 7.87 (m, 1H), 7.70 (d, *J* = 8.3 Hz, 2H), 7.62 – 7.52 (m, 4H), 7.42 (td, *J* = 7.6, 1.1 Hz, 1H), 7.35 (d, *J* = 7.6 Hz, 1H), 6.31 (s, 1H), 5.76 (d, *J* = 16.1 Hz, 1H), 3.76 (s, 3H), 3.73 (s, 3H), 3.70 (s, 3H). **^{13}C NMR** (101 MHz, Chloroform-*d*) δ 168.2, 168.2, 137.7, 136.4, 135.7, 135.7, 132.5, 132.0, 131.8, 131.4, 130.3, 129.9, 129.2, 128.2, 127.6, 127.2 (q), 125.7 (q, *J* = 3.7 Hz), 113.9, 112.9, 52.2, 51.6, 34.1. **^{19}F NMR** (376 MHz, $CDCl_3$) δ -62.5. **IR** (KBr):

2951, 1715, 1614, 1434, 1325, 1288, 1253, 1168, 1124, 1069 cm^{-1}. **HRMS** (ESI): Calculated for $C_{24}H_{20}F_3NO_4Na$ ($M+Na^+$): 466.1237, found: 466.1240.

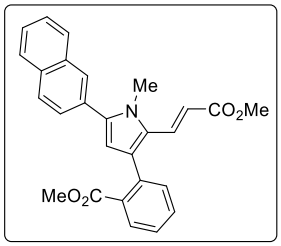

6i: Yellow oil (45%). R_f = 0.4 (toluene/ethyl acetate = 5:1). **^{1}H NMR** (400 MHz, Chloroform-*d*) δ 7.92 – 7.86 (m, 5H), 7.63 (d, *J* = 16.1 Hz, 1H), 7.58 – 7.51 (m, 4H), 7.44 – 7.38 (m, 2H), 6.36 (s, 1H), 5.79 (d, *J* = 16.0 Hz, 1H), 3.82 (s, 3H), 3.75 (s, 3H), 3.71 (s, 3H). **^{13}C NMR** (101 MHz, $CDCl_3$) δ 168.5, 168.4, 139.6, 136.6, 133.4, 132.9, 132.8, 132.0, 131.7, 131.6, 130.1, 129.6, 128.4, 128.2, 128.1, 127.9, 127.5, 127.4, 127.1, 126.7, 126.6, 112.7, 112.6, 52.2, 51.5, 34.2. **IR** (KBr): 2949, 1730, 1712, 1615, 1498, 1432, 1391, 1283, 1250, 1165 cm^{-1}. **HRMS** (ESI): Calculated for $C_{27}H_{23}NO_4Na$ ($M+Na^+$): 448.1519, found: 448.1523.

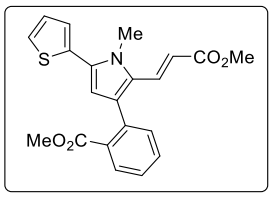

6j: Yellow oil (35%). R_f = 0.3 (hexane/ethyl acetate = 3:1). **^{1}H NMR** (400 MHz, Chloroform-*d*) δ 7.88 (d, *J* = 7.7 Hz, 1H), 7.57 (d, *J* = 16.0 Hz, 1H), 7.55 – 7.49 (m, 1H), 7.43 – 7.39 (m, 1H), 7.37 –7.33 (m, 2H), 7.13 – 7.09 (m, 2H), 6.32 (s, 1H), 5.73 (d, *J* = 16.0 Hz, 1H), 3.82 (s, 3H), 3.72 (s, 3H), 3.69 (s, 3H). **^{13}C NMR** (101 MHz, $CDCl_3$) δ 168.3, 168.3, 136.4, 133.7, 132.6, 131.9, 131.9,

131.7, 131.5, 130.2, 129.7, 127.7, 127.5, 127.5, 126.8, 126.1, 113.2, 113.1, 52.2, 51.6, 33.7. **IR** (KBr): 2949, 1712, 1616, 1434, 1358, 1282, 1253, 1193, 1165, 1079 cm^{-1}. **HRMS** (ESI): Calculated for $C_{21}H_{19}NO_4SNa$ ($M+Na^+$): 404.0927, found: 404.0932.

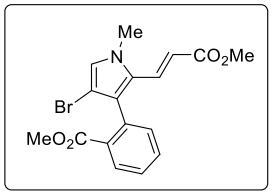

6k: Yellow oil (61%). R_f = 0.3 (hexane/ethyl acetate = 3:1). **^{1}H NMR** (400 MHz, Chloroform-*d*) δ 8.03 (dd, *J* = 7.8, 1.2 Hz, 1H), 7.57 (td, *J* = 7.5, 1.4 Hz, 1H), 7.51 – 7.42 (m, 2H), 7.24 (d, *J* = 1.0 Hz, 1H), 6.83 (s, 1H), 5.54 (d, *J* = 16.0 Hz, 1H), 3.76 (s, 3H), 3.74 (s, 3H), 3.65 (s, 3H). **^{13}C NMR** (101 MHz, $CDCl_3$) δ 168.0, 167.2, 135.0, 132.5, 132.3, 131.7, 131.3, 130.8, 129.0, 128.3, 126.0, 125.8, 114.0, 98.7, 52.3, 51.6, 35.8. **IR** (KBr): 2950, 1715, 1624, 1498, 1434, 1372, 1285, 1254, 1193, 1176 cm^{-1}. **HRMS** (ESI): Calculated for $C_{17}H_{16}BrNO_4Na$ ($M+Na^+$): 400.0155, found: 400.0158.

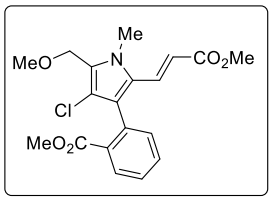

6l: Light yellow oil (71%). R_f = 0.3 (hexane/ethyl acetate = 2:1). **^{1}H NMR** (400 MHz, Chloroform-*d*) δ 8.03 (dd, *J* = 7.8, 1.2 Hz, 1H), 7.56 (td, *J* = 7.5, 1.4 Hz, 1H), 7.53 – 7.44 (m, 2H), 7.27 – 7.25 (m, 1H), 5.57 (d, *J* = 16.0 Hz, 1H), 4.57 – 4.47 (m, 2H), 3.76 (s, 3H), 3.72 (s, 3H), 3.66 (s, 3H),

3.35 (s, 3H). **^{13}C NMR** (101 MHz, $CDCl_3$) δ 168.0, 167.3, 134.2, 132.6, 132.3, 131.6, 131.3, 130.8, 128.7, 128.3, 125.8, 125.6, 115.1, 114.7, 62.9, 57.6, 52.2, 51.6, 32.3. **IR** (KBr): 2950, 1716, 1624, 1574, 1455, 1434, 1404, 1367, 1283, 1193 cm^{-1}. **HRMS** (ESI): Calculated for $C_{19}H_{20}ClNO_5Na$ ($M+Na^+$): 400.0922, found: 400.0927.

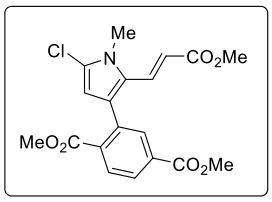

6o: Light yellow solid (71%). R_f = 0.2 (hexane/ ethyl acetate = 1:1). Mp = 146.5– 146.9 °C. **^{1}H NMR** (400 MHz, Chloroform-*d*) δ 8.05 (dd, *J* = 8.1, 1.7 Hz, 1H), 7.96 – 7.90 (m, 2H), 7.42 (d, *J* = 16.1 Hz, 1H), 6.13 (s, 1H), 5.60 (d, *J* = 16.1 Hz, 1H), 3.92 (s, 3H), 3.73 (s, 3H), 3.72 (s, 3H), 3.66 (s, 3H). **^{13}C NMR** (101 MHz, $CDCl_3$) δ 167.9, 167.3, 166.1, 136.1, 135.3, 132.9, 132.9, 131.7, 130.2, 128.7, 127.7, 125.4, 122.2, 113.6, 109.8, 52.6, 52.5, 51.6, 32.2. **IR** (KBr): 2952, 1726, 1623, 1460, 1430, 1348, 1283, 1248, 1193, 1173 cm^{-1}. **HRMS** (ESI): Calculated for $C_{19}H_{19}ClNO_6$ ($M+H^+$): 392.0895, found: 392.0902.

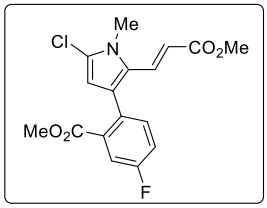

6p: Light yellow solid (69%). R_f = 0.3 (hexane/ ethyl acetate = 3:1). Mp = 127.0– 127.4°C. **^{1}H NMR** (400 MHz, Chloroform-*d*) δ 7.62 – 7.57 (m, 1H), 7.43 (d, *J* = 16.1 Hz, 1H), 7.25 – 7.20 (m,

2H), 6.08 (s, 1H), 5.61 (d, *J* = 16.1 Hz, 1H), 3.72 (s, 3H), 3.72 (s, 3H), 3.68 (s, 3H). **^{13}C NMR** (101 MHz, Chloroform-d) δ 168.1, 166.6 (d, J = 2.6 Hz), 161.8 (d, J = 248.6 Hz), 133.7 (d, J = 7.6 Hz), 132.8 (d, J = 7.4 Hz), 132.0 (d, J = 3.5 Hz), 131.9, 127.9, 125.3, 122.1, 119.1 (d, J = 21.1 Hz), 117.3 (d, J = 23.5 Hz), 113.2, 109.9, 52.4, 51.6, 32.2. **^{19}F NMR** (376 MHz, $CDCl_3$) δ -113.5. **IR** (KBr): 2951, 1734, 1716, 1622, 1491, 1426, 1353, 1283, 1249, 1195 cm^{-1}. **HRMS** (ESI): Calculated for $C_{17}H_{15}ClFNO_4Na$ ($M+Na^+$): 374.0566, found: 374.0570.

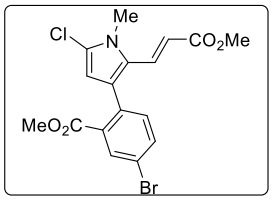

6q: Light yellow solid (72%). R_f = 0.3 (hexane/ ethyl acetate = 3:1). Mp = 120.5– 120.9 °C. **^{1}H NMR** (400 MHz, Chloroform-*d*) δ 8.02 (d, *J* = 2.1 Hz, 1H), 7.62 (dd, *J* = 8.2, 2.1 Hz, 1H), 7.42 (d, *J* = 16.1 Hz, 1H), 7.14 (d, *J* = 8.2 Hz, 1H), 6.08 (s, 1H), 5.66 (d, *J* = 16.1 Hz, 1H), 3.72 (s, 3H), 3.72 (s, 3H), 3.69 (s, 3H). **^{13}C NMR** (101 MHz, $CDCl_3$) δ 168.0, 166.5, 134.8, 133.5, 133.2, 132.8, 131.8, 127.6, 125.2, 122.3, 121.6, 113.5, 109.7, 52.5, 51.7, 32.3. **IR** (KBr): 2950, 1734, 1716, 1622, 1482, 1457, 1426, 1351, 1284, 1245 cm^{-1}. **HRMS** (ESI): Calculated for $C_{17}H_{15}BrClNO_4Na$ ($M+Na^+$): 433.9765, found: 433.9768.

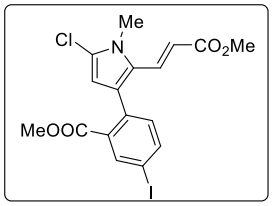

6r: Light yellow solid (51%). R_f = 0.3 (hexane/ ethyl acetate = 3:1). Mp = 126.9– 127.2°C. **^{1}H NMR** (400 MHz, Chloroform-*d*) δ 8.20 (d, *J* = 1.9 Hz, 1H), 7.82 (dd, *J* = 8.1, 1.9 Hz, 1H), 7.42 (d, *J* = 16.1 Hz, 1H), 7.00 (d, *J* = 8.1 Hz, 1H), 6.08 (s, 1H), 5.68 (d, *J* = 16.1 Hz, 1H), 3.72 (s, 3H), 3.72 (s, 3H), 3.70 (s, 3H). **^{13}C NMR** (101 MHz, $CDCl_3$) δ 168.0, 166.4, 140.7, 139.0, 135.4, 133.6, 132.9, 131.8, 127.7, 125.2, 122.3, 113.6, 109.7, 92.8, 52.5, 51.7, 32.3. **IR** (KBr): 2949, 1716, 1622, 1507, 1480, 1424, 1351, 1282, 1248, 1192 cm^{-1}. **HRMS** (ESI): Calculated for $C_{17}H_{15}ClINO_4Na$ ($M+Na^+$): 481.9626, found: 481.9621.

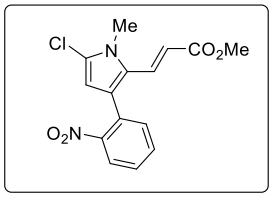

6s: Yellow solid (50%). R_f = 0.3 (hexane/ ethyl acetate = 2:1). Mp = 128.3– 128.7 °C. **^{1}H NMR** (400 MHz, Chloroform-*d*) δ 7.90 (dd, *J* = 8.1, 1.1 Hz, 1H), 7.60 (td, *J* = 7.6, 1.3 Hz, 1H), 7.50 (td, *J* = 7.9, 1.4 Hz, 1H), 7.45 (d, *J* = 16.1 Hz, 1H), 7.36 (dd, *J* = 7.6, 1.3 Hz, 1H), 6.12 (s, 1H), 5.65 (d, *J* = 16.1 Hz, 1H), 3.73 (s, 3H), 3.69 (s, 3H). **^{13}C NMR** (101 MHz, $CDCl_3$) δ 167.8, 149.9, 132.9, 132.7, 131.5, 129.8, 128.9, 125.6, 124.5, 124.1, 122.6, 114.3, 109.4, 51.7, 32.3. **IR** (KBr): 2950, 1714, 1623, 1528, 1483, 1425, 1353, 1283, 1250, 1194 cm^{-1}. **HRMS** (ESI): Calculated for $C_{15}H_{13}ClN_2O_4Na$ ($M+Na^+$): 343.0456, found: 343.0459.

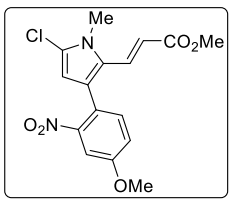

6t: Light yellow solid (48%). R_f = 0.3 (hexane/ ethyl acetate = 2:1). Mp = 188.5– 188.9 °C. **^{1}H NMR** (400 MHz, Chloroform-*d*) δ 7.47 – 7.41 (m, 2H), 7.24 (d, *J* = 8.5 Hz, 1H), 7.13 (dd, *J* = 8.6, 2.7 Hz, 1H), 6.08 (s, 1H), 5.66 (d, *J* = 16.1 Hz, 1H), 3.91 (s, 3H), 3.72 (s, 3H), 3.69 (s, 3H). **^{13}C NMR** (101 MHz, $CDCl_3$) δ 167.9, 159.6, 150.2, 133.7, 131.6, 125.7, 124.2, 122.5, 121.8, 119.3, 113.8, 109.6, 109.4, 56.1, 51.7, 32.2. **IR** (KBr): 2917, 1712, 1654, 1623, 1560, 1530, 1497, 1353, 1281, 1173 cm^{-1}. **HRMS** (ESI): Calculated for $C_{16}H_{15}ClN_2O_5Na$ ($M+Na^+$): 373.0562, found: 373.0561.

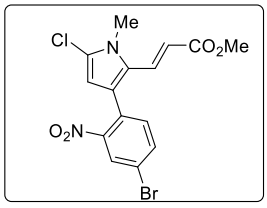

6u: Light yellow solid (44%). R_f = 0.3 (hexane/ ethyl acetate = 3:1). Mp = 164.3– 164.5°C. **^{1}H NMR** (400 MHz, Chloroform-*d*) δ 8.04 (d, *J* = 2.0 Hz, 1H), 7.72 (dd, *J* = 8.2, 2.0 Hz, 1H), 7.42 (d, *J* = 16.1 Hz, 1H), 7.24 (d, *J* = 8.2 Hz, 1H), 6.09 (s, 1H), 5.69 (d, *J* = 16.1 Hz, 1H), 3.72 (s, 3H), 3.71 (s, 3H). **^{13}C NMR** (101 MHz, $CDCl_3$) δ 167.6, 135.8, 134.2, 133.8, 131.2, 128.7, 127.5, 125.6, 122.8, 122.8, 122.0, 114.9, 109.2, 51.8, 32.4. **IR** (KBr): 2360, 2342, 1716, 1532, 1507, 1481, 1427, 1353, 1310, 1282 cm^{-1}. **HRMS** (ESI): Calculated for $C_{15}H_{12}BrClN_2O_4Na$ ($M+Na^+$): 420.9561, found: 420.9554.

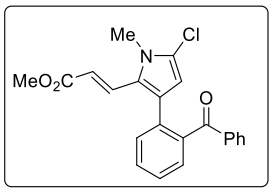

6v: Light yellow oil (68%). R_f = 0.3 (hexane/ ethyl acetate = 3:1). **^{1}H NMR** (400 MHz, Chloroform-*d*) δ 7.64 – 7.59 (m, 2H), 7.56 – 7.50 (m, 2H), 7.47 – 7.41 (m, 2H), 7.41 – 7.34 (m, 2H), 7.30 (t, *J* = 7.7 Hz, 2H), 5.98 (s, 1H), 5.78 (d, *J* = 16.1 Hz, 1H), 3.70 (s, 3H), 3.52 (s, 3H). **^{13}C NMR** (101 MHz, $CDCl_3$) δ 198.0, 168.0, 139.8, 137.5, 134.2, 132.7, 131.9, 131.3, 130.6, 129.8, 129.1, 128.3, 128.0, 127.5, 125.5, 122.4, 113.4, 110.7, 51.6, 32.2. **IR** (KBr): 2949, 1715, 1667, 1622, 1597, 1480, 1449, 1424, 1352, 1314 cm^{-1}. **HRMS** (ESI): Calculated for $C_{22}H_{18}ClNO_3Na$ ($M+Na^+$): 402.0867, found: 402.0874.

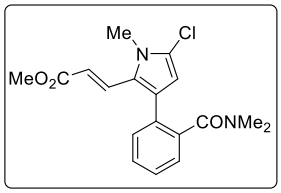

6w: Light yellow oil (61%). R_f = 0.3 (toluene/ acetone/triethylamine = 15:4:1). **^{1}H NMR** (400 MHz, Chloroform-*d*) δ 7.55 (d, *J* = 16.2 Hz, 1H), 7.42 – 7.34 (m, 3H), 7.28 (dd, *J* = 6.2, 2.4 Hz, 1H), 6.25 (s, 1H), 5.96 (d, *J* = 16.2 Hz, 1H), 3.74 (s, 3H), 3.71 (s, 3H), 2.94 (s, 3H), 2.64 (s, 3H). **^{13}C NMR** (101 MHz, $CDCl_3$) δ 171.0, 168.2, 137.0, 132.2, 131.7, 131.2, 129.1, 128.5, 128.0, 127.2, 125.2, 122.9, 113.1, 109.9, 51.7, 38.7, 34.9, 32.8. **IR** (KBr): 2949, 1714, 1623, 1462, 1423, 1395, 1352, 1283, 1249, 1193 cm^{-1}. **HRMS** (ESI): Calculated for $C_{18}H_{19}ClN_2O_3Na$ ($M+Na^+$): 369.0976, found: 369.0972.

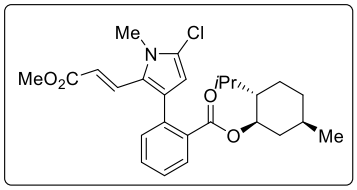

6x: Yellow solid (70%). R_f = 0.3 (hexane/ ethyl acetate = 3:1). Mp = 117.2– 117.6 ºC. **^{1}H NMR** (400 MHz, Chloroform-*d*) δ 7.85 (dd, *J* = 7.7, 1.2 Hz, 1H), 7.53 – 7.38 (m, 3H), 7.25 (dd, *J* = 7.8, 1.2 Hz, 1H), 6.10 (s, 1H), 5.61 (d, *J* = 16.0 Hz, 1H), 4.73 (td, *J* = 10.9, 4.4 Hz, 1H), 3.72 (s, 3H), 3.66 (s, 3H), 1.94 – 1.87 (m, 1H), 1.73 – 1.61 (m, 3H), 1.43 (dddq, *J* = 12.0, 9.8, 6.7, 3.4 Hz, 1H), 1.29 – 1.21 (m, 1H), 1.01 (qd, *J* = 13.3, 12.7, 3.7 Hz, 1H), 0.87 (d, *J* = 6.5 Hz, 3H), 0.81 (t, *J* = 6.7 Hz, 4H), 0.77 – 0.71 (m, 1H), 0.69 (d, *J* = 6.9 Hz, 3H). **^{13}C NMR** (101 MHz, $CDCl_3$) δ 168.1, 167.4, 135.5, 132.6, 132.0, 131.6, 131.5, 130.0, 129.3, 127.8, 125.2, 121.9, 112.9, 110.2, 74.9, 51.5, 47.2, 40.6, 34.4, 32.1, 31.4, 26.0, 23.2, 22.2, 21.0, 16.1. **IR** (KBr): 2953, 1716, 1622, 1457, 1424, 1352, 1281, 1250, 1172, 1127 cm^{-1}. **HRMS** (ESI): Calculated for $C_{26}H_{32}ClNO_4Na$ ($M+Na^+$): 480.1918, found: 480.1919.

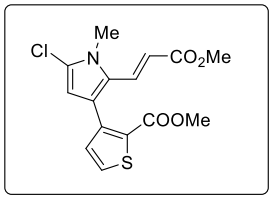

6y: Yellow oil (30%). R_f = 0.3 (hexane/ ethyl acetate = 2:1). **^{1}H NMR** (400 MHz, Chloroform-*d*) δ 7.47 – 7.39 (m, 2H), 6.90 (d, *J* = 5.0 Hz, 1H), 6.17 (s, 1H), 5.67 (d, *J* = 16.1 Hz, 1H), 3.71 (s, 3H), 3.66 (s, 3H), 3.63 (s, 3H). **^{13}C NMR** (101 MHz, $CDCl_3$) δ 168.1, 162.1, 141.4, 132.2, 131.9, 130.7, 128.3, 126.0, 123.4, 122.2, 113.5, 110.3, 52.1, 51.7, 32.4. **IR** (KBr): 2950, 1716, 1623, 1559, 1459, 1435, 1401, 1282, 1249, 1172 cm^{-1}. **HRMS** (ESI): Calculated for $C_{15}H_{14}ClNO_4SNa$ ($M+Na^+$): 362.0224, found: 362.0225.

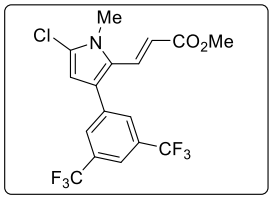

6ah: White solid (69%). R_f = 0.3 (toluene/ethyl acetate = 10:1). Mp = 139.4– 139.8 °C. **^{1}H NMR** (400 MHz, Chloroform-*d*) δ 7.74 (s, 1H), 7.71 (s, 2H), 7.49 (d, *J* = 16.2 Hz, 1H), 6.23 (s, 1H), 5.93 (d, *J* = 16.2 Hz, 1H), 3.69 (s, 3H), 3.68 (s, 3H). **^{13}C NMR** (101 MHz, Chloroform-*d*) δ 167.5, 137.4, 134.0, 132.1 (q, *J* = 33.4 Hz), 131.4, 130.2, 129.0, 127.1, 125.4, 124.7, 123.4, 122.0, 120.9 (dt, *J* = 7.8, 3.8 Hz), 115.7, 109.1, 51.9, 32.9. **^{19}F NMR** (376 MHz, $CDCl_3$) δ -62.9. **IR** (KBr): 2955, 1709, 1622, 1473, 1429, 1418, 1342, 1286, 1174, 1120 cm^{-1}. **HRMS** (ESI): Calculated for $C_{17}H_{12}ClF_6NO_2Na$ ($M+Na^+$): 434.0353, found: 434.0348.

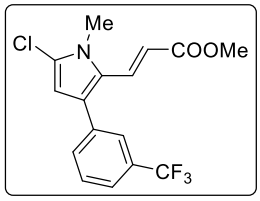

6af: white solid (37 %). R_f = 0.3 (hexane / ethyl acetate =5 :1). Mp = 116.2–116.7 °C. **^{1}H NMR** (400 MHz, Benzene-d_6) δ 7.69 (d, *J* = 16.2 Hz, 1H), 7.63 (s, 1H), 7.26 (dd, *J* = 15.7, 7.8 Hz, 2H), 6.90 (t, *J* = 7.8 Hz, 1H), 5.94 (d, *J* = 16.2 Hz, 1H), 5.85 (s, 1H), 3.44 (s, 3H), 2.74 (s, 3H). **^{13}C NMR** (101 MHz, Benzene-d_6) δ 167.37, 136.38, 132.43, 131.95, 131.47, 129.39, 128.92, 125.91 (q, *J* = 3.8 Hz), 125.24, 124.00 (q, *J* = 3.8 Hz), 123.56, 122.56, 114.90, 109.13, 51.22, 31.72. **^{19}F NMR** (376 MHz, C_6D_6) δ -62.4. **IR** (KBr): 2953, 1714, 1624, 1485, 1466, 1426, 1324, 1285, 1249, 1170 cm^{-1}. **HRMS** (ESI): Calculated for $C_{16}H_{14}ClF_3NO_2$ ($M+H^+$): 344.0660, found: 344.0659.

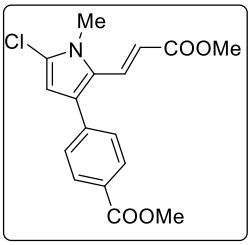

6aa: Light yellow solid (49 %). R_f = 0.3 (hexane / ethyl acetate =5:1). Mp = 132.3–132.8 °C. **^{1}H NMR** (400 MHz, Chloroform-*d*) δ 8.18 (d, *J* = 8.4 Hz, 2H), 7.83 (d, *J* = 16.2 Hz, 1H), 7.34 (d, *J* = 8.4 Hz, 2H), 6.11 – 6.02 (m, 2H), 3.59 (s, 3H), 3.52 (s, 3H), 2.81 (s, 3H). **^{13}C NMR** (101 MHz, C_6D_6) δ 167.5, 166.5, 140.0, 132.2, 130.4, 129.6, 129.5, 129.1, 125.4, 122.5, 115.0, 109.2, 51.6, 51.2, 31.7. **IR** (KBr): 2917, 1719, 1623, 1466, 1428, 1384, 1275, 1175, 1100, 1019 cm^{-1}. **HRMS** (ESI): Calculated for $C_{17}H_{17}ClNO_4$ ($M+H^+$): 334.0841, found: 334.0840.

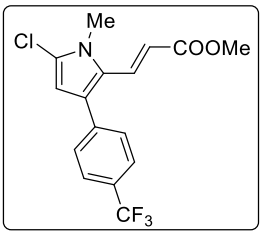

6z: white solid (65 %). R_f = 0.3 (hexane / ethyl acetate =5 :1). Mp = 110.6–111.2 °C. **^{1}H NMR** (400 MHz, Chloroform-*d*) δ 7.71 (d, *J* = 16.2 Hz, 1H), 7.31 (d, *J* = 8.0 Hz, 2H), 7.13 (s, 2H), 6.04 – 5.87 (m, 2H), 3.44 (s, 3H), 2.74 (s, 3H). **^{13}C NMR** (101 MHz, Benzene-*d*6) δ 167.0, 163.1, 138.7, 131.7, 129.0, 128.7, 125.5 (q, *J* = 3.7 Hz), 125.0, 122.3, 114.8, 108.7, 50.9, 31.5. **^{19}F NMR** (376 MHz, C_6D_6) δ -62.1. **IR** (KBr): 2918, 1718, 1623, 1466, 1429, 1384, 1325, 1276, 1170, 1126 cm^{-1}. **HRMS** (ESI): Calculated for $C_{16}H_{14}ClF_3NO_2$ ($M+H^+$): 344.0660, found: 344.0660.

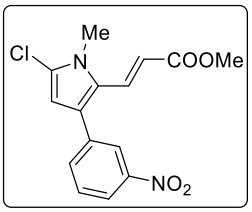

6aq: Light yellow solid (47 %). R_f = 0.3 (hexane / ethyl acetate =5 :1). Mp = 173.9–174.4 ºC. **^{1}H NMR** (400 MHz, Benzene-d_6) δ 8.09 (t, *J* = 1.9 Hz, 1H), 7.72 – 7.67 (m, 1H), 7.63 (d, *J* = 16.2 Hz, 1H), 7.22 (d, *J* = 7.7 Hz, 1H), 6.71 (t, *J* = 8.0 Hz, 1H), 5.93 (d, *J* = 16.2 Hz, 1H), 5.81 (s, 1H), 3.44 (s, 3H), 2.73 (s, 3H). **^{13}C NMR** (101 MHz, C_6D_6) δ 203.82, 167.31, 148.93, 136.77, 134.43, 131.73, 129.41, 125.28, 123.73, 122.70, 121.96, 115.26, 109.10, 51.30, 31.74. **IR** (KBr): 2917, 1710, 1625, 1540, 1522, 1431, 1353, 1293, 1193, 1178 cm^{-1}. **HRMS** (ESI): Calculated for $C_{15}H_{14}ClN_2O_4$ (M+H+): 321.0637, found: 321.0635.

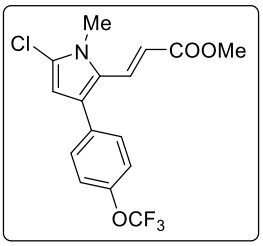

6ac: white solid (36 %). R_f = 0.3 (hexane / ethyl acetate = 5:1). Mp = 104.4–104.9 ºC. **^{1}H NMR** (400 MHz, Benzene-d_6) δ 7.72 (d, *J* = 16.2 Hz, 1H), 7.11 – 7.06 (m, 2H), 6.90 (d, *J* = 8.0 Hz, 2H), 5.96 (d, *J* = 16.5 Hz, 2H), 3.45 (s, 3H), 2.74 (s, 3H). **^{13}C NMR** (101 MHz, Benzene-d_6) δ 167.5, 148.7 (d, *J* = 1.9 Hz), 134.3, 132.1, 130.6, 129.3, 125.2, 122.5, 121.4, 120.0, 114.6, 109.2, 51.2, 31.8. **^{19}F NMR** (376 MHz, C_6D_6) δ -57.6. **IR** (KBr): 2952, 1708, 1623, 1501, 1466, 1427, 1351, 1274, 1213, 1170 cm^{-1}. **HRMS** (ESI): Calculated for $C_{16}H_{14}ClF_3NO_3$ ($M+H^+$): 360.0609, found: 360.0609.

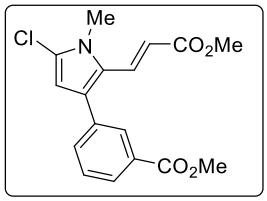

6ae: Light yellow oil (52 %). R_f = 0.3 (hexane / ethyl acetate =5 :1). **^{1}H NMR** (400 MHz, Benzene-*d6*) δ 8.31 (s, 1H), 8.03 (d, *J* = 7.8 Hz, 1H), 7.76 (d, *J* = 16.2 Hz, 1H), 7.39 (d, *J* = 7.7 Hz, 1H), 7.06 (t, *J* = 7.7 Hz, 1H), 6.05 – 5.93 (m, 2H), 3.49 (s, 3H), 3.43 (s, 3H), 2.75 (s, 3H). **^{13}C NMR** (101 MHz, C6D6) δ 167.5, 166.5, 136.0, 133.5, 132.2, 131.4, 130.5, 129.8, 129.0, 128.7, 125.3, 122.5, 114.5, 109.3, 51.7, 51.2, 31.7. **IR** (KBr): 2951, 1720, 1623, 1464, 1431, 1384, 1354, 1278, 1214, 1173 cm^{-1}. **HRMS** (ESI): Calculated for $C_{17}H_{17}ClNO_4$ ($M+H^+$): 334.0841, found: 334.0840.

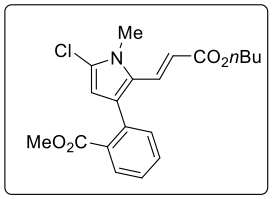

6ak: Light yellow oil (79%). R_f = 0.3 (hexane/diethyl ether = 2:1). **^{1}H NMR** (400 MHz, Chloroform-*d*) δ 7.88 (dd, *J* = 7.8, 1.2 Hz, 1H), 7.51 (td, *J* = 7.5, 1.4 Hz, 1H), 7.47 – 7.37 (m, 2H), 7.28 (d, *J* = 1.0 Hz, 1H), 6.12 (s, 1H), 5.68 (d, *J* = 16.1 Hz, 1H), 4.08 (t, *J* = 6.7 Hz, 2H), 3.73 (s, 3H), 3.72 (s, 3H), 1.62 – 1.56 (m, 2H), 1.35 (dt, *J* = 14.9, 7.4 Hz, 2H), 0.91 (t, *J* = 7.4 Hz, 3H). **^{13}C NMR** (101 MHz, $CDCl_3$) δ 168.0, 167.8, 135.8, 132.0, 131.9, 131.8, 131.3, 130.3, 129.2, 127.7, 125.3, 122.1, 113.5, 109.7, 64.3, 52.2, 32.4, 30.9, 19.3, 13.9. **IR** (KBr): 2957, 1732, 1710, 1621, 1485, 1461, 1431, 1352, 1280, 1252cm^{-1}. **HRMS** (ESI): Calculated for $C_{20}H_{22}ClNO_4Na$ ($M+Na^+$): 398.1130, found: 398.1124.

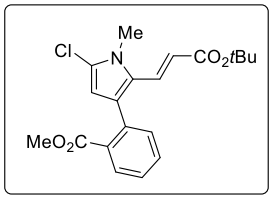

6al: Light yellow oil (70%). R_f = 0.3 (hexane/diethyl ether = 2:1). **^{1}H NMR** (400 MHz, Chloroform-*d*) δ 7.86 (dd, *J* = 7.8, 1.2 Hz, 1H), 7.50 (td, *J* = 7.6, 1.4 Hz, 1H), 7.42 – 7.33 (m, 2H), 7.28 (dd, *J* = 7.6, 1.0 Hz, 1H), 6.11 (s, 1H), 5.66 (d, *J* = 16.1 Hz, 1H), 3.73 (s, 3H), 3.72 (s, 3H), 1.44 (s, 9H). **^{13}C NMR** (101 MHz, $CDCl_3$) δ 168.1, 167.1, 135.8, 132.0, 131.7, 131.4, 131.1, 130.2, 128.9, 127.6, 125.4, 121.9, 115.3, 109.5, 80.2, 52.2, 32.5, 28.3. **IR** (KBr): 2977, 1732, 1699, 1621, 1485, 1460, 1391, 1367, 1285, 1253 cm^{-1}. **HRMS** (ESI): Calculated for $C_{20}H_{22}ClNO_4Na$ ($M+Na^+$): 376.1310, found: 376.1314.

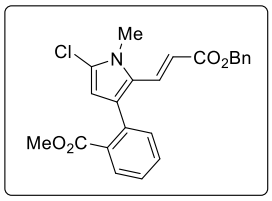

6am: Light yellow oil (77%). R_f = 0.3 (hexane/diethyl ether = 2:1). **^{1}H NMR** (400 MHz, Chloroform-*d*) δ 7.88 (dd, *J* = 7.8, 1.2 Hz, 1H), 7.53 – 7.48 (m, 2H), 7.41 (td, *J* = 7.6, 1.3 Hz, 1H), 7.37 – 7.30 (m, 5H), 7.27 (dd, *J* = 7.7, 1.0 Hz, 1H), 6.13 (s, 1H), 5.74 (d, *J* = 16.1 Hz, 1H), 5.14 (s, 2H), 3.73 (s, 3H), 3.70 (s, 3H). **^{13}C NMR** (101 MHz, $CDCl_3$) δ 167.9, 167.6, 136.4, 135.7, 132.5, 131.9, 131.8, 131.3, 130.3, 129.5, 128.6, 128.2, 128.2, 127.8, 125.3, 122.4, 112.7, 109.8, 66.1, 52.2, 32.4. **IR** (KBr): 2953, 1736, 1712, 1621, 1484, 1458, 1431, 1375, 1351, 1279 cm^{-1}. **HRMS** (ESI): Calculated for $C_{23}H_{20}ClNO_4Na$ ($M+Na^+$): 432.0973, found: 432.0978.

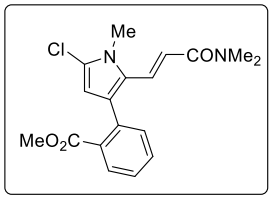

6ao: Light yellow oil (65%). R_f = 0.3 (diethyl ether / ethyl acetate = 2:1). **^{1}H NMR** (400 MHz, Chloroform-*d*) δ 7.88 – 7.84 (m, 1H), 7.54 – 7.45 (m, 2H), 7.38 (td, *J* = 7.6, 1.0 Hz, 1H), 7.31 (d, *J* = 7.6 Hz, 1H), 6.09 (s, 1H), 5.92 (d, *J* = 15.4 Hz, 1H), 3.70 (s, 3H), 3.68 (s, 3H), 2.92 (s, 3H), 2.62 (s, 3H). **^{13}C NMR** (101 MHz, $CDCl_3$) δ 167.9, 166.9, 137.0, 131.9, 131.8, 131.4, 130.0, 129.1, 127.3, 126.1, 125.7, 120.2, 114.2, 109.4, 52.1, 36.7, 35.8, 31.3. **IR** (KBr): 2922, 1731, 1645, 1600, 1487, 1460, 1432, 1416, 1389, 1266 cm^{-1}. **HRMS** (ESI): Calculated for $C_{18}H_{20}ClN_2O_3$ ($M+H^+$): 347.1157, found: 347.1162.

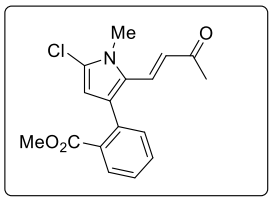

6ap: Light yellow oil (51%). R_f = 0.2 (diethyl ether / hexane = 4:1). **^{1}H NMR** (400 MHz, Chloroform-*d*) δ 7.88 (dd, *J* = 7.8, 1.2 Hz, 1H), 7.52 (td, *J* = 7.5, 1.4 Hz, 1H), 7.42 (td, *J* = 7.6, 1.3 Hz, 1H), 7.32 – 7.26 (m, 2H), 6.15 (s, 1H), 6.02 (d, *J* = 16.2 Hz, 1H), 3.73 (d, *J* = 10.0 Hz, 6H), 2.11 (s, 3H). **^{13}C NMR** (101 MHz, $CDCl_3$) δ 198.0, 168.0, 135.7, 131.9, 131.8, 131.4, 130.6, 130.2, 130.0, 127.9, 125.3, 123.0, 122.3, 110.0, 52.3, 32.5, 27.8. **IR** (KBr): 3381, 2918, 1728, 1579, 1512, 1460, 1426, 1358, 1258, 1085 cm^{-1}. **HRMS** (ESI): Calculated for $C_{17}H_{16}ClNO_3$ ($M+Na^+$): 340.0711, found: 340.0712.

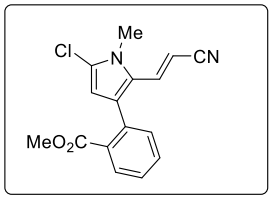

6aq: Light yellow solid (65%). R_f = 0.3 (hexane/ ethyl acetate = 1:1). Mp = 149.0– 149.3 °C. **^{1}H NMR** (400 MHz, Chloroform-*d*) δ 7.92 (dd, *J* = 7.8, 1.3 Hz, 1H), 7.54 (td, *J* = 7.5, 1.4 Hz, 1H), 7.45 (td, *J* = 7.6, 1.3 Hz, 1H), 7.24 (dd, *J* = 7.6, 1.1 Hz, 1H), 7.05 (d, *J* = 16.6 Hz, 1H), 6.12 (s, 1H), 4.92 (d, *J* = 16.6 Hz, 1H), 3.76 (s, 3H), 3.69 (s, 3H). **^{13}C NMR** (101 MHz, $CDCl_3$) δ 167.4, 136.9, 135.5, 132.2, 131.8, 131.1, 130.5, 129.5, 128.2, 124.6, 123.0, 119.6, 110.2, 90.6, 52.3, 32.0. **IR** (KBr): 2951, 2209, 1730, 1609, 1483, 1423, 1355, 1293, 1253, 1127 cm^{-1}. **HRMS** (ESI): Calculated for $C_{16}H_{13}ClN_2O_2Na$ ($M+Na^+$): 323.0558, found: 323.0560.

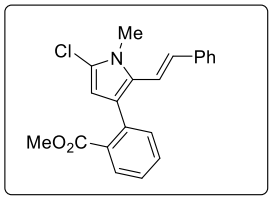

6ar: Light yellow solid (53%). R_f = 0.3 (hexane/ ethyl acetate = 5:1). Mp = 128.8– 129.1 °C. **^{1}H NMR** (400 MHz, Chloroform-*d*) δ 7.70 (d, *J* = 7.8 Hz, 1H), 7.39 (t, *J* = 7.5 Hz, 1H), 7.30 – 7.23 (m, 2H), 7.20 – 7.16 (m, 4H), 7.10 (dq, *J* = 5.6, 3.2 Hz, 1H), 6.71 (d, *J* = 16.5 Hz, 1H), 6.36 (d, *J* = 16.6 Hz, 1H), 6.04 (s, 1H), 3.63 (s, 3H), 3.58 (s, 3H).**^{13}C NMR** (101 MHz, $CDCl_3$) δ 168.8, 137.7, 136.5, 132.1, 131.8, 131.4, 129.8, 128.7, 128.7, 127.7, 127.3, 126.8, 126.0, 123.4, 118.6, 117.2, 108.4, 52.1, 32.3. **IR** (KBr): 2948, 1732, 1632, 1597, 1487, 1452, 1432, 1350, 1292, 1250 cm^{-1}. **HRMS** (ESI): Calculated for $C_{21}H_{18}ClNO_2Na$ ($M+Na^+$): 374.0918, found: 374.0920.

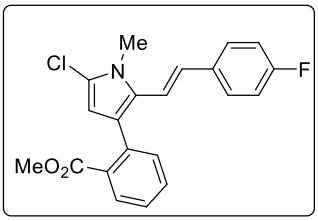

6as: Light yellow solid (55 %). R_f = 0.3 (hexane / ethyl acetate = 5:1). Mp = 93.4–93.9 °C. **^{1}H NMR** (400 MHz, Chloroform-*d*) δ 7.81 – 7.75 (m, 1H), 7.47 (td, *J* = 7.8, 1.4 Hz, 1H), 7.37 – 7.32 (m, 2H), 7.23 – 7.18 (m, 2H), 6.96 (t, *J* = 8.7 Hz, 2H), 6.69 (d, *J* = 16.5 Hz, 1H), 6.38 (d, *J* = 16.5 Hz, 1H), 6.12 (s, 1H), 3.70 (s, 3H), 3.65 (s, 3H). **^{13}C NMR** (101 MHz, Chloroform-*d*) δ 168.83, 162.21 (d, *J* = 246.9 Hz), 136.50, 133.93 (d, *J* = 3.4 Hz), 132.07, 131.83, 131.44, 129.80, 127.57, 127.49, 127.48, 127.42, 126.84, 123.35, 118.59, 116.99 (d, *J* = 2.4 Hz), 115.75, 115.54, 108.40, 52.13, 32.23. **^{19}F NMR** (376 MHz, $CDCl_3$) δ -114.7. **IR** (KBr): 2949, 1730, 1635, 1599, 1508, 1488, 1463, 1436, 1293, 1251 cm^{-1}. **HRMS** (ESI): Calculated for $C_{21}H_{18}ClFNO_2$ ($M+H^+$): 370.1005, found: 370.1004.

7.4.5 General Procedure of Vicinal Difunctionalization of Furans

Scheme 7.11. Vicinal Difunctionalization of Furans

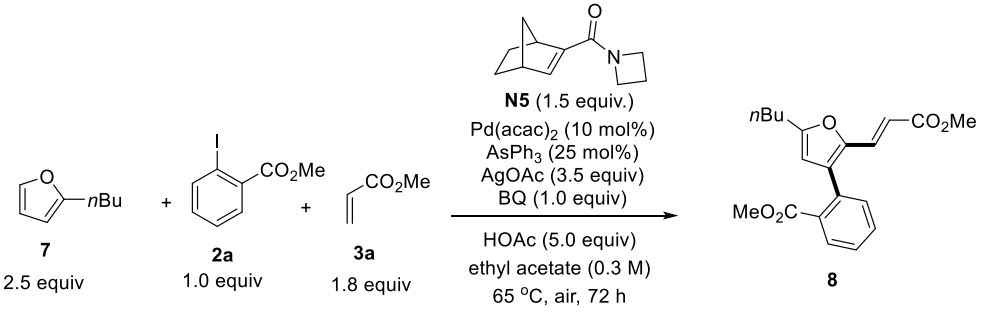

A flame-dried 4.0 mL vial was charged with $Pd(acac)_2$ (3.0 mg, 0.01 mmol, 10 mol%), $AsPh_3$ (7.6 mg, 0.025 mmol, 25 mol%), BQ (10.8 mg, 0.1 mmol, 1.0 equiv), **N5** (26.6 mg, 0.15 mmol, 1.5

equiv), AgOAc (58 mg, 0.35 mmol, 3.5 equiv), furan **7** (0.25 mmol, 2.5 equiv) and aryl iodide **2** (0.1 mmol, 1.0 equiv) in air. Ethyl acetate (0.3 M, 0.33 mL) was then added. After HOAc (30 mg, 0.5 mmol, 5.0 equiv) and acrylate **3** (0.18 mmol, 1.8 equiv) was added, the vial was tightly sealed and stirred on a pie-block preheated to 65 ^{o}C for 72 hours. After completion of the reaction, the mixture was filtered through a thin pad of silica gel. The filter cake was washed with ethyl acetate and the combined filtrate was concentrated under reduced pressure. The residue was loaded to a small amount of silica gel and subjected to flash column chromatography to deliver the desired product **8**.

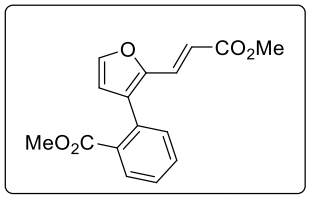

8a: Light yellow solid (50 %). R_f = 0.2 (hexane / ethyl acetate = 10:1). Mp = 86.7 – 87.2 ^{o}C. **^{1}H NMR** (400 MHz, Chloroform-*d*) δ 7.92 (d, *J* = 7.8 Hz, 1H), 7.55 – 7.51 (m, 1H), 7.48 – 7.42 (m, 2H), 7.28 – 7.23 (m, 2H), 6.49 – 6.45 (m, 1H), 6.36 – 6.30 (m, 1H), 3.73 – 3.70 (m, 6H). **^{13}C NMR** (101 MHz, Chloroform-*d*) δ 167.8, 167.7, 147.0 (d, *J* = 3.0 Hz), 143.6, 132.8 (d, *J* = 3.4 Hz), 131.9 (d, *J* = 2.7 Hz), 131.9, 131.1 (d, *J* = 4.1 Hz), 130.6 (d, *J* = 2.1 Hz), 130.1 (d, *J* = 3.4 Hz), 129.9, 128.4 (d, *J* = 2.8 Hz), 115.9 (d, *J* = 3.3 Hz), 114.7 (d, *J* = 2.7 Hz), 52.3 (d, *J* = 3.0 Hz), 51.7 (d, *J* = 2.3 Hz). **IR** (KBr): 2950, 1719, 1635, 1435, 1292, 1260, 1193, 1170, 1116, 1083 cm^{-1}. **HRMS** (ESI): Calculated for $C_{16}H_{15}O_5$ ($M+H^+$): 287.0914, found: 287.0912.

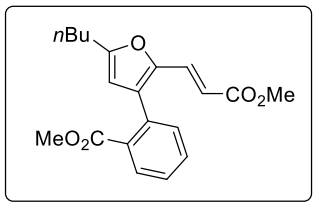

8b: Light yellow oil (80%). R_f = 0.2 (hexane / ethyl acetate = 10:1). **^{1}H NMR** (400 MHz, Chloroform-*d*) δ 7.94 (dd, *J* = 7.8, 1.2 Hz, 1H), 7.58 (td, *J* = 7.6, 1.4 Hz, 1H), 7.48 (td, *J* = 7.6, 1.3 Hz, 1H), 7.37 – 7.27 (m, 2H), 6.32 (d, *J* = 15.6 Hz, 1H), 6.17 (s, 1H), 3.78 (s, 3H), 3.78 (s, 3H), 2.74 (t, *J* = 7.6 Hz, 2H), 1.73 (p, *J* = 7.5 Hz, 2H), 1.52 – 1.42 (m, 2H), 1.00 (t, *J* = 7.4 Hz, 3H).**^{13}C NMR** (101 MHz, $CDCl_3$) δ 168.1, 167.9, 158.7, 145.5, 133.0, 131.8, 131.7, 131.4, 131.3, 130.4, 130.0, 128.1, 114.1, 110.4, 52.3, 51.6, 30.0, 28.0, 22.4, 13.9.**IR** (KBr): 2954, 1719, 1632, 1588, 1541, 1434, 1257, 1193, 1167, 1131 cm^{-1}. **HRMS** (ESI): Calculated for $C_{20}H_{23}O_5$ ($M+H^+$): 343.1540, found: 343.1542.

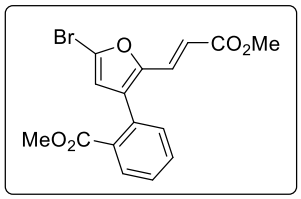

8c: Light yellow solid (54 %). R_f = 0.2 (hexane / ethyl acetate = 10:1). Mp = 139.5– 140.0 °C. **^{1}H NMR** (400 MHz, Methylene Chloride-d_2) δ 7.95 (dd, *J* = 7.8, 1.1 Hz, 1H), 7.59 (td, *J* = 7.5, 1.4 Hz, 1H), 7.50 (td, *J* = 7.6, 1.3 Hz, 1H), 7.31 – 7.28 (m, 1H), 7.11 (d, *J* = 15.6 Hz, 1H), 6.48 (s, 1H), 6.31 (d, *J* = 15.6 Hz, 1H), 3.75 (s, 3H), 3.70 (s, 3H). **^{13}C NMR** (101 MHz, CD_2Cl_2) δ 167.7, 167.5, 149.4, 132.5, 132.2, 131.9, 131.7, 131.6, 131.1, 129.3, 128.8, 125.3, 116.9, 116.7, 52.7, 52.1. **IR** (KBr): 2918, 2346, 1719, 1654, 1630, 1578, 1432, 1384, 1273, 1170 cm^{-1}. **HRMS** (ESI): Calculated for $C_{16}H_{14}BrO_5$ ($M+H^+$): 365.0019, found: 365.0014.

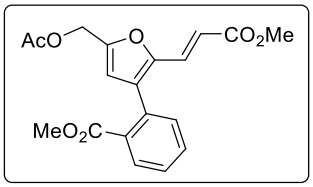

8d: Light yellow solid (59 %). R_f = 0.2 (hexane / ethyl acetate = 5:1). Mp = 89.2 – 89.6 °C. **^{1}H NMR** (400 MHz, Chloroform-*d*) δ 7.94 (dd, *J* = 7.8, 1.1 Hz, 1H), 7.55 (td, *J* = 7.5, 1.4 Hz, 1H), 7.46 (td, *J* = 7.6, 1.3 Hz, 1H), 7.28 (dd, *J* = 7.6, 1.0 Hz, 1H), 7.23 (d, *J* = 15.7 Hz, 1H), 6.50 (s, 1H), 6.37 (d, *J* = 15.7 Hz, 1H), 5.09 (s, 2H), 3.75 (s, 3H), 3.73 (s, 3H), 2.12 (s, 3H). **^{13}C NMR** (101 MHz, $CDCl_3$) δ 170.60, 167.59, 167.52, 150.56, 147.38, 132.46, 132.01, 131.91, 130.93, 130.72, 130.68, 129.55, 128.50, 116.53, 115.14, 58.17, 52.31, 51.79, 21.01. **IR** (KBr): 2952, 1725, 1636, 1601, 1435, 1378, 1315, 1294, 1263, 1233 cm^{-1}. **HRMS** (ESI): Calculated for $C_{19}H_{18}O_7Na$ ($M+Na^+$): 381.0945, found: 381.0947.

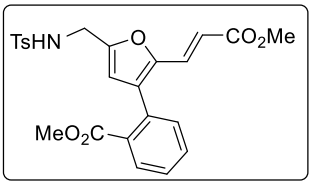

8e: Light yellow solid (75 %). R_f = 0.2 (hexane / ethyl acetate = 5:1). Mp = 120.6 – 130.0 °C. **^{1}H NMR** (400 MHz, Chloroform-*d*) δ 7.95 – 7.88 (m, 1H), 7.74 (d, *J* = 8.2 Hz, 2H), 7.53 (td, *J* = 7.5, 1.3 Hz, 1H), 7.47 – 7.42 (m, 1H), 7.29 – 7.26 (m, 2H), 7.16 – 7.06 (m, 2H), 6.22 (s, 1H), 6.08 (d, *J* = 15.6 Hz, 1H), 5.18 (s, 1H), 4.24 (d, *J* = 5.3 Hz, 2H), 3.74 (s, 3H), 3.73 (s, 3H), 2.38 (s, 3H). **^{13}C NMR** (101 MHz, $CDCl_3$) δ 167.52, 167.48, 151.17, 146.77, 143.77, 137.04, 132.39, 131.98, 131.78, 130.75, 130.71, 130.68, 129.83, 129.31, 128.49, 127.23, 116.25, 115.87, 113.17, 52.37,

51.78, 40.33, 21.59. **IR** (KBr): 2952, 2374, 1719, 1654, 1630, 1598, 1458, 1437, 1269, 1160 cm^{-1}. **HRMS** (ESI): Calculated for $C_{24}H_{23}NO_7SNa$ ($M+Na^+$): 492.1087, found: 492.1085.

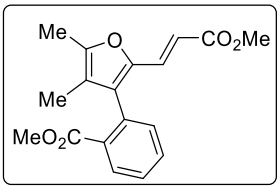

8f: Light yellow oil (45%). R_f = 0.2 (hexane / ethyl acetate = 10:1). **^{1}H NMR** (400 MHz, Chloroform-*d*) δ 8.00 (dd, *J* = 7.8, 1.1 Hz, 1H), 7.55 (td, *J* = 7.5, 1.3 Hz, 1H), 7.46 (td, *J* = 7.7, 1.3 Hz, 1H), 7.22 – 7.18 (m, 1H), 7.09 (d, *J* = 15.6 Hz, 1H), 6.20 (d, *J* = 15.6 Hz, 1H), 3.74 (s, 3H), 3.70 (s, 3H), 2.31 (s, 3H), 1.71 (s, 3H). **^{13}C NMR** (101 MHz, $CDCl_3$) δ 168.1, 167.3, 150.3, 144.7, 133.2, 133.1, 132.3, 132.1, 131.1, 130.7, 130.2, 128.3, 118.2, 113.1, 52.2, 51.6, 12.2, 8.6. **IR** (KBr): 2918, 1726, 1634, 1607, 1434, 1295, 1258, 1163, 1134, 1087 cm^{-1}. **HRMS** (ESI): Calculated for $C_{18}H_{19}O_5$ ($M+H^+$): 315.1227, found: 315.1224.

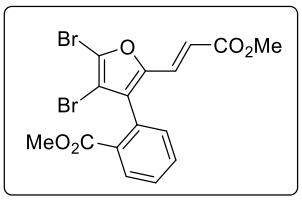

8g: Light yellow solid (40 %). R_f = 0.2 (hexane / ethyl acetate = 10:1). Mp = 140.5 – 140.9 °C. **^{1}H NMR** (400 MHz, Acetone-d_6) δ 8.12 (dd, *J* = 7.8, 1.1 Hz, 1H), 7.77 (td, *J* = 7.5, 1.4 Hz, 1H), 7.68 (td, *J* = 7.7, 1.3 Hz, 1H), 7.44 (dd, *J* = 7.6, 1.0 Hz, 1H), 7.05 (d, *J* = 15.7 Hz, 1H), 6.29 (d, *J* = 15.7 Hz, 1H), 3.76 (s, 3H), 3.69 (s, 3H). **^{13}C NMR** (101 MHz, Acetone) δ 167.0, 166.9, 149.4, 133.5,

133.2, 133.1, 132.1, 131.8, 130.9, 130.7, 128.8, 126.7, 118.0, 108.0, 52.8, 52.1. **IR** (KBr): 2950, 1724, 1634, 1580, 1510, 1434, 1384, 1273, 1200, 1169 cm^{-1}. **HRMS** (ESI): Calculated for $C_{16}H_{13}Br_2O_5$ ($M+H^+$): 442.9124, found: 442.9116.

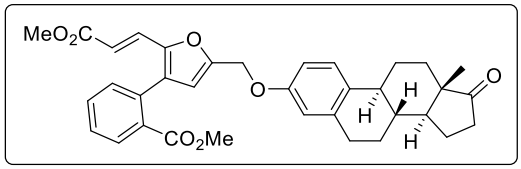

8h: White solid (43 %). R_f = 0.2 (hexane / ethyl acetate = 5:1). Mp = 107.0 – 107.5 °C. **^{1}H NMR** (400 MHz, Chloroform-*d*) δ 7.97 (dd, *J* = 7.8, 1.3 Hz, 1H), 7.57 (dd, *J* = 7.5, 1.3 Hz, 1H), 7.50 (dd, *J* = 7.6, 1.1 Hz, 1H), 7.32 (dd, *J* = 7.6, 1.1 Hz, 1H), 7.30 (d, *J* = 2.7 Hz, 1H), 7.27 (s, 1H), 6.85 – 6.73 (m, 2H), 6.54 (s, 1H), 6.40 (d, *J* = 15.6 Hz, 1H), 5.07 (s, 2H), 3.77 (s, 3H), 3.74 (s, 3H), 2.94 (dd, *J* = 9.6, 4.6 Hz, 2H), 2.54 (dd, *J* = 18.7, 8.5 Hz, 1H), 2.44 (dd, *J* = 10.2, 5.8 Hz, 1H), 2.33 – 2.26 (m, 1H), 2.19 – 1.98 (m, 4H), 1.65 – 1.48 (m, 6H), 0.95 (s, 3H). **^{13}C NMR** (101 MHz, CDCl3) δ 221.1, 167.7, 167.6, 156.4, 151.9, 147.2, 138.1, 133.1, 132.6, 132.0, 131.9, 131.0, 130.8, 130.7, 129.7, 128.5, 126.6, 116.2, 115.2, 114.3, 112.6, 62.7, 52.3, 51.8, 50.5, 48.1, 44.1, 38.5, 36.0, 31.7, 29.8, 26.6, 26.1, 21.7, 14.0. **IR** (KBr): 2929, 1732, 1634, 1605, 1574, 1498, 1454, 1434, 1374, 1261 cm^{-1}. **HRMS** (ESI): Calculated for $C_{35}H_{36}O_7Na$ ($M+Na^+$): 591.2353, found: 591.2350.

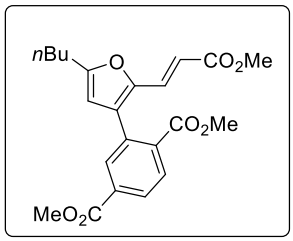

8i: Light yellow oil (71 %). R_f = 0.3 (hexane/ethyl acetate = 5:1). **^{1}H NMR** (400 MHz, Chloroform-*d*) δ 8.08 (dd, *J* = 8.1, 1.7 Hz, 1H), 7.97 – 7.90 (m, 2H), 7.15 (d, *J* = 15.5 Hz, 1H), 6.28 (d, *J* = 15.5 Hz, 1H), 6.14 (s, 1H), 3.94 (s, 3H), 3.75 (s, 3H), 3.73 (s, 3H), 2.69 (t, *J* = 7.5 Hz, 2H), 1.72 – 1.65 (m, 2H), 1.46 – 1.38 (m, 2H), 0.96 (t, *J* = 7.3 Hz, 3H). **^{13}C NMR** (101 MHz, $CDCl_3$) δ 167.8, 167.5, 166.0, 159.0, 145.7, 135.3, 133.2, 132.9, 132.6, 130.4, 130.1, 129.5, 129.1, 114.6, 110.2, 52.7, 52.6, 51.7, 30.0, 28.0, 22.4, 13.9. **IR** (KBr): 2954, 1727, 1634, 1588, 1435, 1251, 1193, 1168, 1115, 1084 cm^{-1}. **HRMS** (ESI): Calculated for $C_{22}H_{25}O_7$ ($M+H^+$): 401.1595, found: 401.1592.

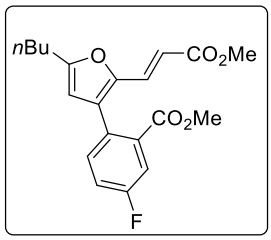

8j: Light yellow oil (74 %). R_f = 0.2 (hexane/ethyl acetate = 10:1). **^{1}H NMR** (400 MHz, Chloroform-*d*) **^{1}H NMR** (400 MHz, Chloroform-*d*) δ 7.60 (dd, *J* = 9.0, 2.4 Hz, 1H), 7.27 – 7.23 (m, 2H), 7.17 (d, *J* = 15.6 Hz, 1H), 6.27 (d, *J* = 15.6 Hz, 1H), 6.09 (s, 1H), 3.74 (s, 3H), 3.73 (s, 3H), 2.68 (t, *J* = 7.6 Hz, 2H), 1.72 – 1.64 (m, 2H), 1.45 – 1.37 (m, 2H), 0.95 (t, *J* = 7.3 Hz, 3H). **^{13}C NMR** (101 MHz, Chloroform-*d*) δ 167.9, 166.8 (d, *J* = 2.5 Hz), 163.3, 160.9, 145.6, 133.6 (d, *J* = 7.7 Hz), 132.9 (d, *J* = 7.5 Hz), 130.3, 129.7, 129.2 (d, *J* = 3.6 Hz), 118.9 (d, *J* = 21.2 Hz), 117.5 (d, *J* = 23.7 Hz), 114.3, 110.4, 52.5, 51.7, 30.0, 28.0, 22.4, 13.9. **^{19}F NMR** (376 MHz, $CDCl_3$) δ -112.9. **IR** (KBr): 2955, 1721, 1634, 1608, 1591, 1544, 1436, 1302, 1271, 1196 cm^{-1}. **HRMS** (ESI): Calculated for $C_{20}H_{22}FO_5$ ($M+H^+$): 361.1446, found: 361.145.

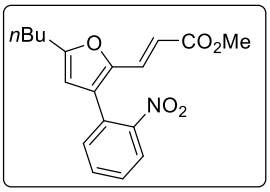

8k: Yellow oil (36 %). R_f = 0.3 (hexane / ethyl acetate = 5:1). **^{1}H NMR** (400 MHz, Chloroform-*d*) δ 7.94 (dd, *J* = 8.1, 1.1 Hz, 1H), 7.63 (td, *J* = 7.6, 1.3 Hz, 1H), 7.53 (td, *J* = 8.0, 1.4 Hz, 1H), 7.38 (dd, *J* = 7.6, 1.3 Hz, 1H), 7.22 (d, *J* = 15.5 Hz, 1H), 6.33 (d, *J* = 15.5 Hz, 1H), 6.09 (s, 1H), 3.74 (s, 3H), 2.68 (t, *J* = 7.6 Hz, 2H), 1.70 – 1.65 (m, 2H), 1.45 – 1.39 (m, 2H), 0.95 (t, *J* = 7.3 Hz, 3H). **^{13}C NMR** (101 MHz, $CDCl_3$) δ 167.7, 159.5, 149.4, 145.9, 132.8, 132.8, 129.2, 127.3, 127.2, 124.7, 115.4, 109.3, 51.8, 29.9, 28.0, 22.4, 13.9. **IR** (KBr): 2956, 1716, 1634, 1613, 1587, 1530, 1435, 1353, 1305, 1261 cm^{-1}. **HRMS** (ESI): Calculated for $C_{18}H_{20}NO_5$ ($M+H^+$): 330.1336, found: 330.1333.

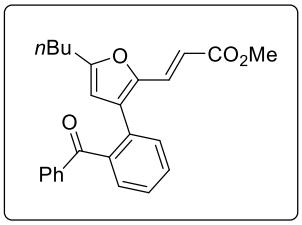

8l: Light yellow oil (69 %). R_f = 0.2 (hexane/ethyl acetate = 10:1). **^{1}H NMR** (400 MHz, Chloroform-*d*) δ 7.54 – 7.51 (m, 2H), 7.47 (ddd, *J* = 8.9, 7.5, 1.4 Hz, 2H), 7.42 (dd, *J* = 7.3, 1.1 Hz, 1H), 7.38 – 7.34 (m, 1H), 7.30 – 7.27 (m, 1H), 7.26 – 7.19 (m, 3H), 6.10 (d, *J* = 15.5 Hz, 1H), 5.85 (s, 1H), 3.67 (s, 3H), 2.38 (t, *J* = 7.4 Hz, 2H), 1.41 – 1.35 (m, 2H), 1.13 – 1.06 (m, 2H), 0.78 (t, *J* = 7.3 Hz, 3H). **^{13}C NMR** (101 MHz, CDCl3) δ 198.17, 167.87, 159.04, 145.70, 139.65, 137.29, 133.10, 131.32, 130.74, 130.67, 130.47, 129.85, 129.69, 129.01, 128.20, 128.14, 114.56, 110.67,

51.69, 29.81, 27.71, 22.07, 13.85. **IR** (KBr): 2955, 1716, 1667, 1631, 1585, 1449, 1434, 1314, 1261, 1193 cm^{-1}. **HRMS** (ESI): Calculated for $C_{25}H_{25}O_4$ ($M+H^+$): 389.1747, found: 389.1750.

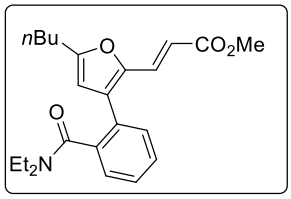

8m: Brown oil (78 %). R_f = 0.2 (hexane / ethyl acetate = 1:1). **^{1}H NMR** (400 MHz, Chloroform-*d*) δ 7.44 – 7.37 (m, 3H), 7.35 – 7.32 (m, 1H), 7.31 – 7.28 (m, 1H), 6.35 – 6.30 (m, 2H), 3.75 (s, 3H), 3.71 (s, 1H), 3.12 (s, 1H), 2.94 (s, 1H), 2.81 (s, 1H), 2.63 (t, *J* = 7.6 Hz, 2H), 1.67 – 1.60 (m, 2H), 1.41 – 1.35 (m, 2H), 1.03 (t, *J* = 7.1 Hz, 3H), 0.94 (d, *J* = 7.3 Hz, 3H), 0.84 (t, *J* = 7.1 Hz, 3H). **^{13}C NMR** (101 MHz, $CDCl_3$) δ 170.1, 168.0, 159.0, 145.7, 137.3, 130.5, 130.3, 129.8, 129.1, 129.0, 128.5, 126.9, 114.5, 110.6, 51.7, 42.6, 38.6, 30.0, 28.0, 22.4, 13.9, 13.7, 12.4. **IR** (KBr): 3332, 2957, 1715, 1629, 1512, 1462, 1435, 1383, 1304, 1247 cm^{-1}. **HRMS** (ESI): Calculated for $C_{23}H_{29}NO_4Na$ ($M+Na^+$): 406.1989, found: 406.1987.

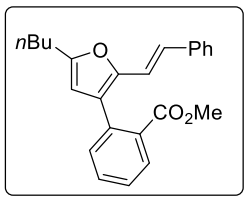

8n: Light yellow oil (78 %). R_f = 0.2 (hexane / ethyl acetate = 20:1). **^{1}H NMR** (400 MHz, Chloroform-*d*) δ 7.86 – 7.80 (m, 1H), 7.53 (td, *J* = 7.5, 1.3 Hz, 1H), 7.43 – 7.36 (m, 4H), 7.29 (t,

J = 7.6 Hz, 2H), 7.19 (t, *J* = 7.3 Hz, 1H), 7.02 (d, *J* = 16.1 Hz, 1H), 6.73 (d, *J* = 16.1 Hz, 1H), 6.09 (s, 1H), 3.72 (s, 3H), 2.71 (t, *J* = 7.6 Hz, 2H), 1.75 – 1.68 (m, 2H), 1.46 (dt, *J* = 14.8, 7.4 Hz, 2H), 0.98 (t, *J* = 7.4 Hz, 3H). **^{13}C NMR** (101 MHz, $CDCl_3$) δ 169.1, 156.1, 147.4, 137.5, 133.9, 131.8, 131.6, 131.5, 130.1, 128.7, 127.4, 127.3, 126.4, 126.4, 124.6, 115.1, 109.2, 52.3, 30.2, 28.0, 22.5, 14.0. **IR** (KBr): 2954, 1732, 1599, 1450, 1432, 1384, 1293, 1261, 1129, 1084 cm^{-1}. **HRMS** (ESI): Calculated for $C_{24}H_{25}O_3$ ($M+H^+$): 361.1798, found: 361.1800.

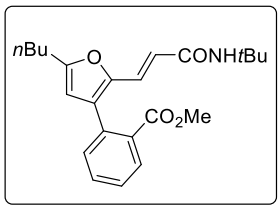

8o: Light yellow solid (51 %). R_f = 0.2 (hexane / ethyl acetate = 3:1). Mp = 129.7–130.0 °C. **^{1}H NMR** (400 MHz, Chloroform-*d*) δ 7.84 (d, *J* = 7.7 Hz, 1H), 7.50 – 7.44 (m, 1H), 7.38 (t, *J* = 7.5 Hz, 1H), 7.29 (d, *J* = 7.5 Hz, 1H), 7.18 (d, *J* = 15.1 Hz, 1H), 6.20 (d, *J* = 15.1 Hz, 1H), 6.07 (s, 1H), 5.41 (s, 1H), 3.72 (s, 3H), 2.65 (t, *J* = 7.5 Hz, 2H), 1.70 – 1.63 (m, 2H), 1.42 (dd, *J* = 14.9, 7.6 Hz, 2H), 1.37 (s, 9H), 0.94 (t, *J* = 7.3 Hz, 3H). **^{13}C NMR** (101 MHz, CDCl3) δ 168.2, 165.6, 157.4, 146.0, 133.2, 131.8, 131.7, 131.1, 130.3, 129.7, 127.9, 126.1, 118.5, 110.1, 52.1, 51.5, 30.1, 29.0, 28.0, 22.4, 13.9. **IR** (KBr): 2960, 1732, 1653, 1621, 1591, 1552, 1454, 1433, 1333, 1272 cm^{-1}. **HRMS** (ESI): Calculated for C23H30NO4 (M+H+): 384.2169, found: 384.2173.

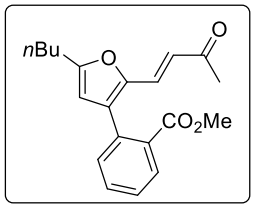

8q: Light yellow oil (52 %). R_f = 0.3 (hexane/ethyl acetate = 5:1). **^{1}H NMR** (400 MHz, Chloroform-*d*) δ 7.89 (d, *J* = 7.5 Hz, 1H), 7.54 (t, *J* = 7.3 Hz, 1H), 7.44 (t, *J* = 7.5 Hz, 1H), 7.29 (d, *J* = 7.6 Hz, 1H), 7.07 (d, *J* = 15.7 Hz, 1H), 6.59 (d, *J* = 15.7 Hz, 1H), 6.15 (s, 1H), 3.73 (s, 3H), 2.70 (t, *J* = 7.4 Hz, 2H), 2.24 (s, 3H), 1.68 (q, *J* = 7.2 Hz, 2H), 1.47 – 1.38 (m, 2H), 0.96 (t, *J* = 7.1 Hz, 3H). **^{13}C NMR** (101 MHz, $CDCl_3$) δ 198.0, 168.2, 159.2, 145.5, 132.9, 132.5, 131.8, 131.6, 131.4, 130.4, 128.2, 128.2, 123.2, 110.7, 52.3, 30.0, 28.1, 28.0, 22.4, 13.9. **IR** (KBr): 2956, 2872, 1731, 1683, 1664, 1615, 1577, 1433, 1293, 1255 cm^{-1}. **HRMS** (ESI): Calculated for $C_{20}H_{23}O_4$ ($M+H^+$): 327.1591, found: 327.1590.

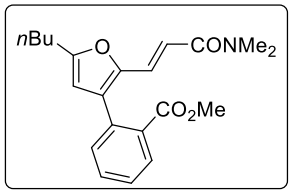

8p: Brown oil (63 %). R_f = 0.2 (hexane/ethyl acetate = 1:1). **^{1}H NMR** (400 MHz, Chloroform-*d*) δ 7.86 (dd, *J* = 7.8, 1.1 Hz, 1H), 7.51 – 7.47 (m, 1H), 7.39 (td, *J* = 7.6, 1.3 Hz, 1H), 7.30 – 7.26 (m, 2H), 6.73 (d, *J* = 15.0 Hz, 1H), 6.09 (s, 1H), 3.73 (s, 3H), 3.06 (s, 6H), 2.68 (t, *J* = 7.6 Hz, 2H), 1.71 – 1.65 (m, 2H), 1.46 – 1.39 (m, 2H), 0.95 (t, *J* = 7.3 Hz, 3H). **^{13}C NMR** (101 MHz, CDCl3) δ 168.2, 167.0, 157.6, 146.3, 133.3, 131.9, 131.7, 131.1, 130.3, 130.0, 128.1, 127.9, 113.7, 110.2,

52.2, 37.2, 36.1, 30.1, 28.0, 22.4, 13.9. **IR** (KBr): 2955, 1730, 1651, 1614, 1585, 1388, 1292, 1266, 1134, 1085 cm^{-1}. **HRMS** (ESI): Calculated for $C_{21}H_{26}NO_4$ ($M+H^+$): 356.1856, found: 356.1852.

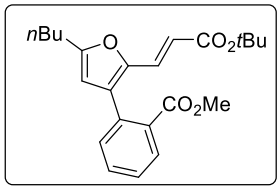

8r: Light yellow oil (65 %). R_f = 0.2 (hexane / ethyl acetate = 10:1). **^{1}H NMR** (400 MHz, Chloroform-*d*) δ 7.86 (dd, *J* = 7.8, 1.1 Hz, 1H), 7.51 (td, *J* = 7.5, 1.4 Hz, 1H), 7.41 (td, *J* = 7.6, 1.3 Hz, 1H), 7.31 – 7.27 (m, 1H), 7.17 (d, *J* = 15.5 Hz, 1H), 6.23 (d, *J* = 15.5 Hz, 1H), 6.10 (s, 1H), 3.73 (s, 3H), 2.67 (t, *J* = 7.6 Hz, 2H), 1.71 – 1.64 (m, 2H), 1.47 (s, 9H), 1.45 – 1.38 (m, 2H), 0.95 (t, *J* = 7.4 Hz, 3H). **^{13}C NMR** (101 MHz, CDCl3) δ 168.20, 166.96, 158.30, 145.74, 133.10, 131.72, 131.69, 131.30, 130.70, 130.34, 128.97, 128.00, 116.52, 110.21, 80.20, 52.22, 30.04, 28.33, 28.03, 22.40, 13.94. **IR** (KBr): 2957, 1729, 1703, 1631, 1588, 1541, 1455, 1433, 1367, 1293 cm^{-1}. **HRMS** (ESI): Calculated for $C_{23}H_{28}O_5Na$ ($M+Na^+$): 407.1829, found: 407.1828.

7.4.6 General Procedure of Ortho Methylation and Alkynylation

Scheme 7.12. Ortho Methylation of Pyrrole 5a

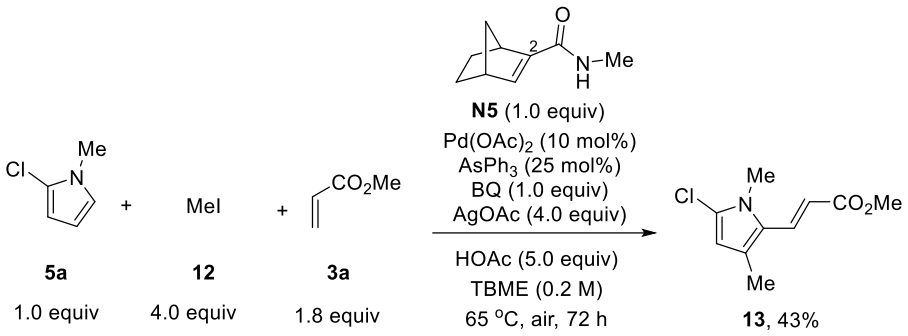

A flame-dried 4.0 mL vial was charged with $Pd(OAc)_2$ (4.6 mg, 0.02 mmol, 10 mol%), $AsPh_3$ (15.2 mg, 0.05 mmol, 25 mol%), BQ (21.6 mg, 0.2 mmol, 1.0 equiv), NBE-CONHMe (30.2 mg, 0.2 mmol, 1.0 equiv), AgOAc (132 mg, 0.8 mmol, 4.0 equiv), Pyrrole **5a** (23.2 mg, 0.2mmol, 1.0 equiv) and MeI **12** (50 ul, 0.8 mmol, 4.0 equiv). Then, 1.0 mL TBME was added. After acrylate **3a** (31 mg/36 µL, 0.36 mmol, 1.8 equiv) and AcOH (60 mg/56 µL, 1.0 mmol, 5.0 equiv) and was added, the vial was tightly sealed and stirred on a pie-block preheated to 65 °C for 72 hours. After completion of the reaction, the mixture was filtered through a thin pad of silica gel. The filter cake was washed with ethyl acetate and the combined filtrate was concentrated. The residue was loaded to a small amount of silica gel and subjected to flash column chromatography to give the desired difunctionalization product **13**.

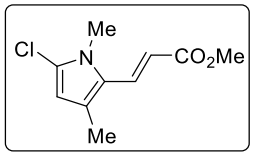

10: Light yellow oil (40 %). R_f = 0.3 (hexane/ethyl acetate = 20:1). **^{1}H NMR** (400 MHz, Chloroform-*d*) δ 7.62 (d, *J* = 15.9 Hz, 1H), 6.02 – 5.95 (m, 2H), 3.78 (s, 3H), 3.63 (s, 3H), 2.21 (s, 3H). **^{13}C NMR** (101 MHz, $CDCl_3$) δ 168.7, 132.3, 125.6, 121.6, 111.7, 110.3, 106.8, 51.7, 31.7,

14.0. **IR** (KBr): 2955, 1770, 1759, 1616, 1384, 1246, 1170, 1057, 913, 744 cm^{-1}. **HRMS** (ESI): Calculated for $C_{10}H_{13}ClNO_2$ ($M+H^+$): 214.0629, found: 214.0629.

Scheme 7.13. Ortho Methylation of Thiophene 9a

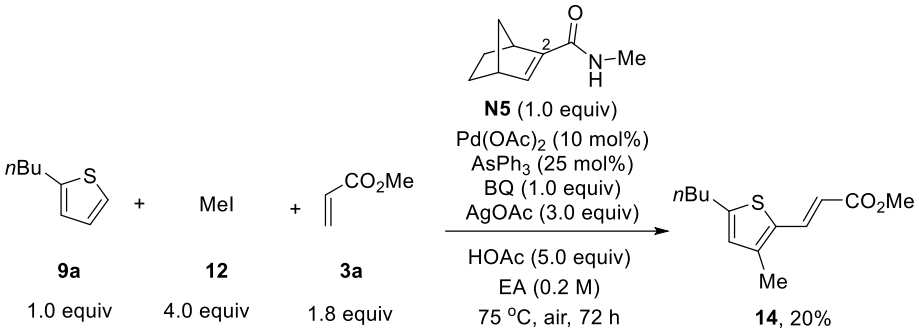

A flame-dried 4.0 mL vial was charged with $Pd(OAc)_2$ (4.6 mg, 0.02 mmol, 10 mol%), $AsPh_3$ (15.2 mg, 0.05 mmol, 25 mol%), BQ (21.6 mg, 0.2 mmol, 1.0 equiv), NBE-CONHMe (30.2 mg, 0.2 mmol, 1.0 equiv), AgOAc (100 mg, 0.6 mmol, 3.0 equiv), 2-butylthiophene **9a** (28.0 mg, 0.2mmol, 1.0 equiv) and MeI **12** (50 ul, 0.8 mmol, 4.0 equiv). Then, 1.0 mL ethyl acetate was added. After acrylate **3a** (31 mg/36 µL, 0.36 mmol, 1.8 equiv) and AcOH (60 mg/56 µL, 1.0 mmol, 5.0 equiv) and was added, the vial was tightly sealed and stirred on a pie-block preheated to 75 °C for 72 hours. After completion of the reaction, the mixture was filtered through a thin pad of silica gel. The filter cake was washed with ethyl acetate and the combined filtrate was concentrated. The residue was loaded to a small amount of silica gel and subjected to flash column chromatography to give the desired difunctionalization product **14**.

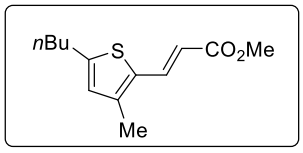

12: Light yellow oil (20 %). R_f = 0.3 (hexane / ethyl acetate =20 :1). **^{1}H NMR** (400 MHz, $CDCl_3$) δ 7.80 (d, *J* = 15.5 Hz, 1H), 6.56 (s, 1H), 6.04 (d, *J* = 15.5 Hz, 1H), 3.77 (s, 3H), 2.77 – 2.70 (m,

2H), 2.27 (s, 3H), 1.66 (d, *J* = 0.9 Hz, 2H), 1.43 – 1.34 (m, 2H), 0.94 (d, *J* = 7.3 Hz, 3H). **^{13}C NMR** (101 MHz, $CDCl_3$) δ 168.0, 148.6, 141.9, 136.1, 131.4, 128.7, 114.0, 51.7, 33.5, 30.2, 22.3, 14.3, 13.9. **IR** (KBr): 2955, 2930, 1717, 1618, 1466, 1432, 1308, 1287, 1266, 1192 cm^{-1}. **HRMS** (ESI): Calculated for $C_{13}H_{19}SO_2$ ($M+H^+$): 239.1100, found: 239.1102.

Scheme 7.14. Ortho Alkynylation of Pyrroles and Thiophenes

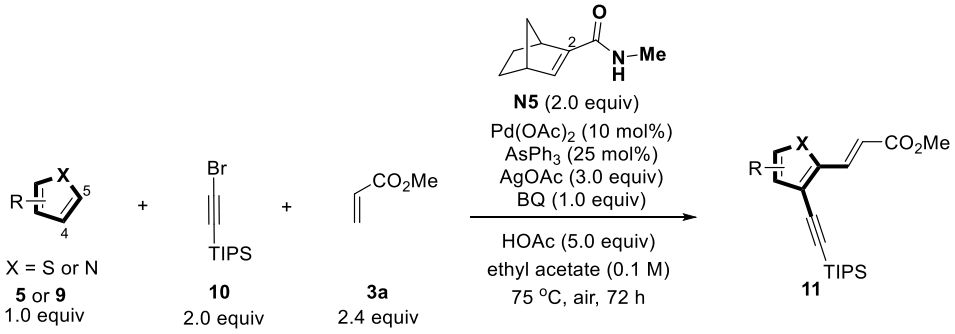

A flame-dried 4.0 mL vial was charged with $Pd(OAc)_2$ (4.6 mg, 0.02 mmol, 10 mol%), $AsPh_3$ (15.2 mg, 0.05 mmol, 25 mol%), BQ (21.6 mg, 0.2 mmol, 1.0 equiv), NBE-CONHMe (60.4 mg, 0.4 mmol, 2.0 equiv), AgOAc (100 mg, 0.6 mmol, 3.0 equiv), heteroarene **5** or **9** (0.2 mmol, 1.0 equiv) and alkynyl bromide **10** (104.5 mg, 0.4 mmol, 2.0 equiv). Then, 1.0 mL ethyl acetate was added. After acrylate **3a** (41 mg/48 µL, 0.48 mmol, 2.4 equiv) and AcOH (60 mg/56 µL, 1.0 mmol, 5.0 equiv) and was added, the vial was tightly sealed and stirred on a pie-block preheated to 75 °C for 72 hours. After completion of the reaction, the mixture was filtered through a thin pad of silica gel. The filter cake was washed with ethyl acetate and the combined filtrate was concentrated. The residue was loaded to a small amount of silica gel and subjected to flash column chromatography to give the desired difunctionalization product **11**.

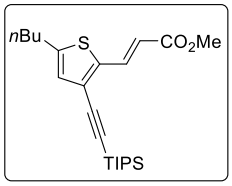

11a: Light yellow oil (53 %). R_f = 0.6 (hexane / ethyl acetate =20 :1). **^{1}H NMR** (400 MHz, $CDCl_3$) δ 7.98 (d, *J* = 15.8 Hz, 1H), 6.76 (d, *J* = 1.0 Hz, 1H), 6.22 (d, *J* = 15.7 Hz, 1H), 3.77 (s, 3H), 2.80 – 2.69 (m, 2H), 1.71 – 1.61 (m, 2H), 1.40 (dt, *J* = 14.8, 6.9 Hz, 2H), 1.14 (s, 22H), 0.93 (t, *J* = 7.3 Hz, 4H). **^{13}C NMR** (101 MHz, $CDCl_3$) δ 167.43, 148.41, 140.18, 136.17, 128.27, 125.86, 116.31, 100.54, 51.74, 33.34, 30.15, 22.23, 18.81, 13.89, 11.42.

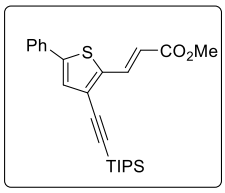

11b: Yellow oil (52 %). R_f = 0.4 (hexane / ethyl acetate =20 :1). **^{1}H NMR** (400 MHz, CD_2Cl_2) δ 7.92 (d, *J* = 15.8 Hz, 1H), 7.54 – 7.49 (m, 2H), 7.35 – 7.30 (m, 2H), 7.29 – 7.24 (m, 1H), 7.22 (s, 1H), 6.26 (d, *J* = 15.8 Hz, 1H), 3.67 (s, 3H), 1.09 (s, 21H). **^{13}C NMR** (101 MHz, CD_2Cl_2) δ 166.76, 145.51, 141.11, 135.28, 132.79, 129.09, 128.80, 126.60, 126.56, 125.87, 117.29, 99.98, 97.89, 51.52, 18.43, 11.29.

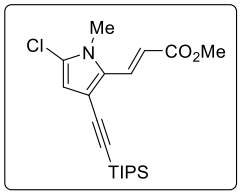

11c: Colorless oil (50 %). R_f = 0.2 (hexane / ethyl acetate =20 :1). **^{1}H NMR** (400 MHz, $CDCl_3$) δ 7.57 (d, *J* = 15.8 Hz, 1H), 7.01 (d, *J* = 15.7 Hz, 1H), 6.27 (d, *J* = 0.5 Hz, 1H), 3.77 (s, 3H), 3.62 (s, 3H), 1.13 (s, 22H). ^{13}C NMR (101 MHz, $CDCl_3$) δ 168.53, 131.05, 130.51, 121.28, 115.97, 112.32, 108.11, 101.14, 96.96, 51.71, 31.40, 18.81, 11.45.

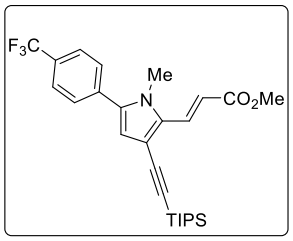

11d: Yellow solid. R_f = 0.3 (hexane / ethyl acetate =10 :1). **^{1}H NMR** (400 MHz, CD_2Cl_2) δ 7.65 – 7.58 (m, 3H), 7.43 (dt, *J* = 7.9, 0.8 Hz, 2H), 7.00 (d, *J* = 15.8 Hz, 1H), 6.39 (s, 1H), 3.67 (s, 3H), 3.57 (s, 3H), 1.07 (s, 22H). **^{13}C NMR** (101 MHz, CD_2Cl_2) δ 167.96, 136.76, 135.21, 133.13, 130.57, 129.29, 125.52, 122.82, 116.37, 115.05, 108.20, 101.84, 96.25. **^{19}F NMR** (376 MHz, CD_2Cl_2) δ -62.94.

7.4.7 Synthetic Utility

Scheme 7.15. Gram-scale Preparation

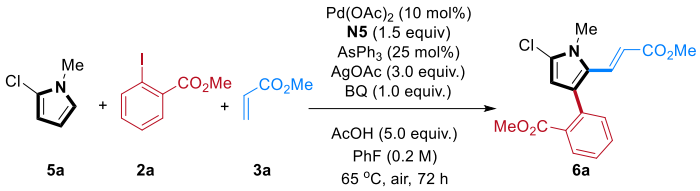

open flask

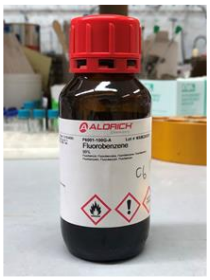

solvent

A flame-dried 100 mL round bottom flask was charged with $Pd(OAc)_2$ (0.16 g, 0.7mmol, 10 mol%), $AsPh_3$ (0.53g, 1.75 mmol, 25 mol%), BQ (0.76 g, 7.0mmol, 1.0 equiv), **N5** (1.86 g, 10.5 mmol, 1.5 equiv), AgOAc (3.5 g, 21 mmol, 3.0 equiv), Pyrrole **5a** (0.81 g, 7 mmol, 1.0 equiv) and aryl iodide **2a** (3.67 g, 14 mmol, 2.0 equiv). Then, 35 mL fluorobenzene was added. After acrylate **3a** (1.8 g, 21 mmol, 3.0 equiv) and AcOH (1.96 ml, 35.0 mmol, 5.0 equiv) and was added, the vial was tightly sealed and stirred on a pie-block preheated to 65 ^{o}C for 72 hours. After completion of the reaction, the mixture was filtered through a thin pad of silica gel. The filter cake was washed with ethyl acetate and the combined filtrate was concentrated. The residue was loaded to a small amount of silica gel and subjected to flash column chromatography to give the desired difunctionalization product **6a** (1.77 g, 76%).

Scheme 7.16. Total Synthesis of (±)-Rhazinilam

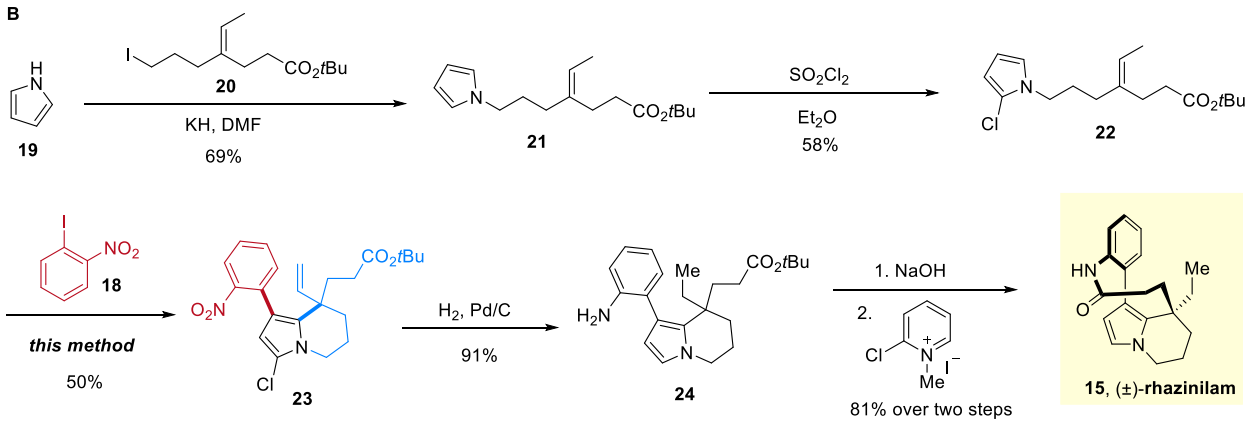

20 was synthesized according to a literature reported procedure.[19]

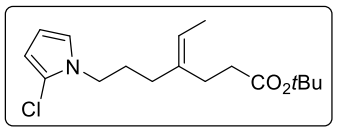

22: Light yellow oil (58 %). R_f = 0.3 (hexane/ethyl acetate =15 :1). **^{1}H NMR** (400 MHz, Chloroform-*d*) δ 6.59 (dd, *J* = 2.9, 2.0 Hz, 1H), 6.08 (t, *J* = 3.4 Hz, 1H), 6.01 (dd, *J* = 3.7, 1.9 Hz, 1H), 5.27 (q, *J* = 6.7 Hz, 1H), 3.84 (t, *J* = 7.3 Hz, 2H), 2.36 – 2.30 (m, 2H), 2.28 – 2.22 (m, 2H), 2.00 (t, *J* = 7.4 Hz, 2H), 1.84 (q, *J* = 7.7 Hz, 2H), 1.61 (d, *J* = 6.8 Hz, 3H), 1.45 (s, 9H). **^{13}C NMR** (101 MHz, $CDCl_3$) δ 172.8, 137.0, 120.9, 120.3, 115.6, 107.7, 106.4, 80.4, 46.6, 34.2, 33.4, 29.1, 28.2, 25.2, 13.4. **IR** (KBr): 2978, 2932, 1790, 1478, 1442, 1367, 1290, 1153, 1088, 703 cm^{-1}. **HRMS** (ESI): Calculated for $C_{17}H_{27}ClNO_2$ ($M+H^+$): 312.1725, found: 312.1725.

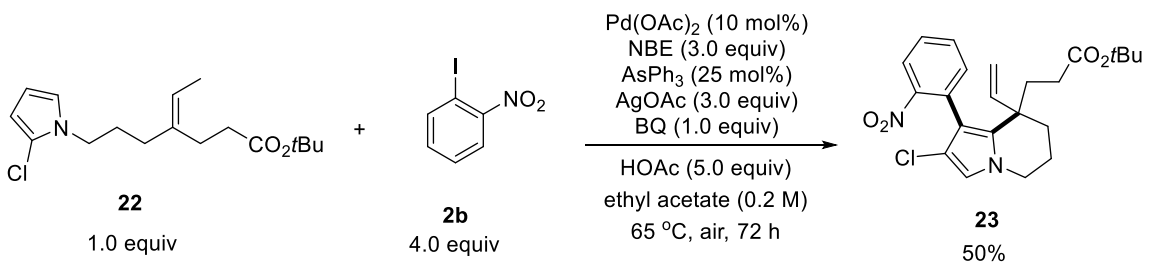

A flame-dried 4.0 mL vial was charged with $Pd(OAc)_2$ (2.3 mg, 0.01 mmol, 10 mol%), $AsPh_3$ (7.6 mg, 0.025 mmol, 25 mol%), BQ (10.8 mg, 0.1 mmol, 1.0 equiv), NBE (28.3 mg, 0.3 mmol, 3.0 equiv), AgOAc (50 mg, 0.3 mmol, 3.0 equiv), pyrrole **22** (46.8 mg, 0.1 mmol, 1.0 equiv) and 2-iodonitrobenzene **2** (99.6 mg, 0.4 mmol, 4.0 equiv) in air. After ethyl acetate (0.2 M, 0.5 mL) and HOAc (30 mg, 0.5 mmol, 5.0 equiv) were added, the vial was tightly sealed and stirred on a pie-block preheated to 65 °C for 72 hours. After completion of the reaction, the mixture was filtered through a thin pad of silica gel. The filter cake was washed with ethyl acetate and the combined filtrate was concentrated under reduced pressure. The residue was loaded to a small amount of silica gel and subjected to flash column chromatography to deliver the desired product **23**.

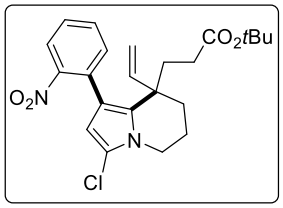

23: Light yellow solid (50 %). R_f = 0.3 (hexane / ethyl acetate =10 :1). Mp = 166.7–170.2 °C. **^{1}H NMR** (400 MHz, Chloroform-*d*) δ 7.72 (d, *J* = 7.3 Hz, 1H), 7.54 (d, *J* = 7.5 Hz, 1H), 7.44 (td, *J* = 7.5, 1.3 Hz, 1H), 7.37 (td, *J* = 7.8, 1.4 Hz, 1H), 5.94 (s, 1H), 5.80 (dd, *J* = 17.3, 10.5 Hz, 1H), 5.13 (d, *J* = 10.0 Hz, 1H), 4.75 (d, *J* = 17.3 Hz, 1H), 4.04 (ddd, *J* = 12.2, 5.5, 2.5 Hz, 1H), 3.64 (dt, *J* = 11.9, 6.0 Hz, 1H), 2.23 – 2.06 (m, 3H), 1.95 – 1.86 (m, 2H), 1.76 – 1.69 (m, 1H), 1.64 – 1.55 (m, 2H), 1.31 (s, 9H). **^{13}C NMR** (101 MHz, $CDCl_3$) δ 172.9, 150.2, 145.6, 133.7, 131.7, 131.2, 128.3, 127.8, 123.8, 115.6, 115.1, 115.0, 108.0, 80.0, 43.8, 43.3, 32.3, 30.8, 30.5, 28.1, 18.6. **IR** (KBr): 2918, 1725, 1685, 1654, 1618, 1541, 1528, 1458, 1384, 1365 cm^{-1}. **HRMS** (ESI): Calculated for $C_{23}H_{28}ClN_2O_4$ ($M+H^+$): 431.1732, found: 431.1730.

24 and **25** were synthesized according to literature reported procedures.[19]

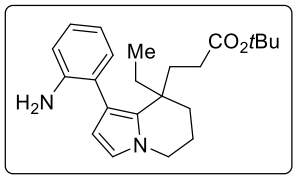

24: Brown oil (91 %). R_f = 0.3 (hexane / ethyl acetate =5 :1). ^{1}H NMR (400 MHz, Chloroform-*d*) δ 7.10 (t, *J* = 7.3 Hz, 2H), 6.76 – 6.69 (m, 2H), 6.56 (d, *J* = 2.6 Hz, 1H), 6.01 (d, *J* = 7.1 Hz, 1H), 3.91 (t, *J* = 5.7 Hz, 2H), 3.75 – 3.42 (m, 2H), 2.14 (dt, *J* = 30.3, 7.1 Hz, 2H), 2.01 – 1.84 (m, 3H), 1.69 (ddt, *J* = 36.0, 12.1, 7.2 Hz, 5H), 1.41 (d, *J* = 24.9 Hz, 9H), 0.83 – 0.70 (m, 3H). ^{13}C NMR (101 MHz, Chloroform-*d*) δ 173.6 (d, *J* = 9.0 Hz), 145.2 (d, *J* = 49.2 Hz), 131.7 (d, *J* = 7.8 Hz), 131.4 (d, *J* = 9.4 Hz), 128.0, 124.8 (d, *J* = 15.7 Hz), 119.0 (d, *J* = 8.6 Hz), 117.9 (d, *J* = 12.6 Hz), 116.0 (d, *J* = 10.2 Hz), 115.0 (d, *J* = 45.5 Hz), 80.1 (d, *J* = 6.1 Hz), 46.3, 39.4 (d, *J* = 8.9 Hz), 35.7 (d, *J* = 142.0 Hz), 34.1 (d, *J* = 92.9 Hz), 32.1 (d, *J* = 27.6 Hz), 29.9 (d, *J* = 17.1 Hz), 28.2 (d, *J* = 5.4 Hz), 21.5 (d, *J* = 28.2 Hz), 9.4 (d, *J* = 14.5 Hz). **IR** (KBr): 2964, 2873, 1725, 1613, 1500, 1482, 1451, 1367, 1297, 1146 cm^{-1}. **HRMS** (ESI): Calculated for $C_{23}H_{33}N_2O_2$ ($M+H^+$): 369.2537, found: 369.2528.

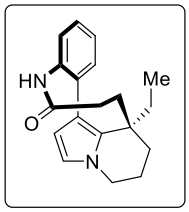

15: White solid (81%). **^{1}H NMR** (400 MHz, $CDCl_3$) δ 7.42 (dd, *J* = 7.3, 1.9 Hz, 1H), 7.37 – 7.27 (m, 2H), 7.20 (dd, *J* = 7.5, 1.7 Hz, 1H), 6.70 (s, 1H), 6.50 (d, *J* = 2.7 Hz, 1H), 5.75 (d, *J* = 2.7 Hz, 1H), 4.01 (ddt, *J* = 12.1, 5.5, 1.8 Hz, 1H), 3.79 (td, *J* = 12.1, 4.8 Hz, 1H), 2.51 – 2.33 (m, 2H), 2.31 – 2.15 (m, 1H), 2.00 – 1.91 (m, 1H), 1.86 (dh, *J* = 11.2, 2.4 Hz, 1H), 1.72 (td, *J* = 13.4, 3.1 Hz, 1H), 1.58 – 1.41 (m, 3H), 1.26 (d, *J* = 7.4 Hz, 1H), 0.71 (t, *J* = 7.4 Hz, 3H). **^{13}C NMR** (101 MHz, $CDCl_3$) δ 177.53, 140.49, 138.16, 131.56, 130.69, 128.12, 127.35, 126.93, 119.25, 117.42, 109.68, 46.21, 39.00, 36.73, 33.20, 30.24, 28.22, 19.55, 8.29. Both ^{1}H NMR and ^{13}C NMR match with literature reported data.[19]

7.4.8 Kinetic Study

Scheme 7.17. Parallel KIE of Indole

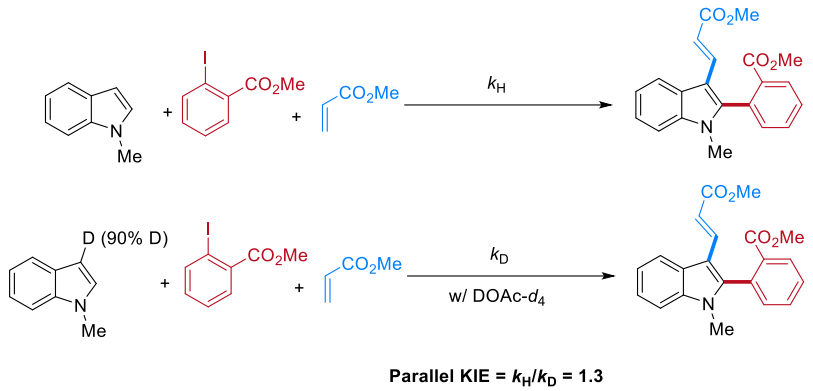

Parallel KIE = k_H/k_D = 1.3

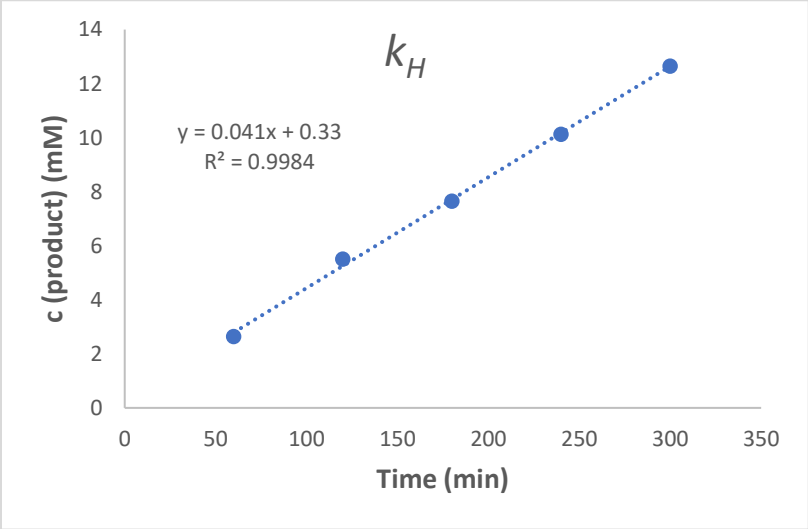

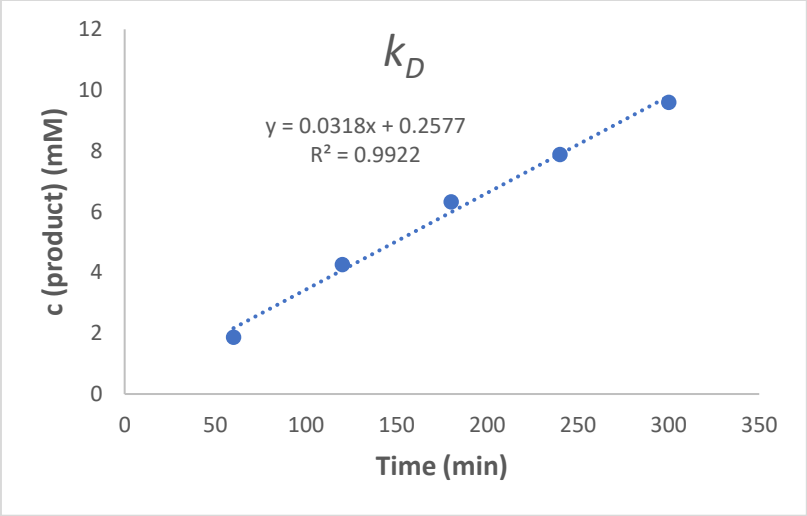

Scheme 7.17. Parallel KIE of Indole (continued)

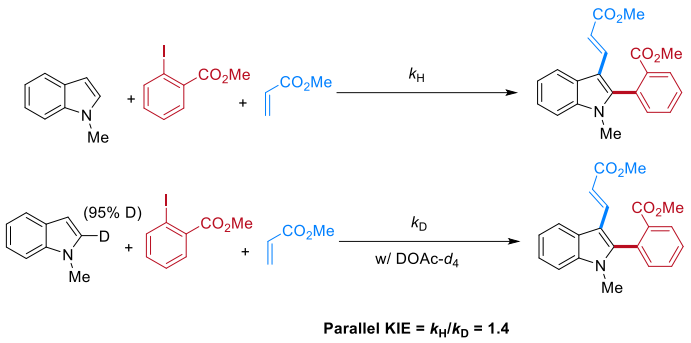

Parallel KIE = k_H/k_D = 1.4

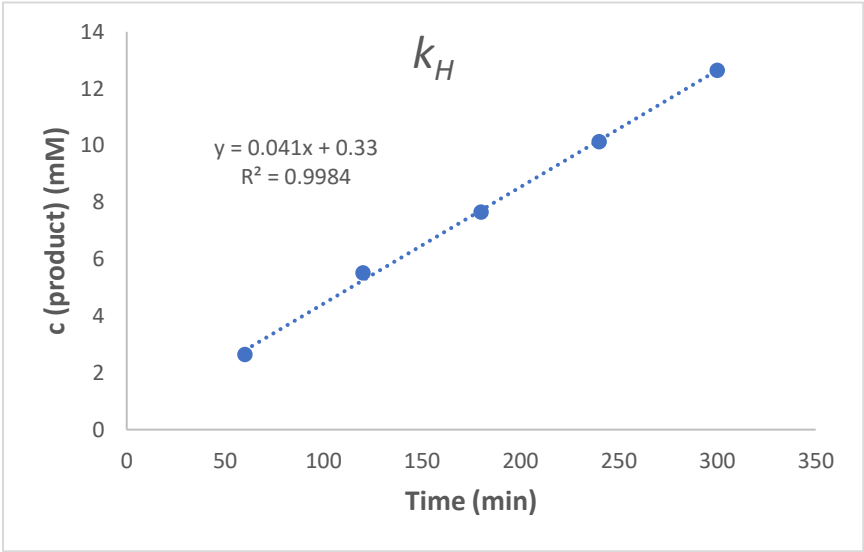

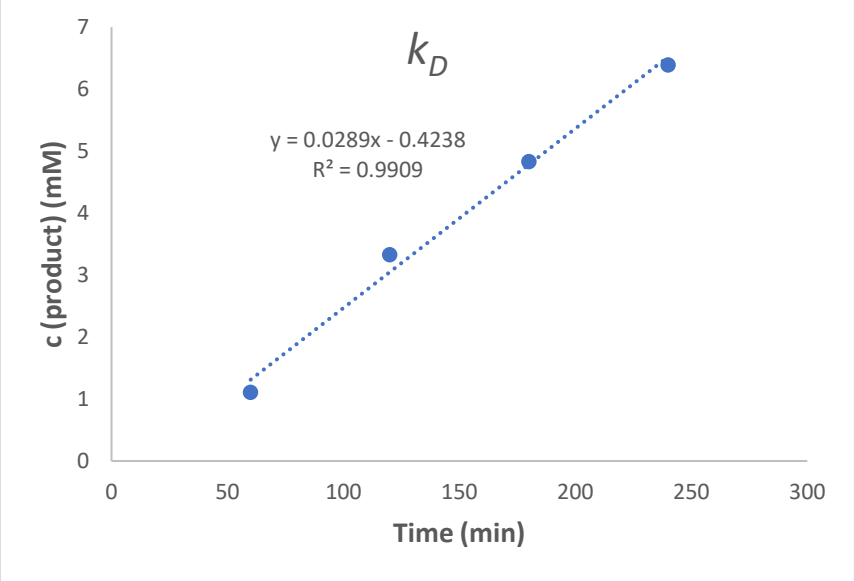

Figure 7.4. Initial-Rate Dependence on N2

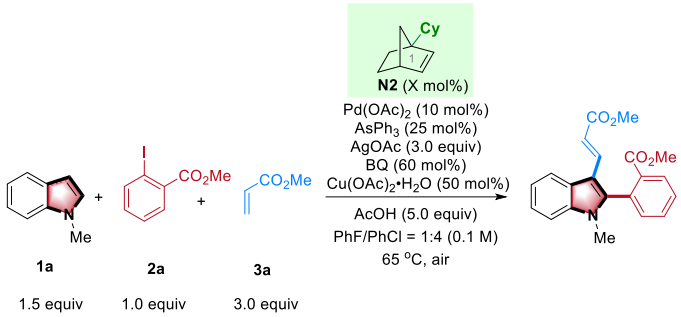

Equivalency of **N5**	0.05	0.1	0.15	0.2	0.4	0.8
[**N3**]/M	0.005	0.01	0.015	0.02	0.04	0.08
[**1a**]/M	0.15	0.15	0.15	0.15	0.15	0.15
[**2a**]/M	0.1	0.1	0.1	0.1	0.1	0.1
[**3a**]/M	0.3	0.3	0.3	0.3	0.3	0.3
[$Pd(OAc)_2$]/M	0.01	0.01	0.01	0.01	0.01	0.01
[$AsPh_3$]/M	0.025	0.025	0.025	0.025	0.025	0.025
[AgOAc]/M	0.3	0.3	0.3	0.3	0.3	0.3
[BQ]/M	0.06	0.06	0.06	0.06	0.06	0.06
[$Cu(OAc)_2$•H_2O]/M	0.05	0.05	0.05	0.05	0.05	0.05
[HOAc]/M	0.5	0.5	0.5	0.5	0.5	0.5
initial rate/mM·min^{-1}	0.0126	0.0195	0.00253	0.031	0.0409	0.0429

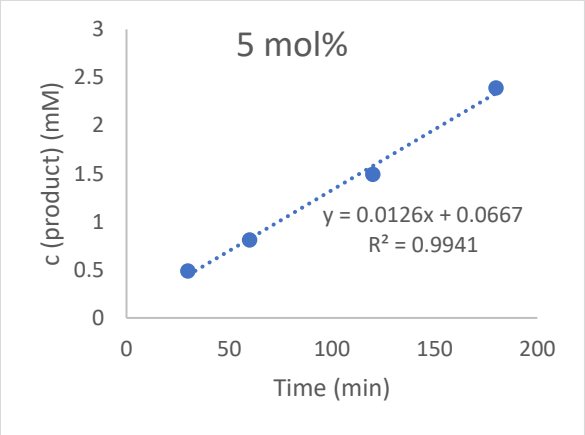

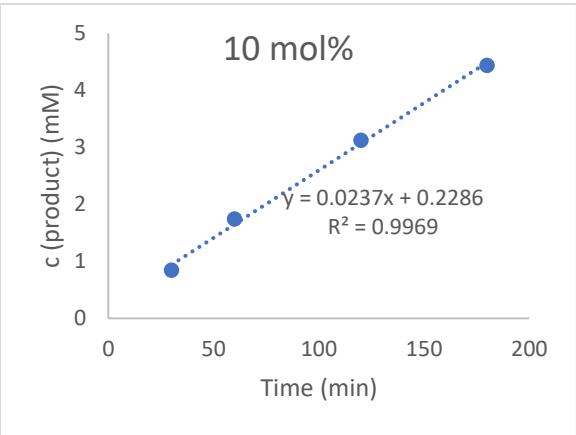

Figure 7.4. Initial-Rate Dependence on N2 (continued)

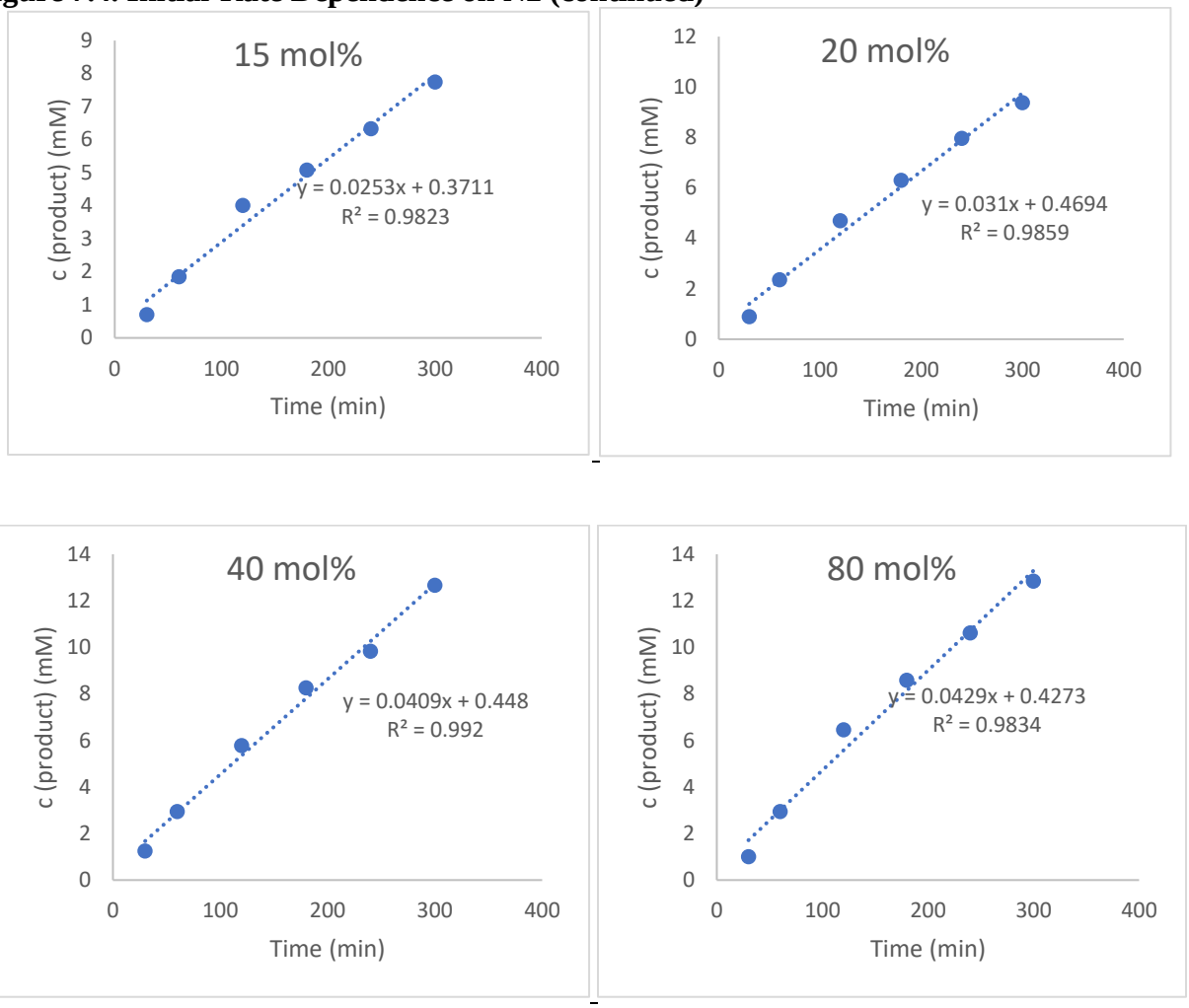

N2: <u>Saturation Dependence</u>

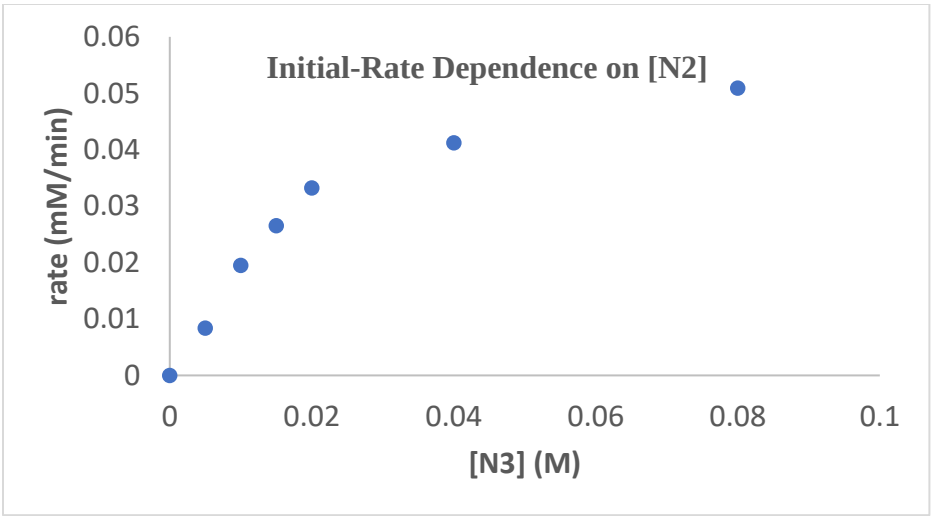

Figure 7.5. Initial-Rate Dependence on N2 (Formation of Direct Alkenylation Side Product)

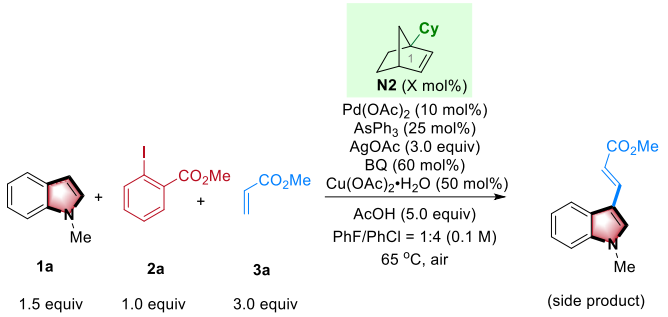

Equivalency of **N3**	0.1	0.15	0.2	0.4	0.8
[**N2**]/M	0.01	0.015	0.02	0.04	0.08
[**1a**]/M	0.15	0.15	0.15	0.15	0.15
[**2a**]/M	0.1	0.1	0.1	0.1	0.1
[**3a**]/M	0.3	0.3	0.3	0.3	0.3
[$Pd(OAc)_2$]/M	0.01	0.01	0.01	0.01	0.01
[$AsPh_3$]/M	0.025	0.025	0.025	0.025	0.025
[AgOAc]/M	0.3	0.3	0.3	0.3	0.3
[BQ]/M	0.06	0.06	0.06	0.06	0.06
[$Cu(OAc)_2$•H_2O]/M	0.05	0.05	0.05	0.05	0.05
[HOAc]/M	0.5	0.5	0.5	0.5	0.5
initial rate/mM·min^{-1}	0.6222	0.4772	0.3673	0.1066	0.0379

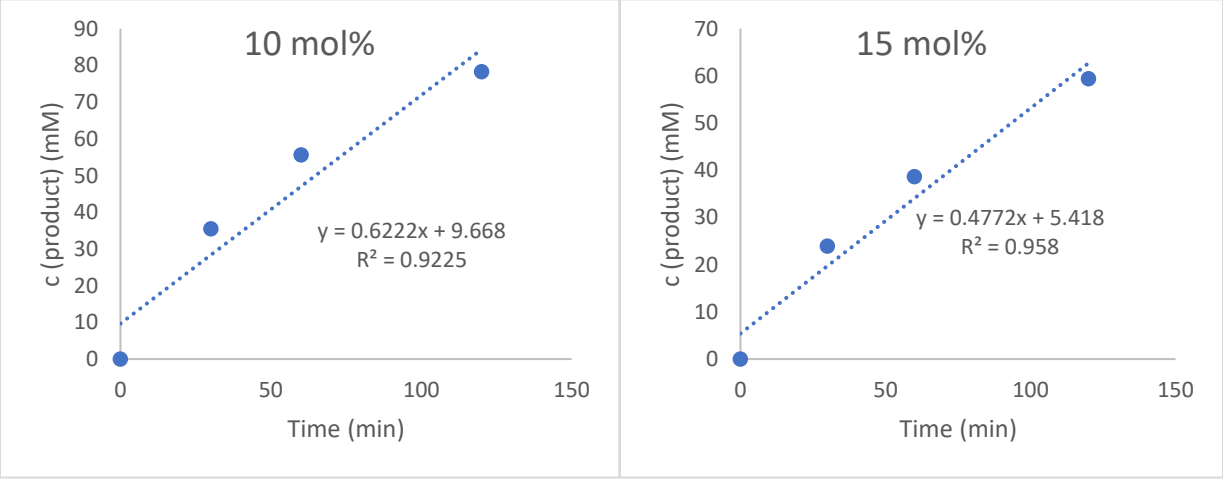

Figure 7.5. Initial-Rate Dependence on N2 (Formation of Direct Alkenylation Side Product) (continued)

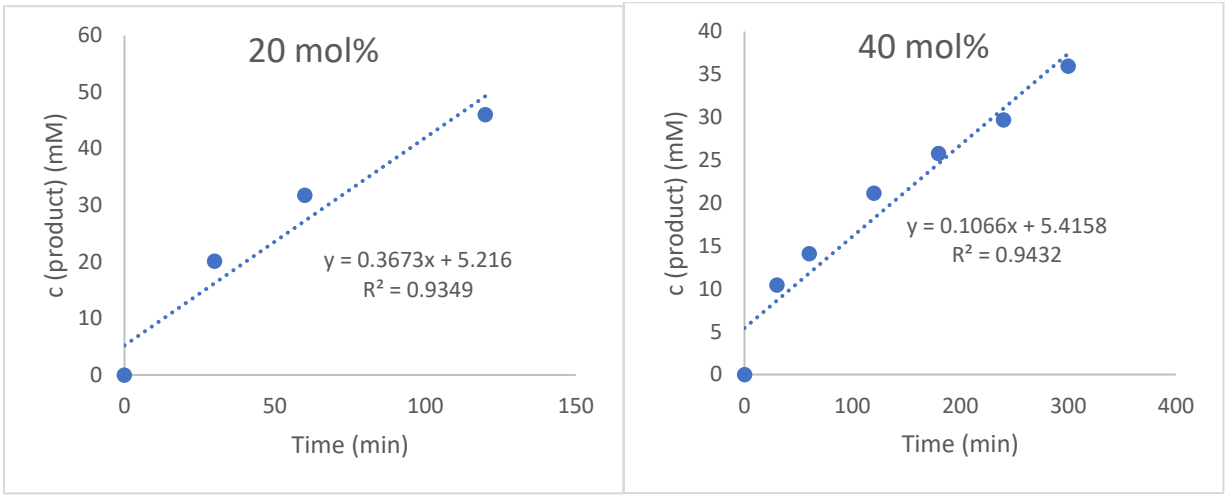

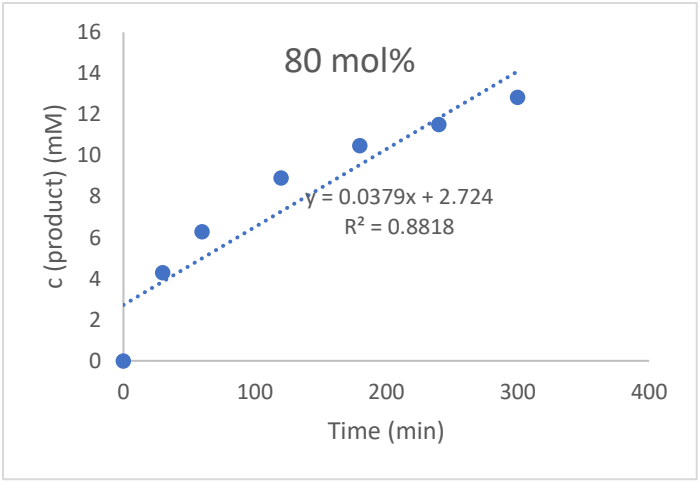

Figure 7.5. Initial-Rate Dependence on N2 (Formation of Direct Alkenylation Side Product) (continued)

N2: <u>Reverse First Order</u>

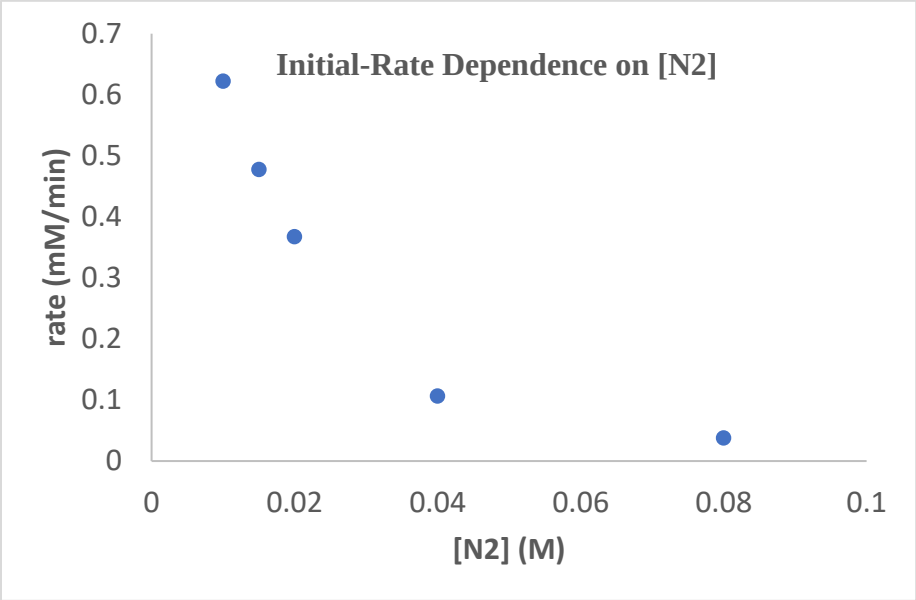

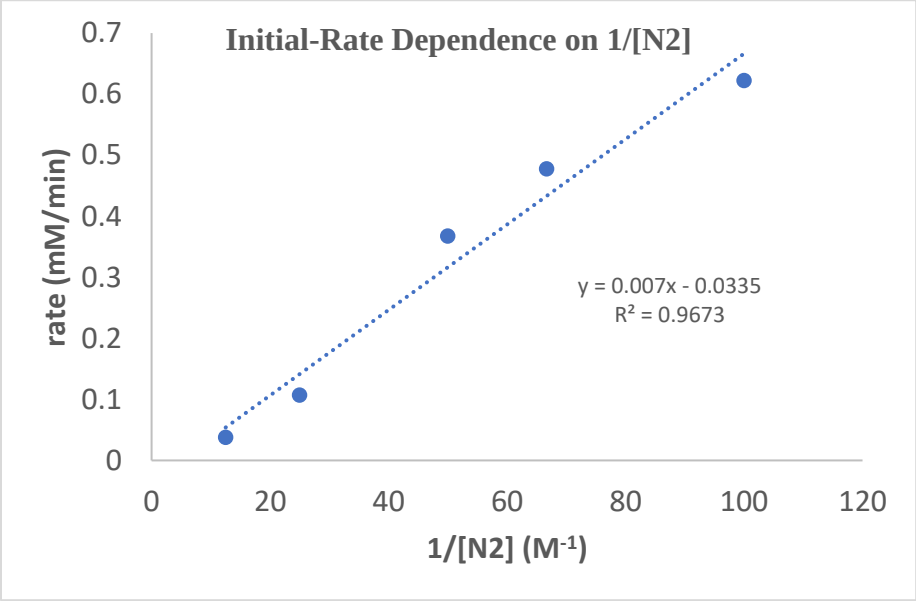

Figure 7.6. Initial-Rate Dependence on 1a

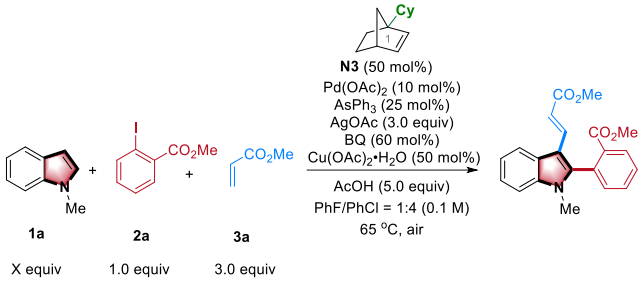

Equivalency of **1a**	0.125	0.25	0.5	0.75	1.0	1.25
[**1a**]/M	0.0125	0.025	0.05	0.075	0.1	0.125
[**2a**]/M	0.1	0.1	0.1	0.1	0.1	0.1
[**3a**]/M	0.3	0.3	0.3	0.3	0.3	0.3
[**N2**]/M	0.05	0.05	0.05	0.05	0.05	0.05
[$Pd(OAc)_2$]/M	0.01	0.01	0.01	0.01	0.01	0.01
[$AsPh_3$]/M	0.025	0.025	0.025	0.025	0.025	0.025
[AgOAc]/M	0.3	0.3	0.3	0.3	0.3	0.3
[BQ]/M	0.06	0.06	0.06	0.06	0.06	0.06
[$Cu(OAc)_2$•H_2O]/M	0.05	0.05	0.05	0.05	0.05	0.05
[HOAc]/M	0.5	0.5	0.5	0.5	0.5	0.5
initial rate/mM·min^{-1}	0.017	0.0232	0.0361	0.0386	0.0402	0.0431

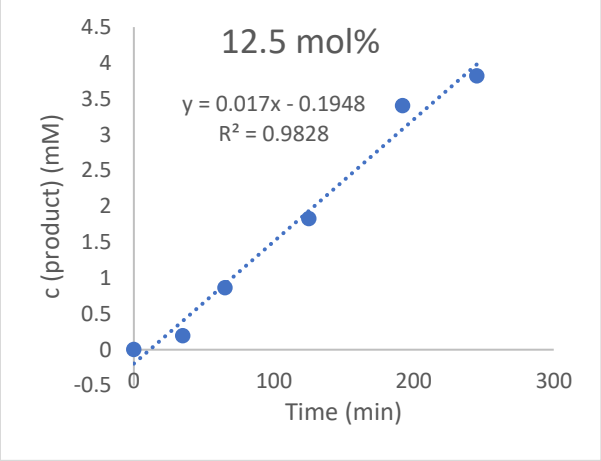

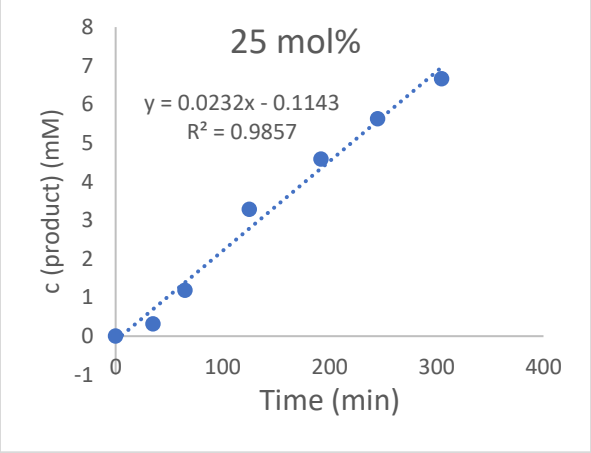

Figure 7.6. Initial-Rate Dependence on 1a (continued)

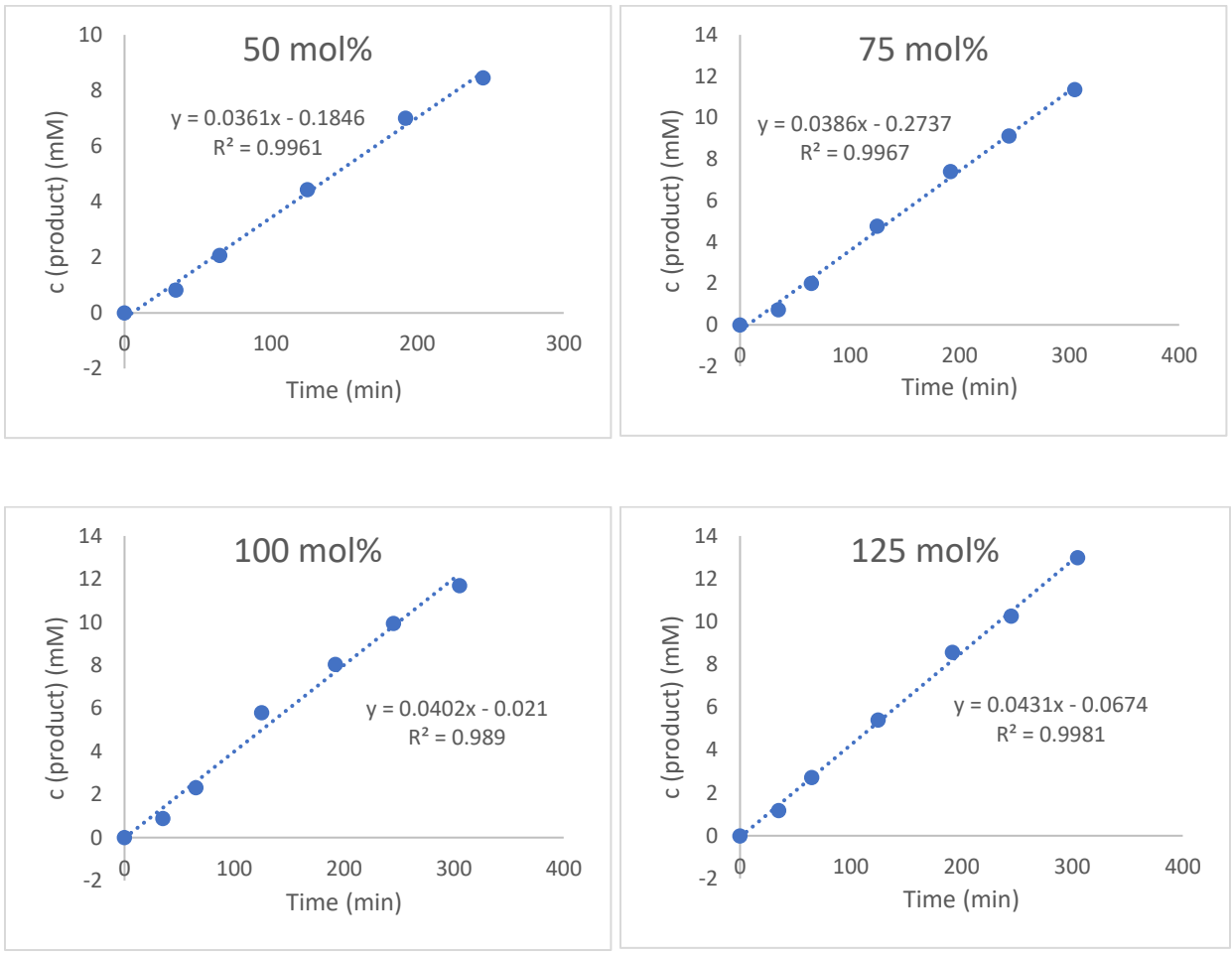

1a: <u>Saturation dependence</u>

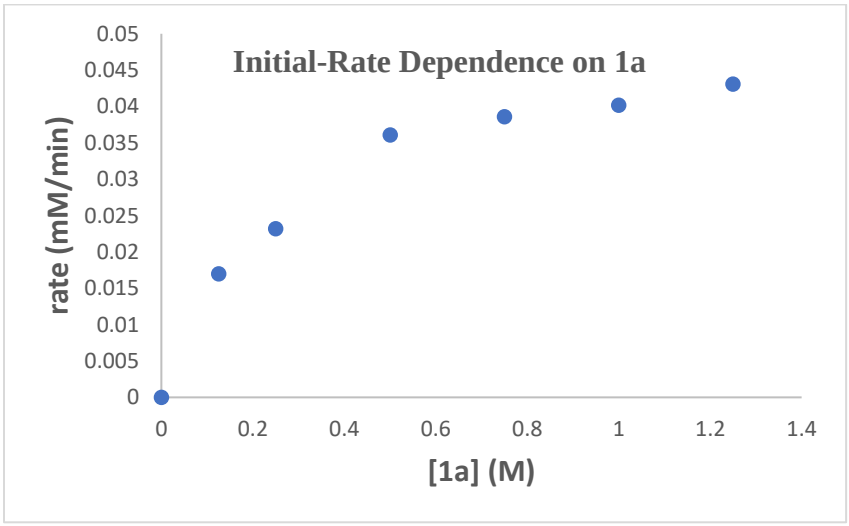

Figure 7.7. Initial-Rate Dependence on 2a

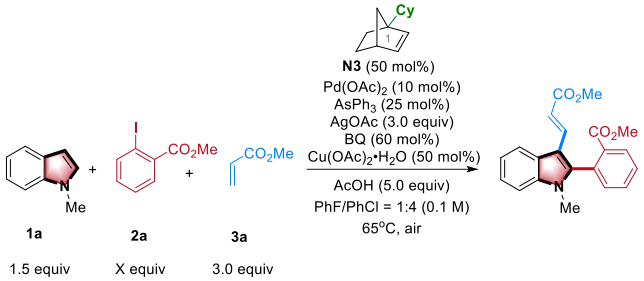

Equivalency of 2**a**	0.125	0.25	0.5	0.75	1.0
[**2a**]/M	0.0125	0.025	0.05	0.075	0.1
[**1a**]/M	0.15	0.15	0.15	0.15	0.15
[**3a**]/M	0.3	0.3	0.3	0.3	0.3
[**N2**]/M	0.05	0.05	0.05	0.05	0.05
[$Pd(OAc)_2$]/M	0.01	0.01	0.01	0.01	0.01
[$AsPh_3$]/M	0.025	0.025	0.025	0.025	0.025
[AgOAc]/M	0.3	0.3	0.3	0.3	0.3
[BQ]/M	0.06	0.06	0.06	0.06	0.06
[$Cu(OAc)_2$•H_2O]/M	0.05	0.05	0.05	0.05	0.05
[HOAc]/M	0.5	0.5	0.5	0.5	0.5
initial rate/mM·min^{-1}	0.0085	0.0152	0.028	0.039	0.0445

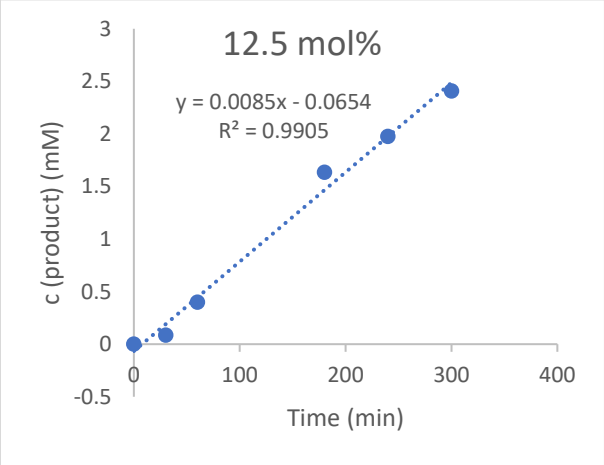

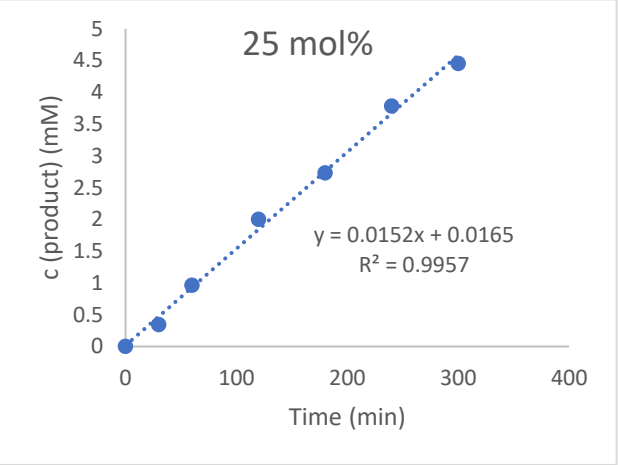

Figure 7.7. Initial-Rate Dependence on 2a (continued)

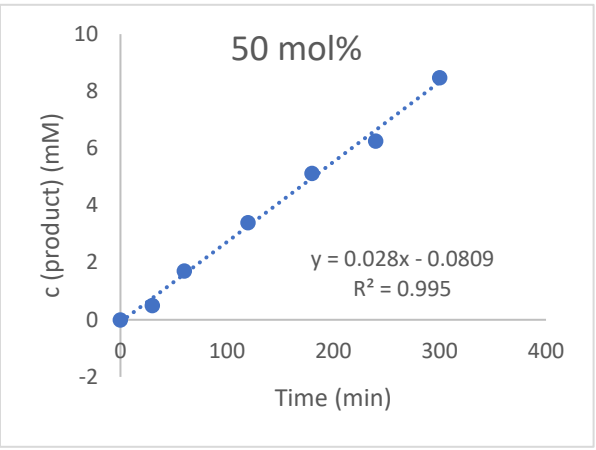

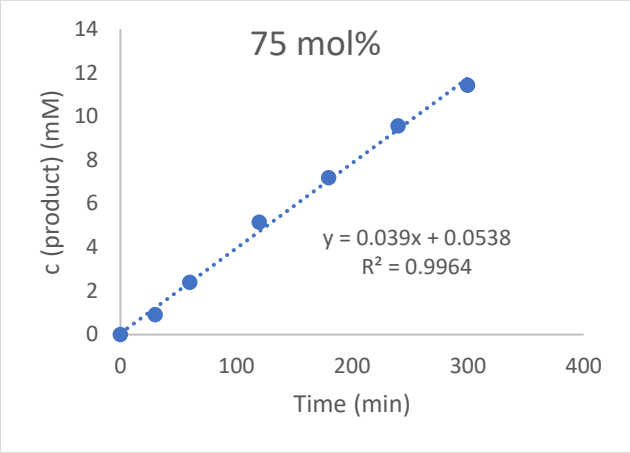

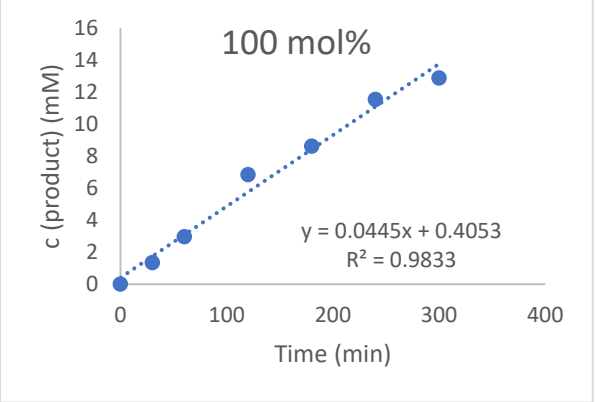

2a: First Order

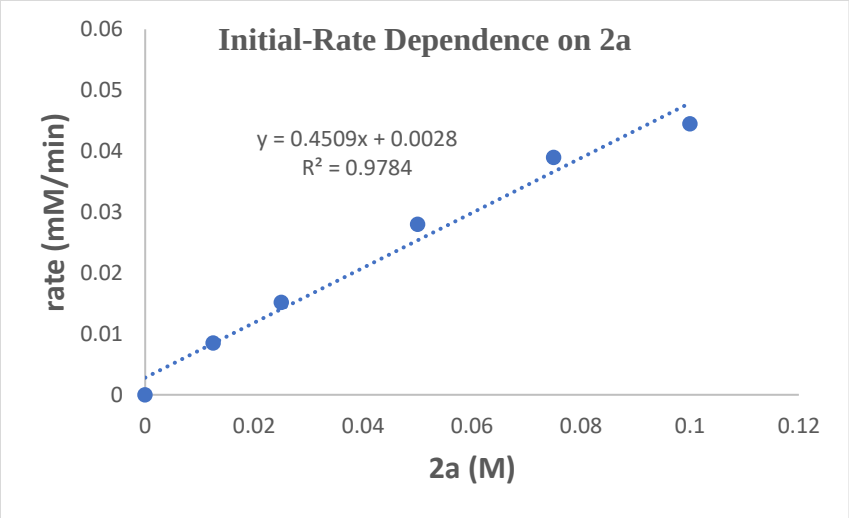

Figure 7.8. Initial-Rate Dependence on 3a

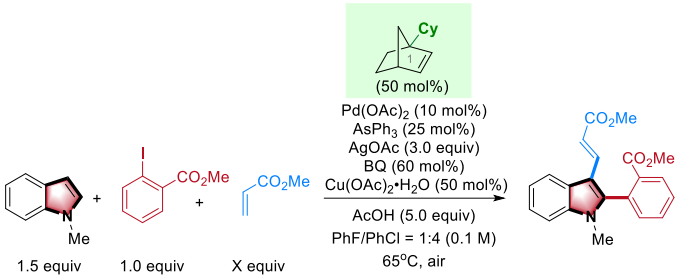

Equivalency of 3**a**	1.0	1.5	2.0	2.5	3.0
[3**a**]/M	0.1	0.15	0.2	0.25	0.3
[**1a**]/M	0.15	0.15	0.15	0.15	0.15
[**2a**]/M	0.1	0.1	0.1	0.1	0.1
[**N2**]/M	0.05	0.05	0.05	0.05	0.05
[$Pd(OAc)_2$]/M	0.01	0.01	0.01	0.01	0.01
[$AsPh_3$]/M	0.025	0.025	0.025	0.025	0.025
[AgOAc]/M	0.3	0.3	0.3	0.3	0.3
[BQ]/M	0.06	0.06	0.06	0.06	0.06
[$Cu(OAc)_2$•H_2O]/M	0.05	0.05	0.05	0.05	0.05
[HOAc]/M	0.5	0.5	0.5	0.5	0.5
Initial rate/mM·min^{-1}	0.0379	0.0416	0.0431	0.0453	0.0451

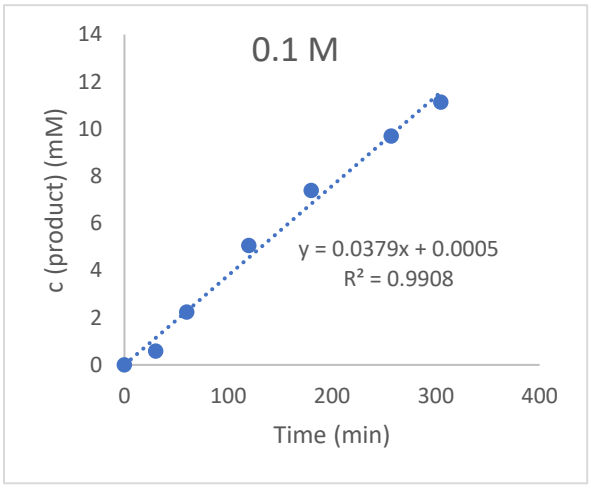

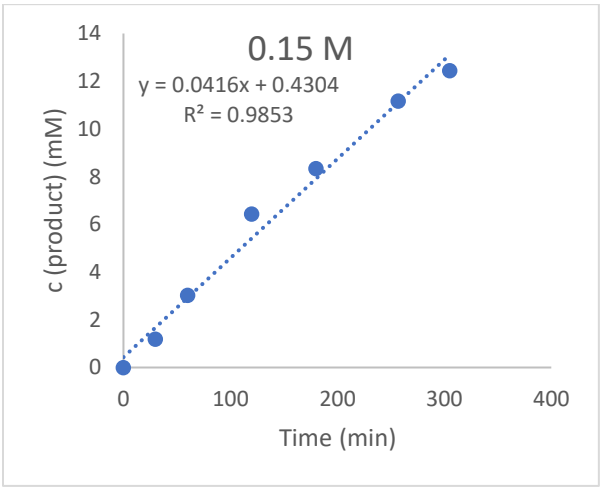

Figure 7.8. Initial-Rate Dependence on 3a (continued)

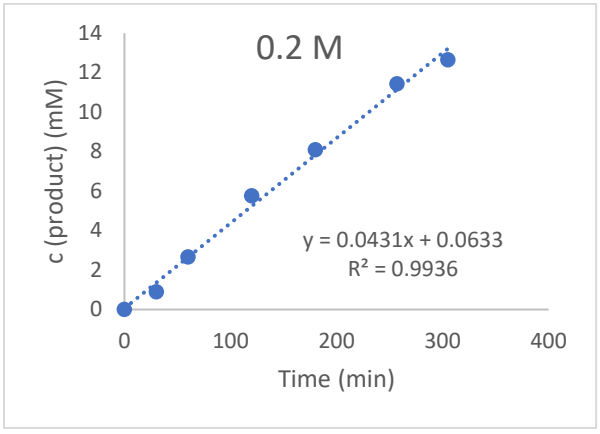

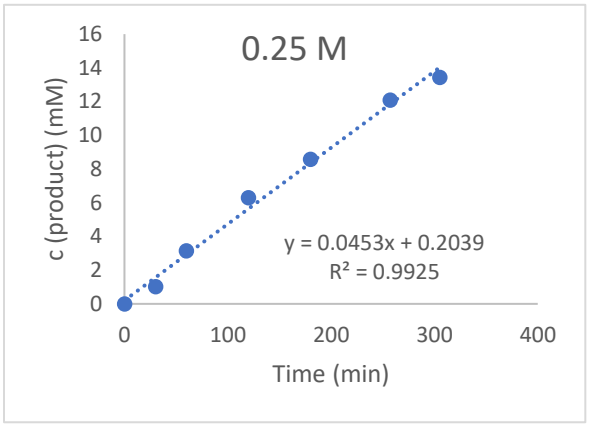

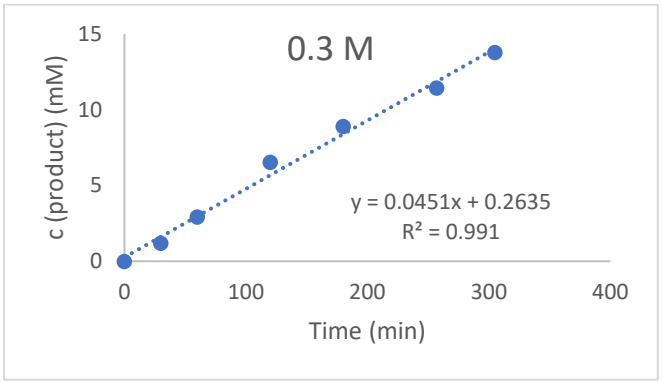

3a: <u>Saturation dependence</u>

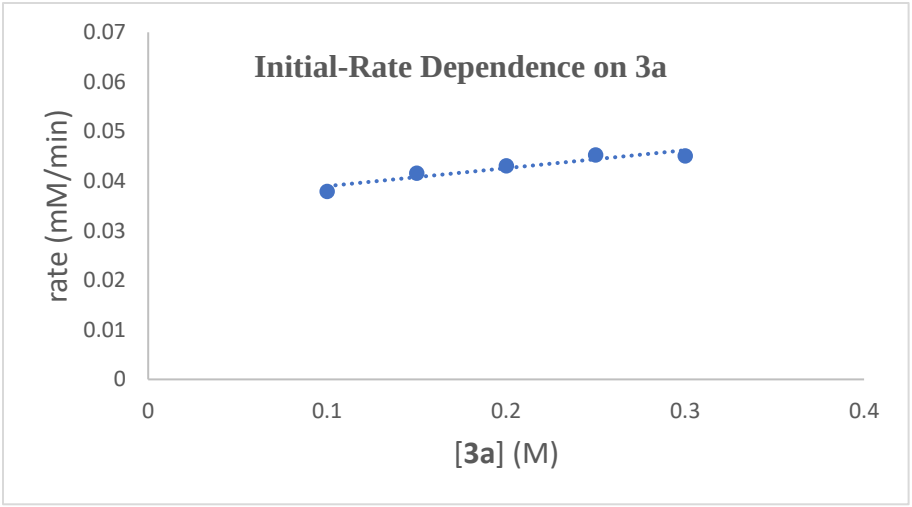

Figure 7.9. Initial-Rate Dependence on [Pd]

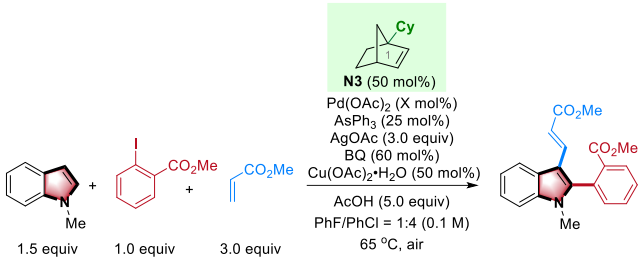

Equivalency of [Pd]	0.025	0.05	0.075	0.1	0.125
Equivalency of [AsPh3]	0.0625	0.125	0.1875	0.25	0.3125
[Pd]/M	0.0025	0.005	0.0075	0.01	0.0125
[AsPh3]/M	0.00625	0.0125	0.01875	0.025	0.03125
[**1a**]/M	0.15	0.15	0.15	0.15	0.15
[**2a**]/M	0.1	0.1	0.1	0.1	0.1
[**3a**]/M	0.3	0.3	0.3	0.3	0.3
[**N2**]/M	0.05	0.05	0.05	0.05	0.05
[AgOAc]/M	0.3	0.3	0.3	0.3	0.3
[BQ]/M	0.06	0.06	0.06	0.06	0.06
[$Cu(OAc)_2$•H_2O]/M	0.05	0.05	0.05	0.05	0.05
[HOAc]/M	0.5	0.5	0.5	0.5	0.5
Initial rate/mM·min^{-1}	0.0087	0.0231	0.0338	0.043	0.051

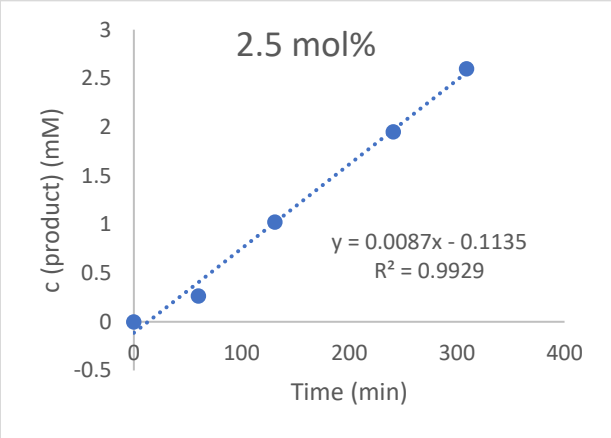

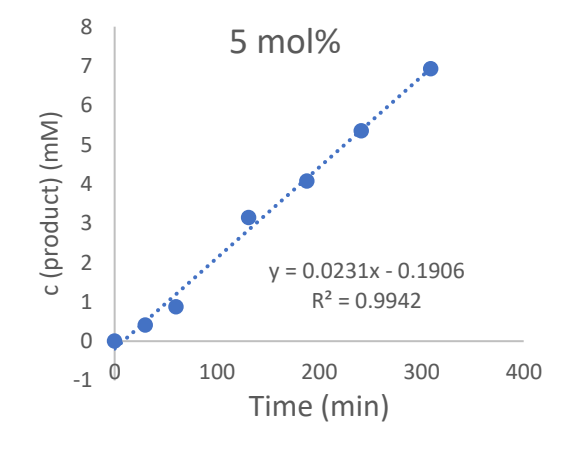

Figure 7.9. Initial-Rate Dependence on [Pd] (continued)

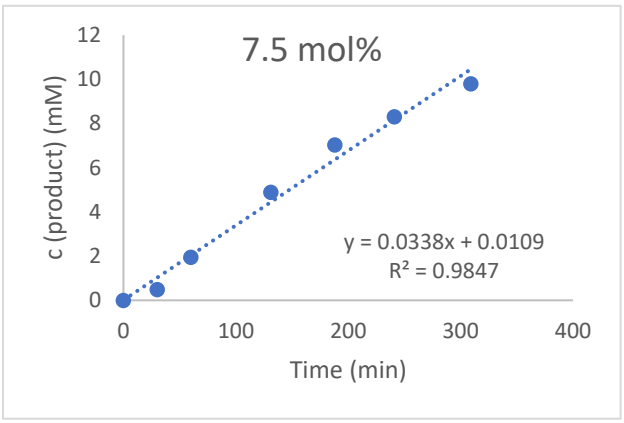

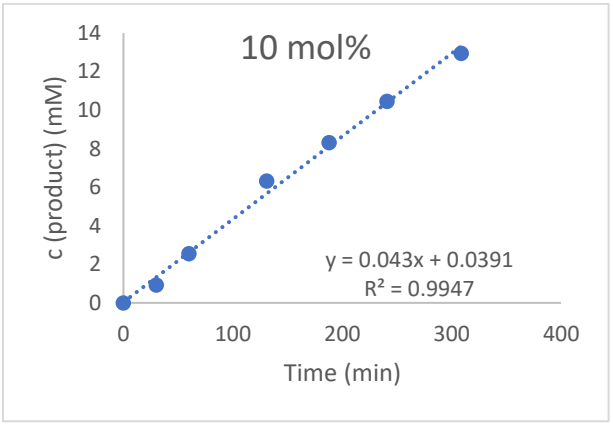

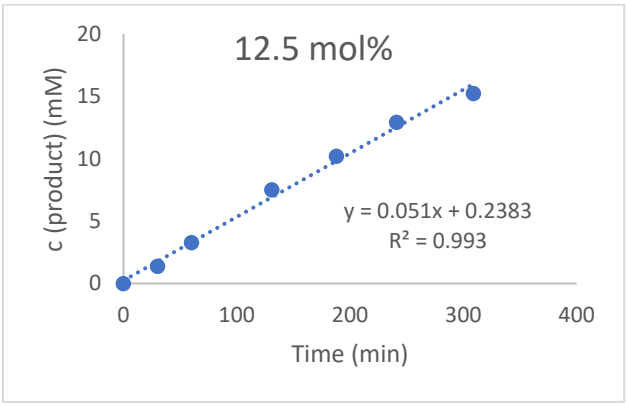

[Pd]: <u>First Order</u>

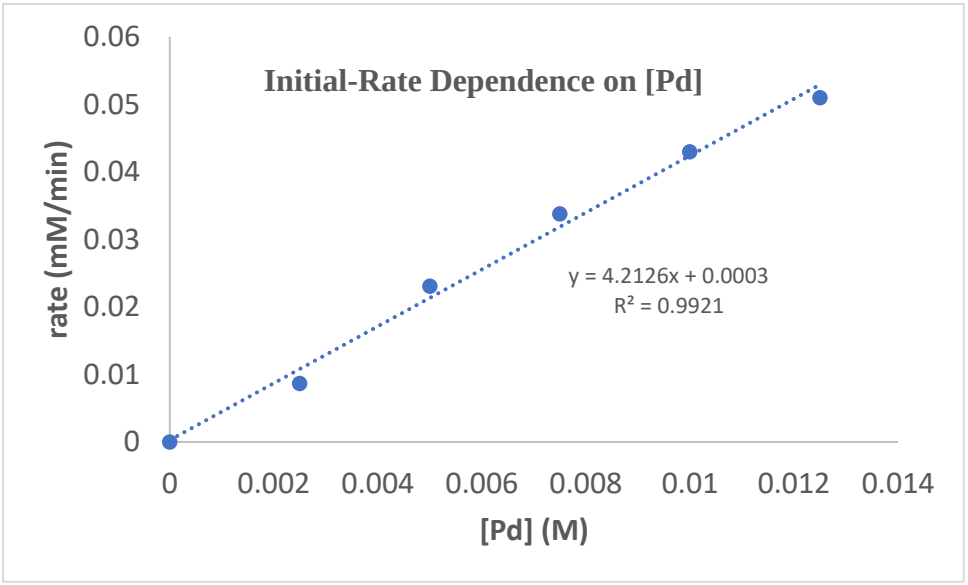

7.5 NMR Spectra

Figure 7.10. ^{1}H NMR Spectrum of 1l

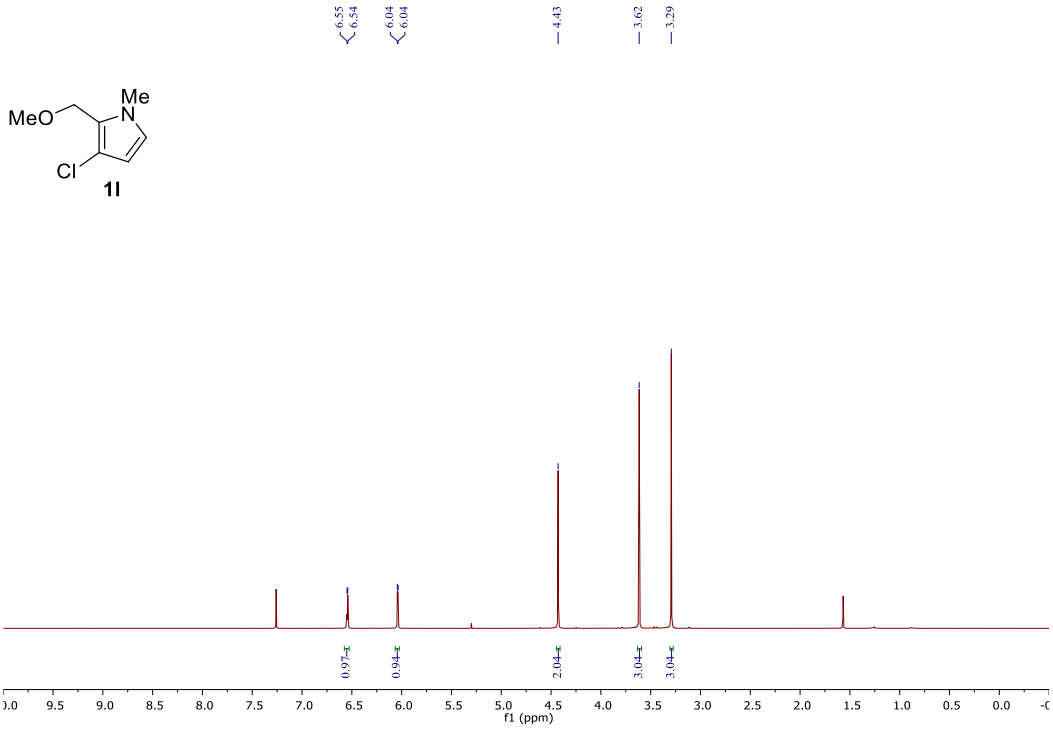

Figure 7.11. ^{13}C NMR Spectrum of 1l

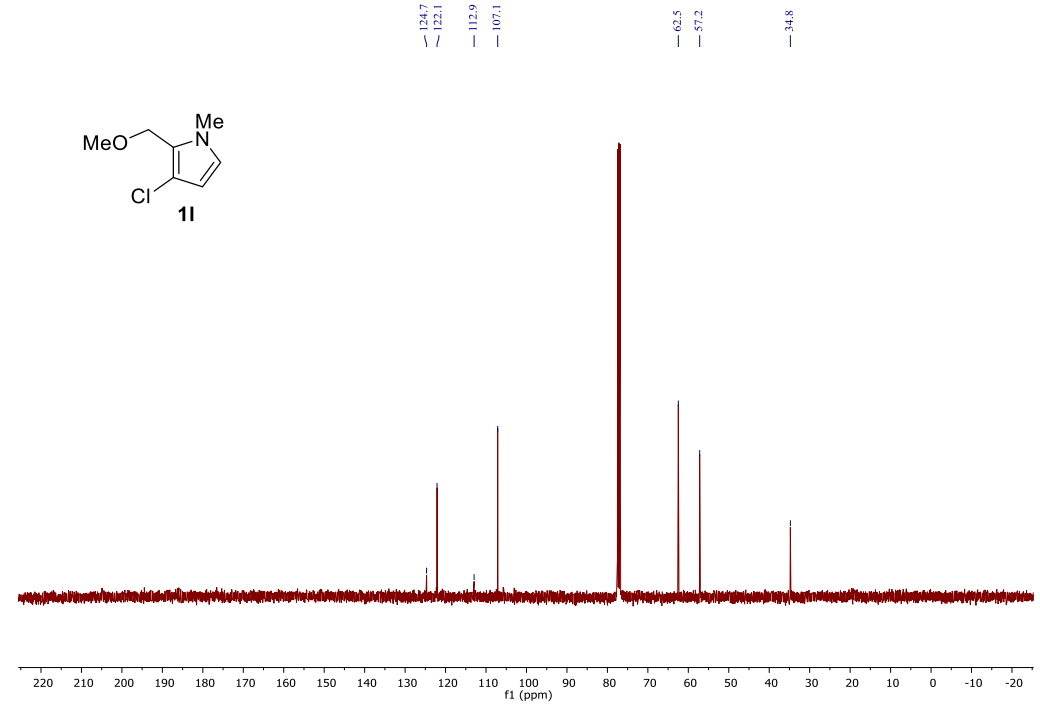

Figure 7.12. ^{1}H NMR Spectrum of 7h

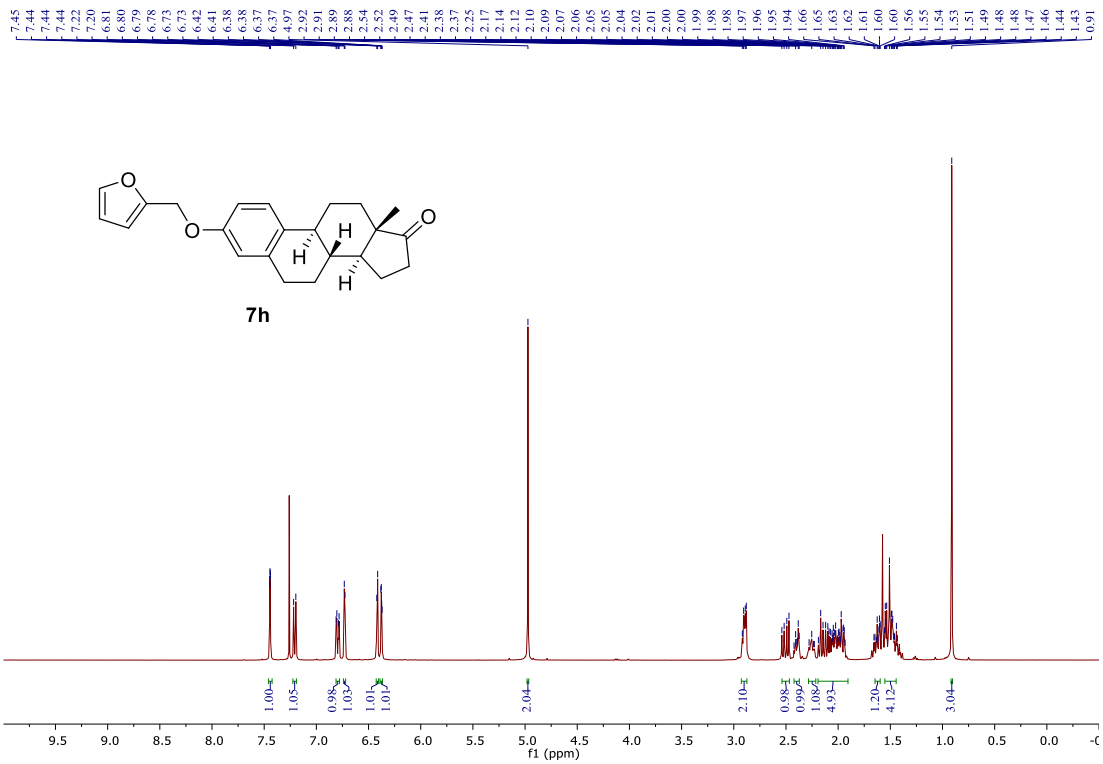

Figure 7.13. ^{1}H NMR Spectrum of 7h

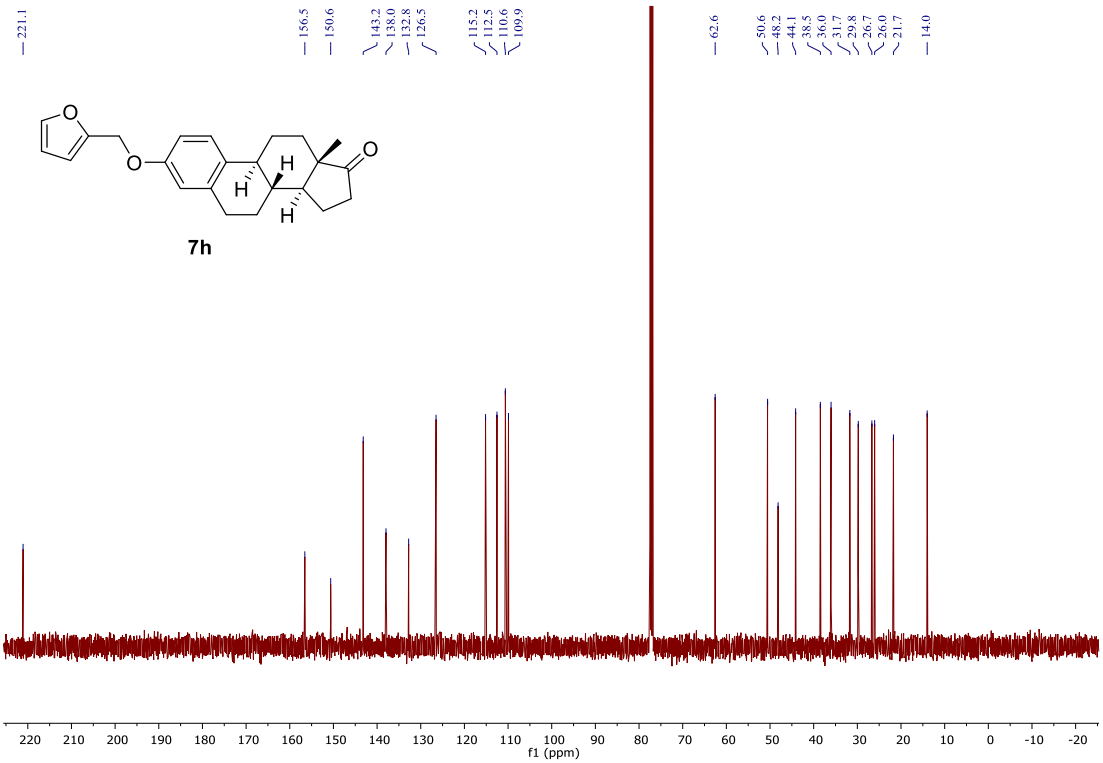

Figure 7.14. ^{1}H NMR Spectrum of 6m

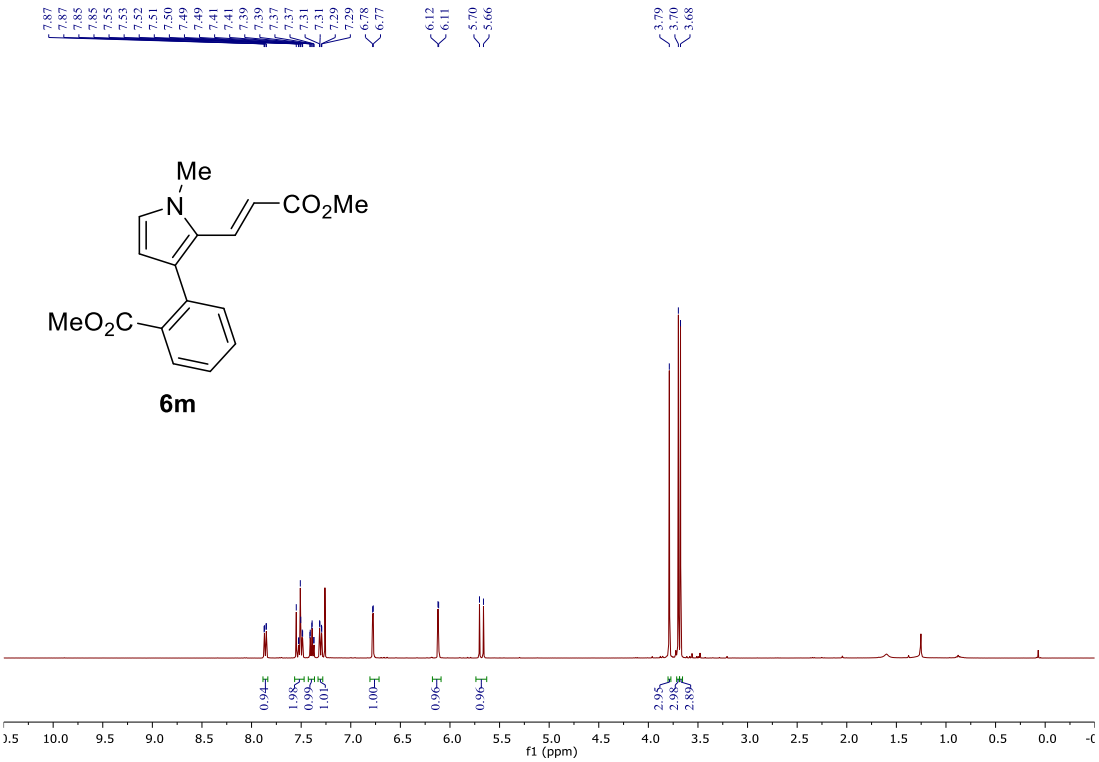

Figure 7.15. ^{1}H NMR Spectrum of 6m

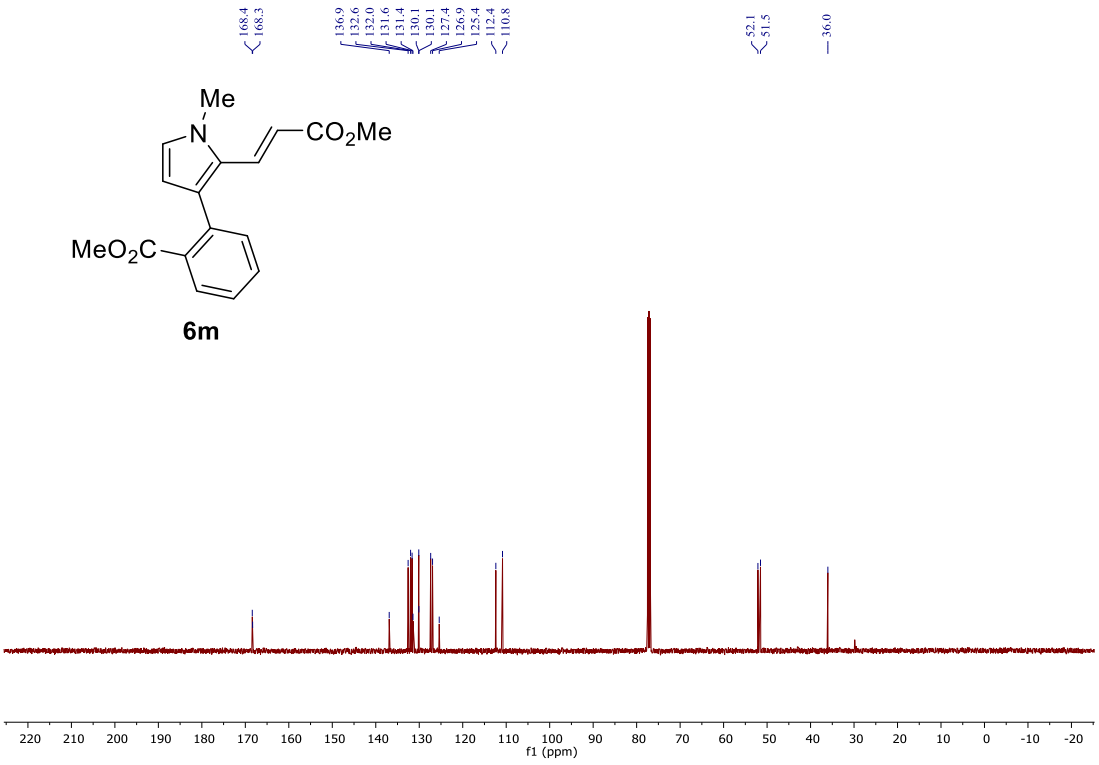

Figure 7.16. ^{1}H NMR Spectrum of 6n

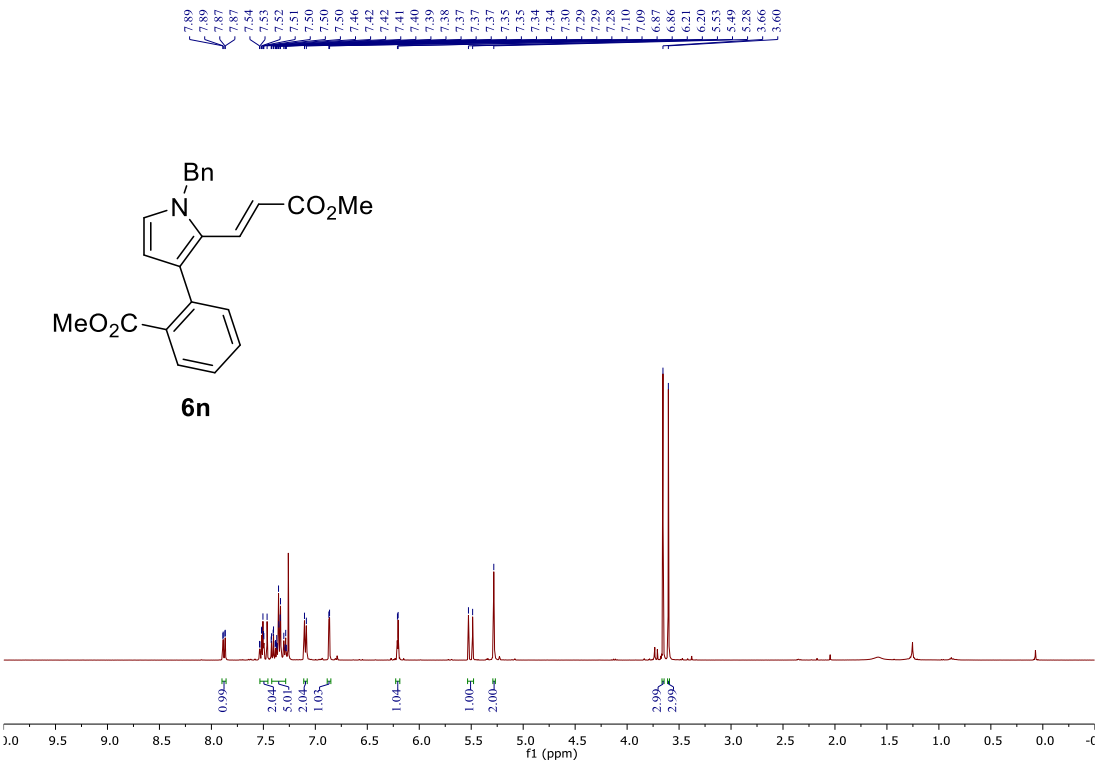

Figure 7.17. ^{1}H NMR Spectrum of 6n

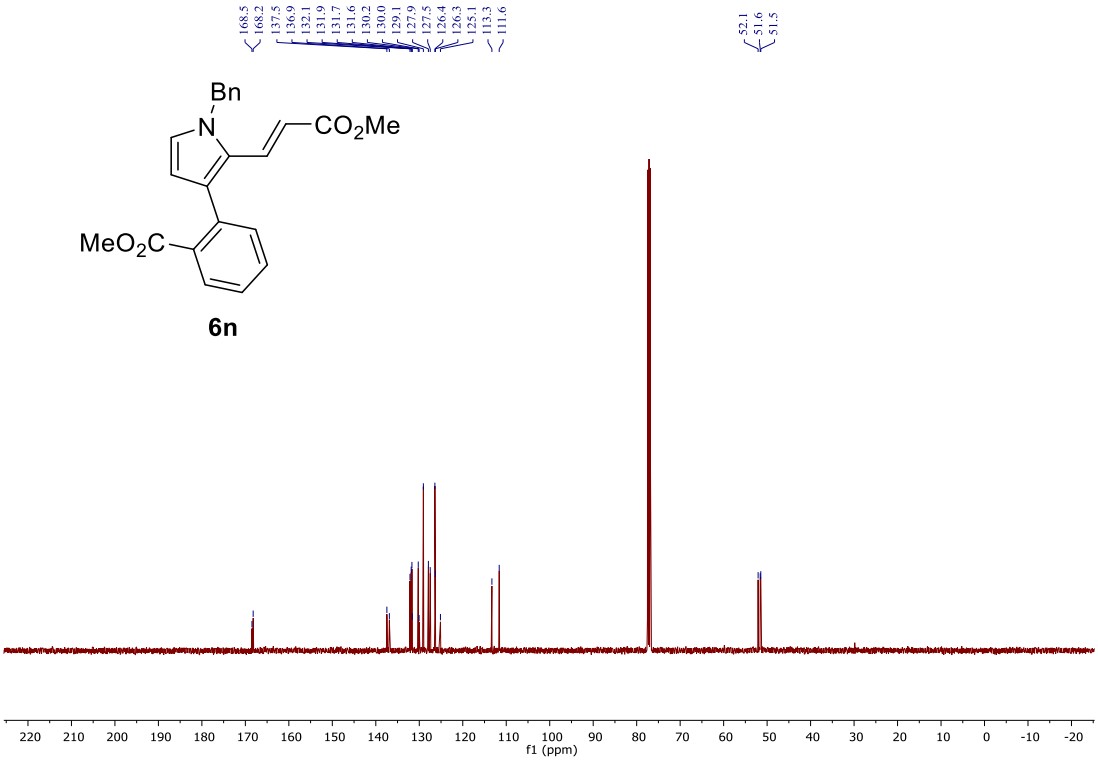

Figure 7.18. ^{1}H NMR Spectrum of 6a

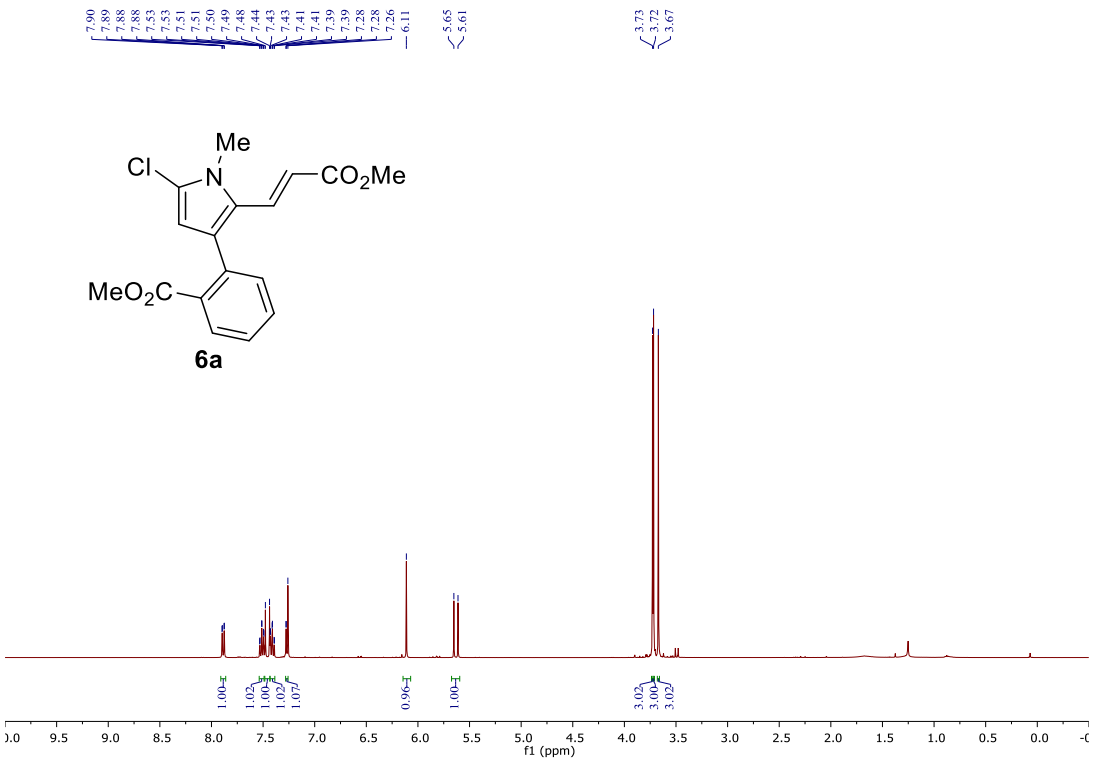

Figure 7.19. ^{1}H NMR Spectrum of 6a

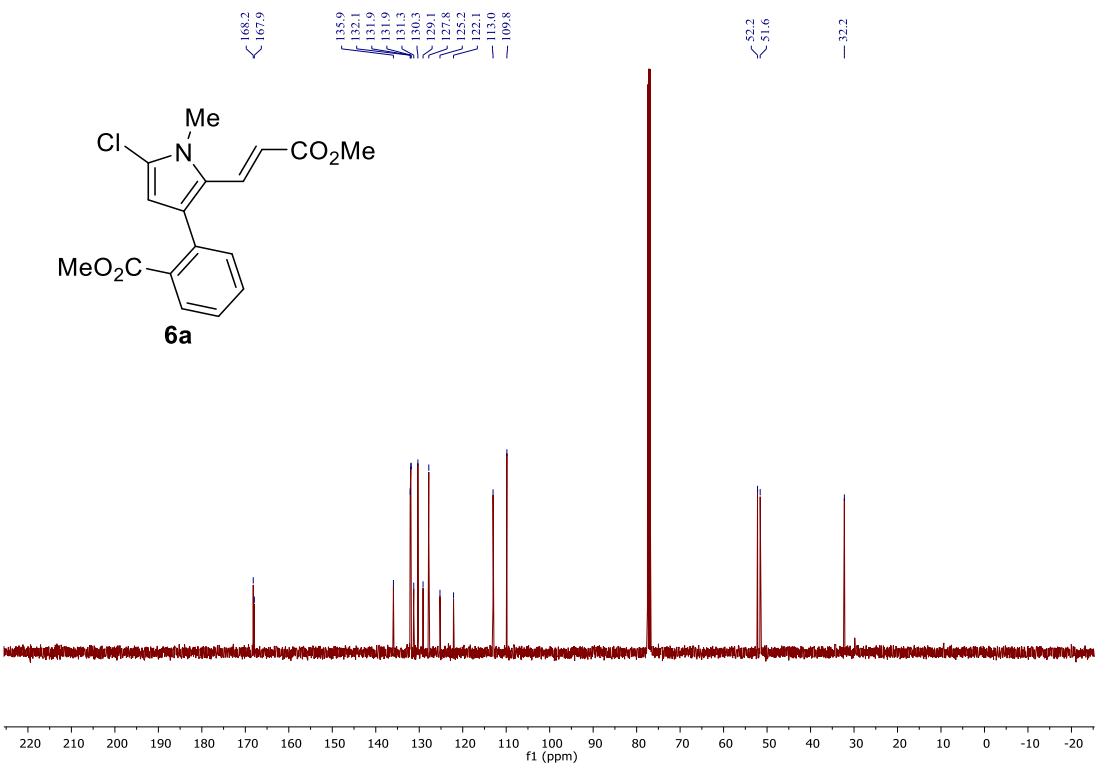

Figure 7.20. ^{1}H NMR Spectrum of 6b

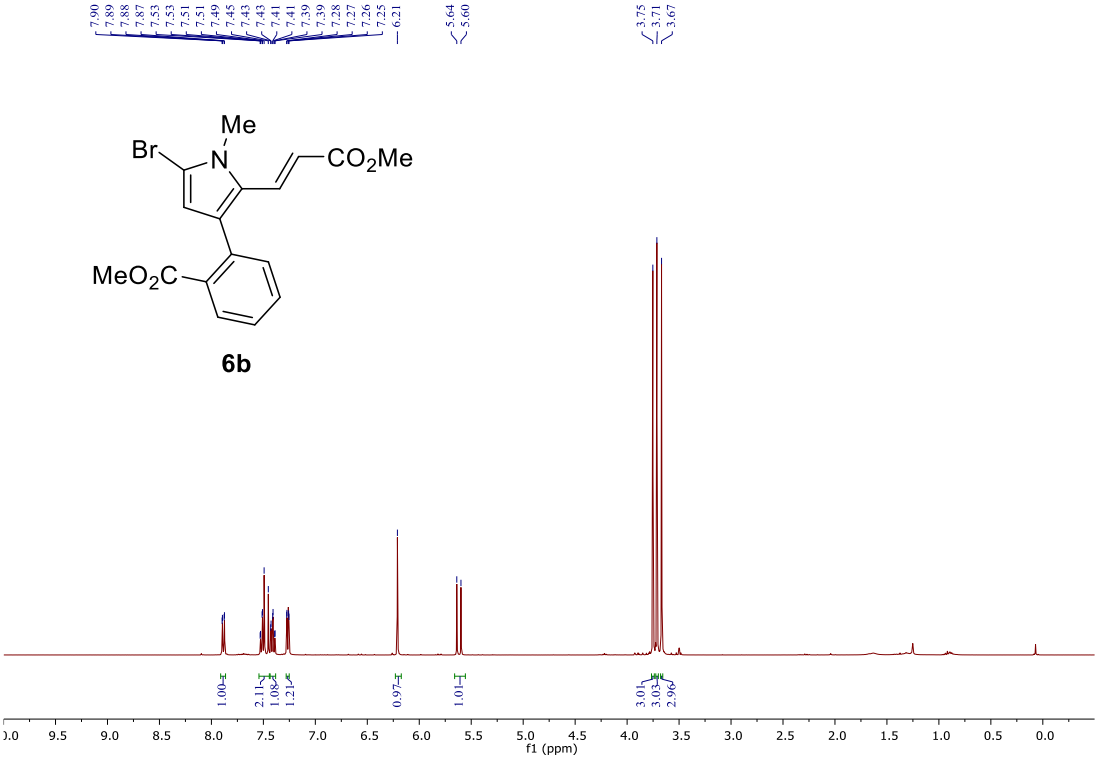

Figure 7.21. ^{13}C NMR Spectrum of 6b

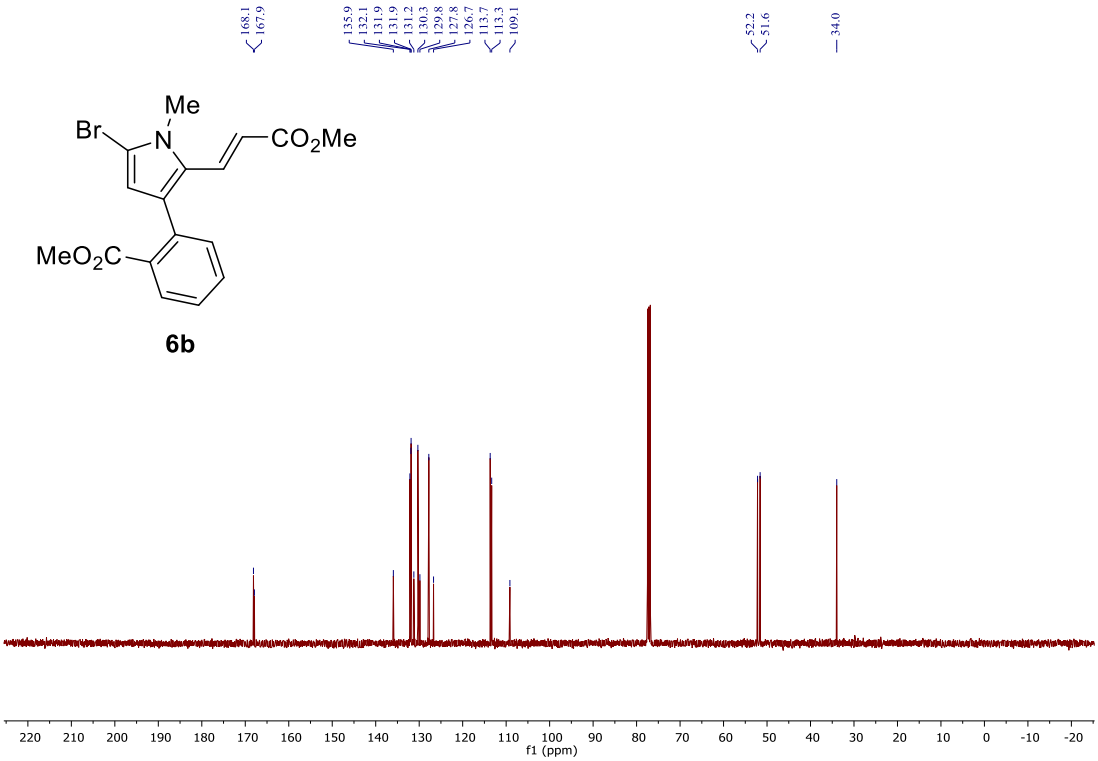

Figure 7.22. ^{1}H NMR Spectrum of 6c

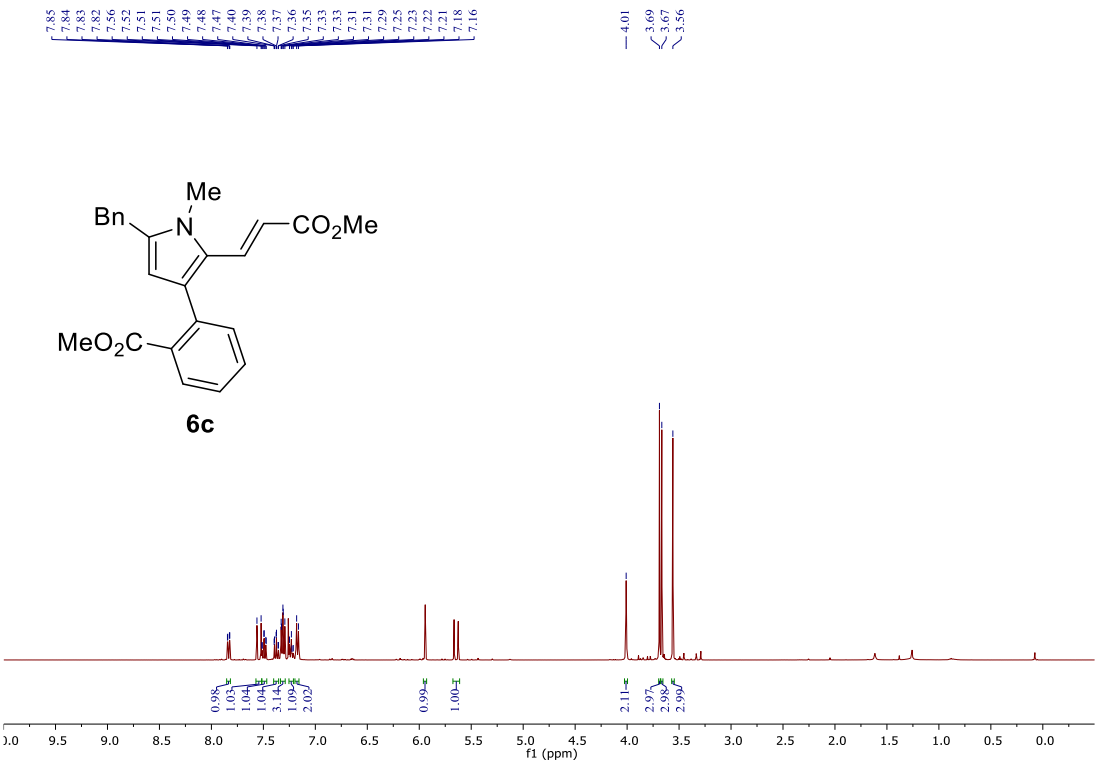

Figure 7.23. ^{13}C NMR Spectrum of 6c

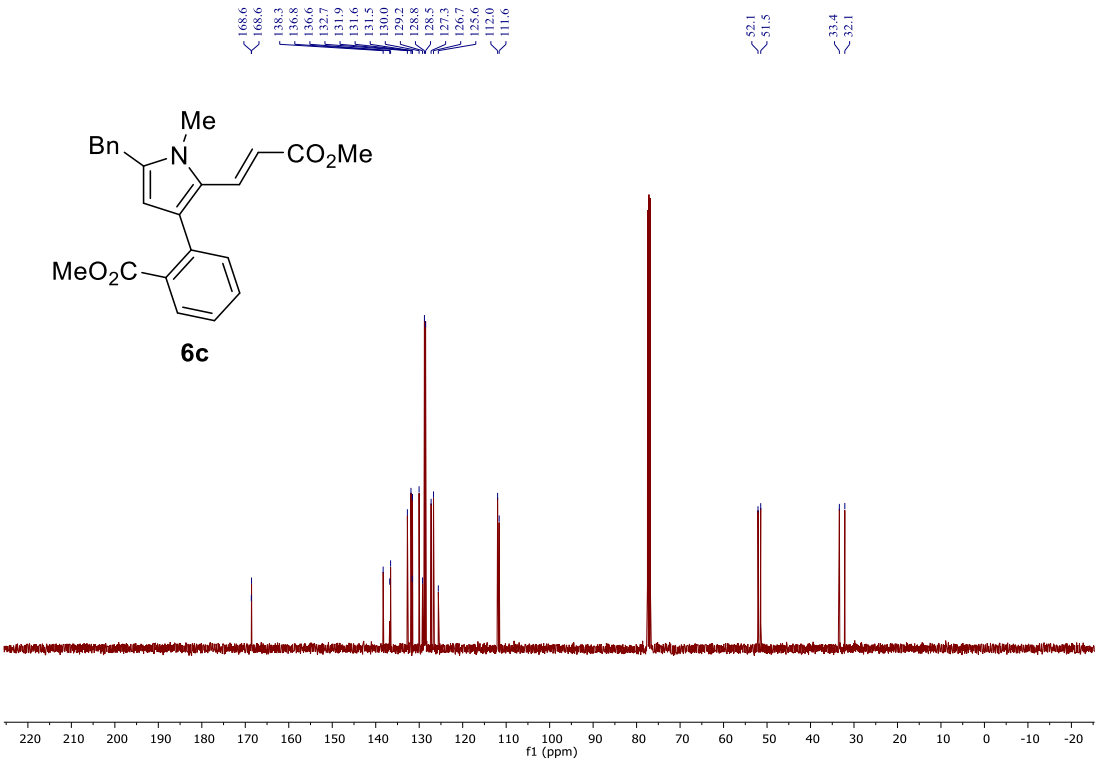

Figure 7.24. ^{1}H NMR Spectrum of 6d

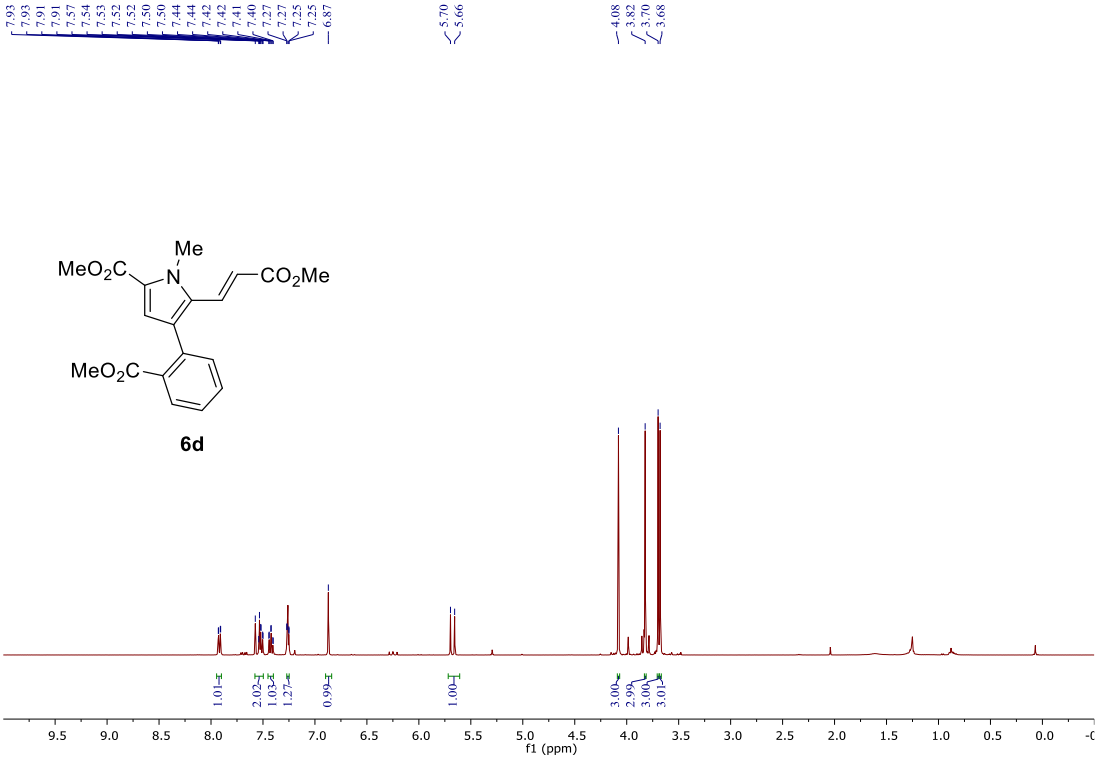

Figure 7.25. ^{13}C NMR Spectrum of 6d

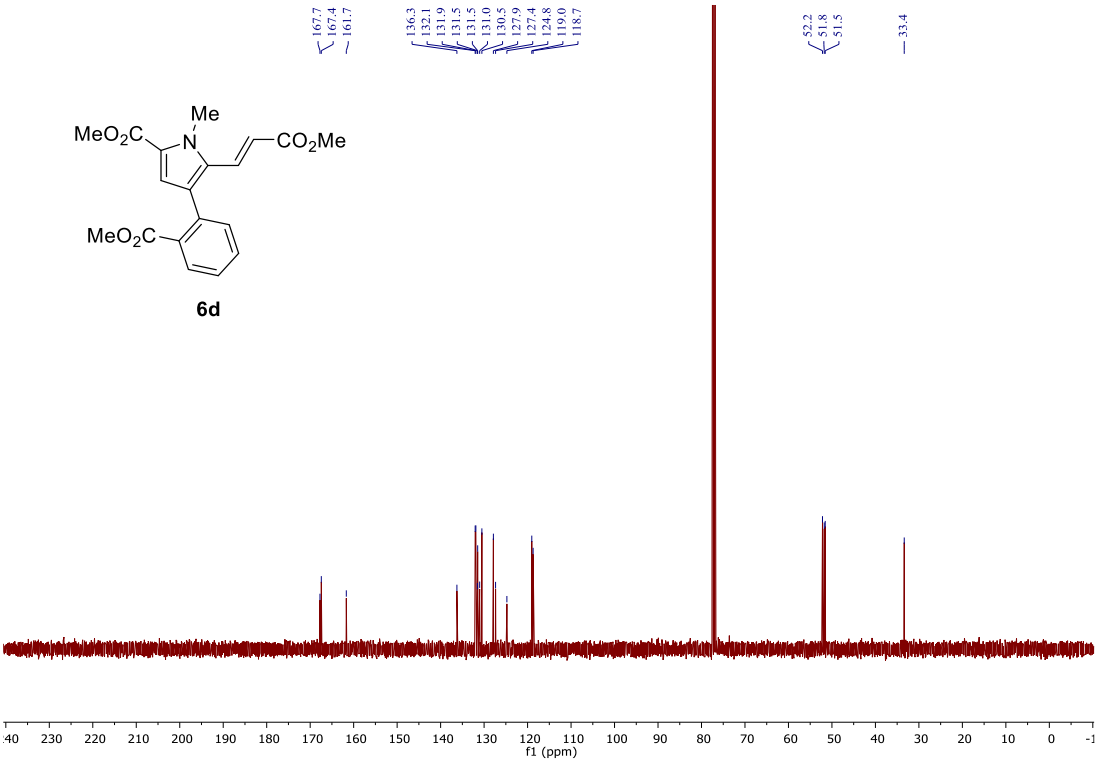

Figure 7.26. ^{1}H NMR Spectrum of 6e

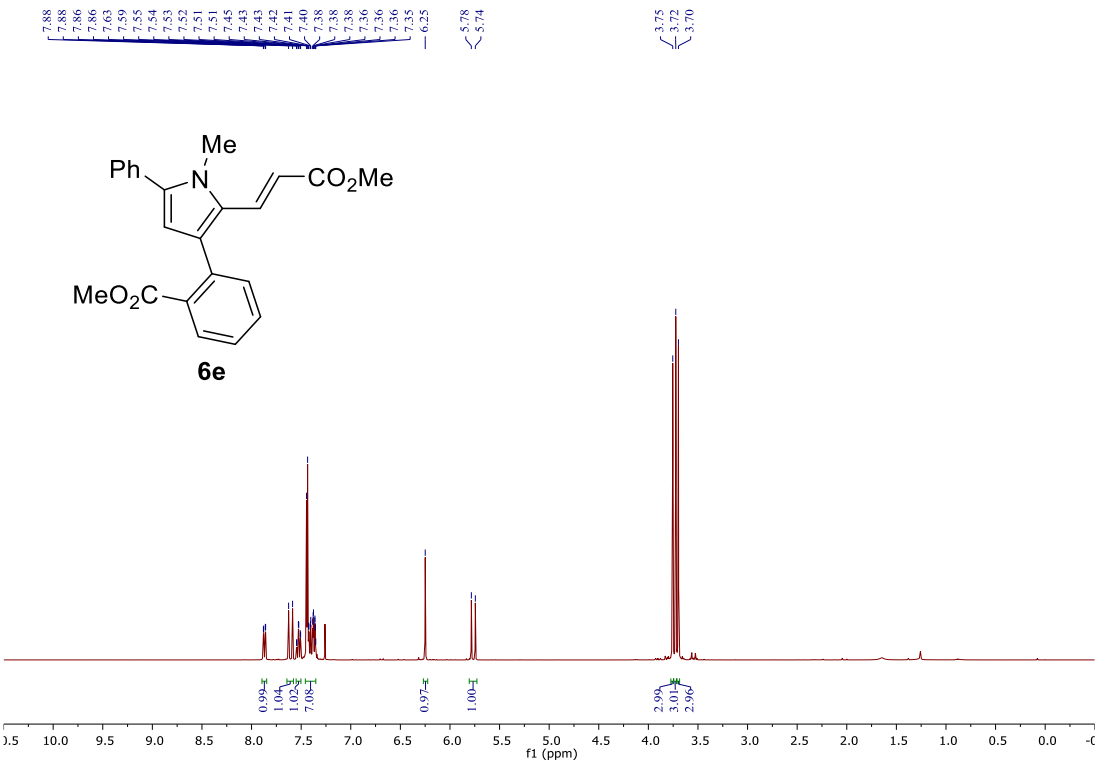

Figure 7.27. ^{13}C NMR Spectrum of 6e

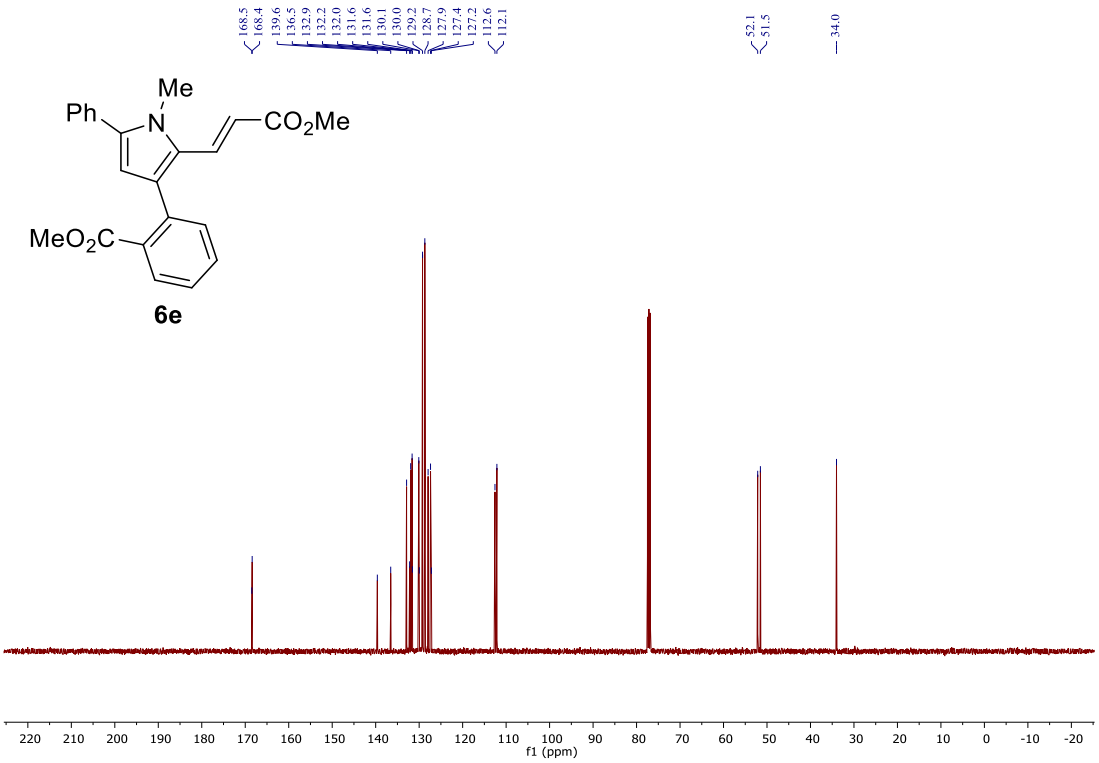

Figure 7.28. ^{1}H NMR Spectrum of 6f

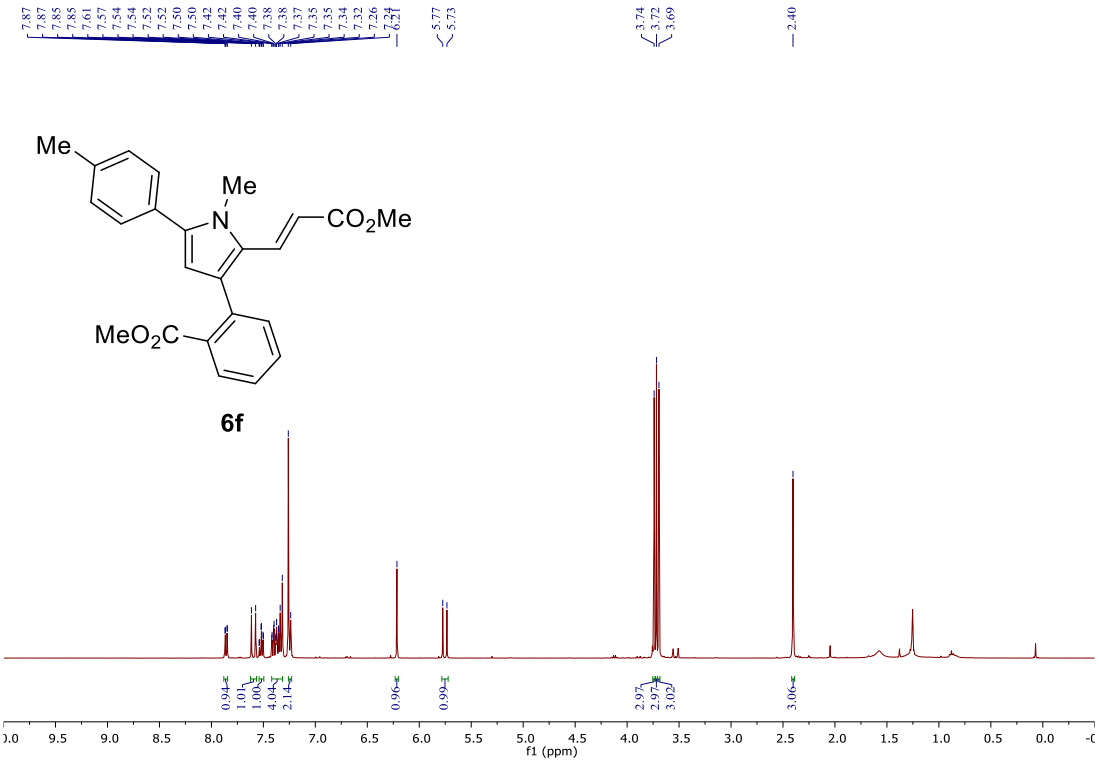

Figure 7.29. ^{13}C NMR Spectrum of 6f

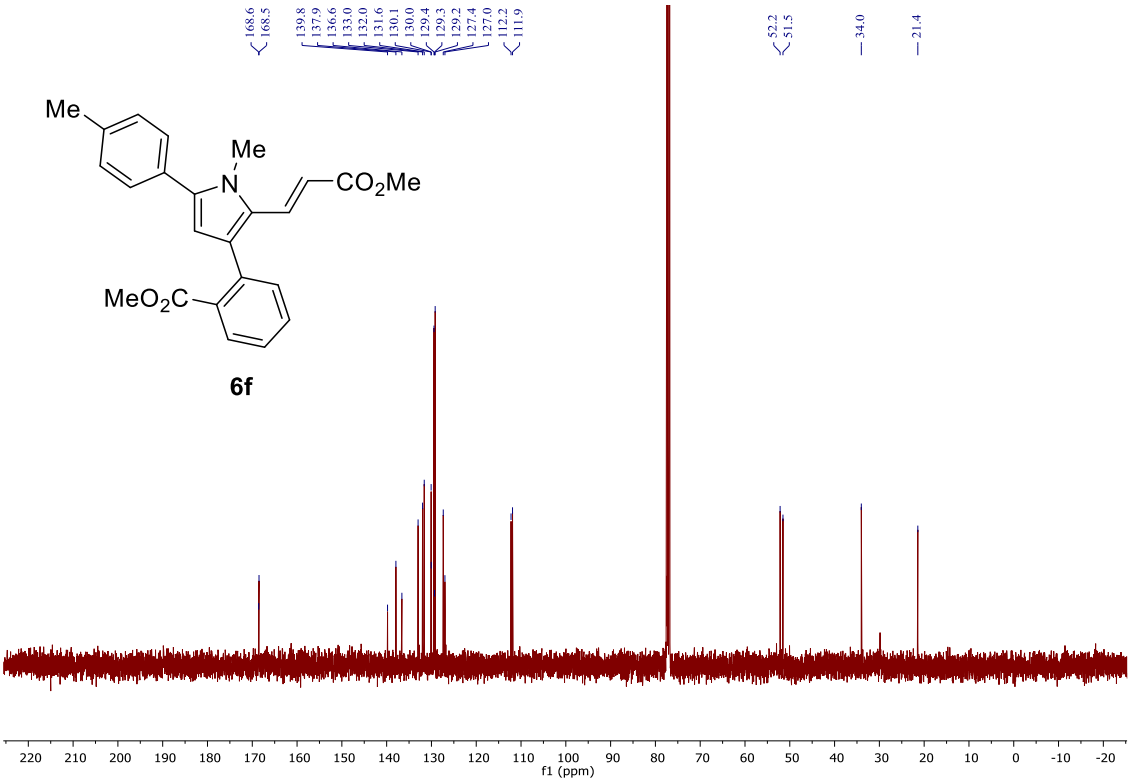

Figure 7.30. ^{1}H NMR Spectrum of 6g

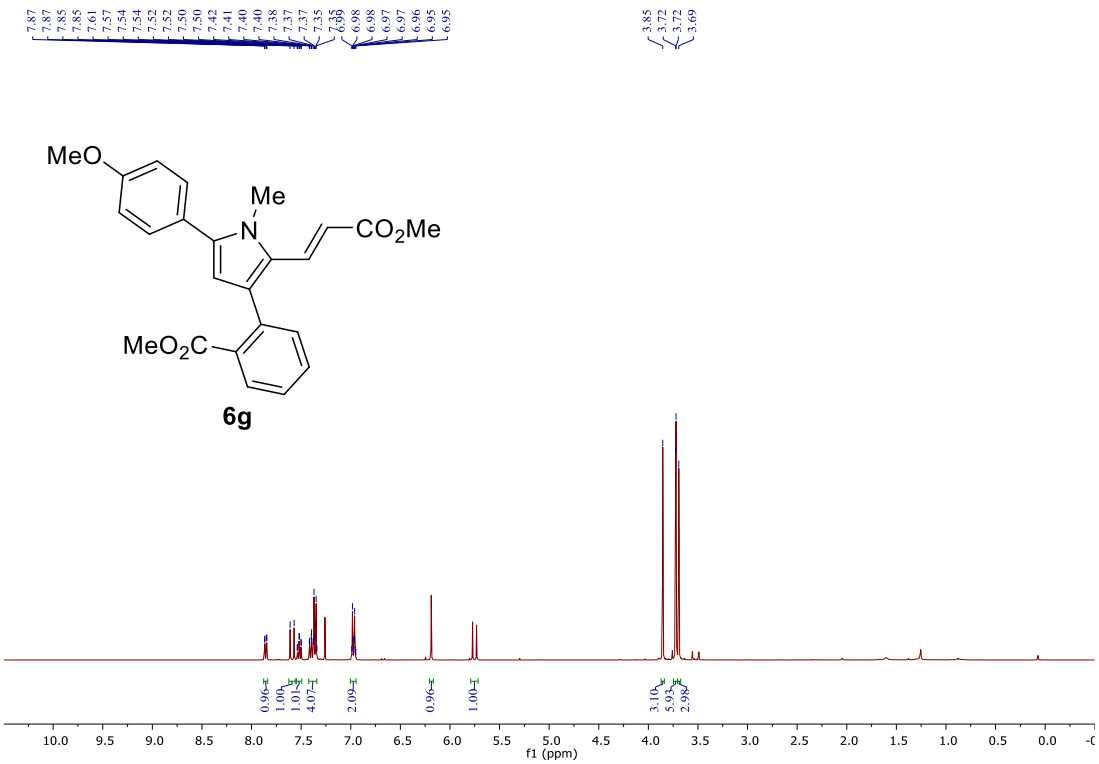

Figure 7.31. ^{13}C NMR Spectrum of 6g

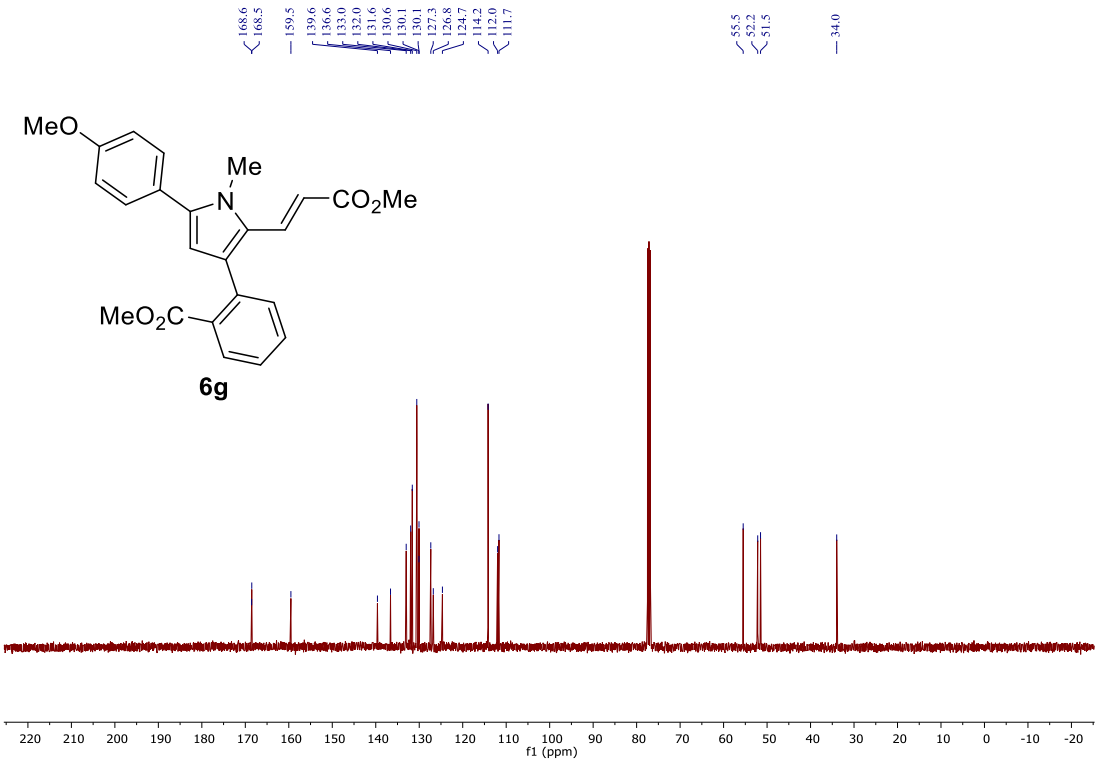

Figure 7.32. ^{1}H NMR Spectrum of 6h

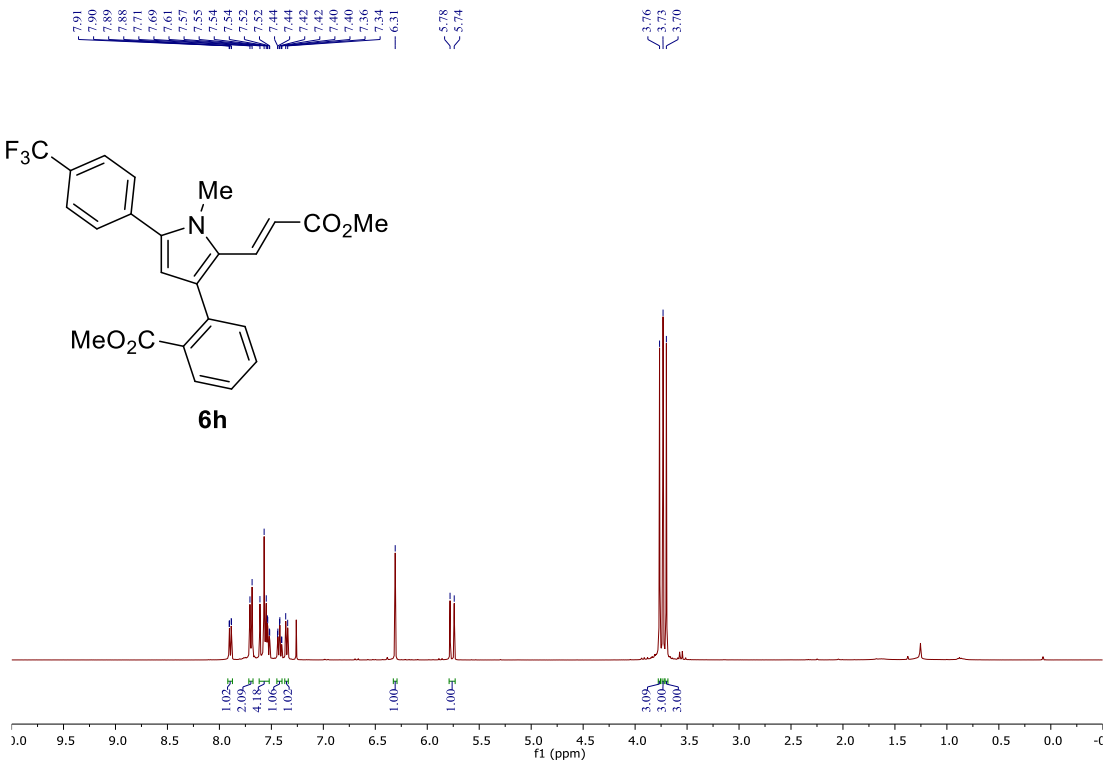

Figure 7.33. ^{13}C NMR Spectrum of 6h

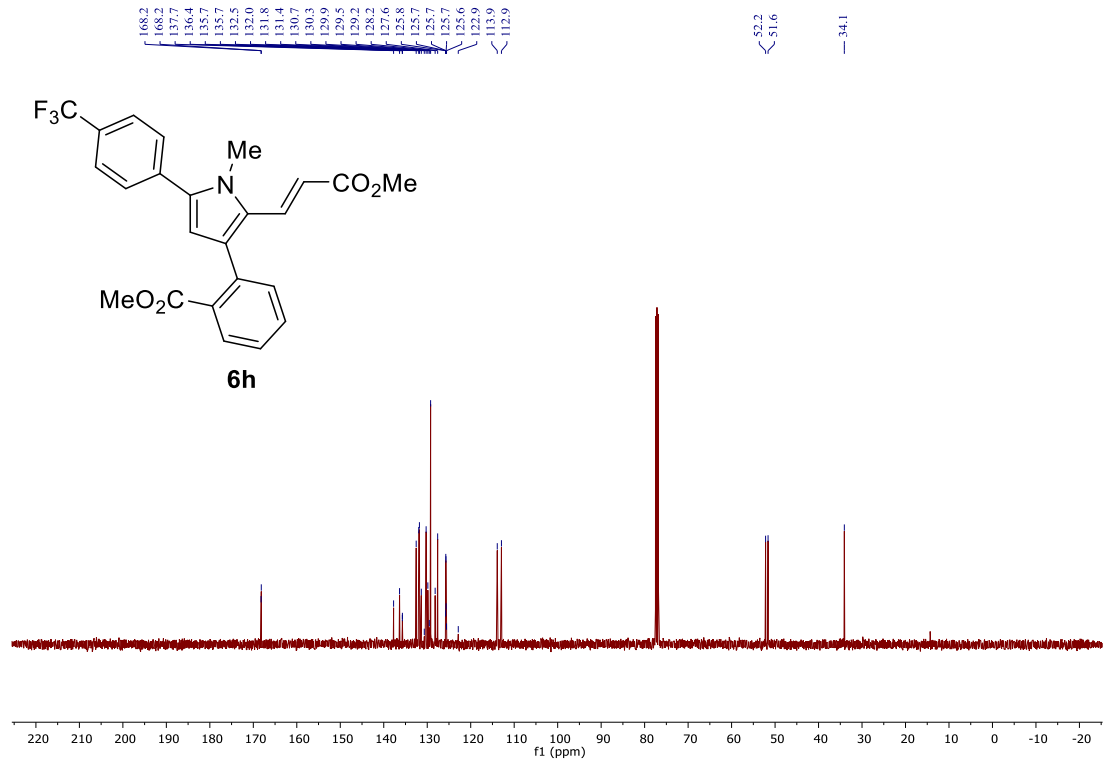

Figure 7.34. ^{19}F NMR Spectrum of 6h

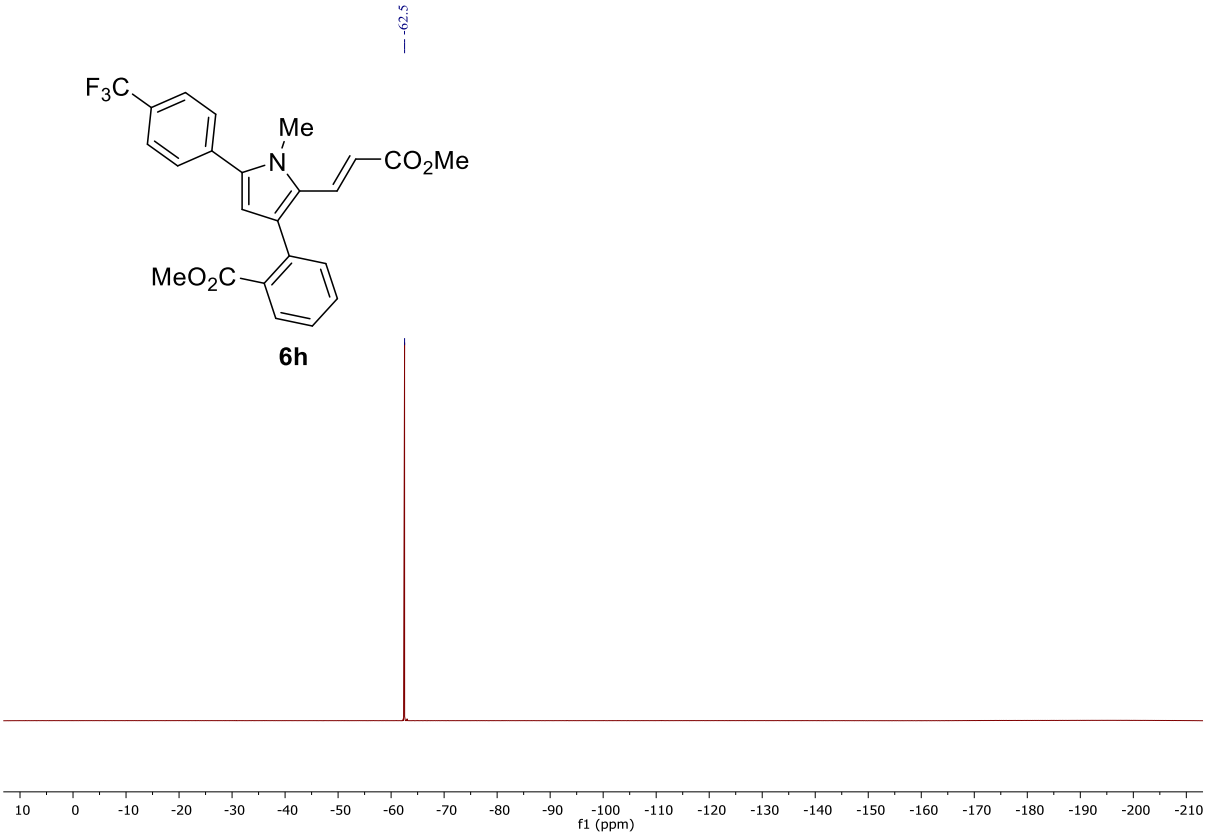

Figure 7.35. ^{1}H NMR Spectrum of 6i

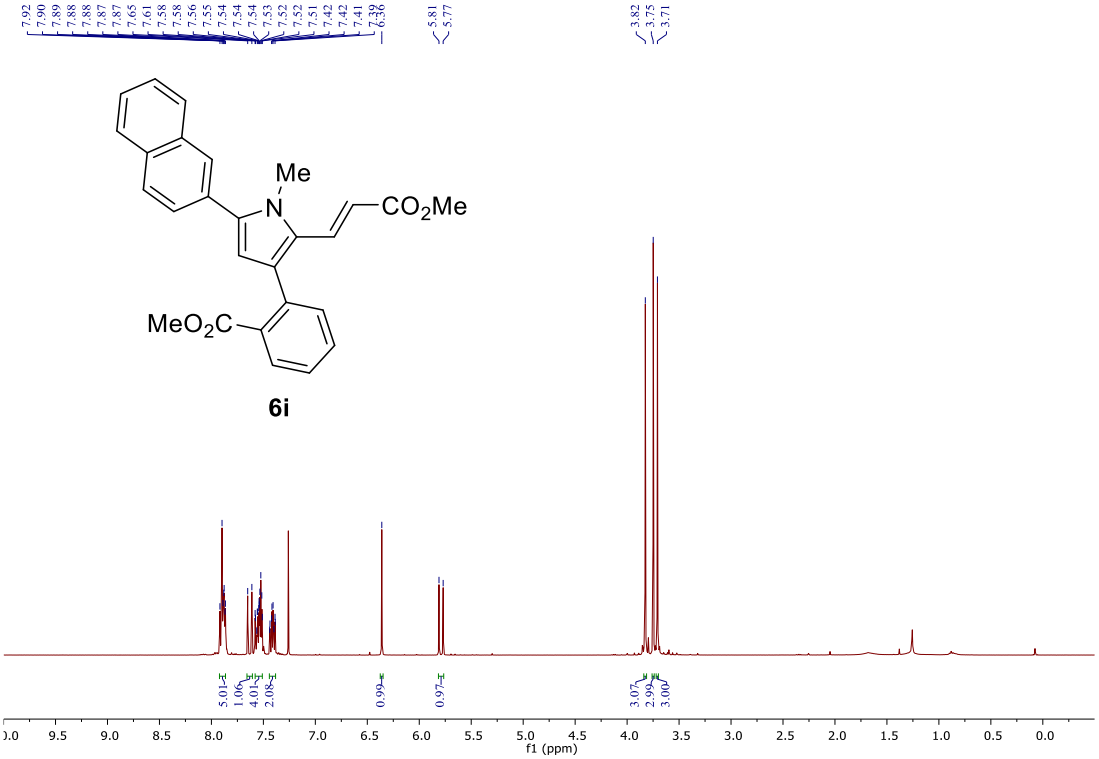

Figure 7.36. ^{13}C NMR Spectrum of 6i

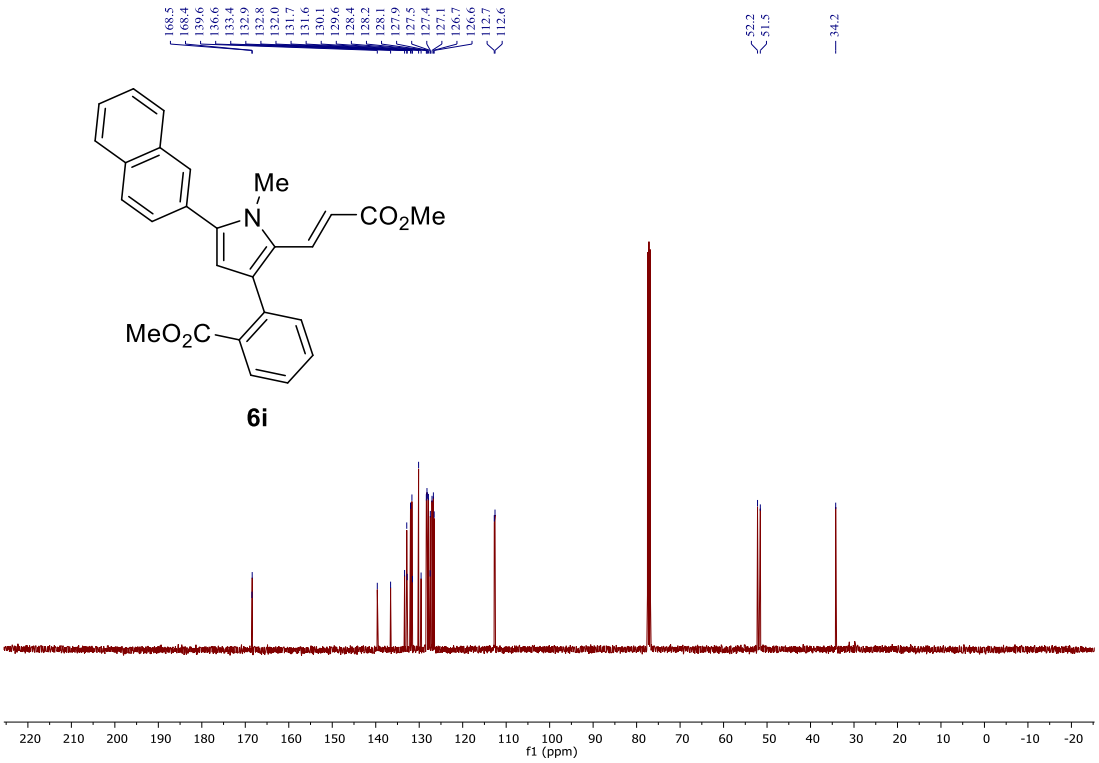

Figure 7.37. ^{1}H NMR Spectrum of 6j

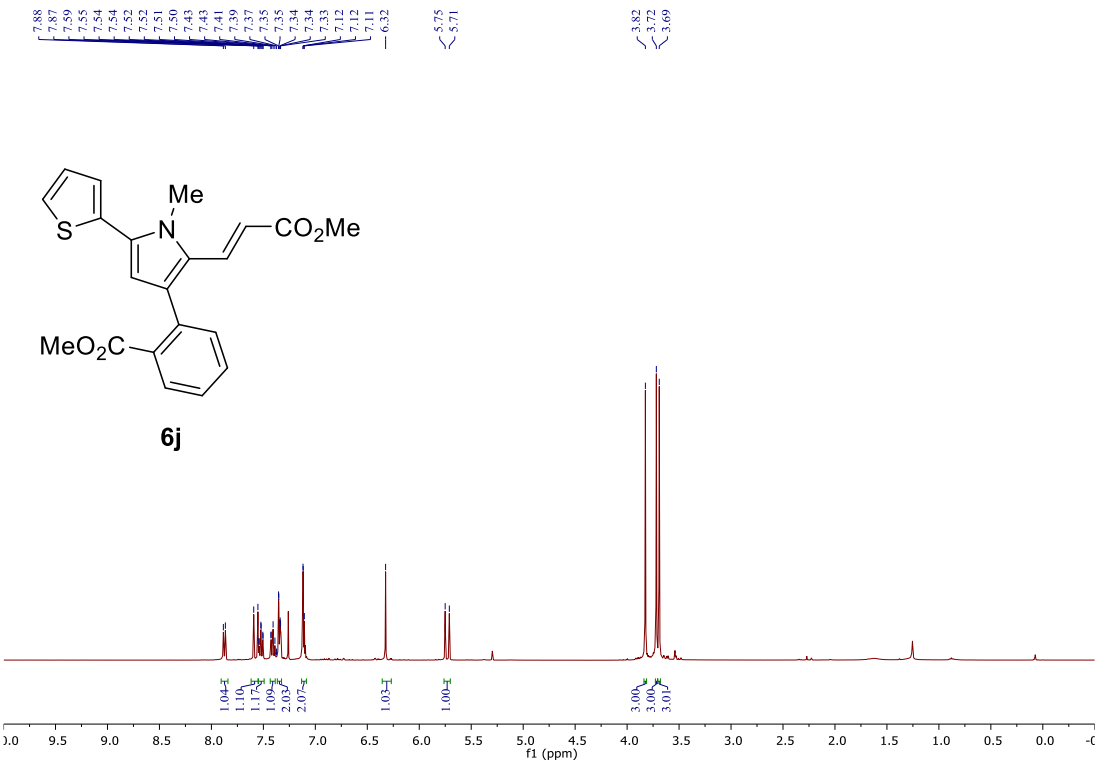

Figure 7.38. ^{13}C NMR Spectrum of 6j

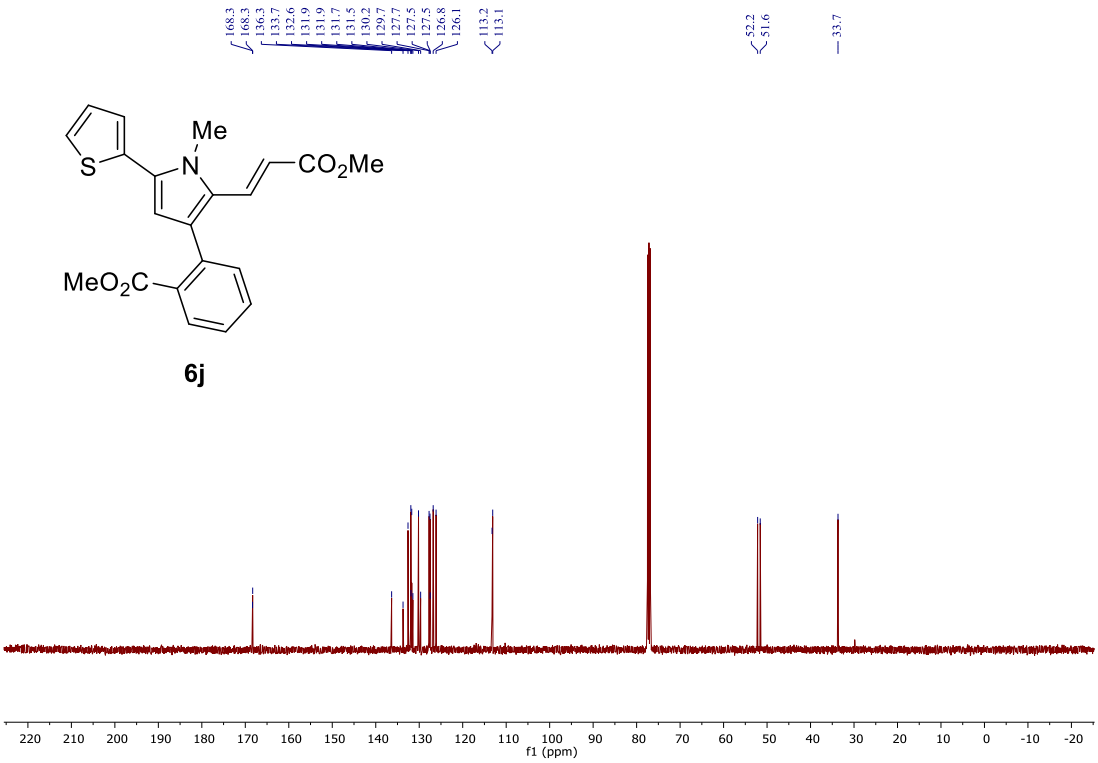

Figure 7.39. ^{1}H NMR Spectrum of 6k

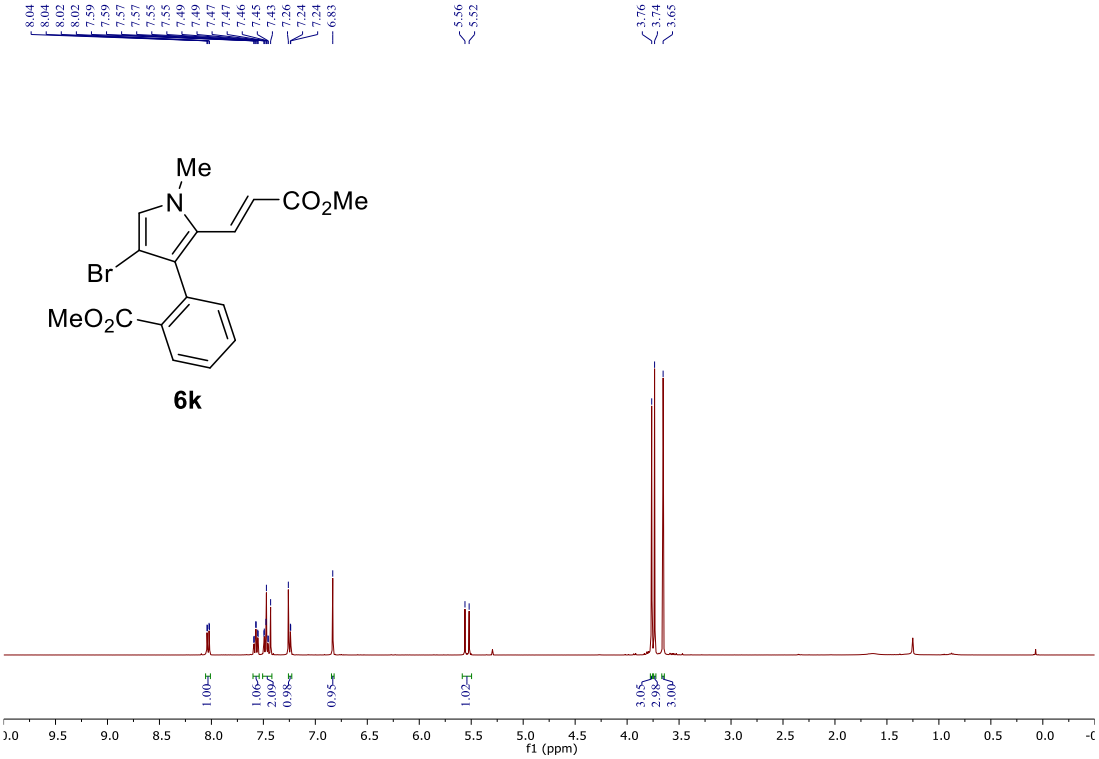

Figure 7.40. ^{13}C NMR Spectrum of 6k

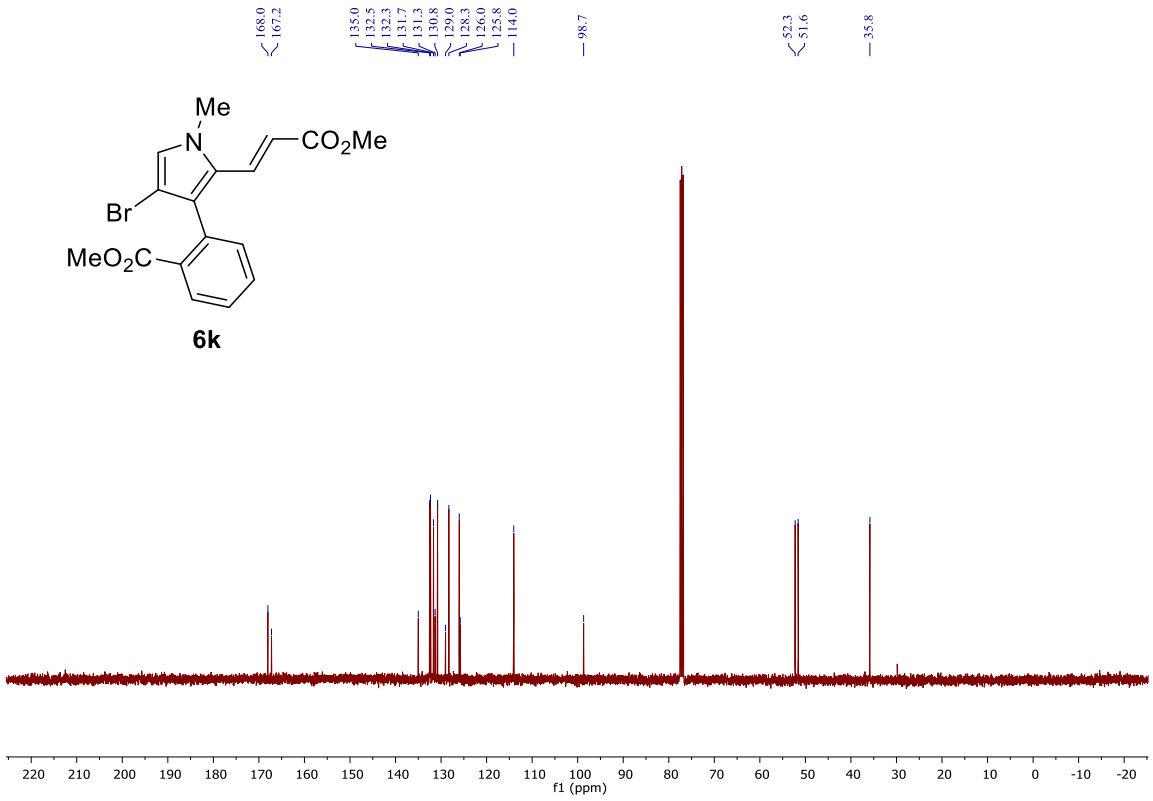

Figure 7.41. ^{1}H NMR Spectrum of 6l

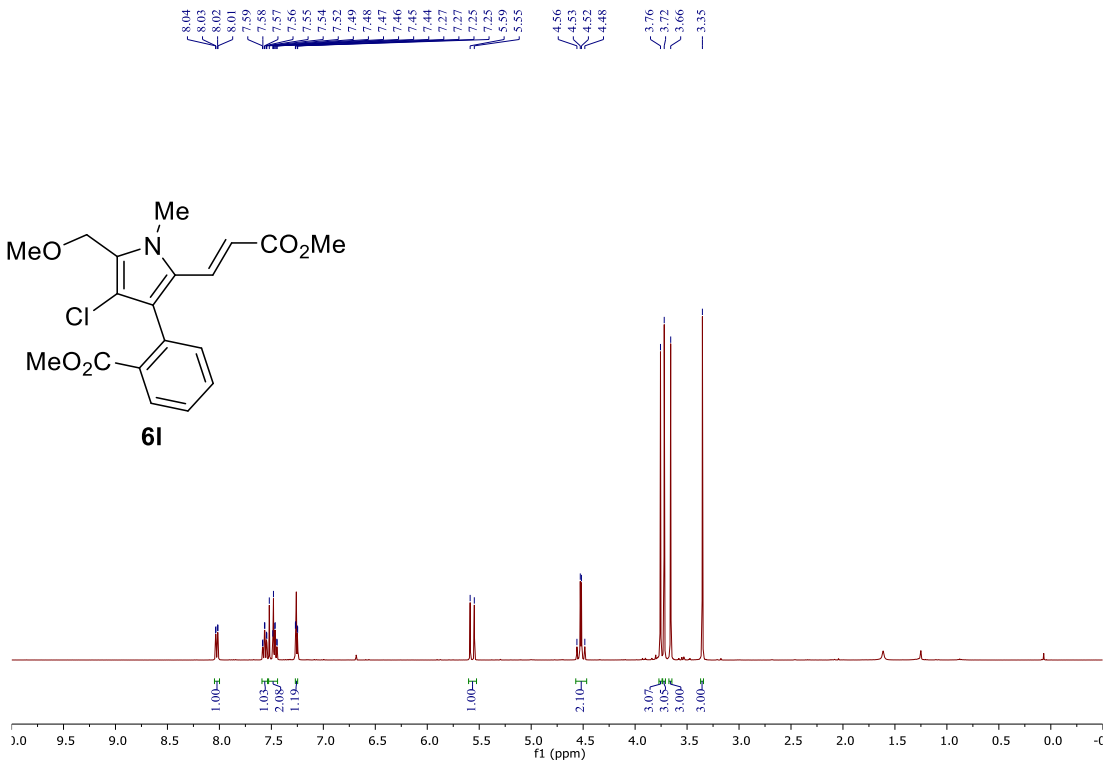

Figure 7.42. ^{13}C NMR Spectrum of 6l

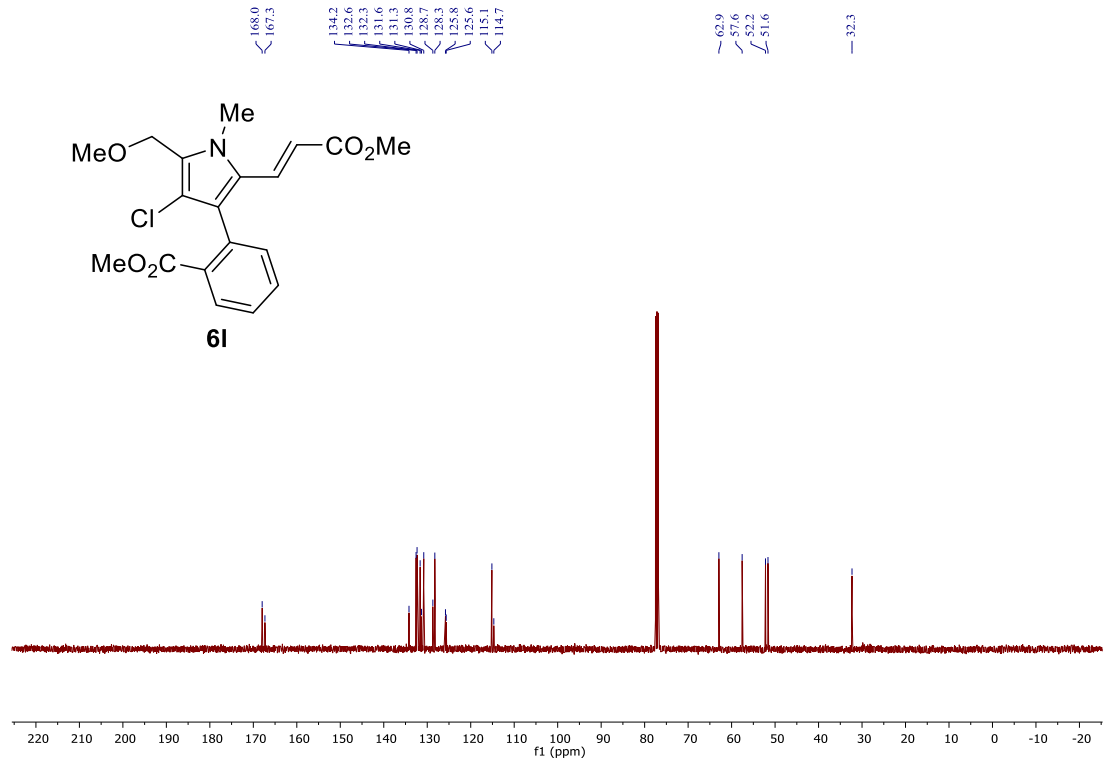

Figure 7.43. ^{1}H NMR Spectrum of 6o

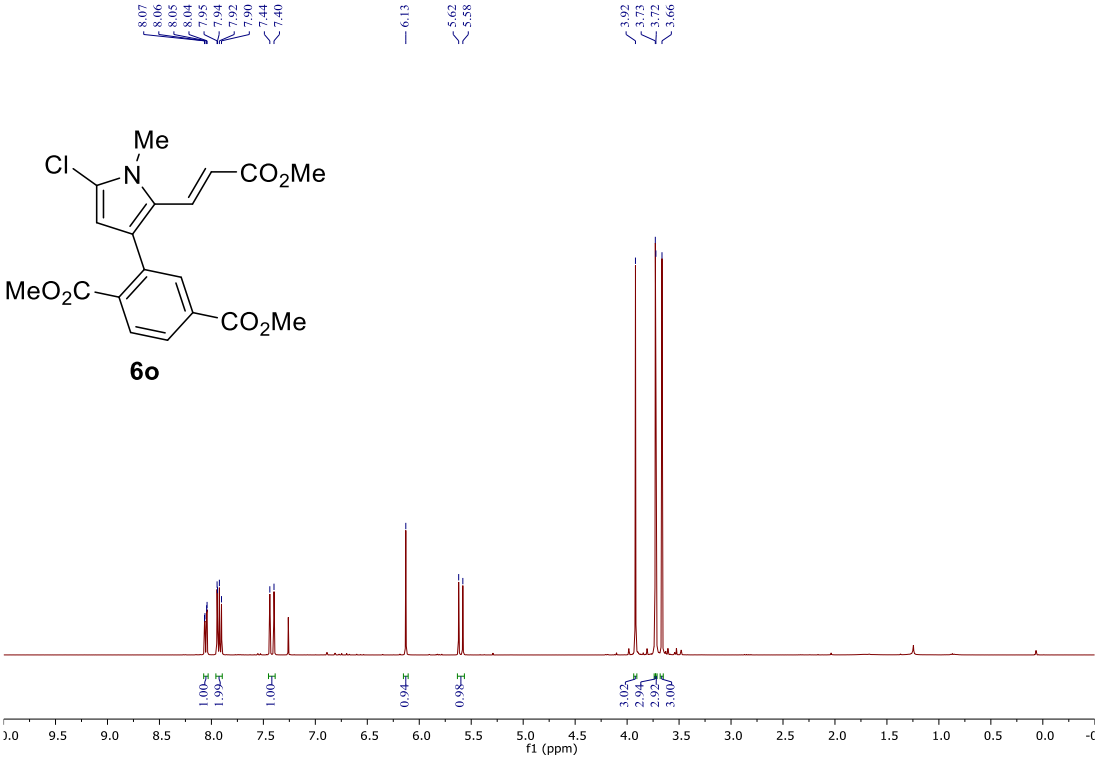

Figure 7.44 ^{13}C NMR Spectrum of 6o

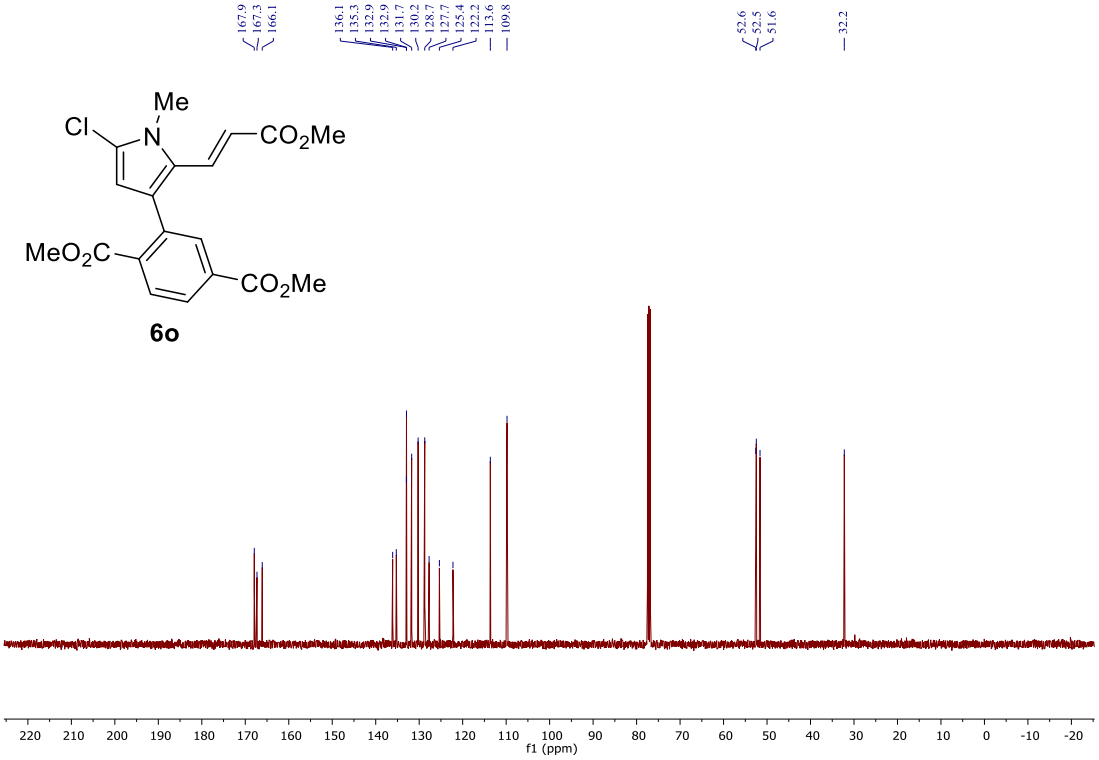

Figure 7.45. ^{1}H NMR Spectrum of 6p

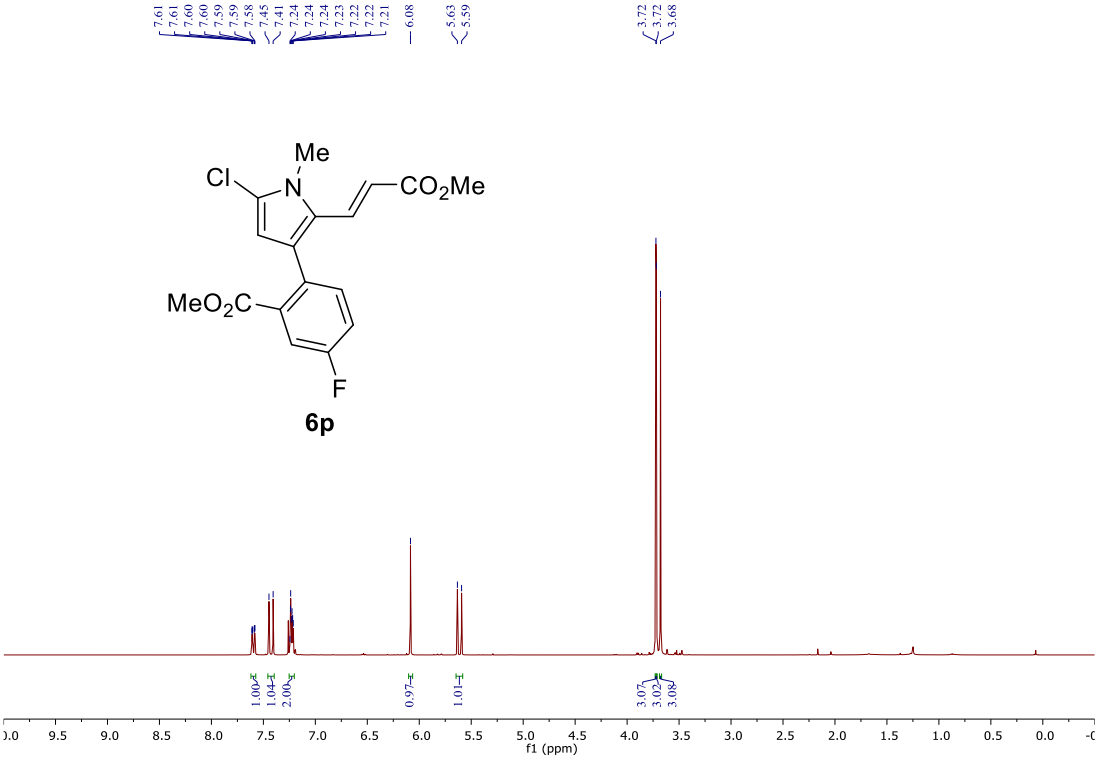

Figure 7.46. ^{13}C NMR Spectrum of 6p

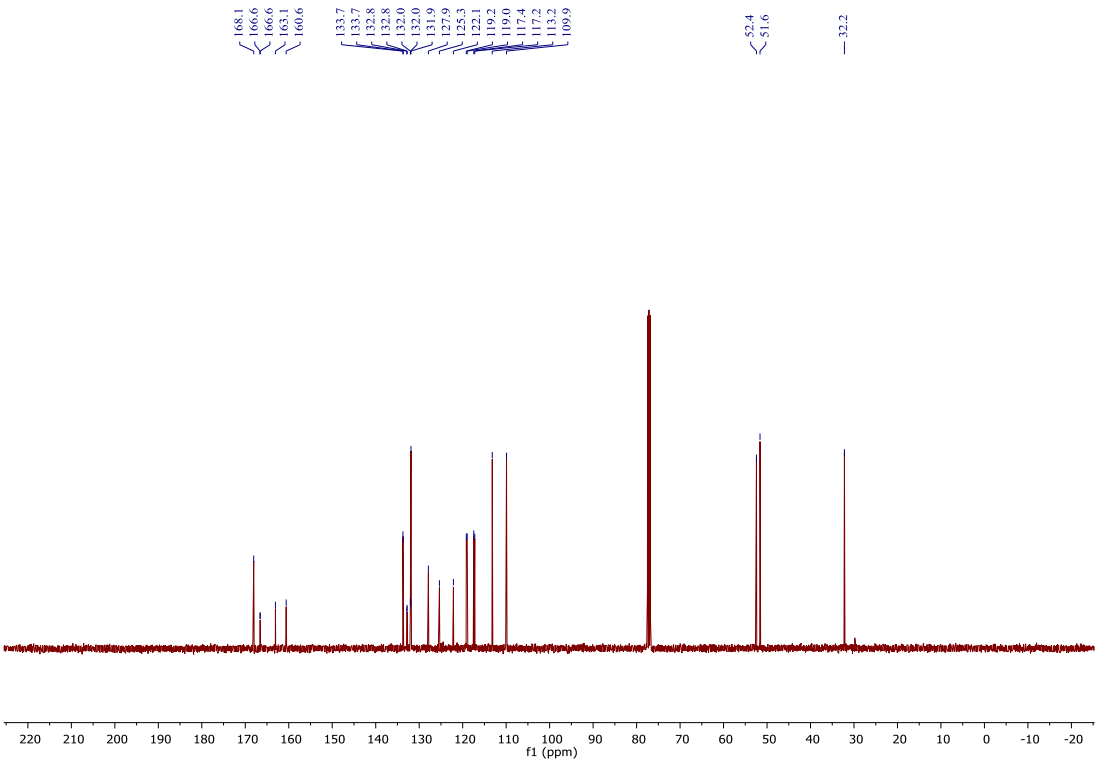

Figure 7.47. ^{19}F NMR Spectrum of 6p

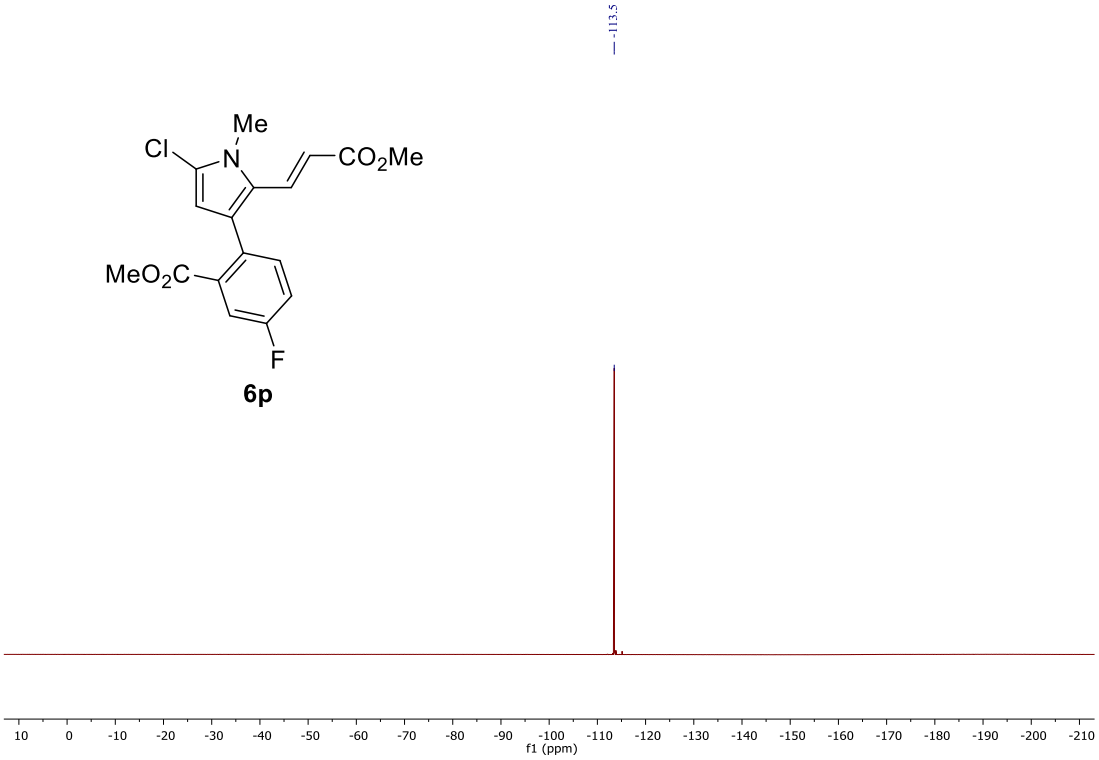

Figure 7.48. ^{1}H NMR Spectrum of 6q

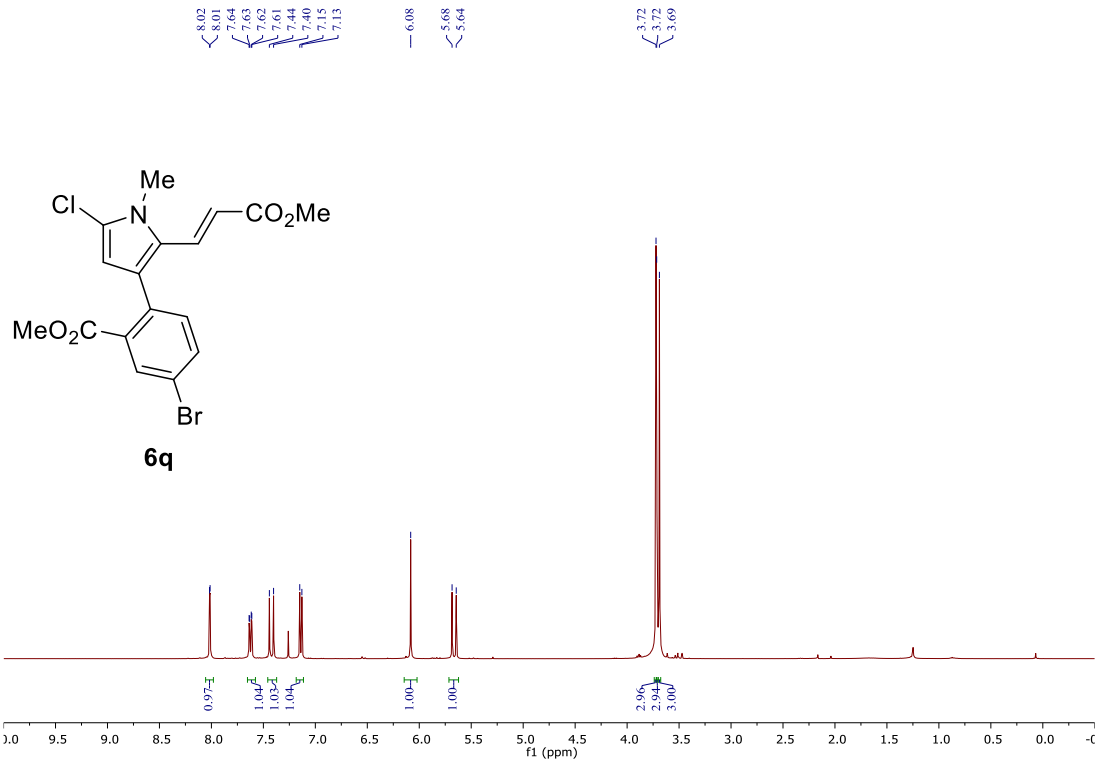

Figure 7.49. ^{13}C NMR Spectrum of 6q

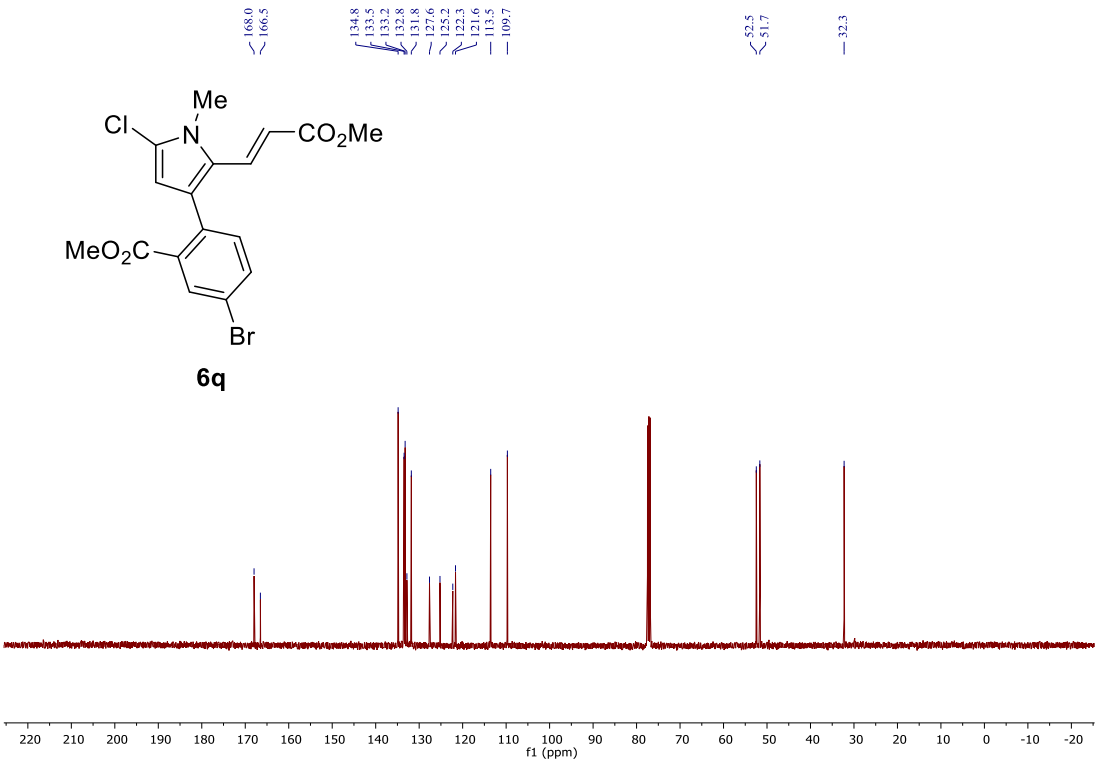

Figure 7.50. ^{1}H NMR Spectrum of 6r

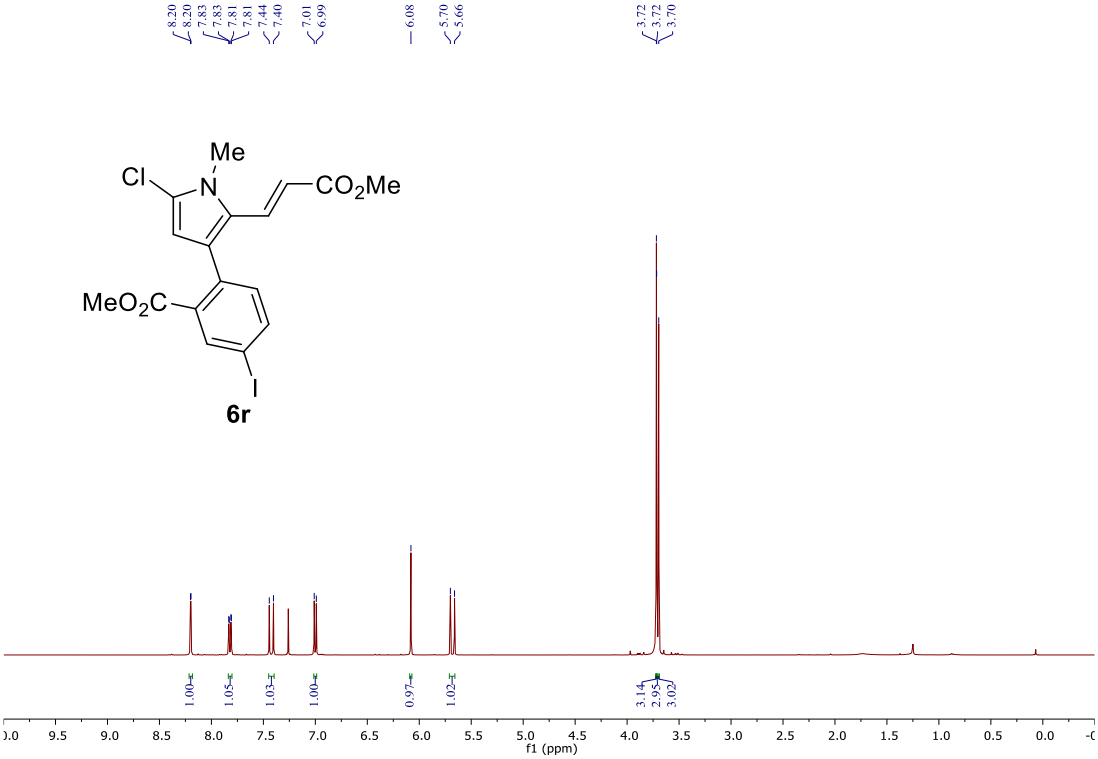

Figure 7.51. ^{13}C NMR Spectrum of 6r

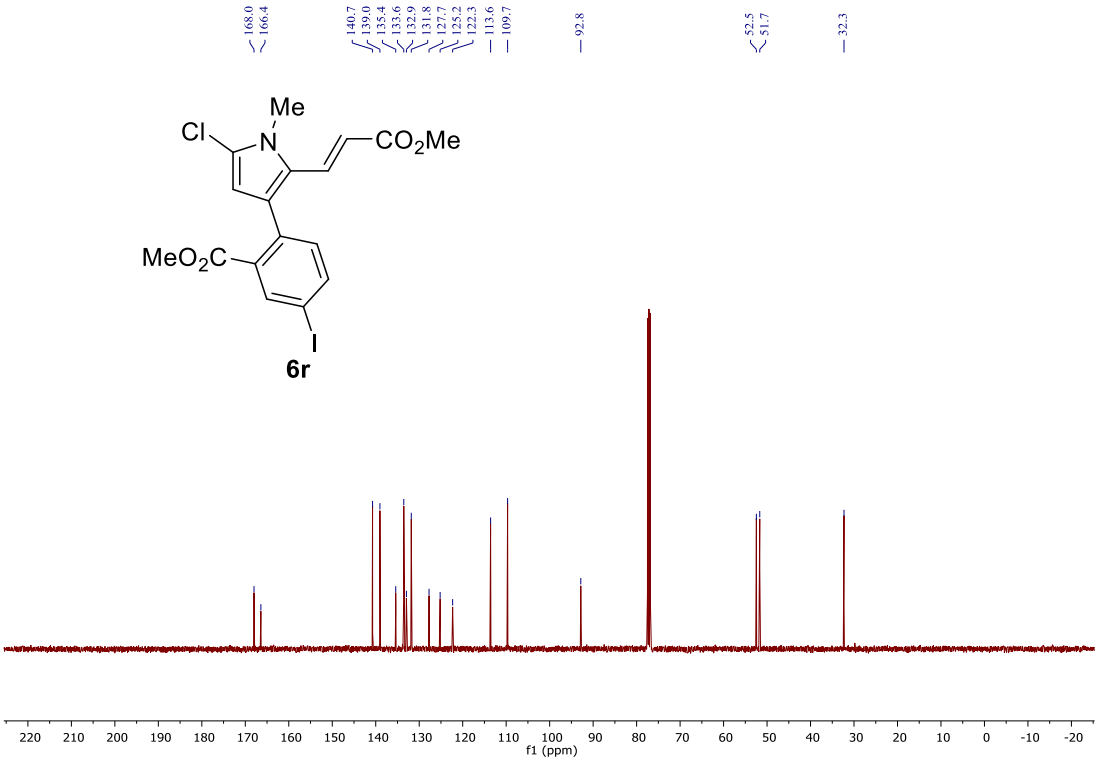

Figure 7.52. ^{1}H NMR Spectrum of 6s

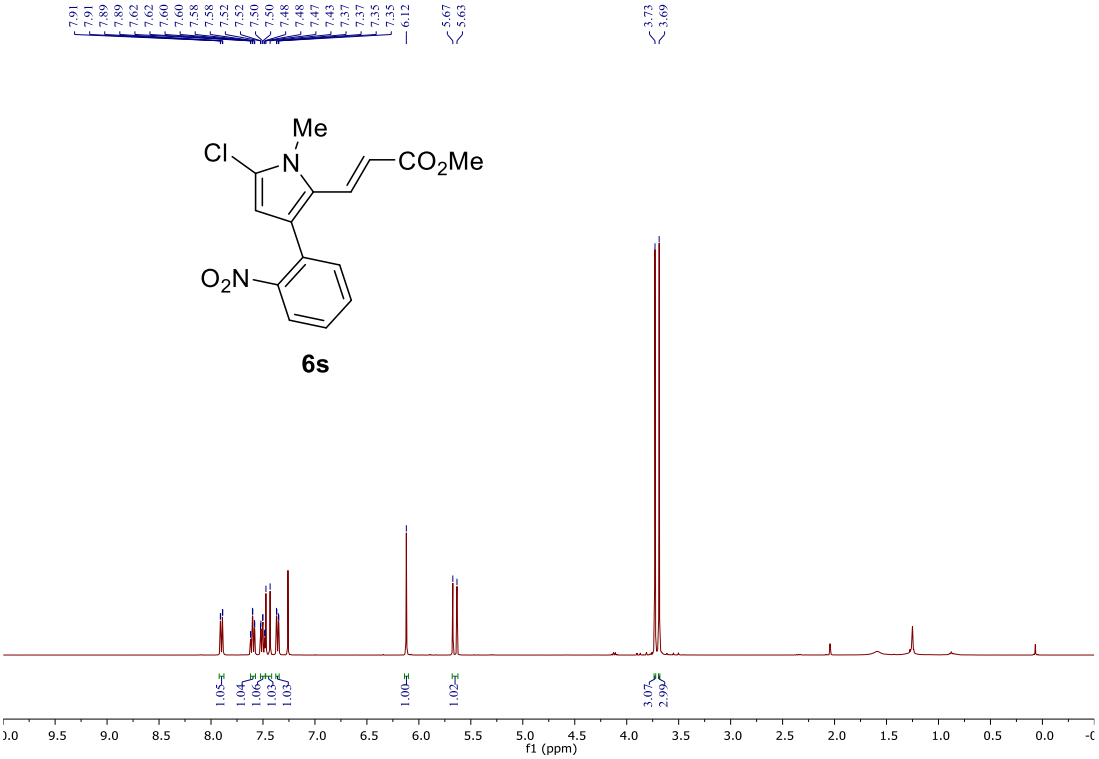

Figure 7.53. ^{13}C NMR Spectrum of 6s

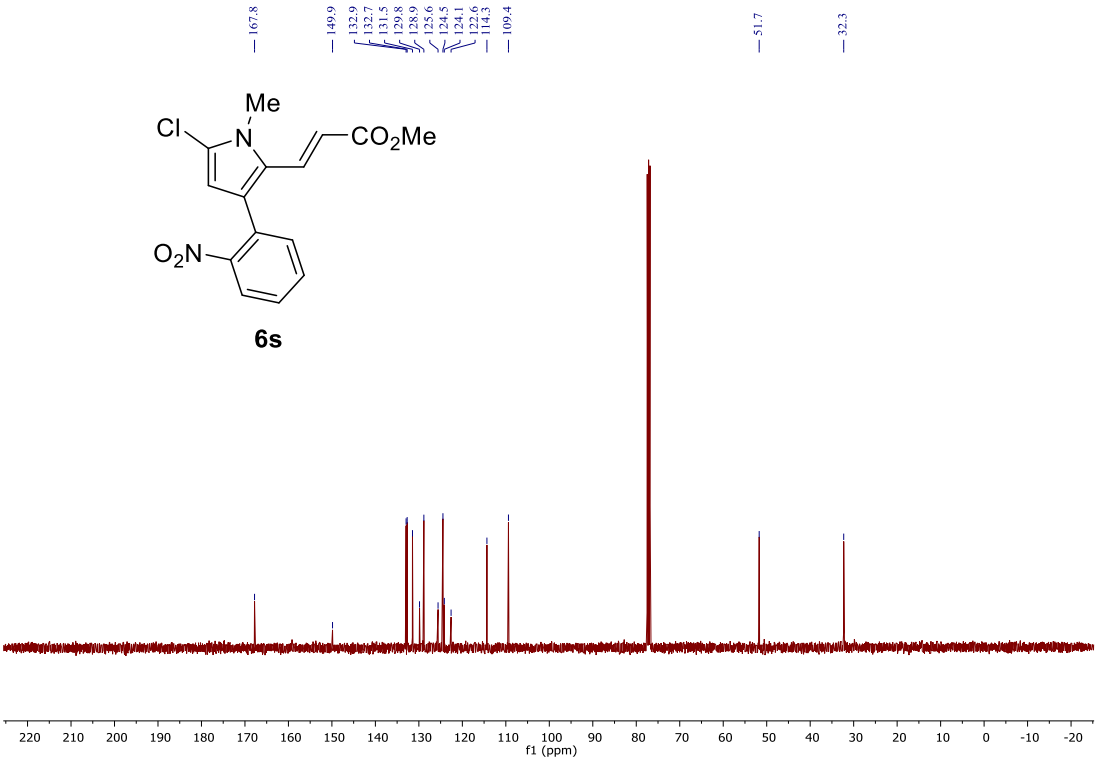

Figure 7.54. ^{1}H NMR Spectrum of 6t

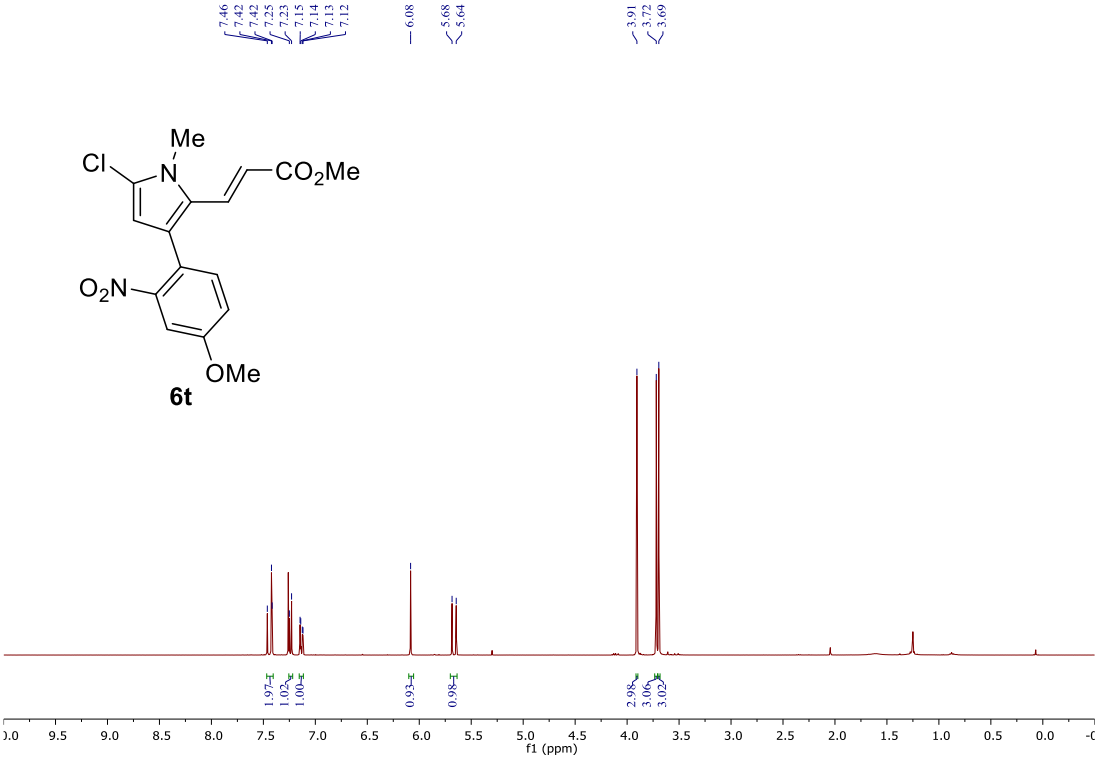

Figure 7.55. ^{13}C NMR Spectrum of 6t

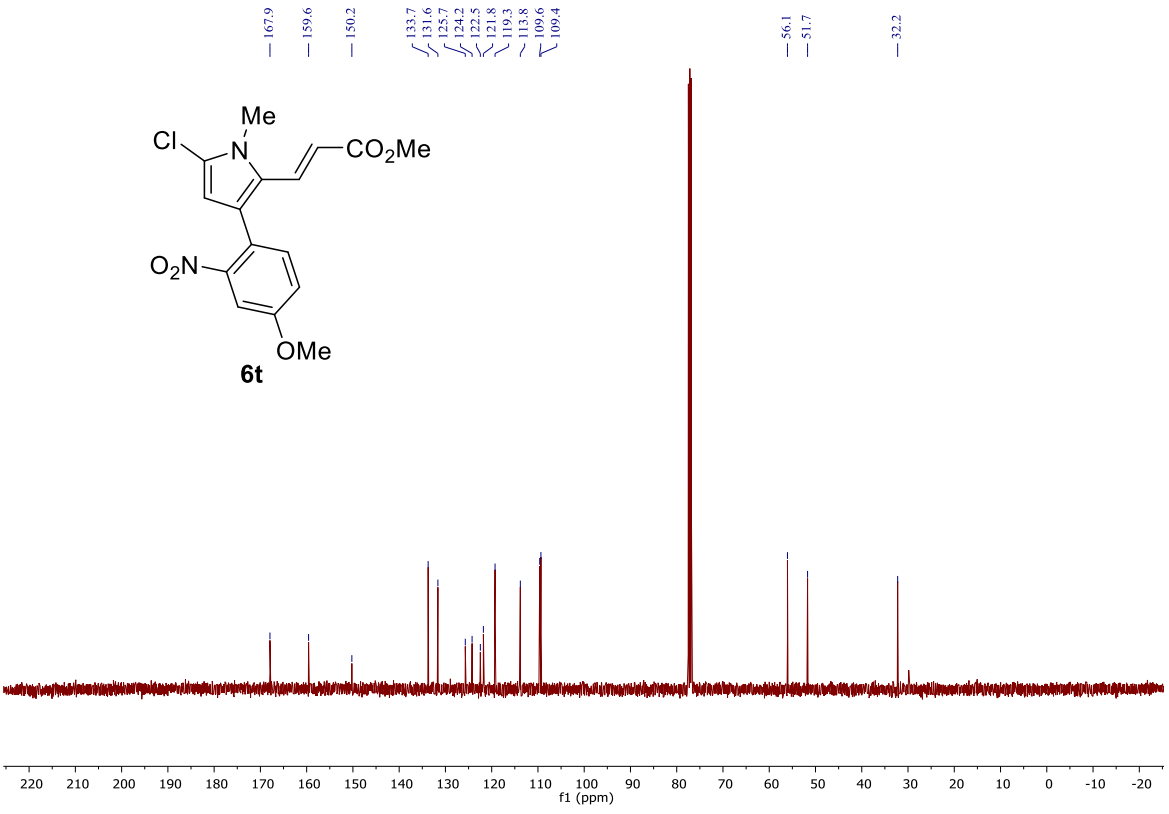

Figure 7.56. ^{1}H NMR Spectrum of 6u

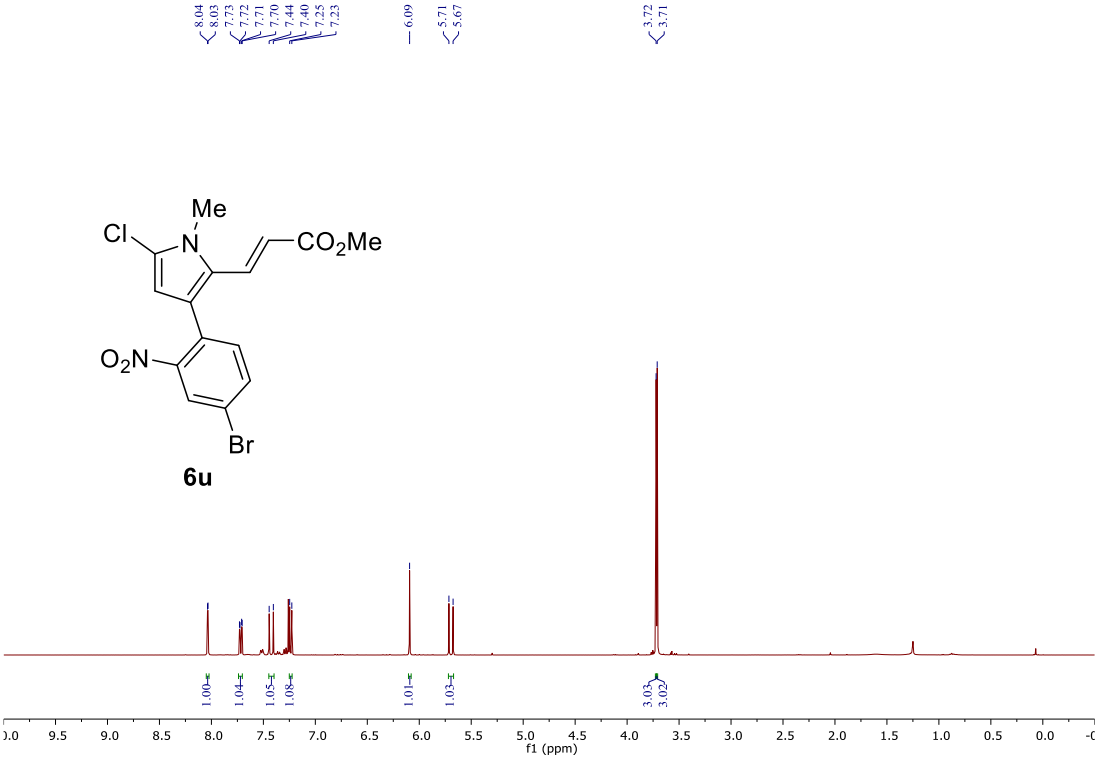

Figure 7.57. ^{13}C NMR Spectrum of 6u

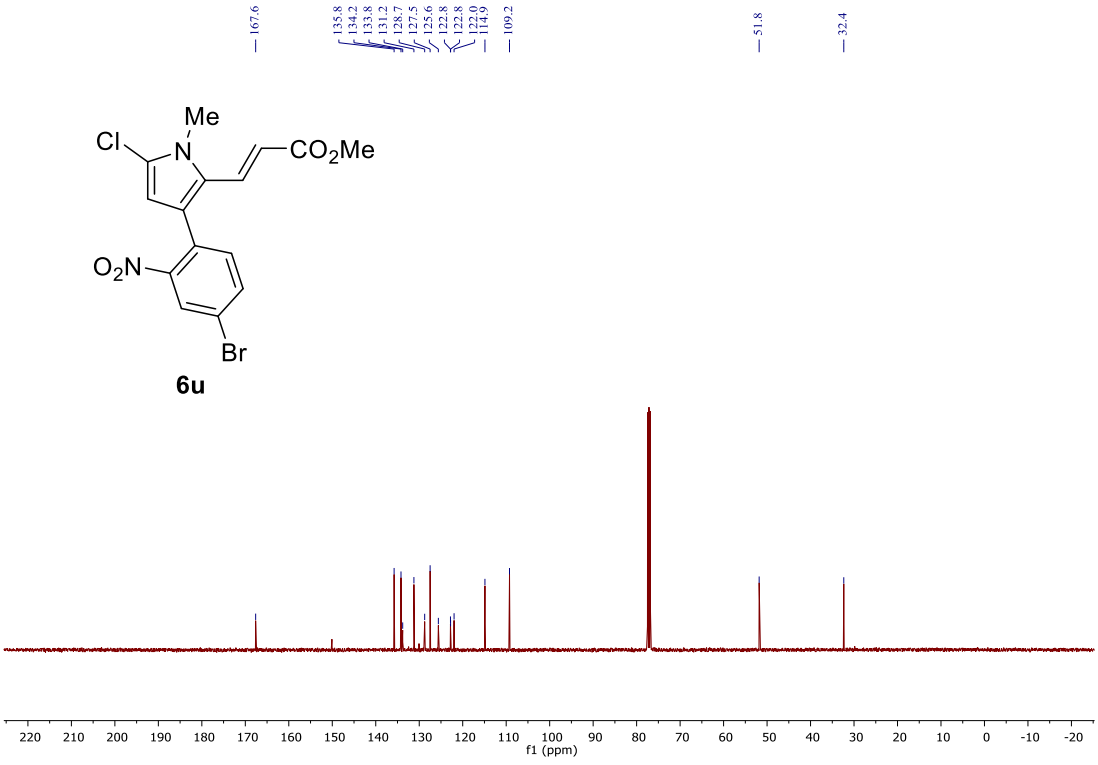

Figure 7.58. ^{1}H NMR Spectrum of 6v

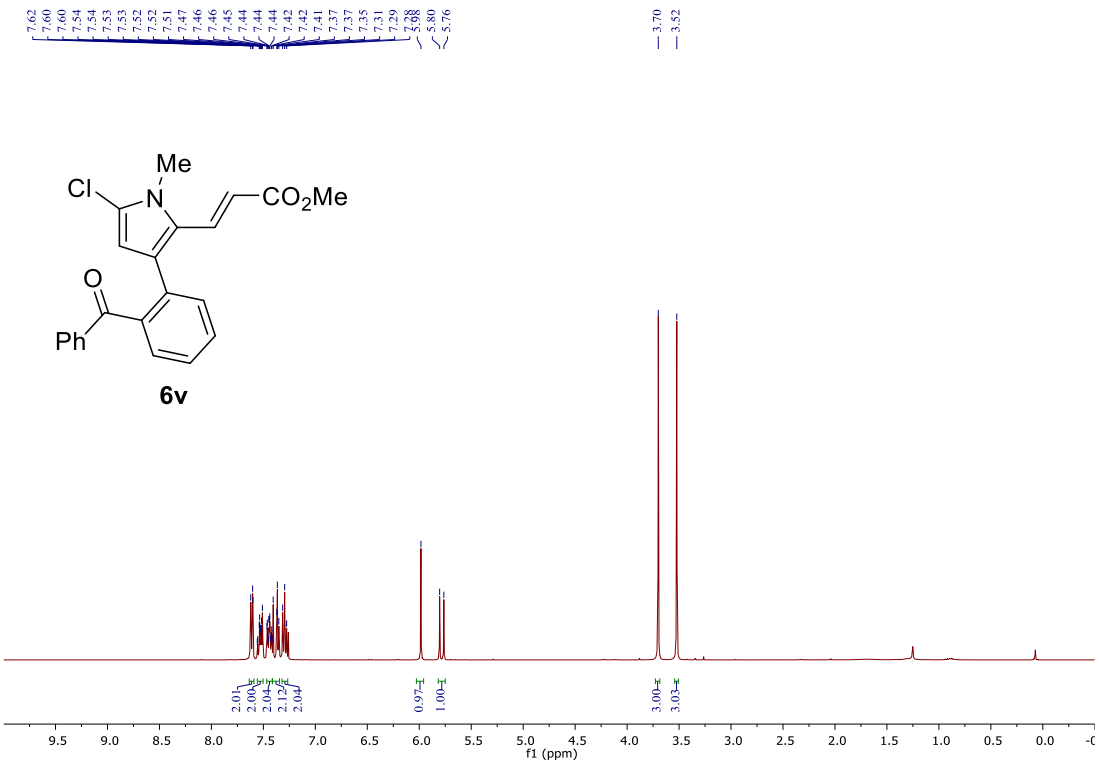

Figure 7.59. ^{1}H NMR Spectrum of 6v

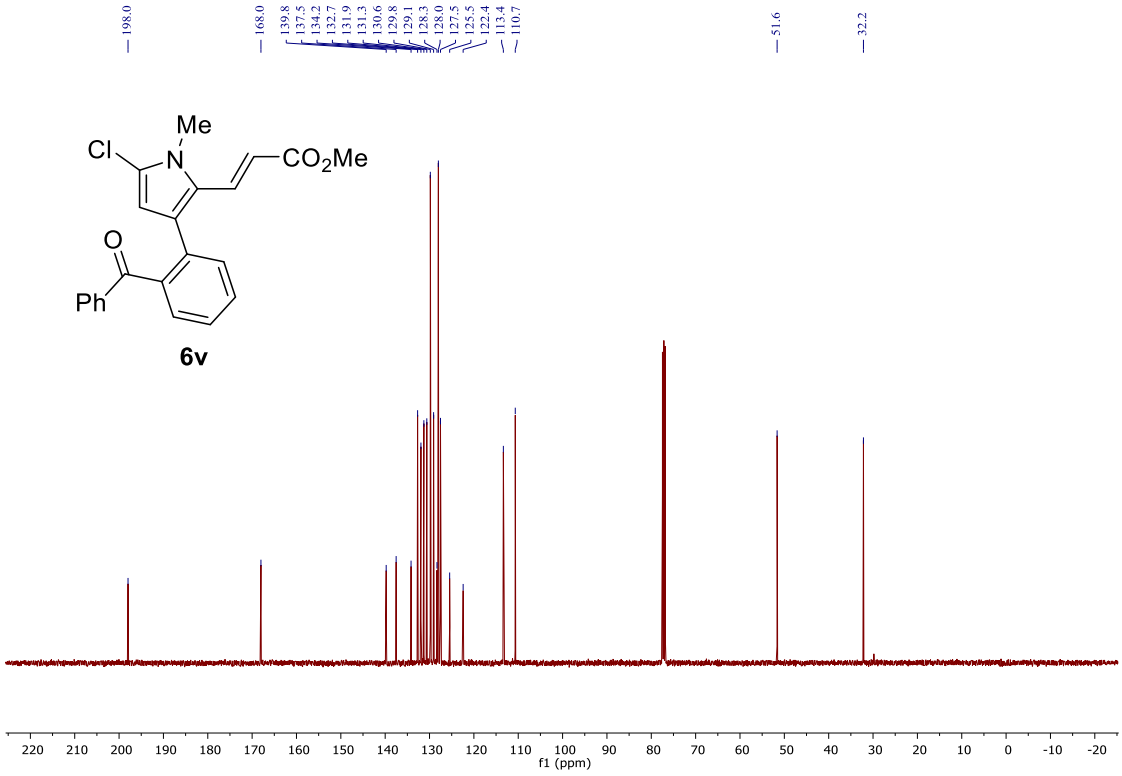

Figure 7.60. ^{1}H NMR Spectrum of 6w

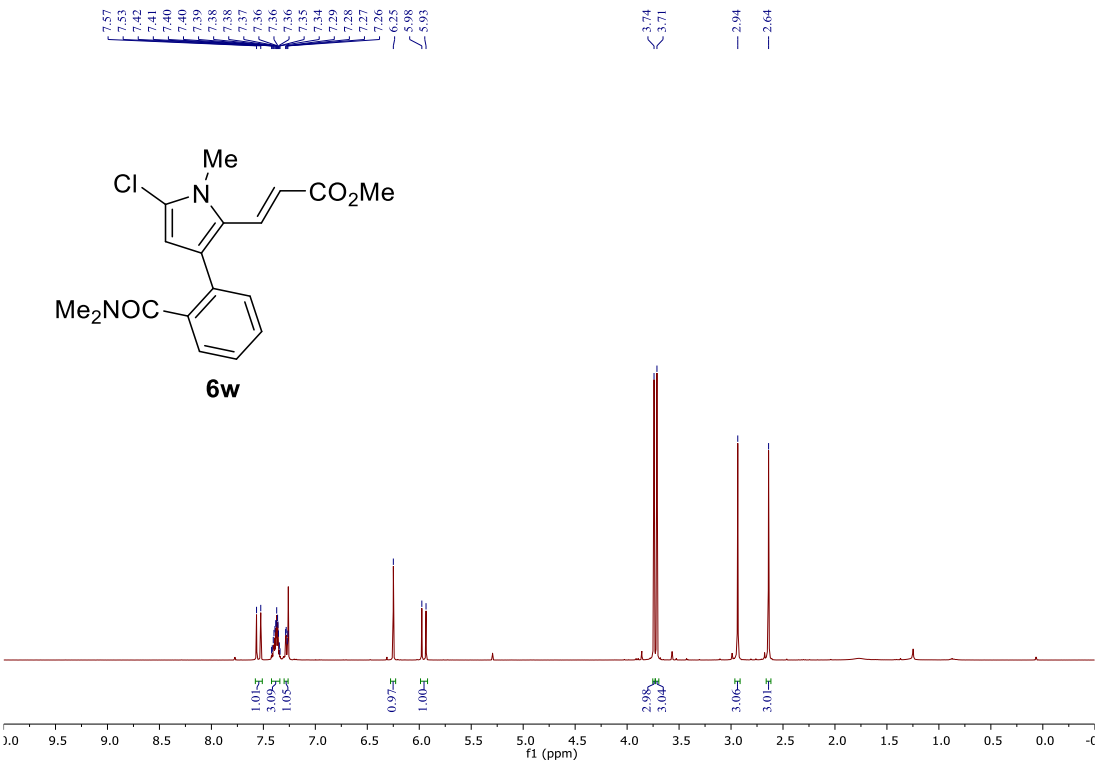

Figure 7.61. ^{13}C NMR Spectrum of 6w

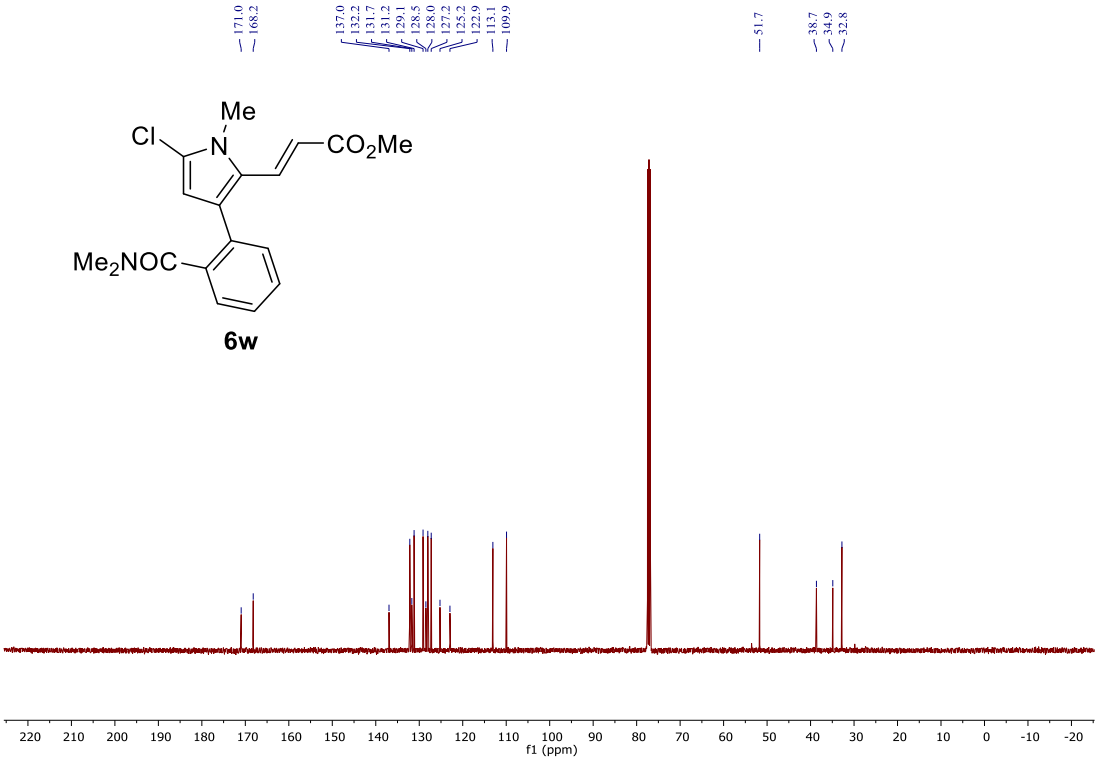

Figure 7.62. ^{1}H NMR Spectrum of 6x

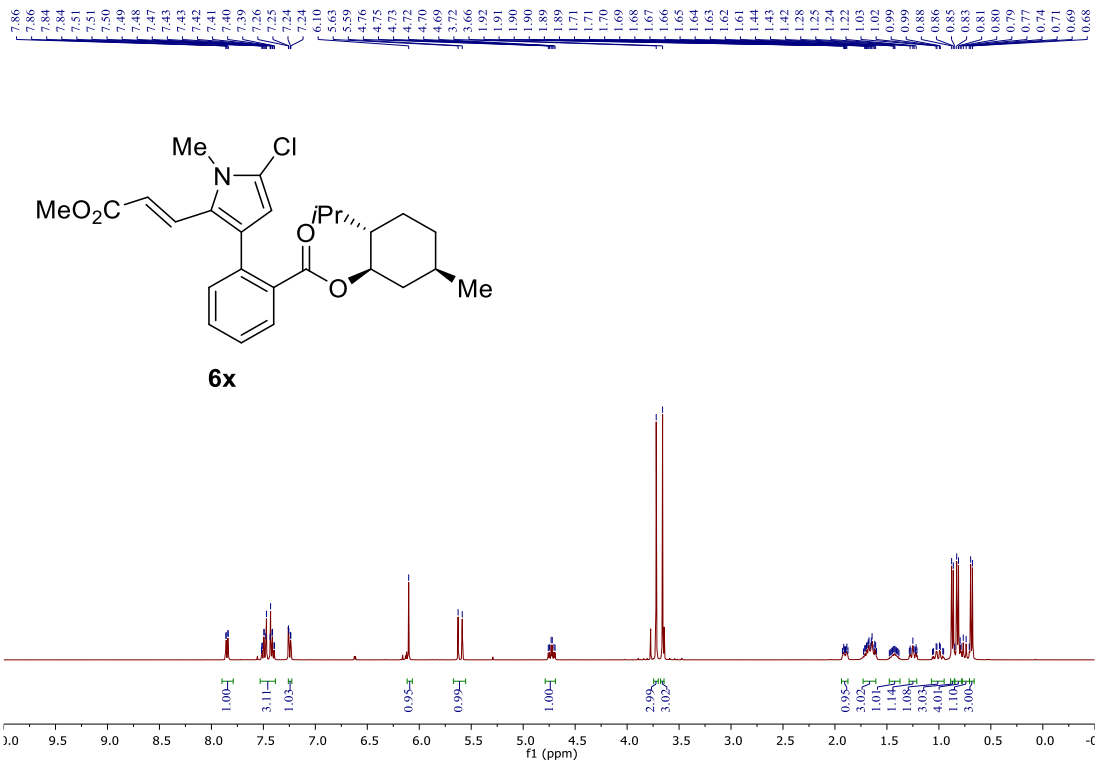

Figure 7.63. ^{13}C NMR Spectrum of 6x

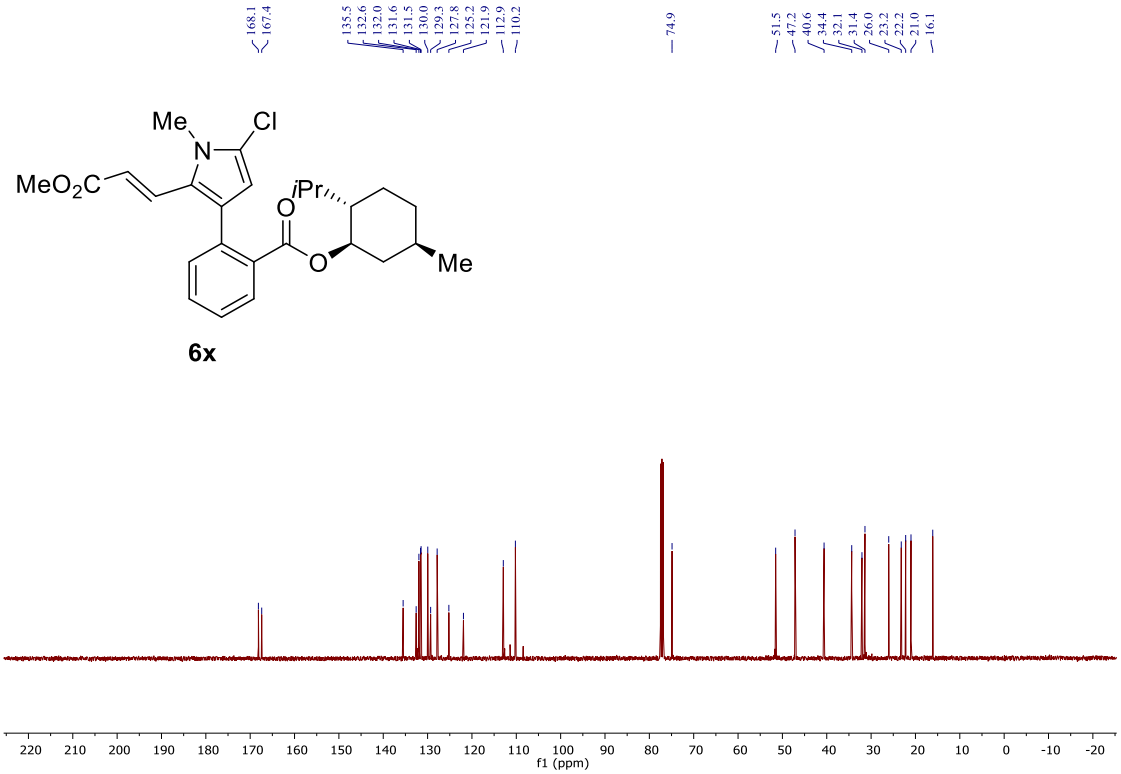

Figure 7.64. ^{1}H NMR Spectrum of 6y

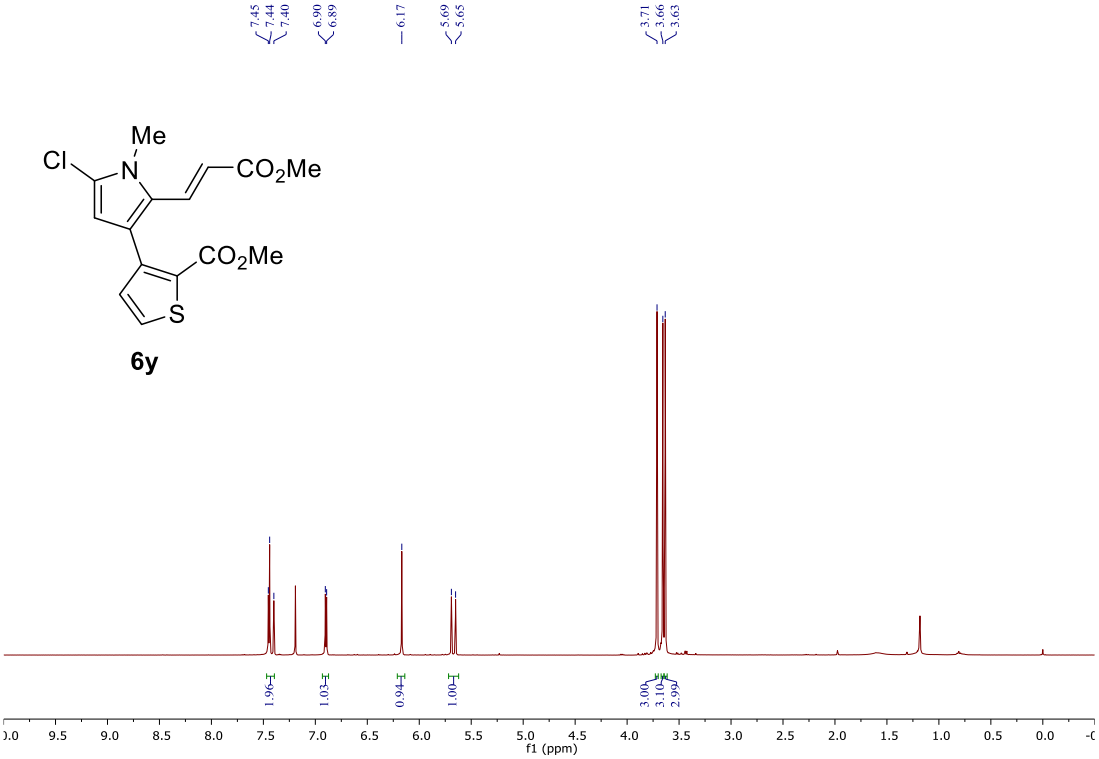

Figure 7.65. ^{13}C NMR Spectrum of 6y

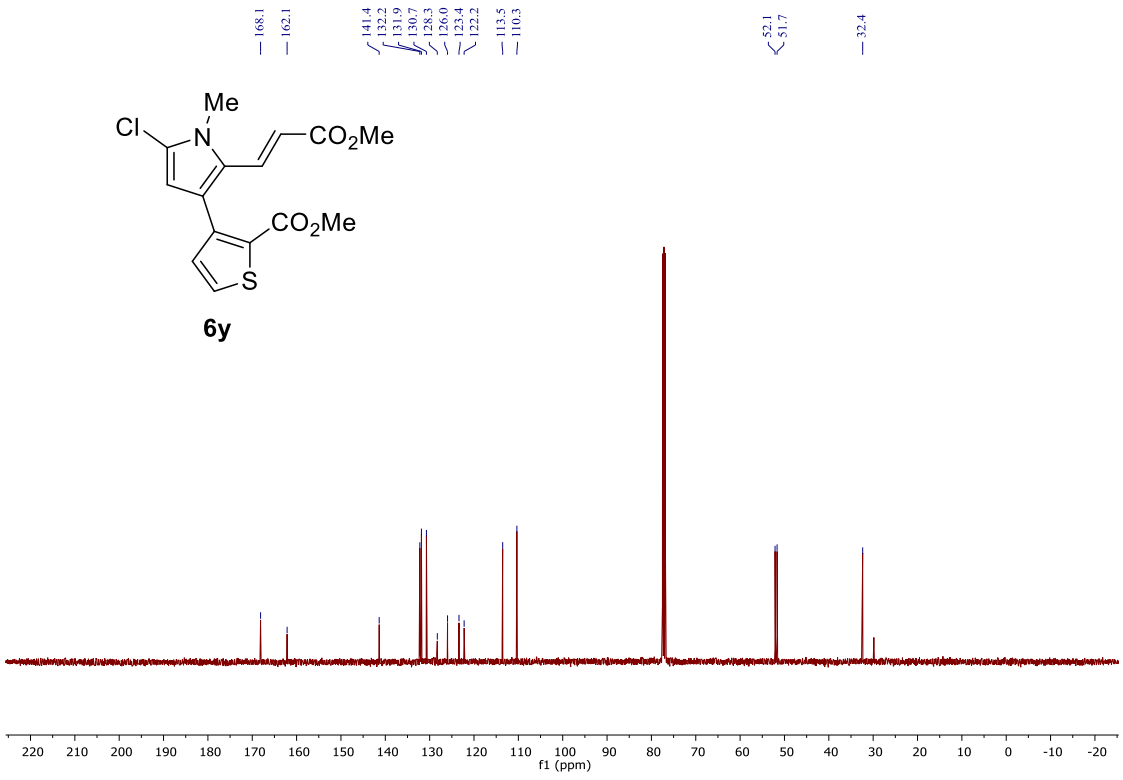

Figure 7.66. ^{1}H NMR Spectrum of 6ah

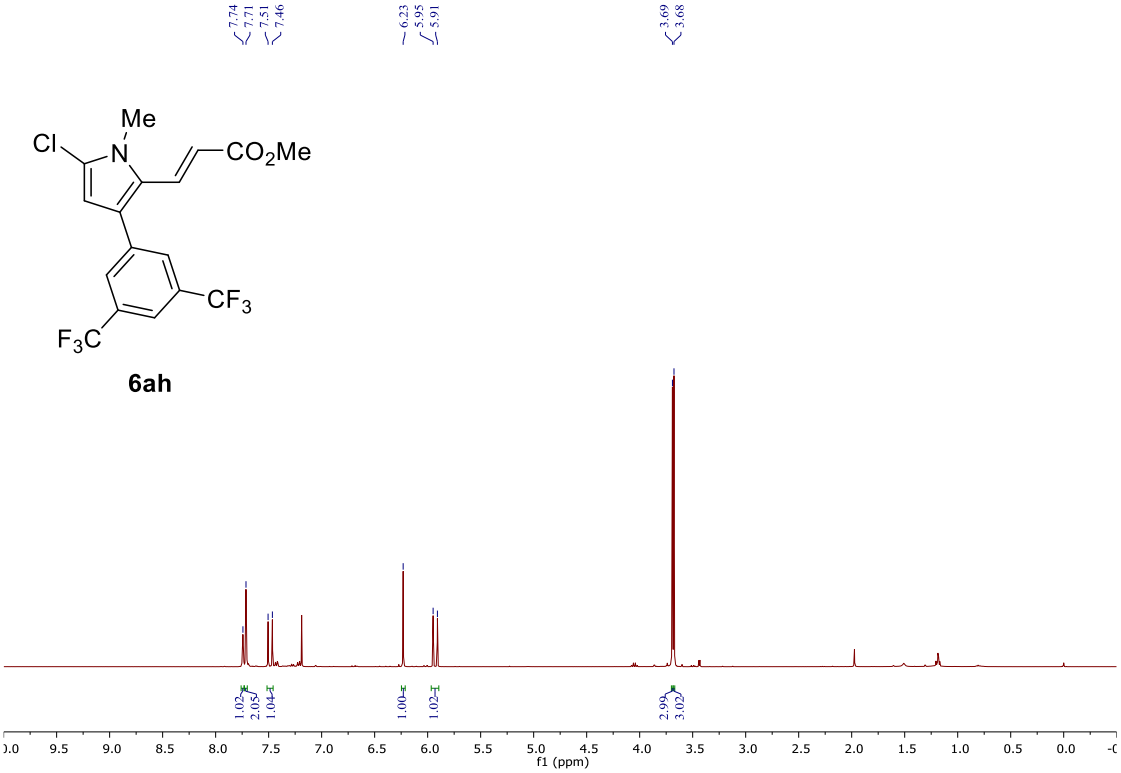

Figure 7.67. ^{1}H NMR Spectrum of 6ah

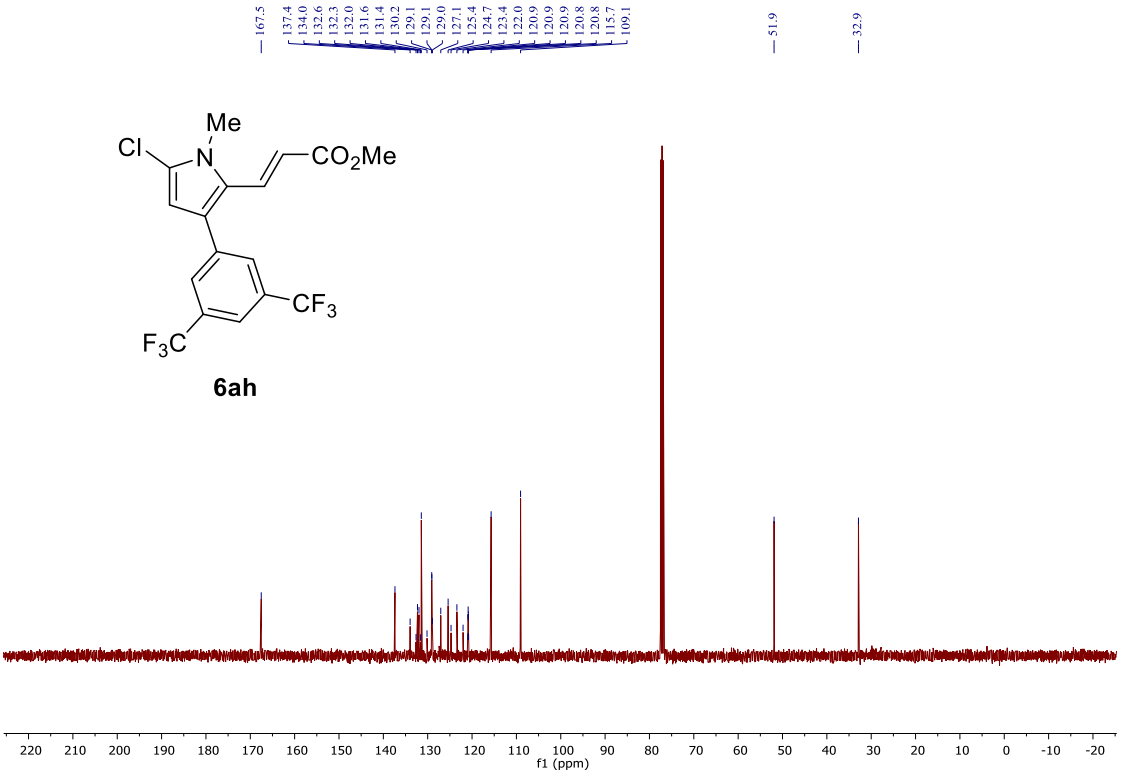

Figure 7.68. ^{19}F NMR Spectrum of 6ah

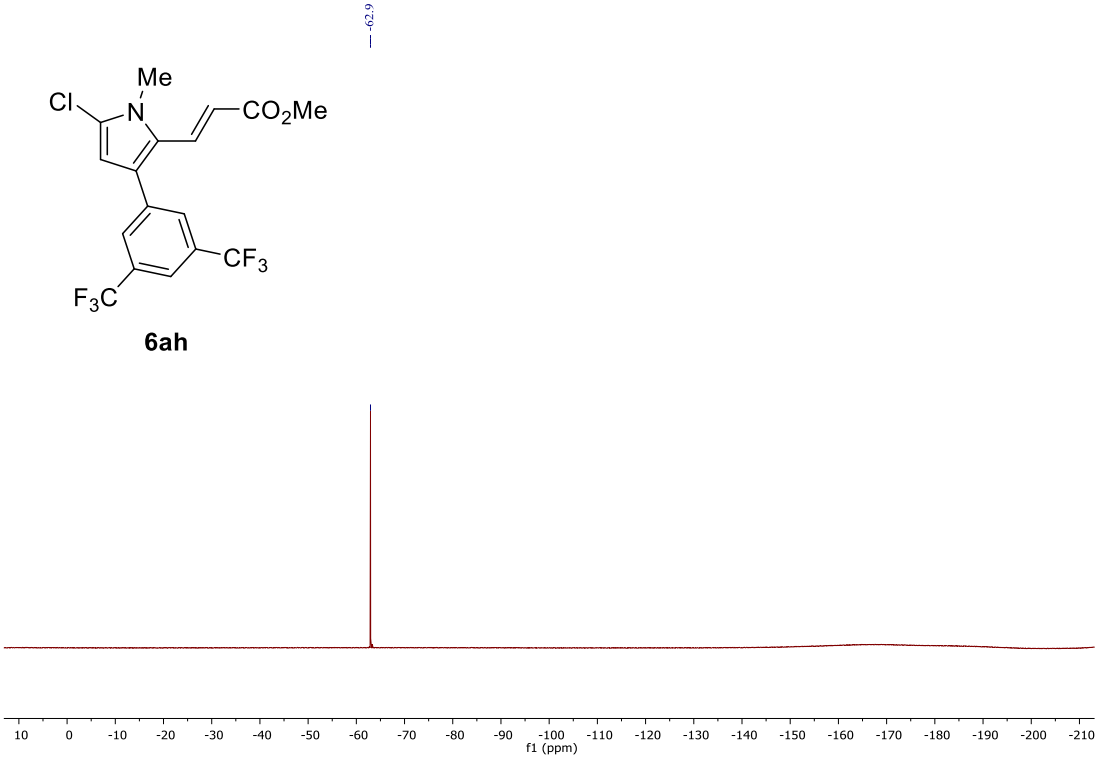

Figure 7.69. ^{1}H NMR Spectrum of 6af

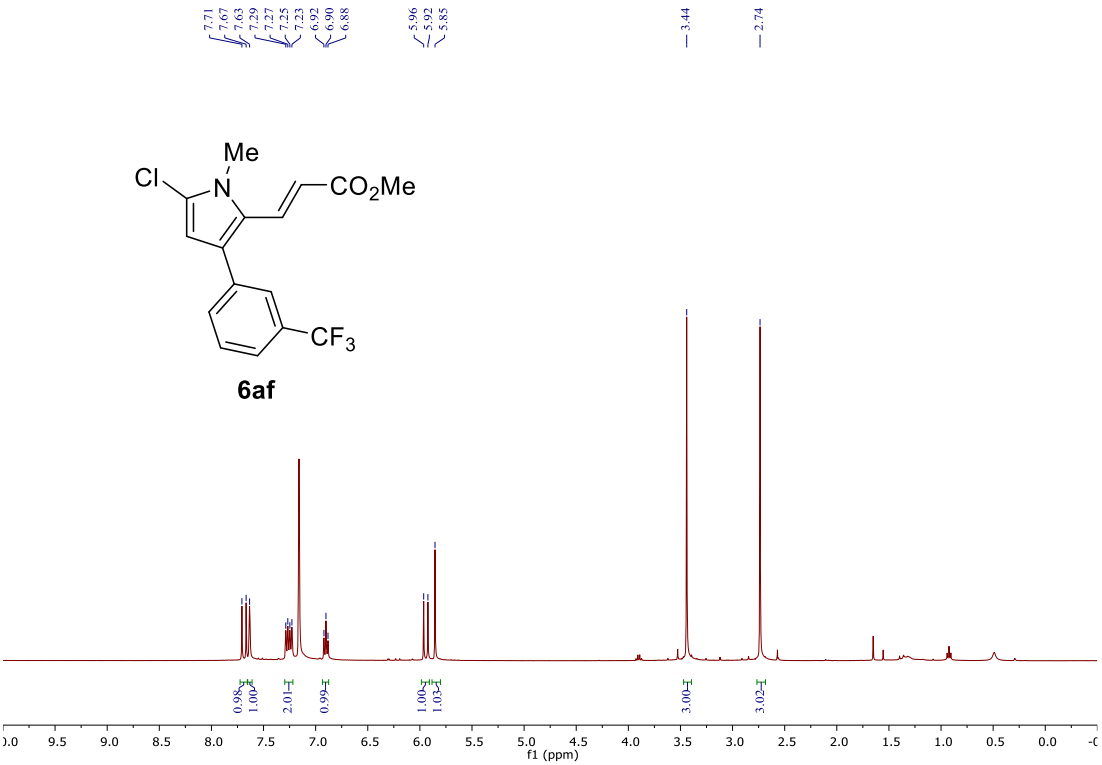

Figure 7.70. ^{13}C NMR Spectrum of 6af

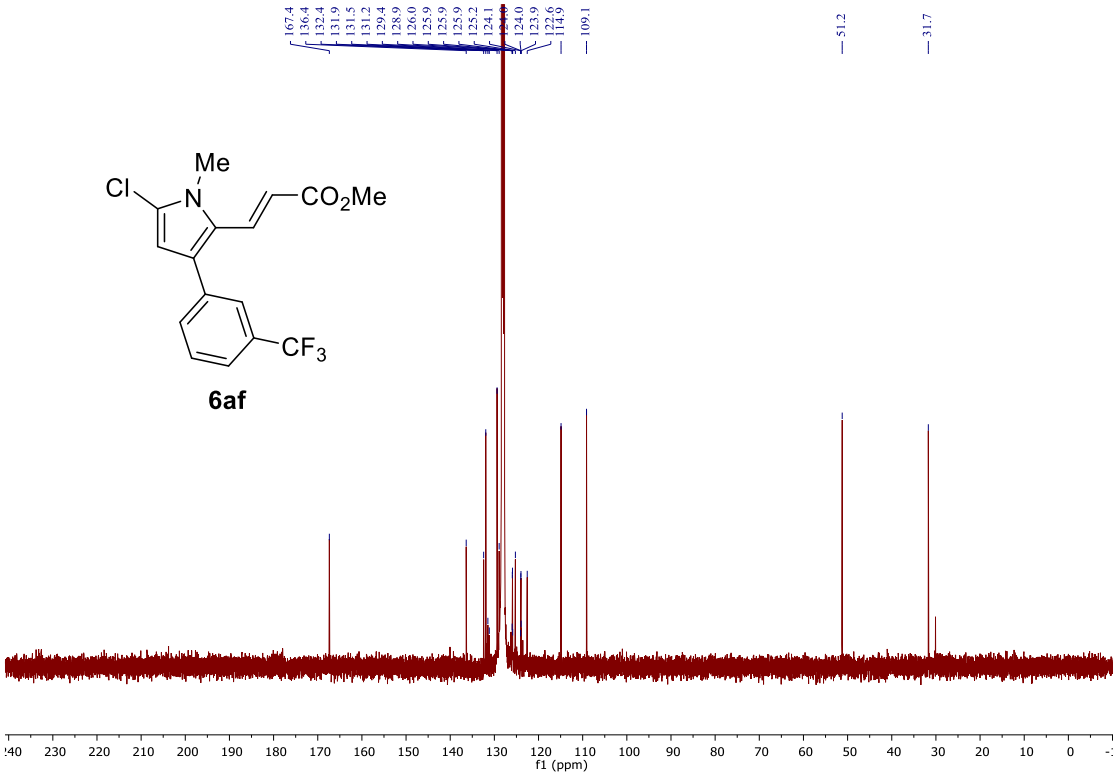

Figure 7.71. ^{19}F NMR Spectrum of 6af

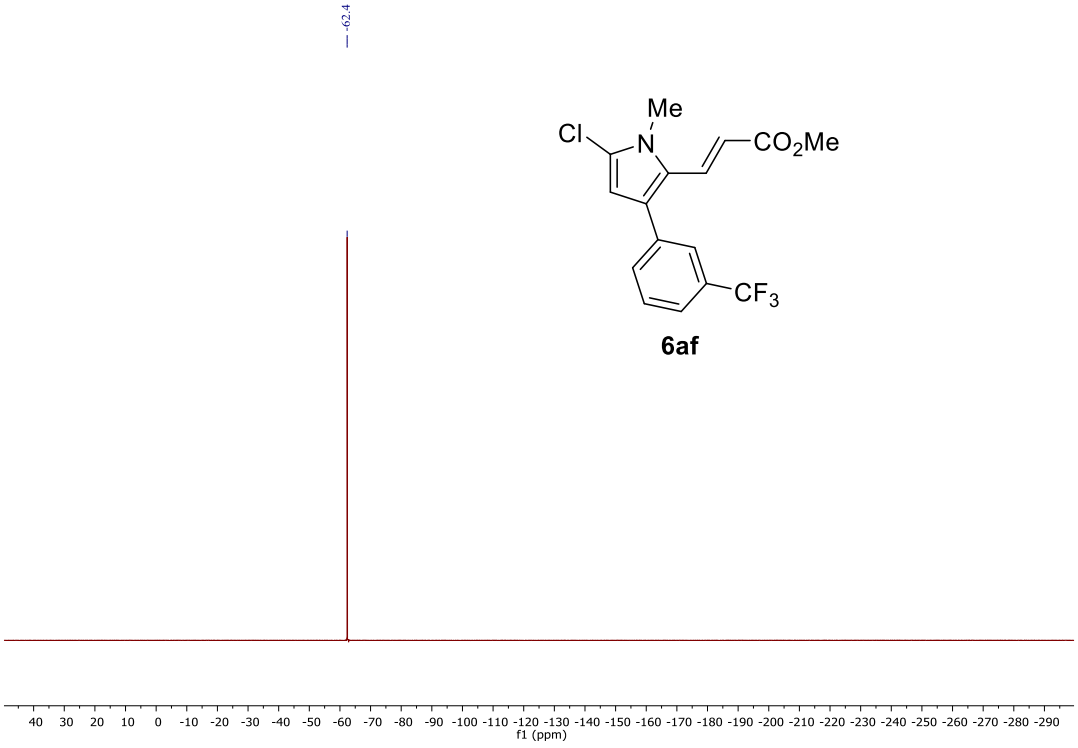

Figure 7.72. ^{1}H NMR Spectrum of 6aa

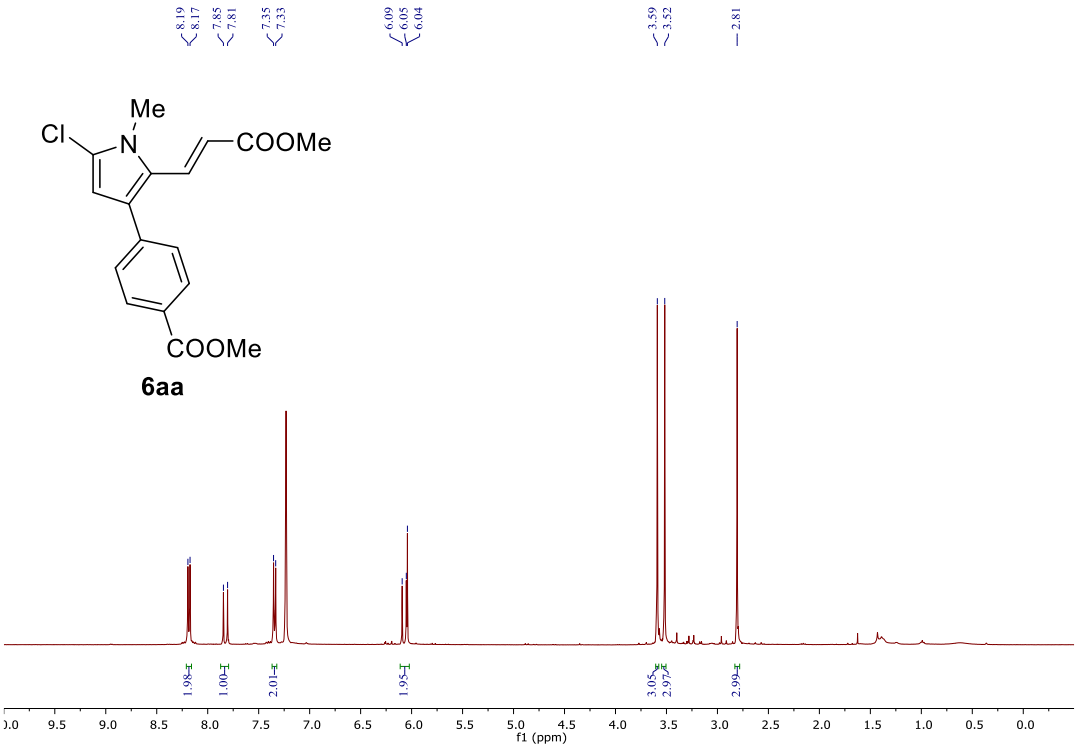

Figure 7.73. ^{13}C NMR Spectrum of 6aa

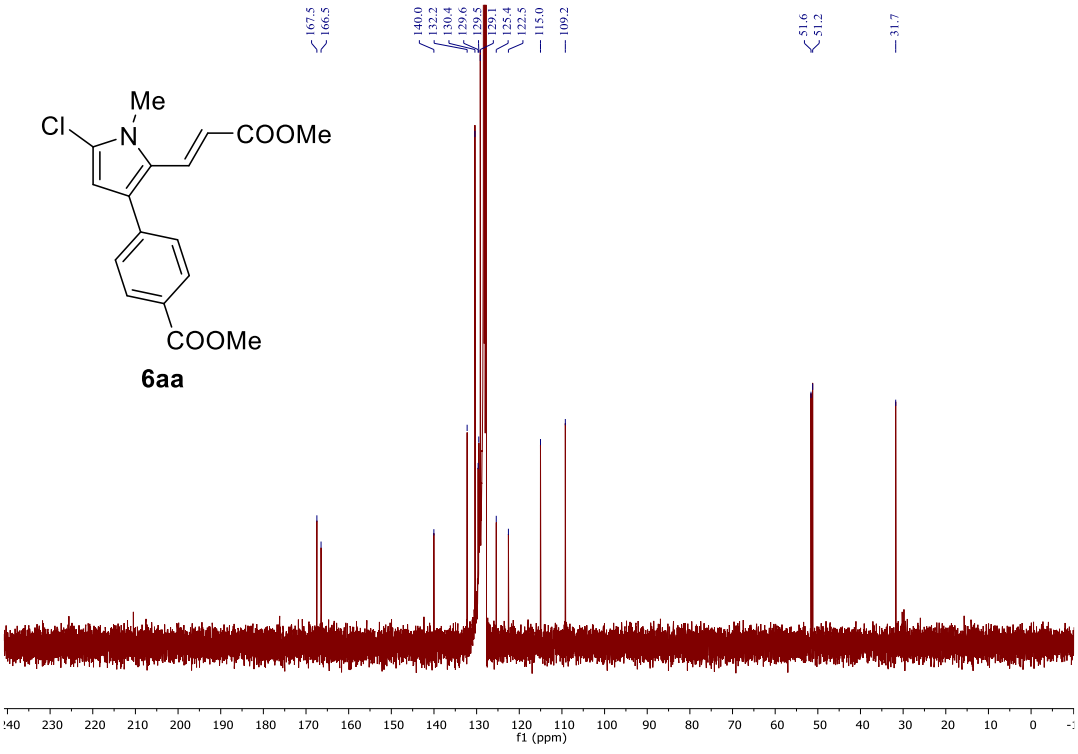

Figure 7.74. ^{1}H NMR Spectrum of 6z

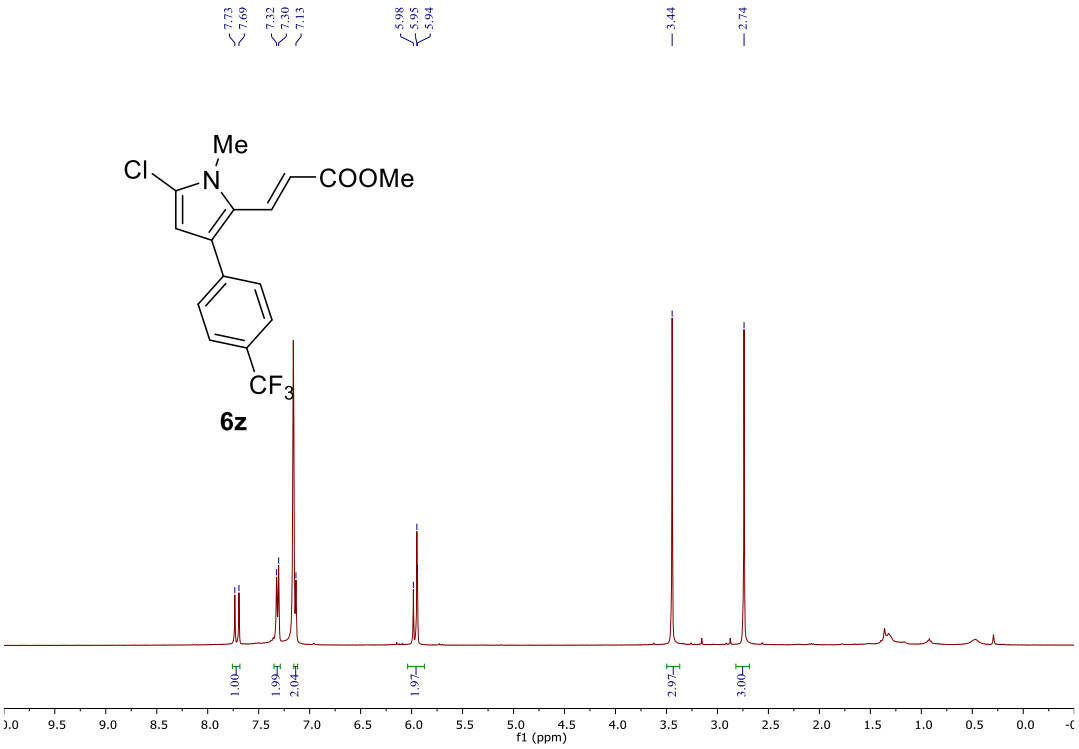

Figure 7.75. ^{13}C NMR Spectrum of 6z

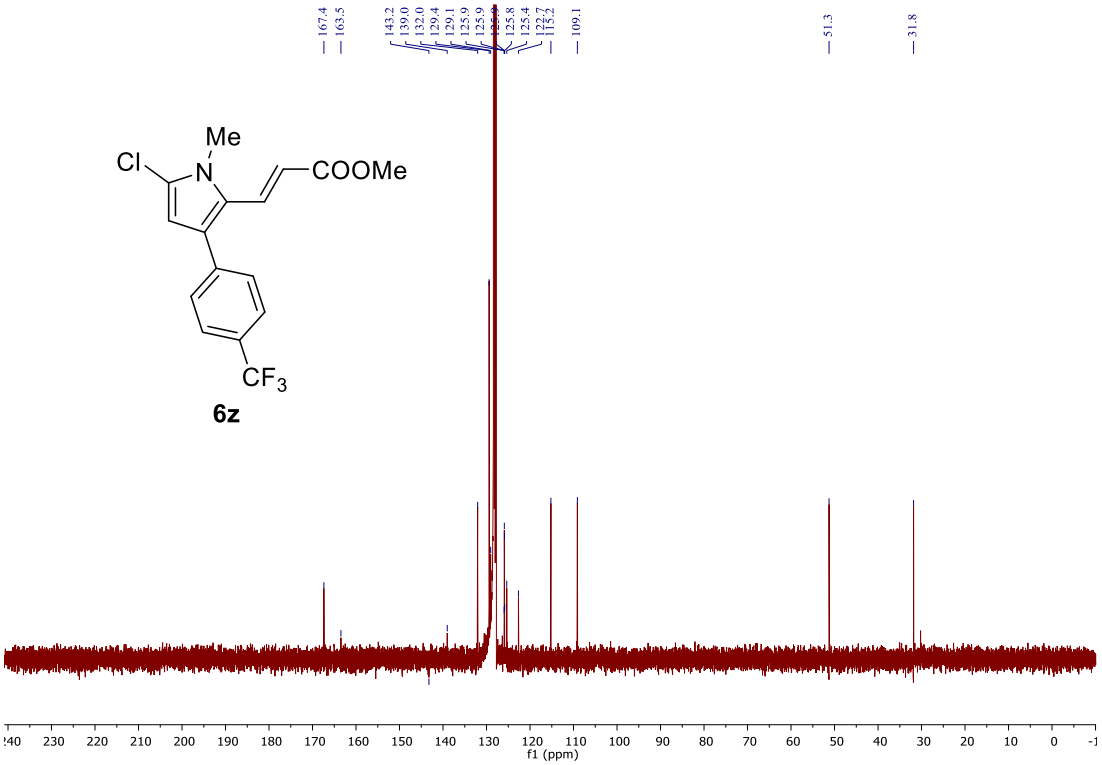

Figure 7.76. ^{19}F NMR Spectrum of 6z

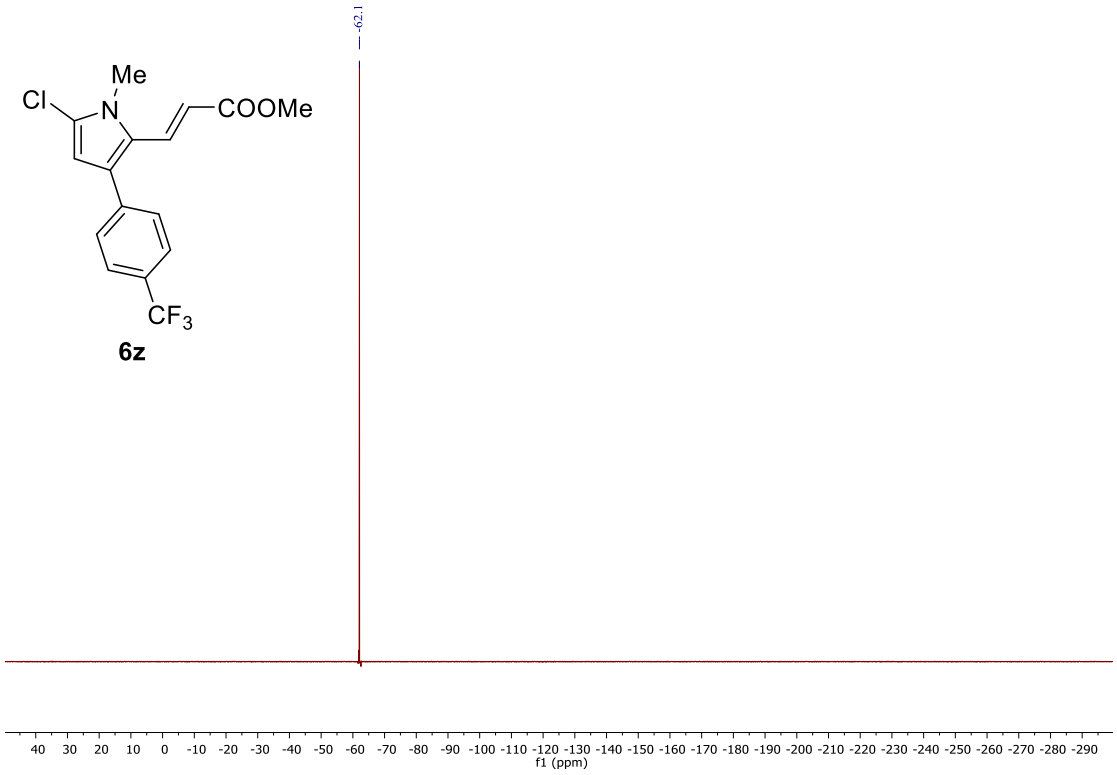

Figure 7.77. ^{1}H NMR Spectrum of 6ag

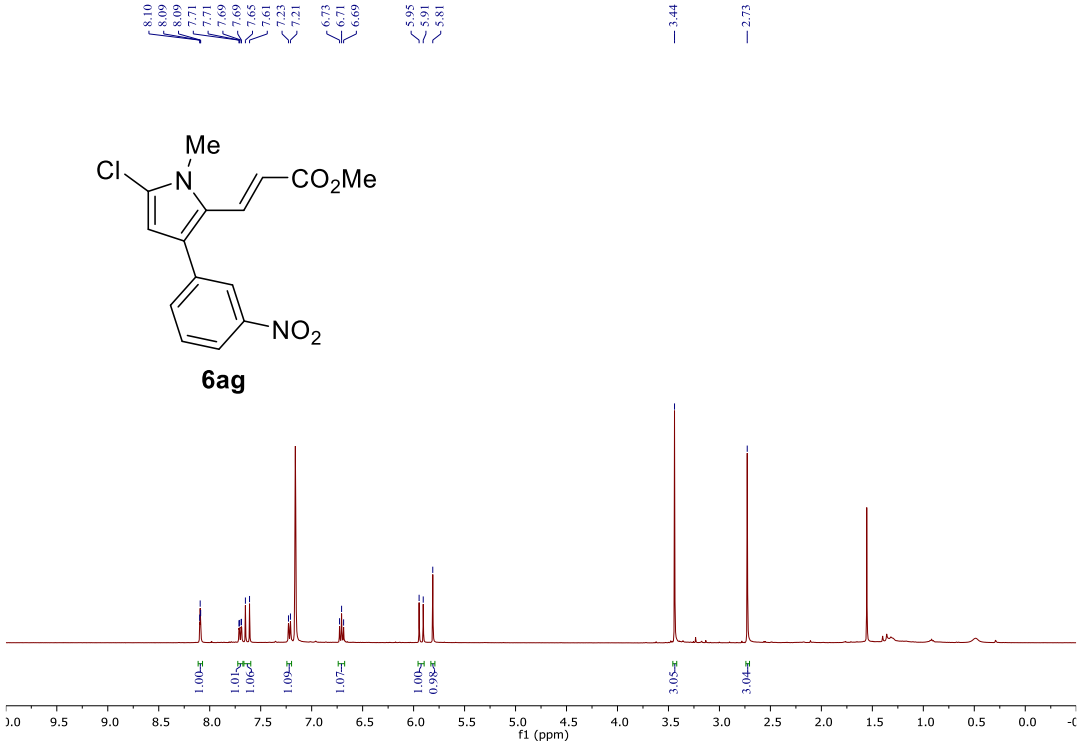

Figure 7.78. ^{13}C NMR Spectrum of 6ag

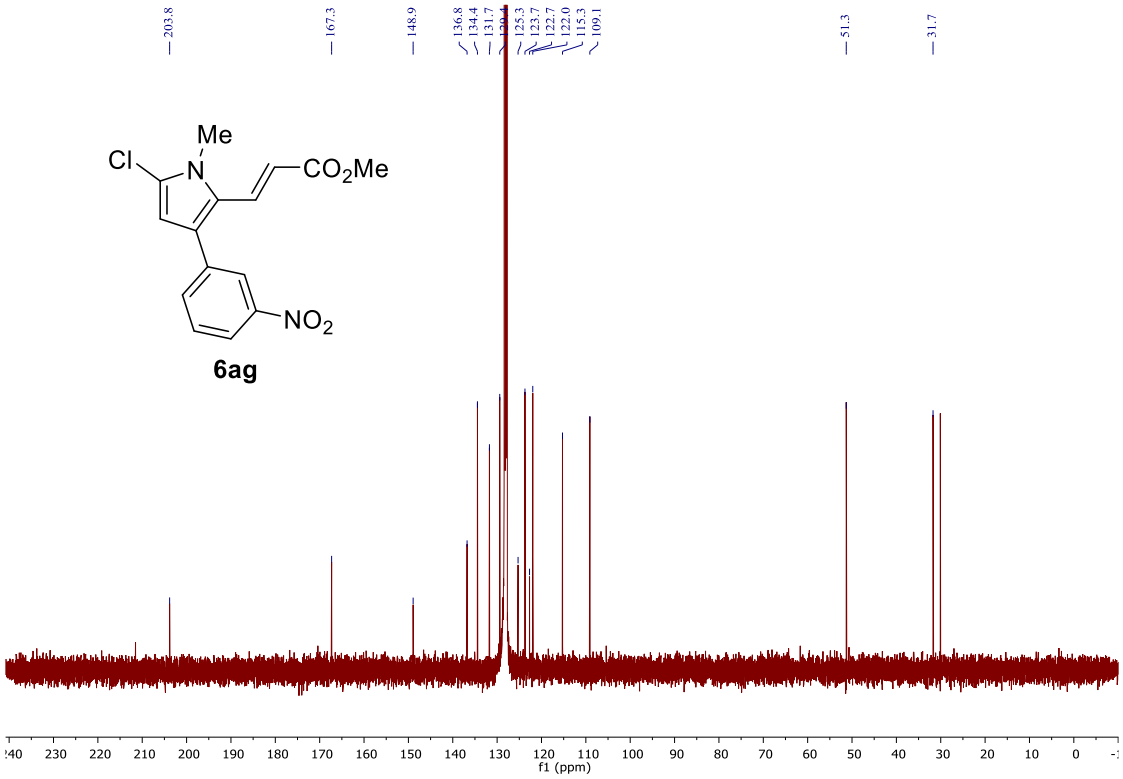

Figure 7.79. ^{1}H NMR Spectrum of 6ac

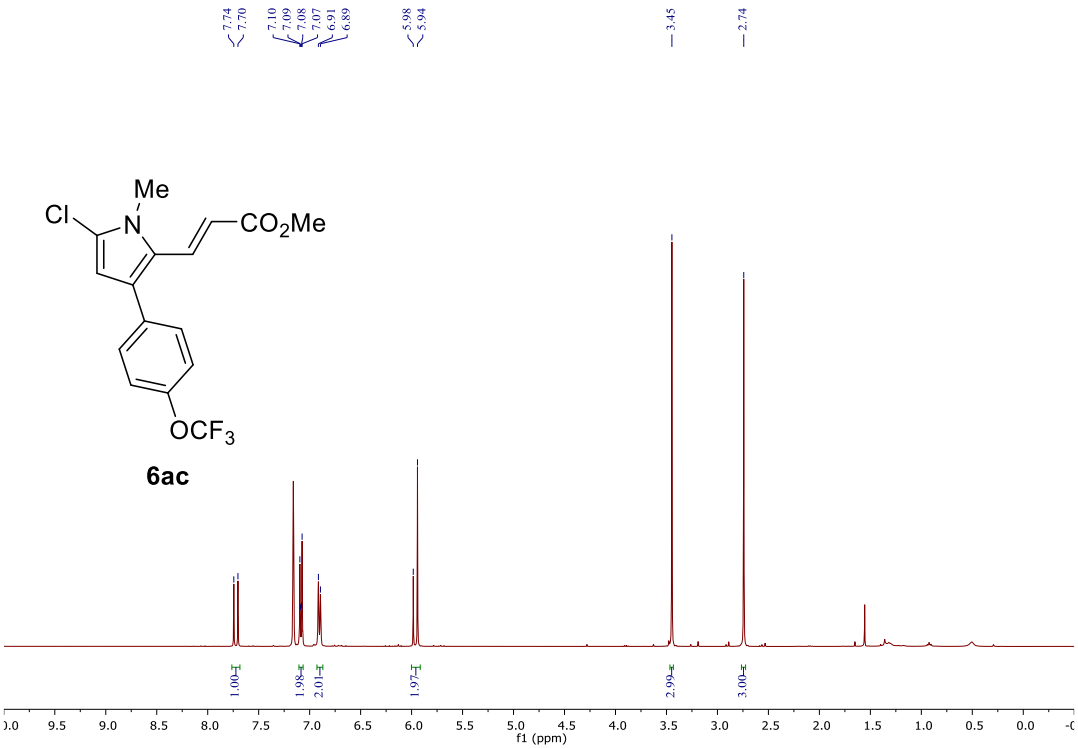

Figure 7.80. ^{13}C NMR Spectrum of 6ac

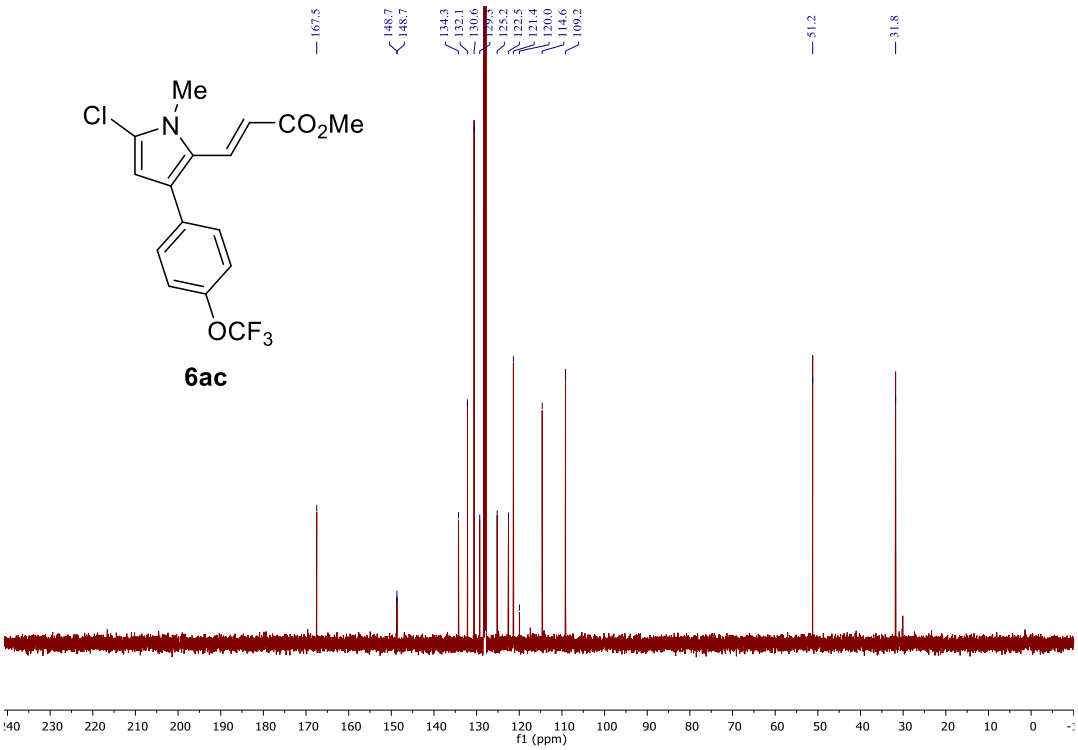

Figure 7.81. ^{19}F NMR Spectrum of 6ac

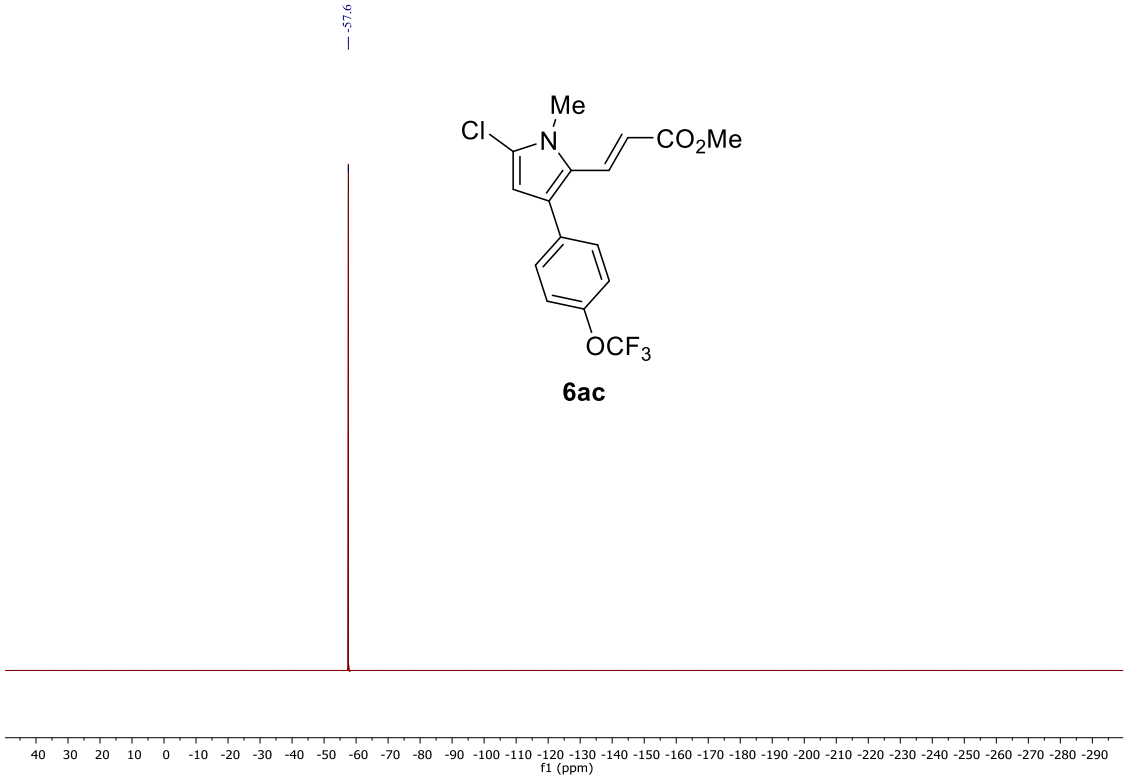

Figure 7.82. ^{1}H NMR Spectrum of 6ae

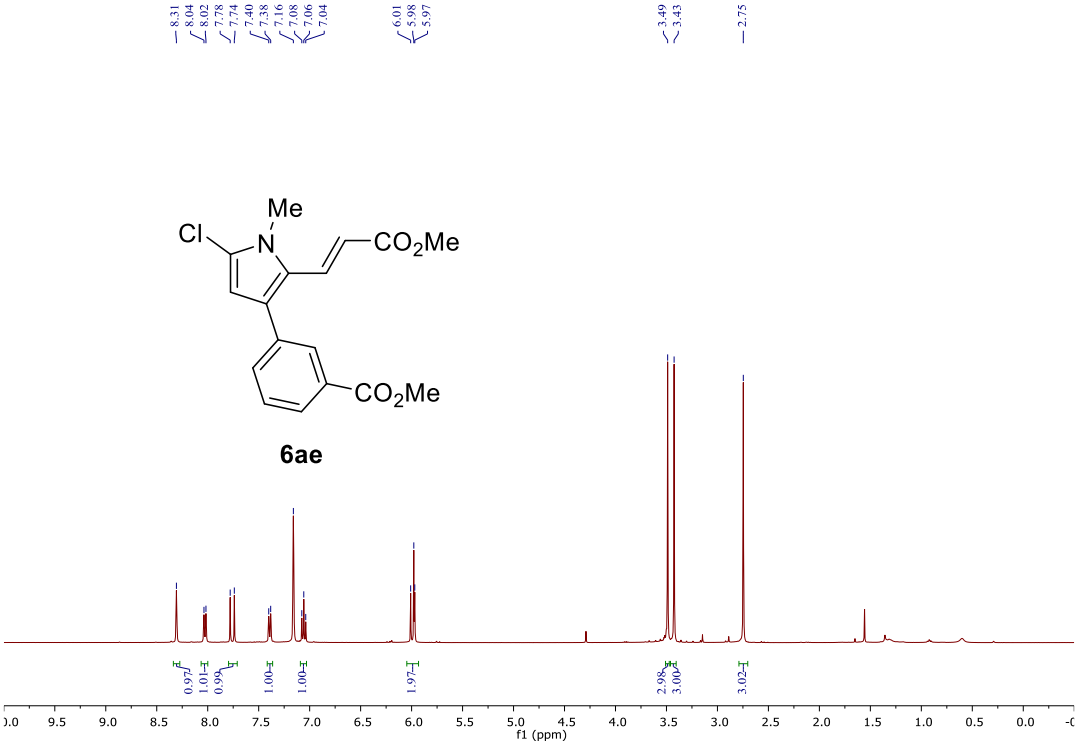

Figure 7.83. ^{13}C NMR Spectrum of 6ae

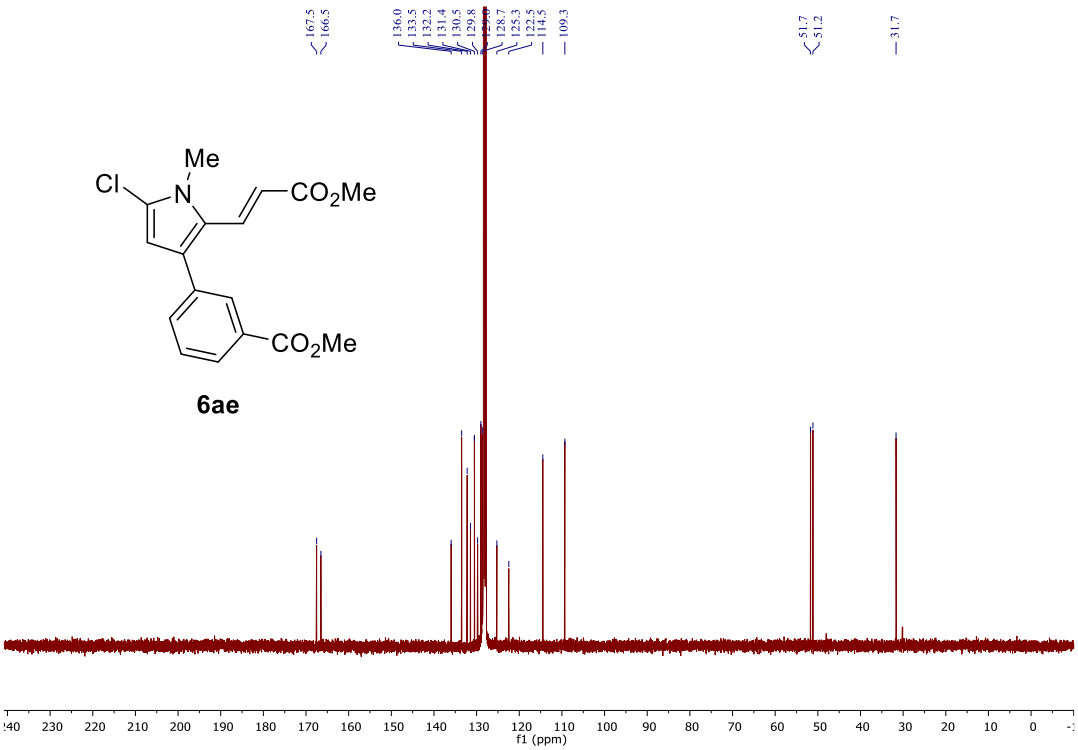

Figure 7.84. ^{1}H NMR Spectrum of 6ak

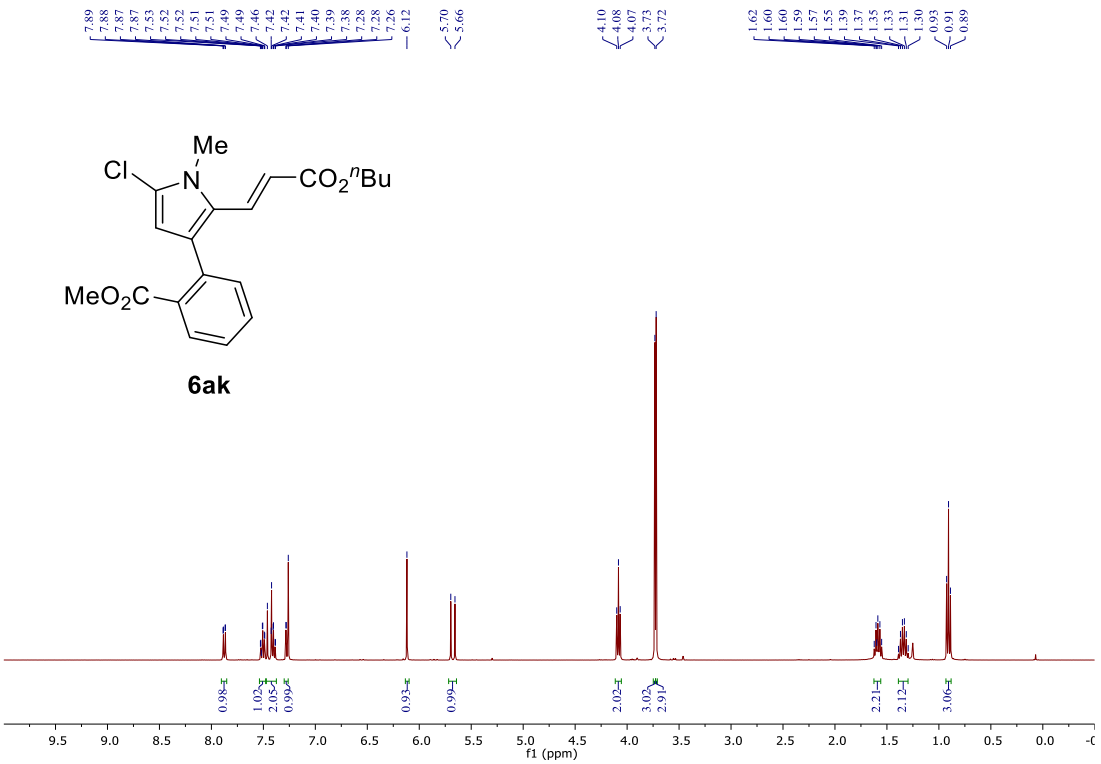

Figure 7.85. ^{13}C NMR Spectrum of 6ak

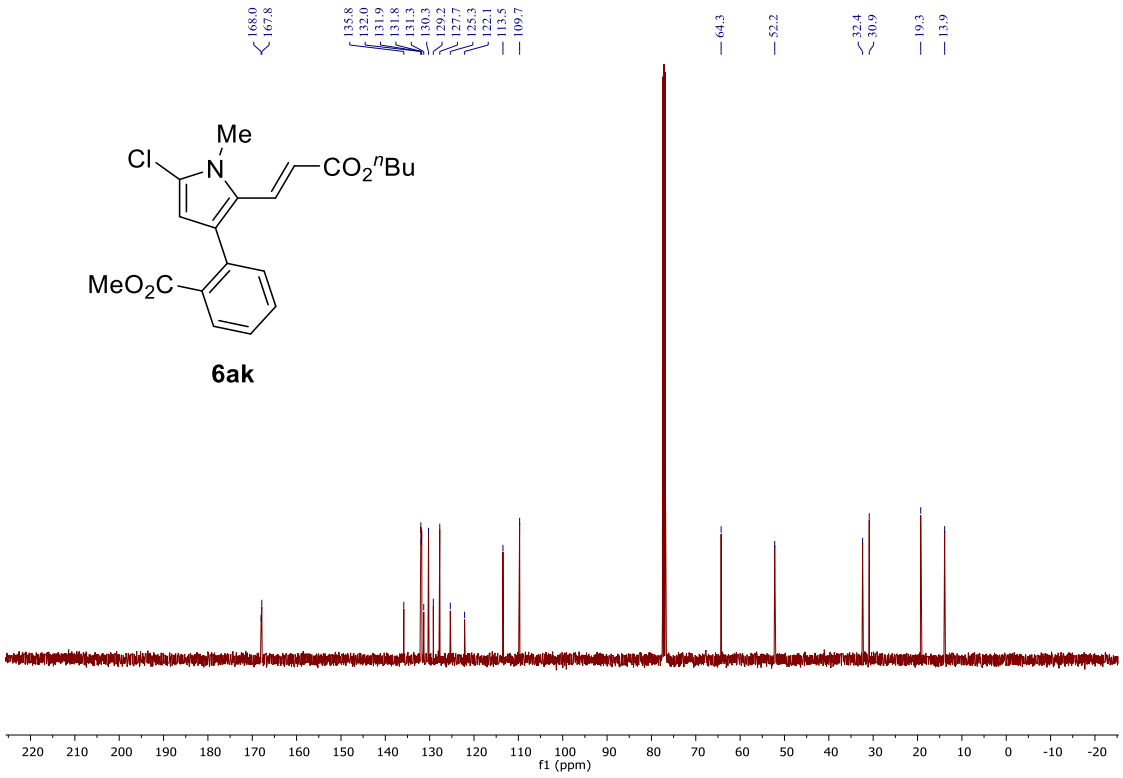

Figure 7.86. ^{1}H NMR Spectrum of 6al

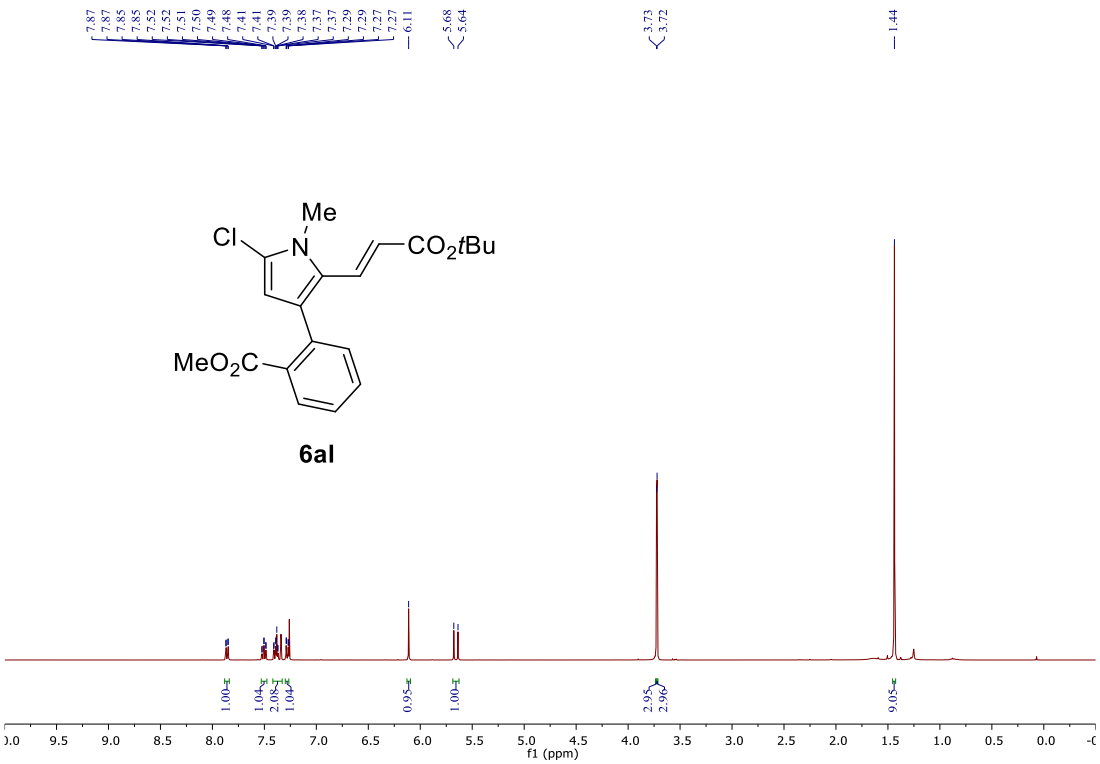

Figure 7.87. ^{13}C NMR Spectrum of 6al

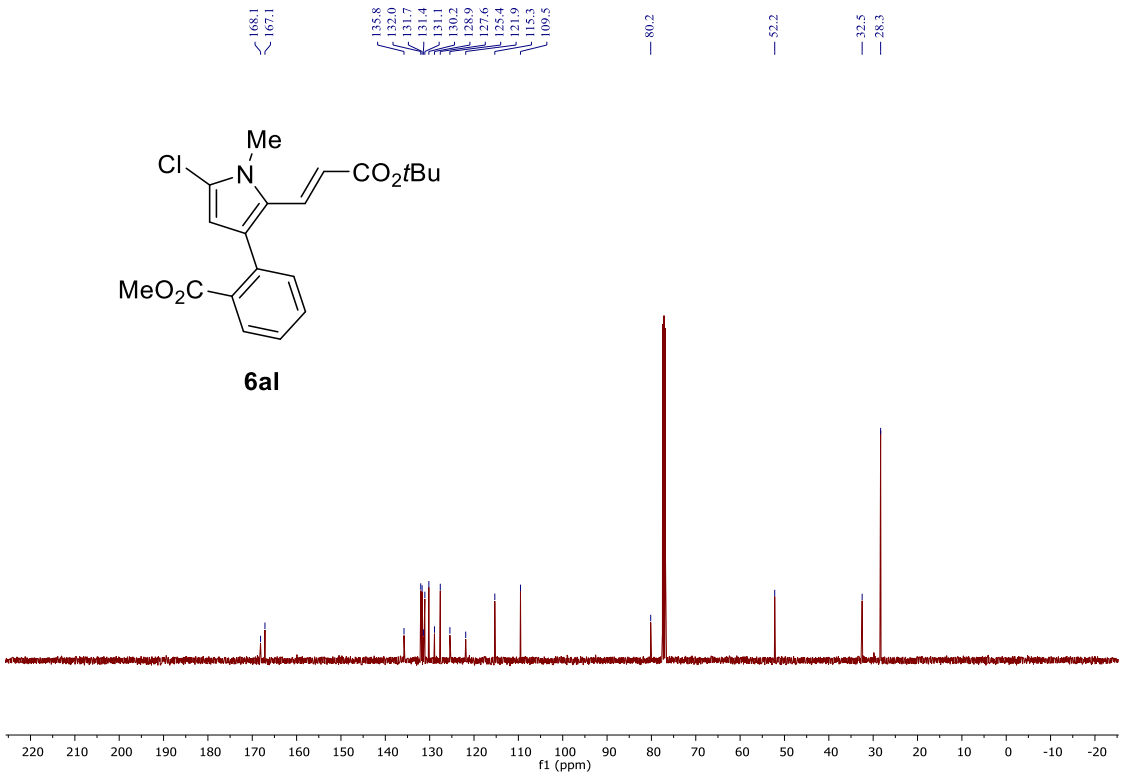

Figure 7.88. ^{1}H NMR Spectrum of 6am

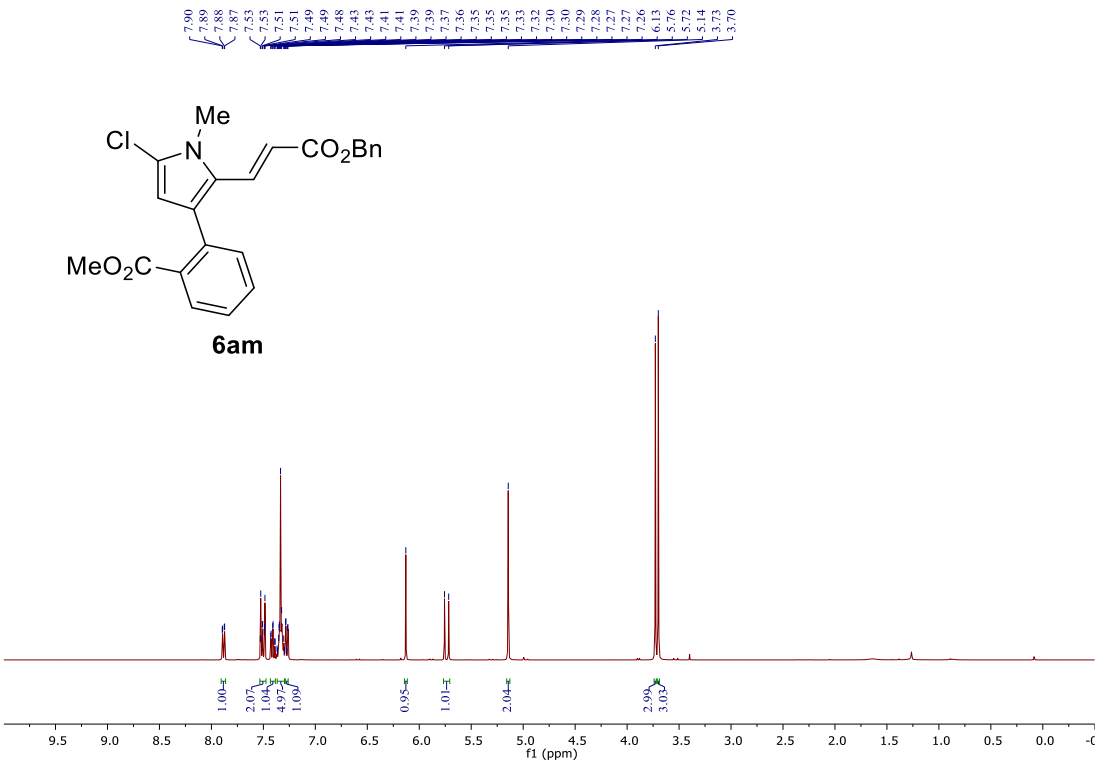

Figure 7.89. ^{13}C NMR Spectrum of 6am

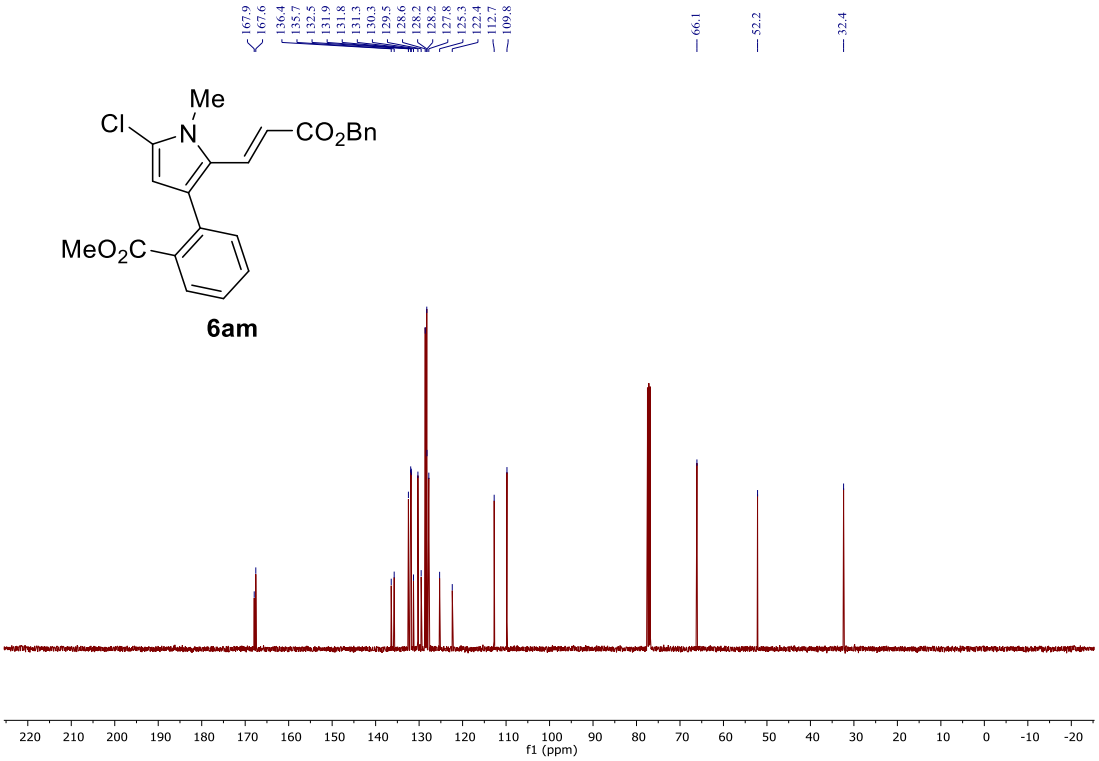

Figure 7.90. ^{1}H NMR Spectrum of 6ao

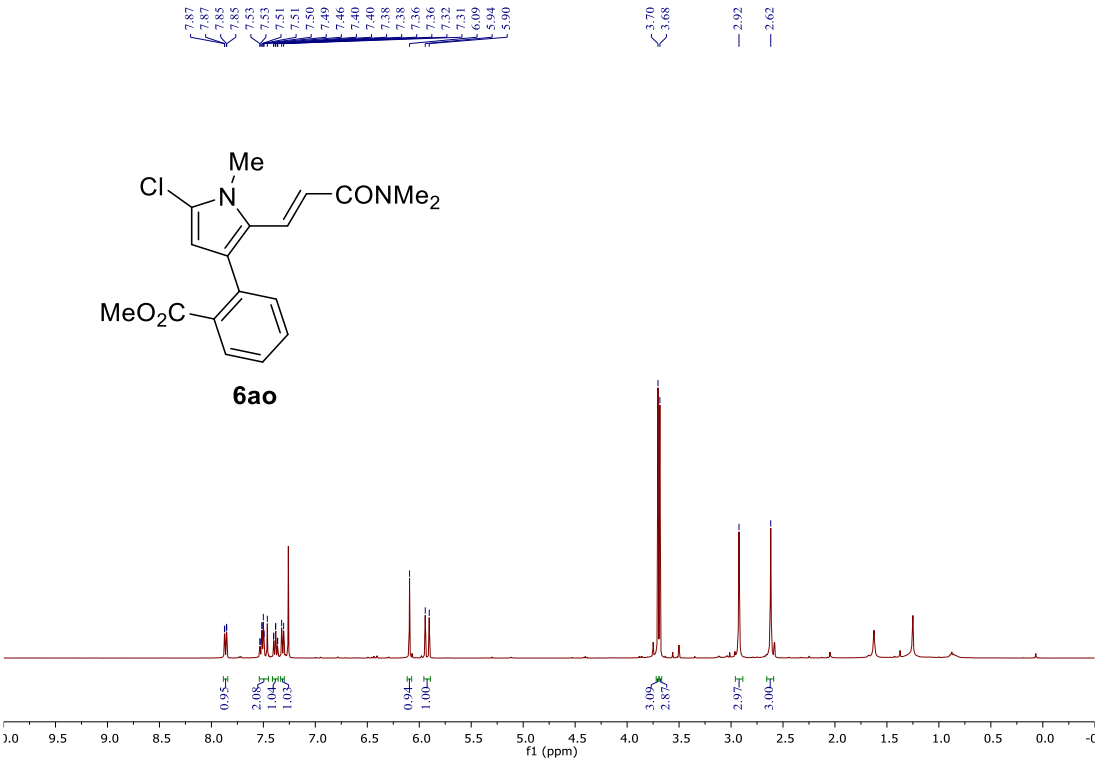

Figure 7.91. ^{13}C NMR Spectrum of 6ao

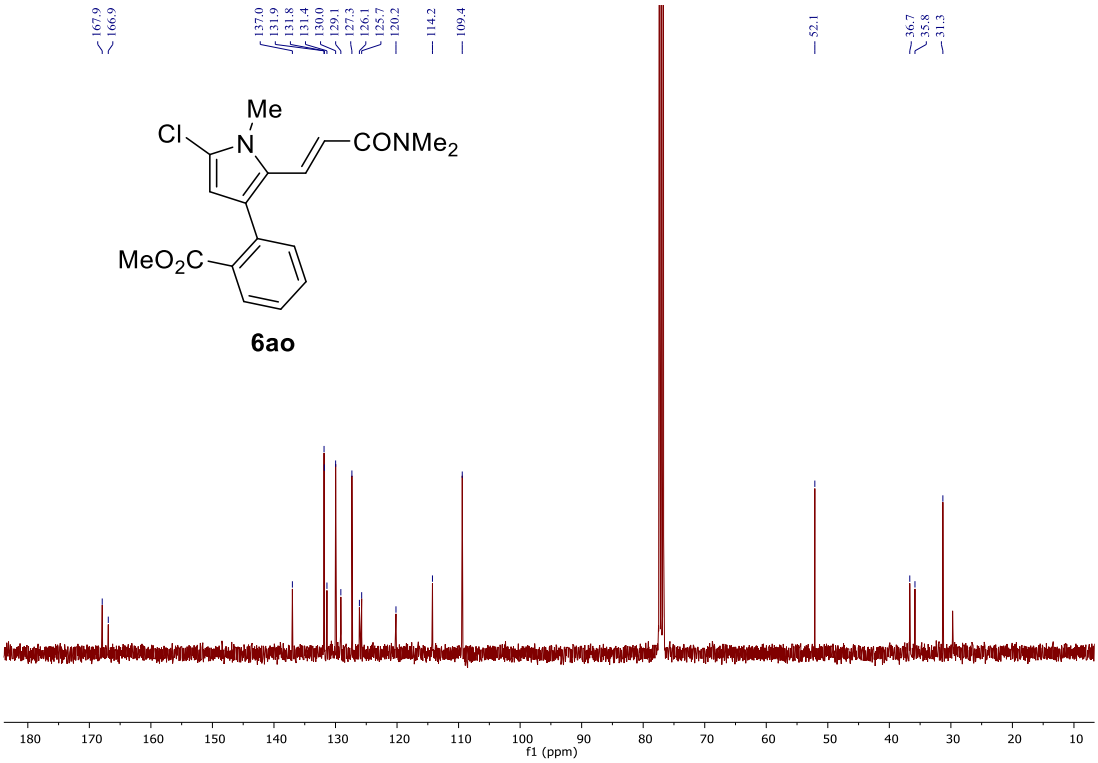

Figure 7.92. ^{1}H NMR Spectrum of 6ap

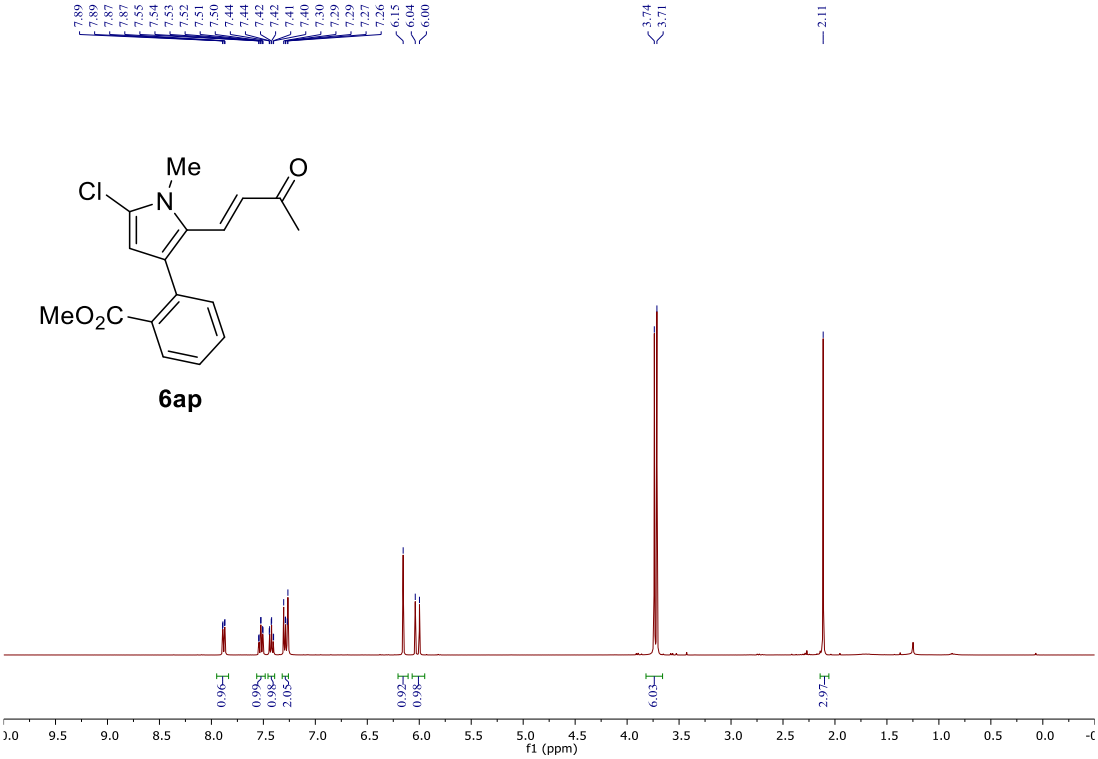

Figure 7.93. ^{13}C NMR Spectrum of 6ap

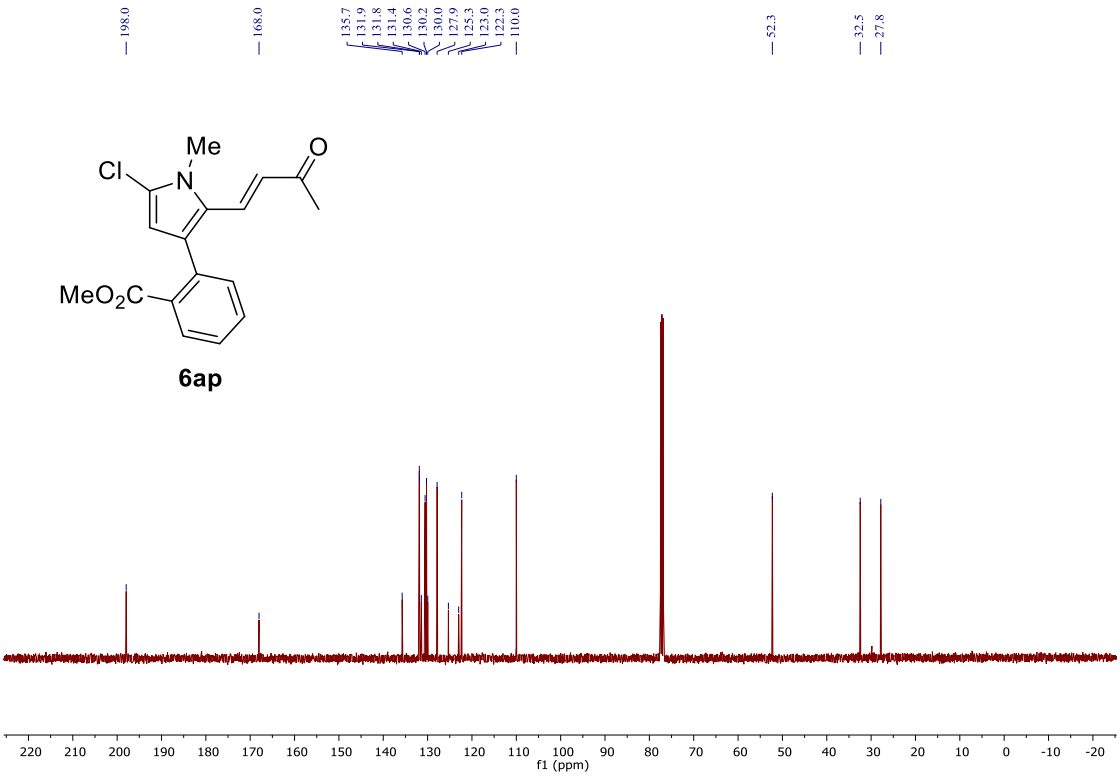

Figure 7.94. ^{1}H NMR Spectrum of 6aq

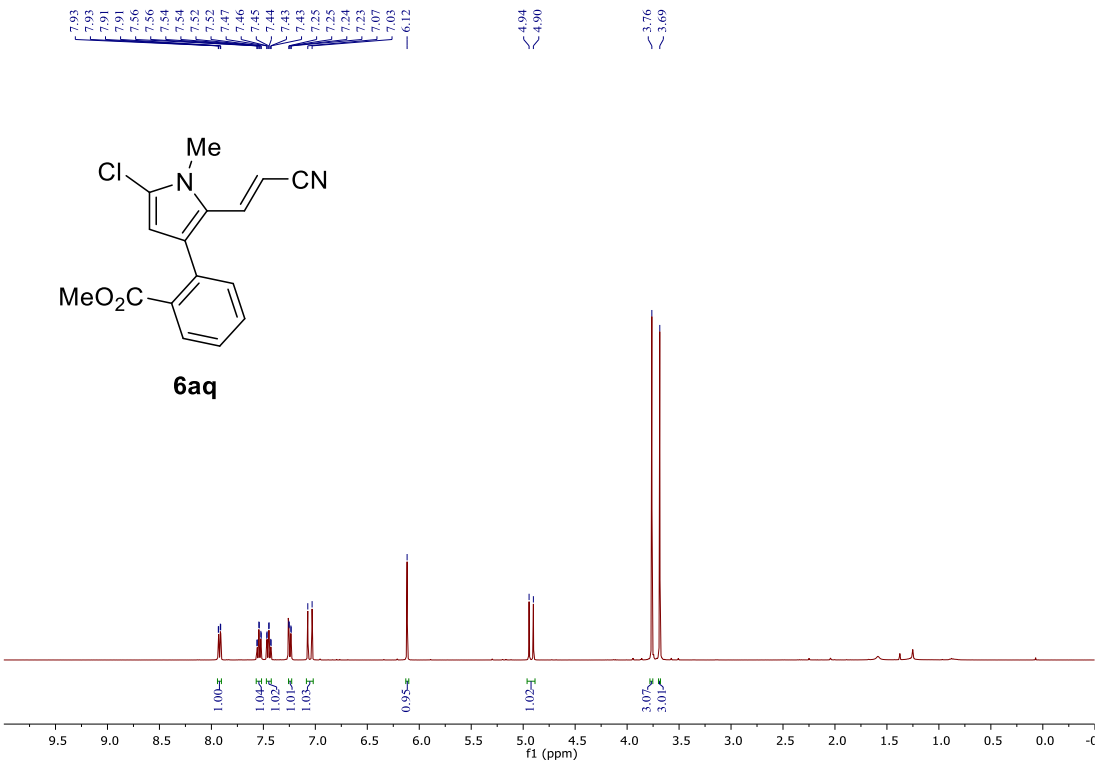

Figure 7.95. ^{13}C NMR Spectrum of 6aq

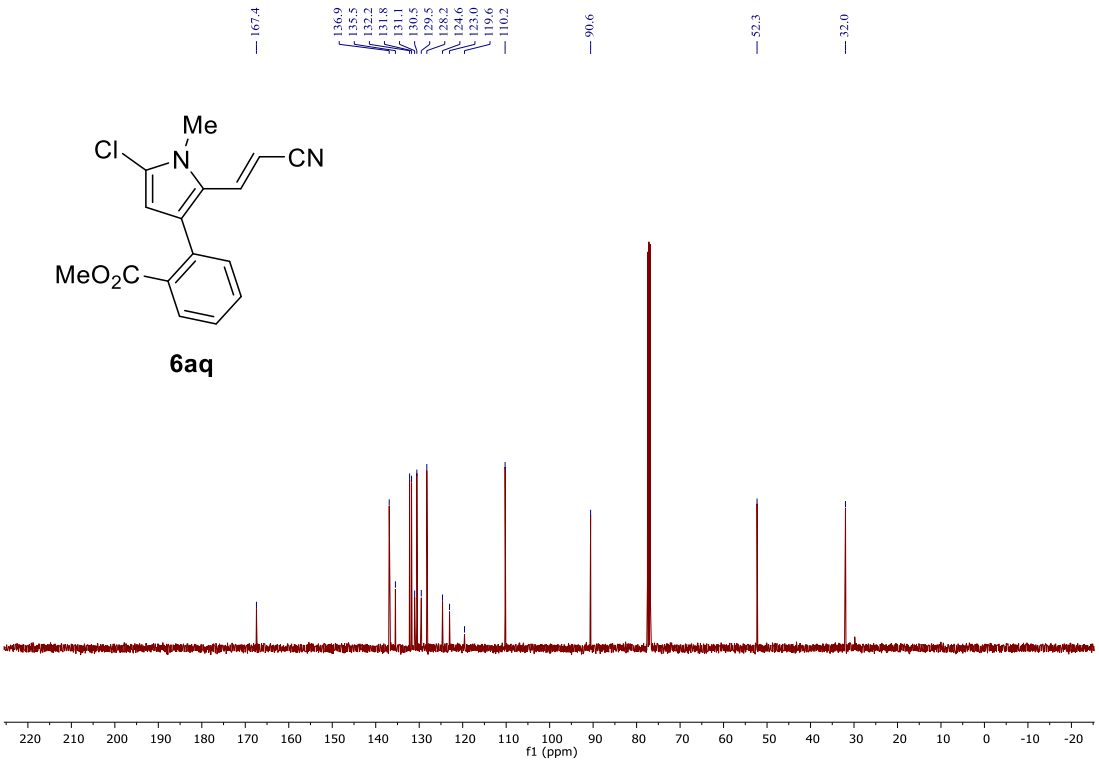

Figure 7.96. ^{1}H NMR Spectrum of 6ar

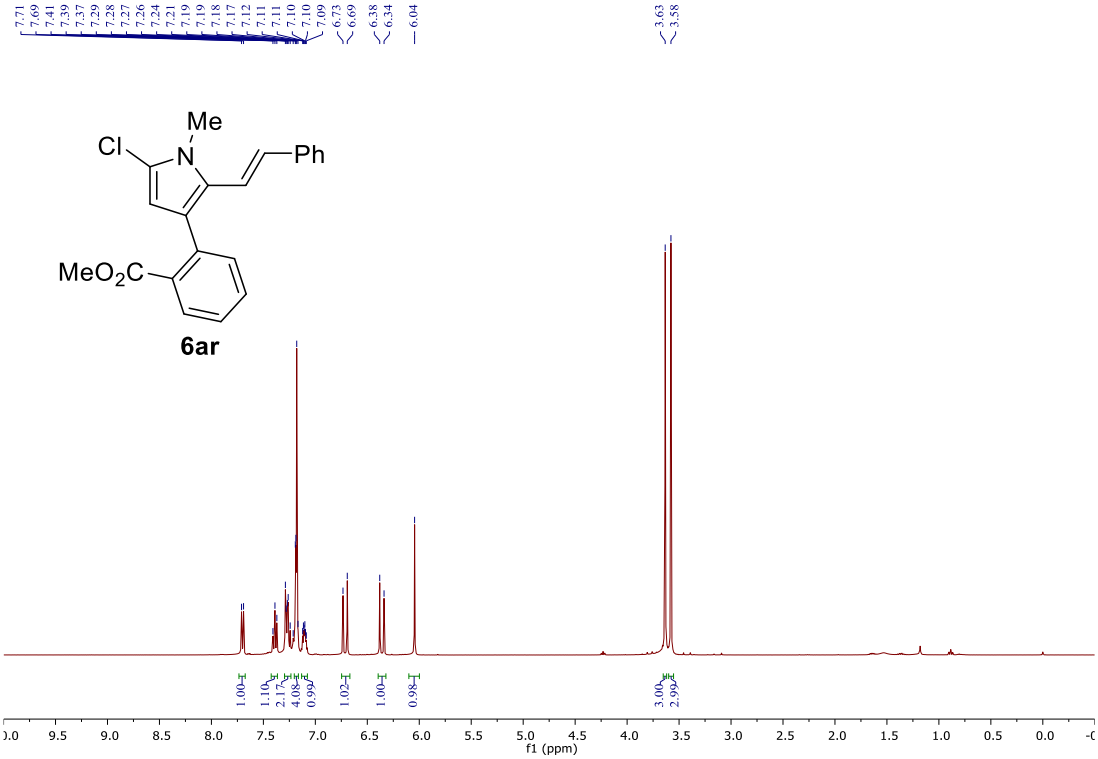

Figure 7.97. ^{13}C NMR Spectrum of 6ar

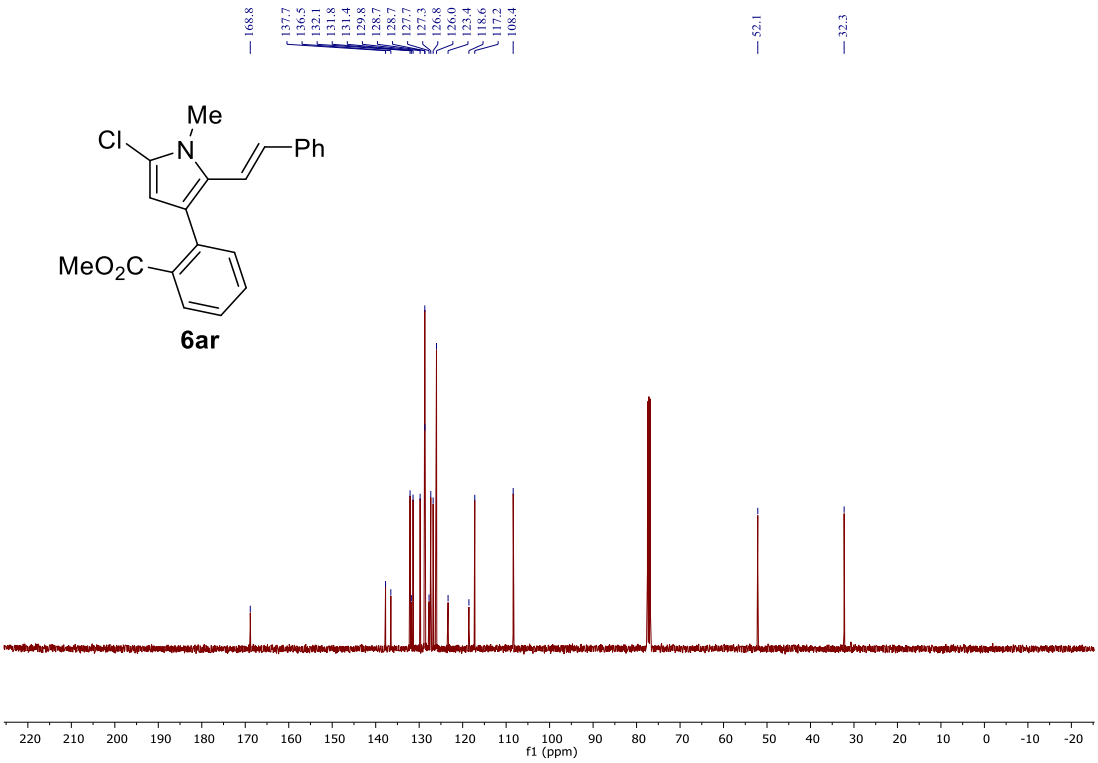

Figure 7.98. ^{1}H NMR Spectrum of 6as

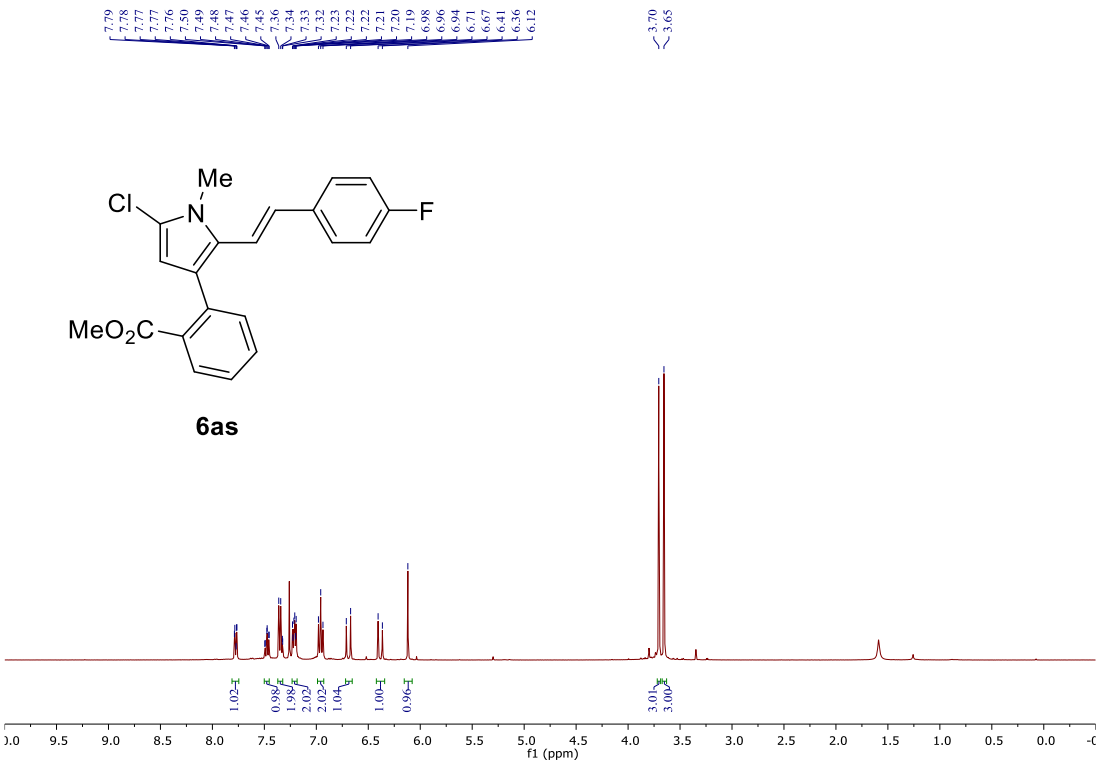

Figure 7.99. ^{13}C NMR Spectrum of 6as

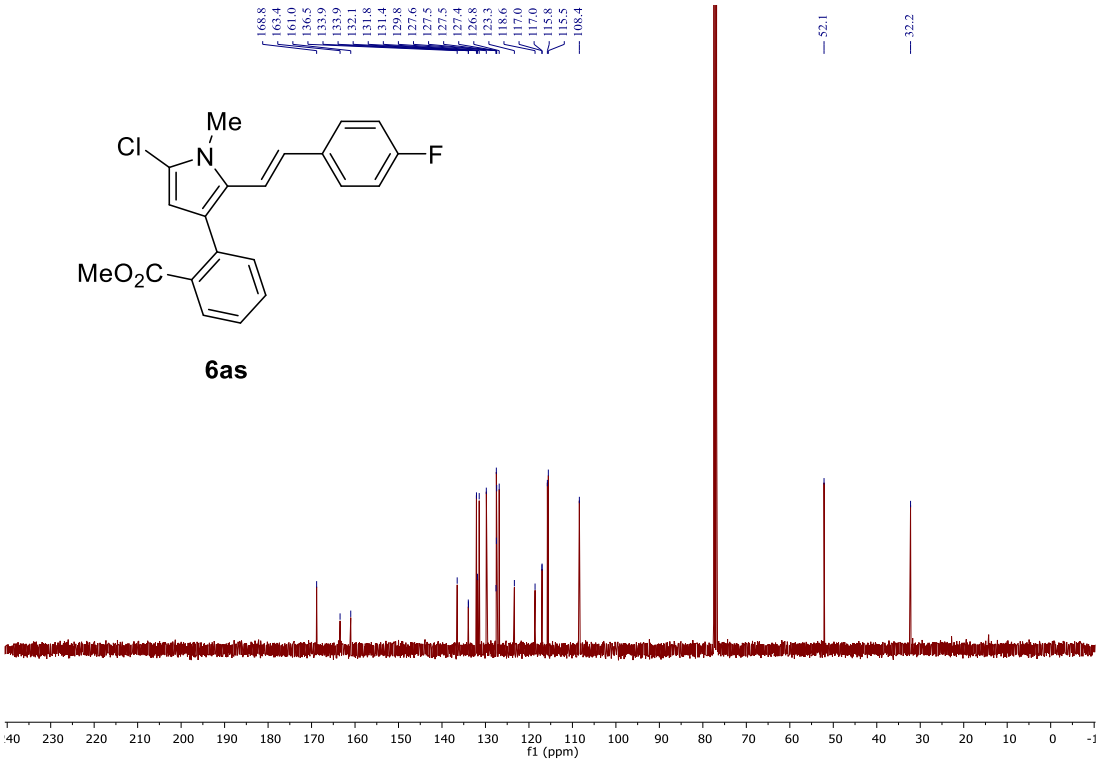

Figure 7.100. ^{19}F NMR Spectrum of 6as

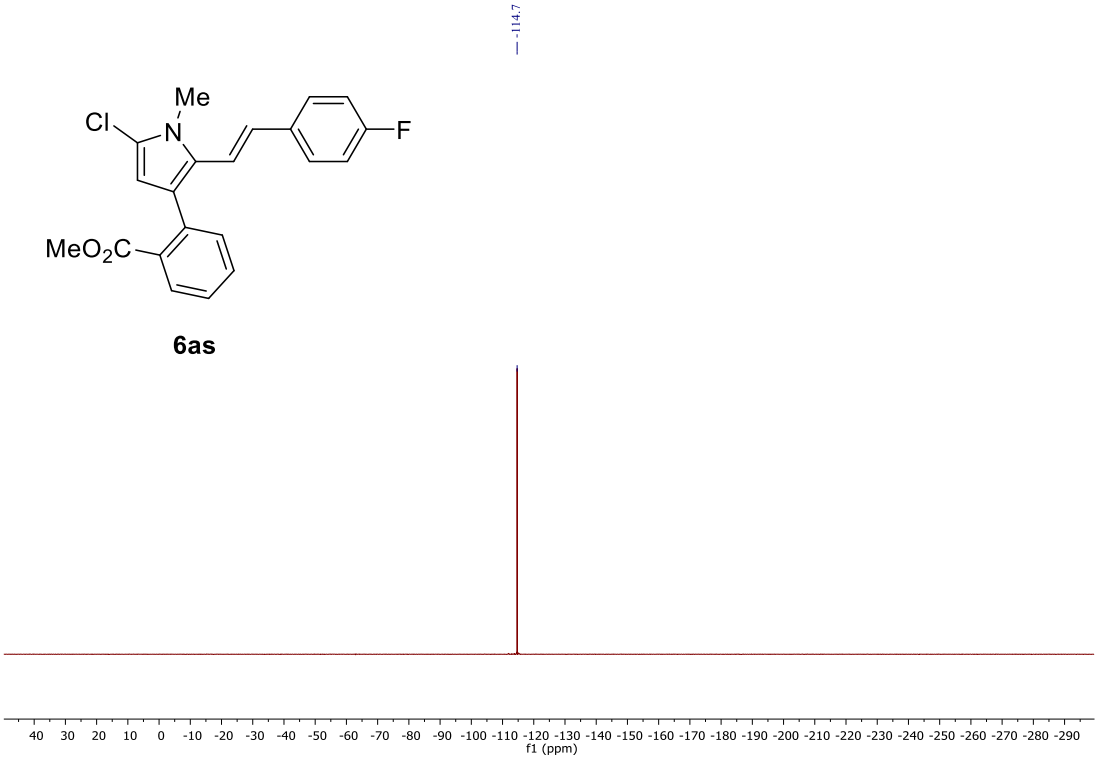

Figure 7.101. ^{1}H NMR Spectrum of 4a

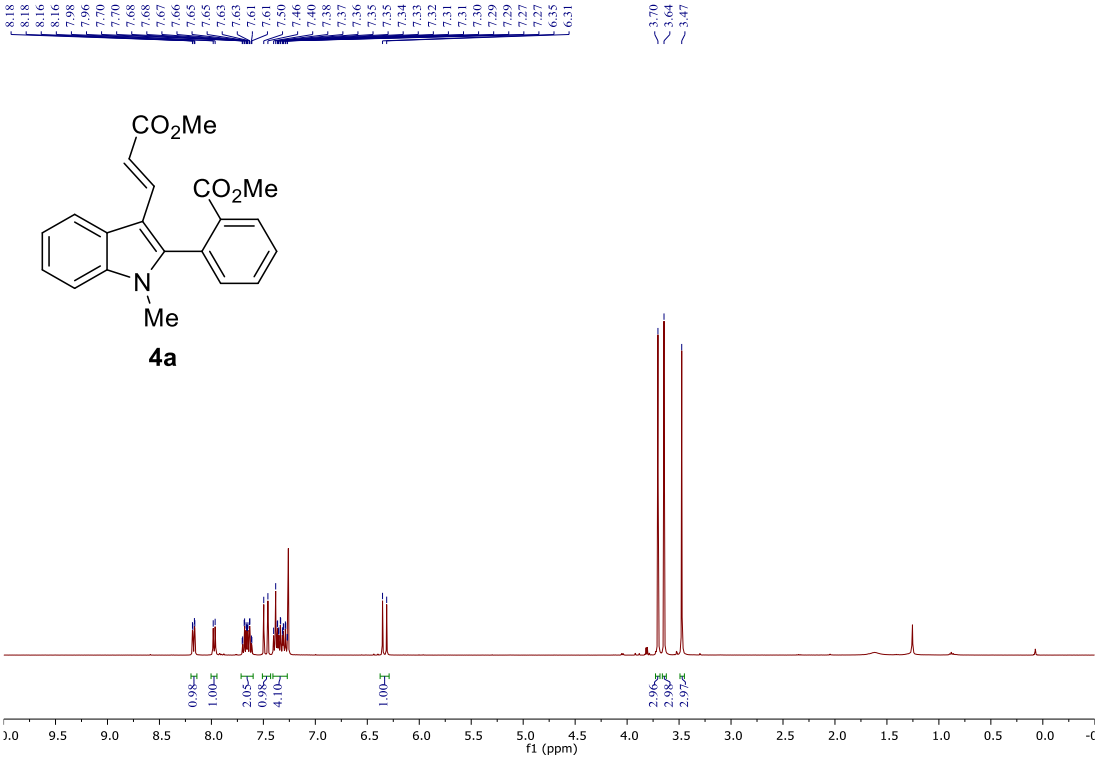

Figure 7.102. ^{13}C NMR Spectrum of 4a

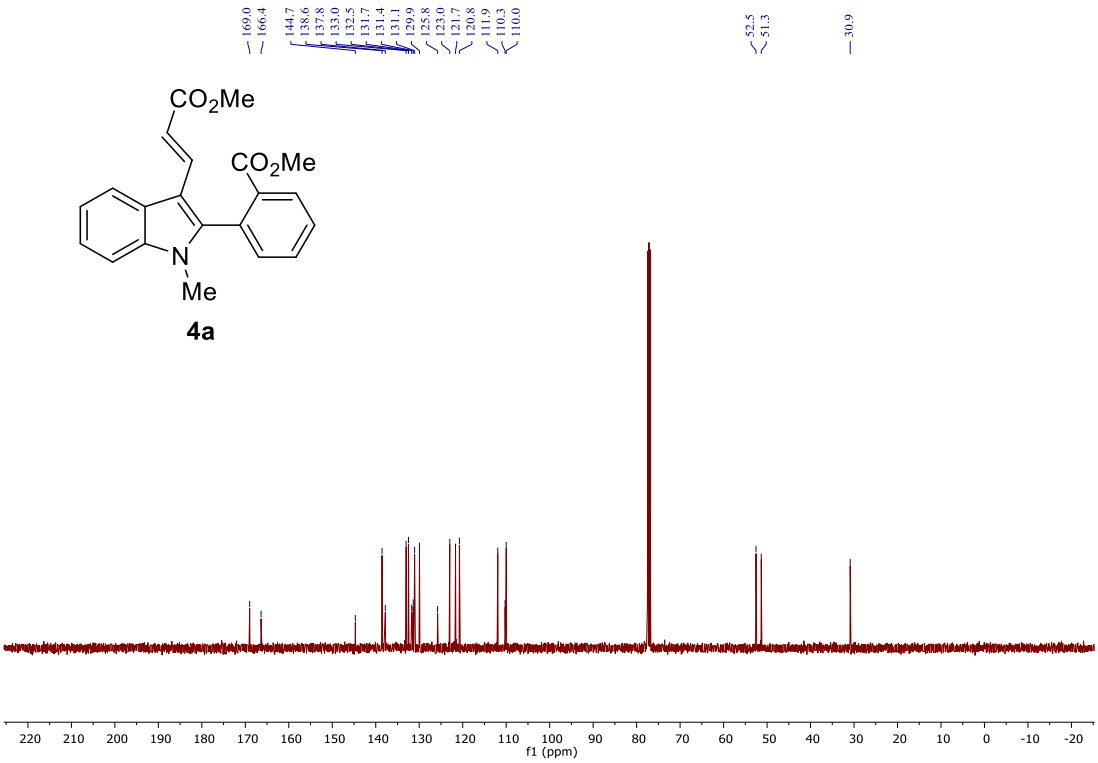

Figure 7.103. ^{1}H NMR Spectrum of 4b

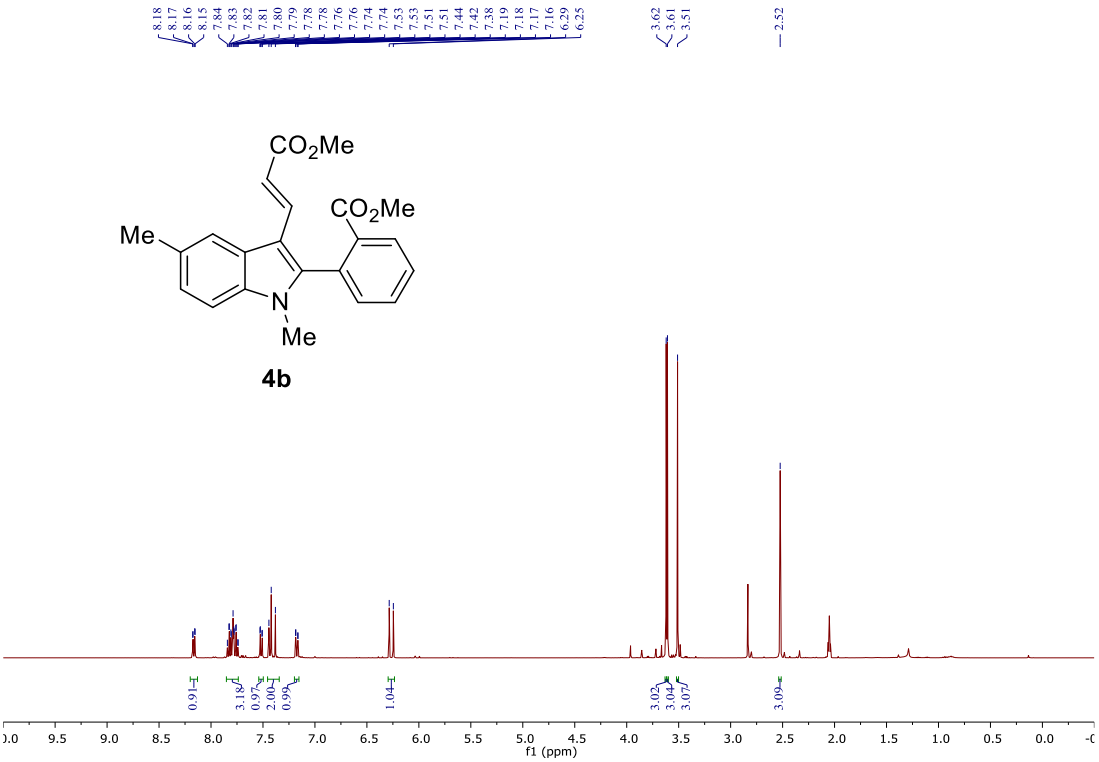

Figure 7.104. ^{13}C NMR Spectrum of 4b

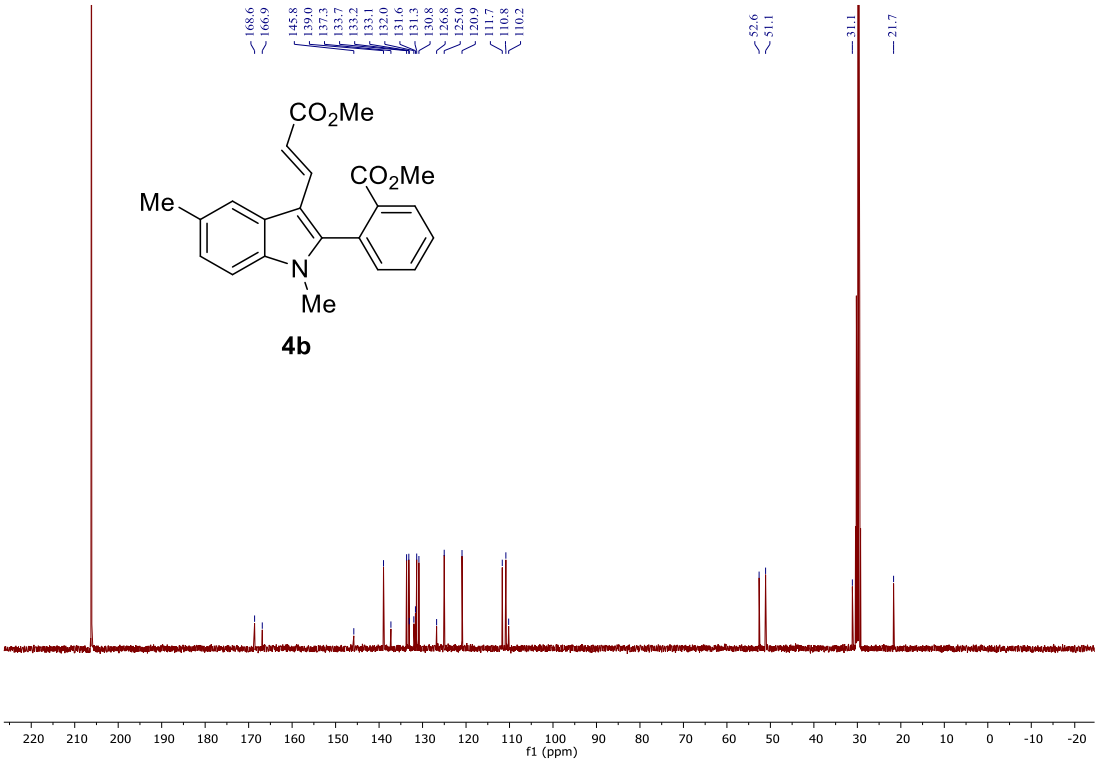

Figure 7.105. ^{1}H NMR Spectrum of 4c

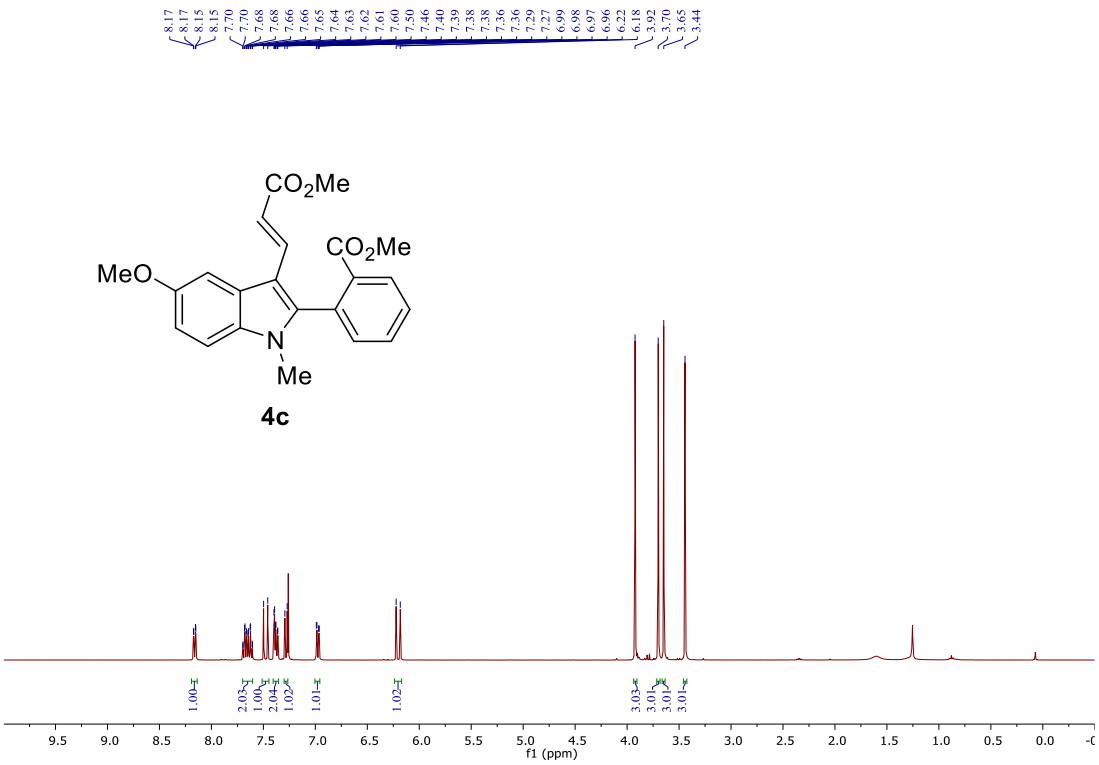

Figure 7.106. ^{13}C NMR Spectrum of 4c

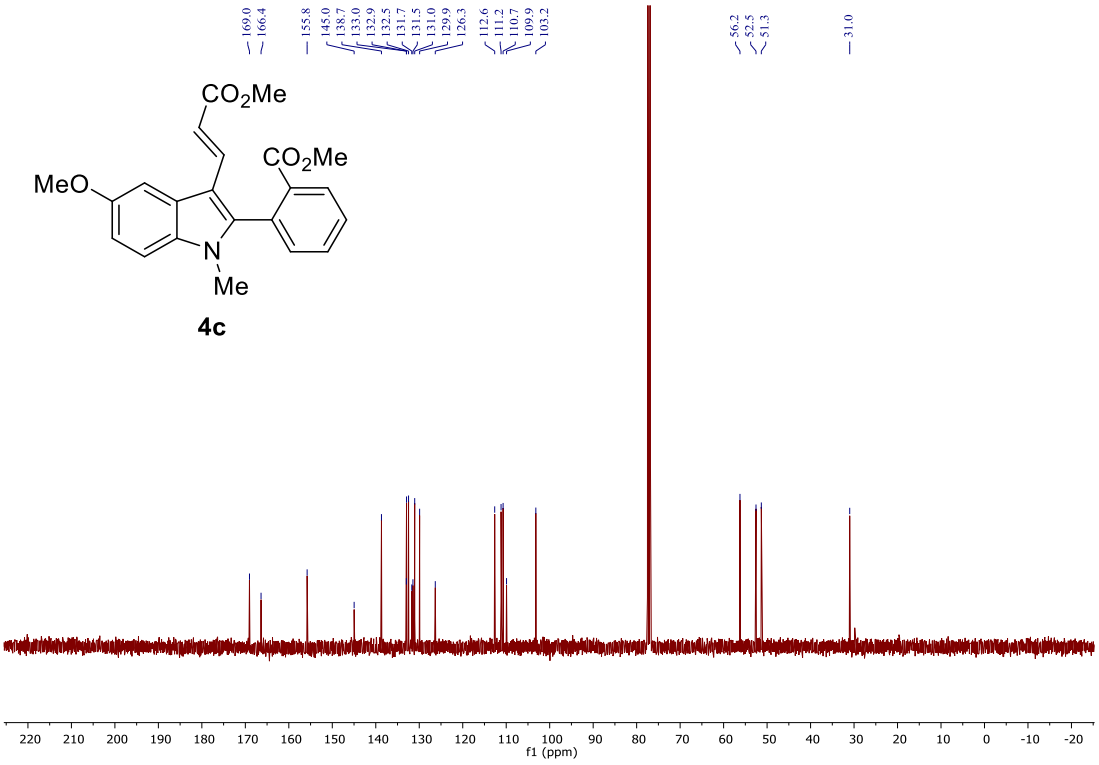

Figure 7.107. ^{1}H NMR Spectrum of 4d

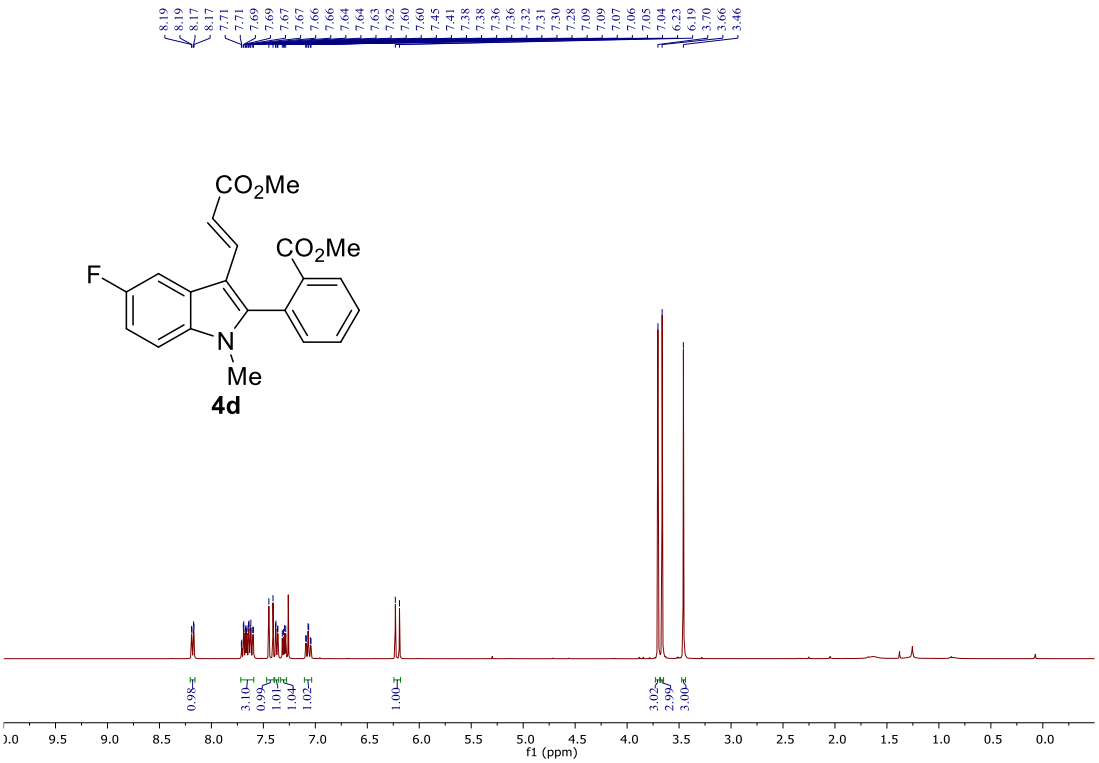

Figure 7.108. ^{13}C NMR Spectrum of 4d

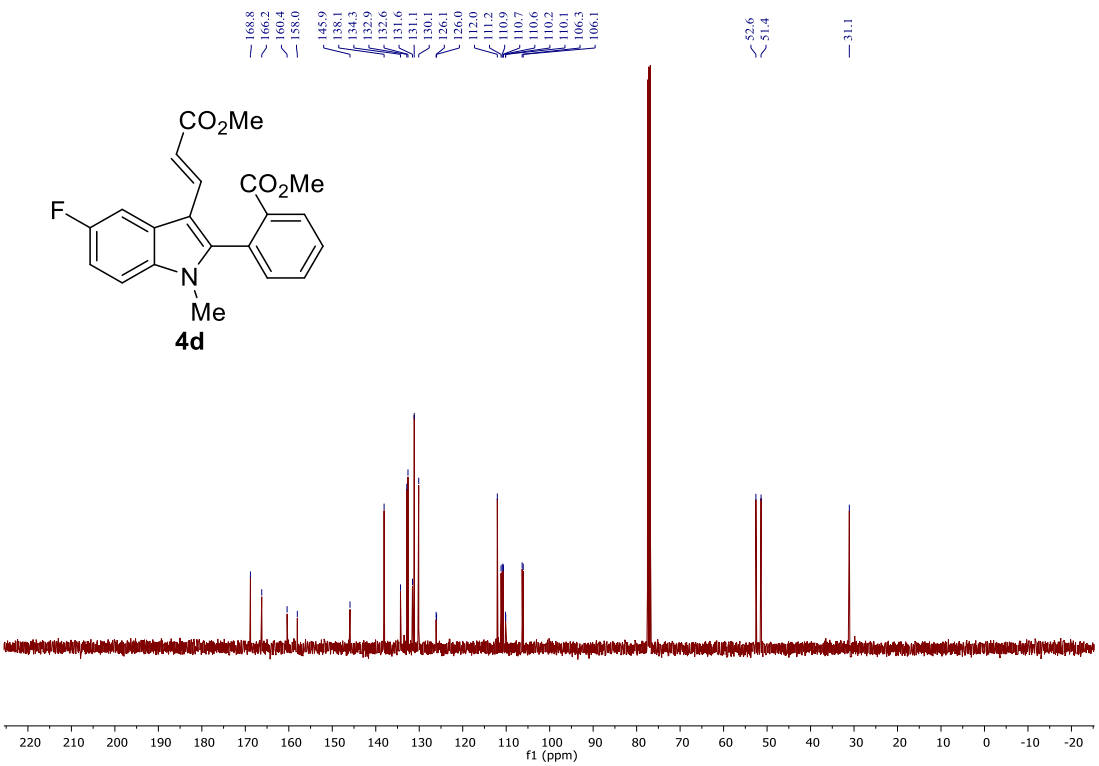

Figure 7.109. ^{19}F NMR Spectrum of 4d

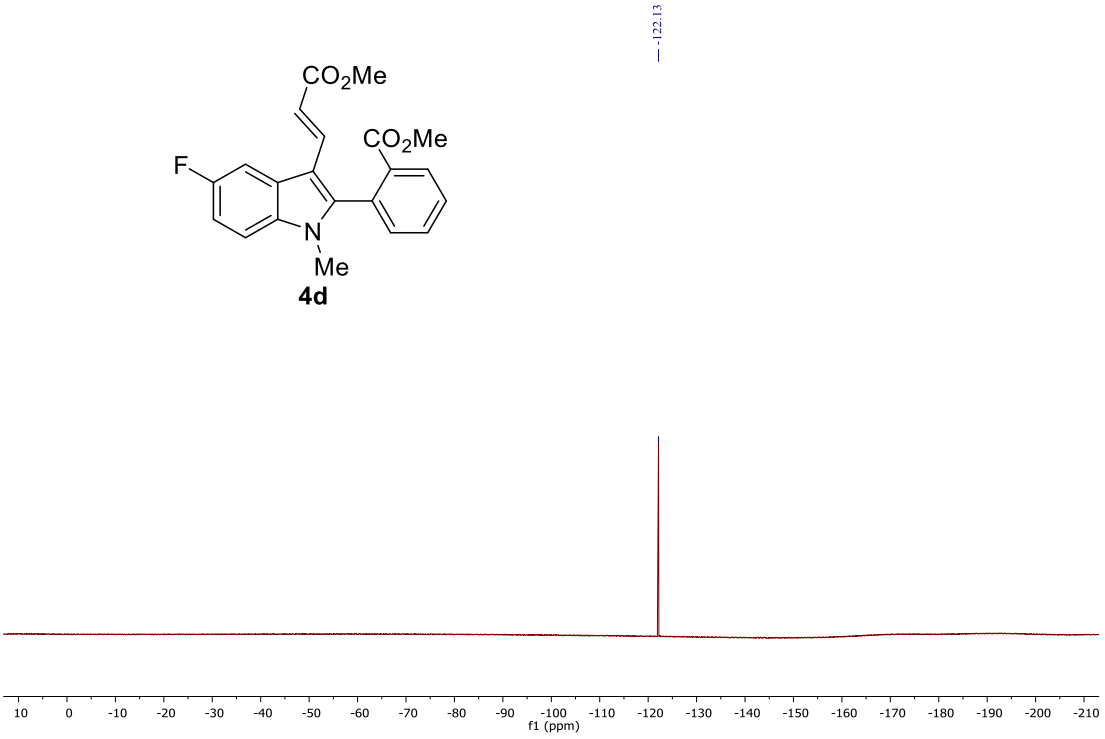

Figure 7.110. ^{1}H NMR Spectrum of 4f

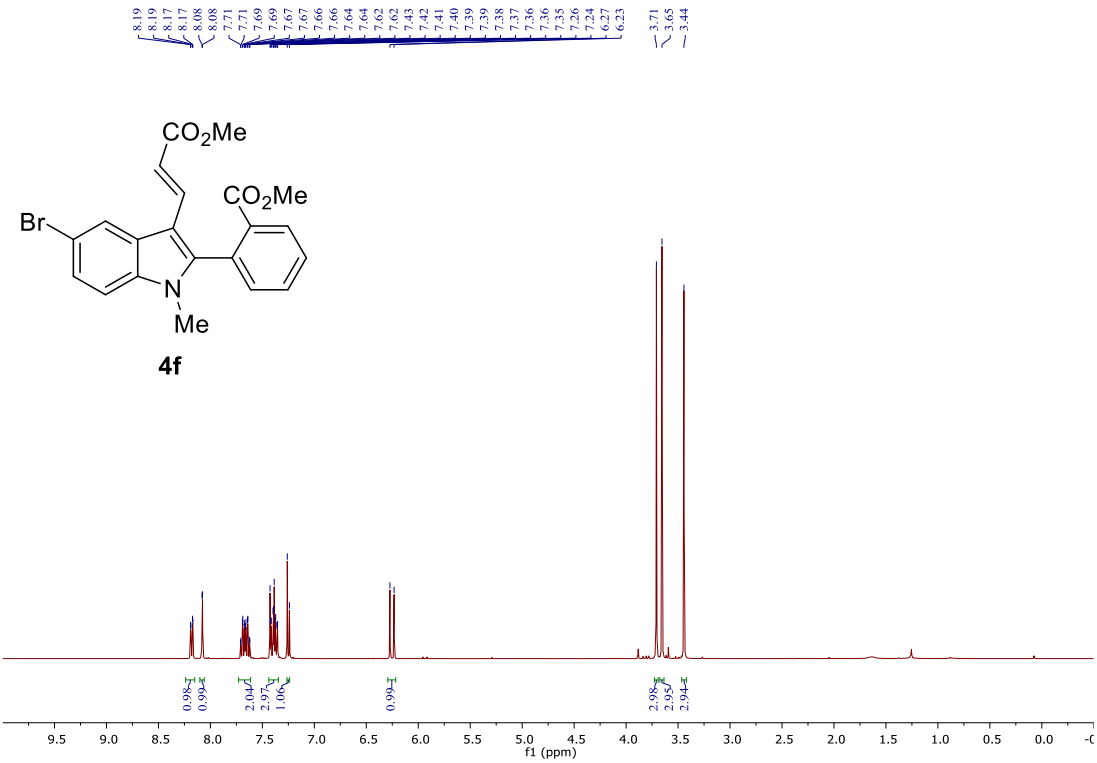

Figure 7.111. ^{13}C NMR Spectrum of 4f

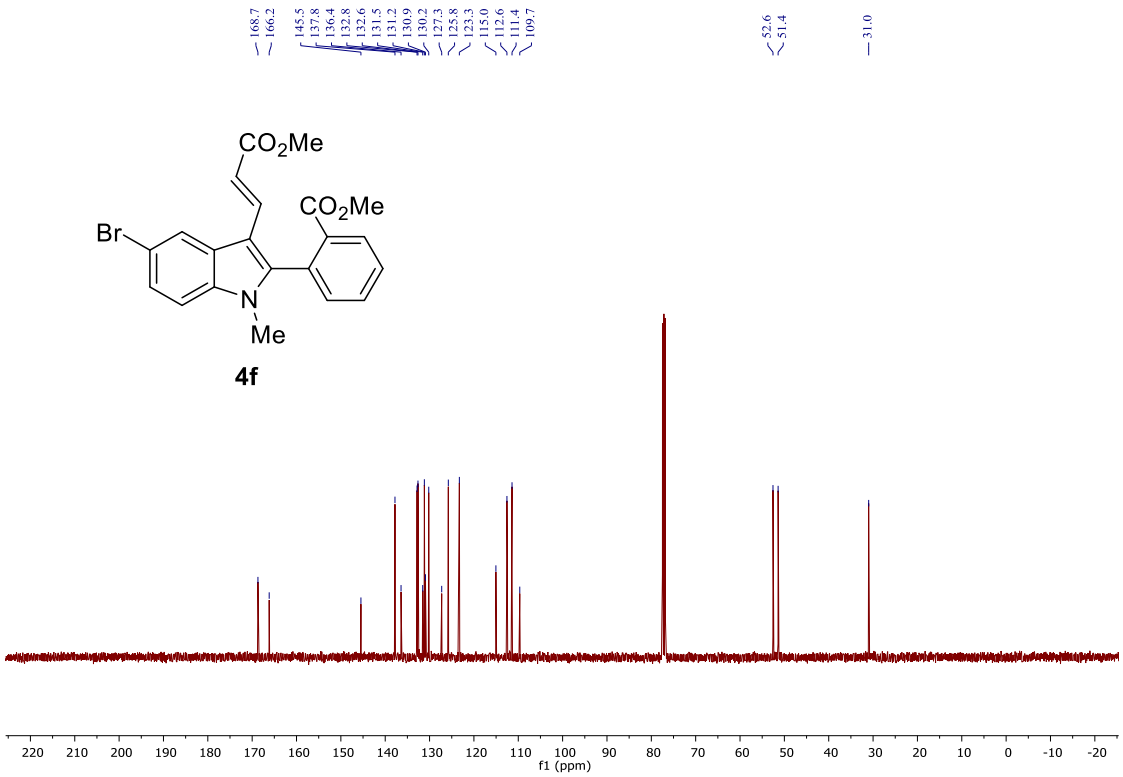

Figure 7.112. ^{1}H NMR Spectrum of 4e

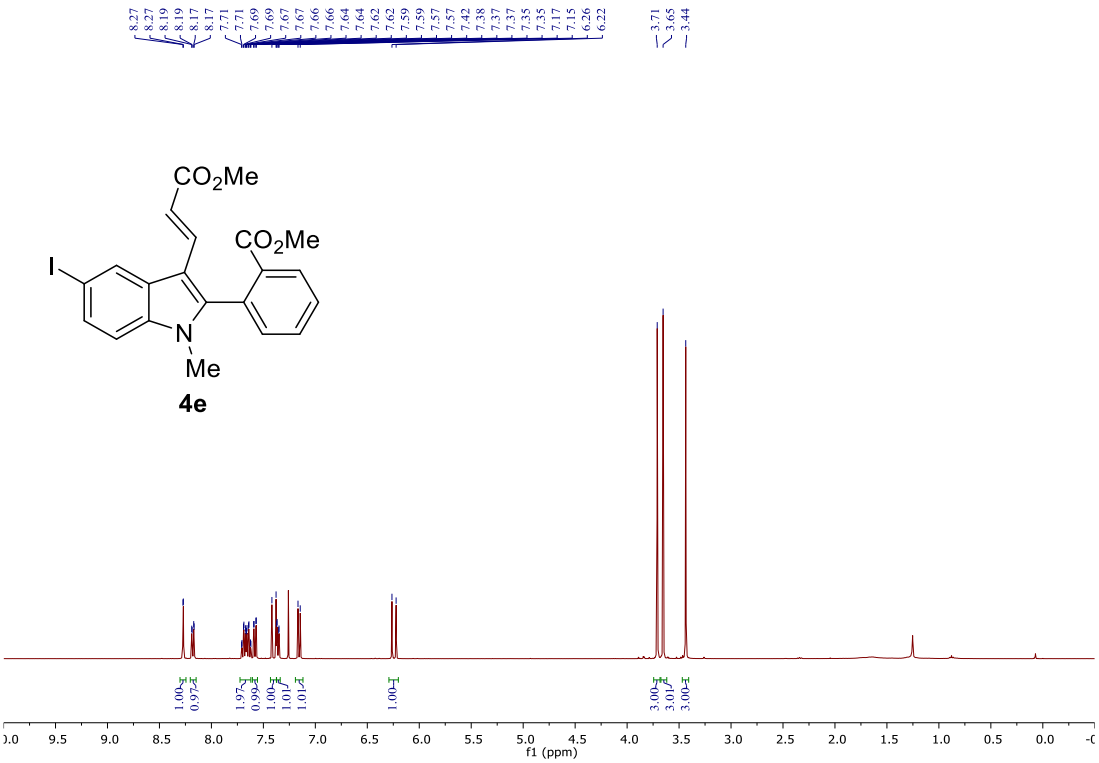

Figure 7.113. ^{13}C NMR Spectrum of 4e

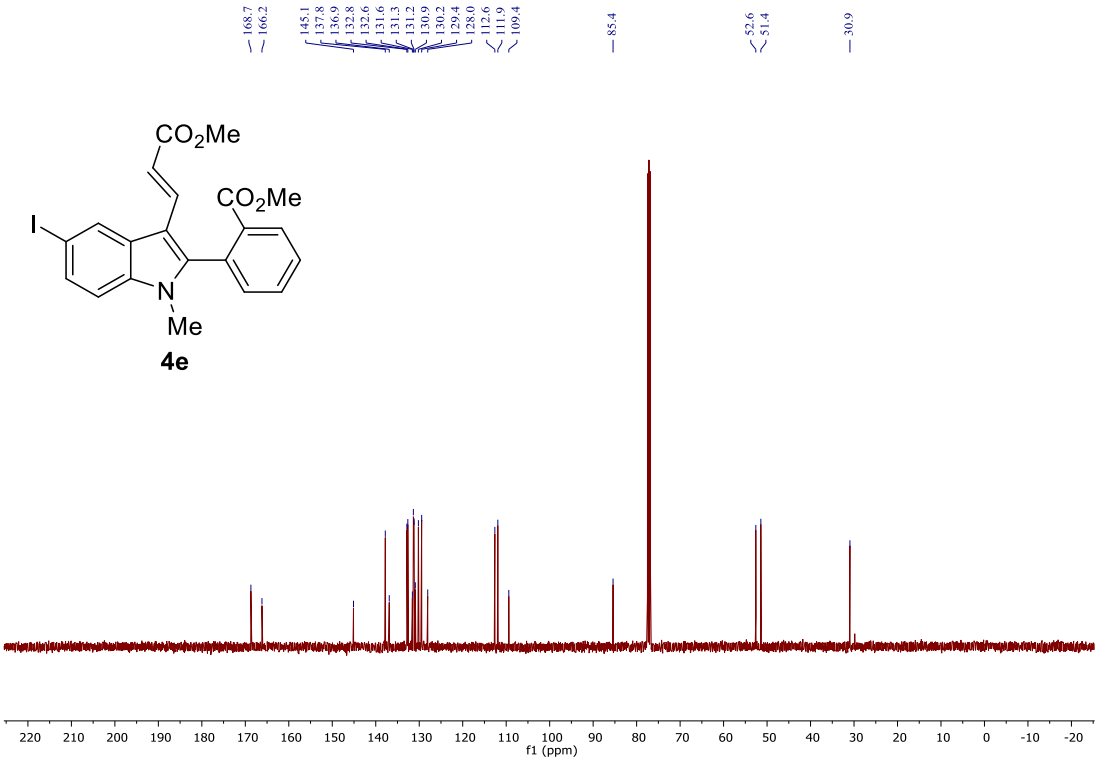

Figure 7.114. ^{1}H NMR Spectrum of 4g

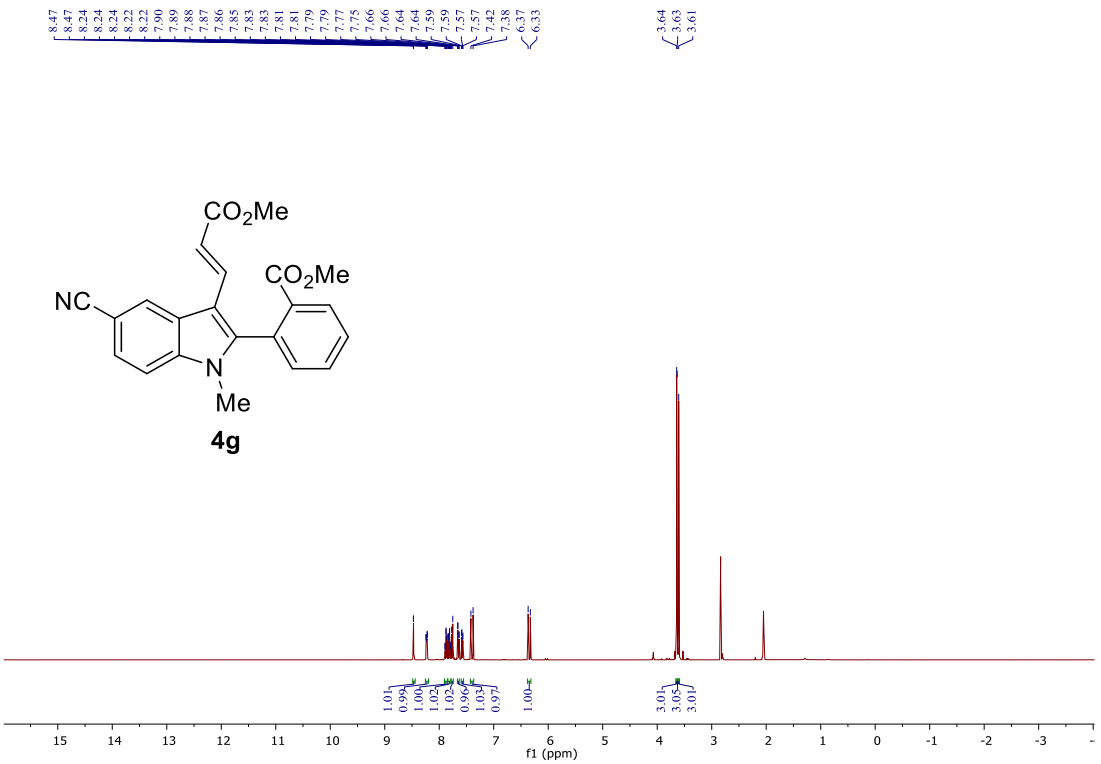

Figure 7.115. ^{13}C NMR Spectrum of 4g

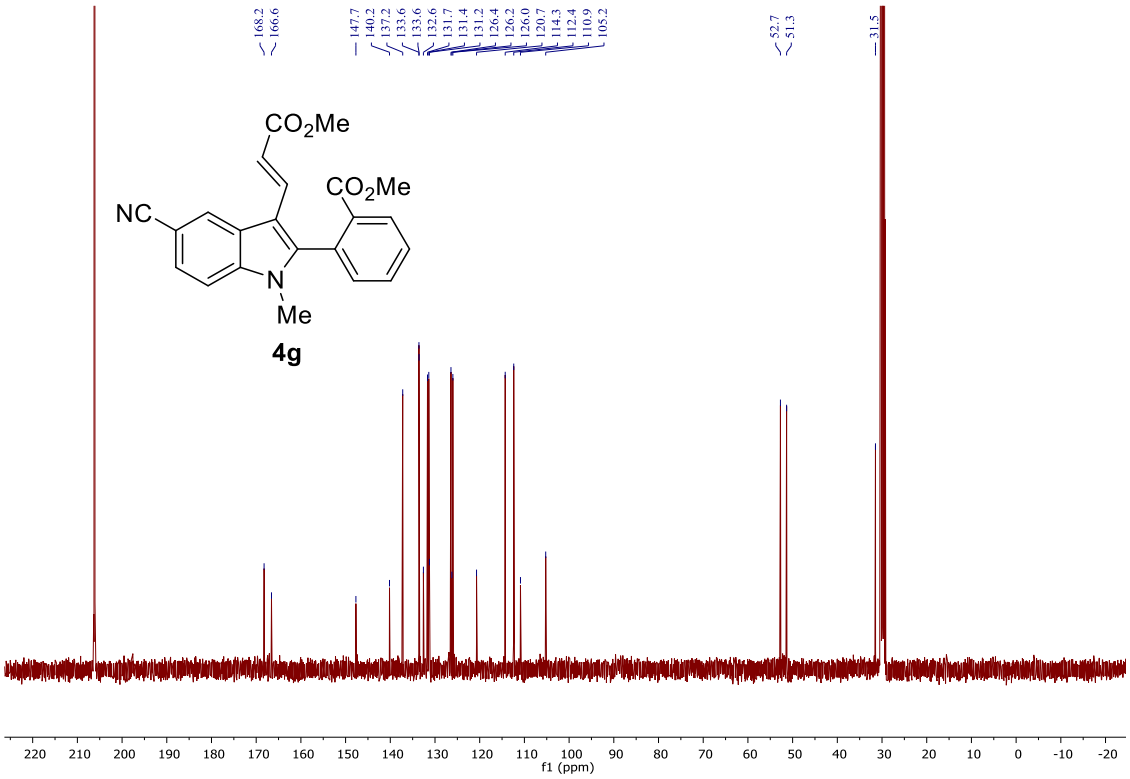

Figure 7.116. ^{1}H NMR Spectrum of 4h

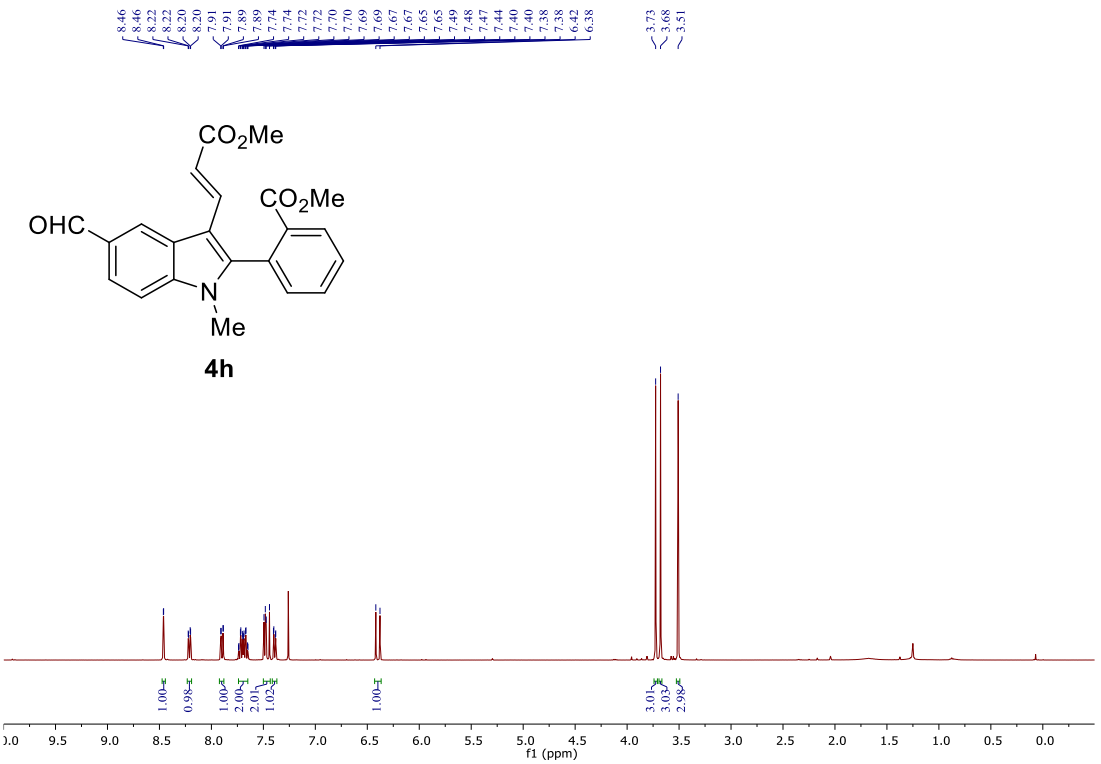

Figure 7.117. ^{13}C NMR Spectrum of 4h

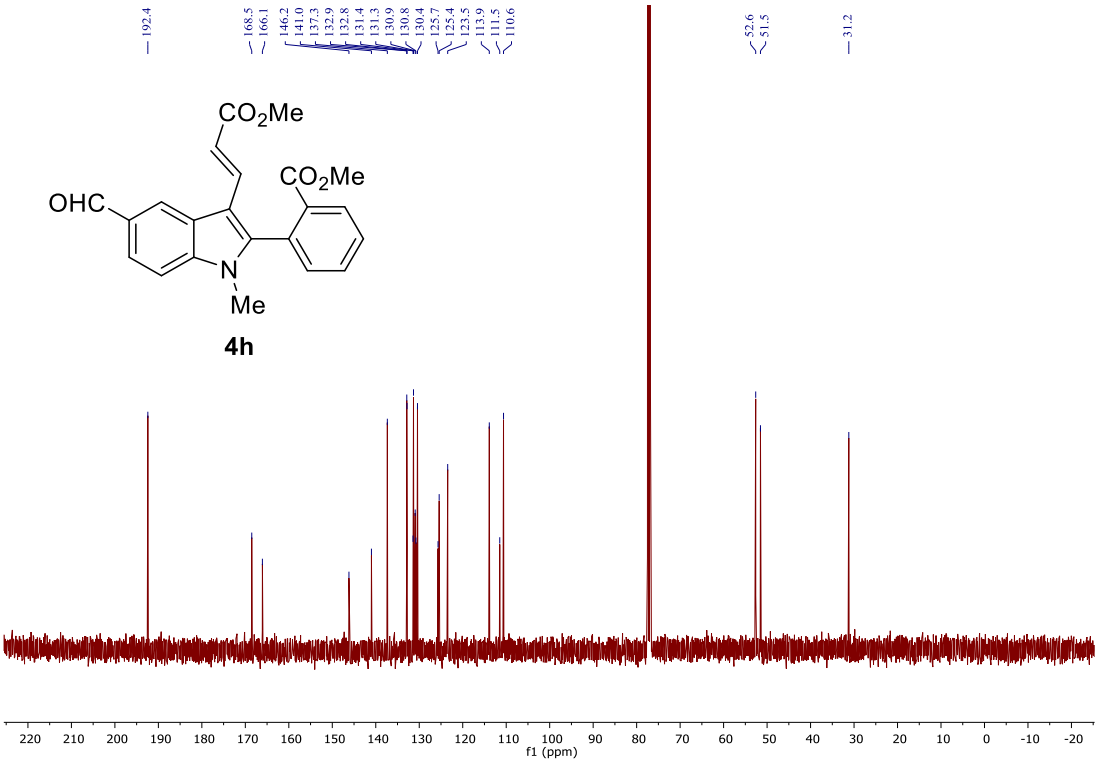

Figure 7.118. ^{1}H NMR Spectrum of 4i

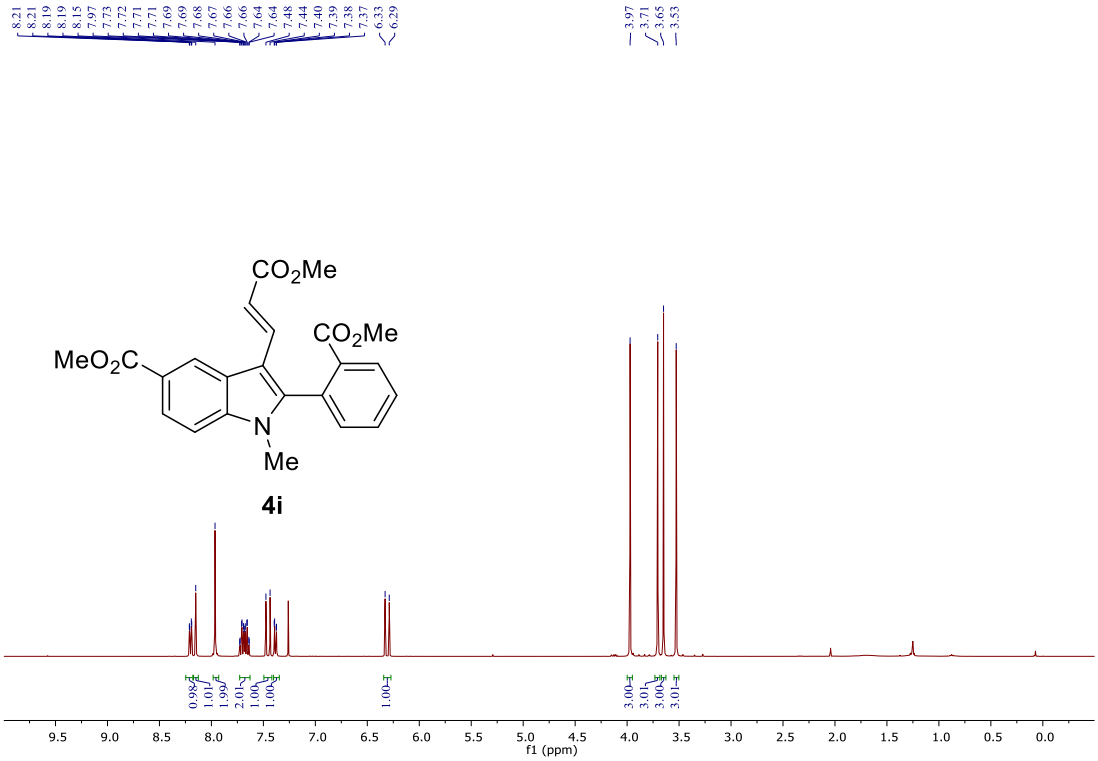

Figure 7.119. ^{13}C NMR Spectrum of 4i

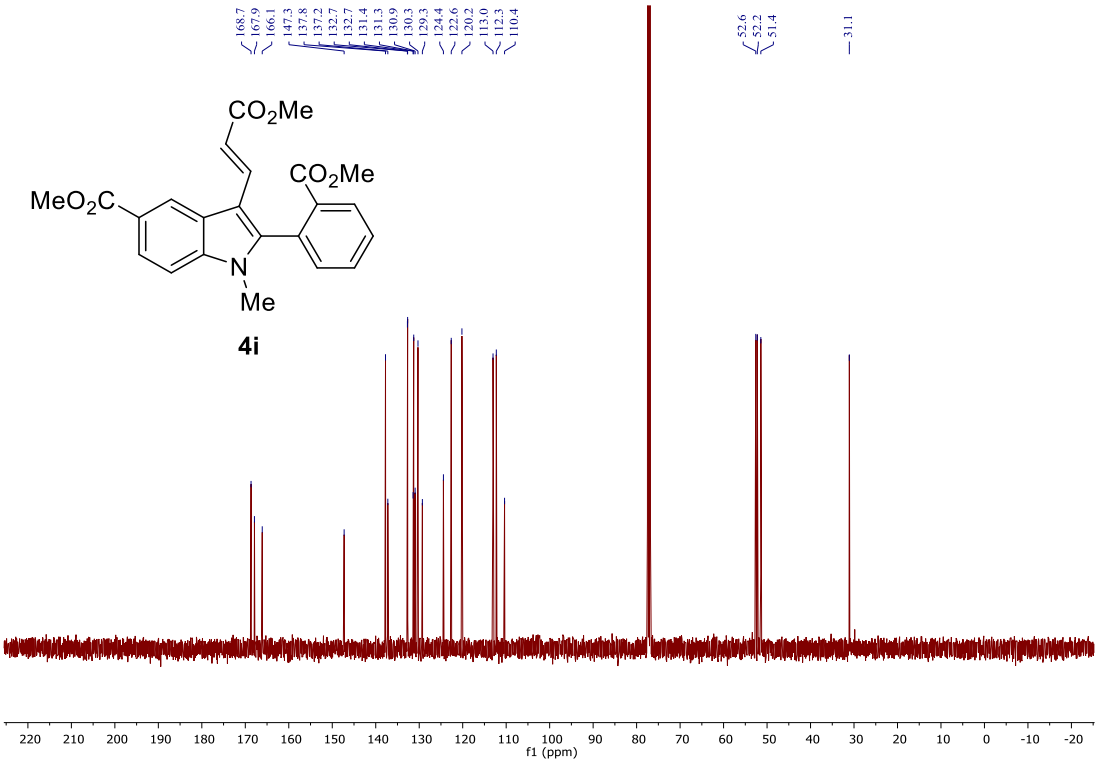

Figure 7.120. ^{1}H NMR Spectrum of 4j

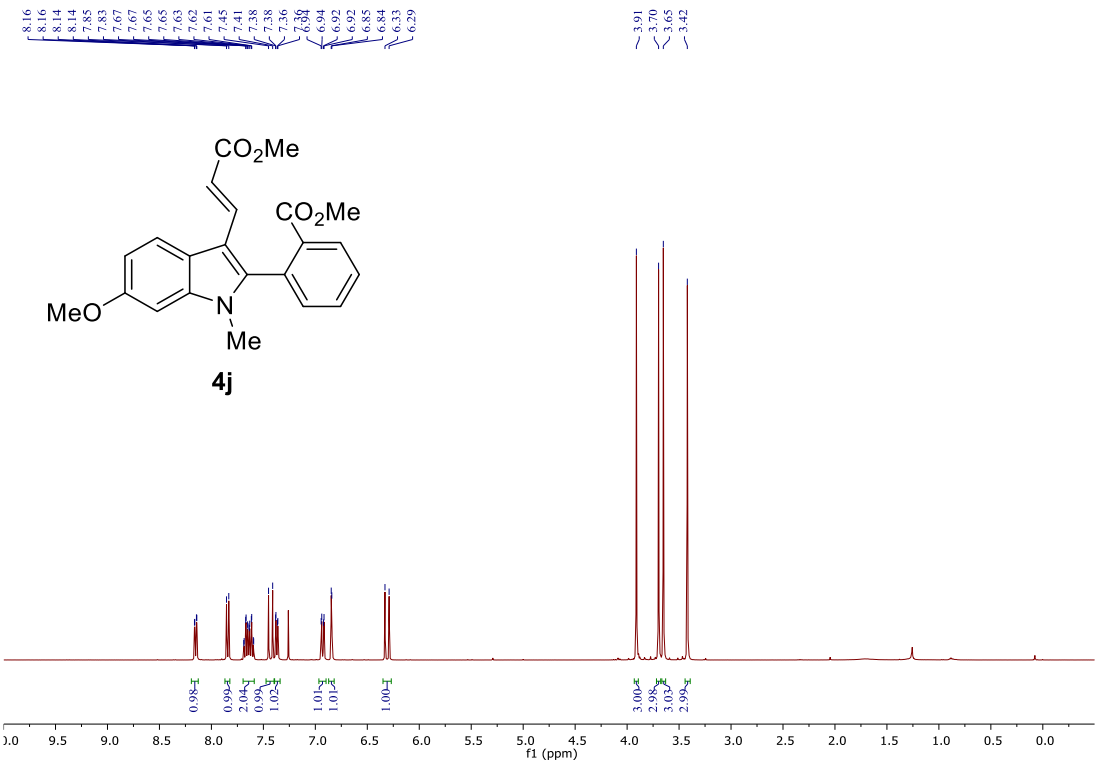

Figure 7.121. ^{13}C NMR Spectrum of 4j

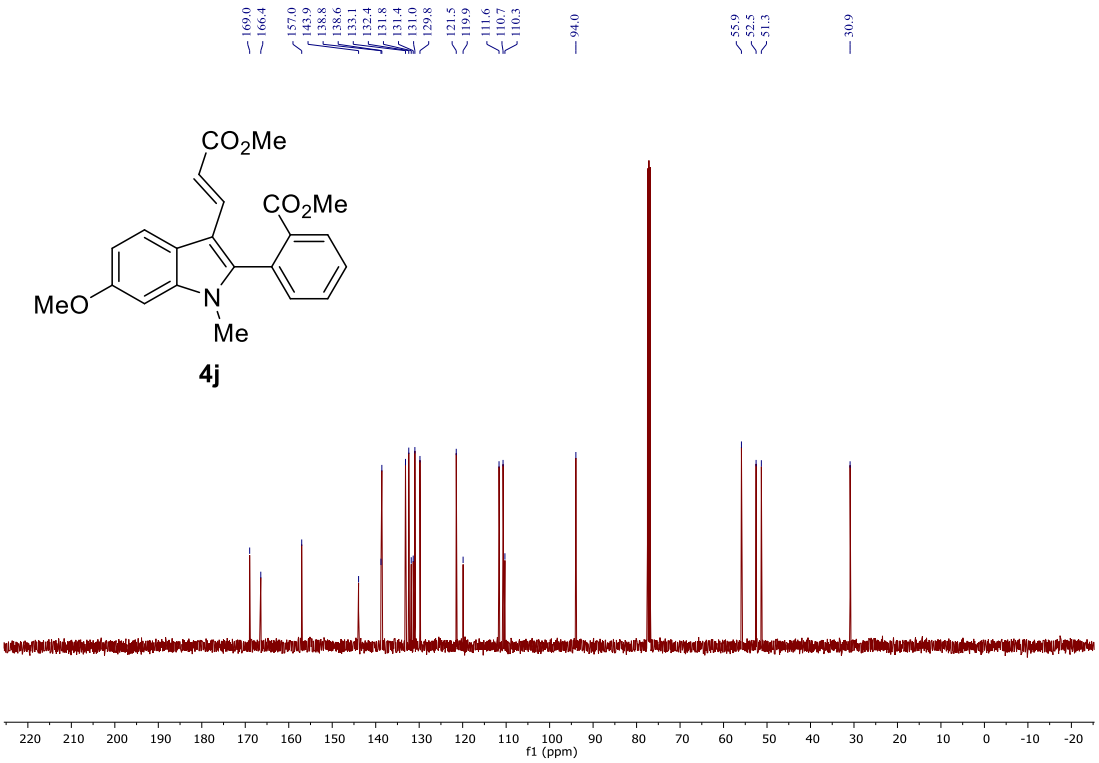

Figure 7.122. ^{1}H NMR Spectrum of 4k

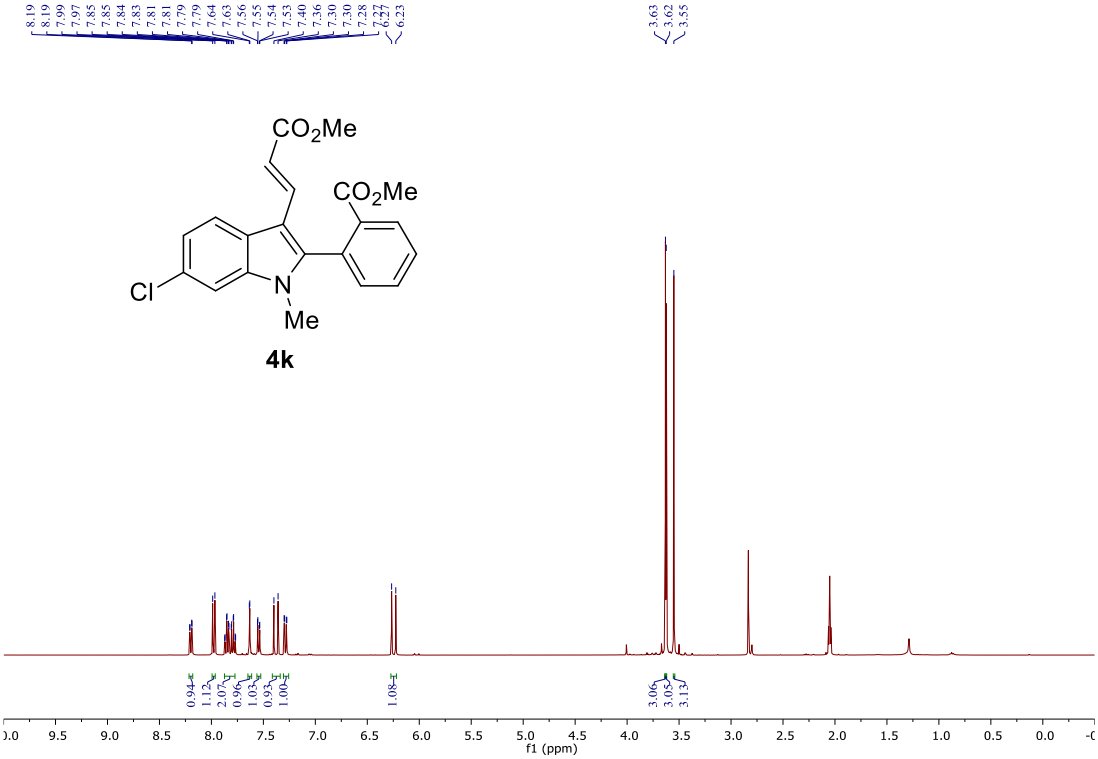

Figure 7.123. ^{13}C NMR Spectrum of 4k

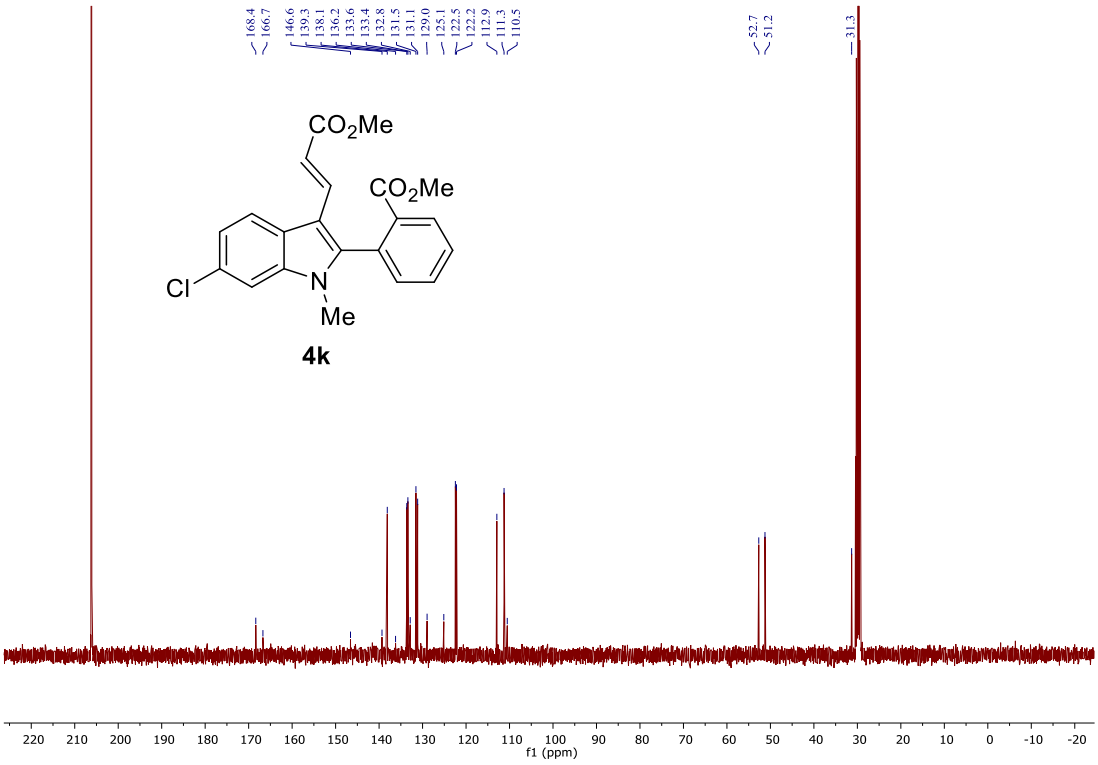

Figure 7.124. ^{1}H NMR Spectrum of 4l

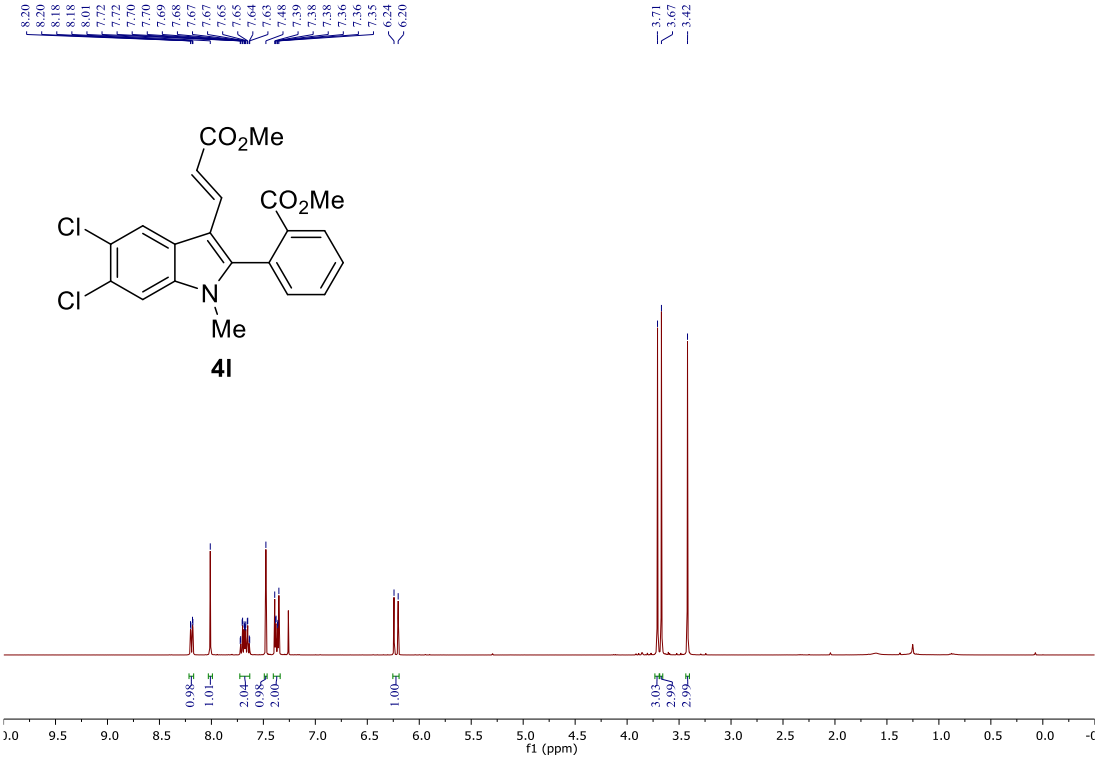

Figure 7.125. ^{13}C NMR Spectrum of 4l

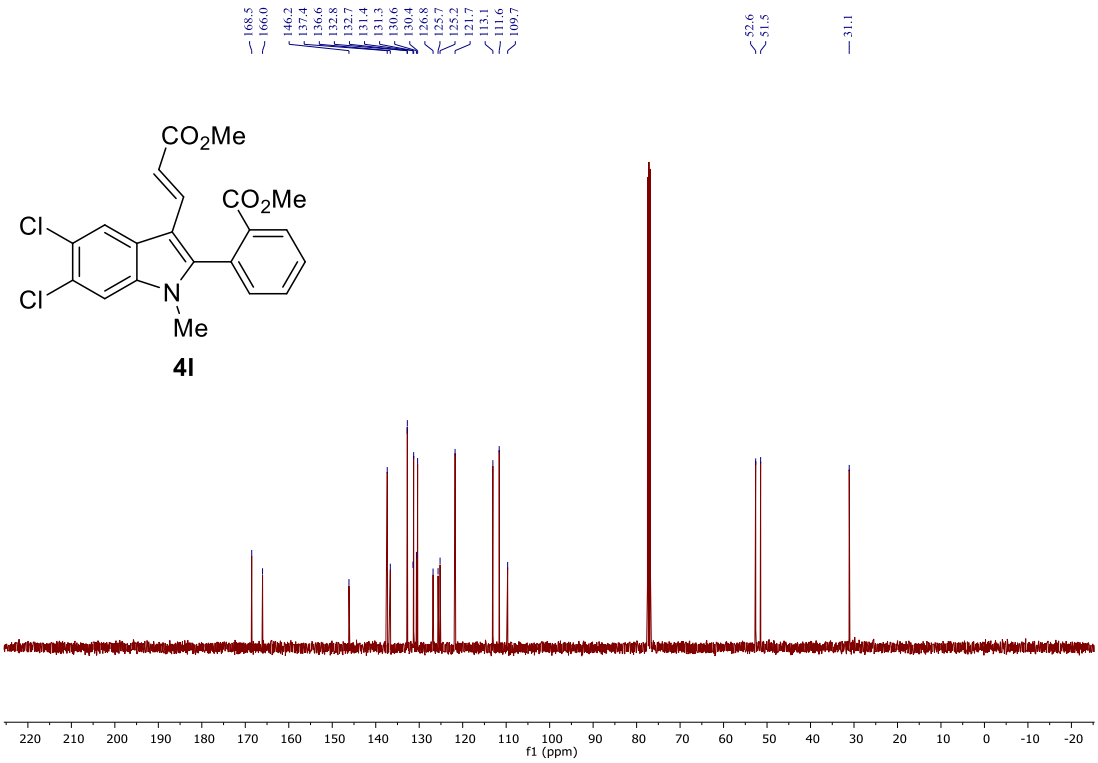

Figure 7.126. ^{1}H NMR Spectrum of 4n

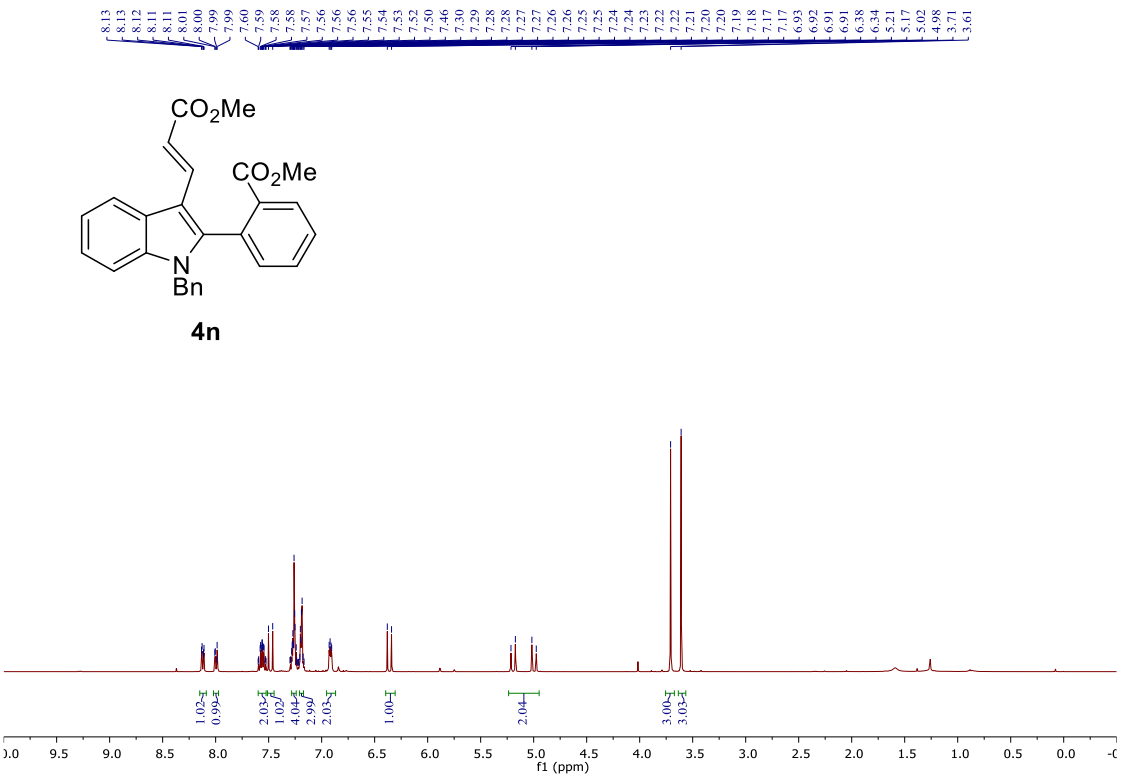

Figure 7.127. ^{13}C NMR Spectrum of 4n

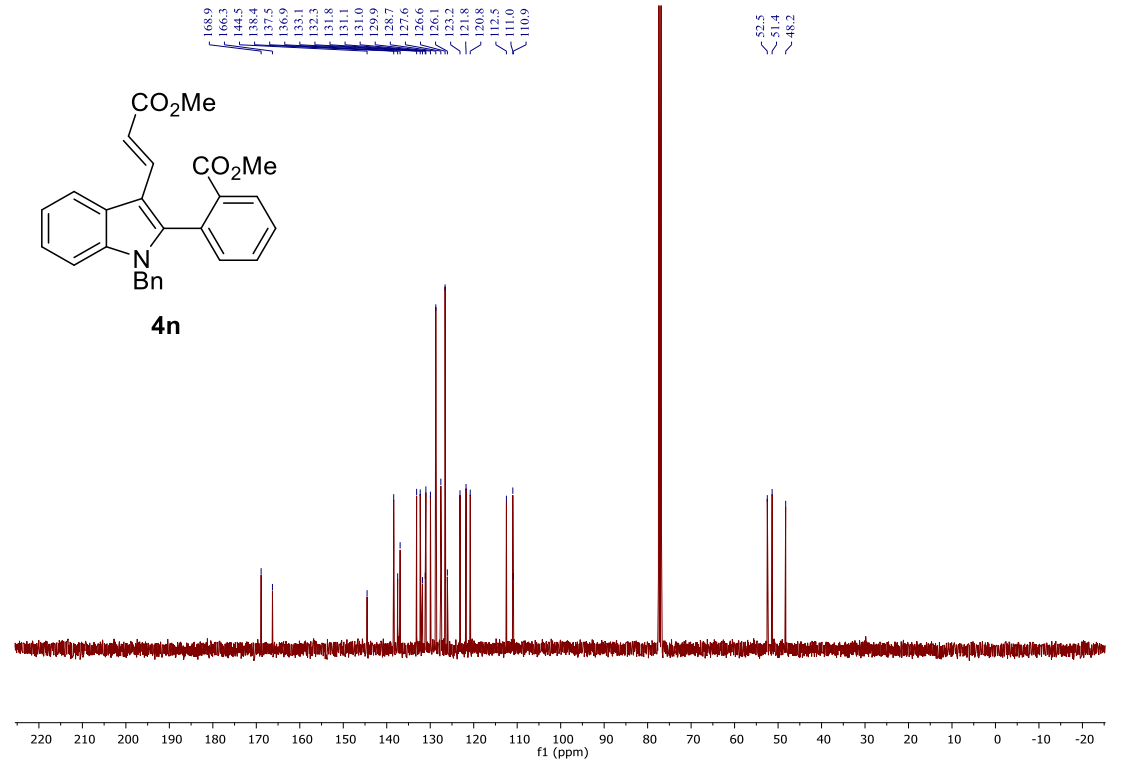

Figure 7.128. ^{1}H NMR Spectrum of 4m

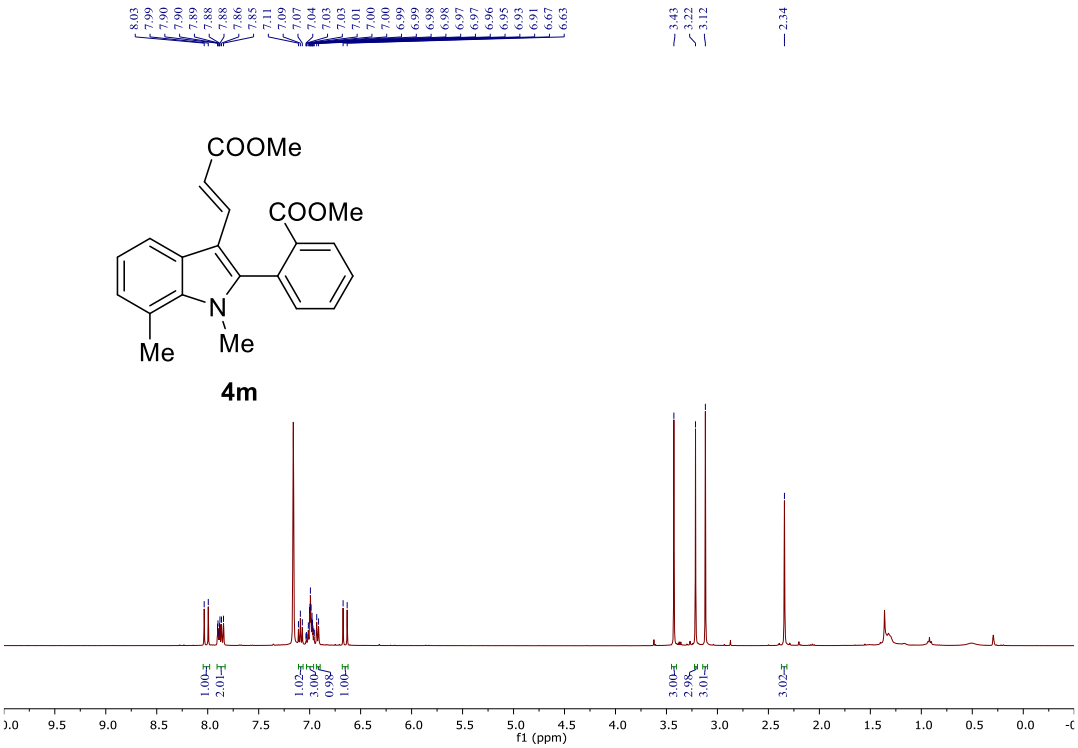

Figure 7.129. ^{13}C NMR Spectrum of 4m

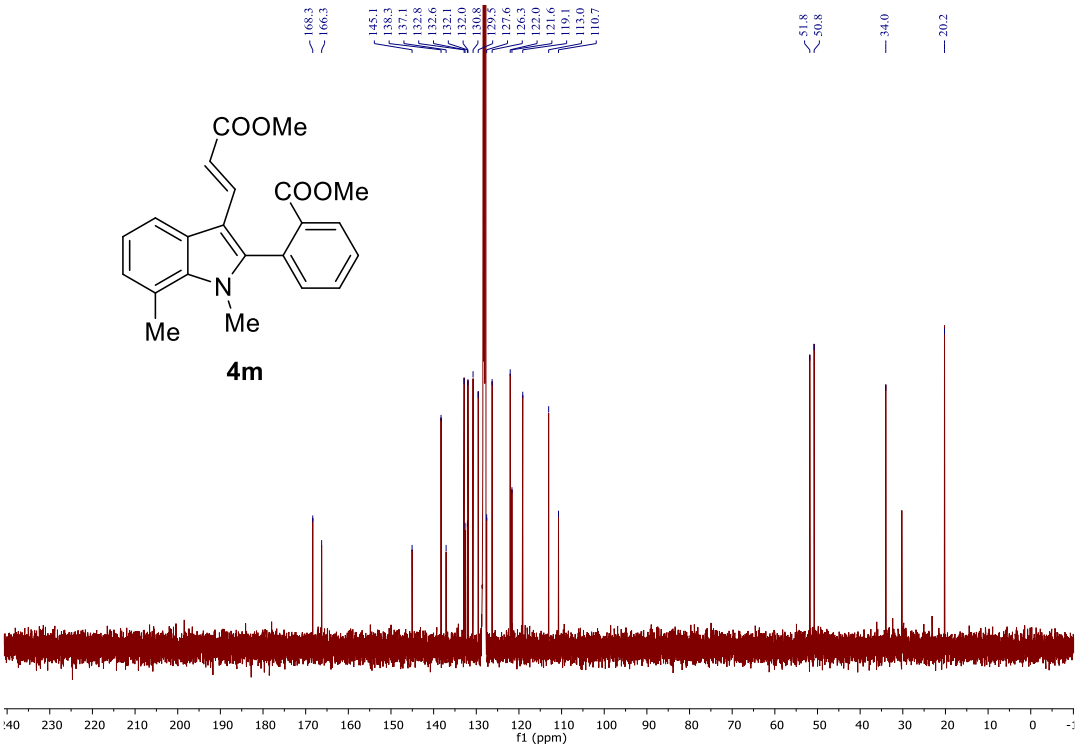

Figure 7.130. ^{1}H NMR Spectrum of 4o

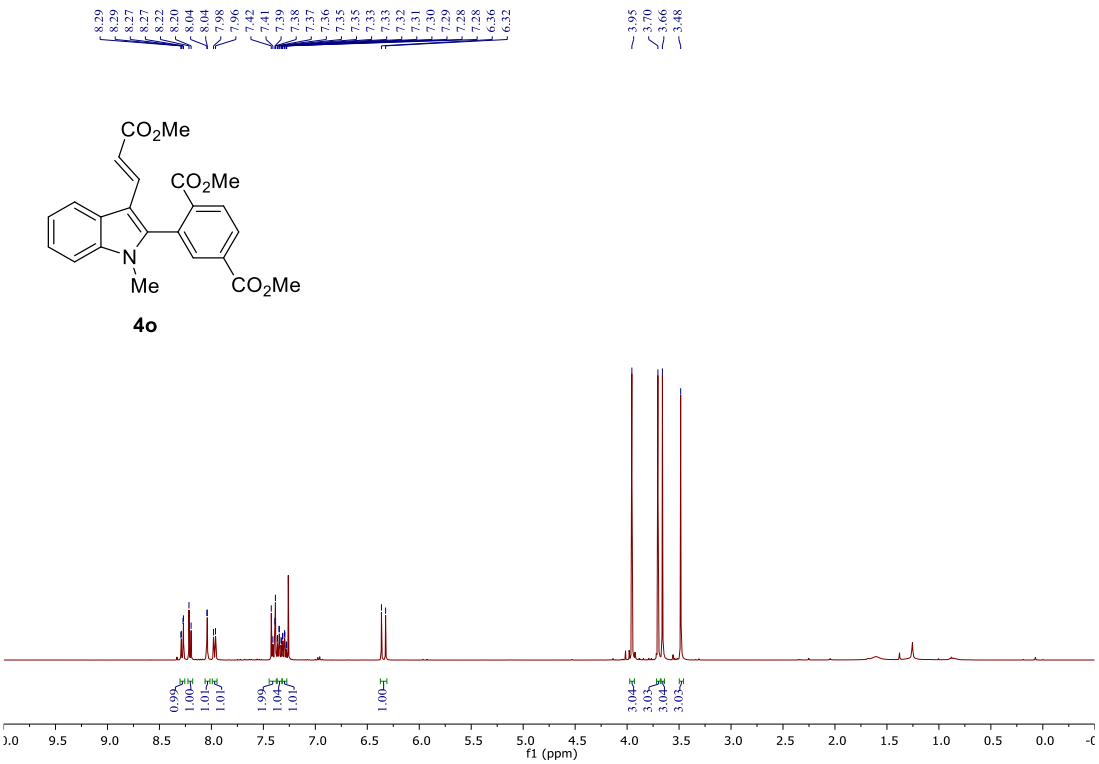

Figure 7.131. ^{13}C NMR Spectrum of 4o

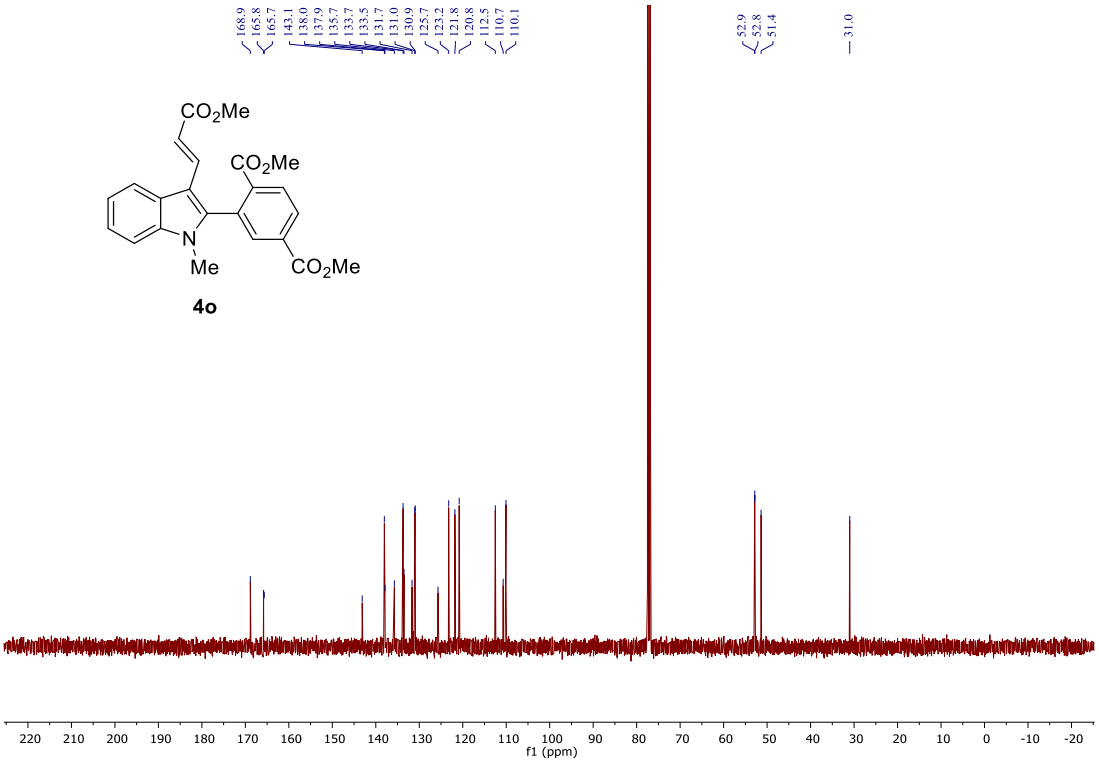

Figure 7.132. ^{1}H NMR Spectrum of 4p

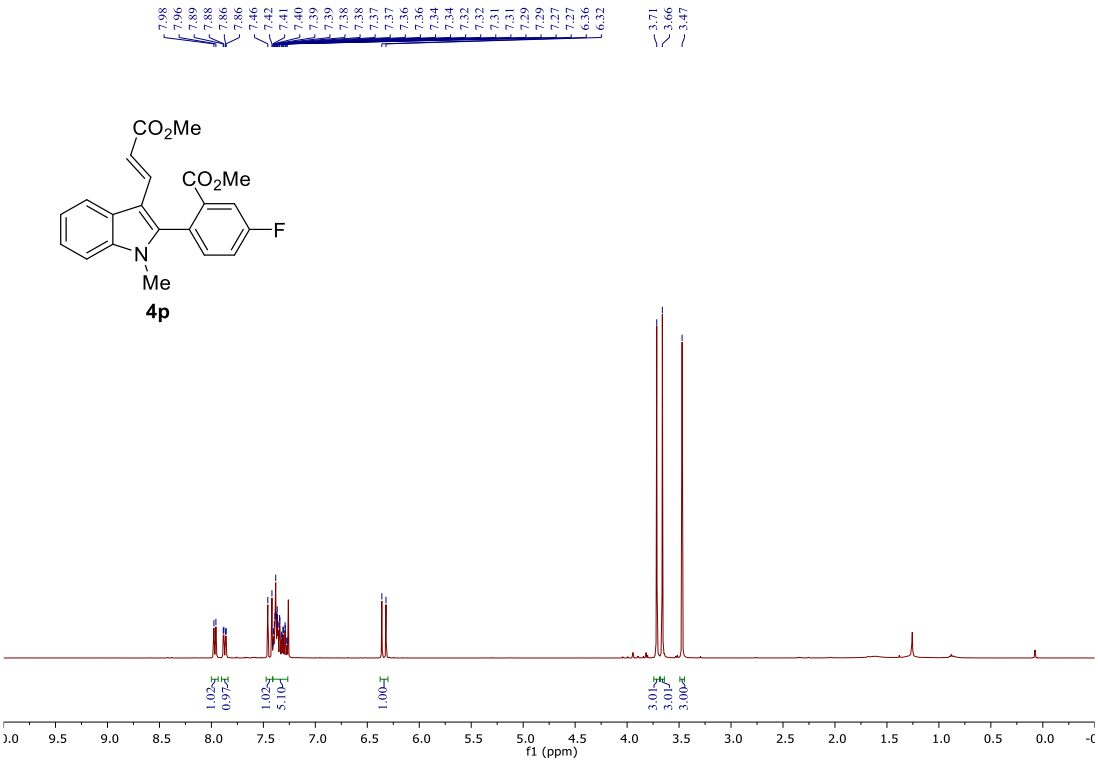

Figure 7.133. ^{13}C NMR Spectrum of 4p

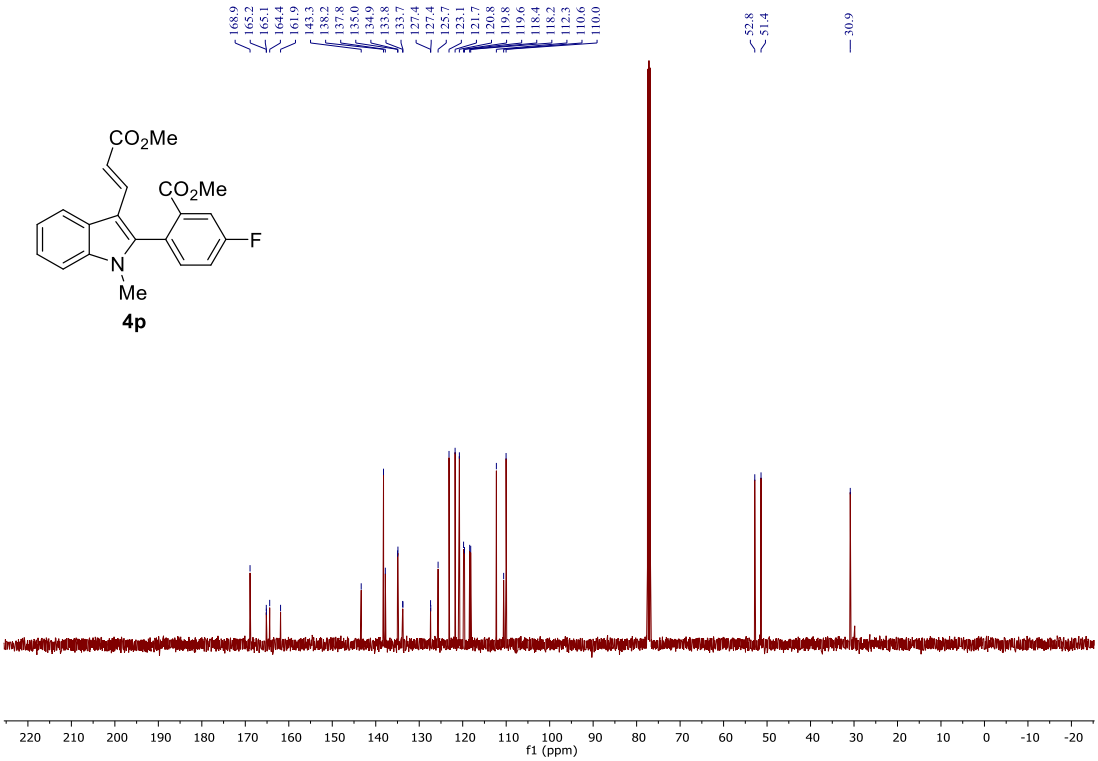

Figure 7.134. ^{19}F NMR Spectrum of 4p

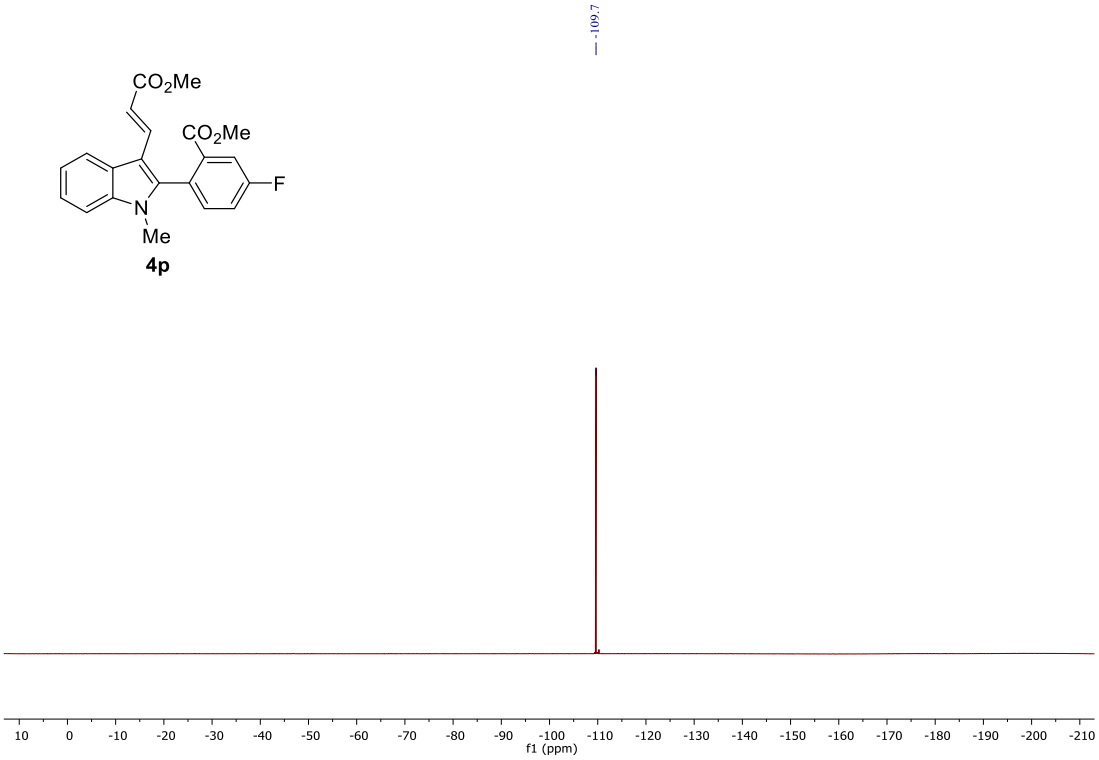

Figure 7.135. ^{1}H NMR Spectrum of 4q

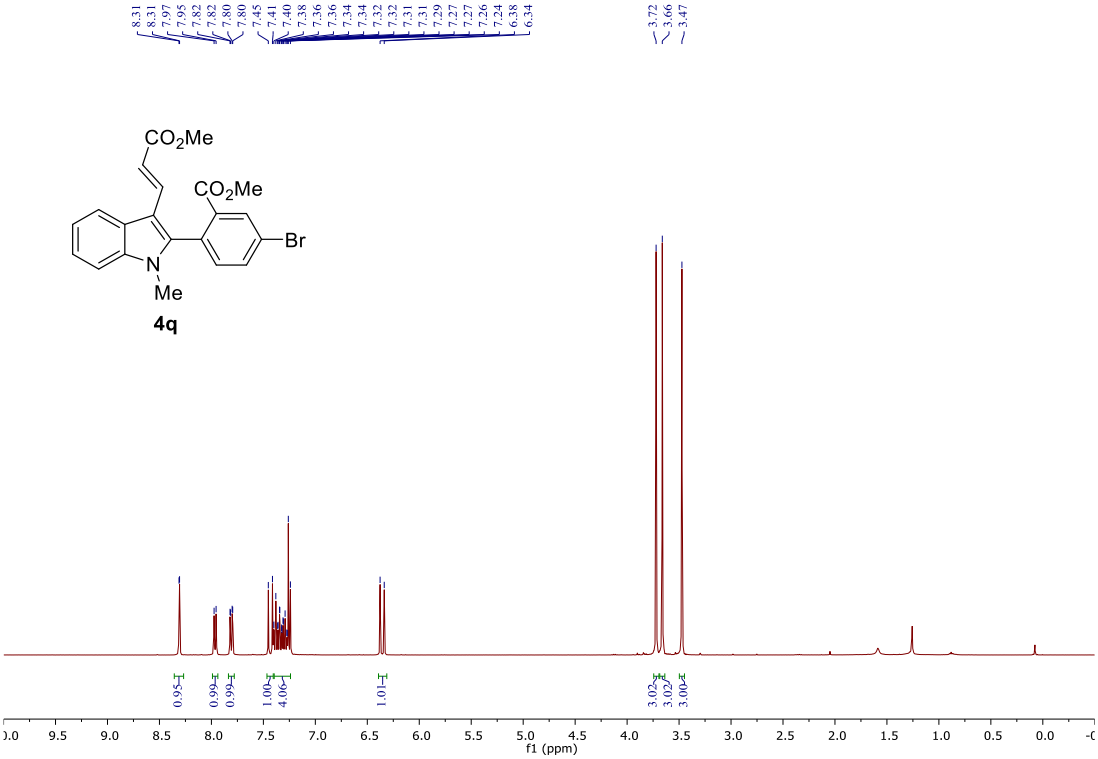

Figure 7.136. ^{13}C NMR Spectrum of 4q

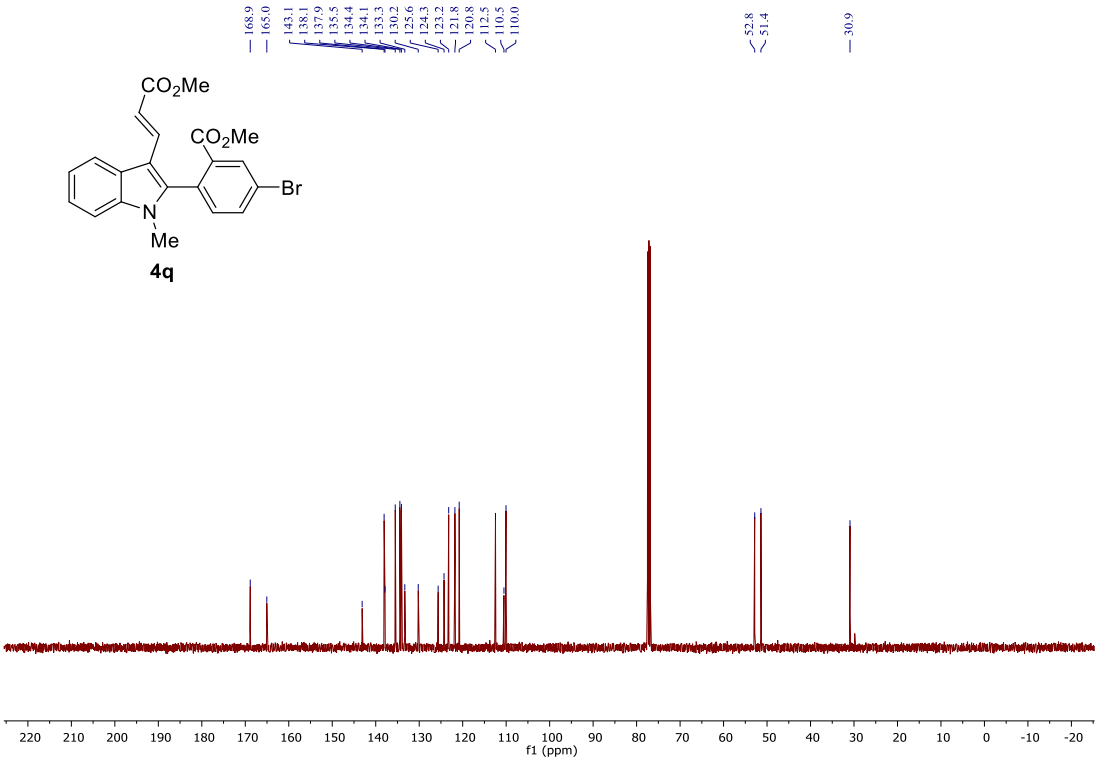

Figure 7.137. ^{1}H NMR Spectrum of 4r

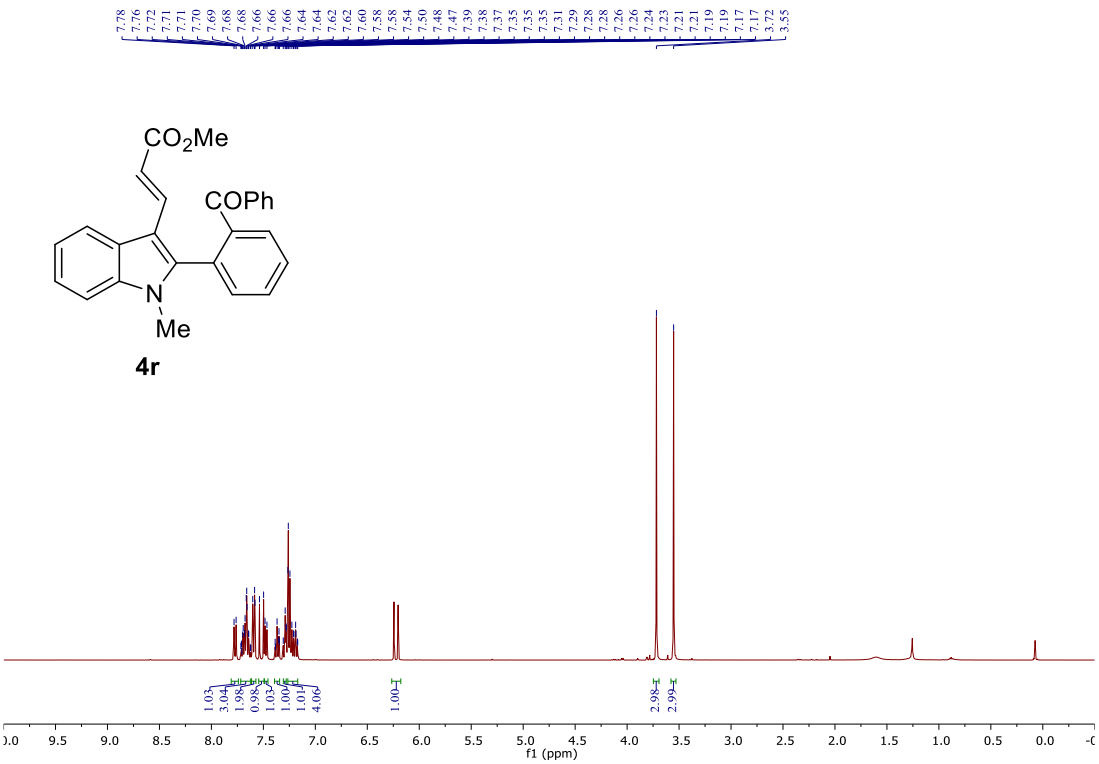

Figure 7.138. ^{13}C NMR Spectrum of 4r

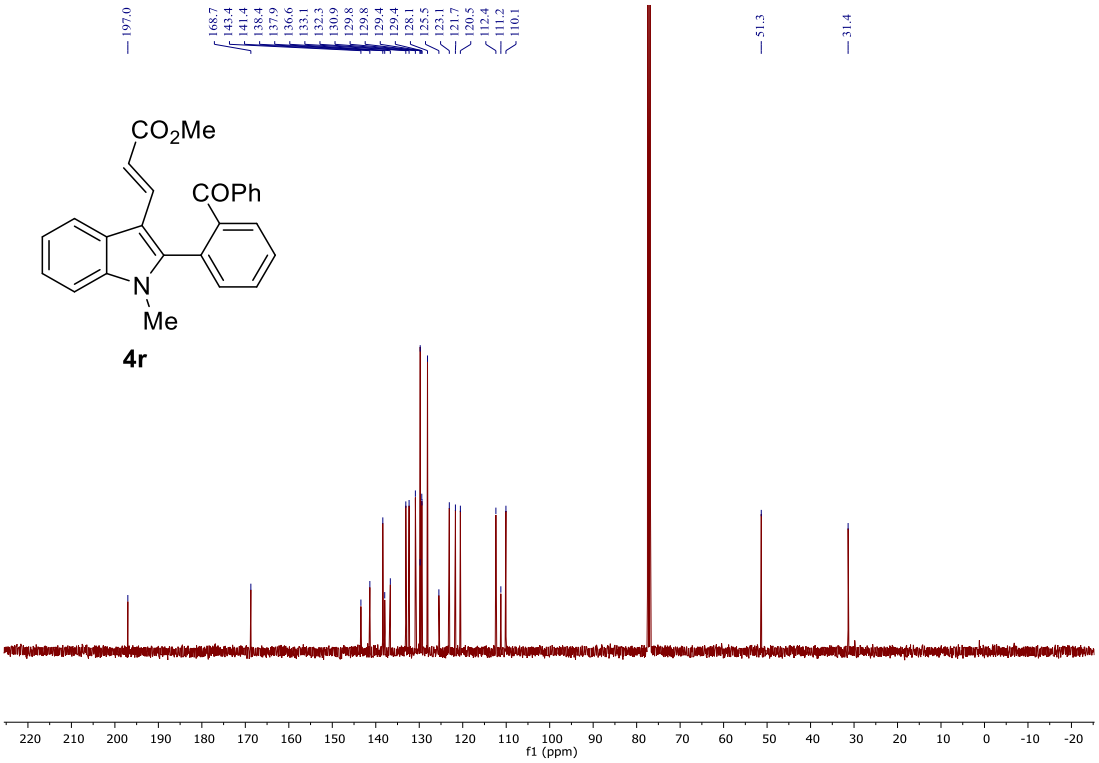

Figure 7.139. ^{1}H NMR Spectrum of 4s

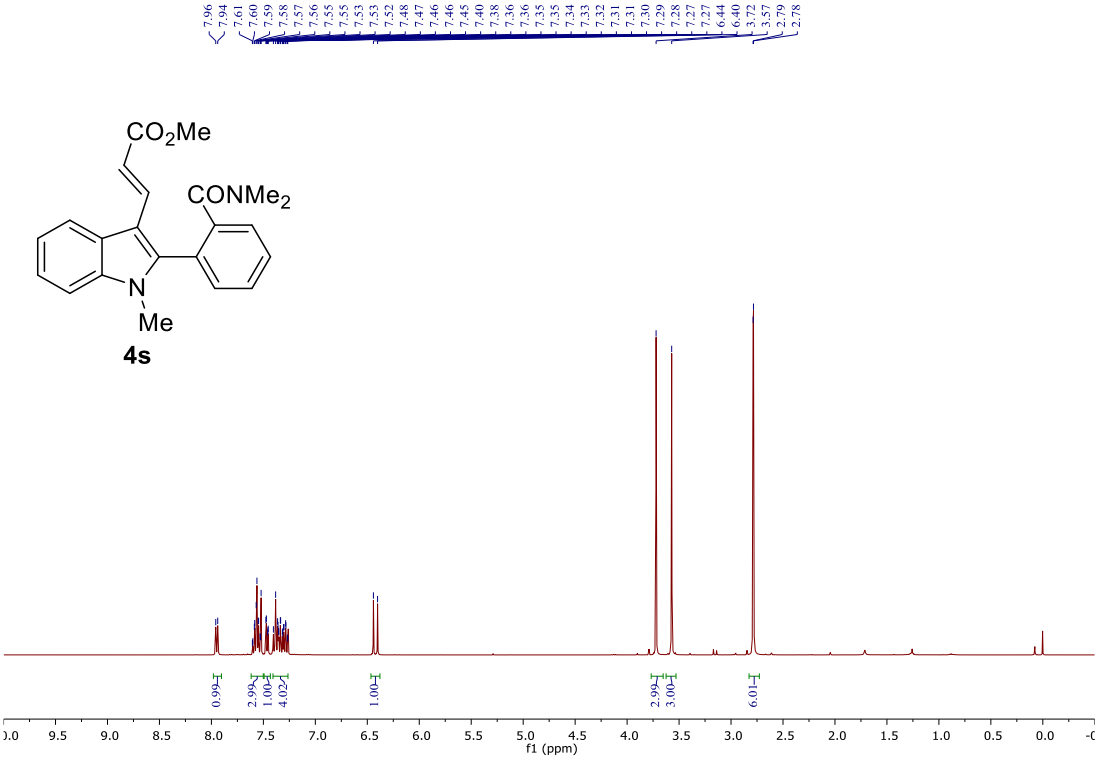

Figure 7.140. ^{13}C NMR Spectrum of 4s

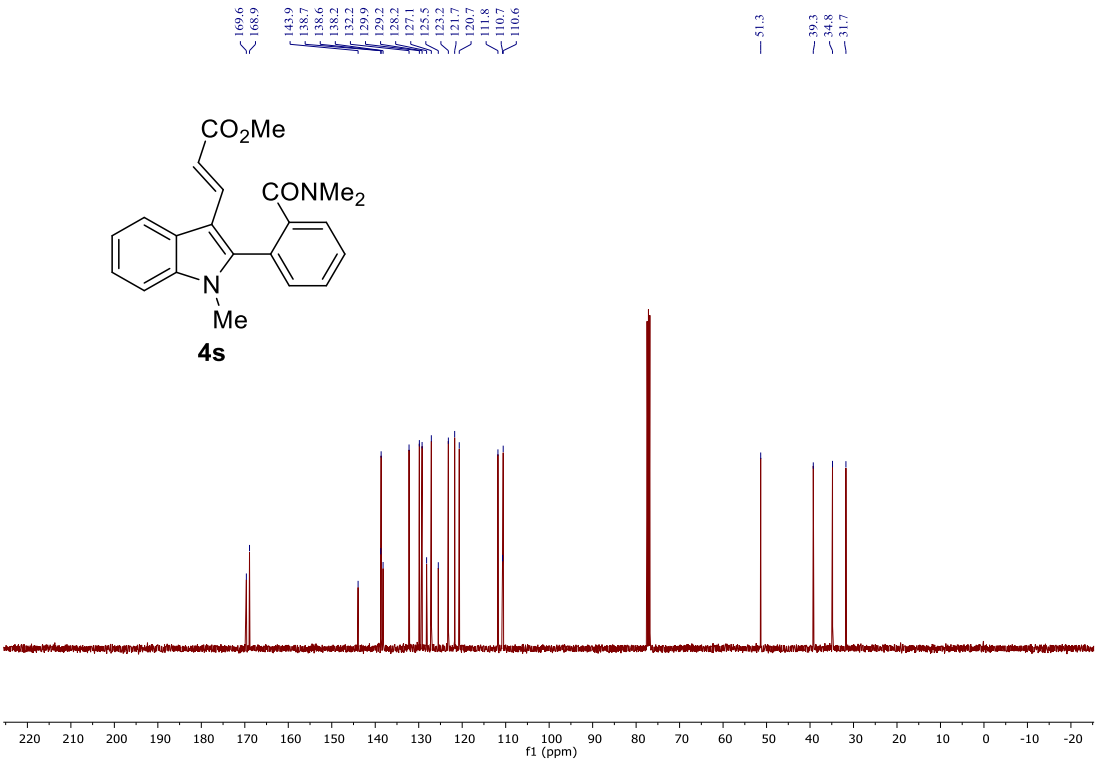

Figure 7.141. ^{1}H NMR Spectrum of 4t

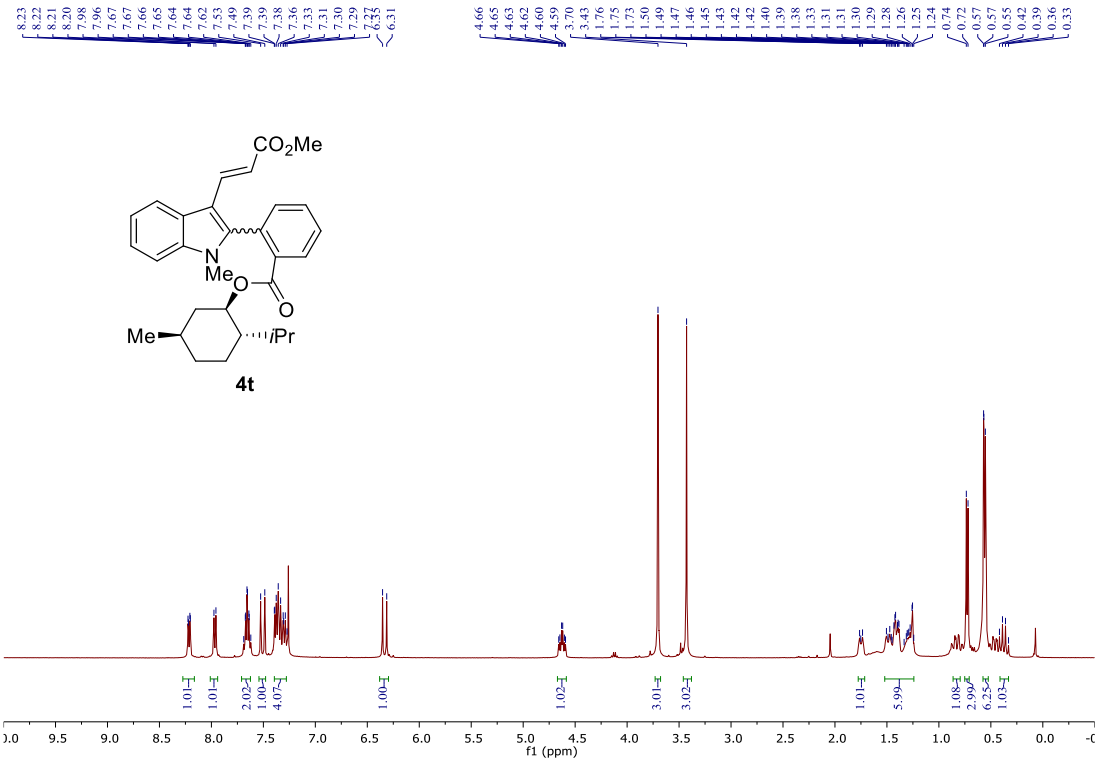

Figure 7.142. ^{13}C NMR Spectrum of 4t

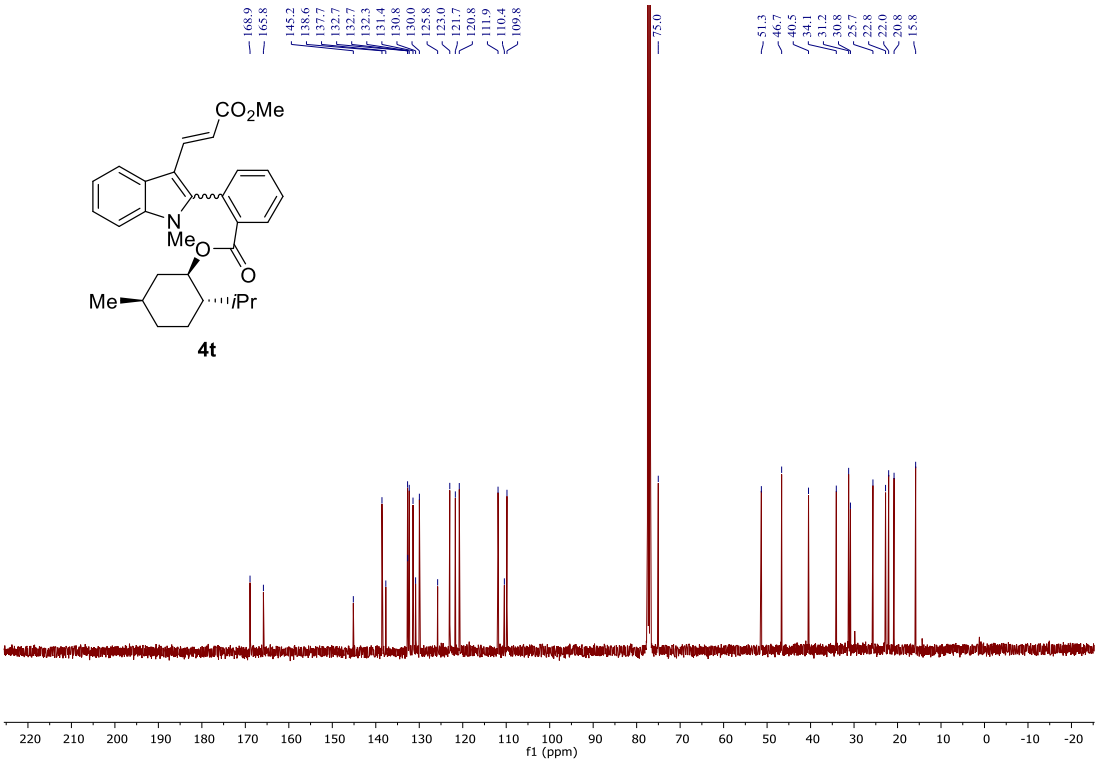

Figure 7.143. ^{1}H NMR Spectrum of 4t'

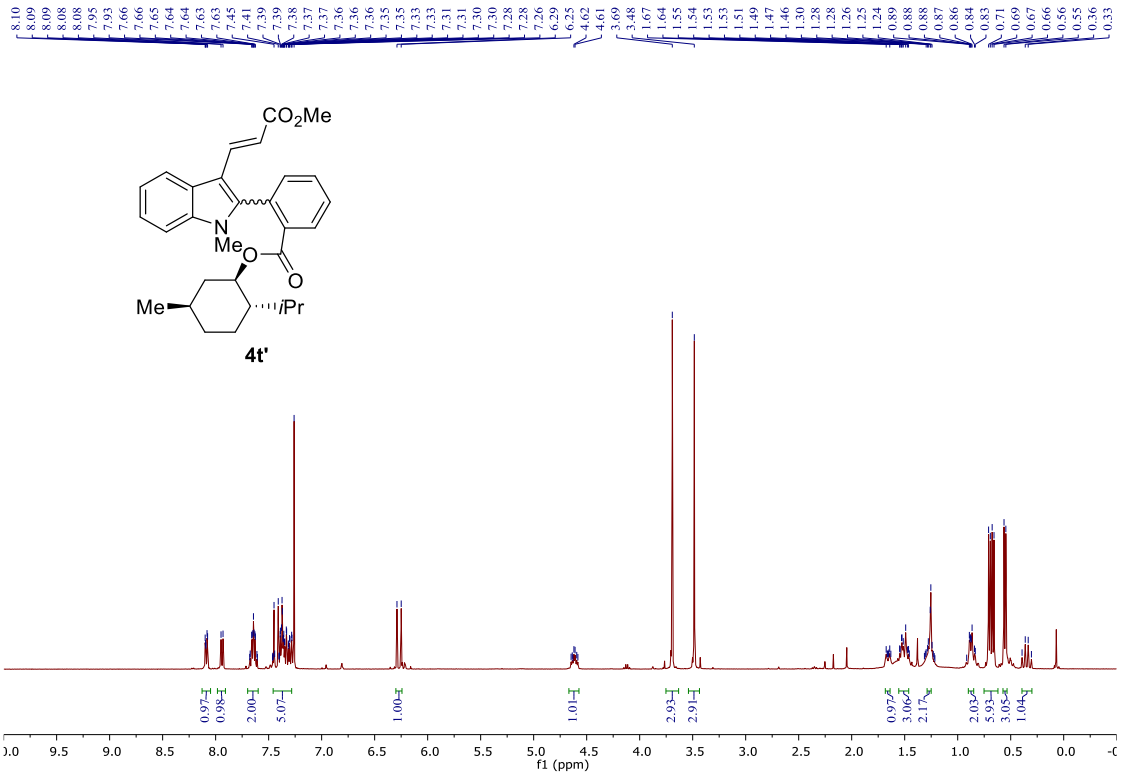

Figure 7.144. ^{13}C NMR Spectrum of 4t'

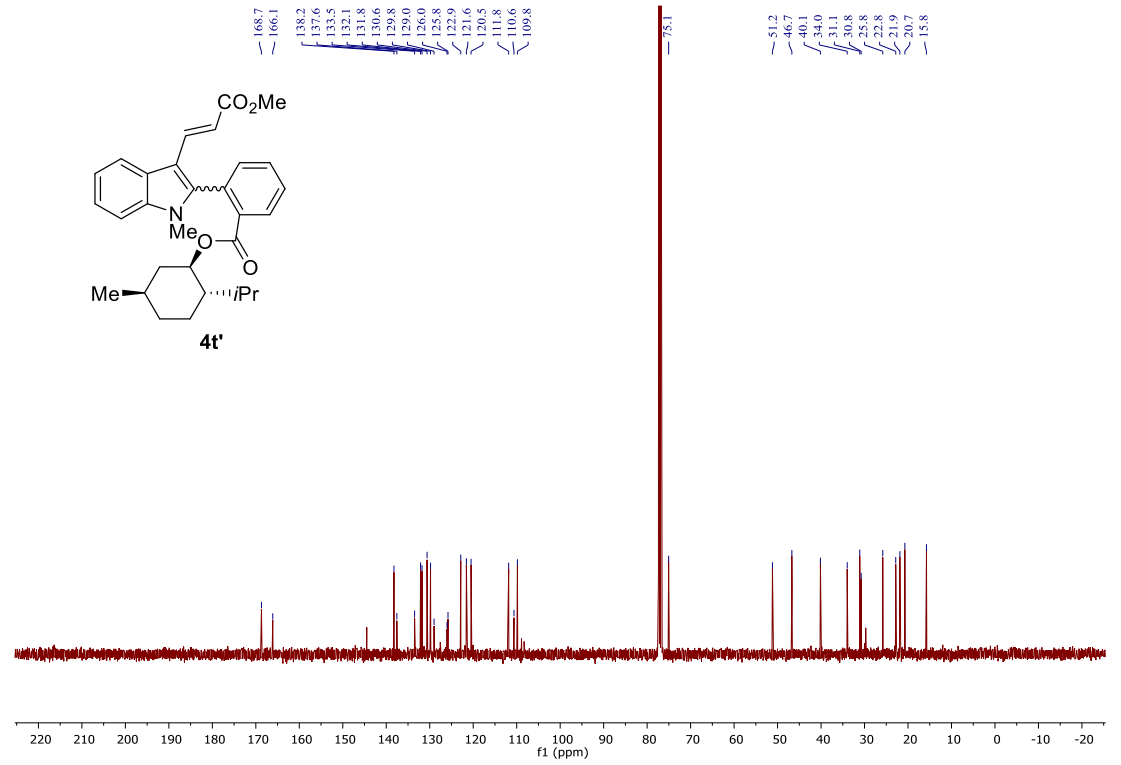

Figure 7.145. ^{1}H NMR Spectrum of 4u

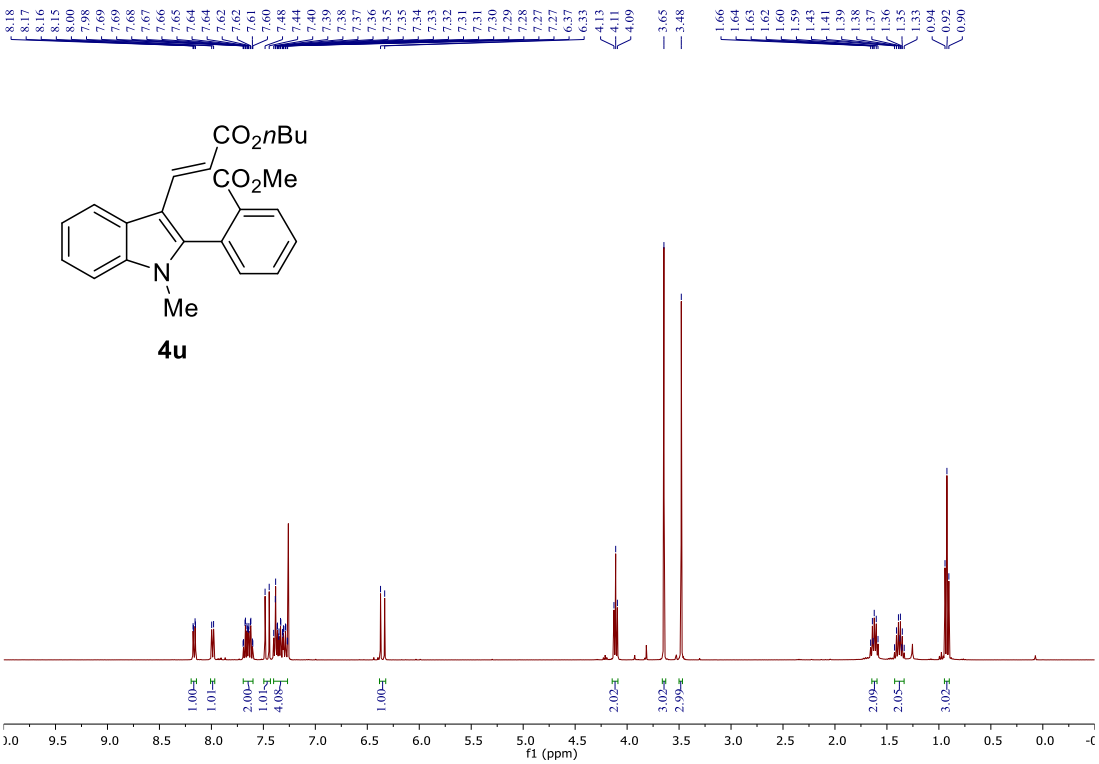

Figure 7.146. ^{13}C NMR Spectrum of 4u

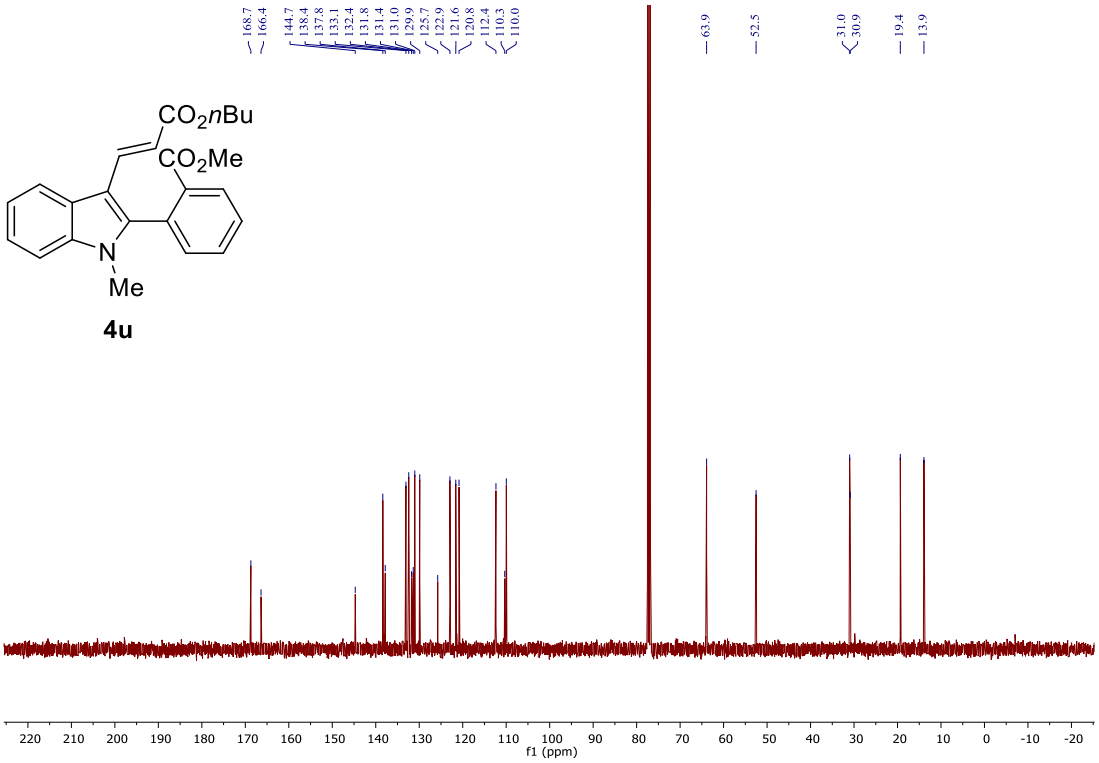

Figure 7.147. ^{1}H NMR Spectrum of 4v

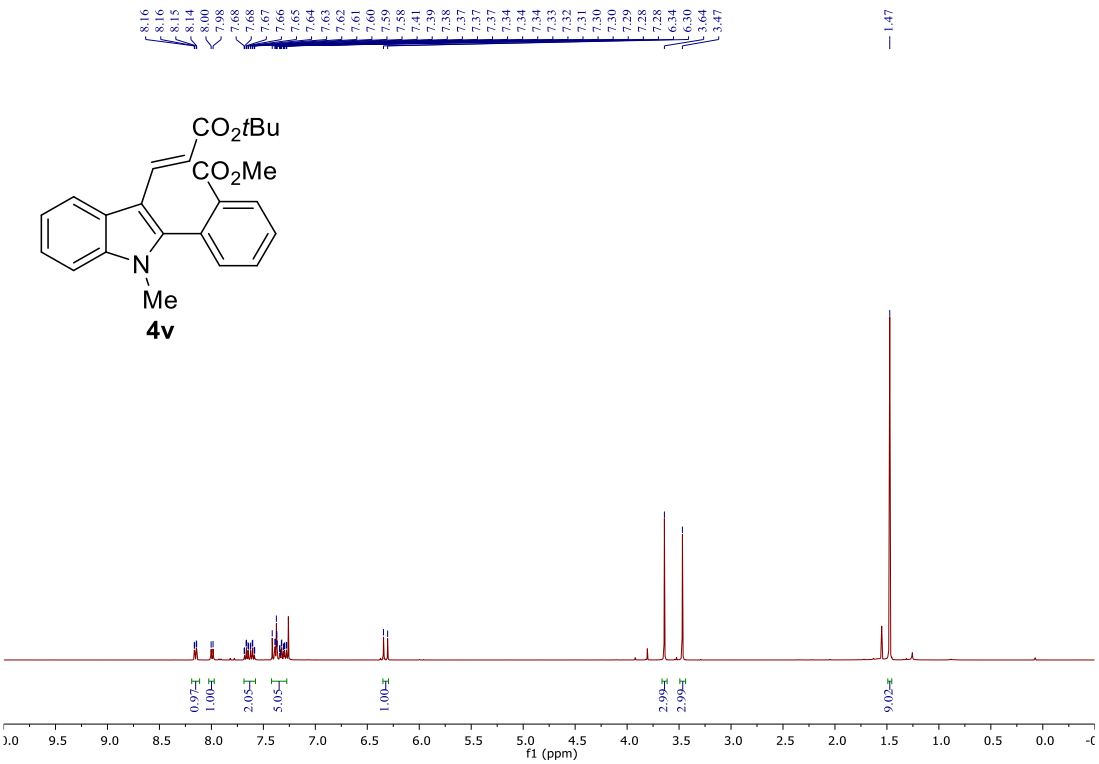

Figure 7.148. ^{13}C NMR Spectrum of 4v

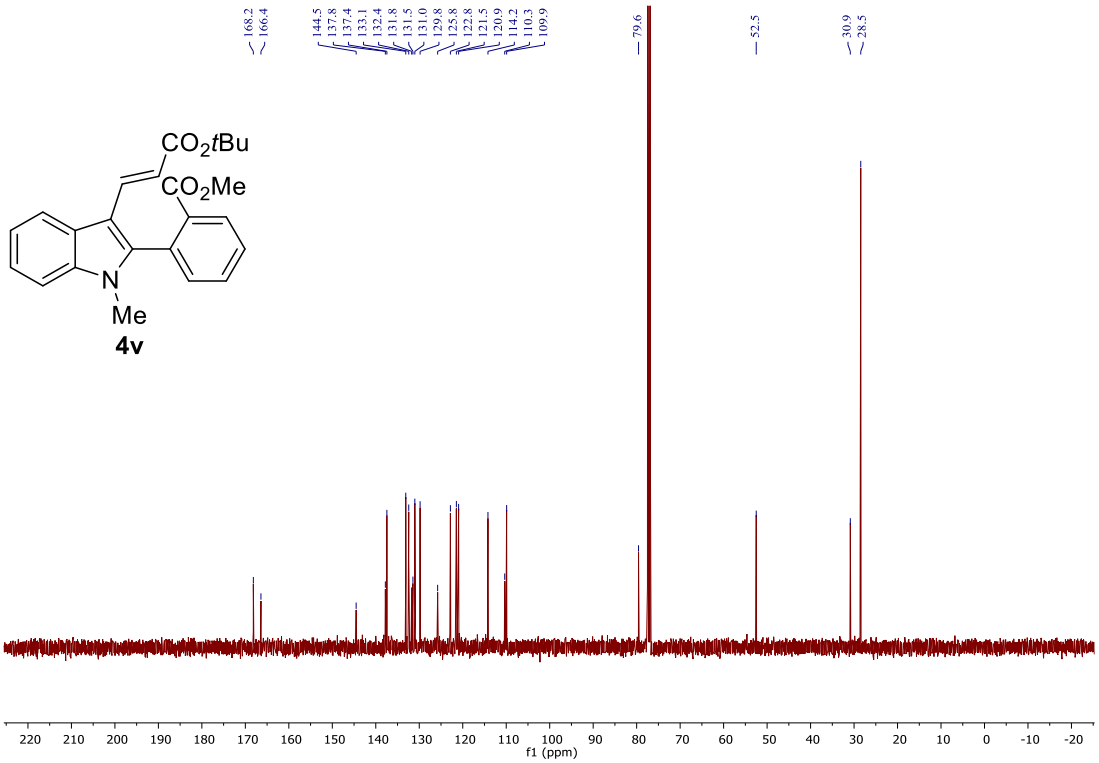

Figure 7.149. ^{1}H NMR Spectrum of 4w

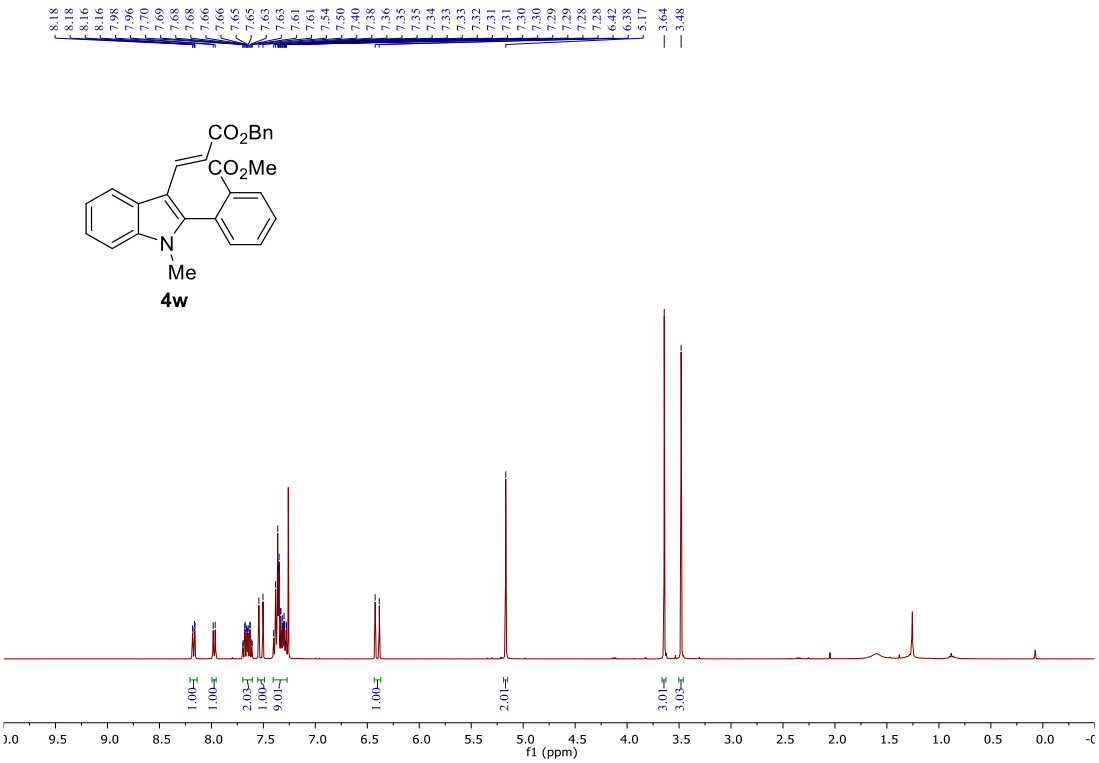

Figure 7.150. ^{13}C NMR Spectrum of 4w

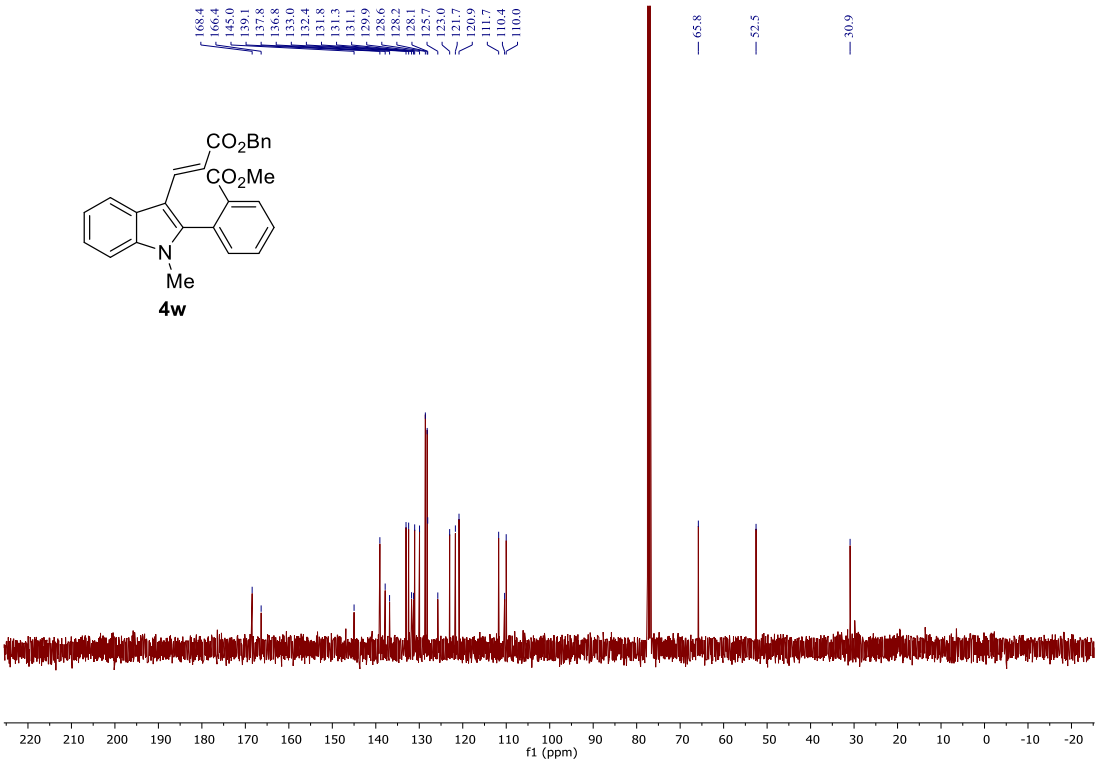

Figure 7.151. ^{1}H NMR Spectrum of 4x

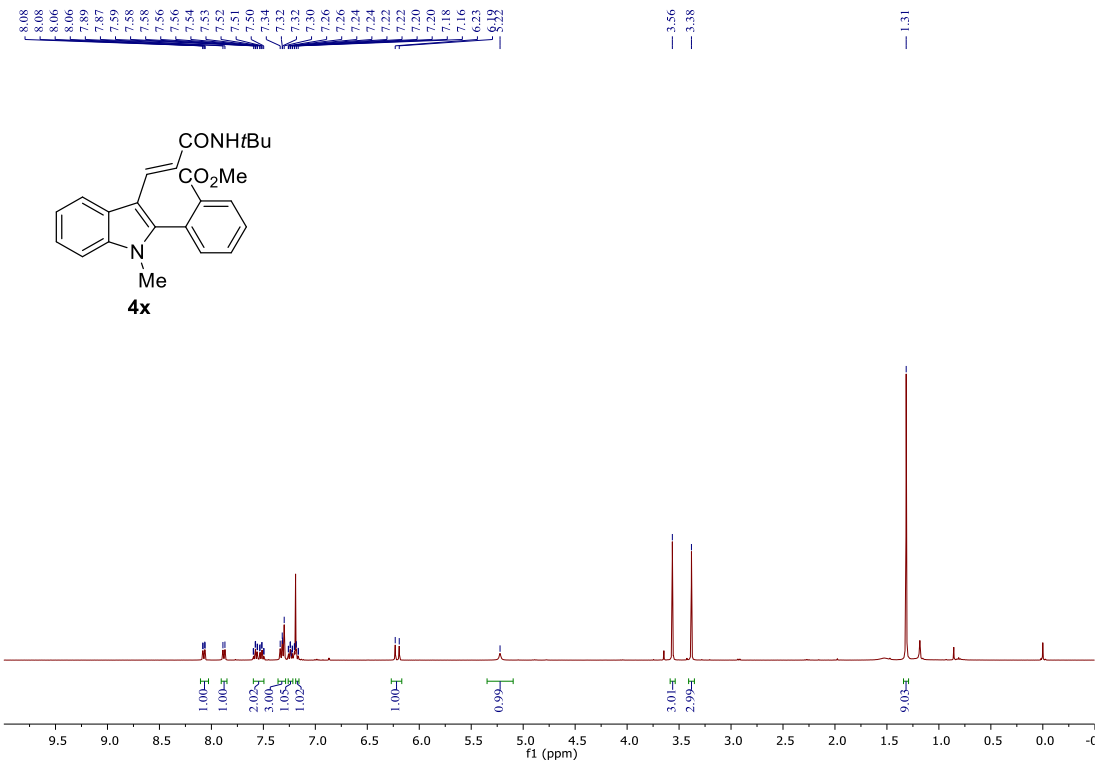

Figure 7.152. ^{13}C NMR Spectrum of 4x

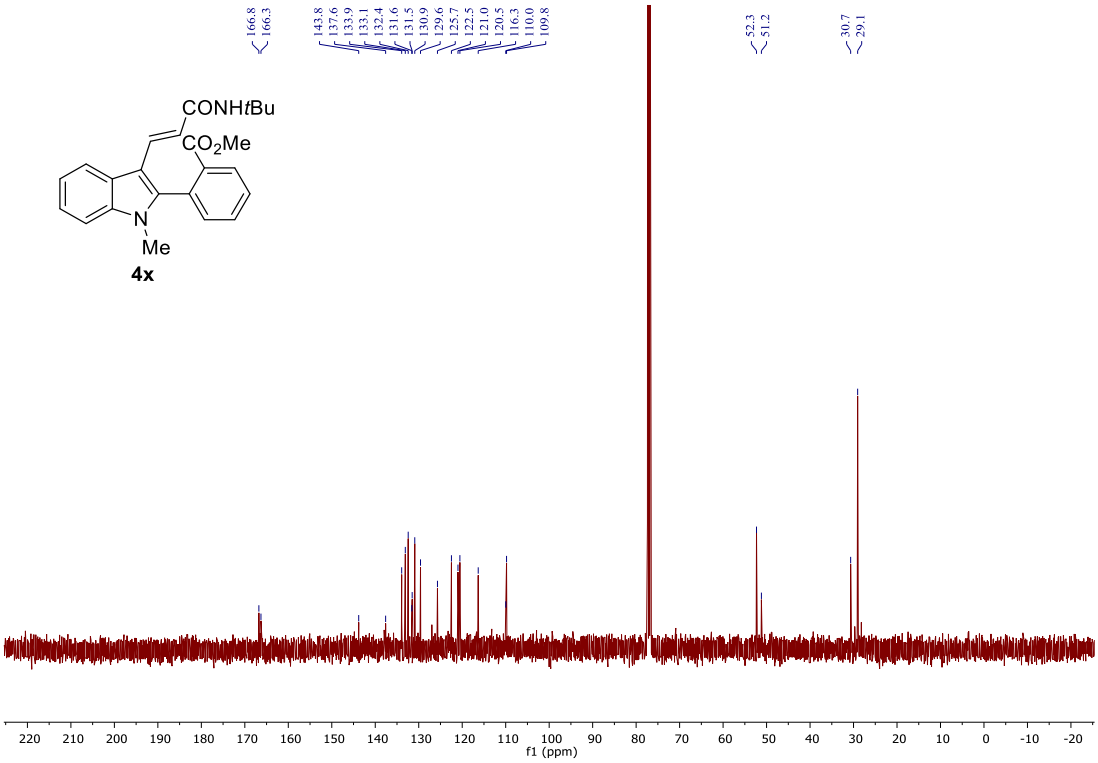

Figure 7.153. ^{1}H NMR Spectrum of 4y

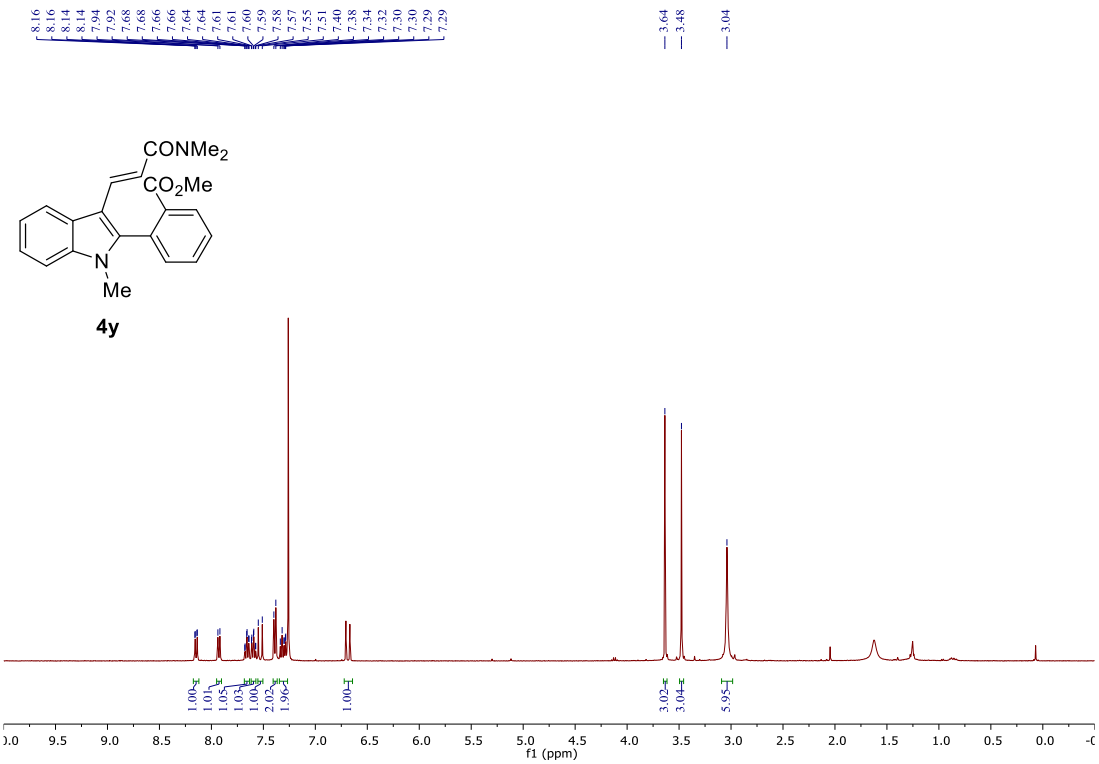

Figure 7.154. ^{13}C NMR Spectrum of 4y

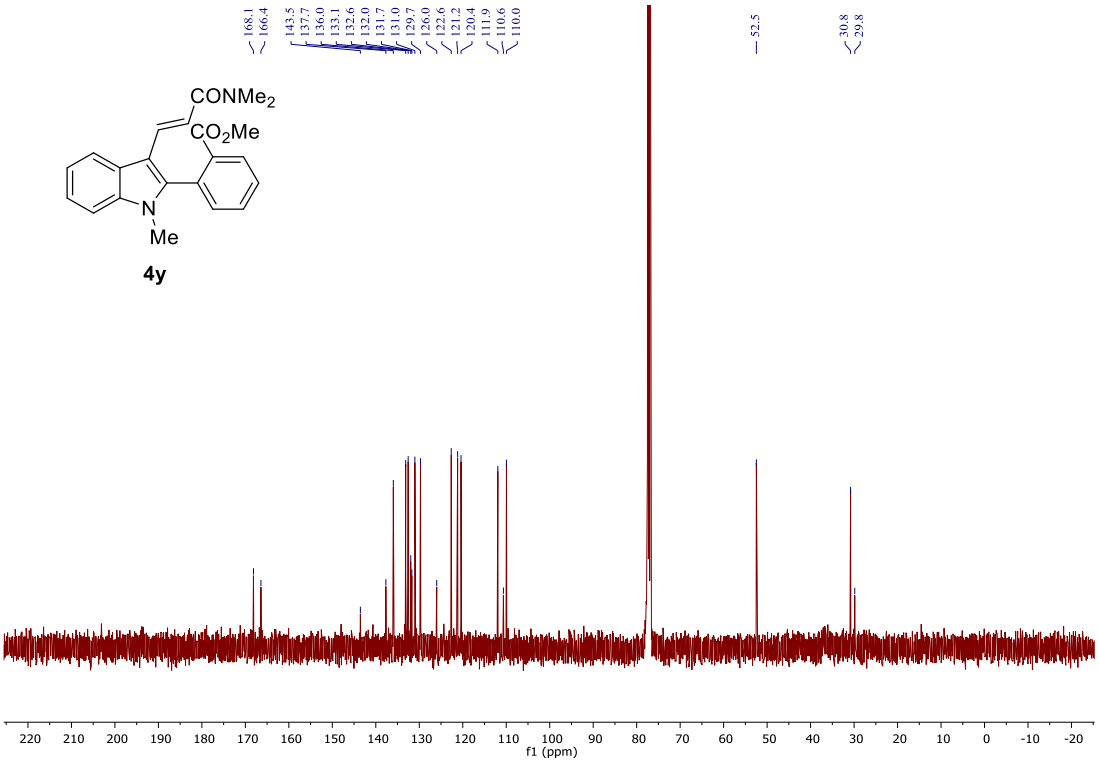

Figure 7.155. ^{1}H NMR Spectrum of 4z

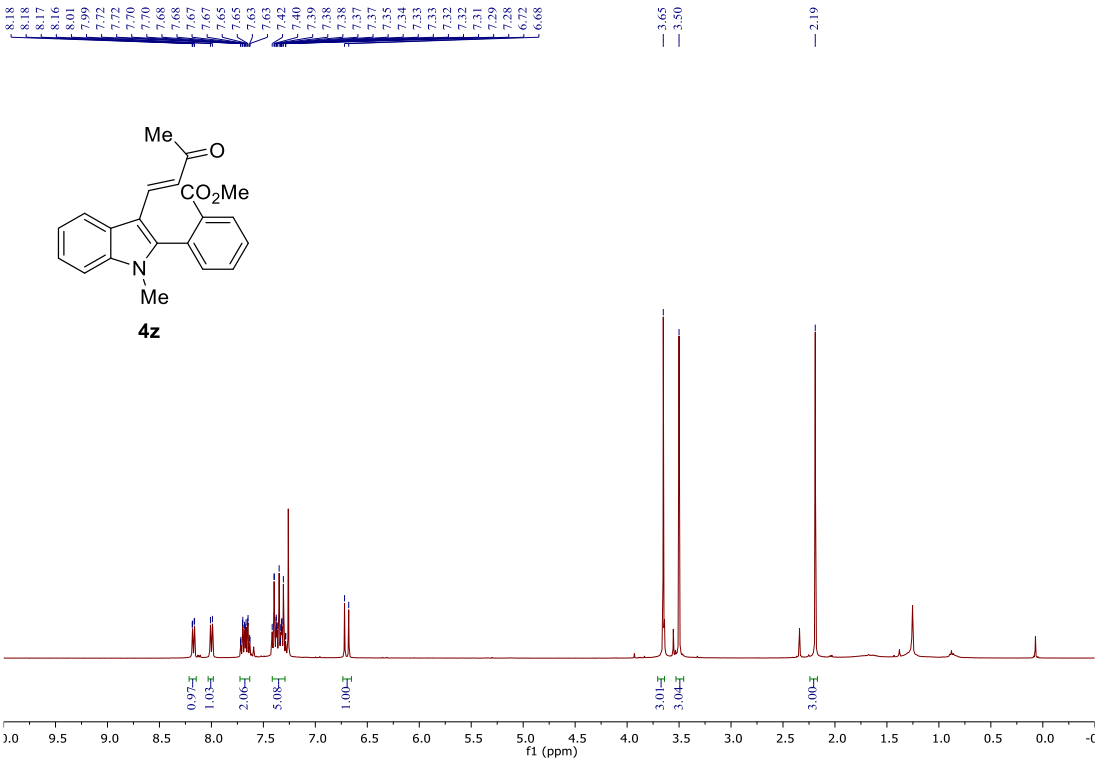

Figure 7.156. ^{13}C NMR Spectrum of 4z

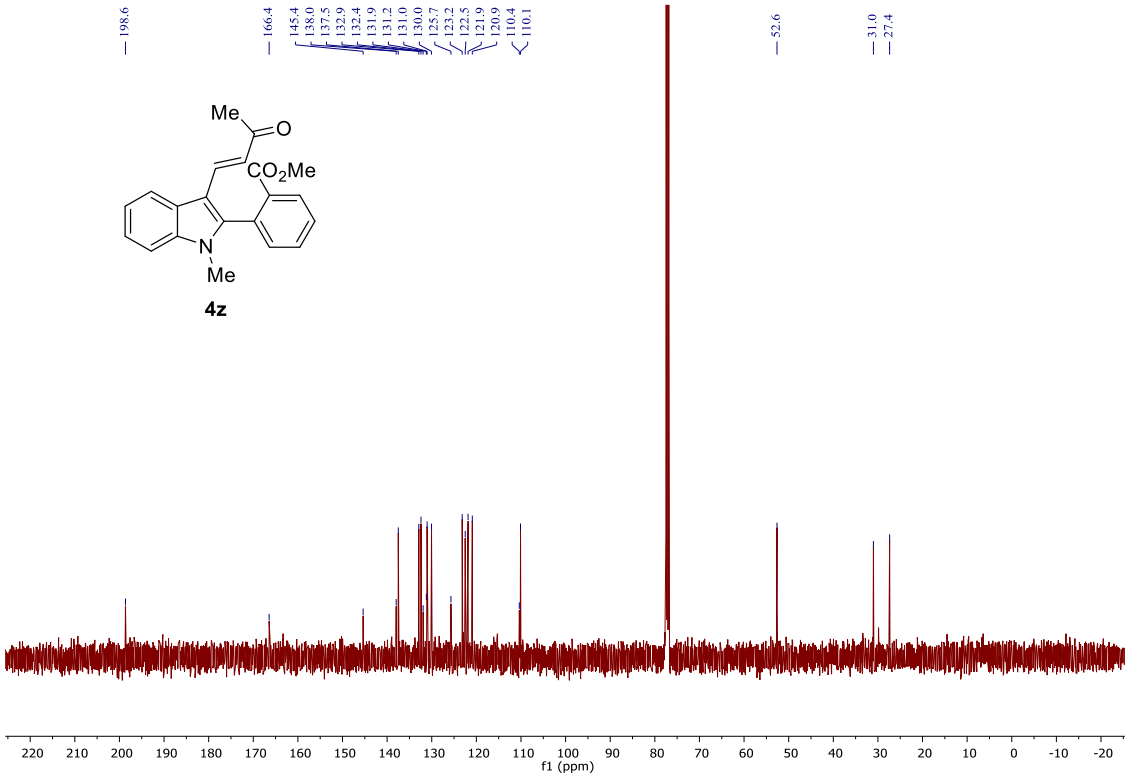

Figure 7.157. ^{1}H NMR Spectrum of 8a

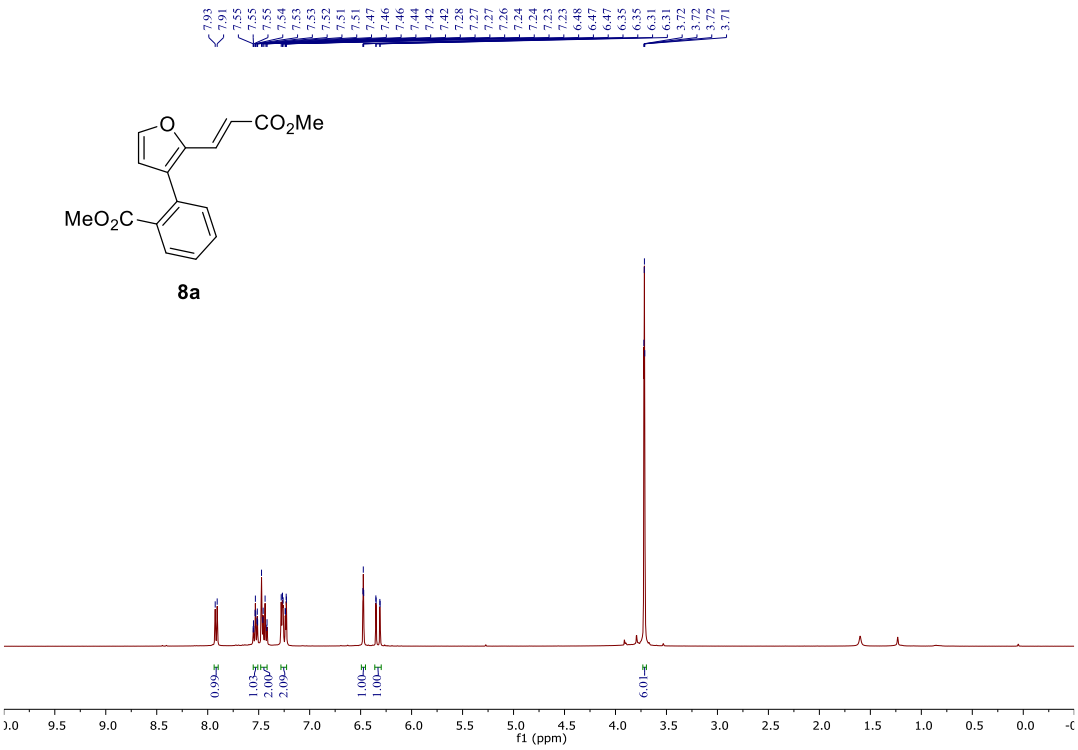

Figure 7.158. ^{13}C NMR Spectrum of 8a

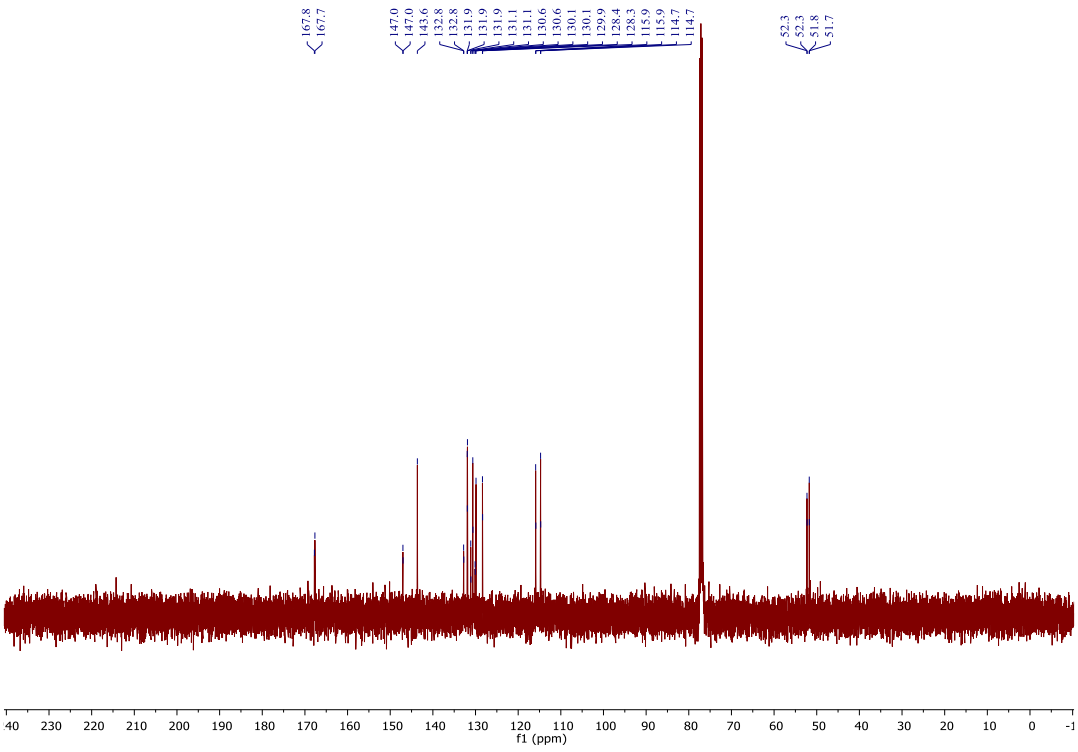

Figure 7.159. ^{1}H NMR Spectrum of 8b

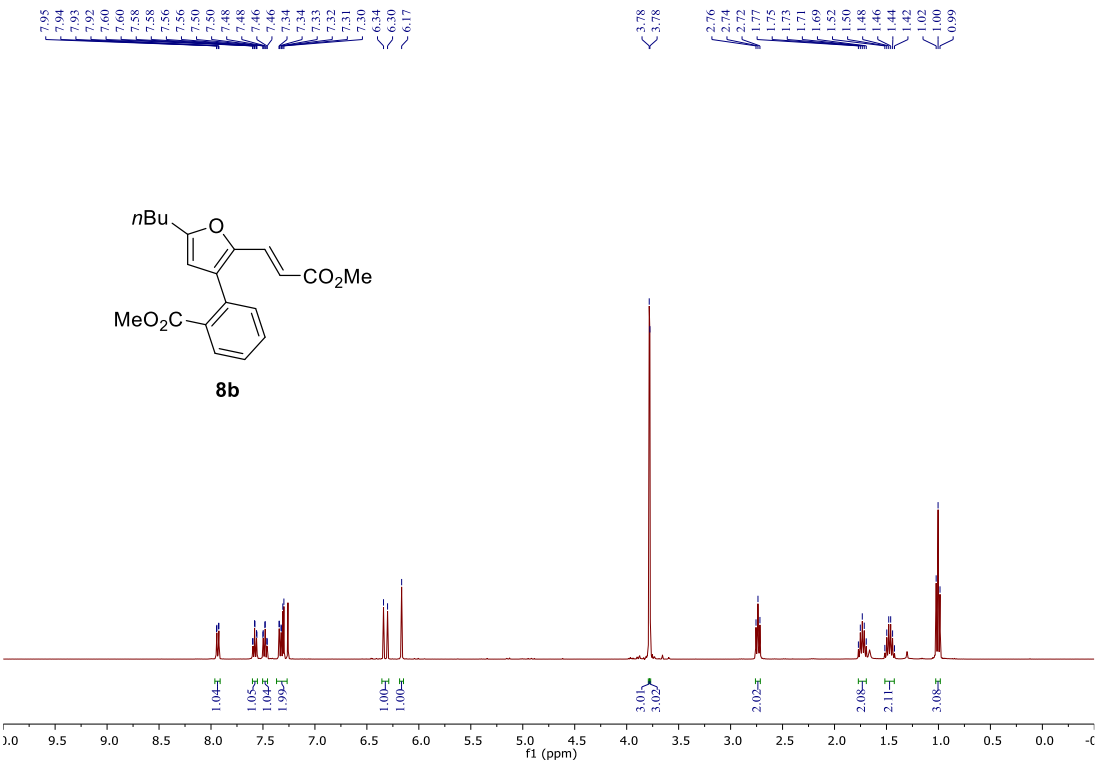

Figure 7.160. ^{13}C NMR Spectrum of 8b

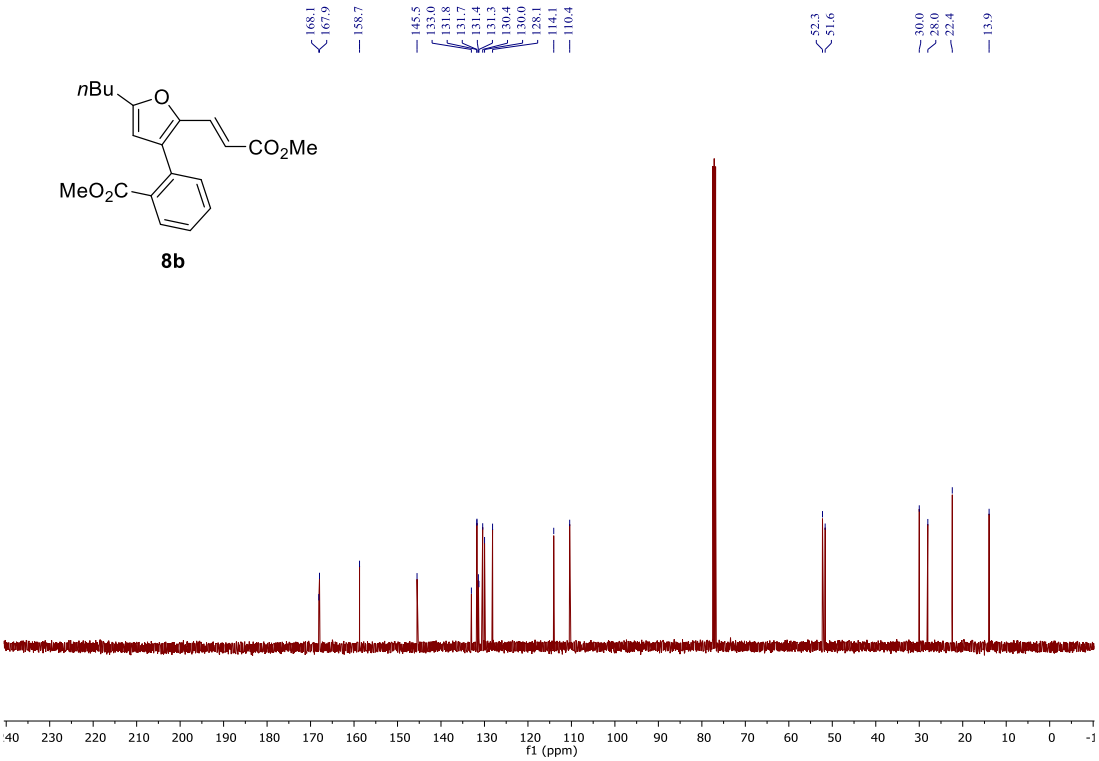

Figure 7.161. ^{1}H NMR Spectrum of 8c

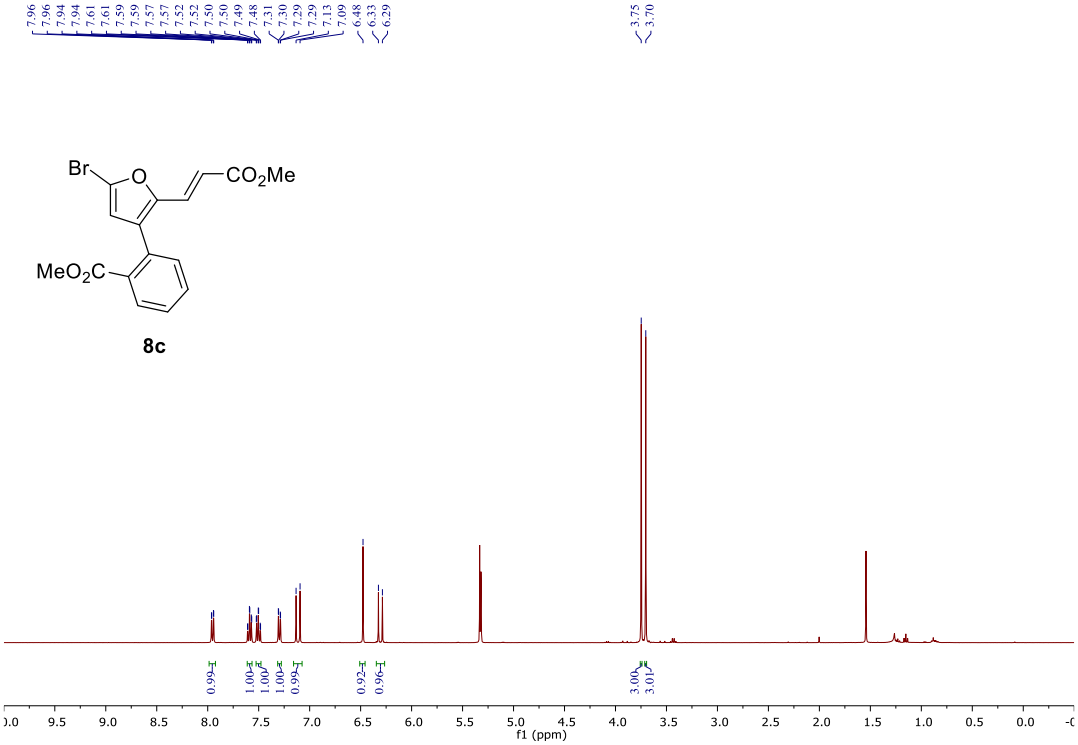

Figure 7.162. ^{13}C NMR Spectrum of 8c

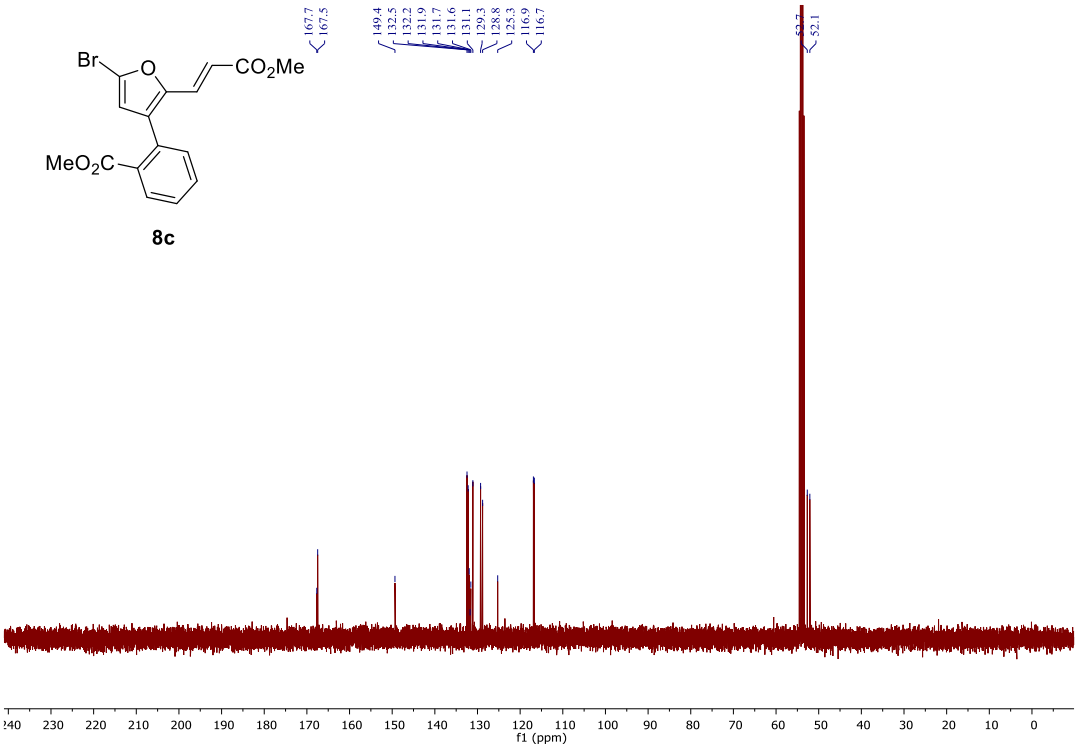

Figure 7.163. ^{1}H NMR Spectrum of 8d

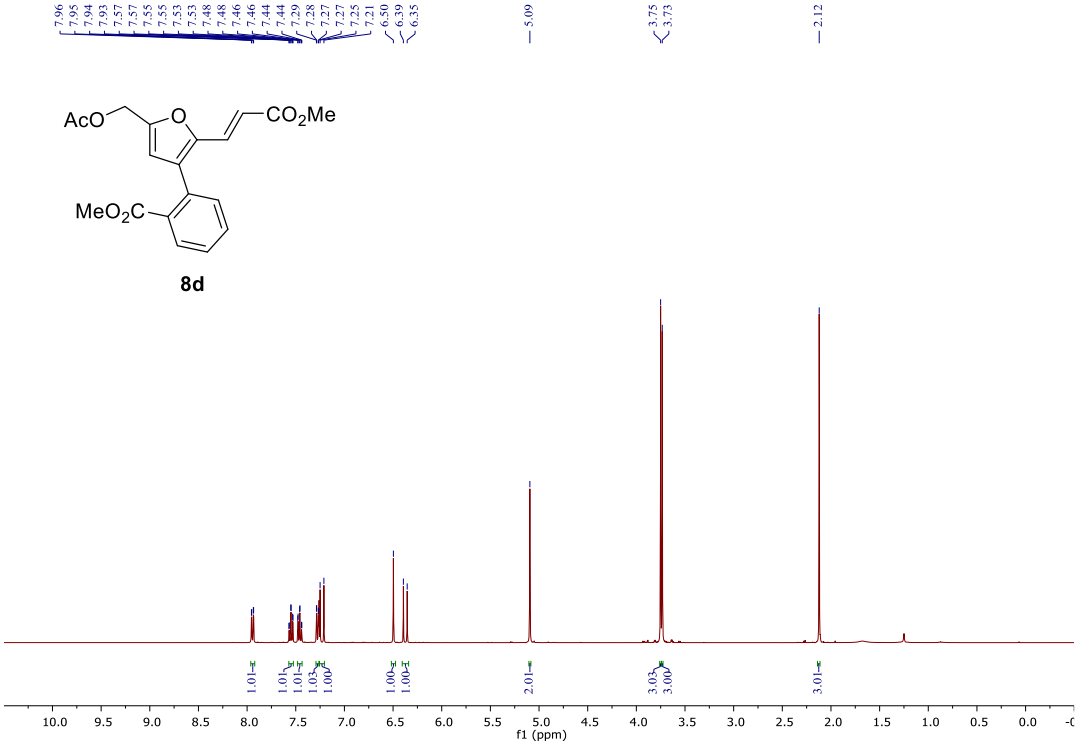

Figure 7.164. ^{13}C NMR Spectrum of 8d

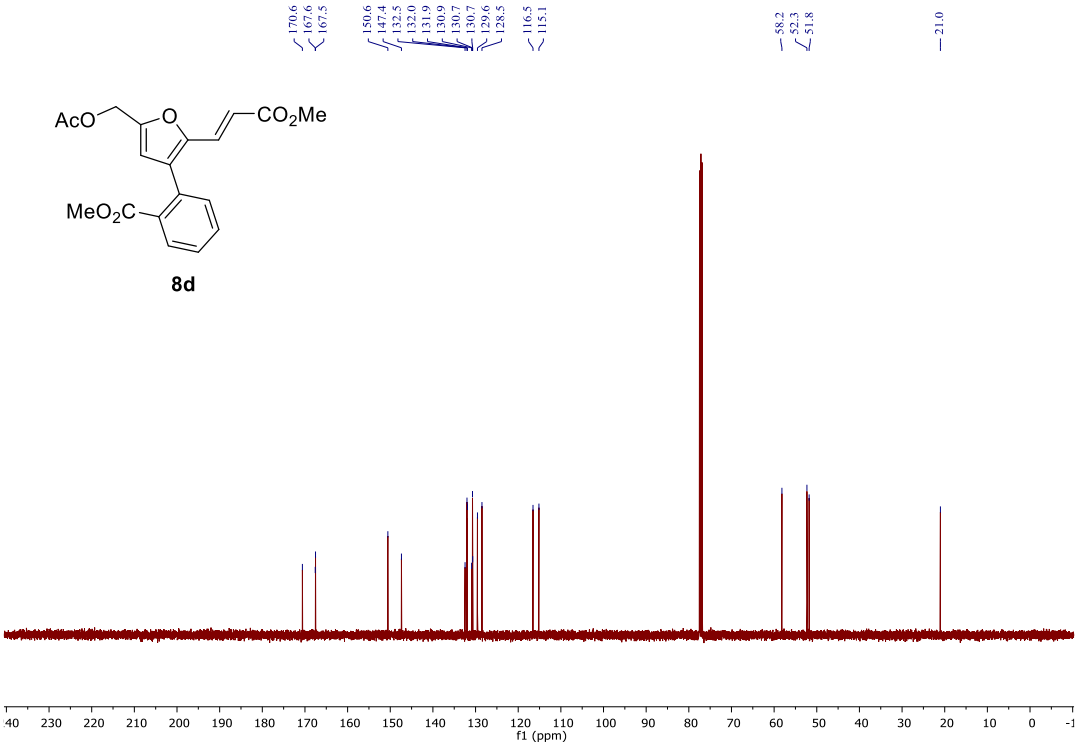

Figure 7.165. ^{1}H NMR Spectrum of 8e

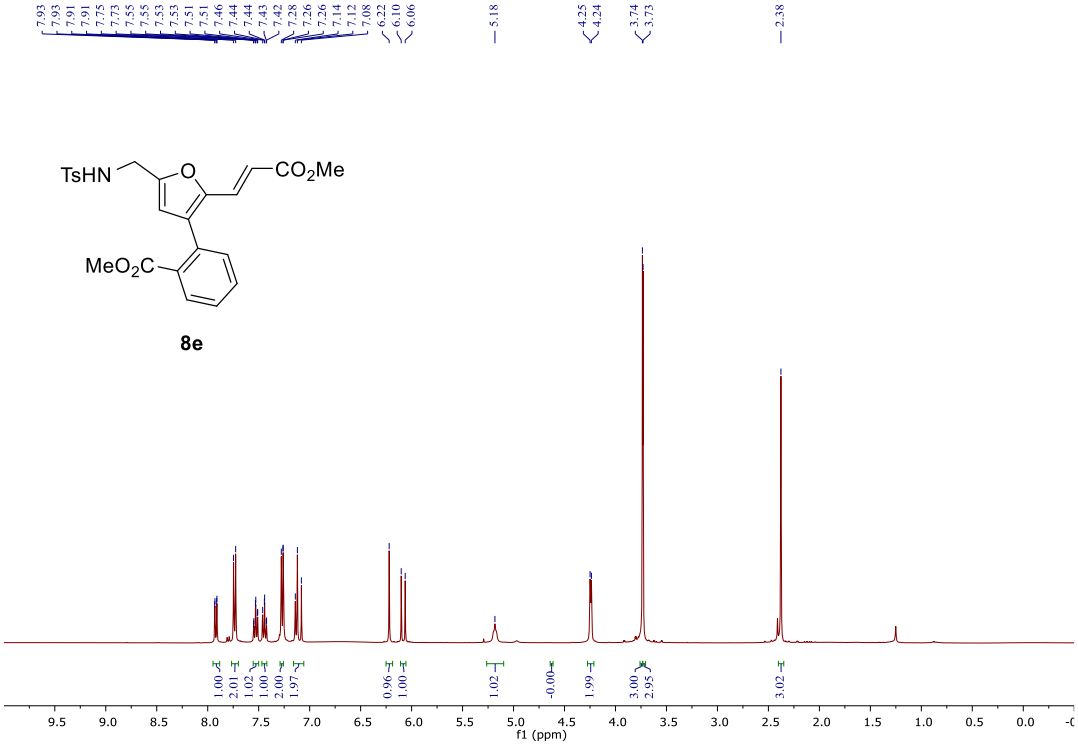

Figure 7.166. ^{13}C NMR Spectrum of 8e

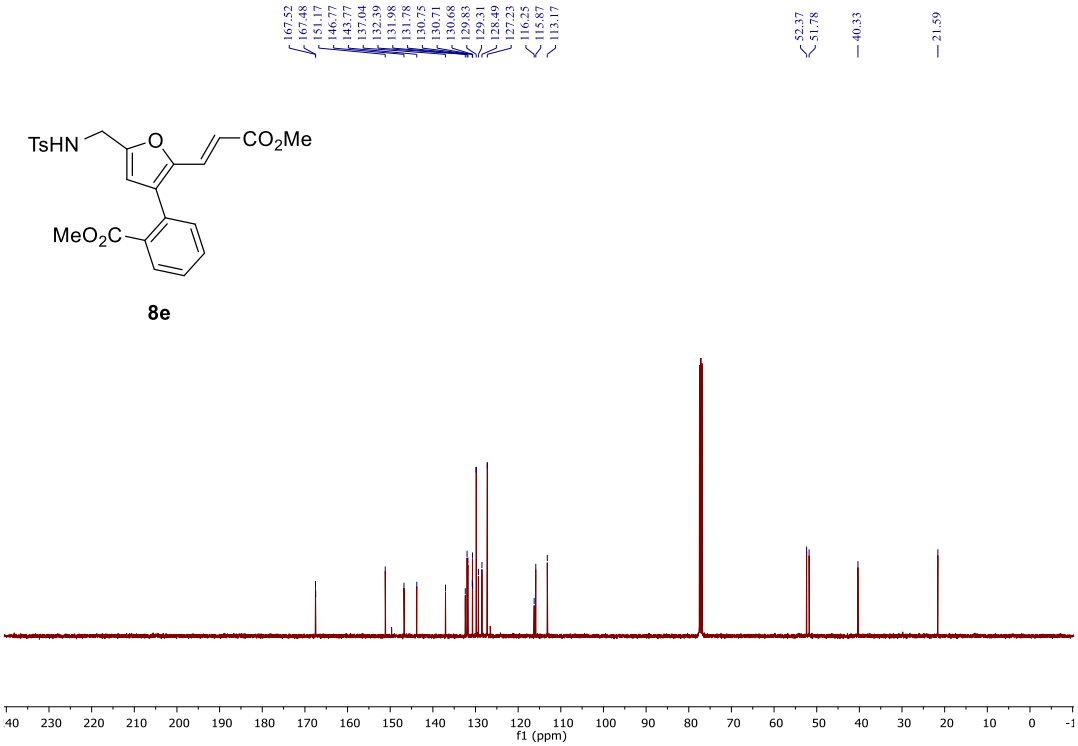

Figure 7.167. ^{1}H NMR Spectrum of 8f

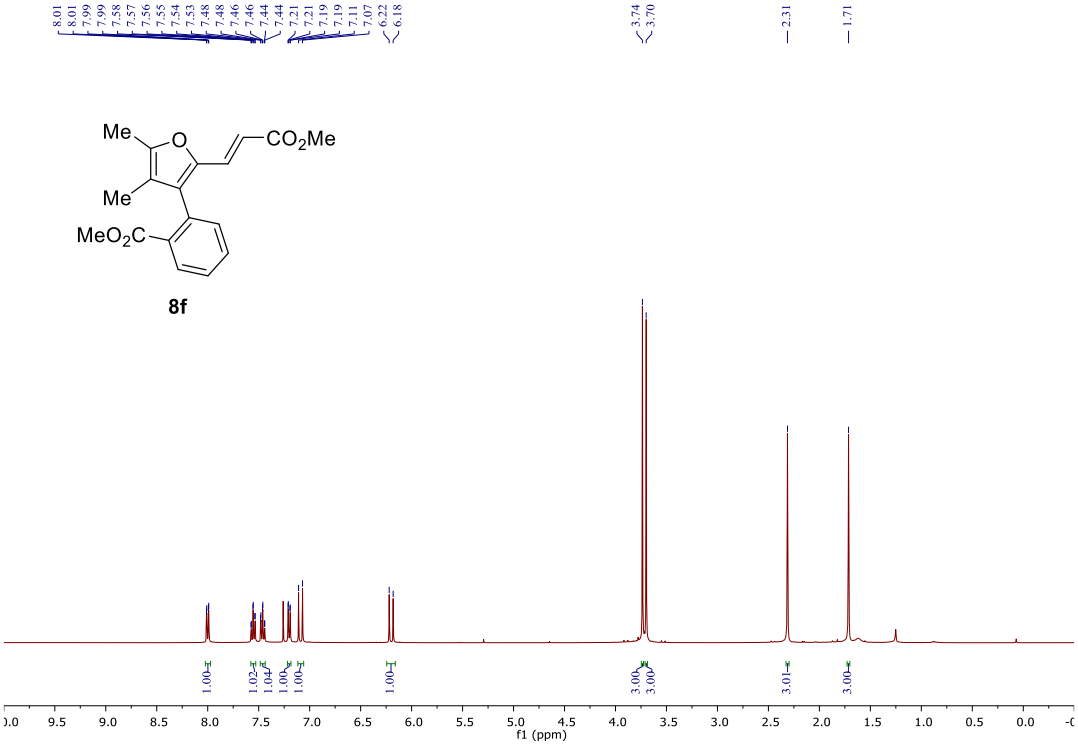

Figure 7.168. ^{13}C NMR Spectrum of 8f

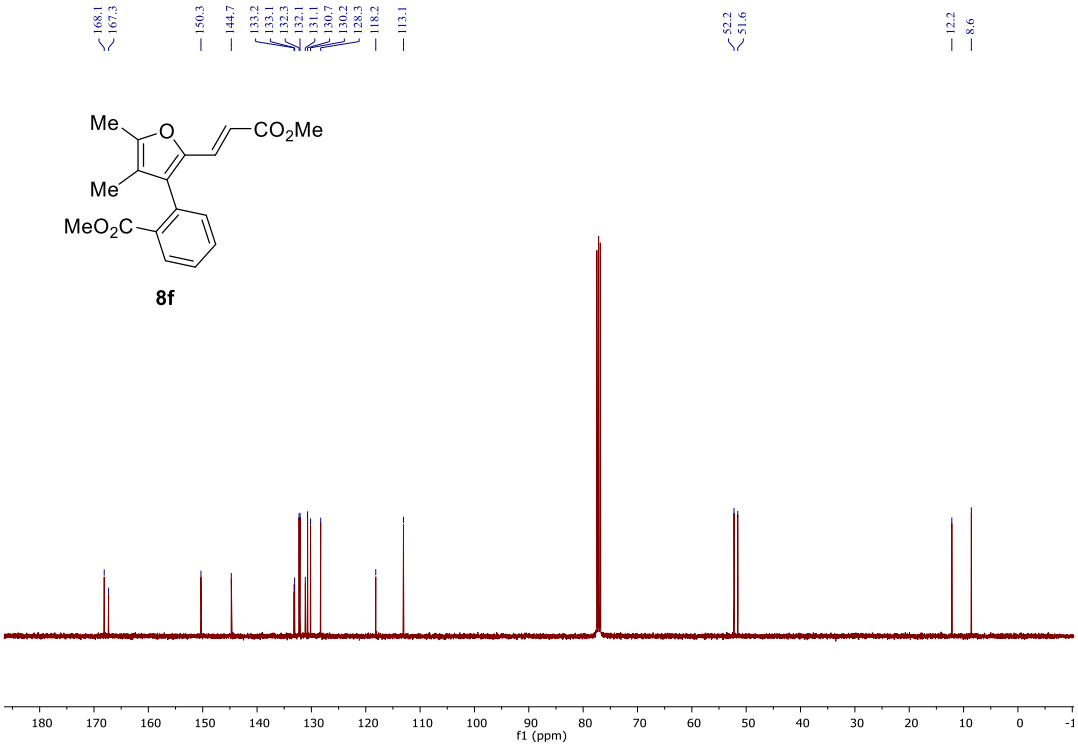

Figure 7.169. ^{1}H NMR Spectrum of 8g

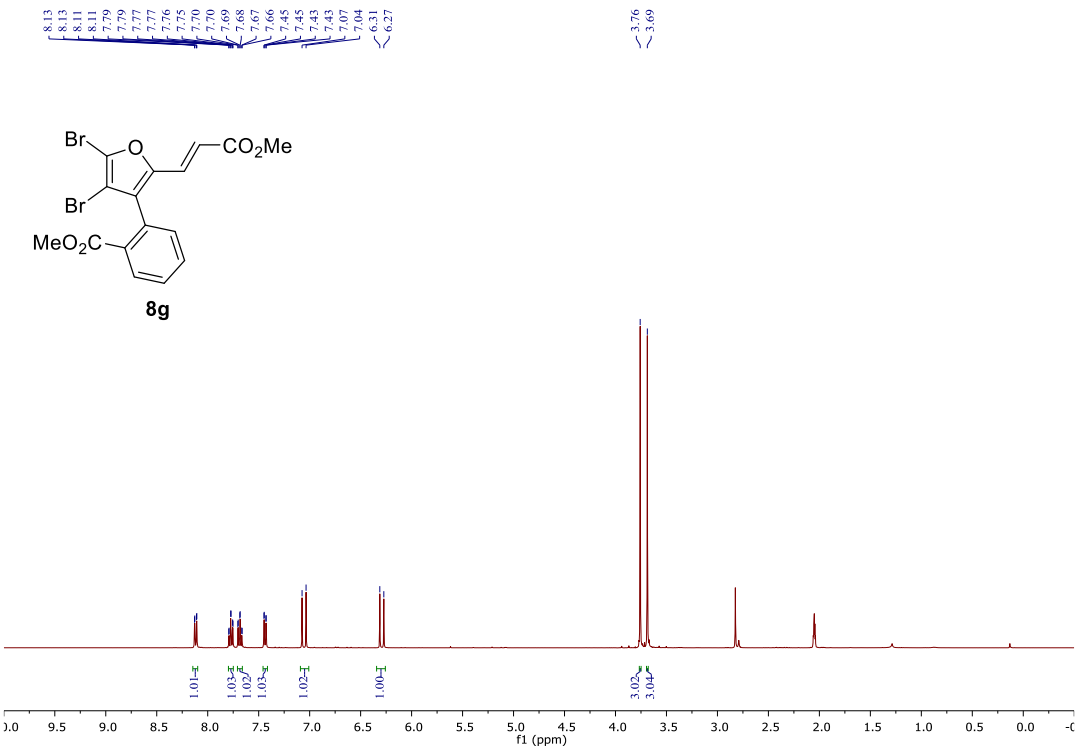

Figure 7.170. ^{13}C NMR Spectrum of 8g

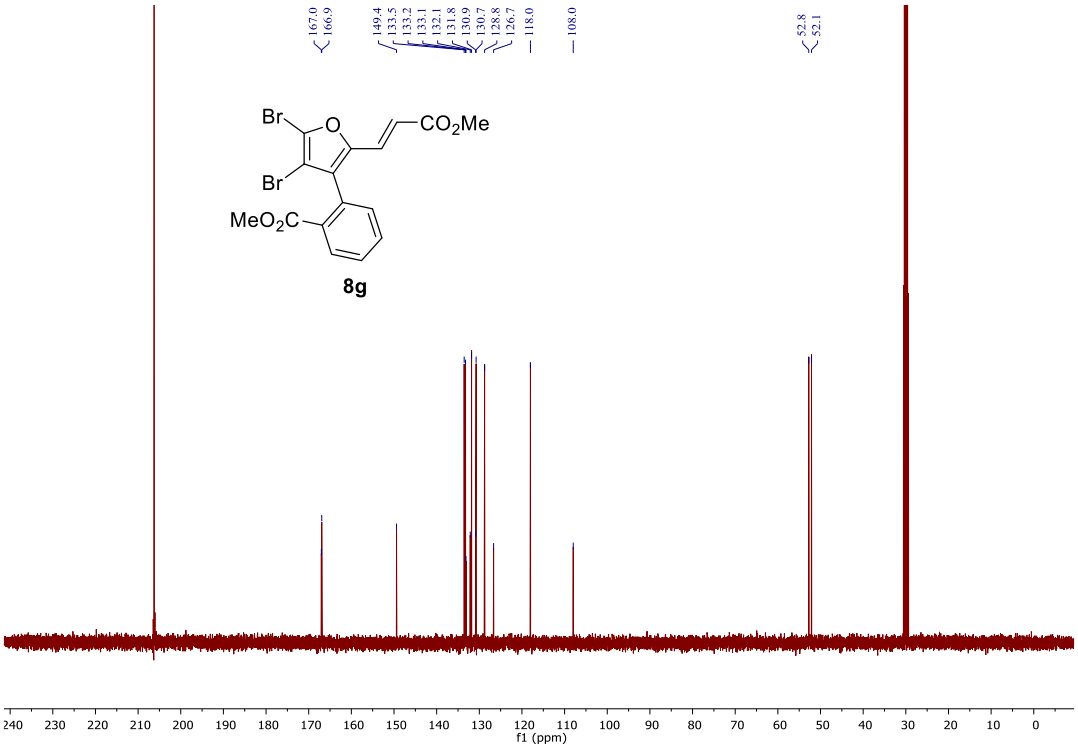

Figure 7.171. ^{1}H NMR Spectrum of 8h

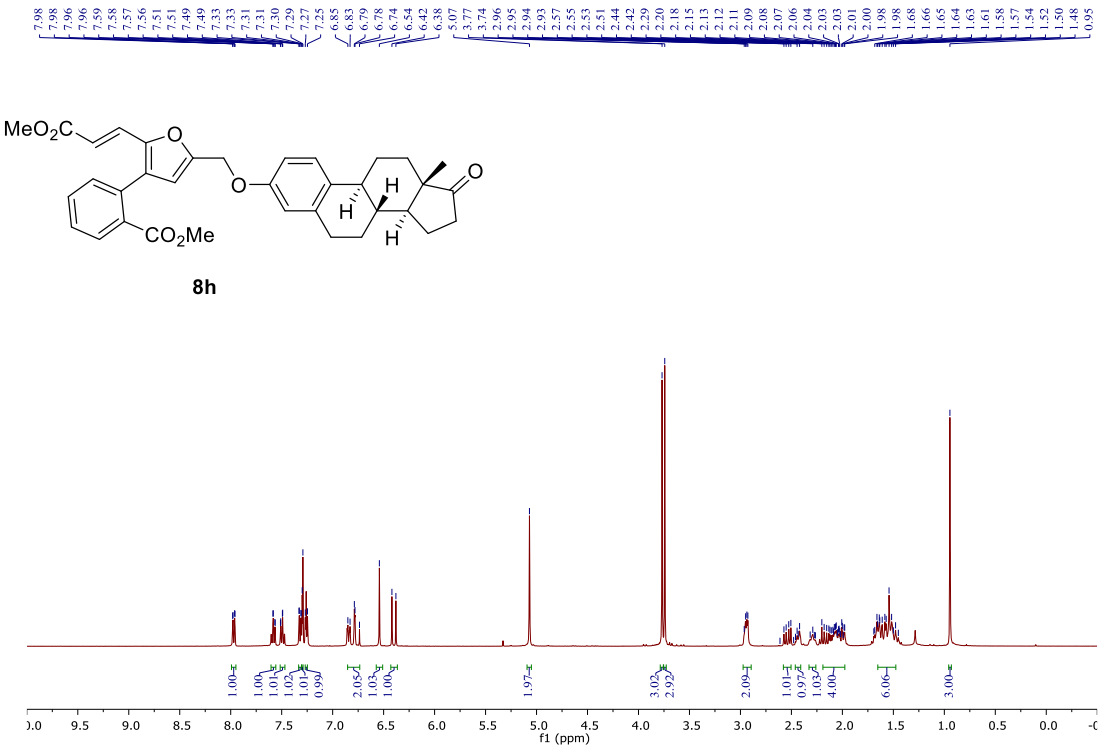

Figure 7.172. ^{13}C NMR Spectrum of 8h

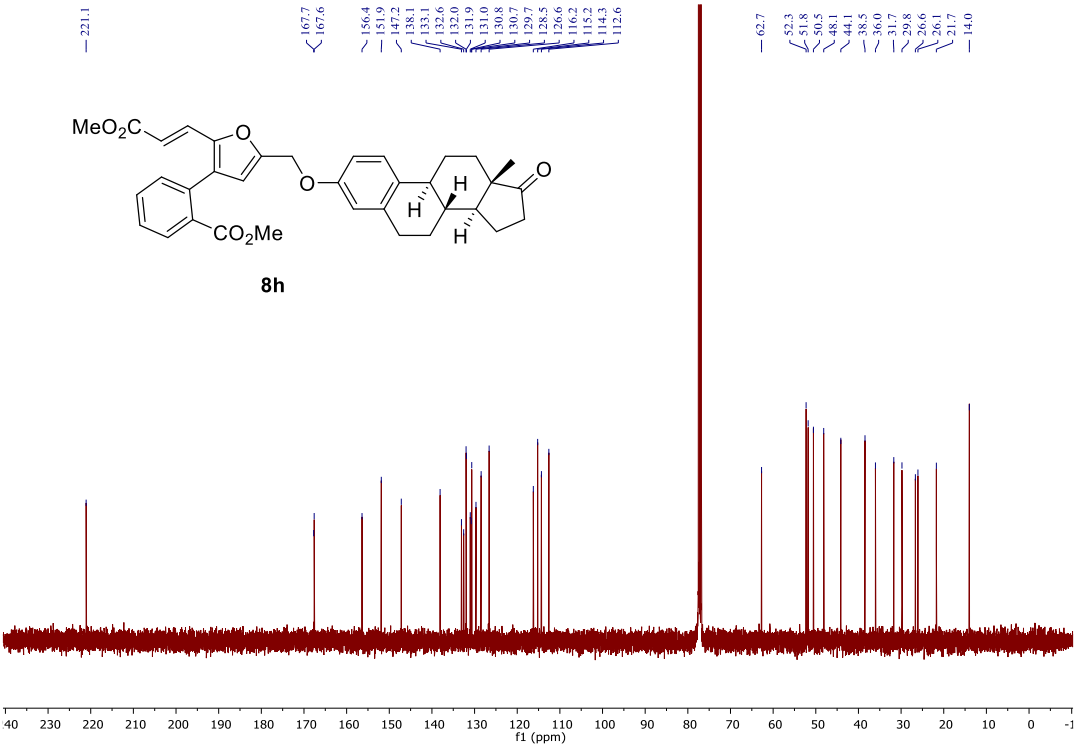

Figure 7.173. ^{1}H NMR Spectrum of 8i

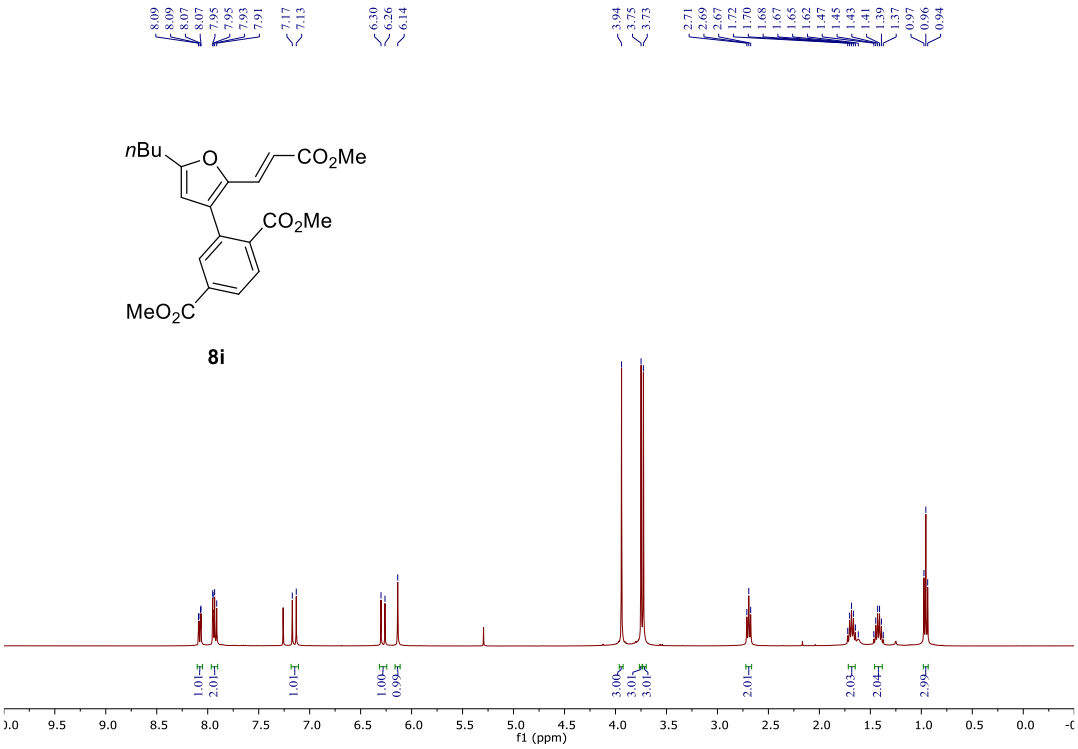

Figure 7.174. ^{13}C NMR Spectrum of 8i

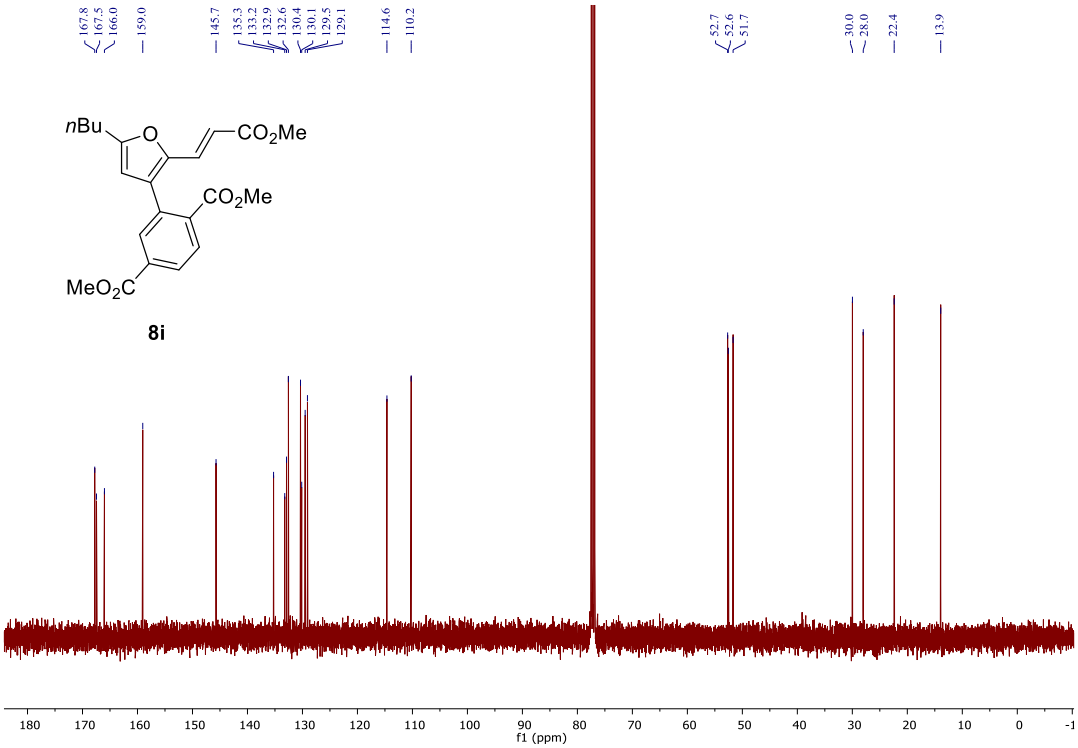

Figure 7.175. ^{1}H NMR Spectrum of 8j

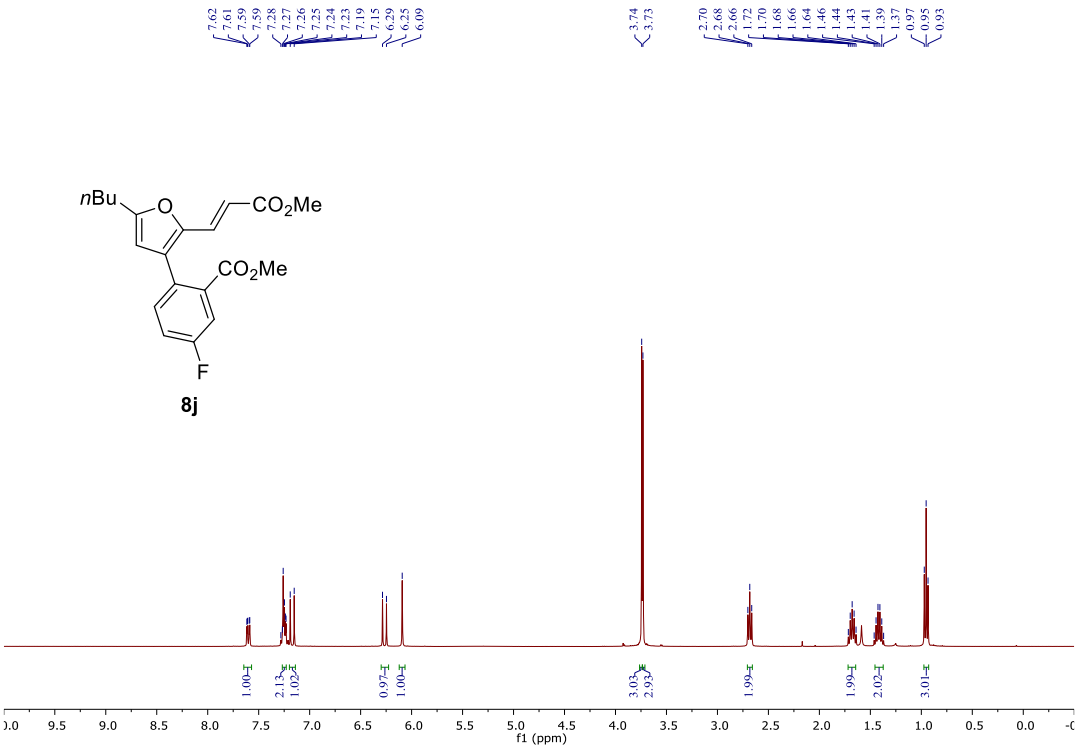

Figure 7.176. ^{13}C NMR Spectrum of 8j

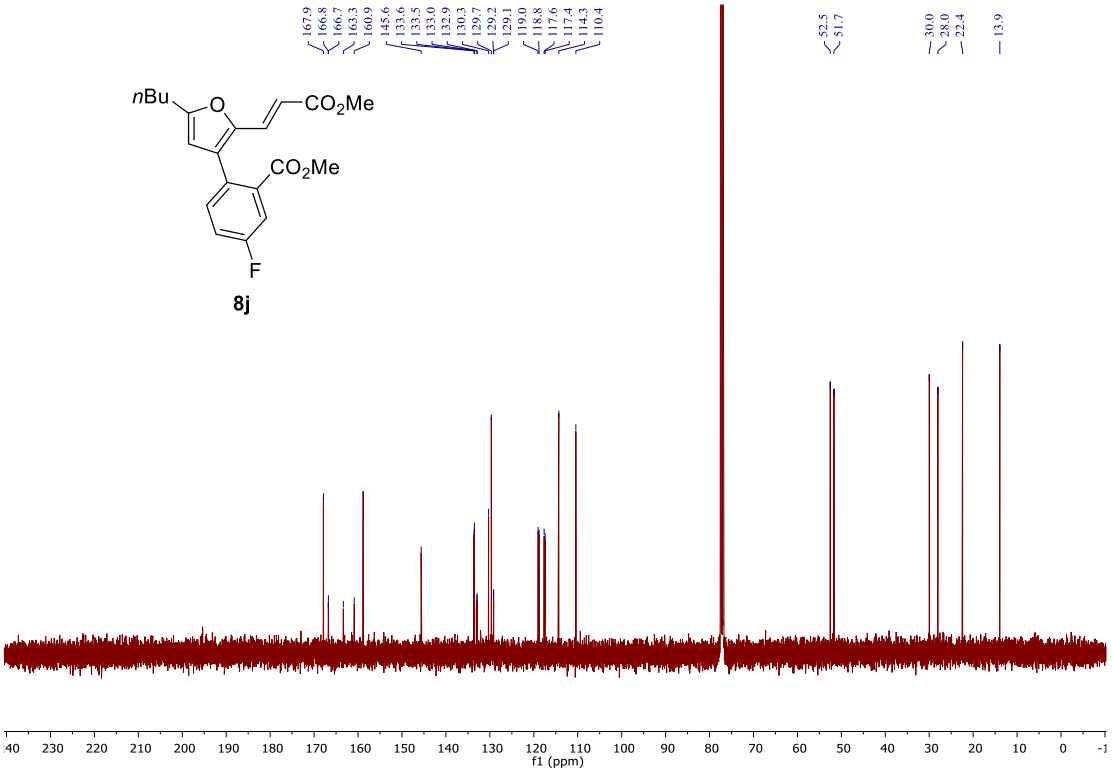

Figure 7.177. ^{19}F NMR Spectrum of 8j

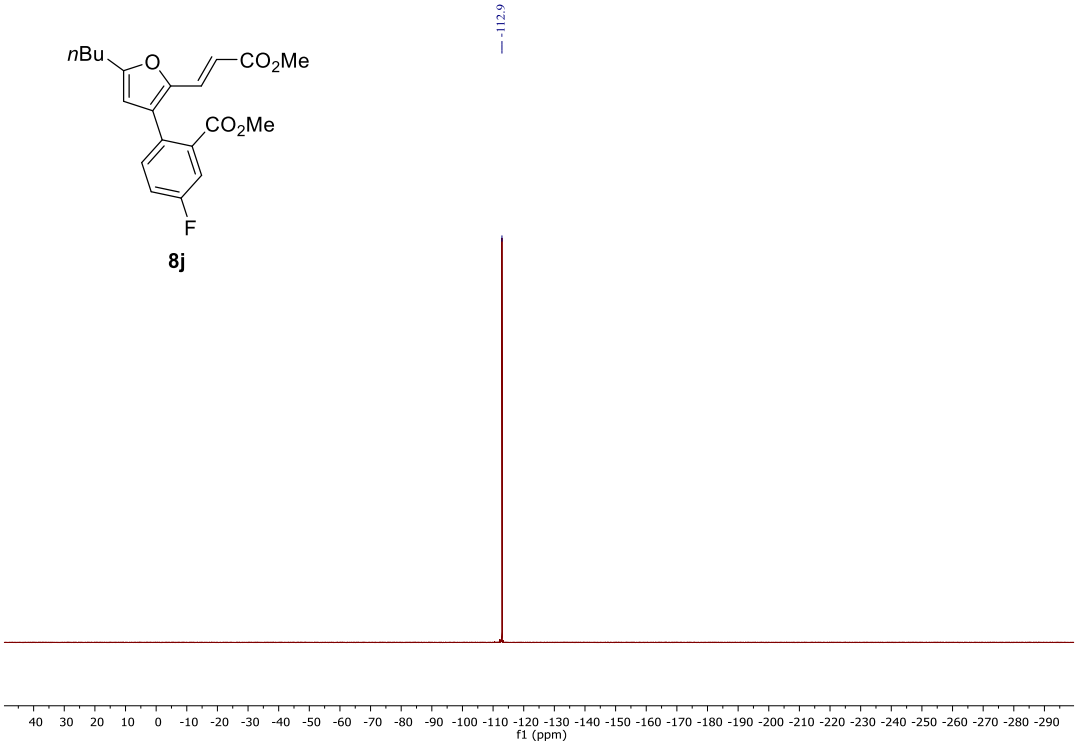

Figure 7.178. ^{1}H NMR Spectrum of 8k

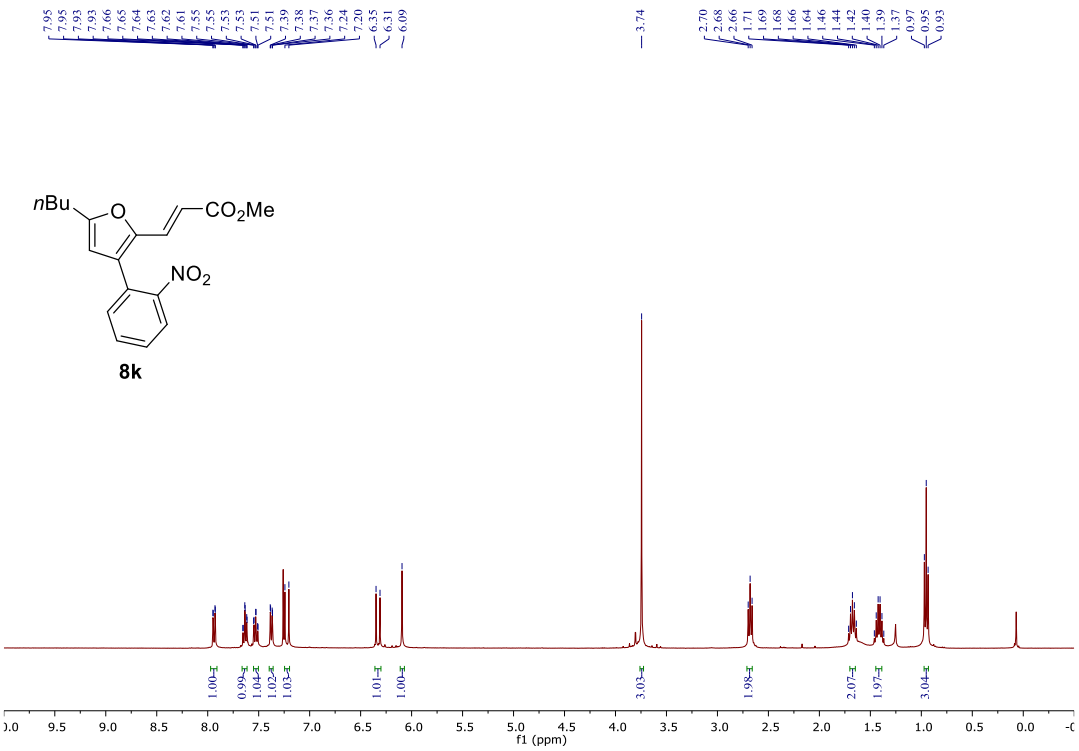

Figure 7.179. ^{13}C NMR Spectrum of 8k

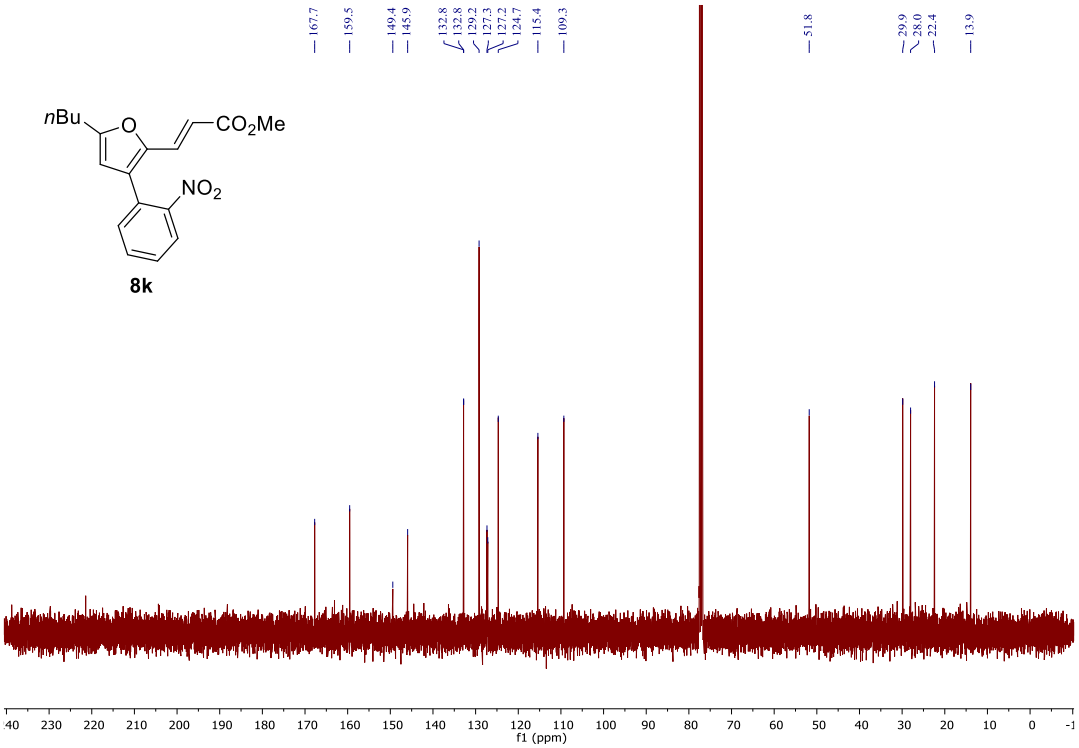

Figure 7.180. ^{1}H NMR Spectrum of 8l

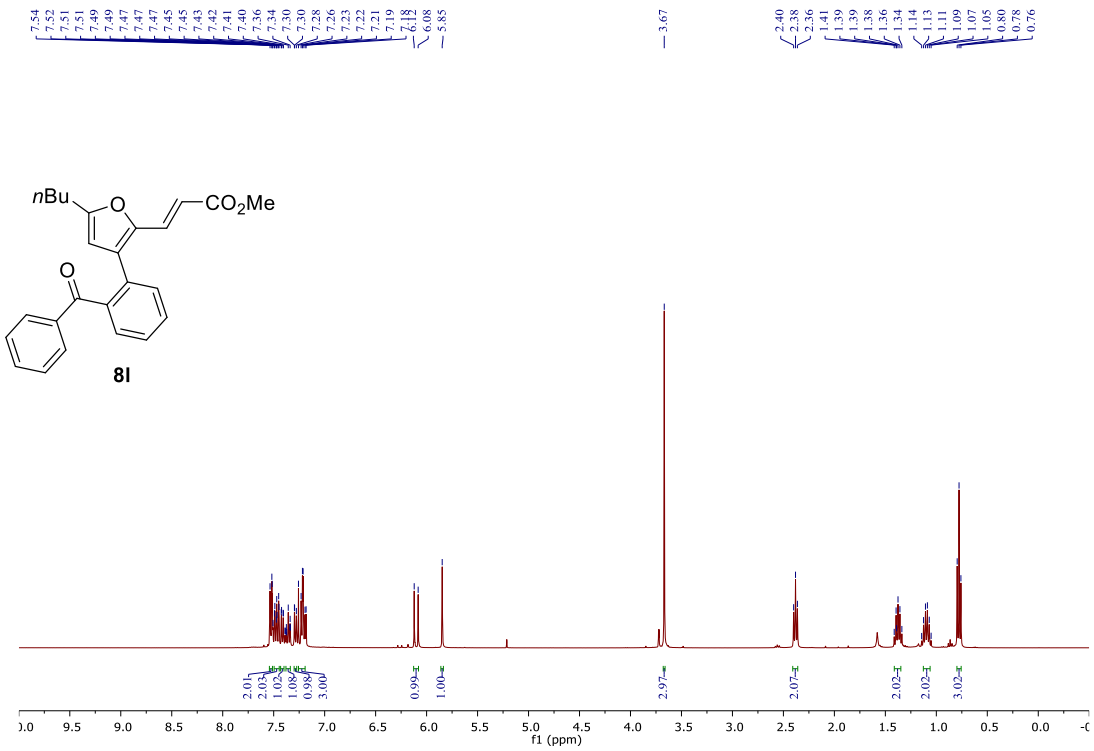

Figure 7.181. ^{13}C NMR Spectrum of 8l

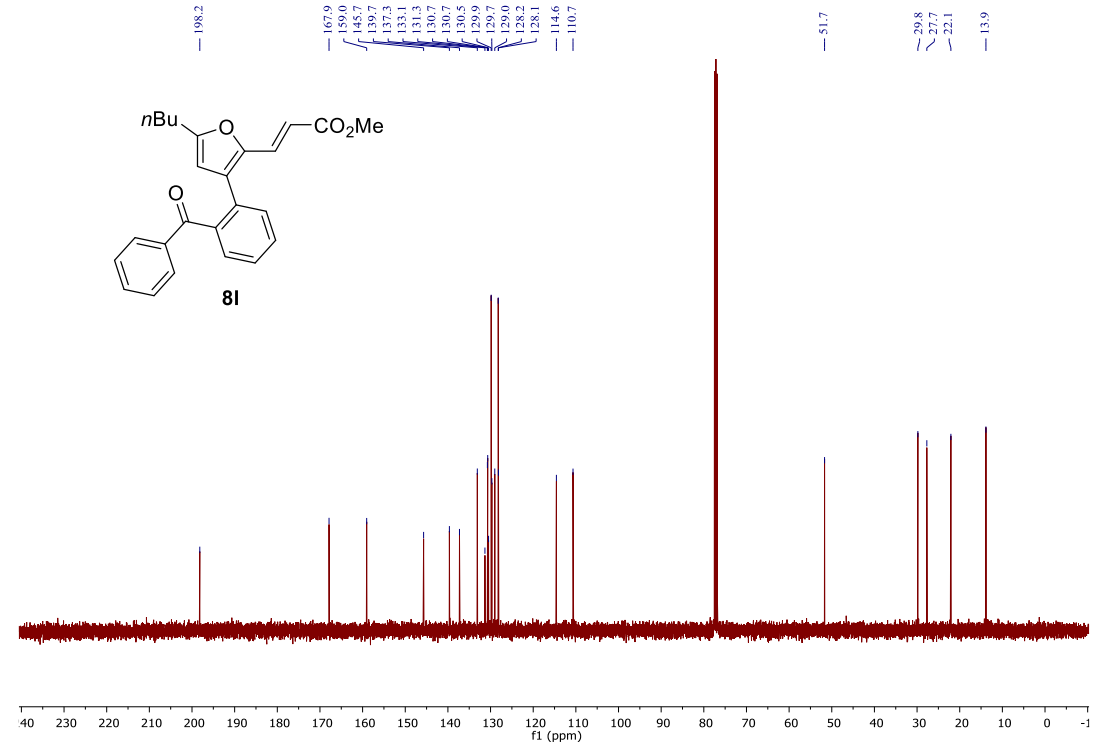

Figure 7.182. ^{1}H NMR Spectrum of 8m

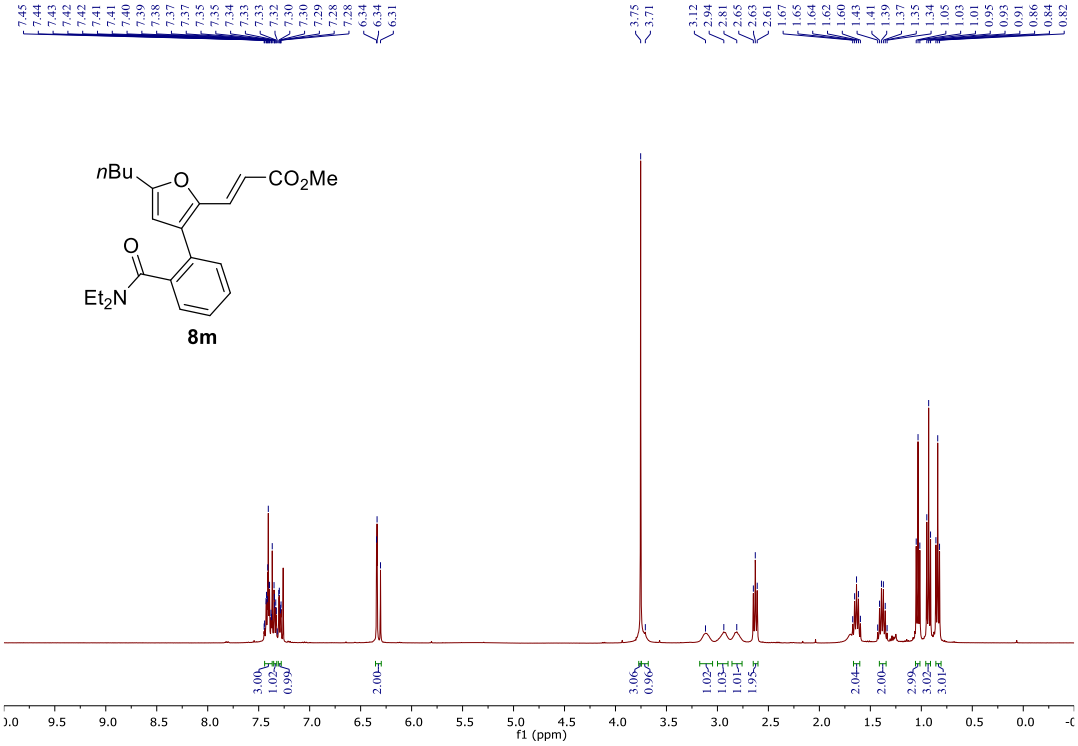

Figure 7.183. ^{13}C NMR Spectrum of 8m

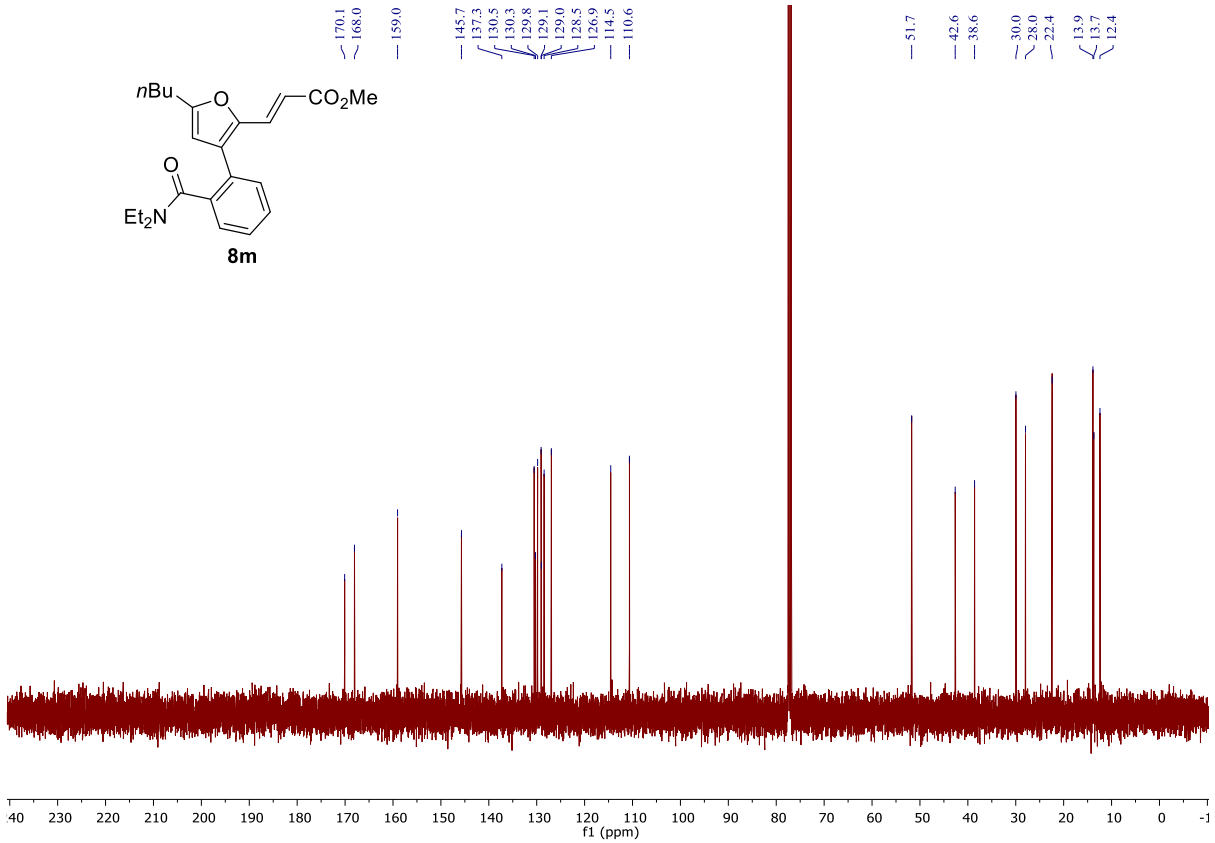

Figure 7.184. ^{1}H NMR Spectrum of 8n

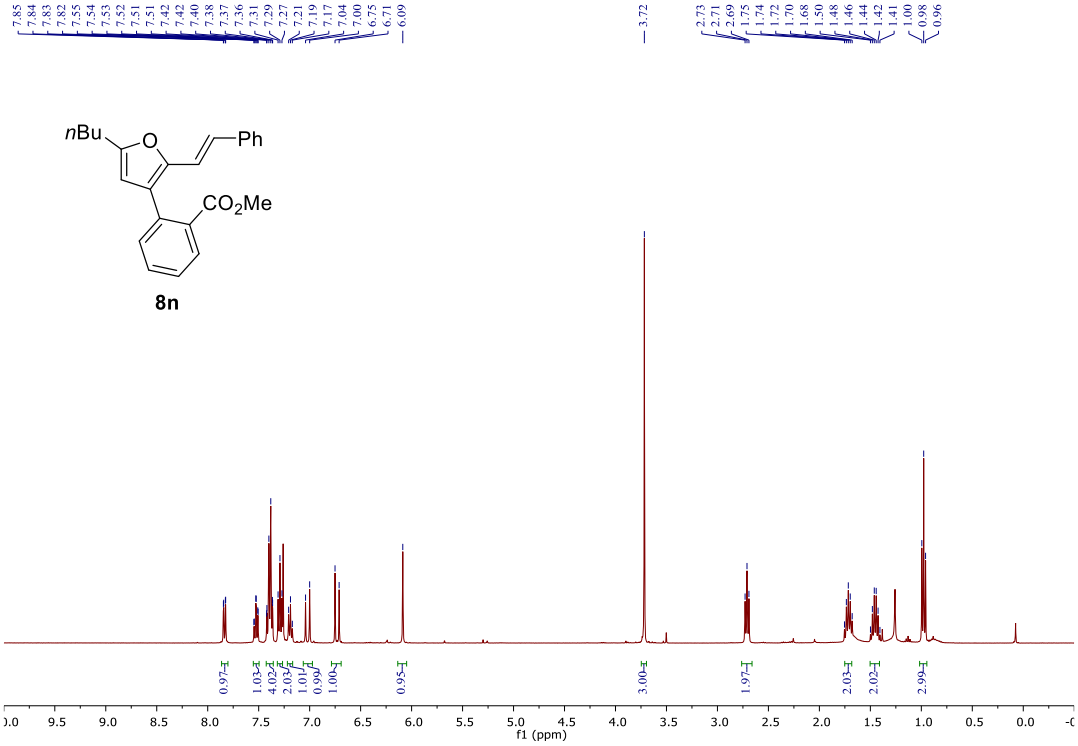

Figure 7.185. ^{13}C NMR Spectrum of 8n

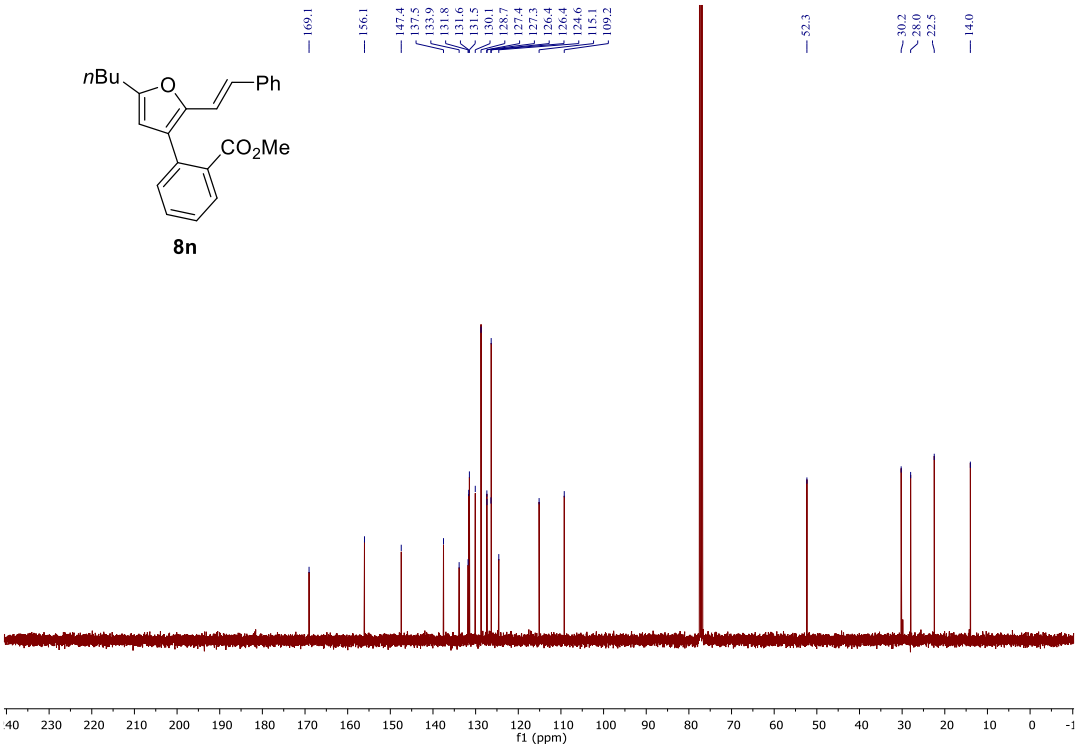

Figure 7.186. ^{1}H NMR Spectrum of 8o

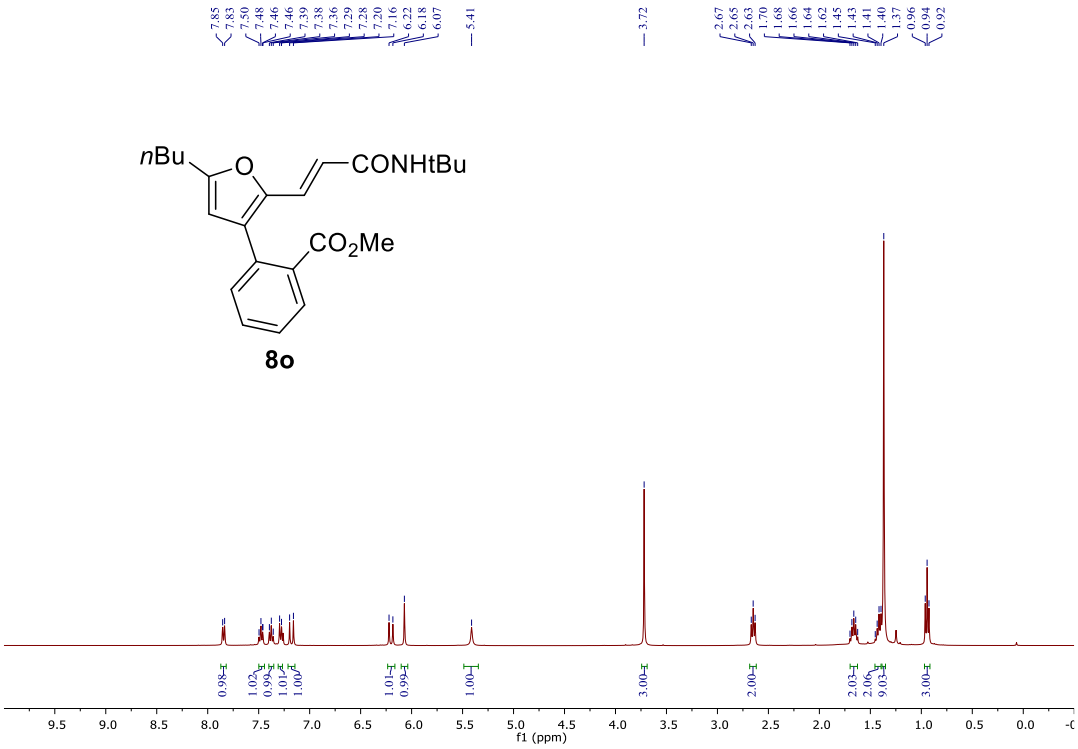

Figure 7.187. ^{13}C NMR Spectrum of 8o

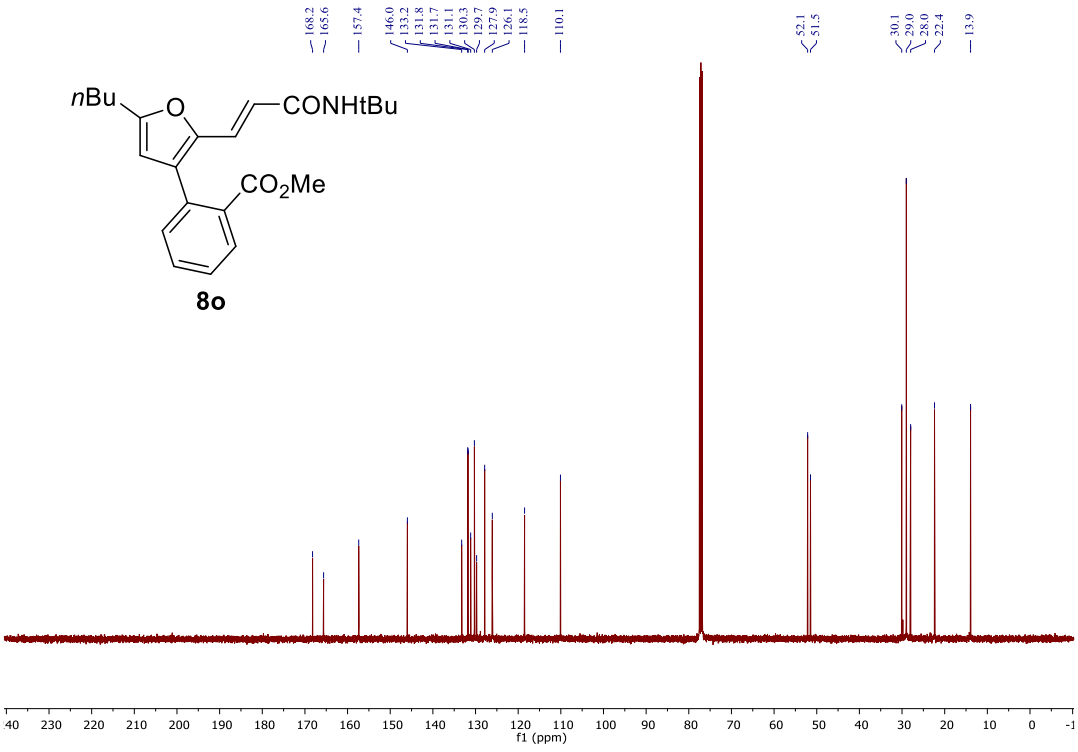

Figure 7.188. ^{1}H NMR Spectrum of 8q

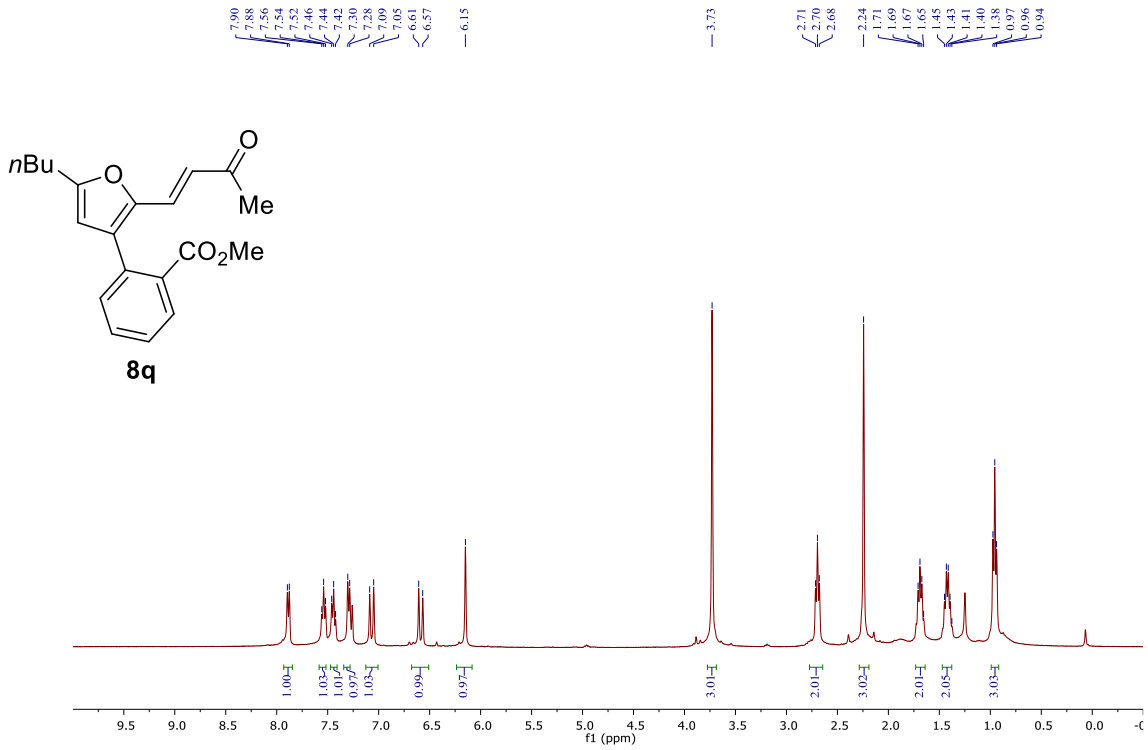

Figure 7.189. ^{13}C NMR Spectrum of 8q

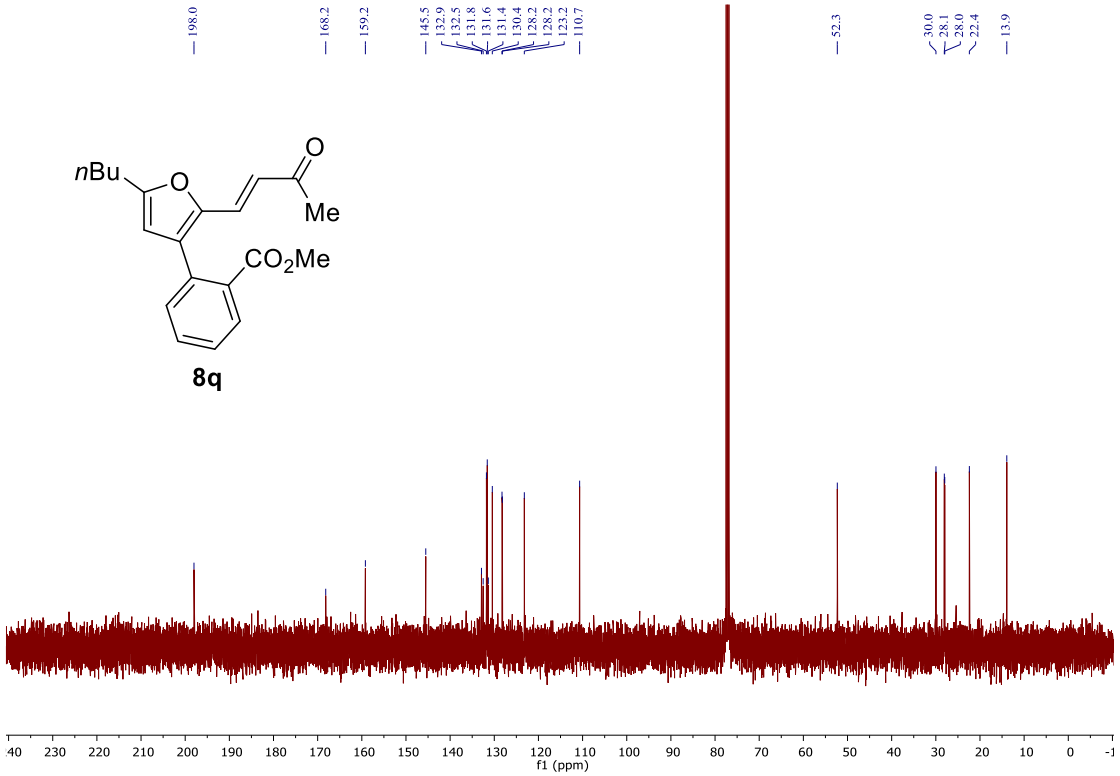

Figure 7.190. ^{1}H NMR Spectrum of 8p

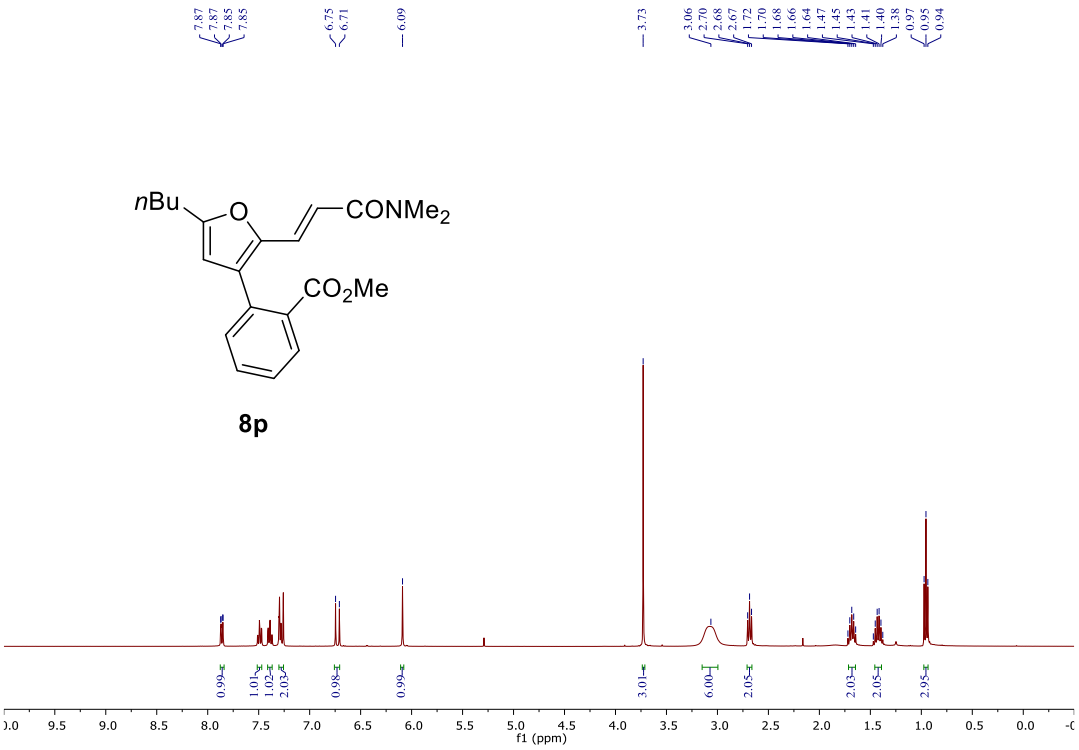

Figure 7.191. ^{13}C NMR Spectrum of 8p

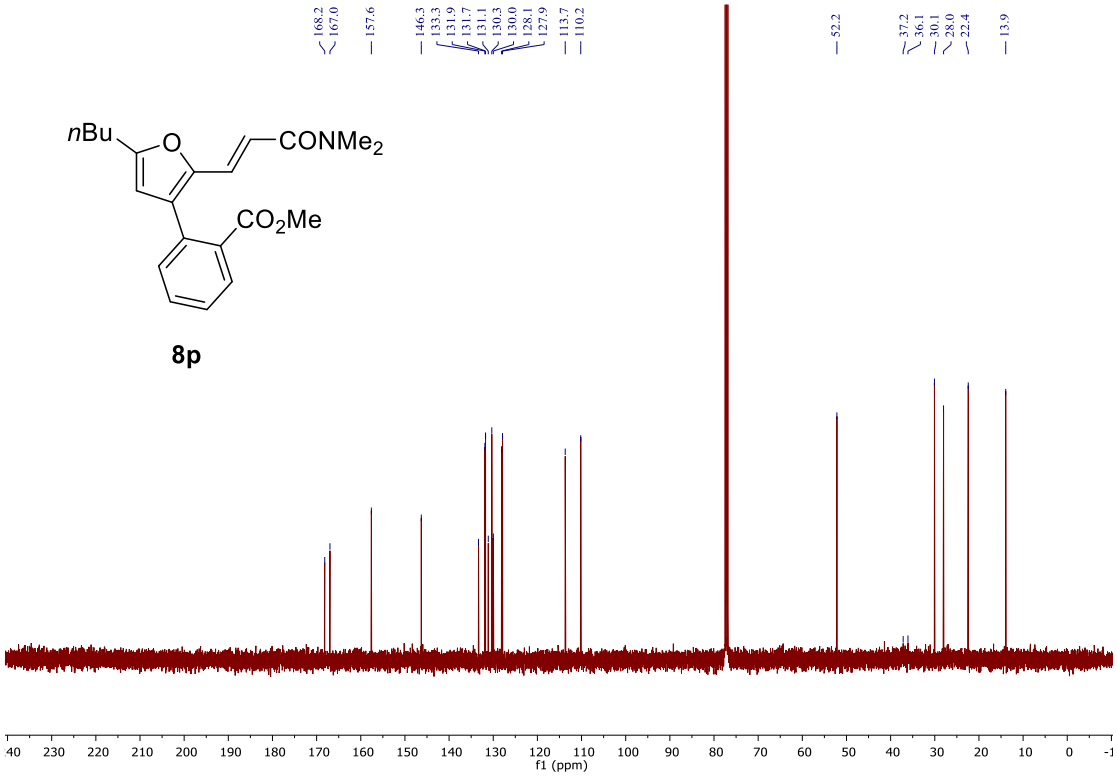

Figure 7.192. ^{1}H NMR Spectrum of 8r

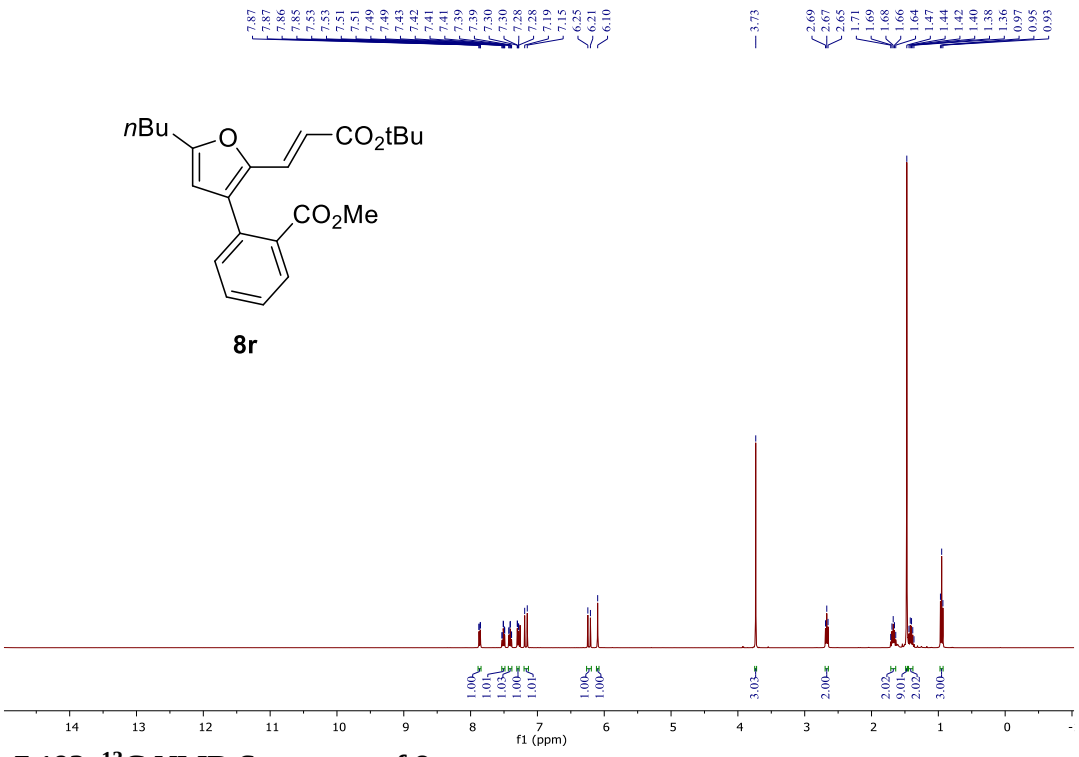

Figure 7.193. ^{13}C NMR Spectrum of 8r

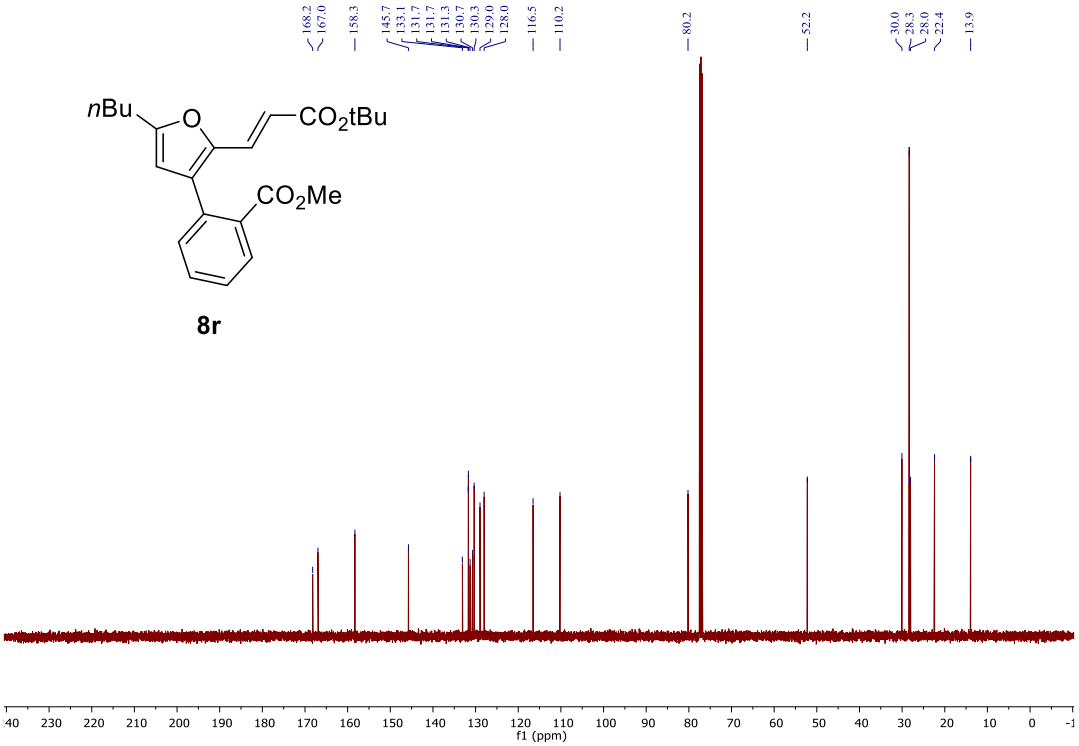

Figure 7.194. ^{1}H NMR Spectrum of 13

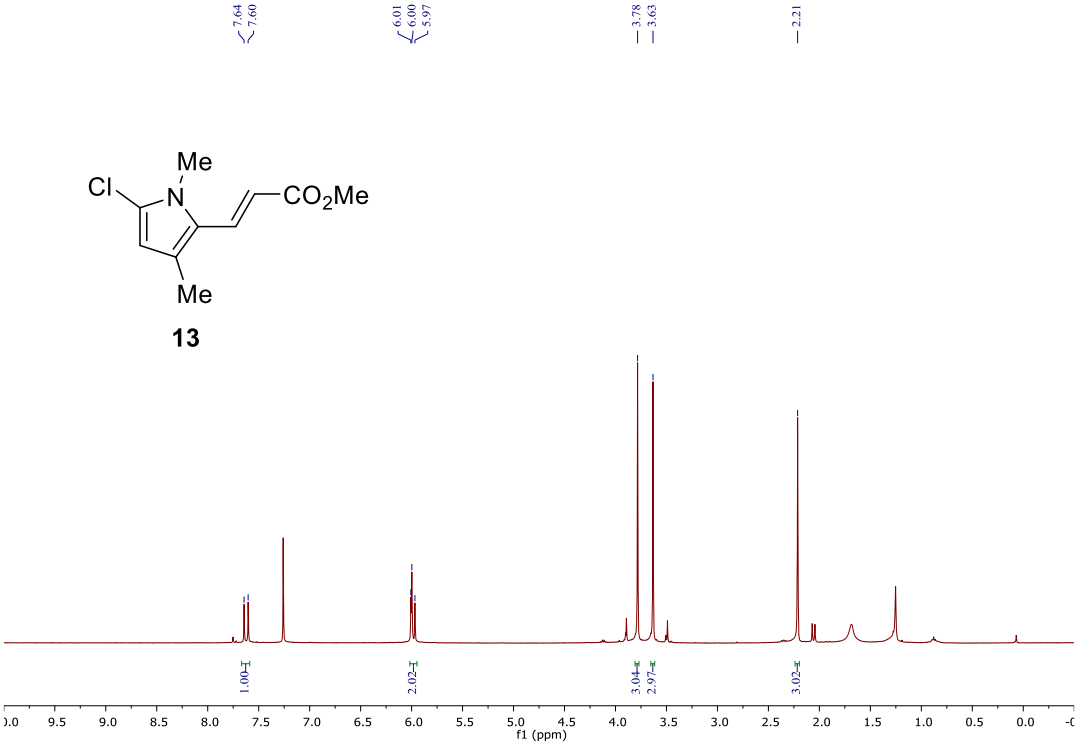

Figure 7.195. ^{13}C NMR Spectrum of 13

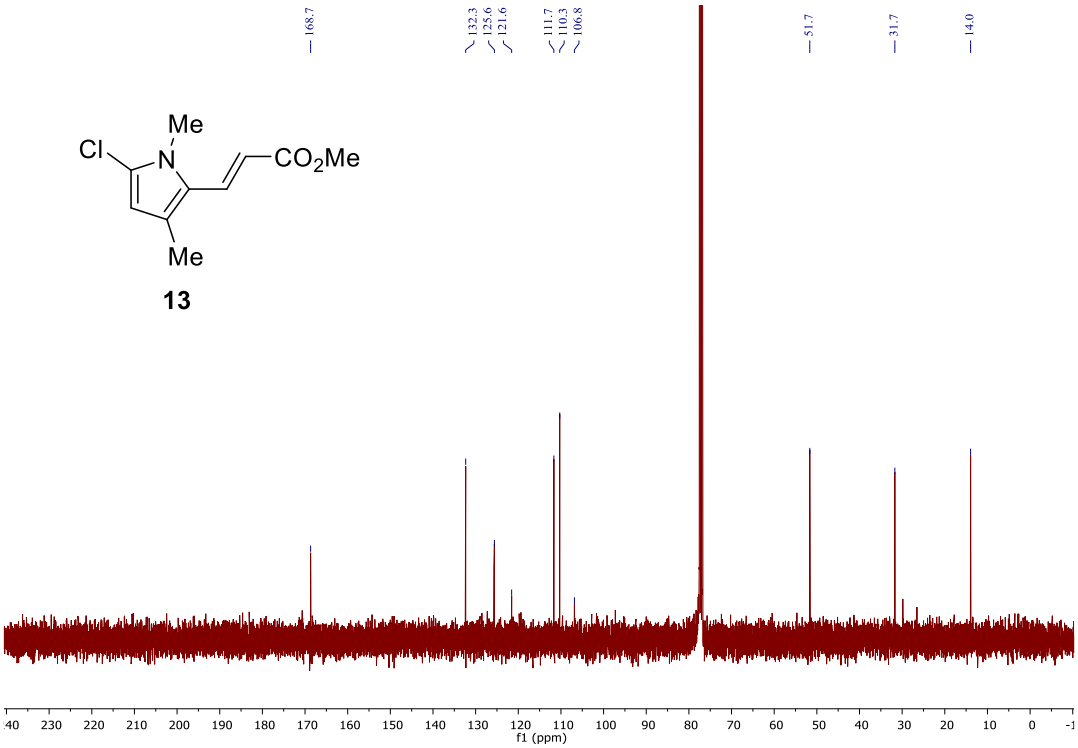

Figure 7.196. ^{1}H NMR Spectrum of 14

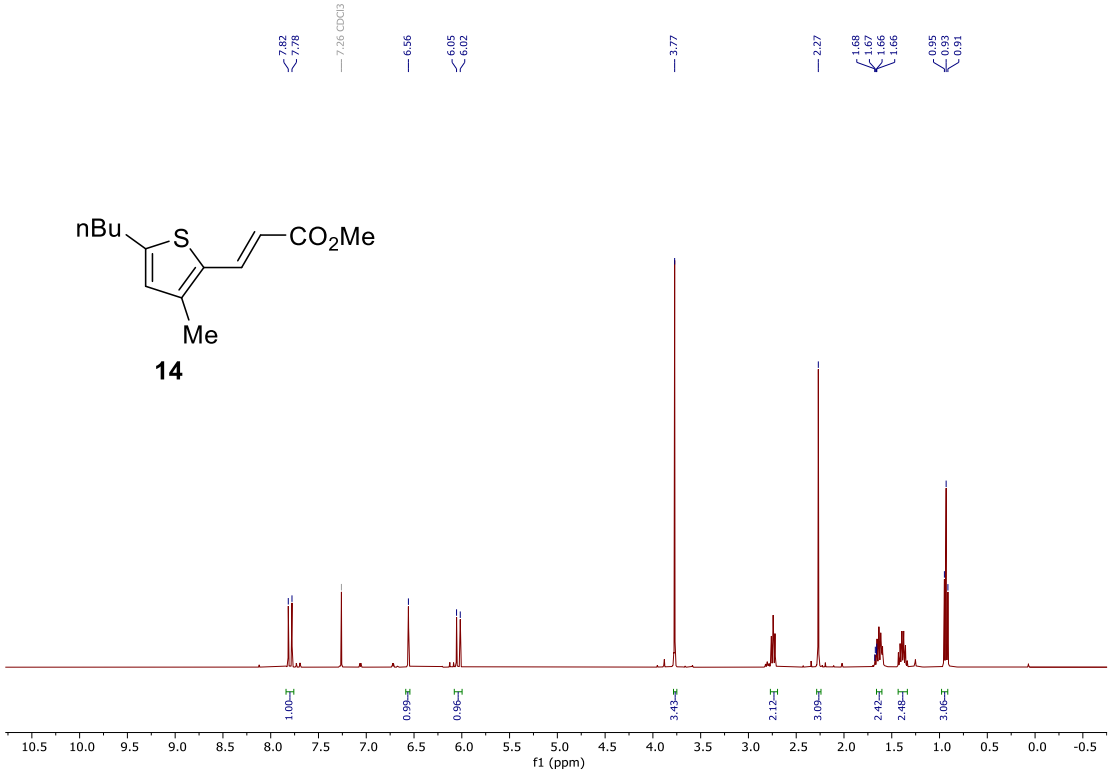

Figure 7.197. ^{1}H NMR Spectrum of 14

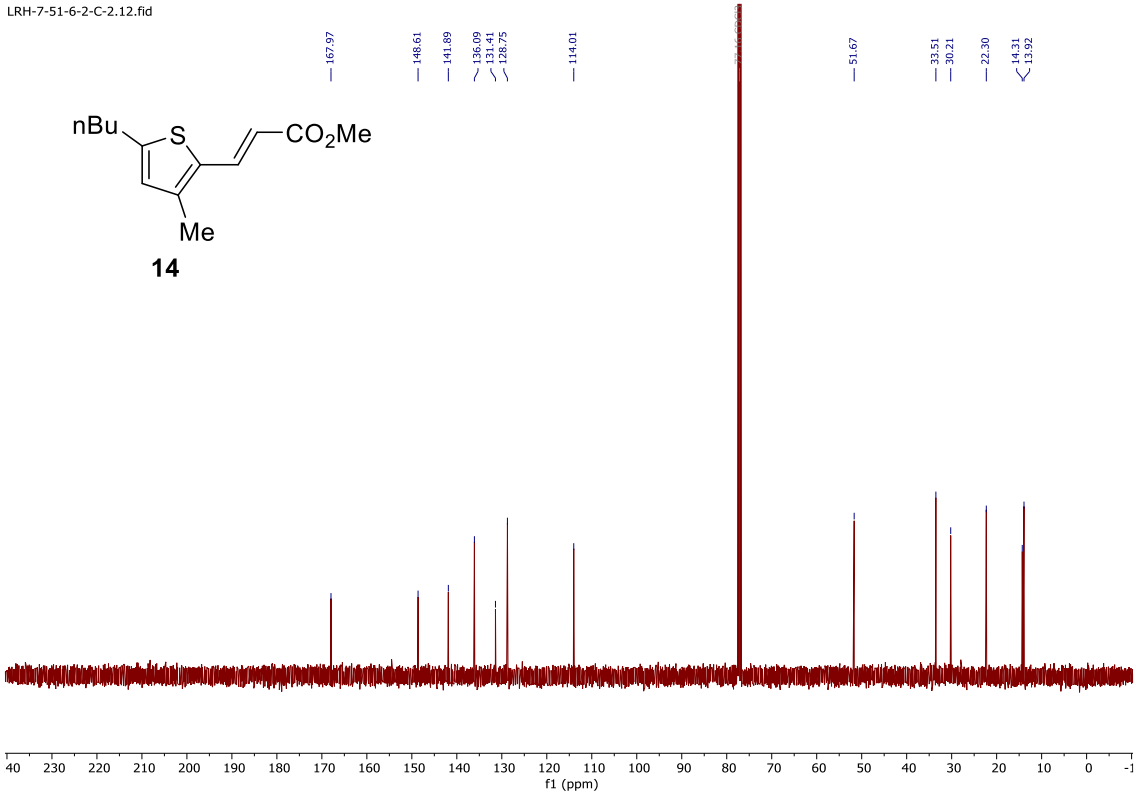

Figure 7.198. ^{1}H NMR Spectrum of 21

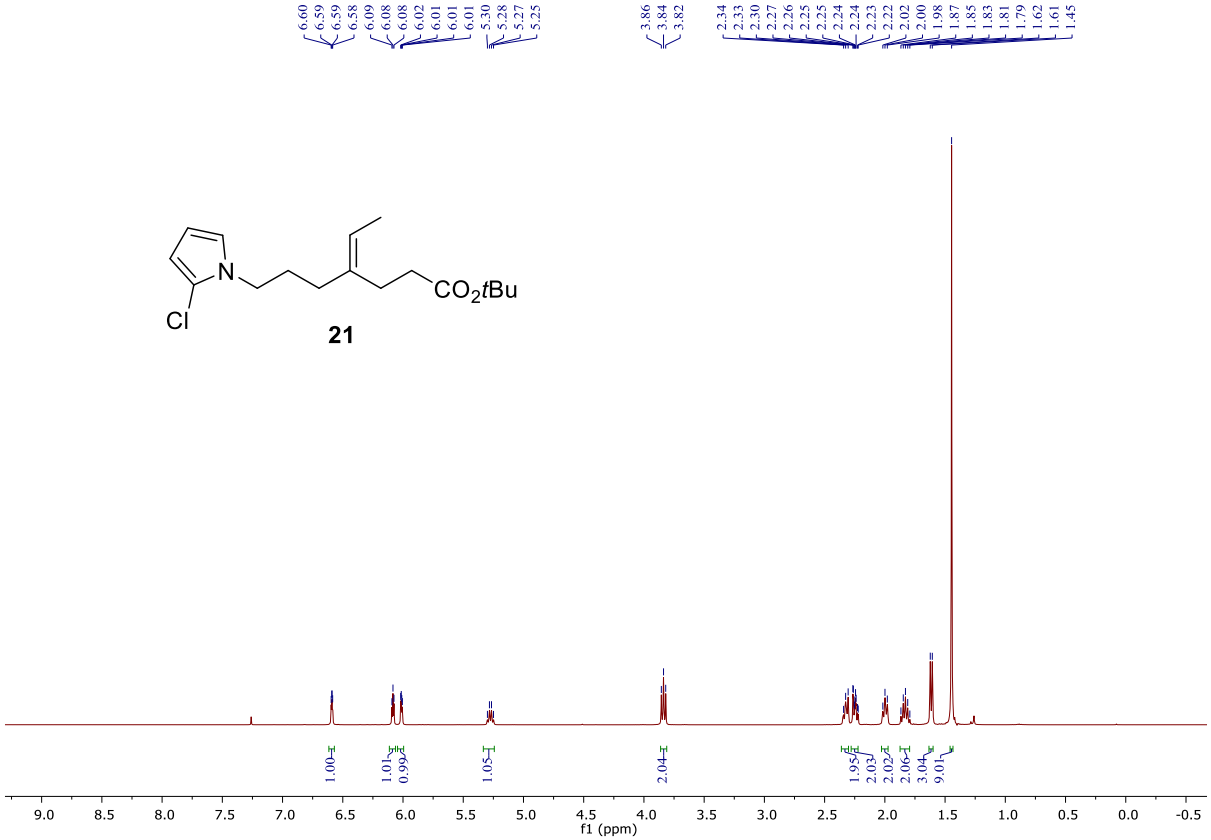

Figure 7.199. ^{13}C NMR Spectrum of 21

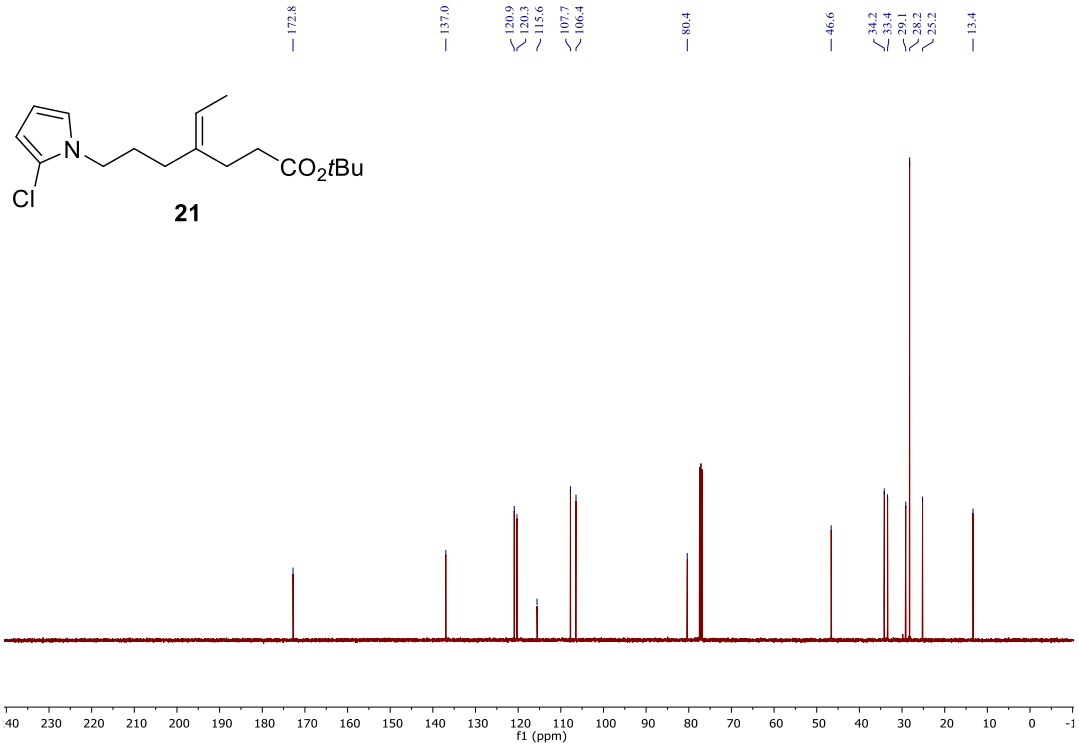

Figure 7.200. ^{1}H NMR Spectrum of 23

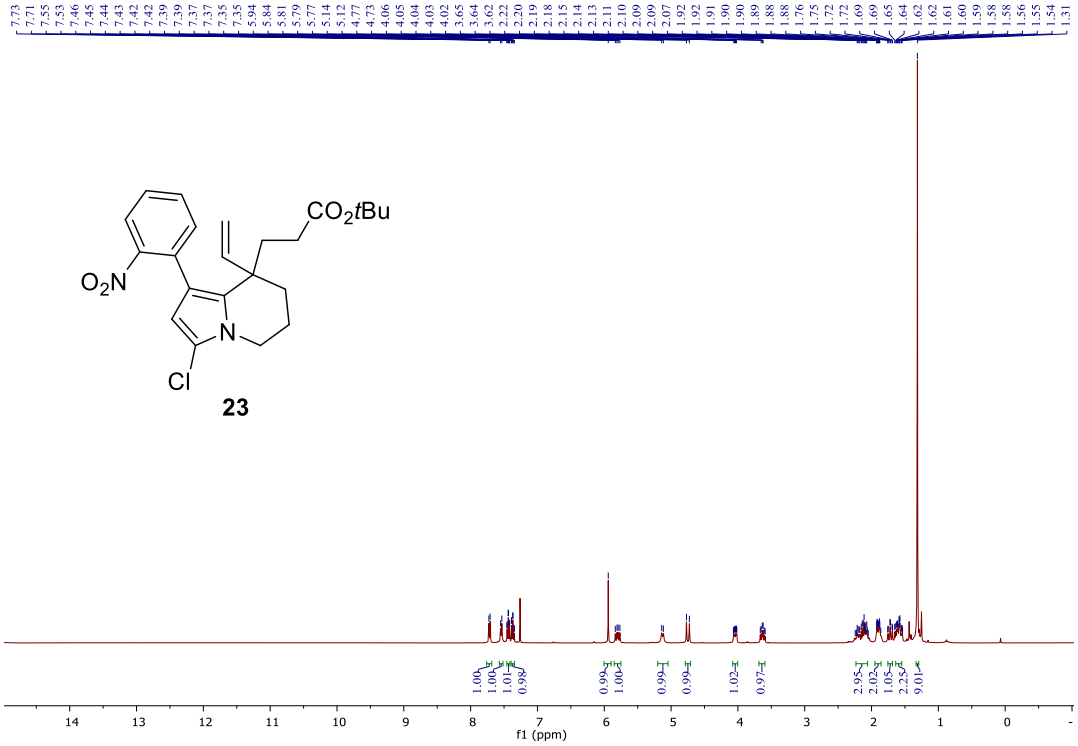

Figure 7.201. ^{13}C NMR Spectrum of 23

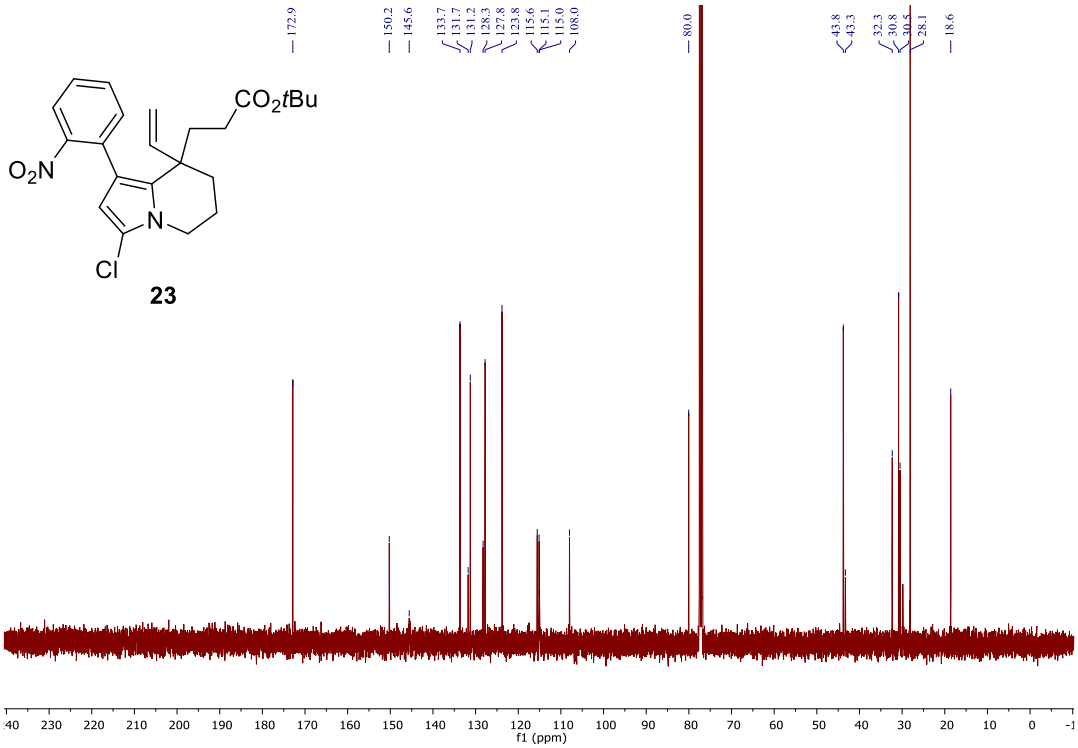

Figure 7.202. ^{1}H NMR Spectrum of 24

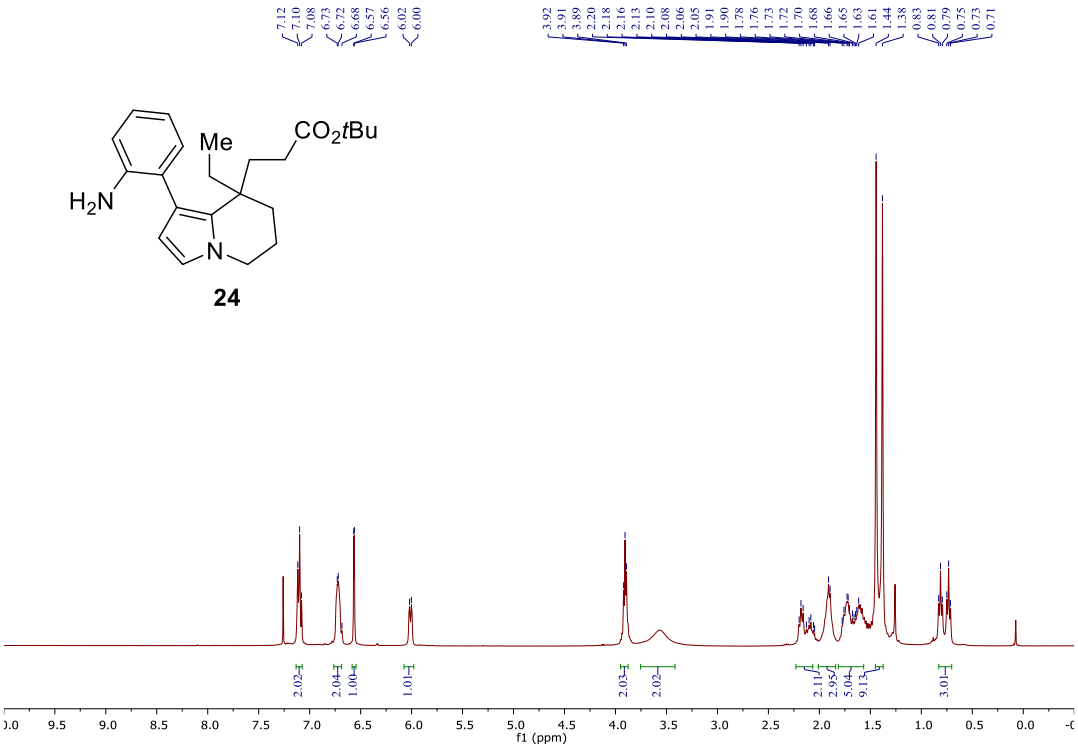

Figure 7.203. ^{13}C NMR Spectrum of 24

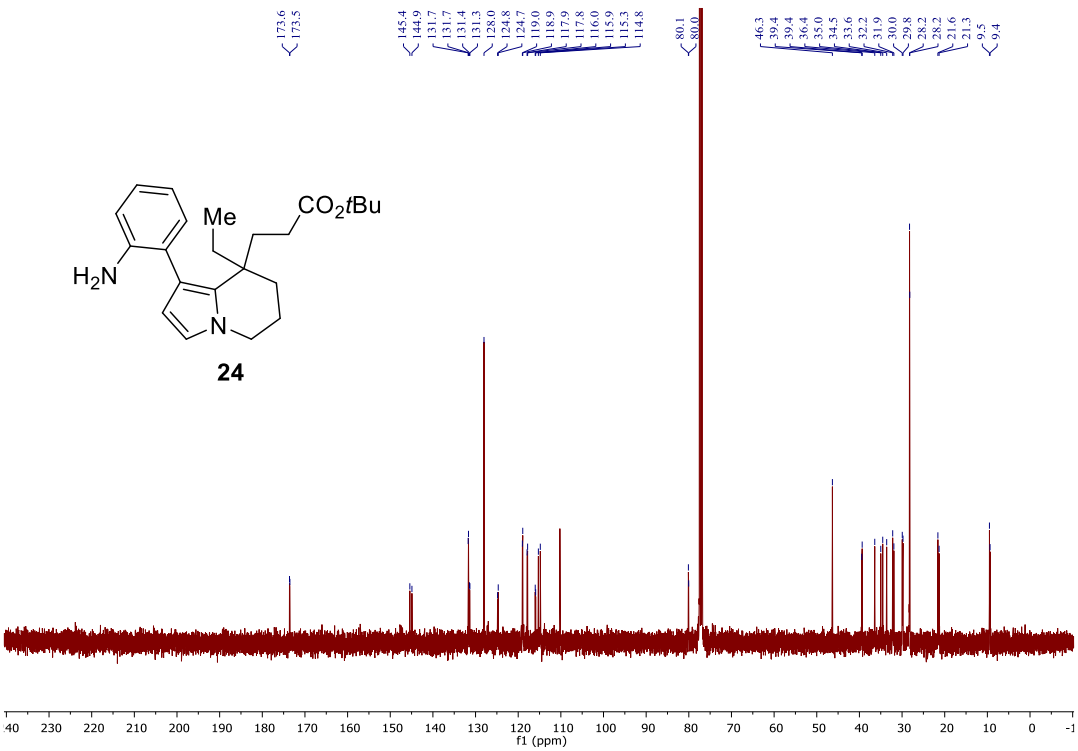

Figure 7.204. ^{1}H NMR Spectrum of 15

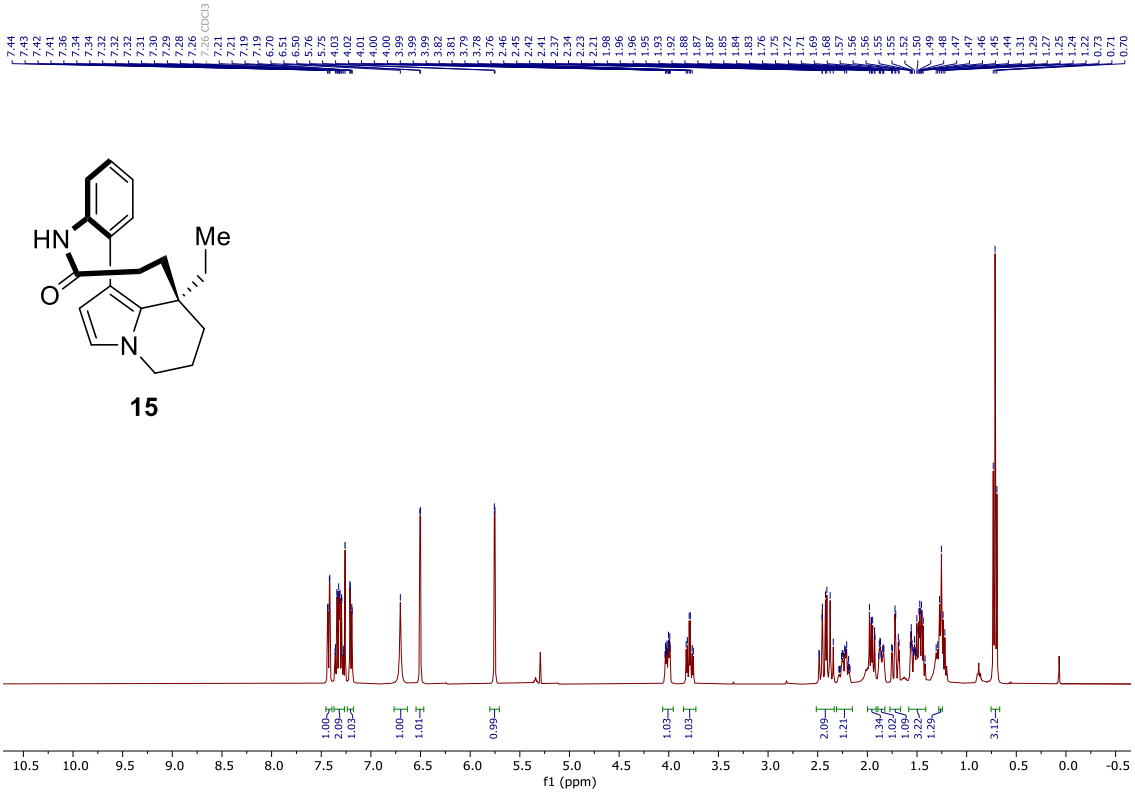

Figure 7.205. ^{13}C NMR Spectrum of 15

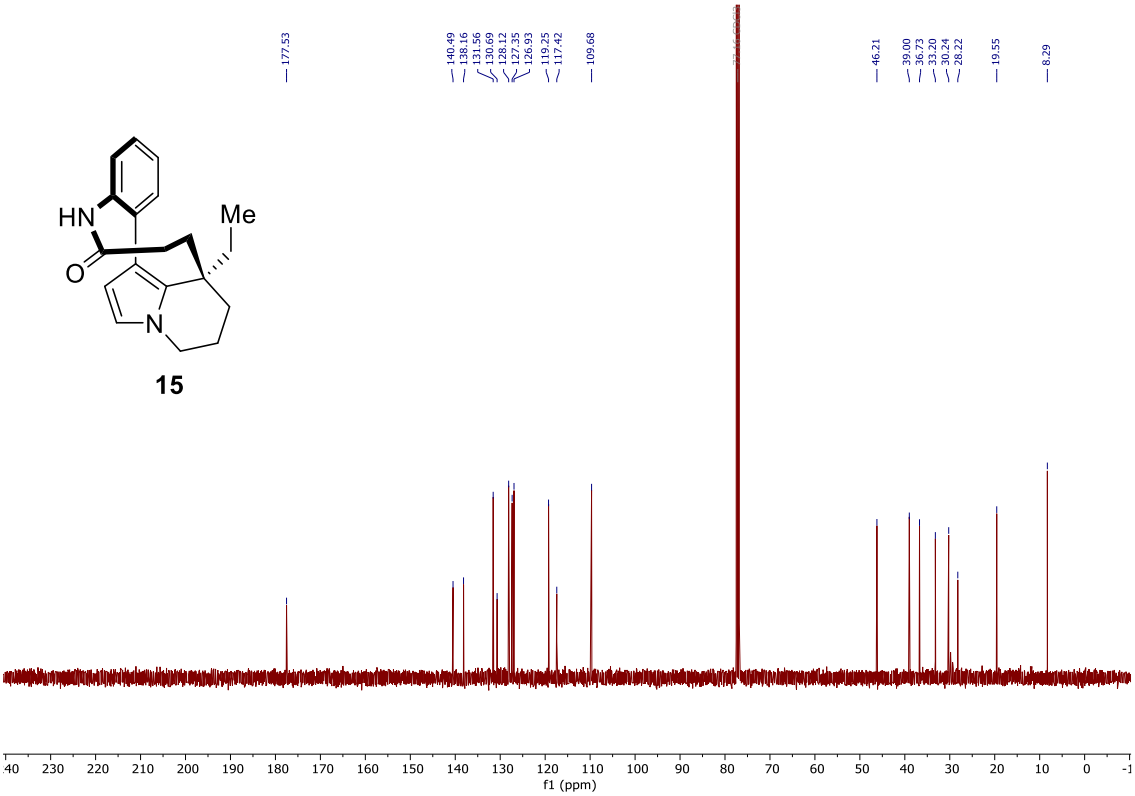

7.6 Crystallographic Data

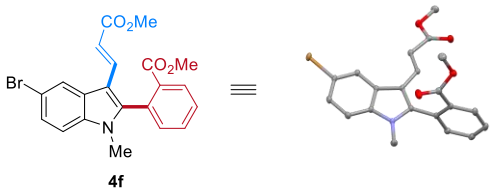

Table 7.7. Crystallographic Data of 4f

Crystal data and structure refinement for ZY-indole.

Identification code	ZY-indole
Empirical formula	$C_{21}H_{18}BrNO_4$
Formula weight	428.27
Temperature/K	100(2)
Crystal system	triclinic
Space group	P-1
a/Å	7.6550(8)
b/Å	10.3036(10)
c/Å	11.9510(12)
α/°	94.916(2)
β/°	99.295(2)
γ/°	102.025(2)
Volume/Å^3	902.85(16)
Z	2
ρ_{calc}g/cm^3	1.575
μ/mm^{-1}	2.304
F(000)	436.0
Crystal size/mm^3	0.441 × 0.254 × 0.162
Radiation	MoKα (λ = 0.71073)
2Θ range for data collection/°	5.02 to 59.268
Index ranges	-10 ≤ h ≤ 10, -14 ≤ k ≤ 14, -16 ≤ l ≤ 16
Reflections collected	27134
Independent reflections	5085 [R_{int} = 0.0206, R_{sigma} = 0.0143]
Data/restraints/parameters	5085/0/247
Goodness-of-fit on F^2	1.069
Final R indexes [I>=2σ (I)]	R_1 = 0.0234, wR_2 = 0.0598
Final R indexes [all data]	R_1 = 0.0255, wR_2 = 0.0609

Largest diff. peak/hole / e Å^{-3} 1.02/-0.21

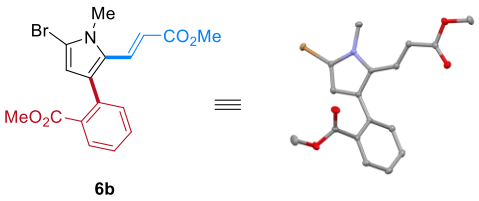

6b

Table 7.8. Crystallographic Data of 6b

Crystal data and structure refinement for ZY-Pyrrole-Br-2.

Identification code	ZY-Pyrrole-Br-2
Empirical formula	$C_{17}H_{16}NO_4Br$
Formula weight	378.22
Temperature/K	100(2)
Crystal system	monoclinic
Space group	C2/c
a/Å	19.2003(13)
b/Å	11.4922(8)
c/Å	16.3272(18)
α/°	90
β/°	119.2540(10)
γ/°	90
Volume/Å^3	3143.2(5)
Z	8
ρ_{calc}g/cm^3	1.598
μ/mm^{-1}	2.636
F(000)	1536.0
Crystal size/mm^3	0.473 × 0.434 × 0.326
Radiation	MoKα (λ = 0.71073)
2Θ range for data collection/°	4.298 to 59.31
Index ranges	-26 ≤ h ≤ 26, -15 ≤ k ≤ 16, -22 ≤ l ≤ 22
Reflections collected	47274
Independent reflections	4447 [R_{int} = 0.0248, R_{sigma} = 0.0104]
Data/restraints/parameters	4447/0/211
Goodness-of-fit on F^2	1.050
Final R indexes [I>=2σ (I)]	R_1 = 0.0206, wR_2 = 0.0529
Final R indexes [all data]	R_1 = 0.0222, wR_2 = 0.0538
Largest diff. peak/hole / e Å^{-3}	0.46/-0.22

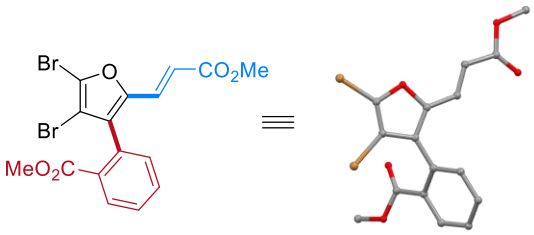

8g

Table 7.9. Crystallographic Data of 8g

Crystal data and structure refinement for 0806-RH.

Identification code	0806-RH
Empirical formula	$C_{16}H_{12}Br_2O_5$
Formula weight	444.08
Temperature/K	100(2)
Crystal system	monoclinic
Space group	$P2_1/c$
a/Å	16.3841(11)
b/Å	20.8818(14)
c/Å	15.0960(11)
α/°	90
β/°	110.165(2)
γ/°	90
Volume/Å^3	4848.2(6)
Z	12
ρ_{calc}g/cm^3	1.825
μ/mm^{-1}	5.038
F(000)	2616.0
Crystal size/mm^3	0.291 × 0.177 × 0.121
Radiation	MoKα (λ = 0.71073)
2Θ range for data collection/°	4.716 to 54.146
Index ranges	-20 ≤ h ≤ 20, -26 ≤ k ≤ 26, -19 ≤ l ≤ 19
Reflections collected	186082
Independent reflections	10571 [R_{int} = 0.0679, R_{sigma} = 0.0361]
Data/restraints/parameters	10571/0/628
Goodness-of-fit on F^2	1.033
Final R indexes [I>=2σ (I)]	R_1 = 0.0350, wR_2 = 0.0632
Final R indexes [all data]	R_1 = 0.0647, wR_2 = 0.0707
Largest diff. peak/hole / e Å^{-3}	0.74/-0.39

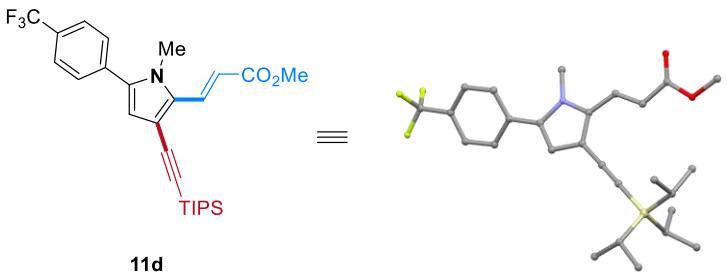

11d

Table 7.10. Crystallographic Data of 11d

Crystal data and structure refinement for mo_0927_XIN_RH_0m.

Identification code	mo_0927_XIN_RH_0m
Empirical formula	$C_{27}H_{34}F_3NO_2Si$
Formula weight	489.64
Temperature/K	100(2)
Crystal system	triclinic
Space group	P-1
a/Å	7.7780(8)
b/Å	9.2572(9)
c/Å	18.5862(19)
α/°	104.059(2)
β/°	91.572(3)
γ/°	94.280(3)
Volume/Å^3	1293.1(2)
Z	2
ρ_{calc}g/cm^3	1.258
μ/mm^{-1}	0.136
F(000)	520.0
Crystal size/mm^3	0.187 × 0.12 × 0.108
Radiation	MoKα (λ = 0.71073)
2Θ range for data collection/°	4.524 to 57.95
Index ranges	-10 ≤ h ≤ 10, -12 ≤ k ≤ 12, -25 ≤ l ≤ 25
Reflections collected	37943
Independent reflections	6827 [R_{int} = 0.0673, R_{sigma} = 0.0612]
Data/restraints/parameters	6827/0/315
Goodness-of-fit on F^2	1.013
Final R indexes [I>=2σ (I)]	R_1 = 0.0499, wR_2 = 0.1035
Final R indexes [all data]	R_1 = 0.0920, wR_2 = 0.1182
Largest diff. peak/hole / e Å^{-3}	0.54/-0.22

7.7 References

(1) (a) Joule, J. A.; Mills, K., *Heterocyclic Chemistry*. Wiley: Weinheim: 2013; (b) Taylor, R. D.; MacCoss, M.; Lawson, A. D. G., Rings in Drugs. *J. Med. Chem.* **2014**, *57*, 5845-5859.

(2) Catellani, M.; Frignani, F.; Rangoni, A., A Complex Catalytic Cycle Leading to a Regioselective Synthesis of o,o′ -Disubstituted Vinylarenes. *Angew. Chem. Int. Ed.* **1997**, *36*, 119-122.

(3) Lautens, M.; Piguel, S., A New Route to Fused Aromatic Compounds by Using a Palladium-Catalyzed Alkylation – Alkenylation Sequence. *Angew. Chem. Int. Ed.* **2000**, *39*, 1045-1046.

(4) (a) Catellani, M.; Motti, E.; Della Ca', N., Catalytic Sequential Reactions Involving Palladacycle-Directed Aryl Coupling Steps. *Acc. Chem. Res.* **2008**, *41*, 1512-1522; (b) Della Ca', N.; Fontana, M.; Motti, E.; Catellani, M., Pd/Norbornene: A Winning Combination for Selective Aromatic Functionalization via C–H Bond Activation. *Acc. Chem. Res.* **2016**, *49*, 1389-1400; (c) Ye, J.; Lautens, M., Palladium-catalysed norbornene-mediated C–H functionalization of arenes. *Nat. Chem.* **2015**, *7*, 863; (d) Wang, J.; Dong, G., Palladium/Norbornene Cooperative Catalysis. *Chem. Rev.* **2019**, *119*, 7478-7528.

(5) Li, R.; Zhou, Y.; Xu, X.; Dong, G., Direct Vicinal Difunctionalization of Thiophenes Enabled by the Palladium/Norbornene Cooperative Catalysis. *J. Am. Chem. Soc.* **2019**, *141*, 18958-18963.

(6) (a) Tetsuya, S.; Masahiro, M., Catalytic Direct Arylation of Heteroaromatic Compounds. *Chem. Lett.* **2007**, *36*, 200-205; (b) Gorsline, B. J.; Wang, L.; Ren, P.; Carrow, B. P., C–H Alkenylation of Heteroarenes: Mechanism, Rate, and Selectivity Changes Enabled by Thioether Ligands. *J. Am. Chem. Soc.* **2017**, *139*, 9605-9614; (c) Liégault, B.; Lapointe, D.; Caron, L.; Vlassova, A.; Fagnou,

K., Establishment of Broadly Applicable Reaction Conditions for the Palladium-Catalyzed Direct Arylation of Heteroatom-Containing Aromatic Compounds. *J. Org. Chem.* **2009**, *74*, 1826-1834.

(7) (a) Mitsudo, K.; Thansandote, P.; Wilhelm, T.; Mariampillai, B.; Lautens, M., Selectively Substituted Thiophenes and Indoles by a Tandem Palladium-Catalyzed Multicomponent Reaction. *Org. Lett.* **2006**, *8*, 3939-3942; (b) Dong, Z.; Wang, J.; Dong, G., Simple Amine-Directed Meta-Selective C–H Arylation via Pd/Norbornene Catalysis. *J. Am. Chem. Soc.* **2015**, *137*, 5887-5890.

(8) Wang, J.; Li, R.; Dong, Z.; Liu, P.; Dong, G., Complementary site-selectivity in arene functionalization enabled by overcoming the *ortho* constraint in palladium/norbornene catalysis. *Nat. Chem.* **2018**, *10*, 866-872.

(9) Wang, J.; Zhou, Y.; Xu, X.; Liu, P.; Dong, G., Entry to 1,2,3,4-Tetrasubstituted Arenes through Addressing the "Meta Constraint" in the Palladium/Norbornene Catalysis. *J. Am. Chem. Soc.* **2020**, *142*, 3050-3059.

(10) Wang, J.; Dong, Z.; Yang, C.; Dong, G., Modular and regioselective synthesis of all-carbon tetrasubstituted olefins enabled by an alkenyl Catellani reaction. *Nat. Chem.* **2019**, *11*, 1106-1112.

(11) Shen, P.-X.; Wang, X.-C.; Wang, P.; Zhu, R.-Y.; Yu, J.-Q., Ligand-Enabled Meta-C–H Alkylation and Arylation Using a Modified Norbornene. *J. Am. Chem. Soc.* **2015**, *137*, 11574-11577.

(12) Dong, Z.; Wang, J.; Ren, Z.; Dong, G., *Ortho* C–H Acylation of Aryl Iodides by Palladium/Norbornene Catalysis. *Angew. Chem. Int. Ed.* **2015**, *54*, 12664-12668.

(13) Li, R.; Liu, F.; Dong, G., Redox-Neutral *ortho* Functionalization of Aryl Boroxines via Palladium/Norbornene Cooperative Catalysis. *Chem* **2019**, *5*, 929-939.

(14) Chen, M. S.; Prabagaran, N.; Labenz, N. A.; White, M. C., Serial Ligand Catalysis: A Highly Selective Allylic C−H Oxidation. *J. Am. Chem. Soc.* **2005**, *127*, 6970-6971.

(15) Wang, P.; Li, G.-C.; Jain, P.; Farmer, M. E.; He, J.; Shen, P.-X.; Yu, J.-Q., Ligand-Promoted meta-C–H Amination and Alkynylation. *J. Am. Chem. Soc.* **2016**, *138*, 14092-14099.

(16) (a) Sui, X.; Zhu, R.; Li, G.; Ma, X.; Gu, Z., Pd-Catalyzed Chemoselective Catellani Ortho-Arylation of Iodopyrroles: Rapid Total Synthesis of Rhazinal. *J. Am. Chem. Soc.* **2013**, *135*, 9318-9321; (b) Zhao, K.; Xu, S.; Pan, C.; Sui, X.; Gu, Z., Catalytically Asymmetric Pd/Norbornene Catalysis: Enantioselective Synthesis of (+)-Rhazinal, (+)-Rhazinilam, and (+)-Kopsiyunnanine C1–3. *Org. Lett.* **2016**, *18*, 3782-3785.

(17) Fang, Z.; Liao, P.-C.; Yang, Y.-L.; Yang, F.-L.; Chen, Y.-L.; Lam, Y.; Hua, K.-F.; Wu, S.-H., Synthesis and Biological Evaluation of Polyenylpyrrole Derivatives as Anticancer Agents Acting through Caspases-Dependent Apoptosis. *J. Med. Chem.* **2010**, *53*, 7967-7978.

(18) Li, R.; Zhou, Y.; Yoon, K.-Y.; Dong, Z.; Dong, G., Sulfenamide-Enabled *Ortho* Thiolation of Aryl Iodides via Palladium/Norbornene Cooperative Catalysis. *Nat. Commun.* **2019**, *10*, 3555.

(19) Gu, Z.; Zakarian, A., Total Synthesis of Rhazinilam: Axial to Point Chirality Transfer in an Enantiospecific Pd-Catalyzed Transannular Cyclization. *Org. Lett.* **2010**, *12*, 4224-4227.

CHAPTER 8

Site-Selective Vicinal Double C−H Functionalization of Five-Membered Heteroarenes with Dual Electrophiles

8.1 Introduction

Arenes and heteroarenes with multiple different substituents are prevalent in functional molecules, such as drugs and organic materials (Figure 8.1).[1] While various arene-functionalization approaches have been established, site-selective installation of *multiple different* functional groups via sequential C−H activation,[2] which is arguably one of the most straightforward approaches, remains a formidable challenge.[3] Recently, the palladium/norbornene (Pd/NBE) cooperative catalysis, originally discovered by Catellani,[4] has emerged as an increasingly useful method for introducing vicinal functional groups (FGs) to aromatic rings in one step.[5] In a typical Catellani reaction, through forming a unique aryl-norbornyl-palladacycle (ANP) intermediate, an electrophile and a nucleophile (or an olefin) are coupled regioselectivity at the arene ortho and

ipso positions, respectively (Scheme 8.1A). This is because the ortho position in the ANP intermediate is more electron-rich, therefore more reactive with electrophiles, whereas the ipso carbon tends to undergo regular cross-couplings with nucleophiles in the reaction.[5j] However, the need of both electrophilic and nucleophilic reactants present in the same reaction vessel has inevitably raised concerns of compatibility, which further limits the type of FGs that can be tolerated. In addition, the presence of the nucleophile can also render regular cross couplings to compete with the Catellani process.

Figure 8.1. Examples of Polysubstituted Heterocycles

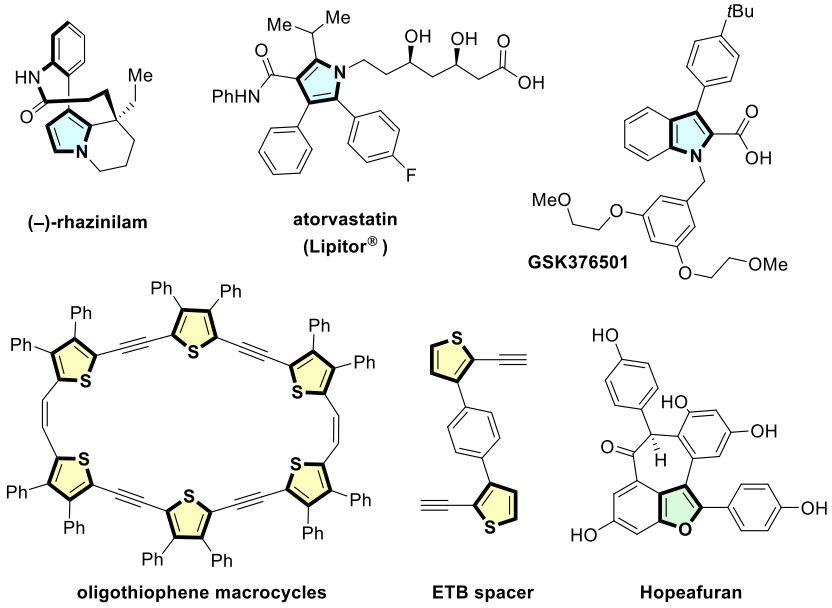

On the other hand, the *nucleophile-free* Pd/NBE catalysis has been developed through a Pd(II)-initiated N−H palladation[6], C−H activation[7] or transmetallation[8] processes, in which protodepalladation takes place at the arene ipso position to regenerate the Pd(II) catalyst, though only one type of FGs can be introduced at once in these reactions (Scheme 8.1B). Thus, one intriguing question is whether two *different aprotic electrophiles* could be coupled site-selectively through the Pd/NBE-catalyzed vicinal double C−H functionalization, which, to the best of our

knowledge, has not yet been established (Scheme 8.1C). In 2009, Lautens reported the only example of terminating the arene ipso position with a tethered carbonyl electrophile based on aryl iodide substrates (Scheme 8.1D), whereas additional reductant was added for Pd(0) reformation.[9] Recently, elegant work by Luan shows two different electrophiles can be coupled in a sequential manner at both ortho positions, though nucleophiles are still needed for ipso quench.[10] In this article, we describe the development of the Pd/NBE-catalyzed vicinal double C−H functionalization of five-membered heteroarenes, including pyrroles, furans and thiophenes, at their C4 and C5 positions through coupling with aryl and alkynyl electrophiles, respectively (Scheme 8.1E). This new transformation provides streamlined synthesis of polysubstituted heteroarenes in an efficient and redox-neutral manner.

In comparison to the conventional Catellani reactions, substantial challenges associated with this double-electrophile coupling could be envisioned (Scheme 8.2). First, it is nontrivial to differentiate the reactivity between two electrophiles in one reaction. In particular, success of this transformation requires one electrophile to selectively react with the ANP and the other one to react with the aryl-Pd(II)-X (X: anionic ligand) intermediate after NBE extrusion (Step C vs Step F). By contrast, the prior ipso protonation reactions (vide supra, Scheme 8.1B) do not have such a selectivity issue as the competing reaction between the ANP and proton will generate the previous intermediate instead of leading to a side-reaction. Second, success of this double-electrophile coupling requires facile ipso C−H palladation to initiate the reaction (step A); from the microscopic reversibility viewpoint, the reverse ipso protodepalladation should also have a low kinetic barrier.[11] Thus, the ipso protonation can compete with the second electrophile to give mono-ortho-functionalized side-products (Step G vs Step D). Third, given that the second electrophile needs to efficiently react with the aryl-Pd(II)-X intermediate, it thus can compete with the NBE insertion

for the direct mono-ipso-functionalized side-product (Step E vs Step B). Therefore, to realize the proposed double C−H functionalization with dual electrophiles, the following three criteria must be met: a) the first electrophile needs to be more reactive than the second one when reacting with the ANP; b) the second electrophile should prefer to react with the aryl-Pd(II)-X intermediates, instead of the ANP; c) The NBE insertion with the aryl-Pd(II)-X intermediate should be faster than its reaction with the second electrophile.

Scheme 8.1. The General Reaction Modes of the Pd/NBE Cooperative Catalysis

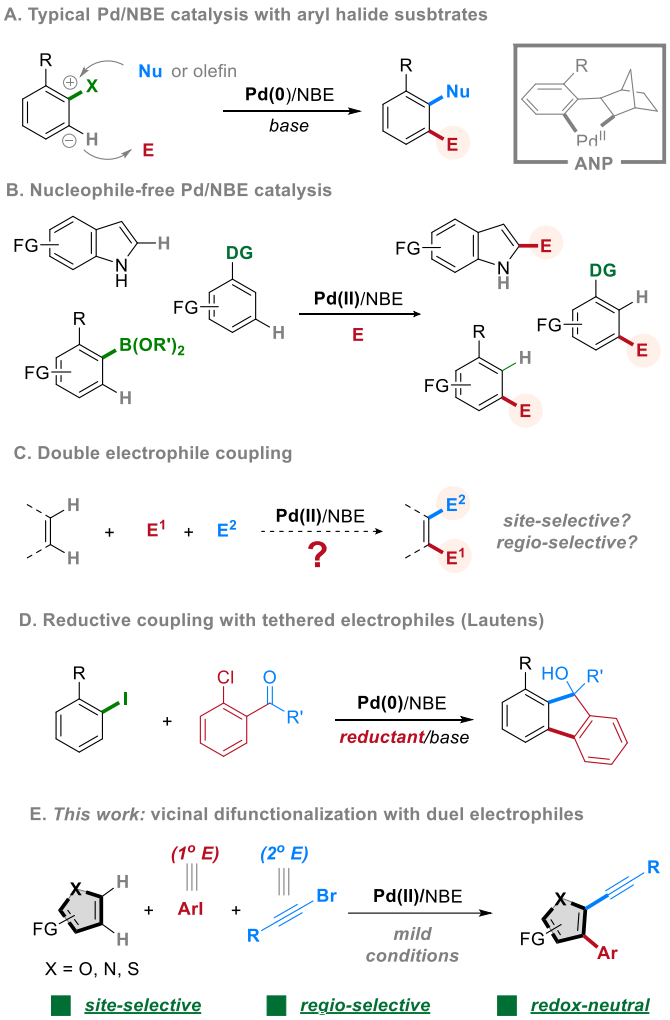

Scheme 8.2. Potential Challenges Associated with the Proposed Reaction

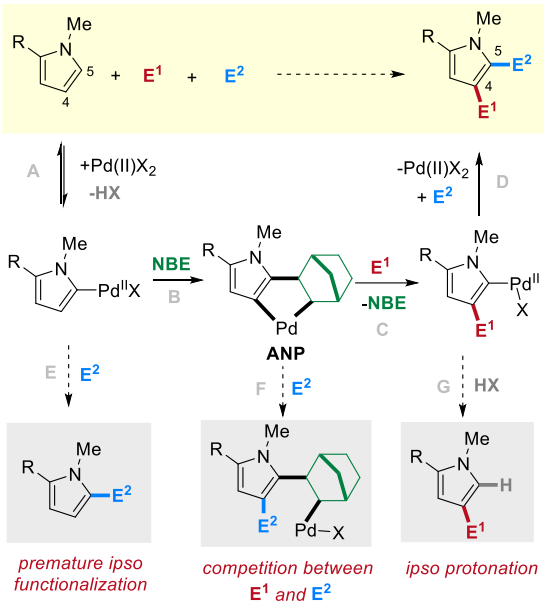

8.2 Results and Discussion

8.2.1 Reaction Discovery and Optimization

We hypothesized one key for the success of this transformation would be the choice of the second electrophile, which should react in a *different reaction mode* from the first electrophile. Given that linear aryl-Pd(II)-X intermediates are generally less electron-rich and less rigid than the corresponding five-membered ANP, they are expected to undergo faster migratory insertion with alkenes or alkynes than the ANP.[12] Hence, π-type electrophiles that require an addition/elimination process could be most suitable as the second electrophile, as they would react faster with the aryl-Pd(II)-X than the ANP. In addition, structurally modified NBEs that give faster migratory insertion could be beneficial to minimize premature ipso functionalization.[5k]

To test the hypothesis, alkynyl bromide **3a**,[13] known to react with aryl-Pd(II)-X species through 2π-insertion followed by a unique *trans* β-bromide elimination,[13e, 14] was employed as the second electrophile. Methyl 2-iodobenzoate (**2a**) was chosen as the first electrophile, as the coordinating ester moiety should promote the selective reaction with the ANP.[2h, 7b] The reaction was first explored with 2-chloro-1-methylpyrrole (**1a**) as the model substrate (Table 8.1). After careful evaluation of various reaction parameters, the desired direct ortho arylation/ipso alkynylation product **4a** was ultimately isolated in 78% yield (entry 1). First, the $Pd(OAc)_2$/$AsPh_3$ combination proved to be optimal;[2h, 7b, 8a] no desired product was observed in the absence of Pd or the ligand (entries 2 and 3). Phosphine-based ligands were much less effective (entries 4 and 5). NBE also proved to be essential (entry 6). The C2 trifluoroethyl amide-substituted NBE (**N1**) was found most efficient and most selective for the model reaction (entry 7). While other C2-substiuted NBEs[15] also gave relatively good yields, their selectivity was worse, giving more direct ipso alkynylation and other side-products. This is consistent with our prior mechanistic study that found

C2-amide NBEs exhibit lower migratory insertion barriers.[16] In contrast, much reduced reactivity was observed with C1-substituted NBEs (**N7** and **N8**)[17], likely due to their increased steric hindrance. The C5-substituted **N9**[18] and C5,C6-disubstituted **N10**[19] also gave inferior results. Although simple NBE (**N11**) appears to produce the desired product in good yield with minimal side-product **4a'**, it nevertheless generated a notably amount of multi-alkynylation side-products (7%), which indicates poorer selectivity than **N1**. The silver salt was beneficial, likely serving as the halide scavenger to promote the oxidative addition of aryl iodide **2a** and/or the coupling with alkynyl bromide **3a** (entry 8).[20] Reducing the loading of **2a** and AgOAc to one equivalent in a 1:1 ratio can still afford 57% yield (entry 9) and replacing AgOAc with CsOAc under an N_2 atmosphere still provided 18% yield (entry 10), suggesting that the role of AgOAc is unlikely to be an oxidant. Finally, the addition of 5 equivalents of HOAc improved the yield (entry 11) possibly through promoting the initial C−H palladation on the pyrrole substrate.[21] It is noteworthy that the reaction is not sensitive to air and water. The system is in principle redox neutral. To exclude the role of air in the reaction, the reaction operated under carefully degassed conditions provided nearly identical results (entry 12).

Table 8.1. Control Experiments

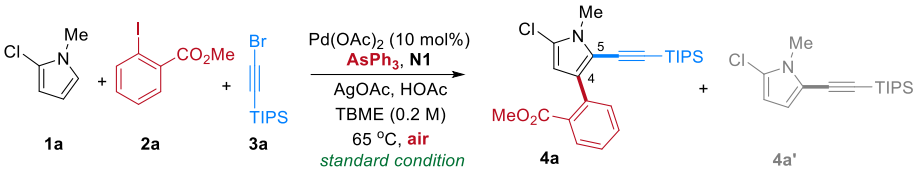

Entry	Change from the *"standard condition"*	yield of **4a** (%)[a]	yield of **4a'** (%)[a]
1	**none**	**78(78)**	2
2	w/o $Pd(OAc)_2$	0	0
3	w/o $AsPh_3$	0	10
4	TFP instead of $AsPh_3$	6	14
5	PPh_3 instead of $AsPh_3$	48	13
6	w/o **N1**	0	21
7	NBE Effect (50 mol% NBE used instead)		*see below*

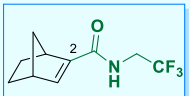

N1
4a, **72%**
4a', 2%

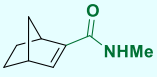

N2
4a, 69%
4a', 7%

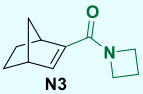

N3
4a, 64%
4a', 5%

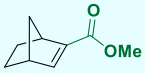

N4
4a, 65%
4a', 5%

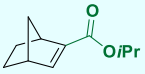

N5
4a, 57%
4a', 10%

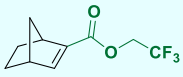

N6
4a, 66%
4a', 10%

N7
4a, 13%
4a', 29%

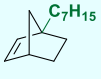

N8
4a, 3%
4a', 29%

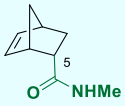

N9
4a, 58%
4a', 13%

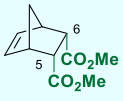

N10
4a, 40%
4a', 26%

N11
4a, 62%
4a', 1%

8	w/o AgOAc	6	1
9	1.0 equiv **2a**, 1.0 equiv AgOAc	57[b]	7[b]
10	CsOAc (5.0 equiv) instead of AgOAc	18[b,c]	<1[b,c]
11	w/o HOAc	64	9
12	under N_2	80	2

[a]The reaction was run with 0.1 mmol **1a**, 0.2 mmol **2a**, 0.18 mmol **3a**, $Pd(OAc)_2$ (0.01 mmol), **N1** (0.15 mmol), $AsPh_3$ (0.025 mmol), AgOAc (0.3 mmol), and HOAc (0.5 mmol) in 0.5 mL TBME (*tert*-butyl methyl ether) for 72 h. Yields were determined by ^1H NMR analysis using dibromomethane as the internal standard. [b]The reaction was set up under N_2. [c]The reaction time was 96 h.

8.2.2 Substrates Scope

With the optimized reaction condition in hand, the scope with respect to aryl iodides was examined first (Table 8.2). Generally speaking, aryl iodides with an ortho electron-withdrawing group (EWG) were most efficient, which should benefit from their selective oxidative addition with the ANP.[22] A series of functional group, including ester (**4a**-**4e**), aryl halides (**4c**-**4e**), nitro (**4f**), ketone (**4j**), amide (**4l**) groups were all well tolerated in this dual-electrophile-coupling reaction. Notably, a second iodide moiety (**4e**) not ortho to the EWG was compatible, which can serve as a handle for future derivatization. The reaction is not limited to the use of ortho-substituted aryl iodides. Ortho-unsubstituted aryl iodides (**4g**-**4i**), including simple phenyl iodide (**4h**) and the one containing an electron-donating group (**4i**), can still be employed as the first electrophile, albeit with diminished yield.

Besides pyrroles, thiophenes and furans are also excellent substrates. A range of thiophenes with various substituents at the C2 position, including protected primary alcohols (**5a**-**5c**), methoxy (**5d**), halogens (**5e** and **5f**), alkyl groups (**5g** and **5h**) and substituted aryl moieties (**5i** and **5j**), were all compatible in this transformation. In particular, both electron-rich (**5d** and **5i**) and electron-deficient (**5k**) thiophenes can deliver the corresponding products in moderate to good yields. The C2 and C3 disubstituted thiophenes (**5l**-**5o**) also proved to be suitable substrates, giving fully substituted products that are nontrivial to be prepared via conventional approaches. Reactions with duloxetine (**5v**) and estrone (**5w**) derivatives worked smoothly to afford the desired difunctionalized products in good yields, indicating the potential synthetic utility of this method toward the late-stage functionalization of bioactive compounds. Pyrrole with a moderate EWG (**5p**) was also compatible. In addition, a series of furans with alkyl (**5u**) and aryl (**5q**-**5t**) substituents at the C2 position were also competent substrates.

Table 8.2. Substrates Scope[a]

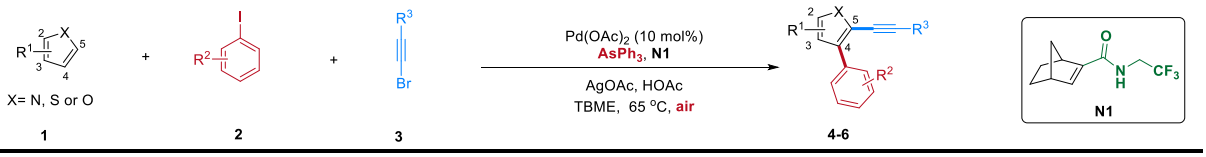

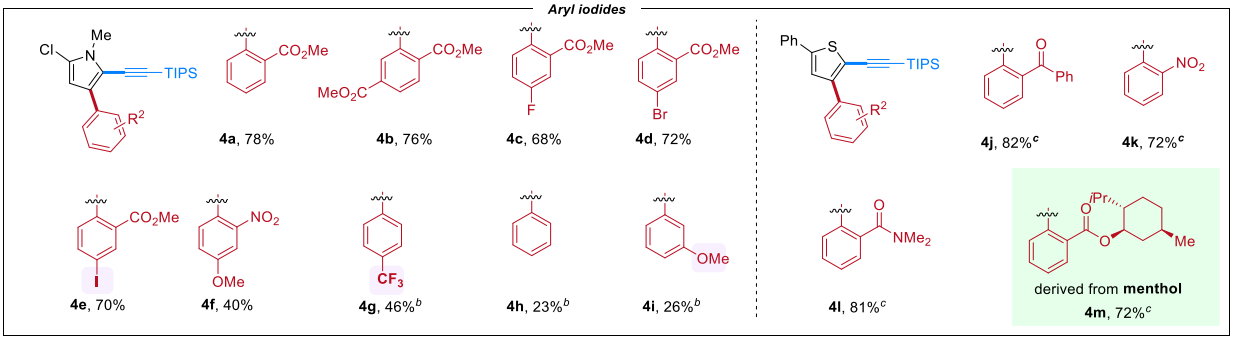

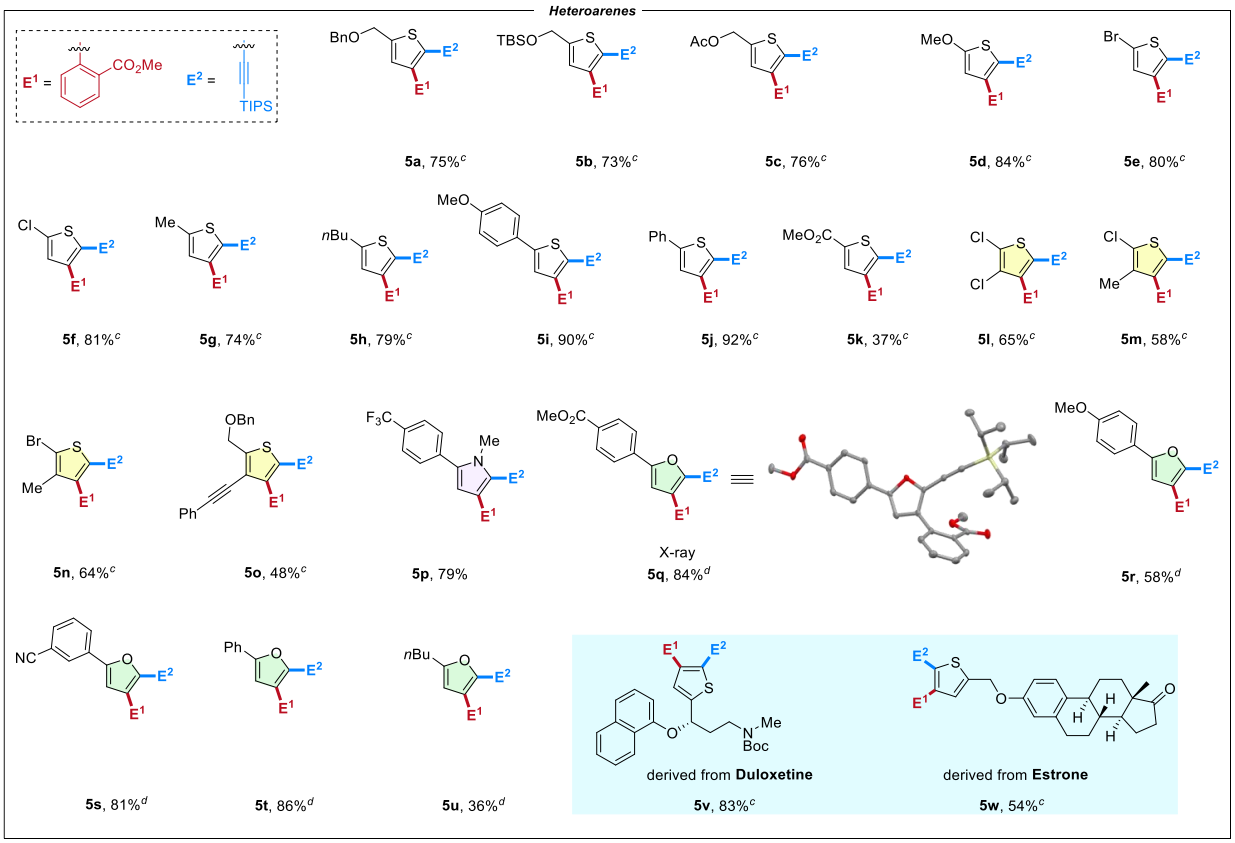

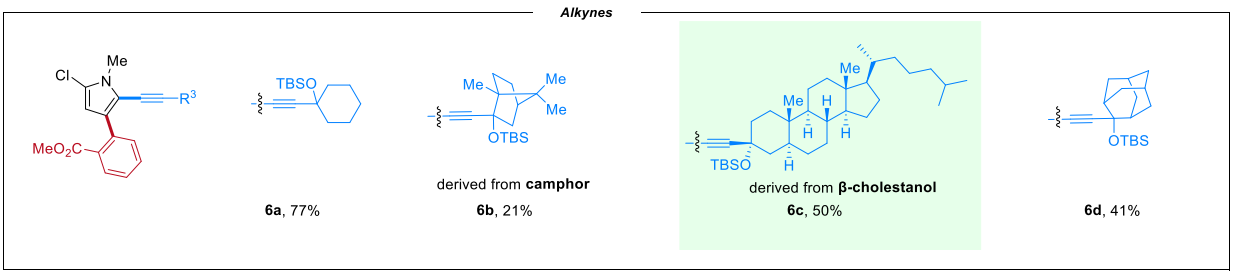

Table 8.2. Substrates Scope[a] (continued)

[a]Unless otherwise noted all reactions were run with 0.2 mmol **1**, 0.4 mmol **2**, 0.36 mmol **3a** and 0.3 mmol **N1** in 1.0 mL TBME for 72 h. [b]**N10** was used instead of **N1**. [c]**N6** and ethyl acetate was used instead of **N1** and TBME. [d]$Pd(acac)_2$, **N3**, and ethyl acetate were used instead of $Pd(OAc)_2$, **N1** and TBME.

Regarding the scope of the second electrophile, besides the commonly used TIPS-substituted alkynyl bromide (**3a**), a number of bulky bromopropargyl silyl ethers were also reactive. Encouragingly, more complex alkyne coupling partners derived from camphor (**6b**) and β-cholestanol (**6c**) were also coupled at the pyrrole C5 position in moderate yields. Given the good substrate scope, it becomes evident that high complexity can be quickly introduced to the products through this three-component coupling strategy.

Beyond using aryl iodides as the first electrophile, preliminary success on employing methyl iodide as the first electrophile has been achieved. When 2-chloro-1-methylpyrrole (**1a**) was subjected to the standard reaction condition with 1.5 equiv of **N2**, the desired C4 methylated/C5-alkynylated pyrrole (**8**) was isolated in 34% yield (Eq. 1). Further optimization of the reaction is underway in our laboratory.

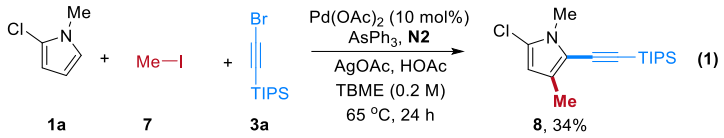

8.2.3 Exploration of the Reaction Pathway

To gain some mechanistic insights of this reaction, a number of control experiments were carried out (Scheme 8.3). First, in the absence of the second electrophile (**3a**), the C4-arylated product **9**

was isolated in 64% yield under the standard conditions (with 50 mol% **N1**), suggesting that ipso protodepalladation occurred when only aryl iodide **2a** was used as the electrophile (Eq. 2). Using alkynyl bromide **3a** alone as the electrophile, the direct mono-ipso-alkynylation product (**4a'**) was dominant even in the presence of NBE **N1**, along with minor multi-alkynylation products **10** (Eq. 3). For comparison, with both electrophiles **2a** and **3a** in the reaction, side-products **4a'** and **10** were only formed in a small amount (Eq. 4). These results indicate that: (i) NBE must react faster with the Ar-Pd-X species than **3a**; otherwise, direction ipso alkynylation would dominate in Eq. 4. (ii) NBE insertion with the metalated pyrrole (or the ANP formation) should be reversible under the reaction conditions; otherwise, ipso alkynylation product **4a'** cannot be the major product in Eq. 3. (iii) Unlike aryl iodide **2a**, alkynyl bromide **3a** favors ipso functionalization instead of reacting with the ANP, probably through Ar-Pd-X migratory insertion followed by β-bromide elimination based on the prior computational study.[14b]

Scheme 8.3. Control Experiments

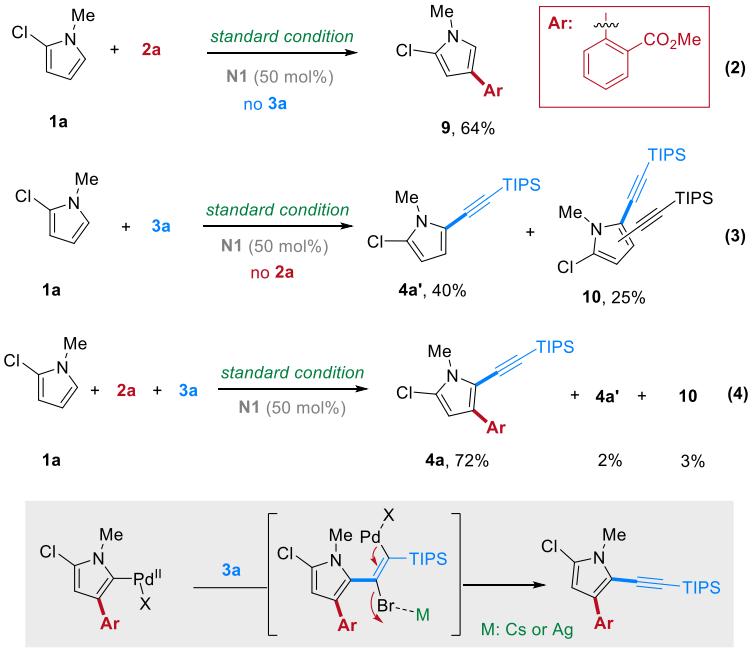

Considering that ipso protonation can also occur under the reaction conditions (Eq. 2), one interesting question is whether the protodepalladation is faster than the coupling with the alkynyl bromide at the ipso position, especially when the reaction contains excess HOAc. If the ipso protonation is faster under the standard conditions, one could imagine that the C4-arylated product (**9**) should accumulate at the early stage of the reaction and gradually be converted to the difunctionalized product (**4a**). To explore this question, the kinetic profile of the model reaction was measured (Figure 8.2), which shows that **4a** was formed rapidly at the beginning of the reaction and the concentration of **9** was low throughout the whole reaction. The lack of buildup of intermediate **9** suggests that **9** is not the kinetic product and the Ar-Pd-X intermediate after the C4 arylation/NBE extrusion reacts faster with the alkynyl bromide than with the acid.

Figure 8.2. Kinetic Profile of the Model Reaction

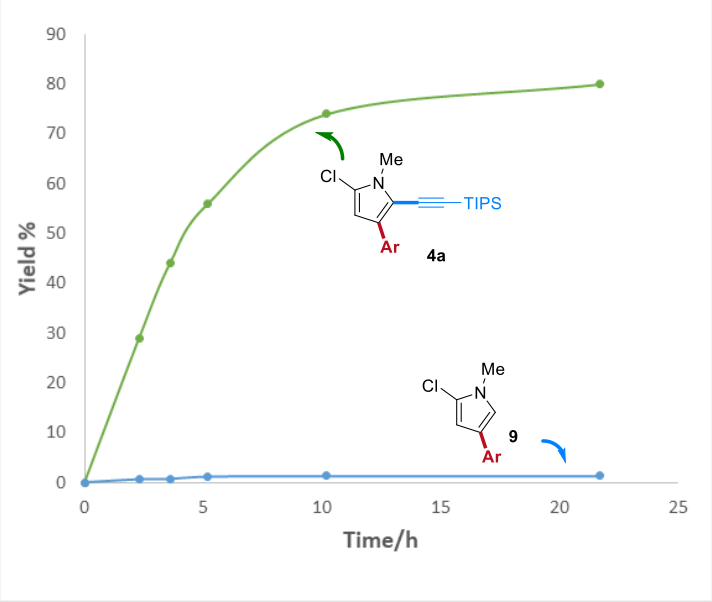

Altogether, the control experiments and the kinetic profile of the reaction imply that the origin of the high selectivity of this dual electrophile coupling reaction is due to the unique reactivity of alkynyl bromides. First, they undergo slower migratory insertion than NBE, thus allowing smooth

formation of the ANP intermediate. Second, alkynyl bromides react much slower with the ANP than aryl iodides, thereby permitting selective arylation at the C4 position. Third, alkynyl bromides react faster with the Ar-Pd-X intermediate after NBE extrusion than protons and aryl iodides; as such, the C5 protonation or arylation can be suppressed or minimized.

8.2.4 Synthetic Utility

The synthetic utility of this method was then explored. From the scalability prospect, it is encouraging that the reaction appears to be roust. On a gram scale, excellent yield can be obtained with an open-flask setup and untreated solvent (Eq. 5). In addition, reduction of the Pd loading to 1 mol% only slightly diminished the yield (Eq. 6).

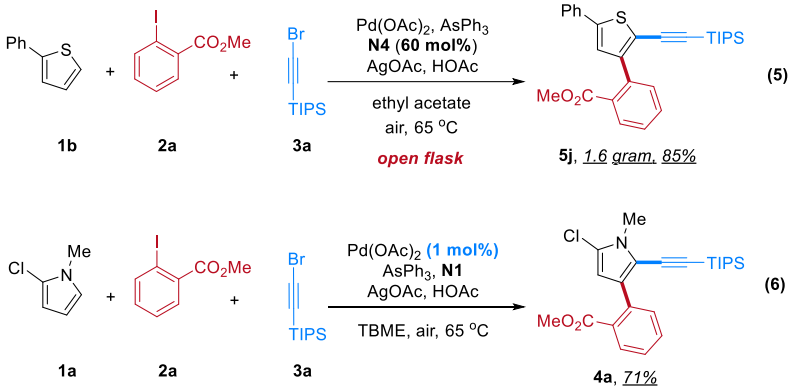

Owing to the versatility of the alkyne moiety, the difunctionalized product can be readily converted to various other structural motifs (Scheme 8.4A). First, the silyl group on the alkyne can be easily removed under mild conditions with tetrabutylammonium fluoride (TBAF). The resulting terminal alkyne (**11a**) can then serve as a convenient handle to install other functional groups to the heteroarene. For example, hydrogenation of the triple bond provided the alkyl moiety (**11d**), and hydrate gave the ketone product (**11e**). In addition, the copper-catalyzed "click" reaction generated

the biaryl linkage through the triazole formation (**11b**). Moreover, internal alkynes (**11c**) can be constructed by a Sonogashira coupling.

Scheme 8.4. Product Derivatizations

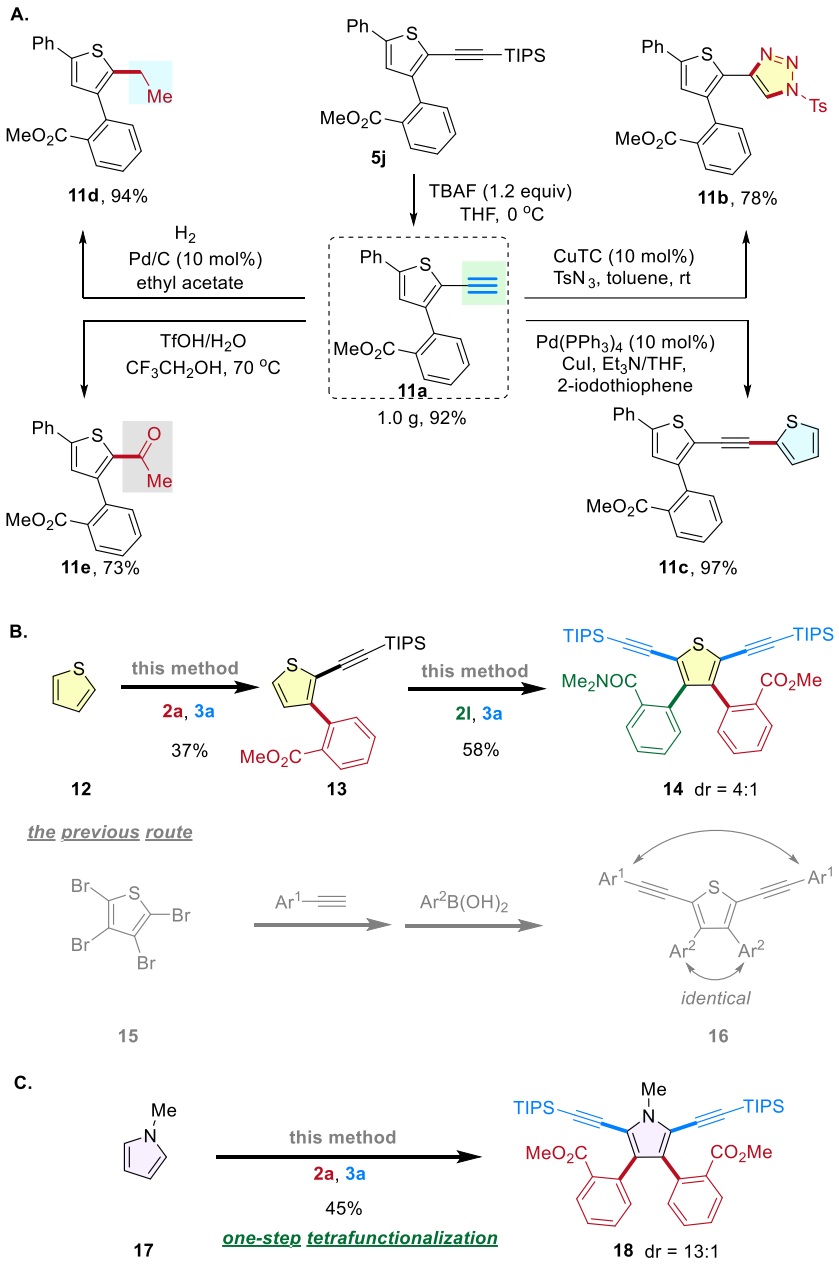

On the other hand, starting from simple thiophene, two sequential double-electrophile couplings can be operated, resulting in a tetra-substituted thiophene (Scheme 8.4B). Compared to the

previous route, our method does not rely on highly pre-functionalized thiophene,[23] and different substituents can be easily installed. Besides thiophene, simple *N*-methylpyrrole (**17**) can undergo the direct tetra C−H-functionalization smoothly, affording fully substituted pyrrole **18** in 45% yield in a regioselective manner. Interestingly, due to restricted rotation of the two aryl substituents, the products (**16** and **18**) were isolated as a pair of diastereomers.

Scheme 8.5. Synthetic Applications

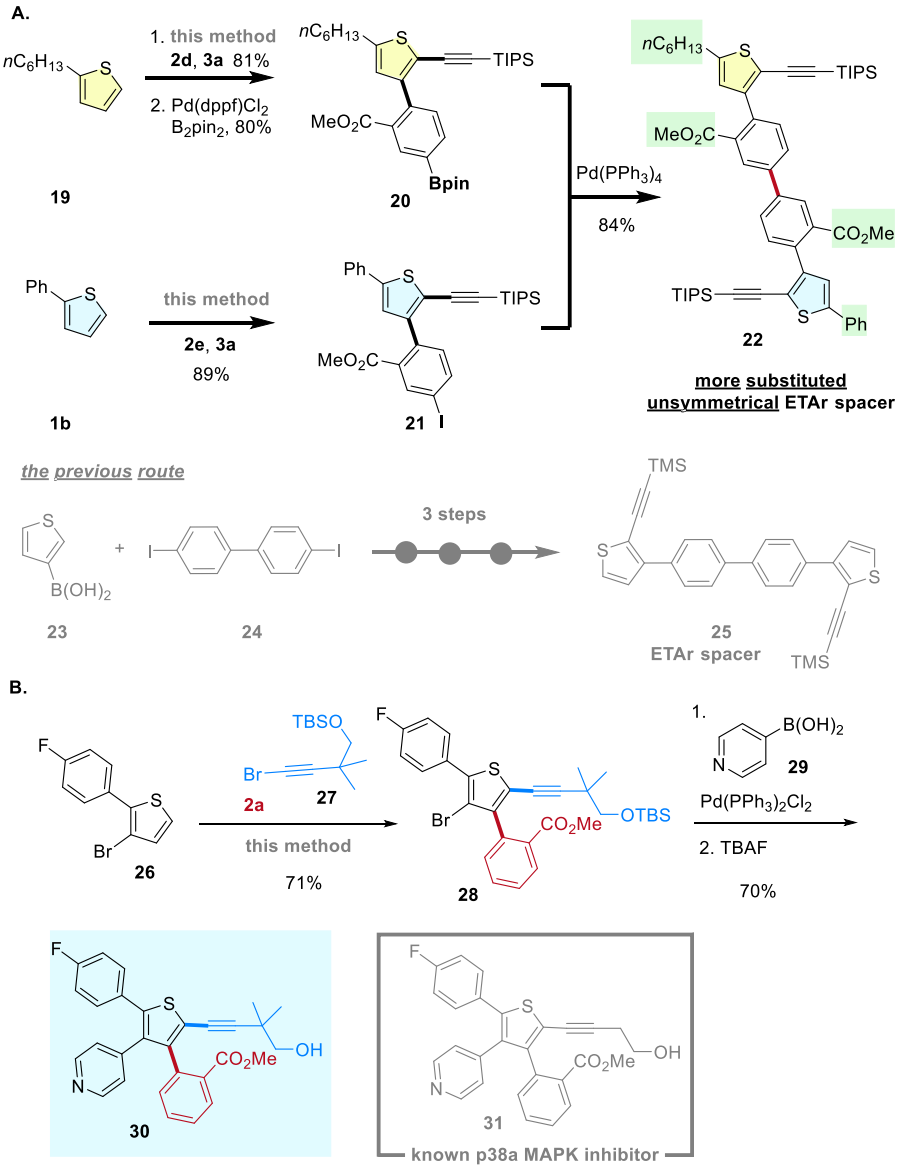

Taking advantage of the high site-selectivity and functional group tolerance, the ortho arylation/ipso alkynylation of two thiophene substrates gave the Br- and I-substituted products (Scheme 5A). The Br-substituent was then converted to the corresponding pinacolboronate (**20**) via the Miyaura borylation, which further coupled with the I-substituted product (**21**) to give a rigid linear compound (**22**) in good yield. Compound **22** could be considered as an ETAr [4,4'-bis(2-ethynyl-3-thienyl)biphenyl] spacer that is a peptide-inspired and easily tunable spacer consisting of 4,4'-biphenyl axis and 3-thienyl moieties at both ends of the axis.[24] Comparing to the previous route, this approach is more modular and provides more-substituted and unsymmetrical ETAr compounds.

Finally, this three-component coupling reaction was employed in the synthesis of an inhibitor analogue for P38α mitogen-activated protein kinase (MAPK).[25] Besides TIPS- and TBS-protected tertiary alcohol-derived alkynyl bromides, a new type of alkynyl bromide (**27**) with a tertiary alkyl substituent was found to be suitable for this double-electrophile coupling, resulting in the desired tetrasubstituted thiophene (**28**) in 71% yield (Scheme 8.5B).[26] The bromo moiety in **28** then underwent smooth Suzuki−Miyaura coupling with boronic acid **29**. After deprotection of the silyl group, the P38α MAPK inhibitor analogue (**30**) was isolated in good overall yield.

8.3 Conclusion

In summary, a site-selective vicinal double C−H functionalization of five-membered heteroarenes with two different electrophiles has been developed through the Pd/NBE cooperative catalysis. As the typical Catellani-type reactions use one electrophile and one nucleophile, the transformation discovered here, therefore, represents a new reaction mode. Capitalizing on the unique reactivity of alkynyl bromides, the three-component coupling reaction proceeds with complete regio- and site-selectivity. In addition, the reaction conditions are mild and robust with tolerance of air, moisture, and a broad scope of functional groups. Thus, it could be attractive for late-stage modification and modular synthesis of complex heteroarene-containing molecules. The mechanistic insights gained in this study could provide useful implications for developing other Pd/NBE-catalyzed double-electrophile-coupling reactions. Efforts on expanding the substrate scope to other arenes/heteroarenes and other classes of electrophiles for more general double C−H functionalizations are ongoing.

8.4. Experimental Procedures and Characterization Data

8.4.1 General Information

Unless noted otherwise, all solvents were dried by filtration through a Pure-Solv MD-5 Solvent Purification System (Innovative Technology). *tert*-Butyl methyl ether (TBME) and ethyl acetate was purchased from Fisher and used directly without further purification. Reaction temperatures were reported as the temperatures of the bather surrounding the flasks or vials. Sensitive reagents and solvents were transferred under nitrogen into a nitrogen-filled glovebox with standard techniques. Analytical thin-layer chromatography (TLC) was carried out using 0.2 mm commercial silica gel plates (silica gel 60, F254, EMD chemical). Vials (15 x 45 mm 1 dram (4 mL) with PTFE lined cap attached) were purchased from Qorpak and flame-dried and cooled in a desiccator prior to usage. High resolution mass spectra (HR-MS) were recorded on an Agilent 6530 LC Q-TOF mass spectrometer using electrospray ionization with fragmentation voltage set at 115 V and processed with an Agilent MassHunter Operating System. Infrared spectra were recorded on a Nicolet 380 FTIR using neat thin film technique. Nuclear magnetic resonance spectra (^{1}H NMR and ^{13}C NMR) were recorded with a Bruker DMX 400 (400 MHz, ^{1}H at 400 MHz, ^{13}C at 101 MHz) or Bruker Model DMX 500 (500 MHz, ^{1}H at 500 MHz, ^{13}C at 126 MHz). Chemical shifts were reported in parts per million (ppm, δ), downfield from tetramethylsilane (TMS, δ=0.00ppm) and were referenced to residual solvent ($CDCl_3$, δ=7.26 ppm (^{1}H) and 77.160 ppm (^{13}C)). All the ^{19}F chemical shifts were not referenced. Coupling constants were reported in Hertz (Hz). Data for ^{1}H NMR spectra were reported as follows: chemical shift (ppm, referenced to protium, s = singlet, d = doublet, t = triplet, q = quartet, quin = quintet, dd = doublet of doublets, td = triplet of doublets, ddd = doublet of doublet of doublets, m = multiplet, coupling constant

(Hz), and integration). All other materials were obtained from Sigma-Aldrich Corporation or Combi-Blocks Inc and were used as received.

8.4.2 Preparation of Alkynyl Bromide Substrates

Alkynyl bromides **3a**[27], **3b**[28], **3c**[28] and **3e**[28] are known compounds, which were prepared according to the literature reported procedures.

Scheme 8.6. Preparation of 3d

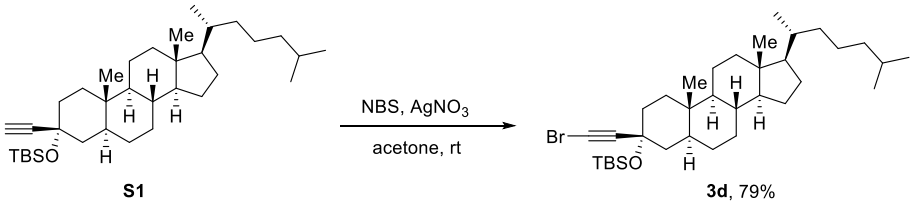

S1 was prepared according to the literature reported procedures.[29] Following a known procedure,[27] to a solution of **S1** (679 mg, 1.3 mmol) in 7 mL acetone were added *N*-bromosuccinimide (NBS) (232 mg, 1.3 mmol) and $AgNO_3$ (21.7 mg, 0.13 mmol). The reaction mixture was stirred for 3 h at room temperature, then poured into 50 mL cooled water. The solution was extracted with hexane (50 mL x 3). The solvent was removed under reduced pressure and the residue was purified by flash chromatography to yield compound **3d** as a white solid (620 mg, 79%).

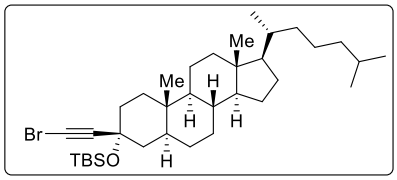

3d: White solid (79%). m. p. = 147.2 – 148.4 °C. R_f = 0.6 (hexane/ethyl acetate = 40:1) **^{1}H NMR** (400 MHz, $CDCl_3$) δ 1.96 (dt, *J* = 12.4, 3.1 Hz, 1H), 1.89 – 1.75 (m, 2H), 1.69 – 1.60 (m, 2H),

1.60 – 1.44 (m, 6H), 1.33 (q, *J* = 8.7 Hz, 5H), 1.29 – 1.18 (m, 5H), 1.11 (tt, *J* = 16.0, 6.9 Hz, 6H), 1.05 – 0.95 (m, 3H), 0.90 (d, *J* = 6.6 Hz, 3H), 0.88 – 0.84 (m, 15H), 0.78 (s, 3H), 0.75 – 0.66 (m, 1H), 0.65 (s, 3H), 0.14 (s, 6H). **^{13}C NMR** (101 MHz, $CDCl_3$) δ 84.6, 72.3, 56.6, 56.5, 54.2, 44.2, 43.71, 43.67, 42.8, 40.2, 39.7, 37.5, 36.3, 36.2, 36.0, 35.65, 35.61, 32.1, 28.4, 28.2, 25.9, 24.4, 24.0, 23.0, 22.7, 21.4, 18.8, 18.1, 12.3, 12.2, -2.7. **IR** (KBr): υ 2931, 2855, 1471, 1255, 1093, 867, 837, 777, 739 cm^{-1}. **HRMS** (ESI): Calculated for $C_{35}H_{62}BrOSi$ ($M+H^+$): 605.3748, found: 605.3750.

8.4.3 Preparation of Structurally Modified Norbornenes (smNBEs)

SmNBEs **N2**[15d], **N3**[15d], **N4**[15b], **N5**[15b], **N7**[17], **N8**[17], **N9**[18] and **N10**[19] are known compounds, which were prepared according to the literature reported procedures.

Figure 8.3. Structurally Modified Norbornenes

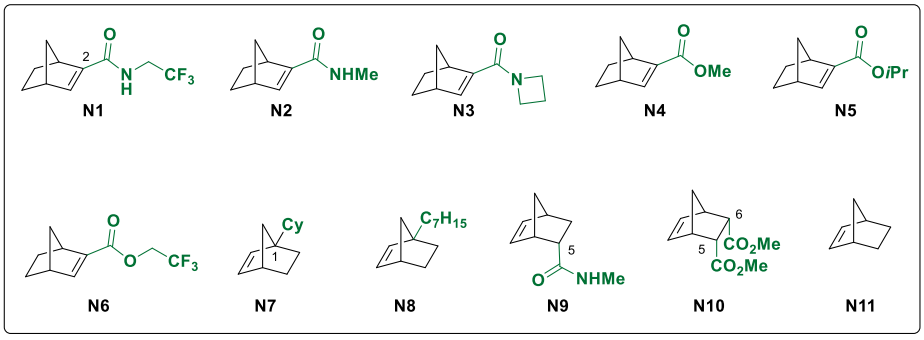

Scheme 8.7. Preparation of N1

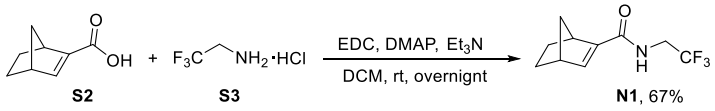

S2 was prepared according to the literature reported procedures.[15b] **S2** (1.38 g, 10.0 mmol, 1.0 equiv), 2,2,2-trifluoroethylamine hydrochloride (2.03 g, 15.0 mmol, 1.5 equiv), 1-ethyl-3-(3-dimethylaminopropyl)carbodiimide hydrochloride (2.88 g, 15.0 mmol, 1.5 equiv), 4-dimethylaminopyridine (122 mg, 1.0 mmol, 10 mol%) and triethylamine (1.52 g, 15.0 mmol, 1.5 equiv) were dissolved in dichloromethane (50 mL). Then, the reaction mixture was stirred at room temperature. After 12 h, it was diluted with diethyl ether, washed with water and brine, dried over $MgSO_4$, and then purified on silica gel (hexanes/acetone = 2:1) to afford **N1** as a white solid (1.5 g, 67%).

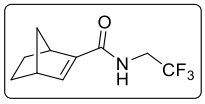

N1: White solid (67%). m. p. = 98.7 – 99.6 ^{o}C. R_f = 0.2 (hexane/acetone = 5:1). **^{1}H NMR** (400 MHz, $CDCl_3$) δ 6.72 (d, *J* = 3.2 Hz, 1H), 6.02 (s, 1H), 3.96 (qd, *J* = 9.1, 6.6 Hz, 2H), 3.20 (s, 1H), 3.03 (d, *J* = 1.5 Hz, 1H), 1.77 (dtdd, *J* = 9.5, 7.3, 5.9, 3.4 Hz, 2H), 1.50 (dq, *J* = 6.3, 2.0 Hz, 1H), 1.26 – 1.18 (m, 1H), 1.16 – 1.03 (m, 2H). **^{13}C NMR** (101 MHz, $CDCl_3$) δ 164.9, 143.1, 142.5, 124.3 (q, *J* = 278.4 Hz), 48.4, 43.6, 42.2, 40.6 (q, *J* = 34.6 Hz), 25.0, 24.7. ^{19}F NMR (376 MHz, $CDCl_3$) δ -72.45. **IR** (KBr): υ 3267, 2955, 2876, 1645, 1538, 1158, 834, 741, 669 cm^{-1}. **HRMS** (ESI): Calculated for $C_{10}H_{13}F_3NO$ ($M+H^+$): 220.0944, found: 220.0941.

Scheme 8.8. Preparation of N6

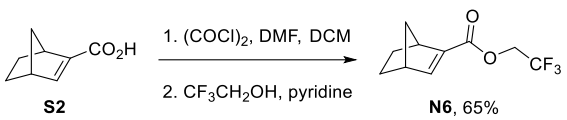

To a solution of **S2** (1.29 g, 9.3 mmol, 1.0 equiv) in DCM (10 mL) with 3 drops of DMF was added oxalyl chloride (1.19 g, 9.3 mmol, 1.0 equiv) dropwise at 0 ^{o}C. The reaction mixture was

stirred at room temperature for another 1 h until the bubbling stopped. Then a mixture of 2,2,2-trifluoroethanol (1.86 g, 18.6 mmol, 2.0 equiv) and pyridine (2.94 g, 37.2 mmol, 4.0 equiv) was added dropwise. The reaction mixture was stirred at room temperature for another 3 h until the reaction was completed. The organic layer was washed with 1 M hydrochloric acid and then concentrated under vacuum. The corresponding ester substituted NBE was isolated after silica gel chromatography (hexane/Et_2O = 20:1) as a colorless oil.

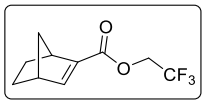

N6: Colorless oil (65%). R_f = 0.3 (hexane/ethyl acetate = 20:1). **^{1}H NMR** (400 MHz, $CDCl_3$) δ 7.08 (d, *J* = 3.1 Hz, 1H), 4.50 (qd, *J* = 8.5, 3.9 Hz, 2H), 3.29 (s, 1H), 3.06 (s, 1H), 1.85 – 1.70 (m, 2H), 1.55 – 1.47 (m, 1H), 1.27 – 1.20 (m, 1H), 1.09 (qd, *J* = 8.1, 2.1 Hz, 2H). **^{13}C NMR** (101 MHz, $CDCl_3$) δ 163.0, 150.0, 139.2, 123.3 (q, *J* = 277.1 Hz), 60.2 (q, *J* = 36.4 Hz), 48.3, 43.9, 42.0, 24.6, 24.5. **^{19}F NMR** (376 MHz, $CDCl_3$) δ -73.78. **IR** (KBr): υ 2974, 2884, 1749, 1413, 1287, 1260, 1171, 1095, 975 cm^{-1}. **HRMS** (ESI): Calculated for $C_{10}H_{12}F_3O_2$ ($M+H^+$): 221.0784, found: 221.0774.

8.4.4 General Procedure of Direct Difunctionalization of Pyrroles

Scheme 8.9. Pyrrole Difunctionalization with Ortho-Substituted Aryl Iodide

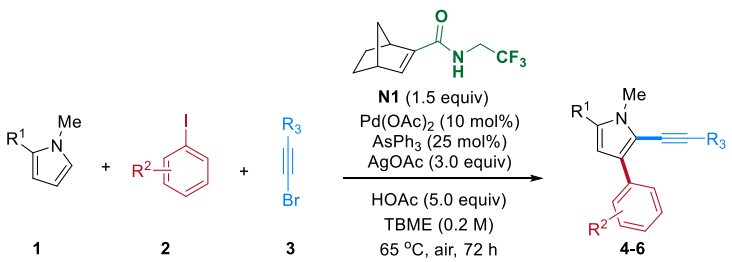

A flame-dried 4.0 mL vial was charged with $Pd(OAc)_2$ (4.6 mg, 0.02 mmol, 10 mol%), $AsPh_3$ (15.2 mg, 0.05 mmol, 25 mol%), **N1** (65.8 mg, 0.3 mmol, 1.5 equiv), pyrrole **1** (0.2 mmol, 1.0 equiv), aryl iodide **2** (0.4 mmol, 2.0 equiv) and AgOAc (100 mg, 0.6 mmol, 3.0 equiv) in air. TBME (1.0 mL) was then added. After alkynyl bromide **3** (0.36 mmol, 1.8 equiv) and HOAc (60 mg, 1.0 mmol, 5.0 equiv) were added, the vial was tightly sealed and stirred on a pie-block preheated to 65 ^oC for 72 hours. After completion of the reaction, the mixture was filtered through a thin pad of silica gel. The filter cake was washed with ethyl acetate and the combined filtrate was concentrated under reduced pressure. The residue was loaded to a small amount of silica gel and subjected to flash column chromatography to give the desired product **4**-**6**.

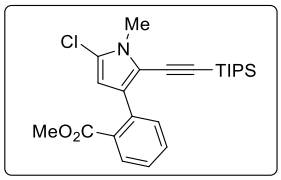

4a: Colorless oil (78%). R_f = 0.4 (hexane/ethyl acetate = 20:1). **^{1}H NMR** (400 MHz, $CDCl_3$) δ 7.78 – 7.72 (m, 1H), 7.63 – 7.58 (m, 1H), 7.42 (td, *J* = 7.6, 1.5 Hz, 1H), 7.30 (td, *J* = 7.6, 1.3 Hz, 1H), 6.06 (s, 1H), 3.78 (s, 3H), 3.66 (s, 3H), 1.04 (d, *J* = 3.1 Hz, 21H). **^{13}C NMR** (101 MHz, $CDCl_3$) δ 169.0, 134.8, 131.2, 130.9, 130.8, 129.6, 128.6, 126.6, 117.8, 114.1, 107.1, 97.5, 97.3, 52.1, 32.1, 18.6, 11.3. **IR** (KBr): υ 2944, 2865, 2141, 1734, 1462, 1270, 1252, 1125, 883, 677 cm^{-1}. **HRMS** (ESI): Calculated for $C_{24}H_{33}ClNO_2Si$ ($M+H^+$): 430.1964, found: 430.1961.

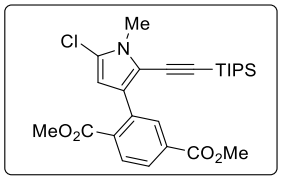

4b: Colorless oil (76%). R_f = 0.2 (hexane/ethyl acetate = 20:1). **^{1}H NMR** (400 MHz, $CDCl_3$) δ 8.20 (d, *J* = 1.7 Hz, 1H), 7.96 (dd, *J* = 8.1, 1.7 Hz, 1H), 7.80 (d, *J* = 8.1 Hz, 1H), 6.08 (s, 1H), 3.90 (s, 3H), 3.80 (s, 3H), 3.67 (s, 3H), 1.01 (d, *J* = 4.1 Hz, 21H). **^{13}C NMR** (101 MHz, $CDCl_3$) δ 168.4, 166.4, 135.3, 134.9, 132.5, 132.3, 129.8, 127.8, 118.2, 114.5, 107.2, 98.0, 97.0, 52.5, 52.4, 32.3, 18.7, 11.3. **IR** (KBr): υ 2946, 2891, 2865, 2142, 1728, 1464, 1436, 1285, 1247, 1114 cm^{-1}. **HRMS** (ESI): Calculated for $C_{26}H_{35}ClNO_4Si$ ($M+H^+$): 488.2018, found: 488.2024.

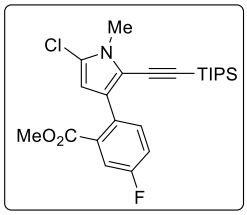

4c: Colorless oil (68%). R_f = 0.4 (hexane/ethyl acetate = 20:1). **^{1}H NMR** (400 MHz, $CDCl_3$) δ 7.54 (dd, *J* = 8.6, 5.6 Hz, 1H), 7.47 (dd, *J* = 9.2, 2.8 Hz, 1H), 7.13 (ddd, *J* = 8.6, 7.9, 2.8 Hz, 1H), 6.03 (s, 1H), 3.78 (s, 3H), 3.65 (s, 3H), 1.03 (d, *J* = 3.1 Hz, 21H). **^{13}C NMR** (101 MHz, $CDCl_3$) δ 167.7, 162.6, 160.1, 133.2 (d, *J* = 7.6 Hz), 132.4 (d, *J* = 7.3 Hz), 131.3 (d, *J* = 3.5 Hz), 127.8, 118.1 (d, *J* = 20.6 Hz), 116.7 (d, *J* = 23.5 Hz), 114.4, 107.3, 97.8, 97.3, 52.4, 32.3, 18.7, 11.4. **^{19}F NMR** (376 MHz, $CDCl_3$) δ -115.20. **IR** (KBr): υ 2944, 2891, 2865, 2142, 1724, 1494, 1436, 1298, 1072, 797 cm^{-1}. **HRMS** (ESI): Calculated for $C_{24}H_{32}ClFNO_2Si$ ($M+H^+$): 448.1869, found: 448.1872.

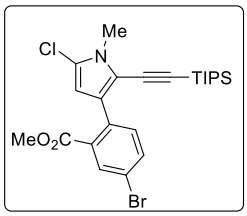

4d: Colorless oil (72%). R_f = 0.4 (hexane/ethyl acetate = 20:1). **^{1}H NMR** (400 MHz, $CDCl_3$) δ 7.89 (d, *J* = 2.1 Hz, 1H), 7.54 (dd, *J* = 8.3, 2.1 Hz, 1H), 7.48 (d, *J* = 8.3 Hz, 1H), 6.03 (s, 1H), 3.79

(s, 3H), 3.65 (s, 3H), 1.04 (d, *J* = 3.3 Hz, 21H). **^{13}C NMR** (101 MHz, $CDCl_3$) δ 167.7, 133.9, 132.9, 132.7, 132.5, 127.4, 120.5, 118.2, 114.3, 107.1, 98.4, 98.3, 97.1, 52.5, 32.3, 18.7, 11.4. **IR** (KBr): υ 2944, 2890, 2865, 2141, 1738, 1484, 1286, 1244, 1093, 792 cm^{-1}. **HRMS** (ESI): Calculated for $C_{24}H_{32}BrClNO_2Si$ ($M+H^+$): 508.1069, found: 508.1072.

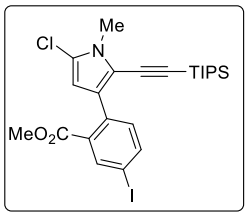

4e: Colorless oil (70%). R_f = 0.4 (hexane/ethyl acetate = 20:1). **^{1}H NMR** (400 MHz, $CDCl_3$) δ 8.07 (d, *J* = 1.9 Hz, 1H), 7.73 (dd, *J* = 8.2, 1.9 Hz, 1H), 7.35 (d, *J* = 8.2 Hz, 1H), 6.03 (s, 1H), 3.78 (s, 3H), 3.65 (s, 3H), 1.05 (s, 21H). **^{13}C NMR** (101 MHz, $CDCl_3$) δ 167.6, 139.9, 138.5, 134.5, 132.9, 132.6, 127.5, 118.3, 114.3, 107.1, 98.3, 97.1, 91.4, 52.5, 32.3, 18.7, 11.4. **IR** (KBr): υ 2943, 2864, 2140, 1736, 1482, 1434, 1284, 1242, 1085, 791 cm^{-1}. **HRMS** (ESI): Calculated for $C_{24}H_{32}ICINO_2Si$ ($M+H^+$): 556.0930, found: 556.0933.

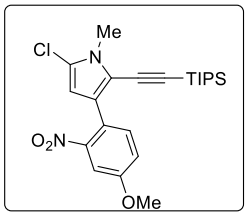

4f: Yellow oil (40%). R_f = 0.2 (hexane/ethyl acetate = 20:1). **^{1}H NMR** (400 MHz, $CDCl_3$) δ 7.56 (d, *J* = 8.6 Hz, 1H), 7.31 (d, *J* = 2.7 Hz, 1H), 7.05 (dd, *J* = 8.6, 2.7 Hz, 1H), 6.03 (s, 1H), 3.86 (s, 3H), 3.65 (s, 3H), 1.04 (d, *J* = 3.8 Hz, 21H). **^{13}C NMR** (101 MHz, $CDCl_3$) δ 158.8, 149.7, 133.4, 124.4, 121.5, 118.6, 118.6, 114.5, 108.9, 106.5, 98.6, 96.8, 56.0, 32.3, 18.7, 11.4. **IR** (KBr): υ

2943, 2891, 2865, 2142, 1533, 1499, 1350, 1299, 1236, 805 cm^{-1}. **HRMS** (ESI): Calculated for $C_{23}H_{32}ClN_2O_3Si$ ($M+H^+$): 447.1865, found: 447.1866.

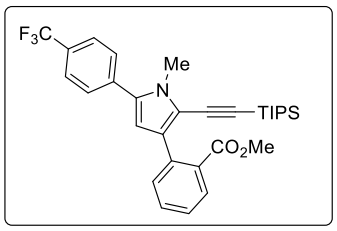

N1 (0.2 mmol) was used and the reaction time was 24 h.

5p: Pale yellow oil (79%). R_f = 0.2 (hexane/ethyl acetate = 20:1). **^{1}H NMR** (400 MHz, $CDCl_3$) δ 7.77 (dd, *J* = 7.8, 1.1 Hz, 1H), 7.73 – 7.69 (m, 1H), 7.67 (d, *J* = 8.2 Hz, 2H), 7.54 (d, *J* = 8.1 Hz, 2H), 7.45 (td, *J* = 7.6, 1.4 Hz, 1H), 7.35 – 7.29 (m, 1H), 6.29 (s, 1H), 3.78 (s, 3H), 3.77 (s, 3H), 1.06 (d, *J* = 3.2 Hz, 21H). **^{13}C NMR** (126 MHz, $CDCl_3$) δ 169.4, 136.2, 135.2, 134.3, 131.4, 131.0, 131.0, 129.8, 129.3 (q, *J* = 32.5 Hz), 129.2, 128.8, 126.7, 125.7 (q, *J* = 3.7 Hz), 124.3 (q, *J* = 271.9 Hz), 117.3, 110.4, 98.9, 98.1, 52.2, 33.7, 18.8, 11.5. **IR** (KBr): υ 2944, 2865, 2139, 1728, 1324, 1125, 1069, 763, 679 cm^{-1}. **HRMS** (ESI): Calculated for $C_{31}H_{37}F_3NO_2Si$ ($M+H^+$): 540.2540, found: 540.2538.

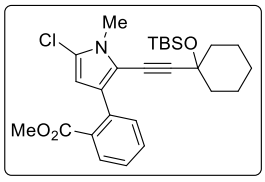

6a: Colorless oil (77%). R_f = 0.4 (hexane/ethyl acetate = 20:1). **^{1}H NMR** (400 MHz, $CDCl_3$) δ 7.77 (dd, *J* = 7.8, 0.9 Hz, 1H), 7.49 (ddd, *J* = 7.7, 1.5, 0.5 Hz, 1H), 7.44 (td, *J* = 7.5, 1.4 Hz, 1H), 7.31 (td, *J* = 7.5, 1.5 Hz, 1H), 6.07 (s, 1H), 3.77 (s, 3H), 3.63 (s, 3H), 1.83 – 1.72 (m, 2H), 1.66 – 1.55 (m, 4H), 1.50 – 1.25 (m, 4H), 0.82 (s, 9H), -0.03 (s, 6H). **^{13}C NMR** (101 MHz, $CDCl_3$) δ

168.9, 135.3, 131.5, 131.1, 131.0, 129.8, 128.4, 126.9, 117.6, 113.5, 107.4, 99.6, 76.0, 70.0, 52.1, 41.1, 32.2, 25.9, 25.4, 22.8, 18.2, -2.9. **IR** (KBr): υ 2934, 2856, 1735, 1290, 1252, 1090, 836, 774, 759 cm^{-1}. **HRMS** (ESI): Calculated for $C_{27}H_{37}ClNO_3Si$ ($M+H^+$): 486.2226, found: 486.2224.

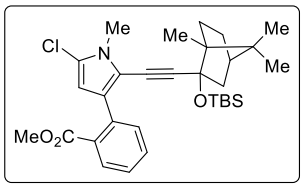

6b: Colorless oil (21%). R_f = 0.4 (hexane/ethyl acetate = 20:1). **^{1}H NMR** (400 MHz, $CDCl_3$) δ 7.83 – 7.75 (m, 1H), 7.51 – 7.41 (m, 2H), 7.32 (ddd, *J* = 7.8, 6.4, 2.3 Hz, 1H), 6.07 (s, 1H), 3.75 (s, 3H), 3.64 (s, 3H), 2.14 (ddd, *J* = 13.1, 4.4, 3.1 Hz, 1H), 1.88 – 1.77 (m, 2H), 1.72 (t, *J* = 4.4 Hz, 1H), 1.63 (ddq, *J* = 11.7, 7.7, 4.0 Hz, 1H), 1.38 (ddd, *J* = 13.2, 11.6, 4.9 Hz, 1H), 1.04 (s, 4H), 0.84 (d, *J* = 5.8 Hz, 6H), 0.78 (s, 9H), -0.07 (s, 3H), -0.12 (s, 3H). **^{13}C NMR** (101 MHz, $CDCl_3$) δ 168.9, 135.5, 131.7, 131.2, 131.1, 129.9, 128.7, 126.9, 117.5, 113.7, 107.5, 99.8, 79.5, 76.0, 52.1, 50.8, 45.8, 32.3, 32.3, 26.9, 25.9, 21.8, 21.7, 18.3, 11.2, -3.09, -3.11. **IR** (KBr): υ 3026, 2951, 2856, 2211, 1735, 1722, 1461, 1252, 1077, 837 cm^{-1}. **HRMS** (ESI): Calculated for $C_{31}H_{43}ClNO_3Si$ ($M+H^+$): 540.2695, found: 540.2694.

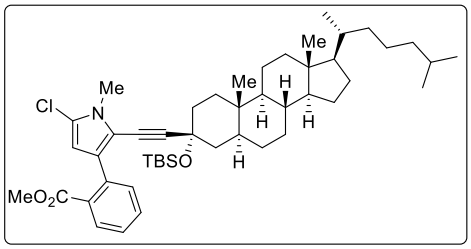

6c: Colorless oil (50%). R_f = 0.5 (hexane/ethyl acetate = 10:1). **^{1}H NMR** (400 MHz, $CDCl_3$) δ 7.81 – 7.76 (m, 1H), 7.49 – 7.41 (m, 2H), 7.31 (ddd, *J* = 7.7, 6.8, 2.0 Hz, 1H), 6.07 (s, 1H), 3.77 (s, 3H), 3.64 (s, 3H), 1.96 (d, *J* = 12.3 Hz, 1H), 1.88 – 1.74 (m, 2H), 1.67 – 1.57 (m, 2H), 1.57 –

1.47 (m, 5H), 1.45 – 0.93 (m, 20H), 0.91 (d, *J* = 6.5 Hz, 3H), 0.87 (dd, *J* = 6.6, 1.8 Hz, 6H), 0.81 (s, 9H), 0.75 (s, 3H), 0.64 (s, 3H), 0.48 (td, *J* = 11.6, 4.0 Hz, 1H), -0.00 (s, 6H). **^{13}C NMR** (101 MHz, $CDCl_3$) δ 168.8, 135.5, 131.6, 131.15, 131.06, 129.9, 128.5, 127.0, 117.5, 113.6, 107.5, 99.3, 77.5, 77.2, 76.8, 76.2, 71.8, 56.6, 56.5, 54.2, 52.1, 43.83, 43.77, 42.8, 40.2, 39.7, 37.5, 36.3, 36.2, 36.0, 35.6, 35.5, 32.3, 32.1, 28.5, 28.4, 28.2, 25.8, 24.4, 24.1, 23.0, 22.7, 21.3, 18.8, 18.1, 12.24, 12.21, -2.67, -2.69. **IR** (KBr): υ 2947, 2933, 2856, 1736, 1723, 1290, 1251, 1088, 837, 775 cm^{-1}. **HRMS** (ESI): Calculated for $C_{48}H_{73}ClNO_3Si$ ($M+H^+$): 774.5043, found: 774.5038.

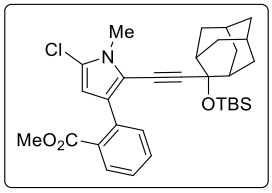

6d: Colorless oil (41%). R_f = 0.4 (hexane/ethyl acetate = 10:1). **^{1}H NMR** (400 MHz, $CDCl_3$) δ 7.77 (dd, *J* = 8.0, 1.0 Hz, 1H), 7.50 – 7.45 (m, 1H), 7.43 (td, *J* = 7.5, 1.4 Hz, 1H), 7.35 – 7.28 (m, 1H), 6.07 (s, 1H), 3.76 (s, 3H), 3.64 (s, 3H), 2.19 (dd, *J* = 12.9, 3.0 Hz, 2H), 2.07 – 1.99 (m, 2H), 1.85 (s, 2H), 1.76 – 1.64 (m, 6H), 1.48 (d, *J* = 12.4 Hz, 2H), 0.84 (s, 9H), -0.07 (s, 6H). **^{13}C NMR** (101 MHz, $CDCl_3$) δ 168.8, 135.5, 131.7, 131.1, 131.0, 129.8, 128.6, 126.9, 117.6, 113.6, 107.5, 99.5, 77.9, 74.4, 52.1, 39.9, 38.1, 35.3, 32.3, 31.9, 27.04, 26.98, 26.1, 18.6, -3.0. **IR** (KBr): υ 2927, 2904, 2855, 1735, 1291, 1252, 1076, 851, 775 cm^{-1}. **HRMS** (ESI): Calculated for $C_{31}H_{41}ClNO_3Si$ ($M+H^+$): 538.2539, found: 538.2538.

Scheme 8.10. Pyrrole Difunctionalization with Ortho-Unsubstituted Aryl Iodide

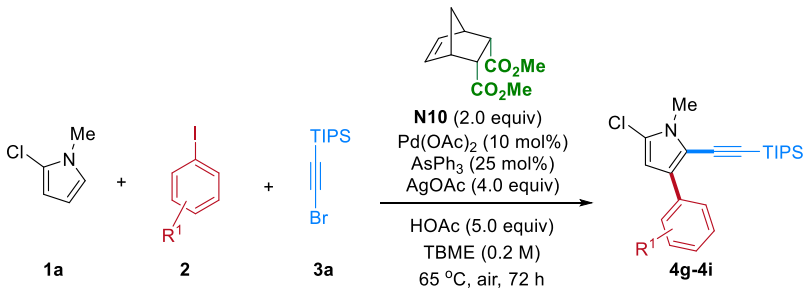

A flame-dried 4.0 mL vial was charged with $Pd(OAc)_2$ (4.6 mg, 0.02 mmol, 10 mol%), $AsPh_3$ (15.2 mg, 0.05 mmol, 25 mol%), **N10** (63.2 mg, 0.3 mmol, 1.5 equiv), **1a** (23.2 mg, 0.2 mmol, 1.0 equiv), aryl iodide **2** (0.4 mmol, 2.0 equiv) and AgOAc (100 mg, 0.6 mmol, 3.0 equiv) in air. TBME (1.0 mL) was then added. After alkynyl bromide **3a** (94 mg, 0.36 mmol, 1.8 equiv) and HOAc (60 mg, 1.0 mmol, 5.0 equiv) were added, the vial was tightly sealed and stirred on a pie-block preheated to 65 °C for 24 hours. Then another portion of **N10** (21.1 mg, 0.1 mmol, 0.5 equiv) and AgOAc (33 mg, 0.2 mmol, 1.0 equiv) were added to the reaction mixture and the vial was heated at 65 °C for another 48 h. After completion of the reaction, the mixture was filtered through a thin pad of silica gel. The filter cake was washed with ethyl acetate and the combined filtrate was concentrated under reduced pressure. The residue was loaded to a small amount of silica gel and subjected to flash column chromatography to give the desired product **4g-4i**.

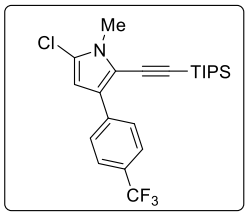

The reaction was run with 0.1 mmol **1a**, 0.2 mmol **2g** and 0.18 mmol **3a**.

4g: White solid (46%). m. p. = 68.0 – 68.8 °C. R_f = 0.5 (hexane/ethyl acetate = 20:1). **^{1}H NMR** (400 MHz, $CDCl_3$) δ 7.92 (d, *J* = 8.3 Hz, 2H), 7.56 (d, *J* = 8.9 Hz, 2H), 6.34 (s, 1H), 3.68 (s, 3H),

1.15 (s, 21H). **^{13}C NMR** (101 MHz, $CDCl_3$) δ 138.0, 128.3 (q, *J* = 32.4 Hz),127.2, 126.5, 125.4 (q, *J* = 3.8 Hz), 124.5 (q, *J* = 271.7 Hz), 119.4, 113.6, 105.4, 100.0, 98.0, 32.2, 18.8, 11.5. **^{19}F NMR** (376 MHz, $CDCl_3$) δ -62.34. **IR** (KBr): υ 2944, 2892, 2866, 2140, 1616, 1463, 1325, 1165, 1124, 1068 cm^{-1}. **HRMS** (ESI): Calculated for $C_{23}H_{30}ClF_3NSi$ ($M+H^+$): 440.1783, found: 440.1781.

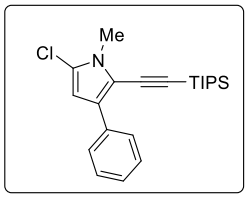

4h: Colorless oil (23%). R_f = 0.5 (hexane/ethyl acetate = 20:1). **^{1}H NMR** (400 MHz, CD_2Cl_2) δ 7.84 – 7.78 (m, 2H), 7.37 – 7.30 (m, 2H), 7.26 – 7.19 (m, 1H), 6.32 (s, 1H), 3.67 (s, 3H), 1.15 (s, 21H). **^{13}C NMR** (101 MHz, CD_2Cl_2) δ 134.7, 129.0, 128.8, 126.9, 126.8, 119.2, 113.2, 105.3, 99.4, 98.7, 32.3, 18.9, 11.8. **IR** (KBr): υ 2942, 2864, 2139, 1461, 1452, 1384, 882, 792, 756, 661 cm^{-1}. **HRMS** (ESI): Calculated for $C_{22}H_{31}ClNSi$ ($M+H^+$): 372.1909, found: 372.1913.

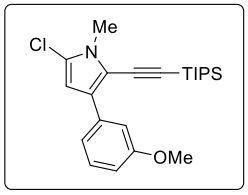

4i: Colorless oil (26%). R_f = 0.3 (hexane/ethyl acetate = 20:1). **^{1}H NMR** (400 MHz, CD_2Cl_2) δ 7.49 – 7.41 (m, 1H), 7.30 – 7.21 (m, 2H), 6.81 – 6.74 (m, 1H), 6.31 (s, 1H), 3.81 (s, 3H), 3.66 (s, 3H), 1.14 (d, *J* = 3.3 Hz, 21H). **^{13}C NMR** (101 MHz, CD_2Cl_2) δ 160.3, 136.0, 129.7, 128.8, 119.4, 119.1, 113.3, 112.7, 112.2, 105.5, 99.5, 98.6, 55.6, 32.4, 18.9, 11.8. **IR** (KBr): υ 2942, 2890, 2864,

2139, 1610, 1602, 1463, 1251, 773, 677 cm^{-1}. **HRMS** (ESI): Calculated for $C_{23}H_{33}ClNOSi$ ($M+H^+$): 402.2014, found: 402.2017.

8.4.5 General Procedure of Direct Difunctionalization of Thiophenes

Scheme 8.11. Thiophene Difunctionalization with Ortho-Substituted Aryl Iodide

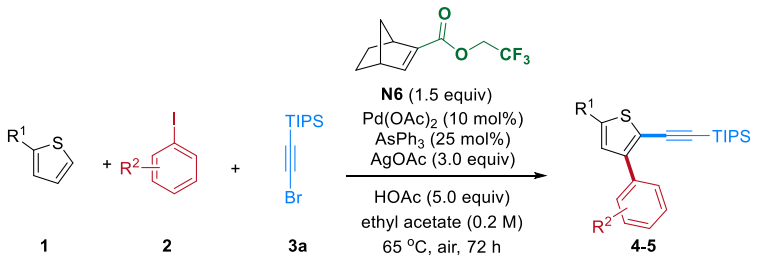

A flame-dried 4.0 mL vial was charged with $Pd(OAc)_2$ (4.6 mg, 0.02 mmol, 10 mol%), $AsPh_3$ (15.2 mg, 0.05 mmol, 25 mol%), **N6** (66.1 mg, 0.3 mmol, 1.5 equiv), thiophene **1** (0.2 mmol, 1.0 equiv), aryl iodide **2** (0.4 mmol, 2.0 equiv) and AgOAc (100 mg, 0.6 mmol, 3.0 equiv) in air. Ethyl acetate (1.0 mL) was then added. After alkynyl bromide **3a** (94 mg, 0.36 mmol, 1.8 equiv) and HOAc (60 mg, 1.0 mmol, 5.0 equiv) were added, the vial was tightly sealed and stirred on a pie-block preheated to 65 °C for 72 hours. After completion of the reaction, the mixture was filtered through a thin pad of silica gel. The filter cake was washed with ethyl acetate and the combined filtrate was concentrated under reduced pressure. The residue was loaded to a small amount of silica gel and subjected to flash column chromatography to give the desired product **4** or **5**.

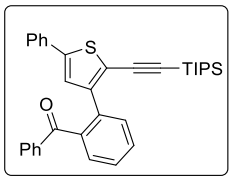

4j: Colorless oil (82%). R_f = 0.4 (hexane/ethyl acetate = 10:1). **^{1}H NMR** (500 MHz, $CDCl_3$) δ 7.72 (dd, *J* = 7.6, 1.3 Hz, 1H), 7.62 – 7.58 (m, 3H), 7.55 (td, *J* = 7.6, 1.6 Hz, 1H), 7.49 (td, *J* = 7.5, 1.3

Hz, 1H), 7.38 – 7.34 (m, 3H), 7.32 (ddd, *J* = 7.7, 6.7, 1.4 Hz, 2H), 7.27 (t, *J* = 1.5 Hz, 1H), 7.22 (dd, *J* = 8.2, 7.4 Hz, 2H), 6.91 (s, 1H), 1.11 – 1.06 (m, 21H). **^{13}C NMR** (126 MHz, $CDCl_3$) δ 198.7, 145.7, 143.7, 138.9, 137.3, 134.3, 133.4, 132.8, 130.8, 130.2, 129.6, 128.9, 128.7, 128.1, 128.0, 127.9, 125.8, 125.5, 119.7, 99.1, 98.3, 18.6, 11.3. **IR** (KBr): υ 3061, 2942, 2864, 2139, 1666, 1288, 935, 882, 752, 705 cm^{-1}. **HRMS** (ESI): Calculated for $C_{34}H_{37}OSSi$ ($M+H^+$): 521.2329, found: 521.2332.

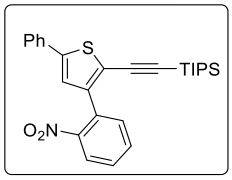

4k: Yellow solid (72%). m. p. = 90.0 – 91.2 °C. R_f = 0.4 (hexane/ethyl acetate = 10:1). **^{1}H NMR** (400 MHz, $CDCl_3$) δ 8.02 – 7.96 (m, 1H), 7.65 – 7.55 (m, 4H), 7.50 (ddd, *J* = 8.2, 6.0, 2.9 Hz, 1H), 7.42 – 7.35 (m, 2H), 7.35 – 7.29 (m, 1H), 7.15 (s, 1H), 1.00 (q, *J* = 4.0 Hz, 21H). **^{13}C NMR** (101 MHz, $CDCl_3$) δ 149.0, 144.6, 142.6, 133.5, 132.7, 132.6, 130.8, 129.2, 128.8, 128.4, 126.1, 124.6, 123.5, 120.1, 99.8, 98.1, 18.7, 11.3. **IR** (KBr): υ 3064, 2942, 2864, 2140, 1529, 1350, 882, 744, 678, 628 cm^{-1}. **HRMS** (ESI): Calculated for $C_{27}H_{32}NO_2SSi$ ($M+H^+$): 462.1918, found: 462.1921.

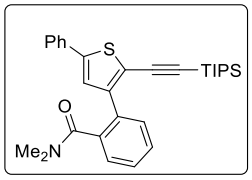

4l: Colorless oil (81%). R_f = 0.2 (hexane/ethyl acetate = 5:1). **^{1}H NMR** (400 MHz, $CDCl_3$) δ 7.77 – 7.71 (m, 1H), 7.62 – 7.55 (m, 2H), 7.44 – 7.35 (m, 5H), 7.34 – 7.28 (m, 2H), 2.88 (s, 3H), 2.55 (s, 3H), 1.02 (d, *J* = 3.7 Hz, 21H). **^{13}C NMR** (101 MHz, $CDCl_3$) δ 171.1, 145.6, 144.0, 136.0, 133.5, 132.3, 130.7, 129.2, 129.0, 128.5, 128.3, 127.0, 126.0, 124.7, 119.3, 99.2, 98.4, 38.2, 34.9,

18.7, 11.4. **IR** (KBr): υ 2942, 2864, 2139, 1641, 1463, 1394, 1068, 882, 754, 690 cm^{-1}. **HRMS** (ESI): Calculated for $C_{30}H_{37}NOSSiNa$ ($M+Na^+$): 510.2257, found: 510.2264.

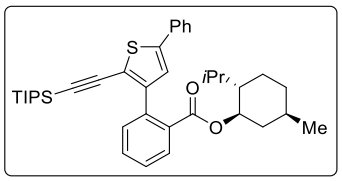

4m: Colorless oil (72%). R_f = 0.7 (toluene). **^{1}H NMR** (400 MHz, $CDCl_3$) δ 7.98 (d, *J* = 7.6 Hz, 1H), 7.60 – 7.54 (m, 2H), 7.53 – 7.46 (m, 2H), 7.44 – 7.40 (m, 1H), 7.40 – 7.34 (m, 2H), 7.29 (t, *J* = 7.4 Hz, 1H), 7.12 (s, 1H), 4.70 (td, *J* = 10.7, 4.4 Hz, 1H), 1.99 (d, *J* = 11.7 Hz, 1H), 1.71 (pd, *J* = 6.9, 2.7 Hz, 1H), 1.56 (d, *J* = 8.8 Hz, 2H), 1.39 (dddd, *J* = 12.6, 9.4, 6.6, 3.5 Hz, 1H), 1.13 – 1.04 (m, 1H), 0.95 (d, *J* = 3.0 Hz, 22H), 0.78 – 0.70 (m, 7H), 0.65 (d, *J* = 7.0 Hz, 4H). **^{13}C NMR** (101 MHz, $CDCl_3$) δ 167.3, 148.1, 142.9, 136.6, 133.9, 131.5, 131.4, 131.3, 129.1, 128.1, 127.9, 125.9, 125.3, 119.0, 99.1, 98.1, 75.1, 47.0, 40.5, 34.3, 31.4, 26.2, 23.3, 22.0, 21.0, 18.6, 16.3, 11.3. **IR** (KBr): υ 3063, 2955, 2865, 2141, 1708, 1454, 1290, 1253, 1128, 751 cm^{-1}. **HRMS** (ESI): Calculated for $C_{38}H_{51}O_2SSi$ ($M+H^+$): 599.3374, found: 599.3368.

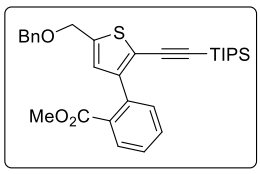

5a: Colorless oil (75%). R_f = 0.2 (hexane/diethyl ether = 20:1). **^{1}H NMR** (400 MHz, $CDCl_3$) δ 7.93 (d, *J* = 7.5 Hz, 1H), 7.54 – 7.47 (m, 2H), 7.42 – 7.28 (m, 6H), 6.85 (s, 1H), 4.68 (s, 2H), 4.60 (s, 2H), 3.72 (s, 3H), 0.98 (d, *J* = 3.5 Hz, 21H). **^{13}C NMR** (101 MHz, $CDCl_3$) δ 168.3, 146.0, 141.0, 138.2, 137.0, 131.8, 131.8, 130.9, 130.7, 128.9, 128.3, 128.3, 128.2, 128.0, 120.5, 99.3, 98.0, 72.2,

67.0, 52.5, 18.9, 11.6. **IR** (KBr): υ 3063, 3030, 2943, 2864, 2141, 1729, 1462, 1292, 1254, 1073, 752 cm^{-1}. **HRMS** (ESI): Calculated for $C_{31}H_{39}O_3SSi$ ($M+H^+$): 519.2384, found: 519.2383.

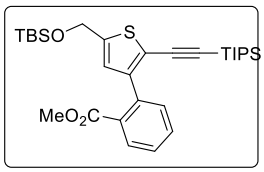

5b: Colorless oil (73%). R_f = 0.3 (hexane/diethyl ether = 10:1). **^{1}H NMR** (400 MHz, $CDCl_3$) δ 7.90 (d, *J* = 7.5 Hz, 1H), 7.54 – 7.45 (m, 2H), 7.37 (ddd, *J* = 7.8, 6.2, 2.5 Hz, 1H), 6.74 (s, 1H), 4.84 (d, *J* = 1.1 Hz, 2H), 3.71 (s, 3H), 1.01 – 0.92 (m, 30H), 0.13 (s, 6H). **^{13}C NMR** (101 MHz, $CDCl_3$) δ 168.1, 145.7, 145.1, 136.8, 131.44, 131.43, 130.7, 130.4, 127.6, 125.0, 118.9, 99.2, 97.1, 61.0, 52.2, 26.0, 18.6, 18.5, 11.3, -5.1. **IR** (KBr): υ 3064, 2945, 2891, 2864, 2143, 1732, 1463, 1292, 1254, 838 cm^{-1}. **HRMS** (ESI): Calculated for $C_{30}H_{47}O_3SSi_2$ ($M+H^+$): 543.2779, found: 543.2777.

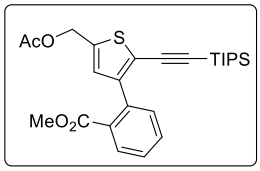

5c: Colorless oil (76%). R_f = 0.2 (hexane/diethyl ether = 10:1). **^{1}H NMR** (400 MHz, $CDCl_3$) δ 7.93 (dd, *J* = 7.8, 1.3 Hz, 1H), 7.53 – 7.44 (m, 2H), 7.39 (ddd, *J* = 7.7, 6.9, 1.8 Hz, 1H), 6.92 (s, 1H), 5.20 (s, 2H), 3.72 (s, 3H), 2.10 (s, 3H), 0.96 (d, *J* = 3.7 Hz, 21H). **^{13}C NMR** (101 MHz, $CDCl_3$) δ 170.6, 167.7, 145.6, 137.2, 136.3, 131.4, 131.3, 130.4, 130.3, 129.4, 127.7, 121.0, 98.5, 98.1, 60.6, 52.1, 20.9, 18.5, 11.2. **IR** (KBr): υ 2944, 2865, 2142, 1733, 1462, 1232, 1073, 781, 753, 677 cm^{-1}. **HRMS** (ESI): Calculated for $C_{26}H_{35}O_4SSi$ ($M+H^+$): 493.1839, found: 493.1833.

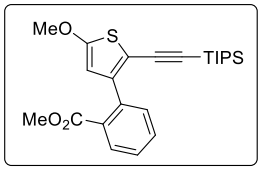

5d: White solid (84%). m. p. = 56.2 – 56.5 °C. R_f = 0.2 (hexane/diethyl ether = 10:1). **^{1}H NMR** (400 MHz, $CDCl_3$) δ 7.88 (d, *J* = 7.7 Hz, 1H), 7.48 (d, *J* = 3.9 Hz, 2H), 7.37 (dt, *J* = 7.7, 4.5 Hz, 1H), 6.09 (s, 1H), 3.90 (s, 3H), 3.75 (s, 3H), 0.95 (d, *J* = 2.6 Hz, 22H). **^{13}C NMR** (101 MHz, $CDCl_3$) δ 168.1, 164.7, 144.6, 137.0, 131.4, 131.2, 130.8, 130.3, 127.7, 106.2, 106.1, 99.4, 95.1, 60.2, 52.2, 18.6, 11.4. **IR** (KBr): υ 2942, 2891, 2864, 2136, 1728, 1498, 1254, 995, 750, 677 cm^{-1}. **HRMS** (ESI): Calculated for $C_{24}H_{33}O_3SSi$ ($M+H^+$): 429.1914, found: 429.1922.

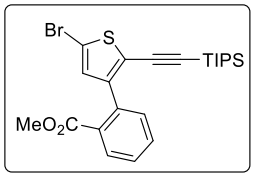

5e: Colorless oil (80%). R_f = 0.4 (hexane/diethyl ether = 10:1). **^{1}H NMR** (400 MHz, $CDCl_3$) δ 7.98 – 7.91 (m, 1H), 7.54 – 7.48 (m, 1H), 7.46 – 7.37 (m, 2H), 6.91 (s, 1H), 3.75 (s, 3H), 0.99 – 0.89 (m, 21H). **^{13}C NMR** (101 MHz, $CDCl_3$) δ 167.6, 146.5, 135.7, 131.7, 131.5, 131.4, 130.6, 130.5, 128.1, 121.4, 111.4, 98.8, 97.7, 52.3, 18.6, 11.3. **IR** (KBr): 2943, 2890, 2865, 2142, 1731, 1462, 1291, 1255, 1072, 750 υ cm^{-1}. **HRMS** (ESI): Calculated for $C_{23}H_{29}BrO_2SSiNa$ ($M+Na^+$): 499.0733, found: 499.0736.

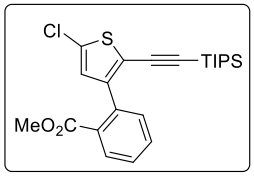

5f: Pale yellow solid (81%). m. p. = 56.6 – 57.2 ^{o} C. R_f = 0.4 (hexane/ethyl acetate = 10:1). **^{1}H NMR** (400 MHz, $CDCl_3$) δ 7.98 – 7.91 (m, 1H), 7.54 – 7.47 (m, 1H), 7.46 – 7.37 (m, 2H), 6.78 (s, 1H), 3.75 (s, 3H), 0.95 (d, *J* = 3.9 Hz, 21H). **^{13}C NMR** (101 MHz, $CDCl_3$) δ 167.6, 145.7, 136.0, 131.7, 131.4, 130.6, 130.5, 128.9, 128.1, 127.9, 118.5, 98.2, 97.8, 52.3, 18.6, 11.3. **IR** (KBr): υ 2944, 2865, 2142, 1731, 1484, 1291, 1255, 1072, 750, 673 cm^{-1}. **HRMS** (ESI): Calculated for $C_{23}H_{30}ClO_2SSi$ ($M+H^+$): 433.1419, found: 433.1417.

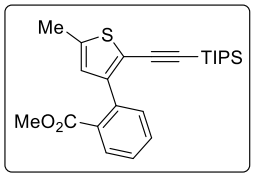

5g: Colorless oil (74%). R_f = 0.3 (hexane/diethyl ether = 10:1). **^{1}H NMR** (400 MHz, $CDCl_3$) δ 7.92 – 7.87 (m, 1H), 7.50 – 7.44 (m, 2H), 7.36 (ddd, *J* = 7.8, 6.2, 2.6 Hz, 1H), 6.61 (d, *J* = 1.2 Hz, 1H), 3.73 (s, 3H), 2.47 (d, *J* = 1.1 Hz, 3H), 0.96 (d, *J* = 3.0 Hz, 21H). **^{13}C NMR** (101 MHz, $CDCl_3$) δ 168.1, 146.2, 139.7, 137.0, 131.4, 131.4, 130.7, 130.3, 127.5, 127.1, 117.6, 99.3, 96.4, 52.2, 18.6, 15.6, 11.4. **IR** (KBr): υ 2943, 2865, 2140, 1732, 1463, 1292, 1255, 1125, 752, 677 cm^{-1}. **HRMS** (ESI): Calculated for $C_{24}H_{33}O_2SSi$ ($M+H^+$): 413.1965, found: 413.1966.

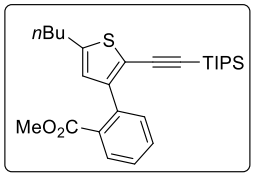

5h: Colorless oil (79%). R_f = 0.4 (hexane/diethyl ether = 10:1). **^{1}H NMR** (500 MHz, $CDCl_3$) δ 7.88 (dd, *J* = 7.8, 1.3 Hz, 1H), 7.54 – 7.43 (m, 2H), 7.37 (ddd, *J* = 7.8, 6.9, 1.8 Hz, 1H), 6.62 (s, 1H), 3.71 (s, 3H), 2.86 – 2.74 (m, 2H), 1.72 – 1.62 (m, 2H), 1.41 (dq, *J* = 14.7, 7.4 Hz, 2H), 1.03 – 0.92 (m, 24H). **^{13}C NMR** (126 MHz, $CDCl_3$) δ 168.3, 145.8, 145.8, 136.9, 131.4, 131.4, 130.8,

130.3, 127.5, 126.0, 117.2, 99.4, 96.4, 52.2, 33.7, 30.0, 22.2, 18.7, 13.9, 11.4. **IR** (KBr): υ 2943, 2865, 2140, 1724, 1463, 1291, 1254, 1125, 883, 752, 677 cm^{-1}. **HRMS** (ESI): Calculated for $C_{27}H_{38}O_2SSiNa$ ($M+Na^+$): 477.2254, found: 477.2250.

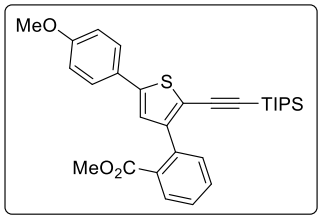

5i: Yellow oil (90%). R_f = 0.3 (hexane/ethyl acetate = 10:1). **^{1}H NMR** (400 MHz, $CDCl_3$) δ 7.96 – 7.90 (m, 1H), 7.55 – 7.47 (m, 4H), 7.40 (ddd, *J* = 7.8, 6.2, 2.5 Hz, 1H), 7.05 (s, 1H), 6.93 – 6.88 (m, 2H), 3.83 (s, 3H), 3.72 (s, 3H), 0.98 (d, *J* = 3.5 Hz, 21H). **^{13}C NMR** (101 MHz, $CDCl_3$) δ 168.1, 159.7, 147.0, 143.4, 136.7, 131.5, 131.3, 130.8, 130.4, 127.8, 127.2, 126.7, 123.6, 118.1, 114.5, 99.2, 97.9, 55.5, 52.2, 18.7, 11.4. **IR** (KBr): υ 2943, 2864, 2138, 1728, 1608, 1513, 1293, 1254, 1036, 827, 753 cm^{-1}. **HRMS** (ESI): Calculated for $C_{30}H_{36}O_3SSiNa$ ($M+Na^+$): 527.2047, found: 527.2039.

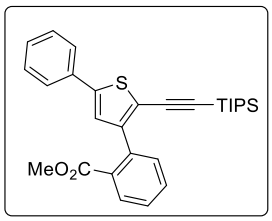

5j: Yellow oil (92%). R_f = 0.3 (hexane/diethyl ether = 10:1). **^{1}H NMR** (400 MHz, $CDCl_3$) δ 7.95 (d, *J* = 7.7 Hz, 1H), 7.64 – 7.57 (m, 2H), 7.57 – 7.49 (m, 2H), 7.45 – 7.35 (m, 3H), 7.34 – 7.27 (m, 1H), 7.17 (s, 1H), 3.73 (s, 3H), 0.98 (d, *J* = 3.6 Hz, 21H). **^{13}C NMR** (101 MHz, $CDCl_3$) δ 168.1, 147.1, 143.4, 136.6, 133.9, 131.6, 131.4, 130.8, 130.5, 129.1, 128.1, 127.8, 125.9, 124.7, 119.1,

99.0, 98.4, 52.3, 18.7, 11.4. **IR** (KBr): υ 3063, 2944, 2865, 2139, 1731, 1455, 1292, 1255, 1073, 752, 678 cm^{-1}. **HRMS** (ESI): Calculated for $C_{29}H_{35}O_2SSi$ ($M+H^+$): 475.2122, found: 475.2109.

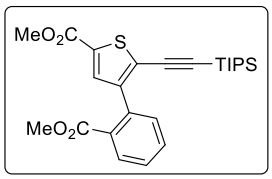

5k: Colorless oil (37%). R_f = 0.2 (hexane/ethyl acetate = 20:1). **^{1}H NMR** (400 MHz, $CDCl_3$) δ 7.98 (dd, *J* = 8.1, 1.5 Hz, 1H), 7.63 (s, 1H), 7.55 – 7.49 (m, 1H), 7.43 (ddd, *J* = 7.9, 6.7, 1.5 Hz, 2H), 3.89 (s, 3H), 3.72 (s, 3H), 1.00 – 0.92 (m, 21H). **^{13}C NMR** (101 MHz, $CDCl_3$) δ 167.4, 162.2, 146.5, 135.9, 134.5, 131.8, 131.5, 131.4, 130.8, 130.4, 128.2, 126.3, 101.0, 98.1, 52.5, 52.3, 18.6, 11.2. **IR** (KBr): υ 2946, 2865, 1722, 1437, 1290, 1251, 1077, 750, 677 cm^{-1}. **HRMS** (ESI): Calculated for $C_{25}H_{32}O_4SSi$ ($M+H^+$): 457.1863, found: 457.1861.

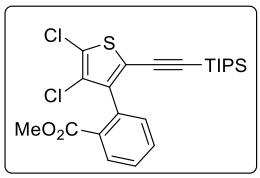

5l: Colorless oil (65%). R_f = 0.4 (hexane/ethyl acetate = 10:1). **^{1}H NMR** (400 MHz, $CDCl_3$) δ 8.06 (dd, *J* = 7.8, 1.4 Hz, 1H), 7.56 (td, *J* = 7.5, 1.4 Hz, 1H), 7.47 (td, *J* = 7.6, 1.4 Hz, 1H), 7.36 (dd, *J* = 7.5, 1.4 Hz, 1H), 3.76 (s, 3H), 0.92 (dq, *J* = 3.5, 1.9 Hz, 21H). **^{13}C NMR** (101 MHz, $CDCl_3$) δ 166.7, 144.3, 134.7, 132.1, 132.0, 130.8, 130.6, 128.8, 124.3, 123.7, 117.1, 99.5, 97.3, 52.3, 18.5, 11.2. **IR** (KBr): υ 2944, 2890, 2865, 2146, 1731, 1462, 1290, 1260, 1126, 744 cm^{-1}. **HRMS** (ESI): Calculated for $C_{23}H_{29}Cl_2O_2SSi$ ($M+H^+$): 467.1029, found: 467.1028.

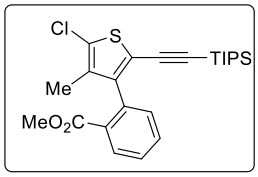

5m: Colorless oil (58%). R_f = 0.4 (hexane/diethyl ether = 10:1). **^{1}H NMR** (400 MHz, $CDCl_3$) δ 8.02 (dd, *J* = 7.8, 1.1 Hz, 1H), 7.54 (td, *J* = 7.5, 1.4 Hz, 1H), 7.42 (td, *J* = 7.7, 1.3 Hz, 1H), 7.26 (dd, *J* = 7.7, 0.9 Hz, 1H), 3.72 (s, 3H), 1.89 (s, 3H), 0.89 (d, *J* = 2.6 Hz, 21H). **^{13}C NMR** (101 MHz, $CDCl_3$) δ 167.0, 147.1, 137.0, 134.3, 132.1, 131.6, 130.7, 130.7, 128.2, 124.5, 116.4, 98.3, 97.6, 52.2, 18.5, 13.2, 11.2. **IR** (KBr): υ 2944, 2865, 2144, 1732, 1462, 1291, 1257, 1127, 1083, 738 cm^{-1}. **HRMS** (ESI): Calculated for $C_{24}H_{32}ClO_2SSi$ ($M+H^+$): 447.1575, found: 447.1567.

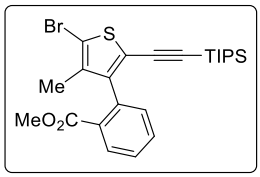

5n: Colorless oil (64%). R_f = 0.4 (hexane/diethyl ether = 10:1). **^{1}H NMR** (500 MHz, $CDCl_3$) δ 8.02 (dd, *J* = 7.8, 1.5 Hz, 1H), 7.54 (td, *J* = 7.5, 1.4 Hz, 1H), 7.42 (td, *J* = 7.6, 1.3 Hz, 1H), 7.25 (dd, *J* = 7.3, 1.1 Hz, 1H), 3.72 (s, 3H), 1.90 (s, 3H), 0.92 – 0.86 (m, 21H). **^{13}C NMR** (126 MHz, $CDCl_3$) δ 166.9, 147.3, 137.1, 136.9, 132.1, 131.6, 130.7, 130.7, 128.2, 119.4, 109.3, 98.4, 98.1, 52.2, 18.5, 14.8, 11.2. **IR** (KBr): υ 2943, 2865, 2142, 1732, 1462, 1291, 1258, 1127, 732 cm^{-1}. **HRMS** (ESI): Calculated for $C_{24}H_{32}BrO_2SSi$ ($M+H^+$): 491.1070, found: 491.1071.

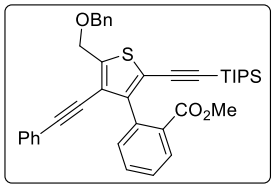

5o: Yellow oil (48%). R_f = 0.2 (hexane/diethyl ether = 10:1). **^{1}H NMR** (400 MHz, $CDCl_3$) δ 8.05 (d, *J* = 7.6 Hz, 1H), 7.59 – 7.51 (m, 2H), 7.47 – 7.39 (m, 3H), 7.36 – 7.28 (m, 3H), 7.23 (dtd, *J* = 12.4, 4.5, 1.7 Hz, 5H), 4.94 – 4.81 (m, 2H), 4.65 (s, 2H), 3.68 (s, 3H), 0.98 (d, *J* = 3.0 Hz, 21H). **^{13}C NMR** (101 MHz, $CDCl_3$) δ 167.6, 147.3, 143.7, 137.9, 135.6, 132.3, 131.7, 131.5, 130.8, 130.5, 128.6, 128.4, 128.3, 128.09, 128.05, 127.9, 122.9, 121.6, 119.2, 98.6, 98.3, 93.9, 82.7, 72.1, 65.9, 52.2, 18.6, 11.3. **IR** (KBr): υ 3063, 3030, 2943, 2864, 2144, 1730, 1289, 1256, 1077, 756, 677 cm^{-1}. **HRMS** (ESI): Calculated for $C_{39}H_{43}O_3SSi$ ($M+H^+$): 619.2697, found: 619.2689.

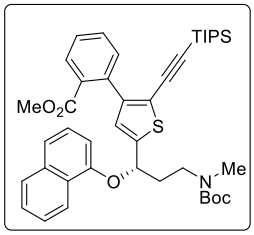

5v: Pale yellow oil (83%). R_f = 0.3 (hexane/ethyl acetate = 5:1). **^{1}H NMR** (400 MHz, $CDCl_3$) δ 8.42 – 8.30 (m, 1H), 7.89 (d, *J* = 7.7 Hz, 1H), 7.83 – 7.76 (m, 1H), 7.54 – 7.45 (m, 4H), 7.42 (d, *J* = 8.2 Hz, 1H), 7.40 – 7.35 (m, 1H), 7.30 (t, *J* = 8.0 Hz, 1H), 6.95 – 6.83 (m, 2H), 5.60 (s, 1H), 3.53 (s, 5H), 2.88 (s, 3H), 2.47 (s, 1H), 2.34 (dtd, *J* = 13.8, 7.6, 4.5 Hz, 1H), 1.37 (s, 9H), 0.95 (d, *J* = 3.3 Hz, 21H). **^{13}C NMR** (101 MHz, $CDCl_3$) δ 168.0, 155.9, 153.1, 145.7, 144.2, 136.2, 134.7, 131.44, 131.42, 130.7, 130.4, 127.8, 127.7, 126.6, 126.3, 126.1, 125.8, 125.5, 122.1, 121.0, 119.2, 106.7, 98.7, 98.0, 79.7, 73.6, 52.0, 45.9, 37.4, 34.7, 28.5, 18.6, 11.3. **IR** (KBr): υ 3054, 2944, 2865, 2142, 1725, 1696, 1397, 1263, 1157, 771, 754 cm^{-1}. **HRMS** (ESI): Calculated for $C_{42}H_{53}NO_5SSiNa$ ($M+Na^+$): 734.3306, found: 734.3304.

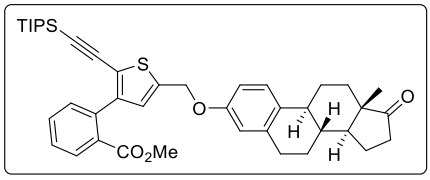

5w: Colorless oil (54%). R_f = 0.2 (hexane/ethyl acetate = 5:1). **^{1}H NMR** (400 MHz, $CDCl_3$) δ 7.95 – 7.90 (m, 1H), 7.53 – 7.45 (m, 2H), 7.39 (ddd, *J* = 7.8, 6.2, 2.5 Hz, 1H), 7.22 (d, *J* = 8.2 Hz, 1H), 6.92 (s, 1H), 6.79 (dd, *J* = 8.6, 2.8 Hz, 1H), 6.73 (d, *J* = 2.7 Hz, 1H), 5.16 (s, 2H), 3.69 (s, 3H), 2.90 (dd, *J* = 8.0, 3.3 Hz, 2H), 2.56 – 2.46 (m, 1H), 2.44 – 2.34 (m, 1H), 2.31 – 2.20 (m, 1H), 2.21 – 1.91 (m, 4H), 1.69 – 1.39 (m, 7H), 0.96 (d, *J* = 3.5 Hz, 21H), 0.91 (s, 3H). **^{13}C NMR** (101 MHz, $CDCl_3$) δ 220.9, 167.8, 156.2, 145.6, 139.2, 137.9, 136.4, 132.8, 131.42, 131.36, 130.5, 130.3, 127.75, 127.67, 126.4, 120.2, 115.1, 112.5, 98.7, 97.8, 65.1, 52.0, 50.4, 48.0, 44.0, 38.3, 35.9, 31.6, 29.7, 26.5, 25.9, 21.6, 18.5, 13.9, 11.2. **IR** (KBr): υ 2942, 2864, 2142, 1736, 1291, 1254, 752, 677 cm^{-1}. **HRMS** (ESI): Calculated for $C_{42}H_{52}O_4SSiNa$ ($M+Na^+$): 703.3248, found: 703.3250.

8.4.6 General Procedure of Direct Difunctionalization of Furans

Scheme 8.12. Furan Difunctionalization with Ortho-Substituted Aryl Iodide

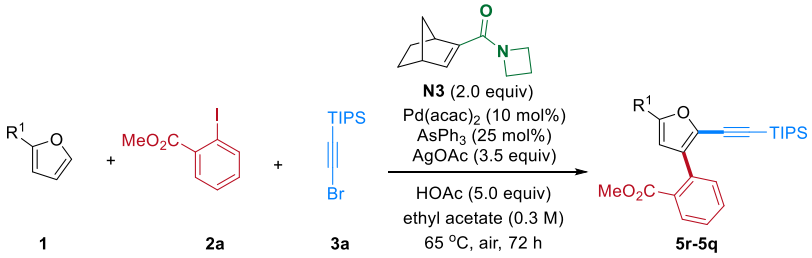

A flame-dried 4.0 mL vial was charged with $Pd(acac)_2$ (6.0 mg, 0.02 mmol, 10 mol%), $AsPh_3$ (15.2 mg, 0.05 mmol, 25 mol%), **N3** (70.8 mg, 0.4 mmol, 2.0 equiv), furan **1** (0.5 mmol, 2.5 equiv), aryl iodide **2a** (52.4 mg, 0.2 mmol, 1.0 equiv) and AgOAc (116 mg, 0.7 mmol, 3.5 equiv) in air. Ethyl acetate (1.0 mL) was then added. After alkynyl bromide **3a** (94 mg, 0.36 mmol, 1.8 equiv)

and HOAc (60 mg, 1.0 mmol, 5.0 equiv) were added, the vial was tightly sealed and stirred on a pie-block preheated to 65 °C for 72 hours. After completion of the reaction, the mixture was filtered through a thin pad of silica gel. The filter cake was washed with ethyl acetate and the combined filtrate was concentrated under reduced pressure. The residue was loaded to a small amount of silica gel and subjected to flash column chromatography to give the desired product **5r-5q**.

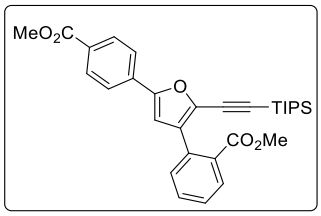

5q: Yellow solid (84%). m. p. = 119.1 – 121.0 °C. R_f = 0.2 (hexane/ethyl acetate = 10:1). **^{1}H NMR** (400 MHz, $CDCl_3$) δ 8.06 (d, *J* = 8.6 Hz, 2H), 7.91 (dd, *J* = 7.8, 1.4 Hz, 1H), 7.78 (d, *J* = 8.6 Hz, 2H), 7.60 (dd, *J* = 7.7, 1.4 Hz, 1H), 7.51 (td, *J* = 7.6, 1.5 Hz, 1H), 7.41 (td, *J* = 7.6, 1.4 Hz, 1H), 6.85 (s, 1H), 3.93 (s, 3H), 3.79 (s, 3H), 1.04 (d, *J* = 4.7 Hz, 21H). **^{13}C NMR** (101 MHz, $CDCl_3$) δ 168.1, 166.8, 152.2, 134.8, 134.1, 132.9, 132.7, 131.6, 131.4, 130.7, 130.5, 130.2, 129.2, 128.1, 124.0, 110.1, 100.3, 95.8, 52.3, 52.3, 18.7, 11.3. **IR** (KBr): υ 2946, 2865, 2144, 1723, 1610, 1280, 1180, 761, 700 cm^{-1}. **HRMS** (ESI): Calculated for $C_{31}H_{37}O_5Si$ ($M+H^+$): 517.2405, found: 517.2408.

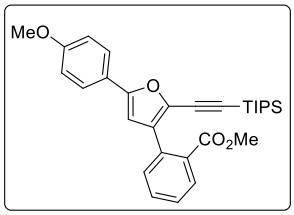

5r: Yellow oil (58%). R_f = 0.3 (hexane/ethyl acetate = 10:1). **^{1}H NMR** (400 MHz, $CDCl_3$) δ 7.87 (dd, *J* = 7.8, 1.4 Hz, 1H), 7.70 – 7.61 (m, 3H), 7.49 (td, *J* = 7.5, 1.5 Hz, 1H), 7.39 (td, *J* = 7.6, 1.4

Hz, 1H), 6.95 – 6.90 (m, 2H), 6.57 (s, 1H), 3.84 (s, 3H), 3.78 (s, 3H), 1.05 (d, *J* = 4.2 Hz, 21H). **^{13}C NMR** (101 MHz, $CDCl_3$) δ 168.6, 159.7, 153.6, 133.2, 133.0, 132.8, 131.4, 131.3, 130.9, 130.3, 127.8, 125.9, 123.3, 114.3, 106.4, 99.2, 96.4, 55.5, 52.3, 18.7, 11.4. **IR** (KBr): υ 2944, 2865, 2142, 1728, 1497, 1254, 1176, 761, 677 cm^{-1}. **HRMS** (ESI): Calculated for $C_{30}H_{37}O_4Si$ ($M+H^+$): 489.2456, found: 489.2462.

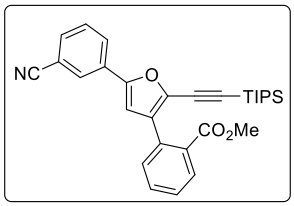

5s: White solid (81%). m. p. = 97.2 – 98.6 °C. R_f = 0.1 (hexane/ethyl acetate = 10:1). **^{1}H NMR** (400 MHz, $CDCl_3$) δ 8.02 – 7.98 (m, 1H), 7.96 – 7.89 (m, 2H), 7.61 – 7.47 (m, 4H), 7.42 (td, *J* = 7.6, 1.4 Hz, 1H), 6.81 (s, 1H), 3.80 (s, 3H), 1.10 – 1.00 (m, 21H). **^{13}C NMR** (101 MHz, $CDCl_3$) δ 168.0, 150.7, 134.9, 132.8, 132.6, 131.7, 131.4, 131.3, 131.1, 130.6, 129.7, 128.2, 128.16, 127.7, 118.6, 113.3, 109.8, 100.5, 95.6, 52.3, 18.7, 11.3. **IR** (KBr): υ 2944, 2865, 2231, 2145, 1728, 1292, 1258, 760, 678 cm^{-1}. **HRMS** (ESI): Calculated for $C_{30}H_{34}NO_3Si$ ($M+H^+$): 484.2302, found: 484.2306.

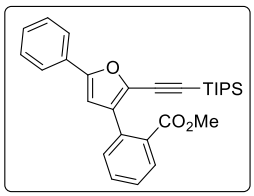

5t: Pale yellow oil (86%). R_f = 0.3 (hexane/ethyl acetate = 20:1). **^{1}H NMR** (400 MHz, $CDCl_3$) δ 7.89 (dd, *J* = 7.8, 1.1 Hz, 1H), 7.77 – 7.70 (m, 2H), 7.68 – 7.61 (m, 1H), 7.50 (td, *J* = 7.6, 1.4 Hz, 1H), 7.43 – 7.37 (m, 3H), 7.29 (t, *J* = 7.4 Hz, 1H), 6.71 (s, 1H), 3.78 (s, 3H), 1.05 (d, *J* = 4.3 Hz,

21H). **^{13}C NMR** (101 MHz, $CDCl_3$) δ 168.5, 153.4, 133.8, 132.8, 132.7, 131.5, 131.3, 130.8, 130.3, 130.2, 128.8, 128.1, 127.9, 124.4, 107.9, 99.5, 96.2, 52.3, 18.7, 11.4. **IR** (KBr): υ 2944, 2891, 2865, 2144, 1727, 1291, 1256, 759, 678 cm^{-1}. **HRMS** (ESI): Calculated for $C_{29}H_{35}O_3Si$ ($M+H^+$): 459.2350, found: 459.2351.

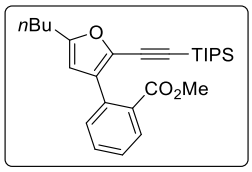

5u: Colorless oil (36%). R_f = 0.4 (hexane/ethyl acetate = 10:1). **^{1}H NMR** (400 MHz, $CDCl_3$) δ 7.81 (dd, *J* = 7.8, 1.4 Hz, 1H), 7.65 – 7.60 (m, 1H), 7.45 (td, *J* = 7.6, 1.5 Hz, 1H), 7.35 (td, *J* = 7.6, 1.4 Hz, 1H), 6.03 (s, 1H), 3.77 (s, 3H), 2.64 (t, *J* = 7.6 Hz, 2H), 1.73 – 1.62 (m, 2H), 1.45 – 1.36 (m, 2H), 1.09 – 0.99 (m, 21H), 0.94 (t, *J* = 7.4 Hz, 3H). **^{13}C NMR** (101 MHz, $CDCl_3$) δ 168.8, 157.0, 133.1, 132.6, 131.4, 131.3, 131.2, 130.8, 130.1, 127.5, 108.1, 98.0, 96.5, 52.2, 30.1, 28.1, 22.4, 18.7, 13.9, 11.4. **IR** (KBr): υ 2944, 2865, 2146, 1725, 1463, 1290, 1254, 761, 677 cm^{-1}. **HRMS** (ESI): Calculated for $C_{27}H_{39}O_3Si$ ($M+H^+$): 439.2663, found: 439.2665.

8.4.7 General Procedure of Ortho Methylation of Pyrrole 1a

Scheme 8.13. Ortho Methylation of Pyrrole 1a

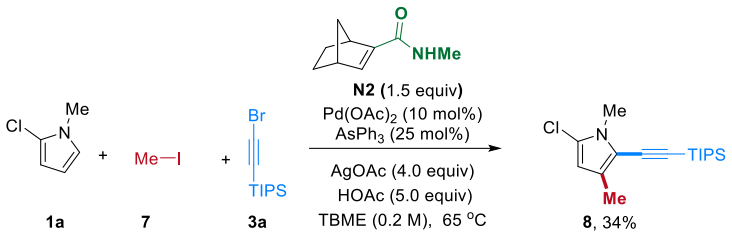

A flame-dried 4.0 mL vial was charged with $Pd(OAc)_2$ (4.6 mg, 0.02 mmol, 10 mol%), $AsPh_3$ (15.2 mg, 0.05 mmol, 25 mol%), **N2** (65.8 mg, 0.3 mmol, 1.5 equiv), **1a** (23.2 mg, 0.2 mmol, 1.0 equiv) and AgOAc (132 mg, 0.8 mmol, 4.0 equiv) in air. TBME (1.0 mL) was then added. After methyl iodide **7** (50 µL, 113.5 mg, 0.8 mmol, 4.0 equiv), alkynyl bromide **3a** (94 mg, 0.36 mmol, 1.8 equiv) and HOAc (60 mg, 1.0 mmol, 5.0 equiv) were added, the vial was tightly sealed and stirred on a pie-block preheated to 65 °C for 24 hours. After completion of the reaction, the mixture was filtered through a thin pad of silica gel. The filter cake was washed with ethyl acetate and the combined filtrate was concentrated under reduced pressure. The residue was loaded to a small amount of silica gel and subjected to flash column chromatography to give the desired product **8** as a colorless oil.

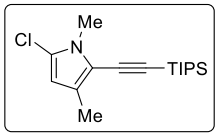

8: Colorless oil (34%). R_f = 0.8 (hexane/ethyl acetate = 20:1). **^{1}H NMR** (400 MHz, $CDCl_3$) δ 5.85 (s, 1H), 3.56 (s, 3H), 2.12 (s, 3H), 1.12 (s, 21H). **^{13}C NMR** (101 MHz, $CDCl_3$) δ 125.8, 117.2, 114.6, 107.4, 97.6, 97.4, 32.0, 18.8, 12.2, 11.4. **IR** (KBr): υ 2943, 2891, 2865, 2141, 1463, 1204, 882, 820, 676, 660 cm^{-1}. **HRMS** (ESI): Calculated for $C_{17}H_{29}ClNSi$ ($M+H^+$): 310.1752, found: 310.1756.

8.4.8 Mechanistic Study

Scheme 8.14. Control Experiments

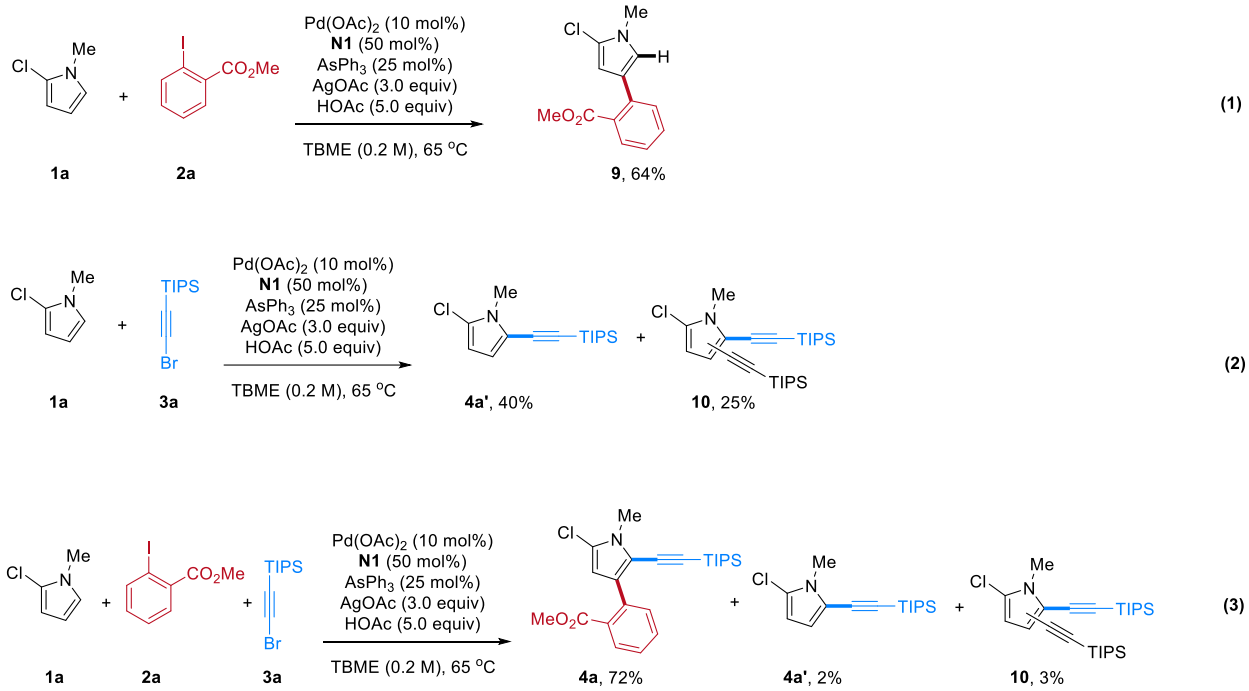

A flame-dried 4.0 mL vial was charged with $Pd(OAc)_2$ (2.3 mg, 0.01 mmol, 10 mol%), $AsPh_3$ (7.6 mg, 0.025 mmol, 25 mol%), **N1** (11.0 mg, 0.05 mmol, 50 mol%), **1a** (11.6 mg, 0.1 mmol, 1.0 equiv), **2a** (52.4 mg, 0.2 mmol, 2.0 equiv) and AgOAc (50 mg, 0.3 mmol, 3.0 equiv) in air. TBME (0.5 mL) was then added. After HOAc (30 mg, 0.5 mmol, 5.0 equiv) was added, the vial was tightly sealed and stirred on a pie-block preheated to 65 °C for 72 hours. After completion of the reaction, the mixture was filtered through a thin pad of silica gel. The filter cake was washed with ethyl acetate and the combined filtrate was concentrated under reduced pressure. The residue was loaded to a small amount of silica gel and subjected to flash column chromatography to give the desired product **9** as a colorless oil.

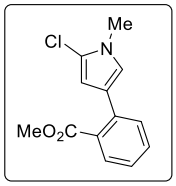

9: Colorless oil (64%). R_f = 0.2 (hexane/ethyl acetate = 20:1). **^{1}H NMR** (500 MHz, $CDCl_3$) δ 7.62 – 7.57 (m, 1H), 7.45 – 7.40 (m, 1H), 7.39 – 7.34 (m, 1H), 7.29 – 7.24 (m, 1H), 6.72 (d, *J* = 2.2 Hz, 1H), 6.14 (d, *J* = 2.2 Hz, 1H), 3.81 (s, 3H), 3.60 (s, 3H). **^{13}C NMR** (101 MHz, $CDCl_3$) δ 170.2, 134.9, 131.0, 130.8, 129.8, 129.1, 126.1, 122.6, 119.6, 117.0, 107.0, 52.3, 34.0. **IR** (KBr): υ 2949, 1727, 1489, 1293, 1251, 1124, 1084, 761, 723 cm^{-1}. **HRMS** (ESI): Calculated for $C_{13}H_{13}ClNO_2$ ($M+H^+$): 250.0629, found: 250.0627.

A flame-dried 4.0 mL vial was charged with $Pd(OAc)_2$ (2.3 mg, 0.01 mmol, 10 mol%), $AsPh_3$ (7.6 mg, 0.025 mmol, 25 mol%), **N1** (11.0 mg, 0.05 mmol, 50 mol%), **1a** (11.6 mg, 0.1 mmol, 1.0 equiv) and AgOAc (50 mg, 0.3 mmol, 3.0 equiv) in air. TBME (0.5 mL) was then added. After **3a** (47 mg, 0.18 mmol, 1.8 equiv) and HOAc (30 mg, 0.5 mmol, 5.0 equiv) were added, the vial was tightly sealed and stirred on a pie-block preheated to 65 ^oC for 72 hours. After completion of the reaction, the mixture was filtered through a thin pad of silica gel. The filter cake was washed with ethyl acetate and the combined filtrate was concentrated under reduced pressure. The residue was loaded to a small amount of silica gel and subjected to flash column chromatography to give the desired product **4a'** and **10** as a colorless oil.

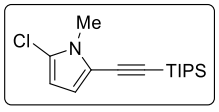

4a': Colorless oil (40%). R_f = 0.8 (hexane/ethyl acetate = 20:1). **^{1}H NMR** (400 MHz, $CDCl_3$) δ 6.39 (d, *J* = 4.0 Hz, 1H), 5.98 (d, *J* = 4.0 Hz, 1H), 3.61 (s, 3H), 1.12 (s, 21H). **^{13}C NMR** (101 MHz,

$CDCl_3$) δ 117.9, 116.0, 114.6, 106.4, 98.1, 95.2, 32.0, 18.8, 11.5. **IR** (KBr): υ 2943, 2891, 2865, 2848, 1455, 1435, 883, 779, 750, 676 cm^{-1}. **HRMS** (ESI): Calculated for $C_{16}H_{27}ClNSi$ ($M+H^+$): 296.1596, found: 296.1599.

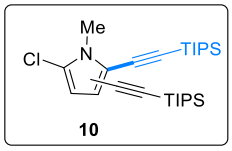

10

10: Colorless oil (25%). R_f = 0.5 (hexane/ethyl acetate = 20:1). Major: **^{1}H NMR** (400 MHz, $CDCl_3$) δ 6.11 (s, 1H), 3.58 (s, 3H), 1.12 (s, 21H), 1.10 (s, 21H). **^{13}C NMR** (101 MHz, $CDCl_3$) δ 120.2, 117.8, 117.4, 110.0, 100.2, 99.3, 96.3, 92.5, 32.4, 18.9, 18.8, 11.5, 11.4.

A flame-dried 4.0 mL vial was charged with $Pd(OAc)_2$ (2.3 mg, 0.01 mmol, 10 mol%), $AsPh_3$ (7.6 mg, 0.025 mmol, 25 mol%), **N1** (11.0 mg, 0.05 mmol, 50 mol%), **1a** (11.6 mg, 0.1 mmol, 1.0 equiv), **2a** (52.4 mg, 0.2 mmol, 2.0 equiv) and AgOAc (50 mg, 0.3 mmol, 3.0 equiv) in air. TBME (0.5 mL) was then added. After **3a** (47 mg, 0.18 mmol, 1.8 equiv) and HOAc (30 mg, 0.5 mmol, 5.0 equiv) were added, the vial was tightly sealed and stirred on a pie-block preheated to 65 °C for 72 hours. After completion of the reaction, the mixture was filtered through a thin pad of silica gel. The filter cake was washed with ethyl acetate and the combined filtrate was concentrated under reduced pressure. The yields of desired difunctionalization product **4a**, ipso alkynylation side-product **4a'** and multi-alkynylation side-product **10** were determined by crude ^{1}H NMR using dibromomethane as the internal standard.

Figure 8.4. Kinetic Profile

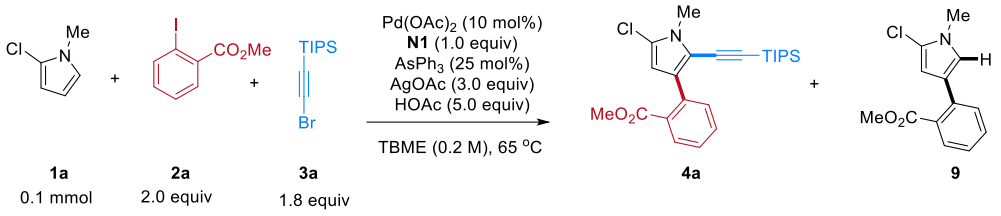

1a 0.1 mmol | **2a** 2.0 equiv | **3a** 1.8 equiv | **4a** | **9**

Time	0 h	2.3 h	3.6 h	5.2 h	10.2 h	21.7 h
4a[a]	0%	29%	44%	56%	74%	80%
9[a]	0%	0.7%	0.8%	1.3%	1.4%	1.4%

[a]Yields were determined by ^{1}H NMR analysis using dibromomethane as the internal standard.

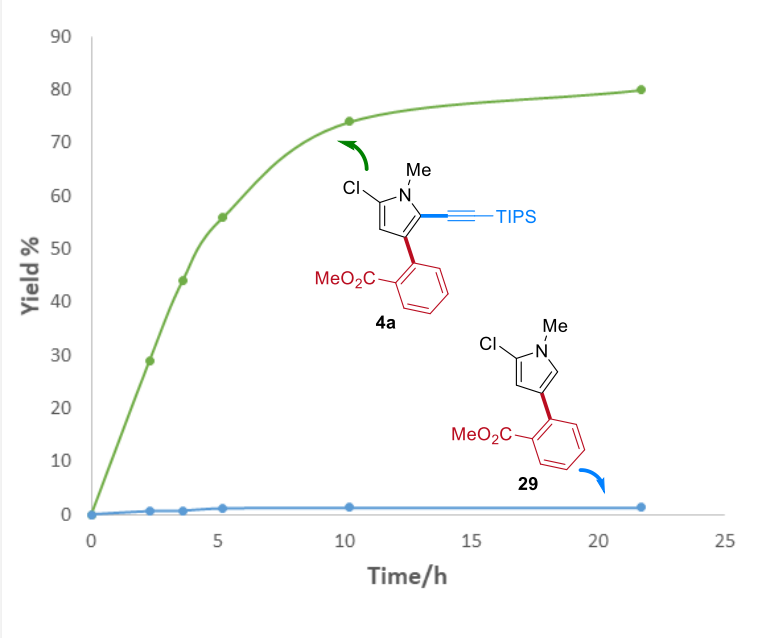

8.4.9 Synthetic Utility

Scheme 8.15. Gram-Scale Preparation

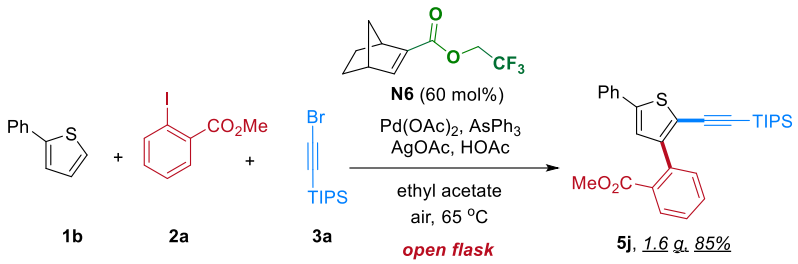

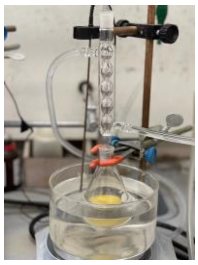

open flask

solvent

A oven-dried 100 mL round bottom flask was charged with $Pd(OAc)_2$ (92 mg, 0.4 mmol, 10 mol%), $AsPh_3$ (304 mg, 1.0 mmol, 25 mol%), **N6** (530 mg, 2.4 mmol, 60 mol%), **1b** (641 mg, 4.0 mmol, 1.0 equiv), **2a** (2.1 g, 8.0 mmol, 2.0 equiv) and AgOAc (2.0 g, 12.0 mmol, 3.0 equiv) in air. Ethyl acetate (15.0 mL) was then added. After **3a** (1.88 g, 7.2 mmol, 1.8 equiv) and HOAc (1.2 g, 20 mmol, 5.0 equiv) were added, the flask was equipped with a reflux condenser and stirred on an oil bath preheated to 65 °C for 72 hours. After completion of the reaction, the mixture was filtered through a thin pad of silica gel. The filter cake was washed with ethyl acetate and the combined filtrate was concentrated under reduced pressure. The residue was loaded to a small amount of silica gel and subjected to flash column chromatography to give the desired product **5j** as a yellow oil.

Scheme 8.16. Using 1 mol% $Pd(OAc)_2$

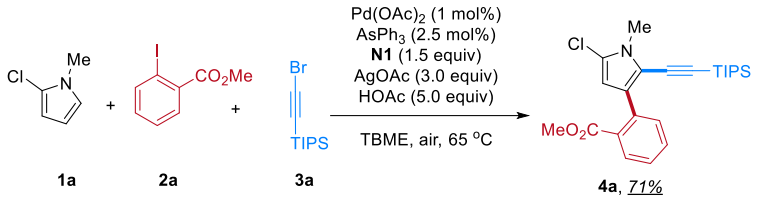

Stock solutions of $Pd(OAc)_2$ (0.01 M in TBME) and $AsPh_3$ (0.025 M in TBME) were prepared prior the reaction. A flame-dried 4.0 mL vial was charged with **N1** (32.9 mg, 0.15 mmol, 1.5 equiv), **1a** (11.6 mg, 0.1 mmol, 1.0 equiv), **2a** (52.4 mg, 0.2 mmol, 2.0 equiv) and AgOAc (50.0 mg, 0.3 mmol, 3.0 equiv) in air. TBME (0.5 mL) was then added. After $Pd(OAc)_2$ (0.1 mL, 0.001 mmol, 1 mol%), $AsPh_3$ (0.1 mL, 0.0025 mmol, 2.5 mol%), **3a** (47 mg, 0.18 mmol, 1.8 equiv) and HOAc (30 mg, 0.5 mmol, 5.0 equiv) were added via micropipette, the vial was tightly sealed and stirred on a pie-block preheated to 65 °C for 72 hours. After completion of the reaction, the mixture was filtered through a thin pad of silica gel. The filter cake was washed with ethyl acetate and the combined filtrate was concentrated under reduced pressure. The residue was loaded to a small amount of silica gel and subjected to flash column chromatography to give the desired product **4a** (71%) as a colorless oil.

Scheme 8.17. Product Derivatizations

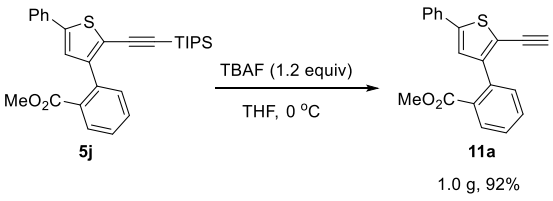

Following a literature reported procedure,[30] to a solution of **5j** (1.62 g, 3.4 mmol, 1.0 equiv) in dry THF (40 mL) was added a TBAF solution (1M in THF) (4.1 mL, 4.1 mmol 1.2 equiv) dropwise at 0 °C under nitrogen atmosphere. Then the reaction mixture was stirred for additional 1 h at 0 °C

until all the starting material was consumed. The reaction was quenched by adding H_2O (20 mL) and the mixture was extracted with Et_2O for three times. The combined organic layers were dried over anhydrous Na_2SO_4, filtered and the solvent was evaporated under reduced pressure. The residue was purified by flash column chromatography through silica gel to give **11a** as an orange solid.

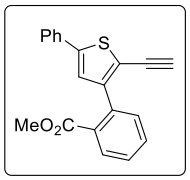

11a: Orange solid (92%). m. p. = 109.7 – 110.5 ºC. R_f = 0.1 (hexane/ethyl acetate = 20:1). **^{1}H NMR** (400 MHz, $CDCl_3$) δ 7.95 (dd, *J* = 7.8, 1.4 Hz, 1H), 7.64 – 7.54 (m, 3H), 7.53 – 7.43 (m, 2H), 7.42 – 7.37 (m, 2H), 7.36 – 7.30 (m, 1H), 7.20 (s, 1H), 3.76 (s, 3H), 3.29 (s, 1H). **^{13}C NMR** (101 MHz, $CDCl_3$) δ 168.4, 147.3, 144.3, 136.0, 133.6, 131.7, 131.1, 131.0, 130.5, 129.2, 128.4, 128.1, 126.0, 124.7, 117.4, 83.9, 76.6, 52.5. **IR** (KBr): υ 3290, 1724, 1293, 1255, 1072, 757, 695 cm^{-1}. **HRMS** (ESI): Calculated for $C_{20}H_{15}O_2S$ ($M+H^+$): 319.0787, found: 319.0788.

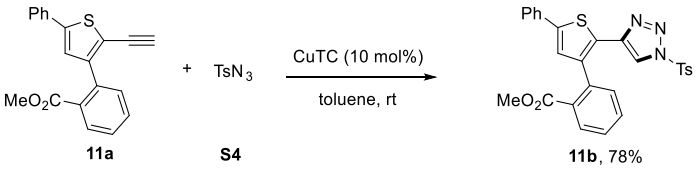

Following a literature reported procedure,[31] copper(I) thiophene-2-carboxylate (CuTc) (1.9 mg, 0.01 mmol, 10 mol%),

sulfonyl azide (21.7 mg, 0.11 mmol, 1.1 equiv), **11a** (31.8 mg, 0.1 mmol 1.0 equiv) in wet toluene (0.25 mL) was stirred at room temperature until the total consumption of **7a**. The mixture as then diluted with 10 mL of saturated NH_4Cl solution and then extracted with ethyl acetate for three times. The combined organic layers were dried over $MgSO_4$ and concentrated under reduced

pressure. The residue was purified by flash column chromatography through silica gel to give **11b** as an orange solid.

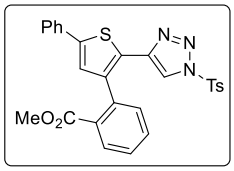

11b: Orange solid (78%). m. p. = 67.1 – 69.2 °C. R_f = 0.7 (hexane/ethyl acetate = 1:1). **^{1}H NMR** (400 MHz, CD_2Cl_2) δ 8.03 – 7.98 (m, 1H), 7.86 (d, *J* = 8.5 Hz, 2H), 7.67 (dd, *J* = 7.3, 1.3 Hz, 2H), 7.65 – 7.55 (m, 2H), 7.44 – 7.38 (m, 4H), 7.37 – 7.30 (m, 2H), 7.24 (s, 1H), 7.18 (s, 1H), 3.54 (s, 3H), 2.45 (s, 3H). **^{13}C NMR** (101 MHz, CD_2Cl_2) δ 167.5, 148.1, 144.0, 142.1, 140.9, 137.1, 133.9, 133.2, 132.7, 131.4, 131.3, 130.9, 130.9, 129.4, 129.0, 128.9, 128.5, 126.5, 126.0, 125.9, 119.0, 52.4, 22.0. **IR** (KBr): υ 3061, 1726, 1295, 1196, 1177, 1091, 983, 759, 670, 590 cm^{-1}. **HRMS** (ESI): Calculated for $C_{27}H_{22}N_3O_4S_2$ ($M+H^+$): 516.1046, found: 516.1048.

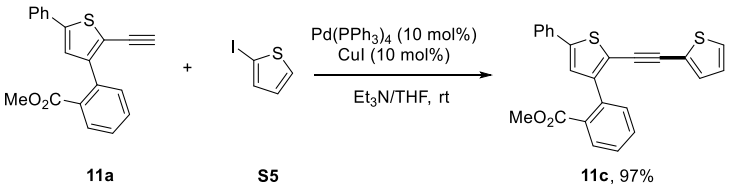

A flame-dried 4.0 mL vial was charged with $Pd(PPh_3)_4$ (11.6 mg, 0.01 mmol, 10 mol%), CuI (1.9 mg, 0.01 mmol, 10 mol%), **11a** (31.8 mg, 0.1 mmol, 1.0 equiv) and 2-iodothiophene (25.2 mg, 0.12 mmol, 1.2 equiv). Then the vial was directly transferred into a nitrogen-filled glovebox without caps. After degassed triethylamine (0.4 mL) and THF (1.0 mL) were added, the vial was tightly sealed, transferred out of glovebox and stirred on a pie-block at room temperature for 12 hours. After completion of the reaction, the mixture was filtered through a thin pad of silica gel. The filter cake was washed with ethyl acetate and the combined filtrate was concentrated under

reduced pressure. The residue was loaded to a small amount of silica gel and subjected to flash column chromatography to give the desired product **11c** as a yellow oil.

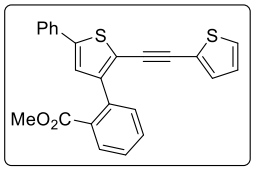

11c: Yellow oil (97%). R_f = 0.2 (hexane/ethyl acetate = 10:1). **^{1}H NMR** (400 MHz, $CDCl_3$) δ 7.97 – 7.91 (m, 1H), 7.64 – 7.60 (m, 2H), 7.59 – 7.51 (m, 2H), 7.47 – 7.36 (m, 3H), 7.35 – 7.29 (m, 1H), 7.27 (s, 1H), 7.26 – 7.23 (m, 1H), 7.18 (dd, *J* = 3.6, 1.2 Hz, 1H), 6.95 (dd, *J* = 5.2, 3.6 Hz, 1H), 3.75 (s, 3H). **^{13}C NMR** (101 MHz, $CDCl_3$) δ 168.6, 146.1, 144.4, 136.0, 133.7, 132.3, 131.6, 131.2, 131.0, 130.5, 129.2, 128.3, 128.0, 127.8, 127.2, 125.9, 124.8, 123.0, 118.4, 89.0, 86.1, 52.5. **IR** (KBr): υ 3061, 2947, 1726, 1293, 1266, 1118, 851, 758, 691 cm^{-1}. **HRMS** (ESI): Calculated for $C_{24}H_{17}O_2S_2$ ($M+H^+$): 401.0664, found: 401.0673.

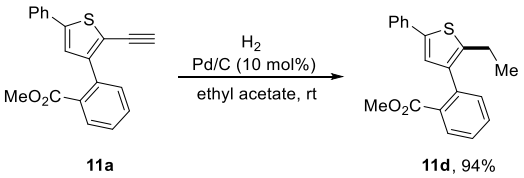

11a **11d**, 94%

A flame-dried 20 mL vial was charged with Pd/C (10 wt. %) (10.6 mg, 0.01 mmol, 10 mol%), **11a** (31.8 mg, 0.1 mmol, 1.0 equiv) and ethyl acetate (0.5 mL). The vial was degassed and refilled with H_2 for three times, then stirred at room temperature until all the starting material **11a** was consumed. After completion of the reaction, the mixture was filtered through a thin pad of silica gel. The filter cake was washed with ethyl acetate and the combined filtrate was concentrated under reduced pressure. The residue was loaded to a small amount of silica gel and subjected to flash column chromatography to give the desired product **11d** as a colorless oil.

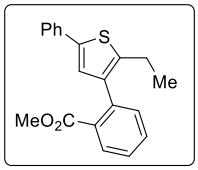

11d: Colorless oil (94%). R_f = 0.3 (hexane/ethyl acetate = 10:1). **^{1}H NMR** (400 MHz, $CDCl_3$) δ 7.92 – 7.86 (m, 1H), 7.60 – 7.56 (m, 2H), 7.53 (td, *J* = 7.5, 1.5 Hz, 1H), 7.41 (td, *J* = 7.6, 1.4 Hz, 1H), 7.38 – 7.30 (m, 3H), 7.27 – 7.20 (m, 1H), 7.08 (s, 1H), 3.68 (s, 3H), 2.64 (q, *J* = 7.5 Hz, 2H), 1.20 (t, *J* = 7.5 Hz, 3H). **^{13}C NMR** (101 MHz, $CDCl_3$) δ 168.5, 142.2, 139.6, 138.0, 137.5, 134.7, 131.5, 131.5, 131.4, 130.1, 128.9, 127.5, 127.2, 125.5, 125.2, 52.2, 22.0, 16.3. **IR** (KBr): υ 3062, 2966, 1732, 1293, 1252, 1124, 1084, 757, 693 cm^{-1}. **HRMS** (ESI): Calculated for $C_{20}H_{19}O_2S$ ($M+H^+$): 323.1100, found: 323.1102.

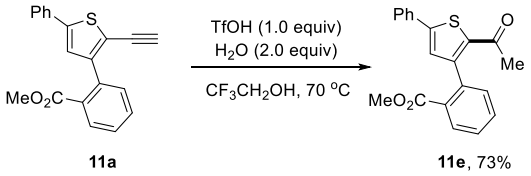

Following a literature reported procedure,[32] to a 4 mL vial were added alkyne **7a** (31.8 mg, 0.1 mmol, 1.0 equiv), H_2O (4 μL, 0.2 mmol, 2.0 equiv), TfOH (10 μL, 0.1 mmol, 1.0 equiv) and CF_3CH_2OH (0.5 mL). Then the tube was sealed and stirred at 70 °C until all the starting material **11a** was consumed. After the reaction was completed, the volatile was removed under reduced pressure and the residue was subjected to flash column chromatography to give the desired hydration product **11e** as a yellow solid.

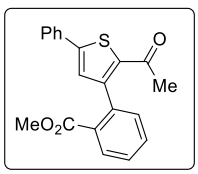

11e: Yellow solid (73%). m. p. = 96.1 – 97.9 °C. R_f = 0.2 (hexane/ethyl acetate = 5:1). **^{1}H NMR** (400 MHz, $CDCl_3$) δ 8.05 (dd, *J* = 7.8, 1.2 Hz, 1H), 7.67 (dt, *J* = 8.5, 2.0 Hz, 2H), 7.59 (td, *J* = 7.5, 1.4 Hz, 1H), 7.51 (td, *J* = 7.6, 1.3 Hz, 1H), 7.44 – 7.33 (m, 4H), 7.18 (s, 1H), 3.71 (s, 3H), 2.06 (s, 3H). **^{13}C NMR** (101 MHz, $CDCl_3$) δ 191.3, 167.2, 149.0, 146.6, 138.4, 138.0, 133.3, 132.0, 130.7, 130.6, 130.4, 129.2, 129.1, 128.6, 127.4, 126.3, 52.4, 28.8. **IR** (KBr): υ 1725, 1647, 1426, 1369, 1259, 1079, 760, 695 cm^{-1}. **HRMS** (ESI): Calculated for $C_{20}H_{17}O_3S$ ($M+H^+$): 337.0893, found: 337.0892.

Scheme 8.18. Stepwise Tetrafunctionalization of Thiophene 12

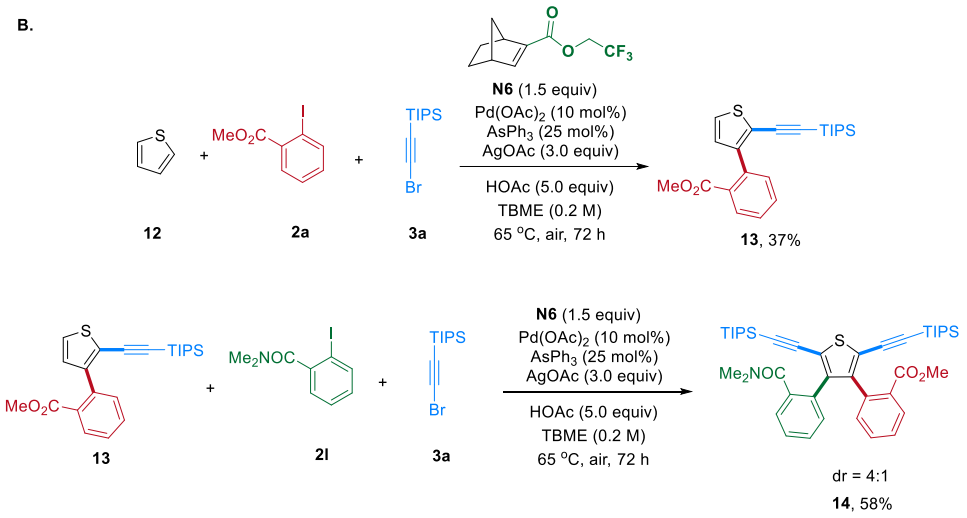

A flame-dried 4.0 mL vial was charged with $Pd(OAc)_2$ (2.3 mg, 0.01 mmol, 10 mol%), $AsPh_3$ (7.6 mg, 0.025 mmol, 25 mol%), **N6** (33 mg, 0.15 mmol, 1.5 equiv), **12** (21.0 mg, 0.25 mmol, 2.5 equiv), **2a** (26.2 mg, 0.1 mmol, 1.0 equiv) and AgOAc (50 mg, 0.3 mmol, 3.0 equiv) in air. TBME (0.5 mL) was then added. After **3a** (47 mg, 0.18 mmol, 1.8 equiv) and HOAc (30 mg, 0.5 mmol, 5.0 equiv) were added, the vial was tightly sealed and stirred on a pie-block preheated to 65 °C for 72 hours. After completion of the reaction, the mixture was filtered through a thin pad of silica gel.

The filter cake was washed with ethyl acetate and the combined filtrate was concentrated under reduced pressure. The residue was loaded to a small amount of silica gel and subjected to flash column chromatography to give the desired product **13** as a yellow oil.

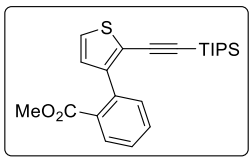

13: Yellow oil (37%). R_f = 0.6 (hexane/ethyl acetate = 5:1). **^{1}H NMR** (400 MHz, $CDCl_3$) δ 7.96 – 7.90 (m, 1H), 7.53 – 7.46 (m, 2H), 7.39 (ddd, *J* = 7.9, 5.8, 3.0 Hz, 1H), 7.20 (d, *J* = 5.2 Hz, 1H), 6.93 (d, *J* = 5.2 Hz, 1H), 3.71 (s, 3H), 0.97 (d, *J* = 3.4 Hz, 21H). **^{13}C NMR** (101 MHz, $CDCl_3$) δ 168.0, 146.1, 136.7, 131.5, 130.7, 130.6, 130.4, 128.8, 127.7, 125.1, 120.0, 98.9, 97.4, 52.2, 18.6, 11.3. **IR** (KBr): υ 2943, 2891, 2865, 2142, 1724, 1293, 1253, 755, 730, 663 cm^{-1}. **HRMS** (ESI): Calculated for $C_{23}H_{31}O_2SSi$ ($M+H^+$): 399.1809, found: 399.1811.

A flame-dried 4.0 mL vial was charged with $Pd(OAc)_2$ (4.6 mg, 0.02 mmol, 10 mol%), $AsPh_3$ (15.2 mg, 0.05 mmol, 25 mol%), **N6** (66 mg, 0.3 mmol, 1.5 equiv), **13** (119.6 mg, 0.3 mmol, 1.5 equiv), **2l** (55 mg, 0.2 mmol, 1.0 equiv) and AgOAc (100 mg, 0.6 mmol, 3.0 equiv) in air. TBME (1.0 mL) was then added. After **3a** (94 mg, 0.36 mmol, 1.8 equiv) and HOAc (60 mg, 1.0 mmol, 5.0 equiv) were added, the vial was tightly sealed and stirred on a pie-block preheated to 65 °C for 72 hours. After completion of the reaction, the mixture was filtered through a thin pad of silica gel. The filter cake was washed with ethyl acetate and the combined filtrate was concentrated under reduced pressure. The residue was loaded to a small amount of silica gel and subjected to flash column chromatography to give the desired product **14** as a yellow oil.

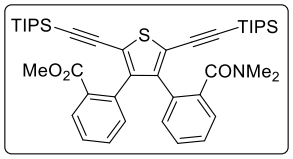

14: Yellow oil (58%, dr = 4:1). R_f = 0.2 (hexane/acetone = 5:1). **^{1}H NMR** (400 MHz, $CDCl_3$) δ 7.76 – 7.66 (m, 1H), 7.63 – 7.51 (m, 1H), 7.48 – 7.38 (m, 1H), 7.35 (d, *J* = 7.7 Hz, 1H), 7.27 – 7.14 (m, 4H), 3.63 (s, 3H), 2.87 (s, 3H), 2.67 – 2.43 (m, 3H), 0.94 (d, *J* = 4.7 Hz, 42H). **^{13}C NMR** (101 MHz, $CDCl_3$) δ 169.7, 167.1, 144.6, 135.7, 133.3, 133.0, 131.5, 131.2, 130.5, 129.9, 128.7, 127.8, 127.6, 127.5, 120.5, 120.2, 99.6, 99.0, 98.1, 98.0, 52.0, 39.3, 35.1, 18.6, 18.6, 11.32, 11.26. **IR** (KBr): υ 2943, 2891, 2865, 2143, 1729, 1645, 1463, 1256, 750, 678 cm^{-1}. **HRMS** (ESI): Calculated for $C_{43}H_{59}NO_3SSi_2Na$ ($M+Na^+$): 748.3646, found: 748.3649.

Scheme 8.19. Direct Tetrafunctionalization of Pyrrole 17

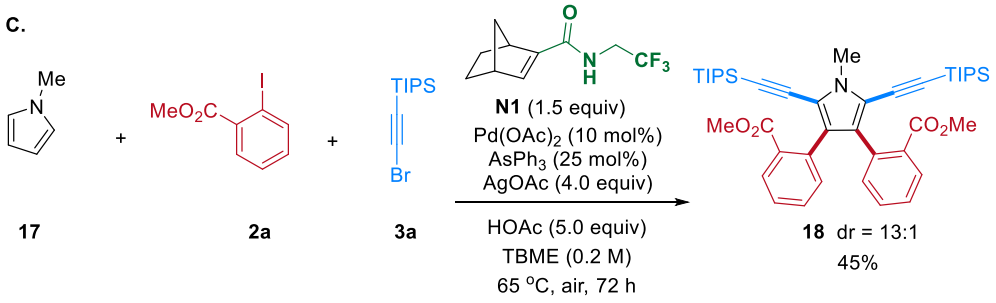

A flame-dried 4.0 mL vial was charged with $Pd(OAc)_2$ (2.3 mg, 0.01 mmol, 10 mol%), $AsPh_3$ (7.6 mg, 0.025 mmol, 25 mol%), **N1** (32.9 mg, 0.15 mmol, 1.5 equiv), **17** (8.1 mg, 0.1 mmol, 1.0 equiv), **2a** (104.8 mg, 0.4 mmol, 4.0 equiv) and AgOAc (66.7 mg, 0.4 mmol, 4.0 equiv) in air. TBME (0.5 mL) was then added. After **3a** (65.3 mg, 0.25 mmol, 2.5 equiv) and HOAc (30 mg, 0.5 mmol, 5.0 equiv) were added, the vial was tightly sealed and stirred on a pie-block preheated to 65 °C for 72 hours. After completion of the reaction, the mixture was filtered through a thin pad of silica gel.

The filter cake was washed with ethyl acetate and the combined filtrate was concentrated under reduced pressure. The residue was loaded to a small amount of silica gel and subjected to flash column chromatography to give the desired product **18** as a colorless oil.

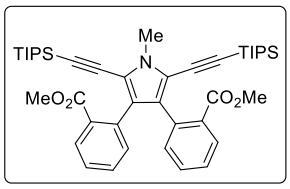

18: Colorless oil (45%, dr = 13:1). R_f = 0.2 (hexane/acetone = 20:1). **^{1}H NMR** (500 MHz, $CDCl_3$) δ 7.67 (d, *J* = 7.7 Hz, 2H), 7.43 (d, *J* = 7.7 Hz, 2H), 7.35 (t, *J* = 7.5 Hz, 2H), 7.22 (t, *J* = 7.6 Hz, 2H), 3.82 (s, 3H), 3.54 (s, 6H), 1.02 (s, 42H). **^{13}C NMR** (126 MHz, $CDCl_3$) δ 168.0, 135.0, 133.4, 131.2, 131.1, 129.8, 127.9, 126.5, 116.1, 97.8, 97.3, 51.9, 33.5, 18.7, 11.4. **IR** (KBr): υ 2943, 2891, 2865, 2142, 1731, 1289, 1253, 1123, 882, 675, 596 cm^{-1}. **HRMS** (ESI): Calculated for $C_{43}H_{60}NO_4Si_2$ ($M+H^+$): 710.4055, found: 710.4053.

Scheme 8.20. Synthesis of ETAr Spacer 22

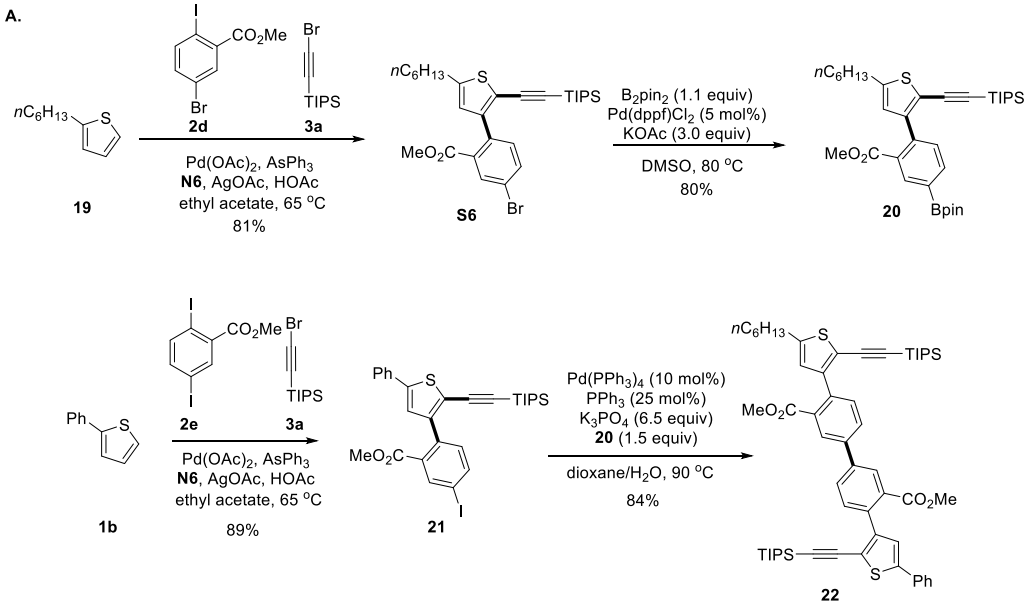

A flame-dried 4.0 mL vial was charged with $Pd(OAc)_2$ (4.6 mg, 0.02 mmol, 10 mol%), $AsPh_3$ (15.2 mg, 0.05 mmol, 25 mol%), **N6** (66.1 mg, 0.3 mmol, 1.5 equiv), **19** (33.7 mg, 0.2 mmol, 1.0 equiv), **2d** (136.4 mg, 0.4 mmol, 2.0 equiv) and AgOAc (100 mg, 0.6 mmol, 3.0 equiv) in air. Ethyl acetate (1.0 mL) was then added. After **3a** (94 mg, 0.36 mmol, 1.8 equiv) and HOAc (60 mg, 1.0 mmol, 5.0 equiv) were added, the vial was tightly sealed and stirred on a pie-block preheated to 65 °C for 72 hours. After completion of the reaction, the mixture was filtered through a thin pad of silica gel. The filter cake was washed with ethyl acetate and the combined filtrate was concentrated under reduced pressure. The residue was loaded to a small amount of silica gel and subjected to flash column chromatography to give the desired product **S6** as a yellow oil.

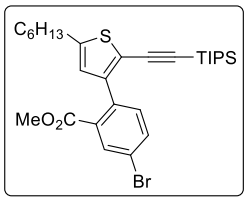

S6: Yellow oil (81%). R_f = 0.4 (hexane/ethyl acetate = 10:1). **^{1}H NMR** (400 MHz, $CDCl_3$) δ 8.02 (d, *J* = 2.1 Hz, 1H), 7.60 (dd, *J* = 8.3, 2.1 Hz, 1H), 7.37 (d, *J* = 8.2 Hz, 1H), 6.59 (s, 1H), 3.72 (s, 3H), 2.77 (t, *J* = 7.5 Hz, 2H), 1.67 (p, *J* = 7.5 Hz, 2H), 1.42 – 1.35 (m, 2H), 1.30 (dt, *J* = 7.1, 3.7 Hz, 4H), 0.98 (d, *J* = 2.9 Hz, 21H), 0.92 – 0.84 (m, 3H). **^{13}C NMR** (101 MHz, $CDCl_3$) δ 166.8, 146.3, 144.5, 135.9, 134.3, 133.1, 132.9, 132.4, 125.6, 121.4, 117.6, 99.1, 97.1, 52.4, 31.7, 31.6, 30.3, 28.9, 22.7, 18.6, 14.2, 11.4. **IR** (KBr): υ 2941, 2929, 2864, 2140, 1739, 1726, 1284, 1244, 882, 767 cm^{-1}. **HRMS** (ESI): Calculated for $C_{29}H_{42}BrO_2SSi$ ($M+H^+$): 561.1853, found: 561.1854.

Following a literature reported procedure,[33] a flame-dried 4.0 mL vial was charged with $Pd(dppf)Cl_2$ (11.0 mg, 0.015 mmol, 5 mol%), potassium acetate (88.3 mg, 0.9 mmol, 3.0 equiv), **S6** (169 mg, 0.3 mmol, 1.0 equiv) and B_2pin_2 (83.8 mg, 0.33 mmol, 1.1 equiv). Then the vial was

directly transferred into a nitrogen-filled glovebox without caps. After degassed anhydrous DMSO (1.5 mL) was added, the vial was tightly sealed, transferred out of glovebox and stirred on a pie-block preheated to 80 ^{o}C for 12 hours. After completion of the reaction, the mixture was filtered through a thin pad of silica gel. The filter cake was washed with ethyl acetate and the combined filtrate was concentrated under reduced pressure. The residue was loaded to a small amount of silica gel and subjected to flash column chromatography to give the desired product **20** as a yellow oil.

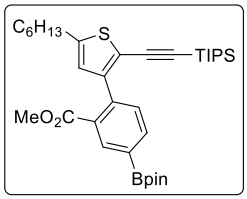

20: Yellow oil (80%). R_f = 0.6 (hexane/ethyl acetate = 5:1). **^{1}H NMR** (400 MHz, $CDCl_3$) δ 8.32 – 8.27 (m, 1H), 7.89 (dd, *J* = 7.6, 1.3 Hz, 1H), 7.52 (d, *J* = 7.6 Hz, 1H), 6.61 (s, 1H), 3.72 (s, 3H), 2.77 (t, *J* = 7.5 Hz, 2H), 1.67 (p, *J* = 7.5 Hz, 2H), 1.36 (s, 14H), 1.30 (dt, *J* = 7.2, 3.7 Hz, 4H), 0.97 (s, 21H), 0.89 (t, *J* = 6.9 Hz, 3H). **^{13}C NMR** (101 MHz, $CDCl_3$) δ 168.4, 146.0, 145.6, 139.5, 137.5, 136.6, 130.7, 130.3, 128.7, 125.9, 117.4, 99.4, 96.7, 84.2, 52.1, 31.7, 31.6, 30.3, 28.9, 25.0, 22.7, 18.7, 14.2, 11.4. **IR** (KBr): υ 2930, 2864, 2140, 1733, 1358, 1281, 1245, 1144, 768, 678 cm^{-1}. **HRMS** (ESI): Calculated for $C_{35}H_{53}BO_4SSiNa$ ($M+Na^+$): 631.3419, found: 631.3427.

A flame-dried 4.0 mL vial was charged with $Pd(OAc)_2$ (4.6 mg, 0.02 mmol, 10 mol%), $AsPh_3$ (15.2 mg, 0.05 mmol, 25 mol%), **N6** (66.1 mg, 0.3 mmol, 1.5 equiv), **1b** (32.0 mg, 0.2 mmol, 1.0 equiv), **2e** (155.2 mg, 0.4 mmol, 2.0 equiv) and AgOAc (100 mg, 0.6 mmol, 3.0 equiv) in air. Ethyl acetate (1.0 mL) was then added. After **3a** (94 mg, 0.36 mmol, 1.8 equiv) and HOAc (60 mg, 1.0 mmol, 5.0 equiv) were added, the vial was tightly sealed and stirred on a pie-block preheated to

65 °C for 72 hours. After completion of the reaction, the mixture was filtered through a thin pad of silica gel. The filter cake was washed with ethyl acetate and the combined filtrate was concentrated under reduced pressure. The residue was loaded to a small amount of silica gel and subjected to flash column chromatography to give the desired product **21** as a yellow oil.

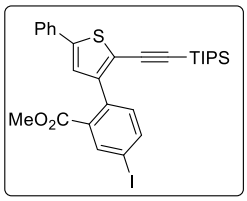

21: Yellow oil (89%). R_f = 0.3 (hexane/ethyl acetate = 10:1). **^{1}H NMR** (400 MHz, $CDCl_3$) δ 8.28 (d, *J* = 1.8 Hz, 1H), 7.84 (dd, *J* = 8.1, 1.9 Hz, 1H), 7.62 – 7.56 (m, 2H), 7.38 (t, *J* = 7.5 Hz, 2H), 7.32 (d, *J* = 7.4 Hz, 1H), 7.26 (d, *J* = 8.1 Hz, 1H), 7.14 (s, 1H), 3.73 (s, 3H), 1.00 (d, *J* = 3.7 Hz, 21H). **^{13}C NMR** (101 MHz, $CDCl_3$) δ 166.5, 145.9, 143.7, 140.4, 139.2, 136.2, 133.7, 133.0, 132.4, 129.1, 128.3, 125.9, 124.2, 119.4, 99.1, 98.7, 92.9, 52.5, 18.6, 11.4. **IR** (KBr): υ 2943, 2890, 2864, 2139, 1733, 1463, 1288, 1238, 761, 677 cm^{-1}. **HRMS** (ESI): Calculated for $C_{29}H_{34}IO_2SSi$ ($M+H^+$): 601.1088, found: 601.1092.

A flame-dried 8.0 mL vial was charged with $Pd(PPh_3)_2$ (5.8 mg, 0.005 mmol, 10 mol%), PPh_3 (3.3 mg, 0.0125 mmol, 25 mol%), K_3PO_4 (68.9 mg, 0.325 mmol, 6.5 equiv), **21** (30.0 mg, 0.05 mmol, 1.0 equiv) and **20** (45.7 mg, 0.075 mmol, 1.5 equiv). Then the vial was directly transferred into a nitrogen-filled glovebox without caps. After degassed water (1.2 mL) and dioxane (3.0 mL) were added, the vial was tightly sealed, transferred out of glovebox and stirred on a pie-block preheated to 90 °C for 12 hours. After completion of the reaction, the mixture was filtered through a thin pad of silica gel. The filter cake was washed with ethyl acetate and the combined filtrate was

concentrated under reduced pressure. The residue was loaded to a small amount of silica gel and subjected to flash column chromatography to give the desired product **22** as a yellow oil.

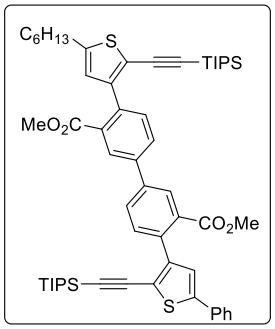

22: Yellow oil (89%). R_f = 0.4 (hexane/ethyl acetate = 10:1). **^{1}H NMR** (400 MHz, $CDCl_3$) δ 8.19 (dd, *J* = 16.7, 1.9 Hz, 2H), 7.76 (ddd, *J* = 9.5, 7.8, 1.7 Hz, 2H), 7.68 – 7.59 (m, 4H), 7.40 (t, *J* = 7.5 Hz, 2H), 7.32 (t, *J* = 7.3 Hz, 1H), 7.23 (s, 1H), 6.68 (s, 1H), 3.77 (d, *J* = 2.8 Hz, 6H), 2.81 (t, *J* = 7.5 Hz, 2H), 1.71 (p, *J* = 7.6 Hz, 2H), 1.44 – 1.38 (m, 2H), 1.34 (dd, *J* = 9.6, 5.7 Hz, 4H), 1.00 (q, *J* = 4.7 Hz, 42H), 0.91 (t, *J* = 6.8 Hz, 3H). **^{13}C NMR** (101 MHz, $CDCl_3$) δ 168.1, 167.9, 146.7, 146.1, 145.5, 143.5, 139.6, 139.1, 136.4, 136.0, 133.8, 132.14, 132.09, 131.5, 131.4, 129.9, 129.7, 129.1, 129.0, 128.9, 128.2, 125.9, 125.8, 124.5, 119.3, 117.5, 99.4, 99.0, 98.7, 96.8, 52.4, 52.3, 31.7, 31.6, 30.4, 28.9, 22.7, 18.67, 18.66, 14.2, 11.39, 11.37. **IR** (KBr): υ 2942, 2891, 2864, 2139, 1734, 1281, 1246, 760, 677, 634 cm^{-1}. **HRMS** (ESI): Calculated for $C_{58}H_{75}O_4S_2Si_2$ ($M+H^+$): 955.4640, found: 955.4642.

Scheme 8.21. Preparation of Alkynyl Bromide 27

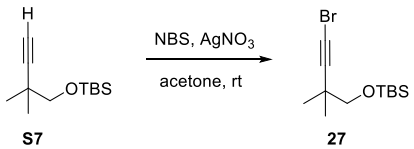

S7 was prepared according to the literature reported procedure.[34] Following a known procedure,[27] to a solution of **S7** (850 mg, 1.0 mmol, 1.0 equiv) in 16 mL acetone were added *N*-bromosuccinimide (NBS) (720 mg, 4.0 mmol, 1.0 equiv) and $AgNO_3$ (66 mg, 0.4 mmol, 10 mol%). The reaction mixture was stirred for 3 h at room temperature, before poured into 50 mL cooled water. The solution was extracted with hexane (50 mL x 3). The combined organic phase was concentrated under reduced pressure and the residue was purified by flash chromatography to yield the compound **24** as a colorless oil (970 mg, 83%).

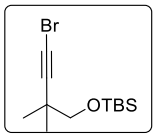

27: Colorless oil (83%). R_f = 0.8 (hexane/ethyl acetate = 20:1). **^{1}H NMR** (400 MHz, $CDCl_3$) δ 3.43 (s, 2H), 1.17 (s, 6H), 0.90 (s, 9H), 0.05 (s, 6H). **^{13}C NMR** (101 MHz, $CDCl_3$) δ 86.2, 71.2, 38.6, 35.1, 26.0, 25.2, 18.5, -5.3. **IR** (KBr): υ 2957, 2930, 2898, 1858, 1472, 1253, 1110, 838, 776 cm^{-1}. **HRMS** (ESI): Calculated for $C_{12}H_{24}BrOSi$ ($M+H^+$): 291.0774, found: 291.0773.

Scheme 8.22. Preparation of Thiophenyl Bromide 26

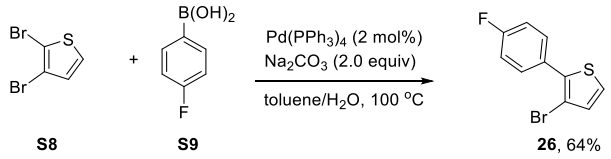

A flame-dried 40 mL vial was charged with $Pd(PPh_3)_4$ (231 mg, 0.2 mmol, 2 mol%), Na_2CO_3 (2.12 g, 20 mmol, 2.0 equiv), 2,3-dibromothiophene (2.4 g, 10 mmol, 1.0 equiv) and 4-fluorophenylboronicacid (1.68 g, 12 mmol, 1.2 equiv). Then the vial was directly transferred into a nitrogen-filled glovebox without caps. After degassed water (12 mL) and toluene (12 mL) were

added, the vial was tightly sealed, transferred out of glovebox and stirred on a pie-block preheated to 100 ^{o}C for 20 hours. After completion of the reaction, the mixture was poured into 50 mL water and then extracted with diethyl ether for three times. The combined organic layers were dried with anhydrous MgSO4 and concentrated under reduced pressure. The residue was loaded to a small amount of silica gel and subjected to flash column chromatography to give the desired product **26** as a colorless oil.

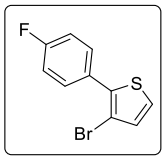

26: Colorless oil (64%). R_f = 0.8 (hexane/ethyl acetate = 10:1). **^{1}H NMR** (400 MHz, $CDCl_3$) δ 7.65 – 7.57 (m, 2H), 7.28 (d, *J* = 5.4 Hz, 1H), 7.13 (ddt, *J* = 8.8, 6.7, 2.6 Hz, 2H), 7.05 (d, *J* = 5.4 Hz, 1H). **^{13}C NMR** (101 MHz, $CDCl_3$) δ 162.8 (d, *J* = 248.6 Hz), 137.3, 131.7, 131.1 (d, *J* = 8.2 Hz), 129.0 (d, *J* = 3.4 Hz), 125.1, 115.7 (d, *J* = 21.7 Hz), 107.9. **^{19}F NMR** (376 MHz, $CDCl_3$) δ -113.06. **IR** (KBr): υ 3110, 3088, 1603, 1559, 1532, 1494, 1232, 1160, 834, 705 cm^{-1}. **HRMS** (ESI): Calculated for $C_{10}H_7BrFS$ ($M+H^+$): 256.9430, found: 256.9425.

Scheme 8.23. Synthesis of P38α MAPK Inhibitor Analogue 30

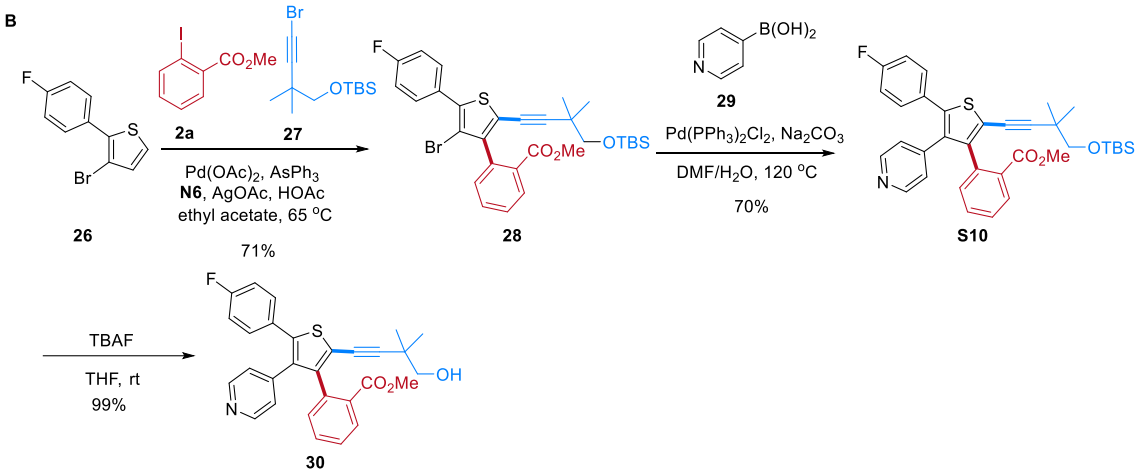

A flame-dried 4.0 mL vial was charged with $Pd(OAc)_2$ (2.3 mg, 0.01 mmol, 10 mol%), $AsPh_3$ (7.6 mg, 0.025 mmol, 25 mol%), **N6** (33 mg, 0.15 mmol, 1.5 equiv), **26** (25.7 mg, 0.1 mmol, 1.0 equiv), **2a** (52.4 mg, 0.2 mmol, 2.0 equiv) and AgOAc (50 mg, 0.3 mmol, 3.0 equiv) in air. Ethyl acetate (0.5 mL) was then added. After alkynyl bromide **27** (52.4 mg, 0.18 mmol, 1.8 equiv) and HOAc (30 mg, 0.5 mmol, 5.0 equiv) were added, the vial was tightly sealed and stirred on a pie-block preheated to 65 °C for 72 hours. After completion of the reaction, the mixture was filtered through a thin pad of silica gel. The filter cake was washed with ethyl acetate and the combined filtrate was concentrated under reduced pressure. The residue was loaded to a small amount of silica gel and subjected to flash column chromatography to give the desired product **28** as a yellow oil.

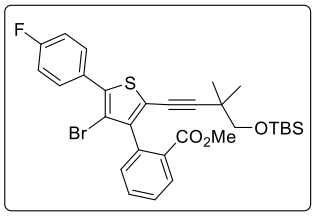

28: Yellow oil (71%). R_f = 0.6 (hexane/ethyl acetate = 5:1). **^{1}H NMR** (400 MHz, $CDCl_3$) δ 8.07 (dd, *J* = 7.8, 1.1 Hz, 1H), 7.68 – 7.62 (m, 2H), 7.59 (td, *J* = 7.5, 1.4 Hz, 1H), 7.48 (td, *J* = 7.7, 1.3 Hz, 1H), 7.41 – 7.35 (m, 1H), 7.13 (t, *J* = 8.7 Hz, 2H), 3.75 (s, 3H), 3.30 (d, *J* = 1.9 Hz, 2H), 1.05

(d, *J* = 1.1 Hz, 6H), 0.87 (s, 9H), -0.00 (s, 6H). **^{13}C NMR** (101 MHz, $CDCl_3$) δ 167.3, 162.9 (d, *J* = 248.9 Hz), 146.0, 136.3, 135.9, 132.2, 131.7, 131.3 (d, *J* = 8.3 Hz), 131.1, 130.5, 129.2 (d, *J* = 3.4 Hz), 128.3, 119.8, 115.7 (d, *J* = 21.8 Hz), 109.4, 103.8, 72.9, 70.9, 52.3, 34.5, 26.0, 25.0, 18.4, -5.3. **^{19}F NMR** (376 MHz, $CDCl_3$) δ -112.61. **IR** (KBr): υ 2953, 2929, 2897, 2857, 1732, 1602, 1257, 1100, 838, 768 cm^{-1}. **HRMS** (ESI): Calculated for $C_{30}H_{35}BrFO_3SSi$ ($M+H^+$): 601.1238, found: 601.1234.

A flame-dried 40 mL vial was charged with $Pd(PPh_3)_2Cl_2$ (3.5 mg, 0.005 mmol, 7 mol%), Na_2CO_3 (42.4 mg, 0.4 mmol, 5.7 equiv), **28** (42.1 mg, 0.07 mmol, 1.0 equiv) and 4-pyridylboronic acid (18.4 mg, 0.15 mmol, 2.1 equiv). Then the vial was directly transferred into a nitrogen-filled glovebox without caps. After degassed water (0.2 mL) and DMF (0.8 mL) were added, the vial was tightly sealed, transferred out of glovebox and stirred on a pie-block preheated to 120 °C for 12 hours. After completion of the reaction, the mixture was filtered through a thin pad of silica gel. The filter cake was washed with ethyl acetate and the combined filtrate was concentrated under reduced pressure. The residue was loaded to a small amount of silica gel and subjected to flash column chromatography to give the desired product **S10** as a yellow oil.

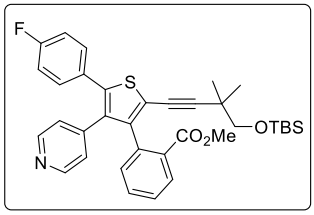

S10: Yellow oil (70%). R_f = 0.2 (hexane/ethyl acetate = 2:1). **^{1}H NMR** (400 MHz, $CDCl_3$) δ 8.32 (s, 2H), 7.86 (dd, *J* = 7.6, 1.5 Hz, 1H), 7.40 – 7.29 (m, 2H), 7.20 – 7.14 (m, 2H), 7.03 (dd, *J* = 7.4, 1.3 Hz, 1H), 6.94 (t, *J* = 8.7 Hz, 2H), 6.87 (d, *J* = 4.6 Hz, 2H), 3.71 (s, 3H), 3.35 – 3.26 (m, 2H), 1.05 (d, *J* = 5.9 Hz, 6H), 0.87 (s, 9H), 0.00 (d, *J* = 1.5 Hz, 6H). **^{13}C NMR** (101 MHz, $CDCl_3$) δ

167.4, 162.6 (d, J = 248.7 Hz), 149.5, 145.7, 144.1, 138.9, 136.5, 134.7, 131.9, 131.55, 131.53, 131.3 (d, J = 8.2 Hz), 130.2, 129.4 (d, J = 3.4 Hz), 127.7, 125.5, 120.3, 115.8 (d, J = 21.7 Hz), 103.3, 72.9, 70.8, 52.3, 34.5, 26.0, 24.9, 18.4, -5.3. **^{19}F NMR** (376 MHz, $CDCl_3$) δ -113.21. **IR** (KBr): υ 3028, 2954, 2929, 2856, 1728, 1597, 1257, 1098, 837, 777, 562 cm^{-1}. **HRMS** (ESI): Calculated for $C_{35}H_{38}FNO_3SSiNa$ ($M+Na^+$): 622.2218, found: 622.2222.

To a solution of **S10** (31.6 mg, 0.05 mmol, 1.0 equiv) in dry THF (1 mL) was added a TBAF solution (1M in THF) (0.06 mL, 0.06 mmol 1.2 equiv) dropwise at room temperature under nitrogen atmosphere. Then the reaction mixture was stirred for additional 4 h until all the starting material was consumed. The reaction was quenched by adding H_2O (5 mL) and the mixture was extracted with Et_2O for three times. The combined organic layers were dried over anhydrous Na_2SO_4, filtered and the solvent was evaporated under reduced pressure. The residue was purified by flash column chromatography through silica gel to give **30** as a colorless oil.

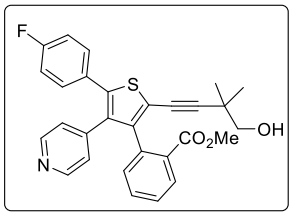

30: Colorless oil (99%). R_f = 0.2 (hexane/ethyl acetate = 1:1). **^{1}H NMR** (400 MHz, $CDCl_3$) δ 8.36 – 8.29 (m, 2H), 7.90 – 7.80 (m, 1H), 7.42 – 7.32 (m, 2H), 7.23 – 7.13 (m, 2H), 7.00 – 6.85 (m, 5H), 3.75 (s, 3H), 3.37 – 3.16 (m, 2H), 2.10 (s, 1H), 1.13 (s, 3H), 1.07 (s, 3H). **^{13}C NMR** (101 MHz, $CDCl_3$) δ 168.5, 162.7 (d, J = 249.0 Hz), 149.7, 146.0, 143.8, 139.4, 136.1, 134.7, 132.1, 131.6, 131.4, 131.3 (d, J = 8.2 Hz), 130.0, 129.2 (d, J = 3.5 Hz), 128.1, 125.4, 119.8, 115.9 (d, J = 21.8 Hz), 102.2, 73.8, 71.6, 52.6, 35.4, 25.1 (d, J = 18.3 Hz). **^{19}F NMR** (376 MHz, $CDCl_3$) δ -

112.88. **IR** (KBr): υ 3272, 3066, 2969, 2927, 1725, 1601, 1507, 1292, 1260, 1077, 736 cm^{-1}. **HRMS** (ESI): Calculated for $C_{29}H_{25}FNO_3S$ ($M+H^+$): 486.1534, found: 486.1540.

8.5 NMR Spectra

Figure 8.5. ^{1}H NMR of 3d

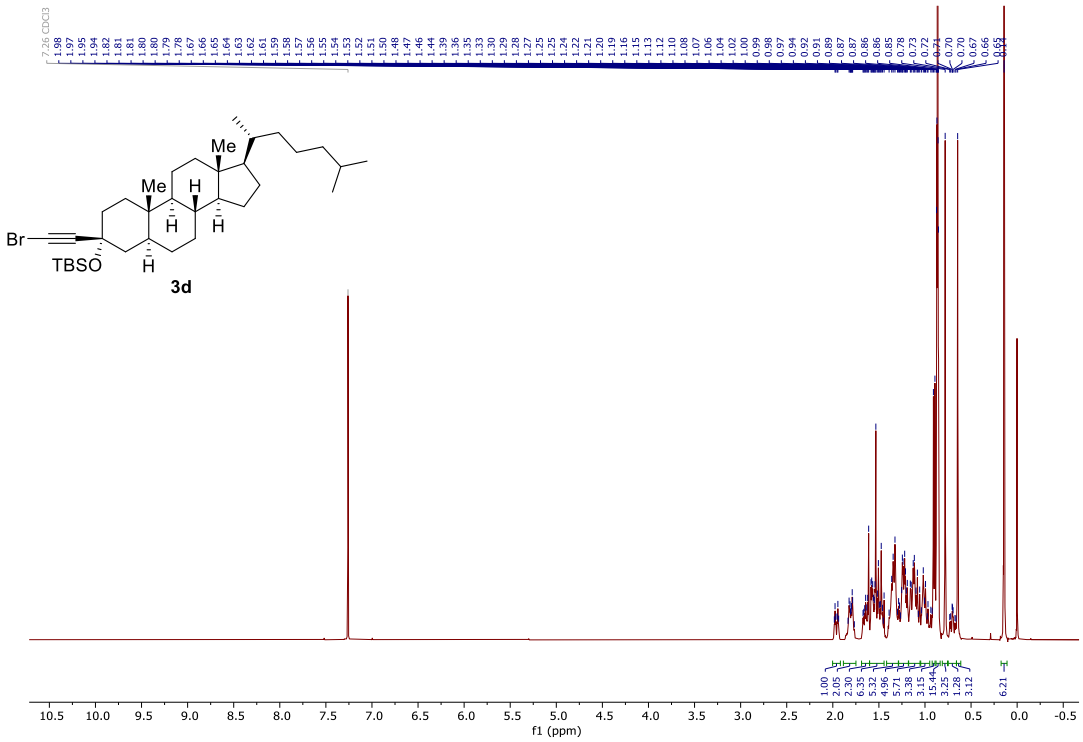

Figure 8.6. ^{13}C NMR of 3d

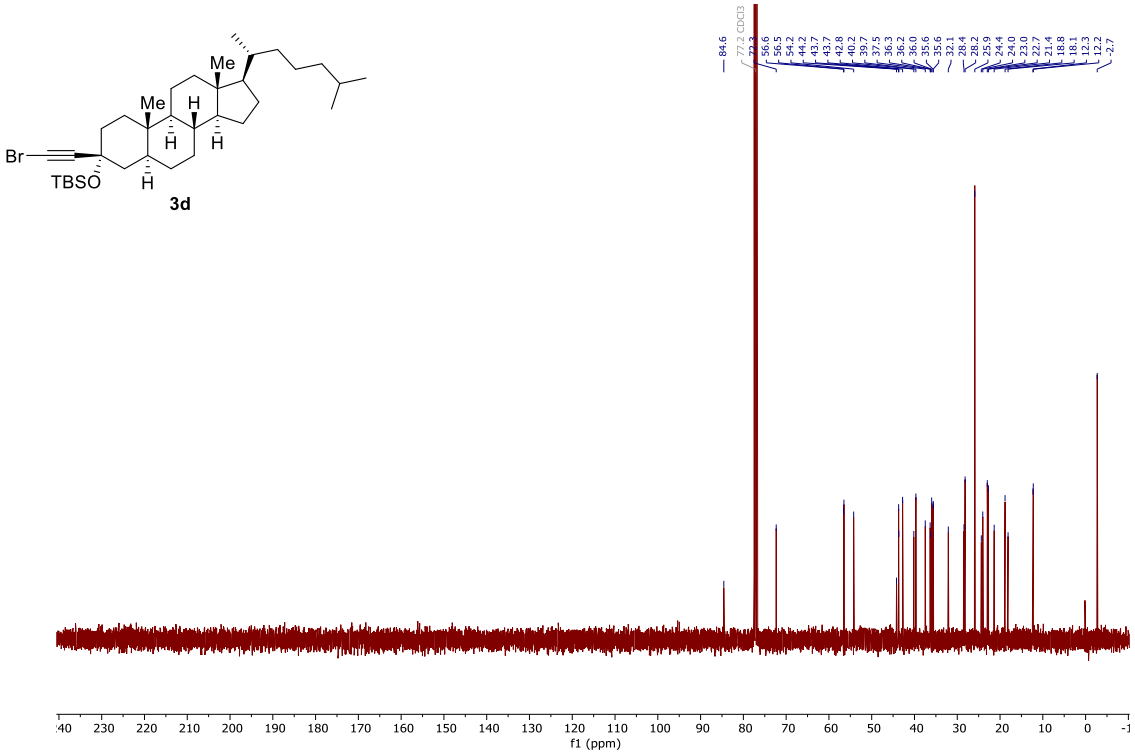

Figure 8.7. ^{1}H NMR of N1

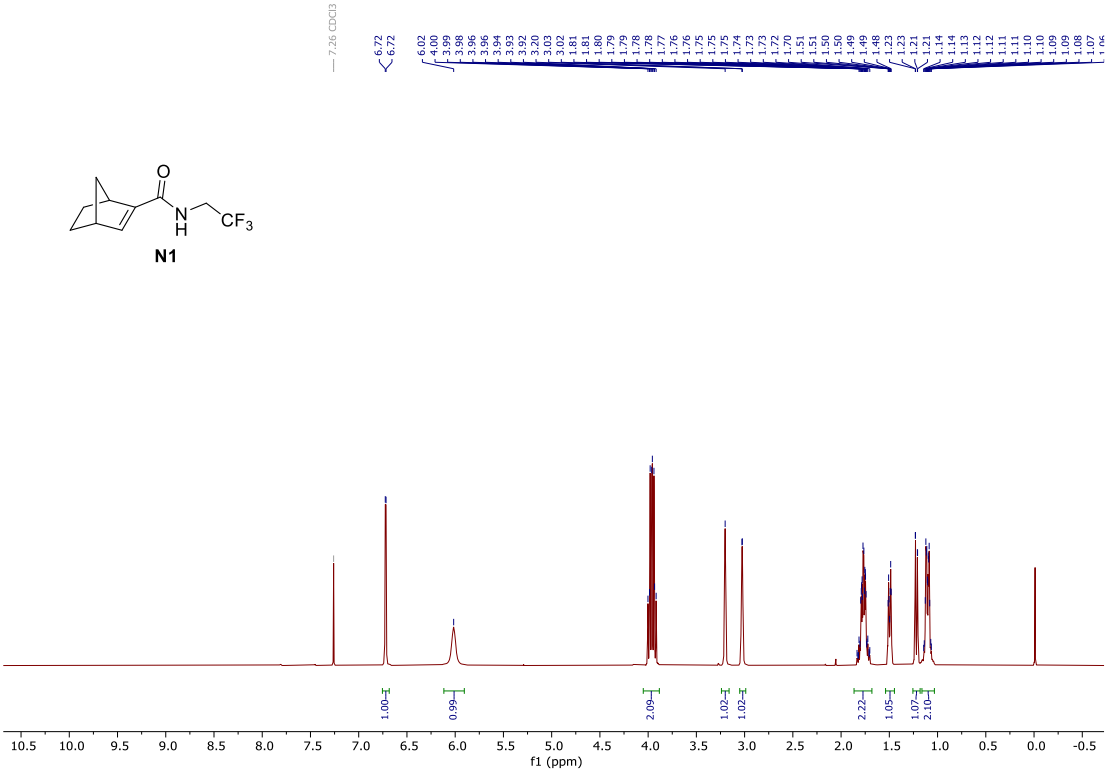

Figure 8.8. ^{13}C NMR of N1

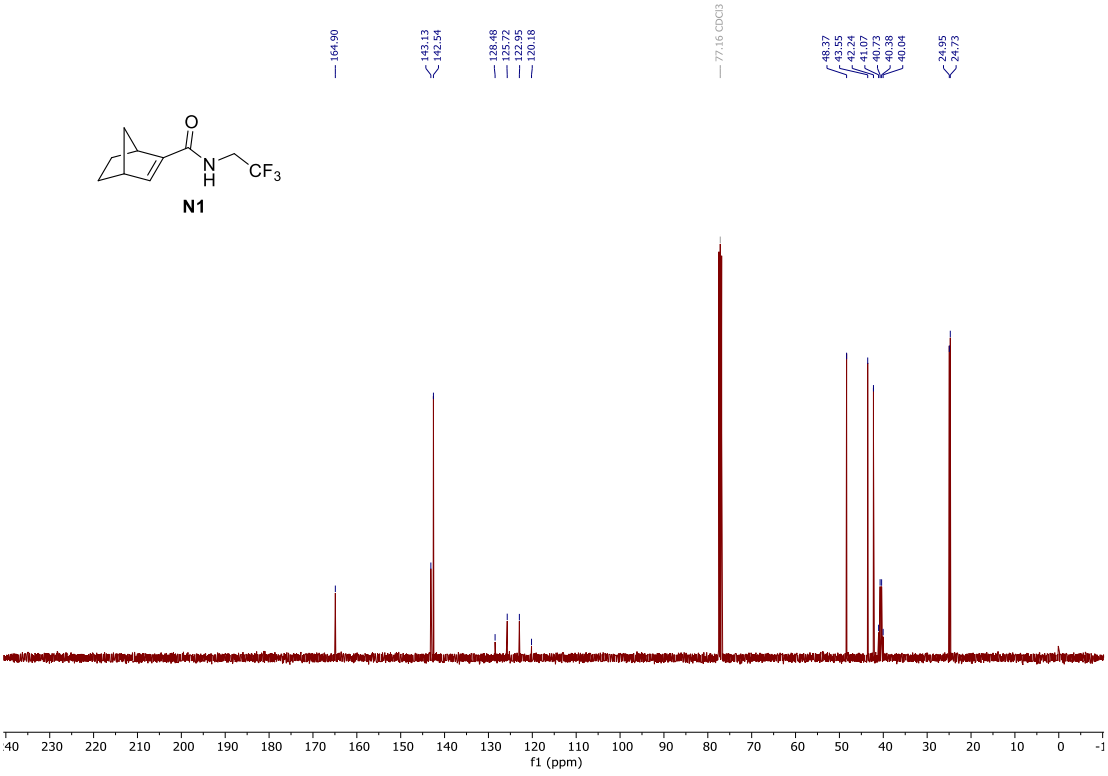

Figure 8.9. ^{19}F NMR of N1

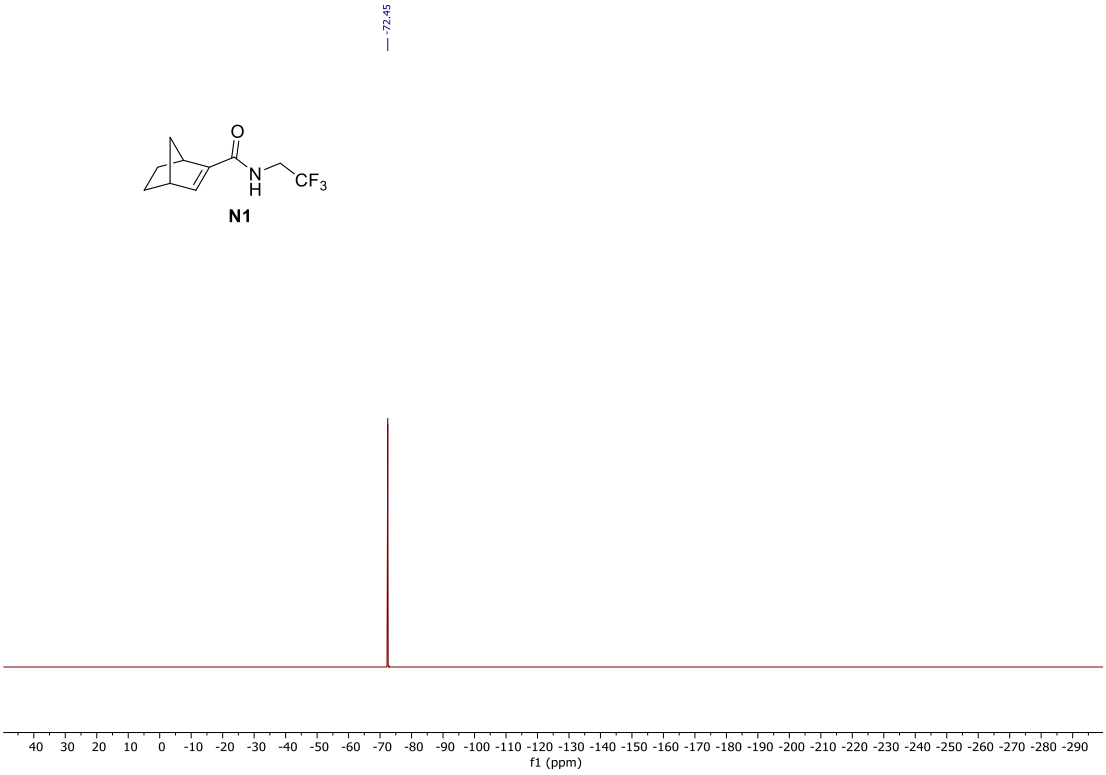

Figure 8.10. ^{1}H NMR of N6

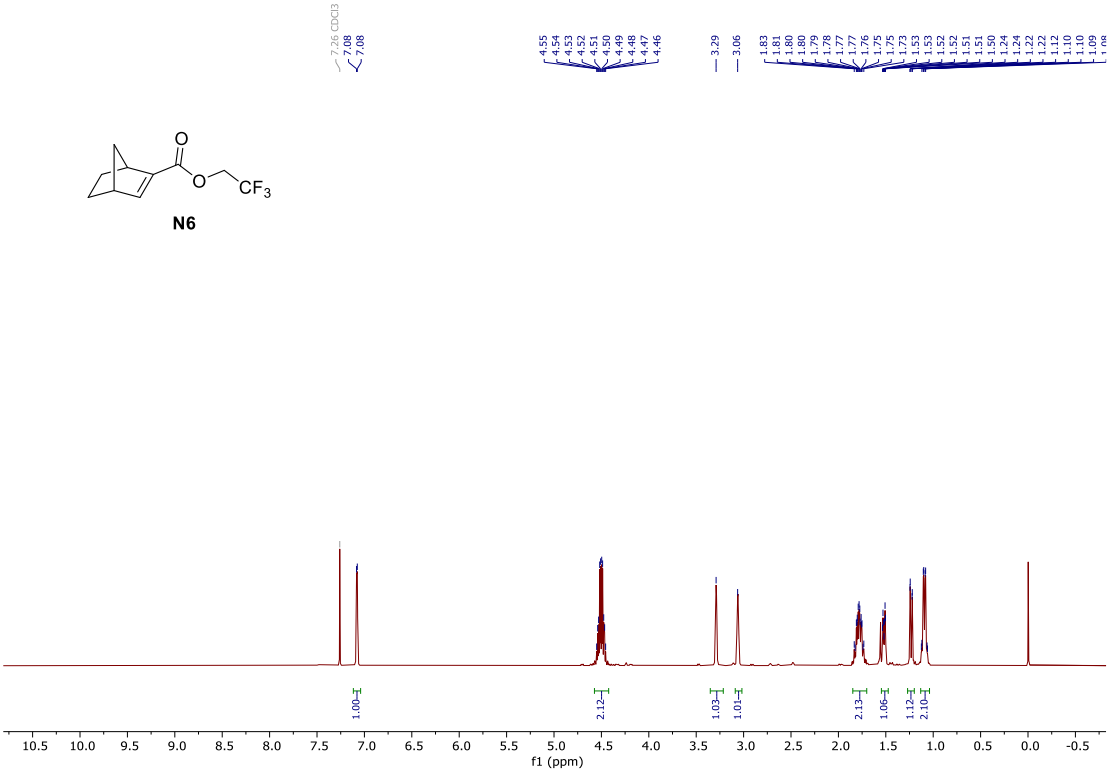

Figure 8.11. ^{13}C NMR of N6

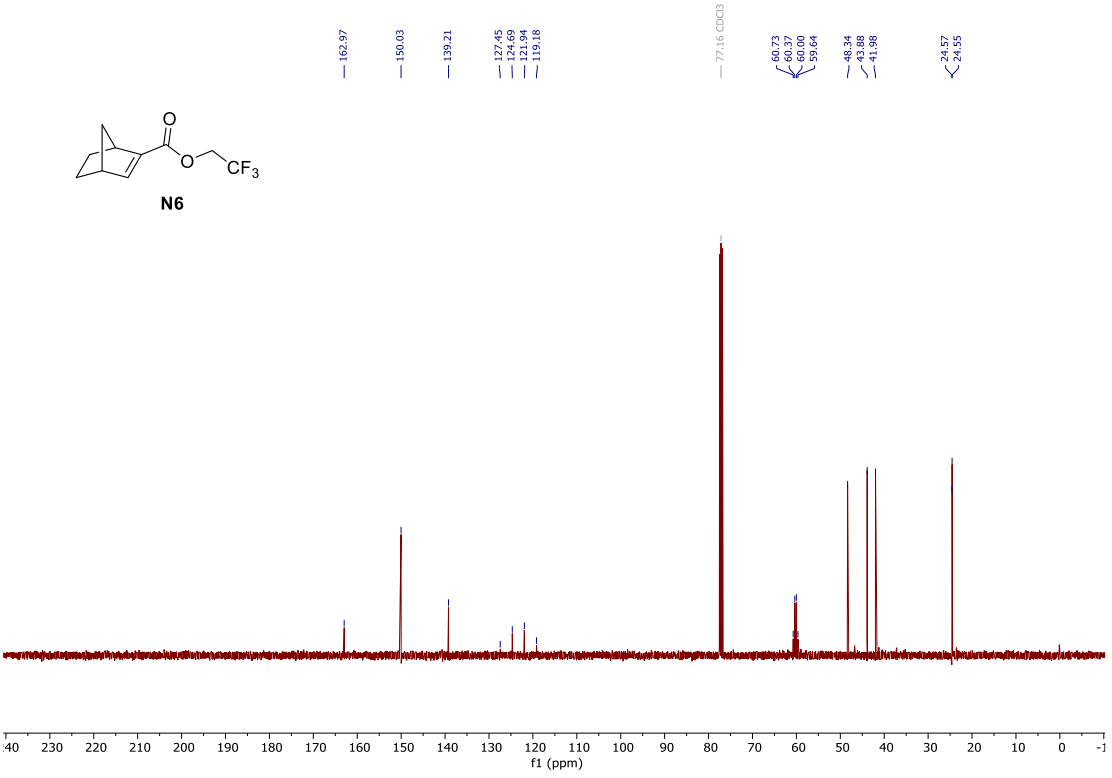

Figure 8.12. ^{19}F NMR of N6

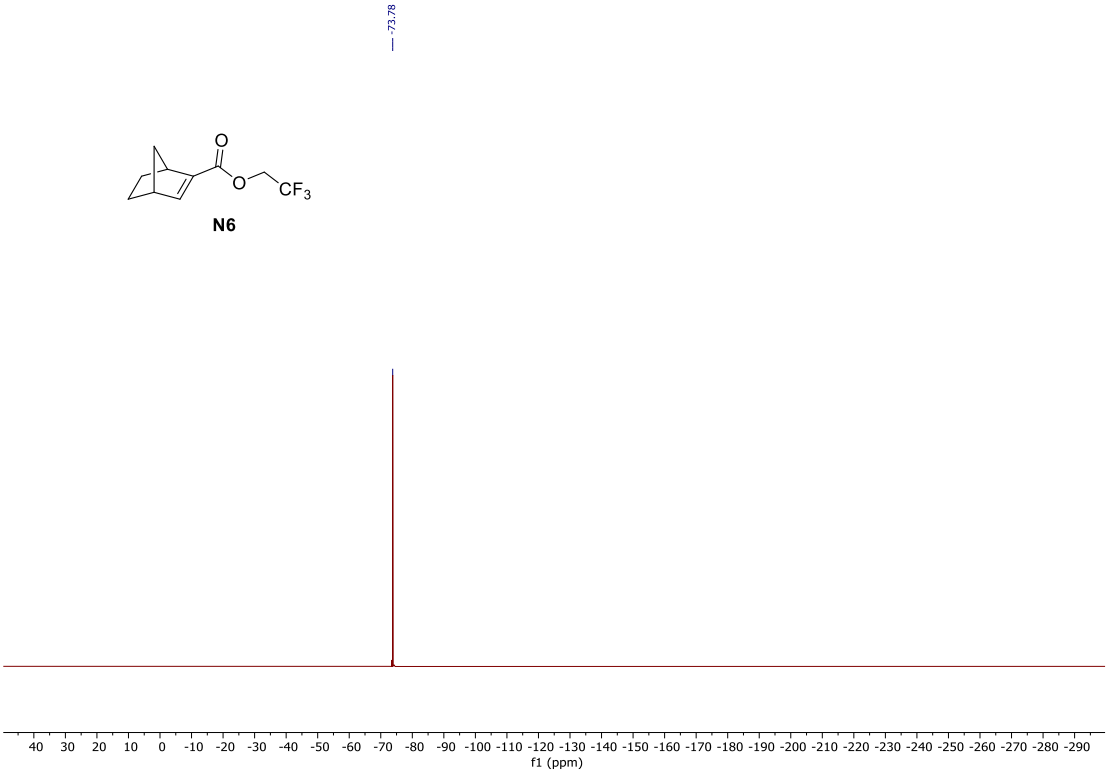

Figure 8.13. ^{1}H NMR of 4a

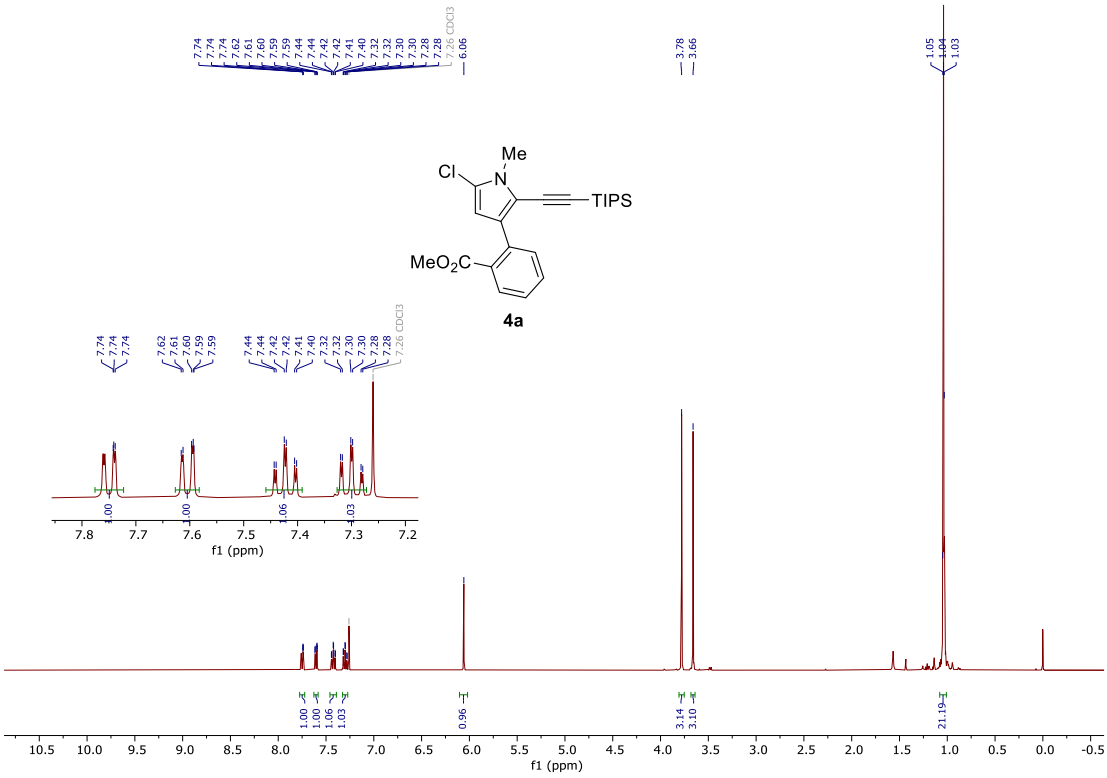

Figure 8.14. ^{13}C NMR of 4a

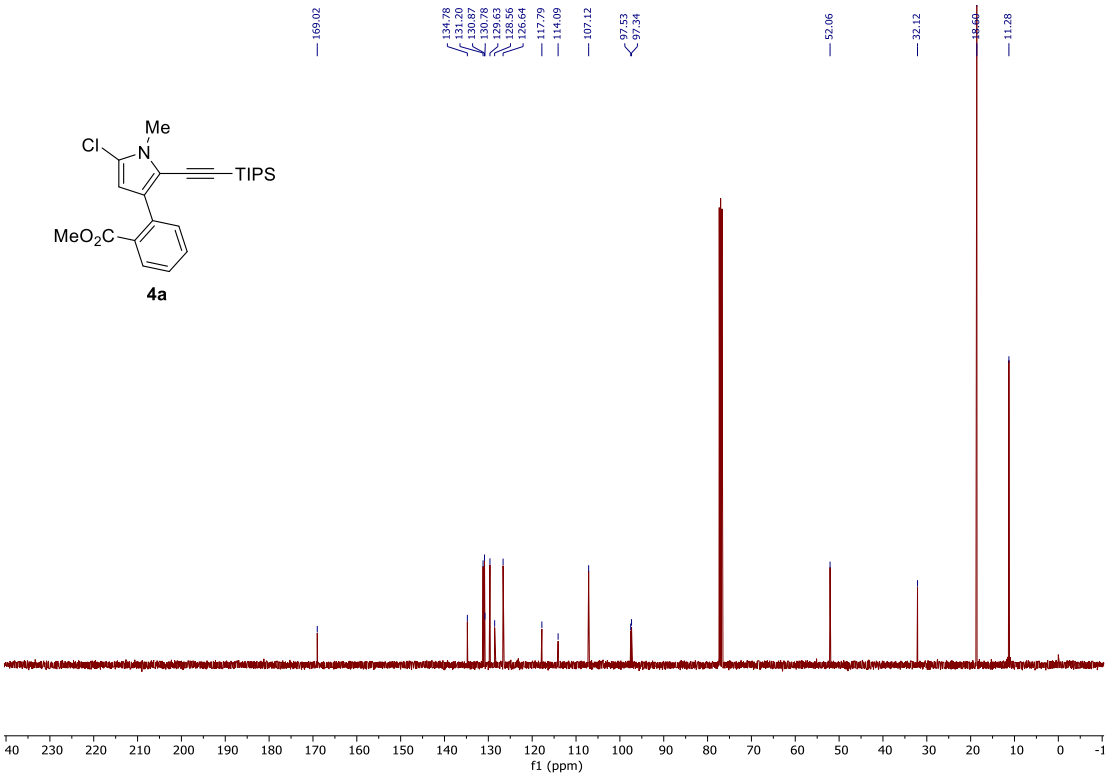

Figure 8.15. ^{1}H NMR of 4b

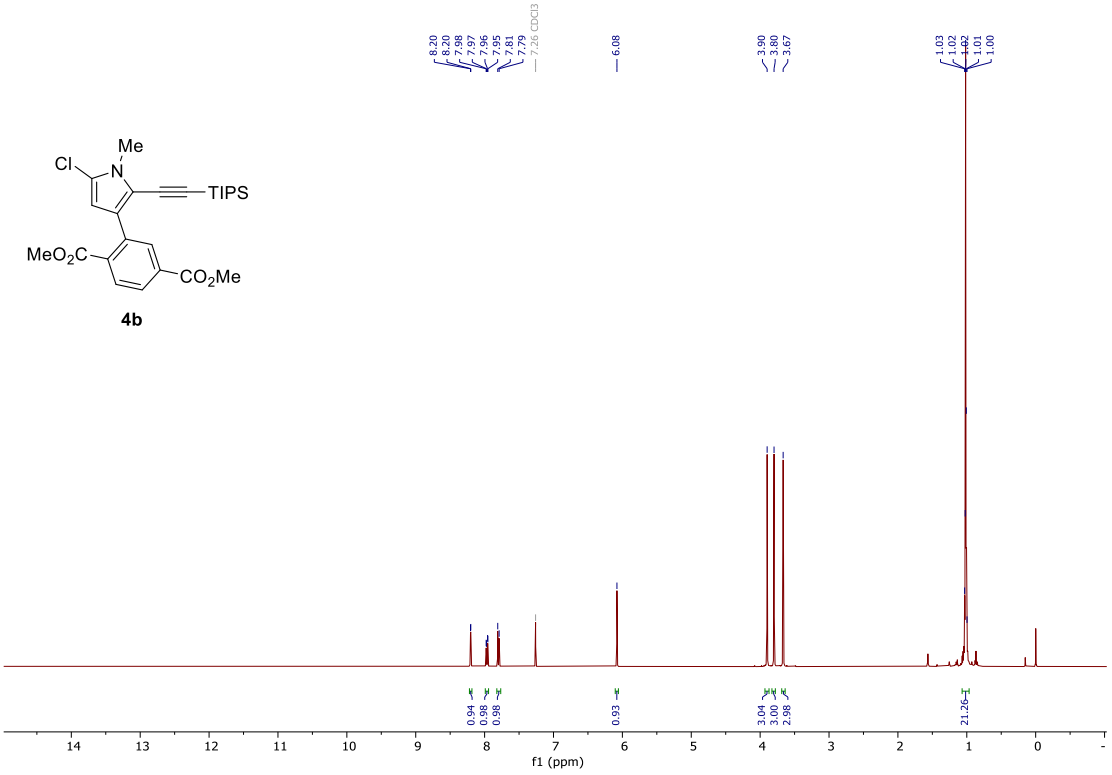

Figure 8.16. ^{13}C NMR of 4b

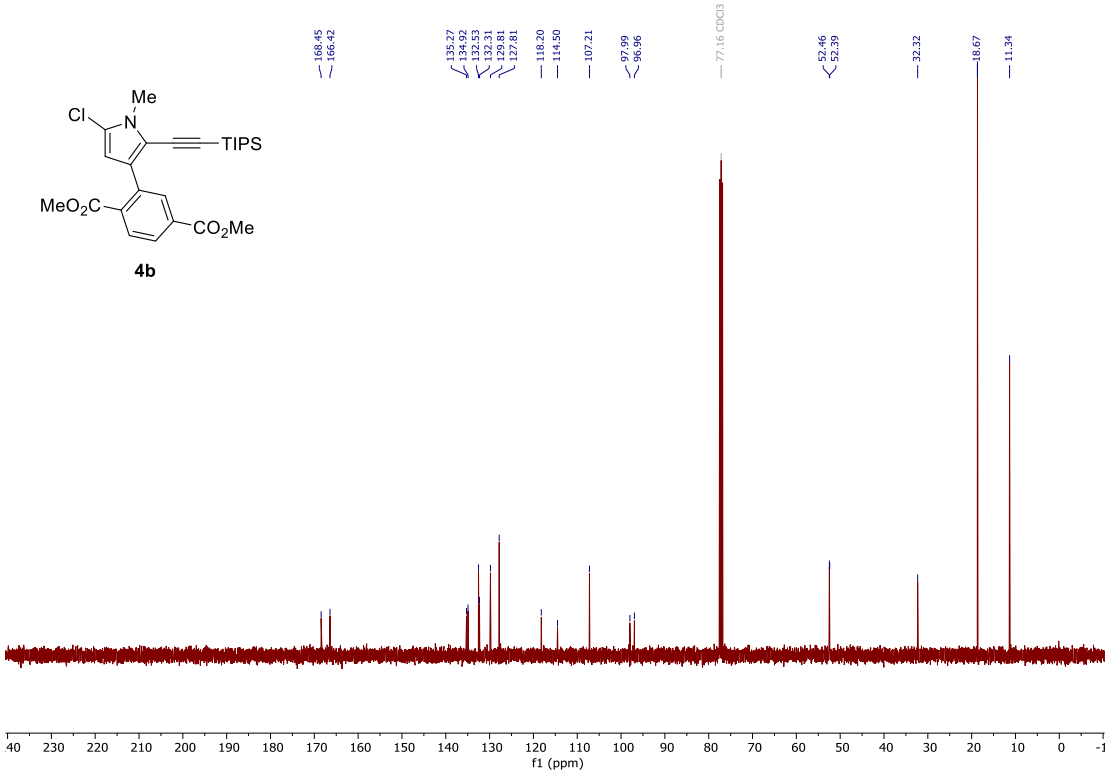

Figure 8.17. ^{1}H NMR of 4c

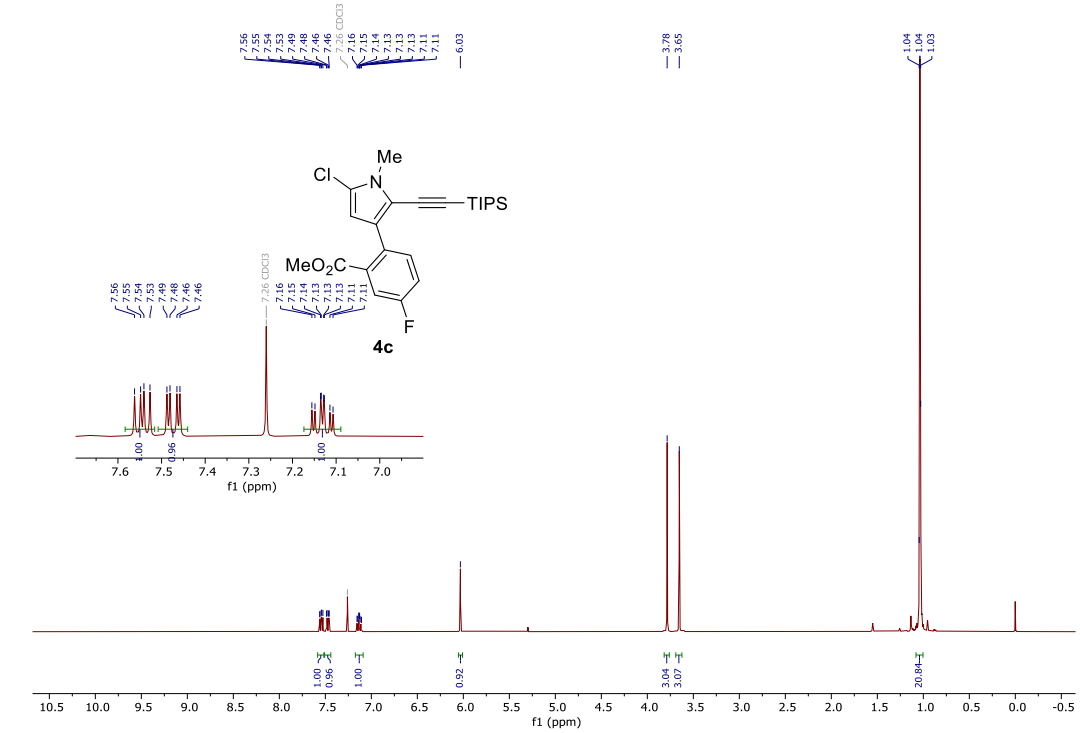

Figure 8.18. ^{13}C NMR of 4c

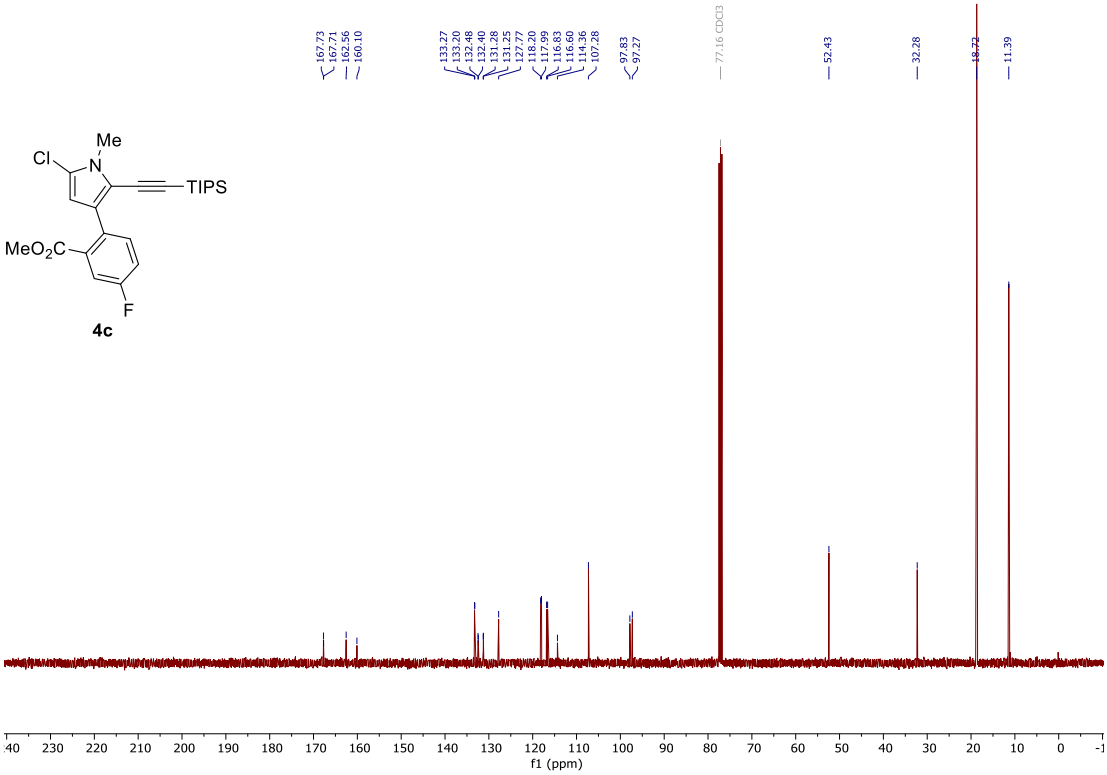

Figure 8.19. ^{19}F NMR of 4c

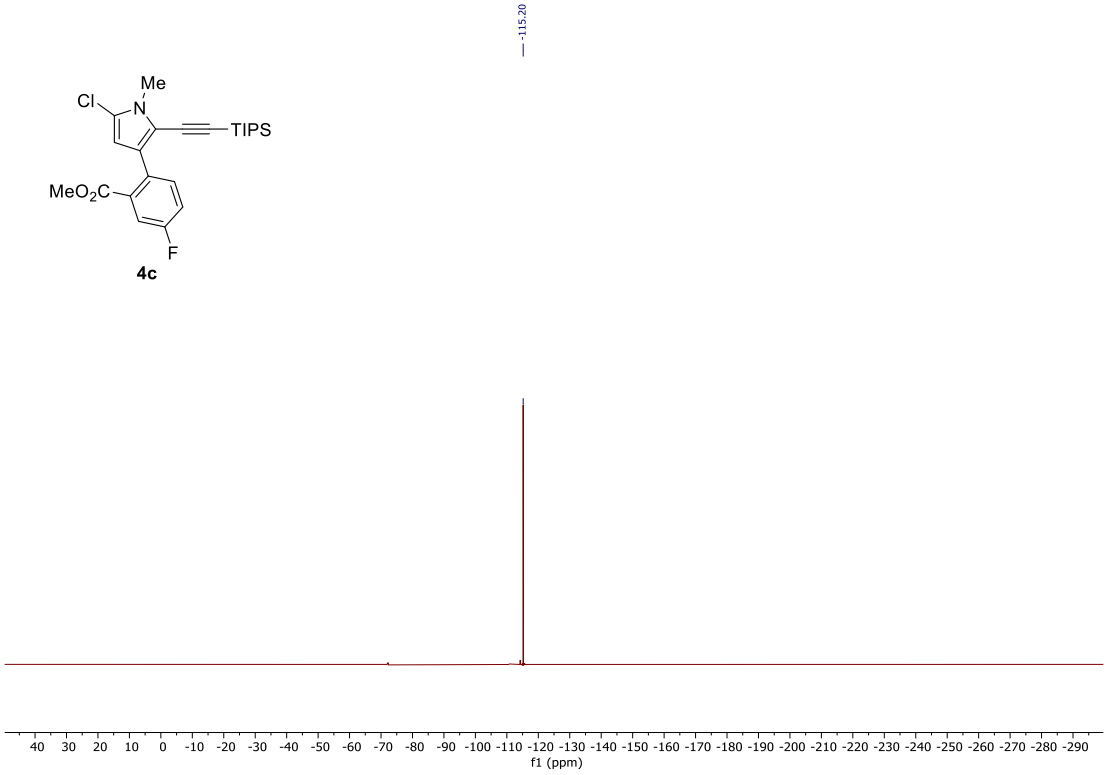

Figure 8.20. ^{1}H NMR of 4d

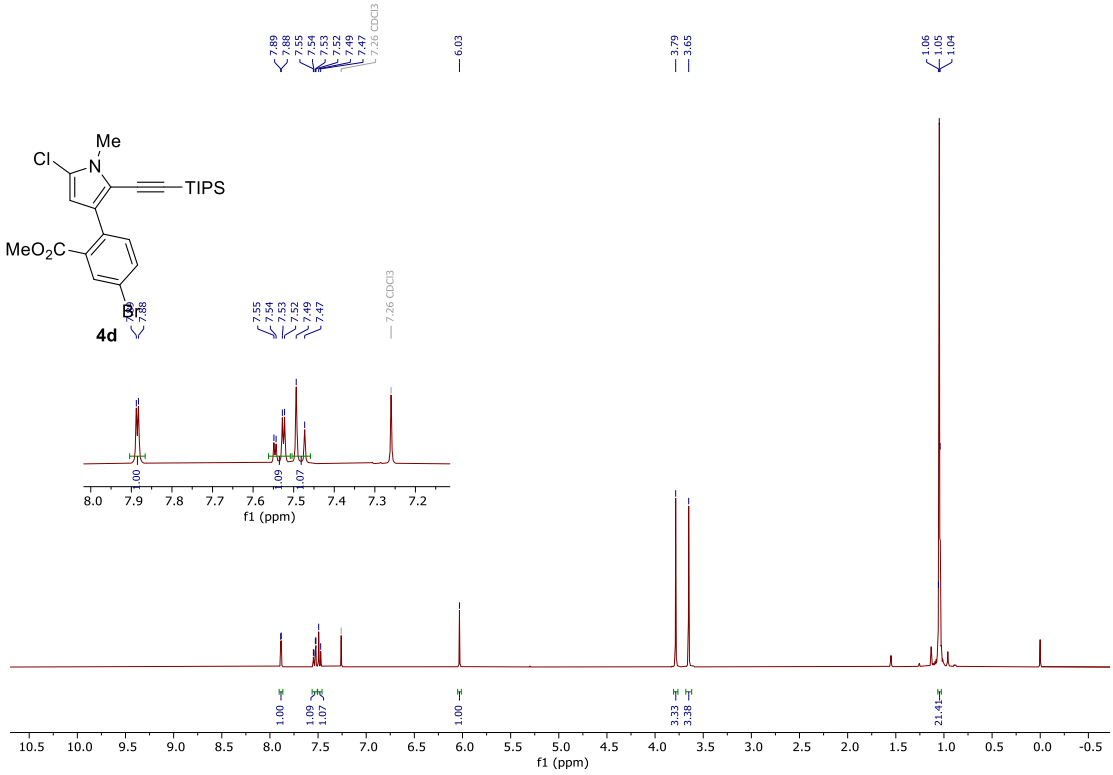

Figure 8.21. ^{13}C NMR of 4d

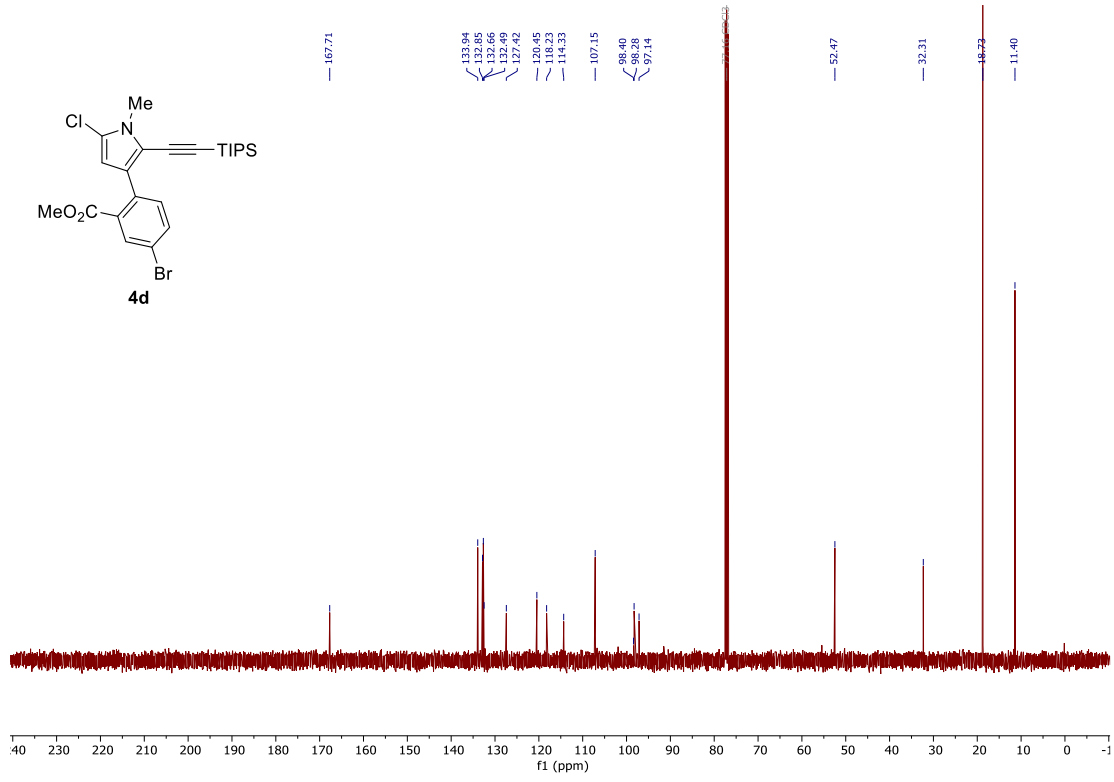

Figure 8.22. ^{1}H NMR of 4e

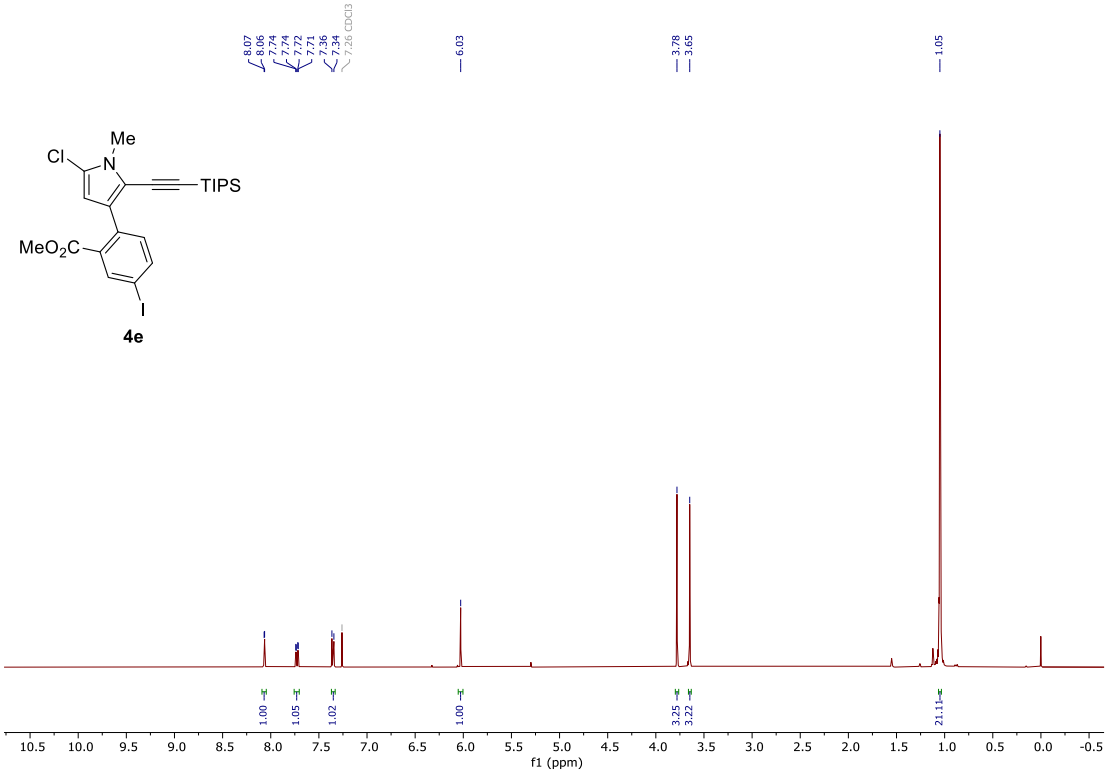

Figure 8.23. ^{13}C NMR of 4e

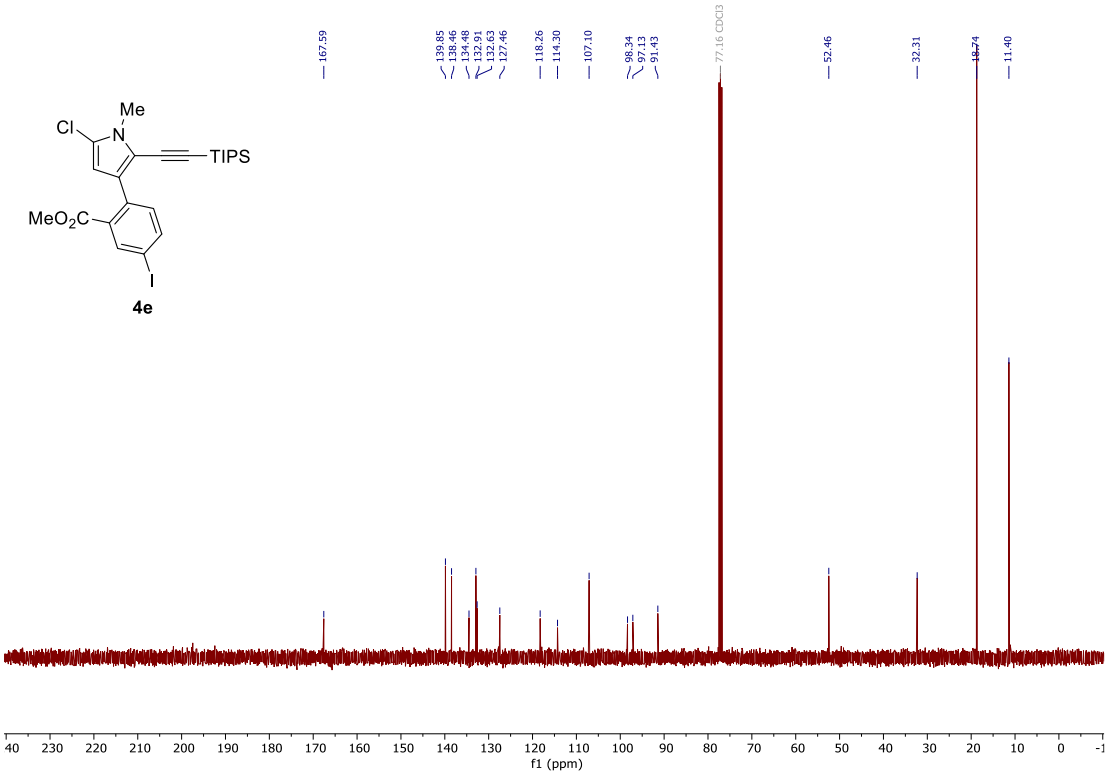

Figure 8.24. ^{1}H NMR of 4f

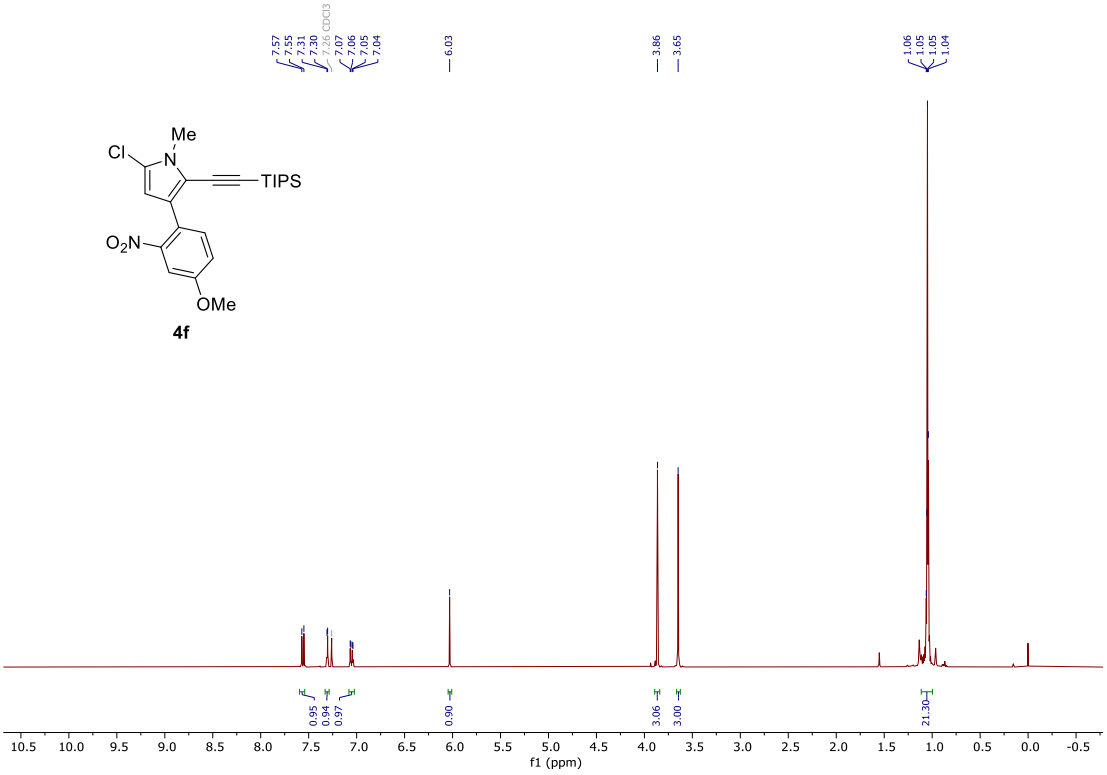

Figure 8.25. ^{13}C NMR of 4f

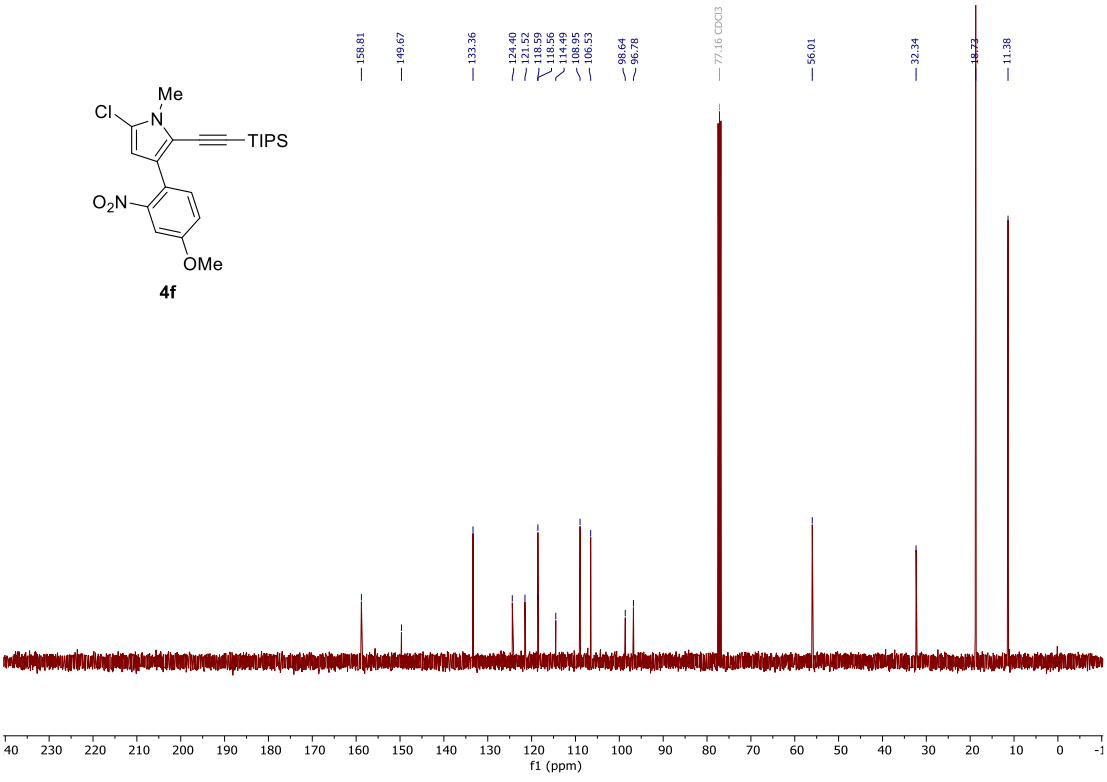

Figure 8.26. ^{13}C NMR of 4g

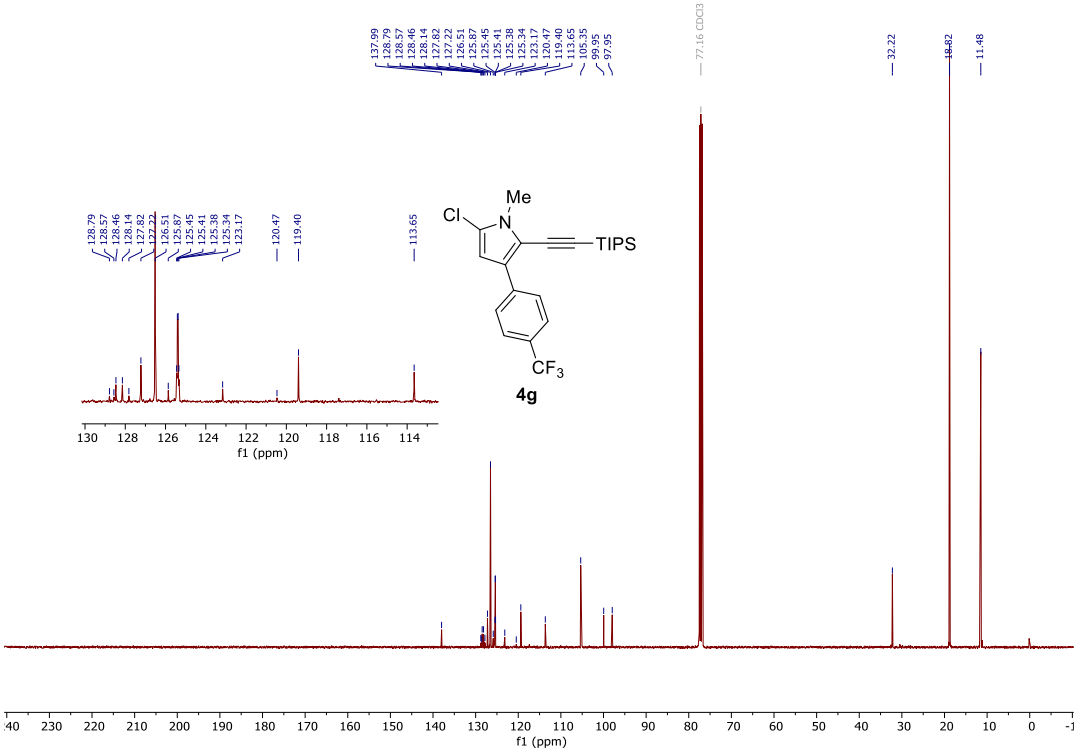

Figure 8.27. ^{1}H NMR of 4g

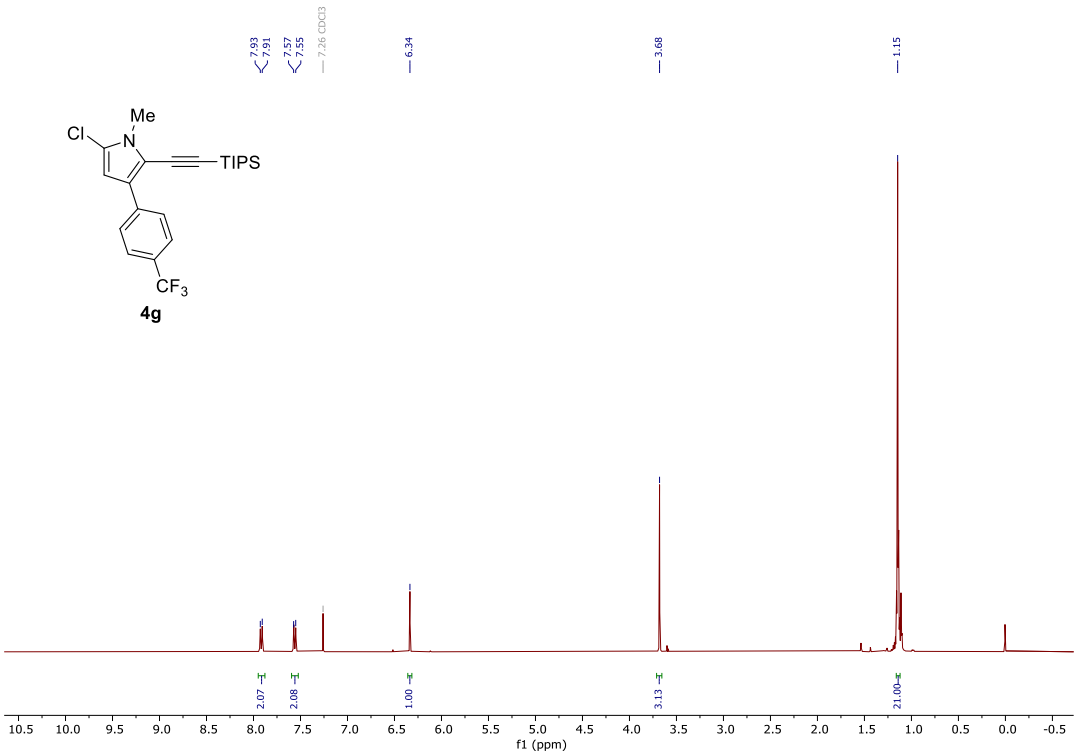

Figure 8.28. ^{19}F NMR of 4g

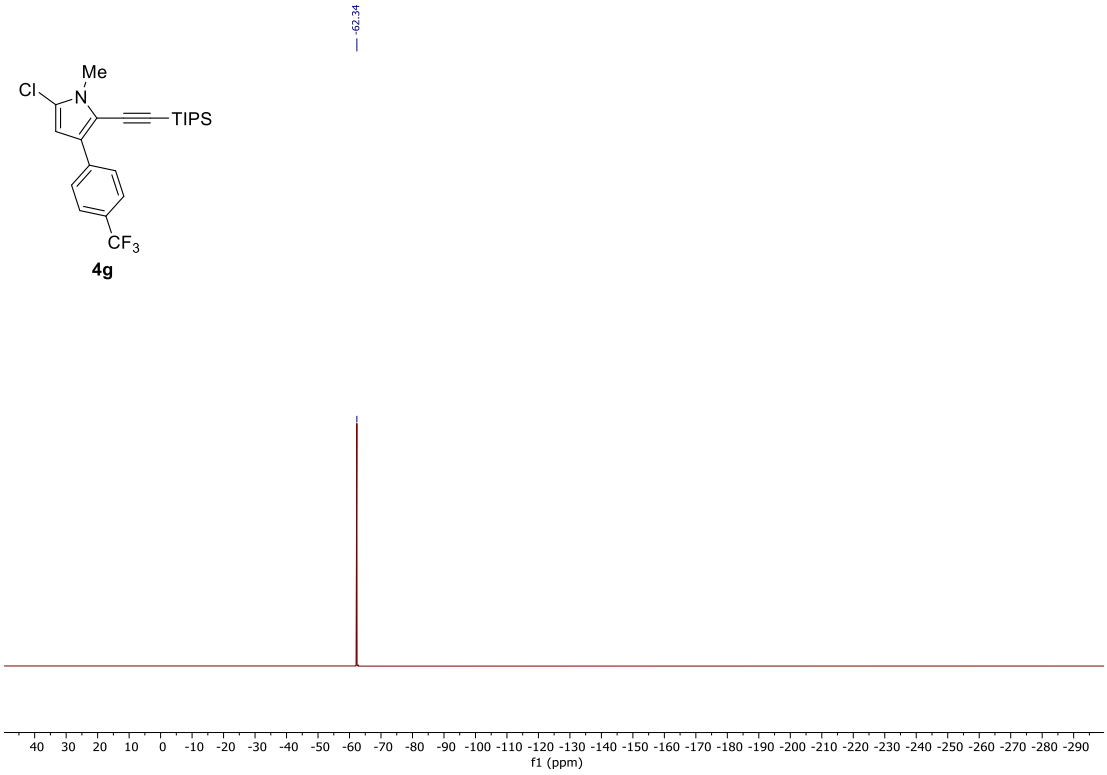

Figure 8.29. ^{1}H NMR of 4h

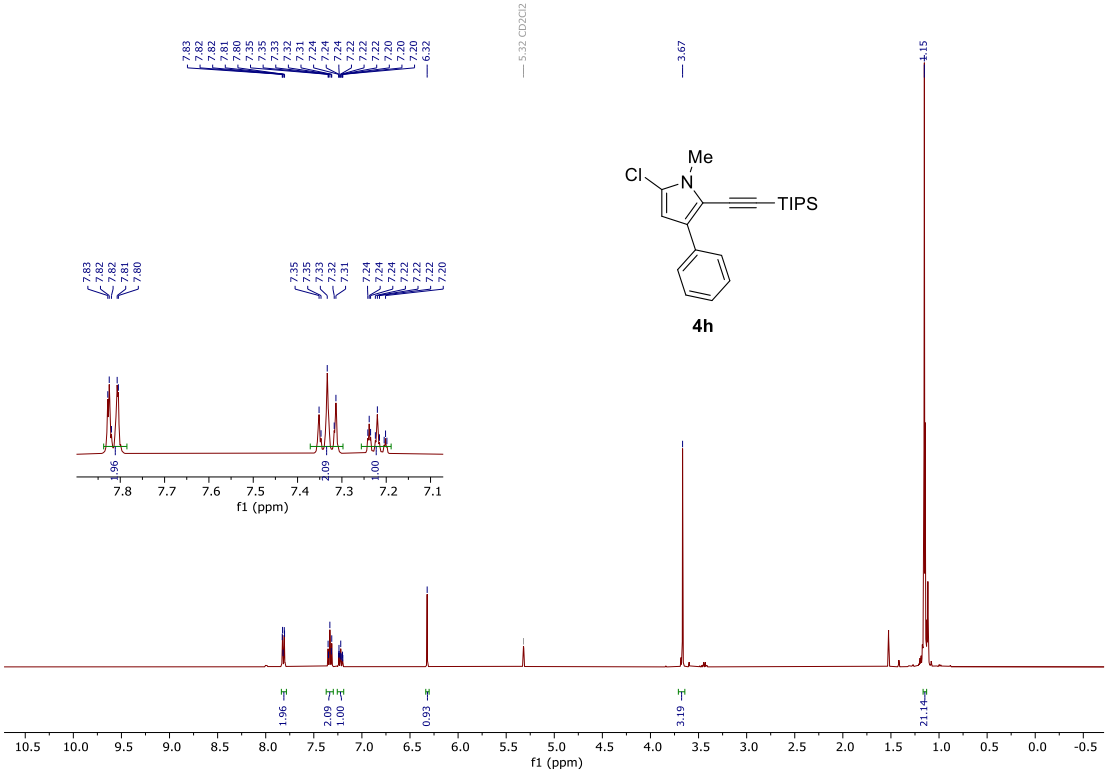

Figure 8.30. ^{13}C NMR of 4h

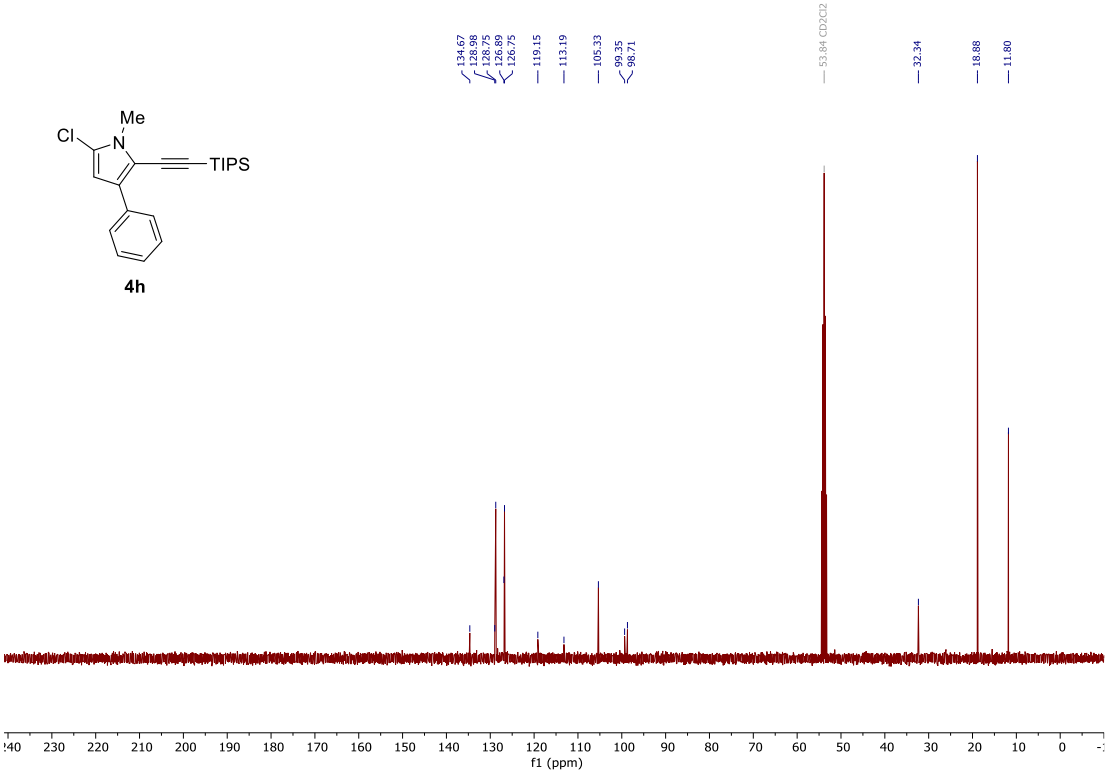

Figure 8.31. ^{1}H NMR of 4i

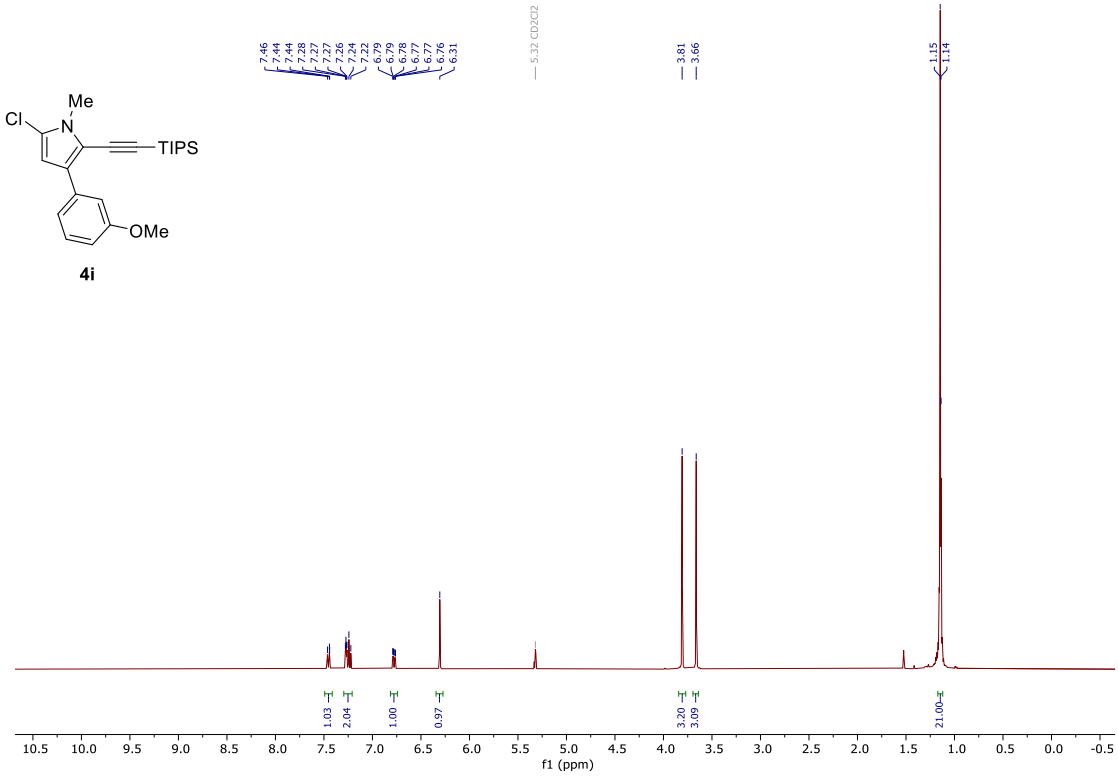

Figure 8.32. ^{13}C NMR of 4i

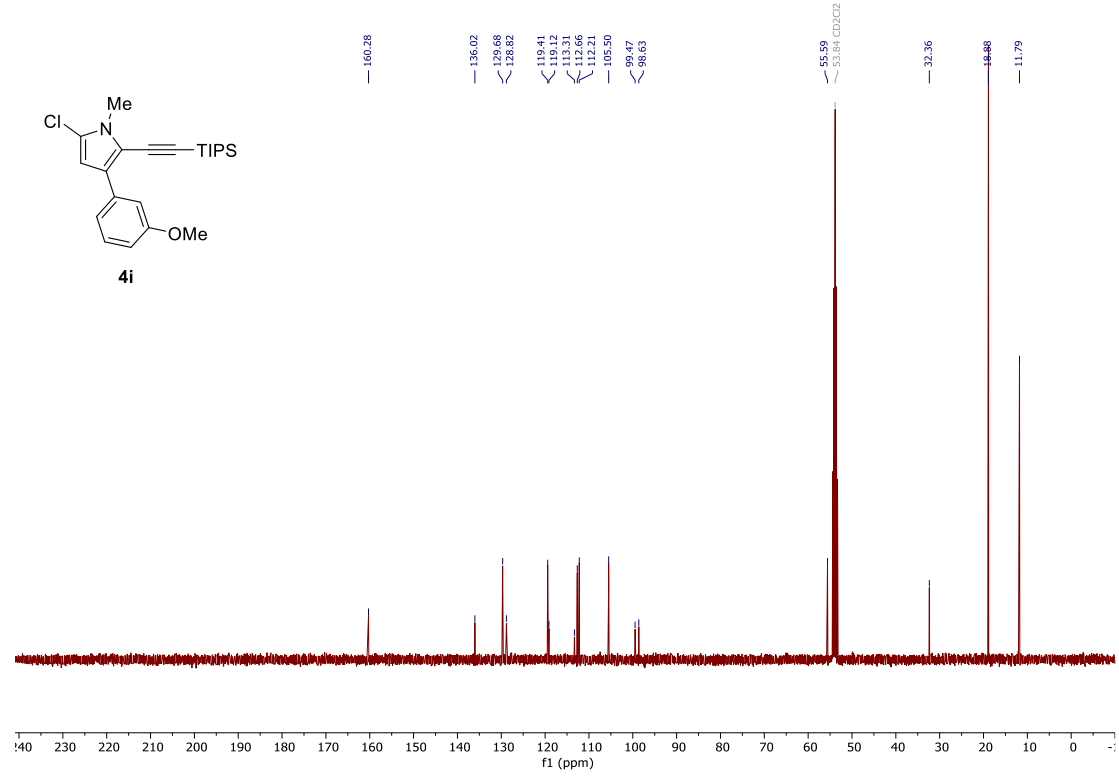

Figure 8.33. ^{1}H NMR of 4j

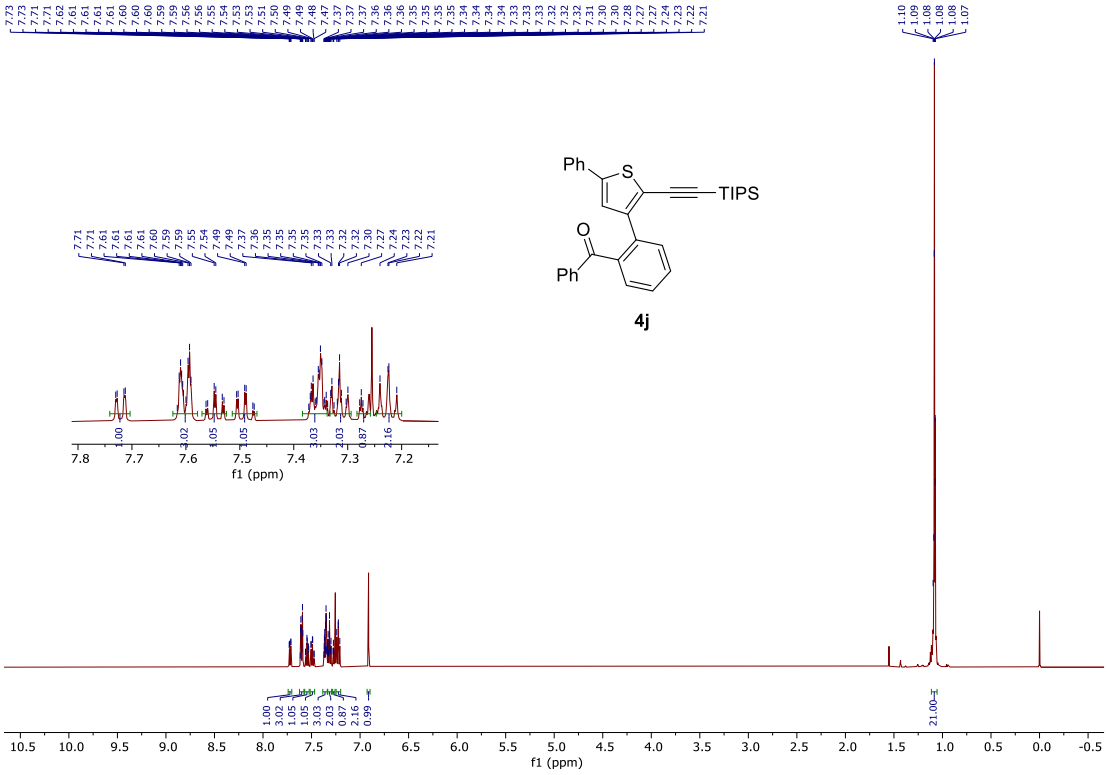

Figure 8.34. ^{13}C NMR of 4j

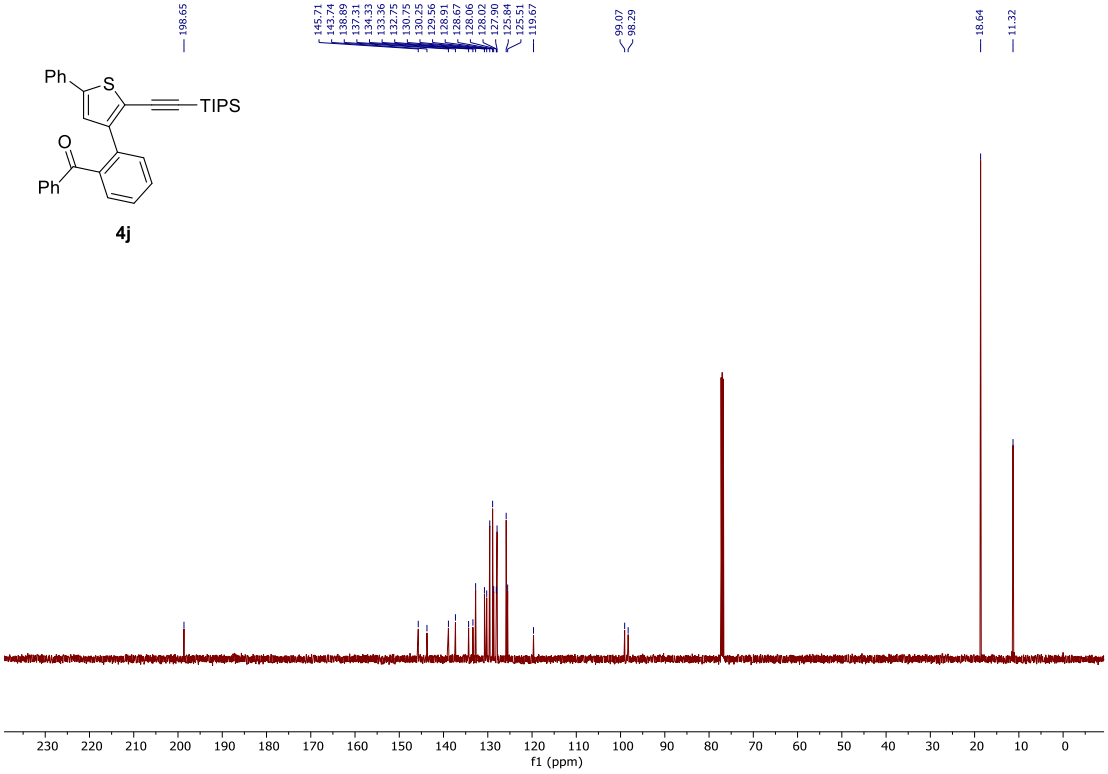

Figure 8.35. ^{1}H NMR of 4k

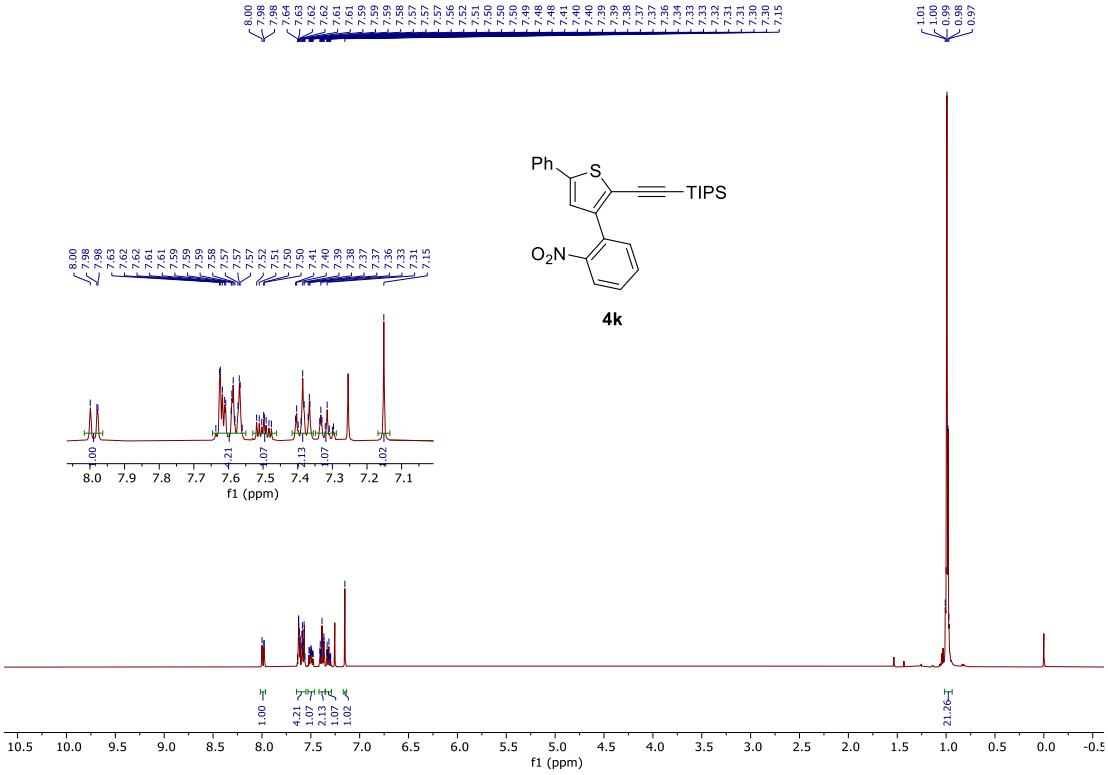

Figure 8.36. ^{13}C NMR of 4k

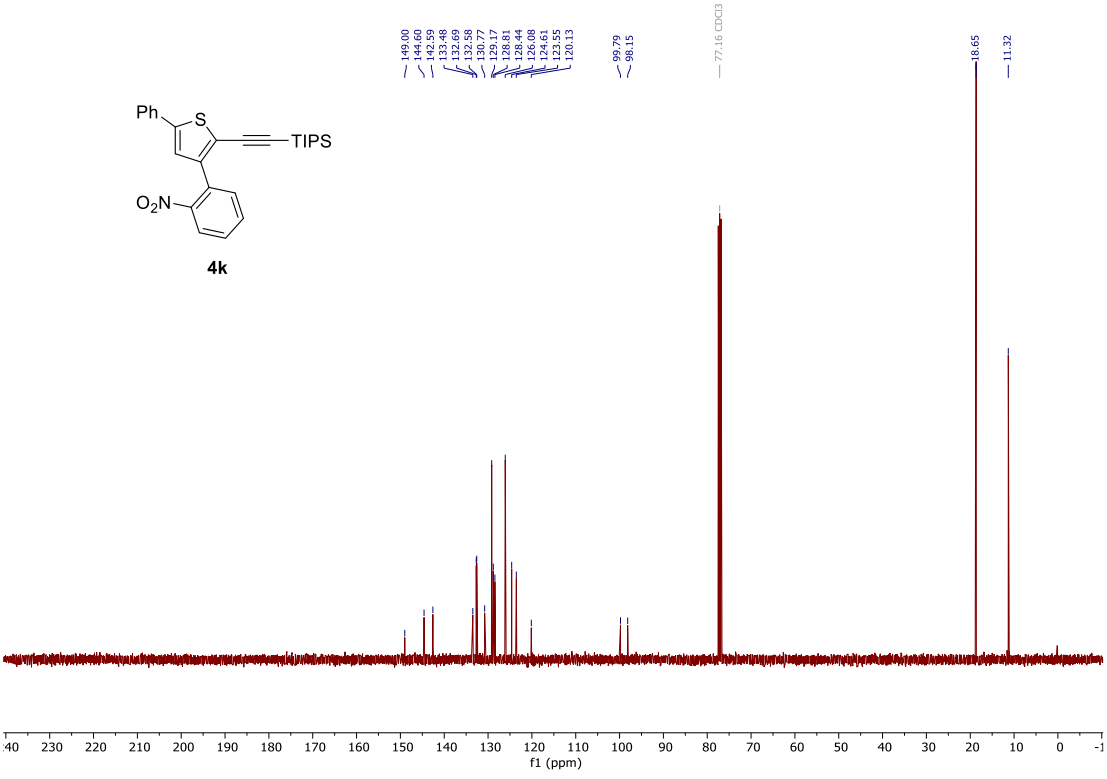

Figure 8.37. ^{1}H NMR of 4l

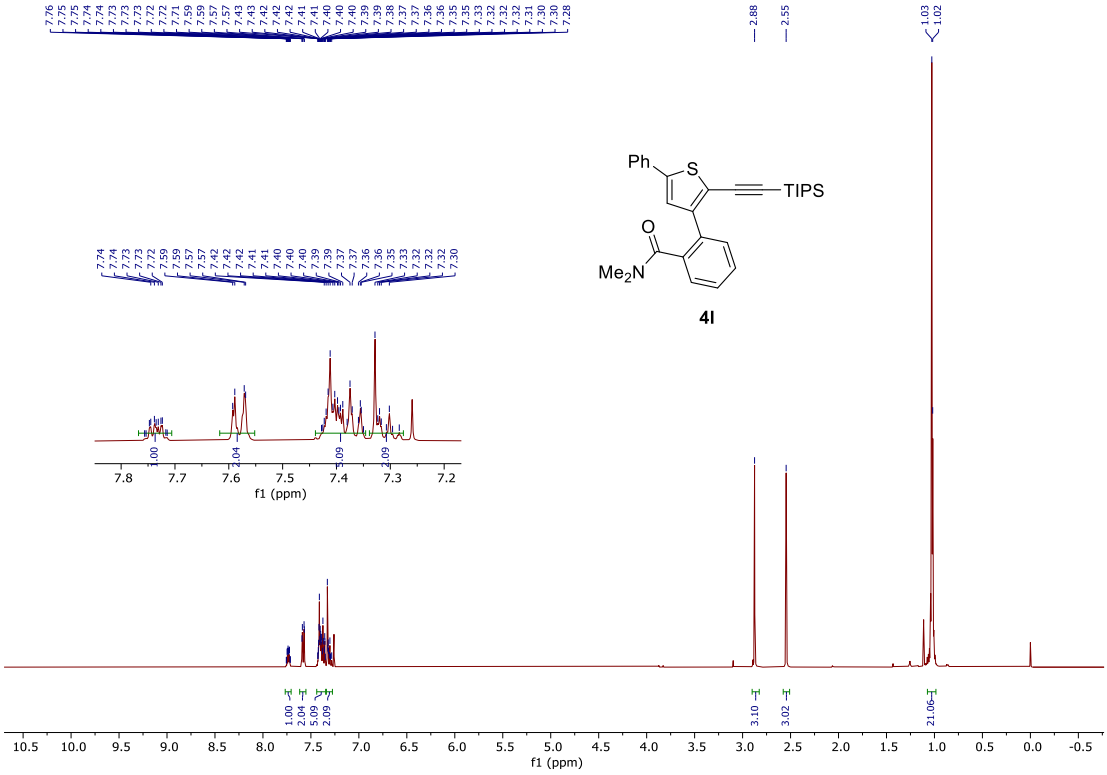

Figure 8.38. ^{13}C NMR of 4l

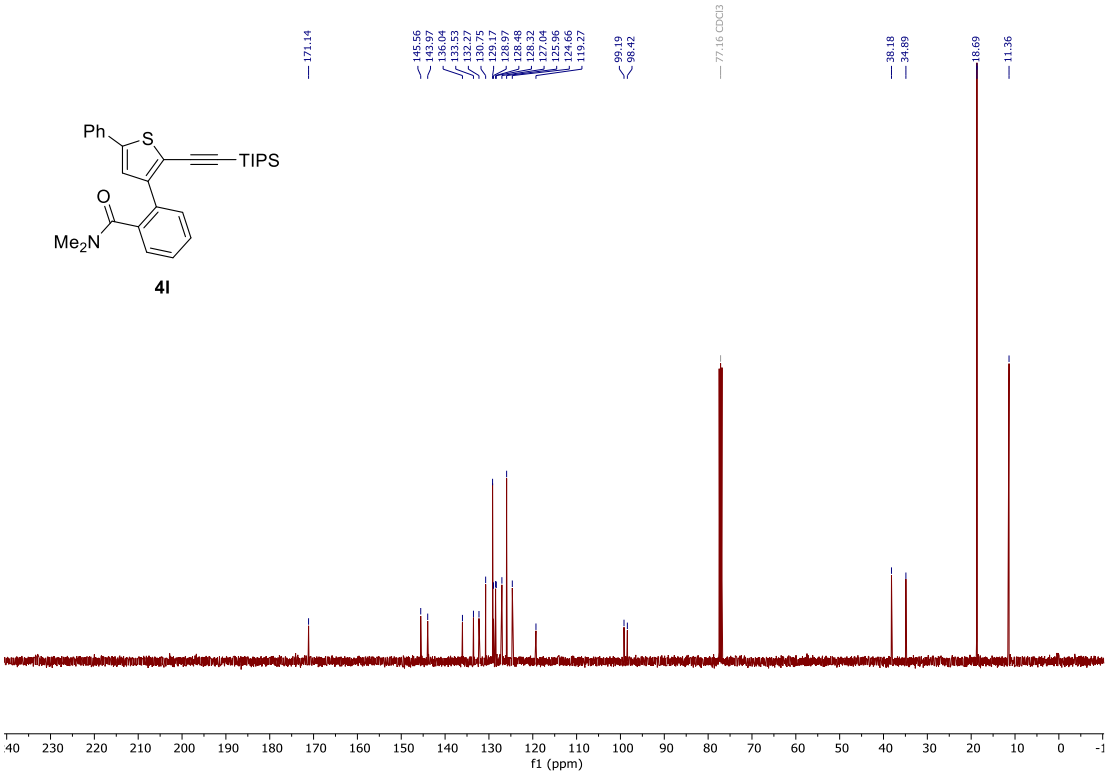

Figure 8.39. ^{1}H NMR of 4m

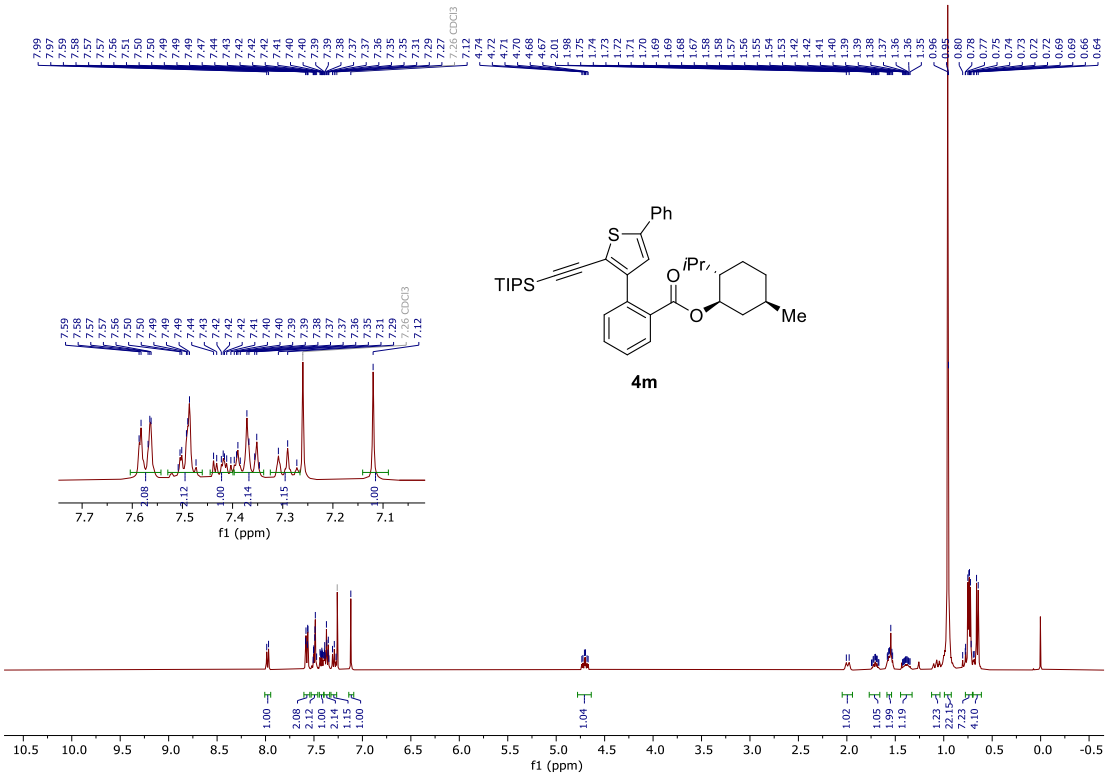

Figure 8.40. ^{13}C NMR of 4m

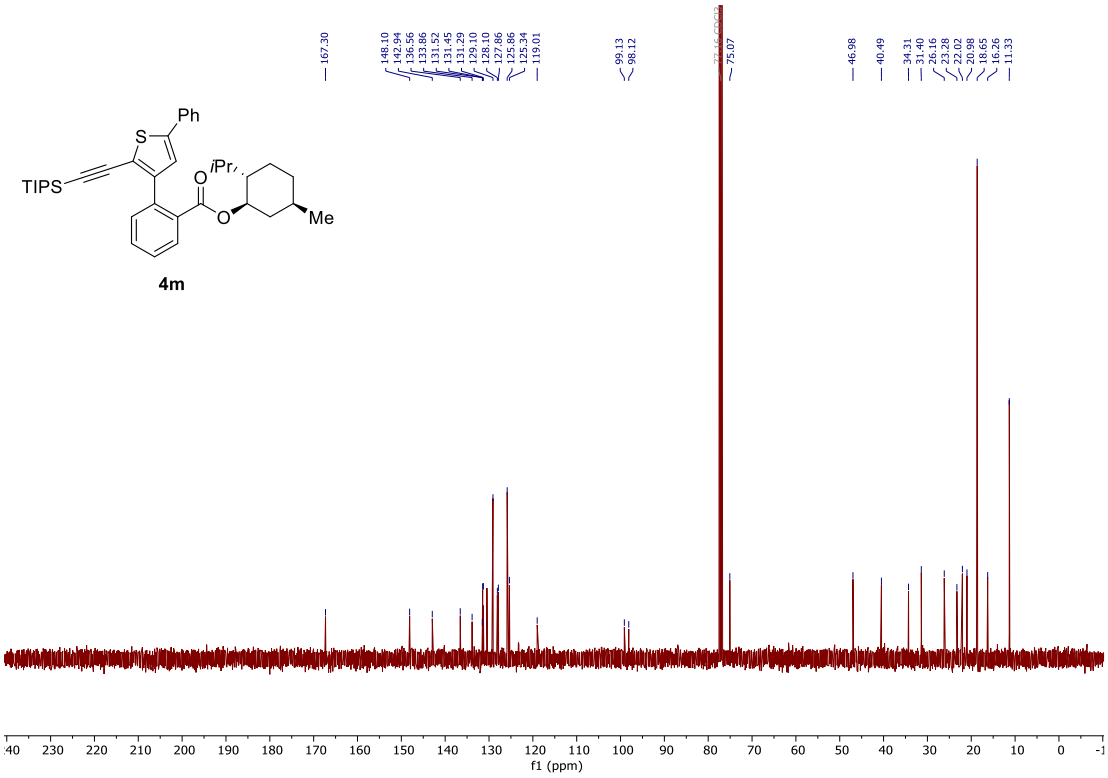

Figure 8.41. ^{1}H NMR of 5a

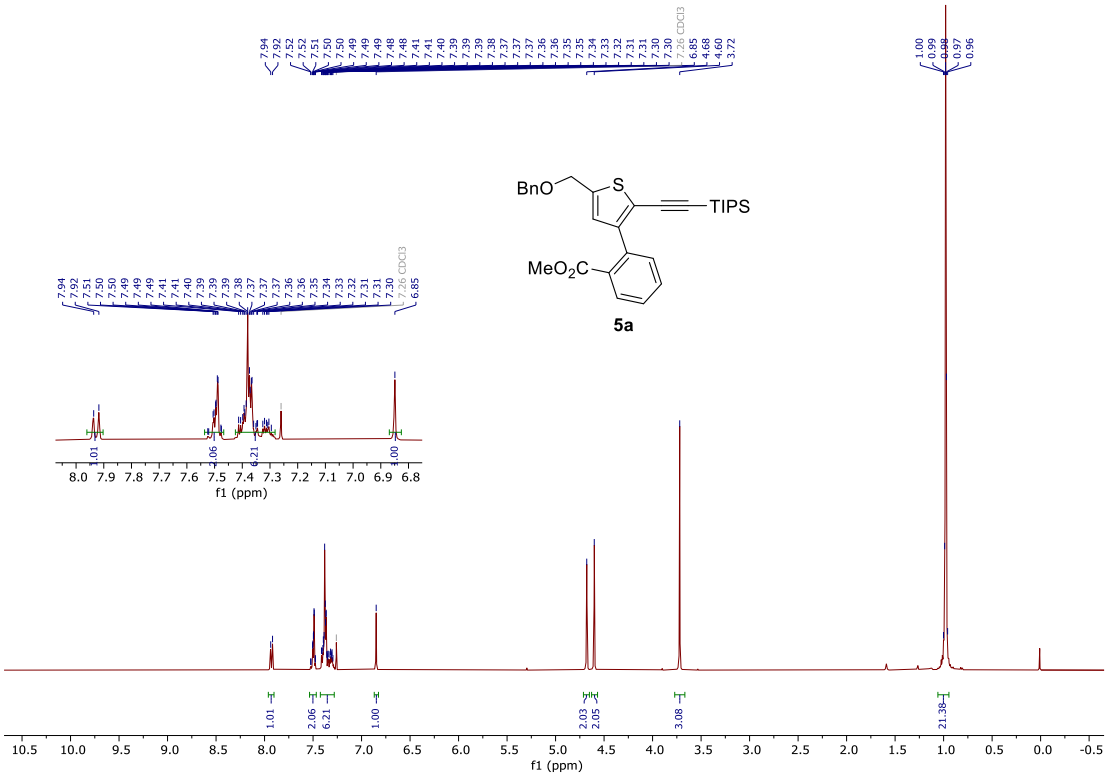

Figure 8.42. ^{13}C NMR of 5a

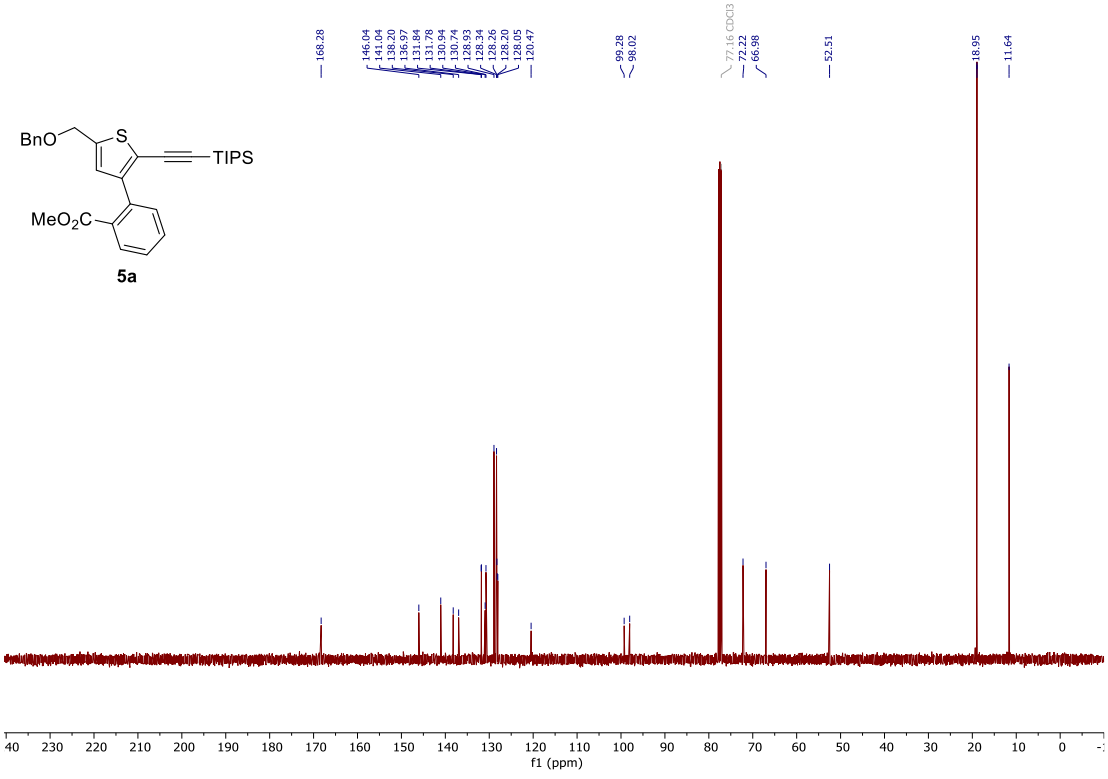

Figure 8.43. ^{1}H NMR of 5b

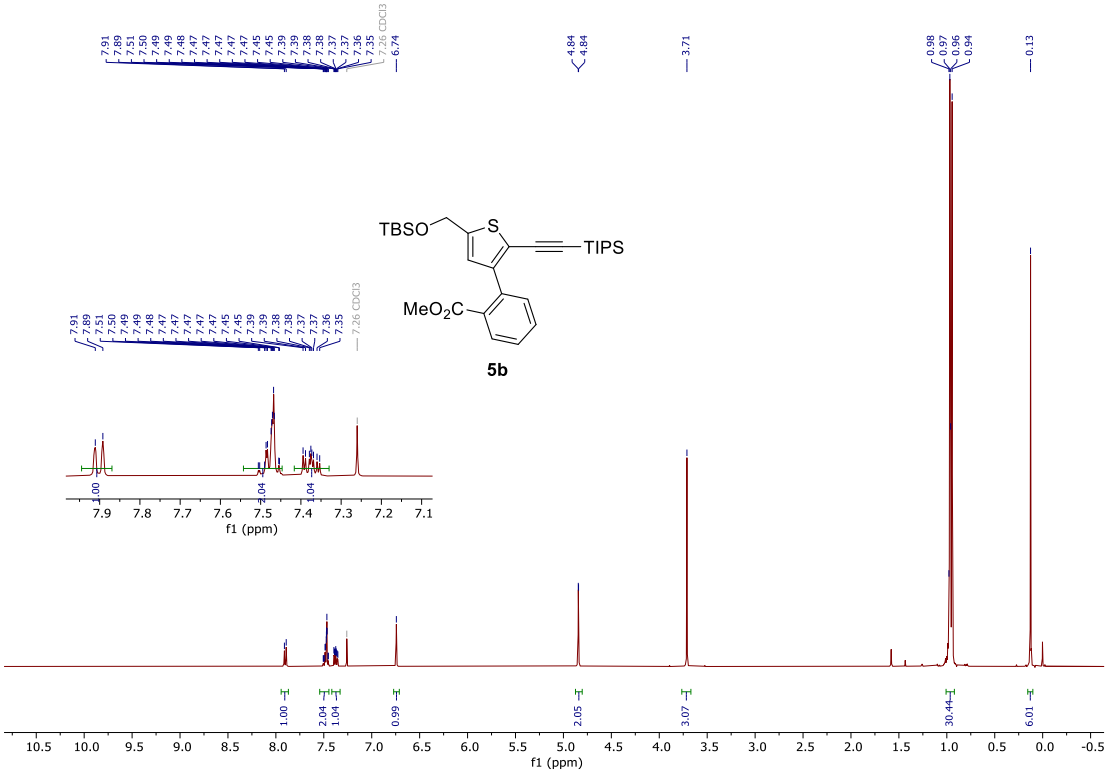

Figure 8.44. ^{13}C NMR of 5b

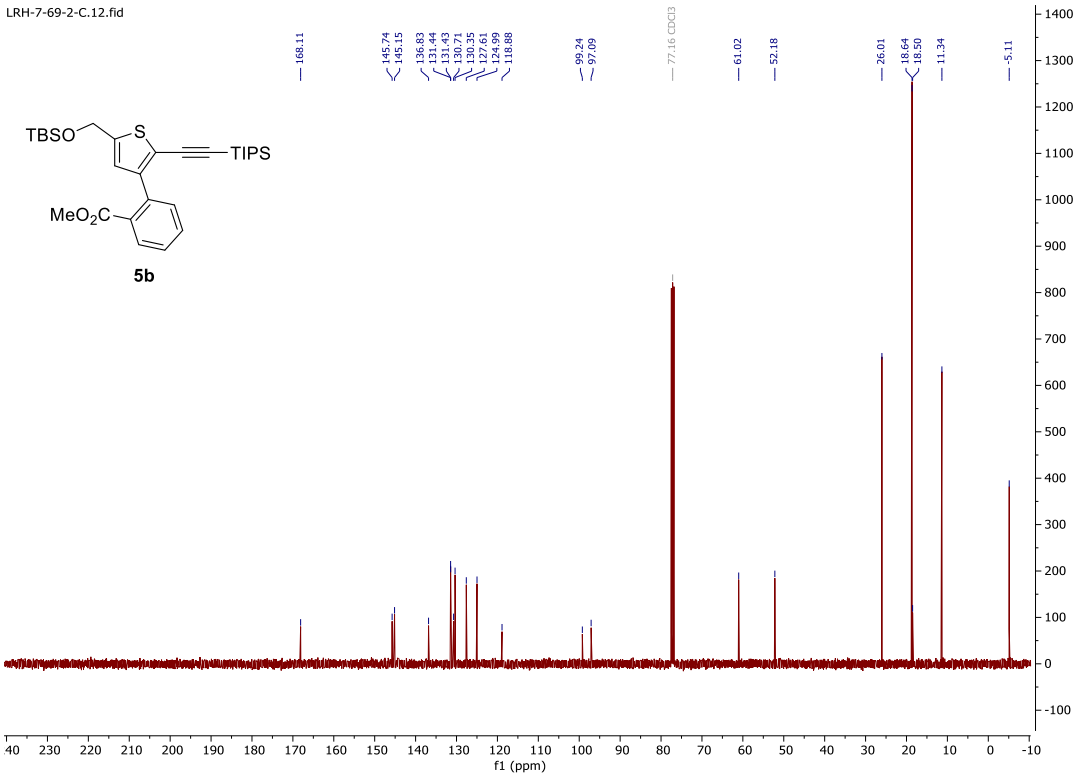

Figure 8.45. ^{1}H NMR of 5c

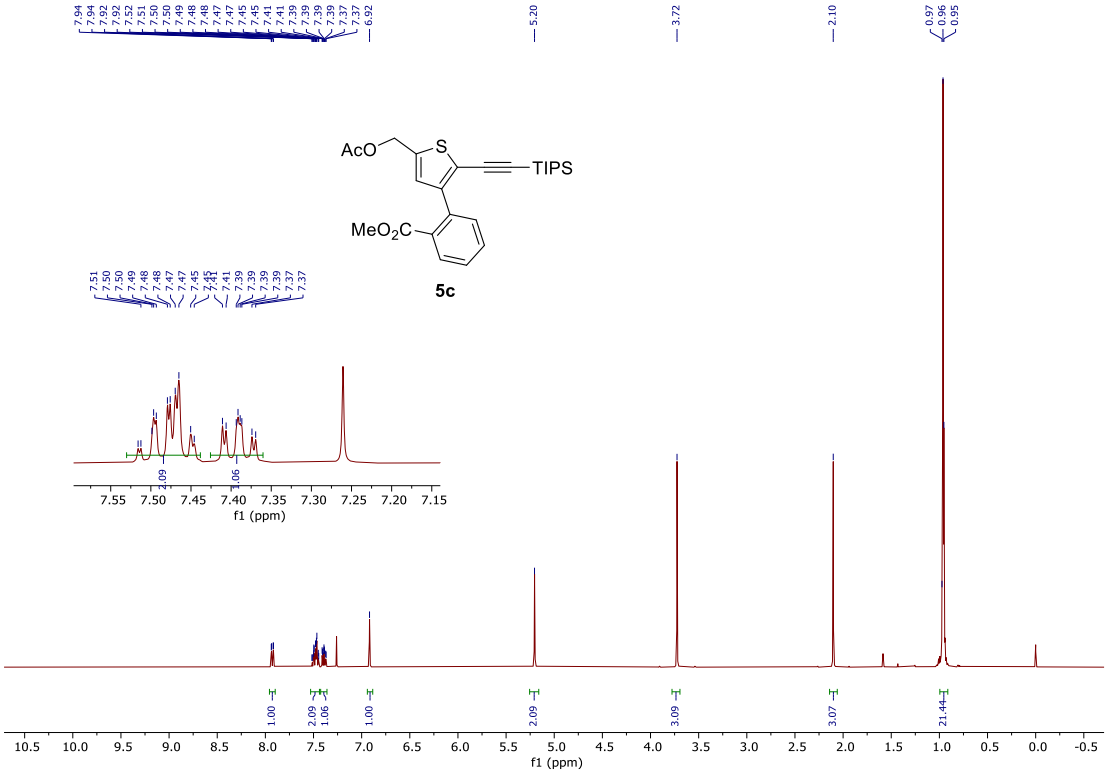

Figure 8.46. ^{13}C NMR of 5c

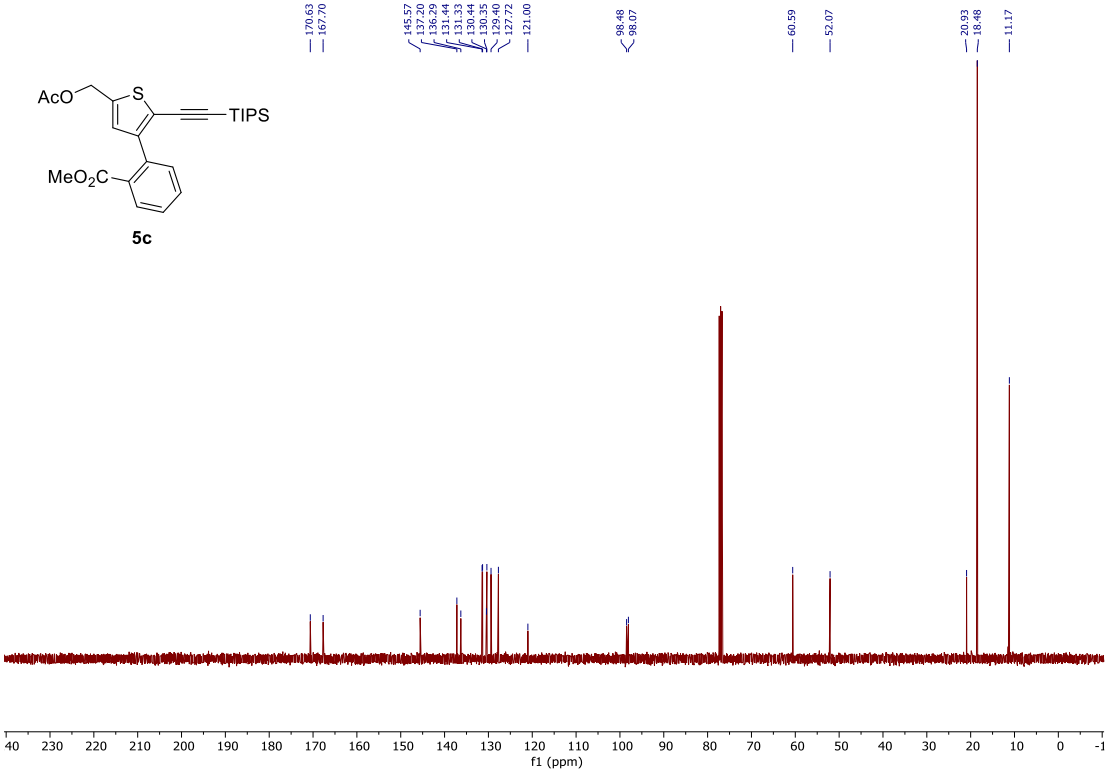

Figure 8.47. ^{1}H NMR of 5d

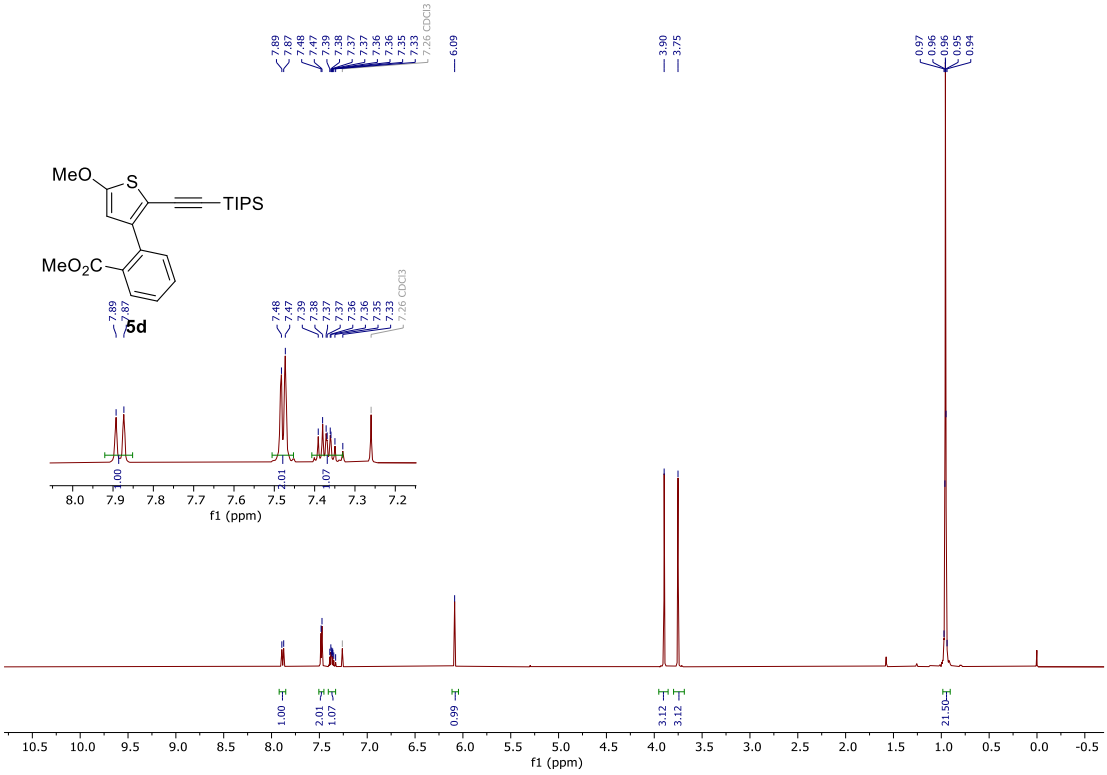

Figure 8.48. ^{13}C NMR of 5d

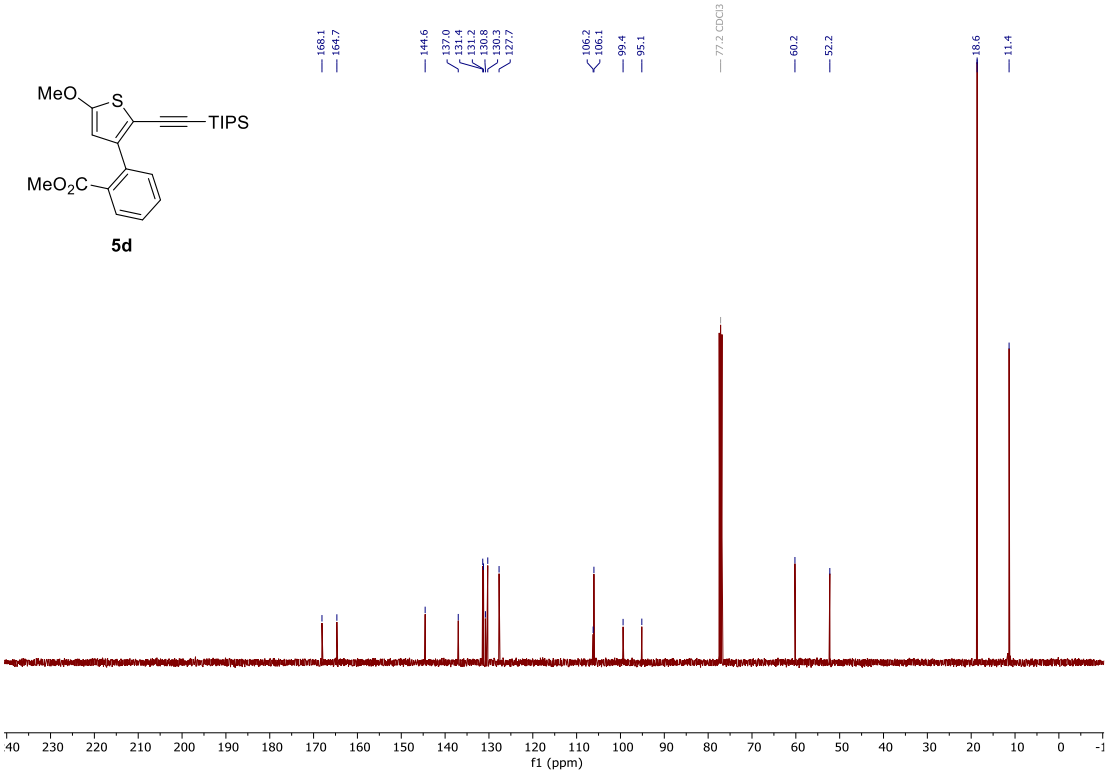

Figure 8.49. ^{1}H NMR of 5e

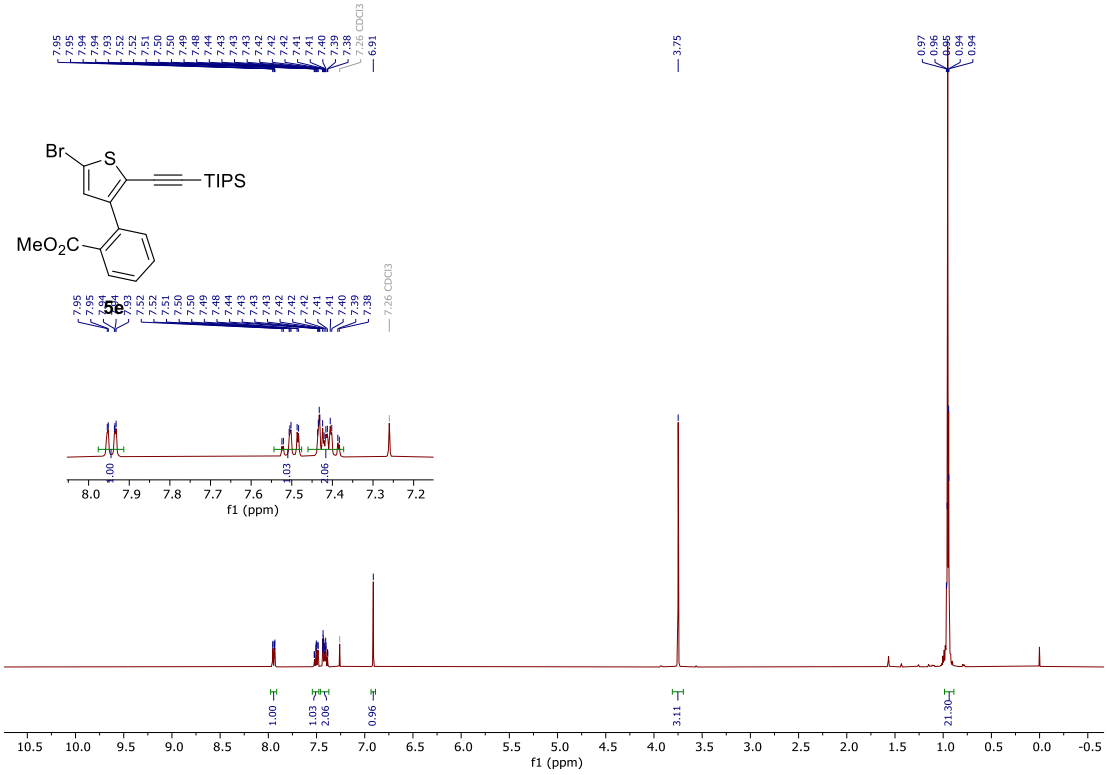

Figure 8.50. ^{13}C NMR of 5e

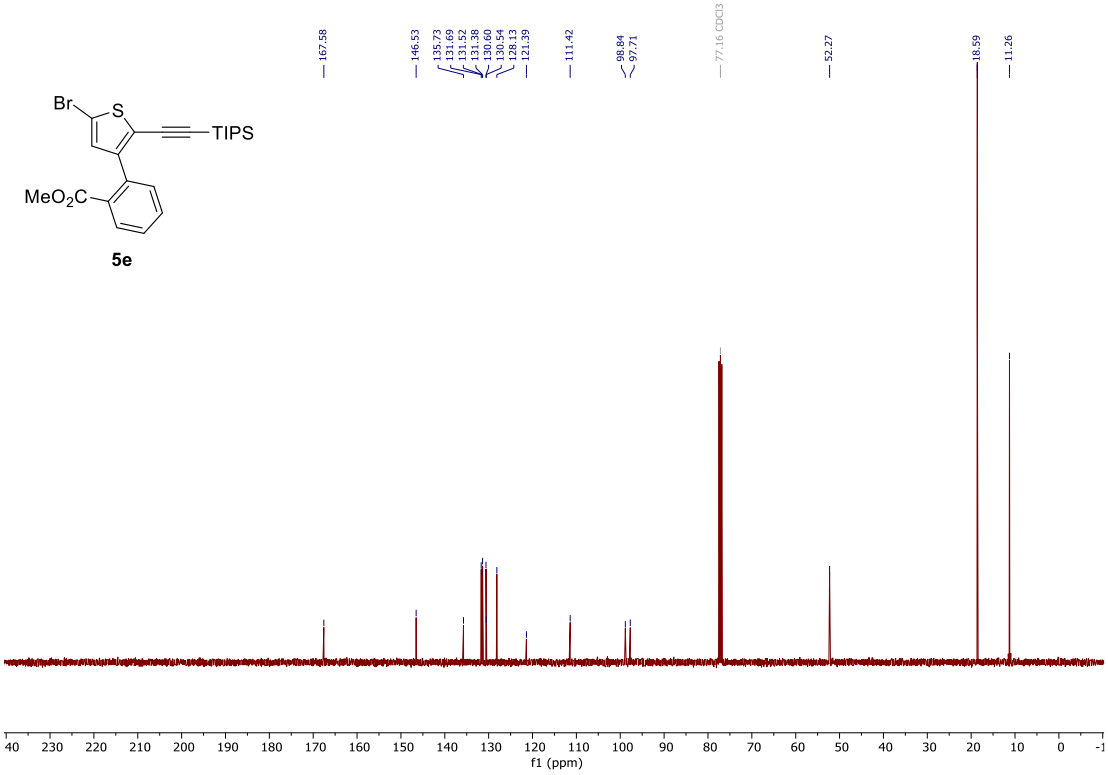

Figure 8.51. ^{1}H NMR of 5f

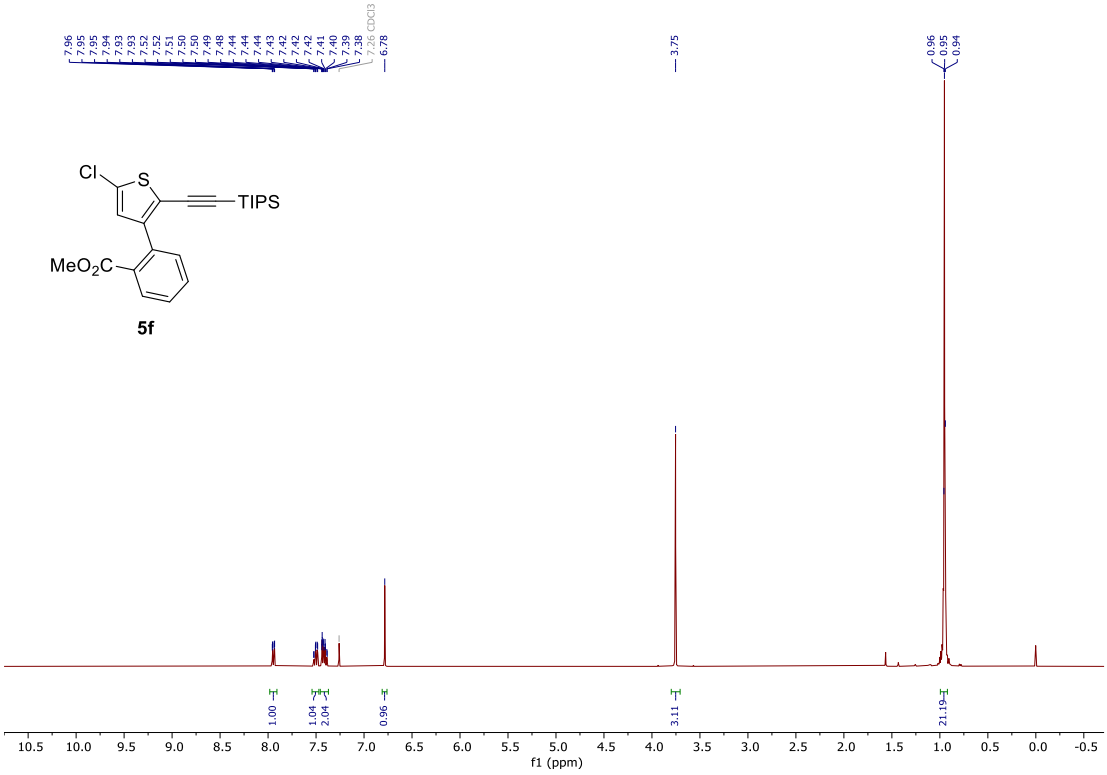

Figure 8.52. ^{13}C NMR of 5f

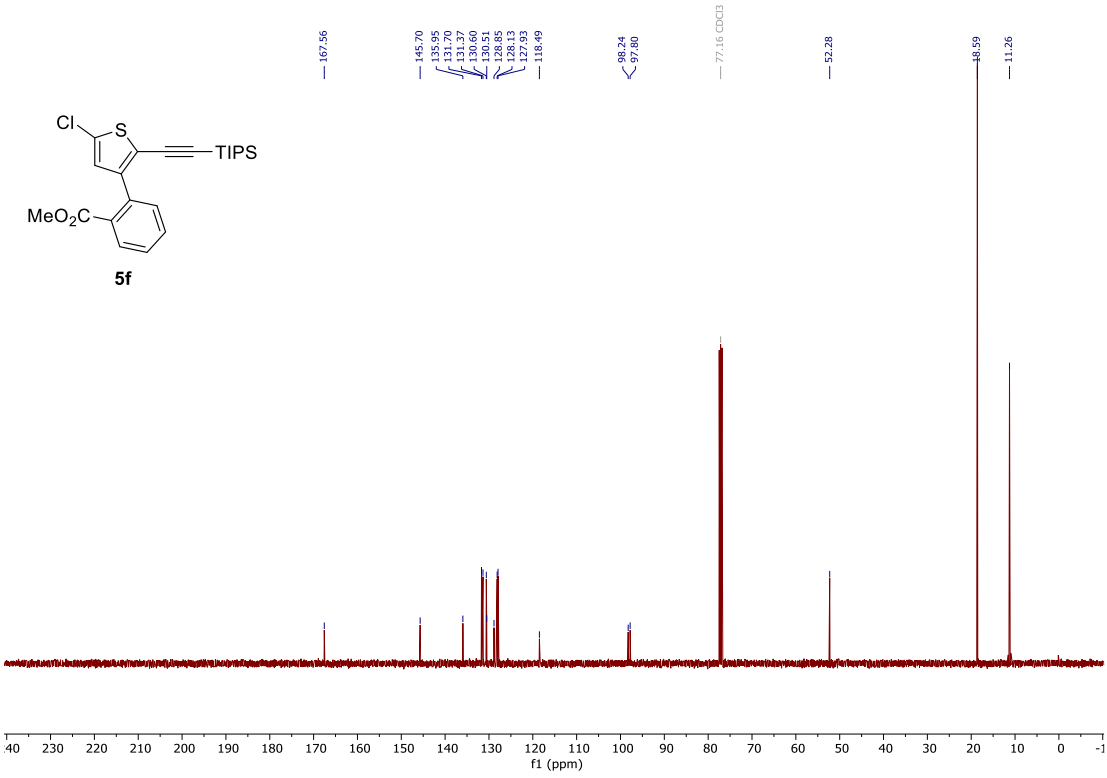

Figure 8.53. ^{1}H NMR of 5g

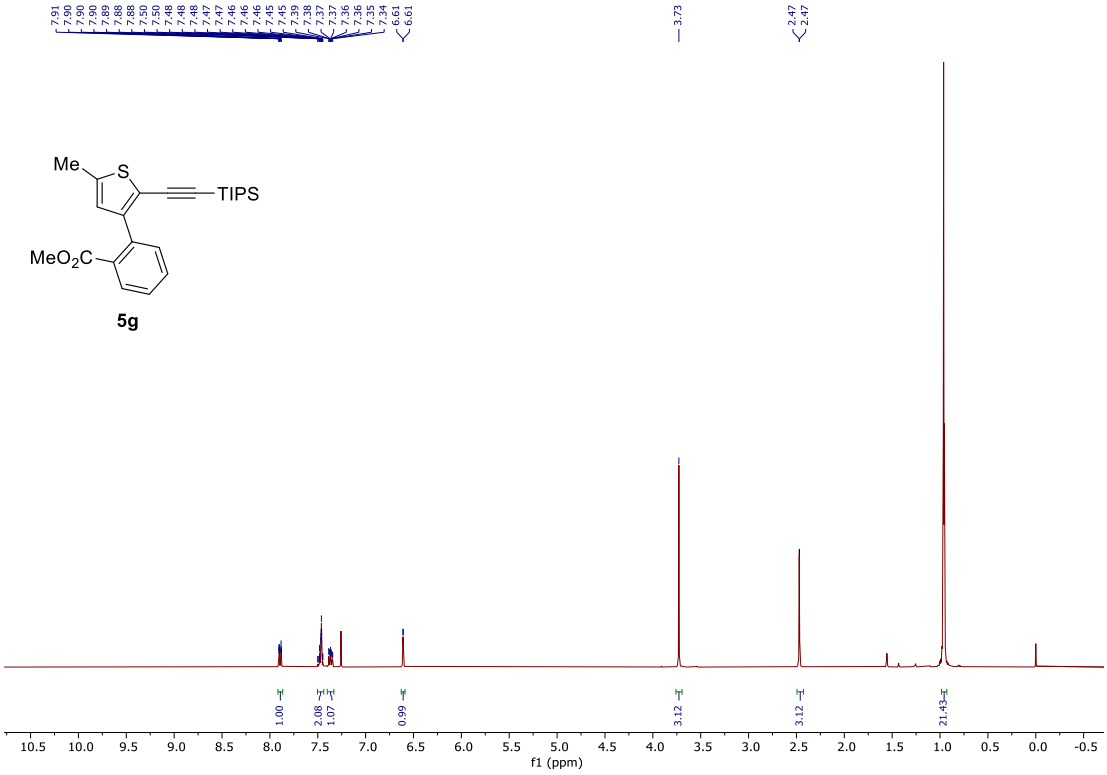

Figure 8.54. ^{13}C NMR of 5g

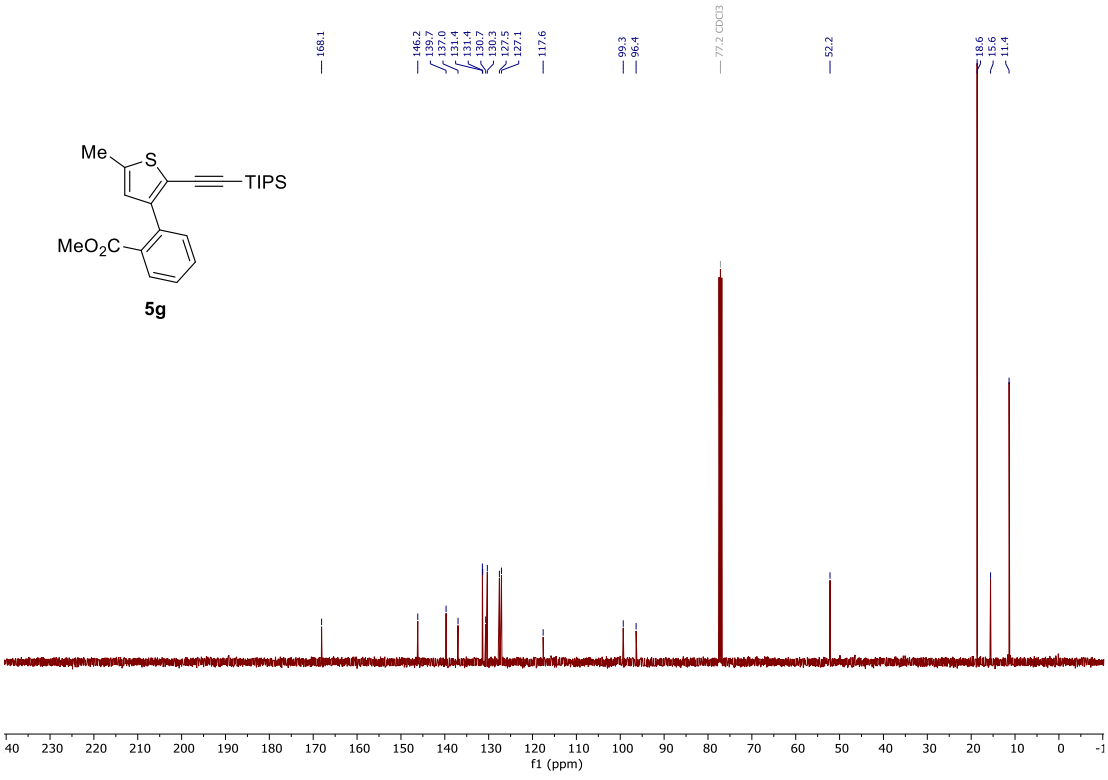

Figure 8.55. ^{1}H NMR of 5h

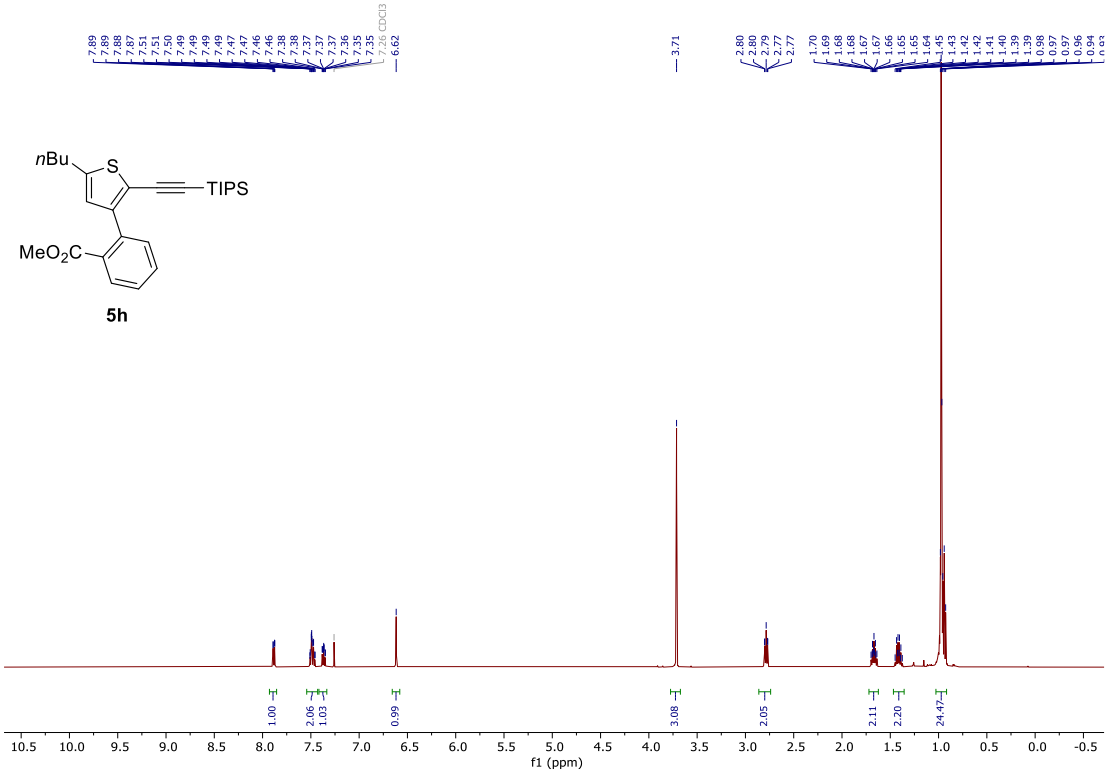

Figure 8.56. ^{13}C NMR of 5h

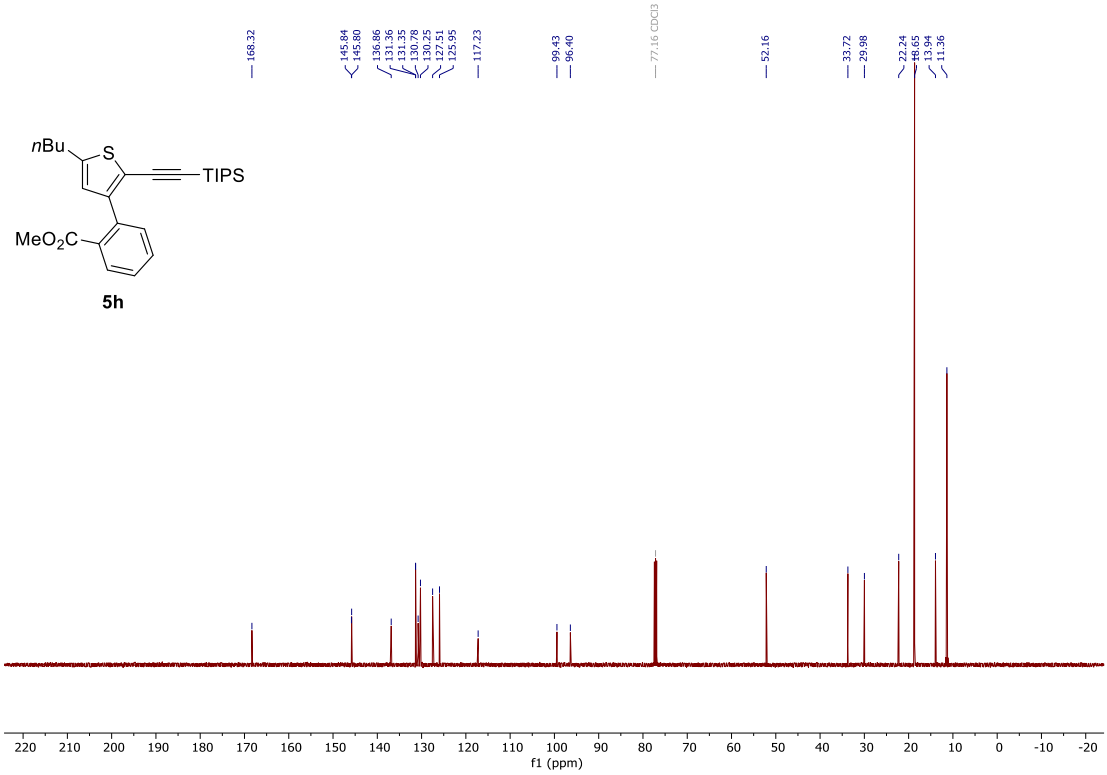

Figure 8.57. ^{1}H NMR of 5i

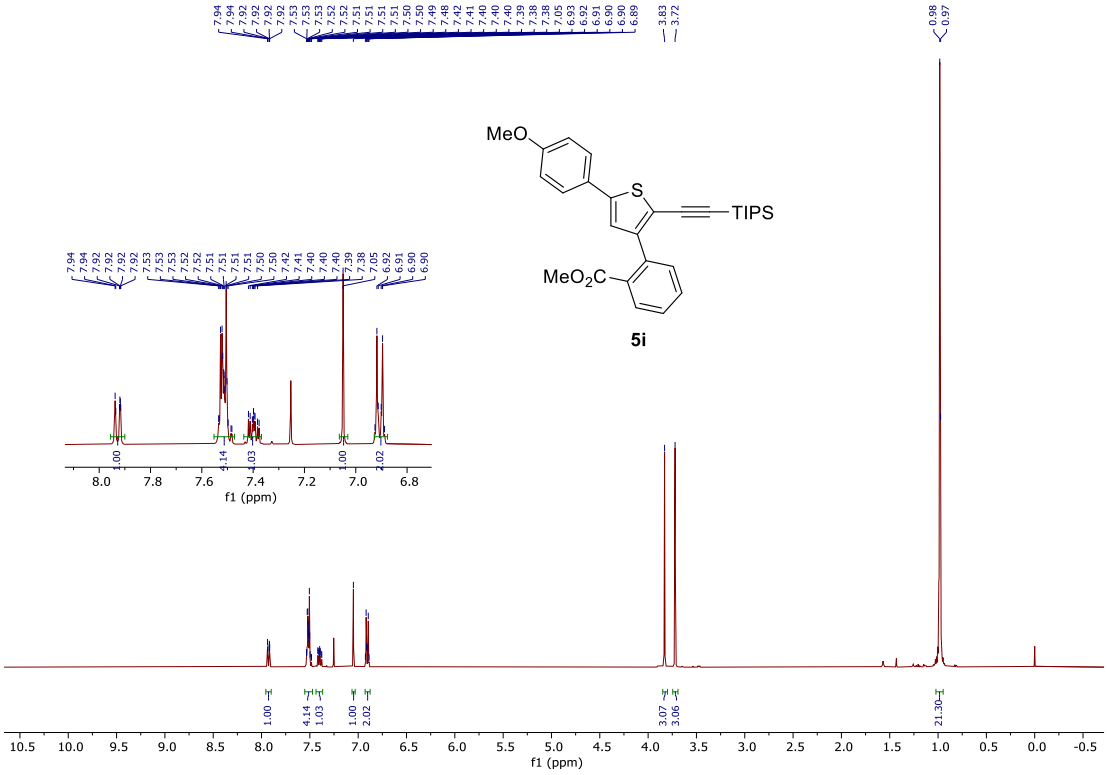

Figure 8.58. ^{13}C NMR of 5i

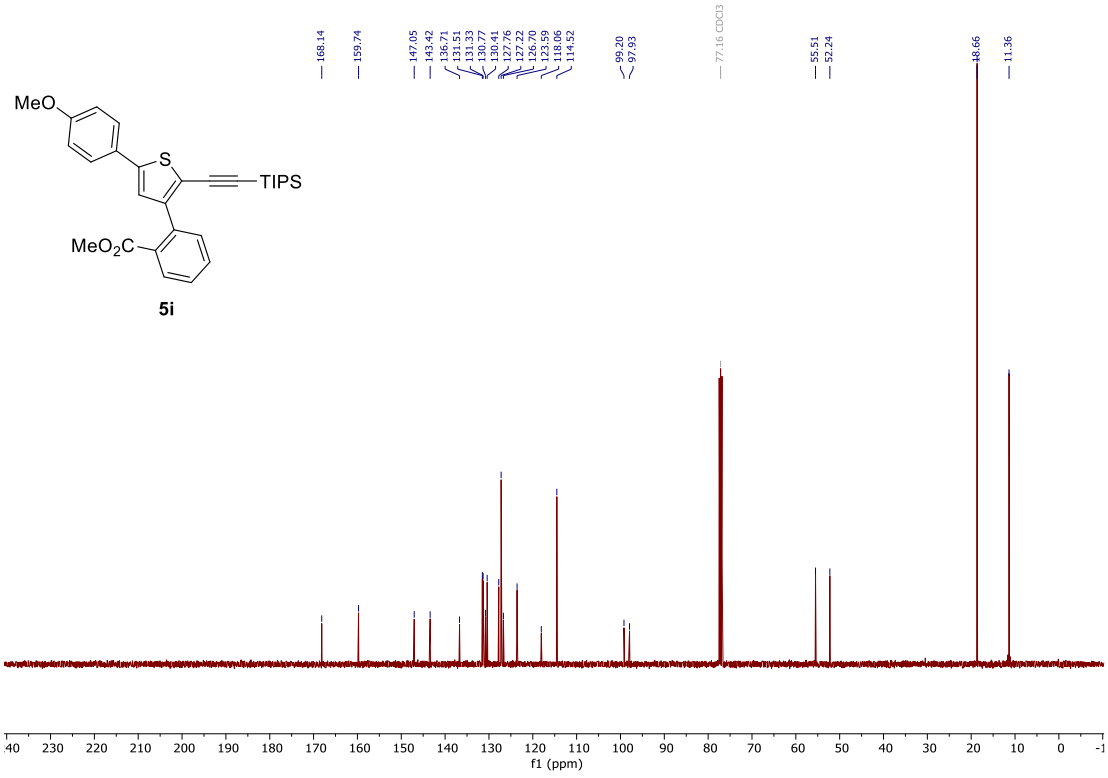

Figure 8.59. ^{1}H NMR of 5j

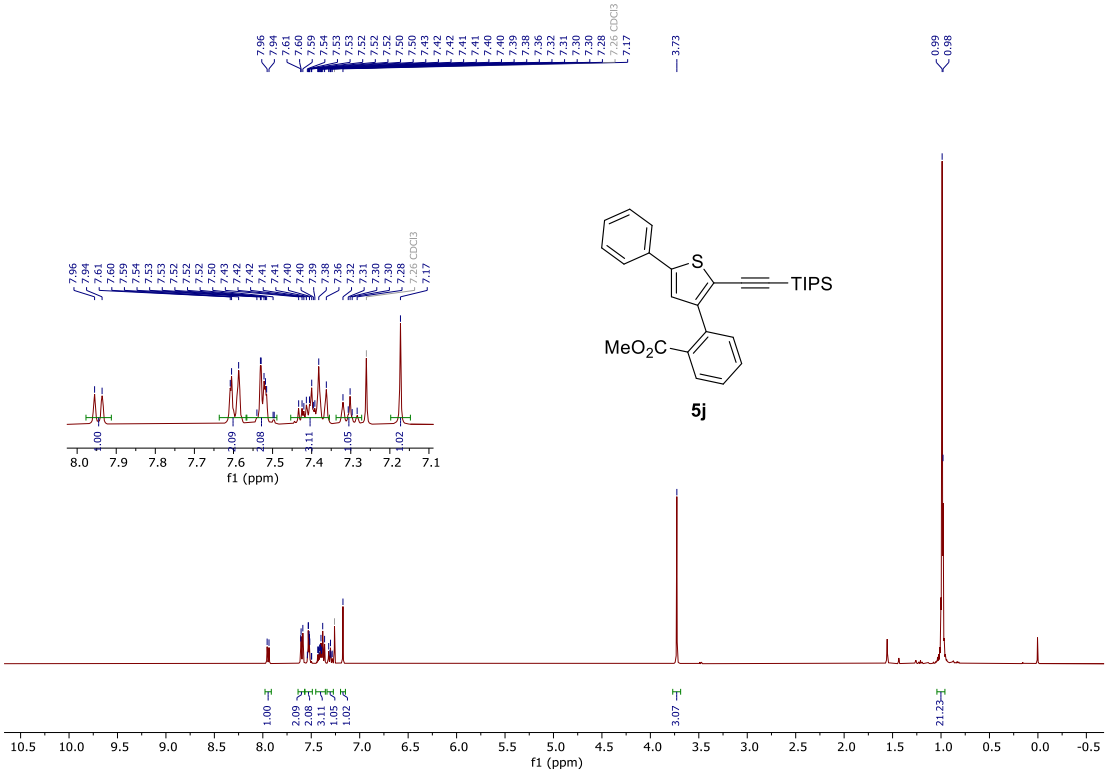

Figure 8.60. ^{13}C NMR of 5j

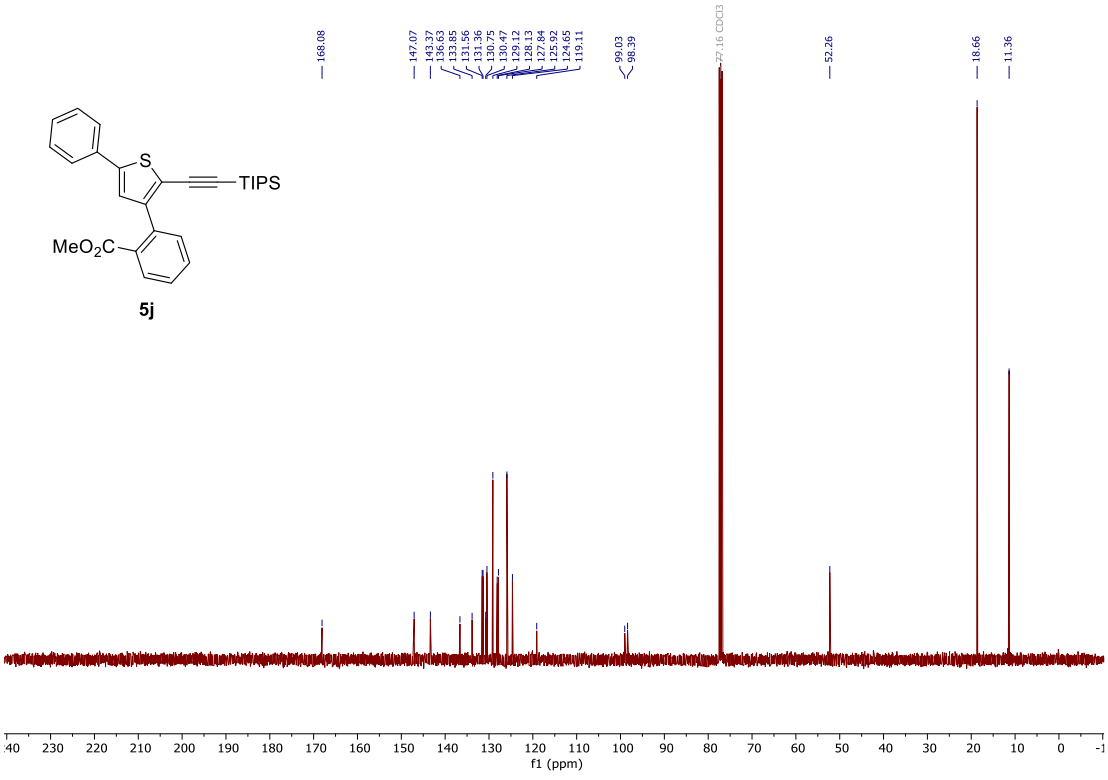

Figure 8.61. ^{1}H NMR of 5k

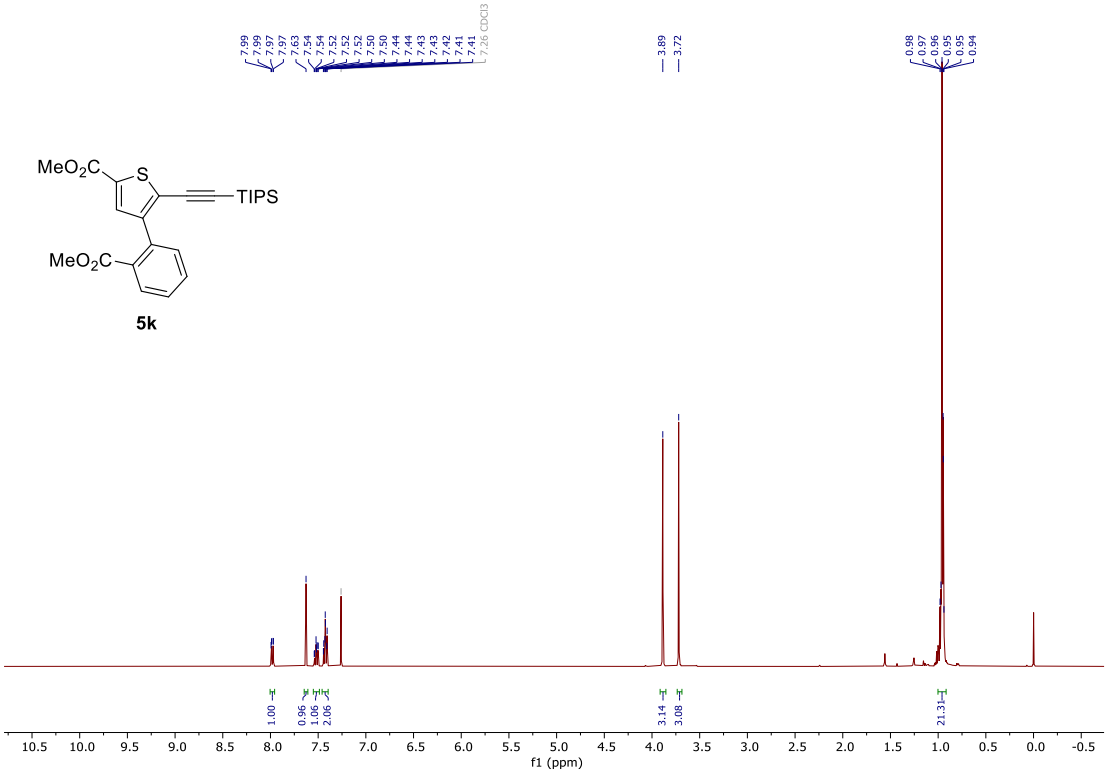

Figure 8.62. ^{13}C NMR of 5k

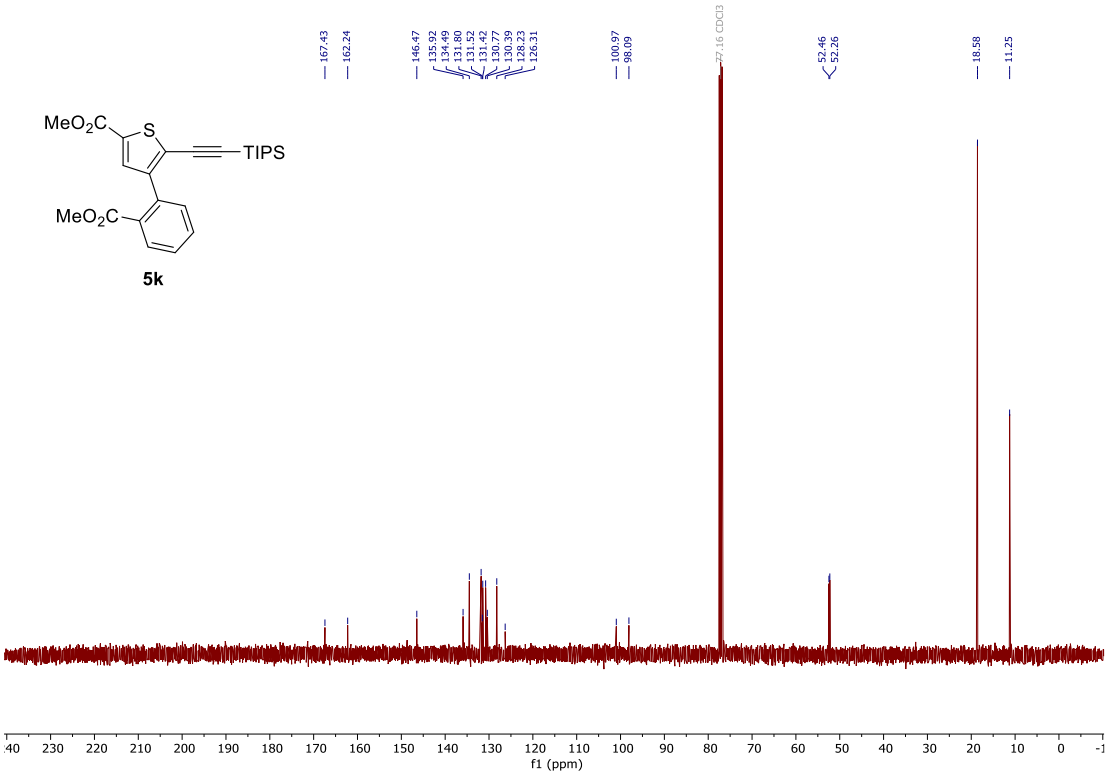

Figure 8.63. ^{1}H NMR of 5l

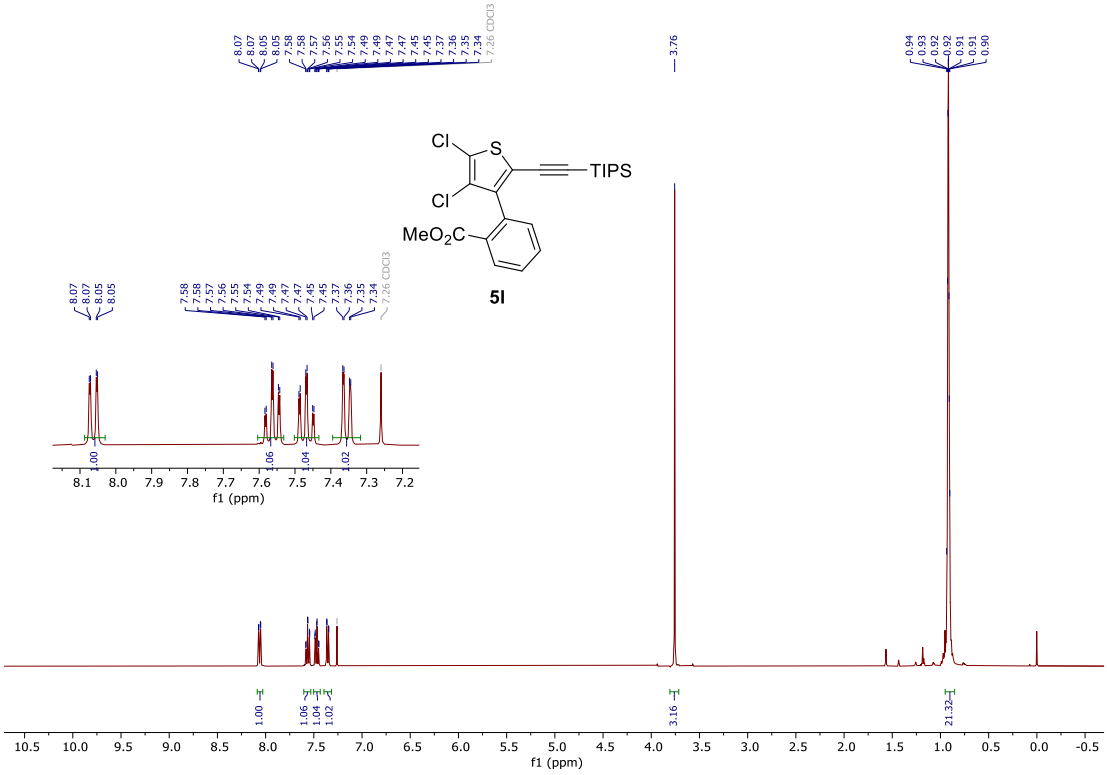

Figure 8.64. ^{13}C NMR of 5l

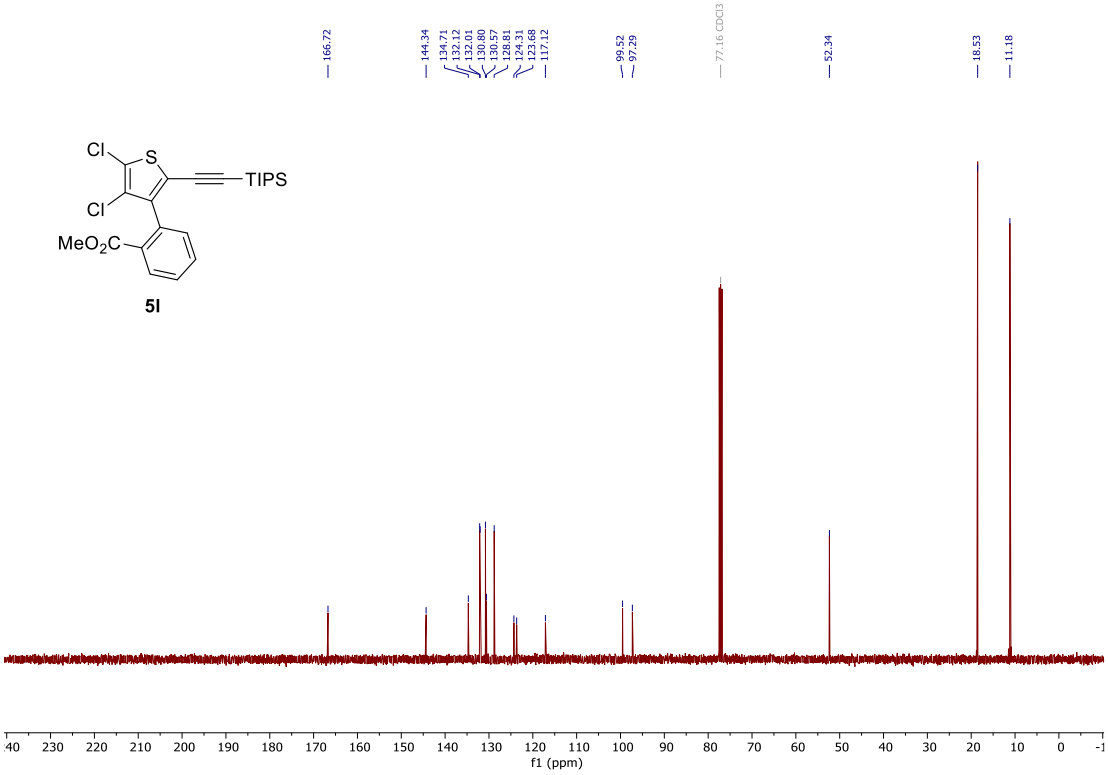

Figure 8.65. ^{1}H NMR of 5m

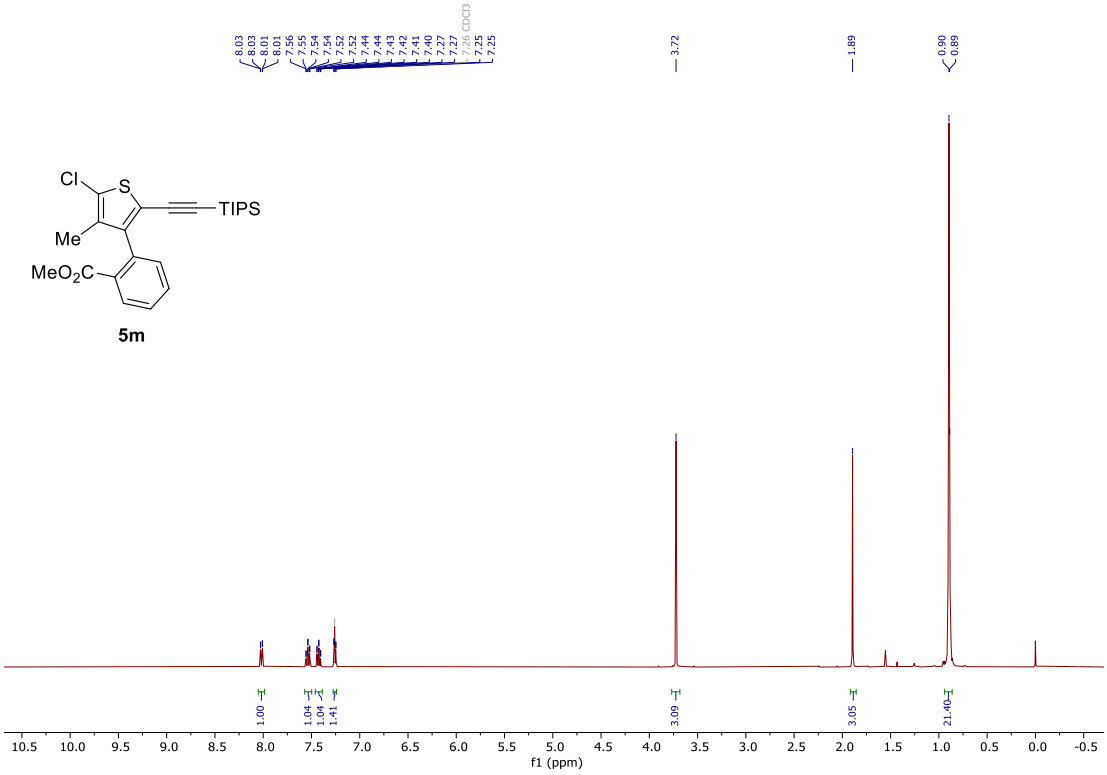

Figure 8.66. ^{13}C NMR of 5m

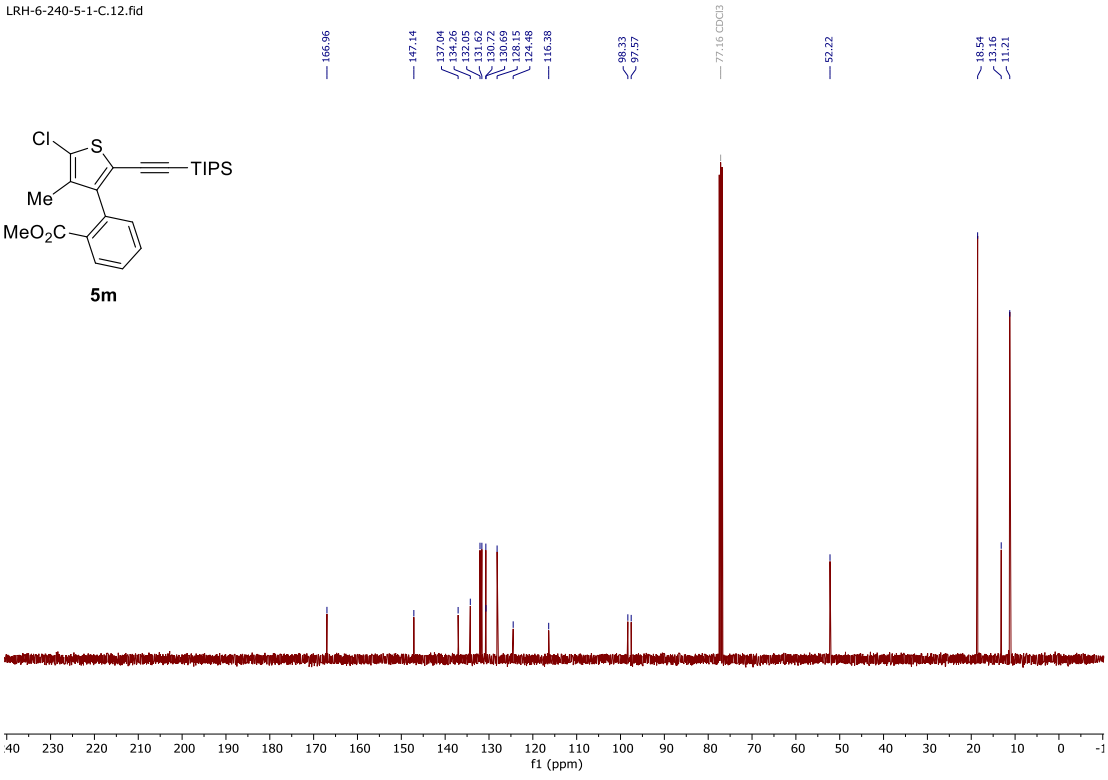

Figure 8.67. ^{1}H NMR of 5n

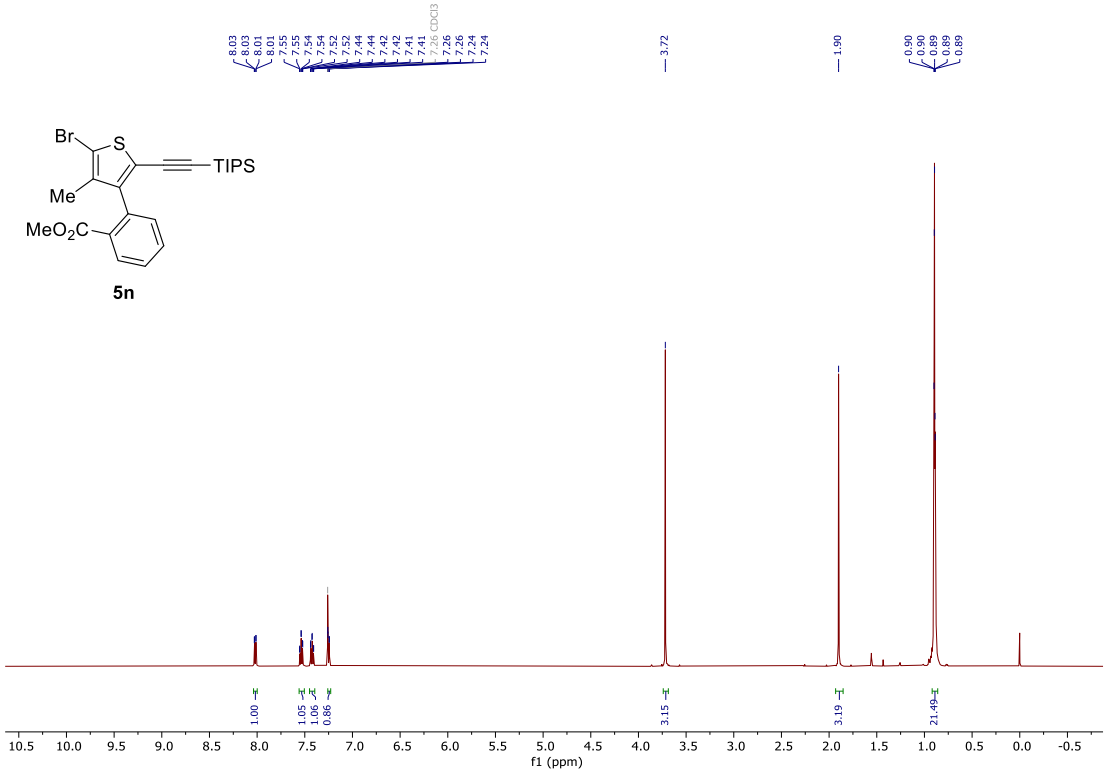

Figure 8.68. ^{13}C NMR of 5n

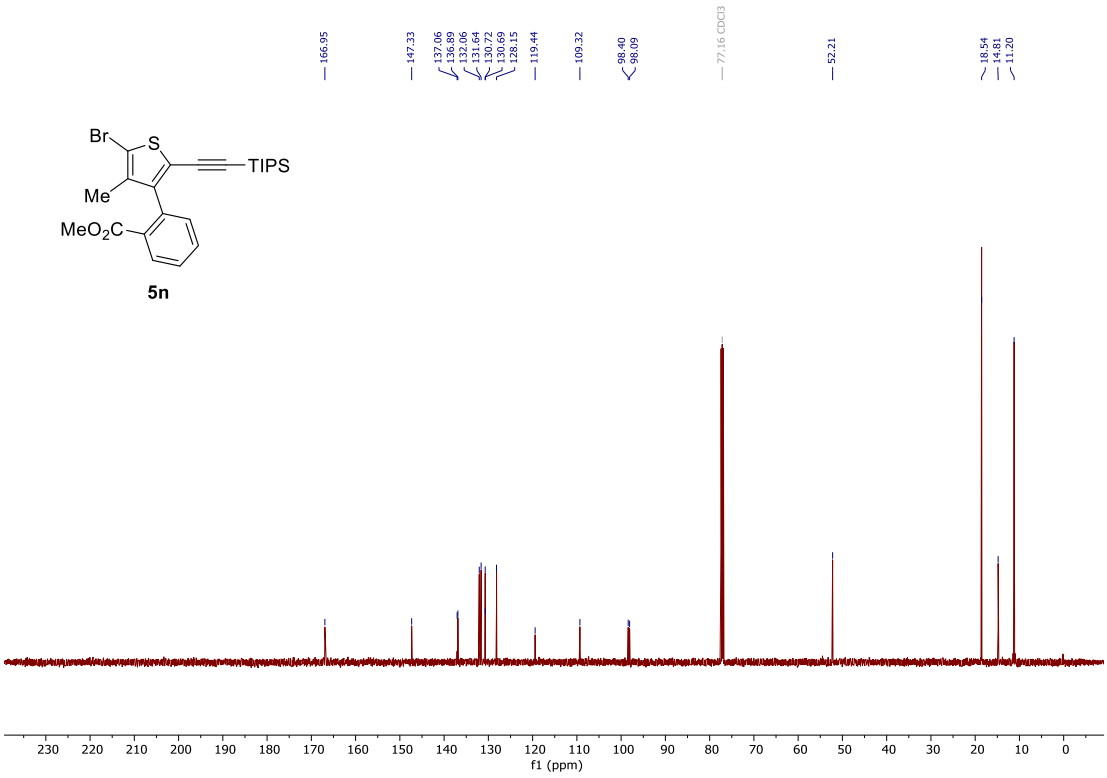

Figure 8.69. ^{1}H NMR of 5o

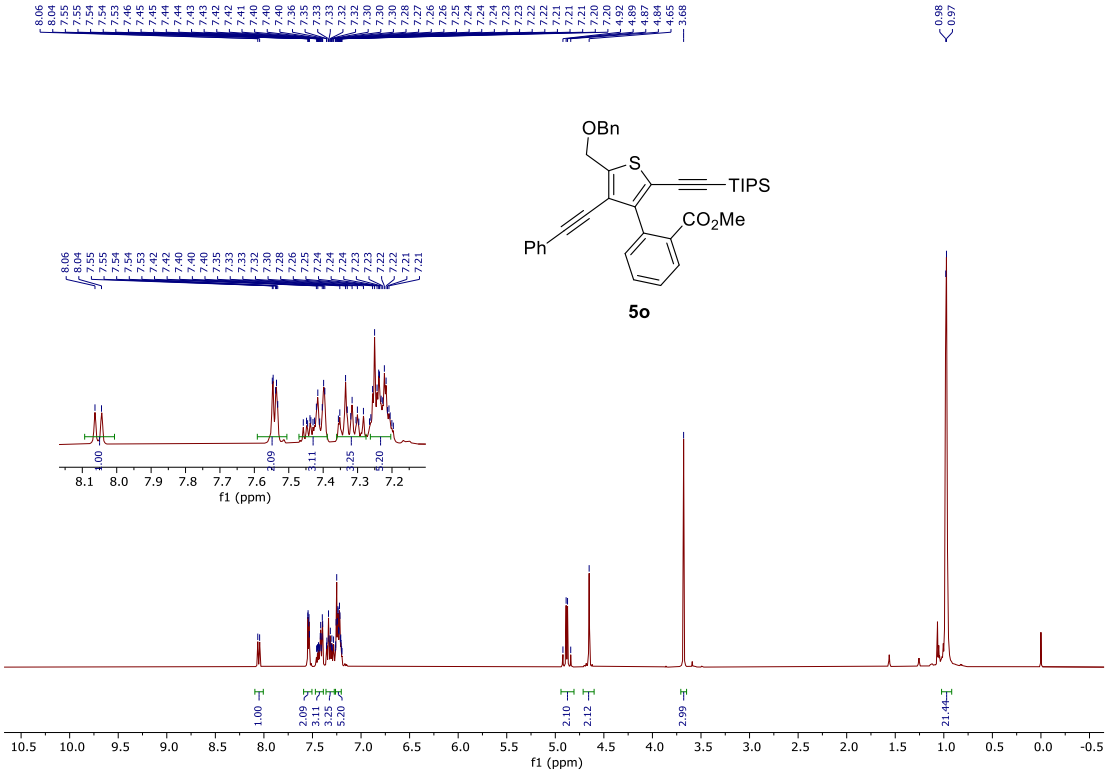

Figure 8.70. ^{13}C NMR of 5o

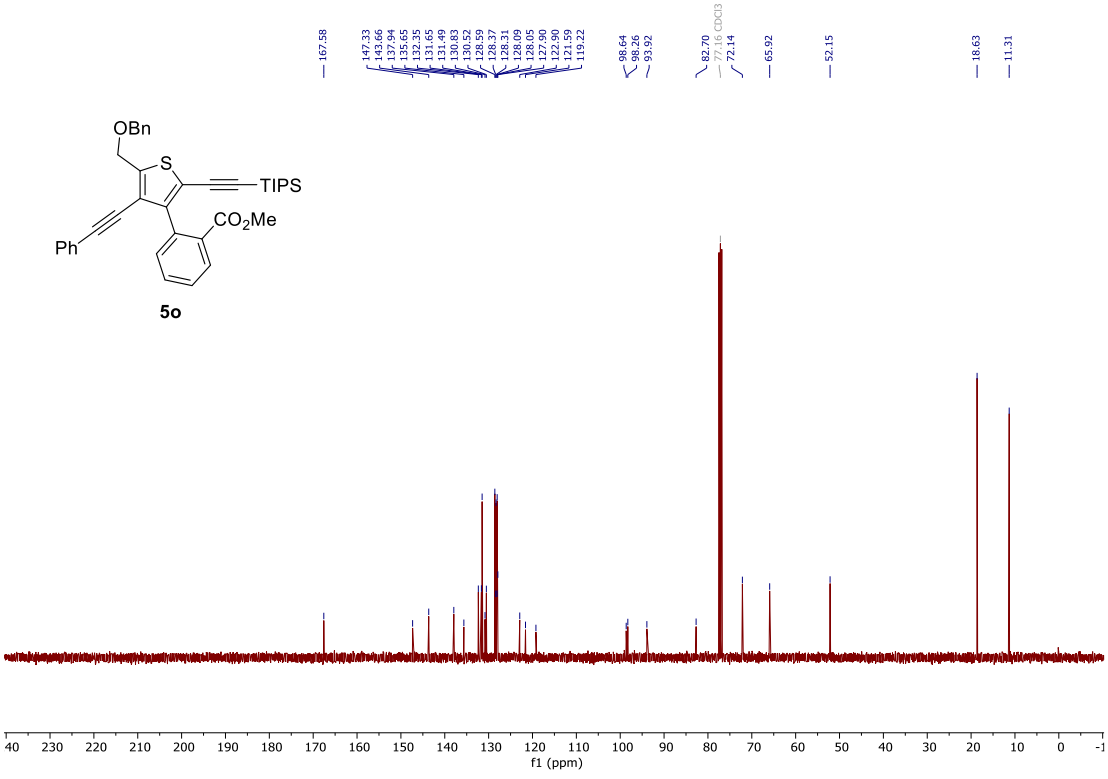

Figure 8.71. ^{1}H NMR of 5p

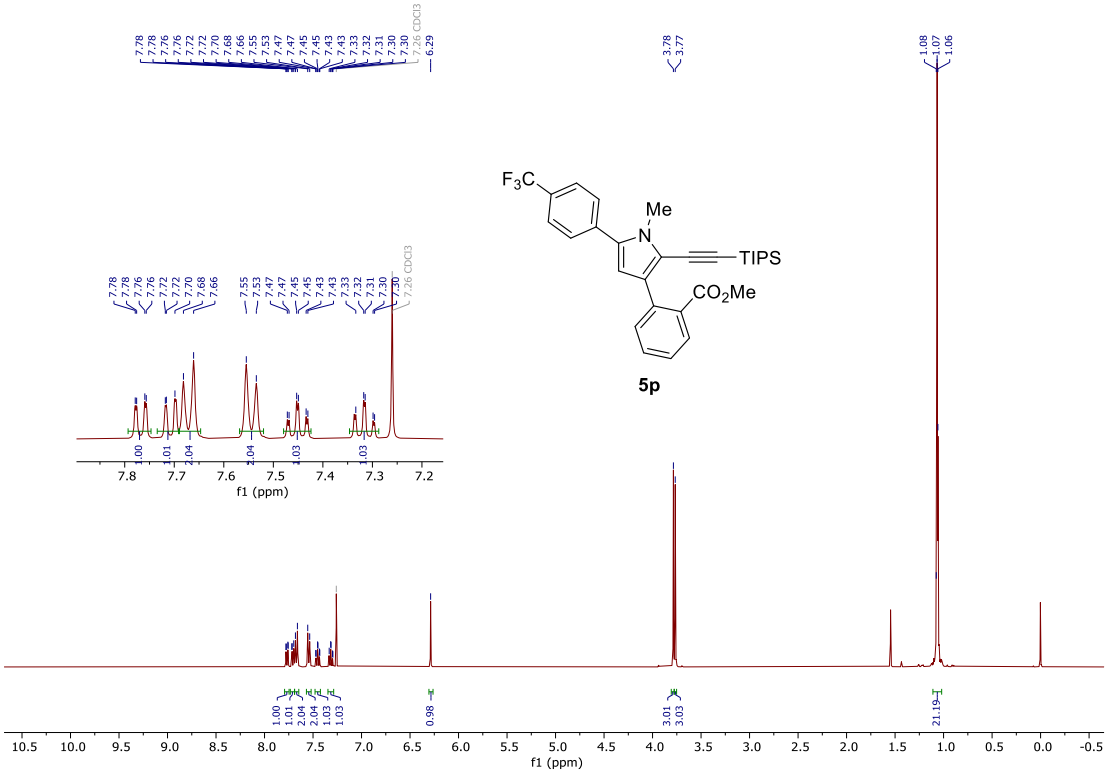

Figure 8.72. ^{13}C NMR of 5p

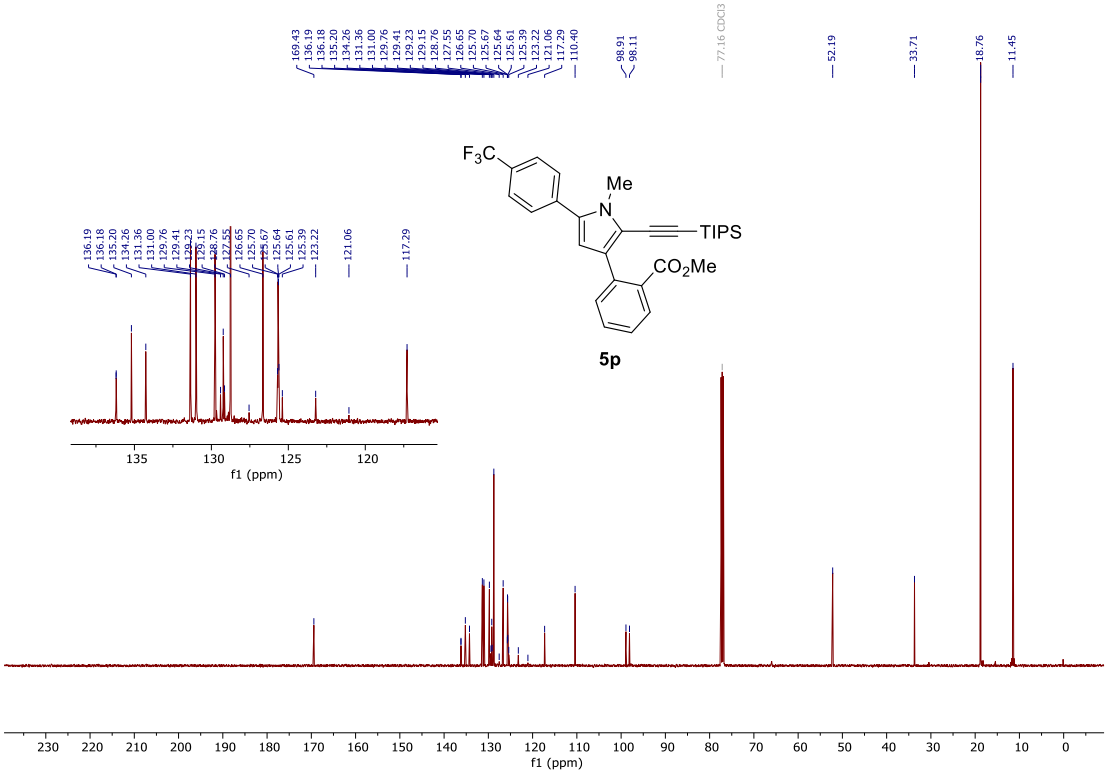

Figure 8.73. ^{1}H NMR of 5p

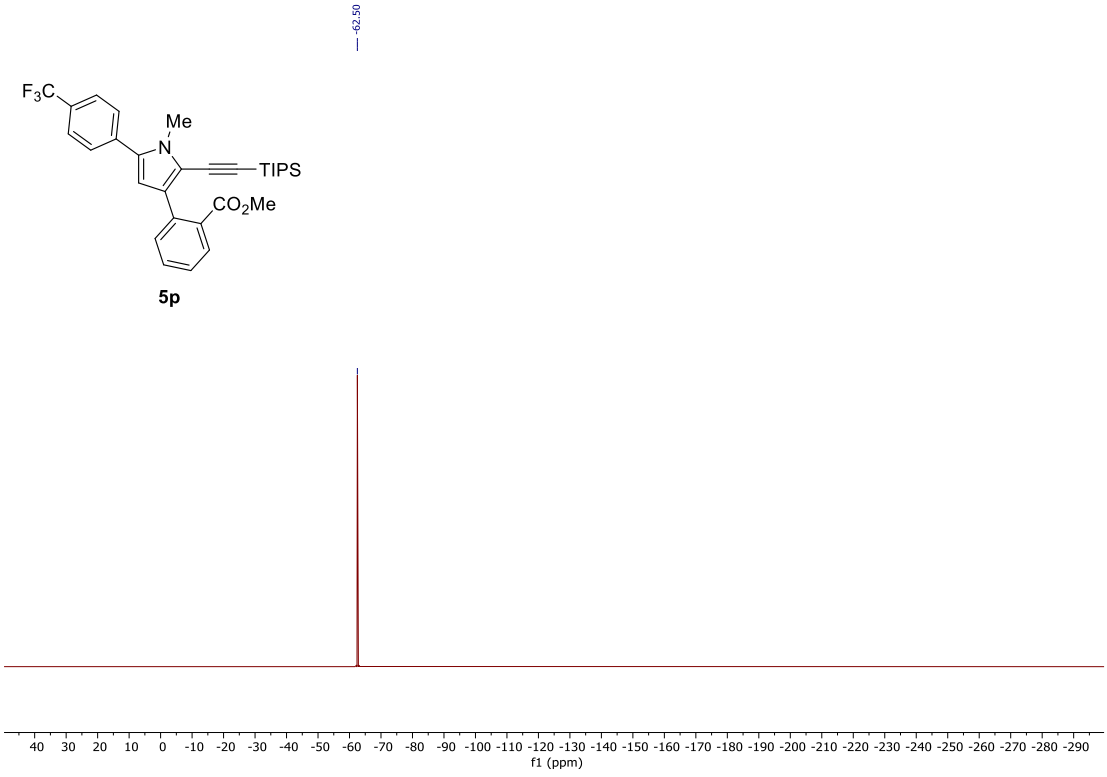

Figure 8.74. ^{1}H NMR of 5u

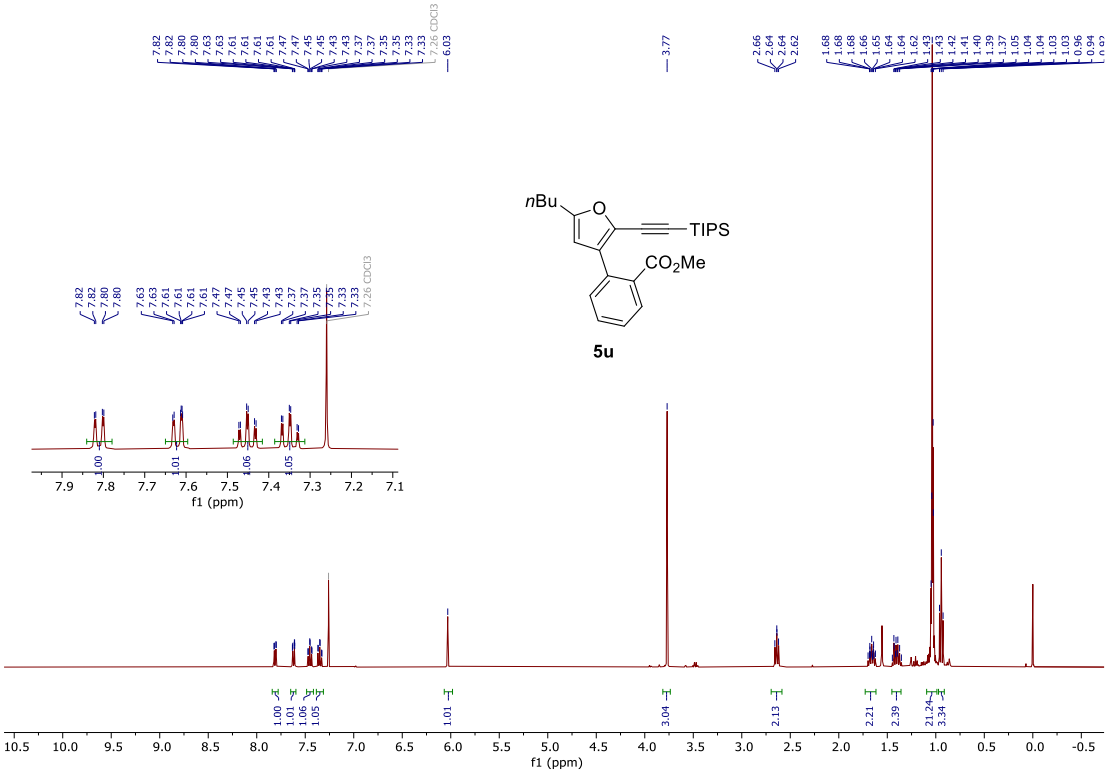

Figure 8.75. ^{13}C NMR of 5u

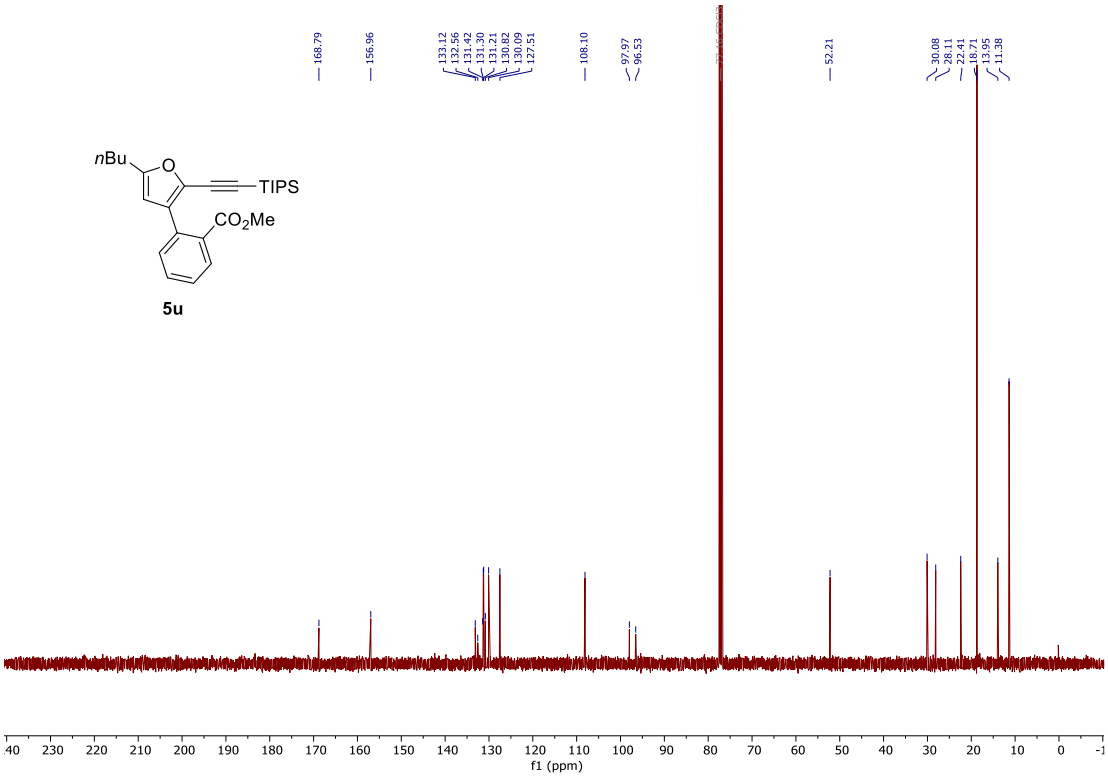

Figure 8.76. ^{1}H NMR of 5q

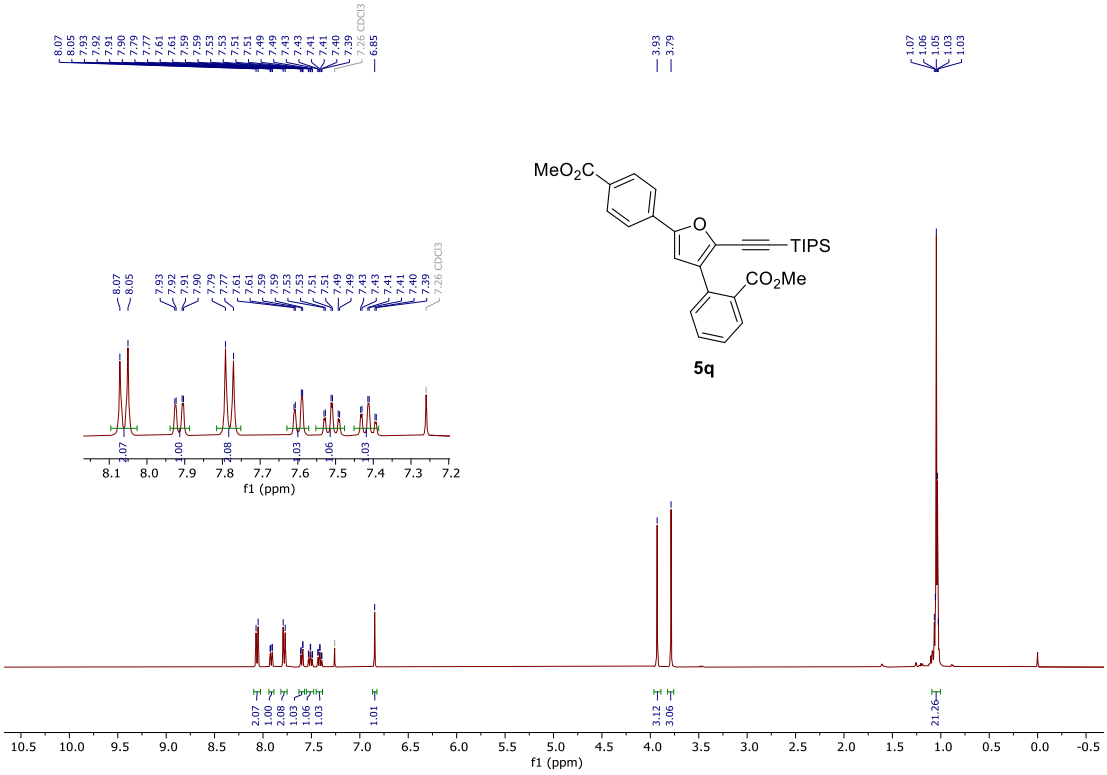

Figure 8.77. ^{13}C NMR of 5q

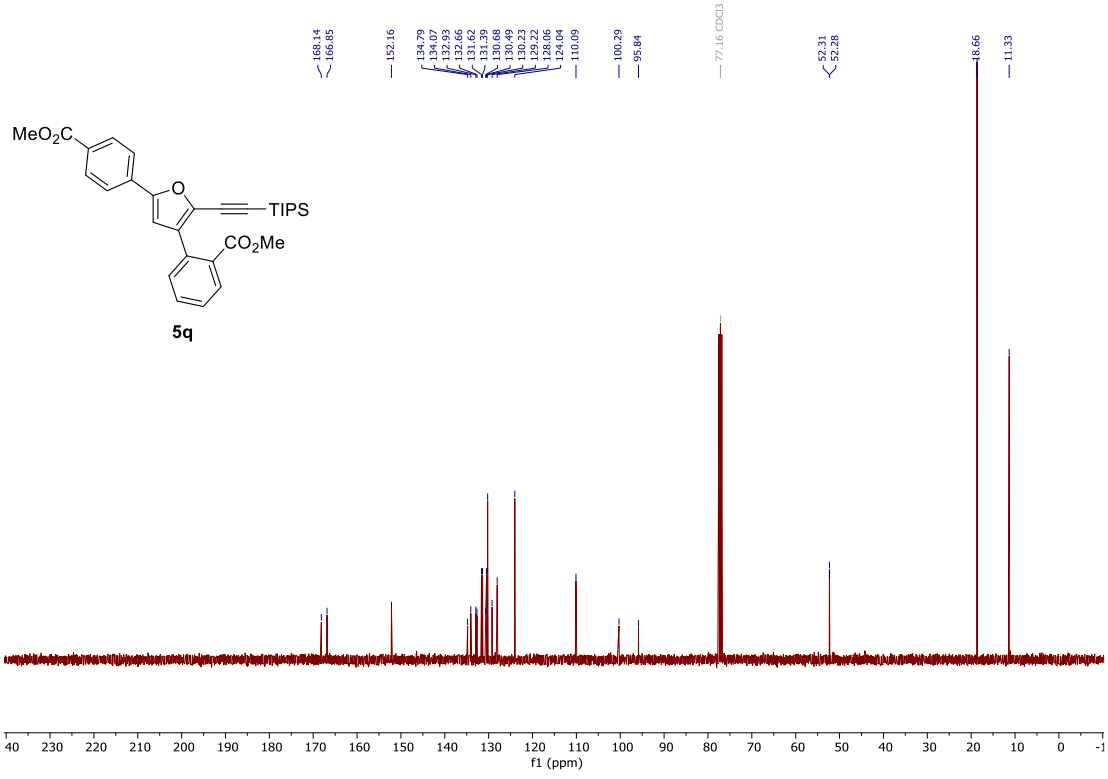

Figure 8.78. ^{1}H NMR of 5r

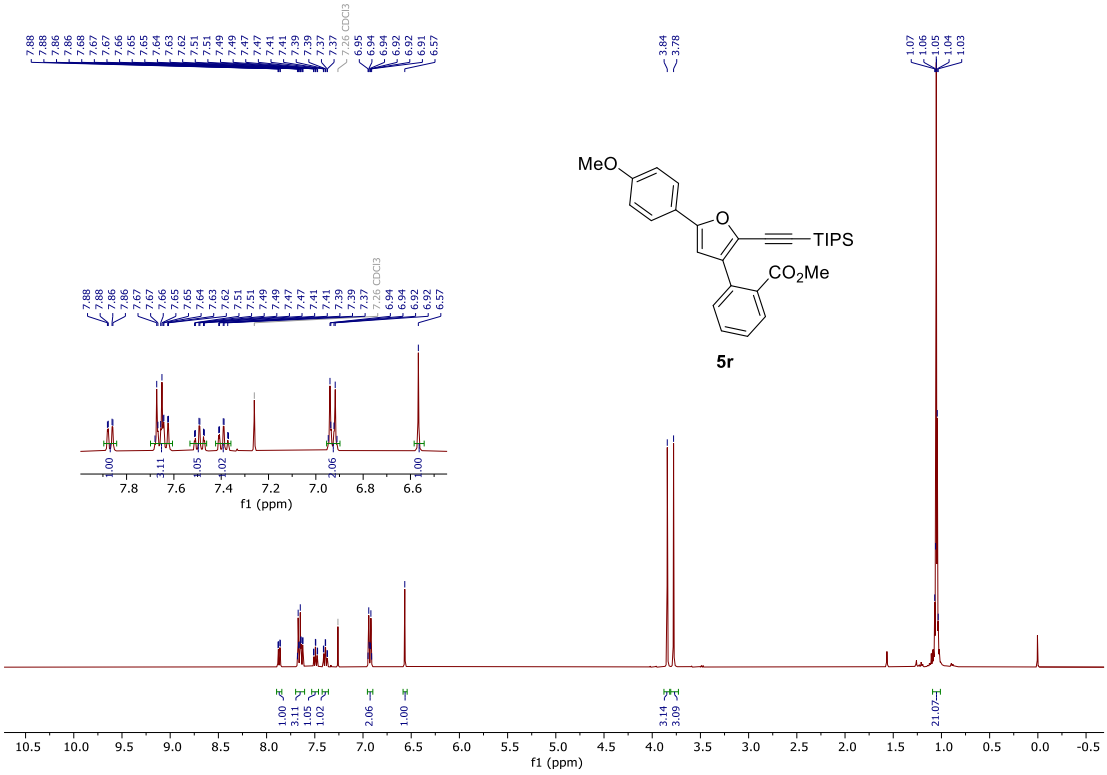

Figure 8.79. ^{13}C NMR of 5r

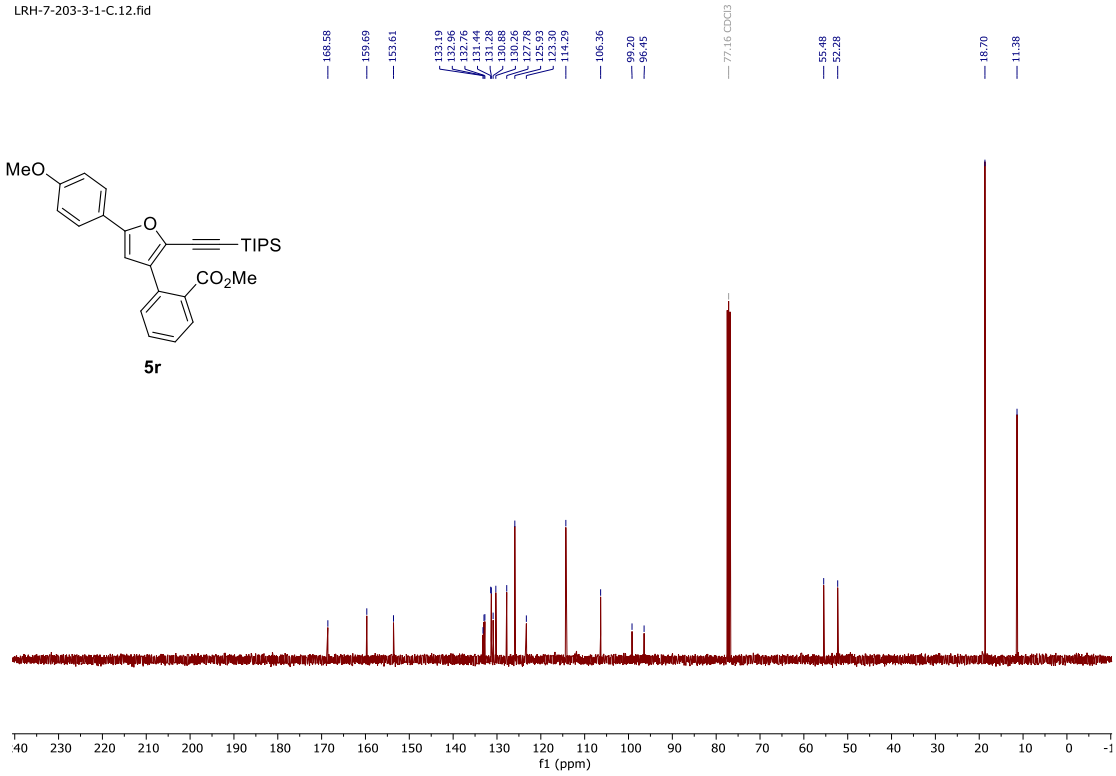

Figure 8.80. ^{1}H NMR of 5s

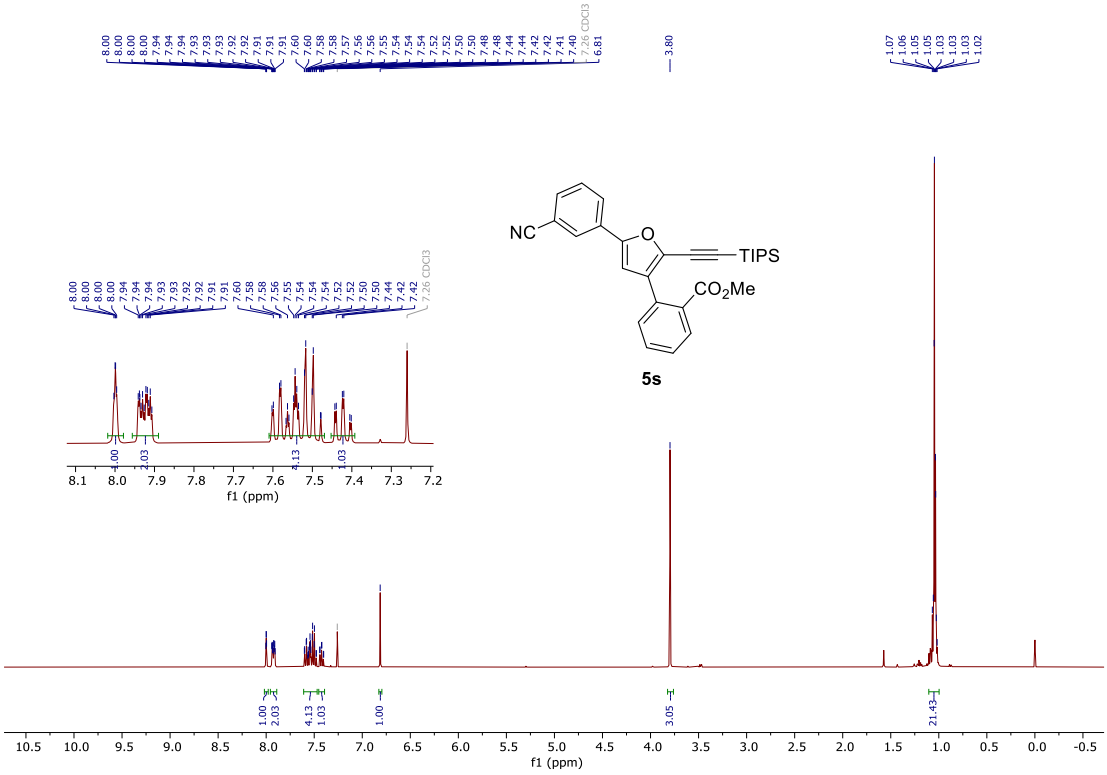

Figure 8.81. ^{13}C NMR of 5s

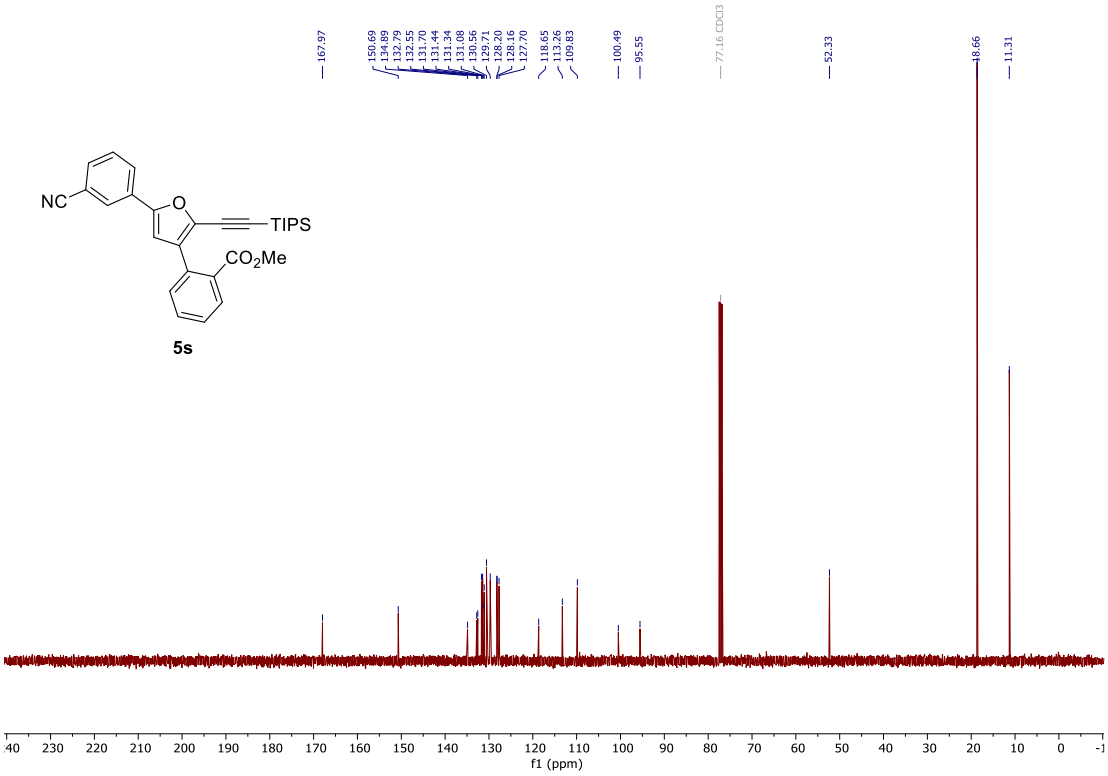

Figure 8.82. ^{1}H NMR of 5t

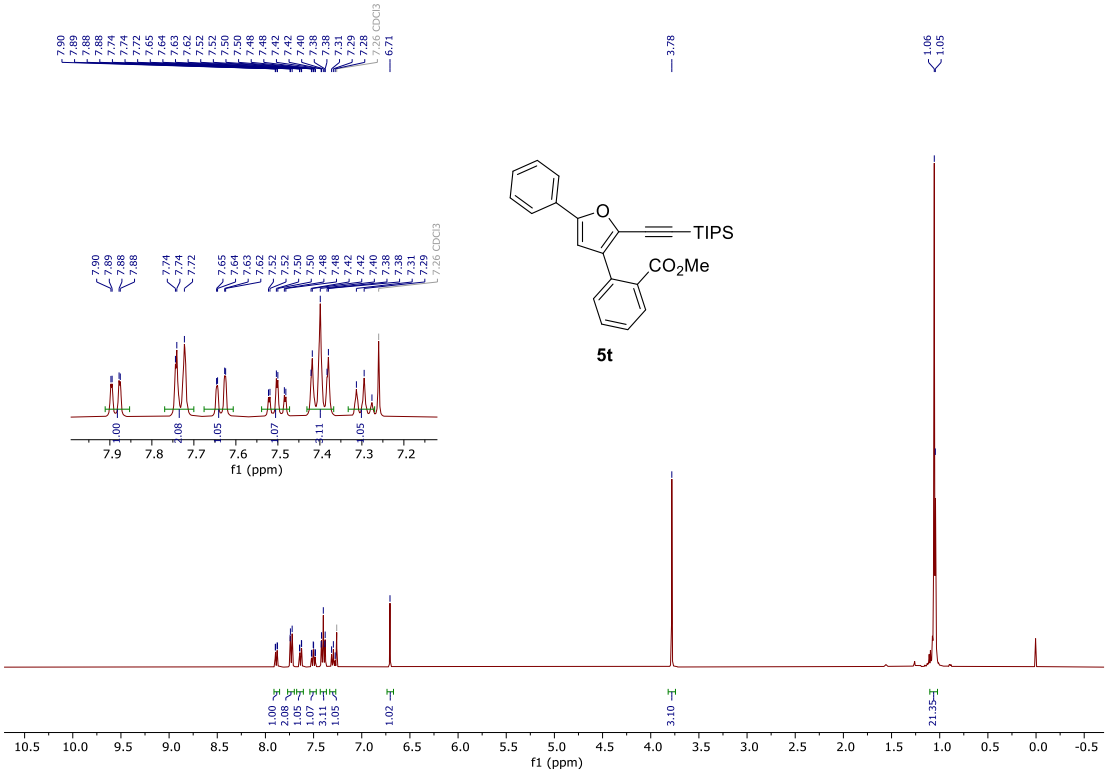

Figure 8.83. ^{13}C NMR of 5t

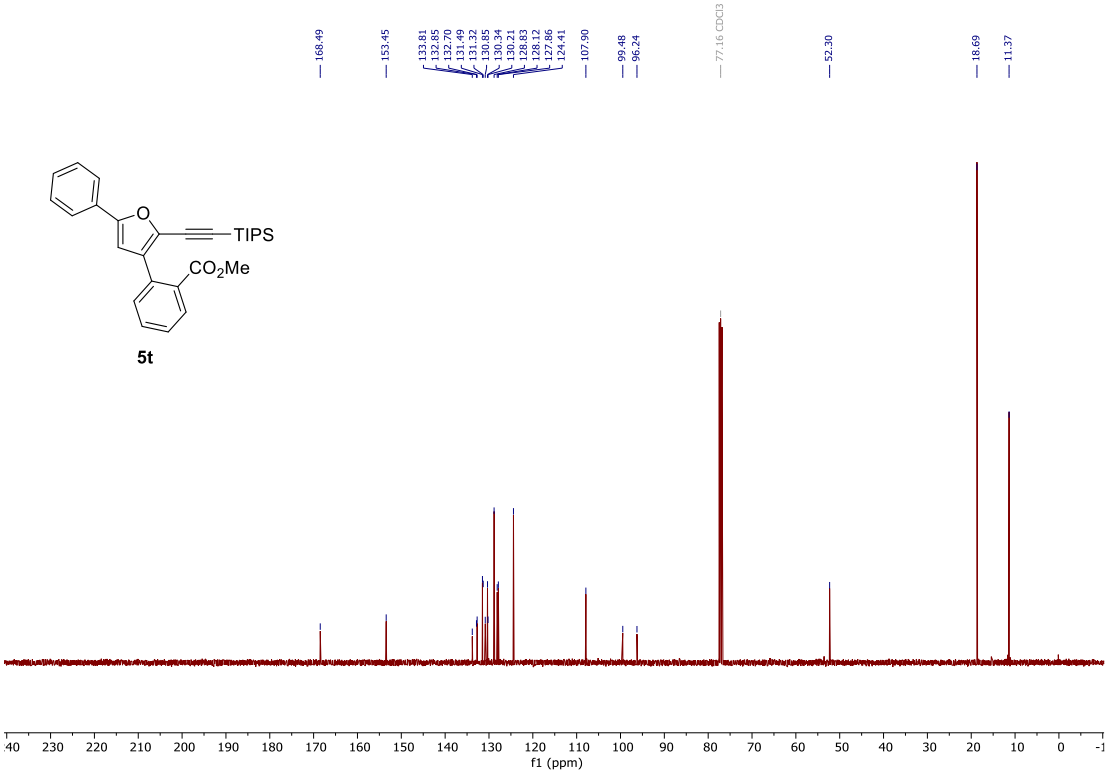

Figure 8.84. ^{1}H NMR of 5v

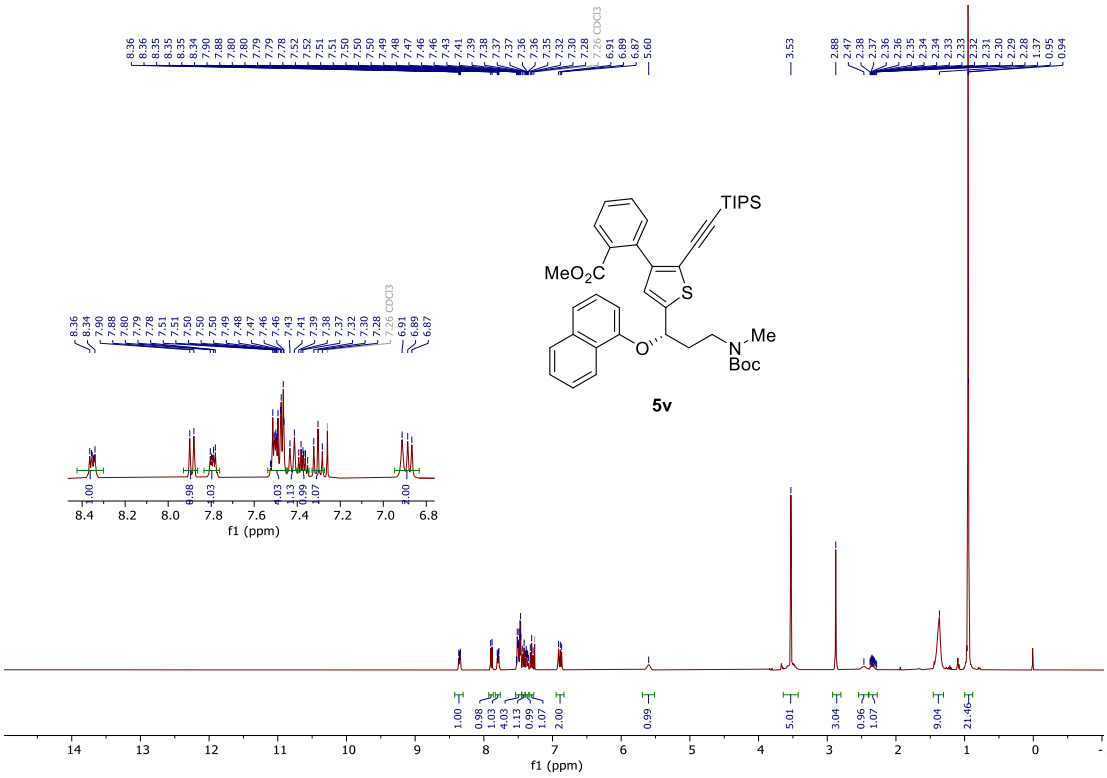

Figure 8.85. ^{13}C NMR of 5v

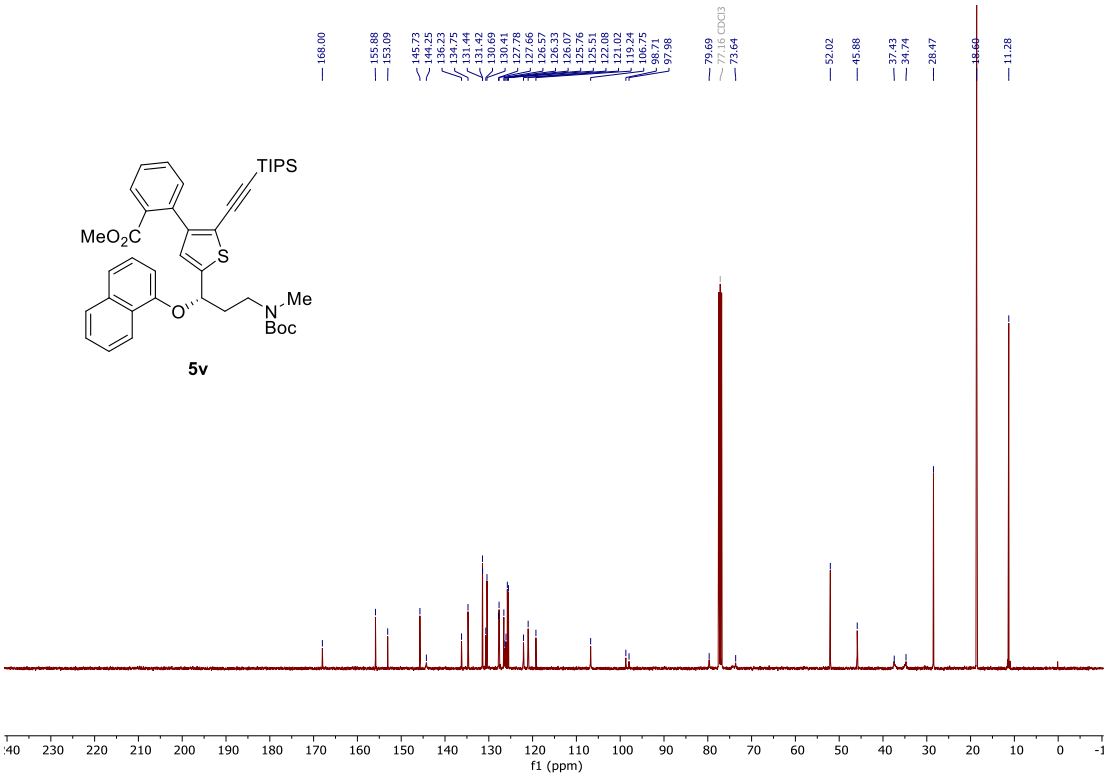

Figure 8.86. ^{1}H NMR of 5w

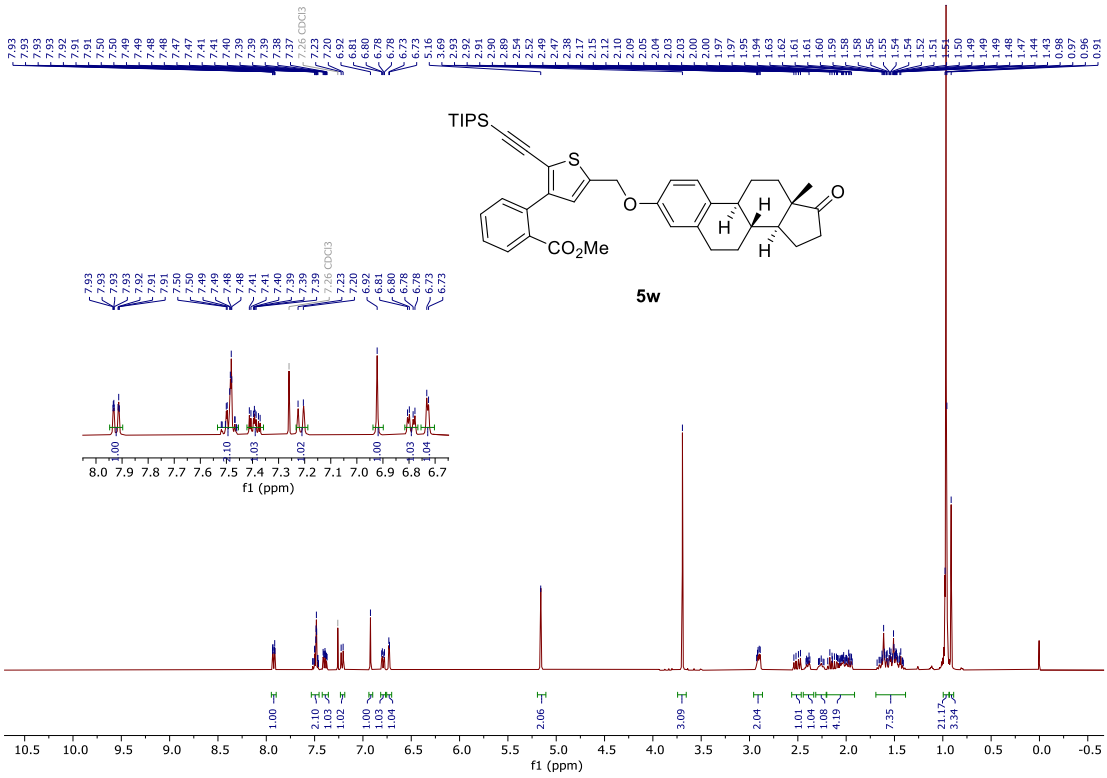

Figure 8.87. ^{13}C NMR of 5w

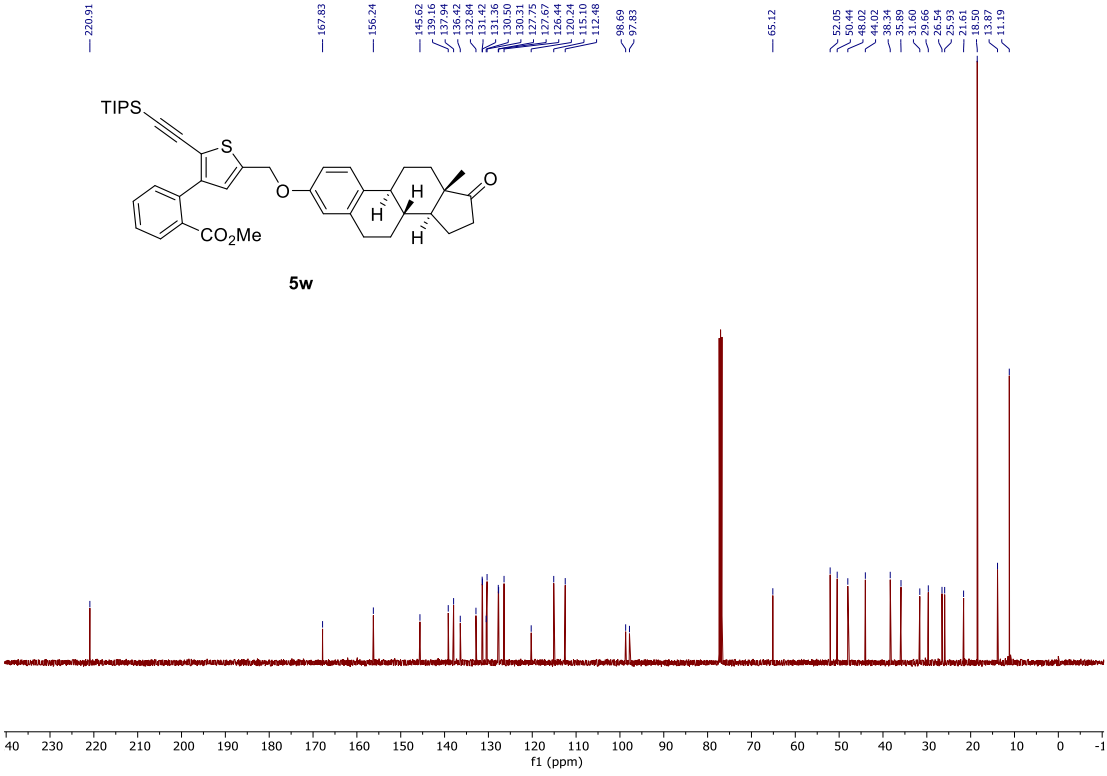

Figure 8.88. ^{1}H NMR of 6a

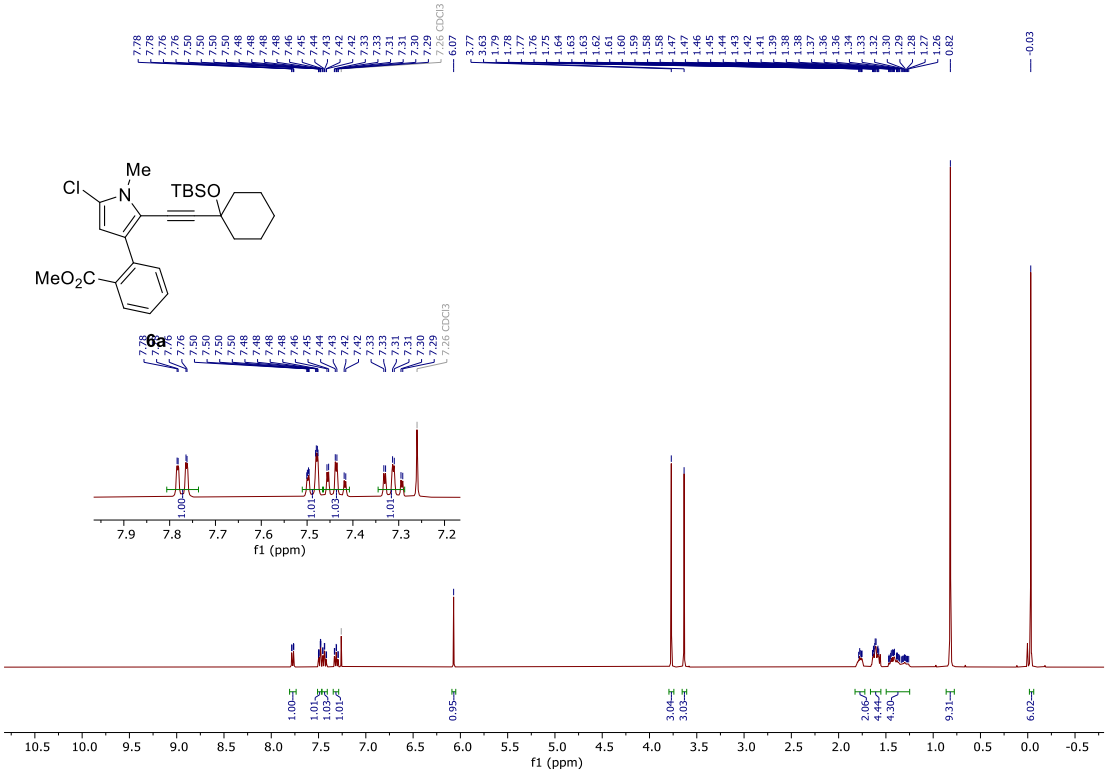

Figure 8.89. ^{13}C NMR of 6a

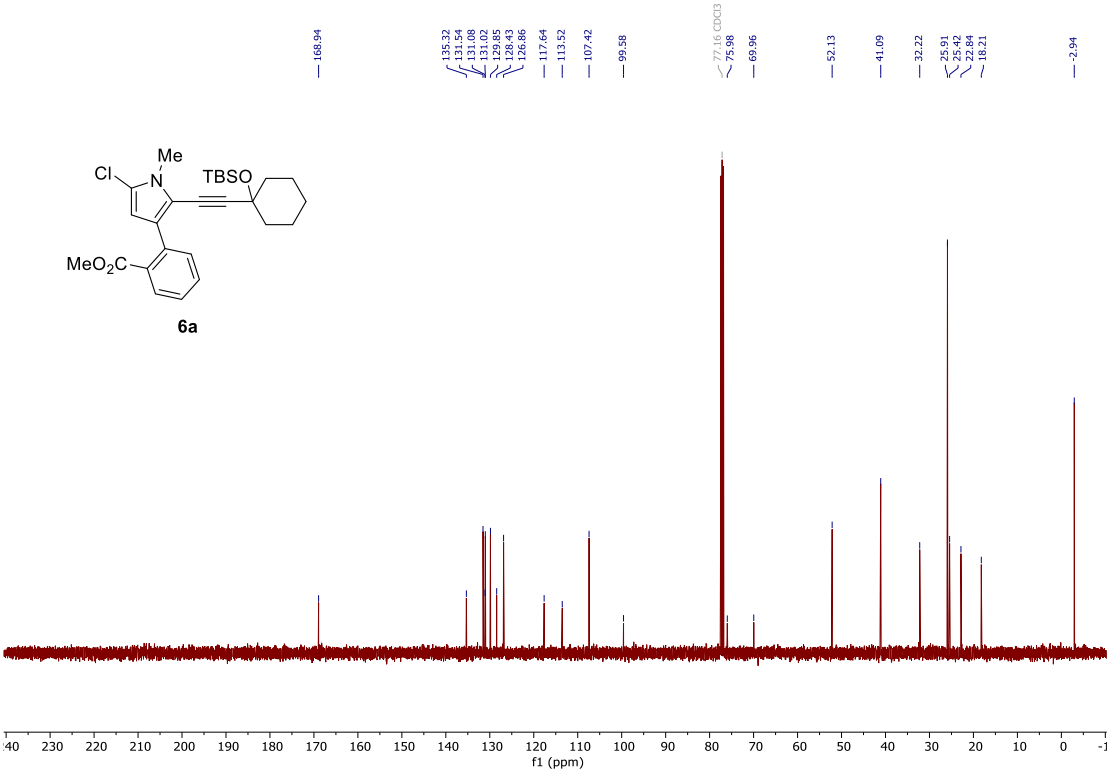

Figure 8.90. ^{1}H NMR of 6b

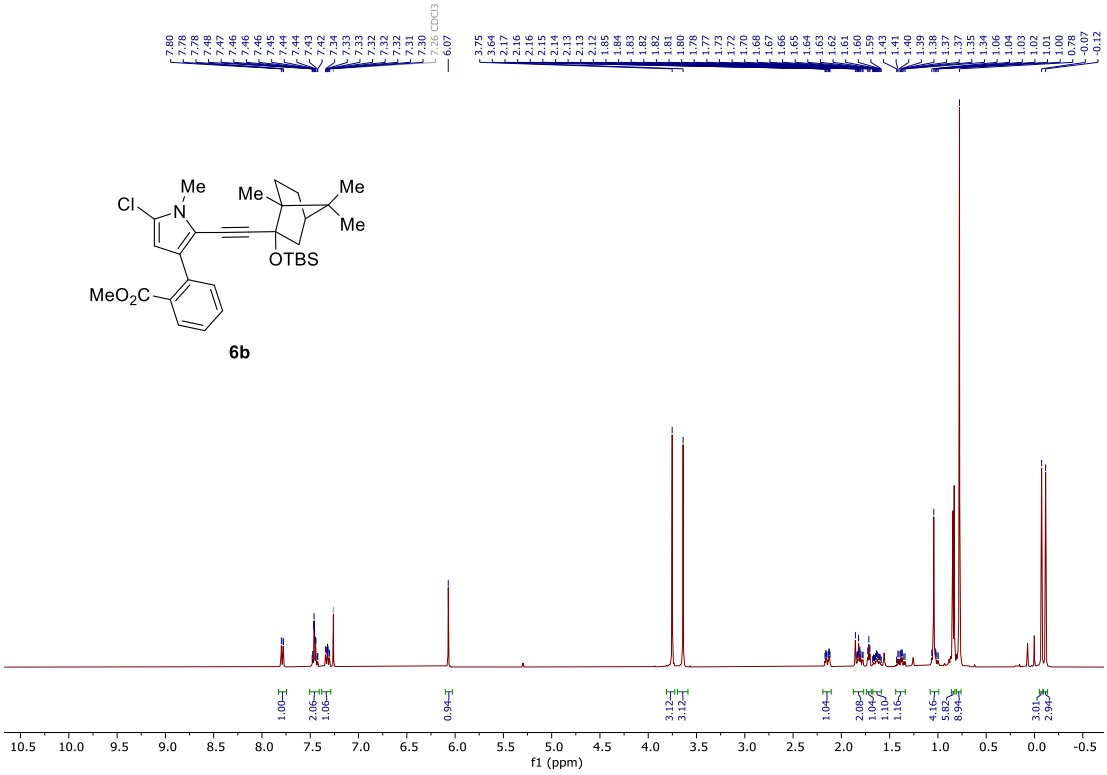

Figure 8.91. ^{13}C NMR of 6b

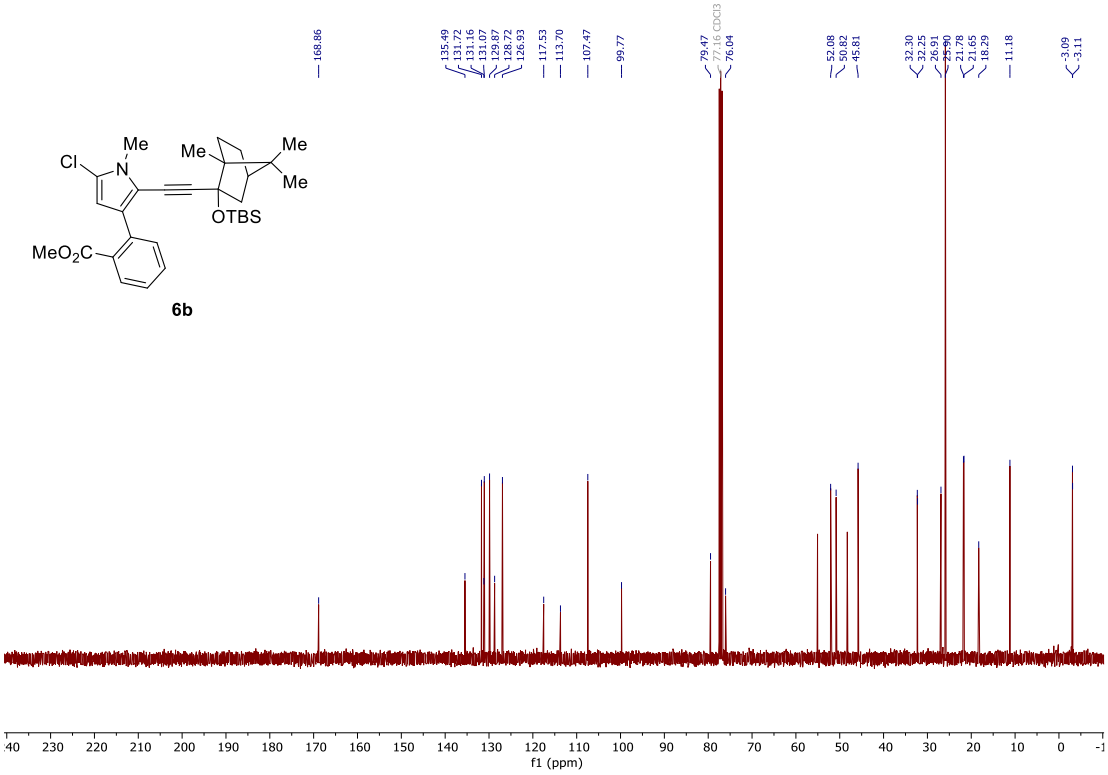

Figure 8.92. ^{1}H NMR of 6c

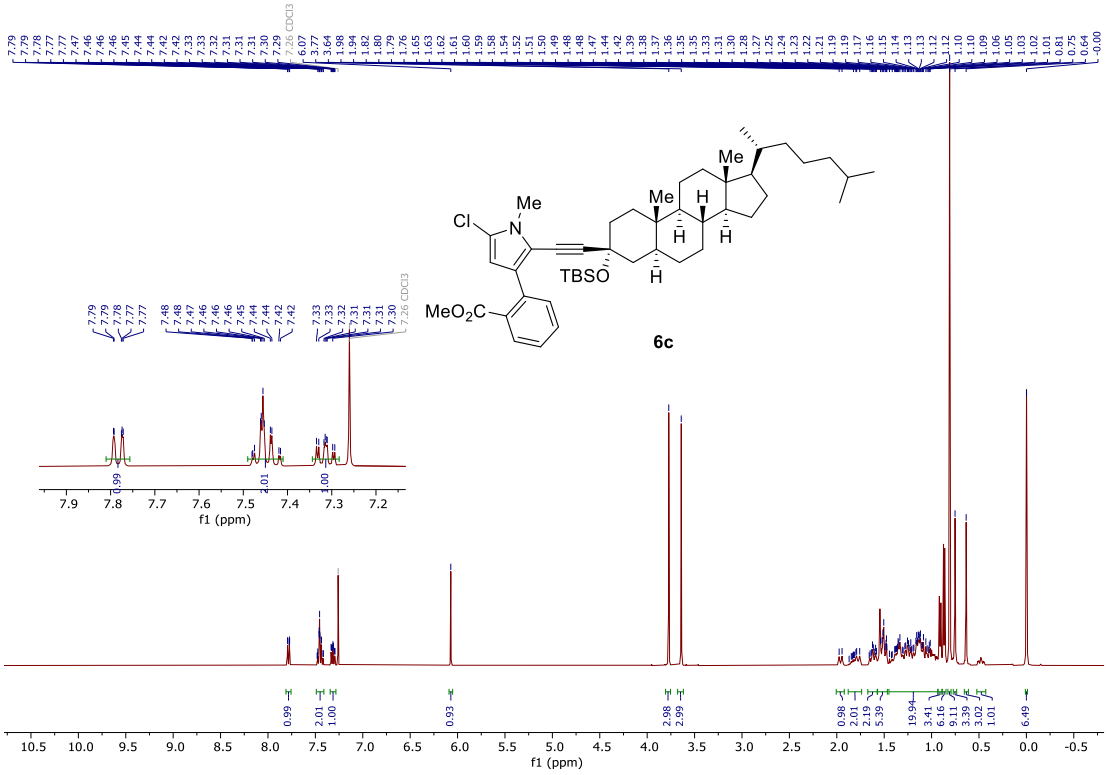

Figure 8.93. ^{13}C NMR of 6c

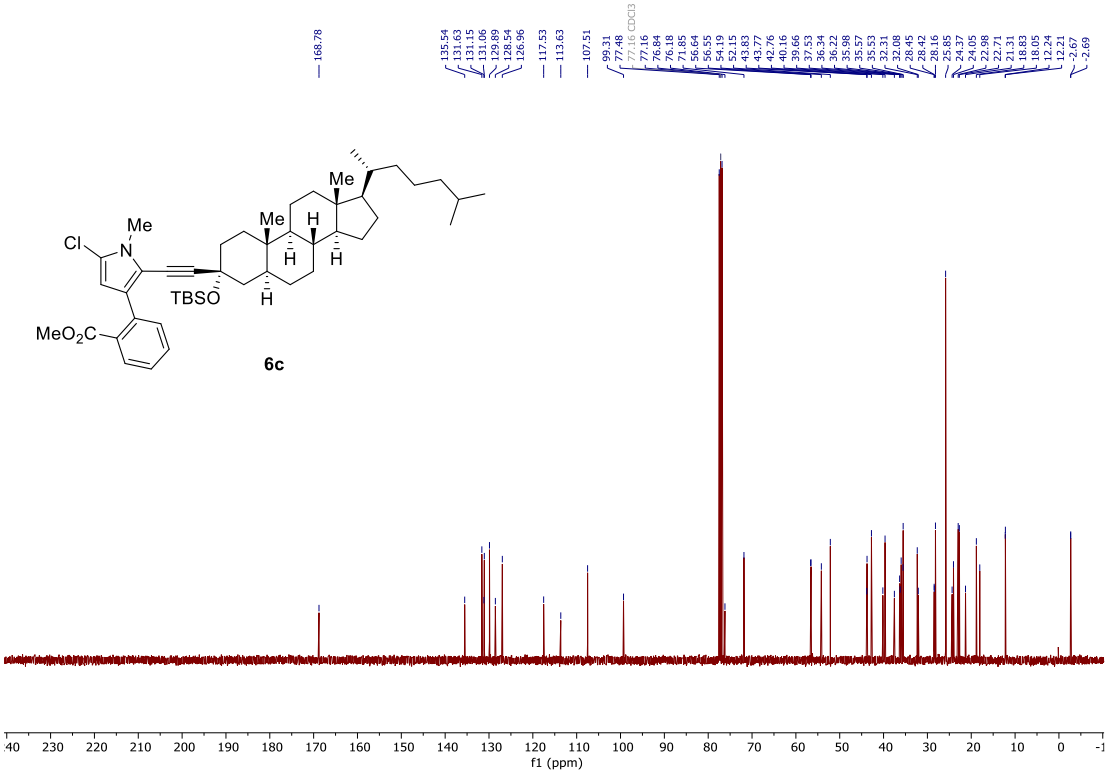

Figure 8.94. ^{1}H NMR of 6d

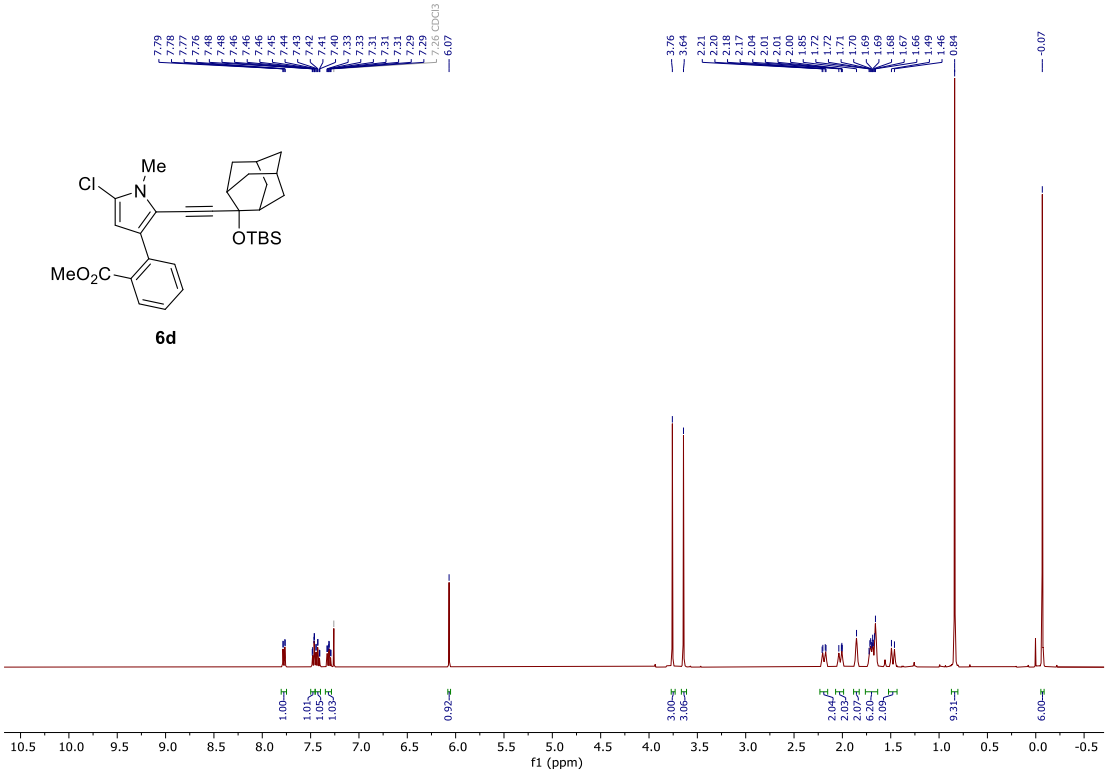

Figure 8.95. ^{13}C NMR of 6d

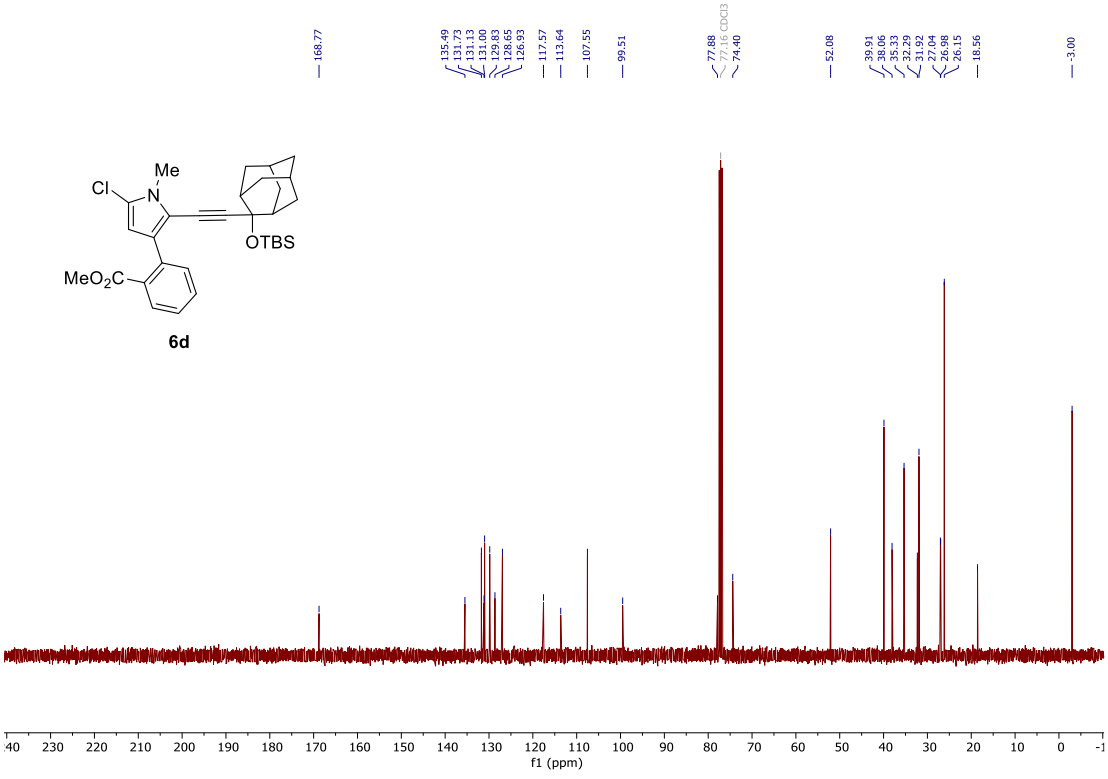

Figure 8.96. ^{1}H NMR of 11a

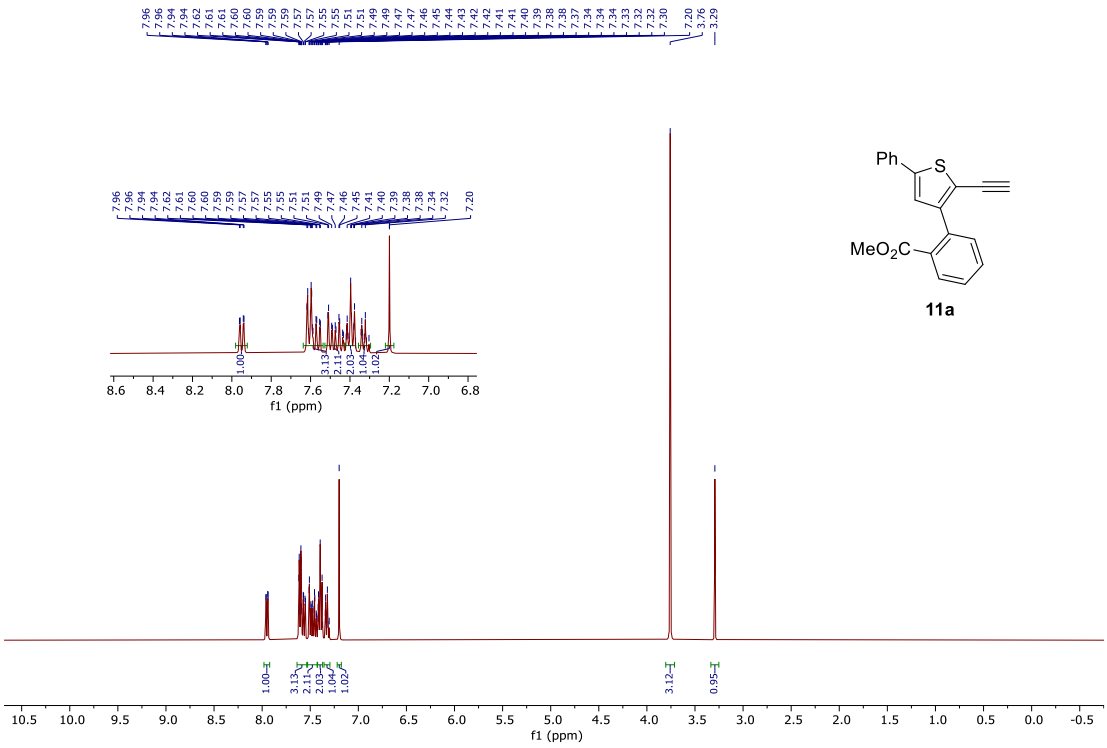

Figure 8.97. ^{13}C NMR of 11a

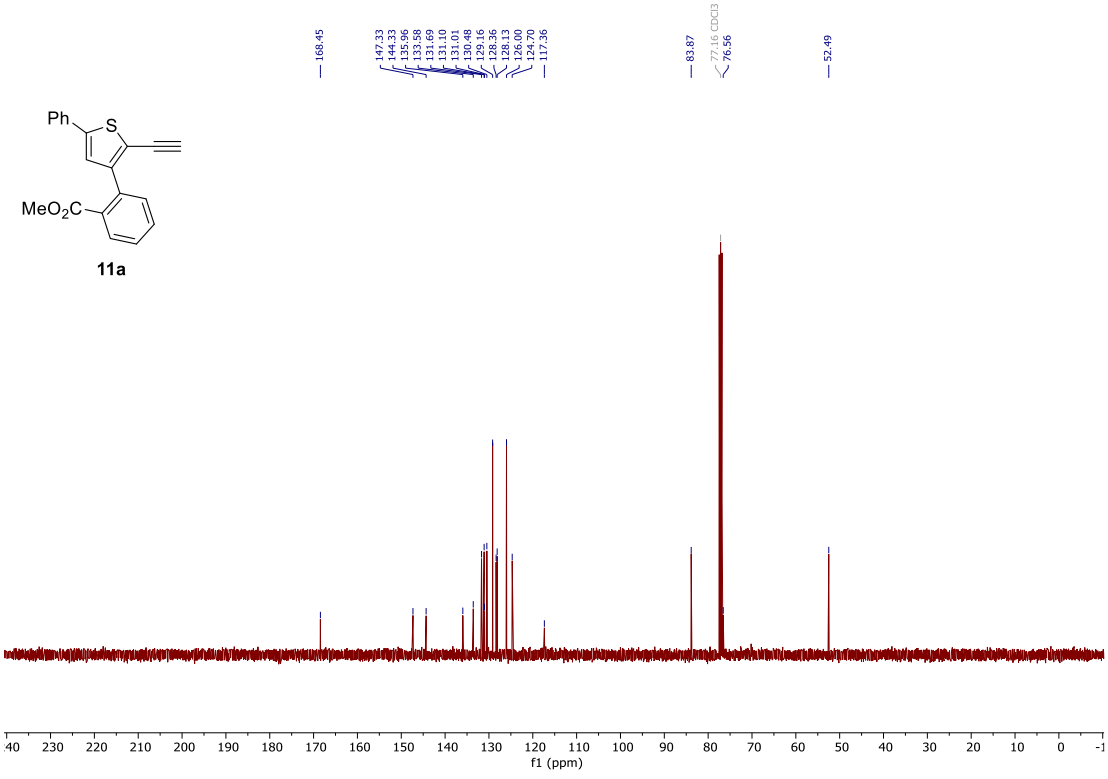

Figure 8.98. ^{1}H NMR of 11b

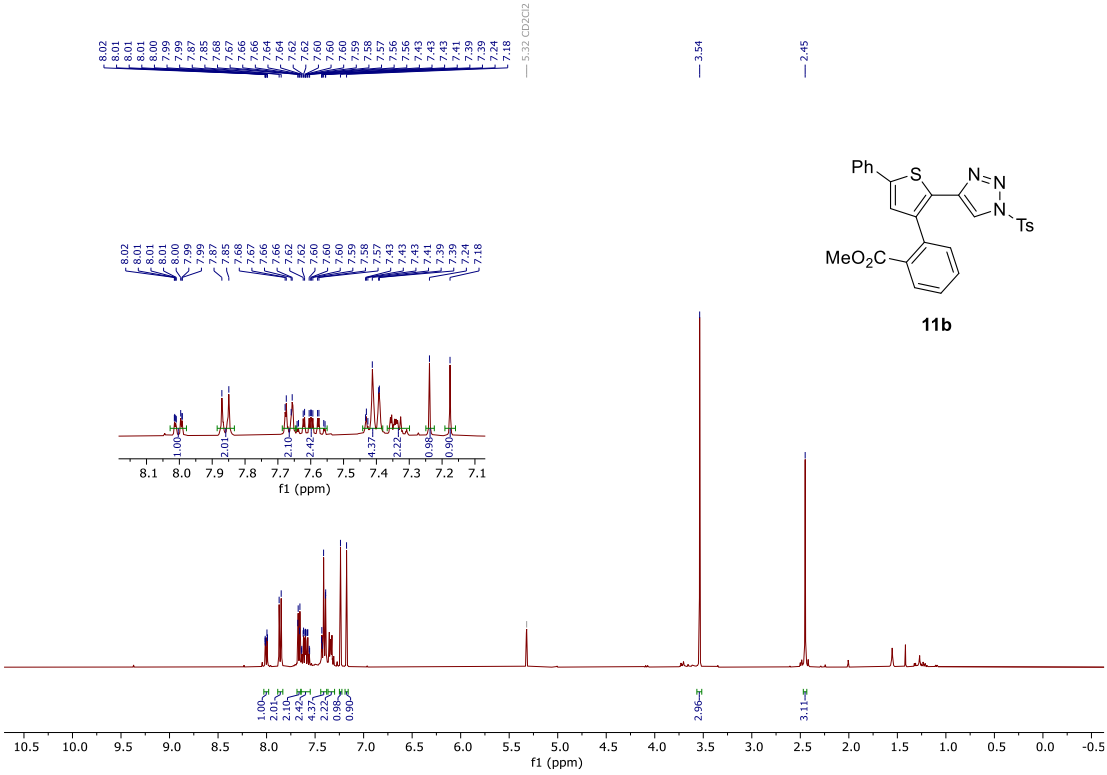

Figure 8.99. ^{13}C NMR of 11b

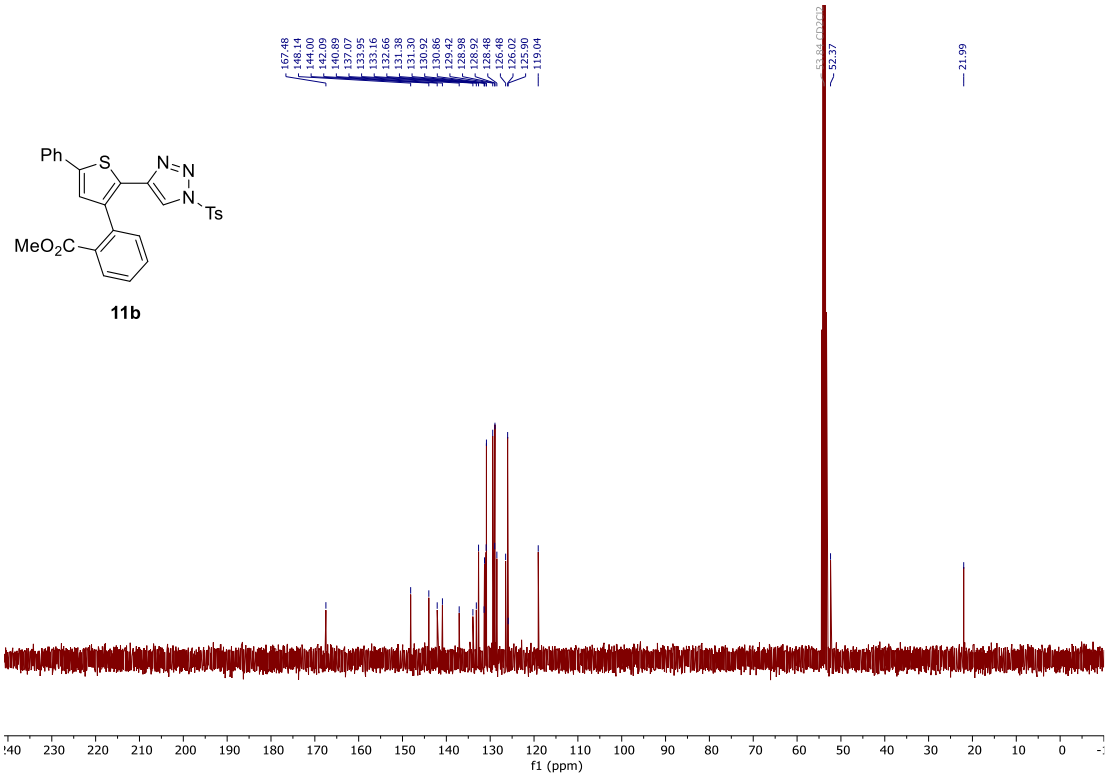

Figure 8.100. ^{1}H NMR of 11c

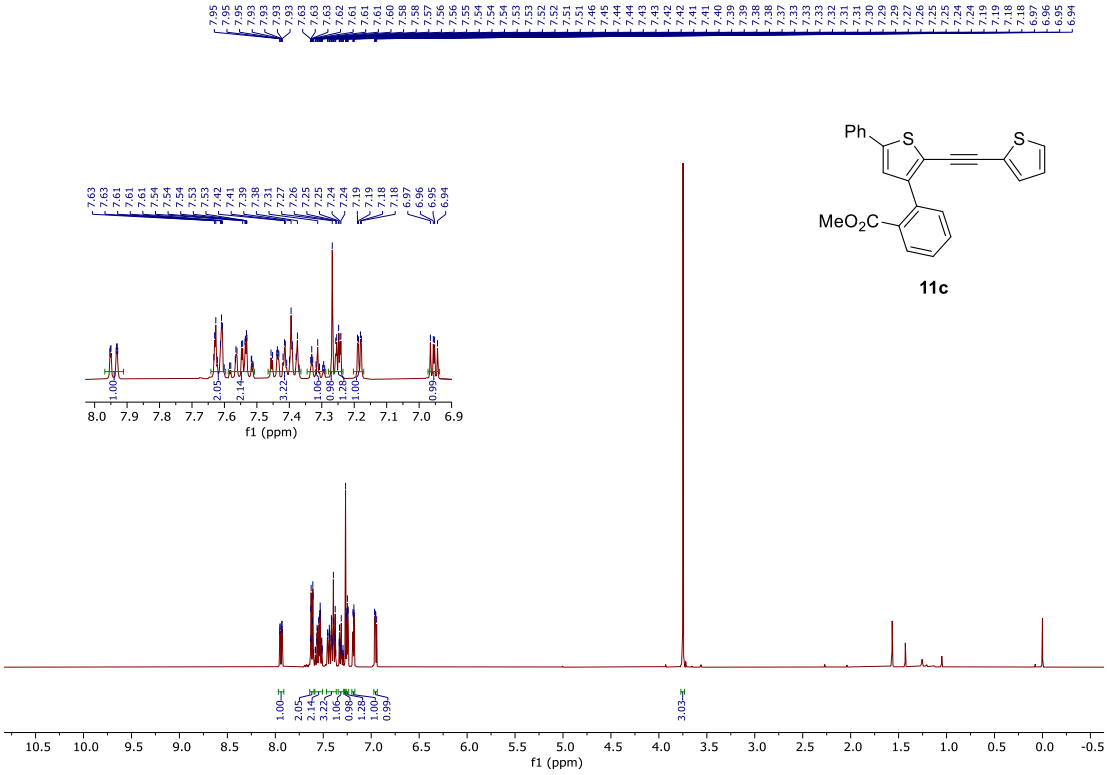

Figure 8.101. ^{13}C NMR of 11c

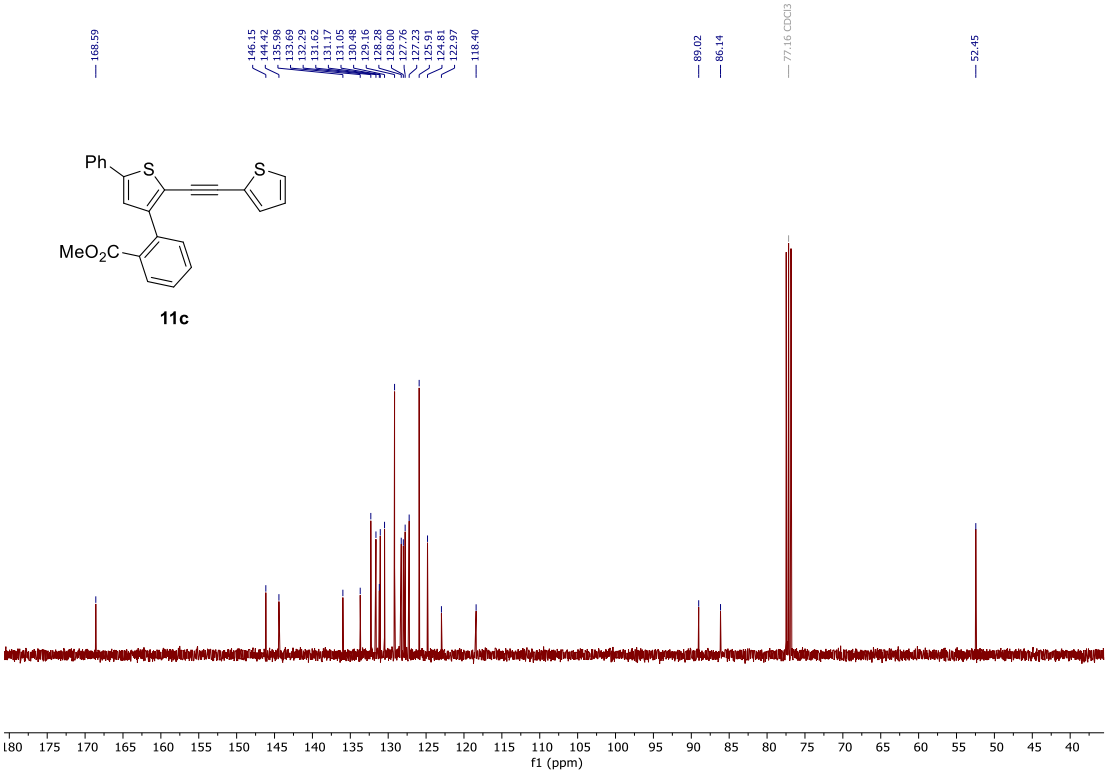

Figure 8.102. ^{1}H NMR of 11d

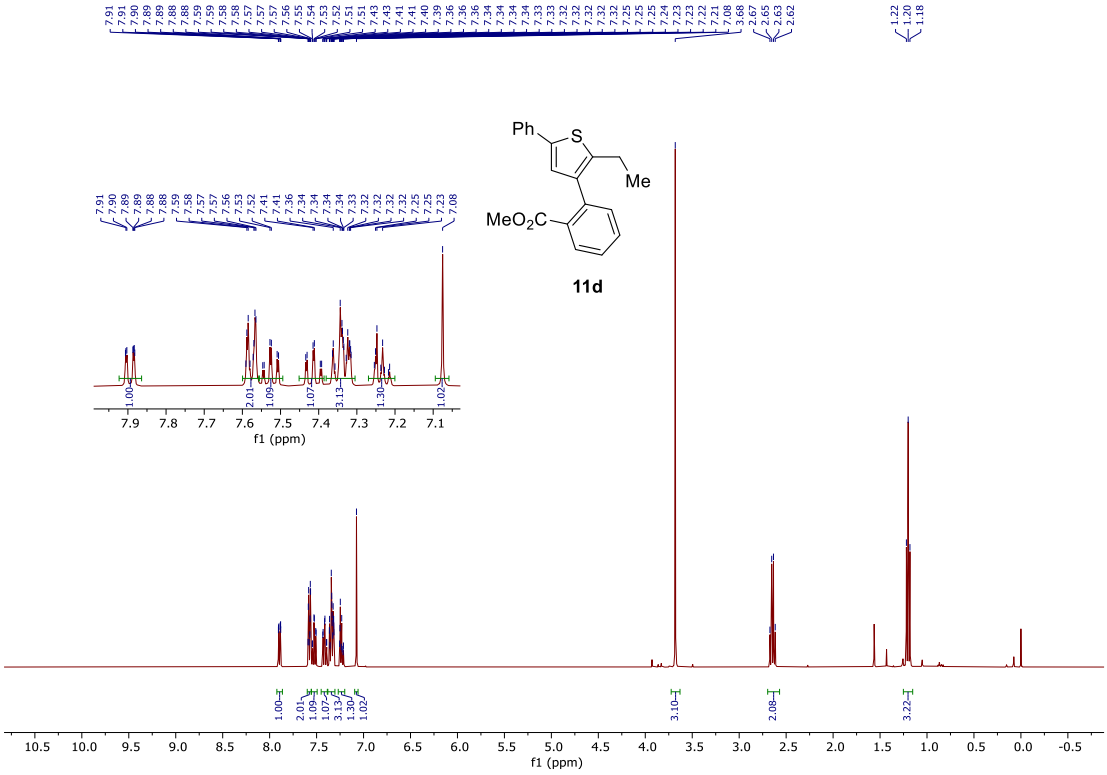

Figure 8.103. ^{13}C NMR of 11d

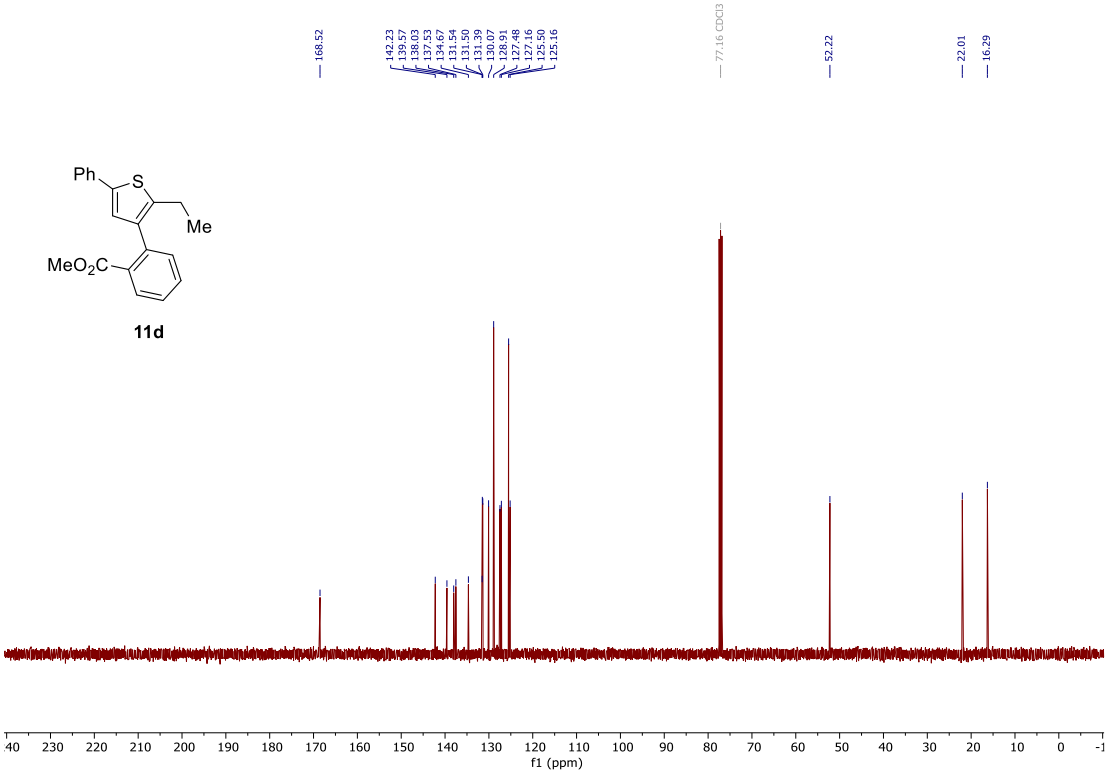

Figure 8.104. ^{1}H NMR of 11e

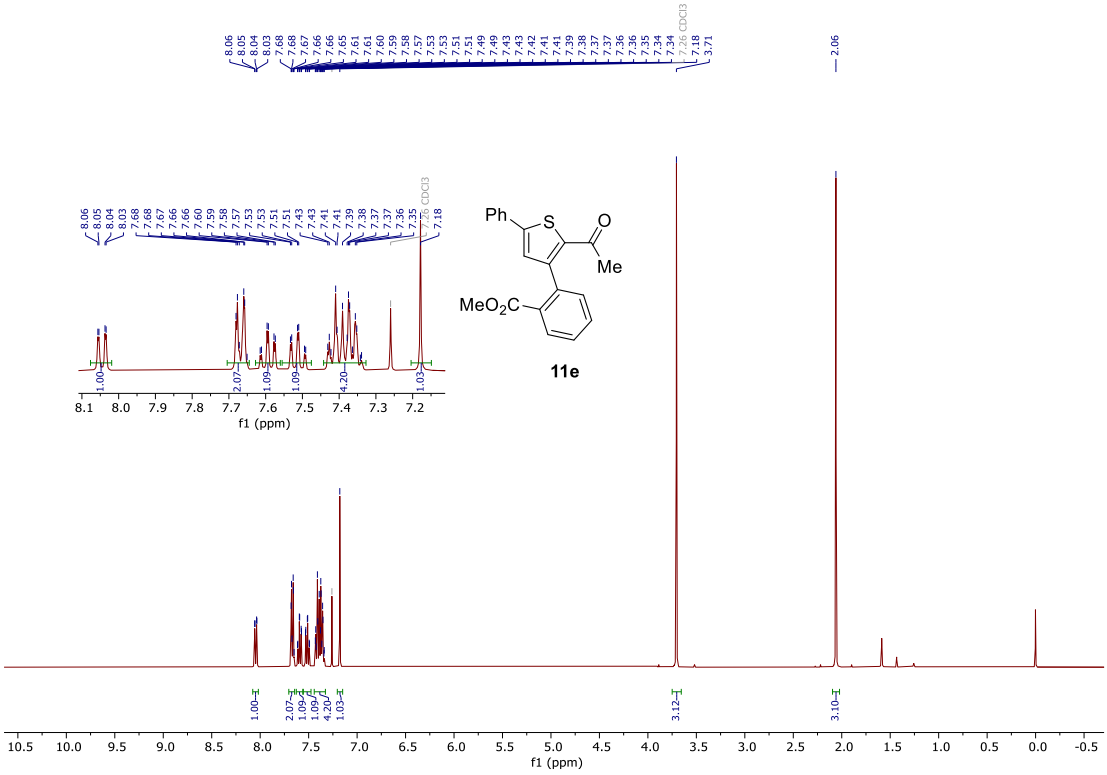

Figure 8.105. ^{13}C NMR of 11e

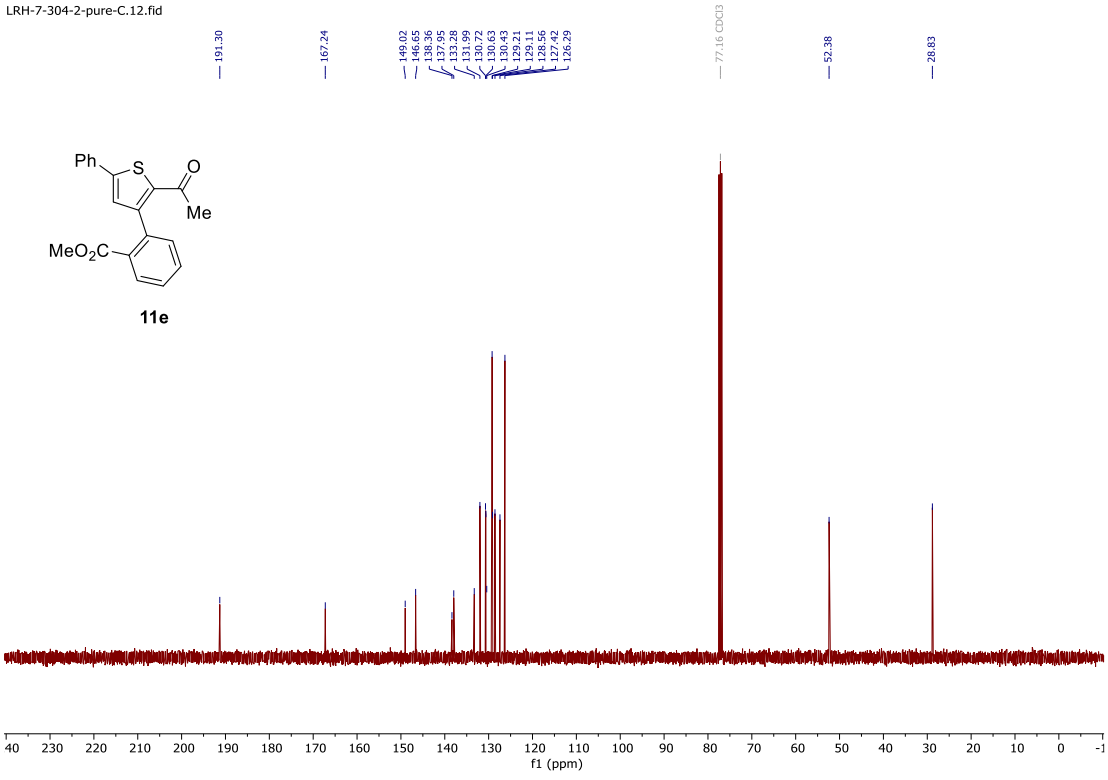

Figure 8.106. ^{1}H NMR of 13

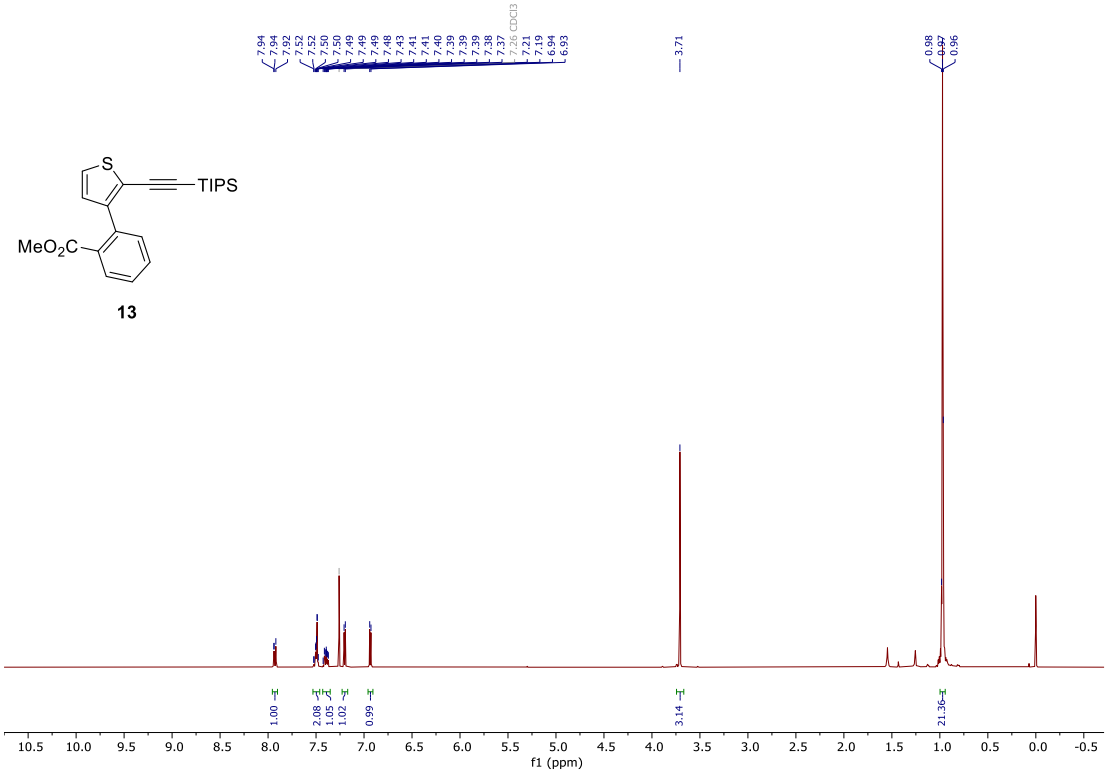

Figure 8.107. ^{13}C NMR of 13

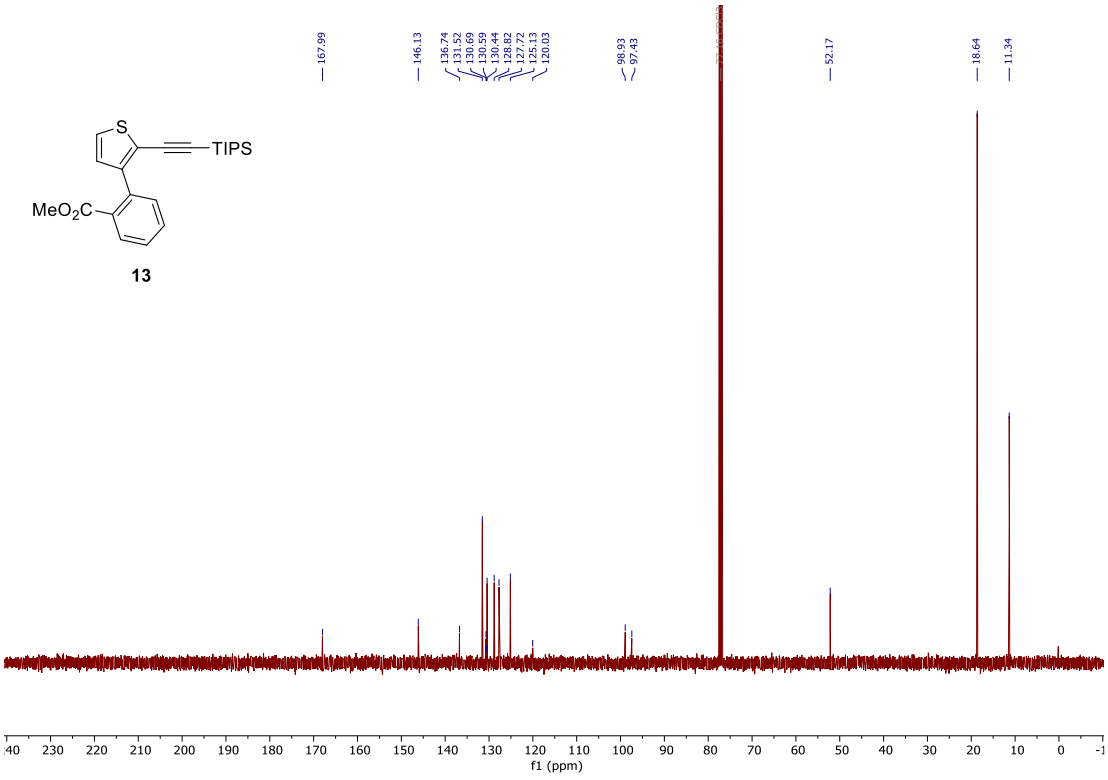

Figure 8.108. ^{1}H NMR of 14

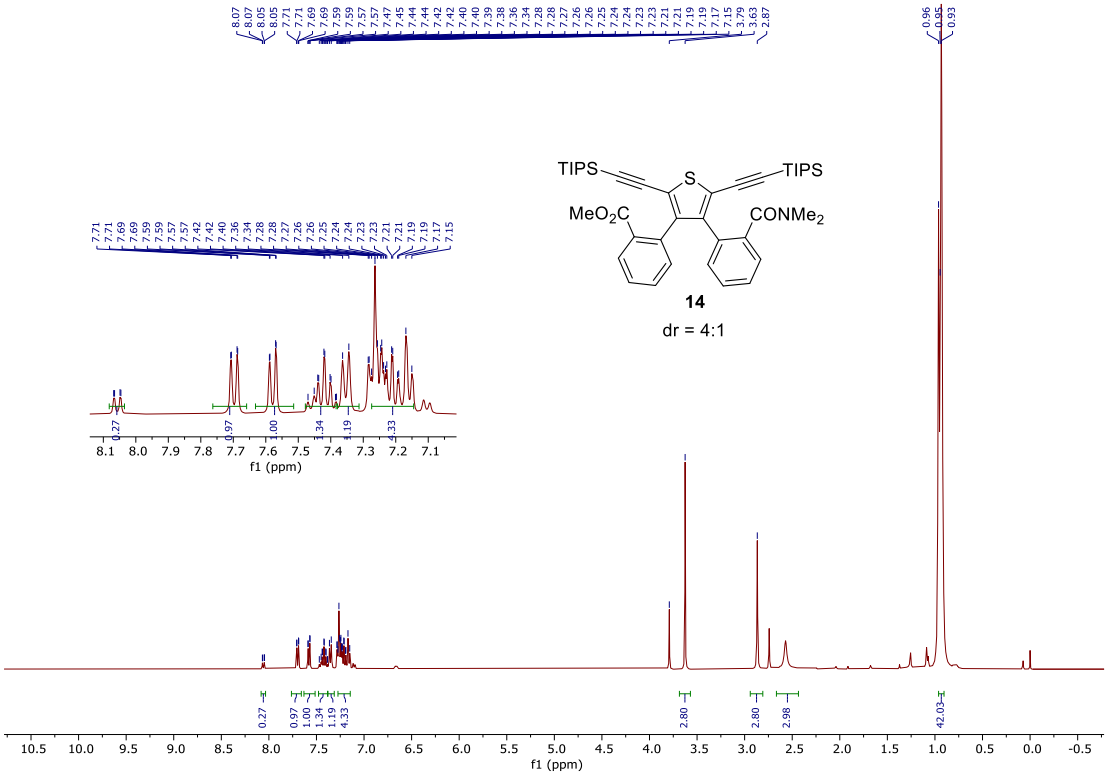

Figure 8.109. ^{13}C NMR of 14

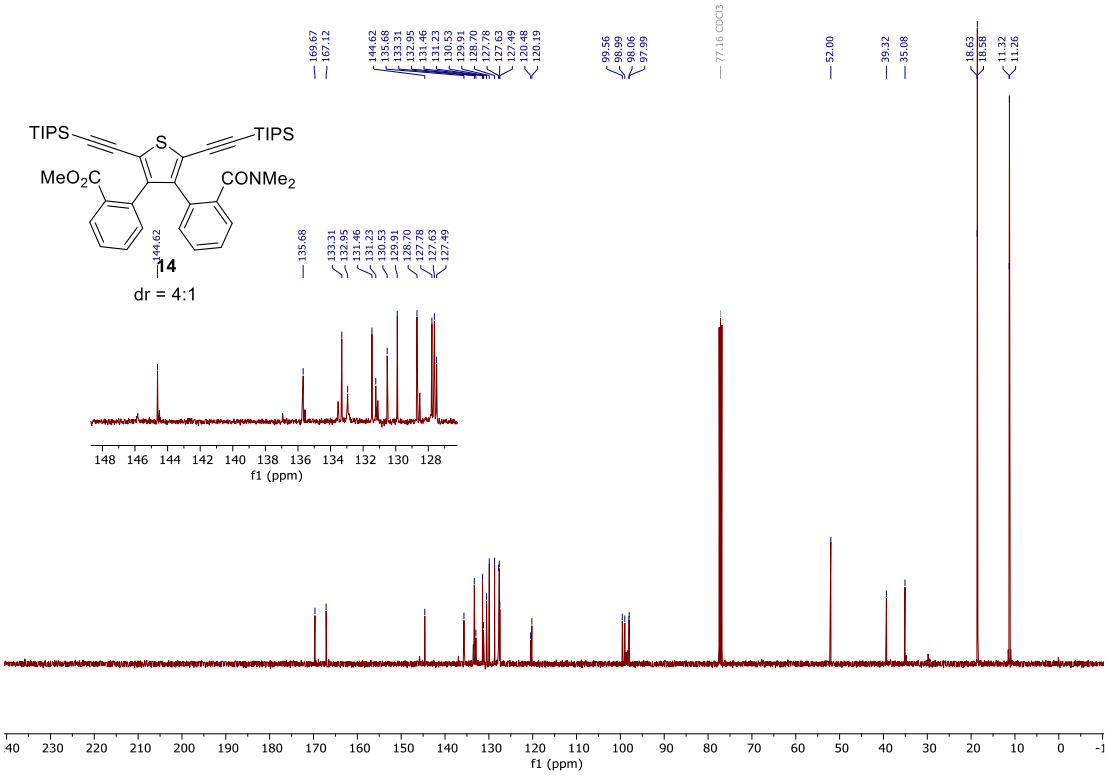

Figure 8.110. ^{1}H NMR of 18

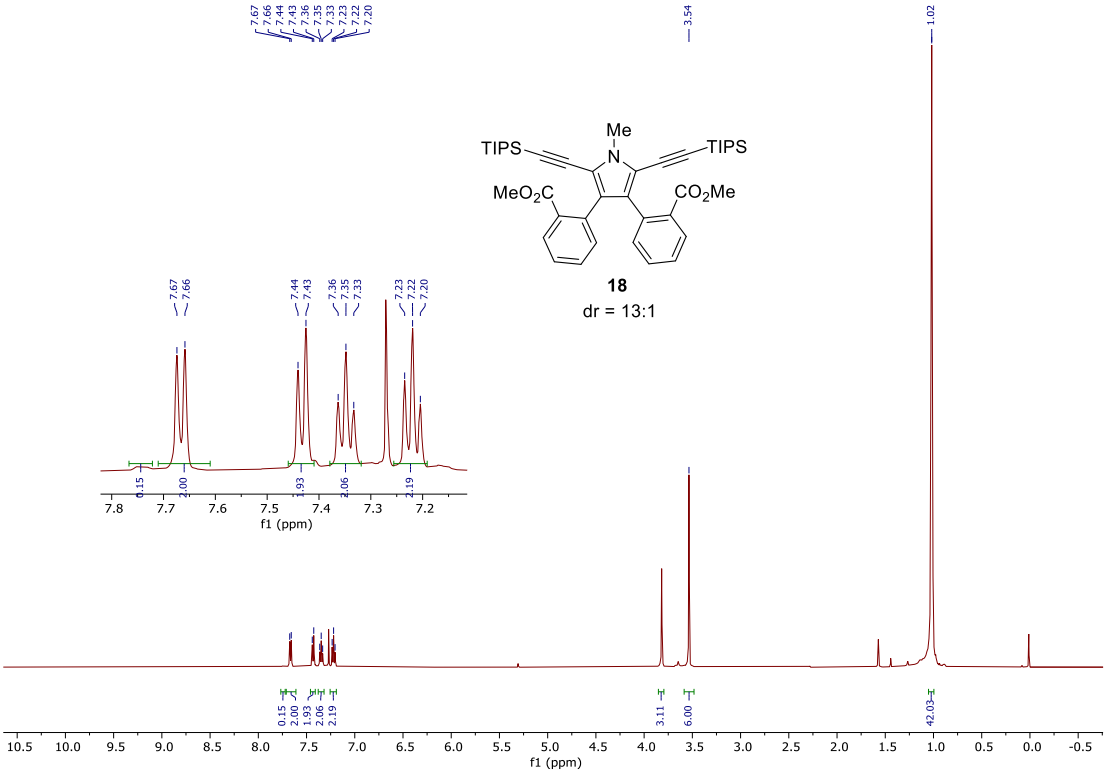

Figure 8.111. ^{13}C NMR of 18

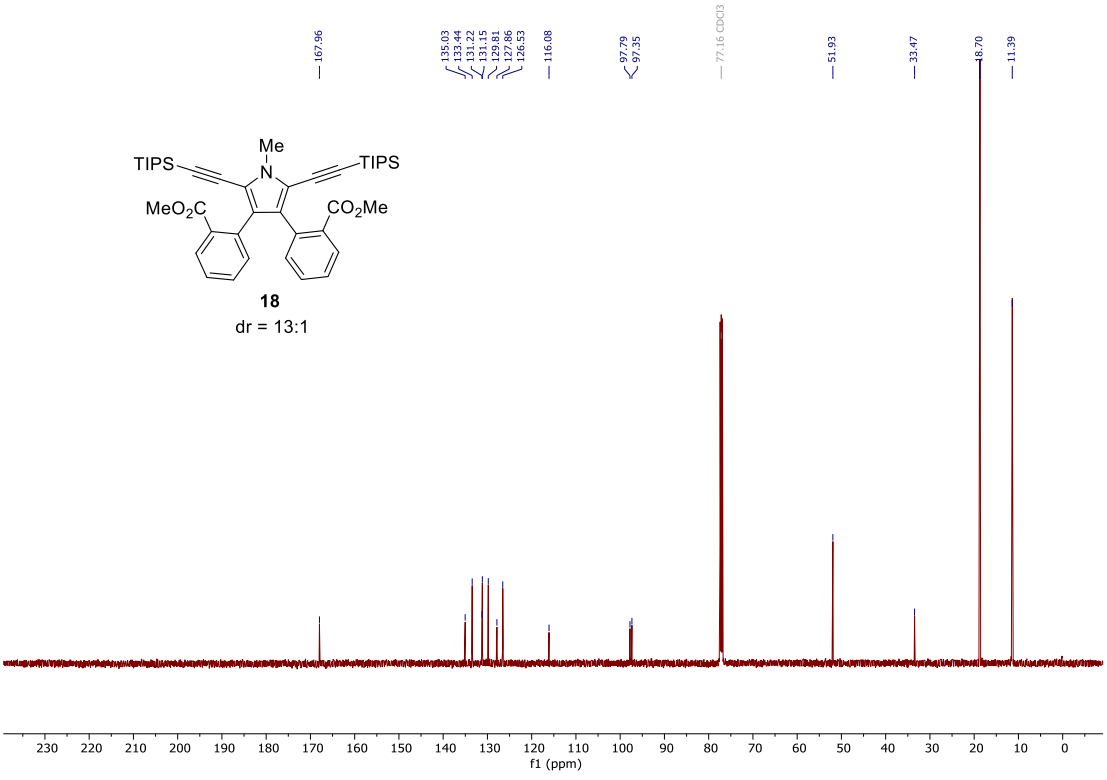

Figure 8.112. ^{1}H NMR of S6

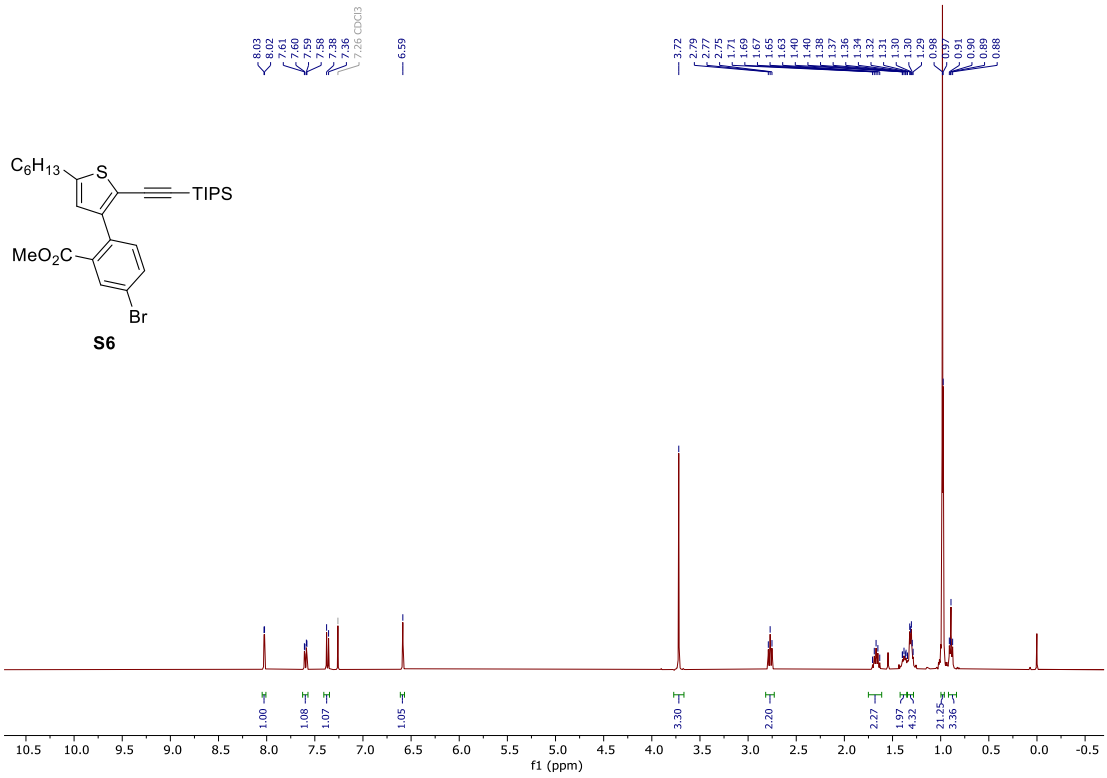

Figure 8.113. ^{13}C NMR of S6

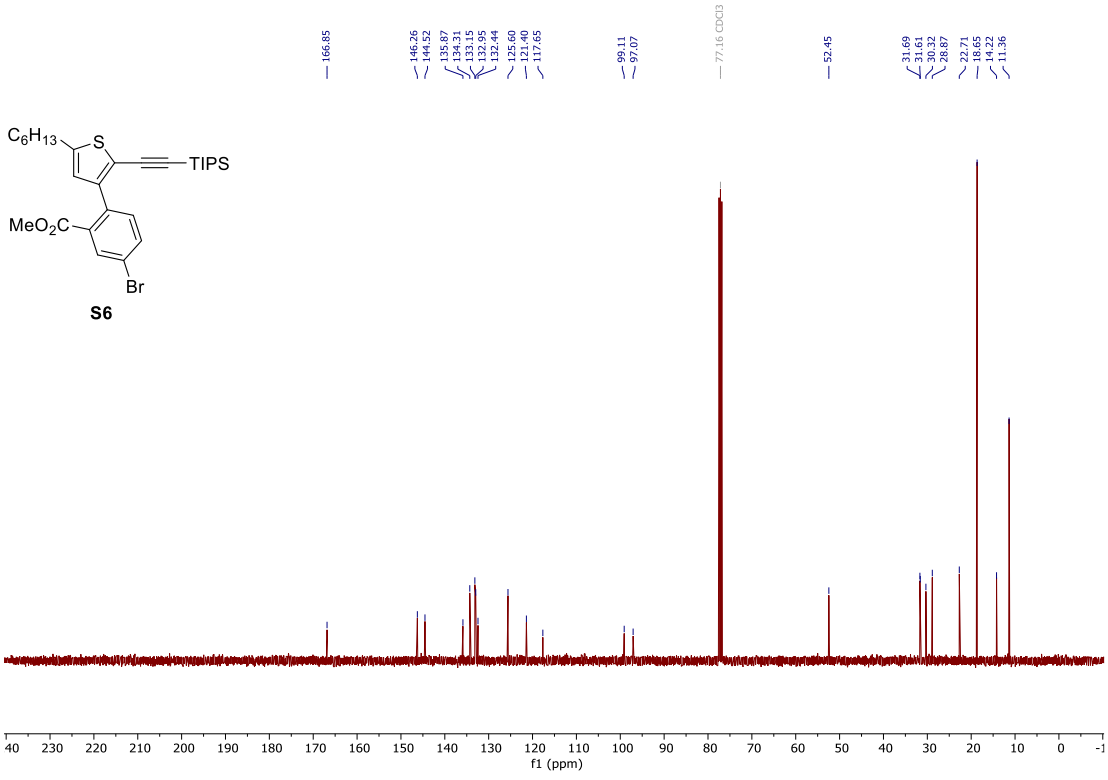

Figure 8.114. ^{1}H NMR of 20

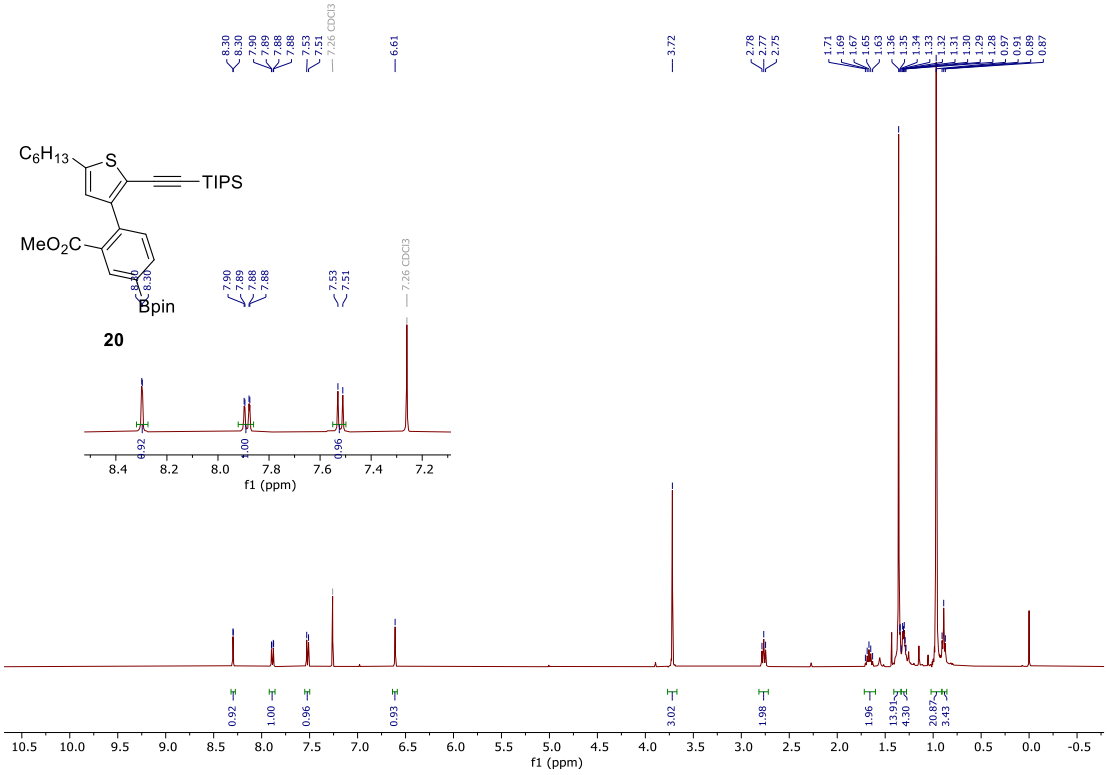

Figure 8.115. ^{13}C NMR of 20

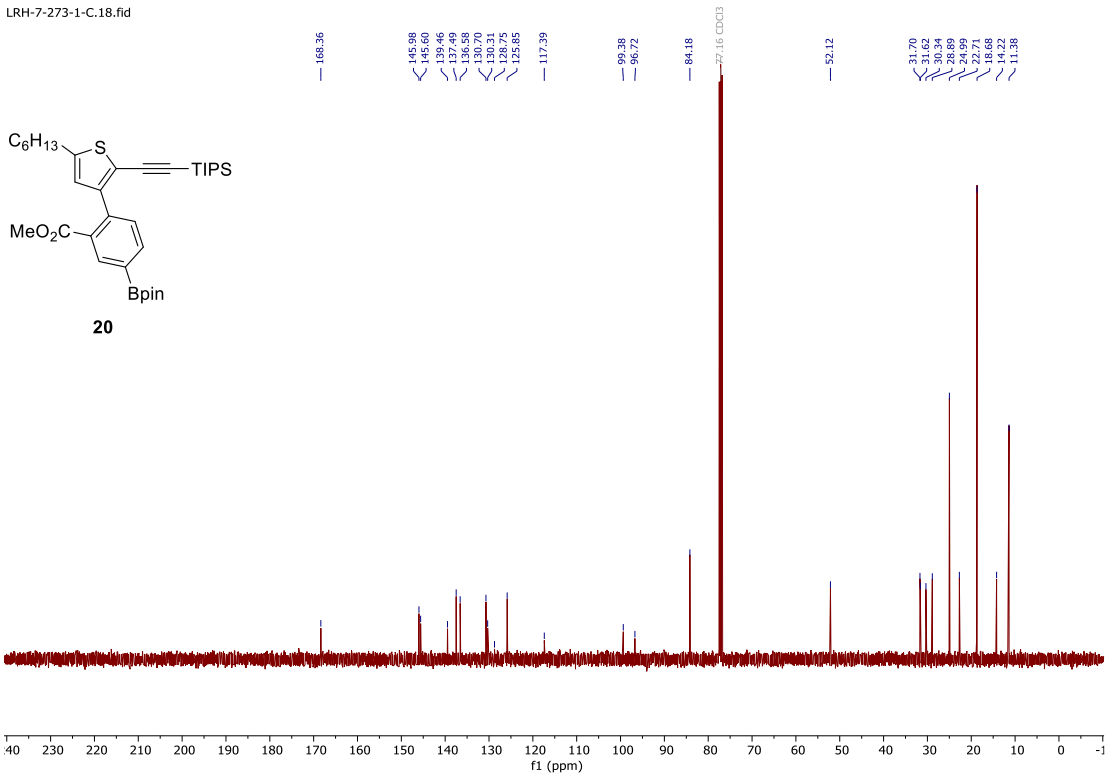

Figure 8.116. ^{1}H NMR of 21

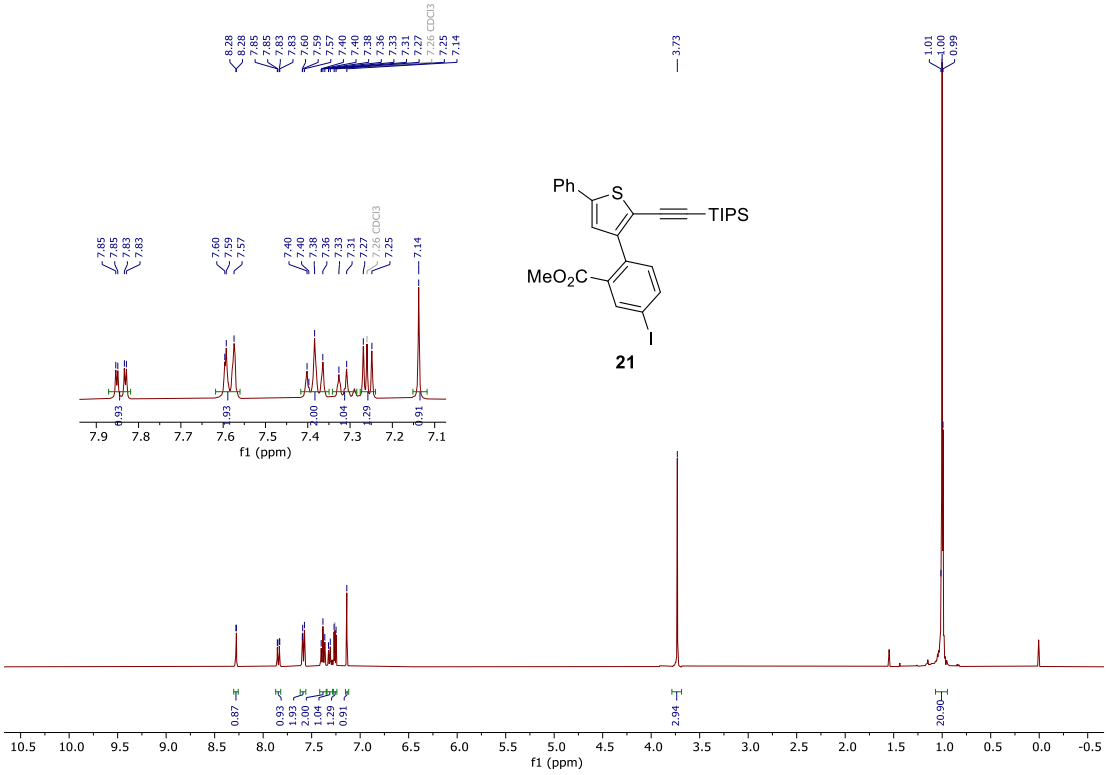

Figure 8.117. ^{13}C NMR of 21

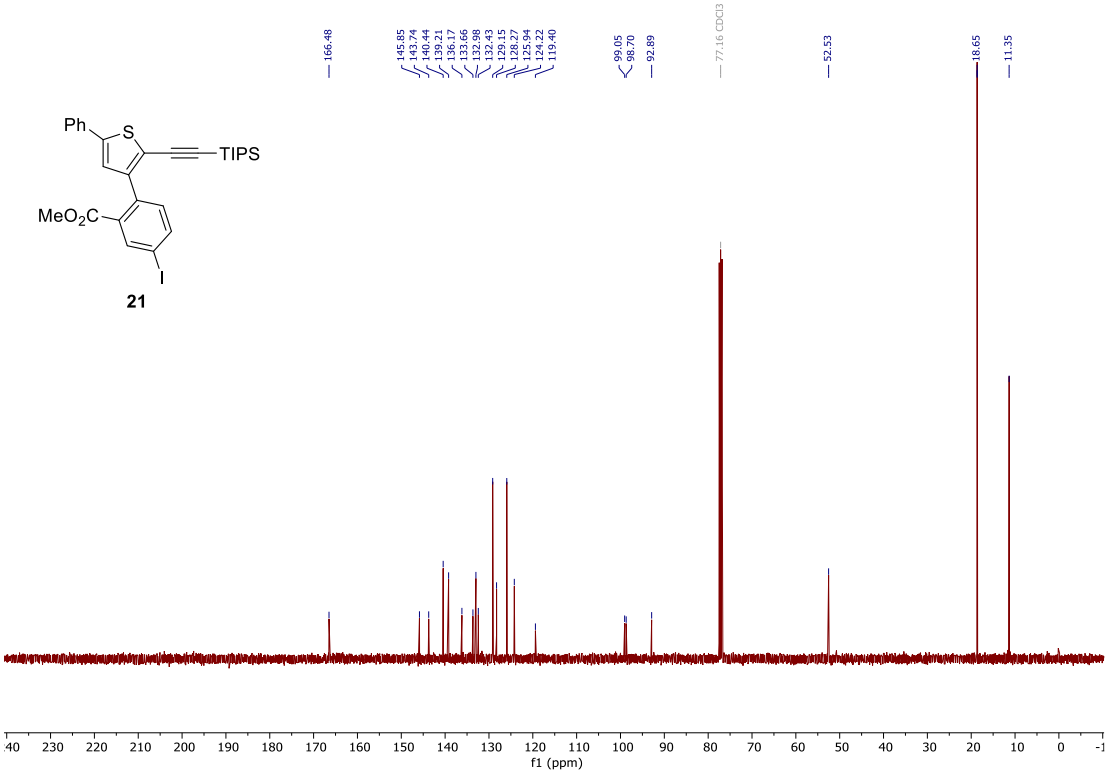

Figure 8.118. ^{1}H NMR of 22

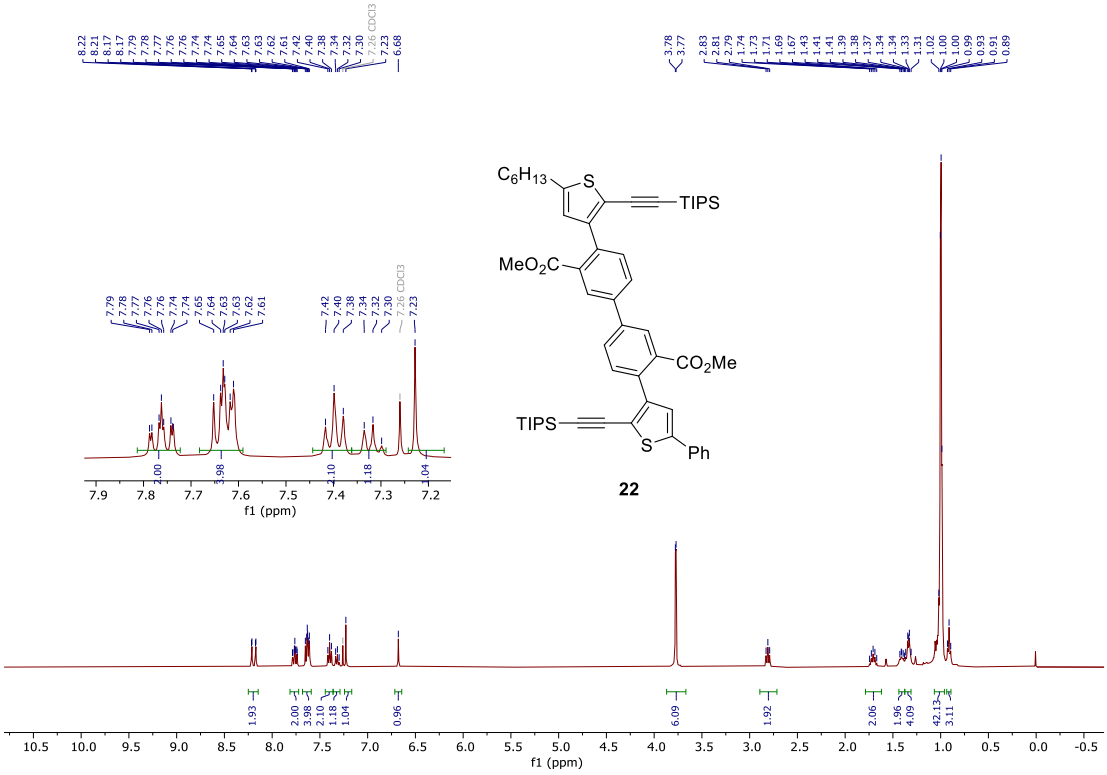

Figure 8.119. ^{13}C NMR of 22

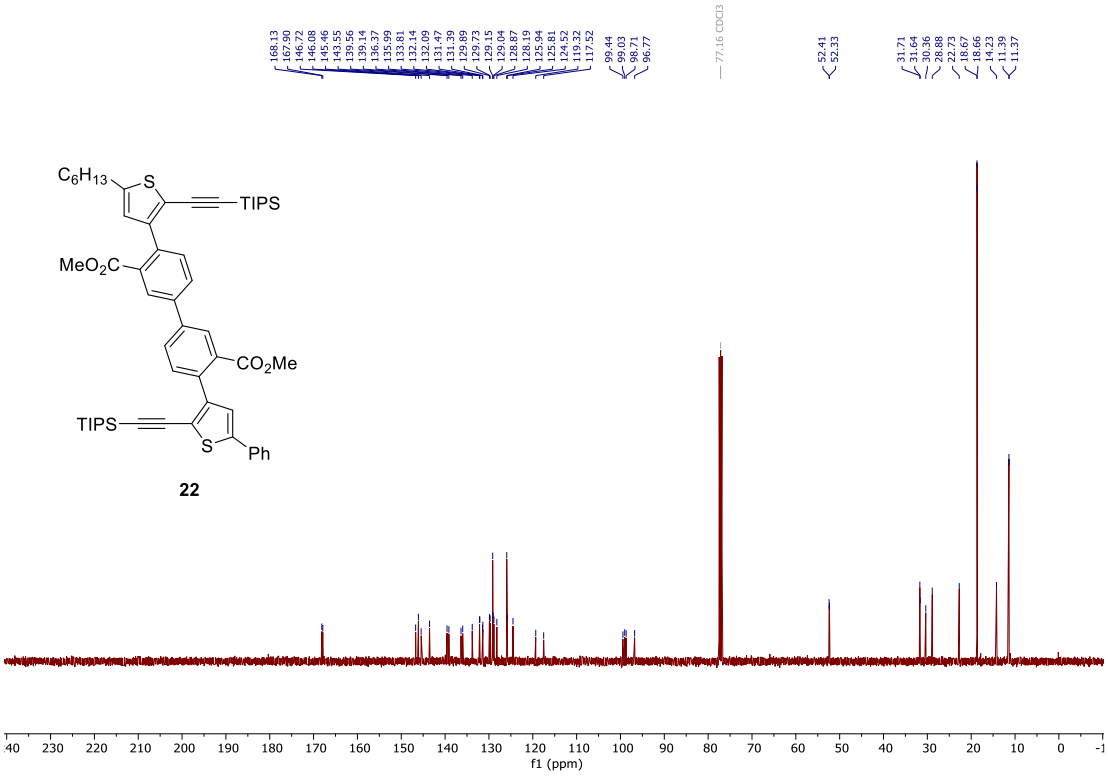

Figure 8.120. ^{1}H NMR of 26

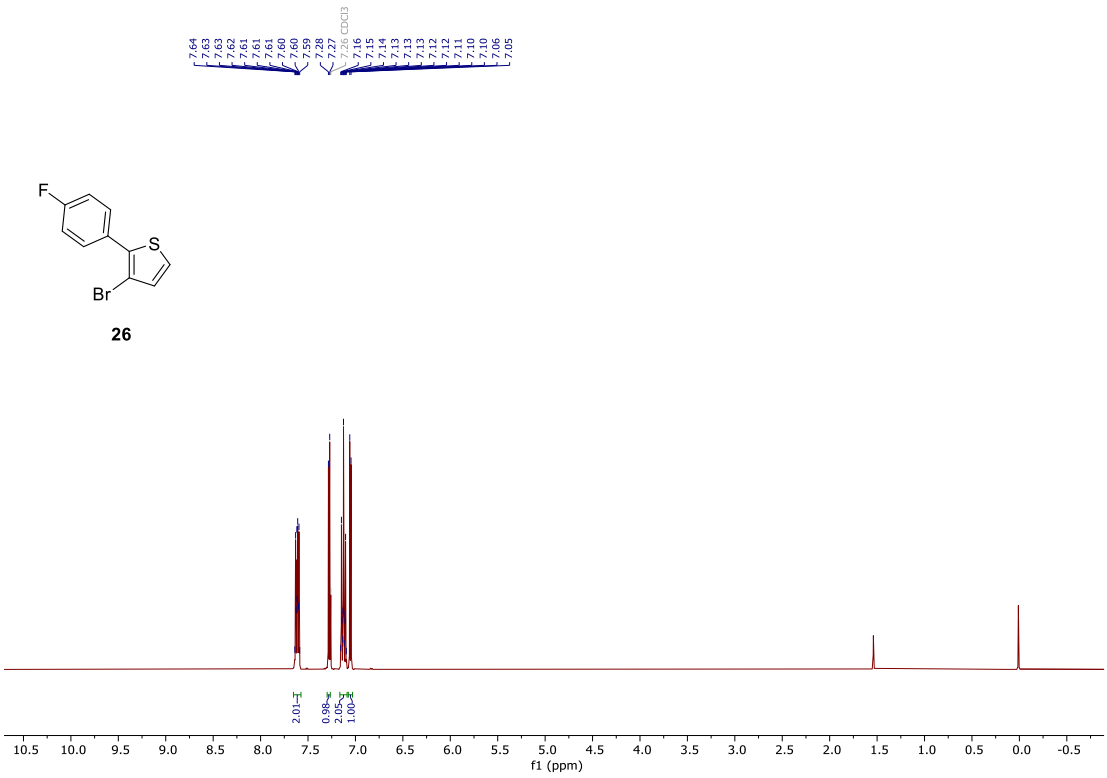

Figure 8.121. ^{13}C NMR of 26

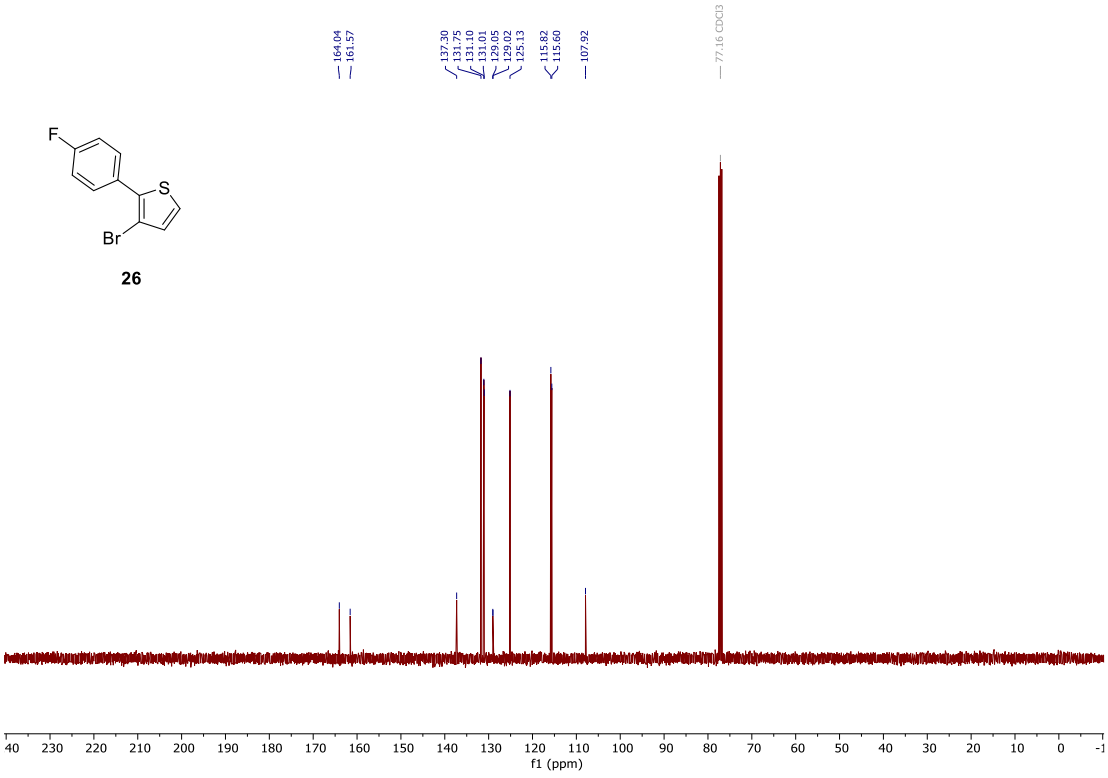

Figure 8.122. ^{19}F NMR of 26

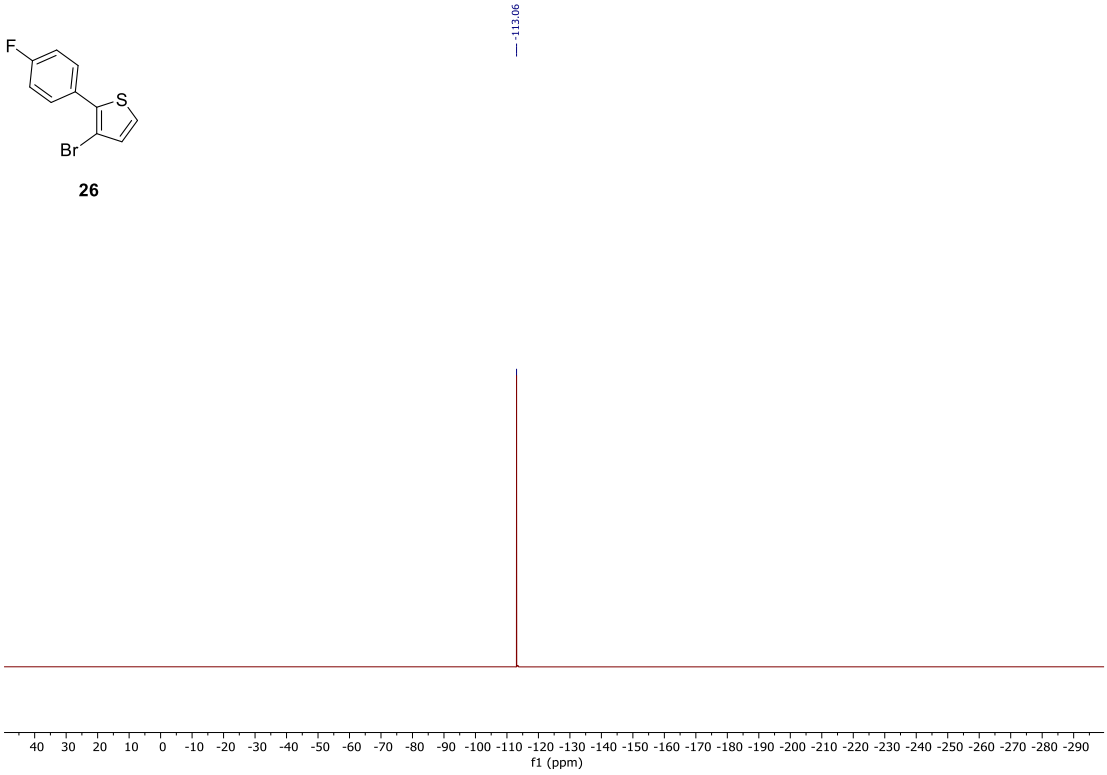

Figure 8.123. ^{1}H NMR of 27

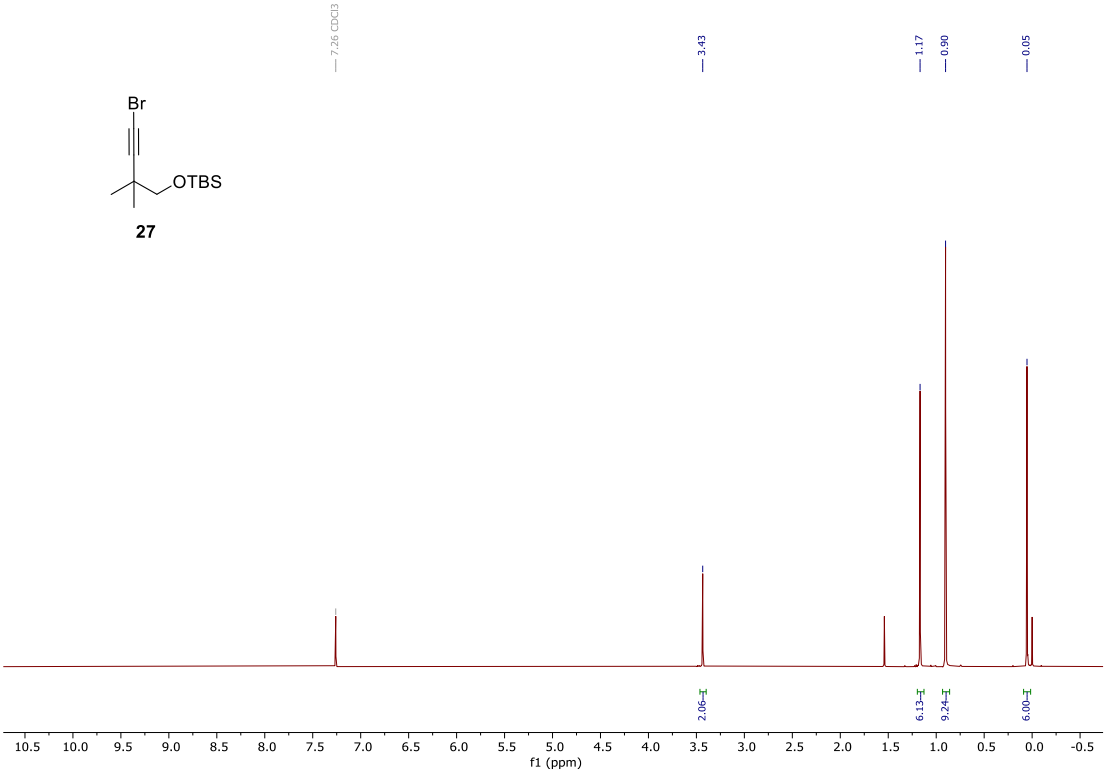

Figure 8.124. ^{13}C NMR of 27

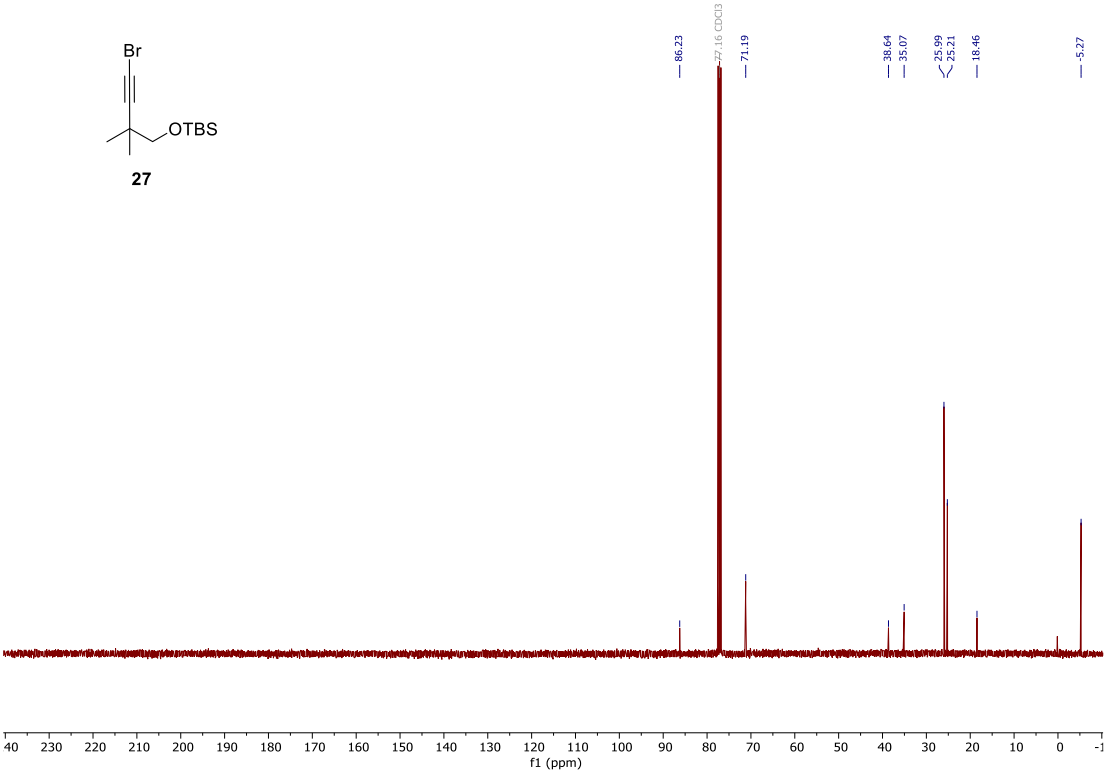

Figure 8.125. ^{1}H NMR of 28

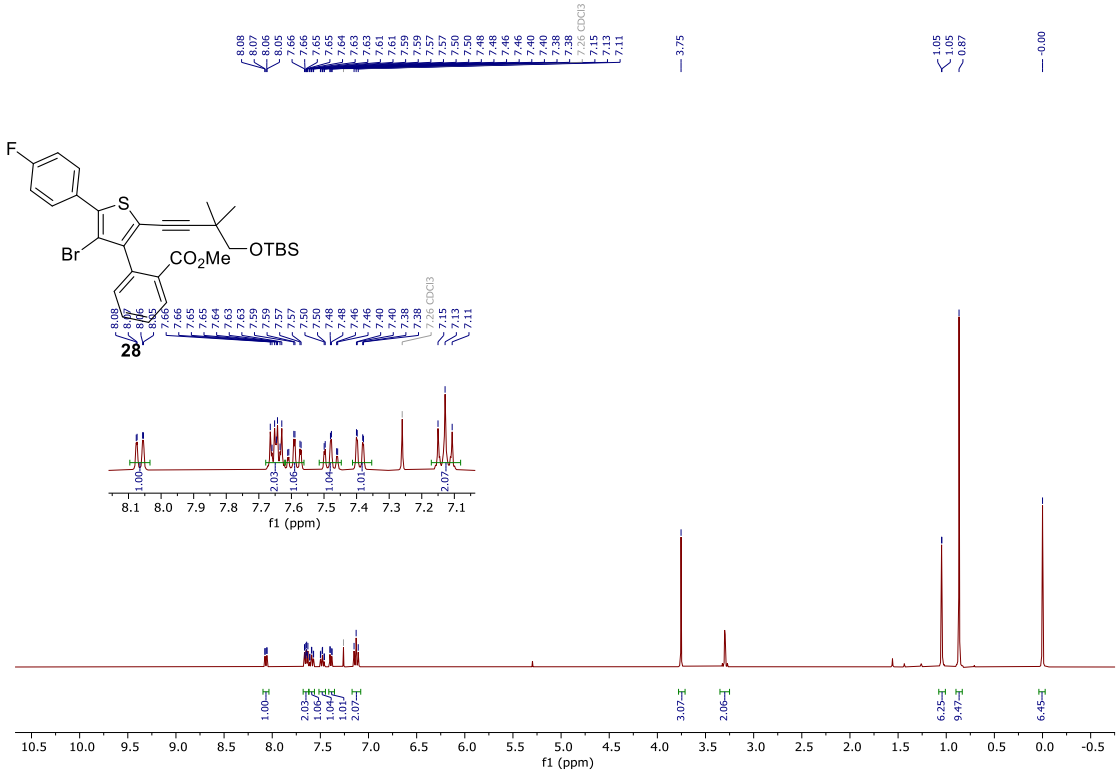

Figure 8.126. ^{13}C NMR of 28

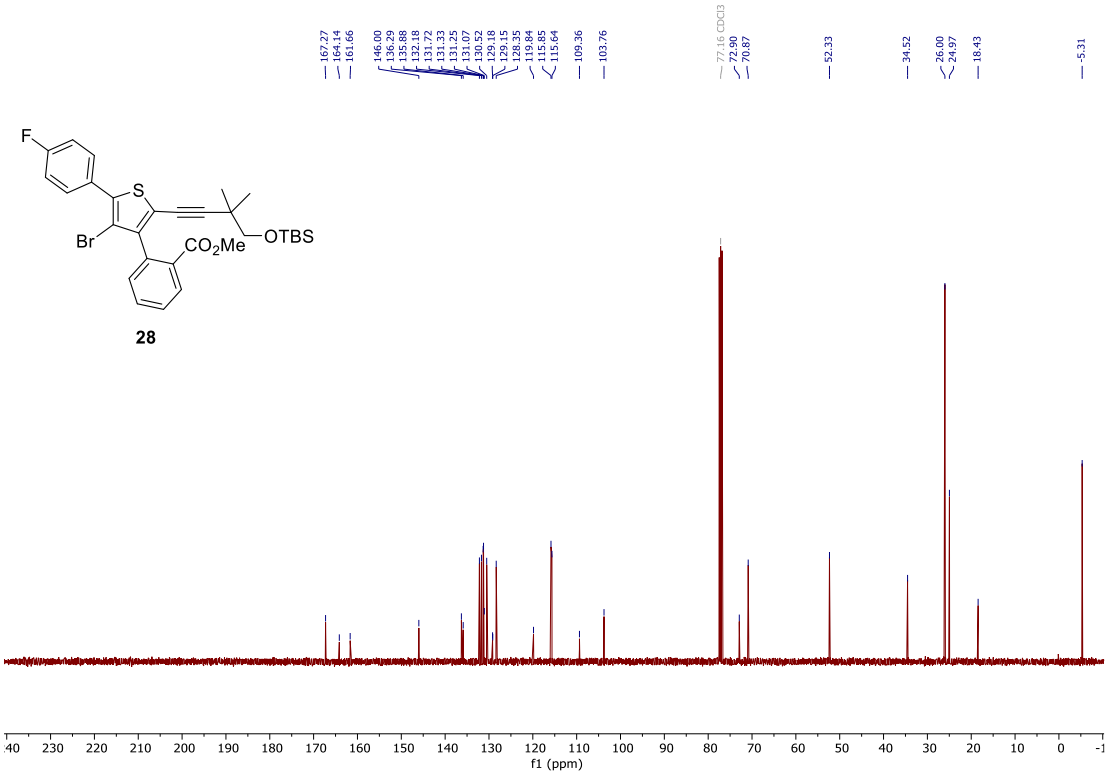

Figure 8.127. ^{19}F NMR of 28

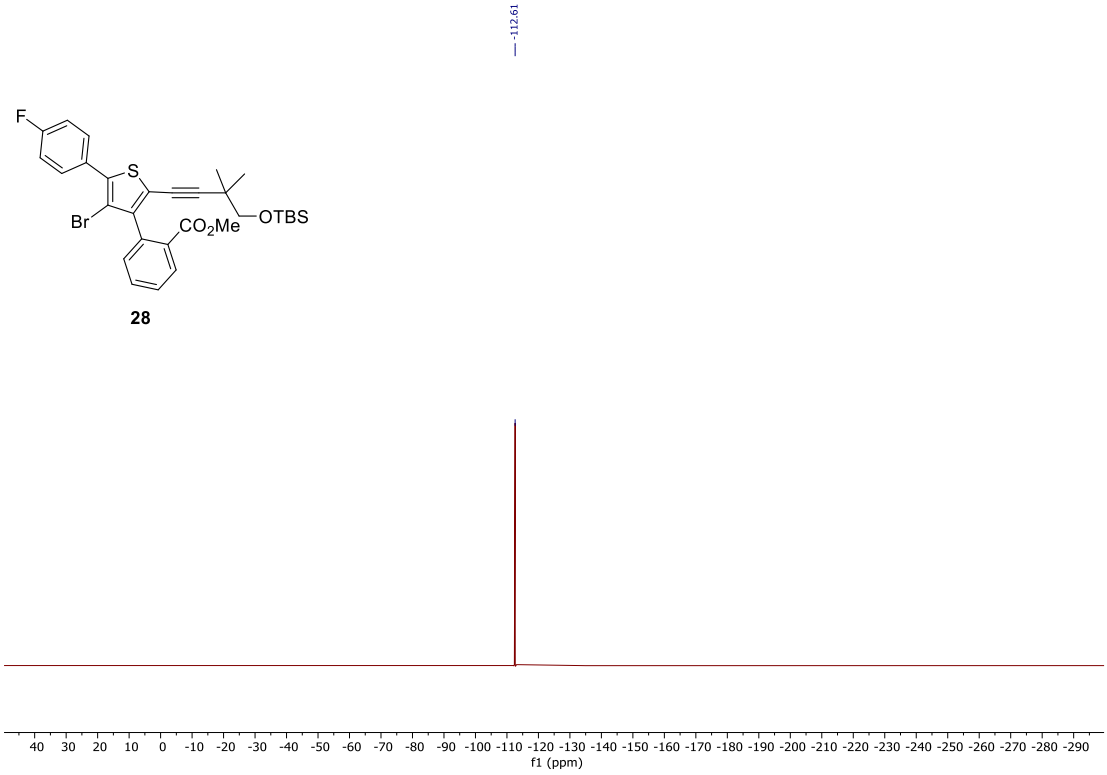

Figure 8.128. ^{1}H NMR of S10

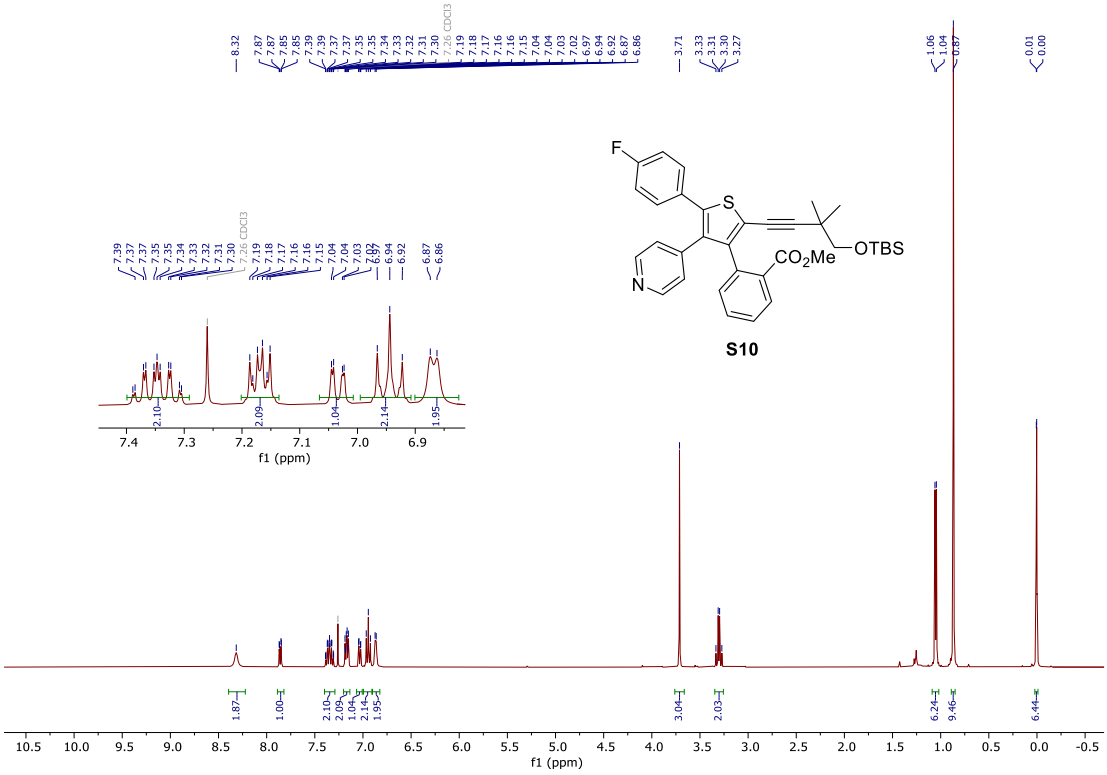

Figure 8.129. ^{13}C NMR of S10

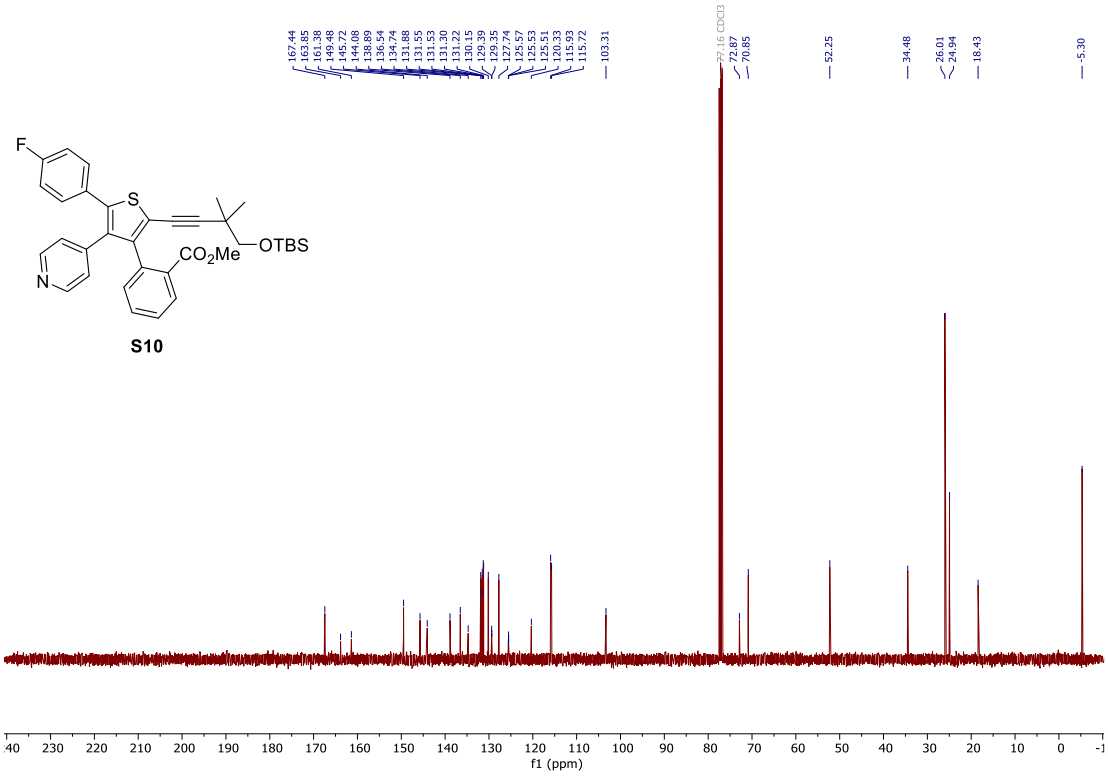

Figure 8.130. ^{19}F NMR of S10

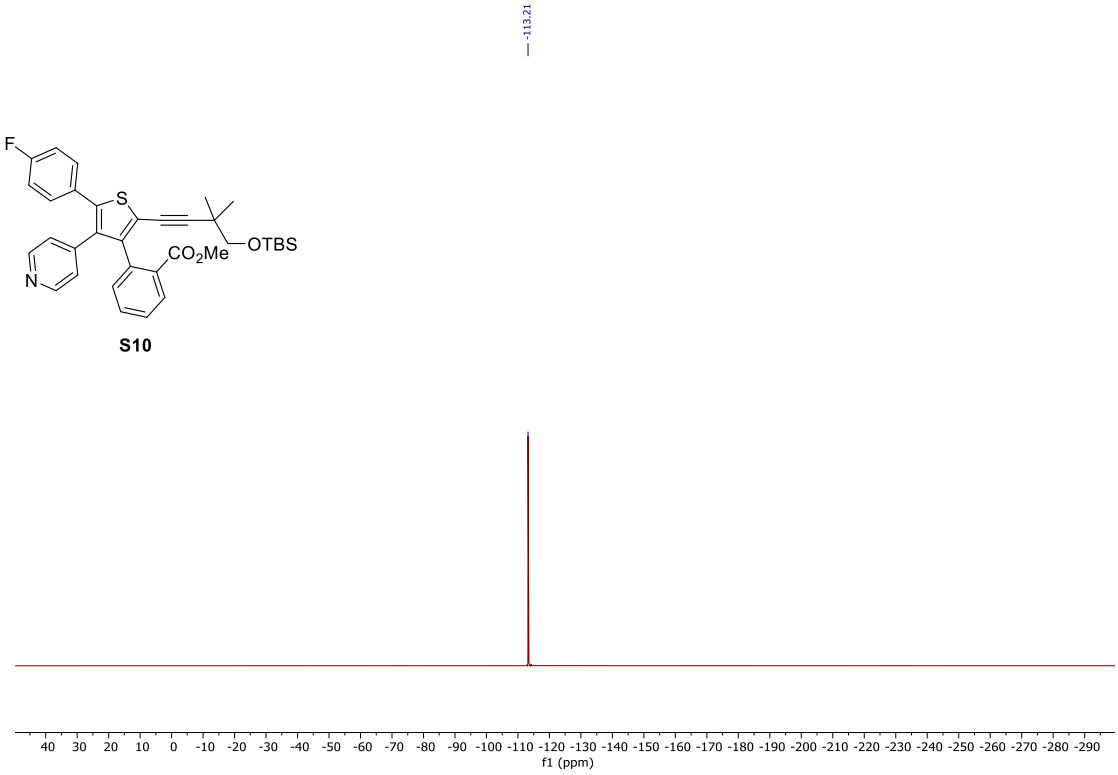

Figure 8.131. ^{1}H NMR of 30

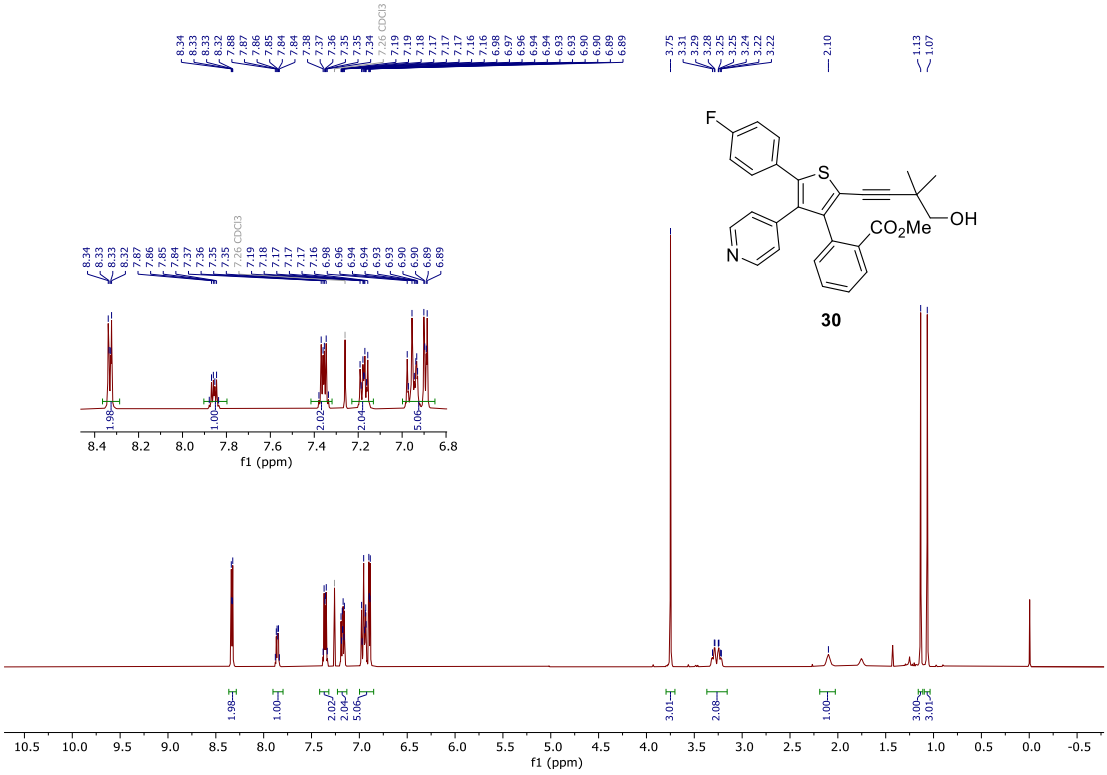

Figure 8.132. ^{13}C NMR of 30

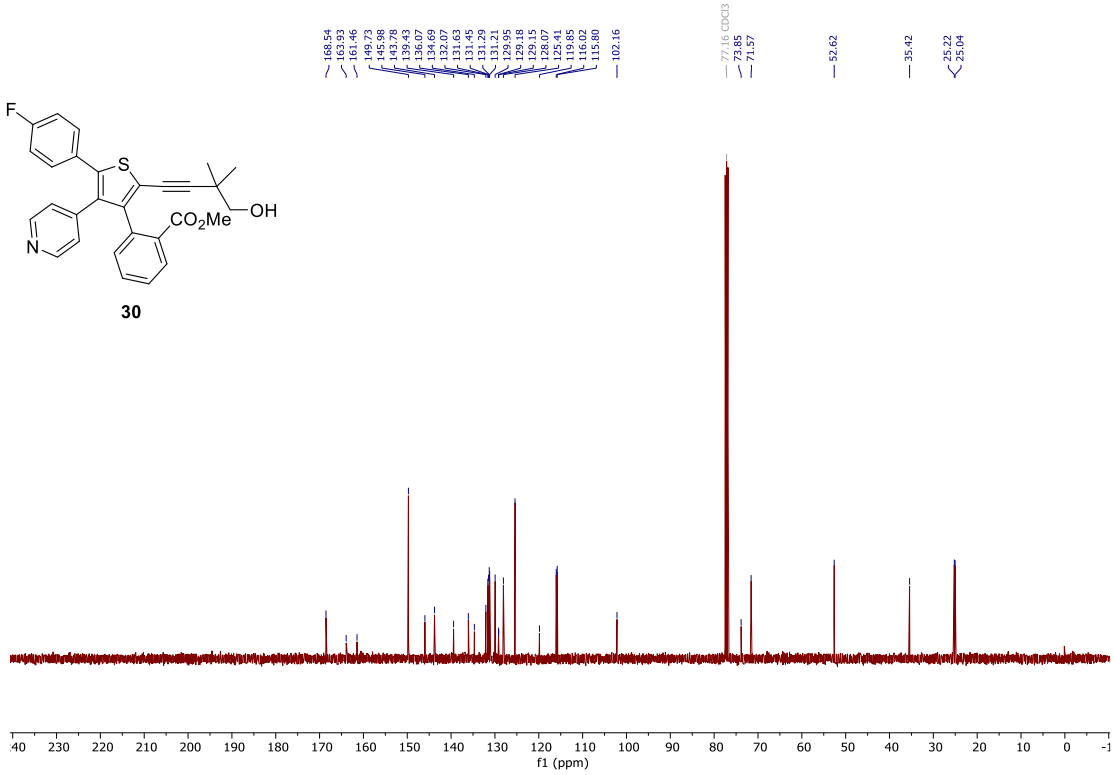

Figure 8.133. ^{19}F NMR of 30

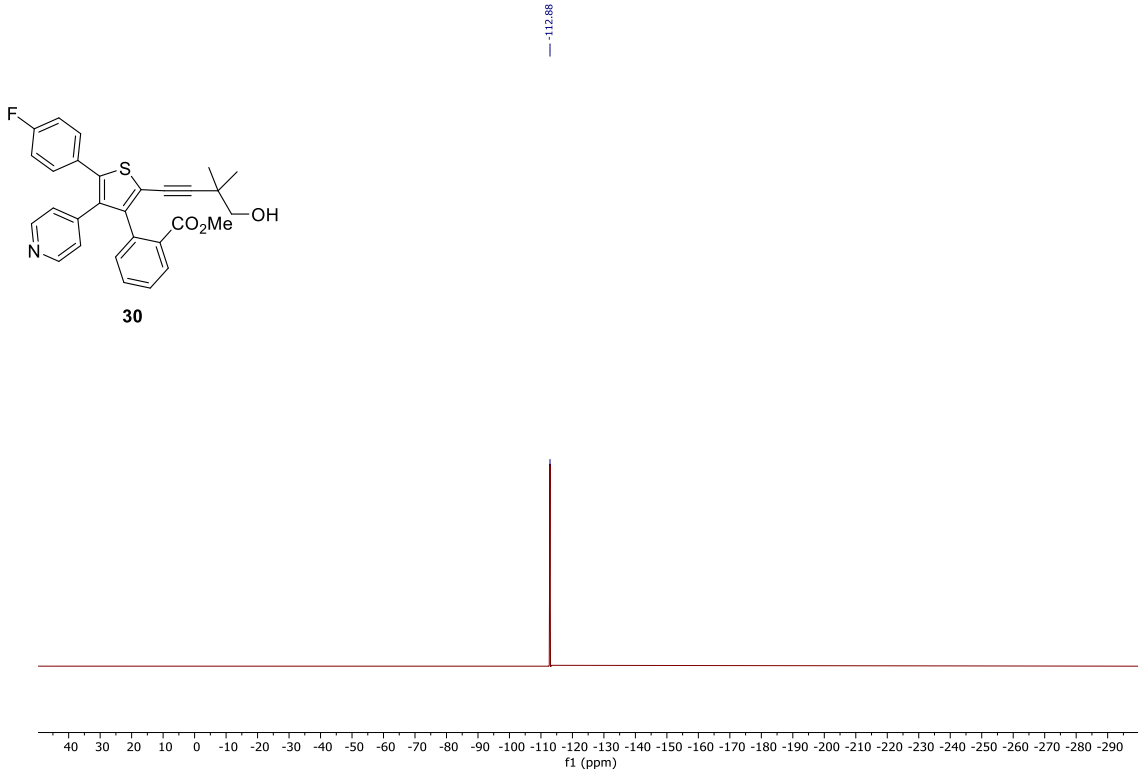

30

Figure 8.134. ^{1}H NMR of 9

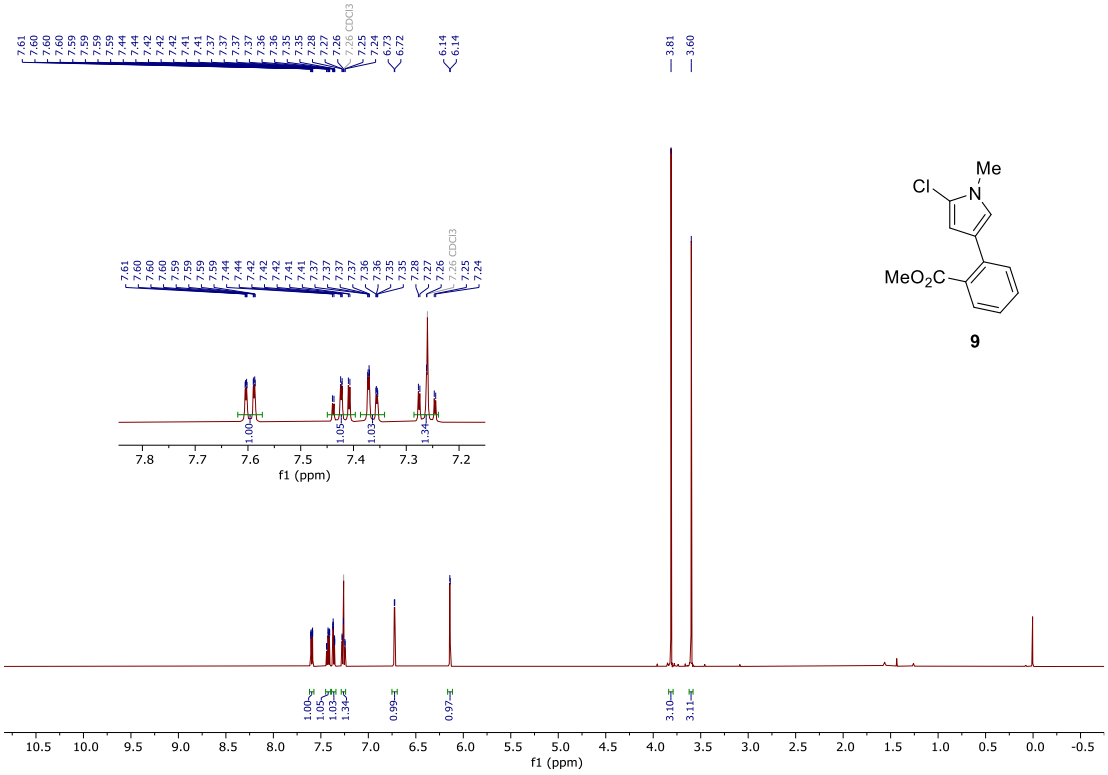

Figure 8.135. ^{13}C NMR of 9

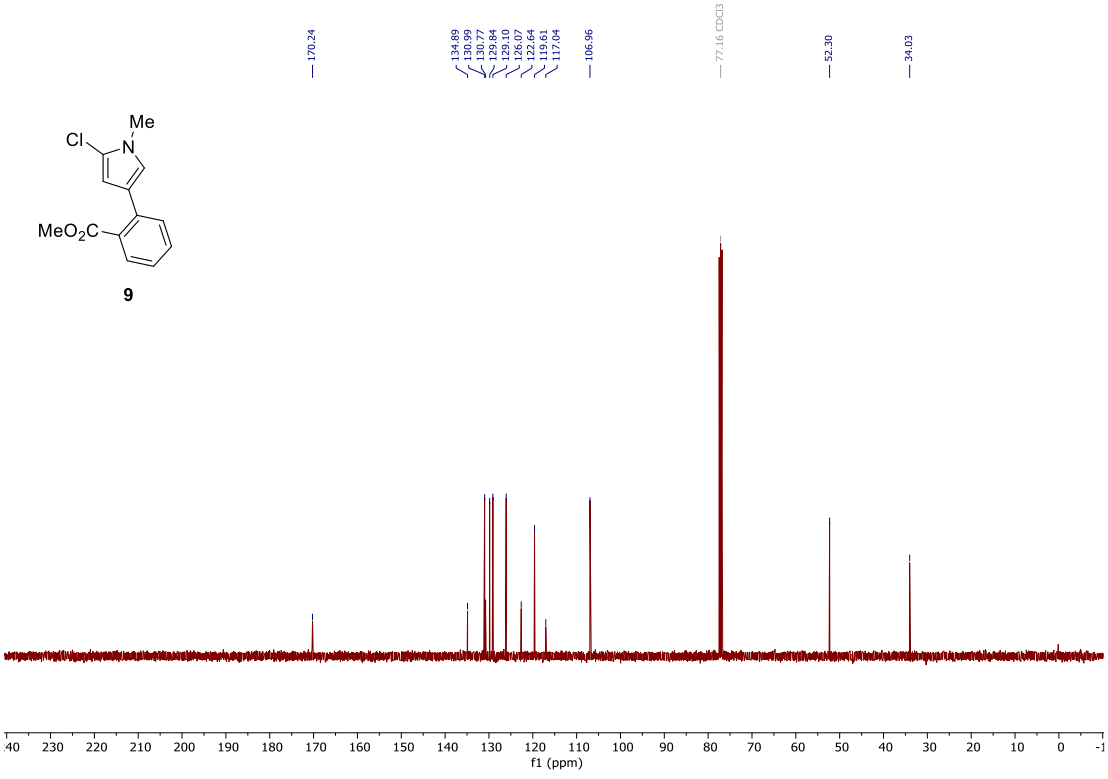

Figure 8.136. ^{1}H NMR of 10

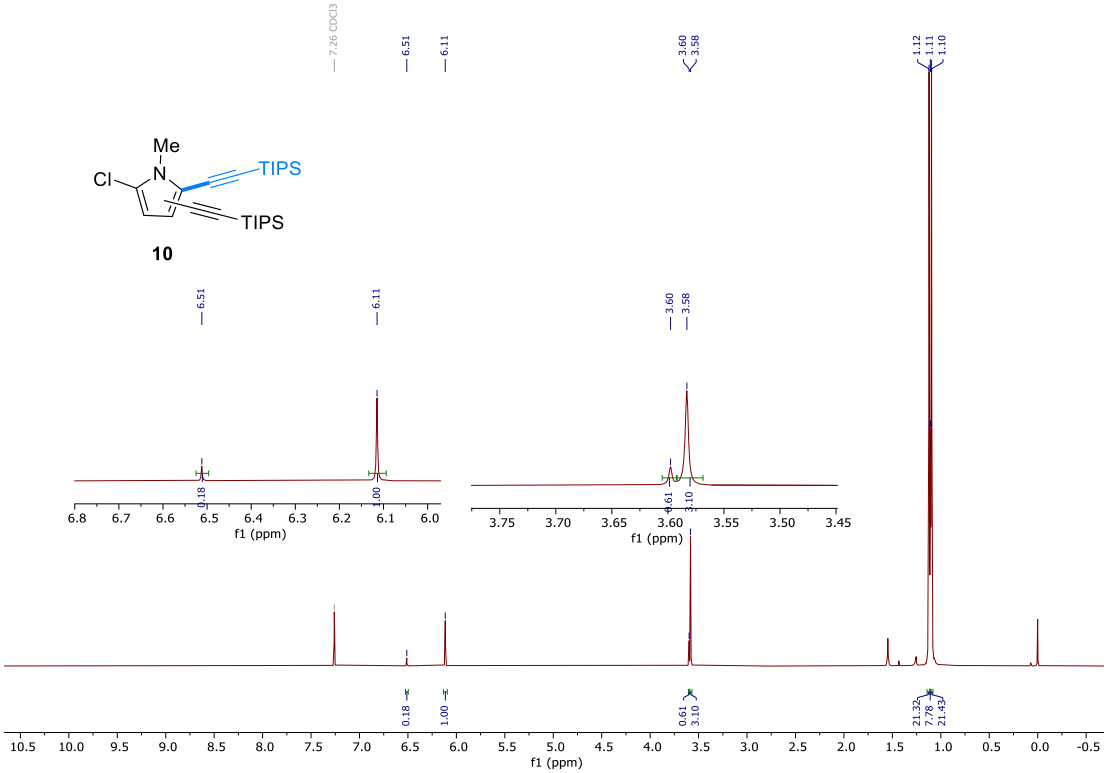

Figure 8.137. ^{13}C NMR of 10

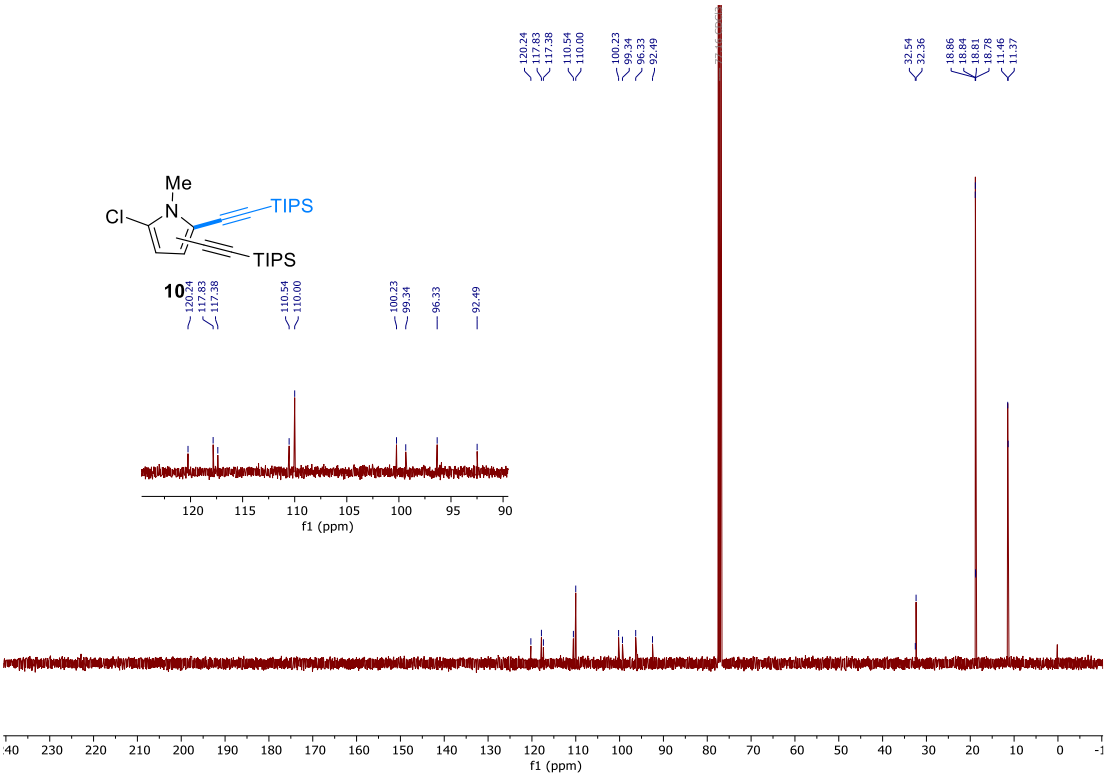

Figure 8.138. ^{1}H NMR of 4a'

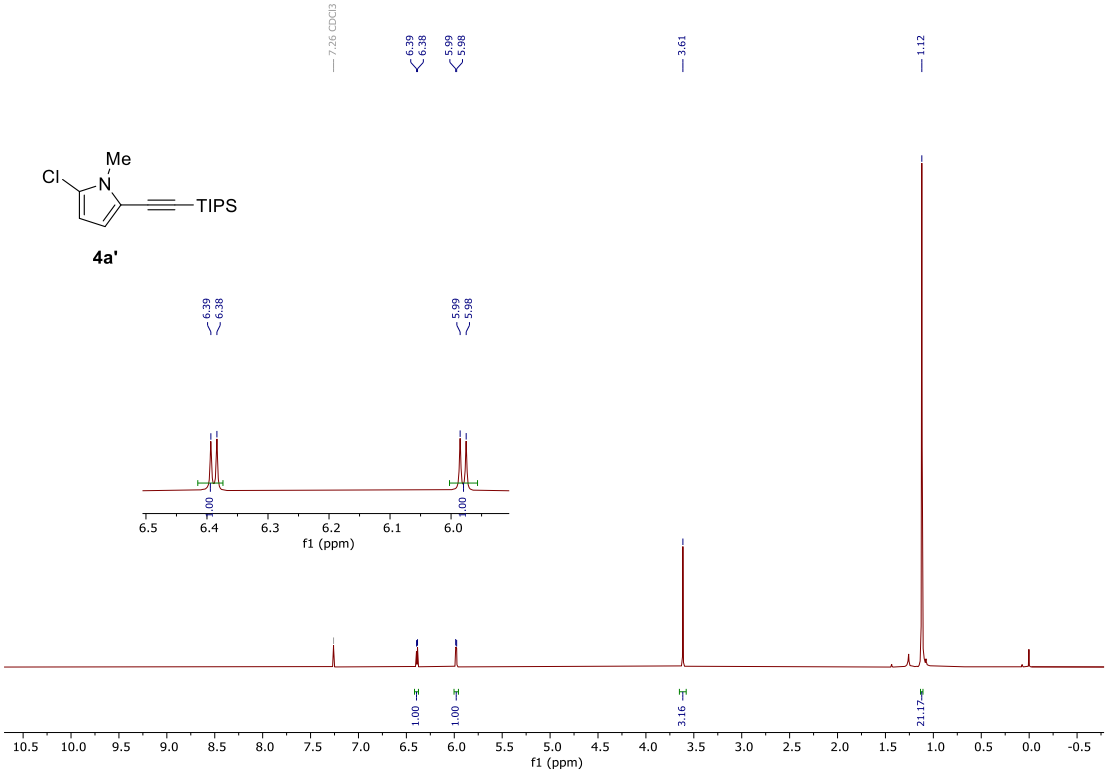

Figure 8.139. ^{13}C NMR of 4a'

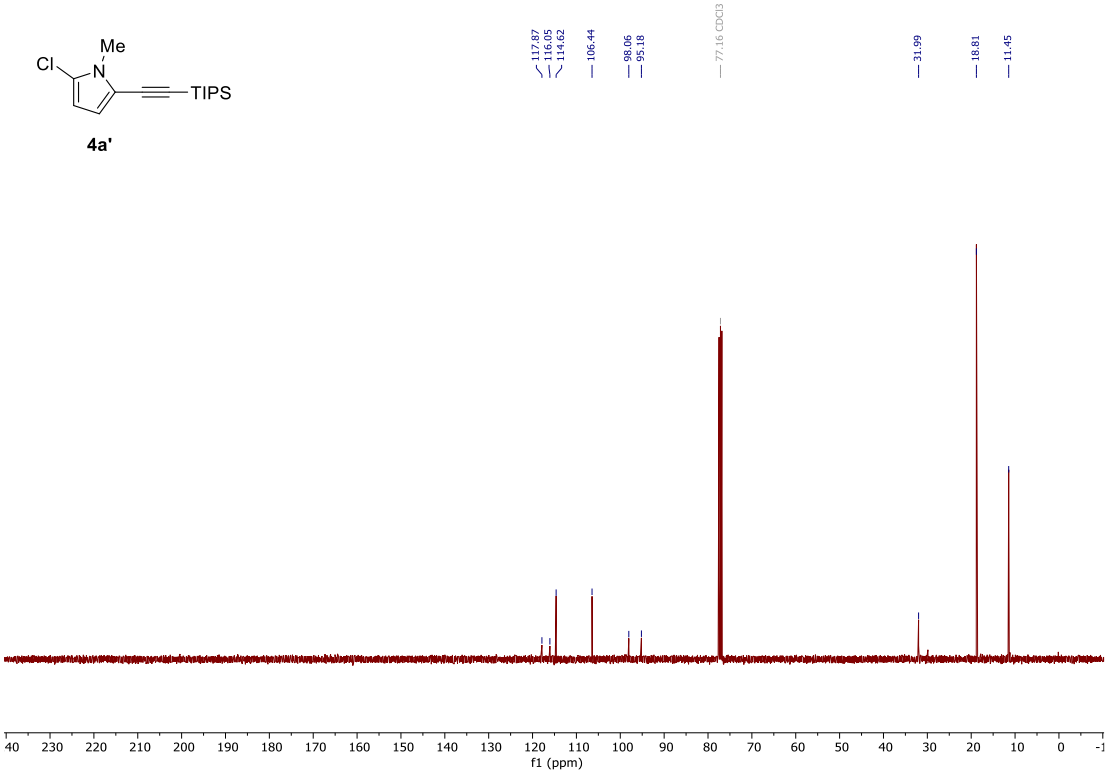

Figure 8.140. ^{1}H NMR of 8

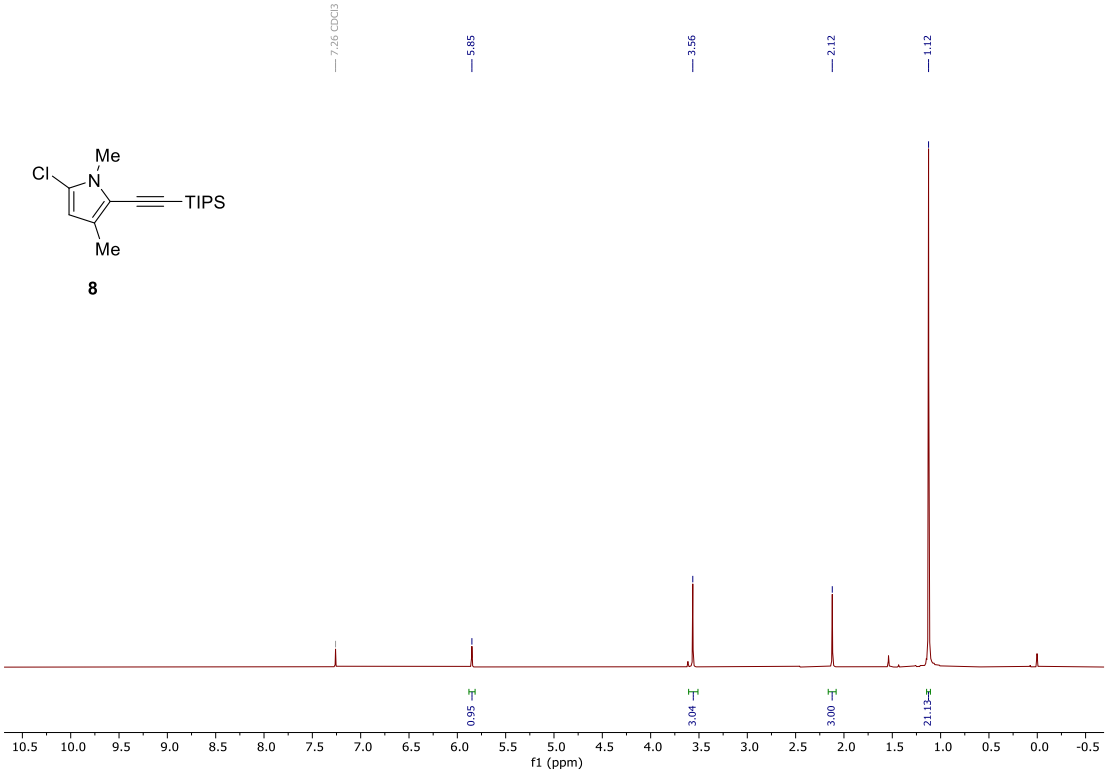

Figure 8.141. ^{13}C NMR of 8

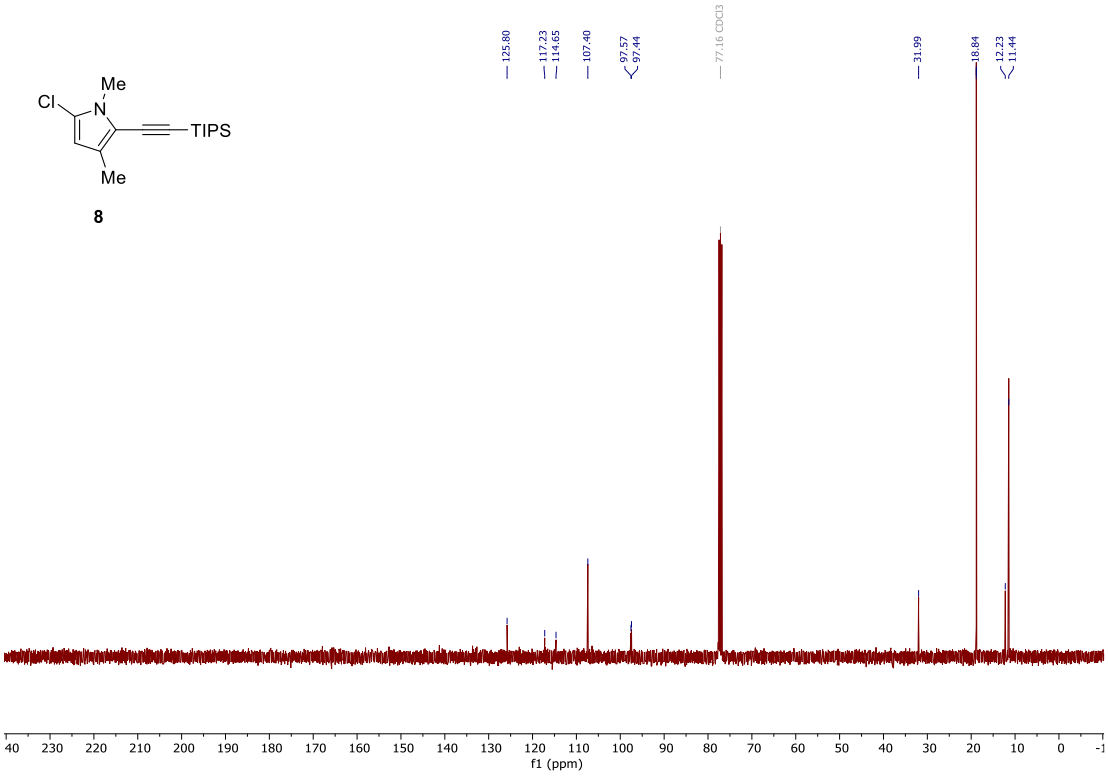

8.6 Crystallographic Data

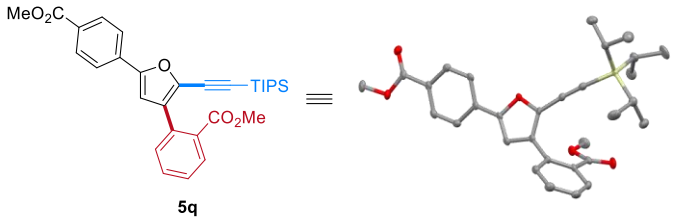

5q

Table 8.3. Crystal Data of 5q

Crystal data and structure refinement for 5q.

Identification code	test-1
Empirical formula	$C_{31}H_{36}O_5Si$
Formula weight	516.69
Temperature/K	100(2)
Crystal system	triclinic
Space group	P-1
a/Å	7.9988(12)
b/Å	8.6246(13)
c/Å	20.360(3)
α/°	85.711(4)
β/°	81.436(4)
γ/°	87.457(4)
Volume/Å^3	1384.2(4)
Z	2
ρ_{calc}g/cm^3	1.240
μ/mm^{-1}	0.123
F(000)	552.0
Crystal size/mm^3	0.364 × 0.133 × 0.115
Radiation	MoKα (λ = 0.71073)
2Θ range for data collection/°	4.738 to 49.752
Index ranges	-9 ≤ h ≤ 9, -10 ≤ k ≤ 10, -23 ≤ l ≤ 24
Reflections collected	28363
Independent reflections	4786 [R_{int} = 0.1029, R_{sigma} = 0.0822]
Data/restraints/parameters	4786/0/342
Goodness-of-fit on F^2	1.039
Final R indexes [I>=2σ (I)]	R_1 = 0.0573, wR_2 = 0.1119
Final R indexes [all data]	R_1 = 0.1087, wR_2 = 0.1294
Largest diff. peak/hole / e Å^{-3}	0.55/-0.32

8.7 References

(1) (a) Joule, J. A.; Mills, K., *Heterocyclic Chemistry*. Wiley: Weinheim: 2013; (b) Taylor, R. D.; MacCoss, M.; Lawson, A. D. G., Rings in Drugs. *J. Med. Chem.* **2014**, *57*, 5845-5859.

(2) (a) Okazawa, T.; Satoh, T.; Miura, M.; Nomura, M., Palladium-Catalyzed Multiple Arylation of Thiophenes. *J. Am. Chem. Soc.* **2002**, *124*, 5286-5287; (b) Goikhman, R.; Jacques, T. L.; Sames, D., C−H Bonds as Ubiquitous Functionality: A General Approach to Complex Arylated Pyrazoles via Sequential Regioselective C-Arylation and N-Alkylation Enabled by SEM-Group Transposition. *J. Am. Chem. Soc.* **2009**, *131*, 3042-3048; (c) Yanagisawa, S.; Ueda, K.; Sekizawa, H.; Itami, K., Programmed Synthesis of Tetraarylthiophenes through Sequential C−H Arylation. *J. Am. Chem. Soc.* **2009**, *131*, 14622-14623; (d) Joo, J. M.; Touré, B. B.; Sames, D., C−H Bonds as Ubiquitous Functionality: A General Approach to Complex Arylated Imidazoles via Regioselective Sequential Arylation of All Three C−H Bonds and Regioselective N-Alkylation Enabled by SEM-Group Transposition. *J. Org. Chem.* **2010**, *75*, 4911-4920; (e) Iaroshenko, V. O.; Gevorgyan, A.; Davydova, O.; Villinger, A.; Langer, P., Regioselective and Guided C–H Activation of 4-Nitropyrazoles. *J. Org. Chem.* **2014**, *79*, 2906-2915; (f) Kim, H. T.; Ha, H.; Kang, G.; Kim, O. S.; Ryu, H.; Biswas, A. K.; Lim, S. M.; Baik, M.-H.; Joo, J. M., Ligand-controlled Regiodivergent C−H Alkenylation of Pyrazoles and its Application to the Synthesis of Indazoles. *Angew. Chem. Int. Ed.* **2017**, *56*, 16262-16266; (g) Ghosh, I.; Khamrai, J.; Savateev, A.; Shlapakov, N.; Antonietti, M.; König, B., Organic semiconductor photocatalyst can bifunctionalize arenes and heteroarenes. *Science* **2019**, *365*, 360; (h) Li, R.; Zhou, Y.; Xu, X.; Dong, G., Direct Vicinal Difunctionalization of Thiophenes Enabled by the Palladium/Norbornene Cooperative Catalysis. *J. Am. Chem. Soc.* **2019**, *141*, 18958-18963.

(3) (a) Mkhalid, I. A. I.; Barnard, J. H.; Marder, T. B.; Murphy, J. M.; Hartwig, J. F., C−H Activation for the Construction of C−B Bonds. *Chem. Rev.* **2010**, *110*, 890-931; (b) Lyons, T. W.; Sanford, M. S., Palladium-Catalyzed Ligand-Directed C−H Functionalization Reactions. *Chem. Rev.* **2010**, *110*, 1147-1169; (c) Toste, F. D.; Sigman, M. S.; Miller, S. J., Pursuit of Noncovalent Interactions for Strategic Site-Selective Catalysis. *Acc. Chem. Res.* **2017**, *50*, 609-615; (d) Rouquet, G.; Chatani, N., Catalytic Functionalization of C(sp2)−H and C(sp3)−H Bonds by Using Bidentate Directing Groups. *Angew. Chem. Int. Ed.* **2013**, *52*, 11726-11743; (e) Huang, Z.; Dong, G., Site-Selectivity Control in Organic Reactions: A Quest To Differentiate Reactivity among the Same Kind of Functional Groups. *Acc. Chem. Res.* **2017**, *50*, 465-471.

(4) Catellani, M.; Frignani, F.; Rangoni, A., A Complex Catalytic Cycle Leading to a Regioselective Synthesis of o,o′ -Disubstituted Vinylarenes. *Angew. Chem. Int. Ed.* **1997**, *36*, 119-122.

(5) (a) Catellani, M., Novel Methods of Aromatic Functionalization Using Palladium and Norbornene as a Unique Catalytic System. *Top. Organomet. Chem.* **2005**, *14*, 21-53; (b) Catellani, M.; Motti, E.; Della Ca', N., Catalytic Sequential Reactions Involving Palladacycle-Directed Aryl Coupling Steps. *Acc. Chem. Res.* **2008**, *41*, 1512-1522; (c) Martins, A.; Mariampillai, B.; Lautens, M., Synthesis in the Key of Catellani: Norbornene-Mediated *ortho* C–H Functionalization. *Top. Curr. Chem.* **2009**, *292*, 1-33; (d) Ye, J.; Lautens, M., Palladium-catalysed norbornene-mediated C–H functionalization of arenes. *Nat. Chem.* **2015**, *7*, 863; (e) Della Ca', N.; Fontana, M.; Motti, E.; Catellani, M., Pd/Norbornene: A Winning Combination for Selective Aromatic Functionalization via C–H Bond Activation. *Acc. Chem. Res.* **2016**, *49*, 1389-1400; (f) Wegmann, M.; Henkel, M.; Bach, T., C–H alkylation reactions of indoles mediated by Pd(ii) and norbornene: applications and recent developments. *Org. Biomol. Chem.* **2018**, *16*, 5376-5385; (g) Liu, Z.-S.;

Gao, Q.; Cheng, H.-G.; Zhou, Q., Alkylating Reagents Employed in Catellani-Type Reactions. *Chem. Eur. J.* **2018**, *24*, 15461-15476; (h) Zhao, K.; Ding, L.; Gu, Z., Development of New Electrophiles in Palladium/Norbornene-Catalyzed *ortho*-Functionalization of Aryl Halides. *Synlett* **2019**, *30*, 129-140; (i) Cheng, H.-G.; Chen, S.; Chen, R.; Zhou, Q., Palladium(II)-Initiated Catellani-Type Reactions. *Angew. Chem. Int. Ed.* **2019**, *58*, 5832-5844; (j) Wang, J.; Dong, G., Palladium/Norbornene Cooperative Catalysis. *Chem. Rev.* **2019**, *119*, 7478-7528; (k) Li, R.; Dong, G., Structurally Modified Norbornenes: A Key Factor to Modulate Reaction Selectivity in the Palladium/Norbornene Cooperative Catalysis. *J. Am. Chem. Soc.* **2020**, *142*, 17859-17875.

(6) Jiao, L.; Bach, T., Palladium-Catalyzed Direct 2-Alkylation of Indoles by Norbornene-Mediated Regioselective Cascade C–H Activation. *J. Am. Chem. Soc.* **2011**, *133*, 12990-12993.

(7) (a) Wang, X.-C.; Gong, W.; Fang, L.-Z.; Zhu, R.-Y.; Li, S.; Engle, K. M.; Yu, J.-Q., Ligand-enabled meta-C–H activation using a transient mediator. *Nature* **2015**, *519*, 334; (b) Dong, Z.; Wang, J.; Dong, G., Simple Amine-Directed Meta-Selective C–H Arylation via Pd/Norbornene Catalysis. *J. Am. Chem. Soc.* **2015**, *137*, 5887-5890.

(8) (a) Li, R.; Liu, F.; Dong, G., Redox-Neutral *ortho* Functionalization of Aryl Boroxines via Palladium/Norbornene Cooperative Catalysis. *Chem* **2019**, *5*, 929-939; (b) Chen, S.; Wang, P.; Cheng, H.-G.; Yang, C.; Zhou, Q., Redox-Neutral *ortho*-C–H Amination of Pinacol Arylborates via Palladium(ii)/Norbornene Catalysis for Aniline Synthesis. *Chem. Sci.* **2019**, *10*, 8384-8389.

(9) Zhao, Y.-B.; Mariampillai, B.; Candito, D. A.; Laleu, B.; Li, M.; Lautens, M., Exploiting the Divergent Reactivity of Aryl–Palladium Intermediates for the Rapid Assembly of Fluorene and Phenanthrene Derivatives. *Angew. Chem. Int. Ed.* **2009**, *48*, 1849-1852.

(10) Wang, J.; Qin, C.; Lumb, J.-P.; Luan, X., Regioselective Synthesis of Polyfunctional Arenes by a 4-Component Catellani Reaction. *Chem* **2020**, *6*, 2097-2109.

(11) O'Duill, M. L.; Engle, K. M., Protodepalladation as a Strategic Elementary Step in Catalysis. *Synthesis* **2018**, *50*, 4699-4714.

(12) Rago, A. J.; Dong, G., Unexpected *ortho*-Heck Reaction under the Catellani Conditions. *Org. Lett.* **2020**, *22*, 3770-3774.

(13) (a) Seregin, I. V.; Ryabova, V.; Gevorgyan, V., Direct Palladium-Catalyzed Alkynylation of N-Fused Heterocycles. *J. Am. Chem. Soc.* **2007**, *129*, 7742-7743; (b) Dudnik, A. S.; Gevorgyan, V., Formal Inverse Sonogashira Reaction: Direct Alkynylation of Arenes and Heterocycles with Alkynyl Halides. *Angew. Chem. Int. Ed.* **2010**, *49*, 2096-2098; (c) Dorel, R.; Echavarren, A. M., Gold(I)-Catalyzed Activation of Alkynes for the Construction of Molecular Complexity. *Chem. Rev.* **2015**, *115*, 9028-9072; (d) Tan, E.; Quinonero, O.; Elena de Orbe, M.; Echavarren, A. M., Broad-Scope Rh-Catalyzed Inverse-Sonogashira Reaction Directed by Weakly Coordinating Groups. *ACS Catal.* **2018**, *8*, 2166-2172; (e) Tobisu, M.; Ano, Y.; Chatani, N., Palladium-Catalyzed Direct Alkynylation of C−H Bonds in Benzenes. *Org. Lett.* **2009**, *11*, 3250-3252.

(14) (a) Tan, E.; Konovalov, A. I.; Fernández, G. A.; Dorel, R.; Echavarren, A. M., Ruthenium-Catalyzed Peri- and *Ortho*-Alkynylation with Bromoalkynes via Insertion and Elimination. *Org. Lett.* **2017**, *19*, 5561-5564; (b) Usui, K.; Haines, B. E.; Musaev, D. G.; Sarpong, R., Understanding Regiodivergence in a Pd(II)-Mediated Site-Selective C–H Alkynylation. *ACS Catal.* **2018**, *8*, 4516-4527.

(15) (a) Shen, P.-X.; Wang, X.-C.; Wang, P.; Zhu, R.-Y.; Yu, J.-Q., Ligand-Enabled Meta-C–H Alkylation and Arylation Using a Modified Norbornene. *J. Am. Chem. Soc.* **2015**, *137*, 11574-

11577; (b) Li, R.; Dong, G., Direct Annulation between Aryl Iodides and Epoxides through Palladium/Norbornene Cooperative Catalysis. *Angew. Chem. Int. Ed.* **2018**, *57*, 1697-1701; (c) Liu, L.-Y.; Qiao, J. X.; Yeung, K.-S.; Ewing, W. R.; Yu, J.-Q., meta-Selective C−H Arylation of Fluoroarenes and Simple Arenes. *Angew. Chem. Int. Ed.* **2020**, *59*, 13831-13835; (d) Wang, J.; Dong, Z.; Yang, C.; Dong, G., Modular and regioselective synthesis of all-carbon tetrasubstituted olefins enabled by an alkenyl Catellani reaction. *Nat. Chem.* **2019**, *11*, 1106-1112; (e) Li, R.; Zhou, Y.; Yoon, K.-Y.; Dong, Z.; Dong, G., Sulfenamide-Enabled *Ortho* Thiolation of Aryl Iodides via Palladium/Norbornene Cooperative Catalysis. *Nat. Commun.* **2019**, *10*, 3555; (f) Li, R.; Liu, F.; Dong, G., Palladium-catalyzed asymmetric annulation between aryl iodides and racemic epoxides using a chiral norbornene cocatalyst. *Org. Chem. Front.* **2018**, *5*, 3108-3112.

(16) Wang, J.; Zhou, Y.; Xu, X.; Liu, P.; Dong, G., Entry to 1,2,3,4-Tetrasubstituted Arenes through Addressing the "Meta Constraint" in the Palladium/Norbornene Catalysis. *J. Am. Chem. Soc.* **2020**, *142*, 3050-3059.

(17) Wang, J.; Li, R.; Dong, Z.; Liu, P.; Dong, G., Complementary site-selectivity in arene functionalization enabled by overcoming the *ortho* constraint in palladium/norbornene catalysis. *Nat. Chem.* **2018**, *10*, 866-872.

(18) Dong, Z.; Wang, J.; Ren, Z.; Dong, G., *Ortho* C–H Acylation of Aryl Iodides by Palladium/Norbornene Catalysis. *Angew. Chem. Int. Ed.* **2015**, *54*, 12664-12668.

(19) Wang, P.; Chen, S.; Zhou, Z.; Cheng, H.-G.; Zhou, Q., Chemoselective Borono-Catellani Arylation for Unsymmetrical Biaryls Synthesis. *Org. Lett.* **2019**, *21*, 3323-3327.

(20) Porey, S.; Zhang, X.; Bhowmick, S.; Kumar Singh, V.; Guin, S.; Paton, R. S.; Maiti, D., Alkyne Linchpin Strategy for Drug:Pharmacophore Conjugation: Experimental and

Computational Realization of a Meta-Selective Inverse Sonogashira Coupling. *J. Am. Chem. Soc.* **2020**, *142*, 3762-3774.

(21) Gorsline, B. J.; Wang, L.; Ren, P.; Carrow, B. P., C–H Alkenylation of Heteroarenes: Mechanism, Rate, and Selectivity Changes Enabled by Thioether Ligands. *J. Am. Chem. Soc.* **2017**, *139*, 9605-9614.

(22) Cárdenas, D. J.; Martín-Matute, B.; Echavarren, A. M., Aryl Transfer between Pd(II) Centers or Pd(IV) Intermediates in Pd-Catalyzed Domino Reactions. *J. Am. Chem. Soc.* **2006**, *128*, 5033-5040.

(23) Saini, K. M.; Saunthwal, R. K.; Verma, A. K., Pd-Catalyzed one-pot sequential cross-coupling reactions of tetrabromothiophene. *Org. Biomol. Chem.* **2017**, *15*, 10289-10298.

(24) Toyota, K.; Okada, K.; Katsuta, H.; Morita, N., Preparations of bis[2-(2-arylethynyl)-3-thienyl]arenes and bis[2-{2-(trimethylsilyl)ethynyl}-3-thienyl]arenes. *Tetrahedron* **2009**, *65*, 145-151.

(25) Vinh, N. B.; Devine, S. M.; Munoz, L.; Ryan, R. M.; Wang, B. H.; Krum, H.; Chalmers, D. K.; Simpson, J. S.; Scammells, P. J., Design, Synthesis, and Biological Evaluation of Tetra-Substituted Thiophenes as Inhibitors of p38α MAPK. *ChemistryOpen* **2015**, *4*, 56-64.

(26) The alkynyl bromide without the gem dimethyl groups was not suitable for this coupling under the current conditions likely due to isomerization of the triple bond.

(27) Yamasaki, R.; Morita, K.; Iizumi, H.; Ito, A.; Fukuda, K.; Okamoto, I., N-Ethynylation of Anilides Decreases the Double-Bond Character of Amide Bond while Retaining trans-Conformation and Planarity. *Chem. Eur. J.* **2019**, *25*, 10118-10122.

(28) Liu, T.; Qiao, J. X.; Poss, M. A.; Yu, J.-Q., Palladium(II)-Catalyzed Site-Selective C(sp3)−H Alkynylation of Oligopeptides: A Linchpin Approach for Oligopeptide–Drug Conjugation. *Angew. Chem. Int. Ed.* **2017**, *56*, 10924-10927.

(29) Choo, K.-L.; Lautens, M., Rhodium-Catalyzed Asymmetric Conjugate Alkynylation/Aldol Cyclization Cascade for the Formation of α-Propargyl-β-hydroxyketones. *Org. Lett.* **2018**, *20*, 1380-1383.

(30) Jiang, Y.; Pan, J.; Yang, T.; Zhao, Y.; Koh, M. J., Nickel-catalyzed site- and stereoselective reductive alkylalkynylation of alkynes. *Chem* **2021**, *7*, 993-1005.

(31) Ma, X.; Xie, X.; Liu, L.; Xia, R.; Li, T.; Wang, H., Facile synthesis of pyrroloindoles via a rhodium(ii)-catalyzed annulation of 3-benzylidene-indolin-2-ones and α-imino carbenes. *Chem. Commun.* **2018**, *54*, 1595-1598.

(32) Liu, W.; Wang, H.; Li, C.-J., Metal-Free Markovnikov-Type Alkyne Hydration under Mild Conditions. *Org. Lett.* **2016**, *18*, 2184-2187.

(33) Gerbino, D. C.; Mandolesi, S. D.; Schmalz, H.-G.; Podestá, J. C., Introduction of Allyl and Prenyl Side-Chains into Aromatic Systems by Suzuki Cross-Coupling Reactions. *Eur. J. Org. Chem.* **2009**, *2009*, 3964-3972.

(34) (a) Wu, H.; Andres, R.; Wang, Q.; Zhu, J., Catalytic Enantioselective α-Ketol Rearrangement. *Angew. Chem. Int. Ed.* **2019**, *58*, 499-503; (b) Wang, Q.; Lübcke, M.; Biosca, M.; Hedberg, M.; Eriksson, L.; Himo, F.; Szabó, K. J., Enantioselective Construction of Tertiary Fluoride Stereocenters by Organocatalytic Fluorocyclization. *J. Am. Chem. Soc.* **2020**, *142*, 20048-20057.